Proceedings of 37th PLEA Conference,
26-28 June 2024 Wrocław, Poland

PLEA 2024: (RE)THINKING RESILIENCE

The book of proceedings

Editors: Barbara Widera, Marta Rudnicka-Bogusz,
Jakub Onyszkiewicz, Agata Woźniczka

PLEA 2024: (RE)THINKING RESILIENCE

Proceedings of 37th PLEA Conference, Sustainable Architecture and Urban Design

26-28 June 2024 Wrocław, Poland
Wrocław University of Science and Technology

Editors: Barbara Widera, Marta Rudnicka-Bogusz, Jakub Onyszkiewicz, Agata Woźniczka

Organised by: PLEA, Fundacja PLEA 2024 Conference

Honorary Patronage: Rector of Wrocław University of Science and Technology,
Prof. Arkadiusz Wójs, DSc, PhD, Eng.

Scientific Patronage: The Committee for Architecture and Town Planning of the Wrocław Branch
of the Polish Academy of Sciences

Wrocław University of Science and Technology Publishing House
Wybrzeże Wyspiańskiego 27, 50-370 Wrocław
http://www.oficyna.pwr.edu.pl
e-mail: oficwyd@pwr.edu.pl
zamawianie.ksiazek@pwr.edu.pl

ISBN 978-83-7493-275-2
https://doi.org/10.37190/PLEA_2024

Local Organizing Committee

Barbara Widera PhD HDr

PLEA 2024 DIRECTOR

Architect, researcher, expert for the European Commission and European Parliament

Research focus: bioclimatic design, nature-based solutions, underwater research and climate resilience

PLEA Associate
Associate Professor at Wrocław University of Science and Technology, Faculty of Architecture
Member of the Mission Board of EU Mission Adaptation to climate change
New European Bauhaus Preparatory Action Dimension Lead Expert

Jakub Onyszkiewicz PhD

PLEA 2024 SECRETARY

Licensed architect, researcher and academic teacher

Research focus: biomimetics in geometry and architecture, natural building materials in modern architecture, energy management and sustainability in building renovation and building information modelling (BIM)

Adjunct at Wrocław University of Science and Technology, Faculty of Architecture
Member of International Association of Shell and Spacial Structures (IASS)

Marta Rudnicka-Bogusz PhD

PLEA 2024 SECRETARY

Architect, researcher and academic teacher

Research focus: preservation of material heritage with complex parentage, cultural landscape as an outcome of overlapping patronages, sustainable cultural landscape

Adjunct at Wrocław University of Science and Technology, Faculty of Architecture
Member of INTBAU and European Architectural Envisioning Association

Aleksandra Marcinów PhD

PLEA 2024 SECRETARY

Architect, researcher, academic teacher, expert in the research of historical objects

Research focus: contemporary adaptations of historic buildings, especially residences, reconstructions of castles and palaces in Silesia in the 19th and early 20th centuries

Adjunct at Wrocław University of Science and Technology, Faculty of Architecture

International Advisory Board

Scientific Committee

Acknowledgements

Local Organising Committee acknowledges and very much appreciates the invaluable help and constant support of PLEA President Heide Schuster, PLEA v-ce President Joana Carla Soares Gonçalves, PLEA Board, International Advisory Board and Scientific Committee. We are extremely grateful for the Honorary Patronage of Rector of Wrocław University of Science and Technology, Prof. Arkadiusz Wójs, DSc, PhD, Eng. and for resulting help of WUST provided at each step of organisation of PLEA 2024. We truly value the Scientific Patronage of The Committee for Architecture and Town Planning of the Wroclaw Branch of the Polish Academy of Sciences.

We acknowledge the role of PLEA 2024 Partners, and Sponsors without whom the organisation of PLEA 2024 would be impossible. We want to express our thanks to our Strategic Partners: The Museum of Architecture and Państwowa Szkoła Muzyczna II stopnia im. Ryszarda Bukowskiego we Wrocławiu. The multidimensional support of the VELUX Group as the Main Industrial Partner of PLEA 2024 was critical for the successful organisation of the conference. Mercedes-Benz GRUPA WRÓBEL helped us to reduce the environmental impact from mobility, in line with our sustainability targets.

In honour of the late Jeffrey Cook, Society of Building Science Educators awards Jeffrey Cook Student Travel Scholarship to PLEA 2024 to support students presenting papers at the PLEA Conference. Funding for this opportunity has been generously provided by the Jeffrey Cook Charitable Trust.

The full list of Contributors, Media Partners and Parter Journals is provided on next pages. We are also truly grateful to all Students, PhD Candidates and young Researchers who assisted participants throughout the whole conference and who made this event vivid and unforgettable experience.

Strategic Partners

Museum of Architecture
in Wrocław

Państwowa Szkoła Muzyczna
II stopnia im. Ryszarda Bukowskiego

Sustainable Mobility Partner

Mercedes-Benz GRUPA WRÓBEL

Main Industrial Partner

VELUX Group

Media Partner

Akademickie Radio Luz

Student Workshop Partner

National Institute of Architecture
and Urban Planning

Partner Journals

Energy and Buildings |
Journal | ScienceDirect.com
by Elsevier

Buildings &Cities |
Community

Architectus | Journal |
architectus.pwr.edu.pl/en/

Table of Contents

3.2. Architecture for human resilience and well-being (including e.g., biophilic design, nature-based solutions, climate adaptation strategies for buildings and spaces)

3.5. Building resilience with innovation and technology (e.g., innovative materials and sustainable technologies)

(RE)THINKING RESILIENCE

Foreword

At the beginning of the third decade of the twenty-first century, the urgent need to counteract the negative effects of climate change has been one of the top priorities of international organizations worldwide. On 11 March 2024, the European Environment Agency published the European Climate Risk Assessment (EUCRA) [1], which provides the latest analysis of how climate change is affecting the planet. This document highlights that in the 12-month period between February 2023 and January 2024 the average global temperature exceeded pre-industrial levels by 1.5°C. Moreover, Europe became the fastest-warming continent in the world, and we already witness alarming phenomena resulting from climate change, which are increasing every year. Disturbances in precipitation patterns brought several catastrophic floods while Southern Europe is struggling with recurrent heatwaves resulting in fatalities. A long-term lack of rainfall causes droughts, leading to the desertification of some European regions [2]. Building resilience to climate change has become a necessity that applies largely to the built environment.

Reacting to the findings highlighted by the EUCRA and to the latest Copernicus reports, on 12 March 2024 the European Commission published a Communication on Managing Climate Risks [3], which sets out how the EU can effectively get ahead of the growing climate-related risks and build resilience to the impacts of climate change. The Communication emphasizes that the EU Mission on Adaptation to Climate Change serves as best practice for all interested parties, and it will be further leveraged to respond to Europe's climate risks. Moreover, it acknowledges the role of Research and Innovation to provide us with knowledge and solutions to the greatest challenges ahead. For this reason, the focus of PLEA 2024 is on the EU Missions addressing priorities of resilience that will determine the life standard of our children.

Understanding how, with knowledge and experience, we can support the development of innovations aimed at effectively managing climate risk is a necessary condition for improving living standards, combating inequalities, and protecting people. Growing environmental awareness is followed by concerns about the depletion of non-renewable resources and excessive GHG emissions. As the building industry is currently responsible for 40% of GHG emissions and similar level of energy consumption, the energy efficiency and CO_2 emissions from the buildings are perceived as important issues. This in turn leads to the enhanced research on more effective application of renewable energy in construction sector and the development of suitable practices of sustainable architectural and urban design. Strategies and methods of daylighting and improved thermal performance are studied with aim to provide optimal comfort and reduced energy consumption.

Renewable energy applications and minimisation of energy consumption are also recognized as solutions to energy poverty [4]. The topic of energy efficiency is analysed together with vernacular and bioclimatic strategies allowing to combine traditional knowledge with innovation and contemporary technology. Equally important to the proper design of the built environment are issues of inclusiveness as well as human resilience and well-being. In this edition of PLEA conference, we refer to the New European Bauhaus initiative, underpinning the importance of architectural education and the training of future leaders in this field.

There are several reasons why we decided to bring PLEA to central Europe. We strongly believe it is time to share responsibilities and spread PLEA mission which remain underestimated in Poland, Czechia, Slovakia, Ukraine, Hungary, and Baltic countries. This opens new prospects for discussion and mutual learning how we advance the building stock and set focus on users in buildings, indoor climate, health, air quality etc.

PLEA theme and vision always reflects the most up-to-date issues. The discussion about how resilient our buildings are, and how well they can support our health and well-being is vivid amongst professionals and stakeholders. Thus, the theme of PLEA 2024 is directly linked to the title of William E. Rees book *Thinking "Resilience"* to continue important changes that were initiated during previous PLEA conferences.

PLEA 2024 conference was held in four parallel series of sessions, identified by the names of the four EU Missions: *Mission Adaptation to climate change, Mission 100 Climate neutral and smart cities by 2030, Mission restore our ocean waters by 2030* and *Mission a Soil deal for Europe*. To further promote the goals of the EU Missions and disseminate knowledge about them, the rooms where the sessions took place were given the Mission names.

All contributions followed one of the proposed research tracks:

1. Sustainable Architecture and Urban Design – together for climate resilience
2. Architecture for human resilience and well-being (including e.g., biophilic design, nature-based solutions, climate adaptation strategies for buildings and spaces)
3. Analysis and methods for resilience and sustainability (e.g., new design and simulation tools, evaluation methods)
4. Re-thinking resilience through renovations and adaptations of buildings and spaces (including cultural and natural heritage retrofitting, methods to improve performance of existing buildings and spaces)
5. Building resilience with innovation and technology (e.g., innovative materials and sustainable technologies)
6. Together we can – think, learn, teach, and take the leadership (e.g., education and training, environmental activism).

These tracks defined the chapters in the proceedings.
In addition to the plenary and general sessions, the conference offered two Technical Sessions:

1. **The New European Bauhaus, Resilience and Architectural Education**
2. **Nature-based solutions and bio-based materials.**

The invitation to participate in the conference was accepted by the most outstanding researchers and professionals, who gave their keynote lectures: John Schellnhuber, Mat Santamouris, Ewa Maria Kuryłowicz, Klaus Loenhart and Joana Carla Soares Gonçalves, whose lecture opened the conference during informal event in the Museum of Architecture in Wrocław. Their keynotes inspired scientists participating in the conference together with their mentees - PhD students, Master students and young researchers, who are our hope for the development and continuation of the process of positive changes for the planet and climate.

The side events of PLEA 2024 included students design competition and workshop, project presentations and exhibition in the Museum of Architecture, Academia Europea roundtable "Science-Region" *EU Climate Neutral, Smart Cities and Adaptation to Climate Change*, as well as several other meetings and discussion panels.

We are deeply convinced that this year's conference has not only become a platform for discussion, exchange of knowledge, best practices, and peer learning, but also contributed to further positive transformation, of which PLEA is the leader and a role model. When organizing the conference, we have taken all the efforts to reduce any negative environmental impact by refraining from printing conference materials. We allocated the funds saved in this way to create the PLEA 2024 Biodiversity Garden in Wrocław. All information on the conference and proceedings has been available online. QR codes allowed downloading the conference program and speaker abstracts in real time. In order to reduce the environmental and economic costs of participation, we created a hybrid event and enabled online participation of speakers.

We sincerely hope that PLEA 2024 in Poland will become an inspiration for all participants and a milestone in the decarbonization of our country.

Barbara Widera

PLEA 2024 Director

PhD, HDr, Eng. Arch.

Associate Professor at Wroclaw University of Science and Technology, Faculty of Architecture

Member of the Mission Board of EU Mission on Adaptation to Climate Change

REFERENCES

[1] European Environment Agency (2024), *The European Climate Risk Assessment (EUCRA)*, EEA Report 01/2024.

[2] Ferreira, C.S., Seifollahi-Aghmiuni, S., Destouni, G., Ghajarnia, N., Kalantari, Z. (2022), *Soil degradation in the European Mediterranean region: Processes, status and consequences*, Science of The Total Environment, Vol. 805, 2022, 150106, https://doi.org/10.1016/j.scitotenv.2021.150106.

[3] European Commission (2024), *Communication from the Commission to the European Parliament, the Council, the European Economic and Social Committee and the Committee of the Regions: Managing climate risks - protecting people and prosperity*, Strasbourg, 12.3.2024.

[4] Santamouris, M. (2019), *Minimizing Energy Consumption, Energy Poverty and Global and Local Climate Change in the Built Environment: Innovating to Zero Casualties and Impacts in a Zero Concept World*, Elsevier, http://dx.doi.org/10.1016/C2016-0-01024-0.

Keynote Speakers

Hans Joachim „John" Schellnhuber

Prof. dr. dr. h. c. mult.

Hans Joachim Schellnhuber studied physics and mathematics and completed his doctorate at the University of Regensburg. After a postdoctoral position at the Institute for Theoretical Physics, Santa Barbara, he held professorships at the Universities of Oldenburg and Potsdam, as well as at the University of East Anglia, Norwich. In addition, he held numerous visiting professorships (e.g. Oxford University, University of California, Santa Cruz; Oxford University; and Santa Fe Institute).

As founding director of PIK, Schellnhuber led the institute from 1991 until 2018. From 2001 to 2005, he was also research director at the Tyndall Centre for Climate Change Research in Great Britain. As leading scientist, he was appointed various positions, such as Co-Chair of the German Advisory Council on Global Change (WBGU), Governing Board Chair of the Climate-KIC of the European Institute of Innovation and Technology (EIT) and Chair of the Standing Committee on Climate, Energy and Environment of the German National Academy of Sciences (Leopoldina). Schellnhuber has been a long-standing member of the Intergovernmental Panel on Climate Change (IPCC) which was awarded the Nobel Peace Prize in 2007. He served as Chief Government Advisor on climate and related issues during the German G8/EU twin presidency in 2007 and as scientific advisor to a number of eminent political and religious leaders, including the German Chancellor Angela Merkel, European Commission President José Manuel Barroso and Pope Francis. He is a member of numerous national and international panels addressing scientific strategies and sustainability issues. Since 2019, he has been intensively engaged in the creation of a „Bauhaus of the Earth".

Rebalancing the Weights of Civilization and Nature

Abstract

A recent paper (Elhacham et al. 2020) revealed that the mass of man-made materials now exceeds all living biomass on Earth. The built environment accounts for most of that disturbing imbalance, which epitomizes the Anthropocene era that started after World War II and generates unprecedented risks to humanity.

In particular, evidence from climate science indicates that anthropogenic global warming will transgress the Paris guardrails of 1.5°C and 2°C, respectively, in the next few decades. To limit the associated dangerous tipping dynamics like the irreversible melting of the Greenland Ice Sheet, greenhouse gas emissions from the global economy must be reduced to almost zero by 2050. Furthermore, *negative emissions* will be needed to re-establish the benign climate of the Holocene, which fostered the rise of our civilization. Nature-based approaches to large-scale CO_2-extraction from the atmosphere are being discussed in various publications. The most interesting option is the *forestry-construction pump*. It shall re-enhance living biomass on Earth and convert harvested biomass into long-lasting elements of the built environment.

This demineralization of settlements is a central goal of the New European Bauhaus (NEB), but the agenda of that initiative is broader: Cities and villages shall become resilient to extreme weather events, recreate spaces where people can meet and discuss freely, and provide beautiful and healthy environments for everyday living. The guiding principle for all this is the *re-entanglement of natural and anthropogenic systems* in shared spaces.

Mattheos Santamouris

Scientia Distinguished Professor of High-Performance Architecture at UNSW Sydney; former professor at the University of Athens, Greece; PhD on Energy Physics

Santamouris is the Anita Lawrence Professor of High Performance Architecture in the University of New South Wales in Australia. He is a past professor at the University of Athens, Greece and visiting Professor at the Cyprus Institute, Metropolitan University of London, Tokyo Polytechnic University, Bolzano University, Brunnel University and National University of Singapore. Past President of the National Center of Renewable and Energy Savings of Greece.

Editor in Chief of the Energy and Buildings, Past Editor in Chief of the Journal of Advances Building Energy Research, Associate Editor of the Solar Energy Journal and actual or past Member of the Editorial Board of the International Journal of Solar Energy, Journal of Buildings and Environment, Journal of Sustainable Energy, Journal of Low Carbon Technologies, Journal of Open Construction and Building Technology, Sustainable Cities and Society and of the Journal of Ventilation. Editor of the Series of Book on Buildings, Energy and Solar Technologies published by Earthscan Science Publishers in London.

Editor and author of 15 international books on topics related to heat island, solar energy and energy conservation in buildings published by Earthscan, Springer, etc. Guest editor of twelve special issues of various scientific journals. Scientific coordinator of many international research programs and author of almost 290 scientific papers published in peer reviewed international scientific journals. Reviewer of research projects in 15 countries including USA, UK, France, Germany, Canada, Sweden, etc. Expert in various International Research Institutions. Highly Cited researcher according to Clarivate in 2017 and 2018.

Awards

Grand Award, Professional Green Building Council, PGBC, 2006, Hong Kong IA Research Award, 2006, National Energy Globe Award 2006, Sustainable Energy Europe Award 2007, Best and Outstanding Paper Award published in Solar Energy Journal during 2005-2006, Nominated for The Sir Robert McAlpine International Book Award', London, 1997, National Award for Environ-

mental Research, ECOCITY 2008, PROSE Award 2012, Reference Work: Best Multivolume Reference/ Science, by the American Association of Publishers, 2013, European Award on Energy Efficient Buildings, European Competition, 2014, ECOCITY Award for Best Scientific Study on Environment, 2015

Member of international research committees

Member of the following International Research and Development Committees:
Advisory Group of the European Union on Energy, Advisory Group of the European Union on Science for the Society, National Committee preparing the Greek Mitigation and Adaptation Plan to Climate Change , Working Committee of the European Community on the „Energy Efficiency and Indoor Environment", European Commission, JRC Ispra, National Representative to the European Standing Committee : „Indoor Air Quality and Its Impact on Man", European Commission, JRC Ispra, European Thematic Network on Energy Efficiency and Indoor Air Quality, of the European Commission, (JRC Ispra), Environmental Committee of the European Network Building Research Institutes, ENBRI, European Working Committee on 'Critical Review of Ventilation Requirements', JRC Ispra, European Commission, European Working Committee on 'Economic Implications of Inappropriate Indoor Air Quality', JRC Ispra, European Commission, Coordinator of the EEC Task on Research Indicators for the Sector of the Built Environment

Expert to international and national scientific bodies

Former Vice President of the Air Infiltration and Ventilation Center, International Energy Agency, United Nations, 2007.Vice President of the World Society of Sustainable Energy Technologies, 2008, Invited Research Expert to the Chinese University and to the Government of Hong Kong on Urban and Built Environment, Invited Theme Editor of the UNESCO – EOLLS Encyclopaedia on Natural Sciences, Invited Expert by the International Solar Energy Society Group to prepare the State of the Art on 'Solar Energy in Buildings' Invited Associate to the PLEA, (Passive and Low Energy Architecture), Organisation, Invited Member of the National Committee to prepare the Building Energy Program, Greece, Invited Expert of the World Health Organisation on Heat Protection, 2006, Invited Member of the Scientific Committee του Canadian Solar Buildings Research Network, Canada, 2006, Invitation to the Konwakai meeting of experts of Daikin Co, JAPAN, 2008-2015.

Recent Developments On Urban Overheating And Heat Mitigation Technologies

Abstract

Overheating of the Built Environment is the most documented phenomenon of climate change impacting the human life in many ways. There are more than 13,000 cities exhibiting serious problems of higher urban temperatures in the world. The magnitude of overheating depends strongly on the local climatic and local landscape conditions. Studies have shown that the average magnitude of the intensity of urban overheating in Asian and Australian cities is close to 4.1°C, while the corresponding value for 110 European cities is close 6°C. Actually, the magnitude of the urban overheating may be as high as 11°C in some cities, and it gets its maximum during anticyclonic weather conditions while the landscape, land use and the morphological and construction characteristics of cities influence highly the magnitude of overheating.

This lecture will present the most recent developments on the magnitude and the characteristics of the urban overheating and the potential synergies with the global climatic change. It will analyse the latest qualitative and quantitative data on the impact of higher urban temperatures on the building's energy supply and demand, heat related mortality, morbidity and well-being, human productivity, survivability of low-income population and environmental quality of cities. The impact of the actual urban overheating as well as of the expected future increase of the urban temperature, on the energy consumption of buildings and their environmental quality is quantified and analysed. The challenges around the dramatic increase of the cooling energy demand in the developing countries and the corresponding impact on environment and economy are presented in detail. Proper adaptation techniques aiming to respond to the overheating challenge, decrease the energy consumption of buildings, improve environmental quality and produce added value to the local economies are analysed. The combined impact of advanced adaptation and mitigation technologies is depicted.

It will present and describe the state of the art on the development of innovative mitigation materials, advanced urban greenery, heat dissipation and evaporative techniques, as the main mitigation and adaptation technologies to offset the impact of urban overheating Recently developed, efficient heat mitigation technologies implemented in large scale urban projects, able to decrease the peak ambient temperature of cities up to 5°C, will be presented. The monitored energy and environmental performance of innovative heat mitigation technologies like super cool materials for buildings and urban structures, thermally adapted greenery combined with anthropogenic heat

reduction techniques and soil humidity boosting technologies, are presented. Results from large scale urban heat mitigation projects show that implementation of the innovative mitigation technologies can reduce the cooling energy consumption of buildings up to 40 %, decrease the concentration of harmful pollutants up to 50 %, reduce heat related mortality up to 35 % and improve the survivability levels of vulnerable urban population considerably. Finally, it will present the main future challenges related to urban overheating and proposes a specific research agenda to alleviate and counterbalance its impact on human life.

Joana Carla Soares Gonçalves

Architect & urbanist, MSc., PhD

Joana´s interests in environmental design has led her to the involvement with research, teaching and practice focusing on the applicability of technical knowledge and design methods in creative architectural and urban design solutions, for various geo-political and socioeconomic contexts and environmentally-related challenges.

Joana Carla Soares Gonçalves is an Architect and Urbanist graduated from the Faculty of Architecture and Urbanism of the Federal University of Rio de Janeiro (UFRJ) in 1993. As a young practicing architect, she worked in Oscar Niemeyer´s office, in Rio de Janeiro. In 1996 she was awarded her master's degree in Environment and Energy from the AA Graduate School in London and in 2003 she earned her PhD degree from FAUUSP.

Currently, Joana is a Course Master at the Master in Sustainable Environmental Design, at the Architectural Association School of Architecture in London and the Course Tutor at the AA Environmental Technical Studies. In London, she also contributes to the Bartlett School of Architecture (BSc in Architecture) and is a visiting Associate Professor at the School of Architecture in Central Saint Martins, where she teaches environmental design disciplines.

Joana Gonçalves was an Associate Professor of Environmental Design at the Faculty of Architecture and Urbanism at the University of São Paulo (FAUUSP), where she taught between 1998 and 2019 and was the Head of the Technology Department between 2015 and 2019 and where she still contributes to the graduate programme of Architecture and Urbanism. In 2011 she was a guest lecturer at the Graduate School of Design (GSD) in Harvard University.

She is the author of a number publications including the book The Environmental Performance of Tall Buildings (2010) with Earthscan; Joana was one of the coordinators of the Buildings' chapter in the UNEP Green Economy Report (2011). She contributed to various technical publications, including Buildings for Extreme Environments: Tropical (2017), organized by CIBSE-UK.

She is also the author of more than 50 scientific articles and is currently working the book The Environmental Architecture of Brazilian Modernism: Culture, History and Performance in São Paulo, to be published by Routledge in 2024. In environmental and sustainability consultancy, one of the recent and prominent projects is the Methodology for Retrofit of Social Housing in Brazil, for the Brazilian Ministry of Housing (2021); among others dealing with offices and residential buildings, as well as urban design.

In January 2022, Joana was made Vice-President of the PLEA international network – Passive and Low Energy Architecture.

Sustainable Cities – South meets Central' on issues of sustainable urban development and renovation of cities in Latin America and Europe

Abstract

The peripheral urban sprawl and verticalization of more central neighbourhoods in Latin American cities is a well-known wide-spread urban phenomena that started in the last decades of the 20th century, in response to socioeconomic and market pressures in cities of growing economies, with various impacts on the quality of the built environment. In spite of the arguments that justify taller buildings and urban density as means for urban regeneration, the densification through verticalization is a complex process of urban transformation, which has often created places of poor urban and environmental quality, often coupled with energy demand and, or health issues. The compromise of urban quality due to verticalization is commonly seeing in cities of emerging economies, such as São Paulo, where planning rules and urban growth are strongly influenced by market forces, with little control by the local authorities. Since the early 2000s, a number of Latin American cities are revising their Urban Development Plans, including the parameters related to built density and the ground conditions at pedestrian level. This talk starts with the presentation of a series of technical studies that investigated the relationship between urban form and buildings environmental response in different climatic contexts, putting side by side Latin America and European cases, including São Paulo, London and Barcelona. Such studies are used as tools to critically review current urban policies. In the sequence, on the second part of talk, the attention is moved to the space between buildings, particularly the public space. Design strategies, urban policies and real-life initiatives to improve and guarantee the quality of the pedestrian realm in the city of São Paulo, in Brazil, and Ponte Vedra, in Spain, are discussed and compared. As an outcome, strategic planning and design measures are established based on the inter-relationships between walkability, socioeconomic factors, pedestrian comfort and behaviour, in urban spaces of different built densities. Clearly, the vast range of research work on topics related to the environmental quality of the built environment in general, found in the decades of publications of the PLEA Conferences, for example, is an indication that the specific knowledge to improve the environmental quality of our cities already exists, as well as the design and technological resources to reduce energy demand in buildings. However, the embodiment of such knowledge in the several processes that make the built environment is part of a design and planning culture that has yet to be established in most cities around the world. In this respect, the talk concludes with the proposition of some methodological and conceptual design ideas and proposals that can contribute to this operational change.

Klaus K. Loenhart

Univ.-Prof. Dipl.-Ing. Architect, MLA Landscape Architecture Harvard GSD, MDesS History & Theory Harvard GSD

Klaus Klaas Loenhart is passionate eco-innovator, founder of terrain: integral designs, terrain.cloud and Professor at ia&l Landlab TU Graz, Austria. As a multi-disciplinarian, he and his teams are envisioning nature-inspired and impact-focused design solutions for reconnecting urban society with our living world.

Klaus considers urban agglomerations to be a living biome. His systemic and passionate mission for an integral and eco-based societal practice was established during his multidisciplinary studies at the Munich University of Applied Sciences and at the Harvard Graduate School of Design in Cambridge, Massachusetts.

Current projects of his studio terrain: integral designs envision living systems of people, space and ecosystem performance, that aim for transformative co-creation between ecological agents and human endeavours to inform the fields of human health, biodiversity, and social urban practices in times of changing climates.

As proof of the concept 'imagining cities that grow air,' he and his team.breathe.austria implemented the Austrian Pavilion at the 2015 EXPO World Fair in Milan—a natural/techno-logical hybrid, whose ecological and atmospheric performance takes centre stage—and were recently awarded the UNESCO City of Design Award – Grand Award.

DASEIN IS CO-DESIGN
Discovering the Collective Agencies of Nature-Based Solutions for Societal Change

Abstract

As this conference calls for a "(re)thinking together" to become an instrument for change, there is nothing better than to invite Nature into the conversation. Plants, animals, matter, and diverse natural phenomena such as air and atmosphere, now claim a seat in the planetary parliament, fostering a new sense of togetherness. The meeting venue itself evolves, shifting from exclusive, extraction-driven boardrooms to a nature-based entangling setting across many sectors.

How such a parliament of nature-based thinking and acting should be organized will not remain a theoretical question. The acknowledgment of the magnitude and severity of the current planetary condition compels us to fundamentally reassess not only the extent of the systemic transformations required in our built environment but also in society at large.

Amidst this challenge, nature-based solutions emerge as a formidable yet underutilized ally in design. The quest for nature-entangled planetary transformations then comes with immense potential: In enabling us to rediscover Nature in architecture, landscape architecture and urban design as a most impactful transformative agency for societal creativity, invention and governance.

Ewa Maria Kuryłowicz

Architect PhD Hdr Professor

General Designer, V-ce President at the Architectural Studio APA Kuryłowicz & Associates. Chairperson of Stefan Kuryłowicz Foundation Council, member of Scientific Award Chapter of POLITYKA, member of Architecture and Urban Planning Committee of Polish Academy of Sciences, member of the National Accessibility Council at the Ministry of the Economy.

Graduate of the Faculty of Architecture, Warsaw University of Technology and Faculty of Architecture Iowa State University, Ames Iowa, USA, visiting professor at the University of Detroit Mercy, USA.

From 2000 to 2008 Director of the Working Programme „Spiritual Places" of the International Union of Architects UIA, based in Paris. President of numerous national and international competitions juries, including SARP jury.

Author of multiple publications (book and journal articles). Co-author, together with the Kuryłowicz & Associates design teams, of many projects (completed and under construction): Building of the Faculty of Modern Languages and Applied Linguistics at the University of Warsaw (2022); Research Station of the Polish Academy of Sciences on the King George Island, Antarctica (completion deadline: 2024), public utility buildings, office buildings, housing estates, single-family houses, industrial infrastructure facilities, etc. Winner of many national and international architectural competitions (with the teams of APA Kuryłowicz & Associates www.apaka.com.pl).

Laureate of numerous prestigious awards, including:
Accessibility Leader competition for lifetime achievement (2022), Honorary Award of SARP (2021), Special Award for lifetime achievement in the field of architecture of the PTPW portal (2018), Gold Badge of SARP (2017), *Bene Merentibus* medal of SARP (2014), Polish HERKULES medal (2012), Silver Cross of Merit of the President of the Republic of Poland (2008), Medal „Friend of Children's Health Centre (2007), Medal Friend of Integration (2002).

Resilience as a climate adaptation strategy.
What can we learn from extreme conditions?

Abstract

As humankind, we have now reached the difficult moment of recognising the inevitability of change in our relationship with nature. There is a need for hope and concrete, grassroots initiatives. This is achievable by adopting a strategy of resilience, which helps transform challenges into opportunities. New types of buildings, designed using this strategy, with a genuine rather than declarative respect for nature, demonstrate that authentic sustainable solutions generate a unique alphabet of architectural forms and that deficits can be turned into potential. One example of such a building is the new pavilion of the Arctowski Polish Antarctic Station, currently under construction (general designer: Kuryłowicz & Associates). The design and layout of this facility are influenced by several factors, including climatic conditions (such as water, snow, wind, and temperature), logistical requirements for the construction and operation of the building, and the mental well-being of polar explorers. Solutions developed for extreme conditions can often be useful in less demanding situations. Adaptation to climate change can be informed by lessons learned from projects implemented in extremely cold conditions, as demonstrated in the case described. It is important to closely examine these experiences as more of them become available over time. This approach will undoubtedly benefit both our planet and its population.

3. PROCEEDINGS

3.1 Sustainable Architecture and Urban Design – together for climate resilience

How Climate Resilient Are Cities in Central Europe?

Leipzig as Case Study for Assessing Climate Comfort in 2022 and 2050 in Neighbourhoods with Different Urban Characteristics

MONICA ROSSI-SCHWARZENBECK[1] FABIAN GÖRGEN[1,2,] PHILIPP MAGIN[1]

[1]Leipzig University of Applied Sciences, Leipzig, Germany
[2]Brandenburg University of Technology, Cottbus, Germany

ABSTRACT: Urban climate change, resulting in rising temperatures, an increase in tropical nights and heat islands, is also becoming a problem in Central Europe. The negative effects of this phenomenon, which are currently visible in isolated periods, will surely increase in duration and intensity in the upcoming decades. In order to reverse this trend, this research, starting from the analysis of current conditions, aims to predict future scenarios and develop efficient climate mitigation strategies in the medium-long-term future for middle European cities. To achieve this goal, three neighbourhoods in Leipzig, Germany, with very different characteristics were taken as case studies and their comfort level in 2022 as well as in 2050 (with morphed climate data) was simulated with the software EnviMET. The model was validated using in-situ measurements from three weather stations located in each of the areas. The aim of this work is to create, based on the simulation results, knowledge of the microclimate in central European neighbourhoods. By investigating different urban environments in the present as well as in the medium-term future, adequate and efficient climate mitigation strategies as well as design and construction practices in order to counter urban overheating can be developed in an early planning phase.
KEYWORDS: Urban climate change, Heat island, validation of simulation, PET, mitigation strategies.

1. INTRODUCTION

Global climate change in recent decades is resulting in increasingly frequent extreme heat events. Particularly in cities characterized by a growing number of inhabitants and high densification, negative effects of climate warming are most evident. Apart from increase of urban densities, several other issues influence the magnitude of urban climate change and heat islands. These include factors as actual design and construction practices using concrete, asphalt or other highly absorbing materials, as well as changing inhabitants' lifestyles like an increased use of air conditioners and using private cars instead of public transportation [1-2].

As extreme events, such as tropical nights (defined from days when daily minimum temperature remains above 20 °C [3]), become more frequent, a trend which is expected to continue growing over the next 30 years, even central European cities that previously did not experience such events are now affected. For this reason, many cities in Europe, including those in central and north Europe, are carrying out studies to monitor current and predict future outdoor microclimate conditions in their urban areas in order to highlight problems and develop climate mitigation strategies.

This paper aims to analyse present (year 2022) and future (year 2050) microclimatic conditions of three study areas that characterize the urban structure of the city of Leipzig, Germany in order to identify criticalities and propose appropriate microclimatic mitigation strategies. In particular, the level of outdoor comfort and temperature curve during day and night is assessed in order to identify criticalities and propose appropriate microclimatic mitigation strategies and consequently suitable design and construction practices.

1.1 Study areas

Leipzig (N 51.341, E 12.375) is a city in Saxony, formerly East Germany, with a rapidly growing population (625.000 inhabitants as of 2022) characterized by an inhomogeneous urban structure. The Office for Environmental Protection, City Planning Office of the City of Leipzig, Germany, carried out in 2021 a study analysing the climate change that has taken place in its territory since 1900. Furthermore, based on two-dimensional simulation models, the study of the City of Leipzig analysed two different possible climate scenarios in its entire municipality up to 2100 [4].

The research presented in this paper, building on the analyses carried out by the city of Leipzig, aims to analyse in more detail, particularly problematic areas of the city. To achieve this goal, three main types of neighbourhoods have been identified: 1. dense and historic city centre, 2. expansion area with typical

large inner courtyards and 3. “Plattenbau” housing settlement with oversized buildings in large green areas. Three areas representing these three typologies have been chosen as study areas (figure 1).

Figure 1: Study areas: downtown (1), Lindenau (2) and Grünau (3)

The first area is the down town of Leipzig, a compact neighbourhood largely rebuilt after World War II. It includes the inner city, the surrounding ring road and adjacent neighbourhoods. While the core of the area features mostly sealed surfaces, in particular the large market square, the areas close to the ring road include vegetation and trees. The building constructions differ from historic lime stone buildings to modern glass facades. Alleyways are mostly narrow. Area 1 has a total size of 1540 m x 1690 m.

The second area is Leipzig-Lindenau, a district west of the inner city consisting of residential buildings with typical multi-story buildings, positioned to form a rectangular with a large greened or in some cases partially paved courtyards. Area 2 has a total size of 1100 m x 995 m.

The third area is Leipzig-Grünau, also west of the city centre and one of the symbolic neighbourhoods of post-war reconstruction characterized by very high multi-story residential building built using the “Plattenbauten” construction technique, surrounded by green recreational areas. Area 3 has a total size of 1510 m x 1135 m.

2. METHODOLOGY

The study is structured according to the following phases:

1) Development of one CFD Model for each area, using microclimate simulation tool ENVI-met [5].
2) Calibration of the models using in-situ measurements from three weather stations located in each of the areas, the simulated air temperatures and relative humidity were validated.
3) Simulation of microclimate condition of the three models in a summer representative day in 2022 and in 2050 as a future scenario, using weather data morphed with the Climate Change World Weather File Generator [6].
4) Validation of the simulation results through a comparison with corresponding measured values.
5) Evaluation of simulation results, particularly of environmental comfort level, and development of short- and medium-term climate mitigation strategies.

2.1 CFD model development

ENVI-met (Version 5.1.1) was used to create models corresponding to the three study areas. The grid size for all models was 5 m x 5 m x 5 m and the grid dimensions were 308 x 338 x 20 (Area 1), 231 x 209 x 20 (Area 2) and 302 x 227 x 20 (Area 3).

Figure 2: ENVI-met model of Area 1 (Leipzig-City)

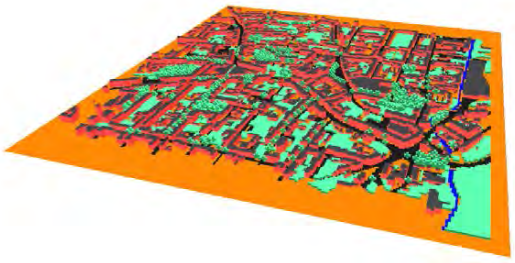

Figure 3: ENVI-met model of Area 2 (Leipzig-Lindenau)

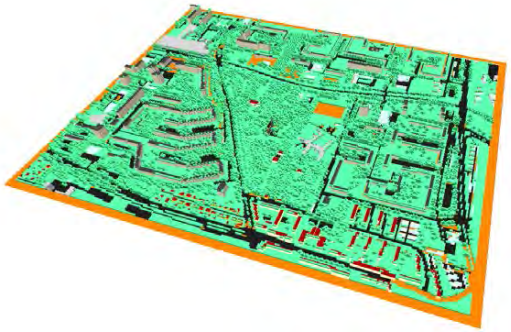

Figure 4: ENVI-met model of Area 3 (Leipzig-Grünau)

The building materials used in the model were brick (yellow), insulated brick (red), glass (transparent) and insulated concrete (grey). For the roofing, red and black tiles as well as flat roofs were

used. The ground surfaces were asphalt road (black), dark granit pavement (grey) and loamy soil (orange). For the vegetation grass (height: 0.15 m, average density) and little leaf limes (middle) were used.

2.2 Calibration process

For the validation of the models, the Root Mean Square Error (RMSE) and the coefficient of determination (R^2) was used (see equations (1) and (2)). Hourly simulated air temperature and relative humidity values were compared to corresponding hourly measured values obtained from local weather stations situated within each study area.

$$RMSE = ((\Sigma (m_i - s_i)^2) / n)^{0.5} \quad (1)$$

where *RMSE* - Root Mean Square Error (-);
m_i - measured value at time step i (-);
s_i - simulated value at time step i (-);
n - total number of time steps (-).

$$R^2 = 1 - (\Sigma (m_i - s_i)^2/(m_i - m)^2) \quad (2)$$

where R^2 - Coefficient of determination (-);
m_i - measured value at time step i (-);
s_i - simulated value at time step i (-);
m - mean value of the measurements (-).

2.3 Simulation: model applications

Following validation, the model application involves microclimate simulations for a base case scenario (2022), and a future scenario (2050). All simulations were executed on a representative and critical summer day, specifically the 21st of June Summer solstice, the day with the greatest hours of sunshine in the year 2022. ENVI-met Full Forcing was employed for these simulations.

2.3.1 Base Case (2022)

The Base Case Scenario used the three initial models to simulate the urban microclimate in each respective area. For Area 1, the input weather data was sourced from a weather station situated in Area 2. Similarly, the input weather data for Areas 2 and 3 originated from an inner city weather station located in Area 1. Subsequently, two .epw files were generated for use in ENVI-met Full Forcing. The evaluation primarily centres on the Physiological Equivalent Temperature (PET), encompassing various parameters such as air temperature, humidity, wind, and radiation to quantify outdoor thermal comfort.

2.3.2 Future Scenario (2050)

The Future Scenario used the same ENVI-met model as the Base Case Scenario with the distinction that the input weather data files were morphed to reflect future weather conditions. The morphing was conducted using the Climate Change World Weather File Generator introduced by Jentsch et al. [9]. Both .epw files underwent morphing, focusing exclusively on air temperature and relative humidity, given uncertainties in predicting changes in wind speeds and radiation for 2050. The evaluation also focused primarily on PET levels in the study areas. The exact ranges defined for the PET can be seen in table 1.

Table 1: Physiological Equivalent Temperature (PET) ranges

PET (°C)	Thermal perception	Grade of physiological stress
< 4.1	Very cold	Extreme cold stress
4.1 – 8.0	Cold	Strong cold stress
8.1 – 13.0	Cool	Moderate cold stress
13.1 – 18.0	Slightly cool	Slight cold stress
18.1 – 23.0	Comfortable	No thermal stress
23.1 – 29.0	Slightly warm	Slight heat stress
29.1 – 35.0	Warm	Moderate heat stress
35.1 – 41.0	Hot	Strong heat stress
> 41.0	Very hot	Extreme heat stress

4. RESULTS

The results include the comprehensive validation process, the assessment of both the base case and future scenarios, and a comparative analysis, emphasizing specific locations experiencing severe heat stress. This comparison serves as a foundation for devising future mitigation strategies.

4.1 Validation

The validation process involved calculating the Root Mean Square Error (RMSE) and coefficient of determination (R^2) through a comparison of hourly simulated values of air temperature and relative humidity with corresponding measured values. The results indicate a strong correlation between simulated and measured values, instilling confidence in the model's ability to reliably simulate microclimatic parameters. Consistent with previous research on the validation of ENVI-met models [6-7], the calculated error values presented in Table 2 align with the required standards, affirming the trustworthiness of the model.

Table 2: RMSE and R^2 values for all areas

	Area 1		Area 2		Area 3	
	T_a	RH	T_a	RH	T_a	RH
RMSE	1.29	5.24	1.28	5.09	1.31	5.67
R^2	0.92	0.90	0.92	0.91	0.91	0.87

4.2 Base case microclimate evaluation (2022)

Upon successful validation of the model, the Base Case Scenario concentrated on the climatic evaluation of all three study areas. The objective was to identify heat islands and quantify outdoor thermal comfort using the Physiological Equivalent Temperature.

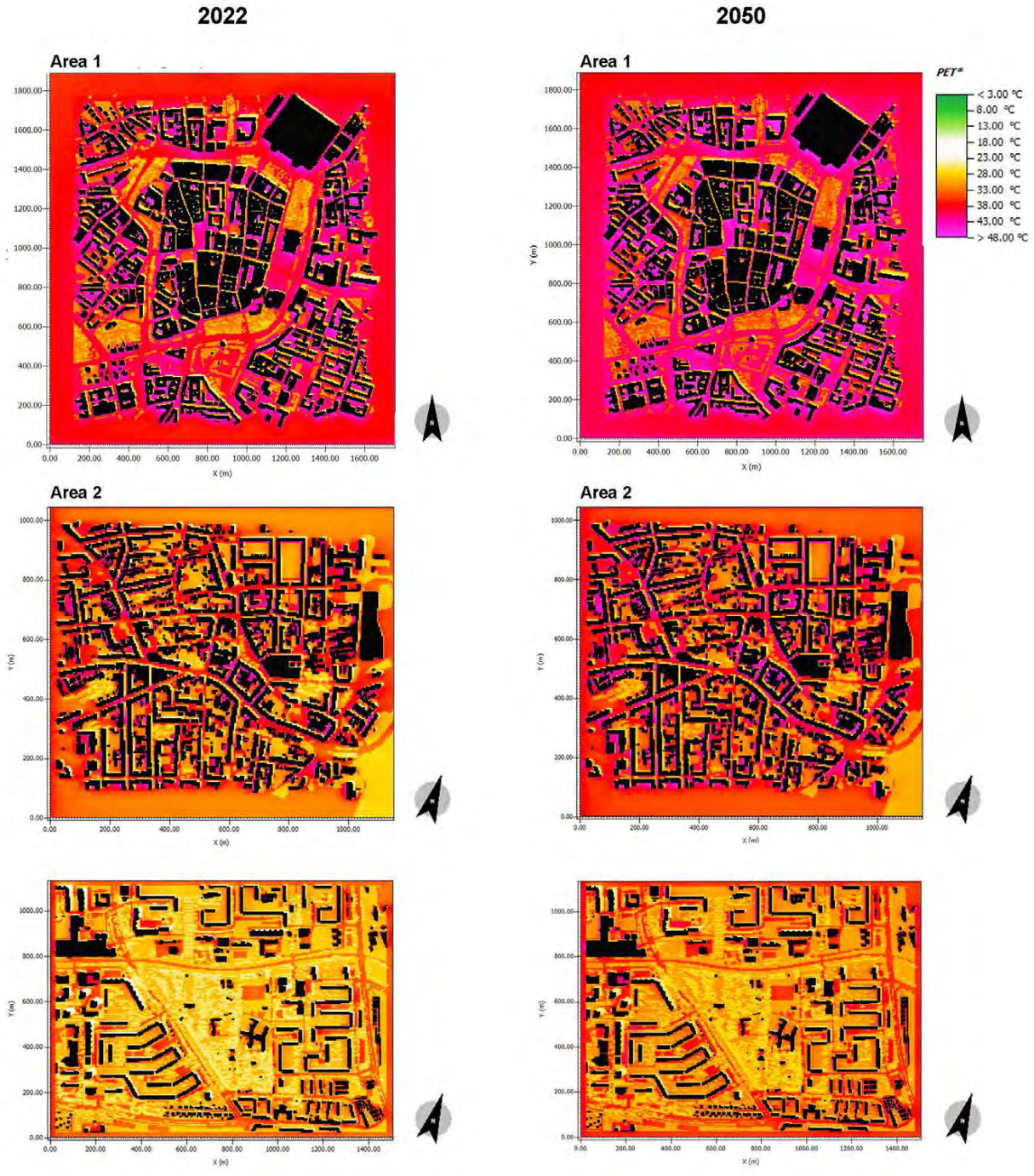

Figure 5: PET levels for area 1,2 and 3 on 21.02.2022 02:00 p.m. and on 21.02.2050 02:00 p.m. at a height of 2.5 m above the ground.

Figure 5 illustrates the results of the simulation, in particular the level of outdoor comfort expressed as Physiological Equivalent Temperature (PET) on 2022 and on 2050 on 21.02.2022 at 02:00 p.m. at a height of 2.5 m above the ground.

Starting with Area 1 on 2022, the findings reveal cause for concern, with maximum PET levels reaching 57.68 °C and minimum levels as low as 23.57 °C. Referring to Table 1, every grid in the investigated area experiences at least slight heat stress. Green spaces exhibit PET levels between 29 °C and 33 °C, indicating moderate heat stress, while the impact of shading from both trees and buildings offers the most comfortable zones in Area 1, with PET levels between 23.57 °C and 29 °C, indicating slight heat stress. Narrow alleys, particularly those with a maximum width of 10m, provide comfortable zones. Wider alleys, however, allow incoming solar radiation, heating up ground surfaces and resulting in elevated PET levels. The most uncomfortable areas are open squares with sealed surfaces, such as the market square in the centre of the study area, or vegetation-

free courtyards where the distribution of hot and humid air is impeded.

In the Area 2 on 2022 the maximum observed PET was very high ($PET_{max,area2}$ = 56.65 °C), signifying extreme heat stress. Only a few locations in Leipzig-Lindenau exhibited PET levels lower than 23°C, indicating no thermal stress. These areas were predominantly situated north of buildings in shaded zones and in close proximity to vegetation. Despite the challenging results, the area appears to be more comfortable than the inner city, primarily attributed to the presence of green infrastructure in this residential district. Courtyards, which posed significant issues in area 1, exhibit lower PET levels when adorned with green spaces and trees. In area 2, streets adjacent to many buildings emerge as the primary concern, as they lack shading from buildings and have the capacity to accumulate substantial heat.

Area 3 on 2022 emerges as the most comfortable among those investigated. The maximum PET, although still indicative of extreme heat stress, is recorded at 46.53 °C, however, limited to a few specific locations. Conversely, a considerable number of spots exhibit PET levels below 23 °C, indicating no thermal stress. Several factors contribute to this comfort. The tall buildings provide shading, and the less dense construction allows for semi-open courtyards that facilitate ventilation, preventing the formation of local heat islands. Notably, Leipzig-Grünau is characterized by abundant greenery, evident in the PET heat map where substantially lower PET levels are observed in the vegetated areas.

4.3 Future microclimate evaluation (2050)

The results of the Future Scenario reveal significant increases in both Physiological Equivalent Temperature (PET) and air temperature across all three study areas.

PET levels for Area 1 in 2050 depict a noteworthy change. Although the maximum PET only slightly increased by +0.2 K compared to the 2022 scenario, the minimum PET experienced a substantial rise of 1.39 K. Notably, considering that in 2022 no spot was thermally comfortable, the current situation has considerably deteriorated. With a minimum PET of 24.96 K across the entire study area, there is no location exhibiting minimal thermal stress. The maximum change in PET reached +5.62K. Furthermore, the findings suggest that the increases in PET are more pronounced in open spaces and less significant in shaded areas such as narrow alleyways.

The maximum PET for area 2 in 2050 increased to 57.41 °C (+0.76 K), while the minimum PET rose to 24.19 °C (+1.86 K), extinguishing the last comfortable spots that were under 23 °C PET in the 2022 scenario. This escalation leaves no zones without thermal stress according to PET. The maximum change in PET was simulated to be 6.49K, indicating a substantial shift in thermal conditions within this area. This emphasizes the urgency of proactive measures to address the heightened thermal stress in the future scenario.

The maximum PET for area 3 in 2050 has increased to 47.99 °C (+1.46 K), while the minimum PET has risen to 23.66 °C (+2.10 K), eliminating the previously existing comfortable zones that registered under 23 °C PET in the 2022 scenario. Consequently, no areas remain without thermal stress according to PET. The maximum change in PET was simulated to be 2.61 K, underscoring the considerable alteration in thermal conditions within this area. These findings accentuate the imperative need for strategic interventions to address the escalating thermal stress anticipated in the future scenario.

4.4 Local outdoor comfort comparison

To examine the thermal behaviour of specific locations within the study areas throughout a 24-hour period, three critical spots experiencing severe heat stress in Area 1, identified as the most uncomfortable area, were analysed. These spots include a narrow alley in the north-west of the city core (A), the main square in the centre (M), and a courtyard in the south-east of the city core (C). Figure 11 illustrates the variation in air temperature and Physiological Equivalent Temperature (PET) between the two scenarios over the course of 24 hours.

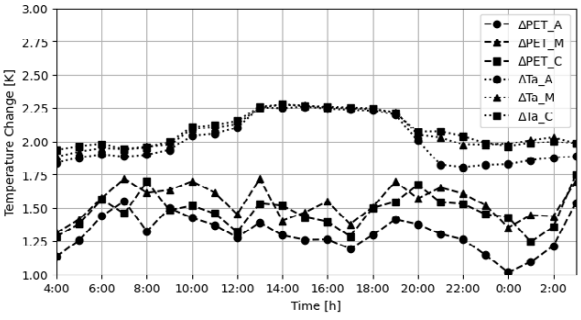

Figure 11: ΔPET and ΔT_a for key locations A,M and C

The results reveal that the maximum change in Physiological Equivalent Temperature (PET) at the three key locations was +1.75 K when comparing the 2022 scenario to the 2050 scenario. The increases remain relatively stable throughout the day, ranging between +1.02 to +1.55 K (A), +1.31 to +1.72 K (M), and +1.25 to +1.75 K (C). This indicates a notable overall increase, yet the comfort levels do not fluctuate significantly between day and night. Examining the change in air temperature, the maximum variation observed was +2.28 K. Similar to PET, the increases remain stable throughout the day, ranging from +1.81 to +2.26 K (A), +1.89 to +2.28 K (M), and +1.94 to +2.28 K (C). Notably, despite the relatively moderate increase during the night, the

temperature exceeds 20 °C. Although not reaching tropical night conditions ($T_a \geq 20$ °C) due to morning temperature drops, these findings raise concerns about the potential for tropical nights in the future. The local outdoor comfort comparison indicates a worsening situation in the future scenario, particularly in vulnerable locations, emphasizing the need for active mitigation strategies in these areas.

5. CONCLUSION

This study focused on the validation of a numerical model to assess and analyse the urban microclimate in various urban settings within the city of Leipzig. The model demonstrated effective validation with favourable RMSE values ranging from 1.28 to 1.31 for air temperature and 5.09 to 5.67 for relative humidity across all three study areas. Additionally, the coefficient of determination showed a strong correlation, with values ranging from 0.91 to 0.92 for air temperature and 0.87 to 0.91 for relative humidity. Subsequently, the validated models were used to evaluate the urban climate in two scenarios, revealing severe heat stress in all areas, quantified using Physiological Equivalent Temperature (PET).

Area 1 exhibited extreme heat stress with PET levels reaching up to 57.68 °C. Local heat islands were primarily observed in large open squares with sealed surfaces and courtyards lacking greenery. Narrow streets, however, served as relatively comfortable zones. Area 2 displayed maximum PET levels of 56.65 °C, displaying the positive impact of greening in residential areas. The green courtyard in this region contrasted with ungreened courtyards in area 1, which proved problematic. Despite being the most comfortable area investigated, area 3 still experienced maximum PET levels of up to 46.53 °C. The tall buildings in this zone provided shade, and semi-open courtyards facilitated ventilation, creating cooler zones within the built environment. However, all three areas exhibited overheating, with PET levels dropping only slightly during midday, and very few locations remaining under 23 °C (no thermal stress).

Evaluation of the future scenario indicated significant increases in PET, with up to 5.62 K (Area 1), 6.49 K (Area 2), and 2.61 K (Area 3). Notably, Leipzig-Grünau (Area 3) emerged as the most resilient area, characterized by tall buildings offering shade, abundant vegetation, and a less densely built environment with semi-open courtyards facilitating air exchange.

Concluding the local outdoor comfort comparison, three selected overheating-prone spots experienced air temperature changes between 1.81 K and 2.28 K over 24 hours. In the same period, PET levels increased between 1.01 K and 1.75 K, highlighting the urgency and the imperative need for intervention. This study promote resilience in overheated cities and serves as a foundational exploration for the development of urban mitigation strategies and urban design measure.

ACKNOWLEDGEMENTS

This research was co-funded by tax funds according to the budget approved by the Saxon State Parliament. A thank you to the The Office for Environmental Protection, City Planning Office of the City of Leipzig who made the results of previous climate studies available and provided the three-dimensional model of the city of Leipzig to be used as a basis for the simulations.

REFERENCES

1. Nakicenovic, N. and Swart, R. Eds. (2000), Emission scenarios, Cambridge University Press, p. 570.
2. Paolini, R. and Santamouris, M. Eds. (2023), Urban Climate Change and Heat Islands, Characterization, Impacts and Mitigation, Cambridge University Press, p. 1-7.
3. Wasem, P. (2021), Leipzig Klimaanalyse – Phase II Erweiterung der Planungshinweiskarte, Stadt Leipzig, Dezernat für Umwelt, Klima, Ordnung und Sport.
4. Copernicus Climate Change Service (2021), Climate and energy indicators for Europe from 2005 to 2100 derived from climate projections. Copernicus Climate Change Service (C3S) Climate Data Store (CDS). DOI: 10.24381/cds.f6951a62.
5. Bruse, M. and Fleer, H. (1998). Simulating surface–plant–air interactions inside urban environments with a three dimensional numerical model. *Environmental Modelling & Software*, *13*(3-4), 373–384. https://doi.org/10.1016/S1364-8152(98)00042-5
6. Jentsch, M.F.; James, P.A.; Bourikas, L. and Bahaj, A.S. (2013). Transforming existing weather data for worldwide locations to enable energy and building performance simulation under future climates. *Renewable Energy*, *55*, 514–524, doi:10.1016/j.renene.2012.12.049
7. Acero, J. A. and Arrizabalaga, J. (2018). Evaluating the performance of ENVI-met model in diurnal cycles for different meteorological conditions. *Theoretical and Applied Climatology*, *131*(1-2), 455–469. https://doi.org/10.1007/s00704-016-1971-y
8. Salata, F.; Golasi, I.; de Lieto Vollaro, R. and de Lieto Vollaro, A. (2016). Urban microclimate and outdoor thermal comfort. A proper procedure to fit ENVI-met simulation outputs to experimental data. *Sustainable Cities and Society*, *26*, 318–343, doi:10.1016/j.scs.2016.07.005.

Climate Resilient Vertical Green Façades
Shading Strategies for Vegetation on Building Skins

CANSU IRAZ SEYREK ŞIK[1,2], BARBARA WIDERA[2]

[1]Doctoral School of Wroclaw University of Science and Technology, Wroclaw, Poland
[2]Wroclaw University of Science and Technology, Faculty of Architecture, Wroclaw, Poland

ABSTRACT: Vertical green façades provide many benefits to the urban biotope, such as improving air quality, reducing the urban heat island effect, providing sustainable stormwater management, creating habitat for insects and animals, contributing to food production, and positively affecting the psychology of urban residents. However, these façades are also adversely affected by extreme climatic events. In this paper, the authors examine shading strategies to increase climate resilience of these façades, and in particular to protect them from sudden heat waves. Three main strategies identified by authors, i.e. passive shading, kinetic self-shading and shading with kinetic layer, are qualitatively analysed and their compatibility to vertical green façades is evaluated. The research results shown that shading with kinetic layer has been the most effective strategy in terms of function, aesthetics, adaptability, and protection. Kinetic shading layer can provide various shading scenarios such as equal, full or partial shading unlike passive shading and require less energy compared to the kinetic self-shading. The paper underlines the gap in the literature on this subject and emphasises the importance of future works on conceptual framework and parametric design for shading strategies.
KEYWORDS: Vertical green façades, Shading strategies, Climate resilience, Kinetic shading

1. INTRODUCTION

Climate change and global warming affect negatively the quality of life of human and non-human inhabitants of ecosystems. Architects and urban planners come up with design ideas that can reduce the energy demand in buildings and mitigate urban heat island effect, while increasing user comfort and safety. Abundant living systems introduced in urban zones are among key drivers towards reduction of Anthropocene impact on climate. Vertical green façades in the urban tissue, improve air quality, increase relative humidity, and decrease the temperature, thus lowering the need for cooling. Further benefits of green façades include sustainable rainwater management and grey water treatment, noise reduction, enhanced biodiversity, and potential for urban farming [1].

Even though vertical green façades contribute to climate change mitigation, they are affected by the heat waves. Unpredictable temperature changes and exposure to extreme solar radiation cause heat stress in plants. Extreme climatic events, such as heat waves, frost, drought, and flooding, can affect plant production and induce mortality. Moreover, even if plants survive the heat extremes, they close their stomata, which means cooling by evapotranspiration decreases, and depress photosynthesis. Plants can change their physiology in response to drought to adapt and survive, for example by elongating their roots [2]. However, this biological adaptation feature is not effective on many vertical green façade types since the depth of the growth medium is limited. This means that artificial irrigation must be increased to prevent drying. Furthermore, the excessive direct solar radiation increases water loss of growth medium. This makes vertical green façades consume a lot of water, which is undesirable [3]. Therefore, it is necessary to protect the façades' vegetation from excessive heat causing drought through solutions that can enhance their climate resistance.

Heat waves reduce yields in agricultural crops. In corn plants, the heat wave causes significant reductions in cob length and mass of the cob as well as the husk which in turn leads to a significant reduction in total reproductive biomass by 16% [4]. In the experimental vineyard studied by Martínez-Lüscher et al. [5] the Cabernet Sauvignon grapes were exposed without shade to a 4-day heat wave 21 days before harvest, resulting in 25% of the clusters being damaged, regardless of irrigation amount. Furthermore, the study indicates that berries in the vineyard suffered a great loss of anthocyanins and flavonoids even if they were not damaged by direct solar exposure. The study concludes that partial shading can have a positive role in the retention of the grape's skin flavonoids in a high-temperature scenario. These results indicate that, taking precautions such as partially shading against extreme heat and inadequate irrigation, especially in vertical gardens used for urban farming, can improve vegetation diversity and quality. However, the existing literature on this topic is scattered and fragmented. Thus, the strategies to ensure climate resilience of vertical green façades need to be further explored.

The authors of this paper propose and discuss design strategies that can boost climate resilient vertical green façades. These approaches are based on three main objectives: plant loss prevention, water savings and increased variety as well as quality of crops when used for urban farming. In line with these objectives, three shading strategies aimed at providing more stable and comfortable living conditions for vertical green façades, are analysed.

2. DESIGN STRATEGIES FOR CLIMATE RESILIENT VERTICAL GREEN FAÇADES

Within the scope of the study, the extensive literature review on existing shading methods and technologies applicable to building skins was carried out. Journal articles, conference proceedings and reports about 'Shading strategies for building façades', 'Shading and passive cooling' or 'Climate resilience of vertical green façades' have been searched in Web of Science database for the last ten years. The first observation from the review is that there is a lack of research on the climate resilience of vertical green façades. This issue has been widely addressed in terms of the climate resilience provided by vertical greenery to the urban environment rather than in relation to design strategies that can provide climate resilience for vertical green façades. The idea of shading to vertical green façade has not been extensively explored so far. The limited number of shading solutions for greenery has been mentioned in this study. To diversify the alternatives and identify the most suitable one to provide climate resilience, the most promising shading solutions, for vertical green façades have been selected for further comparative analysis. This qualitative comparison is focused on advantages and disadvantages of the shading strategies as well as on their compatibility to requirements of vegetation on building skins. The first aspect considered in this analysis was that the plants need to be able to reach 400-700 nm spectral range of daylight necessary for photosynthesis, while being protected from excessive solar radiation and overheating during the summer season and occasional heatwaves. The preliminary research revealed that the key element in the design strategy is the light transmittance of shading elements which should be selected according to the requirement of the plant species. Moreover, even in shading stage, the plants should still be provided with sufficient ventilation. Finally, the influence of moisture from plants evapotranspiration and substrate surface evaporation on the shading elements' behaviour must be considered.

Three of the main solar control strategies for buildings, which are self-shading via the building envelope, passive shading with external or internal devices [6] and active shading with movable shading devices [7], have been adopted to the vertical green façades.

The first analysed strategy is passive shading. Passive systems involve horizontal and vertical shading elements placed at regular intervals according to the orientation of the vertical green façade to provide constant shading for plants. Shading devices such as overhangs, horizontal or vertical louvers and panels, various egg-crate systems, vertical outer planes, horizontal multiple blades or panels and combination of these different solutions exemplified by Kirimtat et al. [8] and Valladares-Rendón et al. [6] are generally used for passive shading on building façades. These devices might be built as integrated modules to vertical green systems or as a second layer in front of greenery to create a secondary skin as shown respectively in Figure 1a and Figure 1b. The VertiKKA project [9] represents an example of the aforementioned strategy. The photovoltaic films are placed in front of the vegetation, aiming to protect the greenery from extreme weather and high levels of solar radiation while allowing for energy generation in the system. In order to provide homogenous shading to the vertical green façades, *mashrabiya* style shading devices, traditionally used in the warmer regions, especially in Middle East, can be applied as shown in Figure 1c [10].

The second strategy focuses on self-shading of the building envelope achieved by the protrusions on the envelope to place transparent surfaces more inward [6]. In order to provide self-shading to vertical green

Figure 1: Passive shading strategies: (a) Horizontal shading panels attached to vertical greenery (b) Horizontal shading panels as secondary skin (c) Mashrabiya style shading for greenery (Source: Authors).

façades, these protrusions can be formed through the movement of the vegetated façade modules with adjustable angles, as shown in Figure 2. In such systems, modules can be positioned horizontally and vertically depending on the orientation of the vertical green façade. During winter, when the sun's position is lower these vegetated modules can mimic the sun-capturing motion as seen on the Adaptive Solar Façade developed in ETH Zurich [11]. In summer, the panels can move to the opposite direction to avoid exposure to excessive solar radiation during heat waves.

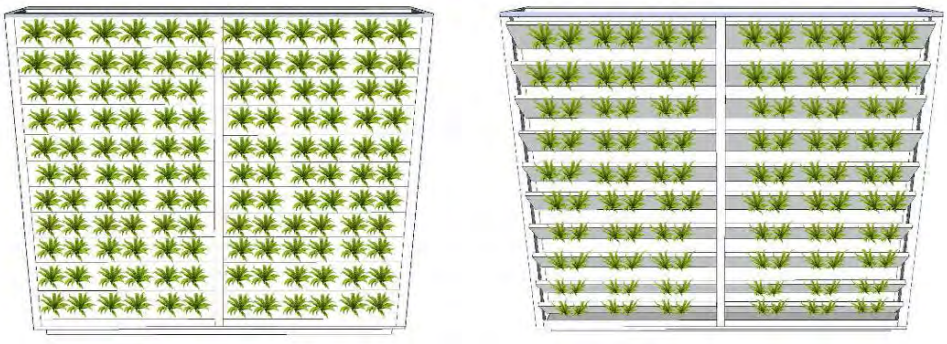

Figure 2: Kinetic self-shaded planted panels (Authors).

The third strategy is based on the kinetic shading layer added to the vertical green façade systems as presented in Figure 3. This kinetic shading layer can be constructed from various materials and controlled either automatically by sensors, manually by the user via a central computer or by interconnected panels consisting of units working as sensing and activating elements [12]. Shading elements can perform different types of movements such as flapping, folding, rotating, sliding according to the design of the system [13]. These elements can change the pattern and transparency ratio (e.g., the Tessellate system) [14]. Sliding foldable louvres that allow airflow and provide partial shading or wings that flutter on the vertical or horizontal axis (e.g., kinetic façade of Campus Kolding designed by Henning Larsen Architects [14]) can be used to create a shading layer. These shading elements can also be constructed using natural materials, such as wood and bamboo, as seen in the kinetic façade of the Aalen University Extension building designed by MGF Architekten [14] and the Carabanchel Social Housing building designed by FOA (Foreign Office Architects) [14].

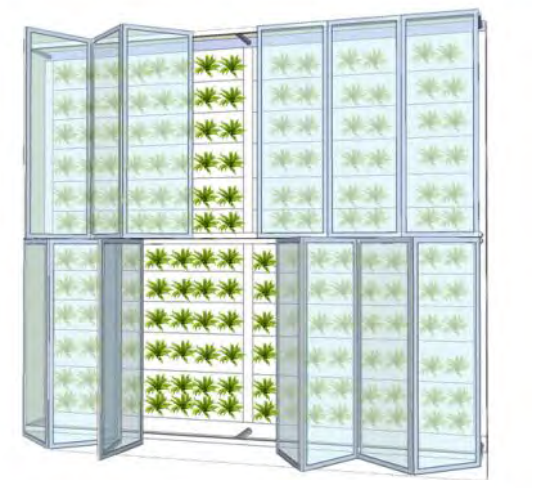

Figure 3: Kinetic shading layer on green façade (Authors)

3. COMPARATIVE ANALYSIS OF DESIGN STRATEGIES

3.1 Advantages and disadvantages of design strategies

The passive shading method is based on traditional façade shading concepts used e.g. in Mediterranean countries. In traditional shading systems applied for agricultural purposes on horizontal fields, the plants are fully covered with light cloth or porous fabric. If the shading material selection does not properly consider the needs of plants, satisfactory yield cannot be obtained due to insufficient amount of daylight and fresh air [5]. Such an uninterrupted stable shading layer is not necessary for vertical planting surfaces. Passive shading devices can provide sufficient shading without completely disconnecting the vertical green façades from the external environment.

Passive ventilated shading is easy to implement and relatively inexpensive [15]. Solar panels, such as in the VertiKKA project mentioned above can be integrated with vertical green systems to generate electricity [9]. However, the disadvantage of these shading elements is that their position cannot be changed. This hinders the system's response to user requests and sudden changes in weather conditions [15].

In kinetic self-shaded modules proposed by the authors, the plants can be shaded, when necessary (e.g. during hot periods), while receiving sufficient daylight during colder periods (when sun rays fall at a more oblique angle). In addition to the effective utilisation of daylight, another advantage of this strategy is the ease of access for humans and animals since the system is not interrupted by an external fixed shading layer. If different modules respond individually and move in the opposite directions within

the same time frame, plants that require different amounts of sunlight can be grown in parallel. This practice may help increase the variety of crops obtained from the system. On the other hand, the system has several limitations. Variables due to the requirements of plant biology and the mobility of the system create design complexity. System movement requires extra energy consumption. The possible weight of vegetated modules is another disadvantage. The costs of maintenance and repair of the mechanical parts may increase the price of kinetic systems [16].

Among analysed shading strategies for vertical green systems, the kinetic shading layer demonstrates the highest adaptability to the climatic changes. Unlike passive shading devices, kinetic layers can respond in multiple ways to heat waves, sudden precipitation and strong winds. This concept can provide equal, full or partial shading for plants and growth medium. If plants with diverse light requirements are located in the same vertical green system, with the application of kinetic layer several shading scenarios can be created for different plant species. Depending on the material and the design of the shading element, the kinetic shading layer systems are lighter than kinetic self-shaded green façades and the movement of elements requires less energy. If the kinetic shading layer is designed without consideration of the requirements of plant biology, human and animal interaction and the external environmental conditions, problems arise in the functionality of the system. This results in high maintenance and repair costs. However, if the necessary requirements are applied into design, maximum efficiency can be obtained with the kinetic shading layer compared to other strategies.

3.2 Design requirements of shading strategies

The types and sizes of shading devices used in building façades should be designed considering the altitude and angle of the solar radiation (in relation to location and façade orientation), the required amount of daylight and the size of shaded area [15, 17]. These considerations establish the basis for design of passive shading devices for vertical green façades too. Design configurations for these devices should be determined taking into consideration the plants' needs and the maintainability requirements of the system. Accessibility for maintenance purposes such as cleaning and repair, gardening and plant care, irrigation and drainage should be provided to users [18]. If shading devices are integrated into the vertical green façade, the distance required for the growth of the plants should be considered. Especially, there should be a gap between the horizontal panels and the first row of plants according to the maximum growth distance of the plant type. Where fixed shading elements or *mashrabiya* style shading devices are used to form a second skin, a gap should be left between the shading layer and the green façade to allow human access to these façades for maintenance, planting, and harvesting. Due to the inability to change position of passive shading devices, the light requirements of the plants must be assessed when selecting the materials or shade-loving species should be preferred.

The module's angle should be arranged considering the plant metabolism in a shading condition of kinetic self-shaded systems. In order to prevent damage to the plants during the module's movement, the size of the modules and the gaps between them should be designed taking into account the maximum dimensions of plants and their growth processes. Furthermore, materials that tend to fall cannot be used for this system. Drainage must be designed according to the movement of water for the various module positions. The weight of the planted modules and the energy required for their movement needs to be considered and sustainable energy generation methods should be integrated into the system.

The design parameters of the kinetic shading layer include geometric shape and motion type, technology, structure and material [12, 19]. The choice of geometry and movements of kinetic façades are influenced by numerous factors such as the function of the system, the required indoor conditions of the building, the requirements of the designer and users as well as environmental and climatic conditions. In order to design geometric shape of kinetic shading devices, architects utilise design methods such as parametric design, performance-based design, generative design, approaches such as biomimicry and patterns such as origami or criss-crossed patterns of latticework in *mashrabijas* [13, 20, 21]. In the same way, different design methods and inspirations can be used by designers for the kinetic shading layer of vertical green façades.

The technologies applied in kinetic façades consist of control, sensing and actuating elements. Façade movement can be activated via pneumatic, hydraulic, material-based, passive actuators or servomotors. Control can be provided via hand-operation, via central computer or interconnected panels by microcontrollers (decentralized control) [22]. In material-based technologies all the sensing, actuating and control features are provided by material itself. These materials include shape memory alloys, shape memory materials, etc. [12].

User interaction with the control mechanism of kinetic shading devices is beneficial for climate resilience and maintainability of vertical green façades. In addition, it is advantageous to open the kinetic shading layer to allow user access during planting and harvesting. This may represent a challenge in the case of material-based technologies that automatically respond to changing environmental

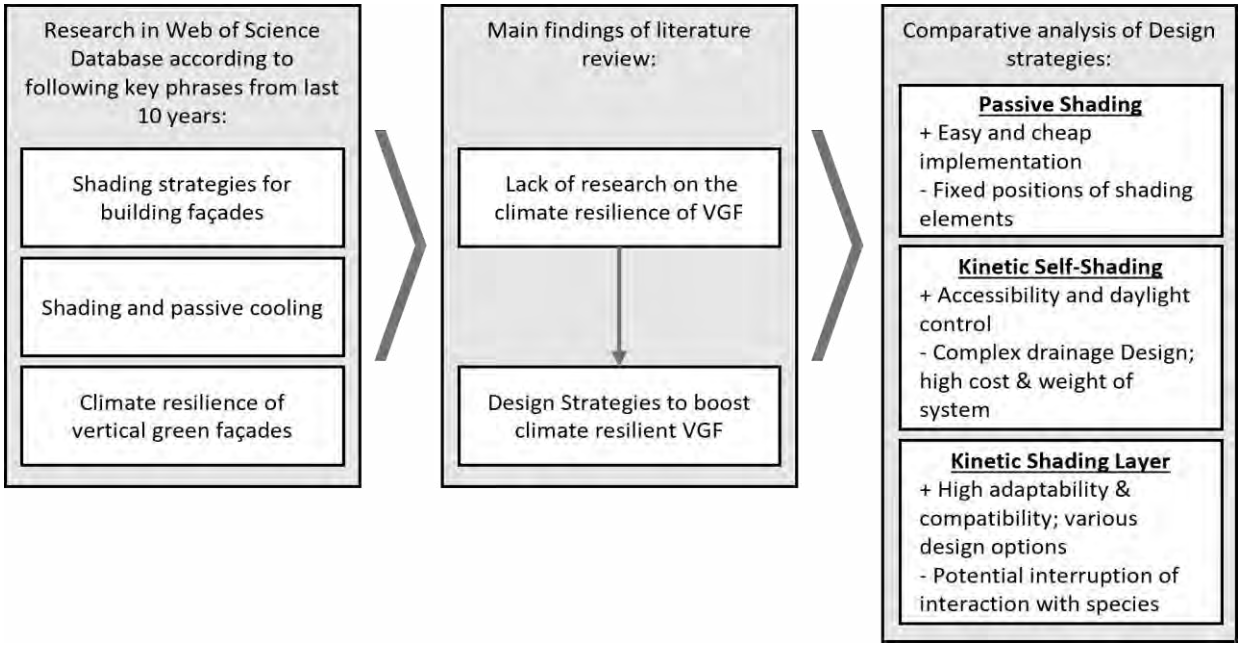

Figure 4: Methodology and main findings of the study (Authors).

conditions since their actions cannot be programmed by the user.

The advantage of these technologies is performing all sensing, actuating, controlling actions and reducing the complexity, cost of construction, maintenance, production of kinetic façades. Moreover, this technology mostly does not require an extra energy source [23]. Therefore, the integrated use of material-based technologies with other technologies that allow user interaction can provide a shading layer that can be controlled when it is necessary but still requires a minimum of energy use. The evapotranspiration and evaporation effects of the vertical green façades should be considered during the material selection.

The shading elements must enable the air flow even in the fully closed position when still providing protection against strong winds. For the healthy growth of the plants and the comfort of other living creatures on the vertical green façades, an optimum gap should be left between the kinetic shading layer and the vertical green façades. The materials of the shading modules affect the durability and functionality of the system. Pirouz et al. [24] integrated a mesh into the vertical green façade surface for fog harvesting and have proven that atmospheric water harvesting for green façade irrigation is possible. Similarly, the fog harvesting mesh can be integrated into the kinetic shading layer and prevent vertical green façades from being dependent on tap water in periods of insufficient precipitation. Materials should be corrosion resistant. It is possible to conclude that the kinetic shading layer strategy allows for more flexible design options.

4. CONCLUSION

Shading systems aimed at protecting vertical green façades against the negative effects of global warming have been comparted. Because the initial analysis revealed that this concept remains largely under-investigated. In this study, this research gap has been identified and addressed. The methodology and main findings of the study have been visualized in Figure 4.

The result of this study revealed that passive shading strategies have lower initial cost and are easy to build but their response to changing climatic conditions is limited. When passive shadings are used for green façades, it is important to ensure that shading effect will reach to the rooting medium such as containers or plant pots to protect them from overheating the and water loss.

Kinetic self-shading demonstrates adequate climate responsiveness. With the absence of an extra layer in front of vegetation, the interaction of human and non-human beings with vegetation is possible and remains uninterrupted. Due to the higher weight of kinetic modules, the mechanical and electrical elements require more maintenance and repair while increasing the total energy consumption of the system. Kinetic shading layers offer more flexibility in terms of design (e.g. in relation to function, aesthetics, adaptability and protection). This system, when properly designed, requires less energy than kinetic self-shading solutions. Kinetic shading layers provide various shading scenarios such as equal, full or partial shading. Furthermore, the design of irrigation and drainage is less complex than the kinetic self- shading solution since the vertical green system is stable. Therefore, it is indicated as the most effective solution in this study.

However, the complexity of kinetic systems in terms of design and construction as well as potential high cost of maintenance compared to the passive systems should be considered. In the case of full shading, further observation on the prototype in the real-life conditions if the kinetic shading layer does not interrupt the interactions of the plants with birds, pollinators, etc.

Further research is necessary to develop conceptual frameworks allowing for correct system adjustment to climate and functional requirements. The effects of shading strategies should be investigated by simulative or experimental studies.

REFERENCES

1. Radić, M., Brković Dodig, M., Auer, T., (2019). Green Façades and Living Walls – A Review Establishing the Classification of Construction Types and Mapping the Benefits. *Sustainability*, 11, 4579. Doi: 10.3390/su11174579.
2. Niu, S., Luo, Y., Li, D., Cao, S., Xia, J., Li, J., Smith, M.D., (2014). Plant growth and mortality under climatic extremes: An overview. *Environmental and Experimental Botany*, 98: p. 13–19. Doi: 10.1016/j.envexpbot.2013.10.004.
3. Pan, L., Wei, S., Chu, L.M., (2018). Orientation effect on thermal and energy performance of vertical greenery systems. *Energy and Buildings,* 175: p. 102-112. Doi: 10.1016/j.enbuild.2018.07.024.
4. Siebers, M.H., Slattery, R.A., Yendrek, C.R., Locke, A.M., Drag, D., Ainsworth, E.A., Bernacchi, C.J., Ort, D.R., (2017). Simulated heat waves during maize reproductive stages alter reproductive growth but have no lasting effect when applied during vegetative stages. *Agriculture, Ecosystems & Environment,* 240: p. 162-170. Doi: 10.1016/j.agee.2016.11.008.
5. Martínez-Lüscher, J., Chen, C.C.L., Brillante, L., Kurtural, S. K., (2020). Mitigating Heat Wave and Exposure Damage to "Cabernet Sauvignon" Wine Grape With Partial Shading Under Two Irrigation Amounts. *Frontiers in Plant Science,* 11. Doi: 10.3389/fpls.2020.579192.
6. Valladares-Rendón, L.G., Schmid, G., Lo, S.L., (2017). Review on energy savings by solar control techniques and optimal building orientation for the strategic placement of façade shading systems, *Energy and Buildings,* 140: p. 458-479. Doi: 10.1016/j.enbuild.2016.12.073.
7. Konstantoglou, M., Tsangrassoulis, A.E., (2016). Dynamic operation of daylighting and shading systems: A literature review, *Renewable and Sustainable Energy Reviews,* 60: p. 268-283. Doi: 10.1016/j.rser.2015.12.246.
8. Kirimtat, A., Kundakci Koyunbaba, B., Chatzikonstantinou, I., Sariyildiz, S., (2016). Review of simulation modelling for shading devices in buildings, *Renewable and Sustainable Energy Reviews,* 53: p. 23-49. Doi: 10.1016/j.rser.2015.08.020.
9. VertiKKA: Die vertikale Klimaanlage, [Online], Available: https://vertikka.de [23 August 2020].
10. Bagasi, A.A., Calautit, J.K., Karban, A.S., (2021). Evaluation of the Integration of the Traditional Architectural Element Mashrabiya into the Ventilation Strategy for Buildings in Hot Climates, *Energies,* 14(3):530. Doi :10.3390/en14030530.
11. Adaptive solar façade, [Online], Available : https://systems.arch.ethz.ch/research/adaptive-solar-façade [17 December 2023].
12. Matin, N., Eydgahi, A., (2019). Technologies used in responsive façade systems: a comparative study, *Intelligent Buildings International*, 14: p. 1-20. Doi: 10.1080/17508975.2019.1577213.
13. Hosseini, S.M., Mohammadi, M., Rosemann, A., Schröder, T., Lichtenberg, J., (2019). A morphological approach for kinetic façade design process to improve visual and thermal comfort: Review, *Building and Environment,* 153: p. 186-204. Doi: 10.1016/j.buildenv.2019.02.040.
14. Aelenei, L., Aelenei, D., Romano R., Mazzucchelli, E.S., Brzezicki, M., Rico-Martinez, J.M., (2018). Case Studies: Adaptive Façade Network, *TU Delft Open*, p. 64-67, 136-139, 220-227.
15. Mohammed, A., Tariq, M.A.U.R., Ng, A.W.M., Zaheer, Z., Sadeq, S., Mohammed, M., Mehdizadeh-Rad, H., (2022). Reducing the Cooling Loads of Buildings Using Shading Devices: A Case Study in Darwin. *Sustainability*, 14(7):3775. Doi: 10.3390/su14073775
16. Attia, S., Bilir Mahcicek, S., Safy, T. & Struck, C., Loonen, R., Goia, F., (2018). Current Trends and Future Challenges in the Performance Assessment of Adaptive Façade Systems, *Energy and Buildings*, 179. Doi: 10.1016/j.enbuild.2018.09.017.
17. Heidari, A., Taghipour, M., Yarmahmoodi, Z., (2021). The Effect of Fixed External Shading Devices on Daylighting and Thermal Comfort in Residential Building. *Journal of Daylighting*, 8: p. 165-180. Doi: 10.15627/jd.2021.15.
18. Chew, M., Conejos, S., Azril, F., (2019). Design for maintainability of high-rise vertical green façades. *Building Research and Information*, 47: p. 453-467. Doi: 10.1080/09613218.2018.1440716.
19. Al-Masrani, S., Al-Obaidi, K.M., (2019). Dynamic shading systems: A review of design parameters, platforms and evaluation strategies, *Automation in Construction,* 102: p. 195-216. Doi: 10.1016/j.autcon.2019.01.014.
20. Sharaidin, K., Salim, F., (2012). Design Considerations for Adopting Kinetic Façades in Building Practice. *The 30th International Conference on Education and research in Computer Aided Architectural Design in Europe (eCAADe 2012)* 12-14 September, Prague, Czech Republic. Doi: 10.52842/conf.ecaade.2012.2.629.
21. Le-Thanh, L., Le-Duc, T., Ngo-Minh, H., Nguyen, Q.H., Nguyen-Xuan, H., (2021). Optimal design of an Origami-inspired kinetic façade by balancing composite motion optimization for improving daylight performance and energy efficiency, *Energy,* 219, 119557. Doi: 10.1016/j.energy.2020.119557.
22. Grobman J., Yekutiel T., (2013). Autonomous Movement of Kinetic Cladding Components in Building Façades, *ICoRD´13 International Conference on Research into Design*, 7-9 January, Chennai, India. Doi: 10.1007/978-81-322-1050-4_84.
23. Sommese, F., Badarnah, L., Ausiello, G., (2023). Smart materials for biomimetic building envelopes: current trends and potential applications, *Renewable and Sustainable Energy Reviews,* 188, 113847. Doi: 10.1016/j.rser.2023.113847.
24. Pirouz, B., Turco, M., Palermo, S.A., (2020). A Novel Idea for Improving the Efficiency of Green Walls in Urban Environment (an Innovative Design and Technique), *Water,* 12, 3524. Doi: 10.3390/w12123524.

PLEA 2024 WROCŁAW
(Re)thinking Resilience

Redefining Urban Spaces:
Quantifying the Impact of Green Infrastructure on Ambient Air Pollution in an Urban Context

FABIAN GÖRGEN[1,2,4] JAKOB BECKER[3,4] RANA SAADALLAH[3] MONICA ROSSI-SCHWARZENBECK[1]

[1]Leipzig University of Applied Sciences, 04277 Leipzig, Germany
[2]Brandenburg University of Technology, 03013 Cottbus, Germany
[3]Bauhaus-Universität Weimar, 99423 Weimar, Germany
[4]Komfortscape GmbH, 10827 Berlin, Germany

ABSTRACT: In response to increasing and alarming levels of ambient air pollution in urban areas, this study focuses on the validation and application of a numerical model to assess air pollution levels in an urban context. Using microclimate simulation tool ENVI-met, a three-dimensional numerical model was developed and validated against in-situ measurements. After the validation process, two green infrastructure scenarios, designed and proposed by a local environmental protection organisation, were assessed focusing on the improvement of NO_2 levels, in contrast to the existing status quo. The results revealed a robust and noteworthy decrease in NO_2 levels up to 40 %, especially in densely populated and high-traffic areas within the inner city. The implementation of these green infrastructure scenarios not only led to a remarkable reduction in pollutant concentrations, demonstrating the tangible impact of these measures on improving urban air quality but also improved thermal comfort by up to 6.04 K (PET). This validated model equips cities and municipalities with a valuable tool for informed decision-making, facilitating the effective implementation of practical green infrastructure solutions to mitigate air pollution and foster more sustainable urban environments.
KEYWORDS: Air Quality, Air Pollution, Green Infrastructure, ENVI-met, Urbanism

1. INTRODUCTION

According to the World Health Organization (WHO), air pollution represents one of the biggest environmental risks to human health [1]. Particularly, modern forms of pollution such as ambient air pollution and toxic chemical pollution have increased by 66 % since 2000, leading to 4.5 million premature deaths worldwide attributed to ambient air pollution alone in 2019 [2]. Referring to the European Environment Agency (EAA) [3], approximately 97 % of the urban population in Europe is exposed to Particulate Matter ($PM_{2.5}$) levels exceeding the air quality guidelines (AQG) set by the WHO [1]. Similarly, around 90 % of the urban population is exposed to elevated nitrogen dioxide (NO_2) levels. The city of Leipzig, in particular, faces a challenge with NO_2 levels, as the concentrations consistently exceeded the AGQ on 336, 335, 328, 311 and 298 days in the pre-COVID years (2015-2019). Several studies have provided evidence on the effectiveness of mitigation strategies to combat ambient air pollution in urban areas. Nowak et al. investigated the effect of urban trees on air pollution and found tree management to be a viable strategy to improve air quality [4]. A study by Tomson et al. demonstrated the positive impact of green infrastructure on improving air quality in street canyons [5]. Tang highlighted the positive influence of green walls on mitigating air pollution in urban areas [6]. As for Leipzig, local environmental protection organisation, *Ökolöwe e.V.,* has developed a systematic mitigation strategy. The ongoing implementation of a bike lane along the inner city ring, replacing a car lane, started in 2022 and is expected to be completed by 2025. The next phase proposes a green promenade ring, envisioned as a car-free urban park with trees, playgrounds and a continuous dedicated bicycle lane [7]. This study focuses on the quantification of the impact of the planned redevelopments on improvements in air quality, using numerical simulations for detailed assessment. For the simulations, ENVI-met [8], a three-dimensional microclimate simulation tool, often used and validated for microclimate assessment [9-10], was used. In the context of air pollution modelling, Sun et al. found that ENVI-met was a reliable software to simulate $PM_{2.5}$ concentrations [11]. However, literature on validated ENVI-met models, specifically focusing on NO_2, is scarce. Therefore, this study aims to adopt a holistic approach, not only validating the model for quantifying air pollution but also applying it to understand the impacts of green infrastructure scenarios. The goal is to enhance the understanding of air quality dynamics and provide insights for evidence-based strategies in cities with similar challenges, contributing to the development of more sustainable and healthier urban environments.

2. STUDY AREA

The study was conducted in Leipzig, Germany (N 51.341, E 12.375), with a focus on an area including the inner city, the surrounding ring road and adjacent neighbourhoods. With a total size of 1130 x 1265 meters, the study area represents a dynamic urban environment with a mix of commercial, residential, and recreational spaces. The ring road serves as a significant traffic route, surrounding the core of the city. Figure 1 illustrates the study area, highlighting the traffic volumes of the investigated roads (see table 1), as well as the locations of a weather station (A), two traffic-counting stations (B and C) and three specific locations within the study area selected as key points for scenario evaluation (D, E and F).

Figure 1: Study area including traffic categories per street segment and key locations A-F

3. METHODOLOGY

For the quantification of the ambient air pollution in the study area a three-dimensional numerical model (CFD) was developed. Subsequently, the model was undertaken a calibration process, comparing the results to in-situ measurements. After validation, the model was applied to quantify NO_2 levels and compare the status quo with the developed green infrastructure scenarios. This approach allowed for a comprehensive analysis of their effectiveness in mitigating air pollution.

3.1 CFD model development

The CFD model for this study was created using microclimate simulation tool ENVI-met (Version 5.1.1). ENVI-met uses the Reynolds-Averaged non-hydrostatic Navier-Stokes equations and integrates the k-ε turbulence model to estimate turbulence, ensuring accurate representation of complex environmental dynamics. The model's grid size was set at 5 m x 5 m x 5 m, resulting in a total model size of 246 x 273 x 20 grids (including an additional 10 grids on each side). Various ground surfaces, including *asphalt road*, *dark granite pavement*, and *sandy loam*, were applied. The vegetation component included grass (h = 0.15 m) and trees *(little leaf lime (middle)*). The used building and roof materials are shown in Figure 2. Simulations were conducted on a representative day known for high traffic density, specifically the beginning of the summer holiday period on 5th July 2019. This day was also representative of the local climate, featuring sunny weather conditions and an average temperature of 21.32 °C. The year 2019 was selected as the reference year, considering irregular traffic patterns in subsequent years due to COVID-19-induced reductions. Using ENVI-met Full Forcing a weather data set from a local weather station (A, see figure 1) was used. For simulating air pollution distribution, ENVI-met sources was used. Traffic volume data were collected from two traffic counting stations alongside the inner ring (B and C). The assumed emission factors per vehicle class for NO_2 for the initial model were as follows: Passenger Cars (PC): 0.176 g/km, Light Duty Vehicles (LDV): 0.304 g/km, Bus (B): 1.365 g/km, Heavy Duty Vehicles (HDV): 0.360 g/km, and Motorcycles (MC): 0.081 g/km. Details regarding traffic categories and their contributions per vehicle category to the overall traffic can be found in table 1.

Table 1: Traffic categories

Cat.	Veh/24h	Vehicle class distribution [%]				
		PC	LDV	B	HDV	MC
I	46.772	88	8	1	2.5	0.5
II	28.386	88	8	1	2.5	0.5
III	5.000	88	8	1	2.5	0.5
IV	500	59	30	1	10	0

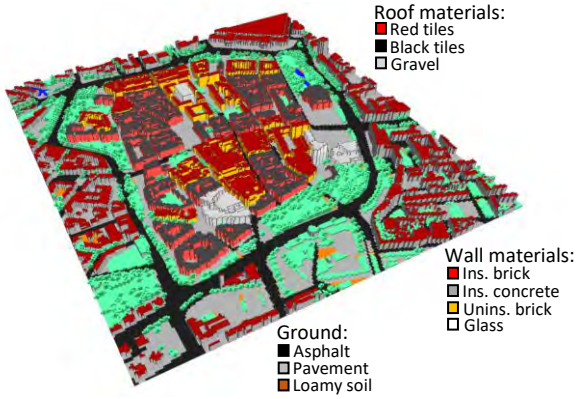

Figure 2: ENVI-met model of the study area

3.2 Calibration process

The validation of the CFD model was conducted in three stages. The simulation results of the status quo were compared to the in-situ measurements

obtained at the designated measurement location (A), calculating the errors as the Root Mean Square Error (RMSE) and the Mean Absolute Error (MAE), as specified in equations (1) and (2), respectively. After evaluating the RMSE and MAE values per stage the model was refined to improve the correlation between measurements and simulation results.

$$RMSE = ((\Sigma (m_i - s_i)^2) / n)^{0.5} \quad (1)$$

where *RMSE* - Root Mean Square Error (-);
m_i - measured value at time step i (-);
s_i - simulated value at time step i (-);
n - total number of time steps (-).

$$MAE = ((\Sigma |(m_i - s_i)|) / n) \quad (2)$$

where *MAE* - Mean Absolute Error (-);
m_i - measured value at time step i (-);
s_i - simulated value at time step i (-);
n - total number of timesteps (-).

3.3 Application of green infrastructure scenarios

In the application phase, the study simulated two distinct green infrastructure scenarios to assess the corresponding impact on NO_2 levels in the study area compared to the existing status quo. The investigated scenarios included the current state (Status Quo Scenario *SQ*), the conversion of an existing car lane into a dedicated bicycle lane (Bike Lane Scenario *BL*), and the implementation of green corridors with increased vegetation (Green Promenade Ring Scenario *GR*). Figure 3 illustrates the design and layout of these scenarios, offering visual representations of the three simulated developments. The simulation period was 24 hours, starting on 4th July 2019, at 09:00 p.m.

3.3.1 Status Quo Scenario

Based on the validated model, the Status Quo Scenario focused on the evaluation of NO_2 concentrations in the existing urban configuration, serving as a benchmark for comparison with the subsequent green infrastructure scenarios. Traffic distribution for this scenario was based on the four categories outlined in table 2. Figure 3a shows an example of the setup, featuring three car lanes in each direction.

3.3.2 Bike Lane Scenario

The ongoing implementation of the bike lane on the inner city ring unfolds in four distinct phases, strategically targeting different locations for the lane conversion from car lane to bike lane. The simulation in this study represents the anticipated final state after the completion of all four phases in 2025. As the bike lane implementation only applies to the ring, adjustments in traffic volume and car lanes were only made to categories I-III. The overall traffic volume was reduced by 10 %, as revealed by comparing the traffic volume before and after the bike lane implementation at traffic counting station B. This reduction was applied to the traffic volume for the other sections as well. Additionally, one car lane per direction was removed in the model, reflecting the reality where it is replaced by a bike lane. The vehicle class distribution and emission factors remained consistent for each category. An example of the bike lane implementation on a three-lane road can be seen in figure 3b.

3.3.3 Green Promenade Ring Scenario

The Green Promenade Ring represents a forthcoming initiative aimed at establishing open green spaces, serving as a green corridor and recreational area. Envisioned as an auto-free urban park with trees, playgrounds, and a continuous dedicated bicycle lane, the green promenade ring, which includes both grass, trees, and green tracks, is set to offer a cooling effect, with urban trees providing shade and purifying the air by filtering pollutants. In this way, the ring seeks to mitigate the impacts of the climate crisis while enhancing the well-being of the residents. The initiative aims to transform the existing car lanes of the inner ring road into a green space. As part of this transformation, the entire traffic flow in both directions will be shifted to the outer ring road. The model was adjusted, compared to the bike lane scenario, by incorporating additional grass and 93 trees along the remaining inner car lanes. Traffic distribution, emission factors, and vehicle class distribution for the outer car lanes, now accommodating both directions, remained unchanged. A visualization of the Green Promenade Ring Scenario can be seen in figure 3c.

Figure 3: Scenario set-up for Status Quo (a), Bike Lane (b) and Green Promenade Ring (c) Scenarios

4. RESULTS

In this section, the outcomes of the study are presented. After completing the calibration process, the validated model was applied to investigate the impact of the green infrastructure scenarios on NO_2 concentration.

4.1 Calibration

After stage 1, it became evident that the simulated NO_2 concentration values were considerably lower than the measurements, resulting in large RMSE and MAE values of 28.91 and 28.37, respectively. The initial model had a set background concentration of 0 µg/m³ for NO_2. Despite allowing a 3-hour lead time for simulation initialization, where the model could establish its own background, this approach failed. The NO_2 concentration tended to approach the artificially set background level of 0 µg/m³ during times of minimal emissions, rather than maintaining a distinct pattern. Although some small similarities in the curves were observed, such as the rush hour peak at 07:00 a.m., the values were consistently too low, indicating a discrepancy in fitting the curve to the actual data. To address the observed behaviour where the simulated curve tended to approach the background concentration during periods of low emissions, the background concentrations were adjusted to the lowest point of the measurements in stage 2 (16 µg/m³). This adjustment significantly improved the errors, reducing the RMSE to 13.57 and the MAE to 12.43. However, it is essential to note that while this adjustment lifted the entire curve, aligning it more closely with the measured data, the simulation pattern still did not closely resemble the actual curve. To address the shortcomings identified in the previous stages, it became evident that adjusting the hourly emission rates was crucial. ENVI-met offers three distribution scenarios for allocating the total vehicle emissions throughout the day. However, recognizing the need for more specific adjustments, manual modifications were made to the hourly emission rates. This involved calculating the percentage difference between the measurements for a particular hour and the stage 2 simulation results for the same hour. The percentage difference, indicating that the measurements were higher, was manually added to the hourly emission rates. This targeted adjustment significantly improved the simulation, resulting in a RMSE of 6.72 and a MAE of 6.02.

The identified errors in stages 1 and 2 underscore the necessity of a rigorous calibration process. Through systematic refinement, the model exhibited the potential for reliable validation, instilling confidence in its ability to simulate air quality dynamics in the specific study area. The successfully calibrated model was subsequently applied for detailed analysis. Nonetheless, for applications in diverse contexts, a comprehensive calibration process is recommended to address potential inaccuracies. Table 2 shows the RMSE and MAE values for NO_2 concentrations throughout the stages.

Table 2: RMSE and MAE per calibration stage (NO_2)

	Stage 1		Stage 2		Stage 3	
	RMSE	MAE	RMSE	MAE	RMSE	MAE
NO_2	28.91	28.37	13.57	12.43	6.73	6.02

4.2 Scenario evaluation

After the calibration process, the validated model after stage 3 was used for further investigations to evaluate NO_2 concentrations in the study area. The simulations focused on three different scenarios, as described in 3.3. For the scenario evaluation the same time period, starting at 09:00 p.m. on the 4th of July and ending at 09:00 p.m. on the 5th of July. While air temperature, relative humidity and global radiation values were kept, as they represented the area, the wind values were changed to get more representative results. A wind direction of 225° (south-west), which is typically for the area, was used. Also, constant wind speeds of 2.5 m/s were included.

4.2.1 Status Quo Scenario

The Status Quo Scenario represents the as-is state on 5th July 2019. In figure 4, the NO_2 concentrations at 07:00 a.m., during the morning rush hour, are visualized across the study area. Simulated NO_2 levels reached a maximum of 32.13 µg/m³, with minimum levels observed at 9.70 µg/m³. Significantly exceeding the air quality guidelines set by the WHO at 5 µg/m³, not a single grid cell simulated in this scenario achieved levels below that goal. As expected, the ring road was identified as the primary source, exhibiting maximum NO_2 concentrations up to 290.6 µg/m³, 233 % higher than on inner-city streets (up to 87.18 µg/m³). However, certain sections of the ring road exhibited lower pollution levels despite similar traffic volumes. This discrepancy is attributed to factors beyond the emission source, such as wind speed and wind direction. Figure 4 shows that in areas without emission sources and buildings to their south-west, lower wind speeds led to decreased NO_2 concentrations. Conversely, despite buildings acting as windbreaks on the west side of the ring, high NO_2 levels persisted due to low wind speeds hindering effective dispersion. This finding underscores that low wind speeds are advantageous in areas without pollution sources but less advantageous when close to emission points, impeding pollutant distribution. In summary, NO_2 levels across the city are alarmingly high, stressing the imperative need for mitigation strategies. It is important to note that the simulated values are still below the actual measured values, as indicated by the validation.

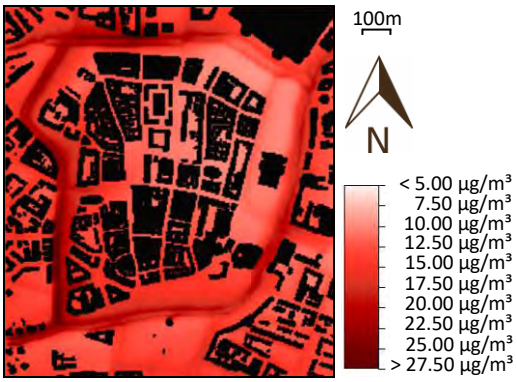

Figure 4: Total NO_2 concentration at 07:00 a.m. (Status Quo Scenario)

4.2.2 Bike Lane Scenario

Applying the Bike Lane Scenario resulted in a decrease in NO_2 levels of up to 4.99 µg/m³ (-15.53 %). However, slight local increases of up to 2.49 µg/m³ (+7.75 %) were noted. This was primarily due to the shift in traffic from three lanes to two lanes (and two lanes to one lane). Figure 5 illustrates the difference in NO_2 concentration during the morning rush hour at 07:00 a.m., compared to the Status Quo Scenario at the same time. While the impact of the bike lane implementation on the city centre was negligible, decreases in NO_2 concentration could be observed within a distance of up to 60 meters, especially in the most polluted areas visualized in figure 4: the north-western and western parts of the inner city ring road. Therefore, in addition to promoting sustainable transport, the bike lane redevelopment also has a positive impact on air quality, particularly in close proximity to the ring road.

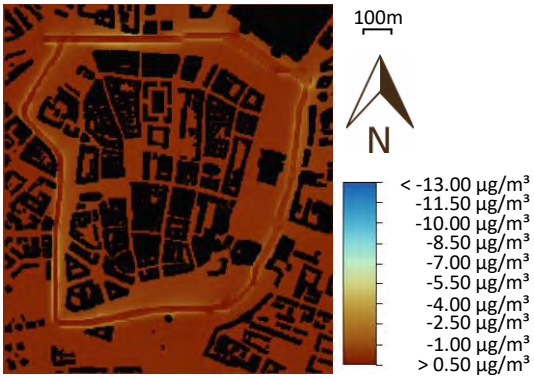

Figure 5: NO_2 concentration difference at 07:00 a.m. (Bike Lane Scenario)

4.2.3 Green Promenade Ring Scenario

The Green Promenade Ring Scenario demonstrated the significant impact that green infrastructure can have on urban air quality. The simulation indicated a maximum decrease in NO_2 concentration of 12.99 µg/m³ (-40.43 %) when comparing the Status Quo Scenario to the Green Promenade Ring Scenario, while the increase due to lane shifting was 2.29 µg/m³ (+7.13 %) as explained in section 4.2.2. Figure 6 visually represents the difference in NO_2 concentration at 07:00 a.m., showing substantial air quality improvements alongside the inner ring where vegetation replaced car lanes.

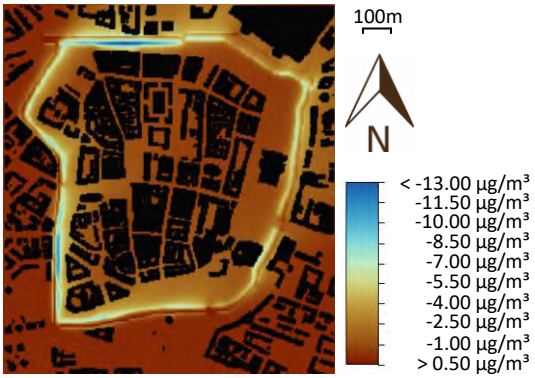

Figure 6: NO_2 concentration difference at 07:00 a.m. (Green Promenade Ring Scenario)

Apart from air quality, the assessment of outdoor thermal comfort using the Physiological Equivalent Temperature (PET) was conducted to evaluate thermal well-being attributed to green infrastructure. The Status Quo Scenario revealed significant heat stress in the study area, with maximum PET levels of 46.34 °C ($PET_{max,SQ}$) at 01:00 p.m. Analysing PET levels after the implementation of the green infrastructure scenario, it was observed that maximum PET levels remained similar ($PET_{max,GR}$ = 46.18 °C). However, the introduction of vegetation and additional trees created comfortable zones around the inner city ring, resulting in a maximum PET decrease of up to 6.04 K. This decrease shifted PET levels from 41.01 °C (indicating strong heat stress) to 34.97 °C (indicating moderate heat stress). Therefore, the Green Promenade Ring Scenario emerges as a promising solution, positively affecting both air quality and outdoor thermal comfort in the urban environment.

4.3 Local scenario comparison

This section focuses on the local assessment of NO_2 concentrations at key locations D to F within the study area (refer to figure 1). Key Location D, the Richard-Wagner-Platz (RWP), situated in the north-west, near a tram station and shopping mall, experienced significant NO_2 changes due to its proximity to the ring road. The bike lane implementation had a minimal impact (up to -0.387 µg/m³), whereas the Green Promenade Ring Scenario resulted in more substantial decreases (up to -2.815 µg/m³). Key Location E, the Kurt-Masur-Platz (KMP), in the southern area near the university campus, saw minor air quality changes with the bike lane scenario (up to -0.263 µg/m³). The Green Promenade Ring Scenario resulted in more pronounced changes (up to -1.488 µg/m³). Key Location F, the Augustusplatz (AP), a major city

square, experienced a slight decrease after the bike lane implementation (up to -0.149 µg/m³), while vegetation and trees enhanced NO_2 concentration by up to 0.862 µg/m³. Figure 7 illustrates the 24-hour difference for both implemented scenarios across all three key locations.

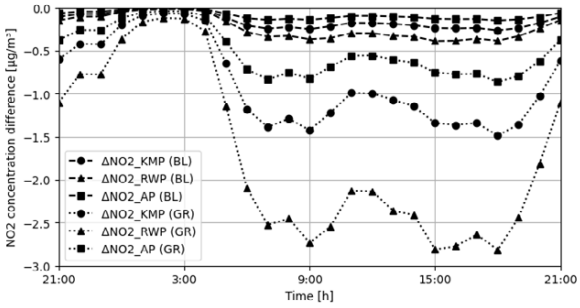

Figure 7: Differences in NO_2 concentration for locations D-F

The local scenario comparison showed that, although the most significant effects of the implemented scenarios were observed in close proximity to the ring road, the interventions also had an impact on frequented squares, indicating positive outcomes beyond immediate pollutant sources.

5. CONCLUSION

In this study, a comprehensive model was established and rigorously validated with in-situ measurements to evaluate the impact of green infrastructure on air quality. The outcomes from calibration stages 1 and 2 underscored the critical importance of calibration for achieving satisfactory performance metrics, as evidenced by the final values of RMSE = 6.47 and MAE = 5.32. The Status Quo Scenario revealed elevated NO_2 levels, surpassing recommended guidelines. The Bike Lane Scenario demonstrated a notable decrease of up to -4.99 µg/m³ (-15.53 %), while the Green Promenade Ring had the most substantial impact with a maximum decrease of -12.99 µg/m³ (-40.43 %). In selected inner-city areas, the Bike Lane scenario showed reductions of up to 3.21 %, 2.28 %, and 1.49 % compared to the status quo, while the Green Promenade Ring Scenario demonstrated significant reductions of up to 18.97 %, 12.88 %, and 8.61 %. Additionally, the simulation indicated a potential decrease in Physiological Equivalent Temperature (PET) by up to 6.07 K, emphasizing the creation of comfortable zones that encompass both enhanced air quality and improved thermal comfort. Nevertheless, it is crucial to acknowledge the study's limitations. Firstly, the reliance on two traffic counting stations, although effective, required the categorization of the study area, introducing a level of simplification. Additionally, only vehicle traffic was considered as a source of NO_2. These limitations should be taken into account when interpreting the results and planning future studies. Despite these constraints, the study highlighted the importance of green infrastructure planning in addressing air quality concerns and improving urban environments. Further research with expanded data sources, varying wind directions and different mitigation scenarios could offer deeper insights into the dynamic impact of green infrastructure on air quality.

ACKNOWLEDGEMENTS

This research was co-funded by tax funds according to the budget approved by the Saxon State Parliament.

REFERENCES

1. World Health Organization. (2021). WHO global air quality guidelines: particulate matter (PM2.5 and PM10), ozone, nitrogen dioxide, sulfur dioxide and carbon monoxide. World Health Organization. https://iris.who.int/handle/10665/345329. Licence: CC BY-NC-SA 3.0 IGO

2. Fuller, R. et al. (2022). Pollution and health: A progress update. *The Lancet. Planetary Health*, *6*(6), e535-e547. https://doi.org/10.1016/S2542-5196(22)00090-0

3. European Environment Agency (2023). Europe's air quality status 2023. Briefing: no. 05/2023. [Luxembourg]: [Publications Office of the European Union].

4. Nowak, D. J., Crane, D. E., and Stevens, J. C. (2006). Air pollution removal by urban trees and shrubs in the United States. *Urban Forestry & Urban Greening*, *4*(3-4), 115–123. https://doi.org/10.1016/j.ufug.2006.01.007

5. Tomson, M., et al. (2021). Green infrastructure for air quality improvement in street canyons. Environment International, 146, 106288. https://doi.org/10.1016/j.envint.2020.106288

6. Tang, K. H. D. (2023). Green Walls as Mitigation of Urban Air Pollution: A Review of Their Effectiveness. *Research in Ecology*, *5*(2), 1–13. https://doi.org/10.30564/re.v5i2.5710

7. Ökolöwe – Umweltbund Leipzig e.V. EIN GRÜNER PROMENADENRING FÜR LEIPZIG. Retrieved December 15, 2023 from https://mehrgruen.oekoloewe.de/gruener-promenadenring-fuer-leipzig/

8. Bruse, M. and Fleer, H. (1998). Simulating surface–plant–air interactions inside urban environments with a three dimensional numerical model. *Environmental Modelling & Software*, *13*(3-4), 373–384. https://doi.org/10.1016/S1364-8152(98)00042-5

9. Acero, J. A. and Arrizabalaga, J. (2018). Evaluating the performance of ENVI-met model in diurnal cycles for different meteorological conditions. *Theoretical and Applied Climatology*, *131*(1-2), 455–469. https://doi.org/10.1007/s00704-016-1971-y

10. López-Cabeza, V. P., Galán-Marín, C., Rivera-Gómez, C., & Roa-Fernández, J. (2018). Courtyard microclimate ENVI-met outputs deviation from the experimental data. *Building and Environment*, *144*, 129–141. https://doi.org/10.1016/j.buildenv.2018.08.013

11. Sun, D., Wu, S., Shen, S. and Xu, T. (2021). Simulation and assessment of traffic pollutant dispersion at an urban signalized intersection using multiple platforms. *Atmospheric Pollution Research*, *12*(7), 101087. https://doi.org/10.1016/j.apr.2021.101087

Analysis of the thermal and energy performance of hybrid ventilated offices in the face of climate change: a case study in Belo Horizonte, Brazil

ROBERTA VIEIRA GONÇALVES DE SOUZA[1] ANA CAROLINA DE OLIVEIRA VELOSO[1]

[1] School of Architecture, Federal University of Minas Gerais, Belo Horizonte, Brazil

ABSTRACT: This study assesses of climate change effects on the thermal and energy performance of a hybrid-ventilated office in Belo Horizonte, Brazil. By utilizing current and future climate data, an analysis was conducted on a 46.6 m² office space with casement windows, employing both natural ventilation and air conditioning. Facade modifications, including solar protection, absorptance, and glazing type, were made for present climate, RCP 2.6 and RCP 8.5 scenarios in 2050 and 2080 per IPCC AR6. Results showed a 25% and 40% average energy consumption increase in 2050 and 2080, respectively, in the unmodified archetype, with a 35% reduction when using natural ventilation. Given these findings, adopting architectural strategies is considered crucial to minimize climate change impact, ensuring future comfort and energy efficiency.
KEYWORDS: Climate change, Thermal Performance, Energy Consumption, Hybrid-ventilation.

1. INTRODUCTION

Global climate change is a growing concern due to its significant impact on the built environment and in the energy demand of buildings. Increasing average temperatures, the occurrence of extreme weather events, and seasonal variations directly affect the thermal and energy performance of constructions worldwide. In this context, it is essential to assess energy consumption in buildings, given their significant contribution to global energy demand [1], and to understand how architectural strategies can mitigate the impact of climate change and ensure greater energy efficiency in the construction sector [2].

In Brazil, a country with a population of approximately 212 million inhabitants, the construction sector plays a relevant role in electricity consumption. Residential, commercial, and public buildings account for 42.7% of the country's total electricity consumption [3], with offices and other commercial buildings representing 13.1% of this value. During the COP26 held in Glasgow in 2021, Brazil committed to implementing the Paris Agreement, promoting energy efficiency strategies to reduce greenhouse gas emissions. The country has set a goal to reduce emissions by 40% by 2030 compared to 2005 levels and aims to achieve carbon neutrality by 2050 [4]. In this context, buildings play a significant role in reducing greenhouse gas emissions as they consume a substantial amount of electricity and contribute significantly to global emissions [5].

For the assessment of the effects of climate change, the Intergovernmental Panel on Climate Change (IPCC) defines prospective scenarios regarding climate alterations, allowing for the analysis of mitigation or adaptation strategies. The IPCC's Assessment Report AR6 [6] presents different future climate change scenarios known as Representative Concentration Pathways (RCPs). These scenarios represent different trajectories of greenhouse gas emissions and serve as a basis for modeling and projecting climate impacts. The RCPs cover a wide range of possibilities, from low-emission scenarios (RCP 2.6) to high-emission scenarios (RCP 8.5). Each RCP is characterized by different levels of atmospheric greenhouse gas concentrations over time. These scenarios provide a set of tools for researchers to assess and compare the potential impacts of climate change, enabling the analysis of various mitigation and adaptation scenarios. Based on the RCPs, it is possible to investigate the effects of climate change in various areas, such as temperature, precipitation, sea-level rise, and ecosystems, providing essential information to guide policies and decision-making towards climate change mitigation and adaptation.

Mitigation involves limiting the impact of global warming by reducing greenhouse gas emissions (GHGs). On the other hand, adaptation refers to measures taken by vulnerable systems in response to current or projected climate conditions, to minimize the damages caused by climate change [7,8].

To understand the impact of architecture on energy consumption, computational simulation is an essential tool. Building thermal environmental simulation, using annual meteorological files at hourly intervals, allows for more accurate prediction of the current and future performance of buildings,

considering climatic conditions [9]. Currently, researchers have three climate transformation tools at their disposal: WeatherShift [10], Weather Morph [11], and CCWorldWeatherGen [12]. Among these tools, CCWorldWeatherGen is the most widely used in research; however, it has not been updated since 2017, using data from the IPCC's AR3 report. In face of that, Rodrigues et al. (2023) [13] have published a tool called the "Future Weather Generator," which is open access, free, and multi-platform, capable of generating future climate files with more recent IPCC data, which will be used in this study.

According to Neves, Melo, and Rodrigues (2019) [14], building envelope characteristics such as window type, presence of shading devices, and window-to-wall ratio are important parameters in buildings that adopt hybrid ventilation. In general, it is possible to reduce energy consumption in buildings through investment in technologies or by understanding user behavior. Therefore, implementing energy efficiency strategies and understanding user behavior in buildings can not only reduce peak energy demand but also decrease overall energy consumption and reduce environmental impacts. Improving energy efficiency can also reduce the need for new investments in energy generation, transmission, and distribution systems [15].

In regions with a mild temperate climate, harnessing natural ventilation can play a significant role in reducing energy consumption [8]. Approximately 30% of the Brazilian population lives in cities with this type of climate, where buildings can operate during winter without the need for heating systems and typically rely on artificial air conditioning for cooling only during the hottest days of summer. Therefore, understanding the effect of architectural variables on the energy performance of these buildings, especially in the face of climate change, can encourage designers to use passive strategies in the early stages of the design process.

The objective of this study is to assess the effects of climate change using current and future climate data on the thermal and energy performance of a hybrid-ventilated office archetype located in Belo Horizonte, Brazil, considering multiple architectural strategies. Belo Horizonte presents many office buildings that use hybrid ventilation but with a tendency to implement fully conditioned buildings from the year 2000, as noted by Alves *et al.* [16]. Analyzing if a hybrid operation will still be worth in the future is therefore considered to be an important assessment for the implementation of future city policies.

2. METHODOLOGY

The methodology employed in this study to analyze the thermal and energy performance of an office room archetype in a building in Belo Horizonte, Brazil (19° 54' S, 43° 56' W), consisted of four steps: 1) selection of an individual office space from the office building archetype developed by Veloso et al. (2023) [17]; 2) selection of elements to be modified in the building façade; 3) selection of climate files from future scenarios; 4) comparative analysis of the data.

2.1 Archetype

The office from the hybrid ventilated office building archetype developed by Veloso et al. (2023) [17] was used in this study. Its office spaces have an average area of 46.6 m² and are equipped with two maxim-air windows, allowing for natural ventilation of the interior spaces during occupied hours. The windows are operated only during occupancy; therefore, the spaces can be naturally ventilated only during working hours. The selected office space is in the East orientation.

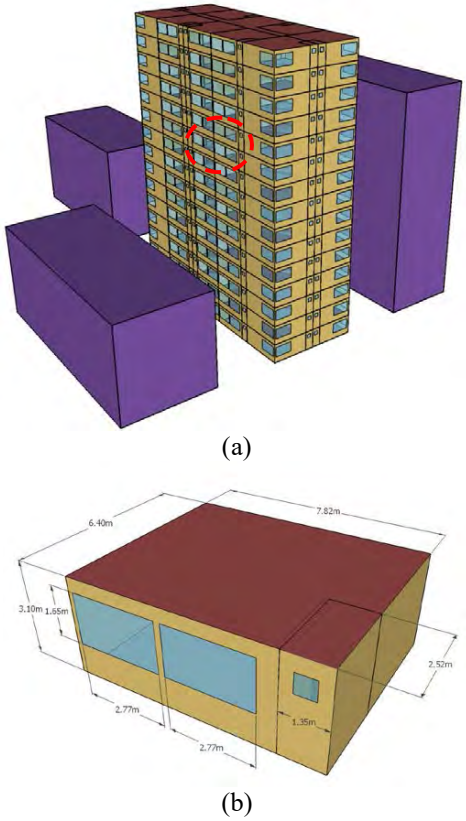

Figure 1: (a) Building archetype and (b) study office space. Source: Authors' own elaboration.

The base building façade is composed by glass with a Solar Heat Gain Coefficient of 0.87, and the external walls are made of concrete blocks with mortar coating. The external walls have a solar absorptance of 0.50 and an emissivity of 0.90. Natural ventilation was modeled using the multizone Airflow Network (AFN) model. The Energy Management System (EMS) module was used to control the opening and closing of windows based on internal temperatures: (1) The air conditioning system activates when the occupied zone's operative temperature is outside the adaptive comfort limits, as

per ASHRAE Standard 55; (2) The air conditioning system deactivates when the zone is occupied, the operative temperature is within the adaptive comfort limits, and the outdoor temperature is below the zone operative temperature; (3) The air conditioning system deactivates when the zone is unoccupied, and the windows are closed. Figure 1 illustrates (a) the archetype developed by Veloso et al. (2023) [17] and (b) the office space analyzed in this study.

Table 1: Schedule and power density of lighting and equipment.

Systems and routines	Unit	Value Used
Office spaces Lighting (LPD)	W/m²	11.9
Bathrooms lighting (LPD)	W/m²	5
Corridors lighting (LPD)	W/m²	5
Equipment	W	720
Air Conditioning COP	W/W	3.2
Occupant density	persons/space	6
Occupation routine	h/day	10:20
Lighting Routine	h/day	4:00

This analysis was conducted for Belo Horizonte, MG, located in southeastern Brazil. The city has a temperate climate (Cwa) characterized by hot summers and mild winters, with average temperatures of 24°C and 19°C, respectively. The prevailing winds consistently come from the east and southeast throughout the year.

2.2 Façade Modifications

A total of 270 simulations were conducted for each scenario (current and climate change - 2050 and 2080) with the following modifications:

1) Three glazing types: type 1 - U-value of 5.6 and SHGC of 0.87; type 2 - U-value of 5.6 and SHGC of 0.5; and type 3 - U-value of 5.6 and SHGC of 0.36.
2) Three solar shading angles: 30°, 65°, and 60°.
3) External walls absorptance with values of 0.2, 0.5, and 0.8 (0.9 emissivity).
4) The simulation identification codes are presented in Table 2.

Table 2: Codes of the parameters analyzed in the simulations.

Solar Shading	Angle External Wall Solar Absorptance	Glass Type
AP30 – 30°	**A20** – α=0,20	**V1** – FS 0,87
AP45 – 45°	**A50** – α=0,50	**V2** – FS 0,50
AP60 – 60°	**A80** – α=0,80	**V3** – FS 0,36

The thermal performance evaluation was conducted using the concept of adaptive comfort based on the outdoor mean temperature, with an acceptability rate of 80% established by the ASHRAE 55 Standard of 2020. The Energy Use Intensity (EUI), typically defined as the energy consumption per usable floor area in kWh/m².year, was selected as the performance indicator to analyze the data sample.

2.3 Climate Data

For this study, computational simulations were performed using EnergyPlus 23.1 software in an office space of a hybrid ventilated building archetype developed by Veloso et al. (2023) [17]. The climate data used was obtained in TMYx 2007-2021 format for the city of Belo Horizonte, acquired from the Climate.OneBuilding website [18]. Additionally, the future climate files were generated using the "Future Weather Generator" developed by Rodrigues et al. (2023) [13].

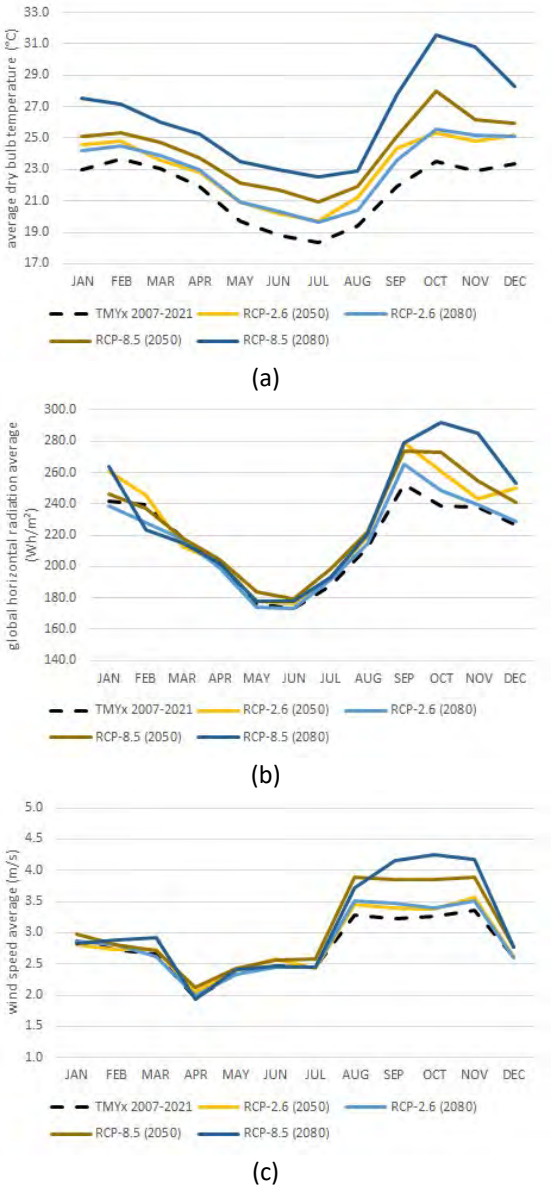

Figure 2: Comparative graph of (a) temperature, (b) solar radiation, and (c) wind speed in Belo Horizonte for the current, RCP2.5, and RCP 8.5 scenarios for the years 2050 and 2080. Source: Authors' elaboration.

For the analysis of future climate, two extreme scenarios presented in the IPCC AR6 report [6] were considered: RCP 2.6 and RCP 8.5. Figure 2 presents a comparison of temperatures, solar radiation, and wind speed between these two scenarios for the years 2050 and 2080.

These scenarios represent different greenhouse gas emissions trajectories. RCP 2.6 depicts a future with low greenhouse gas emissions, characterized by the adoption of clean energy sources, energy efficiency improvements, and significant changes in human behavior. On the other hand, RCP 8.5 represents a future with high greenhouse gas emissions, where mitigation measures are insufficient or not adequately implemented.

The choice of these scenarios is due to their widespread use in studies aiming to assess the impact of climate change on building performance and energy consumption, enabling result comparisons and a better understanding of the effects of climate change.

3. RESULTS

From the analysis of the climatic data presented in Table 3, significant variations in the average external temperature over the years were observed. In the optimistic scenario (RCP 2.6), an average increase of 7% was observed compared to the reference climatic data from 2007-2021. In the pessimistic scenario (RCP 8.5), the variations were even larger, with increases ranging from 12% to 22%. Regarding solar radiation, an average increase of 5% was found in both scenarios analyzed when compared to the reference climatic data. As for wind speed, an increase of 2% was observed in the optimistic scenario (RCP 2.6) and 10% in the pessimistic scenario (RCP 8.5).

Table 3: Variations in Temperature, Radiation, and Wind Speed of Current and Future Climatic Data.

	TMYx 2007-2021	RCP-2.6 (2050)	RCP-2.6 (2080)	RCP-8.5 (2050)	RCP-8.5 (2080)
Annual Average Temperature (°C)	21.6	23.1	23.0	24.2	26.4
Annual Average Solar Radiation (Wh/m²)	217.3	226.8	218.2	227.6	232.0
Annual Average Wind Speed (m/s²)	2.8	2.8	2.8	3.0	3.1

These variations in climatic parameters indicate a scenario of climate change where average temperatures are expected to increase, and solar radiation shows a general increment. Additionally, wind speed also undergoes changes, although with more pronounced differences between the analyzed scenarios.

Based on the variations identified in the climatic files corresponding to the selected scenarios, energy simulations were conducted to compare the hours of comfort and energy consumption of the chosen office archetype. The four future climatic files were considered, as well as design modifications, in order to analyze possible enhancements to mitigate the impact of climate variations. All these design improvement simulations were also conducted with the current climatic file.

Table 4: Variations of the scenarios in terms of the percentage of thermal comfort hours from the current and future climatic files.

		RCP 2.6		RCP 8.5	
Codigo	**2020**	**2050**	**2080**	**2050**	**2080**
CURRENT	75%	64%	65%	58%	45%
AP30_AB20_V1	81%	72%	73%	68%	54%
AP30_AB20_V2	83%	78%	78%	74%	61%
AP30_AB20_V3	83%	80%	80%	78%	65%
AP30_AB50_V1	80%	70%	71%	65%	52%
AP30_AB50_V2	82%	76%	76%	72%	58%
AP30_AB50_V3	83%	79%	79%	76%	62%
AP30_AB80_V1	79%	68%	69%	63%	50%
AP30_AB80_V2	81%	74%	75%	70%	56%
AP30_AB80_V3	83%	77%	77%	73%	59%
AP45_AB20_V1	82%	75%	76%	71%	57%
AP45_AB20_V2	83%	79%	79%	77%	63%
AP45_AB20_V3	83%	81%	81%	80%	67%
AP45_AB50_V1	81%	73%	74%	69%	55%
AP45_AB50_V2	83%	78%	78%	74%	61%
AP45_AB50_V3	84%	79%	80%	77%	64%
AP45_AB80_V1	81%	71%	72%	66%	53%
AP45_AB80_V2	83%	76%	77%	72%	58%
AP45_AB80_V3	83%	78%	78%	75%	61%
AP60_AB20_V1	84%	78%	80%	75%	61%
AP60_AB20_V2	84%	81%	81%	79%	67%
AP60_AB20_V3	83%	83%	83%	82%	69%
AP60_AB50_V1	83%	77%	77%	73%	59%
AP60_AB50_V2	84%	80%	80%	77%	64%
AP60_AB50_V3	84%	81%	81%	79%	66%
AP60_AB80_V1	82%	75%	75%	71%	57%
AP60_AB80_V2	84%	79%	79%	75%	61%
AP60_AB80_V3	84%	80%	78%	77%	64%

Regarding the percentage of thermal comfort hours, as presented in Table 4, the results show a decrease over time in relation to the current scenario. There was an average reduction of 12% in the hours of comfort in the optimistic scenario, and a decrease of 28% in 2030 and of 66% in 2080 in the pessimistic scenario. However, when implementing mitigation strategies to the office building, an increase in the hours of comfort was observed for 93% of the tested strategies. The most effective strategy to increase the thermal comfort hours in the

space was the one that involved a solar protection of 60°, an external wall absorptance of 20%, and solar control glass (FS=0.35), identified as AP60_AB20_V3. These strategies resulted in a 53% increase in the hours of comfort in the pessimistic scenario in 2080 when compared to the base building.

These results indicate that the implementation of mitigation strategies in architecture, can significantly contribute to increasing the hours of comfort in a context of climate change.

In terms of energy consumption, as shown in Table 5, the results indicate an expected increase in electric energy consumption over time in the current configuration of the office space. In the optimistic scenario (RCP 2.6), a 24% increase in energy consumption is projected for 2050 and a 25% increase for 2080. In the pessimistic scenario (RCP 8.5), the increase is even higher, with a projected 30% increase in 2050 and 40% increase in 2080. However, the simulated strategies demonstrated the ability to significantly reduce energy consumption.

In the simulations conducted, it was found that regarding the operation of windows and the hours of air conditioning use, there was an increase of 19% in the RCP2.6-2050 and RCP2.6-2080 scenarios, 32% in the RCP 8.5-2050 scenario, and 47% in the RCP8.5-2080 scenario. This increase justifies the average rise in energy consumption over the years. In the scenario without architectural changes, the use of air conditioning increases in 35% of the hours, being utilized in 90% of the operating hours. These results emphasize the importance of design improvement strategies to mitigate the increase in energy consumption and enhance the energy efficiency of the space.

Among the analyzed strategies, the most effective one for the current scenario again involved a solar protection angle of 60°, external wall absorptance of 20%, and glass with solar control (SHGC=0.35), identified as AP60_AB20_V3. This strategy aligns with the results obtained in the thermal comfort analysis, as it significantly increased the thermal comfort hours in the office space. By implementing these architectural strategies, a 15% reduction in energy consumption was achieved.

This same strategy demonstrated superior efficiency in all scenarios, achieving average savings of 30% compared to the reference scenario. Even in the pessimistic scenario, the energy consumption can be nearly equivalent to that of a scenario without any mitigation strategy.

Table 5: Variations of the scenarios in terms of electric energy consumption from the current and future climatic files.

		RCP 2.6		RCP 8.5	
Codigo	**2020**	**2050**	**2080**	**2050**	**2080**
CURRENT	104.86	138.03	139.07	149.73	175.50
AP30_AB20_V1	94.43	118.22	119.29	122.43	147.70
AP30_AB20_V2	92.31	111.39	112.51	120.59	137.22
AP30_AB20_V3	91.03	104.68	105.80	113.53	129.09
AP30_AB50_V1	95.46	122.42	123.50	132.18	152.59
AP30_AB50_V2	93.30	115.24	116.39	124.63	141.98
AP30_AB50_V3	92.02	108.56	109.67	117.59	133.86
AP30_AB80_V1	96.55	126.75	127.84	136.67	157.72
AP30_AB80_V2	94.36	119.24	120.39	128.81	146.99
AP30_AB80_V3	93.08	112.53	113.67	121.75	138.90
AP45_AB20_V1	92.97	112.03	113.07	121.28	139.30
AP45_AB20_V2	91.23	107.00	108.12	115.97	131.76
AP45_AB20_V3	90.23	101.38	102.50	110.03	125.09
AP45_AB50_V1	93.96	116.15	117.20	125.60	144.09
AP45_AB50_V2	92.20	110.82	111.95	119.97	136.45
AP45_AB50_V3	91.17	105.19	106.29	114.02	129.77
AP45_AB80_V1	95.02	120.41	121.49	130.03	149.14
AP45_AB80_V2	93.24	114.75	115.88	124.08	141.39
AP45_AB80_V3	92.22	109.11	110.21	118.15	139.73
AP60_AB20_V1	91.41	103.05	104.05	111.84	128.10
AP60_AB20_V2	90.06	100.21	101.28	108.81	123.80
AP60_AB20_V3	89.37	95.94	97.01	104.25	119.00
AP60_AB50_V1	92.31	106.88	107.88	115.85	132.56
AP60_AB50_V2	90.94	103.85	104.90	112.62	128.12
AP60_AB50_V3	90.21	99.48	100.54	108.00	123.34
AP60_AB80_V1	93.30	110.84	111.84	120.00	137.36
AP60_AB80_V2	91.91	107.58	108.65	116.56	132.70
AP60_AB80_V3	91.16	103.18	104.20	111.86	127.93

4. CONCLUSION

This study presented an investigation of an office space that operates in a hybrid mode located in a commercial building in Belo Horizonte, Brazil, to assess the effects of climate change on its thermal and energy performance. The conducted simulations demonstrated that over time, the thermal comfort hours decrease and energy consumption increases, particularly in the pessimistic scenario. Natural ventilation shows to still be an interesting feature to this kind of space as, although comfort hours diminish, they are still high in all analyzed scenarios.

Even more, architectural improvement strategies, such as adopting adequate solar protection, low external wall absorptance, and selecting solar control glazing, proved to be effective in mitigating these impacts. These strategies were able to increase thermal comfort hours and reduce energy consumption in all scenarios, resulting in a more efficient and comfortable working environment.

Therefore, it can be concluded that considering architectural design from the early stages, taking into account climate change and adopting sustainable design strategies, is crucial. These conclusions are relevant not only for the studied city but also for other regions affected by climate change, providing guidelines for the design and construction of more resilient and energy-efficient buildings.

ACKNOWLEDGEMENTS

The authors would like to thank the National Council for Scientific and Technological Development (CNPq) and Minas Gerais State Research Support Foundation (FAPEMIG) for providing financial support for this research.

REFERENCES

1. Geraldi, M. S., Ghisi, E. (2020). Mapping the energy usage in Brazilian public schools. Energy and Buildings, 224, 110209, https://doi.org/10.1016/j.enbuild.2020.110209.

2. Wong, S.L., Wan, K.K.W., Li, D.H.W., Lam, J.C. (2010). Impact of climate change on residential building envelope cooling loads in subtropical climates. Energy and Buildings, 42, 2098-2103, https://doi.org/10.1016/j.enbuild.2010.06.021

3. MME - Balanço Energético Nacional 2022: Ano base 2021. Empresa de Pesquisa Energetica, Rio de Janeiro (2022). Available on: https://www.epe.gov.br/pt/publicacoes-dados-abertos/publicacoes/balanco-energetico-nacional-2022 (Access in: 29 April 2022).

4. NDC Registry, disponível em: https://www4.unfccc.int/sites/NDCStaging/Pages/All.aspx, 2021.

5. IEA. World energy outlook 2018: The future is electrifying. International Energy Agency, 2018.

6. IPCC, 2022: Summary for Policymakers [H.-O. Pörtner, D.C. Roberts, E.S. Poloczanska, K. Mintenbeck, M. Tignor, A. Alegría, M. Craig, S. Langsdorf, S. Löschke, V. Möller, A. Okem (eds.)]. In: Climate Change 2022: Impacts, Adaptation and Vulnerability. Contribution of Working Group II to the Sixth Assessment Report of the Intergovernmental Panel on Climate Change. Cambridge University Press, Cambridge, UK and New York, NY, USA, pp. 3–33, doi:10.1017/9781009325844.001.

7. Amaripadath, D., Rahif, R., Zuo,W., Velickovic, M.,Voglaire, C., Attia, S. (2023). Climate change sensitive sizing and design for nearly zero-energy office building systems in Brussels, Energy Buildings. 286, 112971, doi: 10.1016/j.enbuild.2023. 112971.

8. Füssel, H.M. (2007). Adaptation planning for climate change: concepts, assessment approaches, and key lessons, Sustainability Science 2, 265–275, https://doi.org/10.1007/s11625-007-0032-y.

9. Triana, M.A., Lamberts, R., Sassi, P. (2018). Should we consider climate change for Brazilian social housing? Assessment of energy efficiency adaptation measures, Energy and Buildings 158, 1379–1392, https://doi.org/10.1016/j.enbuild.2017.11.003.

10. WeatherShift, March 30, 2022), https://www.weathershift.com/.

11. Jiang, A., Liu, X., Czarnecki, E., Zhang, C. (2019). Hourly weather data projection due to climate change for impact assessment on building and infrastructure, Sustainable Cities and Society. 50, 101688, https://doi.org/10.1016/j.scs.2019.101688.

12. Jentsch, M.F., James, P.A.B., Bourikas, L., Bahaj, A.S. (2013). Transforming existing weather data for worldwide locations to enable energy and building performance simulation under future climates, Renew. Energy 55, 514–524, https://doi. org/10.1016/j.renene.2012.12.049.

13. E. Rodrigues, M.S. Fernandes, D. Carvalho. (2023). Future weather generator for building performance research: an open-source morphing tool and an application. Building and. Environmental, 233, 110104, https://doi.org/10.1016/j.buildenv.2023.110104

14. Neves, L.O., Melo, A.P., Rodrigues, L.L. (2019). Energy performance of mixed-mode office buildings: Assessing typical construction design practices. Journal of Cleaner Production, 234, 451-466, https://doi.org/10.1016/j.jclepro.2019.06.216.

15. Haase, M., Amato, A. (2009). An investigation of the potential for natural ventilation and building orientation to achieve thermal comfort in warm and humid climates. Solar Energy, 83, 389–399, https://doi.org/10.1016/j.solener.2008.08.015.

16. Alves, T. P, Souza, R. V. G, Machado, L, Wilde**,** P. (2018) Assessing the energy saving potential of an existing high-rise office building stock. Energy and Buildings, v. 173, p. 547-561. https://doi.org/10.1016/j.enbuild.2018.05.044

17. Veloso, A.C.O.; Filho, C.R.A.; Souza, R. V. G. (2023) Desenvolvimento de arquétipo de edifício de escritórios com ventilação híbrida: abordagem metodológica para desenvolvimento de modelo. VII Congresso Latino-Americano de Simulação de Edifícios – IBPSA LATAL 2023.

18. Climate One Building, c2020. Available at: < http://climate.onebuilding.org/>. Accessed in: April, 2023.

PLEA 2024 WROCŁAW
(Re)thinking Resilience

Floating platforms for generating emission-free electric energy

JANUSZ RĘBIELAK[1]

[1]Wroclaw Branch of the Polish Academy of Sciences, Wroclaw, Poland

ABSTRACT: The article presents two concepts of constructing floating platforms at sea intended for emission-free production of electricity. In the first one, electricity is generated using photovoltaic panels placed along the edge of a large circular floating platform. In the second and most important concept each platform consists of two main parts stacked horizontally on top of each other, the lower of which is a floating platform. These two separate components of the platform are connected to each other using special support nodes. Each of these nodes has the general shape of a cone and is free to rotate around the vertical axis of the cone. The kinetic energy of sea waves is absorbed by the lower platform floating on the water, setting it in motion, which motion is transmitted to the upper platform via support nodes. The rotating support nodes are connected to electric current generators. The energy generated in this way can be sent directly to external recipients or temporarily stored in the platforms themselves. The paper includes drawings showing examples of appropriate design solutions.
KEYWORDS: Sea, Platform, Energy, Electricity, Emission-Free.

1. INTRODUCTION

In the era of rapidly progressing climate change there is an intensive development of modern electricity generation technologies with significantly reduced levels of greenhouse gas emissions or complete elimination of such gas emissions. The efficiency of new energy technologies can be significantly increased by applying new structural solutions.

The paper presents proposals for shaping platforms designed as artificial floating islands, which can also be the basis for the food and energy self-sufficient residential habitats, where electricity is generated from the movement of sea waves.

2. STRUCTURAL CONCEPT OF SYSTEM OF COMPOSITE FOUNDATION

The composite foundation system has been developed for the foundation of heavily loaded buildings, including high-rise buildings, located on ground with very low load-bearing capacity and in areas of seismic activity or mining damage, which is presented in detail in paper [1]. Module of its intermediate system has a lenticular shape, see Fig. 1a, and it is constructed of straight members, under axial compression or tension, located in a narrow space between two beams parallel to each other or located on two sides of one beam (1) placed on a horizontal base plate (2). The intermediate system is connected to the material of each beam (1) by means of joint nodes of the types (Cn) and (Ce) distributed evenly along the neutral axis of the beam. Nodes of type (C) or (B) connect adjacent lenticular modules of the indirect system and not join the beam matter (1).

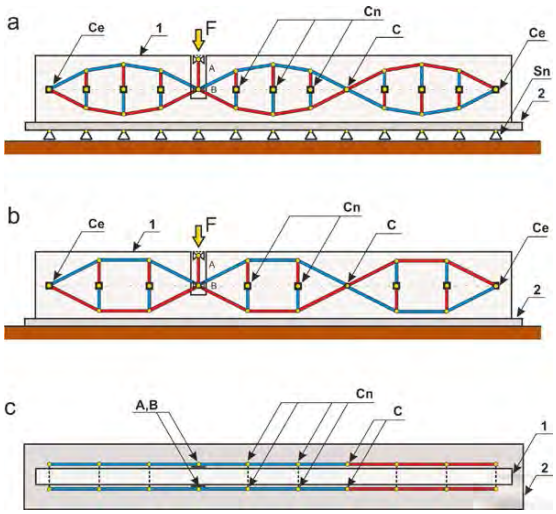

Figure 1: General schemes of structure of the system of composite foundation together with suggested arrangement of special support nodes (Sn).

The lenticular modules connect to the matter of the beams (1) via nodes (Cn) and (Ce). The forces loading (F) the overall foundation structure are applied to type nodes (B, C, Ce) via a short vertical member, placed in appropriate guides, capable of the small vertical displacements. This lenticular module can take simplified shapes, see Fig. 1b, and be replicated endlessly along the horizontal direction due to which surface of the foundation can be theoretically

unlimited and stresses in the ground below this foundation can be very small. A top view of such a structural system is shown in Fig. 1c. Beams (1) can be arranged along different directions to form, for example, orthogonal structures like units shown in Fig. 2 and in Fig. 3.

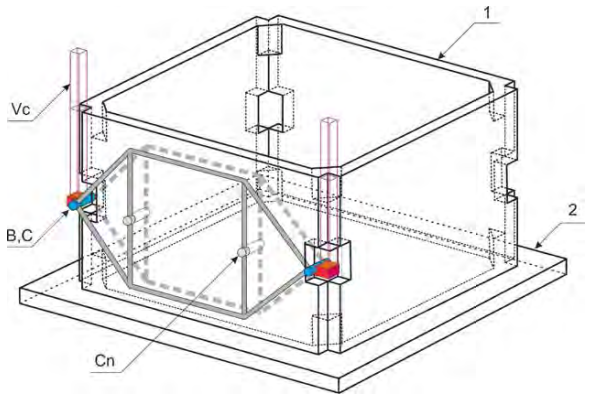

Figure 2: A simple one-story shape of a rectangular unit of the system of composite foundations.

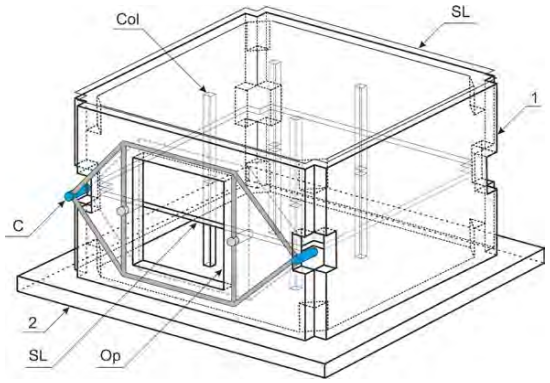

Figure 3: An example of a two-storey shape of a rectangular unit of the system of composite foundations.

It is assumed that a square will be the most favorable shape for the base of an orthogonal unit. If the horizontal geometric dimensions of such a unit are quite large, an appropriate number of columns (Col) should be placed inside it, see Fig. 3. In these cases the construction depth of the beams (1) can also be big. Therefore, for structural and functional reasons, it will sometimes be necessary to design horizontal ceilings (SL) for at least two floors. Their spaces can be intended to perform various functions. For them to be met effectively, technical openings (Op) must be properly arranged in the materials of the basic beams (1).

As mentioned earlier, beams (1) can be placed in different directions, for example creating orthogonal structures composed of large watertight boxes which, when properly connected to each other, can form large artificial floating islands as it is shown in Fig. 4. Such artificial islands with large geometric dimensions, suitably anchored in the bottom of the coastal zone of the tropical sea, can be the bases for objects of numerous utility functions, such as e.g., residential, commercial, warehouse, industrial function or others.

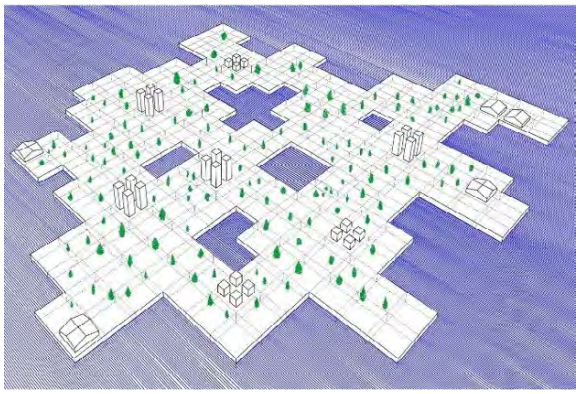

Figure 4: Bird view of floating habitable and industrial artificial island.

3. ARTIFICIAL ISLAND CALLED OCEAN AGAVE

The Ocean Agave, see Fig. 5 - Fig. 10, is planned as an artificial island floating in subtropical ocean areas, in a far distance from land, the sailing direction of which can be controlled by means of set of ship propellers moved by electric engines together with set of rudders. It is indented as an independent settling unit that is self-sufficient in terms of energy and food supply and able to house a group of less than 200 persons [2]. The main bearing structure of the Ocean Agave is exactly the system of composite foundation. Although it has been developed for foundation of the very heavily loaded structures constructed on unstable background but due its structural features, like having a small construction depth, it can get numerous and various applications.

Figure 5: Bird view of the Ocean Agave.

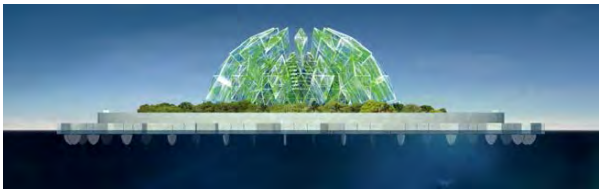

Figure 6: Simplified elevation of the Ocean Agave.

The platform of the Ocean Agave has the structural system of composite foundation having a circular shape, see Fig. 5, and it is built by using properly connected, sealed, steel-reinforced concrete boxes, having mostly trapezoidal shapes with construction depth of 15 meters. Between them are located component parts of the intermediate system having various structural forms. The interior area of this artificial island is protected by the main reinforced concrete breakwater running along its perimeter and having height of ca. 25 meters. The boxes form a circle, having slightly more than 400 meters in diameter, surrounded by perimeter breakwater, which is supplemented with a set of triangular, reinforced concrete elements forming loading bays, constructed similarly to the boxes themselves and with properly placed trapezoidal reinforced concrete elements, which act not only as the circumferential breakwaters, but also they are basic parts of engineering devices able to obtain energy from movement of the sea waves. Another source of electric energy are the photovoltaic panels situated on the oblique internal surface of the circular breakwater.

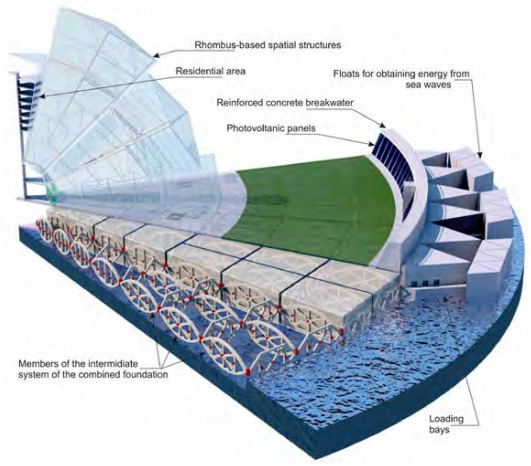

Figure 7: General scheme of arrangement of structural component parts inside whole space of the Ocean Agave.

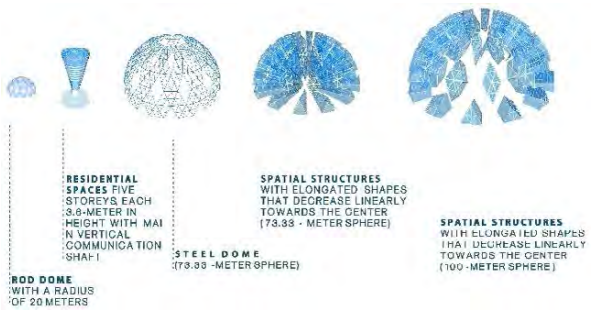

Figure 8: Spatial structures forming the Structural Agave.

Species of trees, shrubs and grass having high resistance to the increased amount of salt contained in the air are in a wide ring belt located between the central part of the Ocean Agave and its coastal zone.

The assumed shape of central part of the Ocean Agave is dictated by the pursuit of allowing the best possible lightning conditions for plants with low tolerance for presence of salt in the air in proximity of the sea water. For this reason, they were placed in enclosed, air-conditioned glass spatial structures with elongated shapes. The plants are grown in appropriate pots that contain fertile soil and are watered by drop irrigation. The pots are evenly placed within each structure and are stably mounted into proper nods by rods and ties.

The lower parts of the spatial structures are mounted onto the nodes of a smaller lattice dome with a radius of 20 meters. Other supporting nodes of these structures are proper indirect nodes that also function as openwork nodes of steel dome with radius equal to 73.33 meters. The residential spaces for permanent inhabitants of Ocean Agave are situated in its middle on five storeys, each 3.6-meter in height.

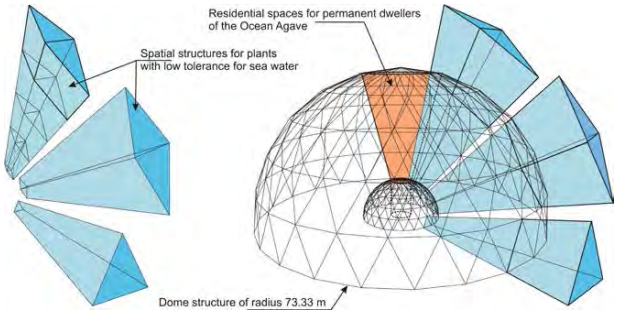

Figure 9: Shapes of the main types of spatial structures located in the center of the Ocean Agave.

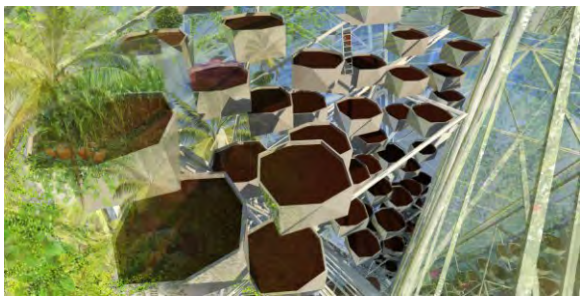

Figure 10: Interior view of spaces of the elongated structures.

The center of the artificial island houses a structure called Structural Agave, divided into several dozen spatial structures with elongated shapes that decrease linearly towards the center, and whose axes converge in the central point of the whole settlement. Their cross-sections are mostly rhombus-based, while only these directly connected to the upper platform's level have their cross-sections shapes into triangles. A structure built this way

possesses a form that closely relates to a shape of 100-meter sphere. These spatial structures are made of stainless steel and covered with appropriate glass panels, which are covered finally by semi-transparent photovoltaic foils.

The permanent dwellers can obtain the protein food from fish in waters surrounding Ocean Agave or bred along with other species of sea animals within appropriate underwater devices, available from numerous loading bays. External re-supplying is to be handled by means of keelboats transporting goods between Ocean Agave and a ship located nearby. Although the Ocean Agave theoretically may not possess its own propulsion, but the potentially huge amount of electric energy generated by devices installed on it induces to equip the floating structure with sets of electric engines used to drive ship propellers immersed in water at an appropriate depth.

4. STRUCTURE OF SPECIAL TYPE OF SUPPORT NODE

The composite foundation system, together with a special type of support node, constitute an unified structural unity and have been developed for the safe foundation of dynamically loaded objects. This mostly concerns the foundation of buildings placed in seismically active areas or located in areas of mining damage. The structural system of one of the basic types of such a support node is shown in Fig. 11-14.

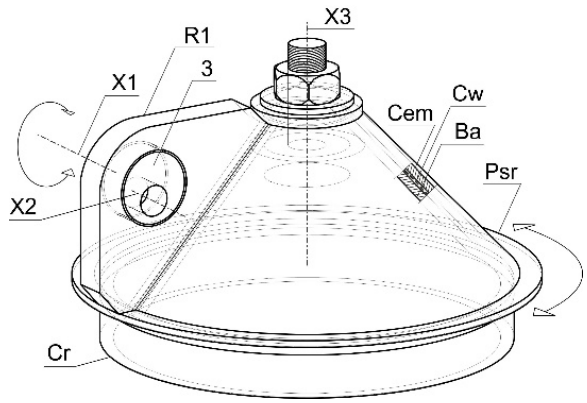

Figure 11: Conical form of main body of special support node with a single rib.

The basic type of the support node structure is made of two sets of conical bodies, while each set consists of two conical modules, of which the basic one (Ba) is fixed permanently by means of a circular ring (Cr) in the upper (Up) or in the lower (Lo) part of the floating platform. Each conical support node is fitted with a conical external module (Cem), which is fully rotatable around the vertical axis X3. Between the basic inner conical module (Ba) and the conical external module (Cem) there is a conical washer (Cw), made for example of Kevlar, which facilitates the rotation of the conical external module (Cem) on the

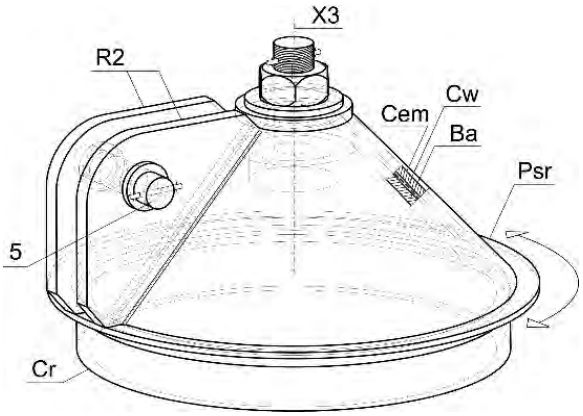

Figure 12: Conical form of main body of special support node with double ribs.

internal module (Ba) around the vertical axis X3. The first set of conical body, see Fig. 11, has a conical external module (Cem) equipped with a single vertical rib (R1) located along an element of a cone and is permanently connected to the conical outer module (Cem). The single vertical rib (R1) has a relatively large thickness and has a circular opening in which a circular roller (3) is accommodated in a fitted manner, for which the axis of rotation is the horizontal axis X1. Within the roller (3) there is a cylindrical hole, for which the axis of rotation is the X2 axis, also located horizontally and parallel to axis X1. Each conical external module (Cem) is equipped with a perimeter stabilizing ring (Psr). The second set of conical body has a similar structure, see Fig. 12, except that this time two vertical ribs (R2) are permanently connected to the conical outer module (Cem), and the thickness of each is half that of single rib (R1). In each of the two ribs (R2) there is a cylindrical hole for placing a horizontal pin (5), whose task is to join in an articulate way the two sets of conical bodies into a single support node, see Fig. 13 and Fig. 14.

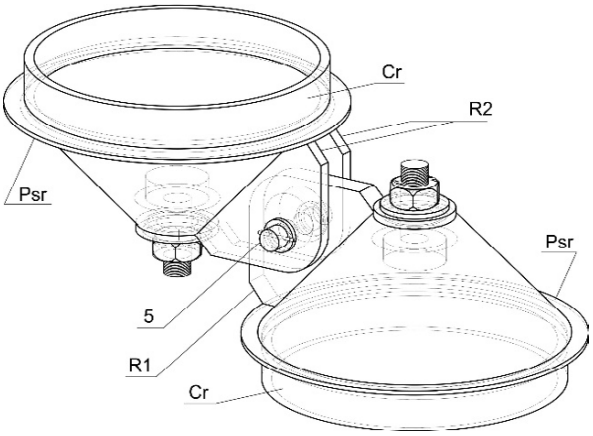

Figure 13: *General view of basic variant of the support node made of two conical bodies.*

The support nodes built in this way and properly connected to the composite foundation system, compare Fig. 1a, can constitute a horizontal dilatation

of the structure of the object from its ground and thus meet the main requirements for the structures of objects loaded dynamically, which include buildings located in zones seismically active or erected in the areas of mining damage, as it is presented in [3-7].

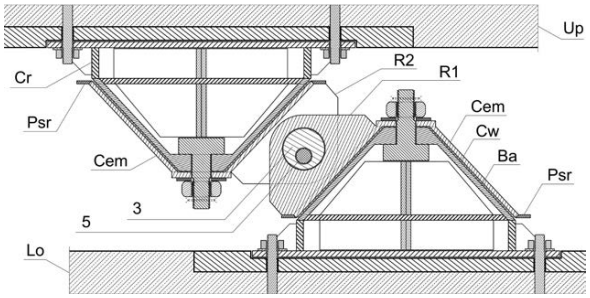

Figure 14: Vertical section of the support node with conical forms of the main bodies.

In each single foundation sector, the arrangement of single (R1) and double (R2) ribs must be identical, and the number of such support nodes will be quite large [8]. Thanks to this and due to use of appropriate conical washers (Cw), the deviations of the vertical axes (X3) of these nodes will be insignificant and their impact on the deformations of the components of the structure will be negligible, due to which the values of these deformations can be within the acceptable dimensional tolerance of the entire structure.

5. FLOATING ELECTRIC POWER STATION

The concept of a floating electric power station just presented has been formulated by application of the basic variant of the support node designed for dynamically loaded objects. In this case the set of nodes must provide effective separation of the two main components of the floating platform, the upper one (Up) and the lower one (Lo), which are located on top of each other. This set enables them to move smoothly between each other only in horizontal directions within a specific range of these displacements.

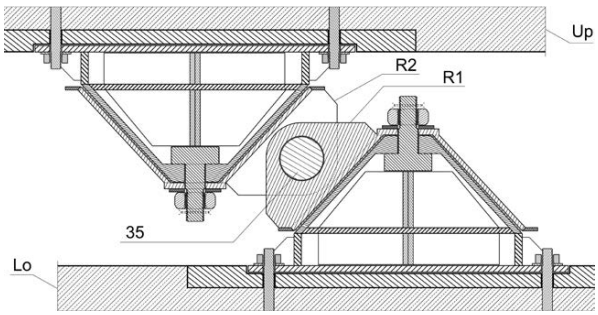

Figure 15: Vertical section of the support node for floating platform designed as a base of the electric power station.

Since in this case there is no need to ensure the possibility of mutual displacements in the vertical direction of the lower and upper parts of the floating platform, the presence of the horizontal pin (3) was eliminated and only the horizontal circular roller (5) was used, which has this time the diameter of the hole located in the single rib (R1) and passing through the all vertical ribs (R1 and R2). In Fig. 15 and in Fig. 16 such a new shape of the horizontal circular roller is marked with the symbol (35). It may be permanently connected to the matter of the two vertical ribs (R2), for example by welding it along its peripheral contact edges with the outer surface of the two vertical ribs (R2).

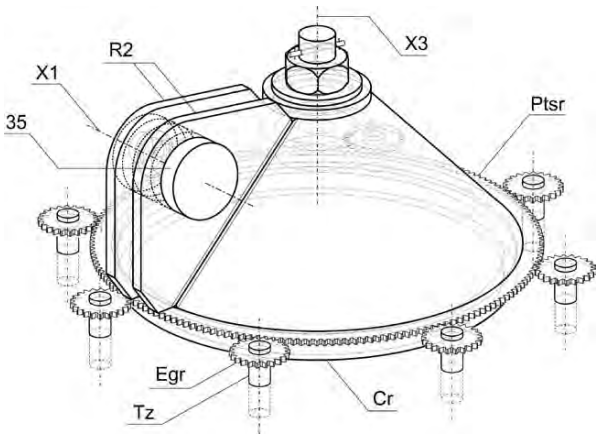

Figure 16: The conical body of the support node with a circumferential gear and a set of external gears.

The main task of the structure of the conical support node is the effective damping of vibrations caused by the dynamic load applied from any direction through the controlled movement of the lower and upper parts of the object connected with a set of such nodes. At the very high values of dynamic loads, these displacements, in this case only in the horizontal plane, consisting in the mutual rotation of the basic conical bodies relative to the vertical axes, sometimes can be extremely fast, which may be dangerous for the whole device.

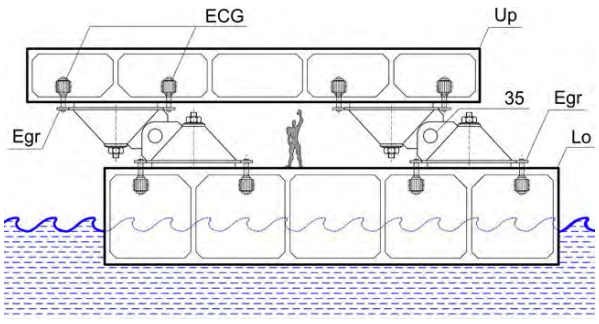

Figure 17: Scheme of the vertical section of the floating platform structure.

To make the vibration damping processes more effective it will be beneficial to transfer the kinetic rotational energy of each of the conical bodies to as

many outside devices as possible (Egr), see Fig. 16, which will be able to absorb this energy in a safe, controlled, and useful manner.

This can be achieved, for example, by making the circumferential stabilizing ring (Ptsr) in the form of a toothed wheel cooperating with external gears (Egr) appropriately spaced around the circumference of this wheel. If the vertical members (Tz) are connected directly to the electric current generators (ECG), they will transmit the kinetic energy from the rotation of the conical bodies to these generators, appropriately connected to the upper part (Up) and lower part (Lo) of the floating platform, see Fig. 17 [8]. The mutual rotation of the upper (Up) and lower parts (Lo) of the floating platform will be caused by the energy of sea waves coming from any direction to its lower part (Lo). The platform can be of various sizes, it can form groups of platforms, be anchored in the coastal zones of seas and oceans, and can also be repositioned in sea basins. The electric energy generated in this way can be stored in battery packs located in the spaces of the lower and upper parts of these platforms or sent via electric cables to other users.

Initial verifications of the design and technological assumptions and preparation of appropriate drawing documentation were carried out based on numerical models of the designed structural systems defined in the Formian programming language [9].

6. CONCLUSIONS

The structural system of the composite foundation can take many different forms and be the basis for the safe positioning of heavily loaded objects, even on very unstable ground. Being made of waterproof boxes properly connected to each other, it can be the main supporting structure of artificial islands located in seas and oceans. The specially designed support node, as an integral part of the composite foundation system, allows for safe and useful absorption of the dynamic loads. Thanks to this sets of such support nodes can be used in the construction of the floating platforms applied to generate emission-free electricity due to the appropriate absorption of sea wave energy.

The proposed structural systems and equipment of the floating platforms must be subjected to thorough and comprehensive static, dynamic and strength analyzes as well as testing of the objects carried out on a natural scale, it also means the test studies of the structural system on a scale of 1:1, to assess their practical suitability for the proposed purposes.

ACKNOWLEDGEMENTS

I would like to thank Wojciech Kocki and Maciej Rębielak for technical assistance in preparation of drawings and visualizations for the Ocean Agave design made for the international architectonic competition eVolo2015.

REFERENCES

1. Rębielak, J,. (2012). System of combined foundation for tall buildings, *Journal of Civil Engineering and Architecture*, 6(12): p. 1627-1634.
2. Rębielak J,. (2018). System of combined foundation as base for mega-structures. In *Proceedings of IABSE Spring Conference: Engineering the Developing World*. Kuala Lumpur, Malaysia, April 25-27.
3. Charleson, A., (2008). Seismic design for architects. Outwitting the quake: Elsevier Ltd.
4. Das, B.M,. (2014). Principles of Foundation Engineering: 5th Edition, Pacific Grove, Thomson/Brooks/Cole.
5. Coduto, D.P,. (2001). Foundation Design: Principles and Practices, 2nd Edition: Prentice Hall.
6. Tomlinson M.J., (2001). Foundation Design and Construction: 7th Edition, Prentice Hall.
7. Elnashai, A. S. and Di Sarno L,. (2008). Fundamentals of Earthquake Engineering: John Wiley & Sons, Ltd.
8. Rębielak, J., (2023). Structural node of foundation for buildings located in seismic areas. In *Proceedings of International Association for Shell and Spatial Structures Annual Symposium*. Melbourne, Australia, July 10-14.
9. Nooshin, H. and Disney P., (2000). Formex configuration processing, *International Journal of Space Structures*, 15(1): p. 1-52.

PLEA 2024 WROCŁAW
(Re)thinking Resilience

Improving the outdoor thermal comfort by solar shading and evaporative cooling in a nursery school in Rome, Italy

MICHELE ZINZI[1], ANDREA CANDUCCI[2], LUNA CIARINI[3], DANILA SEVERA[4], ALESSANDRA BATTISTI[2]

[1] ENEA Italian National Agency for New Technologies, Energy and Sustainable Economic Development, Rome, Italy
[2] Department of Planning, Design, Technology of Architecture – Sapienza University of Rome, Rome, Italy
[3] Free lance pedagogist, Rome, Italy
[4] Municipality of Rome, Rome, Italy

ABSTRACT: The urban overheating is a well-known phenomenon fuelled by the global and local climate change. Solutions to mitigate the severe heat conditions are highly beneficial for pupils who cannot enjoy the outdoor spaces for playing during the warm season. This study documents the impact of outdoor solar shading devices, alone or in combination with an evaporative cooling system, to improve the outdoor thermal comfort conditions in a nursery school in Rome, Italy, and it stands as a pioneering study for climate adaption measures to be installed in schools. The activities were carried out in the second half of July 2023. The instrumental monitoring took place under two gazebos, one equipped with the misting system, and in an open-air reference spot. The sole effect of the solar shading did not significantly improve the outdoor thermal conditions; instead, the average and peak air temperatures dropped by 5 and 8.5°C, respectively, under the misting system, also the thermal comfort index dropped by 0.5 on average, scoring 0.9 as absolute vote. The subjective monitoring took place by submitting an ad-hoc questionnaire to 2/3 years old pupils, whose majority positively evaluated the misted outdoor environment in terms of heat perception and well-being.
KEYWORDS: Outdoor thermal comfort, evaporative cooling, solar shading, monitoring, schools, pupils

1. INTRODUCTION

The urban overheating is a well-documented phenomenon, which originates from global and local warming, in particular the urban heat island for the latter [1, 2]. The trend is continuing to rise due the massive increase of the world population living in urban areas, bound to reach 68% by 2050 [3]. The risk is related to the increase of average and peak temperatures, as well as of extreme events, such as heat waves and hot spells [4]. Thus, cooling down the cities is critical to tackle the consequent social, economic and environmental threats [5, 6].

Many studies were carried out to identify suitable technologies and strategies to tackle the phenomenon; they include cool materials, green infrastructure and water-based technologies [7]. Such solutions are able to reduce the air temperature in the outdoor built environment, as shown from more than 200 projects [8]. Outdoor temperature mitigation allows the reduction of cooling energy or the improvement of thermal comfort in buildings [9, 10], while improving the outdoor thermal comfort conditions [11]. It must be noted that urban solar shading systems can also be used for improving thermal comfort conditions [12].

As the energy prices are subject to sudden variations due to well-known international factors, a large part of the population is experiencing energy poverty. This is particularly true for southern countries, where the need for cooling is more and more needed [13]. The problem is relevant also for non-residential buildings, especially in schools where the main occupants - pupils - deserve special attentions and care [14]. In this perspective, several studies are approaching the pedagogical and sociological importance of outdoor spaces, defined as the prerequisite to trigger processes of change in contexts where pupils are encouraged to relate to themselves and others in a different way than in the indoor environment [15]. Activities raise awareness on issues of respect for the environment, self-perception in the world and health of body and mind [16].

The case of the city of Rome, Italy, is emblematic: the overheating risk guidelines require that pupils cannot stay outdoors during days with temperature above certain values. This approach has two drawbacks, especially for the well-being of nursery school pupils:

i) the overheating risk moves from the outdoor to the indoor environment, which is not adequately cooled in practically all Italian school buildings;
ii) pupils cannot enjoy and play outdoors most of the time during the hottest months, even if such moments should be pursued as much as possible.

Several studies are carried out to assess the cooling potential and thermal comfort improvement thanks to evaporative misting systems, a water-based mitigation technology that is gaining attention [17, 18]. After testing the potential of evaporative cooling installations [19, 20], this research aims to evaluate the potential of outdoor solar shading devices combined with evaporative misting cooling and how these technologies are received by 2/3 years old pupils in terms of comfort and well-being. The field study is based on instrumental measurements and users' subjective preferences in a nursery school in Rome.

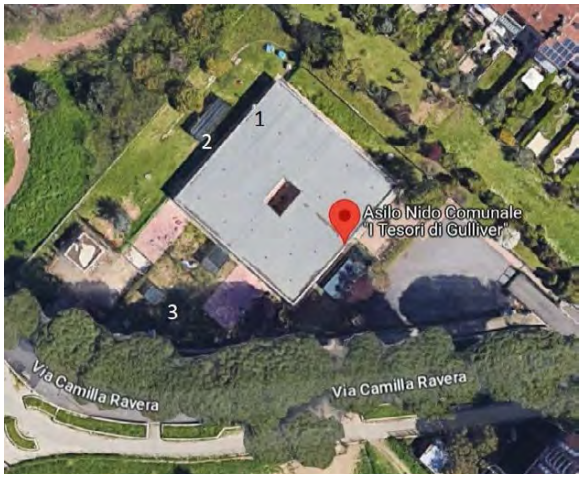

Figure 1: Aerial view of the school and its garden. Monitoring spots: 1 reference spot on the roof, 2 gazebo with the evaporative system, 3 gazebo with shading only.

2. MATERIALS AND METHOD

The study is structured in the following steps:

1. Identification of the case study to carry on the analysis on the mitigation technology potential;
2. Characterisation of the above technologies in the selected urban context;
3. Description of the experimental procedure, performance indicator and subjective questionnaire for thermal comfort and mitigation;
4. Run of the field study and analysis of the results.

2.1 The case study

I Tesori di Gulliver is a nursery school located in the northern outskirts of Rome. The city belongs to the *Csa* class, Mediterranean climate, according to the Köppen-Geiger climate classification. The school hosts about 40 pupils from two to three years old and about 8 adults among technical and teaching staff on daily basis. Nursery schools are generally open until the end of June, but selected ones are open until the end of July to support families, generally low-income and with both parents fully employed.

Being in outskirts, the school is surrounded by green areas and has a wide garden for open-air activities, see the aerial view of the school in Figure 1. The school is selected for being open in July, the hottest month in Rome with August. In addition, the rotation of teaching and technical staff during the period allows a good number of potential interviewees. It is important to note that the thermal conditions experienced in July in the outskirts of Rome are observed much earlier in the central districts of the city because of the severe urban heat island phenomenon [21].

2.2 Thermal comfort technologies: the misting cooling system and the solar shading

The school has installed several gazebos made of a wooden structure and a dark green plastic textile that provides 85 % solar protection. Two are selected for the thermal comfort assessment: S3 (gazebo 3, Figure 1) to test the impact of solar shading, S2 (gazebo 2, Figure 1) to test the combined effect of solar shading and evaporative cooling. The undisturbed microclimatic data are measured on the roof (spot 1).

The latter is achieved by a misting system consisting of 28 nozzles, with 90cm inter-nozzle, covering a misted area of 5.0x2.6m^2. The nozzles are secured to the horizontal wood beams at the top of the gazebo to ensure a vertical emission of the nebulised water; the nozzles are mounted at about 2.3m height from the ground, so the cooled volume is about a 30 m^3. It should be noted that in normal conditions, the height of the nozzles might wet a standing adult. However, this did not happen as the area is used by 2-3 years pupils and the teachers mainly seated. The water circulation is activated by a 70 bar self-compensating pump, with constant electric absorption of 0.6kW. Each nozzle has a standard flow rate of 4.72 litres per hour.

2.3 Quantitative evaluation of thermal comfort

The monitoring set-up consists of three observation spots. The measured quantities and the sensors' specifications are reported in Table 1 and Table 2, respectively. In addition to the measuring spots in the S2 and S3 gazebos, the unaltered microclimatic conditions are measure on the roof (S1) at 3 meters from the ground. The performance indicator used for the assessment is the MOCI (Mediterranean Outdoor Comfort Index), an indicator developed and validated ad-hoc for the Mediterranean area and based on the ASHRAE 7 vote classes (-3/+3) [22]. MOCI is a function of air temperature (AT) and relative humidity (RH), radiant mean temperature (MRT), wind speed (WS) and clothing. It is used for the measuring station under the shaded gazebos. The mean radiant temperature (MRT) is calculated from air speed, air temperature and globe

temperature (GT). The corrected MOCI, in which the MRT is replaced by the global solar irradiation (GSI) [23], is used for the undisturbed station, as fast-response pyrometers are more effective than slow-response globe-thermometers under dynamic outdoor conditions. MOCI is calculated in S3 assuming the same wind conditions as S1.

Table 1: Sensors mounted in the three measuring spots

Quantity	Abbr.	S1	S_2	S3
Air temperature	AT	X	X	X
Air relative humidity	RH	X	X	X
Wind speed	WS	X	X	
Wind direction	WD	X	X	
Solar irradiation	GSI	X		
Globe temperature	GT		X	X

Table 2: Specifications of the installed sensors

Parameter	Unit	Range	Resolution	Accuracy
Air temperature	°C	-40 /60	0.1	± 0.3
Air relative humidity	%	0-100	1	± 1.5
Wind speed	m/s	0-30	0.01	0.3
Wind direction	°	0-359	1	±5
Solar irradiation	W/m^2	0-1000	0.1	±3%
Globe temperature	°C	-30/120	0.1	± 0.3

The monitoring is carried out during 12 days (18-21 and 24-31) of July 2023. Data are acquired 24 hours per day with 10 minutes resolution step. The misting system is activated automatically when the MOCI reaches 1, which represents the start of the thermal discomfort zone, and it is switched off at 16:00 local time (15:00 CET), when the pupils leave the school. The results are evaluated for the hours in which the misting system is switched on for comparison purposes.

Figure 2: Teachers and pupils under misting in spot 2.

2.4 Pupil subjective evaluation of thermal comfort

Given the age of the pupils, the qualitative test is implemented with the aid of images characterising each individual gradient of the question asked. For the first question, the key element is the colour, as the 2/3 years old pupils know and distinguish the primary colours. For the second and third questions, images are used so that the children can encode the question posed (word and image). The test, implemented with the collaboration of the educators, consists of three questions presented with the support of the images presented in Figure 3. The questions refer to the following:

- ✓ Heat perception (a - a lot, a red sun; b - a little, an orange sun; c - neutral, a yellow sun);
- ✓ Well-being perception (a - "I am well", a smiling face; b - "I am not well", a sad face);
- ✓ Experiencing space (a - playing outside, a garden; b - play in the classroom, a school).

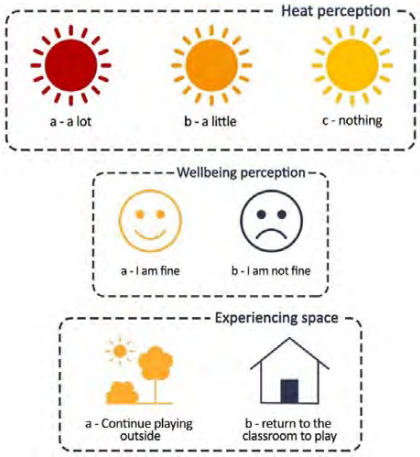

Figure 3: Questionnaire prepared to the school pupils.

3. RESULTS

The results of the two investigation topics are reported in next sub-sections.

3.1 The quantitative monitoring

Table 3 reports the average monitored data and the calculated indicators (mean radiant temperature and MOCI) during the period of not-operation of the misting system. The considered data refer to the hours in which the misting system was typically operated (30 hours in total). This information is useful to compare the performance of the shading devices in the two gazebos (S1 and S2) with respect to the reference zone (S3). In S2, where the wind speed is not calculated, the indicators are calculate assigning the wind speed of spot 1(*) and spot 2(**), respectively. In both cases it can be observed that the thermal comfort is similar under the two gazebos, as the air temperature and relative humidity differences fall in the measurement error of the sensors.

The difference in MOCI thus depends on the different mean radiant temperature, which is a function of the globe temperature. The latter measurement, in

turn, is affected by the geometry of the gazebo, the sky vault viewed by the sensor, the solar irradiation filtering through the shading device and the shadows projected by the high trees on the gazebos. Such context variability explains the differences (however small) in measured globe temperature and calculated MRT in the two zones.

Significant differences are instead observed between the reference spot on the roof and the two gazebos. This is due to the higher wind speed measured on the roof compared to that measured in the garden (S2) for a small amount; the high discrepancy is here introduced by the different contribution of the TMR, which in the corrected MOCI is replaced by the global solar irradiation. In fact, replacing the GSI with MRT calculated for S2 the MOCI in the two spots gives the same result. For the reason explained above, the corrected MOCI had to be used in S1 for the purpose of a more correct measurement even if this probably brings an underestimation of thermal comfort conditions in S1 and, contextually, requires a revision of the thermal comfort indicator.

This is a limit for the study and it can be noted that MRT calculated with the globe thermometer under the sun would have led to higher reference MOCI and made it possible to compare the thermal comfort improvement due to the solar shading alone. This consideration applies for the next results as well.

Table 3: Average values of the measured quantities and calculated indicators when the misting system is switched off

Spot	WS (m/s)	AT (°C)	RH (%)	MRT/GSI (°C/ W/m²)	MOCI (-)
S1	1.1	32.4	46	717.0	1.3
S2	0.7	31.7	48	43.9	1.6
S3*		31.3	48	47.7	1.8
S3**		31.3	48	45.5	1.7

Table 4 reports the monitoring results during the activation of the misting system in the gazebo S2. It can be observed that the average values of the measured quantities are very close in the two periods and the MOCI accordingly. The only noticeable difference concerns the MRT in S3, about 2°C lower in this period compared to the previous one, which determines the lower MOCI by about 0.2.

In terms of measured quantities, the misted area shows a relevant average drop in temperature by about 5°C, corresponding to an increase in relative humidity by 17%. As in the previous monitoring, the average wind speed under the gazebo is lower than that on the roof, about 0.5m/s in this period. The temperature reduction and the humidity increase lead to 0.5 MOCI reduction in the cooled gazebo. The result is quite impressive considering that the MOCI is 0.3 higher than the reference zone when the misting system is switched off. Considering the latter difference as an off set, the misting causes 0.8 drop of MOCI and, more important, the shift from the discomfort to the relative comfort zone (being the indicator below 1).

Table 4: Average values of the measured quantities and calculated indicators when the misting system is switched on

Spot	WS (m/s)	AT (°C)	RH (%)	MRT/GSI (°C/ W/m²)	MOCI (-)
S1	1.3	33.0	46	716.3	1.4
S2	0.8	27.9	69	37.4	0.9
S3*		31.9	48	45.4	1.6
S3**		31.9	47	43.4	1.5

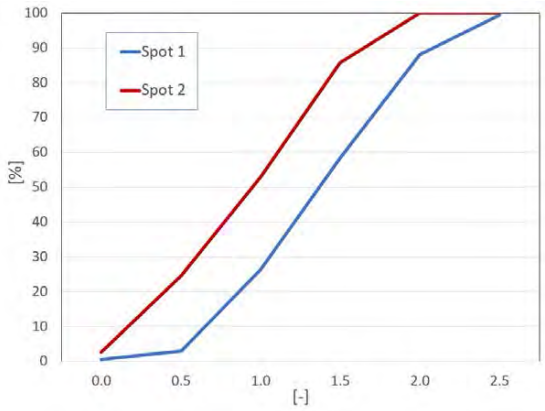

Figure 4: Cumulative distribution of the MOCI indicator in the reference spot and under gazebo S2 when the misting system is activated

Concerning the temperature drop, the minimum difference between the reference and the misting zone is 0.6°C, while the maximum peak 8.5°C; moreover, the difference is above 7°C during 10% of the observation period. It is also interesting to observe the impact of wind on the cooling potential of the misting. In fact, the average temperature drop rises from 5.1 during the whole period up to 6.3°C considering the hours with wind speed below 1m/s in the reference spot S1.

The strong temperature reduction is accompanied by the increase of the relative humidity, which negatively affect thermal comfort conditions above some level. These contrasting effects combine in the results of the comfort indicator, whose difference between the reference and cooled zones is lower than zero in three hours of the period (meaning that it is warmer in the misting area) and peaks 1.3 as maximum. Figure 4 reports the cumulative distribution of MOCI in the two zones and helps understanding the improvement achievable with the evaporated water. Best thermal comfort conditions are obtained for MOCI in the 0-0.5 range, which are achieved in about 25% of the period in the misted zone and only in the 3% of the

monitoring hours in the reference spot. MOCI up to 1 can still be accepted under severe climatic conditions and the hours below this threshold are calculated for 26 and 53% of the period in the reference and in the cooled zones, respectively.

Finally, substantial differences are observed under conditions of high thermal stress. MOCI rises above 1.5 in 14% of the period and never exceeds 2 in the misting zone. In contrast, MOCI is above 1.5 in 40% of the period in spot 1 and still it is above 2 (corresponding to significant thermal discomfort) in 12% of the time.

3.2 The pupils' subjective response

The results of this test campaign are grouped in 3 different test phases and the results are summarised in the Table 4. The first test takes place on 21st of July between 11:00 and 13:00. The sample consists of 13 male and female children playing under the gazebo with the misting switched on. The data shows that, for the heat perception, the majority feels it little (31%) or no (31%) heat, 38% experience high heat perception. The period average temperature is 34.9°C but it drops to 30.8°C in the misted zone. The majority of the sample expresses well-being conditions and prefers playing outside (54%) rather than going back to the classroom. It is important to emphasise that the misting system is a novelty compared to the pupils' daily routine, thus the misting itself becomes an element of play. It is here interesting noting 8% different between the sample that has little or null heat perception, and that expressing well-being conditions.

Table 4: Answers of pupils during the 3 testing days

Answer	Test 1	Test 2	Test 3
	Heat perception		
A lot	38	25	44
A little	31	33	31
Nothing	31	42	25
	Well-being		
I am fine	54	58	69
I am not fine	46	42	31
	Experiencing Space		
Continue play outside	54	58	56
Back to classroom	46	42	44
Average temperature (°C)	30.8	25.4	26.3
Average relative humidity (%)	63	62	49

Such difference increases surprisingly in the second test, run during the same hours of the previous test on the 26th and 28th of July with 12 pupils involved. No heat perception is experienced by 75% of the sample, in line with the milder average temperatures (below 30°C outdoor and about 25°C in the cooled zone). However, only 58% of the sample prefers playing outside.

The third test is carried out the 9th of October and involves 16 pupils, playing under the gazebo without the misting activation. The average temperature during the test is 26.3°C. The sample with high thermal sensation is 44%, which is the highest of the 3 test despite run in autumn; surprisingly, close to 70% of the pupils declare a well-being condition which is the highest during the three test.

Unfortunately, it was not possible to run test 1 without the misting system activation, so the response at high temperature (about 35°C on average) was not collected. This task would have provided interesting data for comparison and it is planned for next summer. However, some interesting information are collected:

- ✓ Pupils' will to play outside moves in a narrow range in the three tests, suggesting that the answer is quite independent from thermal conditions and heat/well-being perception, as well as the role of mitigation strategies.
- ✓ Well-being also seems not much linked to the thermal conditions, as a not clear trend is observed.
- ✓ It seems that pupils mostly enjoy low temperature with high humidity (test 2), might be interesting exploring the impact of *wetting* while playing.

According to the above results, further considerations will be made to understand if and how the proposed questionnaire can really help to understand the feeling of 2/3 years old human beings with respect to the urban overheating.

4. CONCLUSIONS

This paper presents the results of a case study quantifying the benefits of the heat mitigation of a nursery school garden through outdoor shading and evaporative cooling misting in the city of Rome, adding for the first time the feedback of young pupils too.

The quantitative analysis shows that the thermal comfort conditions extend to half of the monitoring period under the misting zone, while they are only achieved in a quarter of the time in the reference zone. The comfort indicator MOCI drop by 0.5 on average and the air temperature by 5°C, peaking at 8.5°C; in parallel, the relative humidity increases by 17% on average.

The subjective comfort evaluation was conducted on pupils 2/3 years with an ad-hoc developed questionnaire. The results are interesting as they witness the will of the majority of the pupils to play outside even with temperature close the 35°C in the reference zones. The preferences of the pupils under the misting zone in very hot conditions resulted similar to those expressed in October in milder conditions, proving the potential of the water-based technologies in creating comfortable and pleasant outdoor environment, even under severe heat conditions.

ACKNOWLEDGEMENTS

Research funded by Project 1.7 “Technologies for the efficient penetration of the electric vector in the final uses” within the “Electrical System Research” Programme Agreements 22-24 between ENEA and the Ministry of Environment (PTR 22-24).

REFERENCES

1.IPCC. Sixth Assessment Report 2023. https://www.ipcc.ch/assessment-report/ar6/.

2.Se Woong Kim, Robert D. Brown, (2021) Urban heat island (UHI) intensity and magnitude estimations: A systematic literature review, *Science of The Total Environment*, Volume 779, 146389,

3.UN-HABITAT. Why Metropolitan Management n.d. https://unhabitat.org/topic/metropolitan-management.

4.Yadav, N., Rajendra, K., Awasthi, A., Singh, C., (2023) Systematic exploration of heat wave impact on mortality and urban heat island: A review from 2000 to 2022, *Urban Climate*, Volume 51, 101622. https://doi.org/10.1016/j.uclim.2023.101622.

5.M.E. Gonzalez-Trevizo, K.E. Martinez-Torres, J.F. Armendariz-Lopez, M. Santamouris, G. Bojorquez-Morales, A. Luna-Leon, Research trends on environmental, energy and vulnerability impacts of Urban Heat Islands: An overview, Energy Build 246 (2021), 111051, https://doi.org/10.1016/j.enbuild.2021.111051.

6.Santamouris M. (2020) Recent progress on urban overheating and heat island research. Integrated assessment of the energy, environmental, vulnerability and health impact. Synergies with the global climate change. Energy Build 2020; 207. https://doi.org/10.1016/j.enbuild.2019.109482.

7.Santamouris, M., 2014. Cooling the cities–a review of reflective and green roof mitigation technologies to fight heat island and improve comfort in urban environments. *Sol. Energy* 103, 682–703. https://doi.org/10.1016/j.solener.2012.07.003

8.M. Santamouris, L. Ding, F. Fiorito, P. Oldfield, P. Osmond, R. Paolini, D. Prasad, A. Synnefa, (2017) Passive and active cooling for the outdoor built environment – Analysis and assessment of the cooling potential of mitigation technologies using performance data from 220 large scale projects, *Solar Energy*. Volume 154, pp, 14–33. https://doi.org/10.1016/j.solener.2016.12.006.

9.C. Li, J. Zhou, Y. Cao, J. Zhong, Y.u. Liu, C. Kang, Y.i. Tan, Interaction between urban microclimate and electric air-conditioning energy consumption during high temperature season, Appl Energy 117 (2014) 149–156.

10.M. Santamouris, R. Paolini, S. Haddad, A. Synnefa, S. Garshasbi, G. Hatvani-Kovacs, et al., Heat mitigation technologies can improve sustainability in cities. An holistic experimental and numerical impact assessment of urban overheating and related heat mitigation strategies on energy consumption, indoor comfort, vulnerability and heat-related m, Energy Build 217 (2020), 110002, https://doi.org/10.1016/j.enbuild.2020.110002.

11.N. Nasrollahi, A. Ghosouri, J. Khodakarami, M. Taleghani, Heat-Mitigation Strategies to Improve Pedestrian Thermal Comfort in Urban Environments: AReview, Sustainability (2020) 12, https://doi.org/10.3390/su122310000.

12.Garcia-Nevado, E., Beckers, B., Coch, H., (2020), Assessing the cooling effect of urban textile shading devices through time-lapse thermography, *Sustainable Cities and Society*, Volume 63, 102458, https://doi.org/10.1016/j.scs.2020.102458.

13.A. Mastrucci, E. Byers, S. Pachauri, N.D. Rao, Improving the SDG energy poverty targets: Residential cooling needs in the Global South, Energy Build 186 (2019) 405–415, https://doi.org/10.1016/j.enbuild.2019.01.015.

14.N. Nasrollahi, A. Ghosouri, J. Khodakarami, M. Taleghani,Fuad Mutasim Baba, Hua Ge, Radu Zmeureanu, Liangzhu (Leon) Wang, Optimizing overheating, lighting, and heating energy performances in Canadian school for climate change adaptation: Sensitivity analysis and multi-objective optimization methodology, Building and Environment, Volume 237, 110336, https://doi.org/10.1016/j.buildenv.2023.110336.

15.Farné R., Bortolotti A., Terrusi M., (2018). Outdoor Education: prospettive teoriche e buone pratiche. Carrocci editore, Roma.

16.5. Azzolini, D., Bazzoli, M., Burlacu, S., Rettore, E., (2023). Valutazione di impatto di Arcipelago Educativo 2022, Save the Children Italia, Fondazione Agnelli e Fondazione Bruno Kessler.

17.G. Ulpiani, Water mist spray for outdoor cooling: A systematic review of technologies, methods and impacts, Appl Energy (2019) 254, https://doi.org/10.1016/j.apenergy.2019.113647.

18.X.i. Meng, L.i. Meng, Y.i. Gao, H. Li, A comprehensive review on the spray cooling system employed to improve the summer thermal environment: Application efficiency, impact factors, and performance improvement, Build Environ 217 (2022) 109065.

19.G. Ulpiani, E. Di Giuseppe, C. Di Perna, M. D’Orazio, M. Zinzi, Thermal comfort improvement in urban spaces with water spray systems: Field measurements and survey, Build Environ 156 (2019) 46–61, https://doi.org/10.1016/j.buildenv.2019.04.007

20.G. Ulpiani, M. Zinzi Experimental assessment of the heat mitigation potential of an urban cooling shelter: Combining water misting with solar shading, wind shield, and smart control, Energy & Buildings 299 (2023) 113623. https://doi.org/10.1016/j.enbuild.2023.113623.

21.Michele Zinzi, Emiliano Carnielo, Benedetta Mattoni, On the relation between urban climate and energy performance of buildings. A three-years experience in Rome, Italy (2018) Applied Energy, Volume 221, Pages 148-160, doi.org/10.1016/j.apenergy.2018.03.192.

22.Salata F, Golasi I, de Lieto Vollaro R, de Lieto Vollaro A. Outdoor thermal comfort in the Mediterranean area. A transversal study in Rome, Italy. Build Environ (2016) 96:46–61. doi.org/10.1016/j.buildenv.2015.11.023.

23.S. Falasca, V. Ciancio, F. Salata, I. Golasi, F. Rosso, G. Curci, High albedo materials to counteract heat waves in cities: An assessment of meteorology, buildings energy needs and pedestrian thermal comfort, Build Environ 163 (2019), 106242, https://doi.org/10.1016/j.buildenv.2019.106242.

PLEA 2024 WROCŁAW
(Re)thinking Resilience

Urban Weather and Climate Correlation Model to Predict Indoor Temperature: A Case of Yangon

MAY ZUNE[1] THET PAING TUN[2] MARIA KOLOKOTRONI[3]

[1]Department of Civil and Structural Engineering, University of Sheffield, United Kingdom.
[2] Department of Electronic and Electrical Engineering, Brunel University London, United Kingdom.
[3] Department of Mechanical and Aerospace Engineering, Brunel University London, United Kingdom.

ABSTRACT: Urbanisation in Yangon has increased by 31% in 2019 compared to 1990; however, limited studies exist to understand the impacts of urban settings and climate change on the existing building stock found in downtown Yangon, Myanmar. The urban heat island effects vary by location; hence, we present a prediction framework for cooling energy demand and thermal performance to understand retrofit design strategies to fit future urban weather conditions in downtown Yangon. The Urban Weather Generator tool was deployed to create the contemporary and future urban weather files to take into account the effects of urban air temperatures and urban materials on indoor environments. For the contemporary weather conditions, the result showed that the UHI effects result in daytime annual mean temperatures areas about 1.4°C higher than temperatures in rural areas and nighttime temperatures of about 4.4°C higher whereas the intensity of urban air temperatures was profound in the future urban weather prediction. The results of this work show the importance of considering future microclimatic external conditions in retrofit interventions for the existing urban building stock to maintain necessary indoor environmental quality with a lower energy demand for cooling and ventilation.

KEYWORDS: Urban heat island; Urban weather generator; Housing retrofit, Thermal and energy performance.

1. INTRODUCTION

The thermal performance of a building is designed and evaluated from its fabric-energy efficiency in response to ambient conditions. The values of ambient conditions are often based on either typical and historical or predictive weather data which portray the anticipated annual weather stream of a location for its short-term and long-term climates. The elevated urban temperatures compared to its rural surroundings are particularly different at night-time as the heat retained by artificial surfaces is slowly released, keeping temperatures higher than the rural areas, a phenomenon known as the urban heat island (UHI) effect. Several case studies have revealed the impact of the UHI effect on current and future energy consumption [1], and those works are location-specific [2, 3].

Understanding the impact of UHI effects is fundamental to investigating retrofitting urban building stock for future weather scenarios; however, most weather files do not account for characteristics of the urban settings that modify urban air temperature and urban wind [2]. The purpose of this work is to (i) present a model to generate urban weather files, (ii) investigate how the urban settings of the selected case study location impact future thermal and energy performances of the existing building stock, and (iii) review potential retrofit strategies to adapt to future urban climate conditions.

2. METHODOLOGY

We present a method to predict indoor temperatures for an urban setting, using the Urban Weather Generator [4, 5] and the climate correlation model [6, 7], for contemporary and future climate scenarios. We used neighbourhood-scale building energy modelling to justify location-specific climate influences on cityscape geometry and energy consumption from different types of buildings. We used physics-based building-scale simulation modelling to identify the threats and challenges associated with the bioclimatic design processes and further retrofit actions to achieve necessary thermal comfort in current and future weather scenarios.

2.1 Case study location and case study room

We selected Yangon, the business capital of Myanmar, as a case study location. Yangon is home to more than 5.6 million people, and urbanisation in Yangon had about 31% increase in 2019 compared to 1990 [8]. The downtown areas have the highest population densities in Yangon, each with more than 100,000 per square mile. This study covered an area of 2300m in length and 250 to 800m in width of downtown Yangon, as shown in Figure 1; this is more

than a 250m radius, as suggested for local urban climate studies [2].

An apartment model (Figure 2) which is typically found in downtown Yangon [9] was selected to test building performance in different weather conditions. Whilst the plan of narrow apartments is common for downtown and across the city, the architectural design in windows, doors and verandas could be slightly different from one to the other. In this work, we considered a south-facing apartment at the 5th storey which is overshadowed by adjacent buildings, the row of apartments in this street has 8 storeys.

2.2 Weather files

Yangon has a tropical monsoon climate. Rural weather files for Yangaon consist of weather data measurements at an operational weather station located in an open area outside a city. Three rural weather files (contemporary and future RCP8.5 scenarios for 2050s and 2080s weather) were obtained from the *Meteonorm*.

The Urban Weather Generator (UWG) [4, 5] was deployed in this work to combine (i) the effect of sensible heat fluxes at the weather station, (ii) vertical profiles of air temperature above the rural site, (iii) air temperatures above the urban canopy layer, and (iv) urban sensible heat fluxes and urban canyon air temperature and humidity to calculate air temperatures inside urban canyons found in Yangon. The building areas of the case study location were defined in the Autodesk Revit massing model according to building types, i.e., residential, schools, retail shops, banks, hotels, restaurants, supermarkets etc. The building density was calculated from the ratio of the total building area to the total site area. The vertical-to-horizontal ratio of the location is calculated from the ratio of the total facade area to the total site area. Green (tree and vegetation) area, road area, river area, etc. were calculated through the Revit area scheme. The urban weather files were generated by co-simulating using (i) Matlab, (ii) a sourced file (.xlsm) which information was fed from the Revit schedules and (iii) three rural weather files, following [2, 4, 5]. The output is a morphed weather file [.epw] that captures the UHI effects from the selected location.

2.3 Methods

Building operation and equipment use schedules for the case studied room were referred to in Table 1, and the constructions of the room were assumed considering locally found available data, as shown in Table 2. For retrofit design strategies, we tested two contrast approaches: external louvre shading for the passive cooling approach and insulation-added scenario for improving the fabric-energy efficiency approach. This allows us to understand vernacular passive design for external retrofit construction and the possibility of retrofitting internally by adding insulation.

First, using the results from the UWG, three rural weather files and three urban weather files are compared, which captured the UHI effects of downtown Yangon. Secondly, the climate correlation model, following [6, 7], was applied to predict an indoor environment by correlating internal environmental variables and external climatic variables. The indoor temperature predictions were calculated using the forecasted external weather data that informs a cross-sectional snapshot of the next 24 hours for different scenarios. Hence, these correlation equations are versatile to predict daily temperatures at any time of the year. Third, the indoor temperatures for the current and year 2080 weather year are compared for rural and urban weather conditions. Finally, the impacts of urban settings on cooling loads are reviewed against the rural weather data.

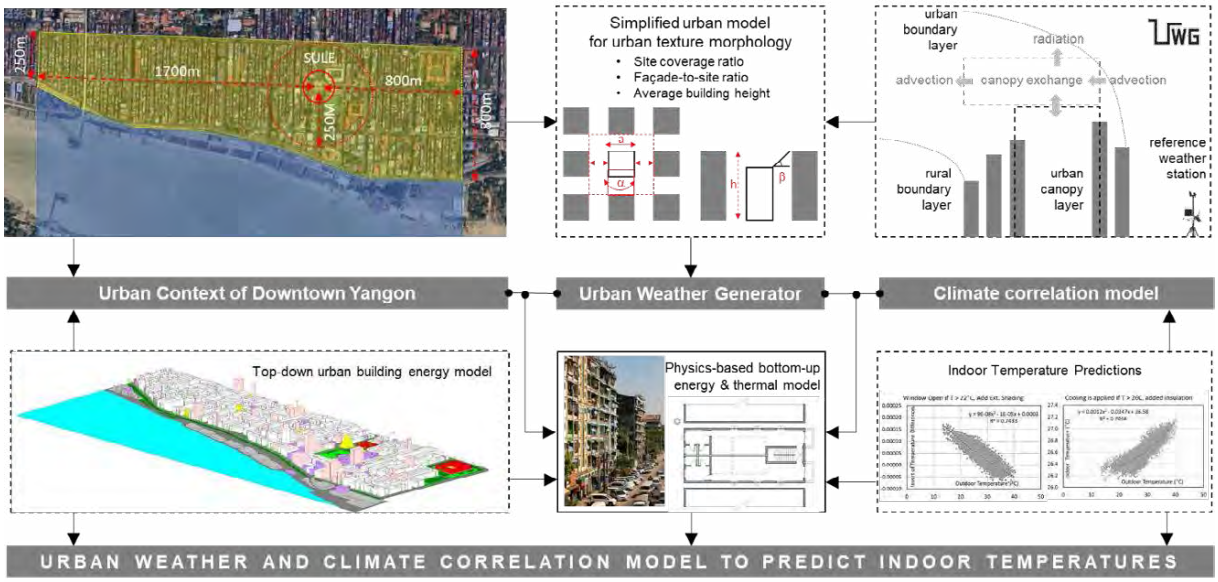

Figure 1. Urban parameters considerations in indoor condition predictions (adapted from [2, 4, 6, 7])

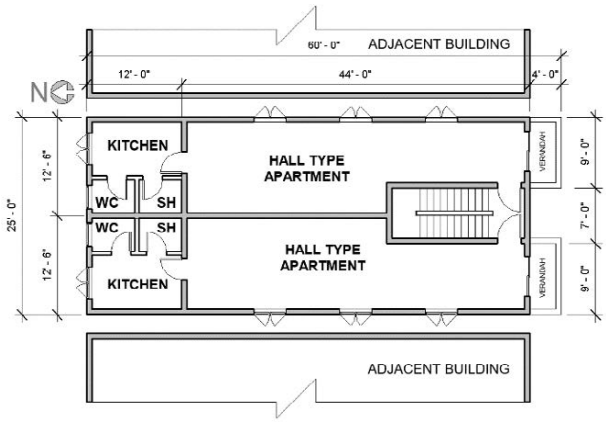

Figure 2. Plan view of the case studied apartment, adapted from [9].

Table 1. Building operation and equipment use schedules.

Parameters	Values	Ref.
Indoor operative temperature		
Heating	Not applied.	
Cooling (Category II)	on if T > 26°C	[10]
Natural ventilation	Window open if T > 22°C	
Building usage and schedules		
No. of occupants	3	
Occupancy / Equipment	Studio type	[11]
Equipment and lighting	Follow the room	[11]
Internal heat gain	2.1 W/m^2 (assume)	
Internal shading: Assume shading is on during daytime if solar radiation is> 90 W/m^2; and the nighttime for privacy.		

Table 2. Building construction data and retrofit options.

Construction	Description and U-value (W/m^2-K)	
Roof	Uninsulated concrete slab	1.55
Ground floor	Uninsulated concrete slab	2.28
Internal floor	100mm concrete floor slab with screed	2.93
External wall (reference)	9" thickness brick with dense plaster on both sides	2.18
External wall (Insulated)	Added 100mm EPS insulation inside	0.34
Window (reference)	Single glazing	5.78
Window (for insulated wall)	Double glazing with Argon filled	2.55

3. RESULTS

3.1 Comparison of weather files

Figure 3 presents a comparison of diurnal and annual outdoor dry bulb temperatures. For contemporary weather, the UHI effect results in daytime annual mean temperatures in downtown Yangon areas about 1.4°C higher than temperatures in its rural area and nighttime temperatures about 4.4°C higher. BS-EN 16798 suggests 23°C~26°C for cooling set point temperatures to maintain the normal level of expectation for thermal comfort whereas the adaptive thermal comfort perceptions could extend about 26°C~31°C in tropical countries [12]. Figure 4 presents the temperature distributions for a year from different weather files. The frequency of temperature distribution below 26°C was reduced when the UHI effects were taken into account if the weather file from the meteorological station was compared to the UWG weather files. The UHI effect is more pronounced during the night than during the day, while it almost disappears in the morning around 09:00; Figure 5 for the UWG program results agrees with the theory of the UHI study [3]. Slightly higher temperatures were found in both the 2050s and 2080s weather files against the contemporary weather files.

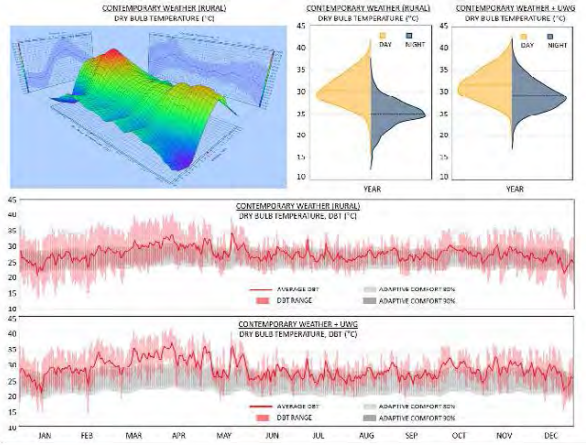

Figure 3. Comparison of diurnal and annual outdoor dry bulb temperatures

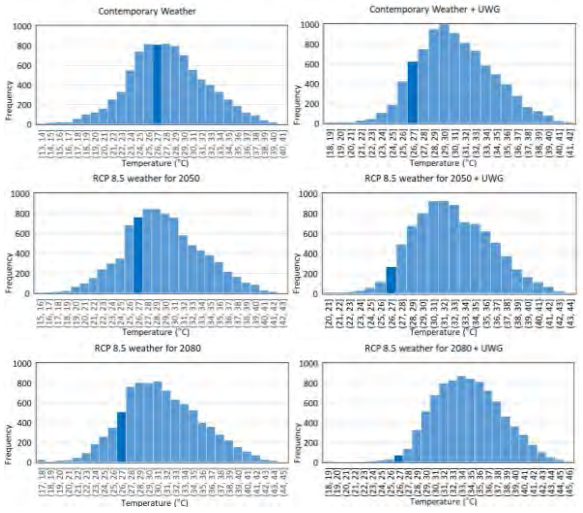

Figure 4. Comparison of temperature distribution for a year

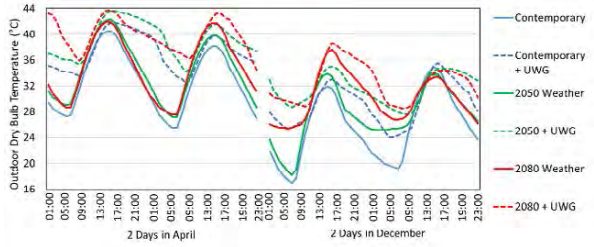

Figure 5. Comparison of hourly outdoor temperatures in April and December

3.2 Correlation results from contemporary weather

Following the framework of the CCM, the correlation equations were derived from different

scenarios predefined in a model and generated using a contemporary weather file. The indoor operative temperatures were correlated by the outdoor dry bulb temperature and the inverted values of temperature differences between the indoor and the outdoor, as presented in Figure 6. Understandably, the strength of the temperature correlation was affected by indoor and outdoor temperature differences in a free-running apartment. The correlation equations were used as prediction equations where the outdoor temperatures from different weather files, generated from the *Meteonorm* database and the UWG programs, were used as independent values in those equations.

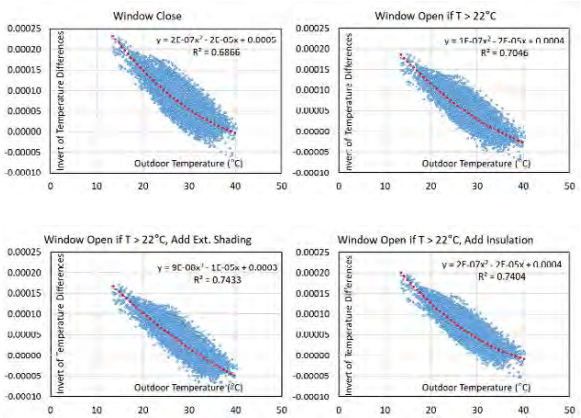

Figure 6. Thermal correlations between external temperatures and inverted values of external and internal temperature differences

3.3 Comparison of retrofit strategies

Figure 7 and Figure 8 present the prediction results for contemporary and year 2080s weather files against respective UWG weather files, for two days in April and two days in December, considering the warmer and colder times of the year. Diurnal temperature variations for a tropical climate city Yangon are typically smaller than in other climates; however, increments in nighttime temperature even cause a decrease in the diurnal temperature range. Therefore, the impacts of warmer temperatures at nighttime in downtown Yangon can be seen on the daily temperature profiles. The predictions of indoor temperatures have predominantly relied on the function of correlations; therefore, similar indoor temperature profiles were found for respective outdoor dry bulb temperatures.

Closing windows (shown as red lines) in the tropical apartment caused warmer indoor temperatures, and the temperature could drop by using natural ventilation (shown as blue lines) for passive cooling, as shown in Figure 7 and Figure 8. Adding insulation could be beneficial to improve fabric energy efficiency whereas the lack of ventilation in an insulated apartment could affect higher indoor air temperatures due to its outdoor tropical weather, as well as there were other internal heat gains. Adding external shading to the apartment, which also has internal blinds, was more effective in maintaining lower indoor air temperatures than adding insulation alone to the apartment.

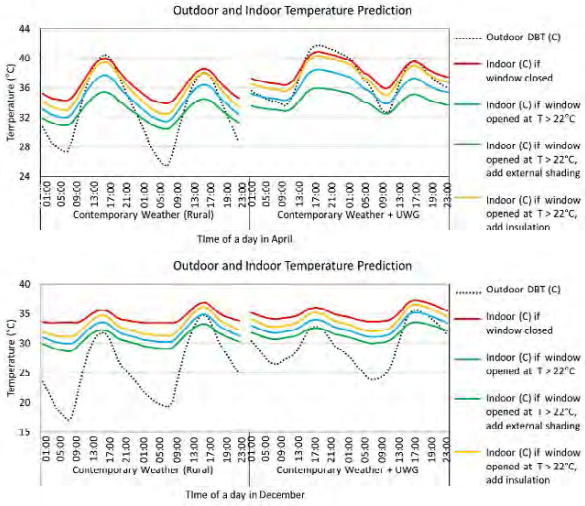

Figure 7. Prediction results for the contemporary weather file compared to the UWG file.

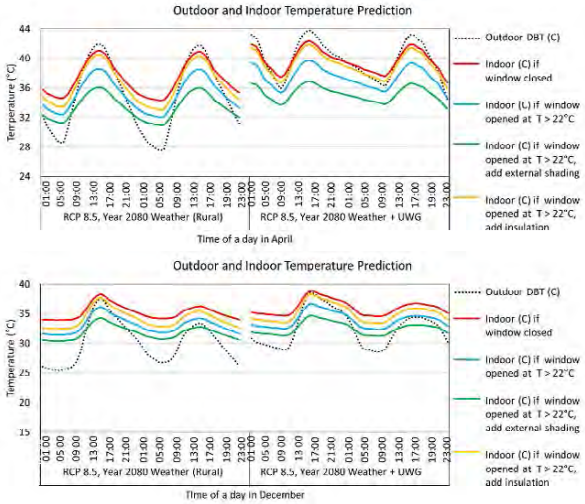

Figure 8. Prediction results for future 2080 weather files compared to the UWG file.

3.4 Comparison of indoor temperature predictions and simulation results

The prediction results from correlation equations predominantly rely on the value of an independent variable; the stronger the relationship between the variables, the more accurate the prediction, but estimating the causal effects was limited in the correlation study. Figure 9 presents the results of simulated indoor temperatures for a contemporary weather file. Therefore, the limitations of temperature prediction can be noted by comparing Figure 7, Figure 8 and Figure 9, despite the prediction results seeming to have good agreement with the simulated results. One important thing to highlight from this comparison was the impact of UHI effects was more profound in the simulated results, showing higher temperatures against the predicted

temperatures. Whilst increases in indoor temperatures have a strong correlation with outdoor temperature, other causation factors need to be considered in examining the UHI effects for indoor air temperature predictions.

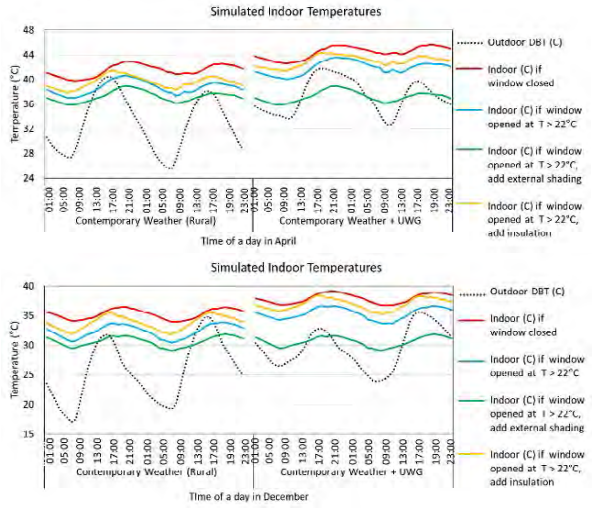

Figure 9. Simulated indoor temperature results for the contemporary weather file compared to the UWG file.

3.5 Cooling loads comparison

Figure 10 presents simulated results of monthly outdoor and indoor temperatures for different scenarios; it compares how the presence and absence of insulation impacted daily cooling loads. The simulated results showed that adding insulation to a free-running apartment (as shown in a yellow line) could cause higher daily indoor temperatures than adding an external shading to the apartment (as shown in a green line).

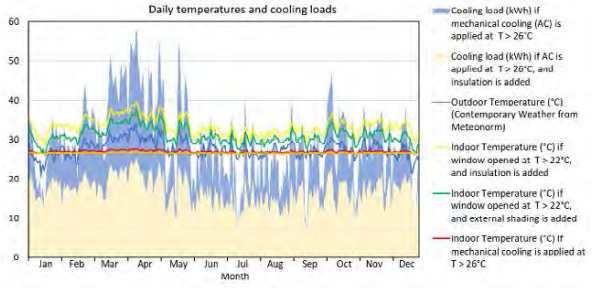

Figure 10. Comparison of daily temperatures and cooling loads, the results for contemporary weather data.

Adding insulation into a building can restrict the transfer of heat by keeping the building stays warm in the winter whereas it can take longer to cool down in the summer. In the tropical climate, the lack of mechanical ventilation or cooling in the apartment led to higher daily temperatures throughout the year. However, adding insulation could maintain lower annual cooling loads (about a 58% reduction compared with the uninsulated scenario) if mechanical cooling was added; as a result, daily temperatures throughout the year can be maintained around 26°C, as shown in an orange line.

4. DISCUSSION

4.1 UHI effects from urban neighbourhood-scale

The UHI effects on downtown Yangon were captured by using the UWG which estimates the effects of urban morphology, geometry, and surface materials on temperature and energy consumption. Significantly increased values in night-time temperatures and increased frequency of temperature distribution above 26°C were found in the results of neighbourhood-scale energy balances from the UWG program against its original rural weather file data. As the outputs of the UWG program solely rely on location-specific climate influences on cityscape geometry and energy consumption from different types of buildings, the resulting UWG weather files can help inform the future energy demand of the downtown Yangon building stock, although the lack of disaggregation at individual levels has been acknowledged, and this could cause different UHI results in different areas of Yangon, similar to [3].

4.2 UHI effects in building-scale

The UHI effects on the studied apartment were investigated by using the correlation model which predicts indoor temperatures for different boundary conditions, i.e., free-running modes and controlled modes, by adding either insulation or external shading. The impacts of UHI effects on the outdoor temperatures were more profound than the indoor temperature predictions (Figure 7 and Figure 8) and the simulated indoor temperatures (Figure 9). The results showed that solar heat gain protection via external shading is more effective than adding insulation for a retrofit option whereas the benefit of cooling load reduction by improving fabric-energy-efficiency via insulation was noted. As the outputs of the predicted indoor temperatures solely rely on the boundary conditions of the correlation model and the strength of correlation equations, the impacts of other causal effects in indoor temperatures were acknowledged by comparing the simulated indoor temperatures.

4.3 Limitations of the study

Current limitations pertain to the UWG's algorithm which only morphs the dry bulb temperatures and relative humidity as the urban wind velocity does not capture the turbulence inside the street canyon. During the development of the UWG program, the mean radiant temperatures calculation for the urban infrastructure such as roads and green areas, and also for the external surface temperatures of walls, roads and roofs had been validated; nonetheless, careful input data is necessary for generating UWG files, as highlighted in [4, 5]. The indoor temperature predictions from the correlation model provide sensible results whereas the predictive

accuracy of the correlation equations is in the process of evaluation to validate with the measured data, as reported in [6, 7].

5. CONCLUSION

We present a method to take into account the UHI effects in indoor temperature predictions, using the UWG program and the correlation model. The methodology is applied to downtown Yangon, the central business district in Myanmar. The presented method helps to realise the UHI effects for contemporary and future weather conditions and predict indoor temperatures for different scenarios. The results demonstrate how the day and night temperatures in this metropolitan area are significantly altered by the urban settings and the UHI effects.

This study compared two distinct retrofit strategies (external shading and insulation) to realise how the indoor environmental conditions could change in future urban weather conditions. Comparisons of the contemporary and future weather scenarios confirmed that the effectiveness of external shading will be more profound in future weather scenarios whilst the complexity of using insulation for fabric energy efficiency is reported. The advantage of insulation and fabric-energy efficiency is found in reducing cooling load. However, it is essential to apply passive design first in retrofitting to protect solar heat gain using shading, which is a means of reducing the risk of indoor overheating; particularly the windows need to be shaded from the sun and protected from rain. Adding insulation is uncommon in the tropical building stock; however, the salient of high-performance building envelope needs to be realised for extreme weather conditions whilst the unintended consequences of superinsulation and airtight construction in retrofit construction need to be addressed, for instance, adding low energy and energy recovery mechanical ventilation. Concurrently, the use of potential solar energy needs to be applied in housing retrofit for Yangon to achieve maximum energy cost savings. This will also help to raise awareness of whether and why the retrofitting of the existing building stock in downtown Yangon needs to make them fit for future climates. Future developments of this method need to investigate how the indoor environment conditions could be altered by the resulting impacts of retrofit construction, occupant behaviours building operations schedule, as the accuracy of the prediction equations relies on the boundary condition of the correlation model.

The presented method is an example of combining a neighbourhood-scale building model and the UWG program to generate urban weather files. Autodesk Revit massing model was used in this work to generate data for a sourced file (.xlsm) to use in Matlab for the UWG program. Recent "Bing Maps Global Building Footprints" derived from satellite imagery by Microsoft Maps [13] can bring technological advancement to generate data for necessary source files to use in the UWG program. That can bring further advantages in applying the presented method for deep learning and machine learning for indoor environmental predictions in different locations where the UHI effects are concerned.

REFERENCES

1. M. Kolokotroni, X. Rena, M. Davies, and A. Mavrogiann (2012) *London's urban heat island: Impact on current and future energy consumption in office buildings.* Energy and Buildings. 47(2012): p. 302-311.
2. A. Salvati and M. Kolokotroni (2023) *Urban microclimate and climate change impact on the thermal performance and ventilation of multi-family residential buildings.* Energy and Buildings. 294(2023): p. 113224.
3. Giannaros et al. (2023) *Numerical study of the urban heat island over Athens (Greece) with the WRF model.* Atmospheric Environment. 73(2013): p. 103-111.
4. B. Bueno, L. Norford, J. Hidalgo, and G. Pigeon (2013) *The urban weather generator.* Journal of Building Performance Simulation. 6(4): p. 269-281.
5. B. Bueno, A. Nakano, L.K. Norford, and C. Reinhart (2015) *Urban Weather Generator - a Novel Workflow for Integrating Urban Heat Island Effect within Urban Design Process.* BS2015(2015-12).
6. M. Zune and M. Kolokotroni (2022) *Climate correlation model to forecast thermal comfort and IAQ in naturally ventilated residential buildings.* in *42nd AIVC conference: Ventilation Challenges in a Changing World, 5th-6th October 2022*. Rotterdam, Netherlands.
7. M. Zune and M. Kolokotroni (2022) *Correlation model to evaluate climate effect on indoor air quality and thermal comfort in houses* in *CATE2022, 5th-6th September 2022*. Edinburgh, UK.
8. Fan et al. (2022) *Urbanization, economic development, and environmental changes in transitional economies in the global south: a case of Yangon.* Ecological Processes. 11(65).
9. MMC, *Architectural Detailing and Yangon Flat (n/a)* in *Myanmar Architect Council*: Yangon.
10. BSI (2019) *BS EN 16798-1 Energy performance of buildings. Ventilation for buildings*, The British Standards Institution: UK.
11. CIBSE (2017) *Design methodology for the assessment of overheating risk in homes*, The Chartered Institution of Building Services Engineers UK.
12. R.J. deDear, K.G. Leow, and S.C. Foo (1991) *Thermal comfort in the humid tropics: Field experiments in air conditioned and naturally ventilated buildings in Singapore.* International Journal of Biometeorology. 34(1991): p. pages259–265
13. Microsoft, *Bing Maps Global Building Footprints Released (2023)*: https://github.com/microsoft/GlobalMLBuildingFootprints.

PLEA 2024 WROCŁAW
(Re)thinking Resilience

Climate-Responsive Design Guidelines for Urban Open Spaces in Hot Arid Climates

MOHAMMED A. ALHARTHI[1], SANDA LENZHOLZER[1], JOÃO CORTESÃO[1]

[1]Wageningen University and Research, Wageningen, The Netherlands

ABSTRACT: Urban heat is a common challenge for many cities, especially in hot arid climate regions as they experience high average air temperatures compared to other climate types. Hot arid cities also have common climate issues such as drought and flash floods. Climate-responsive design can be implemented by spatial designers (i.e., landscape architects and urban designers) to address these issues and, hence, improve outdoor thermal comfort. Design guidelines can assist spatial designers when designing urban open spaces in hot arid. The goal of this study is to develop climate-responsive design guidelines for urban open spaces in hot arid regions. Two methods were employed to fulfil the goal of this study: 1. A systematic literature review; 2. Research for Design. The results show that different street aspect ratios and orientations require careful selection of climate-responsive design strategies in urban open spaces in hot arid cities to provide daytime and night-time outdoor thermal comfort. Also, it is essential to incorporate common climate issues such as drought and flash floods in climate-responsive design guidelines. Presenting design guidelines spatially was considered useful to communicate these guidelines to spatial designer.
KEYWORDS: Climate-responsive design, Design guidelines, Urban open spaces, Hot arid climate

1. INTRODUCTION

Urban heat has been acknowledged as a hazard to health and wellbeing as well as outdoor thermal comfort of urban populations. Some climatic regions are more severely affected by the impacts of urban heat than others. An example is hot arid climate regions, also known as BWh according to Köppen-Geiger climate classification (Fig.1) [1], where temperatures are per se extremely high in summer. In addition, many of the growing cities worldwide are located in hot arid climate regions [2].

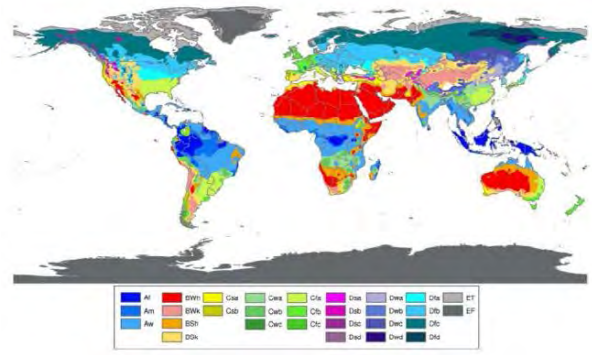

Figure 1: Koppen-Geiger climate type map of the World, where the hot arid climate (BWh) is colored in red [1].

Next to health hazards, climatic conditions, especially when harsh, have an impact on residents' engagement with urban open spaces and in hot arid climates, people often avoid urban open spaces during noon and afternoon hours because of high solar radiation and air temperatures. This is a suboptimal use of urban open spaces, which should thus be designed to minimize the impacts of heat stress especially for extreme heat periods. Apart from that, it is essential to consider other common climate challenges in hot arid climates such as drought and flash floods.

Climate-responsive design can be implemented by spatial designers (i.e., landscape architects and urban designers) to address these issues and, hence, improve thermal comfort and safety conditions. Design guidelines can assist spatial designers in this task for urban open spaces in hot arid climates by providing guidance based on scientific knowledge.

A limited number of studies has been conducted for urban open spaces in hot arid climates and the information is scattered. Still, some studies do provide valuable design strategies to cope with heat stress in these climatic regions. Synthesizing this knowledge is needed for two reasons: (1) to have a holistic view on existing climate-responsive design guidelines for urban open spaces in hot arid climate regions; (2) to develop and test new design guidelines for these regions.

Motivated by these needs, this paper addresses the question: which climate-responsive design guidelines can be implemented in urban open spaces in hot arid climates?

The aim of this study is to contribute to filling in the knowledge gap on climate-responsive design in hot arid climate regions by presenting climate-responsive design guidelines extracted from a systematic literature review on climate-responsive design in urban open spaces in hot arid climate regions.

2. METHODS

Two methods were employed to fulfil the goal of this study:

- A systematic literature review was conducted using the Preferred Reporting Items for Systematic Review Recommendations (PRISMA) method [3]. The Google Scholar search engine was used to search for relevant studies, and 17 studies were found out of 2815.
- Research for Design (RfD). Because this research approach helps to inform design to improve its quality [4], RfD was used to generate climate-responsive design guidelines not distilled from the literature review.

Eventually the design guidelines resulting from this process were synthesized and represented spatially for recurrent urban open spaces in hot arid climate regions.

3. RESULTS AND DISCUSSION

3.1 Systematic literature review

The literature review identified six main types of climate-responsive design interventions for hot arid climate cities. These design interventions are urban form, shading devices, vegetation, water elements, materials, and combined design interventions.

3.1.1 Urban form

Urban form has been addressed in previous studies as having a significant impact on microclimatic parameters and outdoor thermal comfort through changing shade patterns and wind directions. Urban form parameters include aspect ratio (H/W), street orientation and sky view factor (SVF).

It was found that low H/W ratio (e.g., 0.42) increases the temperature and the intensity of the urban heat island due to the high solar exposure [5]. A low H/W ratio does not provide shade [6] and H/W = 0.5 requires shading strategies at the street level [7]. Deep street canyons (H/W ≈ 2) in high-density neighbourhoods were found to be cooler and more humid compared to those in lower H/W values [8]. Street canyons with H/W values between 1 and 2 can be a good compromise as they provide shade and prevent the trap of reflected solar radiation [9].

The North-South (N-S) orientation is reported as the providing the best conditions for thermal comfort as exposure to direct solar radiation is limited. In some cases, the north-orientated urban open spaces are preferred for ventilation as the prevailing wind direction is parallel [10]. The N-S, North-eastern-Southwestern (NE-SW) and North-western- South-eastern (NW-SE) orientations show similar physiological equivalent temperature (PET) patterns [7]. NW-SE oriented streets presented reduced PET values in two case studies in Egypt [11,12] and provided lower air temperature and higher values of humidity [8]. A study in Egypt showed that the most thermally uncomfortable orientations were East-West (E-W) and NE-SW although the NE-SW orientation was slightly better [12].

High SVF values close to 1 in urban open spaces enhance air flow [10,13]. In turn, in low SVF spaces wind speed is lower [10] and, therefore, placing horizontal shading elements (e.g., shade devices or trees) should not hinder the airflow [14].

3.1.2 Shading devices

In general, shaded spaces have lower PET values compared to non-shaded spaces [15] and are more likely to be used. Shading devices can provide shade when buildings do not provide enough shade for pedestrian, especially at midday and afternoon hours. However, placing too many shading devices could hinder night-time time heat release and cause thermal discomfort at night. A possible solution is placing retractable shading devices to accelerate heat release [16].

3.1.3 Vegetation

Vegetation – trees in particular - is one of the most effective heat mitigation strategies. Trees can minimize thermal discomfort and provide cooling effects through evapotranspiration and shade. Trees in streets with H/W ratio of 1 can provide good microclimates similar to deep H/W ratio (H/W=2) streets [8].

Planting small and large trees can similarly provide adequate shade for people. However, large trees can prevent the release of heat at night, leading to a warmer air temperature [17]. This is more likely to happen in narrow streets and small squares. Thus, it is essential to maintain enough spaces around trees for ventilation and night-time heat release.

Drought is a common climate challenge in hot arid climates and can increase stress and mortality risk for trees. Also, trees need adequate amount of water to grown and survive. Thus, implementing stormwater retention strategies can provide water resources for irrigation, and mitigate the risk of flash flooding.

3.1.4 Water elements

The use of water elements can provide cooling effects in urban open spaces. Water mists, for example, can lower the main radiant temperature by 8.2 °C and the air temperature by an average of 3.5 °C, and that can lower the PET value [18]. However, it is not wise to use water elements as there are environmental and cost concerns because many hot arid climate regions suffer from drought and water scarcity.

3.1.5 Materials

The use of high-albedo materials in urban open spaces has positive and negative impacts. High-albedo materials can lower the daytime air temperature but can increase the night-time air temperature [19]. High-albedo materials can increase the mean radiant temperature values [20], and a possible solution is to shade high-albedo materials [9]. To this end, the use of materials, especially high-albedo materials, is not effective as other climate-responsive design interventions in hot arid climates.

3.1.6 Combined design interventions

Previously mentioned climate-responsive design interventions can be combined to provide better cooling effects and outdoor thermal comfort. The shade of trees and buildings can lower the predicted mean vote (PMV) [20]. While the shade of trees and shading devices can provide low mean radiant temperature and PMV [21].

Overall, the combination of design interventions can enhance the cooling effects in urban open spaces in hot arid climate cities and need to be considered to develop effective design guidelines.

3.2 Research for Design (RfD)

Based on the outcomes of the literature review, some design guidelines were developed with the RfD. These design guidelines take into account effective daytime and night-time heat mitigation strategies (Fig.2).

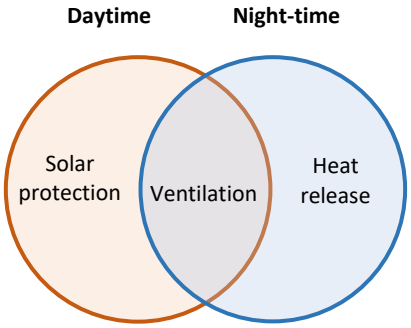

Figure 2: Effective daytime and night-time heat mitigation strategies in urban open spaces in hot arid climate cities.

Providing shade in urban open spaces is essential since urban heat is a common issue in hot arid climates, especially during afternoon hours in summer because of high air temperatures and intense solar radiation.

In addition, other common climate challenges such as drought and flash floods should be incorporated in the design guidelines. Excessive stormwater should be retained to mitigate flooding and can then also be used for irrigation, especially during drought periods. Incorporating such stormwater management strategies help making better design guidelines and eventually prevents an inefficient step-wise rebuilding of streetscapes to deal with separate climate challenges.

To combat urban heat, shading strategies should be wisely chosen and placed based on understanding different shading patterns in different common urban forms. A shading simulation was conducted with Sketch-Up (Fig.3) for the 1st of July 2023 (a typical summer day) and latitude of 24.00°N, where many hot arid climate regions in the northern hemisphere can be found.

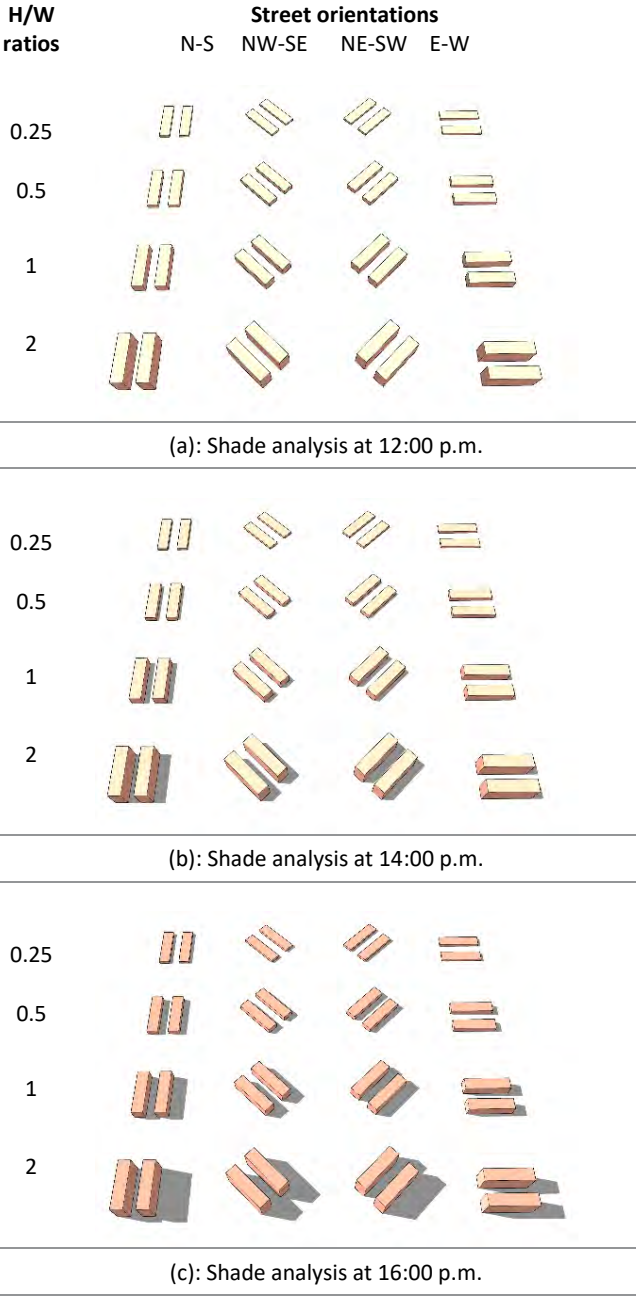

Figure 3: Shading simulation of different H/W ratios of street canyons and street orientations in noon and afternoon hours (between 12:00 p.m. and 16:00 p.m.) on a typical summer day.

Fig.3a shows that there is insufficient shade at 12:00 p.m. in all street canyons with different H/W ratios and street orientations. Thus, providing shade by placing trees or shading devices can ameliorate thermal discomfort, and more likely support people's outdoor physical and social activities.

Fig.3b shows that different street canyons with different H/W ratios or orientations can offer shade at 14:00 p.m. However, low H/W ratio of 0.25 and E-W oriented streets provide very limited shade in different scenarios.

Fig.3c illustrates that buildings can offer more shade at 16:00 p.m., especially, if the H/W ratio is high (H/W=2) in N-S, NE-SW, and NW-SE oriented streets. However, E-W does not provide shade in H/W ratios ≤1.

Overall, shading strategies should be provided in urban open spaces with high and low H/W ratios and different street orientations. Shade analyses can help to wisely place shading interventions, especially for the hot afternoon hours in summer.

The following climate-responsive design guidelines aimed at mitigating increased daytime and night-time temperatures (heat mitigation strategies) by providing adequate shade (vertical shade from buildings and horizontal shade from trees and shading devices) and allowing spaces for ventilation and night-time heat release.

These design guidelines are:

- While shading from buildings can be adequate during most of the daytime hours in hot arid climates, at 12:00 p.m. (midday) this shade is limited in all H/W ratios and street orientations, (see Fig.3a). Therefore, shading from buildings should be complemented with that of horizontal shading devices or trees (Fig. 4).

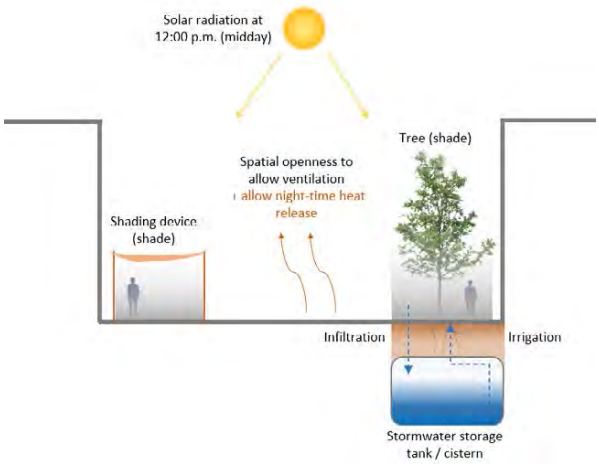

Figure 4: Shading devices and trees can provide shade when urban open spaces are used at 12:00 p.m. This street canyon has a low H/W ratio of 0.5, and these shading strategies can be applied in different street orientations (N-S, NW-SE, NE-SW, and E-W).

- Retractable shade canopies can be used in E-W, NE-SW, and NW-SE street orientations to accelerate the heat release at night, especially if it is difficult to plant trees (e.g., due to underground infrastructure, street functions or limited street width) (Fig. 5).
- Shade should be implemented in in streets with a low H/W ratio and E-W oriented streets with trees or shading devices as they can provide shade and decrease the amount of solar radiation, which can be similar to the effects of high H/W values (≥ 1). However, care should be taken to not obstruct neither air flow nor night-time heat release (Fig. 6).
- Afternoon sun tends to be stronger in hot arid climates. Thus, the placement of climate-responsive design interventions should take into account the possibility of providing cooling effects for afternoon activities in urban open spaces.

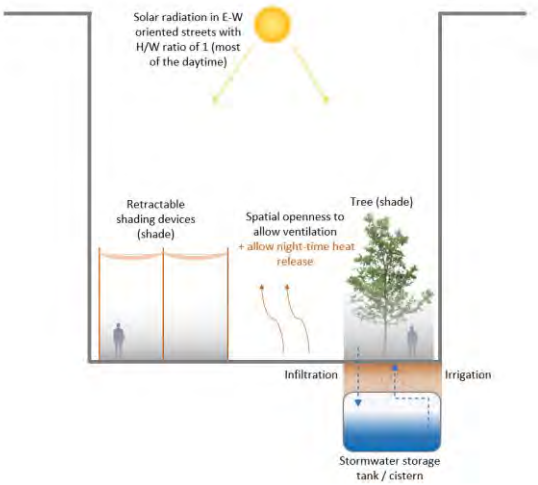

(a): Retractable shading devices provide shade at daytime.

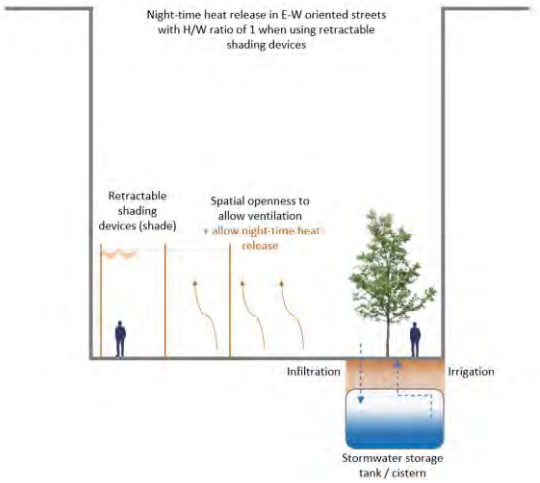

(b): Retractable shading can accelerate heat release.

Figure 5: Retractable shading devices can used to provide shade and accelerate night-time heat release, especially in narrow streets with low SVF values.

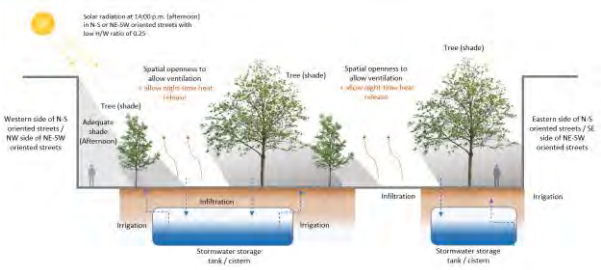

Figure 6: The placement of trees in wide streets with low H/W ratio of 0.25 in N-S and NE-SW oriented streets to provide shade at 14:00 p.m. (afternoon).

- The placement of trees on the western side of N-S oriented streets may not be necessary as buildings can provide adequate shade during harshest hours of the day, from afternoon until the sunset (Fig.7).
- If the shade of trees is needed and the width of a street is limited, place tree pits in the parking space next to the sidewalk. These tree pits can be used to manage stormwater runoff and provide a sustainable source of water for irrigation as drought is a common issue in hot arid climates (Fig.8). However, it is essential to consider the size of the tree pit as small tree pits may lack the needed volume of soil for growing trees to reach the mature size.

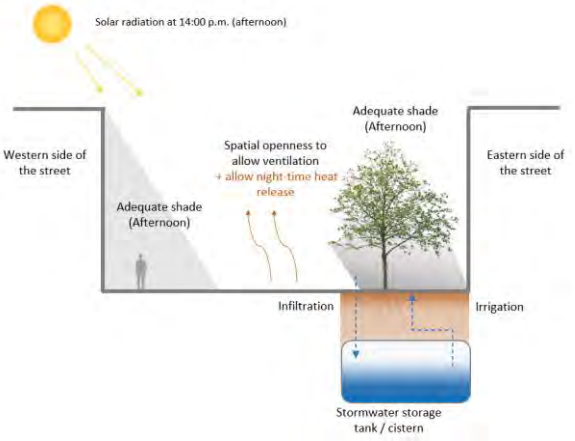

Figure 7: The placement of trees on the western side of north-south oriented streets may not be necessary as buildings can provide adequate shade from afternoon until the sunset.

- In wide streets (around 25 meters or more), there are two possible designs for trees to provide adequate shade and proper ventilation: 1) place a single row of large trees on each side of the wide street, 2) place double rows of small trees on each side of the street (Fig.9). Also, it is possible to combine them by placing a single row of large trees on one side, and place double rows of small trees on the other side.

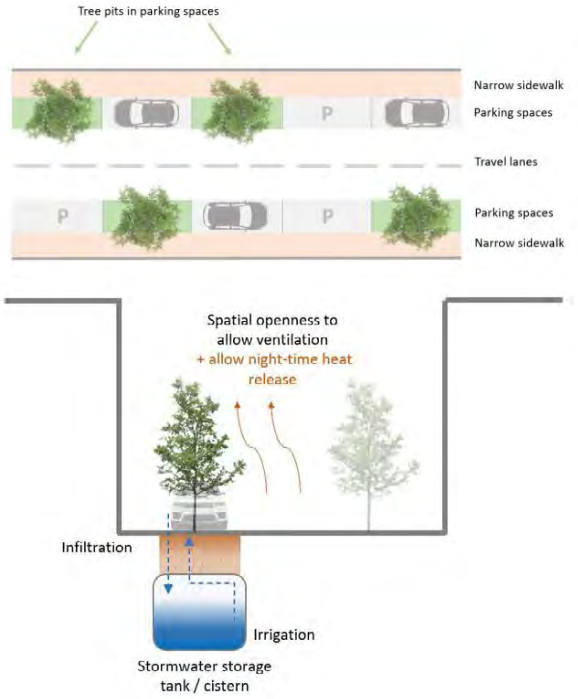

Figure 8: The placement of tree pits in parking spaces to provide adequate shade for pedestrians in narrow E-W oriented streets.

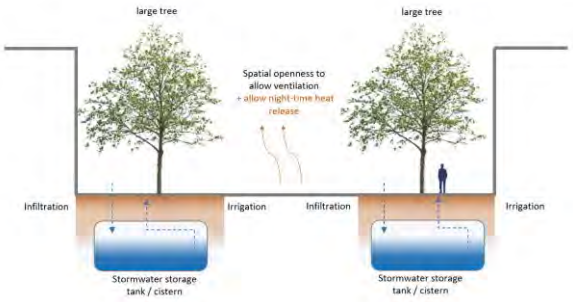

(a): Single row of large trees

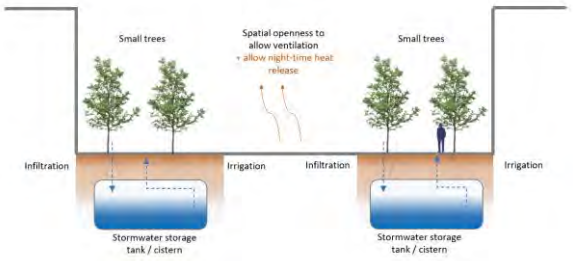

(b): Double rows of small trees

Figure 9: The placement of small and large trees in wide streets to provide adequate shade and proper ventilation.

- Planting heat and drought-tolerant tree species is recommended in hot arid climates as these tree species can withstand the harsh climatic conditions.

These design guidelines are promising in improving outdoor thermal comfort conditions in urban open spaces in hot arid climates. Some of these design guidelines can also address other common

climate issues in hot arid climates (e.g., drought, flashing flooding) and provide water resources for irrigation which is essential for trees.

4. CONCLUSION

The information accessed through the literature review was scarce and indicated the need to extend the existing design guidelines. The previous studies on climate-responsive design in hot arid climates that were found mainly focused on urban form and less on other solutions.

The RfD conducted was a first attempt to create design guidelines from the studies accessed with the literature review, also considering stormwater issues. Presenting these guidelines spatially was considered useful to communicate these guidelines to spatial designers.

The cooling effects delivered by the implementation of the design guidelines presented in this study should be tested through numerical simulations using models such as ENVI-met. In particular, further research is needed to extend the integrated design solutions and test the cooling effects of placing trees and shading devices in different H/W ratios and street orientations. This testing will allow having a better grip on the outdoor thermal comfort requirements in hot arid climates.

It is essential to consider climate-responsive design guidelines at the early design stage of any urban open space project in hot arid climates as these design guidelines provide guidance for spatial designers to achieve outdoor thermal comfort and minimize thermal discomfort, especially in summer.

ACKNOWLEDGEMENTS

This paper is part of PhD study funded by King Abdulaziz University in Jeddah, Saudi Arabia.

REFERENCES

1. Peel, M. C., Finlayson, B. L., & McMahon, T. A. (2007). Updated world map of the Köppen-Geiger climate classification. *Hydrology and Earth System Sciences*, 11(5), 1633–1644.
2. Brown, R. D., Vanos, J., Kenny, N., & Lenzholzer, S. (2015). Designing urban parks that ameliorate the effects of climate change. *Landscape and Urban Planning*, 138, 118–131.
3. Liberati, A., Altman, D. G., Tetzlaff, J., Mulrow, C., Gotzsche, P. C., Ioannidis, J. P. A., Clarke, M., Devereaux, P. J., Kleijnen, J., & Moher, D. (2009). The PRISMA statement for reporting systematic reviews and meta-analyses of studies that evaluate healthcare interventions: explanation and elaboration. BMJ, 339.
4. Lenzholzer, S., Duchhart, I., & Koh, J. (2013). 'Research through designing' in landscape architecture. *Landscape and Urban Planning*, 113(0), 120-127.
5. Bakarman, M. A., & Chang, J. D. (2015). The Influence of Height/width Ratio on Urban Heat Island in Hot-arid Climates. *Procedia Engineering*, 118, 101–108.
6. Mouada, N., Zemmouri, N., & Meziani, R. (2019). Urban morphology, outdoor thermal comfort and walkability in hot, dry cities: *International Review for Spatial Planning and Sustainable Development*, 7(1), 117–133.
7. Ali-Toudert, F., & Mayer, H. (2004). Planning-oriented assessment of street thermal comfort in arid regions. *The 21st Conference on Passive and Low Energy Architecture.* Eindhoven, Netherlands, 19–22.
8. Elbondira, T. A., Tokimatsu, K., Asawa, T., & Ibrahim, M. G. (2021). Impact of neighborhood spatial characteristics on the microclimate in a hot arid climate – A field based study. *Sustainable Cities and Society*, 75, 103273.
9. Othman, A., Abdin, A., Amin, A., & Mahmoud, A. (2020). A bioclimatic design approach for the urban open space design at business parks. *Journal of Engineering and Applied Science.* Faculty of Engineering, Cairo University, 67(8), 1883–1901.
10. Elgamal, N. F. (2017). Impact of Street Design on Urban Ventilation in Hot Dry Climate Using Envi-Met, Case of Greater Cairo Region. *1st International Conference on Towards a Better Quality of Life*.
11. Abdelhafez, M. H. H., Altaf, F., Alshenaifi, M., Hamdy, O., & Ragab, A. (2022). Achieving Effective Thermal Performance of Street Canyons in Various Climatic Zones. *Sustainability*, 14(17), 10780.
12. Abd Elraouf, R., Elmokadem, A., Megahed, N., Abo Eleinen, O., & Eltarabily, S. (2022). The impact of urban geometry on outdoor thermal comfort in a hot-humid climate. *Building and Environment*, 225, 109632.
13. Abaas, Z. R. (2020). Impact of development on Baghdad's urban microclimate and human thermal sensation. Alexandria Engineering Journal, 59(1), 275–290.
14. Alsabbagh, N. (2019). Walkability in Dubai: Improving Thermal sensation [PhD thesis, The Open University].
15. Elnabawi, M. (2016). Assessment of Thermal and Visual Micro-climate of a Traditional Commercial Street in a Hot Arid Climate [PhD thesis]. Newcastle University.
16. Elnabawi, M., and Hamza, N. (2020). A Behavioural Analysis of Outdoor Thermal sensation: A Comparative Analysis between Formal and Informal Shading Practices in Urban Sites. *Sustainability*, 12(21), 9032.
17. Abu Ali, M., Alawadi, K., and Khanal, A. (2021). The Role of Green Infrastructure in Enhancing Microclimate Conditions: A Case Study of a Low-Rise Neighborhood in Abu Dhabi. *Sustainability*, 13(8), 4260.
18. Vanos, J. K., Wright, M. K., Kaiser, A., Middel, A., Ambrose, H., and Hondula, D. M. (2022). Evaporative misters for urban cooling and comfort: effectiveness and motivations for use. *International Journal of Biometeorology,* 66(2), 357–369.
19. Emmanuel, R., and Fernando, H. (2007). Urban heat islands in humid and arid climates: role of urban form and thermal properties in Colombo, Sri Lanka and Phoenix, USA. *Climate Research*, 34, 241–251.
20. Salman, A. M., and Saleem, Y. M. (2021). The effect of Urban Heat Island mitigation strategies on outdoor human thermal sensation in the city of Baghdad. *Frontiers of Architectural Research*, 10(4), 838–856.
21. Ridha, S., Ginestet, S., and Lorente, S. (2023). Adopting a sustainable urban design to improve thermal sensation in an arid climate. *Journal of Engineering and Sustainable Development*, 27(2), 171–179.

PLEA 2024 WROCŁAW
(Re)thinking Resilience

Coupling future weather files and urban heat islands

Analysing Housing Buildings Across Different Socioeconomic Districts

RAFAEL EDUARDO LÓPEZ-GUERRERO[1], AMANDA KRELLING[2], MANUEL CARPIO[1,3]

[1] Department of Construction Engineering and Management, School of Engineering, Pontificia Universidad Católica de Chile.
[2] Laboratory for Energy Efficiency in Buildings, Federal University of Santa Catarina, Florianopolis, Brazil
[3] Centro Nacional de Excelencia para la Industria de la Madera (CENAMAD), Chile

ABSTRACT: Cities grapple with the challenges posed by global warming and urban heat islands (UHIs), with far-reaching socio-environmental and economic consequences, compromised thermal comfort and increasing energy consumption. These issues are particularly exacerbated in buildings located in socioeconomically disadvantaged urban areas. This study examines how UHI affects the energy efficiency of residential buildings in different socioeconomic districts. For this purpose, the UHI effect was modelled using UWG software. Heating loads and uncomfortable hours were analysed through EnergyPlus simulation in a low-income (LID) and a high-income district (HID). To assess future climates, the RCP8.5 scenario was selected to model future weather files for four periods (years 2020, 2030, 2050 and 2080). Also, two window parameters were tested, leading to several test scenarios. The UWG models yielded an annual average UHI intensity of 1.7°C and 1.5°C for LID and HID, respectively. However, across four periods, variations in heating loads for LID houses ranged between 17% and 22% less than those for HID houses. Housing models located in an LID exhibited 68% higher heating loads than those in an HID. Also, a new local energy standard may increase discomfort in summer due to its oversight of UHI, global warming effects, and socioeconomic differences across districts.
KEYWORDS: Sustainable construction, Urban heat island, Future climate files, Socioeconomic differences, Housing models

1. INTRODUCTION

The rapid pace of urbanization poses significant challenges, heightening cities' vulnerability and affecting a larger segment of the population. Furthermore, cities play a substantial role in both local and global climate change phenomena [1]. Among the various contributors to climate change, buildings assume a considerable responsibility, accounting for 35% of global energy consumption and 38% of greenhouse gas emissions [2]. In addition, cities face the challenge of urban heat islands (UHIs), characterized by higher temperatures in urban areas compared to surrounding rural regions [3]. UHIs result in socio-environmental and economic repercussions, compromised thermal comfort conditions and increasing energy consumption in buildings. The cooling penalty resulting from a one-degree increase in temperature or UHI intensity for surface buildings is estimated at 6.63 kWh/m^2/year/K for residential use [4]. This translates to an average of a 23.2% increase in cooling energy consumption and an average 18% decrease in heating energy [4], [5]. Moreover, the combined effects of global warming and UHI may further accentuate these impacts on buildings and urban environments [6].

Issues related to thermo-energy are more pronounced in buildings located in socioeconomically underprivileged areas, especially in poorer urban regions. The correlation between socioeconomic conditions and the likelihood of experiencing the UHI effect was highlighted in the study by Sarricolea et al. [7]. Socioeconomic inequalities pose significant challenges for Latin American cities, exacerbated by urban development models that promote social segregation, real estate speculation and unfavourable environmental conditions [8]. Numerous studies have demonstrated a clear link between urban inequalities and the potential formation of UHI in South America [7], [9]–[11]. Importantly, this issue is not exclusive to developing countries; developed nations also face similar challenges [12]. Despite an abundance of research on the UHI phenomenon, there is still a scarcity of studies that comprehensively assess how the UHI effect impacts the thermo-energy performance of buildings based on their socioeconomic status. Thus, the main objective of this research is to analyse the effects of UHI on the thermal and energy load performance of residential buildings located in different socioeconomic districts. Moreover, to assess the effect of global warming on urban buildings'

performance, modified climate files by UHI were coupled with future climate scenarios.

2. METHODOLOGY

In this work, the city of Temuco, situated in southern Chile (latitude 38.76°E; longitude 72.63°S), was selected as the study case. Based on the Köppen–Geiger climate classification, the city falls under the Csb category [13], [14].

To estimate urban weather data, this study utilized the Urban Weather Generator V 4.1 (UWG) tool [15]. Previous research has extensively used and validated this software [16]–[18]. Considering the input requirements for UWG, the most critical ones are the average building height, site coverage ratio and façade-to-site ratio [16]. Table 1 shows the main simulation parameters in UWG. These values were manually estimated using official local data [19], high-resolution satellite images, field verification and Google Street View. Similarly, urban vegetation coverage, urban area vegetation trees and sensible anthropogenic heat were estimated.

Table 1: Main UWG simulation parameters.

Satellite urban image	District	Low-income (LID)	High-income (HID)
 Low-income	Average building height (m)	3	3.05
	Site coverage ratio (%)	52	28
	Façade-to-site ratio (%)	39	44
	Anthropogenic heat from traffic (peak) (W/m²)	14.18	5.99
 High-income	Vegetation coverage (%)	8	25
	Socioeconomic levels (Chilean classification, from lowest to highest: D–E–C1–C2–ABC1)	D–E	ABC1–C2
	Models contained for EnergyPlus simulation	L_OGUC and L_PDA	H_PDA

Table 2: Main building simulation parameters.

Building geometry	Socioeconomic level	Low-income		High-income
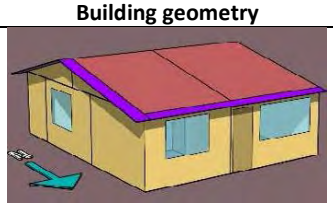 Low-income model	Model house_Standard	L_OGUC	L_PDA	H_PDA
	Surface (m²)	59.5	59.5	108
	Wall building material	Wood	Wood	Wood
	Wall U (W/m²*K)	1.32	0.45	0.45
 High-income model	R100 floor (m²K/W)*100	-	91	91
	Roof U (W/m²*K)	0.3	0.27	0.27
	Window U (W/m²*K)	5.8	2.8	2.8
	Infiltration rate (50p)	24.6	7	7
	Heating setpoint (°C)	20	20	20
	Cooling setpoint (°C)	36	36	36
	Occupation (Nº people)	3	3	3
	Maximum AFN ventilation temperature setpoint schedule (°C)	25	25	25

Table 3: Building model case parametrization.

Case	L_OGUC	L_PDA	H_PDA
A	Full WWR = 25%, WOF = 0.45	Full WWR = 25%, WOF = 0.45	Full WWR = 35%, WOF = 0.45
B	Full WWR = 25%, WOF = 0.8	Full WWR = 25%, WOF = 0.8	Full WWR = 35%, WOF = 0.8
C	-	WWR east/west facade = 42%, WWR north façade = 50%, WOF = 0.45	WWR east/west facade = 42%, WWR north façade = 50%, WOF = 0.45
D	-	WWR east/west facade = 42%, WWR north façade = 50%, WOF = 0.8	WWR east/west facade = 42%, WWR north façade = 50%, WOF = 0.8

Anthropogenic heat from vehicular traffic was calculated using a previously proposed method [20], [21]. Building surfaces were determined using high-resolution satellite images and computer-aided drafting (CAD) urban maps from previous local research [19]. Building properties were customized based on Chilean local standards [22], [23] for the thermal zone corresponding to Temuco (zone 5-F). Notably, cooling demands in Temuco are very low [24] hence, cooling setpoints were consistently set at 36°C throughout the day.

To create future and historical weather files, dynamically downscaled regional climate multi-year projections from the CORDEX database [25] were utilized. The selected scenario was RCP8.5, depicting a future marked by continuously increasing emissions and minimal climate mitigation efforts, leading to a radiative forcing of 8.5 W/m^2 by 2100 [26]. Future weather files were generated using the methodology outlined by researchers in the IEA EBC Annex 80 – Resilient Cooling of Buildings [27]. Four distinct weather data periods were considered for energy simulation, representing typical years in the 2020s (historical), 2030s, 2050s, and 2080s (future). All weather files were adjusted to reflect the influence of the UHI using the Urban Weather Generator V 4.1 (UWG) tool [15] (F_UHI).

Building simulations were carried out using EnergyPlus software V22.2 [28]. The AirflowNetwork (AFN) model was used to simulate natural ventilation during occupied periods, while the thermal comfort ASHRAE 55 adaptive model [29] was used to calculate uncomfortable hours, particularly in summer conditions.

2.1 Building models

The residential building models chosen represent typical detached houses in Temuco, situated in two different socioeconomic districts: a low-income (LID) and a high-income district (HID) [30]. Table 2 provides an overview of the key characteristics for each model. Considering the weather climate files modified according to the UHI effect, in the present analysis, the district's location and characteristics play a significant role. Thus, the whole city was sectorized into local climate zones (LCZs) [31] and the methods applied to LCZ classification and final maps are described in [32]. It is important to highlight that, currently, LID is composed mainly of houses with unique mandatory national thermal standards [22], which are not very restrictive; however, in 2015, a new official decontamination atmospheric plan (PDA) [23] was proposed with new and more restrictive building energy parameters. The adoption of the PDA standard is sparse in LIDs and more prevalent in HIDs. For the purposes of this analysis, we assume that in the medium term (before 2050), all houses in the city will comply with the PDA standard. Consequently, OGUC standard houses (L_OGUC) were simulated only in 2020 and 2030, and PDA standard houses (L_PDA and H_PDA) were simulated in all years.

In this research, the analysis of heating loads and uncomfortable hours focused exclusively on the thermal zones that are most frequently occupied, namely the main room and living area. To assess these variables, two window parameters were tested, window-to-wall ratio (WWR) and the window opening factor (WOF), resulting in four study cases. Case A is a base case, representing the most common WWR and WOF values used across all districts. Conversely, cases B, C and D involve higher values for WWR, WOF or both. The upgraded Chilean standard for Temuco [33] permits increased WWR values, allowing up to 42% for the east/west façade and 76% for the north façade, when the window transmittance is ≤2.8 W/m^2*K. Table 3 outlines the configurations for each case.

2.2 Validation process

According to national statistics, 79.47% of houses in Temuco rely on firewood as their primary heating fuel during winter [34], and the use of electricity for cooling purposes is relatively low [24]. Validating the model poses a challenge due to the diverse factors influencing firewood consumption among families (e.g. type and humidity of firewood, usage schedules, stove efficiency, etc.). To simplify this process, field verification with neighbourhood council chiefs was conducted to confirm the quantity of wood consumed in each studied district. On average, the consumption of firewood was determined to be 9 m^3/year, 4.5 m^3/year and 8 m^3/year for L_OGUC, L_PDA and H_PDA, respectively. Utilizing these quantities and applying the method proposed by [34] for real firewood consumption, the simulated models demonstrated a deviation in heating loads of −8.8% for houses in LIDs and −13.85% for those in HIDs. These differences could be attributed, among other factors, to the non-consideration of the internal loads from electrical equipment, as recommended by the National Sustainable Standard [35].

It is important to highlight that the verification process was carried out with the F_UHI file (year 2020). For this, an exclusively heating season simulation was made (between April and November), and the AFN model with windows closed was set. In addition, considering that ground temperature could strongly affect the buildings' performance [36], field measurements of thermal conductivity and density of soil were made for both

districts. For thermal conductivity, a KD2 Pro Thermal Properties Analyzer, model TR-1, was used. For density calculation, the method of hydrostatic balance proposed by [37] was performed. Therefore, the optimized finite difference model was used in EnergyPlus to calculate ground temperatures [36].

3. RESULTS

The UWG models yielded an annual average UHI intensity of 1.7°C for LID and 1.5°C for HID. Regarding building simulations, Figure 1 shows the simulation outcomes encompassing each F_UHI weather file and model within both districts. The heating load results are derived solely from the heating season in Temuco, whereas uncomfortable hours originate exclusively from the remaining summer months (December to March). This decision was taken considering that in the evaluated city residential buildings are naturally ventilated in summer and only use energy to keep warm in the winter season [24].

As expected, LID and HID have some important differences in both measured outputs. The L_OGUC standard performed 68% more heating loads than H_PDA, and 106% more than the house in the same district (L_PDA) in 2020; however, uncomfortable hours were −28% less than L_PDA and −27.8% less than H_PDA (Case A). For both L_PDA and H_PDA, across four distinct periods, variations in heating loads for LID houses ranged between 17% and 22% less than HID. Nevertheless, differences in uncomfortable hours during the summer season exhibited minimal variability, ranging from 0.2% to 2.7% when compared to L_PDA and H_PDA. These differences have a similar tendency from 2020 to 2080.

As the climate warms over time, it is possible to note the heating loads reducing either in L_PDA or H_PDA, ranging from −5.1% to −29.4% between 2020 and 2080. Similarly, uncomfortable hours varied from 1.7% to 19% during all periods. Considering winter season results, heating load reduction might mean a drop of firewood consumption between 0.2 and 1.1 m^3/kg/year and 0.39 and 2.35 m^3/kg/year for LDI and HDI, respectively.

Reductions in uncomfortable hours resulting from changes in WOF were minimal. In L_PDA, these differences ranged from −3% to −3.9% across the four periods, while in H_PDA, they ranged from −3.2% to −5.2%. Conversely, increases in WWR led to higher heating loads within L_PDA, approximately 7.8% across all periods between cases A and C and when compared with cases B and D. Simultaneously, discomfort hours increased between 2.6% and 6.4% with elevated WWR. Similarly, H_PDA exhibited slight disparities, with discomfort hours rising between 1.8% and 4.5%, and heating loads

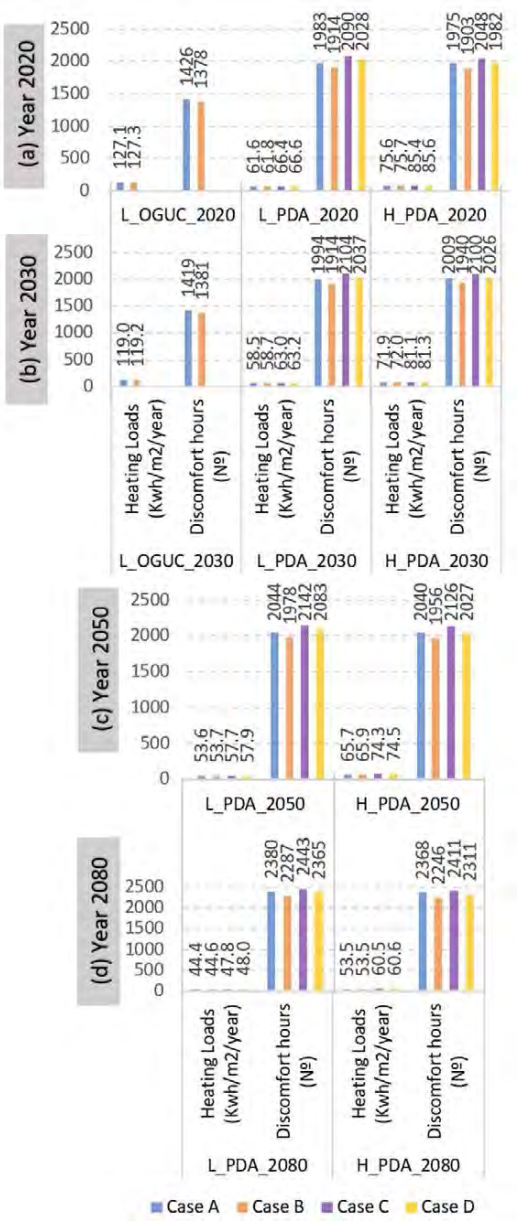

Figure 1: Heating loads and discomfort hours for simulation cases. Years (a) 2020, (b) 2030, (c) 2050 and (d) 2080.

increasing by around 13%. Increased discomfort hours may occur when the WWR is higher, possibly due to solar heat gains by windows. These findings also suggest that H_PDA could be more sensitive to changes in WWR. Moreover, Figure 1 also indicates that variations in WWR might have a lesser impact on discomfort hours in the long-term climate (2080).

4. CONCLUSIONS

The findings of this research lead to the conclusion that the thermo-energy performance of residential buildings could be affected in different ways, depending on district characteristics and building construction properties. Parameters associated with districts, such as high site coverage ratio, limited urban vegetation coverage or

increased anthropogenic heat, may result in higher UHI intensities, particularly in vulnerable socioeconomic districts. Consequently, this can adversely affect buildings with poorer thermo-energy building conditions. These problems are aggravated in socioeconomically vulnerable areas, where a scarcity of urban vegetation and a high building density are often prevalent [7], [38].

Typically, residential buildings in low-income areas are not updated to newer energy standards in southern Chile, suffering from energy poverty, and this issue is still common in most Latin American cities [39]. The significance of this problem is underscored by the fact that L_OGUC, for instance, exhibited 68% more heating loads than H_PDA. In addition, if the warming effect and UHI are simultaneously considered (F_UHI), cooling loads will tend to rise, introducing a new socioeconomic problem related to the use of HVAC systems in summer. Moreover, this phenomenon could increase anthropogenic heat in urban environments, creating a vicious circle of UHI and increased cooling loads.

On the other hand, although new restrictive energy standards are necessary, they should consider seasonal conditions in every region. In this research, it was possible to see that L_OGUC, according to the results of discomfort hours, performed better in summer conditions, but when the same house located in LID is updated to a new restrictive standard (PDA), the uncomfortable time rises considerably in naturally ventilated buildings, even with different WWR and WOF. This issue is also noted with heating loads and discomfort hour increments when both parameters (WWR and WOF) are increased. These problems could be even worse if people leverage the maximum WWR allowed by updated standards in Chile [33], considering that this research used 50% but it is possible to set 76% in north facades. The current standards in Chile permit an increase in WWR without accounting for either the UHI effect or global warming phenomena in future scenarios. Moreover, these standards apply to new buildings and retrofits in LIDs or HIDs. Thus, the problems mentioned above may exacerbate, given that the PDA standard, primarily designed to reduce heating consumption, does not address the broader implications.

Finally, some limitations can be highlighted. This research used AFN and the thermal comfort ASHRAE 55 adaptive model [29] to analyse uncomfortable hours, which might not represent real conditions in Temuco; thus, future research should aim to develop local comfort adaptive models. Additionally, cooling loads were not modelled in this work. To comprehensively assess the combined effects of global warming and UHI, future research could incorporate a holistic analysis that includes cooling loads.

ACKNOWLEDGEMENTS

This work was funded by the National Agency for Research and Development (ANID)/Scholarship Program/DOCTORADO BECAS CHILE/2020–21201032, ANID FONDECYT 1201052 and ANID BASAL FB210015 CENAMAD.

REFERENCES

1. A. Khan, S. Chatterjee, and Y. Wang, “Context and background of urban heat island,” in *Urban Heat Island Modeling for Tropical Climates*, 2021, pp. 1–35. doi: 10.1016/B978-0-12-819669-4.00001-5.

2. UNEP, “Global Status Report for Buildings and Construction: Towards a Zero-emission, Efficient and Resilient Buildings and Construction Sector,” Nairobi, 2020. [Online]. Available: https://wedocs.unep.org/bitstream/handle/20.500.11822/34572/GSR_ES.pdf?sequence=3&isAllowed=y

3. T. R. Oke, G. Mills, A. Christen, and J. A. Voogt, *Urban climates*, First publ. Cambridge University Press, 2017.

4. R. E. López-Guerrero, K. Verichev, G. A. Moncada-Morales, and M. Carpio, “How do urban heat islands affect the thermo-energy performance of buildings?,” *J Clean Prod*, vol. 373, pp. 1–21, Nov. 2022, doi: 10.1016/j.jclepro.2022.133713.

5. X. Li, Y. Zhou, S. Yu, G. Jia, H. Li, and W. Li, “Urban heat island impacts on building energy consumption: A review of approaches and findings,” *Energy*, vol. 174, pp. 407–419, 2019, doi: 10.1016/j.energy.2019.02.183.

6. M. Santamouris, “On the energy impact of urban heat island and global warming on buildings,” *Energy Build*, vol. 82, pp. 100–113, 2014, doi: 10.1016/j.enbuild.2014.07.022.

7. P. Sarricolea, P. Smith, H. Romero-Aravena, R. Serrano-Notivoli, M. Fuentealba, and O. Meseguer-Ruiz, “Socioeconomic inequalities and the surface heat island distribution in Santiago, Chile,” *Science of the Total Environment*, vol. 832, no. October 2021, p. 155152, 2022, doi: 10.1016/j.scitotenv.2022.155152.

8. UN-HABITAT, “STATE OF LATIN AMERICAN AND CARIBBEAN CITIES 2012 Towards a new urban transition,” Kenia, 2012. Accessed: Apr. 11, 2023. [Online]. Available: https://unhabitat.org/sites/default/files/download-manager-files/State%20of%20Latin%20American%20and%20Caribbean%20cities.pdf

9. D. Montaner-Fernández *et al.*, “Spatio-temporal variation of the urban heat island in Santiago, Chile during summers 2005–2017,” *Remote Sens (Basel)*, vol. 12, no. 20, pp. 1–19, Oct. 2020, doi: 10.3390/rs12203345.

10. P. Sarricolea and O. Meseguer-Ruiz, “Urban climates of large cities: Comparison of the urban heat Island effect in Latin America,” in *Urban Climates in Latin America*, Springer International Publishing, 2019, pp. 17–32. doi: 10.1007/978-3-319-97013-4_2.

11. R. G. P. da Silva, C. L. Lima, and C. H. Saito, “Urban green spaces and social vulnerability in Brazilian metropolitan regions: Towards environmental justice,” *Land use policy*, vol. 129, pp. 1–12, Jun. 2023, doi: 10.1016/j.landusepol.2023.106638.

12. T. Chakraborty, A. Hsu, D. Manya, and G. Sheriff, “Disproportionately higher exposure to urban heat in lower-income neighborhoods: A multi-city perspective,” *Environmental Research Letters*, vol. 14, no. 10. Institute of Physics Publishing, pp. 1–10, Oct. 01, 2019. doi: 10.1088/1748-9326/ab3b99.
13. M. C. Peel, B. L. Finlayson, and T. A. Mcmahon, “Updated world map of the Köppen-Geiger climate classification,” *Hydrol Earth Syst Sci*, vol. 11, no. 5, pp. 1633–1644, 2007.
14. Climate data, “Climate data.” Accessed: Apr. 06, 2023. [Online]. Available: https://es.climate-data.org/america-del-sur/chile/ix-region-de-la-araucania/temuco-6152/
15. B. Bueno, L. Norford, J. Hidalgo, and G. Pigeon, “The urban weather generator,” *J Build Perform Simul*, vol. 6, no. 4, pp. 269–281, 2013, doi: 10.1080/19401493.2012.718797.
16. A. Salvati, P. Monti, H. Coch Roura, and C. Cecere, “Climatic performance of urban textures: Analysis tools for a Mediterranean urban context,” *Energy Build*, vol. 185, pp. 162–179, 2019, doi: 10.1016/j.enbuild.2018.12.024.
17. B. Bueno, M. Roth, L. Norford, and R. Li, “Computationally efficient prediction of canopy level urban air temperature at the neighbourhood scale,” *Urban Clim*, vol. 9, pp. 35–53, Sep. 2014, doi: 10.1016/j.uclim.2014.05.005.
18. J. Mao, J. H. Yang, A. Afshari, and L. K. Norford, “Global sensitivity analysis of an urban microclimate system under uncertainty: Design and case study,” *Build Environ*, vol. 124, pp. 153–170, Nov. 2017, doi: 10.1016/j.buildenv.2017.08.011.
19. Municipalidad de Temuco, “ESTUDIO DE PAISAJE E IMAGEN URBANA,” Temuco, 2015. Accessed: Mar. 27, 2023. [Online]. Available: https://legacy.temuco.cl/wp-content/uploads/2018/12/Cap5-Imagen-Urbana.pdf
20. A. K. L. Quah and M. Roth, “Diurnal and weekly variation of anthropogenic heat emissions in a tropical city , Singapore,” *Atmos Environ*, vol. 46, pp. 92–103, 2012, doi: 10.1016/j.atmosenv.2011.10.015.
21. C. S. B. Grimmond, “The suburban energy balance: Methodological considerations and results for a mid-latitude west coast city under winter and spring conditions,” *International Journal of Climatology*, vol. 12, no. 5, pp. 481–497, 1992, doi: 10.1002/joc.3370120506.
22. Chile, *Ordenanza General de Urbanismo y Construcciones*. Chile, 2022.
23. Ley Chile, *Ministerio del Medio Ambiente*. Chile: Biblioteca del Congreso nacional de Chile, 2015. Accessed: Mar. 28, 2023. [Online]. Available: https://www.bcn.cl/leychile/navegar?idNorma=1084085&idVersion=2018-03-10&idParte=
24. Corporación de Desarrollo Tecnológico, “Informe final de usos de energía de los Hogares Chile 2018,” 2019.
25. F. Giorgi, C. Jones, and G. R. Asrar, “Addressing climate information needs at the regional level: the CORDEX framework,” 2009. [Online]. Available: http://wcrp.ipsl.
26. K. Riahi *et al.*, “RCP 8.5-A scenario of comparatively high greenhouse gas emissions,” *Clim Change*, vol. 109, no. 1, pp. 33–57, Nov. 2011, doi: 10.1007/s10584-011-0149-y.
27. EA, “IEA EBC Annex 80 on Resilient Cooling for Residential and Small Non-Residential Buildings Annex Text,” 2019. Accessed: Mar. 26, 2023. [Online]. Available: https://annex80.iea-ebc.org/Data/Sites/10/media/documents/supporting/ebc-annex-80-annex-text-190616.pdf
28. D. B. Crawley *et al.*, “EnergyPlus: creating a new-generation building energy simulation program,” *Energy Build*, vol. 33, pp. 319–331, 2001.
29. ANSI/ASHRAE, “Thermal Environmental Conditions for Human Occupancy,” *ASHRAE*, Art. no. Standard 55-2010, 2010, [Online]. Available: www.ashrae.org
30. INE, “Instituto Nacional de Estadística,” Proyecciones de población. Accessed: Mar. 25, 2023. [Online]. Available: https://regiones.ine.cl/araucania/estadisticas-regionales/sociales/demografia-y-vitales/proyecciones-de-poblacion
31. I. D. Stewart and T. R. Oke, “Local climate zones for urban temperature studies,” *Bull Am Meteorol Soc*, vol. 93, no. 12, pp. 1879–1900, 2012, doi: 10.1175/BAMS-D-11-00019.1.
32. López-Guerrero *et al.*, “How do urban form and socioeconomic differences affect the temperature of the residential district?,” 27th International Congress on Project Management and Engineering, Ed., Donostia, Jul. 2023, pp. 2–027.
33. MINVU, “Ministerio de Vivienda y Urbanismo,” Estándar Higrotérmico Zona Térmica F y G. Accessed: Aug. 10, 2023. [Online]. Available: https://www.minvu.gob.cl/ditec/
34. BES, “Consumo de leña y otros biocombustibles sólidos en la región de la Araucanía: nuevas cifras y tendencias,” 2020. [Online]. Available: www.infor.cl
35. MINVU, “Estándares de Construcción Sustentable para Viviendas - Energía. Tomo II,” 2015.
36. V. González, G. Ramos Ruiz, and C. Fernández Bandera, “Ground characterization of building energy models,” *Energy Build*, vol. 254, pp. 1–11, Jan. 2022, doi: 10.1016/j.enbuild.2021.111565.
37. Determinación de la densidad de un suelo. Método de la balanza hidrostática., *AENOR*. España: ASOCIACION ESPANOLA DE NORMALIZACION Y CERTIFICACION, 1994.
38. M. García-Lamarca, I. Anguelovski, and K. Venner, “Challenging the financial capture of urban greening,” *Nature Communications*, vol. 13, no. 1. Nature Research, pp. 1–4, Dec. 01, 2022. doi: 10.1038/s41467-022-34942-x.
39. R. Calvo, N. Álamos, M. Billi, A. Urquiza, and R. Contreras Lisperguer, “‘Desarrollo de indicadores de pobreza energética en América Latina y el Caribe’ serie Recursos Naturales y Desarrollo, N° 207 (LC/TS.2021/104),” Santiago, 2021. [Online]. Available: www.cepal.org/apps

Evaluating the impact of urban form and GDP on CO_2 emissions through the Geographically Weighted Regression model

YIHAN LI[1]

[1]Shandong Jianzhu University, Jinan, China

ABSTRACT: As the global warming trend worsening currently, researchers' attention was gradually draw to cities seeing that they have the absolute dominant role in CO_2 emission. As the main villain behind global warming, yet little has been done to see how urban forms can influence CO_2 emission of cities. Aiming to fill this gap, this article primarily concentrated on the evaluation of three different urban forms (urban constructive land, rural settlement, other lands) as well as other three auxiliary variables (Gross Domestic Product Per Capita, Road Density, Public Car ownership) to see how they are affecting CO_2 emission of cities individually and aggregately. The result was intriguing to indicate that merely other lands (industrial, transportation, etc) was positively related to CO_2 emission, while the other five variables were all bidirectionally related to CO_2 emission. Additionally, the result also manifested significant discrepancy among different region of China, owing to the fact that the country is still now not evenly developed. This can consequently aid in the process of policy-making, based on the uniqueness of different regions to achieve low-carbon development.
KEYWORDS: Urban Forms, Rural Settlement, Geographically Weighted Regression, China, CO_2 emissions.

1. INTRODUCTION

Climate change is one of the most pressing issues demanding attention. As recorded, global CO_2 emissions remained stable until the first Industrial Revolution which marks the massive exploitation and implementation of fossil-fuel energy, and has continuously been the main contributor to CO_2 emissions [5]. To control the future rise of temperature under 1.5 degrees Celsius, researchers have been striving to address this problem from various perspectives. Cities are constantly the most significant contributor of CO_2 emissions. They are responsible for approximately 70% of global CO_2 emissions, even though they just occupied less than 5% percent of all lands [3,4]. Additionally, it has been reported that during the past century, China has witnessed its significant rise in CO_2 emissions and currently accounted for 27% of the global emissions [5]. Urban areas were thus of great importance in tackling the excessive carbon emission so as to achieve the promise made during the 2015 Paris Agreement on climate change, in which China guarantee to reduce its carbon emission by 60% per unit of GDP.

Even though extensive studies have been conducted to evaluate the drivers behind cities' CO_2 emissions [2,8,9], certain crucial factors, such as the form of rural settlements, remain overlooked. The main reason for choosing this particular form is that rural areas still accounted for considerably amounts of the overall land scope, the participation of this factor can profoundly deepen the result's insight, since for the elaboration of the Paris Agreement cities should not be the only focal point, despite their dominant role in the carbon emission. To adequately address this gap, this article will mainly concentrate on both urban and rural areas' influence on China's excessive amount of greenhouse gas emissions. By combining Ordinary Least Squares (OLS) as well as Geographical Weighted Regression (GWR), the relationship between CO_2 emissions and urban forms can be evaluated. Those factors included three disparate urban forms which are urban construction land (UCL), rural settlement (RS), other lands (OL) (industrial, airport, transportation site and etc.) Additionally, to draw a more comprehensive result, Gross Domestic Product per capita (GDPPC), road density (RD) and public car ownership (PCO) were added. This can consequently aid in policy-making regarding the future development patterns of cities.

2. MATERIALS AND METHODS

2.1 Study area and data availability

The data of CO_2 emissions, Gross Domestic Product (GDP) were obtained from China City Greenhouse Gas Working Group; public car ownerships and road density data were from China City Statistical Yearbook; land use data was from Chinese Academy of Sciences. Consequently, the study area encompassed all cities in China to investigate how selected factors contributed to CO_2 emissions in the year 2020. The table below showed the basic component of the data including its unit, mean, median and Std. Dev.

Table 1: Description statistics of variables

Name	Mean	Median	Std. Dev
GDPPC (10^4 yuan)	6.218	5.245	3.281
UCL (hc)	2294758.424	1235650	2858778.446
RS (hc)	4661064.228	2639200	5401104.264
OL (hc)	1471175	1064000	1592629
RD (Km/Km^2)	5.941	6.600	3.313
PCO (unit/Per 10^4 people)	7.571	7.3	5.610

2.2 Z-score standardization

As shown in the previous section, the chosen variables were of significant discrepancy since they originated from different fields and had different units. In order to make the coefficient of each variable in GWR more comparable, data went through Z-score standardization before it was used for analysis.

Z-score standardization was generally employed in statistical analysis that specifically aimed to solve the situation mentioned before. The equation (1) of it is shown below:

$$x_{new} = (x-\mu)/\sigma \quad (1)$$

where x_{new} – new data;
x – original data;
μ – mean of the data;
σ – standard deviation of the data;

By applying Z-score standardization, heterogeneity of different data was eliminated, therefore making them directly comparable where the magnitude of the coefficient can represent their impact more objectively in order to facilitate policy-making more accurately.

2.3 Research process

2.3.1 Spatial autocorrelation

Spatial autocorrelation was used to estimate the dependence and heterogeneity among CO_2 emissions, which was generally indicated by Moran's I [2]. It comprised two indices, Global Moran's I and Local Moran's I. Global Moran's I represented the global autocorrelation between different geographical regions while Local Moran's I evaluated the autocorrelation with one's proximate cities. They both ranged from -1 to 1, in which negative suggested degrees of heterogeneity and positive suggested degrees of dependence. Two variables of z-score and p-value respectively referred to the level of spatial autocorrelation with proximate cities and its corresponding significance level. In addition to this, global mean and local mean were used to classify spatial clusters. Global mean referred to the overall z-score of all cities while Local mean was the z-score of observation's neighbors. A High-High (HH) cluster comprised of whose local mean was higher than the global mean, while whose local mean was lower than the global mean was classified as Low-Low (LL) cluster. For those that possessed a z-score that was higher than the local mean was defined as High-Low (HL) cluster while the other way around read as Low-High (LH) cluster [11].

2.3.2 Urban form calculation

Three different land use types were selected to evaluate their impacts on CO_2 emissions. They were UCL, RS and OL as mentioned before.

The rudimentary data was Raster which contained all land use of China. Then, Fragstats was applied to extract UCL, RS and OL into new Rasters. Finally, Rasters calculated by the index under Class Metrics named Total Area (CA/TA) was chosen as the embodiment of urban forms. Based on the administrative boundaries of cities, patches under each city's boundary were aggregated, generating a new number representing the total area of a specific urban form in hectares of each city.

2.3.3 Regression analysis

To adequately address the impacts of the selected independent variables on CO_2 emissions, geographically weighted regression (GWR) was therefore applied for the analysis.

In the process, OLS was initial employed to evaluate the goodness-of-fit of the chosen factors' impact on CO_2 emission. Provided with a relatively promising R-square by the OLS, GWR was then employed to show the spatial heterogeneity among cities. The equation (2) of GWR was as followed:

$$yi = \beta_0(u_i, v_i) \sum_{k=1}^{p} \beta_k(u_i, v_i) x_{ik} + \varepsilon_i \quad i = 1,2 \cdots, n. \quad (2)$$

Where ε_i – error item that satisfies the spherical disturbance hypothesis
$\beta_0(u_i, v_i)$ – the intercept items;
k – number of factors;
$i - i$ - th cities;
$\beta_k(u_i, v_i)$ –local regression parameter;

GWR model estimated the exhaustive coefficients of different factors. In terms of the famous geographical law, everything is related to another, and more related with nearer ones rather than distant ones [10], GWR showed decent respect for this concept. Compared with ordinary least squares (OLS), the GWR model can evaluate the local impacts of each independent variable on the dependent variable to articulate spatial heterogeneity, providing us with a more profound insight into this topic.

3. RESULTS

3.1 CO_2 emissions

During the analysis process, our evaluation was limited to 336 cities due to the deficiency of data in those cities.

In summary, cities with high CO_2 emissions were mainly located in eastern China where regions had witnessed considerably growth of urban expansion and populations growth during the past few decades owing to the reform and opening up policy. They primarily concentrate around Beijing-Tianjin-Hebei Urban Agglomeration (BTH), Shandong Peninsular, Yangtze River Delta (YRD), Peral River Delta (PRD) and spotted throughout Chongqing Province. However, Cities in the Northern China with high emissions were probably rendered by the additional consumption of fossil-fuel energy in winters for the purpose of interior heating [6].

Simultaneously, cities in the western area of China emitted way less CO_2 than the eastern area owing to their possession of relatively less populations and low urbanization rate. Most of those cities were unsuitable for human settlement due to severe natural environment. Nevertheless, a few exceptions were located in the north of Xinjiang province around the city called Karamay, owing to the massive exploitation of petroleum. CO_2 emissions of different cities are shown in Fig 1:

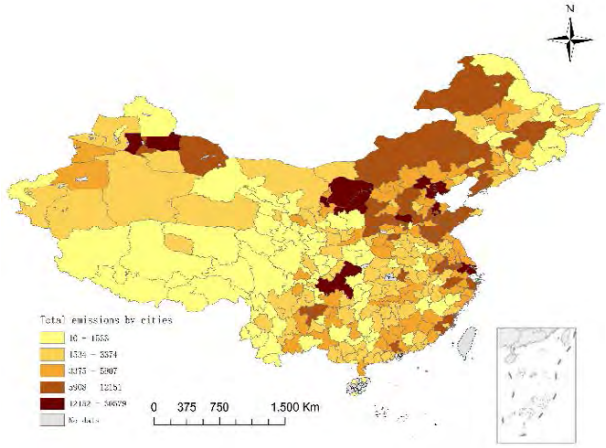

Figure 1: Distribution of CO_2 emissions of 336 cities

3.2 Moran's I

The global Moran's I of CO_2 emissions of the calculated 336 cities of China was 0.200, and the p (< 0.05), indicating that the spatial autocorrelation was statistically significant and of great dependency.

The results of Local Moran's I mainly fell into four different distribution categories as mentioned before. HH clusters were primarily located around the Bohai Sea, YRD, and central of Inner Mongolia; LL clusters were located in the central southern areas; HL cluster spotted in Chongqing and Wuhan city, while LH cluster spotted in the north of Xinjiang province. The spatial distribution of clusters is shown in Fig. 2:

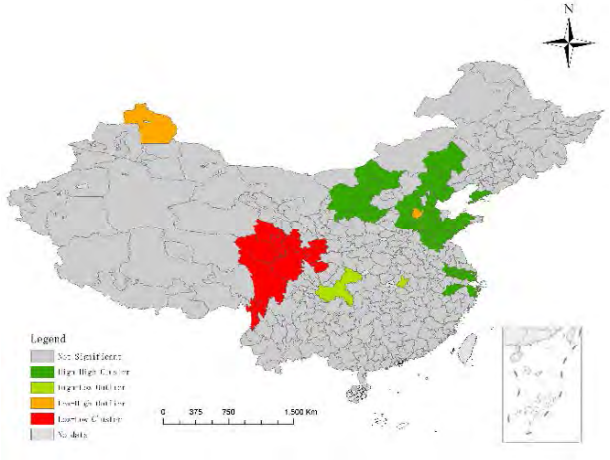

Figure 2: Distribution of Local Moran's I cluster

3.3 OLS

The OLS model was first applied to evaluate the overall impacts of the selected factors on CO_2 emissions before GWR in order to examine the global linear relationship.

The p-value (< 0.05) indicated that the model was statistically significant, while the adjusted R-square (0.612) demonstrated a relatively strong correlation. Additionally, the variance inflation factors (VIF) were all below 10, denying multicollinearity.

Table 2: Global regression analysis (OLS)

Name	Coefficient	Pr. (t)	VIF
Constant	3108.977	36.88	
GDPPC	865.764	0.015*	1.713
UCL	1486.463	0.000*	2.458
RS	504.044	0.000*	1.762
OL	1525.272	0.036*	1.200
RD	222.440	0.127	1.219
PCO	-153.733	0.567	1.659

Adjusted R^2 :0.612 *: Significance

3.4 GWR

The results drawn by GWR showed great heterogeneity that the exhaustive R2 varied across different regions of China, with the highest reaching 0.767 and the lowest falling to 0.408. The areas with high R2 were sporadically scattered in the southeastern coastal areas around YRD, central north areas, north of Xinjiang province and Heilongjiang province. Whereas those with lower R2 lied in the central northwestern areas, the southern section of Yunnan province and cities around the Bohai sea.

In the GWR model, approximately half of the cities possessed a higher R-square compared with the OLS model, indicating a more reliable result. The GWR model further unveiled the spatial non-stationarity of the relationships compared with OLS. It also showed that variables defined to be positively related to CO_2

emissions in OLS can instead be bidirectional in GWR and of significant difference among different regions.

The spatial distribution of R2 is shown in Fig. 3; the coefficients of each variable are shown in Fig. 4; table 3 also marked the coefficients in numbers. They are as followed:

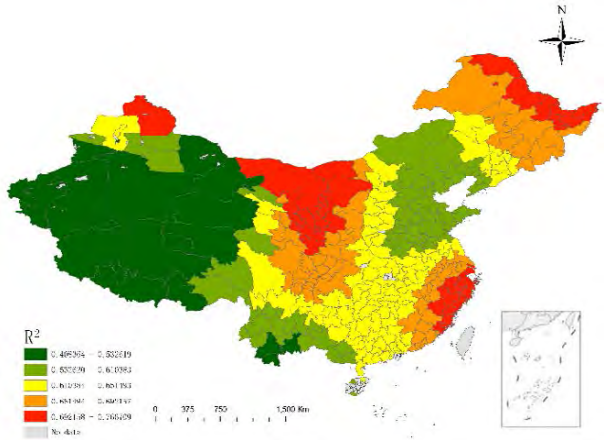

Figure 3: Distribution of R^2 of different cities draw by GWR

Table 3: GWR coefficients

Name	Max	Min	Mean
GDPPC	4139.597	-795.263	714.012
UCL	2647.449	-1577.773	1181.586
RS	6272.139	-350.439	412.819
OL	3249.929	376.881	1625.877
RD	1100.978	-2997.886	193.886
PCO	2677.523	-749.796	21.705

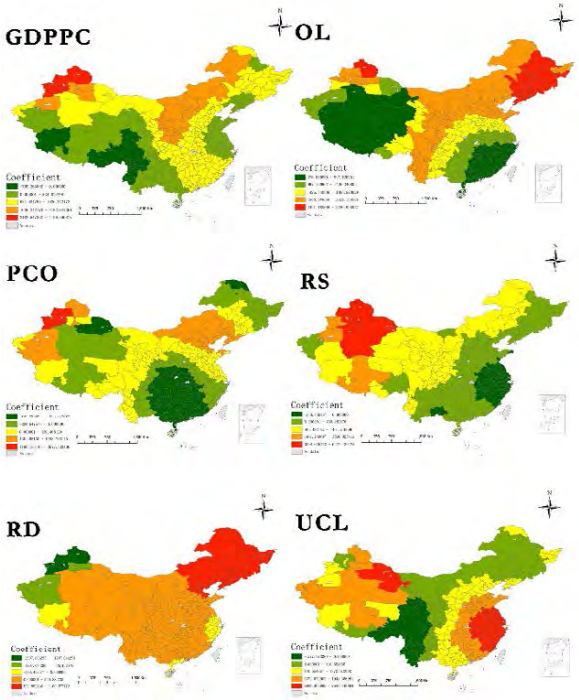

Figure 4: Distribution of Coefficient of variables

As shown in Fig. 4, **GDPPC** was playing a mostly positive role towards CO_2 emissions in which the most significant areas lied in the north of Xinjiang province and central northeast, including Ningxia province and east of Inner Mongolia, except for the southwest section of China, including the west of Sichuan and Yunnan province, the south of Qinghai Province and the south of Tibet province where economic growth could instead alleviate CO_2 emissions.

UCL was also found to be bidirectional, in which the areas of significance formed a gradient tendency, with the most significant core areas concentrating on the YRD region, the heavily developed areas of China, and gradually descend as it moved east. The north of Xinjiang Province also demonstrated great significance. The most insignificant areas were southwest China, especially west of Yunnan and Sichuan province, where UCL was instead playing a negative role towards CO_2 emissions.

The result of **RS** showed a gradient tendency, with the significance ascending from east to west, and even aggregately showed negative in the YRD region which referred to the most developed regions of China. The most significant areas primarily concentrated in central Xinjiang province.

OL manifested a strong positive correlation with CO_2 emissions; the most slightly significant areas lie in the western and southeast coastal section of China, which refers to Xinjiang, Tibet, Guangdong and Fujian Province. Whereas the most significant area lies in the three northeastern provinces and central China covering tons of cities.

RD showed a relatively flat result, in which the majority of cities showed a slight significance; the exception lied in the northeastern section of China, where RD was playing a relatively positive role towards CO_2 emissions. It was worth mentioning that it showed negative in the YRD, Pearl River Delta (PRD) and the east of Xinjiang Province.

PCO showed an intriguing result where almost half of the CO_2 emissions of cities were found to be negatively related to it, which aggregately concentrated in the southern region of China and distributed in the northeastern peripheral areas adjacent to Russian as well as the east of Xinjiang province. It also showed slight significance in the cities near the Bohai sea and the west of Xinjiang province.

4. DISCUSSIONS

Coefficients of the six variables showed significant spatial discrepancy among different regions. This is highly relevant to the unevenly developing stage of Chinese cities, and further discussions were required to demonstrate the reasons behind it in addressing them with expedient policies for the elaboration of low carbon development.

Studies had confirmed that the correlation between **GDP** and CO_2 emissions can roughly be explained by an invert-U shape [7], which means that heavily developed regions may instead emit less CO_2 than those economically undeveloped regions. And

the coefficient did relatively conform with this correlation, where Jiangsu province, Shandong peninsula and YRD showed slight significance seeing that these regions were heavily developed, and also in Tibet, Yunnan province where economic was not heavily developed. Yet the significance concentrated towards the central of China, where the inverted-U shape was likely in its zenith.

UCL is the most emphatic factor to indicate the developed stage of cities in China. Cities with high scope of UCL basically all demonstrated high CO_2 emissions, especially in the YRD region. This was highly relevant to the relentlessly horizontal expansion of cities during the past few decades, which increased transportation distance, causing vehicles to consume more fossil fuel energy. Yet some studies also found that the increased UCL could instead reduce CO_2 emissions by altering the built environment such as mixed use, job density, etc [9]. This may provide some explanations for its negative coefficient in GWR.

RS was one vital point of this research, and it did show great significance in affecting CO_2 emission. The distribution of coefficient basically conformed with the developing stage of cities. Even under the rapid urban expansion of Chinese cities during the past few decades, rural populations still accounted for approximately 35% of the overall population, and rural rejuvenation is currently under high frequency among Chinese urban studies. The massive application of unprocessed fossil fuel energy and stalks for the purpose of cooking, interior heating, etc not only increased CO_2 emissions but also contaminated the air, causing air pollution in winters especially in the 2010s. Now under the supervision of government, individuals living in RS can also have access to cleaned energy like electricity in replacement of fossil-fuel energy, this can consequently reduce CO_2 emission, and restriction banning the burning of stalk was also coming to see its efficiency. However, given the vast scope of China and evenly developed stage, the undeveloped region such as western China may still cling to the traditional energy and were tricky for restriction to reach, which explains the great significance.

OL was found to be the only factor that was positively related to CO_2 emission. Yet it also demonstrated great discrepancy across cities. This is of high relevance to the industrial structure of those regions. While OL includes multiple land use, the one that can significantly contribute to CO_2 emissions is industrial land. In the southern region of China, the shift of industrial structure has lifted high-tech industries to a dominant stage, and the innovative technology that came along with them was not demanding excessive consumption of fossil fuel energy, which meaned environmental-friendly [2,12]. In comparison, OL in the northern region of China was positively related to CO_2 emissions, owing to its reliance on traditional industries which refers to heavy industries with significant fossil fuel energy consumption that can tremendously increase CO_2 emissions.

The increase of **RD** can help avoid traffic congestion and subsequently reduce the invalidate time during transportation, as reported in the previous thesis indicating that transportation of vehicles is one of the major driving factors behind carbon emission [6]. And it is also worth mentioning that in the YRD region, transportation planning may be conducive for the CO_2 alleviation seeing that those cities merged under relatively innovative planning principles, whereas the configuration of the northeastern cities were mostly determined in the 1960s, a time when climate change had rather not been of such an issue as it is today and urban planning had a strong inclination towards the use of vehicles.

The result of **PCO** had also left us with tons of space for discussion. The negative correlation of it with the majority of southern region indicated that it also had some rough relation with the development stage. In the southern regions, under the simultaneous influence of both the tightening restriction on the purchase of traditional vehicles and advocation of public transportation including metro, bus, etc, residents were drove to purchase electrical vehicles and use public transportation as alternatives, explaining the negative coefficient in those regions. Whereas cities in the northern region near the Bohai sea were still clinging to traditional type of cars possibly owing to the low efficiency of battery in electrical cars when faced with extreme temperature in winter.

As for the policy-implications, there are two effective methods that hold transformative potential in achieving the long-term goal of reducing carbon emissions. On the national scale would be the top-down approach in which the local government set forth new regulations that help to alleviate carbon emissions, for instance the restrictions of expansions of UCL and development of high-tech industries can be accomplished through this method; on the regional scale would be the bottom-up methods, where local residents participate in alleviating emissions voluntarily. While the promotions of low-carbon lifestyles and electrical vehicles can substantially increase peoples' aptness towards using them, they can simultaneously bring incentives for the further development of them. The former one can be immediately effective while the latter one may take tremendous time yet it truly guarantees a sustainable future.

5. CONCLUSIONS AND LIMITATIONS

This study adopted the GWR model to analyse the impact of urban, rural, and transportation forms on

carbon emissions in China considering the heterogeneity of development stage of different region. Collectively speaking, the priority of all Chinese cities will undoubtedly lie on economic growth, regardless of their developing stage. GDPPC will thus inevitably still be on an ascending trend. Yet it is still eligible for planners to optimize the policy-making process so as to accomplish low-carbon development based on their relative position in the inverted-U shape. First, cities should find their alternatives for urbanization process instead of the traditional horizontal expansion to stop UCL from further ascending. In fact, new planning policy was already employed which demarcated the boundaries between urban and rural area and emphasized the importance of compact development, which had been proven to be conducive for reduction of CO_2 emissions if treated properly [12]. However, household consumption was also of great significance relating to carbon emission [6], which draws our attention to RS. Recently under the supervision of governments, this situation was basically erased, but effect still has to be made in western region especially Xinjiang Province where cities were less developed compared to the east. OL was another vital factor that affected CO_2 emission. Since its coefficient in GWR showed that it is already playing a slight tendency towards alleviation of CO_2 emissions in developed regions where high-tech industries flourished, it would be expedient for all cities to employ this strategy, which means to develop high-tech industries in replacement of traditional industries for the emancipation from massive fossil-fuel energy.

Apart from urban forms, vehicles were also another factor worth taking into consideration. The advocation of public transportation already showed slight effect in the southern part of China, since it reduced people's willingness of using private vehicles, and the electrical vehicles were also of indispensable assistance. So predictably it would also do the same when it spread to all nations. It is worth mentioning that China is currently pioneering in terms of the field of electrical vehicles, the advocation of electrical buses and private cars simultaneously further assist in the development of high-tech industries, which was proven to be beneficial for estimating CO_2 emissions. Additionally, reasonably increasing RD is also another conducive method of alleviating CO_2 emission as well as the ongoing replacement of traditional vehicles by electrical ones. In other words, those two factors focused more upon the built environment of cities, which was already proven by multiple thesis that it had the potential of estimating CO_2 emission by shaping how residents go out through built environment, such as the density of bus stop. In sum, this article covered both macro-scale planning as well as micro-scale strategies in realizing low-carbon development.

Nevertheless, few limitations still existed during analysis. Among them, the most telling one would be the ignorance of three-dimensional urban forms. Proven by multiple thesis, compactness of an area can pose impact on CO_2 emissions owing to its potential dominance over the micro-climate of urban areas, which made it imperative to be understood for the elaboration of urban renewal strategies [8,12]. Moreover, OLS and GWR were both linear analytical methods which initially had their incompetence when faced with nonlinear models, since not all data can be explained simply by linear analytical methods.

REFERENCES

1. IPCC. (2022), Impacts of 1.5°C Global Warming on Natural and Human Systems. *Global warming of 1.5°C*, 175-312.

2. Wang S, Shi C, Fang C, Feng K. (2019), Examining the spatial variations of determinants of energy-related CO_2 emissions in China at the city level using Geographically Weighted Regression Model. *Applied Energy,* 95-105, 235

3. GEA. (2012), Global energy assessment – Toward a sustainable future. Cambridge, *UK: Cambridge University Press;* p. 1888.

4. IEA. (2012), World Energy Outlook. *Paris: International Energy Agency (IEA);* p. 700.

5. Hannah Ritchie, Max Roser and Pablo Rosado (2020) - "CO_2 and Greenhouse Gas Emissions", [Online], Avaiable: 'https://ourworldindata.org/CO_2-and-greenhouse-gas-emissions'

6. Shudi Zuo, Shaoqing Dai, Jiaheng J, Fanxin Men, Yin Ren, Yunfeng Tian, Kaide Wang, (2022), The importance of the functional mixed entropy for the explanation of residential and transport CO_2 emissions in the urban center of China, *Journal of Cleaner Production*, 380.

7. Jeon H. (2022), CO_2 emissions, renewable energy and enonomic growth in the US. *Electricity Journal;* 35(7).

8. Wang S, Wang J, Fang C, Li S. (2019), Estimating the impacts of urban form on CO_2 emission efficiency in the Pearl River Delta, China. *Cities,* 117-129, 85

9. Ma J, Liu ZL, Chai YW (2015), The impact of urban form on CO_2 emissions from work and non-work trips: a case study in Beijing, China. *Habitat;* 1-10, 47.

10. Tobler WR. (1970), A computer movie stimulating urban growth in the Detroit region. *Econ Geogr;* 234-40, 46.

11. Yongxian Su, Xiuzhi Chen, Yong Li, Jishan Liao, Yuyao Ye, Hongou Zhang, Ningsheng, Huang, Yaoqiu Kuang, (2014), China's 19-year city-level carbon emissions of energy consumption, driving forces and regionalized mitigation guidelines. *Renewable and Sustainable Energy Reviews;* 231-243, 35.

12. Ou J, Liu X, Wang S, Xie R, Li X, (2019), Investigating the differentiated impacts of socioeconomic factors and urban forms on CO_2 emissions: Empirical evidence from Chinese cities of different developmental levels, *Journal of Clearer Production,* 601-614, 85.

PLEA 2024 WROCŁAW
(Re)thinking Resilience

GIS-Based Remote Sensing Approach for Urban Studies:
Locating and Mapping Vulnerable Areas in Hot Climates

JAVIER SOLA-CARABALLO[1], ANTONIO SERRANO-JIMÉNEZ[2], CARLOS RIVERA-GOMEZ[1], CARMEN GALAN-MARIN[1]

[1] Departamento de Construcciones Arquitectónicas I, Seville, Spain.
[2] Departamento de Construcciones Arquitectónicas, Granada, Spain.

ABSTRACT: Urban settlements in warm regions are facing the consequences of the current increases in temperatures. Due to their geometry, materials, and human activities, some urban areas suffer higher heat exposure than others. Moreover, in the current energy crisis, families that are already exposed to these high temperatures also suffer fuel poverty. This research provides an accessible approach to detect and locate vulnerable climatic areas in warm cities. Land surface temperature heatmaps are obtained from remote sensing imagery, which is overlapped with urban plans and income indicators in GIS environment. This proposed guideline allows one to easily identify graphically and with data, especially vulnerable areas, that can be usable for further analysis and prioritise interventions. The results of this contribution have identified the climate-vulnerable areas of Seville, one of the most populous and warmest cities in Spain, where according to this study, nearly 23% of the population lives in climate-vulnerable areas. These zones mainly correspond to neighbourhoods in the suburbs, originally low-income developments built during the second half of the 20th century. This preliminary analysis can be reproduced in other cities providing valuable information for administrations and urban planners.
KEYWORDS: GIS analysis, Remote sensing, Land surface temperature, Climatic vulnerability, Fuel poverty.

1. INTRODUCTION

Cities are the main geographical entity where the society concentrates its activity. According to last UN report [1], their population represent more than 55% of the global. Due to their geographical configuration, the buildings, the urban materials, and the anthropomorphic activities [2], urban settlements are affected by risky phenomena such as the urban heat island, and general urban overheating . Currently, with cities becoming larger and denser [3], this issue has affected the life and health of people [4]. However, with the present situation of global overheating, and the worse future projections of climate change (CC) [5], this problem is becoming a crucial issue to be addressed and mitigated. Public administration, as the society common regulator, has the opportunity and the duty to ensure more climate-resilient public spaces and cities in general [6].

One of the consequences of extreme climate is the economic cost to householders of the energy consumption derived from the use of active HVAC systems [7]. Historically, these issues have been addressed for winter weather in cold climates. The first definition of fuel poverty was made by Boardman [8], who defined it as when a family has to spend more than the 10% of the monthly income for heating. In recent decades, with the mentioned global overheating and the development of new research, some studies have focused on the cooling energy [9] consume. With the current climate, and the present energy crisis and inflationary period, it has become an important problem in warm regions. The same authors estimated that currently there is a 30% percentage of European families in situation of energy vulnerability finding it difficult to face the costs of the necessary energy consume to have the houses in healthy and comfort conditions. Due to that, in recent years, several studies and administrations have developed diverse vulnerability and fuel poverty indexes [10] which combine multiples social, economic and energy parameters. Although these indexes help to quantify and identify the problem, the privacy policy and the multiple variables of these sensitive data hinders to know specific results, and only macro data are known. Therefore, new studies are currently developing new methods to gain knowledge about areas of climatic vulnerability [11], and so, this research. These results serve as relevance preliminary data for pre-diagnosis operations, and to prioritise possible in-depth studies and public urban improvement actions.

To better understand how diverse urban areas are more exposed or affected by extreme hot climate, it is important to study urban climate and the cities overheating. Historically, the literature has mostly studied the UHI phenomenon and its effects [12]. It has been addressed in various ways; the most common method is to measure the differences in air temperature (AT) existing between urban and rural areas [13]. However, to properly characterise the UHI, conscious and repetitive measurement campaigns are

required, with fixed devices or mobile transect [14]. Therefore, because of the complexity and costs that entails, it is commonly used only in the scientific field.

However, according to scientific literature, there are other ways to consider urban heat. One of these is the surface UHI or SUHI [15]. That is, the differences of temperature between the urban materials surface and the temperature of the surface of the rural surface, so the land surface temperature (LST) is analysed instead of the AT [16]. The LST is closely related to materiality but also with the sky view factor (SVF) or urban geometry [17]. Moreover, LST also influences AT [15] and therefore human thermal comfort [18]. On the other hand, although the most common studied phenomenon is the UHI, it is only produced at night, which in some aspects limit the results interpretations. On the contrary, the warmest hours and so the cooling electric energy consumption occur during the central day hours. Therefore, this study focusses on urban heat and the differences of LST within a city, specifically in the overheated areas that are more prone to suffer more extreme heat conditions because of their urban characteristics.

In contrast to complex systems to study the urban heat, the last satellite remote sensing developments provide high-quality thermal land images of a wide range of territory [19]. This relatively new technology with high-resolution thermal sensors obtains a LST heatmap over land but also of city fabrics, which is much faster and more economical than the classic on-site surveys [20]. Among all free accessible satellite, the last launches by NASA in 2021, Landsat 9, could be the one that more valuable data provide for urban studies [21]. Landsat 9 satellite has a thermal infrared sensor 2 (TIRS-2) that captures LST in a spectral resolution (SR) of 30x30 m and with an accuracy of 0.4-1.98 K [22]. On the contrary, an important limitation is the revisit time, about 16 days over the same point.

Complementarily, if these remote sensing tools and their results are integrated into geographical information system (GIS) technology, it is possible to obtain a huge amount of cross-data of the urban environment. GIS allows to visualise all kind of data in a graphic way on the urban environment. Moreover, the open source and free software QGIS [23], enables to develop various urban analysis contrasting diverse official statistical data that are also provided in open access by public Administrations. Social data are usually provided for each census unit, that is, the smallest statistical unit. However, complete urban data is provided for each building thanks to the cadastral open data libraries. This environment allows to develop very relevant studies using official and open data processed by a standard PC, becoming a very powerful and accessible urban analysis tool.

The aim of this research is to propose an easy-applicable methodology based on GIS with remote sensing images to obtain urban vulnerable zones. By outlining the methodology and showcasing its practicality in a city as a real case study, the broad potential of these tools in urban studies becomes evident. The research locates and maps urban heat hotspots, thanks to the LST satellite image, and crosses them with low-income areas. This obtains especially vulnerable zones to face hot extreme climates. Although this study constitutes a simplified approach to urban heat current problematic, it draws the potential of these tools to detect opportunities areas in a given city.

2.METHODOLOGY

The methodology is established as a guideline to locate and map urban areas particularly vulnerable to hot climates. This is made by detecting heat hotspots in the residential urban fabric and crossing them with low-income data of city areas. It is organised in the following steps that could be easily achieved by architects, urban planners, and policy makers. All the data and information are usually available open access, provided by official organizations. Moreover, all the analysis and results extractions are also made with an open-source software, QGIS, which further reinforces the accessibility and usefulness of this study.

2.1. Selection of city and date

For the urban target, medium and large cities in warm regions are recommended to appreciate considerable overheating effects. Moreover, in order to obtain enough contrasts, a warm summer day is suggested. It must coincide with the day of satellite acquisition, which can be consulted in the official Landsat programme website [24].

2.2. Setup of GIS environment

The selected case study city geographic information needs to be loaded into QGIS software environment. The following data are loaded:

- Natural-colour satellite image [25].
- Cadastral blocks and buildings plan, and the associated data with information of heights and year of construction.
- Maps of census units with associated population data. These data are provided by national or local statistical offices.
- Mean income level associated with each census unit. This is the minimum statistical entity for which this information is provided.

2.3. Urban LST

The LST for the entire city was acquired from Landsat 9 thermal images from the USGS website [26]. Some adjustments are made according to the official product guide [27], and the original grid size of 30 m

can also be statistically interpolated using the bicubic method in QGIS. This method obtains a higher quality final image with a resolution of 5x5 m. The raster is cut with the city's administrative limits, providing a thermal heatmap that is overlapped with the city's geographical information, that is, the blocks and buildings map. By combining it with a solid path of all the buildings, the LST of the public and open urban spaces is obtained.

2.4. GIS Analysis

Crossing the LST heatmap raster data with the other GIS layers, several analyses are developed.

- Residential areas scope: non-residential areas have higher LST due to their typical materials [28], and are no representative of the lived urban areas. Therefore, as residential areas are the focus of this research, they are extract and isolated from the rest of non-urban nor residential zones. This provides a more homogeneous fabric that can be studied in depth.
- Thermal hotspots: The LST heatmap is cut with the limits of the residential areas, while the new limits of temperatures are set. This allows for the detection of urban hotspots. To better visualise the warmer areas, using the QGIS rendering tools, temperature values above the 60th percentile of all residential area temperature data are plotted. This provides a new raster with several red spots on the urban fabric plan.
- Low-income levels: As the existing poverty indexes entail more complex analysis based on non-accessible socio-economic data, this research, as an easily reached pre-diagnostic approach, uses the known mean income level per household, that is, an open data provided by each census unit. These data are associated with graphical polygons, and they are represented in a gradient scale. For that, based on the rendering QGIS tools, the gradient colour uses the standard deviation obtained from the total census units mean income data. By adjusting the number of divisions or steps, a certain level of extreme values can be selected. In this case, values especially below the mean are the searched. Thus, the low-income areas are represented over the map and are overlapped with the especially hot areas. This easy visual cross-evaluation, by matching the zones which have both problems, determines the vulnerable areas, which have severe hot exposure and are more prone to have low economic resources.
- Buildings age: These data are analysed on the already known vulnerable areas. It is represented graphically, but also statistically, all in GIS software that provides the histogram distribution of the buildings age. This factor is also strongly related to the climate exposition risks and the tendency to suffer from fuel poverty.
- Affected population: Based on the population data per each census unit, it is possible to obtain the total number of persons affected by these risk conditions and which percentage of the total city population they represent.

These guidelines allow to obtain especially vulnerable areas where the population is more likely to suffer fuel poverty and climate awareness. The following section shows the results of applying this methodology on a specific case study city: Seville, Spain. This proves the feasibility on these combined tools and the relevance of the results that can be obtained.

3. RESULTS AND DISCUSSION

Appling the exposed methodology over a real case study, the following results are obtained, whether geographical and analytical. The selected case study city is Seville, the most populous city in southern Spain (Fig. 1) with more than 650.000 inhabitants. It has a *Csa* climate according to the *Köppen* climate classification [29], characterised by warm and dry summers and mild winters. The selected day is 13 August, a warm day during the summer of 2023, when the Landsat 9 satellite acquired an aerial image over the city. The maximum AT that day was 37.7 ° C and the minimum 20.0°C, recorded by the official airport station, outside the city.

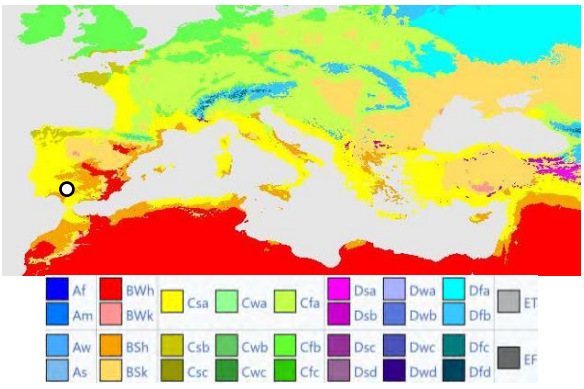

Figure 1. Location of Seville on the Köppen climatic zones map of Europe. Obtained from [30].

The first results can be seen in the Figure 2a, which corresponds to the LST taken by Landsat 9 on 13 August 2023 at 11 a.m. As shown, the warmest areas are, on the one hand, industrial and infrastructure zones, and on the other hand, rural and crop areas.

This is mainly due to two reasons. First, the high exposure level of these areas; either big industrial roofs or crops or fallow with no trees, but completely exposed to sun radiation. In addition, it is also due to the typical materials used in industrial areas, where constructions are made with metal and concrete, and the streets are vast asphalt surfaces.

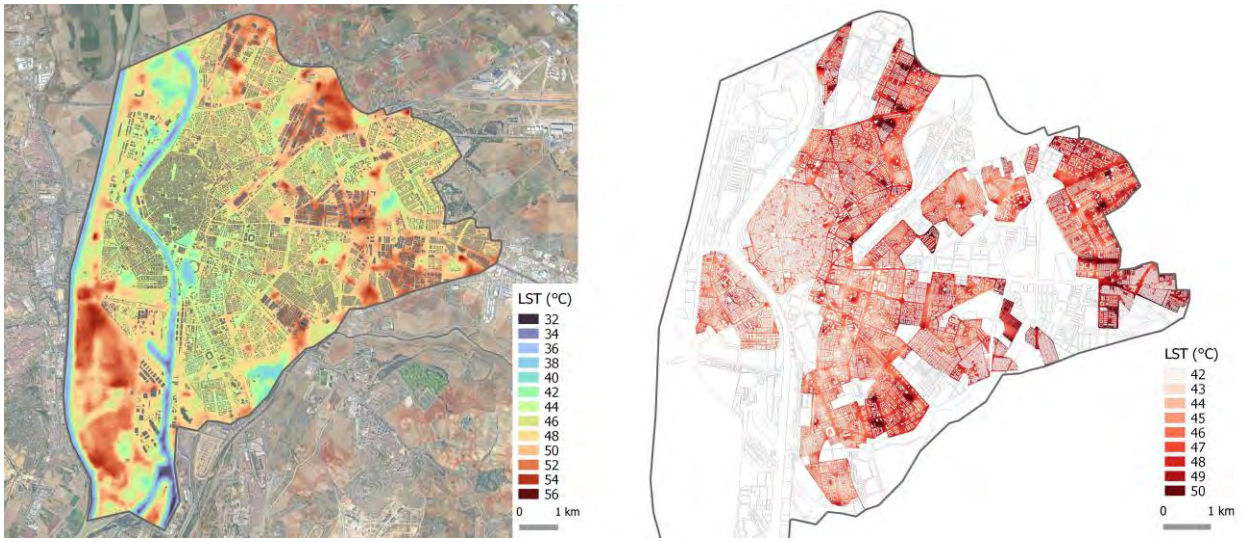

(a) (b)

Figure 2. LST of Seville taken by Landsat 9 on 13 August 2023 at 11 a.m. (a): Whole city LST heatmap. (b): Residental areas LST and heat hotspots in red.

On the contrary, in Figure 2a, residential areas appear to have a more homogeneous temperature range. Therefore, according to the methodology, the first analysis is focused on residential areas. This is made by cutting the thermal image with these areas drawn on GIS, while the boundaries temperatures and the new range are reassigned. This is shown in Figure 2b, where LST higher differences of 9°C, can be observed in residential areas. From this image it is possible to visualise and locate several urban hotspots that in this case are mostly in the suburbs. It is partly influenced by the high temperatures of close industrial or rural areas, as seen in the previous image (Fig. 2a). However, it is also strongly related to the urban morphology of these neighbourhoods. An important percentage of them are sparsely high-rise developments with large hardscape open public spaces, typical of mid-20th century urbanism [31].

The next step consists of mapping the heat hotspots appreciated in the previous image and overlapping them with the low-income areas. Firstly, for the thermal hotspots and according to the methodology, LST values above the 60th percentile have been selected (Fig. 3).

Secondly and following again the exposed guideline, the census units, provided by the Spanish Cadastre [32], have been discretised according to the standard deviation of their average income level, obtained from [33]. In this case, census units with an average income value lower than 0.5 times the standard deviation of the total units are selected. These areas are considered the more economically vulnerable and they are graphically represented on the city fabric, shown in Figure 3. Then, by a visual survey over the map, the coincidence of thermal hotspots and the selected areas sign the existence of target areas.

These zones, already intuited in Figure 3, but clearly isolated in Figure 4, are the zones with higher diurnal temperatures and less economic level. Therefore, they are more vulnerable and more prone to suffer energy poverty under hot conditions. Again, most of the located areas are in the suburbs, which not only have a higher exposure to heat, but due to the social trend in European cities, are more prone to poverty and, therefore, more exposed to climate risks.

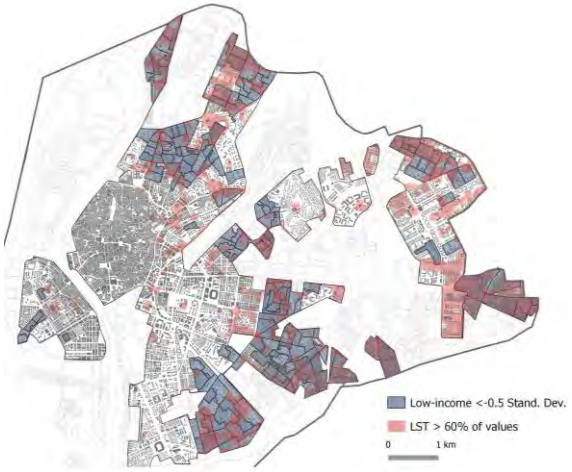

Figure 3. Overlap of heat hotspots and low-income areas.

Finally, the age of the buildings, obtained from [32], is characterized as other relevant parameters of

the located area. The buildings are rendered in colours according to the year of their construction (Fig. 4). Figure 5 also shows the predominance of buildings from the mid-20th century, according to the biggest housing construction stage of the after-war years. This also has an important relationship with the tendency to suffer from energy poverty, as the characteristics of the buildings' envelope have a direct impact on the poor energy performance. It is because at this latitude, insulated envelopes started to be used only in the 80s. Therefore, it results that most of the affected buildings do not have an adequate envelope to face severe climates, which still worsen the exposure to climatic vulnerability. Furthermore, the affected population who lives in these zones is calculated according to the official register, obtaining that the 23% of the total city inhabitants live in these specially affected areas.

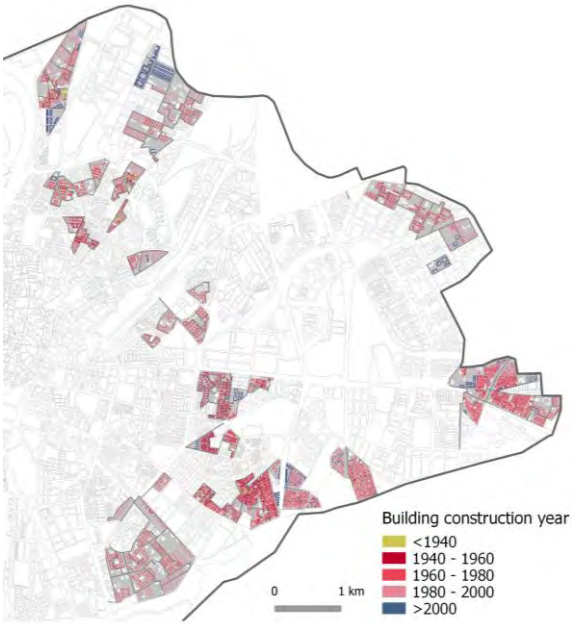

Figure 4. Climatic vulnerable area and their age of construction.

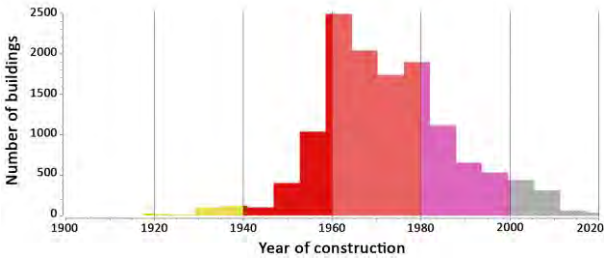

Figure 5. Histogram of the buildings' construction year.

These results map critical areas and zones of opportunity, helping to focus on deeper analysis and improvements of urban resilience.

4. CONCLUSION

This research, through the exposed guidelines and their practical application in a real case study, has shown the potential possibilities of GIS tools and remote sensing thermal imagery applied to urban studies. Thanks to this easy and quick approach, the research responses to the current social demand for detecting vulnerable areas and achieving more resilient cities.

The results obtained from the case study city of Seville have mapped the climate vulnerable areas based on heat exposure, income level, and building age. The results shown that about 23% of population lives in vulnerable areas, most of them mid-20th century neighbourhoods built as low-income districts. These results will also support further research about architectural, urban, and social performance of these areas leading to a to better understanding their climate resilience.

Despite the limitations of these tools, they offer a powerful method for a first preliminary urban diagnostic. The exposed results invite other researchers or technicians to develop new studies or deeper methods that optimise the information obtained. Further research should be deepened on more open access data on urban and socioeconomic indexes that can lead to increase the knowledge of urban vulnerabilities.

In conclusion, this research provides a powerful method that allows to detect and focus vulnerable urban areas that need to be targeted. Furthermore, this and other future in-depth research allows public Administrations to plan the improving urban interventions from a better technical perspective that enables prioritising most critical areas. This issue becomes important in order to achieve the Sustainable Development Goals (SDGs) of the United Nations, especially SDG 11: Make cities inclusive, safe, resilient, and sustainable, in the current climate change and overheating situation.

ACKNOWLEDGEMENTS

This work has been supported by the project PID2021-124539OB-I00 funded by MCIN/AEI/ 10.13039/501100011033; and by "ERDF A way of making Europe", project TED2021-129347B-C21 funded by MCIN/AEI/ 10.13039/501100011033 and by the "European Union NextGenerationEU/PRTR", and grant US.22-07, funded by Junta de Andalucía (Consejería de Fomento, Articulación del Territorio y Vivienda); and predoctoral contract granted to J.S.C. (FPU21/02458). Authors want to knowledge USGS-NASA for providing images; to INE and Catastro, for open data.

REFERENCES

1. United Nations. World Urbanization Prospects-Population Division. 2018. https://population.un.org/wup

2. Oke TR. City size and the urban heat island. Atmospheric Environment (1967). 1973;7:769–79.
3. Maiullari D, Gherri B, Finizza C, Maretto M, Naboni E. Climate change and indoor temperature variation in Venetian buildings: The role of density and urban form. J Phys Conf Ser. IOP Publishing Ltd; 2021.
4. Buscail C, Upegui E, Viel J-F. Mapping heatwave health risk at the community level for public health action.2012.
5. IPCC. Fifth assessment report. Climate change 2014. 2014.
6. Heris MP, Middel A, Muller B. Impacts of form and design policies on urban microclimate: Assessment of zoning and design guideline choices in urban redevelopment projects. Landsc Urban Plan. 2020;202.
7. Halkos GE, Gkampoura EC. Evaluating the effect of economic crisis on energy poverty in Europe. Renewable and Sustainable Energy Reviews. 2021;144:110981.
8. Boardman B. Opportunities and Constraints Posed by Fuel Poverty on Policies to Reduce the Greenhouse Effect in Britain. Appl Energy. 1993;44:185–95.
9. Thomson H, Simcock N, Bouzarovski S, Petrova S. Energy poverty and indoor cooling: An overlooked issue in Europe. Energy Build. 2019;196:21–9.
10. Martín-Consuegra F, Gómez Giménez JM, Alonso C, Córdoba Hernández R, Hernández Aja A, Oteiza I. Multidimensional index of fuel poverty in deprived neighbourhoods. Case study of Madrid. Energy Build. 2020;224:110205.
11. Sanchez-Guevara C, Peiró MN, Taylor J, Mavrogianni A, González JN. Assessing population vulnerability towards summer energy poverty: Case studies of Madrid and London. Energy Build. 2019;190:132–43. https://doi.org/10.1016/j.enbuild.2019.02.024
12. Voogt JA. How Researchers Measure Urban Heat Islands Vancouver-Sunset Urban Flux Tower View project BUBBLE-Basel Urban Boundary Layer Experiment View project.
13. Stewart ID. A systematic review and scientific critique of methodology in modern urban heat island literature. International Journal of Climatology. 2011;31:200–17.
14. Romero Rodríguez L, Sánchez Ramos J, Sánchez de la Flor FJ, Álvarez Domínguez S. Analyzing the urban heat Island: Comprehensive methodology for data gathering and optimal design of mobile transects. Sustain Cities Soc. 2020;55.
15. Oke TR. The distinction between canopy and boundary-layer urban heat islands. 2010. https://www.tandfonline.com/action/journalInformation?journalCode=tato20
16. Hidalgo García D, Arco Díaz J. Modeling of the Urban Heat Island on local climatic zones of a city using Sentinel 3 images: Urban determining factors. Urban Clim.2021;37:100840.https://doi.org/10.1016/j.uclim.2021.100840
17. Sharmin T, Steemers K, Matzarakis A. Microclimatic modelling in assessing the impact of urban geometry on urban thermal environment. Sustain Cities Soc. 2017;34:293–308.
18. Nikolopoulou M. Urban open spaces and adaptation to climate change. 2012. https://onlinelibrary.wiley.com/doi/10.1002/9781444345025.ch9
19. Martin M, Chong A, Biljecki F, Miller C. Infrared thermography in the built environment: A multi-scale review. 2022.
20. Voogt JA, Oke TR. Thermal remote sensing of urban climates. Remote Sens Environ. 2003;86:370–84.
21. Masek JG, Wulder MA, Markham B, McCorkel J, Crawford CJ, Storey J, et al. Landsat 9: Empowering open science and applications through continuity. Remote Sens Environ. 2020. https://landsat.gsfc.nasa.gov/satellites/landsat-9/
22. Wang M, Li M, Zhang Z, et al. Land Surface Temperature Retrieval from Landsat 9 TIRS-2 Data Using Radiance-Based Split-Window Algorithm. IEEE J Sel Top Appl Earth Obs Remote Sens. 2023;16:110012.
23. OSGeo. QGIS project. https://qgis.org/en/site/index.html
24. U.S. Geological Survey. Landsat Acquisition. https://landsat.usgs.gov/landsat_acq
25. Google LLC. Google Earth. https://www.google.com/intl/es/earth/
26. U.S. Geological Survey. EarthExplorer. https://earthexplorer.usgs.gov/
27. U.S. Geological Survey. Landsat 8-9 Collection 2 Level 2 Science Product Guide.
28. Woong Kim S, Brown RD. Urban heat island (UHI) intensity and magnitude estimations: A systematic literature review. 2021. https://doi.org/10.1016/j.scitotenv.2021.146389
29. Chazarra Bernabé A, Lorenzo Mariño B, Romero Fresneda R, Moreno García JV. Evolución de los climas de Köppen en España en el periodo 1951-2020. 2022.
30. Beck HE, Zimmermann NE, McVicar TR, Vergopolan N, Berg A, Wood EF. Present and future köppen-geiger climate classification maps at 1-km resolution. Sci Data. 2018;5.
31. Sola-Caraballo J, Patricia Lopez-Cabeza V, Roa-Fernandez J, et al. Assessing the microclimatic adaptation of a Modern Movement 1960s neighbourhood through its urban evolution. 18th IBPSA International Conference Buildings Simulation 2023. Shanghai; 2023.
32. Sede Electrónica del Catastro - Difusión de datos catastrales.
33. INE. Instituto Nacional de Estadística.
34. MITMA. Análisis de las características de la edificación residencial en España (2001). 2013.

PLEA 2024 WROCŁAW
(Re)thinking Resilience

The Resilience of Typical Andean Roofs in The Face of New Construction Trends

JONNATHAN VILLA[1] JEFFERSON TORRES[2] ALEX SERRANO[1] BORIS ORELLANA[1]

[1]Universidad de Cuenca, Cuenca, Ecuador
[2] CONSISO lab, Universidad Católica de Cuenca, Cuenca, Ecuador

ABSTRACT: Globally, most bioclimatic strategies have focused on the vertical envelope. However, in low-latitude countries such as Ecuador, the roof is the surface responsible for the greatest heat gains and losses of the building. Although this country should have a warm climate throughout its territory because it is crossed by the Andes Mountain range it also has a cold-mountainous climate. As in other regions, new roofing technologies, both heavy and light, have replaced the vernacular roof (VR), characterized by the use of tiles, mud and reed. Additionally, insulating materials, which have not yet been widely used in the region, are beginning to be discussed in local regulations, although they lack a solid theoretical foundation. Therefore, this study undertakes a comparative analysis between the VR of the Andean region and the new roof typologies, both with and without insulation. The methodology applied to this study based on digital simulations. The results demonstrate the importance of the thermal mass of the VR in the regulation of thermal oscillations and its advantage over some current and more expensive construction systems. Furthermore, the study suggests that insulation may not be necessary in certain building systems.

KEYWORDS: Heat Flow, Thermal oscillation, Thermal mass.

1. INTRODUCTION

The building envelope is the physical element that directly interacts with external climate conditions. It serves as a protective barrier against inclement weather. Studies around the world have primarily focused on the vertical envelope, as it accounts for 33% of heat loss [1]. However, in low latitude countries like Ecuador, the roof is the element with the highest heat exchange. Due to their geographical location, these regions are exposed to high levels of solar radiation [2,3] and experience significant radiative exchange with the sky [4]. Furthermore, the low-rise building typology that predominates in these areas means that the roof is responsible for 60% of the indoor-outdoor heat exchange [5,6].

Ecuador's geographical location would suggest a climate characterized by high temperatures. However, due to the Andes Mountain range crossing the country, there is also a region with a cold mountain climate with minimum temperatures of up to 6.4°C [7]. Several of the country's most important cities are located in this region and are home to 35% of the total population. Cuenca is the third most populated city in Ecuador, situated at an altitude of 2560 masl. The average temperature of this city is 15°C, with a low annual thermal oscillation of 2°C. However, there is a significant daily thermal oscillation of 10°C, which can cause discomfort at night and result in high daytime temperatures due to the high solar gain.

In recent decades, this region has experienced a significant change in its construction systems. These changes have caused vernacular construction to be replaced by industrialized systems that aim to increase productivity in terms of construction time and costs. However, the climatic characteristics of the region are not taken into account [8]. As a result, there has been a transition from thick adobe walls to thin concrete or gypsum board walls, from multi-layer envelopes to single-layer elements, etc.

In regards to the roof, the thickness and number of layers of this element have been significantly reduced. Thus, the typical roofs of the Andean region (Fig.1), which were characterized by the use of ceramic tiles, mud, reeds, and air chambers, have been replaced by other roof typologies that prioritize ease of construction [9].

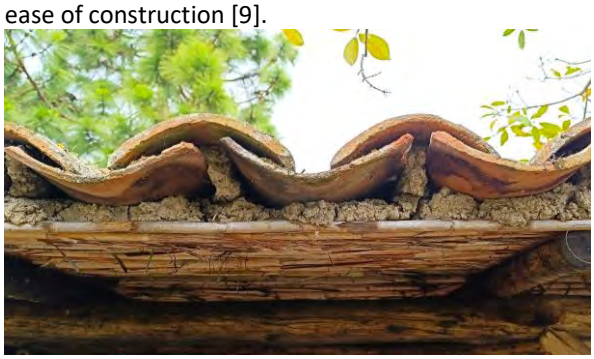

Figure 1: Vernacular Roof. Photo taken by the authors

In these days, the most commonly used roofing typology in the region is the lightweight painted fiber cement roof, of 10 mm thickness. This typology is

used in 65% of new local buildings [10], and omits the use of tiles and, in many cases, the air chamber and the internal ceiling. Another widely used typology, introduced in the last two decades, is the two-way ribbed concrete roof with pumice block lightening, which is used in 21% of new buildings [10]. This type of roof is more expensive and time-consuming, but it has a higher thermal mass and lower U-value. Additionally, in the last decade, the use of steel decking concrete roof has become popular to increase productivity and reduce the weight of the building [10].

Building systems in Ecuador, like in other countries, tend to reduce thermal mass [9]. However, in other regions, thermal mass has been replaced by thermal insulation. The implementation of this material is a commonly used bioclimatic strategy worldwide [11]. The thermal behavior of an envelope, which considers insulation, aims to reduce energy gains or losses between the interior and exterior [12]. In warm, low latitude climates, thermal insulation is crucial to prevent high temperature fluctuations and indoor overheating. Studies have shown that thermal insulation is a passive strategy for roofs to prevent excessive solar radiation during the day and to retain energy (heat) during the night [13, 14].

Although Ecuador has not yet implemented any strategies or regulations for the use and application of thermal insulation, this material is beginning to emerge as a potential solution to the problem of thermal discomfort. However, it is important to thoroughly analyze these decisions beforehand.

Given the constant technological changes that have transformed our cultural heritage, it is important to consider the adaptability of vernacular roof typology. Despite its reduced use, some buildings still employ this construction system and remain operational. It is evident that this typology is less productive than industrialized construction systems. However, it is crucial to assess its resilience to current climatic conditions and the interior thermal discomfort associated with new architectural models. Additionally, it is necessary to evaluate its insulation level and heat retention capacity.

Therefore, this study proposes to compare the thermal behavior of the new roofing systems implemented in the last decades with the typical Andean model of Ecuador.

2. METHODOLOGY

The methodology used in this study is based on digital thermal simulations using Design Builder software [16] and the Energy Plus calculation engine [17]. The study will analyze the typical vernacular roof of the region (VR) and three types of roofs that have been introduced in recent decades: Lightweight Fiber Cement Roof (FR), Heavy Concrete Roof with lightening block (CR_1), and Concrete Roof with metal deck (CR_2). The study will simulate all identified roof typologies in two scenarios: their original state and with the use of insulation. The original state refers to each typology that includes a ceiling separated by a non-ventilated air space. When thermal insulation is implemented, it refers to the original state with an additional 5 cm layer of fiberglass with a thermal conductivity of 0.046 W/mK.

Fig. 2 and Table. 1 show the morphological and material configuration of the 4 study cases. Additionally, Table 1 specifies the thermal mass and U-value of each roof.

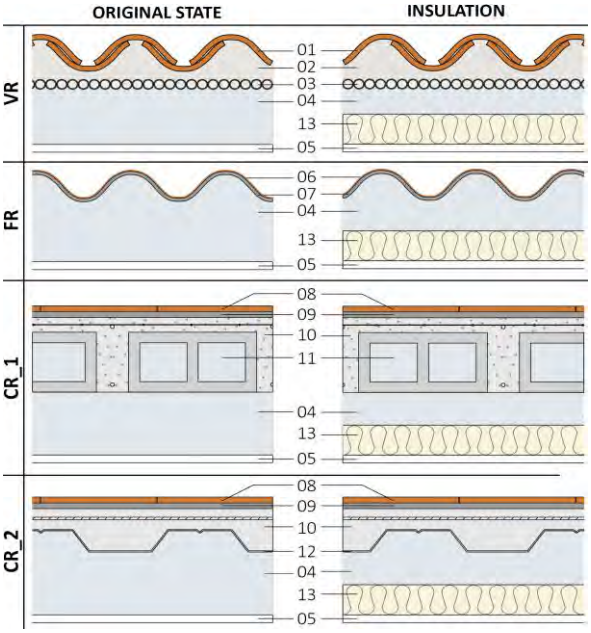

Figure 2: Construction detail of the 4 study cases.

Table 1: Thermal characteristics of the 4 study cases.

TYPE		LAYERS	THERMAL MASS (kJ/m2.K)	U-VALUE (W/m2.K)
VR	ORIGINAL STATE (OS)	01_Ceramic tile (2cm) 02_Clay (2cm) 03_Ceiling reed (2cm) 04_Air chamber (10cm) 05_Plaster (1cm)	75	1.6
	OS + INSULATION	13_Fiber glass (5cm)	77	0.6
FR	ORIGINAL STATE (OS)	06_Paint 07_Fiber cement (1cm) 04_Air chamber (20cm) 05_Plaster (1cm)	15	2.9
	OS + INSULATION	13_Fiber glass (5cm)	17	0.7
CR_1	ORIGINAL STATE (OS)	08_Ceramic 09_Bondex mortar 10_Concrete (5cm) 11_Pumice Hollow Block(15cm) 04_Air chamber (20cm) 05_ Plaster (1cm)	258	1.5
	OS + INSULATION	13_Fiber glass (5cm)	260	0.6

CR_2	ORIGINAL STATE (OS)	08_Ceramic 09_Bondex mortar 10_Concrete (5cm) 12_Metal deck 04_ Air chamber (20cm) 05_ Plaster (1cm)	35	2.6
	OS + INSULATION	13_Fiber glass (5cm)	37	0.7

A simulation base model (Fig. 3) was constructed for the roof study, representing the most common housing typology in the city of Cuenca. The model's morphological characteristics were defined based on the minimum dimensions required by the city's current regulations [7]. The model consists of a two-level attached block with a surface area of 7x10m, with a free height of 2.40m on each level. The glazing percentage is 15% of the floor area. The upper floor is designated for use as a bedroom, with an occupancy rate of 0.057 people per square meter and a usage schedule from 6:00 pm to 6:00 am. The infiltration rate is set at 1.2 air changes per hour [4]. The house is oriented in a North-South direction, which represents the least favorable case in terms of solar gain. For the simulation results, only one bedroom on the first floor (Bedroom 3) was considered. The analysis periods correspond to the conditions of the coldest and hottest months of the year. The software's climate file was used to conduct a statistical analysis of the outdoor air temperature throughout the year, which resulted in the establishment of Cold Day and Hot Day. Cold Day, defined as the 12th of September with a minimum temperature of 6°C and a maximum temperature of 18°C, and Hot Day, defined as the 19th of November with a temperature of 11°C and a maximum temperature of 23°C, according to the EPW file.

The indoor air temperature (Ti) is the reference parameter for these comparisons. According to the Ecuadorian Construction Standard (NEC) [15], the interior comfort range is 18°C to 26°C, which is used as a reference for the analysis.

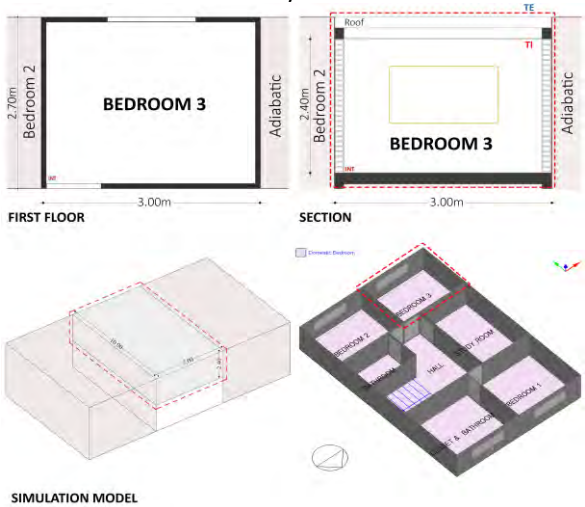

Figure 3: Simulation base model

3. RESULTS

3.1 Original State

Figure 4 shows the indoor air temperature results for the four study cases in the original state for Cold Day (a) and Hot Day (b).

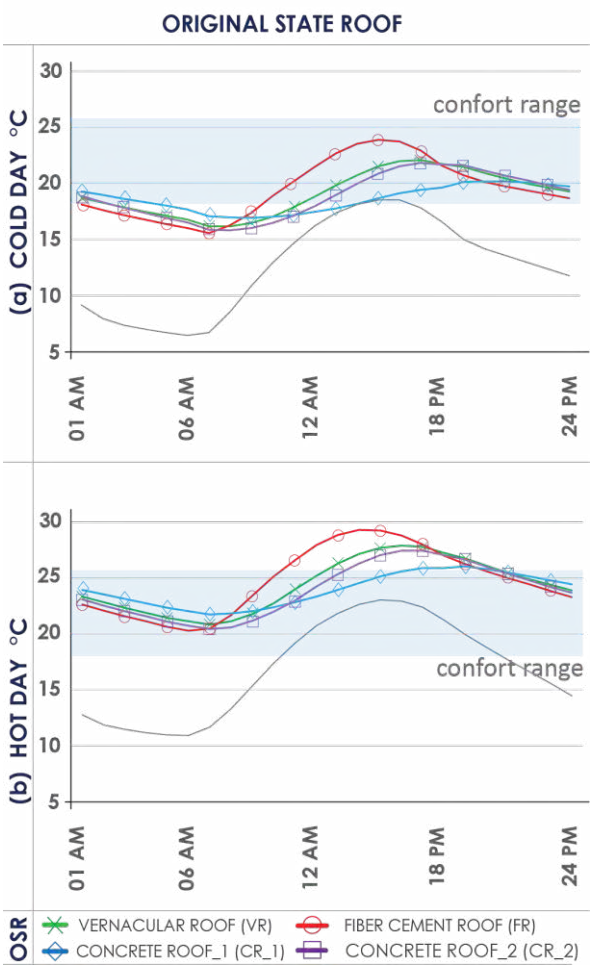

Figure 4: Indoor temperature of the 4 cases studies in the original state on a) Cold Day and b) Hot Day.

On Cold Day (Figure 4a), the lightweight fiber cement roof (FR) presents the most unfavorable conditions of the four studied cases. The temperature acts below the comfort range for half of the night period in this roof, reaching a minimum Ti of 15.5°C. However, during most of the day, the temperature remains within the comfortable range, with a maximum of 23.9°C. During the hot day (Figure 4b), although the discomfort is resolved during the night period, another thermal problem appears, caused by an internal overheating during the diurnal period when it reaches a maximum Ti of 29°C. It is important to note that this roof, unlike the other roofs analyzed, does not show any lag with respect to the external temperature. This is evidence of the low thermal mass of this roof.

On the contrary, the roof that is closest to the comfort range among the four case studies is the heavy concrete roof (CR_1). On Cold Day, this roof

reaches a minimum Ti of 17°C and a maximum of 20.2°C. On Hot Day, the temperature oscillation is between 21.8 and 26°C. It is important to note that the maximum Ti during the two days of analysis is reached during the night period (20h00-21h00). This reflects the high thermal mass of this typology.

Regarding the concrete roof over metal deck (CR_2), on a cold day, the minimum Ti is 15.8°C, which is 2.2°C below the comfort range. The maximum Ti is 21.8°C, indicating that thermal issues occur at night during cold days. Conversely, on hot days, discomfort is due to interior overheating, with a maximum Ti of 27.5°C and a minimum Ti within the comfort range.

Finally, the typical vernacular roof (VR) has a minimum Ti of 16.2°C on Cold Day, only 1.8°C below the comfort range, and a maximum Ti of 22.1°C. This suggests that thermal discomfort occurs at night on this day, although not in an extreme way. Similarly, on a Hot Day, discomfort is caused by overheating, as VR reaches a maximum Ti of 28.1°C.

It is important to note that VR better controls heat gains and loss, thus significantly reducing thermal discomfort compared to FR. Moreover, VR has a thermal performance almost equal to that of CR_2.

3.2 State with Insulation.

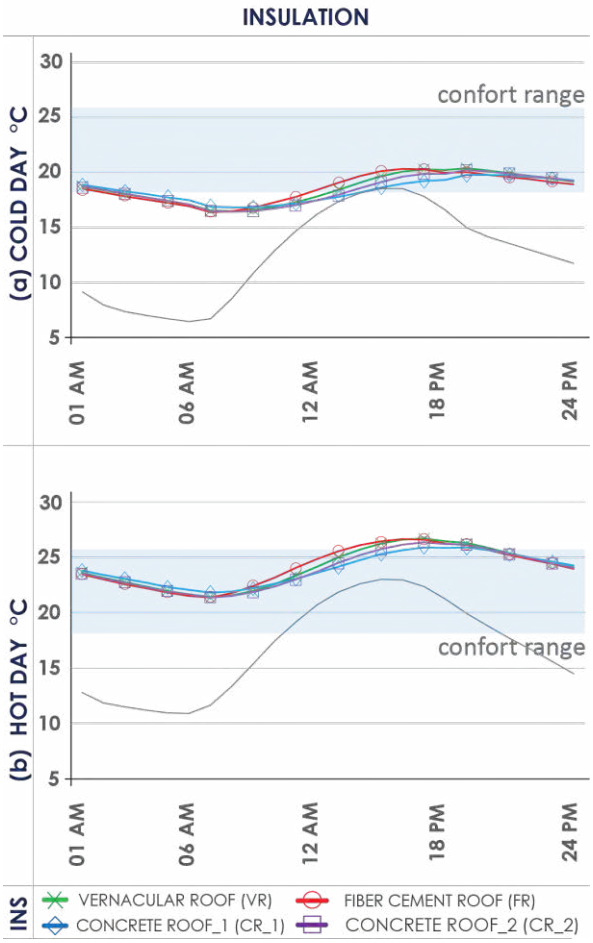

Figure 5: Indoor temperature of the 4 cases studies in the state with insulation on a) Cold Day and b) Hot Day.

Figure 5 shows the indoor air temperature of the four study cases with the use of thermal insulation for the analysis days.

Adding a layer of thermal insulation means that the behavior of all roofs is very similar. On the Cold Day (Figure 5a), Ti reaches a maximum of approximately 20.1°C and a minimum of 16.5°C in all four case studies. On the Hot Day (Figure 5b), Ti reaches a maximum of 26.4°C and a minimum of approximately 21.5°C. The results indicate that the use of thermal insulation eliminates the influence of the different thermal masses, so that the four study cases have practically the same thermal oscillations, delays and temperatures. This is due to the fact that the use of insulation results in all roofs achieving a U-value below 0.7 W/m2. K.

It is important to note the impact of the insulation strategy on each roof's condition. For FR, insulation reduced nighttime discomfort from 4 to 3 hours and overheating from 8 to 5 hours during the day. VR reduced nighttime discomfort from 3 to 2 hours and overheating from 7 to 4 hours. CR_2 reduced nighttime discomfort from 3 to 1 hour and overheating from 6 to 3 hours. Nonetheless, in CR_1, adding insulation did not improve indoor comfort during the day or at night.

To better understand, we provide a detailed analysis of each roof type's thermal oscillations below.

Figure 6 shows a comparative graph of the thermal oscillation and the average Ti between the 4 study cases in Cold Day (Figure 6a) and Hot Day (Figure 6b), taking the two states of analysis, the original case and with the use of insulation.

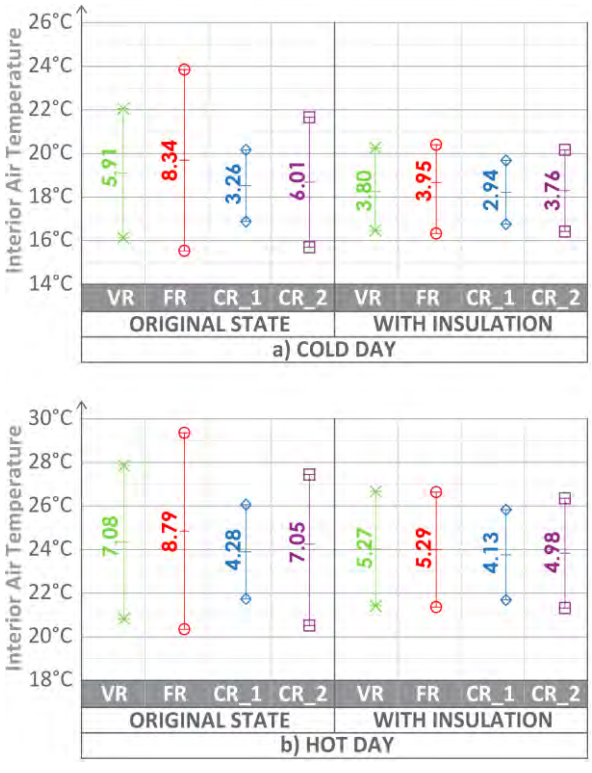

Figure 6: Average indoor temperature and thermal oscillation of the 4 study cases in the original state (left) and the state with insulation on a) Cold Day and b) Hot Day.

According to this comparison in the original state, VR, which is also a light roof, has a lower thermal oscillation than FR in the two analysis days. On the Cold Day, VR shows a lower oscillation of up to 2.43°C than FR due to the higher thermal mass presented by the vernacular typology. This indicates that the uncontrolled reduction of layers in the horizontal envelope significantly increases the thermal oscillation of buildings in this region. During the daytime period, the interior areas of FR become considerably overheated due to high solar radiation and outdoor temperature increase. During the night period, the roof experiences high heat losses due to its high thermal transmittance, causing a drastic drop in temperature.

On the other hand, CR_1, which is the roof with the highest thermal mass, shows an advantage over VR. In its original state, the thermal oscillation of CR_1 is 2.65°C and 2.8°C lower than the thermal oscillation of VR in the Cold Day and Hot Day, respectively. However, the thermal oscillations of VR are not too far from the comfort range, and also its minimum and maximum temperature do not differ much from the results of CR_1. During the Cold Day, when thermal discomfort is experienced at night, VR falls 1.8°C below the comfort range, while CR_1 falls 1°C below this range. Therefore, CR_1 has an advantage of 0.8°C over VR. However, during the hot day, VR is 2°C above the comfort range while CR_1 remains within the upper limit.

Finally, if we compare VR with CR_2, the thermal performance of these two roofs is practically the same. VR has a lower thermal oscillation than CR_2 and a slightly higher average temperature, even on Cold Days.

By comparing the performance of these roofs in their insulated state, it is evident that this strategy has a high impact on the lightweight roofs and on CR_2. However, the effect of this strategy on CR_1 is practically null on both Cold and Hot Days.

The effect of this strategy in CR_1 is reflected in a reduction of the thermal oscillation of 0.3°C and 0.15°C in Cold Day and Hot Day, respectively.

The most representative impact of the use of insulation is seen in FR, with a reduction of 4.39°C and 3.5°C in the Cold and Hot Day, respectively. This means that the use of this strategy in this roof reduces its oscillation by almost 50%. Similarly, in CR_2, the thermal oscillation was reduced by 2.25°C and 2.07°C in the two days of analysis. Finally, in VR, the effect of insulation reduces its oscillation by 2.11°C and 1.81°C in the Cold and Hot Day.

It is important to note that this strategy has a greater impact on reducing heat inputs than losses. As a result, the reduction in maximum Ti is more noticeable than the increase in minimum Ti. In the VR scenario, insulation reduces the maximum Ti by approximately 1.8°C and increases the minimum Ti by 0.3°C over the two-day analysis period. In the FR scenario, this strategy results in a decrease of 3.6°C in maximum Ti and an increase of 0.8°C in minimum Ti. In CR_1, the maximum Ti decreased by 0.4°C and the minimum Ti decreased by 0.1°C. In CR_2, the maximum Ti decreased by 1.6°C and the minimum Ti increased by 0.6°C. Therefore, this strategy will have a greater impact on days with higher temperatures, as it significantly affects the maximum Ti. However, on cold days, even though the insulation causes the minimum Ti to increase, it also causes the maximum Ti not to exceed 20.2°C in all the cases studied.

Finally, it is important to discuss the results of the hot day, where all the roofs, except CR_1, show an overheating of the interior, even considering the maximum allowed (26°C) of the upper limit of the comfort zone. These results indicate the need for cooling, which contradicts the climate of this region. Although VR, which characterizes Andean vernacular architecture, mitigates the high heat input that a light roof can generate, the simulation model has not considered the high thermal mass of the vertical envelope. This influences the increase in heat input through walls and therefore a higher temperature.

4. CONCLUSION

This article addresses the adaptability of the vernacular roof typology of the Andean region of Ecuador to the current climatic conditions, in comparison with the three new roofing systems that have appeared in recent decades. From the study, the following conclusions have been drawn.

The research presented in this paper supports that the thermal performance of roofs in this region depends mainly on their thermal mass and not on their thermal transmittance value. In this region, a low thermal mass roof, such as the fiber cement roof (FR), is not a feasible option because it causes high thermal discomfort during both day and night periods.

On the other hand, a heavy Concrete Roof with lightening block (CR_1), the roof with the highest thermal mass, is the construction system with the best thermal performance, which means that temperatures remain within the comfort range for most of the day. The vernacular roof (VR), which is a light roof typology with a considerable thermal mass, does not differ too much from the values of CR_1 and its performance is practically the same as a metal deck concrete roof (CR_2).

Finally, this article supports that the most important parameter to reduce the thermal discomfort in this region is the high thermal mass, it is

even more relevant than the thermal insulation, which can have a negative impact on the night temperatures. In this context, the vernacular roof is a resilient and feasible option to be adapted in new construction solutions due to its insulation level, its high thermal mass, and the moderate cost it represents compared to a concrete roof.

ACKNOWLEDGEMENTS

This work was supported by Construction master program of University of Cuenca. JT-Q acknowledges to the Catholic University of Cuenca and the Research Program DAMA II with the code PICODS21-35.

REFERENCES

1. Al-Tamimi, A. S., Baghabra Al-Amoudi, O. S., Al-Osta, M. A., Ali, M. R., & Ahmad, A. (2020). Effect of insulation materials and cavity layout on heat transfer of concrete masonry hollow blocks. Construction and Building Materials, 254. https://doi.org/10.1016/j.conbuildmat.2020.119300.

2. Edmonds, I. R., and Greenup, P. J. (2002). Daylighting in the tropics. Solar Energy, 73(2), 111–121. https://doi.org/10.1016/S0038-092X(02)00039-7

3. Vieira, R. G., Guerra, F. K. O. M. V., Vale, M. R. B. G., & Araújo, M. M. (2016). Comparative performance analysis between static solar panels and single-axis tracking system on a hot climate region near to the equator. *Renewable and Sustainable Energy Reviews*, *64*, 672-681.

4. Torres Quezada, J., Coch, H., & Isalgué, A. (2019). Assessment of the reflectivity and emissivity impact on light metal roofs thermal behaviour, in warm and humid climate. Energy and Buildings, 188, 200-208.

5. Mohan Rawat, R. N, (2022), A study on the comparative review of cool roof thermal performance in various regions. Energy and Built Environment, Volume 3, Issue 3, Pages 327-347, ISSN 2666-1233, https://doi.org/10.1016/j.enbenv.2021.03.001.

6. Torres-Quezada, J., Coch, H., Isalguè, A., and López, J. (2018). The roof impact on the heat balance of low height buildings at low latitudes. PLEA 2018 - Smart and Healthy within the Two-Degree Limit: Proceedings of the 34th International Conference on Passive and Low Energy Architecture, 3(December), 937–938.

7. GAD Municipal del Cantón Cuenca. (2022). Plan Uso Y Gestión Del Suelo (Pugs), 200–285. Retrieved from https://www.cuenca.gob.ec/content/pdot-pugs-2022.

8. Torres-Quezada, J., Torres, A., Isalgué, A. & Pages, A. (2022). The evolution of embodied energy in andean residential buildings. Methodology applied to Cuenca-Ecuador. Energy&Buildings, 259, 111858. https://doi.org/10.1016/j.enbuild.2022.111858.

9. Torres-Quezada, J.&Torres, Ana. (2023). Green Energy and Technology Energetic Characterization of Building Evolution A Multi-perspective Evaluation in the Andean Region of Ecuador. (J. E. Torres-Quezada, Ed.). Cuenca, Ecuador: Springer Nature Switzerland AG. https://doi.org/https://doi.org/10.1007/978-3-031-21598-8.

10. ESED (2021). INEC, Estadística de edificaciones. Retrieved from:https://app.powerbi.com/view?r=eyJrIjoiZTBiYWNhMDYtNzk5YS00MTI0LThjZTctOTFiZGJhNDIzMA4IwidCI6ImYxNThhMmU4LWNhZWMtNDQwNi1iMGFiLWY1ZTI1OWJkYTExMiJ9. Date Access: April 3, 2023.

11. Allard, I., Nair, G., and Olofsson, T. (2021). Energy performance criteria for residential buildings: A comparison of Finnish, Norwegian, Swedish, and Russian building codes. Energy and Buildings, 250, 111276. https://doi.org/10.1016/j.enbuild.2021.111276

12. Tariku, F., Shang, Y., and Molleti, S. (2023). Thermal performance of flat roof insulation materials: A review of temperature, moisture and aging effects. Journal of Building Engineering, 76(March), 107142. https://doi.org/10.1016/j.jobe.2023.107142

13. Lee, S. W., Lim, C. H., Chan, S. A., and Von, K. L. (2017). Techno-economic evaluation of roof thermal insulation for a hypermarket in equatorial climate: Malaysia. Sustainable Cities and Society, 35(June), 209–223. https://doi.org/10.1016/j.scs.2017.08.011

14. Dylewski, R., and Adamczyk, J. (2011). Economic and environmental benefits of thermal insulation of building external walls. Building and Environment, 46(12),2615–2623. https://doi.org/10.1016/j.buildenv.2011.06.023

15. MIDUVI. (2011). Eficiencia energética en la construcción en Ecuador, 51. Retrieved from https://inmobiliariadja.files.wordpress.com/2016/09/nec2011-cap-13-eficiencia-energc3a9tica-en-la-construccic3b3n-en-ecuador-021412.pdf

16. DesignBuilder 7.0.2.006 (2020-2022) .DesignBuilder Software Ltd - Home. Available at: https://www.designbuilder.co.uk/ (Accessed: 20 abril 2023).

17. ENERGYPLUS (2015) .EnergyPlus TM Documentation Auxiliary EnergyPlus Programs Extra programs for EnergyPlus, pp. 1–144.

Investigating The Interactional Synergies Between Urban Overheating (UO) And Synoptic Scale Weather Patterns During Heatwaves In A Coastal City.

HASSAN SAEED KHAN[1,2], MAT SANTAMOURIS[2], PAVLOS KASSOMENOS[3], RICCARDO PAOLINI[2], PETER CACCETTA[3]

[1]School of Engineering and Technology, Central Queensland University, Sydney, Australia
[2]School of Built Environment, The University of New South Wales, Sydney Australia
[3]Department of Physics, University of Ioannina, GR-45110, Ioannina, Greece
[4]Data-61, The Commonwealth Scientific and Industrial Research Organization (CSIRO), Perth, Australia

ABSTRACT: Heatwaves' frequency and intensity have increased over time. The potential synergy between local-scale urban overheating (UO) and global weather patterns could have severe consequences for climatic conditions at the local, regional, and global levels. The relationship between atmospheric variables and UO has been the subject of considerable investigation. However, the correlation between UO and global-scale weather patterns, particularly in the context of heatwaves, has yet to be extensively investigated. The present work used the recently developed gridded weather type classification (GWTC) to investigate the influence of global-scale weather patterns (WPs) on UO during heatwaves in a coastal city (Sydney). The impact of humid warm (HW) and warm (W) weather patterns (WPs) was found to be more significant during heatwaves, with both WPs transpiring over 76% of the time and increasing the mean UO magnitude by 6 to 9°C in western Sydney and 3.8 to 5.4°C in inner Sydney. Dry (D) and seasonal (S) WPs predominated during non-heatwave (background), with mean UO magnitudes varying from 2.4 to 4.0°C in western Sydney and 0.6 to 1.0°C in inner Sydney. The weather patterns HW and W indicates dualistic synoptic systems situated on the contrasting sides of the metropolis. Based on the findings of this study, appropriate adaptation and mitigation solutions for extreme heat conditions can be developed.
KEYWORDS: Synoptic-scale weather patterns, global circulation, urban overheating, heatwaves, gridded weather typing classification

1. INTRODUCTION

The localized phenomenon known as urban overheating (UO) is employed as a metric to assess the extent of urbanization. The term "UO" refers to the temperature gradient that exists between urban and rural areas [1]. Changes in the urban fabric (including surfaces, vegetation, configuration, and population density), increased levels of anthropogenic heat and pollutants in urban areas, and synoptic-scale weather conditions are factors that contribute to UO [2]. A heatwave is a phenomenon that occurs at the regional scale and is commonly linked to anomalies in the mid-troposphere. It is characterized by a prolonged duration of clear sky and an increased ambient temperature throughout the entire region [3,4].

Additionally, influencing the UO magnitude are synergistically interacting atmospheric variables such as temperature, humidity, cloud cover, wind patterns, and atmospheric pressure. Considerable research has examined the correlation between UO and meteorological characteristics, specifically focusing on wind speed and cloud cover [5–7].

Typically, low wind speed and clear sky conditions, specifically at nighttime, were associated with exacerbated UO [7]. The clear sky conditions at night enhance the radiative cooling in rural areas, and the low-speed regional winds reduce the secondary air circulation. Both conditions amplify the UO magnitude. As opposed to low-speed regional winds, advection from high-speed continental winds during heatwaves was concluded to be the prime reason behind exacerbated UO magnitude [8–11]. During the daytime, the urban-rural moisture contrast was mostly associated with amplified UO, which is regulated by land use and synoptic climatology [12].

A few studies have investigated the association between UO and global-scale WPs [6,13,14]; however, the synergistic interactions between UO and global-scale WPs during heatwaves are largely unexplored. The association between both phenomena is examined using the circulation-pattern-based classification (CPC) or multivariate weather-typing classification (WTC). In CPC, amplified UO magnitude was typically related to anticyclonic conditions, whereas decreased UO magnitude or urban cooling (UC) was associated with cyclonic

conditions [15,16]. In WTC, dry tropical conditions at nighttime were concluded to be responsible for higher UO [17,18], and moist conditions contributed to diminished UO. Generally, clear and calm meteorological conditions were linked to anticyclonic conditions in the CPC or dry tropical conditions in the WTC [17,19]. Conversely, overcast meteorological conditions were connected with the CPC's cyclonic conditions and the WTC's moist conditions [20].

The present study examined the association between UO and global-scale weather patterns during heatwaves in a coastal city (Sydney) near a desert landmass. Further, this is the extended version of our work published in [21]. The investigation was conducted using the recently established Gridded weather-typing classification (GWTC) to ascertain the correlation between the two phenomena. The GWTC also thoroughly considers geographical and seasonal relativity, making the classification more suitable for bioclimatological and urban climatological studies.

2. DATA AND METHODS

2.1 Climatic Conditions and Meteorological Stations

Sydney is the largest city in Oceania from a geographical and demographic standpoint. In the east, the city is situated along the South Pacific Ocean coastline; in the west, it is encircled by the Blue Mountains. From east to west, the metropolis stretches for around 70 kilometers. The local climate is humid subtropical (Cfa classification under the Koppen-Geiger climate).

The present study divided Sydney into three major zones based on its proximity to the coast: eastern Sydney, inner Sydney, and western Sydney. Eastern Sydney and the Central Business District (CBD) of Sydney are situated near the coast. In inner Sydney, Olympic Park and Canterbury Station were examined, while in eastern Sydney, Observatory Hill (OBS Hill) was explored. Penrith Lakes, Campbelltown, and Liverpool in western Sydney were investigated (Figure 1).

The extent of potential vegetated land and tree canopy coverage in Sydney is greater in the western region compared to the city's eastern side. From the continental to the coastal regions of Sydney, the population density rises from its minimum in western Sydney. Further details about station locations and site characteristics are provided in [21].

2.2 Methods

The Australian Bureau of Meteorology (BOM) provided half-hourly temperature data from 1999 to 2017. In accordance with the validation procedures proposed in [22], the null values and outliers were removed from the dataset. Triangulation and linear interpolation techniques were utilized to fill up the gaps. The hourly averages were calculated with semi-hourly temperature data collection.

The UO was calculated using the ambient temperature differential between the inland locations and the Sydney Central Business District ($\triangle T = T_{inland} - T_{CBD}$), given that the overheating significantly impacted the inland sites. The suitable daily weather patterns for Sydney were obtained from (https://www.personal.kent.edu/~cclee/gwtc2global.html). The WPs under the GWTC are presented in Table 1. The definitions and characteristics of these WPs can be found in [23,24]. The correlation between local and global-scale occurrences was investigated by contrasting the daily maximum UO with the daily GWTC. The circulation-to-environment approach was primarily utilized to investigate the association between both phenomena. The heatwave definition was utilized as proposed in [8]. Further details about the selected heatwave and non-heatwave spells are provided in [21].

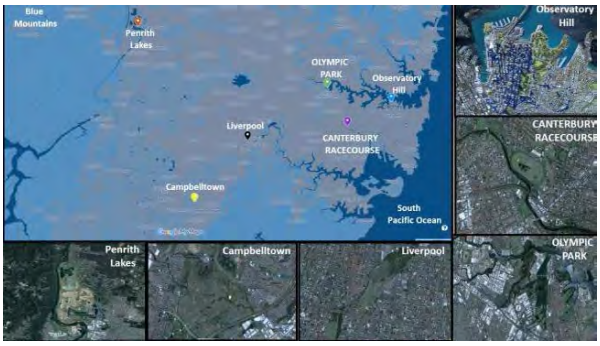

Figure 1. Studied locations in various zones of Sydney (Image source: Google Maps).

Table 1: The weather patterns (WPs) under GWTC

Sr No.	Symbol	WTs
1	HC	Humid Cool
2	H	Humid
3	HW	Humid Warm
4	C	Cool
5	S	Seasonal
6	W	Warm
7	DC	Dry Cool
8	D	Dry
9	DW	Dry Warm
10	CFP	Cold Front Passage
11	WFP	Warm Front Passage

3. RESULTS

While examining the weather patterns frequency during heatwaves, humid-warm (HW), warm (W), and dry-warm (DW) conditions were observed occurring with higher frequency- around 88% of the heatwave time (Figure 2A). Further, while assessing the event-wise frequency of weather patterns, it was also

observed that the HW conditions have also increased over time, particularly after the 2009 heatwaves (Figure 2B).

While studying the WP's frequency during non-heatwaves, seasonal (S) WPs were identified as occurring for around 34% of the time, followed by the dry (D) conditions (25%), as shown in Figure 3A. Further, it was also observed that the frequency of D conditions has increased over time during non-heatwaves (Figure 3B).

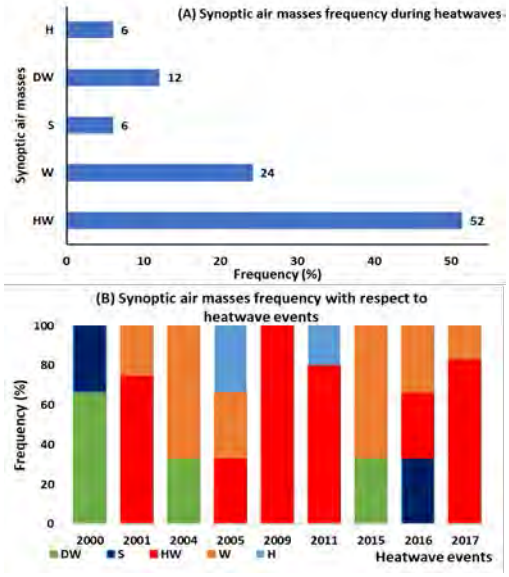

*Figure 2: WPs frequency during heatwaves, **A)** overall (1999-2017), **B)** event-wise. Image reproduced from [21]*

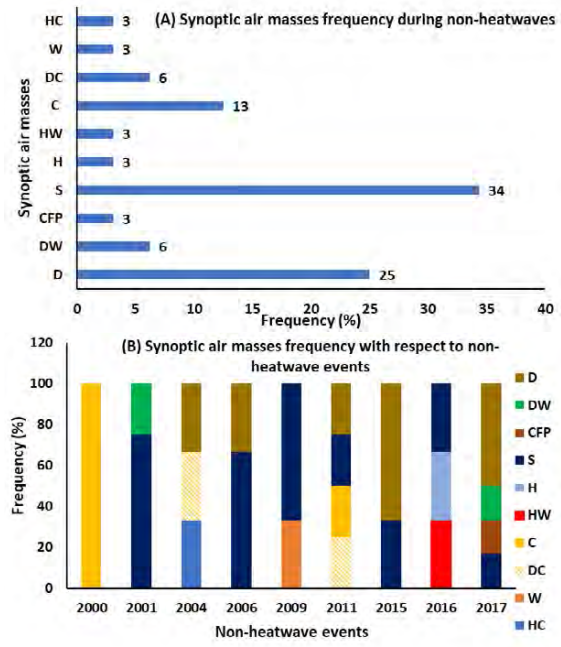

*Figure 3: WPs frequency during non-heatwaves, **A)** overall (1999-2017), **B)** event-wise. Image reproduced from [21]*

An investigation into the UO magnitude across different zones of Sydney revealed that, despite the greater proportion of tree canopy coverage and non-urban land at inland sites, the UO magnitude during heatwaves became more severe during the day as it moved further from the coast towards inland (Figures 4 A-E). Additionally, while examining the correlation between UO and weather patterns during heatwaves, HW and W conditions were mostly accountable for amplified daytime UO in addition to DW and humid (H) conditions (Figure 4 A-E). The mean UO magnitude during heatwaves due to dominant conditions (HW and W) was between 6°C and 9°C in western Sydney and 3.8°C and 5.4°C in inner Sydney. More into it, the HW conditions were comparatively more aggressive than the W, DW, and H conditions. The tropical maritime Tasman airmass, which is warm, moist, and unstable and originates north of the Tasman Sea, may account for the HW conditions in Sydney. These moist conditions reduce the latent heat potential at inland sites during the daytime and increase the inland daytime temperature by partitioning more energy into sensible heat. The W and DW conditions can be ascribed to tropical continental airmasses, which are very hot, dry, and unstable. These airmasses arise over central Australia, and advection from such dry and warm air in the daytime may increase the temperature at inland sites.

The temperate maritime WPs, which bring very moist air from the sea, are mainly responsible for H conditions. These conditions may increase the ambient temperature at inland sites due to adiabatic warming caused by Foehn-like winds on the leeward side of blue mountains. At nighttime, the inland sites cool down quickly due to radiative cooling, which is attributed to higher potentially plantable surfaces. More into it, the impact of W and DW conditions are not pronounced due to lower wind speed. On the other hand, Sydney CBD, being under the influence of coastal winds during any of these weather conditions, maintains a stable temperature (comparatively) during both daytime and nighttime. Thus, the UO magnitude is higher during the daytime and lower at nighttime. Urban shading also keeps the temperature lower in Sydney CBD in the daytime and increases it at night due to longwave emissions.

During non-heatwaves, D weather patterns were accountable for amplified UO at western Sydney, and the UO magnitude ranged between 2.4-4.0 °C (Figures 5A-C). Similarly, at inner Sydney during non-heatwaves, both D and S WPs were predominant, and the UO magnitude was between 0.6-1.0°C (Figures 5 D-E).

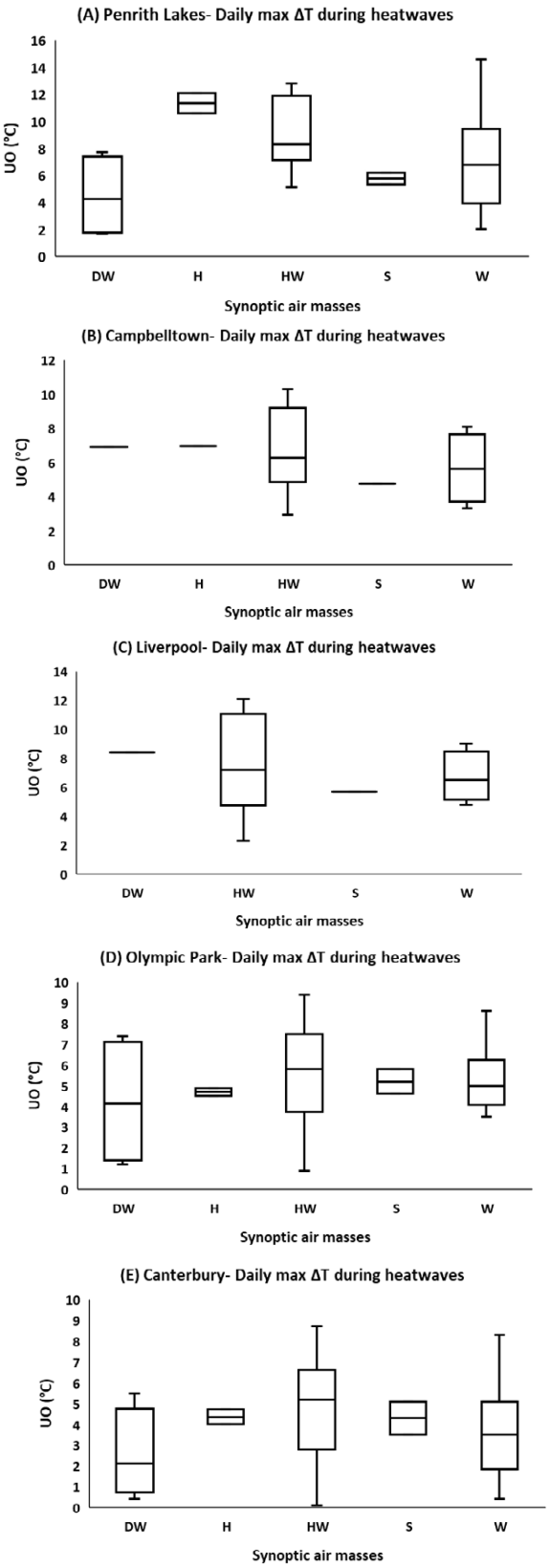

*Figure 4: Global-scale WPs and daily max ΔT during heatwaves, **A)** Penrith Lakes, **B)** Campbelltown, **C)** Liverpool, **D)** Olympic Park, **E)** Canterbury. Image reproduced from [21]*

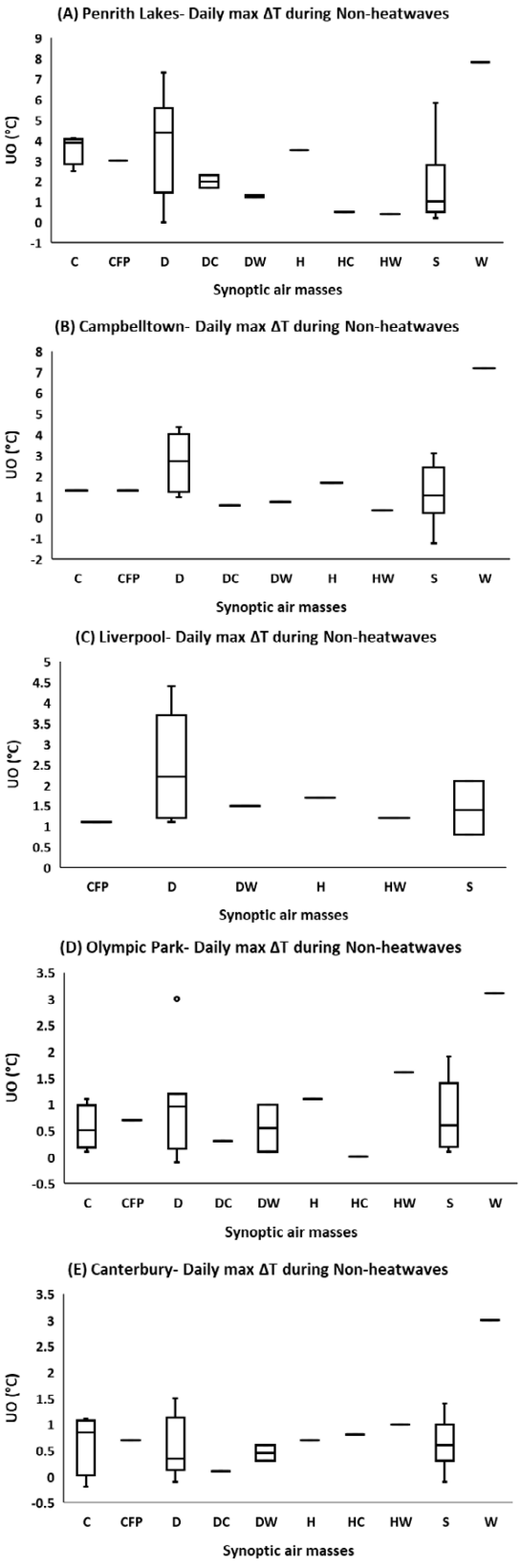

*Figure 5: Global-scale WPs and daily max ΔT during non-heatwaves, **A)** Penrith Lakes, **B)** Campbelltown, **C)** Liverpool, **D)** Olympic Park, **E)** Canterbury. Image reproduced from [21]*

4. DISCUSSION AND CONCLUSION

Urbanization modifies land-atmosphere interactions and influences local, regional, and global climate conditions. Sydney had a notable surge in daytime UO magnitude, reaching 9°C during heatwaves, which was attributed to HW and W/DW conditions. The HW, W/DW conditions indicate the dualistic weather patterns present on the opposite side of the city, which is primarily activated during heatwaves. The advection from continental winds (W/DW) keeps the inland sites warmer when the cool sea breeze can not reach the inland sites, particularly during heatwaves. The findings presented here align with the research conducted in Los Angeles, where the inland sites were more thermally affected due to the non-penetration of coastal winds during heatwaves [25]. Further, our results are also aligned with other studies carried out in Sydney, where continental winds were found responsible for exacerbated UO magnitude when the association between UO and heatwaves was investigated [8,9].

Enhanced daytime UO magnitude was observed under HW conditions during heatwaves; this was ascribed to a compromised latent heat flux at inland sites. These findings comply with the study conducted in northeastern states in the USA [17], where moist conditions resulted in higher daytime temperatures at both urban and rural sites. However, in this case study, the daytime temperatures at Sydney CBD were lower due to the impact of coastal wind.

In Phoenix [18], the northeastern United States (New York, Philadelphia, and Baltimore) [17], and Atlanta [12], it was previously determined that dry tropical weather patterns worsened the amplitude of nocturnal UO. Typically, clear and calm conditions accompany dry tropical weather patterns. Radiative cooling is enhanced in the periphery during periods of clear and calm nighttime conditions, while urban shadowing is of utmost importance in maintaining the temperature of urban areas by the entrapment of longwave emissions. These results are consistent with our study, which found that under the W/ DW conditions, nocturnal temperatures were lower at inland sites than in Sydney CBD.

An examination of the UO-heatwave association revealed that the stored heat flux at nighttime [26,27] and urban-rural moisture differential during the day [28] were the most significant linkages between UO and heatwave, in addition to anthropogenic heat flux [29,30]. In the present study, the activation of both the heating and the cooling mechanism simultaneously during the heatwaves is linked with global-scale circulations and is identified as the major association between UO and heatwaves. Positive interactions between soil moisture, continental-scale circulations, and temperatures were also concluded by [31], and the extreme temperatures in the summer of 2003 in Europe were associated with atmospheric circulation.

REFERENCES

1. *Santamouris, M.; Haddad, S.; Fiorito, F.; Osmond, P.; Ding, L.; Prasad, D.; Zhai, X.; Wang, R. Urban heat island and overheating characteristics in Sydney, Australia. An analysis of multiyear measurements. Sustain. 2017, 9, 712.*

2. Oke, T.R.; Mills, G.; Christen, A.; Voogt, J.A. Urban Climates; Cambridge University Press: Cambridge, 2017; ISBN 9781139016476.

3. Meehl, G.A.; Tebaldi, C. More intense, more frequent, and longer lasting heat waves in the 21st century. Science 2004, 305, 994–7.

4. Miralles, DG; Teuling, A.J.; van Heerwaarden, C.C.; Vilà-Guerau de Arellano, J. Mega-heatwave temperatures due to combined soil desiccation and atmospheric heat accumulation. Nat. Geosci. 2014, 7, 345–349.

5. Morris, CJGG; Simmonds, I.; Plummer, N. Quantification of the Influences of Wind and Cloud on the Nocturnal Urban Heat Island of a Large City. J. Appl. Meteorol. 2001, 40, 169–182.

6. Morris, C.J.G.; Simmonds, I. Associations between varying magnitudes of the urban heat island and the synoptic climatology in Melbourne, Australia. Int. J. Climatol. 2000, 20, 1931–1954.

7. Garratt, J.R. Boundary layer climates. Earth-Science Rev. 1990, 27, 265.

8. Khan, H.S.; Santamouris, M.; Paolini, R.; Caccetta, P.; Kassomenos, P. Analyzing the local and climatic conditions affecting the urban overheating magnitude during the Heatwaves (HWs) in a coastal city: A case study of the greater Sydney region. Sci. Total Environ. 2021, 755, 142515.

9. Khan, H.S.; Paolini, R.; Santamouris, M.; Caccetta, P. Exploring the Synergies between Urban Overheating and Heatwaves (HWs) in Western Sydney. Energies 2020, Vol. 13, Page 470 2020, 13, 470.

10. Khan, H.S.; Paolini, R.; Santamouris, M. Synergies and exacerbations—effects of warmer weather and climate change. Urban Clim. Chang. Heat Islands 2023, 73–121.

11. Khan, H.S. On the climatic synergies at the local, regional, and global scales. The impact on the built environment., Ph.D. dissertation, UNSW Sydney, 2022.

12. Grady Dixon, P.; Mote, T.L. Patterns and causes of Atlanta's urban heat island-initiated precipitation. J. Appl. Meteorol. 2003, 42, 1273–1284.

13. Sheridan, S.C.; Kalkstein, L.S.; Scott, J.M. An evaluation of the variability of Air mass character between urban and rural areas. Biometeorol. Urban Climatol. Turn Millenn. 2000, 487–490.

14. Bejarán, R.A.; Camilloni, I.A. Objective method for classifying air masses: An application to the analysis of Buenos Aires' (Argentina) urban heat island intensity. Theor. Appl. Climatol. 2003, 74, 93–103.

15. Zhang, F.; Cai, X.; Thornes, J.E. Birmingham's air and surface urban heat islands associated with lamb weather types and cloudless anticyclonic conditions. Prog. Phys. Geogr. 2014, 38, 431–447.

16. Mihalakakou, G.; Flocas, H.A.; Santamouris, M.; Helmis, C.G. Application of neural networks to the simulation of the heat island over Athens, Greece, using synoptic types as a predictor. J. Appl. Meteorol. 2002, 41, 519–527.

17. Hardin, A.W.; Liu, Y.; Cao, G.; Vanos, JK Urban heat island intensity and spatial variability by synoptic weather type in the northeast US Urban Clim. 2018, 24, 747–762.
18. Brazel, A.; Gober, P.; Lee, S.; Grossman-Clarke, S.; Zehnder, J.; Hedquist, B.; Comparri, E. Determinants of changes in the regional urban heat island in metropolitan Phoenix (Arizona, USA) between 1990 and 2004. Clim. Res. 2007, 33, 171–182.
19. Szegedi, S.; Kircsi, A. The effects of the synoptic conditions on development of the urban heat island in Debrecen, Hungary. Acta Climatol. Chorol. 2003, 36–37, 111–120.
20. Unger, J. Heat island intensity with different meteorological conditions in a medium-sized town: Szeged, Hungary. Theor. Appl. Climatol. 1996, 54, 147–151.
21. Khan, H.S.; Santamouris, M.; Kassomenos, P.; Paolini, R.; Caccetta, P.; Petrou, I. Spatiotemporal variation in urban overheating magnitude and its association with synoptic airmasses in a coastal city. Sci. Rep. 2021, 11, 6762.
22. Estévez, J.; Gavilán, P.; Giráldez, J. V. Guidelines on validation procedures for meteorological data from automatic weather stations. J. Hydrol. 2011, 402, 144–154.
23. Lee, C.C. The development of a gridded weather typing classification scheme. Int. J. Climatol. 2015.
24. Lee, C.C. The gridded weather typing classification version 2: A global-scale expansion. Int. J. Climatol. 2020.
25. Vahmani, P.; Ban-Weiss, G.A. Impact of remotely sensed albedo and vegetation fraction on simulation of urban climate in WRF-urban canopy model: A case study of the urban heat island in Los Angeles. J. Geophys. Res. Atmos. 2016, 121, 1511–1531.
26. Li, D.; Sun, T.; Liu, M.; Yang, L.; Wang, L.; Gao, Z. Contrasting responses of urban and rural surface energy budgets to heat waves explain synergies between urban heat islands and heat waves. Environ. Res. Lett. 2015, 10, 054009.
27. Imran, H.M.; Kala, J.; Ng, AWM; Muthukumaran, S. Impacts of future urban expansion on urban heat island effects during heatwave events in the city of Melbourne in southeast Australia. Q. J. R. Meteorol. Soc. 2019, 145, 2586–2602.
28. Pyrgou, A.; Hadjinicolaou, P.; Santamouris, M. Urban-rural moisture contrast: Regulator of the urban heat island and heatwaves' synergy over a mediterranean city. Environ. Res. 2020, 182, 109102.
29. Ao, X.; Wang, L.; Zhi, X.; Gu, W.; Yang, H.; Li, D. Observed Synergies between Urban Heat Islands and Heat Waves and Their Controlling Factors in Shanghai, China. J. Appl. Meteorol. Climatol. 2019, 58, 1955–1972.
30. Zhao, L.; Oppenheimer, M.; Zhu, Q.; Baldwin, J.W.; Ebi, KL; Bou-Zeid, E.; Guan, K.; Liu, X. Interactions between urban heat islands and heat waves. Environ. Res. Lett. 2018, 13, 9326.
31. Fischer, E.M.; Seneviratne, SI; Vidale, P.L.; Lüthi, D.; Schär, C. Soil moisture-atmosphere interactions during the 2003 European summer heat wave. J. Clim. 2007, 20, 5081–5099.

Anti-sargassum system for the manufacture of artisanal bricks

JAVIER AGUIRRE CONTRERAS[1], MIGUEL ARZATE PEREZ[1], JAVIER AGUIRRE MUÑOZ[2], GERARDO ARZATE PEREZ[1]

[1]Autonomous Metropolitan University, México, México

[2]Secretary of Public Education, México, México

ABSTRACT: This article presents the design, production, and installation of an anti-sargassum system, to use sargassum in the manufacture of bricks, using a mixture of sargassum, sand, cement in a proportion of 0.81, 0.27 and 0.12 kg respectively in 450 ml of water, producing a brick of 250X125X45 mm with a weight of 1.2 kg. The impact on the manufacture and distribution of sargassum brick when using cement was 9.27168e-06 kg CO_{2eq}. If we compare it with the production and distribution of a red brick which is 0.152620 kg CO_{2eq}. Sargassum brick is 99.99999% less polluting than red brick. It is proposed to develop this project to contain in advance the successive arrivals of this type of macroalgae, using a deployment mesh to later carry out its drying and grinding, with the above being possible to manufacture artisan bricks.
KEYWORDS: anti-sargassum, sargassum brick, cement, red brick, polluting.

1. INTRODUCTION

Climate change (CC) directly affects oceanic waters due to the gradual increase in temperatures in the pelagic areas of the coasts, favouring the multiplication of macroalgae that will eventually become sargassum, causing severe economic impacts on the coasts of Quintana Roo, being that the tourism sector represents 90% of the economic activities of the state [1]. The arrival of sargassum is a phenomenon that as of 2009 grew exponentially throughout since that date to actually [2].

This fact represents a scientific challenge to contain it to the probable minimum, to reduce its catastrophic effects in all the economic branches dependent on the mentioned sector. Its detection begins when the "Great Atlantic Sargasso Belt" starts to expand significantly towards the coasts of the islands of the Caribbean Sea and the State of Quintana Roo [3]. By 2018 and 2019, the volume and extension of this sargassum in the Atlantic had already become alarming. It was estimated that in June 2018 its live weight at sea was more than 20 million tons, distributed along an extension of more than 8,850 km [3].

Among the environmental and economic consequences of sargassum on the beaches of Cancun, Riviera Maya, Playa del Carmen and Tulum, the following are mentioned:

- To this it should be added that the massive sargassum massacres also represent severe public health problems, since when decomposed it generates hydrogen sulfide, methane and ammonium.
- The effect of sargassum produces an immediate environmental effect on current coastal ecosystems, especially the Mesoamerican Reef System, sea grasses, mangroves, and wetlands in general.

Sargassum is a brown or blackish green macroalgae that is kept afloat by gas-filled vesicles. These algae can grow several meters long, are hard in texture and easily interlaced, creating strong and flexible sargassum islands capable of surviving among the strong currents of the Caribbean Sea. In addition, when sargassum reaches the beach, it has a rotten smell and generates hydrogen sulfidic, methane and arsenic that can contaminate soils and ecosystems. [3].

The Sargasso Sea is named after the floating mats of Sargassum algae, first reported by Christopher Columbus in the 15th century. These algae attract fish, shrimp, crabs, birds, and turtles, provide essential habitats, and serve as hotspots for biodiversity and productivity. There are two prevailing species of sargassum, which are Sargassum fluitans and Sargassum natans, are the most abundant in the Sargasso Sea and the Gulf of Mexico, which are connected by ocean currents [3]. "The Sargasso Sea is recognized as an important open-ocean ecosystem, most of which lies outside national jurisdiction, and deserves recognition by the international community given its great ecological and biological importance, cultural significance, and its outstanding universal value" [4]. This background sets the tone and offers options for how to approach the formation of the New Sargasso Sea.

The "New Sargasso Sea", which started in 2011 with a relatively minor biomass, has grown steadily to reach 20 million tonnes of sargassum in June 2018 [3]. One way to measure this amount of sargassum is

to compare it with the national fishing catch in 2017, with a total of 2.16 million tons [5], of which 4,837 tons were algae and giant sargassum. In the summer of 2018, Quintana Roo experienced extraordinary accumulations of sargassum [1].

Studies have been carried out to learn about the formation of this new Sargasso Sea. The results of these scientific investigations have given rise to some preliminary hypotheses of the probable factors that have influenced the explosive increase in the number and volume at successive and uninterrupted arrival of the sargassum conglomerates. Within these hypotheses we can mention the following (not ranked) [3]:

- Increase in surface temperatures of ocean waters.
- Modification of the directions and speed of the ocean currents that occur in the Caribbean Sea.
- Increase in the availability of nutrients due to natural phenomena, in view of the change in the circulation of coastal and inland winds from various regions of the Atlantic, mainly at the mouths of the Orinoco and Amazon rivers.
- The deposition of soluble solids with the arrival of sewage from the domestic sanitary networks of the main population centres of the Quintana Roo coast.
- The sustained confluence of new environmental conditions: temperature, nutrients, light, winds, and currents, which have fostered an optimal environment for the growth and proliferation of these species of pelagic sargassum.

To take advantage of the sargassum that accumulates on coastal beaches and that retained in the pelagic zone, some scientists have sought innovative commercial applications from its residues, such as: fertilizer, construction materials, designer shoes, craft paper, biogas, and the extraction of chemical products for the food or pharmaceutical industry, among others [6].

The objective of this study is that through the design, production, and installation of an anti-sargassum system, it is intended to use the collected sargassum as raw material to manufacture bricks. This will prevent this macroalgae accumulate in mounds in the first 10 m within coastline, which allow tourists to rest and sunbath as well as swim and dive in the 50 m offshore.

Design a short, medium, and long-term strategy that makes the development of a value chain (reuse of the collected sargassum) feasible from sargassum, to obtain the brick. The general objective of this project is to develop a low-cost anti-sargassum system, with the following characteristics.

- Stop early all sargassum islands that come from offshore.
- Do not harm the marine flora or fauna, specifically the coral reefs that are found near the coastline of the state of Quintana Roo.
- Build the anti-sargassum system with recyclable and low-cost materials.
- With the sargassum colected and dried, made of a brick utilizing a small quantity of cement as a binder the mix it.

2. MATERIALS AND METHODS

The method for developing the project is grinding to obtain powder and mixing it with three quarters of sargassum and one quarter of paste made with a mix of sand and cement adding water to it. Done the above obtain a malleable mass for the elaboration of the handmade sargassum brick with specific measurements and volume. Before doing the above, the following steps must be followed:

- Sargassum monitoring.
- Collect sargassum in specific areas.
- Drying with sun exposure.
- Ground sargassum.
- Manufacture of brick.
- Life Cycle Assessment (LCA) of Sargassum brick

2.1 Monitoring

With the National Earth Observation Laboratory (NEOL), the movement of sargassum (Fig. 1) throughout the ocean can be monitored, this is done using an algorithm based on satellite images to know the displacement of the annual arrivals [7].

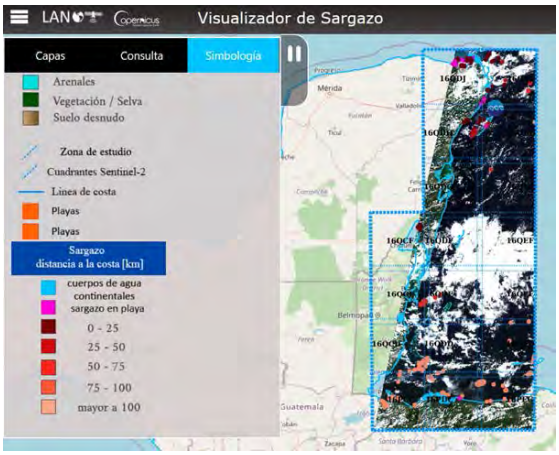

Figure 1. Sargasso viewer utilysing LANOT.

Using an algorithm, sargassum can be detected in the maritime zone near the coast of Quintana Roo, extending to Belize, Guatemala, and part of Honduras, covering an approximate area of 150,000 km^2. Images from the Sentinel-2 satellites of the COPERNICUS Constellation of the European Space Agency are used. A mosaic is generated from 18

satellite images, this occurs every 5 days. To cover the gap of five days between the availability of Sentinel 2 images and thus provide an estimate of the movement of the centroids identified in the sargassum detection process, ocean current data provided by HYCOM (Hybrid Coordinate Ocean Model) is used. [8].

2.2 Collect sargassum in specific areas.

To collect sargassum, you must first register on the Collected Sargassum Monitoring System platform [9] that monitors sargassum for SEMARNAT to know in depth the sargassum phenomenon and thus design better protocols for attention to this problem and obtain permits for the collection of sargassum [9].

The anti-sargassum system is built using a containment barrier (Fig. 2), which has proven to be a great tool if they operate efficiently.

Figure 2. Set of Anti-sargassum system.

2.3 Drying with sun exposure.

After the collection of the sargassum, it is cleaned from the beach sand, later rinsed with seawater, and deposited in sacks to be transferred to the processing workshop. In a clear area, the sargassum is distributed to dry it using sunlight.

2.4 Ground sargassum

When the sargassum is already dry, it is passed through a special mill for it to obtain a finer texture (Fig. 3).

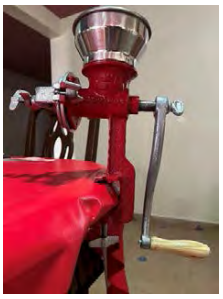

Figure 3. Grain mill.

After grinding the sargassum, we pass it through a 2 mm sieve to separate the fine and coarse parts or to clean it of impurities.

2.5 Manufacture of brick

The geometric dimensions of the finished brick are:

- Length: 250 mm.
- Width: 125 mm.
- Height: 45 mm.
- Weight: 1.2 kg

The composition of the mixture for the brick is as follows.

- Sargassum: 67.5% (0.81 kg)
- Sand: 22.50% (0.27 kg)
- Cement: 8% (0.12 kg)
- Water: 2% (450 ml)

The mixture is poured into the mold (Fig. 4) with the dimensions and compressed with a specifical mechanical press (Fig. 5) made for this purpose, thus reducing the humidity of the mixture.

Figure 4. Brick mold.

Figure 5. Mechanical press.

After being poured into the mold, the mixture is compressed with a mechanical press made for this purpose, thus reducing the humidity of the mixture. Finally, the brick is obtained (Fig. 6).

Figure 6. Sargassum brick.

2.6 Life Cycle Assessment (LCA) of Sargassum brick

As previously mentioned, 0.12 kg of cement was used to produce brick, so a LCA of the production and distribution of the cement was carried out to know the impact that this will have on the production of the sargassum brick. sargassum brick. In accordance with the ISO-14025 methodology, the processes are subdivided into modules. The LCA was carried out

from cradle to gate and covers the production and use stage (module A2-B1) [10].

The inputs and outputs (Table 1) for the manufacture of 1,000 kg of cement are the following [11].

Table 1. Inputs and outputs to produce 1,000 kg of cement.

Life Cycle Inventory (LCI)	*Values*
Inputs	
Stone	600 kg
Clay	100 kg
Limestone	300 kg
Plaster	10 kg
Water	0.2 m^3
Sand	700 kg
Gravel	800 kg
Coal	300 kg
Natural gas	0.2 m^3
Fuel oil	0.0004 m^3
Diesel	0.0 MJ
Electric power	18.0 MJ
Product transportation	100 km
Outputs	
SO_2	2.048 kg
NO_X	0.0212 kg
PM-10	0.00001
PST	0.0032
CO	0.0213
CO_2	0.0956
COV	0.0024
CH_4	0.0011
Hydrocarbons (HC)	0.0026

The openLCA software was used to evaluate the environmental impacts in the manufacture of 0.12 kg of cement. It was used the method CML-IA baseline is developed by the Center for Environmental Studies, Leiden University, The Netherlands in 2001 [12]. Table 3 shows Life Cycle Impact Assessment (LCIA) of the transportation and manufacture a of 0.12 kg of cement.

Table 3. LCIA of 0.12 kg of cement.

Indicator	*0.12 kg of concrete*	*units*
Abiotic depletion	6.71381e-11	kg Sb_{eq}
Abiotic depletion (fossil fuels)	6.53400e-4	MJ
Acidification	2.99133e-4	kg SO_{2eq}
Eutrophication	3.74495e-7	kg PO_{4eq}
Freshwater aquatic ecotox.	1.90954e-7	kg 1,4-DB_{eq}
Global warming (GWP100a)	9.27168e-5	kg CO_{2eq}
Human toxicity	3.33376e-5	kg 1,4-DB_{eq}
Marine aquatic ecotoxicity	8.37763e-3	kg 1,4-DB $_{eq}$
Ozone Layer Depletion (ODP)	3.55770e-12	kg CFC-11_{eq}
Photochemical oxidation	1.19629e-5	kg C_2H_{4eq}
Terrestrial ecotoxicity	3.55049e-8	kg 1,4-DB_{eq}

3. ANALYSIS AND DISCUSSION OF RESULTS

It is essential to present technological alternatives to control and mitigate the economic damage, public health and environmental imbalance caused by sargassum swarms before it is established in the beach area. The benefit of this project is to collaborate in reducing the impact on the tourist image caused by sargassum on our beaches, by developing activities of culture of care and protection of the environment. The achievements during the project development process were:

- Raise awareness in the community to help care for the environment.
- The product was marketed locally.
- Continuity of diversification to the ideas of predecessors who have used sargassum as a source of raw material.

To must, the environmental impact of sargassum brick was compared to the manufacture of a red brick (the environmental impact of red brick was taken from the study conducted by Arzate 2023 [13])

The total emissions of kg CO_{2eq} on the manufacture and distribution of sargassum brick when is used cement as a binder was at 9.27e-6 compared with 152.62e-3 of a red brick [13]. Sargassum brick is 99.99999% less polluting than red brick (Fig. 7).

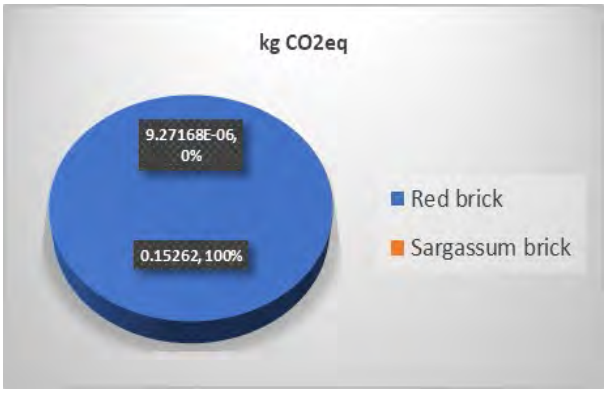

Figure 7. Comparison in percentage between red and sargassum brick.

The advantages of using cement in a sargassum brick making are:

- More than 67% of the material used is organic and low cost.
- It offers multiple advantages, from lower energy consumption in its production, greater durability, and resistance.
- The cement will help the brick achieve a long useful life.
- Other benefits, this organic material improves acoustics, has thermal characteristics and is biodegradable since it is made 67% with sargassum, 24% with other organic matter, and 8% with cement.

The disadvantage of using cement is that its production process has a great environmental impact, which is why it is intended to reduce the percentage of this material.

4. CONCLUSION

Sargassum is good, since it is extremely effective in trapping heavy metal ions that are highly harmful in the food chain, but the excess of this is harmful, so it must be used for the benefit of human beings.

It is important to remove sargassum from beaches and coasts before it decomposes, to prevent the metals and elements it contains from accumulating in the marine area and continuing to harmful the fauna and flora of the Mexican coasts. The main purpose of the above is to reduce both its environmental impact and human health, by reducing the emission of hydrogen sulfidic, carbon dioxide and methane, which are released when the sargassum decomposition process begins. By preventing the sargassum islands from reaching the beach area, large areas of it are released, which can be used as nesting areas for different endemic species of turtles. It is proposed to develop this project to contain in advance the successive arrivals of this type of macroalgae, using a deployment mesh to later carry out its drying and grinding, with the above being possible to manufacture artisan bricks.

According to the results obtained, the following general conclusions can be established:

- The best percentage of cement, for reinforcing sargassum brick, is 8%, since cement percentages greater than 8% decrease the compressive strength.
- It would be advisable to make buttresses or structural reinforcements to the walls or increase the thickness.
- Cement only produces improvements in increasing flexural strength.

ACKNOWLEDGEMENTS

We thank the Secretaría de Educación Pública and the Universidad Autónoma Metropolitana Azcapotzalco for their support for supporting this project entitled "Anti-sargassum system for the manufacture of artisanal bricks".

REFERENCES

1. BID (Banco Interamericano de Desarrollo). (2022). El impacto económico del sargazo: Evidencia de la costa mexicana, [Online], Available: http://dx.doi.org/10.18235/0004470. [21 July 2023]
2. Aguirre Muñoz Alfonso. (2019). El sargazo en el caribe mexicano: de la negación y el voluntarismo a la realidad, [Online], Available: https://www.conacyt.gob.mx/sargazo/images/pdfs/El_Sargazo_en_el_Caribe_Mexicanopdf.pdf [16 July 2023].
3. Wang Mengqiu, Hu Chuanmin, Barnes B.Brian, Mitchum Gary, Lapointe Brian Lapoint, Montoya P. Joseph. (2019). The great Atlantic Sargassum belt, [Online], Available: https://www.science.org/doi/10.1126/science.aaw7912 [16 July 2023].
4. Alegre, L. (2019). In: Redacción, 2019. Este año no habrá solución para el sargazo: Luis Alegre. La Jornada Maya, [Online], Available: https://www.lajornadamaya.mx/2019-06-10/Este-ano-no-habra-solucion-para-el-sargazo--Luis-Alegre [16 July 2023].
5. SECTUR (Secretaría de Turismo). (2019). El Espíritu del Tren Maya, [Online], Available: http://sistemas.sectur.gob.mx/dgots/16-espiritu-tren-maya.pdf [12 November 2023].
6. SEGOB (Secretaría de Gobernación). (2019). ACUERDO por el que se expide el Programa de Ordenamiento Turístico General del Territorio. Diario Oficial de la Federación (DOF): 05/08/2019, [Online], Available: https://www.dof.gob.mx/nota_detalle.php?codigo=5567142&fecha=05/08/2019#gsc.tab=0 [20 July 2023].
7. Sargasso Sea Commission. (2014). The Hamilton Declaration, [Online], Available: http://www.sargassoseacommission.org/meet-the-commission/hamilton-declaration [06 August 2023].
8. CONAPESCA (Comisión Nacional de Acuacultura y Pesca). (2017). Anuario Estadístico de Acuacultura y Pesca 2017. Gobierno de México. Mazatlán, Sinaloa, [Online], Available: https://www.gob.mx/conapesca/documentos/anuario-estadistico-de-acuacultura-y-pesca [02 September 2023].
9. Robles de Benito, R. (2019). Sargazo: ¿situación o problema? De arribazones masivas a las playas de Quintana Roo. La Jornada Maya, [Online], Available: https://www.lajornadamaya.mx/2019-06-28/Sargazo----situacion-o-problema- [20 July 2023].
10. UNAM. 2021. PROYECTOS LANOT MONITOREO DE SARGAZO, [Online], Available: http://sargazo.lanot.unam.mx/lanot/sargazo/ [16 July 2023].
11. SIMSAR. (2021). Sistema de monitoreo de sargazo, [Online], Available: https://app.semarnat.gob.mx/sargazo/#/login [16 July 2023].
12. SEMARNAT. (2021). Lineamientos Técnicos y de Gestión para la Atención de la Contingencia Ocasionada por Sargazo en el Caribe Mexicano y el Golfo de México, [Online], Available: https://www.gob.mx/cms/uploads/attachment/file/636709/SEMARNAT-INECC-SARGAZO-2021.pdf [16 July 2023].
13. EPD, The international EPD System, [Online], Available: https://www.environdec.com/all-about-epds. [16 July 2023].
14. Espinoza López Cesar Alejandro (2005). Inventario de análisis del ciclo de vida para el cemento en México. Tesis para optar el grado de Maestro en Ciencias en Desarrollo Sostenible. Instituto Tecnológico de Monterrey, Campus Estado de México, [Online], Available: https://repositorio.tec.mx/bitstream/handle/11285/628460/CEM276576.pdf?sequence=1&isAllowed=y [16 July 2023].
15. GREENDELTA. (2016). LCIA methods: Impact assessment methods in Life Cycle Assessment and their impact categories, [Online], Available: https://www.openlca.org/wp-content/uploads/2016/08/LCIA-METHODS-v.1.5.5.pdf [16 July 2023].
16. Arzate Pérez Miguel, Aguirre Contreras Javier, Arzate Pérez Gerardo, Aguirre Muñoz Javier. (2023). LIFE CYCLE ASSESSMENT OF A RED BRICK IN SAN LUIS HUEXOTLA, TEXCOCO, STATE OF MEXICO, MEXICO, [Online], Available: https://www.s-arch.net/ [16 July 2023].

Concrete vs adobe: an environmental comparison for a cultural building.

MIGUEL ARZATE PÉREZ[1], JAVIER AGUIRRE CONTRERAS[2], GERARDO ARZATE PÉREZ[3]

[1,2,3] Universidad Autónoma Metropolitana, Ciudad de México, México.

ABSTRACT: Life Cycle Assessment (LCA) enables the determination of the inputs and outputs of matter and energy for a process and/or product throughout its useful life or a part thereof. This analysis provides a standarized framework for information, allowing for comparisons, analysis, and the determination of environmental impacts in kilograms (kg) of carbon dioxide equivalent (CO_{2eq}.). This study aims to present an LCA and evaluate global warming (GW), water consumption (WC), and other indicators by identifying a brutalist building in Mexico in the second half of the 20th century (Museo Tamayo) and its predominant construction material, following the International Organization for Standardization (ISO) 14040:2006 standard. The GW employs an LCA approach, considering all input and output flows resulting in greenhouse gas (GHG) emissions throughout the entire supply chain. The GW is quantified based on the manufacturing, distribution, and construction of the already built museum (concrete) and a potential scenario, using a more sustainable material (adobe). The obtained results indicate that the GW for concrete and adobe is 8.94E+6 and 8.44E+5 kg of CO_{2eq}, respectively. The LCA results can be considered as indicators of management and sustainability, serving as a baseline for implementing strategies and actions that can be directed towards the development of green buildings.
KEYWORDS: Materials, life cycle assessment, global warming, buildings, sustainability.

1. INTRODUCTION

Since the Industrial Revolution, our methods of energy and food production and consumption have modified the atmospheric composition. This is primarily a result of fossil fuel combustion and ecosystem degradation, leading to an elevation in greenhouse gases (GHG), levels in the atmosphere, consequently causing climate change (CC) on Earth [1]. Currently, in Mexico, some effects of CC are noticeable: since 1960, the country has experienced, with national average temperatures rising by 0.85ºC and winter temperatures by 1.3ºC. There has been a decline in the number of cool days, an increase in warmer nights, and a reduction in rainfall in the southeast of the country [2].

In 2015, Mexico emitted 683 million tons of carbon dioxide equivalent ($MtCO_{2eq}$) of GHG due to human activities. The industrial processes that generate GHG result from the transformation of raw materials through chemical and physical processes, as well as fugitive emissions from coal mining and handling (mining). Among the subsectors that generate the most emissions in the industrial sector in the country are cement, steel, and chemicals. Cement emitted 11,404.451 Gg of CO_{2eq} in 2015 [3]. Additionally, the uncontrolled use of natural resources, such as water to supply productive activities like agriculture or industry, leads to the generation of wastewater, degradation of ecosystems, loss of biodiversity, and the depletion of this vital liquid. The three main sectors that have the granted use of this resource are agriculture, public supply, and self-supplied industry, the latter consuming 4.3 km^3 increasing its volume between 2010 to 2017 by 26.9% obtained mainly from groundwater. To measure its extraction, the degree of water resource pressure indicator is used, showing various contrasts due to climate, population size, and service demand. In the north, it fluctuates between 40 and 85%. In the south less than 8%, and in the central part of the Mexico City it's 142% [4].

The construction industry is a crucial sector for the social and economic development of the country, as it provides basic elements of well-being in society, such as schools, hospitals, roads, social interest housing and residential types among others. This economic activity relies on inputs from various industries, including steel, iron, cement, sand, lime, wood, and aluminum; therefore, the construction industry serves as one of the main engines of the country's economy. In 2019, there were 19,501 companies dedicated to construction [5] with 115 involved in cement manufacturing and 725 in concrete [6]. Indeed, one of the primary products used in the Mexican construction industry and globally is ready-mixed concrete. This material is produced with cement, aggregates of different sizes (gravel, grit, and sand), and water [7]. It is utilized on-site or prefabricated for constructing buildings. For example, iconic structures like Estadio Azteca, Universidad Autónoma Metropolitana, Museo Nacional de Antropología, Museo Tamayo, Auditorio Nacional, and Torre Reforma designed respectively by the architects Pedro Ramírez Vázquez, Teodoro

González de León, Abraham Zabludovsky, and Benjamín Romano, have utilized concrete as the primary construction material. However, the use of it in these buildings, like many others, has environmental implications throughout their life cycle, involving the use of raw materials and natural resources, emitting GHG, contributing to global warming (GW), promoting CC, and causing biodiversity loss.

In Mexico, there are local materials that can be explored and utilized in the construction industry, such as products derived from the earth. Examples included blocks made of adobe or rammed earth walls, both produced with local soil, clay, sand, and water. For instance, in Oaxaca, the School of Visual Arts, covering 2,200 square meters, and, designed by architect Mauricio Rocha in 2007 [8], serves as an illustration. Adobe has been employed worldwide, from the Neolithic period to vernacular architecture in the 19th and 20th centuries. Its promotion for use in 21st-century architecture is viable due to its low environmental throughout its life cycle. This results in reduced pollutant emissions (CO_2) and diminished use of natural resources (water), aligning with the sustainability principles in construction [9].

It is important to know the negative impacts associated with the extraction of raw materials, their manufacture and distribution, their usage and the end of their useful life in construction. These impacts can be assessed through the GW metric, which measures the direct or indirect emissions of GHG from obtaining raw materials to the waste generated by a product or service [10]. Due to this, there is a growing in developing methods that provide a more comprehensive evaluation of GW throughout the life cycle. This helps determine improvements in the energy efficiency of each production process stage, aiming to reduce energy consumption and mitigate environmental impact as much as possible. One such technique developed for this purpose is the LCA, a tool that allows us to understand the emissions of the construction sector [11].

The selection of the materials used in constructing can play a pivotal role in reducing the impact generated during each life cycle stage, particularly in extraction, construction, and use. Therefore, evaluating the GW footprint of construction materials becomes a strategic tool to mitigate the impact on CC [10].

The LCA involves compiling the inputs and outputs of mass and energy used throughout the entire life cycle of a product. This encompasses extraction of raw materials, production, use, final treatment, recycling, until its final disposal, following the “cradle to grave” approach. The outcome of the LCA provides insights into potential negative environmental impacts such as GW, acidification, ozone depletion, eutrophication, pollution, and effects on human health [12].

In this study, the LCA was conducted following the ISO 14040:2006. This standard necessitates the use of a flow representation to characterize a unit, as illustrated in Figure 1 [13].

Since the Industrial Revolution, our methods of

impacts such as GW, acidification, ozone depletion, eutrophication, pollution, and effects on human health [12].

In this study, the LCA was conducted following the ISO 14040:2006. This standard necessitates the use of a flow representation to characterize a unit, as illustrated in Figure 1 [13].

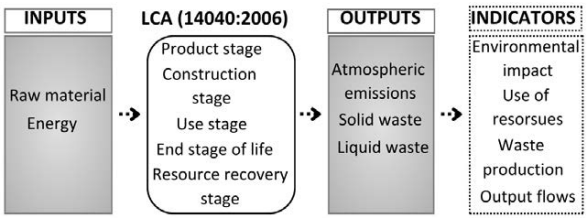

Figure 1. LCA Methodology according to ISO-14040:2006.

The aim of this study was to assess the environmental impact generated by concrete in an already constructed building in the second half of the 20th century (brutalist avant-garde) through LCA and compare it with a potential scenario using a local material called adobe. The emphasis was placed on evaluating GW and resource usage, particularly WC.

2. MATERIALS AND METHODS

The international standards that provide the framework for LCA are ISO 14040:2006 [14] which defines the general principles, and ISO 14044:2006 [15], which further specifies the requirements. As described by ISO 14040:2006 and ISO14044:2006, the LCA methodology consists of four phases: 1) goal and scope, 2) inventory analysis, 3) impact assessment and 4) interpretation of results [16].

According to ISO 14044:2006, Life Cycle Impact Assessment (LCIA) determines the magnitude of a system's environmental impacts throughout the entire product life cycle. In this case, it was conducted from cradle to gate and covers production (A2-A3) (Fig. 2) [10].

Product stage			Construction process stage		Use stage							End stage of life				Resource recovery stage
Raw material extraction	Transport	Manufacture	Transportation to the site	Construction	Use	Maintenance	Repair	Replacement	remodeling	Operational energy use	Operational water use	Demolition	Waste transport	waste deposit	Disposal	Reuse-recover-recycling-potential
A1	A2	A3	A4	A5	B1	B2	B3	B4	B5	B6	B7	C1	C2	C3	C4	D
MND	X	X	MDN	MDN	MND	MND	MND	MND	MND	MND	MND	MND	MND	MND	MND	MND

X: included in the LCA
MND: module not declared or NR: not relevant

Figure 2. Scope of the LCA.

2.1. System limits

The GW analyzed in this study considers a life cycle approach, with boundaries extending from distribution to manufacturing.

- Manufacturing encompasses all processes or requirements through which the raw materials, along with chemicals and other elements such as electricity, water, and fuels, are used to create the new one.
- Transportation represents the output of the constructed system.
- Temporary Limits: The reference year for the data used in preparing the Life Cycle Inventory (LCI) will correspond to the representative information of the production of each material from the factory.
- Geographical Limits: The study area is delimited to the Mexican national territory.
- Impact categories. This study is focus on analyzing the GW and WC using the Recipe 2016 Midpoint method.

2.2 openLCA

The software used was openLCA, with the version employed in this study being 1.11 [17] alongside the ecoinvent 3.7 [18] database for transportation and manufacturing processes related to concrete and adobe, considering all potential environmental impacts that can be generated.

The characteristics of concrete [10] are detailed below:

- Concrete Supplier: XELLA de México.
- Plant location: Garza García, Nuevo León.
- Materials used in the manufacture of concrete: 58% sand, 20% cement, 15% lime, 6% plaster.

Table 1 displays the LCI of materials used in the manufacture of 1 kg of concrete [10].

Table 1. LCI of 1 kg of Concrete.

Input	Unit	Quantity
Electricity	MJ	2.60E-1
Water	kg	2.07E+0
Natural gas	kg	1.56E+0
Diesel	MJ	6.35E-2
LP Gas	kg	4.64E-4
Cement	kg	2.19E-1
Lime	Kg	1.62E-1
Sand	Kg	6.27E-1
gypsum	Kg	6.90E-2
Transport	tkm	2.92E-1
Output	**Unit**	**Quantity**
Carbon dioxide*	kg	9.23E-2
Nitrogen oxide*	kg	2.10E-7
Methane*	kg	1.91E-6

*The supplier has not registered its outputs, so the calculation is made based on the reported use of natural gas [19].

The characteristics of adobe are outlined as follows [10]:

- Adobe supplier: Paquimé
- Plant location: Cuernavaca, Morelos
- Materials used for the manufacture of adobe: 79% bank tepetate, 12% mine sand, 7% cement and 2% limestone.

Table 2 represents the LCI of materials used in the production of 1kg of adobe [10].

Table 2. LCI of 1 kg of Adobe.

Input	Unit	Quantity
Water	kg	2.05E-1
Diesel	MJ	6.45E-2
Oil	MJ	3.10E-3
Bench of Tepetate	kg	1.20E+0
Sand	kg	1.75E-1
Calhydra	kg	3.43E-2
Cement	kg	1.04E-1
Bank tepetate *	tkm	3.00E-1
Output	**Unit**	**Quantity**
Nitrogen oxides**	kg	4.77E-3
Carbon dioxide**	kg	3.87E-8
Methane**	kg	1.93E-7

*The supplier of the adobe is carried out in the same place where the property will be built, so it looks for a tepetate bank that is less than 25 km in radius.

**The supplier has not registered its outputs, so the calculation is made based on the use of natural gas [19].

2.3 Recipe 2016 Midpoint method

ReCiPe is a method for LCA, that converts emissions and resource extractions into a concise set of environmental impact scores using so-called characterization factors [20]. Midpoint indicators focus on specific environmental issues, such as fine particulate matter, land use, freshwater ecotoxicity, ozone formation, global warming, or water consumption [18].

3. RESULTS AND DISCUSSION

Figure 3 shows LCIA of the transportation and manufacture of 1 kg of concrete and 1 kg of adobe.

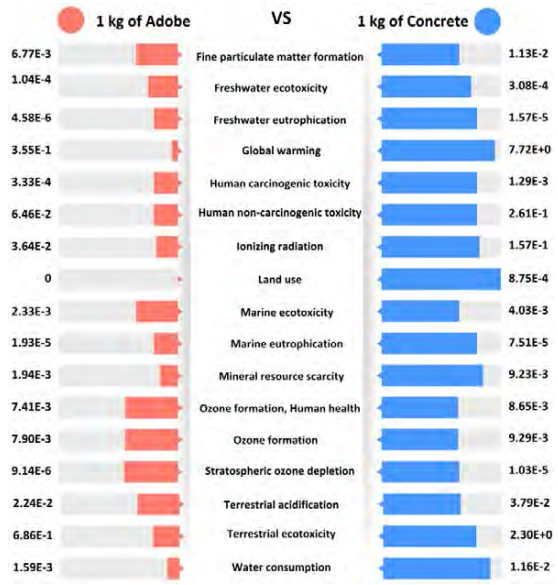

Figure 3. LCIA of 1 kg of concrete and 1 kg of adobe.

This study has a scope from cradle to gate, which implies that, in terms of LCA, the impacts generated during the use and final disposal stage of each of the systems analysed are not considered. The impacts of the use stage are related to the specific characteristics of the design, location, and climatic conditions of the building.

The results of the GW obtained from the openLCA software for each material are presented in Table 3.

Table 3. Global warming in kg of $CO_{2eq.}$ per kg of each material, considering a life cycle approach.

Material	Global warming	Units
1 kg of concrete	7.72E+0	Kg $CO_{2eq.}$
1 kg of adobe	3.55E-1	Kg $CO_{2eq.}$

To calculate the mass required for covering one square meter (m^2) with concrete or adobe, the quantity of kg of each material was separately quantified to construct that. The values were obtained directly from suppliers, technical sheets and reports of the inventories conducted by the Mario Molina Center, located in Mexico City. The results are presented in Table 4 [10].

Table 4. Equivalence: weight in kg/m^2 of concrete and adobe.

Construction System	Materials	Kg/m^2
Concrete wall	Concrete on construction site f´c= 200 kg/cm^3	226.60
Adobe wall	Adobe (made with cement, tepetate, sand and calhydra)	247.50

The LCA of the manufacturing of building materials at the Museo Tamayo (Fig.4), was conducted from the cradle to the gate.

Figure 4. Museo Tamayo

The manufactured material for the institution has the following LCA information:

LCA information for the Museo Tamayo [21] [22].

- Geographic location: Paseo de la Reforma 51, Polanco, Bosque de Chapultepec, CDMX.
- Functional unit-declared unit: 5,100 m^2 [23] of concrete (each square meter requires 226.60 kg/m^2, so a total of 1,115,600 kg was required).
- Functional unit-declared unit: 5,100 m^2 of adobe (each square meter of adobe requires 247.50 kg/m^2, 1,262,250 kg was required).
- Reference useful life: not applicable.
- Database and LCA software used: openLCA, version 1.11, and ecoinvent version 3.7 database.
- This system includes transportation and manufacturing: A scenario of 100 km distance was considered.

Figure 5 shows the GW of the distribution and manufacturing of the Museo Tamayo, using concrete and the Figure 6 shows if adobe were used.

Figure 5. GW in Kg of $CO_{2eq.}$ in the distribution, manufacture to of the Rufino Museum with concrete.

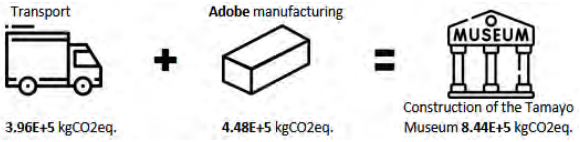

Figure 6. GW in Kg of $CO_{2eq.}$ in the distribution, manufacture to of the Rufino Museum with adobe.

The comparison of GW and WC between adobe and concrete in the Museo Tamayo is shown in Figure 7 and 8.

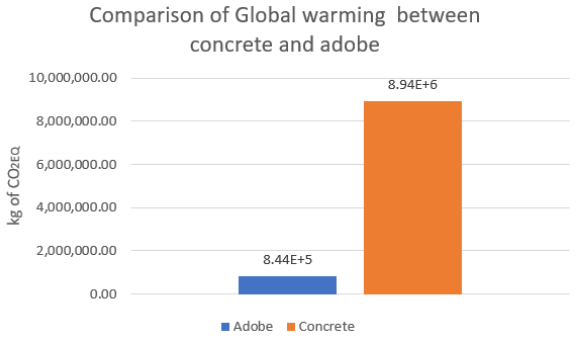

Figure 7. Comparison of GW impacts (kg of $CO_{2eq.}$) between concrete and adobe.

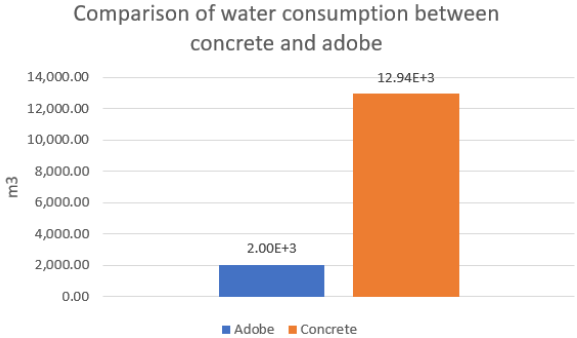

Figure 8. Comparison of the water consumption between concrete and adobe.

4. CONCLUSION

The goal of this study was to identify the brutalist avant-garde in a building in Mexico [24] in the second half of the 20th century (Tamayo Museum) characterized by emphasizing the expressive character of its materials by giving it the predominant shape in its exterior and interior volume (concrete), quantify this material and investigate its environmental impact, comparing it with a probable scenario proposing a local and traditional material from the region (adobe).

The LCA focused on modules A2 (transport) and A3 (manufacturing) to highlight the environmental impact that construction materials can exert at these stages (table 5), spurred by a brutalist movement that advocated for its use without consideration for environmental consequences. Future research will address the review of all stages, including construction and structural materials, maintenance, recovery processes, and recycling methods.

Table 5. GW emissions and water consumption

Material	Global warming	Water consumption
Concrete	8.94E+6 kg of CO_{2eq}.	12.94E+3 m^3
Adobe	8.44E+5 kg of CO_{2eq}.	2.00E+3 m^3

The use of concrete in the building construction emitted 90.55% more $kgCO_{2eq}$. compared to adobe, a natural resource indispensable for biodiversity on the planet, contributing to GHG that lead to GW and, consequently CC. Additionally, is used 85.49% more water compared to adobe.

Understanding the life cycle of materials and their environmental impact, along with the exploitation of resources and the generation of waste, should be one of the first steps in designing a sustainable building. The construction industry emits many pollutants and utilizes significant natural resources essential for the ecosystem, resulting in CC and loss of biodiversity.

In Mexico, the culture of analysing the life cycle of materials in construction is very recent. Architecture schools still do not integrate this topic into their curriculum. Consequently, entire generations of graduates do not apply this methodology at a professional level. Furthermore, the government does not require companies to declare the environmental impact of their products through life cycle assessment, leading to a lack of environmental impact information for many products. Moreover, it is necessary to promote research and development of materials and products that are more sustainable throughout their lifecycle. Disseminating this information to society is crucial, fostering awareness and encouraging the demand for sustainable production that decouples economic growth from environmental degradation. It's essential to increase resource efficiency, advocate for efficient lifestyles, mitigate poverty, and transition towards greener and low-carbon economies. In short, the goal is to achieve more and better with less, as suggested by Sustainable Development Goal number 12: Ensure sustainable consumption and production patterns, particularly under its target 12.8: By 2030, ensure that people everywhere have the relevant information and awareness for sustainable development and lifestyles in harmony with nature [25].

The findings of this study lead to the following conclusions:

- The baseline system, comprising a concrete wall, exhibits the highest GW among examined systems.
- With only: 8.44E+5 kg of $CO_{2eq.}$, adobe has the least impact on the environmental impact.
- The processes with the most significant relevance to the environmental impact of the analysed materials, based on the results obtained, include the use of cement and natural gas, technology employed, transportation of raw materials and electricity consumption.
- It is noteworthy that the cement and concrete industry in our country is actively working to minimize its environmental impact. Strategies such as co-processing, utilizing waste-derived fuels instead of fossil fuels, employing low-carbon cements with alternative raw materials, enhancing energy efficiency in processing kilns, adopting electric transportation, and redesigning the production process with low CO_2 content are being implemented.
- Emphasizing the role of transportation in emissions, it is crucial to acknowledge that they increase with the distance between material manufacturing locations and construction sites.
- The water consumption for material transformation and processing is a vital factor, potentially leading to water stress and scarcity at an industrial level. Exploring sustainable water use practices is essential.
- The computational tool provided in this study enables a detailed examination of these emissions.
- Traditional construction materials like adobe, by creating local jobs, can contribute to sustainable development.
- Promote the use of environmentally friendly technologies and alternative fuels in material manufacturing.
- Use materials that are sourced as close to the construction site as possible to minimize impacts.

- Consider the appropriateness materials for each location, taking transportation into account.

ACKNOWLEDGEMENTS

Thanks to the Universidad Autónoma Metropolitana, Unidad Azcapotzalco. Especially to the Environment Department for the support provided in the preparation of this article.

REFERENCES

1. Instituto Nacional de Ecología y Cambio Climático. Efectos del cambio climático, [Online], Available: https://www.gob.mx/inecc/acciones-y-programas/efectos-del-cambio-climatico. [15 October 2023].
2. México ante el Cambio Climático. ¿Que es el Cambio Climático?, [Online], Available: https://cambioclimatico.gob.mx/que-es-el-cambio-climatico/ [15 October 2023].
3. Instituto Nacional de Ecología y Cambio Climático. Inventario Nacional de Emisiones de Gases y Compuestos de Efecto Invernadero, [Online], Available: https://www.gob.mx/inecc/acciones-y-programas/inventario-nacional-de-emisiones-de-gases-y-compuestos-de-efecto-invernadero. [20 October 2023].
4. Secretaría de Medio Ambiente y Recursos Naturales. Informe del Medio Ambiente, AGUA, [Online], Available: https://apps1.semarnat.gob.mx:8443/dgeia/informe18/tema/cap6.html. [20 October 2023].
5. Instituto Nacional de Estadística y Geografía. Construcción, [Online], Available: https://cuentame.inegi.org.mx/economia/secundario/construccion/default.aspx [16 July 2023].
6. Instituto Nacional de Estadística y Geografía. La industria minera ampliada, [Online], Available: http://internet.contenidos.inegi.org.mx/contenidos/productos/prod_serv/contenidos/espanol/bvinegi/productos/nueva_estruc/702825198848.pdf. [28 October 2023].
7. A. Navas de García, R. Reyes Gil and L. Galván Rico. (2015). Aspects and environmental impacts associated with the production of concrete, Enfoque UTE, vol. 6, [Online], Available: https://doi.org/10.29019/enfoqueute.v6n4.79. [28 de July 2023]
8. ARCHDAILY. Escuela de Artes Visuales de Oaxaca, [Online], Available: https://www.archdaily.mx/mx/750038/escuela-de-artes-visuales-de-oaxaca-taller-de-arquitectura-mauricio-rocha. [24 October 2023].
9. Elias Christoforou, Angeliki Kylili, Paris A. Fokaides and Ioannis Ioannou. (2016). Cradle to site Life Cycle Assessment (LCA) of adobe bricks. Journal of Cleaner Production, vol. 112, pp. 443-452, [Online], Available: https://doi.org/10.1016/j.jclepro.2015.09.016 [28 de July 2023]
10. Instituto de Ingeniería UNAM. Evaluación de la Huella de Carbono con enfoque de Análisis de Ciclo de Vida para 12 Sistemas Constructivos, [Online], Available: https://novaceramic.mercari.com.mx/wp-content/uploads/2021/06/emisiones_co2.pdf [16 July 2023].
11. Aristizábal Alzate E. Carlos, Gonzales Monosalva L. José, Gutiérrez Cano C. Juan. (2020). Life Cycle Assessment and Carbon Footprint Calculus for a PET Bottles Recycling Process at Medellin (ANT). Producción + Limpia. Vol. 15. pp. 7-24, [Online], Available: https://doi.org/10.22507/pml.v15n1a1. [16 July 2023].
12. North Carolina Cooperative Extension Service. LIFE CICLE ASSESSMENT (LCA) DESCRIPTION AND METHODOLOGY, [Online], Available: https://content.ces.ncsu.edu/life-cycle-assessment-description-and-methodology [16 July 2023].
13. Hernández Moreno, Silverio. (2015). Comparative life cycle analysis of three types of indoor luminaries used in buildings. Nova Scientia. vol. 7. pp: 53 -559, [Online], Available: https://www.scielo.org.mx/pdf/ns/v7n14/2007-0705-ns-7-14-00538.pdf [5 November 2023].
14. International Organization for Standardization. ISO 14040:2006, [Online], Available: https://www.iso.org/obp/ui/#iso:std:iso:14040:ed-2:v1:en. [5 November 2023].
15. International Organization for Standardization. ISO 14044:2006, [Online], Available: https://www.iso.org/obp/ui/#iso:std:iso:14044:ed-1:v1:en. [5 November 2023].
16. Yogitha Miriyala, Amanda Thounaojam, Prasad Vaidya and Amol Mangrulkar. (2022). Opportunities and challenges for LCA in India for innovative. PLEA, SANTIAGO vol. 1, pp. 486-491, [Online], Available: https://plea2022.org/wp-content/uploads/2023/03/PROCEEDING-ONLINE-FINAL-MARZO.pdf [5 November 2023].
17. GreenDelta. openLCA, [Online], Available: https://www.openlca.org/greendelta/ [16 July 2023].
18. Ecoinvent. Database, [Online], Available: https://ecoinvent.org/the-ecoinvent-database/ [16 July 2023].
19. Comisión Nacional para el Uso Eficiente de la Energía. Metodologías para la Cuantificación de Emisiones de Gases de Efecto Invernadero y de Consumos Energéticos Evitados por el Aprovechamiento Sustentable de la Energía, [Online], Available: https://www.conuee.gob.mx/work/files/metod_gei_cons_evit.pdf [16 July 2023].
20. NEHPI, LCIA: the ReCiPe model/2018/National Institute for Public Health and the Environment, [Online], Available: https://www.rivm.nl/en/life-cycle-assessment-lca/recipe [16 July 2023].
21.Museo Tamayo. Arquitectura, [Online], Available: http://old.museotamayo.org/el-museo/arquitectura/ [30 Junuary 2024]
22. Liga-Archivos, Archivo Museo Tamayo, [Online], Available: https://www.liga-archivos.org/museo-tamayo [30 January 2024]
23. ArchDaily, Clásicos de Arquitectura: Museo Tamayo/Abraham Zabludovsky & Teodoro Gonzalez, [Online], Available: https://www.archdaily.mx/mx/02-104069/clasicos-de-arquitectura-museo-tamayo-abraham-zabludovsky-teodoro-gonzalez [30 January 2024]
24. Secretaría de Cultura, INBAL, [Online], Available: https://inba.gob.mx/multimedia/prensa/galerias/19225/19225-bol._1749_brutalismo_arquitectonico_en_mexico,_una_mirada_a_la_busqueda_de_la_arquitectura_en_la_segunda_mitad_del_siglo_xx_y_el_xxi.pdf [15 December 2023]
25. Sustainable Development Goals. Ensure sustainable consumption and production patterns, [Online], Available: https://www.un.org/sustainabledevelopment/sustainable-consumption-production/ [10 November 2023]

PLEA 2024 WROCŁAW
(Re)thinking Resilience

Air Infiltration Testing and Energy Simulation of Green Dwellings in a Social Housing Project in Egypt

RANA RAAFAT,[1] SALMA ALLAM,[1] HEND FAROUH ,[2] FARAH SHOUKRY,[1] SHERIF GOUBRAN,[1]

[1]The American University in Cairo, Cairo, Egypt
[2] Housing and Building National Research Center, Giza, Egypt

ABSTRACT: This study investigated the air infiltration characteristics and energy performance of green dwellings within a social housing project in Egypt. This study aimed to evaluate the effectiveness of sustainable building practices in mitigating energy consumption and enhance building resilience facing future climate challenges. The first phase of this research involved comprehensive air infiltration testing using Blower-door testing to assess the airtightness of the building envelope. Subsequently, energy simulations were conducted using state-of-the-art modelling tools, such as Grasshopper, to predict the annual energy consumption of the dwellings. These simulations will account for various factors, such as climate and building design, providing insights into the potential energy savings achievable through sustainable architectural interventions. The social housing context introduces a socioeconomic dimension to the study, considering the affordability and feasibility of implementing green strategies. The findings of this study contribute to the growing body of knowledge on sustainable housing in emerging economies, providing evidence-based insights for policymakers, architects, and developers. Ultimately, this research seeks to promote a holistic approach to building design and construction, emphasizing the importance of air infiltration testing in creating energy-efficient and resilient housing solutions for marginalized communities in Egypt.
KEYWORDS: Air Infiltration, Energy Simulation, Green Dwellings, Social Housing, Egypt

1. INTRODUCTION

Air infiltration is the uncontrolled flow of air into and out of a building through cracks, gaps, and other openings in the building envelope [1]. Residential buildings are the most common buildings in the world, with approximately two billion dwellings [2]. In Egypt, residential buildings consumed approximately 40.5% of the total electricity consumption during 2020/21 [3]. The government is taking proactive measures to address climate concerns. Social housing programs, which aim to provide low-income households with affordable homes, are no exception. It was Egypt's first national green-building effort and the region's first green social housing initiative. The Green Pyramid Rating System (GPRS) [4] has been implemented by the program, which scores at least seven areas: sustainable site and design quality, construction materials and resources, water efficiency, energy efficiency, health and wellness, management, and innovation [5]. One strategy seeks to reduce energy losses through the envelope by improving heat transmission by conduction, which has been extensively solved by using more and better thermal insulation. This study presents the results of air infiltration testing using blower door tests in 8 green dwellings in a social housing project in Egypt. The infiltration values were used in an energy simulation to estimate the energy consumption of the dwellings. The findings of this study suggest that air infiltration testing can be used to identify and quantify air leakages in buildings, revealing not only the potential for significant energy savings, but also a key to unlocking building resilience in social housing.

1.1 Fundamentals of Air Infiltration through Building Envelopes

The airflow as a function of the pressure gradient across the building envelope is represented using the Power Law Equation (1):

$$Q=C_L (\Delta P)^n \quad (1)$$

Where Q - the average airflow rate of pressurization and de-pressurization (m^3/h);

C_L - the air leakage coefficient ($m^3/(h \cdot Pa^n)$);

ΔP - the pressure difference between interior and exterior (Pa) ;

n - the flow exponent that characterizes the flow and is usually in the range from 0.5 to 1 (dimensionless).

The parameters that constitute Equation (1) must be extracted from all infiltration tests to estimate the air leakage quantity and characteristics. To compare different envelopes' performance, airflow, Q, is normalized according to ISO 9972 [6], using the following building parameters: exterior envelope surface area (AE in m^2), net floor surface area (AF in m^2), and internal volume (V in m^3). The resulting infiltration parameters are detailed in (Table 1).

Table 1: Standardized airtightness parameters at 50 Pa

Parameter	Description	Equation	Unit
Q_{50}	Average airflow	CL (50)n	m^3/h
n_{50}	Air change rate	Q_{50}/V	h^{-1}
w_{50}	Specific leakage	Q_{50}/AF	$m^3/h{\cdot}m^2$
q_{50}	Air permeability rate	Q_{50}/AE	$m^3/h{\cdot}m^2$

1.2 Testing methods for air infiltration

The measurement of air leakage through a building envelope is crucial for assessing its energy performance and identifying the potential energy waste. Two commonly employed methods for this purpose are the fan pressurization method, Blower Door Testing (BDT), and the tracer gas method. The blower door test has a variable speed fan to adjust the pressure difference and an aluminium frame to seal the fan tightly into the doorjamb. It measures both the airflow through the fan and the pressure difference between the house inside and outside. Tracer gas testing, as described in ASTM E741 [7] offers an alternative method for measuring air leakage. This method involves injecting a small amount of tracer gas into space and allowing it to mix with the interior air. The tracer gas concentration is monitored over time, and airflow and air change rates are determined based on a mass balance equation. Given its practicality and ease of implementation, the blower door testing method has been selected for this study.

To quantify air infiltration in buildings under specific pressure differences across the building envelope, ISO 9972:2015 [6] and ASTM E779:2010 [8] are the most widely used standards for field measurements of air permeability of buildings or parts of buildings. The test method is conducted by creating mechanical pressurization or de-pressurization of a building until reaching a specific pressure difference between indoors and outdoors and measuring the airflow rate.

2. METHODOLOGY

This study employs the blower door test methodology according to ISO 9972 standard [6] to quantify air infiltration. Consequently, building energy simulation is used to predict energy consumption. The integration of information from energy simulations, air infiltration testing, and a socioeconomic analysis form the basis for a thorough study. This analysis's depth and scope are increased by comparative field testing conducted within the same local context and benchmarked against international knowledge.

2.1 Description of tested dwellings

The present work collectively analyses pressurization tests carried out in 8 dwellings located in the New Administrative Capital in Egypt. Geographically, the dwellings are located in the hot dry climatic zone (Bwh) according to the Koppen climate classification [9]. The selected units comprised green buildings, with identical six-story frame areas, floor areas, and volumes, as depicted in (Figure 1). The dwelling area is 65.50 m^2, with a volume of 178.81 m^3, and an envelope area of 94.14 m^2. with a frame area of 11.50 m^2, and a total frame length of 34.60 m^2. The construction of green dwellings differs from conventional dwellings in using cement bricks and concrete floors and slaps instead of clay bricks. The fenestration elements are PVC window frames with low E glass instead of wooden windows in conventional dwellings.

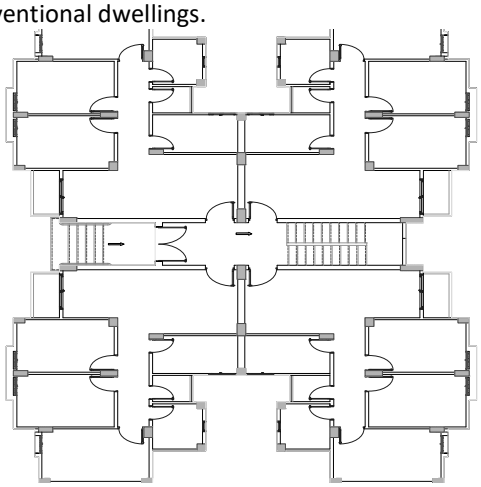

Figure 1: Green housing dwellings floor plan

2.2 Data Validation

All the tests reported in this study meet the requirements of ISO 9972 [6]. Namely, (1) the indoor–outdoor temperature differential multiplied by the building height was less than 250 mK; (2) the wind speed near the ground was lower than 3.0 m/s during the time of the testing; (3) the correlation coefficient between ΔP and the airflow was greater than 0.96 when determining the airflow coefficient C and airflow exponent n using a least squares technique; and (4) the airflow exponent ranged between 0.5 and 1.0.

The first two conditions were checked using the ambient condition measurements completed for each test. To check Conditions 3 and 4, the corrections for zero flow pressure difference, actual and observed airflow through the fan, and internal/external air density differences were applied to the measured pressure differences and airflow rates. Then, the corrected airflow rate through the building envelope was plotted on a log–log plot against the corresponding pressure difference. (Figure 2) shows an example of the graphs produced with a correlation coefficient of 0.999. In conclusion, all the measurements fulfil the corresponding requirements in ISO 9972, and thus the test results were considered valid.

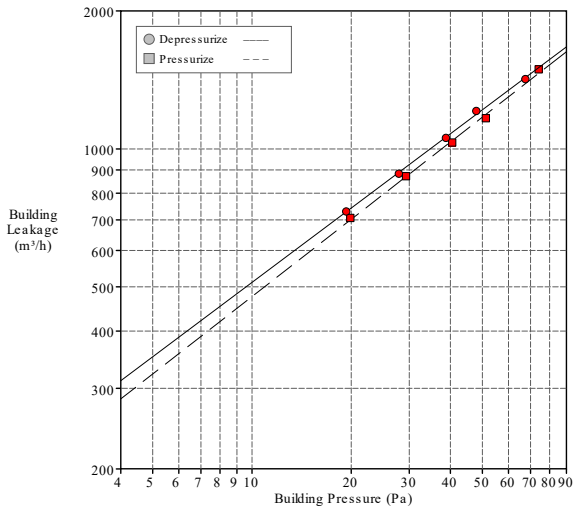

Figure 2: log-log plot against the corresponding pressure difference.

2.1 Air Infiltration Testing

The tested dwellings weren't furnished or occupied during this study. All units' electric, network, and communication systems were already installed, and their exterior doors and windows were installed and functional. The exterior windows and doors were all closed during the test, while the internal doors were all open. The drainage traps in toilets, sinks, and showers were filled with water before the test. To assess air infiltration in the housing units, blower door tests were performed using the Minneapolis Blower Door TM System [10] following the guidelines outlined in ISO 9972:2015 [6] as shown in (Figure 3). During the tests, the applied pressure difference over the building envelope was adjusted in ten-point increments (at 10 to 15 Pa intervals), starting at 10 Pa and ending at 75 Pa, for both pressurization and de-pressurization.

Figure 3: Blower door configuration on tested dwellings.

2.1 Energy simulation input

Following the blower door tests, simulation modeling [11] was conducted to examine the impact of air infiltration on energy consumption. Grasshopper is the simulation program used for the study. A modelling and simulation engine called Energy Plus is used to examine how much energy is used in buildings based on the heating and cooling loads as well as the available heating or cooling systems. Spaces must be converted into thermal zones to identify the attributes required for calculating the energy loads. The program used to determine the building load uses the thermal balancing method advised by ASHRAE for midrise residential buildings [12]. The simulation uses hourly values of climatic data, such as temperature and humidity, for Cairo, Egypt. By integrating these parameters, the simulation models aimed to analyze and quantify the relationship between air infiltration and energy consumption in the studied housing units. The simulation process considered the region's specific climatic conditions, the building envelope's thermal characteristics, and the HVAC systems' efficiency to accurately evaluate the energy performance as shown in (Table 2). This combined approach of field measurements and simulation modelling enables a thorough evaluation of air infiltration and its impact on energy consumption. The data collected during blower door tests provides precise measurements of air infiltration rates. The simulation models, on the other hand, provide a more comprehensive understanding of the impact of air infiltration on energy consumption under varying conditions.

Table 2: Simulation Parameters Input

Characteristics	Specifications
Building Model	Midrise Residential
Window	Glazing: Single 3mm Clear Glass
Walls	Exterior: Cement Brick, Interior: Cement Brick
Floor	Concrete slab, tile flooring
Lighting Schedule	3 W/m^2
Occupancy	0.02 ppl/m^2
Load Schedule	6 W/m^2
HVAC	Split Units

3. RESULTS AND DISCUSSION

3.1 Airtightness

The measurements were carried out in a social housing building to determine building properties such as average airflow, air change rate, air permeability, and Specific Leakage rate (n_{50}, q_{50}, and w_{50}) of the buildings using BDT. Table 3 shows the BDT results of the selected dwelling. The results presented in (Table 3) indicate that:

- The average air change rate and the air permeability rate for the tested sample were 8.44 h^{-1} and 15.50 $m^3/(h \cdot m^2)$, respectively.
- Higher Floor levels in tested dwellings have a higher average value of airtightness parameters.

In a study carried out by Ramos et al. [13] the airtightness of 49 units of two different social housing neighbourhoods was tested. A sample of 25 flats was organized for the rehabilitated case and one with 24 flats for the non-rehabilitated case. The sample was divided into two groups: rehabilitated and non-rehabilitated neighbourhoods, as well as modified and unmodified units. The second case presented an average n_{50} of 8.86 h^{-1} with an average n_{50} of 8.56 h^{-1} for the units with modifications and 9.21 h^{-1} for the units without modifications. Since this study investigates green dwellings, which are considered modified units, it can be compared to the non-rehabilitated modified units.

Table 3: The Airtightness parameters results of Blower Door Testing

Dwelling	Floor	Q_{50} (m^3/h)	n_{50} (h^{-1})	q_{50} ($m^3/h \cdot m^2$)	w_{50} ($m^3/h \cdot m^2$)
G1	0	1195.00	6.68	12.69	18.24
G2	0	1431.00	8.09	15.20	21.85
G3	1st	1324.00	7.49	13.64	20.21
G4	1st	1267.00	7.16	13.05	19.34
G5	3rd	1685.00	9.53	17.36	25.73
G6	3rd	1691.00	9.56	17.42	25.82
G7	4th	1599.00	9.04	16.47	24.41
G8	5th	1765.00	9.98	18.18	26.95
Mean		**1494.62**	**8.44**	**15.50**	**22.81**
Median		**1515.00**	**8.56**	**15.83**	**23.12**
Std. Dev.		**218.28**	**1.24**	**2.16**	**3.33**

Another study in Spain done by Fernández-Agüera et al. [14] on 45 homes in seven open gallery-type social housing buildings in southern Spain. The sample consisted of reinforced concrete frame, and continuous slab buildings with ceramic or cement tile flooring. Only kitchens and bathrooms had continuous suspended ceilings. Vertical envelope consisted of cavity-insulated walls: ceramic-brick wall outside, air chamber with insulation panel, and thin ceramic-brick plastered inner sheeting. Party walls consisted of thin hollow brick (approximately 15 cm thick) partitions, plastered on both sides. All windows, whether side-hinged or horizontal-sliding, had aluminium frames and double glazing and were fitted with built-in roller blinds ('Monoblock' system). The field study consisted of pressurisation/de-pressurization tests performed with a Blower Door device supplemented with infrared thermography and smoke tests. The highest n_{50} value was 8.7 h^{-1}, whereas the lowest, was 3.2 h^{-1}. The mean value was 5.72 h^{-1}, which is slightly better than the case studies in this paper.

Field measurements were performed in the same local context as this study by Raafat et al. [15], which focused on 20 residential dwellings built with heavy construction materials and subjected to extensive characterization and testing. The average air leakage and the air permeability rate for the tested sample were 6.14 h^{-1} and 17.3 $m^3/(h \cdot m^2)$, respectively. The sample selected was a random group of newly constructed dwellings in New Cairo that represent the typical characteristics of the available residential stock in this location. The sample was chosen to feature dwellings in the same development projects, others completed by the same contractors in different locations, and a group of randomly selected dwellings with different finishing qualities and properties. Despite that, the tested dwelling in this study is not considered green or modified but the average value is tighter than the dwellings in the social housing project.

Comparing the results with the literature, see (Figure 4), the average values found are not distant from the non-rehabilitated modified units in the social housing project in Portugal. The study conducted in Spain and Egypt shows better air tightness values than this paper's case studies.

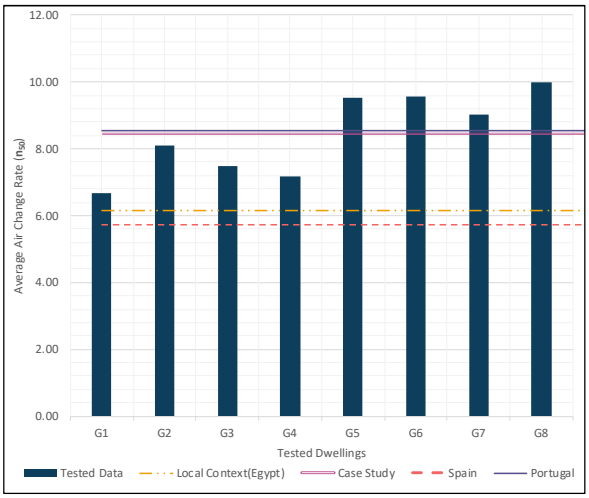

Figure 4: Airtightness variability found in international studies.

3.2 Air Infiltration impact on energy consumption

By performing an energy simulation using Rhinoceros 3D and Grasshopper software for air infiltration testing results, the results are depicted in (Table 4), and (Figure 5) show the energy chart balance for the total energy consumption of the building. The simulations were conducted to estimate the energy consumption of the buildings under the given temperature settings. The study considers temperature range from 20 °C to 27 °C, within the recommended range as per ASHRAE Guideline [13]. By analyzing the simulated energy consumption, the study aims to evaluate the energy implications associated with the air infiltration characteristics observed in the green units.

Table 4: Annual Simulation Results for Tested and the Corresponding Dwellings

Dwelling	Façade Orientation	Floor Level	Cooling Load (KWh)	Heating Load (KWh)
G1	NW	0	2370.6	3035.2
G1 – C*	SW	0	1909.0	3012.9
G2	SE	0	2737.7	2665.6
G2 – C*	NE	0	3088.2	2626.8
G3	NW	1st	4887.1	3111.7
G3 – C*	SW	1st	4523.1	2930.8
G4	SE	1st	5770.7	3254.7
G4 – C*	NE	1st	6087.8	3279.1
G3 – C*	NW	2nd	5560.1	3281.0
G3 - C	SW	2nd	5213.2	3060.3
G4 - C*	SE	2nd	6509.7	3705.3
G4 - C*	NE	2nd	6825.0	3741.0
G5	NW	3rd	5831.2	3477.9
G5 - C*	SW	3rd	5517.0	3262.6
G6	SE	3rd	6753.1	4006.5
G6 - C*	NE	3rd	7038.3	4039.2
G7	NW	4th	6217.1	3707.8
G7 - C*	SW	4th	5933.0	3472.2
G8 - C*	SE	4th	7106.1	4242.8
G8 - C*	NE	4th	7351.4	4281.2
G7 - C*	NW	5th	9056.7	5441.2
G7 - C*	SW	5th	8909.6	5196.9
G8	SE	5th	9901.7	5290.4
G8 - C*	NE	5th	9986.1	5271.6
Mean			**6045.1**	**3724.8**
Median			**6010.4**	**3475.0**
Std.Dev.			**2168.4**	**845.1**

*C: Corresponding simulated Unit

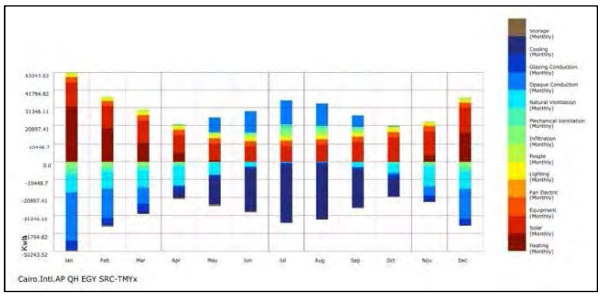

Figure 5: Energy Balance Chart for the whole building.

The energy simulation model takes air infiltration values as input. Because there were 8 tested units, their values were used as input for their corresponding unit in terms of façade orientation and dwelling floor level within the building. The average annual energy consumption for cooling load is 6045.10 KWh, and for heating load is 3724.8 KWh. To compare it to other studies, the EUI (Energy Use Intensity) parameter is used, indicating 92.29 KWh/m^2·yr for cooling load, and 56.87 KWh/m^2·yr. Also, Comparing the cooling and heating demand in relation to the air change rate (n_{50}), Pearson's significance as shown in (Table 5) and (Figure 6) is < .001.

Table 5: Correlation Table

Variable		Cooling Load	Heating Load
Air Change Rate	Pearson's r	0.648	0.644
	p-value	< .001	< .001

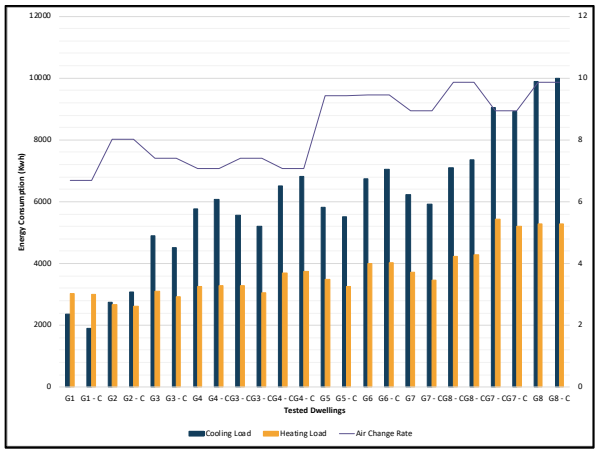

Figure 6: Relation between Energy Consumption and Air Change Rate

A study done in Spain [16] analyzed pressurization tests carried out in 13 dwellings located in residential blocks in the center and north of Spain, which is exposed to mesothermal, and continental climate, indicating that the focus of the energy demands of air conditioning should be on the coldest months. Then, the research was conducted by using computer simulation software: the infiltration modeling started with geometry creation for the buildings in Design Builder. Winter demand ranged from 72.32-30.76 KWh/m^2 and summer demand ranged from 33.11-2.75 KWh/m^2. The results show that infiltration accounts for between 10.5 and 27.4% of winter energy demand in buildings built under the current Spanish Building Code, between 21.9 and 27.0% in buildings subject to CT-79, and between 11.3 and 13.0% in old buildings without energy regulation (but restored by their owners). These values develop better results than the investigated dwellings presented in this study.

4. CONCLUSION

This study's findings demonstrate how air infiltration affects energy consumption in new green social housing dwellings in Egypt. The testing was conducted in eight residential structures. The average air change rate and the air permeability rate for the tested sample were 8.44 h^{-1} and 15.50 m^3/(h·m^2), respectively. Comparing the results with the literature, the average values found are not distant from the non-rehabilitated modified units in the social housing project in Portugal, which was 8.56 h^{-1}. The study conducted in Spain and Egypt shows better air tightness values than this paper's case studies with an average value of 5.72, and 6.14 h^{-1}, respectively.

Using the Rhinoceros 3D and Grasshopper software, the energy performance analysis confirms

the potential for energy savings linked to decreased air infiltration. The average annual energy consumption for cooling load is 6045.10 KWh, and for heating load is 3724.8 KWh. To compare it to other studies, the EUI (Energy Use Intensity) parameter is used, indicating 92.29 KWh/m^2·yr for cooling load, and 56.87 KWh/m^2·yr. Comparing the results with a study done in Spain, Winter demand ranged from 72.32 - 30.76 KWh/m^2 and summer demand ranged from 33.11 - 2.75 KWh/m^2, which is much better than the results investigated in this study. Climate zone is considered a major factor as a difference between the context of the two studies.

Significant energy savings can be achieved by reducing air leakage through enhanced building envelope design, shown as per Pearson's correlation test between energy consumption and air change rate, which showed a significance of <0.001. Improving the building envelope to reduce air infiltration not only results in immediate energy savings but also strengthens a building's resilience to future challenges. A tightly sealed building minimizes the energy required for heating and cooling by fostering stable indoor temperatures and reducing reliance on external climate conditions. A smaller carbon footprint, cheaper energy costs, and a reduced dependency on fossil fuels are all results of this enhanced thermal performance. The findings of this study show that minimizing air infiltration in social housing units has the potential to save energy and enhance building resilience in low-income communities. By creating a more tightly sealed building envelope, air infiltration reduction strategies can help these units better withstand extreme weather events, power outages, and other climate challenges. This can lead to increased safety, reduced damage, and faster recovery times, ultimately protecting vulnerable communities and minimizing the economic and social costs of climate-related hazards. Future investigation is required to examine the location and orientation of dwelling variances and building-specific elements that affect air infiltration rates, to provide evidence-based guidance for policy and program development aimed at improving building resilience and energy efficiency in social housing. Identifying key factors influencing air infiltration rates will help prioritize interventions and allocate resources most effectively.

ACKNOWLEDGEMENTS

The research team organized by the Housing and Building National Research Center "HBRC" and the American University in Cairo "AUC" would like to acknowledge the support received from the Social Housing and Mortgage Finance Fund and the funding received from the Office of the Associate Provost for Research, Innovation, and Creativity at the American University in Cairo. The team would also like to thank the many research assistants and interns who helped in the data collection and site testing.

REFERENCES

1. ASHRAE, ASHRAE Handbook of Fundamentals. (2017).
2. J. Feijó-Muñoz et al., (2019). Energy impact of the air infiltration in residential buildings in the Mediterranean area of Spain and the Canary Islands, Energy Build., doi: 10.1016/j.enbuild.2019.02.023.
3. Egypt Electricity Holding Company (EEHC), (2021). Egypt Electricity Holding Company Annual Report, pp. 1–90, [Online]. Available: http://www.moee.gov.eg/test_new. Accessed 1 Feb 2022
4. S. Attia, (2014). The usability of green building rating systems in hot arid climates, 1st Int. Conf. Energy Indoor Environ. Hot Clim., pp. 65–72.
5. W. Bank, (2020). Report No: pad3356 program paper on a proposed additional loan in the amount of us $ 500 million to the Arab republic of Egypt and a proposed restructuring of the inclusive housing finance program-for-results finance, Competitiveness and Innovation Glob.
6. International Organization for Standardization (ISO), (2015). ISO 9972:2015: Thermal performance of buildings — Determination of air permeability of buildings — Fan pressurization method. ISO/TC 163/SC 1.
7. American Society for Testing and Materials International,(2008). ASTM E 741 Standard Test Method for Determining Air Change in a Single Zone by Means of a, ASTM Int. Stand., vol. 00, no. 2006, pp. 1–17, doi: 10.1520/E0741-11R17.ization.
8. American Society of Testing and Materials, "ASTM Standard E779-87 Standard Test Method for Determining Air Leakage Rate by Fan Pressurization, (2010). ASTM B. Stand., vol. 4, pp. 1–11, [Online].
9. M. Kottek, J. Grieser, C. Beck, B. Rudolf, and F. Rubel, (2006). World map of the Köppen-Geiger climate classification updated, Meteorol. Zeitschrift, vol. 15, no. 3, pp. 259–263, doi: 10.1127/0941-2948/2006/0130.
10. B. Ring, "THE ENERGY CONSERVATORY MODEL 3 MINNEAPOLIS BLOWER DOOR".
11. E. Elbeltagi and H. Wefki, (2021). Predicting energy consumption for residential buildings using ANN through parametric modeling, Energy Reports, vol. 7, pp. 2534–2545, doi: 10.1016/j.egyr.2021.04.053.
12. T. Weston et al., (2007). Energy-efficient design of low-rise residential buildings," ASHRAE Stand., vol. 2018, no. STANDARD 90.2, pp. 1–52.
13. N. M. M. Ramos et al., (2015). Airtightness and ventilation in a mild climate country rehabilitated social housing buildings – What users want and what they get, Build. Environ., doi: 10.1016/j.buildenv.2015.04.016.
14. J. Fernández-Agüera, S. Domínguez-Amarillo, J. J. Sendra, and R. Suárez, (2016). An approach to modelling envelope airtightness in multi-family social housing in Mediterranean Europe based on the situation in Spain," Energy Build., doi: 10.1016/j.enbuild.2016.06.074.
15. R. Raafat, A. Marey, and S. Goubran, (2023). Experimental Study of Envelope Airtightness in New Egyptian Residential Dwellings, Buildings, vol. 13, no. 3, p. 728 doi: 10.3390/buildings13030728.
16. A. Meiss and J. Feijó-Muñoz, (2015). The energy impact of infiltration: a study on buildings located in north central Spain, Energy Effic., doi: 10.1007/s12053-014-9270-x.

PLEA 2024 WROCŁAW
(Re)thinking Resilience

The Carbon Impact of Buildings' Slabs:
Hotspots, Challenges, and Opportunities

YASMINE DOMINIQUE PRIORE,[1,2] LUCILE SCHULTHESS,[1] THOMAS JUSSELME[1]

[1]Energy Institute, University of Applied Science of Western Switzerland (HEIA-FR, HES-SO), Fribourg, Switzerland
[2] Chair of Sustainable Construction, ETHZ, Zürich, Switzerland

ABSTRACT: Considering the urgent call to tackle climate change, reducing greenhouse gas emissions from the built environment becomes a priority. Slabs in multi-family houses are responsible for a high share of building's life carbon emissions due to their intrinsic multi-functional nature and high quantity of materials. This research evaluates the impact of the different functional layers within a slab component, compares alternative materials with regards to the functional requirements, and assesses promising solutions in the context of element-based carbon budgets. Life cycle assessment, following established standards, is applied to a representative library of slab components. Results reveal that material choices for the structural layer significantly influence the environmental impact, with wood structure exhibiting five times lower carbon emissions compared to a traditional concrete slab and meeting the most stringent carbon budgets for the structural layer. The screed layer is identified as a significant contributor to the overall impact, holding an important relationship between its thickness and mass and the level of acoustic insulation. Only limited options are available to replace the cement-based screed in its functionality and although the acoustic performance and thickness hold a non-linear relationship, further studies are needed to confidently replace this layer with alternative materials.
KEYWORDS: Carbon, Slabs, Life-Cycle, Emissions, Buildings

1. INTRODUCTION

As underscored in the latest IPCC report [1], the climate is undergoing unprecedented changes with tangible impacts on societies. Urgent and reinforced efforts are imperative to reduce the rise in emissions and mitigate further global warming, necessitating a fast transition towards climate-resilient development. The built environment holds an important role in addressing climate concerns, contributing approximately 40% of annual anthropogenic greenhouse gas (GHG) emissions through both operational and construction activities. Although improvements on the operational side are noticeable [2], mastering the embodied impact remains crucial for achieving overarching climate goals [3]. Within this context, multi-story building's slabs have emerged as a critical environmental hotspot, constituting 12% to 32% of a building's overall carbon footprint due to their extensive surface area, structural function, and reliance on carbon intensive materials [4]. Slabs in buildings serve multiple functions beyond structural support, i.e. thermal inertia, technical systems distribution, and acoustic properties. Given the complexity of this element, the following research questions arise: which functional layers or performance requirements most significantly contribute to this elevated impact? How do alternative materials and design options compare in terms of emissions reduction while meeting performance requirements? Finally, considering element-based carbon budgets [5], which solutions show promise for optimizing the environmental impact of slab elements? In the literature, the topic of slab elements and their environmental contribution is mainly discussed with regards to their structural function [6,7]. A research gap is identified in the relation of other functional requirements of slabs to the overall carbon impact and the challenges of using alternative materials and designs in fulfilling these requirements.

2. METHODOLOGY

To tackle the opportunities of slabs in reducing the environmental impact of multi-family buildings, a first review of existing slab systems and common practices is conducted. This review focuses on systems available in Switzerland such as those proposed in annex D of the SIA 2032 [8] and the lignum database [9] for wood-based structures but the library could be extended with further typologies and the same methodology applied. In a second step, the whole system is decomposed into functional layers following the eCCC categorization [10] to allow a straightforward comparison and to be able to pinpoint the hotspots inside each system. Intermediate slabs are comprised, as shown in *Figure 1*, of a structure (C04.01), a floor covering (G02), and a ceiling finish (G04). The floor covering is further subdivided into support G02.01 (screed and insulation) and finishing G02.02 (ex: parquet or ceramics). The screed serves multiple functions; it provides acoustic mass, it can accommodate the heating distribution, and acts as a levelling layer to prepare for the finishing layer.

Suspended ceilings can contain technical installations and provide a finishing to the lower structure.

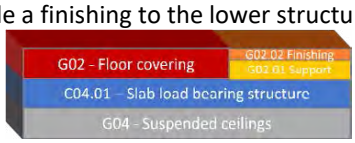

Figure 1: Decomposition of the slab into categories following the eCCC classification.

Then, a comparative life cycle assessment (LCA) is conducted by varying parameters such as thickness and materials. Results are discussed in terms of challenges and opportunities in achieving performance requirements while reducing carbon impacts. Finally, systems are compared with carbon budgets based on allocation of global budgets to Swiss buildings [11] and element-based decomposition [5].

2.1 System boundaries

The slab system, encompassing all layers from the lower to the upper finishing, is considered. Heat distribution is discussed, as floor heating systems are often part of the upper finishing, in terms of screed materials and limitations but no analysis on efficiency or carbon impacts is conducted. Horizontal distribution of ventilation ducts, electrical cables, and sanitary systems are also often integrated in the slab (either directly in the structural layer or in the false ceiling) but displacement in vertical distribution is also possible, therefore impacts are not included in the boundaries for this study. The comparison of solutions throughout the paper is made possible by accounting for equivalent fixed functional requirements and varying one parameter at the time. Functional requirements are defined based on SIA and ISO standards. These can vary depending on the national context and would affect the feasibility of the proposed solutions, but the function to carbon relationships are not affected.

2.2 Carbon impact and storage

Life Cycle Assessment is conducted following the standard SIA 2032. The assessment includes phases A1 to A3, B4, and C1 to C4 as per definition in EN15804. The impact category chosen is GWP100 and the unit is $kgCO_{2eq}$ per functional unit. The quantification of embodied emissions is reported in $kgCO_{2eq}$ per square meter of building element (BE) and year. Emission factors for construction materials are taken from the Swiss KBOB database 2022 version 4 (2023). EPDs or other databases can be used for the analysis to better reflect impact factors outside the Swiss context. The biogenic carbon content of materials, in kgC, is also extracted from the KBOB database and converted into an amount of CO_2 sequestered according to EN 16449:2014. The GWP_{bio} method [12] is also employed for the evaluation of the different systems. The method determines the benefits of delaying biogenic emissions through storage by defining indexe according to lifetime of components (SIA2032 - AnnexC) and rotation of the species utilized. The rotation periods are determined based on literature 70 years for wood products [13] and 1 year-crop rotations for fast growing materials.

2.3 Parametrization and analysed variations

The following four main functional parameter have been analysed:

- Structural layer
- Acoustic requirements
- Floor finishing materials
- Heating distribution.

For each parameter, variations in terms of material and/or thickness have been implemented to grasp the potential opportunities of decreasing the carbon impact while fulfilling the functional requirements.

Thermal requirements are not accounted for as the focus is on intermediate slabs and no specific therma requirement is specified. An insulation layer is sti present but for acoustic performance.

Dimensioning of structural materials for equivalen spans are taken from the Lignum database. Acousti requirements are evaluated based on ISO norm 12354 1/2 by combining the screed and the insulation laye and by varying thickness and materials. Alternative materials for floor finishings are examined based on commonly built systems. Finally, incorporation of the heating distribution in the screed layer is discussed through different screed materials and thicknesses.

3. RESULTS AND DISCUSSION

Results are presented first as a general overview o the systems commonly implemented in the marke and then by comparing alternative materials and/o dimensions with regards to the main functiona requirements: structural, acoustical, floor finishings and heating distribution. Finally, analysed variation are compared with element-based carbon budgets.

3.1 Current practices - overview

Overall, the six slab systems depicted in *Figure* are considered as common current practices. The structure typically consists of a 25cm concrete slab o a wood-concrete composite. Alternatively, it can b entirely made of wood, employing a joist system tha entails a main structure with robust beams supportin thinner planks to form a solid floor. The ceilin finishing is usually direct paint cover (in the case of concrete slab) or a suspended gypsum ceiling. The floor finishing is mainly composed by either parquet o ceramics while the support tends to always use a 7cm cement screed with 2cm EPS acoustic insulation.

In new constructions in Switzerland, concrete slab remain the most widely used system. This is usuall

due to cost of materials, easier integration of horizontal distribution of systems, and general culture.

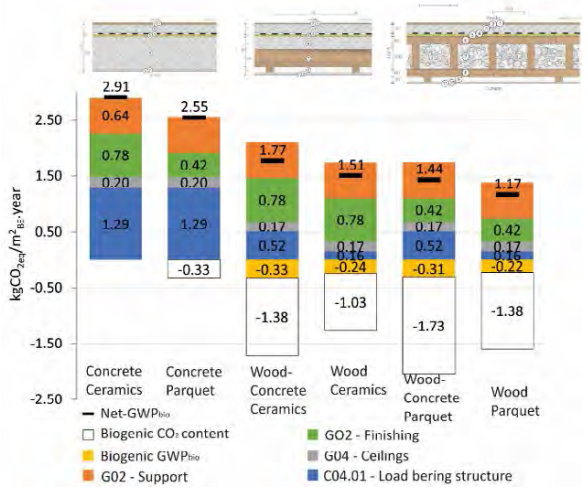

Figure 2: Main slab systems analysed – three structural materials; two types of ceiling; two types of finishing.

A difference of 1.74 $kgCO_{2eq}/m^2_{BE}$.year can be observed in net-GWP_{bio} from the concrete slab with ceramic finishing to the wood slab with parquet, corresponding to a 60% reduction from the standard. The impact of the concrete slabs is dominated by the structural layer while the wood and wood-composite shift their impact to the finishing and the support.

3.2 Structural function

The primary function of the intermediate slab is structural. Designed to withstand vertical loads, slabs also play a crucial role in transferring horizontal forces, such as those induced by wind or seismic activity, to the walls. These walls, in turn, transmit these forces to the foundations. Several parameters come into play for the sizing and selection of a specific type of slab.

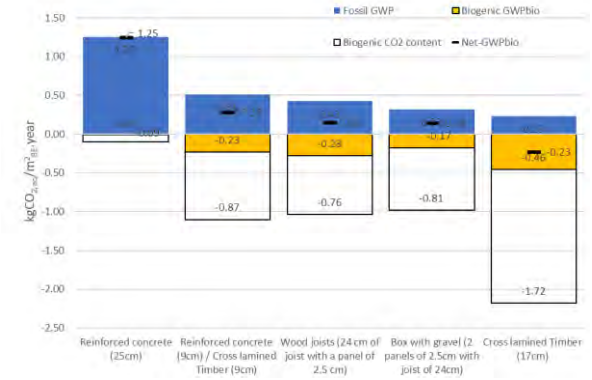

Figure 3: Example of structural layer based on Lignum database for a span of 6m [9].

For equivalent span capability (*Figure 3*), Cross Laminated Timber (CLT) holds five times lower carbon impact than a traditional reinforced concrete system. A wood-concrete composite structure, with a 50/50 ratio, presents an interesting middle option with less than half the impact compared to the base. This system could also be further optimized in its concrete-wood ratio to further decrease its environmental impact. Opting for a wooden structure instead of concrete can significantly reduce Global Warming Potential (GWP), decreasing from 1.25 to 0.23 $kgCO_{2eq}/m^2_{BE}$.year (See *Figure 3*). Additionally, when factoring in biogenic carbon, the environmental benefits become even more pronounced. The biogenic CO_2 content of the systems containing wood surpasses in all cases the fossil GWP and when applying the GWP_{bio} method, the CLT system reaches a negative net- GWP_{bio}, implying a positive impact on the climate.

However, mitigating the carbon footprint of the structural layer extends beyond material choice. Proper structural design is crucial. The thickness of the elements varies depending on the spans, the structural design, and the loads. Reducing the weight of functional layers above the structural layer also contributes to lighter support structures [14].

Furthermore, it must be noted that the dimensioning of the structural layer not always only relates to its structural function. More than half of the commonly implemented 25cm height of the reinforced concrete slab often serves as space for integration of technical horizontal distribution with ventilation ducts' diameters of up to 16cm. Therefore, the impact of the concrete slab depicted in *Figure 3* could be reduced if only the structural requirements were considered.

3.3 Acoustic function

Beyond its structural function, the slab must provide sound insulation. The purpose is to minimize the transmission of airborne noise, which includes sounds propagated through the air, as well as impact noises transmitted through the structure. This function is usually performed by the structure (C04.01) in homogeneous systems and by the support (G02.01) in "sandwich" systems.

For a moderate indoor sound emission, typical of residential and office spaces, with average sensitivity and considering a weighted evaluation level, the accepted values are L' <= 53 dB for impact noise and Di >= 52 dB for airborne noise [15]. For a homogeneous structure, the impact sound level ($L_{n,e,eq}$) and the weighted reduction index (R_w) can be calculated simply using the equation [16,17]:

$$L_{n,e,eq} = 164 - 35\log(m') \quad (1)$$

$$R_w = 37.5\ log(m') - 42 \quad (2)$$

Where m' is the mass per unit area of the structural slab (kg/m²). With the goal of maximising R_w and minimizing L, it is evident the important role that mass has on acoustic performance. Therefore, giving a net advantage to concrete structures (ca. 600kg/m²) in contrast to average wood structures (ca. 120kg/m²).

The decoupling of the screed from surrounding elements and the use of insulating material creates a

"sandwich" effect that dampens noise. A poured floating screed, with a flexible intermediate layer, follows the mass-spring-mass principle to prevent the transmission of floor vibrations to the supporting structure and vice versa. These techniques are commonly employed to minimize noise propagation and enhance acoustic comfort within spaces. In this scenario, the level of impact sound is:

$$L_{n,d,w} = L_{n,e,eq} - \Delta L_w \quad (3)$$

To increase impact noise insulation, two crucial parameters are the dynamic stiffness of the insulation material (s') and the mass of the floating screed (m') [18] as depicted in the formula for the weighted reduction in sound impact (ΔL_w). Reinforcing, again, the importance of mass (of the screed in this case) to the acoustic performance. Explaining the wide use of thick cement-based screeds (ca. 130kg/m^2).

$$\Delta L_w = 13log_{10}(m') - 14.2log_{10}(s') + 20.8 \quad (4)$$

It must be noted that this analysis does not delve into different frequencies and indirect noise effects and the focus is given to direct impact noise attenuation. However, indirect effects, can be significantly mitigated with meticulous planning and well-thought-out connections.

3.3.1 Insulation material

The dynamic stiffness refers to the ability of a material to respond to sound vibrations within a specific frequency range. More specifically, it measures the resistance of the material to deform in response to sound waves. A lower dynamic stiffness indicates an increased ability of the material to attenuate vibrations and, consequently, to provide better sound insulation.

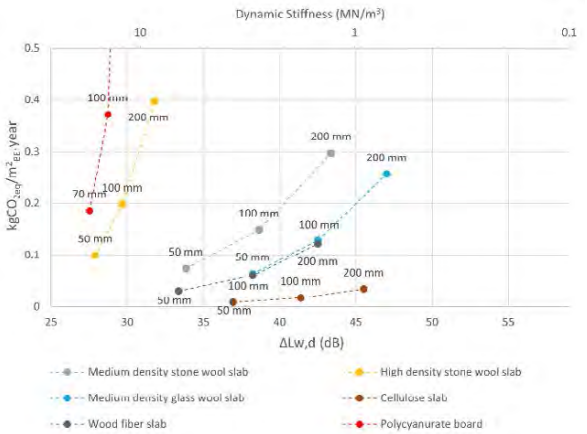

Figure 4: Direct impact sound reduction versus carbon impact for different insulation materials with a concrete slab and a floating screed [19].

The dynamic stiffness involves considering the Young's modulus, the thickness of the insulating material, the airflow resistivity, and the density. Generally, the greater the material thickness and density, the higher the dynamic stiffness, consequently resulting in higher carbon impacts.
Using wood-based materials, such as cellulose, proves beneficial. In addition to a favourable carbon footprint, cellulose offers good acoustic insulation with a low thickness. For instance, choosing a cellulose insulation of 50mm thickness instead of the commonly used stone wool reduces carbon emissions by 0.07 $kgCO_{2eq}/m^2_{BE}$.year and increases acoustic insulation by 3dB. This not only ensures lower environmental impact but also enhanced acoustic performance (see Figure 4). Finally, it is worth noting that not all materials present the same slope and that the thickness is not linearly correlated to the acoustic reduction.

3.3.2 Screed thickness

It has been observed that increasing the thickness of the screed has only a minimal impact on acoustics beyond a certain thickness [7].

30 MN/m^3 represents the maximum dynamic stiffness limit for insulation materials according to the standard. Dynamic stiffness between 6 MN/m^3 and 9 MN/m^3 are typical values for glass wool of 30mm, with different densities. However, specific values from suppliers are often challenging to obtain.

Thus, it can be observed that for the same weighted reduction in sound impact of ΔL_w=35 dB, with s'=6 MN/m^3 the screed has a thickness of 46 mm compared to 73.1 mm with s'=9 MN/m^3. This result decreases the carbon emissions from 0.26 to 0.17 $kgCO_{2eq}/m^2_{BE}$.year, translating to a 0.09 $kgCO_{2eq}/m^2_{BE}$.year reduction for the same level of insulation depending on the insulation material and reducing the screed thickness (*Figure 5*).

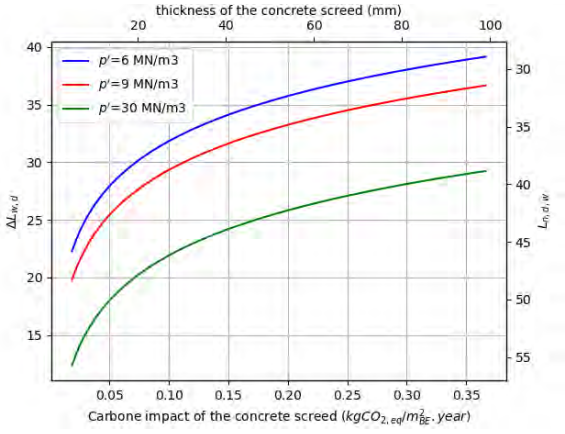

Figure 5: Direct impact sound reduction level comparison for a concrete screed in a floating floor for different dynamic stiffness of the insulation.

It's also interesting to note that the choice of finishing can significantly impact the total load exerted on the structure. Minimizing thickness of the screed is advantageous. A lighter screed allows for a smaller structure as it needs to support less weight. Reducing

the weight of the screed contributes to lowering both the carbon footprint of the screed and that of the overall structure. Although accepted values for direct impact noise are below 53 dB, indicating that the thickness could potentially be drastically reduced, it must be noted that a minimal thickness of 40mm for cement-based screed is defined in the SIA 251 to avoid the risk of cracks.

Screed's materials are not compared in terms of acoustic performance in this article, but acoustic insulation depends on mass. Anhydrite screeds have a better volumetric mass. Thus, at equal weight, potentially similar acoustic insulation can be achieved, leading to a better carbon footprint with a lower thickness (kg/kgCO_{2eq}: 0.12 for concrete vs. 0.09 for anhydrite).

Other initiatives in the market are currently being proposed and evaluated such as earth-based materials which is promising in providing the necessary mass and low carbon impact, but a lack of acoustic studies has been observed to confidently assess its implementation.

3.4 Finishings

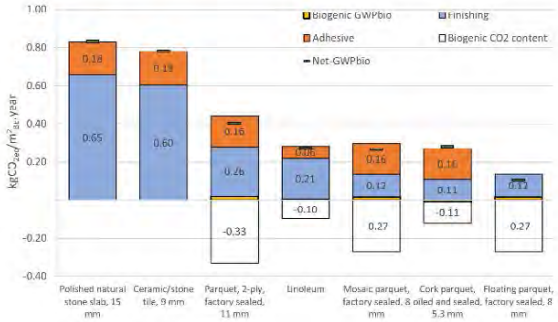

Figure 6: Variations of the finishing layer.

In terms of fossil carbon emissions, linoleum has less impact than certain types of parquet. Choosing parquet over ceramic saves approximately 0.5 $kgCO_{2eq}/m^2_{BE}$.year (see *Figure 6*), a noteworthy reduction. Homes often incorporate a mix of both materials to leverage the benefits of ceramics in bathrooms or kitchens, but minimizing the use of ceramic is worthwhile to decrease the overall carbon footprint.

Adhesives significantly contribute to the carbon footprint. With a floating floor, the carbon impact of the finishing decreases over 0.16 $kgCO_{2eq}/m^2_{BE}$.year. However, it is not compatible with floor heating systems.

3.5 Heating distribution

In addition to providing floor levelling, a screed can incorporate the heating distribution. For this purpose, various types of screeds are possible.

Anhydrite screeds are increasingly being employed as alternatives to cement screeds. However, their installation can be more challenging due to a longer drying time and precise condition requirements. Nevertheless, thanks to their increased strength, they provide the advantage of being able to achieve reduced thickness.

A dry screed, despite its thin thickness, can still have a significant carbon impact (*Figure 7*). But it avoids the need for a drying period, as the entire construction process is dry.

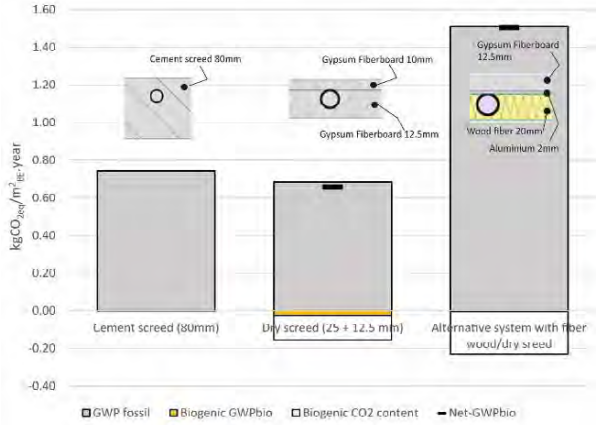

Figure 7: Systems to integrate heat distribution in screed.

3.6 Carbon Budgets

Looking at the next decades and considering carbon budgets until 2050 reveals the precarious position of concrete slabs, becoming obsolete towards the 2040 budget. More importantly, common finishings already face obsolescence now, necessitating a focused examination of these materials and designs (*Figure 8*).

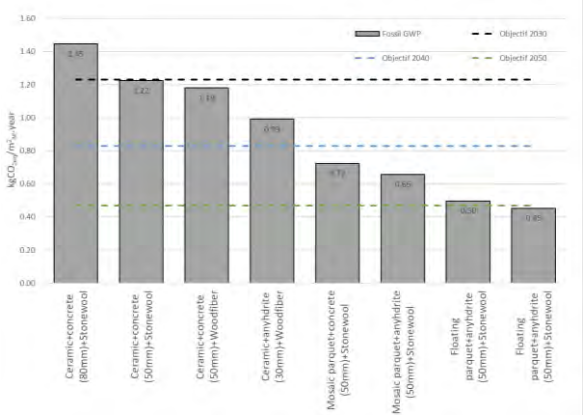

Figure 8: Comparison of finishing systems impact with finishing layer carbon budgets for 2030, 2040, and 2050.

4. CONCLUSION

In conclusion, the identified hotspots in a multi-family house intermediate slab underscore the critical role of this element. The structural layer being on the forefront of the overall impact in case of commonly used reinforced concrete slabs but being surpassed by floor finishing in case of wood-based structures with the screed layer resulting in a determining layer in the slab both for its function and its carbon impact.

Considering these hotspots, the main challenge lies on the fact that heavier structures (ex: concrete structure with cement-based screed) tend to have improved acoustic insulation, making the definition of alternatives a considerable hurdle. The complexity of functional requirements (acoustic insulation, heat distribution) for the screed, a lack of comprehensive data from the suppliers, and limitations on the assessment methods impede the implementation of alternative materials and reduced thicknesses for the finishing layer. The highest challenge, in terms of carbon budget lies in the other functional layers (finishings) with current systems surpassing the budget by circa 20%.

Nevertheless, this study highlighted some preliminary opportunities to decrease the carbon impact of slabs by up to two thirds compared to traditional systems. Notably, the 7cm cement-based screed is usually used for its acoustic insulation ability but the study reveals that reducing the thickness has minimal impact on acoustic performance but a high reduction on carbon impact (logarithmic relationship).

In light of these findings, a call for a more integrated and holistic approach to address all functional requirements of slab elements in multi-family houses becomes imperative. This shift is crucial to recognizing the challenges, fully understanding and implementing the opportunities available, and ensuring a smooth transition to a net-zero built environment.

ACKNOWLEDGEMENTS

The authors would like to thank the iTEC institute (Prof. Daia Zwicky) for the fruitful conversations on the topic of slabs in the frame of the EconBioLA project. Financial support is gratefully acknowledged from the HEIA-FR Smart Living Lab research program.

REFERENCES

1. Shukla, P.R.; Skea, J.; Slade, R. IPCC, 2022: Summary for Policymakers. *Climate Change 2022: Mitigation of Climate Change. Contribution of Working Group III to the Sixth Assessment Report of the Intergovernmental Panel on Climate Change* 2022, doi:10.1017/9781009157926.001.
2. Röck, M.; Saade, M.R.M.; Balouktsi, M.; Rasmussen, F.N.; Birgisdottir, H.; Frischknecht, R.; Habert, G.; Lützkendorf, T.; Passer, A. Embodied GHG Emissions of Buildings – The Hidden Challenge for Effective Climate Change Mitigation. *Applied Energy* 2020, *258*, 114107, doi:10.1016/j.apenergy.2019.114107.
3. Priore, Y.D.; Jusselme, T.; Habert, G. Exploring Long-Term Building Stock Strategies in Switzerland in Line with IPCC Carbon Budgets. *IOP Conf. Ser.: Earth Environ. Sci.* 2022, *1078*, 012023, doi:10.1088/1755-1315/1078/1/012023.
4. John, V. Derivation of Reliable Simplification Strategies for the Comparative LCA of Individual and "Typical" Newly Built Swiss Apartment Buildings. *ETH Dissertation* 2012, doi:https://doi.org/10.3929/ethz-a-007607252.
5. Rezaei Oghazi, N.; Jusselme, T.; Andersen, M. Carbon Budgets at the Component Scale and Their Impacts on Design Choices: The Façade as a Case Study. *CISBAT 23 conference, Lausanne* 2023.
6. Mahboob, A.; Hassanshahi, O.; Hakimi, A.; Safi, M. Evaluating the Performance of Hollow Core Slabs (HCS)-Concrete and Simplifying Their Implementation. *Recent Progress in Materials* 2023, *5*, 1–15, doi:10.21926/rpm.2302016.
7. Ferreira, F.P.V.; Tsavdaridis, K.D.; Martins, C.H.; De Nardin, S. Steel-Concrete Composite Beams with Precast Hollow-Core Slabs: A Sustainable Solution. *Sustainability* 2021, *13*, 4230, doi:10.3390/su13084230.
8. S. suisse des ingénieurs et des architectes SIA 2032 2010.
9. Lignum- Holzwirtschaft Schweiz Lignumdata Available online: https://lignumdata.ch/?page=home (accessed on 20 July 2023).
10. S. suisse des ingénieurs et des architectes Element-Based Cost Classification for Building Construction eCC-BC 2020.
11. Priore, Y.D.; Habert, G.; Jusselme, T. Exploring the Gap between Carbon-Budget-Compatible Buildings and Existing Solutions – A Swiss Case Study. *Energy and Buildings* 2023, *278*, 112598, doi:10.1016/j.enbuild.2022.112598.
12. Guest, G.; Cherubini, F.; Strømman, A.H. Global Warming Potential of Carbon Dioxide Emissions from Biomass Stored in the Anthroposphere and Used for Bioenergy at End of Life. *Journal of Industrial Ecology* 2013, *17*, 20–30, doi:10.1111/j.1530-9290.2012.00507.x.
13. Lippke, B.; Oneil, E.; Harrison, R.; Skog, K.; Gustavsson, L.; Sathre, R. Life Cycle Impacts of Forest Management and Wood Utilization on Carbon Mitigation: Knowns and Unknowns. *Carbon Management* 2011, *2:3, 303–333*, doi:10.4155/cmt.11.24.
14. Oh, J.-W.; Park, K.-S.; Kim, H.S.; Kim, I.; Pang, S.-J.; Ahn, K.-S.; Oh, J.-K. Comparative CO2 Emissions of Concrete and Timber Slabs with Equivalent Structural Performance. *Energy and Buildings* 2023, *281*, 112768, doi:10.1016/j.enbuild.2022.112768.
15. S. suisse des ingénieurs et des architectes SIA 181 - Schallschutz Im Hochbau 2020.
16. International Organization for Standardisation ISO 12354-1:2017 Building Acoustics Estimation of Acoustic Performance of Buildings from the Performance of Elements Part 1: Airborne Sound Insulation between Rooms 2017.
17. International Organization for Standardisation ISO 12354-2:2017 Building Acoustics Estimation of Acoustic Performance of Buildings from the Performance of Elements Part 2: Impact Sound Insulation between Rooms 2017.
18. Schiavi, A. Improvement of Impact Sound Insulation: A Constitutive Model for Floating Floors. *Applied Acoustics* 2018, *129*, 64–71, doi:10.1016/j.apacoust.2017.07.013.
19. Hongisto, V.; Saarinen, P.; Alakoivu, R.; Hakala, J. Acoustic Properties of Commercially Available Thermal Insulators − An Experimental Study. *Journal of Building Engineering* 2022, *54*, 104588, doi:10.1016/j.jobe.2022.104588.

PLEA 2024 WROCŁAW
(Re)thinking Resilience

Influence of Urban Space Types on Airflow Patterns and Air Pollutants

JIAYING LI[1], MINGJIE ZHANG[1],
[1]Nanjing University, Nanjing, China

ABSTRACT: Air pollution has become a global problem. The movement of air pollutants mainly depends on the airflow pattern, which is directly affected by urban spatial form. Understanding the effect of urban spatial form on airflow patterns and air pollutants can help urban designers and planners improve urban ventilation by adjusting the urban form. Most present studies focused on the impacts of a single morphological feature on ventilation performance. However, the form features affected ventilation in real cities are more complex. Therefore, this study attempts to investigate the effect of space types on airflow patterns and air pollutants. The space types are defined by three main factors related to urban ventilation (i.e., the relationship between space and wind direction, the variation of spatial height, and the enclosing degree of space). The study has provided different space types to predict flow patterns and pollutant emission capacities in real urban spaces.
KEYWORDS: Space Type, Airflow Pattern, Air Pollutant, Ventilation, Urban Morphology

1. INTRODUCTION

Since the first Industrial Revolution, the physical environment has been significantly affected by human activities, and air quality is more fragile than before. The World Health Organization has found that air pollution is becoming a major threat to human health and a global issue [1].

It has been found that the movement of air pollutant mainly depends on the airflow pattern in urban space. When a canyon forms a channelling flow, wind speed increases and pollutants leave rapidly. However, when a corkscrew vortex is formed, air pollutants accumulate in the space [2-3]. When multiple vertical vortices are formed within a canyon, the pollutants increase significantly [2].

The urban spatial form characteristics directly affect the airflow patterns. Some scholars indicated that the complex spatial features of street intersections can cause airflow collisions [2]. Some scholars have focused on the effects of high-rise buildings on flow patterns. When incoming wind collides with a high-rise building, the airflow is obstructed and redirected toward the ground, forming a powerful downdraft [4-5].

To sum up, urban spatial form can directly affect airflow pattern, and airflow pattern can affect air pollutant movement. It can be understood that the urban spatial form can directly affect airflow pattern, thus indirectly affecting air pollutant movement [5]. Therefore, understanding the effect of urban spatial forms on airflow patterns and air pollutants can help urban designers and planners improve urban ventilation by optimizing urban spatial forms.

Many scholars have studied on the urban spatial form characteristics that can affect the airflow patterns and air pollutants. These spatial form characteristics can be divided into the relationship between space and wind direction, the height variation of space, and the enclosing degree of space. Regarding the relationship between space and wind direction, it can be judged that the space and wind direction are vertical, parallel, or inclined according to the angle between the spatial axis and wind [2]. Regarding spatial height variation, scholars have put forward some parameters such as aspect ratio and building height ratio [2,6]. Regarding the enclosing degree of the space, scholars put forward the sky view factor, separation degree, spatial continuity, etc [4,7,8]. Most previous studies focus on the effect of a single form factor on ventilation in ideal form spaces [2,6-8]. However, due to the more complex and various spatial forms, a single form factor can not reflect all the effects on ventilation from real urban spaces. Therefore, this study hypothesizes that space types based on these three spatial morphological characteristics related to ventilation performances to predict airflow patterns and air pollutants.

This study explores the influence of space types on airflow patterns and air pollutants, using an urban centre as a study case. First, the continuous space in the study area is divided into subspaces with virtual boundaries to for space classification. Second, subspaces are classified based on three main spatial morphological characteristics related to ventilation performances. Then, CFD simulation is conducted to obtain ventilation data. Finally, the effects of space types on airflow patterns and air pollutants are explored, respectively.

2. STUDY CASE

In China, spaces can be divided into homogeneous spaces in residential areas [9] and inhomogeneous spaces in commercial districts [4]. In the residential areas, the building types are relatively singular, and the layouts are relatively neat, forming relatively simple spaces. Moreover, in commercial districts, the building forms are more multiple, and the layouts are more complex, forming various spaces with different heights and shapes. In order to explore the influence of various and different space types on airflow patterns and air pollutants, this study focuses on the spaces in commercial districts.

Nanjing is a representative megacity and an important hub within the high-density in the Yangtze River Delta, China (Figure. 1). Xinjiekou is the most important commercial district in Nanjing, which is located in the geometric centre of Nanjing. It combines commerce, culture, entertainment, and office buildings, exhibiting a complex spatial form. As Xinjiekou is the earliest Central Business District (CBD) prototype in China, it has typical form morphological characteristics of Chinese commercial districts. Therefore, this study takes Xinjiekou, Nanjing, as a study case.

Figure 1: Study case.

3. METHOD

3.1 Space division method according to wind direction

Because the real urban space is continuous, complex and indescribable, this study obtains subspaces with virtual boundaries by space division. Li et al. (2022) explored the relationship between the SVF and the wind velocity ratio based on three division results. The analysis the method based on three division results has been proven effective, but the correlation degree greatly depends on the space division method [4]. The previous three division results are based on spatial continuity or Gestalt psychology. However, these three division methods do not consider the effect of wind direction on ventilation. So, the optimization of the division method should be considered from the wind direction.

Generally, the airflow maintains the inertial movement along the wind direction until a spatial boundary, then moves along the spatial boundary. It is like Gestalt psychology which also follows an underlying inertia of motion. People tend to extend their inertial vision in the movement direction until a clear architectural interface to complete the non-holotype into a holotype mentally. Therefore, we optimize the division method considering wind direction based on Gestalt psychology. First, the possible linkage points are determined, which are divided into explicit vertices (i.e., corner points of the building) and implicit vertices (i.e., points where the building edge extension lines intersect with the building interface) (Figure. 2(a)). Then, the edges of the subspace, which are obtained by connecting the nearest vertices, are chosen according to the wind direction (Figure.2(b)(c)).

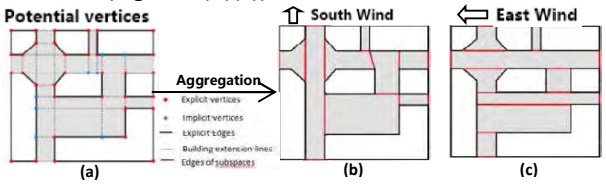

Figure 2: Space division process according to wind direction.

3.2 The spatial classification method

3.2.1 Acquisition method of spatial geometric informations

Previous studies have shown that the relationship between space and wind direction, the height variation of space, and the enclosing degree of spatial can affect the airflow pattern and air pollutant in space. In order to obtain these three spatial morphological characteristics, we need to obtain the vertical and horizontal spatial morphological characteristics of space.

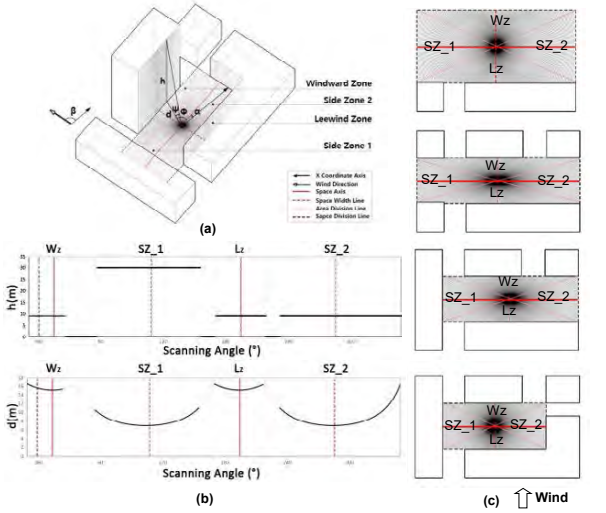

Figure 3: Acquisition method of geometric informations.

In order to express the morphological characteristics that affected ventilation performance, this study should build a platform for acquiring morphological informations. The acquiring geometry data platform has been built by python, as detailed in a previously published paper by our team [10]. In the method, the coordinate system is created by setting the measuring point at the centre of space. The space boundary and building height around the point are scanned to obtain the geometric information of spaces (Figure 3. (a)(b)).

For measuring the relationship between space and wind direction, spatial axis and spatial partition zone are defined. The spatial axis is parallel to the main spatial interfaces. And the line perpendicular to the axis can be regarded as the space width line. Connecting the four corner points of the space, it is possible to divide the space into four zones, namely the windward zone (W_Z), the leeward zone (LZ), and the other two side zones (SZ_1,SZ_2) (Figure 3.(c)).

3.2.2 Spatial morphological characteristics related to ventilation performance for space classifications

(1) The relationship between space and wind direction

The relationship between space and wind direction is the key factor affecting the flow pattern. When the flow is nearly parallel to the space, the flow is mainly governed by a space-axis flow. When the flow is perpendicular to the space, the clockwise vortex structure forms in the space section. When the flow enters the space obliquely, the flow in the space becomes spring-like [2]. The angle between the space axis and wind direction (Θ) represents the relationship between space and wind direction. The angle between the axis (α) or wind direction (β) and the x-axis could be obtained in Section 3.2.1 (Figure. 3).

If α and β are of the same sign, the Θ is calculated using Equation (1):

$$\Theta = |(|\alpha| - |\beta|)| \quad (1)$$

If α and β are of the different sign, the Θ is calculated using Equation (2):

$$\Theta = |(|\alpha| + |\beta|)| \quad (2)$$

If $0°\leq\Theta<30°$ or $150°<\Theta\leq180°$, the space is parallel to the flow,which is recorded as P;

If $30°\leq\Theta<45°$ or $135°<\Theta\leq150°$, the space is at an angle to the flow, which is recorded as A;

If $45°\leq\Theta<135°$, the space is perpendicular to the flow, which is recorded as C.

(2) The variation of spatial height

Oke (1988) proposed that the airflow patterns in symmetry space could be predicted by the H/W [6]. However, when there is a height difference between the two sides of the space, the building height difference has a greater impact on the flow pattern. The building height ratio (BHR) is often used to represent the building height variation. Since building heights are diverse in real cities, BHR is chosen in this study. It is the ratio of windward building height (H_W) to leeward building height (H_L) [11], which is calculated using **Equation (3)**:

$$BHR = \frac{H_W}{H_L} = \frac{\Sigma_{WZ} hi}{\Sigma_{LZ} hi} \quad (3)$$

Where i is any scanning angle, hi is the building height in the direction i, and Σ_{wz}hi and Σ_{Lz}hi are the sums of heights in W_Z and L_Z, respectively.

When BHR≈1, the space is a symmetry space (H0);

When BHR>1, the space is an ascending space (H1);

When BHR<1, the space is a descending space (H2).

In addition, the flow pattern in the space is influenced by the location of the high building. When a space is adjacent to a high building, its flow movement would change under the influence from a strong "downwash" effect, resulting in a better pollution emission capacity. However, BHR cannot represent the characteristics of spaces on one side of the high building. Therefore, this space type is added to this study, named H3. Based on the scanning information (Figure 3), it can be determined whether the space has any high buildings on two sides (SZ_1, SZ_2). If any high building exists, the space would be classified as H3 rather than others.

(3) The enclosing degree of space

It has been shown that the enclosing degree of space affects urban ventilation, which can be represented by different form indicators, such as SVF, separation degree, spatial continuity, number of enclosing edges, etc [4,7,8]. Among them, the number of enclosing edges may have a more direct effect on the flow pattern.

The number of enclosing edges is chosen to characterize the enclosing degree of space. As described in section 3.2.1, this study can obtain building height information on four zones by scanning. Whenever height information appears in a zone, the zone is considered enclosed by buildings. According to the number of enclosing sides, subspaces can be classified as one-sided (L1), two-sided (L2), three-sided (L3), and four-sided enclosures (L4). The enclosing degree is L4>L3>L2>L1.

3.2.3 Space classification based on ventilation Performance

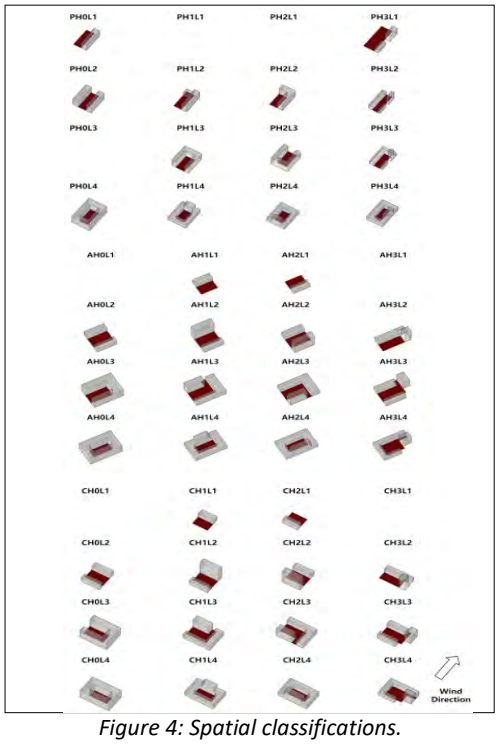

Figure 4: Spatial classifications.

In principle, based on the above three spatial characteristics mentioned, 36 spatial types can be obtained. However, some spatial types do not exist due to the limitation of the number of spatial edges (i.e., CL1H0, CL1H3, PL1H1, PL1H3, AL1H0, AL1H3). For example, when the space is enclosed on only one side and parallelled to the wind direction, it is impossible to be an ascending space or a descending space. So there must be no PH1L1 and PH3L1 type. Therefore, there are 30 types of spaces (Figure 4).

3.3 The ventilation data acquisition method

3.3.1 CFD modelling

The experimental data for the wind environment in the Xinjiekou area are obtained from the computational fluid dynamics (CFD) simulation. The CFD model setup followed the major simulation requirements provided by the Architectural Institute of Japan guidelines [12]. Table 1 shows the CFD setting. In order to verify the accuracy of the simulation results, a model is constructed at a scale of 1:400 (consistent with wind tunnel conditions), with boundary conditions conforming to wind tunnel experiment conditions. Based on the AIJ wind tunnel test standards [12], α=0.14, the boundary layer thickness zr = 0.005 m (2m at real scale), and the reference wind speed Vzr = 3 m/s. The simulation results are validated by comparison with wind tunnel experiments, which has been published in paper by Li et al[4].

Table 1: CFD simulation condition settings.

Calculation conditions		**Solver settings**
Turbulent model		Standard k-e model
Mesh		Tetrahedral grid
Scheme		SIMPLE
Spatial discretization		Second order, Second order upwind
Boundary condition	Inflow	$V(z)=Vzr(z/zr)^{0.231}$
	Outflow	Pressure-outlet
	Side	Wall
	Top/ground	Symmetry
Convergence residual		1e-5
Wind direction		South wind

Many previous studies have used canyons perpendicular to the wind direction as study samples [13-14] because canyons perpendicular to the wind exhibit poorer pollutant discharge capabilities [3]. For the form management in urban planning, it is most important to avoid the worst ventilation conditions in design practice. Therefore, a wind perpendicular to most of the spatial interfaces in the urban space is chosen as the wind direction, which is south wind.

3.3.2 The air pollutants parameter

Many researchers have proposed various ventilation indicators to evaluate pollutant emission capacity. Among different ventilation parameters, the average pollutant concentration (C_{ave}) has been widely used to reflect the impact of urban morphology on the wind flow distribution, which is chosen by this study. The bigger the C_{ave} is, the worse pollutant discharge capacity is. The smaller the C_{ave} is, the smaller the pollutant discharge capacity is. In addition, this study focuses on the wind field (flow pattern and ventilation performance) in the 0-2m pedestrian area (0-0.005m at reduced-scaled) because people often move near the ground in real cities. It could be calculated using Equation (4):

$$C_{ave}= \frac{\sum_{i=1}^{n} C_i dx_i dy_i dz_i}{\sum_{i=1}^{n} dx_i dy_i dz_i} \quad (4)$$

4. RESULTS

4.1 The Results of space division and CFD simulation

Figure 5 shows the spatial division and simulation results of the study case. After overlaying the division result with the simulation, it is found that the transition position of the airflow status is close to the edges of the subspace divided. The division method is reliable.

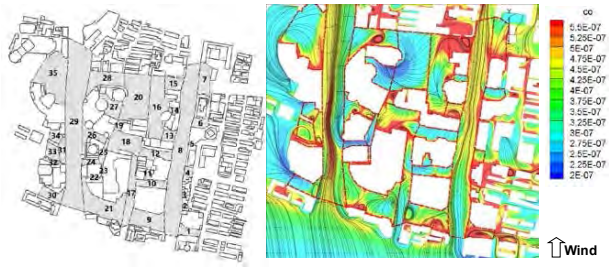

Figure 5: Spatial division and simulation results.

4.2 The Results of Space Types and CFD Simulation

Based on the partition result, the spaces are classified based on the ventilation performance. There are only 13 space types in the study area. Figure 6 shows the classification results.

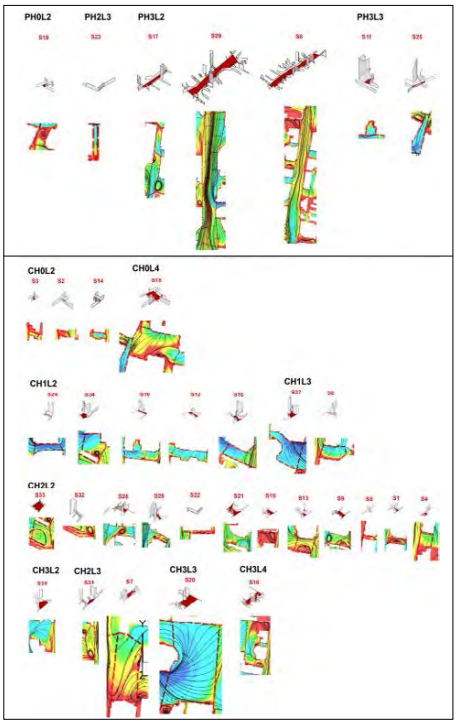

Figure 6: The Classification Results and CFD Simulation.

5. ANALYSIS

5.1 The influences of spatial types on airflow status

After a detailed analysis of space types and airflow patterns in Section 4.2, it is found that spaces with the same type have similar airflow patterns. Table 2 shows the different airflow patterns of 13 spatial types.

In the P types, most airflow movements are mainly controlled by the spatial axises, forming a channel flow, except for S19 (Figure. 6). The variation of spatial height can affect the airflow pattern of the space. When the space is a descending space (H2 type), the airflow is mainly from the surrounding wind rather than the incoming wind. When there is a high-rise building on one side of the space (H3 type), the high-rise can lead the incoming wind into the adjacent space as the main airflow (such as S25) or as a stream of flow into the main airflow of the space (such as S29). When the buildings on both sides of the space are equal in height (H0 type), the airflow depends on the comprehensive result of the incoming wind and surrounding wind. For example, the S19 is parallel to the incoming wind, so a flow moves along the interfaces of the S19. However, the airflow is blocked by a strong flow from a adajent south square, a vortex formed and occupies the entire space in S19. This is because S19 is short. For the enclosing degree of space, the airflow can leave out quickly and smoothly from a space with two enclosing sides (L2 type) (i.e. S17, S29), and the airflow is easy to form a vortex after meeting the windward building building in a space with three or four enclosing sides (L3 and L4 type). To sum up, the length of space also affects the airflow pattern. The airflow pattern of long space is more stable, and the airflow pattern of short space is more affected by the surrounding environment (e.g., S19).

In the C types, the flow patterns are relatively complex. The height variation obviously affects the airflow pattern in the space. When the space is a space consist of two buildings with equal heights (H0 type), most airflows mainly come from the incoming wind, forming a clockwise vortex structure. However, due to the influence of the length of the spaces, the airflow of short space can be affected by the surrounding wind (e.g., S2, S3). When the space is an ascending space (H1 type), the airflow of spaces comes from the windward building building (e.g., S24, S27). When the space is a descending space (H2 type), the flow of the space is affected by the surrounding wind, resluting in forming vortices (e.g., S33, S7). When the space is located on the side of a high-rise building, the airflow enters from the side of the high-rise (e.g., S20). In addition, the enclosing degree can also affect the flow pattern. When the space has three enclosing sides (L3 type), the coming or leaving of the airflow may be affected by the spatial boundary (e.g., S20, S18). When the space has four enclosing sides (L4 type), it is easy to form airflow collisions.

Table 2: Flow pattern results of different space types.

Angle	Spatial Type	PH0L2	PH1L2	PH2L2	PH3L2
P	Airflow Status		/	/	
	Spatial Type	PH0L3	PH1L3	PH2L3	PH3L3
	Airflow Status	/	/		
C	Spatial Type	CH0L2	CH1L2	CH2L2	CH3L2
	Airflow Status				
	Spatial Type	CH0L3	CH1L3	CH2L3	CH3L3
	Airflow Status	/			
	Spatial Type	CH0L4	CH1L4	CH2L4	CH3L4
	Airflow Status		/	/	

5.2 The influences of spatial types on ventilation performance

Section 5.1 has proved that different spatial types have different airflow patterns. Moreover, different sizes and lengths of spaces may also affect the pollutant emission capacities. Therefore, this study groups spaces can analyze the impact of different space types on pollutant emission capacities according to length and area. In urban microclimate studies, scholars often use the length/width ratio (L/W) to represent the length of space. Therefore, the spaces are divided into three length groups according to L/W: T1 group with L/W ≤ 1, T2 group with 1<L/W≤5, and T3 group with L/W>5. Moreover, every group can be further divided into five groups (A1-A5) based on area from small to large. The subspaces in this study area can be divided into 12 groups (Figure 7).

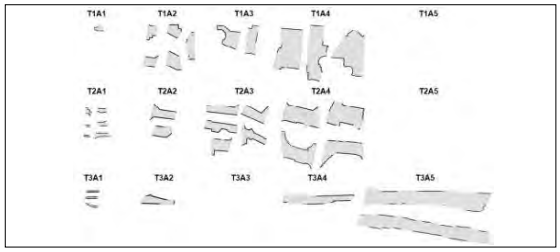

Figure 7: Groups by the lengths and areas of spaces.

Based the 12 groups, the C_{ave} values of subspaces are ranked from smallest to largest in Figure 8. The results show that building height has the most significant influence on pollutant emission capacities. Most of the descending spaces (H1 type) have poor pollutant emission capacities, while ascending spaces (H2 type) and spaces next to any high-rise building (H3 type) have better pollutant emission capacities. For example, in groups T1A2, T1A3, and T1A4, the spaces with the highest C_{ave} values are S4, S7, and S16. Their ventilation spatial types are CL2H2, CL3H2, and CL4H2, respectively. The Spaces with the lowest C_{ave} values are S34, S27 and S20. Moreover, their ventilation spatial types are CL2H1, CL3H1 and CL3H3, respectively. The effects of enclosing degrees on pollutant emission capacities are not significant.

However, the C_{ave} values of the spaces with four sides (L4 types) are greater than that of other spaces, such as S16 in T1A4 and S18 in T2A4. In the relationship between space and wind direction, it is found that the C_{ave} values of spaces parallel to wind direction (P type) are lower than that of other spaces with similar length and area, such as S23 in T2A1. In addition, the lengths of the spaces also affect the pollutant emission capacities. Most short spaces have lower C_{ave} values.

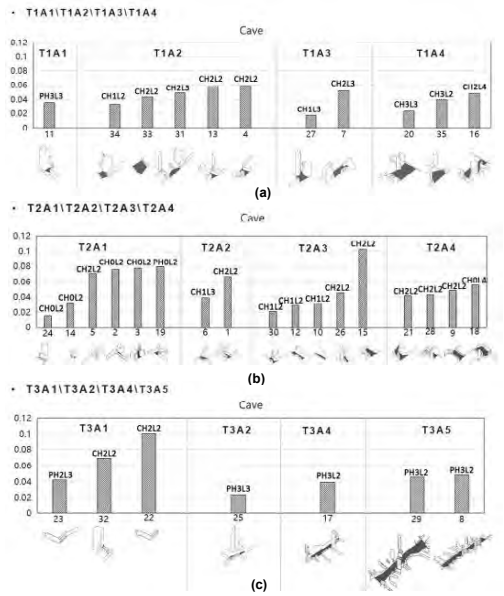

Figure 8: Sort the space according to the C_{ave} values

To sum up, the highest C_{ave} values in three groups tend to be found in PL2H0, CL2H2, CL3H2, CL4H3, or CL4H0 spaces. The low C_{ave} values tend to be found in the CL2H1, CL3H1, or CL3H3 spaces.

6. CONCLUSION

This study shows that space types can directly affect airflow patterns and pollutant emission capacities. PL2H0, CL2H2, CL3H2, CL4H3, and CL4H0 spaces have the worst pollutant emission capacities, because these type spaces are descending spaces (H2 type) or enclosed by four edges (L4 type). In contrast, CL2H1, CL3H1, and CL3H3 spaces have better pollutant emission capacities, because these spaces are an ascending space (H1 type) or adajent to any high-rise building (H3 type). Regarding the relationship between space and wind direction, most the airflow movement in the space parallel to the wind direction is mainly controlled by the spatial axis. In contrast, the airflow in the space perpendicular to the wind direction is more complicated, which depends on other spatial morphological characteristics. Spaces parallel to the incoming flows have better pollutant discharge capacities than spaces perpendicular to the incoming flows. The height variation of the space has the greatest influence on the pollutant emission capacity. The ascending spaces and spaces next to any high-rise building have better pollutant emission capacities. However, descending spaces are prone to form vortices, having the worst pollutant emission capacities. Regarding enclosing degrees, spaces with four enclosing sides have poorer pollutant emission capacities. In addition, the spatial lengths also affect the pollutant emission capacities. Spaces with L/W ≤ 1 show better pollutant emission capacities.

ACKNOWLEDGEMENTS

This work was supported by Postgraduate Research & Practice Innovation Program of Jiangsu Province, and the Shanghai Key Laboratory of Urban Design and Urban Science, NYU Shanghai, Open Topic Grants [grant number 2022JYLi_LOUD].

REFERENCES

1. Thunis, P. (2018). On the validity of the incremental approach to estimate the impact of cities on air quality. Atmospheric Environment, 173, 210–222.
2. Voordeckers, D., (2021). Guidelines for passive control of traffic-related air pollution in street canyons: An overview for urban planning. *Landscape and Urban Planning*, 207: 103998.
3. Huang, Y., (2019). Effects of Wind Direction on the Airflow and Pollutant Dispersion inside a Long Street Canyon. *Aerosol and Air Quality Research*, 19: p. 1152-1171.
4. Li, J., (2022). Exploring urban space quantitative indicators associated with outdoor ventilation potential. Sustainable Cities and Society. 79, 103696.
5. Yang, J.Y., (2020), Air pollution dispersal in high density urban areas: Research on the triadic relation of wind, air pollution, and urban form., Sustainable Cities and Society , 54, 101941.
6. Oke, T.R. (1988). Street Design and Urban Canopy LayerClimate, Energy and Buildings, 11, 103 - 113.
7. Shen, J.L., (2017). An investigation on the effect of street morphology to ambient air quality using six real-world cases. Atmospheric Environment , 164, 85–101.
8. Ng, W.-Y., (2014). A modeling investigation of the impact of street andbuilding configurations on personal air pollutant exposure in isolated deep urban canyons, Sci. Total Environ. 468–469, 429–448.
9. Zhang, M.J., (2021). Effect of urban form on microclimate and energy loads: Case study of generic residential district prototypes in Nanjing, China. 70, 102930.
10. Ji, H.M., (2022). A quantitative study of urban spatial morphology based on the correlation with wind environment, 6th ISUFitaly International Conference.
11. Zajic, D., (2011). Flow and Turbulence in an Urban Canyon. Journal of Applied Meteorology and Climatology, 50(1), 203–223.
12. Tominaga, Y., (2008). AIJ guidelines for practical applications of CFD to pedestrian wind environment around buildings. Journal of Wind Engineering and Industrial Aerodynamics, 96(10–11), 1749–1761.
13. Chew, L. W., (2018). Flows across high aspect ratio street canyons: Reynolds number independence revisited. Environmental Fluid Mechanics, 18(5), 1275–1291.
14. Yang, J., (2021). Influence of urban morphological characteristics on thermal environment. Sustainable Cities and Society, 72, 103045.

PLEA 2024 WROCŁAW
(Re)thinking Resilience

Evaluation The Amount of Sustainable Urban Development Based on Different Types of Urbanization Process

Comparison 20 Years of Urbanization in Seville (Spain) And Ghazvin (Iran)

NADIA FALAH[1], JAIME SOLIS-GUZMAN[2], NAHID FALAH[3]

[1] Ph.D. student in Architecture and Urbanism at the University of Seville, Spain
[2] Professor of Architectural Constructions, School of Building Engineering, Department of Architectural Constructions II, University of Seville, Spain
[3] Regional planner, Administrative District Harburg, Germany

ABSTRACT: The urbanization process promotes rapid changes in structure of metropolises and cities, this research delves into the critical challenge of achieving sustainable urban development by evaluating the pattern of urbanization processes in Seville, Spain, and Ghazvin, Iran, over a 20-year period as a two different city with two different contexts and level of development. With Focus on minimizing negative environmental impacts of rapid urbanization on the limited urban resources (such as land). the study employs Land Use and Land Cover (LULC) modelling to simulate and analyse urbanization patterns in diverse urban contexts, that which one city is more sustainable in keeping natural resource untouchable for long time, therefore is essential to study about city and surrounded area of them also analysing population flow over time. Our findings contribute to the discourse on urban planning strategies, offering insights to address global sustainability concerns.
KEYWORDS: Sustainable Urban Development, Urbanization Processes, Land Use and Land Cover Modelling, Normalized Difference Built-Up Index (NDBI), change detection modelling

1. INTRODUCTION

Urbanization as multifaceted process involves the growth and expansion of urban areas [1], typically characterized by shifting population (Migration-Driven Growth, and Natural growth rate[2]), infrastructure development, Industrial Urbanization, Economic-Induced Growth[3] and changes in land use and land cover [4] (the conversion of land cover into urban areas) in different types of physical development, which is the main factor of sustainable urbanization [1]. The specific type of urban growth in each area often results from a combination of these factors and can change over time due to various environmental, economic, social, and policy-related influences[5]. many urban areas may experience a combination of these factors over time [6].The effective definition of urban development is the basis of understanding urban sustainability [1] Sustainable urbanization and sustainable urban development apply towards the suitable conditions. Sustainable urban development may be defined as a process of synergetic integration and co-evolution among the great subsystems making up a city [5], that consists of to maintain the balance among the "Triple Bottom Lines" of sustainability (economic, environmental, and social as an equal concern) [7]. Therefore, based on these definition, sustainable urbanization targets be used to assess sustainable development which guarantees the local population a non-decreasing level of wellbeing in the long term, without compromising the possibilities of development of surrounding areas and contributing by this towards reducing the harmful effects of development on the biosphere[8] . Sustainable development in cities is reflected in the sustainability of urban systems [1], [9]. In general, the effective detection of urban development is the basis of understanding urban sustainability.

One of the most important factors of sustainable urbanization back to the keeping the natural sources safe, therefore changing in land cover of surface has a direct effect on all 3 dimensions of sustainability, as a result can be said a place with less challenging in land cover or sustainable changes in LCLU can be a more stable case because in long term sustainable changes in LULC will make a balance between social and economic dimensions with environment.

Physical types of urban growth refer to the spatial and structural patterns of development within urban areas. These patterns can vary based on factors such as historical development, planning policies and factors, economic activities, and geographical constraints [10]. Based on the data gathered, different physical classifications of urban growth and development are included:

- Compact Growth and Infill Development: characterized by high population density and a

concentration of buildings (vertical development) in a limited existing developed area (repurposing of underutilized land) [4].

- Ribbon Development and Infrastructure-Led Growth: it occurs when urbanization follows transportation routes (linear patterns of development), such as transportation networks and communication systems resulting [6].
- Sprawl and Dispersed Growth: the outward expansion of urban areas, leading to low-density development. This pattern is often associated with suburban or exurban areas and can result from suburbanization[3].
- Informal Urbanization; unplanned growth of informal settlements or slums within urban areas, often due to rapid urbanization and low level of economy[11].
- Smart Growth: Urban growth is guided by principles of sustainability and follows the main goals of "new urbanism", such as increasing the density, public transportation, environmental considerations and Technological Integration[3].
- Regenerative Growth and Preservation emphasizes the restoration of ecosystems and Conservation initiatives and the adaptive reuse of historical buildings in the urban context[12].
- Mixed Development: This means each part of urban area faced with one type of development over time. in total a city area faced with multi types of growth and development.

it must be mentioned in different conditions, such as level of development in contexts the result will be different, the main aim of this research is how differences growth influence sustainability of the urban development (especially on environment and natural resources). recognizing this process and classify types of urbanization for different city and evaluation it with factors of sustainable LULC changes is essential even for predicting future trends.

2. APPROACH AND METHODOLOGY

the Methodology is based on the mixed approach (descriptive and analytic) [8] to evaluation condition of urban development over a period of 20 years (between 2003 and 2023) is sustainable or not (based on sustainability of LCLU change detection) and compare long-term trends of two different case studies (based on their different contexts). Statistical analysis, data visualization and spanning techniques (remote sensing technology and geographic information system (GIS)) will be used to examine trends and patterns in the urban development and monitor temporal and spatial variations of intensive or diffuse urbanization process the process of acting in methodology is explained in (Figure 1). The main data are satellite images (Landsat 5(TM) for Seville 2003, Landsat 7 (ETM+) for Ghazvin 2003, Landsat 8 (OLI)) for Seville and Ghazvin 2023).

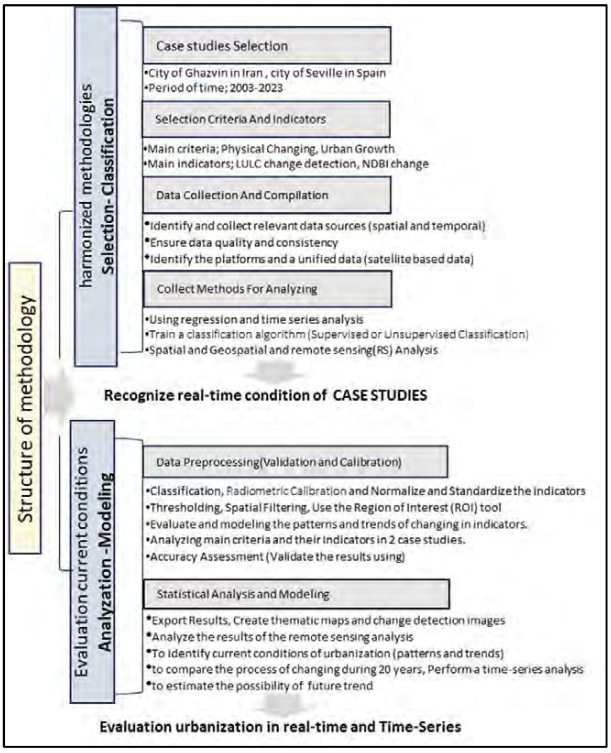

Figure 1: Structure of methodology

the statistics related to the population and general conditions of case studies. Also, software's, such as; SPSS19 for statistics analyse, ENVI 5.3 for Remote sensing and ArcGIS 10.8.2 for Spatial Analysis, will be used. For Simulation, evaluation and comparison outcomes, produce analytical maps based on change detection technique. Four classes of LULC are determined: including built-up area (BUA) levels (cities, villages, roads, industrial areas, etc.), water Bodies (WB) levels (rivers, canals and swamps), forest and agricultural lands, and vegetation(A/V/F), Barren Soil (BS)[8], [13], [14] by using ROI tools (accurate methods for the classification) all images will be normalized and calibrated (Figure 1).the physical development indexes over time are selected and determined by using resource review, which show in (*Table 1*):

Table 1. The effective indexes of urban growth

Indexes	Definition
NDBI	Normalized Difference Built-Up Index
LULCC	Land Use and Land Cover Change
Urban/non-urban area	Recognize only urban area pixels

Here is the explanation of the main indexes:

- NDBI

The Normalized Difference Built-Up Index (NDBI) is a remote sensing index used to identify built-up areas or urban extent in satellite imagery. The formula for NDBI is typically derived from the reflectance values in the near-infrared (NIR) and shortwave infrared (SWIR) bands of the satellite data (Landsat). The NDBI formula is expressed in Equation (1).

$$NDBI = \frac{(SWIR-NIR)}{(SWIR+NIR)} \quad (1)$$

In this formula:
SWIR is the reflectance value in the shortwave infrared band.
NIIR is the reflectance value in the near-infrared band.

The resulting NDBI values range from -1 to 1. Positive values indicate a higher likelihood of built-up areas, while negative values suggest non-built-up areas, such as vegetation or water bodies. it's crucial to note that the effectiveness of the NDBI for mapping built-up areas may depend on the characteristics of the study area, the spatial resolution of the satellite imagery, temporal resolution, and the presence of factors such as shadows or mixed land cover types[4].

- LULCC formula using NDBI

Land Use and Land Cover (LULC) change detection involves comparing two or more images acquired at different times to identify and analyse changes in the landscape[8], [10] and monitoring urban expansion, deforestation. One common method for LULC change detection involves computing the Normalized Difference Built-Up Index (NDBI) for each period and then subtracting one from the other [4]. The change detection formula by using NDBI is expressed in Equation (2).

$$NDBI\ change = \frac{NDBI_i - NDBI_j}{NDBI_i + NDBI_j} \quad (2)$$

In this formula:
$NDBI_i$ is the NDBI value for the post-change (last) image
$NDBI_i$ is the NDBI value for the pre-change (first) image

To identify areas undergoing urban growth over time, the maps of the physical development produce based on those indexes that show the limitations of developing land, amount and direction of the growth over time and analyse and compare similarities and differences in case studies based on their contexts.

- Urban/ non-urban area

In this index, aims is to clarify amount of urban area in the case studies, in this article the red colour is for all types of urban area and other type of land cover and land uses show in white.

3.DISCUSSION

To Determine which city is more sustainable in urbanization process over 20 years with less negative point to environment and less changing in natural land covers, two cities with distinctive characteristics and development trajectories selected, Ghazvin in Iran as a developing country and Seville in Spain as a developed country. Both have a rich history and cultural significance dating back to Roman times, the experience of centuries of residents, and both had undergone significant rapid growth in urbanization and population. Also, they are committed to sustainable development goals and aims. Seville is a city demonstrated to all actions related to Agenda 21 and 2030, and Ghazvin was nominated for city development strategy plan between all cities in developing country (CDS 2006-2010) [4], [13]. also, there is a basic difference in "their context" of development. the location of these two cities shows in (Figure 2).

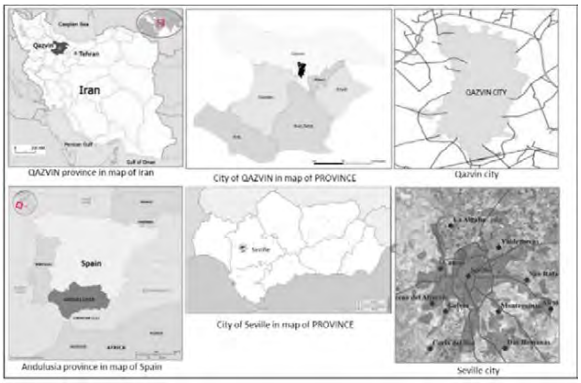

Figure 2; Location of case studies

3.1 population trend in city and urban area

The general trend of population over time for 2 case studies compare in the (Figure 3), these Histogram shows pattern of changing is same in the last decade of 20 century. Seville faced with decline in population growth and experience negative growth rate in the city (losing populations), in Ghazvin dropped the growth rate was observed but the total rate was positive. histogram shows that Seville has bounced back after experiencing these losses. also, in (Figure 4) as a predicting model and formula, based on linear model the population growth rate is calculated for the specified multi-year interval.

The population growth rate in the city of Ghazvin is significantly higher than Seville. However, a comparison of the growth rates within the urban area indicates that the urban area of Seville has experienced a considerable increase in population even more that Ghazvin urban area. This suggests a trend of migration and population movement from city of Seville to the suburb or the attraction of population from surrounding villages to the around of the city (metropolitan). This phenomenon is also prevalent in Ghazvin, where both cities exhibit population dynamics rooted in their economic roles and structural changes in their economic functions.

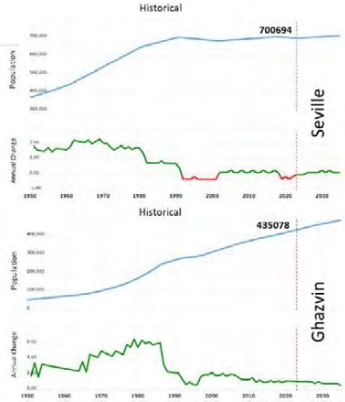

Figure 3;population trend in 2 case studies over 20 years

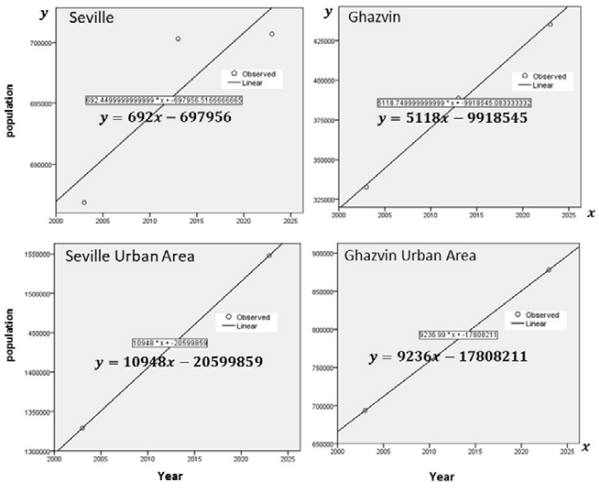

Figure 4;the linear formula for predicting changes in cities and urban area population trend, processing in SPSS.

it can be stated that Ghazvin city and its urban area (metropolitan area) are migrant-receptive same as the Seville urban area with a Signiant increasing of population, while Seville city acts as a source of migrants. That data of population growth in urban area (metropolitan) proves this point in (Table 2). therefore, the growth rate in urban area and metropolitan in both cities have significant growth for 20 years, especially comparing the rate between Seville city and metropolitan these results are very important factor for understanding pattern of urban growth.

3.2 Urban growth trend

Based on steps of methodology, the satellite images of this two cities during 20 years processing , the result of NDBI is classify in (Table 3), Both cities experience a decrease in mean NDBI values (Seville during 20 years change -0.19-point decrease in compare to Ghazvin is almost twice), suggesting a trend towards a decrease in built-up or urban areas or a relative increase in non-built-up areas or natural areas in (Figure 5) are mentioned.

Table 2: cities and urban area population growth rate

City	year	Population	period	Growth rate
Seville	2003	686,845	2003-2023	+0.692%
	2023	700,694		
Seville Urban area	2003	1328985		+10.94%
	2023	1547945		
Ghazvin	2003	332703		+5.119%
	2023	435000		
Ghazvin Urban area	2003	693500		+9.236%
	2023	878240		

Table 3: main data of NDBI analyzing

City	year	Min	Max	Mean	StdDev
Seville	2003	-1	0.9967	-0.56094	0.153
	2023	-1	0.9990	-0.75633	0.112
Ghazvin	2003	-1	0.9977	-0.66286	0.380
	2023	-1	0.9980	-0.7368	0.105

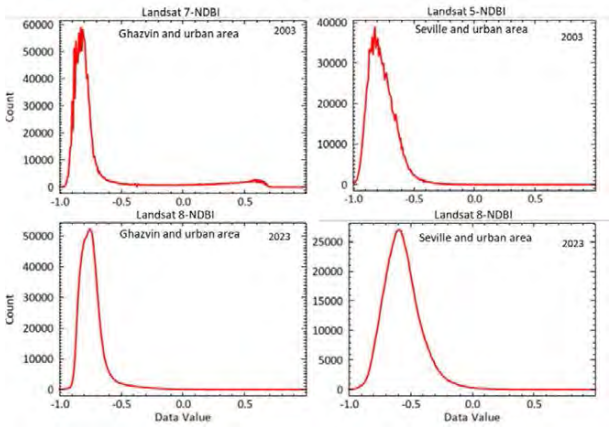

Figure 5; NDBI histogram for 2003 and 2023 in case studies, processing in ENVI based on Landsat satellite images

The means of NDBI values are close in 2023, indicating a similar condition in both cities and In compare with LCLUC the mean of NDBI will be proved. Based on analysing LCLUC (Figure 6), Seville urban area experienced significant changes in the distribution of land use, with a substantial increase in A/V/F area (increased from 73,837 m2 in 2003 to 112,278 m2 in 2023, showing a 52.1% increase**)**.and marking a significant decrease in BS area (45.8% compare to 2003). Ghazvin urban area, on the other hand, saw a decrease in BS (23.6%).and A/V/F area (with 10.1% decrease from 29.40% to 26.20%), WB did not have significant changes but the percentage of BUA has significant increased relative to the total area in both case study. in (Figure 7) normalizes the percentage of LULC class (that covering case studies surface for 2003 and 2023.

3.3 evaluation urbanization process

Based on all above, for evaluation trend and direction of urbanization the amount of Urban/Non-urban area (area which faced with changes in LCLU) is classified and shows the pattern of changing in case studies is different, in Seville urban area experienced sprawl and Ribbon development in suburb area and city border, but in Ghazvin infill and ribbon development especially in north of the city is obvious and metropolitan working as a magnet which increase the number of town or small cities around main cities during 20 years .

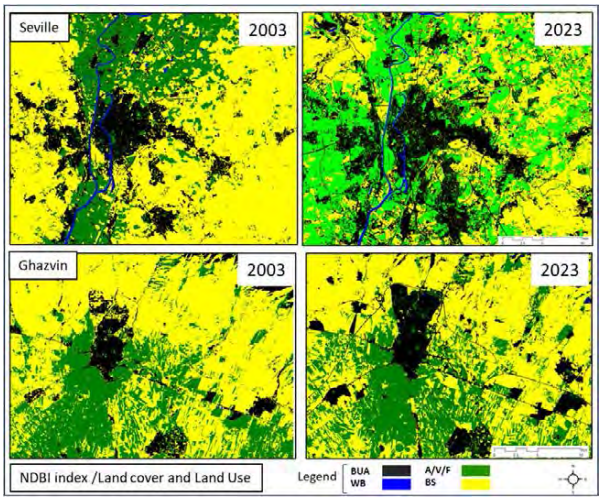

Figure 6; LCLUC and NDBI index, processing; Http://glovis.usgs.gov and processing in ENVI and ArcGIS

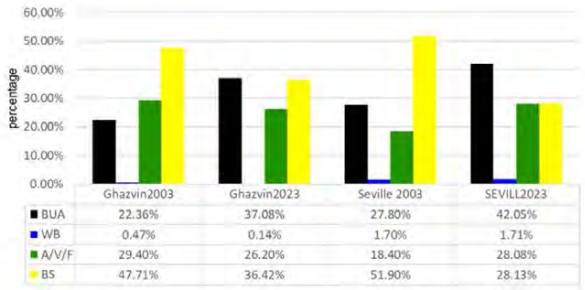

Figure 7;LCLUC Detection during 20 years in total area, processing; in ENVI and GIS and Normalize in SPSS

Therefore, to modeling maps based on (Figure 6) and statistics in (Figure 7) and (*Table 4*), in Seville urban area, the percentage of BUA changing relative to the total area increased over this period by 51.1% and for Ghazvin urban area is 65.9%. it means Both case studies experienced a significant increase in the urban growth, but Seville is more sustainable in LULCC (Figure 8).

Table 4; urban BUA changing, based on ENVI and ARCGIS

BUA changing rate	Ghazvin			Seville		
	2003	2023	20 Years	2003	2023	20 Years
	M^2		%	M^2		%
BUA	24594	40790	65.9%	111273	168113	51.1%

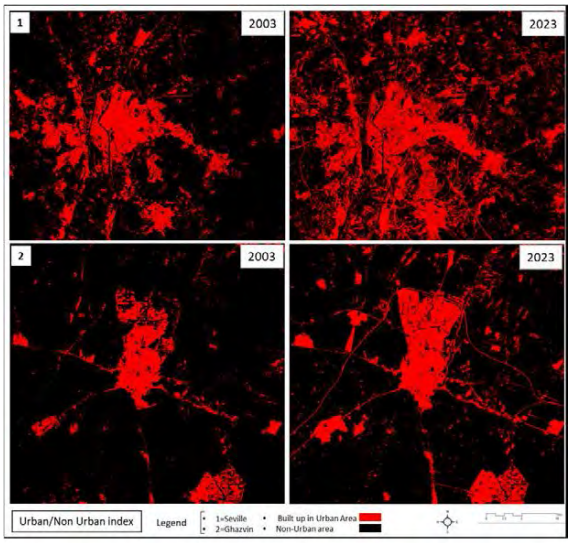

Figure 8; urban Urban/non-urban index in case studies in 2003 and 2023. processing in ENVI and ArcGIS

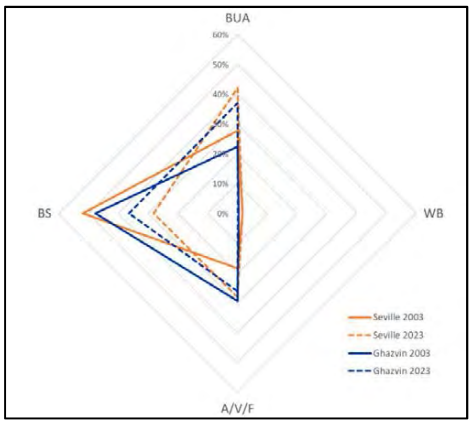

Figure 9; comparing amount of LCLU changing trend.

For comparing the trend in total, result of 2 case studies gathering in (Figure 9), in total the increase in BUA in both Seville and Ghazvin indicates urban expansion and infrastructure development over the years. The increase in A/V/F in Seville suggests efforts to promote green spaces, possibly through afforestation or urban planning initiatives. The decrease in A/V/F in Ghazvin indicate changes in agricultural practices, deforestation, or land conversion for other purposes.

The significant decrease in barren land in both cities suggests land has been repurposed or reclaimed, possibly for urban development (in Ghazvin) or agriculture (Seville) and this is the main different between 2 study areas, that shows changing in LCLU in both of them happened but in Seville area, changing is more sustainable because of types of that (increasing A/V/F land) but in Ghazvin area, all the changes are in order to increasing BUA. Another point is related to population trend these amounts of changing and pattern of growth completely follow the population Shift and Growth, Ghazvin area experienced higher amount of changing but as an infill development (growth rate in city) but Seville faced with negative

growth rate, therefore pattern of changing around the city because of growth rate is acceptable. Infrastructure Development and increasing network connection shaped structure of them with 2 different forms, in Seville increase Ribbon development and in Ghazvin increase link and node connection (with suburb area). Historical Preservation make some limitation of infill growth in Precious historical site(centre of Seville), because of that Ghavin only growth from north of city (because of the preservation of historical garden around the city).Economic Diversification same as; Tourism destination Impact to Seville (need for tourism-related infrastructure and cause shift in residence of city to suburb area based on cost of living) and Industrial cities, make changing in Ghazvin (need for housing Infrastructure, encourage more people for migration to the city) and suburbs (because of the price of living in main city), also, using idea of smart cities in Seville such as the use of technology to enhance liveability and accessibility that increase tend to move to suburb. At the same time informal and poor economic area (in both of Ghazvin and Seville) increase in some Outer Urban Periphery growth. Based on all of types, it can be said Both cities may witness a trend toward mixed developments.

4. CONCLUSION

This comprehensive study delved into evaluating the Sustainability conditions in two different case studies and provides context-specific insights into sustainable urban practices. Through meticulous monitoring, simulation, and data analysis, this research aimed to evaluate sustainable urbanization, particularly in different urban contexts and efforts to recognize and compare the trend of physical development and amount of sustainability of LULC changing in Seville and Ghazvin between 2003 and 2023.

Overall, LULCC over time reflect the dynamic nature of urbanization and clarify which city experienced more sustainable changing based on less negative effects on natural resources. Therefore, based on results, city of Seville in compare to the Ghazvin is more sustainable.

The study's findings underscore that Both cities likely face their unique challenges and opportunities in pursuing urban development. there are lots of other factors that paly vital roles in sustainable urbanization process, such as; topography, climate parameters, the price of land, Quality of agricultural land, Limitation (risk of flood and disasters), Low and policies, and a lot of other economic and social condition. The future analysis of the implementation of these strategies can monitor and evaluate the effects of them on urbanization process. These insights serve as valuable guidance for urban planners, policymakers, and architects in their quest to develop sustainable cities.

REFERENCES

1. A. I. Almulhim, S. E. Bibri, A. Sharifi, S. Ahmad, and K. M. Almatar, “Emerging Trends and Knowledge Structures of Urbanization and Environmental Sustainability: A Regional Perspective,” *Sustainability (Switzerland)*, vol. 14, no. 20, Oct. 2022, doi: 10.3390/su142013195.
2. United Nations, “World Urbanization Prospects - Population Division - United Nations.” Accessed: Dec. 04, 2023. [Online]. Available: https://population.un.org/wup/Country-Profiles/
3. L. Shen, Y. Peng, X. Zhang, and Y. Wu, “An alternative model for evaluating sustainable urbanization,” *Cities*, vol. 29, no. 1, pp. 32–39, Feb. 2012, doi: 10.1016/J.CITIES.2011.06.008.
4. E. J. Gago, S. E. Berrizbeitia, R. P. Torres, and T. Muneer, “Effect of Land Use/Cover Changes on Urban Cool Island Phenomenon in Seville, Spain,” *Energies 2020, Vol. 13, Page 3040*, vol. 13, no. 12, p. 3040, Jun. 2020, doi: 10.3390/EN13123040.
5. World Bank, “Urban Development Overview.” Accessed: Dec.
05,2023.[Online].Available:https://www.worldbank.org/en/topic/urbandevelopment/overview
6. I. Lopez-Carreiro and A. Monzon, “Evaluating sustainability and innovation of mobility patterns in Spanish cities. Analysis by size and urban typology,” *Sustain Cities Soc*, vol. 38, pp. 684–696, Apr. 2018, doi: 10.1016/J.SCS.2018.01.029.
7. S. Ala-Mantila, A. Kurvinen, and A. Karhula, “Measuring sustainable urban development in residential areas of the 20 biggest Finnish cities,” *npj Urban Sustainability 2023 3:1*, vol. 3, no. 1, pp. 1–12, Aug. 2023, doi: 10.1038/s42949-023-00127-8.
8. N. Falah, A. Karimi, and A. T. Harandi, “Urban growth modeling using cellular automata model and AHP (case study: Qazvin city),” *Model Earth Syst Environ*, vol. 6, no. 1, 2020, doi: 10.1007/s40808-019-00674-z.
9. H. Yan and Z. Liu, “A New Perspective on the Evaluation of Urbanization Sustainability: Urban Health Examination,” *Sustainability 2023, Vol. 15, Page 9338*, vol. 15, no. 12, p. 9338, Jun. 2023, doi: 10.3390/SU15129338.
10. S. H. Hosseini and M. Hajilou, “Drivers of urban sprawl in urban areas of Iran,” 2018, doi: 10.1111/pirs.12381.
11. K. Stiphany, “Informal urbanization in Latin America, by Christian Werthmann,” *J Urban Aff*, vol. 45, no. 8, pp. 1534–1535, Sep. 2023, doi: 10.1080/07352166.2022.2162785.
12. A. Yavuz and A. Yavuz, “The Relationship Between Sustainable Urbanisation and Urban Renewal: An Evaluation of Trabzon City Sample,” *Sustainable Urbanization*, Sep. 2016, doi: 10.5772/62951.
13. D. López-Casado and V. Fernández-Salinas, “The Expression of Illegal Urbanism in the Urban Morphology and Landscape: The Case of the Metropolitan Area of Seville (Spain),” *Land 2023, Vol. 12, Page 2108*, vol. 12, no. 12, p. 2108, Nov. 2023, doi: 10.3390/LAND12122108.
14. Y. Zheng, L. Tang, and H. Wang, “An improved approach for monitoring urban built-up areas by combining NPP-VIIRS nighttime light, NDVI, NDWI, and NDBI,” *J Clean Prod*, vol. 328, p. 129488, Dec. 2021, doi: 10.1016/J.JCLEPRO.2021.129488.

PLEA 2024 WROCŁAW
(Re)thinking Resilience

Beyond the Footprint:
The Impact of Infrastructure and Siteworks on the Embodied Carbon of Housing in Ireland

PHILIP COMERFORD[1], OLIVER KINNANE[1], KAVYA MADHU[1], JOSELYN LOPEZ-PELAYO[1], SAWSAN BASSALAT[1]

[1]Department of Architecture, Planning, and Environmental Policy, University College Dublin, Ireland

ABSTRACT: In common with many European countries, plans to decarbonise the construction industry in Ireland focus mainly on reducing the operational energy of buildings and associated greenhouse gas (GHG) emissions, rather than the full life cycle emissions of construction. In order to meet national housing targets, while also reducing emissions in line with the government's Climate Action Plan, other life cycle stages will need to be accounted for. Although there is a growing body of data that measures the embodied energy of different housing types, existing studies to date have mainly assessed materials within the building envelope, with limited measurement of the external areas that serve these buildings. This research fills this gap by proposing a holistic methodology of Life Cycle Assessment (LCA) that includes external areas and siteworks in the embodied carbon calculations of new housing developments. The results indicate that these elements make up a significant proportion of the total embodied carbon of new housing, highlighting the importance of such a methodology. In addition, by integrating external areas and siteworks into LCA calculations, the research highlights the relationships between residential density, and embodied carbon emissions.
KEYWORDS: Embodied carbon, Life Cycle Assessment (LCA), Housing, Residential Development

1. INTRODUCTION

The provision of secure and sustainable housing is fundamental to the UN Sustainable Development Goals [1], yet meeting housing needs through relentless urban expansion can be in direct conflict with climate goals. With 68% of the world's population projected to live in cities by 2050 [2], finding low-carbon strategies for the provision of housing is an urgent issue. In Ireland, an acute housing crisis has given rise to national targets for the production of 33,000 new housing units per year, that are to be achieved in the context of carbon emissions reductions of 45% across the construction sector by 2030, as part of the government's Climate Action Plan [3]. It is clear that meeting both these targets will be impossible under business-as-usual scenarios where new housing demand is largely satisfied by construction on greenfield or peripheral urban sites, generating low-rise urban sprawl, in addition to locking in car-dependant travel patterns and related carbon emissions.

Until now, the true carbon impact of new construction in Ireland has not been entirely assessed, as current regulations only require the reporting of the operational energy used to run buildings through the Building Energy Rating (BER) system, and national regulations provide operational energy targets only for new construction. This situation is mirrored in the academic literature, where at an urban scale the focus to date has largely been on the operational phases of whole life cycle emissions. As the operational energy efficiency of buildings improves, due to improved construction techniques and renewable energy measures, the impact of other life cycle stages that measure embodied carbon (EC) becomes proportionally greater [4].

Furthermore, much existing literature to date that includes embodied carbon in Life Cycle Assessment (LCA) has focused on the individual building, with construction at the urban scale either partially included or entirely omitted. This study seeks to fill this gap, concluding that significant embodied carbon is contained in the roads, footpaths and external surfaces of a new development. Accordingly, the research analyses the scale of the urban block and neighbourhood, developing an LCA methodology that combines building, external hard landscaping, and road infrastructures. This scale is sufficiently detailed to allow comprehensive LCAs of real-world building typologies and also of the external areas that serve them. By considering the whole life cycle emissions of buildings in an urban planning context, the research suggests how claims for the sustainability of higher densities and compact urban growth might be assessed.

2. LITERATURE REVIEW

In order to transition to low-carbon construction, studies have shown that the choice of housing typology and resultant urban form can have a

significant impact on operational GHG emissions [5][6]. More recent studies have also measured the embodied carbon of housing types, finding variations according to factors such as height, structural system, and density [7][8]. As noted above, to date this existing literature has mainly considered the embodied carbon of materials within the building envelope, with limited measurement of associated external areas.

2.1 Literature at building scale

There is an expanding body of information that records the embodied carbon of various building types, such as the Ramboll embodied carbon database [9]. In the academic literature recent studies have sought to understand the sources of embodied carbon although the scope of study is generally confined to buildings only. Drewniok *et al*. [7] compared the efficiency of residential buildings at different heights, finding that heights of between four and storeys are the most efficient in terms of embodied carbon. De Wolf *et al*. [10] focused on structure as the highest contributing element to overall embodied carbon, and discovered a wide range of emissions depending on the structural material and system chosen.

2.2 Literature at urban scale

Expanding from the individual building scale, a study by Stephan *et al.* [8] analysed a low-rise suburban neighbourhood in Melbourne over a period of 100 years under various scenarios including operational carbon, embodied carbon, and transport related emissions. The authors found that embodied and operational carbon emissions were comparable, representing approximately one third of total emissions each, with transport emissions accounting for the remaining third. Alternative scenarios based on these results showed that the replacement of 50% of the single low-rise dwellings by apartment buildings would create a whole life carbon saving. This is in spite of the initial increase in embodied carbon due to demolition and rebuilding.

Other research has adopted an approach of high-level parametric modelling to assess urban neighbourhoods under various scenarios of density and energy intensity. The study by Pomponi *et al.* [11] discovered that while taller urban environments increase GHG emissions, building similarly dense low-rise neighbourhoods can provide savings.

An larger scale study by Kayacetin and Tanyer [12] analyses three social housing projects in Ankara, Turkey, and includes the construction of infrastructure in addition to building-related emissions and transport. This is the most comprehensive study to date in the literature in terms of its scope for accounting embodied carbon at the urban scale. The study divides areas outside the building into transport infrastructure (24% of total emissions) and structural landscape (9%), in line with the findings of this study. The research by Kayacetin and Tanyer calculates life cycle emissions for the construction of external hard surfaces, and also includes transport-related emissions.

Is clear that there is a need for studies that provide detailed LCAs of actual building typologies, in addition to comprehensive assessment of the external areas infrastructures that serve them. This case study fulfils this gap in the current literature, as it operates at the intermediate scale of the urban block, where detailed bottom-up LCAs can be carried out. It should therefore provide more accurate results than some of the urban scale research listed above, that are dependant on abstracted or parametric models of buildings and urban areas.

3. METHODOLOGY

3.1 Scope of LCA

The case study presented here is a recently-built housing development for 112 dwellings on the outskirts of Dublin, whose layout may be considered typical for contemporary housing production on the edge of an Irish town or city. The majority of the units are two storey houses, arranged either in pairs (semi-detached) or as row housing (terraces) (Fig. 1). All dwellings have on-site parking, and are served by a network of newly-built road infrastructure.

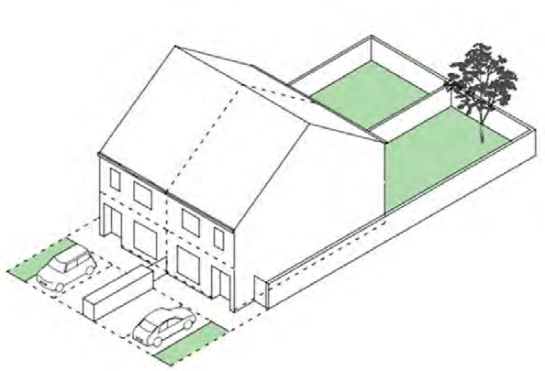

Figure 1: Typical semi-detached house type from case study

The research has been carried out according to EU Levels system Stage 2 'Detailed Design and Construction', and in accordance with reference standard EN 15978:2011 [13]. The study analysed life cycle stages A1-A5, that includes the manufacture of materials, their transport to site, and ancillary construction works. It was considered that insufficient data was available to allow for assessment of later life cycle stages. It is however worth noting that in residential construction, stage B can have a high overall life cycle contribution, largely due to domestic heating systems and appliances, and their operation, maintenance and replacement.

3.2 LCA Methodology

The methodology used is a tool called 'Upfront', developed by the Irish Green Building Council (IGBC) as part of INDICATE, an EU funded project to develop building-level data for Whole Life Carbon (WLC) in Europe [13]. This tool is an Excel-based spreadsheet that calculates WLC by construction element and life cycle stages for according to standards set out in reference document EN 15978 [13]. Environmental Product Declarations (EPDs) have been used where available in order to estimate the global warming potential (GWP) of materials used. Where possible, EPDs used are from the Irish construction industry, or else the closest European equivalents are used. The GWP of other materials where no EPDs are available are calculated using carbon factors from the Inventory of Carbon and Energy (ICE) database, that are included in the Upfront tool.

The results of the buildings were checked using a second methodology, OneClick LCA, that is currently the industry-standard software used in Ireland and the UK. OneClick has assumptions as to construction build-ups and materials built in to the software, and these assumptions are not always visible or editable by the user. Although easier to use than Upfront, less input data is required so it does not give results that are as accurate or as suited to the Irish Construction Industry.

3.3 Scope of Study: LCA by Urban Morphology

As outlined in the above literature review, an innovative aspect of this study is the inclusion of external areas in the LCAs, and these have been calculated separately to the buildings. In order to clarify the scope of the study, a methodology was developed that breaks the development down according to categories of urban morphology with separate LCAs used to measure buildings, plot (front and back gardens), and the urban block and external public areas (Fig. 2). An advantage of breaking down LCAs into these scales is that it allows comparison with other projects and studies, for example those that estimate the buildings only, or developments on infill urban sites where the public external areas and road infrastructure are already existing, and therefore not counted.

For the external areas and services, drawings were prepared to estimate the surface areas of roadways, footpaths and external landscaping. A siteworks Bill of Quantities (BoQ) was then prepared that quantified these external surfaces in a form that could be used for the embodied carbon assessment. Having carried out the LCA for the external surfaces and infrastructure, the final step in the methodology is to assess the proportion of this figure due to each individual dwelling.

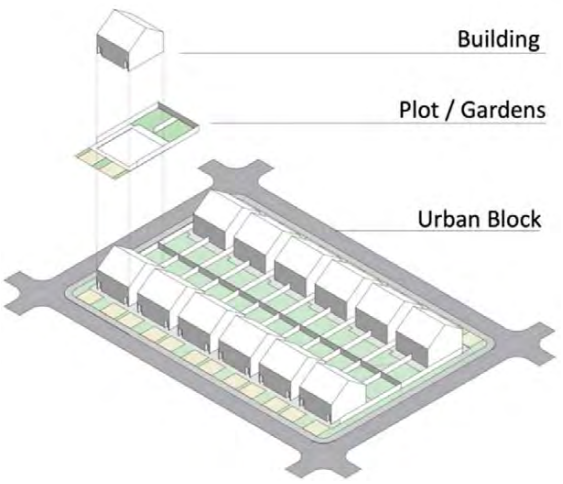

Figure 2: LCA analysis by Scales of Urban Morphology

4. RESULTS

The first results presented here is the LCAs for the house type analysed. Following this, the breakdown of external public areas is shown. Finally, the two sets of results are combined, showing the impact of external works on the overall embodied carbon of the house.

4.1 LCA of Dwellings

Total Stage A1-A5 Emissions in kgCO2e per dwelling
House: 43,169 kgCO2e
Total Stage A1-A5 Emissions in kgCO2e/m2
House: 366 kgCO2e/m2

This result is broken down by building element and material (Fig. 3), and it can be seen that significant carbon is expended in the ground floor, substructure, and external walls. Concrete is the most carbon intensive material, closely followed by insulation, which is mostly of the PIR type. The buildings are finished externally in concrete block or brick, and these high carbon materials are visible in the results. Given these results we could question the logic of cladding timber frame buildings in rendered concrete block and brick, given the high relative contributions of these materials to the carbon count. The roof is also a significant source of carbon emissions, due to the concrete tile finish, and the amount of material generally required to create the large volume of the pitch structure. This suggests that this house type could be made more carbon efficient either by providing a simpler structure such as a low pitch for flat roof, or providing for the possibility of future upwards extension into the roof space. It is worth noting that the overall igure for services (M&E) is low as only stages A1-A5 were analysed. This figure would rise considerably if Stage B (in-use) carbon was included, as replacement figures for mechanical plant, and refrigerant leakage for heat pumps can be considerable.

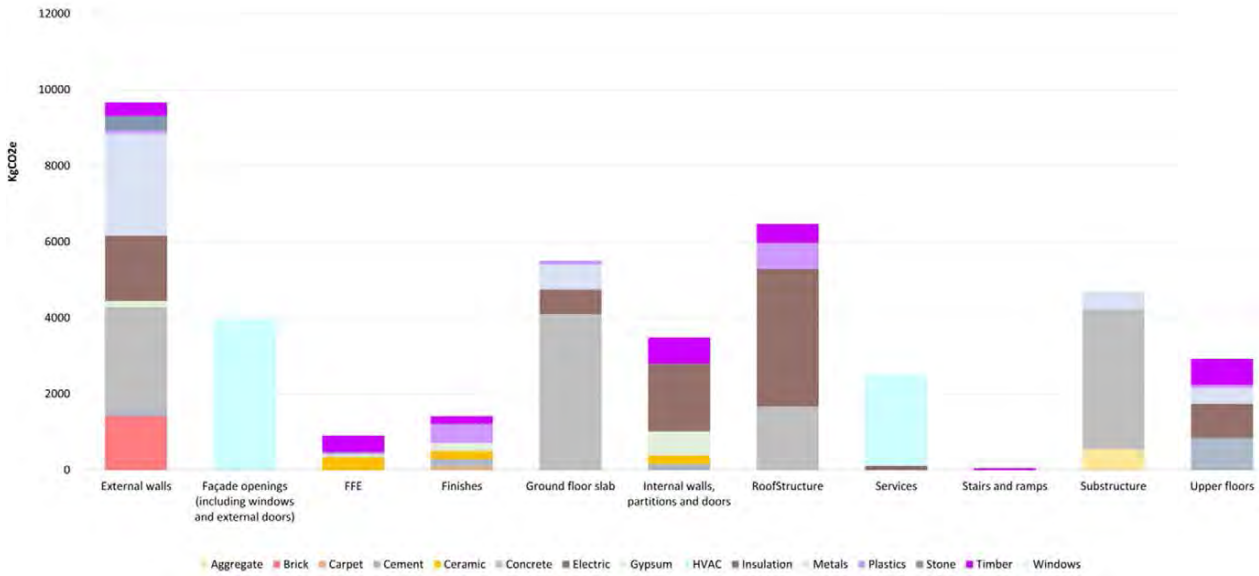

Figure 3: Stage A1-A5 embodied carbon breakdown of individual dwellings by element and material

As noted above these results were also calculated in OneClick LCA software for checking purposes and the result was 318 kgCO2e/m2. While similar in range, this result is slightly lower than that given in Upfront, and the difference could be accounted for by the fact that the principal results used Irish based EPDs and construction build-ups specific to the local industry, whereas OneClick has UK based assumptions built in.

4.2 LCA of External Public Areas

The embodied carbon of the public external areas, has been calculated, the majority of which are either asphalt roadway or concrete footpath (Table 1). Assessing the results, it can be seen that the largest sources of carbon emissions by material are due to concrete and asphalt. Crushed stone aggregate – also known as hardcore – is also a significant figure, as is used for filling siteworks after excavations. Although aggregate has a relatively low carbon factor and therefore low A1-A3 results, it has a high result for stage A4, transport, due to the amount of heavy vehicle movements. The concrete footpaths also represent a high overall figure as these are required to withstand vehicular traffic, and so have a robust and carbon-intensive construction.

Material	Total kgCO2e	kgCO2e/house
Metals	5362	48
Concrete	185321	1655
Asphalt	116122	1037
Aggregate	43561	389
Grand Total	**350366**	**3128**

Table 1: Stages A1-A5 Embodied Carbon of Public External Areas by material

4.3 Combined Results

The results below show that the external areas form a significant part of the embodied carbon of residential construction (Table 2). For low-rise houses, this represents an additional 18% of greenhouse gas (GHG) emissions on top of emissions for the dwellings themselves. The two-storey houses have a high EC figure for external surfaces in both private and public areas due to the quantity of surface given over to vehicle traffic, mostly composed of asphalt and concrete.

Table2: Stages A1-A5 Embodied Carbon of External Areas

Results per Dwelling Unit

	Total KgCO2e Per Dwelling Unit	Total KgCO2e External Areas – Siteworks: Plot	Total KgCO2e External Areas - Siteworks: Public	Total KgCO2e Building + Siteworks	% Increase due to Siteworks
House per unit	43,168	4,742	3128	51,039	18%
House per m2	366	40	27	433	18%

The combined results have been broken down in to dwelling, siteworks (plot), and siteworks (public), as per the categories of urban morphology as described in section 3.2 above. Considering this breakdown, we can see that the external works associated with the private plot create an additional 11% embodied carbon, and those of the public external works an additional 7%. The high figure of 11% for the private plot around the houses – essentially the front and back gardens – is mainly due to the two parking spaces in concrete paving and associated construction build-up.

The combined results for external works furthermore suggest that this form of housing is inefficient in its use of land, as an equivalent apartment building could occupy a similar footprint of site area, yet accommodate more residents.

4.4 Assumptions and Limitations

Finding sufficient data to carry out detailed Life Cycle Assessments (LCA) proved difficult, and certain assumptions have had to be made as a result. It was not possible to obtain Mechanical and Electrical (M&E) services drawings or detailed specifications for any of the projects so information based from studies carried out by the Chartered Institute of Building Surveyors (CIBSE) using their methodology TM65 [14] which provided embodied carbon estimation for stages A1-A5 of projects with similar service installations. It is also noted that service installations can add a high carbon count for in-use life cycle stages B, due to factors such as the replacement of parts, or refrigerant leakage from air-source heat pumps.

Information on the internal finishes of the units was not provided, so these had to be estimated using standard specifications, referring to online estate agents' brochures for visual information. Bills of Quantities (BoQ), where provided were not sufficiently detailed to be useful, so this required the creation of BoQs for both buildings and siteworks elements.

5. DISCUSSION POINTS

Having generated baseline data for a 'business-as-usual' development scenario, the research points towards areas for future decarbonisation strategies.

Analysing the embodied carbon breakdown of individual dwellings shows the high impact of certain external elements such as brickwork cladding and concrete roof tiles. These could easily be substituted for other materials, although regulatory constraints could be encountered, such as the planning authority's requirement to use brick.

An assessment of transport emissions associated with the development was considered beyond the scope of this study. In addition, detailed information on transport modes used was not available due to the development being completed after the most recent national census that records this data. This is a fertile area for future research however, as the dominant two-storey dwelling types has two-car parking spaces, so will generate a high amount of tailpipe emissions. Future research might compare this suburban development with denser equivalents closer to the urban core, where the use of public transport or other soft modes of travel is likely to be more prevalent.

6. CONCLUSION

These results have demonstrated that low-rise, low-density development patterns represent an inefficient use of both land and infrastructure, with consequently increased embodied carbon emissions. The case study therefore provides a basis for future research into denser urban forms with a more compact footprint and use of external space, in order to assess potential savings in emissions. The methodology shows the importance of incorporating LCAs of external works and infrastructure together with the measurement of building, suggesting that future policy should expand the scope of LCAs required for new developments beyond the dwellings themselves to include the entire site and its infrastructure. In order to propose truly low-carbon solutions methods that provide a holistic assessment of life cycle emissions will be required.

ACKNOWLEDGEMENTS

This work was funded by the Sustainable Energy Association of Ireland (SEAI) Research Development and Demonstration (RDD) funding scheme and by AHARDD Construct Innovate funding. These projects are run in collaboration with the Irish Green Building Council (IGBC).

REFERENCES

1. 'Cities - United Nations Sustainable Development Action 2015', United Nations Sustainable Development. Accessed: Dec. 27, 2023. [Online]. Available: https://www.un.org/sustainabledevelopment/cities/
2. 'World Urbanization Prospects - Population Division - United Nations'. Accessed: Dec. 19, 2023. [Online]. Available: https://population.un.org/wup/
3. R. O. Hegarty and O. Kinnane, 'A whole life carbon analysis of the Irish residential sector - past, present and future', *Energy Clim. Change*, vol. 4, p. 100101, Dec. 2023, doi: 10.1016/j.egycc.2023.100101.
4. P. Rode, C. Keim, G. Robazza, P. Viejo, and J. Schofield, 'Cities and Energy: Urban Morphology and Residential Heat-Energy Demand', *Environ. Plan. B Plan. Des.*, vol. 41, no. 1, pp. 138–162, Feb. 2014, doi: 10.1068/b39065.
5. B. Cody, W. Loeschnig, and A. Eberl, 'Operating energy demand of various residential building typologies in different European climates', *Smart Sustain. Built Environ.*, vol. 7, Sep. 2018, doi: 10.1108/SASBE-08-2017-0035.
6. P. Rode, C. Keim, G. Robazza, P. Viejo, and J. Schofield, 'Cities and Energy: Urban Morphology and Residential Heat-Energy Demand', *Environ. Plan. B Plan. Des.*, vol. 41, no. 1, pp. 138–162, Feb. 2014, doi: 10.1068/b39065.

7. M. P. Drewniok *et al.*, 'Mapping material use and embodied carbon in UK construction', *Resour. Conserv. Recycl.*, vol. 197, p. 107056, Oct. 2023, doi: 10.1016/j.resconrec.2023.107056.
8. F. Pomponi, R. Saint, J. H. Arehart, N. Gharavi, and B. D'Amico, 'Decoupling density from tallness in analysing the life cycle greenhouse gas emissions of cities', *Npj Urban Sustain.*, vol. 1, no. 1, Art. no. 1, Jul. 2021, doi: 10.1038/s42949-021-00034-w.
9. M. Röck *et al.*, 'Towards embodied carbon benchmarks for buildings in Europe - #2 Setting the baseline: A bottom-up approach', Zenodo, Mar. 2022. doi: 10.5281/ZENODO.5895051.
10. C. De Wolf, F. Yang, D. Cox, A. Charlson, A. S. Hattan, and J. Ochsendorf, 'Material quantities and embodied carbon dioxide in structures', *Proc. Inst. Civ. Eng. - Eng. Sustain.*, vol. 169, no. 4, pp. 150–161, Aug. 2016, doi: 10.1680/ensu.15.00033.
11. N. C. Kayaçetin and A. M. Tanyer, 'Embodied carbon assessment of residential housing at urban scale', *Renew. Sustain. Energy Rev.*, vol. 117, p. 109470, Jan. 2020, doi: 10.1016/j.rser.2019.109470.
12. E. Standards, 'BS EN 15978:2011 Sustainability of construction works. Assessment of environmental performance of buildings. Calculation method', https://www.en-standard.eu. Accessed: Aug. 30, 2023. [Online]. Available: https://www.en-standard.eu/bs-en-15978-2011-sustainability-of-construction-works-assessment-of-environmental-performance-of-buildings-calculation-method/
13. 'INDICATE- INDICATE accelerator offering a project framework and co-funding to support efforts to generate much-needed building-level Whole Life Carbon (WLC) data in Europe.', INDICATE. Accessed: Dec. 22, 2023. [Online]. Available: https://www.indicatedata.com
14. 'Embodied carbon in building services: a calculation methodology (TM65) | CIBSE'. Accessed: Dec. 22, 2023. [Online]. Available: https://www.cibse.org/knowledge-research/knowledge-portal/embodied-carbon-in-building-services-a-calculation-methodology-tm65

PLEA 2024 WROCŁAW
(Re)thinking Resilience

AQUA-PUNCTURES

Rainwater Harvesting for Urban Cooling through Vegetation and Evaporation in Izmir

THANOS N. STASINOPOULOS[1] NAZLI SÖZER ÇAKIR[1]

[1] Izmir University of Economics, Izmir, Turkey

ABSTRACT: Global warming and urban heat island [UHI] have become interconnected issues related to dehydration in many regions across the globe. To mitigate UHI, it is essential to transform solar heat into latent heat through evaporation rather than allowing it to contribute to the sensible heat in urban areas. This can be achieved by promoting vegetation-based evapotranspiration and implementing evaporative cooling techniques. One effective approach is rainwater harvesting, which moderates the water loss to the sea and facilitates evaporation during dry periods. Furthermore, the collected water can support plant growth and enhance their evapotranspiration process. In Izmir, a Mediterranean city in need of urban cooling, implementing a concept called 'Aquapuncture' can be beneficial. This concept involves creating multiple hubs throughout the city that utilize rainwater for passive cooling. This work focuses on describing the practical aspects and design strategies of these cooling units implemented as attractive and refreshing elements in urban design. The aim is to address the challenges faced by warm cities like Izmir and provide effective cooling solutions. By adopting these measures, it is possible to combat the adverse effects of global warming, mitigate the UHI effect, and create more pleasant and comfortable conditions in warm cities.
KEYWORDS: New water paradigm, urban cooling, rainwater harvesting, cooling stations, evaporative cooling.

1 INTRODUCTION

The Urban Heat Island phenomenon [UHI] has become an increasingly significant issue in modern cities. It has negative implications on various aspects, including energy consumption and public health. As a result, cooling has become a crucial priority in the fields of architecture and urban design.

One effective method to reduce outdoor air temperature is through evaporation, which can be achieved by incorporating various water features in the urban environment. These water features not only provide thermal relief but also enhance the visual appeal of the surroundings. Another cooling strategy involves the evapotranspiration process of plants, which provides shade and further contributes to temperature reduction. However, it is important to note that both of these "green" cooling options heavily rely on "blue" fresh water, which is a resource that is increasingly scarce worldwide. This work proposes a technique to tackle UHI by implementing Rainwater Harvesting (RWH) in a dense urban setting on the Mediterranean coast.

2 BACKGROUND

Extensive research has been conducted to investigate the effectiveness of incorporating green and blue elements in urban design to mitigate the negative impacts of urban overheating. However, it is essential to address a fundamental requirement for supporting vegetation and enabling evaporative cooling: the availability of freshwater. While some existing research as 9 or 11 focuses on evaluating strategies without considering this prerequisite, it is crucial to acknowledge alternative water sources beyond tap water, which often comes from distant locations. Rainwater and stormwater present viable non-conventional water sources that can be harnessed to facilitate urban cooling initiatives 14. By recognizing and utilizing these resources, cities can make significant progress in combating urban heat and promoting sustainable urban environments.

In warm regions with limited fresh water resources on or beneath the ground, utilizing atmospheric water as a supply source is a potential solution. Rainwater and stormwater harvesting are sustainable methods for water supply that can be applied in such areas to supplement other fresh water sources. This work proposes a scheme that combines cooling techniques with rainwater harvesting (RWH) to improve the urban microclimate without the need for a central water distribution network provided by the municipality.

The issue of urban overheating and its associated problems, along with potential solutions, have been extensively studied, including programs like the ESMAP program by the World Bank 5. Proposals by

Kravčík et al. 10 have paved the way for a *"new water paradigm"* that emphasizes local interventions related to the small water cycle. Kimic & Ostrysz 9 present a comprehensive list of urban cooling techniques that *"aim to reintegrate water into a nature-oriented water cycle within the city."* Similarly, Langie et al. 11 examine various forms of water elements in public spaces and highlight the influence of appropriate water element design on cooling effects in the immediate vicinity. Surprisingly, both of these works do not mention the potential use of RWH.

This paper introduces a practical method to enhance the water availability in the city by reducing the wasteful flow of water to the sea and utilizing the latent heat of vapour released into the atmosphere to reduce the sensible heat of the city. An additional objective is to improve the comfort of city dwellers through passive "cooling stations."

3 COOLING STATIONS

Cooling stations or cooling centres are facilities that play a crucial role in providing a safe and cool environment for the public during periods of high air temperatures, especially for those who lack sufficient private cooling options and are more vulnerable to the health impacts of excessive heat. These facilities serve as refuges from excessive heat, allowing individuals to cool down, stay hydrated, and protect themselves from the adverse effects of heatwaves. Cooling stations are vital for ensuring public health and can be an integral part of local heat emergency response plans. The implementation of cooling stations for health reasons has been extensively surveyed in the US by Widerynski et al. 16.

These stations can be integrated into designated indoor community centres, such as libraries, religious buildings, or shopping malls, which are equipped with active cooling systems. They can also be situated in outdoor public parks or community pools.

Such facilities are often indoor spaces and rely on energy-intensive air conditioning. In contrast, this study proposes the creation of a network of semi-outdoor 'oases' that utilize RWH to create cool environments through shading and evaporative cooling.

By utilizing RWH in the design and operation of cooling stations, it becomes possible to reduce the energy demand typically associated with air conditioning systems that intensifies UHI. The collected rainwater can be used for evaporative cooling, effectively lowering the ambient temperature and providing a sustainable and energy-efficient cooling solution. This approach aligns with the goal of creating cool and comfortable environments while minimizing the environmental impact.

4 THE CONTEXT

The work focuses on the city of Izmir, a rapidly growing metropolis located on the west coast of Turkey, with a population of over 4 million. Izmir has a hot-summer Mediterranean climate (Köppen climate classification: Csa) 13. These climatic characteristics make it suitable for implementing evaporative cooling techniques [Figure 1].

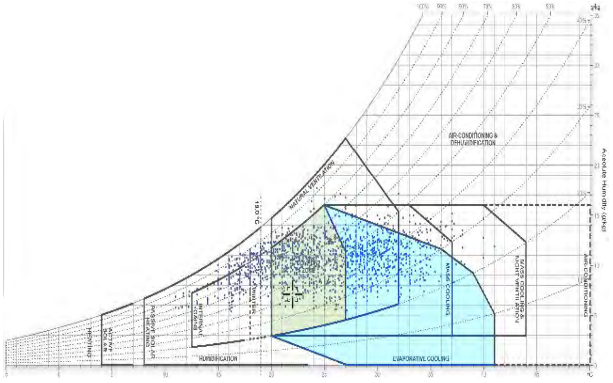

Figure 1: Psychrometric chart for Izmir for the period June-September. The dots show the hourly combination of air temperature and relative humidity. The cyan area indicates the extension of the basic comfort zone (green) by means of evaporation. 42% of the displayed points are in the extended comfort zone. Graph from 12 with climate data from 7.

Izmir receives an average annual rainfall of approximately 700mm, which provides a satisfactory amount of water RWH applications. Many parts of Izmir are densely built with materials that contribute to the UHI effect, leading to discomfort during the summer months. While coastal areas of the city benefit from sea breezes, other areas rely primarily on greenery for cooling, sometimes supplemented by shading or evaporation methods [Figure 2].

Figure 2: Evaporative cooling and shading elements in Baris Selcuk Park in a dense area of central Izmir. Photo by Google Maps Street View.

Green infrastructure, such as vegetation and trees, can help mitigate the UHI effect by providing shade and facilitating evapotranspiration, which contributes to cooling the surrounding environment.

Considering Izmir's climatic conditions, the availability of rainfall, and the challenges posed by the UHI effect, the proposed implementation of evaporative cooling techniques and rainwater

harvesting can offer potential solutions to enhance the urban microclimate and create more comfortable and sustainable environments in the city.

5 INTRODUCING AQUA-PUNCTURE

The urban green areas of metropolitan Izmir are on average about 5% of the built-up areas, ranging from 1% (Gaziemir) to 17% (Narlidere) 6. Maintenance of those areas requires large amounts of water every year, of which nearly 60% comes from groundwater resources 8, 15. There are several good examples of well-equipped and maintained parks of various sizes around the city, the protagonist being the lengthy seafront that many locals fully embrace as an appealing setting for fresh air and coolness.

Besides the neighbourhoods that are near green amenities, there are others less lucky that have no relief from the effects of concrete thermal mass. The present work addresses that situation through 'passive cooling stations' at various spots of the city, which will utilise RWH to alleviate the effects of heat waves and improve the local microclimate around them in a way more friendly to the environment and the city budget than the usual cooling stations.

A network of such structures will spread their cooling effects across the city as a kind of cooling 'acupuncture', a word that in this case can be modified to '*aqua*-puncture' given that its key element is the water. The proposed cooling stations are oasis-like installations where the evapotranspiration of lush vegetation is combined with various methods of evaporative cooling like fountains, misting devices, or passive downdraft systems [PDEC], utilising water collected by RWH systems and stored in the given area. Depending on the location, the collected water can be used for supporting the surrounding green features. A generic example of such a cooling station and its typical components is described next.

6 SYSTEM COMPONENTS

The Basic Aquapuncture Unit [BAU] must possess the main Vitruvius attributes of *"firmitas, utilitas, venustas"* (firmness, usefulness, beauty). In addition, its construction cost and maintenance needs should be minimised, and also it should emanate an ecological identity promoting the benefits of RWH. Based on these specifications, a natural cooling system has been devised aiming at alleviating the distress by urban overheating. It is a green-blue practical application being also an attractive urban feature, preferably in arid neighbourhoods. The basic components of the system are schematically shown in Figure 3 and include:

1. A RWH scheme including catchment and storage.
2. A pergola structure.
3. Vegetation for shading and evapotranspiration.
4. Additional passive cooling systems.
5. Seating facilities.

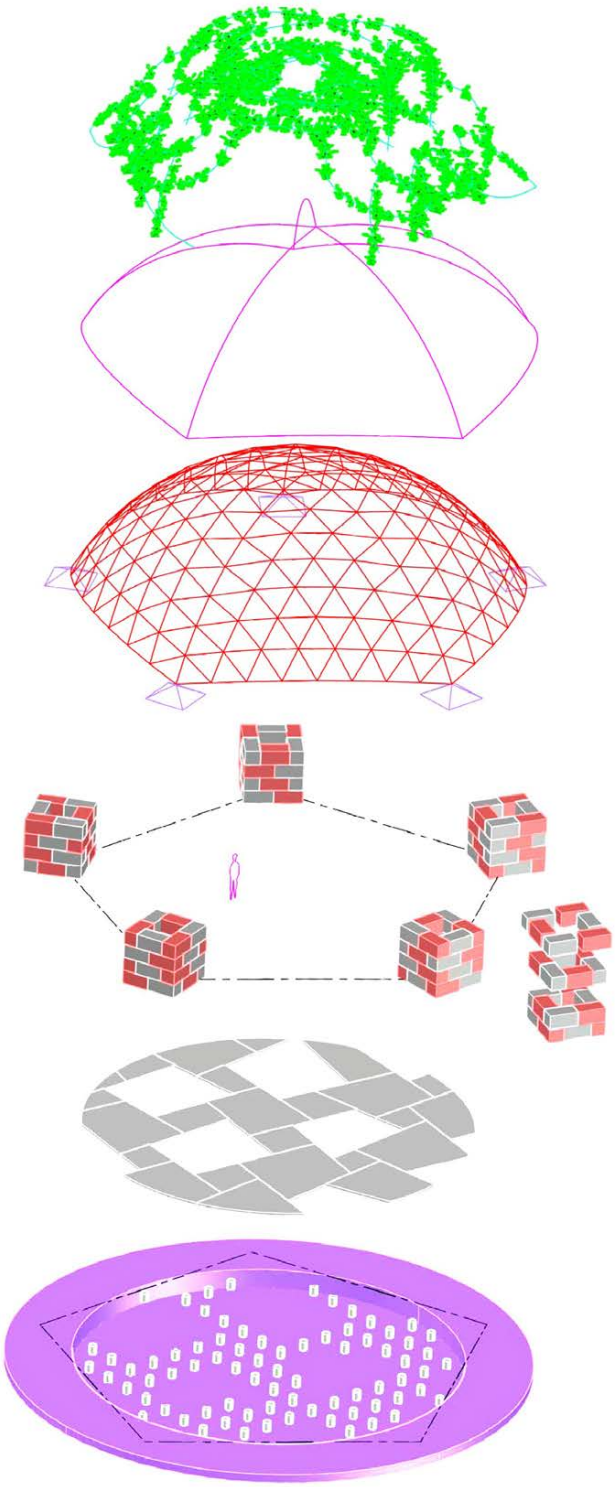

Figure 3: A generic example of an 'aquapuncture' hub. Components 1 and 5 are not shown in the image, as well as additional facilities for functions unrelated to cooling.

6.1 RWH system

The catchment surface is the surrounding pavements, depending on the particular context. The surface runoff reaching the BAU is collected by a grill-covered canal and guided to the water storage after an initial filtration to remove unwanted particles. The

storage can be concrete or synthetic water tanks under the BAU floor, or exposed water ponds, or combination. The capacity of the storage depends on the intended use (cooling, irrigation) and the rainwater potential of the specific area.

In the example illustrated in Figure 3, the water is collected in a circular concrete pond, covered by prefabricated slabs with decorative patterns that rest on low columns in a way reminiscent of the Roman 'hypocaust' system. The water mass depends on the bottom depth and can be fully covered or partially exposed with decorative elements, floating plants, small fountains, lights, etc. Similar creative designs are envisioned in the other examples too.

In addition to concrete, as shown in this example, water storage can be constructed using materials such as steel, synthetic, or composites. Each material has its own advantages and drawbacks, like cost, installation requirements, maintenance needs, and resistance to corrosion or degradation. The choice of material depends on factors such as budget, desired lifespan, site conditions, and legal requirements for water storage.

Water quality, specifically regarding pollutants or contaminants, is a subject for careful consideration. Deng 4 has studied pollution issues related to RWH in urban farming, while Abbasi 1 provides an analysis of water pollution on rooftops caused by chemical, microbiological, and physical agents. Since the water is not to be used for drinking, the main objecting of filtering is to avoid blocking the used pipes, especially if a misting system is employed. In the latter case, the potential health risks require even more attention. That underlines the importance of the proper filtering installation in the materialization of the proposal.

6.2 Pergola top

The top cover is basically a pergola-like structure for supporting climbing vegetation, evaporation systems, lighting, etc. The structure shown in example 1 is a geodesic surface constructed by steel tubes that offer strength and lightweight with a small mass of materials, as sustainability principles instruct. Its high ceiling in the middle offers a spacious feeling and at the same time the low perimeter reduces solar penetration.

The roof frame is resting on massive pillars made of gabion steel baskets filled with crashed stones on a concrete underlay. The cube-like pillars of all the examples shown have a cavity in the middle containing soil for plants growth. Steel pyramids anchored on the pillar tops hold the roof.

This design concept addresses sustainability principles like the least possible use of materials, low construction and maintenance cost, and recycling materials. The same principles can of course be applied using other geometries and materials, as in the examples shown in Figure 4, Figure 5, Figure 6.

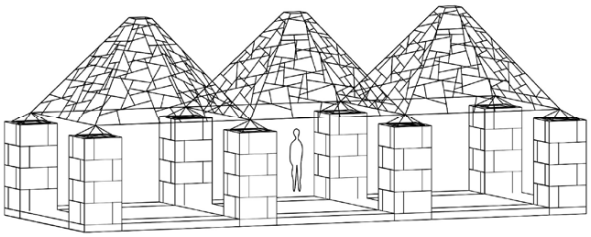

Figure 4: This example is a linear interpretation of the basic 'gabion pillars + steel pergola' concept. The square modules can be repeated along a path, and adjusted to a sloping terrain. The water tanks can be underneath the pavement or nearby. The top opening of the shown pyramidal roof can be combined with a PDEC system.

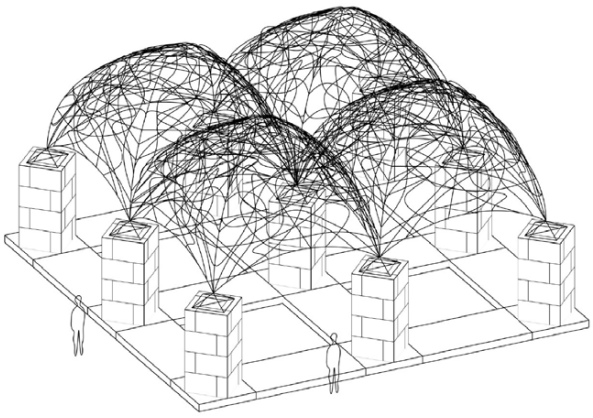

Figure 5: The roof can take various forms always using welded steel bars. The repetition of the square modules can be in two directions.

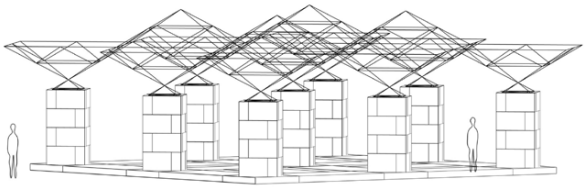

Figure 6: One of the numerous pergola variations can consist of space-frame modular elements.

6.3 Vegetation

Apart from the aesthetic aspects, plants are used in a dual role for cooling through their shade and evapotranspiration. Fast growing climbers like *Wisteria sinensis, Clematis armandii, Ipomoea purpurea*, *Parthenocissus quinquefolia*, etc. can grow on the soil in the pillars and eventually cover the entire roof and the pillars (Figure 7) becoming a source of cool air, while the warm air escapes passing through their foliage. The selection of the most appropriate plants depends on parameters like growing speed, evapotranspiration potential, watering and maintenance needs, effects on human health and on wildlife, etc. Further to the roof, vegetation can grow in the gaps of the gabions, eventually converting the pillars into large green blocks.

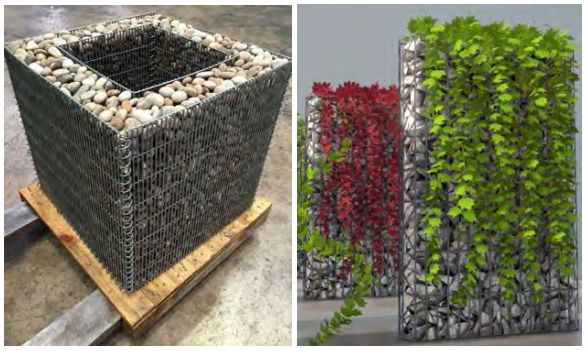

Figure 7: Examples of a hollow gabion planter (left), and gabion pillars covered with climbers (right).

6.4 Cooling systems

Further to the shade and evapotranspiration of the green roof, BAU is a passive mechanism for evaporative cooling by assorted means like: misting sprinklers attached to the roof frame, water dripping on the gabion pillars, small fountains on the cistern cover, etc. These systems are supported by the harvested rainwater, which also sustains the irrigation of the green roof and possibly of the surrounding vegetation.

6.5 Water use

The water collection has a triple objective:

- to withhold stormwater runoff instead of letting it flow freely to the sea;
- to support vegetation and evapotranspiration;
- to feed evaporative cooling applications, in addition of the results of evapotranspiration.

The capacity of the water tank depends on the amount of collected water required for the intended uses. In any case, the use of a filtering system and a pump is essential, requiring the provision of such equipment, housed in one of the pillars or next to the water tank. The filtering requirements are even more intense for using misting nozzles, in which case the issue of the biological agents in the collected water is of prime importance.

6.6 Additional features

In addition to the basic components above, certain other elements can improve the functionality and efficiency of a BAU, such as

- fans to boost evaporation; even better, passive downdraft evaporative cooling systems attached to the pergola;
- seating provision for visitors resting;
- lights to extend use during nights, and to add aesthetic qualities through colour;
- drinking water and refreshments dispensers.

The use of pumps, fans, lights, etc. implies the need for electricity connection, with the relevant installation housed in one of the pillars.

6.7 Financial considerations

The appeal of the scheme depends not only on its performance but also on its costs incurred. The proposed superstructure consists of low-cost materials -mostly crushed stones and a relatively small amount of steel. The substructure cost depends on the type and capacity of the water tank. The water features (misting, dripping, fountains) are not in a high-cost category and their pumps consume a low amount of electricity. The extra cost by additional features depends on their design and it is beyond the cooling role of a BAU.

7 METHODOLOGY

The materialisation of the proposed scheme in urban locations requires the cooperation of the municipal authorities in two parallel directions. Firstly, to develop and monitor a couple of pilot structures; secondly, to formulate an action plan across the city fabric based on the thermal and hydrological conditions of various selected locations.

The scheme matches some of the actions proposed in the report “Izmir Green City Action Plan” 3, namely WCM1.5, WCM1.11, LU1.7, facilitating the integration of Aquapuncture in the municipal activities.

Starting from a review of existing water applications in urban open spaces, the objective is to develop a network of urban ‘oases’ utilising and promoting RWH in the urban setting of metropolitan Izmir, in cooperation with the local authorities. The basic concept is to add cooling installations in selected spots of the city, offering oasis-like spaces for the public. The ultimate aim is triple:

- to provide comfortable conditions in public outdoor spaces during hot periods, mostly in areas far from main green zones;
- to mitigate the negative effects of UHI at local level;
- to advertise the environmental benefits of RWH so to broaden its use and lessen the water stress.

At the present point, the aim is to establish the framework for incorporating the proposal in forthcoming municipal activities and organise its wider implementation after a preliminary period.

8 APPLICATION STEPS

A survey, conducted in collaboration with local authorities, will explore various typologies for cooling hubs, including their space requirements, water demand, construction options, feasibility in legal and financial terms, and the optimal integration within the city. To serve as prototypes for potential replication, one or two pilot projects will be implemented in selected locations in Izmir. These case studies will be crucial in demonstrating how the general concept can be practically applied, following

a meticulous assessment of numerous design parameters.

In order to promote the significance of RWH for the environment and the people, the municipality could organize design contests among professionals and students, inviting them to propose compelling versions of the cooling stations that enhance the cityscape. Such initiatives could potentially attract funding from the private sector and European programs. An example of a similar contest is the "Cool Abu Dhabi Challenge" held in 2020, which invited global proposals for improving outdoor conditions in Abu Dhabi's extreme climate 2.

Drawing from the experience gained in Izmir, the "aquapuncture" model could be adapted and implemented in other locations with similar climatic conditions and comparable annual rainfall. Modifications would be made to suit the specific local context.

9 CONCLUSION

This work introduces the concept of "aquapuncture," which involves the creation of cooling "oases" throughout metropolitan Izmir to enhance the urban environment in a sustainable manner. These installations will not only provide thermal benefits but also contribute to the visual appeal of the cityscape, being also an observable manifestation of the advantages of RWH.

Going one step further, the BAU hubs can evolve into integral components of a "green-blue" network that gradually extends throughout the city. This network serves as a natural and visually appealing solution for addressing the consequences of global warming, particularly by mitigating one of its underlying factors: the aridity prevalent in today's urban landscapes, which disrupts the functioning of the local water cycle.

8. REFERENCES

1. Abbasi T., & Abbasi S. A. (2011). Sources of Pollution in Rooftop Rainwater Harvesting Systems and Their Control. Critical Reviews in Environmental Science and Technology, 41(23), 2097–2167.
2. Abu Dhabi Department of Municipalities and Transport (2020). Cool Abu Dhabi Challenge [online]. https://www.coolabudhabi.com.
3. AECOM (2020). Izmir Green City Action Plan [online]. http://tinyurl.com/ye2a4tp5.
4. Deng Y. (2021). Pollution in rainwater harvesting: A challenge for sustainability and resilience of urban agriculture. Journal of Hazardous Materials Letters, 2, 100037.
5. ESMAP (2020). Primer for Cool Cities: Reducing Excessive Urban Heat. Energy Sector Management Assistance Program (ESMAP) Knowledge Series 031/20. Washington, DC: World Bank.
6. Hepcan, Ş. (2012). Analyzing the pattern and connectivity of urban green spaces: A case study of Izmir, Turkey. Urban Ecosystems, 16(2), 279–293.
7. https://climate.onebuilding.org [online data].
8. Kaya A. (2017). The Adventure of Water in İzmir. İzmir Metropolitan Municipality [online]. http://tinyurl.com/mrywfajw.
9. Kimic K., Ostrysz K. (2021). Assessment of Blue and Green Infrastructure Solutions in Shaping Urban Public Spaces—Spatial and Functional, Environmental, and Social Aspects. Sustainability 2021, 13, 11041.
10. Kravčík M., Pokorný J., Kohutiar J., Kováč M., Tóth E. (2007). Water for the Recovery of the Climate – A New Water Paradigm. Typopress-Publishing House Košice, Slovakia: People and Water NGO.
11. Langie K., Rybak-Niedziółka K., Hubačíková V. (2022). Principles of Designing Water Elements in Urban Public Spaces. Sustainability 2022, 14, 6877.
12. Marsh A. (2018). Psychrometric Chart [online]. https://drajmarsh.bitbucket.io/psychro-chart2d.html.
13. Rubel F., Kottek M. (2010). Observed and projected climate shifts 1901-2100 depicted by world maps of the Köppen-Geiger climate classification. Meteorol. Zeitschrift. 19(2) (2010), pp. 135-141.
14. Tsatsou A., Frantzeskaki N., Malamis S., (2023). Nature-based solutions for circular urban water systems: A scoping literature review and a proposal for urban design and planning, Journal of Cleaner Production, Volume 394, 2023, 136325.
15. Velibeyoğlu K., Yazdani H., Baba A. (2017). Groundwater in local development strategies: case of Izmir. Water Science and Technology: Water Supply, 18(4), 1339–1349.
16. Widerynski S., Schramm P., Conlon K., Noe R., Grossman E., Hawkins M., Nayak S., Roach M., Hilts A. S. (2017). The Use of Cooling Centers to Prevent Heat-Related Illness: Summary of Evidence and Strategies for Implementation, Climate and Health Technical Report Series, Climate and Health Program, Centers for Disease Control and Prevention.

PLEA 2024 WROCŁAW
(Re)thinking Resilience

Investigating The Resilience of the Largest Capital Worldwide

Is Egypt's new capital resilient and can withstand future challenges?

TAMER GADO[1], AKRAM YOUSSEF[2]

[1] Duncan of Jordanstone College of Art & Design, Architecture + Urban Planning, University of Dundee, Scotland
[2] Department of Architecture, Faculty of Fine Arts, Minia University, Egypt

ABSTRACT: From Brasilia to Songdo to the yet-unnamed Egypt's new capital, the world has been facing a surge in the development of planned new capitals across the globe since the mid-1950s. In the MENA region alone, more than ten planned cities are currently being constructed, one of which is a new capital. In 2015, the Egyptian government announced a plan to build a new capital called the New Administrative Capital (NAC) to replace the over-thousand-year-old capital known for its Giza plateau and famous historic mosque skyline. Previous work did not investigate the economic feasibility or categorically conclude whether the NAC will be smart or sustainable and, thus, potentially be resilient. This paper investigates the NAC's smartness, economic feasibility, and sustainability. It was found that the NAC is not economically viable, does not yet have the potential to be smart, and will not perform highly on the three folds of sustainability.
KEYWORDS: MENA region, New Administrative Capital of Egypt, New planned capitals, Resilience, Sustainable cities

1. INTRODUCTION, MAIN AIM, AND RESEARCH IMPORTANCE

More than half of the earth's population lives in cities, and this number is expected to peak in 2050. Much of this population is estimated to be in Africa and the MENA region, with 2.5 billion, constituting 25% of the world's population, expected to live in Africa by 2050 [1]. Developing existing cities and planning new cities to absorb this increase in population in Africa and elsewhere is essential if the global net-zero target is to be met to keep global temperature increase below 1.5°C.

The MENA region is witnessing an unprecedented development of planned cities. The Line in Saudi Arabia and Egypt's New Administrative Capital (NAC) are the most ambitious projects in the region. However, the number of new planned cities in Egypt has surpassed other countries in the area and worldwide. Since the 1970s, the government has built 22 satellite cities and plans to develop 37 more [2]. Arguably, Egypt has the most ambitious new planned cities programme worldwide, surpassing the visions of China and India [3]. The problem is that the population of all those satellite cities sits at only one-fifth of the original plan, making them known as the 'desert ghost towns' [4]. It is not the most successful attempt to house the growing population. Most of those cities are far from Cairo, lack amenities and essential services and are difficult to reach and travel around. According to Nick Arese, people want to live in those new cities, but this requires owning a car, meaning only a particular social group can afford this move. He added that "governments think they can just move people to new areas, but actually, people go where they want to go" [5].

The Egyptian government announced in 2015 the plan to build a new capital, some 72 km east of Greater Cairo, over 700 km2 with a capacity of 6.5 million inhabitants. It is known as the New Administrative Capital of Egypt (NAC) (Figure 1). It is equal to the size of Singapore and four times the size of Washington, D.C. This makes it the largest purpose-built capital in human history.

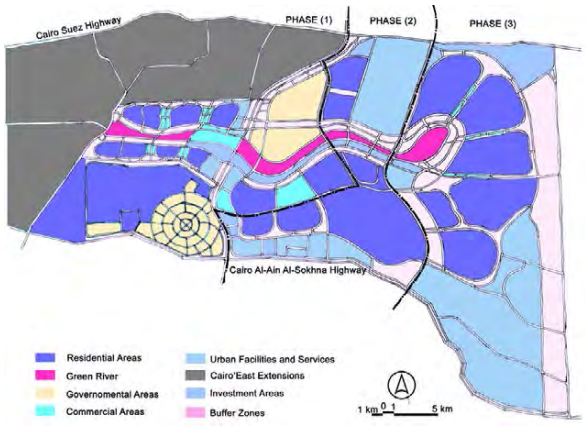

Figure 1: The NAC's planning of its three stages.

The seat of government is relocating to the NAC, with many ministries already moved there in May 2023, even before the completion of the first phase. We argue that rushing the government's relocation

was a political decision to increase consumers' and developers' confidence in the project.

The ambition to create 'smart' and 'sustainable' cities in the MENA region has long been politically pushed to attract global investments and develop new economies to reduce dependence on oil and gas and address the challenges of urban living in existing cities. It is unknown whether the NAC will perform as a smart city as claimed by the government. The NAC's developer (ACUD) claims that the city will be smart because it will have smart traffic, utilities, buildings, and energy management and will be connected and safe. They also claim the city will be smart because the housing blocks use PVC panels.

The resilience of an urban system is its ability to maintain continuity through shocks and stresses while transforming towards sustainability [6]. This is why the sustainability of cities is closely related to their resilience. Shocks and stresses, including economic downturns and social challenges, are significant in Egypt's case. On the other hand, the sustainability of cities includes their society, economy, and environment. It was thus important to study the economic feasibility and sustainability of the NAC, to investigate its resilience and be able to propose ways to enhance it.

This paper aims to investigate the NAC's economic feasibility and sustainability and whether it could be smart as an example of planned purpose-built capital in the MENA region.

In section four, we looked at the NAC's economic feasibility, in section five, we looked into whether it could be a smart city; and in section six, we investigated the city's sustainability with the aim of investigating the city's resilience.

2. RESEARCH LENS AND METHODOLOGY

Global interest in sustainable city planning started with the UN definition of sustainability in 1987, then the Rio Summit in 1992, followed by the Millennium Development Goals, and ended with establishing the Sustainable Development Goals in 2015, which value the role of urban inclusiveness, resilience, and sustainability. However, since the Aalborg Charter 1994, there has been no single 'ideal' model or blueprint for sustainable cities that we could use to investigate the sustainability of the NAC.

From the literature review, including studying the New Urban Agenda [7], we concluded that sustainable cities must offer better places to live and work, and their planning must be about people. They should adapt to population and economic growth and be resilient, especially to global warming. New planned cities should invest in good governance and adopt integrated urban development approaches and technologies such as transit-oriented development, AI, and the Internet of Things if this is affordable and will make the city more sustainable. They need to be walkable and free of cars as much as possible. They should boost the circular and blue economies to consume responsibly. They must promote energy efficiency at macro and micro levels, including building levels. This includes applying net zero carbon policies, technologies, and the use of renewable energy. We applied this research lens to the NAC to assess its sustainability. Then, we applied the three folds of sustainability to investigate the city's sustainability.

We adopted Yolles' definition of sustainability, which is "the ability of human activity to persistently achieve improvement through development" [8]. In this definition, "human activity" encompasses the entire range of human activities, including city planning and operations. We considered employing several sustainability models, including Mitchell's three-nested-dependencies model, the egg of wellbeing model, and the prism model. However, we chose to use the Venn diagram model because it overcomes many of the limitations of previous models despite its limitations, as discussed by Carter & Moir [9]. Besides discussing the NAC's sustainability, we debated its economic viability and potential to be smart (sections 4 and 5, respectively).

3. LITERATURE REVIEW

A systematic critical review was conducted for all primary peer-reviewed references that studied the NAC. Only three references [10-12] studied one or more of the NAC's sustainability in-depth. Only the findings of the references that studied the city's sustainability are briefly discussed here. More in-depth analysis will be presented in future work.

Elmouelhi [10] attempted to theorise urban trends in Egypt and focused on the NAC within the framework of neoliberalism. He discussed how the government and the developers promoted the NAC to higher-income people. He looked at how the city could be inclusive to change the social class gap. He concluded that the government had decoupled the NAC's urban development from social development. On the other hand, Loewert and Steiner [14] studied the NAC's sustainability in depth by conducting qualitative interviews with thirty-six project participants. The authors doubted the city's feasibility and showed how it could lack economic sustainability. Bolleter and Cameron argued that the NAC "will be highly detrimental to existing cities, their inhabitants and the natural environment" [12].

We could not find a common theme supporting a point of view across the previous work regarding the project's sustainability or economic feasibility. None of the previous work critically studied the NAC's feasibility or holistically investigated its sustainability, and none commented on its potential to be smart.

4. ECONOMIC FEASIBILITY

The Egyptian government promotes the NAC as the centre of the "new republic, " an expression used to denote the government's image of the revived country it is trying to rebuild. However, despite the severe economic crisis the country has been facing since 2011, the government justifies building the NAC as a means of taking the pressure off Greater Cairo and other existing cities and as an essential jewel of the crown for the new republic. The government also promotes the NAC as a flagship for smart cities across the region [13]. We could not find evidence that the NAC is economically feasible after studying all available economic indications since 2011 and the preceding period. The country was in almost complete idleness for over thirty years under Mubarak Regime (1981-2011), which was keen to create a state of 'economic equilibrium' promoted as a state of 'economic stability'. But, in reality, it was a state of stagnation. By 2011, human rights would have suffered severely, traffic was highly congested, the train services were dilapidated, transportation was terrible, and the pre-university, higher education, and health systems were dire. So, in response, people protested on the streets shouting the famous revolution slogan "bread, freedom and social justice". Since the Revolution, successive governments have made considerable investments to improve the situation. However, the road is still far from short. Instead, after several megaprojects, the country is left in 2023 with an external debt exceeding 164 billion USD compared to 26.1 billion USD in 2001. People suffer from massive inflation, increased food and fuel prices, especially proteins, scarcity of strategic food, and low average income despite the government's increase in wages and pensions. At the same time, people's savings have depreciated several fold recently due to successive currency flotation and other economic factors. Despite the government agreeing to slow down megaprojects, the regime insists on moving forward quickly with the NAC. This and many other factors concerning rising rents and real estate prices lead us to believe that an imminent bubble is about to burst. So, it is very challenging to justify building the NAC in such a fragile economic climate (more to support this argument under section 6.1).

5. SMART ASPIRATIONS OF THE NAC

The ACUD is promoting the NAC as a smart city. Many technical and policy preconditions must have been in place for this to be possible. None of these were seen during the site visit in August 2023 or were identified in the literature and data. There are no signs of implementing any smart features across the NAC. For example, there is no evidence of implementing Internet of Things infrastructure, including a 5G network or high-speed fibre optics infrastructure. Instead, the focus is on installing surveillance cameras, speed cameras, and advertisement boards. During the site visit, the experience of using the 3G network and the ADSL were unreliable. Also, as many smart cities propose, any services drones could provide will not be possible as drones are prohibited across the country. There is no clear smart transportation strategy, and the focus is on the monorail and the LRT only, which do not connect all parts of the city but connect the city to other parts of the country. There is no plan for using autonomous transportation, rental cars, bikes, or scooters. Lately, the government has taken a good step towards streamlining the movement of passengers across the LRT and the monorail by using a contactless payment card system. Apart from the LRT and the monorail, the fuel used for transportation across the city is mainly fossil-based, with some natural gas buses. The primary source of electricity powering the whole city is natural gas. This means that the carbon dioxide emissions of the NAC will be very high compared to other smart cities.

No web-based technology was found to provide citizens with a one-stop online platform to access all government services. A limited website that can provide some services is in operation. Despite the government's plans to transform Egypt into a digital society, most of the dealings with the government cannot be done online or even via post or phone. It is unclear how this will be different in the NAC. Cairo and other cities suffer from significant solid waste management issues, including collection and disposal. No clear strategy was found for how this will occur across the NAC. For example, no waste incineration plant has been built to produce energy, and no smart methods for waste collection systems have been proposed or built. We are concerned that this means that solid waste could end up in an open dump.

6. ASSESSING THE NAC'S SUSTAINABILITY

The Egyptian government cooperated with the UN to fulfil the SDGs. Egypt's Sustainable Development Strategy (SDS) states that it aligns its goals with the SDGs, although this is unclear in the document. At the 2023 High-Level Political Forum on Sustainable Development, Egypt announced that renewable energy production will increase to 42% by 2030. However, it did not discuss how its SDS will ensure that the NAC will achieve any of the SDGs. Although this paper did not investigate how the NAC will do so, it studied how the city will potentially perform across the three folds of sustainability.

6.1 The NAC's economic sustainability

The NAC's economic sustainability is doubted due to seven issues identified through analysing the

economic indicators of the project and the context of the whole country. Two main issues are presented in this sub-section.

The NAC's financial viability and the effect on the whole country's economy - The first issue relating to how the construction of the NAC could affect the rest of the country's economy relates to how it contributes to increasing the general external and internal debts and putting a massive strain on the general budget. We argue that the project is not economically viable due to the limited economic ability of the country, the timing of the project, how long it takes to complete, and how its different stages are completed and incompatible with the country's financial ability, including its ability to service the related external loans. Those loans are taken to build specific parts of the city, like the central business district, the light rail transit, the high-speed rail project, and the monorail.

We argue that Egypt, which limps through a very fragile economy, cannot afford this megaproject despite the government's claims that no funds from the general budget have been invested in constructing the city. They claim that all the funds are raised from selling the land. However, the government admitted investing five billion Egyptian pounds in the NAC since 2015.

Egypt has faced many economic challenges since the January Revolution in 2011, including an economic crisis that has been escalating to date. The country has a middle-income with a high rate of poverty. The poverty rate increased from 27.8% in 2016 to 32.5% in 2019 [14], with the latest figures from the World Bank showing that 60% of Egyptians are either poor or vulnerable [15].

The Egyptian currency is ranked the 6th worst performing and suffered extreme devaluation. The currency lost 50% of its value in 2022 due to steep devaluation since March and 20% by the beginning of 2023, with expectations that it will plummet even further in 2024 [16]. In November 2023, the US$ price exceeded 50EGP (6.88EGP in November 2013). This deterioration in currency value is due to the damaging financial and economic policies since the 2011 Revolution. These policies were mainly in response to the IMF recommendations. Compliance with these policies was to allow for more borrowing from the fund. This led the country to suffer from a high annual urban inflation rate that rose from 21.3% year-on-year in December 2022 [17] to 35.7% in July 2023 and a core inflation of 41% [18]. The cost of food increased by 73.60% in September 2023 compared to the same month in 2022 [19] and is increasing further.

Egypt has the third highest total external debt in the MENA region after Lebanon and Bahrain [20], reaching $165.3 billion (end of March 2023) [21]. Its debt percentage to GDP was 87.20% in December 2022, which is expected to reach 92.7% in 2023 [22]. This debt level is likely to increase due to the Israel-Gaza war that affected tourism, gas imports, and the Suez Canal. This crisis led the IMF to consider augmenting the 3 billion US$ loan programme, the fourth loan Egypt has received from the IMF since 2016 [23]. This will further increase the total debt by around six billion US$.

We believe a country with this economic performance should not have invested in a mega-scale project like the NAC. Instead, new developments should have targeted lower socio-economic groups, as the World Bank report recommended in 1987 [24], which suggested that Egypt's economic development should focus on microenterprises and midsize enterprises rather than mega-scale developments. Despite this, since the report was published, the government has prioritised the mega-scale project model, and developing satellite cities has become the leading trend since the late 1970s [24]. More than thirty satellite cities across the country have been developed, with only 2.5 million people relocated to those cities, leaving 12 million dwellings vacant [25] and 18 million people living in informal settlements [26], most of which are around Cairo. Regardless of this significant urban development failure and dire economic position, the government is building the largest planned capital worldwide. This disregards the current economic downturn, the financial risks associated with investing in the city, and the risks associated with the Chinese loans taken to build the central business district. The investment made in the NAC should have been directed towards the needs of vital sectors that suffer from massive insufficient funding, such as agriculture, water, energy, industry, education, health, transportation, and social security.

Effect of the NAC on the social inclusiveness of the capital - The second economic issue relates to the affordability of the residential and commercial units across the city and how this will define the demographics of its inhabitants. We argue that the city will not be inclusive. The NAC economic base focuses mainly on business hubs, luxury retail developments, and luxury residential units for sale for 8 to over 40 million EGP, which is not affordable to most Egyptians. NAC provides only for the upper-upper social class instead of prioritising the middle and lower classes that constitute the higher percentage of the population. Talking to the locales during the site visit, the NAC is known among the public as the "city of al Kobar (elite)". In other words, it is the "Billionaires' Row" of Cairo. This approach will divide the capital society into two cities: the historical capital for the poor and middle class and the NAC for the elite and expatriates, the high government

officials, and the high military ranks, affecting the coherence of the country's capital society.

6.2 Assessing the NAC's social sustainability

There is an expected overlap between the NAC's economic and social issues. The focus here is on four socio-economic issues that lead to social segregation and, thus, poor sustainability performance.

NAC does not allow for the lower classes - The main social issue of the NAC is how the city only concentrates on the upper-upper social classes at the expense of the lower and middle classes, including the poor. For example, the price of a small flat in the NAC starts from about 0.9 million EGP, and a small separate house starts from about 5.8 million EGP. These prices will lead the majority of Cairo's high-class, high-middle, and middle-middle classes to migrate to the NAC, where they can find a higher quality of life that they can afford, leaving the lower-middle and lower classes living in Cairo. Besides the negative effect this migration might have on Cairo physically, it will further divide the society. There is no doubt that Cairo is facing massive socio-economic and environmental problems. It is feared that these problems will be overlooked, with all the investment redirected to the NAC. This will potentially cause severe social segregation between the Cairenes across the NAC and the historic metropolis [27], where most of the urban poor reside. It will make the NAC a city for the elite, changing the demographics of one of the world's oldest capitals.

Poor attention to housing needs for all social classes - Social segregation will further take place because very little attention is paid to the housing requirements of the lower-middle and lower classes from the design and typology points of view. There is an evident lack of appropriate residential typology of affordable prices, appropriate size, design and urban design that fulfils the needs of people from the lower classes. Extended families, for example, have no appropriate housing options, such as large-family affordable houses, multi-story family blocks, or plots of land that they can use to build their homes in phases. On the other hand, the design of streets and public spaces does not satisfy the needs of lower-class social interaction, entertainment, or celebrations they usually have on their streets.

Transportation and social segregation - The NAC is located 72km away from Cairo's city centre. According to Google Maps, the fastest route takes 75 mins (not during rush hour) from the NAC's Government Quarter to Al-Tahrir Square in Cairo, making the round trip 144km, taking at least two and half hours. This means that only people with access to private cars or who can afford expensive public transportation will have easy access to the city and its amenities [28]. As a rough indication of how much it will cost to travel this distance, an Uber fair is about 250EGP. This is unaffordable to many people in Cairo and will further enforce social segregation.

Urban planning - Another major social issue is adopting the 'American dream urban model', which separates the urban services and the residential areas and creates a mono-land use [29]. This transforms the city activities from continuous and dynamic to temporary depending on the time of the day and makes the city centres less safe [29] and inactive during the evening. This model has been tested in many planned cities across Egypt and proved socially and economically unsustainable. Another American model adopted widely across the NAC is the gated communities, which are popular among the higher social classes and are very lucrative to developers. However, it is very unaffordable for the lower classes, kills street life and divides society across the city.

6.3 Assessing the NAC's environmental sustainability

Lack of strategy - The major environmental issue facing the NAC is the lack of strategic thinking and planning. Egypt's Vision 2030 does not have any details of how the NAC will achieve the UN SDGs. The NAC does not have a sustainable strategy dealing with integrated transportation, air quality, noise control, solid waste management, sustainable infrastructure, freshwater demands, mitigating climate change, carbon emissions, and climate change resilience.

The effect of the Green River - The second issue relates to the city's planning, which is based on a central spin: Green River, a 35km waterway, and green area. All neighbourhoods are connected to this waterway through further networks of green axes. This vast area is water-hungry and expensive ($500 million first stage). It contradicts Egypt's problem of freshwater scarcity. Egypt is one of the top eleven countries suffering from water stress, scoring a water stress score of 160% in 2018 [30]. Each person only has 600 m^3 (WHO water poverty is 1000 m^3 per person). This figure will decrease to 400 m^3 by 2050. The country's rapidly increasing population, climate change, poor solid waste management and the effect of this on the waterways, poor irrigation systems, and limited water resources put the whole country at risk, making the Green River very unsustainable despite the use of recycled water.

Lack of building energy efficiency standards and high carbon emissions - The third environmental problem relates to building standards and design. The current building standards cannot ensure the construction of sustainable buildings regardless of building typology, as no building energy efficiency code is yet in place. In addition, previous work [31-33] found that walk-up housing blocks and schools built by the government are not climatic responsive,

lack energy efficiency, and are not thermally or visually comfortable. The government plans to build similar buildings in the city. Additionally, proposed commercial and office buildings in such a hot-dry climate, in the form of multistorey fully glazed buildings constructed across the city, do not promise to be sustainable by design despite using efficient centralised cooling plant room. We expect most buildings will not be environmentally conscious and will be fully air-conditioned. Suppose buildings across the NAC are built without, for example, thermal insulation or any consideration for natural ventilation, passive cooling, or protection from solar radiation due to the lack of building energy efficiency codes and sustainable design innovation, the cooling loads and, thus, the energy consumption across the city will be very high. This will significantly impact the carbon footprint of the whole city.

7. CONCLUSIONS AND FURTHER WORK

This work aimed mainly to investigate the sustainability of the NAC as an example of planned capital constructed in the MENA area and to investigate its economic visibility and smartness.

The study argued that the current economic situation in Egypt, with the challenges ahead, does not allow for the building of such a megaproject without negatively affecting people's lives across the country. The work also concluded that the NAC would not potentially be smart and would perform poorly across the three folds of sustainability.

Further work recommends a reform roadmap for the NAC, managed by the Egyptian House of Representatives and its various Standing Committees in collaboration with the relevant practitioners.

References

1. A. Stanley, *African century, A demographic transformation in Africa has the potential to alter the world order*. 2023, IMF.
2. Hassen, A., *In numbers, we publish the plans for the fourth generation cities* in *Al Youm Al Sabaa*. 2021, Al Youm Al Sabaa: Cairo.
3. R. Keeton and M. Provoost, *New cities in the sand: inside Egypt's dream to conquer the desert*, in *The Guardian*. 2019, The Guardian.
4. Y. Shawkat. *New cities are unsustainable*. 2016; Available from: https://bit.ly/481LtLc.
5. P. Kingsley. *A new New Cairo: Egypt plans £30bn purpose-built capital in desert*. 2015 30.11.2023; Available from: https://bit.ly/4a3wgL4.
6. UN Habitat. *What is Urban Resilience*. 2023 [cited 2023 30.11.2023]; Available from: https://bit.ly/3RoXcNG.
7. UN, *New Urban Agenda*. 2017, UN: Quito.
8. M. Yolles, *Sustainability development: exploring the dimensions of sustainability development.* Int. J. Markets and Business Systems, 2018. 3(3): p. 257–275.
9. Carter. and Moir., *Diagrammatic Representations of Sustainability - a Review and Synthesis*, in *28th Annual ARCOM Conference*. 2012, ARCOM: Edinburgh, UK. p. 1479–89.
10. H. Elmouelhi, *New administrative capital - Cairo: Power, urban development and social injustice - the official Egyptian model of neoliberalism*, in *Neoliberal urbanization, Urban development processes in the Arab world*, A. Al-Hamarneh, J. Margraff, and N. Scharfenort, Editors. 2019, Transcript Verlag.
11. P. Loewert and C. Steiner, *The New Administrative Capital in Egypt: The political economy of the production of urban spaces in Cairo.* META J., 2019. 12(1): p. 66-75.
12. J. Bolleter and R. Cameron, *A critical landscape & urban design analysis of Egypt's new Administrative Capital City.* J. of Landscape Architecture, 2021. 16(1): p. 8-19.
13. ACUD. *The Capital Egypt - Smarter future*. 2023 [cited 2023 1.11.2023]; Available from: http://www.acud.eg/.
14. CAPMASS, *2017-2018 Income, Expenditure, and Consumption Survey*. 2019: Cairo.
15. The World Bank, *2015-2019 Country Partnership Framework*. 2015: Washington, D.C.
16. L. Shan. *Egypt's pound is among the worst performing currencies in 2023. And it's expected to plummet further*. 2023 [cited 2023 15.10.2023]; Available from: https://bit.ly/3QByU2D.
17. The World Bank. *The World Bank in Egypt*. 2023 [cited 2023 30.10.2023]; Available from: https://bit.ly/3v2gd01.
18. A. Makary, et al. *Egypt's headline inflation climbs to all-time high of 35.7% in June*. 2023.
19. Trading Economics. *Egypt food inflation*. 2023 [cited 2023 30th October 2023]; Available from: https://bit.ly/467Fpix.
20. A. Mazarei *Debt clouds over the Middle East - Parts of the Middle East & North Africa stand at the brink of a debt crisis*. 2023.
21. Central Bank of Egypt, *External position of the Egyptian economy* 2023.
22. IMF *Egypt database*. 2023.
23. Al Jazeera Media Network. *IMF could augment Egypt's loan programme over effects of Gaza war*. 2023 [cited 2023 18.11.2023]; Available from: https://bit.ly/3MRPLMt.
24. The World Bank, *World Development Report 1987*. 1987.
25. CAPMASS, *Egypt Census 2017*. 2017.
26. GOPP and UNDP Egypt Country Office, *The national strategic planning for urban development - Egypt Vision 2052*. 2014.
27. Unknown, *What happens to Cairo after Egypt builds its new capital?*, in *Haaretz Daily,*. 2018.
28. D. Sims, *Egypt's desert dreams: Development or disaster?* 2014, Cairo: AUC Press.
29. J. Jacobs, *The death & life of great American cities*. 1961: Random House.
30. FAO, *Clean water & sanitation*. 2018: UN.
31. T. Gado, *A parametric analysis of the thermal comfort & cooling in walk-up housing blocks in the Arab Republic of Egypt*. 2001, Cardiff University.
32. T. Gado and M. Mohamed, *Assessment of thermal comfort inside primary governmental classrooms in hot-dry climates*, in *2nd International (SUE-MoT) conference*. 2009.
33. T. Gado and M. Osman, *Investigating natural ventilation inside walk-up housing blocks in the Egyptian desert climatic design region.* Int. J. of Ventilation, 2010. 8(2).

Urban Heat Islands in the Himalayas: Investigating Land Use Land Cover Change Effects in Shimla City, Himachal Pradesh

A Spatio-Temporal Analysis of Urban Climate Dynamics in a Himalayan Setting

RANJEET VERMA[1], HARSIMRAN KAUR[2,] AMRITA DWIVEDI[1]

[1]Department of Humanistic Studies, Indian Institute of Technology (Banaras Hindu University), Varanasi, India.
[2] Department of Architecture, Planning and Design, Indian Institute of Technology (Banaras Hindu University), Varanasi, India.

ABSTRACT: Population growth in the Himalayan urban centres is crucial for planners and researchers worldwide. In the Himalayan region, more than 150 million people live directly, but 1.5 billion people live within its water basins, and during the last three decades, the region has experienced rapid urban population growth. Rapid urbanization demands infrastructural development, significantly altering land use and land cover (LULC) patterns within cities. The alteration of LULC has numerous environmental impacts, most notably an increase in land surface temperature (LST) resulting from the built-up impermeable surface. The increase in LST within the city leads to the prevalence of urban heat island UHI) effects. Understanding UHI dynamics in urban areas is essential for sustainable development and mitigating the negative impacts of urbanization in the Himalayan cities. This study uses remote sensing Landsat 5 and 8 data from 1990 to 2022 and GIS approaches to investigate the spatiotemporal dynamics of LULC from 1990 to 2022 and its impact on UHI in Shimla City, Himachal Pradesh, India. The result of this work shows a significant change in different LULC classes. The built-up cover increased from 5.08 KM² to 13.8 KM² and UHI from 1% to 10% during 1990 to 2022.
KEYWORDS: Land surface temperature, LULC, UTFVI, UHI, Built-up.

1. INTRODUCTION

The Himalayas hold immense importance for human civilization, profoundly influencing various aspects of life and culture across the Indian subcontinent. Their role in supporting life through the provision of water, biodiversity, and climate regulation is indispensable. In recent years, the Himalayas have been subject to rapid changes in their natural landscapes due to the challenges posed by the rapidly growing urbanization process in the regions. In the Himalayan region, more than 150 million people live directly, but 1.5 billion people live within its water basins [1], and during the last three decades, the region has experienced rapid urban population growth [2-3]. This rapid urbanization demands more infrastructural development, leading to significant alterations in land use and land cover (LULC) patterns within the region.

LULC changes have numerous environmental impacts, most notably the rise in land surface temperature (LST) resulting from the built-up cover of impermeable surfaces [4-5]. Compared to natural landscapes, impervious surfaces have a lower albedo, causing them to absorb more solar radiation and, consequently, contributing to an escalation in LST and the prevalence of Urban Heat Island (UHI) effects. LST has been used to investigate urban heat islands locally, regionally, and globally to examine the impact of urbanization impact on the local climate [6-7]. UHIs are areas within the urban environments where temperatures are significantly higher than the surrounding areas. The impact of higher surface temperatures in urban areas is a phenomenon in the surroundings [8]. In urban areas, impervious surfaces like concrete and asphalt absorb and retain heat, and a lack of green space can also contribute to this [9]. The increase in temperature in urban areas affects regional climate, increases energy consumption, causes environmental pollution, and significantly impacts human health and well-being [10]. It can exacerbate residents' discomfort and pose a health risk, particularly during high temperatures [11]. Understanding the LULC pattern UHI dynamics in urban areas is essential for sustainable development and mitigating the negative impacts of urbanization in the Himalayan cities.

Much work has been done on UHI; Du. H. et al., 2016: the impact of LULC on UHI in the Yangtze River Delta urban agglomeration, Li. Y. et al., 2012: monitoring of UHI in the fast-growing Shanghai metropolis, Gogoi P. P. et al., 2019: impact of LULC on LST over Northeastern India, but there is lack of studies which focuses on LULC impact on UHI in the fast-growing Himalayan Cities. This study utilizes

remotely sensed data and geographical information system (GIS) approaches to investigate the spatiotemporal dynamics of LULC change and its impact on LST and UHI in Shimla City, Himachal Pradesh, India, from 1990 to 2022. Additionally, the study will focus on understanding how changes in LULC in mountainous cities lead to an increased urban heat island effect in the region's microclimate. The findings of this research would not only help for policy purposes but also help urban planners and researchers develop sustainable urban design tools for Himalayan cities in the climate change era.

2. METHODOLOGY

2.1 Study area

Shimla City, located in the southwestern part of the Middle Himalayas, graces an average altitude of 2,130 meters above mean sea level (MSL) and is situated between 31˚4′N to 31˚10′N latitude and 77˚5′ E to 75˚15′E longitude (refer to Fig. 1). The city spans a total geographical extent of 35.34 km². According to Census India, in 1991, the population of Shimla City was 129,827; in 2001, 174,789; and in 2011, 235,970 (Table 1). The projected population of 2021 was 3,204,760. The city is a prominent tourist place. According to the Draft Development Plan Shimla Planning Area 2041, on average, 4000 tourists per day visit the city, and during peak season, the number reaches 10,000 per day.

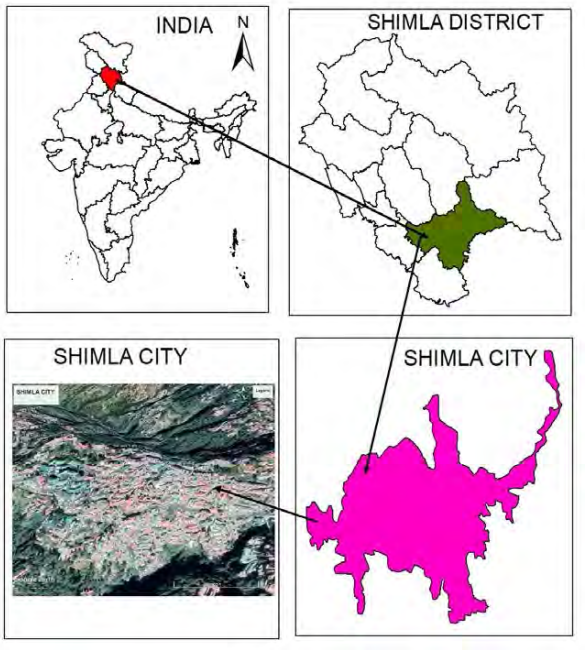

Figure 1: Location map of the study area.

The city experiences an average annual rainfall of 999.4 mm, with approximately 75% of this precipitation occurring during the monsoon period from June to September. The average temperature in Shimla City exhibits a notable range, fluctuating between -1 °C to 10 ˚C during the winter months and 19 °C to 28 ˚C during the summer season.

Table 1: Population growth of Shimla City.

Year	Population	Growth (%)
1981	95,851	---
1991	129,827	35
2001	174,789	35
2011	235,790	18
2021	307,404	30

**Projected population.*
Source: Draft Development Plan Shimla Planning Area, 2041.

2.2 Database

For LULC change mapping and LST calculation, the LANDSAT products provided by the USGS Earth Explorer website (https://earthexplorer.usgs.gov/) were used for this study. The description of the data used for this study is given below;

Table 2: Description of Datasets used for this study;

Sensor	Acquisition Year	Row & Path
Landsat-05	08-04-1990	147/038
Landsat-05	10-04-2001	147/038
Landsat-05	15-05-2010	147/038
Landsat-08	11-04-2017	147/038

2.3 Pre-processing of data

Landsat Collection 2 Level 1 products have been taken from the USGS Earth Explorer website for the present study. Before being used for UHI studies, the Landsat thermal products must undergo a series of pre-processing techniques [12]. The Landsat thermal and optical products were pre-processed using the QGIS plugin semi-automatic classification (SCP) based on the dark object subtraction-1 (DOS-1) algorithm.

2.4 Land use land cover (LULC) supervised classification

Supervised classification is a technique that classifies data points into predefined classes based on labelled training data. A lot of supervised techniques and approaches have been used for satellite imagery classification, such as maximum likelihood classification (MLC), random forest classifier (RF), neural network classification, K-means clustering, and support vector machine (SVM) classification [13]. The present study utilizes SVM classification. SVM is a powerful supervised machine learning-based technique used for classification and regression work. The SVM is well-suited to find the best possible line to classify different classes [14]. In the present study, the supervised SVM technique was performed under the ArcGIS-10.8 environment to classify the images into different classes.

2.5 Calculation of land surface temperature (LST)

This study used Landsat Satellites' thermal bands of Thermal Infrared Sensors (TIRS) to derive LST and Urban Therma Field Variance Index (UTFVI). The Landsat program uses different TIRS band combinations to derive surface temperature data [15]. In Landsat 5, band 6 (spatial resolution 60 meters) and in Landsat 8, bands 10 and 11 (spatial resolution 100 meters) were collected. Each of these bands has been resembling a 30-meter spatial resolution. Although Landsat 8 has two thermal bands, band 10 and 11, in the present study, band 10 is used to derive the LST because band 11 has calibration and stray light error, and researchers do not recommend this to retrieve LST [16]. In the present study, LST is calculated using the mono window technique. For the calculation of LST and UTFVI Landsat 5 (1990, 2001, and 2011) and Landsat 8 (2022), 2 level 1 data were collected from the USGS Earth Explorer website. The following equations (1)-(7) given in the USGS Handbook, step-by-step were followed to calculate LST [17];

Calculation of top of atmospheric radiance

$$Ly = ML*Qcal + AL \quad (1)$$

Where Ly stands for the top of the atmosphere (TOA) spectral radiance, ML stands for Band-Specific Multiplicative re-scaling factor, Qcal is quantised and calibrated standard product pixel value DN, and AL stands for Band-Specific additive re-scaling factor.

$$Ly = \left(\frac{Lmax^{\lambda} - Lmin^{\lambda}}{Qcalmax - Qcalmi}\right)*(Qcal - Qcalmin) + Lmin^{\lambda} \quad (2)$$

Where Ly=sensor radiance, $Lmax^{\lambda}$ =maximum radiance of thermal band, $Lmin^{\lambda}$=minimum radiance of thermal band, Qcal=quantized calibrated pixel value in Digital Number (DN), Qcalmax=maximum quantised calibrated pixel value in DN, Qcalmin=minimum quantised calibrated pixel value in DN.

Calculation of NDVI

$$NDVI = \frac{NIR - RED}{NIR + RED} \quad (3)$$

NDVI stands for Normalised Difference Vegetation Index, and NIR stands for Near Infrared.

Calculation of Fractional Vegetative Cover (FVC) Index

$$FVC = \left(\frac{NDVI - NDVImin}{NDVImax - NDVImin}\right)^2 \quad (4)$$

Calculation of surface emissivity (Ɛ)

$$Ɛ = 0.004*FVC + 0.986 \quad (5)$$

Calculation of Brightness Temperature (BT)

$$BT = \frac{K2}{In\left(\frac{K1}{L_\lambda} + 1\right)} - 273.15 \quad (6)$$

Where K1 and K2 are the calibration constants of thermal bands.

Calculation of Land Surface Temperature (LST)

$$LST = \left(\frac{BT}{1 + \left(0.00115 * \frac{BT}{1.4388}\right) Ln(Ɛ)}\right) \quad (7)$$

In this study, for the calculation of LST from Landsat 5 band 6, equations (2) and (6) were used to convert radiance into temperature.

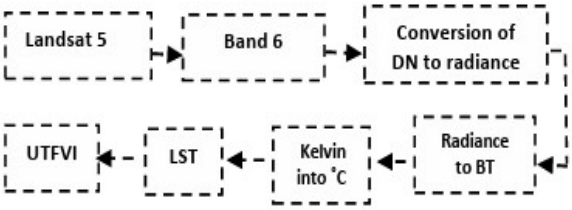

For the retrieval of LST from Landsat 8 band 10, equations (1) and (3 – 7) have been used to convert the digital number (DN) value into temperature.

2.6 Estimation of urban thermal field variance index (UTFVI)

UTVFI is one of the most accepted indicators for characterizing a city's surface urban heat island effect [18]. UTFVI is a quantitative measure to assess the intensity and spatial variability of UHI effects in a city. It shows how hotter the zone is and how unevenly those hotspots are distributed within a city. Table 3 shows the relationship between the UTFVI and UHI phenomena.

Table 3: Relationship between UTFVI and UHI.

UTFVI	UHI Phenomena
-0.50 – 0.000	None
0.00 – 0.100	Weak
0.100 – 0.200	Moderate
0.200 – 0.300	Strong
0.300 – 0.500	Very strong

For the present study, UTFVI is calculated using the following formula:

$$UTFVI = \frac{Ts - Tmean}{Tmean} \quad (8)$$

Where *Ts*= *LST* at a particular point and *Tmean*= the mean *LST* of the study area. Based on the calculated value of UTFVI, the study area is divided into five different regions, as recommended by Zhou et al. (2014), as mentioned in the table.

3. RESULTS

3.1 Land use land cover (LULC) dynamics analysis

The land use land cover (LULC) maps of Shimla City show the continuous growth in the built-up area from 1990 to 2022 (refer to Fig. 2). LULC change analysis was done in Shimla City for 42 years using Landsat satellite images for 1900, 2001, 2011, and 2022. Landsat 5 and 8 multispectral cloud-free data for April and May were taken at 10-year intervals to classify LULC using SVM-supervised classification techniques under the ArcGIS 10.8 environment. The city was classified into four classes: built-up area, dense vegetation, sparse vegetation, and fallow land (refer to Fig. 2). Table 4 shows the temporal statistics of different classes of LULC for the study period. In terms of changes, the most substantial is the

increased built-up area, which was 15.6% in 1990 and increased to 41.4% by 2022, as well as the decrease in fallow land from 4.9% to 1.1%. In addition, dense vegetation cover decreased from 42.4% in 1990 to 36.0% in 2022, while sparse vegetation cover decreased from 39.1% in 1990 to 21.6% in 2022.

Table 4: Temporal statistics of different LULC classes

Land use Class	1990 (%)	2001 (%)	2011 (%)	2022 (%)
Built-up	15.6	25.1	35.6	41.4
Dense V[a]	42.4	54.6	39.5	36.0
Sparse V	39.1	14.1	17.6	21.6
Fallow L[b]	4.9	5.7	7.3	1.1

[a] Vegetation [b] Land

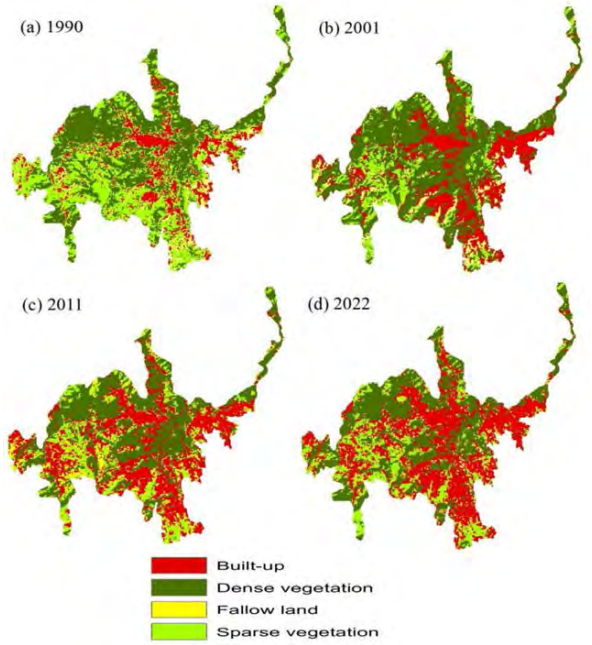

Figure 2: LULC classification map for (a) 1990, (b) 2001, (c) 2011, and (d) 2022

3.2 Changes in land surface temperature (LST)

LST was calculated using the mono window algorithm in the ArcGIS-10.8 environment from 1990 to 2022. April and May months were taken for LST calculation. The description of the data and date are mentioned in Table 2. Figure 3 represents the LST maps of the study area for 1990, 2001, 2011, and 2022. Table 5 shows that the minimum LST was recorded at -1.30 ˚C in 1990 and a maximum of 37.6 ˚C in 2011. This trend is also evident in mean LST; the mean LST increased from 16.3 ˚C in 1990 to 28.6 ˚C in 2011. The most notable change in maximum LST can be seen from 27.6 ˚C in 1990 to 37.6 ˚C in 2011. Figure 3 shows that high LST zones were located in densely built-up areas. The period from 1990 to 2011 was when built-up areas increased by 20%, indicating that the transformation of the natural landscape into a built-up landscape has increased LST.

Table 5: Descriptive statistics of LST from 1990 to 2022.

Year	1990	2001	2011	2022
Min	-1.30	6.5	19.7	10.9
Max	27.6	32.6	37.6	30.4
Mean	14.2	19.6	28.6	20.2

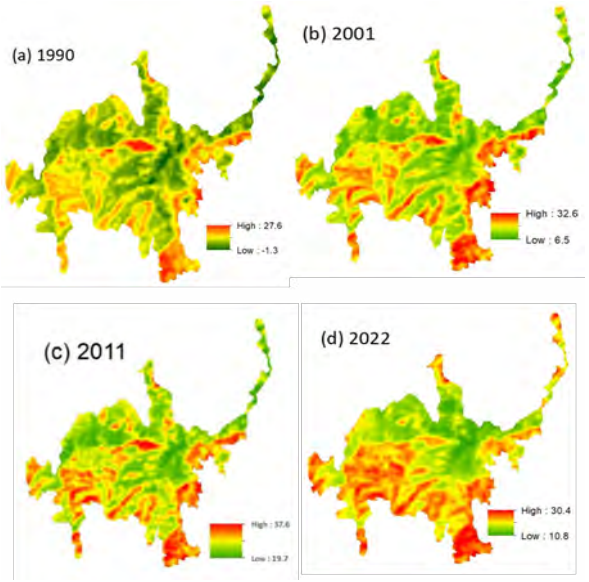

Figure 3: LST maps of Shimla City for a. 1990, b. 2001, c. 2011, and d. 2022.

3.3 Urban thermal field variance index (UTFVI) calculation and urban heat island (UHI) phenomena

In this study, the urban thermal field variance index (UTFVI) is used to quantify the status of urban heat islands (UHI) in the study area. UTFVI is calculated by using equation (8) in ArcGIS-10.8 software using a raster calculator. The UTFVI values of the selected years vary between -0.50 to 0.54. Figure 4 shows the UTFVI for 1990, 2001, 2011, and 2022.

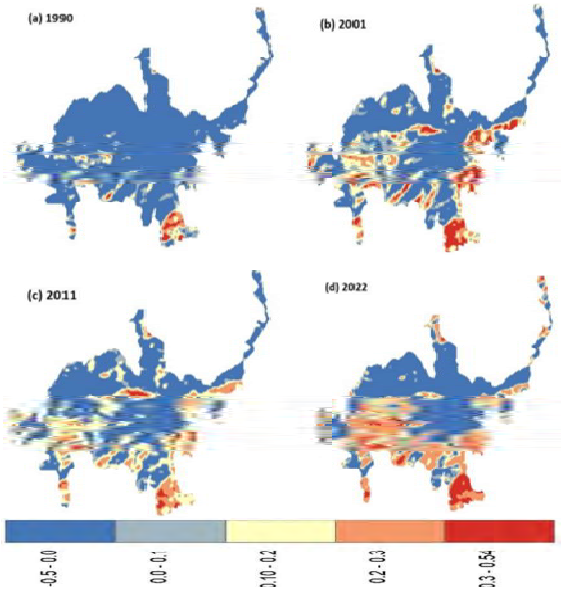

Figure 4: UTFVI maps of Shimla City for a. 1990, b. 2001, c. 2011, and d. 2022.

According to this range, we have divided the UHI effect into weak, moderate, strong, and very strong (refer to Table 3). The impact of the UHI phenomenon is more prevalent during the summer season. Since Shimla City is a mountainous city, the winter is too cold, and the summer is hot, and these situations mask the actual result. In this study, we have preferred the April and May months for calculating LST and UTFVI because these two months are neither too cold nor too hot.

Table 6: UTFVI and UHI phenomenon.

Year	None		Weak		Moderate		Strong		Very Strong	
	KM²	%	KM²	%	KM²	%	KM²	%	KM²	%
1990	27.06	83	2.91	9	1.53	5	0.73	2	0.30	1
2001	17.72	54	4.71	14	5.19	16	2.99	9	1.90	6
2011	17.21	53	3.95	12	4.60	14	5.34	16	1.42	4
2022	15.71	48	3.36	10	3.66	12	6.45	20	3.34	10

Table 6 represents the categorization of Shimla City into five different classes, which determines the spatial distribution of UHI impacts inside the city. The result shows that the non-UHI area from 1990 to 2022 reduced from 27.06 Km² to 15.71 Km². The very strong UHI area significantly increased from 0.30 Km² to 3.34 Km². In 1990, only 1% of the city's area was under a very strong UHI effect, which increased to 10% in 2023. It can be observed from Table 5 that weak and moderate UHI areas showed fluctuation in terms of increase and decrease during the analysis period. In 2001, the weak UHI area increased by 4.71 Km², but in 2022, it decreased to 3.36 Km². The strong UHI area increased from 0.73 Km² to 6.45 Km² from 1990 to 2022. The 2023 UTFVI map (refer to Fig. 4) shows that 2022 has experienced high UHI effects in the densely built-up regions (refer to Fig. 2). The comparative analysis of Figures 2 and 4 shows that dense vegetation areas show none or weak UHI effects, whereas dense built-up areas experience very strong UHI effects.

4. DISCUSSION

In the present study, the spatiotemporal dynamics of LULC and its impact on LST were calculated and compared for the Himalayan mountainous city of Shimla. The study investigates the effect of LULC change and UHI dynamics in the city for 32 years between 1990 and 2022. This study focused on identifying the change in LULC for Shimla City and quantifying the UHI phenomena using UTFVI in remote sensing and ArcGIS environments. This paper aims to achieve two objectives: one, to monitor LULC change dynamics over Shimla City during the analyzed period, and second, to investigate spatial and temporal dynamics of UHI using UTFVI in the city.

The analysis of LULC change was done using Landsat 5 and 8 images, using a machine learning-based SVM algorithm in an ArcGIS-10.8 environment. The city was classified into four classes: built-up, dense vegetation, sparse vegetation, and fallow land. The findings of this paper show that there was a significant change in all LULC classes over the study area during the period 1990 to 2022. Built-up area increased from 15.6% in 1990 to 41.4% in 2022. A notable change in dense vegetation cover class can also be seen. It changed from 42.4% in 1990 to 36% in 2022. Sparse vegetation cover reduced substantially from 39.1% in 1990 to 21.6% in 2022. Fallow land slightly decreased from 4.9% in 1990 to 1.1% in 2022 (Table 4). A significant change in built-up cover between 1990 and 2011 was linked to high population growth in the city. From 1990 to 2011, the city's decadal population growth was 35%. During this period, the built-up cover doubled.

The analysis of the April and May months shows a notable increase in LST of the study area. The calculated minimum, mean, and maximum values of analyzed LST vary from -1.30 ˚C to 10.9, 14.2 ˚C to 28.6 ˚C, and 27.6 ˚C to 37.6 ˚C from 1990 to 2022, respectively (Table 4). The result shows that the densely built-up areas experienced an increase in LST over the years. The reason behind the rise in LST in densely built-up areas is that the built-up cover increased from 15.6% in 1990 to 41.4% in 2022. As the built-up cover expanded, dense and sparse vegetation cover was replaced by roads, buildings, and impervious surfaces. These surfaces absorb and retain heat more than the natural land covers, leading to increased LST.

UTFVI was calculated using the LST of the April and May months of the selected years to quantify the UHI effect in the city. Table 3 shows that UTFVI is classified into five classes: none, weak, moderate, strong, and very strong. The result indicates that extreme UHI zones have increased. Table 6 shows that the strong region has risen from 1% to 10%, while the non-UHI region has reduced from 83% to 48% from 1990 to 2022. The strong UHI region has also seen a notable change from 2% to 20% during the analyzed period. In accordance with the results indicated by the maps, there have been significant changes in LULC classes between 1990 and 2022, primarily the increase in built-up cover, including roads, buildings, and other infrastructure. The increase in built-up cover leads to an increase in the strong UHI zone.

5. CONCLUSION

This study aims to analyze the LULC and examine the temporal dynamics of LST and UHI in Shimla City using multi-temporal Landsat satellite images from 1990 to 2022. Based on the results, it can be seen that built-up cover has increased significantly, with a

decrease in all other land cover classes. It is observed from the result that LST is rising in densely built-up zones and showing that the region is experiencing very strong effects of UHI. As a result of the conversion of natural landscape features into built-up cover, the city's weather conditions have been adversely affected, contributing to an increase in temperature. The dense vegetation covering part of the city is cooler than the other parts. It shows that vegetation cover can be adopted to mitigate the UHI effects within the city. It is also indicated that LULC plays a significant role in LST and UHI dynamics within the city. Based on the spatiotemporal analysis of the LULC and LST, it has been clearly demonstrated that the environmental and ecological conditions in the city are deteriorating and affecting the city's weather conditions. Therefore, the study indicates the necessity of sustainable urban planning strategies to mitigate UHI effects, especially in rapidly urbanizing mountainous cities. For future studies, it is recommended to evaluate the variability of UHI by considering other climatic factors such as wind speed, solar radiation, air and industrial pollutants.

ACKNOWLEDGEMENTS

The authors thank the USGS Earth Explorer for free satellite data. The authors are also thankful to the Indian Institute of Technology (Banaras Hindu University), Varanasi, for providing the necessary infrastructure to carry out this work.

REFERENCES

1. ICIMOD, (2007). Climate Change and the Himalayas: More Vulnerable Mountain Livelihoods, Erratic Shifts in Climate for the Region and the World. Sustain. Mt. Dev. Gt. Himal. Reg. (No.53), no. 53, p. 7.

2. R. Anbalagan (1993). Environmental hazards of unplanned urbanisation of mountainous terrains: a case study of a Himalayan town. *Q. J. Eng. Geol.*, vol. 26, no. 3, p. 179–184.

3. P. Tiwari, A. Tiwari, and B. Joshi (2018). Urban Growth in Himalaya: Understanding the Process and Options for Sustainable Development. *J. Urban Reg. Stud. Contemp. India*, vol. 4, no. 2, p. 15–27.

4. P. Mohammad, A. Goswami, and S. Bonafoni (2019). The impact of the land cover dynamics on surface urban heat island variations in semi-arid cities: A case study in Ahmedabad City, India, using multi-sensor/source data. *Sensors (Switzerland)*, vol. 19, no. 17.

5. K.J. Gohain, P. Mohammad, and A. Goswami (2021). Assessing the impact of land use and land cover changes on land surface temperature over Pune city, India. Quant. Int., vol. 575-576, p. 259-269.

6.Bokaie M, Zarkesh MK, Arasteh PD, Hosseini A (2016). Assessment of urban heat island based on the relationship between land surface temperature and land use/land cover in Tehran. Sustain Cities Soc 23:94–104.

7. Khan AA, Ul Hassan SN, Baig S, Khan MZ, Muhammad A (2019). The response of land surface temperature to the changing land-use landcover in a mountainous landscape under the influence of urbanisation: Gilgit City as a case study in the Hindu Kush Himalayan Region of Pakistan. Int J Econ Environ Geol 10(3): 40–49.

8. Singh, B., Venkatramanan, V., and Deshmukh, B. (2022). Monitoring of land use land cover dynamics and prediction of urban growth using land change modeler in Delhi and its ppenvirons, India. Environmental Science and Pollution Research, 29(47), 71534–71554.

9. Makwinja, R., Kaunda, E., Mengistou, S., and Alamirew, T. (2021). Impact of land use/land cover dynamics on ecosystem service value—a case from Lake Malombe, Southern Malawi. Environmental Monitoring and Assessment.

10. Hishe, H., Giday, K., Van Orshoven, J., Muys, B., Taheri, F., Azadi, H., Feng, L., Zamani, O., Mirzaei, M., and Witlox, F. (2021). Analysis of land use land cover dynamics and driving factors in desa's forest in Northern Ethiopia. Land Use Policy, 101, 105039.

11. Santamouris, M., Cartalis, C., Synnefa, A., and Kolokotsa, D. (2015). On the impact of urban heat island and global warming on the power demand and electricity consumption of buildings—a review. Energy. Buildings 98, 119–124.

12. Stewart, I. D. and Mills, G. (2021). The urban heat island. The Urban Heat Island.

13. Khatami, R., Mountrakis, G. and Stehman, S. V. (2016). A meta-analysis of remote sensing research on supervised pixel-based land-cover image classification processes: General guidelines for practitioners and future research. Remote Sensing of Environment, 177, 89–100.

14. Abdi, A. M. (2020). Land cover and land use classification performance of machine learning algorithms in a boreal landscape using sentinel-2 data. Geosciences and Remote Sensing, 57(1), 1–20.

15. Kumar, M. and Biswas, V., (2013). Identification of Potential Sites for Urban Development Using GIS-Based Multi Criteria Evaluation Technique. A Case Study of Shimla Municipal Area, Shimla District, Himachal Pradesh, India. *Journal of Settlements & Spatial Planning*, *4*(1).

16. Barsi, J. A., Schott, J. R., Hook, S. J., Raqueno, N. G., Markham, B. L., and Radocinski, R. G. (2014). Landsat-8 thermal infrared sensor (TIRS) vicarious radiometric calibration. Remote Sensing, 6(11), 11607– 11626.

17. USGS. (2018). Landsat surface temperature (ST) product guide (Issue October).

18. Jiang, Y., & Lin, W. P. (2021). A comparative analysis of retrieval algorithms of land surface temperature from landsat-8 data: A case study of Shanghai, China. International Journal of Environmental Research and Public Health.

PLEA 2024 WROCŁAW
(Re)thinking Resilience

Thermal performance analysis of traditional timber houses in tropics based on parametric modeling

REZUANA ISLAM[1] KHANDAKER SHABBIR AHMED[2]

[1]Assistant Professor, Department of Architecture, Chittagong University of Engineering & Technology (CUET), Chittagong, Bangladesh
[2] Professor, Department of Architecture, Bangladesh University of Engineering & Technology (BUET), Dhaka, Bangladesh

ABSTRACT: The study evaluates thermal performance of wall envelopes of traditional timber houses, Bangladesh regarding rural thermal comfort. Field investigation integrated detailed observation and day-long environmental monitoring during hot-humid period. From the field data, a three-dimensional study model having three zones (front, middle and rear) has been prepared and validated for parametric study. Three major variables: i) material, ii) thickness and iii) cavity air gap have been considered for parametric studies. Simulations conducted for ten different external wall types and results have been interpreted statistically. It is observed that zone-wise fluctuation of AT has similar pattern where middle zone shows higher indoor temperature compared to outer zones. Wood with its high thermal inertia performs better compared to plain-sheet material. Increasing thickness has little influence on overall mean indoor AT and an increase in thickness by 6.25mm results in decrease in temperature by 0.4°C. For cavity wall construction fluctuation rate is higher when inner leaf is thin despite the size of cavity. An increase in inner leaf of 6.25mm results in a decrease in indoor temperature by 0.3-0.6°C. Linear regression analysis shows a positive correlation between AT and MRT and AT and OT for the values of 0.98 and 0.99 respectively.
KEYWORDS: Traditional timber house, Wall envelope, Parametric study, Thermal performance, Topics.

1. INTRODUCTION

Comfortable indoor thermal environment is crucial to occupiers' health and well-being. Building envelope, being exposed to direct sun and weather, thermally interacts with the constantly shifting outdoor, since, has direct bearing on indoor thermal performance. Regional tropical houses feature distinct physical traits that transformed in response to regional resource barriers, building techniques, and climatic conditions [1-2]. These ventilation-intensive houses used a variety of passive techniques and design strategies to provide residents with the necessary comfort senses. In addition, residents have distinct lifestyles that may have led to the achievement of thermal comfort within the house [1-3]. Knowledge of these traditional building methods is gained through experimentation and passed down through generations, which has been overlooked in a comprehensive understanding of humanity [4]. Traditional timber house of Bangladesh is one of such examples which are commonly found near Sothern coastlines areas of the country. These houses have wooden envelope system which is supposed to be comfortable which needs scientific justification in the changing climatic scenario. Field investigation reveals that indoor thermal environment have not remains within the comfort range the whole day. However, certain discrepancies may arise due to air leakage between the roof, floor and exterior walls which are currently out of scope of the study. Additionally, because of challenges such as industrialization and economic benefits brought about by advances in design, growing popularity of manufactured materials coupled with mass customization wooden envelope is gradually replacing by manufactured material locally known as plain sheet. Moreover, a sense of worth and purchasing power contributes to the decline of traditional timber houses. In the changing construction and climatic scenario this traditional house envelope needs pragmatic and logical rationalization regarding indoor thermal comfort. Therefore, considering limited time and scope, the purpose of this study is to evaluate the thermal performance of the wall of this tropical house.

2. METHODOLOGY

Fig. 1 illustrates the methodology of the study. Timber houses of Bangladesh lack necessary architectural documentation, hence, documentation is needed prior to study. Therefore, a reconnaissance is conducted to select the ideal case study houses. To understand the existing thermal condition of the house and comfort field investigation has been conducted. Prevailing indoor thermal condition and overview of external wall design criteria have been attained. Qualitative data regarding house form and

layout, occupants living pattern, construction materials, technique and passive design strategies has been collected to develop parametric model and interpret results. Day long qualitative data on indoor and outdoor thermal parameter i.e. air temperature (AT°C), mean radiant temperate (MRT°C), relative humidity (RH%) etc. has been done with data loggers (HOBO ware Pro. U30) at the houses' midpoint at two different heights: 750mm above the ground which is the minimum height of working plane used in residential living and near ceiling level.

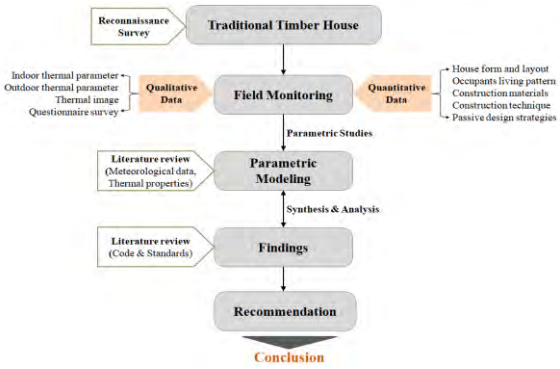

Figure 1: Research structure

To carry out parametric study with EnergyPlus, initially using Google sketch-up with OpenStudio plug-in software, a three-dimensional model has been developed. Parametric studies have considered three major variables: i) material, ii) thickness and iii) cavity air gap. Through changing parameters a couple of experiments were performed to investigate efficient envelope approaches regarding local climate. There is no specific standard regarding thermal comfort for rural areas of Bangladesh. Hence, a literature survey has been conducted to clarify the rural thermal comfort range and to identify thermal properties of the materials. Table 1 [5-6] presents the specified standard comfort range for people wearing simple summer clothing and engaged with light/sedentary activities which have been identified as a basis for the validation and evaluation process.

Table 1: Specified thermal comfort standard [5-6]

Comfort range (°C)	RH (%)	Wind speed (ms^{-1})
Summer: 24–32 Winter: 17–32	50–90	little or no air movement

Finally results have been analyzed and synthesized on the basis of local comfort standard to expand correlation matrix and recommendation towards enhancing thermal comfort.

3. FIELD OBSERVATION

During reconnaissance survey two types of traditional timber house has been identified: single-storied and double-storied. Emphasizing on the construction and residing periods necessary for occupants' acclimatization, initially about 15 from each types have been surveyed and 6 typical cases from each type have been selected and considered for detailed survey. Again, one single and one double-storied house have been considered for day long environmental monitoring during hot-humid period. Data collected provided basic details about current indoor thermal environment (Table 2) and overview of external envelope design strategies (Fig. 2).

Field survey shows that both single and double-storied houses follow a basic zoning and planning strategies. The only difference is: double–storied house has an upper story used for living and storage facilities. Houses are rectangular in shape having three different zones: front socializing, middle living and back service zone. Settlement pattern is detached houses facing N-S direction. Construction is prefabricated in nature having earthen floor or cement concrete flooring and other parts are prepared elsewhere and assembled on site [7]. Hipped roof is placed over the structural frame at an angle of 30° with C.I. (corrugated iron) sheet covering. Roof is provided with a wooden false ceiling and '*Chadoa*' (a piece of fabric) beneath it which creates an attic space of average 1.07m high at the centre position. Middle zone has an average height of 3.2m and front and back zones it is 2.5m. Wall envelope is attached to a frame having average thickness of 100-125mm. Wall envelopes used teak with an average thickness of 12.5mm. Overall opening area takes up approximately 20-25% of the total wall area and swing system makes the opening 100% effective on four sides. Openings are kept open all day and remain closed during night for security purposes, hence, requires mechanical support to ensure comfort at night. Occupancy mapping reveals that it remains empty most of the daytime when the house is hot and remains occupied during night while it becomes cool. Fig. 2 illustrates typical section and envelope details of the case study houses whereas Fig. 3 presents the summery of occupancy schedule inside the houses for a typical summer day [3-4].

Table 2: Surface temperature (mid-day:12:00 pm–4:00 pm) differences of timber house envelope.

House/Level		Floor (°C) (avg.)	Wall (°C) (avg.)		Roof/Ceiling (°C) (avg.)		Outdoor Air Temp. (°C)
			Exterior	Interior	Exterior	Interior	
Single-storied		35.3	42.2	37.7	58.1	42.0	35.42
Double-storied	Ground Floor	31.5	35.5	33.5	46.1	33.3	32.3
	First Floor	37.0	38.2	37.8		41.6	

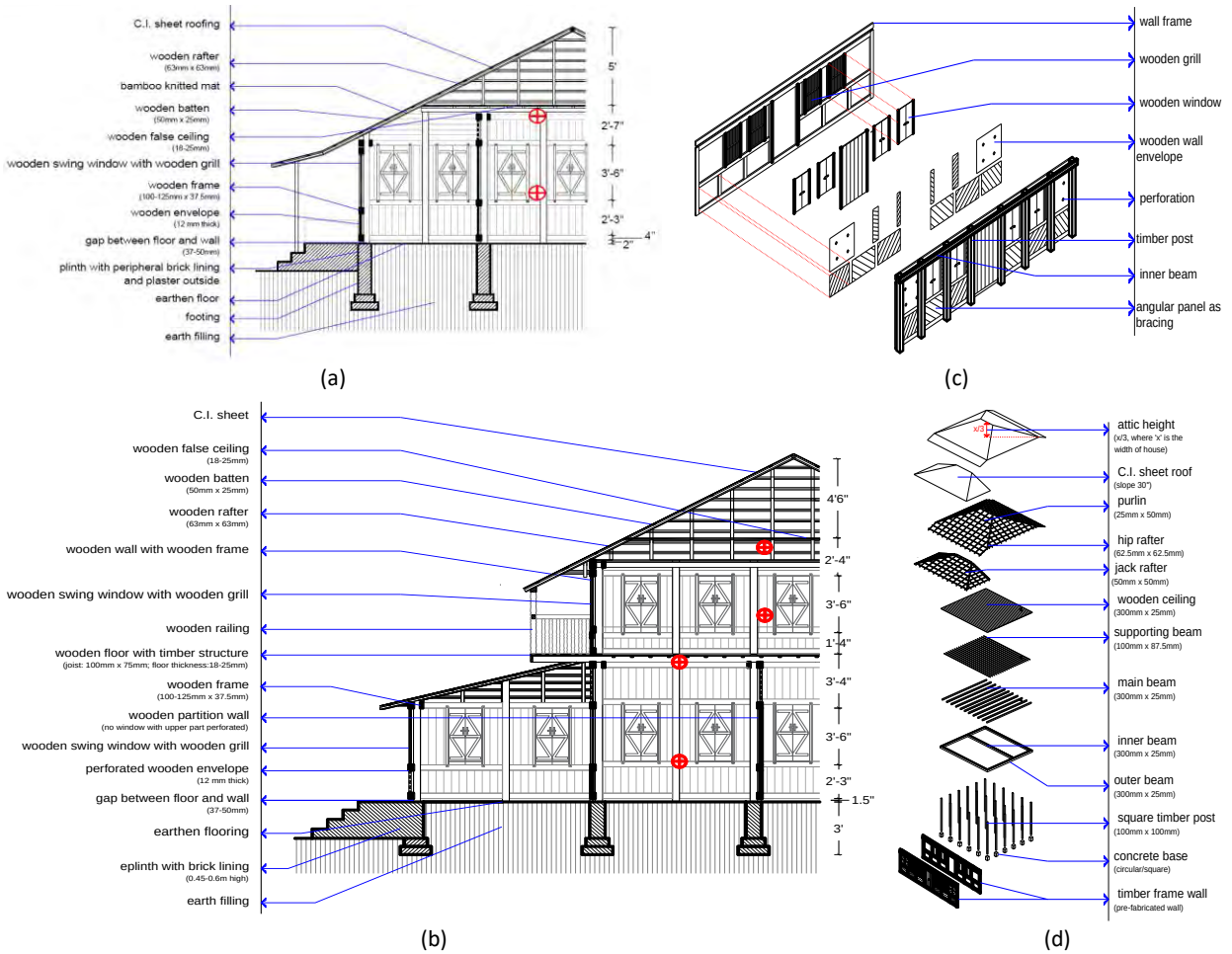

Figure 2: typical section and envelope details: (a) single-storied house; (b) double-storied house; (c) prefabricated wall envelope and (d) exploded view of house components

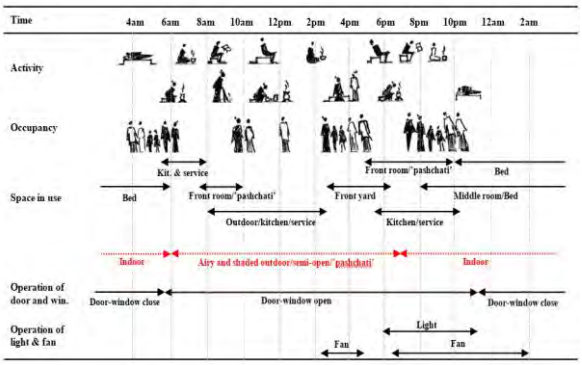

Figure 3: Occupancy mapping of the case study house

4. PARAMETRIC MODEL & VALIDATION

Several studies have validated the numeric outcomes of "EnergyPlus" software towards field data to demonstrate its efficacy [3, 8]. Hence, a three-dimensional model was created based on the findings using "EnergyPlus" and Open-studio Plug-in software to run a couple of simulations to investigate potential envelope techniques to optimize indoor thermal comfort. Table 3 illustrates the traditional timber house parameters considered for parametric study. Modifying variables and material properties enables an evaluation of strategies for reducing indoor temperature. Finally, outcomes are evaluated and synthesized in relation to the regional climate and comfort standards in order to guide future design advancement for improved indoor thermal comfort.

For parametric study weather data file available at Energy-Plus official website is used. All simulated data has been validated with actual data (error ±0.3-5.5%). For parametric studies databases for material, construction, different schedules etc. have been prepared based on field result. A study model of 43.64 sqm area has been prepared having three different zones: Z-1, Z-2 and Z-3 having an average height (h) of 3.2m, 2.65m and 2.65m respectively (Fig. 4) same as case study house for easy comparison of the simulated result with the monitored field data. The site location represents rural fabric of Barisal and weather represents climate of southern coastal zone of Bangladesh. The occupancy load, lighting, electrical equipment, and door-window opening schedule are all like the house surveyed (Fig. 3). Construction considered for model is similar to case surveyed and material properties [11-14] are collected from literature survey (Table 4). As field survey was conducted during the month of August but to reflect most discomfort periods, simulation run period has

been scheduled for the high temperature and high humidity month of June [5-6, 9-10].

Table 3: Test model parameters for simulation study

Parameter	Description
Location	Barisal division
Geographical Location:	i) Longitude 21° 25'(North) ii) Latitude 91° 58' (East)
Time Zone	{GMT +6.0 Hours}
Elevation above sea level	4m
Simulation period	July-August, 2019
Condition	High AT & RH
Sky Model	Clear sky
ASHRAE Climate Zone	1A
ASHRAE Description	Very Hot-Humid
Orientation	Front facing South
Plan Shape	Rectangular
Roof shape & angle	Hipped, 30°
Number of storey	1
Floor to Floor Height	Z-1 Avg. 3.2m Z-2 & 3 Avg. 2.65m
Z-1 (Middle zone)	Gross wall: 14.89m2 Gross window: 2.38m2
Z-2 (Front zone) & Z-3 (Back zone)	Gross wall: 21.04m2 Gross window: 4.77m2
Floor Area	43.97 m2
Construction materials	Floor : Earthen Roof: C.I. sheet Wall: Timber (Teak) Door-window: Wooden swing, 100% operable
Ventilation method	Natural Ventilation Simple (Operable simple window)
Occupancy schedule	Residence occupancy
Number of people	5
Lighting Design level (W)	120 (Cal. method: W/Area)
Equip. Design level (W)	450 (Cal. method: W/Area)

A few cases of changing envelope materials, thickness and construction strategies have been considered (Table 5) and assessed regarding local thermal comfort standard for rural areas of Bangladesh. Timber houses are conventionally built with wooden (teak) walls which are now gradually replacing by plain iron sheet. Therefore, simulation studies considered these two materials: wood and plain iron sheet for performance evaluation. Again, from the field survey it has been observed that wooden wall thickness is 18.75mm whereas frame thickness is 37.5mm. Therefore, changing thickness@12.5mm within maximum value of 37.5mm four different thicknesses between 18.75mm- 37.5mm and cavity air gap of 6.25mm, 12.5mm and 18.75mm have been considered for study. Other parameters i.e. economic impact, structural stability, night ventilation, air-leakage, impact of roof shading, energy related issues, fire safety, security, etc. is out of scope of the research. Finally, thermal performance data of thirteen walls is summarized statistically.

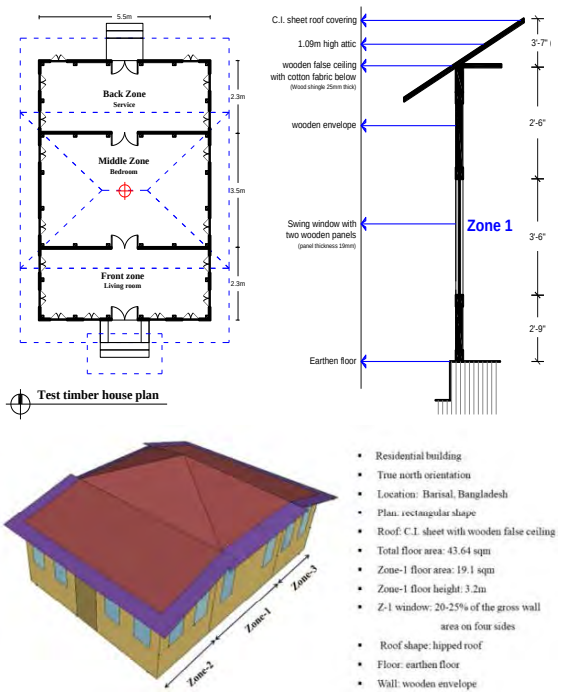

Figure 4: Simulation details of test house

Table 4: Thermal properties of envelope materials [11-14]

Name	material	Conductivity (W/m-K)	Density (Kg/m3)	Specific heat (J/kg-K)
Floor	Earthen	1.4	1460	879
Window & door	Sal	0.96	660	1880
Ceiling	Raintree	0.74	480	1880
Chadoa	Fabric	0.04	225	1380
Roof	CI sheet	65	7300	235
	Teak	1.28	710	1880
Wall	Plainsheet	237	2700	890
	Cavity	*Resistance 0.14-0.17 m2-K/ W		

5. FINDINGS AND CONCLUSION

Table 6 outlined statistical summary of parametric study. Outdoor mean AT and RH were same for all the wall types studied which is 27.83°C and 86.91% with a standard deviation (SD) of 2.03 and 7.84 respectively. It is found that changes in materials, thickness and configurations have significant impact on indoor environment. Simulation result reflects that wood with its high thermal inertia performs better compared to plain-sheet material. Plain sheet wall envelope exhibits low resisting capacity against outdoor temperature and maximum temperature of 39.03°C to 41.10°C with a SD of 0.1 was observed for plain sheet envelope design. It has been observed that increase in thickness of wooden wall has little influence on overall mean indoor AT as insulating property of wood contributes towards low heat gain during day and low heat release during night. Statistical value reflects a decrease in temperature by 0.4°C for an increasing in thickness by 6.25mm.

Table 5: Wall types considered for parametric study

Parameter	Code	Type/ Thickness			Construction	Graphical illustration
Material (WM-1)	WM-1a	12.5 mm			wooden wall	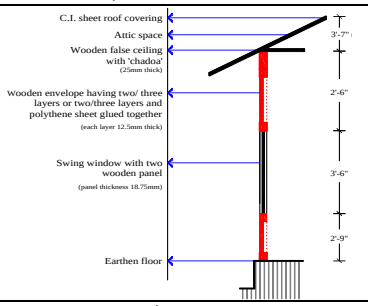
	WM-1b	--			plain sheet wall	
Thickness (WT-2)	WT-2a	18.75 mm			Traditional timber frame wooden wall: 12.5-37.5mm thick	
	WT-2b	25 mm				
	WT-2c	31.25 mm				
	WT-2d	37.5 mm				
Cavity air-gap (WC-3)		Inner leaf	cavity	Outer leaf	12.5-18.75mm two wooden leaf with cavity. Total wall thickness 37.5-50mm	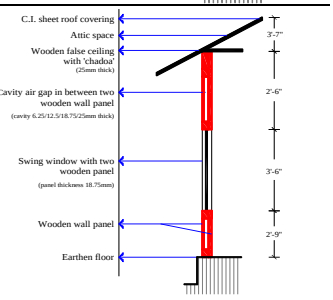
	WC-3a	12.5 mm	6.25 mm	18.75 mm		
	WC-3b	12.5 mm	12.5 mm	12.5 mm		
	WC-3c	18.75 mm	12.5 mm	12.5 mm		
	WC-3d	25 mm	12.5 mm	12.5 mm		
	WC-3e	12.5 mm	18.75 mm	12.5 mm		
	WC-3f	18.75 mm	18.75 mm	12.5 mm		
	WC-3g	12.5 mm	25 mm	12.5 mm		

For cavity wall, fluctuation rate is higher when inner leaf is thin despite of the size of cavity. Maximum AT of Z-1 rises up to 38.91°C-40.72°C where at Z-2 and Z-3 AT is 0.5-1.5°C lower compared to Z-1. W-3d results in lowest maximum temperature which ranges between 36.68°C-38.91°C in different zones whereas highest maximum temperature results for W-3c and W-3e (39.3°C-40.72°C). From the simulation data it is observed that an increase in inner leaf of 6.25mm results in a decrease in temperature by 0.3-0.6°C.

Zone-wise fluctuation of AT has similar pattern where Z-1 shows higher temperature gradients compared to Z-2and Z-3 (Fig. 5). Z-1 AT and OT was nearly 0.5-0.8°C higher than the upper limit of comfort temperature. Both mean MRT and OT is higher for Z-1 by 0.5-1.14°C whereas decrease from Z-2 to Z-3 by nearly 0.2-0.6°C (Table 6). Zone temperature gradients remains 0.5-2.3°C higher than the upper value of comfort where Z-1 shows higher and Z-3 shows comparatively lower temperature gradients compared to others.

Fig. 6 (a) illustrates the overall probability density function (PDF) for different zones. Cumulative density function for different wall types defines frequency distribution of fluctuating variables (Fig. 6(b)). From the figure it is seen that cavity construction performs better compared to plain sheet and wooden wall but with the increase in temperature nearly above 34°C performance of cavity wall decreases. Table 7 shows correlation matrix among temperature gradients. Linear regression analysis shows that a positive correlation among AT and MRT has been obtained for the value of 0.98 whereas for the correlation AT and OT the value is 0.99 (Table 7).

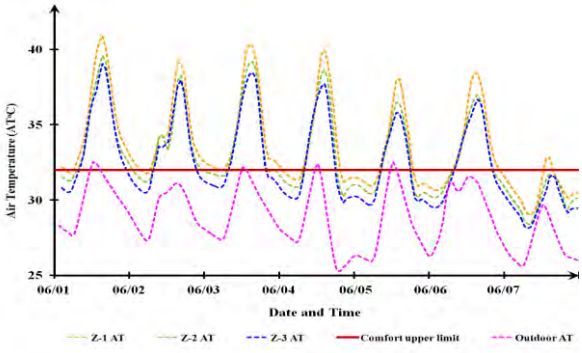

Figure 5: Zone wise fluctuation of air temperature (AT°C)

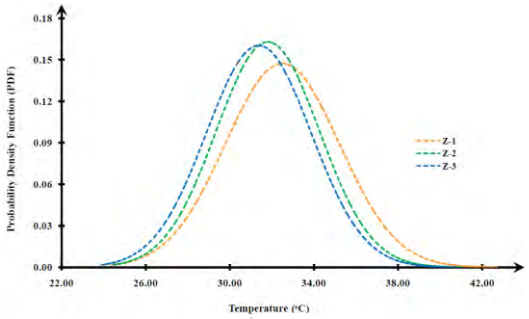

(a)

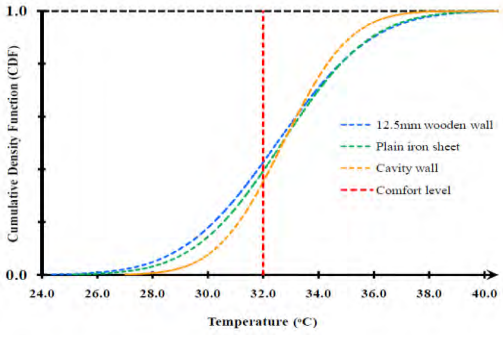

(b)

Figure 6: (a) Zone PDF and (b) CDF for simulated walls

Table 6: Statistical summary of thermal performance of walls considered for parametric study

Wall	Mean Air Temperature (AT°C)			Mean Radiant Temp. (MRT°C)			Operative Temperature (OT°C)		
	Z-1	Z-2	Z-3	Z-1	Z-2	Z-3	Z-1	Z-2	Z-3
WM-1a	32.46	31.80	31.36	31.73	31.37	31.04	32.10	31.58	31.20
WM-1b	34.31	33.36	33.01	33.41	32.84	32.56	33.84	33.10	32.78
WT-2a	32.50	31.81	31.38	31.75	31.37	31.04	32.12	31.59	31.21
WT-2b	32.52	31.84	31.41	31.77	31.38	31.04	32.15	31.61	31.22
WT-2c	32.51	31.81	31.41	31.75	31.35	31.02	32.13	31.58	31.21
WT-2d	32.50	31.78	31.38	31.74	31.34	30.99	32.12	31.56	31.19
WC-3a	32.69	31.91	31.38	31.96	31.47	30.94	32.33	31.69	31.16
WC-3b	32.52	31.84	31.41	31.77	31.38	31.04	32.15	31.61	31.22
WC-3c	32.73	31.95	31.35	32.01	31.49	30.90	32.37	31.72	31.12
WC-3d	32.72	31.96	31.34	32.02	31.50	30.89	32.37	31.73	31.12
WC-3e	32.52	31.84	31.41	31.77	31.38	31.04	32.15	31.61	31.22
WC-3f	32.73	31.95	31.35	32.01	31.49	30.90	32.37	31.72	31.12
WC-3g	32.77	31.97	31.34	32.06	31.51	30.88	32.42	31.74	31.11

Table 7: Correlation matrix among AT, MRT and OT

	Out. Temp	AT	MRT	OT
Out. temp.	1	0.88	0.90	0.90
AT	0.88	1	0.97	0.99
MRT	0.90	0.97	1	0.99
OT	0.90	0.99	0.99	1

6. CONCLUSION

Study on traditional timber house of Bangladesh is still marginal. Hence, the study evaluates thermal performance of wall envelopes of traditional timber house with limited design strategies. From the study the following conclusion can be made:

i. Changes in materials, thickness and configurations have significant impact on zone indoor environment where middle zone shows higher temperature gradients compared to outer zones.
ii. Wooden envelope performs better over plain sheet material. However, Increase in thickness of wooden wall has little influence on overall mean indoor AT and an increase in thickness by 6.25mm results in decrease in temperature by 0.4°C.
iii. Fluctuation rate is higher when inner leaf is thin despite of the size of cavity. Increasing inner leaf by 6.25mm results in a decrease by 0.3-0.6°C.
iv. Positive correlation exists among AT, MRT and OT. Best fitted model can be obtained for AT-MRT and AT-OT for the value of 0.98 and 0.99 respectively.

This study presents insight into thermal performance of wall envelope design which will help built-environmental professionals and policymakers develop passive design strategies to improve occupants' well-being in future.

ACKNOWLEDGEMENTS

This research is part of 1st author's M. Arch thesis.

REFERENCES

1. Islam, R. and K. S. Ahmed, (2021). Indoor Thermal Environment and Occupant's Living Pattern of Traditional Timber Houses in Tropics. *Designs*, 5(1): p.10.
2. Islam, R., (2022). Study on thermal performance of traditional timber houses in Bangladesh, [Unpublished masters' thesis].
3. Chowdhury, S.; K. S. Ahmed and Y. Hamada, (2015). Thermal performance of building envelope of readymade garments factories in Dhaka, Bangladesh. *Energy & Building*, 107: p. 144–154.
4. Salman, M., (2018). Sustainability and vernacular architecture: Rethinking what identity is. In *Urban and architectural heritage conservation within sustainability*. IntechOpen.
5. Mallick, F.H., (1996). Thermal comfort and building design in the tropical climates. *Energy and Buildings*, 23(3): p. 161-167.
6. Sharma, M.R. and S. Ali, (1986). Tropical summer index—a study of thermal comfort of Indian subjects. *Building and Environment*, 21(1): p. 11-24.
7. Islam, R.; K. S. Ahmed and S. Chowdhury, (2023). Exploring traditional timber houses of Bangladesh from the perspective of rural culture and environmental experience. In *6th International Conference on Smart Villages and Rural Development*. Assam, India, 04-05 December 2023.
8. Casini, M., (2021). Construction 4.0: Advanced Technology, Tools & Materials for Digital Transformation of the Construction Industry. *Woodhead Publishing*.
9. Khan M. A. S. et al . , (2011). Indoor thermal condition of factory building in Bangladesh, *Journal of Architecture and Built Environment*, 38(2): p. 55-62.
10. Ahmed K. S., (2003). Comfort in urban spaces: Defining boundaries of outdoor thermal comfort for tropical urban environments, *Energy and Buildings*, 35(1): p. 103–110.
11. Hadden, R. M., A. I. Bartlett, et al. (2017). Effects of exposed cross laminated timber on compartment fire dynamics. *Fire Safety Journal*, 91: p. 480-489.
12. Thakare, K. A., H. G. Vishwakarma, et al. (2015). Experimental investigation of possible use of HDPE as thermal storage material in thermal storage type solar cookers. *Journal of Research in Engineering and Technology*, 4: p. 92-99.
13. Vasubsbu, M., B. Nagaraju, et al. (2015). Experimental measurement of thermal conductivity of wood species in india: effect of density and porosity. *International Journal of Science, Environment and Technology*, 4(5): p. 1360-1364.
14. Clarke, J.A., Yaneske, P.P. and Pinney, A.A., (1991). The harmonisation of thermal properties of building materials.

PLEA 2024 WROCŁAW
(Re)thinking Resilience

Respond to Heatwaves:
A review of urban planning and governance approaches for mitigating public health crises

XINYUE LI[1]

[1]Guangdong University of Technology, Guangzhou, China

ABSTRACT: Under the combined effects of climate change and urbanization, weather extremes such as heatwaves seriously impact ecosystems and human health. Moreover, future climate change scenarios indicate that heatwaves in specific regions (e.g., subtropical/tropical regions) will become more frequent, persistent and severe, exacerbating local public health problems. Hence, there is an urgent need to find strategies to mitigate heatwaves in urban management and planning. The purpose of this paper is to summarize, analyze and discuss heatwave-related research from a planning and design perspective, covering four main areas: advances in heatwave-related research, definitions of heat waves, planning and architectural design recommendations to cope with heatwave problems, and some application examples. This review hopes to provide a comprehensive reference point for planners, architects and government officials to cope with the negative impacts of heatwaves.
KEYWORDS: Heatwaves, Planning strategy, Policy, Mitigation, Built environment

1. INTRODUCTION

As a dual effect of climate change and urbanization, there is a rising trend of extreme weather events in frequency, intensity and duration, which impacts ecosystems and human health. On July 16, 2023, China broke the highest temperature in history, reaching 52.2°C. Heatwaves during 2022 lasted 64 days, the most extended duration since 1961. Heatwave events are proven to significantly affect public health, energy consumption and socioeconomic activities [1]. When exposed to high temperatures, the human thermoregulatory system responds to counteract the adverse effects of heat. However, once the heat exceeds a specific limit, the risk of disease and death increases dramatically on the day of exposure or in the following days. The health effects of sustained extreme temperatures, i.e., heat waves, have been extensively studied [2-4]. In addition to this, extreme weather events caused by the increasing intensity and duration of heat waves are leading to significant numbers of energy system failures, especially in urban areas. This drastically affects the reliability and normal operation of power distribution grids around the world, with high financial costs and huge negative impacts on people's lives [5]. The number of heat-related deaths caused by intense exposure to high temperatures and the risk of heat-related health of vulnerable populations like the elderly will be likely to increase as the world population is aging [6]. The "AR6 Synthesis Report: Climate Change 2023" released by the IPCC states that the best estimate of the global temperature rise will reach 1.5°C between 2021 and 2040. The current situation is compounded by future climate change scenarios that indicate more frequent, long-lasting, and severe heat waves in specific locations (e.g., subtropical/tropical regions), exacerbating public health issues. Hence, it is essential for us to take appropriate measures to cope with the heatwave and to improve human habitats for a healthier living environment for all.

Many studies already exist to assess the causes, influences, characteristics (e.g., magnitude, frequency, duration), and spatial distribution of heatwave disasters from the perspectives of disaster science, meteorology, and ecology, and these studies have been carried out more in developed countries and less in developing countries, especially in the Asia-Pacific region. There are also some reviews of the measurement, occurrence and changes in heatwaves [7-8]. Some researchers review the effects of heatwaves and mechanisms to mitigate the effects [9-11], which may be less direct for practical implementation. Very few studies systematically look at how planners and architects perceive heatwaves from a planning and design perspective.

Therefore, a systematic review of existing heatwave-related planning policies and strategies is a timely research. This paper aims to summarize, analyze and discuss heatwave-related studies from the planning and design perspective, mainly covering four aspects: the advances in research related to heatwaves; the definition of heatwaves; recommendations for planning and building design in response to heatwave problems; some examples of applications. This review hopes to provide planners, architects and government officials with

comprehensive reference points to combat the negative impacts of heatwave.

2. DEFINITION OF HEATWAVES

A heatwave normally refers to high-temperature and high-humidity weather events with two or more consecutive days, bringing negative impacts on public health, energy consumption and socioeconomic activities. Because heatwaves are influenced by various factors, like geographic, social and economic factors, definitions vary greatly across regions and countries [12]. The World Meteorological Organization (WMO) defines a heatwave as “A period of marked unusual hot weather over a region persisting for at least three consecutive days during the warm period of the year based on local climatological conditions, with thermal conditions recorded above-given thresholds” [13]. For Adelaide, a heatwave is defined as five days with a maximum air temperature over 35 ◦C or three days over 40 ◦C, and for Perth, three days over 35 ◦C [14]. Canada, the United States, Israel and other countries define it as two consecutive days when the daytime temperature is over 40.5 ◦C and lasts for more than 3 hours or more. In China, a heatwave is defined by the China Meteorological Administration (CMA) as at least three days with a daily maximum surface air temperature over 35 ◦C [15]. At the same time, some countries do not consider duration and periodicity when defining heatwaves, such as India and Pakistan [16-17].

3. EVALUATION OF HEATWAVE-RELATED RISK

Crichton’s risk triangle is the most commonly used method to evaluate heat risk [18]. According to its analytical framework, the heatwave-related risk depends on the severity, frequency and duration of the hazard, the exposure of the population of interest and the vulnerability of the exposed population. Therefore, the heat health risk is often expressed as a function of hazard, exposure and vulnerability [19]. Vulnerability has also been defined as a combination of exposure, sensitivity and adaptive capacity [20]. However, scholars applied various weighting and integration methods during calculation. Table 1 summarizes some of the common evaluation factors for each part of the risk triangle.

3.1 Heat hazard

In the context of heat health risk assessment, heat hazards are usually considered as the average daily temperature rise [21-22], which can be measured or predicted [23]. Scholars mainly employed temperature indicators to represent the heat hazard, such as daytime and nighttime temperatures [24-26], heatwave duration [27], and frequency and magnitude of heatwaves [28-29]. Besides, in cities with complex geographic contexts, where land surface features affect the spatial variability of weather factors [30], the method improved based on the conventional "land-use regression" is used [31]. Compared with the traditional land-use regression method, the improved one not only utilizes land-use types but also combines urban surface aerodynamic characteristics, building morphological factors, weather data from monitoring networks and upper-air sounding data as predictor variables. Therefore, this method can detect the urban thermal environment and its interactions with land surface characteristics [32].

3.2 Heat exposure

For heat health risk assessment, if there are no people, there is no exposure and no risk [33]. Therefore, population density has been often used as an indicator to quantify exposure in risk assessment studies [34-35]. The DMSP/OLS Nighttime light (NTL) data is a powerful tool for detecting nighttime lights and human nocturnal activities; therefore, it is widely used as an effective proxy for population density and population distribution at a global scale [36-38]. Because of the saturation effect of DMSP/OLS data, the elevation-adjusted human settlement index (EAHSI), which integrates data from multiple sources, is often used to decompose and map the spatial distribution of the human exposure index [23,34].

Additionally, data from the Census and Statistics Department can be used if conditions permit. Demographic data represent population density more accurately than other media, such as the NTL [39].

3.3 Heat vulnerability

Both urban environmental factors and socioeconomic conditions have been shown to influence the relationship between heatwaves and health [40-41]. The economic level of different regions determines, to some extent, the ability of local residents to cope in the event of a hazard. Factors commonly assessed include low-income households, the population living in public rental housing, households living in low-quality areas, the population aged 65 years and above, and the population aged 15 years and above with low education levels [32,42]. Factors in the urban environment of different areas also objectively determine residents’ abilities to cope with, mitigate, and recover from heatwaves [33]. Common evaluation factors include the area of vegetation and water bodies, topographical conditions, transportation conditions, medical facilities, housing conditions, etc [22,43].

3.4 Adaptation capacity

Adaptation to the risk of heatwaves is commonly assessed by factors such as the level of the economy, the greenness of the city, the distribution of healthcare facilities, and the number of health technicians [20]. Adaptation and vulnerability indices are often combined, showing a blurred concept of these two in heat health risk evaluation.

3.5 Evaluation model

Researchers construct risk assessment models related to heatwaves with varying weights for every evaluation factor for different regions. Some scholars use the entropy method to determine the weight of indicators and the natural breaks method to classify different layers [44]. Some scholars have also applied principal component analysis (PCA) for dimensionality reduction, using a variance-weighted approach where the percentage of the variance of each indicator was used as weights for aggregation [22,46]. There are other methods, such as the overlay method, subjective empowerment method, objective empowerment method and combined weighting method.

Table 1: Evaluation Factors for Heat Hazards, Heat Exposure, Heat Vulnerability and Adaptive Capacity.

Layer	Evaluation factors
Heat hazard	- Daytime temperatures - Nighttime temperatures - Heatwave duration - Air quality - Land-use types - Urban surface aerodynamic characteristics - Building morphological - Weather data - Upper-air sounding data
Heat exposure	- DMSP/OLS data - Census data
Heat vulnerability	- Low-income households - Population living in public rental housing - Households living in low-quality areas - Population aged 65 years and above - Population aged 15 years and above with low education level - Vegetation and water bodies - Topographical conditions - Transportation conditions - Medical facilities - Housing conditions
Adaptation capacity	- Level of the economy - Greenness of the city - Distribution of health-care facilities - Number of health technicians

4. HEATWAVE MITIGATION AND MANAGEMENT

Existing scientific studies and planning practices proved that the following planning strategies can mitigate the adverse effects of heatwaves: (1) Green infrastructure, such as green spaces, parks, trees and vegetated areas, which can mitigate the effects of heatwaves by providing shade and cooling the air through evapotranspiration. Incorporating such green infrastructure in cities can help lower temperatures and increase the overall climate resilience of cities [46]. (2) Urban form, such as building density and urban spatial layout. Compact urban forms, limited green spaces and high building densities can exacerbate the urban heat island effect, leading to higher temperatures during heatwaves [47].

In some developed countries and some pioneer cities in China, there are cases and experiences of dealing with heatwaves, like policies and planning guidelines. The Cool Neighbourhoods NYC uses a three-pronged strategy to address the challenges posed by heatwaves. The first is the heat mitigation strategy. The strategy focuses on enhancing green infrastructure such as parks, street greening, and green roofs to provide effective shade and reduce the urban heat island effect. The second is the Heat Adaptation Strategy, which emphasizes community engagement and community resilience, such as Home Health Aides (HHAs), caring for the vulnerable and the Low-Income Home Energy Assistance Program (LIHEAP). The third is the monitoring strategy. Over time, it ensures that implemented strategies are evaluated, enabling timely adjustments to be made. In the central Spanish city of Zaragoza, an interactive map has been launched that clearly shows the location of the shadows cast by buildings on the street at a given date and time, making it easier for citizens to plan their travel routes in advance and avoid roads exposed to the hot sun. The municipal government of Madrid has developed a mobile application called "Madrid Móvil" where people can find the locations of fountains throughout the city. In May 2023, Japan launched a new policy to reduce the number of deaths from heat stroke, which calls for the flexible application of the heat stroke warning issued by the Meteorological Agency, the rational use and improvement of the emergency transportation and emergency medical care system, and visits to the homes of the elderly.

Several strategies have not yet been applied in reality but are supposed to be effective in mitigating the impact of heatwaves on cities. These planning strategies can be divided into two categories: the first is urban planning and design recommendations that can mitigate heatwaves based on factors such as greening, urban geometry, materials and energy consumption. The second category consists of public

management approaches based on factors such as heatwave early warning systems, public education, and the promotion of knowledge about heat mitigation and adaptation. After a systematic review, two general planning categories can be further grouped into green and blue infrastructure, land use and land cover, urban geometry, energy consumption, public awareness and advertising and public health warning.

4.1 Green and blue infrastructure

Nature-based solutions (NBS), such as green (vegetation) and blue (water bodies) infrastructure, are being promoted as cost-effective and sustainable strategies for managing heatwave risk. Scholars have examined their cooling efficiency and found a combination of green-blue NBS had the highest spatial cooling effect, followed by waterbodies, woodland and grassland areas [48]. The proposed strategies include (1) Modification of existing urban plans or new development decisions, such as zoning regulations, transportation, etc. Existing land use patterns should be evaluated to prioritize investments in green-blue infrastructure, especially in vulnerable areas such as those suffering from heat islands [49]. (2) Calculation of thresholds for the maximum cooling effect based on the size of the city and population and configuration of the appropriate amount of blue-green infrastructure and appropriate spatial arrangement. (3) Engagement of community and multi-sectoral stakeholders (e.g., government, business corporations, academia) to collaborate in designing and formulating policies for blue-green infrastructure through, for example, meetings and voting. Since the city centre is often the “hottest” area and increasing its blue-green infrastructure may change the land functions, such a decision involves multiple stakeholders and requires a careful evaluation of economic efficiency.

4.2 Land use and land cover

Previous studies have utilized eddy covariance measurements to demonstrate differences in the performance of different land cover types in the cooling process. Scholars compared the heat flow measurements over urban and rural areas and showed that under the same high humidity conditions, the urban site tends to have increased sensible heat flux, while the rural site tends to have increased latent heat flux [50]. One of the strategies is to develop integrated urban agriculture, which not only helps retain water, promotes cooling effects through evaporation, and prevents soil dehydration during heatwaves but also promotes biodiversity, which contributes to ecosystem resilience and adaptation in the face of climate stress [51]. Another strategy is to use highly reflective materials on pavements and roofs to achieve a cooling effect [52]. However, the development of urban agriculture can be challenging because of limited space and water availability in cities. Highly reflective pavement materials can also be difficult to apply to urban road construction because of high implementation costs and maintenance challenges.

4.3 Urban geometry

The interaction of climate change and urbanization is exacerbating extreme weather conditions in urban environments and affecting urban populations even more. It has been shown that urban permeability and ventilation corridors aligned parallel to the prevailing wind direction can effectively mitigate urban heat stress, and future policy directions should promote adaptive thermal comfort lifestyles towards net-zero carbon emissions [53].

4.4 Energy consumption

The implementation of rooftop photovoltaic panels (RPVPs) is an effective strategy for mitigating the urban heat island effect and utilizing renewable energy sources to alleviate the city's energy demand [54]. Solar energy generated by rooftop photovoltaic panels replaces electricity generated by fossil fuels that emit greenhouse gases. Nowadays, a large number of PV panels have been deployed, but for better results, more advanced technology is needed to improve the conversion efficiency of solar energy.

4.5 Public awareness and advertising

Some studies have proposed related strategies: (1) Heat warnings can be disseminated not only through traditional media, such as television and radio, but also through social media [55]. (2) Measures should be introduced regularly to cope with heat hazards for heat-sensitive people.

4.6 Public health warning

Urban planners and policymakers should promote the construction of a heat warning system, as there are significant differences in the adaptive capacity of people with various income levels, job types and ages to extreme summer heat. It is necessary to gradually solve the problem of unequal distribution and irrational planning of public resources such as medical care, transportation, and space for cooling during high-temperature environments. Subsidies should be provided to economically disadvantaged families or individuals, cooling equipment should be distributed, the working hours of outdoor workers should be adjusted, and appropriate medical incentives should be formulated for heat-induced diseases [44].

5. DISCUSSION

Despite the progress in heatwave-related studies, current studies have several limitations. First, the heatwave evaluation method may result in different spatial distribution patterns for the same study target due to the uncertainty brought by the overlaying approach for constructing heatwave risk indexes. Second, most studies on planning strategies and design recommendations for heatwave risk are carried out in developed regions in Europe and the United States. Studies on local measures for cities in the Asia-Pacific region are still scarce, while those cities are projected to face more severe heatwave events in the future. Third, since some of the planning strategies mentioned in the paper that have not been applied to practice are proposed on a theoretical basis, the application premise and the target service users are still uncertain, and the results obtained cannot be well guaranteed. Future research is recommended to fill in the above gaps if relevant data are available.

6. CONCLUSION

This study systematically summarizes the risks of heat waves from a planning and design point of view, which can provide a powerful reference for planners and architects and a basis for creating cool communities in the future.

REFERENCES

1. Ye, X., (2012). Ambient temperature and morbidity: a review of epidemiological evidence. Environ. *Health Perspect*. 120, 19–28.
2. Tong, S., (2014, February). The impact of heatwaves on mortality in Australia: a multicity study. *BMJ Open,* 4(2), e003579.
3. D'Ippoliti, D., (2010, July 16). The impact of heat waves on mortality in 9 European cities: results from the EuroHEAT project. *Environmental Health*, 9(1).
4. Kovats, R. S. (2004, November 1). Contrasting patterns of mortality and hospital admissions during hot weather and heat waves in Greater London, UK. *Occupational and Environmental Medicine*, 61(11), 893–898.
5. Atrigna, M., Buonanno, A., Carli, R., Cavone, G., Scarabaggio, P., Valenti, M., Graditi, G., & Dotoli, M. (2023). A Machine Learning Approach to Fault Prediction of Power Distribution Grids under Heatwaves. *IEEE Transactions on Industry Applications*, 1–11.
6. Lutz, W., (2008, January 20). The coming acceleration of global population ageing. *Nature,* 451(7179), 716–719.
7. Perkins, S. E. (2015). A review on the scientific understanding of heatwaves—Their measurement, driving mechanisms, and changes at the global scale. *Atmospheric Research,* 164-165, 242–267.
8. Rossiello, M. R., & Szema, A. (2019, May 28). Health Effects of Climate Change-induced Wildfires and Heatwaves. *Cureus.*
9. Zuo, J., Pullen, S., Palmer, J., Bennetts, H., Chileshe, N., & Ma, T. (2015, April). Impacts of heat waves and corresponding measures: a review. *Journal of Cleaner Production,* 92, 1–12.
10. Adnan, M. S. G., Dewan, A., Botje, D., Shahid, S., & Hassan, Q. K. (2022, October). Vulnerability of Australia to heatwaves: A systematic review on influencing factors, impacts, and mitigation options. *Environmental Research*, 213, 113703.
11. Sharma, A., Andhikaputra, G., & Wang, Y. C. (2022, May 4). Heatwaves in South Asia: Characterization, Consequences on Human Health, and Adaptation Strategies. *Atmosphere*, 13(5), 734.
12. Sharma, A., Andhikaputra, G., & Wang, Y. C. (2022, May 4). Heatwaves in South Asia: Characterization, Consequences on Human Health, and Adaptation Strategies. *Atmosphere*, 13(5), 734.
13. Wilkinson, H. UK. (2018) The Global Warming Policy Forum: London, UK, *Heatwaves (GWPF Factsheet 3)*, p. 2.
14. Zuo, J., Pullen, S., Palmer, J., Bennetts, H., Chileshe, N., & Ma, T. (2015, April). Impacts of heat waves and corresponding measures: a review. *Journal of Cleaner Production*, 92, 1–12.
15. Zhi, G., Meng, B., Wang, J., Chen, S., Tian, B., Ji, H., Yang, T., Wang, B., & Liu, J. (2021, October 13). Spatial Analysis of Urban Residential Sensitivity to Heatwave Events: Case Studies in Five Megacities in China. *Remote Sensing*, 13(20), 4086.
16. Zahid, M., & Rasul, G. (2012, January 3). Changing trends of thermal extremes in Pakistan. *Climatic Change*, 113(3–4), 883–896.
17. Azhar, G.S.; Mavalankar, D.; Nori-Sarma, A.; Rajiva, A.; Dutta, P.; Jaiswal, A.; Sheffield, P.; Knowlton, K.; Hess, J.J. (2014, September 25). Correction: Heat-Related Mortality in India: Excess All-Cause Mortality Associated with the 2010 Ahmedabad Heat Wave. *PLoS ONE*, 9(9), e109457.
18. Crichton, D. (1999). The risk triangle. *Natural disaster management*, 102(3), 102-103.
19. Tomlinson, C. J., Chapman, L., Thornes, J. E., & Baker, C. J. (2011). Including the urban heat island in spatial heat health risk assessment strategies: a case study for Birmingham, UK. *International Journal of Health Geographics*, 10(1), 42.
20. Weber, S., Sadoff, N., Zell, E., & de Sherbinin, A. (2015, September). Policy-relevant indicators for mapping the vulnerability of urban populations to extreme heat events: A case study of Philadelphia. *Applied Geography*, 63, 231–243.
21. Krstic, N., Yuchi, W., Ho, H. C., Walker, B. B., Knudby, A. J., & Henderson, S. B. (2017). The Heat Exposure Integrated Deprivation Index (HEIDI): A data-driven approach to quantifying neighborhood risk during extreme hot weather. *Environment International*, 109, 42-52.
22. Inostroza, L., Palme, M., & De La Barrera, F. (2016). A heat vulnerability index: spatial patterns of exposure, sensitivity and adaptive capacity for Santiago de Chile. *PLOS one*, 11(9), e0162464.
23. Chen, Q., Ding, M., Yang, X., Hu, K., & Qi, J. (2018). Spatially explicit assessment of heat health risk by using multi-sensor remote sensing images and socioeconomic data in Yangtze River Delta, China. *International Journal of Health Geographics*, 17(1), 1-15.
24. Song, J., Huang, B., Kim, J. S., Wen, J., & Li, R. (2020, May). Fine-scale mapping of an evidence-based heat health risk index for high-density cities: Hong Kong as a case study. *Science of the Total Environment*, 718, 137226.
25. Amaya, M. A., Mohammed, M., Pingitore, N. E., Aldouri, R., & Benedict, B. (2016, February 10). Community

Exposure to Nighttime Heat in a Desert Urban Setting, El Paso, Texas. *International Journal of Advanced Remote Sensing and GIS*, 5(1), 1507–1513.
26. Obradovich, N., Migliorini, R., Mednick, S. C., & Fowler, J. H. (2017). Nighttime temperature and human sleep loss in a changing climate. *Science advances*, 3(5), e1601555.
27. Unal, Y. S., Tan, E., & Mentes, S. S. (2013). Summer heat waves over western Turkey between 1965 and 2006. *Theoretical and Applied Climatology*, 112, 339-350.
28. Goyal, M. K., Gupta, A. K., Das, J., Jain, V., & Rakkasagi, S. (2023, August 24). Heatwave magnitude impact over Indian cities: CMIP 6 projections. *Theoretical and Applied Climatology*, 154(3–4), 959–971.
29. Brown, S. J. (2020, December). Future changes in heatwave severity, duration and frequency due to climate change for the most populous cities. *Weather and Climate Extremes*, 30, 100278.
30. Shi, Y., Ren, C., Cai, M., Lau, K. K. L., Lee, T. C., & Wong, W. K. (2019). Assessing spatial variability of extreme hot weather conditions in Hong Kong: A land use regression approach. *Environmental research*, 171, 403-415.
31. Hoek, G., Beelen, R., De Hoogh, K., Vienneau, D., Gulliver, J., Fischer, P., & Briggs, D. (2008). A review of land-use regression models to assess spatial variation of outdoor air pollution. *Atmospheric environment*, 42(33), 7561-7578.
32. Hua, J., Zhang, X., Ren, C., Shi, Y., & Lee, T. C. (2021). Spatiotemporal assessment of extreme heat risk for high-density cities: A case study of Hong Kong from 2006 to 2016. *Sustainable cities and society*, 64, 102507.
33. Buscail, C., Upegui, E., & Viel, J. F. (2012). Mapping heatwave health risk at the community level for public health action. *International journal of health geographics,* 11(1), 1-9.
34. Hu, K., Yang, X., Zhong, J., Fei, F., & Qi, J. (2017). Spatially explicit mapping of heat health risk utilizing environmental and socioeconomic data. *Environmental Science & Technology,* 51(3), 1498-1507.
35. Verdonck, M. L., Demuzere, M., Hooyberghs, H., Priem, F., & Van Coillie, F. (2019). Heat risk assessment for the Brussels capital region under different urban planning and greenhouse gas emission scenarios. *Journal of environmental management,* 249, 109210.
36. Ma, H., Shao, H., & Song, J. (2014). Modeling the relative roles of the foehn wind and urban expansion in the 2002 Beijing heat wave and possible mitigation by high reflective roofs. *Meteorology and Atmospheric Physics,* 123, 105-114.
37. Tan, M., Li, X., Li, S., Xin, L., Wang, X., Li, Q., ... & Xiang, W. (2018). Modeling population density based on nighttime light images and land use data in China. *Applied Geography,* 90, 239-247.
38. Savory, D. J., Andrade-Pacheco, R., Gething, P. W., Midekisa, A., Bennett, A., & Sturrock, H. J. (2017). Intercalibration and Gaussian process modeling of nighttime lights imagery for measuring urbanization trends in Africa 2000–2013. *Remote Sensing*, 9(7), 713.
39. Liu, Q., Sutton, P. C., & Elvidge, C. D. (2011). Relationships between nighttime imagery and population density for Hong Kong. Proc. Asia-Pac. Adv. *Netw*, 31, 79.
40. Johnson, D. P., Stanforth, A., Lulla, V., & Luber, G. (2012). Developing an applied extreme heat vulnerability index utilizing socioeconomic and environmental data. *Applied Geography*, 35(1-2), 23-31.
41. Tapia, C., Abajo, B., Feliu, E., Mendizabal, M., Martinez, J. A., Fernández, J. G., ... & Lejarazu, A. (2017). Profiling urban vulnerabilities to climate change: An indicator-based vulnerability assessment for European cities. *Ecological indicators*, 78, 142-155.
42. Cutter, S. L., & Finch, C. (2008, February 19). Temporal and spatial changes in social vulnerability to natural hazards. *Proceedings of the National Academy of Sciences*, 105(7), 2301–2306.
43. Bencheikh, H., & Rchid, A. (2012). The Effects of Green Spaces (Palme Trees) on the Microclimate in Arides Zones, Case Study: Ghardaia, Algeria. *Energy Procedia*, 18, 10–20.
44. Yang, L., Yang, H., Fan, Q., Zhao, G. (2023). Vulnerability Assessment and Planning Response to High-temperature Wave in Large Cities: The Case of Chengdu. *Planners* (02),38-45.
45. Zhang, W., Zheng, C., & Chen, F. (2019, May). Mapping heat-related health risks of elderly citizens in mountainous area: A case study of Chongqing, China. *Science of the Total Environment*, 663, 852–866.
46. Wong, N. H., Tan, C. L., Kolokotsa, D. D., & Takebayashi, H. (2021, January 26). Greenery as a mitigation and adaptation strategy to urban heat. *Nature Reviews Earth & Environment*, 2(3), 166–181.
47. Duan, S., Luo, Z., Yang, X., & Li, Y. (2019, February). The impact of building operations on urban heat/cool islands under urban densification: A comparison between naturally-ventilated and air-conditioned buildings. *Applied Energy*, 235, 129–138.
48. Sahani, J., Kumar, P., & Debele, S. E. (2023, September). Efficacy assessment of green-blue nature-based solutions against environmental heat mitigation. *Environment International*, 179, 108187.
49. Dong, Y. R., Cheng, Y., Qin, L., Wang, Y. Y., & Bai, G. L. (2022). Spectrum characterization and assessment method of long-periodic ground movements. *Soil Dynamics and Earthquake Engineering,* 152, 107002.
50. Li, D., Sun, T., Liu, M., Yang, L., Wang, L., & Gao, Z. (2015, May 1). Contrasting responses of urban and rural surface energy budgets to heat waves explain synergies between urban heat islands and heat waves. *Environmental Research Letters,* 10(5), 054009.
51. Nassary, E. K., Msomba, B. H., Masele, W. E., Ndaki, P. M., & Kahangwa, C. A. (2022, May). Exploring urban green packages as part of Nature-based Solutions for climate change adaptation measures in rapidly growing cities of the Global South. *Journal of Environmental Management*, 310, 114786.
52. Heshmat Mohajer, H. R. H., Ding, L., & Santamouris, M. (2022, June 25). Developing Heat Mitigation Strategies in the Urban Environment of Sydney, Australia. *Buildings*, 12(7), 903.
53. Kwok, Y. T. (2021). Mesoscale Urban Climate Modelling of High-Rise, High-Density Cities: Implications for Urban Heat Mitigation in Hong Kong (Order No. 29186049). (2650275585).
54. Shen, L., Li, H., Guo, L., & He, B. J. (2022). Thermal and energy benefits of rooftop photovoltaic panels in a semi-arid city during an extreme heatwave event. *Energy and Buildings*, 275, 112490.
55. Hatvani-Kovacs, G., Bush, J., Sharifi, E., & Boland, J. (2018, September). Policy recommendations to increase urban heat stress resilience. *Urban Climate*, 25, 51–63.

A Contemporary Vernacular for the Tropical Savanna Climate:
Designing a Learning Centre for a Resilient Future

SURABHI AGARWAL[1], JOANA CARLA SOARES GONÇALVES[1]

[1]Architectural Association School of Architecture, London, United Kingdom

ABSTRACT: With the advancement of technology, buildings have been wired to function with minimal interaction with their occupants to provide steady-state environments all year round. Constant thermal conditions in buildings have led occupants to grow less and less resilient to seasonal changes and climate shifts. The research reported in this paper looks at ways to re-kindle interaction between the environment and its inhabitants using passive design strategies, extending comfort conditions through the use of adaptive opportunities and the pleasure of experiencing thermal delight. The paper explores the potential of alliesthesia in architecture by studying the gradual variation in operative temperature in a series of indoor and transitional spaces.
KEYWORDS: Resilience, Interaction, Comfort, Alliesthesia

1. INTRODUCTION

When earlier, a home or shelter was built to suit the climate, contemporary buildings today are designed to rely on heating and air conditioning systems [1]. The adoption of uniform codes of comfort for all occupants further reduces opportunities to locally modify the environment to suit individual requirements. Furthermore, exposure to controlled uniform temperatures all-year round has made building occupants less resilient to seasonal changes and temperature fluctuations. This has increased energy demands worsening the global warming situation causing a vicious cycle.[2]

This paper puts forward alternative proposals that focus on passive design strategies and performance optimizations through adaptive techniques. The aspects of thermal delight have also been discussed as a layer at understanding and appreciating varying states of thermal environments.

The site chosen is in Kolkata a city with rich cultural heritage and a vernacular architecture that uses local materials and functional transitional spaces as passive strategies. The building typology studied for this research was that of a Learning Centre.

2. METHODOLOGY

After carrying out background studies to understand how humans interact with their built environment, an extensive study was carried out to understand the climate of Kolkata (Fig. 1). It was found that the climate exhibited traits of both a hot-dry as well as a warm-humid climate. This dual nature of the climate made analytical studies extremely crucial for the research in addition to looking at precedents and the vernacular of the region.

The strategies derived from the analytical studies conducted using Ladybug Tools [3] were applied to the design of a Learning Centre to further test and quantify how adaptive opportunities can contribute to comfort conditions within a space. Additionally, the design also acted as an instrument for testing the contribution of alliesthesia in architecture. By definition, alliesthesia is a psychological and physiological phenomenon that describes the dependent relationship between the internal state of an organism and the perceived pleasure or displeasure of stimuli.[4] Though it's a known fact that extra physiological effort is required to adjust to thermal stimuli, people tend to enjoy a range of temperatures, characterized by an inherent sense of thermal delight rather than steady state environments.[5] Tests were also performed to investigate this experience of alliesthesia.

3. CLIMATE ANALYSIS

The climate of Kolkata exhibits a Tropical Wet and Dry or Savanna (Aw) climate according to the Köppen climate classification. Figure 1 illustrates the diurnal variations across the year for Dry Bulb Temperature and Relative Humidity for the region. The 'Hot Periods' start from the month of March and last until October, consisting of months of both hot-dry and warm-humid periods. The rest of the year from November to February exhibits mostly comfortable temperatures during the day making the Hot Period the main months of concern. Based on traits displayed by the different periods, the passive strategies for each of the three different periods have been summarized in Table 1. As it may be observed that the two hot periods require rather contradicting sets of strategies; while some can be easily catered to through providing adaptive opportunities like shading or ventilation, while others like thermal mass and size of openings require a more in-depth understanding to establish its properties and percentages.

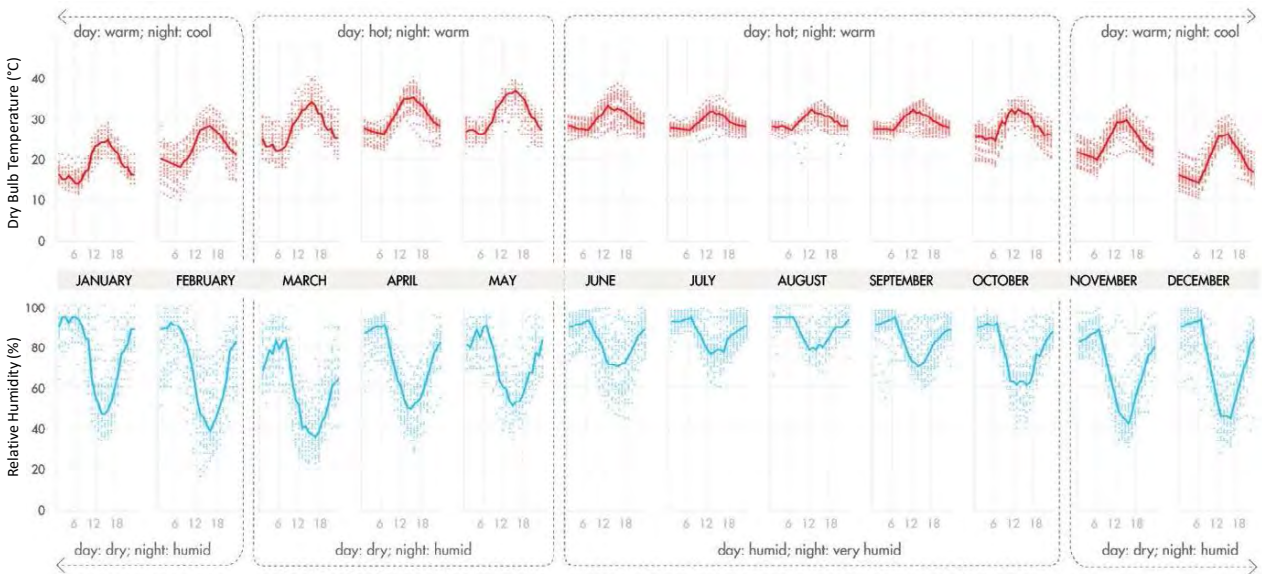

Figure 1: Graph showing Diurnal Climate Variations for Dry Bulb Temperature (°C) and Relative Humidity (%) [6]

Table 1: Climate Summary

Periods		Hot Dry Period (March – May)	Warm Humid Period (June – October)	Cool-Dry Period (November – February)
Climate Summary	Dry Bulb Temperature	Average DBT: 29°C % hours DBT > 30°C: 38% Avg. diurnal swing: 10K	Average DBT: 28°C % hours DBT > 30°C: 28% Avg. diurnal swing: 6K	Average DBT: 22°C % hours DBT < 24°C: 33% Avg. diurnal swing: 11K
	Relative Humidity	Average RH: 67% % hours RH > 70%: 45%	Average RH: 83% % hours RH > 70%: 86%	Average RH: 70% % hours RH > 70%: 27%
	Wind	South; Average 1.8m/s	South; Average 1.5m/s	North; Average 0.8m/s
Passive Strategies	Shading	all day	all day	controlled
	Openings	minimized	maximized (except noon)	maximized at noon
	Ventilation	night ventilation	maximized (except noon)	maximized at noon
	De Coupling	all day	at noon	at night
	Thermal Mass	high thermal mass	low thermal mass	

4. ANALYTICAL STUDIES

4.1 Indoor Comfort

To establish the design considerations and envelope properties for optimizing indoor comfort, the following steps were undertaken:

Step 0 | Base Case Establishment: Driven by the current scenario and industry trends for building spaces in the region, a base case was established. Table 2 lists the specificities of the envelope considered to form a base case for further analysis. The space considered has an exposed roof with a west-facing window, exposed to outdoors and three adiabatic walls and floor condition.

For internal loads associated with the base case, three types of spaces were established based on the typology in question, i.e. a 'Learning Centre'. Derived from standards for densities for various activities in a learning centre [7] the occupancy, equipment and lighting (only during non-daylit hours) loads were determined (Table 3). A schedule was also formulated for each of these spaces for the study based on the programme of the building.

Table 2: Base Case Envelope Specificities

Geometry	l x b x h: 12m x 8m x 3m
Orientation	Longside facing East-West
Exposed Roof	U value: 3.9 W/m^{2}K; 200mm thick RCC Roof
Floor Slab	U value: 2.8 W/m^{2}K; 200mm thick RCC slab
External Wall	U value: 1.72 W/m^{2}K; 200mm thick Brick Wall with 12mm plaster inside
Internal Walls	U value: 2.25 W/m^{2}K; 100mm thick Brick Wall with 12mm plaster inside
Window Wall Ratio	West Facing, 40%
Window	U value: 5.60 W/m^{2}K; 4mm glass; SHGC: 0.7, VT: 0.8

Table 3: The three types of spaces in the centre and their corresponding Internal Loads considered

N.	Space	Occupancy	Equipment	Lighting
1	Classrooms	0.5 ppl/m^2	10 W/m^2	12 W/m^2
2	Workshops	0.3 ppl/m^2	10 W/m^2	12 W/m^2
3	Collab Hub	0.2 ppl/m^2	27 W/m^2	12 W/m^2

Upon testing for this Base Case envelope with the 'Classrooms' typology considered for internal loads in a free-running state and no natural ventilation, it was observed that, temperatures were higher by 6K (Figure 2) on an average from the outdoors, making the space uncomfortable for as much as 92% hours (Figure 4) of the year considering the Indian Model for Adaptive Comfort (IMAC). [8]

Step 1 | Design Optimization: To improve comfort hours for the space, various design optimization tests (Table 4) were undertaken in an iterative manner for orientation, shading with varying depths and spacing, impact of ventilation and window to wall ratios. This provided the necessary takeaways for design requisites of the built form. Figure 2 shows how the correct set of design decisions can help significantly reduce the operative temperature indoors to improve comfort by as much as 65% (Table 6).

Table 4: Various options tested iteratively for Step 1

Orientation	Shading	Ventilation	WWR
• West Facing • East Facing • North Facing • South Facing	• Horizontal • Vertical • Horizontal +Vertical	• No natural ventilation • Yes, natural ventilation; 24 °C set point	• 40% • 60% • 75%

Step 2 | Elemental Optimization: This step sets out to understand the envelope elementally i.e , the roof, the floor and the walls. The materials chosen for the study were based on the vernacular locally available materials such as earth, bamboo (for added roof) and terracotta in filler slabs. (Table 5)

Table 5: Various options tested iteratively for Step 2

Roof	Floor	Walls
• 0.2m RCC slab (3.9 W/m^{2}K) • 0.1m Filler Slab (2.2 W/m^{2}K) • 0.2m RCC Slab (3.9 W/m^{2}K) + Added Roof • 0.1 Filler Slab (2.2 W/m^{2}K) + Added Roof	• 0.2m RCC slab (2.8 W/m^{2}K); Adiabatic • 0.2m RCC slab (2.8 W/m^{2}K); Ground contact • 0.2m Rammed Earth Floor (1.5 W/m^{2}K); Ground contact	• 0.2m Brick Wall (1.72 W/m^{2}K) • 0.3m Rammed Earth Wall (1.5 W/m^{2}K)

It was observed that the treatment of the roof played a major role. Switching to a double roof system with a filler slab improved comfort by over 22% from the optimized Step 1 case. The switch from brick wall to rammed earth wall, exposed concrete roof to a filler slab double roof and a concrete floor to a rammed earth floor on the ground led the comfort to reach 92% annually, for the occupied hours, 8 am to 8 pm. (Table 6)

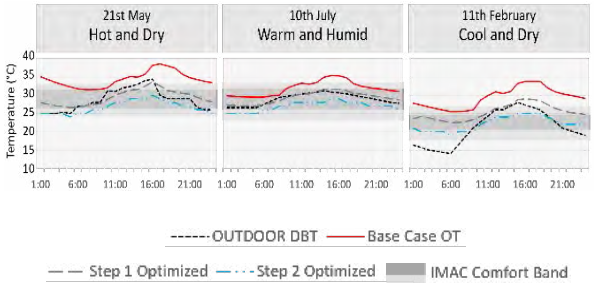

Figure 2: Comparison between the temperatures plotted for different steps of the analytical work

Table 6: Table showing obtained inputs for optimizing comfort at each step and its corresponding comfort hours

Dry Bulb Temperature Outdoor		
Base Case Condition		
STEP 1	Orientation	North South
STEP 1	Shading	South; 0.75m deep
STEP 1	Ventilation	Yes; Set Point: 24°C
STEP 2	WWR	South Facing; 75%
STEP 2	Roof	Filler Slab + Added Roof
STEP 2	Floor	Rammed Earth, Ground
STEP 2	Walls	300mm Rammed Earth

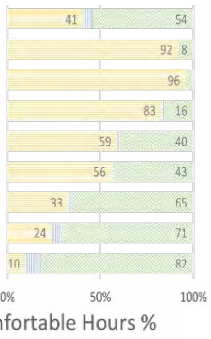

Step 3 | Density Study Iterations: A simple sensitivity test was carried out to understand the impact of density and occupancy on the comfort of the new optimized space obtained. It was observed that though comfort appears to reduce with decreasing density, the percentage of cold hours increase. (Table 7) These additional % of cold hours provide the necessary flexibility for design decisions to be made based on functional spatial needs of the programme.

Table 7: Comparison of achieved comfort hours for varying occupancy densities for the optimized envelope at Step 3

Space	Occupancy Density	Comfort Hrs %	Hot Hrs %	Cold Hrs %
Classrooms	0.5 ppl/m^2	82	10	8
Workshops	0.3 ppl/m^2	81	10	9
Collab Hub	0.2 ppl/m^2	79	9	12

4.2 Outdoor Comfort

It was important to understand periods of outdoor comfort to pave ways to incorporate them into the design to allow for more opportunities for thermal delight and experience of alliesthesia. Based on

vernacular studies carried out for the region, a hierarchy of types of outdoor spaces was established.

Starting from the directly adjacent semi-open space to the indoors, the 'verandas' form an integral part of the hierarchy acting as a thermal buffer between the interior spaces and the 'outdoor'. The 'outdoor' in this case is formed by the courtyard, with a spatial property of forming an enclosure, it is both functionally and climatically essential.

The Verandas: For this purpose, shading studies were carried out for verandas in the four orientations and compared for UTCI comfort levels annually.

Figure 3 shows the results of the studies carried out for the different orientations tested and shading strategies applied. It can be observed that for East and West Orientations a horizontal shading device along with horizontal louvres can help achieve an annual comfort of about 57% whereas in the South facing verandas, equal hours of comfort can be achieved by a roof and a vertical awning of about 0.7m. For the north-facing verandas it was observed that 58% of the time, comfort could be achieved without the need for any shading.

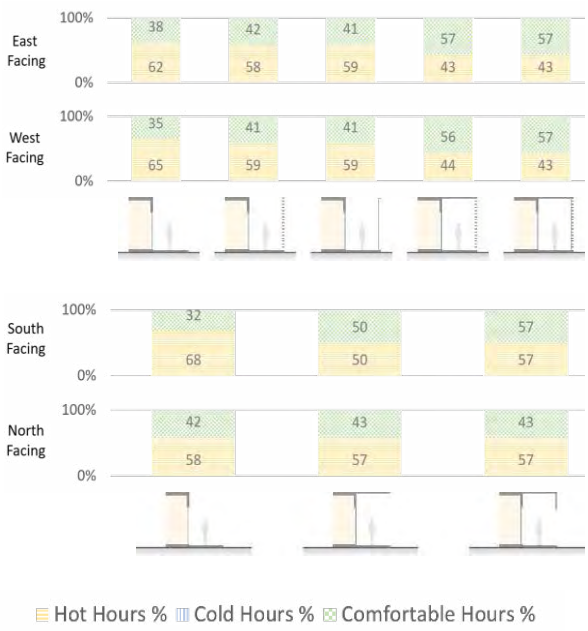

Figure 3: Graphs showing achievable comfort conditions for verandas in different orientations using shading devices

The Courtyards: Courtyards not only help provide shade to the adjacent blocks and open areas but can also be instrumental in inducing wind flow and air movement at the pedestrian level. For the climate in question, which has issues of high humidity levels, it becomes crucial to improve airflow as much as possible. Three different courtyard aspect ratios were tested; amongst which the aspect ratio with 0.3<H/W≤1.0 showed the best results, allowing the creation of a circular whirlwind centred in the middle of the courtyard filling the whole space and obtaining good air renewal. Though the wind velocities were relatively better, they can be further improved through punctures in the enclosed volume (Figure 4).

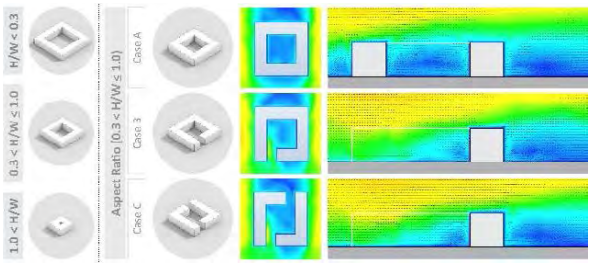

Figure 4: The three types of aspect ratios for courtyards tested and the impact of airflow in the courtyard due to punctures in the form

5. DESIGN APPLICATION

5.1 Programme

The spatial requirements of the programme for the learning centre were divided into three types of spaces. Each of the three spaces were massed based on a certain clustering principle (see Table 8).

Table 8: Clustering Principle for the various spaces forming the programme of the learning centre

Type of Space	Clustering Principle
i. Direct Learning: Classrooms	formal, organized, with breakout spaces
ii. Applied Learning: Workshops	organic, clustered with outdoor activity areas
iii. Interpersonal Learning: Collaborative Hub	mixed, semi-formal, quiet and interactive spaces

5.2 Form Development

Some of the key aspects that were kept in mind while developing the various spaces were: reducing radiation on the envelope; ensuring maximum circulation of wind; forming a hierarchy of outdoor spaces of varying scales and enclosures starting from verandas to small and mid-sized courtyards to a large central courtyard; materiality based on conclusions derived from the analytical studies.

Figure 5: The developed base form for the Learning Centre

5.3 Thermal Comfort

With the overall mass of the buildings and campus plan catered for, the aspect of thermal comfort was looked at in closer detail. Design as well as performance-based decisions such as window-to-wall ratios, and shading designs were derived from analytical studies as well as further optimized for case specific situations. Upon optimizing the envelope as much as possible, adaptive opportunities pertinent to the climate were applied and tested to further improve comfort in the spaces. Figure 6 shows an exploded isometric of one of the three types of learning spaces designed, i.e. the Applied Learning Spaces or the Workshops.

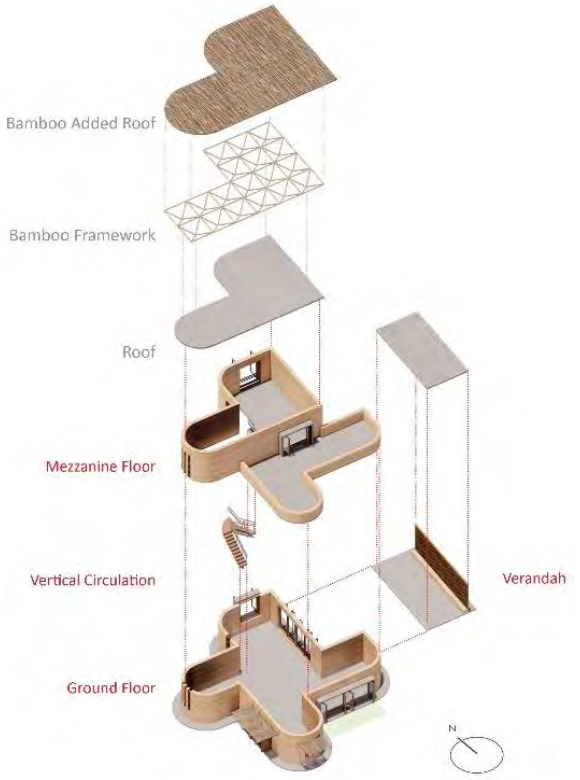

Figure 6: An exploded isometric showing the Applied Learning Space/Workshop spaces with niches, verandas and adjacent courtyard spaces

Figure 7 shows the results of the thermal studies carried out for the space. Two scenarios have been plotted: existing and adaptive. The 'existing' scenario was based on the typical behaviour of people in warm climates (for naturally ventilated buildings), where the tendency is to keep the windows open in the summers with fans on, to ventilate and closed in the winters to store the heat. It was observed that in the 'existing' scenario with the two warm periods always ventilated and the windows closed during the cool period, occupied hours show a comfort percentage of 72% annually. However, by using night ventilation, thermal mass and stack effect, the comfort for the hot and dry period alone showed a rise of almost 9%. In the case of the humid months, the adaptive opportunity of being able to ventilate along with fans allows the temperature to sit within the comfort band. For the cooler months, due to the internal gains, the space heats up making ventilation necessary for comfort. Therefore, it can be seen that by using the available adaptive opportunities correctly and knowing how to interact with the building can help improve comfort annually by over 6% in occupied hours for this case.

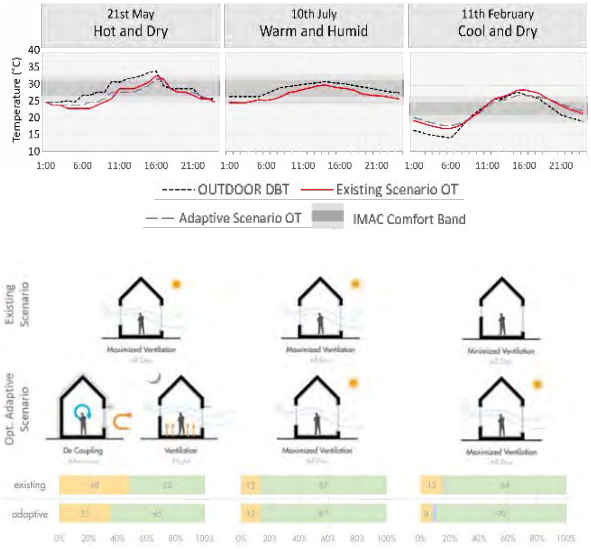

Figure 7: Graphs showing a comparison between the 'Existing' case and the 'Adaptive' case

Table 9: Visuals showing the experiential quality achieved for the learning centre designed

Shaded courtyard spaces	
Indoor workshop space with adjoining semi-open space	
Shaded veranda spaces	

5.4 Thermal Delight

Figure 8 cuts a section across the various indoor and outdoor spaces around the designed workshop spaces and plots the temperature at each of the different spaces for the three typical days. Starting from the open spaces exposed to the sun, to the shaded pathways, the courtyards, the verandas and finally the indoors, the spaces provide a range of temperatures in the various seasons. These instances of positive alliesthesia for an occupant provide moments of thermal delight and pleasure of experiencing comfortable temperature moving from a relatively higher temperature outdoors. Furthermore, the feeling of low surface temperatures with hygroscopic rammed earth walls and floor enhances the pleasures of feeling and being in direct contact with the built.

6. CONCLUSION

The paper shows how passive design strategies accompanied by the use of correct set of adaptive opportunities can help optimize the building envelope for comfort. Furthermore, passive design strategies can also be instrumental in providing the users an experience of alliesthesia to achieve thermal delight which comes in stark contrast with current scenarios in hot tropical cities, where issues of thermal shock and monotony of constant temperatures dominate the city's experience.

To conclude, the experience of increased human interaction between man and the built through active participation by learning how to modify their environment and through involuntarily experiencing thermal delight within a space can positively impact their physiological being, hence paving ways for a more robust, a more resilient future.

REFERENCES

1. H Hawkes, D., McDonald, with J., & Steemers, K. (2013). The Selective Environment. *Taylor and Francis*.
2. Nicol, F., H.B. Rijal & S. Roaf (2022). Routledge Handbook of Resilient Thermal Comfort. *Routledge. London.*
3. Sadeghipour Roudsari, M., Pak, M. (2013). Ladybug: a parametric environmental plugin for grasshopper to help designers create an environmentally-conscious design. *In: Proceedings of the 13th International IBPSA Conference Held in Lyon, France Aug 25–30th.* (http://www.ibpsa.org/proceedings/BS2013/p_2499.pdf)
4. Cabanac, M. (1971). Physiological Role of Pleasure. PubMed. *National Library of Medicine.*
5. Heschong, L. (1979). Thermal Delight in Architecture. *The MIT Press.*
6. Betti, G., Tartarini, F., Nguyen, C, Schiavon, S. (2023). CBE Clima Tool: A free and open-source web application for climate analysis tailored to sustainable building design. *Build. Simul*. https://doi.org/10.1007/s12273-023-1090-5. Version: 0.8.17
7. Neufert, E., Neufert, P., Baiche, B., & Walliman, N. (2006). Architects' data: Neufert. Blackwell Science
8. Manu, S., Y. Shukla, R. Rawal, L.E. Thomas & R. de Dear (2015). Field Studies of Thermal Comfort Across Multiple Climate Zones for the Subcontinent: India Model for Adaptive Comfort (IMAC). *Building and Environment.*

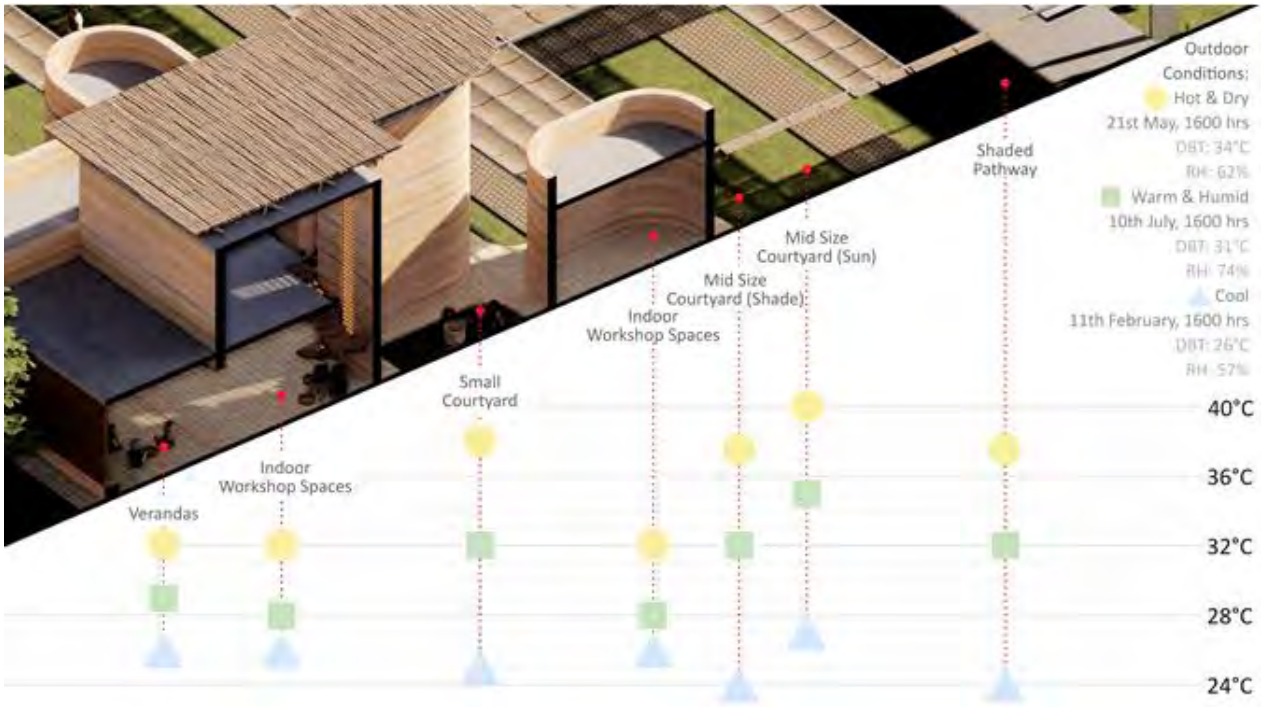

Figure 8: Section through the various outdoor and indoor spaces showing alliesthesia in architecture

PLEA 2024 WROCŁAW
(Re)thinking Resilience

Winery Design in Temperate Continental Climates:
Form and Materiality in the Spotlight.

CAROLINA GANEM-KARLEN[1,2,3], GUSTAVO JAVIER BAREA-PACI[1], HELENA COCH-ROURA[3]

[1] Institute of Environment, Habitat & Energy (INAHE – CONICET), Mendoza, Argentine Republic
[2] Arts & Design School, University of Cuyo, Mendoza, Argentine Republic
[3] Architecture, Energy & Environment (AiE), Polytechnic University of Catalonia (UPC), Barcelona, Spain

ABSTRACT: In a winery energy demand is mostly due to temperature control. Energy flux exchange and thermal inertia of the envelope are crucial because of the constant need for stabilized temperatures. Underground cellars represent a resilient solution thinking in the future, as they can provide temperature peaks dampening and thermal wave phase shifting breaking down temperature variation. Sustainable wine production fills a research gap, identifying emerging trends for business model innovation. In this research, potential design improvements are simulated and discussed regarding the form and the materiality, with the objective to improve internal higro-thermal conditions and energy efficiency. A case study is presented as an example. It includes a partially underground cellar, thermal asymmetries and green roofs. 5 alternatives to improve the envelope are presented. The first 4 modify the thermal resistance of the opaque envelope. Their combination leads to a reduction of 27% of the annual energy demand. The 5th strategy proposes the improvement of the transparent envelope. This strategy requires active management of the envelope during the operation of the winery. The reduction in energy demand reaches 37% (from 80 to 50 kWh/m².year) of the initially estimated energy requirements.
KEYWORDS: underground cellars, envelope, thermal resistance, energy efficiency.

1. INTRODUCTION

The industrial environment is one of the most intensive systems that humankind has created. It consumes substantial proportions of natural resources for its establishment and operation. It also contributes to a large extent to the waste that is deposited in the biosphere. By 2050 environmental challenges are expected to become even more critical and intense. [1] Industry should be conceived as a management of energy and material resources, as part of the continuous flows and exchanges of energy and materials within the biosphere. Industries are required to develop solutions either to address the negative impacts of consumption and production processes or generate positive spill overs [2].

The wine sector is highly vulnerable to climate change, especially due to the dependence of vine growing on specific climatic and environmental conditions. For this reason, adaptation and mitigation measures are important for the future of the wine industry. According to Lichy et al. [3], even though sustainable wine production aligns with the United Nation Sustainable Development Goals (UN-SDGs), no universally accepted approach exists to evaluate sustainable wine production attributes and variables.

In a winery energy demand is mostly due to temperature control. Energy flux exchange and thermal inertia of the envelope are crucial because of the constant need for stabilized temperatures. As a consequence, energy consuming systems are frequently used. All wineries usually include serpentine pipes inside tanks to control temperature during fermentation; and air-conditioned equipment to maintain the appropriate microclimate (temperature & humidity) in oak breeding barrels rooms, wine stowage and bottle storage. In temperate continental climates with important daily and seasonal variations this includes both: heating and cooling.

Recent research [4-7] demonstrate that traditional underground wine cellars are good examples of bioclimatic construction, achieving optimum conditions with almost no energy consumption for cooling.

Mendoza, a major regional wine-producer, needs to shift towards sustainable production to minimize environmental impact and ensure its continuity.

The vernacular practice of underground cellars may represent a resilient solution when thinking in the future. They characterise by temperature peaks dampening and thermal wave phase shifting, breaking down temperature variation.

Even though architects, engineers and investors are aware of the benefits of underground designs in this climate, recent investigations [8-11] have demonstrated that in most cases, if a part of the building is underground, these spaces are usually integrated to others that are highly glazed. Thermal asymmetries between elements of the envelope are frequent and as a result they do not perform as underground spaces. Also, some wineries integrate green roofs as a part of a sustainable image, but their materiality is poor and as a consequence, the desired thermal stability is not met. Even though there is a growing interest in achieving a bioclimatic

performance in wineries, the physical phenomena are not fully understood to work as expected.

Project design is an opportunity to align on ideas, processes, and improve energy efficiency. Dynamic simulation has the advantage to explore design variables that will lead to wise decision-making.

Ferri et al. [12] present resent research regarding internal drivers of eco-innovation in wineries. As a result: willingness to improve, consciousness about the importance of protecting natural resources, and personal responsibility towards the stakeholders and community; were the main impulses for the implementation of sustainable practices; which ranged from an initial product innovation (i.e., a switch to organic and/or biodynamic wine) to process innovation (i.e., adoption of passive and/or active solar energy technologies).

Organic and/or biodynamic wine are more sensible to changes in higro-thermal conditions as they do not use chemicals or additives. They don't add yeast to the fermentation process, and they don't employ sulfites to stabilize the wines. This is a main reason form and materiality of the project become crucial to secure thermal stability in wineries.

Sustainable wine production fills a research gap, identifying emerging trends for business model innovation. In this research, potential design improve -ments are simulated and discussed regarding the form and the materiality, with the objective to upgrade internal higro-thermal conditions and energy efficiency in wineries. A case study is presented as an example. It includes a partially underground cellar, thermal asymmetries and green roofs.

2. METHODOLOGY

Better prediction, characterization and quality assurance of building energy performance is essential to realise the anticipated world-wide energy reductions in buildings and community systems. [13-14] The way programs should be used to address a particular purpose has been termed a Performance Assessment Method (PAM). Well documented procedures for using programs need to be developed to fulfil a real need by increasing consistency of performance assessment, aiding in training, allowing improvement of procedures and promoting quality assurance. Documentation is essential so that, firstly, the assumptions in currently adopted methods can be made explicit and thus open to analysis, secondly, that quality assurance can be carried out, and thirdly, that portions of the assessment method for one application can be re-used for different applications.

A PAM is a guide to evaluate the building performance through the energy simulation of a building, which requires: establishment of a basic design case, calibration of the model, evaluation of the boundary conditions, identification of problems, generation of possible solutions and their evaluation.

Dynamic models consider the time variable and the effects of the thermal capacity of the materials involved through which the energy transfer takes place. Computational simulation methods require an exhaustive load of information and yield accurate information. The EnergyPlus software [15] was used for the analysis of this project. This is a thermal-energy simulation software developed by the National Renewable Energy Laboratory (NREL) of the US Department of Energy (DOE). The EnergyPlus software is one of the most advanced programs in energy efficiency analysis and is the most widely used in the scientific community worldwide.

The exogenous variables that affect the thermal performance of the project (outdoor temperature, solar radiation power in a given plane, wind speed, etc.) vary over time. A TMY3 climate file must be prepared on an hourly basis in order to incorporate them into the dynamic simulation. For this purpose, statistical data are used for the site location.

At the same time, the effect of these variations on the interior space of the building is not immediate, but there is a time delay between cause and effect that varies for each building. Therefore, the energy exchange between a building and the external environment is considered a dynamic system. In order to study them, it is necessary to incorporate the form and materiality aspects of the project by generating a geometric physical model in Open Studio Application and the development of an ad hoc library of physical properties of materials.

Thermal zones are a set of enclosures that are used as the basis or calculation unit for the energy simulation. The calculation is performed at "zone" level based on morphology, i.e. spaces that have the same morphological characteristics: the same height, the same envelope resolutions and the same interactions between spaces. Thermal zones are also defined, depending on the hygrothermal require-ments associated with the use: thermal loads, interior temperatures and schedules.

2.1. Case Study

A project for a partially underground winery was selected as case study. It is located in de DOC wine zone of Luján de Cuyo, Mendoza. The first and only wine-zone of Argentina that has DOC for Malbec (-33° 10´ 29.73 SL, -68° 52´ 55.54´´ WL, 958 masl).

Mendoza has a continental temperate-cold desert climate with significant daily and annual variations. According to 1936 Koeppen's classification adapted by Beck et al. [16], it corresponds to the climatic nomenclature "BWk". The letter "B" defines a dry climate, the letter "W" refers to precipitation below 250 mm per year, and the letter "k" is related to mean annual temperatures below 18 °C. Therefore, the nomenclature "BWk" refers to an arid temperate-cold climate.

2.1.1 Form

The winery is designed on a site characterized by a pronounced slope. This morphological feature is used to partially bury the winery on three of its facades (North, East & South). Figure 1 shows the step-shaped layout of the project, following the natural slope of the land. Each step is related to the natural terrain through a north-south porticoed structure that gives place to the vertical exposed envelope. The staggered horizontal terraces that are then created have green roofs with local vegetation, giving visual continuity to the natural site morphology. This relative position was chosen to bring multiple thermal-energy benefits: stability in the interior environmental conditions and less exposure to the inclement weather outside. The winery is embraced by the natural terrain and opens up to the imposing views of the Andes Mountain to the West.

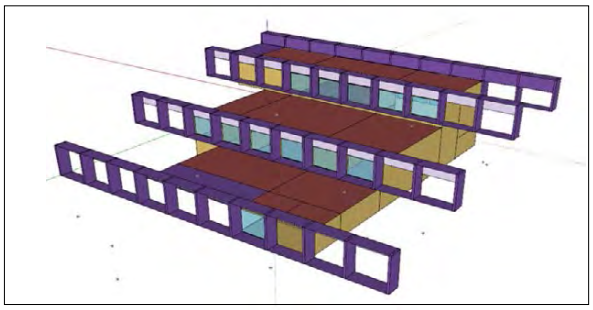

Figure 1. Geometric model showing the step-shaped layout.

2.1.2 Materiality

Table 1 shows the thermal transmittance of the main constructive systems of the winery project.

Table 1. Thermal transmittance of main constructive systems.

CONSTRUCTIVE SYSTEM	THERMAL TRANSMITTANCE [W/m²K]
Interior partition walls and ceilings: 0.30 m thick concrete.	3.08
Exterior ceilings: 0.20 m thick concrete + 0.025 m ceiling insulation, expanded polystyrene 25kg/m3 + 0.20 m module of green roof. Reinforced concrete structure.	0.80
Walls in contact with the ground: Double wall of 0.30 m, air chamber, ground.	1.23
Exterior walls: 0.30 m thick concrete.	3.08
Carpentry with aluminum frame, DVH: 3+3/12/3+3.	3.30

2.1.3 Form and Materiality

The winery envelope is geometrically classified according to the following variables:

- The position with respect to the natural ground plane, either vertical or horizontal.
- The properties of its materiality with respect to the passage of visible light, whether opaque or transparent.
- The contact with the outside air or with the natural terrain as exposed or buried respectively.
- Whether it has a green roof.

There are 4 possible combinations in the project: transparent vertical envelope, buried opaque vertical envelope, exposed opaque vertical envelope, horizontal envelope with green roof. Each possible combination is listed below, detailing the amount of envelope surface with these characteristics, the percentage it represents of the total envelope and the annual gains and losses involved in this type of envelope.

- *Transparent vertical envelope*

With an area of approximately 373.10 m2, it represents 14% of the total envelope. The annual heat gains through the transparent vertical envelope are 46%. Heat losses are 27%.

- *Buried opaque vertical envelope*

With an approximate area of 666.20 m2, it represents 25% of the total envelope. The annual heat gains through the buried opaque vertical envelope are 3%. Heat losses are 37%.

- *Exposed opaque vertical envelope*

With an area of approximately 160.80 m2, it represents 6% of the total envelope. The annual heat gains through the exposed opaque vertical envelope are 7%. And the heat losses are 6%.

- *Horizontal envelope with green roof*

With an area of approximately 1,469.60 m2, it represents 55% of the total envelope. The annual heat gains through the horizontal envelope with green roof are 33%. And the heat losses are 30%.

3. THERMAL AND ENERGY DYNAMIC SIMULATION

3.1 Thermal Zones

The complexity in this case is due to the presence on the 1st level and on the 2nd level of double and triple height spaces, which implies air movement between them and stratification within the same zone. This circumstance leads to the need to disaggregate spaces for analysis according to their interior height. 15 thermal zones were identified:

- 10 thermal zones on the 1st level.
- 3 thermal zones on the 2nd level.
- 2 thermal zones on the 3rd level.

For example, the barrel room was subdivided into three interrelated areas, in order to be able to work with three different ceiling heights. Also, this space is interrelated with the exterior and with other spaces of different shapes on each level. These morphological characteristics required a detailed three-dimensional relational analysis for each space.

Figure 2 shows graphically the thermal zones identified for the project in terms of morphology and hygrothermal requirements.

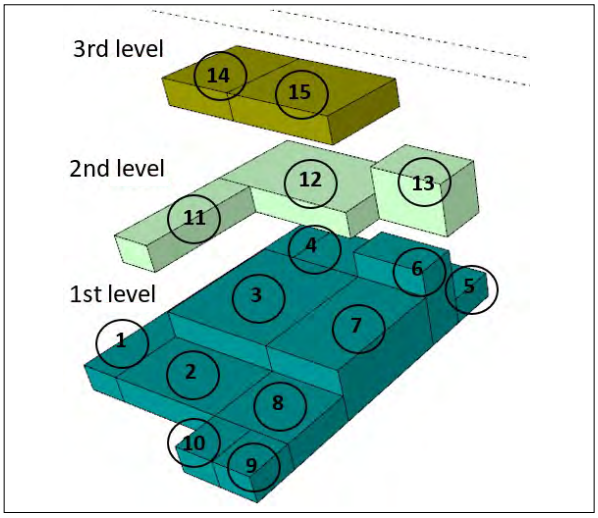

References

First Level	
1 - Staff	6 - Ageing 2 (3 heights)
2 - Press	7 - Ageing 1 (2 heights)
3 - Fermentation 1 (2 heights)	8 - Cellaring 1
4 - Fermentation 2 (1 height)	9 - Cellaring 2
5 - Ageing 3	10 - Tourism
Second Level	
11 - Offices and laboratory	13 - Tourism (VIP) (2 heights)
12 - Crushing and Pressing	
Third Level	
14- Staff	15- Tourism

Figure 2. Thermal zones.

3.2 Thermostats

The thermostats were set according to requirements:
- Fermentation. Air temperature 10°C to 30°C.
- Ageing and cellaring. Air temperature 16°C to 18°C.
- Tourism, offices and staff rooms. Air temperature: 20°C to 24°C.
- 1 constant air change rate (ACH)

3.3 Simulation procedure synthesis

For each analysis case to be evaluated:
- A library of physical properties of materials was developed.
- A general free run in Energy Plus software for 1 year (8760 hours).
- The Ideal HVAC was determined to calculate the energy demand in each case:
  - Heating energy demand assessment
  - Evaluation of the energy demand for cooling
  - Evaluation of the annual energy demand for space conditioning.

4. RESULTS AND DISCUSSION

4.1 Project evaluation

Figures 3 and 4 show the comparative annual energy gain and loss per envelope element.

The highest losses occur in the horizontal envelope with green roof due to the large amount of surface area (55% of the total envelope) responsible for more than 30% of the energy exchanges in both heat loss and heat gain. However, the transparent envelope represents 15% of the exposed envelope and is responsible for approximately 45% of the energy gain and almost 30% of the heat losses.

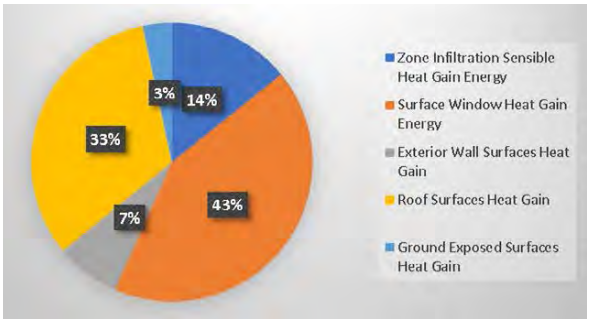

Figure 3 Heat gains annual breakdown.

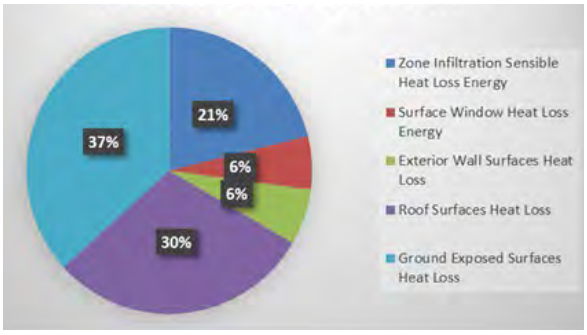

Figure 4 Heat loss annual breakdown.

4.1. Definition of proposals for improvement

4.1.1 Improvement in construction systems

The horizontal envelope has the largest surface area of the total envelope (55%). These are the roofs in contact with the exterior and with a green roof. This element is already insulated and consists of a 0.20 m reinforced concrete slab + 0.025 m expanded polystyrene 25kg/m3 + 0.50 m of green roof module.

It is proposed to increase the thickness of the insulation to 0.075 m and replace the expanded polystyrene with polyurethane.

The change in the material chosen for the insulation responds, on the one hand, to the properties of the insulating material. By using polyurethane, greater thermal resistance is obtained with less thickness.

On the other hand, expanded polystyrene attracts various insects, which after some time undermine the material, eliminating it and thus leaving the architectural element without insulating material. Given the location of the warehouse, this is an important aspect to consider. Based on the analysis carried out, it was decided to evaluate the improvement in the different envelope systems identified in the winery project.

Tables 2 to 4 show the details of the construction systems with the proposed improvements for each opaque element of the envelope:

Table 2. Horizontal opaque envelope. Thermal resistance: 4.37 m²K/W. Thermal transmittance: 0.23 W/m²K

Construction System layers from inside to outside	**Thickness [m]**	**Thermal Conductivity [W/mK]**	**Thermal Resistance [mqK/W]**	**Specific Heat [J/kg K]**	**Density [kg /m³]**
Concrete wall	0.200	1.630		1000	2400
Rigid polyurethane	0.075	0.019		1700	20
Green Roof	0.200	1.200		800	1750

Table 3. Buried vertical opaque envelope. Thermal resistance: 3.47 m2K/W. Thermal transmittance: 0.29 W/m²K

Construction System layers from inside to outside	**Thickness [m]**	**Thermal Conductivity [W/mK]**	**Thermal Resistance [mqK/W]**	**Specific Heat [J/kg K]**	**Density [kg /m³]**
Concrete wall	0.300	1.630		1000	2400
Rigid polyurethane	0.050	0.019		1700	20
Air chamber	0.100		0.14	1	1225
Concrete wall	0.300	1.630		1000	2400
Natural ground	0.200	1.200		800	1750

Table 4. Vertical opaque envelope. Thermal resistance: 2.96 m²K/W. Thermal transmittance: 0.33 W/m²K

Construction System layers from inside to outside	**Thickness [m]**	**Thermal Conductivity [W/mK]**	**Thermal Resistance [mqK/W]**	**Specific Heat [J/kg K]**	**Density [kg /m³]**
Concrete wall	0.300	1.630		1000	2400
Rigid polyurethane	0.050	0.019		1700	20

Table 5 shows a summary of the thermal transmittance with the proposed improvements.

ELEMENT OF THE ENVELOPE	**ORIGINAL THERMAL TRANSMITTANCE** [W/m²K]	**PROPOSED THERMAL TRANSMITTANCE** [W/m²K]
Interior partition walls and ceilings	3.08	3.08
Exterior ceilings	0.80	**0.23**
Walls in contact with the ground	1.23	**0.29**
Exterior walls	3.08	**0.33**
Carpentry with aluminum frame	3.30	**2.90**

Given that the improvement in the thermal resistance of the opaque elements does not imply a change in the architectural aesthetics, 4 alternatives for intervention in the opaque envelope are evaluated. These are presented in cumulative variations, up to the point of intervening on the entire opaque envelope.

It was also decided to include 1 alternative for intervention on the transparent envelope. The latter, in order to assess the reduction in energy requirements by intervening on the resistance of the entire envelope, including transparent and opaque elements.

4.1.2 Proposals

C1: Improvement in the insulation of the horizontal envelope.

C2: Improvement in the insulation of the horizontal and vertical opaque buried envelope.

C3: Improved insulation of buried and exposed opaque vertical envelope.

C4: Improved insulation of the horizontal and vertical opaque buried and exposed envelope.

In addition to the improvement of all the opaque elements of the enclosure (C4), mobile insulation is incorporated into the transparent enclosure. This insulation requires operation by the cellar staff or the incorporation of an automation system.

Good results depend on the opening/closing according to the recommended winter and summer use:

In winter: the movable insulation should cover the openings at times of the day when there is no solar radiation.

In summer: the movable insulation should cover the openings at times of the day when there is direct radiation on the opening.

The analysis of the 5 proposal results gave investors and architects elements of judgement to define the balance point in the cost-benefit of the architectural project, related to the form and materiality of the envelope.

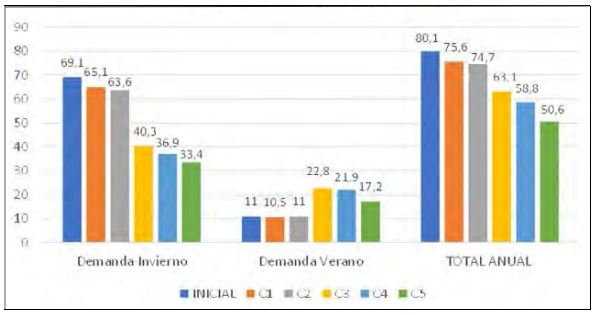

	PROJECT	1	2	3	4	5
WINTER	69.1	65.1	63.6	40.3	36.9	33.4
SUMMER	11.0	10.5	11.0	22.8	21.9	17.2
ANNUAL kWh/m².year	80.1	75.6	74.7	63.1	58.8	50.6

Figure 5. Comparative results. Project and 5 improvements.

The results obtained for alternatives C1, C2, C3, C4 and C5 are presented in Figure 5. The initial project is included as a reference. Final results show a reduction of 37 % (from 80 to 50 kWh/m^2.year) of the initially estimated energy requirements.

5. CONCLUSIONS

In this paper, 5 possibilities for the application of passive strategies integrated into architecture are comparatively evaluated. The proposed alternatives present progressive improvements for the use of the natural energies available on site. This integration contributes to the energy efficiency of the complex and to the reduction of the use of auxiliary energy for the thermal conditioning of spaces in the winery.

Cases C1, C2, C3 and C4 present different alternatives that modify the thermal resistance of the chosen construction systems, given the need to conserve the architectural form.

In the first 3 cases some of the envelope elements are improved. In case C4 the result of combining all the proposed improvements in the opaque envelope is presented. In C4 the annual energy demand decreases by 27%. The improvements in the opaque building systems do not require any management during the operation of the building.

In strategy C5 it is proposed to improve the transparent envelope, i.e. the windows. This will require night-time protection in winter to increase their thermal resistance and reduce energy exchanges, and daytime protection in summer to prevent the entry of solar radiation. By incorporating this strategy, which requires active management of the envelope during the operation of the winery, the reduction in energy demand reaches 37%.

Finally, strategies that are positive in winter do not always have the same effect in summer. For this reason, reductions in winter energy consumption can increase summer energy consumption. In the case of this winery, by reducing the energy flow of the envelope, heat dispersion in summer is also avoided. As the reduction in winter is much more beneficial than the increment that occurs in summer because of the low annual mean temperature (-2.7 °C), it is recommended to move forward with the increase of thermal resistance in the building envelope construction systems.

However, if it is desired to counteract this effect in summer, a night ventilation strategy could be incorporated. In this case it would be possible to reduce the annual energy requirements by 45%.

It is worth mentioning that the latter strategy will depend on the architectural possibilities of having windows opening on opposite sides of the spaces to allow for cross ventilation. It is therefore possible that it can only be applied in some of the cellar spaces. In this case, it is also necessary to manage the opening and closing of windows when required.

REFERENCES

1. European Environmental Agency (2020). State of Nature in the EU. Results from Reporting under the Nature Directives 2013-2018. EEA Report No 10/2020. Publications Office of the European Union. 2. UNGC (2023) Just Transition and Renewable Energy: A Business Brief United Nations Global Compact (UNGC), New York.

3. Lichy, J.; Kachour, M. and Stokes, P. (2023) Questioning the business model of sustainable wine production: The case of French “Vallée du Rhône” wine growers. Journal of Cleaner Production 417: p. 137891.

4. Mazarrón, F. R. and Cañas, I. (2019) Seasonal analysis of the thermal behaviour of traditional underground wine cellars in Spain. Renewable Energy 34: p. 2484–2492.

5. Tinti, F. et al (2014) Experimental analysis of shallow underground temperature for the assessment of energy efficiency potential of underground wine cellars. Energy and Buildings 80: p. 451–460.

6. Jia Yu, J.; Kang, Y.; Zhai, Z.J. (2020) Advances in research for underground buildings: Energy, thermal comfort and indoor air quality. Energy and Buildings 215: 109916.

7. Navia-Osorio, E.G.; Porras-Amores, C.; Mazarrón, F.R. and Cañas I. (2023) Impact of climate change on sustainable production of sherry wine in nearly-zero energy buildings. Journal of Cleaner Production 382: p. 135260.

8. Ganem, C. and Coch, H. (2017) Thermal and Energy Audits in Existent Wineries. A Case Study. Proceedings of 33rd International PLEA Conference. Edinburgh.

9. Ganem, C. and Barea, G. (2020). Assessing buildings’ adaptation to climate change. The case of a winery at design project stage. Proceedings of 35th International PLEA Conference. A Coruña.

10. Ganem, C. and Barea, G. (2022) The complex challenge of sustainable architectural design. Assessing climate change impact on passive strategies and buildings’ opportunities for adaptation. Proceedings of 36th International PLEA Conference. Stgo de Chile.

11. Ganem, C. and Barea, G. (2023) Passive design strategies in focus: Implications of climate change on new buildings and renovations. J. Eng. Sustain. Bldgs. Cities. 4(4): 041004.

12. Ferri, L.M.; De Bernardi, C. and Sydow, A. (2024) Intra-family succession motivating eco-innovation: A study of family firms in the German and Italian wine sector. Journal of Cleaner Production 434: p. 140261.

13. Machard, A.; Inard, C.; Alessandrini, J.M.; Devys-Peyre, F.; Martinez, S.; Ribéron, J. and Pelé, C. (2023) Climate change influence on buildings dynamic thermal behavior during summer overheating periods: An in-depth sensitivity analysis. Energy and Buildings 284: p. 112758

14. Clarke, J. (2016) Energy simulation in building design. Oxford: Butterworth-Heinemann, 2nd edition.

15. Crawley, D.B.; Lawrie, L.K.; Pedersen, C.O. y Winkelman, F.C. (2000). EnergyPlus: Energy Simulation Program. ASHRAE Journal.

16. Beck, H. E., Zimmermann, N. E.; McVicar, T. R., Vergopolan, N.; Berg, A. and Wood, E. F. (2018) Present and Future Köppen-Geiger Climate Classification Maps at 1-km Resolution. Sci. Data, 5(1), p. 180214.

PLEA 2024 WROCŁAW
(Re)thinking Resilience

Green facades plus

Added value of building and solar technology by combinations with plants in the vertical

ROLAND KRIPPNER[1]

[1] Nuremberg Institute of Technology/Faculty of Architecture, Nuremberg (Germany)

ABSTRACT: In addition to the numerous positive properties of green façade surfaces for the local environmental conditions in the outdoor space, the effects of a combination with building services systems, for example decentralised façade ventilation (DFV) or the use of photovoltaic (PV) in the vertical plane, have hardly been known to date. Two research projects at the Nuremberg Institute of Technology have produced extensive results in experimental studies and accompanying building simulations.
In the "EnOB: GreenFaBS" project the investigations with four different greening systems for the green façade and DFV interface demonstrate significant savings in cooling energy requirements and the influence of reduced surface temperatures on room conditioning. For this reason, the smaller "GreenPV" study carried out additional investigations into the combination of green façades (three different greening systems) with crystalline PV modules. Effects such as reduced surface temperatures on the back of the modules can be observed here; however, these hardly lead to additional yields from photovoltaics. The research forms an important basis for façade solutions for climate adaptation and climate neutrality. Important findings are also emerging that are highly relevant to the issue of competition for space, particularly in the façade sector.
KEYWORDS: Façade greening; building technology; ventilation technology; photovoltaics

1. INITIAL SITUATION

In concepts for future climate-neutral cities neighbourhoods and settlements are becoming ever greener. Roofs in particular are mutating into flowering meadows or even tree-covered park landscapes. But in recent years, green façades have also been increasingly used worldwide in the construction of modern, energy-efficient buildings because plants, as a multifunctional design element, are ideal for an ecological concept. Due to adiabatic cooling processes, green façades can be used as natural air conditioning systems in urban planning and counteract the effect of urban heat islands. (Fig. 1) They also fulfil a number of other functions such as natural air filtration of fine dust, absorption of carbon dioxide and improvement of the thermal insulation properties of external walls in winter. The temperatures on their surfaces can also be reduced.

In addition to these numerous positive properties of green façade surfaces for the local environmental conditions in the outdoor space, the effects of a combination with building services systems, for example decentralised façade ventilation (DFV) and/or the use of photovoltaics (PV) in the vertical plane, have hardly been known to date.

In two research projects at the Nuremberg Institute of Technology under the direction of the Faculty of Architecture, extensive results were obtained in experimental studies on façade test stands and accompanying building simulations.

Figure 1: Santiago de Chile- Bellavista, Façade greening (wall-mounted system) (11/2022)

2. MULTIFUNCTIONALITY AND PLUS USES

In the context of sustainable and energy-efficient building concepts, the building envelope has gained enormously in importance over the last two decades. This is reinforced by the global growth of large cities and the resulting increasing relevance of vertical envelope surfaces. Increased surface sealing also has a direct influence on the urban microclimate and leads to urban heat islands - the rise in temperatures in urban centres.

Against this background, the expansion of the protective and control functions of the façade and

Figure 2: Façade test stand. Reference office with decentralised façade ventilation (DFV) (left) and structure with façade greening "Variant 1" and DFV (right, 10/2019)

Figure 3: Façade test stand. Reference office with decentralised ventilation unit (DFV)/ room side (09/2019).

the use of combinations, particularly with building services systems, offer great, previously untapped potential. In view of the requirements for energy generation close to the building, compact ventilation technology and effective climate adaptation strategies, three technologies have become increasingly relevant: decentralised ventilation [1], photovoltaics [2, 4] and greenery in the façade [3].

However, the potential uses of façades, especially in dense urban structures, are often severely limited and characterised by a multitude of additional (multi-)functional requirements compared to roof surfaces. And as the most important structural subsystem with a wide range of protection and control tasks for energy efficiency and user comfort, there is often competition for space. This increasingly requires the investigation of possible combinations and synergies in order to realise the most effective and efficient façade solutions for buildings and neighbourhoods on limited building areas.

The term "green façades plus" was introduced for this work in order to emphasise the additional performance potential of greening systems.

2. ENOB: GREENFABS (02/2019 – 07/2021)

Solution strategies were initially developed in the joint project [5]. The broad spectrum of greening typologies was to be utilised as far as possible. One of the main distinguishing criteria for façade greening is permeability. This means that the (sub)structure of wall-mounted systems can also be designed to be permeable to light and/or air. This is particularly important in the area of transparent and translucent façade surfaces.

As part of the project, a (mobile) façade test stand was set up on an open area of the technical centre of the Nuremberg Institute of Technology (THN) in Rednitzhembach. [6] (Fig. 2) This provided the structural facilities in conjunction with a small weather station and a high level of measurement equipment for experimental studies.

This demonstrator with two identical (small) office rooms makes it possible to investigate new approaches to façade technologies on a 1:1 scale. While one room demonstrates the 'state of the art' as a reference size, various systems can be combined and installed in front of the neighbouring twin room. This makes it possible to directly compare their potential in terms of building physics and design under real weather conditions.

The following variants were analysed: (Fig. 4 + 5):

- two wall-mounted systems (Vertiko GmbH, Buchenbach and Verticalgreendesign (VGD) GmbH, Berlin)
- Mixing/racking system (Kramer Gartenbau, Munich)
- Ground-based system (Jakob Rope Systems, Ostfildern with climbing plants)

During the tests, outside air for the DFV devices (Fig. 3) was drawn in once at the top and once at the bottom of the parapet (Fig. 6). Measurement periods in Rednitzhembach are from May to July 2020 and from June to July 2021. At the same time, detailed models were created in the thermal-energetic building simulation environment TRNSYS and the numerical flow simulation environment ANSYS/ FLUENT at the Institute for Energy and Building - ieg at THN.

2.1 First Results

Both the experimental studies with the four greening systems and the simulation calculations confirm a potential saving in cooling energy requirements and CO_2 emissions of between 23 % and 43 % for the model rooms of the test stand in the cooling period from May to September. (Fig. 7) Compared to the results for the façade test stand, however, the savings potential for a simulated

Figure 4: Greening systems: Variant 1 - Vertiko GmbH, Buchenbach (left / 08/2020) Variant 2 - Verticalgreendesign GmbH, Berlin (right / 06/2020)

Figure 5: Greening systems: Variant 3 - Kramer Gartenbau, Munich (left / 07/2020) Variant 4 - Jakob GmbH, Ostfildern, with climbing plants (right / 06/2022)

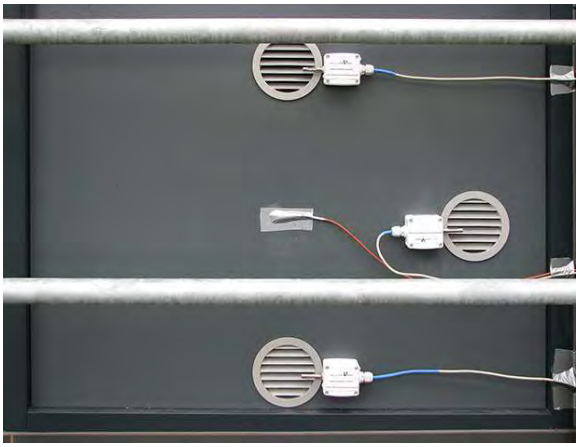

Figure 6: Façade test stand. Reference office with decentralised ventilation unit (DFV)/ room side (09/2019).

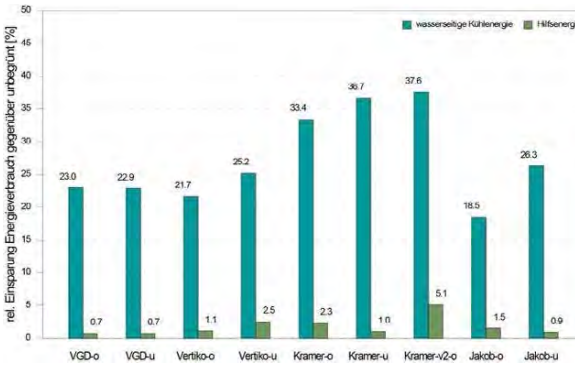

Figure 7: Relative savings of the greening systems in cooling energy (water-side) and auxiliary energy compared to the reference case during the respective series of measurements - results of the Rednitzhembach façade test stand. (Source: THN-ieg)

individual office is lower (7 % to 25 %) due to deviating building design parameters.

This means that the energy requirement and thus the savings potential compared to a façade without greenery also depends on the room behind it (geometry, proportion of window area, heat transfer coefficient, etc.) and its utilisation. For example, a better heat transfer coefficient of the façade behind the greening system leads to a lower savings potential.

The different results of the individual greening systems are due to their geometric, biophysical and spectral properties as well as the plant species considered in each case. The surface resistance of the leaves and the degree of water saturation of the substrate play a particularly important role here. Therefore, the wall-mounted systems showed the greatest cooling potential in the test series and thus the highest savings.

Figure 8: Energy twin rooms at the test facility for energy and indoor climate investigations (VERU). Reference office (left) and structure with façade greening from Vertical-greendesign (VGD) (09/2020) (right / source: IBP)

2.2 Further investigations

Following these initial assessments of the façade combination based on measurement results and simulation studies, further tests were carried out with a selected greening system at the Fraunhofer IBP's VERU test facility for energy and indoor climate analyses. (Fig. 8) On the south side of the 2nd floor of

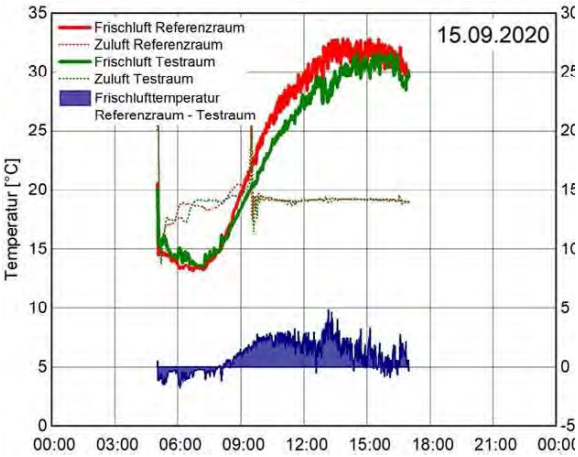

Figure 9: Result of the measurements at the VERU test stand in Holzkirchen. Intake or fresh air and supply air temperature on 15 September 2020 (source: IBP).

Figure 10: Façade test stand. Installation of centre vertical PV module in front of Kramer greening system / variant 1 (06/2022).

the building there are two identical test rooms of 20 m² each, which are specially designed for comparative energy measurements. [7]

The measurements were mainly carried out in September 2020 and between the beginning of August and mid-September 2021.

These further investigations demonstrate two effects of the plants, among others. On the one hand, the greenery leads to a reduction in the intake air temperature of the DFL units (by up to 3 - 4 K lower than in the reference room). (Fig. 9) On the other hand, the shading contributes to a lower façade temperature, which reduces the solar input into the room. [8]

3. GREENPV (04/2021 – 08/2022

As part of a small project study [9], the test work was extended to include the combination of greening and PV. Semi-transparent PV modules from aleo solar GmbH in Prenzlau were used on the THN façade test stand. The frameless construction and the transparent rear side ensure sufficient solar radiation for the plants arranged behind them.

Three variants (wall-mounted and ground-mounted greening, mixed/racking system) were used for the project work. Two wall- mounted systems in particular, which have a higher cooling capacity than climbing plants: (see Fig. 4, left+5)

- Wall-mounted system (Vertiko GmbH, Buchenbach)
- Mixing/racking system (Kramer Gartenbau, Munich)
- Ground-based system (Jakob Rope Systems, Ostfildern with climbing plants)

The test series were carried out with two different distances between the PV modules and the greenery: first with 33 cm, then with 52 cm. (Fig. 10)

The approach aims to achieve synergy effects by utilising the positive properties of both façade systems: Photovoltaics as a technical component and essential building block of a decentralised energy supply close to the building and vertical greening to improve the living environment with the potential for passive cooling.

The aim of the experimental investigation of the combinations was to clarify the extent to which solar yields can be increased by reducing the module temperature through the cooling effects of wall-bound façade greening in particular. The effects of the façade cavity behind the PV module on the plants were also observed.

3.1 Results

The results show that the greening systems reduce the surface temperatures on the back of the PV modules by up to 4.0 K at maximum. It is also clear that the Kramer mixed system and the Vertiko wall-mounted system achieve a slightly greater reduction in surface temperatures than the Jakob ground-mounted system with climbing plants. This is due to the additional cooling effect caused by the moist substrate (Kramer) or the moist geotextile (Vertiko).

In all systems, an influence of the distance between the PV modules and the greening system on the surface temperature can be recognised. A greater distance results in at least a slightly greater reduction in the maximum surface temperatures. However, these temperatures are strongly dependent on the climatic conditions at the time of measurement; higher outside temperatures lead to a higher temperature difference in the **m**aximum values. (Fig. 11)

The individual greening systems also lead to a reduction in the air temperatures between the PV modules and the greening systems compared to the ungreened reference case. Here too, it can be seen that the two wall-mounted systems Kramer and Vertiko achieve a slightly greater reduction than the Jakob system with climbing plants. This also confirms that the PV modules reduce the heat stress of the

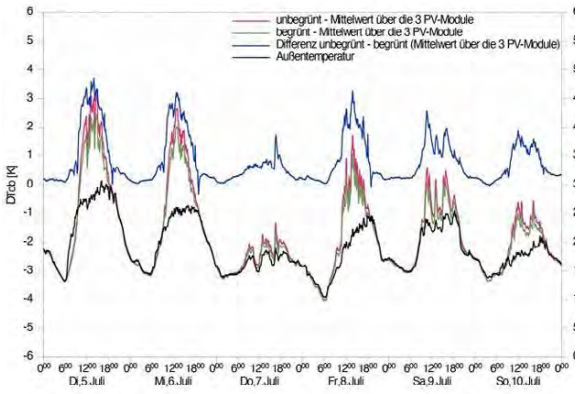

Figure 11: Course of the average surface temperature on the back of the PV modules for the unplanted and planted case and their temperature difference - Kramer system / variant 1 (small distance between the PV modules and the greenery) (top right) (source: THN-ieg)

Figure 12: Façade test stand. Reference office with photovoltaic modules (PV) (left) and structure with Kramer greening system / variant 2 and inclined PV modules (30 °) (right) (09/2023)

plants. During the measurements in the summer of 2022 and 2023, almost no negative effects on growth were observed in either test arrangement, despite the strong decoupling from the ambient climate.

In addition, the greening (in all six variants analysed) also results in a reduction in the perceived room temperatures. On average, the room temperatures can be lowered by up to 1.1 K (Vertiko system). The distance between the PV modules and the greening system does not play a significant role here.

Nevertheless, only slight additional PV yields can be determined by the respective greening systems. The Kramer system with a small distance between modules and façade greening provides the highest value with an increase of around 0.5 %. The measured values are so low that they are within the measurement error of the measurement sensors. This means that the respective greening systems can reduce the surface temperatures on the back of the PV modules to a certain extent, but this has no major influence on the achievable PV yields.

3.2 The interface between green facades and PV

With regard to the combination of greenery and photovoltaics in the façade, however, another aspect is of central importance: the effective evaporation capacity of the plants in the vertical plane in the urban space.

If photovoltaic modules are installed densely and parallel to the wall in front of green façade surfaces, evapotranspiration is significantly restricted and thus the cooling capacity for reducing temperatures in the street space is greatly reduced.

There are many options for the arrangement and design of the two façade systems. The distance between the PV modules and the greenery can be extended to create a façade with more space, and the inclination of the photovoltaics improves accessibility and evaporation performance, while the optimised exposure of the module to the sun should also increase yields.

The design of the positional relationship between the photovoltaic system and the green façade could ultimately only be analysed in initial basic considerations as part of the project work. In addition, test set-ups with two different inclination angles of the PV modules with the Kramer greening system were analysed from various sample set-ups of the three greening systems.

Regarding the changes to be documented in terms of appearance, a decision was made in favour of a more strongly flared variant (based on the optimum orientation for south-facing buildings in Central Europe) (Fig. 12) and a variant with a comparatively flat inclination, which extends the flat character of the original vertical arrangement in a nuanced way.

The results confirm higher yields for the flatter angle of attack (around 11 % in the period under consideration) compared to the vertical arrangement. However, due to the specific installation conditions at the test site, the greater inclination with the 30° variant also led to self-shadowing of the PV modules and thus to significant yield losses. However, an optimised setup (module spacing and/or inclination) can be expected to produce significantly higher yields compared to vertical installation.

4. CURRENT STATUS - OUTLOOK

Many planners in the façade sector still shy away from the use of both greening (especially wall-mounted systems) and photovoltaics, often due to their high degree of complexity and the sometimes difficult coordination of additional trades. However, in view of the social challenges of the energy transition and climate adaptation strategies, both technologies, possibly in conjunction with decentralised façade ventilation, are gaining enormous relevance. Their

diverse combination options also open up an additional spectrum of positive effects.

The results of the thermal-energetic building simulation carried out in the GreenFaBS project show that a greening system installed over the entire surface (storey-high, one façade grid) has a greater effect than a system installed only in the parapet area. However, this effect is essentially low in terms of energy requirements. For example, a completely greened façade area 'only' leads to a 4.0 % lower cooling energy requirement. This opens up certain degrees of freedom when planning functional areas in the façade (under the given framework conditions such as the U-value of the construction). For example, reducing the greening area of a storey-high façade panel to the parapet area by around two thirds results in a comparatively low additional cooling energy requirement.

These areas could also be used for the installation of photovoltaic modules. This is because in the case of an area-parallel arrangement, issues of accessibility for the regular care of plants and maintenance of the system technology must be taken into account. The positive influence of the cooling capacity of the greenery on the exterior of the building also decreases when photovoltaics are used on large areas of the façade.

In view of the upcoming central tasks in the construction sector, both in new buildings and in the refurbishment of existing buildings, the issue of façade competition (e.g. greening in conjunction with photovoltaics) is significant: what areas do the various interfaces or plus uses require in order to optimise the proportion of the various façade technologies? Therefore, the development of multifunctional energy façades, especially on the basis of ventilated rainscreen façades (VHF), must be expanded to include greening techniques. The aim of initial concepts and collaborations is to create a kind of façade construction kit in order to be able to adapt the potential of future solutions more effectively to the respective site-specific characteristics.

ACKNOWLEDGEMENTS

The project "EnOB: GreenFaB" was funded by the BMWi - Federal Ministry for Economic Affairs and Energy, Berlin (via Projektträger Jülich, Fachbereich Energieeffizienz in Gebäuden (ESN1)); Project team including among others Wolfram Stephan and Mario Franz (both Institute for Energy and Buildings - ieg at Nuremberg Institute of Technology [THN-ieg]), Almuth Schade and Herbert Sinnesbichler (both Fraunhofer Institute for Building Physics IBP, Holzkirchen site)

The project study "GreenPV" received financial support from the STAEDLER Foundation, Nuremberg; Project team including among others Wolfram Stephan und Mario Franz (both THN-ieg).

REFERENCES

1. Herzog, T., Krippner, R., Lang, W. (3/2021): Green facades. *Facade Construction Manual*. Munich: DETAIL Business Information GmbH: p. 336-341.

2. Herzog, T., Krippner, R., Lang, W. (3/2021): Integrated facades. *Facade Construction Manual*. Munich: DETAIL Business Information GmbH: p. 322-327

3. Herzog, T., Krippner, R., Lang, W. (3/2021): Solar energy. *Facade Construction Manual*. Munich: DETAIL Business Information GmbH: p. 294-321

4. Krippner, R. (Ed.) (2017): *Building Integrated Solar Technology. Architectural design with photovoltaics and solar thermal*. Detail green books. Munich: DETAIL Business Information GmbH

5. The rectangular structure of a Tiny House has external dimensions of 6.80 m x 2.48 m (l x w). The monopitch roof (3.91 m; 2.77 m [h1; h2]) is covered with a double standing seam sheet made of titanium zinc. The U-value of the exterior walls in timber frame construction complies with the 2016 Energy Saving Ordinance.

6. In co-operation with the Institute for Energy and Building - ieg at Nuremberg Institute of Technology and the Fraunhofer Institute for Building Physics IBP in Holzkirchen; supported by BuGG Bundesverband GebäudeGrün e. V., Berlin (Gunter Mann and Nicole Pfoser) and TROX GmbH, Neukirchen-Vluyn (Klaus-Dieter Wolf) [https://www.th-nuernberg.de/fakultaeten/ar/forschung/konstruktion-und-technik/abgeschlossene-forschungsprojekte/enob-greenfabs/ <30.12.2023>]

7. Sinnesbichler, H. (2018): *Energetische Zwillingsräume. Informationsflyer. [Energetic twin rooms. Information flyer]* Holzkirchen. [and https://www.pruefstellen.ibp.fraunhofer.de/de/energieeffizienz-und-raumklima/veru.html <30.12.2023>]

8. See also Krippner, R. (9/2023): *Der Kühleffekt begrünter Fassaden. The Cooling Effect of Green* Facades. In: Detail, p. 14–17

9. In co-operation with the Institute for Energy and Building - ieg at Nuremberg Institute of Technology [https://www.th-nuernberg.de/fakultaeten/ar/forschung/konstruktion-und-technik/laufende-forschungsprojekte/green-pv/ <30.12.2023>]

PLEA 2024 WROCŁAW
(Re)thinking Resilience

Stuttgart 210
thinking ahead – building ahead

STEFAN KRÖTSCH[1] ROMAN KREUZER[1]

[1]Author1 University of Architecture and Design (HTWG), Constance, Germany

ABSTRACT: The "Stuttgart 210" research project shows the need to reduce the ecological footprint in the construction industry by tackling the challenge of a circular economy. As the main consumer of resources and a significant source of emissions and waste, the project aims to achieve sustainable change through the reuse and upcycling of building components. The focus is on the innovative use of formwork elements from the new Stuttgart 21 main station, which are used in real labs as primary building materials for the construction of new buildings. These laboratories act as experimental platforms to test innovative approaches under real conditions and to further develop the legal framework. The project follows an integrative approach that combines architectural quality, ecological accounting and legal framework conditions and implements the principles of the circular economy in practice. In particular, the research project concentrates on the almost closest possible material cycle, the use of building components, and thus represents a pioneering model for sustainable construction that shows how circular and resource-efficient construction can emerge from a throwaway society.
KEYWORDS: circular, real labs, reuse, sustainability, timber architecture

1. INTRODUCTION

The construction sector is responsible for 40 % of primary energy demand and greenhouse gas emissions, 50 % of materials extracted from the earth and 60 % of waste. [1] The transition to a closed-loop circular economy is therefore particularly relevant in the construction industry. The "Stuttgart 210" research project points the way to the future by planning the reuse and upcycling of the construction materials (formwork elements) originally intended for disposal at the new Stuttgart 21 (fig. 1) main station. This is because the multiple block-glued 8-axis milled formwork elements are of extremely high quality.

Figure 1: New train station Stuttgart 210
©ACHIM BIRNBAUM

Therefore they are predestined for upcycling to use as primary components. The research project presents practical projects in which buildings are planned and constructed from the complex solid wood formwork elements. This does not only create special architecture through the geometric uniqueness of the formwork.

The research project prepares practical projects in which buildings are planned and constructed from the complex solid wood formwork elements. This does not only create special architecture through the geometric uniqueness of the formwork, but also ads value in terms of sustainability. The combination of research and practice makes it possible to test the theoretical concepts of the circular economy directly in reality. This not only calls conventional design strategies and construction processes into question, but also the existing legal and economic framework conditions.

2. GOAL OF THE RESEARCH PROJECT

The aim of the research project is to contribute to a sustainable transformation of the construction sector. The life cycle of timber components is to be extended by not treating components or - as in the case of the formwork elements for Stuttgart 21 main station - construction materials as waste at the end of their first use, but rather as valuable resources for new buildings in real laboratories integrated into the research project.

In itself, timber is a recyclable and CO_2-neutral building material (fig. 2). If it is thermally recycled or decomposes at the end of its useful life, the majority of the material substance is released as CO_2. Trees can metabolize this CO_2 via photosynthesis back into wood, which can then be used again. In this way, the building material is also usually considered to be almost climate-neutral in the life cycle assessment.

If noadditives (glues, varnishes, paints, wood preservatives,…) are added to the timber as a material, it is fully recyclable. With regard to combating the climate crisis, however, it makes a lot of sense to keep the CO_2 stored in wood bound for as long as possible and to

prevent its release in order to relieve the climate over a long period of time. In principle, this can be done in three ways (fig. 2):

1. Use of waste timber to produce new wood-based materials (OSB boards, chipboard, etc.)
2. Re-Use of entire compounds (walls, ceilings, roof constructions, ...)
3. Preservation of entire buildings through further use or conversion

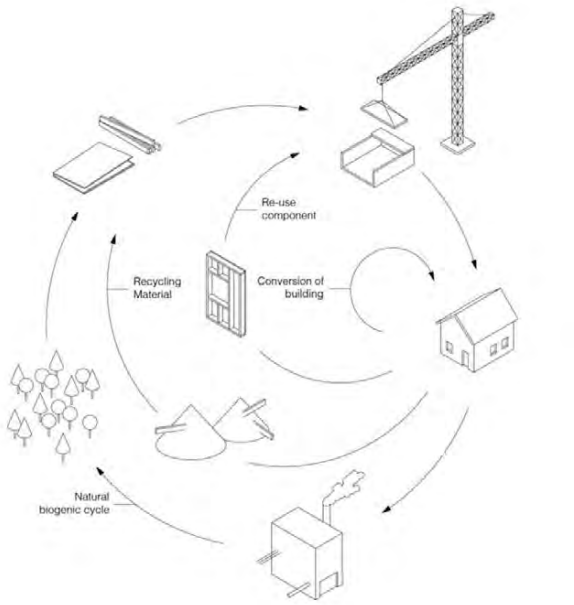

Figure 2: Different cycles in the circular economy of timber building products © HTWG Konstanz, Fachgebiet Baukonstruktion und Entwerfen (Prof. Stefan Krötsch).

The approach according to 1) is appropriate and practicable, but usually leads to inferior use (downcycling) and the addition of additives (glues, etc.). Building in existing structures according to 3) is an important part of architecture and in Europe the most important component of the resource turnaround in the construction industry. As it has an important and long tradition, there are clear framework conditions for dealing with old building components and materials. In Germany, the reuse of entire building components in new contexts according to 2) is largely unclear in terms of its technical and legal classification.

At the same time, however, there is great potential here, as the use of building components usually allows the material to be used in an equivalent way - and in the case of timber, the stored CO_2 can be completely preserved. In the case of construction aids such as highly complex formwork, significant upcycling is even possible if they are used in their second purpose as a primary supporting structure. This is the highest quality and most value-preserving reuse that is possible in this case. By following precisely this path, the "Stuttgart 210" research project is attempting to develop generalizable findings on a reuse process in the sense of upcycling using the example of the wooden concrete formwork of the new Stuttgart 21 main station. By preparing and carrying out 4 trial designs ("real labs") in and near Stuttgart, the project exposes itself to the requirements of actual construction. The knowledge gained from this can in turn be transferred and generalized in a planning aid (roadmap re-use).

3. DESIGN PROCESS

The use of complex, predetermined components requires the design process in architecture to be rethought and restructured. Usually, the function of the building is the starting point of the design considerations, followed at a later stage by a materialization that is as close as possible to the design. When using the formwork elements, this process is reversed: The reused components, as the primary supporting structure shape the possibilities of the spatial design from the outset. In order to be able to exploit the design potential of the elements, the unique geometry of the formwork elements became the determining parameter. This is because potential clients were naturally unable to develop an idea of the type of buildings that could be constructed with them based solely on a catalog of the available components. The project team therefore developed various designs that could be created from the available elements, while the potential use was left largely open.

On the one hand, use-neutral spaces were created that could be used by future clients in a variety of ways (real lab Mannheim). On the other hand, the shape of the formwork elements resulted in very plausible building geometries for which very specific users were found (real labs Stuttgart Vaihingen and Ingersheim). The search for building tasks must therefore precede the design of buildings without a specific use.

After the development of potential designs, which were verified by drawings, 3D models, physical models and renderings, these were published and distributed via various local networks. The aim was to find clients from the public sector. Initially, the plan was to make the catalog of available elements available for finding construction tasks within the framework of competition procedures (architectural competitions). However, the lengthy nature of these procedures and the need for rapid removal from the construction site made this procedure impossible.

As the further use of the formwork was only suggested later in the course of the research project, the processes at the Stuttgart station construction site were not designed for this. Storage areas on the construction site or elsewhere were not available. The key design parameter was therefore the current availability of elements. Potential clients had to be found within a few months so that the formwork could be transported to the new site as quickly as possible.

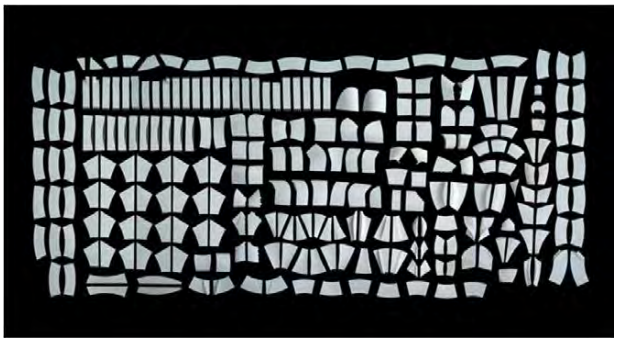

Figure 4: 3D printed formwork elements in scale 1:50 ©Stuttgart210

Precise 3D production drawings of the automated milling process were available for all formwork elements. On the one hand, this was an excellent and absolutely reliable basis for planning. On the other hand, these were highly complex drawings and huge amounts of data, which made it difficult to work intuitively, which is necessary for the design process. The initial plan was therefore to use artificial intelligence to generate random geometric combinations of the amorphous formwork elements, from which useful building designs could then be selected. However, preparing and programming this AI would have taken far too long and during this time most of the formwork elements would have already been destroyed (see above). In order to be able to design quickly, effectively and intuitively, the design team therefore created one of the oldest tools in architectural design by printing out all formwork elements as 3D models at a scale of 1:50 (fig. 3). This not only made it possible to design quickly and purposefully, but also to discuss projects with the clients.

4. LEGAL FRAMEWORK CONDITIONS

The reuse of building components or construction aids affects a whole range of legal fields - from waste law and construction product law to building regulations law and various related legal fields such as contracts for work and services and public procurement law as well as questions of warranty and liability (fig. 4).

With regard to waste legislation, the classification of formwork elements in the legal sense is a key issue, so that they are not understood as waste according to their original use/purpose. According to the German Circular Economy Act, this could be the case if materials lose their first intended use (here specifically as formwork elements) and no further intended use is defined. It is then difficult to reuse the elements as components. This is because in order to be able to leave the area of waste legislation again and become a new construction product, a new definition of the component as a construction product is required, including all product certificates (product data sheet, CE certification, etc.). The person in whose possession the product is at this point in time is therefore responsible for the performance comparable to a building material manufacturer.

The strategy of the research project is therefore to prevent the formwork elements from becoming waste in the first place. Initially, they will be stored temporarily as construction aids, i.e. in accordance with their first purpose, for any necessary reworking at Stuttgart station, such as rectifying defects. They will then be used directly as load-bearing components in the real labs in accordance with their second purpose, so that they can never be regarded as waste.

However, as the formwork was never intended by the manufacturer to be used as building components such as ceilings, roofs or walls, a technical review of its suitability for this purpose is required. With regard to the load-bearing structure, a structural analysis for the new intended use was carried out as part of the research project, which will form the basis for an approval in individual cases under building regulations by the local authorities.

The verification was carried out based on the calculation of the first intended use as formwork - with corresponding checks regarding the new use. The structural analysis should be carried out as purely mathematically as possible, as destructive examinations counteract the aim of reusing the elements. However, they may be necessary in some cases. In addition to the theoretical consideration of the load-bearing capacity, it is particularly important to check the current condition of the formwork elements. For this purpose, visual inspections and other tests should be carried out, as they are common and known from the renovation of old buildings.

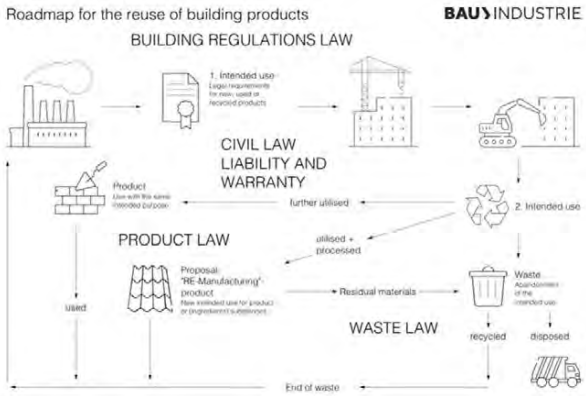

Figure 4: Roadmap - reuse of construction products © Hauptverband der Deutschen Bauindustrie e. V.

Suitability in terms of fire protection, sound insulation and thermal insulation must also be guaranteed. Here, however, the requirements can be kept so low due to the type of use that the verification is relatively unproblematic.

The research project also addresses the challenges arising from the current legal framework, which is often geared towards the use of new materials and rarely takes into account the special features of recycled building components. By overcoming legal hurdles in areas such as public procurement law, building regulations law and works contract law, but especially in construction products law, the possibility is created to use recycled materials in a legally secure manner and at the same time to guarantee the quality and safety of the buildings.

The legally compliant preparation of the real laboratories forces all those involved in the test buildings to contribute their expertise and concerns to the discussion in good time and to find a common approach that does not impose unacceptable risks on clients, planners or contractors. These findings and best practices will be collected, evaluated and generalized as part of the research project.

5. LIFE CYCLE ASSESSMENT

Timber as a building material is the most important representative of the so-called "biogenic raw materials". In contrast to all other building materials (minerals, metals, plastics, glass, etc.), these have a fundamentally different behavior, especially with regard to CO_2 emissions: In the case of non-biogenic building materials, all CO_2 emissions are generated directly during the production process and are already in the atmosphere when the building is completed. With biogenic (renewable) building materials, on the other hand, CO_2 is bound during growth and remains bound in the corresponding building component over the entire period of use. If the focus is placed exclusively on the production of the building, the calculation for biogenic building materials results in negative CO_2 emissions, as their use as a building component prevents natural decomposition and the associated return of CO_2 from growth into the atmosphere. The building acts as a CO_2 reservoir, which is all the greater the more biogenic building materials are incorporated. [2] However, as the entire life cycle is usually considered in a life cycle assessment, a so-called "end-of-life scenario" must be defined. For the end-of-life scenario, it is typically assumed that biogenic components are thermally recycled after dismantling. In this case, the CO_2 bound in the material is completely returned to the atmosphere, which means that renewable building materials only have a neutral balance with regard to the bound CO_2 in the overall characteristic value. Although an energy credit can be calculated for thermal utilization via the recycling potential in Module D, this only compensates for part of the CO_2 emissions. In addition, fossil energy sources are also used for harvesting and processing in the production of biogenic materials, meaning that wood components also cause CO_2 emissions in the life cycle assessment.

As mentioned above, the result of a life cycle assessment with a high proportion of timber building materials is significantly influenced by which end-of-life scenario is used. The standard scenario of thermal utilization is the current basis for all LCA calculations according to the auditing procedures (in Germany DGNB, BNB etc.). In general, this also corresponds to common building practice, but it does not necessarily make sense to use the status quo for scenario considerations that relate to an event in 50 years' time (this is the typical scope of a life cycle assessment).

Applied to the research project, this means that standard calculations of the GWP (Global Warming Potential) come to the conclusion that reusing the wooden formwork elements as long-term components would be worse than thermal utilization. However, this result cannot be a true representation of the CO_2 storage potential. For this reason, the research project is developing a proposal for a balancing system that includes the time of emission or storage of CO_2 by building materials in the balancing. This is because, on the one hand, it is definitely relevant whether the emissions are generated at the beginning of the balance and can then act in the atmosphere for 50 years, or whether they only enter the atmosphere at the end of the cycle. Above all, however, this difference causes a shift in responsibility: in the case of non-biogenic building materials, the emissions arise directly during production and are the responsibility of those involved in planning. In the case of biogenic building materials, those involved in planning organize the storage of CO_2 and future generations have several options in the event of deconstruction as to whether and to what extent these bound emissions are released back into the atmosphere.

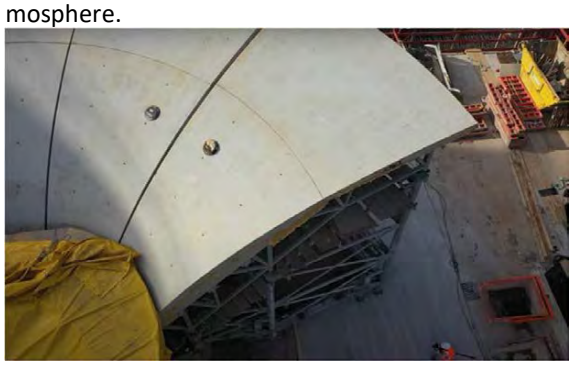

Figure 5: Image: formwork elements from the main station Stuttgart building site ©DB AG

6. PRESENTATION OF THE REAL LABS

The concept behind the real-world laboratories is based on the premise that sustainable building must be researched and promoted not only in theory, but above all in practice. By constructing real buildings from the reused formwork elements, the entire process from planning to implementation and completion of the building is considered. This enables not only the technical and material aspects to be evaluated, but also the social, economic and legal framework conditions to be enforced.

"Real labs as test spaces for innovation and regulation make it possible to test innovative technologies, products, services or approaches under real conditions that are only partially compatible with the existing legal and regulatory framework. The results of such temporally and often spatially limited experimental spaces provide the basis for the evidence-based further development of the legal framework." [3]

The following three real labs designs for new buildings show the architectural potential associated with the shell elements of Stuttgart station.

Figure 6: Image: Removal transportation of formwork elements from the main station Stuttgart building site ©DB AG

6.1 REAL LAB MULTIFUNCTIONAL ROOM MANNHEIM

The real lab Multifunctional Room Mannheim has a floor area of around 10 x 12 meters. The special feature of the building is its spatial structure, which consists of 100% reused materials. The self-supporting building envelope made of HKT elements are edge shell elements from the new Stuttgart railroad station. These have strong ribs on their rear side, which resemble a multi-planked rafter roof construction.
This design feature makes it possible to position the elements in such a way that, from the outside, they reproduce the geometry of an ordinary gable roof building, while inside, their curved shape creates the impression of a textile-like tent, resulting in an extremely aesthetic and high-quality space

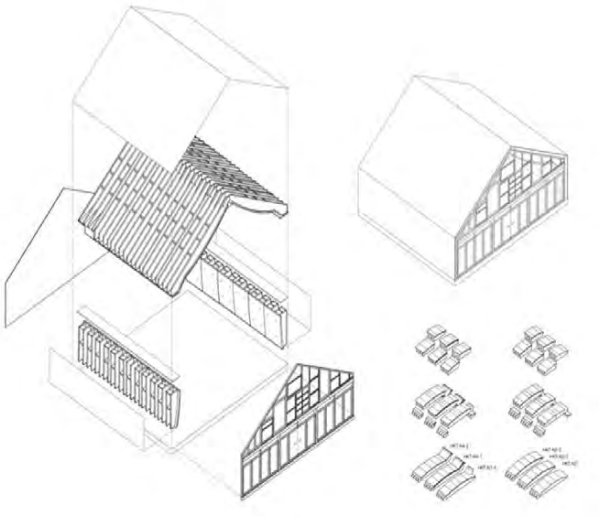

Figure 7: Axonometry Reallab Multifunction Room Mannheim ©Stuttgart210

This column-free space allows for a wide range of conversions for different user groups. These range from a canteen for schoolchildren to an exercise room for a kindergarten or a forest kindergarten to a warm-up room for the homeless or a rehearsal room for the Mannheim National Theatre. An office use for "Next Mannheim" on the edge of Herzogenriedpark in Mannheim is currently being planned.

Figure 9: Rendering Reallab Multifunction Room Mannheim ©Stuttgart210

6.2 REAL LAB ROTUNDA CIRCULEUM VAIHINGEN

The real lab Circuleum consists of two sets of lower formwork with which the iconic chalice columns of Stuttgart's new main railway station were concreted. By assembling and inverting the standard goblet formwork, a self-contained roof structure is created which, thanks to the self-supporting formwork elements, results in a round, column-free space with a diameter of 14 meters. The total diameter of the experimental building is 22 meters. The bulkheads of the rotunda required for the supporting structure create niches that can be used flexibly.

Figure 8: Axonometry and Rendering Round Building Circuleum Vaihingen ©Stuttgart210

As part of the research project, a user was found for the rotunda who operates an arts center for citizens of the surrounding area on an area located at the train station in Stuttgart-Vaihingen. There is currently a temporary circus tent there in the summer. This is to be replaced by the real lab in the long term, so that the thermally closed shell of the rotunda can also be used in winter. In addition, the rotunda will not only be available for the artists' center, but also for a number of other clubs that offer sporting and cultural activities for their own community. Due to the multiple curved shell elements and the room geometry, the room will also be acoustically very interesting for possible chamber music concerts. The shell elements required for this have already been transported to the site and will now be stored there until construction begins.

Figure 10: Rendering Round Building Circuleum Vaihingen ©Stuttgart210

6.3 REAL LAB YOUTH CENTER INGERSHEIM

The real lab Youth Center Ingersheim with a floor area of 10 x 8 meters and a height of 6 meters, the Ingersheim Youth Center is very special in many respects.
It consists of four large, multi-curved formwork elements that were required as special formwork for a pedestrian access tunnel for the new Stuttgart Main Station. These are now set up in such a way that they form a star-like interior, which has a very special, textile appearance thanks to its organic shape. A new building envelope is placed over the elements, which resembles a cube from the outside. As soon as one enters the cube, one experiences the fascinating space. The resulting hollow spaces in the corners of the cube are converted into usable side rooms.

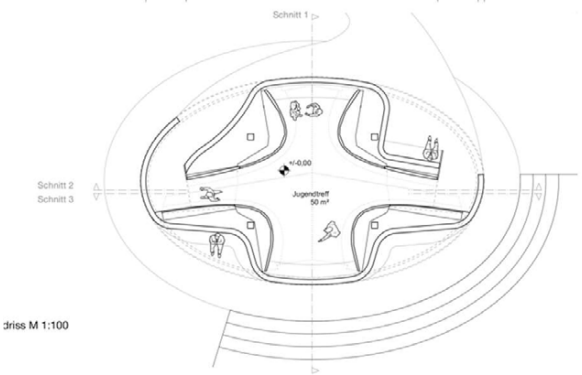

Figure 12: Floor plan and section Youth Center Ingersheim Vaihingen ©Stuttgart210

The elements for this are already in Ingersheim and will be erected in summer 2024 with the help of young people from Ingersheim, architecture students and the municipality of Ingersheim, so that the space will be built by young people and architecture students and will later be available as a meeting place for them.

Figure 11: Rendering Youth Center Ingersheim Vaihingen ©Stuttgart210

7. CONCLUSION

The reuse of construction materials such as the formwork for Stuttgart 21 station as building components is the optimal use from a sustainability perspective. The CO2 bound in the wood is thus stored for a long time and relieves the climate. A new method of life cycle assessment is being developed in the Stuttgart 210 research project in order to accurately map this effect.

But beyond this, the designs of the research project are intended to demonstrate the architectural and design potential of using used components. The resulting interior spaces are reminiscent of textile architecture (tent constructions) due to the geometry of the re-use elements, but consist of solid wood elements, some of which are several meters thick. This transfer of a specific structural form into a new application not only makes the previous use of the formwork tangible, but also creates a unique, unrepeatable architectural identity that cannot be detached from the creation process. An architectural expression that is detached from any free invention, but only follows the necessities and conditions of the existing building.

Even for simple uses, geometrically complex rooms made of solid wood elements could be developed and implemented, which would be unaffordable as new buildings.

The preparation of the practical projects also ensures that very concrete solutions are found for the problems of building with re-use elements - in terms of architectural, technical and also legal issues.

8. REFERENCES

1. TU Darmstadt, (2007). Energieatlas Werkbericht 1: Zukunftskonzept Erneuerbares Wilhelmsburg / IBA Hamburg GmbH; Umweltbundesamt. (Energy Atlas Plant Report 1)
2. BAK Berlin, (2022). Entwurf der EU-Kommission zur Richtlinie über die Gesamtenergieeffizienz von Gebäuden (energy performance of buildings directive, epbd)
3. BMWK - Reallabore – Testräume für Innovation und Regulierung. (Reallabs - Test Spaces for Innovation and Regulation).

PLEA 2024 WROCŁAW
(Re)thinking Resilience

Re-designing the Indian Urban Village

The Case of New Delhi, India

SHREYA ANEJA[1], SIMOS YANNAS[1], JOANA CONCALVES[1]

[1]Architectural Association School of Architecture, London, United Kingdom

ABSTRACT: Migration from small towns to city centres has exploded across India, creating high-density neighbourhoods that are known as urban villages. The inhabitants of these urban villages experience inhuman conditions, caused by extreme high density, lack of ventilation, little or no daylight, thermal discomfort and lack of space and privacy. This paper proposes a prototype for environmentally responsive urban villages in New Delhi. The studies deal with air movement, solar protection, and inhabitant thermal comfort, concluding with design proposals. The fieldwork conducted as part of this project revealed positive microclimatic characteristics of the traditional compact form that contain peak temperatures. In-depth analytical work at urban and building level has shown that inhabitant thermal comfort can be ensured for some 60% of annual hours in the city's sub-tropical climate. The paper highlights the analysis undertaken at urban masterplan level, with an indication of the key strategies derived for the building scale. The results show that acceptable living environments can be achieved. The results of the research can be used to develop a framework for the elaboration of context-specific, environmentally comfortable dense neighbourhoods for the warm regions of the world.
KEYWORDS: Urban Village, Density, Passive Design, Ventilation, Thermal Comfort

1 INTRODUCTION

Migration due to urbanisation from neighbouring towns to city centres has exploded in the last few decades creating high-density neighbourhoods that exist between urban centres and villages, referred to as Urban villages [2,3]. In developing countries like India, such neighbourhoods are populated by people living in inhumane conditions created by high density and precarious built environment (lack of ventilation, little to no daylight, extreme thermal discomfort due to soaring temperatures and lack of space and privacy [3]. However, using traditional elements, these spaces also contain intuitive and close-knit architecture that creates potential for intervention.

New Delhi is selected as the location due to its rapid surge in population (201 registered urban villages as of 2021) and growing economic disparity, elevating the role and importance for better urban villages [1]. According to UN estimates, India will add 400 million urban residents by 2050. Between 1991 and 2011, Delhi's geographic area nearly doubled, with a doubling of urban families and a halving of rural housing. Therefore, it's inevitable that the impact of this growth will be significant and is already raising concerns. It's imperative to examine this urban growth with a critical lens and with importance on ensuring environmental comfort and energy efficiency in these buildings. This research proposes interventions at the urban level. The paper reports on the analysis of air movement and solar radiation conducted by literature review and quantitative analysis.

2 CONTEXT

2.1 Climate

Delhi's climate is classified as humid sub-tropical. It sees a hot, rainless phase from April to June averaging 32°C with wide temperature swings. November to February experience cooler temperatures around 16.5°C. July to mid-September stays warm and humid, averaging just under 30°C. Temperatures swing from highs near 44°C in May and June to lows around 0°C in December and January can be observed. New Delhi gets significant horizontal radiation, 2,050 kWh/m2 yearly. Wind speed averages 1.8 m/s, peaking at 3.9 m/s, mainly from the North-West, and variable during the humid period. In addition, climate change is impacting Delhi, raising temperatures by 0.3°C per decade and worsening air quality due to increased temperatures, changed wind patterns, and more dust storms. Delhi's high urban density adds to humidity, requiring cooling solutions in architectural designs. To combat this climate, designs prioritize shading for radiation and ventilation for humidity control. [4]

2.2 Social

The main user group of these villages are migrants from rural areas who prefer close-knit, communal living in these neighbourhoods akin to their rural experiences. It suggests constructing densely packed, low-rise spaces with semiprivate and public areas for daily interactions, echoing cultural familiarity and promoting community bonds. This helps to suggest a

guideline for the analysis: low rise, densely packed urban villages.

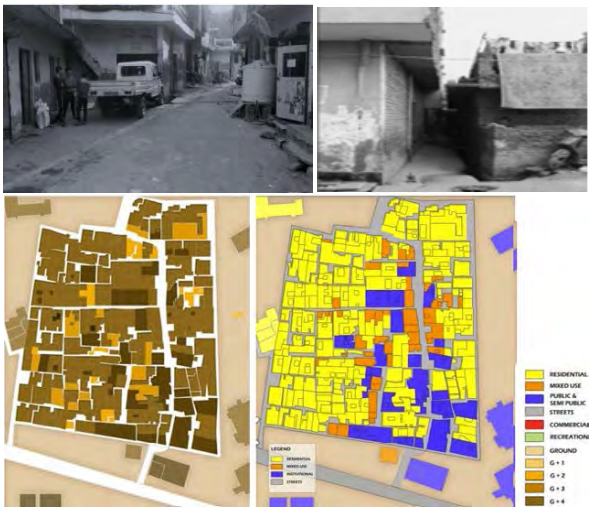

Figure 1: Typical urban village [Pictures by [Author 6]

2.3 Vernacular Aspects

Traditional elements from surrounding architecture hints at different possibilities for analysis including 1. Thresholds, 2. thermal buffer zones, 3. reed/bamboo screens with water sprinkled on them which help reduce temperature due to evaporative cooling etc.

3 METHODOLOGY

This research pro-design study is divided into 3 phases- preliminary research and base case analysis, detailed analysis to formulate a guide for future design and a final prototype proposal with proof of comfort achieved.

Phase 1: This paper begins by examining existing conditions of urban villages in Delhi – exploring environmental and climate factors, living conditions of its inhabitants and vernacular aspects as explained above.

Phase 2: Based on this, the study then identifies key focus areas in terms of the climate and a typical urban village in Delhi: its environmental factors were explored by fieldwork (spot measurements and site survey) and wind and solar studies using CFD software [5] and Ladybug tools [6]. The study is focused on the urban masterplan level and helps identify the existing features that define the positives, negatives, and potential of such an urban hub. Potential passive design techniques have also been explored at the individual house level like potential of increasing indoor ventilation through Optivent studies [7]; decreasing temperature in indoor spaces through evaporative cooling on locally sourced materials (like reed, bamboo); the potential of thermal buffer zones during high summer months – on a site etc.

Phase 3: A chosen site aims to serve as a model for a newly developed urban village, potentially replicable in diverse contexts. The form of the new village is driven from a study of the vernacular elements and the analysis conducted. This section utilizes findings from prior research to outline guidelines for creating an environmentally adaptive prototype of an urban village in India.

4 ENVIRONMENTAL ANALYSIS

Keeping these aspects in mind, Jia Sarai, a typical urban village out of the 200+ neighbourhoods in Delhi was chosen. Studies on wind, outdoor comfort and solar analysis were conducted. This would help inform the guideline for the prototype of similar comfortable neighbourhoods.

4.1 Fieldwork

Field work, which included taking spot measurements and interviews, was carried out to understand the difference in the air temperature inside the urban village and its peripheral areas and correlation with wind, if any. Spot measurements were taken between 27th – 31st October 2022 at 9am, 12pm, 3pm, 8pm using instruments to test dry bulb temperature and wind speeds.

Figure 2 key:

1. *Peripheral road: Busy vehicular road with parking on one side and shophouses on the other. 8m wide street.*
2. *Inside road: narrow street with residences on both sides. 3m wide street.*

Figure 2: Spot measurement points inside the neighbourhood [Fieldwork carried out by Author]

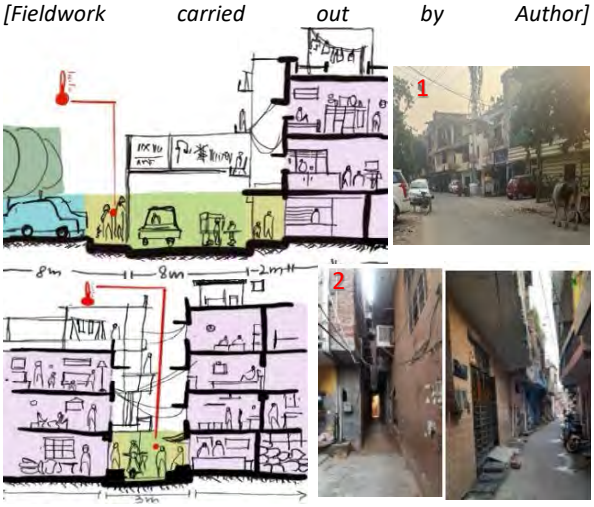

Figure 3: Section and pictures of the spot measurement points. [Sketches by Author]

The two points at which the measurements were taken are shown in the Fig. 2 & 3.
Wind speed obtained on these spots through the device varied from 0.8m/s to 1.5m/s. The latter was only observed inside the village at night which can be attributed to the wind tunnelling effect due to the narrow streets.

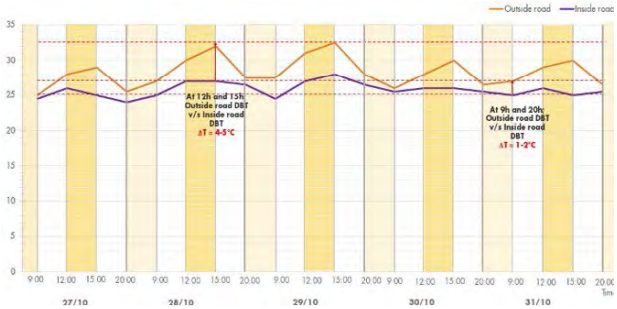

Figure 4: Temperature graph obtained through spot measurements.

Figure 5: Comfort percentage in and around dense neighbourhoods. [Ladybug Tools [6]*]*

There is a 4–5° C difference in temperatures at peak hours during the day and 1 -2° C difference at night between the two spots. Therefore, it can be concluded that there is an advantage to the density as the entire village acts as a single built mass which helps facilitate a better micro-climate overall.
This hypothesis is further confirmed by UTCI studies done using Ladybug tools (Fig. 5). This shows that the comfort percentage on the spot measurement day to be higher inside the village than outside it.
However, upon site visit and while interviewing the people inside the village – disadvantages also emerge. Some streets are too narrow for any wind or light to pass through and thereby are dark with very low air speeds.

4.2 Air Movement

As highlighted in section 1.1, ventilation is a major problem inside urban villages. Therefore, air movement was studied in detail. Givoni [8] demonstrated that air speed has a significant impact on comfort both inside and outside a building. He stated that to allow for wind flow between and around structures, open spaces between building blocks should take regional wind directions into account. It is concluded that with an increase of 1 m/s wind a cooling effect that is equivalent to a 2°C drop in temperature is generated. [8] Hence, wind plays a vital role in not only improving ventilation but also reducing temperature.


Figure 6: Concept sketch to optimise wind pacing through the built mass.

Predominant wind direction on site: *Northwest and West*
Wind simulation studies were done using Autodesk CFD software for the existing urban canyons of Jia Sarai.
The three typical streets: 3m, 6m and 10m are chosen – with two different building heights of 10m and 15m. The same is also analysed for when wind is not perpendicular to the built mass.

The conclusion of the study is as follows: -

a) Wind funnels are observed in the 3m streets. Maximum wind can be observed in urban canyon: 1:1 (Fig.7). Maintaining minimum 3-4m is optimum.

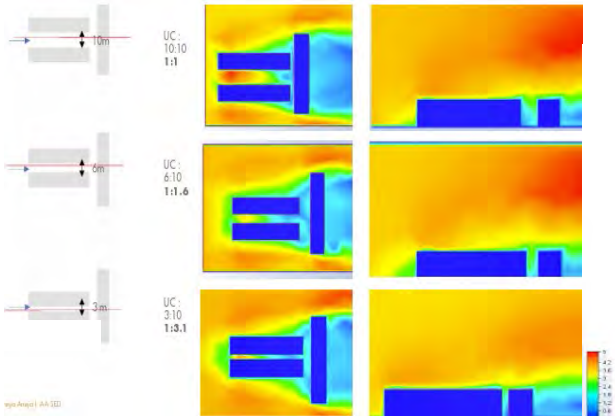

Figure 7: Wind movement through different urban canyons [CFD software]

b) When wind is perpendicular to the façade – the speed is higher and volume between the two groups of buildings is filled with a significant amount of turbulence. When compared to pressure coefficients on parallel faces, a face that is perpendicular to the wind direction will have larger pressure coefficients. As a result, it is determined that adding voids and openings can help facilitate wind flow, even if the urban canyons are narrow.

c) Wind speed inside the canyons is higher when the built mass is at a 15–30° angle to the wind.

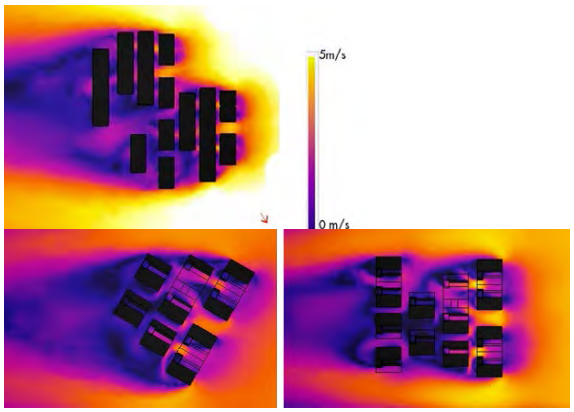

Figure 8: Optimised wind movement through a dense neighbourhood [CFD software [5]]

Wind Chimney/Ventilation Towers

Ventilation towers or wind chimneys can further help create ventilation inside the individual houses. This study determines optimum heights for these low to mid rise developments.

After conducting multiple iterations using Optivent tool [5] for different heights and number of floors, an optimum height of 20m and 24m for the wind chimney for a G+3 house and G+4 was respectively determined (Fig. 9). A wind analysis was also run on these wind chimneys to see the effect inside the space (Fig. 10). It was also observed that the windows should be placed parallel to the wind chimneys.

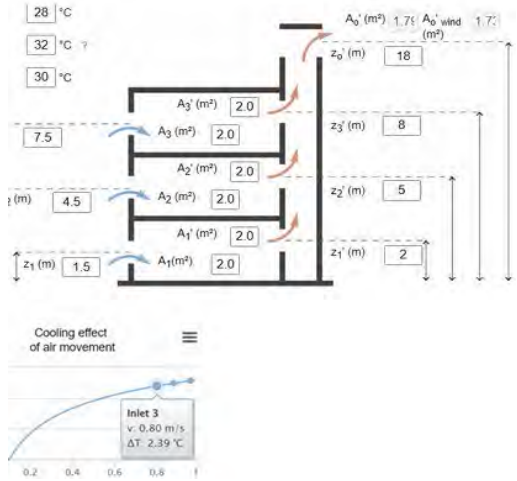

Figure 9: Optimising wind chimney dimensions [Optivent [7]]

It is concluded that there would be an approximate 2.5°C temperature difference in comparison to outside on the street near the window of the wind chimney – because of stack effect. The indoor spaces are expected to cool down further during windy days.

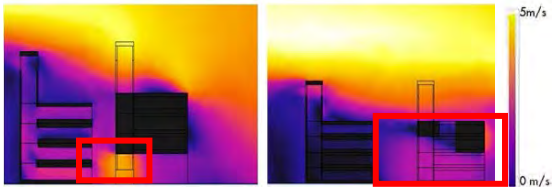

Figure 10: Wind movement through the voids to reach ventilation towers [CFD]

4.3 Solar Study

The density of these urban villages also contributes to reduction in solar radiation on the facades of the buildings due to the self-shading. The rest of the radiation can be combatted by optimising the dimension of shading devices. Otherwise, radiation (which is caused by the high angle summer sun) could lead to overheating. Therefore, different shading options are explored. Based on the wind direction and sun, the ideal orientation of the streets is facing Northwest. Hence the radiation studies are run on buildings facing NW and SE for the smaller urban canyons and SW and NE for the larger urban canyons in the existing village. South façades generally require horizontal shading and the east west facade, vertical fins. Both these strategies are explored in the studies. The study is done for hot periods of the year i.e., the summer months of April to June.

The result is as follows:

a) Higher radiation - SW façade > SE> NW > NE.

b) The buildings with height 15m have unbearably high radiation on top 2 floors, and same can be observed for the houses on the periphery of the street due to lack of self-shading. (Fig. 11). Therefore, it is best to recess the top floors for any façades facing south.

c) For North facing façades: 1.5m overhang on top floor, 1.2m on rest of the floors cuts down the radiation adequately.

d) An analysis of vertical fins was also carried out and in the taller buildings, the south facades ideally require both horizontal and vertical shade. The vertical fins here can also be substituted with reed screens at alternate intervals to make a workable adaptive strategy.

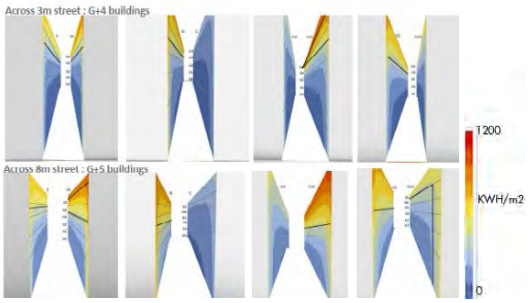

Figure 11: Solar radiation across different urban canyons and shading options [Climate Studio *[9]*]

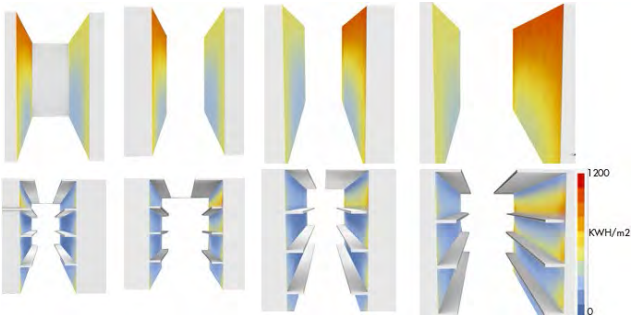

Figure 12: Solar radiation across optimised urban canyons and shading options [Climate Studio *[9]*]

e) For the shorter buildings, 1.2m overhang and 1.5m overhang on the top floor is suggested. The optimized result can be seen in the Fig. 12.

5 BUILDING DESIGN: PASSIVE STRATEGIES

Increasing indoor thermal comfort:

The main passive techniques that can be utilised based on the vernacular aspects in and around the site are as follows: i) Evaporative cooling through sprinkling water on reed and bamboo screens during hot summer hours; ii) Adding thermal buffer zones through thresholds, balconies and roofs that act as rest stops for pedestrians and alternative sleeping areas during hot summer nights respectively since temperatures reduce during winter nights (Fig. 13).

As a collective result of all interventions, a significant difference in temperature in the interior spaces can be expected in comparison to the outside street during peak summer hours.

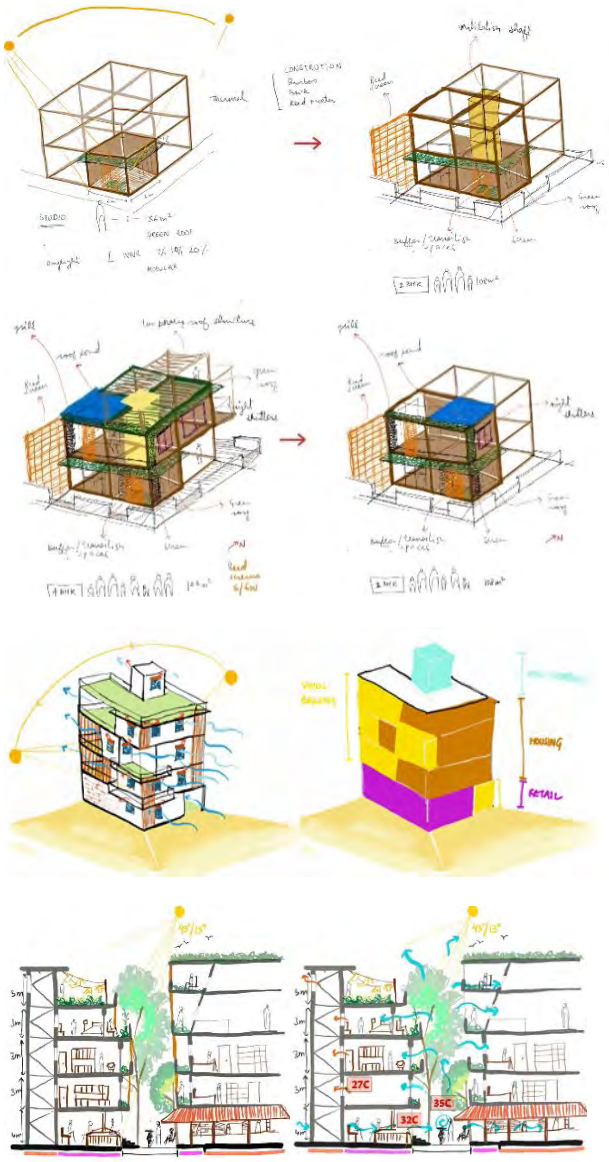

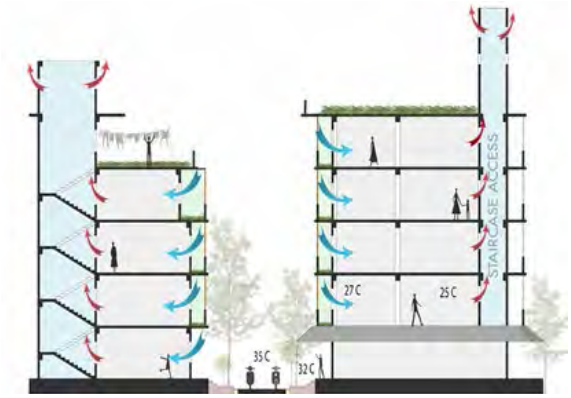

Figure 13: Concept sketches highlighting final design and passive techniques. [Sketches by Author]

6 DESIGN PROPOSAL: MASTERPLAN AND BUILDING FORM

The chosen site on which the prototype has been designed is a rectangle shaped flat plot. It has an approximate area of 4.26 acres (115 m x 150 m).

By translating the previously explored strategies into an overall urban neighbourhood design, a building mass is devised that has less solar gains. It also has, better ventilation due to the facilitation of wind which helps make outdoor spaces walkable and ensure reduced temperatures in the indoor spaces. Overall, this results in a more comfortable urban village.

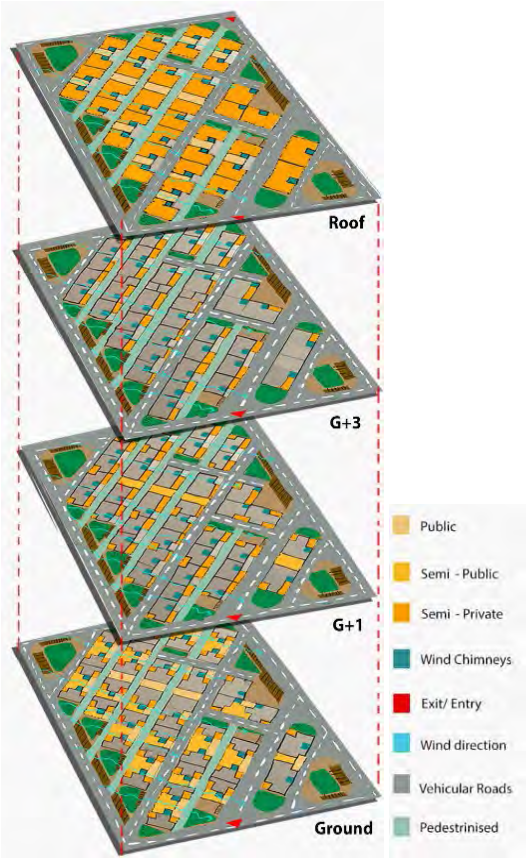

Figure 14: Exploded plans of selected site

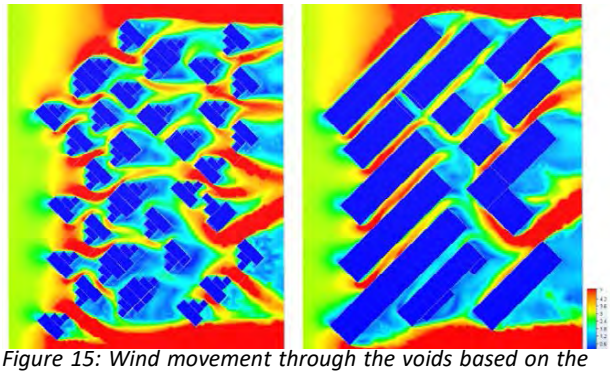

Figure 15: Wind movement through the voids based on the analysis conducted during phase 2 [5]

Key features of the design based on the analysis:

- Incorporation of an amalgamation of contemporary and vernacular elements on the outside and in the indoor spaces respectively.
- Organic public space design that can enhance social interaction as well as wind and microclimate control through thresholds, voids and calculated urban canyon ratios. The wind direction is NW which is the orientation in which the houses were placed. Due to their staggered position (ground floor – is oriented in a way to allow maximum wind to pass to the next few blocks) a typical wind speed of minimum 1.5m/s and going up to 4.5m/s is observed throughout the site (Fig 15). The wind chimneys are oriented in the direction of these voids inside the houses, decreasing temperatures by a further 2-3°C due to stack effect.
- Transient zones are created which act as climate modifiers from the street to inside.
- Through adjustable reed screens, self-shading and extended chajjas (sunshades) - the apartments are well shaded throughout summer. On the periphery and top floors of the buildings, where this shading is not adequate, the apartments are recessed, and balconies are added. This also allows for more flexible shared spaces to be created.
- Utilising density of the villages as a tool to enhance user comfort and enable future expansion. The difference in temperature on the streets inside the dense urban village is 4-5°Cs lower as compared to that on the streets outside during peak summer days. This helps establish that density can enable an increase in comfort.

Overall, an estimated 7°C drop can be obtained inside the houses if these guidelines are followed, ensuring comfort for at least 60% of the year [1].

7 CONCLUSIONS

Catering to site and environmental conditions, this study realises the creation of a prototype methodology and design that can provide user comfort for approximately 60% of the year.

Figure15: Illustration of final proposal

The result stems from solar and wind studies, fieldwork, passive design for evaporative cooling, night ventilation and buffer zones. This study showcases that even with a high population density, soaring temperatures and large diurnal swings, a comfortable living environment can be achieved. This prototype caters to future population expansion and increase in temperature due to climate change.

This research can further be used to analyse the passive design techniques of the individual houses and then develop a framework for creating context-specific, environmentally comfortable dense neighbourhoods around the world.

REFERENCES

1. Author. (2023). “Re-imagining highly dense urban villages, Delhi, India”.
2. Nolan, L.B. (2015) Slum definitions in Urban India: Implications for the measurement of Health Inequalities, Population, and development review.
3. Sharma, H. (2015). “Analysis of masterplan Delhi – 2021, w.r.t. ground reality and housing in Delhi.”
4. Betti, G., Tartarini, F., Nguyen, C, Schiavon, S. (2023). CBE Clima Tool. https://doi.org/10.1007/s12273-023-1090-5. Version:0.8.16
5. Autodesk, Autodesk CFD [Software], Available: https://www.autodesk.com/products/cfd/overview
6. Mostapha (2012), Ladybug Tools, [Software], Available: https://www.ladybug.tools/
7. Juan Vallejo and Pablo Aparicio, OptiVent (Version 2.0) [Online], Available: https://optivent.tools/.
8. GIVONI, B. “Climate Considerations in Building and Urban Design”
9. Solemma, Climate Studio [Software], Available: https://www.solemma.com/climatestudio
10. Author. (2021). “Comparing and analysing public spaces in urban villages in and around Delhi.”, ICAB.
11. Baker, N. (2019). “Heat, Cool and Climate Change. Health Wellbeing and Comfort.” Architectural Association

PLEA 2024 WROCŁAW
(Re)thinking Resilience

Going against Energy Poverty in Coastal Areas
A Sustainable Housing Approach for Climate Displaced People

AHSAN ULLAH[1], ASHIKUR RAHMAN JOARDER[1]

[1]Department of Architecture, Bangladesh University of Engineering and Technology (BUET), Dhaka, Bangladesh

ABSTRACT: In Bangladesh, a large group of people live in coastal rural areas and are below the poverty level. It is critical to fulfil their household energy needs, e.g. electricity, gas, or other utilities altogether, with their limited income. In addition, due to natural calamities, many people are losing their homes and are displaced from their original homes. Khurushkul in Cox's Bazar district, Bangladesh, is one of the examples where coastal people are displaced for a better life and provided housing facilities. However, a portion of their income is spent on bearing the energy cost, which is fuelling the poverty loop. The objective of this research is to demonstrate the result of integration of some key features of sustainable housing approach in place of existing practices to manage energy and poverty issues. Field surveys, questionnaire surveys, building simulation and optimisation, and calculation methods were used to propose effective solutions to the existing problem. The result shows that technological innovation, both in terms of building materials and systems, can be used to advance the level of energy efficiency and resiliency in homes' design and built form to put an end to an uncertain life.

KEYWORDS: Energy poverty, coastal area, rehabilitation program, energy use, climate displaced.

1. INTRODUCTION

Energy poverty has become a pressing issue in developing countries, such as Bangladesh. Fuller [1] says, *"There is no energy crisis, only a crisis of ignorance."* Therefore, the energy problem must be solved from different angles as it is connected to various aspects, such as the availability and management of resources, as well as income and quality of life of the households. Taking initiative at present can actively shape the future instead of being passively dictated by it. Affordability becomes a great concern for low-income groups. On top of that, the income versus the expenditure for energy consumption should be compared to understand the actual scenario. For example, 58 per cent of rural households are energy poor, whereas 45 per cent are income poor in Bangladesh [2].

Energy poverty happens when energy bills become a high percentage of consumers' income, which affects their capacity to cover other expenditures. If consumers are forced to reduce their household energy consumption, that is also termed poverty, which affects their physical and mental health and well-being. Under the "10% Boardman rule," energy poverty occurs when a household is "unable to get an adequate amount of energy services for 10% of disposable income" [3]. The rule recognises that not all households need to make the same effort to pay for their energy needs, which has a more severe effect on lower income households.

Considering Bangladesh's geographical location and climate, where heating costs are negligible, and cooling costs can be minimised with effective natural ventilation, energy poverty can be redefined as a household being "unable to secure sufficient energy services within 7% (excluding 30% of heating costs) of disposable income" [3]. Factors contributing to the escalating poverty of some rural families include unemployment, large family size, low and unstable income, and poor planning of natural resources. Notably, these issues stem from economic conditions, exacerbating their financial struggles. To address this situation, controlling expenditure on essential energy-related bills (e.g. electricity and water) becomes a crucial step.

2. BACKGROUND

With a population of 160 million, Bangladesh is highly vulnerable to climate change and rising sea levels, particularly in its coastal regions, where 28% of the population resides. Future projections indicate a growing number of climate refugees, with a World Bank (WB) report estimating over 19 million people in Bangladesh becoming climate refugees by 2050 [4].

Bangladesh, a low-lying, disaster-prone river delta, annually experiences the displacement of around one million people, resulting in losses of approximately 1% of its GDP due to cyclones, floods, and riverbank erosion [5]. While the government implements rehabilitation programs, the poverty issue persists due to the energy expenditure in daily life. To address energy poverty, rehabilitation housing should prioritise energy preservation, efficiency, and renewable features, such as passive design, provision for natural light and ventilation, rainwater harvesting,

and use of energy-saving equipment and photovoltaic panels. Unfortunately, these considerations are often overlooked while implementing housing projects, necessitating comprehensive attention from policy to construction levels for effective relief.

3. CASE STUDY FOR BASE CASE MODELLING

Khurushkul Ashrayan Prokolpo, in the Cox's Bazar district, Bangladesh, was selected for the investigation. Climate refugees are shifting and will shift to Khurushkul or towards other refugee projects, and they are facing or will face some difficulties. The accommodation in the project is a sharp contrast to their previous house at Kutubdia Para, Cox's Bazar. At present, they are living in an apartment in a five-story building (Figure 1) with two rooms, one kitchen space, and one toilet and bathroom. A few basic problems for the community are unemployment, drinking water, transportation, and, finally, the need to pay energy bills.

Figure 1: *Khurushkul Housing Area*

4. METHODOLOGY

The objective of the study is to bring attention to the impoverished conditions in the coastal rehabilitation zones of Bangladesh and their correlation with energy-related challenges. The issues faced by the chosen community were discerned through an exploration of background information, relevant definitions, and associated theories. A field survey was conducted to gain insights into the actual challenges faced in everyday life. The analysis of data from both the literature review and questionnaire survey was utilised to formulate practical and efficient solutions for the identified problem.

Various improvements to enhance energy efficiency in the existing layout were assessed using different software and plugins. The wind simulation tool in Autodesk Flow was utilised to determine the optimal arrangement for placing buildings on the site. ClimateStudio was employed to quantify radiation levels on each side of the buildings. Ladybug, a Grasshopper plugin, conducted a comprehensive simulation to achieve a balanced approach between maximising natural light and minimising radiation exposure across different seasons. The effective window to wall ratio (WWR) for the site was determined through multi-objective optimisation using the Galapagos plugin in conjunction with ClimateStudio. Calculation methods assessed the feasibility of the integration of renewable energy.

5. FINDINGS

5.1 Energy consumption

The purpose of the survey was to identify the imbalance between income and energy bill expenses. Forty-four families from four different income ranges (profession) were questioned about their income, expenditure and appliances to identify the reason behind their poverty. The result is in Table 1.

Table 1: Monthly Energy consumption based on four categories of family units.

Surveyed items		Family 1	Family 2	Family 3	Family 4
Occupation		Business	Day labour	Business	Business
Family member (nos.)		05	09	08	06
Monthly income ($)		91.23	182.42	255.38	145.93
Monthly expenditure ($)		91.23	164.17	228.02	145.93
Bills ($)	Electricity	2.74	6.38	10.95	7.30
	Gas	11.86	13.68	16.87	13.68
	Water	0.55	0.91	2.74	1.83
Bills to income ratio (%)		16.6	11.5	11.96	15.63

** 1 $ = 109.64 Bangladeshi Taka*

The survey results show that the percentage of energy bills the families are paying against their monthly income are 16.6%, 11.5%, 11.96% and 15.63%, respectively, which means an average of 13.9%. In the case of a tropical climate, this cost should be less than 5% [3]. That is why these climate displaced people are not getting out of the endless poverty loop. The energy consumption data from the questionnaire survey is shown in Table 2.

Table 2: Energy consumption based on equipment types and operation hours in a day.

Family	Equipment	Unit usage (W)	No of Equipment	Operation hours	Total usage (kW)	Lighting cost %
Family type 1	Fan	45	2	13	2.9	83.3
	Light	23	4	19		
	TV	-	-	-		
	Fridge	-	-	-		
	Others	-	-	-		
Family type 2	Fan	45	2	16	4.7	82.8
	Light	23	6	23		
	TV (CRT)	80	1			
	Fridge	-	-	-		
	Others	-	-	-		
Family type 3	Fan	45	2	17	6.8	43.3
	Light	23	5	20		
	TV (LED)	45	1	2		
	Fridge	120	1	24		
	Others	-	2	4		
Family type 4	Fan	45	2	15	6.9	65
	Light	23	5	22		
	TV (CRT)	80	1	2		
	Fridge	120	1	24		
	Others	-	1	2		

From the survey, it was noticed that some of the houses use energy-efficient bulbs, i.e., light-emitting diode (LED) bulbs. In most families, the highest energy consumption occurred due to lighting equipment. In some cases, the Incandescent bulbs

that consume 100W per luminary are used. For calculation, the equipment's energy consumption is made average. The fan takes 45W, the fridge 120W, TV (CRT) 80W, TV (LED) 45W, LED lights 23W, and incandescent bulbs 100W [6]. The operation hours are calculated from the survey report. The four families are selected from different floors to get the diversified data and averaged.

Figure 2 shows the comparison between the expenditure on equipment. In this process, the total cost of energy from different sources is calculated, and then the percentage of cost for a particular equipment is calculated from the total energy cost. The per unit cost is $ 0.05 [7]. One unit of energy is equivalent to one kilowatt-hour (kWh). In every case, the amount of energy consumed by fans and lights is more than that of other equipment. Some common problems identified for high energy consumption are related to building orientation, window location, window size and window use.

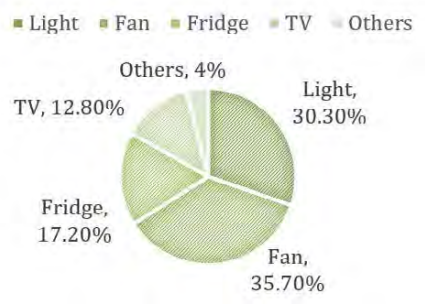

Figure 2: Comparison of expenditure from different equipment.

5.2 Building material

Traditional houses, built with vernacular architecture, local materials, and construction techniques, were more energy efficient. In contrast, the new government-provided housing (Figure 1) is costly to maintain, leading to higher energy bills.

Local materials were abundantly available, with mud plinths and bamboo-woven facades allowing air circulation. Tin was commonly used for roofs, and wood served as columns and lintels in most cases. As the project is low-cost housing, the material should be provided from locally available resources. A prototype design was created from wood, bamboo, tin, and concrete (Figure 3). The structure was made of concrete, and the other façade and fenestration were made using the local material. Thus, they can create their own house, which will reduce the cost of making it and create a sense of identity.

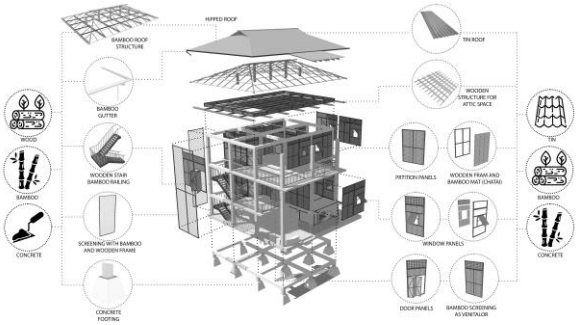

Figure 3: Rethinking fenestration with local material sources

5.3 Building placement

Existing building placement analysis was conducted (Figure 4) to address the site's vulnerability near the confluence of the River Bakkhali and the Bay of Bengal. Autodesk Flow's wind simulation tool was employed, incorporating local weather data and precise geographical coordinates from Google. The simulation results played a crucial role in identifying issues in the current layout and determining the optimal arrangement for such conditions (Figure 5). This strategic approach emphasises not only mitigating potential hazards and ensuring community safety during adverse weather but also guaranteeing sufficient wind access.

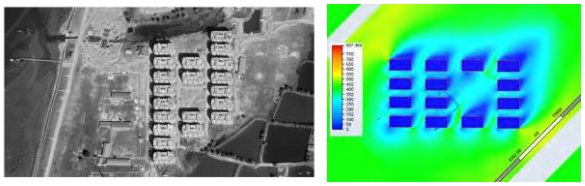

Figure 4: Existing site plan of Khurushkul Housing Area [8] (left) and restricted wind passage during a cyclone (right).

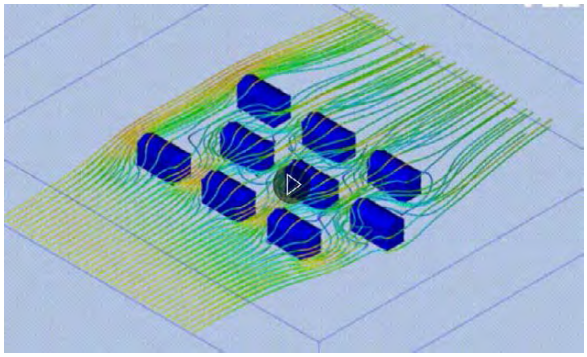

Figure 5: Autodesk Flow – optimal layout determination.

If building placements are done in an iron grid, not all buildings receive sufficient airflow, and during a cyclone, wind passage is restricted (Figure 4). The alternative pattern shown in Figure 5 allows cyclone force to pass through and provides air to most of the building masses.

5.4 Building orientation

In the case of solar radiation, the city of Cox's Bazaar gets usable radiation for solar panels almost

throughout the year and almost 1.1 KW/m^2 during the daytime (Figure 6). Leveraging local weather data, a simulation was conducted using ClimateStudio to quantify radiation levels on each side of the buildings situated at the site precisely. To optimise energy efficiency, the orientations of the buildings were adjusted to minimise heat gain from radiation to enhance overall thermal performance.

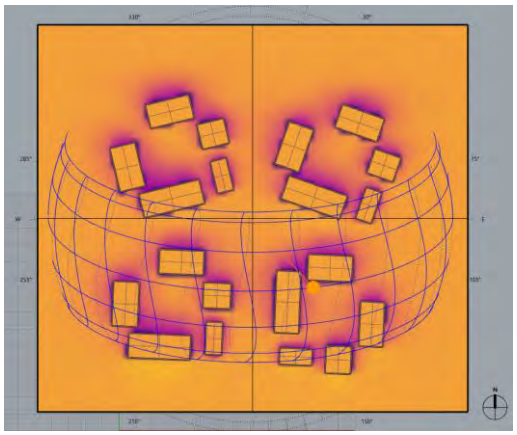

Figure 6: Radiation analysis of the buildings at the site.

Ladybug, a Grasshopper plugin, was employed to conduct an extensive simulation aimed at striking a harmonious balance between maximising natural light and minimising radiation exposure throughout different seasons. The script, which is shown in Figure 7, is designed to evaluate various orientations for the site. Out of numerous possibilities, the top 60 results were chosen, considering radiation levels and light availability.

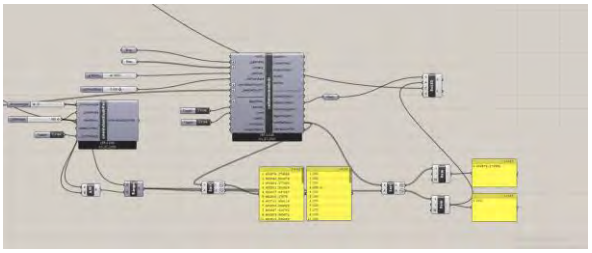

Figure 7: Grasshopper script to evaluate various orientations for the site

Energy usage for lighting and cooling loads was calculated to prioritise the orientation with the most favourable performance, emphasising sustainable design that minimises energy consumption and environmental impact. An anticlockwise rotation of 18 degrees from the existing orientation was performed effectively (Figure 8).

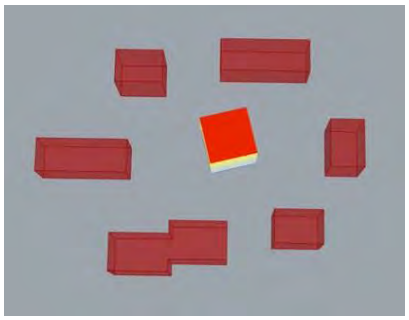

Figure 8: Radiation analysis to prioritise the orientation with the most favourable performance

5.5 Window to wall ratio (WWR)

Inadequate window placement forces constant use of artificial lighting, leading to high energy consumption. Some rooms lack windows (Figure 9).

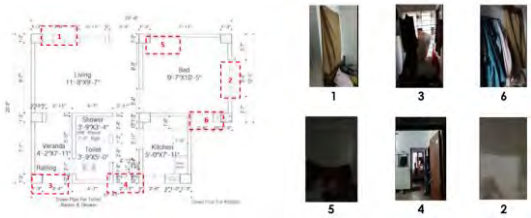

Figure 9: An example of the existing unit plan showing window locations (left) and views (right)

Bangladesh National Building Code (BNBC, 2020) Chapter 8 (Section 8.1.5) presents guidelines for the standard illumination requirement in bedrooms, which is ambient 50 lux and, at bedhead, 150 lux. The illumination measured from the field was in the living room, 3 lux; in the kitchen, 12 lux; at the toilet, 1 lux; and in the bedroom with a window, 87 lux. Introducing alternative fenestration and connecting rooms to the corridor may ensure ample light while preserving privacy and reducing energy usage.

To determine the effective WWR for the site, multi-object optimisation was done through a plugin named Galapagos through ClimateStudio. Galapagos genomes are north, south, east, and west WWR and shading depths. The fitness value is to minimise energy use intensity (EUI) with a maximum stagnant value of 50, population 20, and an initial boost of 02.

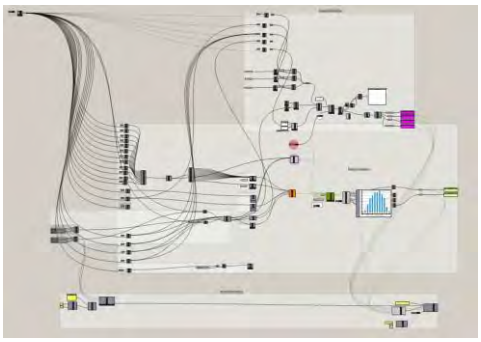

Figure 10: Grasshopper script for optimal WWR

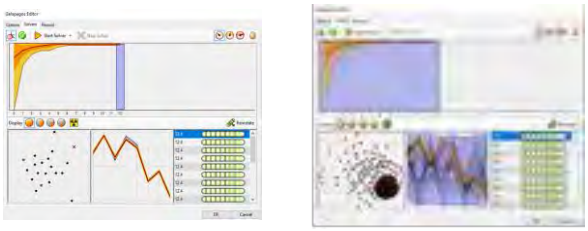

Figure 11: Optimal WWR by Galapagos

Figure 12 shows the Design Explorer analysis. The results were: WWR for North 38%, East 30%, South 25%, and West 10%. In the case of shading, the depth of north shading was 0.11m, east shading was 0.57m, south shading was 1.54m, and west shading was 0.86m.

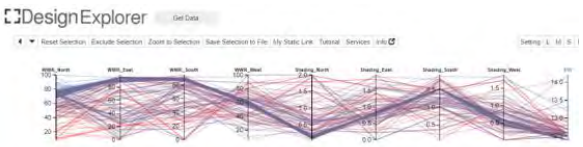

Figure 12: Design Explorer analysis for optimal WWR and shading depth

5.6 Renewable energy production feasibility

The feasibility of using wind turbines, PV panels, biogas, and rainwater is checked from the site's wind characteristics, radiation intensity, amount of required waste, and annual precipitation, respectively.

5.6.1 Wind turbine

In the case of aero leaf, the minimum velocity needed is 2m/s. Figure 12 shows that the site gets the required velocity only a few times or more, except during cyclones or disaster periods [9]. The installation cost of the aero leaf is also huge, which is not feasible for low-cost housing. Finally, the altitude cannot be achieved to get high-velocity wind as the area is prone to cyclones, and high structures are vulnerable here. So, wind turbines were not feasible in these housing areas.

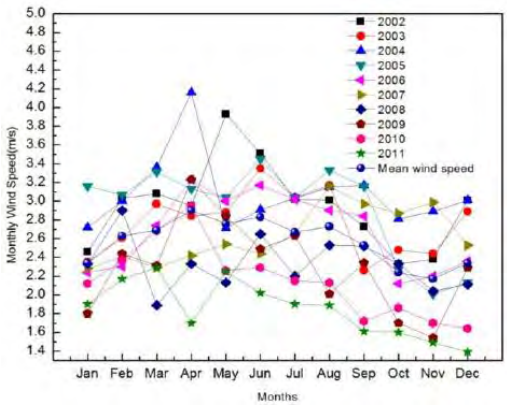

Figure 13: Average monthly mean wind speed [9]

5.6.2 PV panels

The average daily energy consumption per person is 0.775 kWh/day. The total probable roof area used for PV panels is 2725 m² (Figure 14). The size of one panel is 1.5 m^2. So, the total number of panels required was 1800. Panel energy productivity is 300 watts/h, peak sunlight hour is 6, and the unit area is 1.5m x 1m. Total daily productivity 1800×1.8=3240 units. Considering the population of 3360 (current), total energy requirements are 3360×0.775 =2604 units, and extra electricity is 3240-2604 = 636 units. Extra income 636×0.05 = $35.8 per day [10]

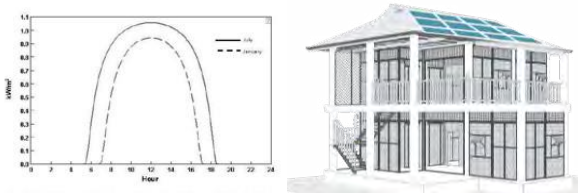

Figure 14: Highest and lowest intensity of direct radiation in W/m^2 (left) and use of PV panels on facing south roof (right)

5.6.3 Biogas plant

The amount of waste needed to generate enough biogas is not feasible in urban areas. Table 3 shows that the most efficient source of biogas is cow dung, which is easily available in Khurushkul. 1 m^3 biogas is equivalent to 0.46 kg liquid petroleum gas (LPG). Daily gas production is 135.47 kg/day [11]. So monthly production is 4064.1 kg. The price of 1 kg LPG is $0.09. So, the price of biogas from monthly production is $3627.02.

Table 3: Gas production from different organic waste

Type	Number	Waste Disposal Rate (kg/head/day)	Gas Production Rate (m^3/kg)	Amount of Gas (m^3/day)
Cow	540	11.5	0.03	186.3
Human Waste	3360	0.4	0.07	94.08
Rural Food Waste	3360	0.07	0.06	14.11
Overall				294.50

The average per capita monthly gas bill is $2 (from the survey). As the overall population is 3360, the total monthly gas bill is $6720. So, by using biogas, the gas bill can be reduced by up to 46.02%. Figure 15 presents a schematic diagram showing the collection layout of waste for biogas.

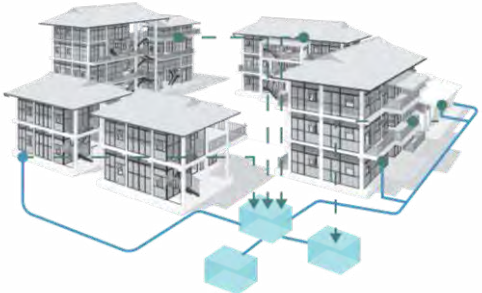

Figure 15. Schematic diagram showing the collection layout of waste for biogas

5.6.4 Rainwater tower

There is enough rain in the site from May to October, and it is highest in the monsoon season (Figure 16). However, the storage problem needs to be solved by design [Figure 3].

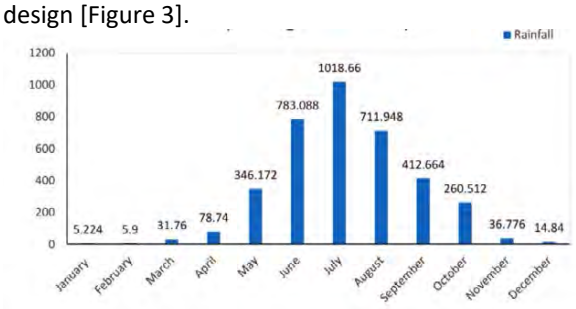

Figure 16: Average monthly rainfall (mm)

Considering the population of 3360 (current), with an average daily drinking water consumption of 3.5L per person. The total water need is 11,760 L/day. Each net shown in Figure 17 can produce an average of 400L daily, so approximately 30 nets of 40 m² size can fulfil the daily drinking water needs [12].

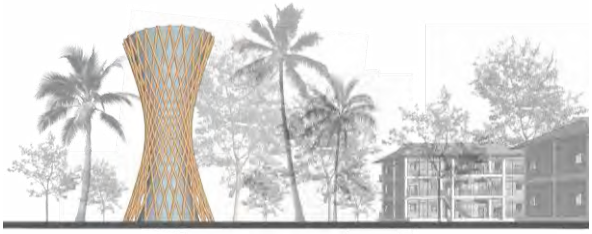

Figure 17: Placement of water tower on the dam

The total cost for 30 nets is $9545.5. The average per capita water bill is $0.007/day, resulting in a total daily water bill of $24.4. In 10 years, the total amount will be $21,993. With 30 nets, a saving of $1244.7/year can be achieved. [13]

6. CONCLUSION

The rising number of climate refugees due to global warming demands careful consideration in rehabilitation programs. Addressing energy poverty is crucial, not only for improving the quality of life in poor coastal communities but also for preventing negative impacts on the national economy by conserving valuable energy resources. While the focus of this research is on the Khurushkul project, it is essential to recognise that other factors may affect poverty in different rehabilitation initiatives. The utilisation of renewable energy is widely ignored due to the rural population's lack of awareness, even though it can be a cost-effective and primary energy source for them.

The outcome of this research shows that careful selection of building materials, placement, orientation and WWR with the incorporation of renewable energy sources, e.g. PV panels, biogas, and rainwater harvesting, holds the potential to elevate the energy efficiency and resilience of homes' design and construction. By increasing people's consciousness and promoting mass awareness, existing conditions can be improved. Comprehensive planning, regular inspections, and environmental considerations are key to making these effective solutions to the climate refugee problem without exacerbating issues.

ACKNOWLEDGMENT

This research was carried out in the Department of Architecture, BUET, Dhaka. The authors gratefully acknowledge the support and facilities provided by BUET.

REFERENCES

1. Meisen, P. (2001). A GENI Opinion-Editorial: A Crisis of Ignorance. Global Energy Network Institute. Available at: http://www.geni.org/globalenergy/library/geni/a-crisis-of-ignorance [Accessed 22 May 2022]
2. Barnes, D.F., Khandker, S.R. and Samad, H.A. (2010) Energy Access, Efficiency, and Poverty: How Many Households are Energy Poor in Bangladesh. 1 June. World Bank Policy Research Working Paper No. 5332, Available at SSRN: https://ssrn.com/abstract=1620783.
3. Boardman, B., 1991. Fuel Poverty: From Cold Homes to Affordable Warmth. London: Belhaven Press.
4. Matsui, K. and Kisinger, C. (2021). Responding to Climate Induced Displacement in Bangladesh: A Governance Perspective. Sustainability, 13(14).
5. UNFCCC (2012). Climate Displacement in Bangladesh: The Need for Urgent Housing, Land and Property (HLP) Rights Solutions. Displacement Solutions. Available at: https://cutt.ly/bwGggV1G [Accessed 17 May 2022]
6. Rahman, M., Rakib, M.F.H. and Howlader, S. (2017). Assessment of Average Household Utility Consumption in Khulna City of Bangladesh. Journal of System and Management Sciences. 7 (4), pp. 17-31.
7. Hasan, M. (2023) Bangladesh Electricity Bill Per Unit 2022. Bdelectricity. Available at: https://cutt.ly/iwDstPTF. [Accessed: 15 July 2022]
8. Bangladesh National Portal. Khurushkul Special Ashrayan Project. Available at: http://www.ashrayanpmo.gov.bd, [Accessed: 25 October 2020]
9. Islam, A., Hasan, M., Islam, M. S. and Khan A.H. (2013). Analysis of Wind Characteristics and Wind Energy Potential in Coastal Area of Bangladesh: Case Study -Cox's Bazar. ELEKTRIKA, 15(2), 1-10.
10. Koons, E. (2023). Solar Energy in Bangladesh: Current Status and Future. Energy Tracker Asia. Available at: https://energytracker .asia/solar-energy-in-bangladesh-current-status-and-future [Accessed 11 March 2024]
11. Hasan, A. S. M., Kabir, M.A., Hoq, M.T., Johansson, M.T. and Thollander, P. (2023). Drivers and barriers to the implementation of biogas technologies in Bangladesh. Biofuels. https://doi.org/10.1080/17597269.2020.1841362
12. Yusuf, F. M.S. (1999) Rainwater harvesting potential in Bangladesh. Master of Engg In Civil Engg, BUET, Dhaka.
13. Cho, R. (2011) The Fog Collectors: Harvesting Water from Thin Air. Climate, Earth and Society, Columbia Climate School. Available at: https://news.climate.columbia.edu /2011/03/07/the-fog- collectors-harvesting-water-from-thin-air/[Accessed 15 July 2023]

PLEA 2024 WROCŁAW
(Re)thinking Resilience

Linking urban warming with city life:
The case of mobility axes in São Paulo - Brazil

DANIELA WERNECK[,1] ULISSES CASTRO[,1] DENISE DUARTE[,1]

[1]University of São Paulo, São Paulo, Brazil

ABSTRACT: Cities are at the center of the discussion about the global climate emergency, since they comprise more than half of the world's population, making urgent plans for mitigation and adaptation to climate change, under the current and future urban and climate scenarios. To this end, our objective is to link some of the spectral indices obtained by remote sensing, mainly Land Surface Temperature (LST) and Enhanced Vegetation Index (EVI), with city life, focusing on the high and medium-capacity public transportation mobility axes of the city of São Paulo - Brazil, in this paper starting with the demarcated areas along the subway system, used by 2.61 million people daily. The methodological procedures encompass the Landsat 8 dataset and Google Earth Engine to retrieve the spectral indices. We observed that the subway stations located in high-rise building areas or surrounded by green areas presented lower LST. Also, the green areas are distributed in a fragmented way in this urban fabric, more concentrated farther from the city center. Thus, it is expected to support adaptation actions at the scale of urban design based on the different climatic responses of the urban space, including the effects of urban heating concerning life in the city.
KEYWORDS: Climate adaptation, Urban planning, Land surface temperature, Enhanced Vegetation Index, Sustainable mobility

1. INTRODUCTION

As urban temperatures continually increase, people will be at greater risk of adverse heat health impacts and other consequences to cities, like loss of economic activity [1, 2]. Since urban areas interact with large-scale weather systems and associated extremes, including storms, droughts, and heat waves, it is urgent to support adaptation plans to climate change, in the current and future scenarios [3, 4].

Typically, the urban area produces a thermal pattern with high and low Land Surface Temperature (LST) zones, corresponding to low and high reflectivity surfaces, green coverage, and water bodies. A high reflective impervious surfaces and green areas absorb less solar radiation bringing a lower LST. Locally, those surfaces can contribute to cool urban environments and reduce building heat gains [1, 3, 4].

In this ongoing study, we focus on the Axes of Structuring Urban Transformation of the city of São Paulo, demarcated by the municipality. The axes are areas along the public transportation systems of high and medium capacity, such as subway, train, and bus corridors.

According to the Strategic Master Plan of the Municipality of São Paulo, published in 2014, and recently revised in 2023, these areas should be organized to increase land use, based on Transit Oriented Development – TOD principles. The strategies include qualification of public spaces, incentives for mixed-uses, and fostering demographic, housing, and urban activities densification along the public transportation system [5].

In 2023, a new version of the Master Plan was released, as a mid-term review, reflecting an ambition of the Real Estate Market, and supported by the current municipal administration to intensify the built density, not necessarily perceived in practice as housing density. An increase in the area of influence around the transport axes from 400 meters to 700 meters was approved in a time of intense land-use speculation.

This discussion also fits into the importance of public spaces, where users, whether pedestrians, tourists, or outdoor workers, are exposed to different conditions in a thermal environment. Public spaces are functioning as social spaces in urban areas, where people experience city life while shopping, traveling to transit stops, or walking around [6]. On that account, changes in microclimate conditions due to urban warming have emerged as a factor of interest in determining the attractiveness of public urban spaces.

Therefore, the objective of this work is to link the spectral indices of vegetation and surface temperature obtained by remote sensing over the areas following the mobility axes of the city of São Paulo. We highlight the axes of the subway stations, used by 2.61 million people daily [7], for a first sight reading of the urban experience under a climate and green bias for subway users.

2. METHODS

The use of remote sensing has proven to be a useful method for monitoring urban surface

parameters [1, 3, 4, 8]. Those data are provided by reflective and thermal signals of the urban texture. In this work, the methods consist of the identification of the study area and the estimation of the correspondent satellite indices. The Landsat 8 data was used to retrieve the Enhanced Vegetation Index (EVI) and daytime LST. Each step is presented in the following sections.

2.1 São Paulo background

The city of São Paulo is located in the southeastern region of Brazil, at latitude 23° and longitude 46°, with altitude ranging between 720 and 850 meters above sea level, approximately 50 km far from the coast, and is crossed by the Tropic of Capricorn (Fig. 1). According to the KOPPEN classification, the city falls under the humid subtropical climate - Cfa, with a rainy period in summer and a dry period in winter [9].

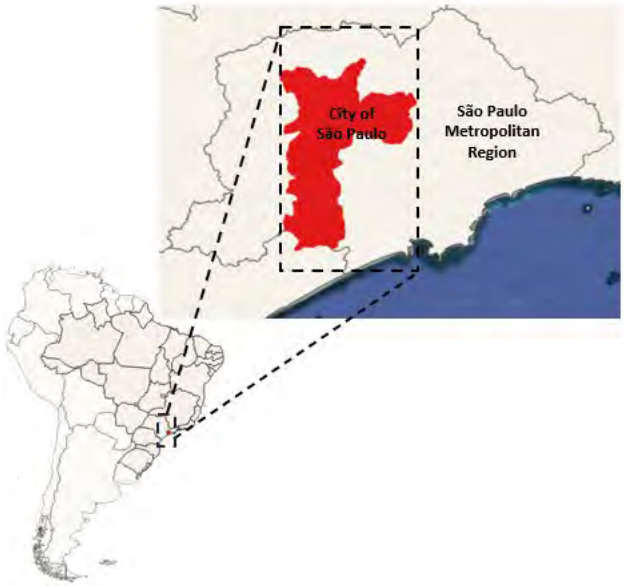

Figure 1: Location of the City of São Paulo and São Paulo Metropolitan Region.

In addition to being the most populous city in Brazil, São Paulo is also the richest city, with a GDP (Gross Domestic Product) per capita of R$60,750.09 (circa US$ 12,364.76) and around 11 million inhabitants inserted in a metropolitan area of 22 million inhabitants [10]. However, from the perspective of urban warming, climate change and extreme events, the rich city emerges as the most unequal, presenting the greatest risk to its population [2].

In São Paulo, periods of extreme heat did not reach 15 days per year during the 1960s and 1970s but reached about 40 days in 2010 and 50 days in 2014 [11]. In 2023, the city experienced extreme heat during the spring season, breaking many local high-temperature records, reaching 37,7° C in November [12]. Another interesting fact is that of the 90 days of last spring, 43 of them recorded temperatures above average, equal to or greater than 30° C [12]. São Paulo was under alert of great danger for a strong heat wave with an estimated increase of 5º C to the average temperature in the period [12].

Also, for future scenarios from 2030-2040, an increase in the average temperature, an increase in the number of hot nights, a decrease in the number of cold nights, and an increase in heatwave events are expected [11]. These forecasts of temperature increase overlap, on the local scale, to the urban heat island effects, caused by urbanization.

Concerning the urban form, previous remote sensing studies developed for the city of São Paulo and the Metropolitan Region of São Paulo [3, 13, 14] indicated a lack of urban vegetation and high values of LST (with 1 Km² spatial resolution, corresponding to a MODIS sensor pixel). The city center encompasses the highest built and population densities transformed by the intense real estate market developments [14].

Thus, the urban fabric is not only short on vegetation and public open spaces but also presents a challenge for sustainable transportation comprising active modes of transport such as walking and cycling. In addition, the presence of highly valuable historical sites in the city center reinforces the importance of improving the thermal environment for people alongside the conservation of their heritage.

2.2 Satellite indices

The second step employs the Google Earth Engine (GEE) to run two open codes to retrieve the mean LST and EVI indices for the years 2014 and 2022, corresponding to the time frame of the Master Plan´s mid-term review. The Landsat 8 imagery was masked by clouds covering up to 10% of the scene (Table 1). The observation time of each Landsat 8 scene for São Paulo was close to 13:00 UTC.

Table 1: Landsat-8 images adopted in this study.

Date	Season	Date	Season
23/01/2014	Summer	02/03/2022	Summer
08/02/2014	Summer	19/04/2022	Fall
28/03/2014	Fall	21/05/2022	Fall
02/07/2014	Winter	22/06/2022	Winter
03/08/2014	Winter	10/09/2022	Winter

Note: Path/row of all images: 220/072.

To obtain the LST, data from the visible, infrared, and thermal bands are required. The Operational Land Imager (OLI) sensor acquires data in the visible (band 4) and shortwave infrared (band 5) range, and the Thermal Infrared Sensor (TIRS) provides the thermal data (band 10).

The code developed in JavaScript was based on the Radiative Transfer Equation (RTE) method (code available at: https://github.com/LissesCastro/LST-

from-Landsat8-TOA/blob/de93b265a3b2e93155da750e9b6f9dfa9789dbb5/LST-L8-TOA-Calculation.js). The RTE method retrieves the LST from the emitted radiation by the surfaces and is widely used in climate studies [1, 3, 8, 13].

The EVI index is similar to the Normalized Difference Vegetation Index (NDVI), frequently used in urban climate research to quantify vegetation greenness. However, EVI corrects for some atmospheric conditions and canopy background noise is more sensitive in areas with dense vegetation [15].

The estimation of EVI requires the bands that correspond to the blue, red, and near-infrared intervals. The formula used in the code for EVI calculation was implemented according to Landsat Surface Reflectance-derived Enhanced Vegetation Index Specifications [15] (code available at: https://github.com/danielawerneck/EVI).

It incorporates coefficients to adjust for canopy background, atmospheric resistance, and values from the blue, red, and near infrared bands. These enhancements allow for index calculation as a ratio between the red and NIR values (Equation 1)

$$EVI = 2.5 * ((Band\ 5 - Band\ 4) / (Band\ 5 + 6 * Band\ 4 - 7.5 * Band\ 2 + 1)) \quad (1)$$

where EVI - Enhanced Vegetation Index;
Band 5 - near infrared band;
Band 4 – red band;
Band 2 – blue band.

3. RESULTS

Figures 2 and 3 present the LST results with mean images of the years 2014 and 2022, respectively. Urbanized areas presented higher daytime surface temperatures compared to less urbanized regions. The mean images are useful to inform the intra-urban distribution of LST, where it is possible to point out that the urbanized area thermal pattern is not homogeneous. This finding was observed in other studies for São Paulo with different sensors and spatial resolution for several years of observation [3, 13, 16].

The predominance of higher surface temperature along the subway axes (above 24.5°C) was observed in more densely populated areas, such as the city center, East and South axes. Those areas are occupied by compact morphologies, few or no trees, and land cover mostly paved. Lower temperatures (below <22°C) were identified in the west axis of the subway and dense vegetation areas. Comparing Figure 2 and Figure 3, an increase in LST is presented in the peripheral areas of the city, mainly the South area.

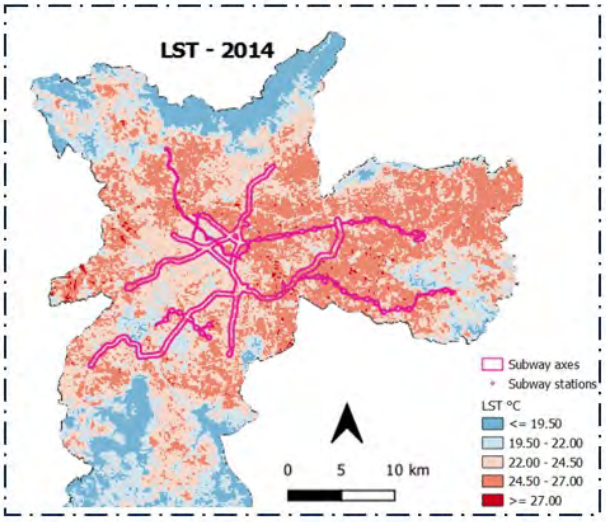

Figure 3: São Paulo - LST image of the urban area for 2022.

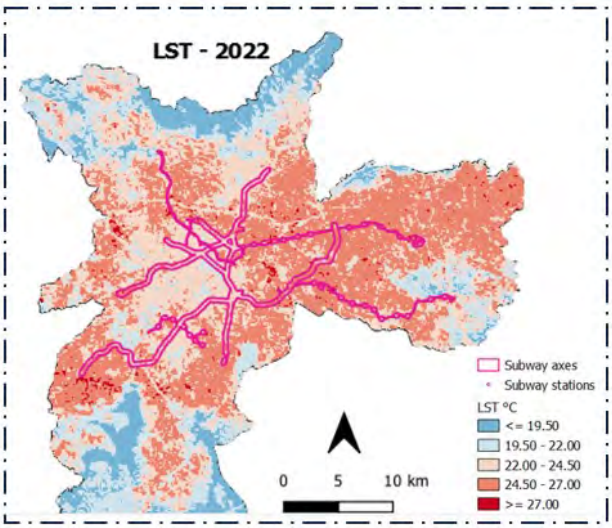

Figure 2: São Paulo - LST image of the urban area for 2014

The subway stations surrounded by green and shaded areas presented lower LST. The Trianon-MASP Station (Fig.4) shows one of the coolest performances from the pixel perspective. Another example is the open arrangement of the Clínicas Station which is surrounded by a cemetery, a Faculty of Medicine, and gardens (Fig. 5). The São Lucas Station and the Belém Station are examples of warm areas (Fig. 4).

Linking LST and urban form, compact typologies such as midrise or low-rise building types with few open spaces and sparse or absence of vegetation have a higher surface temperature (Fig. 6 and Fig. 7). During the day, the areas with compact high-rise buildings have a lower surface temperature than the low-rise building types, indicating the influence of the shade of tall buildings which can reduce the LST viewed by sensors (Fig. 8).

However, other studies conducted for São Paulo based on night-time satellite images pointed out that those areas have a higher nocturnal surface temperature that tends to intensify surface urban

heat island [3, 11, 13]. It can provide an implication for the current urban policy promoting verticalization around the stations.

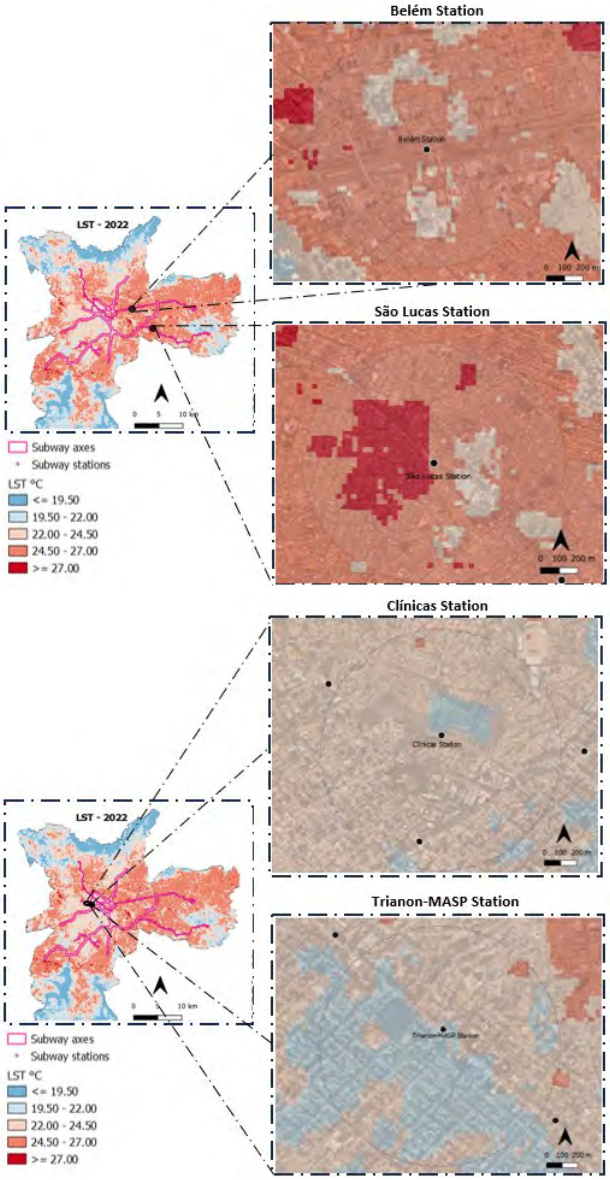

Figure 4: LST of the area of influence of 700 meters around the subway stations – examples of daytime cool and warm areas from the pixel perspective.

Figure 5: Street view image of Clínicas Station. Source: Google Street View, accessed online on the 14th of November 2023.

Figure 6: Street view image of São Lucas Station. Source: Google Street View, accessed online on the 14th of November 2023.

Figure 7: Street view image of Belém Station. Source: Google Street View, accessed online on the 14th of November 2023.

Figure 8: Street view image of Trianon Station. Source: Google Street View, accessed online on the 14th of January 2024.

Noticing other aspects such as urban connections and social interactions, the highlighted areas need a design approach to integrate climate resilience co-benefits for the pedestrian level. Many local streets in the city are not friendly to pedestrians, as on-street parking is ubiquitous, and sidewalks are often occupied by signage, and other permanent obstacles. With globally and locally rising temperatures, active modes of transport such as walking and cycling may become less favorable, particularly on hot days during spring and summer [17, 18].

Analysing the presence of vegetation, Figure 9 presents the results for the vegetation index – EVI. As expected, the urbanized area presents lower values of vegetation index EVI, both in 2014 and 2022 (Fig.4). The green areas are distributed in a fragmented way in this urban fabric, more concentrated in the wealthy neighborhoods and preserved green areas, farther from the city center.

Likewise, the LST image informs lower values in green areas (Fig.2 and Fig.3).

The cooling effect of vegetation on urban environments was pointed out in several studies [1, 2, 3, 4, 6]. Once vegetation can lower surface and air temperatures by providing shade and increasing evaporation, tree coverage is an effective way to mitigate the exposure of the urban population to heat stress.

However, the examples present several challenges regarding the available space in the streets and within blocks for urban vegetation and other types of nature based-solutions implementations (Fig. 6, 7, and Fig.8). Despite considerable differences in its heterogeneous urban fabric, the city of São Paulo shares global and local challenges to tackle inequalities for climate change adaptation due landscape fragmentation caused by rapid growth, urban sprawl, and unsustainable development.

of the thermal environment on the areas of influence of the São Paulo subway stations.

It was observed that the green areas are fragmented in the urban fabric, including in the axes of urban transformation. By establishing the climate dimension for the Strategic Master Plan, actions must also dialogue with the inequalities related to the most sensitive populations. Thus, the EVI and LST can help in the planning of strategies, especially those involving the increase of urban green and aimed at reducing temperature.

We highlight the issues that limit and require additional studies. The variability of the indices also results from the selection of satellite images, since the available sensors do not fully meet the needs of research in urban areas.

For future studies, the indices will be evaluated according to the different months of the year to identify the aspects related to seasonality. Other studies would encompass air temperature data, wind speed, and mean radiant temperature to link the public space more directly to an indicator connected to thermal comfort at microscale.

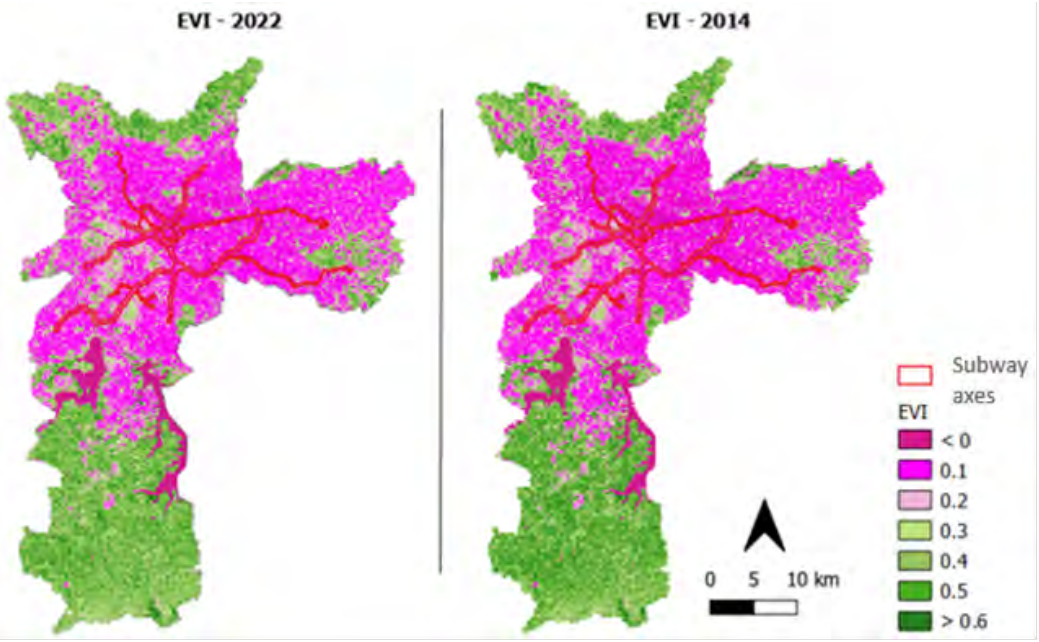

Figure 9: São Paulo - EVI image of the city.

Thus, the need for local warming information is considered crucial to localize vulnerable areas to develop an urban redesign plan, considering the particularities of each zone and the climate consequences.

Considering the ongoing climate emergency, there is a demand for urgent responses from the agents involved in the planning, design, and construction of urban spaces and buildings to adapt to the present and warmer future to the extreme events that climate change has potentiated.

4. CONCLUSION

Urban areas and their climate impacts have been the focus of studies in several fields, sharing climate data and methodology. Thus, to study the urban climate in the field of social sciences, remote sensing presents new possibilities for reading the urban fabric, going beyond the visible spectrum, and providing indicators to analyse the urban ecosystem. In this study, surface temperature and a vegetation index were used to investigate the diurnal variations

ACKNOWLEDGEMENTS

This research was supported by Coordination for the Improvement of Higher Education Personnel - CAPES (grant #88887.688961/2022-00), by the National Council for Scientific and Technological Development (CNPq) - grant #312592/2021-3 and by the São Paulo Research Foundation (FAPESP) – grants

#2022/08401-3 and #2021/11762-5.

REFERENCES

1. Iungman T, Cirach M, Marando F, Pereira Barboza E, Khomenko S, Masselot P, Quijal-Zamorano M, Mueller N, Gasparrini A, Urquiza J, Heris M, Thondoo M, Nieuwenhuijsen M. (2023). Cooling cities through urban green infrastructure: a health impact assessment of European cities. Lancet. 401(10376):577-589. doi: 10.1016/S0140-6736(22)02585-5.

2. Travassos, L. et al., (2021). Why do extreme events still kill in the São Paulo Macro Metropolis Region? Chronicle of a death foretold in the global south. *International Journal of Urban Sustainable Development*, 13:1, p. 1-16.

3. Ferreira, L. S., Duarte, D. H. S. (2022). How hot is your city design? Surface temperature portrait of São Paulo Metropolitan Region. Proceedings of 36th PLEA International Conference, Santiago, Chile: Will cities survive? V. I, p. 532-536.

4. Massaro, E., Schifanella, R., Piccardo, M. et al. (2023). Spatially-optimized urban greening for reduction of population exposure to land surface temperature extremes. Nat Commun 14, 2903. https://doi.org/10.1038/s41467-023-38596-1

5. São Paulo (cidade). Plano Diretor Estratégico do Município de São Paulo. Lei n° 16.050 de 31 de julho de 2014. Diário Oficial Cidade de São Paulo, n° 140. (2014). Available: https://gestaourbana.prefeitura.sp.gov.br/marco-regulatorio/plano-diretor/ [10 June 2023].

6. Gehl, J. (2011). Life between Buildings: Using Public Space, 6th ed.; Island Press: Washington, DC, USA.

7. São Paulo. Companhia do Metropolitano de São Paulo – Metrô. (2022). Relatório Integrado 2022. Available: https://www.metro.sp.gov.br/wp-content/uploads/2023/05/relatorio-integrado-2022.pdf

8. Sekertekin, A. (2019). Validation of Physical Radiative Transfer Equation-Based Land Surface Temperature Using Landsat 8 Satellite Imagery and SURFRAD in-situ Measurements. Journal of Atmospheric and Solar-Terrestrial Physics, V. 196. Available: https://doi.org/10.1016/j.jastp.2019.105161.

9. IAG/USP. Universidade de São Paulo. Seção Técnica de Serviços Meteorológicos – Instituto de Astronomia, Geofísica e Ciências Atmosféricas da Universidade de São Paulo. Boletim Climatológico Anual da Estação Meteorológica do IAG/USP. (2017). Available: http://www.estacao.iag.usp.br/Boletins/2017.pdf

10. IBGE. Instituto Brasileiro de Geografia e Estatística. https://www.ibge.gov.br/estatisticas/economicas/contas-nacionais/9088-produto-interno-bruto-dos-municipios.html?t=pib-por-municipio&c=3550308

11. São Paulo. Plano de Ação Climática do Município de São Paulo 2030 - 2050 (PlanClima SP). Available: https://www.prefeitura.sp.gov.br/cidade/secretarias/governo/secretaria_executiva_de_mudancas_climaticas/acesso_a_informacao/acoes_e_programas/planclimasp/?p=315991

12. INMET – Intituto Nacional de Meteorologia. (2023). Balanço da primavera 2023: São Paulo (SP) registrou chuva e temperaturas acima da media. Available: https://portal.inmet.gov.br/noticias/balan%C3%A7o-da-primavera-2023-s%C3%A3o-paulo-sp-registrou-chuva-e-temperaturas-acima-da-m%C3%A9dia

13. Ferreira, L. S., Duarte, D. H. S. (2019). Exploring the Relationship Between Urban Form, Land Surface Temperature and Vegetation Indices in a Subtropical Megacity, Urban Climate, [S. l.], v. 27, p. 105-123.

14. Muñoz, L.S.; Crevatin, L.; Luz, P.; Shinzato, P.; Duarte, D. (2022). Urban heating, lack of green and lack of space: the contribution of urban vegetation to the improvement of environmental quality in open urban spaces in the city of São Paulo, Brazil. In: 3rd International Conference on: Comfort at the Extremes: Covid, Climate Change and Ventilation, 5th – 6th September 2022, Edinburgh, Scotland. Proceedings [...] Edinburgh: Ecohouse Initative, 2022, p. 263-282.

15. Vermote, E., Justice, C., Claverie, M., & Franch, B. (2016). Preliminary analysis of the performance of the Landsat 8/OLI land surface reflectance product. Remote Sensing of Environment, 185, 46-56.

16. Lombrado, M. A. (1985). Ilha de Calor nas Metrópoles. O exemplo de São Paulo. São Paulo: Hucitec.

17. Sylliris, N.; Papagiannakis, A.; Vartholomaios, A. (2023). Improving the Climate Resilience of Urban Road Networks: A Simulation of Microclimate and Air Quality Interventions in a Typology of Streets in Thessaloniki Historic Centre. Land, 12, 414. https://doi.org/10.3390/land12020414

18. Erell, E.; Pearlmutter, D.; Boneh, D.; Kutiel, P.B. Effect of High-Albedo Materials on Pedestrian Heat Stress in Urban Street Canyons. Urban Clim. 2014, 10, 367–386.

PLEA 2024 WROCŁAW
(Re)thinking Resilience

Open space heat stress in social housing districts

The role of trees depending on urban form

CARLOS LOPEZ-ORDONEZ[1] ELENA GARCIA-NEVADO[1] HELENA COCH[1] MICHELE MORGANTI[2]

[1]Universitat Politécnica de Catalunya – Architecture, Energy and Environment, Barcelona, Spain
[2] Sapienza Università di Roma – SOS Urban Lab, DICEA, Rome, Italy

ABSTRACT: As global warming worsens, understanding the vulnerability of urban areas to extreme heat becomes crucial. Social housing districts, due to their urban form and demographic composition, are identified as high-risk areas for heat stress. This study investigates the impact of trees on mitigating outdoor heat stress in social housing districts, focusing on the Mediterranean region, particularly the metropolitan area of Barcelona. Using mean radiant temperature (MRT) as a key parameter, we use simulations to assess the influence of trees on heat stress in two districts differing in building types: linear blocks vs towers. Our results point out that, in the absence of trees, the latter is more vulnerable to heat stress, since it lacks long-term shaded spaces, such as the corridors generated by the linear blocks. In contrast, when trees are considered, tree-induced shading significantly decreases MRT and shifts its distribution pattern so that both fabrics exhibit similar performances, achieving the same percentage of open space with moderate heat stress (22%). Our findings underscore the importance of a performance-based design approach, emphasizing the need to consider both urban form and tree cover for effective heat stress mitigation in social housing districts.
KEYWORDS: Urban Heat Stress, Thermal Comfort, Mean Radiant Temperature, Urban Vegetation, Urban Overheating.

1. INTRODUCTION

Human-induced global warming is causing climate change, which is resulting in an increased frequency of extreme weather events across the globe [1]. This trend is predicted to intensify over the coming years, leading to severe impacts on people and ecosystems [2]. In this context, the mitigation of the effects of extreme heat events in urban areas has become a growing concern due to their significant negative impacts on public health and well-being [3].

Among the various factors that affect thermal comfort, the mean radiant temperature (MRT) has been identified as the most influential parameter in heat stress in outdoor environments [4]. Some of the causes of a high MRT in urban environments are the absorption and re-radiation of heat from urban components made of concrete, asphalt, and metal, among others, as well as the lack of green and blue infrastructure [5]. A highly effective strategy to reduce MRT is shading. At an urban level, this goal is achieved mainly through the urban form itself or through the presence of trees. The former usually remains stable through time, whereas the latter is sensitive to diverse factors: climate, water availability, and maintenance, among others.

Identifying the most vulnerable areas in cities becomes crucial for counteracting heat stress in open spaces and prioritising climate-sensitive urban regeneration. Social housing districts, usually adopting open urban forms, have been spotted as areas especially prone to heat stress due to limited protection against excessive solar radiation during the warm season compared to the historic city and the XIX century city textures [2]. Additionally, social housing districts are usually home to marginalized and fragile communities, making them even higher-risk areas. In these cases, using trees can be an effective solution as they can create shaded areas in open spaces, providing more comfortable spaces for occupants. In addition, trees promote a cooling effect through evapotranspiration, making the environment more pleasant.

Our study aims to assess analytically and spatially the impact of trees on heat stress in the open space of social housing districts depending on their urban form. For this purpose, we compare the role of trees in two neighbourhoods with different urban forms, using MRT as the key parameter. The results would be useful to guide performance-based design solutions.

2. CASE STUDY

Most climate projections foresee an amplified warming and drying in the Mediterranean compared to the large-scale climate behaviour [6]. As climate change progresses, heat-related problems in the Mediterranean region are expected to worsen, making this location a hotspot and an interesting case study. To conduct our research, we selected two case studies in *L'Hospitalet de Llobregat*, the second biggest city within the Barcelona metropolitan area.

L'Hospitalet has a hot summer Mediterranean climate (Csa, Köppen climate classification), with an annual mean temperature of 16.1°C and a mean relative humidity of 69%. The city presents hot summers and mild winters, with monthly temperatures ranging 9°C and 24.5°C. However, during the summer months, the average maximum temperatures can reach up to 28.5°C (Table 1), and episodes with daily maximums over 30°C are becoming recurring. Moreover, recent studies have confirmed an increment in the occurrence, severity and length of heatwaves in the region since 1970 [7].

Table 1: L'Hospitalet de Llobregat monthly data of average maximum temperature (AMT), mean temperature (MT), average minimum temperature (AmT), relative humidity (%) and daily global horizontal radiation (kWh/m²) [8]

Month	AMT	MT	AmT	RH	Gh
JAN	13.6	9.2	4.7	70	2.2
FEB	14.3	9.9	5.4	70	3.1
MAR	16.1	11.8	7.4	70	4.3
APR	18.0	13.7	9.4	69	5.7
MAY	21.1	16.9	12.8	70	6.5
JUN	24.9	20.9	16.8	68	7.1
JUL	28.0	23.9	19.8	67	7.3
AUG	28.5	24.4	20.2	68	6.1
SEP	26	21.7	17.4	70	4.8
OCT	22.1	17.8	13.5	73	3.3
NOV	17.3	13.0	8.6	71	2.3
DEC	14.3	10.0	5.7	69	1.9

Our work focuses on *Bellvitge* (1964) and *Gornal* (1972), two contiguous social housing districts (Fig. 1) considered as socio-economically vulnerable and listed in the Spanish Catalogue of Vulnerable Neighbourhoods [9]. These two settlements are examples of the implementation of modern-city experimental master plans across Europe. Like many others, *Bellvitge* and *Gornal* follow an urban form model based on zoning principles, high-rise (↑L) and low compactness (↓GSI), as described by the plot in Fig. 2.

Even though urban metrics are alike (Table 2), the selected cases differ in building types and urban layout. *Bellvitge* has mainly linear blocks that define street-like outdoor spaces, whereas *Gornal* has a higher presence of towers, generating open spaces with large squares.

Another preeminent feature of such social districts is over-dimensioned and undefined in terms of land use and ownership of public spaces. In the case of *Bellvitge* and *Gornal*, both have a high open space ratio (↑OSR), relevant green areas and similar tree density. However, the pervious/impervious area ratio is higher in the former.

Figure 1: Location of studied cases (a). Aerial view of Gornal (b) and Bellvitge (c). (Source: Google Earth).

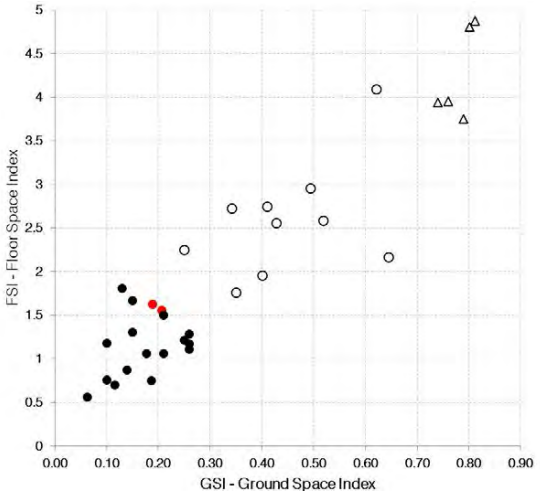

Figure 2. Urban form metrics for case studies (red dots) compared with other European social housing districts (black dots), compact urban textures (white dots) and historical urban textures (triangles).

Table 2: Urban form metrics of case studies (B: Bellvitge; G: Gornal). For definitions see [10, 11].

	A (m^2)	*C (m^2)*	*F (m^2)*	*V (m^3)*
B	40232	8282	62753	191213
G	40232	7573	65639	203267
	L	GSI	FSI	OSR
B	7.58	0.21	1.56	1.96
G	8.67	0.19	1.63	2.01
	Tree density (unit/ha)	Green space index	Pervious surface fraction	
B	67	0.076	0.192	
G	83	0.103	0.013	

3. METHOD

Urban heat stress in both neighbourhoods is analysed through simulations of MRT in UMEP (version 3.20.9), an open-source QGis plugin [12]. MRT calculations in UMEP are based on the SOLWEIG model v2022a, able to compute spatial variations of solar (K) and longwave (L) radiation fluxes from six directions in complex 3D environments, considering the sky, buildings, ground, and vegetation components separately (Fig. 3).

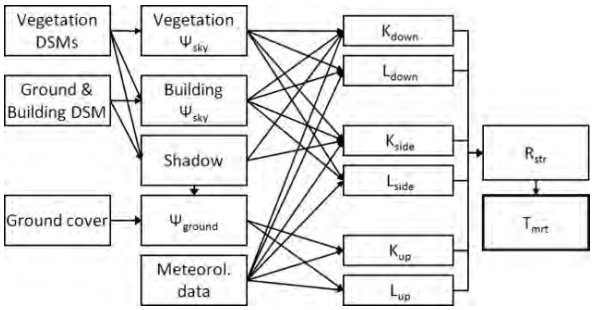

Figure 3: Overview of the SOLWEIG model [12].

UMEP requires several kinds of raster files as input to compute MRT. In this work, those corresponding to the terrain (DEM, Digital Elevation Model) were downloaded from the Barcelona Metropolitan Area (AMB) database [13]. The rasters containing information about buildings, vegetation, and surface covers were developed by the authors: DSM (Digital Surface Model) terrain elevation, building footprints, and height; CDSM and TDSM (Canopy Digital Surface Model and Trunk Digital Surface Model) tree data; Land Cover (lawn, water, buildings, paved surfaces, among others). Utilising the UMEP SVF calculator tool, we calculated the Sky View Factor (SVF) to produce the two last rasters required for MRT calculations, one without trees (using the DSM file) and another with them (using the DSM, CDSM, and TDSM files).

We run pixel-by-pixel simulations to generate high-resolution (1px= 1m²) MRT maps of the open spaces under study in two scenarios: with and without trees. Our simulations focus on a 500 x 500m study area containing a morphologically uniform urban fabric. Our analysis centres on the most critical time of the year: the central hours of the day of the warmest week of the summer in the epw file used for simulations (August 3 to 9, from 10 a.m. to 4 p.m.). The MRT is calculated for each of the indicated hours, and finally, an average is obtained.

We set the emissivity and albedo values of the model as follows: walls 0.90 and 0.5, asphalt 0.95 and 0.18, grass 0.94 and 0.16, bare soil 0.94 and 0.25. The wind speed used was 3.0 m/s, and a light transmissivity through vegetation of 3%.

Within the study area, we selected a 4-ha region of interest (black square in Fig. 4) for deeper quantitative analysis of MRT data, relying on the zonal statistics and raster layer histograms tools of QGIS. Finally, we used the UTCI index to calculate the stress category utilizing our results data.

4. RESULTS

The simulation results show that, in the absence of trees, MRTs range between similar values in both areas (Table 3). However, the range was slightly wider in *Bellvitge* (41-72°C) compared to *Gornal* (43-71°C). On average, the MRT values were also similar, but slightly higher in *Gornal* (58°C) than in *Bellvitge* (57°C).

If the effect of trees is accounted for, there is a decrease in MRT due to an expansion of the shaded area in both neighbourhoods. Trees cause the average MRTs of the studied areas to decline by 6°C in *Bellvitge* and 8°C in *Gornal* compared to the no-trees scenario. Additionally, minimum MRT values decrease by 5°C and 8°C, respectively (Table 3). In quantitative terms, the two neighbourhoods seem to behave similarly if trees are accounted for, though *Gornal* would be slightly cooler (-1°C in MRT_{max}, MRT_{min}, and MRT_{ave}).

Table 3: Summary of key MRT values of the study area.

MRT range	**Bellvitge**		**Gornal**	
	Without trees	*With trees*	*Without trees*	*With trees*
Max.	72	72	71	71
Ave.	57	51	58	50
Min.	41	36	43	35

Much more significant differences arise between the two neighbourhoods when analysing the spatial distribution of MRTs using the maps in Fig.5.

The no-trees scenario (Fig. 5a) evidences that the differences in the urban form itself lead to uneven MRT patterns between studied cases. In *Bellvitge*, the presence of linear blocks creates shaded corridors close to the north side of buildings, which remain significantly colder (MRTs around 41°C).

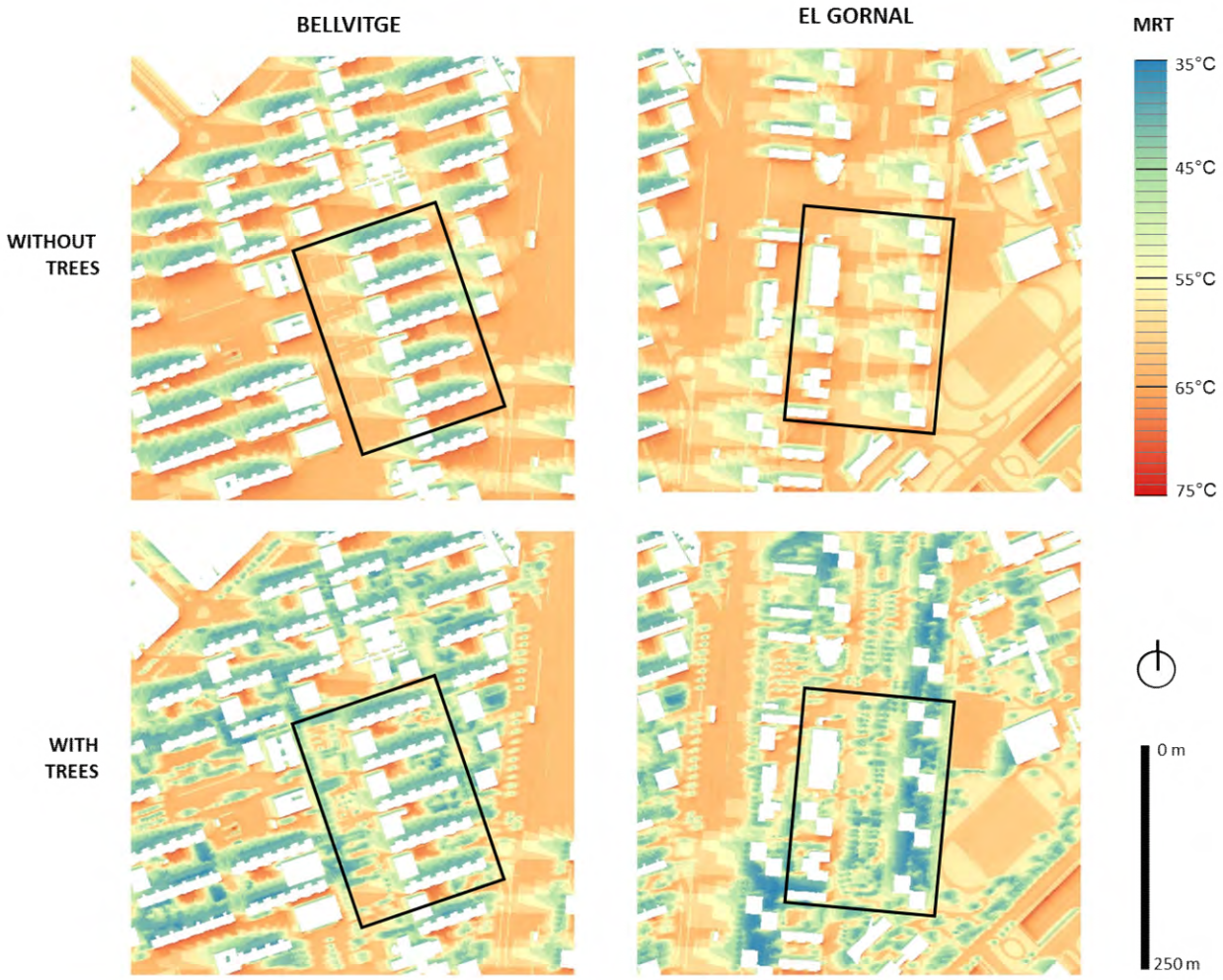

Figure 5: Maps of the average MRT values obtained for Bellvitge and Gornal districts during the simulation period (August 3 to 9, 10:00-16:00 h) with and without trees.

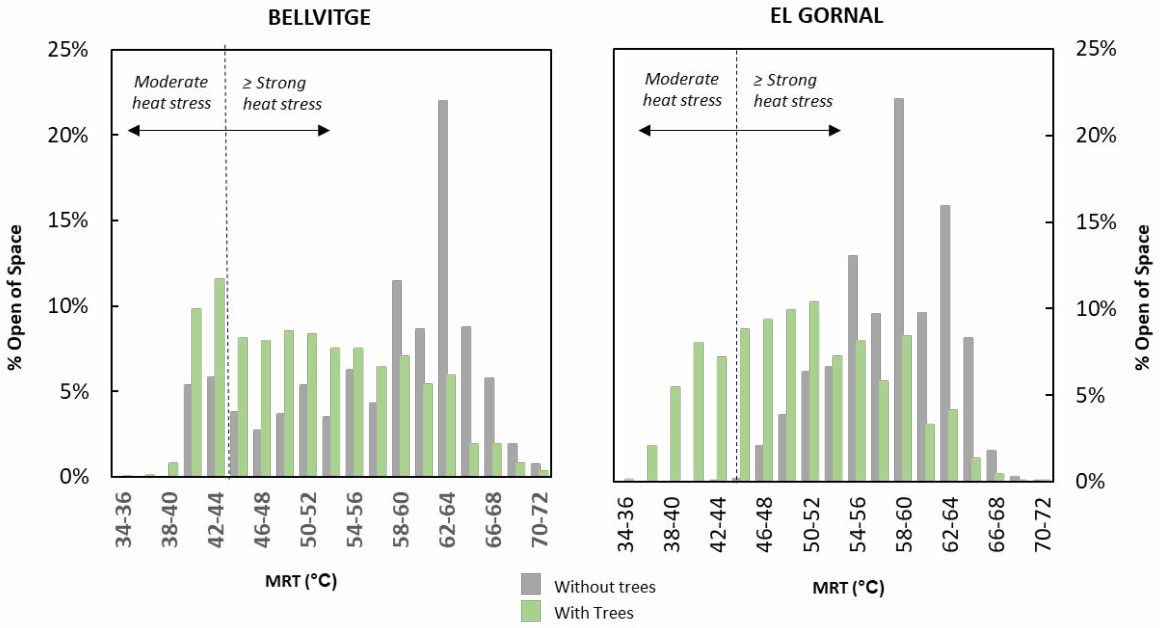

Figure 6: Percentage of open space according to its MRT for Bellvitge and Gornal districts during the simulation period (August 3 to 9, 10:00-16:00 h) with and without trees.

These areas contrast with the zones close to the south side of buildings, much warmer (MRTs up to 72°C) due to both the high levels of direct radiation and the effect of reflections from buildings. In *Gornal*, tower buildings create a less defined shadow pattern, which results in open spaces with higher and more uniform MRTs compared to *Bellvitge*. Moreover, the coolest areas are located on the northwest side of the tower blocks and present MRTs that generally do not go below 46°C.

Simulations with trees show significant changes in the MRT map distribution pattern in both neighbourhoods (Fig. 5b). The tree shadows generate cool areas along the park avenues and between buildings with MRT values that remain between 35 and 45°C. The benefits of vegetation are more noticeable in the tower-type district (*Gornal*) than in the linear-block type one (*Bellvitge*), where the urban form itself creates cool shaded zones. The inclusion of trees in urban fabric like *Gornal* allows for generating new shaded corridors between the towers, spaces scarcely sheltered by the buildings' shadow.

To better quantify the impact of trees on the radiant environment of each neighbourhood, we created histograms describing the percentage of open space by MRT, with and without trees (Fig. 6). Without trees, data show a non-symmetric bimodal distribution in *Bellvitge*, indicating the presence of two different behaviours. The smaller cluster, with mean radiant temperatures (MRTs) between 41 and 46°C, is associated with shaded areas that make up 15% of the open space in this neighbourhood. The larger cluster is associated with sunlit zones, which make up 85% of the open space and have MRTs ranging from 46 to 72°C. This cluster peaks at the 62-64°C bin, indicating that nearly a quarter of the open space area (22%) has MRTs within this range.

However, considering the effect of trees, the data distribution becomes quite right-skewed, suggesting that trees help to keep most of the open space cooler, with fewer areas having extreme MRT values.

Regarding *Gornal*, MRT data for the no-trees scenario present a symmetric unimodal distribution, with most of the values concentrated between 46 and 68°C. Results show that 70% of the open space presents MRT over 54°C, and almost a quarter (22%) has MRTs between 58-60°C (higher peak). The chart shape and its range evidence that sun-drenched open spaces are predominant and there are no long-term shaded areas. In contrast, considering the trees, the dataset shifts toward lower MRTs: 68% of the open space presents MRT below 54°C, and almost a third of them have MRT below 46°C, a value associated with long-term shaded spaces.

5. DISCUSSION

To further discuss the impact of MRT on heat stress, we examined the correlation between this parameter and the comfort levels using the Universal Thermal Climate Index (UTCI [14]), considering the average thermal conditions of simulations (T_{air}=28.7°C, RH=65%, and V_{air}=3 m/s).

Based on our findings (Fig. 7), we observed that the range of MRTs in our study areas is associated with equivalent temperatures that always fall out of the comfort range, being associated with moderate or strong heat stress levels. We also determined that a critical MRT of 45°C exists, beyond which the perception of heat stress shifts from moderate to strong (marked as a dashed line in Fig.6). Our simulations indicated that only shaded areas (by trees or buildings) had MRTs below 45°C, suggesting that direct solar radiation is the dominant variable.

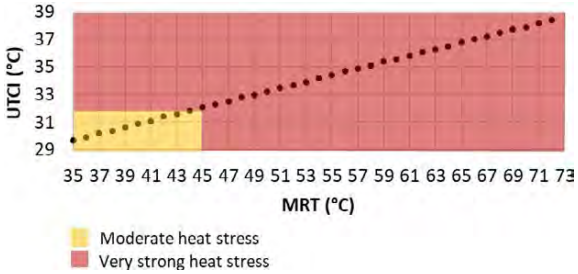

Figure 7: Correlation between MRT and UTCI values.

Using this MRT threshold, we calculated the percentage of open space under moderate and very strong heat stress levels in the two cases (Fig. 8). Results show that, without trees, most of the open space in both neighbourhoods (88.8% for *Bellvitge* vs 99.9% in *Gornal*) falls within the category of strong heat stress. In contrast, when trees are considered, there is an expansion of the shaded area in both neighbourhoods that significantly decreases in MRT and, consequently, in heat stress. Thanks to trees, both cases achieve virtually the same percentage of open spaces classified as having moderate heat stress (≈22%), showing the compensatory role of vegetation in mitigating heat stress.

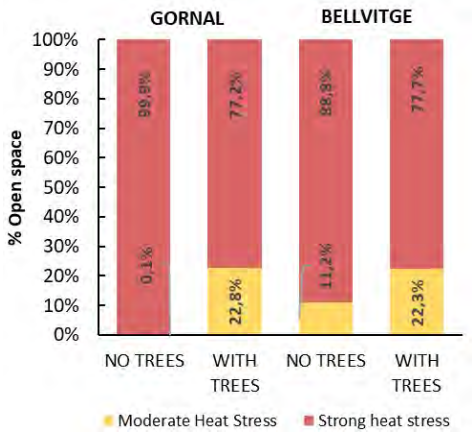

Figure 8: Comfort perception UTCI values.

Results show that trees allow for a more noticeable improvement in comfort in *Gornal* than in *Bellvitge*, taking the no-tree scenario as a baseline. Even though tree density in *Gornal* is higher than in *Bellvitge* (83 vs 67 trees/ha), this difference does not explain the relatively small benefits obtained from trees in *Bellvitge* (+11,1%) compared to *Gornal* (+22,7%).

This divergence can be associated with the smaller size of trees in *Bellvitge* and the location of some of them in areas already shaded by buildings. These findings highlight the importance of shadow-related design factors to maximize the cooling potential of vegetation. In this regard, it is worth noting that our simulations consider tree height and canopy height and diameter for the trees existing in the studied area individually. However, due to software limitations, we assumed the light transmissivity to remain constant among species.

6. CONCLUSION

Introducing a performance-based design approach to counteract open space heat stress is of paramount importance in social housing districts, where the urban form has a limited effect in obstructing solar radiation in the hot season. Trees are powerful tools for this purpose.

Results in this work demonstrated the effectiveness of trees in improving outdoor thermal comfort and a workflow for analysing it from a double perspective. On the one hand, MRT maps allow for a qualitative discussion on how urban form and the use of trees affects the spatial distribution of this parameter. On the other, numerical charts support a deeper analysis of the simulation results from a quantitative perspective.

Our study indicates that low-density/high-rise urban forms with tower-block morphologies are more dependent on the availability of an appropriate tree cover to achieve more comfortable outdoor spaces than neighbourhoods made up of linear blocks. Nevertheless, thanks to the complementary role of trees, both neighbourhoods can achieve similar outdoor comfort levels, even though the starting conditions in the no-tree scenario were different among them.

As shown in our work, achieving full thermal comfort through the use of trees is not always possible. However, creating spaces with milder conditions, which act as urban havens, should be a priority for urban designers in the context of extreme heat periods.

The findings in this paper show the interest in conducting a two-phase assessment in the study of tree-related cooling effectiveness. In the early stage of design, the analysis of the no-trees scenario helps to investigate how urban form itself affects the heat stress of open spaces and detect hotspots where tree use can be most beneficial. This also allows for establishing a baseline to understand and quantify the additional benefits provided by trees depending on the pre-existing urban form, investigated in a second phase.

ACKNOWLEDGEMENTS

Funded by the *European Union – NetxGenerationEU*, *Ministry of Universities and Recovery, Transformation and Resilience Plan*, through a call from *Universitat Politècnica de Catalunya* (Grant Ref. **2021UPC-MS-67534**). This research is also part of the projects: "QFRACLIM – Climate-proof neighbourhoods" - **RP12117A88299 F81**, and the project **PID2020-116036RB-I100**, funded by the *Spanish Ministry of Science and Innovation*.

REFERENCES

1. IPCC, (2023). Climate Change 2023: Synthesis Report. Contribution of Working Groups I, II and III to the Sixth Assessment Report of the Intergovernmental Panel on Climate Change.
2. Maragno, D. et al., (2020). Mapping Heat Stress Vulnerability in Risk Assessment at the Neighborhood Scale to Drive Urban Adaptation Planning. Sustainability, 12:1056.
3. Hatvani-Kovacs, G. et al., (2018). Policy recommendations to increase urban heat stress resilience. Urban Climate, 25: p. 51-63.
4. Kántor, N. and J. Unger, (2011). The most problematic variable in the course of human-biometeorological comfort assessment - The mean radiant temperature. Central European Journal of Geosciences, 3: p. 90-110.
5. Koch, K. et al., (2020). Urban heat stress mitigation potential of green walls: A review. Urban Forestry & Urban Greening, 55:126843.
614. Cos, J. et al. (2022). The Mediterranean climate change hotspot in the CMIP5 and CMIP6 projections. Earth System Dynamics, 13: p.321–340.
7. Serra, C. et al. (2023) Summer Heatwaves Trends and Hotspots in the Barcelona Metropolitan Region (1914-2020), Theoretical and Applied Climatology (preprint).
8. AEMET, (2023). Valores climatológicos normales. Aeropuerto Barcelona. Available: https://www.aemet.es/
9. Ministerio de Transportes, Movilidad y Agenda Urbana, (2021). Atlas de la Vulnerabilidad Urbana. Available: https://atlasvulnerabilidadurbana.mitma.es/
10. Morganti M. et al., (2017). Urban morphology indicators for solar energy analysis. Energy Procedia, 134: p. 807-814.
11. Morganti M. et al., (2023). Heat vulnerability digital mapping at neighbourhood level in the compact city. J. Phys.: Conf. Ser. 2600 082032
12. Lindberg, F. et al., (2019). Urban Multi-scale Environmental Predictor (UMEP) Manual. Available: https://umep-docs.readthedocs.io/en/latest/
13. Àrea Metropolitana de Barcelona, (2023). Geoportal de Cartografía. Available: http://geoportalcartografia.amb.cat/
14. Universal Thermal Climate Index (UTCI): Documents. Available: http://www.utci.org/utci_doku.php

PLEA 2024 WROCŁAW
(Re)thinking Resilience

Urban parks and microclimatic conditions:
Comparative evaluation of geospatial indicators of São Paulo, Brazil.

IARA NOGUEIRA LIGUORI[1], LUCAS RAFAEL FERREIRA[1], NARA GABRIELA DE MESQUITA PEIXOTO[1], LEONARDO MARQUES MONTEIRO[1].

[1]University of São Paulo, Rua do Lago, Butantã, São Paulo / SP, Brazil.

ABSTRACT: Urban parks represent important solutions for resilience against the threats from climate change and urban expansion. In this context, the main goal is to compare the urban thermal situations of a 30-year historical series. The method used is remote sensing analysis, using images from Landsat satellites and data of Normalized Difference Built-Up Index (NDBI), Normalized Difference Vegetation Index (NDVI) and Land Surface Temperature (LST). The object of study is parks and immediate surroundings located in São Paulo - SP, Brazil. Statistical comparisons and map analysis of variations in NDVI, NDBI, and LST values over the years pointed out an attenuation of up to 9ºC in the urban parks compared to their immediate surroundings.
KEYWORDS: Urban Parks, Remote Sensing, Landsat, Surface Temperature, Normalized Difference Vegetation Index (NDVI).

1. INTRODUCTION

The urban growth, boosted in the 20th century, resulted in the formation of large urban centers. The World Cities Report 2022, published by UN-Habitat, points out that 68% of the population in 2050 will live in urban areas [1]. In addition, the Sixth Assessment Report (AR6) of the Intergovernmental Panel on Climate Change (IPCC) predicts that climate changes will result in a transformation in the climate regime, such as an increase in extreme events and temperatures [2].

The high population concentration combined with climate changes can amplify the socio-environmental vulnerabilities, resulting in fragmentation of landscapes and environmental degradation [3].

In this context, urban green spaces represent important solutions for resilience against the threats from climate change and urban expansion [4]. The presence of vegetation and bodies of water reduces the air and surface temperatures and improves the air humidity [5].

The development and maintenance of urban parks improve the population's quality of life, while protecting the biodiversity of local fauna and flora [6].

Based on the scenario presented above, the object of study is parks and immediate surroundings located in São Paulo - SP, Brazil.

The main objective is to compare urban thermal situations over a 30-year historical series. The method used is remote sensing analysis, using images from Landsat satellites and data of vegetation quality, density of built-up areas and surface temperatures.

2. METHOD

The remote sensing data have been obtained from the Landsat 8-9 OLI/TIRS and Landsat 4-5 TM satellites. The images are provided free of charge in the United States Geological Survey (USGS) site [8].

The initial selection criterion is usage of cloudless atmosphere images, obtained between 1992 to 2022 years, a time frame of 30 years.

After the initial analysis, it was observed that most of cloudless atmosphere images were from winter season (June to September in the southern hemisphere). The analyzed area, during winter season, has a dry climate and lower rainfall rates. Therefore, the second selection criterion was limiting the image selection in the winter season. It provided a consistent time basis and minimized seasonal variability, leading to a better comparison and interpretation of the results.

The final selection criterion was the exclusion of images with Normalized Difference Vegetation Index (NDVI) and Normalized Difference Built-Up Index (NDBI) values higher than 1 or lower than -1. Such interference, potentially caused by the presence of bodies of water or metallic surfaces, could compromise the accuracy of the results.

After applying the selection criteria, 20 images were obtained and processed in QGIS software v.3.28.4 for geospatial analysis (Table 1).

The urban parks were delimited and a buffer of 500 meters was applied around their boundaries. After this delimitation, the NDVI, NDBI and Land Surface Temperature (LST) values were analyzed.

Table 1: Selected days based on the established criteria.

Year	Date
1992	07/05 | 07/21 | 09/23
1993	06/22
1999	08/26 | 09/27
2001	06/12 | 08/15
2003	08/05 | 08/21 | 09/06
2004	09/08
2006	09/14
2007	08/16
2008	07/17 | 08/18
2009	08/05
2010	08/24
2017	08/27
2022	09/02

The NDVI corresponds to changes in vegetation cover, and can be used to measure the urbanization process. It is calculated using the near-infrared band and the red band [9]. The Band 5 Near-Infrared (0.85 - 0.88 µm) and Band 4 Red (0.64 - 0.67 µm) of Landsat 8-9 (Equation 1) and the Band 4 Near-Infrared (0.76 - 0.90 µm) and Band 3 Visible Red (0.63 - 0.69 µm) of Landsat 4-5 TM have been used (Equation 2) [10, 11].

$$NDVI = (Band\ 5 - Band\ 4) / (Band\ 5 + Band\ 4) \quad (1)$$

$$NDVI = (Band\ 4 - Band\ 3) / (Band\ 4 + Band\ 3) \quad (2)$$

The NDBI is necessary to understand the urbanization process and it corresponds to the density of the built-up area in the urban site. It is calculated using the shortwave infrared (SWIR) and near-infrared band (NIR) [9], obtained from Band 6 SWIR 1 (1.57 - 1.65 µm) and Band 5 Near-Infrared (0.85 - 0.88 µm) of Landsat 8-9 (Equation 3), and from Band 5 Near-Infrared (1.55 - 1.75 µm) and Band 4 Near-Infrared (0.76 - 0.90 µm) of Landsat 4-5 TM (Equation 4) [10, 11].

$$NDBI = (Band\ 6 - Band\ 5) / (Band\ 6 + Band\ 5) \quad (3)$$

$$NDBI = (Band\ 5 - Band\ 4) / (Band\ 5 + Band\ 4) \quad (4)$$

The LST refers to the radiative changes in surfaces and allows measuring differences in surface temperatures in the analyzed areas [12]. The result is obtained from the analysis of the thermal infrared band. The Band 10 TIRS 1 (10.6 - 11.19 µm) of Landsat 8-9 and Band 6 Thermal (10.40 - 12.50 µm) of Landsat 4-5 [11] have been used.

3. OBJECT OF STUDY

The object of study is parks and immediate surroundings located in São Paulo - SP, Brazil (Fig. 1). The city coordinates are latitude 23.5º S and longitude 46.6º W, approximately 750 meters above sea level. The climate is humid subtropical, classified as Cwa in the Köppen-Geiger system, with hot and rainy summers and moderately cold and dry winters.

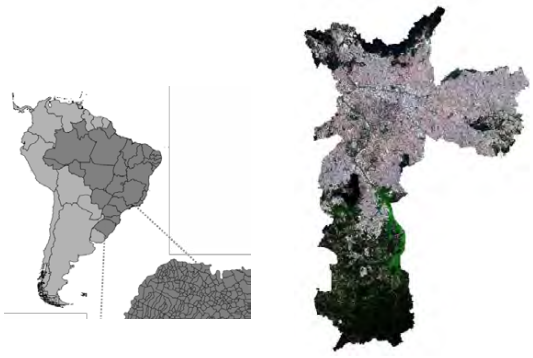

Figure 1: Location of São Paulo city. Data collected from Landsat 8, on 09/12/2017, composition performed in Qgis software v.3.28.4.

The selected parks are:

- Carmo Olavo Egidio Setubal Park: The Carmo Olavo Egidio Setubal Park was inaugurated in 1976, and later Carmo Farm was included in the park perimeter. The total area is 68,527.1 km² and it is located in the eastern region of São Paulo [7] (Fig. 2).

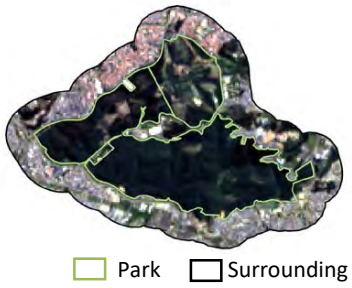

Figure 2: Carmo Olavo Egidio Setubal Park. Data collected from Landsat 8, on 09/12/2017, composition performed in Qgis software v.3.28.4.

- Anhanguera Park: Inaugurated in 1979 the park's total area is 18,116.2 km². It is located in the northern region of the city and it is considered as a wildlife refuge area [7] (Fig. 3).

Figure 3: Anhanguera Park. Data collected from Landsat 8, on 09/12/2017, composition performed in Qgis software v.3.28.4.

- Ibirapuera Park: The park has an area of 12,418.5 km² and it was founded in 1954. It is located in the central region of the city and it is an important tourist attraction of São Paulo city [7] (Fig. 4).

Figure 4: Ibirapuera Park. Data collected from Landsat 8, on 09/12/2017, composition performed in Qgis software v.3.28.4.

4. RESULTS

Each park was individually assessed and the data was used to create graphs of the NDVI, NDBI and LST values. The graphs provide a comprehensive view of changes in vegetation, density of built-up areas and surface temperature over time.

In order to demonstrate the evolution in the last three decades, the maps on 07/05/1992 and 09/02/2022 were created, corresponding to the first and last images analyzed.

4.1. Carmo Olavo Egidio Setubal Park

Carmo Olavo Egidio Setubal Park stands out as the largest of the three parks analyzed. The NDVI analysis revealed similar values throughout the period studied, as shown in Graph 1. However, a more detailed observation using satellite images reveals a progression in the quality of the vegetation at the same period.

The maps indicate an average difference of 0.25 in NDVI values between the park and its surroundings (Figs. 4 and 5). The park area has high NDVI values, indicating a denser and healthier vegetation cover compared to the surrounding areas.

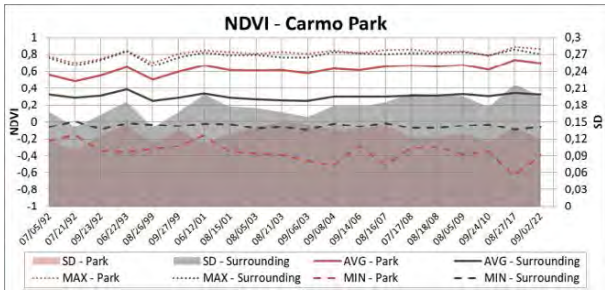

Graph 1: NDVI statistical values of Carmo Olavo Egidio Setubal Park.

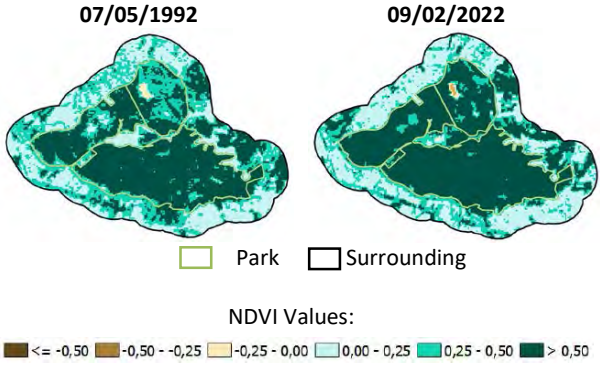

Figures 5 and 6: NDVI maps corresponding to Carmo Olavo Egidio Setubal Park in 1992 and 2022, respectively. Composition performed in Qgis software v.3.28.4.

The NDBI values have a similar indication of the NDVI values (Graph 2). The satellite images demonstrate an increase in building density in the surrounding area over the years, whereas, for the park area, there is a decrease in NDBI values (Figs. 7 and 8).

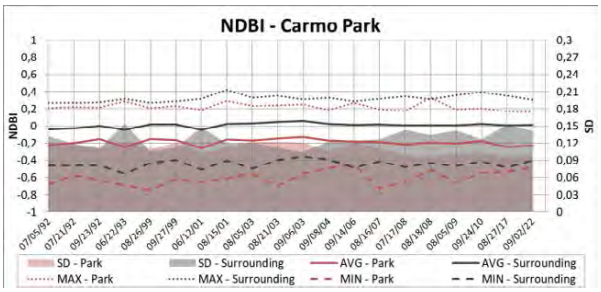

Graph 2: NDBI statistical values of Carmo Olavo Egidio Setubal Park.

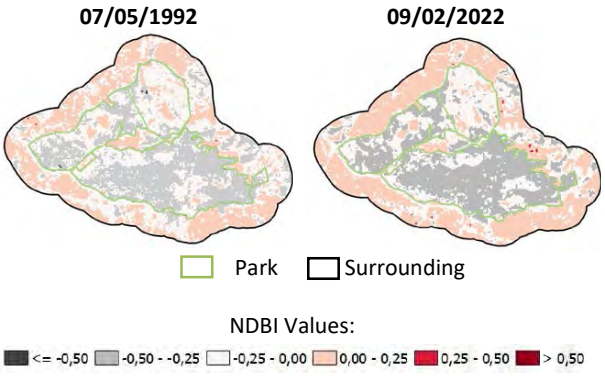

Figures 7 and 8: NDBI maps corresponding to Carmo Olavo Egidio Setubal Park in 1992 and 2022, respectively. Composition performed in Qgis software v.3.28.4.

The LST values have significant variation. The trend line of the average indicates a slight increase in temperature over the analyzed period (Graph 3).

In addition, the temperature difference between Carmo Olavo Egidio Setubal Park and its surroundings is up to 9ºC (Figs. 9 and 10).

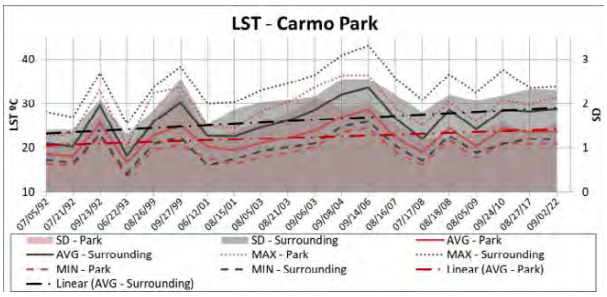

Graph 3: LST statistical values of Carmo Olavo Egidio Setubal Park.

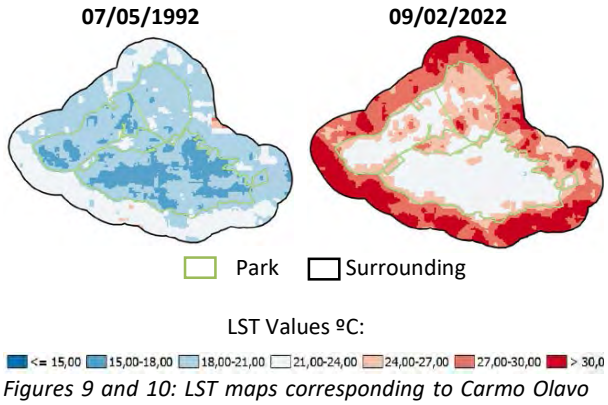

Figures 9 and 10: LST maps corresponding to Carmo Olavo Egidio Setubal Park in 1992 and 2022, respectively. Composition performed in Qgis software v.3.28.4.

4.2. Anhanguera Park

Anhanguera Park is the most isolated from the urban center of the three analyzed parks. The NDVI analysis shows both park and its surroundings have high vegetation quality and density values (Figs. 11 and 12 and Graph 4).

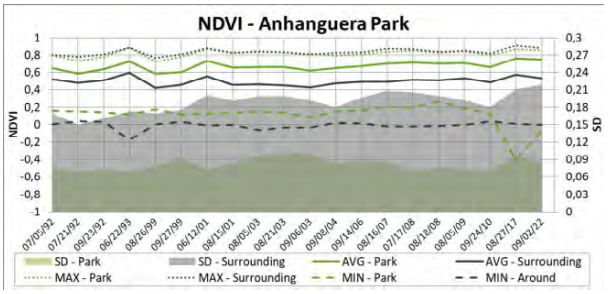

Graph 4: NDVI statistical values for Anhanguera Park.

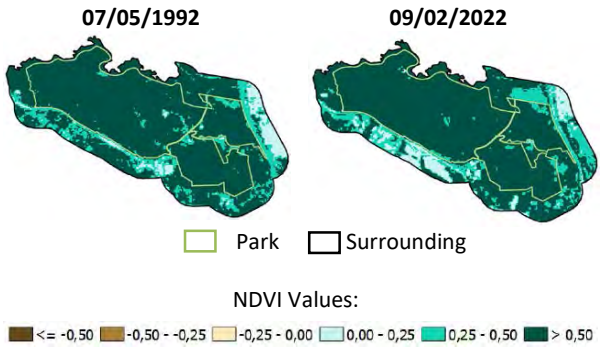

Figures 11 and 12: NDVI maps corresponding to Anhanguera Park in 1992 and 2022, respectively.

The NDBI values have a similar indication of the NDVI values, with slight variation over the years (Graph 5).

However, the analysis of the maps of Figures 13 and 14, indicates an increase in the NDBI values at the far east park area.

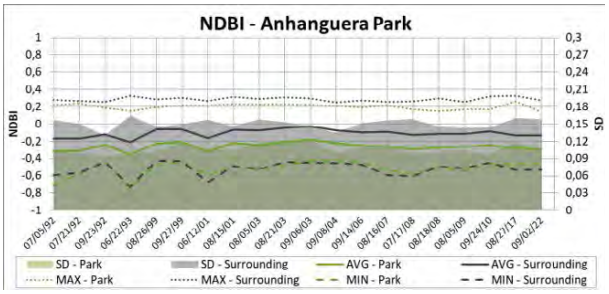

Graph 5: NDBI statistical values of Anhanguera Park.

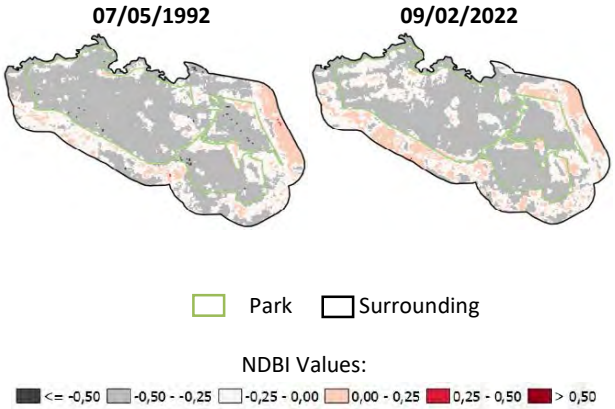

Figures 13 and 14: NDBI maps corresponding to Anhanguera Park in 1992 and 2022, respectively. Composition performed in Qgis software v.3.28.4.

The LST values reflect a clear difference in temperature between the park and its surroundings (Figs. 15 and 16), with a difference up to 9ºC, similar to the results of Carmo Olavo Egidio Setubal Park.

Graph 6 reveals a tendency to temperature increase in the park and its surroundings.

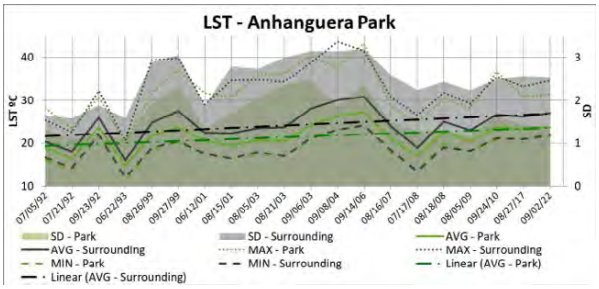

Graph 6: LST statistical values of Anhanguera Park.

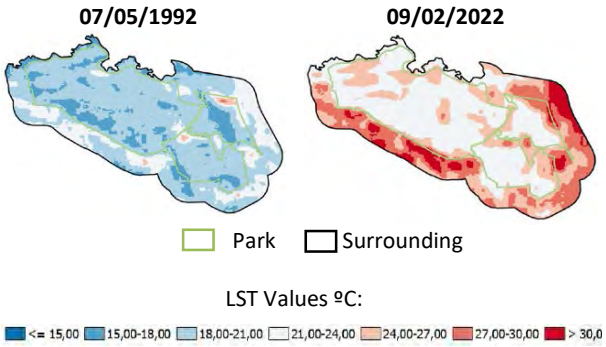

Figures 15 and 16: LST maps corresponding to Anhanguera Park in 1992 and 2022, respectively. Composition performed in Qgis software v.3.28.4.

4.3. Ibirapuera Park

Ibirapuera Park is the smallest of the three parks and the one with the most tourist attractions. Therefore, it is possible to observe a similarity in the built-up density of the park area and its surroundings.

Analyzing the statistical data (Graph 7), there is an increasing tendency of NDVI values of both the park and its surroundings. The increase in vegetation density is also shown in the 1992 and 2022 maps (Figs. 17 and 18).

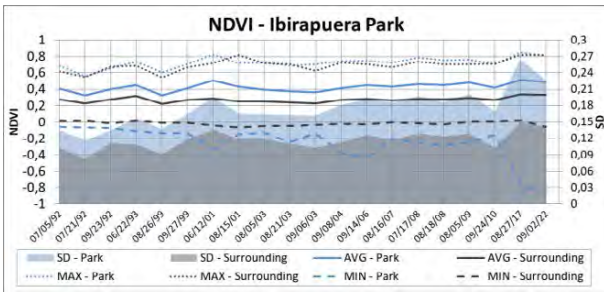

Graph 7: NDVI statistical values of Ibirapuera Park.

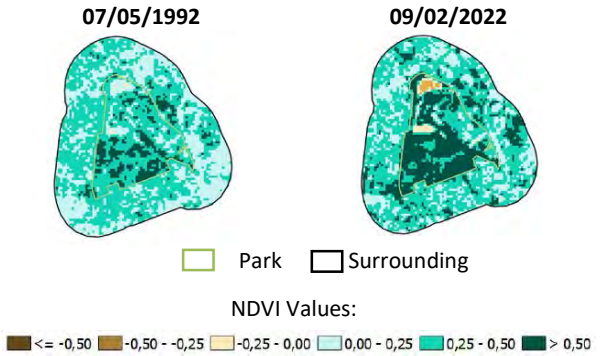

Figures 17 and 18: NDVI maps corresponding to Ibirapuera Park in 1992 and 2022, respectively.

The similarity between the park and its surroundings is corroborated by the similarity of maximum and average NDBI values (Figs. 19 and 20). However, there are divergences in the minimum NDBI values, indicating discrepancies in specific areas (Graph 8).

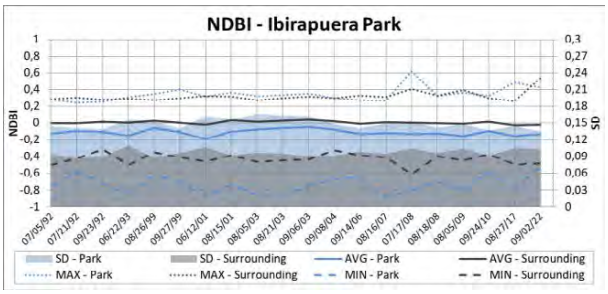

Graph 8: NDBI statistical values for Ibirapuera Park.

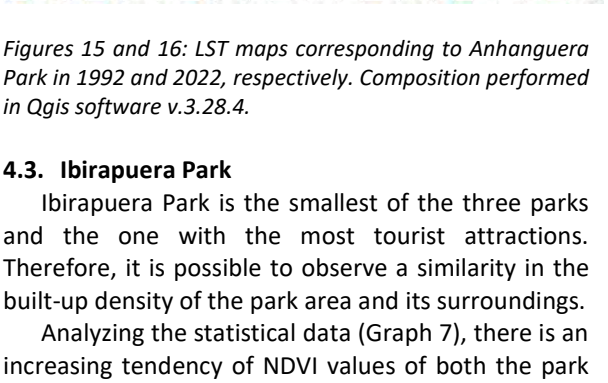

Figures 19 and 20: NDBI maps corresponding to Ibirapuera Park in 1992 and 2022, respectively. Composition performed in Qgis software v.3.28.4.

Ibirapuera Park has the lowest surface temperature attenuation and temperature amplitudes up to 6ºC (Figs 21 and 22). The attenuation of surface temperature is up to 6ºC and the LST average values indicate an upward trend line for both areas (Graph 9).

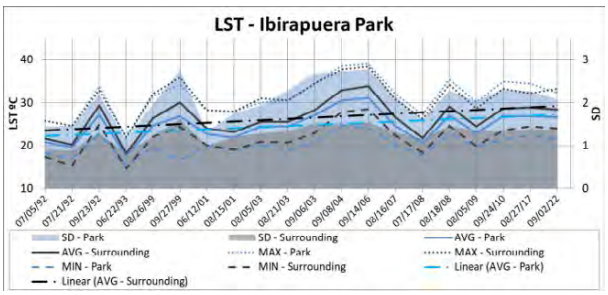

Graph 9: LST statistical values of Ibirapuera Park.

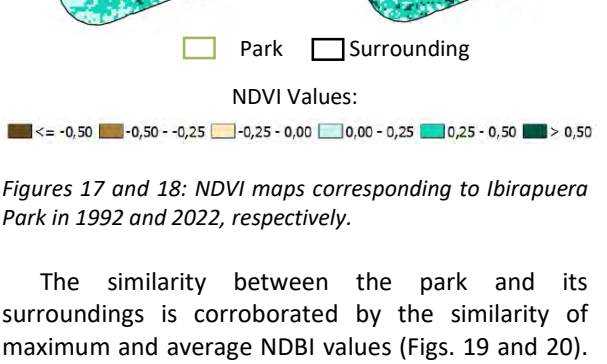

Figures 21 and 22: LST maps corresponding to Ibirapuera Park in 1992 and 2022, respectively.

5. CONCLUSION

In order to compare the urban situation of parks and their immediate surroundings, a 30-year historical series of Landsat satellite images has been evaluated. The values of Normalized Difference Vegetation Index (NDVI), Normalized Difference Built-Up Index (NDBI) and Land Surface Temperature (LST) were computed and analyzed for both areas.

The overall analysis of the objects of the study demonstrated the importance of parks in increasing the environmental quality of urban sites. In addition, it was also possible to identify a significant reduction in surface temperature of the park areas compared to their immediate surroundings.

The analysis of Carmo Olavo Egidio Setubal Park revealed an increase in building density of the surrounding area over the years, including a downward trend in the NDBI values for the park and an increase in the NDBI for the surrounding area. The temperature difference between the park and its surroundings is up to 9ºC.

The Anhanguera Park has the highest NDVI values, indicating a high density and quality of the vegetation both in the park and in its surroundings. The LST values were similar to Carmo Olavo Egidio Setubal Park, and the temperature difference between the areas is also up to 9ºC.

Finally, Ibirapuera Park has similarities in the built-up density of the park area and its surroundings. The attenuation of surface temperature is up to 6ºC and the LST average values indicate an upward trend line.

The presented results corroborate to point out the importance of parks and their benefit in reducing the surface temperature in urban sites.

Future work will advance in the investigation of the park surroundings, subdividing the nearby areas into different proximities. The results will corroborate a deep understanding of the impact of the green spaces in the urban sites.

ACKNOWLEDGEMENTS

Financed by Fundação de Amparo à Pesquisa do Estado de São Paulo (FAPESP - 2022/02552-0 and 2021/02915-2) and Coordenação de Aperfeiçoamento de Pessoal de Nível Superior - Brazil (CAPES - 88887.704300/2022-00).

REFERENCES

1. United Nations Human Settlements Programme (UN-Habitat). Envisaging the Future of Cities.; 2022.
2. IPCC - INTERGOVERNMENTAL PANEL ON CLIMATE CHANGE (2023). Climate Change 2023: Synthesis Report. IPCC Working Group, 2023.
3. LOMBARDO, M. A. Análise das mudanças climáticas nas metrópoles o exemplo de São Paulo e Lisboa. In: CORTEZ, A., and ORTIGOZA, S., orgs. Da produção ao consumo: impactos socioambientais no espaço urbano [online]. São Paulo: Editora UNESP; São Paulo: Cultura Acadêmica, 2009.
4. Santamouris, M. (2001) Energy and Climate in the Built Environment. James & James, London, 2001.
5. Shinzato P. Impacto da vegetação nos microclimas urbanos em função das interações solo-vegetação-atmosfera. Tese doutorado. FAUUSP, São Paulo, 2014.
6. Sunita, Kumar D, Shahnawaz, Shekhar S. Evaluating urban green and blue spaces with space-based multi-sensor datasets for sustainable development. Comput Urban Sci. 2023;3(1).
7. Prefeitura de São Paulo. GeoSampa. Disponível em: <https://geosampa.prefeitura.sp.gov.br/PaginasPublicas/_SBC.aspx>. Acesso em: 27 ago. 2023.
8. USGS. Science For a Changing World. Disponível em: <https://earthexplorer.usgs.gov/> . Acesso em: 20 ago. 2023.
9. HALDER, B. et al. Investigating the relationship between land alteration and the urban heat island of Seville city using multi-temporal Landsat data. Theoretical and Applied Climatology, v. 150, n. 1–2, p. 613–635, 2022.
10. ZHA, Y.; GAO, J.; NI, S. Use of normalized difference built-up index in automatically mapping urban areas from TM imagery. International Journal of Remote Sensing, [s. l.], v. 24, n. 3, p. 583–594, 2003.
11. USGS. Science For a Changing World. Disponível em: <https://www.usgs.gov/landsat-missions> . Acesso em: 20 ago. 2023.
12. ZHANG, Y.; ODEH, I. O. A.; HAN, C. Bi-temporal characterization of land surface temperature in relation to impervious surface area, NDVI and NDBI, using a sub-pixel image analysis. International Journal of Applied Earth Observation and Geoinformation, v. 11, n. 4, p. 256–264, 2009.

PLEA 2024 WROCŁAW
(Re)thinking Resilience

Incidence of overheating in Irish homes for the range of building energy rated dwellings

FAHIMEHSADAT SAJADIRAD,[1] RICHARD O'HEGARTY,[1] OLIVER KINNANE,[1]

[1]School of Architecture, Planning and Environmental Policy, University College Dublin, Ireland

ABSTRACT: As buildings become more energy-efficient in cold climates, the unintended consequence of increased overheating risk during warmer seasons necessitates urgent attention. In this context, there is a significant absence of research addressing the assessment of overheating risks in residential buildings in Ireland. This study examines overheating risk in 1100 social housing units in Dublin, Ireland, considering indoor temperature data and outdoor climate reports for 2022. Evaluating static and adaptive criteria, alongside Building Energy Ratings (BER), the research identifies dwellings at risk and assesses correlations between BER and overheating. The findings reveal that 4% and 42% of dwellings face overheating based on static criteria (CIBSE Guide A and Passivhaus, respectively). Analysis using adaptive criteria (CIBSE TM59) demonstrates minimal overheating instances. Notably, a correlation emerges between poorer BER ratings and higher overheating risks. This study demonstrates that the conclusions one might draw vary depending on the criteria applied for assessing overheating.
KEYWORDS: Overheating Risk, Residential Buildings, Adaptive Criteria, Building Energy Rating, Retrofit Interventions

1. INTRODUCTION

The trend toward airtight and well-insulated buildings, primarily designed to reduce heat loss in colder climates, has inadvertently amplified the risk of overheating during warmer seasons. This elevation in temperatures can significantly impact indoor comfort, occupant health, and overall building energy efficiency.

The International Panel on Climate Change (IPCC) foresees a rise in global temperatures and solar radiation in the upcoming decades [1]. Moreover, the currently sporadic occurrence of unusually high summer temperatures is predicted to become more common, potentially becoming the standard by 2060, based on a medium emissions scenario [2]. As a result, Ireland's climate is anticipated to experience elevated temperatures, especially during the summer months [3]. Consequently, this increase in temperature is expected to raise the internal temperatures of residential buildings. On the other hand, the residential buildings are intensively subjected to reduce greenhouse gas emission in the climate action plans of many countries, particularly Ireland by 2030 and 2050 [4]. In this regard, performance evaluation of residential building in Ireland has been attracted extensive attention.

In this context, it is Important to identify and mitigate the risk of overheating in the residential buildings. To address this gap, this paper assesses overheating risk in a large simplest of dwellings on the east coast of Ireland. Specifically, indoor temperature data for 2022 from 1100 social housing units in Dun Laoghaire Rathdown (DLR), within Dublin City's County in Ireland, were obtained. Concurrently, monthly, daily, and hourly outdoor temperature reports for 2022 in Ireland were analysed. The overheating risk of the dwelling is evaluated through both static and adaptive criteria [5-7]. In addition, this work evaluates the correlation between the Building Energy Rating (BER) and the overheating risk. The number of dwellings that face the risk of overheating in different BER rating (A-G) are determined. This evaluation will be used for selecting the dwellings for retrofit procedures to improve energy efficiency. This approach offers a methodology to evaluate the potential for overheating in residential dwellings in the Irish context.

2. LITRATURE REVIEW

This section involves a review of the method used to analyse overheating and the criteria for overheating referenced in the existing literature. Prior studies have employed a range of dynamic simulation tools, empirical methods, and meta-analyses to examine this matter. Despite the considerable research on housing in the UK, there is a notable lack of literature concerning the evaluation of overheating risks in residential buildings in Ireland. The most commonly employed methods for evaluating overheating are static and adaptive approaches. Several studies conducted the adaptive approach to assessing overheating and considered both the outdoor conditions and human adaptation based on a running mean of external temperature and the quality of the thermal comfort required [8-14]. In the case of the static approach, fixed

temperature thresholds are considered for defining overheating in a building. McGill et al. analysed the indoor temperatures in 60 selected low-energy housing based on the Chartered Institution of Building Services Engineers (CIBSE) approach [7,8]. Moreover, it has been reported to comprehensively understand the occurrence of overheating in the monitored dwellings, it is essential to utilize both fixed and adaptable methods [12-14].

3. METHODOLOGY

This section outline the assessment methodology employed in this study, where a previous paper [16] presented a details methodologies for assessing overheating in three specific Irish dwellings. The primary focus of this research is the analysis and assessment of overheating risk within a large sample set. The procedure of methodology is presented in Fig. 1.

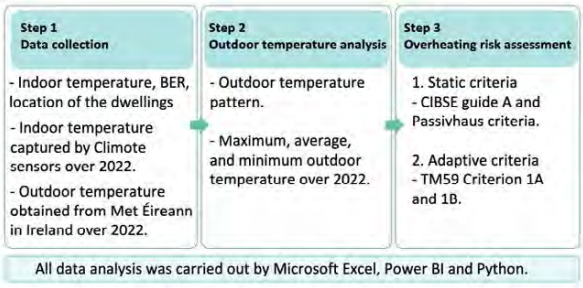

Figure 1: Flowchart of the research methodology.

3.1. Data collection

An extensive collection of 1100 pre-retrofits and retrofit housing in Dublin is provided by DLR. As listed in Table 1, these data consist of the Indoor temperature profile in 8 different zones over 2022 (e.g., bedroom, living room), BER Rating of dwellings, and Geographic Information System data (latitude and longitude) of the buildings. The location of the building is shown in Fig. 2. Indoor temperature measurements within the different zones of the dwellings were captured using temperature sensors developed by the Climote smart technology company [17].

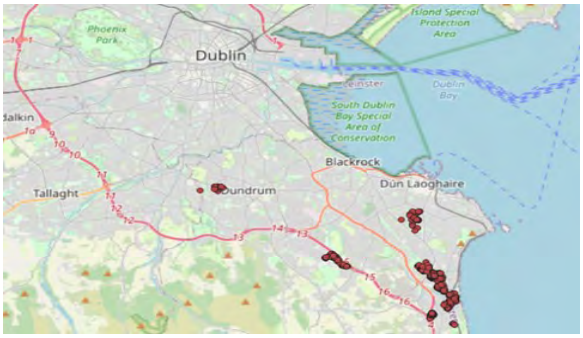

Figure 2: The geographical arrangement of the dwelling sample set in Dublin, Ireland.

The assessment of overheating risk utilized indoor temperature data from 1100 dwellings, consistently recorded over the full year of 2022. Following data filtration for the summer period (May 1 to September 30, 2022), analysis was conducted on 943 dwellings, comprising a total of 949 zones—898 living rooms, 3 bedrooms, 43 heating areas, and individual zones for living rooms 1 and 2, kitchen, Herve, and house. In this study, living rooms, bedrooms, kitchen, and Herve met criteria as occupancy rooms for evaluating overheating risk and occupants' thermal comfort, while heating and house zones were excluded due to their heat transfer functions. It should be noted that the 'Herve' zone refers to the guest room and it is a kind of occupancy room. Therefore, this study considered as a separate bedroom. The details of different zones are presented in Table 1.

Table 1: Name and number of zones after filtration data for the summer period (May 1 to September), over 2022.

No	Name of zones	Number of zones
1	Bedroom	3
2	Heating	43
3	Livingroom	898
4	Livingroom 1	1
5	Livingroom 2	1
6	kitchen	1
7	Herve	1
8	House	1
Total number of zones		949

As depicted in Table 1, the number of zones in this study exceeds the number of dwellings, indicating that some dwellings have multiple zones.

The assessment involved determining the percentage of homes within each BER rating range facing overheating risk, alongside an evaluation of the overall percentage of homes out of the total 943 dwellings that demonstrated overheating. All data analysis was conducted using Microsoft Excel, PowerBI, and Python.

3.2 Outdoor temperature pattern

Meteorological data related to outdoor temperatures was obtained from weather Dublin airport stations on Met Éireann's monthly, daily, and hourly weather reports in Ireland throughout the year 2022. The results of this section will be presented in section 4.2.

3.3 Assessment of overheating risk

The overheating risks in standard residential buildings were evaluated through the criteria provided by the CIBSE. The overheating risk of the dwelling is evaluated through both static (CIBSE Guide A [7] and Passivhaus [6]) and adaptive criteria (TM59) [5]. Both CIBSE Guide A and Passivhaus analyse the overheating by considering fixed

thresholds for various zones and occupancy percentages. The Passivhaus Institute defines overheating in homes as operative temperatures exceeding 25°C for more than 10% of the year [6]. CIBSE Guide A refers to a fixed definition of overheating where 'the internal operative temperature should not exceed 25°C for more than 5% of occupied hours and 28°C for more than 1% of occupied hours.

CIBSE TM 59 presents criteria and calculation methods for evaluating the overheating of naturally and mechanically ventilated residential buildings during summertime [18]. The CIBSE TM 59 adaptive criterion is based on CIBSE TM 52 [5] and CIBSE Guide A [7]. This applies to homes that are predominantly naturally ventilated, a condition met by all the homes in our sample. TM52 criteria are evaluated as follows:

$$\Delta T = T_{OP} - T_{MAX} \quad (1)$$

To calculate the value of ΔT required to evaluate overheating risk, the hourly indoor operative temperature (℃), T_{OP}, and the upper limit temperature for Category III for existing buildings from EN16798-1 (℃), T_{MAX}, are used [19]. The upper limit temperature represents the absolute maximum daily temperature for a room. Operative temperature (T_{OP}) is the average of indoor air temperature (T_A), and the mean radiant temperature (T_{MRT}) [5,12], as follows:

$$T_{OP} = (T_A + T_{MRT})/2 \quad (2)$$

It should be noted that the above equation is valid where the air velocity is less than 0.1m/s, as is typical in buildings [20]. T_{MRT} is a measure of the average temperature of the surfaces that surround a particular point, with which it will exchange thermal radiation. In many spaces, with low air velocity and where air temperature and mean radiant temperature may be similar, air temperature alone can be a reasonable indicator of thermal comfort [12,20]. Consequently, data in this study only include the T_A.

T_{MAX} is calculated using the exponentially weighted running mean of the daily mean outdoor temperature (℃), T_{RM}, via the following formula:

$$T_{MAX} = 0.33T_{RM} + 22.4 \quad (3)$$

$$T_{RM} = (T_{OD-1} + (0.8*T_{OD-2}) + (0.6 * T_{OD-3}) + (0.5 * T_{OD-4}) + (0.4 * T_{OD-5}) + (0.3* T_{OD-6}) + (0.2 * T_{OD-7})) / 3.8 \quad (4)$$

where $T_{OD\text{-}nth\ days}$ (℃) is the daily mean outdoor temperature of the *n*-th day before. where T_{od-1} is the daily mean external temperature for the previous day; T_{OD-2} is the daily mean external temperature for the day before, and so on.

TM59 uses the first criterion for overheating from TM52, which defines the Hours of Exceedance (H_e), representing the duration of overheating, as follows:

$$He=\sum h \forall \Delta T \geq 1℃ \quad (5)$$

The summation is performed over all occupied hours (h) as defined for the type of building. TM59 refines this criterion for domestic application, as shown in Table 2. H_e should not exceed 3% of occupied hours for the months of May to September inclusive based in criterion 1A.

Table 2: CIBSE TM 59 criteria for assessing overheating risk.

Criterion 1A	Criterion 1B
For living rooms and bedrooms: - Occupied hours are set from 9 a.m. to 10 p.m. for living rooms, living rooms1, living rooms2 and kitchens. - Occupied hours are set 24 h per day for bedrooms and herve.	For bedrooms and herves: - During sleeping hours from 10 p.m. to 7 a.m. shall not exceed 26℃ for more than 1% of occupied hours

4. RESULT

4.1 BER Rating of dwellings

The result of the BER Rating of dwellings is shown in Fig. 3. The distributions of the dwelling's BER show that 0.1%, 3%, 41%, 11%, 4%, 1%, 0.3%, and 40% of dwellings possess the BER ratings of A, B, C, D, E, F, G and nocodelisted, respectively. Nocodelisted refers to dwellings without a BER rating. Notably, a significant majority of dwellings hold a nocodelisted and C rating. This underscores the need for retrofitting to reach at least a B rating or higher.

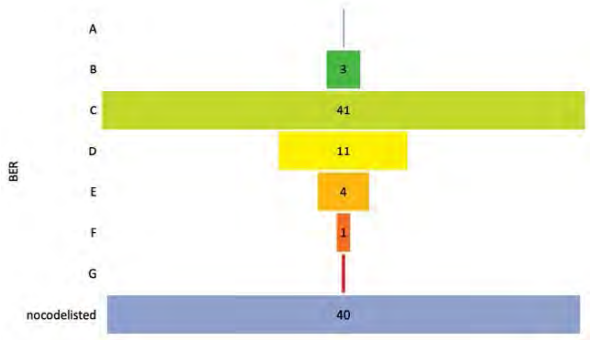

Figure 3: The BER distributions (percentage %) of 943 dwellings within the DLR sample set.

4.2 Outdoor temperature pattern

Fig. 4 illustrates the daily outdoor temperatures recorded from May to September 2022. During this period, August and July registered the highest temperatures. The maximum outdoor temperature recorded at the weather station was 29.1℃ on July 18th at 12:00 pm, while the minimum temperature of 2.7℃ occurred on May 29th at 04:00 am. The average outdoor temperature over the five months stood at

approximately 14.3℃, with a standard deviation of approximately 6.6℃. Temperatures exceeded 20℃ for 246 hours (7%) and 22℃ for 115 hours (3%). The observed outdoor temperatures suggest a mild climate, despite it being summer. Most of these temperatures aligned closely with the average, with slightly higher readings observed in July and August compared to the other months.

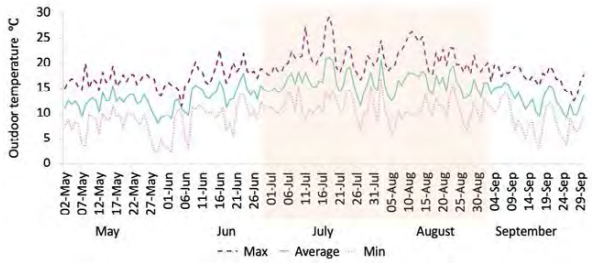

Figure4: Daily Max, average and Min outdoor air temperatures during the summers from 2022 in Ireland. Summers are evaluated between May and September.

4.3 Evaluation of overheating risk in the sample set

Aligned with the definitions used in static criteria for overheating analysis such as CIBSE Guide A and Passivhaus, occupied hours were specified as 07:00 am to 23:00 pm in the living room, living room 1, a living room 2, while for bedrooms and Herve zones, it was defined as 23:00 pm to 7:00 am. It should be note that ddetermining occupied hours for bedrooms and living rooms based on occupant sleep and activity patterns is challenging due to limitations in direct occupant assessment and the scale of dwellings under study. However, an approximation of 8 sleeping hours for bedrooms and 16 activity hours for living rooms is an acceptable occupied hours for overheating analysis that was utilized in this research. This approach is consistent with similar methodologies found in related studies (e.g., [8]) and reflects common residential patterns of night-time rest and daytime activity. The occupied hours in TM59 criterion1A and 1B are shown in Table 2.

4.3.1 Evaluation of overheating risk based on static criteria

The analysis determined the number and percentage of dwellings facing the risk of overheating based on CIBSE Guide A and Passivhaus criteria within the dataset of 943 dwellings. Out of these, 40 dwellings (4%) were identified as facing overheating risk based on the CIBSE Guide A criteria, while 394 dwellings (42%) met the criteria for overheating risk according to the Passivhaus standards, during the 5 non-heating months of 2022 (1st of May to 30th Sep). The differing approaches between CIBSE Guide A and Passivhaus criteria in assessing overheating risks in residential buildings revolve around their evaluation scopes. CIBSE focuses on specific room temperatures, especially bedrooms, while Passivhaus assesses the entire building's compliance with a fixed internal temperature limit. This difference led to a significant contrast in identified risks. This underscores the necessity of balancing overall building performance, emphasized by Passivhaus, with the consideration of room-specific comfort and adaptive approach, crucial for a comprehensive overheating risk assessment.

According to CIBSE Guide A's criteria, 58% of hours in bedrooms and 91% of hours in Herve exceeded 24°C (5%). Additionally, 1.2% of hours occupied in bedrooms surpassed 26°C (1%). In living rooms, 34% of hours and 12.5% of hours in living room 2 exceeded 25°C (5%), while 5% of living room hours exceeded 28°C (1%). In Passivhaus criteria, 52% of hours in bedrooms, 59% in Herve, 48% in living rooms, and 13.5% in living room 2 exceeded 25°C (10%). Despite living rooms being more numerous compared to other zones, higher proportions of hours in bedrooms exceeded static overheating thresholds. The determined number of each dwelling zone based on static criteria is illustrated in Table 3. Among the sample set, the total percentage of living rooms is 95%, with 39% facing overheating based on Passivhaus and 4% facing overheating based on CIBSE Guide A.

Table 3: The number of each zone of dwellings are facing the risk of overheating in both CIBSE Guide A and Passivhaus criteria throughout the 5 non- heating months (1st of May -30th Sep) of 2022.

Name of zones	Number of zones	Passivehous criteria	CIBSE Guide A criteria
Bedroom	3	2	1
Heating	43	19	2
Livingroom	898	372	36
Livingroom 1	1	-	-
Livingroom 2	1	1	-
kitchen	1	-	-
Herve	1	1	1
House	1	1	-
Total no	949	396	40

The correlation of dwelling percentage faced overheating risk under both CIBSE Guide A and Passivhaus criteria and BER is depicted in Fig. 5. The results demonstrate that dwellings with worse BER (C, D, E) shows more overheating risk. 19% of overheating risk happens in 40% of dwellings with no BER. In this regard, the determination of BER for these dwellings can change the distribution and correlation of overheating risk with other BER ratings.

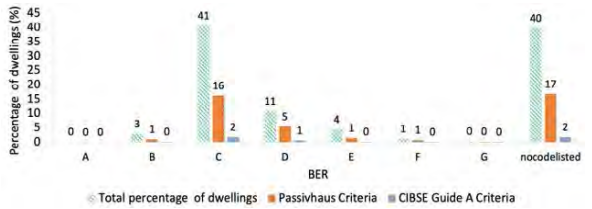

Figure 5: The percentage of dwellings, BER, and overheating risk in both CIBSE Guide A and Passivhaus criteria throughout May to September 2022.

4.3.2 Evaluation of overheating risk based on adaptive comfort CIBSE TM59

In this section, the overheating risk of existing dwellings are assessed using TM 59 criteria. In the overheating calculation results for Criterion 1A, the living room, living room 1, living room 2, and kitchen zones were evaluated over 14 activity hours based on CIBSE TM 59. The results indicated no ΔT greater than or equal to 1 ℃ in living room 1, living room 2, and kitchen zones, signifying the absence of overheating in these areas. Among 898 cases in living rooms, 26 exceeded or equal ΔT by 1 ℃, yet only 1 case exceeded criterion of 3% of occupied hours. The average percentage of overheating across all cases was approximately 0.4%. The distribution of BER for living rooms with ΔT ≥ 1 ℃ evaluated and found 54% as C, 15% as D, 4% as F, 4% as G, and 15% as nocodelisted. Regarding bedrooms and herve zones, evaluated across the entire day (24 hours), no ΔT greater than or equal to the specified criterion was observed, indicating no overheating in these zones.

Fig. 6(a) and (b) illustrate the frequency of hours where ΔT satisfies the threshold of ≥1℃ and the percentage of overheating, respectively. The results indicate that most exceedance hours are below 10 hours, as shown in Fig. 6(a). Additionally, only one dwelling exhibited an overheating percentage of 3.25%, surpassing the 3% threshold of Criterion 1A in TM59's adaptive approach. Fig. 6(b) displays those 26 dwellings had overheating percentages below 1%.

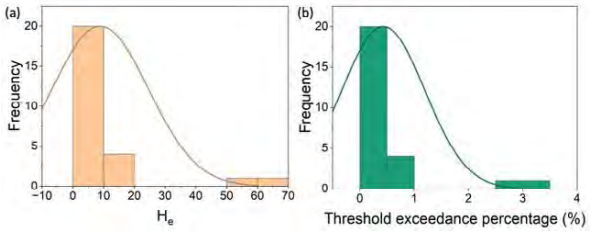

Figure 6: The frequency of hours that the ΔT satisfy the threshold of ≥1 and the percentage of overheating for living rooms using Criterion 1A.

Criterion 1B in CIBSE TM 59 employs a more stringent assessment, focusing on indoor temperatures observed in bedrooms for 9 hours sleeping hours. Overheating is identified if the indoor bedroom temperature exceeds 26°C for more than 1% of the observed period. In total, 1 out of 3 bedroom cases exceeded 26°C, accounting for a percentage of 0.5%. Thus, no instances surpassed 26°C for more than 1% of occupied hours. The distribution of BER in bedrooms indicates 2 nocodelisted and 1 C rating. In the herve zone with a C BER, 3 hours exceeded 26°C during sleeping hours, constituting 0.3% of the observed period, which does not exceed the 1% threshold for overheating in this zone. Consequently, all 4 bedrooms and herve zones could not satisfy the criterion 1B.

5. DISCUSSION

The discussion section delves into the insights collected from the examination of residential buildings in Ireland, focusing on overheating risks and energy performance. The analysis of BER ratings revealed a striking prevalence: 40% of dwellings lacked a BER rating (nocodelisted), while 41% held a C rating. This emphasizes an urgent need for retrofitting to elevate ratings to at least a B or higher. Outdoor temperature patterns demonstrated a generally mild climate during the summer months, with 7% of the time exceeding 20℃ and 3% surpassing 22℃. July and August had slightly higher temperatures, potentially posing challenges in maintaining thermal comfort during these periods.

Assessment through static criteria such as CIBSE Guide A and Passivhaus revealed varying perspectives on overheating risks. CIBSE Guide A identified 4% of dwellings at risk, whereas Passivhaus indicated a higher percentage of 42%. This disparity highlights the importance of balancing overall building performance with room-specific comfort for a comprehensive overheating risk assessment.

The correlation analysis between overheating risks and BER ratings showed a clear association: lower BER-rated dwellings faced higher risks of overheating. Notably, 19% of overheating risk occurred in dwellings without a BER rating, indicating the potential impact of improving BER ratings in mitigating overheating concerns. Further evaluation through adaptive comfort criteria like CIBSE TM59 unveiled nuanced insights. While sporadic instances of potential overheating were observed in living rooms (with ΔT ≥ 1 ℃ in 26 cases), minimal occurrences were noted in bedrooms and other zones, emphasizing the importance of adaptive strategies in addressing overheating risks.

In the realm of overheating analysis, existing literature showcases a broad spectrum of overheating occurrences, influenced significantly by factors such as the criteria employed for analysis, the characteristics of the buildings under study, the density of occupants, and the duration of the research period [8,9,11-14,21]. In our case, the causes of overheating remain less clear. There are a range of possible causes which could be attributed to

various potential factors including building characteristics, design, insulation, ventilation, and occupancy patterns. This underscores the need for a comprehensive approach to address overheating issues in building design and management.

6. CONCLUSION

In conclusion, the examination of a sample of residential buildings in Ireland has shown the challenges and opportunities for enhancing energy efficiency and occupant comfort. Outdoor temperature patterns, although generally mild during the summer, reveal specific challenges during peak months like July and August. The evaluation of overheating risks using static criteria (CIBSE Guide A and Passivhaus) and adaptive comfort criteria (CIBSE TM59), highlights the importance of a balanced approach in assessing overall building performance and room-specific comfort. In addressing the multifaceted causes of poor performance (such as building characteristics and etc,.) a holistic approach to building design and management is crucial.

The evidence emphasizing the need for a nuanced approach to address temperature concerns in specific zones within homes, particularly bedrooms, and living spaces. For retrofitting Irish residential properties, the evidence calls for a tailored approach. It highlights the importance of considering room-specific comfort alongside overall building performance to effectively mitigate overheating risks during retrofit procedures. Regarding future climate change impacts, the evidence underscores the urgency of adapting residential properties. It emphasizes the necessity of designing buildings that can withstand increasingly extreme temperatures while ensuring occupants' comfort and well-being amidst changing environmental conditions.

ACKNOWLEDGEMENTS

Authors are thankful for the technical support and giving the housing sample set data of Chekkala Vijit from Housing of Dun Laoghaire Rathdown.

REFERENCES

1. The Intergovernmental Panel on Climate Change (IPCC), [Online], Available: https://www.ipcc.ch/ar6-syr/[2023].
2. McLeod, R. S., Hopfe, C. J., & Kwan, A. (2013). An investigation into future performance and overheating risks in Passivhaus dwellings. *Building and Environment, 70*p. 189-209.
3. Attia, S., Benzidane, C., Rahif, R., Amaripadath, D., Hamdy, M., Holzer, P., Petersen, S. (2023). Overheating calculation methods, criteria, and indicators in European regulation for residential buildings. *Energy and Buildings, 292*p. 113170.
4. O'Hegarty, R., & Kinnane, O. (2023). A whole life carbon analysis of the Irish residential sector-past, present and future. *Energy and Climate Change, 4*p. 100101.
5. CIBSE TM52, The limits of thermal comfort: Avoiding overheating in European buildings, chartered institute of building services engineers, [Online], Available:https://www.cibse.org/knowledge-research/knowledge portal/tm52-the-limits-of-thermal-comfort-avoiding overheating-in-european-buildings [Oct 2013].
6. Institut, P. (2012). The passive house planning package (PHPP). In: BRE Passivhaus Watford.
7. Environmental design: CIBSE guide A. 8th ed. London: CIBSE. [online], Avalaible: https://www.cibse.org/knowledge-research/knowledge-portal/guide-a-environmental-design-2015 [March 2015 updated 2021].
8. McGill, G., Sharpe, T., Robertson, L., Gupta, R., & Mawditt, I. (2017). Meta-analysis of indoor temperatures in new-build housing. *Building Research & Information, 45*(1-2):p. 19-39.
9. Finegan, E., Kelly, G., & O'Sullivan, G. (2020). Comparative analysis of Passivhaus simulated and measured overheating frequency in a typical dwelling in Ireland. *Building Research & Information, 48*(6):p. 681-699.
10. Finegan, E. (2022). An empirical investigation into current and future overheating frequency in nZEB and Passivhaus dwellings in Ireland. p.
11. Gupta, R., Gregg, M., & Irving, R. (2019). Meta-analysis of summertime indoor temperatures in new-build, retrofitted, and existing UK dwellings. *Science and Technology for the Built Environment, 25*(9):p. 1212-1225.
12. Jang, J., Natarajan, S., Lee, J., & Leigh, S.-B. (2022). Comparative Analysis of Overheating Risk for Typical Dwellings and Passivhaus in the UK. *Energies, 15*(10):p. 3829.
13. Morey, J., Beizaee, A., & Wright, A. (2020). An investigation into overheating in social housing dwellings in central England. *Building and Environment, 176*p. 106814.
14. Gupta, R., & Gregg, M. (2020). Assessing the magnitude and likely causes of summertime overheating in modern flats in UK. *Energies, 13*(19):p. 5202.
15. Sajadirad, F., O'Hegarty, R., & Kinnane, O. (2023). *Analysis Overheating in Irish houses: Result from a large sample set*. Paper presented at the 8th International Conference on Carbon Accounting 2023, Edinburgh, UK.
16.Climote smart technology, [Online], Available: https://www.climote.ie/heating/ [March 2024].
17. Bonfigli, C., Chorafa, M., Diamond, S., Eliades, C., Mylona, A., Taylor, B., & Virk, D. (2017). TM59: Design methodology for the assessment of overheating risk in homes. *CIBSE, London*p.
18. CEN, E. (2019). 16798-1: 2019 Energy Performance of Buildings—Ventilation for Buildings—Part 1: Indoor Environmental Input Parameters for Design and Assessment of Energy Performance of Buildings Addressing Indoor Air Quality. *Thermal Environment, Lighting and Acous*p.
19. Lomas, K., Watson, S., Allinson, D., Fateh, A., Beaumont, A., Allen, J., Garrett, H. (2021). Dwelling and household characteristics' influence on reported and measured summertime overheating: A glimpse of a mild climate in the 2050's. *Building and Environment, 201*p. 107986.
20. Jones, R. V., Goodhew, S., & de Wilde, P. (2016). Measured indoor temperatures, thermal comfort and overheating risk: Post-occupancy evaluation of low energy houses in the UK. *Energy Procedia, 88*p. 714-720.

PLEA 2024 WROCŁAW
(Re)thinking Resilience

Reducing Whole Life Carbon Emissions with Mass Timber Construction

Exploring Design Strategies and Material Choices

AGOSTINO ANSELMO[1], JUAN A. VALLEJO[1]

[1]School of Architecture and Cities, University of Westminster, London, United Kingdom

ABSTRACT: Mass timber construction is gaining momentum every year, driven by the urgency to reduce carbon emissions in the construction industry. Some of the advantages of this material include remarkable structural performance with low weight, ease of construction and a variety of options to suit different applications. One of the most critical aspects of conducting a whole life carbon analysis of a timber building is the confusion surrounding the inclusion of biogenic carbon in the calculations. In addition, previous studies show how the low weight of wood can lead to higher heating and cooling demand due to a scarce thermal mass capacity of this material. A literature review was conducted on these issues and a case study of a community building was analysed. Life Cycle Analyses and thermal simulations were carried out to compare alternative scenarios focusing on material substitutions: changing the materials of the structural frame, slabs, external walls and core to certain mass timber solutions led to significant embodied and operational carbon reductions. The results show how careful mass timber design can lead to significant whole life carbon savings.
KEYWORDS: Mass Timber, Whole Life Carbon, Embodied Carbon, Carbon emissions, Thermal Mass

1. INTRODUCTION

The current climate emergency is arguably the greatest challenge the whole humanity ever faced. According to the latest IPCC report [1], keeping the temperature of the Earth's atmosphere below 1.5 °C above pre-industrial levels is still pragmatically possible, although it requires a strong and coordinated effort by all of humanity. The carbon footprint of building construction and operation is extremely high, accounting for around 37% of global greenhouse gases emissions, while emissions from the production of cement, steel, and aluminium alone account for 13% [2]. The potential for reducing materials-related greenhouse gases (GHG) emissions is growing every day, thanks to a remarkably fervent research activity and an increasing awareness of environmental issues that is driving both the industry and its clients to reduce the impact of the built environment. Together with other viable actions in the architecture and construction sector, a reduction in the amounts and the embodied carbon (EC) of materials will facilitate the achievement of our global environmental goals.

The aim of this paper is to assess the environmental performance of mass timber construction (MTC), with the specific focus of understanding its contribution to a non-domestic building's whole-life carbon (WLC) emissions. As a case study, a community building in King's Cross, London, is analysed by assessing the emissions related to the embodied and operational stages. In the current scenario, the building makes use of MTC for the structural frame and the slabs, while alternative construction scenarios were evaluated, exploring the consequences of different engineered wood product (EWP) choices and the addition of a mass timber (MT) layer to the external walls. Moreover, the study explores the relationship between embodied and operational carbon to understand the holistic environmental implications of MTC, considering possible implications on all life stages.

2. METHODOLOGY

This paper aims to get to an understanding of how employing MTC techniques into a design affects the WLC emissions of the building. A community building in London is going to be analysed as case study: firstly, its building elements will be examined and LCAs will be conducted, focused on the global warming potential (GWP) linkable to MTC. In addition, operational energy will also be considered: by performing thermal simulations, its heating and cooling loads (and the resulting carbon emissions) will be estimated. A climate model based on the IPCC RCP 8.5 [1] for 2100 will be used to test a future-proof scenario and at the same time to heighten the risk of overheating. Several scenarios will be selected to represent designs with different approaches to MTC and will be compared with the base case through LCAs and thermal simulations. By analysing the heating and cooling loads with different construction scenarios, the contribution of MTC to the building's operational energy will be identified.

Through a series of thermal simulations in free running mode, the passive operational temperatures of the building will also be analysed to understand if some slab constructions can bring operational carbon savings thanks to their thermal mass.

Finally, the data gathered from the literature review, LCAs and thermal simulations will be considered to propose a cumulative "environmental best case" scenario, combining different MTC techniques to achieve the most carbon emission reductions.

W3, a community building recently completed in London, was chosen as a case study for this work, in collaboration with Haptic Architects, to test the findings of the literature review and to better understand the environmental impact of this building and its components. This is a 13.50 metres high building with three floors above the ground and a lower ground with basement shared with the rest of the development area.

3 THEORETICAL BACKGROUND

Comparing different MT types and products is an essential step for selecting the right EWP for each application: two of the main distinguishing factors are structural characteristics and environmental impact. The literature shows how materials such as glued laminated timber (glulam or GLT) and laminated veneer lumber (LVL) are particularly suitable for structural elements such as beams and columns, as they are made of parallel strands of wood, giving the product high strength in the grain direction. On the other hand, in cross-laminated timber (CLT) each layer is laid crosswise, perpendicular to the adjacent ones, giving the product isotropy and making it ideal for surfaces such as walls and slabs.

A MT manufacturer can carry out LCAs for their products to disclose their specific environmental impacts: these assessments are then third-party reviewed and published in a standardised Environmental Product Declaration (EPD).

For this study, several EPDs have been selected for glulam, CLT and LVL products to compare them and find average emissions (expressed as Global Warming Potential, GWP) values for each typology in the 2024 MT market. The calculated average upfront carbon (UC, stages A1-A3) emissions of CLT is of 121.75 $kgCO_2e/m^3$, while glulam and LVL have average GWPs of 172.18 and 210.22 $kgCO_2e/m^3$ respectively. Nonetheless, it was found that the actual EC of each product can be far from these numbers: for example, a third of the glulam products have GWPs lower than 65 $kgCO_2e/m^3$, while a tenth of them is above 350 $kgCO_2e/m^3$, without relevant differences in the manufacturing processes or final product. The same also happens in CLT (from 34 to 330 $kgCO_2e/m^3$) and LVL (91 to 361 $kgCO_2e/m^3$). Comparing LVL and glulam, though, requires deeper, case-specific analyses, as the first is much stronger than the latter, allowing for smaller cross sections to be used [6].

4 LITERATURE REVIEW

As MT is a relatively lightweight construction material, the literature shows that a building with MT internal walls and slabs, without the addition of heavier materials, could result in higher energy requirements for heating and cooling compared to RC or clay bricks. Although these materials have a much higher embodied carbon, they are able to store heat through their thermal mass in a way that reduces the need for active heating and cooling systems more effectively than wood [4].

As Diaz suggested in 1995, in lightweight buildings "most of the long term storage of heat (one day or more) will occur through the envelope while the internal mass will store heat for a few hours only. This may not always be desirable as heat storage in internal elements can be significant for the overall thermal performance of the building". In MTC, this can be especially relevant with CLT panelised construction, where the internal elements do not have a strong thermal mass performance. Some literature review context is now proposed.

In 2020, Jensen, Norford and Grinham conducted a study which found that in their case studies, the thermal mass performance of mass timber in the summer season was very poor compared to their concrete equivalents. Regarding overheating risk mitigation, "when comparing decrement in peak temperature, the mass timber design provided about 44% of the decrement of an equivalently scaled concrete case across the cooling season, and about 42% of the decrement on peak days. When comparing cooling energy, the mass timber design provided about half the savings in cooling energy (45-56%) from thermal mass compared to an equivalently proportioned (volume and surface area) concrete case, depending on operational strategy". Yet, the WLC carbon of their MTC scenarios was still less than the RC equivalents – "60% reduction in Los Angeles, and a 27% reduction in Seattle" [3]. Through post-occupancy evaluation surveys and simulations, another study also revealed how lightweight MTC can lead to higher risks of extreme summertime overheating in the UK compared to heavyweight materials, although the occupants satisfaction rate generally stays at a high level [4].

Some studies proposed solutions for this problem: Tonelli and Grimaudo in 2014 conducted an experiment inspired by how the houses in warm climates such as the Mediterranean area traditionally use heavy construction in their fabric. During the 2012 Solar Decathlon event in Madrid, they proposed

a wall stratigraphy with not only insulation, but also heavy materials, achieving a "mass value that is nearly double the value of a normal framed wall, and therefore very close to a traditional masonry wall". High-density fibreboard, PCM boards or concrete can be used to add thermal mass to a MT structure to help mitigate overheating issues. With the same thickness, "the mass of concrete is 75% higher than the mass of" the high-density fibreboard, while boards made with the latter "are much simpler to integrate to a wall than concrete". In different amounts, all these thermal mass addition strategies are effective in reducing overheating, but need to be integrated with other passive strategies [5].

In 2017 Pajek et al. investigated various examples of ways to enhance the summertime thermal performance of lightweight construction. Several improvements were investigated (e.g., clay boards, wood wool thermal insulation, PCM, etc.) and compared with the performance of a conventional thermally insulated high mass wall. Finite element model was created and dynamic thermal performance of enhanced lightweight external walls was analysed in three different European locations: Helsinki (Finland), Vienna (Austria) and Madrid (Spain). Their findings are that "in Southern European locations (e.g., Madrid), summertime thermal comfort in LWCs is much harder to achieve, despite the enhancements presented and analysed in the study", therefore "the use of [lightweight construction] enhancements with low environmental impact, such as wood wool thermal insulation and PCMs, should be encouraged". Moreover, in order to further improve thermal performance, application of high intensity ventilation was found to be necessary.

These cited studies were focused on the energy consumption of buildings during the use phase, but if the reason for reducing energy demand is sought is to cut CO2e emissions, the proposed solutions should also take into account the embodied carbon, both in the upfront and EOL phases. In many cases, the higher upfront emissions of layers added for thermal performance improvement are balanced out in a few years with the operational carbon savings (Hacker et al., 2008). However, in other scenarios, the products used to reduce heating or cooling loads are found to have such a high embodied carbon profile that their use becomes pointless, if not detrimental, to reducing WLC carbon emissions (De Toldi, Craig, Sushama, 2022; Ferreira et al., 2023).

5 ANALYTICAL WORK

5.1 Analysis of the existing building

The structural frame of the W3 building is mostly made of glulam columns and beams, manufactured by the Austrian company Wiehag. This EWP has an UC of 54 $kgCO_2e/m^3$, well below the average glulam UC of 172.18 $kgCO_2e/m^3$. The glulam elements in W3 have a total UC of 11.8 tCO_2e.

36 columns and 37 beams between the ground and first floor are made of steel due to a structural constraint: some recessions in the plan at the ground floor only cause a misalignment between a set of columns on the ground floor and the upper. This creates horizontal loads that, in an all-glulam scenario, would have required large sections of the affected beams and columns, deemed too wide for the architectural design. Indeed, too large frame sections can lead to difficulties in the layout and systems and services runs. Therefore, steel was chosen for these elements, with sections that are much smaller than the glulam equivalent. Despite them being just 1.60 m^3 or slightly more than 1% of the frame, the steel parts have a total UC of 15 tCO_2e. The reason for this wide difference is the 6,100 $kgCO_2e/m^3$ UC of steel, more than 100 times higher than the Wiehag timber. The UC of the entire frame of W3 is therefore 26.8 tCO_2e.

Figure 1: Steel columns and beams in the hybrid mass timber structure of W3

The sections of the upper floors and the roof are based on a 220 mm-thick cross-laminated (CLT) slab, made by the German company Derix. This EWP is also a very carbon efficient material compared to the rest of the market. Moreover, the production centre of this EWP is located 520 km south-east from London, a relatively close location compared to other European MT manufacturers, making the transport emissions low as well. In both the internal slabs and the roof, the design involves the MT slab as the main structural element, while different layers are laid above it to improve the acoustic and fire performance, together with providing a stable and walkable finishing. On top of the 220 mm CLT slab, 270 mm are available for services and finishes, depending on the occupant's preference. The standard predicted floor construction consists, top to bottom, of a timber flooring, screed, plywood, fibre cement boards, a floating floor system and the CLT. The total UC of the internal floors is 36.9 tCO_2e: the CLT slabs contribute with 17 tCO_2e, but the

role of the plywood and fibre cement boards layers was found to be important as well, with respective GWPs of 6.7 and 12 tCO_2e, while the wood flooring adds 1.2 tCO_2e to the total.

Figure 2: View from the second floor of W3

The external walls are made of cassettes where the layers are (outside to inside) cladding with decorative fins, a breather membrane, a sheathing layer of OSB, 230 mm of mineral wool insulation, another layer of OSB, a vapour control membrane, a high thermal performance plasterboard and a finishing to be chosen by the tenants. The cladding and fins on the west, south and a southern part of the east façade, are made of treated radiata pine. On the north and the northern part of the east façade, aluminium was used for the cladding and fins, while a ventilated cavity and an additional plasterboard acting as a sound and fire barrier are added on the inside of the wall.

The foundations, basement, ground floor slab and core of W3 are made with reinforced concrete (RC) - the first two are parts of a substructure shared with the surrounding buildings. The original design featured a CLT core, but a structural analysis showed how its uncentered position in the plan would have required extensive shear occupying a larger part of the plan, reducing the area available for the community functions. Since using RC allowed for a smaller core, this became the preferred choice.

5.2 Analysis of the proposed scenarios

The existing structural frame of W3, consisting of glulam and steel elements, can be compared to alternative scenarios where one or both materials are replaced with different EWPs. While different UC results are expected by the alternatives, an impact on the building's operational energy demand is not anticipated since the frame is on the inside of the walls and does not have a relevant thermal mass capacity. The existing steel beams and columns were considered first. Using the comparison table made by Pollmeier for BauBuche [6], an equivalent volume of MT beams and pillars can be estimated: 1.60 m^3 of steel corresponds to 40 m^3 of glulam, 23.40 m^3 of softwood LVL or 16 m^3 of hardwood LVL. The first scenario tested was a structural frame made entirely of Wiehag glulam: the amount of material required to replace the steel columns and beams with glulam is approximately 25 times higher, while the sections would be 2.5 times larger. Another solution, satisfying an architectural desire for smaller structural elements and emissions savings was hardwood LVL: BauBuche by Pollmeier is the only hardwood (beech) EWP found with enough structural and environmental data to elaborate a scenario. Finally, a third scenario with softwood LVL, less strong than hardwood but more available on the market, was also evaluated.

A strategy that has been evaluated to improve the thermal mass performance of W3 while at the same time keeping a low UC is designing alternative slab constructions. Different scenarios and materials were considered for this possibility, using a simple CLT slab with a thin and lightweight flooring system (such as a suspended timber flooring system), or the same slab with a layer of compressed earth above it. Lastly, a slab entirely made of concrete was tested to compare these solutions to a more diffused, "business-as-usual" industry standard. It needs to be noted that although the specific weight of each solution was calculated, structural feasibility was not considered for this study: some solutions, being heavier than others, might require a stronger structural support, leading to an increase in material use and consequent UC. For this reason, the final environmental impacts of these scenarios would require deeper and larger-scale structural analyses to be properly unveiled.

The composite CLT and concrete solution was inspired by the SOM "Timber Tower" concept [7]. In this research project, a 70 mm thick concrete layer was placed on top of the CLT slabs to improve the poor sound insulation performance of CLT [8]. Earthen floors are made with a mixture of sand, clay soil and fibre. One or more of these elements are normally obtained on site or in the close proximities. The finishing sealing is usually made with linseed oil, tung oil, pine rosin, beeswax and dipentene, making the final surface durable and washable. The final colour is influenced both by the materials used and possible pigmentations that can be added during the process. Although an EPD of this kind of product was not found, clay and rammed earth (RE), being materials similar to earth flooring, were used as substitutes in the LCAs and thermal simulations.

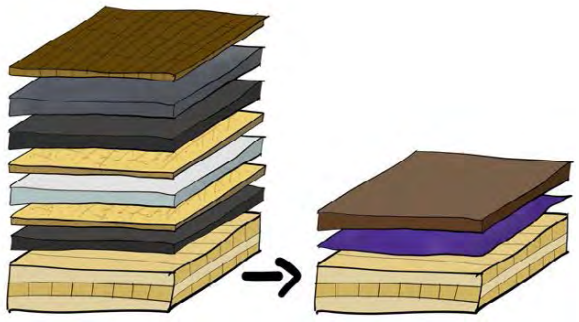

Figure 3: Scheme of slab alternative

An alternative scenario for the construction of the external walls was considered: while the current case involves a cassette system attached to the frame, the considered alternative was a load-bearing CLT wall substituting the external glulam columns. This could bring relevant UC reductions due to the removal of the outer 20 glulam columns of each floor, corresponding to 29.57 m^3. Moreover, the plasterboard can be discarded since visual grade CLT can be used as a finishing material and a fire protection layer if adequately sized. At the same time, its thermal insulation contribution to the wall allows for a reduction of the thickness of the mineral wool layer. With a 140 mm thick CLT layer and the mineral wool insulation thickness reduced from 200 to 155 mm, the U-value of the external wall was kept unchanged (0.20 W/m^2K).

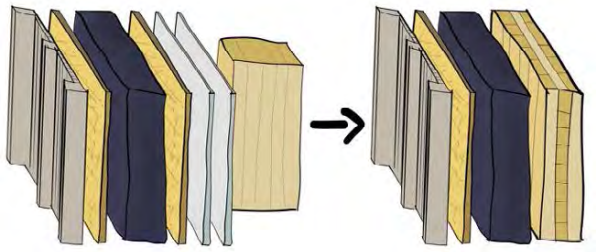

Figure 4: Scheme of wall alternative

5. RESULTS AND DISCUSSION

The environmentally weakest point of the structure consists in the steel elements: although the amount of material required to fulfil the function is almost 15 times higher for LVL and 25 times higher for glulam, in both cases the UC of the structure is lower. If Wiehag glulam was chosen instead of steel, the resulting GWP would be 3.5 tCO_2e, 76% less than the GWP of the base case scenario with steel, saving 11.5 tCO_2e.

If BauBuche LVL was chosen instead, the UC of it would be approximately 4.5 tCO_2e, with a reduction from the base case of 10.5 tCO_2e. Using BauBuche for the entire frame, instead, brings to an increase in WLC emissions due to the higher EC of LVL: instead of the current 11.8 tCO_2e of the GLT structure, the UC would rise to 14.5 tCO_2e. A sensible reduction in size of the columns and beam would therefore cost 2.7 tCO_2e. So, a compromise can be to keep the Wiehag glulam beams and columns as they are while choosing beech LVL as substitution for the steel parts, obtaining small sections with one added tonne of EC as a trade-off compared to the all-glulam solution. The final UC of such frame would be 16.3 tCO_2e, 40% less than the base case, with a saving of 10.5 tCO_2e.

Regarding the new walls, the solution of reducing the mineral wool layer and removing the plasterboard, the finishing and the outer glulam columns in favour of a CLT layer would bring an estimated EC saving of 12.63 tCO_2e, while not having an impact on operational energy due to the U-value being unchanged. However, despite the removal of several columns, the augmented thickness of the external walls would cause a reduction of surface area of 2.46 m^2 per floor (7.39 m^2 in total). Considering how this solution can be generally applied to different projects, a specific value of $kgCO_2e/m^2$ was estimated. The removal of a part of mineral wool insulation, an OSB sheet and the plasterboard brings a reduction of 22.7 $kgCO_2e/m^2$, while the addition of the CLT layer adds 12 $kgCO_2e/m^2$. Therefore, the saving is of 10.7 $kgCO_2e$ per m^2 of wall - without considering the narrowing of the frame elements consequent to the CLT structural contribution.

The slab scenarios were subsequently tested. The simpler one only includes a CLT slab and wood flooring (essential for practical use but not relevant to the thermal analysis): this solution led to higher thermal energy demand in all seasons than the base case, but halving its EC (from 36.90 to 18.20 tCO_2e), with a WLC saving of 15.06 tCO_2e. Adding an earthen layer onto the CLT increments the heating demand but lowers the cooling of a higher amount, bringing reductions in both operational (-4.41 tCO_2e/year) and embodied carbon (-16 tCO_2e/year), for a total of 18.66 less tCO_2e. The “SOM-type” CLT+concrete scenario still brought a slight EC reduction due to the narrow thickness of the concrete layer and a reduction in the cooling load, but an almost equal increase in heating load as well, with a WLC reduction of 7.83 tCO_2e. Lastly, the full concrete slab scenario tested as a comparison caused the most extreme heating load increase (+88.31 $kgCO_2e$/year) and cooling load decrease (-180.28 $kgCO_2e$/year) due to its high thermal mass, but as expected, it also had the highest EC, resulting in the smaller WLC emissions reduction of just 6.10 tCO_2e.

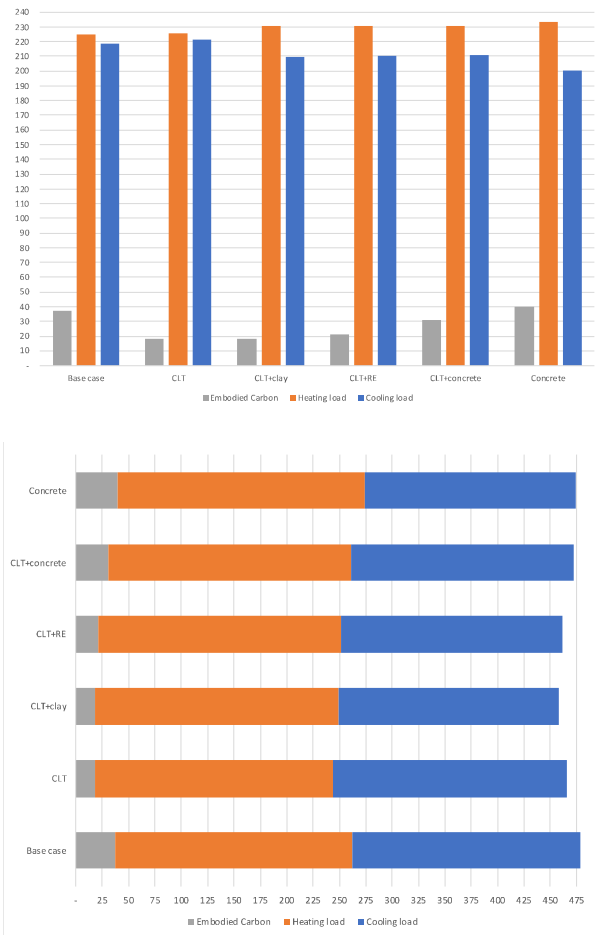

Figure 5: Graphs showing the WLC emissions of the proposed solutions (GWP, tonnes of CO_2e). In the top graph, embodied carbon, and the operational carbon due to heating and cooling loads for 100 years are separated to show the differences, while in the bottom one they are summed to highlight the WLC aspect.

By combining the best performing scenarios (an all-glulam structure, the CLT+earthen slabs, together with the walls and core proposals), the final carbon emissions reduction from the base case is of 62.90 tCO_2e, or 4.70 $kgCO_2e/m^2$.

6. CONCLUSIONS

As seen in the analysis, an efficient design of building elements with MT and a thorough product selection can lead to CO_2e emissions reductions throughout all life cycle stages. Variables that make a sensible difference in the environmental performance of the building include the specific choice of EWPs, where to use them, how the building and its structure are designed, and how to couple timber with other materials to compensate possible weaknesses.

Therefore, designers should take a good amount of care in such choices if a high sustainability level is desired. Literature shows that glulam and LVL are more indicated for structural frame elements, both from an EC and a structural point of view – although it is essential to conduct precise analyses of the specific considered EWPs to understand which one would bring the biggest CO_2 reduction. For surface elements, CLT is demonstrated to be a very carbon-efficient and structurally sound material with great versatility.

The results show how replacing steel and concrete with mass timber elements results in a significant reduction in EC. Adding earthen flooring to CLT slabs proves to be a successful strategy, improving the thermal mass performance with a low carbon profile. Regarding the external walls, replacing the outer columns and the inner layers of a lightweight cassette wall construction (plasterboard and part of the insulation) with a load bearing CLT layer can bring significant EC reductions, around 10.5 $kgCO_2e/m^2$, while maintaining the same U-value. All in all, the carbon emission reduction opportunities with MTC are mostly located in the upfront stage more than in the operational carbon one.

REFERENCES

1. IPCC (2023) *Climate Change 2023: Synthesis Report. A Report of the Intergovernmental Panel on Climate Change. Contribution of Working Groups I, II and III to the Sixth Assessment Report of the Intergovernmental Panel on Climate Change.* Geneva, Switzerland: IPCC. Available at: https://www.ipcc.ch/report/ar6/syr/

2. United Nations Environment Programme (2022a) *2022 Global Status Report for Buildings and Construction: Towards a Zero-emission, Efficient and Resilient Buildings and Construction Sector*. Nairobi: UNEP. Available at: https://globalabc.org/resources/publications/2022-global-status-report-buildings-and-construction

3. Jensen, A., Norford, L. and Grinham, J. (2020) 'Mass(ive) Timber: Examining the Thermally Massive Behavior of Mass Timber Construction', *Technology architecture + design*, 4(2), pp. 186-199 Available at: https://doi.org/10.1080/24751448.2020.1804763.

4. Adekunle, T.O. and Nikolopoulou, M. (2016) 'Thermal comfort, summertime temperatures and overheating in prefabricated timber housing', *Building and environment*, 103, pp. 21-35 Available at: https://doi.org/10.1016/j.buildenv.2016.04.001.

5. Rodrigues, Sougkakis, Gillott (2015) Investigating the potential of adding thermal mass to mitigate overheating in a super-insulated low-energy timber house, *International Journal of Low-Carbon Technologies 2016*, 11, 305–316

6. Pollmeier (2023a) *06: Comparison of BauBuche and other building materials.* Available at: https://www.pollmeier.com/downloads/ (Accessed: 29 March 2023).

7. SOM (2013) *Timber Tower research project*. Skidmore, Owings & Merrill LLP. Available at: https://www.som.com/research/timber-tower-research/

8. Vardaxis, N., Bard Hagberg, D. and Dahlström, J. (2022) 'Evaluating Laboratory Measurements for Sound Insulation of Cross-Laminated Timber (CLT) Floors: Configurations in Lightweight Buildings', *Applied sciences*, 12(15), pp. 7642 Available at: https://doi.org/10.3390/app12157642.

PLEA 2024 WROCŁAW
(Re)thinking Resilience

(Re)thinking Buildings as Carbon Assets:

How can design and construction technologies ensure a resilient return on carbon investment?

MARTIN MURRAY,[1] SHANE COLCLOUGH,[1] PHILIP GRIFFITHS[1]

[1]Ulster University, Belfast, Northern Ireland, United Kingdom.

ABSTRACT: Carbon has become a currency of great significance as we seek to reduce our greenhouse gas emissions to zero by 2050. The intent to create (nearly) zero energy buildings has matured into a focus on zero emission buildings (ZEB), which in turn has focused on the carbon emissions which constitute 75% of our overall greenhouse gas emissions, (GHG). The Paris Agreement (2016) established carbon emission budgets within which we must operate to avoid catastrophic global temperature extremes. To date these have not been complied with. Buildings 'fit for 2050' must consider both embodied and operational carbon, as the guiding metrics by which sustainable validity is measured. Emissions within the built environment, must focus on the return to be achieved in terms of energy saving and energy creation, calibrated against the carbon expended to achieve these. The research case-study investigates how a virtuous carbon circle encompassing (a) improved low embodied carbon fabric leading to (b) improved surplus of return from onsite renewable energy systems, can lead to (c) maximum onsite use and peak grid support. Policy must follow science, and such a science-based policy requires significant transformation toward a ZEB solution.
KEYWORDS: Carbon-budget, Zero-emission Building, embodied-carbon, operational-carbon, PH

1. INTRODUCTION

The Paris Agreement of 2015/2016 (COP21) created a legally binding international treaty defining the estimated carbon emission limits, necessary to reduce global warming. In this context the Intergovernmental Panel on Climate Change, (IPCC) estimated, that to have a 67% chance of limiting the global temperature increase to 1.5°C, the remaining global carbon budget (GCB) from 2018 onwards, would need to be limited to between -500 and 1,340 $GtCO_2$ (bn tonnes); with 420 $GtCO_2$ identified as being the most probable GCB. In 2020 this budget was re-estimated to 400 $GtCO_2$ of CO_2. This is equivalent to an average of only 11 years further years of emissions based on that year's emissions profile, [1].

Ireland also faces this reality of a fast-diminishing CO_2 budget, and one of the principal reasons identified is the ignoring of embodied carbon, [2]. Glynn et al., (2018), attempting a useful understanding of what a zero-carbon energy system pathway for Ireland, (consistent with the Paris Agreement), might be like, suggested that the cumulative carbon budgets remaining for use in Ireland, range from 128$MtCO_2$ to 766$MtCO_2$, (from 2015 through to 2070), reflecting a 0.064% share of the remaining global carbon budget, proportional to Ireland's global population, [3]. All literatures identify a need for immediate action as there is an increasing awareness of the time value and benefit of carbon spend reduction now.

This urgency however must respect the fine balance to be achieved between the immediate carbon expended to lower emissions now, whilst calculating the benefit of such early movement, against this carbon cost. In this context carbon 'spent' must be effective, and efficiently so, to achieve a net zero carbon status, as noted by the World Green Building Council, (WGBC), (2019), [4].

Rovers, (2019) estimated that in the Netherlands the national carbon budget figures required to retrofit all of their old housing stock to reduce carbon emissions, would have used their entire national carbon budget up to 2050, [5]. Rovers' comments are noteworthy in the context that heretofore he had been a significant supporter for radical and swift energy upgrades of Dutch housing, such as Energiesprong, (energy jump). Therefore his warning that high embodied carbon solutions created to reduce carbon emissions, without considering the effective return, may well be counterproductive and warrants serious consideration.

This research paper, which is case study based, is therefore focused on how a *'(re)thinking of buildings as carbon assets'* would transform our understanding of the relationship between fabric priorities and mechanical and electrical technologies, particularly onsite renewable energy systems (RES), so as to ensure a resilient return on the carbon investment and achieve a built environment fit for 2050.

*Table 1: Indicating how 225m² of PV solar array gives an annual output of 30,816kWh, (indicated in blue). Indicated in yellow are the various months where **surplus** PV generation vs building need is available for DEAP, PH (res), NEAP and PH (non-res).*

	Jan	Feb	Mar	April	May	June	July	Aug	Sept	Oct	Nov	Dec	Total
DEAP	8587	7669	7018	5506	**3629**	**2262**	**1619**	**1547**	**2205**	4709	7108	8883	**60,742**
PH (res)	3363	2941	**2327**	**1730**	**1293**	**1186**	**1167**	**1166**	**1185**	**1609**	2704	3584	**24,257**
PV (225m2)	**844**	**1251**	**2417**	**3476**	**4406**	**4242**	**4197**	**3763**	**2812**	**1814**	**1007**	**590**	**30,816**
NEAP	9624	8752	8279	6813	4833	**3248**	**2463**	**2350**	3076	5705	8092	9855	**73,089**
PH. (non res)	3830	3422	2821	**2255**	**1830**	**1728**	**1712**	**1711**	**1726**	2089	3155	4051	**30,328**

2. THE CHALLENGE

The principal activity areas giving rise to carbon emissions within Ireland, are Industry, Agriculture, Power Generation, Transport, and the Built Environment, [2]. These emission areas overlap, and each area fights for the validity of its position, and its right to maintain commercial output. In 2020, Ireland's annual GHG emissions were estimated to be 57.72 million tonnes of carbon dioxide equivalent ($MtCO_2e$). The GHG emissions figure for 2021 had increased to 61.95$MtCO_2e$, while preliminary 2022 emission figures reflect a 1.9% reduction to 60.76$MtCO_2e$. In 2020, Agriculture was the single largest contributor at 37.1%, with transport, energy industries and the residential sector being the next largest, at 17.8%, 15.1% and 12.3%, respectively. These figures combined, confirm Ireland in 2022, as having the third highest GHG emissions per capita within the EU/EEA member states, as noted by the Environmental Protection Agency, (EPA), (2023).

These trends are important, as 2021 is the first year to be used as evidence of compliance with EU targets under the Effort Sharing Regulations, (ESR) regarding emissions which are outside the Emissions Trading Scheme. These targets set the emission budgets to 2030 and 2050, and EU financial penalties will accrue if these are not met. Unfortunately the EPA notes that Ireland is currently running at best, 0.801 $MtCO_2e$ behind target, which will necessitate an average of 8.4% additional reductions across the remaining years (2022 – 2025), to stay within the EU limits. Adherence to such carbon budgets is therefore now a serious issue for Ireland. National policy requires not just an approach related to national trajectories, but one related to science and the direct control of emissions.

In the built environment, Ireland currently has a nearly Zero Energy Building (nZEB) policy approach to climate change, which derives its focus from only a statistical viewpoint, when it actually needs an nZEB science-based approach. Such an approach sees building as carbon assets, the construction and renovation of which, needs to justify all carbon spent. Refurbishments in particular need to be deep, to meet the needs of 2050, not to do so now will require further carbon expenditure in the years ahead.

The Irish Green Building Council, (IGBC), (2016), have estimated that if Ireland wants to keep its 2050 climate-change targets on track, deep-retrofits to a BER level of A2, not B2, are needed for 75% of the existing residential housing stock, [6].

To date the built environment metrics for low energy buildings in Ireland have been determined by the nZEB standard(s) which have been characterised by poor climate definition, moderate fabric performance, and poor performance alignment across building typologies, (residential and non-residential). This is reflected most clearly in the residual kWh surplus achieved from the PV array investment, when the case study building design is aligned with a passive house (PH) building standard, as opposed to an nZEB building standard, (Table 1).

The nZEB buildings designed in accordance with DEAP software for residential, and NEAP for non-residential, reflect a very poor return on both the carbon invested in the PV, and the fabric, resulting in surplus output across only five and three months respectively, when the PV produces enough power to render the buildings zero emission. By contrast the improved building standard of PH allows eight and six months respectively of surplus and zero emission use.

The case study (Fig. 1), research data was purposed to investigate if this step change was a valid approach to achieving the new zero emission building (ZEB) standard, [7], and thus creating a carbon asset with optimal and integrated construction and renewable energy principles, which could be adapted within the construction industry in Ireland.

Figure 1: Overview of case study site from south-west.

2.1 Buildings as carbon assets

Understanding buildings as carbon assets necessitates an understanding of operational and embodied carbon, ensuring that the relative dynamics of each together, justify the carbon spend. The research evolves from the case study buildings being defined across a range of specifications to meet three specific criteria: (i) Improved fabric, including airtightness, (ii) Significant onsite renewable energy systems, (RES), all assessed against (iii) the embodied carbon necessary to achieve these improved performance metrics. Each building was also assessed against both residential and non-residential use, the underlying premise being that an improved level of fabric performance, particularly for commercial buildings, would guarantee such buildings a long-life utility, ensuring that any increased embodied carbon expenditure on the fabric would achieve a significantly beneficial return across time.

2.2 The case study

The case study consists of a campus of three individual buildings, totalling 425m2 set across two and three stories, orientated south, and designed specifically to be loose-fit and calibrated beyond the basic legislative requirements set by the statutory nZEB standard, to the PH standard, (Fig. 1). The case study fabric was specified to meet both the passive house (PH) and the nearly zero energy building (nZEB) standard. The key differential between the two standards is emphasised by the airtightness to be achieved. The passive house planning package, (PHPP), sets a natural lineage toward the new Zero Emission Building (ZEB) standard as defined by the 2023 Energy Performance of Building Directive (EPBD), [7]. The campus is supported by onsite RES in the form of heat pumps and the power output from a PV array of 225m2, the excess output of which increases with improved fabric performance and allows significant benefits across the life expectancy of its operation, (Table 1) and (Table 4). Thus an important virtuous carbon cycle is created.

3. DEFINING A VIRTUOUS CARBON CIRCLE

Understanding buildings as carbon assets necessitates an improved design methodology which corelates the improved fabric with the improved onsite renewable energy systems, leading to the creation of a virtuous carbon circle. This achieves an energy-plus operational profile by facilitating surplus low carbon electrical support for the peak, and off-peak power grid, and the charging of onsite heat pumps, batteries, and electric cars. The need to upgrade fabric to meet our Paris obligations has been identified by civil society groups such as LETI, the RIBA and RIAI, [8]. There is therefore a direct validity in changing fabric from nZEB to PH, (Fig. 2), (Fig. 3).

3.1 Fabric performance

Fabric performance is central to establishing the sustainability credentials of zero emission buildings. However fabric needs consideration across not just a criteria of energy reduction, but also its embodied carbon, and airtightness. Additional fabric necessitates additional embodied carbon, and the case study data investigates if the increased fabric is justified, (Table 2) and (Table3).

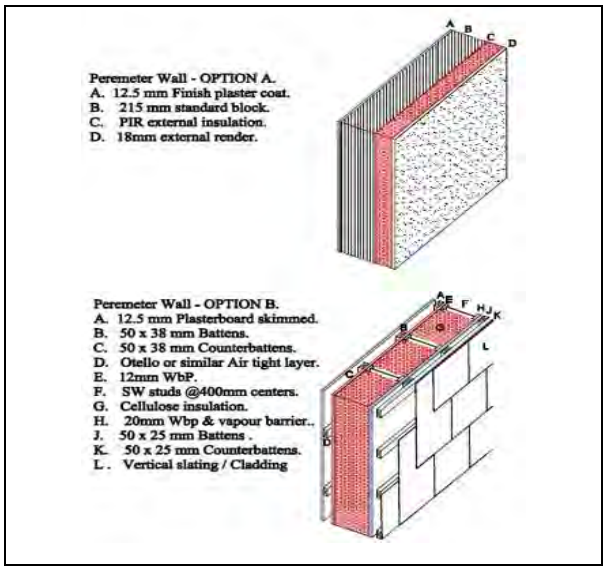

Figure 2: Indicating two contrasting fabric approaches used to estimate additional embodied carbon cost of insulation required to achieve PH standard over the nZEB standard and compare specifications for the commercial (non-res) use against those required for the residential (res) use.

The fabric was considered across three variables (a) the validity of adapting a low embodied carbon timber structure versus a more traditional concrete block structure (Fig. 3), (b) the embodied carbon implications of achieving the improved PH performance, (typically the floor/roof being 0.10 W/m^2K and walls 0.11 W/m^2K), (Fig. 3), and the additional embodied carbon required to meet res use over non-res use, (Table 2) and (Table 3).

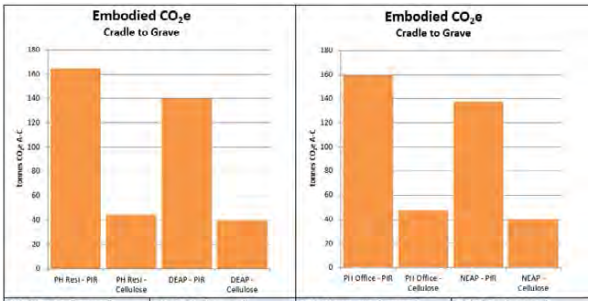

PH (res): (tonnes)		DEAP: (tonnes)		PH (non-r): (tonnes)		NEAP: (tonnes)	
164.3	44.8	139.9	40.0	159.4	47.6	137.4	40.1
PIR	Cellulose	PIR	Cellulose	PIR	Cellulose	PIR	Cellulose

. Data in KgCO2e (tonnes). (Ref AECB Carbon calculator)

Figure 3. Embodied carbon (equivalent) across nZEB (DEAP and NEAP), and PH standards, using traditional concrete block construction and low embodied carbon timber frame construction methodologies across the entire site.

Altering the fabric make-up from traditional masonry construction to timber framed has a significant effect on reducing the overall embodied carbon of the development fabric, as analysed using the AECB carbon calculator, (Fig. 3). This move from a high to a low embodied carbon fabric solution results in a reduced carbon payback period, for both res (DEAP) use, (Table 2), and for non-res (NEAP) use, (Table 3). The payback periods, (measured in $kgCO_2e$ saved), across a 60-year life cycle are low; therefore as low embodied carbon construction becomes common place, it is reasonable to improve the fabric performance at such a low carbon cost.

Table 2: DEAP: Additional embodied carbon within fabric based on Figure 3 set against the reduced heat demand indicating resultant carbon payback times.

DEAP vs PH Standard	Total heat demand use (kWh) (Ref table 5.	Embodied Carbon (Kg CO_2e) of Fabric (across two construction methods)	
DEAP	21,693 per year	139.9	40.0
PH (Domestic)	7,248 per year	164.3	44.8
Savings / Extras	14,445 kWh (Saved per year)	24,400 Kg CO_2e (Extra)	4,800 Kg CO_2e (Extra)
Payback period (yrs.) for embodied carbon used based	**14,445 kWh (@ 0.224kgCO_2e /kWh) = 3,235 kg CO_2e**	**7.54 years Payback period**	**1.48 years Payback period**

Timber construction as a low carbon solution necessitates also the need for carefully considered airtightness, to prevent interstitial condensation within the fabric of the building. Airtightness is therefore a significant aspect of fabric quality, allied with the additional benefit of ensuring an efficiency of operation for heat recovery ventilation, which is necessary for good indoor air quality, (IAQ).

Table 3: NEAP: Additional embodied carbon within fabric based on Figure 3 set against the reduced heat demand indicating resultant carbon payback times.

NEAP vs PH Standard	Total heat demand use kWh	Embodied Carbon of Fabric (across two construction methods)	
NEAP	29,401	137.4	40.1
PH (non-res)	6,377	159.4	47.6
Savings /Extras	23,024 kWh Saved	22,000 Kg CO_2e Extra	7,500 Kg CO_2e Extra
Payback period for embodied carbon	23,024 kWh (@ 0.224 kg/kWh) – 5,157 kg CO_2e	4.3 years	1.45 years

Introducing heat recovery ventilation into residential settings has been proven to be beneficial in both energy terms and IAQ, provided that it is managed well, [9]. However what is generally not discussed are the potential benefits that accrue from the presence of such ventilation, in allowing domestic settings to be capable of commercial use, and vice versa, and the potential dual-use of heat pumps for both winter heating, and summer cooling, the latter being particularly helpful if PV arrays are present.

Such flexibility of use is beneficial in an era where Covid 19 and the Internet together, have disrupted the fixed nature of the workplace. This change in workplace activity is significant as the energy profile of the typical day is altered, and the use profile of home, office, and public/private transportation, transforms. This creates an opportunity for optimal onsite use of renewable energy within the home setting, if available from onsite renewables like PV.

3.2 Onsite renewable energy systems.

The carbon emissions evident within all aspects of our western lifestyle suggests that this very lifestyle must change if we are to create a meaningful reduction in carbon emissions ongoing. The case study research suggests that this is achievable if the virtuous carbon circle of fabric, reduced embodied carbon and RES can be adhered to across our urban building stock.

The case-study addresses the need for onsite low carbon renewable energy in two ways, by the use of heat pumps, and by the installation of PV arrays. The principle of linking low demand with significant supply has been researched before by the PH Institute (PHI) in Darmstadt, which has given rise to two developed energy plus PH standards, (beyond the classic PH standard), PH 'Plus' and PH 'Premium'.

The principle of an energy plus building, (Fig. 4) is the underlying premise of a building as a carbon asset. This principle is further validated by the electrification of the transport sector through EVs, and the heating sector through heat pumps. This in turn effects a transfer of CO_2 emissions from the non-Emissions Trading Schemes (NETS) to the Emissions Trading Scheme (ETS) as part of the GHG emissions accounting norms. However the large, embodied carbon of PV arrays is difficult to justify in the context of a reduced power grid Primary Energy Factor, (PEF).

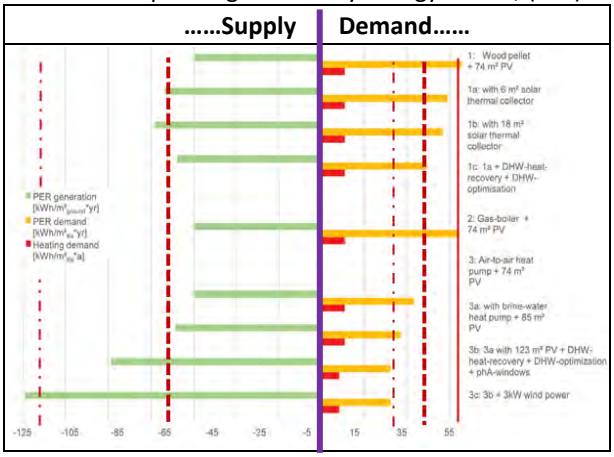

Figure 4: Increased renewable energy generation (green, LHS) set against reduced demand (red is heat demand and yellow overall demand, RHS) reflect the metrics of the PH Plus (vertical dash line) and PH Premium (vertical dot/dash line). The PH Classic is noted to the RHS, (solid vertical red line) and reflects no onsite renewable energy.
(Illustration ref: Passivehouse Plus)

3.3 The embodied carbon of onsite RES.

As the PEF of the main power grid reduces it becomes increasingly difficult to justify the embodied carbon of onsite micro-generation. In regard to PV arrays, a significant bonus can be the surplus energy generated on site, resulting from an improved fabric performance, and the life expectancy of the array. A key insight resulting from the research arises then from the fact that the improved fabric performance does not just save energy, and create comfortable interiors with good IAQ, rather it also allows for a reduced operational size of mechanical and electrical equipment resulting in their lower embodied carbon.

This is significant, as the embodied carbon of a single heat pump over the life of a typical house can equate to the embodied carbon of the fabric itself, due mainly to its anticipated much shorter lifespan, (17 years), as compared to the lifespan of the fabric (60 years). Additionally, as the case study indicates, by communalising the heat pump installation into one significant installation, in lieu of facilitating individual heat pumps to each of the six units, the overall embodied carbon of the installation can be reduced by 70%, 42.0 tonnes to 12.8 tonnes, (Fig. 5).

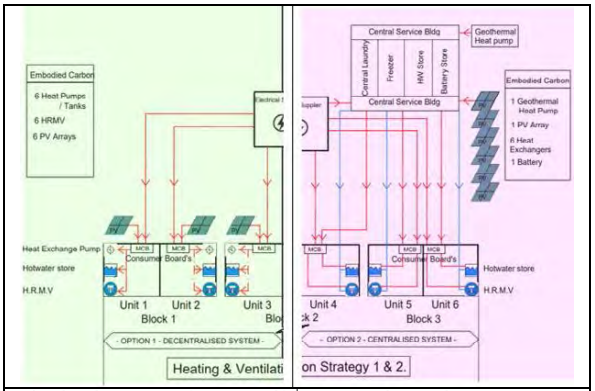

Six 6kW heat pumps (one per unit) each containing 1.75 tonnes of embodied carbon (equivalent) replaced three times over 60-year life (every 20 years). (Total 24 across 60 years). **Equals 42.0 tonnes of embodied carbon (e)**	One ground source heat pump containing 3.2 tonnes of embodied carbon replaced three times over 60-year life (every 20 years) (Total 4 over 60 years). **Equals 12.8 tonnes of embodied carbon (e)**

Figure 5: Schematic arrangement across case study site indicating embodied carbon resulting from the use of six heat pumps (LHS) versus one centralised ground source.

The case study PV array generates 30,816kWh per annum. The carbon intensity is calculated at 61,875 $kgCO_2e$, (Table 5), which effectively sets a neutral carbon intensity for onsite electricity of below 0.1004$KgCO_2e$ per kWh generated, averaged across 20 years of operation.

Of greater benefit still is the realisation that notwithstanding potential gradual inefficiencies, this carbon intensity reduces by a further 33% to .0669$KgCO_2e$ after 30 years, of operation, (Table 4). Life cycle awareness and timing is therefore crucial to understanding the overall embodied carbon lifecycle of a building and its services, and how it might best align with a circular economy.

Table 4: Carbon Intensity of onsite electricity across various PV array life expectancies, of 20, 25 and 30 years.

(PV generation (kWh) per year: 30,816)	20 years	25 years	30 years
Entire generational output	616,320 kWh	770,400 kWh	924,480 kWh
Carbon intensity of PV array at 61,875 $kgCO_2e$ across various life expectancies.	0.1004kg/kWh (Baseline 100%)	0.0803kg/kWh (80%)	0.0669 kg/kWh (67%)

While the calibration of the carbon payback period for the PV array is directly related and dependent on the PEF of the main power grid, nevertheless the payback periods of either 8.96 years based of a power grid PEF of .224kg/kWh, or 4.91 years, based on a PEF of .409kg/kWh, (Table 5), indicate a clear carbon argument for renewable power. There is also great benefit to be gleaned from having the generation directly on site, supporting the power grid locally, avoiding transmittance losses, and facilitating the resilience inherent in being decentralised and calibrated to local needs.

Table 5: Carbon payback calculated based on heat demand savings only, (carbon equivalent) set against the embodied carbon of the PV array itself.

PV Standard		Total generated kWh	Carbon payback period for PV embodied carbon used (based on heat demand only)
PV generation (yr)	=	30,816 kWh	(a) 30,816kWh = 6,903kg CO_2 *(@ 0.221 kg/kWh)*
(PV power =32.25kWp)			(b) 30,816kWh = 12,604kg CO_2 *(@ 0.409 kg/kWh).*
Estimated embodied carbon of PV array. (Based on UK studies by Allen et al (2008) and Hammond et al (2012))	=	61,875Kg CO_2e (225m2 by 275 $KgCO_2e$)	Payback period (dependant on PEF) (a) 8.96 years OR (b) 4.91 years

The recent emergence of electric vehicles (EVs) has also brought an immediate added value to the generated electricity of a PV array. Acting as residual batteries the EVs have the capacity to provide power grid support on the demand side, as is happening in mature electric car areas like California, as noted by Listgarten, (2022), [10]. EV manufacturers have recognised this potential with the introduction of bidirectional charging cars, (V2H), into Ireland, since 2022, leading to their potential future use in peak shaving of electricity within the home and across energy districts. The PV arrays, proposed within the case study site generating 30,328 kWh per year, calculated through PHPP, is on its own, enough dedicated power to charge 6 cars daily to 10.5 kWh, reflecting a range of 45 to 70 km. (A 2022 Nissan Leaf for example, has an efficiency rating of 30 kWh/100 miles or 6.8 km/kWh). This would meet the needs of most short journeys and creates a replacement value for a kWh of electricity, (in lieu say of a diesel car running at 50 miles/gallon), at close to 0.60 cents.

This is substantially more than the approximate default value of 0.13 to 0.21 cents currently quoted as the buy-back value to the grid in April 2023.

However the quantum of surplus energy from the case study PV arrays is directly related to the building's energy demand and therefore its fabric performance. The case study data quantifies the divergence between the heat demand loads for the nZEB and the PH standards and calibrates the increased resilience inherent therefore in the PH standard. The 225m^2 PV array direct surplus of 23,568 kWh, achieved under PH design standards, is sufficient to generate approximately 825 therms of heat, enough to heat a standard 100m2 house for about 27 days or a passive house for about 135 days. It is for these reasons that urban infill redevelopment such as the case study project, can be seen as an opportunity to address climate change with buildings performing as carbon assets, rather than contributing to climate change, as carbon sinks.

4. CONCLUSION

Understanding buildings as carbon assets requires designers from the very beginning of the building's commissioning, to place value centrally to where it is of greatest importance, carbon. Such carbon considerations may also include whether to build at all, an existing building being potentially the most sustainable building of all. The expenditure of carbon and its associated emissions must be justified both by reduced operational energy use, but also by a return on the embodied carbon invested.

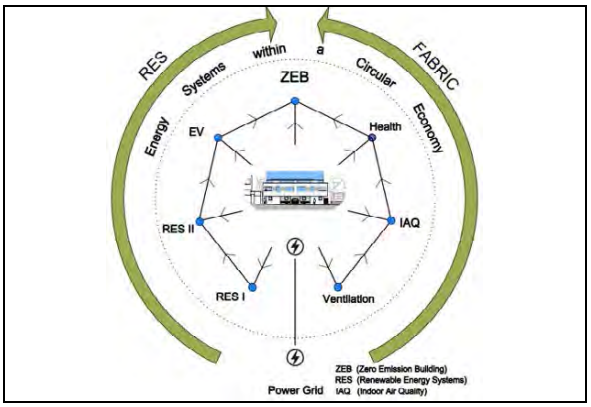

Figure 6: The case study operational diagram manifesting as an optimal balance between RES and fabric, leading to the potential for a zero-emission building across an operational year.

As the research indicates, the alignment of low carbon exemplary fabric with optimising onsite renewable energy systems creates a carbon asset which can be a positive contribution to the ongoing challenge of GHG emissions reduction, (Fig. 6). One particular insight gained from the case study relates to the benefits accruing from, the use of the PH standard over nZEB to achieve the ZEB standard.

However the real insights relate to the potential for reduced embodied carbon within the mechanical and electrical services. The high embodied carbon of the PV array (225m2) is quickly offset by an improved performance of fabric, which ensures that the surplus power from the array is maximised in use. Additionally by maximising the fabric performance the associated heat pumps can be reduced in size and their embodied carbon minimised. If management protocols allow for the centralisation, or communisation of the heat pumps, greater reductions in onsite embodied carbon metrics are possible. This is effective and resilient (re)thinking.

The case study insight is that by careful and improved carbon considerations, we can radically re-assess the relationship of fabric with onsite renewable energy systems (RES), against the return on embodied carbon, thus justifying the long-term carbon invested and meeting the zero emissions need of a post 2050 world.

ACKNOWLEDGEMENTS

The body of research which constitutes the mainstay of this paper was conducted as part of a PhD dissertation completed in 2023. I would like to thank PLEA for their ongoing platform of conversation and debate, Ulster University for its support and my supervisors from that time, Dr Shane Colclough and Prof Philip Griffiths for their helpful and considered insights into these matters.

REFERENCES

1. IPCC, (2019) Special Report on Global Warming of 1.5 ºC. (*https://www.ipcc.ch/sr15/*.
2. O'Hegarty, R., Wall, S., Kinnane, O., (2022). Whole Life Carbon in Construction and the Built Environment in Ireland. *Today, 2030, 2050. (Draft v4), on behalf of the IGBC.*
3. Glynn J., Gargiulo M., Chiodi A., Deane P., Rogan F., Ó Gallachóir, B., (2018). *Zero carbon energy system pathways for Ireland consistent with the Paris Agreement.* Climate Policy, 19:1, 30-42, DOI: 10.1080/14693062.2018.1464893
4. World Green Building Conference, (2019). Downloads/WorldGBC Bringing Embodied Carbon Upfront.pdf
5. Rovers R., (2019). People vs Resources: Restoring a world out of balance. *Eburon, Utrecht.*
6. Irish Green Building Council (IGBC), (2017), Towards large scale deep energy renovation. Unlocking Ireland's Potential. *https://www.igbc.ie/wp-content/ uploads/2017/03/IGBC-*
7. Energy performance of buildings (recast) Amendments adopted by the European Parliament on 14 March 2023, *(COM (2021)0802 – C9-0469/2021 – 2021/0426(COD))1 (Ordinary legislative procedure – recast) P9_TA (2023)0068.*
8. LETI, (2017). London Energy Transformation Initiative. *Now known as Low Energy Transformation Initiative. https://www.leti.uk/about*
9. Sharpe T., Farren P., Howieson, S., Tuohy P., McQuillan J., (2015). Occupant Interactions and Effectiveness of Natural Ventilation Strategies in Contemporary New Housing in Scotland, *UK. Int. J. Environ. Res. Public Health, 12, 8480-8497; doi:10.3390/ijerph120708480*
10. Listgarten, S., (2022). A New Shade of Green. Uploaded: Dec11th.https://www.paloaltoonline.com/blogs/p/2022/12/11/yes-an-app-can-charge-your-ev-better-than-you-can.

PLEA 2024 WROCŁAW
(Re)thinking Resilience

Modelling and Predicting CO2 Emissions in China Using Urban Form and Geographically Weighted Regression

YEEYI NG[1]

[1]China Europe Design Association, Triple Helix Community, Hong Kong, China

*ABSTRACT: This study addresses the urgent need for high-resolution carbon dioxide (CO2) emission inventories in China to tackle climate change. By integrating "top-down" methods, night-time light data (NTL), population aggregation, and urban form indicators, a high-resolution CO2 inventory for 2020 at a 1km*1km scale was developed. Utilizing geographically weighted regression (GWR), the model indicates that the CO2 emission variation can be explained by urban form, population aggregation, and NTL. The model's enhanced accuracy was evident in regions with higher urbanization. The resulting high-resolution emissions mapping offers detailed insights into emission hotspots and distribution patterns, providing crucial support for precise emission analyses at a small scale. The study's findings underscore the importance of considering urban form and population aggregation data alongside NTL in estimating CO2 emissions. This enhanced CO2 grid estimation model not only surpasses traditional NTL-based methods but also offers valuable insights for formulating effective emission reduction strategies.*
KEYWORDS: CO2 emissions, Urban form, Geographically weighted regression model, Emission inventory, China

1. INTRODUCTION

Climate refers to the long-term weather patterns of a specific region, while “climate change” denotes shifts in these long-term average temperatures and weather cycles. Human activities are the primary cause of recent climate changes. If greenhouse gas emissions continue, temperatures will keep rising, leading to persistent changes in the climate system. This increases the likelihood of severe, widespread, and irreversible impacts on both humans and natural systems. As the world’s largest emitter of carbon dioxide (CO_2), China faces significant challenges in addressing climate change [1]. The substantial variations in economic and social development, as well as the diversity in energy consumption structures among different cities in China, contribute to significant disparities in the patterns and trends of CO_2 emissions across these cities [2]. Developing high-resolution CO_2 emission inventories for China can provide essential data, which is crucial for formulating effective mitigation strategies and evaluating the effectiveness of mitigation policies.

Currently, high-resolution gridded CO_2 emissions are generally compiled by two viable urban carbon emissions modeling methods: the "bottom-up" and "top-down" methods. "Bottom-up" methods are suitable for modeling urban carbon emissions in situations where detailed data on individual emissions sources are available, typically used on a small scale [3-5]. In contrast, "top-down" methods rely on proxy data to allocate emissions from a large geographic area to a more specific resolution, which are often used in regional or national greenhouse gas inventories [2].

In addition, existing studies usually estimate gridded CO_2 emissions based on spatial night-time light data (NTL) [6-7]. As NTL intensity plays an important role in detecting artificial lights related to human activities, it can exhibit a robust correlation with socioeconomic variables and reflect CO_2 emissions to some extent [8]. However, there are certain limitations when using NTL, such as underestimating transport and industrial emissions during the daytime, meaning estimation methods that rely solely on NTL may introduce uncertainties and inaccuracies in quantifying emissions [9].

As cities produce over 70% of the global CO_2 emission that results from energy use, it's crucial to understand the relationship between cities and CO_2 emissions. Recent studies have shown that urban form is an important factor influencing carbon emissions. Land use, building environment, development patterns, urban compactness, and other factors related to urban form are commonly regarded as key indicators influencing CO_2 emission [10-13], all of which can be a potential data source for developing high-resolution inventories.

Furthermore, global models, such as the ordinary least squares (OLS), are the most used in the top-down modeling that associates the predictors with carbon emissions. However, as the impact of urban form and NTL on carbon emissions can vary spatially, it is essential to consider the spatial heterogeneity in the effects. Geographically weighted regression (GWR) is a local linear regression method based on

modeling spatially varying relationships in each part of the study area. It produces a regression model that describes the local relationships and thus can well model the local spatial relationships and spatial heterogeneity of the variables [15].

On the basis of previous research, this study aims to model and predict CO_2 emissions in China and develop a high-resolution CO_2 inventory (1km*1km) in 2020 through "top-down" modeling based on GWR regression, and the combination of NTL, population, and urban form indicators, where carbon emissions will be allocated from a city-level scale to grid scale.

2. STUDY AREAS AND DATA SOURCES

2.1 Study area

This study chose the cities in mainland China (without Hong Kong, Macao, and Taiwan) as the study area. In examining mainland China, this study recognizes the substantial economic achievements following the country's reform and opening-up, which is a testament to the country's rapid industrialization and urbanization efforts. However, this progress has been accompanied by increased energy demands and CO_2 emissions, positioning China as a major contributor to global emission figures. Despite these challenges, the varied urban development patterns across China's cities present an opportunity to investigate the complex dynamics between urbanization and environmental impact.

The study area shown in Fig. 1 covered a total of 30 provinces and 371 cities, which represent a spectrum of urban sizes and administrative classifications, from megacities to smaller cities, allowing for an extensive analysis of how different urban forms relate to CO_2 emissions.

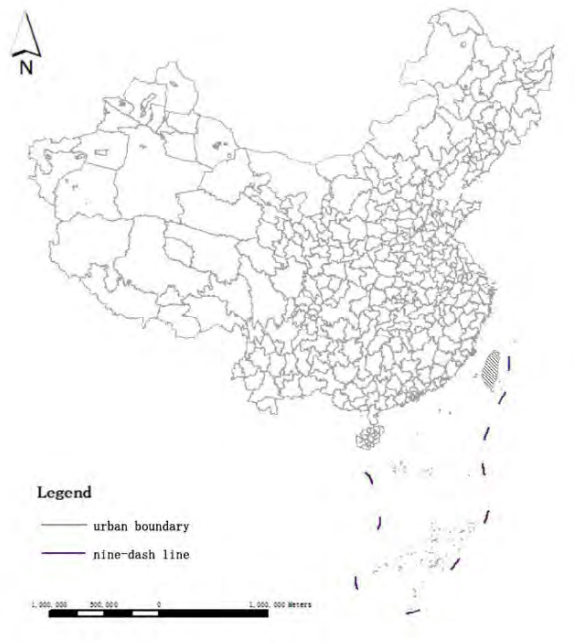

Figure 1: The study area (30 provinces and 371 cities)

2.2 Data sources

Data used in this study include China city CO_2 emissions data, China's national land use and cover change (CNLUCC), population statistics, and VIIRS nighttime light data in 2020. Details of the data are given in Table 1.

The city-level CO_2 emissions data draw on the more mature and widely used international methods of accounting for urban CO_2 emissions, and at the same time combine them with the actual situation of Chinese cities, combining on-site surveys, interviews, telephone consultations, and letters to the relevant parts of the data, but this method only provides CO_2 emission data on the city scale as opposed to a finer spatial scale. This data is used as a reference for modeling CO_2 emissions at the city level of calculation.

The other three types of data have been resampled to a 1 km*1 km grid in this study, which helps construct a CO_2 emission inventory with a resolution of 1 km*1 km. CNLUCC would be transformed in Fragstats 4.2 to obtain urban form data at 1 km*1 km resolution.

Table 1: Data source for estimating CO_2 emissions

Name	Description	Year	Source
China city CO_2 emissions data	Annual city-level data for total CO_2 emissions in China	2020	China City Greenhouse Gas Working Group, CCG
China's national land use and cover change (CNLUCC)	1km*1km land use raster data in China	2020	Data Center for Resources and Environmental Sciences (RESDC), Chinese Academy of Sciences
Population statistics	1km*1km population raster data in China	2020	
VIIRS nighttime light data	Average annual nighttime light on a global scale	2020	Earth Observation Group, NCEI, NOAA

3. METHODOLOGY

3.1 Quantification of urban form

Landscape metrics play an essential role in quantifying diverse characteristics of spatial landscapes, which are intrinsically linked to both ecological integrity and socioeconomic dynamics and are frequently employed to encapsulate the processes and outcomes associated with the spatial configurations of urban environments [14]. Therefore, this study selects the following commonly

used landscape metrics to quantify urban form in China: total area (TA), percentage of landscape (PLAND), largest patch index (LPI), number of patches (NP), contagion (CONTAG), aggregation index (AI), and patch cohesion index (COHENSION). Details of the landscape metrics are given in Table 2.

These seven metrics describe the fundamental dimensions of urban form. TA, PLAND, and LIP were to three land use types: urban land, rural residential areas, and other built-up land. In other words, there were finally 13 kinds of landscape metrics. These indicators were measured with Fragstats 4.2 based on the 1km*1km CNLUCC for 2020, where we could identify and extract the urban land-use regions.

The obtained values served as the independent variables in the spatial modeling of CO_2 emissions. However, while improving the model accuracy, certain variables were removed as not all factors were strongly correlated with the dependent variable. Stepwise regression was used to remove insignificant independent variables to avoid biased results.

Table 2: Description of urban form indicators used in the analysis

Category	Indicator	Abbreviation	Description
Area and Edge metrics	Total Area	TA	TA equals the area (m2) of the landscape, divided by 10,000 (to convert to hectares).
	Percentage of Landscape	PLAND	PLAND equals the percent of the landscape comprised of the corresponding patch type.
	Largest Patch Index	LPI	LPI equals the percentage of the landscape comprised by the largest patch.
	Number of Patches	NP	NP equals the number of patches of the corresponding patch type(class).
Aggregation metrics	Contagion	CONTAG	CONTAG equals the observed contagion over the maximum possible contagion for the given number of patch types.
	Aggregation Index	AI	AI equals the degree to which habitat patches are clumped or aggregated on the landscape.
	Patch Cohesion Index	COHENSION	COHENSION is used to quantify the degree of spatial connectedness within a landscape patch.

3.2 Geographically weighted regression (GWR)

In this study, CO_2 emission statistics of 371 cities in China were selected as the dependent variable, while landscape metrics, population aggregation data, and NTL selected from the stepwise regression were selected as independent variables, to create an optimal city-level model based on R^2 and noncollinearity of variables, further apply to high-resolution CO_2 inventory predictions. The optimal city level model is then applied to the grid scale using GWR and adjusted with national aggregates to obtain the final predictions.

3.3 Spatial autocorrelation

This study adopted spatial autocorrelation to describe the spatial correlation of 1km*1km CO_2 emission data obtained from the forecast. Spatial autocorrelation refers to the degree to which a set of spatial features or their associated values tend to be clustered or dispersed across a geographic space, and it has since become an essential concept in spatial analysis, geography, and related fields. Moran's I is one of the most common statistical methods for measuring spatial autocorrelation. The global Moran's I index [16] represents the spatial autocorrelation in the whole area, while the local Moran's I index [17] represents the local dissimilarities between neighboring cities.

To further explain the types of spatial clusters in local Moran's I, four cluster types are used to reflect a central tendency demonstrated by the regression model: High-High (HH), Low-Low (LL), High-Low (HL), and Low-High (LH).

3. RESULT

3.1 Variable selection

Ten independent variables with significant correlation with the model were finally selected, including eight spatial pattern indicators namely TA (urban land), TA (rural residential areas), TA (other built-up land), LPI (urban land), LPI (rural residential areas), LPI (other built-up land), AI, and NP, as well as population aggregation data and NTL data.

In addition, to ensure the absence of multicollinearity and redundant independent variables in the regression model, the VIF values of the regression variables should not surpass 10 (VIF≤

10) The results, presented in Table 3, demonstrate the absence of multicollinearity among the variables.

Table 3: Assessment of collinearity statistics

Indicator	Tolerance	VIF
TA (urban land)	0.208	4.808
TA (rural residential areas)	0.648	1.543
TA (other built-up land)	0.688	1.453
AI	0.134	7.458
NP	0.348	2.873
population aggregation	0.271	3.694
NTL	0.118	8.447

3.2 CO_2 estimation model by using GWR

After the above steps, the most important independent variables have been identified. Considering the characteristics of the data with repeated attempts, this study chose adaptive bandwidth and optimized it according to the bandwidth parameter. For the entire study area, the R^2 value of the model (R^2=0.928, Adjusted R^2=0.837) shows that 83.7% of the variation can be explained by urban form, population aggregation, and NTL. The results show that the accuracy of the model is improved after improving the model by integrating urban form-related data and population aggregation data.

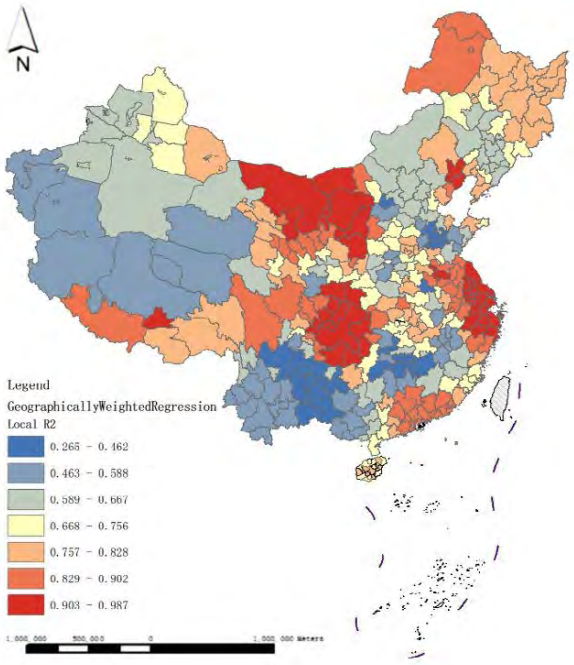

Figure 2: Local R^2 of the GWR model

Fig. 2 reveals that this model is more explanatory in estimating CO_2 emissions in highly urbanized areas like the southeast coast, the region around Sichuan and Chongqing, and the western part of Inner Mongolia. In contrast, rural or less developed areas might not exhibit such strong spatial patterns in relation to CO_2 emissions due to a lack of variability in urban form or other influencing factors not captured by the model. The independent variables of the model influence this, in this study, when selecting the factors related to urban form as independent variables, only the landscape metrics of built-up areas were selected, so that the explanatory degree of the model was commonly higher in areas with higher urbanization.

3.3 High-resolution emissions mapping at the grid scale of 1km*1km

The improved model was used to calculate CO_2 emissions with a resolution of 1 km *1 km in 2020. By utilizing GWR, which accounts for spatial heterogeneity, and building 1km*1km grids, the model provides a more accurate representation of emissions across the grids and a detailed understanding of emission hotspots and distribution patterns, leading to support in China's accurate emission analyses at the small scale.

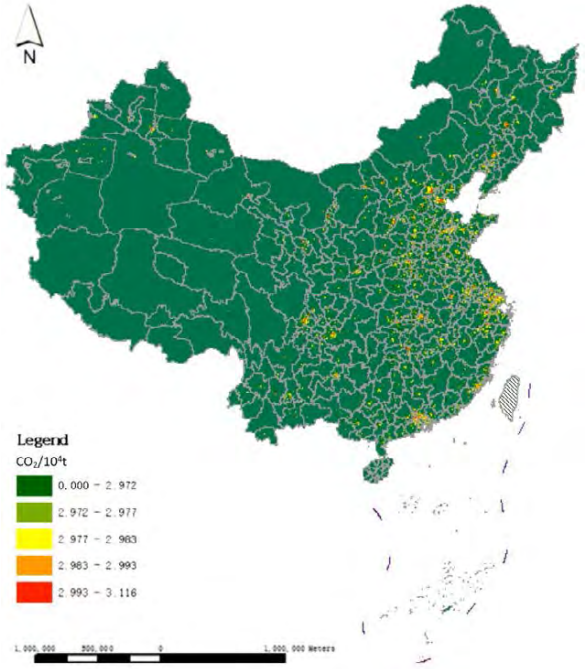

*Figure 3: CO_2 emission distribution at 1 km*1 km grid scale nationwide, 2020*

Fig. 3 shows spatial CO_2 emissions in China in 2020 CO_2 emissions are unevenly distributed, with high-emission grids mainly located in the central and south-eastern coastal areas of China, especially in developed cities such as Beijing-Tianjin-Hebei, the Yangtze River Delta, and the Chengdu-Chongqing urban agglomeration. In contrast, CO_2 emissions grids in northeastern and western China generally have low CO_2 emissions and few high-emission networks, due in part to their sparsely populated areas, low population densities, and low urbanization rates.

In addition, the spatial autocorrelation between multiple grids was considered in this study to measure the effect of city-related data on CO_2 used for prediction as described above. As shown in Fig. 4,

the global Moran's I index is about 0.620 (p-value = 0.000), indicating that spatial CO_2 emissions show clustering patterns.

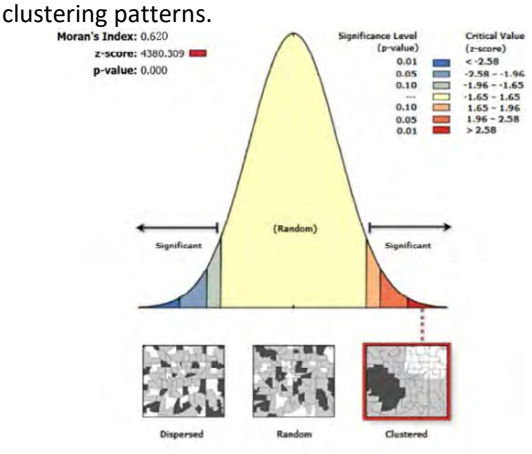

Figure 4: Result of global Moran's I

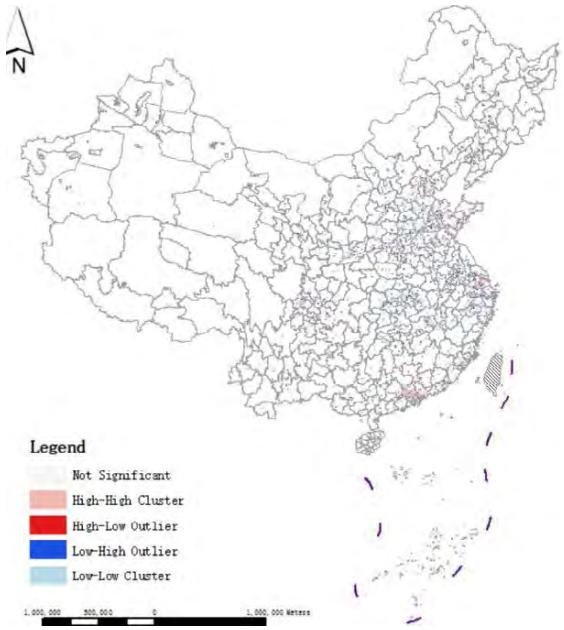

Figure 5: Result of local Moran's I

As it has been shown that spatial correlation exists, the localized Moran's index is further used to help illustrate exactly where spatial clustering exists. Fig. 5 reveals five kinds of clusters. According to Fig. 5, there is significant heterogeneity in spatial patterns of CO_2 emissions. The first-tier cities along the southeast coast are High-High (HH), which means high-emission areas are clustered together. In contrast, the non-first-tier cities in the northwest, southwest, northeast, and central regions are Low-Low, meaning low-emission areas are clustered together. Areas where high carbon emissions are surrounded by low carbon emissions always appear to be surrounded by HH areas. In contrast, areas where low carbon emissions are surrounded by high carbon emissions are more sporadically distributed, mostly scattered among non-first-tier cities in the southeast coast and central China. High-High areas need to be given special attention because they emit large amounts of carbon dioxide and may provide new insights into reducing carbon emissions.

3.4 Comparison with ODIAC emission inventories

To enhance the validation of the emission inventory utilized in this research, we compared the CO_2 emission inventory for 2020 with the Open-Data Inventory for Anthropogenic Carbon dioxide (ODIAC) with a resolution of 1 degree, which focuses on CO_2 emissions from fossil fuel combustion, cement production, and gas flaring.

As shown in Fig. 6, this study selected the Beijing-Tianjin wing region (A), the Yangtze River Delta (YRD) region (B), and the Pearl River Delta (PRD) region (C), whose CO_2 emissions areas are more clustered, to make a comparison of the spatial distribution of CO_2emissions between the high-resolution inventory predicted in this study and ODIAC inventory.

Apparently, this study's 1km*1km resolution inventory demonstrates a more accurate spatial pattern of CO_2 emissions than the ODIAC inventory. This new inventory has greater spatial variation in the predicted values of CO_2 emissions and more spatial detail, not only in resolution but also in spatial detail.

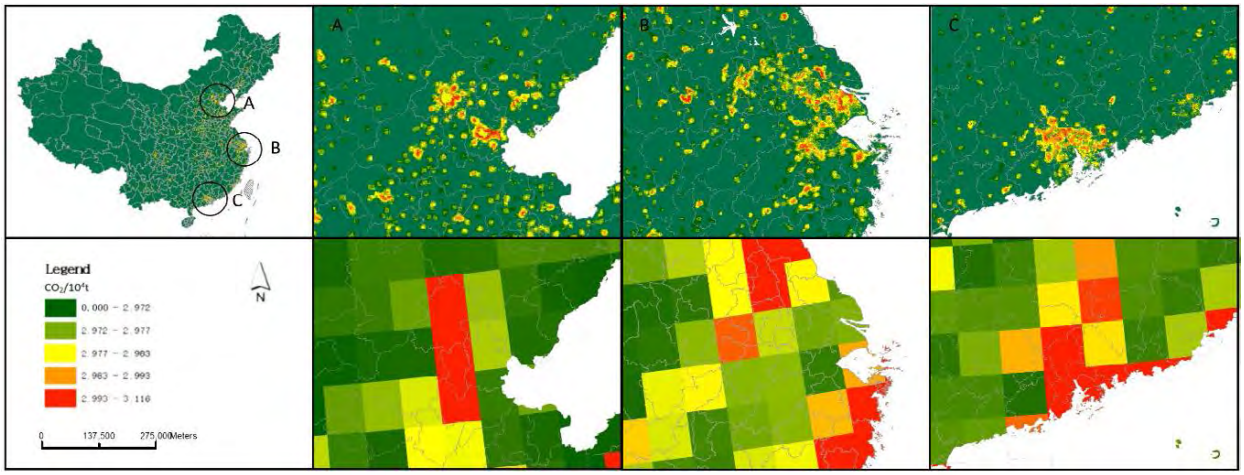

Figure 6: Spatial distribution of CO_2 emissions at the grid scale for predicted inventory in this study and ODIAC

4. CONCLUSION

This study introduced an enhanced CO_2 grid estimation model based on CO_2 energy statistics, NTL, population aggregation, and urban form indicators. The results show that the R^2 of the CO_2 model proposed in this study exceeds 0.90. The improved model assigns higher CO_2 emissions to the grids where urbanization is advanced than to the surrounding grids, compared with the results of spatial assignment using only NTL.

In summary, the high-resolution CO_2 inventory estimated by the model enables a more comprehensive representation of CO_2 emission characteristics, which can further provide support for formulating effective emission reduction strategies. However, there are still some limitations in this study. This inventory cannot accurately estimate CO_2 emissions in areas with little urban built-up land and a lack of human activities.

REFERENCES

1. IEA, (2022). Energy Statistics Data Browser, [Online], Available: https://www.iea.org/data-and-statistics/data-tools/energy-statistics-data-browser

2. Ou, J., Liu, X., Wang, S., Xie, R. and Li, X., (2019). Investigating the differentiated impacts of socioeconomic factors and urban forms on CO_2 emissions: Empirical evidence from Chinese cities of different developmental levels. Journal of Cleaner Production, 226: p. 601-614.

3. Rong, P., Zhang, Y., Qin, Y., Liu, G. and Liu, R., (2020). Spatial differentiation of carbon emissions from residential energy consumption: A case study in Kaifeng, China. Journal of Environmental Management, 271: p. 110895.

4. Zhang, Y., L. Xia and W. X., (2014). Analyzing spatial patterns of urban carbon metabolism: A case study in Beijing, China. Landscape and Urban Planning, 130: p. 184-200.

5. Y. Wu, A. Sharifi, P. Yang, H. Borjigin, D. Murakami and Y. Yamagata, (2018). Mapping building carbon emissions within local climate zones in Shanghai. Energy Procedia, 152: p. 815-822.

6. C.H. Doll, J. P. Muller, C.D. Elvidge, (2000). Night-time: imagery as a tool for global mapping of socioeconomic parameters and greenhouse gas emissions. Ambio, 29: p. 157-162

7. L. Meng, W. Graus, E. Worrell and B. Huang, (2014). Estimating CO_2 (carbon dioxide) emissions at urban scales by DMSP/OLS (Defense Meteorological Satellite Program's Operational Linescan System) nighttime light imagery: Methodological challenges and a case study for China. Energy, 71: p. 468-478

8. Q. Zheng, K. C. Seto, Y. Zhou, S. You and Q. Weng, (2023). Nighttime light remote sensing for urban applications: Progress, challenges, and prospects. ISPRS Journal of Photogrammetry and Remote Sensing, 202: p. 125-141

9. B. Cai, S. Liang, J. Zhou, J. Wang, L. Cao, S. Qu, M. Xu and Z. Yang, (2018). China high resolution emission database (CHRED) with point emission sources, gridded emission data, and supplementary socioeconomic data. Resources, Conservation and Recycling, 129: p. 232-239

10. R. Zhang, K. Matsushima and K. Kobayashi, (2018). A land use planning help mitigate transport-related carbon emissions? A case of Changzhou. Land Use Policy, 74: p. 32-40.

11. Fang, C., Wang, S. and Li, G., (2015). Changing urban forms and carbon dioxide emissions in China: A case study of 30 provincial capital cities. Applied Energy, 158: p. 519-531.

12. Lin, J., Lu, S., He, X. and Wang, F., (2021). Analyzing the impact of three-dimensional building structure on CO_2 emissions based on random forest regression. Energy, 236: p. 121502.

13. Hong, S., E. Hui and Lin, Y., (2022). Relationship between urban spatial structure and carbon emissions: A literature review. Ecological Indicators, 144: p. 109456.

14. X.P. Liu, X. Liang, X. Li, X.C. Xu, J.P. Ou, Y.M. Chen, S.Y. Li, S.J. Wang, F.S. Pei, (2017). A future land use simulation model (FLUS) for simulating multiple land use scenarios by coupling human and natural effects. Landscape and Urban Planning, 168: p.94-116.

15. S. Wang, C. Shi, C. Fang and K. Feng, (2019). Examining the spatial variations of determinants of energy-related CO_2 emissions in China at the city level using Geographically Weighted Regression Model. Applied Energy, 235: p. 95-105.

16. Moran PAP., (1950). Notes on continuous stochastic phenomena. Biometrika, 37: p. 17-23.

17. Anselin L., (1995). Local indicators of spatial association lisa. Geographical Analysis, 27: p. 93-115.

PLEA 2024 WROCŁAW
(Re)thinking Resilience

Carbon footprint of rural and self-built dwellings, in three climate regions of Mexico:

Guanajuato, Colima, and Chiapas.

ISRAEL TOVAR-JIMÉNEZ[1], LUIS VARGAS[1], PAVEL RUIZ[2], VÍCTOR ARVIZU-PIÑA[3], CARLOS ESPARZA[4].

[1]Universidad Iberoamericana León, Guanajuato, México.
[2] Universidad Autónoma de Chiapas, México.
[3]Universidad Iberoamericana CDMX, México.
[4]Universidad de Colima, México.

ABSTRACT:This work develops a comparative study of the incorporated carbon footprint in three cases of rural housing in three different states of Mexico. The three homes located in Chiapas, Colima and Guanajuato, have an area between 45 and 65 sqm and are self-produced dwellings. The incorporated carbon footprint analysis was developed with the OneClick software. The biggest difference between the construction systems is found in the Guanajuato house, which has a concrete slab roofing, and clay brick walls. These differences make it have 2.6 times more Kg CO_2 eq/m^2 than the cases of Chiapas and Colima. This work analyzes the performance of rural homes with the materials currently used in housing programs, and from this analysis seeks to improve their environmental performance, reducing their incorporated carbon footprint.
KEYWORDS: Carbon footprint, social housing, LCA, building materials, self-built dwellings.

1. INTRODUCTION

This paper is part of the work carried out in the National Research and Incidence Project (PRONAII, for its name in Spanish, number 321260), called Development of a Model of replicable social production of dwelling and habitat.

The project objective is to develop a model with a transdisciplinary systemic approach built with the actors involved in the process of social production of Housing and habitat, seeking to strengthen and join efforts in the actions carried out by the National Housing Commission (CONAVI for its name in Spanish) and the Secretariat of Agrarian, Territorial, and Urban Development (SEDATU for its name in Spanish).

Groups from different places of the Mexican Republic collaborate in the project, where the case studies presented in this paper are located, and are part of the different teams: academics, non-governmental organisations, and community groups, among others.

The project PRONAII 321260 is configured with six subsystems: public and legal policy, risks, construction technique, services and resource management, community development, and habitability, the latter being the one in which this work is carried out.

In the last century, there has been a use of conventional construction technologies in the rural context that has transformed the way these constructions interact with the environment. These changes, in addition to reducing the climate adaptability of the houses, increase their carbon footprint by modifying the life cycle of the materials [1-5].

This work seeks to answer two main questions: What is the current carbon footprint of a sample of Mexican rural housing? And based on this analysis in a later stage, how can the footprint of industrial materials be reduced, re-incorporating traditional materials that have been lost? The study cases are located in the states of Chiapas (16.41°N, -93.75°W), Colima (19.5°N, -103.5°W), and Guanajuato (21.15°N, -101.75°W).

2. METHOD

Each working group in its region previously analyzed 10 cases of rural housing, from among these, a house of between 45 to 60 m2 was selected, representative of the materials and construction systems used by region.

This section describes in general terms the case studies considered for the project.

The study case in Chiapas is a 48.34sqm house (figure 1), constructed within the CONAVI social housing program, carried out in the rural community of Monte Sinaí El Fénix II, located in the Sierra Madre of Chiapas, bordering the state of Oaxaca, in the municipality of Cintalapa, which has an altitude of 1300 masl.

Figure 1: Distribution of Chiapas' case.

About the construction elements in this case, here are shortly named and described:

Foundation: concrete slab; Exterior walls: solid concrete block and mortar mix for masonry; Vertical structures: Reinforced concrete columns 15 x 15 cm and 15 x 20 cm; Interior walls: solid concrete block and mortar mix for masonry; Horizontal structures: connecting beam; Floor: concrete slab; Roof: galvanized (zintroalum) roofing sheet; Interior doors: galvanized (zintroalum) steel sheet; Exterior doors: galvanized (zintroalum) steel sheet; Windows: 3mm glass and metal window frame.

In the Colima state study case, the house is self-produced in the rural area to the north of Colima, in the community of El Jaboncillo, Comala (Figure 2). It is located about 800 masl, with a sub-humid tropical climate (Aws); it has an average annual temperature of 25°C, average relative humidity of 65%, and annual rainfall of 900 mm. This house has 61.8 m^2 built.

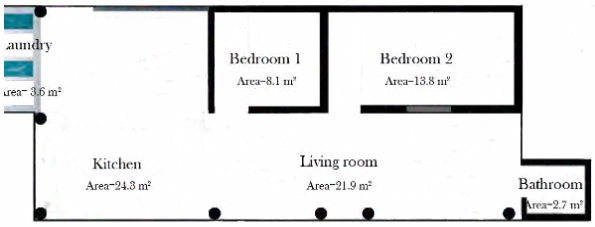

Figure 2: Distribution of Colima's case.

About the construction elements in this case, here are shortly named and described:

Foundation: stone masonry footing; Exterior walls: solid concrete block and mortar mix for masonry; Vertical structures: Reinforced concrete columns 15 x 15 cm and 15 x 20 cm; Interior walls: solid concrete block and mortar mix for masonry; Horizontal structures: connecting beam; Floor: concrete slab; Roof: fiber-cement roofing sheet; Interior doors: galvanized steel sheet; Exterior doors: galvanized steel sheet; Windows: 3mm glass and metal window frame.

In the case of Leon, Guanajuato, the house is self-produced. It is located in the suburban area of the community of Lomas del Suspiro (Figure 3), with an approximate altitude of 1815 masl. The climate is temperate with the sub-humid subtropical variant with summer rains (Cwa). The average temperature is 18.9°C, and the approximate annual precipitation is 621 mm. This house has 64.8 m^2 built.

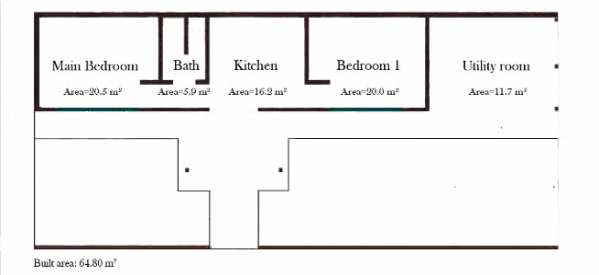

Figure 3: Distribution of Leon's case.

About the construction elements in this case, here are shortly named and described:

Foundation: Isolated Spread Footing; Exterior walls: Clay brick, mortar mix for masonry and cement-sand mortar; Vertical structures: Reinforced concrete columns 15 x 15 cm; Clay brick, mortar mix for masonry and cement-sand mortar; Horizontal structures: connecting beam; Floor: concrete slab; Roof: concrete slab; Interior doors: wooden doors; Exterior doors: wooden doors; Windows: 3mm glass and aluminium window frame.

Cases of Chiapas and Colima share the same material characteristics, except for the roof, which is made of metal for Chiapas and asbestos for Colima.

Leon's house is different from the others in the base material of the walls, with a clay brick partitions and a concrete slab. Likewise, this house has wooden doors, and windows with an aluminium frame.

To quantify the incorporated carbon footprint of the analysed cases, the Life Cycle Assessment (LCA) methodology followed the calculation procedure described by the European standard EN 15978 [6]. The study was limited to the Production phase, which considers the extraction of raw material (A1), its transportation (A2), and the production of materials (A3).

The functional unit used is the square meter of construction of a dwelling. The One Click LCA software was used, taking the production processes of México as the main point of reference. In addition to conducting a comparative analysis between the different case studies, the base cases (baseline) of each type of housing have been established to establish a reference point for each particular case.

Because the One Click LCA software does not have a construction typology for a reference building for

the Mexican context, a reference building from the south of the USA was used (due to its proximity and climatic similarity), considering the ASHRAE 90.1 climatic zones 2 and 3. These climatic zones cover the regions of the case studies analysed in this work: zone 3C for Chiapas (Comitán), zone 3A for Guanajuato (León), and zone 3A for Guadalajara (less than 200 km from Colima).

A 'single-family house' typology was used to generate the baseline for each case. The foundation, envelope, structure and finishes were considered. Electrical, hydraulic or any other installations were not considered. The structural criteria considered for each baseline is a cast-in-place concrete construction, with columns no more than 7.5 m apart. These baseline cases imply compliance with basic standards in terms of structural criteria.

A comparative analysis of each case with the benchmark of a global home has been carried out. For this, the One Click LCA classification has been used. This benchmark accounts for embodied impacts relating to all building parts, except building technology and external areas. Data are included into the benchmarks based on mechanical and manual screening that considers consistency, completeness and plausibility.

The databases used for construction materials are mainly based on Environmental Product Declarations (EPD) with a geographical scope to Mexico. However, data sources from other regions were used when they were not available for the Mexican context.

3. ANALYSIS

In Chiapas housing, the vertical structure, the exterior walls and the roof are the three main construction elements that contribute to the carbon footprint, with 26.0%, 17.8% and 12.9% respectively, concentrating 56.7% of the total. The reinforcing steel and concrete (of columns, beams and floor), the cement block pieces (of the interior and exterior walls) and the sheet metal (of the roof), are the materials that concentrate the largest amount of carbon footprint, with 33.1%, 19.5%, 11.7% and 11.6% respectively. These materials concentrate 75.9% of the total equivalent CO_2 emissions (See figure 4).

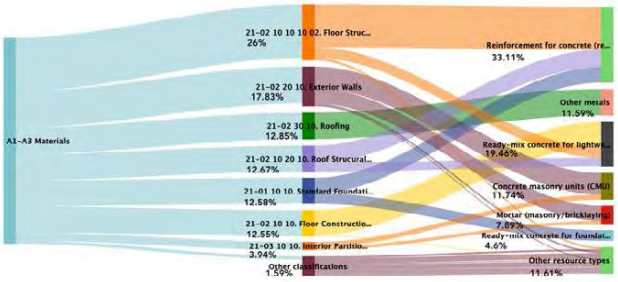

Figure 4: Sankey diagram, incorporated Carbon footprint of Chiapas' case.

In the Colima Housing, the floor, the exterior walls and the vertical structure are the three main construction elements that contribute to the carbon footprint, with 52.5%, 18.5% and 15.2% respectively, concentrating 86.1% of the total. As in the Chiapas case, reinforcing steel and concrete (for columns and floor), pieces of cement block (for interior and exterior walls) and metal sheet (for the roof) are the materials that concentrate the greatest carbon footprint, with 40.6%, 20.6%, 9.9% and 9.9% respectively. These materials concentrate 80.9% of the equivalent CO_2 emissions (See figure 5).

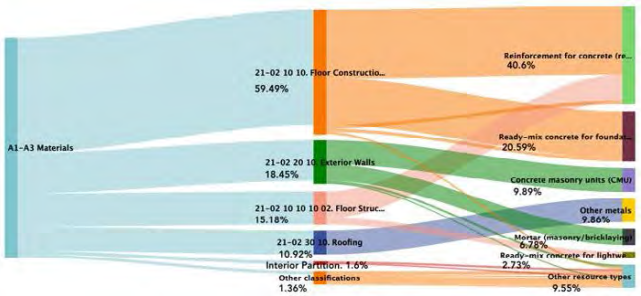

Figure 5: Sankey diagram, incorporated Carbon footprint of Colima's case.

In the Leon House, the floor, the exterior walls and the roof are the three main construction elements that contribute to the carbon footprint, with 30.4%, 27.2% and 22.5% respectively, concentrating 80.0% of the total. Similar to the previous cases, the reinforcing steel (of the floor and roof), the brick pieces (of the interior and exterior walls) and the concrete (of the floor and roof), are the materials that concentrate the largest carbon footprint, with 35.9%, 28.7% and 18.0% respectively. These materials concentrate 82.5% of the equivalent CO_2 emissions (See figure 6).

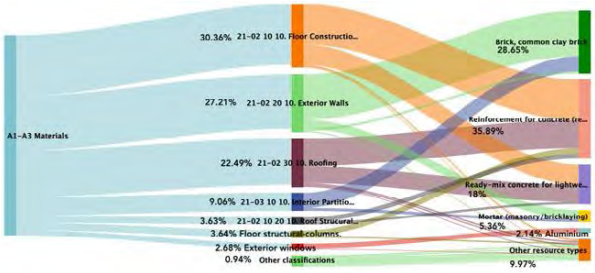

Figure 6: Sankey diagram, incorporated Carbon footprint of Leon case

4. RESULTS

The home in Leon city is the one with the largest incorporated carbon footprint, with 28.2 Ton CO_2 eq. In second place is the house in Colima, with 10.2 Ton CO_2 eq, and in third place is the house in Chiapas, with 8 Ton CO_2 eq. Considering that the home located in León is the one with the highest incorporated

carbon footprint (100%), the home in Colima represents 36.2% of that Carbon footprint, while that in Chiapas represents only 28.4%. However, to effectively compare the cases analyzed, it is necessary to take the functional unit established in the study, the square meter of construction. The order of the results varies slightly with positions 2 and 3: Leon with 435.2 kg CO_2 eq/m^2, Chiapas with 165.5 kg CO_2 eq/m^2, and Colima with 164.9 kg CO_2 eq/m^2. Carrying out the same comparative analysis, and the case of León being the highest (100%), the cases of Chiapas and Colima represent 38% and 37.9% respectively (See figure 7).

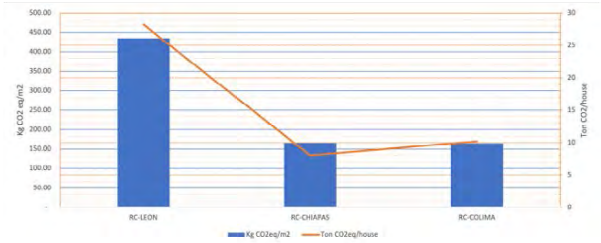

Figure 7: Carbon footprint incorporated into materials in the case studies. Column 1 Leon, 2 Chiapas and 3 Colima.

In order to visualize the impact that these results would have, it is advisable to transform them into something more tangible. The following table shows the forest area that would be necessary for one year to mitigate the CO_2 emitted by each home. An absorption of 0.84 Ton CO_2 eq is considered for each acre of forest for one year (0.40 Has), according to data from the United States Environmental Protection Agency [7]

Table 1: Forest area needed per year to mitigate CO2 for each case study (Has)

Chiapas Case	Colima Case	Leon Case
3.9 Has	4.9 Has	13.6 Has

In the comparative analysis of each real case (RC) with its respective baseline (BL), the house in León has a carbon footprint slightly higher than that of the real case (401.23 ton CO_2/m^2 of the baseline and 435.19 ton CO_2/m^2 of the real case). On the other hand, the real cases of Chiapas and Colima represent a much smaller impact than their respective baselines. For Chiapas, the real case represents 41.4% of its baseline, while for Colima, the real case represents 38.2% of its respective baseline. A possible explanation for this may be that these houses do not necessarily involve a structural design and calculation that would possibly lead to the incorporation of more materials that guarantee their structural resistance and probably promote better thermal performance. Once the results of all the cases considered are available, it is expected to know the influence of the different local materials on the respective carbon footprints and their performance concerning their respective base cases.

Figure 8 shows the comparative analysis of all cases, by construction elements. It can be seen that the floor is the construction element with the greatest environmental impact in the real cases of Colima and Leon, while the columns are in the real case of Chiapas. In the real case of Leon, the exterior walls and the roof are the elements that also represent a considerable embodied carbon footprint (see section 3). In the baseline of each case, the roofs, beams and exterior walls are the elements with the largest carbon footprint. The real case of Leon stands out due to the large amount of reinforced concrete used, since both the roof and the floor are built with concrete, as is considered in the baseline. It is worth mentioning that the concrete used in the analysis of all real cases has been considered concrete and steel with virgin raw materials. That is, the use of recycled raw materials has not been considered. In this sense, it is possible that by considering a certain percentage of recycled raw materials, the carbon footprint of real cases could decrease.

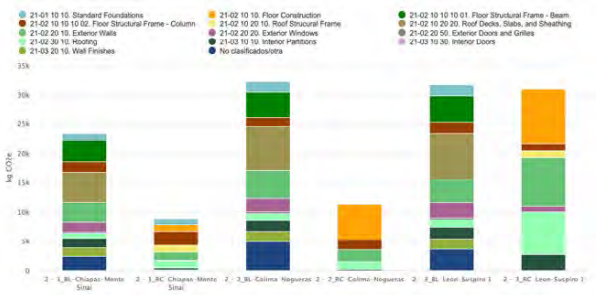

Figure 8: Incorporated Carbon footprint by construction elements in Real and Baseline cases.

The case of the exterior walls also stands out, where in the real case of Leon they are built with mud brick, and in the case of Colima and Chiapas, they are built with cement blocks, which provide a lower embodied carbon footprint. However, even though 70% of the materials used in the analysis correspond to Mexico, it is necessary to mention that for the cement block, a dataset from the United Arab Emirates has been used, since the database available in the software One Click LCA did not have one from Mexico (fig. 9).

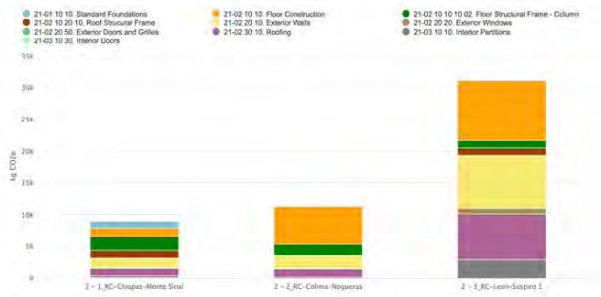

Figure 9: Incorporated Carbon footprint by construction elements in real cases. Column 1 Chiapas, 2 Colima, and 3 Guanajuato.

The benchmark analysis shows that the Leon real case house belongs to category E, as it has an incorporated carbon footprint of 435.2 kg CO_2 eq /m^2, while the cases of Chiapas and Colima belong to category A, with 165 kg CO_2 eq/m^2 (fig. 10).

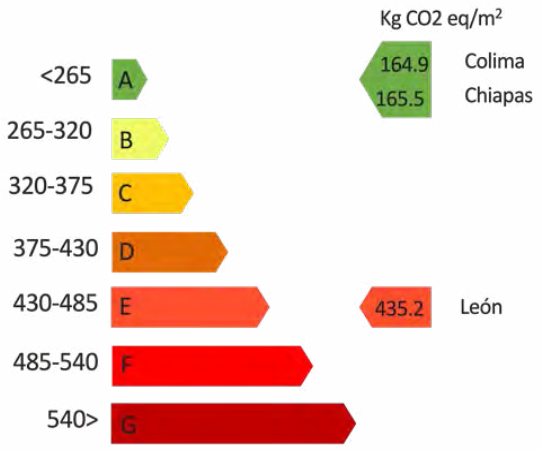

Figure 10: Benchmark analysis of real cases, considering a global home typology.

5. CONCLUSIONS

The building sector represents the main contributor of CO_2 worldwide, and is expected to continue growing as the world population does, mainly in developing countries such as Mexico. Although strategies and policies have been implemented aimed at ensuring a more sustainable and energy efficient housing sector, these actions have focused on the operational phase, leaving aside the rest of its life cycle, even more so, in informal housing. In this work, a diagnosis has been made of the carbon footprint incorporated in the construction materials of peri-urban housing, designed and built informally, that is, without the guidance or support of building specialists.

Although the carbon footprint incorporated in the production phase of the cases presented has been calculated, it is necessary to complete the analysis and cover the complete life cycle of each home. This is necessary to know the implications of the materials in the operational phase of the homes, especially those related to thermal comfort in warm climates such as those found in these cities (Guanajuato, Colima and Chiapas). It will also be important to know the implications that these materials would have in the construction, replacement and maintenance phases.

On the other hand, even though a wide-ranging software at an international level has been used (One Click LCA), which has data on materials in the Mexican context, it has not been possible to know in detail the characteristics of the information on these materials. due to the software configuration itself. Above all, with respect to those materials whose information source comes directly from the "internal database" of the software. Not so when the EPDs are used as a source of information, since these documents specify with sufficient clarity and transparency, the technical and geographical scope aspects that were considered when carrying out the respective LCA studies for those materials.

Likewise, of the 55 construction materials/systems used in the three case studies, 70% have a geographical scope limited to Mexico, while the rest belong to the region of Europe, the United States, or United Arab Emirates. Even though these materials are, essentially, the same as those used in Mexico, the production processes of each one can vary significantly with the processes in Mexico, and with this, its carbon footprint.

Thus, the need to have databases and LCA software for buildings, adapted to the Mexican reality, has to be a highlight of Mexico's construction materials research. This is precisely one of the main barriers that have been pointed out by various authors for the application of LCA in the Latin American region [8-11].

Conventional construction technologies in Mexico, adopted by rural and peri-urban communities in different parts of the country, make it difficult to adapt to each particular context, increasing the carbon footprint generated by one of them, and sometimes the ecological footprint by transferring from one to another.

Solutions adapted to the local context, including materials, technology, and user practices, can move into improved habitat systems appropriate to where they are settled.

This analysis of the carbon footprint on a micro scale, in the national context, will also allow the generation of a macro database in the future, in the construction sector, in which there is a lack of information. Globally, according to the Scopus publication base, a total of 1833 journal articles are revealed with focus on carbon footprint in the field of construction in general, of which only 115 (6% of the total) studies have a macro -level analysis of the construction sector (Cihat, and Kucukvar, 2020), which shows that there is a need to generate a greater amount of data that allows decisions to be made in popular housing policies, particularly in Mexico.

ACKNOWLEDGEMENTS

The authors would like to acknowledge sponsorship from CONAHCYT, of Project 321260, Development of a replicable social production model for housing and habitat.

Also, we would like to thank all of our respective departments and institutions, for the support for this research project, and all the people involved in it.

REFERENCES

1. Global ABC/IEA/UNEP (Global Alliance for Buildings and Construction, I. E. A. and the U. N. E. P. (2020). GlobalABC Regional Roadmap for Buildings and Construction in Latin America.

2. United Nations Environment Programme. (2020). 2020 Global Status Report for Buildings and Construction: Towards a Zero-emission, Efficient and Resilient Buildings and Construction Sector. In Global Status Report for Buildings and Construction. www.iea.org

3. UN HABITAT. (2012). Going Green: A Handbook of Sustainable Housing Practices in Developing Countries. In UN Habitat.

4. Bahramian, M., & Yetilmezsoy, K. (2020). Life cycle assessment of the building industry: An overview of two decades of research (1995-2018). Energy & Buildings, 219, 109917. https://doi.org/10.1016/j.enbuild.2020.109917

5. Cabeza, L. F., Boquera, L., Chàfer, M., & Vérez, D. (2021). Embodied energy and embodied carbon of structural building materials: Worldwide progress and barriers through literature map analysis. Energy and Buildings, 231, 110612. https://doi.org/10.1016/j.enbuild.2020.110612

6. European Committee for Standardization (CEN). (2011). En 15978:2011 Sustainability of Construction works-Assessment of environmental performance of buildings-Calculation method. Sustainability of Construction Works. Assessment of Environmental Performance of Buildings. Calculation Method.

7. EPA. Calculador de equivalencias de gases de efecto invernadero | US EPA. https://espanol.epa.gov/la-energia-y-el-medioambiente/calculador-de-equivalencias-de-gases-de-efecto-invernadero#results (2022).

8. Arvizu-Piña, V. A. & Cuchí Burgos, A. Promoting sustainability in Mexico's building sector via environmental product declarations. International Journal of Life Cycle Assessment (2017) doi:10.1007/s11367-017-1269-z.

9. Arvizu-Piña, V. A., Armendáriz López, J. F., García González, A. A. & Barrera Alarcón, I. G. An open access online tool for LCA in building's early design stage in the Latin American context. A screening LCA case study for a bioclimatic building. Energy Build 295, (2023).

10. Güereca, L. P., Ochoa Sosa, R., Gilbert, H. E. & Suppen Reynaga, N. Life cycle assessment in Mexico: overview of development and implementation. Int J Life Cycle Assess 20, 311–317 (2015).

11. Ochoa, R., Güereca, L. P. & Morillon, D. LCA of buildings in Mexico: Advances, Limits and Catalysts. in Vth International Conference on Life Cycle Assessment, CILCA (2013).

12. Cihat, N., and Kucukvar, Murat. Carbon footprint of construction industry: A global review and supply chain analysis.
Renewable and Sustainable Energy Reviews, ELSEVIER.
Volume 124. (2020).

PLEA 2024 WROCŁAW
(Re)thinking Resilience

Inhabiting Liminal Zones
Design in Urbanised Estuaries in the Climate Emergency

IRENE PEREZ LOPEZ[1]

[1] School of Architecture and Built Environment; College of Engineering, Science, and Environment; University of Newcastle; Newcastle, NSW, Australia.

ABSTRACT: Restoring natural ecosystems and reconnecting natural and built environments might be our best ally in managing the impact and unpredictable effects of a changing climate. Designing a new urban paradigm, with mitigation and adaptation strategies in harmony with living systems at the forefront, will improve urban climate adaptation, resilience, and liveability and help reconnect humans with natural systems. In this context, the paper presents the investigation developed in the Hunter River and its Estuary (Australia), which serves as a model for medium-sized urbanised estuary cities in Australia, to identify critical threats and to propose spatial practices that reconnect natural and built environments at three scales of planning: catchment, urban, and precinct scales. Methodologically, the research is organised into two differentiated phases (i) the spatiotemporal analytical phase, which identifies vulnerabilities, challenges, and opportunities, synthesising key findings through mapping, and (ii) the projective phase, which formulates speculative adaptative design. The results present adaptation and mitigation strategies to respond systemically to areas under threat in a medium-long time frame adapting to sea level rise, preparing for extreme weather events, promoting climate-wise typologies, improving water and energy performance in buildings, and restoring and expanding ecological connectivity.
KEYWORDS: Urbanised Estuary, Climate Change, Adaptation and Mitigation, WSUD.

1. INTRODUCTION

Urbanised estuaries are complex and highly dynamic systems, strongly modified by an intensive history of urbanisation, industrial and agricultural activity, and cultural exchange. Nevertheless, estuaries are a wealth of biodiversity, where fresh and saltwater converge, with invaluable ecosystem and natural values [1]. The consequences of the rapid industrial revolution and urbanisation are responsible for transforming or destroying natural habitats and the rich hydrological systems. Such ecosystems are critical in balancing the territory's sustainability, maintaining ecosystem services, and providing climate buffers [1, 2], amongst other benefits for humans and other species.

The vulnerability in estuaries increases exponentially with the drastic intensification of climate-related events [3]. In Australia, since 1950, the climate patterns have evolved, increasing the frequency, intensity, and unpredictability of droughts and rain episodes, heatwaves, and bushfires, representing additional risks by affecting population health, safety, and lifestyle; the natural environment, and local and regional economies [4]. Moreover, rapid urban expansion means that major storms and floods now affect many more people and threaten the coastal infrastructure – particularly water, waste management, roads, and recreational facilities [5].

Critical climate adaptation challenges include water security and quality issues in human and natural ecosystems [6], evidencing the magnitude of the problem and the vulnerability of estuaries and coastal cities, identified by the Intergovernmental Panel for Climate Change (IPCC) as the most exposed to potential climate change impact. The former situates climate and water issues, flood and drought, at the front of estuary sustainability and resilience debates, bringing attention to the importance of moving toward mitigation and adaptation measures in the built environment while supporting and enhancing nature to recover [7].

The destruction of coastal and riverine ecosystems and climate threats compromise urban security and liveability [2, 8]. The problem is exacerbated in coastal communities oriented towards natural amenities and lifestyle since their "ecosystems have limited capacity to adapt and enhanced climate change impacts, threatened by habitats isolation, fragmentation, and intrusion of invasive species" [5]. Restoring natural ecosystems and reconnecting natural and built environments might be our best defence to manage climate change's impact and unpredictable effects. Designing a new urban and built environment paradigm, with mitigation and adaptation strategies in harmony with living systems at the forefront, will improve urban climate adaptation. Moreover, such strategies will enhance liveability, maintain the provision of other coastal services, including food [2], help reconnect humans with nature and natural systems, improve health and well-being, and ultimately support ecosystems and biodiversity.

Drawing on these critical aspects, this paper presents the investigation developed in the Hunter

Estuary, New South Wales (NSW), Australia, where the City of Newcastle sits. The estuary is threatened by the severe modification of its hydrological and geomorphological systems, urbanisation pressures, air, water, and land contamination due to industrial and port activities, cultural and social challenges, and severe climate extremes. The scenarios under study include low-lying and reclaimed lands, eroded beaches and coastal areas threatened by extreme weather events, stormwater run-off, sea level rise and the risk of a potential tsunami, impacting the natural environment and man-made infrastructures, properties, and facilities. This research aims to identify critical threats and propose climate adaptation and mitigation practices that reconnect the natural and built environment, improve sustainability, and promote climate urban security.

2. METHODS AND LITERATURE REVIEW

The methodology integrates analytic research methods (identification, analysis, and synthesis) and projective-explorative methods (testing scenarios, strategies, and spatial design) [9]. The analytic-research phase promotes a site-specific approach with a long-time span, working across scales to understand the estuary as part of a larger catchment. It incorporates mapping and geospatial data to synthesise and visualise geomorphological and hydrological changes and identify at-risk areas. Subsequently, it moves into a synthesis phase that helps identify spatial and planning challenges and areas of opportunity and, finally, a projective-explorative phase that utilises design as a driver of knowledge. The research methods involved:

(i) Primary archival, cartographic and data documentation – To analyse scientific, environmental and geomorphological studies at catchments and estuary scale [10-12]; and traversed with historiographic surveys and chronicles (The University of Newcastle Cultural Collection, the NSW State Library, and the National Library of Australia); and, geodata [13] and hazard and risk reports and database [14, 15]. Data compilation is translated into mapping to generate cartography that (a) unfolds the estuary evolution starting in early colonial surveys, and (b) interpolates data to identify areas at risk and areas of opportunity for climate adaptation.

(ii) Australian, New South Wales and Local Government climate-related and hazard-related policies and legislation – To discern the national, state, and local statutory planning instruments containing climate change preparedness and mitigation provisions [5, 16-18].

(iii) Australian and international literature on climate change adaptation – To identify best or leading planning and design climate-related theories and practices. It targets practices that counteract inhabitation threats, improving built environments' climate resilience and liveability from technical and engineering approaches [19, 20], environmental and Nature-based Solutions (NbS) [21-23], and speculative adaptative design and planning [20, 24-26].

3. CLIMATE MITIGATION AND ADAPTATION AS PLANNING DRIVERS.

The IPCC alerts that even if mitigation measures were applied systemically and globally to reduce fossil fuel dependency and emissions, “anthropogenic warming and sea level rise would continue for centuries due to the timescales associated with climate processes” [25, 27]. Consequently, adaptation measures – to accommodate humans, built environment and natural systems to the impacts of climate change, and mitigation efforts – to reduce net carbon emissions and to limit climate change over time [5], are complementary for dealing with the impacts of climate change. However, they are not necessarily integrated or do not always work in the same direction and often depend on the scale of planning, as argued by Howard [28, 29].

Despite the efforts of local governments in Australia and internationally to develop and implement innovative planning approaches that indirectly improve resilience to climate change [5], ‘business as usual’ design and planning models are still in place. Standard practices in NSW are land clearing, instead of re-densification and infill, in existing precincts and new development. Often, developments occur in reclaimed and lowlands, such as the Broadmeadow Precinct in Newcastle, adopting minimal and questionable climate adaptation measures. Even though policies are changing rapidly, building codes and guidelines make recommendations for mitigation measures that are not compulsory yet, leaving essential building sustainability performance decisions to developers or individuals [4]. Moreover, urban adaptation strategies, such as water-sensitive urban design (WSUD) or nature-based solutions (NbS), are accepted and validated as efficient methods to increase resilience and are incorporated into policies and practices. However, they are not necessarily implemented systemically and interconnected.

New or existing developments potentially impacted by adverse climate-related effects must be reconsidered at all planning levels, from territorial strategic planning to the master plan, precinct, and architecture policies and guidelines. Moreover, transitioning into a climate-resilient urban and suburban model demands a trans-governmental, trans-disciplinary, trans-agent, and multi-action adaptation and mitigation approach, considering short, medium, and long timeframes and adjusting

flexibly and dynamically to climate change. The research presented here operates at three scales: (i) the upstream Hunter River Basin (NSW, Australia) or catchment scale; (ii) Newcastle Local Governments Area (LGA) or Hunter Estuary scale; (iii) precinct/s and built environment scale. This approach helps to identify non-anticipated areas at risk and, building on these, propose site-specific and tailored mitigation and adaptation measures.

3.1 Catchment scale

For planning and spatial disciplines, it is critical to understand estuaries as part of a larger catchment, informed by their geomorphology, hydrology, and ecology. Devastating floods impacted the Hunter River and its Estuary in 1855, 1955, and 2022. The intensification of oceanic surges and storm events, such as the 2007 NSW Central Coast floods, are an increasing menace. Critical changes in the Hunter are the result of the engineering of the river after the Maitland floods (1955), the impact of deforestation for agriculture, stockbreeding and mining upstream, and land reclamation for port and industrial operations at the estuary. The colonial and capitalist growth destroyed and disconnected terrestrial and hydrologic habitats, depriving the river of new layers of alluvial soil and riparian vegetation [56][10], with severe implications for catchment and settlements' resilience to climate change.

Decisions taken upstream, such as clearing, mining, and agricultural operations, and their countereffects, such as water discharge and contamination, threaten the Hunter Wetland National Park, listed under the Ramstad Convention, Hexham and other unprotected riverine and estuary ecosystems [11]. At the estuary, the Port of Newcastle exports coal responsible for 359.90 Mt of global carbon emissions yearly [42]. The Hunter energy and economy transition is discussed at all levels of governance, and it has international, national, regional, and local implications. Nevertheless, measures to mitigate industrial and agricultural intrusive practices are still under discussion without clear timeframes. The collaboration of local governments, organisations, and community in implementing mitigation and adaptation measures is critical to achieving: (i) The transition of the Hunter from a fossil fuel economy into a sustainable economic system, taking advantage of technological advances such as hydropower, wind, solar power, and biomass; (ii) The restoration of the biodiversity through reforestation, habitat protection, habitat connectivity, and the development of non-polluting and localised industrial and agriculture models, including incentives for carbon capture or storage [5]; (iii) Adaptation and preparedness for extreme weather events like droughts and floods, sea level rise or tsunami, by restoring and expanding riverine ecological corridors and habitats that will act as flood defence and buffers of climate intensification and dramatic drought periods [23].

3.2 LGA or Hunter Estuary scale

The Hunter Estuary is part of the Newcastle's Local Government Area. Critical zones at risk in the estuary result from man-made transformation over 200 years of colonisation and industrialisation. The extraction of coal and the construction of the world's largest coal port generated substantial changes in its hydrology and geomorphology. At this scale, mitigation and adaptation strategies are strongly conditioned by land reclamation, the urbanisation of lowlands, and the changes in flow dynamics and bathymetry. Numerical modelling associated with the Floodplain Risk Management Studies Field [20] assesses vulnerability and potential floodplain risks, measuring the intensity and probability of flood hazards influenced by flash flooding episodes due to rainfalls in the catchment, upstream river flood episodes, and oceanic inundation from high ocean tides and storm surges [72]. These hazards exclude SLR projections [22] and Tsunami projections [21], which have been interpolated in this study and crossed over with Probable Maximum Flood and Risk to Life predictions, as presented in Figure 1. The counterpart of drastic flooding and storm episodes are very intense drought periods, heat islands, and seasonal bushfires.

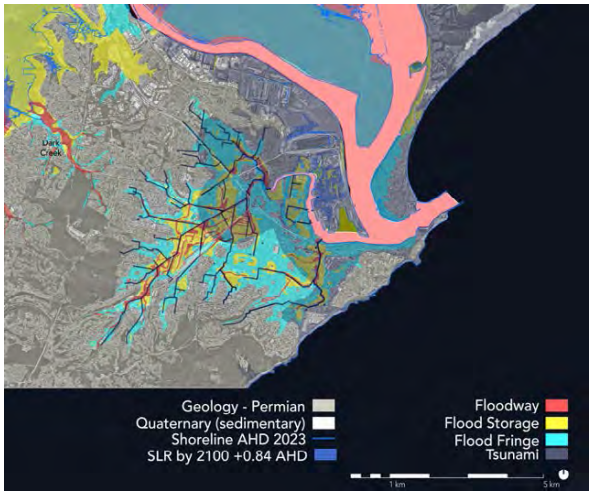

Figure 1: *Flooding Hazard Assessment maps including PMF Floodway, PMF Fringe, and PMF Storage [14]; 2100 Sea Level Rise (AHD +0.84 m); and Tsunami Predictions. Attribution: Irene Perez Lopez, licensed under CC BY-NC-ND 4.0.*

To improve climate security, a range of sustainable and safety measures must be addressed locally. The unpredictability of climate evolution and the cost associated with implementing adaptation and mitigation measures make adaptation at the local scale a real challenge. Actions beyond the local government's legislative and financial capacity often

require a partnership with the state or national government [6] and community engagement through educational programs and incentives.

In the Newcastle LGA, business-as-usual land use regulations promote car dependency, large transportation distances, investment in the infrastructure network, and urban expansion based on clearing and sprawl into forested and/or agricultural land. Changes in land use toward a climate mitigation strategy demand re-densification and infill in consolidated neighbourhoods, the implementation of the 15-minute neighbourhoods, the provision of reasonable alternatives to private mobility, and the increase of vegetation and forest coverage supporting carbon sequestration in peri-urban areas. Such measures are discussed but have not been implemented in Newcastle or outside major capital cities in Australia.

Site-specific adaptation strategies presented in this paper are the result of identifying critical areas at risk in the estuary and the lowlands over a long-time span, recognising the capacity of existing systems to adapt, and proposing new adaptation strategies based on the principles of:

(i) Treating water and natural systems as leverage [28]. The public domain offers opportunities to develop a blue-green public water-sensitive network reconnecting disconnected habitat. The strategy, presented in Figure 2, connects the urban fabric through a network of re-naturalised storm channels with urban public spaces, water bodies, and Nature Reserves. Such actions align well with flood adaptative development strategies to mitigate post-emergency events, acting as buffer zones to protect the urban environment and enhance natural water systems [30, 31]. Measures help control runoff, alleviate urban heat island effects, increase infiltration by re-naturalising, using soft surfaces, and guarantee urban ecological connectivity [11].

(ii) Rethinking water as the ground of settlement [24] by providing a 'Room to the River' [25] instead of fighting against it. Community, public and vacant land, such as BHP's former industrial site, can accommodate room for the river's flash flooding episodes and the predicted SLR footprint, as illustrated in Figure 2. Transformative actions will prepare the LGA for the impact and increase of storm events, coastal flooding, and sea level rise. This buffer provides opportunities to rethink hard edges and infrastructures, construct green embankments and levees, terraced floodable wetlands, and revegetate shores of creeks and floodable parks planted with riverine plants and mangroves that sequester carbon.

More drastic approaches propose that urban hydrology must mimic the pre-urbanised or natural hydrological flows or manage retreat if other adaptation measures cannot protect a precinct.

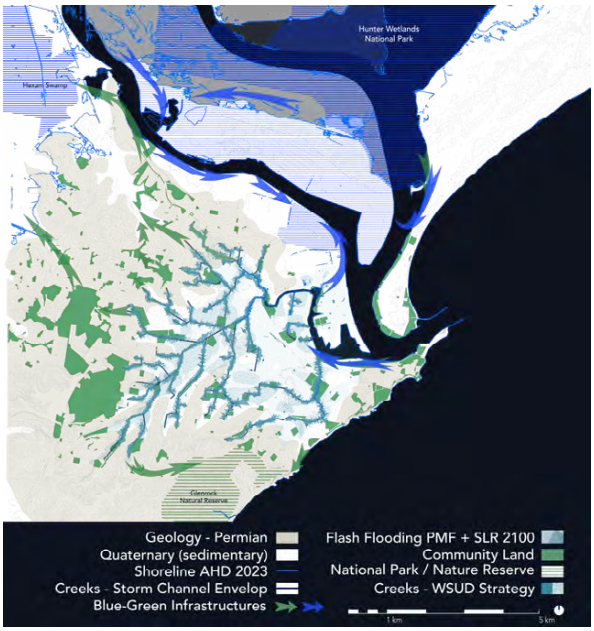

Figure 2: Green and Blue Infrastructure network addressing flood-related hazards and riverine connectivity. Attribution: Irene Perez Lopez, licensed under CC-BY-NC-ND 4.0.

2.3 Precinct and dwelling scale

Reclaim and lowlands, identified in Figure 1a, are at imminent risk of flooding and impacted periodically by ocean storm surges, tidal influences or threats by sea level rise projections that anticipate areas of the estuary permanently below sea level by 2100 [73]. Reclaim lands at Carrington, Maryville, or Stockton, and floodplains such as Hamilton or National Park must address climate issues to reduce the hazards to life and potential future retreats.

At this scale, mitigation measures must consider (i) the implementation of environmental standards, building codes and certification, already in practice in Australia but not compulsory yet; (ii) the optimisation of energy and water consumption through design and better usage; (iii) waste and wastewater regulation; and,(iv) the provision of renewable energy incentives, still below effective mitigation standards [5].

Adaptation requires a multiple-action approach, including responses to weather variability to cope with alternative dry and wet periods. At the precinct scale, areas at risk need to evolve into climate-resilient suburb models through 'water-wise' dwelling typologies integrated within 'water-sensitive' precincts that incorporate WSUD strategies, stormwater, and wastewater management [23, 32, 33]. Such measures increase safety by reducing runoff and peak flow in intense rain periods, decreasing drainage infrastructure costs, and, combined, consolidating a network of urban spaces connected through blue-green corridors to other green areas and local nature reserves that offer amenities and recreational opportunities.

Due to the lowlands and reclaimed lands' strategic location in the estuary, re-densification and infill

developments are under construction, not necessarily responding to sustainable water and climate-related challenges. Innovative architectural design approaches (i.e., “water-wise” dwelling typologies) can help address urban water challenges such as flooding, water security, and urban heat islands. Dwelling and commercial must integrate water servicing technologies to minimise demand, reduce reliance on imported water [31, 34], promote a decentralised urban water system, harvest stormwater for reuse, mitigate the effects of changed hydrology, integrate technology such as water servicing technologies, and connect with a network of blue-green infrastructures [30]. Additional climate resilient measures include raising floor levels, waterproofing openings [35], removing fences, facilitating post-event water storage flows, reducing flood hazards, and incorporating solar energy, amongst other mitigation measures.

Figure 3: Water Sensitive Urban Design. A*ttribution: Irene Perez Lopez, licensed under CC BY-NC-ND 4.0.*

4. DISCUSSION AND FUTURE RESEARCH

The research prompts critical transformations in the urban realm and built environment by integrating adaptation and mitigation strategies to respond systemically to areas under threat at multiple scales, from catchment to urban and precinct scales, and in a medium-long time frame. The climate evolution and the exacerbation of climate-related events claim an urgent need for action incorporating mitigation and adaptation measures in the urban realms and the built environments to resolve climate-related urban security. The alternative to adaptation and mitigation is investing in post-disaster or ‘holding the line’ through hard edges and infrastructures that have probed negatively to solve climate-related hazards. More drastically, the alternative will be a retreat for many coastal and riverine cities in Australia.

One of the key drivers of this research is to probe the importance of understanding estuaries as part of a larger catchment in planning and spatial disciplines. Estuaries are dynamic and complex systems dominated by socioeconomic, spatial, and cultural processes, as well as hydrological and ecological systems. Incorporating such complexity over time and space is fundamental in preparing and adapting cities in the climate century. In this sense, design and spatial disciplines can strongly contribute to climate adaptation by generating site-specific climate-responsive projects while re-establishing the connection between built and natural environments and promoting well-being and cultural values.

The challenge at the river basin scale is understanding the estuary as part of a larger catchment and integrating adaptation and mitigation measures as part of a medium-long-term territorial logic and vision. At the urban scale, the aim is to promote a new urban paradigm connecting hydrological and ecological systems with the built environment through a network of blue-green infrastructure. Finally, at the precinct and built environment scale, the research highlights the importance of reformulating residential/commercial areas into ‘climate-wise’ neighbourhoods harmoniously with a ‘water-sensitive’ urban realm, connecting the built environment with living systems.

All these require investment in adaptation projects to implement and test the effectiveness of speculative and experimental models. Moreover, new interdisciplinary and multi-agent alliances involving the scientific community, policymakers, local and state government, and civil society are needed. it is critical a shift in governance, policies, and planning priorities, working towards spatial adaptation strategies instead of investing in emergency and post-disaster. The approach demands flexibility to adapt to unpredictable and dynamic systems, including reforming planning policies toward flexible tools able to adapt and evolve with climate.

Further research and implementation are essential to promote a new paradigm in the urban realm and architecture in the Anthropocene. In this sense, the study contributes to critical theories of urbanism and climate adaptation, working radically with natural systems and establishing water as a ground of settlement. The final aim is to translate this research and prototyping into guidelines and recommendations, establishing a planning framework for new developments.

ACKNOWLEDGEMENTS

I acknowledge the Traditional Custodians of the Land where the University of (+) resides and pay my respects to Elders past, present, and emerging. Research support funds are provided by the College of (+) at the University of (+).

REFERENCES

1. Costanza, R., et al., The value of the world's ecosystem services and natural capital. Ecological economics, 1998. 25(1): p. 3-15.

2. Spalding, M.D., et al., The role of ecosystems in coastal protection: Adapting to climate change and coastal hazards. Ocean & Coastal Management, 2014. 90: p. 50-57.
3. Reisinger, A., R.L. Kitching, F. Chiew, L. Hughes, P.C.D. Newton, S.S. Schuster, A. Tait, and P. Whetton, Australasia. In: Climate Change 2014: Impacts, Adaptation, and Vulnerability. Part B: Regional Aspects. Contribution of Working Group II to the Fifth Assessment Report of the Intergovernmental Panel on Climate Change. 2014: Cambridge, United Kingdom and New York, NY, USA. p. 1371-1438.
4. Norman, B., Principles for an intergovernmental agreement for coastal planning and climate change in Australia. Habitat International, 2009. 33(3): p. 293-299.
5. Gurran, N., E. Hamin, and B. Norman, Planning for climate change: Leading practice principles and models for sea change communities in coastal Australia. 2008: University of Sydney, Faculty of Architecture Design & Planning.
6. UNESCO and UN-Water, The United Nations World Water Development Report 2020 :water and climate change. 2020, UNESCO: Paris.
7. Oppenheimer, M., et al., Sea Level Rise and Implications for Low-Lying Islands, Coasts and Communities, in The Ocean and Cryosphere in a Changing Climate: Special Report of the Intergovernmental Panel on Climate Change, C. Intergovernmental Panel on Climate, Editor. 2022, Cambridge University Press: Cambridge. p. 321-446.
8. Chausson, A., et al., Mapping the effectiveness of nature‐based solutions for climate change adaptation. Global change biology, 2020. 26(11): p. 6134-6155.
9. Roggema, R., Research by Design: Proposition for a Methodological Approach. Urban Science, 2017. 1(1): p. 2.
10. Albrecht, G., Rediscovering the Coquun: towards an environmental history of the Hunter River, in River Forum 2000. 2000: Wyndham Estate, Hunter River.
11. McVicar TR, P.K., Hodgkinson JH, Barron OV, Rachakonda PK, Zhang YQ, Dawes WR, Macfarlane C, Holland KL, Marvanek SP, Wilkes PG, Li LT and Van Niel TG Context statement for the Hunter subregion. Product 1.1 for the Hunter subregion from the Northern Sydney Basin Bioregional Assessment. 2015, Department of the Environment, Bureau of Meteorology, CSIRO and Geoscience Australia, Australia.
12. Bairstow, D., Hydraulic power and coal loading at Newcastle harbour, New South Wales. The Australian Journal of Historical Archaeology, 1986: p. 57-66.
13. Colquhoun GP, H.K., Deyssing L, Ballard JC, Folkes CB, Phillips G, Troedson AL and Fitzherbert JA 'New South Wales Seamless Geology dataset (Single Layer)', version 2.2 [dataset], D.o.R.N. Geological Survey of New South Wales, Maitland, Editor. 2022.
14. Haines, P., The Newcastle City-wide Floodplain Risk Management Study and Plan Compendium of Maps. 2012, City of Newcastle: Newcastle NSW.
15. Australia, C.R., Coastal Risk Australia; Predicted Coastal Flooding Resulting from Climate Change. 2021.
16. Norman, B. and N. Gurran, Regional Solutions for Multi-level Governance Challenges in Australian Coastal and Climate Change Planning. MULTI-LEVEL GOVERNANCE, 2017: p. 281.
17. Bradley, M., I. van Putten, and M. Sheaves, The pace and progress of adaptation: Marine climate change preparedness in Australia's coastal communities. Marine Policy, 2015. 53: p. 13-20.
18. Brunckhorst, D.J., et al., Hunter & Central Coasts New South Wales - Vulnerability to climate change impacts: Report to the Department of Climate Change and Energy Efficiency, Australia. 2011: Australian Government, Department of Climate Change and Energy Efficiency.
19. Mattei, J.H., Structures of Coastal Resilience. By Catherine Seavitt Nordenson, Guy Nordenson, and Julia Chapman. Washington (DC): Island Press. The Quarterly review of biology, 2019. 94(3): p. 307-308.
20. Roggema, R. and E.C. Proquest, Nature driven urbanism. 2020, Cham, Switzerland: Springer.
21. Morris, R.L., et al., From grey to green: Efficacy of eco‐engineering solutions for nature‐based coastal defence. Global change biology, 2018. 24(5): p. 1827-1842.
22. Cooperative Research Centre for Water Sensitive Cities (CRCWSC). 2021; Available from: https://watersensitivecities.org.au.
23. Wong, T.H.F., Australian Runoff Quality. A guide to Water Sensitive Urban Design. 2006: Engineers Australia.
24. Mathur, A.C.D.d.M.A.U.o.P.S.o.D., Design in the terrain of water. 2014.
25. Meyer, H., Delta Urbanism coming of age: 25 years of Delta Urbanism where are we now? Journal of Delta Urbanism, 2020(1).
26. Meyer, H.A.N., Delta-Urbanism: New Challenges for Planning and Design in Urbanized Deltas. Built Environment (1978-), 2014. 40(2): p. 148-155.
27. Solomon, S., et al., IPCC fourth assessment report (AR4). Climate change, 2007. 374.
28. Jonkman, B. and H. Ovink, On sustainable delta development: Sustainable coastal adaptation is possible - Water as catalyst for sustainable development. Journal of Delta Urbanism, 2020(1).
29. Howard, J. and G. Monbiot, A Critical Perspective on the Adaptation Turn in Urban Climate Planning. Planning for climate change: Strategies for mitigation and adaptation for spatial planners, 2009. 19.
30. Moravej, M., et al., What roles do architectural design and on-site water servicing technologies play in the water performance of residential infill? Water research (Oxford), 2022. 213: p. 118109-118109.
31. Renouf M.A., K.S.J., Bertram N., London G., Todorovic T., Sainsbury O., Nice K., Moravej M., Sochacka B. , Water Sensitive Outcomes for Infill Development: Infill Performance Evaluation Framework. 2020, Cooperative Research Centre for Water Sensitive Cities.: Melbourne, Australia.
32. Design, W.b., The Water Wise House. Water by Design.
33. Moore, R. Private water supply. 2004. Barton, A.C.T: Engineers Australia.
34. London, G., Bertram, N., Sainsbury, O. & Todorovic, T. , Infill typologies catalogue – Revision A. 2020, Cooperative Research Centre for Water Sensitive Cities.: Melbourne, Victoria.
35. Rogers, B., et al., An interdisciplinary and catchment approach to enhancing urban flood resilience: a Melbourne case. Philosophical Transactions of the Royal Society A, 2020. 378(2168): p. 20190201.

PLEA 2024 WROCŁAW
(Re)thinking Resilience

Impact of Aspect Ratio of Alleyways and Water Bodies on the Thermal Microclimate of Modern Pathways

JAWAHAR AL HASHIM[1], HAYDER KHAN[1], HANAN AL-KHATRI[1], SALEH AL SAADI[1]

[1]Sultan Qaboos University, Engineering Department, Al Khoud, Muscat, Sultanate of Oman.

ABSTRACT: In hot, arid countries like Oman, the climate reduces physical activity of residents and increases dependency on car transportation. Improving walkability requires studying outdoor thermal comfort and its relationship with microclimate. This study investigates the effects of alleyway geometry and water bodies on thermal microclimate. Evaporative cooling is a mechanism that can help in achieving a comfortable outdoor environment. This research focuses on the combined effect of evaporative cooling from a water body and the aspect ratio of an alleyway on the temperature at the pedestrian level. For simulation, computational fluid dynamics (CFD) was used, and the results were compared with the base case: an alleyway without a water body. The results showed that water features combined with a high height-to-width ratio can reduce temperature by up to 2.3°C.
KEYWORDS: Outdoor thermal comfort, Alleyways, Evaporative cooling, Shading, Microclimate.

1. INTRODUCTION

Oman is in the southeastern quarter of the Arabian Peninsula and has a hot, dry climate most of the year. The growing densities of urban cities are intensifying global climate change, affecting the microclimatic conditions of cities. The hotter conditions are discouraging people from spending time outdoors. Thermally comfortable pathways are necessary to encourage residents to walk and reduce their dependency on automated transportation. This is essential to achieving a sustainable city, but we are missing the required information to achieve this goal. Traditional Omani villages use passive design strategies like high aspect ratio, overhangs for shading, and water bodies such as Falaj (Figure 1) within the settlements that provide a microclimate with relatively comfortable conditions. The Falaj system is an irrigation infrastructure used in Oman. It consists of a small canal that transports water from one source to another by gravity.

Figure 1: Falaj Al Khatmain, Birkat Al Mouz Village (source: authors)

The thermal microclimate is affected by several environmental parameters like incident solar radiation, air temperature, humidity, and air velocity [1]. One of the passive strategies used to minimize incident solar radiation is shading. The amount of shading in an alleyway is affected by its aspect ratio (height-to-width ratio). A study conducted in a hot-arid city in Algeria compared the urban environment of traditional alleyways and modern urban canyons. The aspect ratios of the alleyways and urban canyons were 2 and 0.6, respectively. Traditional alleyways managed to reduce the air temperature by up to 3 °C, whereas urban canyons resulted in increased air temperature by up to 4 °C [2]. Another research indicated that traditional structures provided better outdoor thermal comfort due to the shading and natural ventilation strategies integrated with their urban forms [3]. These studies validate the role of the high aspect ratio of buildings in protecting from radiation and reducing air temperature.

A study was conducted by Oke (1988), a pioneer researcher in thermal microclimate, on airflow of different aspect ratios. The findings suggested that if the aspect ratio of a canyon is low, the air flows in and out with minimum disturbance. The airflow changes for narrower canyons, and a vortex is created, preventing air from flowing in or out [4].

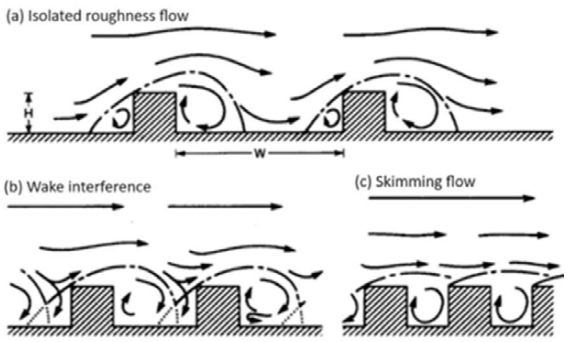

Figure 2: Flow regimes associated with airflow over building arrays of increasing H/W: (a) Isolated roughness flow, (b) wake interference, and (c) skimming flow [4].

Based on the aspect ratio value, flow regimes are divided into three categories [4]:

a. **Isolated roughness flow** (Figure 2. (a)) occurs when the height and spacing between buildings cause disturbance in airflow.
b. **Wake interference** (Figure 2. (b)) occurs when flows are disturbed, and secondary flows are deflected to the canyon.
c. **Skimming flow** (Figure 2. (c)) occurs in a high aspect ratio where a stable circulatory vortex is formed in the canyon.

Therefore, when considering the aspect ratio, it is important to consider how it affects the airflow in an alleyway. Apart from shading, passive cooling strategies are also found in the traditional settlements of Oman. These strategies depend on the evaporation of water from a source, like trees or water features, creating a cooling effect and reducing the air temperature. An investigation of the effect of evaporative cooling from water bodies in an urban environment was conducted in Japan [5]. An experimental simulation was done to mimic the effect of the vapour transport mechanism from a water surface within an array of buildings. A reduction in temperature to a maximum of 2 °C was induced at the pedestrian level. It was concluded that at a wind velocity of 3 m/s and a height of 10 m, the effect of evaporative cooling could extend to an unobstructed distance of 100 m. Potential cooling of water features depends on solar radiation and evaporative cooling. Cooling drops with an increase in solar radiation or humidity.

One of the methods of investigating the effect of these parameters is using a simulation model, such as computational fluid dynamics (CFD). CFD is a numerical simulation method that resolves the interaction of air, mass, and heat transmission with specific impediments, such as buildings. This approach is often used in urban microclimatic studies as it saves time and optimizes and fine-tunes the design.

To the authors' knowledge, no research studies have examined the combined impact of evaporative cooling and aspect ratio at a pedestrian level on urban canyons under a hot and arid climate.

This paper investigates the effect of shading from aspect ratio and evaporative cooling resulting from the existence of a water body. The optimum aspect ratio can be determined through investigation and numerical modelling using CFD. In this study, Star CCM+ software is used to analyse the parameters affecting outdoor urban microclimates.

2. SITE

Oman has many different traditional settlements that have been preserved over the years. For this study, the model dimensions were chosen mainly based on a survey of the average aspect ratio in various villages in Oman (**Table 1**). The aspect ratios are computed by averaging the sum of all individual measurements of height-to-width ratio.

Table 1: Comparison of the aspect ratio of different traditional settlements in Oman.

SETTLEMENT	ASPECT RATIO
Harat Al Khabt	1.17
Misfat Al Abriyeen	1.76
Harat Al Qasra	1.4
Harat Al Msalamat	1.67
Harat Al Saybani	1.5
Harat Saija	1.5

3. METHODOLOGY

This research used CFD to evaluate the effect of evaporative cooling from water bodies on improving thermal comfort at pedestrian levels' alleyways. Two main scenarios were modelled: an alleyway with Falaj and another without Falaj. Several aspect ratios were modelled within each of these scenarios.

An air domain of dimensions (192 m by 160 m by 48 m) was modelled using STAR CCM+ (Figure 3) based on recommendations from a guidebook on CFD simulations [6]. In the case of a single wind direction, the border should be 5H between the inflow boundary and the investigated area and 10H between the outflow along with other boundaries and the investigated area, where H is the characteristic height of the buildings. The investigation was based on steady, incompressible turbulent flow. Reynolds-Averaged Navier-Stokes equations (RANS) and realizable k- epsilon turbulence model were used as a closure for conversion equations [7].

In hot and arid regions, the primary heat source is solar radiation. Gray thermal and surface-to-surface radiation models were used to simulate radiant heat transmission. The solar radiation was computed using the solar calculator within the software by assigning a specific date, time, and geographic location.

For the domain of the air, the left, right, and top boundaries were modelled as slip walls. The inlet was set as velocity inlet, and the outlet was set as pressure outlet. The bottom of the domain was treated as ground soil with a thickness of 0.5 m. To simulate the atmospheric processes at the inflow boundary, the atmospheric boundary layer (ABL) flow of Richard and Hoxey was imposed [8].

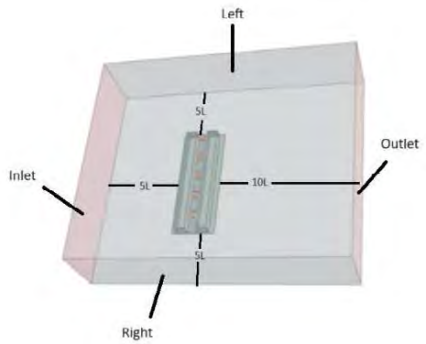

Figure 3: Domain of computational model.

An 80 m-long alleyway was modelled with different widths to vary the aspect ratios. The aspect ratios used were 1.45, 1.6, 1.8, 2, 2.3, and 2.6. Falaj size of 80 m by 0.5 m was used based on the typical geometry of Falaj found in Oman. It was positioned at the centre of the alleyway.

For the domain, blocks, and water body, meshes of cell size 2 m, 0.5 m, and 0.3 m were used, respectively (Figure 4). The edges were applied with further finer mesh sizes. Surface remesher, polyhedral mesher, and prism layer mesher were used to refine the simulation mode. Results from the wind tunnel experiment by Hall are used to validate the mesh size through sensitivity analysis [9]. This was executed by modelling the experiment, running a simulation in CFD, and comparing the velocity profiles with the practical results. This analysis is done to establish a well-defined mesh that facilitates accurate flow simulations and ensures convergence.

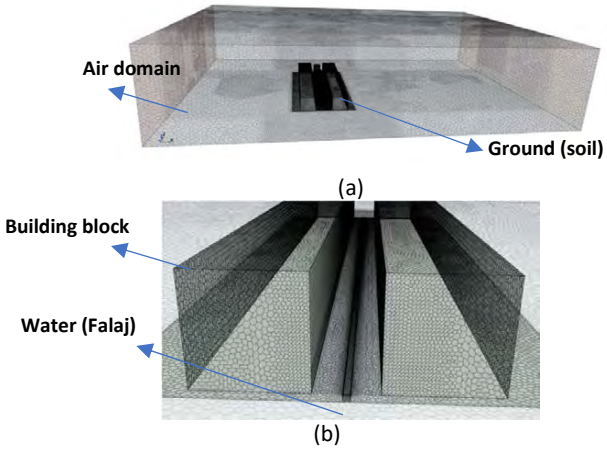

Figure 4: Grid mesh applied on (a) air domain, (b) alleyway.

The falaj was treated as a 0.5 m deep body below ground level. The evaporative cooling was treated the heat exchange of water from the top surface of the falaj. It was evaluated as a source term. This process was divided into three parts: radiant heat transfer to surroundings, evaporative heat dissipation, and convective heat transfer with the air. The total heat exchange of the water surface (ϕ_n) was calculated by [10]:

$$\phi_n = \phi_s + \phi_a - \phi_b - \phi_e - \phi_c \quad (1)$$

$$\phi_s = l(1-\gamma) \quad (2)$$

$$\phi_a = (1-\gamma)\varepsilon_{ac}\sigma(273+t_a) \quad (3)$$

$$\phi_b = \sigma\varepsilon_w(273+t_w) \quad (4)$$

$$\phi_e = f(w_z)(e_w - e_a) \quad (5)$$

$$\phi_e = 0.47f(w_z)(t_w - t_a) \quad (6)$$

$$e_w = e^{2.3026}\left[\frac{aT_d}{T_d+b} + c\right] \quad (7)$$

$$e_w = e^{2.3026}\left[\frac{aT_s}{T_s+b} + c\right] \quad (8)$$

ϕ_s- incoming solar radiation, [W/m^2];
ϕ_a – incoming longwave radiation, [W/m^2];
ϕ_b – longwave radiation, [W/m^2];
ϕ_e- evaporative heat dissipation, (W/m^2];
ϕ_c- heat convection quantity, [W/m^2];
l- average solar radiation, [W/m^2];
γ- reflectivity of water, shortwave;
γ_a- reflectivity of water, longwave;
w_z- wind speed, [m/s];
$f(w_z)$- function of wind, 9.2 + 0.46w$_z$^{2};
e_w- evaporative pressure of water;
e_a- evaporative pressure of air, [mmH$_g$];
σ- Stefan-Boltzmann constant, [W/m^2.K^4];
t_a- air temperature 2 m above the water surface, [°C];
t_w- temperature of water surface, [°C];
T_d- dewpoint temperature, [°C];
T_s- dewpoint temperature, [°C];
a, b and c are constants.

Table 1: Values used in numerical simulation.

Parameter	Value
WIND VELOCITY	1 to 10m/s
ROUGHNESS HEIGHT	0.05
OUTDOOR AIR TEMPERATURE	45°C6
INLET TEMPERATURE	43°C
SURFACE TEMPERATURE	43°C
SOLAR RADIATION	823.6 W/m^2 with solar diffusion of 0.4
TRADITIONAL ALLEYWAY ALBEDO	0.5
Z	10
Σ	5.67 x 10^{-8} W/m^2.K^4
T_s	20°C
T_d	9°C
A	7.5
C	0.6609
BUILDING WALL THICKNESS	0.4m
WALL MATERIAL (BRICK) THERMAL CONDUCTIVITY	1.0 W/m-K
ROOF THICKNESS	0.2m
ROOF MATERIAL THERMAL CONDUCTIVITY	1.0 W/m-K
GROUND (SOIL) THERMAL CONDUCTIVITY	2.7 W/m-K

4. RESULTS

Table 3: Measurements obtained from fieldwork.

Parameter	Value
Air temperature	45°C
Water surface temperature	43°C
Relative humidity	20%
Wind speed	1 m/s
Water temperature	46°C

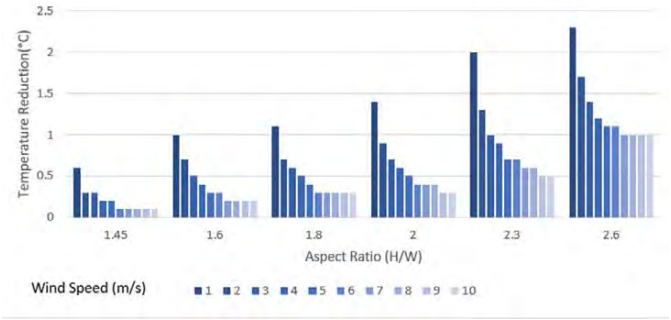

(a)

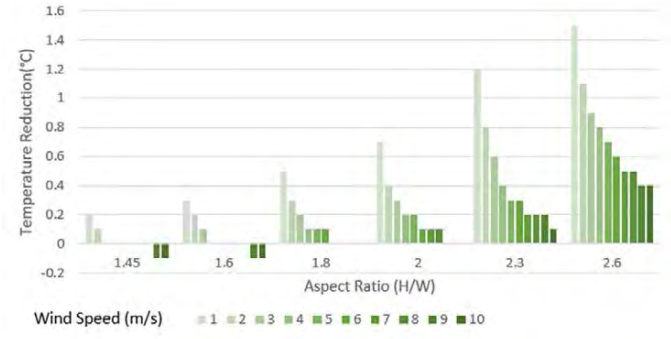

(b)

Figure 5: Temperature reductions in alleyway (a) with Falaj, and (b) without Falaj.

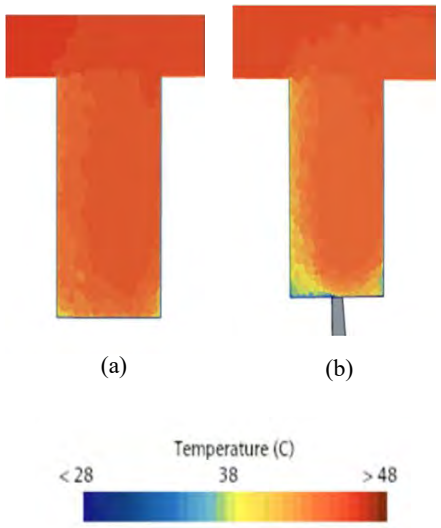

(a) (b)

Figure 6: Temperature within alleyway (a) without water (b) with water.

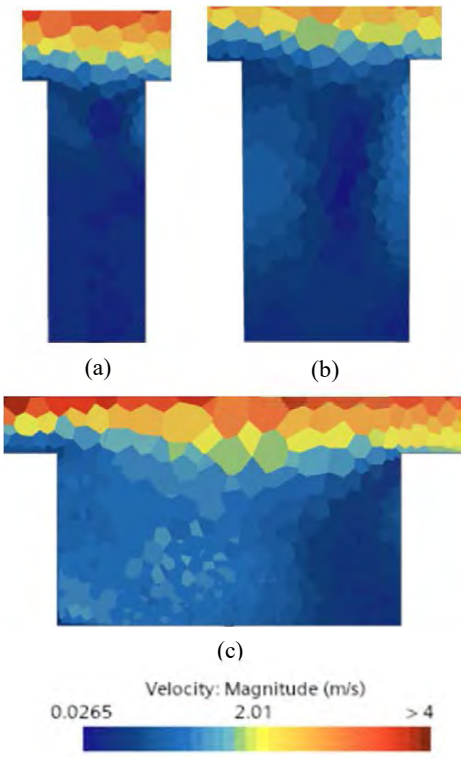

Figure 7: Airflow and velocity in alleyway of aspect ratio (a) 2.6, (b) 1.8. (c) 0.5

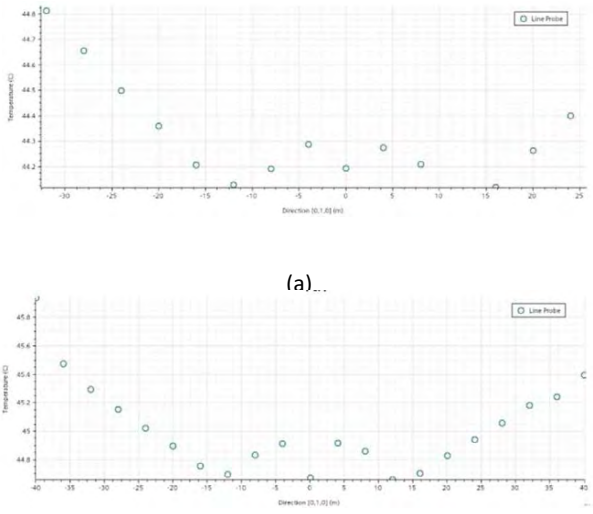

(a)

(b)

Figure 8: Plot of temperature measurement across the alleyway (a)without water, and (b) with water.

The analytic results from Figure 5 show the temperature reductions for the two scenarios. The presence of the water body has a positive impact on the thermal condition of the alleyway. The reductions are highest at a wind speed of 1 m/s. Adding the water body to the model gave further temperature reductions up to 0.8 °C. At higher wind speeds, the effect of evaporative cooling on the temperature defuses. Besides, increasing the aspect ratio improves the thermal conditions due to minimum incoming solar radiation. For example, at an air speed of 1 m/s, the aspect ratio of 1.45 reduced the air temperature by 0.6 °C, whereas the reduction was 2.3°C for an aspect ratio of 2.6. It can be established that a higher aspect ratio of alleyways provides better protection against solar radiation. This effect is enhanced with an increase in wind speed. Figure 6 shows the temperature changes within the alleyway, with and without Falaj. The presence of water cooled the surroundings as the temperature around the building surface reduced due to evaporative cooling. This validates that water bodies provide a cooling effect depending on the proximity of the surroundings.

The effect of different aspect ratios on airflow is shown in Figure at a wind speed of 5 m/s. When the air entered the alleyway, its speed reduced until a vortex was formed. The vortex was larger in narrow alleyways. This prevents the air from flowing in and out, reducing the ventilation rate and airflow at the pedestrian level, which can lower the walkability.

Figure 8 displays the temperature changes across the alleyway measured using a line probe setup within the simulation. The temperature reduction throughout the canyon ranged from 0.5 °C to 1.3 °C. The lengthy shape of the Falaj provided an extended cooling effect across the street.

5. CONCLUSION

The study was conducted to assess the effect of evaporative cooling and shading on the thermal microclimate of an alleyway to improve walkability. The following observations were taken:

- Narrow canyons protect the street against solar radiation, which can reduce the air temperature within the street.
- Depending on the proximity, water features provide a cooling effect to its surroundings. This implies that the closer the water is to the ground, the better effect it has at the pedestrian level.
- Narrow alleyways are also associated with interrupted airflow. This forms a vortex within the canyon, which can cause ventilation issues.
- Numerical simulations provide better and faster insights into the thermal conditions of urban environments.

Overall, combining the effect of shading from aspect ratio and evaporative cooling from water features optimally can help regulate the thermal microclimate for pedestrians. Investigations with further values of aspect ratios and different sizes of water bodies can provide clearer solutions for improving outdoor thermal comfort. After selecting the suitable pathway sizes, the cases can be applied to an urban model for a better and more realistic

understanding of the effects on microclimate. These findings can be used to generate design guidelines for modern urban pathways.

ACKNOWLEDGEMENTS

The research has received funding from Sultan Qaboos University's internal grant program (IG/ENG/CAED/20/02). The authors gratefully acknowledge the university and the Department of Civil and Architectural Engineering for their ongoing support.

REFERENCES

1. Sergey Mijorski, Stefano Cammelli, Johnathan Green, A hybrid approach for the assessment of outdoor thermal comfort, Journal of Building Engineering, Volume 22, 2019, Pages 147-153.

2. Bourbia F., & Awbi H. B. (2004a) Building Cluster and Shading in Urban Canyon for Hot Dry Climate: Part 1: Air and Surface Temperature Measurements. Renewable Energy, 29(2), 249-262.

3. Mozafari, Nadiya & Alimardani, Masoud. (2020). Climate Adaptability of Old and New House in Bushehr's Historical Texture. Civil and Environmental Engineering. 16. 10.2478/cee-2020-0024.

4. T.R. Oke, Street design and urban canopy layer climate, Energy and Buildings, Volume 11, Issues 1–3, 1988, Pages 103-113.

5. Tominaga, Y., Sato, Y., & Sadohara, S. (2015). CFD simulations of the effect of evaporative cooling from water bodies in a micro-scale urban environment: Validation and application studies. Sustainable Cities and Society, 19, 259–270.

6. Franke, Jörg & Baklanov, Alexander. (2007). Best Practice Guideline for the CFD Simulation of Flows in the Urban Environment: COST Action 732 Quality Assurance and Improvement of Microscale Meteorological Models.

7. Benkari, N., & Sallam, I. (2021). Pedestrian Paths as an Indicator of Legibility Aspects of Omani Traditional Settlements. IOP Conference Series: Materials Science and Engineering, 1203.

8. P. J. Richards & R. P. Hoxey, Appropriate boundary conditions for computational wind engineering models using the k-ε turbulence model. Journal of Wind Engineering and Industrial Aerodynamics, (1993).

9. D. J. Hall, S. Walker & A. M. Spanton, Dispersion from courtyards and other enclosed spaces. Atmospheric Environment, 33(8) (1999).

10. Li Yang, Xiaodong Liu, Feng Qian, Research on water thermal effect on surrounding environment in summer, Energy and Buildings, Volume 207 (2020).

PLEA 2024 WROCŁAW
(Re)thinking Resilience

Tepotzotlán: Geodesign and Bioclimatic Architecture

A case of study in the outskirts of Mexico City´s Metropolitan Area

ANIBAL FIGUEROA[1] GLORIA MARIA CASTORENA [2]

[1] Universidad Autonoma Metropolitana, Mexico City
[2] Universidad Autonoma Metropolitana, Mexico

ABSTRACT: This paper analyzes a series of studies and proposals for the municipality of Tepotzotlán in the outskirts of Mexico City, that have been developed using a geodesign methodology and bioclimatic design principles. The area is in the north west entrance to the Valley of Mexico where all major land routes from the north and center of the country are located. For this reason, uncontrolled industrial growth has happened next to the Mexico-Queretaro Highway, producing a major impact in the area of study. Industry has expanded on farmland, isolating the housing area and the historic core from their main communication roads and affecting environmental systems, particularly on its hydrology. A newly developed industrial zone (2015) that borders with the state park is a major concern, as it starts a trend for uncontrolled industrial development in both sides of the highway.
KEYWORDS: Geodesign, Bioclimatic Architecture, Climate Change, Green Corridors, Tepotzotlán

1. INTRODUCTION

Mexico City's Metropolitan Area is one of the largest in the world with a population of 21.8 million [1]. Tepotzotlan´s municipality is located in its north-west edge. From 2005 to 2007, a group of academics and students from the Universidad Autonoma Metropolitana in Mexico City (UAM) developed a joint project with Harvard University´s Graduate School of Design called "Alternative Futures for Tepotzotlan"[2] that foresee three different scenarios for the territory in the future: adopting immediately corrective measures, a late adopting scenario and non-adoptive scenario of continuing development as it was.

Given the fifteen years interval between scenarios of the study, the previous work is a valuable tool that allow us to evaluate past, present and future conditions (2005, 2020, 2035, 2050). Some of the proposals of this early study have been implemented, but others that were fundamental for environmental quality and sustainability of the area were ignored.

Using this work as a base, the UAM team has continued to work in the area of Tepotzotlan for the last 18 years. Academic studies and proposals have slowly turned into environmentally conscious buildings such as a hospital, hotels and hostels, sports facilities and housing; public spaces in the form of linear parks for rivers and ravines' recovery projects; and regional planning official documents such as the land use allocation ordinance that promotes Passive and Low Energy Architecture and GeoDesign as principles to develop climate resilience in the particularly complex and diverse urban environment of the growing edge of Mexico City´s Metropolitan Area.

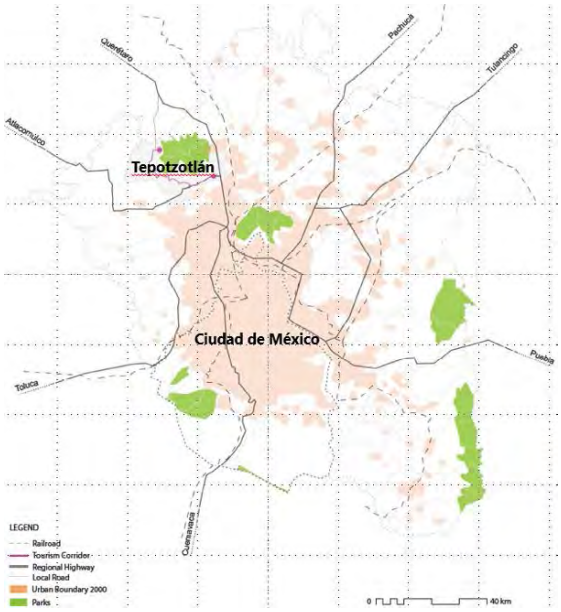

Figure 1: Location of Tepotzotlan, Mexico City's Metropolitan Area parks and main highways

2. GEODESIGN METHODOLOGY AND BIOCLIMATIC ARCHITECTURE PRINCIPLES

In the north west area of Mexico City´s growing rim, some of the biggest challenges for twenty-first century's design are present. Tepotzotlán´s urban zone and buildings need to adapt to social, political and economic challenges, while climate change creates harsh environmental conditions in temperature and rainfall that produce draught some years and landslides and flooding on others. It is important to develop the necessary resilience in the infrastructure and build spaces.

Our approach is based on a design process that takes into account the physical and climatic

conditions of a place and considers the contributions of various professional and social groups, with the support of a methodology originally proposed by Carl Stenitz from Harvard University [3] and geo-referenced information that takes advantage of new calculation and mathematical modeling programs.

The geodesign methodology proposes the analysis and iteration of six models: representation, process, evaluation, change, impact and decision. They are associated to key questions, beginning with How should the study area be described? and ending on questions such as How should the area be changed?

Using this methodology it is possible to identify trends in industrial activity, commercial areas and housing development needs; define a water management plan for rain water, drainage, the aquifer and water treatment plants; a solid waste strategy for recycling; the roll of protected natural areas and parks at a metropolitan level; the creation of "green corridors" that keep alive the natural hydrologic system in the form of linear parks; a comprehensive landscape management plan to preserve the desirability and beauty of the area including a sierra park with low impact activities; reforestation policies for eroded zones, etc..

Geodesign methodology has also been used to promote a participatory process that includes government at all levels, private initiative associated with industry and services, Non-Government Organizations, schools and universities. Several tools have been applied to fine tune the proposals process: workshops and analysis meetings with local groups, public expositions of proposals, site visits, printed material and even an elementary school children's drawing contest called "How Tepotzotlan should be in 20 years", among others.

On specific buildings that belong to the local government and the private sector, bioclimatic architecture principles have been proposed to provide natural ventilation, use local materials with appropriate U values such as a volcanic stone called "tepetate", increase daylighting, reduce energy for climate control and install rainwater harvest systems.

3. POPULATION GROWTH

The accelerated growth of the population is already posing great challenges. Urban development and buildings need to adapt to a massive phenomenon of migration, population aging and new social behaviors. Vehicle traffic is intense and chaotic.

In Tepotzotlán, population growth has increased the inequality of urban development, causing more than 25% of all housing units to be overcrowded. According to the Population and Housing Census of Mexico´s National Institute of Statistics and Geography, in the last 50 years the population increased from 13,000 inhabitants in 1960 to 104,000 in 2020 equivalent to 8 times more inhabitants in just 60 years [4]. This very fast population growth generates increased demand for services, education, employment and infrastructure, which will need to be effectively established to meet current and future needs, and sets an increasing pressure on its territory. That is why it is required an urban development plan using principles of geodesign and passive architecture [5] that can sustain the well-being of its present and future inhabitants.

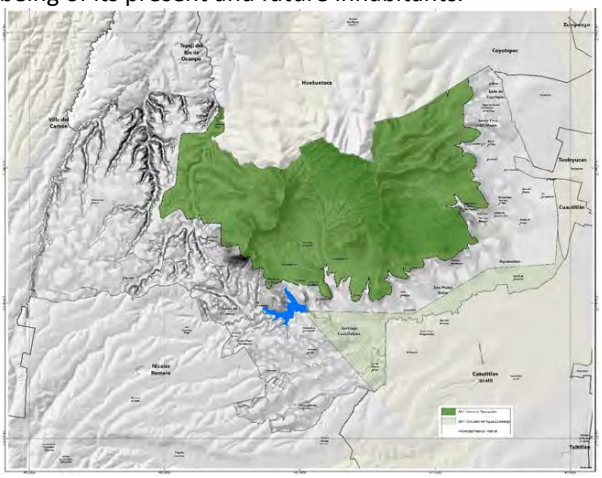

Figure 2: Natural Protected Areas in the municipality of Tepotzotlan

For this reason, Tepotzotlán presents enormous challenges to conserve and protect on its territory the important natural and historical assets of the Municipality. Nearly 50% of the municipality are state parks and productive farmland [6].

At the same time, it houses precious historical buildings from the XVI and XVII centuries including one of the best-preserved baroque churches in the Jesuits College of Tepotzotlán that is now the National Museum of the Viceroy Period.

Figure 3: Baroque Church of the National Museum of the Viceroy Period (XVII and XVIII centuries)

There is enormous economic and political pressure to transform natural areas into urban and industrial uses and modify and sometimes destroy historical elements to give space to new buildings.

4. CLIMATE AND CLIMATE CHANGE

4.1 Normal Weather Conditions

In normal terms climate in the area varies from a lower east side (2220 meters above sea level) to a higher west portion (2880 m). As altitude increases, temperature falls and rainwater increase. In general, climate tends to be temperate in the daytime and cold at night year around, with the highest temperatures in spring months and lower temperatures in dryer and colder winter. There is a clear summer raining season from May to September with an average of 705 mm per year. [7]

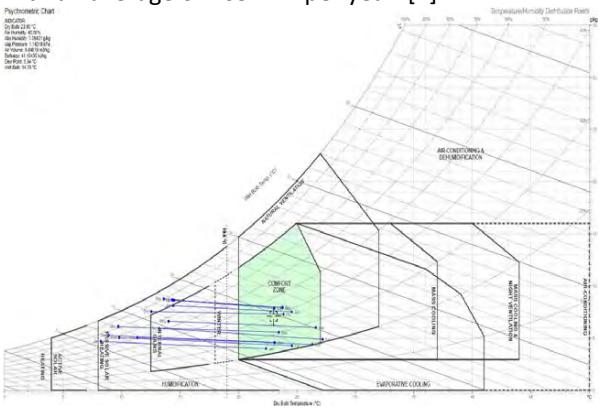

Figure 4: Psychometric Chart of Tepotzotlan (1991-2020), using Andrew Marsh tools

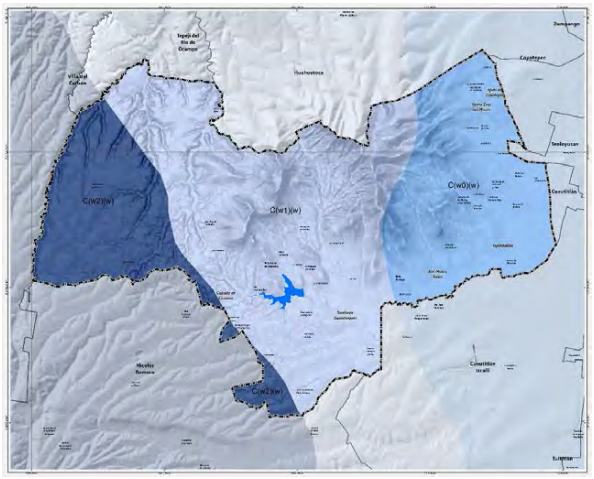

Figure 5: Climate differences in Tepotzotlan's territory

4.2. Climate Change

Climate change is a reality that is increasingly affecting life quality of life in Tepotzotlán. Its short-term consequences can affect large areas of the municipality making some neighborhoods and buildings uninhabitable.

Although temperature increase in the region has been moderate (0.8°C), there is a clear trend on annual rainfall increment. It the last 60 years, there is tendency for 28% more rain water. None the less, yearly variations are very significant: from a severe draught (less than 100 mm) in 1995 to intense rain above 1000 mm in 2002-2003 and from 2013 to 2016.

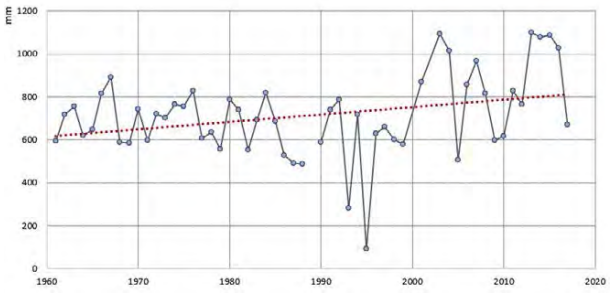

Figure 6: Annual total rainfall 1961-2017

5. FOOD

The municipality has an important reserve of rich agricultural land that produces local food and two Natural Protected Areas that are fundamental for a healthier environment required for agriculture and urban development. None the less, land speculation, illegal invasions and wood extraction are major dangers for them.

Some of the most important consequences of UAM team involvement from 2020 to 2023 are the new urban guidelines for the Municipality Land Use Allocation (Plan de Desarrollo Urbano Municipal 2023) that have been approved as official law to provide protection of farmland in the western part of the municipality. They also mark and define development limits for state parks, woodland and natural areas.

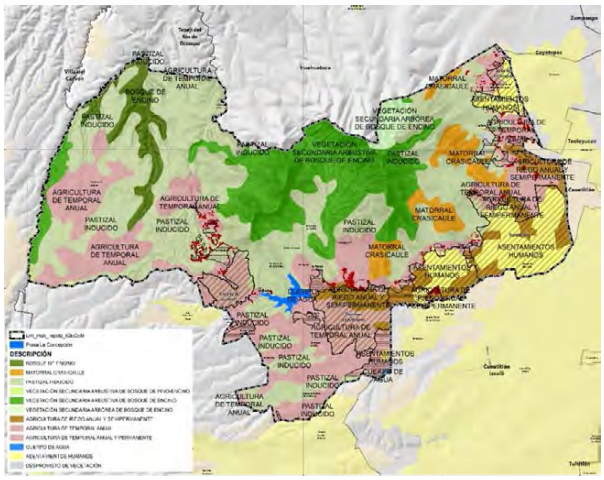

Figure 7: Urban Areas, Farmland and Parks in Tepotzotlan

6. WATER AND ENERGY

Water supply for a fast-growing population is one of the most important local issues as the water consumption approaches the limits of supply [8]. New low-cost water technologies as rainwater harvesting, water reuse systems and water treatment have been tested.

Although energy consumption per capita in the analysed territory (1,140 KWh/person year) is much less that in other parts of the country or Mexico´s City Metropolitan Area (average 2,186 KWh/person year)

[9] , the impact of increasing cost of energy in a low income population is reviewed from the perspective of affordability, life quality, efficiency, consumption and micro generation.

Since 2021 another program to promote site sensitive passive energy housing designs in under way with construction guidelines and build demonstration examples of correct orientation, local materials, greenhouses, rain water harvesting, solar water heaters and other sustainable well know technologies. The main purpose is to generate architectural samples that will guide new urbanization and construction processes applying sustainable principles. This program is associated with the project "A Model of Social Production of Housing and Habitat" financed by the Mexico´s National Council for Science and Technology (CONAHCYT 2021-2024). The goal is not to produce "ideal prototypes" of new housing but to improve and adapt existing constructions and technologies to the local building traditions. At the same time develop in local inhabitants a hands-on experience of the benefits, cost and limitations of a sustainable approach to architecture.

Figure 8: Self build housing units in Flores Magon Neighborhood, Tepotzotlan

This program goals are to test solutions to today's problems in real examples and prevent the necessary adjustments for the immediate future.

6. HEALTH

In relation to respiratory infection deceases (such as SARS-COV-19) that are the main reason for death in the population, the project includes a new hospital, now under construction, to attend basic medical services. Its design has been developed by the UAM team. In this and other build examples air quality, indoor temperature and ventilation rates are top priorities

Figure 9: Tepotzotlan Local Public Hospital under construction (2023)

7. RESULTS

None the less, through the last 18 years with the support of local governments and NGO´s, articles, official documents, divulgation materials and build projects have been produced. Among them the most important are:

7.1 Development Plan 1994-1996.

This plan was one of the first UAM supported works for Tepotzotlan. It was set as an official guiding document for a three years administration. Thoughtfully used by the local government produced good results in public works particularly basic infrastructure (water supply, pavement, electricity). It was awarded a price as one of the three best municipal plans of the State of Mexico.

7.2. Development Plan 2004-2006.

A second Municipal Plan was developed ten years later. Precisely during this administration, the Harvard-UAM project was started and a different approach was taken by local government, commercial activities and housing developers. Local problems associated with fast grow of population and industrial activity were evident and the plan considered a priority to limit the number of industries, improve public services and housing quality.

7.3 Alternative Futures for Tepotzotlan 2005-2010

The Harvard-UAM project had many relevant products. First in 2006 with a large 500 square meters exhibit at the National Museum of the Viceroy Period open for six months to the general public and visited by more than 20,000 people, particularly local inhabitants, primary and secondary local students. It was complemented by guided visits to the Sierra de Tepotzotlan and many of the historic constructions. Its main goal was to create consciousness in local population of their role on the actual problems and the future development.

Later, in 2010, was published "Alternative Futures for Tepotzotlán"[2] with 2,000 copies that were distributed throughout the municipality. This document contains the data that supported the study

and a series of maps that illustrate it on the local territory.

7.4. Municipal Urban Development Plan 2023

Starting in 2019, the UAM team supported urban planning and development ordinances that were finally presented to the public in 2023 and approved by the State of Mexico´s deputies chamber in October of the same year [10].

This extensive document, has to comply with several laws and regulations on its development. However, it is a fundamental instrument for land allocation, as it specifies and limits the type of buildings, height and density of any new construction. It also defines urban and non-urban limits of the 20,907 Hectares of municipal land.

In order to accommodate the future population growth, a moderate increase in density has been proposed for specific parts of the urban area: reducing the minimum lot and increasing construction height from four to six meters. At the same time central historic cores have been defined for the three urban centres, identifying buildings with historic value, limiting height and activities and defining pedestrian areas among other measures to protect their historical character.

7.5. Urban Projects

At a large scale there are some important projects on the guidelines. A series of overpasses on the main highway to facilitate access of automobiles and trucks Others include water ways turned into pedestrian and bicycle roads. Water treatment plants that are required to keep water clean and visitors safe.

A new highway access overpass was developed by the Federal Government with local government support. The overpass facilitates traffic to and from Mexico City, as well as the incoming flow of traffic from the region.

A second highway over pass is now under construction to allow for a direct access from the Queretaro highway to the industrial zone. This element will remove traffic from the downtown area, separating trucks from cars.

7.6. Green Corridors

One of the key elements of the urban and regional proposals was the “green corridor” system. It has been difficult to implement them. However, the one kilometer first stage of “Rio Chiquito” green corridor has recently been finished and two other stages (2.5 km) are currently under of construction. The fourteen kilometer “Zanja Real” linear park project is programed for 2024-2025.

Figure 10: Rio Chiquito Linear Park (2023)

7.7. Architectural Projects

Several architectonic projects have been originated on the guidelines and concepts developed by the Harvard-UAM team. Specific projects were conceptually developed such as the municipal handicrafts market, small scale boutique hotels, a regional chain hotel at the entrance of the municipality from the Mexico Queretaro highway, a new regional bus terminal. All of them have been build.

Figure 11: Polideportivo Tepotzotlan under construction (2023)

The hospital and the multi-sports complex are currently under construction. The architectonic project and field supervision was developed by the UAM team.

8. CONCLUSION

Changing urban trends and architectonic elements is a slow process. Although it is clear, by the data available, that Tepotzotlan needs to adapt to a series of important changes and protect its natural and historic patrimony, the “late adaptive scenario” has been the best possible option.

In some areas the “non-adaptive approach” seems to dominate, particularly in industrial development areas with their large economic and political power and the argument that industry brings

jobs and economic development, underestimating the large environmental impact and diminishing of local residents' quality of life.

None-the-less, as a result of this research, it has been possible to have a direct and indirect effect on the development of large industrial, urban and rural areas, particularly those with environmental and cultural value.

Geodesign and sustainable low-energy architecture approaches are complementary, since it is impossible to talk about bioclimatic architecture without applying these same principles at the neighborhood, city and a regional scale in order to develop resilient places.

There is a lot that has been achieved in the last twenty years. Normative instruments for sustainable development have been approved and are mandatory. The Municipal Urban Development Plan (2023), is now the basis for official normativity and regulation. However, it requires sensitive, well informed and intelligent officials to implement it correctly and sustain it in the mid and long term.

On the other hand, strategic projects have been designed and built, such as the highway overpass, a large highway hotel, the regional bus central, a central market; and more recently, linear parks for the protection and use of natural water sources, a hospital and a multi-sports center.

None-the-less, there are strategic projects that remain in their concept stage, such as the Zanja Real linear park; a large biological water treatment plant; the Rio Hondo pedestrian, bicycle and recreational project; a cycling street system and a truck and heavy traffic independent mobility plan, among others.

There is still a lot of work to do.

ACKNOWLEDGEMENTS

Research studies for Tepotzotlán have been financed by numerous institutions and individuals, among them the Universidad Autonoma Metropolitana, Unidad Azcapotzalco; the H. Ayuntamiento de Tepotzotlán and the CONACHYT-PRONAII program "Development of a Replicable Social Production Model of Housing and Habitat"

REFERENCES

1. Gobierno de Mexico (2023). Data Mexico. [Online], Available:https://www.economia.gob.mx/datamexico/es/profile/geo/valle-de-mexico
2. Stenitz, C. Figueroa, A. Castorena, G. (2010). Alternative Futures for Tepotzotlan. Ed Universidad Autonoma Metropolitana. Ciudad de Mexico, Mexico
3. Stenitz, C. (2012). A Framework for Geodesign: Changing Geography by Design. ESRI Press. USA
4. Instituto Nacional de Estadística y Geografía (INEGI) (2020). Nacimientos en México por año. [Online], Available: https://www.inegi.org.mx/temas/natalidad/
5. Figueroa, A. Fuentes V. (2022). Arquitectura Bioclimatica y Geodiseño: Nuevos Paradigmas. Ed. Universidad Autonoma Metropolitana, Ciudad de Mexico, Mexico
6. IGECEM (2014). Reporte de la Comisión Estatal de Parques Naturales y de la Fauna (CEPANAF). Toluca, Mexico.
7. Comision Nacional del Agua. (2020). Normales Climatologicas. Ed. SARH. Ciudad de Mexico, México.
8. UNESCO (2020). Informe Mundial de las Naciones Unidas sobre el Desarrollo de los Recursos Hídricos 2020. New York, USA.
9. Campos, Leticia (2005). La Electricidad en la Ciudad de Mexico y Area Conurbada. Ed Siglo XXI, Ciudad de Mexico, Mexico.
10. Gobierno del Estado de Mexico (2023). Plan de Desarrollo Urbano de Tepotzotlan. [Online], Available: https://sedui.edomex.gob.mx/sites/sedui.edomex.gob.mx/files/files/planes_municipales/Tepotzotlan/TEPOTZOTLAN-PMDU.pdf

Water-Neutral Systemic Design and Planning Decisions
Across Different Urban Scales

PEPE PUCHOL-SALORT[1,2,3], EDUARDO RICO-CARRANZA[1,2], STANISLAVA BOSKOVIC[1], MAARTEN VAN REEUWIJK[1], JENNIFER K. WHYTE[1,2,4], ANA MIJIC[1,2]

[1] Imperial College London, United Kingdom
[2] Centre for Systems Engineering and Innovation, Imperial College London, United Kingdom
[3] World Economic Forum, Switzerland
[4] University of Sydney, Australia

ABSTRACT: In the next decade, London's planning authorities are aiming to build over half a million new households to meet the UK's surging housing demand. This future scenario poses a significant challenge to urban water security, exacerbated by new development pressures, the climate emergency, and the city's expanding population. Water Neutrality (WN) has emerged as a promising concept for assessing crucial urban water security indicators. However, while various studies have explored WN, there remains limited literature on its practical application across diverse urban scales and how it can inform decisions for the allocation of new urban development and retrofit solutions. This work introduces an innovative, data-driven approach to evaluate water-neutral design options across different urban scales. The Water Neutrality Decision Support Tool (WaNetDST) prototype is presented as a pioneering solution capable of transitioning from city-wide assessments to individual urban development sites. Combining GIS spatial datasets and an aggregated scoring system, WaNetDST facilitates a comparative analysis for water-neutral development. It compares urban planners' preference with the potential for WN retrofit strategies to mitigate new development impacts. The outcomes generated by WaNetDST will reshape decision-making processes for Local Planning Authorities and housing developers, fostering new dialogues among city boroughs.
KEYWORDS: Water Neutrality, Urban Planning, Decision-Support, Evaluation Tool, Spatial Allocation

1. INTRODUCTION

Integrating social and environmental dimensions with urban infrastructure systems is crucial for achieving sustainable urban development [1,2]. Within the decision-making process of the urban planning system, data is a compilation of information collected either in-situ or remotely, which is then transformed into evidence by key decision-makers [3,4]. However, this transformation process is heavily influenced by the governance and policy context that shapes strategic decisions in systemic design [5].

Systemic design is a developing approach that has advanced in recent years [6,7], which combines traditional design principles and systems thinking by encompassing a holistic and exhaustive analysis of the urban form elements. Systemic design sees the planning process as a whole and considers different planning aspects such as urban water management as one of the layers in the design of cities.

With the advent of the digital era, there is a constant increase in the availability of raw spatial datasets in the UK from various sources (e.g., UK and London census, Central Government and local urban planning departments, British Geological Survey, etc.). However, most of these datasets are disaggregated and challenging to comprehend for key urban stakeholders [8]. In the context of urban water security, the available data often cannot be directly used for decision-making purposes as they do not provide direct information about changes in the urban water system, and most infrastructure solutions are based on specific urban scales [9]. Although the Greater London Authority (GLA) and Local Planning Authorities (LPAs) in several boroughs in the capital currently require evidence-based policy-making for water-neutral strategies [8], there is a lack of knowledge on how to realistically implement WN across different urban scales [10,11].

Spatial allocation is a complex problem that involves multiple stakeholders and whole-system uncertainties [12]. Multi-Criteria Decision-Making (MCDM) methods are tools used in infrastructure planning to evaluate the balance between urban planning purposes and systemic design options [13]. While examples in the literature offer valuable indicators for different stakeholders, there is still limited evidence of a tool that integrates strategic decisions of systemic design and evaluates urban planners' preferences for new urban development and potential retrofit opportunities with water-neural design options [14].

Combining the systemic design concept with the decision-making process for urban water neutrality will require integrated evaluation of often conflicting

criteria in a data-driven tool. In this work, a novel prototype of a Water Neutrality Decision-Support Tool (WaNetDST) is developed to inform diverse urban stakeholders about systemic design options and facilitate evaluation for water-neutral development. By assigning aggregated scoring values to selected spatial units, WaNetDST offers a quantitative and spatial approach to allocate new and retrofitting design options across different urban scales in London. Ultimately, the results from WaNetDST have the potential to transform the decision-making process for Local Planning Authorities (LPAs) and housing developers, fostering new dialogues among boroughs within the same city.

2. CASE STUDY AREAS ACROSS SCALES

The novel WaNetDST is intended to operate across different urban scales. From larger to smaller scales, the main areas of study in this work will be city, borough, and urban development site. At the city scale, the focus is on London, which is divided into 32 boroughs, further sub-divided into smaller zones known as Lower Layer Super Output Areas (LSOAs) for statistical purposes. At the proof-of-concept stage of WaNetDST, all the information was collected and processed at the LSOA and borough levels.

At the borough scale, the main case study area is the London Borough of Enfield (LBE) located in North London (Figure 1). Covering approximately 83 km^2, the borough is composed of one-third residential houses, another third mainly consisting of Green Belt areas, and the remaining portion including commerce, industry, shops, transport, and other amenities [15]. LBE is known for its abundance of green spaces, particularly surrounding the Green Belt in the North, as well as water reservoirs in the East side [16].

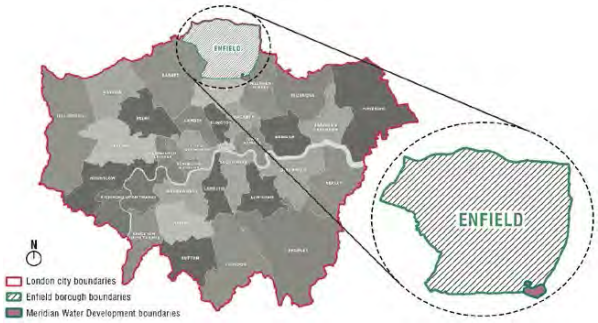

Figure 1: Case study areas in WaNetDST from city to borough to urban development site scale focusing on the London Borough of Enfield (LBE) and Meridian Water Development Plan (MWDP).

Within the LBE, several urban development projects are already underway, with the Meridian Water Development Plan (MWDP) being particularly notable. Spanning across an 85-ha site, this development aims to accommodate a total of 10,000 homes and a railway station. The project is expected to take 20-25 years to complete, divided into four stages, with construction on the first stage already initiated in 2021. The majority of the MWDP site consists of brownfield land that was previously used for industrial purposes.

3. MULTI-CRITERIA INTEGRATED EVALUATION

The main objective of WaNetDST is to optimise the allocation of water-neutral developments. Initially, Local Planning Authorities (LPAs) may utilise the tool to generate scoring maps based on their preferences for new development areas and WN retrofitting opportunities. These quantitative maps then could serve as informative instruments for urban developers, who might initiate the systemic design process at early stages of development [17].

3.1 Water Neutrality Decision-Support Tool

The prototype of WaNetDST includes two types of ruling categories: one based on urban planners' preference for allocating new urban development, and the other based on Water Neutrality (WN) retrofit opportunities (green boxes in Fig. 2). The rules for scoring the WN retrofit opportunity category are derived from literature and expert advice, while the rules for urban planners' preference scoring are based on feedback obtained from participatory workshops conducted as part of two large research programmes (i.e., CAMELLIA and VENTURA). The activities in these participatory workshops followed group model building principles [18].

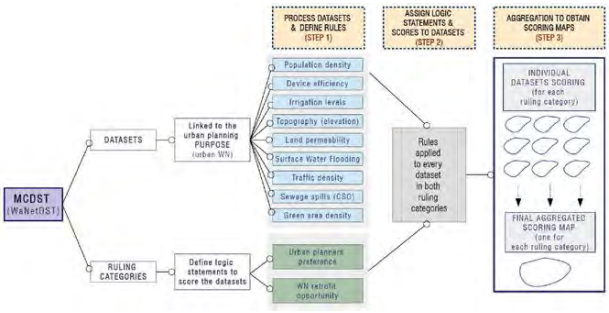

Figure 2: Diagram of the Multi-Criteria Decision-Support Tool (MCDST) based on the urban planning purpose of Water Neutrality (WN).

The functionality of WaNetDST is divided into three main phases, as illustrated in Fig. 2. In the first phase, a series of spatial datasets related to water-neutral urban planning are selected and processed, and scoring rules are defined. These datasets are chosen based on the participatory workshops and meetings with water and geological experts conducted prior to the full development of the tool as part of CAMELLIA and VENTURA research programmes. Among publicly available options, three datasets for each WN indicator were identified as the most relevant (Table 1). Urban consumer demand is linked to population density, device efficiency, and

irrigation levels, while flood risk is linked to elevation, land permeability (represented by runoff coefficient), and surface water flooding. River water quality is linked to traffic density, sewage spills, and green area density.

Table 1: Datasets introduced in WaNetDST, differentiating the type of data, if raw or processed, and its original source. The rows shaded in blue are the datasets that need to be processed from their raw sources.

WN INDICATORS	Dataset	Type of data	Raw / Processed	Source
CONSUMER DEMAND	**Population density**	Vector	Raw	UK Census
	Device efficiency (Directly linked to typology, age, and size of households)	Vector	Processed	Raw datasets: UK Census
	Irrigation levels (Directly linked to private garden and population datasets)	Vector	Processed	Raw datasets: Office for National Statistics
FLOOD RISK	**Elevation**	Raster	Raw	UK Ordenance Survey Open Data
	Land permeability (Linked to Runoff Coefficient, CR)	Raster	Processed	BGS Land-Use map
	Surface water flooding	Vector	Raw	Environment Agency
WATER QUALITY	**Traffic density**	Linear	Processed	Department for Transport - UK Gov
	Sewage spills (Linked to CSO maps)	Point	Processed	The Rivers Trust
	Green area density	Vector	Processed	BGS Land-Use map

In the second phase, after processing the selected datasets (Table 1) and defining the general rules, logic statements and scores are assigned to each dataset in each ruling category. The scores for urban planners' preference in allocating new urban development are based on the physical and environmental properties of the land. On the other hand, the scores for WN retrofit opportunities are based on the potential of a specific site to mitigate urban water security impacts through WN design options implementation [14].

Finally, the third phase involves aggregating the scores obtained previously. This aggregation process results in a series of GIS location maps that will be utilised by housing developers during the early stages of the planning application process. Step 3 is sub-divided in two sub-steps for spatial and numerical assessment (Fig. 2). In Step 3.1, individual maps are generated for each dataset, representing the scores for both the urban planners' preference and WN retrofit opportunity categories. In this first prototype, a total of eighteen individual maps are produced (nine for each ruling category), although this number may vary depending on the selected datasets. Subsequently, in Step 3.2, the scores from each dataset are averaged and combined to generate a single location map for each ruling category. In the proof-of-concept version of the tool, the weights assigned to each dataset are equal. The process for obtaining the aggregated scoring value within each ruling category follows Equation 1:

$$\text{Rul. Cat. SV} = (\Sigma \text{ Dataset 1 SV x Weight 1} + \text{Dataset [X] SV x Weight [X]} + \ldots) / (\text{Total Num. of Datasets [X]}) \quad (1)$$

where Rul. Cat. - Ruling Category;
SV - Scoring Value;
W(x) - Weight.

In this first prototype of WaNetDST, a total of nine datasets linked to urban water security are used, and each dataset is assigned an equal weight of one. Upon completion of the process, users of WaNetDST will have the ability to assess multiple strategic areas or urban development sites within the city.

3.2 Ruling categories visualisation

In Step 2 of WaNetDST process (Fig. 2), after assigning the scoring values, the visualisation of location maps and their corresponding numerical values becomes crucial for the development of WaNetDST. Consistency and clarity are important aspects to ensure coherence across all the maps in WaNetDST. The information from the datasets is divided into five intervals, evenly distributed based on equal counts quantile. This approach, facilitated by the QGIS tool, organises groups with an equal quantity, resulting in evenly distributed shading on quantile-based maps.

Table 2: Colour-coding used in WaNetDST for the Urban Planners Preference and Water Neutrality (WN) Retrofit Opportunity scoring following 5 rating intervals and scoring levels based on equal counts quantile distribution.

WaNetDST scoring colour-coding based on equal counts quantile distribution			
Urban Planners Preference Scoring			
Rating Interval	**Scoring Level**	**Approximate scoring values rates**	**Colour**
1	Very low	0-3	
2	Low	3-4	
3	Medium	4-5	
4	High	5-7	
5	Very high	7-10	
WN Retrofit Opportunity Scoring			
Rating Interval	**Scoring Level**	**Approximate scoring values rates**	**Colour**
1	Very low	0-3	
2	Low	3-4	
3	Medium	4-5	
4	High	5-7	
5	Very high	7-10	

To maintain consistency and facilitate interpretation of the scores across all location maps, a color-coding scheme is employed (Table 2). For the urban planners' preference scoring, a range of oranges and reds is utilised, with darker red indicating lower preference and lighter shades representing higher preference. Conversely, for the WN Retrofit Opportunity scoring, different shades of blue are used, with lighter blue indicating lower opportunity and darker shades indicating higher opportunity.

4. RESULTS

4.1 Visualisation of processed datasets

The processing of datasets in Step 1 of WaNetDST (Fig. 2) involves generating nine individual visualisation maps for each dataset before assigning any scoring value. These maps are considered crucial for understanding the water neutrality (WN) urban form properties. As an example, see the processed datasets for irrigation levels, traffic density and green area density are visually presented in the next Fig. 3.

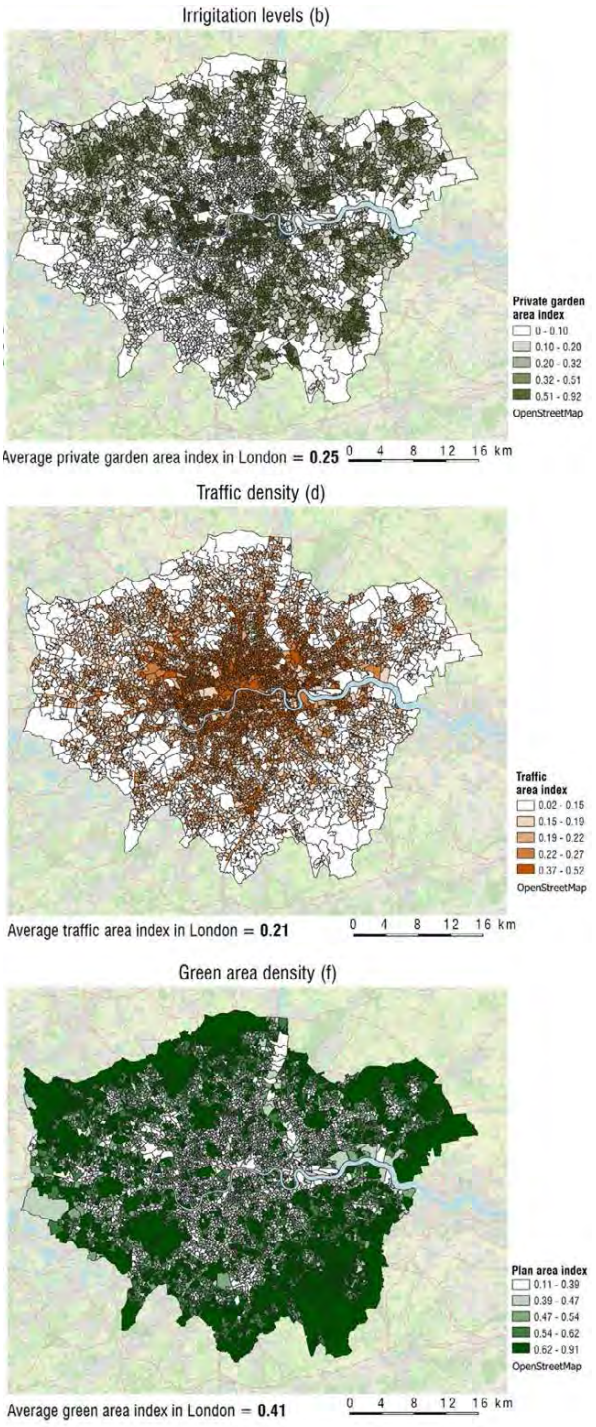

Figure 3: Example of three WaNetDST processed datasets visualisation maps informing about key WN urban form properties for urban water security evaluation and their average values of area index.

4.2 Decision-support aggregated maps

Upon processing the nine maps for each dataset (Section 4.1), scoring values are assigned to each dataset according to the logic statements in the second phase (Fig. 2). Their values are then aggregated using Eq. 1 and two overall aggregated maps are obtained at the city scale (one for urban planners' preference, and one for WN retrofit opportunity; Fig. 4).

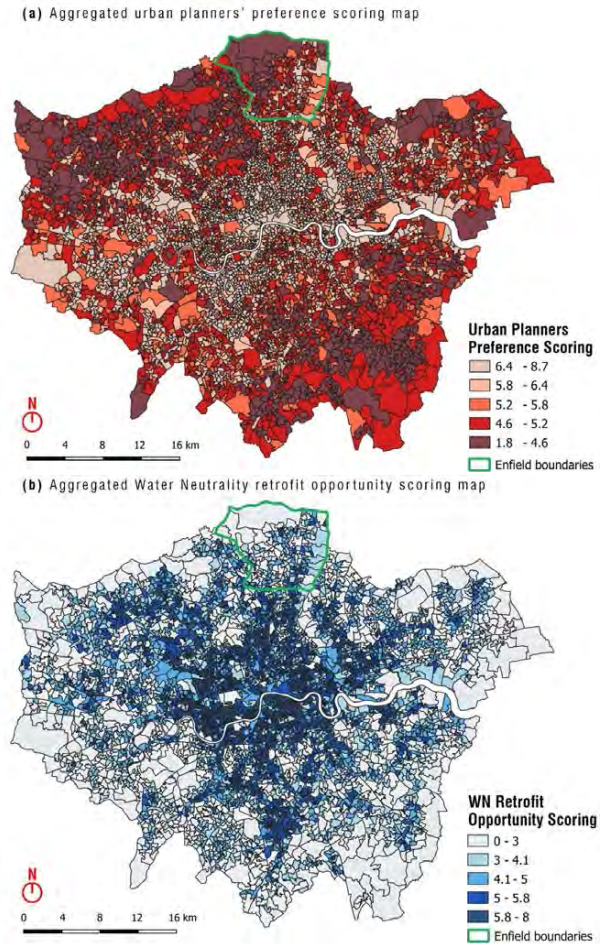

Figure 4: WaNetDST aggregated urban planners' preference scoring map (a) and aggregated Water Neutrality (WN) retrofit opportunity scoring map (b) at London city scale following the aggregation of the nine datasets with London Borough of Enfield (LBE) boundaries marked in green.

While establishing a clear pattern for WN purposes across the entire city is challenging (as each LSOA has its own properties derived from the datasets and rules integrated into the tool), a reduced preference for new urban development in numerous peri-urban zones is observed. These areas typically feature larger green spaces and existing houses (Fig. 4a). Conversely, the opportunities to implement new WN design options receive higher scores in the city centre and densely populated neighbourhoods characterised by paved, impervious areas and ageing infrastructure (Fig. 4b). The overall aggregated maps, like the ones

shown in Fig. 4, are intended to be included in the Local Plans by LPAs in subsequent stages of the work. They are aimed to serve as guidance for urban planners and housing developers in formulating various WN urban planning scenarios.

5. DISCUSSION

WaNetDST offers the capability for cross-scale evaluation, presenting significant potential to inform various urban stakeholders. Once the scoring maps for urban planners' preference and WN retrofit opportunity are obtained at the city scale, a conceptual virtual platform will be developed to seamlessly integrate the aggregated results from both scoring categories. This innovative virtual platform can take the form of a web-based interface or a plugin within QGIS, providing insights into WN synergies resulting from future urban development within a borough and its proposed new urban developments.

WaNetDST serves as an informative decision-support tool, offering both quantitative (numerical scoring results) and qualitative (visualisation maps) information. The results highlight the significance of urban distribution and design parameters in achieving WN targets within and outside development boundaries.

The first prototype of WaNetDST presents, however, a series of limitations. Currently, the datasets used are open-source and publicly available, with manageable data sizes. However, in certain cases, the datasets might need special permission (licence) to be downloaded, be difficult to be shared with the public, or require special software to be processed. Datasets may also differ in resolution, with some boroughs having more detailed data on flood risk while others rely on national studies with larger resolutions.

In the first prototype of WaNetDST, nine datasets are processed grouped by the three UWS indicators, but this number can be expanded in future iterations. Some examples of datasets that could influence the UWS indicators, and therefore WN levels, are orientation (linked to solar radiation and surface reflectance, which influence water quality and nutrients in micro-habitats); amount of rain (linked to the amount of water naturally received, therefore influencing the amount of water consumed from rainwater harvesting systems, and to the level of flood risk); climate (warm temperatures being linked to the amount of water consumed and water supply availability); level of income (linked to the amount of water consumed); or wastewater treatment plant technology (linked to the quality of the water released to the rivers and other natural water bodies); among others.

Another limitation of WaNetDST is the subjectivity of input related to logic statements from experts and urban planners involved in its development. For instance, while most experts in participatory workshops agreed on the logic statement for population density (preferring high-density urban areas due to developed infrastructure and supply networks), some members believed the opposite could be argued, preferring to avoid additional pressure on already stressed areas. Furthermore, the primary users of WaNetDST at this stage are top-level decision-makers like LPAs and housing developers. However, future stages aim to incorporate a more inclusive bottom-up approach involving community groups and non-profit environmental organisations as part of the advisory board.

One direction for future work in WaNetDST involves scoring aggregation at the borough level and the development of a trading system among boroughs within the same city. This would allow LPAs from different departments and governance bodies to trade based on their specific housing targets and current environmental properties. In the context of London, certain boroughs may face challenges in fully achieving their WN targets, such as having high housing targets but low WN retrofit opportunities. By implementing this trading system, boroughs might be able to trade with other planning authorities to implement required WN design options outside their boundaries. This trading system could potentially be transformed into a credit system, similar to nitrogen pollution credits, where boroughs will exchange WN credits based on their WN retrofit opportunity situation.

Table 3: Capacity for water-neutral urban development table comparing the land-use types with the three tactical decision categories, where green tick means developable and red cross means non-developable.

CAPACITY FOR WATER NEUTRAL URBAN DEVELOPMENT				
	Land-Use Types	Greenfield	Brownfield	Existing Buildings
Tactical Decision Categories	Implement WN options in new homes	√	√	x
	Retrofit existing homes	x	x	√
	Add new BG space	x	√	√

Furthermore, while the information in this proof-of-concept stage was collected and processed at the LSOA and borough levels, future stages are expected to employ finer resolution maps and smaller spatial units. This would allow for more accurate opportunity scoring in WaNetDST, which can be linked to different types of land, such as greenfield, brownfield, or existing buildings. Connecting design options with land-use types will provide insights into the development capacity within each spatial unit. For example, implementing WN options in new homes would be feasible in greenfield and brownfield areas (new developable land), while retrofitting would only be possible in existing buildings (see Table 3). This

additional level of complexity and accuracy in the Decision-Support Tool (DST) results would enhance the understanding of the capacity for development in each specific spatial unit.

6. CONCLUSION

This work introduces an integrated evaluation toolkit called WaNetDST. The application of WaNetDST enables the optimal allocation of new urban developments while identifying environmental synergies across various urban scales. Its spatial allocation component has the potential to significantly reduce the environmental impacts of urban development in cities and foster public acceptance of transformative infrastructure interventions [17].

In its initial prototype, WaNetDST incorporates nine datasets linked to the three urban water security indicators (i.e., consumer demand, flood risk, and river water quality) and provides informative visualisations and numerical assessments of systemic conditions for achieving water neutrality in London.

Future stages of the work will involve expanding the DST to include a larger number of more accurate datasets and incorporating input from additional stakeholders, such as Statutory Consultees and community groups, to benefit from their expert advice. Ultimately, the integration of WaNetDST with existing water-neutral infrastructure frameworks [14] will enhance participatory and systemic design approaches for sustainable urban planning.

ACKNOWLEDGEMENTS

This research is part of the CAMELLIA project (Community Water Management for a Liveable London), funded by the Natural Environment Research Council (NERC) under grant NE/S003495/1; and, part of the euPOLIS project, funded by the European Union's Horizon 2020 program H2020-EU.3.5.2., under grant agreement No. 869448. It would not have been possible without funding from the Engineering and Physical Sciences Research Council (EPSRC) Centre for Doctoral Training (CDT) in Sustainable Civil Engineering under grant EP/L016826/1.

REFERENCES

1. United Nations (2015). *Transforming our world: the 2030 Agenda for Sustainable Development.* Department of Economic and Social Affairs. Public Report.

2. Pandit, A., et al. (2017) Infrastructure Ecology: An Evolving Paradigm for Sustainable Urban Development. *Cleaner Production* 163: S19-S27.

3. Hill, T., and Symmonds, G. (2011). Sustained water conservation by combining incentives, data and rates to effect consumer behavioural change. *WIT Transactions on Ecology and the Environment* 153, 409-420.

4. Eggimann, S., et al. (2017). The Potential of Knowing More: A Review of Data-Driven Urban Water Management. *Environ Sci Technol* 51(5): 2538-2553.

5. Hammad, A., et al. (2019). Sustainable Zoning, Land-Use Allocation and Facility Location Optimisation in Smart Cities. *Energies* 12(7).

6. Jones, P., and Kijima, K. (2018). S*ystemic Design: Theory, Methods, and Practice.* Japan, Spinger Nature, 1st Edition.

7. Battistoni, C., et al. (2019). A Systemic Design Method to Approach Future Complex Scenarios and Research Towards Sustainability: A Holistic Diagnosis Tool. *Sustainability* 11(16).

8. Greater London Authority (GLA, 2021). *The London Plan. The Spatial Development Strategy for Greater London.* Retrieved from: https://www.london.gov.uk/what-we-do/planning/london-plan/

9. Bichai, F., et al. (2015). Understanding the role of alternative water supply in an urban water security strategy: an analytical framework for decision-making. *Urban Water Journal* 12(3), 175-189.

10. Marzouk, M., and Othman, A. (2020). Planning utility infrastructure requirements for smart cities using the integration between BIM and GIS. *Sustainable Cities and Society* 57, 102120.

11. Chen, S., et al. (2021). Revisiting China's Sponge City Planning Approach: Lessons From a Case Study on Qinhuai District, Nanjing. *Frontiers in Environmental Science* 9:748231.

12. Ni, J., et al. (2014). A Multiagent Q-Learning-Based Optimal Allocation Approach for Urban Water Resource Management System. *IEEE Transactions on Automation Science and Engineering* 11(1): 204-214.

13. Jato-Espino, D., et al. (2014). A review of application of multi-criteria decision-making methods in construction. *Automation in Construction* 45: 151-162.

14. Puchol-Salort, P.; et al. (2022). Water neutrality framework for systemic design of new urban developments. *Water Res* 219: 118583.

15. Enfield Council (2021). *Enfield Local Plan. Main Issues and Preferred Approaches.* Retrieved from: www.enfield.gov.uk/enfieldlocalplan

16. Bussi, G., et al. (2022). Green infrastructure and climate change impacts on the flows and water quality of urban catchments: Salmons Brook and Pymmes Brook in north-east London. *Hydrology Research* 53(4): 638-656.

17. Puchol-Salort, P., et al. (2021). An urban planning sustainability framework: Systems approach to blue green urban design. *Sustainable Cities and Society* 66: 102677.

18. Richardson, G. P., and Andersen, D. F. (1995). Teamwork in group model building. *System Dynamics Review 11*(2), 113-137.

3.2. Architecture for human resilience and well-being (including e.g., biophilic design, nature-based solutions, climate adaptation strategies for buildings and spaces)

PLEA 2024 WROCŁAW
(Re)thinking Resilience

Comparative Analysis of Urban Heat Island Effects on Building Energy Consumption in the U.S. Midwest

A combined workflow using Urban Weather Generator and Future Typical Meteorological Year Climate Scenarios

FARZAD HASHEMI[1], NEGAR SALAHI[2], SEDIGHEH GHIASI[2], ULRIKE PASSE[2]

[1]School of Architecture + Planning, The University of Texas at San Antonio, San Antonio, United States
[2] College of Design, Iowa State University, Ames, United States

ABSTRACT: Urban areas often experience higher air temperatures than their surrounding rural counterparts, a phenomenon known as the urban heat island (UHI) effect. This significant human-induced alteration of urban microclimates has notable consequences, especially on urban energy consumption and resulting economic implications. This study presents an in-depth analysis of the UHI effect on urban building energy consumption in a US Midwest neighbourhood. Utilizing a three-phase methodology, the research first simulated UHI intensities with current and future Typical Meteorological Year (TMY) data, integrated with the Local Climate Zone (LCZ) classification system and the Urban Weather Generator (UWG) model. The second phase employed the urban modelling interface (umi) for building energy simulation, capturing the UHI impact on both residential and commercial buildings. The third phase demonstrates that UHI effects lead to reduced heating demand but increased cooling requirements in the future, with residential areas being more affected. The study's findings reveal critical challenges for urban planners and policymakers, emphasizing the need for sustainable designs to address fluctuating heating and cooling demands in changing climates.
KEYWORDS: Urban Heat Island, Local Climate Zones, Urban Weather Generator, Urban Modelling Interface, Building Energy Consumption

1. INTRODUCTION

One of the most documented phenomena of urban climate change caused by urbanization is known as the "urban heat island" (UHI), which conventionally refers to the difference between the urban temperature and corresponding rural or suburban areas [1]. Today, UHI effects are a global concern and have been observed in cities regardless of their locations and size; Chicago, IL [2], Phoenix, AZ [3], Houston, TX [4] in the U.S., Beijing [5] and Xian [6] in China, Sydney [7] and Melbourne [8] in Australia, Stuttgart [9] Germany, and Dublin [10] Ireland to name a few. A number of factors contribute to the formation of the UHI; however, it is largely caused by low evapotranspiration, high solar radiation absorption, air flow blockage, and high anthropogenic heat release in cities [11]. The UHI effects threaten the health and productivity of urban populations and cause general discomfort, respiratory difficulties, and heat-related mortality in climatically diverse cities [12-15]. In addition, the rise in urban temperatures has a significant effect on building energy usage, leading to an increase in cooling energy needs by 10% to 120%, and a reduction in heating energy demands by 3% to 45% depending on location [16].

To measure the UHI intensity in different urban contexts, the conventional approach is to compare air temperature data gathered at one to two meters above ground for "urban" and "rural" conditions at two or more fixed sites and/or from mobile temperature surveys [1]. Utilizing this methodology, [17] examined a decade of air temperature data from five Berlin sites, finding pronounced night-time warmth in the city during summer and slight warmth throughout winter days compared to a reference site scattered with trees. Using urban and suburban weather data collected, [18] reported that UHI effects can double cooling loads and triple peak electricity loads for cooling in urban buildings in Athens, Greece. [19] studied the effect of the London Heat Island on heating and cooling energy in an office building across 24 locations, finding a 25% increase in cooling and a 22% decrease in heating needs in urban versus rural areas. [20] discovered that relocating buildings from suburban to urban areas in Manchester, UK, with average summer UHI, raised chiller energy demands by 9.4% to 12.2%, influenced by building design and glazing ratio. The study used data from iButton temperature sensors.

A major challenge caused by the conventional approach of comparing air temperatures in urban and rural areas to analyse the UHI effects is the substantial variation in urban areas in terms of building density, surface types, and green spaces. To address this, the Local Climate Zones (LCZ) classification system [21] offers a standardized

method to categorize urban areas based on their physical and climatic attributes. The LCZ classification scheme recognizes 17 standard classes, 10 built types ranging from LCZ 1 to LCZ 10 and 7 land cover types ranging from LCZ A to LCZ G. Each LCZ type is associated with a typical range of parameter values that describe surface cover, building heights and street aspect ratio, etc.

Another challenge in studying urban heat islands is the need for extensive measuring equipment and effort. To overcome this, modelling tools have been developed, such as the Urban Weather Generator (UWG) [22]. Utilizing the EnergyPlus building energy simulation engine [23] and incorporating the principles of the Town Energy Balance (TEB) model [24], the UWG considers urban characteristics, building properties, and anthropogenic heat for detailed urban temperature simulations. The model calculates hourly air temperature and humidity in urban canyons from measured weather data outside of urban areas. However, determining the ideal model size for accurate urban area simulations and the need for specific data inputs, especially when field data are unavailable, limits the use of the model. This can be particularly challenging for architects and building engineers in the early design phases, where time and resources are limited. To bridge these gaps, a novel methodology was proposed by [25], that couples the LCZ classification with the UWG. This approach generates modified weather data reflecting the unique thermal and morphological characteristics of each LCZ. Using the aforementioned methodology, this study aids in estimating UHI intensity at a neighbourhood scale, thereby enhancing the comprehension of UHI effects on building energy use. The modified weather data, suitable for use in standard energy simulation tools, were generated over a year of simulation at the LCZ scale with UWG providing urban-specific weather data. The data was then combined with Future Typical Meteorological weather data developed by [26]. Subsequently, this UHI-induced weather data, were incorporated into the Urban Modelling Interface (*umi*) developed by [27] to conduct an in-depth energy simulation of urban buildings.

2. METHODOLOGY AND CASE STUDY

Elevated temperatures in urban locales affect building energy performance through significantly increase in cooling loads and to some extent decrease building heating loads. In this context, understanding the intricate relationship between UHI and urban energy consumption is of paramount importance. This study provides a comprehensive understanding of UHI effects on urban building energy consumption, in a scale of urban neighbourhood focusing on the Capitol East, a low-income neighbourhood in the US Midwest city of Des Moines, IA. This neighbourhood was chosen as the pilot study area because of its unique socio-economic characteristics that potentially limit residents' adaptive capacity to regulate indoor temperatures, making it a representative case for many urban areas with similar challenges. The study utilizes both existing Typical Meteorological Year 3 (TMY3) [28] and future projected TMY climate data at the canopy level of the neighbourhood. Fig. 1 depicts the proposed workflow employed in this study, encompassing three fundamental stages:

2.1 Step 1: Weather Data Simulation

The initial phase was centred around hourly simulations of UHI intensities using both current TMY3 and future weather data. This was achieved by coupling the LCZ classification system with the UWG tool. According to the description provided by the LCZ classification dataset, the Capitol East neighbourhood is categorized as Open Low-Rise, LCZ 6 (Fig. 2) in which buildings are small, detached to attached in row, with 1 to 3 stories. Also, scattered trees and abundant plant coverage exist in LCZ 6. After extracting the urban characteristics data such as anthropogenic heat flux, surface albedo, and terrain roughness class from the LCZ dataset sheet, the neighbourhood 3D model [29, 30] was incorporated into the UWG. The UWG was initially developed in MATLAB, with later versions created in Python.

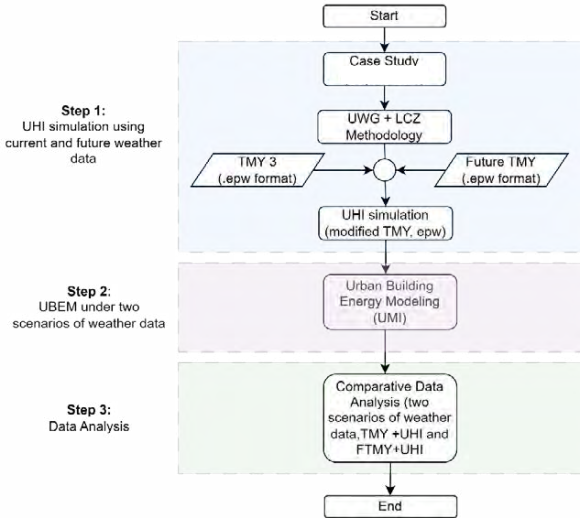

Figure 1. Workflow to study UHI impacts on building energy consumption utilizing both TMY3 and projected Future TMY.

Additionally, the Ladybug tools [31] introduced a user-friendly version of the UWG through Dragonfly, a Grasshopper 3D plugin, enabling urban designers to conduct climate and UHI modelling within the Rhino 3D interface. To ensure a holistic representation of both buildings and trees, spatially explicit data from a complete inventory of 340 existing buildings and

1142 trees (both yard and street trees) and buildings were added into the model.

Figure 2. Images, 3-D illustration, and properties of LCZ6 - Open low-rise, for the Capitol East neighborhood, Des Moines, IA.

Fig. 3 illustrates levels of data that the neighbourhood 3-D model includes. According to the assessor's data collected for 340 buildings in the neighbourhood, 259 buildings had active air conditioning systems and 81 were naturally ventilated. In the UWG model, construction information detailing the material properties and performance of the entire structure was incorporated to represent conditioned buildings and their associated waste heat. Buildings without active air conditioning were treated as shading devices.

Figure 3. Layers added into the neighborhood 3-D model.

Consequently, 21 building templates, 13 for buildings with active AC and 8 for non-AC buildings, were generated in the UWG model to represent both commercial and residential buildings in the neighbourhood. After integrating required data, the UHI simulation were run for two scenarios of weather data; existing TMY 3 data recorded at the Des Moines airport and future TMY created by combining existing TMY data with model-projected changes in climate.

The calendar-year-long simulation showed that the average annual UHI intensity was at 0.54° with the current weather data and 0.56°C for the future weather scenario. Moreover, the maximum UHI peaked at 12.4°C for the current scenario and 13.6°C for the future scenario, both occurring on February 1st in the afternoon post-sunset. This pattern indicates a potential rise in urban heat effects in future conditions due to the changing climate. The generated weather data in this step, tagged as TMY3+UHI and FTMY+UHI formatted in EnergyPlus Weather (EPW), serve as the major input for the subsequent phase of this study.

2.2 Step 2: Urban Building Energy Modelling (UBEM)

To conduct the building energy simulation at the neighbourhood scale, the urban modelling interface (*umi*), a Rhinoceros-based urban modelling design tool, was employed. *umi* utilizes EnergyPlus as a simulation engine for buildings thermal simulation. *umi* is based on the Shoeboxer algorithm, a fully automated, reliable, abstracted, and rapid multizone urban simulation workflow to decrease the geometric complexity of thermal models and facilitate large-scale urban simulations [32, 33]. Several recent studies [34-36] have employed *umi* to simulate energy usage within urban environments including the Grove Park neighbourhood of Atlanta, two neighbourhoods in Boston, MA, USA, and an area in Dublin city centre.

Four main scenarios were designed for this study using four weather files: the current TMY3, TMY3+UHI, align with future projections FTMY and FTMY+UHI. The building construction materials and trees geometry were added in *umi* model based on the data gathered from the Assessor's office of the County.

The city of Des Moines, IA falls under climate zone 5A based on the International Energy Conservation Code (IECC), classifying it as a cold climate. The neighbourhood is characterized predominantly by single-family housing [37], has emerged as a focal point for revitalization efforts, led collaboratively by residents and city planners. Covering an area of 282,778 square meters, the area's housing stock, dating back to the early 1900s, underscores an urgent need for enhancements [38-39].

2.3. Step 3: Comparative Data Analysis

In order to examine the UHI impacts on the energy needs for heating, cooling, and their cumulative demand, an energy simulation framework was developed. This framework utilized four distinct weather data files: the current TMY3 and TMY3+UHI, in conjunction with future projections FTMY and FTMY+UHI. These were instrumental in performing

energy simulations using the *umi* software and the findings from this step are detailed in the following sections.

Fig. 4 demonstrates that the UHI effects resulted in an increase of consumption for cooling by 7.31% in the current weather scenario and 2.77% for future projections for all buildings in the neighbourhood. The most significant rise in cooling energy requirements for all buildings occurred in April and May, a pattern consistent in both the current and future scenarios. In contrast, the heating demand exhibits a decline of 3.17% in the current scenario and 3.23% in the future scenario. This decrease was most pronounced in September and October for both the current and future scenarios. When the impacts of UHI are taken into account, the overall energy consumption (cooling + heating) shows a decrease of 2.23% and 2.29% in the current and future scenarios, respectively. This translates to a fall from 4881 MWh to 4772 MWh in the current, and from 4405 MWh to 4304 MWh in future scenario. The UHI effect consistently caused a decrease in heating requirements while simultaneously increasing the demand for cooling in both scenarios. Additionally, the overall energy consumption, when considering the UHI, is on a downward trend, with the decrease being nearly identical for both the current and future scenarios.

Moreover, a sector-specific analysis of the UHI effect indicates subtle differences in energy consumption for both scenarios. In the residential sector, there was a decline in energy usage for combined heating and cooling purposes from 4094 MWh to 3993 MWh, marking a 2.46% reduction for the current scenario, and from 3649 MWh to 3551 MWh, showing a 2.71% decrease for the future scenario. Conversely, the commercial sector exhibited a modest downturn from 787 MWh to 778 MWh, amounting to a 1.11% decrease in the current scenario, and a marginal decline from 755 MWh to 754 MWh, or 0.18%, in the future scenario.

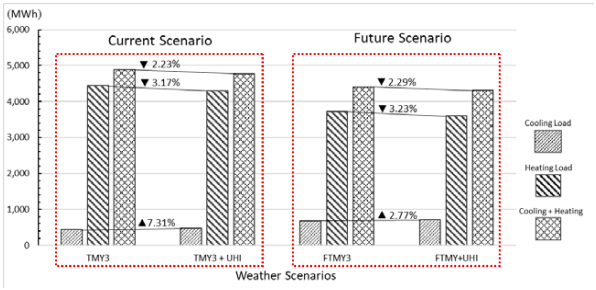

Figure 4. Actual and percentage change in cooling, heating, and combined energy consumption under four weather scenarios

Delving into a comparative analysis between current and future energy scenarios, Fig. 5 depicts patterns of energy consumption for cooling, heating, and their cumulative effect across the four noted scenarios. These scenarios are arranged from the highest to the lowest total energy consumption, considering both the presence and absence of UHI effects.

The initial scenario, using current TMY3 weather data without the UHI effect, shows the highest energy consumption. Simulations suggest a notable reduction of 9.75% in annual energy use when transitioning to the future scenario, with figures dropping from 4881 MWh to 4405 MWh. This change is marked by a 56% increase in cooling load and a 16.27% decrease in heating load for neighbourhood buildings.

Incorporating the UHI effect into both the current TMY3 and future TMY scenarios leads to a decline in total energy consumption, primarily due to a reduction in heating load, which is more significant than the increase in cooling load. By comparing current TMY3 with UHI effects to future TMY with UHI, an estimated 9.81% decrease in overall energy use, a 16.32% reduction in heating loads, and a 49.79% increase in cooling loads are observed. Among these scenarios, the future weather data with the added UHI effect shows the lowest energy use for combined heating and cooling.

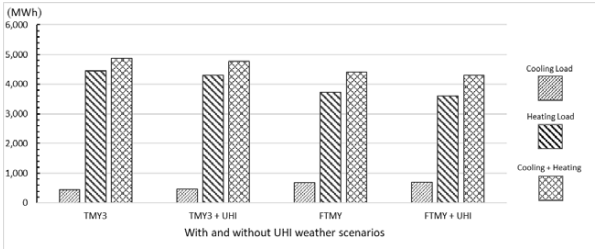

Figure 5. Energy consumption comparison for cooling, heating, and combined energy under current and future weather scenarios with and without the UHI effect.

The analysis between residential and commercial buildings indicates different impacts of projected changes. Under the future TMY scenario, residential buildings' cooling load is anticipated to rise by 75% compared to the current TMY3 scenario. However, this increase is reduced to 62% when the UHI effect is taken into account, comparing the current TMY3 with UHI against the FTMY with UHI. This reduction can be attributed to the fact that the difference between the future TMY and the current TMY3 already accounts for a significant temperature increase, which is further amplified in the scenarios with UHI. Commercial buildings, in contrast, exhibit a 36.4% increase in cooling load when comparing current and future data, with a slight increase to 36.6% when including the UHI effect. For heating, residential buildings are anticipated to have a 15.80% increase in demand from the current TMY3 to the future TMY, and a similar increase from the UHI-influenced current TMY3 to the future TMY.

3. DISCUSSION AND CONCLUSION

This paper offers significant insights into UHI effects and their implications on building energy consumption at an urban scale. It described a three-step methodology that involves simulating UHI intensity using standard TMY data and projected weather data, followed by integrating this modified weather data into urban building energy simulations. This architect-friendly approach highlights the importance of considering UHI effects in studies of building energy.

The Capitol East neighbourhood, characterized as an Open Low-rise area, was modelled in detail, integrating both built and vegetative elements such as trees and grass areas to accurately represent the urban landscape. This detailed modelling, in conjunction with the method of integrating the LCZ classification system with the UWG model, allowed for the creation of weather data that not only reflected present conditions but also anticipated future shifts in UHI intensity.

The following phase of urban building energy modelling provided crucial findings, specifically regarding the UHI's influence on energy consumption within the modelled buildings and the differential impacts on residential and commercial sectors. Specifically, the simulations estimated a 9.81% decrease in overall energy use, a 16.32% reduction in heating loads, and a 49.79% rise in cooling loads when comparing the UHI-influenced current weather data to future projections. Moreover, the UHI effect on the residential sector was particularly notable, as evidenced by an increase in cooling load of 75% in future scenarios, which decreased to 62% with the inclusion of UHI effects. The commercial sector, while also impacted, showed a consistent increase in cooling load of approximately 36% across both current and future scenarios, with and without UHI.

The findings highlight significant challenges that urban planners and policymakers must navigate due to evolving climate conditions, underlining the importance of sustainable design practices that address both heating and cooling requirements. Future research should aim to apply this methodology across diverse climatic regions to uncover the different impacts of UHI in varying settings. Moreover, this study's focus was limited to a selected neighbourhood characterized as LC6-Open Low Rise. Broadening the scope of this research to include other LCZ built types, particularly downtown areas typically comprising compact high or mid-rise buildings, would offer deeper insights into the UHI effect on a range of building typologies, including mixed-use and office buildings.

ACKNOWLEDGEMENTS

This work was partially supported by the US National Science Foundation (NSF), Awards # 1855902 and # 2226880. Any opinions, findings, and conclusions or recommendations expressed in this material are those of the author(s) and do not necessarily reflect the views of the NSF.

REFERENCES

1. Oke, T. R., (1973). City size and the urban heat island. Atmospheric Environment, 7(8): p. 769-779.
2. Ackerman, B., (1985). Temporal March of the Chicago Heat Island. Journal of Applied Meteorology and Climatology, 24(6): p. 547-554.
3. Tarleton, L. F. and Katz, R. W., (1995). Statistical Explanation for Trends in Extreme Summer Temperatures at Phoenix, Arizona. Journal of Climate, 8: p. 1704-1708.
4. Streutker, D. R., (2002). A remote sensing study of the urban heat island of Houston, Texas. International Journal of Remote Sensing, 23(13): p. 2595-2608.
5. Chen, W., Zhang, Y., Pengwang, C., and Gao, W., (2017). Evaluation of Urbanization Dynamics and its Impacts on Surface Heat Islands: A Case Study of Beijing, China. Remote Sensing, 9(5).
6. Lu, L., Weng, Q., Xiao, D., Guo, H., Li, Q., and Hui, W., (2020). Spatiotemporal Variation of Surface Urban Heat Islands in Relation to Land Cover Composition and Configuration: A Multi-Scale Case Study of Xi'an, China. Remote Sensing, 12(17).
7. Santamouris, M. et al., (2017). Urban Heat Island and Overheating Characteristics in Sydney, Australia. An Analysis of Multiyear Measurements. Sustainability, 9(5).
8. Jamei, Y., Rajagopalan, P., and Sun, Q. (Chayn), (2019). Spatial structure of surface urban heat island and its relationship with vegetation and built-up areas in Melbourne, Australia. Science of the Total Environment, 659: p. 1335-1351.
9. Ketterer, C. and Matzarakis, A., (2014). Human-biometeorological assessment of the urban heat island in a city with complex topography – The case of Stuttgart, Germany. Urban Climate, 10: p. 573-584.
10. Alexander, P. J. and Mills, G., (2014). Local Climate Classification and Dublin's Urban Heat Island. Atmosphere, 5(4): p. 755-774.
11. Nuruzzaman, Md., (2015). Urban Heat Island: Causes, Effects and Mitigation Measures - A Review. Environmental Monitoring and Analysis, 3(2): p. 67.
12. Basara, J. B., Basara, H. G., Illston, B. G., and Crawford, K. C., (2010). The Impact of the Urban Heat Island during an Intense Heat Wave in Oklahoma City. Advances in Meteorology, 2010: p. 230365.
13. Mallen, E., Stone, B., and Lanza, K., (2019). A methodological assessment of extreme heat mortality modeling and heat vulnerability mapping in Dallas, Texas. Urban Climate, 30: p. 100528.
14. Dong, J., Peng, J., He, X., Corcoran, J., Qiu, S., and Wang, X., (2020). Heatwave-induced human health risk assessment in megacities based on heat stress-social vulnerability-human exposure framework. Landscape and Urban Planning, 203: p. 103907.
15. Cuerdo-Vilches, T. et al., (2023). Impact of urban heat islands on morbidity and mortality in heat waves:

Observational time series analysis of Spain's five cities. Science of the Total Environment, 890: p. 164412.
16. Li, X., Zhou, Y., Yu, S., Jia, G., Li, H., and Li, W., (2019). Urban heat island impacts on building energy consumption: A review of approaches and findings. Energy, 174: pp. 407-419.
17. Fenner, D., Meier, F., Scherer, D., and Polze, A., (2014). Spatial and temporal air temperature variability in Berlin, Germany, during the years 2001-2010. Urban Climate, 10(P2): pp. 308-331.
18. Santamouris, M., Papanikolaou, N., Livada, I., Koronakis, I., Georgakis, C., Argiriou, A., and Assimakopoulos, D. N., (2001). On the impact of urban climate on the energy consumption of buildings. Solar Energy, 70(3): pp. 201-216.
19. Kolokotroni, M., Zhang, Y., and Watkins, R., (2007). The London Heat Island and building cooling design. Solar Energy, 81(1): pp. 102-110.
20. Skelhorn, C. P., Levermore, G., and Lindley, S. J., (2016). Impacts on cooling energy consumption due to the UHI and vegetation changes in Manchester, UK. Energy and Buildings, 122: pp. 150-159.
21. Stewart, I. D. and Oke, T. R., (2012). Local climate zones for urban temperature studies. Bulletin of the American Meteorological Society, 93(12): pp. 1879-1900.
22. Bueno, B., Norford, L., Hidalgo, J., and Pigeon, G., (2013). The urban weather generator. Journal of Building Performance Simulation, 6(4): pp. 269-281.
23. Crawley, D. B. et al., (2001). EnergyPlus: Creating a new-generation building energy simulation program. Energy and Buildings, 33(4): pp. 319-331.
24. Masson, V., (2000). A physically-based scheme for the urban energy budget in atmospheric models. Boundary-Layer Meteorology, 94(3): pp. 357-397.
25. Hashemi, F., Iulo, L. D., and Poerschke, U., (2020). A Novel Approach for Investigating Canopy Heat Island Effects on Building Energy Performance: A Case Study of Center City of Philadelphia PA. AIA/ACSA Intersections Research Conference, CARBON: p. 30.
26. Patton, S., (2013). Development of a future typical meteorological year with application to building energy use. MSc thesis, Iowa State University, Ames.
27. Reinhart, C., Dogan, T., Jakubiec, J. A., Rakha, T., and Sang, A., (2013). Umi – An Urban Simulation Environment For Building Energy Use, Daylighting And Walkability.
28. Wilcox, S. and Marion, W., (2008). Users Manual for TMY3 Data Sets (Revised). United States.
29. Jagani, C. and Passe, U., (2017). Simulation-based Sensitivity Analysis of Future Climate Scenario Impact on Residential Weatherization Initiatives in the US Midwest. Proceedings of SimAUD 2017, Toronto, CA, Urban Energy; May 22-24: p. 345-352.
30. Hashemi, F., Marmur, B., Passe, U., and Thompson, J., (2018). Developing a workflow to integrate tree inventory data into urban energy models. SimAUD 2018 Symposium on Simulation for Architecture and Urban Design, Tu Delft, Delft, The Netherlands, June 4-7.
31. Pak, M., Smith, A., and Gill, G., (2013). Ladybug: A Parametric Environmental Plugin For Grasshopper To Help Designers Create An Environmentally-conscious Design. Building Simulation Conference Proceedings.
32. Dogan, T. and Reinhart, C., (2017). Shoeboxer: An algorithm for abstracted rapid multi-zone urban building energy model generation and simulation. Energy and Buildings, 140: pp. 140-153.
33. Dogan, T. and Reinhart, C., (2013). Automated Conversion Of Architectural Massing Models Into Thermal 'shoebox' Models. Building Simulation Conference proceedings.
34. Heidelberger, E. and Rakha, T., (2022). Inclusive urban building energy modeling through socioeconomic data: A persona-based case study for an underrepresented community. Building and Environment, 222: p. 109374.
35. Nidam, Y., Irani, A., Bemis, J., and Reinhart, C., (2023). Census-based urban building energy modeling to evaluate the effectiveness of retrofit programs. Environment and Planning B: Urban Analytics and City Science, p. 239980832311545.
36. Buckley, N., Mills, G., Letellier-Duchesne, S., and Benis, K., (2021). Designing an Energy-Resilient Neighbourhood Using an Urban Building Energy Model. Energies, 14(15): p. 4445.
37. Alcivar, J. et al., (2014). Capitol East Neighborhood Charter Plan Update. Accessed: Nov. 17, 2023. [Online]. Available: https://works.bepress.com/jane_rongerude/7/
38. Polk/Des Moines Assessor - Residential Downloads. [Online]. Available: https://www.assess.co.polk.ia.us/web/exports/basic/resl.html
39. City of Des Moines GIS Data City of Des Moines GIS Data. [Online]. Available: https://www.dsm.city/city_of_des_moines_gis_data/

PLEA 2024 WROCŁAW
(Re)thinking Resilience

Self-Sufficient Villages:
Enabling Welfare and Low Carbon Lifestyles in Rural Galicia, NW Spain

JORGE RODRÍGUEZ-ÁLVAREZ[1], JAVIER ROCAMONDE-LOURIDO[1]

[1]Universidade de A Coruña, A Coruña, Spain

ABSTRACT: This research is based on the premise that rural areas offer a wide range of social and environmental opportunities and that they play a key role in the ecological transition. The main objective of this research project is to develop a methodology to plan and regenerate rural settlements introducing a socially informed and circular design approach that considers the local needs and landscape values. This paper presents a methodology to evaluate the energy self-sufficiency in rural areas exploiting community-owned resources. It analyses the potential energy yield from biomass, hydropower, solar and wind infrastructures deployed within the boundaries of the case study, in Canicouva, Spain. It compares the energy production with the demand of the village to calculate the potential surplus that can be fed to the grid and thus improving the local economy while reducing the environmental impact.
KEYWORDS: Energy, Rural, Renewable, Community

1. INTRODUCTION

Mainstream theory on urban sustainability has concluded that models based on concentration, diversity and high density are the most effective to reduce our carbon footprint [1]. They argue that concentration offers environmental, social and economic advantages. Moreover, the conventional approach mixes rural and suburban areas as if they followed similar patterns thus penalizing rural household's energy consumption [2]. However, when we look into strictly rural lifestyles, the trend is reversed and rural regions are revealed and less dependent on fossil fuels [3], [4].

Despite the overwhelming attention to urban issues and progressive abandonment (Figure 1), the fact remains that nearly one third of the European population do not live in cities but in rural areas [5]. The Rural realm has its own challenges as it is currently experiencing radical transformations, not least rising energy prices and low income increase vulnerability and fuel poverty. The research focuses on the potential of rural areas as energy generators to introduce a novel community-based service provision method that enables the environmental and social regeneration of rural settlements, delivering inclusive and self-sufficient habitats with a low carbon footprint.

2. METHODOLOGY

We apply an interdisciplinary approach that combines urban metabolism and a social perspective to investigate, plan and design alternative community-based service delivery. The investigation evaluates the viability of decentralized basic service provision (energy, water and social support) based on geographic, demographic and technical thresholds and parameters. The objective is to develop and test an integrated design methodology based on social and technical innovation as to enhance the implementation of these principles in architecture and urban planning.

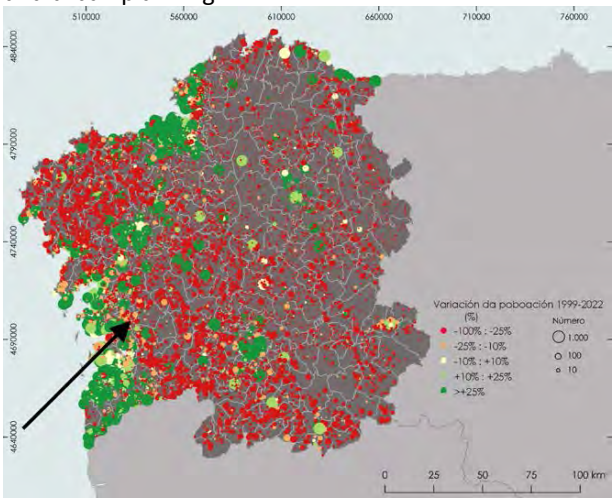

Figure 1 Population dynamics in Galicia between 1999-2022 (each dot represents one settlement). The arrow indicates the location of the case study: Canicouva

In this paper we describe a preliminary methodology to evaluate the potential energy self-sufficiency applied to a case study: Canicouva, which is a small rural village located in Pontevedra, northwest Spain (Figure 1). First, we characterize the demand of the rural settlement, considering the building characteristics and users' profiles. Then we investigate the available community-based systems that can meet the local energy needs and, eventually, generate a surplus. We aim to transcend the numerical exercise to integrate the landscape impact and land use implications of the different technologies.

2.1 Demand characterization

We apply the urban energy model Litheum (litheum.citic.udc.es) to calculate the heating and lighting loads from domestic buildings. This model considers the built form and climatic conditions to produce quick estimates for large study areas. For end-uses other than thermal and lighting we assumed the average values from official statistics [6]. With these parameters we obtained a total annual energy demand of 3,178MWh, half of which is dedicated to space heating (Figure 2.

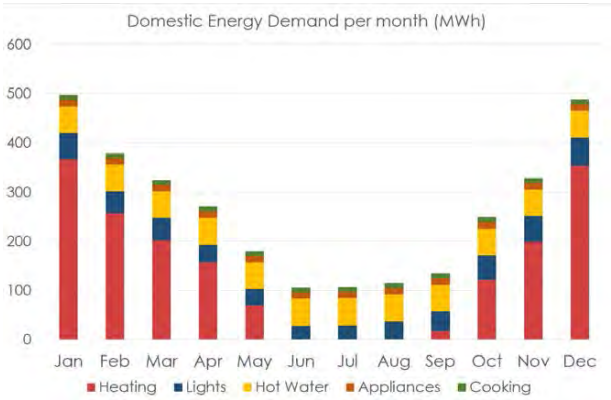

Figure 2 Energy demand per month and end use from all buildings in the study area

Seasonal and daily fluctuations of the energy demand are relevant for the integration of renewable systems, since wind or solar availability vary greatly over these cycles. For the seasonal patterns (Figure 2) the main variation is caused by heating and, to a lesser extent, lighting. For the estimate of hourly loads in typical days we applied occupancy and usage schedules defined by Knight and Kreutzer [7] for European single family houses. When the loads are broken down it is possible to visualize the magnitude and timing of peaks as well as the uses that cause them (Fig. 3).

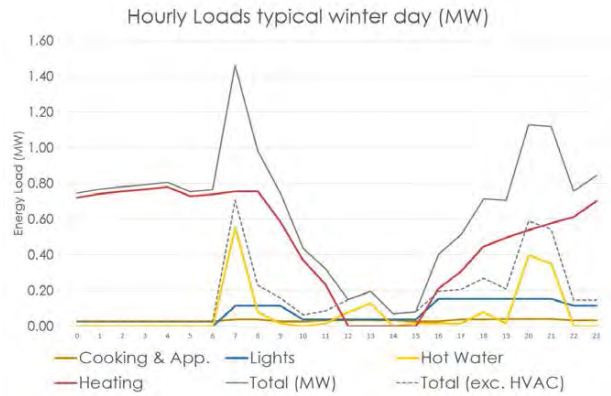

Fig. 3 Hourly load characterization for the whole settlement in a typical winter day (MW)

The demand for the existing buildings in their current state constitutes the base case (Figure 4). It would be illogical to tackle self-sufficiency only from the supply side, without applying energy conservation measures to reduce the demand at the unit level. Therefore, we created two additional demand scenarios:

- **Scenario 1.** It assumes that all houses have been insulated and their systems have been updated, with more efficient technologies (e.g. LED, efficient boilers and appliances)
- **Scenario 2.** To the previous case, we add unit-level energy generation by rooftop solar PVs and collectors. The heat and energy generated would provide a further reduction in the energy demand to be met by the community-based facilities.

The energy breakdown of the three scenarios, together with the energy supply from community systems are illustrated in the next section (Figure 6).

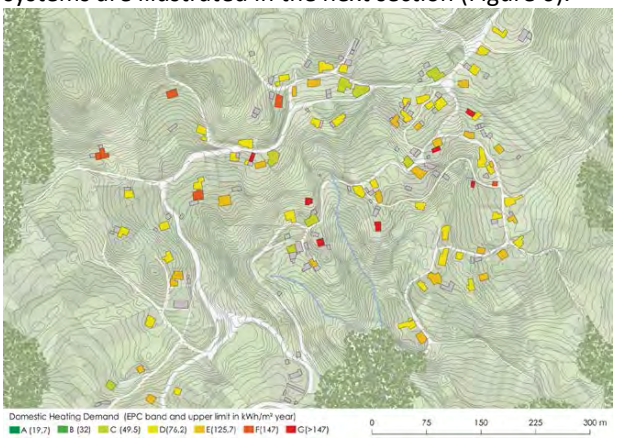

Figure 4 Current energy demand from buildings in Canicouva

2.2 Local energy generation

2.2.1 Estimation of Biomass potential. Biomass is defined as any material of biological origin, including forests, crops and organic waste. Overall, the energy supply from biomass is estimated around 10% [8] and it's been expanding in Europe in the last decade. Biomass can be used to generate heat or electricity. Biomass boilers have an efficiency in the order of 80-90% while biomass fuelled power plants are in the region of 20-30%. When electricity and heat are combined they can reach up to 35% efficiency [9]. Energy biomass in forests can be obtained in two ways: Primary forest biomass, which is a by-product from forestry management (clearing, logging, thinning and cutting…) and energy crops, in which trees are grown with the specific purpose of energy generation [10].

This research integrates a simplified method to estimate the biomass for energy potential in the study area, based on the presence of community owned land and managed forest. Forest Management Communities are organizations at Parish level or below to share and manage the communal land resources (mostly forest and pastures). They have a longstanding tradition in Galicia and membership is automatic for all households living in the parish or hamlet. The opportunities that they present for community led services and resource exploitation are

obvious and as such it has raised academic attention in recent years [11].

An approximate estimate of the biomass energy potential in the territory associated to a rural settlement can be calculated in few steps. First, the land owned by the Forest Management Community (FMC) is identified from the regional registry [12] and mapped in GIS. Then, we use cartographic data from the National Forest Inventory [13] to differentiate the area owned by the FMC that is actually a managed forest. We used a Digital Elevation Model (DEM) to exclude those areas with a slope above 30% as they are not viable for exploitation [14]. We apply specific ratios for each species (*Table 1*) based on empirical studies [15] to calculate the biomass and equivalent energy potential from forest biomass. We also obtain an estimate from energy crops. We designate around 40ha of the common land for this purpose. We apply a density of 20.000 trees/ha, which would produce around 13m³ of wood per hectare and year in this regional context [16].

Table 1 Biomass and energy ratios per hectare for the two main forestry species in Galicia

Species	Biomass ratio (Mg ha^{-1} year)	Energy eq. (Gj Mg^{-1} year)
Pinus Pinaster	0.65	18.1
Eucalyptus Globulus	1.2	18.35

2.2.2 Hydropower potential. Water has been a traditional energy source, mainly transforming kinetic energy into mechanical force applied to mills. The world's first hydroelectric project was built in Northumberland, England in 1878 [17]. The 20th century witnessed an exponential increased of hydroelectric capacity in Spain, reaching over 12,000 installed MW and nearly 30,000 GWh produced by 1975 [18]. Galicia has currently 3,744MW of hydropower potential, 91% corresponding to 45 large plants (over 10MW) and 9% from 111 Micro-Hydro Power (MHP) plants [19]. The smallest registered plant is a generator that provides a net Power of 20kW, while the largest one has a Net Power Capacity of 313MW. In the right conditions, MHP has a low environmental impact. Although it possible to design plants of-the-river (i.e. without changing the river water flow) smalls dams allow flexibility to store water and adapt the generation to the demand. These kind of dams were traditionally built for water-mills.

The power capacity of the MHP plant depends on two factors: head (level difference) and flow. Therefore, the ideal conditions occur along rivers with step profiles and narrow canyons, located in rainy regions. Galicia is on the most humid regions in Spain, with an average rainfall above 1,200 l/m² [20]. The study area has four streams in its territory, three of which converge in Ponte Novo river, which has an annual average flow of 470 l/s [21]. The ecological flow to minimize the impact on the river's biodiversity ranges from 50 to 100l/s in the dry and humid seasons respectively. Leaving that aside we can estimate a potential average usable flow of 400l/s, with a maximum peak of 700l/s (0.7 m²/s) in December.

The next step would be to identify the location of the different elements of the MHP plant with the minimum environmental impact. The turbine is located inside a powerhouse, which must be at a lower level than the intake. To maximize the head and, therefore, the potential energy, we can use a channel to divert the water upriver and a penstock to convey the water from the channel to the turbine. Given the gentle topography and narrow canyon of River Ponte Nova we draft a design that provides a net head of 20m (**Error! Reference source not found.**).

With the previous parameters we can calculate the potential energy generation from the MHP plant using formula F.1 [22] :

$$P = Ef \cdot W_d \cdot g \cdot Q \cdot H \qquad [F.1]$$

Where:

P is the power produced at the turbine shaft in kW
Ef is the hydraulic efficiency of the system (around 0.6-0.8)
g is the acceleration due to gravity (9.81m/s²)
Q is the volume flow rate passing through the turbine (m³/s)
H is the effective pressure head of water across the turbine (m)

The resultant monthly values are summarized in Figure 5. The average power potential is 50kW. If we assume a Capacity Factor of 50-60% to translate the power into energy, we find that a potential generation of nearly 300MWh per year would be within reach. Given the fluctuation of the river flow, the construction of a small dam could both provide more flexible regulation and adaptation to the demand and an additional amenity to the village, as it could be used as a swimming area in summer.

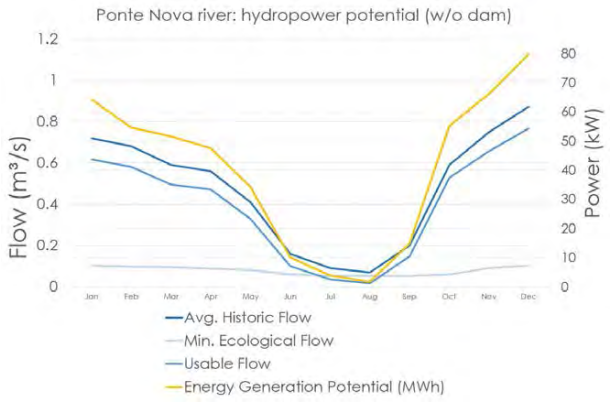

Figure 5 Hydropower potential of Ponte Nova river without water storage

2.2.3. Solar Energy is the most abundant energy source. It is used directly, to passively warm up buildings, and indirectly, to heat up air or water in solar collectors. Although the capacity to create electrical currents from sunlight and semiconductors

was discovered in the 1840s the first commercial solar cells were released in the United States in 1958 [17]. Spain is the one the regions with greater solar potential in Europe but it is behind countries, such as Germany (66GW), Italy (25GW) or Netherlands (22GW), in the installed solar photovoltaic power, reaching 20GW in 2022 [23]. Registered photovoltaics systems in Galicia amount to almost negligible: 136MW of installed power in 8,760 facilities, with an average of 16kW per installation [19]. The largest solar farms in central and south Spain reach up to 500MW while only two plants are above 2MW in Galicia, which suggest a large growth potential. The power of PV modules is given in watts as peak power (Wp), which is the output given for 1000W/m² and 25ºC (typical summer day in north Spain). The daily performance is calculated by combining the available solar radiation and the system efficiency. A wide range of tools have been developed to make quick estimates of solar installations. In this study we selected PVGIS [24] and SMA Sunny Design [25]. We started by designing a 1000m² solar farm in a former football pitch owned by the local community. The plant consists of 450 modules of 300W each for a total peak Power of Wp=135kWp. The annual energy yield, according to Sunny Design is nearly 200MWh. Although PVGIS tends to underestimate the energy generation (by mostly overestimating the system's losses) it provides hourly data, which is useful to draw supply/demand comparisons. For our case, it estimates an annual energy yield of 180MWh. These results will be iterated, increasing the size of the plant with the objective of matching the demand with on-site renewable technologies.

2.2.4. **Wind energy**. Galicia is a windy region, highly exposed to constant northern winds in summer and strong although more irregular southern winds in winter. There are 174 wind farms with a total installed capacity of 3,886 MW [19], which makes an average of 22MW per plant. In 2022 they generated 9,788GWh of electricity (56GWh per wind farm as average). One of these farms could yield nearly 20 times the total energy demand of the study area. It is highly cost-efficient, and it does not cause significant greenhouse emissions, beyond manufacturing. However, the deployment of this technology has been subject of great controversy and local opposition. The visual impact of large turbines in rural landscapes and the acoustic pollution are the most frequent causes of disagreement. The side effects on wildlife, cattle and farming are also among the reasons given by conservationists and rural communities.

The energy generated by wind turbines can be estimated once wind availability is determined and the turbine size and model are defined. We fetched wind data from the regional meteorological agency (meteogalicia.gal). It provides 10-minute data from the station located 10km south of the study area. Wind turbine's suppliers provide information on the dimensions and power curve of commercial models, which can be used to calculate the energy production using formula F.2:

$$P = 1/2 \cdot C_p \cdot k_3 \cdot \rho \cdot A \cdot v^3 \qquad [F.2]$$

Where:

P is the power output of the wind turbine in W
C_p is the power coefficient of the turbine.
k_3 is the cube factor or energy pattern factor.
ρ is air density (assumed as 1.225 kg/m³)
A is the swept area of the blades (m²)
v is wind speed (m/s)

For this analysis we iterated over low and mid power generators as to balance visual impact and efficiency. However, the smallest turbines offering significant output were mid-power 100 kW turbine with 10m blades. We selected the model nED100 by Norvento [26], which generates around 140 MWh in the designed conditions. This is significantly below the average annual energy production of the wind turbines currently installed in the Galician landscape, which have a power capacity of nearly 1MW and generate above 2GWh.

3. RESULTS

The analysis of the community-based energy systems reveals the self-sufficient potential of the settlement since it is possible to generate more energy than the current demand within its associated territory (Figure 6).

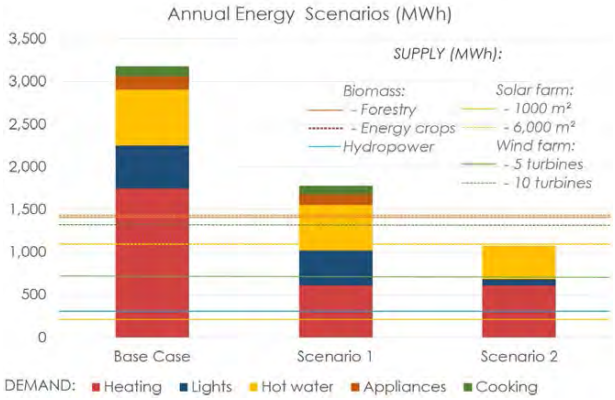

Figure 6 Demand and supply from local energy generation in 3 scenarios

The technology that delivers the greatest yield is biomass, with an annual energy production of 1.4GWh just from conventional forestry operations. A designated energy crop of 42 ha could add another 1.4GWh every year. The second most prolific system would be the wind farm. In a baseline scenario we designed 5 – 100kW turbines, which deliver nearly 700MWh. By doubling the number of generators, it would be possible to obtain up to 1.4GWh of wind energy. It must be noted that the selected turbines

are below the average power that is currently being installed and that a much greater yield is achievable. However, we aimed to balance landscape integration with energy production. The baseline solar farm has 10 modules that produce over 18MWh each, for a total 180MWh per year. It is possible to extend the solar farm beyond the former football pitch to accommodate 50 additional modules, so that the energy yield can increase to 1GWh/year. Hydropower offers a modest production of 290MWh per year, which could be potentially increased with pumped hydropower storage. The local stream is relatively small, but it is representative of the streams of the region (beyond large rivers already exploited).

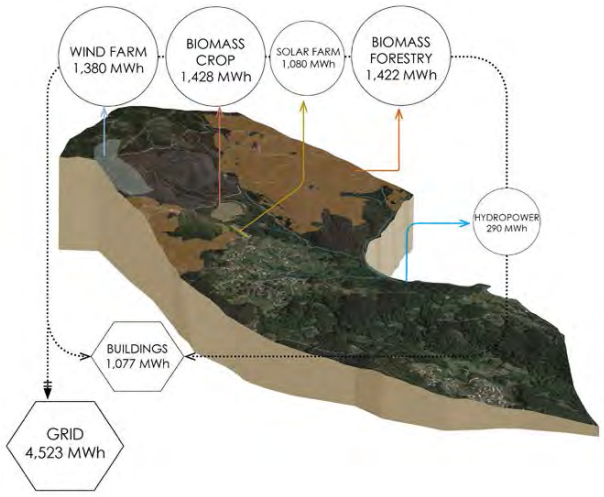

Figure 7 Diagram of the energy infrastructure and potential yield

The total energy generated from all systems in the most productive scenario is 5.6GWh per year (***Figure 7***), which show a 70% excess over the current demand and up to four times larger in scenario 3. If we consider the efficiency of building services as 0.8, the surplus would be approximately reduced to 40% respect to these values.

Table 2 Energy density of the different energy technologies

Technology	Energy (MWh)	Area (Ha)	Energy density (MWh/ha)
Biomass Forestry	1422	241	5.90
Biomass Crops	1428	42	34.00
Hydropower	290	0.6259	463.33
Solar farm 10mod	180	0.17	1058.82
Solar farm 60mod	1080	1.2	900.00
Wind 5 turbines	690	102	6.76
Wind 10 turbines	1380	188	7.34

Interestingly, since we designated the specific location and spatial needs for each system, we can obtain the area of land that each technology requires (Table 2). From this point of view, solar technologies are the most land-efficient, since they yield an energy density around 1GWh/ha. These criteria also favour hydropower, which requires relatively little land as its elements (weir, channel, penstock…) are integrated in the riverbank and are compatible with other uses. Although the remaining systems are far behind, we must consider that low density systems are still viable in these rural regions, where large tracts of land are available.

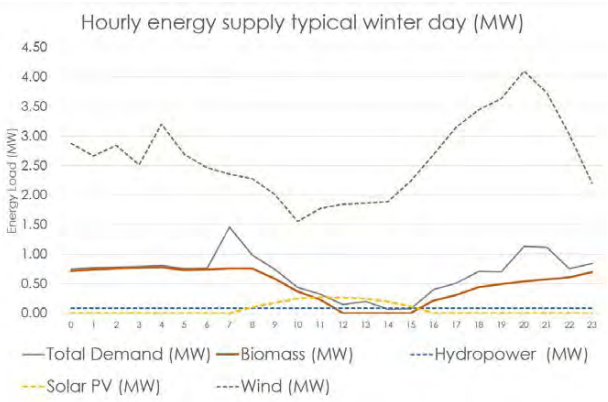

Figure 8 Hourly demand from buildings and potential supply from local energy sources for a typical winter day

Finally, the hourly variation of power availability from the studied systems without energy storage is examined (Figure 8). Solar and wind present the larger fluctuations; hydropower has seasonal variations, but it remains stable on the daily cycle. Biomass is, by definition, energy stored in wood and, therefore, it can be distributed to match the demand. In this case we assume that biomass is used to fuel the heating system. Biomass, Hydropower and Solar could potentially provide enough energy by introducing simple storage (e.g. hot water tanks) that could satisfy the peak demand. Wind energy could then be avoided or fed into the grid.

3. CONCLUSION

This paper has defined a methodology to evaluate the energy self-sufficiency in rural areas based on community systems. It concludes that the land associated to rural settlements has potential to generate an energy surplus that could be exploited to reduce the carbon footprint and increase the welfare of their inhabitants.

ACKNOWLEDGEMENTS

Grant PID2021-123961OA-I00 Funded by MCIN/ AEI/10.13039/501100011033/ and by ERDF A way of making Europe.

REFERENCES

1. E. Glaeser, Triumph of the city: how our greatest invention makes us richer, smarter, greener, healthier, and happier. New York: Penguin Books, 2014.
2. E. L. Navamuel, F. Rubiera Morollón, y B. Moreno Cuartas, «Energy consumption and urban sprawl: Evidence for the Spanish case», Journal of Cleaner Production, vol. 172, pp. 3479-3486, ene. 2018, doi: 10.1016/j.jclepro.2017.08.110.
3. C. Matos, I. Bentes, S. Pereira, A. M. Gonçalves, D. Faria, y A. Briga-Sá, «Which are the factors that may explain the

differences in water and energy consumptions in urban and rural environments?», Science of The Total Environment, vol. 642, pp. 421-435, nov. 2018, doi: 10.1016/j.scitotenv.2018.06.062.
4. G. Vita et al., «GLAMURS Deliverable 7.3: Analysis of current impact of lifestyle choices and scenarios for lifestyle choices and green economy developments»,. GLAMURS: EU SSH.2013.2.1-1 Grant agreement no. 613420., 2016.
5. European Commission, «Rural Voices. A qualitative analysis of the findings from stakeholder workshops contributing to the long-term vision for rural areas». European Network for Rural Development, 2021.
6. INEGA, «Domestic Energy». Accedido: 27 de diciembre de 2023. [En línea]. Disponible en: https://www.inega.gal/eficienciaenerxetica/domestico.html
7. I. Knight y N. Kreutzer, «European Electrical Standard Profiles». IEA - ECBCS, 2007.
8. J. Popp, S. Kovács, J. Oláh, Z. Divéki, y E. Balázs, «Bioeconomy: Biomass and biomass-based energy supply and demand», New Biotechnology, vol. 60, pp. 76-84, ene. 2021, doi: 10.1016/j.nbt.2020.10.004.
9. IEA, «IEA (2007), Biomass for Power Generation and CHP, IEA, Paris». Accedido: 15 de diciembre de 2023. [En línea]. Disponible en: https://www.iea.org/reports/biomass-for-power-generation-and-chp
10. Forest Research, «General biomass information». Accedido: 15 de diciembre de 2023. [En línea]. Disponible en: https://www.forestresearch.gov.uk/tools-and-resources/fthr/biomass-energy-resources/general-biomass-information/
11. R. Fernández-González, F. P. Guillén, O. Manta, S. A. Apostu, y V. Vasile, «Forest Management Communities' Participation in Bioenergy Production Initiatives: A Case Study for Galicia (Spain)», Energies, vol. 15, n.o 19, p. 7428, oct. 2022, doi: 10.3390/en15197428.
12. Xunta de Galicia, «Montes vecinales en man común». Accedido: 15 de diciembre de 2023. [En línea]. Disponible en: https://ovmediorural.xunta.gal/es/consultas-publicas/montes-vecinales-en-man-comun
13. Ministerio para la Transición Ecológica y el Reto Demográfico, «Inventario Forestal Nacional». Accedido: 15 de diciembre de 2023. [En línea]. Disponible en: https://www.miteco.gob.es/es/biodiversidad/temas/inventarios-nacionales/inventario-forestal-nacional.html
14. Biorreg-Floresta, «Atlas de la biomasa forestal primaria en bosques cultivados de Galicia». Asociación Forestal de Galicia, 2006.
15. E. Mateos, F. Garrido, y L. Ormaetxea, «Assessment of Biomass Energy Potential and Forest Carbon Stocks in Biscay (Spain)», Forests, vol. 7, n.o 12, p. 75, mar. 2016, doi: 10.3390/f7040075.
16. ECAS, «Cultivos energéticos espacio atlántico». Asociación Forestal de Galicia, 2007.
17. S. Ruin y G. Sidén, Small-scale renewable energy systems: independent electricity for community, business and home. Boca Raton London New York Leiden: CRC Press, Taylor & Francis Group, 2020.
18. E. Swyngedouw, Liquid power: water and contested modernities in Spain, 1898-2010. en Urban and industrial environments. Cambridge, Massachusetts: The MIT Press, 2015.
19. INEGA, «Power Plants List». Accedido: 23 de diciembre de 2023. [En línea]. Disponible en: https://www.inega.gal/enerxiagalicia/listaxecentrais.html
20. Meteogalicia, «Informe Climatológico 2022». 2023.
21. Augas de Galicia, «Estudo para a determinación do réxime de caudais ecolóxicos das masas de auga superficiais da categoría río da demarcación hidrográfica de Galicia-Costa». Xunta de Galicia, 2013.
22. British Hydropower Association, «A Guide to UK Mini-Hydro Developments». 2012.
23. statista, «World ranking of the countries with the highest installed solar photovoltaic power as of 2022». Accedido: 26 de diciembre de 2023. [En línea]. Disponible en: https://es.statista.com/estadisticas/641225/potencia-solar-fotovoltaica-instalada-por-paises/
24. European Commission, «Photovoltaic Geographical Information System». Accedido: 27 de diciembre de 2023. [En línea. . Disponible en: https://re.jrc.ec.europa.eu/pvg_tools/en/tools.html
25. SMA, «Sunny Design». Accedido: 27 de diciembre de 2023. [En línea]. Disponible en: https://www.sunnydesignweb.com/sdweb/#/
26. Norvento, «Aerogenerador nED100». 2023. Accedido: 27 de diciembre de 2023. [En línea]. Disponible en: https://www.norvento.com/wp-content/uploads/2023/01/I1218-24-39-03-02-V02_02-nED-ESP_OnLine.pdf

PLEA 2024 WROCŁAW
(Re)thinking Resilience

Urban Heat Island Mitigation Strategies:
Microclimate analysis of tree canopies and green surface combinations in Los Angeles and Phoenix

SHAOBO YANG[1] PABLO LA ROCHE[1,2] ARIANNE PONCE[1]

[1]Arcadis, Los Angeles, USA
[2] Cal Poly Pomona University, USA

ABSTRACT: This research addresses the critical issue of urban heat islands, in which urban areas experience significantly higher temperatures than their surroundings, adversely affecting human comfort and well-being. Focusing on Inglewood, a city neighboring Los Angeles, and Phoenix, Arizona, the study uses a comprehensive methodology involving microclimate analysis-based UTCI calculations to assess the impact of horizontal green surfaces and different levels of tree canopies on outdoor thermal stress mitigation. The results demonstrate that these interventions can effectively lower outdoor temperatures, reducing the heat island effect and heat stress levels and enhancing overall thermal comfort in the study areas. While the approach shows substantial mitigations in terms of strong and moderate heat stress, it may have a limited impact on extreme heat stress areas. The study provides urban planning strategies for integrating these interventions to create more sustainable and resilient urban environments, supporting policymakers and urban planners in their efforts to reduce the effects of urban heat islands.
KEYWORDS: Urban Heat Islands, Microclimate Analysis, Outdoor Thermal Comfort, Climate Resilience, Green Infrastructure

1. INTRODUCTION

Global climate change and the urban heat island effect pose a significant threat to human thermal comfort within urban areas. Research shows a rising trend in the intensity, duration, and frequency of heat waves in Los Angeles, attributed to ongoing global climate change [1]. For this reason, architects and urban designers have the responsibility of prioritizing measures to mitigate the Urban Heat Island (UHI) effect in their project designs.

Urban heat islands are distinct areas within cities that exhibit significantly higher temperatures compared to their surrounding rural regions. This phenomenon is caused by various factors, such as insufficient vegetation that limits shade from tree canopies and the prevalence of hardscape surfaces like asphalt and concrete, which elevate both surface and ambient temperatures [2]. These factors contribute to trapping and retaining heat in urban environments, leading to extreme temperatures. Extreme heat can cause heat-related fatalities, increased wildfire risks, and heightened strain on the power grid [3] [4]. Understanding the complex interplay of these factors is important for developing effective sustainable design strategies to mitigate the adverse effects of urban heat islands and promote climate resilience.

This research investigated how different combinations of horizontal green surfaces and tree canopies could address this issue. The primary objective of this study is to quantify the effect of implementing different combinations of horizontal green surfaces and tree canopies on the outdoor thermal comfort of the research area. This is achieved by comparing the heat mitigation potential of horizontal green surfaces and tree canopies utilizing the Universal Thermal Climate Index (UTCI) as the metric and comparing the results with a base case scenario for a typical hot day.

The outcomes of this research provide guidelines for the effectiveness of implementing horizontal green surfaces and increasing tree canopy to alleviate outdoor thermal stress, aiding urban planners and policymakers in creating more sustainable and resilient urban environments.

2. IMPACT OF GREEN SURFACES AND TREE CANOPY ON OUTDOOR COMFORT

Urban environments exacerbate extreme heat conditions by virtue of the disproportionate presence of low-lying constructed surfaces compared to natural, non-manmade landscapes [5] [6].

Previous research demonstrates that neighborhoods with historical redlining tend to have higher temperatures, primarily attributed to their limited access to green spaces and mature tree canopies, which results in inadequate shade [7]. Another study shows that the combination of green infrastructure or green spaces in established urban areas has the potential to alleviate the urban heat island effect [8]. Urban green spaces provide a nature-based remedy for thermal stress, with vegetated areas capable of reducing temperatures in urban environments [9] [10]. Salata et al. stated that in Rome, Italy, street trees and parks reduced air

temperatures by up to 1.34°C, while Yan et al. mentioned that in Beijing, China, they achieved a cooling effect of 2.8°C, and Thorsson et al., said that in Chiba, Japan, the cooling effect was even more substantial at 3.0°C [11] [12] [13].

Another study demonstrates that the vegetation in the canopy layer can improve thermal comfort by blocking direct solar gains and providing some evaporative cooling [14]. Additionally, research also demonstrates the benefits of green roofs in reducing the building cooling load [14] [15]. Further research into green roofs, canopies, and greened surfaces could help establish their role in mitigating urban heat stress.

3. METHODOLOGY

The methodology implemented in this research encompasses study area selection, data collection, ENVI-met modeling, BIO-met calculation, intervention implementation, thermal index comparison, and data analysis (Figure 1).

The first step used Envi-met to construct a base model for Inglewood, Los Angeles. The base model encompasses building geometry, existing site features (roads, tree canopy, and green surfaces), material, and soil settings through data collection from diverse sources, such as geographical information system (GIS) data, satellite imagery, and aerial photographs, providing the required inputs for an accurate representation of the site's geometry and features.

The second step involves the targeted intervention in the base model by modifying the tree canopy, green surfaces, and the weather file to create new case models. This intervention aims to explore the potential impacts of alterations to these components on outdoor thermal conditions.

Subsequently, in the third step, simulations are conducted using both the base model and the modified scenario models. BIO-met facilitates a comprehensive simulation process, allowing for the calculation of the Universal Thermal Climate Index (UTCI).

In the fourth step, results from the simulations of the base model and the modified scenario model are analyzed and compared. This comparative assessment forms the basis for drawing conclusions regarding the effectiveness of the interventions and their implications for outdoor microclimate conditions.

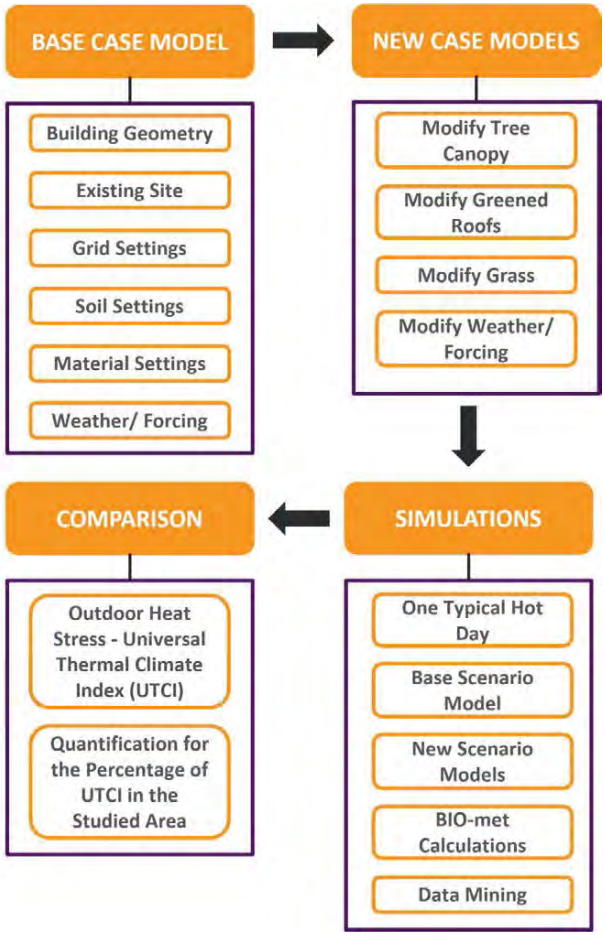

Figure 1 Methodology flow chart for microclimate study

3.1 Simulation model and parameters

ENVI-met is a microclimate simulation software that is used for urban planning [16]. The modeling processes were conducted in ENVI-met Space. The existing site, including its trees, roads, and buildings, is accurately modeled within the software to create the baseline scenario, serving as the model base for subsequent simulations (Table 1).

Modifications are made to the simulated model by incorporating horizontal green surfaces and increasing the tree canopy. The design and placement of these interventions adhere to predetermined guidelines and considerations to ensure their effectiveness in mitigating outdoor thermal stress.

Another set of studies used the same baseline site conditions and modified models but replaced weather forcing by using the Phoenix, Arizona weather file.

Table 1 Model Settings in Envi-Met Spaces.

Model set-up	Settings	Area
Existing trees	29 cylindric medium trunk sparse and	Tree cover= 1827m2

	medium 15 m (deciduous)	Site canopy = 3.52%
Buildings	44 building (4-9 m) Material: moderate insulation wall Tile roof, Clear Float Glass	13143 m2 (25.3 % footprint)
Grid resolution and model domain	x*y*z: 3m*3m*3m	Site:231m*225m (*45m)
Soil	Sandy loam	13788m2 (26.5%)
Horizontal Green Surfaces (applied in roof and ground)	Grass 25cm average dense on ground Greenings with air gap sandy loam substrate on roof	2439 m2 (4.7%)
Road/walkway	Asphalt	22344 m2 (43%)
Weather file	USA_CA_Hawthorne.Muni.AP-Northrop.Field.722956_TMYx.2007-2021.epw	
	USA_AZ_Phoenix-Sky.Harbor.Intl.AP.722780_TMYx.2007-2021.epw	

3.2 Simulation index

The Universal thermal climate index (UTCI) describes the environmental temperature equivalent determined with a reference environment. This index is defined as the reference environment's air temperature that results in an identical strain index value when compared to the response of the reference individual in the actual environment. UTCI is widely acknowledged as one of the most comprehensive metric for assessing heat stress in outdoor thermal comfort. This index was formulated to establish a standardized criterion for evaluating heat stress within the context of human meteorology. UTCI is classified into ten categories, ranging from extreme cold stress to extreme heat stress (Table 2) [17] [18].

Table 2 Universal thermal climate index

UTCI (°C) range	Stress Category heat
above 46	extreme heat stress
38 to 46	very strong heat stress
32 to 38	strong heat stress
26 to 32	moderate heat stress
9 to 26	no thermal stress
0 to 9	slight cold stress
-13 to 0	moderate cold stress
-27 to -13	strong cold stress
-40 to -27	very strong cold stress
below -40	extreme cold stress

BIO-met within the ENVI-met is used to calculate Universal thermal climate index (UTCI) (Figure 2). This provides objective measures of human thermal comfort and serves as the key indicator for evaluating the impact of interventions.

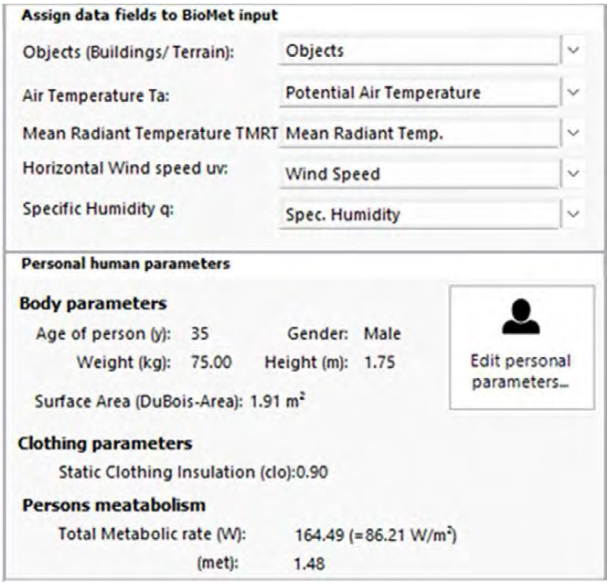

Figure 2 Model setting parameters in Envi-Met Bio-Met.

4. CASE STUDIES

Los Angeles has a Mediterranean climate with mild, wet winters and warm to hot, dry summers, featuring moderate temperature variations. Meanwhile, in the Sonoran Desert, Phoenix experiences a hot desert climate with extreme summer heat, mild winters, low humidity, and minimal precipitation. Despite these differences in climate classification, both cities grapple with the formidable challenge of urban heat stress, which is exacerbated by the scorching temperatures they encounter. By choosing these two cities, the study aims to explore how green infrastructure interventions can address the shared issue of extreme heat and enhance outdoor thermal comfort, offering insights that can be applied not only to these cities but also to other hot desert climate regions worldwide.

With the consideration of the integration of trees, grass, and green roofs within the plannable urban areas, the first segment of the study utilizes the Inglewood weather file in conjunction with nine distinct model configurations, each with varying levels of green surface and tree canopies combinations (Figure 3). The second segment of the research uses the Phoenix weather file and employs an existing model as the baseline, alongside a single modified model that incorporates maximum tree canopy,

maximum grass coverage, and maximum green roof implementation.

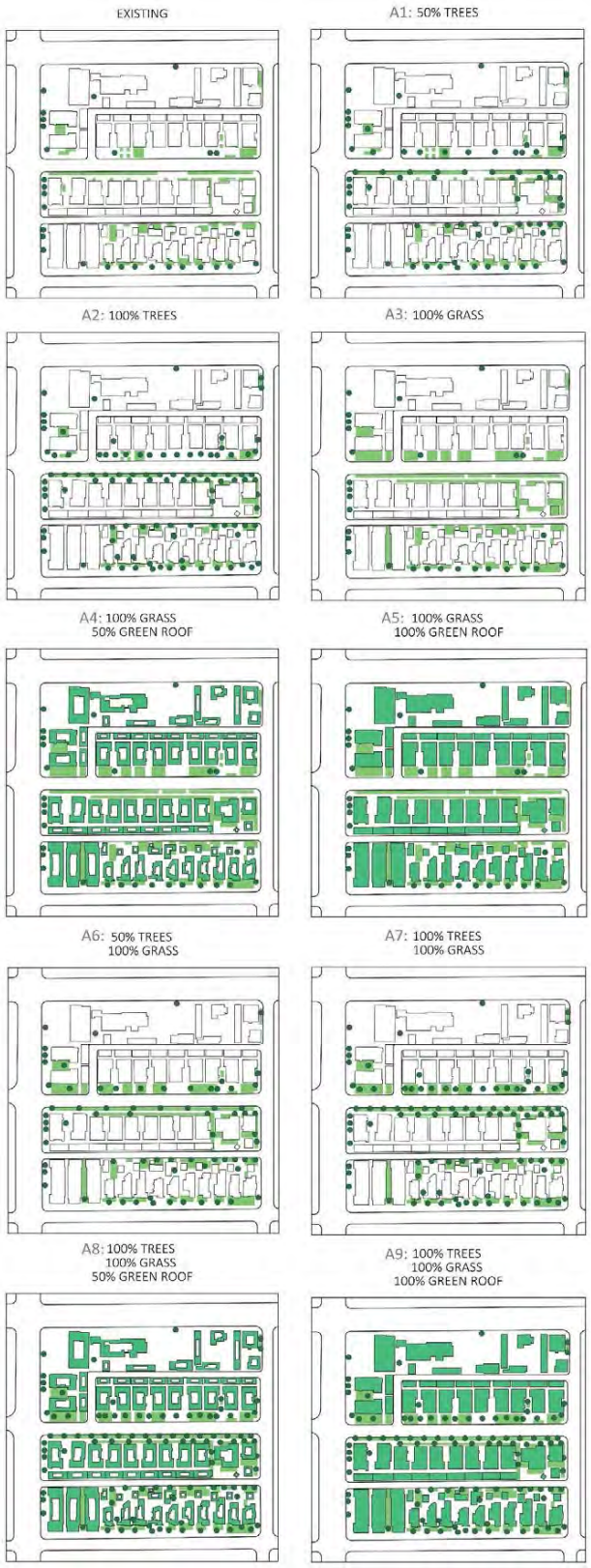

Figure 3 Intervention models used for simulations.

The Universal Thermal Climate Index (UTCI) is calculated for both the baseline scenario and the scenarios with interventions. These models represent an array of urban design configurations, including differing levels of tree canopy, grass cover, and living roofs. Model A1 features a 50% tree canopy, while Model A2 pushes the boundaries with maximum tree canopy coverage. Models A3 and A4 introduce maximum grass coverage and a combination of maximum grass and a 50% living roof, respectively. As progress through the models, they become increasingly complex, culminating in Model A9, which incorporates maximum grass, maximum tree canopy, and maximum living roof coverage. The chosen simulation date is October 15th at 12:00 PM, and the simulation height is 1.5 meter. A comparative analysis is then conducted to assess the level of thermal stress mitigation achieved by the interventions. The results are evaluated and analyzed using data mining and visual representations to make comparisons.

5. RESULTS

To assess the impact of implementing horizontal green surfaces and increasing tree canopy on outdoor thermal stress mitigation, UTCI is calculated for ten different models, including the base model and nine new models with different combinations and levels of intervention of horizontal green surfaces and tree canopies. The calculated UTCI values enable the quantification of the percentage of strong heat stress, moderate heat stress, and no heat stress within the study area, comparing these percentages with those obtained from the base model. The results show the effectiveness of these interventions in reducing heat stress levels and improving thermal comfort in the study area (Table 2, Table 3, Figure 4, and Figure 5).

Table 3 Results and UTCI comparison for Inglewood (Model A1: 50% Tree Canopy, Model A2: Max Tree Canopy, Model A3: Max Grass, Model A4: Max Grass & 50% Living Roof, Model A5: Max Grass & Max Living Roof, Model A6: Max Grass & 50% Tree Canopy, Model A7: Max Grass & Max Tree Canopy, Model A8: Max Grass & Max Tree Canopy & 50% Living Roof, Model A9: Max Grass & Max Tree Canopy & Max Living Roof)

Percentage Reduction of Heat Stress			
Heat Stress Category	Strong	Moderate	None
Model A1	10.68	-10.68	0
Model A2	18.48	-18.4	-0.07
Model A3	0.31	-0.31	0
Model A4	1.02	-1.02	0
Model A5	1.32	-1.32	0
Model A6	10.72	-10.72	0
Model A7	18.31	-18.24	-0.07
Model A8	18.78	-18.69	-0.09
Model A9	18.92	-18.83	-0.09

Figure 4 Results and UTCI false color map (Inglewood)

The microclimate study of outdoor thermal comfort in Inglewood shows that the introduction of green infrastructure elements, such as tree canopies, grass coverage, and greened roofs, can have a substantial mitigating effect on heat stress in urban areas. Specifically, the adoption of a 50% tree canopy model (Model A1) and the maximum tree canopy model (Model A2) shows significant reductions in strong heat stress levels, achieving reductions of 10.68% and 18.48% when compared to the base model, respectively.

Furthermore, the incorporation of green roofs in Model A4 and Model A5 exhibited a promising reduction in strong heat stress of 1.02% and 1.32%, respectively. When these greened roofs were combined with maximum grass coverage, the reduction was even more pronounced, with Model A8 and Model A9 showing reductions of 18.78% and 18.92%, respectively.

Results also indicate that these green infrastructure interventions have the potential to significantly reduce moderate heat stress, with reductions mirroring those observed for strong heat stress.

Table 4 Results and UTCI comparison for Phoenix (Model B1: Max Grass & Max Tree Canopy & Max Living Roof)

		Base Model	Model B1
UTCI (°C)	Heat Stress	Percentage of Heat Stress	
UTCI > 46	Extreme	4.24	6.08
38 < UTCI < 46	Very strong	95.76	93.9
32 < UTCI < 38	Strong	0	0.02
		Average UTCI (°C)	
Average UTCI		42.936	42.896

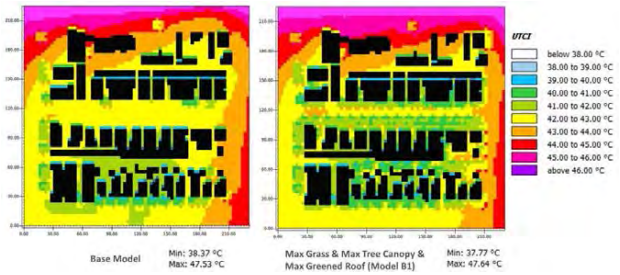

Figure 5 Results and UTCI false color map from ENVI-Met (Phoenix)

In the context of microclimate study on outdoor thermal comfort in Phoenix demonstrates that the introduction of horizontal greened surfaces and an increase in tree canopy, as exemplified by Model B1 (Maximum Grass & Maximum Tree Canopy & Maximum Green Roof Model), can mitigate outdoor thermal stress, particularly in the category of Very Strong Heat Stress. This intervention leads to a reduction in UTCI in the study area, emphasizing its potential to enhance the comfort of individuals exposed to high thermal stress conditions.

However, it is noted that this approach does not yield significant relief for areas already experiencing Extreme Heat Stress and Strong Heat Stress. In these extreme categories, the reduction in UTCI is minimal,

suggesting that additional strategies or interventions may be required to address heat stress effectively in such a climate.

It is important to note that when considering the study area, the inclusion of horizontal green surfaces and increased tree canopy coverage has a positive impact. It results in a lower average UTCI for the entire study area, which highlights the effectiveness of incorporating horizontal greened surfaces and enhancing tree canopy coverage, as exemplified by Model B1, in mitigating outdoor thermal stress, particularly in areas with Very Strong Heat Stress. While this approach may not be a panacea for Extreme Heat Stress and Strong Heat Stress zones, it contributes to a more comfortable outdoor environment on average.

6. CONCLUSION

In conclusion, the microclimate study shows the potential of integrating horizontal green surfaces and increasing tree canopy coverage to mitigate outdoor thermal stress. Across various models, maximizing a combination of different green infrastructure elements significantly reduces both strong and moderate heat stress levels.

In Inglewood, the most effective single strategy is tree canopy; the model with maximum tree canopy achieves an 18.48% reduction. Combining maximum grass and maximum living roof surfaces leads to increased reductions of 18.92%. The potential of these interventions is also evident in the reduction of moderate heat stress. Similarly, the microclimate study in Phoenix demonstrates that the combination of maximum grass, tree canopy, and green roof mitigates Very Strong Heat Stress, showing its potential for enhancing outdoor thermal comfort.

Overall, the findings show the significant and positive impact of implementing strategies involving grass, tree canopy, and green roofs in mitigating heat stress. These green infrastructure elements play a crucial role in enhancing outdoor thermal comfort and the tree canopy is more effective than the horizontal surfaces.

REFERENCES

1. Perkins-Kirkpatrick, S.E., S.C. Lewis. (2020). Increasing trends in regional heatwaves *Nature Communications* 11, No. 3357 https://doi.org/10.1038/s41467-020-16970-

2. Abbas, Y., Oefner, C. M., Polacheck, W. J., Gardner, L., Farrell, L., Sharkey, A., ... & Oyen, M. L. (2017). *A microfluidics assay to study invasion of human placental trophoblast cells*. *Journal of The Royal Society Interface*, 14(130), 20170131.

3. Burillo, D., Chester, M. V., Pincetl, S., & Fournier, E. (2019). Electricity infrastructure vulnerabilities due to long-term growth and extreme heat from climate change in Los Angeles County. *Energy Policy*, 128, 943-953.

4. Mohajerani, A., Bakaric, J., & Jeffrey-Bailey, T. (2017). The urban heat island effect, its causes, and mitigation, with reference to the thermal properties of asphalt concrete. *Journal of environmental management*, 197, 522-538.

5. Voelkel, J., Shandas, V., & Haggerty, B. (2016). Peer reviewed: Developing high-resolution descriptions of urban heat islands: A public health imperative. *Preventing chronic disease*, 13.

6. Ziter, C. D., Pedersen, E. J., Kucharik, C. J., & Turner, M. G. (2019). Scale-dependent interactions between tree canopy cover and impervious surfaces reduce daytime urban heat during summer. *Proceedings of the National Academy of Sciences*, 116(15), 7575-7580.

7. Hoffman, J. S., Shandas, V., & Pendleton, N. (2020). The effects of historical housing policies on resident exposure to intra-urban heat: a study of 108 US urban areas. *Climate, 8*(1)

8. Lehmann, S. (2014). *Low carbon districts: Mitigating the urban heat island with green roof infrastructure. City, Culture and Society*, 5(1), 1-8.

9. Lindberg F, Grimmond CSB (2011) The influence of vegetation and building morphology on shadow patterns and mean radiant temperatures in urban areas: model development and evaluation. *Theor Appl Climatol* 105:311–323. https://doi.org/10.1007/s00704-010-0382-8

10. Shashua-Bar L, Pearlmutter D, Erell E (2011) The influence of trees and grass on outdoor thermal comfort in a hot-arid environment. *Int J Climatol* 31:1498–1506. https://doi.org/10.1002/joc.2177

11. Yan H, Wu F, Dong L (2018) Influence of a large urban park on the local urban thermal environment. *Sci Total Environ 622:882–891.* https://doi.org/10.1016/j.scitotenv.2017.11.327

12. Thorsson S, Honjo T, Lindberg F, Eliasson I, Lim EM (2007) Thermal comfort and outdoor activity in Japanese urban public places. *Environ Behav* 39:660–684. https://doi.org/10.1177/0013916506294937

13. Salata F, Golasi I, Petitti D, de Lieto Vollaro E, Coppi M, de Lieto Vollaro A (2017) Relating microclimate, human thermal comfort and health during heat waves: an analysis of heat island mitigation strategies through a case study in an urban outdoor environment. *Sustain Cities Soc* 30:79–96. https://doi.org/10.1016/j.scs.2017.01.006

14. La Roche, P., & Berardi, U. (2014). Comfort and energy savings with active green roofs. Energy and buildings, 82, 492-504.

15. La Roche, P., Yeom, D. J., & Ponce, A. (2020). Passive cooling with a hybrid green roof for extreme climates. Energy and Buildings, 224, 110243.

16. High-resolution 3D modeling of urban microclimate with Envi-Met Software. (2023).

17. Błażejczyk, K. (2010). UTCI-nowy wskaźnik oceny obciążeń cieplnych człowieka= UTCI-new index for assessment of heat stress in man. *Przegląd geograficzny,* 82(1), 49-71.

18. Young, A. (2017). Universal Thermal Climate Index.

PLEA 2024 WROCŁAW
(Re)thinking Resilience

Resilience in the Passive Standard Buildings:
How hard will global warming hit the passive designs located in the cool-temperate climate of central Europe?

MARTYNA WODO[1] ANDRZEJ KACZMAREK[2]

[1]Cundall Poland, Wrocław, Poland
[2] Cundall Poland, Wrocław University of Science and Technology, Wrocław, Poland

ABSTRACT: The Passive House Standard (PHS) focuses on energy efficiency and thermal comfort. To fulfil the Standard when designing in the central European climate, significant south glazing is crucial, but leads to overheating. This paper investigates the resilience to climate change of two residential PHS buildings located in Poland. By using PHPP (Passive House Planning Package) alongside dynamic energy simulations, we analyse the current and future cooling demand as well as overheating. The results show a significant increase in future cooling demand and overheating time, especially in south-exposed rooms and zones. The comparison of current cooling demand calculated with PHPP and dynamic simulations indicates that PHS's whole-building approach to overheating does not capture all thermal comfort issues. South-facing building zones will either be uncomfortable for up to 20% of the year or rely heavily upon external blinds or active cooling. The results also show potential limitations in Passive House window ventilation methodology (overestimation of the effectiveness of this method). The study helps to understand the climate-specific challenges in achieving PHS while maintaining summer thermal comfort. It also flags up the limitations in overheating methodology that designers should consider at the early design stage to avoid thermal comfort issues.
KEYWORDS: Passive House, Energy efficiency, Resilience, Overheating, Thermal comfort

1. INTRODUCTION

The Passive House Certification is an international building standard developed in Germany in 1988 [1]. Since its beginning, 40,000 units have been certified on six continents, with a rapid increase from 1 000 000 m2 to 3.5000 000 m² in the last seven years [2]. The standard is focused on energy efficiency – the heating demand must be below 15 kWh/m²/a or the heating load must be below 10 W/m². The primary goal is to minimize heat losses from the building through the building envelope; utilise already occurring heat sources, including solar and internal heat gains (people, lights, equipment); reject unwanted thermal energy, such as excess solar in summer; ensure constant and controlled ventilation for healthy indoor air quality [1].

Energy efficiency is not the only aspect incorporated in the Passive Standard design. Passive House Institute underlines the importance of the health and well-being of building occupants by providing high-quality indoor thermal comfort [1]. The thermal comfort indicator is the frequency of overheating (average for the whole building) with the acceptable limit set at max. 10% of temperature above 25°C over a year. To obtain the certificate, the potential of overheating is assessed only for current climate conditions, overheating due to global warming and rising temperatures is currently not taken under consideration for the certification process.

1.1 Overheating problem and its occurrence in Passive House dwellings

Overheating can be defined as *the phenomenon of a person experiencing excessive or prolonged high temperatures within their home, resulting from internal and/or external heat gains, and which leads to adverse effects on their comfort, health or productivity* [3].

During the last twenty years, rising air temperatures and heat waves have become more intense in cool temperate European climates [4]. Climate change projections for Europe show that over the next century, heat waves for northern and eastern Europe will become more frequent, intense and will last longer [5]. According to projections [6], the average summer temperature will rise on similar level in the UK, Germany and Poland.

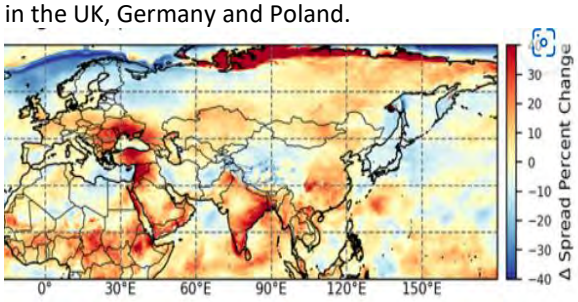

Figure 1: Percentage of temperature increase in July and August (current air *temperature vs future predictions) across the selected continents [6]*

The problem of overheating in Passive Standard Buildings (PSB) is present in the literature with majority of PHS research related to current climate conditions of Germany and the UK [7-9].

Colclough et.al [8] compared the recorded summer performance of five Irish buildings certified with the Passive Standard (PHB) with five buildings built to satisfy current building regulations (DTSB). The indoor temperatures in the living rooms in PHB were higher - on average 1.6°C during the summer months. The overheating (above 24 °C) did not occur in the DTSB, whereas PHB exceeds the threshold by 8.4% of the time and 1.4% of the time for 26 °C. For the bedrooms, the average temp in PHB was 1.5 °C higher, exceeding the 24-degree threshold for 18% of the time (26 °C for 2.2% of the time). The research also includes interviews with the inhabitants, who revealed dissatisfaction with summer comfort in PHB.

Mitchell and Natarajan [9] analysed data (indoor temperature measurements) from 82 Passive Standard dwellings across the UK, showing that 83% of houses meets the overheating target. They pointed out, however that Passive House standard considers whole building instead of each habitable room. When they analysed room data (bedrooms) they found out that only 60% of bedrooms passes max. 10% of overheating. The conclusion was to limit the overheating to 5% and taking into consideration each room instead of the whole house.

Table 1: Monthly average external air temp. for selected locations in Poland, UK and Germany and the heating and cooling demands [kWh/m²/a] for the same building design and characteristics (thermal envelope, systems) located in those regions.

	Poland		UK		Germany	
	Poznań	Warsaw	Midlands	Borders	Kassel	Potsdam
Jan	-1.7	-3.3	4.5	3.7	0.8	0.1
Feb	-0.7	-2.1	4.9	4.1	1.9	1.7
Mar	3	1.9	6.4	5.4	5.2	4.4
Apr	7.9	7.7	8.3	7.2	9.4	9.9
May	13.6	13.5	11.4	9.8	13.6	14.4
Jun	17	16.7	14.4	12.5	16.0	16.9
Jul	18.3	18	16.2	14.5	17.9	19.0
Aug	17.7	17.3	16.7	14.4	18.2	19.1
Sep	13.7	13.1	14.1	12.2	13.9	14.7
Oct	9.1	8.2	10.4	9.0	9.6	10.0
Nov	4.1	3.2	6.8	5.8	5.2	4.5
Dec	0.2	-0.9	4.4	3.6	1.4	0.9
Heating Demand	**15.4**	**18.3**	**7.9**	**8.5**	**11.90**	**12.30**
Cooling Demand	**14.5**	**13.5**	**7.6**	**4.9**	**13.90**	**19.60**

Western European locations require less thermal insulation, airtightness, and solar gains to comply with the Passive House demand of 15 kWh/m²/a than central European locations (including Poland, Czech Republic, Slovakia). Table 1 shows the comparison of selected cool, temperature climate locations of Poland, UK, and Germany, showing the monthly average temperatures (according to PHPP climate data) and the heating and cooling results. The same building (townhouse) with the same envelope and system properties, located in milder (region 2 of 5) climate in Poland (Poznań) barely passed the required 15 kWh/m2/a target, whereas the same building located in the UK or in Germany requires much less energy for heating and (apart from Potsdam which is the closest location to Poland) less energy for cooling.

1.2 Objectives

The purpose of this paper is twofold. Firstly, to investigate how resilient to climate change are the PSB located in the cool, temperate conditions of central Europe. Secondly, to show how the heating demand targets influence the overheating problem in particular (central European) location. Authors believes that this issue is not yet addressed properly, as majority of PHS research focuses on milder climate cases where less south glazing and less strict thermal envelope is required to meet PHS (see table 1).

The research focuses on two scales of residential buildings. Buildings fulfil the demands of Passive House Certification and meet the overheating target. By using dynamic energy simulations and future weather files, we assess the potential of overheating for 2020 (considering the period between the three decades (10s/20s/30s)) and 2050 weather files (considering the period between the three decades (40s/50s/60s)). We looked at overheating potential by assessing not only the whole-building potential but also selected rooms. The results show that for middle-sized and small-sized buildings (townhouses and single-family houses) the whole-building overheating level will rise alongside cooling demand. On average, the cooling demand will be 20% higher in 2020 (10s/20s/30s) and almost 90% higher in 2050 (40s/50s/60s) than current cooling demand. For single family house It will exceed 15 kWh/m²/a PH threshold in 2050, for townhouse it will remain under the 15 kWh/m²/a . The rooms facing south will become more inconvenient, with about 12-13% of hours exceeding 25 ºC in 2020 and 16-17% of hours in 2050.

The research proves that PHPP (Passive House Planning Package) heavily depends on window ventilation as an overheating mitigation strategy. The calculated window air change value in PHPP is twice as big as calculated by dynamic simulations software (IES VE). Further research is needed to fully understand the PHPP calculation methodology.

2. METHODOLOGY

In the first step of the research, we modelled two residential buildings according to PH methodology, using the Passive House Planning Package (PHPP) to

fulfil PH certification criteria. In the second step, with using the same inputs, we created the dynamic energy model using IES-VE (2023) software. Comparing and validating PHPP calculations with dynamic modelling is a method widely used by Passive House Institute - several hundred objects were compared with calculated results using the PHPP and dynamic simulations [10]. Moreover, IES VE is an approved software to assess overheating (for example approved in British TM 59 methodology). In the first step, we compared the current heating and cooling demand results from the static, PHPP simulation with the results from dynamic IES simulation. - The difference between the results was marginal. For single-family building heating and cooling demand difference was within 1% and for townhouse within 3%. The cooling setpoint was assumed at 25ºC as the PH overheating threshold. To validate the dynamic model, we used heating and cooling demand as per the heating and cooling schedule indicated by PHPP. We have also excluded window ventilation, so the only air source was mechanical ventilation with heat recovery (working in bypass mode in summer) and infiltration.

To assess the future cooling demand and overheating potential, we used two weather files for further dynamic modelling – the first one covers the period 2010 to 2040, with the 2020s being the middle of the three decades (10s/20s/30s). The second one covers the period from 2040 to 2060. Both weather files assume the 50th percentile and were created by the climate change world weather file generator (CCWorldWeatherGen). It uses the Intergovernmental Panel on Climate Change Third Assessment Report model summary data of the HadCM3 A2 experiment ensemble [11] and is based on the so-called 'morphing' methodology. [12] We analysed the heating and cooling demand for both weather cases, as well as overheating potential expressed as % of the time a year of indoor temperature above 25ºC. Whereas the Passive House methodology looks at the average overheating value for the whole building (treated as a single zone), we looked at particular rooms to reflect a more realistic approach. We compare our results with (to an extent) an analogical UK study and discuss them as well as potential mitigation strategies in the local climate context.

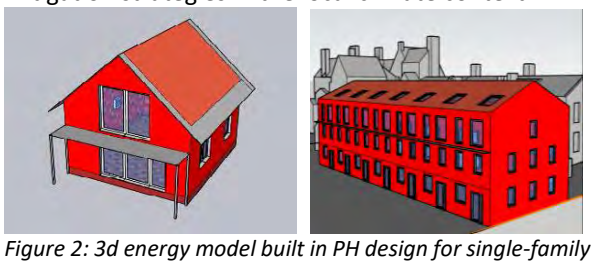

Figure 2: 3d energy model built in PH design for single-family house (Building 1) and townhouse (Building 2)

The analysed buildings differ in size – Building 1 is a single-family house and Building 2 is a townhouse with 7 living units. The PHPP calculations were done for a cool-temperate climate location in Poland (Zone 2, Poznań, Greater Poland). The climate zone was chosen as a temperate case -out of five Polish climate zones, (zone one is the warmest in winter, zone five is the coldest in winter). The summary of building characteristics is presented below. Overheating mitigation measures used for the current and future weather scenarios were window ventilation and overhangs (Figure 2) -1.5 overhang over south glazing in Building 1, 0.6 overhang above first-floor glazing in Building 2 and external, semi-transparent blinds for roof windows.

Table 2: Summary of building characteristics, showing fabric and systems properties.

Building type	Town House	Single Family
Thermal Envelope		
Wall U-value	0.1 W/m²K	0.1 W/m²K
Roof U-value	0.1 W/m²K	0.1 W/m²K
Ground floor U-value	0.1 W/m²K	0.1 W/m²K
Windows - U value glass	N - 0.53 S,E,W -0.64 W/M²k	N - 0.58 W/m²K S,E,W-0.55 W/m²K
Windows - U value frame	0.71	0.69 W/m²K
Windows - g value	N- 0.53 S,E,W -0.6	North - 0.53 Other aspects -0.6
Roof windows - U value glass	0.75 W/m²K	n/a
Roof windows - U value frame	1.1 W/m²K	n/a
Roof windows - g value	0.62	n/a
Doors U values	n/a (glazed)	0.8 W/m²K
Instalation thermal bridges	0.04 W/mK	0.04 W/mK
Thermal bridges - allowance	1.2 kWh/m²/a	0
Internal heat gains	2.7 W/m²	2.6 W/m²
Systems		
Ventilation - designed max.air flow rate	966 m³/h	140 m³/h
Ventilation - ach/h	0.41 1/h	0.47 1/h
Ventilation - Heat recovery efficiency (effective)	81.90%	89.90%
Air tightness [n50]	0.60	0.40
Window ventilation air change rate	1.1/h	1.8 1/h
Building characteristics		
Treated floor area	605.15	92
Nr of occupants (standard PH)	15.1	2.2

3. RESULTS

The results for both building types, located in central Poland indicate that:

- Passive House Planning Package (PHPP) underestimates the current and future cooling demand as well as overheating percentage in both analysed buildings.
- the problem of overheating in PHB will increase significantly over time, especially for the rooms with south exposure.

3.1 Current weather - results

For the single-family house, Passive House indicates 3% of overheating and 6.6 kWh/m²/a cooling demand. Window ventilation in PHPP was assumed - cross-ventilation with tiled windows, 10° open in North-South and East-West direction for 8 hours per day during the summer, wind velocity =1 m/s, temp. difference interior-exterior 4 K (velocity and temp. was set as standard PHPP values). Based on the inputs PHPP calculates a 1.8 1/h window air change rate. In IES windows were set accordingly, assuming open when:

- the internal temperature >22°C, the internal temperature is > external temperature and the external temperature > 15°C progressively (using a ramped profile) with maximum opening of all windows when the internal temperature reaches 24.5°C.
- Window opening restrictors are assumed to limit the maximum opening angle to 10°

The cooling demand is 68% higher than in PHPP when the whole-year period is considered (not only months with cooling demand as calculated in PHPP). Cooling demand in winter months comes from very large south glazing with high g value and no window ventilation (as the assumption made in IES that the windows are open only if the external temperature is above 15°C).

For the townhouse, PHPP indicates 4% overheating and 4.8 kWh/m²/a cooling demand. Window ventilation in PHPP was calculated to 1.09 1/h, assuming cross-ventilation with tiled windows in a North-South direction for 8 hours per day, with standard values for air velocity and interior-exterior temp. difference. In IES windows were set accordingly with effective opening defined as in single-family house. The cooling demand is 90% higher than in PHPP when the whole-year period is considered (not only months with cooling demand as calculated in PHPP).

The first noticeable thing is that whereas PHPP assumed cooling mainly during spring and summer (April-September), IES results show additional cooling demand also in other months. For the townhouses cooling starts in March and lasts until November, and for the single-family house, cooling is present in all months (with marginal values for January and December), however in single family house, PHPP is also showing prolonged cooling demand (March-October). The presence of cooling demand in winter and transition months is related to large south glazing with high g value and limited shading (the overhangs will partially block the summer sun but will let the spring and winter sun in). Large glazing with high g value is crucial to obtain enough solar gains to keep the heating demand below 15 kWh/m²/a.

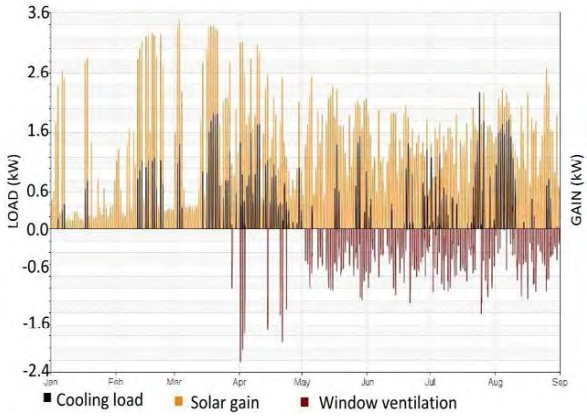

Figure 3: Solar gains and cooling load (above x axis) and window ventilation (below x axis) in January-august (living room in single family house, with 1.5m overhang).

Another factor influencing the cooling demand is the comparison of window ventilation air change rate calculated in PHPP and in IES (based on the same inputs). The calculated air change per hour in PHPP is more than twice as big as the one estimated in the IES Macro Flo module, so a large part of cooling demand in PHPP is offset by windows.

3.2 Future weather predictions-results

The result of the analysis indicates that cooling demand will significantly rise in both buildings (fig 4).

For 2020 weather files cooling demand in single-family house increased by 12% in comparison to IES's current weather results. For the 2050 weather file cooling demand raised by another 50% and exceeded the PHPP maximum cooling demand value (15 kWh/m2/a).

For 2020 weather files cooling demand in townhouses increased by 36 % in comparison to IES's current weather results. For 2050 weather file cooling demand raised by another 60% but did not exceed the PHPP target value of 15 kWh/m2/a.

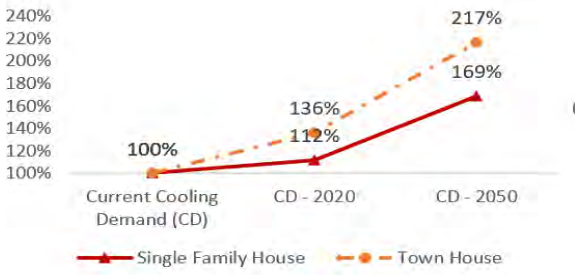

Figure 4: Proportional rise of the cooling demand for single family house and the townhouse, in reference to the current values (in the graph defined as 100% – starting point).

The significant rise in the cooling demand can be explained by rising external temperatures and sun radiation during the summer months. The change in the external temperatures throughout the year limits the possibility of effective window cooling and the rise of the solar radiation-intensive summer solar gains.

3.3 Future weather prediction -overheating in rooms with south exposure.

PHPP considers overheating for the whole building only, without looking at particular rooms or zones. Dynamic simulations suggest that the frequency of overheating in south-exposed, habitable spaces in both – single and townhouses is significantly higher than the average for the whole building.

In the single-family house, we consider the open space (figure 5) -living room, dining space and kitchen, about 36 m^2 -the majority of the ground floor surface, exposed mainly to the south and east. For the current weather conditions, the frequency of overheating (considering overhang for the south windows and openable windows) equals to 11% of hours during the year (in comparison to 3% for the whole building, calculated in PHPP). The overheating rises to 12% in 2020 and 17% in 2040. When considering the overheating only during the summer period (June-August), the results are as follows: 18% for current weather, 25 % in 2020 and 38% in 2050.

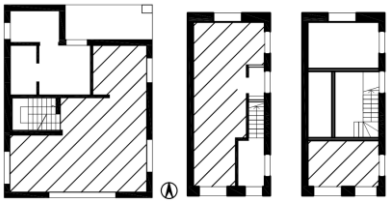

Figure 5: Left side: Single family house, ground floor plan (GF). Middle: townhouse unit GF. Right: side: First floor, townhouse unit. Zone analysed for overheating marked with lines: ground floor (GF=living room, dining area, kitchen) and bedroom in the townhouse).

For the townhouse, the considered area also covered the open-plan ground floor, consisting of the kitchen area, dining, and living room (31 m²). Windows are exposed to south, north, and east (last unit) or to south-north (middle unit). Additionally, the south-exposed bedroom on the first floor is analysed.

Similarly, as in the single-family house, the living space overheats more than the PHPP average for all townhouse units (4%), but the difference is much smaller– 5.4% for the last unit, and 2.4% for the middle unit.

The results for the living area in the townhouse indicate that the problem of overheating is less significant than in the single-family house, especially for the middle units, with fewer windows and sun exposure. It can be explained by much smaller south glazing and fewer wall areas exposed to external conditions. However, if we look at the percentage of overheating only in the summer months (June-August), the results are much more alarming. They are also much higher for the bedroom -reaching 20% for the middle unit and 30% for the last unit for the current weather. The significantly higher results are mostly due to the smaller room size (12 m2), higher glazing percentage and single-side ventilation. For the bedroom, an external shading is considered (0.6 m overhang) as well as window ventilation.

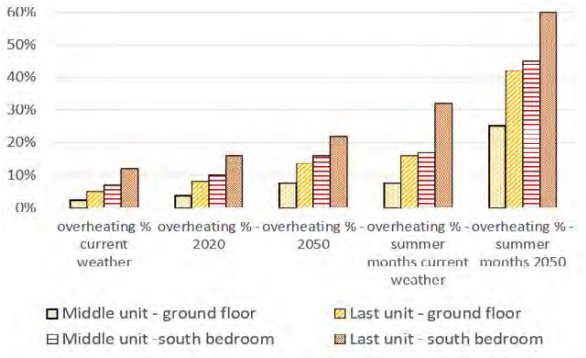

Figure 6: Overheating percentage in selected townhouse areas. Overheating = % of hours exceeding 25 °C during the year and during the summer months (June-September).

4. DISCUSSION

The results for the townhouse obtained in the study are to the extent consistent with the results presented by Mcleold et al [13] who investigated the thermal performance of Passive Standard buildings (townhouses) in the context of climate change in the UK. Their results suggest that the overheating level will rise in the analysed period (1980-2080) assuming the mean warmer year (50th percentile test reference year)), TRY the London weather file. In detail, Mcleold started the analysis with almost no overheating for light and medium construction types (0.4-1.1% respectively for the year 2002). Summer temperatures are reduced by night purge natural ventilation. According to simulations, overheating will rise to 6.2-9.6% in 2080 (circa 900%), but will not extend the 15 kWh/m²/a.

The major climate-related difference between Mcleaold case and our study is the size of the south glazing. The analysed case study has a 33% south glazing-to-wall ratio, whereas both buildings in this analysis have: a 59% south glazing-to-wall ratio. The g value was similarly high in both analyses (0.6).

Mcleod et al proved that south glazing area and external shading are the most influential parameters affecting the overheating in their research, which is also coherent with our study. The issue is that for the analysed location (Poland), the winter solar gains are crucial in keeping the heating demand below the PH target. Table 1 shows the heating demand results for the same building located in the UK, Germany, and Poland. UK and Germany's heating demand is on average 40-50% lower than Polish, so winter solar gains for small-scale buildings are much less important to obtain certification in those locations. In our analysis (as can be seen in Table 2) all other building parameters affecting heating demand are already stringed There is almost no room for further

improvements -apart from taking advantage of solar gains. This should be possible without an overheating penalty, assuming an effective shading strategy. However, based on PHPP analysis, fixed shades (horizontal or vertical) will not fully block the summer sun nor the sun in the transition periods, because their depth needs to be limited to fully capture the winter sun. Other possible solutions would be using moveable shading (external blinds, louvres). They would significantly reduce overheating but will influence several other parameters, such as visual comfort, daylight access or energy used in complementary electric lighting. Their effectiveness relies on users' behaviours, or the necessity to install additional, automatic systems [14]. Another option could be the shading mounted only for the summer period, for example, made from canvas, but this strategy would be reasonable mainly for ground floor, terrace windows. Additional research would be needed to assess the most effective shading strategy.

The second issue is the effectiveness of window ventilation. As noticed in the result section, PHPP heavily depends on window ventilation as an overheating mitigation strategy. The calculated window air change value in PHPP is twice as big as calculated in IES. Further research is needed to fully understand the PHPP calculation methodology, as it is not described in detail in the PH manual. The possible reason of overestimating the air changes is using the average monthly temperatures instead of hourly temperatures to calculate window potential to ventilate the space

4. CONCLUSION

This paper answers two questions - how hard will global warming hit the passive designs located in the cool-temperate climate of central Europe and how serious is the current overheating problem in small-scale, PHS designs. The results show that:

- Passive House Planning Package (PHPP) underestimates the current and future cooling demand as well as overheating percentage in both analysed buildings.
- The problem of overheating in PHB will increase significantly over time, especially for the rooms and zones with south exposure. The PHPP whole-building approach to overheating should be reconsidered.

The cooling demand will rise alongside with climate change and current strategies will not be able to keep the overheating potential below 10%, especially for south-exposed rooms. Either carefully designed, additional shading strategies or active cooling will be needed to improve thermal comfort in summer and transition periods.

Overheating can always be offset by active cooling, but the core idea of Passive House is to avoid any unnecessary electricity demand. The PH criteria for small-scale buildings in central-European climate might need reconsideration in the context of climate change. More research is needed to fully understand the climate-specific challenges in achieving PHS while maintaining summer thermal comfort. The next step of this study is to create digital twins of existing buildings and validate the IES results with the real-time measurements and interviews with building inhabitants.

REFERENCES

1.Passive House Institute, Passive House Principles [Online],Available:httpshttps://passiv.de/en/02_informations/02_passive-house-requirements/02_passive-house-requirements.htm [26 August 2023].

2.Passive House Institute, Passive House certification worldwide,[Online],Available:https://passivehouse-international.org/index.php?page_id=65 [26 August 2023].

3. Zero Carbon Hub, Defining Overheating. Evidence review[Online]https://www.cewales.org.uk/files/2014/4370/9984/Defining_Overheating_Evidence_Review.pdf [10 December 2023]

4. Rahif, R. et al, (2021). Review on Time-Integrated Overheating Evaluation Methods for Residential Buildings in Temperate Climates of Europe. *Energy and Buildings*, 252.

5. D'Ippoliti, D., Michelozzi, P., Marino, C. et al, (2010). The impact of heat waves on mortality in 9 European cities: results from the EuroHEAT project. *Environmental Health,* 9(37).

6. Turnau, R. et al, (2022). Model Projections of Increased Severity of Heat Waves in Eastern Europe. *Geophysical Research Letters*, 49.

7.Passive House Institute, The impact of warming climate conditions on buildings [Online], Available: https://passipedia.org/phi_publications/2021_vol.3_the_impact_of_warming_climate_conditions_on_buildings [26 August 2023].

8. Colclough S. et al. (2017). Summer performance of certified passive houses In Temperate Maritime Climates. In PLEA Conference Proceedings. Edinburgh, UK, July 3-5.

9. Mitchell, R. and N. Sukumar, (2020): UK Passivhaus and the energy performance gap. En*ergy and Buildings,* 224.

10. PHI, Calculating energy efficiency [Online] https://passipedia.org/planning/calculating_energy_efficiency/phpp_-_the_passive_house_planning_package/phpp_-_validated_and_proven_in_practice [26 August 2023].

11. Data Distribution Centre (DDC) of the Intergovernmental Panel on Climate Change (IPCC) [online] Avaible: https://www.ipcc-data.org/ [18 December 2023]

12. Jentsch M.F., James P.A.B., Bourikas L. and Bahaj A.S. (2013) Transforming existing weather data for worldwide locations to enable energy and building performance simulation under future climates, *Renewable Energy*, 55: p. 514-524.

13. Mcleod, R., Hopfe, C. and A.Kwan, (2013). An Investigation Into Future Performance And Overheating Risks In Passivhaus Dwellings. *Building and Environment*,70.

14. Glória Gomes, M. A.J. Santos and M. Calhau, (2022). Experimental study on the impact of double tilted Venetian blinds on indoor daylight conditions. *Building and Environment*, 225.

PLEA 2024 WROCŁAW
(Re)thinking Resilience

Efficacy of passive design strategies for houses in warm-subhumid climates

Architecture for human resilience and well-being

MARIO FILOMENO CABRERA SANDOVAL[1], CARLOS J. ESPARZA-LÓPEZ[1], PEDRO CIPRIANO MAGANA MENDOZA[1], J.C. CAICEDO-MONCAYO[1], JENNIFER JIMENEZ-ANZAR[1]

[1]University of Colima, Colima, Mexico

ABSTRACT: Mass-construction housing is a construction sector essentially governed by the increase in construction costs and the demand for housing, which leads to an increase in the reproduction of architectural models that do not respond to the climatological characteristics of the site. Therefore, it generates an environment of discomfort for the user and affects the excessive use of artificial air conditioning systems. The purpose of this study is to evaluate the effectiveness of passive strategies aimed at improving the interior temperature conditions of homes in the warm subhumid climate zone. The study was carried out through scenario simulations implementing improvements to a typical 57.23m² home. The analysis of the thermal performance improvement was carried out through dynamic simulation based on the building orientation parameters, shading elements in the windows, ventilation and the envelope materials. According to the climate diagnosis, there is a warm season that reflects possible overheating inside the home, which is why the model was analyzed in the summer season. The results are shown as a percentage of the comfort hours following the requirements of the adaptive model. of ASHRAE Standard 55-2021.
Keywords: thermal performance, passive design, solar protection, ventilation, housing

1. INTRODUCTION

Thermal comfort in homes is an important issue for the well-being and health of the people who live there. In a home it is essential to have appropriate air conditioning strategies that allow maintaining a pleasant and constant temperature inside, but the development of mass housing uses a building prototype replicated throughout the country without taking into account the environmental response. In this research work, the energy potential of strategies to improve the interior temperature of the private home in warm subhumid climates that result in reducing electrical energy consumption is evaluated.

At the beginning of the 1990s, the dominant idea was that any designed building could solve its environmental control problems through the use of energy systems; however, in the current situation with fewer resources, it is essential to take into account the climate where it is located [1]. Currently, deficiencies can be observed in buildings that operate in conditions that do not offer thermal comfort for their inhabitants, which in turn causes domestic, commercial or industrial energy waste, since the lack of ideal conditions is resolved through the intervention of artificial air conditioning equipment [2].

To improve the resilience of the interior thermal environment of mass-built homes, they must be designed with greater than average energy efficiency. Such a design could reduce building energy consumption and minimize a family's electricity costs, making adaptability to extreme heat more feasible.

2. BACKGROUND

Continuous efforts are made in research and development to incorporate new passive technologies and processes that achieve buildings that are resilient to changes in the environment. The Intergovernmental Panel on Climate Change (IPCC) has presented scientific evidence on climate change and the challenges ahead [3]. The above has involved international collaboration since the 1990s with results presented through periodic IPCC reports aimed at addressing the current climate situation for adaptation and mitigation; and the integration of sustainable development policies [4].

According to the IPCC, there must be a top priority focus on climate-related actions because CO_2 emissions and additional greenhouse gas (GHG) emissions are the main reason for global temperature changes. Cities that have never felt extreme heat now experience several days of high temperatures, but often lack the infrastructure to combat it [5].

Heat waves are prolonged periods, more than two days, of excessively high daytime temperatures [6]. They can affect society in several ways, including people's health, increased water stress, food, and energy consumption.

The thermal resilience of the built environment can be defined as the ability of a building to withstand disruptive events while maintaining

comfortable conditions inside [7], the most common external stresses being emergencies such as power outages and heat waves. The idea of building thermal resilience is closely related to the concept of passive architecture, which according to [8] is the ability of a building to protect occupants from external climatic events, so that thermal conditions are naturally achieved inside comfort.

When heat wave weather conditions affect a population, the severity of its impacts can differ greatly among the many socioeconomic statuses of people living in the community. Housing conditions can affect a person's adaptability to sharp increases in temperature, especially in urban environments and vulnerable communities [9].

Mexico has highlighted that adaptation measures to climate change must be aimed at reducing vulnerability by increasing adaptive capacities and reducing the risk of climate-related disasters. If GHG emissions decline dramatically over the next decade, adaptation will still be necessary to address the global changes already underway [10]. The architectural design must be carried out with the objective of creating an envelope that functions as protection against extreme weather conditions; spaces must be thought of that take advantage of the potential of the environment and in this way provide comfort conditions to the user.

Currently, meeting comfort conditions is sacrificed for various reasons such as the increase in construction costs and housing demand, which leads to an increase in the development of mass housing and the use of industrialized materials for their low cost and reduced construction time. However, on several occasions these do not respond to the climatological characteristics of the site, which generates an environment of discomfort for the user and, therefore, has an impact on the excessive use of artificial air conditioning systems [11].

3. METHOD

In the research methodology of this study, it is important to point out the literature review that has consolidated passive design strategies as agents of adaptation to the conditions of climate change [12], [13]. The research methodology is quantitative and is based on sampling, data collection and numerical simulation.

In the sampling stage, the characteristics of the object under observation are defined. The mass-constructed home can be presented with different components. For this research, homes of up to 100m2 built will be analyzed. The architectural envelope is made up of different elements which will be classified based on the functions of sun protection, ventilation and thermal insulation.

In Mexico, the official source of climate data is the National Meteorological Service (NMS) (https://smn.conagua.gob.mx/es/). A form of summary of information useful for the calculations of this study are the so-called climatological normals, which consist of statistics, preferably for 30 years. Said in statistical terms, climatological normals are constructed from the averages and extreme values of a period, while the typical year should represent the statistical mode of a sample of one or more decades.

To build the numerical reference model, climate data and data on the materials of the architectural envelope are taken. When the numerical model is calibrated and validated, significant parameters are changed to analyze the interior temperature of the home and it is reviewed with the adaptive model to evaluate the thermal performance.

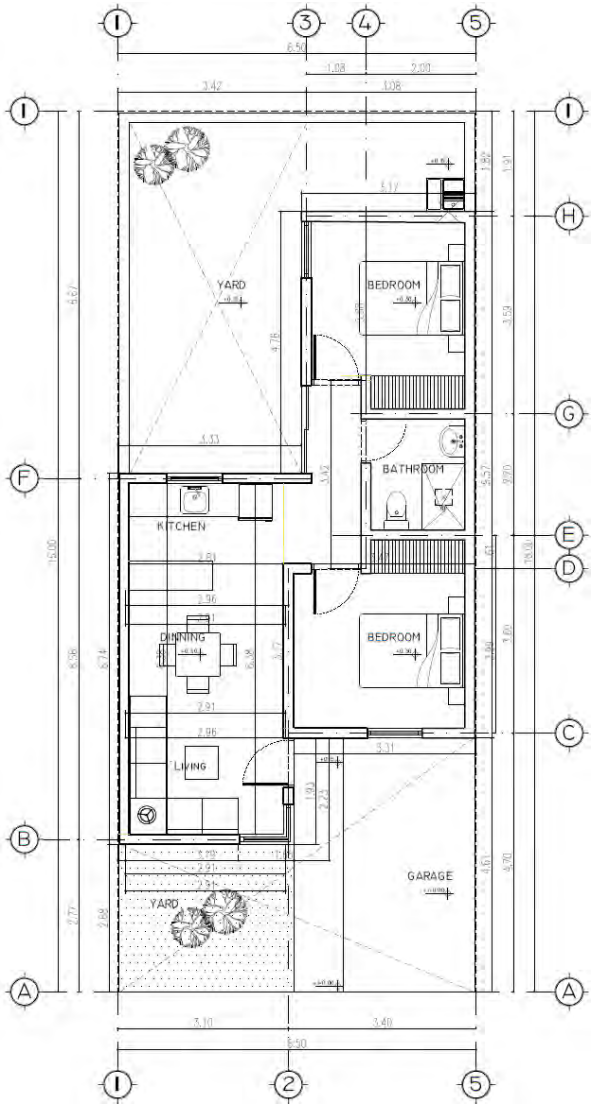

Figure 1: Architectural detail of mass-construction housing in Mexico

The housing model was selected based on several factors: housing type classification, construction period and use layout. The selection according to the

classification of housing type was based on the Housing Building Code (HBC) 2017, which says that a social housing is one that has a constructed area between 40 m2-70 m2 and a range of cost from 118.10 to 00 UMA (Update Measurement Unit, an economic unit for Mexico). The chosen housing prototype has 57.23 m2, distributed in an architectural program of living room-dining, kitchen, full bathroom, two bedrooms with closet, backyard, front yard and garage. The architectural floor plan can be seen in figure 1.

This prototype of housing was selected due to its disposition of use, when an agreement was presented by the construction company and the educational program of the University of Colima to carry out research and take climatic variables during a period of two months, where only the use was exclusive for said actions.

The model of the house was created based on the housing typology proposed by the HBC. The envelope parameters used represent the characteristics of the traditional construction elements in this type of building. On the exterior walls, 140 mm thick annealed red partition walls with 20 mm flattening on the outside and inside were considered. the value U=1.042 $Wm^{-2}K^{-1}$, the flat roof slab is made of 100 mm thick concrete, with asphalt waterproofing on the outside and flattened plaster on the inside, the value U=1.273 $Wm^{-2}K^{-1}$. The thermal simulation was carried out in the Design Builder software, and it was also considered that the house was empty during the observation period.

The climatic parameters recorded in the warm subhumid region show that due to the high levels of direct radiation it receives, as well as the high concentrations of humidity, the environmental conditions are high and considerably stable, since both during the day and at night Humidity and temperature levels are above the comfort zone, and their variation throughout the year is minimal [11]. In a warm subhumid climate, it is necessary to carry out cooling tasks throughout the day, most of the year, to create comfortable conditions in the home, then the thermal envelope must be protected so as not to expose it directly to solar radiation and thus avoiding generating profits, in addition to allowing the capture of the prevailing winds.

The climatic data have been obtained from records open to the public from the National Meteorological Service (SMN in Spanish) of Mexico. The bioclimarq2023 tool [12] was used to generate the climatic characterization, the bioclimatic diagnosis and the climatization recommendations.

Thermal comfort was defined for this climatic zone using the comfort model described in the adaptive version of the ASHRAE Standard 55-2021, and with *bioclimarq*^{2023} [12] the thermal ranges are calculated by reconciling diagnostic variables.

The analysis of the improvement in the thermal performance of the envelope was carried out through dynamic simulation based on orientation, shading and ventilation. These parameters are chosen from previous research on passive house design [7, 12- 17].

Throughout the year, temperature conditions that fall within the comfort zone represent approximately 50% of the time. For the rest, the basic air conditioning strategies that improve the identified requirements are daytime ventilation and nighttime ventilation plus thermal inertia. Furthermore, it is recommended that during 87% of the daytime period, efforts should be made to ensure that the glass openings remain protected from the sun. Figure 2 shows the appropriate air conditioning strategies for the study climatic zone by time of year.

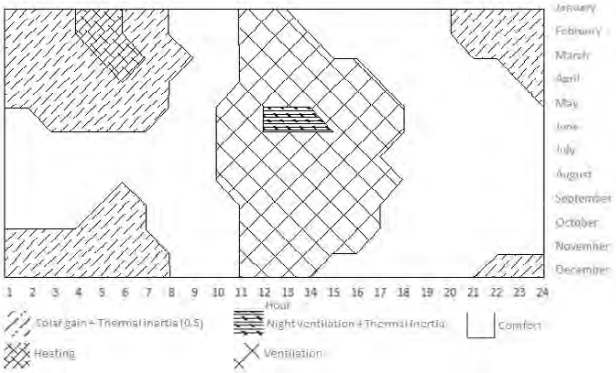

Figure 2: Distribution of air conditioning strategies in the hours of the year.

Taking into account that the factors that affect the thermal performance of the building are the solar radiation gain, insulation and reflectivity [1], the strategies of modifying the orientation, proposing different shading situations and maintaining natural ventilation are situations that are considered they simulated individually. The results were then compared with the base case to determine the efficiency of the selected strategies.

4. RESULTS

Based on the simulated models, the results of the solar heat gain through the windows, walls and roof, the interior ventilation through the windows, the operating temperature of the interior spaces, the percentage of hours that exceed the comfort limit for each case.

The thermal variation in this climatic zone is evident (figure 3), in the summary of the climate diagnosis it is presented as the upper temperature limit of comfort 29°C while the minimum temperature limit of comfort is 20°C, in addition to the representation of temperatures of a typical day

reveals a concern about heating between 10 a.m. and 4 p.m.

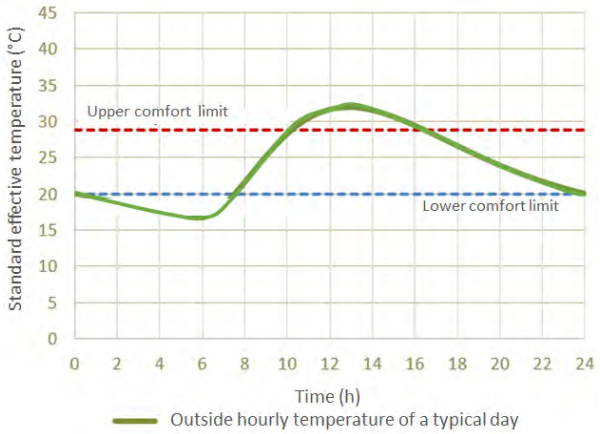

Figure 3: Typical day temperature in the study climatic zone.

Design Builder software was used to calculate the thermal performance of each case study. The base model was simulated with different orientations, the initial orientation is 0° which represents the main façade facing North and with clockwise rotation the orientations of 22.5°, 67.5° and 90° were made, the model is complemented with a couple of adiabatic blocks that represent the adjacent homes as shown in figure 4.

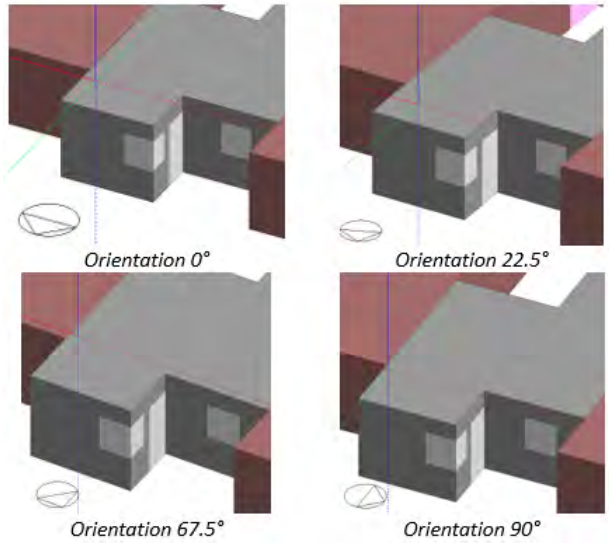

Figure 4: The initial orientation of the main façade is 0°, which represents North

Solar protections simultaneously fulfill two functions, the first is that the shading strategy reduces solar radiation gains, secondly, it is to guarantee ventilation. In warm subhumid climates, ventilation is essential to renew the air inside the home because even in the rainy season the temperatures are above the comfort zone and the overhangs on the windows must even protect from rain to allow the passage of the wind [1] and [18]. The windows of the house were protected with overhangs with different angles of sun protection, which are shown in figure 5.

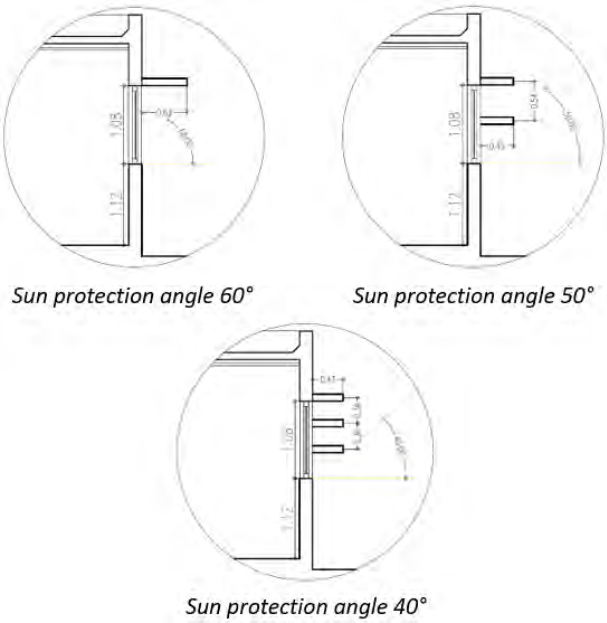

Figure 5: Window ruffle design for different sun protection angles.

The thermal performance of the home was evaluated in the summer season, the calculation of the typical summer week was carried out to then determine the critical day of this time interval. Varying the orientation alone improves thermal performance.

According to the adaptive model, the highest percentage of comfort hours found is observed in the 22.5° orientation while in the other orientations, even with lower solar radiation gain, the percentage of comfort hours are noticeably lower. The results are shown in Table 1.

Based on the previous results of the orientation variation, solar protection will be implemented, with the purpose of increasing the percentage of comfort hours.

As has been widely studied [18-20], the reduction of solar gains through any means of shading in warm climatic zones contributes to improving indoor temperature conditions, but it must also allow the passage of natural ventilation. The design of the ruffles is the result of in-depth analysis so that they can be contemplated from the design of the home.

Table 1: Summary of solar gains and percentage of hours in comfort.

	CASE STUDY ORIENTATION				
	0°	22.5°	45°	67.5°	90°
Max solar gains (kW)	2.126	1.633	1.443	1.295	1.295
Avarage solar gains (kW/h)	0.406	0.367	0.368	0.359	0.359
Percentage of hours in discomfort	63.10%	62.50%	64.29%	63.10%	63.10%
Percentage of hours in comfort	36.90%	37.50%	35.71%	36.90%	36.90%

Of the different proposals, the cantilever with the sun protection angle was not the one with the highest percentage with hours of comfort, in fact, the cantilever with a 40° sun protection angle is the one that presents the best performance. Table 2 shows the results of solar gain and percentage of hours in comfort.

Table 2: Results of the 22.5° orientation plus solar protections.

	CASE STUDY ORIENTATION 22.5° + SHADE		
	60°	50°	40°
Max solar gains (kW)	1.420	1.529	1.229
Avarage solar gains (kW/h)	0.263	0.292	0.259
Percentage of hours in discomfort	55.95%	57.14%	54.76%
Percentage of hours in comfort	44.05%	42.86%	45.24%

The percentage of hours in thermal comfort of the model with 22.5° orientation is a clear reflection of the decrease in the entry of solar radiation due to the configuration of the architectural envelope. The percentage of hours in comfort increased noticeably from 37.5% to 45.24%, when different shading situations were implemented. The main reason is that solar gain was decreased, but importance should be given to natural ventilation. The maximum solar gain of the model with 22.5° orientation is 1,633 kW and by adding the cantilever lattice with a protection angle of 60° the maximum gain decreases to 1,420 kW, but it is not the lowest of the maximum solar gain values.

The lowest value of maximum solar gain is equal to 1,229 kW and occurs in the model with the combination of the 22.5° orientation and the window with the solar protection angle overhang of 40°. With these data it becomes evident that in this climatic zone shade must have ventilation as a necessary complement. But there is also a limit to these benefits because the outside air has the temperature of the outside environment, so sometimes the wind carries hot air. Due to this situation, it is recommended to have plant elements that allow the wind to cool before entering the home, but the configuration of these elements is outside the scope of this study.

5. CONCLUSION

This article studied the effectiveness of passive strategies such as orientation and solar shading to evaluate the influence on the interior thermal performance of mass-built homes. Based on this parametric study, the model simulations produced results that allow influencing the design of the envelope to increase the hours of comfort in the warm subhumid climate zone.

Ventilation is key to achieving comfort conditions in warm subhumid climates, which is why sun protection strategies must provide protection against radiation and even allow the passage of outside air. Since daytime ventilation follows the outside temperature, nighttime ventilation must be included to expel hot air.

For the application of passive design strategies, the climatic characteristics of the site must be taken into account to then evaluate the thermal performance of the home. The tool used in this article for climate characterization was bioclimarq and climate consultant was reviewed for the design of solar protections.

In the present study, the model was complemented with adiabatic blocks that represent neighboring buildings; The current information can be expanded to find out the existence of an effect on thermal performance due to the proximity between these buildings.

This research provides relevant design guidelines for the development of mass housing that reduce energy consumption and increase hours of thermal comfort, so this information can be useful for future design projects. Furthermore, it could guide the improvement of this type of buildings in warm-subhumid climates.

ACKNOWLEDGEMENTS

First author wishes to thank the National Council of Humanities, Science and Technology (CONAHCyT) of Mexico, for the grant provided in the doctoral scholarship.

REFERENCES

1. R. Serra Florensa and H. Coch Roura, (2004). Arquitectura y energía natural, vol. 17. Iniciativa Digital Politécnica
2. A. Tejeda Martínez and G. Gómez-Azpeitia, (2015). Prontuario solar de México. Colima: Universidad de Colima, Universidad Veracruzana, 2015
3. Agencia Internacional de Energía (AIE), (2019). "Informe global de edificios y construcción de 2019: ONU Medio Ambiente y AIE," Atlanta, USA
4. O. Kinnane, T. Grey, and M. Dyer, (2017). "Adaptable housing design for climate change adaptation," Proceedings of the Institution of Civil Engineers - Engineering Sustainability, vol. 170, no. 5, pp. 249–267, doi: 10.1680/jensu.15.00029.
5. IPCC, (2023). "IPCC_AR6_WGIII_Chapter01," in IPCC AR6 WGIII, https://www.ipcc.ch/report/ar6/wg3/downloads/report/IPCC_AR6_WGIII_Chapter01.pdf
6. N. US Department of Commerce, "National Weather Service. NOAA's National Weather Service.," https://www.weather.gov/.
7. S. Attia et al., (2021). "Resilient cooling of buildings to protect against heat waves and power outages: Key concepts and definition," Energy Build, vol. 239, p. 110869, doi: 10.1016/j.enbuild.2021.110869.
8. W. Rahmah, (2012). "Environmental Prospective of Passive Architecture Design Strategies in Terrace Houses," Procedia - Social Behav Sci.
9. A. Y. Lo, C. Y. Jim, P. K. Cheung, G. K. L. Wong, and L. T. O. Cheung, (2022). "Space poverty driving heat stress vulnerability and the adaptive strategy of visiting urban parks," Cities, vol. 127, p. 103740, doi: 10.1016/j.cities.2022.103740.
10. SEMARNAT-INECC, (2018). México. Sexta comunicación nacional y segundo informe bienal de actualización ante la Convención Marco de las Naciones Unidas sobre el cambio climático. México. Accessed: Nov. 20, 2023. [Online]. Available: https:// cambioclimatico.gob.mx/sexta-comunicacion/
11. SEDATU and CONAVI, (2022). ESTRATEGIAS DE DISEÑO ARQUITECTÓNICO CON ENFOQUE BIOCLIMÁTICO: Criterios técnicos para una vivienda adecuada. México: Subdirección General de Análisis de Vivienda, Prospectiva y Sustentabilidad
12. G. Gómez-Azpeitia, A. Tejeda-Martínez, and L. C. Herrera -Sosa, (2023). Arquitectura, confort y cambio climático, Primera edición. México: Puertabierta Editores
13. L. K. Alba Gómez, L. C. Herrera Sosa, and C. J. Esparza López, (2021). "Análisis de costo-beneficio de estrategias de climatización pasiva en vivienda social en Ciudad Juárez, Chihuahua," Vivienda y Comunidades Sustentables, no. 10, pp. 81–91, doi: 10.32870/rvcs.v2i10.165.
14. R. Rivera and G. Ledesma, (2019). "Improvement of Thermal Comfort by Passive Strategies. Case Study: Social Housing in Mexico," International Journal of Structural and Civil Engineering Research, pp. 227–233, doi: 10.18178/ijscer.8.3.227-233
15. S. Pathirana, A. Rodrigo, and R. Halwatura, (2019). "Effect of building shape, orientation, window to wall ratios and zones on energy efficiency and thermal comfort of naturally ventilated houses in tropical climate," International Journal of Energy and Environmental Engineering, vol. 10, no. 1, pp. 107–120, doi: 10.1007/s40095-018-0295-3.
16. C. E. Vázquez-Torres and A. Gómez-Amador, (2022). "Impact of indoor air volume on thermal performance in social housing with mixed mode ventilation in three different climates.," Energy and built environment, vol. 3, pp. 433–443
17. J. Araúz, D. Mora, and M. C. Austin, (2019). "Impact of the envelope layout in the thermal behavior of buildings in Panama: A numerical study," Proceedings - 2019 7th International Engineering, Sciences and Technology Conference, IESTEC 2019, pp. 209–214, doi: 10.1109/IESTEC46403.2019.00-74.
18. P. Serrano, (2023). "Así afecta la tasa de ventilación en la demanda energética de edificios." Accessed: Mar. 05, 2023. [Online]. Available: https://www.certificadosenergeticos.com/afecta-ultima-modificacion-db-hs3-demanda-energetica-edificios
19. B. Givoni, (1998) Climate considerations in building and urban design. John Wiley & Sons
20. S. Szokolay, (1990). House Design for Overheated Environments. Memoria del I encuentro Nacional de Diseño y medio ambiente
21. A. Auliciems and S. V. Szokolay, (200) PLEA Notes. note 3: Passive and Low Energy Architecture-Design Tools and Techniques-Thermal comfort. Retrieved from PLEA in association with Department of Architecture. Brisbane, Queensland, Australia.: The University of Queensland

PLEA 2024 WROCŁAW
(Re)thinking Resilience

Guidebook on the Built Environment for the Elderly in Extreme Hot Weather

Bridging the gap between climatic knowledge and design of indoor and outdoor environments

YILIN LEE[1], KAO GAO[2], EDWARD NG[2]

[1] The Chinese University of Hong Kong, Hong Kong, China
[2] Institute of Future Cities, The Chinese University of Hong Kong, Hong Kong, China

ABSTRACT: Exposure to extreme heat will become more frequent due to global warming. The severity of heat-related illnesses and mortality increases with age. Elderly with low income who cannot afford air-conditioners, are most vulnerable. Although there is abundant scientific knowledge on urban climate, it has had relatively limited impact on improving the design of the built environment. The study, in the form of a guidebook, represents a visual tool that communicates how scientific knowledge can be applied as architectural and urban design strategies for practical implementation to mitigate extreme heat. 13 indoor design strategies were simulated in EnergyPlus. In the optimised combined design strategy, the comfortable time can be increased to 63% (2312 hours) of the total occupancy time from 4% (138 hours) of the base case. The most optimal strategy requires 37% (1358 hours) of total occupancy time of AC cooling, whereas the flat without design improvement requires 96% (3523 hours) of cooling. The most effective strategies are balcony, fully glazed/fully openable window, and cross ventilation, yet insulation and fully glazed window are the poorest strategies.
KEYWORDS: Knowledge transfer, Design implementation, Extreme urban heat, Thermal comfort, Energy efficiency

1. INTRODUCTION

As a result of climate change, extreme heat incidences are becoming increasingly severe and frequent. Numerous studies [1–3] suggest that climate change and extreme heat will predominantly impact cities due to the urban heat-island (UHI) effect. Worldwide, more people live in cities and the rate of urbanization is projected to increase [4]. Antropogenic activites have caused approximately 1 °C rise in temperature compared to pre-industrial levels and is estimated to reach 1.5°C by 2050 [5]. Global warming has serious consequences for people, communities, and the built environment. Cities face unequal distribution of heat burdens due to the spatial heterogeneity of the UHI intensity which affects vulnerable populations the most [6]. Several reports expressed concern about the severe impact of climate change on cities that will disproportionately cause harm to the urban poor. Susceptibility to heat stress varies according to physical exposure to hot climates and corresponds to land cover, weather conditions, demographic characteristics, health status, individual heat sensitivity, and the use of air-conditioning [1,7,8]. The severeness of heat-related illnesses and mortality increases with age. Elderly citizens with low income who cannot afford the use of air-conditioners, are particularly vulnerable. Studies show that the relationship between extreme climate events and health are compelling with a dramatic upsurge in hospital admissions, morbidity, and mortality rates, especially among elderly [6]. In Hong Kong, the mortality rate rose by 1.8% for every 1°C increase for temperatures above 28.2°C [9]. Extreme urban heat poses the deadliest climate hazard in many countries [10]. Thus, it is of critical urgency to adapt measures that cool the built environment and conserve energy while safeguarding the health of vulnerable groups.

Although there is abundant scientific knowledge on urban climate, it has had relatively limited impact on the design of the built environment. Eliasson [11] claims climatologists have not communicated scientific results in a way that is appropriate. He proposed a framework of five variables that explain the reasons for the low impact of urban climatology on planning practice. There is a consensus among researchers that a gap exists between urban climatic knowledge and practical implementation that can cool the urban environment [11,12]. There is an urgency to address the gap between planning, architectural design and urban climatology which would entail transferring climatic knowledge into planning practice [11–13]. Researchers agree that urban climatology awareness is lacking and not in a

form that is easily understood across other disciplines to be integrated into design and planning [14].

This study provides design recommendations and planning guidance in a clear and simple manner relatable to policymakers, designers, planners, and co-professionals. The study, in the form of a guidebook on the built environment for the elderly in extreme hot weather, is intended as a visual tool that communicates how scientific knowledge can be applied as architectural and urban design strategies. The guidebook consists of indoor and outdoor strategies. To keep the study concise, only important indoor strategies will be analysed as follows:

1. Analysis of building simulation results
2. Formulation of design strategies
3. How proposed strategies address Eliasson's framework of explanatory variables

2. METHODOLOGY

To answer the question: *Why despite all the scientific knowledge developed in urban climatology, and building energy conservation, it is not sufficiently implemented in practice?* We use a mixed methods approach combining quantitative analysis qualitative methods. This study will be limited to Task B, developing mitigation strategies for the Built Environment in the form of a guidebook (Figure 1) Emphasis is placed on how to bridge the gap and transfer the knowledge between scientific research (building performance, urban climatology) and practical implementation.

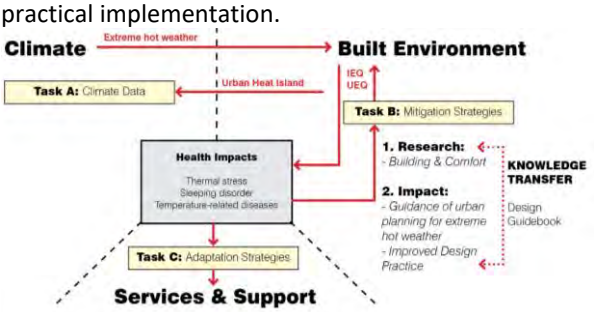

Figure: 1 Methodology of knowledge transfer

Building simulations are conducted in EnergyPlus 9.4 coupled with thermal comfort-based HVAC control scheme. The model (Figure 2) is based on a typical public housing high-rise building. 13 design strategies were analysed against a base case scenario. The simulation period is from 28th April to 1st October with a 5-minute time resolution.

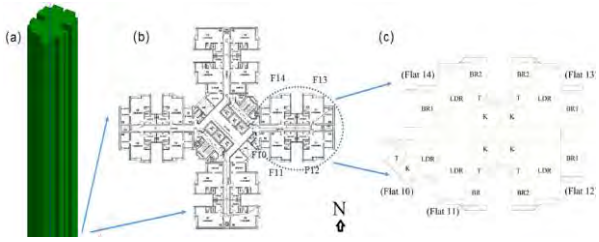

Figure 2: Model layout for (a) the whole residential building (b) the whole floor plan (c) the study area: Flat 10, 11 & 12.

Table 2: Design strategies considered in the simulation.

Strategy	Base case	Changed feature
S1. Ventilation potential	No window on the sidewall of BR1 at Flat 12.	Fully glazed &openable window on same surface.
S2. Vent window	No vent windows.	30% of openable window convert to vent window.
S3. Floor-to-floor height	2.7 m.	3.7 m.
S4. Glass type	Plain glass.	Tinted Low-e glass.
S5. Wall insulation	No wall insulation.	50 mm polystyrene on external wall surface
S6. Balcony	No balcony.	Balcony size 1mx2 m.
S7. Openable window area	Openable window-to-floor area ratio 1/16.	Fully glazed & openable window at LDR & BR
S8. Wall shading	No wall shading.	Hypothetical wall shading (full elimination of solar radiation)
S9. Floor level	5/F floor-to-floor height 2.7 m	25/F.
S10. Window shading	No window shading.	Hypothetical wall shading to all windows.
S11. Cross ventilation	No cross ventilation.	2 ventilation corridors by opening doors & windows at living room of 2 opposite dummy flats (Flat 13, Flat 14).
S12. S1-S12 combined except S5&8	N/A	N/A
S13. S1-S12 combined except S3,5&8	N/A	N/A

Since the efficacy of a specific design strategy is affected by orientation, residents' HVAC usage patterns, and occupancy schedules, the study analysed four orientations (N/S/E/W), four HVAC strategies (no cooling, fan for cooling, air conditioning (AC)+fan for cooling, and AC only), and two occupant behavior patterns (Active/Inactive) for each strategy. Consequently, 32 sub-scenarios were simulated for each strategy. Detailed simulation settings, occupancy schedules, etc. are listed in the supplementary document. Concerning weather data, a summer reference year (SRY) weather dataset is generated taking into account heat extremes by calibrating the typical meteorological year (TMY) weather dataset at a weather station (22.32 N,114.17 E) in Hong Kong, using methods discussed in [15,16]. Four HVAC usage patterns and opening operation behaviours are simulated (a) No HVAC: regardless of thermal comfort. (b) Fan only: operated when indoor PMV > 0.5. (c) Fan-AC mixed cooling: fan operated if indoor environment (PMV < 0.5) can be reached

when indoor PMV > 0.5, if not AC is used. (d) AC cooling: if indoor PMV > 0.5, AC is used to achieve comfortable indoor environment.

3. RESULTS

3.1 Simulation Results

Since elderly spend most of the day at home, the analysis is based on an inactive occupancy schedule, providing a representative building performance assessment in summer.

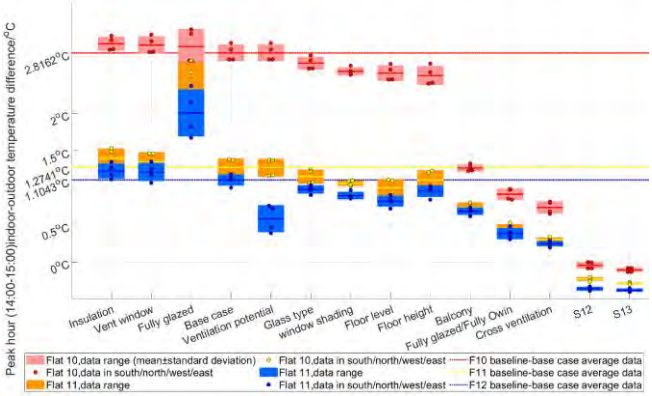

Figure 3: Range of Tpeak_dif for each strategy considering four building orientations, inactive schedule and fan-only.

The simulated results indicate that T_{peak_dif} (difference between the living room air temperature and outdoor ambient temperature at 14-15:00) is a useful indictor for evaluating the efficacy of each design strategy. In the base case of Flat 11 and 12 which are larger flats, T_{peak_dif} reaches approximately 1.5℃ (Figure 3). In a small west-facing fully glazed flat T_{peak_dif} can reach >3℃, which corresponds to a 6% rise in heat-related mortality rate among elderly. It is therefore, strongly discouraged to assign such apartments to the elderly. T_{peak_dif} is reduced as designs improve and becomes minimal for the best strategy S13. Moreover, T_{peak_dif} shows a consistent pattern with that of thermal comfort.

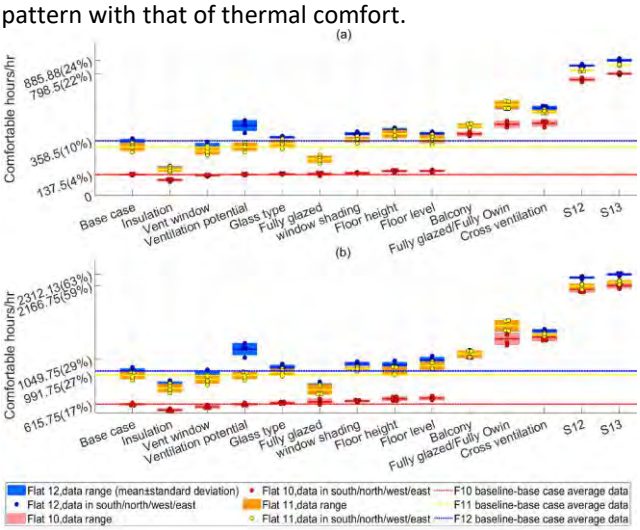

Figure 4: Summer comfortable time (PMV<0.5) of each design strategy considering 4 building orientations, under inactive schedule and (a) no-HVAC situation (b) Fan-only.

Without design improvements, the comfortable time for all flats is less than 10% of the total occupancy time, with smaller flats performing worst. The summer comfortable times for Flat10, Flat11, and Flat12 are 138 hours, 319 hours, and 339 hours, respectively, which correspond to 4%, 9%, and 9% of the total occupied time in the base case (Figure 4). The outcomes suggest that the thermal comfort gap between small and large flats can be narrowed with design improvements, and the best design strategy can increase the summer comfortable times of Flat 10, Flat 11, and Flat 12 to 21%, 23%, and 26% of the total occupied time, respectively (Figure 4). The use of a fan amplified the effects of each design strategy on indoor thermal comfort. By using a fan in the best strategy S13, comfortable times can be increased to 2167 hours, 2214 hours, and 2312 hours, which account for 59%, 60%, and 63% of the total occupancy time, respectively. In other words, the most optimal strategy S13 of Flat 12 with fan only requires 37% of total occupancy time (1358 hours) of AC cooling, whereas the smallest flat without design improvements and no use of fan requires 96% (3523 hours) of cooling. Figure 2 shows the most effective strategies are balcony, fully glazed/fully openable window, and cross ventilation, yet insulation and fully glazed window are the poorest strategies.

For our study it is important to consider both, thermal comfort, and cooling energy efficiency at the same time. This is to reduce the elderly's exposure to the duration and intensity of indoor heat if they do not use AC cooling, and to reduce electricity consumption if they opt to use AC. In practice, however, these two objectives are often conflicting. Figures 3 and 4 show strategies which enhance natural ventilation (increase opening size and create ventilation channels) are the most effective passive design strategies in a subtropical climate. Yet, natural ventilation brings more outdoor air which contains latent heat and inadvertently results in higher cooling loads. On the other hand, energy saving measures, such as adding insulation or reducing window size, results in higher indoor temperatures when air conditioning is not in use, causing even hotter indoor environment for non- air conditioning users. The most optimal strategy S13 yields the highest comfortable hours at around 800 hours for Flats 10-12, yet the cooling energy increases by at least 20-30% for all flat types (Figure 5).

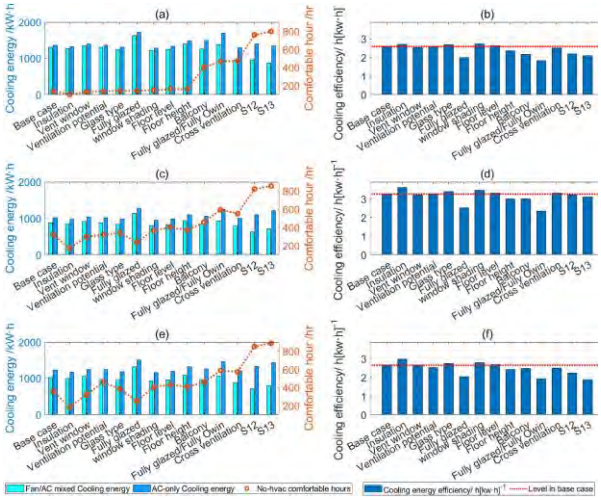

Figure 5: Cooling energy and comfortable hours for each strategy in: (a) Flat 10 (c) 11 (e) 12. Average air conditioning energy efficiency in: (b) Flat 10 (d) 11 (f) 12.

3.2 Knowledge transfer process

To demonstrate how our results can be meaningfully interpreted in the form of a guidebook with practical design strategies, we will only focus on the five indoor strategies that enhance natural ventilation (Figure 7). By translating our scientific results into simple design strategies, it is intended to achieve more impact and implementation in planning and architectural design, addressing Eliasson's framework of constraints. There are several reasons for the weak impact of urban climatology on planning. Eliasson [11] summarized these into 5 categories: conceptual and knowledge, communication, policy, organisational and market. The guidebook intends to fill these gaps in as follows (Figure 6).

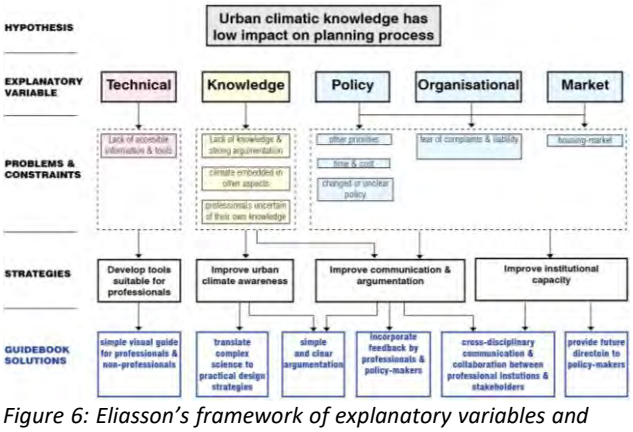

Figure 6: Eliasson's framework of explanatory variables and proposed solutions through the guidebook.

Firstly, the guidebook improves awareness on urban climate. It provides simple and clear argumentation justifying the need for climatic design consideration, translates complex science into simple design strategies, improves cross interdisciplinary communication by involving multiple professional institutions and stakeholders, and provides further consideration for policymakers thereby addressing institutional capacity.

For research to be impactful it should be easily accessible and understood by planners and architects to be implemented in practice. The transfer of scientific research knowledge to professionals and specialists entails practical problems of application. Research findings are challenging to apply in a practical context due to various reasons, such as an architect's formal training consists of graphic and visual medium to address the complexity of generating 3 dimensional designs for buildings and cities. To address the gap between climatology, building and urban design it is necessary to provide practitioners with an interpretation of scientific research that is comprehensible. Simple graphical presentation (Figures 8-11) in the form of a guidebook is an ideal medium to illustrate how professionals can apply research findings realistically during the early design phase.

3.3 Passive design implementation

To increase the impact of climatic knowledge it is thus necessary to enhance communication and argumentation between planners, architects, and policy makers, as well as the public. Scientific researchers must respond to practical needs of designers, architects, and planners by providing good arguments, appropriate visual tools, and methods such as those presented through the guidebook.

INDOOR STRATEGIES	SCORING	
VENTILATION		
Cross-ventilation	+ ❄❄❄❄	
Increase openable window area	+ ❄❄❄❄	
Optimal flat size with at least one bedroom	+ ❄❄❄	
More than one window in bedroom	+ ❄❄	
Maximise vertical opening distance	+ ❄	
Fully glazed facade with small/few openings		− ❄❄❄
SHADING & ORIENTATION		
Balcony	+ ❄❄	
Window shading elements	+ ❄	
Orientation: Living areas not facing west	+ ❄	
Orientation: Living areas facing west		− ❄
WINDOW GLAZING		
Low-E glass / Tinted glass	+ ❄	
OTHERS		
High floor level	+ ❄	
Reduce anthropogenic heat	+ ❄	

OVERALL SCORE	
Outstanding	❄ × 21
Exceeding Expectations	❄ × 14
Meeting Expectations	❄ × 10
Not Meeting Expectations	❄ × 6
Far Below Expectations	❄ × 4

Figure 7: Extracted from the guidebook, the effectiveness of each strategy investigated in the building simulations, is reflected in the scoring. This provides a user-friendly tool for architects and other design professionals.

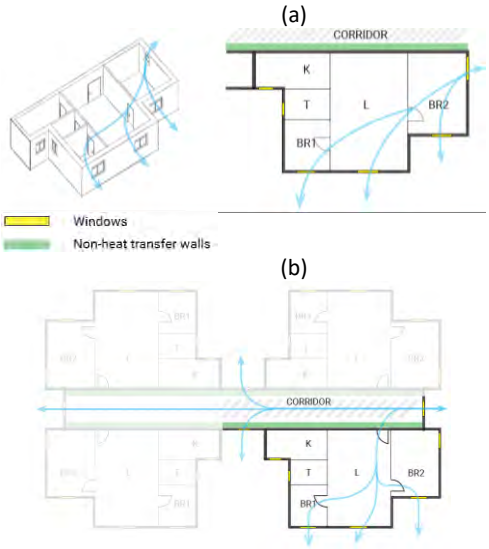

Figure 8: Design strategy illustrations extracted from the guidebook, cross ventilation through openings (a) and through opened door and corridor (b).

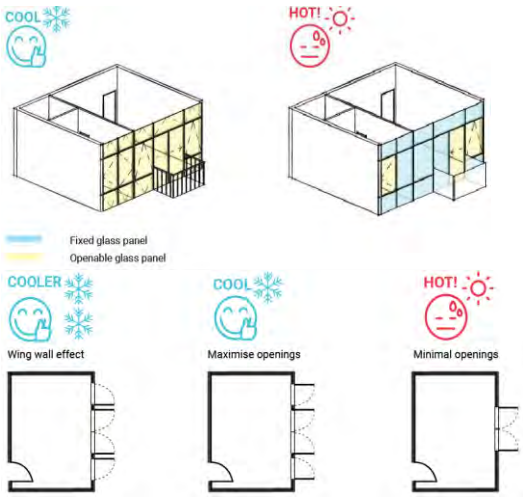

Figure 9: Design strategy illustrations extracted from the guidebook, increase openable window area.

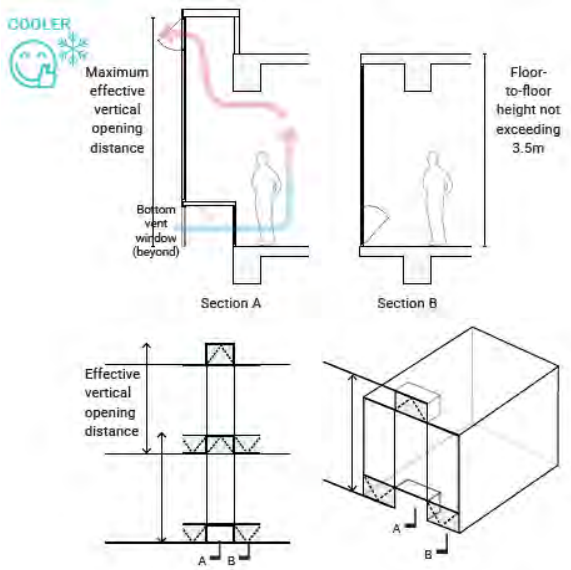

Figure 10: Design strategy illustrations extracted from the guidebook, maximum vertical opening distance.

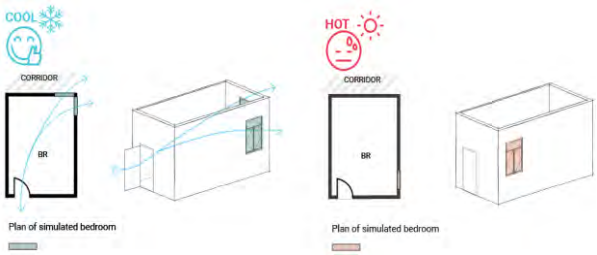

Figure 11: Design strategy illustrations extracted from the guidebook, more than one window in bedroom.

4. DISCUSSION

In the wake of climate change and increasing urban heat phenomena there is a rising demand for increasing knowledge about urban climate and certainly a necessity for improved tools to incorporate climatic knowledge into planning and architectural practice. Design professionals require training that is not purely based on theory but rather based on real world examples that show clearly how knowledge and research can be realistically implemented. Climate is inevitably entangled in broad-ranging context. Insufficient knowledge and a professional's lack of confidence leads to an absence of strong arguments and communication issues. Consequently, planning professionals demand better availability of information, improved methods, and user-friendly tools suitable to the planning process. One important suggestion is for researchers to provide professionals, decision-makers, policy makers and the public with clear arguments why these climatic principles should be employed in the planning and design of cities and buildings.

5. CONCLUSION

This study has provided strong arguments, design recommendations and planning guidance in a clear and simple manner that is user-friendly for architects, designers, developers, and co-professionals. These practical design strategies are based on the technical analysis of building simulation results. In doing so, we translated scientific knowledge in a graphic form suitable for architects, urban designers and other professionals. The guidebook on the built environment for the elderly in extreme hot weather, represents a visual tool that communicates how technical knowledge can be realistically applied as building and urban design strategies. To keep the study concise, we have limited the scope only to indoor strategies that enhance natural ventilation and focused on these to explain the process of knowledge transfer.

The indoor temperature of a 1BR or 2BR apartment without design improvment is around 1.5°C higher than outdoor temperature. For a small self-contained and west-facing studio, the temperature difference is over 3°C. A fully glazed façade with minimum openable window area

increases cooling loads by 20-30%. To protect the elderly from excessive exposure to heat stress, it is discrouaged to assign small studio apartments to them due to poor heat dissipitation. 1 or 2BR flats are more suitable for the elderly, as it allows for better heat dissipation and natural ventilation.

The simulation model is validated through in-situ measurements found in previous studies [17,18]. The simulation results reasonably quantify that proposed design strategies are effective in lowering indoor temperature, increasing comfort time, and reducing the need for AC cooling. Future studies could investigate the optimum flat size where at least two zones could be differently designed according to user behaviour. One room could be optimally designed for reducing cooling loads when air-conditioning is in use (PMV>0.5), where the other room could be optimised for thermal comfort during shoulder season when air-conditioning is not in use (PMV<0.5). This study is only limited to extreme heat in summer and it is necessary to examine an annual scenario since cold weather may cause other health implications, especially for the vulnerable elderly population

ACKNOWLEDGEMENTS

This study was supported by a grant from the Research Grants Council of Hong Kong (No. CU R4046-18F), the Hong Kong PhD Fellowship Scheme (No. PF21-60822) and the Chinese University of Hong Kong's Vice Chancellor's Scholarship.

REFERENCES

1. Luber, G.; McGeehin, M. Climate Change and Extreme Heat Events. *American Journal of Preventive Medicine* 2008, *35* (5), 429–435. https://doi.org/10.1016/j.amepre.2008.08.021.
2. Horton, R. M.; Mankin, J. S.; Lesk, C.; Coffel, E.; Raymond, C. A Review of Recent Advances in Research on Extreme Heat Events. *Curr Clim Change Rep* 2016, *2* (4), 242–259. https://doi.org/10.1007/s40641-016-0042-x.
3. Bell, J. E.; Brown, C. L.; Conlon, K.; Herring, S.; Kunkel, K. E.; Lawrimore, J.; Luber, G.; Schreck, C.; Smith, A.; Uejio, C. Changes in Extreme Events and the Potential Impacts on Human Health. *Journal of the Air & Waste Management Association* 2018, *68* (4), 265–287. https://doi.org/10.1080/10962247.2017.1401017.
4. Meerow, S.; Keith, L. Planning for Extreme Heat: A National Survey of U.S. Planners. *Journal of the American Planning Association* 2022, *88* (3), 319–334. https://doi.org/10.1080/01944363.2021.1977682.
5. Ipcc. *Global Warming of 1.5°C: IPCC Special Report on Impacts of Global Warming of 1.5°C above Pre-Industrial Levels in Context of Strengthening Response to Climate Change, Sustainable Development, and Efforts to Eradicate Poverty*, 1st ed.; Cambridge University Press, 2018. https://doi.org/10.1017/9781009157940.
6. Ho, J. Y.; Shi, Y.; Lau, K. K. L.; Ng, E. Y. Y.; Ren, C.; Goggins, W. B. Urban Heat Island Effect-Related Mortality under Extreme Heat and Non-Extreme Heat Scenarios: A 2010–2019 Case Study in Hong Kong. *Science of The Total Environment* 2023, *858*, 159791. https://doi.org/10.1016/j.scitotenv.2022.159791.
7. Naheed, S.; Eslamian, S. Chapter 17 Urban Vulnerability to Extreme Heat Events and Climate Change. In *Disaster Risk Reduction for Resilience: Disaster Risk Management Strategies*; Eslamian, S., Eslamian, F., Eds.; Springer International Publishing: Cham, 2022. https://doi.org/10.1007/978-3-030-72196-1.
8. Santos Nouri, A.; Costa, J.; Santamouris, M.; Matzarakis, A. Approaches to Outdoor Thermal Comfort Thresholds through Public Space Design: A Review. *Atmosphere* 2018, *9* (3), 108. https://doi.org/10.3390/atmos9030108.
9. Chan, E. Y. Y.; Goggins, W. B.; Kim, J. J.; Griffiths, S. M. A Study of Intracity Variation of Temperature-Related Mortality and Socioeconomic Status among the Chinese Population in Hong Kong. *J Epidemiol Community Health* 2012, *66* (4), 322–327. https://doi.org/10.1136/jech.2008.085167.
10. Oh, K.-Y.; Lee, M.-J.; Jeon, S.-W. Development of the Korean Climate Change Vulnerability Assessment Tool (VESTAP)—Centered on Health Vulnerability to Heat Waves. *Sustainability* 2017, *9* (7), 1103. https://doi.org/10.3390/su9071103.
11. Eliasson, I. The Use of Climate Knowledge in Urban Planning. *Landscape and Urban Planning* 2000, *48* (1–2), 31–44. https://doi.org/10.1016/S0169-2046(00)00034-7.
12. De Schiller, S.; Evans, J. M. Bridging the Gap between Climate and Design at the Urban and Building Scale: Research and Application. *Energy and Buildings* 1990, *15* (1–2), 51–55. https://doi.org/10.1016/0378-7788(90)90115-Y.
13. Ren, C.; Ng, E. Y.; Katzschner, L. Urban Climatic Map Studies: A Review: URBAN CLIMATIC MAP STUDIES: A REVIEW. *Int. J. Climatol.* 2011, *31* (15), 2213–2233. https://doi.org/10.1002/joc.2237.
14. Mills, G. Progress toward Sustainable Settlements: A Role for Urban Climatology. *Theor. Appl. Climatol.* 2006, *84* (1–3), 69–76. https://doi.org/10.1007/s00704-005-0145-0.
15. Lau, K. K.-L.; Ng, E. Y.-Y.; Chan, P.-W.; Ho, J. C.-K. Near-Extreme Summer Meteorological Data Set for Sub-Tropical Climates. *Building Services Engineering Research and Technology* 2017, *38* (2), 197–208. https://doi.org/10.1177/0143624416675390.
16. Jentsch, M. F.; Eames, M. E.; Levermore, G. J. Generating Near-Extreme Summer Reference Years for Building Performance Simulation. *Building Services Engineering Research and Technology* 2015, *36* (6), 701–727. https://doi.org/10.1177/0143624415587476.
17. Liu, S.; Kwok, Y. T.; Lau, K. K.-L.; Ouyang, W.; Ng, E. Effectiveness of Passive Design Strategies in Responding to Future Climate Change for Residential Buildings in Hot and Humid Hong Kong. *Energy and Buildings* 2020, *228*, 110469. https://doi.org/10.1016/j.enbuild.2020.110469.
18. Gao, K.; Fong, K. F.; Lee, C. K.; Lau, K. K.-L.; Ng, E. Balancing Thermal Comfort and Energy Efficiency in High-Rise Public Housing in Hong Kong: Insights and Recommendations. *Journal of Cleaner Production* 2024, *437*, 140741. https://doi.org/10.1016/j.jclepro.2024.140741.

Digital and Spatial Design Considerations in Healthy University Classrooms:

How can we make use of innovative digital tools to safeguard the health and well-being of occupants and improve IAQ?

FARAH SHOUKRY[1], SHERIF GOUBRAN[2,] KHALED TARABIAH[3]

[1]PhD Candidate, Environmental Engineering Program, the American University in Cairo
[2]Assistant Professor, Department of Architecture, the American University in Cairo
[3]Associate Professor, Department of Architecture, the American University in Cairo,

ABSTRACT: This research aims to investigate the design considerations of university classrooms post-pandemic. It investigates the following questions: (1) What are the lessons learned regarding health and well-being in the context of post-pandemic? (2) to what extent can we apply our learnings to design healthy university classrooms? (3) how can we use innovative digital tools to safeguard the health and well-being of occupants? The research employs a two-step qualitative research methodology. (1) Datal collection: which encompasses a brief literature review of recent academic articles and primary data collection through conducting two focus groups and three expert interviews. (2) Data analysis: Transcription of interviews and categorizing emergent topics. The research sets the foundation to develop a framework for classroom design that considers a multi-perspective of identified user needs: classroom interaction, architectural features, use of technology, and prioritizing the health and well-being of occupants, we support the evolving pedagogical approaches in university-level classrooms.
KEYWORDS: Learning Environments, Digital Tools, Spatial Considerations, IAQ guidelines, University, Classroom

1. INTRODUCTION

The COVID-19 pandemic posed transformative repercussions on education facilities around the globe. Schools and universities incurred several stages of adaption: lockdown measures, doors re-opening while applying COVID-19 measures, and incorporating digital solutions in an effort to limit face-to-face presence – including online learning, remote learning and blended learning methods (1).

What we can learn from scholars on the research subject, is that to design a healthy university classroom post the pandemic, we are to adopt health-promoting design principles, incorporate technology for both enabling online learning and to better monitor and improve the indoor conditions – whether it be air quality, thermal comfort or minimizing infections among students and educators. Incorporating the evolving pedagogical needs of the learning process is yet another dimension to consider. Thus, the space needs to accommodate many dynamics: collaborative learning, flexible seating arrangements, and individual study efforts.

This research attempts to clarify the design directions for a healthy university classroom, in an arid climatic zone, taking the perceptions of both students and educators in Cairo, Egypt. To this end, the research paper investigates the following questions: (1) what are our lessons learnt in the context of post-pandemic on health and well-being? (2) to what extent can we apply our learnings to design healthy university classrooms? (3) how can we use innovative digital tools to safeguard the health and well-being of occupants and improve Indoor Air Quality?

2. METHODS

The research adopts qualitative research approach to aggregate insights on optimal spatial design standards for educational buildings through a three-step research methodology: (1) Data collection: a brief literature review of recent academic articles, primary data collection through conducting two focus groups, and four expert interviews. (2) Data analysis: Transcription of focus groups and interviews and categorizing emergent topics in response to the main research question.

2.1 Data Collection

2.1.1 Focus Groups

The selected target group for both the focus group (FG) and interviews are practicing architects, environmental consultants, and health professionals with the necessary expertise to advise on design considerations for well-being in higher educational facilities. Both focus group and semi-structured interviews tackled the following topics: spatial design and its impact on learning, digital dimensions in

learning environments, the impact of COVID-19, design guidelines, and the integration of technology.

The first focus group (FG-01) targeted professionals (2 active participants out of 5). The second group (FG-02) was for young architects at both graduate and undergraduate students (6 active participants out of 7). The two FGs included a brainstorming exercise where participants were asked to visualize their ideas for a healthy university learning spaces that includes the digital dimension for health and well-being of occupants. The FGs were conducted online via Zoom to discuss the digital and spatial design considerations in university classrooms, emphasizing health and well-being. Each FG was 90 minutes long and included a total of 10 participants. The dates by which the FGs were conducted 9th of May and 22nd of May 2023.

2.1.2 Experts Interviews

Three experts' interviews were conducted for validation purposes – architecture and education fields of expertise. A semi-structured interview guide was designed with topics and sub-topics related to the main research questions for research validation. Given the expertise of each interviewee differed, so has the interview narrative. The interviews lasted 50 minutes each and were manually transcribed. All interviews were conducted online via Zoom with cameras open.

2.3 Primary Data Analysis

The analysis of the focus group transcriptions, and expert interviews transcriptions, as well as interview notes were analyzed via Atlas.ti software. The transcriptions were coded according to emergent topics, (32 codes) in total – refer to *Table 1: Transcription Codes*- below. Afterwards, the sub-topics analysed and key themes from reviewed literature were categorized in a tabular format. The results of this qualitative study is then used to inform the key features for classroom design and retrofitting in higher education institutions.

Table 1: Transcription Codes

Transcription Analysis Codes			
accessibility	digital learning	inclusive design	sense of belonging
acoustics	distraction	individual learning	teaching methods
air quality	energy	interactive learning tools	technology
behaviour	furniture	natural lighting	type of learning space
challenges	general comments	natural materials	ventilation
collaboration	greenery	pandemic and health	view
colour scheme	healthy indoors strategies	psychology	workshop objectives
design intervention	higher education	school design	zoning

3. RESULT AND ANALYSIS

3.1 Transcription Analysis

A qualitative analysis was conducted through Atlas.ti software, according to 32 codes, which were identified as the major topics. The sub-topics were then later organized into five main categories: external factors, architecture, technology, education, human-aspects.

3.2 Visual Analysis

The results of the focus group brainstorming activities have led to the generation of 8 conceptual design of classrooms, answering the research's investigation. The participants were engaged in the brainstorming design activity facilitated through the Google Slides platform. The exercise was focused on a virtual representation of a medium-sized classroom measuring approximately 16 meters by 4 meters. Alongside this visual abstraction, four distinct categories of icons were provided, enabling participants to showcase their ideas for creating a healthy university classroom. These categories included (a) furniture, (b) technology elements, (c) indoor air and occupant health-related features, and a (d) miscellaneous category for additional considerations.

The visual analysis, as depicted in *Figure 1*, took the form of a zoning diagram illustrating the spatial distribution of the elements placed by the participants. This diagram serves as a tool to analyze similarities and differences of patterns in the placement of various design elements within the classroom layout. As shown at the top of *Figure 1* a zoning key is present, consisting of ten categories. These categories differentiate between individual and group learning spaces – i.e. individual desk spaces versus a group furniture arrangement either for learning or lounging. Other categories highlight architectural elements: placement of doors and windows, and greenery. Finally, the technology aspects, include three categories: Internet of Things (IoT) controls, and augmented reality (AR), virtual reality (VR) equipment placement, as well as interactive learning tools. By examining this visual representation, insights into the collective preferences and priorities of the participants regarding classroom design emerged. The designs expressed similar themes in terms of user needs, and each had several unique features.

A summary of common trends identified through the visual analysis is presented in *Table 2*. This tabular representation offers a concise snapshot of emergent themes and design principles observed within the participants' design outcomes. Thus, providing valuable insights for informing future research-related discussions and decision-making processes related to classroom design.

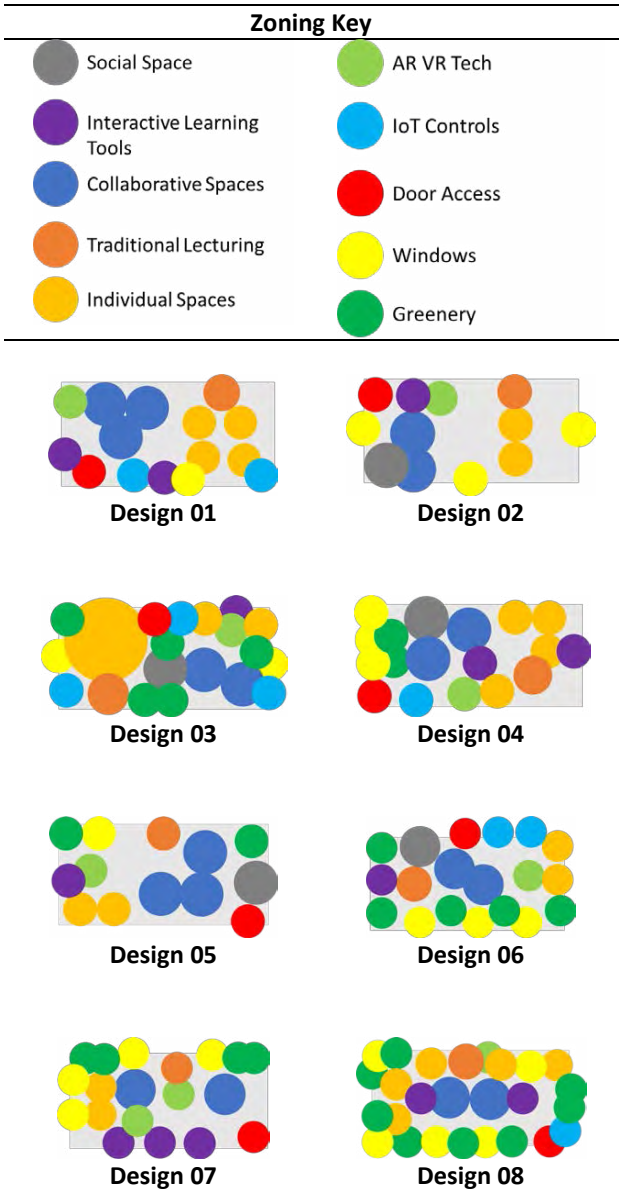

Figure 1: Focus Groups - Classroom Design Activity

Table 2: Focus Groups - Classroom Design Activity - Summary of Key Features

Design Feature	Description	Design Code
Flexible Design of Classrooms	Participants expressed the need for flexible design of classrooms that can accommodate several activities, furniture arrangements, and both individual and collaborative type os learning settings. The placement of doors was considered in terms of circulation, and the zoning of activities in terms of noise levels.	1, 3, 4, 5, 6, 7
Connection to the outdoors – greenery.	Windows placement attempted to maximize the view to the outdoors, assuming it was a good view. Another method was the use of green plants within the classrooms. The outdoors/greens correlated with increased productivity.	4,6,7,8
Cross Ventilation.	The placement of windows again was emphasized as important to encourage cross-ventilation in classrooms. In the case of the window, placement is not an option (retrofitting), use of fans is encouraged, for air change.	2,3,7,8
Hygiene and Personal Space	One interesting perspective that one of the participants voiced is the issue of hygiene. The personnel use of desks is encouraged in schools. It is also associated with the concept of vandalism. To decrease vandalism issues, the design of the classroom encourages students to have their own personal space [a designated desk space] which increases.	8
IOT and switch controls:	The participants expressed several ideas related to the use of switch controls and how having more than one switch control is better for the students. - HVAC. Temperature control - Temperature reading. To know if they should be opening the windows. - Lighting. To be segmented along the classroom activities.	1,3,4,6,8

4. DISCUSSION

When it comes to classroom design, research shows that occupant health, thermal comfort, and indoor air quality are all important factors to consider (2–9). However, the specific priorities may vary depending on the students' and faculty's context and needs. For example, in some cases, promoting occupant health may require prioritizing air filtration and ventilation, while acoustic and lighting design may be more important in other cases. The key is to take a holistic approach to classroom design and consider all factors that can impact occupant well-being and learning outcomes. This variation according to priorities was reflected in the visualization exercise in the conducted focus group. However, the multifaceted priorities do not mean that the design should only meet the top-tier. It means that the optimal design would manage to meet all, the sub-optimal would meet some.

A comfortable, attractive classroom came in as the key design objectives during the expert interview [E2]:

> *[For] building a new classroom, you would definitely need [many factors]. [Natural lighting] and good lighting, ergonomic furniture for communicating learning and, comfort of course. I'm not talking about any of these in any particular order. [Wayfinding]… It's accessible…Classrooms should be attractive to students by all means. It cannot be just focused on energy [performance or efficiency]. [It] has to be attractive and the attractiveness here means that you are comfortable. The light, the level of light inside is good. The chair that you sit on is comfortable ergonomically. There's some technology going around that allows you to interact and present well. It works. Basically, it's an environment that works…I would want to deliver an attractive learning environment for students and faculty. Without this, everything else will collapse [E2].*

Technology has significantly impacted classroom design in recent years, specifically post the pandemic. One of the key considerations is the need to design classrooms that can accommodate hybrid models of learning, such as blended learning and the flip classroom (10–12). This often requires a more flexible design approach accommodating different teaching methods and learning styles. Additionally, technology can be used to support student engagement and active learning, such as through the use of interactive displays and digital tools – E1.

Taking a step back, it is vital to understand the dynamics that takes place in the classroom. There is a wide body of literature which discusses the differences between teaching and learning methods (10–15).

The interview with the education expert has given us some insights on the classroom dynamics, especially with the traditional set-up in a lecture hall:

> *On teaching and learning methods. So for example, let's give the example of lecturing lecture based. OK, so lecture based is the oldest [approach known to humankind]. …. You're lecturing , [as in] the faculty member, has all the knowledge, the student, are listening and by default we assume they're…So just because I'm teaching, I'm assuming my students are learning and this is a false assumption, right? The learning isn't happening except for those students that are very engaged, driven internally, intrinsically motivated, and learning by listening. The short or even the long term retention is like 10 to 15% [of what you have learnt]. So you know that's saying what you remember 10% of what you listen to and 20% of what you watch and 80% of what you [memorize?]…So if a faculty member is lecturing, we call that one way one way transmission of information… the learning space is usually set up as it's been set up for over 150 years, which is like the industrial kind of set up, you know, rows of students [E1].*

We can deduce that teaching and learning are two-way interactions between the learner, educator, and the surrounding space. The dynamics represent interconnected yet distinct dimensions of education. The traditional concept of teaching often conjures the image of an educator imparting knowledge to a group of students within a designated physical space; the lecturing model is the oldest known to humankind. In this model, the teacher serves as the primary source of information, and students act as receptors of that knowledge. However, the effectiveness of teaching is not only judged by the ability of the lecturer to recite information; it is also dependent on the student's capabilities to process information, and thus, the learning happens. Learning is students' active engagement and assimilation of knowledge, transforming information into meaningful understanding (16). Effective teaching is inseparable from learners' dynamic interaction with and absorption of knowledge.

That being said, the recent trends in learning spaces, is moving away from the traditional lecturing set-up, and considering more flexible arrangements to allow for collaborative learning methods to take place; an opinion which was expressed graphically during the classroom visualization exercise, as well by the education expert:

> *The outdated design of lecture halls now is being revisited as being more flexible, so I've been in lecture halls where you can move the table and the chair and kind of zoom in to someone else and work in a pair or turn around completely and work in a group of four or six [E1].*

On the practical side, designing classrooms for hybrid models of learning can be challenging, as it requires balancing the need for technology and digital resources with the need for a physical classroom environment that promotes student engagement and learning outcomes. Some successful strategies include designing flexible spaces that can be easily reconfigured for different teaching and learning needs, and incorporating a mix of digital and physical resources to support learning. The pandemic experience has been very challenging in terms of the timeframe to which the education model had to shift to a remote method at its initial phase, before resorting to a hybrid mode. On this particular point in time, an architectural educator reflects [E3]:

> *The COVID experience has been very challenging, specifically with the architectural practice. The main medium is sketching, and drawing. [learning remotely] has taken away this medium, and it very challenging to be compensated. When learning remotely, [as an educator] you have to do double or triple the effort, in order to communicate effectively with the students. … The positive note, however, is there is time to reflect, for example, when giving feedback. On the students' side, though, I am not sure how they would receive this feedback, as there was no*

discussion to explain the logic…overall very challenging [E3].

Using classroom space efficiently is important for promoting student engagement and active learning. The focus group visualization exercise showed that creating an engaging and interactive learning environment is possible by creative zoning of space. This can be achieved through a variety of design strategies, such as using modular furniture that can be easily reconfigured, designing spaces for group work and collaboration, and incorporating technology that supports different teaching and learning styles – refer to Figure 4. The architectural design discipline is inter-related. For example, while we know that furniture and other classroom features play an important role in promoting student comfort and engagement; we also have to plan for its functionalities. If we design for a collaborative learning space, we have to mitigate the consequences: noise [E1]:

But the more flexible the furniture, the more flexible the learning space, the better the acoustics [has to be]… because collaboration is noisy. So if you're in a room that doesn't have good acoustics,… then there's going to be a lot of noise that is going to be counterproductive to the learning. So students will often say, can we go work outside? it's too noisy [E1].

Moving on to the digital dimension, digital tools and devices can be used to support a variety of classroom activities, such as collaborative learning, real-time feedback, and active engagement. As emphasized by the architectural practitioner [E2], it is essential to distinguish between two types of technologies used inside the classroom. One has to do with teaching and learning, and the other is associated with building controls and infrastructure [E2]. Giving an example on the Leutron Systems within classrooms, [E2] illustrates:

Instructors get in, for example, they put their login ID and password and the room sets itself. It brings the blackout shades down. It sets the dimming. Adjusts the light scenes. And then it opens up the lecture on the projector and you know, brings it up to students by just putting a password The instructor, adjust(s) the whole set of the classroom according. That's called the Lutron system because it combines and integrates physical issues like blackout shades with lighting and with AV audio visual technologies[E2].

This type of technologies – teaching and learning technologies – is significantly different than the ones associated with the smart building controls, for example to monitor indoor air quality. As explained by [E2] the most typical solution is the use of sensors, in the air ducts: "Which will analyse the air that's coming back collected from the classroom. …Analyse that for CO2 levels…. Sends a signal to the Air handling unit to give more fresh air [E2]."

It is high time that we think of conditions to be more personalized. Having individual lighting, even air conditioning outlets. Very small things, that are common in the shared spaces, that are absent in the learning space. For example when you travel on a bus, or the airplane, you get to control the amount of air through the nozzle. But you don't have this level of control in the classroom. This is on the systems level. While keeping, as well, an open and flexible set-up in terms of technology and seating arrangements [FG 02 – Participant].

If we use architectural pedagogy as a practical application for the healthy classroom design conversation post-pandemic, we understand the discipline is continually evolving, and there is a notable departure from the traditional architectural methods. The discipline is being revolutionized by the advances in virtual platforms and artificial intelligence engines. This shift will be further complicated by the expectations of users learning, and the educators teaching. This calls for a re-evaluation of the design expectations and considerations of a healthy university classroom design: a practical application.

5. CONCLUSION

The research set was to investigate the design requirements of a university classroom post-pandemic and validate the following: (1) Students' and educators' health and well-being are at the forefront of objectives when designing a learning space. (2) the expectations of students and educators has exponentially heightened in light of the dramatic digital shift of education post – pandemic, and the focus group summary of key features to consider listed the majority of dimensions we are encouraged to look at the healthy classroom design considerations. Finally, (3) the ever-changing and advancing technologies can both aid in promoting an engaging learning environment and enhance building performance controls that explicitly influence occupants' health and well-being. The research holds its potential to guide several follow-up research investigations – including:

- developing a thorough framework for classroom design considering classroom interaction, architectural features, use of technology, and prioritizing the health and well-being of occupants, as well as support the evolving pedagogical approaches in university-level classrooms.
- testing the validity of the proposed framework in its contextual application,
- generating a gap analysis report to existing standards and guidelines of recent learning spaces manuals at a university level, and
- debating the future of the architectural discourse in light of recent technological advancements and debates.

ACKNOWLEDGEMENTS

We extend our heartfelt gratitude to Engaged Sustainable Futures for their invaluable support throughout this research endeavor. Special appreciation is extended to the Centre for Learning and Teaching at the American University in Cairo for their unwavering dedication to enhancing learning spaces. We also express our sincere thanks to the Department of Architecture and the Architecture Alumni Association for their ongoing initiatives in bringing distinguished lecturers to engage in discussions about the future of architectural discourses. For all, thank you, your perspectives have helped us shape this research outcome. The research received Graduate Support Grant Award | PHD Exchange Grant (R45), from the American University in Cairo. This study was approved by the Institutional Review Board (IRB) of the American University in Cairo. All participants provided written or verbal, informed consent prior their participation in the study (Case# 2022-2023-010).

REFERENCES

1. Daftary MN, Jorden J, Habib M, Pather I, Tofade T. Implementing virtual experiences and remote assessments during the COVID-19 pandemic: A college experience: Innovation in experiential learning or assessment. Pharmacy Education [Internet]. 2020 Sep 6 [cited 2020 Dec 18];54–5. Available from: https://pharmacyeducation.fip.org/pharmacyeducation/article/view/1149

2. Agarwal N, Meena CS, Raj BP, Saini L, Kumar A, Gopalakrishnan N, et al. Indoor air quality improvement in COVID-19 pandemic: Review. Sustainable Cities and Society [Internet]. 2021 Jul 1 [cited 2022 Sep 8];70:102942. Available from: https://www.sciencedirect.com/science/article/pii/S2210670721002274

3. Alonso A, Llanos J, Escandón R, Sendra JJ. Effects of the COVID-19 Pandemic on Indoor Air Quality and Thermal Comfort of Primary Schools in Winter in a Mediterranean Climate. Sustainability [Internet]. 2021 Mar 3 [cited 2021 Sep 23];13(5):2699. Available from: https://www.mdpi.com/2071-1050/13/5/2699

4. Anand P, Cheong D, Sekhar C. A review of occupancy-based building energy and IEQ controls and its future post-COVID. Science of The Total Environment [Internet]. 2022 Jan 15 [cited 2022 Sep 26];804:150249. Available from: https://www.sciencedirect.com/science/article/pii/S0048969721053262

5. Jia LR, Han J, Chen X, Li QY, Lee CC, Fung YH. Interaction between Thermal Comfort, Indoor Air Quality and Ventilation Energy Consumption of Educational Buildings: A Comprehensive Review. Buildings. 2021 Nov 28;11(12):591.

6. Kallawicha K, Wongsasuluk P, Chao HJ. Modern Solutions for Indoor Air Quality Management in Commercial and Residential Spaces. In: Saini J, Dutta M, Marques G, Halgamuge MN, editors. Integrating IoT and AI for Indoor Air Quality Assessment [Internet]. Cham: Springer International Publishing; 2022 [cited 2022 Sep 8]. p. 73–88. (Internet of Things). Available from: https://doi.org/10.1007/978-3-030-96486-3_6

7. Marzouk M, Atef M. Assessment of Indoor Air Quality in Academic Buildings Using IoT and Deep Learning. Sustainability [Internet]. 2022 Jan [cited 2022 Sep 8];14(12):7015. Available from: https://www.mdpi.com/2071-1050/14/12/7015

8. Saini J, Dutta M, Marques G. Indoor Air Quality and Internet of Things: The State of the Art. In: Saini J, Dutta M, Marques G, editors. Internet of Things for Indoor Air Quality Monitoring [Internet]. Cham: Springer International Publishing; 2021 [cited 2022 Sep 8]. p. 33–50. (SpringerBriefs in Applied Sciences and Technology). Available from: https://doi.org/10.1007/978-3-030-82216-3_3

9. Saini J, Dutta M, Marques G. Predicting Indoor Air Quality: Integrating IoT with Artificial Intelligence. In: Saini J, Dutta M, Marques G, editors. Internet of Things for Indoor Air Quality Monitoring [Internet]. Cham: Springer International Publishing; 2021 [cited 2022 Sep 8]. p. 51–67. (SpringerBriefs in Applied Sciences and Technology). Available from: https://doi.org/10.1007/978-3-030-82216-3_4

10. Francis N, Morgan A, Holm S, Davey R, Bodger O, Dudley E. Adopting a flipped classroom approach for teaching molar calculations to biochemistry and genetics students. Biochem Molecular Bio Educ [Internet]. 2020 May [cited 2023 Oct 30];48(3):220–6. Available from: https://iubmb.onlinelibrary.wiley.com/doi/10.1002/bmb.21328

11. Gravett K, Baughan P, Rao N, Kinchin I. Spaces and Places for Connection in the Postdigital University. Postdigit Sci Educ [Internet]. 2022 Jun 18 [cited 2023 Feb 7]; Available from: https://doi.org/10.1007/s42438-022-00317-0

12. Nortvig AM, Petersen AK, Balle SH. A Literature Review of the Factors Influencing E-Learning and Blended Learning in Relation to Learning Outcome, Student Satisfaction and Engagement. Electronic Journal of e-Learning [Internet]. 2018 [cited 2020 Dec 14];16(1):46–55. Available from: https://eric.ed.gov/?id=EJ1175336

13. Davis D. Improving Student Learning With A More Effective Teaching Environment. In: 2005 Annual Conference Proceedings [Internet]. Portland, Oregon: ASEE Conferences; 2005 [cited 2023 Oct 30]. p. 10.731.1-10.731.8. Available from: http://peer.asee.org/15542

14. García-Morales VJ, Garrido-Moreno A, Martín-Rojas R. The Transformation of Higher Education After the COVID Disruption: Emerging Challenges in an Online Learning Scenario. Frontiers in Psychology [Internet]. 2021 [cited 2023 Apr 5];12. Available from: https://www.frontiersin.org/articles/10.3389/fpsyg.2021.616059

15. Kim N. Architectural Design Approach of New Medical Education Building Fit for Pedagogy Changes. Korean Med Educ Rev [Internet]. 2015 Oct 31 [cited 2023 Oct 30];17(3):97–104. Available from: http://kmer.or.kr/journal/view.php?doi=10.17496/kmer.2015.17.3.97

16. Munna AS, Kalam MA. Teaching and learning process to enhance teaching effectiveness: literature review. IJHI [Internet]. 2021 Feb 3 [cited 2023 Dec 3];4(1):1–4. Available from: http://humanistudies.com/ijhi/article/view/102

PLEA 2024 WROCŁAW
(Re)thinking Resilience

Effects of Perceived Housing Environment Qualities on Mental Wellbeing and Satisfaction in a Dense Chinese City

A Cross-sectional Survey during the COVID19 Pandemic

YONG HE[1], DIXIN ZHANG[1], XI ZHANG[2], JIANGTAO DU[2]

[1]College of Architecture and Urban Planning, Tongji University, China
[2] Liverpool School of Architecture, University of Liverpool, Liverpool, UK

ABSTRACT: Housing environment is one of determinants for occupants' physical and mental health, especially during the COVID19 pandemic. This article presents a cross-sectional study of effects of perceived housing environment qualities on mental wellbeing in Shanghai city. A structured survey was administered among 317 adults living in Shanghai during two COVID19 periods (January 2021 & April 2022). Perceived housing environmental qualities investigated were Living and Housing Conditions (12 items), Biophilic Factors (seven items), Indoor Climates (seven items), and Perceived Residential Environmental Qualities (six items). Quality of Life (QoL), Overall Satisfaction (OS), and Psychological Restoration (PRS) were tested as dependent variables. Several key findings were achieved as follows. 1) There were significant correlations between typical housing environmental qualities and dependent variables. 2) The linear regression analyses identified the significant predicting effect of Indoor Climate for QoL, OS, and PRS. 3) The predicting effect of Perceived Residential Environmental Qualities can be found for only OS and PRS. 4) Window view can significantly predict the PRS, while the PRS cannot receive significant impact from the indoor plant. 5) Several housing factors (e.g., home floor, home area, occupancy, and satisfaction of room numbers) can also be the predictors for the three dependent variables.
KEYWORDS: Perceived housing environment, Mental wellbeing, Satisfaction, Residential buildings, Shanghai

1. INTRODUCTION

Recent studies have shown that the increasing urbanization can bring in big challenges to residents' health in various urban areas for both wealthy and poor populations [1, 2, 3]. Typical health problems caused by the urbanization include pollution-related health conditions and communicable diseases, poor sanitation and housing conditions, and related health conditions [1]. As proved by investigations [1, 2], people who have lived in urban houses with poor environmental conditions for a long period may suffer from various health problems, especially for the mental aspects. Therefore, the World Health Organization (WHO) has clearly pointed out that improving housing conditions can save lives, prevent disease, increase quality of life, and help mitigate climate change [3].

Evidence achieved in several countries has shown that the housing environment is one of the determinants for occupants' physical and mental health. Two cross-sectional surveys in USA and Japan found that general housing conditions were associated with residents' respiratory health and sick building syndrome [4, 5]. A survey in Sweden identified that noise, light, odour, and vibration can be the typical stressors for the urban residents living in their homes [6], while maintaining a comfortable thermal environment at home could be critical for residents' mental health in Japan [7]. In addition, with the advent of application of biophilia in buildings, it has been emphasized that biophilic elements (e.g., blue sky, sunlight, and plants) inside one's own home can support integrative health and lifestyle behaviours and promote resilience [8]. To achieve a sustainable and healthy housing quality, two rating systems have been developed in two countries [9, 10]. The Housing Health and Safety Rating System in UK aimed to help local authorities identify and protect against potential risks to health and safety from deficiencies in dwellings [9], whilst the National Healthy Housing Standard in USA was developed to empower and equip local communities to improve residents' health by improving housing quality [10].

Due to the rapid growth of urbanization in China, the residential areas in cities are facing a dramatic degradation of environmental qualities, which may bring in a number of environmental problems relating to residents' health [11]. As pointed out in a nationwide cross-sectional survey in China [11], urban housing factors and neighbourhood conditions were related to health outcomes (physical & mental) whilst their impacts varied across different age groups. As for mental health issues, studies have preliminarily exposed that both indoor and outdoor housing environments can significantly affect the psychological well-being or life satisfaction among city residents [12, 13]. At the moment, there are two national standards which can be used to support the design of healthy

housing in China, including 'Evaluating Standard for Healthy Housing (T/CECS 462-2017)' [14] and 'Assessment Standard for Healthy Community (T/CECS 650-2020)' [15]. However, only general design strategies can be found from these standards and there is still a lack of detailed guidelines used for the achievement of practical solutions. Thus, it could be necessary to carry on collecting more solid evidence on perceived housing environment qualities and their specific effects on mental health among Chinese urban residents.

This article presents a cross-sectional survey of the relationship between perceived housing environment qualities and residents' mental wellbeing and satisfaction in Shanghai city during the period of COVID19 pandemic, aiming to develop useful practical design strategies to promote the health housing in a dense city.

2. METHODS AND MATERIALS

2.1 Online survey: location, approach, and respondents

This survey was conducted among adult residents living in Shanghai city (31.2304° N, 121.4737° E), which is the country's biggest city and a global financial hub.

An online survey was administered through a social media (WECHAT) and a survey tool (Sojump, www.wjx.cn) during two periods of COVID19 (January 2021 & April 2022).

Finally, a total of 317 questionnaires were found as valid (response rate: 66%). Key demographic and socioeconomic status of respondents were as follows: male (42.9%), female (57.1%); age: 41% (18-35 years), 56.2% (36-59 years), 2.8% (≥ 60 years); marital status: married (64%), single (36%).

2.2 Research design and instruments

The research design of this survey can be found in Figure 1, including independent and dependent variables and three research paths. Four types of independent variable and three types of dependent variables were used as the instrument in this survey. The independent variables included 1) Living and Housing Conditions (12 items): housing location (H_loc), the duration of your living (H_dur), the floor of your home (H_flo), total area of your home (H_are), housing ownership (H_own), occupancy of your home (H_occ), number of bedroom (H_bed), satisfaction of room size (H_sa_s), satisfaction of room layout (H_sa_l), satisfaction of room number (H_sa_n), availability of unshared room (H_un_r), room to stay (H_ro), 2) Biophilic Factors (seven items): size of window (W_siz), orientation of window (W_ori), availability of window protection devices (W_pro), amount of indoor plant (In_pla), the first most viewed external content (View1), the second most viewed external content (View2), the third most viewed external content (View3), 3) Indoor Climates (In_cli, seven items), 4) Perceived Residential Environmental Qualities (PREQ, six items). Three dependent variables were applied as: Quality of Life (QoL, five items), Overall Satisfaction (OS, one item), Psychological Restoration (PRS, three items). The covariates comprised five items: age, gender, marital status (Mar_sta), educational status (Edu_sta), and job status (Job_sta).

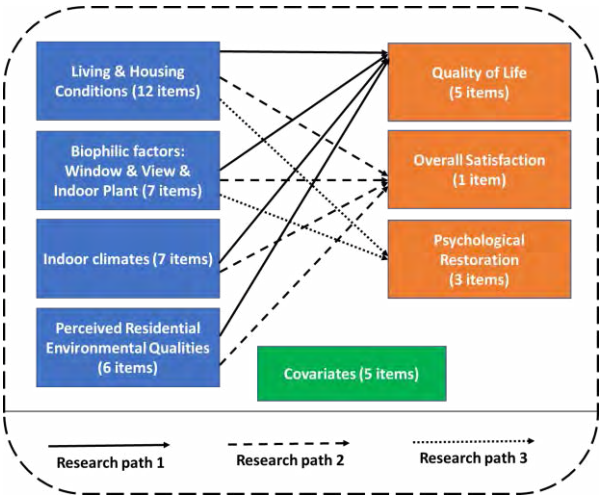

Figure 1: Research design: variables and three research paths. (Blue: independent variables, Brown: dependent variables, Green: covariates).

Three hypothesized research paths were tested as: 1) the association between four independent variables and quality of life; 2) the association between four independent variables and overall satisfaction; 3) the association between living & housing conditions / biophilic factors (window & view & indoor plants) and psychological restoration.

2.3 Statistical analysis

A correlation analysis was applied between independent and dependent variables, while a series of linear regression analyses were conducted to test the three research paths above (as shown in Figure 1).

3. RESULTS

Three parts of key results are presented, including correlation analysis and the effects of perceived housing environmental qualities on Quality of Life, Overall Satisfaction, and Psychological Restoration.

3.1 Correlation analysis: key variables

The correlation analysis was conducted between four types of independent variables (Living & Housing Conditions, Biophilic Factors, Indoor Climates, and Perceived Residential Environmental Qualities) and three dependent variables (QoL, OS, PRS).

Table 1: Significant correlations between four types of independent variables and QoL, OS, PRS. (n=317)

Variables	r	Variables	r
H_dur & OS	0.122*	W_siz & PRS	-0.181**
H_are & OS	0.299**	W_ori & OS	-0.117*
H_are & PRS	0.187**	W_pro & QoL	0.126*
H_own & OS	-0.197**	W_pro & OS	0.133*
H_bed & OS	0.212**	W_pro & PRS	0.148**
H_bed & PRS	0.153**	In_pla & OS	0.116*
H_sa_s & OS	0.364**	In_pla & PRS	0.145**
H_sa_s & PRS	0.319**	View1 & OS	-0.206**
H_sa_l & OS	0.386**	View1 & PRS	-0.271**
H_sa_l & PRS	0.270**	In_cli & QoL	0.258**
H_sa_n & OS	-0.144*	In_cli & OS	0.386**
H_un_r & QoL	0.157**	In_cli & PRS	0.390**
H_un_r & OS	0.264**	PREQ & QoL	0.168**
H_un_r & PRS	0.257**	PREQ & OS	0.574**
W_siz & OS	-0.178**	PREQ & PRS	0.421**

*Significant: **≤0.01, *≤0.05.*

Table1 gives significant correlations between the independent and dependent variables (p≤0.05). Four types of independent variables significantly correlate with QoL, OS and PRS separately.

QoL can positively correlate with only one item of Living & Housing Conditions or Biophilic Factors: QoL & availability of unshared room (r = 0.157, p ≤ 0.01), QoL & availability of window protection devices (r = 0.126, p ≤ 0.05).

OS positively correlates with six Living and Housing Conditions, such as duration of living (r = 0.122, p ≤ 0.05), total area of home (r = 0.299, p ≤ 0.01), number of bedroom (r = 0.212, p ≤ 0.01), satisfaction of room size (r = 0.364, p ≤ 0.01), satisfaction of room layout (r = 0.386, p ≤ 0.01), and availability of unshared room (r = 0.264, p ≤ 0.01). Two items of Biophilic Factors (availability of window protection devices & amount of indoor plant) are also positively correlated with OS (r = 0.133 & r = 0.116, p ≤ 0.05). Negative correlations are found between OS and two Living and Housing Conditions: housing ownership (r = -0.197, p ≤ 0.01) and satisfaction of room number (r = -0.144, p ≤ 0.05). In addition, OS negatively correlates with three Biophilic Factors: size of window (r = -0.178, p ≤ 0.01), orientation of window (r = -0.117, p ≤ 0.05), and the first most viewed external content (r = -0.206, p ≤ 0.01).

PRS can positively correlate with five Living and Housing Conditions: total area of home (r = 0.187, p ≤ 0.01), number of bedroom (r = 0.153, p ≤ 0.01), satisfaction of room size (r = 0.319, p ≤ 0.01), satisfaction of room layout (r = 0.270, p ≤ 0.01), availability of unshared room (r = 0.257, p ≤ 0.01). Two Biophilic Factors are positively correlated with PRS: availability of window protection devices (r = 0.148, p ≤ 0.01) and amount of indoor plant (r = 0.145, p ≤ 0.01). Two Biophilic Factors are negatively correlated with PRS: size of window (r = -0.181, p ≤ 0.01) and the first most viewed external content (r = -0.271, p ≤ 0.01).

Indoor Climates and Perceived Residential Environmental Qualities are positively correlated with QoL, OS and PRS (p ≤ 0.01).

In addition, there were no significant correlations found between the following variables (p > 0.05): QoL & 11 Living and Housing Conditions (housing location, floor of home, occupancy of your home, room to stay, duration of living, total area of your home, housing ownership, number of bedroom, satisfaction of room size, satisfaction of room layout, satisfaction of room number), QoL & six Biophilic Factors (size of window, orientation of window, amount of indoor plant, View1, View2, View3), OS & four Living and Housing Conditions (housing location, floor of home, occupancy of your home, room to stay), OS & two Biophilic Factors (View2, View3), PRS & seven Living and Housing Conditions (housing location, floor of home, occupancy of your home, room to stay, duration of living, housing ownership, satisfaction of room number), PRS & three Biophilic Factors (orientation of window, View2, View3).

3.2 Effects of housing environmental qualities on Quality of Life (QoL)

In Table 2, a regression analysis is presented in terms of the prediction of quality of life from independent variables and covariates.

Table 2: Regression analysis: the prediction of Quality of Life from independent variables and covariates.

	Model1		Model2		Model3	
	B	SE	B	SE	B	SE
Constant	55.7**	11.35	-1.03	20.16	-8.29	23.41
Win_siz	-2.03	1.66	-1.35	1.63	-0.65	1.64
Win_ori	0.58	0.65	0.63	0.65	0.83	0.65
Win_pro	6.96*	3.27	5.83	3.25	6.52*	3.27
In_pla	-0.26	1.47	-0.68	1.44	-1.03	1.44
View1	-3.68	2.88	-2.82	3.01	-3.84	3.00
View2	0.53	2.78	1.32	2.74	1.03	2.75
View3	-1.78	2.60	-1.82	2.59	-1.15	2.58
H_loc			0.61	1.11	0.97	1.13
H_dur			2.17	1.14	1.81	1.18
H_flo			2.43*	1.09	2.18*	1.08
H_are			-5.23**	1.96	-5.41**	1.99
H_own			3.90	3.37	4.84	3.50
H_occ			1.23	2.35	0.33	2.38
H_bed			1.47	2.45	1.76	2.43
H_sa_s			-1.59	1.64	-1.20	1.64
H_sa_l			0.02	1.58	-0.41	1.58
H_sa_n			-2.93	1.68	-3.40*	1.68
H_un_r			3.60	1.90	3.62	1.91
H_ro			-1.65	0.99	-1.35	1.04
In_cli			10.1**	2.82	9.44**	2.84
PREQ			3.16	2.21	3.43	2.19
Age					1.25	2.53
Gender					7.43**	2.69
Mar_sta					-4.18	4.07
Edu_sta					0.47	1.81
Job_sta					-1.58	1.31
R^2		*0.03*		*0.15*		*0.18*

*Significant: **≤0.01, *≤0.05.*

Model1 shows that the availability of window protection devices has a significant positive predicting effect on the Quality of Life (B = 6.96, p ≤ 0.05). When the other three types of housing environmental qualities enter the regression (Model2), the effect tends to be insignificant (p > 0.05). The floor of home and Indoor Climates show positive effects (p ≤ 0.01), while the total area of home has a negative effect (B = -5.23, p ≤ 0.01).

When the covariates are added (Model3), the predicting effects of independent variables in Model2 can still be found as significant. The availability of window protection devices has a positive predicting effect on Quality of Life, while satisfaction of room number shows a negative effect. For the covariates, only the effect of gender is significant (p ≤ 0.01). The variables in Model3 can explain 18% of the variance Quality of Life.

3.3 Effects of housing environmental qualities on overall satisfaction (OS)

Table 3 shows the prediction of overall satisfaction from independent variables and covariates through a regression analysis.

Table 3: Regression analysis: the prediction of Overall Satisfaction from independent variables and covariates.

	Model1		Model2		Model3	
	B	SE	B	SE	B	SE
Constant	8.41**	0.77	1.48	1.14	-0.78	1.33
Win_siz	-0.26*	0.11	-0.12	0.09	-0.10	0.09
Win_ori	-0.05	0.04	-0.05	0.04	-0.04	0.04
Win_pro	0.51*	0.22	0.12	0.18	0.12	0.19
In_pla	0.10	0.10	0.06	0.08	0.04	0.08
View1	-0.73**	0.19	-0.20	0.17	-0.20	0.17
View2	-0.38*	0.19	-0.09	0.16	-0.08	0.16
View3	-0.16	0.18	0.00	0.15	-0.01	0.15
H_loc			0.02	0.06	0.04	0.06
H_dur			-0.01	0.06	-0.02	0.07
H_flo			0.06	0.06	0.05	0.06
H_are			0.05	0.11	0.09	0.11
H_own			-0.32	0.19	-0.45*	0.20
H_occ			0.17	0.13	0.20	0.13
H_bed			-0.06	0.14	-0.06	0.14
H_sa_s			0.09	0.09	0.11	0.09
H_sa_l			0.16	0.09	0.13	0.09
H_sa_n			-0.16	0.10	-0.20*	0.10
H_un_r			0.04	0.11	0.00	0.11
H_ro			0.00	0.06	-0.04	0.06
In_cli			0.33*	0.16	0.31*	0.16
PREQ			1.14**	0.13	1.12**	0.12
Age					0.13	0.14
Gender					0.24	0.15
Mar_sta					0.39	0.23
Edu_sta					0.25*	0.10
Job_sta					0.09	0.07
R^2		*0.11*		*0.45*		*0.47*

*Significant: **≤0.01, *≤0.05.*

It is found in Model1 that four Biophilic Factors can have predicting effects on Overall Satisfaction. The availability of window protection device has a positive predicting role (B = -0.26, p ≤ 0.05), while the size of window has a negative effect (B = 0.51, p ≤ 0.05). The significant predicting effects are also found at View1 (p ≤ 0.01) and View2 (p ≤ 0.05).

When the other independent variables are added (Model2), the predicting effects of the four Biophilic Factors tend to be insignificant (p > 0.05). Both Indoor Climates and PREQ have positive effects on Overall Satisfaction.

When the covariates are added (Model3), the predicting effects of Indoor Climates (B = 0.31, p ≤ 0.05) and PREQ (B = 1.12, p ≤ 0.01) remain significant. The significant predicting role can be also found at education status and two housing conditions (p ≤ 0.05). The variables in Model3 can explain 47% of the variance in Overall Satisfaction.

3.4 Effects of housing environmental qualities on psychological restoration (PRS)

Table 4 indicates the predicting effect on the psychological restoration from independent variables and covariates through a regression analysis.

Table 4: Regression analysis: the prediction of Psychological Restoration from independent variables and covariates.

	Model1		Model2		Model3	
	B	SE	B	SE	B	SE
Constant	4.31**	0.39	1.24	0.65	1.35	0.76
Win_siz	-0.13*	0.06	-0.07	0.05	-0.08	0.05
Win_ori	-0.02	0.02	-0.02	0.02	-0.02	0.02
Win_pro	0.29**	0.11	0.16	0.11	0.18	0.11
In_pla	0.06	0.05	0.04	0.05	0.03	0.05
View1	-0.53**	0.10	-0.4**	0.10	-0.4**	0.10
View2	-0.29**	0.10	-0.20*	0.09	-0.16	0.09
View3	-0.14	0.09	-0.11	0.08	-0.12	0.08
H_loc			-0.04	0.04	-0.03	0.04
H_dur			-0.03	0.04	-0.02	0.04
H_flo			0.08*	0.04	0.08*	0.04
H_are			-0.09	0.06	-0.07	0.06
H_own			-0.04	0.11	-0.10	0.11
H_occ			0.15*	0.08	0.17*	0.08
H_bed			0.00	0.08	0.00	0.08
H_sa_s			0.07	0.05	0.06	0.05
H_sa_l			0.00	0.05	0.01	0.05
H_sa_n			-0.01	0.05	0.00	0.05
H_un_r			0.11	0.06	0.10	0.06
H_ro			-0.04	0.03	-0.06	0.03
In_cli			0.31**	0.09	0.32**	0.09
PREQ			0.36**	0.07	0.35**	0.07
Age					-0.14	0.08
Gender					0.04	0.09
Mar_sta					0.04	0.13
Edu_sta					-0.01	0.06
Job_sta					0.07	0.04
R^2		*0.16*		*0.36*		*0.37*

*Significant: **≤0.01, *≤0.05.*

Model1 shows that four Biophilic Factors have predicting roles for psychological restoration, such as size of window, availability of window protection devices, View1, and View2.

When the other independent variables are added in Model2, the predicting effects of View1 and View2

can still be found as significant. Both Indoor Climates and PREQ can show positive effects on psychological restoration ($p \leq 0.01$). Two housing conditions also express positive predicting effects ($p \leq 0.05$).

After adding the covariates (Model3), the predicting role of View2 is no longer significant ($p > 0.05$). The predicting effects of View1, indoor climates, PREQ, and two housing conditions (floor of home, occupancy of home) can still be found as significant. The variables in Model3 can explain 37% of the variance in psychological restoration.

4. DISCUSSIONS AND CONCLUSIONS

4.1 Housing environmental qualities and QoL

Our findings can support that there is the association between quality of life and several living and housing conditions, biophilic factors, and indoor climates. The positive predictive effect of indoor climates on quality of life was in line with previous studies [7, 16]. The evidence from previous studies found that living on higher floors was associated with worse mental health, possibly due to a lack of social interaction [17, 18]. Recent research has shown that this negative relationship disappeared completely and even became positive after adjusting for the socioeconomic and demographic variables [19]. Poor self-rated health in high-rise residential buildings could be explained by strong demographic and socioeconomic segregation between high-rise and low-rise buildings [19]. In our case, the floor level had a positive effect during the COVID19 pandemic. This could be related to the fact that most high-rise residential housing was equipped with better sanitation conditions than the old multi-storey housing in Shanghai.

4.2 Housing environmental qualities and PRS

As hypothesized, there is the association between psychological restoration and several Living and Housing Conditions, and Biophilic Factors. In addition, the Indoor Climates and PREQ also indicated positive predicting effects. Similar associations can be found between indoor climates, neighbourhood perceived environment and other mental health indicators (psychological distress and self-rated mental health) [7, 11].

As for living and housing conditions, the occupancy of home had positive predicting effects. It could be explained by a result achieved in an investigation across European countries that living alone during the pandemic was reported to be associated with greater loneliness [20]. Company from family members at home could be extremely important to help people stay mentally healthy in the lockdown period.

The present study indicated the only restorative effect of sky (not the plant). It was found that the sky as the most viewed external content would deliver a higher score of psychological restoration than other elements (e.g., plants). This finding was in line with one study also conducted in densely populated cities [21]. However, indoor plants and window view of greenery exposed positive effects in another study without considering sky view [22].

4.3 Housing environmental qualities and satisfaction

Living and housing condition, indoor climates, and PREQ were found associated with overall satisfaction. The association between housing condition, indoor climates, perceived residential environment qualities, and satisfaction has been exposed in previous studies [6, 13, 23]. In a previous study, the number of rooms per person can take positive effect on the housing satisfaction [24]. However, we found a new trend that the satisfaction of the number of rooms had a negative predictive effect on overall satisfaction. In addition, people with higher education status would deliver a higher overall satisfaction score. The finding that the owners other than renters were more likely to be satisfied with their housing environments was also similar as the previous study [11].

4.4 Biophilic factors for mental wellbeing

It can be well supported by this study that housing environmental qualities, especially indoor climates and PREQ, can play an important predicting role in mental health of occupants in a dense city. It could be worth noting that the window view and window protection devices have significant effects on mental wellbeing. Windows with protection devices and a sky view will significantly benefit psychological restoration and quality of life.

Since the impacts of physical housing conditions on health have received attentions [14, 15], it is necessary to promote more studies into the effects of biophilic factors on wellbeing in housing environment in China.

4.5 Research limitation and future work

This study has several potential limitations. First, the questionnaires have been collected from two short periods in 2021 and 2022. The behavioural differences of residents between the two periods were not investigated and analysed in this study. Second, causal claims cannot be drawn from this cross-sectional study in terms of the observed associations. It remains unknown whether the associations between perceived housing environmental qualities and mental health would change after time. Third, the sample size was modest. Limited by sample size, this study did not stratify people with different demographic and socioeconomic status.

The repeated questionnaire survey will be carried out in future work to see if there are changes of the associations between perceived housing environmental qualities and mental health before and

after Covid19 lockdown. Various methods will be adopted to increase the diversity and number of participants. In addition, stratified analysis of people with different socio-economic status and residential areas with different economic conditions will be added.

ACKNOWLEDGEMENTS

The authors acknowledge the financial supports from the National Natural Science Foundation of China (No.51778438) and Tongji Architectural Design (Group) Co., Ltd. (No.2022J-JZ07).

REFERENCES

1. Kuddus, M.A., Tynan, E. & McBryde, E. (2020). Urbanization: a problem for the rich and the poor? Public Health Reviews 4, 1.
2. Pevalin, D. J., Reeves, A., Baker, E., & Bentley, R. (2017). The impact of persistent poor housing conditions on mental health: A longitudinal population-based study. Preventive Medicine, 105, 304–310.
3. World Health Organization (WHO). (2018). WHO housing and health guidelines. Switzerland. Available at https://www.who.int/publications.
4. Gan, W., Sanderson, W. T., Browning, S. R. & Mannino, D. M. (2017). Different types of housing and respiratory health outcomes. Preventive Medicine Reports, 7, 124-129.
5. Suzuki, N., Nakayama, Y., Nakaoka, H., Takaguchi, K., Tsumura, K., Hanazato, M., Hayashi, T., Mori, C. (2021). Risk factors for the onset of sick building syndrome: A cross-sectional survey of housing and health in Japan. Building and Environment, 202, 107976.
6. Pedersen, E. (2015). City dweller responses to multiple stressors intruding into their homes: noise, light, odour, and vibration. International Journal of Environmental Research and Public Health, 12, 3246–3263.
7. Kanno, I., Hasegawa, K., Nakamura, T., Kogure, M., Itabashi, F., Narita, A., Tsuchiya, N., Hirata, T., Nakaya, N., Sugawara, J., Kuriyama, S., Tsuji, I., Kure, S., Hozawa, A. (2022). Relationship between the housing coldness/warmth evaluation by CASBEE Housing Health Checklist and psychological distress based on TMM Community-Based Cohort Study: a cross-sectional analysis. Public Health, 208, 98-104.
8. Kellert, S. R., Heerwagen, J., & Mador, M. (2011). Biophilic design: the theory, science and practice of bringing buildings to life. John Wiley & Sons.
9. The office of the Deputy Prime Minster. (2006). Housing health and safety rating system: operating guidance. London, UK. Available at https://assets.publishing.service.gov.uk. (Final access: 1st August 2022).
10. National Center for Healthy Housing & American Public Health Association. (2014). National healthy housing standard. Columbia, MD: National Center for Healthy Housing. Available at https://nchh.org/resource-library/national-healthy-housing-standard. (Final access: 1st August 2022).
11. Tang, J., Chen, N. Q., Liang, H. L., & Gao, X. (2022). The Effect of Built Environment on Physical Health and Mental Health of Adults: A Nationwide Cross-Sectional Study in China. International Journal of Environmental Research and Public Health, 19(11), 21, Article 6492.
12. Phillips, D. R., Siu, O. L., Yeh, A. G. O., & Cheng, K. H. C. (2005). The impacts of dwelling conditions on older persons' psychological well-being in Hong Kong: the mediating role of residential satisfaction. Social Science & Medicine, 60(12), 2785-2797.
13. Sun, B. D., Liu, J. H., Yin, C., & Cao, J. S. (2022). Residential and workplace neighbourhood environments and life satisfaction: Exploring chain-mediation effects of activity and place satisfaction. Journal of Transport Geography, 104, 10, Article 103435.
14. China Association for Engineering Construction Standardization. (2017). Evaluating standard for healthy housing. Available at https://www.gongbiaoku.com/book/jxf19320hym (Final access: 8th November 2023).
15. China Association for Engineering Construction Standardization. (2020). Assessment standard for healthy community. Available at https://www.gongbiaoku.com/book/l2519854upt (Final access: 8th November 2023).
16. Chen, Y., Li, M., Lu, J. F., & Chen, B. (2023). Influence of residential indoor environment on quality of life in China. Building and Environment, 232, 10, Article 110068.
17. Hannay, D. R. (1981). Mental health and high flats. Journal of Chronic Diseases, 34(9-10), 431–432.
18. Evans G. W. (2003). The built environment and mental health. Journal of urban health: bulletin of the New York Academy of Medicine, 80(4), 536–555.
19. Verhaeghe, P.-P., Coenen, A., & Van de Putte, B. (2016). Is Living in a High-Rise Building Bad for Your Self-Rated Health. Journal of Urban Health-Bulletin of the New York Academy of Medicine, 93(5), 884-898.
20. Keller, A., Groot, J., Matta, J., Bu, F., El Aarbaoui, T., Melchior, M., Fancourt, D., Zins, M., Goldberg, M., Nybo Andersen, A.-M., Rod, N. H., Strandberg-Larsen, K., & Varga, T. V. (2022). Housing environment and mental health of Europeans during the COVID-19 pandemic: a cross-country comparison. Scientific Reports, 12(1), 5612.
21. Masoudinejad, S., Hartig, T. (2018). Window View to the Sky as a Restorative Resource for Residents in Densely Populated Cities. Environment and Behaviour, 52, 401-436.
22. Dzhambov, A. M., Lercher, P., Browning, M. H. E. M., Stoyanov, D., Petrova, N., Novakov, S., & Dimitrova, D. D. (2021). Does greenery experienced indoors and outdoors provide an escape and support mental health during the COVID-19 quarantine. Environmental Research, 196, Article 110420.
23. Braubach, M. (2007). Residential conditions and their impact on residential environment satisfaction and health: results of the WHO large analysis and review of European housing and health status (LARES) study. International Journal of Environment and Pollution, 30(3-4), 384-403.
24. Foye, C. (2017). The Relationship Between Size of Living Space and Subjective Well-Being. Journal of Happiness Studies, 18(2), 427-461.

PLEA 2024 WROCŁAW
(Re)thinking Resilience

Building Performance Analyses in Higher Education:
The Solar Decathlon 21/22 Experience

ISIL KALPKIRMAZ RIZAOGLU[1], KARSTEN VOSS[1]

[1]University of Wuppertal, Faculty of Architecture and Civil Engineering, Chair of Building Physics and Technical Services, Wuppertal, Germany

ABSTRACT: This study shares didactive findings on building performance analyses at Solar Decathlon Europe 2021/2022 (SDE21/22), the recent European edition of an international university-level student competition. The competition aims to educate and train the future actors of Architecture Engineering and Construction, recognizing that they have a key role in the creation of environment friendly, energy efficient and comfortable built environments. First, the integration of the topics of building performance across the curricula of the participating universities and the use of building performance simulation tools in the scope of SDE21/22 are explored by the review of the teams' reports. Second, the results of a survey conducted with the teams are shared, focusing on design-integrated use of building performance simulation tools. Finally, the performance gap task, one of the methods applied in the competition, for the investigation of the difference between anticipated and actual performance of a building, is presented as a showcase of the design-build pedagogical approach in SDE21/22. The study aims to communicate the importance of the design-integrated use of performance simulations in higher education, and thus promote integrated interdisciplinary teaching and learning methods.
KEYWORDS: Solar Decathlon, Higher Education, Building Performance, Didactive Methods, Review, Survey.

1. INTRODUCTION

Recognizing the fact that the challenges in Architecture, Engineering and Construction (AEC) are multidimensional and highly interactive, integrated interdisciplinary analysis and evaluation has become a necessity rather than an option, to increase the flexibility, creativity and efficiency of a design process and thereby increase resilience in the midst of climate change [1,2]. The level of progress towards a more sustainable built environment relates to how well the future AEC actors are being equipped during their higher education [3]. Integrated approaches that incorporate real-life challenges and interdisciplinary workflows have a high potential to enable these future actors to take a more proactive role in creation of more sustainable future [4,5].

In response, this paper shares didactive findings on building performance analyses (BPA) at Solar Decathlon Europe 2021/2022 (SDE21/22) [6], which took place in Wuppertal, Germany in 2022. SDE is the worldwide European edition of the Solar Decathlon (SD) competition [7].

The topics, tools and methods of BPA in the scope of SDE21/22, with a particular focus on Building Performance Simulation (BPS), are analyzed through reviews and a survey to reveal their effectiveness and provide future perspectives for better adoption of BPA in higher education.

2. SOLAR DECATHLON EUROPE 21/22

The competition is distinctive in that it treats design not only as a creative problem-solving exercise, but also as an integrated process where evidence-based methods and practical skills are required. The SDE21/22 was the first edition fully focusing on the existing stock of residential apartment buildings in an urban area to promote energy transition for achieving climate-neutrality. Also, it was the first inspired by the results of Annex 74 - Competition and Living Lab Platform [8] of the International Energy Agency's Energy in Buildings and Communities (IEA EBC) Programme, which encouraged significant updates to the competition rules closely related to BPA [9].

In the scope of SDE21/22, a total of 18 teams from 11 countries with participation of more than 500 students competed through the 10 main contests of the competition: (I) Architecture; (II) Engineering & Construction; (III) Energy Performance; (IV) Affordability & Viability; (V) Communication, Education & Social Awareness; (VI) Sustainability; (VII) Comfort; (VIII) House Functioning; (IX) Urban Mobility; and (X) Innovation. The teams worked on the planning and design of their projects for 3 years. To ensure the gradual continuation of the work and provide feedback, the teams were asked to make a series of submissions, namely "deliverables", to the SDE21/22 organizers, including all documents, drawings, and other materials.

The teams were introduced to two main challenges (1) in the "Design Challenge" (DC), teams created a design and energy concept for the renovation and extension of an existing building, including its urban context; and (2) in the "Building Challenge" (BC), teams designed a House Demonstration Unit (HDU) as a representative for DC and built it in a shared competition space, namely "Solar Campus", in the competition final (Fig. 1).

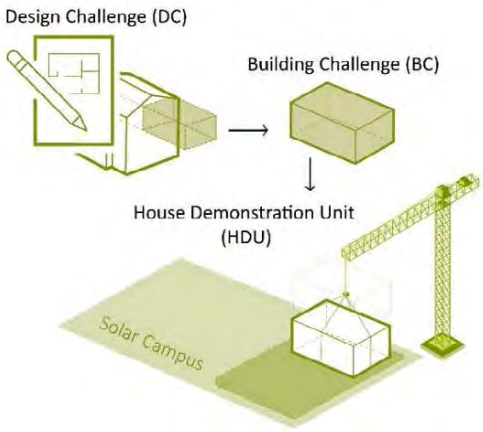

Figure 1: Design Challenge, Building Challenge and House Demonstration Unit in SDE21/22, ©SDE21/22.

Due to the difficulties caused by COVID-19, the competition final was postponed from 2021 to 2022 and 16 out of 18 teams were able to participate in the competition final to build their HDUs. Therefore, 16 HDUs, which are one- to two-story units with up to 110 m^2 of living space, were built by the teams.

3. BUILDING PERFORMANCE ANALYSES

The authors collected the base data of this study via reviews, which are made through the official documents of SDE21/22 and the final reports of the 16 teams took part in the competition final. All the data and documentation of SD, including SDE21/22, are available on ‘‘Building Energy Competition & Living Lab Knowledge Platform” [10]. A further investigation about the use of the BPS tool was carried out through an online survey called "BPS in SDE21/22", which was conducted in an anonymous format with the participation of 12 out of 18 teams, through the online communication platform of SDE21/22, right after the completion of the competition. A total of ten closed-ended questions with single and multiple-choice options were asked. One recent study by the authors [11] provides a comprehensive assessment of the integrated use of BPS tools in the context of SDE21/22.

In SDE21/22, the main method for the estimation of the building performance was BPS throughout the whole process, as well as monitoring and testing during the competition final to evaluate the real performance of the HDUs.

3.1. Building performance in the curricula

The integration of the SDE21/22 topics across the curricula of the teams' universities was explored by the review of their "Communication and Education" reports submitted as part of the competition, with a particular focus on the topics of building performance.

Example structures observed among the teams’ universities for the integration are as follows:

- Elective and/or compulsory courses and bachelor’s and master’s theses that enable students to take part in SDE21/22 as a part of their study program without exceeding the planned period of study.
- Joint courses offered through collaborations between different teaching chairs / departments to enable students from different disciplines to study on the SDE21/22 topics and to bring building physics education closer to design education.
- Councils formed by students and functioning as a link between the faculty bureaucracy and students.

In the scope of the review, the performance topics includes energy, indoor thermal comfort, indoor air quality, ventilation, hygrothermal assessment, lighting, and related building technical equipment, and building integrated renewable energy systems. It was observed that in general the number of courses covering performance topics was higher in teams formed by students from more technical and/or engineering-oriented disciplines compared to design and art. More specifically, it is seen that courses such as sustainable design and lighting design were more common in the architecture programs, while courses related to the thermal and optical properties of a building, such as thermal comfort, were more common in the engineering programs.

The number and weight (in %) of courses covering building performance within the total courses offered at the universities within the scope of SDE21/22 are summarized (Table 1). Some reports mentioned the existence of some courses related to SDE21/22, but did not give details about the topics, so in these cases the information was not applicable (n/a).

Table 1: Number and weight (in %) of the courses covering building performance topics within the total courses offered at the universities within the scope of SDE21/22. The abbreviations refer to the teams, [11].

	Bachelor Courses	Master Courses	In total (%)
NCT	2 out of 18		11%
ROS	5 out of 24	3 out of 7	26%
UPH	2 out of 4	n/a	**50%**
HBC	3 out of 13	1 out of 2	27%
HSD	4 out of 16	7 out of 16	34%
KIT	11 out of 17	n/a	**65%**
FHA	4 out of 16	n/a	25%
GRE	3 out of 5		**60%**
HFT	6 out of 30		20%
TUD	1 out of 4		25%
UPV	7 out of 11	2 out of 5	**56%**

n/a: not applicable

The weight of the courses in the curricula were cross analyzed with the success of the teams in the contests of "Architecture", "Engineering and construction", "Energy performance" and "Comfort", where BPA was intensively applied, in order to see whether the higher weights of the performance

courses in the curricula resulted in higher success in the competition. For each contest, the points collected by the teams are presented as a percentage of the total points that can be earned (e.g., KIT earned 90% of the total points that could be earned for architecture contest.). The first 4 teams in whose curriculum the performance courses had at least 50% weight were evaluated (Fig. 2). It is seen that the teams that had higher success in the contests were the ones from the universities with the higher weights of performance related courses.

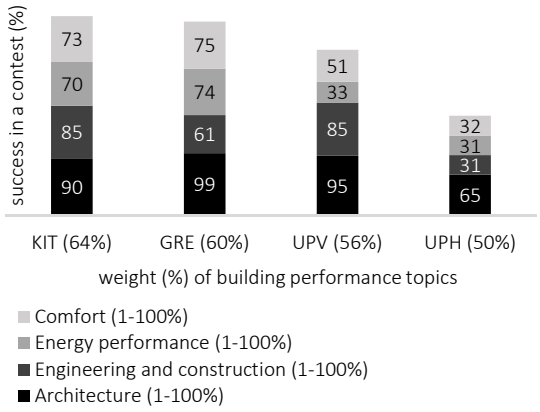

Figure 2: Cross analysis of the teams' success in the contests that BPA were applied and the weight of the courses covering building performance topics in the curricula, [11].

Focusing on opportunities and barriers for better integration of BPA into the curriculum, the review showed that the main threat is rigid curricula. In turn, flexible curricula, adoption of project-based, experiential, and interdisciplinary learning, better use of digital education platforms, and collaborations within and across universities stand out as opportunities.

3.2. Use of BPS tools in the competition

Another review aiming to analyze the use of BPS tools in SDE21/22 is made through the final version of project manuals. This includes detailed analyses of the teams' reports for each contest.

During SDE21/22, the teams were asked to provide simulations to assess the plausibility and efficiency of their energy concepts over the course of a year, continuously via deliverables. Besides that, BPS accompanied to in-situ test and measurements.

BPS studies were deliberately encouraged in SDE21/22 by targeting 3 main didactive points:

- Studying design variations during design development
- Testing the robustness of a design (e.g. against extreme weather conditions such as heat wave effect) and/or extreme/unexpected user behavior (e.g. operation of blinds and windows).
- Producing simulation data to be compared with measurements as a part of the performance gap task.

A wide variety was observed amongst the BPS tools used by the teams, in terms of calculation methods (un-dynamic, dynamic, semi-dynamic), field of application (e.g., domains of energy, comfort, lighting etc.) (Table 2), level of integration with the design tools (i.e., integrated, semi-integrated, independent), as well as intelligent design options provided by the tools (i.e., parametrization and optimization).

When the fields of application of the tools are categorized and the percentage of the teams using a tool for a specific field is analyzed, the energy field has the highest rate of application with 94% of the teams, which is followed by comfort and photovoltaic & photovoltaic thermal (PV/PVT) systems (Fig. 3).

Table 2: List of tools used by the teams according to the fields of application, [12]*, © SDE21/22.*

	FIELDS	BPS TOOLS
Site & Climate	Climate Analyses, Radiation, Shadow.	RESBy, Vi-suite, Ladybug Tools, Climate Consultant, ClimateStudio.
Energy	Use, Cost, Balance.	Design Builder, MATLAB/ Simulink, Ladybug Tools, IDAICE, SimRoom, EN-13790 Tool, Plancal Nova, EnergyPlus, DDS-CAD, TRNLizard, TRNSYS 18, ENERCALC, ETU Sim.Gold, IES-VE, PHPP, OpenStudio, Climatestudio.
Comfort	Thermal Comfort, Air quality, Humidity.	Design Builder, SimRoom, TRNLizard, TRNSYS 18, ENERCALC, ETU Sim. Gold, IES-VE.
PV/PVT System*	Design, Production, Grid integration.	PVlib Python, PVGIS, AutoCalSol, Polysun, TRNLizard, Sunny Design, PV*SOL, T*SOL Valentin, OpenModelica, PV syst 7, POLYSUN, SolarEdge.
Ventilation	Passive, Mechanical.	Ladybug Tools, Plancal Nova, DDS-CAD, TRNFLOW.
Hygrothermal	Heat, Moisture.	WUFI, Lesosai & Flixo, Therm, PsiTherm.
Lighting	Daylight design, Artificial light design, Visual Comfort.	Autodesk Revit, IDAICE, Dialux Evo, Radiance, VELUX, IES-VE, RELUX.
LCA**	Cost, Carbon footprint, Circularity.	UMI Tool, eLCA/Bauteileditor, SimaPro 9.0, Caala OneClickLCA.

*PV: Photovoltaic / PVT: Photovoltaic Thermal System,
**LCA: Life Cycle Assessment

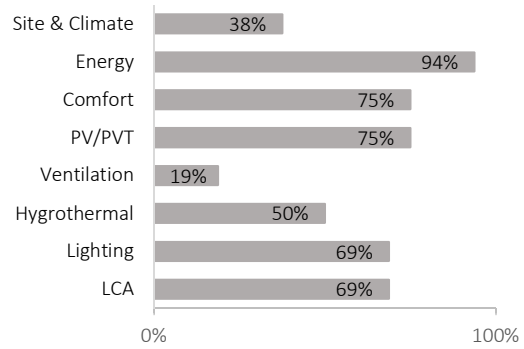

Figure 3: Fields of application according to percentage of teams used a BPS tool in a specific field.

Further analyses are made through the results of the survey. Part of the results are shared here focusing on design-integrated use of BPS tools and the integrative effectiveness of the design and building challenges (DC and BC).

First, the digital design and documentation tools used by the teams were asked in relation to the design phases and the design challenges (Fig. 4). Design phases were described in the survey as early design, design development, and advanced design [13].

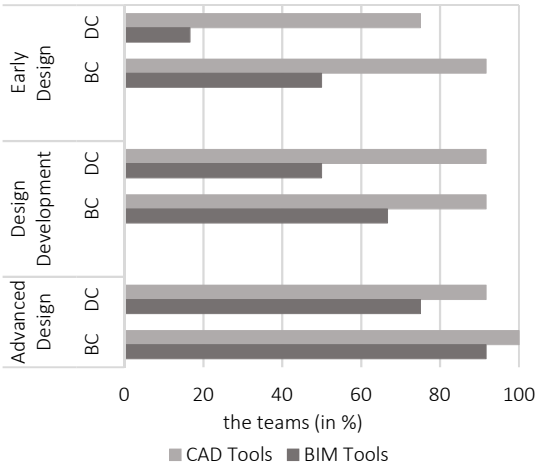

Figure 4: Use of digital design and documentation tools in relation to the design phases (Early, Design Development, and Advanced) and the challenges (DC and BC), © SDE21/22.

While the use of Computer Aided Design (CAD) tools exhibits an intense and stable pattern in the design stages, the use of Building Information Modeling (BIM) tools is seen to increase in the later stages of the design process. In all design phases, the use of BIM tools was higher in BC compared to DC. On the other hand, while the use of BIM increased from early phase to advanced phase, CAD was always the most dominant tool of the whole design process.

Regarding the phase at which the teams started using BPS tools, the teams showed a varying pattern for the DC. On the other hand, for BC, most of the teams (75%) involved BPS in their design workflows starting from early design phase (Fig. 5).

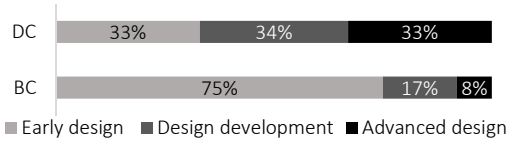

Figure 5: Design phases (of the challenges, DC and BC) in which the teams started using BPS tools, [11]*, © SDE21/22.*

A level of integration of a BPS tool with a design tool, which refers to the physical availability of the BPS tool directly in a digital design environment, was asked. Definitions were provided in the survey as follows (I) non-integrated - all design process and performance simulations are conducted in separate digital environments, (II) Partially integrated - BPS and design tools are in separate digital environments, but file exchange between them to transfer data from one to other is possible, and (III) Integrated - BPS tools are physically available in digital design environment. The results show that teams used BPS tools integrated with design tools more in the planning and design process of BC compared to DC (Fig. 6).

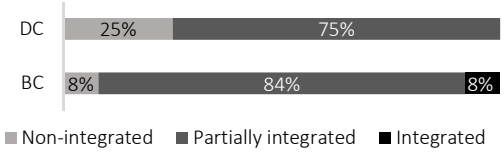

Figure 6: Integration of BPS tools into the digital design environment in relation to the challenges (DC and BC), [11]*, © SDE21/22.*

More than half of the teams stated that the influence of BPS on design decisions was high. Also, the teams mainly agreed that BPS, particularly during early design, was useful for creating design alternatives, raised confidence for decision making and supported creativity.

3.3. Performance gap task

Performance gap analysis is defined as an investigation of the difference between anticipated and actual performance of a building. Two recent studies [9,14], including the authors, report in detail the results of monitoring and measurement of the SDE21/22 units in terms of building physics. In SDE21/22, the performance gap task, which relates and connects design and operation stages in terms of building performance by compiling expectations, simulation, and measurements, stands out as a showcase for the design-build pedagogical approach. The task had two main components: (1) co-heating test and (2) simulation. The teams were requested to deliver their HDUs' performance simulations for the period where the co-heating tests were conducted, and operative temperatures were monitored in the built HDUs to be compared to the simulation results.

The co-heating test is defined as an assessment of the as-built performance of a building by comparing the heat input into a building against the disparity

between temperatures inside and outside the building [15]. During the co-heating tests, the HDUs were homogeneously heated to an elevated steady-state interior temperature, which is well above the outside temperature, using electric fan heaters with an output of 3 kW and an air flow rate of 250 m^3/h running 3 days, June 7- 9, between 12 am and 6 am. Including the pre-conditioning period and co-heating periods, in total 7 days were between the completion of the construction of HDUs and the public visits, therefore the monitoring data was not interrupted with users' interactions. House-hold appliances were the only source of internal gains. Ventilation systems were out of operation. The air-tightness test took place right before the co-heating test, so all ventilation openings were closed. All movable shadings were closed to minimize the effect of passive solar gains. To plan and conduct the co-heating tests in the scope of SDE21/22, research on dynamic test methods for buildings from "Annex 71 - Building Energy Performance Assessment Based on In-situ Measurements" in the IEA EBC program is used as a reference [16].

The task aimed to provide students an overview of building performance at the intersection of indoor thermal comfort and thermal characterization, but also to encourage students to do better work, keeping in mind that their work will be evaluated by comparison of simulated and measured data.

To ensure a homogeneous modeling and simulation process among the teams for indoor climate and energy calculations of HDUs, a simplified single zone BPS tool, namely "SimRoom" [17], had been introduced to the teams by the SDE21/22 organizers during the early design phase of the HDUs. It was preferred for being a free excel-based educational tool that is easy to learn and proved by positive didactive experiences in many schools of architecture and engineering in Germany [18,19]. The use of other BPS tools had also been encouraged for comparison of results and more advanced simulations in both design and operation processes. To achieve consistency with in-situ measurements, simulation settings such as weather data, heating period and power, occupancy, operable blinds, and ventilation were set as pre-defined conditions in a special edition of SimRoom. Some other inputs were adjustable to allow the teams to update the thermo-physical, optical, and geometry-related properties of the HDUs as-built. A comparison of the measured and simulated hourly mean operative temperatures for the main living spaces is presented in Figure 7 [9]. In general, the simulations and the measurements display a similar pattern. Exceptions are (1) some teams (e.g. HFT and FHA) participated late due to construction delays, (2) the harmonized pre-conditioning in all buildings was not achieved and (3) in one case, the automatic switch-off function of a heater (e.g. TUD) failed.

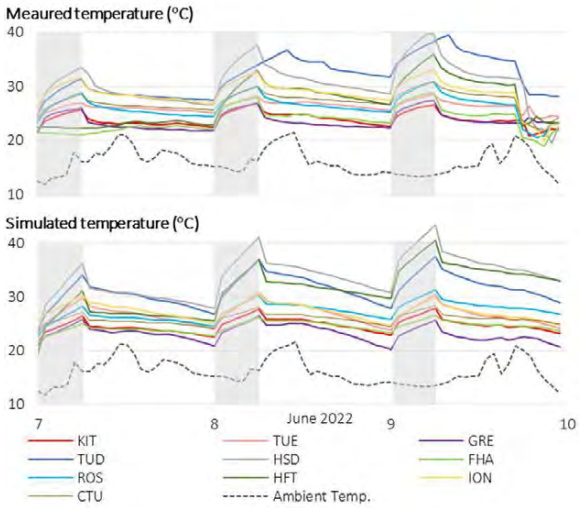

Figure 7: Comparison of the measured and simulated hourly mean operative temperatures of 10 HDUs [9]. *The abbreviations in the legend refer to the 10 SDE21/22 teams.*

The response of the units to the operation time of the heaters, represented by the gray background in the graphs, was an important learning outcome for the teams, not only understanding the dynamics stemming from their own units, but also, for relating the results to the differences between the HDUs. Units with smaller test volumes (HSD and HFT) had higher temperature increases in a shorter time. The different temperature decays, each time after the fan heaters were switched off, reflects the differences in thermo-physical characteristics of the units such as thermal transmittance, air tightness, and thermal mass [11].

4. CONCLUSION

This paper shared the experiences in SDE21/22 to illustrate the potential of incorporating BPA in higher education. (1) Didactic approaches that promote experiential learning and combine different phases of a building project, (2) early integration of performance investigations in a design process with the use of BPS tools, and (3) multidisciplinary and continuous feedback for students during their studies are identified as the aspects for better adoption BPA in higher education.

Comparative evaluations of design and building challenges show that didactive methods that incorporate design, construction and operation steps together are likely to be more effective than those based on design only, for integrating design and performance education.

Although it is not possible to speak of a definitive causality, the cross analysis of the teams' success in the contests that BPS were applied and the level of weight of the building performance topics in the curricula points to the potential of performance-integrated teaching for the creation of a high-performance built environment.

The overall review indicates the necessity of flexible curricula for better integration, where collaborations between different disciplines with diverse knowledge can be established.

Furthermore, the rich variety of BPS applications realized by the teams is an illustrative example of how BPS can be an instrumental tool in solving multidimensional and interactive challenges.

The performance gap analysis appears to be a useful didactic method, demonstrating why simulations, tests, monitoring and measurements are important and interrelated throughout the design and construction phases of a building project, and how important interdisciplinary collaborations are to balance the different requirements. Studies [9,14,20,21] , conducted shortly after the competition, using the performance gap data, shows the high interest and raise expectations for future research.

SDE21/22 – competition source book [22] summarizes the competition, the results, the teams' contributions, and cross analyses of key topics. All the data and documentation provided on the ‘‘Competition Knowledge Platform” [10] provides a source for further research and education.

The findings of the study cannot be generalized on a large scale as they are based on a single experience, but they are noteworthy for providing perspectives on how BPA can be applied in higher education. The study can be used as a reference to communicate the importance of the design-integrated use of BPS in higher education, and to promote integrated interdisciplinary teaching and learning methods.

ACKNOWLEDGEMENTS

The authors thank the German Federal Ministry of Economic Affairs and Climate Action for funding SDE21/22, and to all the teams and the Energy Endeavour Foundation for their intensive and fruitful cooperation.

REFERENCES

1. Kalpkirmaz Rizaoglu, I. and Voss, K. (2020) Building Performance Simulation to Stimulate Architectural Early Design: Integrating Design and Simulation. 35th PLEA Pro., A Coruña, 1525–1530.
2. Kalpkirmaz Rizaoglu, I. and Voss, K. (2022) Building Performance Simulation in Design Education: Design-Integrated versus Additive. BauSim 2022 Pro. https://doi.org/10.26868/29761662.2022.43.
3. Herrera-Limones, R., Rey-Pérez, J., Hernández-Valencia, M. and Roa-Fernández, J. (2020) Student Competitions as a Learning Method with a Sustainable Focus in Higher Education: The University of Seville “Aura Projects” in the “Solar Decathlon 2019.” Sustainability, 12. https://doi.org/10.3390/su12041634.
4. Brown, J.B. and Russell, P. (2022) When Design-Build Met the Live Project – or – What Is a Live-Build Project Anyway? In: Smet, A. De and Pak, B., Eds., Experiential Learning in Architectural Education: Design-Build and Live Projects, Routledge, Abingdon, 9–24. https://doi.org/10.4324/9781003267683-2.
5. Voss, K., Sánchez, S., Russel, P., Arranz, B., Holloway, L., Hendel, S., Amaral, R., Stark, M., Balcerzak, A. and Ingeborg van Luijn, A. (2020) Solar Decathlon Europe - Analysis of the Results.
6. Solar Decathlon Europe 21/22. https://sdeurope.uni-wuppertal.de/en/ [20 November 2023].
7. Solar Decathlon. https://www.solardecathlon.gov/ [13 June 2023].
8. IEA EBC Annex 74. https://annex74.iea-ebc.org/ [15 October 2023].
9. Voss, K., Kalpkirmaz Rizaoglu, I., Balcerzak, A. and Hansen, H. (2023) Solar Energy Engineering and Solar System Integration – The Solar Decathlon Europe 21/22 Student Competition Experiences. Energy and Buildings, Elsevier, 285, 112891. https://doi.org/10.1016/J.ENBUILD.2023.112891.
10. Building Energy Competition & Living Lab Knowledge Platform. https://building-competition.org/ [30 July 2023].
11. Kalpkirmaz Rizaoglu, I. and Voss, K. (2024) Building Performance with an Integrated Simulation Approach: Experiences in Solar Decathlon Europe 21/22 and Future Perspectives. Building and Environment, Elsevier, 254. https://doi.org/https://doi.org/10.1016/j.buildenv.2024.111261.
12. Kalpkirmaz Rizaoglu, I. (2023) Building Performance Simulation Tools. In: Voss, K. and Simon, K., Eds., Solar Decathlon Europe 21/22 – Competition Source Book, Wuppertal, 150–153. https://doi.org/10.25926/svtg-e916.
13. RIBA. (2020). Plan of Work Building Project Stages. https://www.architecture.com/-/media/GatherContent/Test-resources-page/Additional-Documents/2020RIBAPlanofWorkoverviewpdf.pdf [15 June 2023].
14. Voss, K., Hansen, H., Kaliga, M. and Rizaoglu, I.K. (2023) Solar Decathlon Europe 2022 – Bauphysikalische Ergebnisse von Demonstrationsgebäuden. 2023 Bauphysik Kalender, Wiley, 531–550. https://doi.org/10.1002/9783433611289.ch15.
15. Bauwens, G. and Roels, S. (2014) Co-Heating Test: A State-of-the-Art. Energy and Buildings, 82, 163–172. https://doi.org/https://doi.org/10.1016/j.enbuild.2014.04.039.
16. Building Energy Performance Assessment Based on In-Situ Measurements, IEA EBC. https://www.iea-ebc.org/projects/project?AnnexID=71 [15 October 2023].
17. SimRoom 4, SDE 21/22 Special Edition. https://ingefo.de/Werkzeuge/SimRoom/ [15 June 2023].
18. SimRoom as a Learning and Teaching Tool. https://www.ingefo.de/Lehre/ [15 June 2023].
19. SimRoom - Comparison with Different BPS Tools. https://ingefo.de/Werkzeuge/SimRoom/ [15 July 2023].
20. Carbonare, N., Bühler, M., Pfafferott, J. and Wagner, A. (2022) RoofKIT – Building Simulation in Sustainable Housing at the Solar Decathlon Europe 21/22.
21. Weidner, P. and Gerber, A. (2023) Scalable Façade-Integrated PVT-Systems for Upward Extensions in the Urban Context. CISBAT, Lausanne.
22. Voss, K. and Simon, K., Eds. (2023) Solar Decathlon Europe 21/22 – Competition Source Book. Wuppertal. https://elpub.bib.uni-wuppertal.de/receive/duepublico_mods_00000696.

PLEA 2024 WROCŁAW
(Re)thinking Resilience

The potential of vegetation to modify urban climate

Using thermography to evaluate the urban radiant environment

DIEGO-JAVIER PERALTA-LUNA[1], CARLOS ALONSO-MONTOLIO[1], HELENA COCH[1]

[1] Architecture, Energy & Environment (AiE), Polytechnic University of Catalonia (UPC), Barcelona, Spain.

ABSTRACT: This study analyses vegetation as a shading element in urban environments, with a focus on mean radiant temperature and its relationship with outdoor thermal comfort. The methodology was based on measurements taken from thermographic images. A unique representation of the urban radiant environment around a specific point was created by joining multiple thermographic captures. The analysis revealed that exposed surfaces can reach temperatures up to 22ºC higher than those in the shade. Mean radiant temperature was calculated from this image using a script. The calculated mean radiant temperature and the measured air temperature were used to calculate outdoor thermal sensation for two comfort indices: physiological equivalent temperature (PET) and the universal thermal climate index (UTCI). The results showed that mean radiant temperature has a greater influence on thermal sensation than air temperature. Vegetation has proved to be an efficient solution in the outdoor environment, by providing shade and maintaining its own radiant temperature similar to air temperature. This effect is important to reduce mean radiant temperature in urban environments.
KEYWORDS: vegetation, shading device, thermography, urban radiant environment, urban thermal comfort

1. INTRODUCTION

Mitigation actions are needed in response to projected global temperature increases, particularly for the summer period [1]. Cities are the most affected places, in terms of temperature increase and population affected.

Parks, squares and public spaces play a vital role in bringing people closer to nature. To improve the health of inhabitants and increase the city's resilience, it is essential to better understand how thermal conditions influence users' perception of the urban space.

Air temperature, humidity, air movement and radiant temperature are the main parameters that influence thermal perception. Radiant exchange has been identified as a key factor in determining thermal comfort in outdoor urban spaces [2]. Sun is the main source of radiation and has a decisive influence on the radiant characteristics of an outdoor environment.

Studies have shown that the presence of shading elements in cities with hot, sunny periods and high temperatures has a significant impact on the average radiant temperature and, consequently, on the urban climate [3][4]. Shading is a strategy to mitigate solar exposure and improve the liveability of urban spaces [5].

To mitigate radiant exchange, researchers have explored various types of surfaces such as: pavements, building walls and urban objects, considering the presence or absence of shade. Studies have demonstrated that when surfaces are exposed to direct sun radiation, there is a considerable temperature difference. However, with the presence of shade, the temperature variation among different surface finishes becomes less significant [6].

Several studies investigated the correlation between mean radiant temperature (Tmrt) in shaded spaces created by trees and canopies. These studies have demonstrated that trees have a better cooling effect compared to other shading devices [7][8]. Such studies are commonly conducted using a globe thermometer.

Thermographic images can be used as a valuable tool to obtain global information about the radiative environment, rather than just specific measurement points. They lead to better understanding of radiative phenomena.

2. METHODOLOGY

The objective of this study was to evaluate the effect of vegetation and its impact on the mean radiant temperature. To meet this objective, an image of the urban radiant environment was used to allow a global spatial analysis. This image was constructed through several individual thermographic images.

The process that was followed was based on measurements made with a thermographic camera Testo 872s, which has a field of view of 30º x 42º. A Benro TMA37AL tripod was used to stabilise the camera and a Benro GD3WH rotule was used to rotation 360ºC on horizontal axis and 180ºC on vertical axis to capture the radiant surroundings (Fig. 1).

The Testo 872s camera generates a thermographic image and a standard photograph at the same time.

Figure 1: Thermographic camera, rotule and tripod

To capture the environment around a specific point, approximately fifty thermographic images were taken in about fifteen minutes (Fig. 2). All images were taken using the same temperature scale.

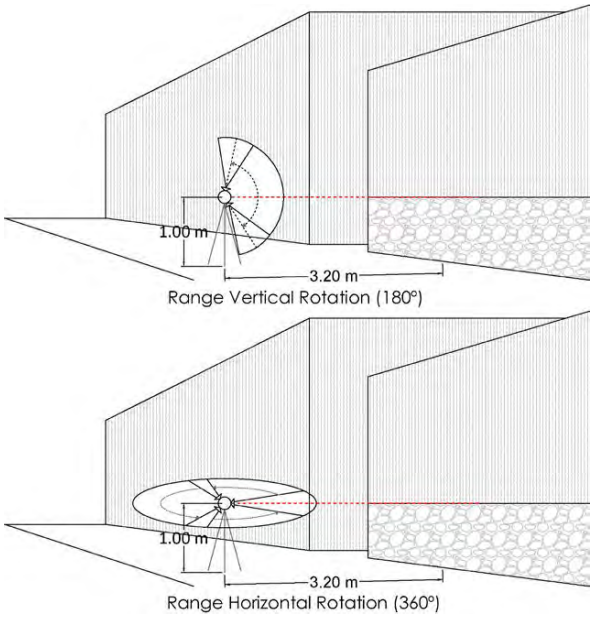

Figure 2: Rotation of the thermal camera around both the vertical and horizontal axes

KolorAutopano software was used to combine the thermographic images and standard photographs. The combination of thermographic and standard images facilitated the analysis and identification of radiant temperature values, and established correlations between vegetation and the shading effects produced.

Using the radiant environment image, we proceeded to calculate the mean radiant temperature for this specific point using a script develop for this purpose.

Subsequently, an analysis was conducted to determine how the mean radiant temperature affects the thermal comfort experienced by pedestrians in a public space. For this purpose, two thermal comfort indices were employed: physiological equivalent temperature (PET) and universal thermal climate index (UTCI).

Using these two thermal comfort indices, we calculated the thermal sensation for this specific urban environment, reducing the effect of the shade provided by vegetation.

This analysis enabled us to compare the influence of mean radiant temperature and air temperature on people thermal comfort.

2.1 Case study

A public space had to be selected with vegetation as a shading element. A point between Carrer de Pascual i Vila and Carrer de Pablo Gargallo in Barcelona, Spain, was chosen for this purpose (Fig. 3).

This street segment has a wide sidewalk (11 m) and a significant number of trees: 38 in total on both sidewalks. All the trees are Celtis Australis. These trees create various shaded areas, so we could analyse the surfaces' radiant temperature. The building walls, pavements, cars and other objects were part of the radiant environment studied.

The images were captured on a clear day, on 16 May at 11:15 h solar hour (13:15 h official hour). The camera was positioned at a height of 1.00 m and 3.20 m away from nearby buildings (Fig. 2).

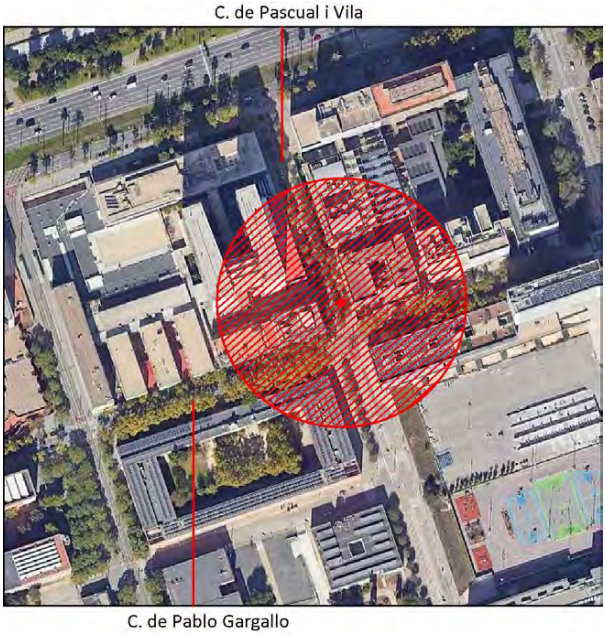

Figure 3: Case study location

2.2 Calculating mean radiant temperature

The mean radiant temperature was determined through an urban radiant environment image. To construct this image, a thermal camera was positioned at a height of 1 m. It was rotated around a point using a rotule. The images were taken in a way that they have an overlapping area so that they can be joined using software.

KolorAutopano was selected as the software to join the images due to its ability to identify common points and seamlessly connect them (Fig. 4). In the urban radiant environment image, a specific temperature scale was employed, with each temperature corresponding to a colour code. With this information and a scripting language, the temperature of each pixel was determined.

A standing position was chosen as the reference to calculate the radiation received by a person in outdoor space. Previous studies have determined that a vertical cylinder approximates the shape of a standing person [9][10]. This shape was used in the present study.

The mean radiant temperature was calculated with the weighted sum of each pixel's temperature in the urban radiant environment image. In this method, each temperature's value was weighted according to its location in space and the angle at which it falls on the vertical cylinder.

Notably, our primary objective was to analyse the influence of vegetation in outdoor environments as a shading element. Therefore, direct solar radiation values were not utilized. The result of the calculation of mean radiant temperature corresponds to a shaded place.

The value of the calculated mean radiant temperature according to the composed thermographic image was 22ºC. This corresponds to a specific point in the urban context.

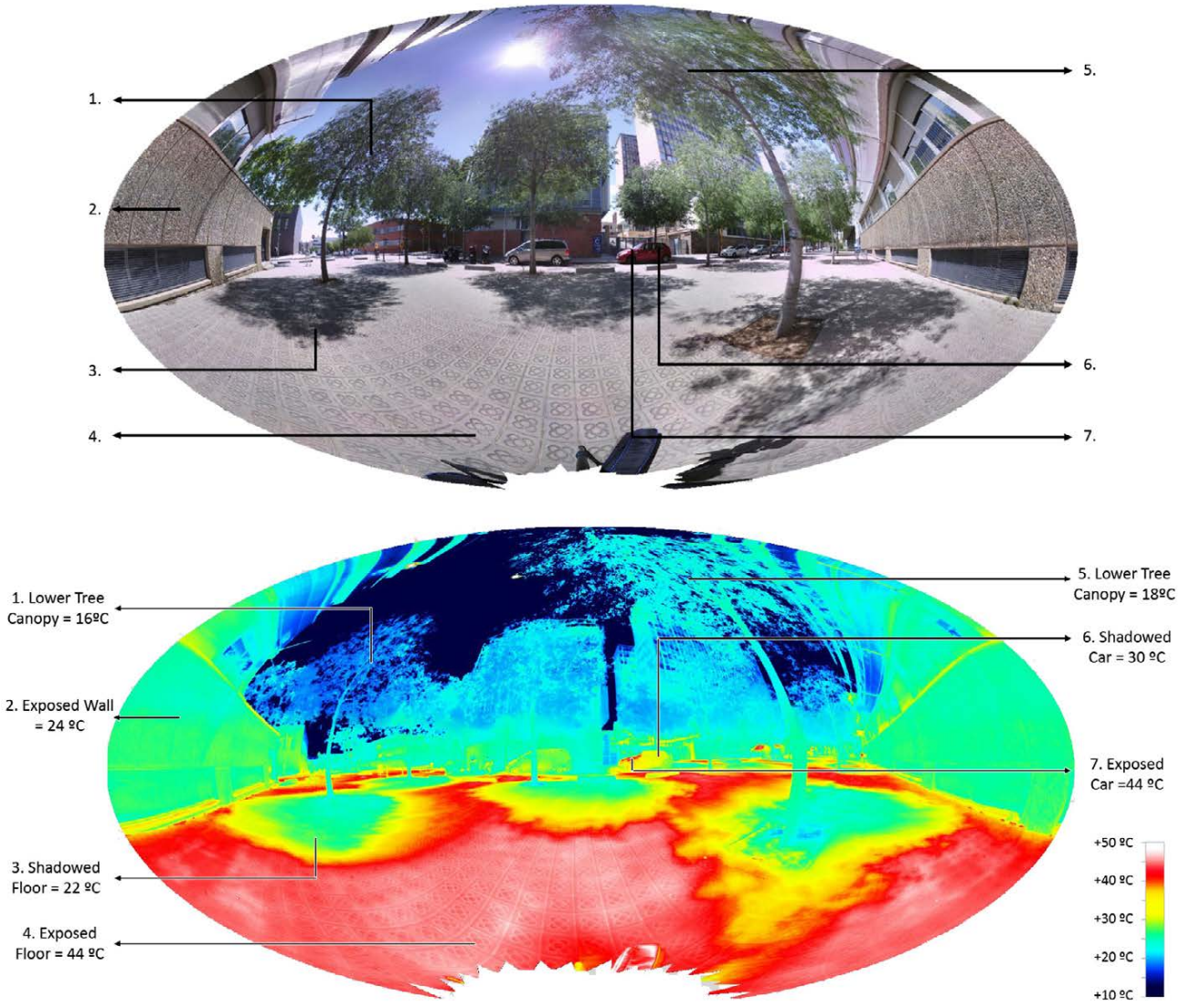

Figure 4: (Up) Composed photograph of the case of study. (Down) Urban radiant environment

2.3 Calculating thermal comfort index

Thermal comfort indices were used as a method to analyse the impact of the mean radiant temperature on people's thermal sensation.

With over 200 thermal comfort indices developed, it was essential to select the ones that best suit our analysis.

In a study by Migliari et al. [11], a graphical methodology was developed to assess the suitability of various thermal comfort indices for different criteria.

For our study, the selected thermal comfort index had to meet two specific criteria: it should consider mean radiant temperature as a climatic factor and it should be applicable in urban environments.

Out of all the thermal indices analysed, 19 met these criteria. We chose two indices for our study: UTCI, which has a strong focus on mean radiant temperature in urban spaces and PET, which not only met the criteria but is also the most used in outdoor thermal perception studies [12][13].

The objective of using the thermal comfort indices was to compare the influence of mean radiant temperature and air temperature on people thermal sensation.

To meet this objective, we calculated the thermal sensation for the real case study, which is a particularly vegetation-shaded place. The climatic factors used were obtained through calculation (mean radiant temperature 22ºC), measurements (air movement 0.5 m/s) and meteorological data (air temperature 22.7ºC and humidity 34%).

Subsequently, we calculated the thermal sensation for the same location, and gradually diminished the impact of the shade provided by vegetation. Two scenarios were employed for this analysis.

We modified only the mean radiant temperature (Tmrt). Previous studies [14][15] suggested that Tmrt can increase up to 25ºC in the absence of shade. We used this range to calculate the thermal sensation for mean radiant temperatures ranging from 22ºC to 47ºC.

We modified only the air temperature (Ta). Previous studies [14][15] suggested that Ta can increase up to 3ºC in the absence of shade. We used this range to calculate the thermal sensation for air temperatures ranging from 22.7ºC to 25.7ºC.

The assessment scales of PET and UTCI are given in Figure 5 [16][17].

Rayman was employed as software to calculate PET and UTCI, as this software has consistently demonstrated reliable results and is freely available.

PET and UTCI assessment Scale			
Thermal Sensation	Pet Range	Thermal Sensation	UTCI range
Very cold	< 4 ºC	Extreme cold stress	< - 40 ºC
Cold	4 to 8 ºC	Very strong cold stress	- 40 to - 27 ºC
Cool	8 to 13 ºC	Strong cold stress	- 27 to - 13 ºC
Slightly cool	13 to 18 ºC	Moderate cold Stress	-13 to 0 ºC
Comfortable	18 to 23 ºC	Slight cold stress	0 to 9 ºC
Slightly warm	23 to 29 ºC	No thermal stress	9 to 26 ºC
Warm	29 to 35 ºC	Moderate heat stress	26 to 32 ºC
Hot	35 to 41 ºC	Strong heat stress	32 to 38 ºC
Vety Hot	> 41 ºC	Very strong heat stress	38 to 46 ºC
		Extreme heat stress	> 46 ºC

Figure 5: PET and UTCI scale

3. RESULTS AND DISCUSSION

The thermographic images revealed that the shadow generated by vegetation (Fig. 6) had a significant impact on the radiant urban environment. The lowest recorded temperature corresponded to the bottom part of the trees, with approximate values of 17ºC.

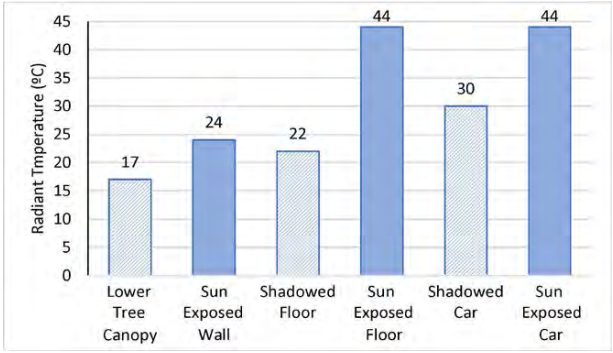

Figure 6: Surfaces' radiant temperature exposed to solar radiation and shadowed

The effect of shadow on horizontal surfaces showed radiant temperatures ranging from 22ºC to 44ºC. These values could be obtained through the thermal camera's software and the individual thermographic measurement. The vertical surface of the building exposed to the sun exhibited a temperature similar to the horizontal surface under the shade, which could be related to the angle of solar radiation incidence on these surfaces (Fig. 4).

Regarding horizontal surfaces, both the car and floor surfaces exhibit similar temperatures when exposed to direct solar radiation. However, these surfaces under shade can display temperature differences of up to 8 ºC.

It was observed that, during this period, the influence of the shadow had a greater impact on horizontal surfaces.

The impact of mean radiant temperature on thermal comfort can be observed in Fig 7. When the mean radiant temperature was increased 25ºC, from 22ºC to 47ºC, corresponding to a less shaded scenario, people thermal sensation increased 12ºC on the PET index and 7.4ºC on the UTCI index.

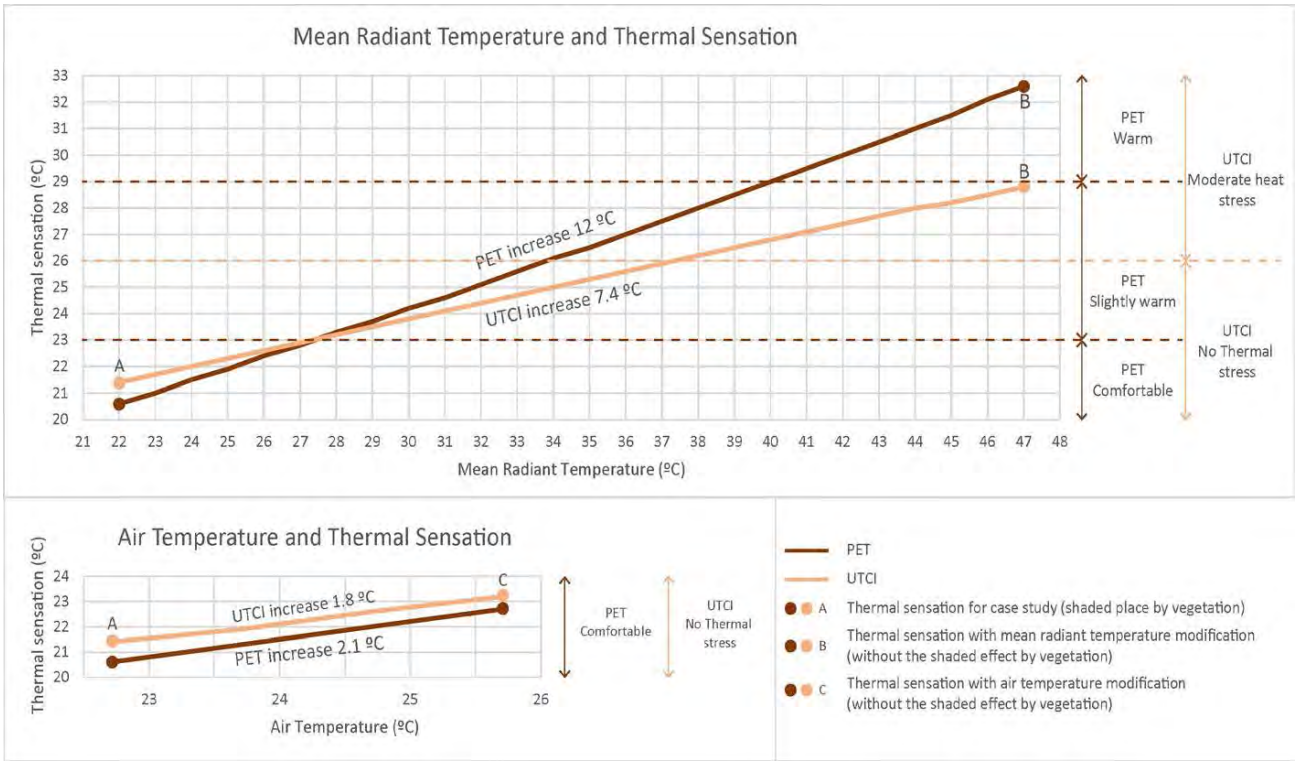

Figure 7: The impact of vegetation on thermal comfort. Comparison between modifying the mean radiant temperature (B) and the air temperature (C).

When the air temperature was increased 3ºC, from 22.7ºC to 25.7ºC, which corresponded to a less shaded scenario, the people thermal sensation increased 2.1ºC on the PET index and 1.8ºC on the UTCI index (Fig. 7).

Changes in thermal sensation can be observed. In PET, the sensation changed from comfortable to warm, and in UTCI, it changed from no thermal stress to moderate thermal stress.

When the results of modifying the mean radiant temperature and air temperature are compared in the calculation of PET and UTCI, it is evident that the mean radiant temperature variation had a greater impact than the air temperature variation (Fig. 8).

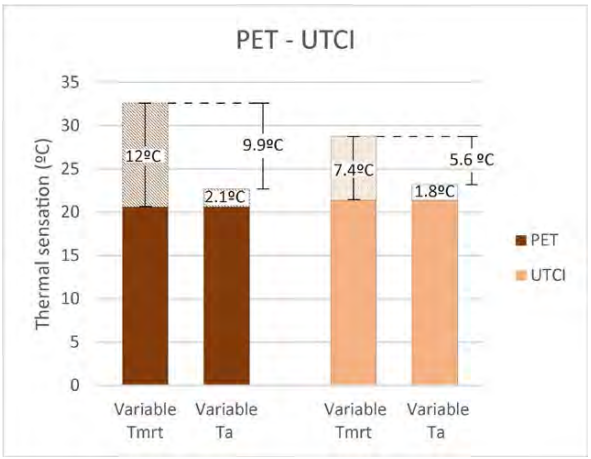

Figure 8: Impact on thermal comfort indices when the mean radiant temperature and air temperature are varied.

This study highlights the importance of considering mean radiant temperature when outdoor environments are designed. To achieve optimal results in warm periods, it is crucial to think not only about surface materials but also about the effect of shading on these surfaces.

Vegetation has proved to be an efficient solution, not only to provide shade to materials but also because it generally maintains a similar radiant temperature to the surrounding air temperature. This effect is significant in achieving a lower mean radiant temperature in the environment.

4. CONCLUSION

Thermographic images of complex urban environments can be a powerful tool to assess and visually observe phenomena that affect urban contexts, to design healthier and more resilient cities.

Spatial thermographic of an urban environment has proven to be a valuable tool for conducting radiation analysis in outdoor spaces. It provides 4π global data that aids in the study of how different surfaces behave within complex radiant environments.

Through the calculation of comfort indices, we could observe the impact of vegetation as a shading element on thermal sensation outdoors, specifically the impact of air temperature (Ta) and the even greater impact of the mean radiant temperature (Tmrt). For the PET index, the thermal sensation

increased by almost 10ºC more when Tmrt was modified rather than Ta. For the UTCI index, the thermal sensation increased around 5.6ºC more when Tmrt was modified rather than Ta (Fig. 8).

In this study, measurements were taken on a day when climatic conditions resulted in a comfortable thermal sensation under shading. However, changing the value of mean radiant temperature in a scenario with less shade can shift the thermal sensation to warm (PET) and moderate heat stress (UTCI).

Through the use of global thermographic images, the importance of vegetation as shading was observed.

For this specific case study, the horizontal surfaces exposed to solar radiation had a radiant temperature significantly higher than shaded surfaces. The canopy tree had a radiant temperature similar to air temperature.

During the months of the year when cities experience heatwaves and considering the influence of mean radiant temperature on thermal sensation, it is essential to implement strategies such as using vegetation as a shading element. Such strategies are crucial in creating urban spaces that remain as far as possible from the heat stress range values.

ACKNOWLEDGEMENTS

This research was carried out under project PID2020-116036RB-I00, funded by the Spanish Ministry of Science and Innovation (MCIN), ref. number MCIN/AEI/10.13039/501100011033.

REFERENCES

1. UNEP, Climate Change 2023: Synthesis Report | UNEP - UN Environment Programme. 2023.

2. M. Nikolopoulou and S. Lykoudis, “Thermal comfort in outdoor urban spaces: Analysis across different European countries,” Build. Environ., vol. 41, no. 11, pp. 1455–1470, Nov. 2006, doi: 10.1016/j.buildenv.2005.05.031.

3. D. Armson, P. Stringer, and A. R. Ennos, “The effect of tree shade and grass on surface and globe temperatures in an urban area,” Urban For. Urban Green., vol. 11, no. 3, pp. 245–255, Jan. 2012, doi: 10.1016/j.ufug.2012.05.002.

4. C. K. C. Lam, J. Weng, K. Liu, and J. Hang, “The effects of shading devices on outdoor thermal and visual comfort in Southern China during summer,” Build. Environ., vol. 228, no. October 2022, p. 109743, 2023, doi: 10.1016/j.buildenv.2022.109743.

5. J. M. Ochoa de la Torre, “La vegetación como instrumento para el control microclimático,” Universitat Politècnica de Catalunya, 1999.

6. J. K. N. Tan, R. N. Belcher, H. T. W. Tan, S. Menz, and T. Schroepfer, “The urban heat island mitigation potential of vegetation depends on local surface type and shade,” Urban For. Urban Green., vol. 62, no. April, 2021, doi: 10.1016/j.ufug.2021.127128.

7. X. Nan, H. Yan, H. Zhu, Q. Han, R. Wu, and Z. Bao, “Assessing the thermal environments of parking lots in relation to their shade design characteristics,” Sustain. Cities Soc., vol. 83, no. May, pp. 1–16, 2022, doi: 10.1016/j.scs.2022.103931.

8. N. Kántor, L. Chen, and C. V. Gál, “Human-biometeorological significance of shading in urban public spaces—Summertime measurements in Pécs, Hungary,” Landsc. Urban Plan., vol. 170, no. September 2017, pp. 241–255, 2018, doi: 10.1016/j.landurbplan.2017.09.030.

9. R. D. Brown and T. J. Gillespie, “Estimating outdoor thermal comfort using a cylindrical radiation thermometer and an energy budget model,” Int. J. Biometeorol., vol. 30, no. 1, pp. 43–52, 1986, doi: 10.1007/BF02192058.

10. S. A. Krys and R. D. Brown, “Radiation absorbed by a vertical cylinder in complex outdoor environments under clear sky conditions,” Int. J. Biometeorol., vol. 34, no. 2, pp. 69–75, 1990, doi: 10.1007/BF01093450.

11. M. Migliari, R. Babut, C. De Gaulmyn, L. Chesne, and O. Baverel, “The Metamatrix of Thermal Comfort: A compendious graphical methodology for appropriate selection of outdoor thermal comfort indices and thermo-physiological models for human-biometeorology research and urban planning,” Sustain. Cities Soc., vol. 81, no. September 2021, p. 103852, Jun. 2022, doi: 10.1016/j.scs.2022.103852.

12. O. Potchter, P. Cohen, T.-P. Lin, and A. Matzarakis, “Outdoor human thermal perception in various climates: A comprehensive review of approaches, methods and quantification,” Sci. Total Environ., vol. 631–632, pp. 390–406, Aug. 2018, doi: 10.1016/j.scitotenv.2018.02.276.

13. P. Kumar and A. Sharma, “Study on importance, procedure, and scope of outdoor thermal comfort –A review,” Sustain. Cities Soc., vol. 61, no. May, p. 102297, Oct. 2020, doi: 10.1016/j.scs.2020.102297.

14. C. L. Tan, N. H. Wong, and S. K. Jusuf, “Outdoor mean radiant temperature estimation in the tropical urban environment,” Build. Environ., vol. 64, pp. 118–129, Jun. 2013, doi: 10.1016/j.buildenv.2013.03.012.

15. H. Lee, H. Mayer, and L. Chen, “Contribution of trees and grasslands to the mitigation of human heat stress in a residential district of Freiburg, Southwest Germany,” Landsc. Urban Plan., vol. 148, pp. 37–50, Apr. 2016, doi: 10.1016/j.landurbplan.2015.12.004.

16. P. Höppe, “The physiological equivalent temperature - a universal index for the biometeorological assessment of the thermal environment,” Int. J. Biometeorol., vol. 43, no. 2, pp. 71–75, Oct. 1999, doi: 10.1007/s004840050118.

17. D. Fiala, G. Havenith, P. Bröde, B. Kampmann, and G. Jendritzky, “UTCI-Fiala multi-node model of human heat transfer and temperature regulation,” Int. J. Biometeorol., vol. 56, no. 3, pp. 429–441, May 2012, doi: 10.1007/s00484-011-0424-7.

PLEA 2024 WROCŁAW
(Re)thinking Resilience

Impact of Window vs Windowless Exam Rooms on Cognitive Performance:
A Field Study During a University Exam

SUNWOO CHANG, STEFANO SCHIAVON[1]

[1]University of California, Berkeley, CA, USA

ABSTRACT: This study aims to measure the impact of having visual connections to nature through windows on the cognitive performance of university students, as assessed by their final exam scores. To build upon prior research conducted in controlled laboratory and climate chamber settings, which may have a gap between findings and real-world contexts, demonstrating the positive effects of window views on occupants, this study addressed the limitations of lab-based experiments by conducting a field test in university lecture rooms with 121 students enrolled in STEM classes, taking their actual final exam. In the field test, we randomly assigned the students to either of two conditions: one with windows and one without, while monitoring indoor environmental factors. The results revealed no significant difference in cognitive performance—whether measured by scores or cognitive efficiency gauged by the time taken to complete the exam—between students in conditions with and without window views. Given the known small effect size of having windows on cognitive performance and the relatively small number of data points, we recognized that further iterations of the field tests are required to accumulate a more substantial dataset and draw more robust conclusions.
KEYWORDS: Window, View, Cognitive performance, Learning, Field test

1. INTRODUCTION

Creating a visual connection to the natural world outside through windows may bring benefits to the occupants [1]. While consistent findings documented the positive effects of human-nature interaction on cognitive performance and stress recovery, Ko et al. (2020) suggested that even providing a visual contact through windows could yield positive outcomes for occupants [2-3]. The study from Ko, et al. (2020) utilized a randomized crossover study design while maintaining identical indoor environmental quality variables, including temperature, lighting, and air quality, known to significantly affect occupants, controlling the confounding variables. However, it was conducted within a climate chamber. Therefore, it would be valuable to investigate whether the positive effects of a visual connection to nature can be replicated in real-world scenarios. There are several limitations in lab studies, including the unrealistic way of assessing cognitive performance. Ko et al. (2020) utilized cognitive tests from Cambridge Brain Sciences to evaluate participants' cognitive performance. In simulated work and learning conditions, it is difficult to determine whether participants were sufficiently motivated to achieve their highest possible achievements and scores. Additionally, considering that the tests were designed by researchers for specific purpose, a potential gap may exist between these assessments and the actual working tasks. To address these concerns, we conducted a field test to assess the impact of providing window views on cognitive performance by analyzing the final exam scores of students enrolled in a large building science class.

2. METHODS

2.1 Experimental design

We conducted a field experiment within existing university lecture rooms, where students are usually engaged in their typical academic activities, including attending lectures and taking exams.

We used the students' exam scores as a metric for assessing their cognitive performance during the test, given their strong motivation to attain the highest possible scores, which differs from other cognitive tests designed in a laboratory setting where participants may not necessarily exert their maximum effort.

We set two distinct conditions: one with windows (WW) and one without windows (WoW). A total of 121 students were randomly assigned to four lecture rooms, with two rooms designated for each condition. WW1 and WW2 represented the WW rooms, while WoW1 and WoW2 represented WoW. Each room accommodated between 27 to 33 students.

The selected lecture rooms used in the field test were equipped with versatile movable wood panels affixed to the walls, allowing for the transformation of the lecture spaces into exhibition areas. For the WoW condition, these panels remained closed during the exam.

WW1 and WoW1 are located next to each other and they shared similar design contexts and spatial

arrangements. WW1 covered an area of 99 m² for 34 students (equating to 2.9 m² per person), while WoW1 had 93 m² for 34 occupants (resulting in 2.7 m² per person). Similarly, WW2 and WoW2 were also located in immediate proximity to each other: WW2 had an area of 93 m² for 30 individuals (3.1 m² per person), and WoW2 spanned 101 m² for 30 occupants (3.3 m² per person).

2.2 Building design, physical and visual attributes of windows, and window view

The building's facade is equipped with an egg crate design, an external shading device featuring both overhangs and vertical fins, across all orientations except the North, ensuring that direct sunlight is blocked from entering the interior spaces year-round, minimizing the potential risks of glare.

For the physical attributes of the windows in both WW1 and WW2, each window had a rectangular design with a fixed width of 1.1 m. However, the windows had different heights depending on the row: 0.9 m for the bottom row, 1.1 m for the middle row, and 1 m for the top row. The window frames were made of metal. These single window units were positioned at fixed intervals of 0.3 m vertically, totalling three windows in height, and repeated horizontally at 0.4 m intervals, totalling six windows across. Consequently, the WW1 wall comprised a total of 18 single windows. The windows are of the operable awning type. During the field test, the windows remained closed. The calculated wall area measures 29.75 m², with a width of 8.5 m and a height of 3.5 m, with 20 m² dedicated to glazing, yielding a WWR of 67%. For their visual attributes, these windows were equipped with single-pane glazing and offered a VLT value of 0.8 when they are clean and new.

There was a difference in finishings between the WW1&WoW1 and WW2&WoW2 conditions. For WW1&WoW1, the horizontal intervals between these windows consisted of wood finishing with a white paint coating. The vertical intervals were constructed from concrete materials with a white paint finish.

For WW2&WoW2, the vertical intervals between these windows consisted of unfinished wood, exposing the material. The horizontal intervals were constructed from concrete materials without a finish. Regarding the window views, for WW1, observers primarily had visual contact with the greenery outside, including trees and grass. For WW2, occupants could have a visual connection with a building featuring a grey facade, which faces the building where the exam is being taken from a distance. At a closer range, the view content seen included land covered with grass.

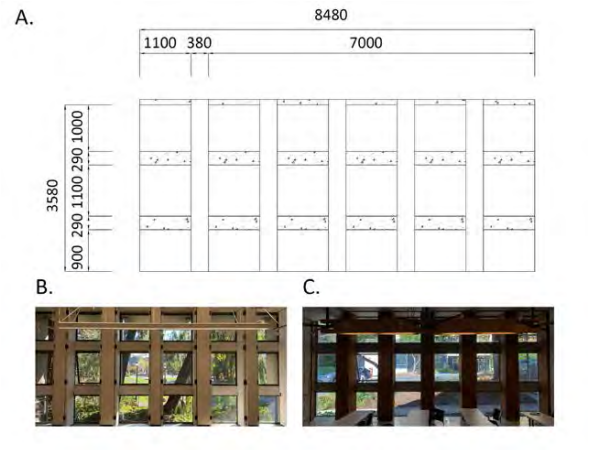

Figure 1. A. Section of walls and windows for both WW1 and WW2; B. The window view as seen in the room, With Window #1; C. The window view as seen in the room, With Window #2.

2.3 Environmental conditions: Pre-measurement

We monitored the temperature, relative humidity, and carbon dioxide concentration (CO2), and light intensity by employing data loggers (Model MX1102, Onset HOBO, USA) and light meter (T-1H, KONICAMINOLTA, Japan and Ds-2000, Sylvania, Hungary). These measurements were taken due to the potential of these variables to act as confounding factors. In addition, in the middle of the semester, we conducted a continuous, week-long pre-measurement for temperature, relative humidity, and CO2. The resulting median and Interquartile range (IQR) values for temperature, RH, and CO2 are as follows:

WW1: 20 °C (IQR=1), 40% (IQR=9), 350 ppm (IQR=30)
WW2: 20 °C (IQR=2), 40% (IQR=6), 430 ppm (IQR=50)
WoW1:21 °C (IQR=1), 40% (IQR=8), 450 ppm (IQR=40)
WoW2:20 °C (IQR=1), 40% (IQR=7), 375 ppm (IQR=50)

We found that the indoor conditions were consistent and meeting guidelines. To measure light intensity, sensors were placed in five different locations within each room, and the mean values were calculated. The results indicated that for WW1 and WoW1, the recorded values were 800 lux and 900 lux, respectively, while for WW2 and WoW2, the values were 300 lux and 350 lux.

2.4 Final exam details

The final exam, having a total of 100 points, comprised a combination of 62 assigned points for conceptual questions, true/false and multiple-choice, and 37 points for calculation questions. 1 point was given to all for acknowledging the school's honor code. To ensure a comprehensive assessment that challenges both theoretical understanding and calculation skills, we meticulously structured our exam. It encompasses conceptual inquiries into several fundamental concepts of building science,

including climate analysis, heat transfer, building energy, solar geometry, daylighting, indoor air quality, acoustics, and HVAC. For instance, we ask questions like: How bright is the brightest part of the overcast sky compared to the darkest part? These questions aim to evaluate students' understanding of well-established knowledge covered in the class and required readings, rather than requiring them to generate their own ideas. In the calculation questions, students are tasked with deriving specific values by correctly selecting and applying the appropriate formulas and input parameters.

2.5 Statistical analysis

We first conducted the Shapiro-Wilk normality test to assess whether the students' final exam scores followed a normal distribution [4]. Following this, we investigated the influence of two experimental conditions, WW and WoW, on students' cognitive performance during the exam using the Mann-Whitney U Test [5]. The Mann-Whitney test, a non-parametric method, was employed, eliminating the need for specific assumptions about normal distribution. Within this test, data from the WW and WoW groups were pooled, ranked in ascending order, and then the sum of ranks for each data point was calculated, resulting in having the U value. When comparing the U values between the two groups (WW and WoW), if one is significantly smaller or larger (two-sided) than the other, it indicates a meaningful difference in final exam scores between the groups.

We used the z-score method and t-test to assess whether there was a significant difference in individual students' relative grade positions before (pre-exam) and after (post-exam) the exam by the conditions. Our hypothesis was that having a visual connection to the outside through windows would increase cognitive performance. Consequently, we expected that students in WW would demonstrate an improved post-exam ranking compared to their pre-exam ranking, and vice versa. To test this, we computed z-scores for each student before and after the exam, calculating the difference between these two z-scores for each student. We then applied a t-test to analyze these difference values by the conditions.

To assess their pre-final exam performance, we aggregated the scores from six in-class quizzes. These quizzes were proctored by the instructor team, similar to the actual exam format and excluding any potential for collaborative work or cheating. The post-exam Z-score for each student was determined using their final exam score. We computed the effect size using Cohen's d, denoted as "r."

We assessed statistical power using GPower. For the effect size, we adopted a value of .2 based on prior literature (Ko et al., 2019), which suggested small effect sizes for cognitive performance—.31 for "Working memory" and .26 for "Concentration." Given that this is our initial field test, we intentionally chose a relatively small effect size. We established a significance level (alpha error probability) as .05, and the sample size for both groups was set at 60. Consequently, our calculated statistical power was .19. We used R as a statistical analysis software to run Mann-Whitney U Test, Shapiro-Wilk Test, standarized score, and t-test.

3. RESULTS

3.1 Environmental conditions

The field test took place on in mid-May, 2023 from 8:00 am to 11:00 am. We monitored several indoor environmental quality factors, including temperature, relative humidity, CO_2 levels, lighting, and acoustic conditions, to ensure similarity across four distinct rooms: WW1, WoW1, WW2, and WoW2. To gather this data, we used two sensors—MX1102 (Onset HOBO, USA) for temperature, relative humidty, and CO2 measurement and MX1104 (Onset HOBO, USA), for measuring temperature and relative humidity while also measuring light data. As a result, the temperature difference between WoW1 and WW1 was found to be $Median_{windowless\text{-}window\_1}$ = 1 °C, with an $IQR_{windowless\text{-}window\_1}$ of .5 °C. Similarly, WoW2 and WW2 showed a temperature difference of $M_{windowless\text{-}window\_2}$ = 1 °C, accompanied by an $IQR_{windowless\text{-}window\_1}$ of .7 °C.

For the lighting conditions at WW1 and WW2, we measured horizontal illuminance levels to assess the lighting condition of two spaces during the test. This was because there might be a potential dynamic influence of direct sunlight and diffuse light on the desk-level illuminance (target illuminance), affecting students taking exams when the movable panels remained open. To ensure consistent data collection, we positioned both sensors on stools at the same height as the desks where students took exams. In WW1, the light intensity increased by ~200 lux compared to the pre-measurement, rising from ~800 to ~1000 lux. Meanwhile, in WW2, the light intensity decreased by ~100 lux, dropping from ~300 to ~200 lux. We conducted two separate acoustic level measurements: the first at 8:30 and the second at 9:00. The resulting average acoustic levels for each room were as follows: 47 dB for WW1, 50 dB for WoW1, 49 dB for WW2, and 44 dB for WoW2.

Table 1: Environmental conditions during the field test

Condition	WW1	WoW1	WW2	WoW2

Temp °C	22 (.5)	23 (.3)	21 (1)	22 (1)
RH %	50 (2)	45 (3)	50 (2)	50 (1)
CO_2 ppm	480 (120)	580 (150)	490 (55)	410 (60)
Light lux	1,000	n/a	200	n/a
Acoustics dB	47	50	49	44

Figure 2. Field experimental conditions: two spaces with windows (left column) and two spaces without windows (right column)

3.2 Cognitive performance by overall, conceptual and calculation question scores

There were no significant differences in students' performance between the condition with and without view (*p-value*>.8, r < .1, a negligible effect). The same was found regardless of question types, whether they were conceptual, calculation, or the sum of the two.

Table 2: Exam score results based on question type and room type.

Type	Conceptual (62 points)	Calculation (37 points)	Overall (99 points)
Entire Class	Mean=43.8 SD=7.5	Median=30 IQR=9	Median=74.5 IQR=17.5
WW	Mean=44.1 SD=7.5	Median=30 IQR=9.5	Median=74.2 IQR=17.6
WoW	Mean=43.52 SD=7.5	Median=30 IQR=7	Median=75 IQR=20
Normally Distributed?	Y (*p-value* >.07)	N (*p-value* <.01)	N (*p-value* <.01)

Since the scores from conceptual questions followed a normal distribution, we employed a t-test. However, when comparing the scores representing the sum of conceptual questions between the two conditions, our analysis did not provide any significant evidence of a difference in means (*p-value* > .9, r < .1, a negligible effect).

Similarly, we did not find that scores obtained from calculation questions from students in the WW condition were higher than those of the students who took the exam in the WoW condition (*p-value*>.7, r<.1, a negligible effect).

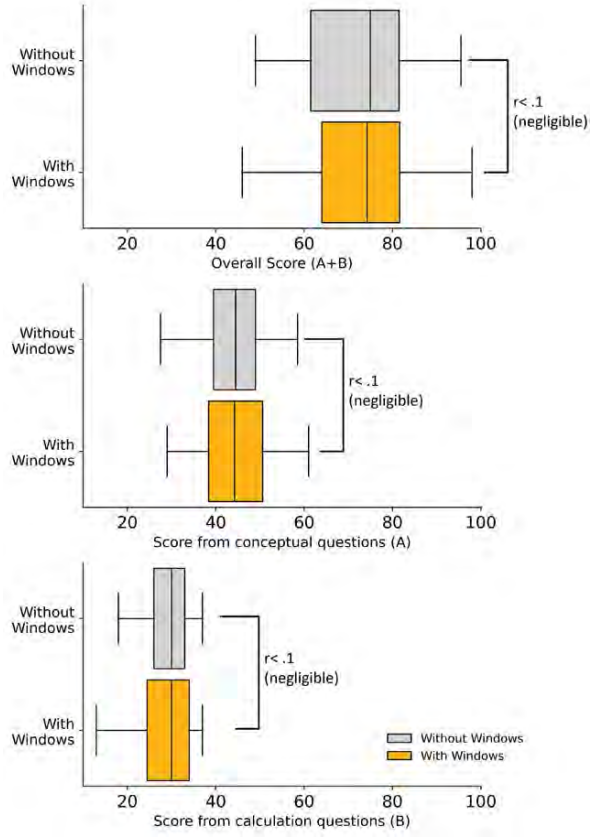

Figure 3. Comparing students' overall scores, their scores on conceptual and calculation questions, depending on the students took the exam in the rooms with or without windows.

3.3 Cognitive performance by pre-and post-exam performance

We observed that the difference between pre-exam and post-exam Z-scores followed a normal distribution, as tested by applying a Shapiro test with a significance level of .05 and a *p-value* of .388. Since students are randomly assigned to either WW or WoW and are independent of each other, we conducted a t-test, which revealed that there was no significant difference in the mean values of Z-score

differences between the conditions (significance level = .05, *p-value* = .485, t = .700, effect size < .2, a negligible effect).

3.4 Cognitive efficiency measured by taken exam time

We analyzed the data in terms of cognitive efficiency. This analysis was based on the assumption that if the students who stayed in the WW condition finished their exam earlier, we could infer higher efficiency, as the outcomes were similar between the conditions. We excluded two students from the WoW1 condition as they arrived late for the exam. Therefore, 119 data points were used for the analysis. The exam time had median and IQR values of 111 min and 40.5 min, respectively, for the overall class. For the students in the WW condition, the time taken to finish the exam was 114.5 min and 42.5 min for the median and IQR, respectively. For the students in the WoW condition, the time taken to finish the exam was 106 min and 34 min for the median and IQR, respectively. Because the time taken for the exam was not normally distributed (significance level = .05, *p-value* < .01), we utilized the Mann-Whitney U test. There was no significant difference in the time taken for the exam between the conditions (U=1528.5, significance level=.05, *p-value*=.200, effect size=.23, indicating a small effect).

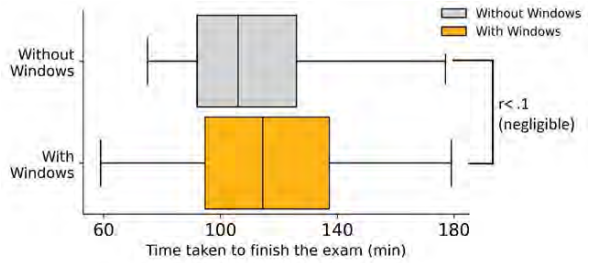

Figure 4. Comparing students' time taken to finish the exam, depending on the condition where students took the exam, the rooms with or without windows.

4. CONCLUSION

We investigated the impact of having a visual connection to the outside via windows on performance of students during their university final exams.

We plan to replicate this study over several years to accumulate a sufficient sample size. Based on our literature review, we expected a .25 effect size in people's enhanced exam performance when they have a visual connection to the outside. To achieve a statistical power of .8 with a significance level of .05, we need 265 data points for both the with window and windowless conditions, which may require up to four years of field experiments.

In this study, we could not find a significant difference in students' performance whether they had a window view out or not. At this stage, it is difficult to explain why our results were inconsistent with previous findings in controlled laboratory experiments. It is unclear whether this gap is due to an insufficient sample size or if the effects of having windows are not substantial enough to boost performance in the real-world contexts. Further research is needed to better understand these outcomes.

REFERENCES

1 . Ko, W., Schiavon, S., Zhang, H., Graham, Lindsay T., Brager, G., Mauss, I., and Lin, Y., (2020). The Impact of a View from a Window on Thermal Comfort, Emotion, and Cognitive Performance., *Building and Environment*, 175.

2 . Berman, Marc G., Jonides, J., and Kaplan, S., (2008). The Cognitive Benefits of Interacting With Nature. *Psychological Science*, 19: p. 1207–1212.

3 . Ulrich, Roger S., Simons, Robert F., Losito, Barbara D., Fiorito, E., Miles, Mark A., and Zelson, M., (1991). Stress Recovery during Exposure to Natural and Urban Environments. *Journal of Environmental Psychology*, 11(3): p.201-230.

4 . Shapiro, Samuel S., and Wilk, M., (1965). An Analysis of Variance Test for Normality (Complete Samples)., *Biometrika*, 52(3): p.591-611.

5 . Mann, Henry B. and Whitney, D. Ransom, (1947). On a Test of Whether one of Two Random Variables is Stochastically Larger than the Other. *Ann. Math. Statist.* 18 (1): p. 50 – 60.

PLEA 2024 WROCŁAW
(Re)thinking Resilience

Development of a New Adaptive Comfort Model for Social Housing in Andalusia

YANET CORONA-MACÍAS[1], EVELYN DELGADO-GUTIÉRREZ[1], MARTA TORRES-GONZÁLEZ[1], DAVID BIENVENIDO-HUERTAS[2], DANIEL SÁNCHEZ-GARCÍA[1], CARLOS RUBIO BELLIDO[1]

[1]University of Seville, Seville, Spain
[2] University of Granada, Granada, Spain

ABSTRACT: An approach with potential benefits in terms of energy efficiency and sustainability is adaptive thermal comfort, which recognizes the variability and subjectivity of individuals' thermal preferences. International standards have included models that allow predicting users' comfort levels based on outdoor temperature, but they are not always applicable, requiring the development of specific models that consider the environmental, economic, and social reality of certain regions and groups of people. This research evaluates the applicability of the UNE-16798-1:2019 standard in social housing located in Mediterranean climate zones during the summer months and develops a new adaptive thermal comfort model according to users' thermal adaptability. The advantage of this proposal is its replicability of the method at an international level. The existence of a specific model constitutes the first step towards making more accurate predictions of energy demands and consumptions, identifying cases of energy poverty in the region and generating more sustainable and conscious investments in energy efficiency. This will also contribute to mitigate health problems associated with high temperatures resulting from climate change.
KEYWORDS: climate change, social housing, adaptive thermal comfort model, mediterranean climate

1. INTRODUCTION

Climate change has led to an increase in extreme temperatures worldwide. Hotter summers can cause homes to become extremely hot, resulting in uncomfortable and, in some cases, hazardous living conditions. The inability to use cooling systems for vulnerable families, combined with energy-inefficient buildings, leads to situations of energy poverty.

To have reliable indicators of energy poverty, it is essential to understand the energy consumption that corresponds to occupants' comfort needs. The main causes of high energy consumption are air conditioning and heating systems [1, 2], which leads users to limit their use and, consequently, reducing thermal comfort.

1.1 Adaptive thermal comfort

For several decades, many researchers have been studying the factors related to thermal comfort in individuals. The first models of thermal comfort emerged from experimental results in laboratories and climatic chambers, with standardized clothing and activity conditions [3]. This approach, based on the Predicted Mean Vote (PMV) and the Predicted Percentage of Dissatisfied (PPD), establishes static setpoint temperatures and has been adopted by numerous regulations such as UNE-EN ISO 7730:2006 [4]. However, various studies have demonstrated that this approach is not the most suitable for addressing the thermal comfort of occupants in a free-running building mode [5-9], as it does not consider the users' ability to control their environment through certain behaviors, in addition to disregarding thermal memory, cultural, social, and climatic factors [7, 8].

In response to this issue, the adaptive approach — supported by numerous field studies such as the Smart Control and Thermal Comfort SCATs project conducted in Europe, and the RP-884 project carried out in various regions of the world — emerges. The adaptive comfort models derived from these studies have been incorporated into the American standard ASHRAE 55-2020 and the European standard EN 16798-1:2019 [10, 11].

These standards establish a mathematical direct relationship between the prevailing mean outdoor temperature and occupants' comfort temperatures, making them attractive due to their relative simplicity [12]. However, these models have certain ranges of application, which means they cannot be used in extreme temperature conditions [13, 14]. Additionally, in the case of the model developed in the EN 16798-1:2019 standard, it is based on a limited database for average outdoor operating temperatures above 25°C, reducing its applicability in warm climates [13].

For this reason, in recent years, there has been a trend towards developing specific adaptive comfort models for specific climates [14, 15]. The Equation (1) proposed by Humphreys [16] has served as a foundation for this, defining a mathematical relationship between comfort temperature and outdoor temperature, where the constants (a and b) vary depending on the context in which the model is developed.

$$T_{comf} = a\, f(T_{ext}) + b \quad (1)$$

where T_{comf} is Neutral comfort temperature (°C); T_{ext} is the prevailing mean outdoor temperature (°C); *a* and *b* are constants.

1.2 The Mediterranean climate in Andalusia

Andalusian cities are characterised by extremely hot summers, classified as 3 and 4 on a range of 1 to 4, during the hot months according to the Technical Building Code (CTE-DB-HE) [17]. These conditions have been intensified in recent years due to climate change. The most common way to control high temperatures within homes in Andalusia is through individual cooling systems, which are operated by users based on their thermal preferences and their ability to handle the subsequent high energy consumption. As a result, many times, the setpoint temperatures for the summer months established in the CTE-DB-HE [17] are lower than the actual operating temperatures recorded in residential buildings. This situation, combined with the thermal memory developed by the inhabitants of these climatic areas, influences the modification of comfort temperature values relative to the neutral temperatures obtained from adaptive comfort models in international standards.

This reality is more evident in social housing, where families are usually in vulnerable situations. In fact, in 2018, Andalusia had the largest stock of protected housing in all of Spain [18], most of which were built before the establishment of the first energy efficiency requirements in Spanish regulations. This, together with the lack of specific studies on poverty in this region, makes it essential to develop models that serve as a basis for subsequently determining levels of energy poverty. In this sense, the objective of this work is to stablish a specific adaptive thermal comfort model that allows predicting energy consumption.

2. METHODOLOGY

This work was carried out in several stages, starting from the study of existing research precedents on the topic and the contextualization of the case study. Secondly, a representative sample of population was selected to answer surveys and monitor environmental parameters to generate the database used in the statistical analysis to determine the applicability of the European standard EN 16798-1:2019 [11] and develop a mathematical model that fits the case study.

2.1 Selection of case studies

To conduct this research, a sample of social housing units in Andalusia promoted by the Andalusian Agency of Housing and Rehabilitation (AVRA). A total of 46 single-family homes within public residential buildings participated in monitoring the indoor environmental conditions and answering the surveys.

2.2 Monitoring of environmental conditions

The selected homes underwent monitoring of internal environmental variables during the warmest months in Seville (Spain), from June to October 2023. The average outdoor temperatures during these months ranged from 21°C to 34°C, being some recordings outside the limits established by the EN 16798-1:2019 standard [11].

The measurement of indoor variables was done on site, recording the dry bulb temperature (T_a), globe temperature (T_g), relative humidity (RH), and air velocity (V_a) using the Delta Ohm model 32.3 device. The data logger was placed in the living room of each home at a height of 1.1m from the floor and the surveys were carried out simultaneously.

For the measurement of outdoor conditions, the Testo 160 IAQ sensor was used, recording air temperature (T_a) and relative humidity (RH) at 5-minute intervals.

2.3 Administration of surveys

Following the Code of Ethics of the World Medical Association (Declaration of Helsinki), informed consent signed by each participant was obtained before responding to the surveys. Anonymity and confidentiality were ensured. The survey model was based on standardized methods [10, 19], initially collecting information about the dwelling, the HVAC systems used, clothing, activity level, and then assessing the thermal sensation and thermal preference of the occupants. Based on the collected information regarding the clothing worn during the survey and the activity level, the thermal insulation (clo) was determined, ranging from 0 to 0.8 clo, and the metabolic rate (MET) with values between 0.8 and 2.4 MET, according to UNE-EN ISO 7730:2006. The values of the Thermal Sensation Vote (TSV) and the Thermal Preference Vote (TPV) were defined using a seven-level scale based on the thermal equilibrium of the human body (Table 1) [4,20].

Table 1: Scale of levels for TSV and TPV.

Question	Answer	Variable	Range
How do you feel now?	Cold (-3), Cool (-2), Slightly cool (-1), Neutral (0), Slightly warm (1), Warm (2), Hot (3)	TSV	From -3 to 3
How would you like to feel?	Much colder (-3), Cooler (-2), Slightly cooler (-1), The same (0), Slightly warmer (1), Warmer (2), Much hotter (3)	TPV	From -3 to 3

A total of 437 surveys were conducted with occupants aged between 17 and 92 years, interviewing 250 women and 187 men. The surveys were conducted at different times depending on the

availability of the individuals. Participants were asked to position themselves as close as possible to the measurement equipment without interfering with its functioning while answering the interview.

2.4 Statistical analysis

The data resulting from the monitoring and surveys were statistically processed to develop the new adaptive comfort model.

Firstly, 22 surveys with inconsistent responses were identified, where the sum of TSV and TPV was ≤ -3 or ≥ 3. Based on the remaining responses, comfort temperatures were determined using the Griffiths Equation (2):

$$T_{comf}=Top-TSV/b \quad (2)$$

where T_{comf} is the Neutral comfort temperature (°C); T_{op} is the Operative temperature (°C); TSV is the Thermal Sensation Vote; and *b* is the Griffiths constant (0.5) [21].

The obtained comfort temperatures were organized according to the average outdoor operating temperatures, and box plots were created, detecting 8 outliers.

To determine the average outdoor operating temperatures (θ_{rm}), Equation (3) was used, which considers the average of the outdoor temperatures of the previous 7 days.

$$\theta_{rm} = (\theta_{ed-1} + 0.8*\theta_{ed-2} + 0.6*\theta_{ed-3} + 0.5*\theta_{ed-4} + 0.4*\theta_{ed-5} + 0.3*\theta_{ed-6} + 0.2*\theta_{ed-7}) /3.8 \quad (3)$$

where θ_{rm} is the prevailing mean outdoor air temperature of a particular day (◦C); and θ_{ed-i} is the average daily outdoor temperature of i previous days (◦C).

A total of 407 points (θ_{rm}, T_{comf}) were obtained after excluding inconsistent surveys and outliers from the comfort temperatures. These values were then compared to the UNE EN 16798-1:2019 standard. To gain a better understanding, the difference between the room's operative temperature and the standard's neutral temperature was determined for each θ_{rm} value. Each difference was then associated with the percentage corresponding to each TSV level. To simplify the analysis, the TSVs were grouped into Cool (TSV < -1), Comfort (-1 ≤ TSV ≤ 1), and Warm (TSV > 1).

Finally, a regression analysis was performed to obtain a new adaptive comfort model based on the points (θ_{rm}; T_{comf}), determining the neutral temperature and the ranges within which an 80% and 90% thermal acceptability could be achieved. Ultimately, the model was evaluated using the TSV values obtained from the field study.

3. RESULTS AND DISCUSSION

3.1 General analysis of the generated database from the surveys and recordings

In the conducted measurements, the mean daily temperature of the outdoor air ranged from 20°C to 34°C, ±3,25°C SD, with the median temperature recorded around 25°C. As a result, 32% of the values for the average θ_{rm}, considering the 7 days prior to the study period, were found to be above 25°C, falling within the reduced applicability range of the EN 16798-1:2019 standard.

On the other hand, regarding the monitoring and TSV of the surveys, it was found that the comfort temperature for the users ranged from 18°C to 34°C, ±3,23°C SD.

From the conducted surveys, the TSV of the users was determined (Fig. 1), with the majority being neutral at 41.79%, followed by a slightly warm sensation at 23.43% of the surveyed cases. The perceptions of slightly cool, warm, and cool occupied 12.08%, 9.18%, and 8.66% respectively. People who expressed feeling hot (2.80%) or cold (1.93%) were isolated cases. This demonstrates that the thermal perception of the users ranges from neutral to slightly warm, representing 65.22% of the cases.

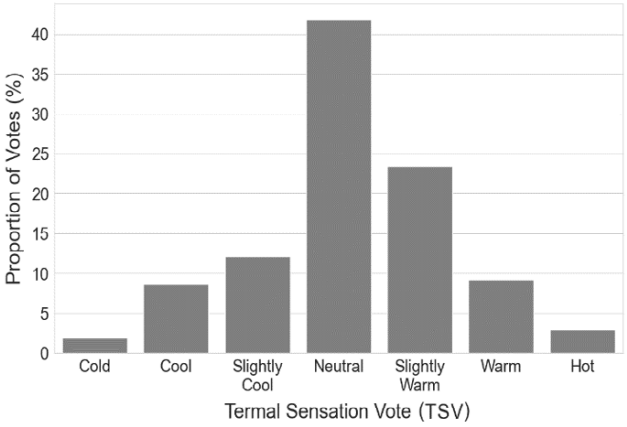

Figure 1: Proportion of TSV retrieved from the surveys.

These results corresponded to the levels of TPV (Fig. 2), with 72.22% of the users preferring to remain the same or be slightly cooler.

Furthermore, if we add that 79.14% of the surveyed individuals on days with average θ_{rm} above 25°C expressed feeling slightly cool, neutral, or slightly warm, and that 76.28% preferred temperatures that were slightly cooler, the same, or slightly warmer, it could be argued that there is a certain adaptability on the part of users to temperatures corresponding to the warm climate in the studied area.

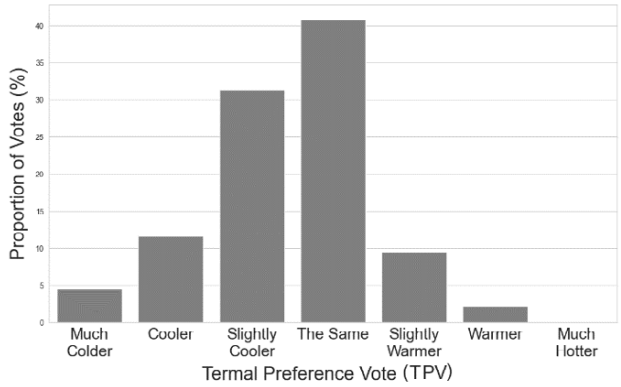

Figure 2: Proportion of TPV retrieved from the surveys.

3.2 Applicability of the EN 16798-1:2019 standard to the study case.

The EN 16798-1:2019 standard defines three Categories based on the expectations of building occupants, as well as other factors that influence comfort perception and the age of the building. These ranges are established using the neutral temperature of the model, which can be determined by Equation (4), and are set between the limits of 10°C and 30°C for θ_{rm}. For temperatures outside of these limits, the comfort temperature can be considered static. Additionally, for average outdoor operating temperatures above 25°C, the applicability of this standard is reduced.

$$T_{neutra} = 0{,}33\ \theta_{rm} + 18{,}8 \qquad (4)$$

where T_{neutra} is the neutral temperature (°C); and θ_{rm} is the prevailing mean outdoor air temperature of a particular day (°C)

During the measurement period, 139 comfort temperature values were obtained when the mean outdoor operating temperature was above 25°C, accounting for 32% of all data points (Fig. 3). Additionally, it was observed that for these cases compared to those with outdoor operating temperatures below 25°C, there was a slight increase in the comfort temperature relative to the neutral temperature calculated according to the EN 16798-1:2019 standard. There was also a narrower range of comfort with a higher concentration of data points towards neutrality, indicating a variation in the thermal response of individuals when exposed to higher temperatures.

This variation was confirmed by establishing the relationship between the percentage of TSV and the deviation of the measured room's operative temperature from the neutral temperature of the standard (Fig. 4).

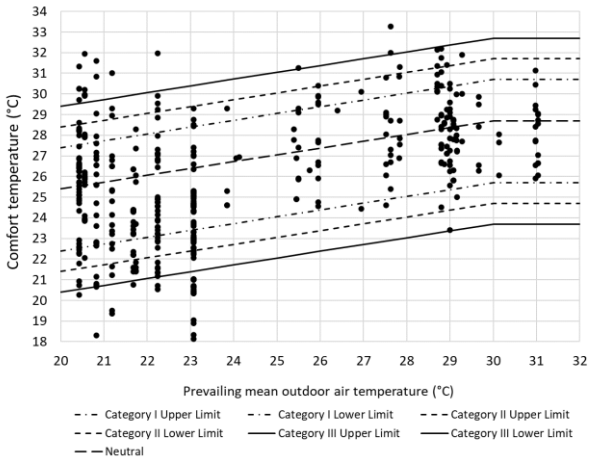

Figure 3: Scatter plot: User comfort temperature and outdoor running mean temperature within the limits of categories I, II and III according to EN 16798-1:2019.

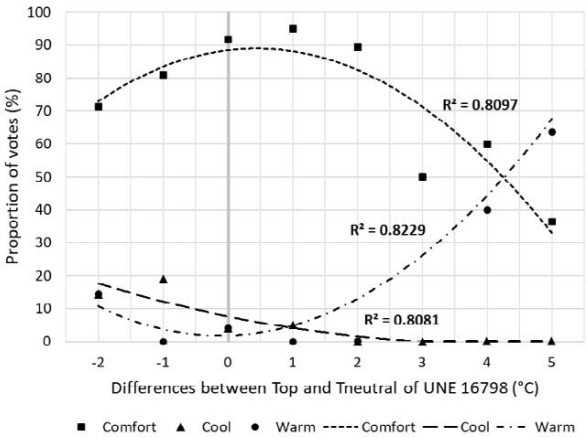

Figure 4: Percentage of TSV corresponding to the deviation of the Top from the neutral temperature of the EN 16798-1:2019 standard.

For this analysis, differences with a very small number of cases were disregarded to avoid misleading evaluations of the model. As a result, it was found that the comfort vote for TSV ranged between 32.98% and 89.01%, and there was a deviation in the regression curve obtained compared to the neutral line of the EN 16798-1:2019 standard of approximately +0.5°C (R^2=0.8097). Furthermore, it can be observed that the 80% threshold is only surpassed by the votes corresponding to comfort, with a high percentage of individuals feeling comfortable when temperatures are between 1.38°C below the neutral temperature of the standard and 2.27°C above it. This represents a much smaller range (3.65°C) compared to Category II of the standard (7°C). As for the 90% threshold for this regression curve, it is not surpassed in any case.

3.3 Development of a new adaptive comfort model.

Given the percentage of data points that fall within the reduced applicability range of the EN 16798-1:2019 standard, the deviation of the maximum point on the comfort curve from the neutral line, and the

decrease in the range of comfort, a new adaptive comfort model was developed for temperatures above 25°C. For this purpose, a regression analysis was conducted to obtain a trendline that relates the average outdoor operating temperature to user comfort temperatures. Through this analysis, the neutral temperature of the new model was defined using Equation (5) when the average outdoor operating temperature is greater than 25°C and less than 31°C, 25°C≤θ_{rm}≤31°C, with an R^2 value of 0.0088.

$$T_{neutra}=0{,}1273\ \theta_{rm}+24{,}526 \qquad (5)$$

where T_{neutra} is the Neutral temperature (◦C); and θ_{rm} is the prevailing mean outdoor air temperature of a particular day (◦C)

The statistics determined for the proposed equation were the Standard Error (SE) with a value of 2.17, the Mean Absolute Error (MAE) which was 1.68, and the p-value. A significance level of 95% was set for the p-value, so the obtained value for this statistic (0.265) indicates a weak correlation between the variables. This can be explained by the small slope of the line, as the neutral temperature remains nearly constant despite the increase in the mean outdoor operating temperature.

To evaluate the new model and obtain the 80% and 90% comfort ranges, the same analysis as conducted for the EN 16798-1:2019 model was performed, this time establishing the relationship between TSV and the difference between the operative temperature and the neutral temperature of the new model (Fig. 5). From this analysis, it was found that the peak of the Comfort curve aligns with the neutral temperature of the model, demonstrating its fit to the thermal response of users to these temperatures.

On the other hand, the 80% acceptability level of the TSV exhibits a shift of ±2.00°C from the neutral line of the new comfort model, corresponding to Category II of the standard. The 90% thermal acceptability for the TSV was obtained within a range of ±0.85°C from the neutrality of the proposed model, corresponding to Category I of the EN 16798-1:2019 standard. Category III of the standard establishes a 65% acceptability limit, which, in the case of the upper limit of the new model, translates to a deviation of 3.20°C from the obtained neutral temperature. This implies that, for the highest average outdoor operating temperature (31°C), a comfort temperature of approximately 32°C is reached, which is too high to be considered comfortable. Therefore, for the new model, only two acceptability ranges have been established: one for 80% with a range of ±2.00°C and one for 90% with a range of ±0.85°C (Fig. 6).

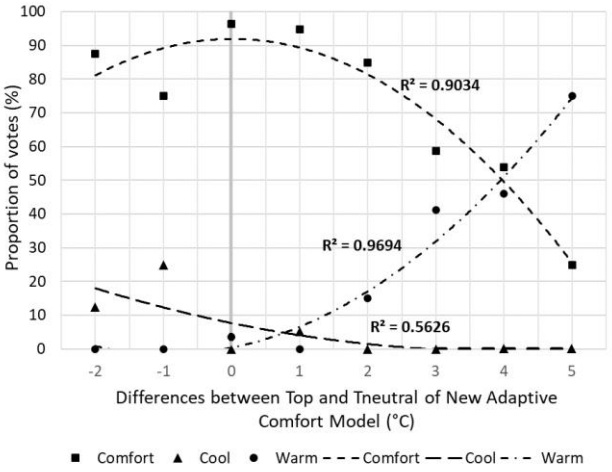

Figure 5: Percentage of Thermal Sensation Votes (TSV) corresponding to the deviation of the operative temperature (Top) from the neutral temperature of the obtained new comfort model.

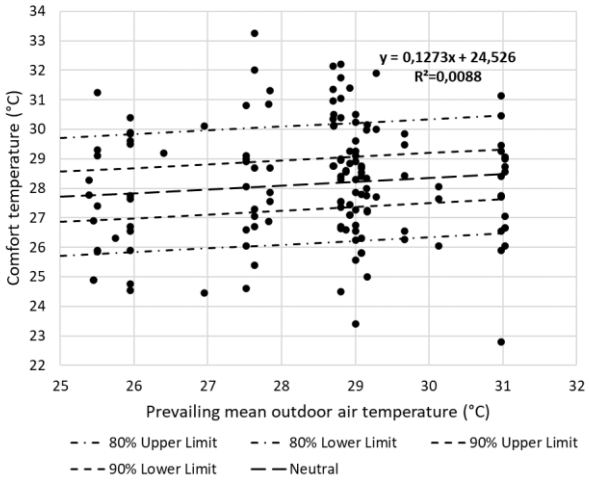

Figure 6: Scatter plot: User comfort temperature and outdoor running mean temperature over the neutral line of the new comfort model and the 80% and 90% ranges.

4. CONCLUSION

In this research, an adaptive comfort model has been developed for vulnerable households in Andalusia, considering mean outdoor operating temperatures where the applicability of the EN 16798-1:2019 standard is reduced. From the conducted analysis, a deviation of approximately +0.5°C was detected in the adjusted neutral temperature based on the comfort levels obtained from the field study compared to the neutral temperature of the standard. Additionally, despite the higher percentages of votes being obtained for Comfort and slightly warm sensations, there was a decrease in the range of acceptability compared to the standard. The 80% of of comfort votes were concentrated within temperatures ±2.00°C of neutrality, indicating that at very high temperatures, the possibilities of taking actions to achieve comfort without the use of conditioning systems are reduced, resulting in narrower

acceptability ranges compared to Category II of the EN 16798-1:2019 standard. The new comfort model will allow predicting energy demands and consumption more accurately through simulation engines like EnergyPlus, considering specific adaptive setpoints. These consumption values can be used to update energy poverty indices in the region during the summer season, taking into account household consumption costs and family income, and generating different combinations for subsequent comparison with the 2M indicator (double the national average energy expenditure), which is considered by the National Strategy against Energy Poverty. Being aware of the reality of this issue will contribute to developing effective construction practices that lead to improvements in people's quality of life.

ACKNOWLEDGEMENTS

This research was part of the project “Implications in the mitigation of climate change and of energy poverty through a new adaptive comfort model for social housing (ImplicAdapt)”, Reference: US.22-02, which is financed by the Junta de Andalucía and has had the collaboration of the Andalusian Housing and Rehabilitation Agency (AVRA) for access to housing and participation of its users, for which the authors acknowledge the support.

REFERENCES

1. Pérez-Lombard, L., Ortiz, J., & Pout, C. (2008). A review on buildings energy consumption information. Energy and Buildings, 40(3), 394–398. https://doi.org/10.1016/j.enbuild.2007.03.007

2. Chua, K. J., Chou, S. K., Yang, W. M., & Yan, J. (2013). Achieving better energy-efficient air conditioning – A review of technologies and strategies. Applied Energy, 104, 87–104. https://doi.org/10.1016/J.APENERGY.2012.10.037

3. Fanger, P. O. (1970) Thermal confort: analysis and applications in environmental engineering (McGraw-Hill (ed.)).

4. UNE-EN ISO 7730:2006. Ergonomics of the thermal environment – Analytical determination and interpretation of thermal comfort using calculation of the PMV and PPD indices and local thermal comfort criteria, 52 (2006).

5. Humphreys, M. A., & Fergus Nicol, J. (2002). The validity of ISO-PMV for predicting comfort votes in every-day thermal environments. Energy and Buildings, 34(6), 667–684. https://doi.org/10.1016/S0378-7788(02)00018-X

6. Humphreys, M. A. (1994). Field studies and climate chamber experiments in thermal comfort research, Thermal Comfort: Past, Present and Future,52–72.

7. Brager, G.S. & de Dear, R.J. (1998). Thermal adaptation in the built environment: a literature review. Energy and buildings, 27(1), 83–96. https://doi.org/10.1016/S0378-7788(97)00053-4

8. De Dear, R. J. & Brager, G.S. (1998). Developing an Adaptive Model of Thermal Comfort and Preference. ASHRAE Transactions, 104(March), 145-167. https://escholarship.org/content/qt4qq2p9c6/qt4qq2p9c6.pdf

9. Dear, R.D., Brager, G. & Cooper, D. (1997). ASHRAE RP- 884 Developing an Adaptive Model of Thermal Comfort and Preference. Database, (March).

10. ANSI/ASHRAE. (2020). ANSI/ASHRAE Standard 55-2020: thermal environmental conditions for human occupancy.

11. EN 16798-1: 2019. (2019). Energy Performance of Buildings—Ventilation for Buildings—Part 1: Indoor Environmental Input Parameters for Design and Assessment of Energy Performance of Buildings Addressing Indoor Air Quality, Thermal Environment, Lighting and Acoustics—Module M1-6.4.

12. de Dear, R. J., & Brager, G. S. (2002). Thermal comfort in naturally ventilated buildings: revisions to ASHRAE Standard 55. Energy and Buildings, 34(6), 549–561. https://doi.org/10.1016/S0378-7788(02)00005-1

13. Sánchez-García, D., Rubio-Bellido, C., Pulido-Arcas, J. A., Guevara-García, F. J., & Canivell, J. (2018). Adaptive Comfort Models Applied to Existing Dwellings in Mediterranean Climate Considering Global Warming. Sustainability (Switzerland), 10(10). https://doi.org/10.3390/su10103507

14. Pérez-Fargallo, A., Pulido-Arcas, J. A., Rubio-Bellido, C., Trebilcock, M., Piderit, B., & Attia, S. (2018). Development of a new adaptive comfort model for low income housing in the central-south of chile. Energy and Buildings, 178, 94–106. https://doi.org/10.1016/j.enbuild.2018.08.030

15. Attia, S., & Carlucci, S. (2015). Impact of different thermal comfort models on zero energy residential buildings in hot climate. Energy and Buildings, 102, 117–128. https://doi.org/10.1016/j.enbuild.2015.05.017

16. Humphreys M. (1978) Outdoor temperatures and comfort indoors, Batiment International, Building Research and Practice, 6:2, 92. https://doi.org/10.1080/09613217808550656

17. Royal Spain, Decree 450/2022 of June 14th, modifying the Technical Building Code, aproved by Royal Decree 314/2006 of March 17th. Available from: https://www.boe.es/boe/dias/2022/06/15/pdfs/BOE-A-2022-9848.pdf

18. AVRA. (2018). Agencia de Vivienda y Rehabilitación de Andalucía. Available from: https://www.juntadeandalucia.es/avra/

19. ISO, I. (2019). 10551: 2019 Ergonomics of the physical environment—subjective judgement scales for assessing physical environments. European Committee for Standard (CEN): Brussels, Belgium.

20. Encuesta Sensación Térmica. Proyecto Implicadapt. https://docs.google.com/forms/d/1rhuYBsjOQeqJ9UhHtgk5sRtmXTB-QAJjB1bWrnRFHH8/prefill

21. Nicol, F., & Humphreys, M. (2010). Derivation of the adaptive equations for thermal comfort in free-running buildings in European standard EN15251. Building and Environment, 45(1), 11–17. https://doi.org/10.1016/j.buildenv.2008.12.013

PLEA 2024 WROCŁAW
(Re)thinking Resilience

How Climate Change Affects the Energy Performance of Single Family Housing

A Statistical Approach to Simulations and Resilient Architecture Design

KRZYSZTOF CEBRAT[1] WERONIKA LECHOWSKA[2] ŁUKASZ NOWAK[1]

[1] Wrocław University of Science and Technology, Poland
[2] SRDK STUDIO PROJEKT sp. z.o.o.

ABSTRACT: The research focuses on how climate changes affect the calculated energy demand of buildings, and on the advantages of a novel method for determining a set of building parameters that facilitate their adaptation to ongoing climate changes. To achieve these goals we study two meteorological data sets from different periods and then analyse the energy calculations made on the basis of a database of 5040 models of buildings. The results of our studies show, that with the increase in the average air temperature of 1.2 C°, nearly 82% of the tested building variants showed a higher total energy demand, all of which show a significantly higher calculated demand for energy for cooling. Buildings with poor envelope energy efficiency will from now on either overheat or need to be actively cooled. Therefore the basic design strategy should be to reduce the area of windows oriented south, along with increasing insulation of partitions. All other features of buildings show a wide range of possible values, and the overall energy demand depends heavily on their inter-relations. Our results also show that dynamic energy analysis should be carried out only on the most current meteorological data prepared for hourly calculations.
KEYWORDS: climate change, randomly generated data, energy performance of buildings, single family housing

1. BACKGROUND AND RESEARCH QUESTIONS

Nowadays, to design a building means a work of meeting architectural needs with actual technical regulations and building code with taking economic, social and environmental aspects into the consideration. A properly designed building should be energy efficient today, but it also should be after 20, 40 or even more years. To predict the impact of changing climate on adopted building design strategy in terms of thermal insulation, window area, thermal mass or airtightness to name a few, we should analyse both: the building energy demand with current weather data and their future predictions.

The work presented here was carried out on a sufficiently large scale, so the results can be the basis for drawing more universal conclusions, regarding design strategies for resilient, energy efficient and comfortable buildings.

Our research focuses on determining how changes in the parameters describing the climate, affect the calculated energy demand; and on formulating preliminary guidelines for the design of resilient buildings. The field of study is now subjected to very thorough analyses so numerous, that it would be pointless to mention even the more important ones. But despite the fact that designing resilient buildings in the environment of climate change is such a 'hot topic' there are relatively little research like [1] or [2] that take into account the interdependencies between significant energy parameters of buildings. Probably due to the time-consuming nature of the procedures or the complexity of the matter, the most common approach is to analyse the impact of selected variables on the energy balance of the building [3, 4]. We show, that this method might be misleading.

The impact of climate change cannot be shown in isolation from location. So even if similar studies were conducted in other locations [5], the conclusions drawn from them will probably not be binding somewhere else. Additionally, in Poland, for some time now, steps have been taken to update the methodology and meteorological data used for calculations [6]. Our research shows how important this can be for simulation results.

2. THE FRAMEWORK OF THE STUDIES

2.1 Building models – the statistical approach

The idea of the research, was to move away from a case study - a strictly defined project - in favour of identifying and describing the general features of a large group of cases in specific external conditions.
Therefore, the research was carried out on a sample of 5040 randomly generated models of single-family buildings with a fixed heated volume (600 m3) and location (Wrocław).

Randomly generated models mean, that they were described by randomly generated parameters necessary for the calculation of the energy demand in accordance with applicable law.

Subsequently, the generated data allowed to characterize and analyse the buildings by a set of their energy performance features, namely:

- A/V ratio (area of external partitions/heated volume of the building ratio) [1/m],
- Share of south-oriented wall area in the overall wall area [%],
- Roof area [m2],
- Area of windows facing south [m2],
- Share of north-oriented window area in the overall window area [%],
- Window area to wall area ratio [-],
- Average (weighted) U-value of all partitions [W/(m2K)],
- Average (weighted) U-value of partitions excluding windows [W/(m2K)],
- Share of heat losses through thermal bridges in overall transmission heat losses [%],
- Air-tightness of the building [1/h],
- Thermal mass of the building [J/K],
- Area of the wall between the unheated and the heated volume of the building [m2],
- Air-tightness of the unheated volume of the building [1/h],
- Ratio of unheated volume to the heated volume of the building [-].

2.2 Meteorological databases

As we wanted the conclusions from our research to be as universal as possible, we chose a location in a temperate climate, one might say "average", not distinguished by extreme temperatures or the amount of solar radiation.

The experiment compared the energy demand of all models, with calculations based on two different sets of climate data for the location of Wrocław, Poland:

- IMGW: a database used for energy performance calculations according to the methodology legally binding in Poland, for which Typical Meteorological Year averages data collected in the years 1971 – 2000 [7, 8, 9].
- IWEC2: a database provided by ASHRAE, based on observations from 1984-2008 [10, 11]. The database is used both for hourly simulations in the Energy Plus program and for monthly energy calculations based on Polish Standards.

Both databases contain typical meteorological years, which are a statistical reflection of the climate in a given place during a selected time period. They contain not only temperature data, but also solar radiation, humidity, rainfall, wind speed and direction data. These are averages prepared on the basis of many years of measurements and mathematical models:

- IMGW: The annual sequence of weather data for energy calculations is generated for 12 months selected from a period of at least 10 years of meteorological observations for a given location. Observations were conducted by the Institute of Meteorology and Water Management (in Polish: Instytut Meteorologii i Gospodarki Wodnej) between 1971 and 2000. The source data are used then to determine typical meteorological years for Poland included several basic 3-hour meteorological parameters and modelled values of solar radiation intensity derived from an mathematical model.

Work is currently underway to determine new typical meteorological years for Poland, calculated on the basis of available meteorological data from synoptic stations of the IMGW and models of repeated backward analysis of the ERA5 database of the Copernicus system covering the years 2001-2020 [6]. They are not available yet, therefore we used the IWEC2 data in our comparative analysis.

- IWEC2: this database contains weather observations of wind speed and direction, sky cover, visibility, ceiling height, dry-bulb temperature, dew-point temperature, atmospheric pressure, and liquid precipitation. For each of these parameters, there are on average at least four observations per day. They extend to 25 years of measurements between 1984 and 2008.
  Because the ISH database contains no measured solar radiation, the hourly total horizontal solar radiation is calculated from an empirical Zhang-Huang Model taking into account the sun-earth geometry, reported cloud cover, the temperature difference compared to three hours before, relative humidity, and wind speed. The model is then adjusted on an hourly basis using the new ASHRAE Clear Sky Model to correct for statistical noise in the hourly profile.

2.3 The analysis

Out of the 5040 building models, the ones in which the change in the amount of energy demand calculated for the IMGW and the IWEC2 climate data did not exceed 1% of the value (in plus or in minus) were chosen for further comparative analysis. As a result it included a total of 659 models for which it was reasonable to assume, that their features

(mentioned earlier in 2.1) make them resistant to climate change.

Subsequently, from the selected group of 659 models, 10% of the most energy-efficient were chosen.

The average values of features of models of the entire population (5040) and of the selected groups were then compared, and on this basis, conclusions were drawn regarding the possible strategies of climate adaptation of buildings.

To verify our findings, and to find possible interdependencies between features, we then reduced the group of 65 building models to a group of 50, and afterwards successively by 10 at each step, until finally we rested with a group consisted of 10 models which simultaneously met the condition of (a) the minimum change in energy consumption and (b) its lowest consumption.

The systematically reduced groups were analysed for changes in the variance of the values of selected features.

Last but not least, we took a look at the parameters of building models whose overall energy demand has decreased in changed climate conditions.

3. RESULTS

3.1 The IWEC 2 versus the IMGW weather data

Our experiment showed some discrepancies between the simulation results based on hourly and monthly data.

The analysis of heat gains on planes facing different directions (N, S, W, E) showed that, for the IMGW data, the gains on the eastern side are greater than on the western side, while for the IWEC2 data these values are almost equal.

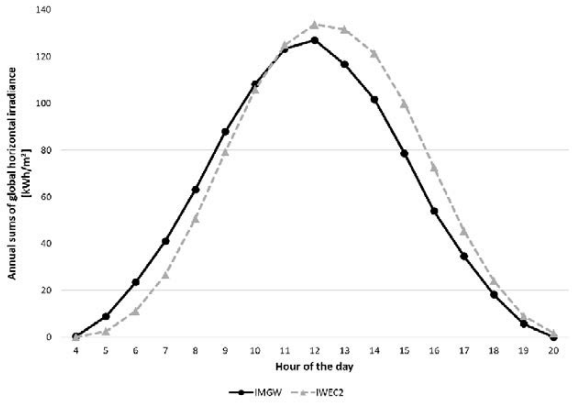

Figure 1: Annual sums of global solar irradiance in each hour during the year: a comparison of the IMGW and the IWEC2 data for Wrocław.

The reason for such results is the global horizontal irradiance in the IMGW data. It is not fully suitable for hourly simulations, because the program reads them with a half-hour shift (Fig. 1), showing higher solar gains on the eastern surfaces than on the western ones.

The IWEC2 data were developed on the basis of more recent measurements than the IMGW data, and show that average air temperatures have increased significantly in recent years.

Figure 2 shows these differences and - as described below - they have a measurable impact on the energy use in buildings.

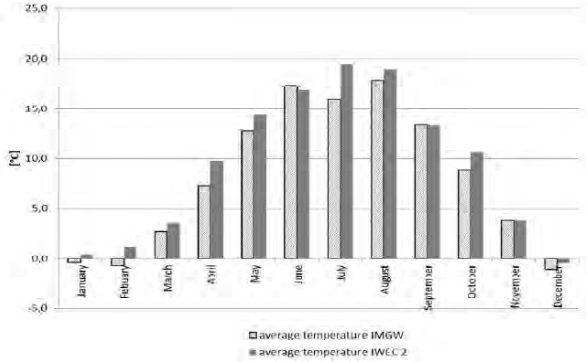

Figure 2: Average monthly temperature shift, between the IMGW and the IWEC2 data for Wrocław.

3.2 Energy performance and design strategies

The results for all 5040 tested models, set in the conditions described by the newer climate database (IWEC2), show a lower calculated demand for energy for heating (EU_H) and a significantly higher calculated demand for energy for cooling (EU_C), which is shown (for the 659 least affected models) in Fig. 3..

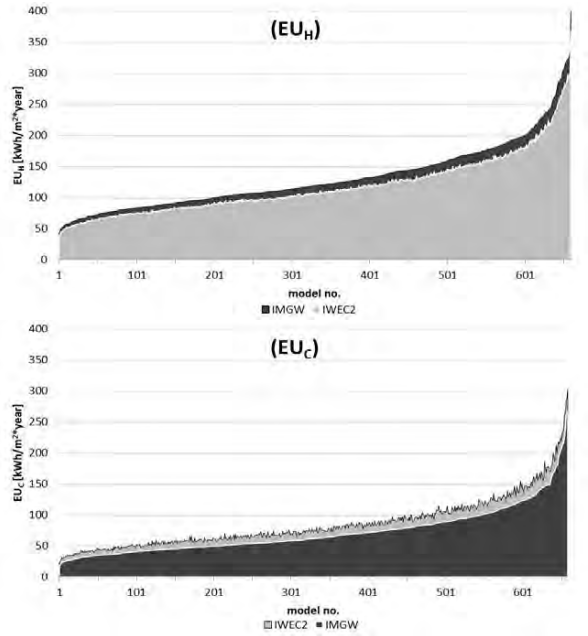

Figure 3: A comparison of energy demand index for heating (EU_H) and cooling (EU_C) for building models simulated with the IMGW and the IWEC2 data for Wrocław. The models were ranked according to the increasing value of energy demand. For visibility, the figures show the 659 models least affected by climate change, but the effect is valid for the whole group of 5040 buildings.

Nearly 82% of the tested building variants showed a higher total demand (heating and cooling) for usable energy: only 909 of the models showed a decrease in total energy demand - these are buildings in which the increase in energy demand for cooling was lower than the decrease in energy demand for heating.

The results indicate that even with the recorded increase in the average air temperature of 1.2 °C in Wrocław, the average increase in energy demand for cooling is 20.0 kWh/m^2/year, and the average decrease in energy demand for heating is 11.9 kWh/m^2/year.

The comparative analysis of the characteristics of building models that were least affected by climate change, and at the same time were the most energy-efficient (the best 10% of the chosen 659 models, based on the IMGW data), brings some interesting results (Table 1).

Table 1: Energy parameters of resilient and standard buildings. The values show how climate change influences the strategies of architectural design. (1): average value for all tested models; (2): average value for energy effective models least affected by climate change, (3): relative parameter value change [%].

	(1)	(2)	(3)
A/V [1/m]	0.78	0.79	**+1.5%**
Thermal mass [J/K]	77.9x10^5	80.6x10^5	**+3.5%**
Area of windows facing south [m^2]	20.50	12.14	**-40.8%**
Window area to wall area ratio [-]	106.49	121.38	**+14.0%**
Air-thightness_n50 [1/h]	5.22	3.96	**-24.2%**
Share of windows facing north [%]	25.06	26.74	**+6.7%**
Average U value of all partitions [W/(m^{2}K)]	0.45	0.25	**-43.6%**
Average U value of partitions excluding windows [W/(m^{2}K)]	0.27	0.21	**-23.2%**
Share of heat loss through thermal bridges in transmission heat loss [%]	10.43	9.45	**-9.4%**

From the first rough analysis it follows that if buildings are to maintain their good energy parameters, then the basic design strategy should be to reduce the area of windows oriented south (by reducing their size or by using blinds), along with increasing insulation of external partitions. The next thing to do would be increasing the air-tightness of the building envelope. Buildings with poor envelope energy efficiency will from now on (calculated for the IWEC2 data) either overheat or need to be actively cooled to maintain comfort.

Interestingly, the requirements for increased insulation applies to windows to a lesser extent than to other partitions.

A more detailed analysis (taking also into account the variance of feature values) of smaller and smaller groups of increasingly energy-efficient buildings indicates that the pointed out features: area of windows facing south and air-tightness are in fact the features that become more consistent and less variable within the in increasingly smaller groups.

This implies that these features of buildings must decrease (or increase) if we want to achieve better energy parameters, while the rest should be considered together, because only when considered together can they give the desired result, even though the range of values (freedom in shaping) remains large or at least constant as in the case of the average U value.

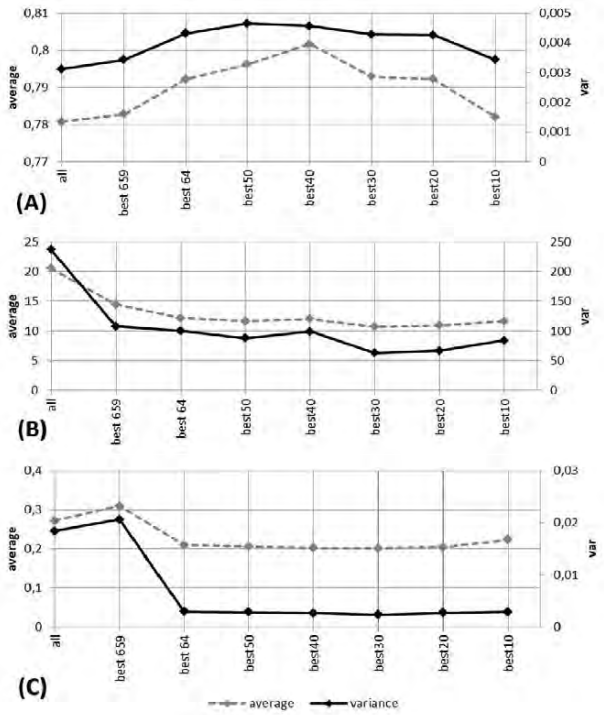

Figure 4: Average values and variance of (A): A/V factor, (B): area of south-facing windows, (C): average weighted U value (excluding windows); for increasingly energy-efficient buildings in successive, increasingly smaller groups of analysed models.

Another words, the decrease in energy demand does not correlate with any single parameter of the models (the correlation coefficient oscillates between -0.61 for the U factor and 0.03 for the percentage of window area facing north). This indicates the need to simultaneously consider all model parameters responsible for the building's energy performance. This is a significant discovery resulting from the conducted analyses. Chosen results are shown in Figure 4.

At the last step of our research, we took a closer look at buildings, which decreased the overall energy demand as the climate data changed.

Comparing the resulting group of 909 buildings that, in a sense, "gained" from climate change, we can be confused: virtually for all features, both the average values and their variances remain without significant changes compared to the entire group of 5040 generated models. Except for two: the area of windows facing south and the average U coefficient. The average value of the first one (windows) decreased significantly, while also significantly decreasing the variance, and the average value of the latter (U), on the contrary, increased, increasing the variance (Table 2).

There is no straightforward answer why this happens, since these two features are uncorrelated (correlation coefficient = 0.25). The simplest advice concerning this result may be that one should never optimize just one parameter at a time. At a deeper insight it turns out, that neither the form of the building, nor its orientation, U values of specific of partitions and other parameters are not common for all those models. Only one element might have an impact on the results: out of 909 models, the overwhelming majority (710) have some form of an unheated buffer zone – either solid or glazed.

Table 2: Differences in average values and variances of parameters of the group of all 5040 building models and the group of 909 building models, that occurred to have a lower energy demand after climate change: (1): area of windows facing south [m^2]; (2): average (weighted) U-value of partitions excluding windows [W/(m^2K)].

	(1)	**(2)**
overall average	20.50	0.27
909 average	14.21	0.39
overall variance	236.48	0.02
909 variance	130.45	0.04

4. CONCLUSIONS

The results of our research show, regardless of the type of simulation (hourly / monthly), that the calculations should be based on current meteorological databases. What more – detailed hourly analysis should not be carried out on meteorological data prepared for monthly calculations.

As for the preferred strategies of climate adaptation of buildings: while the climate changes, maintaining the current parameters of comfort and energy consumption may require, in particular, even greater sensitivity to the size and type of glazed surfaces – especially those facing south and the thermal transmittance of partitions. This is no surprise. But what is interesting is that all other features have quite a wide range of possible values, and the final overall energy demand depends heavily on their inter-relations. So as far as we can tell – also as our other research shows – when considering possible strategies for adapting buildings to climate change, one should always consider interdependency of a set of building parameters, not isolated variables. This is also a strong reason for introducing mandatory energy simulation of buildings.

It is also worth paying more attention (and further research) to the impact of buffer zones. Our results indicate that they may have a significant impact on the energy demand of buildings and may constitute an alternative to standard thermal modernization.

Last, but not least we also know, that buildings that will not be modernised (and currently consume high amounts of energy) will still increase their energy demand - in particular energy for cooling - or will significantly reduce the comfort of use (they will overheat).

5. DISSCUSSION

In our research, we focused on currently used meteorological data, because it is on its basis that energy characteristics are prepared and thus design decisions are made.

To observe differences more accurately, year to year, it would be necessary to analyze the measurement data and perform simulations on their basis [12 – 15]. In order to determine the expected changes in the building's energy demand in the coming years, it would be necessary to prepare a set of weather data expected for the next decades [16, 20]. Such analyses were performed, among others, in Iran [17], Egypt [18], Italy [19], Belgium [20], or Canada [21]. This way, the expected changes in the cooling load of buildings was determined, and allowed planning the modernization of the existing building structure and predicting the most desirable design solutions for the future.

REFERENCES

1. Abbasi Kamazani, M. and Dixit M. K., (2023). Multi-objective optimization of embodied and operational energy and carbon emission of a building envelope. *Journal of Cleaner Production*, 428, 139510.

2. Cebrat, K. and Nowak, Ł., (2018). Revealing the relationships between the energy parameters of single-family buildings with the use of Self-Organizing Maps. *Energy and Buildings*, 178: p. 61-70.

3. Ma, R. and Long, E., (2023). Analysis of the rule of window-to-wall ratio on energy demand of residential buildings in different locations in China. *Heliyon*, vol. 1, 1, e12803.

4. Šadauskienė, J., Šeduikytė, L., Paukštys, V., Banionis, K. and Gailius, A., (2016). The role of air tightness in assessment of building energy performance: Case study of Lithuania. *Energy for Sustainable Development*, 32: p. 31-39.

5. Berardi, U. and Jafarpur P., (2020). Assessing the impact of climate change on building heating and cooling energy demand in Canada. *Renewable and Sustainable Energy Reviews*, 121, 109681.
6. Narowski, P., (2022). TLM2000 – Typowe lata meteorologiczne dla Polski wyznaczone na podstawie danych meteorologicznych i klimatycznych z lat 2001-2020. *Ciepłownictwo, Ogrzewnictwo, Wentylacja*, vol. 53, no. 9: p. 7-20.
7. Typical meteorological years and statistical climatic data for the area of Poland for energy calculations of buildings. [online] Available: https://www.gov.pl/web/archiwum-inwestycje-rozwoj/dane-do-obliczen-energetycznych-budynkow [17 August 2023].
8. Narowski, P., (2008). Obliczenia energetyczne budynków - typowe lata meteorologiczne i statystyczne dane klimatyczne dla obszaru Polski. *Rynek Instalacyjny,* 10: p. 28–35.
9. Narowski, P. and Heim, D., (2008). Dane klimatyczne dla potrzeb modelowania transportu ciepła i wilgoci w przegrodach budowlanych. *Fizyka budowli w teorii i praktyce*, vol. III: p. 85–92.
10. Huang, Y. J., Su, F., Seo, D. and Moncef, K., (2014). *Development of 3012 IWEC2 weather files for international locations (RP-1477)*. Available: The Free Library, https://www.thefreelibrary.com/Development of 3012 IWEC2 weather files for international locations...-a0371282964 [17 August 2023].
11. Available: https://www.ashrae.org/technical-resources/bookstore/ weather-data-center [17 August 2023].
12. Moradi, A., Kavgic, M., Costanzo, V. and Evola, G., (2023). Impact of typical and actual weather years on the energy simulation of buildings with different construction features and under different climates. *Energy*, 270, 126875.
13. Lou, S., Li, D.H.W., Huang, Y., Zhou, X., Xia, D. and Zhao, Y., (2020). Change of climate data over 37 years in Hong Kong and the implications on the simulation-based building energy evaluations. *Energy and Buildings*, 222, 110062.
14. Siu, C. Y. and Liao, Z., (2020). Is building energy simulation based on TMY representative: A comparative simulation study on doe reference buildings in Toronto with typical year and historical year type weather files. *Energy and Buildings*, 211, 109760.
15. Weclawiak, I. A., Tao, Y. X., Nayeem, A., Cho, I. and Gonzalez, J. E., (2023). Viability and accessibility of the Great Lakes microclimate data over current TMY weather data for accurate energy demand predictions. *Urban Climate*, 50, 101593.
16. Hosseini, M., Bigtashi, A. and Lee, B., (2021). Generating future weather files under climate change scenarios to support building energy simulation – A machine learning approach. *Energy and Buildings*, 230, 110543.
17. Reveshti, A. M., Ebrahimpour, A. and Razmara, J., (2023). Investigating the effect of new and old weather data on the energy consumption of buildings affected by global warming in different climates. *International Journal of Thermofluids*, 19, 100377.
18. Mahdy, M., Elwy, I., Mahmoud, S., Abdelalim, M. and Fahmy, M., (2022). The impact of using different weather datasets for predicting current and future energy performance of residential buildings in Egypt. *Energy Reports*, vol. 8, Sup. 3: p. 372-378.
19. Salata, F., Falasca, S., Ciancio, V., Curci, G. and de Wilde, P., (2023). Climate-change related evolution of future building cooling energy demand in a Mediterranean Country. *Energy and Buildings*, 290, 113112.
20. Elnagar, E., Gendebien, S., Georges, E., Berardi, U., Doutreloup, S. and Lemort, V., (2023). Framework to assess climate change impact on heating and cooling energy demands in building stock: A case study of Belgium in 2050 and 2100. *Energy and Buildings*, 298, 113547.
21. Jafarpur, P. and Berardi, U., (2021). Effects of climate changes on building energy demand and thermal comfort in Canadian office buildings adopting different temperature setpoints. *Journal of Building Engineering*, 42, 102725.

PLEA 2024 WROCŁAW
(Re)thinking Resilience

Post Occupancy Evaluation in Educational Spaces: The Impact of Seasonal Discrepancies

ÖZLEM DURAN[1] JILL ZHAO[2] WILLIAM PETTIFER[3]

[1]University of Salford, Salford, UK
[2] University of West of England, Bristol, UK
[3]University of Bath, Bath, UK

ABSTRACT: This paper presents findings from a Post Occupancy Evaluation research of a BREEAM Excellence-rated university building, to understand the experience of the students using university study spaces. This research focuses on winter conditions and the outcome is compared with the outcome of previous research which focused on summer conditions. The research combined qualitative and quantitative methods and focused on occupancy patterns, thermal comfort, air quality, and noise level of the study spaces within the building, as well as the students' preferences and experiences of the study spaces. The research collected over 350 questionnaire surveys in total (over 200 in summer and over 150 in winter), as well as monitored environmental data and observation data over two weeks. (by on-site data recorders and momentary data recordings by manual devices) The findings showed winter and summer behavioural differences and occupants' comfort perceptions, suggesting that the building management decisions have to consider seasonal discrepancies to improve building performance but more importantly, avoid having a negative impact on students' environmental comfort and subsequent learning experience.
KEYWORDS: University buildings, Post-occupancy evaluation, thermal comfort, occupant behaviour, educational spaces

1. INTRODUCTION

Sustainable buildings are crucial for providing quality education [1]. Considering students spend more time in educational buildings than in any other public building [2], it is worth highlighting the importance of adequate performance with the consideration of student's wellbeing and productivity. The built environment is the largest energy consumer and greenhouse gas emitter, and the public sector in particular is associated with poor design and mismanagement [3]. High energy consumption in campus buildings is one of the biggest expenses in the educational sector [4]. Additionally, there is a lack of understanding of energy consumption and its influence on user comfort during building operations [5].

University buildings' occupancy patterns are very different than in other building typologies and are difficult to predict because they are occupied predominantly by a group of students with different daily timetables, study patterns, course requirements, and a wide range of personal preferences [6]. Therefore, to overcome the environmental comfort performance gap (difference between energy and comfort predictions vs and actual performance of a building), understanding the students' behaviour is significant [8]. Additionally, students' intellectual performances are proven to be impacted by environmental factors, thermal comfort in particular [8]. Thermal discomfort causes distraction and reduction in the student's academic performance and mental tasks [8,9, 10]. Therefore, measuring the in-use occupant behaviour and understanding students' environmental evaluation of the study spaces, are critical in predicting and optimising the environmental comfort and performance of university buildings

2. POST OCCUPANCY EVALUATION

Post Occupancy Evaluation (POE) is defined as a structured evaluation of a building's performance post-initial use and provides an understanding of the user's and building's needs, alongside recommending ideas for meeting the needs [11]. Benefits of utilising POE include cost and time savings, and better space utilisation [12]. These benefits would help to improve the daily life of the occupants. However, there are barriers to using POE which has resulted in POEs being underused in educational spaces and thus resulting in potential health implications such as underperformance of users [13].

POE exposes the strengths and weaknesses of projects and design, from which development teams can learn in order to further improve their projects. However, POE is often bypassed to reduce the cost of a project. The barriers include; the absence of compensation for conducting a POE, fear of revealing shortcomings and risking property value [14], lack of time, awareness and specialists and variations in performance indicators, methodology and objectives.

Although secondary school buildings are widely studied, focusing on factors that influence student performance, such as indoor pollutants and thermal conditions such as ventilation rate [15], air quality [16] and thermal comfort [17], there are limited POE studies on university buildings [11, 14, 18]. The lack of consensus on the performance indicators, variations of the aim of the project and the collected data type reduce the comparability of these projects.

Moreover, there is only a very limited number of studies which investigated the impact of seasonal discrepancies in particular in POE studies of university buildings. Serghides et al [19] highlighted the impact of equipment used in summer (negatively) and winter (positively) on thermal comfort due to the internal heat gain from the equipment. On the other hand, Isaac [20] did not report any seasonal discrepancies, suggesting this to be the result of design and construction adaptability to different weather patterns. However, adaptability to seasonal changes requires the identification of weather patterns that have an impact on the occupant's perception and behaviour. The occupancy pattern and energy consumption level of university buildings fluctuate greatly across the year based on seasons that are associated with term times, exam periods and holidays. Therefore, more studies are needed to determine seasonal discrepancies in the post-occupancy use of university buildings.

This paper presents findings from post-occupancy evaluation research of a BREEAM Excellence-rated [21] university building, to understand the experience of the students using university study spaces. The research focuses on winter conditions and the outcome is compared with the preliminary research [22] which focused on summer conditions. This comparison informs on the seasonal discrepancies in study spaces in terms of environmental conditions such as thermal comfort, air quality, noise and variations in occupant behaviours.

3. METHODOLOGY

The studied building is a five-storey, purpose-built university building that has achieved a BREEAM Excellence rating for its design scheme and the design of the building adopted a principle to maximise sustainability through informed decisions . It is located in the East Midlands in the U.K and the construction was completed in March 2021.

The research combined qualitative and quantitative methods and focused on occupancy patterns, thermal comfort, air quality, and noise level of the study spaces within the building, as well as the students' preferences and experiences of the study spaces. The winter and summer data are compared to investigate the seasonal discrepancies. The winter data collection included data from over 150 questionnaire surveys as well as monitored environmental data (by on-site data recorders and momentarily data recording by manual devices) and observation data over two weeks; between 28 February 2023 and 13 March 2023 at 9 am, 12 pm and 3 pm. The external temperature during observation hours varied between 0°C-7°C allowing the observation period to be representative weeks for winter. Summer data was collected from 11 May 2022 to 17 May 2022 on 5 weekdays from 9 am to 5 pm. in one-hour intervals and resulted in 206 questionnaire surveys returned by the students. This period was chosen to maximise the respondent rate, as it was just before the exam period. The external temperature fluctuated between 10°C and 23°C during the studied period.

Figure 1: First-floor (top) and second-floor (bottom) study spaces and surveyed zones

The surveys comprise two sections; Demographics (age, gender, how much time was spent studying per day and week, students' preferred study area, thermal sensitivity, clothing level and metabolism level prior to entering the study space), as well as environmental comfort (thermal comfort, ventilation, humidity, lighting and acoustics). Each category of the environmental comfort questions adopted a similar structure. It asked the occupants to rate their sensations using a seven-point Likert scale [23] and their adaptive behaviour, followed by any further comments they wanted to express. The observation data includes the number of occupants per zone, how many windows were open, as well as temperatures, CO2, and noise levels.

The common study areas are on the first and second floors of the building and can be accessed directly via the main staircase. For the purpose of this research, the study spaces were divided into five different zones that have distinctive characteristics (Figure 1). Zones 1, 2, and 3 are part of the library on the first floor. Zone 1 is dedicated to studying using university computers, with some group work areas. Zone 2 is a quiet study area and Zone 3 is a silent area. Zone 4 is on the second floor and is dedicated to group work comprising eight rooms, among which only two have windows. Zone 5 is a tutorial space, furnished to allow group seating. It also has direct access to the

terrace located on the second floor. The majority of the openable windows face southeast and southwest. Due to the acoustic constraints of the local environment and to achieve compliance with Building Bulletin 93 [24], the use of natural ventilation throughout the year is not possible. Therefore, the study spaces adopt a hybrid ventilation system. The units are provided with a wall-mounted controller with integral temperature and CO2 sensors, accessible by the occupants. The control allows the ventilation system to be boosted temporarily (for an hour) or turned off. There is no separate mode for winter or summer ventilation. All the studied zones are equipped with no active cooling. Learning spaces are heated 24 hours during term times based on a setpoint of 21°C between 7:00-18:00 and 19°C throughout the rest of the day and night.

4. DATA ANALYSIS

The following section compares the winter and summer data to highlight the discrepancies.

4.1 Occupancy

The majority of the respondents were aged between 18 and 25. Both studies showed a larger percentage of female occupants who responded to the questionnaires than their male counterparts. Proportionally, more female participants (45%) were sensitive to cold than males (27%).

Most of the respondents reported a low metabolic rate in all five zones in both studies. This aligns with Bleicher and Maclean [25] where occupants seated at desks typically have a lower metabolic rate. The level of clothing (Figure 2) shows seasonal differences in the comparison, with the majority of respondents wearing 'moderate to light' clothing in summer and 'moderate to heavy' clothing in winter.

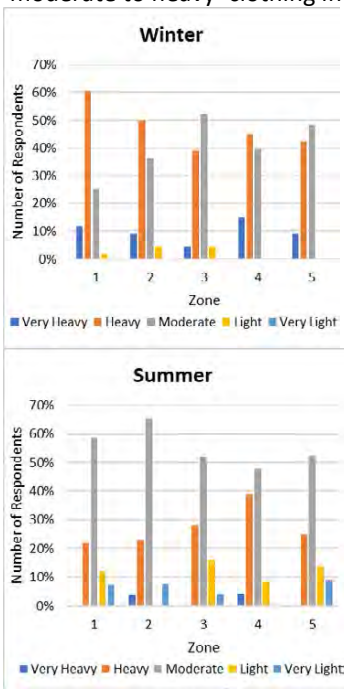

Figure 2: Seasonal difference of clothing level per zone

The occupancy level across zones fluctuates between the two seasons (Figure 3). The group study space (Zone 4) was less popular during exam season (summer) but had a higher level of occupancy during winter. The maximum occupancy in Zone 4 in winter had at times exceeded that of Zone 1, even though Zone 1 is designed to accommodate nearly twice the size of Zone 4 occupants. Winter study also showed the occupancy levels in Zone 5 fluctuating greatly throughout the day, with lunchtime having the highest footfall, due to this zone containing a kitchenette where hot food can be consumed.

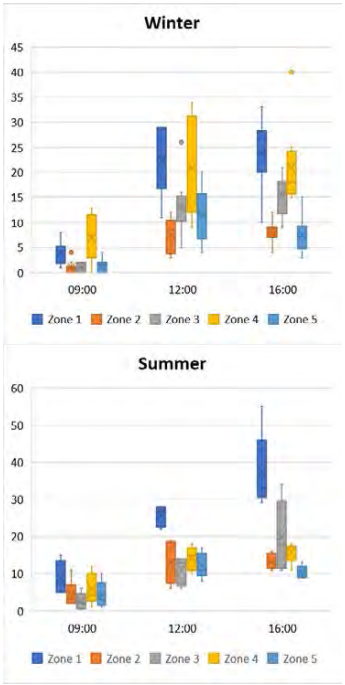

Figure 3: Seasonal occupancy level per zone in three timestamps

4.2 Thermal environment

Similar to the summer study, a bigger proportion of participants found the temperature to be neutral. In the summer study, 23% of the respondents stated it was warm and 10% stated very warm (Figure 4).

The measured temperatures were relatively stable in all zones (Figure 5), despite seasonal changes and occupancy levels. Temperature fluctuation throughout the observed period is more apparent across zones in winter than in summer. Zone 5 had a lower minimum temperature in winter than other zones, corresponding to a higher vote of 'slightly cold' in the thermal satisfaction survey.

Zone 1 is by far the warmest zone in both studies with the highest mean and max temperature. It has the highest occupancy levels on average of the five zones, as well as the provision of computers, both of which had an impact on the zone's temperature [22]. This has been moderately reflected in the thermal satisfaction vote in the summer study. Winter study resulted in a smaller proportion of respondents reporting the environment being warmer than their

preferences across zones except for Zone 4, where 55% of the users reported it to be 'slightly warm' or 'warm'. This might be due to the higher occupancy in Zone 4.

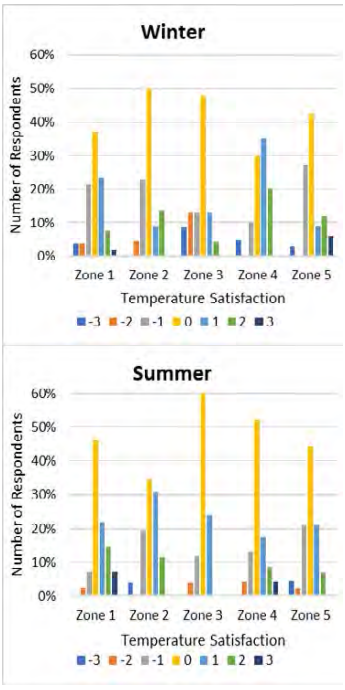

Figure 4: Seasonal temperature satisfaction per zone

In both studies, most students responded to the temperature by changing clothing with 69% doing so in the winter study and 58.2% in the summer study. In the summer study, there was a larger percentage of students opening or closing windows (17%) to adjust indoor temperature than in winter, where only 6.3% of the students opened or closed windows in winter. This suggests that there were less adaptable opportunities in window openings to regulate temperature and ventilation during winter.

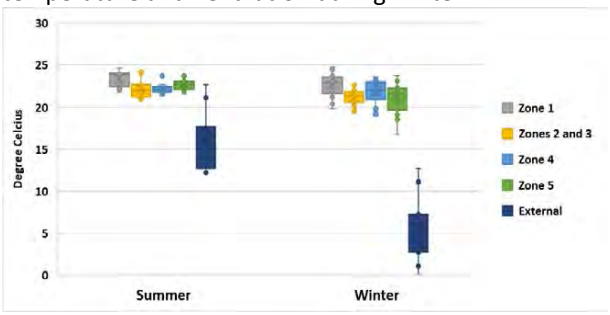

Figure 5: Temperature range by zone by season

4.3 Ventilation and CO2

Corresponding to the window opening behaviour observed, 94% of the time, all windows were closed in the winter study, a much higher proportion in comparison to the summer (66%), contributing to an overall higher CO2 levels measured in doors. (Figure 6). There was a wider gap between the highest and lowest CO2 levels in the winter study with levels ranging between 400 and 1400ppm than in the summer study (between 400 and 900ppm). CO2 levels generally increased throughout the day in both studies, with 9am on average having the lowest CO2 levels and 4 pm generally having the highest. Similar to the summer study, Zones 4 and 5 show higher mean and maximum CO2 level, the peak CO2 level exceeded 1500 ppm on one occasion, indicating risks of inadequate ventilation [26].

Despite the low window opening behaviour, the main method for the occupants to regulate ventilation is still to open or close a window in both studied seasons (62%), followed by 'do nothing' (14%). In the summer study, 17% of the respondents indicated they were unable to adjust the indoor temperature. They found the control to be 'confusing' and were only able to adjust the fan speed rather than temperature.

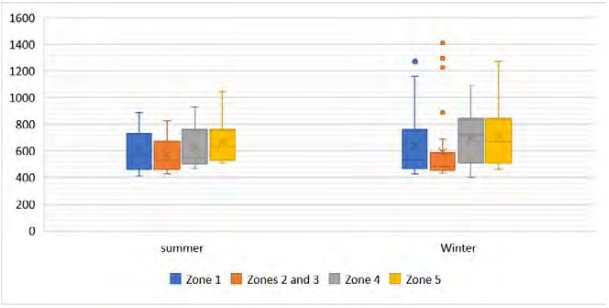

Figure 6: CO2 level by zone by season

A low percentage of respondents encountered odour. However, the proportion of people who reported encountering odour in winter was higher (12%) than in summer (5%). Most of the respondents who encountered odour were in Zones 4 and 5 where the consumption of hot food was permitted, unlike the other zones. This was supported by most of the comments being related to food. In winter seasons, more hot food was consumed, creating higher occupancy in the kitchenette area and a higher proportion of complaints against food odour, suggesting the seasonal usage of the kitchenette and inadequate ventilation during mealtimes.

4.4 Acoustic

45% of the respondents were satisfied with the noise levels. 9 am was generally the quietest time of day in all five zones. Correlating with the occupancy level, Zones 1 and 4, which had higher occupancy levels on average across the observed time period, were also noisier than Zones 2 and 3, which generally had lower occupancy levels. The noise levels in Zone 5 fluctuated and often peaked at noon due to it being popular at lunchtime.

The summer study had a larger percentage of respondents who found that roads/traffic was the dominant source of disruption (20%) than that of the winter study 13%. This could be due to a larger number of windows being open in summer, making

the traffic noise more prominent to building users. The most dominant action in response to noise levels was putting on headphones (75%). The percentages of the other actions between the two studies were also similar to each other, with changing location being the second most dominant action in response to noise levels (18%).

5. DISCUSSION

The previous study reported that during the summer data collection period, which was also predicted to have one of the highest volumes of occupancy, the occupancy level on average across all 5 zones remained far below the design maximum occupancy level. The CO2 level across five zones stayed under 1000 ppm most of the time. Therefore, the hybrid ventilation system, which was set to be triggered by CO2 levels, was activated only once throughout the observation period. However, the questionnaire survey revealed that approximately a third of the surveyed occupants found the spaces warm or very warm, despite the majority of the occupants self-identified as sensitive to cold [22]. Yet the initial simulation model did not predict overheating risk based on CIBSE TM52 [27]. As a result, no cooling was set despite the system having the capability. The occupants mostly used adaptive behaviours, such as opening windows, to regulate the temperature. During the summer observation period, over 50% of the windows were open on the fifth day when the internal temperature across all zones reached 24°C. However, during the time period when the recorded CO2 level in any zone reached over 900ppm (Zones 4 and 5 on day 1 and Zones 5 on day 4), no window was open, suggesting that the occupants were more likely to open windows based on thermal comfort rather than air quality.

This has also been reflected in the winter study. Unlike in the summer, the winter ventilation strategy relied heavily on the mechanical ventilation system to lower the indoor CO2 level. The options of opening windows were much less popular due to a lower external temperature. 94% of the time, all windows were closed despite a higher CO2 level being recorded. On occasions the CO2 measure was bordering 1500 ppm, indicating risks of inadequate ventilation.

This seasonal difference has been accentuated by the report of odour and noise. In summer study, ventilation relied on behavioural adaptations such as window opening to achieve thermal comfort. As a result, the occupants who preferred quiet or silent study zones reported a higher level of traffic noise being carried through the opened windows from the adjacent roads. Whereas in winter study, noise from traffic was less of an issue with the majority of the windows being closed. However, during the winter, the increased consumption of hot food in the kitchenette area and a lack of adaptive behaviours for opening windows to expel foul air, or having sufficient mechanical ventilation resulted in more reports of odour. In both case scenarios, the hybrid ventilation strategy fell short due to different reasons. Therefore, we recommend that the ventilation systems to be reconfigured to consider the seasonal discrepancies in how the study spaces are used. For instance, in the summer, considering the acoustic need and overheating risks, the mechanical ventilation should be programmed to also be able to be activated by temperature, instead of solely taking CO2 into levels account, thus mitigating overheating whilst preserving a good acoustic level for exam preparation. In winter, given the limited adaptation behaviour for window opening, mechanical ventilation settings should consider an extra boost during mealtimes in study areas where hot food is being prepared and consumed to remove extra odour.

Noticeably, in both studies, when asked what actions to take when temperature was not to their preferences, a variety of adaptive behaviours were reported, including ‘change clothing’, ‘having a hot/cold drink’, ‘change location’, ‘turn on heating/cooling’, and ‘opening/closing windows’. No respondent has chosen the ‘do nothing’ option. Whereas when asked what actions to take when ventilation was not satisfactory, ‘opening/closing windows’ was the most popular action, followed by ‘do nothing’ (17%), suggesting that behaviour adaptations responding to ventilation and air quality needs are limited. The occupants either do not know or are not supported with ways to adapt their behaviour to achieve satisfactory ventilation and air quality.

6. CONCLUSION

The result suggests that seasonal differences in how university study areas are used, and the availability of behavioural adaptation options could mean that hybrid ventilation strategies need to be re-evaluated to provide optimum thermal comfort.

The POE study detected seasonal discrepancies in study spaces in terms of environmental conditions and variations in occupant behaviours which impact the students' wellbeing. The building management decisions have to consider these discrepancies and alter strategies based on occupants' seasonal needs (in this case temperature-based triggers in summer and CO2-based triggers in winter) to improve building performance.

We recognise a series of limitations in this study. Firstly, the sample size could benefit from a larger and more diverse range of participants. Due to the majority of the respondents being females in this

study, thermal satisfaction is likely to be affected by the result of their thermal sensations. Secondly, the summer observation period has not captured the highest temperatures, e.g. in July, because students were on term holiday.

ACKNOWLEDGEMENTS

This research is based on previous research which was made possible by the UROS funding provided by the University of Lincoln, UK. This funding allowed four student researchers to participate in summer term data collection. The student researcher William Pettifer then carried out the data collection for the winter term as part of his dissertation "A Study of the Usage and Effectiveness of Post Occupancy Evaluation in Educational Spaces" at the University of Lincoln, UK.

REFERENCES

1. Aghimien, D.O., Adegbembo, T.F., Aghimien, E.I. and Awodele, O.A., 2018. Challenges of Sustainable Construction: A Study of Educational Buildings in Nigeria. *International Journal of Built Environment and Sustainability*, 5(1). Available from https://ijbes.utm.my/index.php/ijbes/article/view/244

2. Zomorodian, Z.S., Tahsildoost, M. and Hafezi, M., 2016. Thermal comfort in educational buildings: A review article. *Renewable and Sustainable Energy Reviews*, 59 895–906.

3. Macmillan, S.(Ed.), 2004. Designing Better Buildings: Quality and Value in the Built Environment. Taylor & Francis.

4. Dias Pereira, L., Raimondo, D., Corgnati, S.P. and Gameiro da Silva, M., 2014. Energy consumption in schools – A review paper. *Renewable and Sust. Energy Reviews*, 40 911–922.

5. Lawrence, R. and Keime, C., 2016. Bridging the gap between energy and comfort: Post-occupancy evaluation of two higher-education buildings in Sheffield. *Energy and Buildings*, 130 651–666.

6. Franceschini, P.B, Neves, L.O., 2022. A critical review on occupant behaviour modelling for building performance simulation of naturally ventilated school buildings and potential changes due to the COVID-19 pandemic, *Energy and Buildings,* 258.

7. Shi, X., Si, B., Zhao, J., Tian, Z., Wang, C., Jin, X., Zhou, X., 2019. Magnitude, Causes, and Solutions of the Performance Gap of Buildings: A Review. *Sustainability* 11. https://doi.org/10.3390/su11030937

8. Ricciardi, P., Buratti, C., 2018. Environmental quality of university classrooms: Subjective and objective evaluation of the thermal, acoustic, and lighting comfort conditions. *Building and Environment*. 127, 23–36. https://doi.org/10.1016/j.buildenv.2017.10.030

9. Jowkar, M., Rijal, H.B., Brusey, J., Montazami, A., Carlucci, S., Lansdown, T.C., 2020. Comfort temperature and preferred adaptive behaviour in various classroom types in the UK higher learning environments. *Energy and Buildings.* 211, 109814. https://doi.org/10.1016/j.enbuild.2020.109814

10. Barbhuiya, Saadia, Barbhuiya, Salim, 2013. Thermal comfort and energy consumption in a UK educational building. *Building and Environment* 68, 1–11. https://doi.org/10.1016/j.buildenv.2013.06.002

11. Mustafa, F.A. (2017) Performance assessment of buildings via post-occupancy evaluation: A case study of the building of the architecture and software engineering departments in Salahaddin University-Erbil, Iraq. *Frontiers of Architectural Research*, 6(3) 412–429.

12. Preiser, W.F.E., 2001. Feedback, feedforward and control: post-occupancy evaluation to the rescue. *Building Research & Information*, 29(6) 456– 459.

13. Ahmed, H., Edwards, D.J., Lai, J.H.K., Roberts, C., Debrah, C., Owusu-Manu, D.-G. and Thwala, W.D. 2021 Post Occupancy Evaluation of School Refurbishment Projects: Multiple Case Study in the UK. *Buildings*, 11(4) 169.

14. Ahmadi, R. T., Saiki, D., Ellis, C., 2016. Post Occupancy Evaluation an Academic Building: Lessons to Learn, *Journal of Applied Sciences and Arts*: Vol. 1 : Iss. 2, Article 4. Available at: http://opensiuc.lib.siu.edu/jasa/vol1/iss2/4

15. Batterman, S., 2017. Review and extension of CO_2-based methods to determine ventilation rates with application to school classrooms, *International Journal of Environmental Research*. Public Health 14 (2) 145.

16. Wargocki, P., Porras-Salazar, J.A., Contreras-Espinoza, S.,Bahnfleth, W.. 2020. The relationships between classroom air quality and children's performance in school, *Building and Environment*. 173

17. Kükrer, E., Eskin, N., 2021. Effect of design and operational strategies on thermal comfort and productivity in a multipurpose school building, *J. of Building Engineering*. 44

18. Tookalooa, A., Smithb, R., 2015. Post Occupancy Evaluation in Higher Education. *Procedia Engineering* 118 515

19. Serghides, D.K. , Chatzinikola, C.K., Katafygiotou, M.C., 2015. Comparative studies of the occupants' behaviour in a university building during winter and summer time, *Intern. Journal of Sustainable Energy*, 34:8, 528-551, DOI:10.1080/14786451.2014.905578

20. Isaac, S., Meir, I., Pignatta, G. (Eds.). 2023. Net-Zero and Positive Energy Communities: Best Practice Guidance Based on the ZERO-PLUS Project Experience (1st ed.). Chapter 1: Post-occupancy evaluation: the missing link. *Routledge*. https://doi.org/10.1201/9781003267171

21. BREEAM, 2023. [Online] Available at: https://bregroup.com/products/breeam/how-breeam-works/

22. Duran, O., Zhao, J., 2022. Post-Pandemic Study Spaces: Post Occupancy Evaluation of BREEAM Excellence Rated University Building. ASA (Architectural Science Association) Conference, Perth, Australia

23. ANSI/ASHRAE 55, 2020. Environmental Conditions for Human Occupancy, Atlanta, GA, USA: ASHRAE American Society of Heat., Refrigeration and Air Conditioning Engineers.

24. BB93, 2015. Building bulletin 93, Acoustic design of schools: performance standards, Department of Education.

25. Bleicher and Maclean (2023) Thermal Comfort (TG 22/2023). BSRIA.

26. HSE, 2023. Using CO_2 monitors - Ventilation in the workplace. [accessed 13 May 2023]. Available at: https://www.hse.gov.uk/ventilation/using-co2-monitors.htm

27. CIBSE TM52. 2013. The limits of thermal comfort: avoiding overheating in European buildings. London: CIBSE

PLEA 2024 WROCŁAW
(Re)thinking Resilience

Transition to Biophilic Hospitals

Key Biophilic Design Parameters in Healthcare Environments

AINHOA ARRIAZU-RAMOS[1] AURORA MONGE-BARRIO[1] JESUS MIGUEL SANTAMARIA[2] ANA SANCHEZ-OSTIZ[1]

[1] School of Architecture - University of Navarre, Pamplona, Spain.
[2] Institute for Biodiversity and Environment (BIOMA) - University of Navarre, Pamplona, Spain.

ABSTRACT: The current trend in healthcare environments is to design spaces which that support the recovery process and well-being of patients. The interest in biophilic design is rising as it considers that exposure to natural environments has positive effects on human health and well-being. This study provides a summary of an initial review about biophilic design in hospitals and its effects on patients health and staff work. A review methodology was followed to analyse relevant published research and case studies in which biophilic design is developed. The results show that biophilic design positively affects the patients' psychological health, well-being and recovery processes, and in relation to the staff; it improves stress, mood, communication and attention levels. In addition, the analysis found that the biophilic design patterns in the first category "Nature in the Space" are the most used ones and have the greatest influence on patients and staff. Among them, we can highlight natural light, views of nature, fresh air and thermal comfort. The use of plants is also very recurrent but not as a first measure. The review may influence standards that regulate hospitals' design, so that biophilic design will be something considered in all future healthcare environments.
KEYWORDS: Biophilic design, Restorative environments, Patients, Staff, Literature review.

1. INTRODUCTION

The term "biophilia" was used for the first time in the 1960s by Erich Fromm, to describe the tendency of humans to be attracted to everything that is alive and vital [1]. However, architecture has often contributed to distancing humans from nature through the use of artificial materials and forms, relegating nature to parks, forests, and natural reserves [2].

In contrast, biophilic design encourages the use of natural elements and processes as design inspiration in the built environment. The idea behind this is that exposure to natural environments and features has positive effects on human health and well-being, which has been supported by a wealth of research [3].

According to Browning et al. [4] the 14 biophilic design patterns, described by Edward O. Wilson [5] can be organized into three categories to illustrate the enhancement of user experience and its biological responses, as well as the potential impacts in different care levels: *(i) nature in the space; (ii) natural analogues; (iii) and nature of the space*. Table 1 shows the 14 patterns of biophilic design in each category.

Table 1: Patterns of biophilic design.

Nature in the space
(P1) Visual Connection with Nature Direct views of nature, such as landscapes, vegetation, or water.
(P2) Non-Visual Connection with Nature Natural sounds, textures, and scents into the environment to engage all senses.
(P3) Non-Rhythmic Sensory Stimuli Sensory experiences, like a gentle breeze, rustling leaves, or the sound of flowing water.
(P4) Thermal and Airflow Variability Natural variations in temperature and airflow, which can mimic outdoor conditions and provide a more comfortable and stimulating environment.
(P5) Presence of Water Water features, such as fountains, ponds… to create a calming effect.
(P6) Dynamic and Diffuse Light Variable levels and qualities of light, including natural daylight and dynamic lighting conditions.
(P7) Connection with Natural systems Incorporating elements that emulate natural processes, such as using sustainable materials, green roofs, rain gardens, plants…
Natural analogues
(P8) Biomorphic Forms and Patterns Shapes inspired by nature, such as organic forms or fractal patterns.
(P9) Material Connection with Nature Using natural materials like wood, stone, or bamboo to create a tactile connection with the environment.

(P10) Complexity and Order
Balancing a level of complexity and order in design to mimic natural patterns and create a visually interesting and stimulating space
Nature of the space
(P11) Prospect
Clear line of sight or views into the distance, which can evoke a sense of exploration and curiosity.
(P12) Refuge/ Privacy
Spaces for privacy or retreat.
(P13) Mystery
Elements that create a sense of curiosity and wonder.
(P14) Risk/Peril
Controlled elements of risk or excitement, such as bridges, climbing features, or dynamic elements, to add a sense of adventure and challenge.

In contrast, the architecture of current hospitals suffers from three major determinates: firstly, they are linked to major roads (noise, poor air quality…) for easy access [6]; secondly, they are often located in dense urban environments where there is no space for green zones or views of nature [6]; thirdly, they prioritise technology and space efficiency over biophilic design [7].

In this line, some studies found that these kind of hospitals are not the most suitable recovery spaces for patients, especially when they are children or adolescents [8]. As a result, the benefits of biophilic design principles are increasingly recognised.

There are different scales in hospital interventions with biophilic design. Three categories of intervention can be defined:

- Total intervention in large hospitals.
- Total intervention in small hospitals.
- Partial interventions through interior design projects

Besides, interventions can be indoors or outdoors or both.

Despite the increasing scientific evidence of the positive effects of biophilia in hospitals, European regulations do not consider biophilic design as something to be recommended or mandatory. For example, in Spain, the recent Technical Building Code (2019) only regulates fire protection, the accessibility of different spaces in hospitals and the incorporation of photovoltaic panels as a source of renewable energy [7].

In this context, the main aims of this study are providing a summary of the knowledge generated about biophilic design in hospitals and its effects on patient health and staff behaviour; and, based on this evidence, establishing which are the most important biophilic design parameters to consider when designing new hospitals.

2. METHODS

This study followed a review methodology in order to find all relevant published research that would answer to the two main objectives set. The search focused on two areas: scientific articles and case studies.

Scientific Articles

The search was carried out in two different databases (Scopus and Web of Science) through a Python script. The language was limited to English and Spanish. In order to avoid biased data, the search was limited to peer-reviewed academic journal publications. The basic search syntax with Boolean operators and through ScopusSearch (python) was: (“biophilic design” OR “biophilia” OR “nature”) AND (“hospital” OR “healthcare” OR “therapeutic environment”) AND (“patients” OR “staff”).

Figure 1 shows the 437 indexed articles resulting from the search, grouped by year of publication. Not all of them have been reviewed for this paper. As this is an initial review, some of them were reviewed, corresponding to the following inclusion criteria: i) papers with results that relate biophilic parameters to people’s health; ii) papers with results focused on patients and staff.

Based on these criteria, the most cited and relevant ones were analysed.

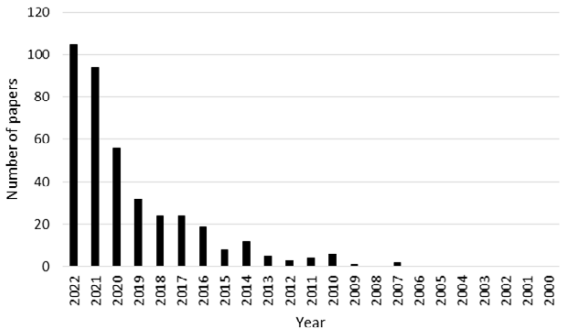

Figure 1: Papers by publication year related to biophilia in hospitals and Healthcare Environments. Own elaboration.

Case studies

The search was focused on hospital case studies where biophilic design had been implemented. It was conducted on the open web, looking for “hospitals with biophilic design”.

The hospitals could be located around the world and respond to the following inclusion criteria: i) be built (not in project or under construction); ii) the biophilic design should be implemented at least partially in some space of the hospital; iii) and it architectural project and a report or article where the spaces were analysed should be advailable.

Thus, 12 case studies were selected for analysis (Table 2). For the evaluation and identification of biophilic design criteria, the plans, reports and photographs of each of them were analysed.

Table 2: Analysed case studies (from oldest to newest).

Name	Type of hospital	Year of intervention	Place
Sarah Kubitschek Hospital	Traumatology Rehabilitation hospital	1994	Salvador (Brasil)
Östra Hospital	Psychiatric facility	2006	Göteborg (Sweden)
Socio-health center Santa Rita	Socio-health center	2009	Menorca (Spain)
Khoo Teck Puat Hospital	General hospital	2010	Singapore (Singapore)
The Royal Children's Hospital	Pediatric hospital	2011	Melbourne (Australia)
New Lady Cilento Children's Hospital	Pediatric hospital	2014	Brisbane (Australia)
Do Rocio Hospital	General hospital	2014	Campo Largo (Brasil)
Kaari Hospital	General hospital	2015	Kuopio (Finland)
Christ Hospital	General hospital	2015	Cincinnati (USA)
Memorial Bahçelievler Hospital	General hospital	2018	Istambul (Turkey)
Strawberry Hill Behavioral Health Hospital	General hospital	2019	Kansas City (USA)
Niño Jesus Hospital	Pediatric hospital	2022	Madrid (Spain)

3. RESULTS AND DISCUSSION

3.1 General results from the initial review

The first general result is that biophilic design in hospitals is a topic with an increasing interest, as it can be seen in the exponential growth of papers related to it through the last 20 years (Figure 1) and the higher number of case studies in the last ten years.

Secondly, considering patients, it was found that the effect of biophilia in hospitals is not being studied in relation to their physical health (there is not much scientific evidence quantifying the direct effect of biophilia on certain diseases or specific pathologies) but there are evidences of its benefits on the mental health and well-being of patients, which has a beneficial effect on their recovery process. In relation to staff, biophilic design is studied in relation to the stress at work, the ability to concentrate and the relationship/mood with patients and between colleagues.

Regarding the methodologies used in the analysed researches, the most common are the ones based on the development of patient and staff questionnaires. However, these post-occupational studies used to quantify the real effect of biophilic interventions are scarce.

Figure 2 shows an example of questionnaires used in the studies.

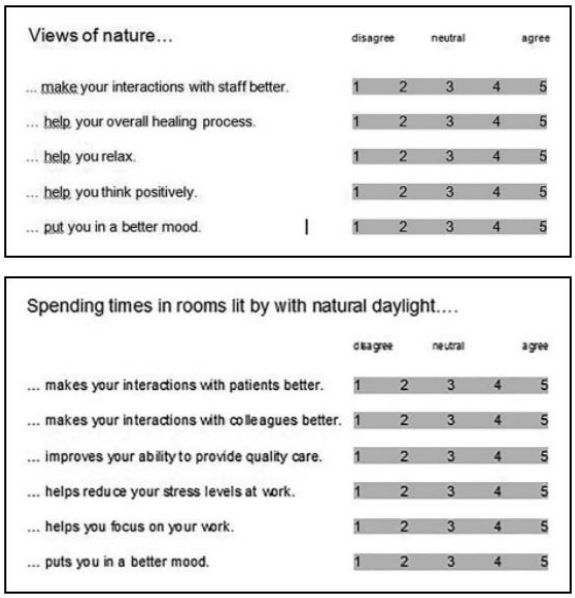

Figure 2: Sample patient (top) and staff (bottom) matrix questions. Extracted from [9].

Finally, it has been found in line with previous studies [10], that biophilia in hospitals is still more theoretical than practical (as it can be seen in the difference between the number of papers (437) and the number of case studies (12)).

3.2 Biophilic design and patients' health/staff development

The following connections between biophilic design and the health of patients and/or the performance of staff were found:

In relation to patients, humanising hospital spaces positively impact patients' psychological health, well-being [11] and recovery processes [6]: patients in hospitals with biophilic design have lower levels of pain, anxiety and fatigue during their recovery process [12], sleep better (better circadian system functioning) [13], are in better mood [14] and recover faster requiring less pain medication [15].

In relation to the staff's rest areas, biophilic design also showed good results in reduction of stress levels [16]. Working areas with biophilic parameters, specially natural light and windows with views, significantly improved mood and communication amongst nurses [17] and helped to improve their satisfaction and attention levels [18].

Within the 12 case studies analysed, post-occupational studies to quantify the effects of biophilia have been carried out in only two: Khoo Teck Puat Hospital and Östra Hospital.

Khoo Teck Puat Hospital (KTPH) [19].

Figure 3: View of hospital's courtyard. Extracted from International Living Future Institute webpage.

This is an example of total intervention in a large hospital, where there is a full biophilic design. The hospital has: 8 roof gardens, 5 levels of corridor planters, 81 balconies planter boxes. These gardens are self-sufficient and environmentally friendly.

In 2016, a comparative post-occupational study was conducted among 200 people [19], either users of the KTPH or of a traditional hospital. The results show that biophilic design contributed to better self-reported wellbeing outcomes for patients, visitors and staff. Besides, more than 80% of people give affirmative answers when asked if hospitals should invest in green elements. The results confirmed KTPH's role as a community hub where 15% of visitors come for social and recreational reasons.

Östra Hospital [20].

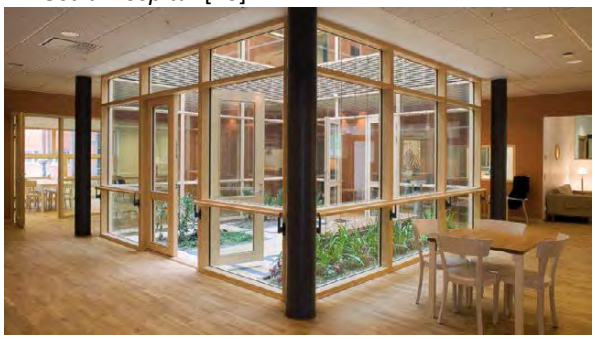

Figure 4: View of one courtyard of the hospital. Extracted from Whitearkitekter (the architects of the project) webpage.

This is an example of total intervention in a small hospital.

Patients and staff moved in 2005 from a traditional hospital to this new one counting with biophilic design. Data collected from the year before the move to the new hospital, compared to the year after it, show an improvement in the number of compulsory injections - down from 23 (2005) to 17 (2007) - and restraints - down from 63 occasions (2005) to 35 (2007) - in patients. Regarding the staff, there is a decrease in sicklisting, from 9% (2005) to 6% (2007) [20].

3.3 Biophilic design criteria

First, in order to establish which biophilic design parameters are most important to consider within hospitals, the patterns implemented in the 12 case studies were analysed. Table 3 shows the patterns of biophilic design developed in each hospital.

Table 3: Patterns of biophilic design implemented in each case study

Name	Patterns of biophilic design
Sarah Kubitschek Hospital	Indoor plants (P7) Multi-sensory environment (P2) Natural light: dynamic and diffuse (P6)
Östra Hospital	Indoor and outdoor plants (P7) Multi-sensory environment (P2) Sounds of nature (P3) Fresh air and thermal comfort (P4) Natural light (P6) Connection with natural systems (P7) Colours and natural materials (P9) Views of nature (P11) Privacy (P12)
Centro socio-sanitario Santa Rita	Indoor and outdoor plants (P1) Multi-sensory environment (P2) Natural light (P6) Biomorphic Forms and Patterns (P8)
Khoo Teck Puat Hospital	Indoor and outdoor plants / green roofs and walls (P7) Multi-sensory environment (P2) Sounds of nature (P3) Fresh air and thermal comfort (P4) Water (P5) Natural light (P6) Views of nature (P11)
The Royal Children's Hospital	Multi-sensory environment (P2) Fresh air and thermal comfort (P4) Water (P5) Natural light: dynamic and diffuse (P6) Complexity and order (P10) Views of nature (P11) Biomorphic Forms and Patterns (P8)
New Lady Cilento Children's Hospital	Green roofs and walls (P7) Natural light (P6) Biomorphic Forms and Patterns (P8)
Do Rocio Hospital	Indoor and outdoor plants/ green roofs and walls (P7) Natural light (P6)
Kaari Hospital	Artificial nature: paintings of landscapes or flowers (P1) Natural light (P6)
Christ Hospital	Green roofs and walls (P7) Natural light (P6)
Memorial Bahçelievler Hospital	Artificial nature: paintings of landscapes or flowers (P1) Natural light (P6) Biomorphic Forms and Patterns (P8)
Strawberry Hill Behavioral Hospital	Indoor plants (P7) Natural light (P6) Colours and natural materials (P9)
Niño Jesus Hospital	Artificial nature paintings of landscapes or flowers (P7)

	Biomorphic Forms and Patterns (P8)

In general, patterns of the first category "*Nature in the space: P1-P7"*, are the most implemented ones.

Then, a classification of the most important parameters of biophilic design to be considered for the transition to biophilic hospitals was developed. This classification of biophilic criteria has been divided according to hospital areas (rooms, treatment areas, waiting areas, work areas and rest areas) and users (inpatients, outpatients and staff). These chosen areas are the optimal ones within a hospital for implementing biophilic design. Table 4 shows the classification.

Table 4: Classification by groups of the biophilic design parameters identified as most important in a hospital.

Inpatients ***Rooms***	1. Fresh air and thermal comfort (P4) 2. Natural light (P6) 3. Views of nature (P1) 4. Refuge and Protection (P12) 5. Plants (P1) 6. Multi-sensory environment (P2) 7. Water (P5) 8. Colours and natural materials (P9)
Inpatients Outpatients ***Treatment areas***	1. Natural light (P6) 2. Views of nature (P1) 3. Fresh air and thermal comfort (P4)
Outpatients ***Waiting areas***	1. Fresh air and thermal comfort (P4) 2. Natural light (P6) 3. Views of nature (P1) 4. Privacy (P12) 5. Plants (P7) 6. Water (P5) 7. Colours and natural materials (P9)
Staff ***Work areas***	1. Natural light (P6) 2. Views of nature (P1) 3. Fresh air and thermal comfort (P4)
Staff ***Rest areas***	1. Privacy (P12) 2. Fresh air and thermal comfort (P4) 3. Plants (P1) 4. Natural light (P6) 5. Views of nature (P1) 6. Water (P5)

This classification has been made on the basis of the literature review: only the most relevant articles are cited in this paper, due to lack of space: [8,9,28,12,21–27]

After both analysis, there are some parameters that are repeated in most areas, users and case studies, therefore, they can be highlighted as the most relevant ones to consider in the designs: natural light (P6), views of nature (P1) and fresh air and thermal comfort (P4).

Plants are also recurrent, but do not occupy the first place, although it seems to be the most associated parameter to biophilic design. Moreover, in some hospitals (i.e. *Complexo Hospitalario de Ourense–Spain; Dorset County Hospital-UK*) plants and flowers have been banned inside rooms, arguing that the bacteria they carry may pose a health risk to patients. However, they may be included in staff rest rooms and in waiting areas.

In addition, it is important to design with natural colours and materials, especially in patient rooms to avoid aseptic and unwelcoming spaces.

There are other patterns that do not even appear in the classification, so they can be considered secondary: Non-Rhythmic Sensory Stimuli (P3), Biomorphic Forms and Patterns (P8), Complexity and order (P10), Mystery (P13) and Risk/Peril (P14).

4. CONCLUSIONS

The initial literature review carried out in this research showed that there is a growing interest in biophilic design in hospitals, but mostly in a theoretical way: there has been a significant increase in publications related to this topic in the last 20 years but there are much less real cases and even fewer case studies where biophilia has been applied and its real impact measured. Therefore, more post-occupational studies are needed to quantify and validate biophilic measures in real case studies.

Biophilia has been found to have a direct relationship with the mental health of patients improving their pain, anxiety, fatigue, mood and sleep during their recovery process. In relation to staff, biophilic design has also shown good results in reducing stress and attention levels and has significantly improved staff's mood and communication.

The main novelty of this study is to provide a classification of the most important biophilic parameters to be considered for each group and hospital area and give design criteria for a real application. This classification is helpful for determining priorities for when designing different spaces in healthcare environments as it is very difficult to apply all the 14 patterns in all interventions. Within the 14 biophilic design patterns, there are three that are fundamental for patients and staff in all areas considered: natural light (P6), views of nature (P1) and fresh air and thermal comfort (P4). Thinking in biophilia, the use of plants is also very recurrent, but it is not revealed as a first measure. However, it is advisable to consider it in staff rest areas and in waiting areas. Besides, it is important to consider natural colours and materials within design, especially in patient rooms to avoid aseptic and unwelcoming spaces.

Future research could investigate how to develop the main parameters to provide an effective and rigorous transition to biophilic design in new and existing hospitals.

This study underlines the importance of biophilic design in hospitals, providing evidence of the influence of the environment in the recovery process of patients and the work/satisfaction of the staff.

These findings may influence regulations related to hospitals design, so that biophilic design will be something considered in all future healthcare environments.

ACKNOWLEDGEMENTS

This research has been carried out by researchers from the CÁTEDRA DE SALUD Y MEDIO AMBIENTE of the University of Navarra promoted by SANITAS.

REFERENCES

1. S. Totaforti, Applying the benefits of biophilic theory to hospital design, City, Territ. Archit. 5 (2018) 1–9. https://doi.org/10.1186/s40410-018-0077-5.

2. Stephen R. Kellert, Building for Life : Designing and Understanding the Human-Nature Connection, 2005.

3. D. Bowler, L. Buyung-Ali, T. Knight, A.S. Pullin, The importance of nature for health: Is there a specific benefit of contact with green space?, CEE Rev. 08-003 (SR40). Environ. Evid. Www.Environmentalevidence.Org/SR40.Html. (2010) 1–57.

4. W. Browning, C. Ryan, J. Clancy, 14 Patterns of Biophilic Design: Improving health and well-being in the built environment, 2014.

5. E.O. Wilson, Biophilia, 1984.

6. M.S. Abdelaal, V. Soebarto, The Death of Modern Hospital: Towards a restorative healthcare architecture Planning and Design of Public Spaces to Support Ageing Well View project, (2018). https://www.researchgate.net/publication/327593839.

7. Amanda C. Cleveland, Symbiosis between biophilic design and restorative healing environments: The impact on overall well-being of urban dwellers, Florida State University, 2014.

8. K. Peditto, M. Shepley, N. Sachs, J. Mendle, A. Burrow, Inadequacy and impact of facility design for adolescents and young adults with cancer, J. Environ. Psychol. 69 (2020) 101418. https://doi.org/10.1016/j.jenvp.2020.101418.

9. M. Tinner, P. Crovella, P.F. Rosenbaum, Perceived Importance of Wellness Features at a Cancer Center: Patient and Staff Perspectives, Heal. Environ. Res. Des. J. 11 (2018) 80–93. https://doi.org/10.1177/1937586718758446.

10. W. Zhong, T. Schröder, J. Bekkering, Biophilic design in architecture and its contributions to health, well-being, and sustainability: A critical review, Front. Archit. Res. 11 (2022) 114–141. https://doi.org/10.1016/j.foar.2021.07.006.

11. J. Soderlund, P. Newman, Biophilic architecture: a review of the rationale and outcomes, AIMS Environ. Sci. 2 (2015) 950–969. https://doi.org/10.3934/environsci.2015.4.950.

12. S.H. Park, R.H. Mattson, Effects of flowering and foliage plants in hospital rooms on patients recovering from abdominal surgery, Horttechnology. 18 (2008) 563–568. https://doi.org/10.21273/horttech.18.4.563.

13. F. Beute, Y.A.W. de Kort, Salutogenic effects of the environment: Review of health protective effects of nature and daylight, Appl. Psychol. Heal. Well-Being. 6 (2014) 67–95. https://doi.org/10.1111/aphw.12019.

14. H. Zhou, R. Chen, J. Wang, J. Lu, T. Yu, X. Wu, S. Xu, Z. Li, C. Jie, R. Cao, Y. Yang, Y. Li, D. Meng, Bringing nature into hospital architecture: Machine learning-based EEG analysis of the biophilia effect in virtual reality, J. Environ. Psychol. (2023) 108947. https://doi.org/10.1016/j.jenvp.2023.102033.

15. R.S. Ulrich, View through a Window May Influence Recovery from Surgery, Science (80-.). 224 (1984) 420–421.

16. D. Putrino, J. Ripp, J.E. Herrera, M. Cortes, C. Kellner, D. Rizk, K. Dams-O'Connor, Multisensory, Nature-Inspired Recharge Rooms Yield Short-Term Reductions in Perceived Stress Among Frontline Healthcare Workers, Front. Psychol. 11 (2020) 1–6. https://doi.org/10.3389/fpsyg.2020.560833.

17. R.S. Zadeh, M.M.C. Shepley, G. Williams, S.S.E. Chung, The impact of windows and daylight on acute-care nurses' physiological, psychological, and behavioral health, Heal. Environ. Res. Des. J. 7 (2014) 35–61. https://doi.org/10.1177/193758671400700405.

18. Terrapin Bright Green, The Economics of Biophilic Design, (2012) 9–22.

19. International Living Future Institute, KHOO TECK PUAT HOSPITAL, (n.d.). https://living-future.org/case-studies/award-winner-khoo-teck-puat-hospital/ (accessed 28 November 2023).

20. W. Architects, Östra Hospital, Terrapin Bright Green Case Study. (2006) 1–4.

21. T.A. Ouf, A. Makram, S.A. Abdel Razek, Design Indicators Based on Nature and Social Interactions to Enhance Wellness for Patients in Healthcare Facilities, Adv. Sci. Technol. Innov. (2021) 449–461. https://doi.org/10.1007/978-3-030-65181-7_36.

22. G.M. Avinç, S.A. Selçuk, An Evaluation of Biophilic Design Parameters in Hospital Buildings, (2021) 1–7. https://orcid.org/0000-0003-1049-2689.

23. K. Gillis, B. Gatersleben, A review of psychological literature on the health and wellbeing benefits of biophilic design, Buildings. 5 (2015) 948–963. https://doi.org/10.3390/buildings5030948.

24. D.K. Brown, J.L. Barton, V.F. Gladwell, Viewing nature scenes positively affects recovery of autonomic function following acute-mental stress, Environ. Sci. Technol. 47 (2013) 5562–5569. https://doi.org/10.1021/es305019p.

25. G. Wiltshire, E. Pullen, F.F. Brown, M. Osborn, S. Wexler, M. Beresford, M. Tooley, J.E. Turner, The experiences of cancer patients within the material hospital environment: Three ways that materiality is affective, Soc. Sci. Med. 264 (2020) 113402. https://doi.org/10.1016/j.socscimed.2020.113402.

26. S. Blaschke, C.C. O'Callaghan, P. Schofield, Nature-based care opportunities and barriers in oncology contexts: A modified international e-Delphi survey, BMJ Open. 7 (2017). https://doi.org/10.1136/bmjopen-2017-017456.

27. S. Blaschke, C.C. O'Callaghan, P. Schofield, Cancer Patients' Recommendations for Nature-Based Design and Engagement in Oncology Contexts: Qualitative Research, Heal. Environ. Res. Des. J. 11 (2018) 45–55. https://doi.org/10.1177/1937586717737813.

28. B.H. Tekin, R. Corcoran, R.U. Gutiérrez, A Systematic Review and Conceptual Framework of Biophilic Design Parameters in Clinical Environments, Heal. Environ. Res. Des. J. 16 (2023) 233–250. https://doi.org/10.1177/19375867221118675.

PLEA 2024 WROCŁAW
(Re)thinking Resilience

Monitoring and Evaluation of Indoor Environmental Quality
in Two Primary Schools with Mixed-mode Ventilation

WEN-JYE LIAO[1], YU-JIE LU[2], WEI-AN CHEN[3], RUEY-LUNG HWANG[2]

[1]Department of Architecture, National Cheng Kung University, Tainan, Taiwan.
[2]Department of Industrial Technology Education, National Kaohsiung Normal University, Kaohsiung, Taiwan.
[3]Institute for a Secure and Sustainable Environment, University of Tennessee, Knoxville, U.S.A.

ABSTRACT: This study describes the environmental monitoring results of two elementary school classrooms located in rural and urban Taiwan, aiming to quantify the comprehensive impact of air conditioning (AC) usage behaviour on thermal comfort (TC) and indoor air quality (IAQ). AC usage behaviour differs between rural and urban schools. In rural classrooms, the teacher decides whether to operate it with a limited allowance, while in urban classrooms, students vote for its activation with a more generous allowance. A long-term monitoring of classroom temperature and CO_2 concentration was conducted from April 1st to June 30th, and Environmental Quality Index (EQI) was used to measure thermal comfort and indoor air quality levels. AC management was found to significantly affect the time fraction of AC usage, EQI_{TC}, and EQI_{IAQ}. In urban classrooms with less stringent management, the AC usage time fraction is 42.2%, which significantly improves EQI_{TC}. However, this benefit is offset by a lower EQI_{IAQ} due to insufficient ventilation during the AC operation period. It was found that EQI_{TC} did not improve in the rural classroom, which focused on electricity conservation and had a 5.7% time fraction for AC operation.
KEYWORDS: School Building, Mixed-mode Ventilation, Indoor Environmental Quality, Thermal Comfort, Indoor Air Quality

1. INTRODUCTION

Students spend most of their day in the classroom, and a good indoor environmental quality (IEQ) is crucial for their academic performance and health [1], highlighting the urgent need for schools to maintain good IEQ in the classroom. Children are more sensitive to the variation of indoor thermal environment than adults and prefer cooler conditions [2-3]. However, the thermal conditions in classrooms are largely determined by teacher choices, with students often being passive recipients, in part because students feel they need permission before intervening [4]. Therefore, tailoring the classroom thermal conditions to students' expectations is critical to positively impact their performance and health.

Primary school classrooms in Taiwan typically rely on natural ventilation to maintain thermal comfort and operate the air conditioning (AC) only as needed to reduce the risk of indoor overheating. This operating mode, known as mixed-mode, involves utilizing natural ventilation or AC based on occupants' preferences and their response to indoor thermal conditions [5]. During the summer, especially on hot days, the use of AC becomes nearly unavoidable to ensure better thermal comfort [6]. On the other hand, classroom doors and windows are typically closed when AC is in use. At this time, if sufficient outdoor air is not introduced using mechanical or natural ventilation, it will lead to the accumulation of indoor CO_2 concentration, resulting in a conflict between thermal comfort and indoor air quality (IAQ) [7-8]. Using monitoring is a simple and reliable way to avoid this conflict situation from occurring. For example, Zapata-Lancaster et al [9] measured CO_2 levels, temperature and relative humidity to ensure that British classrooms provide satisfactory ventilation and thermal conditions for teachers and students. The trade-off between thermal comfort and IAQ is a critical aspect of IEQ in mixed-mode ventilated classrooms [7-9].

Urban areas, affected by the urban heat island effect, often face higher outdoor temperatures and elevated levels of CO_2 and particulate matter compared to rural areas. This leads to increased AC usage and fewer opportunities for maintaining good IAQ [10].

Two classrooms, one in a rural area and the other in an urban area, was selected in this study to conduct an in-depth assessment of their long-term thermal comfort and IAQ levels. Our primary goal was to uncover the factors influencing variations in AC usage between urban and rural schools, considering not only differences in outdoor conditions but also other possible stimuli. Furthermore, we aimed to identify and address thermal and IAQ issues associated with AC operating behaviours in both urban and rural educational environments. Ultimately, this study seeks to provide practical and actionable recommendations for enhancing the IEQ of classrooms.

2. METHODS

2.1 Investigated school

This study conducted field measurements in two primary schools, one in a rural area and the other in an urban area, both equipped with ceiling fans and split air-conditioning units (14.6 kW and 14.8 kW, respectively). These two schools have similar classroom dimensions: 8.8 m × 7.1 m × 3 m (depth × width × height) for the rural school and 9.1 m × 7.5 m × 3.8 m for the urban school. The rural school building is oriented north-south, while the urban school building is oriented east-west. In terms of occupancy, the rural school has 16 occupants, including teachers and students, while the urban school has 30 occupants. Students attend 16 lessons per week in the rural classroom and 17 lessons in the urban classroom. Additionally, students are required to attend 29 lessons per week, each lasting 40 minutes.

Ceiling fans are typically in use during school hours. School authorities recommend, but do not require, the use of AC when the outdoor temperature exceeds 28°C. However, each school sets its own upper limit for electricity charges related to AC use, and any costs exceeding this limit are the responsibility of the student. The upper limit per semester for electricity charges in the rural schools under investigation is NT$3,000, while for the urban schools, it is NT$5,000. To operate the air conditioner, a control card with a pre-deposited amount is required, and the current usage fee balance is displayed on the device screen. In rural classrooms, the decision to use the air conditioner is made by the teacher, whereas in urban classrooms, it is determined by a student vote. Additionally, the urban schools have a reminder that, when using the air conditioner, classroom windows cannot be fully closed, and two windows must remain partially open. The rural schools do not have this reminder.

Table 1 Measurement parameters and equipment specifications

Parameter	Range	Accuracy
Temperature	-40~125℃	±0.4℃
CO_2	0~10,000ppm	±30ppm ±3% of reading

2.2 Data collection and assessment metrics

The field measurements were conducted from April 1st to June 30th, coinciding with Taiwan's transition from cool spring to hot summer, which is also a period that school classrooms often use AC. The measurement parameters included classroom and outdoor temperature as well as CO_2 concentration. The equipment accuracy details are provided in Table 1. Besides, the electricity consumption for AC was calculated based on the pre-deposited card balance.

The Environmental Quality Index (EQI), which can be calculated by Eq. (1) [11], is used as an indicator to quantify thermal comfort and IAQ conditions within classrooms. According to Equation (1), EQI evaluates indoor comfort quality by weighting the fraction of time in the three categories I, II and III outlined in EN15251 [12]. Category I signifies a high level of expectation, scoring 100 points for durations within this range. Category II represents a normal level of expectation, receiving 70 points. Category III indicates an acceptable, moderate level of expectation, warranting 35 points. Exceeding these categories results in a score of 0 without further calculation. Table 2 shows the range of the three categories in EN15251 [12] for thermal comfort and IAQ. Thermal comfort is categorized according to the deviation from the optimal comfort temperature, while IAQ is categorized according to the difference between indoor and outdoor CO_2 concentrations. The comprehensive EQI score of the classroom is then calculated as the weighted average of TC and IAQ, as shown in Equation (2), with weight coefficients of 0.189 and 0.150, respectively [11].

$$EQI_{TC/IAQ} = 100 \times f_{I} + 70 \times f_{II} + 35 \times f_{III} \quad (1)$$

$$EQI_{c} = \frac{0.189 \times EQI_{TC} + 0.150 \times EQI_{IAQ}}{0.189 + 0.150} \quad (2)$$

where f is the time fraction the thermal comfort (TC)/ IAQ level falls into the categories I, II and III; EQI_c, EQI_{TC} and EQI_{IAQ} are the EQI score for the comprehensive, TC and IAQ, respectively.

Table 2 Scope of the three categories in EN 15251

description		Category		
		Ⅰ	Ⅱ	Ⅲ
thermal comfort	temperature deviated from optimal comfort temperature (°C)	±2	±3	±4
indoor air quality	CO_2 concentration above outdoor concentration (ppm)	<350	<500	<800

3. RESULTS AND DISCUSSION

3.1 Outdoor conditions

Figure 1 presents the outdoor temperature distribution measured at both schools during daily school hours and highlights the range of the three categories in EN15251. Rural and urban schools exhibit similar outdoor temperature trends, with rural schools having a slightly wider daily temperature range. Specifically, rural schools experienced outdoor temperatures ranging from 21.5°C to 35.7°C, with an average of 29.4°C. In contrast, urban schools had outdoor temperatures varying between 23.6°C and 36.0°C, with an average of 30.2°C. Overall, Figure 1 illustrates that rural schools generally have broader

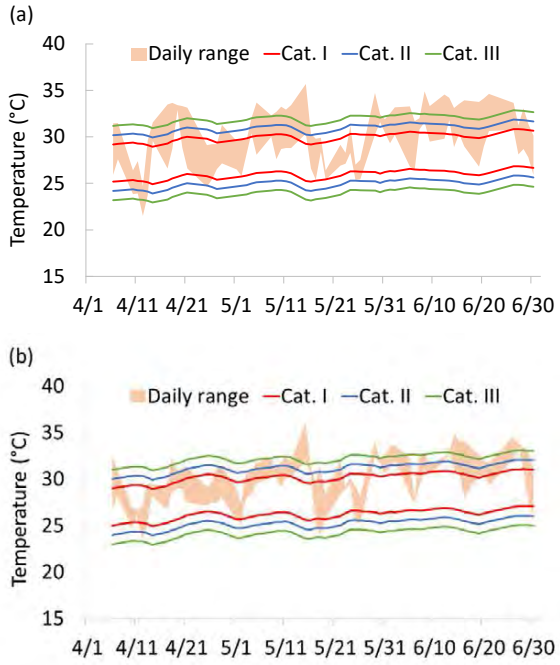

Figure 1: Distribution of outdoor temperature measured in (a) rural and (b) urban school

daily temperature fluctuations.

Table 3 summarizes the fraction of time the outdoor temperature fell within each comfort category and the EQI_{TC} were calculated accordingly. The fraction of time in Table 3 are calculated in time steps of 10 minutes. The maximum acceptable temperature for school buildings is defined by EN 15251 Category II conditions. Rural schools exceeded the upper limit of reference conditions (Category II+) for outdoor temperature in 39.6% of class periods, with 24.7% of class hours exceeding the upper limit of Category III+. In urban schools, these percentages were 37.2% and 16.6%, respectively. Approximately 40% of school hours in both rural and urban schools fall within the high-level expectation category (Category I). Additionally, 24% of rural school hours and 19.5% of urban school hours are categorized as neutral-to-cool (Categories I-, II-, III-, and below).

Under the reasonable assumption that the indoor temperature of naturally ventilated classrooms is close

Table 3 Time fraction of outdoor temperature in EN 15251 categories and the corresponding EQI_{TC}

School		Rural	Urban
warmer-than-neutral	exceed	24.7 %	16.6 %
	Ⅲ+	14.9 %	20.6 %
	Ⅱ+	13.6 %	18.7 %
	Ⅰ+	22.5 %	24.6 %
cooler-than-neutral	Ⅰ-	18.3 %	14.9 %
	Ⅱ-	4.0 %	3.4 %
	Ⅲ-	1.2 %	1.2 %
	below	0.7%	0.0 %
EQI_{TC}		58.8	62.6

to the outdoor temperature, the thermal comfort EQI for urban classrooms is 62.6, which is 3.8 points higher than the 58.8 EQI for rural classrooms. Regarding the fraction of time when school authorities allow AC usage at temperatures ≥ 28°C, rural classrooms can use AC for 75.9% of the time, while urban classrooms can use it for 82.7% of the time. This indicates a longer need for AC in urban classrooms, despite their higher thermal comfort EQI compared to rural classrooms.

3.2 Usage of air-conditioning

Figure 2 presents statistics on daily air conditioner operating minutes from April 1 to June 30, clearly indicating a significantly higher frequency of AC use in urban classrooms compared to rural ones. In urban classrooms, the air conditioner is turned on for 42.2% of the time, nearly matching the 37.2% when the outdoor temperature exceeds the upper limit of EN15251 Class II, but only half of the 82.7% allowed by school authorities for air conditioner use. In comparison, the time fraction of use AC in rural classrooms is 5.7%, which is much lower than the time fraction (39.6%) when the outdoor temperature exceeds the upper limit of EN15251 Category II and the time fraction (75.9%) when school authorities allow AC to be turned on. Under the mixed-mode ventilation strategy, the electricity consumption for AC in rural classrooms and urban classrooms is 73.2 kWh and 589.3 kWh, respectively, translating to electricity costs of NT$868 and NT$4,420, respectively.

We believe that such a significant difference in the proportion of air-conditioning usage time is caused by differences in air-conditioning operation management. A phenomenon was observed that in rural classrooms, it is the teacher's decision whether to turn on the air conditioner or not. Since students do not often use air conditioners at home after school, the teacher subjectively does not encourage students too frequently use air conditioners at school. The teacher was concerned that the free quota might not suffice and could be exhausted quickly. To prevent imposing an extra financial burden on students, the teacher refrained from using air conditioners until the weather remained consistently hot, typically after late May. In contrast, urban students frequently use air conditioners at home and have a higher free quota in

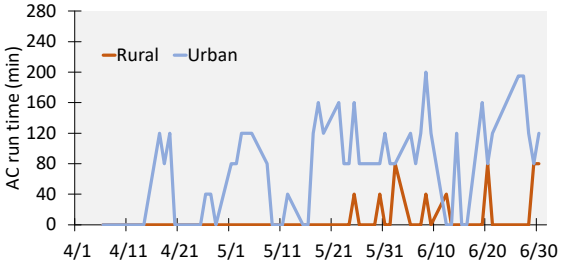

Figure 2: AC operating time in the two schools.

schools. These factors make them less concerned about AC electricity bills and encourage them to use air conditioners more frequently, following their preferences in pursuit of greater thermal comfort.

3.3 Thermal Comfort Assessment

During the measurement period, the indoor temperature in the rural classroom, operating under mixed ventilation mode, ranged from 24.7°C to 35.3°C, averaging 31.1°C. Table 4 summarizes the time fraction of the indoor thermal environment within each comfort category. Rural classrooms generally experienced warmth, with only 2% of school hours below thermal neutral temperatures. In terms of overheating discomfort, 54.2% of school hours exceeded category II+, a 14.6% increase from the 39.6% outdoors. The thermal comfort EQI score for rural classrooms is 47.8, which is 11.0 points lower than the outdoor score of 58.8. This difference arises because the air conditioner is only used for 5.7% of class time, while students' metabolic heat contributes to higher indoor temperatures during natural ventilation.

In the urban classroom, indoor temperatures ranged from 23.6 to 30.3°C, with an average of 26.5°C. Frequent use of the air conditioner in urban classrooms maintains an average indoor temperature of 26.3°C when the air conditioner is active, ensuring a neutral-than-cool thermal environment. As shown in Table 4, 92.7% of the class hours in the urban classroom meet the thermal comfort condition specified by EN 15251 category II, with only 0.7% experiencing overheating discomfort. It is worth noting that 89.9% of class hours fall within the cooler-than-neutral categories I- and II-, likely reflecting students' preference for cooler thermal conditions [3]. Specifically, the urban classroom's EQI_{TC} is 83.8, which is 21.2 higher than the corresponding outdoor EQI_{TC} of 62.6.

The results of the thermal environment measurements indicated that although strengthening AC management in the rural classroom can reduce the energy consumption of AC, it cannot completely alleviate the indoor thermal discomfort. Conversely, urban classroom management, while relatively lax, maintains high thermal comfort but can lead to a cooler or overcooled environment and increased energy consumption. One simple way to prevent overcooling in classrooms is to raise the thermostat's minimum temperature setting above the thermal neutral point. Investigating the ideal trade-off between AC power consumption and thermal comfort remains a significant topic for future research. It is crucial to identify and implement management strategies that effectively manage energy usage while ensuring that students and educators benefit from a comfortable learning environment. Achieving this balance will not only enhance the overall IEQ of classrooms but also contribute to energy conservation efforts.

Table 4 The time fraction in each thermal comfort category and the EQI_{TC}

School		Rural	Urban
warmer-than-neutral	exceed	31.5	0.0
	Ⅲ+	22.7	0.7
	Ⅱ+	19.3	1.2
	Ⅰ+	24.4	8.4
cooler-than-neutral	Ⅰ-	1.8	46.1
	Ⅱ-	0.2	37.2
	Ⅲ-	0.0	6.5
	below	0.0	0.1
EQI_{TC}		47.8	83.8

3.4 Indoor Air Quality

Figure 3 shows the distribution of the average difference in indoor and outdoor CO_2 concentrations per 10 minutes for the two classrooms. First of all, comparing Figure 3 with Figure 2, it becomes evident that the difference in indoor and outdoor CO_2 concentrations is clearly synchronized with the use of air conditioners. In addition, it is noticeable that during natural ventilation, the CO_2 concentration in urban classrooms is higher than that in rural classrooms, primarily because the number of occupants in urban classrooms is almost twice that of rural classrooms. While urban classrooms typically maintain two windows partially open when the air conditioner is in use to ensure necessary ventilation, Figure 3 still reveals that urban classrooms exhibit significant differences in CO_2 concentration. These differences far exceed the thresholds for Category I or II, especially during the AC operation period. This indicates that the ventilation provided through the two partially open windows is insufficient. In the rural classroom, the average CO_2 concentration difference increased by 383 ppm, rising from 12 ppm during natural ventilation to 395 ppm during AC. In the urban classroom, the average CO_2 concentration difference increased by 476 ppm from 57 ppm to 533 ppm when the air

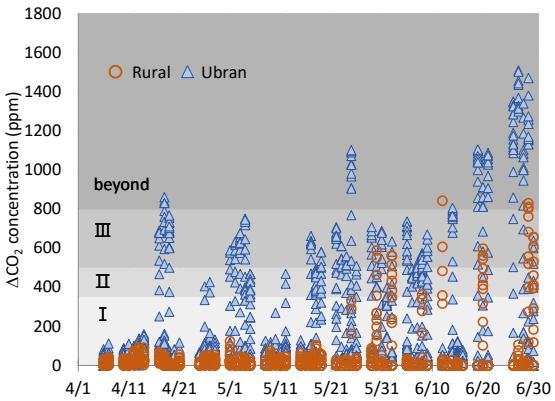

Figure 3: Every 10 minutes distribution and categories of indoor CO_2 concentrations in two schools.

conditioner was activated.

Table 5 summarizes the fraction of time when the CO2 concentration fell into various categories according to EN 15251. In the rural classroom, natural ventilation accounted for 94.3% of class time, resulting in CO_2 concentrations falling within Category I for 96% of that time and only 2% in Category III. Consequently, the EQI_{IAQ} was measured at 97.8. Conversely, in the urban classroom, AC was used for 42.2% of class time, often with inadequate ventilation.This led to CO_2 levels meeting Category I criteria for only 68% of the time, with 22% exceeding Category II, resulting in an EQI of 80, which is 17.2 points lower than that of rural classrooms. The findings highlight the risk of IAQ deterioration in classrooms when air conditioners are used without adequate outside air circulation. Thus, before installing mechanical ventilation equipment, it is essential to install carbon dioxide concentration monitors as they can remind students to open windows to maintain proper ventilation rates.

Table 5 The time fraction in each CO2 category and the EQI_{IAQ}

School		Rural	Urban
Category	Ⅰ	96%	68%
	Ⅱ	2%	10%
	Ⅲ	2%	14%
	beyond	0%	8%
EQI_{IAQ}		97.8	80.0

3.5 Comparative Analysis

After separately evaluating the thermal comfort and IAQ of the classroom, the final analysis centers on the comprehensive EQI_C of the classroom and its comparison with outdoor conditions, as depicted in Figure 4. For rural classrooms, the EQI_C stands at 70.0, which is 7.0 points lower than the outdoor EQI_C of 77.0. Figure 4 illustrates that both the thermal comfort EQI_{TC} and EQI_{IAQ} in rural classrooms are lower than those corresponding to outdoor conditions. This disparity is primarily attributed to teachers' stringent control over air conditioner usage. It is reasonable to speculate that increasing the usage of air conditioner in rural classrooms to alleviate overheating discomfort could lead to an improved EQI_C. In addition, the primary purpose of installing AC in classrooms is to enhance thermal comfort. Excessive focus on air conditioner power consumption and overly stringent usage management for energy conservation purposes may sacrifice thermal comfort, resulting in an overall decline in environmental quality, which should not be encouraged.

The urban classroom achieves an EQI of 82.1, surpassing the outdoor EQI of 79.1 by 3 points. Figure 4 illustrates that this improvement in EQI_C for urban classrooms primarily results from a significant enhancement in thermal comfort. Urban schools

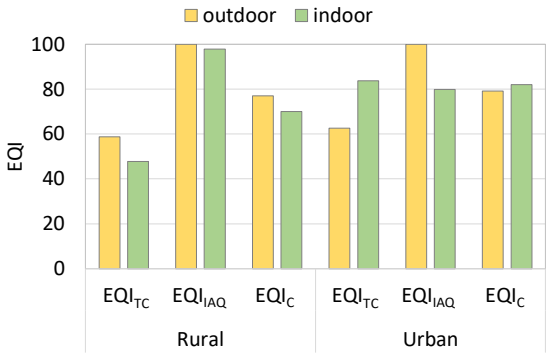

Figure 4: Results of EQI and energy use in two schools.

adopt less stringent air-conditioning controls and offer more generous free quotas, allowing students to pursue their preferred cooler environment. However, it was observed that the thermal environment in urban classrooms tends to be slightly cooler than necessary. By adjusting the temperature set point slightly higher by 1-2°C, it's reasonable to anticipate improved EQI_{TC} and EQI_C scores, along with reduced AC energy consumption and costs. However, Figure 4 also illustrates that the EQI_{TC} bonus gained from using AC is offset by the EQI_{IAQ} deduction due to inadequate ventilation. Hence, it is crucial to furnish students with additional information and reminders, emphasizing the importance of maintaining proper ventilation alongside AC usage to uphold excellent IAQ. This proactive approach ensures that the beneficial intent behind installing air conditioners remains intact.

4. CONCLUSION

This study presents the findings from measurements conducted in two primary schools in Taiwan, with the objective of quantifying the combined impact of thermal comfort and IAQ on IEQ. Additionally, we aim to establish the connection with AC management behaviours. These results underscore the importance of adjusting AC management practices based on a comprehensive assessment of the prevailing conditions of thermal comfort and IAQ within the classroom. We emphasize that environmental control should not be solely governed by energy conservation concerns or individual preferences, since IEQ has a significant impact on the students' health, concentration, and learning performance. In conclusion, there should be a shift in focus within AC investments towards enhancing environmental quality. Therefore, it is recommended that classrooms be equipped with temperature and CO_2 concentration sensors to monitor real-time changes in the classroom environment.

The current study has certain limitations that can offer valuable insights for future research endeavours. Firstly, our research was conducted in a hot and humid climate zone, typical of Taiwan's location. Therefore, the findings may not be directly applicable to regions

with significantly different weather conditions. Secondly, we placed less emphasis on addressing the risk of overcooling, as Taiwan typically experiences extremely hot weather conditions. In light of emerging challenges, such as energy poverty and the increasing frequency of extreme heatwaves attributed to climate change, there is an urgent need to advance our thermal management strategies. To address these imperatives, our forthcoming research endeavors will embark on a comprehensive exploration of the intricate relationships encompassing cost-benefit analysis, building energy efficiency, and the holistic well-being of occupants, with a particular focus on school buildings. Our objective is to undertake a comprehensive examination of a diverse range of thermal management methodologies, incorporating both advanced artificial technologies and innovative passive design strategies. The overarching goal is to formulate strategies that not only reduce energy consumption but also prioritize the comfort, health, and productivity of individuals within indoor environments. In this evolving landscape, achieving the optimal balance between sustainability, energy efficiency, and occupant well-being takes on paramount importance in shaping a more sustainable and resilient built environment.

ACKNOWLEDGEMENTS

We offer our sincere appreciation for grant support from the National Science and Technology Council of Taiwan under the project number MOST 111-2221-E-017-006.

REFERENCES

1. Toyinbo, O., (2023). Indoor Environmental Quality, Pupils' Health, and Academic Performance—A Literature Review. *Buildings*, 13(9): p. 2172.

2. Teli, D., Jentsch, M.F., James, P.A., (2012). Naturally ventilated classrooms: An assessment of existing comfort models for predicting the thermal sensation and preference of primary school children. *Energy and Buildings,* 53: p. 166–182.

3. Liang, H.H., Lin, T.P., Hwang, R.L., (2012). Linking occupants' thermal perception and building thermal performance in naturally ventilated school buildings. *Applied Energy*, 94: p. 355-363.

4. Bernardi, N., Kowaltowski, D.C., (2006). Environmental Comfort in School Buildings: A Case Study of Awareness and Participation of Users. *Environment and Behavior*, 38(2): p. 155-172.

5. Hwang, R.L., Huang, A.W., Chen W.A., (2021). Considerations on envelope design criteria for hybrid ventilation thermal management of school buildings in hot–humid climates. *Energy Reports,* 7: p.5834-5845.

6. Huang, K.T., Hwang, R.L., (2015). Parametric study on energy and thermal performance of Urban School buildings with natural ventilation, hybrid ventilation and AC. *Indoor and Built Environment*, 25: p. 1148-1162.

7. Hwang, R.L., Liao, W.J., Chen, W.A., (2022). Optimization of energy use and academic performance for educational environments in hot-humid climates. *Building and Environment*, 222: p.109434.

8. Liao, W.J., Chen, W.A., Hwang, R.L., (2023). Determination of the Optimal Temperature Set-point and Ventilation Rate for Balancing Energy Consumption and Learning Performance in Primary Schools in Taiwan. *Proceedings of the 5th International Conference on Building Energy and Environment,* p.1829-1834.

9. Zapata-Lancaster, M.G., Ionas, M., Toyinbo, O., Smith, T. A., (2023). Carbon Dioxide Concentration Levels and Thermal Comfort in Primary School Classrooms: What Pupils and Teachers Do. *Sustainability*, 15(6): p. 4803.

10. Catalina, T., Ghita, S.A., Popescu, L.L., Popescu, R., (2022). Survey and Measurements of Indoor Environmental Quality in Urban/Rural Schools Located in Romania. *International Journal of Environmental Research and Public Health*, 19(16): p. 10219.

11. Marino, C., Nucara, A., Pietrafesa, M., (2012). Proposal of comfort classification indexes suitable for both single environments and whole buildings. *Building and Environment*, 57: p. 58-67.

12. CEN (European Committee for Standardization), (2007). Indoor environmental input parameters for design and assessment of energy performance of buildings—addressing indoor air quality, thermal environment, lighting, and acoustics. *Brussels*, EN15251:2007.

PLEA 2024 WROCŁAW
(Re)thinking Resilience

Living Places: Healthy Homes for People & Planet

A single-family home with ultra-low carbon footprint

LUCILE SARRAN[1] NICOLE DI SANTO[1] RASMUS SOEGAARD[2] LONE FEIFER[1] KASPER REIMER[3]

[1] VELUX A/S, Hørsholm, Denmark
[2] Artelia A/S, Copenhagen, Denmark
[3] EFFEKT Arkitekter ApS, Copenhagen, Denmark

ABSTRACT: This research focuses on designing and constructing ultra-low-carbon homes within the Danish building industry. The primary objective was to showcase the feasibility of building homes with significantly reduced carbon footprints while maintaining superior indoor environments and adapting to regulations and market conditions. Two unique houses were designed and constructed to exhibit alternative approaches to achieving a very low carbon footprint while incorporating aesthetic value to promote a sense of community. The study utilised a comprehensive life cycle assessment (LCA) methodology to evaluate the environmental impacts of construction materials and operational energy use. Results indicated that both houses achieved more than a 64% reduction in global warming potential (GWP) compared to a benchmark house, staying well below the maximum threshold established by Danish legislation. The study further emphasised the importance of material selection in reducing carbon footprints and highlighted the availability of a diverse range of low-carbon materials in the market. This research demonstrates that designing cost-effective, ultra-low-carbon homes using existing materials and technologies is feasible, paving the way for higher ambitions in the construction sector to meet climate targets.
KEYWORDS: Ultra-low-carbon homes, Life Cycle Assessment, Global Warming Potential, Building Industry, Design Optioneering.

1. INTRODUCTION

Energy use in the built environment accounted for 27% of the world's CO_2 emissions in 2022 and building materials for an additional 10% [1]. As energy efficiency progresses, the contribution of embodied emissions to the building's whole lifecycle carbon footprint is becoming more apparent. Legislation across Europe is therefore increasingly adopting a lifecycle approach to carbon emissions in buildings: in France, Denmark and the Netherlands, lifecycle global warming potential (GWP) thresholds have already been established for new construction, and more countries are planning to implement such legislative requirements in the years to come [2]. The European Union's (EU) revised Energy Performance of Buildings Directive is expected to bring similar requirements for all European countries by the end of this decade [3]. These initiatives are necessary to bring the European Union on track with its CO_2 reduction commitments, but the few proposed thresholds are not yet ambitious enough to reach the 1.5-degree target set by the Paris Agreement [4].

The construction industry is a key sector in which to intervene and must, therefore, learn how to design and operate buildings with a much lower carbon footprint than what is (or will be) required. The EU is taking a proactive approach to address the urgent challenges of resource depletion and climate change. This involves implementing a new sustainable construction strategy, which aims to consider End-of-Life scenarios from the product design stage and optimise energy efficiency throughout the entire lifespan of constructed assets. The ultimate goal is to extend the useful life of constructed assets and promote environmental sustainability. Therefore, it is crucial to consider Life Cycle Assessment (LCA) when designing future-proof constructions.

The building industry is a slow-moving sector, but its decarbonisation is urgent. Many solutions already exist to build with a very low carbon footprint, but a share of the industry lacks knowledge about these solutions [5]. Cost is often seen as a barrier to the development of green buildings, as many players assume such solutions will be more expensive [5-6]. Finally, while many pilot low-carbon buildings have been built over the years [7], they are not always replicable at scale in an affordable way.

The project described in this article seeks to demonstrate the feasibility of affordable, ultra-low carbon homes with excellent indoor environments, built with today's materials and technologies and adapting to local customs, regulations, and market conditions. This paper introduces Living Places, a single-family home concept developed and built by three players in the Danish building industry (i.e., VELUX, EFFEKT Architects and Artelia Denmark). This article presents the design process, the final concept, and the results in terms of the project's carbon footprint.

2. METHODS

The project's goal and scope were defined, and LCA was performed using a design optioneering approach to calculate the materials' overall impact. From a theoretical viewpoint, this section also explains the methodology used to assess the carbon footprint of the single-family houses executing LCA.

2.1 Construction program and benchmark house

Two single-family houses were designed and built with the goal of showing two alternative ways to reach a very low carbon footprint while maintaining durability and affordability. The houses were intended to host a family of four, with three bedrooms, one bathroom and a combined kitchen-living room. The building design arose from the amalgamation and integration of the partners' expertise and creativity, with a focus on incorporating aesthetic value and creating a communal atmosphere that fosters a sense of belonging.

A benchmark house was also defined, representing a typical Danish single-family house with the same function. The benchmark house was a single-plan, 184 m^2 detached house with three bedrooms. It had a concrete foundation and floor slab, concrete external walls with mineral wool and a brick façade, aerated concrete internal walls, a barred roof construction with roof tiles and a ventilated attic. It had underfloor heating and was connected to district heating. The house also had a balanced mechanical ventilation system with heat recovery and was equipped with a 7 m^2 photovoltaic installation.

2.2. LCA method

The ISO Standard 14040:2006 [8] defines the functional unit in an LCA as the quantified performance of a product system. In this study, the functional unit is a single-family house. LCA was carried out following the methodology adopted in the Danish legislation in January 2023. Three distinct phases were undertaken to conduct a comprehensive LCA of the houses. Firstly, a life cycle inventory analysis (LCI) was conducted, encompassing a thorough review of the product's inputs and outputs from acquiring raw materials to production, use and disposal. The second phase involves the life cycle impact assessment (LCIA), estimating the potential environmental impacts of these inputs and outputs. The final phase, known as life cycle interpretation, involved interpreting the inventory analysis results and impact assessment phases concerning the study's objectives. The system boundary includes the lifecycle stages A1-A3, B4, B6, C3 and C4, which were evaluated using the Danish LCA compliance software LCAbyg according to EN 15978:2012. The evaluation period was 50 years.

LCAbyg's database is modelled after the German ÖKOBAUDAT database for construction products, utilising Environmental Product Declarations (EPD) to represent available products comprehensively. The Federal Ministry for the Environment, Nature Conservation, Building and Nuclear Safety (BMUB) oversees ÖKOBAUDAT for in-depth cradle-to-grave analyses of building products and services. This database contains standardised data sets for various construction materials and processes, organised according to European standards for assessing environmental quality. However, as a result of new Danish regulations, LCAbyg's database now supplements ÖKOBAUDAT data with an additional 10-30% of generic data, as outlined in BR18 annex 2 table 7 [9]. Moreover, transport and site processes are not considered in the calculations and can be entered into the tool in relation to the individual product.

The energy use during the building's lifetime was estimated using the Danish energy frame calculation method and inserted as an input into LCAbyg. The calculation of operational emissions from energy use was done considering an average carbon intensity of electricity of 56 gCO_2/kWh in Denmark between 2021 and 2071 (starting in 2021 with 238 gCO_2/kWh and assuming a greening of the electrical grid reaching 40 gCO_2/kWh in 2040).

The impact categories supported by LCAbyg calculate the environmental profile results describing (1) environmental impacts[1], (2) resource use, primary energy[2], and (3) resource use, secondary materials and fuels, and use of water[3]. This project focuses on optimising the global warming potential (GWP) of the houses; therefore, the results achieved in the other impact categories are not discussed in this article.

The LCA calculation was carried out by the project's engineering consultant and verified by independent researchers via LCAbyg. The buildings' environmental profiles analysed were obtained by combining the environmental impacts associated with the operation and those attributed to building materials.

2.3 Design Optioneering approach

A tool was developed in order to determine the optimal design choices for materials and services iteratively to achieve ultra-low carbon homes. A

[1] GWP = Global Warming Potential; ODP = Ozone Depletion Potential; POCP = Formation potential of tropospheric Ozone; AP = Acidification Potential for Soil and Water; EP = Eutrophication Potential; ADPE = Abiotic Depletion Potential Elements; ADPF = Abiotic Depletion Potential Fossil Fuels.

[2] PENRT = Total Use of non-renewable primary energy resource; PERT = Total Use of renewable primary energy resources.

[3] RSF = Use of renewable secondary fuels; NRSF = Use of non-renewable secondary fuels.

comprehensive list of materials and products utilised in the construction of each building element, including external and internal walls, windows and doors, floors, roofs, and foundations, as well as relevant information regarding operations such as heating systems, ventilation, storage, and PV systems, were meticulously identified. The carbon footprint of each of these construction elements was extracted from environmental product declarations (EPDs) and inserted into the tool developed for this project. Cost information was also included in the tool. This tool enables the selection of design options for various building components, such as foundation, ground floor, external and partition walls, and more. Each choice was already associated with a value in kg CO_2/unit yr. based on an LCA per component and a value in DKK/unit based on market prices. After selecting the desired components and materials, the tool calculates the building's total GWP in kg $CO_2/m^2/yr$. Through this iterative process of selecting and comparing building components, the final materials for the house were chosen in such a way as to reach the carbon footprint goal.

Subsequently, the LCAbyg tool was utilised to calculate multiple impact categories, thereby verifying the construction's overall environmental impact throughout its life cycle.

3. RESULTS

The process described in Section 2 resulted in the design of two distinct houses with mirrored floor plans, one with a timber frame structure and the other with a CLT-based structure.

3.1. Architectural design and services

The houses were designed as 3-story single-family houses with a pitched roof on the two upper floors. The total floor area was 147 m^2, which was purposefully chosen to be slightly smaller than the benchmark house and the Danish average in order to showcase smaller living as one strategy to reduce the overall carbon footprint of the built environment.

Regarding the building services, both houses were equipped with an air-to-water heat pump and radiators. The timber frame house was purely naturally ventilated via automated façade and roof windows reacting to indoor temperature, humidity and CO_2 concentration signals. Windows could also be operated manually by the occupants. A balanced mechanical ventilation system with heat recovery was installed in the CLT house, complementing the manual and automated windows and enabling hybrid ventilation. Both houses had 11 m^2 PV panels located on the flat part of the roof.

The energy frame calculation gave a net yearly electrical consumption from the electrical grid of 5.1 $kWh/m^2/yr$. – the electricity produced onsite by the photovoltaic panels is already deducted from this number. The operational emissions of the house were calculated to be 0,28 $kgCO_2/m^2/yr$.

3.2. Choice of materials

The details of the investigated design options are shown in Table 1. The comparison of the Global Warming Potential of these different options is shown in Figure 1 for each of the main construction element categories. The GWP is shown per m^2 of floor area. Figure 1 and Table 1 also show the chosen options for the timber frame house and the CLT house. The cost of each option was also estimated and considered in the choice of materials but not shown in this article.

Choosing a foundation and floor based on screw piles and a wooden cassette, instead of the traditional concrete-based foundation and floor slab, permitted to divide the carbon footprint of these elements by a factor 2 to 3.

Both houses looked similar from the outside, with untreated wooden cladding, a steel roof and a 3-layer façade and roof windows. However, they were based on different construction principles: one of the houses had a traditional timber frame structure and a wooden skeleton for internal walls, while the other used CLT in external and internal walls, floors and the roof. Paper wool and wood fibre insulation were chosen for external walls and roofs.

3.3. LCA of the two houses

The final results of the LCA in terms of the total Global Warming Potential (GWP) of each house are shown in Table 2.

Table 2: Global Warming Potential results.

GWP ($kgCO_2eq/m^2/yr.$)	Benchmark house	LP timber frame	LP CLT
Embodied	8,2	3.5	3.6
Operational	2,9	0.3	0.3
Total	11,1	3.8	3.9

Table 1: Detail of the investigated design options for each construction element.

Option	Foundation	Floor slab	External wall	External wall cladding	Interior walls	Floor deck	Roof	Roof cladding	Windows
1	Traditional strip foundation in Leca and concrete	Traditional concrete slab + polystyrene insulation	Wooden cassette + mineral wool	Wooden cladding, untreated	Steel skeleton + mineral wool + 2 x gypsum pr. side	Ribbed deck + apparent beams	Light wooden cassette + wood fiber insulation	Roofing felt	3-layer wood-alu façade windows
2	Strip foundation in Leca and concrete + FutureCem	Concrete slab with FutureCem +polystyrene insulation	Wooden cassette + I-joists + wood fiber insulation	Wooden cladding, heat-treated	CLT	Ribbed deck + apparent glulam beams	Light wooden cassette + paper wool insulation	Steel sinus plates	3-layer wood-wood façade windows
3	Screw pile foundation	Concrete slab with FutureCem + Rockwool Terrænbats	Wooden cassette + paper wool insulation	Wooden cladding, painted	Wooden skeleton + mineral wool + 2 x gypsum pr. side	Ribbed deck + gypsum ceiling	CLT with wood fiber insulation	Zinc	3-layer alu façade windows
4	L-element	Light wooden cassette, raised	Wooden cassette + paper wool insulation, thin	Sinus plates, steel + zinc magnesium	Wooden skeleton + wood fiber insulation + 2 x gypsum pr. side	CLT		Roof tiles	3-layer PVC façade windows
5		Light slab + polystyrene insulation	CLT with wood fiber batts	Tiles	Wooden skeleton + wood fiber insulation + OSB and gypsum pr. side			Wooden slats on the roofing felt	3-layer wood-alu sloped roof windows
6		Light slab + Rockwool Terrænbats	Insulated bricks	Slates	Wooden skeleton + wood fiber insulation + 1 x gypsum pr. side			Wooden cladding, untreated	3-layer alu-PU sloped roof windows
7		Light wooden cassette, raised (alternative)	Concrete wall + mineral wool	Fiber cement	Insulated bricks			Wooden cladded, heat-treated	2-layer modular skylight
8			Rockwool RedAir	Plaster	Aerated concrete			Wooden cladding, painted	3-layer modular skylight
9					Wooden skeleton + wood fiber insulation + plywood			Slates	
10								Fiber cement	

Legend:

Chosen option in the CLT house
Chosen option in the timber frame house
Chosen option in both houses

The timber frame house achieved a 65,8% reduction in GPW compared to the benchmark house, while the CLT house achieved a 64,9% reduction. In both cases, the achieved GWP was more than three times lower than the maximum threshold set by the new Danish legislation of 12 $kgCO_2eq/m^2/yr$.

Both houses were built in Copenhagen in 2023, showing the practical feasibility of these designs. Figure 2 shows pictures of the realised houses. Simulations carried out during the design process showed that both design concepts also achieved excellent indoor environmental quality – these results are presented in another contribution to the PLEA 2024 conference.

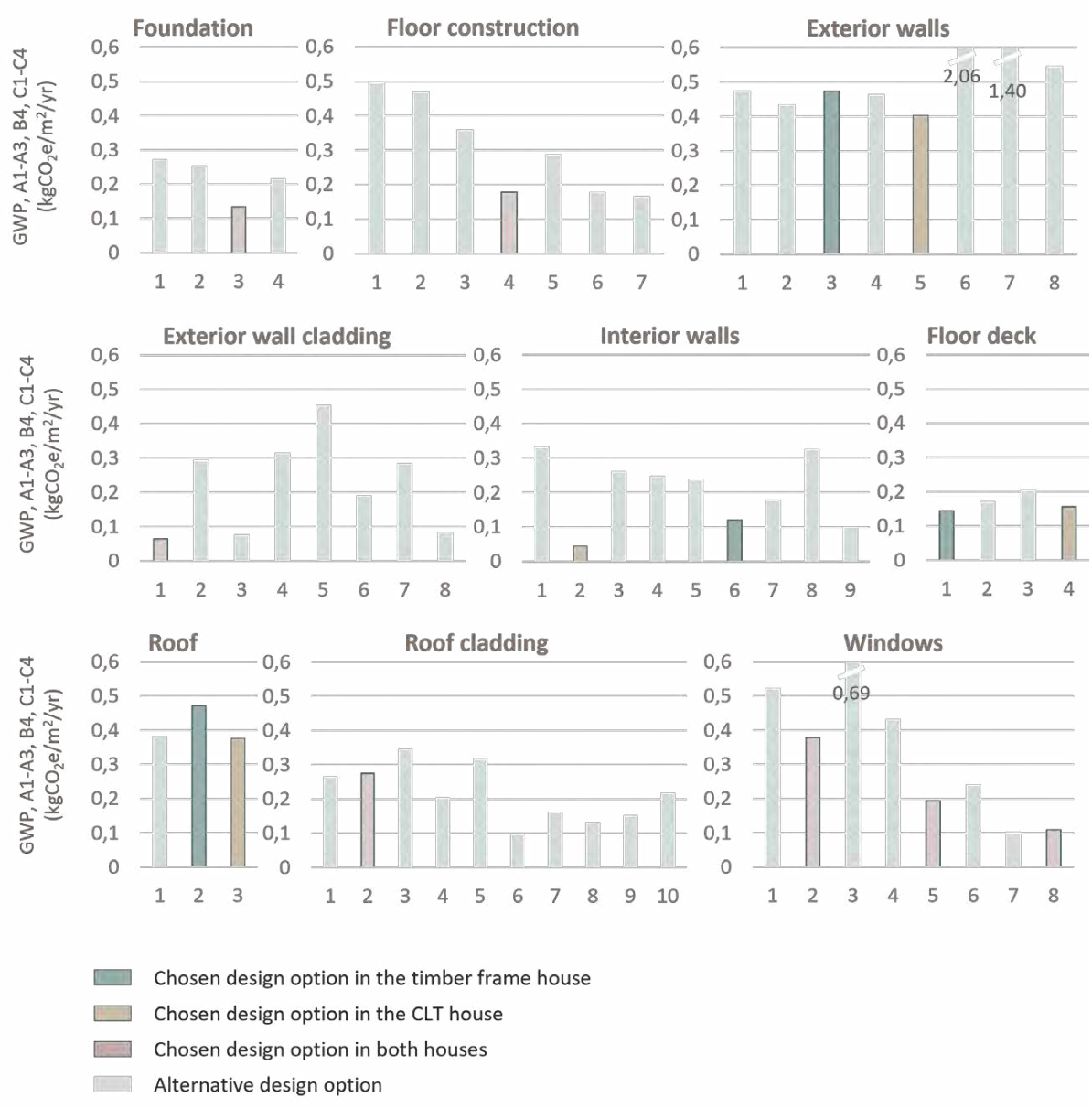

Figure 1: GWP of different design options for each construction element. The numbers on the x-axis correspond to the design option details shown in Table 1.

4. DISCUSSION

This study highlights the importance of carefully selecting building materials in order to achieve a low carbon footprint. The design optioneering approach revealed the significant differences between materials – and even between brands – when it comes to their global warming potential. However, the example of Living Places shows that a large range of low-carbon materials exists today. There is potential for overcoming the current challenge of creating low-carbon pilot buildings that can be economically replicated at various scales. The method used in this study is transparent, and the assessments demonstrate
the practicality of designing cost-effective, ultra-low carbon homes with exceptional indoor environments, utilising today´s materials and technologies.

A limitation of this study resides in the quality of the data used to perform the LCA. It is difficult to find environmental product declarations for all used materials. Therefore, the LCAs conducted for this

project included 22% and 20% generic EPDs for the timber frame and CLT houses, respectively.

Moreover, designing this project and comparing different materials based on their carbon footprint is a time-consuming operation that requires a larger budget as well as close cooperation between the different involved parties – developer, architect, engineer, etc. While this is difficult in most mainstream construction projects, the Living Places case shows the value of a deeper collaboration between parties in the early stages of the building design process.

5. CONCLUSION

With the two presented design concepts, the Living Places initiative showed that it is possible, with today's materials and technologies, to build single-family houses with a lifecycle carbon footprint three times lower than what is currently required by legislation. This paves the way for legislators and the building industry to raise their ambition level in order to bring the construction sector on track to meet the targets set out in the Paris Agreement.

Figure 2: Pictures of the built houses in Living Places Copenhagen. a: Overall view of the area; b and c: Outside view; d: Inside view of the timber frame house; e: Inside view of the CLT house. Photos: Adam Mørk

ACKNOWLEDGEMENTS

The authors wish to acknowledge the invaluable contribution of the project partners – VELUX, EFFEKT Architects and Artelia Denmark.

REFERENCES

1. United Nations Environment Programme, (2022). 2022 Global Status Report for Buildings and Construction
2. One Click LCA, (2022). Construction Carbon Regulations in Europe. Review and best practices.
3. European Commission, (2023). Proposal for a directive of the European Parliament and of the Council on the energy performance of buildings (recast).
4. Reduction Roadmap, (2022). Reduction Roadmap: Preconditions and Methodologies. reductionroadmap.dk.
5. Giesekam, J., J. R. Barrett, and P. Taylor, (2016). Construction sector views on low carbon building materials. *Building Research and Information*, 44(4): p. 423–444.
6. Mata, E., D. Peñaloza, F. Sandkvist, and T. Nyberg, (2021). What is stopping low-carbon buildings? A global review of enablers and barriers. *Energy Research and Social Science,* 82(July).
7. A. Garnow et al., (2021). BUILD Rapport 2023:12 - Boligbyggeri fra 4 til 1 planet: 25 Best Practice Cases.
8. International Organization for Standardization, (2006). ISO 14004:2006. Environmental Management - Life Cycle Assessment - Principles and Framework.
9. Danish Knowledge Center for Energy Savings in Buildings, (2018). Energy requirements of BR18, April, pp. 95–98.

Investigating the Seasonal Impact of Urban Heat Island on PM2.5 for Two Urban Agglomerations in China

YIHANG SU[1]

[1]School of Architecture and Urban Planning,Huazhong University of Science and Technology,Wuhan City, China

ABSTRACT: In recent years, urban areas face two challenging problems caused by urbanization; UHI and air pollution, which have a potential synergistic effect. We explore these interactions in two urban agglomerations; Yangtze River Delta (YRD) and the Pearl River Delta (PRD) using PM2.5 concentrations data and land surface temperature (LST) data for 2022 collected from Moderate Resolution Imaging Spectroradiometer (MODIS). Through regression analysis we found that the relationship between PM2.5 concentrations and UHII of PRD is stronger than which of YRD, which can be attributed to different synoptic weather conditions. PRD is closer to the tropics and less affected by the cold air of the northern cold wave, so there is a significant positive correlation throughout the four seasons. Moreover, there was a substantial seasonal effect on the strength of the correlations between UHI and PM2.5, with some air pollutants showing strong associations with UHI during certain seasons. Thus, the potential interaction between PM2.5 concentrations and UHII warrants cooperation appropriate mitigation measures to solve these two urban problems in a coordinated manner.
KEYWORDS:PM2.5, Urban heat island, Climate change, Urban Agglomeration.

1.Introduction:

Industrialization and urbanization have driven global development in the past few decades while bringing significant environmental issues[1]. Due to the altered underlying surface, urban areas are often warmer than rural areas and suburbs; This phenomenon is widely known as the Urban heat island (UHI) [2]. At the same time, urban activities, such as automobile exhaust, coal, and fuel combustion, are the primary sources of air pollution[3]. In addition, urban morphological factors can affect the air's temperature, humidity, and ventilation, thereby affecting the diffusion, migration, and settlement of pollutants[4-6].

Therefore, urban areas face two challenging problems caused by urbanization; UHI and air pollution, which have become the main challenges in most cities in China [7]. UHI can lead to warmer temperatures and low wind speed, affecting the spatial distribution and concentration of PM 2.5. Therefore, UHI and urban air pollution have a potential synergistic effect. Furthermore, their relationship can vary under different seasons due to the different climatic conditions. Thus, it is necessary to conduct comprehensive research to discover the potential mechanisms of the two in different seasons to solve these two urban problems in a coordinated manner.

By Studying the relationships between urban heat island intensity (UHII) and air pollutants in Seoul, Jack Ngarambe et al. found that O3 concentrations were negatively correlated with UHII. In contrast, CO, SO2, PM2.5, PM10, and NO2 concentrations were positively correlated with UHII. Moreover, there was a substantial seasonal effect on the strength of the correlations between UHI and air pollution[8]. By investigating the spatial-temporal distributions of the daytime and nighttime LST and air pollutant concentrations and their interactions in the Yangtze River Delta urban agglomeration, Yue Jiang et al. showed that the daytime and nighttime LST were positively correlated with O3 concentrations, with the correlation being strongest in spring and autumn. The PM2.5, PM10, SO2, NO2, and CO concentrations show negative correlations with the daytime and nighttime LST, with the strongest interactions in winter[9]. Different contexts, such as climate background and geographical characteristics, can influence the relationship between them, while most previous studies only focus on single cities or regions, which leads to incomplete understanding of the relationship between the two and less target solution. Therefore, this study aims to examine and compare the seasonal effects of UHI on PM2.5 in the two largest urban agglomerations in China.

2. Materials and methods

2.1 Study area

This paper selects the urban agglomeration with the highest urban density and urbanization level in China: the Yangtze River Delta (YRD) and the Pearl River Delta (PRD).[10, 11]. YRD is located in the eastern coastal area of China. It accounts for 1.2% of China's total land area, but contributes 15.9% of its GDP[12]. PRD is located in the coastal area of southern China, accounting for 85% of Guangdong's GDP and 70% of its population[10]. Both urban agglomerations belong to the subtropical monsoon climate, while PRD is closer to the tropics and YRD is more affected by cold air. The distribution of each urban agglomeration is shown in Figure 1.

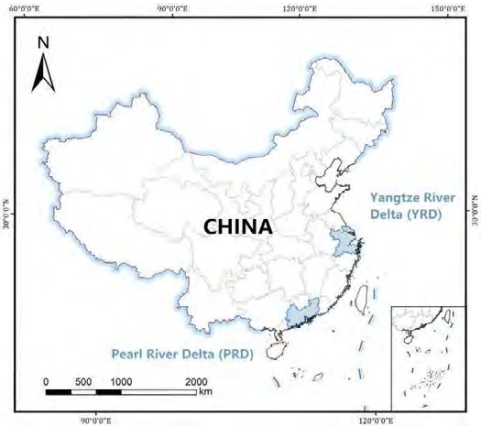

Figure 1: locations of YRD and PRD

2.2 Data

This study includes PM2.5 concentrations data and land surface temperature (LST) data, both of which use Moderate Resolution Imaging Spectroradiometer (MODIS) remote sensing data (resolution of 1 km). The study period is from the 1st of January 2022 to the 31st of December 2022.

2.3 Research steps

2.3.1 Data processing

The original data (spatial resolution of 1 km), including PM2.5 concentration and LST were reprojected to the WGS48 coordinate system. Then, based on the four seasons (spring is from March to May, summer is from June to August, autumn is from September to November, and winter is from December to February), the seasonal grid data was calculated according to the mean value of each pixel.

2.3.2 Calculating urban heat island intensity (UHII)

The seasonal MODIS LST data were converted to degree Celsius using equation(1):

$$T_s = DN * 0.02 - 273.15 \quad (1)$$

Where T_s represents the LST of the unit (◦C); the digital number (DN) is the brightness value of a pixel.
After dividing the research area into urban and rural areas, we calculated each area's average LST of the suburbs. Urban heat island intensity (UHII) was calculated using equation (2).

$$UHII = T_{urban} - T_{rural} \quad (2)$$

Where T_{urban} is the average LST of an urban area [◦C] and T_{rural} is the average LST of rural areas previously calculated.

2.3.3 Spatial autocorrelation analysis

Global autocorrelation and local spatial autocorrelation are applied to explore spatial aggregation characteristics and their evolution patterns.

The global spatial autocorrelation (Global Moran's I) can describe the overall characteristics of the spatial pattern of PM2.5 and UHII, which is calculated as shown below:

$$I = \frac{n\sum_{i=1}^{n}\sum_{j=1}^{n} W_{ij}(x_i-\bar{x})(x_j-\bar{x})}{\sum_{i=1}^{n}\sum_{j=1}^{n} W_{ij}(x_i-\bar{x})^2} \quad (3)$$

$$S^2 = \frac{1}{n}\sum_{i=1}^{n}(x_i-\bar{x})^2 \quad (4)$$

$$w_{ij} = \begin{bmatrix} w_{11} & \cdots & w_{j1} \\ \vdots & \ddots & \vdots \\ w_{i1} & \cdots & w_{jn} \end{bmatrix} \quad (5)$$

Where I is the global Moran index; x_i represents the observed value of region i; n represents the total number of observed samples; w_{ij} represents the spatial weight; $\bar{x}$ is the mean value of x.
In addition, the local indicators of spatial auto-correlation (LISA) reveal the regional variability characteristics of pollutants in each study unit, which was calculated using equation (6):

$$I_i = \frac{(x_i-\bar{x})}{S^2}\sum_{j}(x_i-\bar{x}) \quad (6)$$

Where I_i is the local Moran index, the spatial correlation patterns of local autocorrelation include: Four types of High-High (H–H) aggregation; High-Low (H-L) aggregation; Low-High (L-H) aggregation; Low-Low (L-L) aggregation; H–H and L-L indicate spatially positive correlation features, and H-L and L-H indicate spatially negative correlation features.

2.3.4 Regression analysis

As a typical global linear regression model, the ordinary least squares (OLS) model is a common method to quantify the statistical relationship between independent and dependent variables. This study uses OLS to study the Seasonal Impact of Land surface temperature on PM2.5.
The OLS model can be described using equation (7):

$$S = \beta_n + \sum_{m=1}^{\rho}\beta_m\alpha_m + \varepsilon \quad (7)$$

where S is the dependent variable (PM2.5 concentrations), β_n is the intercept, β_m is the regression coefficient corresponding to the explanatory variable α, and ε is the random error value. This model can represent the intensity of the relationship between PM2.5 concentrations and UHII.

3. Results

3.1 Descriptive statistics

Table 1 shows the descriptive statistics of our dataset upon completing the data processes described

in the section. Regarding PM2.5 concentrations, both regions have the highest concentration in spring and the lowest in summer, and the overall concentration level of YRD is higher than that of PRD. Regarding UHII, the overall PRD level is higher than YRD's.

Table1: Average concentration of PM2.5 concentrations and UHII (units).

	Spring	Summer	Autumn	Winter	Annual average
PM2.5 concentrations (YRD)	32.58	16.98	20.77	32.38	25.68
PM2.5 concentrations (PRD)	27.91	12.59	18.18	26.58	21.32
UHII(YRD)	1.97	1.56	0.43	0.91	1.22
UHII (PRD)	2.97	3.56	2.81	2.46	2.95

3.2 Spatial variation of PM2.5 concentrations and UHII in YRD and PRD

The global and local Moran's indices have been calculated to explore the spatial aggregation characteristics of PM2.5 and UHII in YRD and PRD. The results of global Moran's indices are shown in Table 2. where the global Moran's I index is greater than 0. It passes the significance test, indicating significant global spatial autocorrelation among PM2.5 and UHII in YRD and PRD. PM2.5 and UHII have similar aggregation characteristics in spatial distribution, and the spatial distribution of which tends to be aggregated.

Table2: Global Moran's I indices for PM2.5 and UHII in YRD and PRD

	PM2.5 Spring	PM2.5 Summer	PM2.5 Autumn	PM2.5 Winter	UHII Spring	UHII Summer	UHII Autumn	UHII Winter
Moran's I index(YRD)	0.93	0.89	0.92	0.91	0.56	0.51	0.51	0.62
Moran's I index(PRD)	0.99	1.02	1.03	0.94	0.56	0.76	0.71	0.59
Z-Score(YRD)	153.54	147.62	151.45	148.33	91.83	82.86	82.86	102.27
Z-Score(PRD)	24.51	25.26	25.33	23.09	13.88	18.76	17.35	14.51
P-value(YRD)	<0.05	<0.05	<0.05	<0.05	<0.05	<0.05	<0.05	<0.05
P-value(PRD)	<0.05	<0.05	<0.05	<0.05	<0.05	<0.05	<0.05	<0.05

The spatial aggregation distribution of PM2.5 in YRD is shown in the figure 2. In spring, the High–High aggregation areas are mainly located in the Northen part of YRD, including Shanghai and southern Jiangsu, while the Low-Low aggregation areas are primarily located in Zhejiang Province. In summer, the High–High aggregation areas are expand to the area around Tai Lake. In autumn and winter, the High–High aggregation areas are mainly located in the western part of YRD, while the Low-Low aggregation areas are primarily located in coastal areas including Shanghai.

The spatial aggregation distribution of UHI in the urban area of YRD is shown in the figure 3. In spring, the High–High aggregation areas are mainly located in Shanghai and Suzhou-Wuxi-Changzhou area. In summer, the High–High aggregation areas are located in most of the major cities in YRD. In autumn and winter, the High–High aggregation areas are mainly located in Shanghai and several major cities in Zhejiang Province. In addition, Shanghai belongs to High–High aggregation areas across all seasons.

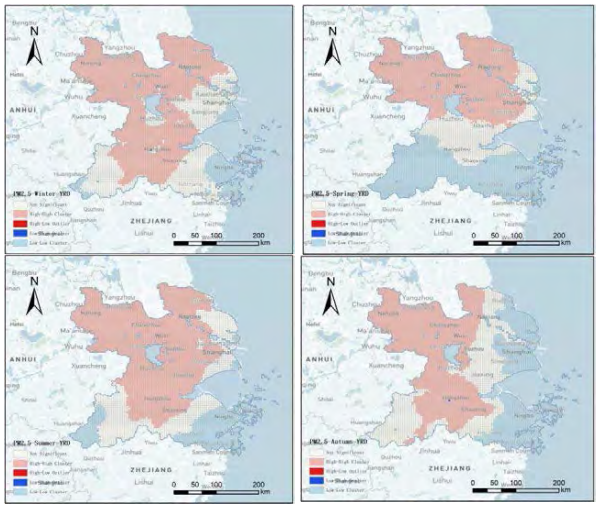

Figure 2: Spatial aggregation distribution of PM2.5 in the YRD

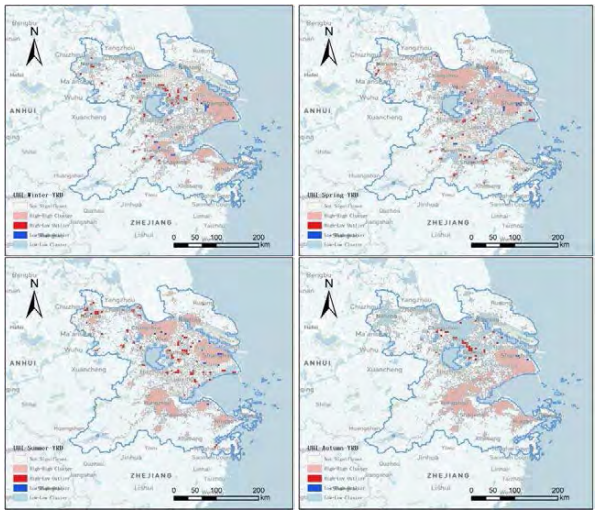

Figure 3: Spatial aggregation distribution of UHI in the urban area of YRD

The spatial aggregation distribution of PM2.5 in PRD is shown in the figure 4. Across all seasons, Southern coastal areas belong to Low-Low aggregation areas, and High–High aggregation areas are mainly distributed in Guangzhou and the northern part of PRD.

The spatial aggregation distribution of UHI in the urban area of PRD is shown in the figure 5. The High–High aggregation areas are mainly located in Guangzhou, Dongguan and Shenzhen across all seasons with tiny seasonal changes.

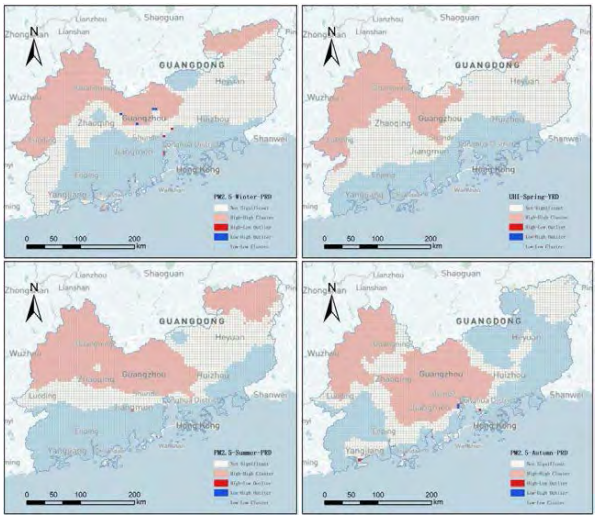

Figure 4: Spatial aggregation distribution of PM2.5 in the PRD

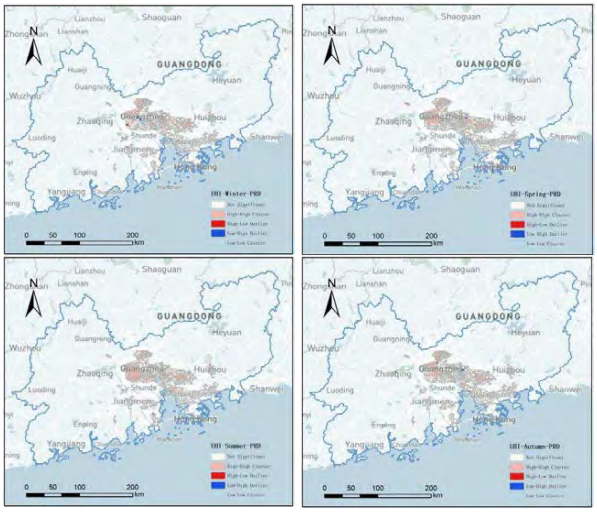

Figure 5: Spatial aggregation distribution of UHI in the urban area of PRD

3.3 Relationship between PM2.5 concentrations and UHII in YRD and PRD

The relationship between PM2.5 concentrations and UHII in YRD and PRD has been analyzed to investigate the potential interaction between PM2.5 concentrations and UHII. In regards to YRD, UHII is positively correlated with PM2.5 in spring and negatively correlated in autumn and winter, while in summer it did not pass the significance tests. In regards to PRD, the correlation coefficient indicates that UHII is positively correlated with PM2.5 across all seasons, which means that PM2.5 concentration increases with increasing UHII.

Comparing YRD and PRD as a whole, the relationship between PM2.5 concentrations and UHII of PRD is stronger than which of YRD, which can be attributed to different synoptic weather conditions. Both YRD and PRD belong to the subtropical monsoon climate, while PRD is closer to the tropics and less affected by the cold air of the northern cold wave, so there is a significant positive correlation throughout the four seasons. The negative correlation between autumn and winter in YRD may be due to the weak heat island in autumn and winter, but PM2.5 concentration remains high due to the stable atmosphere and low wind speeds within the city during winter, so the two are negatively correlated. The inconspicuous summer may be due to the rainy season, where PM2.5 is dispersed or randomly distributed in the local space without specific patterns.

The potential interaction between PM2.5 concentrations and UHII warrants cooperation appropriate mitigation measures to solve these two urban problems in a coordinated manner. For PRD, some measures can be taken to simultaneously alleviate UHI and PM2.5 concentrations. AS for YRD, caution is needed as alleviating one problem may exacerbate the other one, so that it is necessary considers the consequent change of air quality when designing mitigation strategies of UHI and take strategies that are better for both urban thermal environment and air quality.

Table 3: Correlation coefficients between PM2.5 and UHII in YRD and PRD

		Spring	Summer	Autumn	Winter
YRD	R^2	0.243	/	0.161	0.121
	coefficient	(1.395)***	0.015	(-0.725)***	(-0.972)***
PRD	R^2	0.729	0.420	0.355	0.087
	coefficient	(1.301)***	(0.463)***	(0.553)***	(0.667)***

Statistically significant results are marked with an asterisk symbol (*). (Statistical significance is determined at P < 0.001).

4. Conclusion

In the study, we confirmed seasonal impact of UHII on PM2.5. Furthermore, we found that different climatic conditions are one of the reasons affecting the relationship between UHII and PM2.5, which warrants appropriate mitigation measures in different regions. The results presented in the current study serve as a basis for discussing and exploring such processes in order to solve these two urban problems in a coordinated manner.

Reference:

1.Apte, J., *High-resolution air pollution mapping with Google Street View cars: Exploiting big data.* Abstracts of Papers of the American Chemical Society, 2019. **257**.

2.Arnfield, A.J., *Two decades of urban climate research: A review of turbulence, exchanges of energy and water, and the urban heat island.* International Journal of Climatology, 2003. **23**(1): p. 1-26.

3.Pui, D.Y.H., S.-C. Chen, and Z. Zuo, *PM2.5 in China: Measurements, sources, visibility and health effects, and mitigation.* Particuology, 2014. **13**: p. 1-26.

4.Shi, K., et al., *Exploring the relationships between urban forms and fine particulate (PM2.5) concentration in China: A multi-perspective study.* Journal of Cleaner

Production, 2019. **231**: p. 990-1004.
5.Guo, L., et al., *The influence of urban planning factors on PM2.5 pollution exposure and implications: A case study in China based on remote sensing, LBS, and GIS data.* Science of The Total Environment, 2019. **659**: p. 1585-1596.
6.Chen, M., et al., *Effects of urban green space morphological pattern on variation of PM2.5 concentration in the neighborhoods of five Chinese megacities.* Building and Environment, 2019. **158**: p. 1-15.
7.Xu, H.H. and H. Chen, *Impact of urban morphology on the spatial and temporal distribution of PM2.5 concentration: A numerical simulation with WRF/CMAQ model in Wuhan, China.* Journal of Environmental Management, 2021. **290**.
8.Ngarambe, J., et al., *Exploring the relationship between particulate matter, CO, SO2, NO2, O-3 and urban heat island in Seoul, Korea.* Journal of Hazardous Materials, 2021. **403**.
9.Jiang, Y., et al., *Spatio-temporal variation of the relationship between air pollutants and land surface temperature in the Yangtze River Delta Urban Agglomeration, China.* Sustainable Cities and Society, 2023. **91**.
10.Fang, X.Q., et al., *Spatial-temporal characteristics of the air quality in the Guangdong - Hong it Kong - Macau Greater Bay Area of China during 2015-2017.* Atmospheric Environment, 2019. **210**: p. 14-34.
11.Cai, W.B., et al., *Identifying hotspots and management of critical ecosystem services in rapidly urbanizing Yangtze River Delta Region, China.* Journal of Environmental Management, 2017. **191**: p. 258-267.
12.Xu, X.B., et al., *Ecological risk assessment of ecosystem services in the Taihu Lake Basin of China from 1985 to 2020.* Science of the Total Environment, 2016. **554**: p. 7-16.

PLEA 2024 WROCŁAW
(Re)thinking Resilience

School Resilience
Assessment of Environmental Parameters in Classrooms

BEATRIZ PIDERIT-MORENO[1] VALENTINA CHANDÍA-ARRIAGADA[1]

[1] San Sebastián University, Faculty of Engineering, Architecture and Design Concepción, Chile

This research aimed to assess the architectural potential of school classrooms for providing a good integral IEQ, which is one of the factors influencing the physical learning environment. Learning environments should be suitable, safe and comfortable to foster the holistic development of students, especially in contexts with limited energy resources. An Environmental Factors Evaluation Matrix was created, defining 20 architectural factors. A categorization was devised to evaluate the effectiveness of the integration of these factors and to obtain a diagnosis of the weighted environmental quality of the classroom to identify the factors that need improvement, show serious deficiencies, or are missing in the classrooms. The method was applied in 30 school classrooms to validate its application. The research results revealed both environmental strengths and weaknesses. The design parameters of "Acoustic" and "Thermal" showed significant deficiencies in the integration of conditioning to improve both aspects. The incorporation of simplified methods for the evaluation of IEQ based on architectural design is expected to help reduce the gaps for the environmental rehabilitation of these spaces.
KEYWORDS: Learning Environment, Post Occupancy Assessment, School Design, Environmental Comfort

1. INTRODUCTION

Improving the quality of existing educational spaces is imminent, especially in contexts of energy poverty. Schools are often well below internationally defined environmental standards. For this reason, in the context of rethinking resilience and moving towards the reconstruction of educational spaces. It is necessary to deepen and find solutions for the lack of environmental comfort in schools in the region. Research indicates that students are resilient and often adapt to poor environmental conditions. [1, 2].

Schools often fall significantly below internationally defined environmental standards. For this reason, in the context of rethinking resilience and moving towards the reconstruction of educational spaces, this article presents the results of an investigation aimed at assessing the environmental aspects of Chilean school classrooms through an architectural survey as a pilot case. This allowed for identifying the gaps for the environmental rehabilitation of these spaces.

Resilience in schools, considering the quality of the indoor classroom environment, is a crucial aspect for the development and well-being of students. Resilience refers to the ability to adapt and thrive in adverse conditions, and in the school context, this involves creating environments that support students' physical and mental health, as well as their academic performance. The relationship between indoor environmental quality (IEQ) and resilience in schools is evidenced in several studies that have examined how environmental conditions affect student learning and health.

For example, daylight has been shown to have a significant impact on students' academic performance. Heschong et al.[3] y Tanner [4] found positive correlations between daylight and learning progress, highlighting that a well-lit environment can improve students' concentration and well-being, contributing to greater academic resilience. Similarly, classroom air quality is a critical factor. Daisey et al. [5] y Gao et al. [6] note that inadequate ventilation can lead to health problems and poor academic performance, suggesting that improving air quality can help students become more resilient in the face of health and learning challenges.

The acoustic environment also plays an important role. According to Crandell & Smaldino [7] y Shield & Dockrell [8] a noisy or acoustically poor environment can negatively affect children's academic performance and psychosocial well-being, indicating that classroom sound management is essential to foster resilience.

Regarding thermal comfort, studies such as those by de De Dear et al. [9] and Wargocki & Wyon [10] have shown that both extremely low and high temperatures can affect school performance. Porras-Salazar [11] adds that thermal conditions can have a differential impact depending on the socioeconomic background of students, implying that adaptability to different temperature ranges is an aspect of resilience in educational settings.

Taken together, these studies underscore the importance of considering the quality of the indoor environment in schools as a fundamental pillar of student resilience. A comprehensive approach that addresses these aspects can contribute significantly

to students' well-being and academic success, preparing them to face challenges both inside and outside the classroom.

This article aims to assess the environmental aspects of school classrooms through an architectural survey, in order to define the gaps in the environmental quality of Chilean classrooms. This approach enabled the identification of key areas for the environmental rehabilitation of these spaces.

2. METHODOLOGY

This research was designed based on a mixed methodology, where the physical characteristics of the built environment (school classrooms) are related to the environmental quality that they present, this relationship was made through architectural factors.

For the evaluation, an indicative or point-in-time post-occupational evaluation method was designed.

Prior to the design of the evaluation, initial criteria were defined that the instrument had to meet, among which were:

1. Be applicable to existing schools, so that a diagnosis of the current state can be generated.
2. Include the evaluation of the integral environmental quality of the classroom, so thermal, visual, acoustic and air quality aspects are considered, in relation to the comfort of the occupants.
3. Data collection or measurements should not include on-site environmental monitoring equipment or energy simulations.
4. The tool should be simple and quick to use, both in terms of input data and diagnostic results.

The evaluation design was divided into three stages. Initially, the "Environmental Factors Evaluation Matrix" [12] was developed. The second stage focused on the preparation of the necessary information gathering and evaluation tools. In the third phase, the evaluation was applied to 30 classrooms through the classification and weighting of environmental and architectural factors, which provided information on the quality of the environment in the classrooms analyzed, which allowed the validation of the application.

2.1 Case Studies

The criteria established was to evaluate Chilean public educational establishments. Classrooms were selected through a representative sample of educational establishments in the three regions with the most educational establishments in Chile. In total, 30 classrooms belonging to 23 public schools were evaluated. Within the sample, there were traditional classrooms and some classrooms were identified that were recently improved in thermal and acoustic aspects.

2.2 Architectural Factor Characterization

The characterization of the architectural factors allowed the evaluation of environmental parameters in an integrated manner. Two complementary instruments were used, with the aim of collecting as much information as possible from the classrooms to be evaluated, and then categorizing the architectural parameters and thus defining the environmental quality of the classroom.

A checklist was used, it was designed from the lists proposed by Bluyssen [13–15].

It collected both the characterization of general information of the classroom (e.g. identification code, number of occupants, general dimensions of the classroom, shape, orientation), and the elements of the built environment of the classroom (e.g. thermal envelope, types of glazing, optimization of natural lighting, heating and cooling systems, operable window surfaces for ventilation).

The architectural survey was done with a high-resolution 3D space scanning camera, Matterport Pro 2, which virtually reconstructed the original scene. This tool made it possible to extract the classroom measurements, which were analyzed based on the architectural parameters to be evaluated. With this, the time for collecting information and evaluating the classrooms was optimized.

Figure 1: Matterport Pro 2 Rotary Camera & Virtual Scene.

A classification is applied according to the percentages of compliance obtained in each environmental parameter. This made it possible to determine a diagnosis of the environmental quality of the classroom. This classification was previously developed and calibrated through a theoretical model of a classroom that integrates all architectural factors, achieving excellence [12]. (see Figure 7).

Figure 2:Survey of the characteristics of the classroom with a 3D model.

2.3 Environmental evaluation criteria.

In order to evaluate the physical characteristics of the classroom environment, 20 factors related to physical attributes of the indoor environment were identified. Five architectural factors were selected and categorized according to the references studied. To identify each architectural factor, an abbreviated coding was given, with two letters identifying the environmental factor and a number identifying the architectural factor evaluated. In the lighting factor (LI), aspects of Daylighting and Optimization strategies were considered, in the aspects referred to acoustics (AC), factors related to Design of the space and Indoor conditioning were selected, for the thermal environment (TE) the factors to be evaluated were related to Passive and Active strategies, finally, for the air quality (AQ), the factors considered were associated to Ventilation flow rate, Ventilation strategies and Indoor conditioning.

"IEQ Assessment", these were categorized following a scoring system scale divided into three levels (Effective, Adequate, and Inadequate), to evaluate each of the architectural parameters outlined in the evaluation matrix, using the criteria described in a previous article[12]. All architectural parameters were verified and categorized, thus knowing the score obtained in each of the environmental factors. In this way, the general performance of the classroom is shown, visualizing the net score obtained for each environmental factor, without incorporating the specific weight of the environmental aspect.

Then, a classification was made where the specific weights of each environmental factor are applied, this was called "Weighted IEQ Assessment" and details through a pink graph the compliance with each of the architectural parameters, indicating in detail the category obtained by each aspect evaluated, in addition to graphing the weighting or weight that each environmental factor represents. In this way, it is possible to visualize in which parameters there are strengths or shortcomings and how much it affects the integral context.

The weights given to each environmental factor were determined through a panel of experts in the area, through a hierarchical analysis process (AHP) [16, 17], where the following weights were established, for Lighting (12%), Acoustics (22%), Thermal (32%) and Air Quality (36%).

The Weighted IEQ Assessment of the classroom, gives it a percentage of compliance and a classification according to its score. Rating it as Excellent, Satisfactory, Acceptable, Unacceptable or Poor.

Table 1: IEQ Weighted l scoring scale.

	Level of compliance
86- 100 % Excellent	The architectural parameters appear as outstanding in the evaluated space.
71 - 85 % Satisfactory	To achieve optimal environmental quality, only small adjustments should be made.
41 - 70 % Acceptable	Modifications should be made to improve the environmental quality.
26- 40 % Unacceptable	Substantial changes must be made to improve.
0 - 25 % Poor	There is an urgent need for major changes if the environmental quality of the classroom is to be increased.

3.RESULTS

3.1 IEQ Assessment

A general analysis of the 30 classrooms evaluated was conducted. A diagnosis of performance for each of the environmental factors is described below:

The design parameter *"Lighting"*, despite the fact that it is the aspect where there were fewer shortcomings, in any case, none of the classrooms evaluated satisfactorily complied with all the parameters. In the LI01 parameter, 30% of the classrooms achieved the effective range, since they presented a natural lighting coverage between 75-100% of the classroom width, while 70% of the classrooms achieved the adequate range, since the natural lighting coverage was between 50-75%, no classroom presented a coverage of less than 50% of the classroom width. The parameter of distribution of openings (LI02) was the weakest, due to the fact that none of the classrooms had multilateral illumination. 60% of the classrooms reached the adequate range, since they had bilateral lighting, and 40% of the classrooms reached the inadequate range, since they only had unilateral lighting. In LI03, Window-to-Wall Ratio (WWR), 43.3% achieved a range of effective, since the ratio between classroom windows and glazed wall area was greater than 40% of the surface. The architectural factor LI04, which refers to optimization and distribution of lighting, 60% reached the range of adequate, since they presented a curtain as lighting protection, 30% of the classrooms reached the range of effective, since they presented more than one element of optimization of lighting or outdoor solar protection, the remaining 10% did not

present any type of solar protection. Regarding the provision of artificial lighting (LI05), 56.7% of the classrooms had energy-efficient equipment in good condition and working order, while seven classrooms (23.3%) were inadequate, due to the lack of lighting equipment or because they were not in a good state of maintenance.

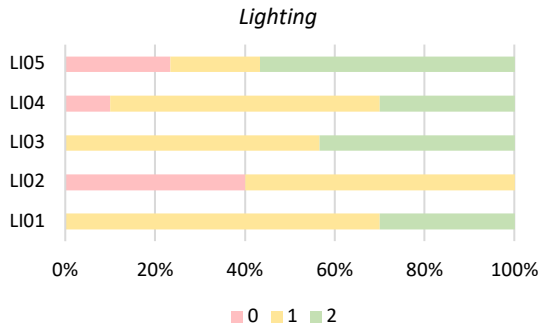

Figure 3: Classroom performance in lighting aspects

The design parameter *"Acoustic"* is the most critical aspect. In parameter AC01, 96.7% of the classrooms reached the adequate range, since the height of the classroom was between 2.4 and 3.5 meters. In AC02, referring to the quality of glazing, 73.3% of the classrooms reached the rank of inadequate, because they had single glazing, while 20.7% had at least DVH without thermal bridges (PVC or RPT frame). In AC03, aspect that evaluates Window-to-Floor Ratio (WFR), two classrooms (6.7%) reached the effective range and 93.3% reached the inadequate range, since the glazed surface was greater than 16% of the classroom surface. In AC04, aspect that refers to the percentage of absorbent material in the ceiling, 83.3% did not present any type of material as acoustic absorbent, so they obtained the rank of inadequate, on the other hand, 5 refurbished classrooms (16.7%) achieved the rank of effective, since they presented more than 40% of the ceiling with absorbent material.

A similar situation occurred with AC05, where 90% of the classrooms did not have absorbent material in the walls, and therefore obtained the rank of inadequate.

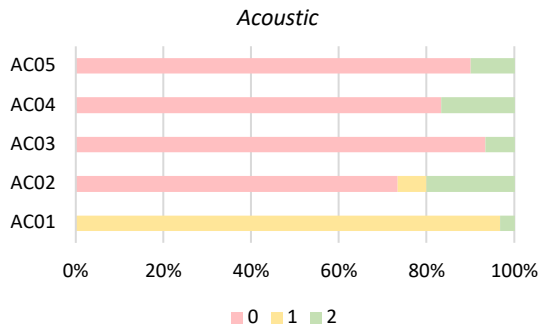

Figure 4: Classroom performance in acoustic aspects

The design parameter *"Thermal"* also showed shortcomings in terms of air conditioning, either due to the absence of insulation in the envelope, the use of simple glass in the windows or because there was no air conditioning system. The TE01 factor referred to solar protection, 66.7% of the classrooms reached the adequate range, since they only had curtains as solar protection elements. In TE02, 50% of the classrooms had an adequate orientation of the glazing, 30% had an inadequate orientation (south facing) and 20% (six classrooms) had a north facing orientation, which gave it an effective rank. Factor TE03, which evaluates the quality of the window frames and glazing, 73.3% of the classrooms were rated inadequate because they had single glazing, 6.7% were rated adequate because they had hermetic double glazing (DVH) but with thermal bridges, and 20% were rated effective because they had DVH glazing without thermal bridges (PVC or RPT frame). In factor TE04, referring to the thermal envelope, 86.7% of the classrooms had no thermal envelope, while four classrooms (13.3%) achieved the effective range because they had EIFS insulation in their envelope. In TE05, 26.7% of the classrooms had some type of air conditioning system, reaching the effective range, and 73.3% of the classrooms evaluated did not have this requirement, therefore, they obtained the inadequate range.

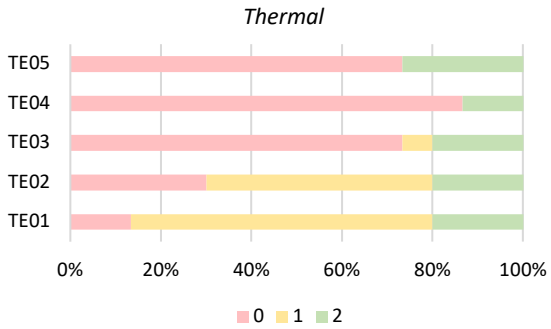

Figure 5: Classroom performance in thermal aspects

Finally, the design parameter *"Air quality"* showed some shortcomings, even in the operable surface for ventilation. Regarding the volume of air per student (AQ01), 76.7% of the classrooms effectively complied with the factor, a situation that guarantees a good environmental quality, together with the operable surface for ventilation (AQ02), an aspect that 70% of the classrooms evaluated effectively complied with, while 6.7% of the classrooms did not comply with the operable surface required to guarantee good ventilation in the classroom. In AQ03, 53.3% of the classrooms had cross ventilation, which placed them in the effective range, while 40% of them only had ventilation through a single opening, which placed them in the inadequate range. For factor AQ04, 70% of the classrooms reached the adequate range, with projecting windows and 26.7% had sliding windows,

which gave them the inadequate range. In AQ05, 86.7% of the classrooms did not have a mechanical ventilation system, so they were rated as inadequate, while 13.3% of the classrooms evaluated were rated as effective because they had this requirement.

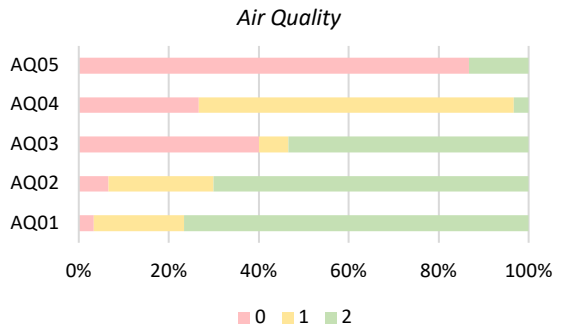

Figure 6: Classroom performance in air quality aspects

3.2 IEQ Weighted Assessment

Out of the 30 classrooms evaluated, the results of the overall weighted compliance were as follows, none of them complied outstandingly in all the factors evaluated. Three of the classrooms, corresponding to 10% of the total, were classified as Satisfactory, reflecting compliance with the objectives, but there are parameters that could improve their condition.

To achieve optimum environmental quality, only minor adjustments should be made. 5 of the classrooms (17%) were classified within the Acceptable range, so their characterization is not detrimental, but neither do they favor the environmental quality of the classroom, so modifications should be made to improve the environmental quality. Sixty-seven percent (20 classrooms) are in the Unacceptable category, which means that the classrooms have serious architectural deficiencies that do not ensure proper environmental quality. There are non-compliances in at least half of the architectural parameters evaluated. Therefore, in order to improve, substantial changes must be made.

Finally, 7% of the classrooms were classified in the Poor category, so the spaces showed severe deficiencies, in terms of environmental quality, there is absence or non-compliance with most of the architectural factors evaluated. Major renovations are urgently needed if the environmental quality of the classroom is to be improved.

Table 2: Result of IEQ Weighted scale.

Category		% Classroom
Excellent	100% - 85%	0
Satisfactory	85% - 71%	10%
Acceptable	70% - 41%	17%
Unacceptable	40% - 26%	67%
Poor	25% - 0%	7%

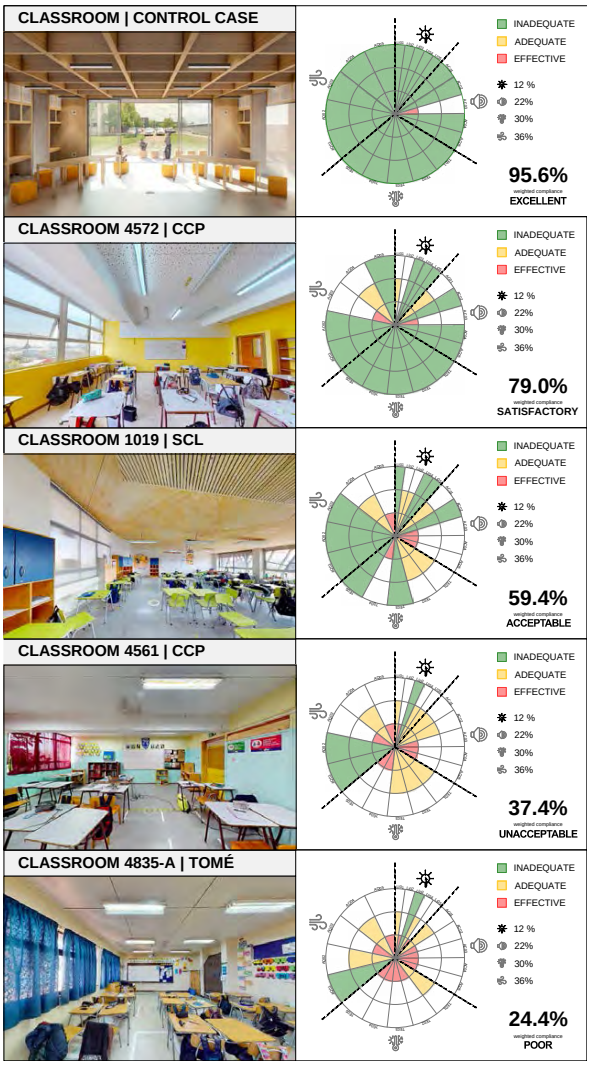

Figure 7: Classrooms classified by environmental factor considering the design parameters.

4. CONCLUSION

The proposed method has made it possible to identify the design parameters that need to be improved or transformed in school classrooms in the Chilean context. The instruments designed allow for a comprehensive diagnosis through visits to the establishments, proving to be an efficient approach.

The characterization of classrooms reveals differences in environmental quality between those with thermal and acoustic improvements and those without. The IEQ Weighted Assessment allows progress towards an integrated diagnosis of environmental factors. However, there are limitations in the proposed classification since it was not possible to include classrooms with better quality infrastructure.

When proposing an integrated assessment, it is crucial to establish criteria that are intertwined and have an impact on more than one environmental aspect, as is the case with glazing, an element that influences all 4 environmental factors. It is therefore

considered as the most significant factor in this integrated assessment.

Similarly, it is recognized that there are certain architectural factors that are in conflict with each other. The acoustic factor (AC03) requires minimizing sound reverberation, which implies limiting glazed surface. However, the lighting factor (LI03) requires maximizing the entrance of natural light, which implies increasing the glazed surface. These two factors are in conflict and pose a challenge for architectural design, as a balance between the two must be sought and their implications understood.

Characterization of the classrooms reveals differences in environmental quality between those with thermal and acoustic improvements and those without. From the sample, it is observed that, for the design parameter of "Acoustic", there are important deficiencies in the integration of conditioning, due to the absence of absorbent material in the ceiling and walls of the classrooms; a similar situation occurs in the thermal environment, due to the fact that neither passive nor active strategies are integrated. The sample studied has revealed the existence of significant gaps that require attention to achieve an effective environmental rehabilitation.

Post-occupational evaluation of educational spaces is a field that requires simplified tools to facilitate its application. By developing these tools, it opens the possibility for non-experts to perform the evaluations, without depending on specific monitoring equipment. This would make it possible to increase the number of classrooms evaluated and to have a systematic control of the environmental conditions of the learning environments. In this way, it could awaken the interest of educational institutions, both public and private, that want to improve the environmental quality of existing classrooms and detect and solve the environmental shortcomings that affect the educational process.

ACKNOWLEDGEMENTS

This work has been funded by Fondecyt 1210701, "Characterization of physical learning environments in school classrooms that promote academic self-esteem and school motivation."

REFERENCES

1. Trebilcock M, Soto-Muñoz J, Yañez M, Figueroa-San Martin R (2017) The right to comfort: A field study on adaptive thermal comfort in free-running primary schools in Chile. Build Environ 114:455–469. https://doi.org/10.1016/j.buildenv.2016.12.036

2. Diaz M, Cools M, Trebilcock M, et al (2021) Effects of climatic conditions, season and environmental factors on co2 concentrations in naturally ventilated primary schools in Chile. Sustainability (Switzerland) 13:. https://doi.org/10.3390/su13084139

3. Heschong L, Wright RL, Okura S (2002) Daylighting impacts on human performance in school. Journal of the Illuminating Engineering Society 31:101–114. https://doi.org/10.1080/00994480.2002.10748396

4. Tanner CK (2009) Effects of school design on student outcomes. Journal of Educational Administration 47:381–399. https://doi.org/10.1108/09578230910955809

5. Daisey JM, Angell WJ, Apte MG (2003) Indoor air quality, ventilation and health symptoms in schools: an analysis of existing information. Indoor Air 13:53–64. https://doi.org/10.1034/j.1600-0668.2003.00153.x

6. Gao J, Wargocki P, Wang Y (2014) Ventilation system type and the resulting classroom temperature and air quality during heating season. In: Lecture Notes in Electrical Engineering. Springer Verlag, pp 203–214

7. Crandell CC, Smaldino JJ (2000) Classroom acoustics for children with normal hearing and with hearing impairment. Lang Speech Hear Serv Sch 31:362–370. https://doi.org/10.1044/0161-1461.3104.362

8. Shield BM, Dockrell JE (2003) The Effects of Noise on Children at School: A Review. BUILDING ACOUSTICS 10:97–116

9. De Dear R, Kim J, Candido C, Deuble M (2015) Adaptive thermal comfort in australian school classrooms. Building Research and Information 43:383–398. https://doi.org/10.1080/09613218.2015.991627

10. Wargocki P, Wyon DP (2013) Providing better thermal and air quality conditions in school classrooms would be cost-effective. Build Environ 59:581–589. https://doi.org/10.1016/j.buildenv.2012.10.007

11. Porras-Salazar JA, Wyon DP, Piderit-Moreno B, et al (2018) Reducing classroom temperature in a tropical climate improved the thermal comfort and the performance of elementary school pupils. Indoor Air 28:892–904. https://doi.org/10.1111/ina.12501

12. Piderit-Moreno MB, Leighton J, Chandia V, Perez-Fargallo A (2023) Method to assess the integration of personalization, stimulus and environmental design principles in school classrooms. J Phys Conf Ser 2600:142010. https://doi.org/10.1088/1742-6596/2600/14/142010

13. Bluyssen PM (2017) Health, comfort and performance of children in classrooms - New directions for research. Indoor and Built Environment 26:1040–1050. https://doi.org/10.1177/1420326X16661866

14. Bluyssen PM, Zhang D, Kurvers S, et al (2018) Self-reported health and comfort of school children in 54 classrooms of 21 Dutch school buildings. Build Environ 138:106–123. https://doi.org/10.1016/j.buildenv.2018.04.032

15. Bluyssen PM (2014) The Healthy Indoor Environment: How to assess occupants' wellbeing in buildings, 1st Edition. Routledge

16. Saaty TL, Vargas LG (2012) Models, Methods, Concepts & Applications of the Analytic Hierarchy Process. Springer US, Boston, MA

17. Saaty TL (1988) What is The Analytic Hierarchy Process?

PLEA 2024 WROCŁAW
(Re)thinking Resilience

Enhancing Patient Experience through Analysis of Indoor Environments in a Maternity Ward

SALAAM HAMAD[1], LUKE HESPANHOL[1], CHRISTHINA CANDIDO[2], SARAH J MELOV[3,4]

[1]School of Architecture, Design and Planning, The University of Sydney, Sydney, Australia
[2]Faculty of Architecture, Building and Planning, University of Melbourne. Melbourne, Australia
[3]Reproduction and Perinatal Centre, The University of Sydney, Sydney, Australia
[4]Westmead Institute for Maternal and Fetal Medicine, Westmead Hospital, Westmead, Australia

ABSTRACT: The research focuses on understanding the patient experience in hospital environments, particularly in maternity wards, where there is limited representation in scientific literature. The study aimed to investigate patient and staff environmental experience in an urban tertiary referral hospital maternity ward. The study employs a mixed-method approach, including surveys, spot measurements, and site observations, conducted in a Sydney hospital over a year. Qualitative data collected from 129 patient surveys and 29 staff surveys highlights issues related to patient thermal comfort and a perceived lack of control over their environment. The quantitative data further indicates that noise levels exceed recommended guidelines, and certain rooms exhibit problems with lighting. Patient dissatisfaction with thermal conditions, confirmed by staff surveys, suggests the need for a more personalized and adaptable hospital environment. The study concludes that addressing these issues can enhance patient comfort, staff efficiency, and overall maternity ward experience.
KEYWORDS: maternity ward, thermal comfort, patient satisfaction, patient safety

1. INTRODUCTION

Hospital buildings are complex, multifunctional environments where creating an optimal indoor setting is crucial for the comfort, safety and well-being of patients and the comfort of the staff. These buildings operate around the clock, with patients at times critically unwell and medical professionals providing care regardless of the time. However, due to the intense nature of medical procedures and patient care, hospitals can quickly transform into high-stress environments.

Understanding the patient experience is an important step towards achieving patient-centred care. This involves examining various aspects of how patients perceive their time within the hospital [1]. By doing so, we can estimate the degree to which patients are receiving care that caters to their individual preferences and needs. Valuing patient experience alongside other critical aspects such as the effectiveness of care, can yield comprehensive and holistic assessment of the quality of a hospital [2].

Thermal comfort and other environmental factors have been extensively discussed in numerous research articles, predominantly employing models like PMV. PMV (Predicted Mean Vote) is a reference index commonly used in the evaluation of thermal comfort conditions in mechanically conditioned environments. It is based on six variables: activity level, thermal resistance of clothing, air temperature, average radiation temperature of the surroundings, air relative humidity, and air velocity [19]. However, the application of PMV in hospital rooms fails to adequately capture the diverse preferences of patients [3]. Furthermore, standardized indoor conditions prove inadequate in meeting the requirements of both medical staff and patients simultaneously. Therefore, using building occupants and study participants to determine thermal comfort enables a clearer comprehension of the interaction between occupants and buildings [4]. This approach also yields a more comprehensive assessment of how thermal comfort connects with various components of indoor environmental quality, ultimately influencing overall occupant experience and satisfaction [5]. This research aims to bridge this gap, particularly in the context of maternity wards, a domain with limited representation in scientific literature. The primary objective is to conduct a comparative analysis between summer and winter, focusing on the evaluation and analysis of indoor environment quality parameters and subjective feedback from women in the maternity ward.

2. METHODS

This study was conducted in the maternity ward of Westmead Hospital, a large health facility in Sydney, Australia, over a span of one year, from July 2022 to June 2023. The patient population (table 1) for this research were women who had given birth within the last few days, most of whom have their newborn rooming-in with them. Field work took

place during two campaigns in December 2022 and then June 2023. A mixed-method approach was used with deployment of an online survey (targeting patients and midwives), IEQ (Indoor Environmental Quality) spot-measurements, and site-observation. The study was conducted with approval from Western Sydney Local Health District Human Research Ethics Committee (Approval number: 2022/ETH00119).

Table 1: Demographics table of patient participants.
**0 days means survey was taken on same day of delivery.*

Age range		%
	18 - 23	8.3
	24 - 33	52.5
	34 - 43	37.5
	44 - 53	1.7
Days postpartum		
	0 days*	10.8
	1 day	43.2
	2 days	27
	3 days	8.1
	4 days	6.3
	5 days	2.7
	6 days	1.8
Delivery mode		
	C-section	52
	Vaginal birth	48
Feeding method		
	Formula	6.3
	Breastfeeding	65.8
	Mixed	27.9

2.1 Qualitative data

In addition to promoting patient surveys through posters featuring QR codes placed on the walls of patient rooms, the research process also involved a personalized approach. Patients were directly approached by the researcher in-person and extended an invitation to participate in the surveys. The surveys included inquiries about satisfaction with various environmental factors such as room temperature, air quality, acoustics, and lighting. Additionally, it included questions regarding the birth outcomes, infant care, and demographic details. Furthermore, ward staff (midwives) were invited to participate in a survey determining their satisfaction with the indoor environment of their workplace, as well as investigating their perception of the patient experience. A total of 129 (64 in summer and 65 in winter) patient surveys and 29 staff surveys (all in winter) were collected and stored using the Qualtrics platform, and these were analysed using Excel.

2.2 Quantitative data

To complement the qualitative survey data, quantitative measurements of indoor environmental quality (IEQ) were conducted twice a year on-site, once during the summer (December 2022) and once in the winter (June 2023). These measurements included variables like air temperature, humidity levels, carbon dioxide concentrations, sound levels, and lighting conditions. Data was collected with hand-held devices from one spot location close to the patient and at bed height. With information available for both summer and winter periods, we could assess any seasonal variations in indoor comfort and quality. Data was then benchmarked against recommended thresholds from the electrical and lighting guidelines of the VHHSBA [6], WHO (World Health Organisation) guidelines [7], the National Asthma Council Australia [8], as well as using the CBE comfort tool [9] to check compliance with ASHREA Standard 55-2020.

3. RESULTS AND DISCUSSION

Quantitative data from IEQ devices reveals that most parameters align with recommended guidelines, indicating a theoretically acceptable indoor environment.

However, minimum and maximum noise levels recorded during the study were 35 – 64 and 36 – 60 dBA for summer and winter respectively, which is much higher than the World Health Organisation (WHO) recommended guideline of < 30 dBA for treatment rooms or hospital wards [7] (Table 3), required to reduce the impact of noise on sleep disruption, irritation, and communication. Studies in the literature have shown that excessive noise has grown to be a serious issue in hospitals worldwide and have reported many independent investigations on the matter [18]. None of the studies that have been published comply with WHO standards, in fact the majority of the studies have reported noise levels that are 20–40 dBA or more over WHO recommendations [10]. Noise has notable detrimental effects on patients' physiological and psychological health, making it one of the main environmental elements that patients most usually complain about [11].

Lighting was observed to be an issue as well. Variability in room lighting is significant, with some rooms benefitting from ample natural light through large windows, needing minimal additional lighting during the day. In contrast, other rooms suffer from darkness due to small windows, requiring substantial artificial lighting. The brightest room measured during the study recorded a mean of 326 lux in summer and 117 lux in winter, whereas the darkest room recorded 47 lux in summer and 26 lux in winter. According to the Victoria Health Building Authority, acceptable lighting levels for patient rooms consist of

160 lux for general use, 240 lux for reading, and 1 lux for night light [6] (table 3).

CO2 levels remain nearly constant throughout the year, with a mean of 650 ppm in summer and 632 ppm in winter (Table 3). Both are considered acceptable levels below the 1,000 ppm threshold [12], although patients commented about the stuffiness and lack of air flow in the rooms, leading them to feel compelled to keep the room door open (table 2). Instead of applying a single fixed value to all places, CO2 thresholds should be determined on a case-by-case basis. The thresholds that were determined from the literature were shown to be extremely sensitive to variables like activity level and community prevalence, causing CO2 thresholds to differ between different indoor environments. Hence, ASHRAE does not recommend a particular threshold value [13].

The relative humidity levels in summer and winter were almost the same, ranging between 34% and 53% (**Error! Reference source not found.** 3) throughout the year, slightly compliant with the safe threshold advised by the National Asthma Council Australia 2016 [8]. For health, productivity, and a decreased risk of illness, a relative humidity range of 30 to 70% is considered safe, while 40 to 60% is considered ideal [14]. Jing et al. suggest that elevated humidity levels may negatively impact an occupant's thermal comfort. To prevent discomfort (table 2), it is crucial to consider a relative humidity limit. The appropriate hospital code should specify a humidity limit within the acceptable air temperature range, enabling effective control of the indoor environment [15].

Table 2: Percentage of patient responses for satisfaction with air movement, humidity and overall IEQ conditions

	Air movement (%)		Humidity (%)		Overall IEQ (%)	
Very dissatisfied	4		2		4	
Dissatisfied	6	24	6	18	9	24
Slightly dissatisfied	14		10		11	
Neutral		20		33		19
Slightly satisfied	15		12		13	
Satisfied	25	56	23	49	33	57
Very satisfied	16		14		11	

Table 3: Minimum, maximum and average measurements of IEQ parameters for summer and winter rounds.

		Min	Max	Avg.	Recommended guideline
Temperature (°C)	Summer	22.4	24.4	23	21 - 24
	Winter	22.3	23.2	23	
Humidity (%)	Summer	34	53	43	30 - 70 (40 - 60 ideal)
	Winter	35	53	43	
CO2 (ppm)	Summer	362	811	650	<1000
	Winter	546	734	632	
Lighting (lux)	Summer	13.6	862	138	160 general
	Winter	1.92	237	69	
Noise level (dBA)	Summer	35	64	44	<30
	Winter	36	60	44	

Thermal comfort emerged as the most significant issue. The responses from the patient survey multiple-choice questions revealed that approximately 20 – 30 % of participants reported neutral to temperature, while a majority ranging from 70 – 80 % experienced sensations of either warmth or coldness that deviated from their preferred temperature (table 4, figure 1).

Notably, the percentage of participants expressing a preference for feeling warmer slightly surpassed those who indicated a preference for feeling cooler, indicating that the ward environment was perceived as cold for most patients (Figure 2).

Table 4: Patient perception of temperature in their hospital rooms at time of survey for winter and summer rounds

	Winter (%)		Summer (%)	
Cold	11.7		18.5	
Cool	3.3	33.3	16.7	46.3
Slightly cool	18.3		11.1	
Neutral		23.3		33.3
Slightly warm	16.7		7.4	
Warm	13.3	43.3	11.1	20.4
Hot	13.3		1.9	

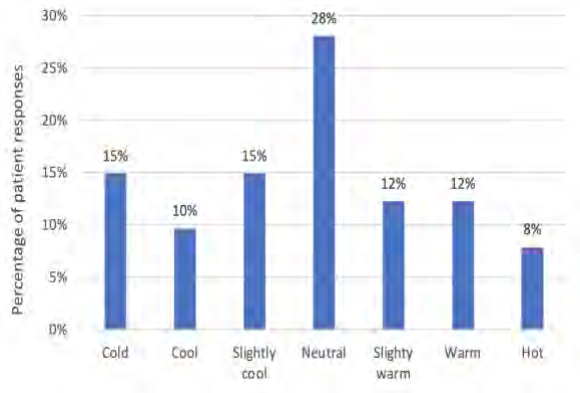

Figure 1: Patient thermal sensation in their hospital room at the time of the survey through full year of study.

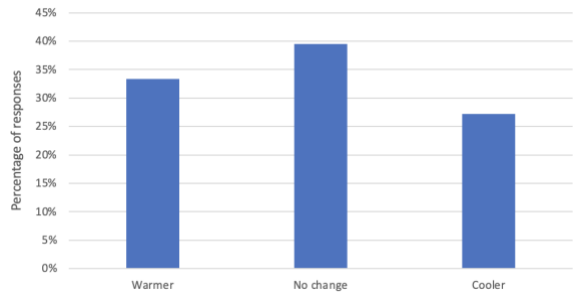

Figure 2: patient thermal preference in their hospital room at time of survey.

This is generally the situation in most instances, particularly in older hospitals such as the study hospital, where the thermal environment is not specifically designed to address the thermal preferences of patients. Instead, they tend to be designed using standard comfort approaches commonly seen in office settings, where a uniform temperature is maintained throughout the entire office space, often neglecting the specific and diverse thermal needs of patients [16]. In the case of the study hospital, the temperature was recorded to be between 21.9-23.3°C in winter and 22.4 – 24.2°C in summer. While these ranges align with ASHRAE Standard 55 [9], they may not offer patients the desired quality of thermal experience they should ideally receive.

Although some degree of temperature dissatisfaction is apparent in patients' responses to multiple-choice questions, where predefined answers are available, comments made by patients emphasise the significance of temperature discomfort as a problem affecting their overall experience. Comments ranged from “it’s very hot” to “it’s freezing” showing a wide range of discomfort between patients. This difference in insights suggests a psychological aspect, where the mothers might not prioritise their own comfort over her baby’s, which could lead them to respond differently. Alternatively, they might attribute their discomfort to the recent childbirth experience or any medication they is taking rather than an uncomfortable environment. This might cause some of the patient survey responses to diverge from their real-time experiences. Meaning, a patient might indicate satisfaction with the temperature in response to multiple-choice questions, which could imply contentment with their baby's comfort or overall satisfaction. However, when provided with an opportunity to comment on their satisfaction with the thermal environment, they may offer more detailed insights into their true experience.

Findings from the survey with staff confirm these observations among patients, as 69% of staff participants highlight patient dissatisfaction with thermal conditions. This dissatisfaction is evident from frequent requests from patients for temperature adjustments, which require maternity staff to engage in a time-consuming process involving building maintenance. This long process of receiving and responding to these requests not only impacts patient comfort directly but also diverts the energy and time that the staff could dedicate to caring for mothers and newborns, ultimately affecting the overall patient experience during their hospital stay. Even if the midwives were to make the temperature adjustments as requested, raising or lowering the temperature based on an individual's request might lead to discomfort for other patients in the ward. Achieving thermal comfort becomes challenging when individuals in a shared environment are involved in various activities and have different needs [17]. This is especially evident in hospitals, where patients are confined to limited spaces and with minimal control over their surrounding temperature and have diverse needs and conditions.

When examining the IEQ spot-measurements and related patient survey findings for both summer and

winter, no significant difference is apparent concerning humidity, CO2 concentrations, and noise levels. However, when considering temperature, the comparison indicates that a greater number of patients expressed preference for being warmer during winter, and conversely, cooler in summer (Figure 3). This observation leads to the conclusion that the building is not effectively delivering a comfortable thermal environment for its occupants.

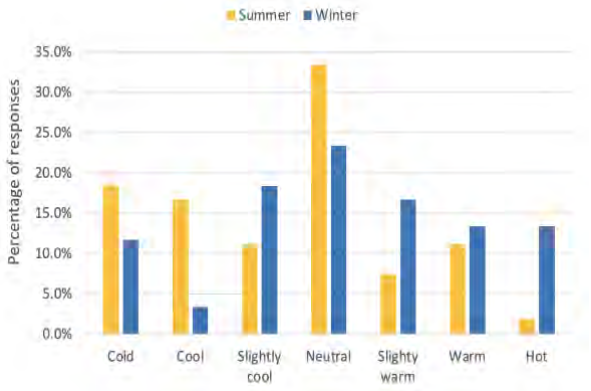

Figure 3: A comparison between summer responses and winter responses of patients about their thermal sensation. More patients felt warm during winter while more patients felt cold during summer.

No statistically significant relationship was identified between the sensation of temperature and either the participants' age or activity level. Additionally, no significant association was observed between temperature perception and the method of delivery (vaginal birth or caesarean section). No trend was observed for patients who breastfed or employed a combination of breastfeeding and formula. However, an invalid trend is evident among patients relying solely on formula to feed their newborns, showing a notable bias towards feeling cold (all respondents reported feeling cold or neutral). Given the limited number of participants who indicated using formula to feed their newborns (only 4 out of 129), this aspect warrants further investigation to be validated.

The results highlight other factors that contribute to patient dissatisfaction with the indoor environment. Most cited reasons other than temperature discomfort include inadequate air movement and stuffiness, drafts from surroundings like windows and air vents, a perceived lack of personal control over IEQ conditions and local discomfort.

3. STUDY SUGGESTION

The study suggests that hospitals should offer patients a more personalised and adaptable environment, giving them the flexibility to modify various aspects of their surroundings to align with their preferences and achieve optimal comfort. This could involve integrating interactive technology that enables patients to log their well-being and satisfaction with the indoor environment, submit specific requests, and have some control over their certain parameters of their surrounding environment. Additionally, it would efficiently inform staff of patient requests and needs in a more streamlined and time-saving manner. Implementing such an approach would not only enhance patient comfort but also alleviate staff workload, allowing them to focus on essential care tasks and therefore improving the overall patient experience.

4. CONCLUSION

In conclusion, the analysis of Indoor Environmental Quality (IEQ) data in the maternity ward shows that while some parameters align with recommended guidelines, notable concerns exist affecting the overall patient experience. Patient feedback indicates discomfort with thermal conditions, particularly experiencing excessive warmth in winter and coolness in summer. Lighting inconsistency and noise levels exceeding recommendations are also concerns. Psychological factors influencing patient responses along with responses from staff surveys, emphasise the need to provide a comfortable thermal environment at the hospital maternity ward. Addressing these issues may enhance patient comfort and staff efficiency, contributing to a more optimal experience for the new mothers.

This study presents an investigation of a potential problem in the maternity ward regarding patients comfort and well-being. However, future efforts will focus on investigating possible solutions and subsequently include the development of prototypes for an interactive system. This system aims to provide patients with flexibility and autonomy to control various environmental parameters within their rooms, with the ultimate goal of enhancing their overall hospital experience.

Enhancing human resilience from infancy has significant long-term health implications. Prioritising a nurturing postnatal environment for infants to foster maternal attachment and comfort may decrease stress levels, thus improving attachment opportunities and reducing overall stress. This approach not only enhances individual resilience by mitigating health-related stressors but also strengthens staff resilience, allowing for greater focus on essential tasks within healthcare settings, ultimately enhancing the overall resilience of the hospital environment and freeing up resources to address other stressors.

ACKNOWLEDGEMENTS

We would like to thank all clinicians and women who gave their precious and valuable time to assist with this research.

REFERENCES

1. Godovykh, M. and Pizam, A., 2023. Measuring patient experience in healthcare. International Journal of Hospitality Management, 112, p.103405.

2. Avlijas, R.N., Squires, R.N., Janet, E., Lalonde, R.N. and Backman, R.N., 2023. A concept analysis of the patient experience. Patient Experience Journal, 10(1), pp.15-63.

3. Rus, T., Cruciat, G., Nemeti, G., Mare, R. and Muresan, D., 2022. Thermal comfort in maternity wards: Summer vs. winter conditions. Journal of Building Engineering, 51, p.104356.

4. Yuan, F., Yao, R., Sadrizadeh, S., Li, B., Cao, G., Zhang, S., Zhou, S., Liu, H., Bogdan, A., Croitoru, C. and Melikov, A., 2022. Thermal comfort in hospital buildings–A literature review. Journal of Building Engineering, 45, p.103463.

5. Faraji, A., Rashidi, M., Rezaei, F. and Rahnamayiezekavat, P., 2023. A Meta-Synthesis Review of Occupant Comfort Assessment in Buildings (2002–2022). Sustainability, 15(5), p.4303.

6. Engineering guidelines for healthcare facilities: Electrical and lighting 2020. Victorian Health and Human Services Building Authority, Vol 2.

7. Coombs, J., Ayub, M., Schultz, T., Weichula, R., Zander, A. and Cusack, L., 2021, February. Noise measurements in an acute Australian hospital. In Proceedings of Acoustics (Vol. 21, No. 23, p. 2022).

8. Koster, L., 2016. Indoor humidity and your family's health. Natl. Asthma Counc.

9. Tartarini, F., Schiavon, S., Cheung, T., Hoyt, T., 2020. CBE Thermal Comfort Tool : online tool for thermal comfort calculations and visualizations. SoftwareX 12, 100563. https://doi.org/10.1016/j.softx.2020.100563

10. West, J.E. and Busch-Vishniac, I., 2005, October. Hospital noise, its role in patient well-being and the challenges for noise engineers. In INTER-NOISE and NOISE-CON Congress and Conference Proceedings (Vol. 2005, No. 2, pp. 443-449). Institute of Noise Control Engineering.

11. Deng, Z., Xie, H. and Kang, J., 2023. The acoustic environment in typical hospital wards in China. Applied Acoustics, 203, p.109202.

12. Lyu, X., Luo, Z., Shao, L., Awbi, H. and Piano, S.L., 2023. Safe CO2 threshold limits for indoor long-range airborne transmission control of COVID-19. Building and Environment, 234, p.109967.

13. Peng, Z. and Jimenez, J.L., 2021. Exhaled CO2 as a COVID-19 infection risk proxy for different indoor environments and activities. Environmental Science & Technology Letters, 8(5), pp.392-397.

14. Wolkoff, P., Azuma, K. and Carrer, P., 2021. Health, work performance, and risk of infection in office-like environments: The role of indoor temperature, air humidity, and ventilation. International Journal of Hygiene and Environmental Health, 233, p.113709.

15. Jing, S., Li, B., Tan, M. and Liu, H., 2013. Impact of relative humidity on thermal comfort in a warm environment. Indoor and Built Environment, 22(4), pp.598-607.

16. Alotaibi, B.S., Lo, S., Southwood, E. and Coley, D., 2020. Evaluating the suitability of standard thermal comfort approaches for hospital patients in air-conditioned environments in hot climates. Building and Environment, 169, p.106561.

17. Khalid, W., Zaki, S.A., Rijal, H.B. and Yakub, F., 2019. Investigation of comfort temperature and thermal adaptation for patients and visitors in Malaysian hospitals. Energy and Buildings, 183, pp.484-499.

18. Hulland, T., Su, A. and Kingan, M., 2020. Noise in an inpatient hospital ward in New Zealand. *Building Acoustics*, *27*(4), pp.299-309.

19. d'Ambrosio Alfano, F.R., Olesen, B.W., Palella, B.I., Pepe, D. and Riccio, G., 2019. Fifty years of PMV model: Reliability, implementation and design of software for its calculation. *Atmosphere*, *11*(1), p.49.

PLEA 2024 WROCŁAW
(Re)thinking Resilience

Thermal comfort and indoor air quality in new social housing in Chile:

The case of Cordilleras de Doña Marta, Puente Alto, Santiago.

GILLES FLAMANT[1,2], WALDO BUSTAMANTE[1]

[1]Centre for Sustainable Urban Development (CEDEUS), Pontificia Universidad Católica de Chile, Santiago, Chile
[2] Research Group Building Physics, Ghent University, Gent, Belgium

ABSTRACT: Ten years ago, the Ministry of Housing and Urban Development in Chile launched a 'Program for Social Housing Regeneration' which introduced stricter thermal standards for new and retrofitted housing than the current mandatory building code. However, studies evaluating the thermal comfort and indoor air quality of such new interventions are lacking. This paper presents the results of an evaluation carried out in a new housing project in Chile, located in the outskirts of the Metropolitan Region of Santiago. Environmental conditions and indoor air quality were continuously monitored in five apartments during the winter. The results showed a high percentage of hours outside the thermal comfort zone in the living and bedrooms, and excessive indoor relative humidity in several bedrooms. Excessive CO_2 levels were also measured in the bedrooms – but not in the living rooms -, indicating inefficient operation and/or design of the installed ventilation system. The formaldehyde concentration measured in the living rooms almost never exceeded the short-term limits. On the contrary, the levels of indoor particulate matter $PM_{2.5}$ largely exceeded the WHO recommended limit value of 15 µg/m³, due to too high outdoor concentrations and some indoor $PM_{2.5}$ emission sources in 2 of the 5 apartments.
KEYWORDS: Social housing, Thermal comfort, Indoor Air Quality, Monitoring, Survey

1. INTRODUCTION

Chilean cities exhibit high levels of socio-territorial inequality. Neighborhoods, typically located on the urban periphery and inhabited by economically and socially disadvantaged residents, show deficiencies in access to basic services, public spaces, and an environment that lacks adequate infrastructure [1]. In addition, housing in these areas often falls well below acceptable quality standards for the well-being of residents [2].

Currently, mandatory standards for the thermal performance of housing (whether social or not) are poor, focusing primarily on the heating season. However, there are programs for the thermal retrofitting of existing homes and the construction of new social housing units that have implemented more rigorous thermal standards, along with systems to improve indoor air quality. These programs have been part of the public policy of the Ministry of Housing and Urban Development (MINVU) in the country [1].

Simultaneously, the Ministry of Environment, in collaboration with MINVU, has established more stringent standards for both new housing and the thermal retrofitting of existing homes in various urban centers throughout the country that are affected by high levels of atmospheric pollution. This pollution is primarily attributed to the use of firewood for both cooking and heating in households [3].

As part of this policy, the MINVU created the Program for Social Housing Regeneration, which has been in charge of various interventions in the country for about 10 years [4]. One of these interventions took place in the Puente Alto commune on the outskirts of the Metropolitan Region of Santiago, involving housing complexes in the Bajos de Mena area. In this area, the regulatory thermal requirements are low: the maximum U-value for walls is 1.9 W/m²K, single glazing is allowed, and there are no mandatory standards for ventilation systems and airtightness of the building envelope. The aforementioned MINVU Regeneration Program has opted to improve these standards, with lower U-values for walls and glazing, as well as the application of mechanical ventilation systems to improve indoor environmental conditions. To the best of the authors' knowledge, no studies are known that have evaluated the impact of these interventions on thermal comfort, indoor air quality (IAQ), and energy consumption, both in thermal retrofitting and in new housing projects in different cities across the country. Moreover, despite the vital importance of maintaining good IAQ in homes to guarantee the comfort, well-being and health of its occupants, studies on IAQ are scarce in Chile.

This paper presents the results of an evaluation carried out in a new housing project in Bajos de Mena, Puente Alto commune, Santiago, Chile, where the environmental conditions and IAQ inside the

dwellings are determined through a monitoring campaign of different variables, as well as through a survey applied to the inhabitants of these dwellings.

2. THE CASE STUDY: A BRIEF DESCRIPTION

The project, Cordilleras de Doña Marta, was inaugurated in February 2023 and includes 280 apartments of about 60 m² each, distributed in a series of 4-story buildings (figure 1). Duplex apartments occupy the third and fourth floors and consist of a living-dining room, kitchen, bathroom and loggia on the third floor and three bedrooms on the fourth floor (figure 2). The apartments do not have central heating. The most common heating systems used by families are unvented portable heaters releasing their flue gases directly inside the house (such as kerosene) or electric heaters.

Figure 1: Picture of the apartment buildings of Cordilleras de Doña Marta. Chile.

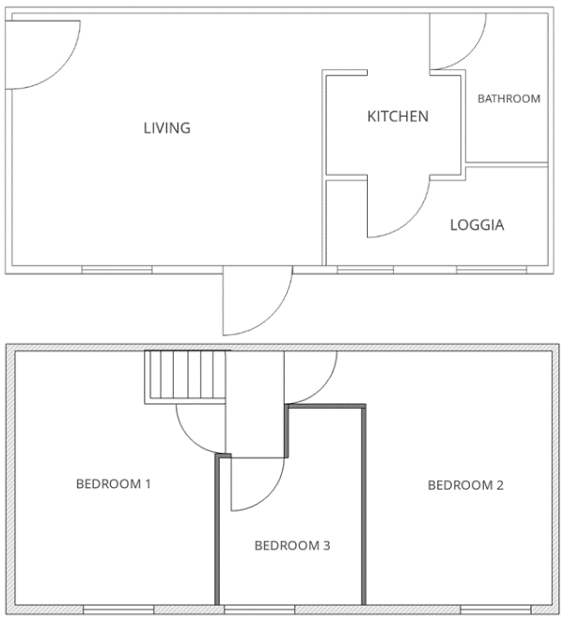

Figure 2: Floor plan view of the third and fourth stories of the building (duplex apartment).

This is one of the first projects built with a combination of good energy efficiency measures: thermal insulation in walls (U-value=0.76 W/m²K) and in roof (U= 0.35 W/m²K), double-glazed windows (U= 3.0 W/m²K), and a mechanically exhaust ventilation system with air extractors in the kitchen and bathroom and air inlets in walls or windows in the living room and bedrooms. No kitchen hood was installed.

These homes are inhabited by families who previously lived in buildings built in the 1990s in Bajos de Mena, in apartments of approximately 40 m² with very low thermal performance standards. The residents of this condominium are classified as having low or very low incomes, according to the latest population census of the country [5].

The city of Santiago has a Mediterranean climate, with minimum and maximum daily average temperatures of, respectively, 2.6°C and 13.6°C in winter (July), and 12.9°C and 29.4°C in summer (January) [6].

3. METHODOLOGY

Five apartments were selected for this study, located in different buildings blocks. Apartment denoted S1 is on the first floor, the other four (S2 to S5) are duplex apartments on the third and fourth floors. Table 1 provides background information on the 5 apartments units.

Table 1: Background information for the selected apartments. Condominium and block nr., number of occupied bedrooms, number of occupants of the dwellings.

Apart.	Block no.	Bedroom no.	Occupant no.
S1	Condo 1, H	1	3
S2	Condo 1, F	2	4
S3	Condo 2, 1	3	4
S4	Condo 2, 1	2	2/3
S5	Condo 3, D	3	4

Continuous environmental monitoring was conducted over a period of one month in winter. Measurements of indoor air temperature and relative humidity (RH) were taken every 10 minutes in the living room, kitchen, bathroom and two (occupied) bedrooms (HOBO MX1101). Carbon dioxide (CO_2) was also measured in the living room and bedrooms (HOBO MX1102). In addition, a short-term continuous IAQ monitoring was carried out in the living room where formaldehyde, light volatile organic compounds (LVOC), and particulate matter ($PM_{2.5}$) were measured every 10 minutes over a one-week period (NEMO IAQ). Apartment S1 was monitored in week 28, S3 and S4 in week 30 and S2 and S5 in week 34. Air temperature, relative humidity and $PM_{2.5}$ were also measured outdoors over the whole monitoring period (NEMO OAM). Calibration of the CO_2 sensors was performed 1 day prior to the start of the monitoring campaign. The estimated measurement

uncertainty of sensors is ±0.21°C for air temperature, ±2% for RH, 100 ppm for CO_2, 15-20% for formaldehyde and ±5% of reading value for $PM_{2.5}$. A survey was also conducted with the occupants (S1, S3, S5) to assess their perceptions of thermal comfort and indoor air quality, household usage patterns, and to identify the type of heating and ventilation system, among other variables.

The level of thermal comfort and IAQ was evaluated based on Exposure Limit Values (ELV) and guidelines available worldwide. The minimum indoor temperature was set at 18°C during the day [7,8] and 16°C at night [9]. A relative humidity range between 30% and 70% was considered comfortable [10]. The risk of mould growth was supposed to occur when the monthly average relative humidity on a typical thermal bridge with a temperature factor of 0.7 exceeded 80% [11]. Four CO_2 concentration classes were defined according to EN16798-1 [7], considering an outdoor reference concentration of 400 ppm: < 950 ppm ('very good'), 950-1200 ppm ('good'), 1200-1750 ppm ('moderate'), >1750 ppm ('insufficient'). For formaldehyde, a short-term (30-minute average) limit value of 100 µg/m³ (WHO) [12] and a long-term (1 year) limit value of 10 µg/m³ (Public Health England) [13] were used. Finally, 24-h average limit values of 15 µg/m³ (WHO) [14] and 50 µg/m³ (legislation in Chile) [15] were considered for $PM_{2.5}$.

4. RESULTS AND DISCUSSION

Table 2 provides the main results from the 1-month environmental monitoring and the 1-week IAQ monitoring.

4.1 Continuous environmental monitoring

The mean outdoor air temperature was 11.4°C during the monitoring period, and the outdoor relative humidity was 70%. The results of the indoor air temperature are plotted in figure 3. The spatially average air temperatures (living room + kitchen + bedrooms) range from 15.8°C to 17.9°C depending on the apartment (mean value = 16.9°C). The bathroom shows the lowest temperatures in all dwellings, with 2.0°C lower than the warmest rooms, on average. The spatially average air temperature of each case is below 18°C for 54% to 94% of the occupancy hours during daytime (7h-22h) (mean = 72%). Occupancy hours are determined based on the survey results for S1, S3 and S5 and on permanent occupancy for S2 and S4 (survey results not available). The average temperature in the bedrooms is below 16°C for 19% to 61% of the night hours (22h – 7h) (mean = 37%).

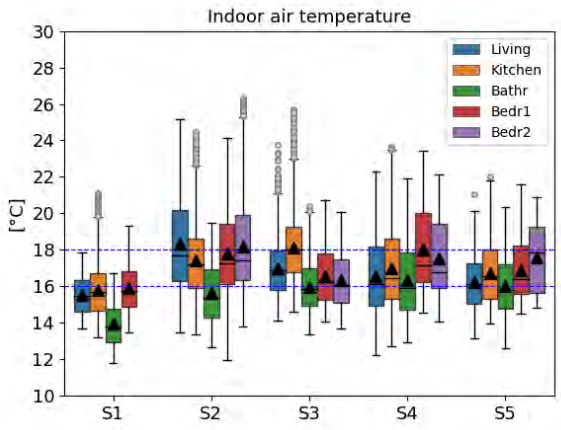

Figure 3: Indoor air temperature in all rooms (living, kitchen, bathroom, bedrooms) across the five apartments under analysis.

The relative humidity is in the comfort range 30%-70% for almost all hours in the living room and at least 80% of the time in the kitchen across all cases. In contrast, humidities above 70% are observed in one of the bedrooms for 99%, 59% and 47% of all hours across cases S1, S3 and S4, respectively (table 2). The monthly average relative humidity on a typical thermal bridge with a temperature factor of 0.7 exceeded 80% in the bathroom for S1 and S3, and also in the main bedroom for S1. Consequently, these rooms show a risk of mould growth.

The indoor CO_2 levels measured in the living room remained below 950 ppm most of the time in all cases (figure 4). In contrast, the mean CO_2 level exceeded 950 ppm in almost all bedrooms. Figure 5 shows the distribution of the mean CO_2 concentration in each hour of the day in the most critical bedroom across the 5 apartments. It can be observed that the highest concentrations occur during the night hours.

Figure 6 provides the percentage of time spent in each of the four previously defined CO_2 classes in the case of the bedroom showing the highest CO_2 concentrations. It shows that the IAQ in these bedrooms may be classified as 'insufficient / bad' (> 1750 ppm) for more than 40% to 70% of the nighttime across S1 to S5. This reveals too low ventilation rates in the bedrooms during the night. Lower CO_2 concentration in the living room is probably due to a lower occupancy but also to airing (opening of the windows) for some hours during daytime according to the survey results (see §4.3).

Table 2: Spatially average temperature, relative humidity in the most critical bedroom, carbon dioxide in the most critical bedroom at night, formaldehyde, LVOC and particulate matter $PM_{2.5}$ in all 5 apartments.

Variable		S1	S2	S3	S4	S5
Temp. (°C)	Mean	15.8	17.9	17.0	17.3	16.7
	P25	14.8	16.3	15.8	15.6	15.4
	P75	16.6	19.4	18.1	18.9	18.0
	% time < 18°C (day)	94%	54%	74%	68%	72%
	% time < 16°C (night)	61%	23%	41%	19%	40%
$RH_{,bed}$ (%)	Mean	82	53	71	68	64
	% time > 70%	99%	0%	59%	47%	24%
$CO_{2,bed,night}$ (ppm)	Mean	2659	1783	1824	1789	1582
	P25	1419	1013	1484	1515	1278
	P75	3782	2438	2134	2072	1948
Formald. (µg/m³)	Mean	39	8	30	9	24
LVOC (ppb)	Mean	173	48	61	93	61
$PM_{2.5}$ (µg/m³)	Mean	98	29	45	43	18
	% time > 15 µg/m³	100%	72%	100%	100%	34%
	% time > 50 µg/m³	92%	16%	24%	25%	14%

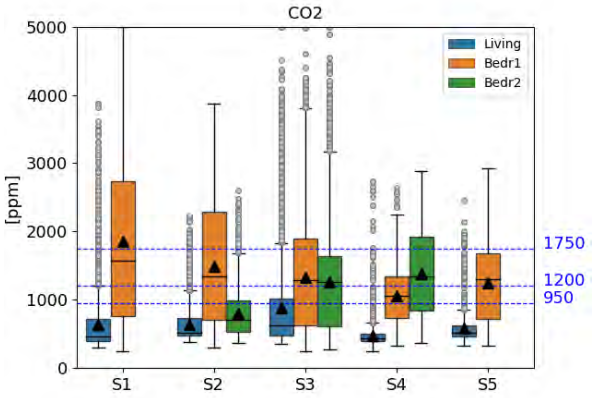

Figure 4: Indoor CO_2 levels in the living and bedrooms across the five apartments under analysis.

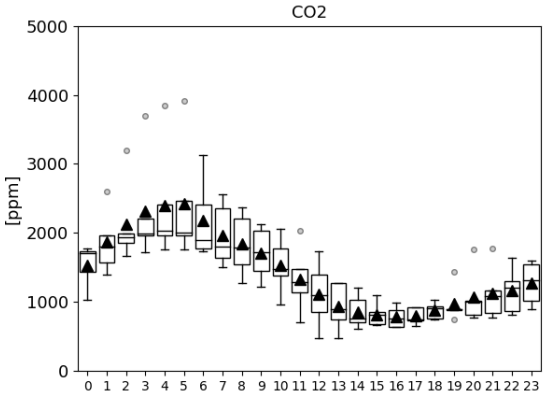

Figure 5: Distribution of the mean CO_2 in each hour of the day concentrations in the most critical bedroom across the 5 apartments.

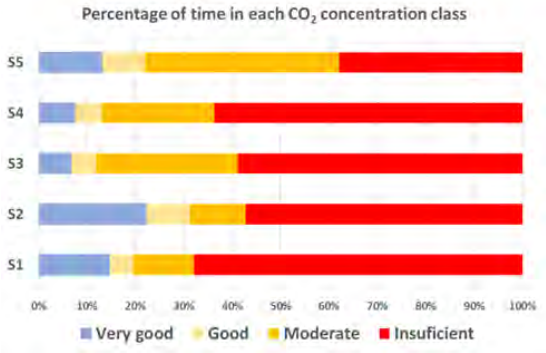

Figure 6: Time spent in each CO_2 concentration class during the night hours in the most critical bedroom across the five apartments under analysis.

4.2 Indoor air quality monitoring

The results of the formaldehyde concentration measured in the living room during one week are plotted in figure 7. The 30-minute average concentrations almost never exceed the limit value of 100 µg/m³ recommended by the WHO. The mean values for S2 and S4 are just below the 1-year limit value of 10 µg/m³ set by *Public Health England*. The values for the three other apartments are around 30 µg/m³. Although the interpretation of the LVOC concentration is less straightforward, the monitoring did not reveal high LVOC concentrations, with values below the 810 ppb for almost all hours, except for S1 (3% of hours > 810 ppb).

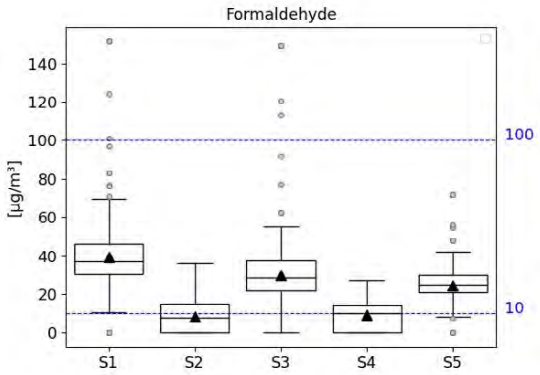

Figure 7: Formaldehyde concentration in the living room across the five apartments under analysis.

Figure 8 shows the indoor concentrations of particulate matter $PM_{2.5}$ measured during 1 week in the living room of each apartment and the corresponding outdoor concentration. S2 and S5 were monitored during the same week, as were S3 and S4. A significant difference in the outdoor $PM_{2.5}$ concentration is observed between the three measurement periods (S1, S2/S5, S3/S4). A high correlation is found between the median values of outdoor and indoor concentrations, except for S1. A significant part of the outdoor particulate matter enters the building through infiltration and ventilation (air inlets and opening of the windows). Added to this is the $PM_{2.5}$ produced by indoor emission sources. S1 and S2 show much higher indoor concentration than outdoors, indicating the non-negligeable generation of particulate matter by indoor emission sources. While exposed to the same outdoor concentration as for S5, case S2 clearly shows higher $PM_{2.5}$ concentrations. The following number of $PM_{2.5}$ concentration peaks (with levels of indoor concentration much higher than the outdoor concentration) were counted: 12, 25, 3, 1 and 3 for the S1, S2, S3, S4 and S5, respectively. These peaks are probably due to indoor emissions related to the cooking activities, knowing that the kitchen is connected to the living room by a large opening (absence of internal door). The resulting $PM_{2.5}$ levels are well above the ELV of 15 µg/m³ (24-h moving average) recommended by the WHO, as shown in table 2. Even considering the much less stringent ELV of 50 µg/m³ applied in Chile, the measured $PM_{2.5}$ levels are above the limit for a significant part of the time.

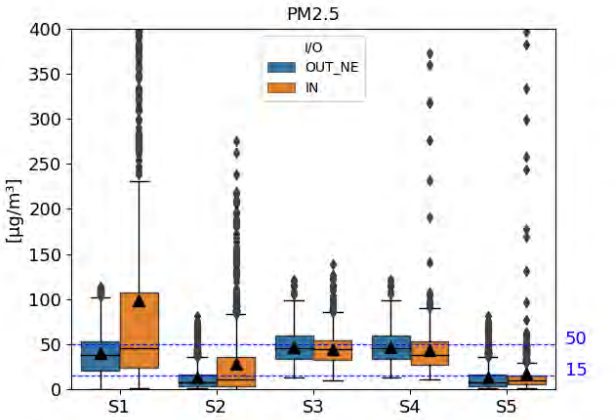

Figure 8: $PM_{2.5}$ concentration in the living room across the five apartments under analysis and corresponding outdoor $PM_{2.5}$ concentration.

4.3 Survey results

The survey reveals that the occupants are equipped with portable heaters (electric or kerosene), but that they use them very little, between 1 and 6 hours per day, only on the coldest days of the winter period. This explains the high percentage of hours outside the thermal comfort zone in the 5 apartments. However, the occupants rated their thermal perception of the indoor environment as acceptable ('not cold' – 'not hot').

Although the occupants reported the absence of mould on the walls, they did report water vapour condensation on the windows in all occupied bedrooms, which is consistent with the high RH levels observed in the bedrooms, particularly in S1 and S3.

Windows (usually in the living room) are opened for about 3 hours a day in S3, all day long in S5, and much less in S1. This probably explains - with a lower room occupancy - the low levels of CO_2 measured in the living room across all cases. All monitored bedrooms are occupied by only 1 person in S3, S4 and S5, 2 persons in S2 and 3 persons (2 adults + 1 newborn baby) in S1. The occupants leave 'sometimes to always' the internal door of the bedroom open, in S3 and S5, and 'never' in S1. This logically leads to higher CO_2 levels in S1 compared to the other cases. We could also conclude that the CO_2 concentration in the bedrooms would be even higher in S3, S4 and S5 if they were occupied by more than one person. All residents rated the indoor air quality in their homes as good to very good, even though measurements showed high levels of CO_2 in the bedrooms.

The survey also indicates that the kitchen extractor is controlled by an ON/OFF switch in all cases, and runs for between 20 min and 2 h (estimated time) a day according to the apartment. The kitchen extractor was removed in S3 and operates for about 2.5 hours in S5 (with the light on) and 5 hours per day in S1 (depending on the RH

level). The extractors do not run at night. The fact that the ventilation system (air extractors) does not operate at night means that the air supply to the bedrooms through the air inlets is dependent on wind and temperature conditions, which probably explains the insufficient supply of outdoor air per person, and consequently the excessive CO_2 levels in the bedrooms.

5. CONCLUSION

The monitoring of the indoor environmental conditions in five new social housing units (apartments) during one month in winter period revealed a high percentage of hours outside the thermal comfort zone. However, the occupants did not report a negative thermal perception of the indoor conditions. Too high indoor RH values were observed in various bedrooms. A risk of mould growth was identified in two bathrooms and one bedroom. In the living rooms, the measured indoor CO_2 levels remained low most of the time in all cases, and the 30 minute-average formaldehyde concentrations - and the LVOC in general - almost never exceeded the short-term limit values. Indoor $PM_{2.5}$ levels in the living room largely exceed the WHO recommended ELV of 15 µg/m³, due to too high outdoor concentration levels and to some indoor $PM_{2.5}$ emission sources in 2 of the 5 apartments. Too high CO_2 levels were observed in the bedrooms, which indicates an inefficient operation and/or design of the installed ventilation system. As a further work, similar analysis will be performed on a larger sample of social housing units and, based on all the monitoring results and IAQ simulations, efficient ventilation systems and/or strategies will be proposed to guarantee the IAQ and the health of the occupants.

ACKNOWLEDGEMENTS

This work was funded by the National Agency for Research and Development (ANID), Chile, under research grant FONDECYT 1221666. The authors also gratefully acknowledge the research support provided by CEDEUS under the research grant ANID/FONDAP 1523A0004.

REFERENCES

1. Fuentes, l., Rasse, A., Bustamante, W., Larraín, C and Perrozi, A. (2022). Regenerando Barrios. Aprendizajes de experiencias nacionales e internacionales para una política de regeneración urbana en Chile. *En Propuestas para Chile*. Pontificia Universidad Católica de Chile. Santiago, Chile
2. Bustamante, W., Cepeda, R., Martínez, P., & Santa María, H. (2009). Eficiencia energética en vivienda social: un desafío posible. *Camino Al Bicentenario - Propuestas Para Chile*.
3. Ministerio del Medio Ambiente. (2023). Planes de prevención y/o descontaminación atmosférica (PPDA). https://ppda.mma.gob.cl
4. MINVU. (2013). Regeneración de Condominios Sociales.
5. Instituto Nacional de Estadísticas. (2018). Censo 2017, Síntesis de resultados.
6. Flamant, G., Bustamante, W., Schmitt, C., Bunster, V. and Osorio, C, (2022). Thermal and environmental evaluation of mid-rise social housing retrofit under different climate conditions. *Journal of Building Engineering*, 46(2022) 103714.
7. EN 16798-1, (2019). Energy performance of buildings - Ventilation for buildings - Part 1: Indoor environmental input parameters for design and assessment of energy performance of buildings addressing indoor air quality, thermal environment, lighting and acou., CEN.
8. World Health Organization, (2018). WHO Housing and health guidelines.
9. Peeters, L., de Dear, R., Hensen, J. and D'haeseleer, W., (2009). Thermal comfort in residential buildings: Comfort values and scales for building energy simulation. *Appl. Energy*, vol. 86, no. 5, pp. 772–780, 2009, doi: 10.1016/j.apenergy.2008.07.011.
10. CIBSE, (2007). Environmental design CIBSE Guide A. London.
11. Caillou, S., Heijmans, N., Laverge, J. and Janssens, A., (2014). Méthode de calcul PER : Facteurs de réduction pour la ventilation à la demande.
12. World Health Organization, (2010). Guidelines for Indoor Air Quality. Selected Pollutants.
13. Public Health England, (2019). Indoor Air Quality Guidelines for selected Volatile Organic Compounds (VOCs) in the UK.
14. World Health Organization, (2021). WHO global air quality guidelines.
15. Ministerio del Medio Ambiente, (2011). Norma Primaria de Calidad Ambiental para material particulado fino respirable MP 2,5. Decreto 12.

PLEA 2024 WROCŁAW
(Re)thinking Resilience

Blurred Edges & Expanded Thermal Comfort:
Integrating Outdoor Environments for Enhanced Well-being and Energy Efficiency in Commercial Office Buildings

ELIZABETH L. MCCORMICK[1,2] LIN WHIPKEY[1], JIANXIN HU[1]

[1]North Carolina State University, Raleigh, NC, United States
[2]University of North Carolina Charlotte, Charlotte, NC, United States

ABSTRACT: The rapid adoption of air conditioning and modern building technologies has significantly impacted global energy consumption and CO_2 emissions, particularly within the building sector. This paper explores the evolution of comfort expectations in response to the widespread embrace of mechanical conditioning and the pursuit of thermal neutrality. Focusing on urban workplace settings, this paper advocates for expanded notions of indoor comfort by integrating principles of biophilia, natural ventilation, thermal variability, and individual control. Through a synthesis of literature and case studies, the study demonstrates how these elements contribute to enhanced thermal satisfaction and energy efficiency. The shift towards adaptive workplace design, influenced by the outdoors, challenges conventional norms, aligns with evolving workplace trends, and promotes a holistic, sustainable approach to building design that prioritizes occupant well-being and environmental responsibility.
KEYWORDS: Thermal comfort, adaptive workplace design, biophilia, indoor-outdoor integration

1. INTRODUCTION

The rapid and widespread adoption of air conditioning, tall buildings, and curtain wall technology has had a profound impact on global energy consumption as the building and construction sector account for more than one third of global energy consumption and CO_2 emissions. With global building and construction growth rates of 3-5% per year [1], the ratio of built space to natural landscape is increasingly shifting. The rapid expansion of interior space also reflects a profound shift in the amount of time humans spend indoors, a transition which corresponds with significant economic shifts from manufacturing to knowledge-based work [2]. This change was facilitated by the introduction and embrace of conditioning technologies in the early 1900s. As humans moved into artificially-conditioned environments, specific interior comfort expectations emerged and forever changed perceptions of thermal satisfaction [3]. In training the body to "hate the heat," anthropologist Gwyn Prins identified the physical addiction to conditioned air as "the most pervasive and least noticed epidemic in modern America" [4,5].

While variability in temperature, light, and humidity significantly shape our perception of space, modern mechanical conditioning seeks to provide consistent and uniform environments, creating a sense of thermal and spatial neutrality independent of the unpredictable factors of weather, climate, and human activity [6–8]. While thermal neutrality may be the simplest approach to conditioning the indoors, it comes at the cost of substantial energy consumption [9] and occupant dissatisfaction [10]. Heating, cooling, and ventilation (HVAC) represent 40% of the energy load in buildings [11], with greater demand in humid climates. However, research shows that building occupants are willing to tolerate a wider range of thermal conditions outside compared with inside buildings due to a number of psychological and physiological factors.

By influencing comfort perceptions through modifications to non-physical conditions, it becomes possible to navigate the delicate balance between energy efficiency, thermal comfort, and occupant satisfaction. As a result, this paper explores the concept of expanded thermal comfort conditions in urban workplace settings. This synthesis of literature addresses how comfort expectations have evolved over time and describes behavioral changes associated with energy consumption in commercial buildings. Ultimately, the goal of this research is to expand notions of indoor comfort, combining the healthful benefits of the outdoors with the functionality of indoor workplaces.

2. BACKGROUND

ASHRAE Standard 55 defines thermal comfort as the "condition of mind that expresses satisfaction with the thermal environment and is assessed by subjective evaluation" [12]. This document is used extensively across the United States to establish indoor environmental conditions in conditioned buildings, defining a temperature and humidity range that attempts to satisfy most (80%) individuals [13]. ASHRAE Standard 55 builds upon the PMV (predicted mean vote) model, which uses Fanger's equation of

thermal regulation theory of the human body, which assumes that human bodies reach thermal equilibrium inside buildings with fixed temperature and air humidity ranges. However, it has been found that this method is only reliable under conditions of thermal neutrality - the more variable or dynamic the thermal conditions, the more biased the approach becomes [14]. Despite the objective of achieving the *least offensive* thermal environment, many factors affect thermal perception, including local climate, gender, age, metabolism, psychological status, and socio-cultural situations [15,16].

In the late 1990s, ASHRAE conducted the Thermal Comfort Database project to explore an *adaptive* thermal comfort model, which was adopted into ASHRAE Standard 55-2010, merging indoor thermal and personal factors to generate an indoor thermal environment suitable to most occupants [17,18]. Similarly, researchers have examined the thermal expectations of naturally ventilated and mixed-mode buildings [19–22]. The more natural variations that are introduced, the greater the variability in the model. Regarding outdoor thermal comfort, researchers have developed numerous indices for the heat exchange between the human body and the environment, including indices from visible temperature, wind-chill index, rational indices, outdoor standard effective temperature, and the Universal Thermal Climate Index (UTCI). However, these metrics still do not consider the psychological factors of outdoor thermal perception [23,24].

Lenzholer and de Vries (2020) expands thermal comfort models by integrating psychological factors into the physical/physiological-psychological model for outdoor thermal perception (PhyPsy model), which assumes that both the physical/physiological and psychological aspects affect thermal perceptions [15]. They argue that people's short-term exposure to thermal experiences can lead to long-term thermal perceptions and memory for a specific environment and form a mental framework that helps the individual organize, process, and store information for a particular outdoor environment.

Despite extensive research on thermal comfort, standardizing this concept proves challenging due to the dynamic and multi-faceted nature of the human condition. Nevertheless, in the following sections, we will describe strategies to enhance thermal comfort conditions beyond the limitations of steady-state thermal comfort modeling without increasing energy consumption.

3. EXPANDED COMFORT ZONES

While mechanical systems can directly affect temperature and humidity, several other factors can influence perceptions of thermal comfort without significant energy expenditure. Cabanac's conceptual model of *alliesthesia,* for example, found that individuals experience enhanced feelings of thermal pleasantness when the environment mitigates thermal stress [25]. By exploring the dynamics of thermal pleasure, Sijie et al.'s (2021) found that pushing occupants beyond conditions of thermal neutrality could establish a basis for increased delight in the thermal environment [7]. This section will address four emerging areas of research that influence thermal comfort *perceptions* without altering physical conditions: biophilia, natural ventilation, variability, and control. Each of these aspects has the potential to broaden expectations of thermal comfort with potentially significant energy implications.

3.1 Biophilia (visual access to nature)

The concept of biophilia suggests that humans respond positively to nature and that a more 'natural' building can evoke positive responses and directly influence occupants' well-being [26]. Biophilic design principles emphasize the integration of features such as natural light, vegetation, and natural materials into buildings, offering both psychological and physiological impacts on perceived comfort [27]. This notion embraces the psychological factors influencing thermal perception beyond those related solely to measurable biometeorological effects [28]. The inclusion of indoor plants, for example, has demonstrated a positive influence on the overall well-being of building occupants, resulting in fewer health complaints and reduced sick leave [29,30].

Similarly, research shows that there is a clear link between visual factors, such as daylight and views, on thermal perceptions in a space [31,32]. Exposure to natural light not only improves visual comfort but also regulates circadian rhythms to promote a sense of alertness during the day and better sleep quality at night. In a 2020 study, Ko et al. found that windows providing a visual connection to the outdoors had a cooling effect as 12% of participants felt more comfortable in the room with windows, despite similar thermal conditions to the room without windows. Through their analysis, they determined that having a window was equivalent to a .74°C (1.33°F) cooling effect, which could achieve an average savings of approximately 8% in cooling energy and 6.5% of total HVAC energy for a medium-sized office building in San Francisco (or 6% in Singapore) [33]. In addition to having a positive impact on the occupants' overall perceptions of the built environment, visual connection to nature has proven to have a positive impact on attention, stress and discomfort, as well as overall health and well-being [34,35], which can also expand tolerances of thermal expectations. However, it is important to note that there are psychological adaptations that are unique to individual subjects, including expectations for 'naturalness', time of exposure, as well as perceived control, and

environmental stimulation, that further influence biophilia-related thermal perceptions [36].

3.2 Natural ventilation (direct access to nature)

Throughout history, humans have employed air movement as a simple yet effective strategy for regulating indoor thermal comfort. However, contemporary conditioning systems largely prioritize the precise control of temperature and humidity over airlow, yet the adjustment of air movement can significantly influence perceptions of indoor thermal comfort [37–39]. Although fans consume energy, occupants experiencing increased airflow are comfortable across a broader range of temperatures, which allows for higher cooling setpoints, compared to rooms without ceiling fans [40]. In a 2008 study, Schiavon et al. found that increased air velocity led to a reduction in cooling energy consumption ranging from 17% in Athens to 48% in Helsinki [37]. Hybrid cooling in particular can lead to significant energy savings, particularly in cooling-dominated climates, which can be incorporated into any building regardless of age. In a separate study, Schiavon found that by integrating fans and adjusting thermostat temperature set points, energy consumption was reduced by one-third [41].

In addition to increased airflow, building occupants frequently express a preference for natural ventilation over mechanical alternatives, driven largely by a strong connection with the outdoors [9,42]. By providing a direct link to outdoor air, it allows occupants to experience natural sounds, scents, and the occasional breeze. Similarly, outdoor air is often perceived as 'fresher' compared with air circulated through mechanical systems [43]. As with biophilic elements, this direct connection to nature is known to have positive effects on mental well-being and can contribute to a more comfortable indoor experience, regardless of physical conditions. Additionally, natural ventilation allows for variable airflow based on outdoor conditions, providing relief from the tedium of conditioned air. Because occupants expect greater temperature fluctuations outdoors, they are willing to accept a greater range of thermal conditions with outdoor air [44]. As before, it's important to note that individual preferences for ventilation can differ, and the perceived comfort of natural ventilation will vary.

3.3 Thermal variability (stimulation)

The outdoor environment is rich with thermal gradients and temporal transitions in temperature, humidity, wind speed, and radiation, whether arising from seasonal transitions or intermittent occurrences. The need for sensory stimulation emerges as a crucial factor in determining an individual's satisfaction indoors, both enhancing perceptions of comfort while also reducing building energy consumption [45]. Arens (2006) emphasizes that under heterogeneous and transient thermal conditions, neutrality can still be perceived as comfortable, however, the most pleasant experiences occur when thermal stimuli actively contribute to alleviating whole-body thermal stress [7,46]. Additionally, the broad range of thermal comfort conditions found in outdoor spaces, coupled with psychological effects of connecting with nature, can contribute to increased thermal satisfaction [47]. Transitional spaces also play a role in individuals' acceptance of a wider range of thermal conditions.

In conditions where natural climatic variations occur, such as in outdoor or transitional spaces, there is a higher tolerance for thermal fluctuations in the physical environment [36]. In fact, Nakano and Tanabe (2004) demonstrated that occupants of semi-outdoor environments could tolerate a temperature range two to three times wider than that predicted by Fanger's PMV-PPD model [48,49]. In terms of psychological adaptation, according to Fountain et al. (1996), after being exposed to variations in indoor conditions that are considered pleasant, a person's comfort expectations may become more relaxed [50]. In workplace settings, individuals will often retreat outside during lunch breaks to stimulate their senses with fresh air and sunlight, an experience which serves as a brief respite from the monotony of the conditioned workplace [36]. Overall, these findings emphasize the positive correlation between spatial and thermal variability and the satisfaction that individuals derive from their thermal environments.

3.4 Control and personal choice

Apart from thermal uniformity, environmental conditions within typical workplace settings are frequently subjected to stringent regulation by a centralized mechanical system with limited opportunity for personalized control. This lack of thermal autonomy is particularly evident in tall buildings where operable windows are either inaccessible or entirely unavailable to occupants. However, research indicates that even without altering ambient thermal conditions, providing occupants with a sense of control of their own microclimate (and specific sources of discomfort) can significantly improve thermal comfort perceptions while simultaneously decreasing building energy consumption [36,51]. Zhou et al. (2013), for example, found that the ability to control the physical environment, which is a purely psychological factor, is a large reason that naturally ventilated buildings have higher acceptable temperature ranges compared with air-conditioned environments [52]. Occupants can improve their perception of their thermal environment by opening a window, using a desk lamp, or using a personal fan. In response to this condition, research initiatives such as those led by UC Berkeley's

Center for the Built Environment (CBE), are advancing the development of personal comfort systems (PCS). These systems, including heated and cooled office chairs, IoT-connected desk fans, and low-energy heating devices, aim to target an occupant's immediate microclimate, empowering individuals with a greater degree of control over their thermal environment [53].

4. EMERGING MODELS OF ADAPTIVE WORKPLACE

Due to the changing nature of office work and worker profiles, the impact of technology, and the growing need for flexibility, workplace design is rapidly changing, particularly in response to the COVID-19 pandemic. There is also a growing trend of work extending beyond the confines of traditional office environments, encompassing settings such as homes, cafes, and trains. This shift results in a notable increase in the flexibility of the physical boundaries associated with office work [54]. Additionally, there are emerging flexible work arrangements (FWA), such as coworking, mobile work, and 'hot desks', that are part of larger social trends in the ownership of space [55]. In a 2019 New York Times article, Jane Margolies states, "Nature aside, outdoor work areas are a logical next step in the evolution of flexible offices" [56].

Ultimately, the aim of this synthesis research is to facilitate the development of a more dynamic indoor environment, while also fostering moments of thermal delight and positive stimulation [45]. This endeavor not only prioritizes occupants' well-being but also contributes to energy savings. However, it is not yet clear whether the connection to outdoor space will remain positive in organizational settings [57]. With an understanding of the evolving landscape of office work and the imperative for adaptable workplace design, the subsequent section delves into pertinent case studies.

4.1 Built works

Completed in 2017, 512 W. 22nd St is an 11-story, 172,700 SF office building in New York City, with nearly 17,000 SF of planted terraces and a common roof. Inspired by the principles of biophilic design, every floor in the building has operable windows and direct access to planted outdoor space. "It's about connecting people to daylight and making [them feel] connected to nature" says architect Rick Cook from New York-based design firm, CookFox. "While improvements used to get paid for by energy savings," Cook says, "it's harder to make the financial argument about quality and comfort" [58]. CookFox has their own office space in the building and their outdoor space is used to keep bees and grow kale.

EskewDumezRipple's (EDR) Center of Developing Entrepreneurs (CODE) building, completed in 2022, is a 215,000 SF mixed-use building in Downtown Charlottesville. The project was design as a spec-office building that embraced the changing nature of work and create a space where "locally-grown innovations in information technology, clean energy, and the like, could blossom into locally-based businesses, rather than relocating outside of the region" [59]. Combined with other efficiency measures, this building offers at 73% energy reduction from comparable buildings.

In 2021, HOK's Center for Academic Medicine at Stanford University in Palo Alto strategically relocated 20% of its program to outdoor spaces, including both work and leisure spaces. Taking advantage of Northern California's mild climate, the team used porches, balconies, skybridges, and covered walkways in what HOK calls a "passive-first design approach" to reduce energy consumption by 85% from baseline while simultaneously addressing physician burnout through biophilic design principles.

4.2 Theoretical projects

Though not all projects can be sited next to a nature preserve, as with the previous project, all of these examples offer outdoor spaces as moments of respite; however, the bulk of office work still occurs indoors. Instead, EDR's award-winning competition entry for the Metals in Construction Magazine Next Generation Façade competition, 'The Ecotone', explores the spatial buffers and thermal gradients between inside and out in a speculative 30-story office building in Brooklyn. Referencing the environmental gradients between ecosystems, this project creates a diverse community of occupiable spaces that generate a gradient of thermal zones. This allows occupants the opportunity to organize their surroundings through contrast and heterogeneity.

Additionally, some academics are pushing for a significant transition in architectural design, challenging the rigid divisions between interior and exterior spaces for the dual benefits of health and energy efficiency. Michael Hensel's *heterogeneous architecture*, for example, introduces semi-interior

Figure 1: The Ecotone, Metals in Construction competition entry, 2018. Image by EskewDumezRipple

conditions to explore the spatial elements of perceived boundary conditions in architecture [60].

5. DISCUSSION & CONCLUSION

Perceptions of human thermal comfort prove to be intricate, characterized by multiple interacting components that continuously adapt and self-organize. The extensive use of mechanical conditioning as the primary thermal strategy and the embrace of thermal neutrality have resulted in a pervasive lack of environmental stimulation in contemporary buildings. This has led to a general disconnection from nature, accompanied by heightened levels of energy consumption, carbon emissions, and extensive ecological degradation.

The influence of the outdoor world, such as access to nature, fresh air, and thermal variability, significantly shapes our perceptions of indoor thermal comfort. As we witness a collective shift toward more adaptive outdoor comfort models, it is clear that the indoor environment would also benefit from a more nuanced approach to thermal comfort modeling. By steering away from the conventional pursuit of thermal neutrality and embracing the concept of thermal pleasure, we can profoundly impact the occupant experience in the indoor environment. This paradigm shift promises enriched experiential qualities within the workplace setting, fostering a broader tolerance for variations in thermal comfort. This, in turn, holds the promise of substantial energy savings, challenging the status quo of thermal neutrality and advocating for a more human-centric approach to indoor thermal comfort.

The incorporation of outdoor spaces in the workplace serves as a tangible embodiment of the evolving understanding of thermal comfort. It not only aligns with the growing appreciation for nature's impact on well-being, but also challenges conventional workplace norms that prioritize thermal neutrality. By introducing elements of the outdoor world indoors, workplaces can become more dynamic, fostering an environment that accommodates the diverse and evolving experiential preferences of the occupants.

As we acknowledge the complex interplay of factors influencing thermal comfort, it becomes apparent that the connection with nature is essential for truly sustainable solutions. The incorporation of outdoor elements within indoor spaces not only addresses occupant well-being but also represents a step toward mitigating the environmental impact of commercial building practices. This holistic approach, driven by an understanding of the multifaceted nature of thermal comfort, is pivotal in shaping a future where sustainable design integrates seamlessly with the natural world. It is a call to action for a more holistic and sustainable approach to design – one that prioritizes the intricate balance between human comfort, energy conservation, and ecological responsibility.

REFERENCES

1. United Nations Environment Programme 2020 Global Status Report for Buildings and Construction: Towards a Zero-Emissions, Efficient and Resilient Buildings and Construction Sector; 2020;
2. Al Horr, Y.; Arif, M.; Kaushik, A.; Mazroei, A.; Katafygiotou, M.; Elsarrag, E. Occupant Productivity and Office Indoor Environment Quality: A Review of the Literature. Building and Environment 2016, 105.
3. Moe, K. Thermally Active Surfaces in Architecture; Princeton Architectural Press, 2010.
4. Prins, G. On Condis and Coolth. Energy and Buildings 1992, 18, 251–258,.
5. Mahdavi, A.; Kumar, S. Implications of Indoor Climate Control for Comfort, Energy and Environment. Energy and Buildings 1996, 24, 167–177.
6. Luo, M.; de Dear, R.; Ji, W.; Bin, C.; Lin, B.; Ouyang, Q.; Zhu, Y. The Dynamics of Thermal Comfort Expectations: The Problem, Challenge and Implication. Building and Environment 2016, 95, 322–329.
7. Liu, S.; Nazarian, N.; Hart, M.A.; Niu, J.; Xie, Y.; de Dear, R. Dynamic Thermal Pleasure in Outdoor Environments - Temporal Alliesthesia. Science of The Total Environment 2021, 771, 144910.
8. Barber, D.A. Modern Architecture and Climate: Design Before Air Conditioning; Princeton Univ. Press, 2020.
9. Liu, S.; Xie, Y.; Zhu, Y.; Lin, B.; Cao, B.; Wong, N.H.; Niu, J.; Fang, Z.; Lai, D.; Liu, W.; et al. Comparative Analysis on Indoor and Outdoor Thermal Comfort in Transitional Seasons and Summer Based on Multiple Databases: Lessons Learnt from the Outdoors. Science of The Total Environment 2022, 848, 157694.
10. Humphreys, M.A.; Hancock, M. Do People like to Feel 'Neutral'?: Exploring the Variation of the Desired Thermal Sensation on the ASHRAE Scale. Energy and Buildings 2007, 39, 867–874.
11. Graham, C.I. High-Performance HVAC Available online: https://www.wbdg.org/resources/high-performance-hvac (accessed on 8 May 2021).
12. ASHRAE ANSI/ASHRAE Standard 55Standard 55-2013 - Thermal Environmental Conditions for Human Occupancy (ANSI Approved) 2013.
13. Givoni, B. Comfort, Climate Analysis and Building Desing Guidelines. Energy and Buildings 1992, 18, 11–23.
14. Van Hoof, J. Forty Years of Fanger's Model of Thermal Comfort: Comfort for All? Indoor Air 2008, 18, 182–201.
15. Lenzholzer, S.; de Vires, S. Exploring Outdoor Thermal Perception - a Revised Model. International Journal of Biometeorology 2020, 63.
16. Schooshtarian, S. Theoretical Dimention of Outdoor Thermal Comfort Research. Sustainable Cities and Society 2019, 47, 1–14.
17. de Dear, R.J. A Global Database of Thermal Comfort Field Experiments. ASHRAE Transactions 1998, 104.
18. de Dear, R.J.; Brager, G.S. Developing an Adaptive Model of Thermal Comfort and Preference. ASHRAE Transactions 1998, 104, 145–167.
19. Rupp, R.F.; Vasquez, N.G.; Lamberts, R. A Review of Human Thermal Comfort in the Built Environment. Energy and Buildings 2015, 105, 178–205.
20. Indraganti, M.; Oaka, R.; Rijal, H.B. Field Investigation of Comfort Temperature in Indian Office Buildings: A Case of Chennai and Hyderabd. Building and Environment 2013, 65, 195–214.

21. Indraganti, M.; Oaka, R.; Rijal, H.B.; Brager, G.S. Adaptive Model of Thermal Comfort for Offices in Hot and Humid Climates of India. Building and Environment 2014, 74, 39–53.
22. Oropeza-Perez, I.; Petzold-Rodriguez, A.H.; Bonilla-Lopez, C. Adaptive Thermal Comfort in the Main Mexican Climate Conditions with and without Passive Cooling. Energy and Buildings 2017, 145, 251–258.
23. Jendritzky, G.; Maarouf, A.; Staiger, H. Looking for a Universal Thermal Climate Index (UTCI) for Outdoor Applications; Windsor, UK, April 5 2001; pp. 353–367.
24. Knez, I.; Thorsson, S.; Eliasson, I.; Lindberg, F. Psychological Mechanisms in Outdoor Place and Weather Assessment: Toward a Conceptual Model. Int J Biometeorology 2009, 53, 101–111,
25. Cabanac, M. Physiological Role of Pleasure. Science 1971, 173, 1103–1107.
26. Ulrich, R.S. Biophilia, Biophobia, and Natural Landscapes. In The Biophilia Hypothesis; Island Press, 1995.
27. Joye, Y. Architectural Lessons from Environmental Psychology: The Case of Biophilic Architecture. Review of General Psychology 2007, 11, 305–328.
28. Lenzholzer, S.; de Vries, S. Exploring Outdoor Thermal Perception—a Revised Model. Int J Biometeorol 2020, 64, 293–300.
29. Han, K.-T.; Ruan, L.-W. Effects of Indoor Plants on Self-Reported Perceptions: A Systemic Review. Sustainability 2019, 11, 4506.
30. Bringslimark, T.; Hartig, T.; Patil, G.G. Psychological Benefits of Indoor Plants in Workplaces: Putting Experimental Results into Context. HortScience 2007, 42, 581–587.
31. Chinazzo, G.; Wienold, J.; Andersen, M. Daylight Affects Human Thermal Perception. Sci Rep 2019, 9, 13690.
32. te Kulve, M.; Schlangen, L.; van Marken Lichtenbelt, W. Interactions between the Perception of Light and Temperature. Indoor Air 2018, 28, 881–891.
33. Ko, W.H.; Schiavon, S.; Zhang, H.; Graham, L.T.; Brager, G.; Mauss, I.; Lin, Y.-W. The Impact of a View from a Window on Thermal Comfort, Emotion, and Cognitive Performance. Building and Environment 2020, 175.
34. Aries, M.B.C.; Veitch, J.A.; Newsham, Guy.R. Windows, View, and Office Characteristics Predict Physical and Psychological Discomfort. Journal of Environmental Psychology 2010, 30, 533–541.
35. Leather, P.; Pyrgas, M.; Beale, D.; Lawrence, C. Windows in the Workplace: Sunlight, View, and Occupational Stress. Environment and Behavior 1998, 30, 739–762.
36. Nikolopoulou, M.; Steemers, K. Thermal Comfort and Psychological Adaptation as a Guide for Designing Urban Spaces. Energy and Buildings 2003, 35, 95–101.
37. Schiavon, S.; Melikov, A.K. Energy Saving and Improved Comfort by Increased Air Movement. Energy and Buildings 2008, 40, 1954–1960.
38. Liu, S.; Yin, L.; Schiavon, S.; Ho, W.K.; Ling, K.V. Coordinate Control of Air Movement for Optimal Thermal Comfort. Science and Technology for the Built Environment 2018, 24, 886–896.
39. Arens, E.; Turner, S.; Zhang, H.; Paliaga, G. Moving Air for Comfort. 2009.
40. Raftery, P.; Douglass-Jaimes, D. CBE Ceiling Fan Design Guide 2020.
41. Vo, K. Hybrid Cooling Leads to Significant Energy Savings in Tropical Office Buildings Available online: https://citris-uc.org/hybrid-cooling-leads-to-significant-energy-savings-in-tropical-office-buildings/.
42. Brager, G.S.; de Dear, R.J. Thermal Adaptation in the Built Environment: A Literature Review. Energy and Buildings 1998, 27, 83–96.
43. Gao, J.; Wargocki, P.; Wang, Y. Ventilation System Type, Classroom Environmental Quality and Pupils' Perceptions and Symptoms. Building and Environment 2014, 75, 46–57.
44. Tan, Z.; Chung, S.C.; Roberts, A.C.; Lau, K.K.-L. Design for Climate Resilience: Influence of Environmental Conditions on Thermal Sensation in Subtropical High-Density Cities. Architectural Science Review 2019, 3–13.
45. Mishra, A.K.; Loomans, M.G.L.C.; Hensen, J.L.M. Thermal Comfort of Heterogeneous and Dynamic Indoor Conditions — An Overview. Building and Environment 2016, 109, 82–100.
46. Arens, E.; Zhang, H.; Huizenga, C. Partial- and Whole-Body Thermal Sensation and Comfort—Part II: Non-Uniform Environmental Conditions. Journal of Thermal Biology 2006, 31, 60–66.
47. Spagnolo, J.; de Dear, R. A Field Study of Thermal Comfort in Outdoor and Semi-Outdoor Environments in Subtropical Sydney Australia. Building and Environment 2003, 38, 721–738.
48. Nakano, J.; Tanabe, S. Thermal Comfort and Adaptation in Semi-Outdoor Environments. ASHRAE Transactions 2004, 110, 543–553.
49. Hwang, R.-L.; Lin, T.-P. Thermal Comfort Requirements for Occupants of Semi-Outdoor and Outdoor Environments in Hot-Humid Regions. Architectural Science Review 2007, 50, 357–364.
50. Fountain, M.; Brager, G.; de Dear, R. Expectations of Indoor Climate Control. Energy and Buildings 1996, 24, 179–182.
51. Nikolopoulou, M.; Lykoudis, S. Thermal Comfort in Outdoor Urban Spaces: Analysis across Different European Countries. Building and Environment 2006, 41, 1455–1470.
52. Zhou, X.; Ouyang, Q.; Zhu, Y.; Feng, C.; Zhang, X. Experimental Study of the Influence of Anticipated Control on Human Thermal Sensation and Thermal Comfort. Indoor Air 2013, 24, 171–177.
53. Lehrer, D.; Arens, E.; Zhang, H.; Fannon, D. Prototyping Solutions to Improve Comfort and Enable HVAC Energy Savings. 2020.
54. Petersson Troije, C.; Lisberg Jensen, E.; Stenfors, C.; Bodin Danielsson, C.; Hoff, E.; Mårtensson, F.; Toivanen, S. Outdoor Office Work – An Interactive Research Project Showing the Way Out. Frontiers in Psychology 2021, 12.
55. Hirst, A. Settlers, Vagrants and Mutual Indifference: Unintended Consequences of Hot-desking. Journal of Organizational Change Management 2011, 24, 767–788.
56. Margolies, J. The Next Frontier in Office Space? The Outdoors. The New York Times 2019.
57. Klotz, A.C.; Bolino, M.C. Bringing the Great Outdoors Into the Workplace: The Energizing Effect of Biophilic Work Design. AMR 2021, 46, 231–251.
58. Weiss, L. NYC Office Buildings Are Buzzing with New Green Spaces. New York Post 2016.
59. EskewDumezRipple Center of Developing Entrepreneurs (CODE) Available online: https://www.eskewdumezripple.com/the-center-of-developing-entrepreneurs.html.
60. Hensel, M.; Turko, J.P. Grounds and Envelopes: Reshaping Architecture and the Built Environment; Routledge, Taylor & Francis Group: London; 2015.

PLEA 2024 WROCŁAW
(Re)thinking Resilience

Sustainable Development of Green School Design in Taiwan

HONGYI SHIH,[1]

[1]Environmental and Interior Design, Texas Tech University, Lubbock, United States

ABSTRACT: This paper advocates for Green Schools as vital in addressing environmental challenges and fostering sustainability education, particularly focusing on Taiwan's universities. The objective is to formulate concise guidelines for Green School design, integrating insights from the study of development processes and LEED-certified case studies. By analysing user expectation data from a targeted redesign, specific design principles are identified, tailored to Taiwan's climate and culture. The research culminates in the practical application of these principles to redesign indoor spaces in Nanhua University's Zhongdao building, aligning with LEED criteria. Beyond enhancing sustainability, this effort also aims to serve as a model, promoting the Green School concept across Taiwan. This comprehensive approach, integrating theoretical insights with practical implementation, contributes to the discourse on sustainable educational infrastructure within a concise framework.
KEYWORDS: Green School, University Design, Well-being, Sustainable Design, Sustainability

1. INTRODUCTION

Environmental issues have been a growing concern in recent years, with pollution, global warming, and climate change reaching alarming levels. The significance of both protecting the environment and teaching younger generations how to live sustainably is increasing [1]. The concept of the "Green School" offers a solution to these problems because schools can model best practices for energy efficiency and sustainable design. Additionally, they can educate students, faculties and staff about the science behind the concepts and encourage them to carry the ideas forward to future generations [2].

Schools are not only great environments for education, practice, and demonstration of sustainability, but they can also provide a healthy, practical, efficient, and environmentally friendly space for teachers and students in their daily lives. As the science behind Green School concepts is applied and taught, the health and well-being benefits are experienced firsthand, with students, faculties and staff as the primary beneficiaries. This paper specifically targets universities among the various levels of schools, given their leading role in education, research, policy formation and the exchange of information essential for achieving the sustainable development goals [3].

The aim of this paper is to establish a set of guidelines for Green School design in Taiwan, by creating a flexible, comprehensive, and universal design system tailored to the unique conditions, culture, and climate of Taiwan.

2. BACKGROUND

Taiwan is a small island situated in tropical and subtropical zones at the edge of the Pacific Ocean. 36,000 KM^2 in size, 70% of the island has mountainous terrain while the majority of the remaining areas consist of plains located on the west coast. Consequently, 70% of the 23-million population resides in the five largest cities located on the west coast, with an additional 15% in other urban areas [4]. In the pursuit of a more sustainable Taiwan, the implementation of Green Schools stands out as a viable solution among various options to address specific environmental issues caused by weather, resources, and society that are derived from Taiwan's geological characteristics.

First, weather. Taiwan's overall weather is hot, humid, and rainy with an average temperature of 75°F year-round. In the summer, temperatures can become sultry hot, reaching up to 104°F, with a daily average of 81°F [5]. Exposure to such heat, especially in high humidity, is dangerous to human health and can lead to heat related illness such as exhaustion, heatstroke, heat cramps, etc. [6]. During winter, the weather becomes cold, windy, smoggy, and rainy. Exposure to smog has been linked to harmful air quality, causing adverse health effects, including heart disease, lung cancer, and respiratory diseases etc. [7]. Therefore, addressing the adverse effects of these specific climatic conditions becomes critical in Taiwan, with a focus on improving indoor air quality and thermal comfort.

Second, natural resources, or a lack thereof. Being a small island, natural resources in Taiwan are scarce. 98% of energy needs are served by imports, with 93% of that reliant on fossil fuels [8]. Being so heavily dependent on imports has inherent security challenges, exposing Taiwan's economy to fluctuating energy prices, sudden supply shocks, instability of reserve margins, and unbalanced energy equity, etc. Therefore, to achieve energy conservation, Taiwanese government agencies have taken action by promoting the implementation of energy conservation policies, such as the Government Office

Energy Saving Policy, hoping to encourage private industry and commerce to adopt them. Past statistics on energy-saving counselling cases indicate that implementing energy-saving improvements in electricity, lighting, air-conditioning, and office equipment could potentially result in a 20% energy-saving in government agencies and 15-20% in schools [9]. Especially for schools, where conservation should be best modelled, taught, and practiced. There have been many years of research into sustainable development in Taiwan, however, only a few universities in Taiwan have started to conceptualize and implement a "Sustainable University" [10].

Third, the society of education. There are 10,931 schools with 4,260,327 students in Taiwan, who spend most of their daily lives at schools [11], and that is almost 20% of Taiwan's entire population. Students spend much more of their waking times at school than in their homes, as Taiwan has a nine-year compulsory education system, along with prep courses given during summer break. Consequently, the resulting energy consumption is enormously huge. In order to address this heavy school energy consumption issue, designing energy-conserving schools in response to Taiwan's hot and humid subtropical weather and students' needs has become a critical task. Among all different levels of schools, universities have the most complex situation not only because students spend a huge amount of time being there but also because it has the most complicated construction process. Unlike secondary school, which may consist of solitary buildings, university is more like a small, self-reliant city with diverse facilities such as classrooms, administrative buildings, research facilities, laboratories, studios, libraries, sports facilities, recreation centers, and dormitories. The multifaceted nature of university campuses makes designing energy-efficient solutions imperative.

3. OBJECTIVES

- To establish a model design criterion for Green Schools as a guideline and methodology in Taiwan.
- To deliver environmental lessons and foster awareness of sustainability in future generations.
- To provide an interior-based alternative solution for new construction or building renovation that meets only partial Leadership in Energy and Environmental Design (LEED) requirements yet fulfils specific crucial sustainability effects.
- To create an inexpensive and quick deployable partial LEED compliant working model that can easily be adapted and applied to renovate every educational building to promote sustainability in Taiwan.
- To set a precedent of Green School building redesign and renovation with a focus on both sustainability and residents' well-being.
- To raise awareness and willingness to government, educational systems, and the construction industry, facilitating the expansion of these practices to more educational buildings.

4. METHODOLOGY

The research was conducted qualitatively in nature, involving the analysis of case studies and survey. The LEED rating system was analysed to create a framework that serves as a reference for developing the design principles and elements for this paper. Case studies was conducted to advance the understanding of green school designs in the United States and to propose methods for evaluating the design principles and elements of successful Green School designs.

A building in Taiwan was selected as the remodel design target and a survey was conducted to understand the residents' needs and expectations for a Green School. The findings were then organized to summarize the design principles and contributing to a successful Green School. In the final phase, partial indoor spaces of the selected building were re-designed incorporating the aforementioned design principles and elements to make each of the selected indoor areas more environmentally friendly.

5. CASE STUDY

5.1 LEED rating system

First, the LEED rating system was analysed to develop design principles and elements necessary to reduce the environmental footprint of the facility and building. Following the completion of the analysis, three categories for design principles and elements were identified: energy, material, and well-being. For energy, the main goals are to maximize the utilization of natural and renewable energy such as sunlight and natural ventilation, as well as to manage water flow in the exterior spaces to reduce the environmental impacts associated with fossil fuel energy consumption and the burden on wastewater systems. For material, the key objectives are to adopt local recyclable materials, reuse existing building materials, and minimize construction waste to lower environmental impacts related to extraction, transportation, and processing. For well-being, the primary targets are to improve the indoor air quality and comfort, provide individuals with control over lighting and ventilation, and establish a connection between outdoor views and indoor spaces.

5.2 Nancy Nicholas Hall: LEED Gold certification

Nancy Nicholas Hall of the University of Wisconsin -Madison was selected as the case study subject because it houses the Design Studies Department, where the author first drafted this research paper as an MFA student, providing access to detailed information for study.

Additionally, the average humidity in Madison is similar to that of Taiwan, averaging around 70% annually [12]. These two features make Nancy Nicholas Hall a great reference. Nancy Nicholas Hall was renovated and expanded in 2012, and now accommodates the School of Human Ecology [13]. It received the Gold LEED certificate in 2013, marking the sixth LEED certification for the University of Wisconsin-Madison [14]. The vision of the project is to provide a sustainable space that encourages and promotes teaching, research, creative scholarship, and outreach. The building serves as a consolidated home for the School of Human Ecology offering programs and extensive research and collaboration spaces for faculties and students. Within the campus community and beyond, this setting promotes the School of Human Ecology's goal, visibility, and accessibility in a sustainable environment. The sustainable approaches include:

- The commitment to water sustainability. The porous pavement facilitates water permeability rather than retention or runoff. In addition, drought-tolerant native landscaping conserves water by using drought-resistant grass native to the area.
- Energy saving is realized through a multifaceted approach. All new equipment is Energy Star rated, accompanied by high-efficiency lighting and HVAC systems to reduce energy consumption. Thermal mass is utilized throughout the summer to minimize day-to-night temperature changes by strategically situating thermally massive objects in the structure, such as exposed concrete, stone, and water. Innovative features like displacement ventilation, indirect evaporative cooling, and indicator lights for open windows contribute to reduction in energy consumption during air conditioning use.
- Sustainable materials. Alongside the 95% of construction waste and materials being reused or recycled, the inclusion of non-toxic finishes and materials additionally reduces the demand for natural resources.
- Occupant well-being priority. Abundant natural light reaches regularly occupied rooms within 20 feet of windows. The use of products emitting low levels of volatile organic compounds (VOCs) enhances air quality, fostering productivity and satisfaction, and reducing health-related absences among building users.
- Open space strategy. The strategic placement of a patio to the north and a Rooftop Terrace on the third floor not only expands usable areas but also achieves a remarkable ratio of open spaces to the development footprint, fostering biodiversity. The innovation commitment earned Exemplary Performance for Maximized Open Space credit.

6. GREEN SCHOOL DESIGN DATA COLLECTION

6.1 Questionnaire development

A questionnaire was developed and randomly distributed to users with the aim to understand their needs and expectations for the Green School, uncovering unmet requirements, identifying new opportunities, and inspiring innovative solutions for the redesign paper. The questionnaire, consisting of both multiple-choice and open-ended questions, sought to identify needs, expectations, and preferences related to sustainable indoor spaces. Specifically, it examined their association with sustainable design strategies within the ZhongDao Building, as reported by occupants based on their firsthand experiences. Areas considered for renovation included the office, lobby, and terrace, as each could be improved to achieve sustainability and a higher degree of human comfort. Multiple selections are allowed. This anonymous questionnaire was randomly disseminated to students, faculties, alumni, and any individuals who had visited the ZhongDao Building. Participation was entirely voluntary.

6.2 Result and findings

The results from the questionnaire, providing valuable insights, were used to guide the future design directions aimed at enhancing the sustainability of the ZhongDao Building for both occupants and the environment.

A total of forty-seven participants completed the survey, all of them are Taiwanese. The majority of the participants are students, followed by faculties and staff, alumni and student's parents.

Figure 1: Demographic characteristics of the participants.

Most participants believe that more appropriate acoustics and better ventilation are needed for the

office. More greenery and access to natural light are needed for the lobby. And access to natural light and more greenery are needed for the terrace.

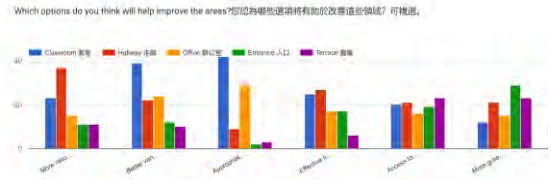

Figure 2: Participants' preferred changes for better sustainability of each of the designated redesign areas.

The improvement of mental health and the increase of creativity are considered as the two most likely benefits of sustainable design to the occupants, followed by better physical health, more effective study, increases in participation, engagement in class, and the increase of productivity.

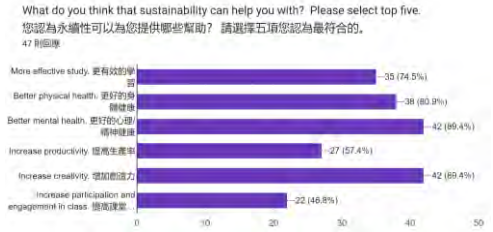

Figure 3: Participants' expectations for the potential benefits of sustainable design.

For material, wood and bamboo are considered the two most suitable materials.

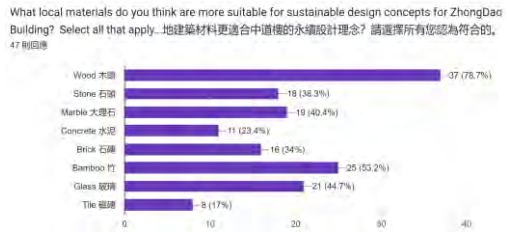

Figure 4: Participants' expectations for sustainable materials.

Energy saving equipment and acoustic control are believed to be the main missing sustainable design strategies in the ZhongDao Building. Two additional comments were received for this question are lack of moisture control and lack of sunshade and rain shelter facilities.

Figure 5: Participants' expectations for sustainable design approaches.

Suggestions additional to the questionnaire are 1) adding grass, paved pedestrian pathways, and leisure area, 2) incorporating more natural elements and natural scenes, and 3) providing more functions than merely a place for academic learning.

7. GREEN SCHOOL DESIGN DEVELOPMENT

The vision of the ZhongDao building renovation is to apply green design principles and elements, analysed and generated from the case studies and the questionnaire, to improve the sustainability scores and increase occupants' comfort levels in the existing three areas of the ZhongDao building. The following design principles and elements are divided into three main categories: energy, materials, and well-being. They are then defined to serve as guidelines to direct the conceptual design planning for the renovation of ZhongDao building and other Green Schools in Taiwan.

7.1 Proposed design principles

The vision of the ZhongDao building renovation is to apply green design with the following principles.

For energy:

- Optimize the use of the building site, location, and environment to reduce energy use and improve interior comfort.
- Adopt the cradle-to-cradle philosophy to design high-quality, healthy, and energy-responsible interior spaces to address the limited natural resources issue in Taiwan.
- Utilize sustainable design to model and promote sustainable concepts, raising environmental awareness among residents.

For materials:

- Create multi-purpose spaces to maximize efficiency in consolidating costs and support.
- Minimize the use of chemical products to reduce the harmful effects of off-gassing on the environment and human well-being.

For wellbeing:

- Foster a supportive working and learning environment to encourage creativity, professionalism, collaboration, and interactions among students, faculties and staff.
- Integrate the surrounding natural environment with the building's interiors to enhance residents' well-being.
- Incorporate modularity and flexibility to allow for changes, especially in coping with future pandemics.

7.2 Proposed design elements

The following design elements represent the approaches used to guide the sustainable strategies of design.

For energy:

- Limit reliance on non-renewable energy.
- Utilize daylighting to create well-lit indoor areas to reduce reliance on artificial lighting and promoting occupants' health.
- Employ natural ventilation for summer cooling to reduce air-conditioning use maximizing occupant comfort and maintaining good indoor air quality.
- Incorporate glass in interior layouts to avoid obstructing visual access to natural light and the outside view from one space to another.
- Adopt operable windows to allow to provide better control over natural ventilation and lighting according to demands.
- Use shading products to protect the interior from summer sun and maximum the use of winter sunlight.

For materials:

- Maximize the use of existing materials, furniture, and fixtures.
- Utilize local non-toxic, low-VOC materials and locally manufactured products to minimize the use of imported materials.
- Use durable and reusable products to minimize maintenance and replacement demands.

For well-being:

- Offer opportunities for natural light and views.
- Develop exterior spaces, allowing views out to the site and to campus.
- Adopt native plants to minimize irrigation, fertilization, pesticide and maintenance demands, and to provide a teaching opportunity to allow students to learn local plants species.
- Adopt natural methods to prevent insects from entering the interior spaces without using chemical insect repellent.
- Incorporate ergonomics solutions to improve posture and alignment and to limit physical stress.

7.3 Design application

The proposed design principles and elements are applied to redesign the Design Department's office, ZhongDao Building's lobby and terrace, but not the entire building due to time constraints.

7.3.1 Office

The office redesign focuses on better ventilation and improved space utilization.

- All windows have tilt-turn parts.
- Ceiling fans are added.
- Most of the materials are existing or used.
- Greenery is adopted.
- Low-VOC and non-toxic materials are included.
- All materials are produced within 500 miles.

Figure 6: Existing office

Figure 7: Proposed design

7.3.2 Lobby

The lobby redesign focuses on improving air circulation and the thermal effect on the whole building.

- All materials are recyclable and chemical-safe.
- Native water-conserving plants are adopted.
- Local CNC prefabrication is utilized.
- Wall-mounted greenery is employed.
- Wood is widely used.
- All materials produced within 500 miles.

Figure 8: Existing lobby

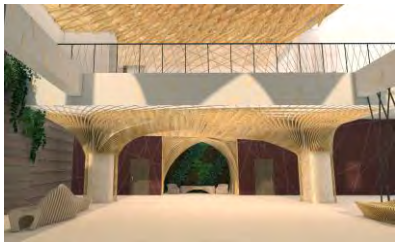

Figure 9: Proposed design

7.3.3 Terrace

The terrace redesign focuses on providing a relaxing open green space.

- Most of the materials used are recyclable.
- Native water-conserving plants are adopted.
- At least 25% of the terrace is vegetated.
- Local CNC prefabrication is utilized.
- All pavers are permeable.
- Wood is widely used.

- All materials are produced within 500 miles.
- Wood pavers are made of recycled wood plastic composites.

Figure 10: Existing terrace

Figure 11: Proposed design

8. CONCLUSION

In conclusion, the paper sheds light on the important role of Green Schools, emphasizing the dual focus on environmental sustainability and the holistic well-being of students, faculties, and staff in Taiwan. A deep dive into survey findings revealed distinct user expectations, centering around acoustics, ventilation, greenery, and natural light. These expectations formed the bedrock of tailored guidelines for sustainable school design. Furthermore, the paper unveiled insightful suggestions from the community, including a desire for natural elements, scenes, pedestrian and leisure areas, and multi-functional spaces beyond academic learning. Integrating these findings, the paper proposed design principles and elements concentrate on optimizing energy use, material choices, and fostering well-being.

Beyond a theoretical framework, the approach of this paper found practical application in the redesign of Nanhua University's Zhongdao building. This not only validated the theoretical stance but also presented a tangible demonstration of the approach's real-world impact. Navigating the complex landscape of sustainable renovations, the paper advocates for a pragmatic solution: fast-tracking partial LEED compliance. This approach concentrates on vital improvements, effectively addressing environmental concerns while aligning with the community's vision for a greener and more functional educational space.

REFERENCES

1. Shivanna, K. R. (2022). Climate change and its impact on biodiversity and human welfare. *Proceedings of the Indian National Science Academy, 88*(2).

2. Boeri, A., & Longo, D. (2013). Environmental quality and energy efficiency: sustainable school buildings design strategies. *International Journal of Sustainable Development and Planning, 8*(2), 140-157.

3. Ashida, A. (2022). The role of higher education in achieving the sustainable development goals. In *Sustainable Development Disciplines for Humanity: Breaking Down the 5Ps—People, Planet, Prosperity, Peace, and Partnerships* (pp. 71-84). Singapore: Springer Nature Singapore

4. Su, Z.-Y., Jeng, J.-H., & Lin, C.-R. (2007). Application of Geographic Information System for Land Use Capability Classification and Land Use Suitability Evaluation. *Journal of Soil and Water Conservation, 39* (4), 333 - 354.

5. Central Weather Bureau. (2023, January 16). https://www.cwb.gov.tw/V8/C/W/OBS_Top.html.

6. Khan, A. (2019). Heat related illnesses. Review of an ongoing challenge. S*audi Medical Journal, 40*(12), 1195–1201.

7. Ko, Y. C. (1996). Air pollution and its health effects on residents in Taiwanese communities. *The Kaohsiung journal of medical sciences, 12*(12), 657-669.

8. Feigenbaum, E. A., & Hou, J. Y. (2020). *Overcoming Taiwan's Energy Trilemma*. Carnegie Endowment for International Peace.

9. Bureau of Energy, Ministry of Economic Affairs. (2016). *Government Agencies Energy Consumption Guidance Manual*.

10. Chuang, Y. (2005). A Green University's Theory and Practice - A Case Study of Evaluation Indicator System. [Master's thesis, National Kaohsiung Normal University of Environmental Education].

11. Coudenys, B., Strohbach, G., Tang, T., & Udabe, R. (2022). On the Path Toward Lifelong Learning: An Early Analysis of Taiwan's 12-Year Basic Education Reform. E*ducation to Build Back Better*, 75–98.

12. World Weather & Climate Information. (n.d.). *Average monthly humidity in Madison (Wisconsin)*, the United States of America. https://weather-and-climate.com/average-monthly-Humidity-perc,madison-wisconsin-us,United-States-of-America.

13. Dorschner & Sasaki, (2008). *Program Document School of Human Ecology*, Addition and Renovation, UW-Madison.

14. Richter, B. (n.d.). *Nancy Nicholas Hall designated LEED Gold*. https://news.wisc.edu/nancy-nicholas-hall-designated-leed-gold/

PLEA 2024 WROCŁAW
(Re)thinking Resilience

Interior architectural design method to enhance the users' emotional and mental well-being

Toward the synergy of selected models of biophilic design and interior architectural design for adaptive reuse

MAGDALENA CELADYN[1], ANNA MICHALEK[1]

[1] Faculty of Interior Design, Academy of Fine Arts in Krakow, Krakow, Poland

ABSTRACT: The application of the concept of biophilia into interior architectural design is analysed in the literature on the subject in the context of its influence on several user-related questions. These combine stress reduction, stimulation of creativity, acceleration of the healing process, as well as improvement of the psychological health of users. Interior architectural design for adaptive reuse includes direct references to the sustainability-oriented requirement for the efficient management of resources. This design scheme concentrates on the exploration of the physical longevity of single artefacts or developed spatial structures featuring indoor environment. It provides users of the newly conceived as well as remodelled internal spaces with multisensorial experience, initiates their emotional engagement with particular interior's components and interior as a whole, and offers possibility to track multidimensional connotations. This article aims at the assessment of synergic application of selected patterns of biophilic design, in particular with its responsiveness-oriented model, and the adaptive-reuse design scheme with the focus on its immaterial aspects. It considers the methodology of interior architectural design used to enhance the users' emotional and mental well-being. The study indicates that Interior Architecture Design for Adaptive Reuse and responsiveness-oriented scheme of biophilic design are the complementary strategies that enhance the health and well-being of the users, through the intensification of their emotional engagement, provision of multisensorial experience and exploration of cultural connotations.
KEYWORDS: biophilic design, responsiveness, interior architectural design, adaptive reuse.

1. INTRODUCTION

The paper discusses the enhancement of psychological health and well-being of occupants of interiors, achieved with the inclusion of patterns of selected biophilic design models, as well as the guidelines for the Interior Architectural Design for Adaptive Reuse (IADfAR) [1], which is based on the reintroduction of reclaimed building materials and products from refurbished or demolished buildings to internal spaces.

The constructive effects of inclusion of biophilia into the design of the built environment are provided by two main approaches. These embrace the close proximity and direct visual contact of the occupants with plants, as well as advanced stimulation of „positive response to artificial creations that follow geometrical rules for the structure of organisms" [2]. The considering of the elements of regenerative design (e.g., improvement of users' health), and methods to support the resilience of natural environment (e.g. implementation of renewable materials) [3] strengthen the position of biophilic design. The selected biophilic design schemes combine attributes that allow to consider this design approach specifically through the multidimensional analysis of material substances completing the built environment in view of their impact on the character and intensity of the beneficial interrelationship between human and nature [4,5].

The IADfAR scheme, concerning the retaining of material substance within the structure of the constitutive components of interior spaces, refers directly to the sustainable demand for the efficient management of resources. Therefore, the conversion of reclaimed building products as deconstruction or demolition waste to valuable structural interior components, can be treated as a complementing design method for the widely recognized concept of adaptive reuse of existing buildings [6, 7]**.** The study, examining the effectiveness of the adaptive reuse design framework in view of the users' psychological comfort, concentrates on its intangible aspect.

This article aims at the assessment of synergic application of selected patterns of biophilic design, in particular with its responsiveness-oriented model [4], and the adaptive-reuse design scheme with the focus on its immaterial aspects, into the methodology of

interior architectural design as means to increase the users' emotional and mental well-being.

2. MATERIAL AND METHODS

The study is based on selected points of the responsive biophilic design model and Interior Architectural Design for Adaptive Reuse of materials and products, discussed in its intangible aspect.

The application of the concept of biophilia into interior architectural design is analysed in the literature on the subject in the context of its influence on several user-related questions. These problems, combining stress reduction, stimulation of creativity, acceleration of the healing process, as well as moderating of psychological health of users, which are solved through the implementation of various design patterns. These include the introduction of the characteristics which directly refer to the nature into internal spaces, the usage of the objects that represent and simulate those present in the nature, formal exploration of the phenomena of natural environment, as well as the examination of the exchange of information between man-made and natural environments. This concept, by Salingaros and Madsen [4], concerns the elevating of the occupants of interiors through the broad exposure of the properties of natural material substances reclaimed and reintroduced to form new objects.

Interior Architectural Design for Adaptive Reuse is directly derived from the sustainability-oriented requirement for the efficient management of resources. This scheme concentrates on the exploration of the physical longevity of single artefacts or developed spatial structures featuring indoor environment. The design model provides users with multisensorial experience, initiates their emotional engagement with particular interior's components and interior as a whole, as well as offers occupants the possibility to track multidimensional connotations. the influencing users' perception and encouraging their emotional connection with the nearest environment is to support their psychological comfort.

3. BIOPHILIC DESIGN GUIDELINES

The main objective of biophilic design, term coined and introduced by Kellert [8], is to translate the biophilia understood as phenomenon of the inherent human affinity to affiliate with the processes and systems within the natural environment [9]. Biophilic design is to transfer this association with nature into the approach for designing the built environment [8,10] in a search for reconciliation of human with nature. The biophilic design allows for overcoming the "separation that architecture placed between itself and nature" [4], and thus reconstructing the connectedness between the habitat and nature. The biophilic design aims to shape artificial environments that have a positive effect on individual's health and well-being [5] and to support improved health, well-being, and performance as measured through the personal biometrics and self-rated mood [11].

The models of biophilic design combine the typology of various categories, patterns, and attributes that organize the interior architectural design methodology. There are several selected schemes to accomplish the concept of biophilia in creating of indoor environment and its components. Among these well-established models are schemes founded on valorisation [10], application [12], as well as responsiveness [4].

3.1 Valorisation scheme

Kellert defines biophilic design as an approach to achieve "long-term sustainability of restoring and enhancing people's positive relationship to nature in built environment" [10], and situates it within the design paradigm identified as a "restorative environmental design". Biophilic design being an essential element within this construct assures, together with the low-environmental-impact design strategy to minimize a negative impact on natural environment, the positive environmental impact of an artificial setting. Biophilic design is identified as an approach that encourages beneficial contact between people and nature raised within the built environment, that is essential for the sustaining of the users' physical and mental well-being.

According to Kellert, enhancement of the users' attachment to buildings and places, which is a condition for the responsible usage and careful maintenance of the built environment in longer perspective, makes specific value of biophilic design.

3.2. Application model

Browning et al. propose biophilic design scheme, named for the purpose of this study as an application model. This scheme is intended to explore and incorporate the nature-design relationships in the creation of built environment, makes a "series of tools for understanding design opportunities including the roots of the science behind each pattern, then metrics, strategies and considerations for how to use each pattern" [12]. The authors underline that their aim is promotion of a creativity in an application of the scientific research on biophilia into design, in order to enhance health and well-being for individuals and society in an effective way. They admit that this approach supports measurable, positive impact of biophilic design on health, while strengthening the empirical evidence for the human-nature connection.

The biophilic design scheme encompasses the category of Natural Analogues, featuring various

classifications of the user's experience of biophilia within the built environment. Among the design patterns which belong to this category is Material Connection with Nature. This pattern enables search for the indirect evocations of nature in the shaping of interior spaces. It examines the possibilities of providing a distinct meaning of a specific place with materials and elements acquired from the local natural sources, processed to a limited extent, and carefully exposed. Recommendations concerning the application of this pattern into design comprise variability of different materials and techniques of their introduction, as well as usage of natural materials of limited processing instead of their synthetic imitations.

According to Browning et al., in spite of still limited evidence to support beneficial relationship between health and biophilic design attributes, the design pattern named as Material Connection with Nature reveals its positive influence on experience of the place, in particular on enhancement of the users' overall psychological comfort.

3.3. Responsiveness-oriented framework

The responsiveness-oriented approach to "support biophilia hypothesis from the independent directions", proposed by Salingaros and Masden [4], underlines the phenomenon of the specific exchange of information between humans and their nearest environment, between natural and artificially conceived surroundings. This process of a mutual communication assures the buildings occupants' emotional engagement, and subsequently the sense of belonging and well-being.

The exchange of information, essential for the designing of artefacts which constitute interiors, is named by the authors as a "neurological nourishment" [4]. This process exercised with the application of diverse technical solutions within the indoor environment, is to emulate the formal complexity of natural objects through the investigation of the physical characteristics of introduced natural, renewable materials. The design model explores ways the material substance is implemented to form objects patterned on nature, to reach the users' neurological connectivity and nourishment, and thus, to provide them with a direct and intense experience of relationship between the built and natural environments.

The scheme, following the biophilia concept, proposes fourteen measures to accomplish the design for responsiveness, which imitates the visual and performative values of natural objects. These steps comprise determinants being related to the physical, as well as intangible aspects of the material substance of which the factors describe the issue of users' neurological connectivity with artefacts.

Among the design methods indicated by authors that address the questions of physical characteristics and structural solutions, while proving their potential in designing interior spaces and their components of clear responsive appeal, are the following:

- Reuse of these locally reclaimed natural materials and products from older buildings, aimed to confirm their high informational content;
- Usage of natural unfinished materials;
- Adjusting design solutions to introduce the available materials of different sizes, and thus to reduce possible production of solid waste;
- Inversion of small-scale construction elements;
- Introduction of small-scale objects into the newly conceived structures of building materials of limited finishing.

The design techniques to exercise this scheme concerns mostly the analysis of physical parameters of reused building products and materials and feasibility problems, as well as information-related questions resulting from the materials aspects.

4. INTERIOR ARCHITECTURAL DESIGN FOR ADAPTIVE REUSE

Interior Architectural Design for Adaptive Reuse of reclaimed building materials and products concerns an essential sustainability-related question of the minimisation of the negative environmental impact of built environment on the natural one. IADfAR features an alternative proposal for retaining the material substance acquired from the locally available existing objects and their reintroduction into the structure of the newly conceived interior components. This design model focusing on the creative absorption of the pre-used products within the newly conceived interior components, allows interior architecture to respond to changing conditions, due to the building's deteriorating performance occurring over time, in an environment-responsible manner. This approach underlines systemic adaptation of the secondary products and objects in forming new interiors or modifying the existing ones. It reveals the discipline's possible role in accomplishing the resilience in designing through the conservation of resources.

4.1. Materiality context

The IADfAR model can be measured within its materiality context. This scheme proposes the accomplishment of an effective management of resources and promoting the closed circuit of natural resources. It is implemented through the reintroduction and formal assimilation of the salvaged building materials and products, without their significant reshaping or reprocessing, into the

building setting in order to create multifunctional constitutive interior components (i.e. external walls accompanied on their inner side by various technical devices or biological finishing to enhance the indoor environment quality parameters, partitions, stationary or mobile space dividers of various dimensions and spatial configurations, raised floors, integrated or suspended ceilings).

Therefore, this interior architectural design scheme allows remanufacturing of the building waste into the valuable interior component being assembled with the secondary materials and products reclaimed from refurbished or demolished buildings. The interior component itself, becomes a "passive design instrument for effectiveness of waste management" [1], playing a specific role in moderating interrelationship of designed and natural environments.

4.2. Intangibility context

The intangible context of discussed design model covers the multidimensional stimulation of the occupants' perception of interior components made with pre-used parts. The reintroduction of salvaged resources complies with the assumption that design concept "endorsed with creatively implemented building technology and selection of building materials offers the inner spaces end-users' multi-sensorial experiences, while forming emotional bonds with their immediate physical environment" [13].

This design model offers the opportunity for an occupants for an individual, subjective interpretation of these interior components featuring single objects as well as complex, functionally and spatially developed structures. This scheme is to establish a kind of the users' re-engagement and "intimate connection" [14] with the objects, defined through their symbolic and meaningful values, source, formation, as well as the maintenance throughout their lifespan.

The emotional experience accompanying the first contact with an object provokes subsequently the developed reflective response. The phenomenon of place attachment involves affirmative and positively experienced connections developed from the affective, and then cognitive responses occurring between individuals and the elements of their physical environment. The reintroduced materials and products featuring interior components strengthen a design concept, while offering opportunities to the occupants to experience it, and to develop their own psychological comfort.

The process of captivating the occupants' attention, moderating their psychological comfort, and influencing their positive reactions toward the interior components completed according to IADfAR, comprises the following:

- Multisensorial experience, enhanced due to the perception of the reclaimed materials' physical attributes and techniques applied to their exposure. The multidimensional exploration of artefacts leads to their recognition and further acceptance of place built with them.
- Emotional engagement, gained through the experience of meaningful and expressive properties of reintroduced secondary products and materials of "charismatic quality" [15] gained over time. This is to evoke the users' emotional attachment caused by the provided services and "information it contains and the meaning it conveys" [15]. The initial affective response is followed by arousing of topophilia understood as individually developed and emotionally-based positive reception of space, as well as the occurrence of emotional durability. This is defined as creating "deeper, more sustainable bonds between people and their material things" [15], accompanied by the readiness to reduce the consumption, decrease in waste production, and finally to offer an alternative for the throwaway society.
- Cultural references, which add meaning to objects allow to discover and then to explore the multitude of their historic and aesthetic considerations. These connotations provide the sense of cultural continuity demonstrated by reintroduced materials and products of historical or aesthetic value. They allow occupants to reach the reflective level of conscious interpretation of experienced emotions, which are caused by interaction with reintroduced objects and build up users-object relationship on specific "layered complexity" rich of various citations, including cultural and historical ones. These condition the occurrence of empathy and attachment toward these objects [15].
- Reflective response based on the semantic analysis of the experience of reintroduction of pre-used materials and products, supplemented with the awareness of environment-friendly practises. This leads to the mature consideration based on "rationalization and intellectualization" [16] of the product-interior component made with pre-used elements and indicates the meaning assigned to their complex inclusion into interiors.
- Behavioural effect, fostering solid user-object relationship due to the recognition of

environmental dimension in the design of interior components. The growth of this attitude determines the development of the product attachment, expressed by the rational and careful usage of objects and their systematic maintenance in long-time perspective.

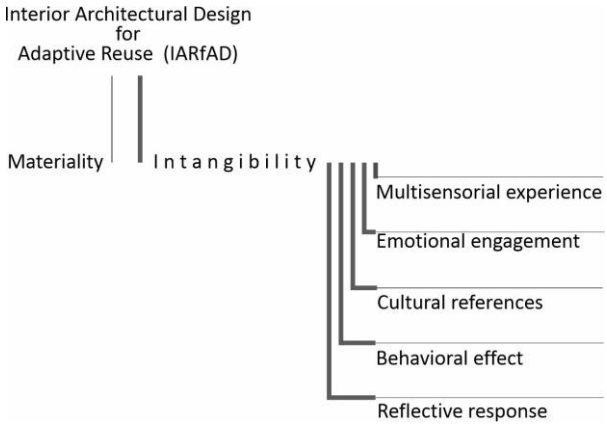

Figure 1: Intangibility context of scheme of interior architecture for adaptive reuse.

The above-mentioned main features associated with the intangibility perspective of IARfAD are displayed in Figure 1. The concept of the substitution of originally conceived components with these made with the reclaimed parts, requires consideration at the very initial stage of design process and the application of critical design approach. It is necessary since this design scheme challenging the well-established and commonly accepted aesthetic conventions "contributes to new ways of thinking about and developing material culture" [17]. This design model involves the development of innovative techniques based on the broad exposition of physical characteristics of the acquired pre-used parts.

The exemplary design techniques to employ the interior architectural design for adaptive reuse with emphasis on its intangible context, comprise the following:

- Exposition of physical imperfections, visible minor physical damages, scratches, stains, cracks of reused salvaged objects of material value as the evidence of constant evolvement of objects and accumulation of the time-related marks
- "Truth windows" placed within the structure of selected interior components (e.g. multifunctional fixed or mobile space dividers) to allow the exposition of the secondary products being in symbiotic relationship with other parts
- Appearance of reclaimed objects of clearly defined original purpose in new functional or spatial contexts
- Distinctive mechanical working and assembling techniques assuring simple dismantling or further replacement of pre-reused parts or products for further reuse, modernisation or reconfiguration according to the users' needs
- Structural honesty revealing the physical solutions applied to incorporate the reclaimed parts forming a component
- Honest materiality to expose the objects' texture and surface achieved through the limitations in the amount of the conservation working on salvaged products before their reintroduction into interior components.

5. DISCUSSION

The biophilic design is to create a positive, multidimensional, and valued human experience of nature within the built environment, in particular in interior spaces. The persistence of biophilic design experience is more likely conditioned by the integration of its patterns with the programming or infrastructure of the place [12].

The intensification of the users' response and increase in the quality of emotional experience for the illustration of human-nature connection in design, can be examined in the context of merging biophilic design interventions with other design guidelines. Interior Architectural Design for Adaptive Reuse is a scheme with the potential to reinforce biophilic design's role in moderating psychological comfort (Fig. 2).

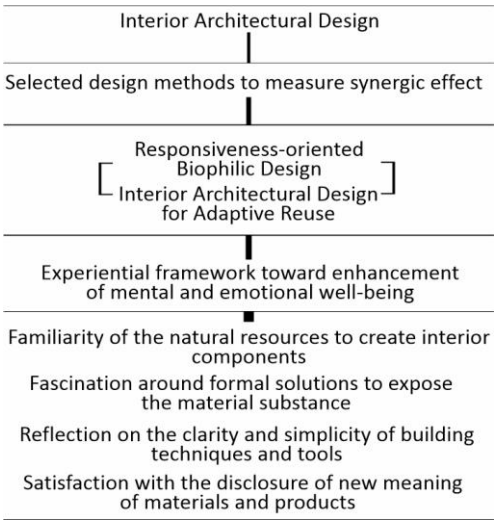

Figure 2: Implementation of responsiveness-oriented biophilic design and IADfAR in view of the users' psychological well-being enhancement.

The concept to execute an adaptive reuse of secondary materials and building products, complies with the sustainability imperative of "resourcefulness

and restraint" [14] in design. This approach emphasizes the build-up of the user-object relationship in a way that extends the initial materiality-related questions, and addresses the problem of perception and appreciation of the cultural values represented by the object.

The qualities and attributes of the natural resources reintroduced into the structure of interior components, in accordance with the IARfAD, are to evoke a "soft fascination" [18] toward these objects embedding the salvaged reclaimed parts, as well as place itself. These reclaimed natural materials that constitute interior components, attract the users' attention offering them information of a similar intensity as in the case of perceiving the attributes of natural environment. Therefore, IARfAD follows the remarks by Berto et al., that the design methods focused on a high level of the environment-related fascination engage processes affording psychological restoration of the occupants.

The interior components of a compound structure (i.e. composition of the new and secondary parts arranged in a way to fulfill functional demands, formal objectives) have the potential to assure emotional restoration, providing users with the experience of nature-related preservation and adaptation of cultural and heritage values expressed in the reclaimed objects.

6. CONCLUSION

This study concerned the question of moderation of psychological health and well-being of the occupants of interiors. It was considered with regard to the attributes of selected biophilic design models, in particular these related to the psychological nourishment, as well as Interior Architectural Design for Adaptive Reuse. The main area of the possible impact of this design scheme on the psychological well-being of users concentrated on the intangible context of the scheme.

IADfAR and the biophilic design for responsiveness were discussed as complementary design strategies for the enhancement of health and well-being of users through their emotional engagement with interior components as the objects of dual structure.

The analysis of this problem revealed that synergetic implementation of both above-mentioned design methods results in the psychological well-being assured with various elements. These combine the intensifying of the multisensorial perception of interiors, moderation of the occupants' sense of continuity in cultural proficiency coming from the reused building parts, improvement of mental retreat as well as the emotional relief within the space filled with objects made with the well-known natural materials of positive cultural connotations.

REFERENCES

1. Celadyn, M., (2019). *Interior architectural design for adaptive reuse in application of environmental sustainability requirements.* Sustainability, 11, 14.
2. Salingaros, N.A., (2019). The Biophilic Healing Index Predicts Effects of the Built Environment on Our Wellbeing, In *Journal of Biourbanism*, 8, 1: p. 13–34.
3. Africa, J., Heerwagen, J., Loftness, V. and C.R. Balagtas, (2019). Biophilic design and climate change: Performance parameters for health, *Frontiers in Built Environ*ment, 56.
4. Salingaros, N.A., and K.G. Masden, (2008). Neuroscience, the Natural Environment, and Building Design. In *Biophilic design: the theory, science and practice of bringing buildings to life*, Kellert, S.R., Heerwagen J., and M. Mador, (eds.). Hoboken, New Jersey: John Wiley & Sons Inc., p. 59-83.
5. Bolten, B. and G. Barbiero, (2020). Biophilic design: how to enhance physical and psychological health and wellbeing in our built environments. *Visual Sustainability,* 13: p. 11-16.
6. Brooker, G. and S. Stone, (2004). *Re-readings. Interior architecture and the design principles of remodelling existing buildings*. London: RIBA Enterprises.
7. Plevoets, B., and K. Van Cleempoel, (2013). Adaptive reuse as an emerging discipline: an historic survey. In *Reinventing architecture and interiors: a socio-political view on building adaptation,* G. Cairns (ed.), London: Libri Publishers, p. 13-32.
8. Kellert, S.R. (2005). *Building for life: Designing and understanding the human-nature connection.* Washington, DC: Island Press.
9. Kellert, S.R. and E.O. Wilson, (1993). *The Biophilia Hypothesis.* Washington, DC: Island Press.
10. Kellert, S.R., (2008). Dimensions, elements, and attributes of biophilic design, In *Biophilic Design. The Theory, Science, and Practice of Bringing Buildings to Life*, S.R. Kellert, J. Heerwagen and P. Mador, (eds.) Hoboken, NJ: John Wiley & Sons, p. 3-19.
11. Ryan, C.O. and W.D. Browning, (2018). Biophilic design. In *Encyclopaedia of Sustainability Science and Technology*, R. Meyers, (ed.), New York, NY: Springer.
12. Browning, W.D., Ryan, C.O., and J.O. Clancy, (2014). *14 Patterns of Biophilic Design*. Terrapin Bright Green, LLC: New York, NY.
13. Celadyn, M. and W. Celadyn, (2022). *Apparent destruction architectural design for the sustainability of building skins.* Buildings, 12, 8.
14. Walker, S., (2006). *Sustainable by Design: Explorations in Theory and Practice*. New York: Earthscan from Routledge.
15. Chapman, J., (2015). *Emotionally Durable Design. Objects, Experiences & Empathy*. London and New York: Routledge Taylor & Francis Group.
16. Norman, D.A., (2004). *Emotional Design: Why We Love (or Hate) Everyday Things*. New York, NY: Basic Books.
17. Walker, S., (2010). Temporal Objects - Design, Change and Sustainability. *Sustainability,* Vol. 2: p. 812-832.
18. Berto, R., Barbiero, G., Pasini, M. and P. Unema, (2015). Biophilic Design Triggers Fascination and Enhances Psychological Restoration, In the Urban Environment, In *Journal of Biourbanism*, p. 27-34.

PLEA 2024 WROCŁAW
(Re)thinking Resilience

Embodied Carbon of Building Enclosures

PROF MARK GORGOLEWSKI[1]

[1]Toronto Metropolitan University, Toronto,

Canada

ABSTRACT: Building enclosure design has until recently focused on thermal performance and its impact on operational carbon emissions. Embodied carbon emissions associated with building enclosure systems are not so well understood but contribute significantly to the emissions over a building's lifespan. This paper outlines a methodology for calculating the embodied carbon of building enclosure systems and presents the results for the embodied carbon intensity of wall, floor and roof systems typically used for larger buildings in Canada. The resulting database will inform design at the earliest stages through the lens of embodied carbon prior to the establishment of detailed design information, enabling designers to choose optimum enclosures that balance embodied and operational carbon emissions across the building's life cycle, and to consider material substitutions to reduce emissions.

1. INTRODUCTION

As operational energy use in buildings and the resulting carbon emissions are reduced by designing high performance buildings and decarbonizing electrical grids, the impact of embodied carbon becomes more significant. The impact on a building's total lifecycle carbon emissions by embodied carbon emitted to create and install all the materials and components required in construction is fast becoming a driving factor. Some predictions suggest that between 2023 and 2050 embodied carbon could represent the majority of a new building's carbon emissions [1].

Building enclosure design has until now mainly focused on thermal performance and its impact on operational carbon emissions. This area is now well understood, and industry-trusted tools exist to evaluate thermal bridging and whole building thermal performance [2]. Conversely, most embodied carbon analysis to date has focused on structural materials such as concrete and steel due to the large quantities required for mid- and high-rise construction and their high embodied emissions impact [3]. Embodied carbon emissions associated with building enclosure systems are not well understood but contribute significantly to the emissions over a building's lifespan. Furthermore, there may be trade-offs between operational and embodied carbon in building enclosure design since these systems are significant for their impact on both an operational and embodied carbon. Decisions made early in the design phase are critical and need to be informed through both an operational and embodied lens. It is important to understand the balance between embodied impacts of various envelope and their operational emissions [4].

This research aims to establish an industry and municipality-accepted methodology for calculating the embodied carbon of building enclosure systems in Ontario, Canada. In addition, utilizing this methodology, the study seeks to quantify the embodied carbon intensity of commonly used enclosure systems used in office, multi-unit residential and institutional buildings (Ontario Building Code (OBC) Part 3 buildings) which typically use high carbon intensity materials [5]. The intention is to provide tools to help design teams to start to consider and address this issue. This data will be used to prepare guidance to design teams to help with decision making on appropriate low carbon enclosure systems. The resulting database will inform design at the earliest stages, prior to the establishment of detailed design information, through the lens of embodied carbon, enabling designers to choose optimum enclosures that balance embodied and operational carbon emissions across the building's life-cycle and consider material substitutions to reduce emissions.

Low energy and low carbon use buildings require a high-performance thermal enclosure to significantly reduce environmental loads; typically, this leads to added number, quality and quantity of materials within the specified assemblies. However, this added material impact must be balanced with low embodied carbon enclosure design. This relies on the use of low carbon materials as well as durable materials that minimize maintenance and replacement needs throughout the building's life cycle.

2. METHODOLOGY

Twenty-six wall, roof and floor systems were chosen for analysis based on their ability to meet the thermal performance of the Toronto Zero Emission

Buildings Framework [6]. These were selected after consultation with industry and review of commonly used building enclosure systems typically used in commercial, institutional, and multi-unit residential buildings in Ontario. The City of Toronto Zero Emissions Building Framework (2017) Appendix C: Parametric modelling results [7] was used as a reference point to set recommended baseline target effective R-values. This helped to establish reasonable thermal performance targets that both meet current needs of designers as well as meeting future performance requirements of local energy codes such as the Toronto Green Standard Version 4 [6]. Thus, all assessed wall enclosures aimed to achieve a thermal performance target of RSI-4.4 m_2K/W (R-25), roofs aimed to achieve RSI-5.3 m_2K/W (R-30) and for the floors RSI-4.4 m_2K/W (R-25) was used.

The effective R-value of each of the selected assemblies was calculated and adjusted to achieve as close as possible to the above targets. This process followed building science best practice principles as well as NECB-2017 [8] and ASHRAE Fundamentals [9]

An example of an effective R-value calculation is provided in Table 1 for wall W01, which includes the assembly description, material thickness, material conductivity, effective R-value and nominal R-value. Assumptions and data sources are included for each material.

Table 1: Example of calculations for R-value of wall assembly

W01 R-Value Calculations:

Assembly Description	t_{si} [mm]	t_{in} [in]	k [W/=mK]	C (USI) [W/m²K]	RSI Effective [m²K/W]	R-effective (ft²·°F·h/BTU)	R-nominal (ft²·°F·h/BTU)
Interior Film					0.12	0.68	
Interior Gypsum Board	12.7	0.5	0.16	27.04	0.04	0.21	
Steel Stud-Framed Wall	63.5	2.5	0.49	7.75	0.13	0.73	
Single-Wythe CMU Wall	203.2	8	1.18	5.81	0.17	0.98	
Self-Adhered Sheet-Applied Air Barrier and Water-Resistive Barrier (WRB) Membrane (Vapour Permeable)	1	0.03	-	-	-	-	
Semi-Rigid Mineral Fiber Exterior Insulation with Intermittent Stainless Steel Masonry Veneer Anchors	152.4	6	0.04	0.24	4.09	23.22	25.80
Air Cavity	25	0.98	0.03	-	-	-	
Anchored Masonry Veneer	90	3.54	0.79	8.78	-	-	
Exterior Air Film					0.03	0.17	
Total	**547.8**	**21.6**			**4.6**	**26.0**	**25.8**

The embodied carbon emissions analysis was carried out using the principles of the European Standard EN 15978:2011 for whole-building LCA, utilizing the Attributional (ALCA) methodology to quantify direct environmental impacts. The volume or mass of material in each layer of the assembly was calculated and then using emissions data from appropriate Environmental Product Declarations (EPDs). Table 2 illustrates the breakdown for wall W01. The material layers that have the greatest impact are highlighted in yellow to identify where most impact can be made by material substitutions. The calculations were made for a functional unit of 9 m^2 of enclosure assembly. This was to account for all assembly components that might be missed in a smaller area, such as studs, insulations pins, and anchorage systems. However, the data is reported both for 9 m^2 and also normalized for 1 m^2 carbon intensity (kg CO_2e/m^2) to simplify early design stage calculations from enclosure area take-offs. The LCA calculations assumed a building life span of 60 years. If components had a shorter lifespan, the emissions associated with replacement were included.

The material EPDs were selected from the One Click LCA database [11], or where necessary other databases such as EC3 were used. In most cases generic or industry average data (for North America where possible) was selected, but in rare cases it was necessary to search specific manufacturer data when no generic data was available or appropriate.

Table 2: Example of calculations for the embodied carbon of a wall assembly

W01 Embodied Carbon Emissions (A1-A3 Life Stages) for 9m²:

Category	Material (RDH Specification)	Description (from EPD)	Thickness [mm]	Volume of Material (m³)	Carbon Emissions (A1-A3) ($KgCO_2E$)	% of Total
Finish	Interior Paint	Eggshell acrylic paint, 1294.29 kg/m³		0.0014	0.6	0.0%
Finish	Interior Gypsum Board	Gypsum plaster board, regular, generic, 6.5-25 mm, 10.7 kg/m², (for 12.5 mm), 858 kg/m³	12.7 (0.5")	0.114	26.0	2.1%
Interior Finish Support	Steel Stud Framing	Steel stud framing for drywall/gypsum plasterboard per sq. meter of wall area (incl. air gaps per m3); 63.5 mm x 30.5 mm, gauge 25	63.5 (2.5")	*	39.0	3.2%
Back-Up Structure	Reinforced Concrete Block Masonry	Concrete masonry unit (CMU), normal weight, 2250 kg/m³ (Canadian Concrete Masonry Producers Association)	203.2 (8")	1.8	468.0	38.1%
Exterior Membrane	Vapour Impermeable Membrane	Latex-based membrane, vapor impermeable, fluid-applied, 40 mils (1mm), 1.15 kg/L, Perm-A-Barrier® NPL 10	1 (0.04")	0.009	22.5	1.8%
Exterior Insulation	Exterior Insulation Mineral Wool (Semi-Rigid)	Heavy density mineral wool board, industry average US (NAIMA), 1 m2K/W, 34 mm (1.3"), 4.2 kg/m², 123.52 kg/m³	152.4 (6")	1.35	241.9	19.7%
Exterior Insulation	Insulation Pins	5 insulation pins per panel - 169 pins in total - Hot-dipped galvanised steel; 80% recycled content - 0.28 kg/m²	-	0.000302	3.7	0.3%
Cladding Anchorage	Stainless Steel Brick Ties	Assumed 4-foot spacing for angle support - 17 anchors in total - Composed from hot-dipped galvanized cold-formed steel, USA industry average, 7769 - 7849 kg/m³ (SFIA)	-	0.001	17.9	1.5%
Cladding	Clay Brick	Clay brick (Acme Brick Company, Belden Brick Company, etc.) 2120 kg/m³	90 (3.5")	0.81	407.4	33.2%
	Total				1227.1	100.0%

*Software calculates the impact based on the area provided

W01 Environmental Emissions (A1 to C4 life stages) for 9m²:

		A1 to C4	A1-A3	A4-A5	B1-B5	C1-C4	A1-A3
Result Category	Units	Total	Construction Materials	Transportation to Site & Construction	Material Replacement & Refurbishment	Deconstruction	A1-A3 % of Total
Global Warming	kg CO_2e	1,480.13	1,221.51	40.35	140.24	78.03	82.5%
Acidification	kg SO	5.69	5.04	0.23	0.28	0.14	88.6%
Eutrophication	kg Ne	1.15	1.04	0.03	0.03	0.043	90.5%
Ozone Depletion	kg CFC11e	0.000079	0.000059	0.000011	0.0000014	0.0000078	74.5%
Formation of Tropospheric Ozone	kg O3e	73.50	59.15	6.51	5.12	2.72	80.5%
Fossil Fuel Primary Energy	MJ	18,376	15,327	1,147	1,338	565	83.4%
Biogenic Carbon Storage	kg CO_2e	0	0	0	0	0	

The focus of the LCA assessment was embodied carbon emissions (GWP) and this is broken down by material layer to highlight where the greatest impacts occur. However, other environmental indicators as defined by the TRACI v2.1 characterization for North America are reported for the assembly as a whole for the various life stages (lower part of Table 2). Default values in OneClick LCA for transport impacts were used. Life cycle stages A1 to A3 (product stage) [10] are the main focus as these tend to dominate and the

data is most reliable. To give some indication of total environmental impact over the full lifecycle, stages A3-A5 (construction), B (use) and C (end of life), are also reported although these are generally a small proportion of the total carbon emissions and can vary by location, site, etc. Biogenic carbon, which refers to the carbon that is taken out of the atmosphere and stored in biological materials such as trees or plants through the process of photosynthesis, is also reported where appropriate.

3. DISCUSSION

The results of the analysis for nine walls and five roofs are summarised in the form of comparative charts (Fig 1, Fig 2).

The charts show the total estimated life cycle stage A1 to A3 emissions, in addition emissions associated with A1 to A5 stages are indicated as well as the estimated reduction in assembly emissions resulting from biogenic carbon (to the left of the vertical axis). The intent of representing the data in this way is for readers to quickly understand assemblies with the highest and lowest embodied emissions, as well as to compare these assemblies with proposed project-specific assemblies. This can help to simplify early-stage decision making.

The pie charts in Figure 3 represents the total embodied carbon emissions for seventeen wall enclosure systems (including the last four (W14 to W17 which are refurbishment options for existing walls). The size of each circle is proportional to the overall impact; large pies show a larger overall carbon emission. The pie slices represent major enclosure component categories.

These pie charts indicate that the embodied carbon emissions of enclosures are generally dominated by the cladding material, insulation layers, and backup structure. Other components such as interior finish, paint, connectors, etc have limited impact. Thus, the attention of designers should be to carefully choose these three components' and look for low emissions alternatives. For example, W06 and W07 are precast concrete panels and the backup structure component is most significant. While for W04 where CLT is the backup structure, it is minor.

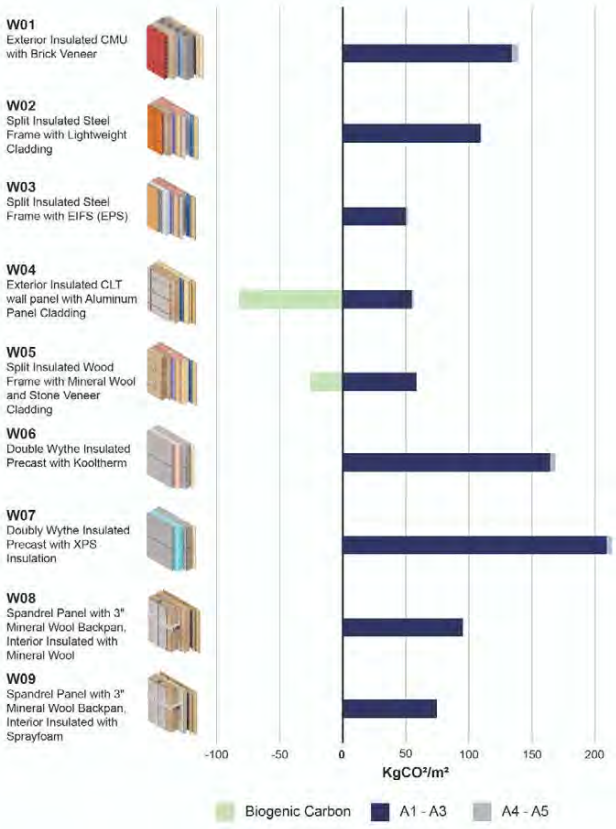

Figure 1: Summary of embodied carbon emissions for nine walls

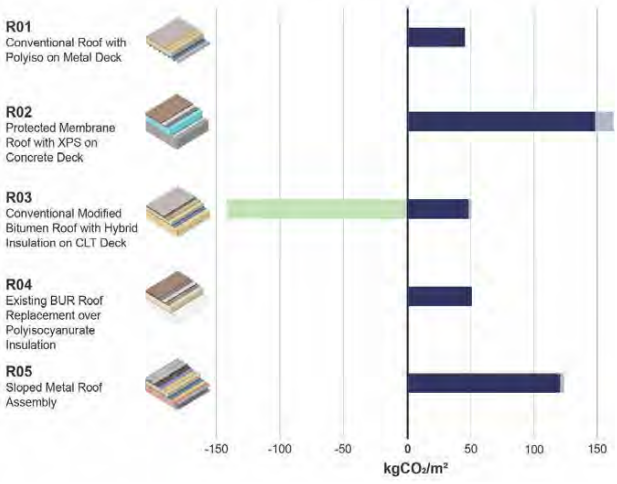

Figure 2: Summary of embodied carbon emissions for five floors

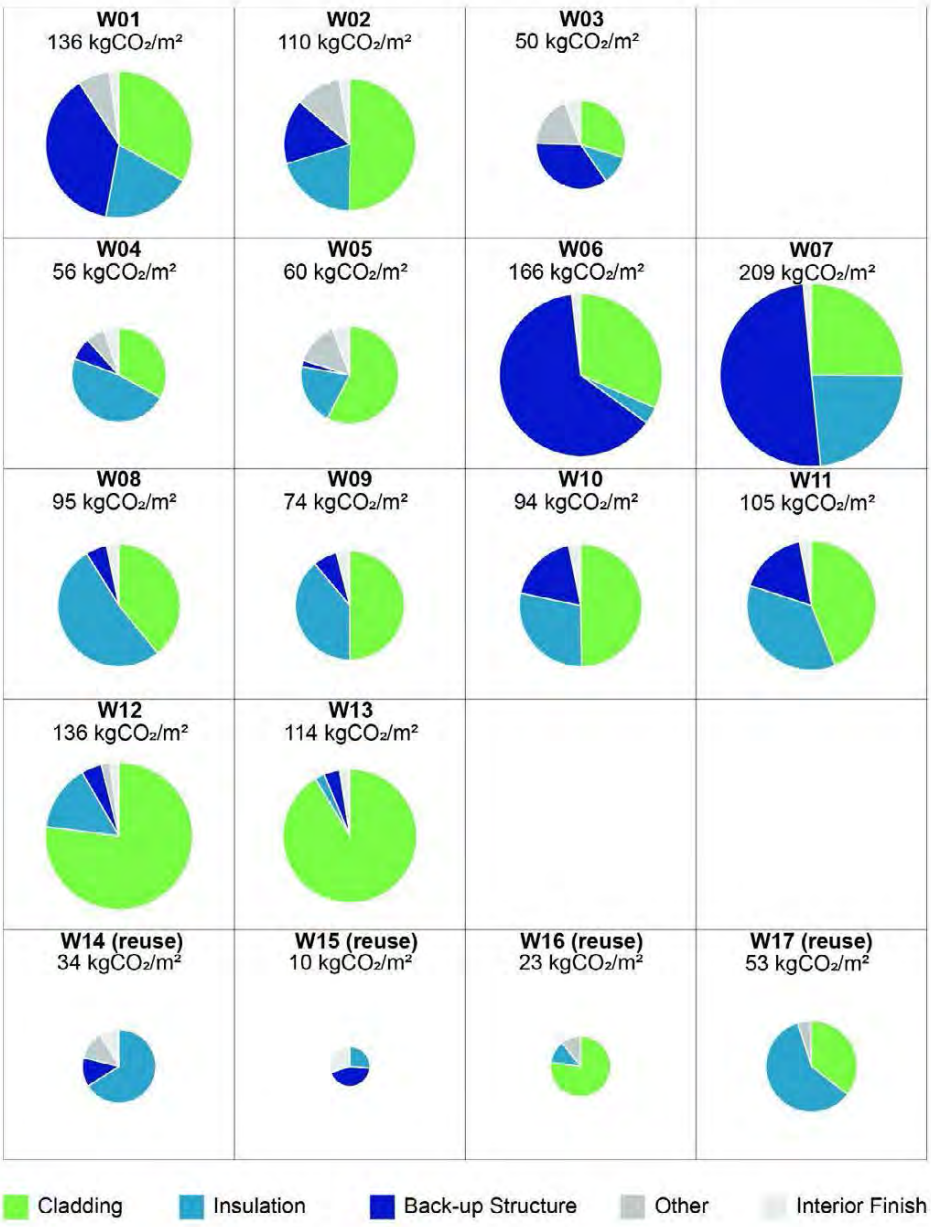

Figure 3: Comparison of the embodied carbon emissions for walls

The data should be viewed as a snapshot since new and updated EPDs are constantly becoming available. Nevertheless, when armed with the embodied carbon breakdown by assembly component, users can readily understand which components have the most significant contribution to whole assembly carbon content, and which layers are most worthwhile to investigate further to seek improvement by selecting project specific materials, substituting these preliminary EPD values with their own sources.

A summary sheet is available for each enclosure system which provides a detailed breakdown of the results (see https://www.rdh.com/blog/embodied-carbon-resources-for-building-enclosures/). This includes a graphic such as the one shown in Figure 4 which illustrates the enclosure system and provides a visual indication of the embodied carbon emissions by layer for wall W01.

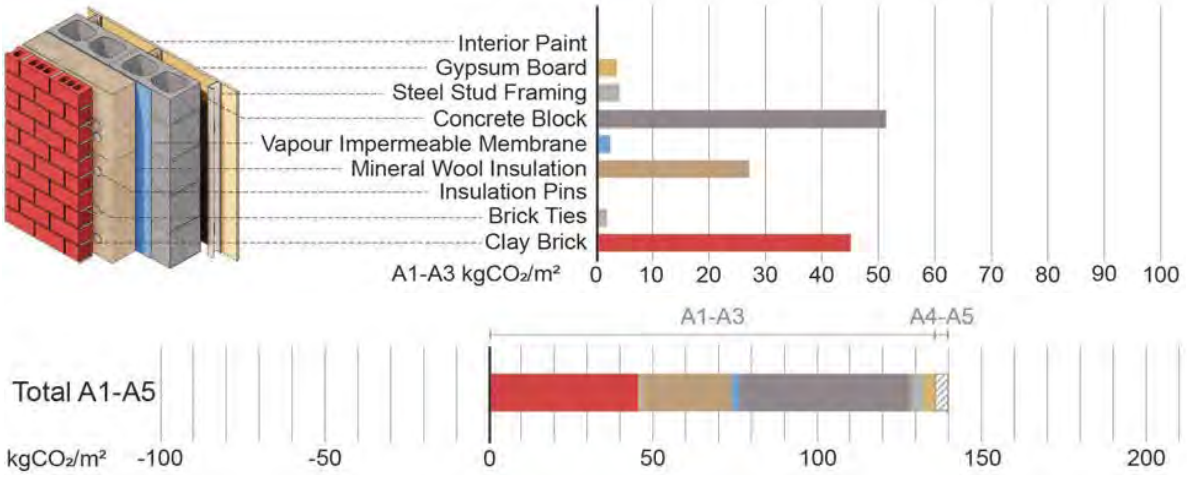

Figure 4: Embodied carbon emissions by layer for wall W01 (kgCO₂/m²)

By looking in more detail at insulation it is clear that careful selection can reduce the overall embodied carbon emissions as there are considerable variations between insulation types, and between manufacturers of the same insulation type. In general, rigid board insulation materials used for external layers outside the structure, both foam based and mineral wool based, have a higher embodied impact compared to batt and loose fill insulations materials used between studs, which are usually less dense.

There are significant opportunities to explore alternative rigid insulation materials such as woodwool board and cork. Also, for batt type insulation there are some low impact alternatives such as cellulose and wool insulation. Thus, the current tendency to use external insulation due to benefits in thermal performance from a reduction of thermal bridging has to be balanced by the additional embodied carbon in these materials.

Since the enclosure systems selected for this study are typically used in larger and taller buildings, the cladding materials tend to be higher embodied impact materials such as aluminium or steel cladding, brick or stone, and EIFs. Thus, in most cases the cladding material layer is a major contributor to embodied carbon. This is an area of investigation of potential alternatives in future.

4.CONCLUSION

The 26 assessments carried out so far provide a useful start for developing a better understanding of embodied carbon issues for enclosure systems. Nevertheless, there are many other enclosure systems and different materials that can be used so design teams will need to use this data as a starting point for further investigation and to demand detailed LCA data from manufacturers. Further analysis of alternative systems using more biobased materials will also provide useful comparisons.

The study highlights the need for increased transparency in data reporting, particularly through the availability of more EPDs for a diverse range of materials. Future research, looking at sensitivity analysis will contribute valuable insights into the environmental performance of insulation and cladding materials, which have a significant impact aiding stakeholders in making informed decisions towards more sustainable building practices.

Embodied carbon analysis of buildings and components is still in its infancy and availability of data is changing quickly. For many materials and components in North America EPDs are often either generic industry level assessments or are not yet available. Data used in EPD assessments and databases are often based on national or even continental averages which do not highlight the differences between particular manufacturers. The global warming potential of materials within the production stage is often regionally specific, and is driven by factors such as the source energy of regional electrical grids, manufacturing processes, regional transportation options, availability of raw materials, etc. The national averages available do not include these critical systemic differences between provinces and industries within provinces, and the resulting global warming potential of the assemblies and materials within these assemblies are subject to change when placed within a specific regional context. Thus, these assessments should not be

treated as complete answers to enclosure selection, but rather to inform a consideration of the different materials that make up an enclosure. They highlight which layers may have significant impact and merit further attention. As manufacturer or even production plant specific EPDs become more widely available, this will allow a more detailed analysis and selection of materials. This will facilitate the careful selection of locally manufactured materials and components.

A guidance document resulting from this project along with the outcomes for all the enclosure assessments and comparisons are available at: https://www.rdh.com/blog/embodied-carbon-resources-for-building-enclosures/

ACKNOWLEDGEMENTS

Thanks to The Atmospheric Fund for supporting this project and to RDH and Toronto Metropolitan University. Those who contributed to this work include: Erica Barnes, Rehanna Devraj-Kizuk, Steve Kemp, Jerry Kim, Fatma Osman, Russell Richman, Kelsey Saunders, YuXin Shi, Bofa Udisi.

REFERENCES

1. UNEP, (2022) Global Status Report for Buildings and Construction
2. BC Housing (n.d.) Building Envelope Thermal Bridging Guide, https://www.bchousing.org/research-centre/library/residential-design-construction-guides/building-envelope-thermal-bridging
3. Zigart, M., Lukman, R. K., Premrov, M., & Leskovar, V. Z. (2018). Environmental Impact Assessment of Building Envelope Components for Low-rise Buildings. Energy, 501-512.
4. Echenagucia, T. M., Moroseos, T., & Meek, C. (2022). On the Tradeoffs Between Embodied and Operational Carbon in Building Envelope Design: The impact of Local Climates and Energy Grids. Energy and Buildings, 1-16.
5. Rock, M., Saade, M. R., Balouktsi, M., Rasmussen, F. N., Birgisdottir, H., Frischknecht, R., . . . Lützkendorf, T. (2020). Embodied GHG Emissions of Buildings – The Hidden Challenge for Effective Climate Change Mitigation. Applied Energy, 1-12.
6. City of Toronto (2017) Toronto Zero Emission Buildings Framework, https://www.toronto.ca/wp-content/uploads/2017/11/9875-Zero-Emissions-Buildings-Framework-Report.pdf
7. City of Toronto (2022) Toronto Green Standard Version 4: Buildings Energy, Emissions & Resilience. Retrieved from The City of Toronto: https://www.toronto.ca/city-government/planning-development/official-plan-guidelines/toronto-green-standard/toronto-green-standard-version-4/mid-to-high-rise-residential-non-residential-version-4/buildings-energy-emissions-resilience/
8. National Research Council of Canada (2017) National Energy Code of Canada for Buildings NECB-2017.
9. ASHRAE (2021) ASHRAE Handbook of Fundamentals.
10. International Organization for Standardization(a). (2006). ISO 14040 Environmental Management - Life Cycle Assessment - Principles and Framework. Geneva: ISO.
11. https://www.oneclicklca.com/

PLEA 2024 WROCŁAW
(Re)thinking Resilience

Evaluating Thermal Comfort in Squares of High-Density Areas in Seville

PEGAH REZAIE[1], JAVIER SOLA-CARABALLO[1], VICTORIA PATRICIA LOPEZ-CABEZA[2], CARMEN GALAN-MARIN[3]

[1] Ph.D. student in Architecture at the University of Seville, Spain
[2] Department of Applied Mathematics, School of Architecture, University of Seville, Spain
[3] Department of Building Constructions, School of Architecture, University of Seville, Spain

ABSTRACT: Squares serve as vital social spaces in urban environments, especially in high-density areas. In cities like Seville, where the weather can be hot and arid, it becomes crucial to evaluate the thermal comfort of plazas to ensure the well-being of residents and visitors. This research comprehensively investigates the thermal comfort conditions in plazas located within high-density areas of the historic centre of Seville, Spain. The study employs a multi-faceted approach, combining meteorological data, environmental measurements, and simulation to assess the thermal comfort levels in selected plazas: San Julian Square and Cristo de Burgos Square. Meteorological data, including air temperature, humidity, surface temperature and wind speed is collected and analysed to characterize the urban microclimates and identify any distinct patterns or anomalies. The presence and characteristics of vegetation, shading structures, and water features in plazas are considered, as they can significantly impact the local microclimate and provide relief during extreme weather conditions. The insights gained from this study can inform urban planners, policymakers, and architects in their efforts to create sustainable and liveable cities that prioritize the thermal well-being of residents and visitors, even in the face of climate change challenges.
KEYWORDS: Squares, Thermal comfort, ENVI-met, High density.

1. INTRODUCTION

Over 50% of the world's population presently lives in cities, and it's estimated that by 2030, nearly 60% will be urban dwellers. Rapid urban expansion in the past 50 years has not only drawn new residents but has also significantly changed the urban environment. This transformation, including landscape changes and urban activities, has impacted local weather patterns and the broader urban climate [1]. Open-air areas and squares play a pivotal role in fostering sustainable cities by facilitating the flow of pedestrian traffic and hosting diverse outdoor activities, thereby significantly enhancing urban liveability and vibrancy. Encouraging greater foot traffic and engagement within these outdoor spaces yields multifaceted benefits for cities, spanning physical, environmental, economic, and social dimensions [2]. Urban areas undergo significant thermal comfort variations due to alterations in the radiation budget, wind patterns, and the arrangement of buildings and urban elements like vegetation. These changes create diverse microclimatic conditions within short distances, affecting how individuals experience local thermal comfort [3]. Green spaces in urban areas play a significant role in enhancing urban environments and establishing high-quality urban landscapes [4]. There is proof that the type of ground cover and the shading provided by artificial structures and trees have a substantial impact on the temperature conditions in an area [5]. Cities consist of various street canyons with different shapes, sizes, and orientations. The overall outdoor comfort within these cities is a combination of comfort experienced within these street canyons. A street canyon refers to a street that is enclosed by buildings on both sides [6]. Researchers have increasingly focused on the significance of shading and planting.

Since the 1980s, there has been a surge in studies focusing on outdoor thermal comfort, largely driven by heightened concern for pedestrians in urban settings like canyons, plazas, and squares. This trend has resulted in an abundance of research endeavours aimed at understanding and implementing microclimate design parameters centred around enhancing pedestrians' thermal comfort [7]. The majority of people tend to visit squares or public spaces when the temperature aligns closely with their comfort range. As a result, the outdoor temperature significantly influences how individuals perceive comfort and utilize outdoor areas. This impact differs based on the varying thermal preferences of people in different climatic regions [8].

The assessment of thermal comfort in these communal spaces extends beyond luxury, emerging as a pivotal necessity in cultivating an environment conducive to social gatherings and community interactions, given the significance of these plazas in the citizens' well-being. In line with this, the exploration of thermal comfort assessment

methodologies within Seville's plazas encompasses an intricate analysis. This includes a comprehensive evaluation of various factors influencing comfort levels. Numerical simulations, executed through the utilization of ENVI-met software [9] are a significant component of this analysis, focusing on understanding the impact of different parameters such as air temperature, relative humidity, wind speed and mean radiant temperature on thermal comfort within the squares. This article endeavours to deeply explore the multifaceted dimensions of thermal comfort assessment within Seville's urban plazas, employing a comprehensive approach that integrates empirical analysis, simulation methodologies, and innovative solutions.

2. METHODOLOGY

The research employs a comprehensive methodology that combines field measurements, simulation, and data analysis to understand the parameters that influence thermal comfort in urban areas and how to improve it when facing high temperatures. To evaluate thermal comfort, various parameters such as air and surface temperatures, globe temperature, wind speed, and relative humidity are measured. With them, thermal comfort and mean radiant temperature are calculated. Numerical simulations utilizing the software ENVI-met (5.1.1) are employed to analyse these parameters and their impact on thermal comfort within the squares at different times. The role of urban design and green spaces in shaping thermal comfort is examined.

2.1 Case Studies in Seville

According to Demuzere et al. [10], in Seville, there are several areas with high-density residential neighbourhoods. The most significant high-density neighbourhood of this city is Casco Antiguo (Old Town) which is the historic centre of Seville. Casco Antiguo is a densely populated area with narrow streets and traditional architecture. It includes neighbourhoods with a mix of residential buildings, shops, and tourist attractions. Two squares have been selected as shown in Figure 1: San Julian Square (PL1) and Cristo de Burgos Square (PL2), in two locations of the Casco Antiguo (Old Town). These squares offer a comprehensive experience of Seville's Casco Antiguo neighbourhood. They cover historical, modern, tranquil, and culturally rich aspects, reflecting the diverse preferences and interests of residents and visitors alike.

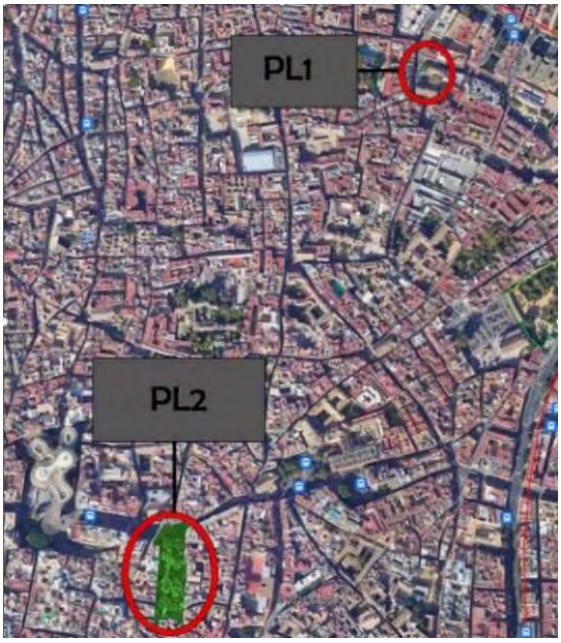

Figure 1: Selected Areas. Source: Rezaie, P. (2023) from Google Earth, https://earth.google.com/web.

- San Julian square (PL1):

In this research, PL1 has been chosen for the assessment of thermal comfort within urban environments due to its geometry characteristics, the absence of water bodies and limited green elements, representative of many small squares in this area. PL1, measuring approximately 28.5 meters in width, 44 meters in length, and a mean height of surrounding buildings of 9.5 meters, exhibits an aspect ratio (the relation between the height and the width) of 0.34 and 0.2 respectively. The surrounding buildings are constructed primarily from brick and concrete materials, and the field floor materials are asphalt and stone, which play a crucial role in shaping the environmental conditions within this area (Figure 2).

Figure 2: PL1. Source: Rezaie, P. (2023).

- Cristo de Burgos Square (PL2):

PL2 is roughly 40 meters wide, 140 meters long, and buildings around stand at a mean height of 10.5 meters, showcasing an aspect ratio of 0.3 and 0.1 respectively. The surrounding buildings primarily use brick and concrete materials, while the ground consists of asphalt and stone (

Figure *3*). These dimensions and materials significantly influence the environmental conditions within the area. The square's design elements—mostly abundant green elements that provide shade—play a substantial role in shaping visitors' thermal

experiences and drive our attention to the analysis of its microclimate and contrasting it with the previous one. Analysing factors such as solar exposure, wind flow, and structural arrangement offers the opportunity to understand the thermal qualities affecting visitors' comfort. This understanding can offer crucial insights for optimising the square's design to enhance thermal comfort and improve the overall quality and usability of public spaces within Seville's urban environment.

Figure 3: PL2. Source: Rezaie, P. (2023).

2.2 Field Measurements

Field observations are essential to validate the applicability of ENVI-met within the research site. Data collection occurred on a representative summer day (23rd of July 2023) at different times, midday, and evening in the two squares. Temperature, humidity, and globe temperature (by a thermo-hygrometer TROTEC TC100), wind speed (by an anemometer TROTEC TA300), and surface temperature (by a thermometer TESTO 905 T2) were measured. Ten points were selected within each square for these measurements. These data are used to calibrate the simulation models in ENVI-met which allows us to measure thermal comfort according to the Universal Thermal Climate Index and extend the implication of the differences found in the squares in relation to urban design and user comfort.

2.3 Simulation set-up

ENVI-met is crafted to examine microclimates by applying the foundational principles of fluid dynamics and thermodynamics. It can replicate the intricate interplays among buildings, soil, greenery, and the atmosphere. Hence, it finds widespread utility in investigating urban microclimates. The software is tailored for 3D modelling, featuring a typical horizontal resolution ranging from 0.5 to 5 meters and a temporal scope of 24 to 48 hours, using time steps of 1 to 5 seconds. This level of resolution facilitates the scrutiny of interactions among individual buildings, surfaces, and vegetation [9].

Following the measurements conducted on-site, the subsequent stage involved simulating the thermodynamic performance of the squares using the ENVI-met software (version 5.1.1). Details regarding the models and boundary conditions for each simulated square are outlined and presented in Figure 4, and Table 2.

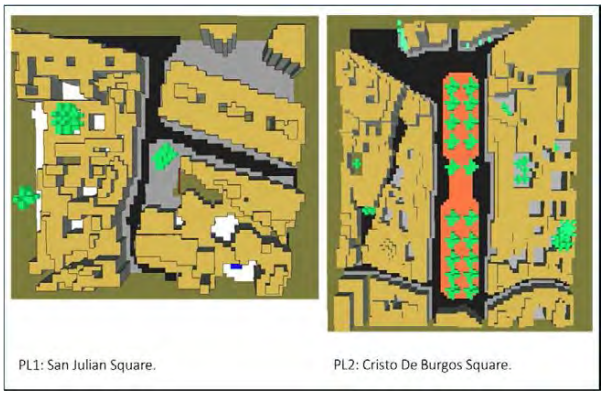

Figure 4: Simulation models.

Table 1:Parameters of each Square.

Parameters	PL1	PL2
Number of grid cells	80*70*15	100*105*30
Size of the cells (m) (x,y,z)	2*2*2	2*2*2
Nesting grids	4	4
Model rotation out of north	0	0

Table 2: ENVI-met materials used in the simulations.

Squares	PL1	PL2
Wall	C2(0200C2)	C2(0200C2)
Roof	R1(0200R1)	R1(0200R1)
	ST (0200ST)	ST (0200ST)
	G2(0200G2)	GS (0200GS)
Soil materials	GS (0200GS)	KK (0200KK)
	PL (0200PL)	
	WW (0200WW)	

The same day of monitoring campaigns was simulated, July 23rd, 2023. The simulation's input parameters included hourly Air Temperature (AT) and Relative Humidity (RH) using simple forcing, along with average wind speed and direction taken from a nearby weather station (Table 3

*Table **3***).

Table 3: Air temperature and Relative Humidity in 24 hours.

Hour	AT(°C)	RH (%)	Hour	AT(°C)	RH (%)
0:00	25.3	43	12:00	29.2	41
1:00	23.6	49	13:00	31.1	37
2:00	22.7	58	14:00	32.9	31
3:00	22.5	64	15:00	34.8	26
4:00	21.7	65	16:00	36	24
5:00	21.8	67	17:00	36.3	26
6:00	21.7	67	18:00	36.5	18
7:00	21.6	66	19:00	37.4	18
8:00	22.1	66	20:00	36.5	19
9:00	24.1	61	21:00	34.5	24
10:00	26.3	54	22:00	32	32
11:00	27.5	49	23:00	29.7	37

3. RESULTS AND DISCUSSION

3.1 Direct monitoring result

The observations of monitoring reveal variations in air temperature (AT), relative humidity (RH), wind speed (WS), and surface temperature (ST) among the two squares.

In PL1, measured at 18:00 hours, the lowest air temperature (AT) is 37.9°C while the highest temperature is 40.8°C (Figure 5). In PL2 which was measured at 13:00 hours, the minimum air temperature was 33.0°C. On the other hand, the maximum temperature was 37.4°C (Figure 6). The highest variations occurred between points at the sun or in the shade.

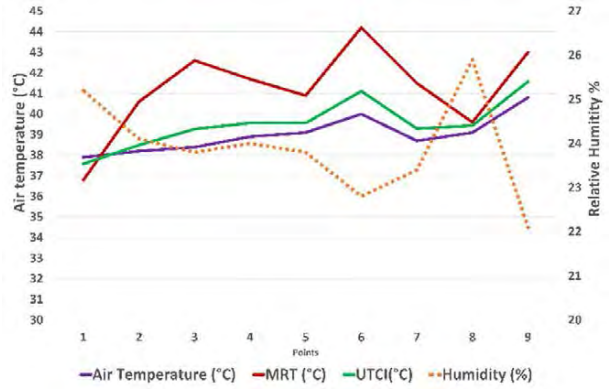

Figure 5: PL1 Air temperature and relative humidity measured and MRT and UTCI calculated in 9 points at 18:00 hours.

Concerning wind speed, the two squares had low values between 0.7 and 1.5 m/s and demonstrated the same variations in wind speed during day and night. This is due to the high urban density in these areas and the presence of vegetation, blocking wind speed.

Last, concerning surface temperature, the highest values are achieved in areas without shading and high thermal capacity materials. Without the cooling effect of shadows and the moisture released from vegetation, the square surfaces store the heat from solar radiation, resulting in elevated temperatures during the evening hours, reaching 57.3 °C in PL1. and 55 °C in PL2. The lowest points are 36.3 °C in PL1 and 30.2 °C in PL2.

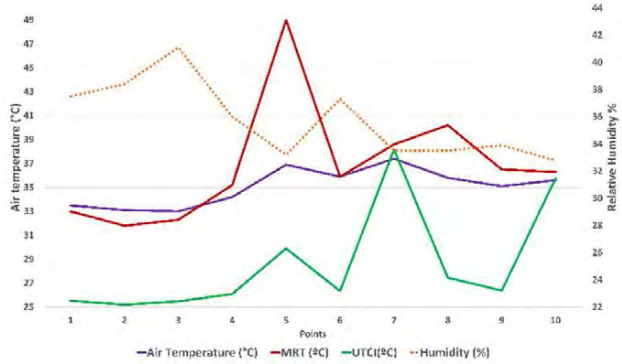

Figure 6: PL2 air temperature and relative humidity measured and MRT and UTCI calculated in 10 points at 13:00 hours.

Understanding the spatial distribution of mean radiant temperature (MRT) is crucial for urban planners to implement design strategies that improve thermal comfort. Integration of shading elements, the use of materials with higher reflectivity or lower thermal conductivity, and the incorporation of green spaces can help to mitigate higher MRT values, thereby creating more comfortable and user-friendly environments. MRT has been calculated from the monitored globe temperature using the standard ISO 7726:2021 [11].

In PL1, the MRT values range from 36.9°C to 44.2°C across the nine points, showcasing a variance in thermal conditions within the square. Points located under direct solar radiation or surrounded by surfaces with materials that absorb and emit more heat exhibited relatively higher MRT values compared to the other points in the shade.

In PL2, MRT spans from 31.8°C to 49.0°C among the ten points, showcasing considerable differences in thermal states within the square, again related to areas receiving direct solar radiation. In this square, the difference among the points is higher, mostly due to the higher presence of vegetation which maintains a larger area of the surfaces in the shade for a longer time, reducing its MRT. The areas with higher MRT values may induce increased thermal discomfort for individuals in those locations due to higher radiant heat emitted by surrounding surfaces. To measure that, the Universal Thermal Comfort Index (UTCI), a metric that represents the perceived temperature experienced, is calculated. It considers air temperature, mean radiant temperature, relative humidity, and wind speed within a human energy model to provide a temperature measure that reflects the heat strain or cold strain perceived by the human body outdoors [12]. In PL1, UTCI range from 37.58°C to 41.58°C, and in PL2 range from 25.2°C to 38.17°C. PL1 generally exhibits higher UTCI values compared to PL2, indicating warmer perceived temperatures. The values correlate with MRT, indicating the high impact of this parameter on thermal comfort.

In order to analyze comfort not only at measured times but throughout the day, simulation is needed. The simulation results are shown in the following section.

3.2 Simulation result

The simulations were performed to analyse the hourly evolution of the different parameters beyond the monitoring times. Figure 7 shows the hourly evolution of the air temperature at the two plazas and the weather station on the simulated day. In PL1, the AT fluctuates between 23.3°C at 6:00 hours and 34.4°C at 19:00 hours. In PL2, the AT varies from its lowest point of 23.1°C at 6:00 to its highest at 32.9°C at 19:00. At the weather station, the AT reaches its lowest point

of 21.6°C at 7:00 in the morning and surges to its highest at 37.4°C by 19:00 hours.

Regarding Relative Humidity (RH) in PL1, the highest RH is 57.5% at 6:00, while at 19:00, it drops to its lowest point of 22.9%. In PL2, RH peaks at 58.4% in the morning at 7:00, contrasting sharply with its lowest point of 25% at 20:00. At the weather station, RH varies between a maximum of 67% and a minimum of 18%, observed respectively at 6:00 and 19:00.

At most times, the air temperature at PL1 tends to be slightly higher than at PL2. Throughout most times, the Relative Humidity at PL1 and PL2 tends to be slightly lower compared to the readings at the weather station.

Focusing on the monitored points, the MRT results varied 6.4 °C in PL1 and 6.6 °C in PL2, and the UTCI varied 1.6°C in PL1 and 1.9°C in PL2. The highest values were provided at the direct sun-exposed points Table 4.

Table 4. Simulation results at monitoring points and times.

PL1				PL2			
AT (°C)	RH (%)	MRT (°C)	UTCI (°C)	AT (°C)	RH (%)	MRT (°C)	UTCI (°C)
34.0	24.7	32.2	32.5	30.2	37.2	35.2	31.6
34.2	24.2	34.9	33.4	30.2	37.2	31.7	30.4
34.3	24.1	35.5	32.8	30.8	35.9	38.3	31.1
34.3	24.1	38.6	34.1	30.3	37.1	32.5	29.7
34.3	24.2	34.0	33.4	30.7	36.7	34.3	30.3

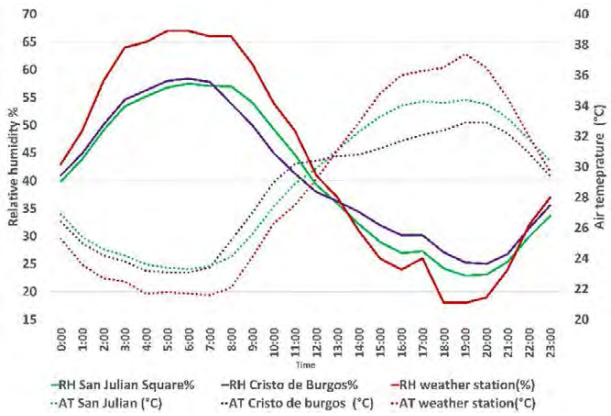

Figure 7: Comparing AT with RH in PL1 and PL2 and weather station.

In order to compare the results of monitoring and simulation, four statistical parameters are selected: the Normalized Mean Bias Error (NMBE), the Mean Absolute Percentage Error (MAPE), the Root Mean Square Error (RMSE) and the Coefficient of Variation of the Root Mean Square Error (CV(RMSE)). The four of them are usually used to evaluate the performance of a forecasting or prediction model. The NMBE, MAPE and CV(RMSE) provide a percentage value that should be close to 0. The RMSE provides temperature results that also should be close to 0. Generally, values under 20% are considered acceptable.

The achieved simulation accuracy is reflected in the lower percentage of 20%, showcasing an acceptable simulation scenario. Both PL1 and PL2 exhibit NMBE, MAPE, and CV(RMSE) values for parameters like AT, RH, MRT, and UTCI, all of which fall below the 20% mark. However, it's worth noting that RMSE, a measure indicating the deviation between observed and simulated data, should ideally be close to zero. In our study, the RMSE registers a higher value, possibly attributed to inaccuracies stemming from either the monitoring process or the simulation model itself (Table 5).

The comparison of the monitoring and simulation results suggests that the monitoring provides a wider range of values in each plaza while the simulation results are much more homogeneous. In addition, relative humidity values provide more accurate results, while UTCI values are less precise. Among the two squares, the most noticeable difference in accuracy occurs in the MRT values, where PL2 provides much more accurate results than PL1, suggesting that the software is more accurate in shaded spaces, being the most significant difference between the two squares.

Table 5. Statistical parameters for the simulations' accuracy.

		NMBE	MAPE	RMSE	CV(RMSE)
AT	PL1	15.2%	12%	5.4	14%
	PL2	16.0%	13%	5.9	17%
RH	PL1	0.4%	0%	1.1	5%
	PL2	-4.6%	4%	2.9	8%
MRT	PL1	17.3%	14%	6.4	16%
	PL2	-1.7%	1%	3.1	9%
UTCI	PL1	19.7%	16%	7.0	18%
	PL2	-8.6%	11%	5.4	19%

The reasons for the discrepancies between monitored and simulated data could stem from many sources. First, the precision of the monitoring instruments used to collect data could be reduced under extreme heat conditions, such as the ones monitored under the sun. On the other hand, simulation with ENVI-met has been previously reported to provide some discrepancies between monitoring and simulation. This stems from the lack of local information to use as boundary conditions in the simulation or the modelling limitations of the software.

However, the methodology followed in this section suggests that ENVI-met is a promising software in order to analyse mitigation strategies such as vegetation or cooling materials in this kind of space so common in the city centres of European cities.

4. CONCLUSION

This comprehensive study delved into evaluating the thermal comfort conditions in two representative Seville's Squares. Through meticulous monitoring, simulation, and data analysis, this research aimed to understand the factors influencing thermal comfort, particularly in high-density urban areas facing hot and arid weather conditions.

Overall, the investigation into air temperature, humidity, wind speed, and surface temperature unveiled distinctive patterns and variations among the plazas PL1 generally depicted higher UTCI values, indicating potentially warmer conditions or increased thermal stress compared to PL2, suggesting that the addition of vegetation is a good strategy to increase thermal comfort.

The study's findings underscore the pivotal role of urban design elements, vegetation, shading structures, and surface materials in shaping thermal comfort within these plazas. The future analysis of the implementation of strategies such as shading elements, materials with higher reflectivity, and green spaces emerges as crucial tactics to mitigate higher thermal values, ensuring more user-friendly and comfortable environments. These insights serve as valuable guidance for urban planners, policymakers, and architects in their quest to develop sustainable and liveable cities, prioritising the thermal well-being of residents and visitors amidst the challenges posed by climatic changes.

ACKNOWLEDGEMENTS

This work has been funded by grant US.22-07 Junta de Andalucía (Consejería de Fomento, Articulación del Territorio y Vivienda) and supported by the project PID2021-124539OB-I00 funded by MCIN/AEI/ 10.13039/501100011033 and by "ERDF A way of making Europe", project TED2021-129347B-C21 funded by MCIN/AEI/ 10.13039/501100011033.

REFERENCES

1. C. Ren, E. Y. Y. Ng, and L. Katzschner, 'Urban climatic map studies: A review', *International Journal of Climatology*, vol. 31, no. 15. pp. 2213–2233, Dec. 2011. doi: 10.1002/joc.2237.
2. L. Chen and E. Ng, 'Outdoor thermal comfort and outdoor activities: A review of research in the past decade', *Cities*, vol. 29, no. 2, pp. 118–125, 2012, doi: 10.1016/j.cities.2011.08.006.
3. J. A. Acero and K. Herranz-Pascual, 'A comparison of thermal comfort conditions in four urban spaces by means of measurements and modelling techniques', *Building and Environment*, vol. 93, no. P2, pp. 245–257, Nov. 2015, doi: 10.1016/j.buildenv.2015.06.028.
4. Dimoudi and M. Nikolopoulou, 'Vegetation in the urban environment: microclimatic analysis and benefits', *Building and Environment*, vol. 35, no. 1, pp. 69–76, Jan. 2003, doi: 10.1016/S0378-7788(02)00081-6.
5. T. P. Lin, Y. F. Ho, and Y. S. Huang, 'Seasonal effect of pavement on outdoor thermal environments in subtropical Taiwan', *Building and Environment*, vol. 42, no. 12, pp. 4124–4131, Dec. 2007, doi: 10.1016/j.buildenv.2006.11.031.
6. T. E. Morakinyo and Y. F. Lam, 'Simulation study on the impact of tree-configuration, planting pattern and wind condition on street-canyon's micro-climate and thermal comfort', *Building and Environment*, vol. 103, pp. 262–275, Jul. 2016, doi: 10.1016/j.buildenv.2016.04.025.
7. M. Taleghani, L. Kleerekoper, M. Tenpierik, and A. Van Den Dobbelsteen, 'Outdoor thermal comfort within five different urban forms in the Netherlands', *Building and Environment*, vol. 83, pp. 65–78, Jan. 2015, doi: 10.1016/j.buildenv.2014.03.014.
8. T. P. Lin, A. Matzarakis, and R. L. Hwang, 'Shading effect on long-term outdoor thermal comfort', *Building and Environment*, vol. 45, no. 1, pp. 213–221, Jan. 2010, doi: 10.1016/j.buildenv.2009.06.002.
9. 'microclimate-simulation-software', Accessed: Nov. 27, 2023. [Online]. Available: https://www.envi-met.com/microclimate-simulation-software/
10. M. Demuzere, B. Bechtel, A. Middel, and G. Mills, 'Mapping Europe into local climate zones', *PLoS One*, vol. 14, no. 4, Apr. 2019, doi: 10.1371/journal.pone.0214474.
11. ISO 7726:2021-03, Ergonomics of the thermal environment. Instruments for measuring physical quantities. 2021.
12. 'https://www.antonellodinunzio.online/web-project/utci-tool/utci-calculator.html'.

PLEA 2024 WROCŁAW
(Re)thinking Resilience

Understanding the Transit Gap:
A Comparative Study of On-Demand Bus Services and Urban Climate Resilience in South End, Charlotte, NC and Avondale, Chattanooga, TN

SANAZ SADAT HOSSEINI,[1] BABAK RAHIMI ARDABILI,[2] MONA AZARBAYJANI,[3]
SRINIVAS PULUGURTHA,[1] HAMED TABKHI[4]

[1]Department of Civil and Environmental Engineering, University of North Carolina at Charlotte, Charlotte, NC, USA
[2]Department of Public Policy, University of North Carolina at Charlotte, Charlotte, NC, USA
[3]School of Architecture, University of North Carolina at Charlotte, Charlotte, NC, USA
[4]Department of Electrical and Computer Engineering, University of North Carolina at Charlotte, Charlotte, NC, USA

ABSTRACT: Urban design significantly impacts sustainability, particularly in the context of public transit efficiency and carbon emissions reduction. This study explores two neighborhoods with distinct urban designs: South End, Charlotte, NC, featuring a dynamic mixed-use urban design pattern, and Avondale, Chattanooga, TN, with a residential suburban grid layout. Using the TRANSIT-GYM tool, we assess the impact of increased bus utilization in these different urban settings on traffic and CO2 emissions. Our results highlight the critical role of urban design and planning in transit system efficiency. In South End, the mixed-use design led to more substantial emission reductions, indicating that urban layout can significantly influence public transit outcomes. Tailored strategies that consider the unique urban design elements are essential for climate resilience. Notably, doubling bus utilization decreased daily emissions by 10.18% in South End and 8.13% in Avondale, with a corresponding reduction in overall traffic. A target of 50% bus utilization saw emissions drop by 21.45% in South End and 14.50% in Avondale. At an idealistic goal of 70% bus utilization, South End and Avondale witnessed emission reductions of 37.22% and 27.80%, respectively. These insights are crucial for urban designers and policymakers in developing sustainable urban landscapes.
KEYWORDS: Urban Design Patterns, Urban Transportation, Demand-Responsive Bus Services, CO2 Emissions, Climate Resilience

1. INTRODUCTION

Urban design pattern significantly shapes transportation behaviors, influencing cities to either promote or hinder public transit. Pedestrian-friendly environments with walkable and bikeable designs lead to reduced car ownership and increased reliance on public transportation. Conversely, many post-World War II American cities, adopted car-dependent designs, leading to a decline in public transit use, notably bus transit. Main challenges plague US urban design and public bus transit, including urban sprawl, reduced bus ridership, rising costs, fleet limitations, inadequate bus stop coverage, and safety concerns, contributing to a shift toward private vehicles and consequently increased carbon emissions. By mid-2022, ridership had fallen to 62% of pre-pandemic levels, with some cities, like Charlotte, experiencing a 75% drop between 2014 and 2022, particularly in post-WWII car-dependent cities (Fig.1) [1-4].

Moreover, the broader availability of personal cars, driven by affordable ownership and low gas prices, contributes to a national decline in public transportation usage, leading to heightened traffic congestion, increased CO2 emissions, and negative environmental impacts, especially impacting underserved communities relying on older, high-emission vehicles. Traditional bus transit systems struggle to adapt to the dynamic nature of modern urban life. Our proposed solution integrates urban design principles with technology, envisioning a demand-responsive public bus system dynamically matching riders with available buses based on real-time demand [5].

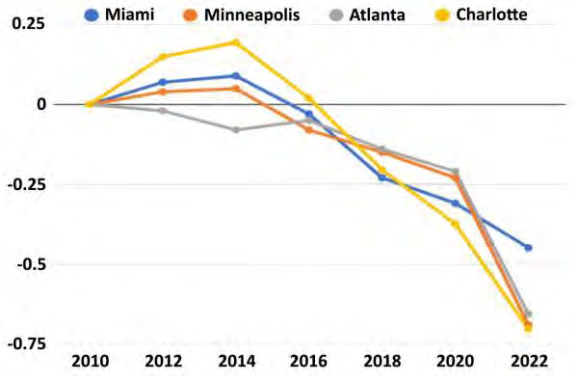

Figure 1: Bus ridership reduction relative to 2010.

We aim to unlock the potential of bus transit, creating an appealing ecosystem for a diverse range of commuters, including underserved communities and overlooked middle-class residents from various urban settings in cities. This study conducts a

comparative analysis of two case studies, South End in Charlotte, NC and Avondale in Chattanooga, TN, utilizing the TRANSIT-GYM simulation tool to model potential impacts of this bus system with increased utilizations on areas with different urban design layouts. Preliminary results show that pedestrian-friendly areas like South End exhibit less transit inequality, with simulations indicating reduced traffic congestion and CO2 emissions. Doubling bus usage reduces daily emissions in South End by 10.18% and Avondale by 8.13%, with overall traffic decreasing by 12.06% in South End and 8.90% in Avondale. At 50% bus utilization, South End sees a 21.45% drop in daily emissions, while Avondale experiences a 14.50% decrease. A 70% bus utilization target results in a 37.22% emissions reduction for South End and a 27.80% decrease for Avondale.

The outcomes of these simulations offer a roadmap for how municipalities might approach urban planning in the future, ensuring that it is both efficient and environmentally conscious. The main contributions of this paper are as follows:

1. Utilizing the TRANSIT-GYM simulation tool to quantify the benefits of increasing bus ridership through the hypothetical demand-responsive bus system and its effects on traffic reduction and CO2 emissions in different urban settings.
2. Investigating how different urban design patterns affect transit behaviour, CO2 emissions, and the feasibility of on-demand bus systems in South End and Avondale.
3. Highlighting the transformative potential of increasing bus ridership in enhancing climate resilience, reducing CO2 emissions, and addressing transportation disparities caused by different urban design patterns.

The paper is structured as follows: Section 2 reviews research on urban design's impact on public transit and sustainability, Section 3 explains the selection of South End and Avondale for impact assessment, Section 4 presents simulation results, and Sections 5 and 6 discusses the implications and future research directions.

2. LITERATURE REVIEW

Recent literature emphasizes the intricate relationship between urban design and public transit efficiency to enhance urban sustainability, particularly through pedestrian-friendly designs that address the 'transit gap.' TRANSIT-GYM, developed by R. Sun et al., serves as a dynamic tool optimizing public transit operations and energy costs, facilitating efficient and equitable planning [6]. Sen et al.'s BTE-Sim offers a simulation environment for rapid modeling and optimization of public transportation systems, empowering urban planners to enhance network performance and cost-effectiveness [7].

Tao Ji et al. stress the urgency of resilient transportation infrastructure in urban areas amidst climate change challenges [8, 9]. Winkler et al.'s study critically evaluates challenges linked to reducing urban transport emissions, underscoring the necessity for comprehensive policies targeting carbon reduction in city-level emissions [10]. Jing et al.'s research delves into the intricate relationship between public transport development and carbon emissions reduction, unveiling an inverted U-shaped curve. Their findings suggest measures such as green infrastructure, government-market coordination, and energy transformation to effectively mitigate carbon emissions [11].

These studies and tools highlight the importance of simulation and AI in creating efficient, demand-responsive transit systems, improving urban resilience, lowering emissions, and informing future research on transit improvements' impacts.

Our research adds to the current body of knowledge by conducting empirical analyses and simulations in South End, Charlotte and Avondale, Chattanooga. We focus on how transitioning from private cars to public transit influences CO2 emissions and transportation efficiency in these different urban settings. This study presents two key research questions that drive our investigation and findings.

1. How significantly will the scenario reduce CO2 emissions and ease traffic in the case study areas?
2. How do each area's urban design and street layouts influence the simulation results?

3. METHODOLOGY

In this section, we explain the rationale behind selecting Charlotte and Chattanooga, discuss data sources and the simulation process, and describe the scenarios under consideration.

3.1 Selection of Case Study Areas

Our study, targeting South End in Charlotte, NC and Avondale in Chattanooga, TN, aims to deliver accurate and comprehensive results by examining these cities' distinct urban designs, bus ridership patterns, and their effects on transit disparities and CO2 emissions. These areas were specifically chosen for their contrasting urban environments and substantial populations, providing a rich context for analysing the impact of urban design and transportation systems on CO2 emissions and community dynamics.

Charlotte, NC, displays the "New South" model with its post-World War II expansion, featuring radial main streets, car-centric suburbs, and denser central areas with pedestrian-friendly grid streets.

Chattanooga, TN, shaped by its geography and history, embraces modern urban planning, like the Complete Streets Ordinance, to create a diverse environment accommodating various modes of transportation and prioritizing neighbourhood safety and interaction.

Charlotte's South End has evolved from a manufacturing district to a dynamic urban area with a blend of modern and historic elements, a comprehensive public transit system, and pedestrian-friendly spaces. Despite this, its bus usage remains low, like Avondale, and our study will analyse bus lines '5', '16', '19', '35', and '41x' [12-16].

In contrast, Avondale, a suburban Chattanooga neighborhood with mid-20th-century roots, presents a mix of older housing in a grid street pattern, facing challenges in carpool reliance and minimal bus usage due to socioeconomic factors. Our study includes bus lines 10A, 10C, and 10G in this area [17-18].

These two neighbourhoods, each with unique characteristics, are crucial for comprehending the environmental consequences of urban planning in their respective cities.

3.2 Simulation and Data Sources

Utilizing the Transit-GYM tool and SUMO software [6], our study replicates traffic dynamics, transportation frameworks, and urban mobility scenarios. Multiple steps were undertaken to create SUMO scenario files for the selected areas and their bus operations, involving crafting trip definitions, establishing networks, determining vehicle configurations, and generating SUMO and GUI files. This approach aids urban transit agencies in assessing the energy implications of different transportation decisions [6]. Data for simulations, sourced from various channels [7], included:

- Map Data from Open Street Maps processed through SUMO's NETCONVERT to create SUMO-compatible road networks.
- A detailed list of public transit vehicle characteristics was compiled for SUMO's vehicle type definition file.
- The latest General Transit Feed Specification (GTFS) data (as of November 25th, 2023) provided real-time route details, bus stop locations, and schedules essential for transit simulation setup [19, 20].
- Origin-Destination (OD) data and Traffic Analysis Zones (TAZ) files were used to record trips and indicate traffic demand between zones. POLYCONVERT converted TAZ files to SUMO TAZs, outlining regions and corresponding edges, crucial for generating personal plans and vehicle trips in SUMO.

3.3 Bus Transit Simulation Workflow

The bus transit simulation workflow, as shown in (Fig.2), follows a structured process using SUMO tools. Initiated by collecting OD Demand matrix data, TAZ files, vehicle parameters, and GTFS, a Domain-Specific Modelling Language (DSML) program interprets these inputs, generating XML files detailing person trips, vehicle types, bus trips, and bus stop locations. Real-time interaction with the optimized network XML file and GTFS data is facilitated by the Traffic Control Interface (TraCI), which accurately positions bus stops throughout the simulation. The NETEDIT tool, a SUMO suite component, serves as an interactive graphical editor for creating and modifying road network maps for simulations. XML files representing daily non-bus traffic, integrated bus and person routes, and detailed edge-based network information are incorporated, along with average daily traffic calculations based on Annual Average Daily Traffic (AADT) and the Traffic Count Database System (TCDS) [21, 22]. These files, along with a SUMO-readable network file, amalgamate into the simulation configuration. Upon execution, the simulation assesses bus operations, providing key performance metrics such as arrival times, wait times, and load factors, offering a comprehensive view of the transport system's efficiency [6].

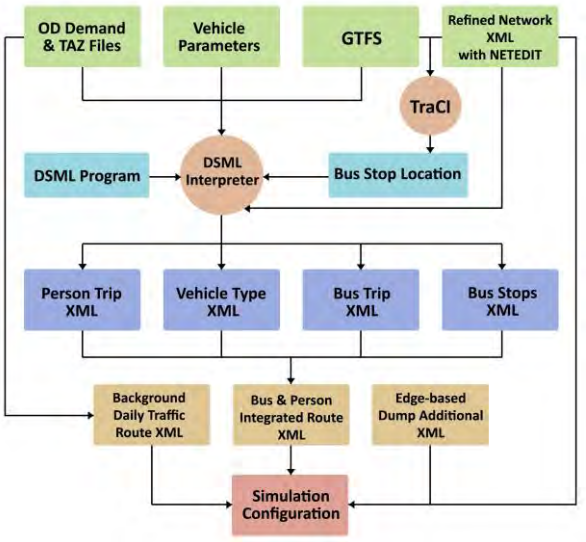

Figure 2: Bus transit simulation workflow with TRANSIT-GYM tool [6].

3.4 Scenario Selection

To assess the impact of On-Demand Bus service and bus ridership improvements on CO2 emissions in two different urban areas, our study compared three scenarios against a baseline, which simulated each case study area's current street network and existing traffic patterns. The baseline reflected CO2 emissions with the current bus system and ridership rate unchanged. In the first scenario, we doubled the current bus utilization within a day by transitioning

private car users to a demand-responsive transit system. This resulted in a 12.06% decrease in South End and 8.90% decrease in traffic in Avondale compared to the baseline. For the second scenario, envisioning a 50% bus utilization (our proposed demand-responsive system's target), we projected a 21.13% decrease in traffic in South End and 18.40% decrease in Avondale. The third scenario assumed an idealistic 70% bus utilization, leading to approximately a 34.41% decrease in traffic in South End and 29.29% decrease in Avondale and The Results section delves into CO2 emissions, examining the impact of these changes in bus trip utilization across scenarios.

4. RESULT

In this section, the preliminary results of the simulations under different scenarios are presented.

4.1 Statistical Analysis

(Table 1) compares car and bus utilization across a baseline and three increased bus utilization scenarios in South End, Charlotte. The baseline scenario captures current traffic, including the number of cars, buses, and passengers that leads to approximately 4386 reductions in car trips which increased the average bus passengers from 6.36 to 12.72. In the same scenario in Avondale, Chattanooga as shown in (Table 2) in next page, 982 unique person IDs using 173 bus line trips detected in Avondale from 5 am to 9 pm. The first scenario in Avondale, causes 660 fewer cars, which increases average bus occupancy from 5.7 to 11.40 passengers, resulting in an 8.90% decrease in traffic congestion without exceeding the current 173 bus line trips. The second scenario for both areas, leads to a significant drop in car trips: in Avondale, car trips decreased to 1363.6 trips, and in South End, from the initial number of 35335 to 28685. Also, the third scenario leads to less car trips for both areas. The necessary bus line trips for both areas remain under the existing number, indicating an enhanced bus system efficiency and no requirement for additional services.

4.2 Simulations Results

In this section, we represent the results of simulations in each scenario following the steps explained in the methodology section. (Fig.3) depicts the daily CO2 emissions for South End, Charlotte, NC, measured from 5 AM to 9 PM across four different traffic scenarios. The base scenario peaks at 6:34 PM with total emissions of 2931.17 tonnes. When simulating Scenario 1, the peak emissions occur earlier at 5:23 PM, with a total of 2632.77 tonnes, indicating a slight decrease in emissions. Scenario 2 shifts the peak to 5:33 PM with total of 2302.41 tonnes emissions. Finally, scenario 3 leads to total of 1840.25 tonnes emissions and the peak at 7:16 PM.

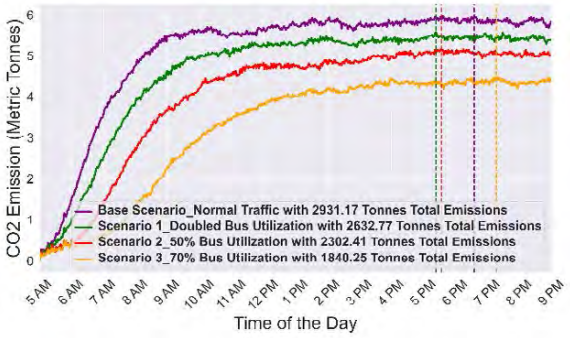

Figure 3: Daily CO2 emissions over time (hours) from 5 AM to 9 PM for different scenarios for South End, Charlotte, NC - With peak emission for base scenario at 6:34 PM, peak emission for scenario 1 at 5:23 PM, peak emission for scenario 2 at 5:33 PM, and peak emission for scenario 3 at 7:16 PM.

(Fig.4) illustrates the daily CO2 emissions in Avondale, Chattanooga, TN, from 5 AM to 9 PM across four different scenarios: the baseline, doubled bus utilization (Scenario 1), 50% bus utilization (Scenario 2), and 70% bus utilization (Scenario 3). The baseline scenario peaks at 4:55 PM with 118.72 tonnes of emissions. Scenario 1, peaks at 2:40 PM with emissions slightly lower at 109.07 tonnes. Scenario 2, peaks at 2:26 PM and the lower emissions from the above scenarios at 101.50 tonnes. Finally, scenario 3, has the lowest emission of 85.71 tonnes. The peaks show the times of day with the highest CO2 emissions for each scenario. As cars are reduced and buses are used more, emissions decrease.

Table 1: Statistical comparison of different scenarios' calculations for South End

Area	Scenario	Bus Utilization Data			Passenger Data		Traffic Reduction Data	
		Current Bus Utilization	Increase Rate of Utilization	New Bus Utilization	Current Person Trips Using Buses	Total Passengers Require Bus Services	Reduction in Car Trips	Total Average Traffic After Reduction
South End	Base Scenario	18.17%	1X	18.17%	6585	6585	0	36370
	Scenario 1		2X	36.34%		13165.2	12.41%	31983
	Scenario 2		3.07X	50%		18112.5	21.75%	28685
	Scenario 3		4.29X	70%		25357.5	35.41%	23855

Table 2: Statistical comparison of different scenarios' calculations for Avondale

Area	Scenario	Bus Utilization Data			Passenger Data		Traffic Reduction Data	
		Current Bus Utilization	Increase Rate of Utilization	New Bus Utilization	Current Person Trips Using Buses	Total Passengers Require Bus Services	Reduction in Car Trips	Total Average Traffic After Reduction
Avondale	Base Scenario	16.28%	1X	16.28%	982	982	0	7412
	Scenario 1		2X	32.56%		1972	9.12%	6752
	Scenario 2		3.07X	50%		3027.5	18.84%	6048
	Scenario 3		4.29X	70%		4238.5	30%	5241

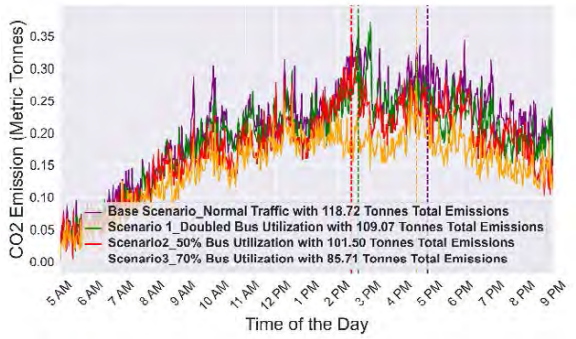

Figure 4: Daily CO2 emissions over time (hours) from 5 AM to 9 PM for different scenarios for Avondale, Chattanooga, TN - With peak emission for base scenario at 4:55 PM, peak emission for scenario 1 at 2:40 PM, peak emission for scenario 2 at 2:26 PM, and peak emission for scenario 3 at 4:33 PM.

The variance in emission trends between two urban areas is influenced by their distinct urban designs. In the South End, a mixed-use area, emission patterns show a steady rise from early morning, peaking around 8 AM, indicative of diverse activities starting the workday, leading to consistent emissions above 5 tonnes post 8 AM. This reflects the area's blend of residential, commercial, and leisure activities, contributing to a steady flow of traffic. In contrast, a primarily residential area shows more pronounced emission fluctuations, aligning with typical suburban patterns. These fluctuations are driven by peak commute hours, with sharp peaks during morning and evening rush hours, illustrating how urban design—whether mixed-use or residential—affects traffic patterns and, consequently, emissions.

5. DISCUSSION

Our study offers a comparative analysis of the Avondale and South End neighborhoods, illustrating the impact of urban design on public transport efficiency and climate resilience. South End, with its organic street network and a mix of activities, shows significant reductions in traffic and CO2 emissions, unlike Avondale's suburban grid layout. However, South End's dense pattern also leads to increased traffic congestion and emissions, as the existing street network struggles with the high volume.

In South End, the mixed-use, pedestrian-friendly environment reduces reliance on private vehicles, aiding in emission reduction. Yet, this benefit is offset by congestion issues arising from its high-density urban pattern. Avondale, with its grid pattern and residential focus, faces challenges of longer trips and higher traffic due to limited local destinations.

This research highlights the dual nature of urban design impacts on public transit and sustainability. South End's design encourages public transport use but also brings congestion challenges, indicating a need for adaptive, demand-responsive transit solutions. Avondale's experience points to the importance of incorporating local amenities in residential areas. Our findings emphasize the need for holistic urban design strategies that balance density, accessibility, and environmental impact, crucial for effective city-wide CO2 emission reduction and climate resilience.

6. CONCLUSION AND FUTURE WORK

The aim of this research is to illustrate how urban design affects public transit effectiveness and sustainability, in particular through the lens of demand-responsive bus services in South End, Charlotte, NC, and Avondale, Chattanooga, TN. It reveals how South End's mixed-use layout and dynamic land use enhance the benefits of increased bus utilization, resulting in greater CO2 emissions reductions than Avondale. As a result, urban design and transit solutions are intricately intertwined, advocating context-specific solutions. While the study relies on simulations and may not capture all real-world complexities, it paves the way for future empirical research in diverse urban settings to solidify these findings. From a policy standpoint, this study reinforces the need for comprehensive urban planning. In such planning, demand-responsive transit systems must be seamlessly integrated with broader urban policies, including zoning, housing, and environmental concerns. An integrated approach is needed to address broader challenges, such as social equity and environmental sustainability. The research sets the stage for multi-disciplinary exploration, emphasizing the importance of a holistic approach to urban development that aligns public transit enhancements with overarching urban development

objectives, thereby fostering a sustainable, equitable, and resilient urban future.

ACKNOWLEDGEMENTS

We are grateful to the Charlotte Area Transit System (CATS) for providing crucial data. We thank everyone who contributed to the development of TRANSIT-GYM tool, particularly Professor Abhishek Dubey and his team at Vanderbilt University for their exceptional assistance. Our special thanks to Professor Srinivas Pulugurtha from UNC Charlotte and his laboratory for their invaluable assistance. Moreover, we appreciate the financial support provided by UNC Charlotte's School of Data Science and College of Engineering.

REFERENCES

1. Erhardt, G. D., Hoque, J. M., Goyal, V., Berrebi, S., Brakewood, C., & Watkins, K. E. (2022). Why has public transit ridership declined in the United States? *Transportation Research Part A: Policy and Practice*, *161*, 68–87. https://doi.org/10.1016/J.TRA.2022.04.006

2. *Product Details R47302*. (n.d.). Retrieved July 30, 2023, fromhttps://crsreports.congress.gov/product/details?prodcode=R47302

3. Berrebi, S. J., Joshi, S., & Watkins, K. E. (2021). On bus ridership and frequency. *Transportation Research Part A: Policy and Practice*, *148*, 140–154. https://doi.org/10.1016/J.TRA.2021.03.005

4. Hosseini, S.S., Azarbayjani, M., Lawrence, J., Tabkhi, H. (2023). Towards Understanding the Benefits and Challenges of Demand Responsive Public Transit-A Case Study in the City of Charlotte, NC. *arXiv preprint arXiv:2304.06467*. https://doi.org/10.48550/arXiv.2304.06467.

5. Rashvand, N., Hosseini, S.S., Azarbayjani, M., Tabkhi, H. (2023). Real-Time Bus Arrival Prediction: A Deep Learning Approach for Enhanced Urban Mobility. *arXiv preprint arXiv:2303.15495*. https://doi.org/10.48550/arXiv.2303.15495.

6. Sun, R., Gui, R., Neema, H., Chen, Y., Ugirumurera, J., Severino, J., Pugliese, P., Laszka, A., & Dubey, A. (2021). TRANSIT-GYM: A Simulation and Evaluation Engine for Analysis of Bus Transit Systems. *Proceedings - 2021 IEEE International Conference on Smart Computing, SMARTCOMP 2021*, 69–76. https://doi.org/10.1109/SMARTCOMP52413.2021.00030

7. Sen, R., Tran, T., Khaleghian, S., Pugliese, P., Sartipi, M., Neema, H., & Dubey, A. (2022). BTE-Sim: Fast Simulation Environment For Public Transportation. *Proceedings - 2022 IEEE International Conference on Big Data, Big Data 2022*, 2886–2894. https://doi.org/10.1109/BIGDATA55660.2022.10020973

8. Ji, T., Yao, Y., Dou, Y., Deng, S., Yu, S., Zhu, Y., & Liao, H. (2022). The Impact of Climate Change on Urban Transportation Resilience to Compound Extreme Events. *Sustainability 2022, Vol. 14, Page 3880*, *14*(7), 3880. https://doi.org/10.3390/SU14073880

9. *Climate Change Impact Urban Transportation Resilience | Encyclopedia MDPI*. (n.d.). Retrieved December 8, 2023, from https://encyclopedia.pub/entry/22953

10. Winkler, L., Pearce, D., Nelson, J., & Babacan, O. (2023). The effect of sustainable mobility transition policies on cumulative urban transport emissions and energy demand. *Nature Communications 2023 14:1*, *14*(1), 1–14. https://doi.org/10.1038/s41467-023-37728-x

11. Jing, Q. L., Liu, H. Z., Yu, W. Q., & He, X. (2022). The Impact of Public Transportation on Carbon Emissions—From the Perspective of Energy Consumption. *Sustainability 2022, Vol. 14, Page 6248*, *14*(10), 6248. https://doi.org/10.3390/SU14106248

12. *The South End: Living the Life on Charlotte's Blue Line - RentCafe rental blog*. (n.d.). Retrieved December 8, 2023, from https://www.rentcafe.com/blog/apartment-search-2/neighborhood-guides/the-south-end-living-the-life-on-charlottes-blue-line/

13. *Charlotte, North Carolina Neighborhoods - December 2023*. (n.d.). Retrieved December 8, 2023, from https://www.zipdatamaps.com/neighborhoods/north-carolina/city/map-of-charlotte-neighborhoods

14. *The Demographic Statistical Atlas of the United States - Statistical Atlas*. (n.d.-a). Retrieved December 8, 2023, from https://statisticalatlas.com/place/North-Carolina/Charlotte/Population

15. *CNU31: Charlotte, NC. South End Spaces*. (n.d.). Retrieved December 8, 2023, from https://www.micnu.org/post/cnu31-charlotte-nc-south-end-spaces

16. Hosseini, S.S., Azarbayjani, M., Tabkhi, H. (2023). Community-Driven Approach for Smart On-Demand Public Transit in Charlotte in Underserved Communities - Pilot Study for User Acceptance and Early Data Collection. *ARCC 2023 International Conference-The Research-Design Interface, pp. 25-32.* https://www.arcc-arch.org/wp-content/uploads/2023/09/ARCC2023ProceedingsFINAL-PW.pdf.

17. *Avondale Chattanooga, TN 37406, Neighborhood Profile - NeighborhoodScout*. (n.d.). Retrieved December 8, 2023, fromhttps://www.neighborhoodscout.com/tn/chattanooga/avondale

18. *The Demographic Statistical Atlas of the United States - Statistical Atlas*. (n.d.-b). Retrieved December 8, 2023, from https://statisticalatlas.com/place/Tennessee/Chattanooga/Population

19. *Transitland • Charlotte Area Transit System (CATS) • GTFS feed details: f-dnq-charlotteareatransitsystem*. (n.d.). Retrieved December 8, 2023, from https://www.transit.land/feeds/f-dnq-charlotteareatransitsystem

20. *Transitland • Chattanooga Area Regional Transportation Authority (CARTA) • GTFS feed details: f-dn5r-carta*. (n.d.). Retrieved December 8, 2023, from https://www.transit.land/feeds/f-dn5r-carta

21. *ArcGIS Web Application*. (n.d.). Retrieved December 8, 2023, from 4https://www.arcgis.com/apps/webappviewer/index.html?id=964881960f0549de8c3583bf46ef5ed4

22. *Traffic Count Database System (TCDS)*. (n.d.). Retrieved December 8, 2023, from https://tdot.public.ms2soft.com/tcds/tsearch.asp?loc=Tdot&mod=TCDS

PLEA 2024 WROCŁAW
(Re)thinking Resilience

Assessment of heat stress hazard at an intra-urban level: A case of Delhi, India

KSHITIJ KACKER[1], MAHUA MUKHERJEE[1,2], PIYUSH SRIVASTAVA[2]

[1]Department of Architecture and Planning, IIT Roorkee, Roorkee, India
[2] Centre of Excellence in Disaster Mitigation and Management, IIT Roorkee, Roorkee, India

ABSTRACT: Heat stress conditions, exacerbated by changing climate patterns, pose significant risks to the health, economy, and overall well-being of city inhabitants. To assess the impact of heat stress on residents is understood by developing a comprehensive heat stress hazard map utilizing the Humidex index for the city of Delhi, India. Employing the Weather Research Forecast Urban Canopy Building Effect Parameterization model, a high-resolution humidex map is generated at a resolution of 333.33m. The map delineates humidex conditions during the summer and monsoon periods in 2023. Alarming findings reveal that 98% of the city falls under the dangerous mark, indicating a heightened hazard of heat stroke for its residents. Even during the monsoon season, the dangerous mark persists for 77% of the city, with the remaining areas experiencing discomfort. All Local Climate Zones are adversely affected by elevated humidex levels, with the Bare Soil and Sand zone exhibiting higher humidex ranges compared to the rest of the city in both seasons. Additionally, the combination of Compact Mid-Rise and Open Low-Rise zones in the eastern part of the city also faces elevated humidex levels. To mitigate these adverse effects, the study concludes by proposing various nature-based solutions that can be implemented to reduce the impact on the city.
KEYWORDS: Humidex, WRF-UCM, Nature-based Solution (NbS), Heat stress

1. INTRODUCTION

Extreme heat conditions under changing climate are risk to health, energy security, economy, and well-being of habitants of built and natural environment. Exposure of the body to extreme thermal conditions results in failure of its thermo-regulatory mechanism. This leads to increased morbidity and mortality rates in vulnerable population. With the current growth rate, the urban population in India is expected to reach 600 million by 2030 and by 2050, 50% of the population will be urbanized [1]. Increased frequency and duration of extreme heat events and unequal development expose the residents of the city to increasing thermal climate change-related mortality and morbidity risks [2-3]. This poses a challenge for policymakers to derive safety mechanisms to protect people.

To address the issue, it is important to gain a comprehensive understanding of the specific hazards within the urban area. Given that global climate models provide a broader perspective of heat stress, they lack to provide details required for localized decision-making within a city. This underscores the necessity to create a detailed hazard maps that focus on the urban environment. These maps serve to illuminate the effects on a smaller, neighbourhood level. Since formulating policies at an individual residence level is impractical, addressing challenges at the Local Climate Zone (LCZ) level offers a more viable approach.

Heat stress maps of cities are crucial as they map the high spatial heterogeneity in cities which helps to understand the heat stress hazard. Intra-urban heat stress studies depicting the variability are rarely considered over Asia, which houses many megacities [4-5]. India is home to many such cities with high population. Urban level subtleties should be taken into consideration by the policy makers and academicians, while mapping thermal hotspots at high spatial resolution [6]. This study intends to address this concern by formulating a novel numerical weather prediction model-based heat stress hazard map for a city at a very fine resolution and discusses Nature based Solution (NbS) to mitigate heat stress and adapt to the intra-urban level heat related hazard.

2. HEAT STRESS INDEX

As per ISO 31010, indices if well understood, can be used for risk classification associated to an activity. It provides a single numeric output by integrating a large range of factors that impact the risk [7]. Single parameter like air temperature only explains a small part of how humans experience heat. Other factors may be equally or more important to understand heat releasing and heating mechanism of human body [8].

'Humidex' is an index developed by Meteorological Service of Canada as an alternative to heat index. It has been used in epidemiology for calculating mortality and morbidity as well as in

weather forecasting. It describes the hotness an average person feels due to weather under combined effects of heat and humidity as a hazard index. It is considered as a sensory index that helps in representing an equivalent temperature for comparison [9].

The humidex formula is in following equation (1):

$$\text{Humidex} = Tdb + [\,0.5555\,(\,Pa - 10)]$$

Or

$$\text{Humidex} = Tdb + 0.5555\,(\,6.11 e^{5417.7530\left(\frac{1}{273.16} - \frac{1}{Tdp+273}\right)} - 10) \quad (1)$$

Tdb = dry bulb temperature (°C),
Pa = vapor pressure (hPa),
Tdp = dew point temperature (°C)

Also, according to [10], the relationship between Dew point temperature, Dry bulb temperature and Humidity can be expressed as equation (2):

$$Tdp = Tdb - ((100 - RH)/5) \quad (2)$$

RH = Relative Humidity (%)

The model describes humidex of 20°C - 29°C as little discomfort, 30°C - 39°C as some discomfort, 40°C - 45°C as great discomfort where exertion should be avoided and 46°C and above as dangerous where possible heat stroke can take place [11]. For this study a new category that is 50°C and above is taken as a layer with higher severity named as highly dangerous.

3. OBJECTIVES

The objectives of the study are to:

- Develop a validated heat stress hazard map of Delhi (India) urban area.
- Understand the relation between LCZ and heat stress of the urban areas

The study is limited to the municipal boundary of Delhi city.

4. STUDY DESIGN

4.1 Study Area

Delhi is situated in the northern part of India. The co-ordinates being at 28.38°N, 77.12°E, at an altitude of 218m above the mean sea level. The area that municipal boundary of Delhi encompasses is between 28° 24' 17" N and 28° 53' 00" N latitude and 76° 50' 00" E and 77° 20' 37" E longitude. Delhi experiences extreme weather conditions, characterized by scorching summers with temperatures ranging from 27.6°C to 44.2°C and chilly winters with temperatures varying between 3.5°C and 22.2°C. The climate in Delhi varies from tropical moist (Koppen-Cwa) to semi-arid (Koppen-Bsh) due to the influence of continental air in the region [12]. According to [13], in 2011 National Capital Territory (NCT)-Delhi had a 98% urbanized population which is quite more than the then national average of 32%. The overall population in NCT-Delhi was 16.79 million in 2011 and is expected to rise to 38.94 in 2030 [14].

4.2 Model and Experimental Design

The study focuses on developing a hazard map by deploying the Weather Research and Forecast – Urban Canopy Building Effect Parameterization Model (WRF-UCM_BEP) to get meteorological variables at a resolution of 333.33m [15]. This is achieved by using the boundary conditions from ERA5 reanalysis data, which is used to downscale the variables to the given resolution and the urban definition is added through the global LCZ data available at 100m resolution [16]. The data output is then validated through in-situ meteorological measurements from the network of weather stations provided by Delhi Pollution Control Committee and Central Pollution Control Board. Utilizing the validated model output, the humidex index is calculated through Equation (1) and presented geospatially.

The research is conducted during the monsoon and summer periods of 2023, selecting a span of 5 days to serve as indicative of respective season. This approach is aimed at encompassing points when temperatures reach their peak and humidity level is low, as well as vice-versa conditions. These factors are crucial inputs for the humidex equation. According to these criteria the peak air temperature in 2023 was 23rd May 2023 and the point with maximum dew point temperature was on 13th July 2023, which made 21st May 2023 to 25th May 2023 and 11th July 2023 to 15th July 2023 as the period of simulation. Also, these values reached their maxima at 14:30 IST, which helped in mapping the heat stress map for the given tenure.

Next, a LCZ map of Delhi is generated using the World Urban Database and Access Portal Tools (WUDAPT) LCZ generator, utilizing designated training areas for model training [17]. This LCZ map is then compared with the heat stress map to discern heat stress impacts across different Local Climate Zones (LCZs) and analyze correlations within the outputs. Based on the comparison of maps, a series of NbS techniques are identified to alleviate heat stress conditions in Delhi.

5. RESULT

5.1 Summer Humidex

Humidex in summer season of 2023 has values reaching to highly dangerous levels over the city. The humidex ranges from 41.5°C to 54.1°C, in which 98% of the city's region is under the highly dangerous mark, i.e., above 50°C. Throughout this highly dangerous marked city a variation of 4.1°C can be

noted with Central, North and South Delhi being under a range of 50°C to 52°C and West and East Delhi being in 52°C to 53°C as shown in Figure 2. The discrete point spider graphs in Figure 1 defines the validation and fit of the usage of simulation, in comparison to real world data at various locations spread across the city of Delhi for the given days.

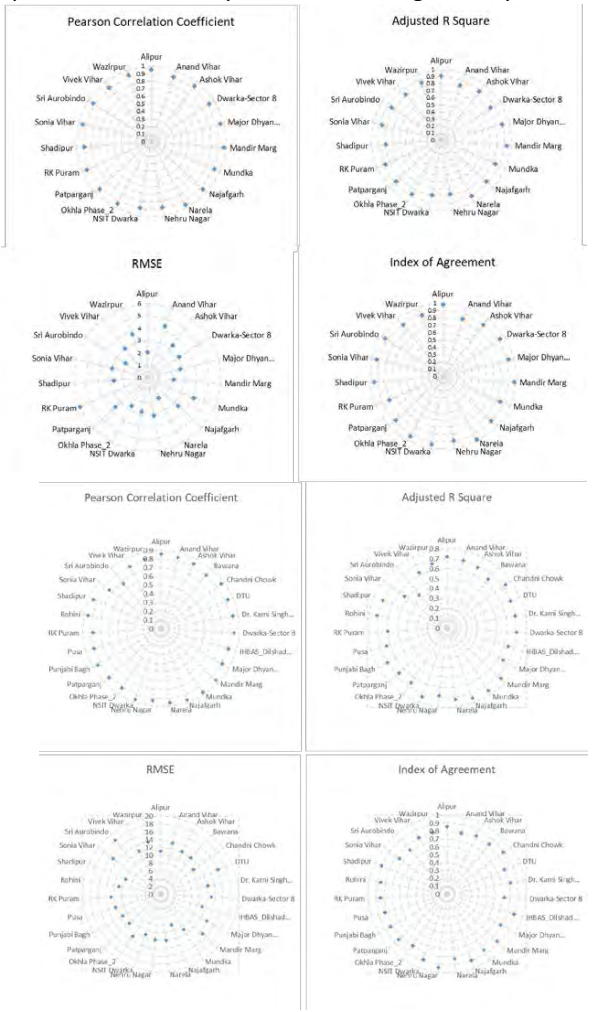

Figure 1: Clockwise from Top Left: Pearson Co-relation; Adjusted R^2; Index of Agreement; RMSE (Above for Temperature at 2m in Summer Period) and (Below for Relative Humidity at 2m in Summer Period)

5.2 Monsoon Humidex

Humidex in monsoon season of 2023 has values reaching to dangerous levels over the city. The humidex ranges from 38.5°C to 50.2°C, in which 77% of the city's region is under the dangerous mark, i.e., above 45°C and rest of the city is under a great discomfort segment. Throughout the city a variation of 11.7°C can be noted with Central Delhi being under a range of 41°C to 43°C, North Delhi being under a range of 45°C to 47°C, West Delhi majorly covered in the patches of 47°C and above and South and East Delhi being in patches of either 41°C to 43°C or 47°C and above; as shown in Figure 4. The discrete point spider graphs in Figure 3 defines the validation and fit of the usage of simulation, in comparison to real world data at various locations spread across the city of Delhi for the given days.

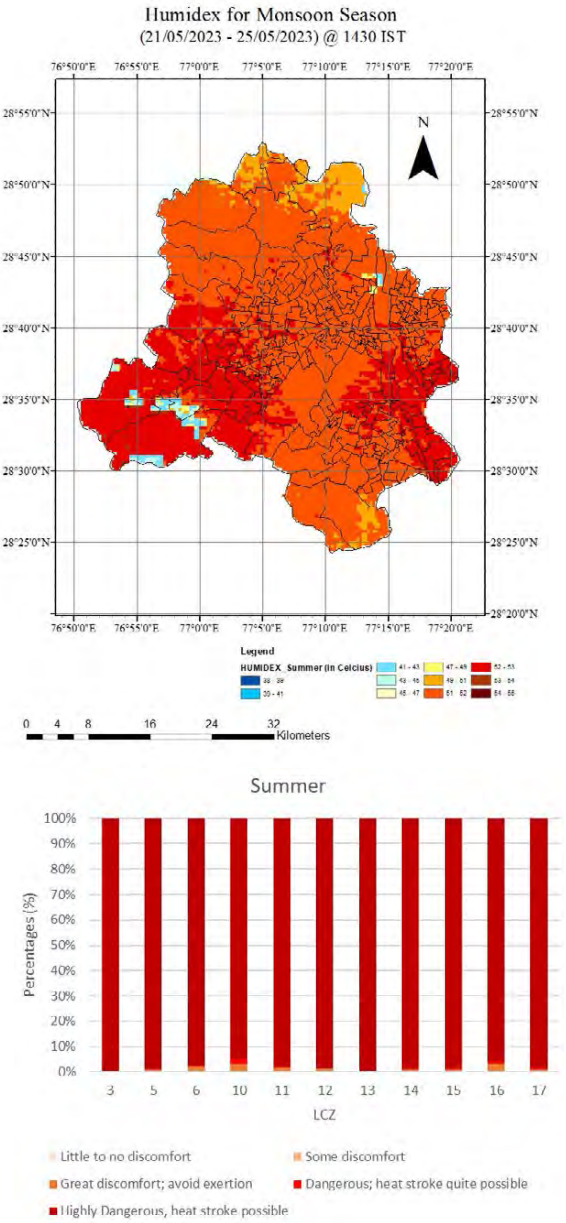

Figure 2: Humidex for summer season (21/05/2023 – 25/05/2023) at 14:30 IST (Above) and Percentage share of heat stress in summer in different LCZs (Below)

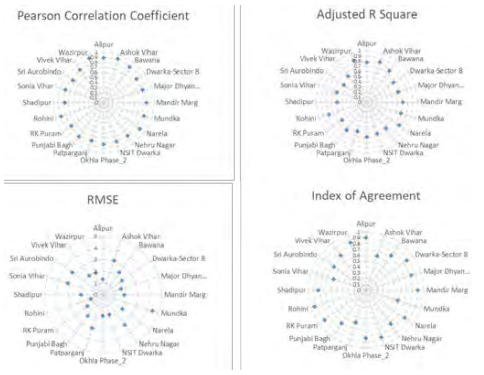

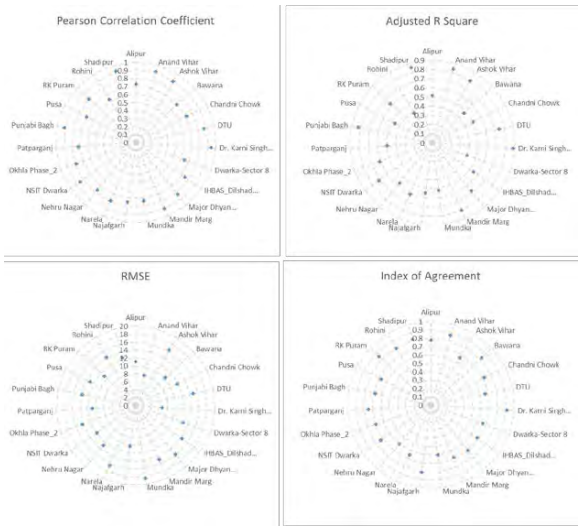

Figure 3: Clockwise from Top Left: Pearson Co-relation; Adjusted R^2; Index of Agreement; RMSE (Above for Temperature at 2m in Monsoon Period) and (Below for Relative Humidity at 2m in Monsoon Period)

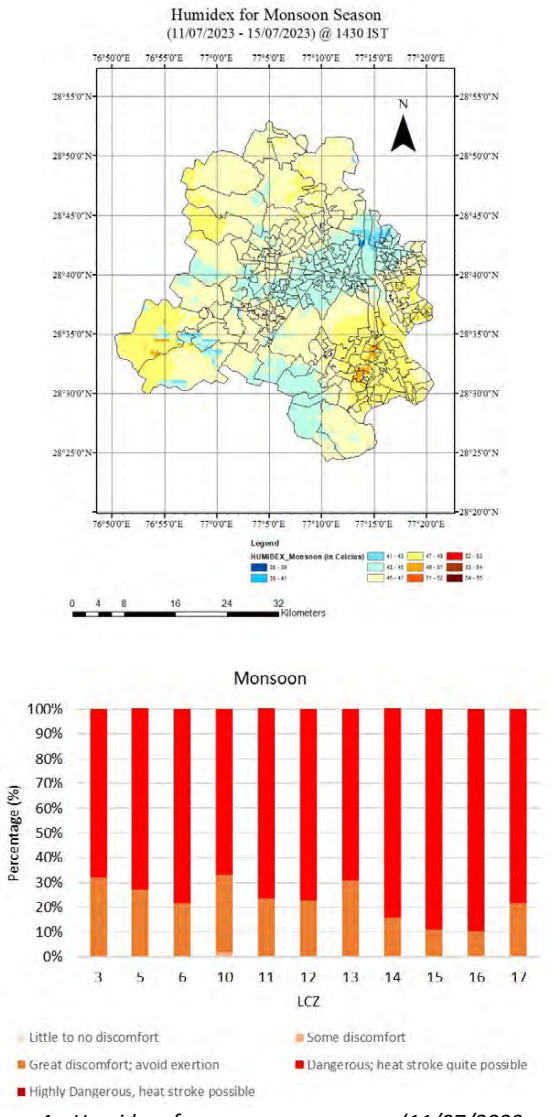

Figure 4: Humidex for monsoon season (11/07/2023 – 15/07/2023) at 14:30 IST (Above) and Percentage share of heat stress in monsoon in different LCZs (Below)

5.3 Local Climate Zone

Figure 5 shows that 58.8% of the area of Delhi falls under the built LCZ zones numbered from 1 to 10, while the unbuilt LCZ zones numbered from 11 to 17, cover 41.2% of Delhi's area. Majority of the built LCZ zones consists of Open Mid-Rise structure (LCZ5), Open Low-Rise (LCZ6), Compact Low-Rise (LCZ3) and Heavy Industry (LCZ10) which share 22.7%, 22.3%, 13.4% and 0.5% respectively of the city's area. The unbuilt LCZ consists majorly of Low Plants (LCZ14), followed by Bare soil and sand (LCZ16), Dense Trees (LCZ11), Bush and Scrubs (LCZ13), Bare Rock or Paved (LCZ15), Water (LCZ17) and Scattered trees (LCZ12) in the percentages of 18.3%, 7.8%, 6.1%, 5.6%, 1.5%, 1.3% and 0.6% of Delhi's area respectively.

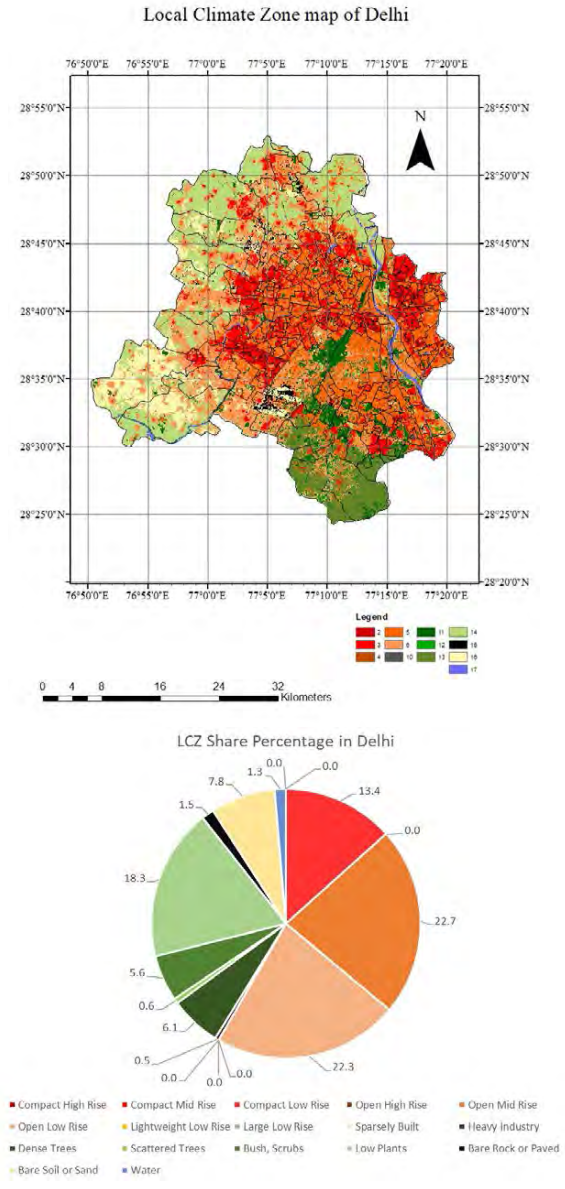

Figure 5: Local climate zone map of Delhi (Above) and Percentage share of LCZ in Delhi (Below)

5. DISCUSSION

5.1 Summer Humidex

Throughout the summer, Delhi has experienced extreme humidex hazard conditions, subjecting the entire city to significant heat stress. To highlight the intensity across different parts of the city, a new segment is incorporated into the traditional humidex indices within the study. A comparison between Figure 2 and Figure 5 reveals that the western part of the city, encompassing Bare Soil and Sand (LCZ16), Open Mid-Rise (LCZ5), and Compact Low-Rise (LCZ3), exhibits highly dangerous humidex levels. Notably, 98% of LCZ 16 registers humidex levels exceeding 50°C. In the eastern part, primarily covered by Open Mid-Rise (LCZ5) and Compact Low-Rise (LCZ3), similar highly dangerous levels are observed.

The northern and southern tips depict relatively cooler zones compared to other parts of the city in Figure 2. Contrasting with Figure 5, these zones fall under Low Plant (LCZ14) in the northern part and Bush and Scrubs (LCZ13) in the southern areas. Despite 30.6% of Delhi's area classified as green in Figure 5, including forested areas constituting 13.15% of the total city area as of 2021 [18], the city still experiences high heat stress, with maximum temperatures nearing 57°C. Even though this green area meets the World Health Organization's (WHO) minimum requirement of 9m² of green space per capita [19], the challenge persists. During the same period, humidity values peak at nearly 33% around 14:30. To alleviate these conditions, it is essential to implement measures addressing the overall air temperature throughout the city, with particular emphasis on the western and eastern regions.

Strategy:

- Deciduous trees that are indigenous to Delhi like Cassia fistula, Neolamarckia cadamba, should be planted in the city center as well as the places that are yet falls in with unbuilt LCZs. As deciduous trees have large foliage that protects the citizens from harsh sun during summer and they shed their leaves in winter, which allows sun to enter during winters.
- Provision of urban forest at locations designated as green areas will also be helpful. This large agglomeration of forest will cool down the incoming hot air. The current green space covers 30.6%, of the city, still the temperature reaches to higher levels, as the LCZ11 is only 6.1%, its growth will improve the heat stress conditions during summer.
- Green wall and green roof can be deployed at building levels to reduce the impact as Compact Low-Rise (LCZ3), provides less space to plant trees on the ground. Due to this technique, the areas with dense growth can be cooled down during the summer.

5.2 Monsoon Humidex

During the monsoon, humidex becomes a bit less harsh, but still the conditions for majority of the spatial extent are dangerous. In Figure 4, the western and eastern part of the city are under the high humidex zones. As the summer heat index this region also stays in a higher hazard value than the whole city. The central part of the dense city stays comparatively less harsh. As per the relative humidity in the central part of the city is less in comparison to the green areas around it clearly shows the Urban Dry Island (UDI) effect. As the maximum air temperature at 2m during 14:30 IST is nearly about 36°C and the city center shows the UDI effect, the humidex tends to become lower in value. The eastern part remains a problem due to its higher air temperature values than that at the central region. Hence to reduce the humidex during the monsoon months it becomes more necessary to reduce the humidity in the region, as the maxima values for humidity are reaching nearly 97% at 14:30 within the city.

Strategy:

- Permeable surfaces are necessary for removal of stagnant water. Gravel or pavers, help water to infiltrate in the ground. This helps to reduce humidity levels and improve ground water condition within the city.
- Naturally as it is difficult to control the humidity levels at an urban scale, the planning of neighbourhood becomes important. The neighbourhood planning should be either remodelled or new planning should promote air movement, as this is one of the techniques to use NbS through technology.
- The Water management also place a crucial role to reduce humidity, the water from places where people are living should be removed by management techniques. It can be delivered to storage areas or to ground water recharge pits. If taken to wetlands, then wetland area will be having a higher humidity, so city can be planned accordingly. Accordingly, retention pond can be designed over areas where less of population is present, like (green LCZ areas).
- The clothing values for monsoon could be altered to make people feel comfortable.

6. CONCLUSION

The paper provides a novel mapping of humidex at 333.33m for summer and monsoon season of 2023 in Delhi, India. The city is under a tremendous heat stress under the summer and monsoon peaks. The conditions in summer are so harsh that a new segment in the humidex range is added to show its

severity. As the humidex is a combination of both temperature and humidity, hence this map shows the discomfort that the residents face. High-resolution model helps in understanding the places where these issues are worse than the other. The Western and Eastern part of the city come out to be facing a high amount of humidex discomfort in both seasons. All the LCZs in summer and monsoon are part of the high humidex values, but particularly LCZ16, Bare soil and sand is present on the western side that faces the harshness of the humidex and the urban cluster on the Eastern part faces the issue. To reduce the humidex level both the air temperature and humidity must be managed. For doing so, there are various NbS that could be deployed. To decrease the impacts through temperature use of deciduous trees, urban forest, green wall and roof system, conversion of unbuilt LCZs to LCZ11, wherever possible can be done. For decreasing the humidity levels, the NbS have to clubbed with various technologies like planning to improve the wind movement and water management or to provide better clothing to the users. Both NbS techniques have to be integrated to provide better results in both the seasons at the same place. It can be observed that NbS can act as a catalyst or a helper to reduce the discomfort, but now the conditions are reaching to certain thresholds that sustainable mechanical techniques must be planned simultaneously. Hence, *Nature-based Technical Solution (NbTS)* should be focussed now. But this should only be planned after a detailed ward level analysis. Hence, this creates a need of future study on selection of high humidex hotspots and to alter or improve their planning at a micro level.

ACKNOWLEDGEMENTS

We acknowledge the National Supercomputing Mission (NSM) for providing computing resources of 'PARAM Ganga' at the Indian Institute of Technology Roorkee, which is implemented by C-DAC and supported by the Ministry of Electronics and Information Technology (MeitY) and Department of Science and Technology (DST), Government of India. Also, KK is thankful to Prime Minister Research Fellowship (PMRF – Grant No. PM-31-22-701) for their support.

REFERENCES

1. NITI Aayog, "REFORMS IN URBAN PLANNING CAPACITY IN INDIA," Government of India, New Delhi, 2021.
2. C. Singh, M. Madhavan, J. Arvind and A. Bazaz, "Climate change adaptation in Indian cities: A review of existing actions and spaces for triple wins," Urban Climate, vol. 36, pp. 1-20, 2021.
3. IPCC, "IPCC_AR6_WGII_FinalDraft_FullReport," WMO, UNDP, 2022.
4. B. Jänicke, A. Holtmann, K. R. Kim, M. Kang, U. Fehrenbach and D. Scherer, "Quantification and evaluation of intra-urban heat-stress variability in Seoul, Korea," International Journal of Biometeorology, vol. 63, pp. 1-12, 2019.
5. J. Bao, X. Li and C. Yu, "The Construction and Validation of the Heat Vulnerability Index, a Review," International Journal of Environmental Research and Public Health, vol. 12, pp. 7220-7234, 2015.
6. D. M. Lapola, D. R. Braga, G. M. D. Giulio, R. R. Torres and M. P. Vasconcellos, "Heat stress vulnerability and risk at the (super) local scale in six Brazilian capitals," Climatic Change, vol. 154, pp. 477-492, 2019.
7. I. Keramitsoglou, C. T. Kiranoudis, B. Maiheu, K. D. Ridder, I. A. Daglis, P. Manunta and M. Paganini, "Heat wave hazard classification and risk assessment using artificial intelligence fuzzy logic," Environmental Monitoring and Assessment, vol. 185, no. 10, pp. 8239-8258, 2013.
8. S. Koopmans, B. Heusinkveld and G. Steeneveld, "A standardized Physical Equivalent Temperature urban heat map at 1-m spatial resolution to facilitate climate stress tests in the Netherlands," Building and Environment, vol. 181, no. 106984, pp. 1-13, 2020.
9. G. Havenith and D. Fiala, "Thermal Indices and Thermophysiological Modeling for Heat Stress," Comprehensive Physiology, vol. 6, no. 1, pp. 255-302, 2016.
10 M. G. Lawrence, "The Relationship between Relative Humidity and the Dewpoint Temperature in Moist Air: A Simple Conversion and Applications," American Meteorological Society, vol. 86, pp. 225-234, 2005.
11. Government of Cananda, "Warm season weather hazards," Government of Cananda, 16 04 2019. [Online]. Available:https://www.canada.ca/en/environment-climate-change/services/seasonal-weather-hazards/warm-season-weather-hazards.html. [Accessed 22 12 2023].
12. Shahfahad, M. W. Naikoo, A. R. M. T. Islam, J. Mallick and A. Rahman, "Land use/land cover change and its impact on surface urban heat island and urban thermal comfort in a metropolitan city," Urban Climate, pp. 1-21, 2022.
13. DDA, "Draft Sub-Regional Plan for NCT Delhi -2021," DELHI DEVELOPMENT AUTHORITY, Delhi, 2021.
14. United Nations, "World Urbanization Prospects," United Nations, New York, 2019.
15. A. Martilli, A. Clappier and M. W. Rotach , "An urban surface exchange parameterization for mesoscale models.," Boundary-Layer Meteorology, vol. 104, pp. 261-304, 2002.
16. M. Demuzere, J. Kittner, A. Martilli, G. Mills, C. Moede, I. D. Stewart, J. v. Vliet and B. Bechtel, "A global map of local climate zones to support earth system modelling and urban-scale environmental science," Earth System Science Data, vol. 14, pp. 3835-3873, 2022.
17. M. Demuzere, J. Kittner and B. Bechtel, "LCZ Generator: A Web Application to Create Local Climate Zone Maps," Frontiers in Environmental Science, vol. 9, pp. 1-18, 2021.
18 Ministry of Environment, Forest and Climate Change, Government of India, "Forest coverage in the country," Ministry of Environment, Forest and Climate Change, 20 07 2023. [Online]. Available: https://pib.gov.in/PressReleasePage.aspx?PRID=1941073#:~:text=As%20per%20latest%20ISFR%202021,geographical%20area%20of%20the%20country.. [Accessed 25 12 2023].
19 World Health Organization, "Health Indicators of Sustainable Cities in the Context of the Rio+20 UN Conference on Sustainable Development," WHO, Geneva, Switzerland, 2012.

PLEA 2024 WROCŁAW
(Re)thinking Resilience

Optimization of Standardized Brazilian School Buildings with Passive Strategies and Cool Coatings

CAMILA MACHADO DE AZEVEDO CORREIA[1], CLÁUDIA NAVES DAVID AMORIM[1], MATTHEOS SANTAMOURIS[2]

[1]University of Brasilia, Brasilia, Brazil
[2]University of New South Wales, Sydney, Australia

ABSTRACT: Standardized replicable buildings can cause discomfort and increased air conditioning usage. Besides, super cool coatings are effective passive solutions. Therefore, this study evaluates thermal comfort in a standardized Brazilian public school in 8 climates, verifies suitable cool coatings and identifies optimal additional passive techniques to meet regulatory requirements without active air conditioning. Methods include pilot simulations with DesignBuilder, thermal comfort analysis considering ASHRAE 55 adaptive model; JEA Algorithm optimization simulations; identification of most influential passive strategies by sensitivity analyses; and evaluation of the ideal opaque envelope through heat balance. Results showed that current model do not meet the Brazilian normative. Thus, different super cool coatings are recommended: thermochromic for heating-dominated; spectrally selective for cooling-dominated dry and high broadband emissivity for extreme-cooling-dominated humid zones. Regarding opaque envelope, thermal mass flat roofs and insulated walls are advised. In 7 of 8 climates, super cool roof was most effective followed by natural ventilation. Optimal combinations include super cool envelope, window shading and natural ventilation 24 hours 7 days a week with 95% aperture for extreme-cooling-dominated zones; super cool roofs, medium reflectivity walls and 5% aperture for cooling-dominated; thermochromic roof and dark walls with natural ventilation during occupancy with 5% aperture for heating-dominated.
KEYWORDS: Super Cool Coatings, Educational Buildings, Energy Efficiency, Building Design, Building Energy Simulation

1. INTRODUCTION

Currently, more than 55% of the world population lives in cities and this percentage is predicted to increase to 68% by 2050 [1]. This continuous growth of built-up areas potentiates the phenomenon of heat islands, reduces the levels of comfort in external and internal spaces. This situation has caused an increase in the use of air conditioning [2], registered mainly after the 2000s with a growth of 130% until 2022 [3]. This scenario is potentiated in standardized public constructions replicated in different climatic contexts, generally planned to overcome constructive deficits, such as public schools in Brazil [4]. In these cases, the low cost and the ease of replicating the models is opposed to the lack of adaptation to the climatic context, which causes discomfort for the occupants and increases the tendency of artificial conditioning [4, 5].

The energy efficiency of buildings and the thermal comfort are fundamental objectives for an adequate performance of buildings [6]. These are targets of numerous building design optimization studies [7]. An optimization study is achieved by a combination of different design variables, such as building geometry, envelope, passive strategies and energy systems [7].

Among the most common passive solutions in optimization studies, super cool coatings stand out, as they have a high potential for cooling buildings [1, 8]. Research on super cool coatings has advanced significantly in recent years, but there are still research gaps, expressed by the following questions:

1) Which super cool coatings are best suited for Brazilian climates?
2) Is it possible to provide comfort and energy efficiency in standardized Brazilian public schools only with passive strategies?

This article, therefore, proposes an analysis of the most suitable super cool coatings for the 8 Brazilian bioclimatic zones and an optimization study of a replicable standardized architectural design of Brazilian public schools, with air conditioning based only on passive strategies and super cool coatings. The objectives of the optimal solutions are: thermal comfort and low energy consumption.

2. METHODS

The optimization process was structured in four stages (Preparation, Algorithm Optimization Simulations, Non-Algorithm Optimization Simulations and Final Step), based on [7].

Section 2.1, focusing on preparation, covers climate, building, occupancy, and soil information for

modelling and simulations, outlining optimization objectives selection, climate grouping, Thermal Comfort Analysis, and adherence to Brazilian normative requirements. The section also covers scenario definition and variable selection based on Heat Balance Analyses, along with the identification of suitable super cool coatings for the Brazilian context through a literature review and consideration of common opaque substrates. Section 2.2 presents Algorithm Optimization Simulations methods, settings, and criteria for interpreting Heat Balance and Sensitivity Results. Section 2.3 explains Non-Algorithm Simulations, detailing tested variables and software settings, while Section 2.4 (Final Stage) outlines criteria for the synthesis of the optimized building by climate groups.

2.1 Preparation

Reference cities from each Brazilian bioclimatic zone were chosen according to [9], and their climatic characteristics are detailed in Table 1.

Table 1: Cities selected and Weather Classification

Zone	City	Koppen-Geiger Classification	ASHRAE Classification
1	Caxias do Sul	Cfb	3A: Warm Humid
2	Nova Friburgo	Cwb	2A: Hot Humid
3	Florianópolis	Cfa	2A: Hot Humid
4	Brasília	Aw	2A: Hot Humid
5	Santos	Af	2A: Hot Humid
6	Goiânia	Aw	1A: Very Hot Humid
7	Picos	Bsh	1A: Very Hot Humid
8	Belém	Am	A0: Extremely Hot Humid

The study focuses on a standardized 1 classroom public school, a project developed by the National Education Development Fund (FNDE), a federal government institution with extensive operations across Brazil. This model is replicated in various Brazilian regions, especially in small municipalities. Data for this school model (Figure 1) were obtained from official government sources [10].

Figure 1: Standardized School Floor Plan and Perspective.

All rooms in the schools were modelled, but thermal evaluation focused exclusively on the classrooms. DesignBuilder Version 7.0.2.4 with EnergyPlus engine was used. The recommended north-south solar orientation by FNDE was adopted. Building thermal and optical properties, based on [9, 11] are detailed in Table 2.

Table 2: Building Materials – FNDE Standard Schools

Building Element	U (W/m².K)	R (%)
External Walls	2.37	60
Internal Walls	2.37	70
Roof	2.05	35
Internal Floor	3.20	40
Glazing	5.70	-

These FNDE projects don't include air conditioning system. The lighting system consists of fluorescent lamps, with power density of 8W/m² [10]. The electrical equipment in the classroom was 5W/m², as used in previous studies [12].

The classroom occupancy, with 30 children reading, follows the schedule outlined by the Brazilian Ministry of Education: February to June and August to December, from 8:00 am to 12:00 pm and 2:00 pm to 6:00 pm.

In simulations, Kiva Basic is employed for calculating ground temperatures, with no floor insulation layer, aligning with the FNDE standards.

Pilot simulations were conducted in all 8 bioclimatic zones for verification of the thermoenergetic performance of current state schools. Occupied hours in thermal comfort were calculated by the adaptive method of ASHRAE 55 with 80% acceptability, which is the method used in the Brazilian Labeling Program (PBE Edifica) [13]. It mandates naturally ventilated public buildings without artificial conditioning to achieve at least 90% occupied hours in thermal comfort during building use, with a 10% tolerance for heat discomfort, neglecting cold discomfort — a concern in cold cities.

Therefore, the main objective function in this study is thermal comfort, with a 10% tolerance for hours in heat discomfort and 10% for cold discomfort, as an adaptation of PBE Edifica requirements. Pilot simulations and an initial evaluation of the main objective function achievement revealed distinct climatic groups: Zones 1, 2, and 3 with more than 10% of cold discomfort and heating needs; zones 4, 5, and 6 with more than 10% of heat discomfort and cooling needs; and zones 7 and 8 with more than 70% heat discomfort, necessitating extreme cooling strategies. These groups, considered as optimization scenarios, were called heating-dominated, cooling-dominated, and extreme-cooling-dominated zones, based on [14] definitions.

Subsequently, to guide the selection of optimization variables, impactful variables were assessed by annual heat balances.

Analysing heat balances, key elements were selected: Roof, Ventilation and Walls. To avoid natural light reduction, local window shadings were only considered in critical cases of heat discomfort (Zones 7 and 8) to reduce window solar gains.

Considering the high impact of the roof on heat gains and discomfort, super cool coatings on roofs were prioritized in all zones. The best option for each Brazilian bioclimatic zone was hypothesized as show in Figure 2, considering variations in average annual temperature and air humidity portrayed bioclimatic chart of [9] and material performance variations described by [15].

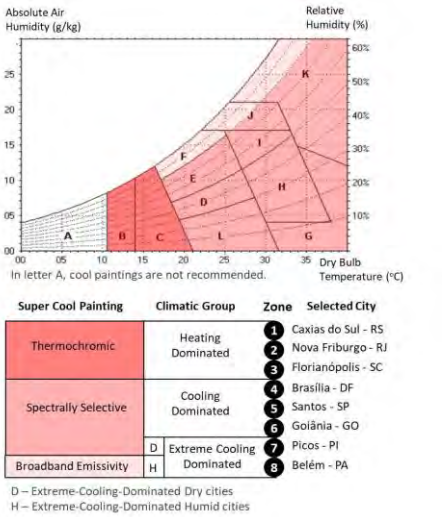

Figure 2: Bioclimatic Chart and suitable super cool coatings.

International research guidelines of super cool coatings [15] indicate that coatings with high emissivity in the atmospheric window or spectrally selective coatings offer superior cooling effect in hot and dry climates (average annual relative humidity under 80%). Thus, the extreme-cooling-dominated zones were subdivided into dry and humid. Due to limitations in DesignBuilder, all simulations employed a uniform setting of emissivity at 90%, without differentiation between spectrally selective and broadband emissivity coatings. As a result, the evaluation of these coatings focused solely on variations in envelope reflectivity.

Thermochromic coatings were explored for mixed Brazilian climates (heating-dominated zones) to modulate heat gains and losses. This option was tested on the roof, simulating different reflectivity values ranging from 10 to 70% in cold and warm months May to October and November to April). For walls, conventional paints with reflectivity from 10 to 50% were simulated. For cooling-dominated zones, super cool coatings with reflectivities of 70 and 90% were tested on roofs and conventional paints of 10 to 70% on walls. In extreme cooling-dominated zones, only super cool coatings with 90% reflectivity was tested for roofs and walls, with local shading using louvres (35°) and sidefins (20°) calculated with Sol-ar Analysis software. To prevent glare, super cool coatings on walls were tested only in extreme-cooling-dominated zones (7 and 8), where schools present extreme cooling needs.

In order to explore diverse thermoenergetic behaviors and identify the ideal substrate for applying super cool coatings in varied climates, different compositions were evaluated (Table 3).

Table 3: Thermal Properties Details of Envelope tested in Optimization Simulations

Substrate Type	Roof		External Wall	
	U (Wm².K)	C (KJ/m².K)	U (Wm².K)	C (KJ/m².K)
Current State	2.25	220.00	2.39	69.73
Insulated	0.57	23.49	0.42	122.00
Light	5.93	55.00	4.40	110.00
Heavy	3.21	220.00	2.93	220.00

For ventilation, optimal solutions were sought in each climatic group, considering two operation schedule options and 5 opening stages. Specifically, in heating-dominated zones, ventilation variables were tested separately for summer and winter. The optimization algorithm variables and scenarios are summarized in Figure 3.

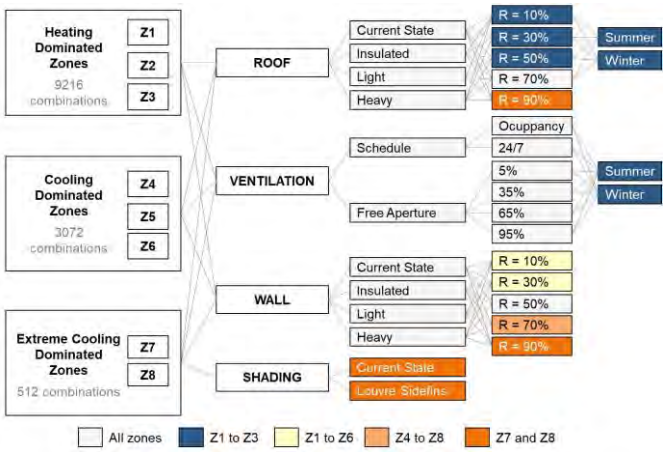

Figure 3: Optimization Variables and Scenarios.

2.2 Algorithm Optimization Simulations

The JEA algorithm was used in optimization simulations for all climates. Cooling and extreme-cooling zones underwent annual simulations, while heating-dominated zones were separately simulated for summer and winter.

The interpretation of the results of thermal comfort and heat balances were complemented with sensitivity analyses: 1. of variables (original and optimized settings of roof, walls, ventilation and shadings) and 2. of roof and walls reflectivities in the optimized model.

In the first step, a comparison between the original school settings and the final optimized model helped identify the most impactful passive strategy for occupied hours in thermal comfort compared to the current state schools.

In the second step, the assessment focused on the influence of super cool coatings on thermal comfort across bioclimatic zones. This was done through variations in reflectivity of roofs and walls from 10% to 90%, considering the final optimized school model. 200 simulations were run per zone per sensitivity analysis.

2.3 Non-Algorithm Optimization Simulations

After algorithm optimizations, only two of the 8 zones failed to meet the target of maximum 10% discomfort from cold or heat: Zone 1 (Caxias do Sul – RS), from heating-dominated group, with 15.4% of cold discomfort and Zone 7 (Picos – PI), from extreme-cooling-dominated group, with 11.8% of heat discomfort.

In these two cases, the last most significant variable for optimization, the ground, was explored. Given the school's single floor horizontal design, the extensive ground contact area plays an important role in thermal balance, further influenced by the surface coverage in adjacent building areas.

However, the DesignBuilder software and the JEA algorithm do not include the external ground as a possible optimization variable. Consequently, an optimization without an algorithm was conducted by testing different reflectivities of the floors adjacent to the building: 30 and 50% for zone 1 and 90% for zone 7. Considering an external concrete surface with 90% emissivity, the final achievement of the optimization objective, focusing on maximum hours in thermal discomfort and annual heat balance, was analysed.

2.4 Final Stage

An optimal school model was synthesized by climate groups, with high thermoenergetic performance provided mainly by super cool coatings and easy replication across the national territory.

3. RESULTS

3.1 Pilots Simulations of Current State School

The results of occupied hours in thermal comfort and heat balance are summarized in Figure 4.

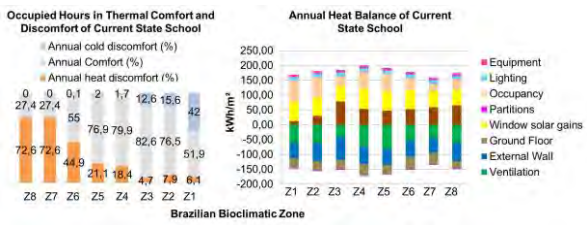

Figure 4: Thermal Comfort and Annual Heat Balance of Current State School.

Schools in zones 2 to 5 present thermal comfort for most of the year, with zone 3 being the most favourable due to milder climates. Zones 1, 2, and 3 exhibit more discomfort from cold than heat during winter when external temperatures are low. The opposite trend is observed in the other zones. Zones 7 and 8 endure extended periods of heat discomfort, lacking cold discomfort, given prevailing external temperatures exceeding 25°C.

Roof is one of the main sources of annual heat gains across all bioclimatic zones, due to the low reflectivity (20%), emphasizing the need for prioritized intervention to reduce heat discomfort. Window solar gains in cities with higher latitudes, Zones 1, 2, 3, and 5 (29, 22, 27, and 24° South, respectively) increase beneficially in winter due to higher solar radiation incidence on the north façade. Classrooms with windows on two opposite sides facilitate cross ventilation, a significant contributor to heat loss in all cases.

In zones 1, 2, and 3, excessive thermal losses due to ventilation contribute to discomfort in winter, making it a key variable for optimization. Zone 1 experiences thermal losses from walls and roofs in winter due to low external temperatures and insufficient thermal insulation of the envelope.

Zone 4 maintains balanced heat gains and losses, leading to a high annual percentage of thermal comfort. While zone 5 shows comparable outcomes, the significant heat discomfort during summer highlights the need to explore cooling strategies and apply super cool coatings.

Zone 6 exhibits significant heat discomfort throughout the year due to relatively high temperatures, reaching above 23°C on average and exceeding 30°C in the hottest hours. Super cool coating on roof is suggested as a potential strategy. Zones 7 and 8 face very high heat discomfort (above 70%) due to elevated temperatures, surpassing 25°C and 30°C. Zone 8's heat discomfort is further intensified by high humidity levels consistently above 80%. Maximum cooling strategies are essential for these two zones.

3.2 Algorithm Optimization

For extreme-cooling-dominated zones, the optimal solution consisted of an insulated wall and heavy roof, both covered by super cool coating, and windows open 24 hours a day with 95% area for ventilation. The thermal comfort objective was achieved only in Belém (Zone 8), with maximum discomfort of 7.3% due to heat and in Picos (Zone 7) it was almost reached, with 11.8% of discomfort.

In cooling-dominated zones, the common optimal solution included an insulated wall with R = 50%, heavy roof with R = 90%, and windows with 5% openings for ventilation. Optimal combinations

included opening windows during occupancy for Brasília (Zone 4) and 24 hours 7 days a week for Santos (Zone 5) and Goiânia (Zone 6). The target objective was achieved in all three cities, with over 90% of occupied hours in thermal comfort.

The optimal model in heating-dominated zones featured an insulated wall with 10% reflectivity, a heavy roof with thermochromic coatings (10/70% in Caxias do Sul and 50/70% in Nova Friburgo and Florianópolis), and 5% window opening for ventilation. In Caxias do Sul (Zone 1), ventilation occurred only during occupancy, while in Florianópolis and Nova Friburgo, it was during occupancy in winter and 24 hours 7 days a week in summer. The optimization objective was achieved only in two cities, with a maximum of 4.4% of occupied hours in thermal discomfort due to heat and 2.3% due to cold in Nova Friburgo, and 0.4% due to heat and 1.5% due to cold in Florianópolis.

Thermal balance of extreme cooling dominated zones (7 and 8) shows that the main factors responsible for thermal losses during the day are: the ground floor (due to the grass cover of the ground adjacent to the building), the wall and the roof covered by the super cool coating. The ground floor has a great influence on the thermal balance due to the horizontality of the building and the larger area in contact with the ground. Ventilation is a heat loss strategy, mainly in the morning and in winter. Specifically in Belém (Zone 8) during the winter, night ventilation provides adequate thermal losses during the night.

3.3 Sensitivity Analysis

The sensitivity analysis reveals that in 7 of 8 climates (Zones 2 to 8), the roof with super cool coating has the most significant impact on thermal comfort, followed by the percentage of window openings for ventilation. Only in Zone 1 (Caxias do Sul), the ventilation is more influential due to higher cold related discomfort in the original model. In extreme-cooling-dominated and cooling-dominated zones, super cool roofs with 90% reflectivity are crucial for optimal results. Super Cool coatings applied on roof plays a significantly more substantial role than that of the walls in all cases.

3.4 Non-Algorithm Optimization

In Picos (Zone 7), the external concrete floor coated with a super cool coating of 90% reflectivity slightly reduced annual thermal gains from the ground floor, providing necessary thermal losses for thermal comfort optimization objective achievement.

The objective was also achieved In Caxias do Sul (Zone 1) with external concrete floor with 50% reflectivity, the option proved more effective, preventing summer thermal gains and reducing winter losses through the ground floor. The final results of thermal comfort and heat balance of optimized schools are shown in Figure 6.

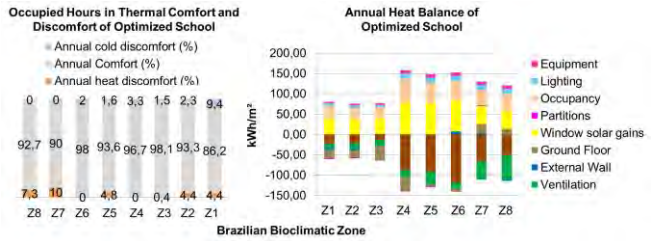

Figure 6: Thermal Comfort and Annual Heat Balance of Optimized School.

3.5 Final Stage

The optimal passive strategies for the standardized 1 classroom school are summarized in Figure 7.

Zone	Wall Refectivity	Roof Reflectivity (Winter/Summer)		Ventilation (Winter/ Summer)		Aditonal Strategies
1	10%	10%	70%	Occupancy 5% Aperture		Concrete ext. Ground R = 50%
2						None
3		50%		Occup. 5% Apert.	24/7 5% Apert	
4	50%	90%		Occupancy 5% Aperture		
5				24/7 5% Aperture		
6						
7	90%	90%		24/7 95% Aperture		Local Shading, Cool ext. Ground R = 90%
8						Local Shading α = 35º and β = 20º

Figure 3: Optimal Solutions by Climatic Group

Variations among different climates primarily involved surface finishes, window shading, and external floor materials adjacent to the building, while the compositions of the opaque and transparent envelope remained consistent across all cities. The opaque envelope materials that offered adequate thermal performance in the 8 bioclimatic zones were insulated wall (U=0.42W/m².K; C=122.00 KJ/m².K) and heavy roof (U=3.21 W/m².K ; C=220.00 KJ/m².K).

Ventilation is recommended for passive climate control in all cases, particularly during operational hours. The variation in ventilation recommendations among regions lies in the percentage of window opening: 95% for extreme cooling- dominated zones (7 and 8) and 5% for other zones (1 to 6). In most cases (zones 2 to 8), a heavy flat roof with a concrete slab proves to be a suitable solution.

Zone 1, characterized by lower temperatures, demands higher thermal insulation of walls and roof and dark colors on the envelope to favor heat absorption. Zones 1 to 3 benefit from a thermochromic roof to ensure comfort in both summer and winter. Zones 4 to 8, experiencing gradually longer periods of higher temperatures, require increased values of roof and wall reflectivity.

Even if window shading is avoided to maintain original natural light conditions in classrooms, it is

necessary for zones 7 and 8 to reduce solar gains and heat discomfort. In these zones, super cool coatings on the envelope are also necessary to enhance heat losses. Specifically in zone 7, covering the external ground with super cool coating is essential to decrease surrounding air temperature and enhance heat losses from the building through ground contact.

4. CONCLUSIONS

This article brings a significant contribution with an evaluation of thermal comfort in a standardized Brazilian public school across 8 climates, suggesting suitable super cool coatings and identifying optimal additional passive techniques to meet regulatory requirements of thermal comfort and low energy consumption without active air conditioning.

The proposed replicable methodology, utilizing thermal comfort and heat balance results from the current state of schools to identify impactful variables and group similar cases for scenario optimization, provided precise guidance for the process, thereby facilitating the achievement of the objective.

The simulations prove the effectiveness of the proposed suitable super cool coatings based on the bioclimatic chart and the literature review: thermochromic for heating-dominated, spectrally selective for cooling-dominated dry zones and with high broadband emissivity for cooling-dominated humid zones.

According to heat balance analyses, the FNDE's standardized model for public schools, featuring a heavy flat roof and insulated walls, aligns with Brazil's climatic diversity. Despite minor adjustments required for each climate, including super cool coatings, envelope reflectivity, and ventilation schedule and openable-window-area-ratio, the model effectively promotes occupant thermal comfort and low energy consumption without artificial climate control. Schools in extreme climates that were not addressed with algorithm optimization require additional passive strategies: moderately reflective external concrete floors (50%) for Zone 1 from heating-dominated group; super cool coatings on external concrete floors Zone 7 from extreme-cooling-dominated cities.

Sensitivity Analyses shows that the super cool coating applied on roof stands out as one of the most effective passive cooling techniques tested, primarily because of the horizontal shape of schools. In cooling-dominated cities, a higher roof reflectivity reduces the necessity for thermal insulation, aligning with previous studies and Brazilian normatives.

In 7 out of 8 Brazilian bioclimatic zones, the second most impactful passive strategy is the free aperture for natural ventilation. Window openings should be larger in extreme-cooling-dominated cities to optimize thermal losses and smaller in heating-dominated cities. These combined powerful and low-cost passive techniques, super cool coating on roof and natural ventilation, should also be investigated in other horizontal Brazilian buildings or in buildings with a similar climatic context.

ACKNOWLEDGEMENTS

This study was supported by CNPq (National Council for Scientific and Technological Development) and by FAP-DF (Foundation for Research Support in the Federal District).

REFERENCES

1. Pisello, A. L. (2017). State of the art on the development of cool coatings for buildings and cities.
2. Gnecco, V. M., Geraldi, M. S., Fossati, M., & Triana, M. A. (2022). Comparison between national and local benchmarking models: The case of public nursery 675 schools in Southern Brazil, . 78.
3. Khan, H. S., Paolini, R., Caccetta, P., & Santamouris, M. (2022). On the combined impact of local, regional, and global climatic changes on the urban energy performance and indoor thermal comfort—The energy potential of adaptation measures, . 267.
4. Kowaltowski, D. C. C. K., Labaki, L. C., & Pina, S. A. M. G. (2001). Conforto e Ambiente Escolar. *Cadernos de Arquitetura, 3*, 1 – 26.
5. Geraldi, M. S., & Ghisi, E. (2020). Mapping the energy usage in Brazilian public schools, . 224.
6. Cabeza, L. F., & Chàfer, M. (2020). Technological options and strategies towards zero energy buildings contributing to climate change mitigation.
7. Ascione, F., Bianco, N., Mauro, G. M., & Vanoli, G. P. (2019). A new comprehensive framework for the multi-objective optimization of building energy design: Harlequin, . 241 .
8. Ascione, F., Masi, R. F. D., Santamouris, M., S. Ruggiero, G. Vanoli, P. (2018). Experimental and numerical evaluations on the energy penalty of reflective roofs during the heating season for Mediterranean climate,. 144.
9. ABNT – Associação Brasileira de Normas Técnicas. (2005). NBR 15220: Thermal performance of buildings. Rio de Janeiro.
10. FNDE, Infraestrutura Física Escolar: Escola 1 sala, (2023).URL:https://www.fnde.gov.br/index.php/programas /par/eixos-de- atuacao/infraestrutura-fisica-escolar.
11. da Silva Weber, F., Melo, A. P., Marinoski, D. L., Guths S., Lamberts, R. (2017). Desenvolvimento de um modelo equivalente de avalição de propriedades térmicas para a elaboração de uma biblioteca de componentes construtivos brasileiros para o uso no programa EnergyPlus.
12. Lopes, A. F. O. (2020). Da simulação ao projeto, Mestrado em arquitetura e urbanismo, Universidade de Brasília.
13. ELETROBRÁS, PROCEL, CB3E, UFSC. (2021). Manual de Aplicação da INI-C, 1 ed., Pbe Edifica.
14. Cory, S., Lenoir, A., Donn, M., Garde, F. (2011) Formulating a building climate classification method, in: Proceedings of Building Simulation,. 1662 – 1669.
15. Feng, J., Saliari, M., Gao, K., Santamouris, M. (2022) On the cooling energy conservation potential of super cool roofs, 112076 –.

PLEA 2024 WROCŁAW
(Re)thinking Resilience

Assessing indoor temperatures in UK social housing dwellings during summer 2022

RAJAT GUPTA[1], YUANHONG ZHAO[1], CHLOE BERRY[1]

[1]Low Carbon Building Research Group, School of Architecture, Oxford Brookes University, Oxford, UK.

ABSTRACT: While UK dwellings are designed to retain heat to increase thermal comfort during winter periods, successively warmer summers and the occurrence of extreme heat periods are a growing concern. This paper empirically assessed the magnitude and duration of summertime overheating during the record-breaking summer of 2022 in the living rooms and bedrooms of 42 existing social houses in West Midlands, UK. To assess the prevalence of summertime overheating, static and adaptive overheating assessment criteria were used following the CIBSE TM59 protocol. Living room mean temperatures were observed to be 1.4°C higher than bedrooms. Static assessment showed that living rooms in 50% of bungalows and 41% of semi-detached dwellings were overheated. About 93% of bedrooms exceeded the static threshold for >1% of occupied hours going up to 10% in nearly half the bedrooms. Using the more forgiving adaptive overheating criteria, the risk of overheating in bedrooms decreased to <1% overall and <0.3% during occupied hours. The adaptive overheating assessment showed that 21% of living rooms overheated. In addition, air change rates were calculated using the CO_2-based decay method. Ventilation levels based on calculated ACH were found to be low (<0.5h^{-1}) indicating inadequate ventilation. The divergences in quantifying overheating risk in dwellings represent variations in overheating metrics used and inconsistencies this causes. Despite the differences, the occurrence of overheating makes a strong case for housing authorities to consider passive adaptations, increase resident awareness and promote behavioural adaptations to minimise the risk of overheating.

KEYWORDS: Overheating, indoor temperature, monitoring, ventilation, social housing

1. INTRODUCTION

Despite the temperate climate of the UK, ever increasing research has revealed global warming is causing successively warmer summers over the last four decades and demonstrating the reoccurrence of extreme periods of heat. The summer of 2022 experienced the UK's record-breaking temperature of 40.3°C on the 19th of July [1]. Excessive exposure to high temperatures can be fatal for many, and the evidence research has identified surrounding the risks to human health is extensive [2]. Overheating in the residential buildings is an increasing concern. In recent years, UK building regulations have emphasised the importance of a reduction in space heating demand through the implementation of higher-level fabric efficiency [3]. Until building regulation revisions were implemented in June 2022 [4], there was little consideration of summertime overheating in UK dwellings, especially in vulnerable social housing dwellings occupied by those on low income.

There were 4.4 million existing socially owned dwellings in England in 2022. In recent years, it has been under obligation to comply with zero carbon standards, particularly for the social sector, since it relies on public funding [5]. However, social housing demographics are inclined to increase the occurrence of overheating.

Taking into consideration the increase in the occurrence of extreme heat periods and the link to the vulnerability of social housing tenants, existing literature offers a small range of studies that use empirical data. Sameni, Gaterell, Montazami and Ahmed [6] monitored 18 social Passivhaus flats and five Passivhaus social houses over three summer periods to assess the extent of overheating. Overheating ranged from 3%-99% and flats were more susceptible to overheating with 72% failing Passivhaus designed criteria. Gupta & Kapsali [7] assessed the overheating risk in six low-carbon dwellings. Results demonstrated that using CIBSE static and dynamic overheating assessments, there were contrasting differences. Vellei, Ramallo-González, Kaleli, Lee, and Natarajan [8] recorded sufficient data in 48 retrofitted well-insulated dwellings to use the CIBSE TM52 adaptive benchmark to examine the extent of overheating. Results concluded that 12% of kitchens, 27% of bedrooms and 2% of living rooms failed the criteria. It is evident that empirical analysis studies have focussed on retrofitted**,** low-carbon and Passivhaus dwellings with very limited studies on the existing housing stock.

Table 1: Specification, resolution and accuracy of monitoring devices

Device	Parameter	Range	Accuracy	Resolution
Airthinx IAQ (Living room)	Temperature (°C)	0 to 99	± 0.5	0.1
	Relative Humidity (%)	0 to 99	± 2	0.1
	Carbon Dioxide (ppm)	0 to 5000	± 50 +5% FS	1
HOBO MX1102a (Bedroom)	Temperature (°C)	-40 to 70	±0.21°C from 0-50°C	0.024°C at 25°C
	Relative Humidity (%)	0 to 100	±2.0% from 20-88%	0.01%
	Carbon Dioxide (ppm)	0 to 5000	±50ppm	-
HOBO MX2301 (External)	Temperature (°C)	-40 to 70	±0.2	0.036
	Relative Humidity (%)	0 to 100	±2.5-3.5 (10% to 90%); ±5 (below 10% and above 90%)	0.01

Existing literature shows a limited number of studies that focus on assessing the risk of overheating in existing social housing dwellings that form a large proportion of the national housing stock. Against this context, this paper systematically conducts empirical measurement and statistical analyses of indoor temperatures in the living rooms and master bedrooms of 42 social housing dwellings (West Midlands, UK) during the record-breaking summer of 2022.

2. METHOD

A socio-technical approach was adopted which included continuous monitoring of indoor and outdoor temperatures as well as indoor CO_2 levels from 1st May 2022 to 30th September 2022. During this time, the UK experienced a record-breaking summer including five defined heatwaves [9]. Time series analysis was conducted at three levels: the *sample* level which included all 42 dwellings, the *typology* level which divided dwellings into four categories dependent on their built form, and *individual dwelling* level. Empirical time series data was gathered in living rooms using Airthinx IAQ sensors, in master bedrooms using Hobo MX1102a, and outdoors using Hobo MX2301. Table 1 above shows the specifications of the sensors.

An in-person household survey was conducted to gather contextual data about household characteristics, occupancy and behaviours. Data on building characteristics (dwelling age, construction type and building fabric) was derived from Energy Performance Certificates (EPC).

To assess the prevalence and extent of summertime overheating, both adaptive and static overheating criteria were used following the CIBSE TM59 protocol [10,11]. Criterion A is a dynamic (adaptive) overheating metric for living rooms using threshold comfort temperatures derived from the daily running mean outdoor temperatures ($T_{rm,}$). Criterion B is static and consists of night time hours in bedrooms which should not exceed 26°C for more than 1% of annual occupied hours.

3. RESULTS

The case study dwellings varied in size ranging from 41m^2 to 111m^2, EPC ratings ranged from EPC C to E, and the mean number of residents per dwelling was 3, with occupancy ranging from one resident to seven residents as detailed in Table 2.

3.1 Living room overheating assessment

During the monitoring period, a record-breaking outdoor temperature of 40.3°C was measured by the Met Office [1]. Monitored outdoor temperatures were found to reach 39.8°C with an overall mean of 17.1°C. At the sample level, indoor living room temperatures reached 37.3°C with a daily mean of 24.1°C. Daily mean living room temperatures largely imitated the daily mean external temperature profile, consistently between 21°C and 30°C indoors and between 10°C and 30°C outdoors. Temperatures greater than the CIBSE [11] recommended upper comfort level of 25°C were marginally exceeded and associated with recognised

Table 2: Household and building characteristics for housing typologies

Characteristic	6 Bungalows (B)	12 Standard semi-detached (S)	21 Triangular semi-detached (TR)	3 Terraced (T)
External dwelling image				
Number of occupants	1-2	1-7	1-6	2-4
Dwelling area	41m^2	79m^2 and 111m^2	96m^2	67m^2 and 77m^2
Age of construction	1976-1982	1930-1949 and 1950-1966	1900-1929	1950-1966
EPC rating	C-D	D-E	D-E	C-D
Wall U-Value	0.37W/m^{2}K	0.37-0.49W/m^{2}K	0.49W/m^{2}K	0.49W/m^{2}K
Roof U-Value	0.18W/m^{2}K	0.22-0.3W/m^{2}K	0.45W/m^{2}K	0.22-0.29W/m^{2}K
Ground floor U-Value	0.78W/m^{2}K	0.78-0.87W/m^{2}K	0.75W/m^{2}K	0.77-0.78W/m^{2}K

heatwave periods. There was little differentiation between occupied and unoccupied hours which had a Pearson's correlation coefficient value of 0.99. The daily mean indoor temperature in the living rooms was 1.4°C higher than that in the bedrooms (Table 3).

Table 3: Descriptive statistics for living room and bedroom indoor temperature at sample level (n: 42 dwellings)

	Device	Mean	Min	Max
Living room	Airthinx IAQ	24.1°C	10.4°C	37.3°C
Bedroom	Hobo MX1102a	22.7°C	11.6°C	40.0°C
Outdoor	Hobo MX2301	17.7°C	3.8°C	39.8°C

Temperatures across five defined heatwave periods at the sample level represented the highest daily average temperature consistently during heatwave four (08/08-17/08, 2022). Diurnal temperatures peaked early evening at 29.1°C and did not drop below 27.7°C at mid-morning, largely presenting discomfort for residents above the recommended 25°C [11]. Heatwave period one experienced the lowest diurnal temperatures reaching 26.3°C during early evening and a low of 24.2°C mid-morning. Figure 1 shows the distribution of indoor temperatures at the sample level across the five heatwave periods. Minor differences were identified between occupied and unoccupied hours suggesting the building's ability to retain heat and poor night time ventilation levels to relieve discomfort. Outside temperatures had a notably lower median compared to indoors, consistently by 4-6°C. Heatwave two experienced the highest outdoor and indoor temperatures yet heatwave four showed the highest indoor median temperatures. This period experienced six successive days of high temperatures with a mean temperature >23°C, not allowing effective cooling to occur, compared to three days during heatwave two.

Figure 1: Distribution of living room temperatures at sample level across occupied and unoccupied hours during the defined heatwave periods.

At the typology level, type B and S experienced the highest daily mean and diurnal temperatures across the monitoring period with an overall mean of 24.8°C and 24.6°C respectively, which may be attributed to their higher number of exposed sides. Typically, typology B had the highest daily mean and diurnal temperatures over the monitoring period, particularly, the heatwave periods. These were predominantly occupied by retired residents who spent extended time indoors contributing to internal gains. The highest temperature recorded was in typology TR reaching 37.3°C, despite this type experiencing the lowest mean of 23.7°C. The lowest daily average temperatures fluctuated between typologies TR and T which had varying construction types, but were the oldest typologies. Maximum temperatures exceeded 34°C across all typologies, implying discomfort.

Figure 2 shows the distribution of temperature in the living rooms of individual dwellings throughout the monitoring period. Median values exceeding 25°C were notably prevalent in 29% of dwellings, with 42% being type S dwellings suggesting the building fabric was responsible. Interestingly, when outdoor temperatures peaked, T03 exhibited a daily mean of 28.2°C, whereas, adjoining dwellings recorded at 26.2°C and 26.5°C respectively, suggesting that resident behaviours might be responsible.

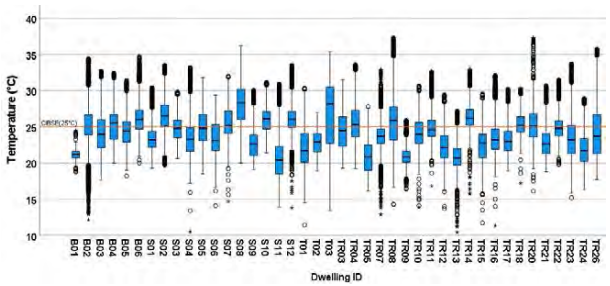

Figure 2: Temperature distribution in the living room of individual dwellings across the monitoring period.

Static CIBSE requirements suggest living room temperatures remain between 23-25°C [11]. Mean living room temperatures showed that 33% of dwellings exceeded 25°C, by proportion, 50% of bungalows and 41% of standard semi-detached dwellings. Very few had south-facing windows but did have high levels of occupancy over the average day. Mean temperatures below 23°C occurred in 29% of dwellings, by proportion, 66% of terraced and 33% of triangular semi-detached dwellings. There were few similarities between resident occupations, indicating considerable variation. This reinforces that higher mean temperatures are influenced by resident behaviours, while lower temperatures are justified through the building fabric and construction. However, overheating assessment using the more forgiving adaptive overheating method (which is based on the running mean outdoor temperatures) at the typology level showed that typology B had the greatest of 0.6% during occupied hours and 0.1% during unoccupied hours.

Individually, 21% of living rooms failed criterion a, exceeding the threshold comfort temperature by at least 1°C for more than 3% of occupied hours. 17 dwellings had an overheating risk between 0.1% and 3% during occupied hours. The most significant was T03, which exceeded 29.2% of occupied hours. This mid-terraced dwelling experienced the influence of

temperatures from adjoining dwellings from the retention of heat through brick walls due to their high thermal mass. Dwelling S08 also experienced significant overheating at 18.8% of occupied hours. The adjoining dwelling, S07, also exceeded the limit for 3.4% of occupied hours. Although identical construction methods were used, resident behaviour and preferences were suggested to create such differences. Results from the adaptive overheating assessment in living rooms suggested resident behaviour, such as window opening, and preferences were the contributing factors regarding the extent of overheating risk, as identical dwellings showed vast differences.

3.2 Bedroom overheating assessment

At the sample level, indoor bedroom temperatures ranged significantly from 11.6°C to 40°C, with a mean value of 22.7°C (Table 3), and remained below CIBSE's threshold of 26°C [10]. Occupied and unoccupied hours showed little difference where temperatures remained high overnight. Figure 3 shows daily mean indoor temperature profiles distinctly following daily mean outdoor temperatures, as well as the five defined heatwave periods notified. Consistently, indoor temperatures remained higher than outdoor temperatures at all times, generally by 3-4°C, although this reduced during heatwave periods.

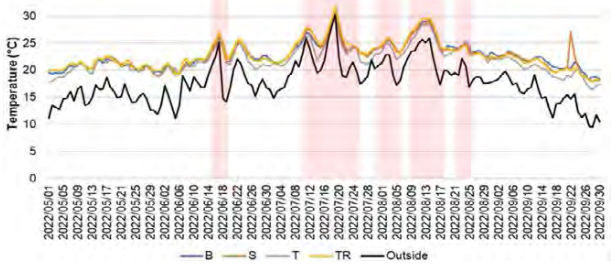

Figure 3: Bedroom daily mean temperature at typology level compared to outside temperature & defined heatwave periods

Diurnal bedroom temperatures, for the most part, were highest in typology TR dwellings by about 1°C higher than other typologies. TR also experienced the greatest temperature variation over the average day compared to other typologies due to a high thermal mass and poor insulation. Terraced dwellings had the lowest diurnal temperature overall and across heatwave periods. Since bedrooms in terraced dwellings were north-west facing so direct sunlight was limited, and most bedrooms had two large windows allowing for high levels of natural ventilation.

Figure 4 shows temperature distribution in the bedrooms of individual dwellings across the monitoring period. Indoor temperatures reached as high as 40°C in dwelling S12 around 14:00 during heatwave periods. This dwelling housed a family of seven residents with many large animals who mostly occupied the dwelling at all times which presented large internal heat gains. In addition, a south-facing bedroom window suggested direct sunlight caused interference. The highest mean temperature was reached in TR22 at 24.7°C due to a large south-facing window. The lowest mean temperature was recorded in TR16 at 16.9°C, since the bedroom was on the ground floor and had the window open at all times. In addition, overgrown shrubbery, copious vegetation and large trees provided constant shading of the entire dwelling.

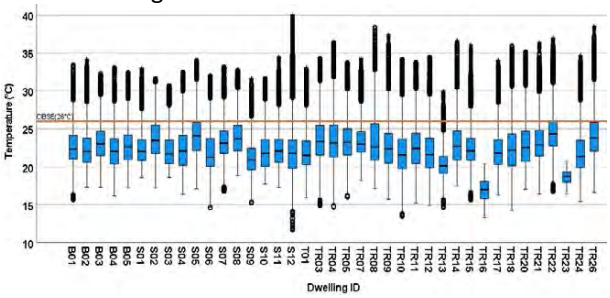

Figure 4: Temperature distribution in the bedrooms of individual dwellings across the monitoring period.

Overheating was found to be prevalent using the static overheating assessment. Nearly 93% of the bedrooms exceeded the static threshold for more than 1% of occupied hours. Of these, 48% experienced >26°C for more than 10% of occupied hours. 60% were associated with south-east, south and south-west facing windows. Typologies TR and S were most susceptible to high temperatures. Static overheating assessment in Table 4 shows typology S and TR overheating during occupied hours at 10.1% and 10.8%. Roof exposed bedrooms with no insulation were most susceptible to high temperatures as well as south-facing windows.

Table 4: CIBSE TM59 overheating assessments at typology level in master bedrooms overall and for occupied hours

Overheating metric	Typology	Overall	Occupied hours (%)	Unoccupied hours (%)
Adaptive assessment (>3% occupied hours)	B	0.4	0.2	0.4
	S	0.7	0.2	1
	TR	0.8	0.2	1.1
	T	0.4	0.2	0.5
Static assessment (>1% occupied hours)	B	9.3	8.3	4.1
	S	11.4	10.1	5.1
	TR	12.7	10.8	5.4
	T	7.3	8	4.0

Individually, dwelling S05 experienced the longest extent of overheating at 26.4% of occupied hours. Dwelling TR13 experienced temperatures greater than 26°C for 1.1% of occupied hours yet the adjoining dwelling with the exact orientation and construction experienced static overheating at 15.5%. All typologies experienced temperatures remaining high or even increasing when occupied leading to discomfort impacting the ability to sleep and quality of life. This was only evident when using CIBSE's static overheating assessment.

Using adaptive overheating risk assessment, the overheating risks in bedrooms at sample and typology levels were lower, <1% overall and <0.3% during occupied hours. The triangular semi-detached dwellings overheated the most at 0.8% overall and 0.2% during occupied hours. Individually, zero dwellings failed the adaptive overheating assessment during occupied hours. In addition, all mean temperatures remained below 26°C. 66% of bungalows, 58% of standard semi-detached and 57% of triangular semi-detached dwellings had mean temperatures below 23°C.

3.3 Air change rates

The CO_2-based decay method calculated air change rates (ACH^{-1}) related to ventilation and infiltration. Living room air change rates at the sample level in Table 5 ranged from $0.02h^{-1}$ to $6.25h^{-1}$ with a mean of $0.24h^{-1}$. Similar means in the region of $0.22\text{-}0.26h^{-1}$ were identified at the typology level, the greatest being associated with the standard semi-detached. This is likely due to 58% of these dwellings had a wall grill present in the living room. Typology S also experienced the maximum of $6.25h^{-1}$, this perhaps derived from three differing construction methods and locations causing variation in ventilation and infiltration. However, typology TR was expected to have the greatest ACH due to the high levels of infiltration incorporated into the construction. Yet a mean of $0.22h^{-1}$ revealed one of the lowest in addition to typology B. Results could differ as CO_2 values were much higher in typology B, due to prolonged occupancy, with a peak recorded value of 5,000ppm and peak mean value >2,000ppm, way beyond recommended threshold. Typology TR had the lowest CO_2 mean at typology level <1,250ppm.

Table 5: Descriptive statistics for living rooms and bedrooms ACH at sample and typology level

Analysis level	Living room			Bedroom		
	Min	Max	Mean	Min	Max	Mean
Sample	0.02	6.25	0.24	0.03	2.82	0.25
B	0.02	1.46	0.22	0.04	2.82	0.25
S	0.03	6.25	0.26	0.33	1.98	0.24
TR	0.03	1.38	0.22	0.04	1.15	0.25
T	0.05	0.9	0.23	0.04	1.37	0.35

Individually, dwelling S11 had the largest interquartile range, greatest median and maximum value. The adjoining dwelling, S12, also had a larger than average interquartile range, therefore suggesting ventilation levels were high likely due to the construction. Previous comments from both residents expressed concerns about poor thermal performance due to airtightness and the leaky building fabric. From this, results suggest infiltration levels were high. Most other dwellings showed the distribution of data to be relatively consistent. 68% showed maximum values below $1h^{-1}$ and interquartile ranges $<0.5h^{-1}$. These results imply poor levels of ventilation occurring which caused CO_2 levels to decrease slowly whilst also suggesting window opening was limited.

Air change rates in master bedrooms at the sample level in Table 5 show a range of $2.79h^{-1}$ and a mean of $0.25h^{-1}$ which infers poor levels of ventilation achieved. Similar mean values were also noted at typology level, between $0.24\text{-}0.25h^{-1}$ with the exception of typology T at 0.35^{-1} which benefitted from two opening windows for increased levels of ventilation. Distinction between the air change rates during defined occupied and unoccupied hours was evident. During occupied hours, continual exhalation of CO_2 from residents meant the opportunity for a decrease in CO_2 in bedrooms overnight was less likely even with the window open. Unoccupied means were higher across all typologies by $0.07h^{-1}$ and $0.16h^{-1}$. This implied ventilation was greater when unoccupied and not contributing to night time cooling to reduce the risk of overheating.

Air change rates $>1h^{-1}$ occurred in 29% of bedrooms. ACH greater than $0.5h^{-1}$ were usually outliers suggesting ventilation was limited. Dwelling B02 experienced the greatest median of $0.4h^{-1}$ and an upper quartile of $0.75h^{-1}$ due to frequent window opening. Where CO_2 levels remained below 1000ppm in bedrooms, these were mostly during unoccupied hours.

4. DISCUSSION

Indoor temperatures frequently exceeded 30°C in individual dwellings. High indoor temperatures generally correspond to high outdoor temperatures, particularly during periods of successively high outdoor mean temperatures. Interquartile ranges and mean temperatures in the living room showed great variation between 20-30°C while bedroom interquartile ranges remained between 20-25°C. Such differences suggest the influence of occupant activities and behaviours.

Statistical analysis revealed overheating to be frequent. Using the adaptive overheating assessment, 21% of living rooms exceeded the threshold comfort temperature by at least 1°C for more than 3% of occupied hours. Following the same criteria, 0% of bedrooms overheated during occupied hours. When applying the static overheating assessment to bedrooms, 93% failed, exceeding the static threshold of 26°C for more than 1% of occupied hours, whilst 48% recorded temperatures >26°C for more than 10% of occupied hours. Overheating in living rooms was generally associated with resident behaviours and thermal preferences. Identical adjoining dwellings experienced contrasting levels of overheating. Overheating in bedrooms was largely dependent on dwelling construction. Bedrooms in typology TR with no insulation, high thermal mass and roof exposure,

experienced the greatest percentage of static overheating. Bedrooms with two windows provided effective ventilation and consequently the lowest risk of overheating.

Estimated air change rate calculations revealed ventilation to be low, $<0.5h^{-1}$. Levels of ventilation and infiltration were found to be mostly consistent throughout dwelling typologies, despite varying built forms. Window opening occurred more so in master bedrooms identified by evident differences in occupied and unoccupied hours. Living room data showed contrasting outcomes between typologies which could be influenced by occupancy. Dwellings which housed mostly retired residents had higher mean indoor temperatures during occupied hours.

5. CONCLUSION

This paper empirically assessed the magnitude and duration of summertime overheating during the record-breaking summer of 2022 in 42 existing social houses located in West Midland, UK. The study sample consisted of four varying typologies that were naturally ventilated. Temperature monitoring was conducted in the living room and master bedroom of each dwelling between May 2022 and September 2022 at 15-minute intervals. Contextual data was collected in the form of household and building characteristic surveys by at least one resident. Empirical data was assessed using CIBSE's static and adaptive overheating assessment criteria. The two different metrics used provided diverging results.

Despite the divergence, it was evident that summertime overheating was prevalent throughout all dwellings, particularly when using static overheating assessment. Using adaptive overheating assessment, most bedrooms passed. Such contrasting results represent significant variations in overheating metrics used and inconsistencies this causes. This needs to be urgently addressed so that the risk of overheating in vulnerable social housing dwellings can be mitigated.

Given that overheating was apparent in social housing, irrespective of construction, it is vital that housing providers consider adequate adaptations to increase the comfort for the 4 million existing social dwellings already inhabited. It is especially vital for residents classified as vulnerable and at increased risk to suffer from adverse health implications derived from high indoor temperatures. Results suggested resident behaviours and activities also affected changes in temperatures. Increasing resident awareness and knowledge regarding behavioural adaptation during periods of extreme heat could alleviate the risk of overheating in vulnerable settings such as social housing.

ACKNOWLEDGEMENT

This study is part of the REFINE project funded by the UK Government's Social Housing Decarbonisation Fund (SHDF) Demonstrator Grant No. 31/5281. We are grateful to the occupants for their help and support in conducting the study.

REFERENCES

1. Met Office. (2022, July 15). UK prepares for historic hot spell: https://www.metoffice.gov.uk
2. UK Health Security Agency. (2022). Heatwave plan for England - Protecting health and reducing harm from severe heat and heatwaves. Department for Health and Social Care.
3. Gupta, R., Gregg, M., & Irving, R. (2019). Meta-analysis of summertime indoor temperatures in new-build, retrofitted, and existing UK dwellings. Science and Technology for the Built Environment, 25(9), 1212-1225.
4. HM Government. (2021). Overheating - Approved document O. RIBA.
5. McManus, A., Gaterell, M., & Coates, L. (2010). The potential of the Code for Sustainable Homes to deliver genuine 'sustainable energy' in the UK social housing sector. Energy Policy, 38(4), 2013-2019.
6. Sameni, S., Gaterell, M., Montazami, A., & Ahmed, A. (2015). Overheating investigation in UK social housing flats built to the Passivhaus standard. Building and Environment, 92, 222-235.
7. Gupta, R., & Kapsali, M. (2016). Empirical assessment of indoor air quality and overheating in low-carbon social housing dwellings in England, UK. Advances in Building Energy Research, 10(1), 46-88.
8. Vellei, M., Ramallo-González, A., Kaleli, D., Lee, J., & Natarajan, S. (2016). Investigating the overheating risk in refurbished social housing. Proceedings of 9th Windsor Conference: Making Comfort Relevant, (pp. 7-10).
9. Office for National Statistics (ONS) and UK Health Security Agency (UKHSA). (2022). Excess mortality during heat-periods: 1 June. Office for National Statistics.
10. CIBSE. (2017). Design methodology for the assessment of overheating risk in homes. London: CIBSE.
11. CIBSE. (2021). Environmental Design: CIBSE Guide A. London: The Chartered Institution of Building Services Engineers.

PLEA 2024 WROCŁAW
(Re)thinking Resilience

Modernist heritage and environmental quality of Nadyr de Oliveira House (1960):

A Corbusian residence in São Paulo, Brasil

EDUARDO GASPARELO LIMA[1,2], LAÍS DE GUSMÃO COUTINHO[1,2,3], JOANA CARLA SOARES GONÇALVES[4], RANNY LOUREIRO XAVIER NASCIMENTO MICHALSKI[1], ALESSANDRA RODRIGUES PRATA SHIMOMURA[1]

[1] School of Architecture and Urbanism of USP, São Paulo, Brazil
[2] Escola da Cidade, São Paulo, Brazil
[3] National Council for Scientific and Technological Development scholarship holder, São Paulo, Brazil
[4] Architectural Association School of Architecture, London, United Kingdom

ABSTRACT: Modernist Brazilian architecture has placed significant emphasis on matters pertaining to comfort and environmental quality. While certain figures within this domain have achieved widespread recognition, there are Brazilian architects who, despite incorporating diverse bioclimatic principles into their modernist projects, have not garnered the recognition they deserve. In this context, Carlos Barjas Millan, a São Paulo-based architect renowned for a series of works demonstrating invaluable environmental quality, stands out. This article seeks to examine the environmental quality of one of Millan's designed residences – the Nadyr de Oliveira Residence – with a focus on thermal, luminous, and acoustic considerations. To accomplish this, a comprehensive case study was undertaken, considering all the characteristics and solutions implemented by the architect. The methodology employed encompassed field analyses and measurements of thermal, lighting, and acoustic aspects during both warm and cold periods. Following the collection and analysis of data, it is apparent that the residence exhibits areas for improvement, particularly in relation to thermal comfort during colder periods. From the perspectives of natural lighting and acoustics, there is no immediate necessity to propose solutions. However, the ongoing maintenance and specific enhancements to buildings with historical and heritage value are consistently encouraged.
KEYWORDS: Environmental quality, Brazilian Modernism, Bioclimatic Project, Corbusian House

1. INTRODUCTION

The Modern Movement emerged in Europe during the 20th century, reflecting the socioeconomic changes originated in the Industrial Revolution. In architecture, it was characterized by the rejection of traditional models, the utilization of prefabricated materials, the geometrization of shapes, the predominance of straight lines, the disassociation between structure and walls, and a focus on functionality.

Brazilian Modernist Architecture, which flourished between 1930 and 1964, placed a special emphasis on considerations related to comfort and environmental quality [1]. During this period, building design sought to address local microclimatic conditions and cultural habits, adhering to bioclimatic principles.

As noted by Marta Romero [2], Bioclimatism involves the consideration of environmental aspects within the local context of a building, with the goal of achieving passive natural environmental conditions through an integrated approach to thermal attributes, daylight, sound, and colour. Therefore, the application of these principles inevitably requires a tailored design that is well-suited to the specific location and utilizes local materials, showcasing historical, cultural, environmental, and technological expertise.

Notable figures associated with this movement include Mies van der Rohe, Frank Lloyd Wright, Walter Gropius, and Le Corbusier, who defined the five points of modern architecture. Several Brazilian architects were significant influenced by the groundbreaking ideas and architectural principles introduced by the French-Swiss personality, especially professionals in the Rio de Janeiro-São Paulo axis.

One notable figure is Oscar Niemeyer, whose iconic modernists designs reflect a profound imprint of Le Corbusier. João Filgueiras Lima, affectionately known as Lelé, stands out as another prominent name in the Brazilian Modernist Movement. Lelé was a dedicated advocate of bioclimatic principles, integrating environmental considerations into his designs and prioritizing architectural solutions that emphasized natural ventilation and controllable daylighting access. While many architects sowed the seeds of modern architecture linked to Bioclimatism in Brazil, not all received the deserved international

recognition. One such noteworthy figure is Carlos Barjas Millan.

Carlos Millan, born in 1927, graduated in 1951 from the School of Architecture of Mackenzie Presbyterian University. According to Villa [3], Millan, years after graduating, had exposure to the School of Architecture and Urbanism of the University of São Paulo (FAUUSP), where the Modern Movement was widely disseminated. Although his architectural production was concise due to his early death in 1964, it played a significant role in the architecture of São Paulo and left a lasting impact on several generations of Brazilian architects.

Against this backdrop, this paper seeks to investigate the environmental quality of a Corbusian house designed by Millan. Furthermore, a discussion is initiated regarding the preservation of modern architecture, encompassing the challenges of maintaining or adapting these structures in the context of ongoing conversations related to environmental quality demands and resilience in the face of a changing climate. This study is part of a broader research project initiated in 2014, with the aim of assessing the environmental performance of iconic architecture in the city of São Paulo, birthplace of the *Escola Paulista* (São Paulo School) of Modern Architecture [4, 5].

2. CASE STUDY – NADYR DE OLIVEIRA HOUSE

In 1960, during a period in which his projects were more mature, Millan designed the Nadyr de Oliveira House (Fig. 1). As reported by Matera [6], some solutions in this residence became recurrent in conceptual designs conceived by the architect after that year, such as: pure and single volumes; building program organized around a central nucleus; different vertical circulations defined by its uses, isolating the service one on an external volume detached from the main body of the house; linear kitchen with reduced area and illuminated by two horizontal windows (the higher one illuminates de centre of the plan and the lower one, the work surface) that also favours the stack effect; service areas closed by *cobogós*, with permanent ventilation, and located close to the bedrooms; exposed concrete structures with lateral overhangs and ribbed slabs filled with perforated ceramic blocks, reducing the U-factor of the construction component; zenithal lighting and convective air movement in a multiple-use bathrooms; and iron frames painted with orange lead.

This project is the first apartment-house designed by Millan, built on a single floor lifted over pilotis and with minimal interference in the original terrain, a classic concept spread by Le Corbusier. On the ground floor there are the servants' bedroom and bathroom, garage, entrance hall, and a social bathroom. The geometric floor plan is organized around the access space and the volume of the bathroom, around which are the three bedrooms, living-room, kitchen, and laundry room, all connected through a peripheral circulation.

Natural ventilation stands out in the thermal environment of the house, being favoured by the design of window frames, strategically positioned. The social areas were integrated with the entrance hall on the lower floor, enhancing the volume of space. This spatial integration fosters convective air movement, facilitating the circulation of fresh air. Cross ventilation is further facilitated by the opening of doors and windows, particularly when the access doors to the service area are opened. This area is enclosed by *cobogós* and, as a result, remains permanently ventilated.

On one facade of the living room (North), the architect designed a floor-to-ceiling frame consisting of upper sliding windows and lower tilting windows, ensuring diverse opening possibilities. The placement of the upper windows was strategic to privilege the views of the area that would later become Parque Alfredo Volpi in 1966, and as such, they did not incorporate shading, relying on the natural shade provided by nearby trees. Conversely, the lower windows are externally shaded by concrete cobogós. In the bedrooms, the shading arrangement is inverted: the smaller lower windows lack shading, while the larger upper windows are equipped with an operable roller blind – a common solution at the time, known as Copacabana shutters.

Additionally, it is noteworthy that the opaque walls of the residence were constructed using cellular concrete blocks, which presents a thermal conductivity more appropriate for the climatic conditions of São Paulo.

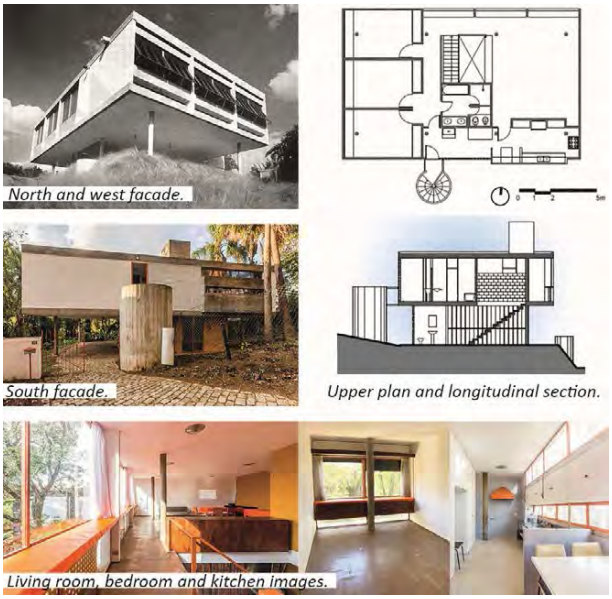

Figure 1: Nadyr de Oliveira House, 1960. Photos: Acrópole Magazine, Rafael Schimidt, and authors.

3. METHOD AND ANALISYS

The methodology employed is experimental and inductive, involving fieldwork and measurements of thermal, daylighting, and acoustic variables. In addition to the data collected on-site, simplified calculations were undertaken, when pertinent.

In the context of thermal ambiance, measurements recorded values of dry bulb air temperature, globe temperature, air movement, and relative humidity. These measurements were taken every 15 minutes using HOBO Onset data loggers, which were installed simultaneously in the living room and a bedroom of the case study during the summer and winter periods of 2019 – for the purposes of this paper, only data related to the living room will be presented. For the warmer period, 15 days between March and April were selected, followed by another 15 days in September to capture a cooler period. External temperatures, humidity levels, and global radiation measurements were recorded in an open space near the house using a Campbell weather station.

For the analysis, data collected over a period of seven consecutive days, covering both weekdays and weekends, were examined. The selected days represented stable conditions, closely resembling typical conditions for each respective period. The results were analysed comparatively and juxtaposed with the comfort zone of 80% acceptability range for occupant-controlled naturally conditioned spaces as defined by ASHRAE 55 [7].

To collect daylight data, HOBO Onset data loggers equipped with photocells were utilized. The devices were positioned in the centre of the room at a height of 75 cm from the finished floor, adhering to the position recommended by Brazilian regulations [8] for daylight simulations. Illuminance levels were recorded every 15 minutes, mirroring the frequency of thermal data collection. To estimate external illuminance levels, Equation (1), developed by the Technological Research Institute of São Paulo (IPT) and presented by Alucci [9], was employed.

$$E = 94 * R \qquad (1)$$

where E – Illuminance level (lux);
R – Solar radiation (W/m²).

As an assessment metric for daylighting data, the useful daylight illuminance ranges (UDI fell-short, UDI supplementary, UDI autonomous and UDI exceeded) established by Nabil and Mardaljevic [10] were considered.

Acoustic measurements were conducted in both internal and external spaces under similar sound conditions, following the sound level meter adjustment recommendations specified by national standards [11, 12]. The measurements were supported by a Larson Davis sound integrator, Class 1, Model 831-RI, equipped with octave and third-octave filters and historical time recording capabilities.

For external data collection, the equipment was mounted on a tripod at a height of 1.20 meters from the floor and 1 meter from the building envelope. Internal measurements involved moving the sound level meter within the room to obtain a more representative sample of the sound ambiance of the evaluated space.

A-weighted continuous sound pressure level data collection extended over a total of ten minutes with a 10-second integration time for internal and external spaces. Additionally, the A-weighted sound pressure level was calculated for the entire measurement period.

Furthermore, an airborne sound insulation measurement was conducted on the facade of the residence's living room. All instruments used in these measurements were from the company HBK, including a dodecahedron, Model 4292, as a sound source, a microphone, Model 4189, to capture the sound pressure level, and a sound level meter, Model 2270, to measure sound levels and reverberation time. The measurements adhered to normative procedures [13], and the method employed involved a sound source with global speakers providing the difference in sound level introduced by a facade when using a real source is not feasible.

Finally, the sound levels and sound insulation of the facade were compared with Brazilian legislative and normative recommendations [14, 11, 12]. For strictly residential areas, as is the case, the recommended external sound pressure level during the daytime is 50 dB, while during the nighttime period, it is 45 dB. Internal measurements recommend RL_{Aeq} values of 40 dB for the living room.

4. CLIMATIC CONTEXT OF SÃO PAULO

Regarding to the climate, the city of São Paulo (Latitude 23.85° S; Longitude 46.64° W; Altitude 792 meters above sea level) is situated in a subtropical region, characterized by warm-humid summer days with predominantly partially cloudy sky, and cool and drier winter days with predominantly sunny sky. The prevailing wind directions throughout the year are South, South-Southeast, and Southeast. Air temperatures are moderate for most of the year with an annual average temperature of 19.3 °C, according to data from the climatological bank of the National Institute of Meteorology [15]. Typical warm days with clear skies can easily result in temperatures exceeding 30 °C in the early afternoon. Conversely, on warm days with cloudy skies, air temperatures hover around 20 °C. During typical cooler days, solar radiation impact can push air temperatures up to 24 °C, whereas on cooler cloudy days, temperatures struggle to rise above 15 °C. According to the Köppen-Geiger Classification, São Paulo's climate is classified

as temperate, featuring no dry season and hot summers (Cfa).

5. RESULTS AND DISCUSSIONS

5.1. Thermal ambiance

The Nadyr de Oliveira House is currently available in the real estate market for purchase or rent, and as a result, it is unoccupied. This fact should be taken into consideration during the analyses of the measurements since it does not present thermal loads from occupation and equipment.

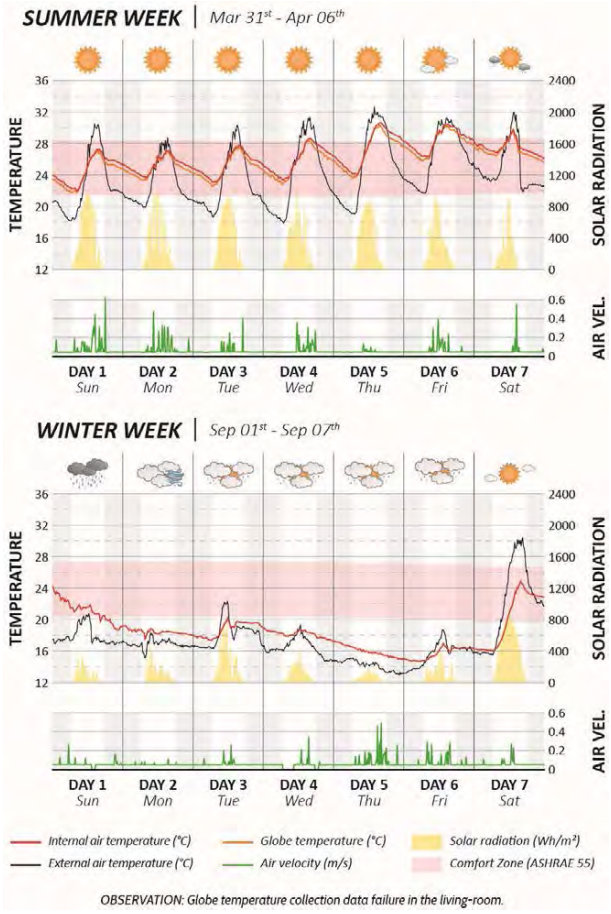

Figure 2: Measurements of dry bulb air temperature, globe temperature and wind speed during warm and cold periods in the living-room with external air temperature and solar radiation.

During periods of thermal gains in the summer week, the highest indoor temperature measured was 30.7 °C, about 3 °C less than the outdoor temperature. When in the absence of solar radiation, the house can store thermal loads, guaranteeing internal temperatures up to 5.5 °C warmer than the external ones.

During the initial three days of the summer week, with external air temperatures ranging between 28.5 °C and 30.5 °C, indoor air temperatures consistently remained within the comfort range of 80% acceptability for naturally ventilated spaces. However, in the subsequent days, external air temperatures rose to values near 32 °C, resulting in elevated internal temperatures that surpassed the upper limit of the comfort zone.

For the climate of São Paulo, controlled ventilation is desired when outdoor temperatures exceed 30 °C, since the outdoor air that penetrates the room arrives at a high temperature, warming it up. The globe temperature in warm periods has a difference of 1 °C between air temperature in the first hours of the day, with a tendency to equalize as solar radiation increases throughout the day.

In the cold period, the lowest measured air temperature was 14.6 °C in the coldest dawn, when the outdoor temperature reached 12.5 °C. Globe and air temperatures tend to be consistent whenever there is an overcast sky. Internal air temperatures generally remained below the lower limit of the comfort zone. On partially cloudy days, when the external air temperature reached 22 °C and available solar radiation approached values close to 800 Wh/m², the internal air temperature approached the comfort range. If the space were occupied, it is likely that temperatures would rise, reaching within the comfort range.

Despite having a thermal lag effect, the peaks of indoor temperature coincide with the outdoor one. This may be related to the amount of glazed area on the facades. To confirm the hypotheses presented, simulation studies on the thermal environment of the residence should be conducted.

5.2. Daylighting ambiance

The natural lighting in the residence (Fig. 3) is abundant due to the high percentage of glazed surfaces, yet not excessive, thanks to the presence of vegetation. Additionally, internal bounces are facilitated by the white-painted walls and ceiling and the unoccupied room.

During the warm season on clear-sky days, internal illuminance levels varied between 1000 and 1200 lux, while on partially cloudy days, levels were around 700 lux. It is noteworthy that, for both sky conditions mentioned, illuminance levels close to or above 300 lux are predominantly observed between 9 am and 4:30 pm. The 300 lux threshold indicates that the daylight itself would be sufficient for executing a significant number of tasks, except for those requiring greater visual acuity. Therefore, artificial lighting would only be necessary from 5 pm until the early morning hours.

Concerning the winter season, on overcast days, illuminances can reach 400 lux during the mornings but hardly exceed 200 lux in the afternoons. On sunny days, however, values can reach 900 lux during the day.

It is important to note that due to limitations in the quantity of equipment, measurements were taken for a central point in the room only, and more

comprehensive simulation studies are necessary to broadly understand the daylighting ambiance of the project. Nevertheless, these assessments already indicate a good natural lighting quality in the house.

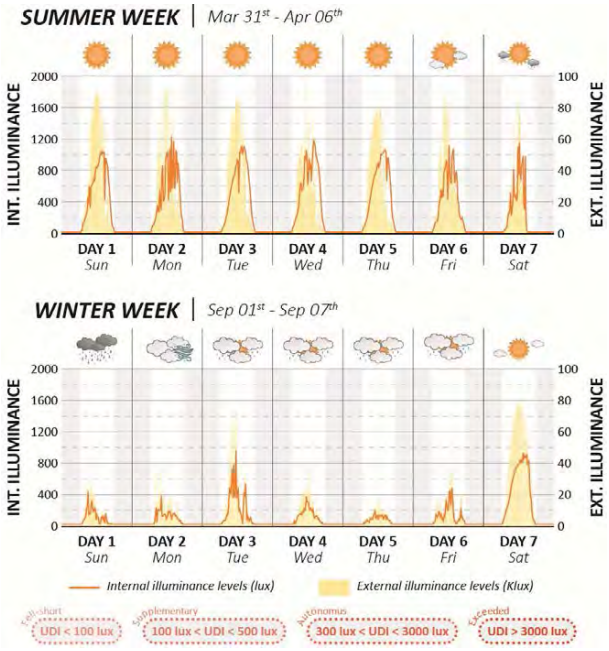

Figure 3: Measurements of illuminance levels during warm and cold periods in the living-room with estimated external illuminance levels.

5.3. Acoustic ambiance

Regarding the acoustic ambiance of the residence (Fig. 4), the measurements indicate values that exceed normative recommendations. However, it is worth noting that the LA90 data reveals values of 49.3 dB for the external environment and 40.1 dB for the internal environment. LA90 is a statistical measure indicating the sound pressure level exceeded during 90% of the measurement period, excluding sound pressure peaks – elevated sound pressure levels result from the proximity of the house to airplane routes and local traffic. Its assessment shows that the external sound pressure level is within the limit recommended by Brazilian regulations, while the internal sound pressure level exceeds the limit by only 0.1 dB.

It is essential to recall that the internal measurements of the residence were conducted with the house entirely unoccupied. The introduction of furniture into the room, representing absorbing components, would diminish the measured sound pressure levels.

Before evaluating airborne sound insulation, it is necessary to classify the area where the project is implemented according to the predominant Noise Class. The values obtained during measurements indicate that Nadyr de Oliveira House is located in a Noise Class I area, in which sound pressure level incident on the facade equal to or less than 60 dB. For this case, the required limits for minimum, intermediate, and superior performances of vertical enclosures in dwellings are 20 dB, 25 dB, and 30 dB, respectively. Therefore, the result of airborne sound insulation for the living room's facade does not even meet the minimum performance level. However, it is emphasized that the evaluation of living rooms, kitchens, laundries, and bathrooms is not compulsory for the Noise Class in question, with its verification being necessary only for Noise Class III.

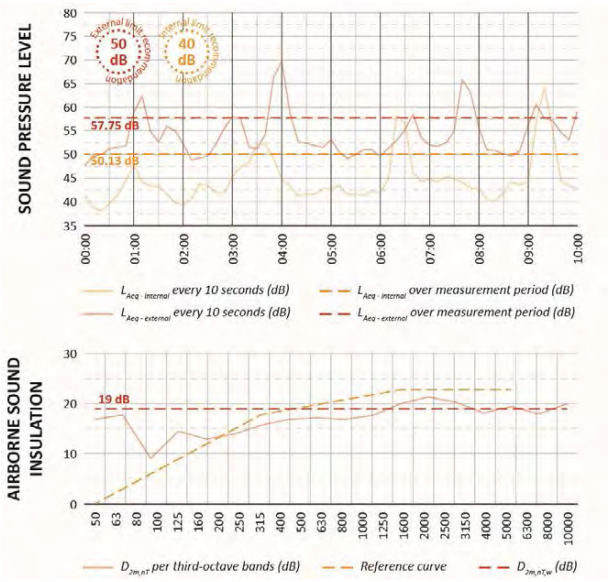

Figure 4: At the top, measurements of internal and external sound pressure levels. At the bottom, airborne sound insulation information, measured by weighted standardized facade level difference of the living room facade.

6. ENVIRONMENTAL ADEQUACY OF MODERNIST ARCHITECTURE

Any heritage building, endowed with historical architecture, and cultural values, poses the unique challenge of achieving a delicate balance between preservation and environmental performance. These discussions gain more prominence when considering the climate changes already experienced. Adapting buildings to meet current demands is an emerging challenge, particularly when they are officially listed, as is the case with the Nadyr de Oliveira House.

New materials and construction systems introduced by industrial development were fundamental to the emerging of the modernist architecture. However, the modernist projects were originated in a time predating the energy and oil crises, when energy resources were perceived as inexhaustible, and sustainable development and energy efficiency were not yet prevalent concerns.

Consequently, a considerable number of structures from this period feature extensive glazed surfaces in their facades. While this design choice ensures excellent natural light levels, it also leads to the overheating of spaces. Moreover, the abundance of window cracks results in high rates of air infiltration, a

characteristic that can be advantageous in São Paulo's climate during warmer periods but contributes to lower temperatures during colder seasons. This also has a detrimental impact on acoustic ambiance, as it diminishes the sound insulation properties of the facades. In these instances, envelope projects typically necessitate upgrades to align with contemporary environmental requirements.

In relation to this case study, the replacement of windows with others of the same design but more airtight and made with innovative materials, such as special glass that prevents the passage of solar radiation, is a desirable solution. Additionally, the use of thermal-acoustic mortars that do not alter the project's characteristics is also advisable. Disassociated structures from the residence could be strategically positioned to block the solar radiation. The use of more efficient lighting sources, only when natural light is insufficient, would also contribute to the reduction of energy consumption and the thermal ambiance of the house.

Finally, an important issue not addressed in the studies but directly tied to the utilization and preservation of this project is the presence of a sole bathroom on the upper floor. Historically, it was customary for a single bathroom to be shared by the entire family, a practice now deemed inappropriate. This factor plays a role in the extended duration the residence spends on the real estate market, consequently contributing to its gradual deterioration. This prompts inquiries about its residential suitability: could an architectural studio, for example, potentially inhabit the project without compromising the design concepts?

7. FINAL CONSIDERATIONS

This paper presented an assessment of the environmental quality of Nadyr de Oliveira House, located in São Paulo, and its preservation as a modernist heritage building. Despite the existence of some areas for improvement, it is crucial to emphasize that environmental quality extends far beyond measurements of environmental comfort variables. The uniqueness of this residence is intricately linked to the appropriate integration of various design strategies, which harmonizes building techniques, site conditions, and environmental strategies on a case-by-case basis. In this study case, the ventilation linked to the envelope characteristics assumes a distinctive role in determining its overall performance. This approach diverges from the notion of relying on predefined rules or optimal solutions for achieving adequate environmental performance, aligning more closely with Bioclimatic principles.

ACKNOWLEDGEMENTS

We express our gratitude to FAPESP (Process No. 2018/19902-8) for supporting this research. Special thanks are extended to Acoustic Engineer Fernando Dias and the company HBK. Additionally, we would like to acknowledge and appreciate the cooperation of the residence owners. Our thanks also go to Fabiana Oliveira for establishing contact with the homeowners.

REFERENCES

1. Corbella, O. & Yannas, S., (2009). Em busca de uma Arquitetura Sustentável para os Trópicos. Rio de Janeiro, Ed. Revan.

2. Romero, M., (2012). Estratégias Bioclimáticas de Reabilitação Ambiental Adaptadas ao Projeto. Brasília: p. 3.

3. Villa, G. F., (2013). O desenho de arquitetura na obra de Carlos Millan: relações entre as soluções técnicas e formais. Scientific Report. IAU. University of São Paulo. São Carlos.

4. Gonçalves, J. *et al.*, (2018). Revealing the thermal environmental quality of the high-density residential tall building from the Brazilian bioclimatic modernism: the case-study of Copan building. *Energy and Buildings*, 175: p. 17-29.

5. Gonçalves, J. *et al.*, (2022). Lessons Learnt from The Brazilian Bioclimatic Modernism: The case-study of the Sul American Bank building (1966). PLEA Conference, Santiago, Chile.

6. Matera, S., (2005). Carlos Millan, um estudo sobra a produção em arquitetura. Masters dissertation. FAUUSP. São Paulo.

7. ASHRAE, (2020). *ASHRAE Standard 55: Thermal environmental conditions for human occupancy*. Atlanta, ASHRAE.

8. ABNT (2021). *ABNT NBR 15575: Edificações habitacionais - Desempenho*. Rio de Janeiro, ABNT.

9. Alucci, M., (2006). *Manual para dimensionamento de aberturas e otimização da iluminação natural na arquitetura*. São Paulo, FAUUSP.

10. Nabil, A.; Mardaljevic, J., (2005). Useful daylight illuminance: a new paradigm for assessing daylight in buildings. *Lighting Res. Technol.* v. 37, n. 1, p. 41-59.

11. ABNT, (2020). ABNT NBR 10151: Acústica – Medição e avaliação de níveis de pressão sonora em áreas habitadas – Aplicação de uso geral. Rio de Janeiro, ABNT.

12. ABNT, (2020). NBR 10152: Acústica - Níveis de pressão sonora em ambientes internos a edificações. Rio de Janeiro, ABNT.

13. ABNT, (2021). ABNT NBR ISO 16283: Acústica - Medição de campo do isolamento acústico nas edificações e nos elementos de edificações. Rio de Janeiro, ABNT.

14. São Paulo, (2016). Lei de Parcelamento, Uso e Ocupação do Solo de São Paulo. São Paulo.

15. Climate data. [Online], Available: http://climate.onebuilding.org [12 December 2023].

PLEA 2024 WROCŁAW
(Re)thinking Resilience

Restorative Experience in Semi-outdoor Spaces
from Thermal Pleasure to Psychological Well-being

KUN LYU[1,2], RICHARD DE DEAR[1], ARIANNA BRAMBILLA[1], ANASTASIA GLOBA[1]

[1] University of Sydney, Sydney, Australia
[2] École Polytechnique Fédérale de Lausanne, Lausanne, Switzerland

ABSTRACT: Biophilic design holds great potentials for improving built environment occupants' psychological wellbeing through its restorative benefits. However, several limitations exist in current biophilic design research and practice, including the lack of considerations for the thermal experience and cultural aspects. This study aims to explore potential links between occupant thermal experience, their cultural backgrounds and psychological restorative benefits from exposure to biophilic inspired semi-outdoor spaces. A multisensory Virtual Reality experiment was conducted to examine the restorative responses to semi-outdoor environments. Findings highlight the relevance and importance of thermal delight for biophilic design in architecture to support occupant psychological well-being.
KEYWORDS: thermal pleasure, psychological well-being, adaptive opportunity, cultural factors, biophilic design

1. INTRODUCTION

With the rapid and continuous process of urbanisation, cities are expanding and densifying rapidly to accommodate the growing population, leading to the potential loss of urban green spaces and biodiversity. Opportunities for urban inhabitants to interact with nature are diminishing [1]. This has direct implications for human health and well-being because of the restorative benefits afforded by the experience of nature[2].

The concept of biophilic design has gained significant relevance over recent years for its potential to improve occupants' health and well-being through the embedded multisensory quality of nature[3]. Despite its recent progresses, there are still limitations.

Firstly, multisensory biophilic qualities are insufficiently discussed in biophilic design literature. The restorative benefits from exposure to biophilic environments, including its effects on attention restoration[4] and stress reduction[5], have been studied almost entirely in the visual domain, instead of other sensory domains, especially the ***thermal sense***. In practice, the introduction of nature has often been reduced to a superficial collection of discrete visual elements instead of a synthetic and immersive experience. For example, indoor living walls with high resource budgets for maintenance and irrigation may be introduced as simple add-ons to an otherwise irrelevant architectural design scheme, just to render a visually pleasant scene.

In thermal comfort research, the thermal pleasure principle, *thermal alliesthesia*[6], can contribute to the understanding of the dynamic thermal experiences in outdoor urban and natural settings. Thermal alliesthesia indicates that the hedonic tone (pleasant or unpleasant) of an environmental thermal stimulus depends on the stimulus itself and the individual's internal thermal state. The adaptive approach to thermal comfort provides an alternative perspective for understanding the rich thermal experiences of our interactions with outdoor environments through its recognition of the active role played by human occupants.

Secondly, ***sociocultural*** contexts have been largely overlooked in biophilic design. This is not surprising considering biophilia hypothesis is built on a biologically evolutionary perspective to human-nature relationships. One might observe an international style of biophilic architecture regardless of cultural origin. Yet, distinctive architectural expressions of nature have evolved in history, for example, the Japanese *Zen Garden* embedded in courtyard versus the formal and symmetrical *French garden*. Individual differences in restorative experiences[7] need to be explored, including not only visual preferences of nature, but also thermal preferences.

Built environment inhabitants with different sociocultural backgrounds may have distinct thermal preferences towards outdoor environments. Knowledge of these differences may contribute to a better understanding of individual experiences in biophilic outdoor environments. Cultural norms can influence an individual's habits, such as clothing and dietary habits, leading to different thermal experiences. Moreover, different cultural backgrounds may be associated with distinct environmental attitudes towards specific weather components, such as sunlight[8].

This paper aims to address the above-mentioned two limitations in biophilic design by exploring the interrelationships between thermal pleasure, cultural influence, and restorative benefits of semi-outdoor environmental experiences.

2. METHOD

This study adopted an empirical approach. An experiment with human subjects was conducted in an immersive Virtual Reality integrated climate chamber, where the visual, auditory, and thermal conditions of two semi-outdoor environmental scenarios were simulated. This includes a nonadaptive scenario where participants were exposed to strong sunlight with breeze but no adaptive opportunity, and an adaptive scenario where opportunities to choose between sunlight exposure and shade exist.

2.1 Research participants

Thirty-eight research participants, consisting of 19 Chinese and 19 Australian participants (male participants:15, female participants:23, average age = 24 ± 5), undertook the study in two experimental sessions. All experimental participants have lived in Sydney, Australia for at least three months to ensure physiological acclimatisation to the local climate.

2.2. Experimental conditions

The creation of the visual and auditory stimuli for the virtual semi-outdoor space was based on an actual roof garden – *SkyPark* in the Central Business District, Melbourne. The visual environment was constructed in VR using *Rhino3D* and *Unity* and delivered to participants via a head-mounted display *Oculus Rift S*. Different sunlight conditions were created for *sunlight only* and *sunlight + shade* scenarios (*Figure 1*). The auditory experience was simulated with *Unity*'s audio system, which enables a head-tracking binaural render of ambisonic audio recording for achieving an interactive urban soundscape experience.

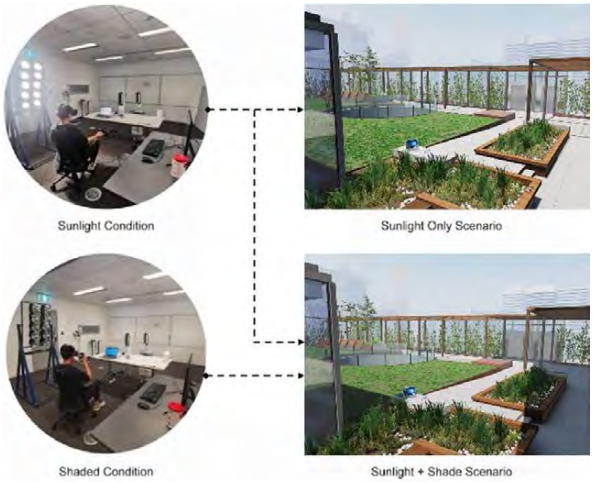

Figure 1: Experimental scenarios

Air temperature, airflow, and solar radiation of the semi-outdoor environment were simulated using the HVAC systems of the climate chambers, an array of halogen heat lamps, and digitally controlled bladeless fans. A summary of the simulated thermal conditions is shown in Table 1.

Table 1 : Thermal Experimental Conditions (T_{air}: air temperature, T_{mrt}: mean radiant temperature, RH: relative humidity, V_{air}: air velocity)

Thermal Condition	T_{air} (°C)	T_{mrt} (°C)	RH (%)	V_{air} (m/s)
Indoor	24.0 ± 0.1	24.0	55	0.05 ± 0.01
Semi-outdoor Sunlight	28.0 ± 0.1	39.7	60	1.00 ± 0.01
Semi-outdoor Shade	28.0 ± 0.1	28.0	60	1.00 ± 0.01

The solar radiation was simulated using a bank of ten quartz tungsten halogen lamps (250 W per lamp). The halogen heat lamps were controlled digitally with *Arduino* microcontroller and power relay, able to respond automatically to the user's actions in VR. The wind conditions were simulated using two digitally controlled bladeless fans to recreate the turbulence characteristics of an actual 30-min outdoor wind time series, as captured by high-speed (1 Hz) thermal anemometer in an urban setting.

2.3 Procedure

The experiment included three phases, pre-test, environmental exposure, and post-test.

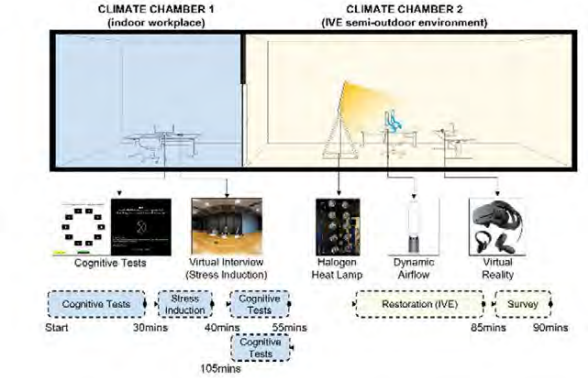

Figure 2: Experimental set-up and procedure

The *pre-test* was conducted in climate chamber 1 (*Figure 2*), simulating a workplace environment. Fatigue and stress inductions were administered to participants, including a series of cognitive tests (Backward Digit-span and Sustained Attention to Response Task), and a Trier Social Stress Test. Participants' cognitive performance and stress level were measured.

The *environmental exposure* took part in climate chamber 2 (*Figure 2*) immediately after the pre-test.

Participants experienced the simulated semi-outdoor environment for 25 min, during which they could freely explore the virtual environment. After the environmental exposure, participants completed a questionnaire regarding their subjective appraisal of the experience.

In the post-test stage, participants returned to chamber 1 and were asked to take the cognitive tests again.

2.4 Data collection

(1) Backward Digit-span Test (BD)

BD has been widely used as an indication of directed attentional capacity. During the test, participants were asked to recall a series of number sequences ranging from 3 to 12 in length in backward order.

(2) Sustained Attention to Response Task (SART)

SART reflects the subject's cognitive capacity to sustain attentional focus over an extended time. During the experiment, SART was administered to participants using Inquisit V6 (Millisecond Software). 225 digits from 1 to 9 were presented to subjects in a pseudo-randomised sequence. Participants were asked to withhold their response to the digit '3' but respond as quickly and accurately as possible by pressing the spacebar button on the keyboard.

(3) Questionnaire

A questionnaire was filled out by participants regarding their subjective experience of the virtual semi-outdoor environment, including perceived sensory pleasantness (visual, auditory, and thermal), perceived environmental influence on mood, and a short-form perceived restorativeness scale. Sensory pleasure was surveyed with seven-point continuous scale questions (*How pleasant did you feel about the visual/auditory/thermal environment? 3: very unpleasant, 0: neutral, +3: very pleasant*). The perceived mood influence was based on five bipolar scale of basic emotional dimensions (*How would you describe the effect of the environment on you in terms of the following emotions: depressed-elated, unsure-confident, grouchy-good-natured, anxious-relaxed, fatigued-energetic.* A five-item short-form perceived restorativeness scale[9] was used, with item for each restorative component from Attention Restoration Theory (*fascination*, *being-away, scope, coherent, compatibility*)[4]. *Fascination* refers to the ability of the environment to engage ongoing effortless attention. Being-away describes the psychological distance of an individual to attention demanding mental activities. *Scope* and *coherent* are important for an environment to have sufficient information for exploration and to have an ordered structure for comprehension. *Compatibility* refers to the mutual fit between an environment's affordance and the individual's purpose.

3. RESULTS

3.1 Thermal pleasure and restorative benefits

Thermal pleasure was significantly associated with restorative benefits in SART performance, as indicated by D-prime ($\beta = 0.24$, $p < 0.05$), subject's sensitivity to task stimuli, CV ($\beta = -0.27$, $p < 0.05$), differences in reaction time produced by lapsing attention (*Table 2*). Visual pleasure was associated with Delta Errors ($\beta = -0.34$, $p < 0.01$).

Table 2: Statistical Association between Sensory Pleasure and SART Performance (p<0.05, ** p<0.01, ns Non-significant)*

	β-Value		
	Delta D-prime	*Delta* CV	*Delta* Errors
Thermal Pleasantness	0.24*	Ns	-0.27*
Visual Pleasantness	ns	-0.34**	ns
Auditory Pleasantness	ns	ns	ns
F	5.12	10.84	6.48
R^2	0.06	0.11	0.07

Stepwise regression using individual sensory pleasantness as predictors for the overall environmental influence on perceived mood (sum of individual emotional dimensions) showed that among the sensory modalities, thermal pleasure was the most significant predictor of environmental influence on perceived mood ($\beta = 0.52$, $R^2 = 0.43$, $p < 0.001$). There was also a significant association between visual pleasantness votes and environmental influence on perceived mood ($\beta = 0.27$, $R^2 = 0.06$, $p < 0.05$), although accounting for much less variance. Auditory pleasantness was not a significant predictor.

Stepwise multiple regression analyses were conducted to examine the relationships of individual sensory pleasantness votes with the perceived restorative components. In Table 4, visual pleasantness was positively associated with fascination ($\beta = 0.50$, $p < 0.001$), being-away ($\beta = 0.37$, $p < 0.01$), coherence ($\beta = 0.30$, $p < 0.01$), scope ($\beta = 0.38$, $p < 0.01$) and compatibility ($\beta = 0.48$, $p < 0.01$). There were positive associations between the sense of being-away and thermal pleasantness ($\beta = 0.25$, $p < 0.05$).

3.2 Cultural influence on thermal experience and restorative benefits

As indicated in *Figure 3*, thermal pleasure assessments between Chinese (Median = − 0.45) and Australian groups (Median = 1.75) differed significantly during *sunlight-only* environmental exposure ($p < 0.001$). Chinese participants were more likely to experience thermal displeasure when exposed to direct sunlight (T_{mrt} = 39.7C°), while the opposite

trend was observed in Australian subjects. In the *sunlight+shade* scenario, the difference between the two cultural groups was not significant (p > 0.05), due to improvement of thermal pleasure for Chinese participants (Median difference = 2.3, p < 0.0001).

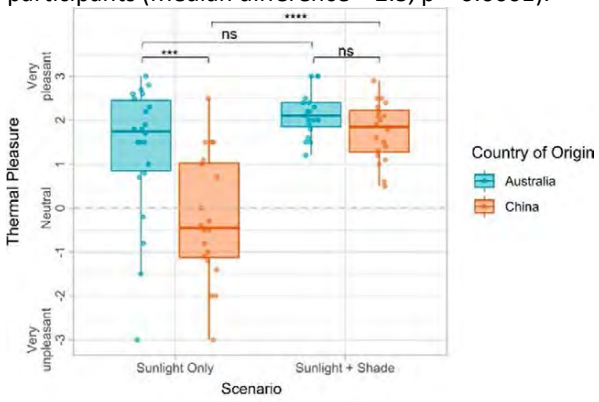

Figure 3: Thermal pleasure between groups and scenarios

Figure 4 shows that Australian participants received more improvement of their cognitive performance than Chinese participants in the *sunlight-only* scenario (Mean difference = 0.85, $p < 0.05$). No significant difference was found between the two cultural groups in the *sunlight + shade* scenario ($p > 0.05$) due to the improvement of cognitive performance for the Chinese group when given adaptive opportunity (Mean difference = 0.84, $p < 0.05$). A mixed-model Analysis of Variance (ANOVA) test on the backward digit-span test performance suggests no statistically significant effect of both Country of Origin, F (1, 72) = 2.67, $p = 0.10$, and Scenario, F (1, 72) = 0.24, $p = 0.62$.

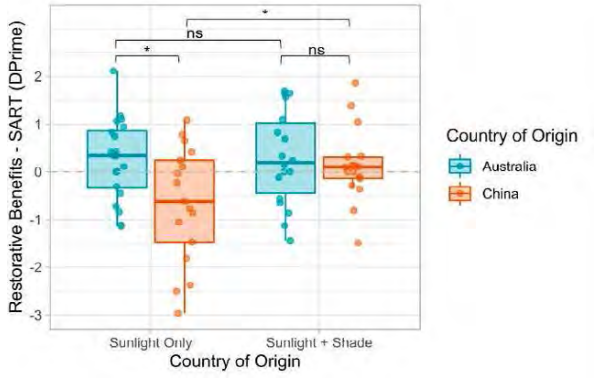

Figure 4: Comparison of SART performance between cultural groups and scenarios.

Figure 5 indicates the perceived environmental influence on mood was significantly positively associated with thermal pleasure rating ($\beta = 2.5$, $R^2 = 0.42$, $p < 0.001$). Given the significant difference in thermal pleasure between *Australian* and *Chinese* cultural groups, the restorative benefit on mood also differed significantly (Median difference = 3, $p < 0.01$). Australian participants had a more positive mood after the semi-outdoor environmental exposure compared to Chinese participants.

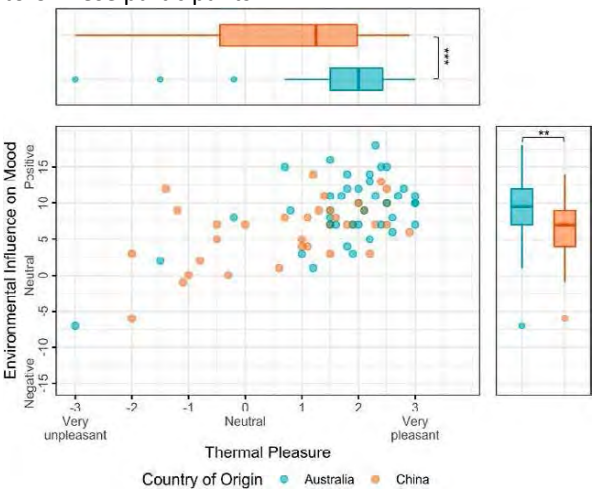

Figure 5: Statistical relationship between cultural group, thermal pleasure and environmental influence on mood.

4. DISCUSSION

This section discusses the results' relevance in the existing literature and synthesizes the findings into a conceptual model, depicting the process of occupant adaptation to the semi-outdoor thermal environment during the restorative experience. The implication of the findings on biophilic design in architecture is also discussed.

4.1 Conceptual model

Immediate environment (*Figure 6*) refers to the thermal milieu of an individual that directly impacts the person's heat balance and includes air temperature, humidity, airflow characteristics, and the radiative fluxes from sun, sky, ground, and nearby objects.

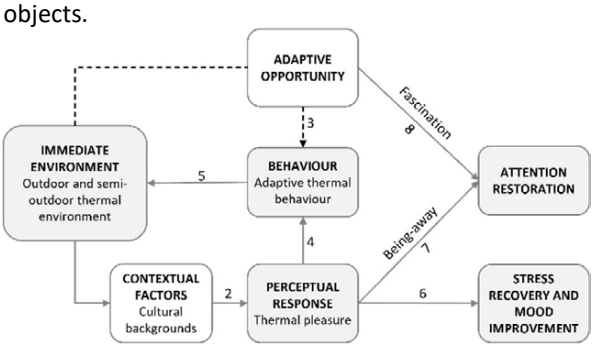

Figure 6: conceptual model - relationships between the thermal realm and psychological restoration

The subjective *perceptual response* to thermal stimuli is determined by the individual's internal thermal state and the capacity of the stimuli to restore heat balance of the body. This response is further shaped by *contextual factors*, such as *cultural backgrounds*. In the present study, significant differences in thermal pleasure responses were observed between *Chinese* and *Australian* participants when exposed to the same semi-outdoor thermal

environment during the *sunlight-only* scenario. This disparity can be potentially explained by a *cultural difference* in the notions of skin beauty (*fair* vs *tanned* skin tone) which shape attitudes towards sunlight exposure. In addition, Australians' affinity to sunshine may also be associated with the Australian beach culture. The beach occupies a significant and multivalent place in Australia and Australian culture. The strong positive thermal pleasure derived from burning sunshine, cold waves, and cool breeze constituents a vital part of the sensory hedonistic alliesthesia experience for beachgoers, and contributes to Australians' affective bond to the place – *topophilia*[10]. In addition to cultural backgrounds, other contextual factors related to personal backgrounds and situations may also be relevant, such as socio-economic status[11], climatic backgrounds[12], purpose and frequency of visit, and perceived control[13].

Depending on the availability of adaptive opportunities in the environment and the individual's current thermal comfort state, adaptive behavioural responses may alleviate thermal displeasure or enhance thermal pleasure (Figure 6 links 3 and 4). The current study observed a significant improvement in thermal pleasure for the Chinese participants when offered choices during the *sunlight + shade* scenario (Figure 3).

Significant associations between thermal pleasure and restorative benefits of semi-outdoor environmental exposure were observed. Thermal pleasure was the strongest predictor of participants' subjective mood improvement resulting from semi-outdoor exposure compared to visual and auditory pleasure. The association between mood improvement and thermal pleasure can potentially be explained through *Stress Recovery Theory* and *alliesthesia* theory. Stress Recovery Theory views stress response and recovery as adaptive processes in which quick-onset emotional reactions to the external environment are necessary to initiate physiological adaptation and motivate avoidance behaviour in relation to environmental challenges or threats. Recovery occurs when the environment is beneficial to human well-being or survival, thereby recharging adaptive resources to sustain energy levels for future events or opportunities [5]. From an evolutionary perspective, it is vital to our species' survival that the alliesthesia mechanism (depending on the thermal stimuli's ability to restore homeostasis) can elicit strong affective responses, including sensory pleasure/displeasure, activation/recovery of stress response, and positive/negative mood.

The relationship between the thermal realm (thermal pleasure, thermal adaptive opportunity) and attention restoration was understood through the lenses of *fascination*, *being-away*, *extent*, and *compatibility* (Figure 6 links 7 and 8). In the current study, thermal pleasure was significantly positively associated with being-away ($\beta=0.25$, $p<0.05$), referred to as the psychological distance or disengagement from the current work task or attention-demanding mental activities. To cope with unpleasant thermal environmental stressors psychological resources are required, thus attenuating the sense of being-away. The results also indicate that access to adaptive opportunity is associated with higher ratings of *fascination* and *being-away*. Environments that are replete with adaptive opportunities promise more diverse experiences to the inhabitants, thereby enhancing the quality of *fascination*.

4.2 Design implication

The relative importance of sensory modalities in human experience has been the subject of much conjecture. Although holding great importance as input to cognitive processing about the external world[14], the visual sense alone may not have the most significant influence on our experience of the world, certainly not emotional experiences. Findings of the current study provide evidence to the theoretical discussions of the active role of the thermal sense in affecting the emotional experiences of built environment inhabitants.

The potential of the built space to engage a rich texture of thermal experiences for its inhabitants has been articulated in the book *Thermal Delight in Architecture*[15] as well as scientifically explored in *Thermal Alliesthesia*[16]. This current study further supports the discussions around thermal delight in architecture with its association with tangible restorative benefits to building occupants. The results suggest that thermal pleasure contributes substantially to the restorative experience, leading to enhanced cognitive performance and improved mood states. The atmosphere created by the active engagement of thermal pleasure in outdoor nature fosters an enhanced sense of well-being in architecture.

Understanding thermodynamics in nature and how we interact with it physiologically, emotionally, and behaviourally has potential application in architectural design conception. Metaphors are regarded as essential tools of thought for design conception that express and articulate human existential experience in the world[17]. A departure of the guiding metaphors for architectural conception from mechanistic images requires a deep understanding and integration of the subtlety and dynamic complexity of biological phenomena in the natural world. Edward Wilson stated in his landmark book Biophilia[18] that "the superorganism of a leaf-cutter ants' nest alone is a more complex system in its performance than any human invention and unimaginably old" (p.37).

Understanding the biological world with the lens of our own biological heritage will bring new models for the contemporary architecture. This understanding cannot be achieved via only visual terms but also the multisensory comprehension of the interactions between humans and the natural world. Aspirations towards an architecture that engages the dynamic thermal interaction in nature can be seen in the works such as Glenn Murcutt's *Simpson-Lee House*, Peter Zumthor's *Thermal Vals* and Philippe Rahm's *Meteorological Architecture*[19].

The current study also emphasises inhabitants' cultural backgrounds as a significant factor in biophilic design. The culturally distinct groups of Chinese and Australian participants showed pronounced differences in their thermal pleasure assessments, adaptive behaviours, and restorative outcomes from exposure to semi-outdoor environments. These findings highlight the need for a shift in biophilic design from a generic one-size-fits-all design guideline to a more contextualised and nuanced framework taking into account local culture, climate, and user's backgrounds. Most of the current biophilic design frameworks propose a collection of discrete design patterns that attempts to introduce natural elements or emulate natural characteristics in the design of the physical environment. The successful integration of these universally-defined design themes, such as thermal & airflow variability, presence of water, and prospect & refuge[20], needs to be grounded in the specific context of place and people to achieve biophilic design's goal of fostering human well-being.

5. CONCLUSION

This study explored the potential relationship between thermal experience and psychological restorative benefits. The findings of current study bring empirical evidence to support the key roles of thermal pleasure and cultural considerations within the biophilia theme in contemporary architecture.

REFERENCE

1. Miller, J. R. (2005). Biodiversity conservation and the extinction of experience. *Trends in Ecology & Evolution*, *20*(8), 430–434. https://doi.org/10.1016/j.tree.2005.05.013

2. Hartig, T., Mitchell, R., de Vries, S., & Frumkin, H. (2014). Nature and Health. *Annual Review of Public Health*, *35*(1), 207–228. https://doi.org/10.1146/annurev-publhealth-032013-182443

3. Kellert, S. R., Heerwagen, J., & Mador, M. (2013). *Biophilic Design: The Theory, Science and Practice of Bringing Buildings to Life*. John Wiley & Sons, Incorporated. http://ebookcentral.proquest.com/lib/usyd/detail.action?docID=818992

4. Kaplan, R., & Kaplan, S. (1989). *The experience of nature: A psychological perspective*. Cambridge University Press.

5. Ulrich, R. S., Simons, R. F., Losito, B. D., Fiorito, E., Miles, M. A., & Zelson, M. (1991). Stress recovery during exposure to natural and urban environments. *Journal of Environmental Psychology*, *11*(3), 201–230.

6. Parkinson, T., & de Dear, R. (2015). Thermal pleasure in built environments: Physiology of alliesthesia. *Building Research & Information*, *43*(3), 288–301. https://doi.org/10.1080/09613218.2015.989662

7. Lyu, K., Brambilla, A., Globa, A., & de Dear, R. (2023). A socio-cultural perspective to semi-outdoor thermal experience and restorative benefits – Comparison between Chinese and Australian cultural groups. *Building and Environment*, *243*, 110622. https://doi.org/10.1016/j.buildenv.2023.110622

8. Tung, C.-H., Chen, C.-P., Tsai, K.-T., Kántor, N., Hwang, R.-L., Matzarakis, A., & Lin, T.-P. (2014). Outdoor thermal comfort characteristics in the hot and humid region from a gender perspective. *International Journal of Biometeorology*, *58*(9), 1927–1939. https://doi.org/10.1007/s00484-014-0795-7

9. Han, K.-T. (2018). A review of self-report scales on restoration and/or restorativeness in the natural environment. *Journal of Leisure Research*, *49*(3–5), 151–176. https://doi.org/10.1080/00222216.2018.1505159

10. Tuan, Y.-F. (1990). *Topophilia: A Study of Environmental Perceptions, Attitudes, and Values* (p. 260 Pages). Columbia University Press.

11. Aljawabra, F., & Nikolopoulou, M. (2010). Influence of hot arid climate on the use of outdoor urban spaces and thermal comfort: Do cultural and social backgrounds matter? *Intelligent Buildings International*, *2*(3), 198–217. https://doi.org/10.3763/inbi.2010.0046

12. Yang, W., Wong, N. H., & Zhang, G. (2013). A comparative analysis of human thermal conditions in outdoor urban spaces in the summer season in Singapore and Changsha, China. *International Journal of Biometeorology*, *57*(6), 895–907. https://doi.org/10.1007/s00484-012-0616-9

13. Nikolopoulou, M., & Steemers, K. (2003). Thermal comfort and psychological adaptation as a guide for designing urban spaces. *Energy and Buildings*, 7.

14. Spence, C. (2020). Designing for the Multisensory Mind. *Architectural Design*, *90*(6), 42–49. https://doi.org/10.1002/ad.2630

15. Heschong, L. (1979). *Thermal delight in architecture*. MIT press.

16. de Dear, R. (2011). Revisiting an old hypothesis of human thermal perception: Alliesthesia. *Building Research & Information*, *39*(2), 108–117.

17. Pallasmaa, J. (2017). Architecture and Biophilic Ethics. Human Nature, Culture, and Beauty. *International Journal of Architectural Theory*, *22*(36), 57–69.

18. Wilson, E. O. (1984). *Biophilia*. Harvard University Press.

19. Rahm, P. (2009). Meteorological Architecture. *Architectural Design*, *79*(3), 30–41. https://doi.org/10.1002/ad.885

20. Ryan, C. O., Browning, W. D., Clancy, J. O., Andrews, S. L., & Kallianpurkar, N. B. (2014). BIOPHILIC DESIGN PATTERNS: Emerging Nature-Based Parameters for Health and Well-Being in the Built Environment. *International Journal of Architectural Research: ArchNet-IJAR*, *8*(2), 62. https://doi.org/10.26687/archnet-ijar.v8i2.436

PLEA 2024 WROCŁAW
(Re)thinking Resilience

Resilience Assessment in School Buildings through Comfort Analysis in Two Brazilian Bioclimatic Zones

LUCAS RAFAEL FERREIRA[1], NARA GABRIELA DE MESQUITA PEIXOTO[1], IARA NOGUEIRA LIGUORI[1], LEONARDO MARQUES MONTEIRO[1].

[1]University of São Paulo, Rua do Lago, 876 Butantã, São Paulo / SP, Brazil.

ABSTRACT: This article explores the resilience of school buildings in the context of thermal, lighting, and acoustic comfort in two Brazilian bioclimatic zones Bioclimatic Zone 1 (Campos do Jordão - SP) and Bioclimatic Zone 3 (São Paulo - SP), with a specific focus on the direct impact of climate on the thermal and lighting characteristics of the structures. Employing a qualitative-quantitative method, the study involves comprehensive measurements and evaluations, incorporating comfort descriptors and the application of questionnaires to assess thermal, lighting, and acoustic perceptions and preferences. The findings highlight the imperative need for interventions aimed at improving the adaptability of buildings to promote resilience. Key insights reveal deficiencies in acoustic insulation, ventilation-related challenges affecting thermal comfort, and deficiencies in natural lighting in both zones. The proposed interventions cover investments in acoustic insulation, ventilation strategies, optimization of lighting design, implementation of lighting control mechanisms, consideration of thermal coatings, and exploration of humidity control solutions.
KEYWORDS: Resilience, Environmental Comfort, Thermal Comfort, Acoustic Comfort, Lighting Comfort.

1. INTRODUCTION

In 2019, approximately 55% of the global population lived in urban areas, with a projected increase of 13% by 2050 [1]. The rapid growth of cities, technological advancements, and industrialization, predominantly stemming from the industrial revolution, have contributed to alterations in global climate patterns [2] and an increase in noise pollution [3]. Many of these alterations are indicated by researchers due to greenhouse gas emissions resulting from the human model of planetary occupation.

The Intergovernmental Panel on Climate Change (IPCC), the scientific-political organization responsible for assessing climate changes due to anthropogenic factors, cautioned in its latest report (AR6) about the alarming repercussions of the heightened emissions of greenhouse gases (GHGs). This increase is directly correlated with the escalation in both the frequency and severity of temperature fluctuations and catastrophic events on a global scale [4].

The building's exposure to climate is directly connected to its thermal and energy performance [5]. Climate change presents new challenges to buildings, cities, and citizens, requiring solutions to enhance constructions' flexibility and adaptability to constant temperature changes. Climate becomes a shaping agent of space.

Considering in this work that resilience in the capacity of the built environment to withstand and adapt to changes or impacts of carious kinds over time [6-9], the resilience of school buildings in terms of environmental comfort becomes a crucial aspect to ensure an environment conducive to learning and occupants' well-being.

In the Brazilian context, which encompasses eight distinct bioclimatic zones (Fig. 1), comprehending and adapting school buildings to face climatic challenges is of paramount importance. This paper discusses the resilience of buildings within the school context concerning thermal, lighting and acoustic comfort in two specific bioclimatic zones: Bioclimatic Zone 1 (Campos do Jordão – SP) and Bioclimatic Zone 3 (São Paulo – SP) considering the direct influence of climate on the thermal and lighting characteristics of the buildings.

Identifying these factors is crucial to enable resilience in the face of climate-derived impacts and changes, as well as other socio-environmental conditions affecting the comfort of the built environment.

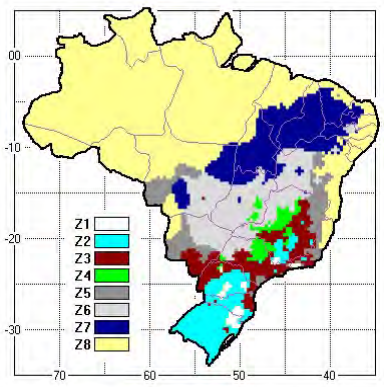

Figure 1: Brazilian bioclimatic zones.

2. METHOD

The established method was qualitative-quantitative through measurement, encompassing the evaluation of comfort descriptors in conjunction with interviews focused on thermal, luminous, and acoustic perception and preference. The equipment was positioned within each designated space: teachers' rooms, computer rooms, and drawing rooms of each building.

Thermal comfort was assessed by recording air temperature, radiant temperature (derived from globe temperature), relative humidity, and airspeed [10]. The evaluation of lighting comfort was conducted through the collection of data from both natural and artificial lighting sources. The gathered data encompassed illuminance (lux) levels at the task plane [11-13]. Acoustic comfort was assessed by measuring the sound pressure level (L_{Aeq}) with a sound level meter [13-14].

The data was collected during a typical operating day for both buildings and the results of the thermal comfort indices were compared with the climatological records of the cities São Paulo – SP and Campos do Jordão – SP and all the comfort data (thermal, lighting and acoustic) with the relevant standards.

Questionnaires were administered to users during the established periods of occupancy for the analysis of comfort perception. Furthermore, an analysis of comfort surroundings and the buildings was conducted, with a focus on the building's resilience and users' well-being.

3. OBJECT OF STUDY

The current study focused on analyzing the resilience of school buildings in two educational institutions:

- The federal Institute of Education, Science and Technology of São Paulo (IFSP) in the city of Campos do Jordão (22°44'33'' S, 45°35'33'' W and 1613 m), belonging to Bioclimatic Zone 1 (Z1);
- The Faculty of Architecture and Urbanism of the University of São Paulo (FAU USP) in São Paulo (23°33'36'' S, 46°43'47'' W and 741 m), belonging to Bioclimatic Zone 3 (Z3).

In each of these buildings, three common places were selected: the teachers' room (TR), the computer room (CR), and the drawing room (DR).

4. RESULTS AND DISCUSSION

4.1 Questionnaire

Questionnaires were employed to evaluate environmental comfort in two distinct Brazilian bioclimatic zones, Zone 1 and Zone 3. The survey tool, officially sanctioned by the Research Ethics Board with CAAE number: 74030723.8.0000.5390, unveiled valuable insights into users' perspectives on various environmental factors, as depicted in Table 1.

Table 1: Statistical data from user responses regarding the comfort within each of the studied rooms.

1. Right now, how do you perceive the temperature in this room? *						
	CR Z1	CR Z3	DR Z1	DR Z3	TR Z1	TR Z3
Mean	6.78	7.83	6.35	8.22	5.71	8.15
Median	6.75	8	6	9	5	8.25
Standard deviation	1.72	1.68	1.73	2.27	1.51	1.66
2. At this very moment, how do you assess the natural ventilation in this room? **						
	CR Z1	CR Z3	DR Z1	DR Z3	TR Z1	TR Z3
Mean	4.06	2.89	3.67	2.02	2.64	1.73
Median	4	2.25	3.5	1	1.5	1.75
Standard deviation	2.56	2.6	2.43	2.4	3.35	1.53
3. Without the fan on, how would you describe the thermal sensation in the room? ***						
	CR Z1	CR Z3	DR Z1	DR Z3	TR Z1	TR Z3
Mean	5.6	2.14	6.1	2.37	5.79	2.04
Median	5	2	6	1.5	5	1.5
Standard deviation	2.69	1.95	2.5	2.91	3.46	2.56
4. How would you rate the artificial lighting in this room? **						
	CR Z1	CR Z3	DR Z1	DR Z3	TR Z1	TR Z3
Mean	7.22	7.69	7.8	7.83	6.5	7.76
Median	7.75	8	8.5	8	5	8
Standard deviation	2.34	1.73	2.1	1.82	3.94	1.96
5. How would you rate the natural lighting in this room? **						
	CR Z1	CR Z3	DR Z1	DR Z3	TR Z1	TR Z3
Mean	5.77	6.75	6.5	7.43	4.29	5.39
Median	5.25	6	6.5	8	2	5
Standard deviation	2.66	2.85	2.01	2.59	3.94	2.69
6. Can you easily carry out all activities without artificial lighting?						
	CR Z1	CR Z3	DR Z1	DR Z3	TR Z1	TR Z3
Yes	31%	50%	60%	43%	71%	25%
No	69%	50%	40%	57%	29%	75%
7. Considering the quantity and intensity of external noises in this room, how do you find it? ***						
	CR Z1	CR Z3	DR Z1	DR Z3	TR Z1	TR Z3
Mean	4.98	6.68	4.33	3.66	4.29	4.76
Median	5	6.75	4.5	3	5	4.75
Standard deviation	2.32	2.26	2.49	2.59	2.55	2.23
8. How often is it necessary to close the windows and doors to achieve good audibility? ****						
	CR Z1	CR Z3	DR Z1	DR Z3	TR Z1	TR Z3
Mean	4.56	5.31	4.98	5.78	4.14	5.05
Median	5	5	5	5	5	5
Standard deviation	2.91	2.81	3.01	3.24	1.38	2.42

* 0 - Very cold, 5 - comfortable, 10 - Very hot; ** 0 - unsatisfactory, 05 - neutral, 10 – satisfactory; *** 0 - uncomfortable, 05 - neutral, 10 – comfortable; **** 0 - always, 05 - sometimes, 10 - never (20)

The comfort average, established at 5 for question 1, acted as a benchmark for evaluating the collected responses. Interestingly, the findings reveal that in Zone 1, participants' responses averaged between 5.71 and 6.78, indicating a closer proximity to comfort. In contrast, respondents in Zone 3 reported

averages ranging from 7.83 to 8.22. Notably, these results suggest that individuals in the latter zone encounter notable discomfort in the analyzed environments.

Concerning ventilation, the average responses reflected a widespread sense of dissatisfaction, with this sentiment being particularly pronounced in Zone 3. Participants in this area communicated a heightened level of discomfort in the environments, particularly when lacking fans.

In terms of artificial lighting, the average responses fell within the range of 6.5 to 7.83, suggesting a reasonably satisfactory evaluation. However, when assessing natural light, a decline in satisfaction is evident, with average responses spanning from 4.29 to 7.43. Notably, Zone 1 exhibited the lowest satisfaction rates in this regard. Surprisingly, a significant majority of respondents deem artificial lighting essential for accomplishing their daily activities.

In terms of acoustic comfort, the average response falls within the range of 3.66 to 6.68, pointing to a generally low perception. In numerous instances, the necessity to shut doors and windows to guarantee good hearing directly affects both ventilation and the sense of thermal comfort, thereby amplifying users' discomfort in the rooms examined.

The results gleaned from the questionnaires offer a comprehensive insight into users' perspectives on environmental comfort in the two Brazilian bioclimatic zones. This information is pivotal for grasping the distinct requirements of each region, facilitating the formulation of interventions and enhancements in the studied environments.

4.2 Acoustic Comfort

Acoustic comfort is a crucial factor in the educational environment, directly influencing the academic performance and well-being of students and teachers. Brazilian Standard NBR 10.152 establishes guidelines for the sound pressure level in classrooms, recommending a maximum of 35 dB to promote an environment conducive to learning. The results of acoustic measurements carried out in selected environments in Zones 1 and 3 of the Brazilian bioclimatic zones revealed significant variations in this recommendation (Figure 2).

In Zone 1, the teachers' room had a measured value of 46.5 dB, exceeding the limit recommended by ABNT NBR 10.152:2017. The computer room in the same zone recorded a higher level, reaching 54.2 dB. The drawing room, in turn, showed an even more significant value, reaching 60.1 dB.

In contrast to Zone 1, Zone 3 showed slightly more favorable results, although still far from the normative recommendation. The teachers' room registered 52.6 dB, while the computer room showed 51.3 dB. The drawing room, although smaller than Zone 1, revealed a level of 53.4 dB.

It is clear that, based on the data obtained, school environments in the two Brazilian bioclimatic zones face challenges in terms of acoustic comfort, especially in computer and design rooms. Exceeding the limits set by the standard suggests the need for interventions and corrective measures to optimize the sound environment and create conditions more conducive to teaching and learning.

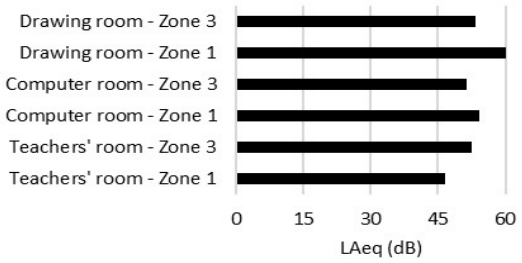

Figure 2: Values measured in L_{Aeq} in each of the rooms.

4.3 Thermal Comfort

The data collected through on-site measurements in the chosen environments in Brazilian Bioclimatic Zones 1 and 3 offers a comprehensive view of thermal comfort, a critical consideration for the resilience of buildings. The operative temperature was obtained by averaging the air temperature and the radiant temperature, and was used as a metric for evaluation, concerning the parameters established by ASHRAE 55 of 2017, which defines the range of 22.5°C to 25.5°C for operative temperature and 65% relative humidity (RH).

Figures 3 and 4 show the results measured indoors, highlighting the variations in operating temperatures throughout the day, relative humidity, and air speed. On 18/09/2023, the outside temperature varied between 17°C and 33°C. In the CR, TR and DR, operating temperatures fluctuated little, but none remained within the parameters set by ASHRAE 55, indicating a thermally uncomfortable environment for users.

No significant variation in internal temperatures, together with the answers to the questionnaire, suggests a consistency between the measured environmental conditions and the users' subjective perception of thermal comfort. It is important to note that the differentiated insolation did not result in large variations, pointing to the effectiveness of the architectural design due to the potential for thermal inertia.

Relative humidity (RH) varied between 46.4% and 56%, reflecting an adequate balance for thermal comfort in Zone 3. The low ventilation speeds of less than 0.05 m/s recorded in all the rooms indicate a deficiency in ventilation, corroborating the

dissatisfaction expressed by users in the questionnaires.

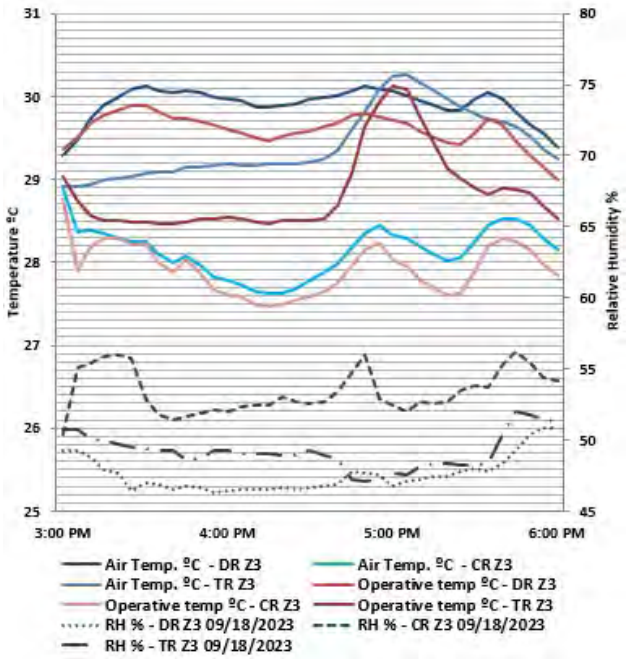

Figure 3: Temperature and relative humidity data collected in São Paulo/SP Zone 3.

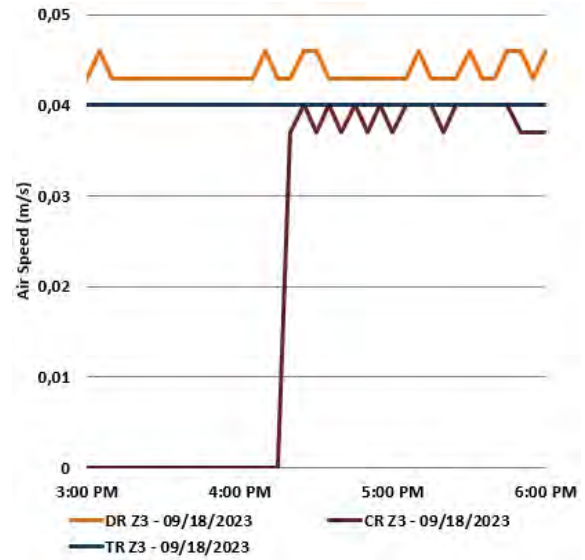

Figure 4: Air speed data collected in São Paulo/SP Zone 3.

In Zone 1, measurements were taken on three different days (09/11/2023, 10/11/2023, and 13/11/2023), reflecting the specific weather conditions. Outside temperatures varied between 22°C and 18°C. The operating temperatures in the DR, CR, and TR remained within the limits set by ASHRAE (Fig.5), demonstrating thermally comfortable conditions.

The variation in Relative Humidity (RH) in Zone 1 was wider, with values in the DR ranging from 57.5% to 72.7%, in the CR from 62.3% to 66%, and in the TR from 38.8% to 46.4% (Fig.5). This variation did not compromise thermal comfort, as indicated by the answers to the questionnaires.

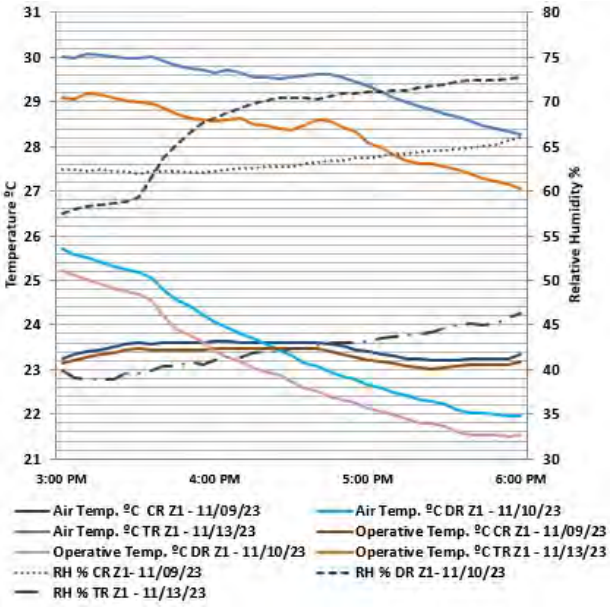

Figure 5: Temperature and relative humidity data collected in Campos do Jordão/SP Zone 1.

Similarly, to Zone 3, inadequate ventilation (below 0.05 m/s) was observed in the rooms studied (Fig.6), coinciding with users' dissatisfaction with ventilation, showing a gap in the efficiency of the ventilation system in the buildings analyzed.

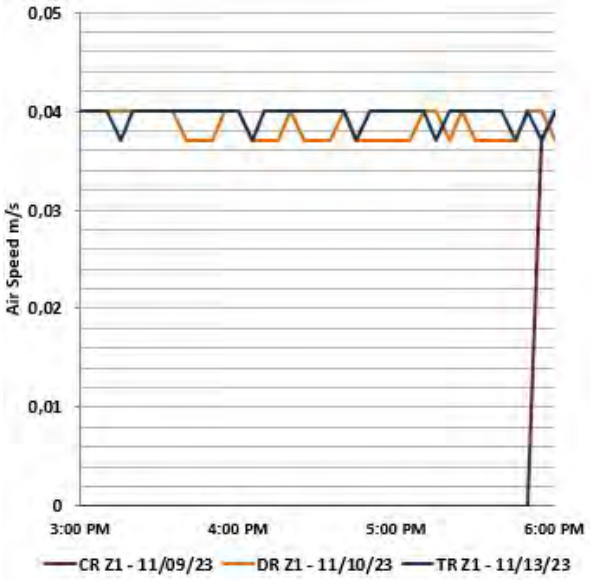

Figure 6: Air speed data collected in Campos do Jordão/SP Zone 1.

The data collected in the two bioclimatic zones did not reveal efficiency and resilience in the buildings analyzed about the factors studied. Interventions and adaptations are needed to satisfactorily meet the needs of users. In Campos do Jordão/SP, Zone 1, characterized by a high-altitude

tropical climate, high relative humidity throughout the year was observed in the measurements, hindering the body's thermal regulation and potentially generating discomfort in the internal environments. In contrast, São Paulo/SP, Zone 3, with a subtropical climate and also high relative humidity, can result in considerable discomfort, especially on hot days, reducing the effectiveness of the body's thermal regulation.

4.4 Lighting Comfort

Lighting comfort plays a crucial role in the educational environment, directly influencing academic performance and the well-being of occupants. The study on lighting comfort in the two Brazilian bioclimatic zones (Zone 1 and Zone 3) has revealed valuable information regarding the lighting conditions in the selected environments (Fig. 3). Measurements were conducted during the use of the rooms in the afternoon, between 03:00 PM and 06:00 PM. This choice of timing allowed for considering the influence of both natural and artificial light, given the significant contribution of both during this time frame.

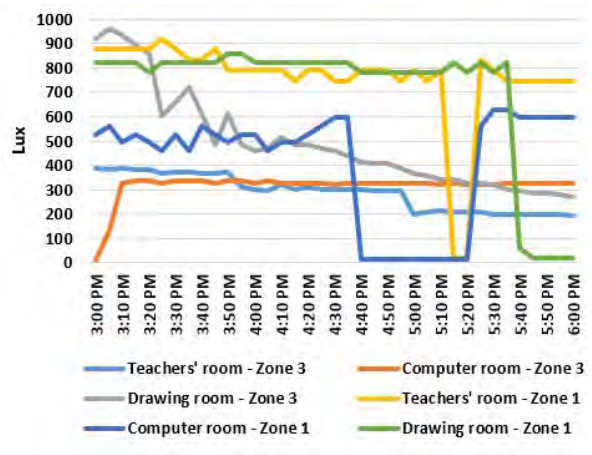

Figure 3: Values measured in lux in each of the environments measured according to the time of day.

Analyzing the drawing room in Zone 3, the limited contribution of natural light stands out, necessitating the indispensable use of artificial lighting. Throughout the measurement period, recommended lux standards were maintained, ranging from 500 lux to 700 lux, underscoring the need for enhanced illumination due to the specific activities conducted in this space.

In the teachers' room in Zone 3, natural lighting is restricted, and artificial light manages to remain within the range of 300 lux to 400 lux, close to the minimum recommended by the Brazilian standard (ABNT NBR 5413:1992). This condition persists almost throughout the measurement period, emphasizing the importance of adjustments or improvements in the lighting of this environment.

In the Zone 3 computer room, stability in lighting was observed, staying above 300 lux throughout the measurement period. Additionally, the presence of sunlight contributes to these values, highlighting the effectiveness of the combination of natural and artificial light in this specific space.

In Zone 1, the teachers' room demonstrates a significant contribution from sunlight, maintaining considerable values between 700 lux and 900 lux during measurements. This result underscores the importance of architectural design and the arrangement of openings to optimize the entry of natural light into this environment.

In the Zone 1 computer room, characterized by smaller openings, the entry of natural light is limited. However, artificial light plays a fundamental role, allowing the illumination to stay between 500 lux and 600 lux for the majority of the measurement period.

Finally, in the drawing room of Zone 1, large openings provide a substantial entry of natural light, complemented by artificial light to meet the specific lighting demands of the space. Measurements indicated that the illumination remained between 700 lux and 900 lux, highlighting the efficiency of the architectural design in promoting ideal conditions for drawing activities.

5. CONCLUSIONS

The results obtained from the on-site measurements indicate that the rooms analyzed had deficiencies in sound insulation, allowing external noise to enter that exceeds the limits established by NBR 10.152 for internal environments. This finding suggests the urgent need for interventions to improve the acoustic insulation of the buildings studied. The use of acoustic insulating materials and the evaluation of physical barriers to reduce external noise are essential recommendations for promoting quieter environments that are conducive to user comfort.

The rooms maintained moderate thermal amplitudes owing to their good thermal inertia; however, the absence or inadequacy of ventilation led to discomfort for the occupants. Despite Zone 1 staying within acceptable temperature parameters for comfort, Zone 3 fell short of meeting these criteria. Enhancing thermal comfort calls for the implementation of effective ventilation strategies, including the adoption of strategic openings, cross ventilation, and the utilization of technologies that support air circulation. Additionally, exploring the application of thermal coatings can contribute to more efficient management of thermal conditions in the rooms.

High relative humidity was observed in Zone 1, indicating the need for ventilation mechanisms to improve thermal comfort. Body thermal regulation

becomes challenging in conditions of high humidity, justifying the implementation of adequate ventilation systems to reduce feelings of discomfort. Strategies such as natural ventilation, dehumidifiers, and mechanical ventilation systems can be considered to optimize humidity management and improve occupants' thermal sensation.

The limited natural light in all the rooms underscores the necessity for interventions to comply with regulatory standards and guarantee ample lighting conditions for users. Evaluating and refining the lighting design is recommended, incorporating more efficient light sources evenly distributed throughout the spaces. The implementation of systems for utilizing natural light and controlling lighting, such as presence sensors, can contribute to resilience and optimize energy consumption and creating well-lit environments.

To promote the resilience of buildings, it is essential to implement strategic interventions that improve their overall efficiency. In this context, investing in acoustic insulation materials is an essential measure to mitigate the entry of external noise, contributing significantly to the quality of the internal environment. In addition, the implementation of ventilation strategies, such as strategic openings and air circulation systems, emerges as a crucial solution for optimizing thermal comfort, considering the thermal inertia already present in the spaces studied. Such enhancements not only fortify building resilience but also underscore the interplay of acoustic and thermal considerations in fostering an environment conducive to occupant well-being.

Evaluating and adjusting the lighting design, incorporating more efficient light sources, as well as introducing lighting control mechanisms, not only meet regulatory requirements but also promote better-lit and energy-efficient environments. In addition, the consideration of the application of thermal coatings aims to improve the management of thermal conditions in environments, while the exploration of specific solutions for humidity control, such as dehumidifiers or mechanical ventilation systems, represents a comprehensive approach to holistically improving environmental comfort. These integrated interventions, when applied in a coordinated manner, have the potential to make buildings more resilient, providing sustainable and comfortable environments for occupants.

ACKNOWLEDGEMENTS

Supported by Coordination of Superior Level Staff Improvement - Brazil (CAPES 88887.704300/2022-00) and The São Paulo Research Foundation (FAPESP 2021/02915-2 e 2022/02552-0).

REFERENCES

1. UNDESA – United Nations Department of Economic and Social Affairs/Population Division (2019). World Urbanization Prospects 2019. New York, United Nations. Available:https://population.un.org/wpp/Publications/Files/WPP2019_Volume-II-Demographic-Profiles.pdf [25 august 2023].

2. Rosenzweig, C. et al (2011). Urban Climate Change in Context. Climate Change and Cities: First Assessment Report of the Urban Climate Change Research Network, *Cambridge University Press*, Cambridge, UK, 3-11.

3. Ferreira, R. F. et al. (2022). Acústica e Eficiência Energética: proposta de atenuação de ruído escolar por meio de barreira acústica composta por módulos fotovoltaicos. *XII Congresso Iberoamericano de Acústica*. Florianópolis, Brazil.

4. IPCC – INTERGOVERNAMENTAL PANEL ON CLIMATE CHANGE (2023). Climate Change 2023: Synthesis Report. IPCC Working Group.

5. De Wilde, P.; Coley, D. (2012). The implications of a changing climate for buildings. *Building and Environment*, v. 55, p. 1-7.

6. Duarte, M.; Almeida, N.; Falcão Silva, M. J.; Rezvani, S. (2021b). Resilience rating system for Building Against natural hazards, *15 WCEAM*, Brazil, Paper ID 94.

7. Garcia, J.; Vale, B. (2017). Unravelling Sustainability and Resilience in the Built Environment. Routledge, London, UK.

8. Rodin, J. (2015). The Resilience Dividend. Great Britain: profile books.

9. Pickett, S. T. A.; McGrath, B.; Cadenasso, M. L.; Felson, A. J. (2014). Ecological resilience and resilient cities, Building Research & Information, 42:2, 143-157. DOI:10.1080/09613218.2014.850600

10. AMERICAN SOCIETY OF HEATING, REFRIFERATING AND AIR-CONDITIONING ENGINEERS (2017). ANSI/ASHRAE Standard 55: Thermal Environmental Conditions for Human Occupancy. 1-52. Atlanta, USA.

11. ASSOCIAÇÃO BRASILEIRA DE NORMAS TÉCNICAS (2005). ABNT NBR 15.125: Iluminação. Rio de Janeiro, RJ, Brazil.

12. ASSOCIAÇÃO BRASILEIRA DE NORMAS TÉCNICAS (1992). ABNT NBR 5413: Iluminância de interiores. Rio de Janeiro, RJ, Brazil

13. ASSOCIAÇÃO BRASILEIRA DE NORMAS TÉCNICAS (2021). ABNT NBR 15.575: Edificações habitacionais - Desempenho. Rio de Janeiro, RJ, Brazil.

14. ASSOCIAÇÃO BRASILEIRA DE NORMAS TÉCNICAS (2017). ABNT NBR 10.152: Acústica – Níveis de pressão sonora em ambientes internos a edificações. Rio de Janeiro, RJ, Brazil.

PLEA 2024 WROCŁAW
(Re)thinking Resilience

CLIMATE SENSITIVE SHADES:
Meteoactive Building Shading in the Architectural Environment

LUISA KATHARINA SANDER[,1] ALEXANDER STAHR[,1]

[1]FLEX | Professional Research Team, Leipzig University of Applied Sciences, Leipzig, Germany

ABSTRACT: A novel approach to understanding the anatomy of wood in more detail in order to quantify the properties relevant to architectural developments forms the core idea of the project. This specifically relies on the active use of the mostly negatively perceived hygroscopic behavior of wood. The concept is based on the moisture-related phenomenon of opening and closing pine cones, which acts as a bionic inspiration for exploring climate-sensitive structures. Based on defined parameters, targeted changes to the wood properties can be brought about in order to combine and produce homogenized and professionally "meteoactive" veneers as so-called bi-layers. Due to the temperature and humidity-dependent swelling and shrinking of the bi-layer veneers, the bending can be controlled, for example in the form of shading elements, without the use of electricity or mechanical systems.
KEYWORDS: bi-layer, veneer, moisture, temperature, resource-efficiency

1. RESEARCH QUESTION

Instead of making mechanical systems more and more efficient, we should work on more economical solutions that approach a zero-energy state. So how can a decentralized system be generated that creates a naturally controlled filter layer, similar to human skin or the breathing organism? This motivating question is the central theme of the research and highlights the author's fascination with circular constructions. Furthermore, the continuous testing of the knowledge already gained is essential for a sustainable architecture and realistic application processes. This includes the research question to be investigated: How can the research parameters for conditioning the wooden elements be selected accordingly in order to make the system more weather-resistant and be able to be used in different climate zones? The hypothesis is the selection of suitable types of wood depending on the climate zone, the thickness of the bilayer veneers and the investigation of a semi-permeable wood coating that simultaneously allows moisture exchange with the environment.

2. STATE OF TECHNOLOGY

The hygroscopic material behavior of wood has been a current topic being tested by research teams at several universities (e.g. University of Stuttgart, Swiss Federal Institute of Technology Zurich) for many years in order to develop methods for the feasibility of movable constructions in architecture. The moisture-dependent protective reaction of pine cones serves as inspiration from nature. The cone scales only open when it is dry and allow the seeds to be spread by the wind; when it is wet, they remain closed to protect their offspring. Similar to the principle of a heated bi-metal strip, the scales consist of two layers of material that react differently to the humidity. In combination, the dimensional change in the lower layer causes a bending and thus closure of the entire scale. When the bottom layer dries, the scale is pulled back down to open. According to findings by *Poppinga* and *Speck* from the University of Freiburg, fossil cones are also capable of bending movements even after millions of years [1]. This interesting behavior of the pine cones acts as an example of bionic and autonomously reacting flap systems.

The first wooden prototypes using the natural influencing factors: temperature and humidity are, for example, the "Urbach Tower" and the HygroSkin" pavillon of the research team at the University of Stuttgart under the leadership of *Menges* and *Knippers* [2]. The desired curvatures of the elements can be achieved through certain drying and swelling processes. The research is based on studies by *Reichert* regarding the potential use of the hygroscopic properties of the complex wood structure and their dimensional changes [3]. This embody a no-tech concept, which can be naturally controlled in the form of wooden control elements. Another invention that uses the hygroscopic material behavior of wood are the "solar trackers" by the scientist *Rüggeberg* from the EMPA research center and the ETH Zurich University. It is a timber-construction, which aligns solar modules towards the sun based on the bi-layer principle [4].

This level of knowledge serves as a valuable thematic template and provides an incentive to investigate further options for optimizing and controlling

the responsiveness of wood, especially for outdoor applications, as well as its bending behavior.

3. APPROACH

The main idea of the research project is the active use of the hygroscopic behavior of wood by combining different types of wood in the form of bi-layer veneers to apply them for instance as sun shading facilities. Therefore, it is essential to analyse the microstructure of the natural material in much more detail.

Regarding to the references [1-4, para. 2.], an aspect to be further developed is the choice of wood species appropriate to the environment. It is important to clarify the criteria according to which the woods are examined individually. For the durability of the products, it is advantageous to choose types of wood that are more suitable for outdoor use (e.g. oak, ash, robinia, eucalyptus). Against the background of the future fundamental restructuring towards resilient mixed deciduous forests, the authors suggests the increased use of deciduous wood species. A further way to specify the bi-layer system is the appropriate choice of components. Instead of being limited to one type of wood, the combination of two different types in form of an active and passive layer (detailed explanation in para. 5. PROJECT FINDINGS) results in higher deformation potential and control over the bending direction.

The research-method relies on a clear concept of consecutive, systematic approach. The first part consists of experiments regarding the targeted analysis of different parameters to describe the material behavior of wood under different temperature and humidity scenarios. The combinatorics and precise analytics of the properties of different types of wood in a flat composite make it possible to control the bending. The strategies consist of examining the wood structure by generating a µCT scan as micro-computed tomography and the deformation of wood veneer samples at different humidity levels at different time intervals using a climate-chamber. At the same time, the bending states of respective humidity stages from 40 to 90 % RH (relative humidity) were recorded using a 3D scan in order to use them to generate a computer-aided parametric simulation model. With this approach, precisely defined values can determine the curvature of the elements and, depending on the selected parameter, generate the desired result.

In the next step, the design potential of the developed solution was examined by projecting it onto a sample façade. The parameters such as the dimension, shape and arrangement can be regulated as desired. This is intended to illustrate the possibilities and limitations of the approach in practical application.

4. PARAMETERS

In order to initially achieve significantly lower scattering results, the deformation behavior can be influenced by the:

- type of wood
- veneer cutting technique
- woodcut areas
- arrangement of the fiber direction
- thickness of the test specimens
- shape and dimension of the test specimens

4.1 Woodcut areas

How much a wooden board shrinks or swells depends on which part of the tree trunk it was cut from and how the cells are arranged. The structure shows extremely developed anisotropic material behavior. The directional dependence is reflected in the following areas: longitudinal (in the direction of the fibers), radial (across the annual rings) and tangential (alongside the annual rings). The swelling and shrinkage behavior is therefore most pronounced in wood that has been cut from the tangential area. This occurs much weaker in woods from the radial zone and least in the longitudinal direction of the fibers [5].

The swelling and shrinkage values differ depending on the type of wood and indicate its staying power. Depending on the area of application, a most suitable wood with appropriate values can be selected. The target (in front of the ongoing and becoming more and more intensive resource efficiency debate) should be to use all the material (leaving the former way of selecting the material) by precisely (automated) analyzing the individual micro-structure and to modify the properties by processing the veneers using laser machining.

4.2 Cutting technique

Depending on the type of preparation, different results and veneer appearances can occur. When flat slicing the halved trunk is cut from the outside. In the outermost area of trunk, veneer leaves lively flake markings (horizontal annual rings) because the annual rings are cut at a shallow angle. If the cut moves closer to the trunk, the veneers show a stripy structure due to the increasingly rectangular cut (vertical annual rings). With the circular peeling technique, the tree trunk is clamped along its central axis and then peeled in spiral shape from the outside. The result of veneer pattern then shows an irregular and flaky pattern similar to the shapes of nests or eyes [6].

In relation to the hygroscopic behavior of wood, the selection of the appropriate cutting technique and thus the cutting area is also of high importance. If you compare these techniques with the swelling and shrinkage zones, the flat sliced veneer reacts more strongly to the ambient humidity with horizontal annual rings than that with vertical rings.

4.3 Type of wood

Due to different raw and drying densities, the types of wood can be divided into two categories: hardwoods and softwoods, which show different reactions the ambient humidity. If the drying density is above 550 kg/m^3, it is considered as hardwood; anything below that is classified as softwood [7].

The moisture behavior was examined with initial experimental tests on veneer samples using a water spray bottle and a hand-held moisture meter. The samples measuring 10 x 12 cm in the cross-grain direction were clamped into a specifically designed holder and sprayed with water from one side. The moisture dose was then gradually increased so that development from the initial stage to around 30 % moisture could be documented photographically.

It became clear that the softwoods (pine and limba) formed a stronger sample curvature than the denser hardwoods (oak and walnut). Based on the results, one can generally assess that the hardwood samples are more resistant to moisture than the softwoods, but still show a pronounced bending reaction (Fig. 1, 2).

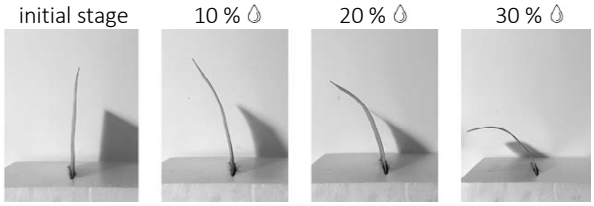

Figure 1: Hardwood moisture test (oak veneer)

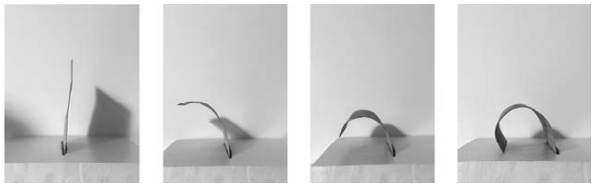

Figure 2: Softwood moisture test (pine veneer)

In order to investigate the reaction in more detail in further experiments, specifically selected veneer was used from the FSG veneer and sawn wood trading company in Borsdorf. Its facility has a large hall where various types of veneer are dried and stored. For the next investigative step, the sliced hardwoods with a tangential cut: larch, oak, ash and beech containing high strength and elasticity properties were chosen, as well as the lighter and easy-to-machine softwoods: spruce (flat sliced, tangential cut), pine (flat sliced, radial cut) and birch (peeled). With this selection, the different types of veneer processing could be checked at the same time and tested in combination in the next phase.

4.4 Fiber direction

When moisture is added, the direction of the grain determines the type of bending of the wood veneer. The wood fibers, as elongated wood cells, not only serve to strengthen the wood, but also act as “muscles” that cause the structure to move actively. The swelling is initiated by the binding of water molecules only along the fiber structure of the cellulose fibers between the stablilizing lignin. If you try this process by adding moisture to one side of the veneer sheet, the fibers swell and stretch the section transversely to the direction of the fibers more than in the longitudinal direction. As a result, the veneer curves towards the wet side because that is where the water binding takes place first.

5. PROJECT FINDINGS

The parameters described above were combined in the next phase in form of a bi-layer – strategy (Fig. 3). This means that the bending direction and the reaction of the respective layer to ambient humidity can be adjusted and then controlled independently without mechanical or electrical influence. Previously, the bending direction of the veneer sheet could only be determined by spraying water from one side. If moisture is applied from all sides when used outdoors, it is not possible to predict or control exactly in which direction the element will bend. This certainty about the curvature behavior is extremely important when using the element as a shading panel in order to allow as much light to pass through by opening the façade when the humidity is high and to shade the building by bending the elements back when the humidity is low and the sunlight is strong.

This principle can be achieved by connecting an active and passive layer. The active layer forms a type of wood that has a high swelling and shrinkage value and can absorb a lot of moisture. The passive layer is a more moisture-resistant type of wood that reacts as little as possible to the ambient humidity and remains rigid. When the air humidity is high during the swelling process, the active layer “pushes” the element in the direction of the passive layer and, during the shrinking process, back in the opposite direction. Within the bi-layer composite, the alignment of the fibers and the woodcut area (tangential/radial) from which the veneer was obtained must also be considered.

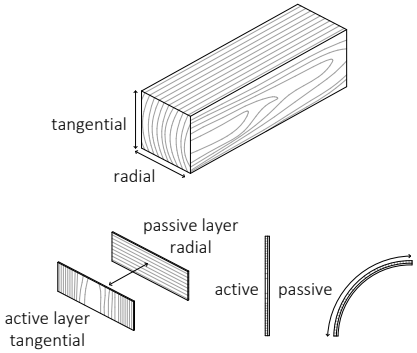

Figure 3: bi-layer strategy

As the knowledge gained was further developed, the application of the system was limited to outdoor areas as a shading system. Therefore, in the next step, only types of wood that were suitable for outdoor use were selected. These include: oak, larch and eucalyptus. The native wood species oak has the highest differential tangential swelling and shrinkage value of this selection at 0,36 %. In addition, it also has high strength and elasticity values (13,000 N/mm^2) [8] and is weather-resistant. The tangentially sliced oak (tangential annual rings) acts as an active element in the bi-layer composite.

The eucalyptus veneer was used for the passive layer. This type of wood is often used in garden furniture construction, as decking or window frames, as it is also very robust, weatherproof and resistant to fungus. Eucalyptus is a tree species that comes from Australian and Tasmanian virgin forests, so it would be irresponsible to use wood from overexploited plantations. As an alternative, FSC-certified eucalyptus wood can be grown sustainably in the European forest area of Galicia, Spain. The tree species Eucalyptus globulus, introduced in the 19th century, was able to adapt well to the Spanish climate and spread massively. The property of rapid growth of 50 cm per year is also particularly sustainable, enabling a growth height of up to 60 m. This type of wood also has a higher raw density of up to 910 kg/m^3 than oak (770 kg/m^3) and is therefore very sustainable for the resistant layer. So that it reacts even less to moisture, the veneer was chosen in a radial cut (vertical annual rings) with a differential swelling and shrinkage value of 0,25%. Its external appearance, with its interesting light reddish-brown colour and gently shimmering grain, also forms a harmonic combination with the light to medium brown oak veneer.

5.1 Microscopic examination

In order to explore the structural components of the two hardwoods of the bi-layer: oak and eucalyptus in relation to their moisture reactions, a microscopic examination was also carried out. For this purpose, support was provided by the Polyclinic for Dental Conservation and Periodontology at Leipzig University Medical Center and its research team made a microcomputed tomography (µCT) scan possible. The one-month study focused on comparing dry and moistened veneer samples. The result of the scanned veneer shows very clear and detailed images in cross section and longitudinal section as well as a 3D model (Fig. 4).

With the help of these representations, the complex "organism" of the two woods can be illustrated and understood very well. Since no visual differences could be found between the dry and wet samples, an analysis of the pore sizes was carried out for both types of veneer. So far, these have shown very different behavior patterns in the volume change of the pores. Only in one wet eucalyptus sample did the pores shrink, as expected. To achieve statistical certainty, more samples would have to be examined in the future. The first insight and investigation approach into the wood structure opens up many interesting facts that still need to be explored.

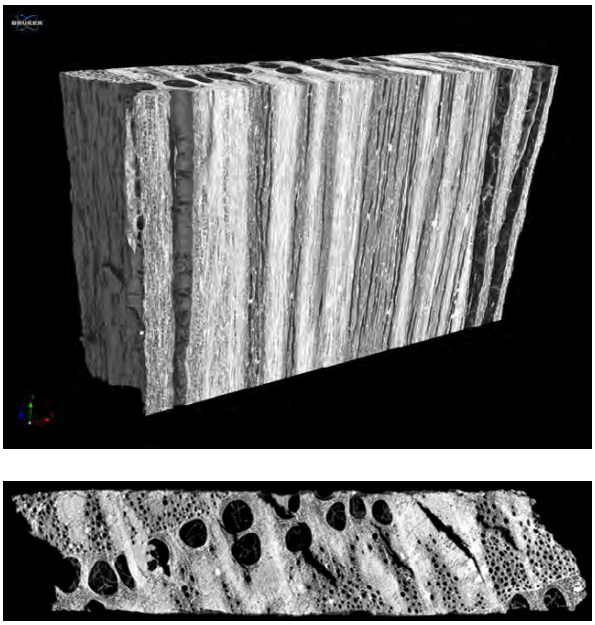

Figure 4: µCT scan - Oak, Polyclinic for Dental Conservation and Periodontology at Leipzig University Medical Center

5.2 Climate chamber experiments

Using the initially applied investigation strategy of the bi-layer principle using water spray bottles, it was only possible to estimate the moisture added to the wood samples and to read the content using the moisture meter. When using the wooden elements outdoors, the humidity in the surroundings and how this affects the wood are of great importance. Therefore, the experiments were moved to a climate chamber with precise measuring methods.

For the investigations, a constant temperature of 20°C was chosen as the average summer temperature in Germany. At the same time, this creates good climatic conditions for a faster development of air humidity, because the warmer the air temperature, the more water it can absorb. In relation to the temperature, the prevailing external humidity, for example in Berlin, was then gradually adjusted from 40 to 90 % RH (relative humidity). In order to determine the point in time at which the moisture content changes in the climate chamber, the equilibrium moisture content of the two veneers oak and eucalyptus, must be determined in advance. If the veneer is adjusted to a new climate too early, residual deformation from the previous moisture state occurs and leads to inaccuracies. As long as the veneer absorbs moisture, its

mass increases; when there are no changes, equilibrium is reached and the time interval for adjustment is known.

After selecting the appropriate wood glue (PUR glue) for a shear-resistant connection of the two wood layers and setting up a sample holder, the moistening in the climate chamber could be started. During the humidification process from 40 to 90 % RH, different bending movements such as curvature and torsion could be examined. This made it possible to check the initial thesis for plausibility (Fig. 5).

The key question to be tackled was how to measure the discontinuous bending of the test specimens contact-free, precise and especially quick. Therefore, a 3D-Scanning-Tool (Artec Leo) has been used to create a parametric simulation model. As a preparatory measure for the scan of the climate chamber tests, the creation of target points on a background poster was essential. These are target points that the 3D scanner captures during the scanning process to place the object in the same position in the coordinate system with each scan (Fig. 6).

Figure 5: climate chamber tests of bi-layer veneers

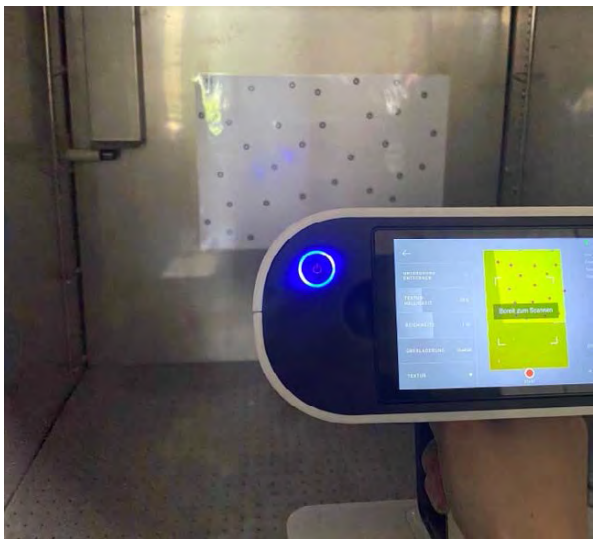

Figure 6: Target points detection of the 3D scanner

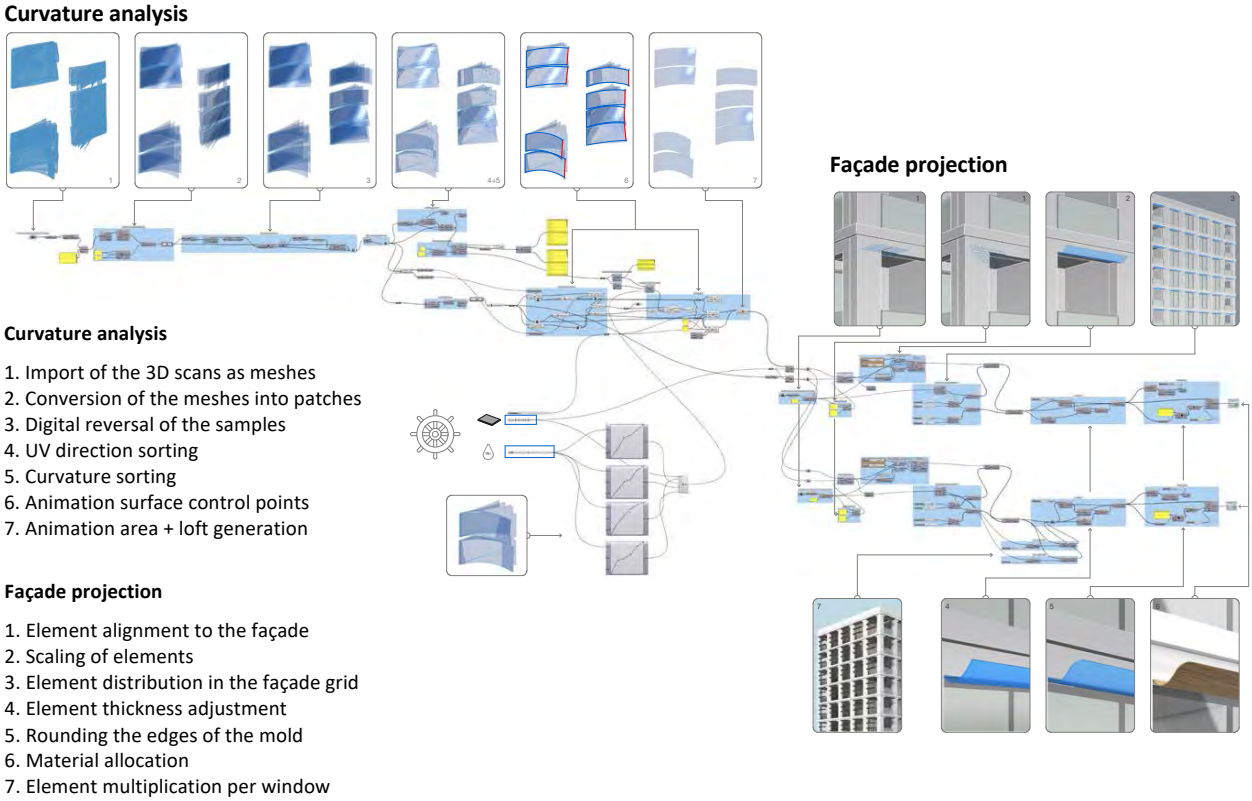

Figure 7: Simulation script of façade shading elements

5.3 Parametric model

In the next step, the processed and optimized 3D scan models were imported into computer-aided modelling software and linked to a self-developed simulation script (Fig. 7). This enabled the generation of an algorithmic bending simulation as a loft surface that can interpolate between the individual phases of the veneer deformations. The created loft surface serves as the basis for projecting the shading elements onto a sample building façade. This can be aligned with the window, scaled accordingly and distributed in the façade grid. Since the interior rooms on the west and east sides are exposed to the highest levels of sunlight in summer, the digital script was supplemented with a parameter that enables the arrangement of several shading elements per window. Basically, the shading elements are intended to protect the window from heat input (shrinkage) when the relative humidity is low and the sunlight is high (Fig. 8) and to open the window front again when the relative humidity is high and the sunlight is low (swelling), (Fig.9).

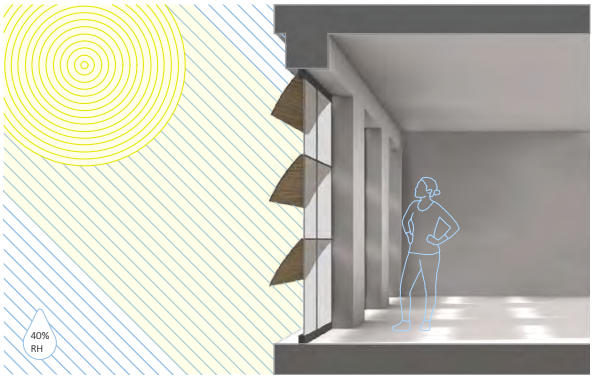

Figure 8: Curvature state of shading at 40 % RH

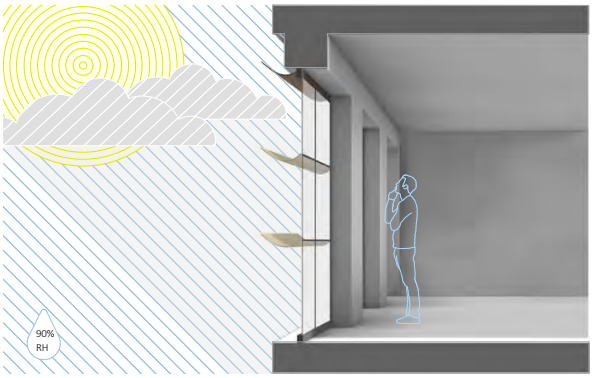

Figure 9: Curvature state of shading at 90 % RH

6. INNOVATION POTENTIAL

The use of renewable resources, the continuous exchange of the material with the surrounding climate and the low material consumption defines the core elements for a sustainable shading solution based on the ingenious use of natural phenomena. Therefore, this research focuses on the topic: Architecture for human resilience and well-being (including biophilic design, nature-based solutions, climate adaption strategies). In contrast to most existing technologies, individual slats can be easily replaced, which ensures minimal maintenance costs. Their meteoactive and noiseless functionality would also contribute to a better indoor climate. The innovative approach to be developed: breathable wood coating + meteosensitive bending of bi-layer slats, also contains a high disruptive potential.

7. FUTURE PROJECT STEPS

Since this is a research in progress, the following options where considered as a outlook for the topic of climate-sensitive shading:

- Testing of bi-layer thicknesses for a more practical and weather-resistant solution
- Multi-seasonal analysis of wood behavior after multiple swelling and shrinking processes
- Functional investigation of the shading system in relation to other climate zones
- Development of an inorganic-organic hybrid layer based on sol-gel systems for wood
- Developing a strategy to affect the bending behavior or veneer based on annual ring analysis and individualized laser processing
- Creation of a digital weather analysis by importing desired weather data into the parametric simulation model of the shading elements

REFERENCES

1. Poppinga, S. *Hygroscopic motions of fossil conifer cones.* [Online], Avaiable: https://www.nature.com/articles/srep40302 [15 June 2023].
2. Knippers, J. and Menges A., Institute for Computational Design and Construction. *HygroSkin - Meteosensitive Pavillon.* [Online], Aviable: https://www.icd.uni-stuttgart.de/projects/hygroskin-meteorosensitive-pavilion/ [15 June 2023].
3. Correa, D., Krieg, O.D., Menges, A., Reichert, S., Rinderspacher, K., University of Stuttgart. *HygroSkin: A Climate-Responsive Prototype Project based on the Elastic and Hygroscopic Properties of Wood.* [Online], Aviable: https://papers.cumincad.org/data/works/att/acadia13_033.content.pdf [11 March 2024]
4. ETH Zürch. *Wooden solar trackers.* [Online], Aviable: https://honr.ethz.ch/en/the-group/facade/wooden-bilayer.html [09 May 2023].
5. Ferrer, C.; Hildebrand, T.; Martinez-Canavate, C., (2023). *Touch Wood – Material, Architektur, Zukunft, Anatomie des Holzes:* p.82-83.
6. Initiative Furnier + natur e.V. *Furnier-Herstellung*. [Online], Aviable: https://www.furnier.de/furnier/furnier-herstellung.html [09 July 2023].
7. Wolf, U., (2022). *Holzhärte: Was ist das und wie wird sie berechnet?* [Online],
Aviable: https://www.ausbaupraxis.de/auch-die-harten-kommen-aus-dem-garten-11102022 [30 December 2023]
8. Ehmke, G. and Grosser, D. *Das Holz der Eiche.* [Online], Aviable: /https://www.lwf.bayern.de/mam/cms04/forsttechnik-holz/dateien/w75_das_holz_der_eiche-eigenschaften_und_verwendung_bf_gesch.pdf [30 July 2023].

Monitoring the prevalence and intensity of overheating in English care homes during summer 2022

RAJAT GUPTA[1], ALASTAIR HOWARD[1], MIKE DAVIES[2], ANNA MAVROGIANNI[2], ELENI OIKONOMOU[2]

[1]Low Carbon Building Research Group, School of Architecture, Oxford Brookes University, Oxford, UK
[2]Institute for Environmental Design and Engineering, University College London, London, UK

ABSTRACT: Summer 2022 was the joint hottest on record in England, with outdoor temperatures >40 °C and five separate Level 3 Heat Health Alerts. During the heat periods excess deaths were 6.2% above the five-year average, with older people being most vulnerable. This paper presents research gathered from 41 care homes across England during summer 2022. Longitudinal monitoring of indoor and outdoor air temperature and relative humidity conducted in multiple locations within each care home allowed investigation of how building characteristics affected propensity for overheating. Spikes in temperature exceeded 40 °C within three care homes and 35 °C within 14 care homes. Mean temperatures in London care homes were nearly 2 °C warmer than those elsewhere. Upper-floor rooms were significantly warmer than ground floor rooms, and urban/suburban care homes significantly warmer than rural care homes. Other characteristics (building age, size, room orientation) showed much less significant differences in temperature distributions between groups. The use of CIBSE overheating metrics (Guide A, TM52 and TM59) revealed endemic overheating across the care homes. This study has identified some differences between rooms/care home types that could help inform the future design and operation of care homes to protect against the negative consequences of overheating.
KEYWORDS: Overheating, residential care, summer, temperature, humidity

1. INTRODUCTION

Summer 2022 was the joint hottest on record in the England, with outdoor temperatures exceeding 40 °C for the first time since records began [1]. The UK Health Security Agency (UKHSA) issued Level 3 Heat Health Alerts for five distinct heat periods from June to August 2022. During these periods, excess deaths were 6.2% above the five-year average [2], with older populations most affected. These statistics are reminiscent of findings from studies following the Europe-wide heatwave of August 2003, when excess mortality during the ten-day heatwave in England was 33% in those aged 75 and over, and only 14% in the under-75's [3, 4], with a quarter of heat-wave-related deaths occurring in care homes and mortality in London increasing by 3% for every 1 °C increase in daily average temperature over 21.5 °C [5].

Public Health England (now UKHSA) identified 24.5°C as the threshold above which excess heat-related mortality may become apparent [6], principally through cardiovascular and respiratory disease. Rising temperatures and heatwaves increase risks to physical and emotional health, but also have significant financial implications in terms of the cost of adapting buildings, operating active cooling systems, and potential reduction in productivity [7].

The Climate Change Committee's 2022 report [8] identified key characteristics that affected whether individual buildings overheat during hot weather: location (London and the south of England experiencing more frequent and intense extreme high temperatures than the rest of the UK); urbanisation (the urban heat island effect); Building type (flats and well insulated buildings having an increased risk of overheating); occupant behaviour (e.g. window-opening and curtain-closing patterns).

The UK Government's Climate Change Risk Assessment report [9] and the 2018 National Adaptation Programme [10] have identified summertime overheating in care settings as a key risk and research priority for the health and social care system. The design and operation of care settings in the UK has historically focussed on keeping residents warm since they are vulnerable to cold [11]. At the same time, there has been a relative lack of attention to the risk of summertime overheating in unprepared care homes [12].

Summertime overheating is widespread, even in newer buildings [13]. The characteristics of new-build energy-efficient housing – airtight and well insulated – can make them particularly prone to this problem. In addition, features such as heated corridors (common in elderly care settings but not normally found in general housing), and the use of window-opening restrictors, may also contribute to overheating. Increasing thermal mass and improving ventilation can help when designing new care homes, with additional ventilation and solar shading strategies also beneficial [14].

Several studies have investigated care homes using computer simulations with predicted climate scenarios. Others have conducted longitudinal monitoring in a small sample of care homes. This paper presents analysis of longitudinal environmental monitoring gathered from 41 care homes across England, allowing consideration of a wide range of

building typologies and characteristics and how these may affect care homes' propensity for overheating.

2. METHODOLOGY

Hobo MX1101 and MX1102A (accuracy of ±0.21 °C, ±2% RH) devices monitored air temperature and RH in indoor rooms categorised as bedrooms (115 resident rooms, occupancy varying from nights only to 24/7; day hours 07:00-22:00), lounges (46 communal rooms used by multiple residents and staff during the day; occupied hours 08:00-20:00), and offices (34 staff-only rooms; occupied hours 09:00-17:00). Weather-proofed Hobo MX2301 (accuracy of ±0.2 °C, ±2.5% RH) devices monitored outdoor temperature and relative humidity (RH) at each care home. The devices were shielded from radiation. Note that whilst operative temperature is the ideal measure to calculate overheating, differences in operative and dry bulb (air) temperature tend to only be significant in indoor spaces with high levels of exposed thermal mass or high indoor air velocity [15], neither of which applied to the case study care homes. Furthermore, the Hobo devices used cost less and were smaller and more discreet than operative temperature monitors, and therefore more appropriate for deploying over long periods.

Care homes serve as both domestic spaces for the residents and non-domestic spaces for the staff. CIBSE's three overheating metrics were investigated with this in mind. CIBSE Guide A defines overheating when 1% or more of occupied hours exceed 28 °C in living areas or 26 °C in bedrooms. Fixed maximum air temperatures do not allow for occupants' ability to adapt to their environment. Therefore, CIBSE TM52 was considered, deriving threshold comfort temperature $T_{threshold}$ from the running daily mean of outdoor temperatures. The metric has three criteria: (1) no more than 3% of occupied hours (May-Sep) more than 1 °C above $T_{threshold}$; (2) daily weighted exceedance W_e <6 (where $W_e = \Sigma(DT \times H_{DT})$, DT=temperature difference above $T_{threshold}$ and H_{DT}=hours spent above DT); (3) maximum indoor temperature <4 °C above $T_{threshold}$. Overheating is deemed to have occurred if at least two of the three criteria are failed. CIBSE TM59 combined dynamic and static criteria: (A) no more than 3% of occupied hours (May-Sep) more than 1 °C above $T_{threshold}$; (B) No more than 1% of overnight hours in bedrooms over 26 °C annually; (C) no more than 3% of occupied hours > 26 °C annually. Overheating is deemed to have occurred if any of these criteria are failed. Criteria B and C consider proportions of annual hours. The data available therefore provide indicative results for TM59 rather than definitive results.

Typology analysis considered the characteristics of the care homes. Building age groups were informed by Standard Assessment Procedure (SAP) building age bands: Pre-1930, 1930-1976, 1977-2002, and Post-2002. 'Locality' consisted of three groups: urban (surrounded by shops, hospitals, offices etc), suburban (residential neighbourhoods), and rural (countryside or small villages). Regional locations were defined as North (from Merseyside to Tyne and Wear); Midlands (Northamptonshire, Warwickshire, Oxfordshire, and Gloucestershire), South (Hampshire, West Sussex, and the Isle of Wight); and Greater London. 'Proximity to coast' defined coastal care homes as those located within 10 km of the coast (a definition used in agriculture to identify the effect of coastal climates). Care home build type considered whether the building was purpose built or converted from a previous use. Care home size was based on number of bedrooms (small: <30, medium: 30-59, large: 60 or more). In addition, the floor and orientation of rooms were considered.

3. RESULTS FOR THE 41-CARE HOME SAMPLE

3.1 Temperature

Monitored indoor temperatures varied widely over the Jun-Aug 2022 period, exceeding 40 °C in three care homes and exceeded 35 °C in 14 care homes (**Error! Reference source not found.**). Outlier low temperatures were in unoccupied (and therefore unheated) bedrooms, indicating that many care homes maintained some level of background heating provision throughout the whole year. Analysis focussed on occupied hours as defined above (all hours for bedrooms). (Average temperatures were 25.2 °C (mean) and 25.0 °C (median), with a quartiles of 23.7 °C and 26.4 °C.

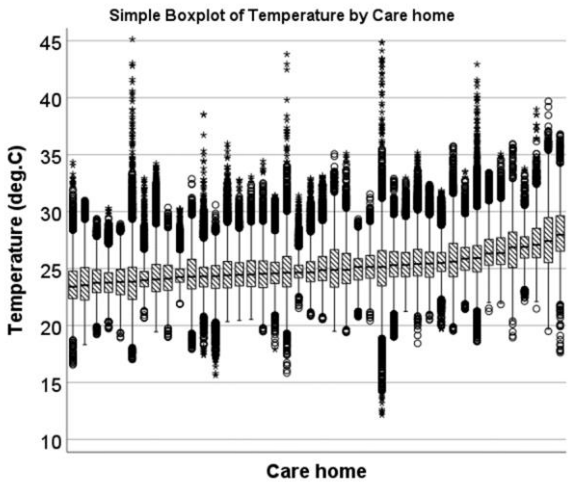

Figure 1 Boxplot showing the distribution of monitored temperatures during occupied hours (lounges and offices) and all hours (bedrooms) across the 41-care home sample.

Analysis of temperatures distributions for monitored locations disaggregated by different

categories revealed interesting findings, both in differences and similarities between the groups.

Disaggregating by location revealed London care homes were 1.8-2.2 °C warmer (mean/median) than those in other regions. The 25th C for London (25.2 °C) was almost the same as the 75th Cs in the north and south care home groups (25.4 and 25.5 °C respectively). Bedroom night-time hours in London were 1.8-2.2 °C (mean) warmer than bedrooms in other regions. There was little to distinguish between temperature distributions in the care homes in the north, midlands and south.

Urban and suburban care homes were 0.8-1.0 °C (mean) warmer than rural care homes. Compared to rural bedrooms, urban and suburban bedrooms were 1.3-1.4 °C (mean) warmer during the day and 1.2 °C (mean) warmer at night. Inland care homes were 1.0 °C (mean) warmer than coastal care homes.

Differences depending on building age were less pronounced. Pre-1930 care homes were 0.5-0.8 °C (mean) cooler than care homes built after 1930. However, these older care homes also had the most extreme outliers, exceeding 45 °C in once instance. Bedrooms in care homes built in the oldest two groups (i.e. pre-1977) experienced the greatest differences between day and night temperatures, a 0.4-0.5 °C drop at night compared to 0.1-0.2 °C drop in bedrooms in the newer care homes, possibly due to thermal mass in older buildings. Grouping care homes by size or build type (purpose built or converted/extended) made no significant difference to indoor temperature distributions.

Ground floor rooms (including rooms in single-storey buildings) were 0.8-0.9 °C cooler than those on middle and top floors. Room orientations were defined thus: rooms facing SE, S or SW were grouped as Southerly, those facing NW, N or NE were Northerly, those facing SE, E or NE as Easterly, and those facing NW, W or SW as Westerly. Some rooms were therefore in two groups, others were internal rooms. Consequently, the sample size was different for this stage of the analysis. Interestingly, southerly orientated rooms were not significantly warmer than northerly rooms, with means, medians and quartiles all within 0.0-0.2 °C of one another. Easterly orientated rooms were around 0.5 °C warmer (mean, median, quartiles) than westerly rooms.

3.2 Relative humidity

Relative humidity (RH) within the monitored care homes varied widely over the Jun-Aug 2022 period, with lows below 30% and highs above 80%. While peaks above 70% were rare, lows below 30% were common and found in all but one care home. During occupied hours, the overall mean and median RH were 45.6% and 45.3% respectively, with a lower quartile of 39.7% and upper quartile of 51.0%. This lower quartile indicates that across the whole dataset, more than a quarter of RH readings were below the recommended 40-60% range during occupied hours.

RH in London care homes was 4.8-10.9% lower (mean) than in other regions. Care homes in the South tended to have higher RH, likely due to their coastal proximity: coastal care homes had mean RH 6.6% higher than inland care homes; inland care homes had RH below 40% for a third of occupied hours compared to only 9% of occupied hours for coastal care homes. Only 48% of occupied hours were within the 40-60% recommended RH range in London care homes, with more than half of occupied hours below 40% (Figure 2). In contrast, rooms in care homes across the rest of England had RH between 40 and 60% for 70-80% of occupied hours.

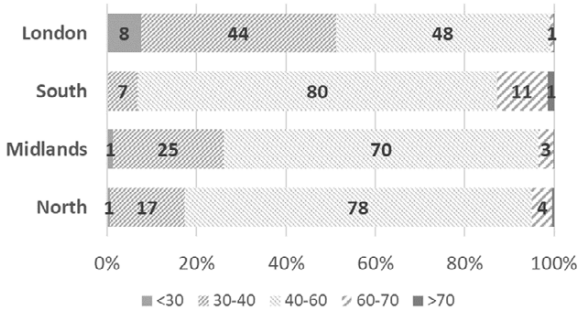

Figure 2 Stacked bar chart showing percentage of occupied hours within the recommended 40-60% RH range, grouped by region.

RH in rural care homes was 3.9-4.8% higher than in urban and suburban localities, and within 40-60% RH for almost 80% of occupied hours compared to 69% (suburban) and 63% (urban). Only 11% of occupied hours were below 40% in rural care homes, compared with 26% (suburban) and 31% (urban). Rural care homes' surroundings (trees, bushes, grass, water etc.) would raise the outdoor RH levels. Pre-1930 care homes had higher RH than those built later. Building size and type made little difference to distributions of RH.

Monitored ground floor rooms had higher RH than those on middle or top floors. More than three quarters of occupied hours in ground floor rooms were in the 40-60% RH range, compared to only 61-63% of occupied hours in middle and top floor rooms. Ground floor rooms were below 40% RH for 17% of occupied hours compared to 31-35% of occupied hours in middle and top floor rooms. Room orientation made no significant difference to RH distribution.

3.3 Overheating

Overheating was investigated for the 33-care homes (149 rooms) sub-set which had monitoring

data covering the full May-Sep 2022 non-heating period. Overheating was endemic during this period, with 95% of rooms failing CIBSE Guide A metric, 62% of rooms failing CIBSE TM52 metric and 99% of rooms failing CIBSE TM59 metric. The binary pass/fail for these overheating metrics did not help identify the severity of overheating. Therefore, analysis also considered how often locations were overheating according to each metric.

CIBSE Guide A found overheating in all 50 monitored locations in London care homes, and in 93-94% of monitored rooms across the rest of England. CIBSE TM52 was much more forgiving: 43-44% of monitored rooms in the Midlands and South overheating compared to 63% in the North and 82% in London (Figure 3). The cooler climate in the north meant lower threshold comfort temperatures and consequently more rooms failing this metric. Whilst London's warmer outdoor temperatures raised threshold comfort temperatures, this was not enough to prevent over 4/5ths of monitored rooms to overheat. Metric TM59 was the least forgiving metric, with all but two monitored locations overheating.

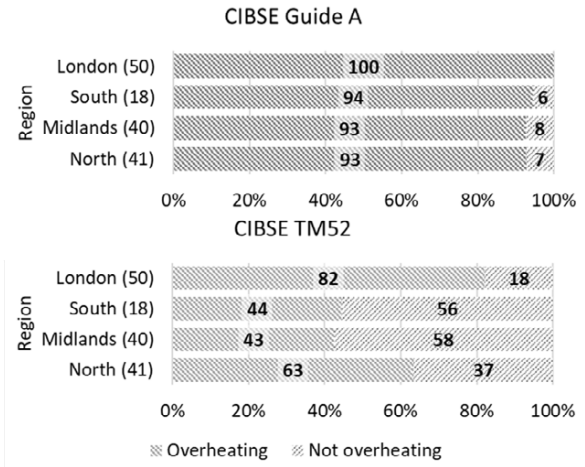

Figure 3 Grouped by region, proportion of monitored locations found to be overheating according to CIBSE Guide A (top) and TM52 (Bottom).

For each overheating metric/criterion, the proportion of monitored occupied hours when the temperature threshold was exceeded has been considered. For CIBSE Guide A, bedrooms were more likely to fail than lounges and offices due to the lower temperature threshold (Figure 4). London bedrooms, lounges and offices exceeded temperature thresholds much more than those in other regions. The three criteria for TM52 produced quite different results, but with similar trends. London bedrooms failed Criterion 1 far more often than bedrooms in other regions. Criterion 2 (daily weighted exceedance) was failed far less often in north and midlands care homes than those in the south and London. Criterion 3 (temperatures <4 °C above $T_{threshold}$) was rarely failed and only for a very small percent of occupied hours.

Whilst most rooms failed CIBSE Guide A, the few that did not fail were in either the oldest Pre-1930 care homes or the newest ones built post-2002. The oldest care homes were more likely to have rooms fail CIBSE TM52 compared to care homes built after 1930. There was little to distinguish between building age groups in terms of how often they exceeded temperature thresholds. More recently built care homes, particularly those purpose built since 2002, were not overheating much more or less than those built in the decades or even centuries before.

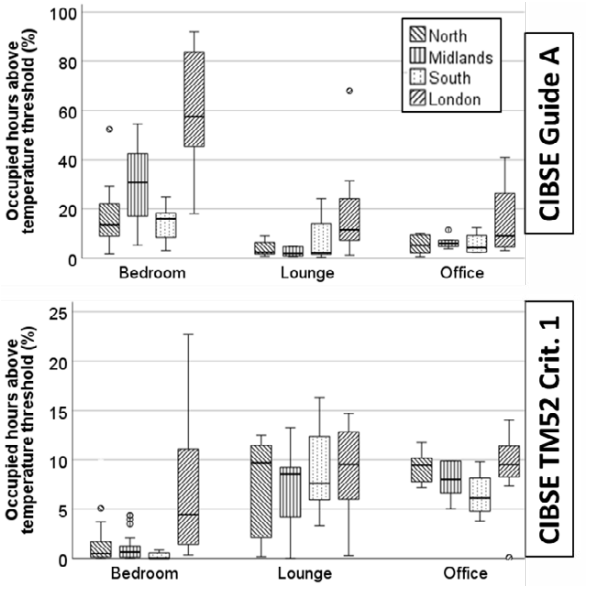

Figure 4 Clustered by region and grouped by room type, proportion of occupied hours above temperature threshold according to CIBSE Guide A (26 ℃ bedrooms, 28 ℃ lounges and offices) and CIBSE TM52, Criterion 1.

Rooms in both purpose-built and converted/ extended care homes were almost equally likely to fail CIBSE Guide A. CIBSE TM52 was failed in a higher proportion of rooms in converted/extended care homes than from rooms in purpose-built care homes. There was very little to distinguish between the two build-type groups when considering CIBSE Guide A in more detail. There was very little to differentiate between lounges and offices in purpose-built and converted/extended care homes for any of the three TM52 criteria. There was little to distinguish between bedrooms in converted/extended and purpose-built care homes with regards to TM59 criterion 2. In summary, the differences between rooms in converted/extended and purpose-built care homes were minimal, with only very subtle differences found for specific criteria.

All seven of the monitored locations to pass CIBSE Guide A were located on the ground floor. Ground and middle floor rooms were significantly more likely

to pass CIBSE TM52 compared to rooms on the top floors (41-42% pass compared to only 26% pass respectively). Both rooms which passed TM59 were both located on the ground floor. Bedrooms on the ground floors exceeded 26 °C much less often than those on middle or top floors. Ground floor bedrooms that exceeded the temperature threshold defined by CIBSE TM52 Criterion 1 did so far less often than bedrooms on middle or top floors. In summary, ground floor rooms – particularly bedrooms – exceeded the temperature thresholds less often than rooms on middle or top floors of the care homes. Although there were subtle differences, rooms on middle and top floors tended to have similar temperatures and overheating results as one another. This contradicts findings of other studies suggesting that top-floor rooms/flats may be more at risk (e.g.[16, 17], although these studies tend to have investigated high-rise apartment blocks rather than buildings such as care homes and hotels with only a few floors and larger footprints).

Despite the southerly orientated rooms experiencing significantly more solar gains than those facing in a northerly direction, the temperature distributions and overheating characteristics of the two groups were remarkably similar. The differences between easterly and westerly rooms were much more significant than differences between northerly and southerly rooms. Bedrooms and lounges that were orientated westerly exceeded the overheating temperature thresholds less often those orientated easterly. Whilst both orientations should in theory receive similar levels of solar gains over the course of a day, easterly rooms will receive these in the mornings. The resulting higher temperatures would remain throughout the day. Westerly orientated rooms would not receive solar gains until later in the day, with the opportunity to purge some of this heat overnight coming much sooner.

4 Discussion

This paper has gathered and analysed temperature and RH data gathered from 41 care homes (195 rooms) from Jun-Aug 2022, and overheating in a subset of 33 care homes (149 rooms) from May-Sep 2022, with a focus on identifying significant differences in these data streams depending on the characteristics of the care homes or rooms. Regarding the overheating metrics, 95% of monitored rooms failed CIBSE Guide A, 99% failed CIBSE TM59, but only 62% failed CIBSE TM52.It is worth considering that since most residents spend most/all of their time indoors, outdoor temperatures may not have much influence on their comfort temperatures, particularly compared to staff who come and go from the building much more often. Furthermore, the ability of elderly residents to adapt physiologically to their local environmental conditions may be reduced, particularly those with underlying health concerns. Key findings can be grouped according to care home locations, care home buildings and individual room characteristics.

With regards to location, rooms in London care homes were around 2 °C warmer than rooms in other regions. Consequently, they were much more likely to fail overheating metrics, particularly TM52, and to exceed the temperature thresholds of these metrics for much greater proportions of occupied hours. Rooms in rural locations were around 1 °C cooler than rooms in suburban and urban locations. Rural rooms were less likely to fail CIBSE Guide A and much less likely to fail TM52. Rural bedrooms exceeded the overheating temperature thresholds less often than bedrooms in suburban and urban care homes. Coastal care homes were around 1 °C cooler than in inland care homes. Consequently, coastal rooms were less likely to fail CIBSE Guide A and TM52, and when they did fail, coastal rooms exceeding overheating temperature thresholds less often than those inland.
With regards to the care home buildings, the oldest age group of care home (Pre-1930) had slightly lower temperatures than care homes built since 1930. However, the relationship between build age and overheating performance was difficult to define: Monitored rooms in Pre-1930 and Post-2002 care homes exceeded CIBSE Guide A temperature thresholds less often than monitored rooms in care homes built in between. This distinction was not seen when measured against TM52. Large care homes experienced less extreme temperatures than small and medium care homes, but their overall temperature distributions were very similar. Differences in how often overheating metrics were failed were only marginal.

With regards to individual rooms, rooms located on ground floors were almost 1 °C cooler than those on middle and top floors. There was little difference between rooms on middle or top floors. There was surprisingly little to distinguish between rooms orientated to the north and rooms orientated to the south. However, rooms orientated to the west were around 0.5 °C cooler and exceeded overheating thresholds less often than those orientated east.

The findings from this study should provide useful insights for those involved in the design of new care homes or the refurbishment of existing care homes. Characteristics that make buildings or individual rooms more vulnerable to overheating should be considered and, where possible, measures taken to mitigate these risks. To minimise installation and running costs, as well as carbon emissions, passive solutions (shading, enhanced natural ventilation, use of thermal mass) should be prioritised over active cooling measures (air conditioning).

5 Conclusion

This study has provided useful insights into which typologies/groupings have the most significant differences in indoor environment/overheating. Clearly, each location has a unique combination of characteristics. The use of CIBSE overheating metrics (Guide A, TM52 and TM59) revealed endemic overheating across the care homes. Peak temperatures exceeded 40°C within three care homes and 35°C within 14 care homes. London care homes were nearly 2°C warmer than those elsewhere. Upper-floor rooms were significantly warmer than ground floor rooms, urban/suburban care homes significantly warmer than rural care homes, and inland care homes significantly warmer than coastal care homes. Other characteristics (building age, size, room orientation) showed much less significant differences in temperature distributions between groups. Identifying precisely which occupancy and building characteristics have the most influence room-by-room with regards to overheating is a complex statistical challenge.

Care homes present several distinctive challenges to designers. The reliability and performance of equipment is paramount since the provision of a comfortable environment is a critical part of providing effective care [11]. However, care home residents tend to find cool air-conditioned air unacceptably cold and draughty. Adaptive behaviours (changing clothing, changing food and drink intake, and opening windows) provide low tech and low-cost alternatives and are more feasible to implement.

One important practical constraint to any potential retrofit measures is the fact that care home buildings are in constant use [18]: even a light-touch retrofit could cause significant disturbance to the frail and sensitive residents. Careful planning could allow some quick-to-deploy retrofit measures to be taken in conjunction with scheduled redecoration/ refurbishment. However, this often occurs piecemeal as and when rooms become available 'between residents', making it difficult to integrate retrofit measures that require physical materials and labour which would be much more efficiently deployed in one go. Another constraint specific to care home settings is that safety regulations mean window openings are limited to a maximum 10 cm, both for security against outsiders coming in and to prevent residents – particularly those with dementia – from climbing out [12].

ACKNOWLEDGEMENTS

The authors would like to thank NERC (Grant ref: NE/T013729/1) for funding the ClimaCare research.

REFERENCES

1. Met Office. *Joint hottest summer on record for England*. 2022 12/07/2023]; Available from: https://www.metoffice.gov.uk/about-us/press-office/news/weather-and-climate/2022/joint-hottest-summer-on-record-for-england.
2. ONS and UKHSA. *Excess mortality during heat-periods: 1 June to 31 August 2022*. 2022 12/07/2023]; Available from: https://www.ons.gov.uk/peoplepopulationandcommunity/birthsdeathsandmarriages/deaths/articles/excessmortalityduringheatperiods/englandandwales1juneto31august2022.
3. Kovats, R.S., H. Johnson, and C. Griffith, *Mortality in southern England during the 2003 heat wave by place of death.* Health Stat Q, 2006. 29(3): p. 6-8.
4. Johnstone, A.M., et al., *Factors influencing variation in basal metabolic rate include fat-free mass, fat mass, age, and circulating thyroxine but not sex, circulating leptin, or triiodothyronine.* The American journal of clinical nutrition, 2005. 82(5): p. 941-948.
5. Hajat, S., et al., *Impact of hot temperatures on death in London: a time series approach.* Journal of Epidemiology & Community Health, 2002. 56(5): p. 367-372.
6. PHE, *Heatwave plan for England - making the case: the impact of heat on health - now and in the future.*, D.o. Health, Editor. 2014: London.
7. Arup, *Addressing overheating risk in existing UK homes (Arup)*, C.C. Committee, Editor. 2022: UK.
8. Climate Change Committee, *Risks to health, wellbeing and productivity from overheating in buildings*. 2022, Climate Change Committee: London.
9. DEFRA, *UK Climate Change Risk Assessment*, F.a.R.A. Department for Environment, Editor. 2017, UK Government: London.
10. DEFRA, *The National Adaptation Programme and the third strategy for climate adaptation reporting*, F.a.R.A. Department for Environment, Editor. 2018, UK Government: London.
11. Guy, S., et al., *Building Comfort for Older Age: Designing and Managing Thermal Comfort in Low Carbon Housing for Older People.* University of Manchester/Housing LIN, 2013.
12. Gupta, R. and M. Gregg, *Do deep low carbon domestic retrofits actually work?* Energy and Buildings, 2016. 129: p. 330-343.
13. Lewis, A., *Energy use in an ageing society: The challenges of designing energy-efficient older people's housing.* Manchester Memoirs–Being The Memoirs and Proceedings of the Manchester Literary and Philosophical Society, 2014. 151: p. 20-32.
14. Botti, A. and M. Ramos, *Adapting the design of a new care home development for a changing climate.* International Journal of Building Pathology and Adaptation, 2017.
15. Mavrogianni, A., et al., *Urban social housing resilience to excess summer heat.* Building Research & Information, 2015. 43(3): p. 316-333.
16. Habitzreuter, L., S.T. Smith, and T. Keeling, *Modelling the overheating risk in an uniform high-rise building design with a consideration of urban context and heatwaves.* Indoor and Built Environment, 2020. 29(5): p. 671-688.
17. Baborska-Narozny, M. and M. Grudzinska, *Overheating in a UK High-rise Retrofit Apartment Block – Ranking of Measures Available to Case Study Occupants Based on Modelling.* Energy Procedia, 2017. 111: p. 568-577.
18. Neven, L., G. Walker, and S. Brown, *Sustainable thermal technologies and care homes: Productive alignment or risky investment?* Energy Policy, 2015. 84: p. 195-203.

PLEA 2024 WROCŁAW
(Re)thinking Resilience

An Analysis of Reflective Roof Insulations, Thermal Comfort and Carbon Emissions for an Elementary School Design in Indonesia

HASNA HANIFA[1], STEPHEN SHARPLES[1]

[1]School of Architecture, University of Liverpool, Liverpool, United Kingdom

ABSTRACT: Indonesia has pledged to achieve net-zero emissions by 2060, as announced at the UN Climate Change Conference in 2021 (COP 26). While the government has put frameworks and policies in place to reach this target, they have primarily focused on large-scale buildings, neglecting smaller ones such as schools. Ensuring that school buildings are optimised is of utmost importance in providing quality education for future generations. This research specifically focuses on the roof of a school, which is a crucial component of a building for reducing energy consumption and handling thermal loads. Additionally, the research investigates the use of reflective insulation in the elementary school building design prototype to enhance thermal comfort and improve the building's performance. The study's method involved computational modelling, building simulations, and life cycle assessments of the buildings. The findings show that reflective insulation improved thermal comfort more than uninsulated roofs. The white metal roof with glass wool insulation and aluminium foil demonstrated the best indoor operative temperatures of all the roof systems examined. However, this design generated significantly higher embodied carbon emissions due to the thermal insulation. These results highlight the need for a balanced strategy to enhance thermal comfort without producing significant carbon emissions.
KEYWORDS: Carbon Emissions, Indonesia, Operative Temperature, Reflective Insulation, Thermal Comfort.

1. INTRODUCTION

Indonesia has a hot and humid equatorial tropical environment, with little seasonal variations in the weather [1]. Indonesia's average land temperatures are approximately 28°C along the coast, 26°C inland, and about 23°C higher up in the mountains [2]. Indonesia also receives high levels of solar radiation, with an average Global Horizontal Irradiation (GHI) of 4.8 kWh/m^2 per day [3]. As a result, buildings acquire the most heat through radiation rather than conduction or convection, and the majority of heat transfers into buildings occur through the roof. As a result, the roof design must incorporate, ideally, a passive cooling approach, such as reflective thermal insulation. In Southeast Asia, reflective insulation is the most effective type of roof insulation and when comparing reflective insulation-covered roofs to uninsulated roof attics, a reduction in ceiling heat flux of 80% has been observed [4]. The use of reflective and radiative roofs, such as white-coloured roofs, is also recommended as a strategy to improve the thermal performance of buildings [5][6].

However, roof insulation has received inadequate attention from the Indonesian government in terms of building standards and regulations. For example, the roof of an Indonesian elementary school building prototype was designed with just clay tiles and no roof insulation, resulting in diminished thermal comfort inside the classroom throughout the day (Figure 1).

Figure 1: An elementary school building in Jakarta, Indonesia, with clay roof tiles with no insulation. Source: author

2. METHOD

This research evaluated the thermal performance of a prototype elementary school building design based on the Technical Guidelines in the Circular Letter published by the Indonesian Ministry of Public Works and Housing. A comparative analysis was undertaken, using DesignBuilder dynamic thermal simulation software [7], to evaluate the school's performance using different roof insulation configurations. EnergyPlus Weather (EPW) files were specifically generated for the designated location (Jakarta), using the climate software Meteonorm [8]. To assess future thermal performance Meteonorm

also generated EPW files for 2050 and 2080 using a Representative Concentration Pathway RCP of 4.5 [9]. Additionally, the study used the life cycle assessment software One Click LCA [10] to evaluate the total (operational and embodied) carbon emissions for each roof option.

3. CASE STUDY – ELEMENTARY SCHOOL BUILDING PROTOTYPE DESIGN

The Indonesian standard school building design prototype employs conventional structural systems, such as on-site reinforced concrete constructions. The school building design standardisation using conventional structures varies based on the type of school. For elementary schools, the design standard for a one-storey classroom is measured at 7m x 8m in plan, with a capacity of 28 students, a total floor area of 56m², and a floor-to-ceiling height of 3.5m [11]. Typically, an elementary school building consists of one or three classrooms with pitched roofs, a connecting corridor in front of the classrooms, and separate building masses for toilets, a library, prayer rooms, and teacher rooms. For a long time, clay tiles with timber trusses have been commonly used as roof construction for school buildings; however, the use of metal roofs with steel trusses is increasing nowadays. The 3D visualisation of the elementary school building design prototype is illustrated in Figure 2. However, for the building simulation, the single classroom building with a clay roof tile is used as the base model.

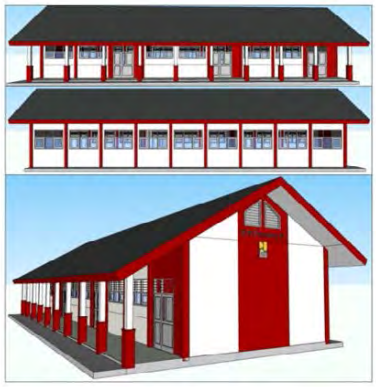

Figure 2: 3D Visualisation of Elementary School Building consists of 3 classrooms based on the prototype design. Source: Technical Guidelines in the Circular Letter published by the Indonesian Ministry of Public Works and Housing.

The roof combinations shown in Table 1 were selected for the school simulations in DesignBuilder after an examination of typical Indonesian school buildings. For each roof simulation, the school model's floor and walls remained unchanged.

3.1 Site Location

Jakarta, Indonesia was chosen as the site location for the building simulation. Jakarta is situated on the northwest coast of Java and has a latitude of -6.13 °N and a longitude of 106.75 °E. It is the largest city in Southeast Asia, one of the world's most populous islands, and serves as the diplomatic capital of the Association of Southeast Asian Nations (ASEAN).

Table 1. Constructional Layers for Building Simulation. Source: DesignBuilder

Case	Roof Constructional Layers	U-Value W/m²K	R-Value m²K/W
1	20mm Clay Tiles Roof	3.226	0.310
2	0.4mm Metal Roof	3.448	0.290
3	0.4mm White Metal Roof,0.8mm Bubble Foil	1.535	0.651
4	0.4mm White Metal Roof,8mm Aluminium Foil,25mm glass wool	0.889	1.125
5	0.4mm White Metal Roof,8mm Aluminium Foil,50 mm rock wool	0.571	1.750

Figure 3: Jakarta is located on Java's northwest coast.

The location was chosen because there is a nearby weather station that ensures accurate and reliable weather data collection. The temperature in Jakarta remains stable year-round, ranging from 27 to 29°C with minimal daily fluctuations. At 9.00 AM, the level of humidity spikes to a high of 88-94%, while at 3.00 PM, it remains uncomfortably high at around 67-77%. It is worth noting that the city's average dew point is approximately 24°C [12].

3.2 Climate Classification

The climate of the site location for the case study is justified using various climate classification sources, which include the ASHRAE and Köppen-Geiger climate maps. The weather files obtained from Meteonorm for use in DesignBuilder classify this case study as belonging to ASHRAE climatic zone 0A, which is classified as very hot and humid. According to the Köppen-Geiger climate classification, the climate of this location is considered a Tropical rainforest (Köppen climate classification: Af). This area has a

tropical climate with consistent precipitation of at least 60mm throughout the year, low wind speeds, and an average temperature above 20°C, as per the Köppen-Geiger climate classification. The sun shines from the south for half the year and from the north for the other half [13].

4. SIMULATION RESULT AND FINDINGS

The impact of each roof configuration on the operative temperature was evaluated during the hottest and coldest months, in October, and February, respectively. The energy consumption of this building was simulated in DesignBuilder based on contemporary weather data for only interior lighting since the building is naturally ventilated. Furthermore, the operative temperature was chosen as it represents the average of the mean radiant temperature and ambient air temperatures.

4.1 Temperature Distribution and Comfort

Table 2 shows that, based on current and projected weather data, Case 2 had the highest operative temperatures and Case 4 had the lowest operative temperatures in both the coldest and hottest months.

Table 1. Mean Monthly Operative Temperature in the Hottest and Coldest Months, source: DesignBuilder

Case	Contemporary		2050		2080	
	Feb (°C)	Oct (°C)	Feb (°C)	Oct (°C)	Feb (°C)	Oct (°C)
1	27.5	28.7	28.3	29.9	28.8	30.3
2	27.6	28.8	28.4	29.9	28.8	30.4
3	27.0	28.1	27.8	29.2	28.2	29.7
4	26.8	27.9	27.6	29.0	28.0	29.5
5	26.8	28.0	27.6	29.0	28.1	29.5

Moreover, these different roof configurations' impacts on the operative temperature were compared during the hottest and coldest months in February and October, respectively. The results (Table 2, Figure 4, and Figure 5) show that all the insulated roofs (Cases 3, 4, and 5) performed better than the uninsulated roofs (Cases 1 and 2) in keeping a lower indoor temperature for both periods. Therefore, Case 2 had the highest operative temperature and Case 4 had the lowest operative temperature in both the coldest and hottest months based on contemporary and future weather data according to RCP 4.5. The data indicates that Case 5, which utilized 50mm rock wool insulation, exhibited a higher operative temperature than Case 4, which only had 25mm glass wool insulation.

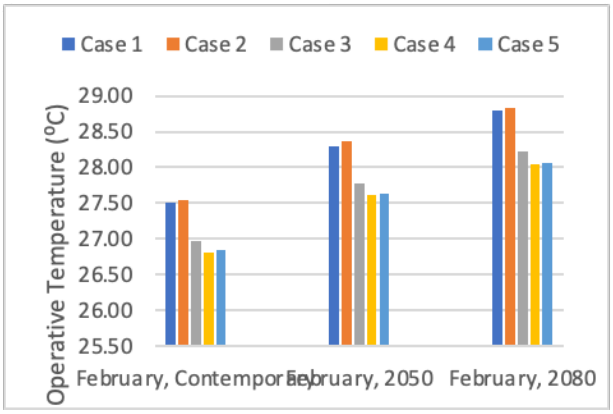

Figure 4: Comparison of the Mean Operative Temperature in February (the coldest month) based on the current and projected weather data. Source: DesignBuilder.

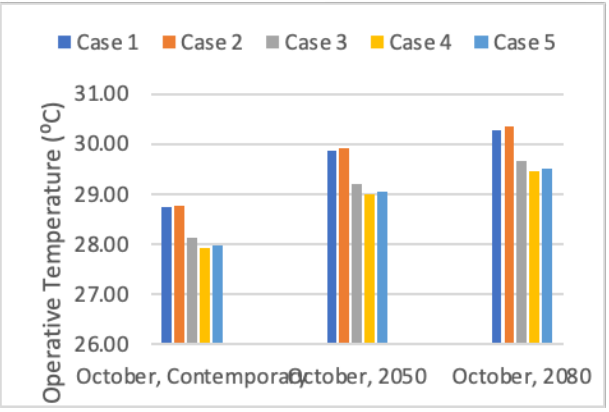

Figure 5: Comparison of The Mean Operative Temperature in October (the hottest month) based on the current and projected weather data. Source: DesignBuilder.

4.2 Overall Life Cycle Assessment

The carbon emissions of the buildings in this section were comprehensively analysed throughout their life stages using the life cycle assessment software in One Click LCA for the contemporary climate. It consists of embodied carbon energy from materials (A1-A3), transportation (A4), construction (A5), energy for maintenance and replacement (B1-B5), operational energy use (lighting only) (B6), and carbon emissions at the end of life (C1-C4). The carbon emissions levels of the building under study using One-Click Life Cycle Assessment software were based on Embodied Carbon Benchmark CH Q3 2021 Global - primary school since there is currently no specifically established benchmark for elementary school buildings in Indonesia. The embodied carbon benchmark results showed that Case 1 building, classed A had 245 $KgCO_2e/m^2$ of greenhouse gas emissions, and Case 2 in. class B, had 259 $KgCO_2e/m^2$ of emissions. On the other hand, Cases 3, 4, and 5 were in class C with 312 $KgCO_2e/m^2$, 316 $KgCO_2e/m^2$, and 320 $KgCO_2e/m^2$ of emissions, sequentially. A summary of the global warming emissions in the life cycle stages is presented in Table 3.

Table 3. Global Warming Life Cycle Stages. Source: One Click LCA

Case	Global Warming Life Cycle Stages ($KgCO_2e$)					
	A1-A3	A4	A5	B1-B5	B6	C1-C4
1	11,362	242	792	1,835	93,135	284
2	12,191	241	902	1,835	93,734	263
3	15,136	245	1,123	1,835	91,278	272
4	15,349	245	1,140	1,835	91,200	272
5	15,546	245	1,156	1,835	91,120	273

A building's life cycle evaluation examines every aspect of the building, including the materials, use, energy use, and end of life. Since this study was limited to the configurations of roof materials, Figure 6 examines the effects of these components on roof elements exclusively. Therefore, the Embodied Carbon of the buildings based on building elements is illustrated in Figure 7. Embodied carbon is the total impact of all greenhouse gas emissions related to a material's life cycle, from its extraction and manufacturing through its end-of-life phases. It is also known as Global Warming Potential (GWP) and is measured in kilogrammes of Carbon Dioxide Equivalent ($KgCO_2e$). The following are included in the calculation of embodied carbon: material extraction (module A1), transport to manufacturer (A2), manufacturing (A3), transport to site (A4), construction (A5), use phase (B1), maintenance (B2), repair (B3), replacement (B4), refurbishment (B5), deconstruction (C1), transport to end of life facilities (C2), processing (C3), and disposal (C4). Therefore, Case 1 had the lowest potential for global warming, while Case 5 had the highest potential for global warming, as shown by Figures 6 and 7.

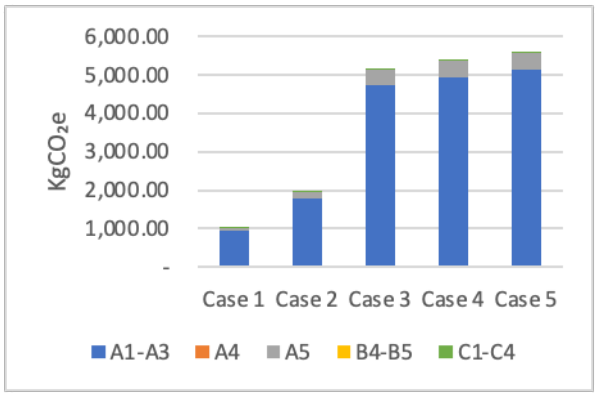

Figure 6: Life Cycle Assessment - Global Warming Potentials (Roofs Only). Source: One Click LCA

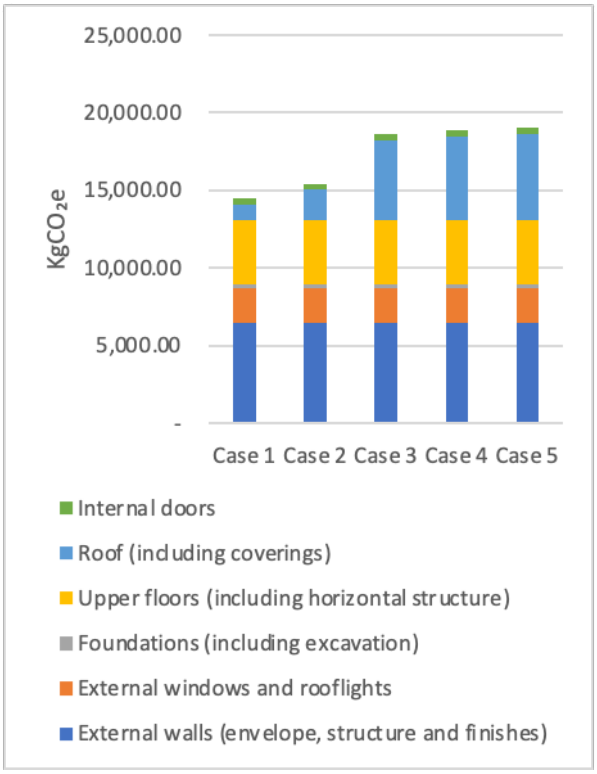

Figure 7: Embodied Carbon based on Building Elements. Source: One Click LCA

5. COMPARATIVE ANALYSIS AND DISCUSSION OF RESULTS

5.1 Indoor Thermal Comfort

The thermal comfort of school buildings is not explicitly regulated in Indonesia. However, earlier thermal comfort studies conducted in Indonesia, demonstrated that citizens of significant cities like Jakarta felt comfortable at air temperatures of 27.7 °C [14]. Therefore, the 27.7 °C temperature was chosen as the upper-end value of the comfort range for the thermal discomfort hours assessment.

Furthermore, as shown in Table 4, Case 2 had the largest percentage of discomfort hours for both current and future climates, while Case 4 had the lowest. Inserting thermal insulation, resulted in a considerable reduction in overall discomfort hours.

Table 4. Annual Discomfort Hours of the Case Study, source: DesignBuilder

	Contemporary		2050		2080	
	Hours at or above 27.7 °C					
Case	Hours	%	Hours	%	Hours	%
1	829.1	49.3	1009.3	60.1	1097.5	65.3
2	837.6	49.9	1018.3	60.6	1105.1	65.8
3	743.2	44.2	933.7	55.6	1031.3	61.4
4	712.4	42.4	905.2	53.9	1006.0	60.0
5	718.6	42.8	912.0	54.3	1012.9	60.3

5.2 Life Cycle Assessment

Following the overall life cycle assessment in section 4.2, it has been determined that Case 5 registered the highest total carbon emissions (operational and embodied) with 110,177 $KgCO_2e$, based on current weather data. It was followed by Case 4 with 110,042 $KgCO_2e$ and Case 3 with 109,890 $KgCO_2e$. Conversely, Case 1 marked the lowest total carbon emissions with 107,651 $KgCO_2e$, followed by Case 2 with 109,167 $KgCO_2e$. Notably, despite having lower total carbon emissions, Cases 1 and 2 consumed more energy (B6) when compared to Cases 3, 4, and 5.

Furthermore, based on Figure 8, it was observed that Case 1 emitted the least total carbon emissions in both current and projected years, while Case 5 had the highest total carbon emissions in current years, and Case 3 produced the most total carbon emissions in 2050 and 2080. However, it was found that Case 2 produced the highest B6 emissions for both current and projected years.

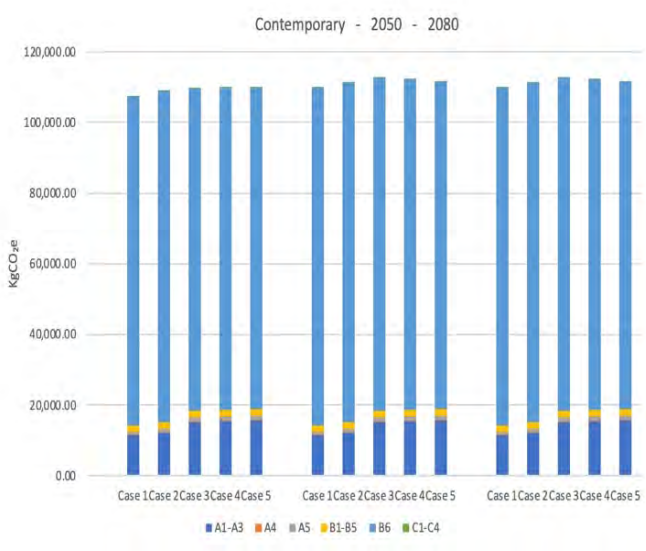

Figure 8: Total Carbon Emissions (embodied and energy) based on Current and Projected Weather Data. Source: DesignBuilder and One Click LCA.

Therefore, this study highlights that electricity generation poses the most significant potential for global warming, consuming no less than 83% of energy across all analysed roof configurations. Apart from electricity, external wall materials (envelope, structure, and finishes), foundations, and roof materials contribute significantly to global warming. Other materials, such as mortar and roof insulations, also have high emission levels. The material contributions to global warming rely on the building's roof system and the amount of material used in the building.

6. CONCLUSION

As analysed using a school case study with contemporary and future weather data, Case 4 provided better thermal comfort than uninsulated roofs. It was found that a building with white metal roofs and glass wool foil (Case 4) had an average of about 53.88% hours above the comfort temperature of 27.7°C, while the base model with clay roof tiles without insulation (Case 1) had 60.08%. A building with the uninsulated metal roof (Case 2) had approximately 60.61% above the same temperature benchmark. In terms of carbon impact, Case 4 had 4,327 $KgCO_2e$ higher embodied carbon than Case 1 which had the least carbon impact on the environment. However, it is essential to note that if the building is designed to install mechanical cooling, Case 1 may not be the most energy-efficient option since it would have a higher energy consumption than Case 4. Case 4 can be a better choice in terms of reducing energy consumption and its impact on global warming. Overall, these findings highlight the importance of a balanced strategy to improve comfort without producing significant carbon emissions.

Moreover, according to the analysis performed using a case study, Case 4 had the roofing that is most suitable for buildings housing elementary schools in tropical regions. The roof configuration for Case 4 consists of a 0.4mm white metal roof, a 10mm higher air cavity, 4mm of aluminium foil, 25mm of glass wool, 4mm of aluminium foil, and 50mm of lower air cavity, which used reflective insulation and radiant barrier as thermal insulation technologies for energy efficiency. As per the findings in Section 4.1, it is observed that 25mm glass wool insulation performed better than 50mm rock wool insulation in building simulation. This suggests that thicker insulation may not be appropriate for this type of building. Consequently, radiant heat transmission was more effectively prevented by thermal insulation that uses reflecting technology, such as radiant barriers and reflective insulation, which employs a very thin coating of low-emittance aluminium foil [15] which is applied on the Case 4 roof configuration. Shrestha and Rijal also discovered that using Glass Wool insulation can reduce the operative temperature of a building by 2°C. [16]

Therefore, based on the overall building life cycle assessment using One Click LCA for the current climate, it is evident that Case 5 is the least sustainable building option. It had approximately 19,056 $KgCO_2e$ of embodied carbon. On the other hand, Case 1 (the base model) is the most environmentally friendly choice, with 14,515 $KgCO_2e$ of embodied carbon. As for the other cases, Case 2 had 15,433 $KgCO_2e$ of embodied carbon, Case 3 had

18,612 $KgCO_2e$ of embodied carbon, and Case 4 had 18,842 $KgCO_2e$ of embodied carbon.

REFERENCES

1. World Atlas, “Indonesia Maps & Facts” [25 February 2023].
2. BMKG Indonesia, *Climate Change Assessment in Indonesia* (2021), 1-2. [3 May 2023].
3. Silalahi et al., (2021). "Solar PV Resource Assessment for Indonesia’s Energy Future," *2021 IEEE 48th Photovoltaic Specialists Conference (PVSC)*, Fort Lauderdale, FL, USA, 2021, pp. 0178-0181, 10.1109/PVSC43889.2021.9518969.
4. Haw and Ashhar, “Reflective Insulation in South-East Asia Region,” in Thermal Insulation and Radiation Control Technologies for Buildings, ed. Jan Ko´sny · David W. Yarbrough (Cham: Springer, 2022): 83-100.
5. Irma Handayani Lubis and Mochamad Donny Koerniawan, (2018). “Reducing Heat Gains and Cooling Loads Through Roof Structure Configurations of a House in Medan,” *IOP Conference Series* 152: 012008, https://doi.org/10.1088/1755-1315/152/1/012008.
6. 6. Azimil Gani Alam et al., (2019). “Building Beneficial Roof Insulation in Vertical Housing: Physical and Economical Selection Method,” *Evergreen* 6, no. 2: 124–33, https://doi.org/10.5109/2321006.
7. DesignBuilder (2023) https://designbuilder.co.uk/
8. Meteonorm (2023) https://meteonorm.com/
9. CoastAdapt (2017) https://coastadapt.com.au/infographics/what-are-rcps
10. One Click LCA (2023) https://www.oneclicklca.com/
11. The Ministry of Public Works and Housing Indonesia, the Circular Letter of The Director General of Human Settlements Number: 47/SE/DC/2020 (Jakarta: The Ministry of Public Works and Housing Indonesia, 2020), 1-18.
12. Agya Utama and Shabbir H. Gheewala. (2009). “Indonesian Residential High-Rise Buildings: A Life Cycle Energy Assessment,” *Energy and Buildings*, Volume 41, Issue 11, pp. 1263–68, https://doi.org/10.1016/j.enbuild.2009.07.025.
13. None Nisrina Dewi Salsabila et al., (2023). “Analyzing the Effects of High-Rise Buildings with Glass Façades on Outdoor Human Comfort in The Jakarta Metropolitan Area,” *Journal of Advanced Research in Applied Sciences and Engineering Technology* 29, no. 2, pp. 91–104, https://doi.org/10.37934/araset.29.2.91104.
14. Tri Harso Karyono, “Thermal Comfort in Indonesia” in Sustainable Houses and Living in the Hot-Humid Climates of Asia, ed, Tetsu Kubota, Hom Bahadur Rijal, and Hiroto Takaguchi. (Singapore: Springer, 2018): 119-120.
15. Sau Wai Lee, Chin Haw Lim, and Elias Bin Salleh. (2016). “Reflective Thermal Insulation Systems in Building: A Review on Radiant Barrier and Reflective Insulation.” *Renewable & Sustainable Energy Reviews* 65, pp. 643–61. https://doi.org/10.1016/j.rser.2016.07.002.
16. Mishan Shrestha and Hom Bahadur Rijal, (2021). “Investigation on Summer Thermal Comfort and Passive Thermal Improvements in Naturally Ventilated Nepalese School Buildings,” *Building and Environment*, *Energies*, Volume 190, pp. 1251. https://doi.org/10.3390/en16031251.

PLEA 2024 WROCŁAW
(Re)thinking Resilience

Occupants' well-being in office buildings:
a field work in Chile

MAUREEN TREBILCOCK-KELLY[1,2], JAIME SOTO-MUÑOZ[3], PAULINA WEGERSTEDER-MARTÍNEZ[1], RAÚL RAMÍREZ-VIELMA[4]

[1]Dept. Design and Theory of Architecture, Universidad del Bío-Bío, Concepción, Chile
[2]Centre for Sustainable Urban Development CEDEUS, Chile
[3]Dept. Building Science, Universidad del Bío-Bío, Concepción, Chile
[4]Dept. Psychology, Universidad de Concepción, Concepción, Chile

ABSTRACT: With humans spending approximately 90% of their time indoors, contemporary architectural design prioritizes the creation of spaces that promote health and well-being. Despite the growing academic discourse, questions persist about the parameters that define occupants' well-being in buildings. The objective of this paper is to explore well-being criteria in office buildings through fieldwork. The research methodology involved conducting a survey encompassing 359 occupants from 8 LEED-certified office buildings in Chile. The questionnaire comprised various sections. One section explicitly prompted respondents to evaluate a specific set of parameters based on their significance for well-being within an ideal office environment. Another section addressed occupants' satisfaction with various aspects of their current office environment, while a final section incorporated a multi-item scale for evaluating eudaimonic well-being. The results indicate that, beyond the typical Indoor Environmental Quality (IEQ) parameters, other crucial aspects include Security, Privacy, Connecting with Nature, Universal Accessibility, and Ergonomics (Furniture and Desk Space). Respondents accord great importance to Security, a local concern related to crime. Privacy is gaining significance due to the rise of open-plan office layouts at the expense of individual offices. Conversely, aspects considered important for occupants' well-being in the literature, such as environmental control and opening windows, are not deemed significant by the respondents.
KEYWORDS: well-being, comfort, occupant, workplace

1. INTRODUCTION

Health has always been at the centre of the delivery of green buildings. However, contemporary society is confronted with novel challenges that require a fresh approach to addressing occupant well-being. This involves adopting a more comprehensive viewpoint that encompasses not only physical health but also broader dimensions of human well-being, including social and psychological aspects [1]. The connection between occupants and nature has become more relevant, where the design and planning of the built environment play an essential role in in promoting both the physical and emotional welfare of those inhabiting them [2-4].

Historically, research in this field primarily aimed to identify characteristics that define "unhealthy buildings," often characterized by symptoms associated with sick building syndrome (SBS) experienced by occupants [5].

Hanc [6] argues that, despite studies often addressing the poor environmental conditions of buildings, a novel and almost parallel movement can now be observed among researchers in the built environment in the pursuit of "well-being."

As humans spend approximately 90 per cent of our time indoors, architectural design is currently expected to generate spaces that promote health and well-being of people to meet the demands of daily life [7].

More recently, a growing body of literature has shifted its focus towards determining factors that contribute to a "healthy building". This refers to a built environment that fosters the multidimensional well-being of the occupants.

In the field of the built environment, the concept of eudaimonic well-being takes on special relevance, originating from neo-Aristotelian philosophy and associated with human flourishing [8]. In other words, eudaimonic well-being refers to a deeper and more meaningful sense of well-being, linked to the full development or comprehensive fulfillment of the individual, where their experiences in the workplace cover a significant portion of their waking hours.

The connection can be addressed by considering various aspects, such as the purpose of work and its

meanings for employees, a positive organizational climate, the balance between work and personal life, and/or the design of the physical space, among others.

Despite an increasing discussion on this topic in academic papers, there are still questions related to how to design, measure and enhance the well-being of living spaces [9]. Designers do not have a systematic process for incorporating strategies that promote occupant well-being within buildings [10]. This is due to the lack of understanding of how the built environment influences health and well-being of people [11].

Some of the early advances in establishing specific well-building criteria for buildings have been made in the field of sustainability. Green building rating systems like LEED, BREEAM, and DGNB incorporate criteria for occupants' health, emphasizing indoor environmental quality. Targeted certification programs, including WELL Building Standard and Fitwel, have emerged globally. These newer systems are designed to comprehensively guide health-focused design, with a particular emphasis on indoor air quality.

Zhang et al. [12] review a large number of studies that recognize the importance of indoor climate, space, furniture, and privacy, as well as the visual quality of nature. Meanwhile, many attributes of the building environment, such as privacy, functional suitability, aesthetics, and social aspects could affect human psychological or physical health as well [13].

New innovative solutions have been introduced and consolidated in the design of workspaces, but with little direct understanding of how occupants experience the space and what characteristics of the building are most valued for their well-being.

2. METHODOLOGY

The aim of this paper is to explore well-being criteria in office buildings through field work. The research methodology involved conducting a survey that encompassed 359 occupants from 8 office buildings located in Chile.

2.1 Office buildings and their occupants

The office buildings selected for this study are LEED certified and were constructed within the last 10 years. The choice of LEED certification specifically represents best practices in terms of Indoor Environmental Quality (IEQ), given the absence of regulations in this field within the country. Moreover, the exclusive focus on LEED certified buildings ensures a standardized and comparable sample.

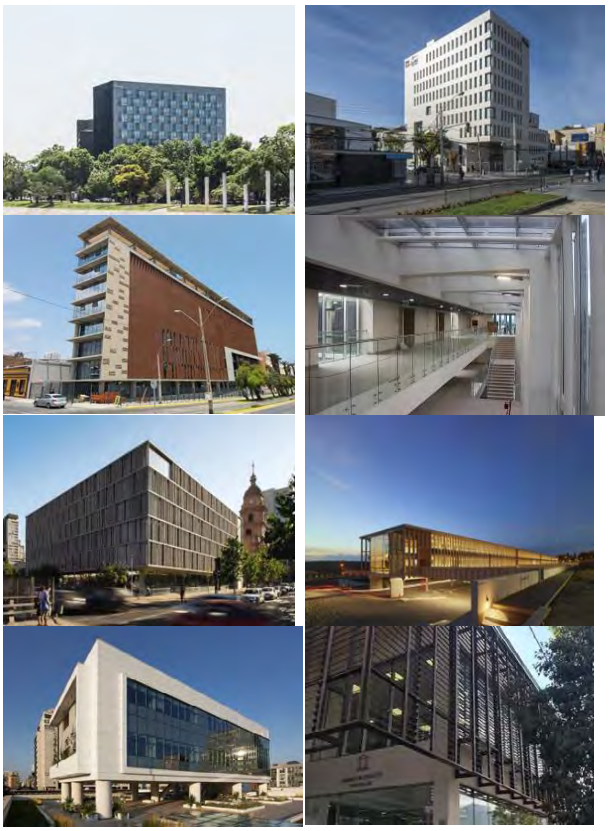

Fig 1: Photographs of the office buildings

The buildings are situated in four different cities in Chile (refer to Table 1). The participants are occupants of these buildings who voluntarily agreed to participate in the study, adhering to research ethics procedures. Among the building occupants, 51.7% are males, and 48.3% are females. Regarding office building layouts, 8% of respondents work in individual offices, 19% share offices with up to 8 co-workers, and 72% work in open-plan office spaces.

Table 1: Characteristics of the office buildings and their occupants

Building Number	City	Construction year	Number of Participants	Average age
1	Antofagasta	2018	29	42.5
2	Viña del Mar	2017	31	43.2
3	Viña del Mar	2017	26	37.8
4	Santiago	2016	49	35.6
5	Santiago	2014	86	37.6
6	Santiago	2016	13	40.0
7	Santiago	2019	9	44.1
8	Los Angeles	2019	116	43.3

2.2 Questionnaire

The questionnaire comprised various sections. One section explicitly prompted respondents to evaluate a specific set of parameters based on their significance for well-being within an ideal office environment. Participants were asked to rate the importance they assign to each aspect for their well-being, according to their preferences for an ideal office environment, without necessarily considering their experience in their office building.

This section of the questionnaire included two different sets of parameters corresponding to different office building scales.

At the workplace scale, the parameters combined sensory qualities of the indoor environment, such as temperature, air quality, noise, and lighting, with more tangible features of the workplace, such as desk space, furniture, views from the window, interior design, option to open windows, and privacy.

At the scale of the entire office building, the parameters encompassed spaces within the architectural program as well as characteristics of the building and its location. These included meeting and socialization spaces, spaces for connecting with nature, presence of daylight, bicycle parking, spaces for sport activities, nursing room, silent room, sustainability strategies, security, universal accessibility, proximity to restaurants, proximity to public transport, proximity to green areas. Each parameter was assessed in a scale from 1 (not important) to 7 (very important). Additionally, respondents were asked to select the top three parameters at each building scale.

Another section of the questionnaire focused on occupants' satisfaction with various aspects of their current office environment, encompassing both indoor environmental qualities and architectural features. Respondents were requested to rate their satisfaction on a scale ranging from 1 (not satisfied) to 7 (very satisfied).

The final section incorporated a multi-item scale for evaluating eudaimonic well-being concerning the building, developed by Watson [14]. This well-being scale for buildings is grounded in the SACRA model, encompassing five components: Satisfaction, Affect, Competence, Relatedness, and Autonomy. The metric includes 22 items rated on a 5-point Likert scale (ranging from strongly disagree to strongly agree). Its formulation was guided by the definition of well-being as flourishing, featuring statements like "I have purpose when I'm in this building" and "I feel valued when I'm in this building" [14].

The questionnaire was developed based on a literature review and the findings from an initial qualitative exploration stage that involved interviews with occupants [15]. A pilot version was administered to a small sample of office workers, allowing to refine the questions, ensuring they were understandable to the participants.

3. RESULTS AND DISCUSSION

The results of the survey are organised in two subsections. The first subsection shows the importance that the occupants give to the specific set of parameters for their well-being, extracted directly from the questionnaire. Therefore, it comprises explicit well-being criteria. The second subsection shows the correlation of data from Watson´s Building Well-being Scale and occupants' satisfaction with different aspects of the office environment. Therefore, it allows to identify building qualities and criteria that occupants implicitly relate to well-being.

3.1 Explicit well-being criteria

The results from the section prompting respondents to explicitly identify parameters contributing to their well-being are presented below. Figures 1 and 2 depict the importance assessment of each parameter at the scale of the workspace.

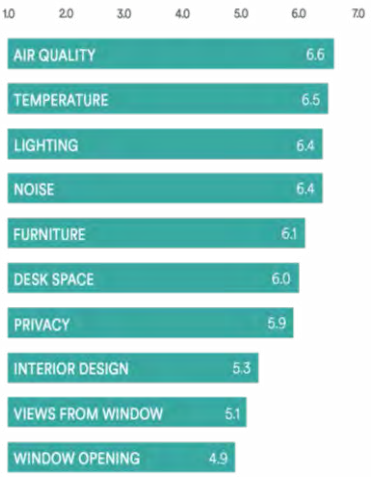

Fig 1: Importance of each feature at the scale of the workspace (1: Not important – 7: Very important)

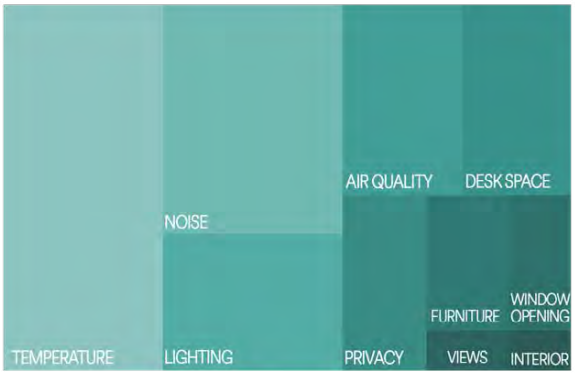

Fig 2: Most important features at the scale of the workspace

The four Indoor Environmental Quality parameters (Air quality, Temperature, Lighting, and Noise) are consistently recognized as the most important, both when respondents were asked to rate their importance on a scale from 1 to 7 (Fig 1) and when asked to select the top 3 parameters from the list (Fig 2). This aligns with expectations, as occupants may associate the term 'well-being' with environmental comfort. In addition, LEED certification gives credits to IEQ strategies, particularly lighting, air quality and thermal comfort, so the design process of these certified office buildings have taken into account IEQ criteria.

The middle of the well-being ranking is comprised by three distinctive parameters: Furniture, Desk Space and Privacy, which relate to the layout of the workspace and ergonomics. Occupants give importance to ergonomics as they relate comfort with physical well-being.

Interestingly, Window Opening is one of the least important features for the occupants. Operable windows are very rare in LEED certified buildings, so half of the case studies have only a few operable windows, while the others are fully air-conditioned, sealed buildings.

Finally, Views Out and Interior Design are not nearly as relevant for occupants' well-being as other features from the list.

On the scale of the entire building, occupants prioritize Safety as their foremost concern (see Fig. 3 and Fig. 4), a result in line with expectations given the rising crime rates experienced in the country, and the seismic nature of the context.

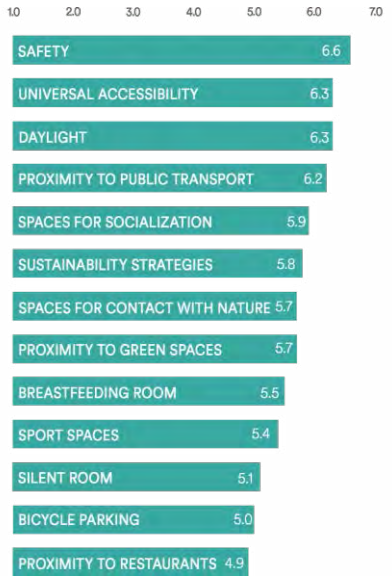

Fig 3: Importance of the feature at the scale of the entire building (1: Not important – 7: Very important)

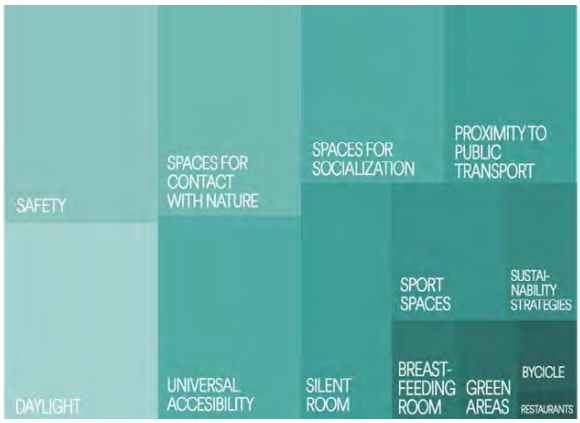

Fig 4: Most important features at the scale of the entire building

A second set of crucial features comprises Daylight, Universal Accessibility, and Spaces for Contact with Nature (see Fig 4). It is noteworthy that, following the prioritization of a practical and critical-for-survival feature like Safety, building occupants emphasize biophilic features, primarily associated with psychological well-being.

On the other hand, Bicycle Parking and Proximity to Restaurants were voted as least important for occupants' well-being.

In the middle, the provision of specific spaces in the building, such a Silent Room, a Breastfeeding Room and Sport Spaces was less valued compared to Socialization Spaces, suggesting that occupants give special importance to social well-being.

3.2 Implicit well-being criteria

This subsection shows the correlation of data from Watson´s Building Well-being Scale and occupants' satisfaction with different aspects of their office environment. Therefore, it allows to identify building qualities and criteria that occupants implicitly relate to their eudaimonic well-being.

The Building Well-being Scale assessed occupants' eudaimonic well-being based on SACRA (Satisfaction, Affect, Competence, Relatedness, and Autonomy) through 22 items on a Likert scale. This multi-item scale produces a single value for occupants' well-being, ranging from 1 to 5.

Tables 2 and 3 display participants' responses to satisfaction with different aspects of their actual workspace. The variables exhibited a normal statistical distribution.

For the quantitative analysis of variables related to occupants' eudaimonic well-being and the office environment, Pearson correlations were employed.

Table 2: Correlation between satisfaction and comfort with the indoor environment and eudaimonic well-being of buildings' occupants.

	Pearson correlation
Job satisfaction	0.521**
Perceived health	0.504**
Overall comfort	0.486**
Perceived productivity	0.453**
Perceived stress	0.213**

** Correlation is significant at the 0.01 level (2-tailed)

Table 2 illustrates the correlations between the multi-item scale of building well-being and variables related to job satisfaction, perceived health, overall comfort, perceived productivity, and perceived stress. As anticipated, the majority of correlations are positive, indicating a consistent alignment between individuals' perceptions of the workplace and the psychosocial factors linked to the building. Notably, stress exhibits a limited correlation with building well-being, suggesting a less pronounced connection in this aspect.

Finally, and to understand which features of the space influence well-being, perceptions of built environment components were correlated with eudaimonic well-being. Interior design and Privacy are single items assessing satisfaction with these aspects. Ergonomics of the workspace comprises satisfaction with Furniture and Space in the desk. Environmental control is a single item addressing satisfaction with the control of window opening, solar shading, thermostat, etc.

Table 3: Correlations between workspace features and eudaimonic well-being of buildings' occupants.

	Pearson correlation
Interior design	0.382**
Privacy	0.327**
Ergonomics of the workspace	0.317**
Environmental control	0.160**

** Correlation is significant at the 0.01 level (2-tailed)

Table 3 shows that Interior Design, Privacy, and Ergonomics of the workspace exhibit a positive and significant relationship with well-being, whereas the control of the environment shows no significant correlation with eudaimonic well-being.

In terms of health, the participants were asked to rate how healthy they felt when they were in the building, on a scale from 1 (less healthy) to 7 (much healthier).

Perceived health showed a high correlation with overall comfort and overall well-being, which is somewhat predictable and suggests that people closely associate the terms health, comfort and well-being. Health showed a higher correlation, but still low, with thermal comfort in both winter and summer than with lighting and noise. It also showed a higher correlation with furniture, interior design and building image.

4. CONCLUSION

Health and well-being in buildings are gaining more attention in times of a climate emergency, where the primary objective is to provide buildings that can keep their occupants healthy. This study contributes to this critical goal by identifying well-being criteria in buildings based on occupants' perceptions and experiences. In addition to the typical Indoor Environmental Quality (IEQ) parameters such as air quality, temperature, lighting, and noise, other aspects are crucial for office workers: security, privacy, connection with nature, universal accessibility, and ergonomics (furniture and desk space).

It is interesting to note the importance that office workers in the country give to Security, which is a local concern that relates to crime and natural disasters. Privacy is gaining interest due to the raise of open plan office layout in detriment of individual cellular offices.

On the other hand, some aspects that have been considered important for occupants' well-being in the literature, such as environmental control and opening windows, are not deemed important for the respondents. This fact can relate to LEED certification criteria that indirectly promotes sealed and fully air-conditioned buildings.

This leads to a final reflection on the challenges that recent rises in global temperature and increasing heat waves events will bring to buildings and society. Buildings will have to prepare to power cuts and heat waves in a much more resilient manner, for occupants' well-being and health.

ACKNOWLEDGEMENTS

This paper is part of the research project Fondecyt Regular 1201456 funded by Agencia Nacional de Investigación y Desarrollo ANID, Chile. The authors would like to thank the research support given by the Research Group on Environmental Comfort and Energy Poverty (+CO-PE) from Universidad del Bío-Bío; and CEDEUS, ANID FONDAP 1523A0004.

REFERENCES

1. Ramanujam, M. (2014). *Healthy Buildings and Healthy People: The Next Generation of Green Building*.

2. Chang, P.-J., & Bae, S. Y. (2017). Positive Emotional Effects of Leisure in Green Spaces in Alleviating Work–Family Spillover in Working Mothers. In *International Journal of Environmental Research and Public Health* V14(7). DOI: 10.3390/ijerph14070757

3. Joseph, R. P., & Maddock, J. E. (2016). Observational Park-based physical activity studies: A systematic review of the literature. *Preventive Medicine*, 89, 257–277. DOI: 10.1016/j.ypmed.2016.06.016

4. Taylor, L., & Hochuli, D. F. (2015). Creating better cities: how biodiversity and ecosystem functioning enhance urban residents' wellbeing. *Urban Ecosystems*, 18(3). DOI: 10.1007/s11252-014-0427-3

5. Ho, D. C. W., et al. (2004). Assessing the health and hygiene performance of apartment buildings. Facilities, 22, 58–69. DOI: 10.1108/02632770410527789

6. Hanc,M, McAndrew, C, & Ucci, M. (2019) Conceptual approaches to wellbeing in buildings: a scoping review, *Building Research & Information*, 47:6, 767-783, DOI: 10.1080/09613218.2018.1513695

7. Collado, S., et al. (2017). Restorative Environments and Health BT - Handbook of Environmental Psychology and Quality of Life Research (G. Fleury-Bahi, E. Pol, & O. Navarro (eds.); pp. 127–148). Springer International Publishing.

8. Mikus, J., & Grant-Smith, D. (2021). Advancing Eudaemonic Design as an Approach to Amplify Health and Well-being in the Built Environment. In *Architecture Media Politics Society (AMPS) Conference: Environments by Design: Health, Wellbeing, and Place*.

9. Zhang, X., Du, J., & Chow, D. (2023). Association between perceived indoor environmental characteristics and occupants' mental well-being, cognitive performance, productivity, satisfaction in workplaces: A systematic review. *Building and Environment*, DOI: 10.1016/j.buildenv.2023.110985

10. Awada M et al (2021). Ten questions concerning occupant health in buildings during normal operations and extreme events including the COVID 19 pandemic. *Building and Environment,* 188. DOI: 10.1016/j.buildenv.2020.107480

11. Hoisington, A. J. et al. (2019). Ten questions concerning the built environment and mental health. *Building and Environment*, 155(March), 58–69. DOI:10.1016/j.buildenv.2019.03.036

12. Altomonte S. et al. (2020). Ten questions concerning well-being in the built environment. *Building and Environment*, 180. DOI: 10.1016/j.buildenv.2020.106949

13. Liu, H, Xu, X, Tam, V, Mao, P (2023). What is the "DNA" of healthy buildings? A critical review and future directions. *Renewable and Sustainable Energy Reviews,* 183. DOI: 10.1016/j.rser.2023.113460

14. Watson, K. (2018). Establishing psychological wellbeing metrics for the built environment. *Building Services Engineering Research and Technology.* Vol 39(2). DOI:10.1177/0143624418754497

15. Trebilcock, M, Soto-Muñoz, J, Wegertseder-Martinez, P, Ramirez-Vielma, R. (2022) Well-being in office spaces from the occupants' perspective: a qualitative approach. PLEA 2022, Santiago.

PLEA 2024 WROCŁAW
(Re)thinking Resilience

Is Service Design the Right Way for Designing with Nature?

A case study on how to design nature-based solutions for resilience.

VIKTOR BUKOVSZKI [1 2], FRANCISCA TAPIA [2 3], LUCA VERESS [2]

[1] Chair for Strategic Landscape Planning and Management, School of Life Sciences,
Technical University of Munich, Germany
[2] Advanced Building and Urban Design Kft, Hungary
[3] Marcel Breuer Doctoral School, Faculty of Engineering and Information Technology,
University of Pécs, Hungary

ABSTRACT: Nature-based solutions (NbS) have emerged in the past years in Europe as critical instruments to achieve climate-resilient cities. Due to their complexity, systemic functioning, contextual embeddedness, and multifunctionality, designing NbS eludes the practice of conventional urban design, architecture, and landscape architecture. This study follows discussions of a participatory design process in Hungary, meeting the standards of NbS scholarship to argue for a new design theory suitable for NbS. Using a grounded theory approach, it is presented that concepts and principles of service design was ubiquitous in the sampled design process, even though the service design framework was never explicitly used. The experiences are leveraged to argue that adopting service design would create a shared language for participatory design, prime designers to apply a systems perspective, and integrate operational requirements from early design phases – all of which are pertinent to overcome the design challenges stemming from NbS complexity. The contribution of this study is providing case evidence for a service design approach to NbS design.
KEYWORDS: Nature-based solutions, Service design, Co-design, Ecosystem services, Design theory

1. INTRODUCTION

Nature-based solutions (NbS) are critical components in hybrid engineered-ecological systems of adaptation for climate-resilient cities. NbS leverage biophysical, biochemical, and ecological processes to perform as in an urban green-and-blue infrastructure. Furthermore, they perform more than one function, in fact, the same NbS can serve different roles simultaneously, for example offering nutrients, regulating urban water cycles, filtering air from pollutants [1]. Furthermore, as they become large, city-shaping features, often public, semi-public spaces, their distribution, and design have a justice aspect, and it is critical to subject them to participatory planning and governance [2].

Of the several barriers hindering NbS uptake, informational barriers are critical. A general lack of information and high degree of uncertainty on NbS performance and design persists [3]. Despite multiple cycles of research projects, NbS knowledge appears unable to penetrate from academic discourse. In practice, NbS are designed by architects, landscape, or urban designers, overseen by public institutions prone to fragmentation of responsibilities. This does not only limit the value and novelty to be captured from NbS [4], but also hinders long-term maintenance, crucial for NbS performance [5]. In short, while NbS researchers highlight the complexity of their object, stemming from multifunctionality, systemic nature, and the need for participation, NbS production is stuck on conventional planning practices led by siloed departments [6].

The objective of this study is to identify a conceptual framework for integrated design process that accounts for NbS complexity and has the potential to bridge the gap between academia and practice. Thus, our research question is how should an NbS design problem be conceptualized to afford effective discourse in a participatory design process?

The research question can be translated to the selection of an appropriate design theory to be fit for integrated and participatory NbS design. This is an ambitious goal, and a definitive answer is beyond the possibilities of this study. What is presented here is an argument to the pertinence of one design theory: service design. Service design is a theory where the design object is one or multiple service(s), and the design discourse is centred around experiences and interactions between the service provider, the service itself, and the user [7]. Our hypothesis is that service design offers the conceptual framework for answering the research question.

2. MATERIALS AND METHODS

2.1 Methodology: grounded theory

To ascertain whether service design provides an adequate conceptual framework for NbS design, we rely on a grounded theory approach, that is, the

systematic coding of qualitative data to arrive at concepts, categories, and eventually, a theory [8]. However, the result of the process in this case is not the development of a new theory, but evidence whether service design is a viable theory for NbS design. The research question is answered by matching the concepts emerging from the grounded theory analysis with concepts of service design.

The data of the study comes from the joint participatory design of two NbS projects, a public park and a nearby schoolyard in the town of Szombathely, Hungary – meaning the findings are not generalizable. The project consisted of a four-part workshop series organized by an international research consortium, with local expert and layperson stakeholders, focusing on: (1) strategic placement of the NbS, and identification of objectives, (2) conceptual programming and design of the NbS, (3) critical evaluation of NbS concept alternatives, and (4) specification of monitoring indicators. What makes this project a suitable case study is that each workshop was preceded by internal discussions of the project team – a single municipal department and commissioned experts – with the exact same scope. The workshop series models a holistic approach, managed by NbS researchers, whereas the internal discussions model a conventional green space development project. The coding itself relies on memos, contents created by workshop participants, and written observations.

2.2 Conceptual framework: service design

The main tenet of service design is a shift from putting material artefacts and goods as the object design to services, originating from a wider service shift in the areas of marketing, economics, engineering, and management [7]. Service is the core concept, which is defined by a set of common characteristics (Figure 1). Most importantly, Shostack's tangibility continuum is used to distinguish goods from services. Anything of value can be described as an interconnected bundle of components, and the dominance, with services being more intangible than tangible [9]. Second, services, though intangible, are encountered through tangible, material experiences, also called evidence [10], service encounters [11], or touchpoints [12], either essential or peripheral to the service. Third, a service does not exist autonomously and continuously, rather it is co-produced by service users and providers in lived, embodied performances in staged environments [13]. This means each service is unique – to an extent – to the actors and context in which it plays out. Finally, due to all the above, activities of a service are split into a domain of interface, where exchange takes place, and a domain of infrastructure, which facilitates it [7]. The service shift in essence is expanding the focus of design from the infrastructural with the interface.

The service characteristics paint a different design practice, which has not yet seeped into all design fields [7]. It calls for a multidisciplinary practice integrating applied behavioural sciences (e.g., marketing), technological expertise (e.g., ICT), and a design field (e.g., graphic design) that allows simultaneous design of material elements and intangible interactions [14]. During service design, the starting point is the service outcome, which helps identifying evidences or touchpoints, where material arrangements can be made [10]. A service outcome can be anything of value for the user, can be tangible or intangible, lasting or temporary. Service outcomes are co-produced with users, as long as the service prerequisites, the necessary resources are in place [15]. What is in control of the designers, is to (1) describe the core and supporting services as the service concept that addresses real user needs, (2) imagine a realistic model of unique user processes as a set of actions that generate service outcomes, and (3) specify the service system, i.e., the resources necessary for the service process to materialize. These three areas form the three main tasks of service design (Figure 1).

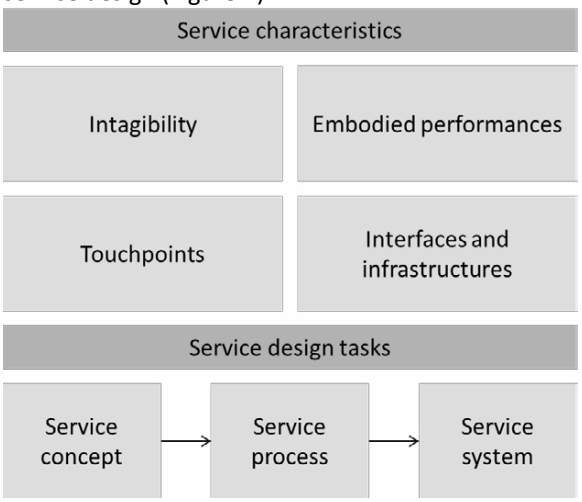

Figure 1: Service design conceptual framework

Each of the three design tasks require a different language. When formulating service concepts, discussions focus on values, form and function, experiences, the service outcomes [16]. Behavioural sciences are used to argue for or against a service concept, evaluating them in terms of perceptions, pleasure, flow of time, memories [17-18]. User processes on the other hand are input-output models, with a flow of user-based and operational activities [19]. They are usually drawn up as scripts, and the main success factor is the fidelity of the design script to the user scripts [20]. Finally, the service system includes the service prerequisites to facilitate the service, including staff, physical and

technical environments, organisational and control activities; and the users themselves, described by their knowledge, capabilities, scripts, and states of mind [15]. The service defines the roles users, staff, and the provider organization assume, and a good service system optimizes their relationships for efficiency, satisfaction, perceived control, and autonomy [13]. The ultimate guiding principle of design is the performance of the service system during the service process. What should happen in broad terms during an encounter with a service is broken into how it should happen in more detail, which provides performance standards for design. Better descriptions of sub-processes are the ones that are more easily relatable to design dimensions, and better fitting to evaluate solution alternatives [19].

3. RESULTS AND DISCUSSION

The results show that the discourse during the workshops bears the hallmarks of the service design framework. In this section, we present the clearest examples of each concept introduced in section 2.2 and opine how this might influence NbS design.

2.3 Identified service design concepts.

Most notably, the workshop discussions reproduced Shostack's **(in)tangibility** continuum and evidence concepts. Stakeholders tend to describe NbS as a sequence of tangible and intangible offerings, where the intangible ones are evidenced by a tangible clue. Places to sit, somewhere to go with a dog, things children can do outside, and protection from traffic noise came up among intangible components, but tangible items, like chess boards, playgrounds, and flower beds were also mentioned. When pressed for what they imagine, intangible components like places to sit were tied to different shreds of evidence, like stone benches or wooden platforms. Landscape designers have a crucial role in decoding intangible experiences to a variety of tangible elements in an open dialogue. For example, during the workshops, the intangible need to interact with nature more than just looking at it was first translated to a rerouted river with aquatic playground elements, then to a barefoot thematic and educational pathway in the schoolyard (Figure 2).

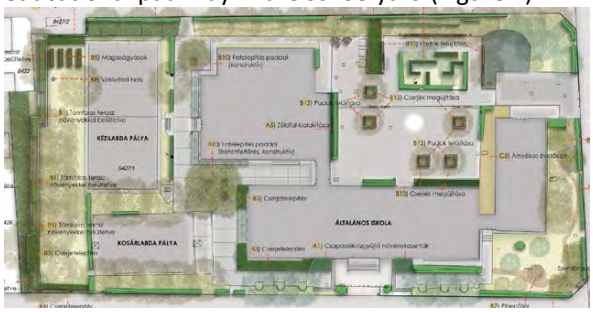

Figure 2: Concept design for the schoolyard. Educational pathway is in the bottom right, the vegetable garden is in the top left corner.

Exposure to users from the start also nudged the designers to think less in terms of design visions are more in terms of **user processes**. For most design choices, like a Miyawaki microforest (Figure 3), and Tetris-style modular benches, the designers had to prove their utility while talking about how it would be used. Specifically with the modular benches, the issue of vandalism came up, conflicting some user scripts of damaging the furniture with the idealized designer scripts of creatively rearranging them. The participatory design sessions led to a gradual shift from rationalizing design choices by adherence to a design narrative, towards by telling stories of what people will be able to do. For example, the designers were instructed earlier to include rainwater harvesting, because it fits the NbS narrative. However, this feature was later evaluated by its ability to reduce maintenance costs by providing irrigation water. It also meant that the designer's attention naturally shifted from the infrastructural to towards the interface domain of their designs.

Figure 3: Concept design for the small park. Miyawaki micro forest is in the top, the river on the right side.

Another notable shift was a better representation of the maintenance perspective. Both the school director and the municipal green space management representatives signalled their inability to operate costly and complicated solutions. For all core components of the interventions, there was an ongoing brainstorming on how to link the exploitation of the new green spaces to distributing maintenance duties. For example, the school received vegetable

gardens, the most popular solution, specifically because they would be tended to by a children's cooking club (Figure 2), whereas a resident with carpentry experience expressed interest in teaching others how to protect timber structures in the small park. This line of discussion fits the design of the **service system**, assigning roles and resources not simply for the upkeep of physical elements (like the timber structures), but specifically to sustain a service (vegetables for the cooking class). The workshop addressed the importance of service system elements, including user competencies, staff competencies, organizational activities, and technical environments. In the schoolyard, elements like the skills of the students, teachers' available time, cooking class schedules, and raised vegetable beds were prioritized. The system also includes educational activities, for which the garden was designed for. No physical element was confirmed before considering maintenance. Aside from landscaping, the design also included the coordination between the school board and director for the organisation of training and planting workshops, the engagement of students, especially teenagers, through diverse activities such as art calls and outdoor events, and the crucial involvement of parents in weekly tasks like watering and planting. One observation included the necessity to broaden the range of activities beyond mere planting workshops. The prospect of implementing such diversified activities on a medium-term basis was considered, with the potential of functioning as an exemplary project for other educational institutions.

An interesting element of the local service system discussed was the role of local fauna, particularly beavers, that ascend rivers and damage trees in public parks. This topic emerged during a workshop with local water authority representatives. In service design, understanding the context isn't just about producing immediate solutions, but fostering relationships between various actors that could influence the transition from the current to future states. This principle implies that actors, even non-human ones like beavers, are integral to the system model. As Kimbell (2010b) asserts, design for services focuses on the relationships between elements and actors within systems, rather than the objects themselves [21]. Consequently, the boundaries of design become blurred, necessitating considerations beyond the intervention site. These include beaver habitat protection efforts, culling policies, and broader ecological relationships. Thus, non-human users also become part of our service system model.

3.2 The value of service design

While service design was not a guiding principle for the design process, the presence of related concepts offered a glimpse into the benefits of explicitly applying the service design framework. In our opinion, the three most important benefits are: (1) having a common language between laypeople and various experts involved in participatory design; (2) introducing a system thinking mindset to the design process, (3) consciousness of operational requirements in early design phases.

The workshops diverted discussions very soon from technical problems to understanding who was involved in the functioning of the NbS, who the users are and what are their needs. This is exactly the starting point of Shostack's service blueprinting, and subsequently every service design [10]. Understanding the users and their perspectives helped guide the formulation of problems and evaluation of design solutions, focusing on interface elements and user experiences. Additionally, the use of service design aids in the development of new services and understanding of user needs. It highlights the significance of adding new functionalities and actors in the NBS context during a service's operational lifetime to assess quality and identify necessary redesigns.

On the one hand, NbS are infrastructural components, managing rainwater, modulating the microclimate, mitigating environmental pollution and hazards. On the other hand, they are interfaces, providing irrigation water, sheltering from summer heat, and dampening traffic noise. Discussions in terms of user processes not only provide useful information for designers to make better choices but also raise the awareness and approval of NbS – a concept unheard of in the study city before the workshops.

Service systems are of particular value for NbS design, given how they also function as systems embedded into larger systems themselves. Conventional landscape architectural practice does not routinely capture the different larger systems suggested by the different NbS roles. For example, it is not common in Hungary for a landscape architect to conduct microclimate simulations to see how specific green and blue arrangements influence outdoor comfort through shading, wind patterns, and evapotranspiration. Similarly, the project team did not consider beavers as potential hazards for trees.

Much like a service, an NbS is an embodied performance of human and non-human actors, not a set of tangible objects with clear boundaries. Adopting service design primes the designers to start asking questions about the systems at play and involve the necessary disciplines as soon as possible.

Finally, talking about user processes and expected benefits, and experiences opened the possibility to discuss NbS operation, use, and maintenance even before the first design concepts emerged. If

embedded into urban infrastructure, the importance of urban greens increases, and the different infrastructural roles prescribe different quality requirements landscape architects may not yet routinely consider. For example, a sedimented bioswale is not only an eyesore, it also impedes runoff reduction. Each of these NbS roles can be reformulated in the language of services, and having operational expertise from public utilities represent the customers would guarantee that a service design approach to NbS systematically responds to diverse operational requirements.

4. CONCLUSION

The research question inquires on an appropriate design theory to conceptualize NbS in a participatory design process. Appropriateness in this sense means that it affords effective communication among designers and stakeholders. According to our case study contrasting conventional and NbS literature-compliant design processes, service design is one possible answer. This is demonstrated in the presence of service design concepts in the holistic, research-led, and participatory design process, as opposed to its absence in the conventional, siloed, linear approach.

The novelty of this study is in suggesting that a grounded theory of NbS design may coincide with service design. The suitability of service design for NbS has not yet been proven – to the knowledge of the authors. The significance of linking an existing, well-known design theory lies in the opportunity that mature concepts, methodologies can be relied on to deliver NbS, meeting the standards of the NbS literature. This allows designers not so close to the research of NbS to engage in NbS, as opposed to conventional landscape projects. More case studies in different contexts, and different NbS types would reinforce this claim, while a dedicated methodology of service design of NbS is warranted to deductively test the suitability of the theory – since grounded theory is an inductive method.

Critical reflection on the way NbS is designed in its best practices is essential to identify design theories that open the process to more practitioners. It would be interesting to see if other design theories could be interpreted from ongoing research projects, and how different NbS they would produce. The link between design and improvement in services is frequently tied to its cross-disciplinary character. When we consider NbS, service design boosts the exchange of information among stakeholders, organizations, and local communities. Implementing service design from the outset is a fluid process. It fosters ongoing innovation among varied groups in ever-changing scenarios. Adopting service design, or other proven design theories could lead to a systematization of designing NbS, accelerating their widespread integration into urban systems, and contributing to improved urban resilience.

ACKNOWLEDGEMENTS

The project (JustNature) leading to this submission has received funding from the European Union's Horizon 2020 research and innovation programme under grant agreement No 101003757.

REFERENCES

1. Calheiros, C. S. C., & Stefanakis, A. I. (2021). Green Roofs Towards Circular and Resilient Cities. Circular Economy and Sustainability, 1 (1), 395–411. https://doi.org/10.1007/s43615-021-00033-0
2. Broto, V. C., Allen, A., & Rapoport, E. (2012). Interdisciplinary Perspectives on Urban Metabolism. Journal of Industrial Ecology, 16(6), 851–861. https://doi.org/10.1111/j.1530-9290.2012.00556.x
3. Kabisch, N., Stadler, J., Korn, H., Bonn, A., Frantzeskaki, N., Pauleit, S., Naumann, S., Davis, M., Artmann, M., Haase, D., et al. (2016). Nature-based solutions to climate change mitigation and adaptation in urban areas. Ecol. Soc., 21.
4. Davis, M., & Naumann, S. (2017). Making the Case for Sustainable Urban Drainage Systems as a Nature-Based Solution to Urban Flooding. In Nature-Based Solutions to Climate Change Adaptation in Urban Areas: Linkages between Science, Policy and Practice (pp. 123–137). Cham, Switzerland: Springer International Publishing. https://doi.org/10.1007/978-3-319-56091-5
5. Wamsler, C. (2015). Mainstreaming ecosystem-based adaptation: Transformation toward sustainability in urban governance and planning. Ecol. Soc., 20.
6. Sarabi, S., Han, Q., L. Romme, A.G., de Vries, B., & Wendling, L. (2019). Key Enablers of and Barriers to the Uptake and Implementation of Nature-Based Solutions in Urban Settings: A Review. Resources, 8, 121.
7. Secomandi, F., & Snelders, D. (2011). The Object of Service Design. Design Issues, 27(3), 20–34. https://doi.org/10.1162/DESI_a_00088
8. Walker, D., & Myrick, F. (2006). Grounded Theory: An Exploration of Process and Procedure. Qualitative Health Research, 16(4), 547–559. https://doi.org/10.1177/1049732305285972
9. Shostack, G. L. (1977). Breaking Free from Product Marketing. Journal of Marketing, 41(2), 73–80.
10. Shostack, G. L. (1984). Designing Services That Deliver. Harvard Business Review, 62(1), 133–9.
11. Cook, L. S., Bowen, D. E., Chase, R. B., Dasu, S., Stewart, D. M., & Tansik, D. A. (2002). Human issues in service design. Journal of Operations Management, 20, 159–174. https://doi.org/10.1016/S0272-6963(01)00094-8
12. Mager, B. (2008). Service design. In M. Erlhoff & T. Marshall (Eds.), Design Dictionary: Perspectives on Design Terminology. Basel: Birkhäuser.
13. Gallouj, F., & Weinstein, O. (1997). Innovation in Services. Research Policy, 26, 537–56.
14. Moritz, S. (2005). Service design. Practical access to an evolving field. http://stefan-moritz.com/welcome/Service_Design_files/Practical%20Access%20to%20Service%20Design.pdf. Accessed 10 Dec 2023.

15. Edvardsson, B., & Olsson, J. (1996). Key Concepts for New Service Development. The Service Industries Journal, 16(2), 140–64.
16. Clark, G., Johnston, R., & Shulver, M. (2000). Exploiting the service concept for service design and development. In New Service Development: Creating Memorable Experiences (pp. 71–91). SAGE Publications, Inc. https://doi.org/10.4135/9781452205564
17. Ariely, D., & Carmon, Z. (2000). Gestalt characteristics of experiences: The defining features of summarized events. Journal of Behavioral Decision Making, 13, 191–201.
18. Roese, J. N., & Olson, J. M. (1995). Counterfactual thinking: A critical overview. In J. N. Roese & J. M. Olson (Eds.), What Might Have Been: The Social Psychology of Counterfactual Thinking (pp. 1–56). Lawrence Erlbaum Associates, NJ.
19. Ramaswamy, R. (1996). Design and Management of Service Processes: Keeping Customers for Life. Reading, MA: Addison-Wesley.
20. Stewart, D. M., & Chase, R. B. (1999). The impact of human error on delivering service quality. Production and Operations Management Journal, 8(3), 240–263.
21. Kimbell, L. (2010b). "Service-dominant logic and design for service."Touchpoint, 1(3), 23-26.
22. Stickdorn, M., & Schneider, J. (2012). This is service design thinking: Basics, tools, cases. John Wiley & Sons.

Indoor temperature in Mediterranean traditional homes

High thermal mass and occupant behaviour

ELISABETTA MARIA PATANE'[1], SUKUMAR NATARAJAN[1], DAVID COLEY[1]
[1]University of Bath, Bath, United Kingdom

ABSTRACT: Traditional Mediterranean homes are known for their passive cooling strategies, relying on natural ventilation and high thermal mass envelopes. However, climate change and occupant behaviour challenge their efficacy. This study explores the real-world interaction between thermal mass and occupant behaviour in three existing dwellings: two traditional heavyweight, one modern mediumweight. Indoor air temperature was longitudinally monitored in 27 rooms of nine apartments from April 2018 to May 2019. 68 questionnaires captured 12 residents' behaviours and thermal perceptions during the same period. T-Tests and Mann-Whitney U Tests were used to estimate the statistical significance of the comparison. Traditional construction consistently maintains cooler temperature due to higher thermal mass, smoothing indoor temperature peaks and reducing fluctuations from solar gain and human activity. Prolonged window opening for ventilation in summer minimizes the passive cooling effect. High thermal mass homes were found comfortable at lower temperatures, and occupants wear more clothing insulation than those in the other existing building. The study suggests the potential of traditional buildings for climate change resilience, future research needs to tackle building and occupant interaction in extreme conditions such as hot summers and/or during heatwaves.
KEYWORDS: Thermal mass, Adaptive Comfort, Residential

1. INTRODUCTION

Traditional Mediterranean homes, constructed with dense materials like stone, clay, or earth in thick walls and horizontal structures, are renowned for their high thermal mass [1]. Empirical evidence extensively demonstrates that these stone buildings remain cool during summer, with temperatures often falling within comfortable ranges without the need for air conditioning [2,3]. Research by [4] further illustrates the impact of thermal mass through simulations, indicating that even a small alteration, such as replacing a masonry stone external wall with a cavity one (transitioning from high to medium thermal mass), can lead to a significant increase in peak hourly temperatures in summer days.

Nighttime ventilation associated with high thermal mass buildings is a strategy widely implemented in buildings for energy saving and thermal comfort [5,6]. The heat stored in the envelope mass during the day is discharged at night when outdoor air is cooler. Research by Givoni et al. [7,8] in desert and arid regions highlights that this strategy is the most efficient when the summer diurnal temperature variation falls between 15–20 °C, with maximum daytime temperatures ranging from 30 to 36 °C. Similarly, Shaviv et al. [9] observed the benefits of this approach in a hot and humid Mediterranean climate, where the typical diurnal temperature variation is around 7 °C. They found that night ventilation coupled with high thermal mass can passively reduce room temperatures by 3 to 6 °C during the summer months.

Currently, Mediterranean cities face the detrimental impacts of climate change. Elevated nighttime temperatures and more frequent heat waves contribute to decreased diurnal outdoor temperature variations, reducing the efficacy of night ventilation and high thermal mass. The risk of long-term overheating in high-thermal mass buildings increases when there is no mechanism to dissipate absorbed heat during the day [10]. Similarly, insufficient ventilation and indoor heat generation from occupant behaviour can further impede the cooling capacity of high thermal mass envelopes. However, no study has previously addressed these conditions in a real-world experiment. Therefore, it is crucial to assess the vulnerability of traditional homes to climate change, by empirically observing their thermal performance and occupant comfort and behaviour.

This study investigates the dynamic interaction between buildings and occupant behaviour in a real-world case study set in the Mediterranean region, where traditional buildings are constructed with stone and rely on natural ventilation. Understanding the thermal performance and occupant behaviour in this context is important as the Mediterranean region is one of the world's most densely populated areas and is particularly vulnerable to the effects of climate change. As a result, homes in this region may undergo retrofitting with energy-intensive systems to adapt to climate change.

The primary objective of this study is to assess the actual thermal conditions through longitudinal measurements of homes with diverse thermal mass envelopes. Additionally, the study aims to survey occupant comfort and behaviour to comprehensively evaluate the building's performance. The research questions addressed are as follows:

(1) Does the envelope thermal mass difference affect air temperatures when rooms have no internal heat gains and windows are closed?

(2) Does the envelope thermal mass difference affect air temperatures when rooms are occupied?

(3) Does occupant activity and overall comfort change when living in traditional high thermal mass homes compared to other existing buildings?

1.1 Case Study

Catania is a coastal Mediterranean city whose climate is classified "Csa" according to the Köppen Climate Classification ("hot dry-summer" - Mediterranean Climate). Catania's yearly average temperature is 17.5°C. August is the hottest month and historical peak temperature are at 26.2°C. The historical daily variation is between 7-20°C, sourced from the Sigonella Airport weather station stored in "SIAS - Servizio Informativo Agrometeorologico Siciliano". These climatic conditions can maximize the cooling potential of night ventilation and high thermal mass. These conditions maximize night ventilation and thermal mass cooling potential. Catania, with 311,584 residents in 182.90 km^2, is prone to urban heat island effect. The city is surrounded to the north by the Etna volcano whose eruptive activity has provided the basalt stone for centuries. Today, the basalt stone is still among the most used construction materials locally.

Figure 1 shows the case study dwellings. They are all located less than 2 km from the historical city centre. Two dwellings were built before the 1960s. In this time, basalt stone was the main material for load-bearing walls, while the horizontal construction is shielded by a decorative false vault that hides the thermal mass of the structure. The third dwelling was built after 1960s when structures were made of concrete and walls with clay hollow bricks. The U-value and the thermal mass classification are widely discussed in the [2]. The traditional dwellings have a heavyweight construction (following the ISO 52016-1:2017 classification), while those built after the 1960s were classified as mediumweight construction. TM2 and TM1 were used as bespoke labels to identify the two traditional buildings (Thermal Mass 2 – TM2) and TM1 for the rest (Thermal Mass 1 – TM1).

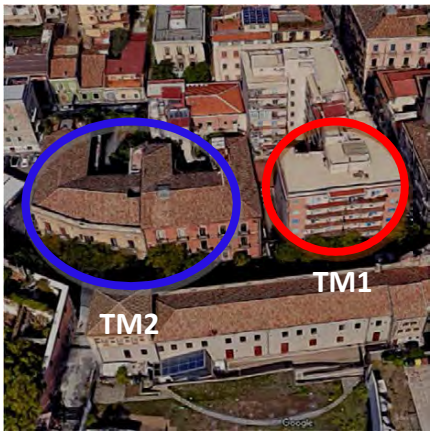

Figure 1: Case study buildings: TM2 (left – traditional high thermal mass buildings) and TM1 (right – modern medium thermal mass building).

2. METHOD

Pairwise tests in a simulation environment were developed to assess the effects of thermal mass under different ventilation models of [11] on room temperature. The baseline case was the TM2, validated against longitudinal measurements of room and surface temperatures. The latter helps to identify the active surface in the heat transfer of a high thermal mass envelope. The infiltration rate was used as a calibration parameter. The methodology has been extensively discussed in [4] study. A change from heavyweight to mediumweight construction was applied on a single external wall. This test was important to establish the role of thermal mass in the overall heat balance of a room in a worst case scenario: when windows are opened and when an external wall thermal mass with a high glazing ratio is reduced. Early simulation results (discussed in section 3.1) showed a significant impact of thermal mass changes on room temperature also when windows were opened, which led to the implementation of the monitoring and survey campaign.

The room air temperature (T_a) was longitudinally monitored in 27 rooms in nine apartments from the 4th of April 2018 to the 1st of May 2019. Four apartments were in the TM2 buildings and three in TM1. The number of apartments monitored was in total 50% of the total number of apartments in use, therefore those selected were considered representative of the case study. The instruments used for the monitoring were the stand-alone IButton sensors. Each apartment was equipped with three IButtons monitoring: a living/kitchen room, a bedroom, and a low-occupied/unoccupied room simultaneously. Living and kitchen rooms as well as unoccupied rooms are exposed to the south, while bedrooms are exposed to the north. The consistency in the space layout across the sample facilitated the implementation of the pair-wise comparison in field settings.

A total of 12 residents aged between 40 and 70 were surveyed and a total of 68 questionnaires were

collected. The survey revealed that the heating system is extensively used from January to March. As the study intends to picture naturally ventilated conditions, this period was excluded from the sample. Meanwhile, the survey revealed also that ACs are rarely used and often just to cover the hottest hours of the day. Therefore, the ACs equipped rooms were kept as part of the sample. Residents, who were likely to influence environmental changes because they spend long hours at home, were surveyed. Each resident completed a questionnaire every two months. The questionnaire design adapted this work [12] to the local practices and building properties (i.e. AC use and Shading). The questionnaire comprises three sections: context, subjective environmental assessment, and pattern of behavior. The context section gathers data on time, date, weather conditions, occupancy, clothing levels, and metabolic activity. The subjective environmental assessment gathers data on concurrent thermal sensation, preference and acceptability, and overall comfort, including aspects such as acoustic, air, and light comfort. The pattern of behaviour section gathers data on window, shading, heating, fan, and AC usage; as well as personal adaptive actions such as consuming warm food or wearing additional clothing. The total number of questions were 63, some answers were reported into a numerical scale (7-point ASHRAE 55 scale for thermal votes), 5-point frequency scale (never, rarely, sometimes, often, always).

The data was then grouped into TM2 and TM1 the continuous normally distributed data (e.g. room air temperature) was analyzed through T-Test comparison; while ordinal data (frequency scores) through the Mann-Whitney U Test for non-normally distributed data. The statistical comparison is significant when the p-value is lower than alpha which is set at 0.1. When a significant difference is observed between the two groups, it indicates that they are independent from each other, thereby establishing evidence of the effects of high thermal mass on rooms and people.

3. RESULTS AND DISCUSSION

This section explores the early simulation tests results (3.1) and the outcomes of longitudinal monitoring and survey campaigns (3.2-3).

3.1. Pairwise Comparison

The model in [4] was used to compare the two different thermal mass levels and their effect on indoor temperatures. The study demonstrates: (i) reducing the thermal mass of a single external wall raises peak temperatures. Here, the sensitivity of (i) to different ventilation modes and prolonged exposure to summer heat is shown in Figure 2. The daily maximum and mean air temperatures were simulated over a summer under different ventilation modes as per [11], and the temperatures were subtracted to the lower thermal mass case scenario (TM1 - cavity wall). All ventilation modes are insufficient to achieve the same relative temperature advantage when windows are closed or opened at night. This underscores the importance of examining occupant behaviour in real-world scenarios, as night ventilation may not always be practical, and opening windows could impact the effectiveness of thermal mass.

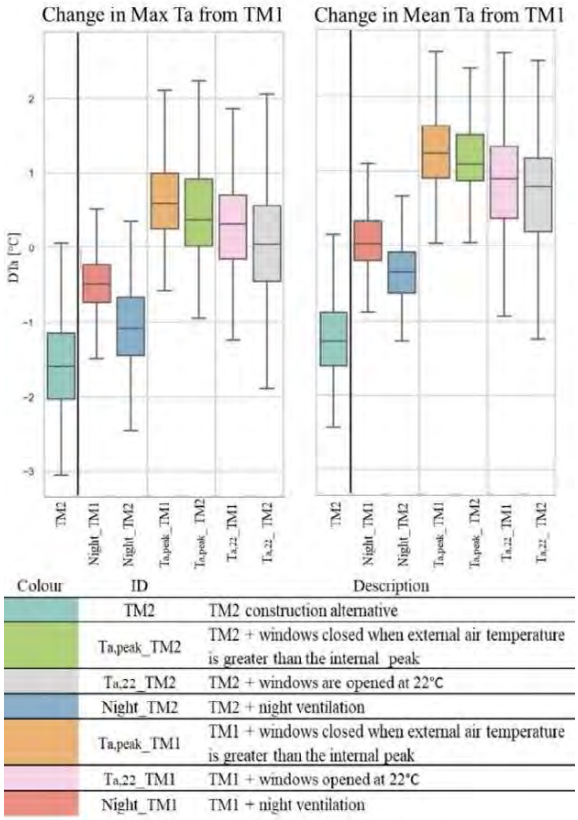

Figure 2: Change in maximum and mean hourly indoor air temperature (T_o) from the base wall model TM1

3.2. Room temperatures

Only unoccupied rooms were selected to validate the simulation results in a real-world setting. Given the absence of internal gains and windows being closed, the observed conditions are predominantly influenced by the thermal mass effect of the building envelope.

Table 1 presents the hourly distributions of unoccupied room temperatures for each season. TM2 rooms exhibit significantly cooler temperatures than TM1. The maximum difference is about 4 °C observed in Autumn. Given the absence of internal gains and windows being closed, the observed conditions are predominantly influenced by the thermal mass effect of the building envelope.

Table 1: t-test results (t and p-value) between room groups of hourly temperature distributions (T_o) for each season

Season	T_a (°C)		t	p-value
$T_{external}$ (°C)	TM2	TM1		

Spring 19±4.2	22±0.7	22.6±0.5	-17	<0.1
Summer 28±3.5	27±1.7	28±1.4	-23	
Autumn 23±2.0	20.7±2.0	24±1.0	-57	
Winter 15±2.8	18.3±1.7	18.9±1.8	-10	

Figure 4 and Figure 3 depict the hourly temperature distribution of bedrooms and living/kitchen rooms. Mean temperatures in both living/kitchen and bedrooms are higher than those in the unoccupied rooms, with the highest mean observed in the living/kitchen rooms. This temperature difference is attributed to internal heat gains. Peak occupancy and peak solar gains occur around lunchtime for living/kitchen rooms as surveyed (Table 2). These rooms remain exclusively reliant on natural ventilation throughout the monitoring period, a factor that, in conjunction with heat gains, contributes to the observed variations in temperature distribution. Bedrooms serve as a means of ventilating the apartment during the daytime, as indicated in Table 4. Moreover, during the summer season, they are actively used for artificial cooling through air conditioning (AC). Notably, the data in Table 3 reveals that AC usage in bedrooms occurs more often during midday than at night suggesting a strategic cooling approach. In autumn, bedrooms have the largest temperature range which is likely attribute to cooler outdoor temperatures (4.7±1.51 oC cooler outdoor temperatures on average – Table 1) and shorter window's opening.

Table 2: Occupancy profile derived from survey data.

	Occupancy in Living/Kitchen		
	Weekday		Weekend
	06 - 16:00	20 - 23:00	
Mean duration in hours	1.6±1.2**	3	
Physical Activity	Light*	Sedentary*	
Presence	Often*	Always*	Often*

** the total number of observations is higher than 90%*
*** covers lunchtime duration*

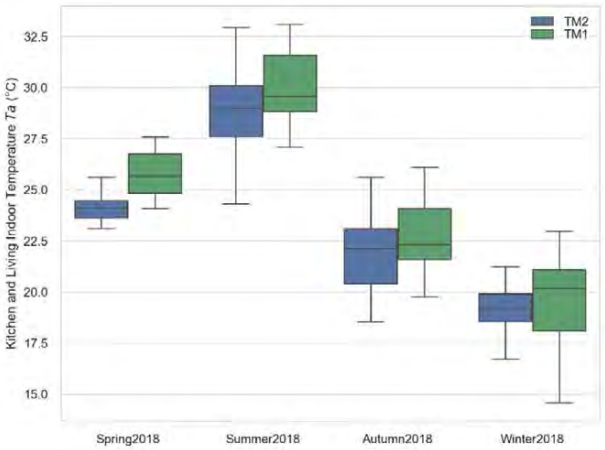

Figure 3: Distribution of hourly living/kitchen air temperature

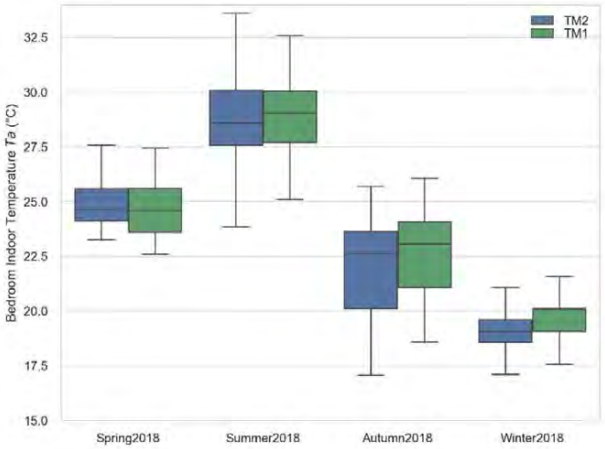

Figure 4: Distribution of hourly bedroom air temperature

Table 3: AC recorded use in Bedrooms.

AC use in Bedrooms		
		Frequency
Mean Setpoint	23 ±1.8°C	
Start and end time	12 - 16:00	Sometimes*
	19 - 23:00	Rarely*

**the total number of observations is higher than 90%*

Table 4: Window's recorded opening use.

	Window's opening	
	Other seasons	Summer
Mean opening duration	1.4±0.15 hours	All day
Start and end time	08-10:00	08-23:00
Rooms used for ventilation	Bedrooms and living/ kitchen rooms*	

**the total number of observations is higher than 90%*

TM2 living/kitchen rooms are significantly cooler than in TM1. Even though living/kitchen rooms are subject to higher solar gains during these seasons, TM2 can rely on more thermal mass to delay daily peaks and absorb excess heat. The temperature distribution in TM1, on the other hand, reflects higher temperatures and greater variability. In contrast, bedrooms, primarily used for natural ventilation and

artificial cooling experience a less pronounced thermal mass effect.

3.3 Thermal adaptation

Thermal sensation votes were grouped by thermal mass levels and outdoor mean running temperature. The average seasonal thermal sensation votes were plotted against the ASHRAE 55 Adaptive thermal comfort model. The mean operative temperatures were derived from the longitudinal measurements of room temperatures and assuming the air speed is below 0.1 m/s.

Figure 5 shows that in winter, TM2 occupants feel warmer than those in TM1. As TM2 room temperatures were significantly lower than those in TM1, this finding highlights a form of thermal adaptation to indoor conditions in high thermal mass buildings. Below 20°C operative temperature, TM1 occupants feel "cold -2" and TM2 feel "slightly cool -1". Furthermore, at 15 °C outdoor running mean temperature, both groups feel "neutral 0" at a much lower temperature than the one specified by the Adaptive Model. The personal adaptive strategies shown in Table 6, reveal that the occupants in TM2 are more likely to use an additional blanked and wear more clothes in winter than those in TM1 buildings.

Interestingly, the summer mean thermal sensation vote did not differ significantly between TM2 and TM1: they both feel "neutral 0" at about 28°C operative temperature. This consistency may be attributed to the practice of prolonged opening of windows in summer which predominantly influences the thermal sensation over the thermal mass effect.

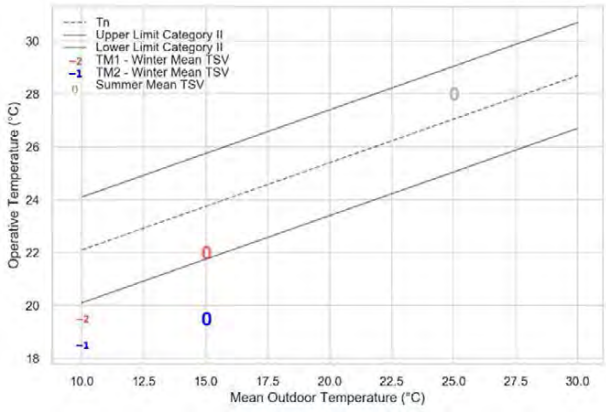

Figure 5: Group Mean Thermal Sensation Vote (TM2 group – blue, TM1 group – red), plotted against the ASHRAE 55 Adaptive Thermal Comfort Model.

Table 6: Frequency scores for the following actions: additional blanket, wear more clothes and windows closed; the comparison between TM2-TM1 via Mann-Whitney U Test.

	No per Score					
	Additional Blanket		*Wear More Clothes*		*Window closed*	
	TM2	TM1	TM2	TM1	TM2	TM1
Never		1		3	1	
Rarely		2				
Sometimes	2	1	2			
Often	5	1	4		5	2
Always	1				1	3
	Mann-Whitney U Test					
U	5.06		6.17		2.78	
p-value			<0.1			

4. CONCLUSION

This study aims to evaluate the passive cooling effectiveness of high thermal mass in traditional buildings compared to medium-weight modern constructions. What distinguishes this comparison is its reliance on real measured data and the integration of occupant behaviour and thermal sensation. As a result, it marks the first comprehensive assessment of traditional Mediterranean homes and their occupants.

The results demonstrate that rooms in traditional buildings consistently maintain cooler temperatures throughout the year, even those with high internal gains like living/kitchen spaces. The higher thermal mass of the traditional envelope appears to play a key role in smoothing indoor temperature peaks caused by solar and internal gains. Bedrooms' temperatures are slightly different as heat gains are limited and windows are used for ventilating the apartment during the day. In summer, the duration of windows opening is excessive as it is opened for all day. This undermines the temperature difference between thermal mass groups. Therefore, the ventilation strategy needs to be addressed and optimize the thermal mass effect.

In winter, the occupants in traditional homes are thermally neutral at lower operative temperatures compared to those in modern homes. They often add extra clothing insulation, even while sleeping, and tend to close windows more frequently. On the other hand, the thermal sensation in summer for both groups reflects the ASHRAE 55 Adaptive Comfort Model. This result shows that the effect of natural ventilation is more significant than the thermal mass difference in summer.

The methodology presents a noteworthy limitation which is the small number of returned answers. This incomplete response pattern poses a potential source of bias in the analysis, as the missing data could impact the comprehensive understanding of occupant behaviours and perceptions. To address this in future research, design fewer but essential questions could help mitigate this limitation.

Passive cooling features such as high thermal mass and natural ventilation offer viable solutions in existing homes but require optimization. Retrofitting with active systems to compensate for inefficient behaviours, as excessive summer ventilation, risks increasing energy bills. Therefore, careful consideration and occupant engagement with passive

cooling strategies are essential to ensure energy-efficient and sustainable solutions for residential buildings.

REFERENCES

1. Zhiqiang Z, Previtali J. M. (2010) Ancient vernacular architecture: characteristics categorization and energy performance evaluation. Energy and Buildings, 42: 357-365. https://doi.org/10.1016/j.enbuild.2009.10.002

2. N. Cardinale, G. Rospi, A. Stazi (2010), Energy and microclimatic performance of restored hypogeous buildings in south Italy: The "Sassi" district of Matera, Build. Environ. 45: 94–106. https://doi.org/10.1016/j.buildenv.2009.05.017.

3. S. Martín, F.R. Mazarrón, I. Cañas (2010), Study of thermal environment inside rural houses of Navapalos (Spain): The advantages of reuse buildings of high thermal inertia, Constr. Build. Mater. 24: 666–676. https://doi.org/10.1016/j.conbuildmat.2009.11.002.

4. Evola G, Marletta L, Maria Patanè E, Natarajan S (2017) Thermal inertia of heavyweight traditional buildings: Experimental measurements and simulated scenarios. Energy Procedia, 133:42–52. https://doi.org/10.1016/j.egypro.2017.09.369

5. M. Santamouris, A. Sfakianaki, K. Pavlou (2010) On the efficiency of night ventilation techniques applied to residential buildings, Energy Build. 42:1309–1313. https://doi.org/10.1016/j.enbuild.2010.02.024.

6. V. Geros, M. Santamouris, S. Karatasou, A. Tsangrassoulis, N. Papanikolaou (2005) On the cooling potential of night ventilation techniques in the urban environment, Energy Build. 37 243–257. https://doi.org/10.1016/j.enbuild.2004.06.024.

7. Givoni B (1991) Performance and applicability of passive and low-energy cooling systems. Energy and Buildings, 17(3):177–199. https://doi.org/10.1016/0378-7788(91)90106-D

8. E. Krüger, E. González Cruz, B. Givoni (2010) Effectiveness of indirect evaporative cooling and thermal mass in a hot arid climate, Build. Environ. 45:1422–1433. https://doi.org/10.1016/j.buildenv.2009.12.005.

9. E. Shaviv, A. Yezioro, I.G. Capeluto (2001) Thermal mass and night ventilation as passive cooling design strategy, Renew. Energy. 24:445–452. https://doi.org/10.1016/S0960-1481(01)00027-1.

10. Roucoult JM, Douzane O, Langlet T (1999) Incorporation of thermal inertia in the aim of installing a natural nighttime ventilation system in buildings. Energy and Buildings, 29(2):129–133. https://doi.org/10.1016/s0378-7788(98)00057-7

11. Coley D, Kershaw T, Eames M (2012) A comparison of structural and behavioural adaptations to future proofing buildings against higher temperatures. Building and Environment, 55:159–166. https://doi.org/10.1016/j.buildenv.2011.12.011

12. Hughes, C & Natarajan, S (2019), Summer thermal comfort and overheating in the elderly, Building Services Engineering Research and Technology, 40(4):426-445. ttps://doi.org/10.1177/0143624419844518

PLEA 2024 WROCŁAW
(Re)thinking Resilience

Outdoor Comfort of Schoolyards in a Hot-arid Climate:
A Forgotten Design Parameter

REEM OKASHA[1,2], CLARICE BLEIL DE SOUZA [1], IAN KNIGHT[1]

[1] Welsh School of Architecture, Cardiff University, Cardiff, UK
[2] Architectural Engineering Department, Zagazig University, Zagazig, Egypt

ABSTRACT: This study investigates the impact of enclosed courtyards on alleviating outdoor thermal stress in public school sites in hot-arid climate zones. A digital workflow is used to gauge the contribution of enclosed courtyards from public school prototypes designed by the Egyptian Government to outdoor thermal comfort (OTC) conditions in the cities of Alexandria, Cairo, and Asyut, respectively situated in the North coast, Delta and Cairo, and Southern Upper Egypt hot-arid zones. Results show enclosed courtyards benefit hot-arid zones in general, but zone-specific design strategies and regulations could improve OTC even further, particularly in the mid-seasons, if OTC is considered a design parameter.
KEYWORDS: Outdoor Comfort, Schools, Hot arid climate, UTCI, Early design stage

1. INTRODUCTION

In Egypt, new cities are planned to extend the urban axis to the desert from large governorates, free from old urban fabric constraints. They offer opportunities for schools with different shapes to be built so they are better integrated with their neighbourhoods and adapted to the climate of these regions. The Egyptian government, through the General Authority of Educational Buildings (GAEB), has designed several public-school prototypes that are built throughout the country with similar structural and construction specifications. These prototypes do not respond to the different hot-arid climate zones existing in Egypt. Regulations specify that 20% shading is required when designing schoolyards [1], regardless of where prototypes is built. However, recent public-school prototypes designed by GAEB contain passive elements such as semi-enclosed and enclosed courtyards, which can potentially enhance the thermal condition of outdoor spaces if appropriately designed and adapted to different climatic regions. It is, therefore, important these new designs respond to the climatic and microclimatic conditions of these new areas, thus allowing schoolyards to play their key roles in enabling appropriate outdoor activities.

Thermal comfort is essential in the design of schoolyards for promoting children's well-being and physical and mental health. It also plays a pivotal role in enhancing children's general performance [2]. To date, little attention has been paid to the appropriate design of schoolyards to achieve outdoor thermal comfort [3], particularly in hot arid regions, where outdoor spaces are subject to high heat and radiation, leading to excessive temperatures during the hot seasons [4]. Findings from field measurements, surveys, and simulations conclude that lack of greenery, shading, and the presence of direct solar radiation are the main causes of outdoor thermal discomfort in Egyptian schools [5]–[7]. Various shading strategies are proposed to enhance the thermal environment of schoolyards and reduce heat stress while improving student thermal comfort, e.g., sun sail shading [7], vegetation [6], and shading units and trees [5]. However, none of these studies considered the role of enclosed courtyards in alleviating heat stress.

Mahmoud and Abdallah [5] and Elgheznawy and Eltarabily [7] assessed the thermal conditions of semi-enclosed schoolyards in Asyut (Southern Upper Egypt zone) and Port Said (North Coast zone), respectively. They concluded these semi-enclosed yards suffered from strong heat stress in a hot Autumn and an early summer day, but they did not examine OTC conditions during the summer as a whole or more comprehensively throughout mid seasons.

This paper explores on an hourly basis the contribution of enclosed courtyards to alleviate thermal stress in school sites in three different hot-arid climate zones and for how many students. It highlights missing opportunities that current prototypes proposed by the Egyptian government could cater for if fine-tuned to different climate contexts.

2. METHODOLOGY

OTC is assessed using the Universal Thermal Climate Index (UTCI), which adopts an advanced human thermal model and is appropriate for all climate zones and seasons [8]. The assessment uses the workflow and post-processing method proposed in [9].

The workflow developed using the Ladybug toolkit for Grasshopper encompasses several key stages.

First, the selected school site, building, and surroundings were modelled in Rhinoceros 3D. Subsequently, the Urban Weather Generator (UWG), through the Dragonfly plugin, is employed to model urban microclimate and urban heat island effects of three climate zones represented by the cities of Alexandria, Cairo, and Assiut. The Mean Radiant Temperature (MRT) was then calculated considering the long and short-wave radiations by using validated simulation engines (Energy Plus and Radiance). MRT was combined with air temperatures, Relative Humidity (RH), and wind speed, to calculate the hourly UTCI for 5m x 5m grid located at 1.1m height throughout the whole school outdoor area. UTCI results were recorded for the three cities during typical school operating hours from 8:00 to 15:00 throughout the year, including summer holidays, to account for summer activities the open and close yards might accommodate beyond the teaching period.

Results were post-processed based on a designer's perspective, similarly to [9], across the seasons for the three cities using the following steps:

- Assessing spatially averaged UTCI value distribution over the seasons to provide insights into the thermal conditions and the characteristics of each climate zone.
- Exploring frequencies of thermal stress categories and comfort to assess if climate zones differ in seasonal OTC conditions.
- Assessing seasonal spatial distribution of MRT side-by-side with the percentage of time in comfort to understand the potential role of the prototype in improving OTC conditions.
- Understanding the role of shading and the overshadowing potential of the prototype to improve annual OTC conditions.
- Exploring the percentage of time the schoolyard is in comfort at each operating hour to assess how effective the prototype is in improving OTC conditions.
- Calculating the number of pupils in comfort for the morning and lunch school break times to assess if the prototype potential to cater for outdoor usage differs in each climate zone.

3. CASE STUDY

A site with 9266 m^2 in Badr city, one of the new cities in Cairo Governorate, was selected for the study. It hosts a GAEB detached courtyard school building prototype. This is the most used prototype in Badr, corresponding to 54% of public-school building shapes in the city (as per observation in Google Earth). The prototype has 3 storeys, 42 classrooms, and two central rectangular courtyards (ratios of 0.9 height/width and 1.14 length/width) with a long axis oriented towards the NW-SE direction in an angle of 14.18° from the north (Figure 1).

Simulation inputs (Table 1) considered geometrical and construction parameters based on the schools' Specs and Bill of Quantities Item prescribed by GAEB [10]. The thermal properties of construction materials were set following the study of [11] and [12]. Schedules and activities were determined based on the Egyptian school year and operating hours. All school spaces are naturally ventilated through openings and have only ceiling fans. Zone loads were set following a study of [11].

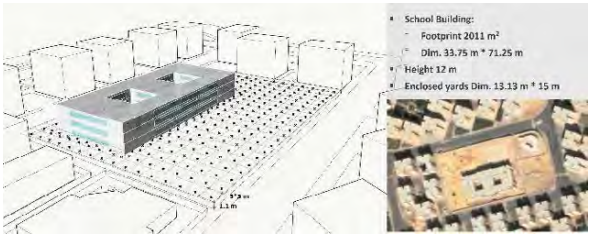

Figure 1: Prototype, site, and surroundings.

Table 1: Simulation inputs considered geometrical and construction parameters prescribed by the GAEB in Egypt.

Parameters	**Value for school**		
Material	THK (cm)	U-value (W/m^2K)	Albedo
Exterior Walls (Red brick)	30	2.809	0.25
Roofs	24.4	0.847	0.15
Typical Floors	21	3.711	-
Ground floor	34.4	1.113	-
School Ground (Dry sand)	30	0.87	0.35
Window (6mm single clear)	SHGC 0.81, U-Value 5.77		
Window-to-Wall Ratio	33%		
Infiltration	0.0003 $m^3/s\text{-}m^2$		

Simulations were conducted using the configuration displayed in Figure 1 and the data in Table 1 for the cities of Alexandria (31.2001°N, 29.9187°E), Cairo (30.0444°N, 31.2357°E), and Asyut (27.1783°N, 31.1859°E), representing the three climate zones which contain most of the cities in Egypt; respectively Northern Coast, Delta and Cairo, and Southern Upper Egypt zones. Although Egypt is characterised by a hot-dessert climate (BWh) according to Koppen's climatic classification, there are variations in climate conditions that enable the country to be further sub-divided into different climatic zones [13].

Figure 2 illustrates the characteristics of each of the three selected cities, showing Asyut has a harsher climate than the others, particularly with lower RH, as low as 24.3%, and relatively high average-hourly radiation rates, both global and direct due to relatively high frequency of clear days. Average annual wind speeds are similar for all three cities. High average summer dry bulb temperatures were observed, with the highest value of 31.2°C in Asyut decreasing by 1.2°C and 2.6°C, respectively, in Cairo and Alexandria.

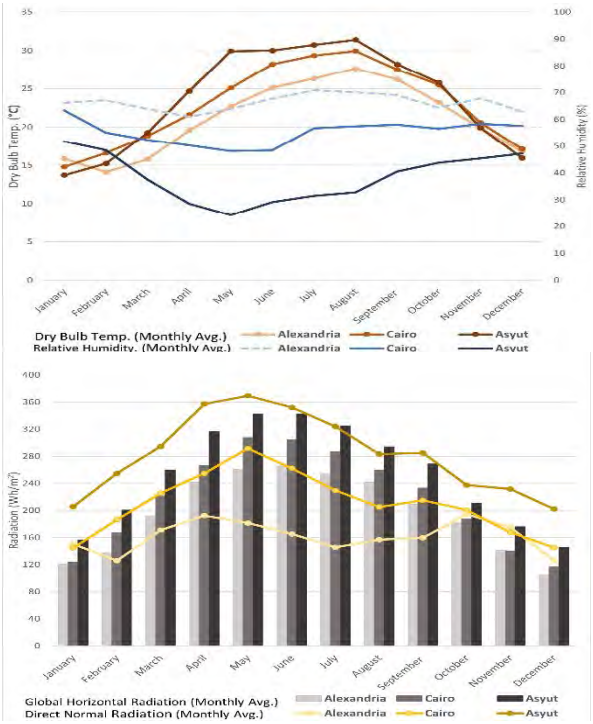

Figure 2: Monthly average Dry Bulb Temperatures and Relative Humidity (Top), Monthly average Global Horizontal Radiation and Direct Normal Radiation (bottom).

4. RESULTS AND DISCUSSION

The distribution of the spatially averaged UTCI results for the three climates is displayed in Figure 3, showing the relationship between UTCI values and the different stress categories, e.g., moderate cold stress, comfort, moderate heat stress, etc.

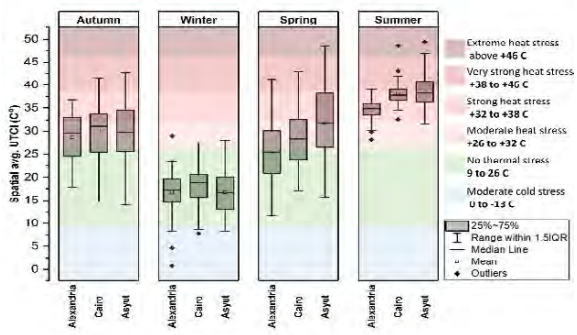

Figure 3: Spatial Avg. UTCI distributions over the seasons.

Results show all cities suffer from heat stress in Summer, whereas they are in comfort during winter. Results vary for the Spring, showing the Median UTCI of Asyut is 2.8°C and 5.07°C higher than Cairo and Alexandria, respectively. Whereas in Autumn, Cairo showed a higher Median value than the two cities. The results highlight that spring conditions have different needs in each zone. Asyut has the highest maximum UTCI within the interquartile range (IQR) over the seasons. While Alexandria showed lower values compared to the other cities. Results also show that UTCI distribution ranges tend to be wider in Asyut, particularly in spring and summer, meaning seasonal and daily variations need to be carefully examined in all zones to ascertain seasonal and hourly needs.

Figure 4 shows the percentage of time each city is in comfort or under different stress categories. This data is taken from each test point in the schoolyard rather than the spatial average results shown in Figure 3. Results discriminate findings from Figure 3 in terms of magnitude of stress, showing comfort percentages are insignificant in the Summer and around 1/3 in the Autumn for all cities. Winter is comfortable more than 2/3 of the time in all cities, whereas spring condition varies from Alexandria to Asyut, showing the former is 1/2 of the time in comfort, whereas the latter is 2/3 of the time under heat stress.

A range of 17-28% of moderate heat stress in mid-season suggests that schoolyards could achieve higher comfort levels if appropriately designed. It also indicates that if moderate heat stress is acceptable, schoolyards will be comfortable around 50% of the time in Cairo and Asyut, while in Alexandria, this could be around 75% of the time. These differences and data from Figure 2 suggest climate zone-based mitigation strategies might be needed potentially due to variations in solar radiation across the three cities. This hypothesis is consistent with sensitivity analyses from a previous study [14], which indicate that MRT is the main contributor to OTC in hot-arid climates.

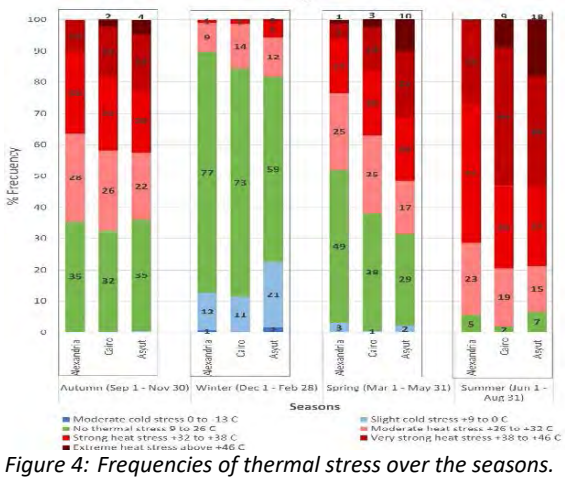

Figure 4: Frequencies of thermal stress over the seasons.

Figure 5 displays green bars from Figure 4 in space, whereas Figure 6 shows the spatial distribution of seasonal average MRTs in an attempt to explain differences across the three climate zones. Maps show that the overshadowing provided by the building significantly alleviates OTC conditions and substantially reduces the average MRT values. They also show significant differences between the open and enclosed yards in all climates, suggesting prototypes with enclosed yards can effectively improve OTC conditions in each investigated climatic zone. These findings agree with Natanian et al. [14], who found that the courtyard building shape had the highest OTC performance in three climatic zones of a

hot climate when compared to the other building shapes.

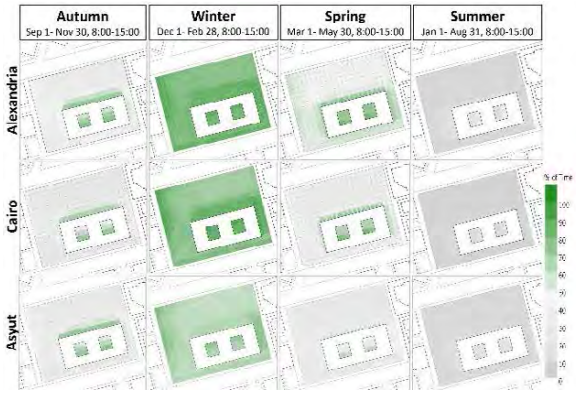

Figure 5: Percentage of time in comfort over the seasons.

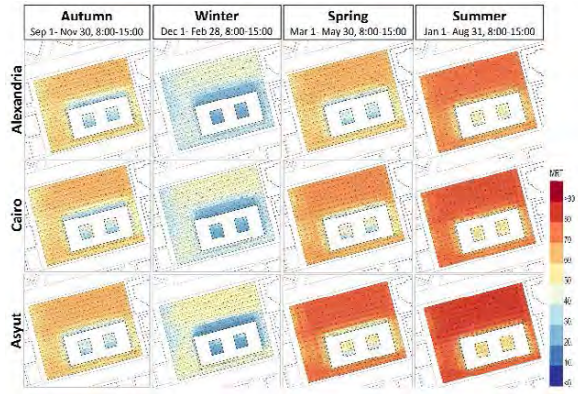

Figure 6: Average MRT over the seasons.

The maps show that the enclosed yards are mostly comfortable in winter, and more than 50% of their area remains comfortable in the autumn. In the spring, the enclosed yards are comfortable in Alexandria, with around a third of their area remaining comfortable in Asyut. However, the enclosed yards represent only 5% of the total schoolyard area, meaning adjustments to their size are needed for this prototype to contribute to OTC conditions more effectively. The maps indicate the limited shading impact of the surroundings, suggesting the need for mitigation strategies in the open yards to enhance their thermal conditions, especially in mid-season and summer.

Thermal stress in all climate zones is severe in the whole schoolyard over the summer. This agrees with the findings from [7], who investigated a semi-enclosed courtyard of a school in a coastal city with a climate like Alexandria and proposed a shading ratio of 60% to mitigate the heat stress recorded on a summer day in the exposed courtyard. However, it is unclear if shading alone can alleviate harsh OTC conditions in this season as average MRTs in the open yards during summer can reach up to 80°C, probably due to higher radiation fluxes. The dry sand used to pave schoolyards potentially contributes to the reflected radiation, which could lead, among other factors, to increased MRT in the exposed parts of the schoolyards. Further investigations are needed to ascertain the potential contribution of shading to alleviate OTC conditions in these climate zones.

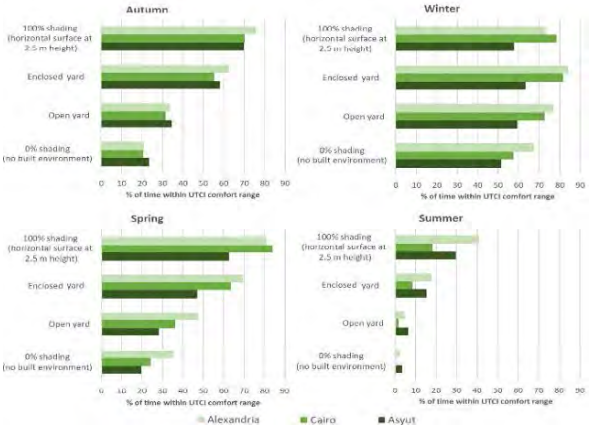

Figure 7: Percentage of time in comfort for different shading conditions.

Table 2: Annual Shade Index Range recorded from the results of the test points in the open and enclosed yards.

	Alexandria	Cairo	Asyut
Enclosed yards	63 - 87%	58 - 86%	54 - 84%
Open yard	2 - 71%	2 - 68%	1 - 66%

Figure 7 illustrates the percentage of time in comfort that can be achieved with no shading or 100% shading for the three climate zones. Full shading was calculated considering a horizontal surface at 2.5 m height above the ground. Shading in the open and enclosed yards considered the amount of shading delivered by both the school building and site surroundings. Extremes are shown as references, with 100% shading highlighting the role of this mitigation strategy in each climate zone. It is evident that shading is beneficial in the mid-seasons and summer, with notable benefits to comfort conditions in Spring (around 65% to 85% of the time) and in autumn (between 70% to 75%), despite the slight decrease in comfort observed in winter. Interestingly, in summer, it seems to benefit Asyut more than Cairo, showing it is difficult to achieve more than 40% to 18% of the time in comfort. In any case, Figure 7 illustrates shading is effective to be used potentially alone in the mid-season but in combination with other strategies in the summer.

Table 2 shows the contribution of the prototype and surroundings in shading conditions in the three climate zones. The shading index (SI) based on [15] was used to assess the shading levels in the schoolyards. Annual SI values were calculated for each test point and converted to percentages for comparability with the reference cases. The open yards exhibit the widest range of annual SI across all cities ranging from 1-2% to 66-71%. Lower values indicate exposure to direct solar radiation, while higher values suggest shaded areas potentially provided by the prototype. In contrast, the enclosed yards show higher annual SI values compared to the

open yards, ranging from 54% to 63% at the minimum and reaching up to 87% at the maximum. This implies that courtyards with an aspect ratio of 0.9 tend to provide shade, reducing direct solar radiation, which positively impact their thermal performance in these three climate zones. Given the proven benefits of shading, prototypes of this kind are worth to be deployed in these climate regions. However, variations in SI among the cities highlight the need for further investigation into courtyard aspect ratio, fine-tuning them to the latitude for higher shading percentages.

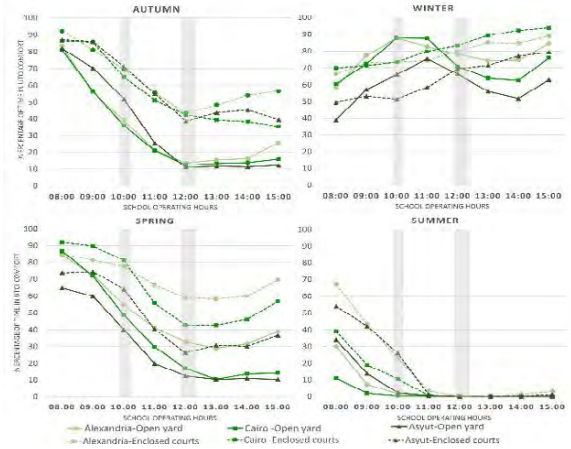

Figure 8: Percentage of time in comfort during school operating hours over the seasons for open and enclosed yards highlighting school break times.

Figure *8* disaggregates findings from Figure 6. It shows the comfort conditions of the open and enclosed yards throughout the school day for the different seasons across the three climate zones. Grey columns highlight morning and lunch break times when most school children are in the outdoor area. Results show clear differences between OTC conditions in the mornings and afternoons, with comfort conditions dramatically dropping from 8am to 12pm, particularly in the mid-seasons.

In the Autumn, open yards are in comfort 40% to 50% of the time during the 10am break time, whereas the enclosed yards are in comfort from 65% to 70% of the time. This difference between the percentage of time in comfort becomes higher at lunchtime when the enclosed yards are around 30% more comfortable than the open yard. During this season, OTC conditions for the three climate zones are fairly similar, and the effect of the prototype is notable, particularly in the afternoon when enclosed yards contribute to increasing the percentage of time in comfort by at least 30% in all climates.

In the Spring, OTC conditions for the open and enclosed yards are similar in pattern but different in magnitude for the three climate zones. Similarly, to the Autumn, during the 10 am break time, open yards are in comfort 40% to 55% of the time, whereas enclosed yards are in comfort between 60% to 80% of the time. At lunchtime, the percentage of time in comfort for the enclosed yard in Asyut is similar to the percentage of time in comfort for the open yard in Alexandria, whereas in the afternoons, the enclosed yard is at least 60% of the time in comfort in Alexandria but no more than 40% of the time in Asyut. During this season, the effect of the prototype is less notable in Asyut, where differences in OTC conditions between the open and enclosed yards are no more than 20%.

In the winter, break times are at least 50% of the time on comfort with the open yard notably better than the enclosed yard in the mornings, and the enclosed yard better than the open yards in the afternoons. In the summer, OTC conditions are very similar for the three climates, with enclosed yards contributing to alleviate thermal stress at the 10 am break by around 15% of the time in Alexandria and Asyut but no more than 10% of the time in Cairo, showing neither the climate zone nor the prototype make a difference in this case.

Table 3: Maximum number of students in comfort outdoors during morning and lunch breaks.

City	Yard	Autumn		Winter		Spring		Summer	
		10:00	12:00	10:00	12:00	10:00	12:00	10:00	12:00
Alexandria	**Open**	**537**	**185**	**1204**	**1071**	**751**	**449**	**21**	**2**
	Closed	**54**	**33**	**57**	**62**	**60**	**46**	**18**	**0**
	Total	591	218	1261	1133	811	495	39	2
Cairo	**Open**	**494**	**173**	**1204**	**973**	**670**	**232**	**4**	**0**
	Closed	**50**	**33**	**57**	**64**	**63**	**33**	**8**	**0**
	Total	544	206	1261	1037	733	265	12	0
Asyut	**Open**	**711**	**153**	**905**	**911**	**550**	**170**	**30**	**0**
	Closed	**55**	**30**	**40**	**54**	**50**	**20**	**20**	**0**
	Total	766	183	945	965	600	190	50	0

Table 3 explores results from Figure 8 in relation to how different climate zones and a prototype with enclosed yards impact the design by showing the number of students in comfort outside at 10am and during lunch breaks. Figures from Table 3 were calculated by dividing the average area in comfort at break times by the minimum area per student share of outdoor space as prescribed by the GAEB ($5m^2$/Student). Considering public school regulations limit the number of students to 40 per cohort [1], it is possible to conclude that the enclosed courtyards can host no more than 1.5 cohorts, a very small number of students. At 10am break times, enclosed yards can host more than 1 but less than 2 cohorts of students in the autumn, winter, and spring but less than half a cohort during summer. At 12pm break times, enclosed yards can host less than 1 cohort of students in the mid-season, except for the spring in Alexandria. Almost no cohort can be hosted in the summer. These numbers show the benefits provided by the prototype with an enclosed yard are very similar to school end-users across the three climate zones.

However, when looking at the OTC conditions of the open yard at 10am, one can see that Asyut can host 5 more student cohorts outside than Alexandra in the Autumn, whereas the exact opposite can happen in the Spring. When looking at OTC conditions at

12pm, one can see that Asyut and Alexandria have similar capacity to host around 4 cohorts of students outside in the Autumn but that the latter can host 5 more cohorts than the former in the Spring. Whereas the summer condition seems almost hopeless in any of the three climate zones, winter capacity to host students outdoor is higher in Alexandria and Cairo compared to Asyut by 8 student cohorts at 10am and between 2 to 4 cohorts at 12pm. These large differences show a higher impact on end-users and justify fit-for-purpose mitigation strategies for each of the three climate zones in the open yard.

5. CONCLUSION

The study shows significant spatial and temporal variations in OTC conditions delivered by the GAEB prototype with enclosed yards when deployed to different hot-arid climate zones. These variations significantly impact the number of end-users that can comfortably perform outdoor activities in each climate zone, justifying fit-for-purpose regulations and design guidelines per zone. These guidelines should be developed considering the following aspects:

- ***Maximise percentage of shading on open yards***, taking advantage of neighbouring buildings and the school building, mainly aiming to provide shading from mid-day throughout the afternoon, when OTC conditions are less favourable in mid seasons and summer;
- ***Deliver specific mitigation measures in addition to shading during the summer season***, as shading alone will not enable almost anyone to stay outdoors during school break times;
- ***Increase the size of enclosed yards*** to cater for more students in them if appropriate, as they notably increase shading and reduce MRTs but are not enough to effectively host more than 1 and a half student cohorts;
- ***Adjust the aspect ratio of courtyards*** when increasing their size to ensure more than 50% of the shading area so they can still provide favourable OTC conditions to cater for outdoor activities.

Further studies should focus on undertaking a sensitivity analysis for this prototype in each of the three climate zones, considering enclosed yards with various aspect ratios to identify the range of courtyard proportions suitable for each climate zone. Ideally, the sensitivity analysis should be tied to the size of the school and the number of student cohorts it can host. This way, massing studies in early design stages would cater for a forgotten design parameter, normally considered a byproduct of design, rather than a design target from the beginning.

ACKNOWLEDGEMENTS

The authors would like to acknowledge the Egyptian Ministry of Higher Education for the scholarship given to the first author to undertake the research and attend the conference.

REFERENCES

1. GAEB (2018). Criteria and requirements for the validity of the site and school buildings in New urban communities. Cairo.
2. Vanos, J. K. (2015). Children's health and vulnerability in outdoor microclimates: A comprehensive review. Environment International, 76, pp. 1–15.
3. Antoniadis, D., Katsoulas, N. and Papanastasiou, D. K. (2020). Thermal Environment of Urban Schoolyards: Current and Future Design with Respect to Children's Thermal Comfort. Atmosphere 2020, 11(11), p. 1144.
4. Cohen, P. et al. (2019). Urban outdoor thermal perception in hot arid Beer Sheva, Israel: Methodological and gender aspects. Building and Environment, 160, p. 106169.
5. Mahmoud, R. M. A. and Abdallah, A. S. H. (2022). Assessment of outdoor shading strategies to improve outdoor thermal comfort in school courtyards in hot and arid climates. Sustainable Cities and Society, 86, p. 104147.
6. El-Bardisy, W. M., Fahmy, M. and El-Gohary, G. F. (2016). Climatic Sensitive Landscape Design: Towards a Better Microclimate through Plantation in Public Schools, Cairo, Egypt. Procedia - Social and Behavioral Sciences, 216, pp. 206–216.
7. Elgheznawy, D. and Eltarabily, S. (2021). The impact of sun sail-shading strategy on the thermal comfort in school courtyards. Building and Environment, 202, p. 108046.
GAEB (2018) Criteria and requirements for the validety of the site and school buildings in New urban communities. Cairo.
8. Broede, P. et al. (2010). The Universal Thermal Climate Index UTCI in operational use. Proceedings of Conference: Adapting to Change: New Thinking on Comfort Cumberland Lodge, Windsor, UK, April 9-11.
9. Okasha, R., Souza, C. B. De and Knight, I. (2023). Informing early-stage design decisions: Comprehensive spatial and temporal analyses of outdoor thermal comfort to maximise the use of schoolyards. In 18th International Conference of the International Building Performance Simulation Association (IBPSA). Shanghai, China, Sep 4-6.
10. GAEB, (2020). Report on Prototype's Specs and Bill of Quantities. General Administration for Systems Development and Decision Support, Cairo, Egypt, .
11. Hammad, H., Abdelkader, M. and Faggal, A. A. (2017). Investigating the thermal comfort conditions in an existing school building in Egypt. JES. Journal of Engineering Sciences, 45(3), pp. 360–379.
12. Ibrahim, Y. et al. (2021). On the Optimisation of Urban form Design, Energy Consumption and Outdoor Thermal Comfort Using a Parametric Workflow in a Hot Arid Zone. Energies, Vol. 14, Page 4026
13. Hamed, M. M., Nashwan, M. S. and Shahid, S. (2022). Climatic zonation of Egypt based on high-resolution dataset using image clustering technique. Progress in Earth and Planetary Science, 9(1), pp. 1–16.
14. Natanian, J. et al. (2020). From energy performative to livable Mediterranean cities: An annual outdoor thermal comfort and energy balance cross-climatic typological study. Energy and Buildings, 224, p. 110283.
15. Aleksandrowicz, O. et al. (2020). Shade maps for prioritizing municipal microclimatic action in hot climates: Learning from Tel Aviv-Yafo. Sustainable Cities and Society, 53, p. 101931.

PLEA 2024 WROCŁAW
(Re)thinking Resilience

Indoor Environmental Quality in the Building Archetypes of Self-built Houses:

A Case Study in San Quintin, Mexico.

ABNER OCAMPO-MENDOZA[1], CRISTINA SOTELO-SALAS[2]

[1]Facultad de Ingeniería, Arquitectura y Diseño, Universidad Autónoma de Baja California, Ensenada, México
[2]Facultad de Arquitectura y Diseño, Universidad Autónoma de Baja California, Mexicali, México

ABSTRACT: Self-built houses offer an affordable housing option in countries like Mexico, where 57% of homes are constructed in this manner. However, the construction characteristics of such homes often lack quality because they are built without professional oversight. This deficiency can adversely affect indoor environmental quality, which has been underexplored in this context. This research evaluates the thermal comfort and indoor air quality of self-built homes in San Quintin, Mexico. House archetypes were developed based on their construction features to achieve this, and the three most common archetypes were selected for further analysis. In situ measurements were obtained in one representative house for each archetype. Dry bulb temperature, relative humidity, and CO2 levels were recorded over 5 days. The recorded levels revealed deficiencies in all the houses, with CO2 levels exceeding 1000 ppm throughout the monitoring period, contravening international standards. While average indoor temperatures were higher than outdoor, most of the time, the temperature remained outside the comfort zone. The gathered information identifies a genuine need for intervention to improve current housing conditions, with overcrowding, poor envelope insulation, and inadequate ventilation being the primary issues.
KEYWORDS: Indoor environmental quality, indoor air quality, thermal comfort, self-built houses, building archetypes

1. INTRODUCTION

Indoor Environmental Quality (IEQ) refers to a building's performance in achieving an indoor environment that meets the needs of its occupants. It is mainly composed of four parameters: thermal comfort, air quality, visual comfort, and acoustic comfort. These parameters have a direct impact on the health, productivity, and well-being of the occupants [1]. The most extensively studied aspects are thermal comfort and indoor air quality. The former is highlighted due to its identified role as the parameter with the greatest impact on an individual's comfort and well-being. The latter is crucial for its implications on health and is also more straightforward to study due to the equipment involved [2]. These are affected by factors inherent to the occupant, such as their physiology and clothing, as well as environmental conditions. Unlike those related to occupants, environmental conditions can be objectively measured with the appropriate equipment. An important factor determining the environmental conditions of a space is the construction characteristics, as they have a direct impact on all IEQ parameters [3].

1.1 Self-built houses

Self-built houses are homes in which families makethe most important decisions about the process, like the design, the location of the land or choosing what materials to use. In Mexico, 57% of the housing stock corresponds to this type of dwelling [4]. It represents a more affordable way to access housing since intermediaries are eliminated, and they are often built progressively, starting with small spaces or deficient materials, and expanding or modifying them over the years.

However, a problem associated with this type of production is the lack of technical knowledge used in construction, which results in unsuitable indoor environments [5]. In this regard, in Mexico, there is the Housing Backlog Index, used by Mexico's National Housing Commission (CONAVI), to determine dwellings that do not meet adequate housing requirements: Overcrowded spaces, building some or all of their walls, roof, or floor with waste materials, and/or limited access to basic services such as drainage or electricity [6]. The research focuses on the San Quintin region on the northwest coast of Baja California, Mexico. There, more than 80% of the homes are identified as inadequate. However, the index does not provide detailed information about the state of the houses, much less about their environmental conditions, which are not taken into account.

This region is predominantly rural, with irrigation agriculture as the primary economic activity. It is located 200 kilometers from the southern border with the United States. Due to these characteristics, migration from other parts of the country has played a significant role in the region's development since the

1970s. Initially, in temporary work camps, and later settling in the area in their own homes. Before this process, the region was practically uninhabited [7]. In recent years, there has been a significant urbanization process and an increase in the number of dwellings.

1.2 Similar studies

A similar study was conducted in La Huasteca, a Mexican region in the south of the country where the annual mean temperature oscillates from 21.5 to 31.9°C. Four different types of housing were identified based on their construction materials: Traditional houses with vegetable materials and construction systems typical of the region, some with a circular floor plan and others with a rectangular floor plan; Hybrid houses that use concrete blocks in walls but retain traditional roofs; and replaced houses that exclusively use concrete in both walls and roof. They monitored 11 houses distributed in 3 localities for 9 months. The results show that during the warm season, houses with vegetal elements exhibited better thermal performance, while those made entirely of concrete responded better in winter [8].

Another study was conducted in the region of the Lower Papaloapan River Basin, located in the southern part of Mexico, where temperatures range from 15°C to 42°C throughout the year. The study examined 77 homes in 17 different communities, characterizing them based on the material of their roofs. Four common types of roofing materials were observed in self-built homes: zinc, asbestos, concrete, and palm leaves. They carried out a comparative study and an indoor thermal comfort analysis, simulating the thermal performance over a year. The findings revealed that homes with palm roofs had the best performance, while housing with zinc roofing produced the worst results. In the case of a false ceiling, a standardizing effect was observed for all types of roofing [9].

A research study focused on the thermal performance of self-built houses in Ulaanbaatar City, Mongolia. Researchers conducted surveys in two areas of the city to identify the most common type of self-built housing. A total of 16 houses were entered and surveyed. The findings revealed that all the self-built houses included in the study were poorly constructed, and this negatively impacted their energy efficiency. This leads to increased consumption of carbon and wood, worsening air pollution levels [10].

Indoor environmental quality (IEQ) in this type of housing is rarely studied due to its very heterogeneous characteristics. Even so, research that addresses it tends to focus solely on thermal performance and leaves aside possible interactions with other components of IEQ.

1.3 Objectives

This research aims to identify deficiencies and problems in self-built houses in San Quintin concerning their thermal comfort and indoor air quality with their construction characteristics. The goal is to pinpoint the most significant opportunities for improvement, generating recommendations to enhance the indoor environmental quality conditions of homes and consequently improve the quality of life for their inhabitants without increasing energy consumption.

2. METHODS

2.1 Study area

Based on the 2020 population census [11], the five largest localities of the San Quintin region had a total of 58,369 inhabitants. Among these, the locality with the highest percentage of inadequate housing conditions was chosen to represent the region. This is the locality of Emiliano Zapata (30°46'N, 116° 0'W) with 9636 inhabitants. According to the same census, Emiliano Zapata comprises 2422 households, out of which 1077 were subject to analysis due to resource availability. The study area is presented in Figure 1.

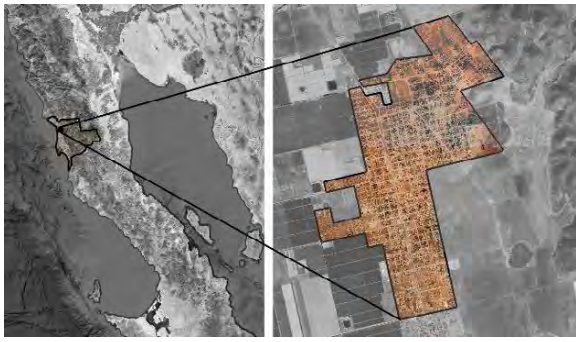

Figure 1: Location of the study area. San Quintin region (left). Emiliano Zapata locality (right).

The climatological conditions are categorized as ‘‘hot desert” (BWh) in the Köppen-Geiger climate classification [12]. The average annual temperature is 17°C, with a relative humidity (RH) of 79%, and an average annual rainfall of 80.4 mm. In the coldest month, the average temperature is 13.7°C, and in the warmest month, it is 21.2°C. The study period falls within the transition from the warm to the cold season, where the average temperature is 16.1°C [13].

2.2 Study design

The methodological design of the research consists of three main phases: (a) Classification of self-built houses into different archetypes based on their constructive features; (b) Measurement of environmental parameters; (c) Analysis of the correlation between the observed indoor environmental parameters and the construction characteristics of the analyzed houses.

2.3 Preliminary study.

A photographic survey of houses was conducted through walking tours across the locality. Google Earth images and drone photographs of the area were also utilized to determine their location and other parameters not visible at street level.

Due to resource availability, a smaller area within the entire locality was surveyed. According to official data, a total of 1761 houses are located in the surveyed area [11]. Out of these, 1308 were photographed, and 231 were discarded due to unclear details. Therefore, the final total of analyzed houses was 1077.

Recorded construction characteristics were limited to those observables from the exterior, including the outline of the architectural floor plan and the materials of walls and roofs. Sets were defined for further analysis by shared construction characteristics.

2.4 Measurement of environmental parameters.

Fieldwork measurements of indoor parameters were carried out on one representative home from the three most common archetypes. Indoor dry bulb temperature (DBT), relative humidity (RH), and CO2 levels were continuously monitored every half hour on an alternating basis for five days in both the social area (SA) and the bedroom (BR) of each house. Two Extech CO210 Data Loggers were utilized one for each room. The equipment was positioned at a height of 1.5 meters following ISO 16000 guidelines to avoid interference from people's respiration [14]. The data loggers (Figure 2) were placed as far from the wall as possible without affecting the normal functioning of the dwelling.

Figure 2: Monitoring equipment on-site: Data logger (left), weather station (Right).

Meteorological data was also collected during the monitoring period using a portable AcuRite Atlas model 06059 weather station. This station was positioned on the roof of a centrally located home in the locality, at a height of 9.5 meters above ground level, to record outdoor dry bulb temperature (DBT) and relative humidity (RH) values. The equipment specifications on both the data logger and the weather station are shown in Table 1.

Table 1: Monitoring equipment specifications.

Parameter	Range	Accuracy
Indoor DBT [1]	-10 to 60°C	±0.6°C
Indoor RH[1]	0.1% to 99.9%	±3% (10 to 90%)
Indoor CO2[1]	0-9999ppm	±(5%rdg+50ppm)
Outdoor DBT. [2]	-40°C a 70°C	±0.55°C
Outdoor RH[2]	1-100 %	±2% HR

Note: (1. Data logger; 2, Weather station)

2.5 Data analysis.

To analyze the temperature and its relationship with the thermal requirements of the population, Neutral Temperature (Tn) is used. In this study, the thermal comfort model of Auliciems and Szokolay [15] was employed, as it is widely accepted globally. Equation (1) allows us to determine Tn based on the average outdoor temperature.

$$Tn = 17,6 + 0,31Tmed \quad (1)$$

where

Tn- Neutral temperature;

Tmed-Monthly mean temperature.

The comfort zone (CZ) is established based on the range recommended by the authors, within ±2.5 °C from the Neutral Temperature (Tn), with a 90% acceptability rate. Relative humidity (RH) was assessed against the ISO 7730 standard which defines an optimal range between 30 and 70% RH [16] and CO2 levels with the ISO 1600 which sets a threshold of 1000 ppm [14].

3. RESULTS

3.1 Preliminary study

The results of the photographic survey reveal that 89% of the houses are single-story. Concerning orientation, 40% face East-West, 37% face North-South, and 23% lack a predominant orientation.

In terms of layout, 50% of the houses have a rectangular floor plan. Additionally, 26.9% feature a porch, 12.8% have an attached volume, primarily used as a bathroom, and 7.2% include a garage. Regarding external wall materials, 79% of the houses use concrete blocks exclusively, 16% use plywood sheets, and 6% employ a combination of both. Other materials such as brick and siding account for less than 1%.

Roofing materials consist of 68% wood, 29% concrete slabs, and 2% metal sheets. The prevalent materials for covering wooden roofs are sanded cardboard and asphalt shingles, together comprising 79%. The primary roof shape is gabled and inclined, while the concrete slabs, with occasional exceptions, are flat. Out of the 1077 houses, only 12 have chimneys, and seven were identified with air conditioning equipment.

3.2. Development of archetypes.

For the development of archetypes, the following criteria were chosen based on observations in the preliminary study: 1) levels, 2) architectural layout; 3) wall materials; 4) roof material; 5) roof shape; and 6) use of porch or garage.

The three most common construction archetypes (AT) were identified as follows:

- AT1: Single-story, rectangular layout, concrete walls, gable wooden roof (84 houses).
- AT2: Single-story, rectangular layout, concrete block walls, flat concrete slab roof (69 houses).
- AT3: Single-story, rectangular layout, plywood sheet walls, gable wooden roof (56 houses).

All of them are without porches or garages. Based on this classification, the case studies were selected and are presented in Figure 3. A determining factor in the selection of these homes was the occupants' willingness to participate in the study.

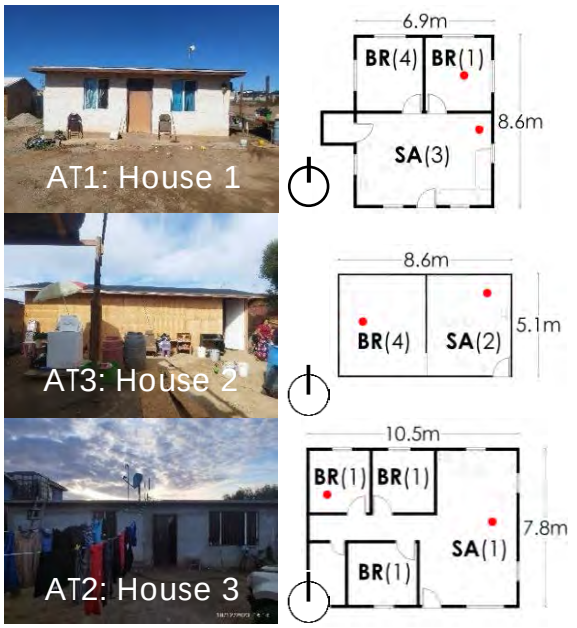

Figure 3: Case studies and equipment placement. (BR: Bedroom; SA: Social Area; number in parentheses indicates the quantity of people sleeping in the room)

House 1 (H1) has a surface area of 63 m2 and 9 occupants; House 2 (H2) has 44 m2 and 6 occupants; House 3 (H3) has 84 m2 and 4 occupants. In all three houses, the SA comprised a single space serving as the kitchen, dining room, living room, and bedroom during the night. The three houses have the same material on the interior and exterior walls. None have a false ceiling or use any climate control devices such as fans or air conditioners. All the doors are of the flush type, except the main door of H3, which is a metal screen door with a fabric curtain. All windows in H1 and H3 are single-pane with aluminum frames. H2 lacks windows; however, it has openings at the junction of the wall and the roof, allowing air exchange with the exterior.

3.3. Thermal comfort

The thermal performance of the three houses is illustrated in Figure 4. A Tn of 22.6 °C was established, with a range from 20.1 to 25.1 °C.

H1 and H2 consistently record temperatures higher than outdoors at all times. H1 exhibits a greater temperature difference when temperatures are cooler, while H2 does so when is warmer outdoors. On average, H1 has temperatures 4.5 °C higher in BR and 4.6 °C in SA compared to the outdoor. As for H2, these figures are 3.3 °C in BR and 2.8 °C in the SA. H3 shows less temperature variation throughout the day than outdoors. The average temperature is higher by 1.2 °C in BR and 1.7 °C in SA compared to the outdoors. Although it manages to reduce the temperature during the afternoon, this result is counterproductive.

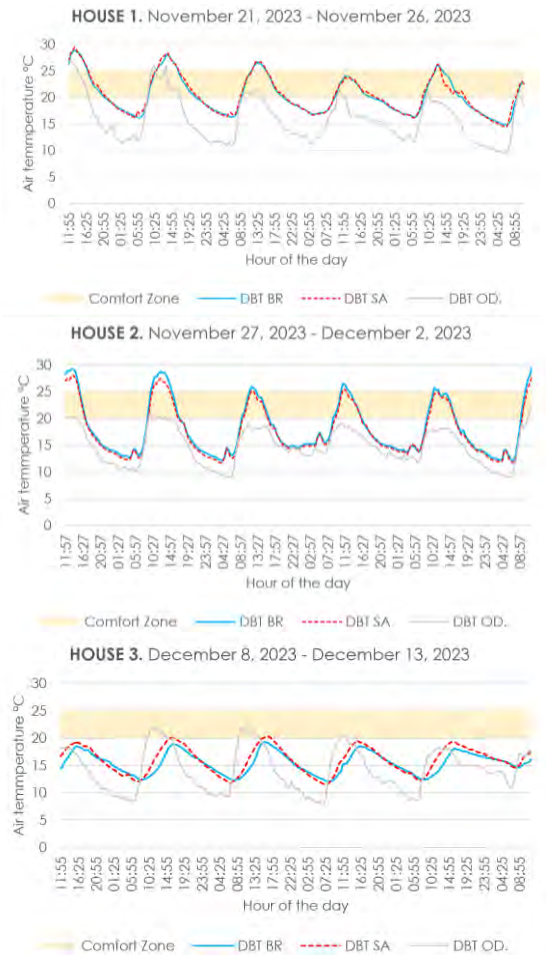

Figure 4: Indoor DBT measurements.

The relative humidity (RH) is depicted in Figure 5. In H1, the average levels are 61% in BR and 59% in SA. For H2, RH has average values of 65% in BR and 68% in SA. H3 exhibits an RH of 81% in BR, 73% in SA, and 75% outdoors. The RH average values are 61% in BR and 59% in SA, both in the optimal range. RH in both BR and SA is outside the optimal range, with an average RH of 81% and 73%, respectively.

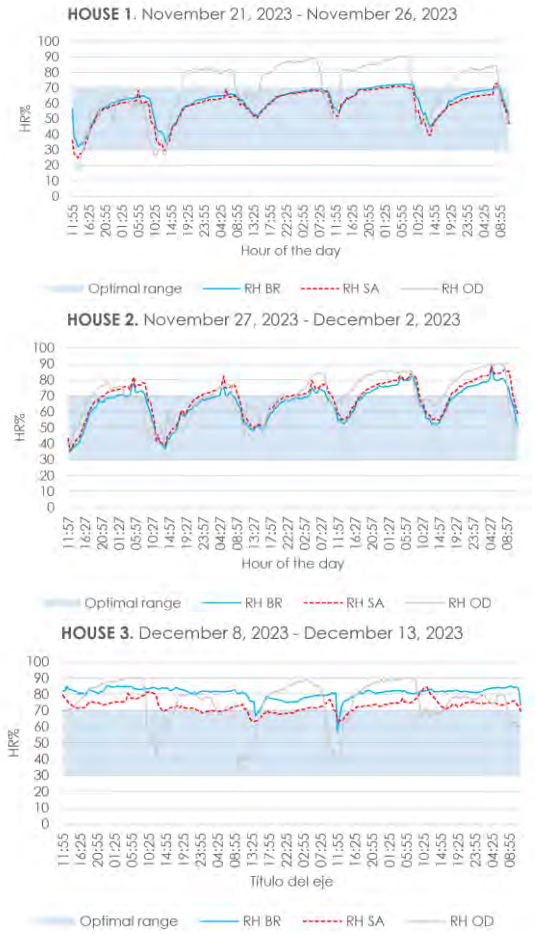

Figure 5: Relative Humidity (HR) measurements.

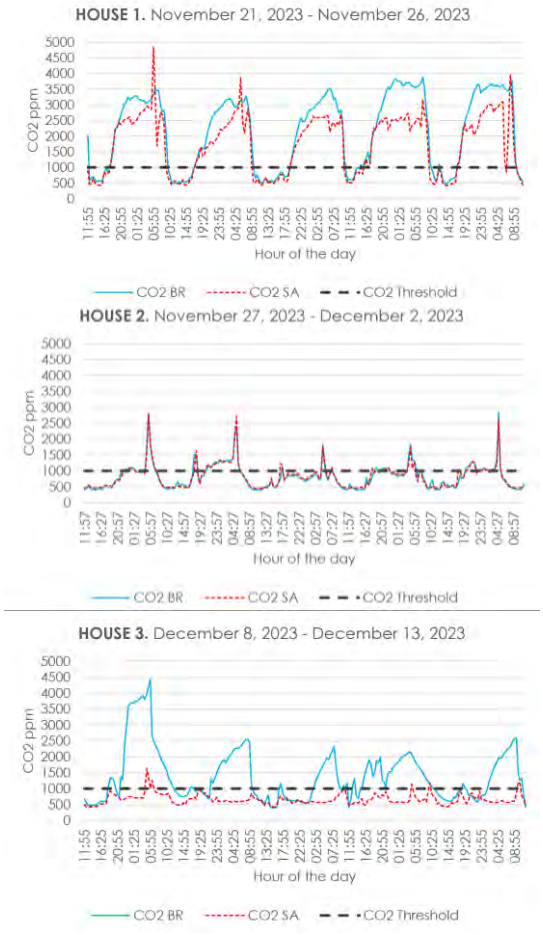

Figure 6: CO2 levels measurements

When analyzing the percentage of time that the conditions are in the comfort range (Table 2), H1 shows the best performance, while H3 has the worst in all the parameters.

Table 2: Percentage of time within the comfort range.

	Comfort zone			RH optimal range		
	OD	BR	SA	OD	BR	SA
House 1	17%	32%	36%	42%	90%	90%
House 2	5%	18%	20%	51%	63%	**47%**
House 3	10%	**0%**	**2%**	30%	**2%**	**22%**

Note: Highlighted values indicate conditions that are worse than outdoor conditions

3.4. Air quality

Figure 6 presents the CO2 levels. H1 shows the highest concentrations in both rooms, averaging 2180 ppm in BR and 1753 ppm in the SA. The maximum recorded concentration reached 4842 ppm, occurring at 6 am in SA. H2 exhibits a similar performance between both rooms, 823 ppm in BR and 825 ppm in SA. Nevertheless, during the nights, the values remain at levels close to 1000 ppm, with occasional peaks around 6 am exceeding 1500 ppm. H3 shows an average concentration of 666 ppm in SA. In contrast, the BR presents average levels of 1400 ppm.

4.DISCUSSION

Differences were observed in all of the registered parameters among the three case studies. H1 with an occupancy density of 7m2 per person presented the highest levels of CO2. During cool nights, windows are closed, promoting the accumulation of CO2. Approximately 70% of the time, the concentration is above the suggested limit of 1000 ppm. Additionally, a peak is recorded in SA around 6 am, likely due to the use of the stove. Indoor temperatures average 20.3°C for the BR and 20.5°C for the SA. While it barely beats the minimum range of the CZ set at 20.1°C, it falls far short of the Tn of 22.6°C.

H2 has a similar occupancy density to H1 (7.3m2 per person). However, 70% of the recorded CO2 levels are below the concentration threshold in both rooms. These relatively low CO2 levels can be attributed to the gaps between the roof and walls, facilitating a constant exchange of air with the exterior, despite the absence of windows. Nevertheless, it shows spikes in CO2 levels around 6 am and 5 pm when the stove is used for cooking. The average temperatures are more than 4°C below the Tn.

H3 has an occupancy density three times lower than H1 and H2 (21m2 per person). This difference is noticeable, as 96% of the registered data in SA is below the 1000 ppm threshold. In BR, it is only 42.5%. This

discrepancy is because the SA has a greater surface area, a higher number of windows, and the presence of a door connecting directly to the outdoors, which enhances ventilation. Mean temperatures in BR and SA are 7.1°C, and 6.6°C below Tn, respectively.

The study presents certain limitations that should be taken into account. During the selection of case studies, characteristics such as interior distribution, door material, thickness of building elements, their thermal properties, and window-to-wall ratio, were not included due to resource constraints. These aspects shall be addressed in future studies to improve representativeness.

5. CONCLUSION

This research aimed to identify deficiencies in self-built houses in San Quintin concerning their thermal comfort and indoor air quality. To achieve this, the houses were categorized into archetypes (AT) based on observed building characteristics. One house was selected for each AT, and monitoring of DBT, RH, and CO2 levels was carried out over 5-days in each case.

The three prevalent housing ATs are single-story with a rectangular outline layout: AT1 features concrete walls with a gable wooden roof, AT2 includes concrete block walls with a flat concrete slab roof, and AT3 exhibits plywood sheet walls with a gable wooden roof. The recorded data indicates that all the houses exhibit conditions of low heating and high concentrations of CO2 for the majority of the time. AT3 stands out with the poorest thermal performance, as 99% of temperature recorded data falls outside the CZ. In contrast, AT1 shows the highest concentrations of CO2, averaging 2180 ppm in BR and 1753 ppm in SA.

Three major issues were identified in these houses: overcrowding, poor envelope insulation, and inadequate ventilation. Overcrowding causes high CO2 concentrations even with constant ventilation. Occupants in the three ATs expressed a desire to expand their homes. However, this alone may not improve the Indoor IEQ of the houses. Materials that increase thermal gains and retain heat for extended periods are necessary. Also, mechanisms facilitating ventilation without substantial heat loss are crucial, both in existing spaces and new constructions.

To achieve a more accurate comparison, it would be optimal to monitor all houses simultaneously throughout an entire year to gain a more comprehensive understanding of IEQ performance. Despite these limitations, the gathered information in this work identifies a genuine need for intervention to improve the current housing conditions. Furthermore, it provides an approach for the development of future studies aimed at proposing cost-effective solutions to the IEQ problem in San Quintin, self-built houses.

REFERENCES

1. Mujan, I., Anđelković, A.S., Munćan, V. Kljajić, M. and Ružić, D. (2019). Influence of indoor environmental quality on human health and productivity - A review. *Journal of Cleaner Production*, 217: p. 646–657.

2. Andargie, M.S., Touchie, M. and O'Brien, W. (2019). A review of factors affecting occupant comfort in multi-unit residential buildings. *Building and Environment*, 160: p. 106182.

3. Mewomo, M.C., Toyin, J.O., Iyiola, C.O., and Aluko, O.R. (2023). Synthesis of critical factors influencing indoor environmental quality and their impacts on building occupants health and productivity. Journal of *Engineering, Design and Technology.* 21(2): p. 619–634.

4. Secretaria de Desarrollo Agrario Territorial y Urbano (2021). *Autoproducción de vivienda adecuada en México.* GIZ.

5. Salazar, T. and Flores-Gutiérrez, A. (2018). Vivienda popular mexicana desde los ojos de la habitabilidad. *SketchIN: Revista de* Arquitectura y Diseño. 2(4): p. 22-34.

6. Comisión Nacional de Vivienda (2020). *Cálculo del Rezago habitacional a nivel municipal. Censo de Población y Vivienda 2020.*

7. Velasco, L., Zlolniski, C. and Coubès, M.L. (2014). De jornaleros a colonos: Residencia, trabajo e identidad en el Valle de San Quintín. 1a edn.

8. Aguillón-Robles, J., Arista-González, G.J. and Cataño-Barrera, A.M. (2020). Comportamiento térmico de la vivienda rural. *Legado de Arquitectura y diseño*, 15(28): p. 102–111.

9. García-Arellano, C., Ramírez-Ibáñez, M. and Luna, B. (2022). Comparative study of the indoor apparent temperature of dwellings with different roofing in the Lower Papaloapan River Basin region. *Indoor and Built Environment.* 31(2): p. 537–551.

10. Gado, T. and Games, T.S. (2018). A Parametric Study to Optimize the Thermal Performance of Mongolian Self-built Houses in Terms of Energy Efficiency: Towards a Cleaner Environment for Ulaanbaatar. In *PLEA 2018*. Hong Kong.

11. Instituto Nacional de Estadísticas y Geografía (2020). Inventario Nacional de Vivienda, [Online], Available: https://www.inegi.org.mx/app/mapa/espacioydatos/?app=inv [4 August 2022].

12. Peel, M.C., Finlayson, B.L. and McMahon, T.A. (2007). Updated world map of the Köppen-Geiger climate classification. *Hydrology and Earth System Sciences,* 13(3): p. 243–249.

13. Comisión Nacional del Agua (2022). Climatic data recorded by the Automatic Weather Station SAN QUINTIN, B.C., period 2000-2022. [Online], Available: https://smn.conagua.gob.mx/es/observando-el-tiempo/estaciones-meteorologicas-automaticas-ema-s

14. International Organization for Standardization (2017). Indoor air — Part 26: Sampling strategy for carbon dioxide (CO2). *ISO 16000.* Ginebra.

15. Auliciemsk A. and Szokolay, S. (1997). Thermal Comfort. *In PLEA 1997*. Brisbane.

16. Olesen, B.W. and Parsons, K.C. (2002). Introduction to thermal comfort standards and to the proposed new version of EN ISO 7730. *Energy and Buildings*, 34(6): p. 537–548.

Housing Habitability Assessment in Vulnerable Urban Areas in Hot-Arid Climate

Case Study: Mexicali, Baja California, Mexico

RAMONA ALICIA ROMERO-MORENO[,1] OSVALDO LEYVA-CAMACHO[,1]
GONZALO BOJÓRQUEZ-MORALES[,1] CRISTINA SOTELO-SALAS[,1] DANIEL ANTONIO OLVERA-GARCÍA[,1]

Facultad de Arquitectura y Diseño, Universidad Autónoma de Baja California, Mexicali, México

ABSTRACT: The challenges concerning the habitability and adequacy of housing in marginalized urban areas are multifaceted, encompassing issues such as resettlement due to urbanization dynamics, the impact of pandemics, and the influence of current and future climatic events. Despite adequate housing being recognized as a human right in international regulations, millions worldwide still lack proper housing. This article analyzes the characteristics of precarious housing and its surroundings based on the perception of habitability conditions in a hot arid climate context. The case study of Mexicali, Mexico is presented. Fieldwork was conducted through the design and implementation of a survey in areas of social deprivation and priority attention. The survey was administered during September-November 2022, where 308 effective records were obtained. The results of the inhabitant's profile, the physical characteristics of the home, the perception of habitability conditions and some aspects of the urban context are shown. The results indicate that inhabitants aged 50 or older are predominant and have constructed their homes through self-construction methods. Additionally, there are significant thermal habitability issues. However, despite these challenges, the majority of individuals express contentment with their housing conditions.
KEYWORDS: Environmental habitability, Precarious Housing, Vulnerable Urban Areas, Hot-Arid Climate

1. INTRODUCTION

The right to adequate housing, as recognized by the United Nations, encompasses various essential conditions such as security of tenure, availability of services, affordability, habitability, accessibility, location, and cultural adequacy [1]. The concept of adequate housing by UN-Habitat focuses on rights and universal standards, emphasizing accessibility and basic services, while habitability considers quality of life and individual perceptions, incorporating cultural aspects. Both aim for human well-being but differ in approach: one normative, the other subjective and contextual. Despite global efforts to address housing inadequacies, challenges persist, with millions lacking adequate housing worldwide [2]. Ensuring access to adequate housing is crucial not only for fulfilling human rights obligations but also for promoting health and social well-being, particularly among vulnerable populations [3, 4].

In Spain, the absence of unified legislation on housing habitability has prompted calls for establishing minimum national standards [5]. Conversely, studies focusing on habitability conditions in Barcelona stress the need for housing rehabilitation programs and user-centric urban planning [6, 7]. These contrasting viewpoints highlight the complexity of addressing housing issues in Spain, where a balance between national legislation and localized interventions is crucial for ensuring livable housing conditions. Various studies have explored the relationship between living space proportions and housing standards, emphasizing the impact of physical dimensions on well-being and social stability.

Conflicting evidence suggests that while some studies in Latin America emphasize the importance of integrating physical and psychosocial aspects in housing design in Argentina [8] other research underscores the significance of habitability factors such as thermal, lighting, acoustic, and olfactory components [9]. This divergence in perspectives highlights the intricate nature of housing design considerations, indicating a necessity for a holistic approach that addresses both the biopsychosocial well-being of residents and the environmental factors contributing to overall comfort and functionality. However, there is a gap in achieving residents' needs satisfaction when housing conditions and urban contexts are precarious [10].

Research on habitability in precarious housing in the Metropolitan Area of Oaxaca reveals that despite the influence of construction materials on dwelling quality, inhabitants do not perceive their housing as

precarious. The study identifies deficiencies in services, sanitation issues, and the crucial role of community solidarity due to limited governmental and non-governmental support [11]. This challenges the conventional understanding of habitability and emphasizes the subjective perception of residents in assessing the quality of their living conditions, highlighting the complex interplay between physical aspects of housing and the social context in which it is situated. By integrating strategies for climate resilience, urban planning, and sustainable housing practices, it is possible to work towards enhancing the habitability and adequacy of housing in marginalized urban areas

In Mexico, the National Housing Plan 2019-2024 prioritizes the attention to social housing, specifically addressing those with social disadvantages [12]. Within the framework of the National Strategic Programs, known as PRONACES (CONAHCYT, 2021), there are National Research and Advocacy Projects, known as PRONAII, the research presented here is part of the Project titled "Adequate housing, sustainable habitat, and social cohesion. Alternatives to impact urban poverty conditions in vulnerable priority areas in three cities in Mexico (Ciudad Juarez, Merida, and Mexicali)" [13].

This article analyzes the characteristics of precarious housing and its surroundings based on the perception of habitability conditions in an extremely hot-dry climate context. The results of the case study in Mexicali, Baja California, are presented.

2. METHOD

2.1 Study area

Mexicali is located in the desert strip of northwestern Mexico, at 32º39´48" N and 115º28´04" W. Based on the Köppen climate classification modified by Garcia, Mexicali's climate is type BW (h") hs (x") (e") which indicates a dry arid hot climate, with extreme thermal oscillation [14]; its mean annual temperature is 23.7°C with winter rains (Fig. 1).

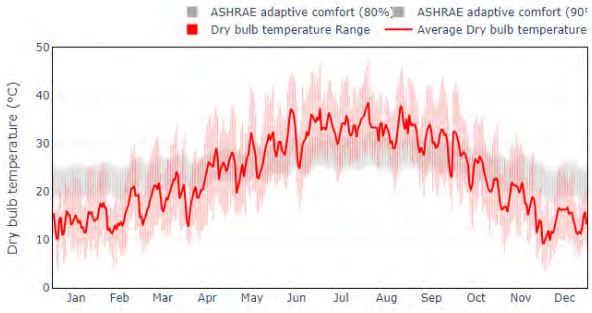

Figure 1: Annual Dry Bulb Temperature, Mexicali. CBE Clima Tool (2024).

Statistical data from 1981-2010 show a critical season due to high temperatures in the months of June through August, with average high temperature of 42.9 °C, and extreme high temperature of 45 °C. Additionally, it presents a cold season in the months of December through February with minimum mean temperature of 6.8 °C and extreme minimums of 3.4 °C, as shown in Fig. 2. Extreme maximum mean temperatures of up to 52 °C were recorded on July 28, 1995 [15].

2.2. Sample space definition

In Mexicali, according to the 2020 Population and Housing Census [16], the 2010 CONEVAL marginalization polygons [17] and the Priority Attention Polygons [18, 19] 27 Basic Geostatistical Areas (BGA) were identified.

Within the tiers of social lag in Mexicali, extreme critical conditions of social lag (low level) are not shown, since high and medium levels of social lag prevail (Table 1).

Table 1: Population and housing, Social Lag (SL) Zones, Mexicali, 2020

Area	Social lag	BGAs	Popula-tion	Housing
Mexicali, Mexicali	High	6925	399	115
Mexicali, Mexicali	High	7228	259	87
Mexicali, Mexicali	High	7779	1060	328
Progreso, Mexicali	High	6304	34	9
Progreso, Mexicali	High	6319	128	43
Progreso, Mexicali	High	7637	76	20
Puebla, Mexicali	High	7798	26	8
Sta. Isabel, Mexicali	High	6395	73	24
Mexicali, Mexicali	Medium	3812	908	307
Mexicali, Mexicali	Medium	3969	3137	986
Mexicali, Mexicali	Medium	5946	537	168
Mexicali, Mexicali	Medium	5965	339	112
Mexicali, Mexicali	Medium	6018	4443	1366
Mexicali, Mexicali	Medium	6910	539	174
Mexicali, Mexicali	Medium	7641	938	295
Mexicali, Mexicali	Medium	768A	246	68
Mexicali, Mexicali	Medium	7694	535	170
Progreso, Mexicali	Medium	5611	213	69
Progreso, Mexicali	Medium	6287	46	14
Puebla, Mexicali	Medium	5700	2241	715
Sta. Isabel, Mexicali	Medium	5113	719	202
Sta. Isabel, Mexicali	Medium	558A	114	32
Sta. Isabel, Mexicali	Medium	6338	486	133
Sta. Isabel, Mexicali	Medium	6342	87	27
Sta. Isabel, Mexicali	Medium	6376	462	133
Sta. Isabel, Mexicali	Medium	686A	50	18
Sta. Isabel, Mexicali	Medium	7529	257	76
Total			18,352	5,699

The main areas of concentration of the population were located in the eastern sector of the city, 5,432 people distributed in 1740 houses in an area of 270.07 hectares; the southern sector with 7,580

people distributed in 2352 homes in an area of 236.33 hectares; and the western sector, where 5,432 people were located, distributed in 1607 homes in an area of 560.39 hectares. Most of these sectors are part of the periphery of the urban area of Mexicali.

2.3. Sample design

We worked with a random sampling of a finite population, composed of the 27 AGEBs of study, leaving 10 areas, according to their proximity by spatial location. To more precisely identify the dynamics of concentration of the urban population in conditions of poverty in relation to housing, the census block was defined as the geographic unit of analysis.

The stratified random sampling technique of the blocks that concentrate the population in overcrowded homes was used, since this variable allows us to observe, as a whole, the concentration of the population and the physical habitability characteristic of the home. For the sample, a population of 18,352 inhabitants grouped in 5,699 homes was taken as a base, separating the cluster by the census variable "Average occupants per room in inhabited private homes" greater than 2%, considered as overcrowded homes.

The free access software STATCALC-Sampling Size Power from Epi Info™ [20] (CDC, 2022) was used to calculate the sample. The design parameters were adjusted to a real prevalence of 50% and 5% as a confidence limit, with a sample size of 90%, yielding a total of 267 surveys, which were adjusted to 300, due to the availability of financial and human resources to reduce field time and increase the accuracy and quality of data in the field.

For the spatial distribution of the survey points, the Sampling Design Tool for ArcGIS [21] was used; This open access tool creates random points stratified in spaces defined by polygons of interest. Once the sample points are generated, they are imported into the Qgis software [22], for analysis and cartographic adjustment, as well as for the design of maps for the work of collecting information in the field. To facilitate the distribution of the survey locations and surveyors, the field maps were exported in KML format, for the location of the sample points on mobile devices such as tablets and cell phones that have data, using the My maps application available at the Google suite.

2.4 Research design and instruments

The survey design was based on the United Nations' concepts of adequate housing. A questionnaire with 114 questions was developed.

In the urban context, the availability of services, materials, facilities, and infrastructure was considered, as well as the urban perception of these elements. Regarding housing, the quantity of spaces, dimensions of the spaces, type, and quality of materials, and construction systems were taken into account. For the analysis of habitability, structural, spatial, environmental, and sanitary aspects were considered.

Environmental habitability considers [9]: a) Thermal habitability, b) Luminous habitability, c) Acoustic habitability, d) Olfactory habitability and e) Spatial habitability. These variables were studied qualitatively.

2.5. Fieldwork

The survey was applied in person, during the months of October to December 2022 (Fig. 2). 308 valid questionnaires were obtained. The survey applied was reviewed and transferred to a digital format in Google Forms.

Figure 2: Fieldwork, Social Lag Zones, Mexicali, 2022.

2.6 Statistical analysis

The statistical analysis was carried out based on frequencies. Mainly the nominal variables related to the profile of the inhabitants, general characteristics of the home, environmental habitability conditions and structural conditions of the home were analyzed.

3. RESULTS

3.1 Profile of the inhabitant of Social Lag Areas

The age range of those interviewed was 2.6% under 19 years of age, 13.7% from 20 to 29 years of age, 14.7% from 30 to 39 years of age, 20.8% from 40 to 49 years of age, 18.9% from 50 at 59 years old and 29.3% aged 60 and over. This means that approximately 50% of the population is 50 years old or older. 62.5% are female and 37.4% are male.

It is observed that 49.1% of the homes are inhabited by two to three people, 36.1% by four to five people, 11.7% by six to seven people and 3.1% by eight or more people.

This means that approximately 50% of the population is 50 years old or older. Around 50% of the homes are inhabited by four or more people,

which generates overcrowding due to the number of rooms available for sleeping.

3.2. Characterization of housing in vulnerable areas

Two large general groups of housing typologies were identified, those self-built or self-produced and those acquired at the Baja California Housing Institute. The first group corresponds to a non-standardized design, use of diverse materials (concrete block and wood, among others); and use of materials in poor condition. The second group corresponds to a standardized housing model, called "progressive model", with an area of 21 square meters.

The inhabitants have not increased the size of their home, especially in the "progressive" model, since around half of the population lives in homes of 20-30 sqm (Fig. 3).

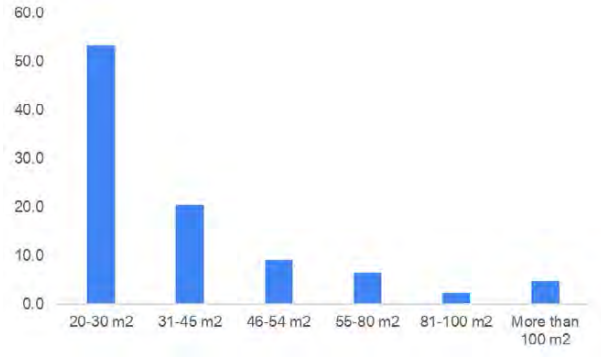

Figure 3: House Construction Area, Social Lag Zones, Mexicali (Percentage)

Regarding the number of rooms, 36.5% have three rooms, 25.7% have four rooms, 15.6% have two rooms. In 97.7% of the homes there is at least one bathroom inside the home, while the rest have none.

Regarding the predominant construction systems in walls, they are concrete blocks (51.5%), followed by wood (20.2%) and brick (16.3%). Meanwhile, 21.5% of roofs are made of wood, 21.2% are made of wood and galvanized sheet metal, and 15% are made of deck insulated concrete. Fig. 4 shows a house built with brick and another with waste materials.

Figure 4: Constructive systems in study area housing, Social Lag Zones, Mexicali

Regarding the services and equipment of the home, in these areas the home has access to drinking water, drainage and sewage services, electricity services, and the use of gas tanks for cooking.

Regarding the equipment of the home, 76.2% have some air conditioning equipment, 7.5% with an evaporative cooler, 8.8% with fans and 7.5% with no equipment. Even though a high percentage has air conditioning equipment, it is generally of low energy efficiency and most houses do not have thermal insulation in walls or ceilings.

3.3. Perception of environmental habitability conditions

Thermal habitability conditions are strongly affected in the warm season, as shown in Fig. 5. It is observed that 67.5% present some problem due to warm conditions, mainly as a consequence of the impact of the climate conditions and the housing's envelope characteristics.

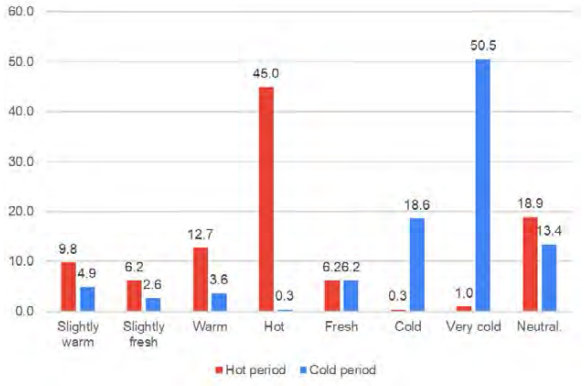

Figure 5: Perception of thermal habitability, precarious housing, Mexicali (Percentage).

Regarding luminic habitability, it is observed that lighting in the house, both natural and artificial, shows good acceptance levels by the inhabitants (Table 2).

Table 2: Perception of natural and artificial illumination.

Ilumination	Perception (Percentage)		
	Good	Regular	Bad
Natural	60.9	32.2	6.8
Artificial	64.5	29.3	6.2

In general terms of acoustic habitability, 40.1% reported that they sometimes hear noises from the outside, and 23.8% reported always hearing them, but they did not consider it a problem (Fig. 6).

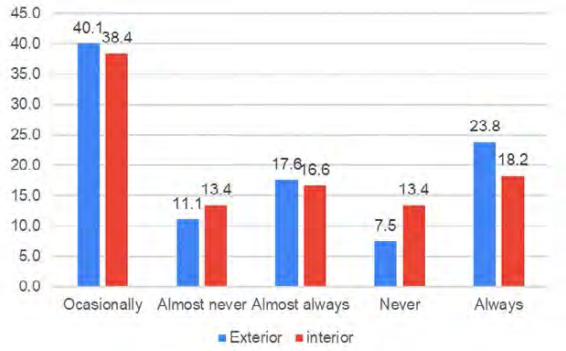

Figure 6: Perception of noise, Outdoor and Indoor, Percentage

Regarding the perception of odors, 30.3% reported that they always or almost always perceive odors from outside, 31.6% mention that occasionally perceive them and 38.1% that they do not perceive discomfort due to odors. The perception of odors was also not reported as a problem.

3.4. Other important aspects for habitability from the inhabitants' perspective

In the perception of the quality of public services in the neighborhoods, the drinking water service has a predominant good perception (67.1%); drainage and sewage is perceived as bad (47.9%) and electricity is perceived as good (70%).

In garbage collection services, 61.6% are perceived as good, 24.1 as average, 12.4 as bad and the rest did not respond. While the conservation of streets, pavements and sidewalks, 71% reported that they were in poor condition, 19.5% in fair condition and 8.1% that they were in good condition.

A relevant aspect in the perception of housing habitability conditions and its immediate context is safety (Fig. 7). At housing level, security is often obtained through guard dogs and the use of metal fences.

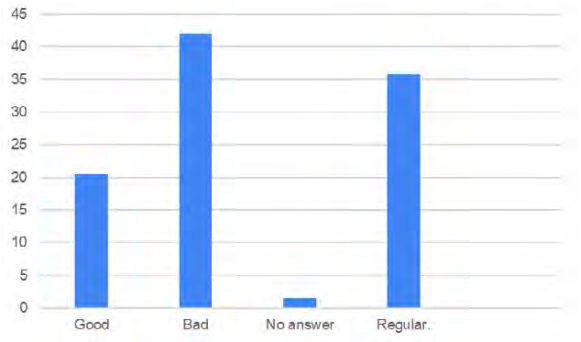

Figure 7: Neighborhood safety, Mexicali, Percentage.

In general, 68% consider that the main problem in these areas is the lack of security; 44.8%, the lack of public transportation; 35.5%, the distance to pay for services; 16.3%, the poor quality of housing; and 8.7% domestic violence, among others.

The inhabitants mentioned that the main reason for living in those areas or neighborhoods, 35.2% answered "because it is my home"; 25.7%, have no other option; 16.9%, because their family is close; 12.7%, because they like it, and only 2.6% mention they live there because its cheap or affordable.

4. CONCLUSIONS

The research findings show that, although in Mexicali, there are no critical conditions of social lag, compared to other areas of the country, effects due to the extreme weather conditions are identified.

Around half of the inhabitants of housing in areas of social lag do not have thermal habitability conditions neither in the hot nor in the cold season. Around 60% report that they perceive a good quality of natural lighting, even when the home feels "dark."

The predominance of self-construction without technical assistance and the lack of financial resources generated serious habitability problems, such as homes with a lack of thermal insulation, a lack of natural lighting, with minimum heights that do not facilitate natural ventilation, a lack of spatial functionality, with the use of materials not suitable for the climate, among others.

Making housing compatible as a human right, which allows inhabitants to have habitable conditions, regardless of socioeconomic level and in an extreme climate, remains a significant challenge.

Future quantitative studies are suggested to contrast with the qualitative responses of the inhabitants through measurements of indoor temperature, indoor relative humidity, lighting levels, air movement patterns, and air quality levels, to determine the indoor environmental conditions.

ACKNOWLEDGEMENTS

To the National Council of Humanities, Sciences, and Technologies (CONAHCYT), for the funding provided to PRONACES Project 321261.

REFERENCES

1. United Nations Human Right, UN Hábitat, (2010). The Right to Adecuate Housing Fact Sheet no. 21 rev1. Avalaible: **The Right to Adequate Housing: Fact Sheet No. 21/Rev.1 | UN-Habitat (unhabitat.org)** .

2. Onapa, H., Sharpley, C. F., Bitsika, V., McMillan, M., MacLure, K., Smıth, L., y Agnew, L. L. (2021). The Physical and Mental Health Effects of Housing Homeless People: A Systematic Review. *Health & Social Care in the Community*. https://doi.org/10.1111/hsc.13486

3. Mitchell, L., Baylis, P., y Randolph, S. (2021). Monitoring Enjoyment of the Rights to Adequate Housing and Health Care and Protection in Aotearoa New Zealand. *SSRN Electronic Journal*. https://doi.org/10.2139/ssrn.3926831

4. Davis, E. E. (2021). Housing as a Human Right Within an Era of International Exceptionalism. Constitutional Review. https://doi.org/10.31078/consrev723
5. Jiménez, M. L. G., y Antonio, V.-Y. (2021). Key Elements for a New Spanish Legal and Architectural Design of Adequate Housing for Seniors in a Pandemic Time. *Sustainability*. https://doi.org/10.3390/su13147838
6. Prószynski, M. B. (2023). The Legal Framework of Public Civil Archives in Spain. *Archiwa Biblioteki I MuzeaKościelne*. https://doi.org/10.31743/abmk.16272
7. Vima-Grau, S., Cornado, C., Ravetllat, P.J., y Garcia-Almirall, P. (2021). Multiscale Integral Assessment of Habitability in the Case of El Raval in Barcelona. *Sustainability*. https://doi.org/10.3390/su13094598
8. Nasir, A., Yusuf, A., Makhfudli, M., Harianto, S., Okviasanti, F., y Kartini, Y. (2023). Living Experiences of People Living With HIV-AIDS From the Client's Perspective in Nurse-Client Interaction in Indonesia: A Qualitative Study. Plos One. https://doi.org/10.1371/journal.pone.0282049
9. Jirón, P., Toro A., Caquimbo S., Goldsack L. Martínez L., Colonelli P., Hormazábal N. y P. Sarmiento (2004). Bienestar Habitacional. Guía de Diseño para un Hábitat Residencial Sustentable. Santiago de Chile.
10. Irving, A. (2021). Exploring the Relationship Between Housing Conditions and Capabilities: A Qualitative Case Study of Private Hostel Residents. Housing Studies. https://doi.org/10.1080/02673037.2021.1928004
11. Caballero, J., Pérez, M. y Gómez, L. (2017). Percepción de habitabilidad en la vivienda precaria: caso Zona Metropolitana Oaxaca, México. *Revista Contribuciones a las Ciencias Sociales.* http://www.eumed.net/rev/cccss/2017/03/vivienda-precaria-mexico.html
12. Gobierno de México, (2019). Programa Nacional de Vivienda 2019-2024 https://www.gob.mx/shf/documentos/plan-nacional-de-vivienda-pnv-2019-2024#:~:text=El%20Programa%20Nacional%20de%20Vivienda%20%28PNV%29%20comprende%20una,de%205%20millones%20de%20familias%20tengan%20un%20hogar
13. Universidad Autónoma de Ciudad Juárez, Universidad Autónoma de Yucatán y Universidad Autónoma de Baja California. (2022). PRONACES Vivienda adecuada, hábitat sustentable y cohesión social. Alternativas para incidir en las condiciones de pobreza urbana en zonas vulnerables de atención prioritaria en tres ciudades de México (Ciudad Juárez, Mérida y Mexicali).
14. Urias, H., García, O., y Bojórquez, G. (2020). Identification and classification of local climate zones in a semi-arid city of northwestern Mexico. *Viviendas y comunidades sustentables* https://doi.org/10.32870/rvcs.v0i9.163.
15. Sistema Meteorológico Nacional https://smn.conagua.gob.mx/tools/RESOURCES/Normales_Climatologicas/Normales8110/bc/nor8110_02033.TXT
16. INEGI. (2020). Censo de Población y Vivienda 2020. Retrieved from https://www.inegi.org.mx/programas/ccpv/2020/#Microdatos. Retrieved 15 de octubre de 2021, from Instituto Nacional de Geografía https://www.inegi.org.mx/programas/ccpv/2020/#Microdatos
17. CONEVAL (2010). Grado de Rezago Social en AGEB, http://www.coneval.gob.mx
18. CONEVAL. (2018). Criterios Generales para la Determinación de las Zonas de Atención Prioritaria, 2019. Consejo Nacional de Evaluación de la Política de Desarrollo Social Retrieved from https://www.coneval.org.mx/Medicion/Documents/Criterios-ZAP-2019.pdf.pdf
19. SEDATU. (2021). Criterios generales para la elaboración del Plan de Acciones Urbanas Prioritarias para la aplicación del Programa de Mejoramiento Urbano2021 vertiente Mejoramiento Integral de Barrios. Secretaría de Desarrollo Agrario, Territorial y Urbano Retrieved from https://mimexicolate.gob.mx/wp-content/uploads/2021/02/Criterios-PAU-PMU-MIB-04-enero-2021.pd
20. CDC. (2022). Epi Info 7: Centers for Disease Control and Prevention, US. Retrieved from https://www.cdc.gov/epiinfo/esp/es_index.htm
21. Buja, K., & Menza, C. (2013). Sampling design tool for ArcGIS: Instruction manual.[for ESRI ArcGIS 10.0 Service Pack 3 or higher]. In: NOAA/National Centers for Coastal Ocean Science.
22. QGIS.org. (2022). QGIS 3.22. Geographic Information System User Guide.: QGIS Association. Retrieved from https://www.qgis.org/es/site/index.htm

PLEA 2024 WROCŁAW
(Re)thinking Resilience

Building Performance Profiles using Neural Networks:
Learned Vector Embeddings for Building Energy & Water Usage Mapping

ANDREW AZIZ[1]

[1]Toronto Metropolitan University / Independent, Toronto, Canada

ABSTRACT: The availability of energy usage, water usage, and carbon emissions data plays a key role in the pursuit of researching sustainable design strategies. However, given that this data includes many different metrics for many buildings, analysing and visualizing this data remains challenging. This paper proposes an unsupervised learning pipeline using neural networks to generate vector embeddings – defined as $f : \mathcal{D} \rightarrow \mathbb{R}n$ where data $\mathcal{D}$ is embedded into an n-dimensional vector – to convert the many metrics of building performance into a singular vector for each building. This paper presents a case study using this methodology on multifamily buildings in New York, USA using the "Energy and Water Data Disclosure for Local Law 84 2022" dataset. From this, 64-dimension vector embeddings are generated for 13,500 multifamily buildings, embedding 26 building performance metrics. The resulting vectors are plotted using a t-SNE dimensionality reduction and analysed using K-Means clustering to group them into categories based on similar building performance. Relative analysis between vectors is also performed by measuring Euclidian distance and Cosine Similarity. This approach offers great potential as a novel methodology for visualizing and analysing building energy usage, water usage, and carbon emissions data for a wide range of stakeholders.
KEYWORDS: Energy and Water Usage Embeddings, Unsupervised Feature Learning, Vector Embeddings, Building Energy Consumption and Emission Profiles, Building Performance Visualization

1. INTRODUCTION

The built environment is a key contributor to worldwide carbon emissions and energy consumption, with research into decarbonization efforts being paramount. However, while access to building energy, water consumption, and carbon emissions data has started to become more accessible for researchers, mapping and drawing insights from this data remains a difficult process. Recent work [1] has sought to create a data sharing platform to catalogue the many building performance datasets. While this process makes it much more seamless to search for relevant building data, it works primarily as a repository. Given that many datasets related to building performance emerging from initiatives such as New York's "Energy and Water Data Disclosure for Local Law 84" contain many discrete measurements and metrics (249 attributes/categories describing ~30,000 buildings for the 2021 dataset) [2], it is important to define a pipeline for mapping and classifying this data such that insights can be drawn efficiently to help inform decision making and research.

At present there exists a key research gap regarding the accessibility of this building performance data by designers, architects, and developers to extract insights from these metrics and put them into action. This gap, which exists both in research and practice has a significant impact on preventing thorough precedent research for stakeholders interested in either finding buildings similar to their proposal from which they can learn from, or to understand the scope and potential opportunity of a given energy retrofit from either a research or business perspective. Having access to a system which provides a relative similarity score (such as a score between 0-1) for energy usage, water usage, and carbon emissions between buildings fills a key research gap and provides pertinent data to the many stakeholders who play a role in the building development process to learn from precedents and to make climate positive decisions.

This paper proposes leveraging a process of unsupervised feature learning on building energy usage, water usage, and carbon emissions datasets to create "building performance profiles". These "profiles" are vector embeddings, created using unsupervised feature learning which is defined as the following: $f : D \rightarrow \mathbb{R}n$ where data D is transformed into an n-dimensional vector in a latent space. This allows for the efficient mapping and comparison of many disparate metrics within a dataset (such as the many energy, water, and carbon metrics) by embedding a series of vectors to each describe an individual object such as a building. These vectors serve as a proxy for energy usage, water consumption, and carbon emission. This approach is chosen due to its proficiency in cataloguing

multidimensional data into a consistent vector which can be compared and studied at scale by measuring the distance and angles between vectors (via Euclidian distance and Cosine Similarity respectively), and from which relative insights can be drawn that would otherwise be hidden in the raw data.

2. LITERATURE REVIEW AND RELATED WORK

An extensive literature review was conducted to study similar work in this area as a point of departure. Literature related to the underlying technological approach for the proposed methodology in this paper, as well as research from other domains that utilized a similar approach was also studied.

2.1 Neural Networks and Building Performance

The use of neural networks in the pursuit of developing sustainable buildings has largely focused on the prediction of building performance and energy consumption. This is largely applied using regression where models are trained to identify the relationship between independent variables and a dependent variable. In the realm of the two key machine learning paradigms – *supervised* and *unsupervised* – regression models are situated in the former, where a model is trained on a labelled dataset with input data corresponding to labelled output data.

This approach can be used to train deep learning models using remotely sensed data or building characteristics – including street view, aerial images, building height data, glazing area, orientation, occupancy, among other variables [3-7] – to understand the relationship between those variables and the building energy usage. This can be used to predict the energy usage/performance of buildings using those aforementioned characteristics. This is done to increase the availability of energy usage data without on-site visits or in areas where access to this data is limited [4]. It is also possible to use these models to identify which of these building characteristics disproportionally contribute to energy inefficiency [3].

Other research in this area has also used this approach to forecast energy usage data from a large set of existing of data points, also known as a *Time Series Forecasting Method* [8, 9]. This data and prediction can be based on long-term data (yearly) [4, 8], or short-term energy usage (hourly) [4, 10, 11]. This predictive data can be used to optimize the performance of existing smart buildings [9, 12].

As neural networks become more successful in predicting and aggregating data, there have been initiatives to catalogue this data [10]. However, it is becoming increasingly important for this data to be available in an accessible format for designers, architects, developers, and other stakeholders such that insights can be extracted. As a result, there exists a research gap in the space of accessible visualization and analysis tools that catalogue building performance data.

Recent work including “The Building Data Genome Directory” [1] begins to bridge this gap by aggregating datasets for building energy performance that can filtered based on a wide range of metrics. While this increases data accessibility, it remains in a tabular form. Similarly, it exists mainly as raw data which renders large scale comparison and analysis between buildings difficult. Also, given the wide range of metrics which define building performance – including energy and water usage, gas emissions, among many others [2] – it is important for any visualization to map all these values to create a comprehensive system of analysis for a building.

Given the multi-dimensional and complex nature of this data and the related metrics, it is necessary to return to neural networks to visualize, process, and analyse them – albeit from the perspective of vector embeddings as opposed to the predictive regression models.

2.2 Vector Embeddings and their Visualizations

Vector embeddings leverage an unsupervised process, where models strive to search for patterns in an unlabelled dataset. As opposed to the supervised models which require a sufficiently large training dataset labelled or categorized by a human reviewer, unsupervised models can find patterns and clusters in large unlabelled datasets from which insights can be drawn [9]. The creation of vector embeddings using unsupervised feature learning is defined as the following: $f : D \rightarrow \mathbb{R}$n where data D is transformed into an n-dimensional vector in a latent space. Vector embeddings use a process of dimensionality reduction, where complex data can be captured in a n-dimension latent space and represented as vectors where processes such as clustering (grouping similar vectors into categories) can occur [9].

Given that this process of vector embedding is very successful at converting raw data into an n-dimensional latent space, it initially emerged in natural language processing research via word2vec [13-15]. Recently it has been adapted for mapping spatial data [16-18], however to the best of the author's knowledge it has yet to be adapted for the purposes of studying building performance metrics.

Vector embeddings have become very effective at capturing complex, multi-dimensional data and allowing it to be synthesized into a singular vector which can then be visualized and processed efficiently. This paper will utilize this approach to synthesize the many relevant building performance metrics for each building into a vector such that buildings can be mapped and analysed in relation to each other.

3. METHODS

This paper utilized the "Energy and Water Data Disclosure for Local Law 84 2022 (Data for Calendar Year 2021)" dataset for New York, NY from NYC OpenData [2]. It consists of 249 attributes/metrics describing 29,842 buildings.

3.1 Data Processing

Of these 249 attributes comprising of metrics ranging from energy use to property address to gross floor area, 26 of the metrics most relevant to overall building energy and water consumption, and carbon emissions were selected as defined in Table 1:

Table 1: Selected Energy and Water Consumption / Emission Attributes from the Energy and Water Data Disclosure for Local Law 84 2022 Dataset for Buildings in New York, NY

Consumption / Emission Attribute	Unit
Largest Property Use Type - GFA	(ft^2)
Year Built	(year)
Site EUI	($kBtu/ft^2$)
Weather Normalized Site EUI	($kBtu/ft^2$)
National Median Site EUI	($kBtu/ft^2$)
Site Energy Use	(kBtu)
Weather Normalized Site Energy Use	(kBtu)
Weather Normalized Site Electricity	(kWh/ft^2)
Weather Normalized Site Natural Gas	($therms/ft^2$)
Source EUI	($kBtu/ft^2$)
Weather Normalized Source EUI	($kBtu/ft^2$)
National Median Source EUI	($kBtu/ft^2$)
Source Energy Use	(kBtu)
Weather Normalized Source Energy	(kBtu)
Natural Gas Use	(kBtu)
Electricity Use - Grid Purchase	(kBtu)
Electricity Use - Grid and Generated from Onsite Renewable Systems	(kWh)
Total GHG Emissions	(MTCO2e)
Direct GHG Emissions	(MTCO2e)
Indirect GHG Emissions	(MTCO2e)
Net Emissions	(MTCO2e)
Property GFA - Calculated (Buildings)	(ft^2)
Indoor Water Use (All Sources)	(kgal)
Outdoor Water Use (All Sources)	(kgal)
Municipally Supplied Potable Water	(kgal)

The 29,842 unique buildings were defined as a variety of different programmatic types including "*Multifamily Housing*", "*K-12 School*", "*Office*", "*Multifamily Housing, Parking*", and "*Multifamily Housing, Retail Store*". For the purposes of this research, 13,500 of the buildings defined exclusively as "*Multifamily Housing*" were selected to comprise the training dataset to minimize the noise from differing programmatic types. For this data to be processed by the neural network, it was also necessary to normalize all the individual metrics to be between 0 and 1 using min-max normalization.

3.2 Generating the Vector Embeddings

As mentioned previously, this paper and methodology uses vector embeddings to map and process building performance data. This technique allows for the efficient mapping and comparison of many disparate metrics within a dataset by embedding a vector to describe each building's energy usage, water usage, and carbon emissions.

In order to create the vector embeddings this paper utilizes an autoencoder, which consists of an encoder and decoder. Mean Squared Error (MSE) is chosen as the loss function and the Adam optimizer is also used. The architecture for the autoencoder is:

- Encoder:
  - 26 → 48 neurons fully connected layer,
  - ReLU activation function,
  - 48 → 64 neurons fully connected layer
- Decoder:
  - 64 → 48 neurons fully connected layer,
  - ReLU activation function,
  - 48 → 26 neurons fully connected layer

In the autoencoder, the encoder takes an input of 26 (which corresponds to the number of unique metrics) and transforms it through two fully connected layers - with the first layer having a hidden representation of 48 dimensions and a ReLU activation, followed by a second layer which maps the representation from 48 to 64 dimensions. The decoder takes this output and reverses the process, eventually mapping it back to the original input dimension. There were 1000 epochs used and the best validation loss for this training was 0.0817.

The resulting embeddings can be reduced in dimensionality (64 to 2 dimensions) using t-SNE, such that the embeddings and resulting vectors can be visualized. This process allows the conversion of many unique datapoints per building representing energy performance into a single consistent 64-dimensional vector for each building, which allows for large scale comparison between buildings as a function of their performance.

For the purposes of replicability, it is important to note that the unsupervised learning nature of this process will likely result in some variation between training iterations. Nonetheless, the general clusters and similarity values should remain consistent. However, it does likely mean that comparing datasets embedded at different times will likely result in some variance and, as a result, buildings should only be compared with those in the same dataset.

4. RESULTS

This paper defined an approach for generating vector embeddings of building energy usage, water usage, and carbon emissions data using unsupervised learning. As more data is being collected by municipalities and cities through open data initiatives, this seeks to define a pipeline for the large-scale analysis and comparison between building performance based on metrics such as energy and water usage, direct and indirect greenhouse gas emissions, among many others [2]. These vectors can be compared to each other and grouped based on Euclidian distance and Cosine Similarity (measuring the angle between vectors).

4.1 Visualizing Data using t-SNE

Using t-SNE, dimensionality can be reduced (64 to 2-dimensions) such that the embeddings and resulting clusters can be visualized (Fig. 1). From this, it is possible to identify which buildings have a similar performance profile. Buildings with good performance (low carbon emissions, low energy and water usage) will appear in the same region, and the opposite will as well, with all other buildings grouped respectively across the vector latent space.

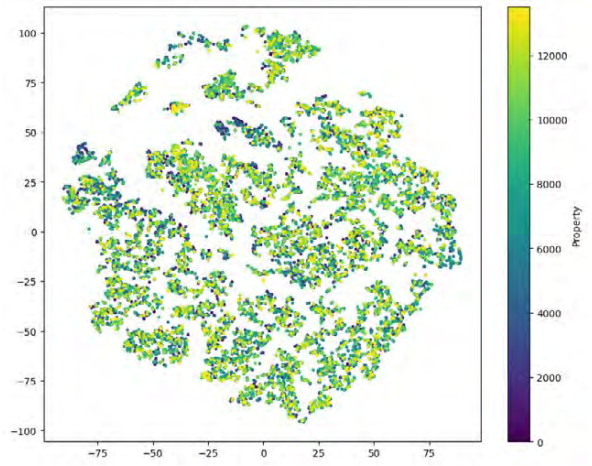

Figure 1: Multifamily Building Energy & Water Usage Embeddings Visualized Using t-SNE Visualization

It is also possible to perform cosine similarity on the vector embeddings to identify buildings with the most similar profiles to a selected building.

Table 2: Cosine Similarity for a selected building (a value closer to 1 means that building is more similar to 750 Riverside Dr.). This table is showing the 4 most similar buildings to 750 Riverside Dr. in the dataset.

As shown in Table 2, the buildings with a similar cosine similarity to 750 Riverside Dr. all appear to have very similar energy usage, greenhouse gas emissions, and property gross floor areas, showing how this approach can successfully map and compare all of these metrics effectively.

Through this approach, identifying a building with good building performance metrics will allow for the identification of other similar performing buildings given that they will be near in the latent space.

4.2 Visualizing Categories using K-Means Clustering

This paper also uses the K-Means algorithm to categorize the resulting vectors into an *k* number of clusters (Fig. 2). K-means groups the data (in this case the building performance vectors) into the prescribed number of clusters based on the Euclidian distance between every vector [19].

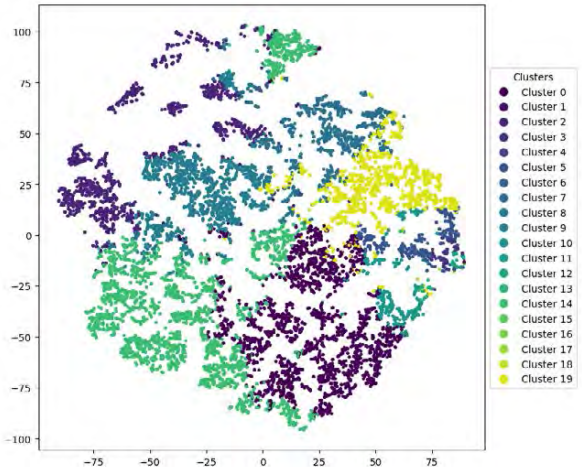

Figure 2: Multifamily Building Energy & Water Usage Embeddings Visualized Using t-SNE Visualization and K-Means Clustering

As a result, the building vectors can be grouped based on their vector similarity where the nearest vectors are grouped together to result in a *k* number of clusters. This paper defined *k* as 20 clusters that the building vectors were grouped into. The resulting graph (Fig. 2) showcases the vector embeddings (which have been reduced to 2-dimensions using t-SNE) classified into the 20 unique clusters.

5. DISCUSSIONS

This methodology provides a pipeline to translate complex and multifaceted data into a consistent and comparable vector. This allows for a much more

Address	Cosine Similarity	Year Built	Site Energy Use (kBtu)	Electricity Use – Grid (kBtu)	Total GHG (MTCO2e)	Direct GHG (MTCO2e)	Indirect GHG (MTCO2e)	Property GFA (ft²)
750 Riverside Dr.	**1**	**1920**	**4439305**	**166418.9**	**247.5**	**205.6**	**41.9**	**43123.0**
2501 Newkirk Ave.	~0.9999861	1931	4541227.3	187933	254.5	207.1	47.3	44800.0
8742 Elmhurst Ave.	~0.9999822	1932	4848383.7	193400.9	271.2	222.5	48.7	45850.0
536 Beach 22nd St.	~0.9999803	1932	4062261.7	136404.7	225.4	191	34.3	36500.0
5801 14th Avenue	~0.9999798	1927	3882438.6	162421.1	217.7	176.8	40.9	38410.0

effective process for conducting precedent research when it comes to analysing building performance. It has great potential to support the work of researchers, architects, designers, developers, and other stakeholders in the pursuit of developing more sustainable buildings. It similarly acts as foundational approach from which many other research trajectories could leverage to synthesize the multi-dimensional data of building performance and predict/understand which variables affect building energy efficiency.

Use cases for this methodology include studying the feasibility of conducting building retrofits using a specific approach, which can be done by studying the number of buildings which sit within a relevant cluster that holds a reference project. Also, it is possible to identify buildings most in need for a retrofit based on their similarity to previously identified buildings.

5.1 Limitations

It is important to mention the potential limitations of this methodology. First relates to the access and availability of data. While the availability of energy usage, water usage, and carbon emissions datasets are becoming more commonplace, not all municipalities and cities publicly release or even collect this data. As a result, it may be difficult for this methodology to be applied to a city that doesn't release this type of data.

The second potential limitation is the issue of inconsistent data. It is common for many cities that do collect this data to do so in either differing units or metrics, or to not collect certain values at all. This inconsistency can require additional pre-processing as well as the removal of relevant data points and metrics which were provided by one municipality but not the other to create a consistent dataset. Both of these limitations, however, help define the next steps of this research.

5.2 Next Steps

The issue of data availability is key as inconsistent or missing data of a given regions renders that entire region unable to be mapped and prevents the subsequent vector embeddings/profiles from being generated. However, one of the key next steps is to invert the pipeline of data → vector embeddings and instead leverage other independent variables to predict the vector embeddings. In lieu of all the necessary energy usage, water usage, and carbon emissions data, it is possible to use other sources of publicly available data – including street view images, aerial images, building orientation, etc. – to train machine learning models to predict the vector embeddings of those buildings. This approach is similar to other regression analysis that has taken place in this area of research [3-7], but instead of trying to predict a singular metric or building energy efficiency score, a vector would be predicted which represents a much more comprehensive capture of building performance. This would require a sufficiently large dataset of vectors for a wide range of buildings (which this paper provides) in a similar climatic region. This proposed pipeline offers an alternative to generating the necessary vector embeddings should the data for a specific municipality be unavailable or not be made public.

This does, however, raise another point of discussion when it comes to the potential limitations of scaling this methodology, especially across different regions around the world and between different program types. Even if similar metrics are present in datasets for two climatically differing cities – such as New York and Amsterdam for example – the respective design strategies to create buildings which suit those climates are different. The design and detailing of buildings in one region will vastly differ from the other (as will the building performance) to even maintain the same level of comfort inside the building. Other lifestyle factors due to both climatic and cultural differences can also have an impact on building performance values and profiles. As a result, for this methodology to be impactful, buildings should only be mapped and compared to other buildings of both a similar programmatic type and in similar regions or climatic environments. As a result, issues of inconsistent data between different municipalities and cities can be of less concern (especially if they are vastly different in climate) since buildings should primarily be compared in similar regions. Datasets within each region are expected to be sufficiently large enough and capture a wide range of metrics to prove fruitful in a relative comparison process, even if not all of the data is consistent between cities. Similarly, since one of the key attributes of vector embeddings is the ability to compress inconsistent data into a consistent n-dimensional vector, a sufficiently large dataset should for suitable for intra-dataset (and subsequently intra-city) comparison and analysis.

Another next step is to integrate this data it into a building genome system which allows for someone to search up a building based on its performance characteristics and metrics, and then find buildings similar to that one. It would also be pertinent to have this data be accessible in a map format so buildings can be more easily studied and compared in a spatial interface. Making this information accessible via an interface or map allows possible stakeholders to have further access to this data and allows them to extract valuable insights without needing a technical background.

6. CONCLUSIONS

This paper proposes an approach for the generation of vector embeddings for building performance data including energy usage, water usage, carbon emissions, and other metrics. This process is used to map many discrete metrics that define building performance and energy efficiency into vectors such that comparisons between building performance "profiles" can be mapped and analysed.

It is also possible to map these vectors against other environmental or social factors to study how they can impact building energy usage, water consumption, and climate emissions. Given that the pursuit of sustainable design is multifaceted, it is important to understand the many other factors which have an impact on building efficiency and performance.

Future work also includes integrating multiple years of datasets into the embeddings to track progress and see if similar buildings are trending in the same direction from a performance standpoint. This can identify which buildings are getting either more or less efficient relative to their peers.

As more building energy usage, water usage, and carbon emissions data gets collected in the pursuit of sustainable design, it is important for this multi-dimensional data to be catalogued and mapped in a way that allows for further comparison and analysis. Using a dataset which catalogues the energy and water usage of 13,500 multifamily buildings in New York, USA, this paper introduced a methodology that leverages a technique known as vector embeddings to generate a 64-dimension vector to capture the building performance and efficiency for each building. This approach allows for building performance vectors to be compared to each other using Euclidian distance, Cosine Similarity, and K-Means clustering. This methodology proposes a novel approach for visualizing and analysing building energy usage, water usage, and carbon emissions data and offers great potential for making this data more accessible in the pursuit of creating more sustainable buildings.

REFERENCES

1. X. Jin et al., "The Building Data Genome Directory -- An open, comprehensive data sharing platform for building performance research," 2023, doi: 10.48550/ARXIV.2307.00793.

2. "Energy and Water Data Disclosure for Local Law 84 2022 (Data for Calendar Year 2021) | NYC Open Data." Accessed: Aug. 30, 2023. [Online]. Available: https://data.cityofnewyork.us/Environment/Energy-and-Water-Data-Disclosure-for-Local-Law-84-/7x5e-2fxh

3. C. E. Kontokosta, "Predicting Building Energy Efficiency Using New York City Benchmarking Data," presented at the 2012 ACEEE Summer Study on Energy Efficiency in Buildings, 2012, pp. 163–174.

4. K. Mayer, L. Haas, T. Huang, J. Bernabé-Moreno, R. Rajagopal, and M. Fischer, "Estimating building energy efficiency from street view imagery, aerial imagery, and land surface temperature data," 2022, doi: 10.48550/ARXIV.2206.02270.

5. M. Rosenfelder, M. Wussow, G. Gust, R. Cremades, and D. Neumann, "Predicting residential electricity consumption using aerial and street view images," Applied Energy, vol. 301, p. 117407, Nov. 2021, doi: 10.1016/j.apenergy.2021.117407.

6. M. Sun, C. Han, Q. Nie, J. Xu, F. Zhang, and Q. Zhao, "Understanding building energy efficiency with administrative and emerging urban big data by deep learning in Glasgow," Energy and Buildings, vol. 273, p. 112331, Oct. 2022, doi: 10.1016/j.enbuild.2022.112331.

7. A. Tsanas and A. Xifara, "Accurate quantitative estimation of energy performance of residential buildings using statistical machine learning tools," Energy and Buildings, vol. 49, pp. 560–567, Jun. 2012, doi: 10.1016/j.enbuild.2012.03.003.

8. J.-S. Chou and D.-S. Tran, "Forecasting energy consumption time series using machine learning techniques based on usage patterns of residential householders," Energy, vol. 165, pp. 709–726, Dec. 2018, doi: 10.1016/j.energy.2018.09.144.

9. H. P. Das et al., "Machine Learning for Smart and Energy-Efficient Buildings," 2022, doi: 10.48550/ARXIV.2211.14889.

10. P. Emami, A. Sahu, and P. Graf, "BuildingsBench: A Large-Scale Dataset of 900K Buildings and Benchmark for Short-Term Load Forecasting," 2023, doi: 10.48550/ARXIV.2307.00142.

11. A.-D. Pham, N.-T. Ngo, T. T. Ha Truong, N.-T. Huynh, and N.-S. Truong, "Predicting energy consumption in multiple buildings using machine learning for improving energy efficiency and sustainability," Journal of Cleaner Production, vol. 260, p. 121082, Jul. 2020, doi: 10.1016/j.jclepro.2020.121082.

12 L. Zhang and Z. Chen, "Opportunities and Challenges of Applying Large Language Models in Building Energy Efficiency and Decarbonization Studies: An Exploratory Overview," 2023, doi: 10.48550/ARXIV.2312.11701.

13. Q. V. Le and T. Mikolov, "Distributed Representations of Sentences and Documents," 2014, doi: 10.48550/ARXIV.1405.4053.

14. Y. LeCun, Y. Bengio, and G. Hinton, "Deep learning," Nature, vol. 521, no. 7553, pp. 436–444, May 2015, doi: 10.1038/nature14539.

15. T. Mikolov, K. Chen, G. Corrado, and J. Dean, "Efficient Estimation of Word Representations in Vector Space," 2013, doi: 10.48550/ARXIV.1301.3781.

16. P. Gramacki, S. Woźniak, and P. Szymański, "gtfs2vec -- Learning GTFS Embeddings for comparing Public Transport Offer in Microregions," 2021, doi: 10.48550/ARXIV.2111.00960.

17. K. Leśniara and P. Szymański, "highway2vec -- representing OpenStreetMap microregions with respect to their road network characteristics," 2023, doi: 10.48550/ARXIV.2304.13865.

18. Z. Wang, H. Li, and R. Rajagopal, "Urban2Vec: Incorporating Street View Imagery and POIs for Multi-Modal Urban Neighborhood Embedding," 2020, doi: 10.48550/ARXIV.2001.11101.

19. P. Arora, Deepali, and S. Varshney, "Analysis of K-Means and K-Medoids Algorithm For Big Data," Procedia Computer Science, vol. 78, pp. 507–512, 2016, doi: 10.1016/j.procs.2016.02.095.

PLEA 2024 WROCŁAW
(Re)thinking Resilience

REVEAL The Unseen:
The Incidence of Air Purifiers on Indoor Air Quality in Classrooms Located in Polluted Urban Areas in Southern Chile

MARÍA ISABEL RIVERA[1-2], VALENTINA GONZALEZ[1], PATRICIA HUERTA[3], PIA MONTSERRAT MELLADO[1], ANGELA JAVIERA CARRASCO[1], MARIA CAMILA CORONADO[3], ALISON KWOK[3], ANDREA MARTÍNEZ[1]

[1] Departamento de Arquitectura, Facultad de Arquitectura, Urbanismo y Geografía, Universidad de Concepción, Chile
[2] Centre for Sustainable Urban Development (CEDEUS), Chile
[3]Departamento de Salud Pública, Facultad de Medicina, Universidad de Concepción, Chile
[4] Department of Architecture, University of Oregon, Oregon, U.S.A.

ABSTRACT: - Providing fresh air in naturally ventilated classroom settings is essential for the health and well-being of students and teachers. However, providing fresh air is not always easy for schools located in polluted outdoor air conditions, such as high concentrations of particulate matter (PM2.5 or PM10) like those located in central and south-central regions of Chile, frequently exceeding international standards frequently. The need for a low-cost intervention to reduce indoor pollutants in classrooms is relevant and urgent. This research aims to investigate the efficacy of low-cost interventions in naturally ventilated schools in southern Chile during the winter season. Fieldwork was undertaken in nine classrooms from two schools in the metropolitan area of Concepción during the winter 2023. Results show a significant improvement in the reduction of particulate matter in the classroom with an air purifier (REVEAL) fabricated for this study compared to manufactured air purifier and control conditions (no intervention in the classroom). This study provides a significant contribution to how IAQ can be improved through low-cost interventions, with significant implications for improving the health and well-being of students and teachers.
KEYWORDS: Indoor air quality, air purifiers, primary schools, energy poverty

1. INTRODUCTION

Providing fresh air in naturally ventilated classroom settings is essential for the health and well-being of students and teachers. The latter became of great importance during the COVID-19 pandemic to reduce airborne transmissions. However, providing fresh air is not always an easy endeavor for schools that are located in polluted outdoor air conditions, such as high concentrations of particulate matter ($PM_{2.5}$ or PM_{10}) like those located in central and south-central regions of Chile, frequently exceeding international standards frequently [1,2]. Firewood is used extensively in these regions for space heating, causing high concentrations of particulate matter indoors and outdoors during the heating season [from May to October]. This is in part due to the lack of energy efficiency standards and stricter building codes on building envelope construction which has led to high thermal transmittance of most residential building envelopes. In addition, the high cost of electricity in Chile has led users to find cheaper forms of space heating, like firewood, for locations in cold Mediterranean and oceanic climates located south of Santiago.

In addition, fresh air can only occur in these types of schools by opening a window, and this is limited during the cold winter season when outdoor temperatures are low, impacting users ʾcomfort when these schools cannot afford to provide heating systems in their classrooms. School design in Chile, as well as residential design, lacks indoor environmental quality (IEQ) standards, such as the international standards ASHRAE 55 or ISO 7730. Most schools do not have heating or cooling systems due to prohibitive associated costs; thus, energy poverty also applies to school buildings [3]. Chilean educational investment capital is limited, and, in many cases, there are no funds to cover such operational costs, particularly in public schools.

Indoor air quality in schools has been evidenced to be poor due to insufficient air ventilation rates and high student density [4 - 7]. Previous studies have shown difficulty in delivering indoor air quality in classrooms with high occupancy, which leads to high CO_2 concentration due to respiration.

CO_2 concentrations can also be used as a proxy for indoor air quality in the classroom, as shown in the study by Chatzidiakou et al. [8,9]. Low CO_2 concentration is correlated with the dilution of indoor pollutants and the purge of airborne particles. Therefore, finding proven and cost-effective methods to reduce indoor pollutants in naturally ventilated classrooms is essential, particularly for children who

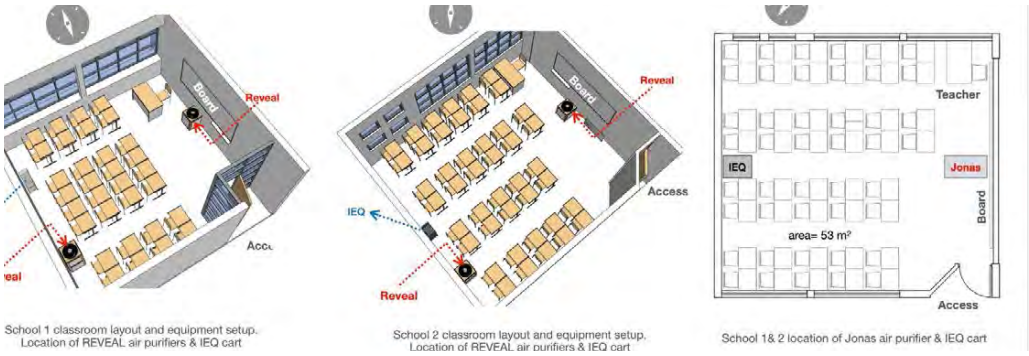

Figure 3: *Classroom layout and equipment setup for school 1 & 2. Image left and middle show location of air purifies REVEAL and IEQ cart at the back of the classroom. Image on the right show floor plant view of location of Jonas air purifier front of the classroom.*

spend a significant amount of their life in school and are more susceptible to long-term health damage due to low IEQ.

The need for a low-cost intervention to reduce indoor pollutants in classrooms is relevant and urgent. This research aims to investigate the efficacy of low-cost interventions in naturally ventilated schools in southern Chile during the winter season. In addition, our understanding of occupants 'adaptive behavior, occupancy patterns, and indoor pollutant characterization can be found in naturally ventilated classrooms.

Figure 1: inside views of classroom topology in both schools. In red square shows the location of IEQ cart.

2. METHODOLOGY

2.1 Field study location

The study design was a pragmatic controlled trial, wherein two classroom interventions were tested against the usual ventilation in three classrooms across two schools—one located in the city of San Pedro de la Paz and the other in the city of Chiguayante—during the winter season of 2023. Both cities are part of the metropolitan area of Concepción, in southern Chile, at 36°49' South Latitude, 73°2' West longitude and 15 meters above sea level. Climate conditions for Concepción, based on the updated Köppen-Geiger climate classification for continental Chile [10], are temperate Csb, with cold, mild winters and mild dry summers. Based on TMYx.2004-2018 data, Concepción has 2044 HDD (18°C), with an annual average temperature of 13°C (55°F), an average minimum of 2°C (36°F), and an average maximum of 26°C (79°F) [11].

2.2 Case Study

The selected criteria for the schools included: 1) accessibility to public/public-subsidized middle school grade levels (6th to 8th); 2) classrooms with the same orientation (i.e., facing north); 3) naturally ventilated classrooms; 4) no HVAC system and limited heating. In addition, occupant density is set to be a minimum of 1.1m2/student (11.8 ft2) and a volume of air of $3m^3$/student [12]. Figure 1.

2.3 Data Collection

Physical measurements of environmental parameters indoors and outdoors (i.e., T, RH, CO_2, $PM_{0.3}$, $PM_{0.5}$, $PM_{1.0}$, $PM_{2.5}$, $PM_{5.0}$, PM_{10}, O_3, and TVOCs) were collected during four consecutive weeks (the most representative of this year's winter) at each school through novel field analysis. A IEQ cart was placed at the back of each classroom, to avoid interference with classroom activities, and avoiding blocking student's view to the board, and access to a wall plug as seen in Figure 2 & 3. Datalogger sensors were placed in accordance with EN15251 & ASHRAE 62.1 and 55. HOBO Onset MX1102, Graywolf 3016 particulate counter, and Graywolf DS-II were used to collect data indoors (Figure 2). For outdoor data, purple air particulate counter datalogger and Onset MX2301 for air temperature and relative humidity were used. Intervention includes using air purifiers, one from a local manufacturer [Jonas] and one designed and built by the research study group [REVEAL], as seen in Figure 4. Particulate matter concentrations were compared with the United States Environmental Protection Agency (EPA) Air Quality Index (AQI), the WHO Air Quality Guidelines (AQG), and local Ministry of Environment (MMA) of Chile.

Figure 2: Top image shows the location of IEQ cart at the back of the classroom. Image below, show thermal comfort and air quality dataloggers used for the study

In addition, building characterization was collected through a checklist, based on the literature review of POE. A summary of the variables collected during classroom visits is shown in table 1.

Table 1: *Architectural description of case studies*

	School 1			***School 2***		
	S1_C1	S1_C2	S1_C3	S2_C1	S2_C2	S2_C3
Classroom seating capacity	36	35	35	46	44	46
Classroom area (m^2)	43.0	43.0	43.0	53.0	53.0	53.0
Occupant density (m^2/student)	1.19	1.22	1.22	1.15	1.20	1.15
Classroom ceiling height	3.0	3.0	3.0	3.0	3.0	3.0
Classroom Volume (m^3)	129	129	129	159	159	159

**S1= School 1, S2= school 2. C1= Classroom 1, C2= Classroom 2, & C3= Classroom 3. Classroom seating capacity is based on the maximum number of tables present in each classroom during fieldwork visits.*

2.4 Design of low-cost Air Purifier

Our study designed and built a new version of Corsi Rosenthal Box, which incorporated local materials and dimensions that could be incorporated in a Chilean classroom setting. The design process included: 1) determining the amount of exterior airflow in the room based on [13]; 2) air exchange per hour (6 ACH); 3) calculation of the amount of CO2 generated in air by specific classroom size based on [14]; and 4) selection of fan dimension and efficiency (minimum of 860m^3/hr.). The final design included a small and a stacked version, which were tested in the field. Figure 4.

2.5 Data Analysis

Data cleaning was done to remove measurements that were lost, and to match corresponding timestamp. Descriptive statistical analysis was done for all measured environmental parameters. For each variable the following was calculated: average, median, minimum, maximum, variance and skewness.

Normality tests were performed, along with visual analyses, to decide whether to use parametric or non-parametric tests of hypotheses. We opted for the latter and utilized the Kruskal-Wallis one-way analysis of variance to assess whether mean differences were significant among the three independent sample groups. Subsequently, to identify which intervention differed significantly from the control (REVEAL or JONAS) in each classroom, the post-hoc Tukey's Honestly Significant Difference (HSD) test was conducted at a significance level of 0.05.

Figure 4: top image, air purifier designed and built by the research study group [REVEAL], bottom image air purifier from a local manufacturer [Jonas]. Image on the bottom right show new and used MERV-13 filters after 4 days of use.

3. RESULTS

3.1 Characterization of IAQ in classrooms

Physical characterization of classroom and architectural attributes are shown in table 1 and 2.

Table 2: *Average N students present at each intervention.*

	Classroom	Control	Int 1	Int 2	Average
School 1	C1	29	21	28	**26**
	C2	35	31	27	**31**
	C3	32	32	25	**30**
School 2	C1	30	38	40	**36**
	C2	33	33	41	**36**
	C3	40	40	40	**40**

**Each intervention consisted in one control evaluation and two interventions. Depending on the schedule each classroom had one week with one air purifier locally manufacture (Jonas) and two low-coast air purifiers developed for this study (REVEAL).*

In general classrooms presented a very high student density compared to other developed countries per square meters for each student, however both schools comply with the minimum area of 1.1 m^2 per student set by local code regulation.

Descriptive statistical summary of indoor and outdoor physical environmental parameters for both schools in all 6 classrooms during control and interventions is summarized in table 3 & 4.

During the fieldwork (2 ½ months in winter), the average outdoor temperature was 10°C, with an average of 81% relative humidity. Particulate matter concentrations were higher than international standards such as ASHRAE 62.1 & WHO. The latter also exceeds the local government's annual average maximum by the Ministry of Natural Environment (MMA) of 20 µg/m3.

Table 3 shows a summary of the IAQ parameters measured. Due to the high density in the classroom, high CO_2 concentration levels were measured, which exceeded the current national regulation of 700 ppm maximum (an average of 2,210 ppm and a maximum of 4,201 ppm). Also, particulate matter concentrations are much higher than outdoor concentrations for PM2.5 and PM10 by more than a factor of 2. The latter can be inferred by the leaky building envelope in the schools, in which higher concentrations were observed at night when students and teachers were not in the classroom. Low outdoor temperatures increase heating demand at night, resulting in more wood-burning usage.

The average indoor air temperature in all classrooms, was 18°C, only 8 degrees higher than the average outdoor temperature. Average indoor relative humidity was 65% during the fieldwork campaign, with a maximum measured value of 80%. Total volatile organic compounds (TVOC) concentration measures the total concentration of all measured VOCs. Indoor VOCs come from many indoor sources, including building materials, furnishings, consumer products, tobacco smoking, people and their activities, and indoor chemical reactions. An average of 1,492 was measured inside the classroom, with a maximum of 13,750.

Kruskal-Wallis one-way test analysis of variance was used to assess whether mean differences were significant among the three independent sample groups, Table 5.

***Table 4**: Descriptive statistics of outdoor environmental parameter measurements*

	T°C	RH%	$PM_{2.5}$	PM_{10}
Average	10.5	80.9	55.73	66.71
Median	11.0	80.8	51.24	61.63
Min	10.9	79.4	10.34	14.72
Max	11.1	82.7	186.20	221.12
SD	2.04	7.29	31.48	36.41
VAR	4.16	53.12	991.20	1325.50

***Table 5**: Summary of test Kruskal-Wallis for different IEQ parameters.*

Null Hypothesis	*Test*	*Sig.*	*Decision*
Air temperature distribution is the same within intervention categories received at the test	Kruskal-Wallis	.000	Reject Null hypothesis
Relative Humidity distribution is the same within intervention categories received at the test	Kruskal-Wallis	.000	Reject Null hypothesis

Continue in next page…

***Table 3**: Descriptive statistics indoor environmental parameter measurements at both schools*

	TVOCs	CO_2	CO	O_3	$PM_{0.3}$	$PM_{0.5}$	$PM_{1.0}$	$PM_{2.5}$	$PM_{5.0}$	PM_{10}	T°C	RH
Average	1492.10	2210	4.99	0.00	7,20	6.67	11.26	71.41	113.90	143.88	18.4	65.2
Median	317.77	1977	4.27	0.00	4.83	3.87	8.82	65.31	100.90	114.78	18.8	67.4
Min	88.19	1504	2.85	0.00	0.48	0.77	1.48	12.15	27.00	31.06	16.2	53.8
Max	13765.48	4201	12.57	-0.01	20.01	19.89	25.99	137.88	298.70	385.40	20.1	80.0
SD	3329.58	786	2.43	0.00	5.49	5.15	5.73	40.98	75.56	99.68	1,1	8.2
VAR	11086145	618102	6.0	0.00	30	26.53	33	1679	5711	9936	1.3	67.0

Particulate Matter 2.5 distribution is the same within intervention categories received at the test	Kruskal-Wallis	.000	Reject Null hypothesis
Particulate Matter 10.0 distribution is the same within intervention categories received at the test	Kruskal-Wallis	.000	Reject Null hypothesis
CO_2 distribution is the same within intervention categories received at the test	Kruskal-Wallis	.000	Reject Null hypothesis

**One-way analysis of variance to assess whether mean differences were significant among the three independent sample groups*

In addition to poor indoor air quality evidenced by this study during winter months, poor thermal comfort measurements were collected. During fieldwork, observation notes were collected, evidencing cold envelope surfaces, which promote interior condensation, mold growth affecting construction materials, and, worse, students' and teacher's health and well-being.

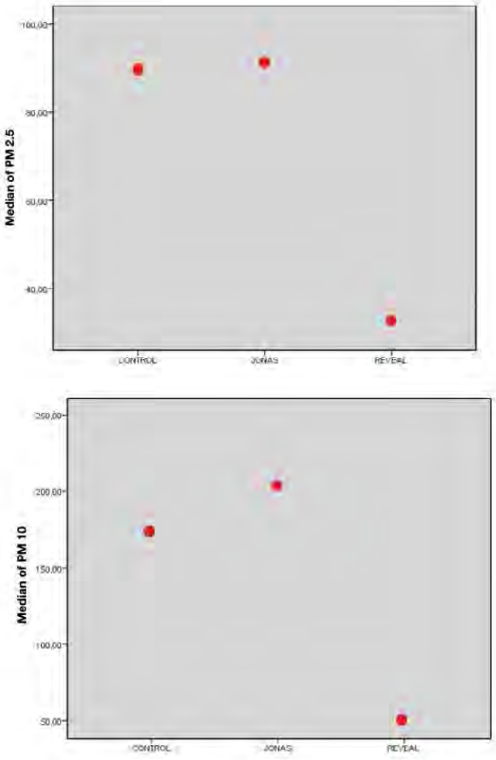

Figure 5: shows the values for particulate matter 2.5 & 10 concentrations for each classroom intervention. The performance of the REVEAL air purifier surpasses that of the control and Jonas by more than 2.5.

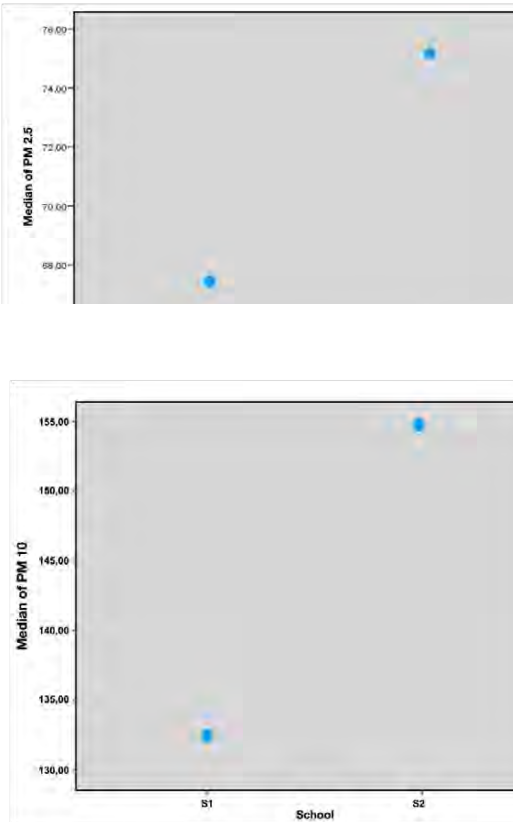

Figure 6: compares the concentrations values for particulate matter 2.5 & 10 at each school (S1 & S2). The performance of school 1 was notorious better in comparison with school 2, where the IAQ was much worse

4. CONCLUSION

As part of the evidence contributed by this research, new attention should be paid to the night-time IEQ conditions inside classrooms for leaky building envelopes. These conditions can be worrisome in the early hours of school if no strategy is implemented to refresh the air before students come in. The incorporation of air purifiers can help mitigate the reduction of indoor pollutants, as seen in Figure 5 & 6. However, more extreme building design retrofit interventions should be implemented for school locations with high outdoor air pollution during winter.

ACKNOWLEDGEMENTS

The authors gratefully acknowledge the research support provided by ANID/FONDECYT 11221255, ANID/FONDAP 1523A0004, ANID/FONDECYT 11240683 and ANID/PAI 77180057.

REFERENCES

1. Molina, C., Toro, R., Manzano, C. and Leiva-Guzmán, M.A. (2017). Particulate matter in urban areas of south-central Chile exceeds air quality standards. Air Quality, Atmosphere & Health, 10:653-667.

2. Reyes, R., Nelson, H., Navarro, F. and Retes, C. (2015). The firewood dilemma: Human health in a broader context of well-being in Chile. Energy for Sustainable Development, 28:75-87.

3. Felmer Plominsky, G., Martínez Arias, A. ., Rivera, M. I. ., & Zepeda-Gil, C. (2023). Pobreza energética en contextos de exclusión urbana: nuevos enfoques para la acción desde América Latina. *Revista INVI*, *38*(109), 1–16. https://doi.org/10.5354/0718-8358.2023.72446

4. Armijo, G.; Whitman, C.J.; Casals, R. Post-occupancy evaluation of state schools in 5 climatic zones of Chile. Gazi Univ. J. Sci. 2011, 24, 365–374.

5. Rivera, M.I.; Kwok, A.G. Thermal comfort and air quality in Chilean schools, perceptions of students and teachers. In Proceedings of the Architecture for health and Well-Being, Toronto, ON, Canada, 29 May–1 June 2019; pp. 709–718.

6. Trebilcock, M.; Bobadilla, A.; Piderit, B.; Figueroa, R.; Muñoz, C.; Sanchez, R.; Aguilera, C.; Hernández, J. Environmental Performance of Schools in Areas of Cultural Sensitivity. In Proceedings of the PLEA2012–28th Conference, Opportunities, Limits & Needs Towards an environmentally responsible architecture, Lima, Perú, 7–9 November 2012; pp. 7–12.

7. Diaz, M.; Cools, M.; Trebilcock, M.; Piderit-Moreno, B.; Attia, S. Effects of Climatic Conditions, Season and Environmental Factors on CO2 Concentrations in Naturally Ventilated Primary Schools in Chile. Sustainability 2021, 13, 4139. https://doi.org/10.3390/su13084139

8. Chatzidiakou, L.; Mumovic, D.; Summerfield, A. Is CO 2 a good proxy for indoor air quality in classrooms? Part 1: The interrelationships between thermal conditions, CO 2 levels, ventilation rates and selected indoor pollutants. Build. Serv. Eng. Res. Technol. 2015, 36, 129–161. [CrossRef]

9. Chatzidiakou, L.; Mumovic, D.; Summerfield, A. Is CO 2 a good proxy for indoor air quality in classrooms? Part 2: Health outcomes and perceived indoor air quality in relation to classroom exposure and building characteristics. Build. Serv. Eng. Res. Technol. 2015, 36, 162–181. [CrossRef]

10. Sarricolea, P.; Herrera-Ossandon, M.; Meseguer-Ruiz, Ó. Climatic regionalisation of continental Chile. J. Maps 2017, 13, 66–73. [CrossRef].

11. Betti, G., Tartarini, F., Nguyen, C, Schiavon, S. CBE Clima Tool: A free and open-source web application for climate analysis tailored to sustainable building design. Build. Simul. (2023). https://doi.org/10.1007/s12273-023-1090-5. Version: 0.8.16

12. Ministerio de Vivienda y Urbanismo. Ordenanza General de Urbanismo y Construcción; Ministerio de Vivienda y Urbanismo: Santiago de Chile, Chile, 2014.

13. INN, I. N. de N. (2013). Norma NCH3308 Chilena - Jonas. Ventilación - Calidad aceptable de aire interior - Requisitos . https://www.jonas.cl/?jet_download=3691

14. Allen, J., Spengler, J., Jones, E., & Cedeno-Laurent , J. (2020). (rep.). *5-step guide to checking ventilation rates in classrooms* (pp. 22–43). Boston, Massachusetts : Harvard Healthy Buildings Program.

PLEA 2024 WROCŁAW
(Re)thinking Resilience

Convertible Urban Shades for Climate Resilience

A Holistic Evaluation

MATTHIAS RUDOLPH[1], MOHAMMAD HAMZA[1,2], CHRISTIAN DEGENHARDT[1], STEPHAN ENGELSMANN[1], OLIVER KAERTKEMEYER[1], INES SCHLECKER[1]

[1]ABK Stuttgart, Germany
[2]Transsolar Energietechnik GmbH, Stuttgart, Germany

ABSTRACT: Cities with high building density increasingly suffer from urban heat islands (UHI) due to climate change, as sealed surfaces retain heat and limited ventilation proves inadequate for cooling. To counteract these effects, our study investigates the potential of Convertible Urban Shades to mitigate UHI by offering a diurnally or seasonally adjustable shading solution for urban areas, thereby fostering resilient urban microclimates. Utilizing a physical mock-up in Stuttgart, Germany, we compared the impact of no, fixed and convertible shades. Results from the measurement campaign carried out during a heatwave period showed that by using the no-shade scenario as baseline, convertible shades outperform fixed shade, by providing peak reduction of street surface temperature of ~16°C during daytime, and up to ~3°C colder at nighttime. The study also explored the architectural impacts of different shading structures in a street canyon. A scaled mock-up of the street canyon was used to involve stakeholders in a participatory design process to discuss design and implementation policies. The findings highlight Convertible Urban Shades' role in promoting resilient urbanism.
KEYWORDS: Convertible Urban Shades, Outdoor Comfort, Urban Microclimate, Sustainable Urban Design, Lightweight Tensile Structures

1. INTRODUCTION

In the face of escalating climate change impacts, urban areas stand at the nexus of both vulnerability and opportunity. Rapid urbanization has led to reduced green cover, compromised air quality, and amplified building energy consumption [1]. Especially for cities with high building density, the high degree of sealed / impervious surfaces retain heat longer while limited urban ventilation often proves insufficient in cooling these surfaces [2]. This affects the quality of public spaces and poses adverse health risks.

This paper presents an introductory, yet holistic, investigation into “Convertible Urban Shades" as a scalable design solution for locally reducing temperatures in high-density urban areas. "Convertible Urban Shades" are lightweight, tensile shading structures designed for urban spaces, such as plazas, courtyards, and wide street-canyons, offering adjustable shade as needed.

These shading structures respond quickly to leverage the diurnal swings of temperature and radiation-balance in the Urban Canopy Layer (UCL). During daytime they deploy to minimize solar gains and retract at night to allow for cooling through long-wave radiation exchange with the night sky and increased convection. Thus, they serve as an agile response to the urgency of stabilizing urban microclimates amidst climate change and intensifying heatwaves.

The research presented in this paper focuses on the applicability of these shading structures in high-density, central and southern European cities, using Stuttgart, Germany, as a case study. It explores three interconnected factors: (i) the potential for improvement in the urban microclimate through the reduction of air and surface temperatures (at the pedestrian and façade level) in the Urban Canopy Layer compared to traditional fixed shading; (ii) the structural and architectural evaluation; (iii) and an integral component focusing on communication and participation strategies. The latter is dedicated to understanding stakeholders' perceptions and facilitating their direct involvement in the design and implementation process.

2. LITERATURE REVIEW

The field of urban climatology has historically concentrated on adaptation strategies that emphasize the influence of blue-green infrastructure [3], and the surface properties of the built environment (albedo, thermal heat capacity) [4]. However most existing sidewalks in dense central European cities like Stuttgart have existing infrastructure such as sewage and electrical systems underneath sidewalks. This urban sub-surface infrastructure poses a hard limit on easy integration of dense tree plantations necessary to achieve required canopy thickness for sufficient shade [5]. Hence alternative adaptation strategies need to be explored for such situations.

In recent years a growing body of research shows that shading of public urban space has also proven to be an effective strategy for reducing the urban heat

island (UHI) effect on the macroclimate level [6], as well as for improving the pedestrian comfort on the microclimate level [7] [8]. Hence urban shading is regarded as an effective strategy for climate adaptation. However, most urban planning research on shading is primarily concerned with the effects of self-shading street canyons and trees, such as the works of [3] [9] [10]. Limited studies focusing on specifically designed urban shading devices are found in literature. [11] [12] [13] investigate the impact of colour, material and geometry of fixed shading structures deployed in streets and plazas and found improvement in the outdoor thermal comfort. The city of Seville, Spain is one example of successful implementation of such seasonally fixed shading devices in urban areas of Europe.

The effectiveness of these shading devices in a plaza typology could also be further improved by making them diurnally adjustable to limit the solar heat gain during daytime and allowing for cooling through radiation to the night sky by retracting these shades at night, as shown by [14]. The large folding umbrellas in the Holy Prophet's Mosque in Medina, KSA are a famous demonstration of this strategy in a plaza typology [15]. While such convertible urban shading devices are also listed as a basic strategy against UHI in [16], limited evaluation of the improvement of thermal environment in a variety of urban typologies is provided. This paper attempts to bridge this gap on convertible urban shades (CUS) by providing measured data on their thermodynamic effectiveness, and by calibrating a TRNSYS thermal simulation model for further analysis of these devices.

3. HOLISTIC EVALUATION

3.1 Proof-of-Concept & TRNSYS calibration

A proof-of-concept mock-up was constructed on the rooftop of the ABK Stuttgart building to collect measured data for air and surface temperature for three configurations – no-shade, fixed shade, and convertible urban shade (CUS). The measurement campaign was carried out in Stuttgart, Germany during the period of summer heatwaves (July to September 2023).

The experimental setup consisted of lightweight boxes with an overall outer dimension of 104 x 136 x 94 cm (width/length/height). The floor consisted of three layers of massive bricks, for a thermodynamic representation of the top layer of a common street surface (brick specification: 240 x 115 x 71 mm, 2000 kg/m^3, 0.96 W/m·K). The brick layers were placed in an OSB wooden box (internal dimension of brick volume: 60 × 60 × 21.3 cm), insulated with an 10 cm layer of hard polystyrene. Such a setup allowed to mimic an isolated section of an infinitely large urban plaza, with negligible heat exchange to surrounding surfaces. Surface temperature sensors were fixed at the top surface of the brick volume, as well as depths of -7,1cm and -14,2cm. Air temperature sensors (rain-protected) were placed in the box. The setup is illustrated in Figure 1.

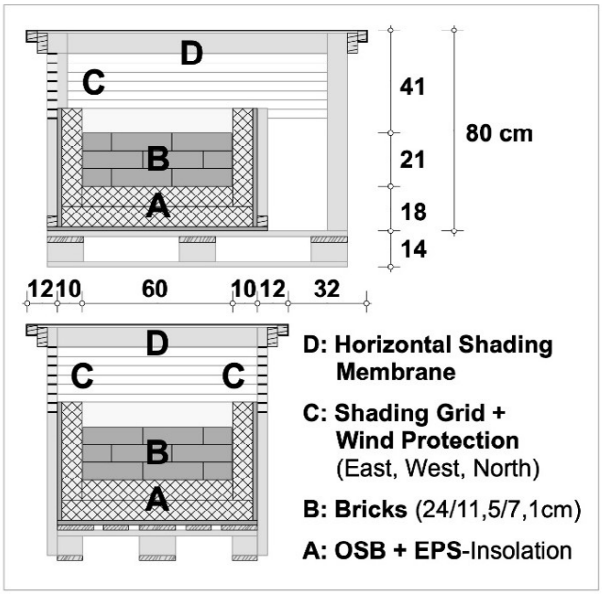

Figure 1: Mock-up cross and longitudinal section.

For the two boxes with shading (fixed and CUS), an identical shading material was used – a white PVC fabric from SergeFerrari (Flexlight Advanced 902-S2; Tsol = 0.07; Rsol = 0.80; ABSsol = 0.13). Additionally for the box with CUS, the shading was retracted everyday around sunset and activated again next morning.

For interpreting sample results of the floor surface temperature measurement campaign presented in Figure 2, the no-shade scenario serves as the baseline, representing status quo. For the fixed shade, it was found that it provides peak reduction of ~14°C during daytime but can get ~1°C warmer at nighttime. The CUS was found to outperform the fixed shade, by providing peak reduction of ~16°C during daytime, and up to ~3°C colder at nighttime, when compared to the baseline no-shade scenario.

Finally, a detailed TRNSYS micro-climate simulation model was setup for the experimental setup, with the goal to calibrate the model with the measured data. Figure 3 shows the final calibrated model achieved an average R2 of over 0.94. This validation sets the ground for more detailed simulations in the future.

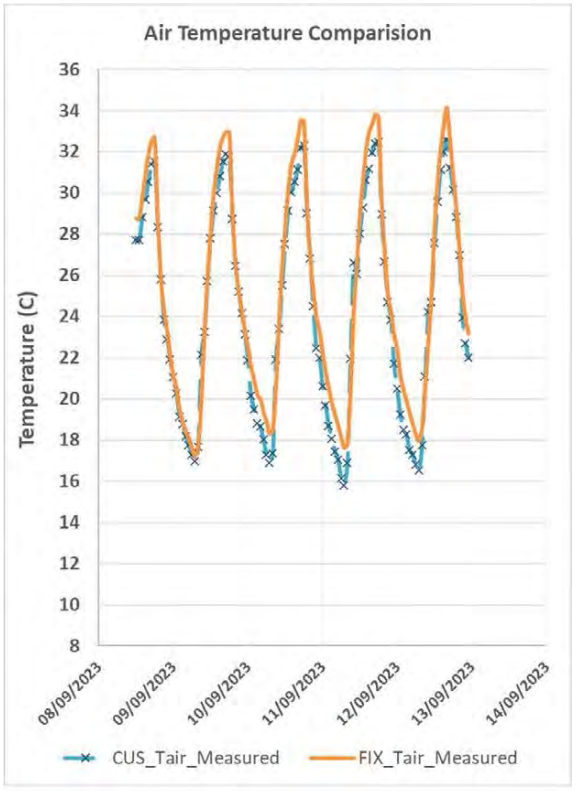

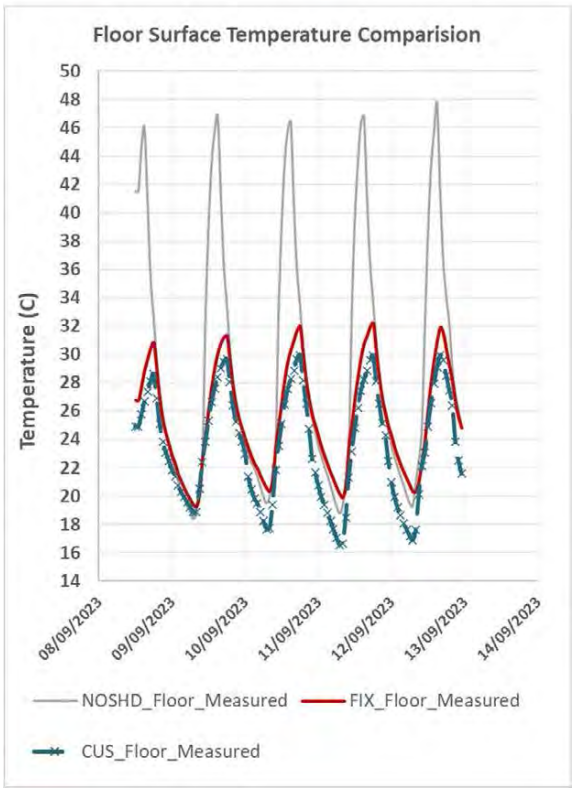

Figure 2: Measured Temperatures – No Shade, Fixed and Convertible Shade.

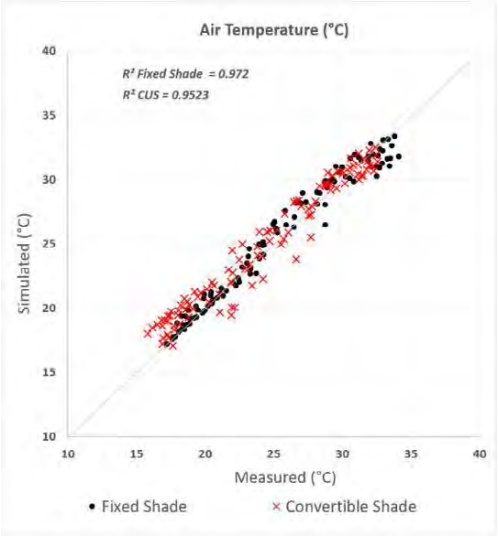

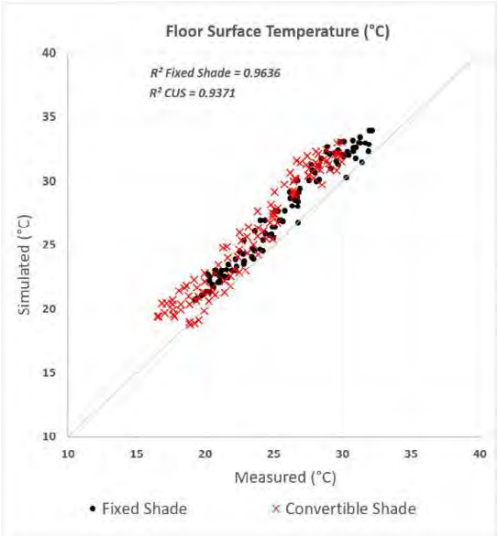

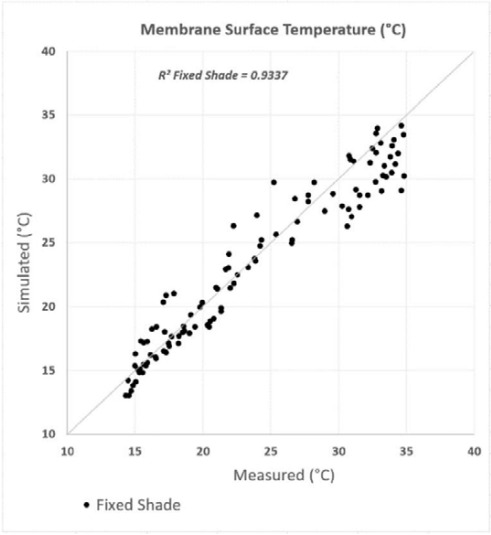

Figure 3: Correlation between Measured and Simulated Temperatures.

3.2 Structural and architectural evaluation

As mentioned in the introduction, "Convertible Urban Shades" are lightweight, load bearing, tensile structures, which allow maximum utilization of the

strength of the material (e.g. membranes). They optimize the mechanical characteristics of the material by eliminating inefficient bending stresses etc [17].

The great advantage of such tensile-only load-bearing structures is the “foldability” that they offer, making them ideally suited in applications such as movable and adaptable shading strategies. They offer a simple, reversible, and complete change in the geometry of a load-bearing component, which allows for swift adaptation of the structure to respond to a myriad of stimuli such as weather changes/climatic factors, acoustic boundary conditions, requirements for thermal behavior, lighting and exposure conditions etc [18] [15]. Such shading structures can also cover large spans without needing space-consuming, bulky supporting structures, making them suitable for use in large urban spaces like public squares etc.

From a structural design perspective, Convertible Urban Shades can be broadly classified into two main categories: (A) pneumatically pre-stressed construction and (B) mechanically pre-stressed construction. Both can be used to realize a variety of transformation principles [18] [19] [20].

(A) Pneumatic pre-stressed construction can be further classified into six sub-categories based on the transformation principle: (i) push-through cushions, (ii) inverting hoses, (iii) tires with membrane retraction in beads, (iv) rolled hoses, (v) cushions, and finally (vi) convertible multi-cells [18].

(B) Mechanically pre-stressed construction can also be further classified into three sub-categories based on their transformation principle: (i) membrane as a convertible component within a non-convertible primary system e.g. centrally gathered roof, (ii) membrane that follows the transformation of the primary structure e.g. umbrella, and finally (iii) membrane as a component of a convertible primary system whereby the membranes change their position in space, but not their geometry, when the primary system moves, e.g. movable roof.

Additionally, mechanically prestressed structures can also be classified into four styles based on the direction of movement during the transformation process: (i) parallel, (ii) central, (iii) circular, and (iv) peripheral moving constructions. The textile membranes are either gathered, folded, or rolled [19] [21].

However, Convertible Urban Shades introduce special constraints on the choice of the membrane material due to changes in shape during the travelling process. Hence high-strength fabrics made of organic fibers, PVC-coated polyester fabrics, PTFE fabrics, and Aramid fabrics are needed for such an application.

Convertible shading structures are also significantly more complex in terms of design, construction, and maintenance, as compared to a typical fixed shading structure [17].

Therefore, from an architectural design perspective, fixed vertical textile lamellas were also briefly studied besides adaptive membrane structures for more holistic evaluation. The advantages of fixed lamellas are their comparatively low planning and execution requirements in comparison to adaptive systems, and they also ensure a continuous ventilation of the street.

Three distinct system geometries were conceived and investigated as seen in Figure 4. The underlying consideration was a street in an east-west orientation in Stuttgart, with a total length of 140 meters, a width of 14.5 meters, and buildings with an average height of 14 meters (eaves height). The variants differ in terms of their horizontal distance and the vertical extension of the membrane. Variant 1 features lamellas at a horizontal interval of 2 meters and a height of 3 meters. In Variant 2, the distance increases to 5 meters and the lamella height to 4 meters. Finally Variant 3 has a horizontal distance of 10 meters with a lamella height of 7 meters.

As a preliminary evaluation, a direct sunlight hours study of the 3 variants demonstrates that all show similarly good shading of the street. Future studies will evaluate the detailed microclimate using the calibrated TRNSYS model from this study.

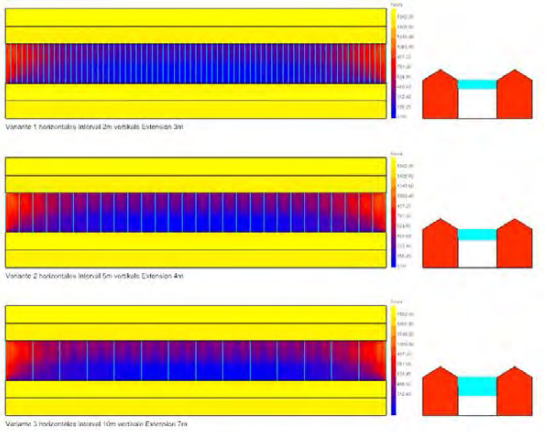

Figure 4: Sun hours study for different vertical lamellas.

Regarding the architectural impact, Variant 3 shows a significant reduction in terms of overall material consumption and assembly effort.

The suspension cable could serve as one of the most efficient structural design solutions that can be used for such fixed shading system – the membrane is simply attached to the suspension cable, and either allowed to hang freely or is stabilized by an additional ballast. Such simple cable structures offer high tensile strength and their low weight enable them to bridge

large spans with minimal material use. Such a rudimentary tensile suspension cable structure can also be easily and firmly anchored into the building façade. Common materials used for suspension cables are galvanized steel, stainless steel, and other high-strength modern composite materials, which significantly contribute to the longevity of the constructions. Further structural options such as frames, tensioning of the membrane, or stiffening with battens, will be examined more closely in future publications as part of the ongoing research process.

3.3 Research-related Communication and Participation

The transformation of urban public spaces towards climate adaptation requires broad acceptance in society, considering a large number of different stakeholders. Based on a stakeholder analysis, specific communication strategies were developed for each target group, adhering to the recommendations of the National Institute for Science Communication (NAWik) [22]. The goal was to engage, involve, and facilitate interdisciplinary exchanges among participating stakeholders. Furthermore, insights were gained through interactions with diverse stakeholders affect the development of individual shading strategies.

First, a dedicated project website communicates climate change challenges, provides updates on current research, and allows for idea contributions. It caters to both experts and laypeople. Second, a public symposium was also organized to spread awareness, featuring lectures and discussions aimed to bring together a diverse array of stakeholders and perspectives, including architects, structural engineers, urban climatologists, city officials, and the public. Third, a large-scale physical model and traveling exhibition format – named “U°CA On Tour”, was created. This platform facilitated participatory evaluation, allowing various interest groups to interact with different design typologies and collect user preferences, concerns as well as, suggestions. The model informs, engages, collects feedback, promotes transparency, and encourages collaboration. The model proves to be particularly accessible, communicative, and inclusive.

Positive feedback from the implemented formats helped to strengthen the efforts in knowledge transfer and stakeholder involvement. In the next phase, a communication strategy will be employed to further involve the city administration and planning stakeholders. This will enable the collection of additional information regarding implementation and planning processes.

Scientific pursuits on climate change adaptation, often remain inaccessible to the common people due to their highly specialized subject matter. Communication and participation strategies accompanying such research can help counteract this, by engaging in public discourse around the opportunities and challenges related to such measures, as evidenced by the paradigm adopted in this work.

Figure 5: Residents and users interacting with the travelling exhibition of Convertible Urban Shades (‘U°CA On Tour’) as part of the participatory design process (Stuttgart, Germany).

4. CONCLUSION

This paper presented a holistic investigation of Convertible Urban Shades, encompassing measurement campaigns, thermodynamic validation of computer models, architectural and structural design considerations as well as participatory engagement.

Climate change exacerbates the urgency of rethinking urban spaces. Traditional architectural interventions pertaining to blue-green infrastructure may fall short due to long implementation timelines and potential disruptions to existing infrastructure. Alternative solutions such as Convertible Urban Shades offer a promising avenue, embodying flexibility, and efficiency. Our measurement campaigns showed their potential to reduce ground surface temperatures at day by 16°C and at night by upto 3°C compared to the status quo. By combining architectural innovation with user-driven acceptability, this research contributes to the discourse of sustainable architecture and urban design for climate resilience.

ACKNOWLEDGEMENTS

This research is funded by the BW Stiftung, Germany.

We would also like to thank Mr. Rainer Kapp from the Amt für Umweltschutz, Stadtklimatologie, Stuttgart, for providing weather data from measurement stations in the city. We express our sincere gratitude to the members of the Project Advisory Council - Prof.

Thomas Auer & Prof. Julian Lienhard, for their valuable input. Finally, we thank architecture students Fabian Striffler, Florian Moritz Klein, Fynnian Schmid and Tim Stempel for their support in building the mockup.

REFERENCES

1. F. Meng, Q. Yu und X. Yang, „Analysis of Influence of Urban Spatial Morphologies on Thermal Microclimate," *Polish Journal of Environmental Studies*, Bd. 30, Nr. 2, pp. 1725-1736, 2021.
2. N. Kartikawati und A. Kusumawanto, „Spatial control to reduce urban heat island effect in urban housing," *Journal of Architecture & Environment*, Bd. 12, Nr. 1, p. 27, 2013.
3. S. E. Gill, J. F. Handley, A. R. Ennos und S. Pauleit, „Adapting Cities for Climate Change: The Role of the Green Infrastructure," *Built Environment*, Bd. 33, Nr. 1, pp. 115-133, 2007.
4. H. Akbari, M. Pomerantz und H. Taha, „Cool surfaces and shade trees to reduce energy use and improve air qulaity in urban areas," *Solar Energy*, Bd. 35, pp. 295-310, 2001.
5. T. Häussermann, „Mittlere Forststraße immer noch ohne Bäume" Stuttgart-West, p. 18, 11 2022.
6. A. Middel, N. Selover, B. Hagen und N. Chhetri, „Impact of shade on outdoor thermal comfort - a seasonal field study in Tempe, Arizona," *International Journal of Biometereology*, Bd. 60, Nr. 12, pp. 1849 - 1861, 2016.
7. R. Paolini, A. G. Mainini, T. Poli und L. Vercesi, „Assessment of Thermal Stress in a Street Canyon in Pedestrian Area with or without Canopy Shading," *Energy Procedia*, Bd. 48, pp. 1570-1575, 2014.
8. N. Kántor, L. Chen und C. V. Gál, „Human-biometeorological significance of shading in urban public spaces—Summertime measurements in Pécs, Hungary," *Landscape and Urban Planning*, Bd. 170, pp. 241-255, 2018.
9. H. Kusaka und F. Kimura, „Thermal Effects of Urban Canyon Structure on the Nocturnal Heat Island: Numerical Experiment Using a Mesoscale Model Coupled with an Urban Canopy Model," *Journal of Applied Meteorology and Climatology*, Bd. 43, Nr. 12, pp. 1899-1910, 2004.
10. F. Bourbia und F. Boucheriba, „Impact of street design on urban microclimate," *Renewable Energy 35*, pp. 343-347, 2010.
11. E. Garcia-Nevado, A. Bugeat, E. Fernandez und B. Beckers, „Using textile canopy shadings to decrease street solar loads," in *PLEA 2020*, A CORUÑA, 2020.
12. M. Alharthi und S. Sharples, „Modelling and Testing Extendable Shading Devices to Mitigate Thermal Discomfort in a Hot Arid Climate - A case study for the Hajj in Makkah, Saudi Arabia," in *PLEA 2020*, A CORUÑA, 2020.
13. A. L. Pisello, V. L. Castaldo, G. Pignatta, F. Cotana und M. Santamouris, „Experimental in-lab and in-field analysis of waterproof membranes for cool roof application and urban heat island mitigation," *Energy and Buildings*, Bd. 114, pp. 180-190, 15 02 2016.
14. K. Wolfgang, M. Engelhardt und D. Kiehlmann, „The human bio-meteorological chart - A design tool for outdoor thermal comfort," Munich, 2013.
15. SL Rasch GmbH, *SL Rasch - The Work of SL*, Leinfelden Echterdingen, 2022.
16. L. A. Ruefenacht und J. A. Acero, „Strategies for Cooling Singapore: A catalogue of 80+ measures to mitigate urban heat island and improve outdoor thermal comfort," 2017.
17. W. Sobek und M. Speth, „Textile Werkstoffe im Bauwesen," *Deutsche Bauzeitung*, Bd. 127, Nr. 9, pp. 74-81, 1993.
18. F. (. Otto und E. Bubner, Institut für leichte Flächentragwerke (IL) - Nr.:12 - Wandelbare Pneus., Stuttgart: Karl Krämer Verlag, 1975.
19. Institut für Leichte Flächentragwerke, Band IL 5, Wandelbare Dächer, Stuttgart: Karl Krämer Verlag, 1972.
20. K. Linkwitz, D. Ströbel und P. Singer, „Die Analytische Formfindung," *Prozess und Form - "Natürliche Konstruktionen" - Der Sonderforschungsbereich 230*, 1996.
21. C. Gengnagel, „Mobile Membrankonstruktionen Zugl.," Techn. Univ. München, München, 2005.
22. Nationales Institut für Wissenschaftskommunikation (NaWik) gGmbH (Hrsg.), „Leitfaden Präsentieren," NaWik, Karlsruhe, 2021.

PLEA 2024 WROCŁAW
(Re)thinking Resilience

Designing a Naturally Ventilated Building in an Air Polluted City

Case study of a library in Milan: challenges, implementation, and energy savings

MATTEO MERLI[1] RAFAEL ALONSO CANDAU[1] FLORENCIA COLLO[1] OLIVIER DAMBRON[1]

[1]Atmos Lab, London, United Kingdom

ABSTRACT: This paper develops the adoption of natural ventilation (NV) as a sustainable solution for cooling in urban environments, with a focus on the challenging context of Milan. Using the European Library of Information and Culture (BEIC, from Baukuh and Onsite Studio with the help of Atmos Lab) as a case study, the paper delves into the practical integration of NV and its impact on energy efficiency. Analysing critical pollutants (PM2.5, PM10, NO_2, O_3) from 2015 to 2023 in Milan, the study compares concentrations against Italian laws and WHO guidelines. The main pollutants significantly decrease during the natural ventilation season, consistently below recommended thresholds, and exhibit decreasing trends over recent years, supporting the safe implementation of NV. Thermal simulations show a 29% increase in cooling demand with the omission of night cooling strategies and up to 64% without NV entirely. This escalation is further pronounced when accounting for electrical fan usage, resulting in a total increase of 72% and 188%, respectively, thus underscoring the importance of NV strategies in resilient urban design.
KEYWORDS: Natural Ventilation, Air Pollution, Energy Efficiency, Air Quality, Passive Design

1. INTRODUCTION

The increasing global temperatures are inducing a rise in the cooling demand in buildings across Europe, making it the fastest-growing use of energy in buildings [1]. During the last decades, an increase in air pollution in cities started to advocate against the use of natural ventilation [2,3] to provide fresh air and ventilate, which coupled with the easiness of calculation and implementation of mechanical ventilation completely discouraged the use of natural means. At the same time, building energy policies are demanding increasingly well-insulated and airtight envelopes which make buildings more susceptible to overheating, thereby escalating the need for increased cooling. This emphasises the urgency to find solutions for the feasibility of natural ventilation in cities where it ceased to be the norm. This also builds on the increasing attention from policymakers towards air quality, growing public awareness and drastic changes in weather conditions. This paper presents the project for a naturally ventilated library in Milan, a city that ranks among the most polluted in Europe: the European Library of Information and Culture (BEIC), designed by Baukuh and Onsite Studio with the help of the authors as environmental consultants, and currently under construction. The paper delves into the challenges found in designing such a naturally ventilated building and the benefits of implementing the strategy.

2. THE CLIMATE OF MILAN

The climate of Milan is humid subtropical with hot and humid summers and relatively cold winters. Predictions for 2050 indicate a significant impact of climate change on Milan's summers, with an expected average temperature increase of 2.5 °C, reaching an average high of above 30 °C. Prevailing winds, characterised by low velocity, consistently come from southern orientations throughout the year.

3. THE CASE STUDY

The BEIC consists of two naves with a trapezoidal cross-section, extensively glazed, for a total area of around 30,000 m². An atrium in the northern volume, provides space for circulation and social interaction, introduces daylight to the building's core, and acts as a buffer space to reduce winter heat losses from the surrounding heated volume. The traditional library space is in the south nave to benefit from the sun, whereas the Media library is in the north nave to avoid direct contact with the sun, thus preventing the coupling of its high internal gains with the solar ones. The book storage is located underground, to benefit from its stable hygrothermal conditions. The atrium's central position enables cross ventilation with the spaces at each level, collecting exhausted air that mixes with fresh air before being released through high openings on the top floor. (Figure 1)

Figure 1: Nuova BEIC, images, typical plan and section presented in the competition.

3.1 Implementation of the natural ventilation strategy

Operable windows are installed on all facades, with the amount determined by facade orientation and function, optimised via thermal simulations.

In general, the design focused on the number of operable windows per facade, as factors such as the type of opening and discharge coefficient had already been maximized within the constraints imposed by the presence of solar protection mesh on the facade. In most of the facades, ¼ of the panes are operable, allowing for granular control of the openings. In the atrium, a larger proportion of operable windows, particularly in the upper part, were necessary to improve air circulation and maintain the neutral pressure plane higher than the last occupied floor, ensuring that hot air is effectively exhausted without being drawn back into occupied areas (Figure 2).

The optimisation through thermal simulations was aimed at enhancing the building's behaviour in free-running mode (no heating nor cooling) and reducing the cooling demand in active mode. Consequently, thermal simulations guided the definition of operation modes tailored to seasonal conditions (Figure 3): in winter, windows remain closed as outdoor temperatures are largely below those required indoors; during the temperate time of the year (mostly spring, autumn, and some milder summer days), outdoor temperatures are acceptable for human comfort and windows can open during the day; while in the hot season, air conditioning is active during the day and windows are closed, however, when outdoor temperature drop at night, windows can open to dissipate residual heat and prepare the building for the following day.

To facilitate the operation of the window when conditions are favourable, a significant proportion of them are automated. This feature is crucial for supporting night cooling strategies and ensuring control over the windows that are out of the occupants' reach.

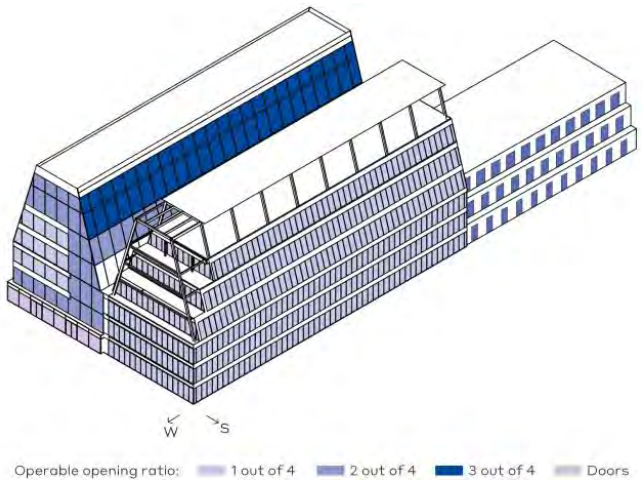

Figure 2: Operable opening ratios by facade.

4. METHODOLOGY

Critical pollutants (PM2.5, PM10, NO_2, O_3) are analysed from 2015 to 2023 using data from ARPA Lombardia´s air quality stations [4], which are classified as Traffic and Background based on proximity to traffic. The urban background station "Milano Pascal Città

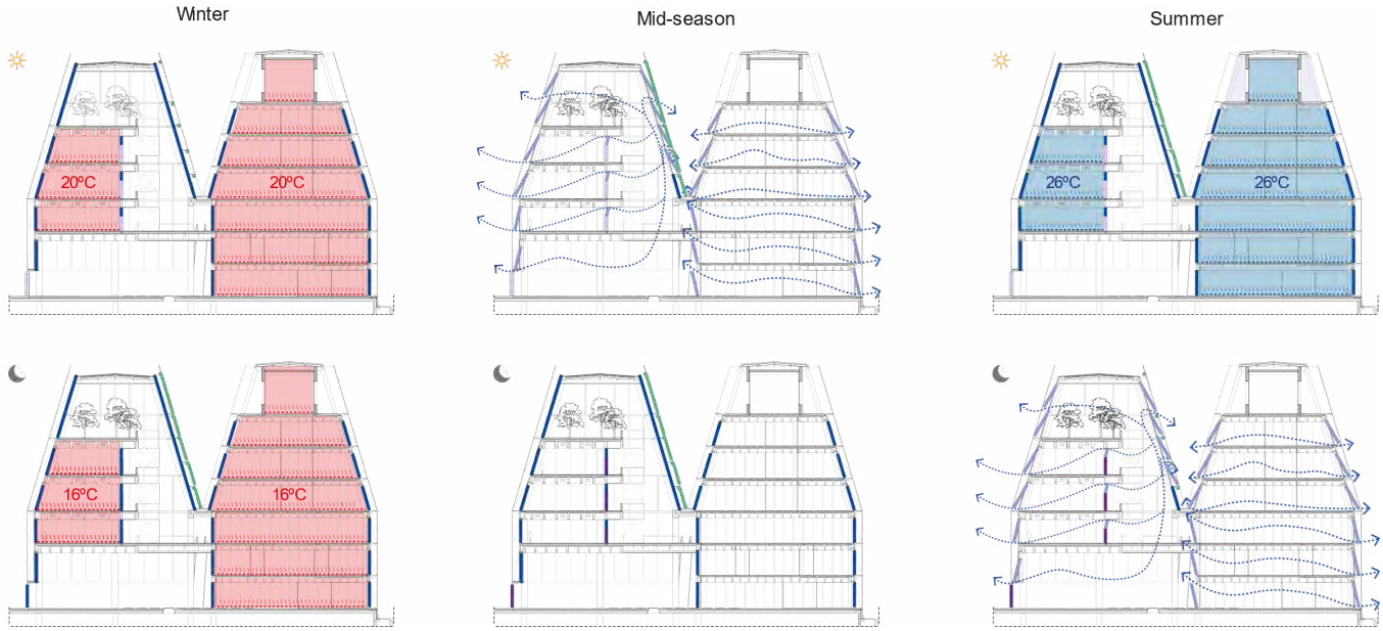

Figure 3: Operation modes of the building during each season of the year.

Studi" is chosen for its comprehensive pollutant collection (not all stations measure all pollutants) and its proximity to the site (2 km). Given the potential discrepancies with urban stations [5], an in-depth examination of all stations was conducted, and no significant differences were observed. Other key pollutants like CO and SO_2 are not reported as they consistently remain well below the recommended limits [6].

Concentrations are compared against Italian legal limits (baseline) and WHO guidelines (target) [3]. While the WHO periodically updates guidelines, the most recent EU (2008) and Italian decrees (2010) [7,8] implement the WHO guidelines from 2005 [9].

Table 1: Italian (and EU) legal limits and recommended AQG targets from WHO Air Quality Guidelines 2021.

Pollutant	Averaging time	Limit value	AQG
PM2.5, µg/m³	Annual	25	5
	24-hour	25[(a)]	15
PM10, µg/m³	Annual	40	15
	24-hour	50	45
NO_2, µg/m³	Annual	40	10
	24-hour	200[(b)]	25
O_3, µg/m³	8-hour[(c)]	120	100

[(a)] Lacking a 24-hour limit, it aligns with the annual limit value and 24-hour WHO interim target 4.
[(b)] The 1-hour limit is adopted.
[(c)] Daily maximum 8-hour mean.

The analysis focuses on the short-term limits (24-hour and 8-hour) to assess the dynamics with precision. The natural ventilation season is considered from the 1st of April to the 30th of September, for a total of 183 days.

The thermal model was built in EnergyPlus v.22.1 via Honeybee [10] for Grasshopper and Rhinoceros. The benefits are evaluated in terms of reduction in energy demand and energy consumption. Three scenarios were simulated:

I. Day and night NV: baseline scenario that represents the final configuration of the building.
II. Daytime NV only, with night ventilation via mechanical systems.
III. No NV: Cooling relies solely on mechanical systems. Night ventilation is carried out via mechanical systems.

For scenarios I and II, windows open when T_{in} > 23 °C and when T_{in} > T_{out}. In scenarios II and III, mechanical systems integrate the use of “free cooling”, an approach to lower indoor air temperature by introducing external air when it is naturally colder, and it is commonly employed to reduce energy consumption. However, in practice, free cooling is not entirely cost-free, as it requires energy for fans. In the model, it activates when T_{in} > 23 °C and when the temperature difference between inside and outside is > 4 °C. This is common practice as it avoids air movement and associated fan energy consumption with little benefit. The efficiency factors for the fans are 1.3 kW/(m³/s) for supply and 0.9 kW/(m³/s) for extraction. The conversion from cooling energy demand to electrical consumption is calculated assuming a coefficient of performance (COP) of 3.5.

5. AIR QUALITY IN MILAN

5.1 Context

Milan is one of the most populous cities in the Po Valley, an area that ranks at the top of the most

polluted in Europe due to aggressive land use, extensive industrialization, high population densities, and resulting high levels of road transport. The natural confinement formed by the Alps to the north and the Apennine chain to the south, makes the wind speed in this area among the lowest in Europe, around 1.5 m/s on average, favouring air stagnation and winter fog events that trap pollution close to the ground. According to a recent study [11], if Po Valley had the same meteorological conditions typical of central-northern Europe, average monthly concentrations of PM10 and NO_2 would be lowered by 60 to 70% [11].

5.2 Air Quality Analysis

Figures 4, 5, 6 and 7 show the concentration levels of PM2.5, PM10, NO_2, and O_3, also reporting the trend of days exceeding the recommended limit. Table 2 summarises the number of days exceeding the limit and guideline values during the natural ventilation season, highlighting their limited occurrence compared to the entire season and the overall reduction trend over recent years.

The measurements of all pollutants show a marked seasonal behaviour. Concentration levels of PM2.5, PM10, and NO_2 reach maximum peaks during winter, as the need for combustion in domestic heating and increased traffic density cause an increase in emissions [12]. During the warmer months, pollutants are at a minimum as there is a decrease in combustion and improved dispersion, aided by rainfall in the mid-seasons. Therefore, during the natural ventilation season, pollution levels are reduced on average by 32% for PM2.5 and NO_2, and 35% for PM10 compared to annual values. Remarkably, a significant number of days within this period fall below both regulatory limits and guideline values, especially demonstrating favourable trends over recent years.

Ozone presents a pronounced seasonal behaviour with peaks during the hot season. It is formed in the atmosphere by photochemical reactions in the presence of sunlight and precursor pollutants, such as NO_x and VOCs, explaining their higher concentrations in summer. During the natural ventilation season, O_3 concentration exceeds the recommended limit for almost 1/4 of the period and 1/2 of the total days when considering the guideline target. However, despite the summer daily average being higher, O_3 is characterized by a strong diurnal variation due to its significant influence on temperature, relative humidity, and sunshine [13]. This variation reduces night-time levels enough to permit the night cooling needed during the hottest period. It's also important to note that the higher presence of NO in cities contributes to the degradation cycle of O_3, resulting in lower concentrations than in mountain and rural areas, where the air quality wouldn't be considered a threat to natural ventilation. Moreover, ozone filters are not typically included in standard mechanical systems, making it a stretch to consider ozone a constraint on NV implementation.

Table 2: Number of days exceeding the limit (and guideline) value during the natural ventilation season (out of 183 days).

	PM2.5	PM10	NO2	O3
2015	29 (95)	5 (9)	0 (108)	43 (87)
2016	18 (82)	9 (13)	0 (130)	50 (87)
2017	13 (61)	0 (4)	0 (92)	64 (106)
2018	10 (61)	1 (3)	0 (86)	62 (112)
2019	4 (40)	1 (1)	0 (66)	49 (97)
2020	5 (40)	0 (1)	0 (29)	48 (110)
2021	3 (34)	0 (2)	0 (40)	37 (80)
2022	1 (14)	0 (1)	0 (56)	44 (111)
2023	1 (21)	0 (1)	0 (39)	32 (79)

5.3 Future projections of the air quality in Milan

Numerous air quality studies support the hypothesis of a generalised decreasing trend in pollutant emissions in the future [6,14,15], attributed to consistent improvements in citizens' vehicle fleets, with a growing prevalence of carbon-neutral vehicles, or changes in the industrial productive system, showing increased consideration for the environment and emissions control. Notably, the Municipality of Milan is proactively enhancing air quality through regulations and measures restricting activities that generate pollution and promoting the adoption of more sustainable practices. These initiatives aim to further diminish air pollution in the upcoming years, creating opportunities for a wider implementation of natural ventilation strategies.

6. BENEFITS OF USING NATURAL VENTILATION

The benefits of adopting natural ventilation strategies are presented in terms of energy savings calculated through thermal simulations (Figure 8):

- The total cooling demand for the building is 10 kWh/m^2, which is considered low. With a COP of 3.5, the annual electrical consumption is equal to 3 kWh_{el}/m^2.
- Opting for mechanical ventilation instead of natural ventilation for night cooling raises cooling energy demand by 29% to 12 kWh/m^2 (4 kWh_{el}/m^2). When factoring in the electrical energy utilised by fans, the total energy consumption increases by 72%.
- If natural ventilation strategies are completely omitted, cooling demand increases by 64% to 16 kWh/m^2 (5 kWh_{el}/m^2) when compared to the baseline, and up to 188% if including the energy for fans.

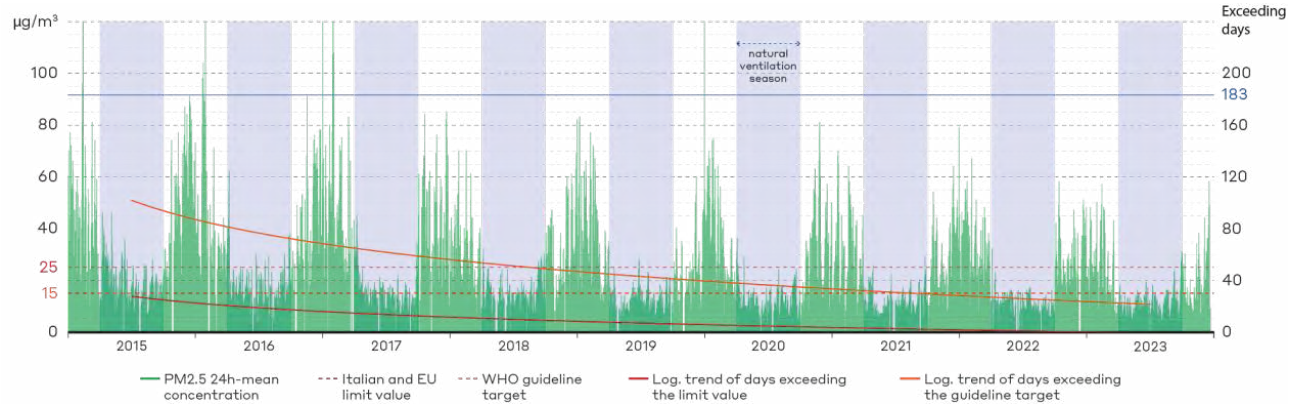

Figure 4: PM2.5 daily mean concentrations, and trend of days exceeding the limit and guideline values from April to September.

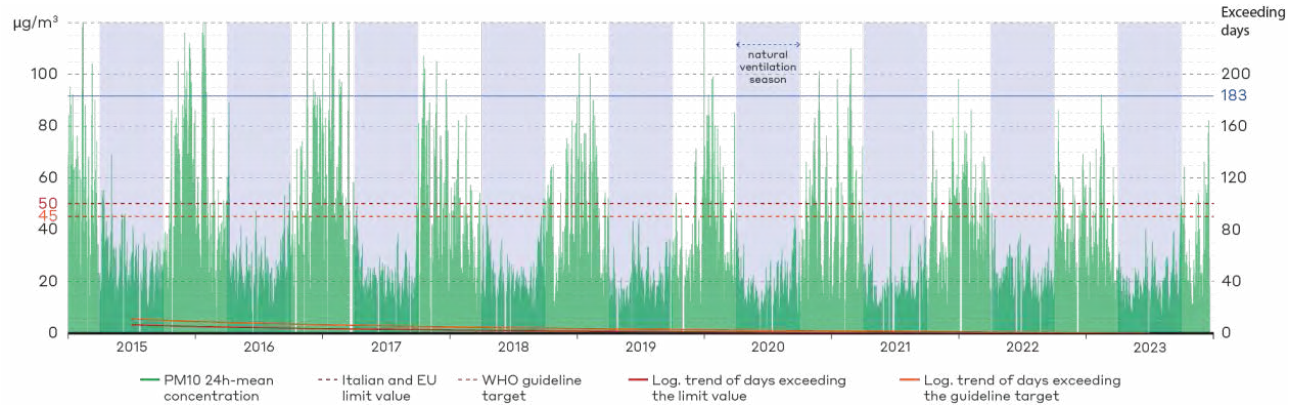

Figure 5: PM10 daily mean concentrations, and trend of days exceeding the limit and guideline values from April to September.

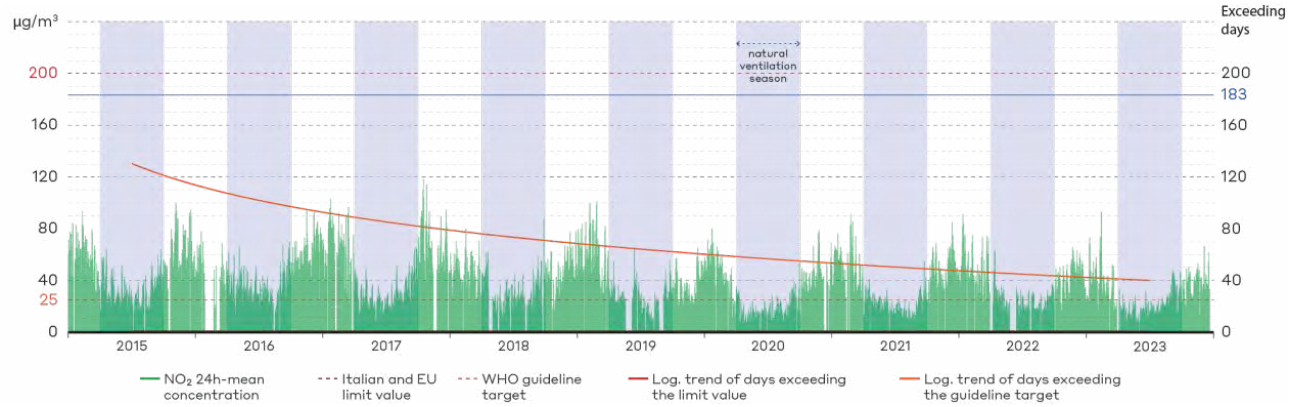

Figure 6: NO_2 daily mean concentrations, and trend of days exceeding the limit and guideline values from April to September.

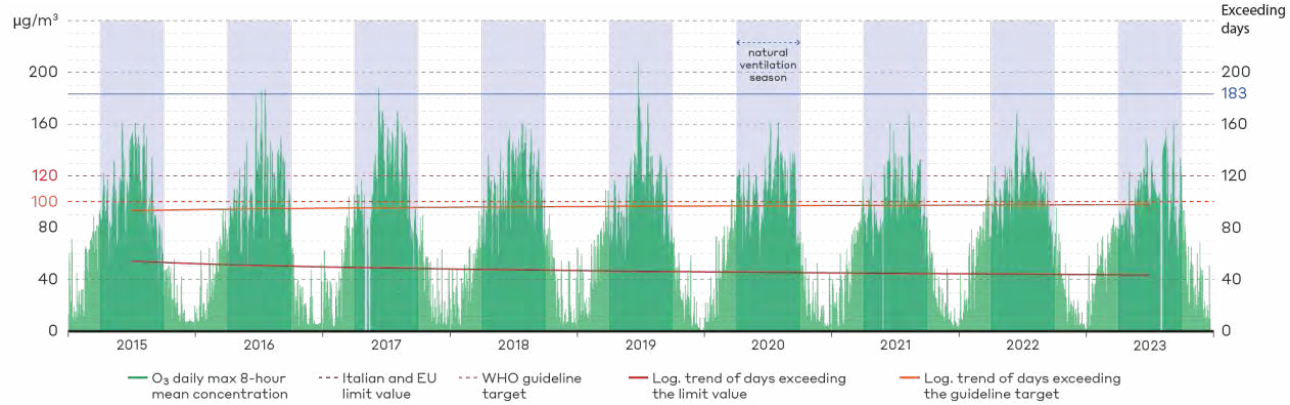

Figure 7: O_3 daily max 8-hour mean concentrations, and trend of days exceeding the limit and guideline values from April to September.

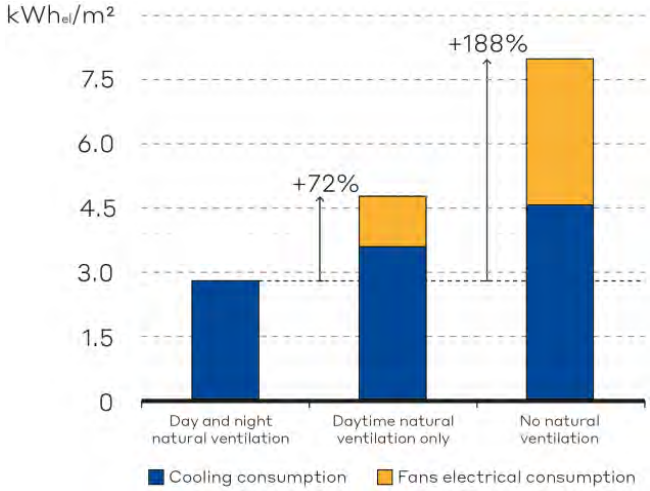

Figure 8: Annual electrical energy consumption in the three ventilation scenarios.

Although scenarios with reduced or absent use of NV integrate free cooling, this does not prove to be as effective as natural ventilation via windows opening, as its operation is limited by more restrictive conditions that prevent the fans from operating for little benefit. Furthermore, the operation of the fans to perform free-cooling proves to be significantly energy-intensive, consuming 25% and 43% of the total electrical consumption, respectively. This increase results in significant operating costs for the building every year, confirming the superiority of natural ventilation in making the building more sustainable and resilient.

7. CONCLUSION

In response to the escalating cooling demand in buildings due to rising temperatures from climate change, this paper supports a transition towards natural ventilation and passive cooling. However, concerns about increased pollutant transport into buildings through open windows necessitate a thorough assessment of air quality during the design process.

The case study of Milan, known for its air pollution challenges, provides the context to assess the feasibility of natural ventilation strategies in urban environments. Analysing critical pollutants (PM2.5, PM10, NO_2, O_3) from 2015 to 2023, the study compares concentrations against Italian and EU limits and WHO guidelines. Despite challenges posed by ozone, potentially limiting natural ventilation implementation during the hottest summer weeks, other pollutants exhibit a marked reduction during the natural ventilation season with values that consistently fall below recommended thresholds for a significant number of days. Results also indicate that Milan's air quality exhibits favourable trends in decreasing pollution levels, supporting a wider implementation of NV strategies in the upcoming years.

A detailed case study of the European Library of Information and Culture (BEIC) illustrates the practical integration of NV. Through thermal simulations, the study quantifies energy savings and underscores the effectiveness of NV in reducing cooling demands. The analysis reveals that choosing mechanical free cooling over NV for night cooling significantly increases cooling energy consumption, and this escalation is further pronounced when accounting for fan usage. When entirely omitting natural ventilation strategies, the impact is magnified.

In conclusion, the BEIC project in Milan serves as a practical example of the effectiveness of natural ventilation in addressing the challenge posed by increasing cooling demands, reducing the reliance on mechanical systems and increasing the resilience of buildings in response to climate change.

REFERENCES

1. IEA (2018), The Future of Cooling, IEA, Paris https://www.iea.org/reports/the-future-of-cooling.
2. Stabile, L.; Dell'Isola, M.; Russi, A.; Massimo, A.; Buonanno, G., (2017). The effect of natural ventilation strategy on indoor air quality in schools. Sci. Total Environ. 595, 894–902.
3. WHO, Global Air Quality Guidelines (2021). Geneva: World Health Organization, 2021.
4. ARPA Lombardia. Open Data Regione Lombardia, 2023.
5. Belias, E.; Licina, D. Influence of outdoor air pollution on European residential ventilative cooling potential, (2023). Energy Build. 289, 113044.
6. ARPA Lombardia, Milano - La Qualità dell'Aria negli ultimi anni - Valutazione sul periodo 2016 – 2021, (2021).
7. European Parliament and Council of the European Union. Directive 2008/50/EC of the European Parliament and of the Council of 21 May 2008 on Ambient Air Quality and Cleaner Air for Europe.
8. Italian Legislative Decree No. 155 implementing Directive 2008/50/EC on ambient air quality and cleaner air for Europe (2010). Gazzetta Ufficiale No. 216, 15 September 2010.
9. WHO, Air Quality Guidelines: Global Update 2005, (2006). Geneva: World Health Organization.
10. Honeybee plugin, part of Ladybug Tools suite, (2023).
11. Raffaelli, K.; Deserti, M.; Stortini, M.; Amorati, R.; Vasconi, M.; Giovannini, G., Improving Air Quality in the Po Valley, Italy: Some Results by the LIFE-IP-PREPAIR Project, (2020). Atmosphere 11, 429.
12. INEMAR ARPA Lombardia, INEMAR Emission Inventory 2019, (2022). Milan, Italy, 2022.
13. Xia, N.; Du, E.; Guo, Z.; de Vries, W. The Diurnal Cycle of Summer Tropospheric Ozone Concentrations across Chinese Cities: Spatial Patterns and Main Drivers, (2021). Environ. Pollut. 286, 117547.
14. Maranzano, P., Air quality in Lombardy, Italy: An overview of the environmental monitoring system of ARPA Lombardia, (2022). Earth 3, 1: 172-203.
15. Lotrecchiano, N.; Trucillo, P.; Barletta, D.; Poletto, M.; Sofia, D. Air Pollution Analysis during the Lockdown on the City of Milan (2021). Processes, 9, 1692.

PLEA 2024 WROCŁAW
(Re)thinking Resilience

Climate Change and Dementia Care:
Impacts on Energy Demand for Residential Assessment Wards.

NEVEEN HAMZA[1] MOHAMED MAHGOUB[2] KEITH REID[3] DAVID ANDERSON[3]
LEIGH TOWNSEND[3]

[1]Newcastle University, Newcastle,United Kingdom
[2] University of Emirates, AlAin, United Arab Emirates
[3]Cumbria, Northumbria, Tyne and Wear Trust, CNTW, UK

ABSTRACT:. In the UK, Dementia residential assessment wards are used to assess needs of people living with late stage dementia and behaviours that challenges, where personalized care plans are drawn. Poor homeostasis is a condition of ageing, people living with late-stage dementia who express thermal discomfort among other heath confounders using agitation and aggression as a proxy. To reduce agitation and provide thermal comfort, indoor temperatures are generally maintained between 22-24C, responding to a higher energy demand than other building typologies. This research investigates the impacts of tight indoor temperatures ranges, scenarios of climate change and a push by legislation to adopt passivehaus standards. An award-winning facility is used as a case study to assess changes on building energy demand per m2 to remove confounders of inappropriate design on results. And provide generalizability to other facilities. Results predict that climate change has a profound effect on reducing heating energy demand. The use of more insulative building fabric can also achieve noticeable energy reductions. A combination of more insulted building fabric and Climate change is predicted to decrease energy demand by 30%, but due diligence needs to maintain indoor air quality.
KEYWORDS: Dementia, Climate change, thermal comfort, agitation, energy demand

1. INTRODUCTION

The UN, World Meteorological Organization announced alarmingly on Thursday the 30th of November 2023, in the Annual Climate Change conference in Dubai (The independent reporting from COP28 Climate summit), that climate change is indisputable and 2023 continued the trend observed over the last decade, reaching the highest hottest year on record. The World Meteorological Organization also warned that the average temperature for the year rose by 1.4 degrees Celsius from pre-industrial times – a mere one-tenth of a degree under a target limit for the end of the century as laid out by the Paris climate accord in 2015.

Climate change is expected to increase the frequency of prolonged heat waves, unpredictable patterns of cold weather, rainfall and draughts, forest fires and concentration of air pollution, and most importantly have implications on health and specifically on an ageing population. Global average warmings are projected to reach about 2.5 °C if emissions continue to rise at the current level, following the projections represented by the IPCC Representative Concentration Pathway 6.0 (RCP6.0) and may reach 8.5C.[1]

Globally, neurological disorders are increasingly recognized, after cardiovascular diseases, as the second cause of death [2]. Dementia Modelling of the UK suggests a 57% increase in the number of people with dementia from 2016 to 2040, with an estimated 1·2 million people living with dementia in 2040 in the UK [3]. This is compounded by the UK's ageing population where The number of people aged 65–74 years in the UK is expected to increase by 20% between 2019 and 2040, and the number of people aged 85 years and over to increase by 114%. The prevalence rate of dementia among older people in the UK is estimated to be 7.1% [4].

Although research has progressed in understanding the core symptoms, of neurodegenerative disease, such as dementia, and their impacts on cognitive deterioration, increasing dependency on care providers and having impaired social functioning, there is meagre research on the impact of thermal comfort on agitation and aggression, and the impact of thermal comfort needs on building energy demand in a context of climate change.

In the past decade studies highlighted the risk of climate change on older populations, reporting predicted increases in incidents of heat stress, heat exhaustion, heart stroke and hypothermia [5-7] People living with Dementia have been found to have significant circadian dysfunction in core body temperature, which may precede the clinical onset. This which underlines a metabolic hypothesis that people living with dementia will be more affected by the phenomenon of global climate change [8-9], and will need to live in air conditioned spaces.

Research on the link between dysfunctional haemostasis due to dementia and its impact on universal neuropsychiatric symptoms, such as apathy, agitation, depression, delusion, agitation, and sleep disturbance remains lacking. Although incidents of aggression are rare, about 1 % of the building occupied time, they can be as burdensome for the person and their carers, as the cognitive deterioration from the disease itself [10-13]. Due to the body's impaired ability to regulate temperature, exposure to fluctuating temperature can lead to increasing the risk of thermal stress on patients and increasing the uptake of harmful psychotropic drug treatment for mental disorders [14].

Although there is an increased interest in published guidelines for the design of Dementia friendly environments [15] that specifies material finishes, colours, and the need to create 'appropriate' thermal, visual, and acoustic measures, quantification of energy use for these environments under climate change is lacking. Thermal guidelines exist for hospital environments [16], less is understood on the range of comfort temperatures for people living with dementia in different climates and cultures, and the impacts of climate change on the need to provide climatically controlled environments for people living with neurodegenerative disease.

This research aims to look at the impacts on heating and cooling energy demand of residential assessment Dementia wards under scenarios of climate change. The paper extends predictive scenarios to look at implications of current trends in constructing and refurbishing the NHS stock to Passivhaus standards under climate change scenarios.

The objectives of the research are:

1- Correlating reliable and validated agitation records and indoor monitored environments to deduct comfort thermal ranges for people living with dementia.

2- To predict changes to cooling and heating energy demand under scenarios of climate change for maintaining environmental conditions that reduce agitation levels

3- To predict changes to cooling and heating demand if Passivhaus standards are pursued in new construction and refurbishment.

2. THE BASE CASE

To reduce the impact of poor design on the assessment of energy demand, the base-case is based on the state of the art, award winning design for a specialized dementia care assessment unit for people living with advanced stage dementia. Figure 1, shows a zonal diagram and isometric of the building. The building is a single storey 'pavilion' designed around three indoor courtyards. Acknowledging that care frameworks are equably important as the physical building environment, in this facility care frameworks are designed on individual basis and are more about a person's needs and individual comfort than a collective medical diagnosis. This leads to a high level of one-to-one patient to nursing staff ratio, in addition to 2 doctors and 4 cleaning staff.

The building comprises two single gender wards with 10 rooms each and 4 (swing) rooms that can be used if more females or male occupants are admitted, totalling 24 rooms.

Spaces are designed to reflect a non-institutional home like interior design with interior decoration relatable to patients such as pictures of football players, movie stars and abstract art of landmarks of the region.

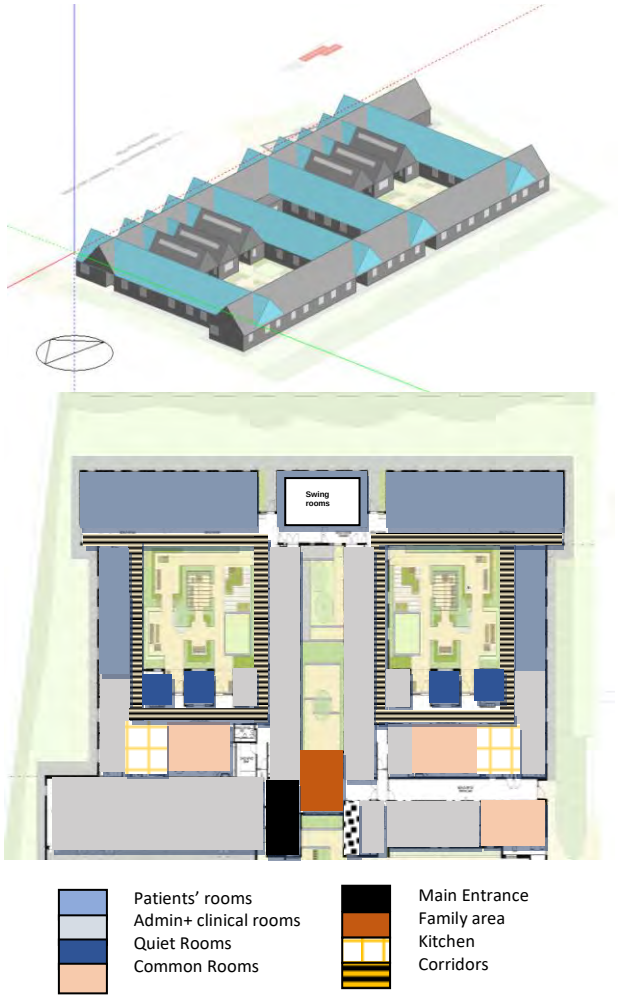

Figure 1I: Isometric and diagrammatic zoning

Key elements of the design are divided into 'patient and care provision' space, and 'staff only' spaces.

Patient and care provision spaces:

- Single occupancy bedrooms with an ensuite toilet.
- An out of ward area for patients to meet with family.
- A common room to encourage social interaction, watching TV, listening to music, and dining.
- Quiet rooms: small-scale areas that accompany the development of person-centred activities, accessible from the common room.
- An entertainment room, where movies and games nights can take place between patients, family, and staff.
- Single sided corridors that circulate around a an enclosed greenspace 'courtyard' for wandering, and in summer for sitting out and gardening activities.
- All indoor spaces provide obstacle free paths that incorporate universal design elements such as wheelchair accessibility, sufficient clearance for turns, and ergonomic accessible railings.
- Dedicated spaces for daily household activities in the therapeutic kitchen, where patients and staff can prepare simple meals.
- An assessment kitchen to assess the person's ability to be self-independent.
- On ward medical assessment room
- A hairdresser

Staff only spaces are:

- On-ward meeting room,
- ward manager room
- next to the common room a nursing station for passive observation and managing patients' clinical requirements.
- Out of ward storage,
- staff changing rooms,
- a larger team meeting room
- laundrettes

The intensive and personalized care frameworks lead to an architectural programme divides the space equally to a 50-50% for patient rooms and for staff.
The indoor garden space is rarely used in winter except for visual relief and a connection with the outdoors. In summer doors are opened to manually purge ventilation or allow patients outside on the rare occasion of a sunny summer day.
There are two mechanical systems.
An underfloor heating system is used throughout to avoid the need for installing radiators that are considered a tripping hazard for patients.

Table 1: Model Data Input		Unit
No. of floors	1	
Plot area	2229	m^2
Pitched roof height	4.5	m
External wall insulation	U-value: 0.52	W/m^2-K
Roof insulation	U-value: 0.51	W/m^2-K
External window	U-value: 1.96	W/m^2-K
Passivhaus triple glazing	U-value: 0.8	W/m^2-K
Passivhaus External wall insulation	U-value: 0.15	W/m^2-K
Passivhaus Roof insulation	U-value: 0.15	W/m^2-K
System type	Variable refrigerant flow (VRF)	
Maximum supply air temp	23°C	
Minimum supply air temp	22°C	
Heating set back	22°C	
Cooling set back	24°C	
CoP	2.5	
Model infiltration	Constant 0.7 ac/h	

In the common area and in quiet rooms a VRF air conditioning is used to control the levels of simultaneous heating and cooling needed.
In summer the nurses have an override control on the air conditioning system to open the upper skylights in the saw-toothed structure to allow for purge ventilation.

3. Methodology

This study looked at a sample population of resident patients in an award winning purpose-built inpatient building for people with severe dementia with associated behavioural and psychological complications of dementia (BPSD). Indoor thermal and humidity levels were measured for a year and correlated to the Cumbria, Northumberland, Tyne and Wear Trust's "Talk First" Dataset which records all incidents of verbal and physical aggression through a robust incident reporting system.

To find the range of indoor operative temperatures that reduce patient agitation, a full year of air and globe temperatures were monitored in 3 minute intervals over a full calendar year from September 2022-September 2023. Areas monitored were the wards common rooms and corridors, bedroom monitoring was trailed then stopped as patients perceived the equipment to be spying on their privacy and they always attempted to dismantle it. Due to the long study period, small, unobtrusive, and self-contained data acquisition devices were used to ensure that they do not interfering with the occupants' regular activities. The HOBO MX1104 Analog/Temp/RH/Light data logger measures and transmit data wirelessly from indoor environments to a mobile device or computer using Bluetooth Low Energy (BLE) technology. The MX1104 also includes one analogue input that was used to measure globe temperature. As the building has a low air velocity of less than 0.3m/sec, operative temperature is

calculated as a mathematical average of air and globe temperature.

Building energy performance analysis were undertaken using Design builder software (version7), with building materiality as specified in Table 1. CIBSE climate change Test Reference Year (TRY) predictive files were used, to simulate the annual changes in heating and cooling energy demand. The weather files use a baseline from 1984-2013. Files are presented for 2020,2050 and 2080. As 2013 was the 6th highest year on record and 2023 is the highest yet on record according to the World Meteorological Organization, with the earth temperature already increasing by 1.4C before the 2030 expected IPCC pledge, therefore this research used the high emission scenario, with emissions predicted to reach a 4C increase by 2080. Cooling is needed for the summer months from May till September.

As our understanding of the climate system and our ability to model it improves, and as computing power increases, it is likely that future projections will be refined. A consequence of these expected improvements is that both the model projections and probability distribution for a given outcome are likely to evolve in the future. This is not a reason for delaying carrying out a risk assessment but may impact on the actions taken to build resilience [16]

4.ANALYSIS AND DISCUSSION

The building HVAC system setpoints for cooling and heating respectively were between 22-24^{0}C. Monitored data indicate that the building fluctuated between 21-25.5^{0}C However, monitoring the indoor environment and the correlations to a database of recorded incidents of agitation (Figure 2) suggests that people living with Dementia and BPSD are less tolerant to temperature fluctuations. Providing a comfortable environment that reduces agitation requires adhering to the narrower range for thermal comfort guidelines for hospitals [17].

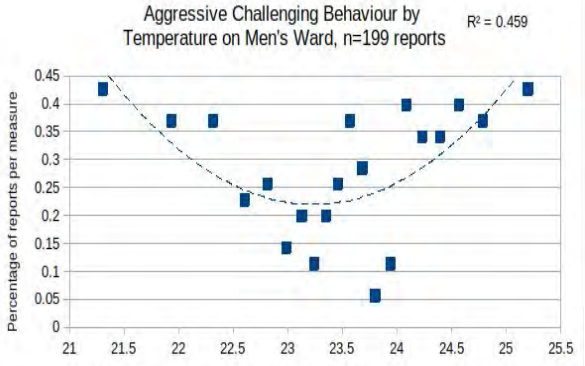

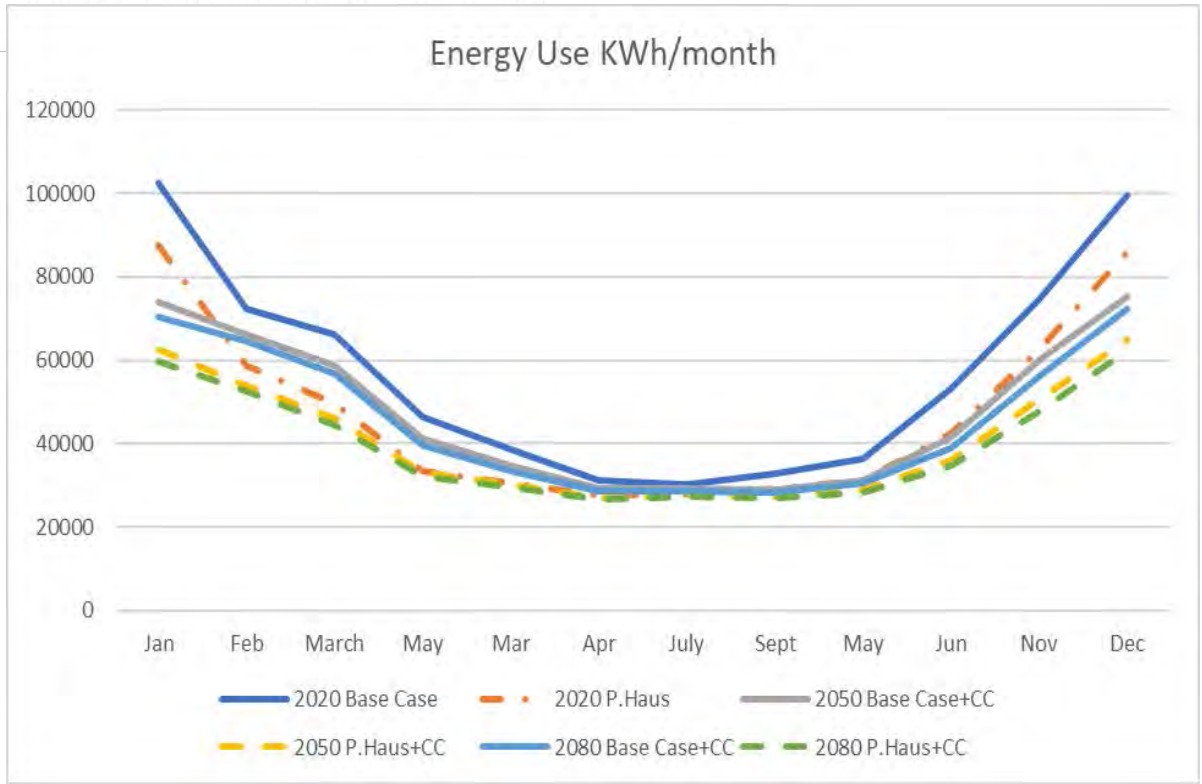

Figure3: Changes in energy demand due to climate change (CC) and application of PassiveHaus standards

Table 2: comparison between effects of Climate change and refurbishment to Passivhaus standard on annual energy demand

Energy Demand in KW/m2/ month- Base Case (BC). Climate Change (CC)

	2020 Base Case (BC)	2020 P.Haus	BC+2050 CC	BC+2050 CC+P.Haus	BC+2080 CC	BC+2080 CC+P.Haus
Jan	45.89	39.27	33.17	28.07	31.62	26.75
Feb	32.34	26.39	29.67	24.19	28.94	23.58
March	29.72	22.30	26.33	20.63	25.47	20.02
April	20.84	15.08	18.57	14.81	17.8	14.47
May	17.33	13.74	15.66	13.52	15.05	13.31
June	14.06	12.40	13.09	12.13	12.86	12.01
July	13.57	12.50	13.07	12.40	12.91	12.31
August	14.70	13.16	12.92	12.23	12.71	12.08
Sept	16.37	14.04	14.07	12.97	13.67	12.75
October	23.81	19.06	18.66	16.13	17.50	15.54
Nov	33.45	28.11	26.96	22.76	25.25	21.41
Dec	44.70	38.52	33.83	29.08	32.42	27.88
Total	306.89	254.56	256.01	218.91	246.21	212.11
% Change from BC		-17%	-16.5%	-28.67%	-19.77%	-30.89%

Figure2, indicates that operative temperatures that coincided with the least agitation recorded incidents, as incidents of agitation tend to increase in severity outside these temperatures. Table2 and Figure 3, show that narrowing down the indoor temperature range to two degrees, can lead to a substantial use of energy for heating and building operation per Kwh/sq,m

However, the warmer ambient temperatures is predicted to decrease heating demand. This paper sought to look into changes in heating demand combining the effect of climate change and a regulatory framework to increase insulation of health care facilities to Passivehaus standards . If passivhaus standards are implemented it would help the reduction of energy demand due to the need to tighten the indoor thermal conditions to only 2C difference from 22-24C

If the current annual trend of increasing earth temperature continues to 4C by 2080, then heating loads are predicted to decrease by 19.77%. Climate change combined with Passivhaus standards will substantially decrease heating loads by 30.89%.

CONCLUSIONS

Energy demand for heating and cooling is increased due to poor homeostasis in older people and the need to constantly provide thermally comfortable environments to reduce behavioural and psychological symptoms of dementia

Incidents of agitation and aggression although amounting to 1% of building occupancy time, have a major effect on staff provision, medication and care frameworks. Our studies show a reduced tolerance to temperature changes by this group, and an increase in behaviours that challenge when indoor temperatures are slightly outside the narrow range of 22-24C. This necessitates an extremely efficient HVAC system and a well-insulated building fabric. Currently air conditioning systems attempting to control indoor temperatures between 22-24C are still inefficient and our monitoring found that the building experiences fluctuations between 18-25C.

There is a substantial energy demand penalty of attempting to control the indoor environment to a narrower range of temperatures of 22-24^{0}C, when compared to other building typologies where temperature is usually controlled between 18-21^{0}C .

As the pavilion design, with its circulation corridor around a courtyard is the most advocated design for Dementia patients to relieve agitation and wandering syndrome effects, this leads to a higher exposed building fabric. Refurbishment to a higher standard of insulation such as Passivhaus standard will lead to a substantial energy saving around 18%, However, this comes with a caveat of increased refurbishment cost, as current wall systems may not accommodate the levels of thicknesses of insulation, and in addition, a with tighter infiltration control, there is a needs to monitor for indoor air quality.

Table 2 and Figure 3, indicate that climate change scenarios are impactful on reducing the overall building energy demand in 2050, and more in 2080. This decrease is equal to increasing the insulative properties of the building envelope to the stringent passivhaus standard under current climatic

conditions. The decision of not to refurbish to passivehaus standard and rely on sustainable renewable energy generation from solar panels maybe considered as an alternative but with a caveat that mounted renewable systems need a substantial roof space and a southerly orientation.

Therefore, a combination of insulating the building to passivhaus standard and the predicted tendency of increased ambient temperatures due to climate change may decrease energy demand. It is worthwhile considering that the changes in ambient temperatures have adverse effects on increasing the rainy season and flooding effects in temperate climates, these will need to be considered in refurbishment of healthcare buildings

ACKNOWLEDGEMENTS

This research is jointly funded by the Wellcome Trust-small grant scheme and the Architectural Research Collaborative research group (ARC), School of Architecture, Planning and Landscape, Newcastle University. The project was registered for ethical approval by Newcastle University Medical Ethics Committee as a Service Evaluation Approval SER-19-047 - Evaluating the impact of environmental conditions on agitation levels for patients with Dementia in hospital wards (ARCADIA)

REFERENCES

1. Associated Press (2023) 2023 set to be hottest year on record, Secretary general reporting in COP 28 Dubai, https://www.cbc.ca/news/science/un-cop28-record-heat-1.7040807

2.Vos,T., Lim,S., C Abbafati,C., et al(2020) Global burden of 369 diseases and injuries in 204 countries and territories, 1990–2019: a systematic analysis for the Global Burden of Disease Study 2019. *The Lancet*, Vol.396,p.1204-1222

3.Livingston G, Huntley J, Sommerlad A, et al (2020). Dementia prevention, intervention, and care: 2020 report of *the* Lancet *Commission.* Lancet

4.Alzheimer's Society (2020) *Alzheimer's Society's view on demography*. Alzheimer's Society. https://www.alzheimers.org.uk

5.Zanobetti, A., O'neill,M., Gronlund,C., Schwartz, J. (2012) Summer temperature variability and long-term survival among elderly people with chronic disease. Proceedings of the National Academy of Sciences, Vol 109, pp.6608-6613

6.Shi, L., Kloog, I., Zanobetti, A. et al.(2015) Impacts of temperature and its variability on mortality in New England. *Nature Climate Change, Vol* **5**, p.988–991

7. Andrews,O., Le Quéré,C., Kjellstrom,T.,et al *(2018).* Implications for workability and survivability in populations exposed to extreme heat under climate change: a modelling study. *Lancet Planet Health*, p. 540-547

8.Whittington,R., Papon,M.,Chouinard-Decorte, F. and Planel,E. (2010) Hypothermia and Alzheimer's Disease Neuropathogenic Pathways. *Current Alzheimer's Research*, 7(8), p.717 – 725

9.Carrettiero,D., Santiago, F., Motzko-Soares,A.,and Almeida, M. (2015) Temperature and toxic Tau in Alzheimer's disease: new insights. Temperatures, 2:4, p.491-498

10. Gresham M, Morris T, Min Chao S, Lorang C, Cunningham C. Specialist residential dementia care for people with severe and persistent behaviours: A ten-year retrospective review. *Australas J Ageing*. 2021;40:309–316.https://doi.org/10.1111/ ajag.12964

11. Louis S., Carlson, A., Abhilash Suresh, A., Joshua Rim, J., Mays,M., Ontaneda,D., Dhawan, A.(2023) Impacts of Climate Change and Air Pollution on Neurologic Health, Disease, and Practice, A Scoping Review. *Neurology*, 100 (10) 474-483

12. Doan, J. and Dhawan, A. (2023) Neurology and climate change: what we know and where we are going. *The Journal of Climate Change and Health*, in press,100284

13. Bongioanni, P., Del Carratore, R., Corbianco, S., et al (2021) Climate change and neurodegenerative diseases, *Environmental Research,* Volume 201,111511

14. Cheshire, W. (2016) Thermoregulatory disorders and illness related to heat and cold stress. *Autonomic Neuroscience: Basic and Clinical* 196.p. 91–104

15. Health Building Notes (2015) Dementia-friendly health and social care environments, HBN 0802, Department of Health, UK

16. Fung F, Lowe J, Mitchell JFB, Murphy J, Bernie D, Gohar L, Harris G, Howard T, Kendon E, Maisey P, Palmer M and Sexton D (2018). UKCP18 Guidance: Caveats and Limitations. Met Office Hadley Centre, Exeter.

17. Chartered Institute of Building Services Engineering (2016) CIBSE Guide A:Environmental Design, CIBSE, UK

PLEA 2024 WROCŁAW
(Re)thinking Resilience

Perceptions of physical well-being in work-from-home settings

A preliminary analysis

SANYOGITA MANU[1] , ADAM RYSANEK[1]

[1] Faculty of Applied Sciences, University of British Columbia, Vancouver, Canada.

ABSTRACT: In late March 2020, around 4.7 million Canadian workers transitioned to remote work due to the pandemic, reflecting a worldwide shift. As remote work becomes increasingly common, it is important to understand its impact on personal well-being. This paper explores how working from home affects physical activity, physical symptoms, and sleep -related problems. The research, conducted in summer 2022, involved 94 participants. A significant majority, at least 80%, reported high to moderate weekly physical activity, with consistent activity levels over time. Common physical complaints included sleep disturbances, low energy, muscle pain, backache, and fatigue, affecting at least 18% of participants. The most prevalent sleep-related issues were of daytime drowsiness, early awakening, sleep duration, and difficulty falling asleep. The overall analysis suggests that the participants experienced a moderate to high level of physical well-being while working from home. Notably, there was a clear link between physical symptoms and sleep issues, though these did not correlate strongly with other measured aspects. None of the physical well-being metrics were significantly correlated with how participants perceived their work performance, well-being, or satisfaction while working from home. This study highlights the critical relationship between remote work, physical health, and sleep, offering valuable insights for the evolving work landscape.
KEYWORDS: Indoor environmental quality (IEQ), Work-from-home (WFH), Physical well-being, Physical symptoms, Sleep

1. INTRODUCTION

The advent of remote work has revolutionized traditional work paradigms, enabling employees to perform their duties from the comfort of their homes. While this transition offers newfound flexibility and convenience, it has also raised concerns about the impact on the physical well-being of at-home workers. This research aims to delve into the various factors that influence the physical health of individuals engaged in remote work setups.

Recent studies have suggested a complex interplay between remote work, sedentary behaviour and screen usage, and its repercussions on overall health [1]. Prolonged sitting, reduced physical activity, and inadequate ergonomic setups have been identified as potential contributors to musculoskeletal discomfort and other health issues [2,3]. Furthermore, the blurring boundaries between work and personal life in remote setups might lead to extended working hours and increased stress, potentially exacerbating health concerns [4,5].

This study is a part of a doctoral research project that was initiated in March 2022 to systematically evaluate the indoor environmental quality (IEQ) and perceived well-being and productivity of at-home workers. While the project is ongoing, the objective of this study is to present a preliminary analysis of the at-home workers' perception of their physical well-being.

2. METHODS

Ninety-four study participants (or WFH sites) were recruited through convenience and snowball sampling from Metro Vancouver (Canada) and Seattle Metropolitan (U.S.) regions for a period nearly two months in the summer of 2022. The inclusion criteria required that participants be working from home for at least two days a week, carrying out sedentary, computer-based work. Individuals planning to move houses, carry out home renovations, or change their working location during the study period were excluded from the study. Each participant was given an indoor, desktop IEQ monitor to be installed in their WFH offices [6,7].

A battery of survey instruments was used in this study for subjective assessment of comfort, well-being, and productivity. The variables of interest being presented in this paper come from three standard questionnaires. The first is the International Physical Activity Questionnaires – Short Form (IPAQ-SF) [8], which was used to assess the types of intensity of physical activity that people do as part of their daily lives. It comprises seven items pertaining to the time spent doing vigorous and moderate activities, walking and sitting, based on last 7-day recall. This instrument allows estimation of total physical activity in terms of "low", "moderate" and "high" categories of individual

activity patterns. The IPAQ has been tested extensively for reliability and validity across 12 countries [9].

The second questionnaire is the Cohen-Hoberman inventory of physical symptoms (CHIPS) [10,11] which lists 33 common physical symptoms. Each item is rated for how much that problem bothered or distressed the individual during the past two weeks. Items are rated on a 5-point scale from "not at all (0)" to "extremely (4)". The total CHIPS score is computed by adding the scores across the 33 items ranging from 0 (representing absence of any symptoms) to 132 (denoting severe distress from the symptoms).

The third questionnaire is the Athens Insomnia Scale (AIS) [12] which comprises eight items. The first five items pertain to sleep induction, awakenings during the night, final awakening, total sleep duration, and sleep quality; while the last three refer to well-being, functioning capacity, and sleepiness during the day. Each item of the AIS can be rated from 0 to 3, (with 0 corresponding to "no problem at all" and 3 "very serious problem"). The respondents are asked to rate positive if they had experienced the sleep difficulty described in each item at least three times a week during the last month. The total AIS score is computed by adding the scores across the 8 items and can range from 0 (denoting absence of any sleep-related problem) to 24 (representing the most severe degree of insomnia).

ANOVA and Kruskal-Wallis or Friedman tests were used to compare different groups of data. The Shapiro-Wilk test and Levene's tests were used to check whether the assumptions of normal distribution and homogeneity of variances were met for ANOVA. Spearman's rank correlation was used to assess the association between variables. Data analysis was done in Python using Pandas to process the data and provide descriptive statistics; SciPy for statistical tests; and Matplotlib to create plots.

3. RESULTS

When interpreting the results of this analysis, it is important to keep in mind that on average participants worked from home (WFH) for at least 3 days a week for the duration of the survey period, starting from May 23 until July 15, 2022. At least 67% were WFH for minimum of 3 days and at least 43% were WFH for a minimum of 4 days.

3.1 Physical activity

Figure 1 illustrates the distribution of survey participants' weekly physical activity engagement across three categories: low, moderate, and high. The values represent the percentage of participants in each category per week. In Week 1, 18% were low, 39% moderate, and 43% high in activity. The trend shows variability across weeks. For instance, by Week 4, low activity increased to 20%, while high activity decreased to 32%. Notably, in Week 5, a significant 67% reported high activity, contrasting with only 19% in low activity. Overall, the data suggest fluctuating patterns in physical activity levels among the participants throughout the 8 weeks.

To test for statistically significant differences between weeks the Friedman test, which is a non-parametric equivalent to the repeated measures ANOVA, was used since the activity scores are categorical data. The categorical scores were converted into numerical ranks: "1" for "low", "2" for "moderate" and "3" for "high". The output from the Friedman test indicates that the null hypothesis may be rejected X^2 (7, N = 60) = 18.47, p < .05. This suggests that there are statistically significant differences in the activity scores across the weeks.

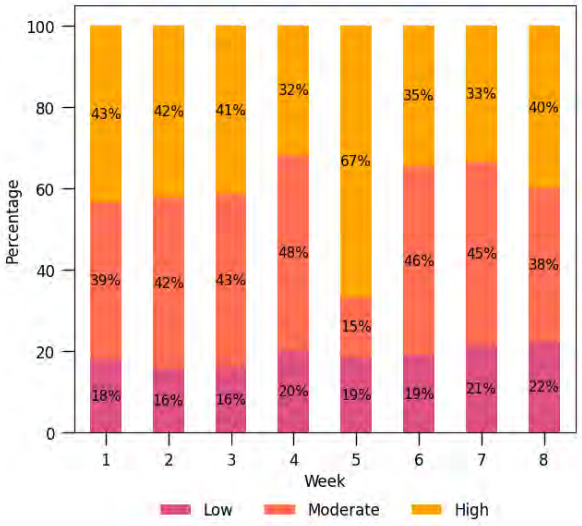

Figure 1: A weekly distribution of votes for physical activity categories

3.2 Physical symptoms

The statistical summary in Figure 2 provides an insight into the CHIPS scores, representing the experience of physical health symptoms reported every two weeks. The median scores were generally low. Initial scores at week 2 and week 4 showed a slight increase, suggesting a potential trend. However, scores then decreased notably at week 6 and slightly at week 8, indicating a potential improvement in physical well-being. Dispersion, measured by standard deviation, was relatively high across all time points, reflecting significant variability in symptom experiences among participants. Notably, the maximum scores varied considerably - 45 (week 2), 60 (week 4), 57 (week 6), and 74 (week 8), indicating the range of symptom severity. In conclusion, the data suggests an initial increase followed by a subsequent decrease in physical symptom experiences among participants, with substantial variability across all time points.

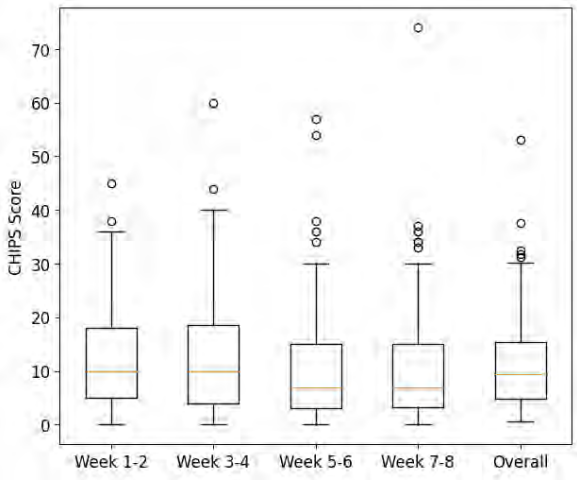

Figure 2: A bi-weekly visual summary of the CHIPS scores

The bi-weekly datasets met the assumption of homogeneity of variances but were not normally distributed. Despite that, ANOVA was performed on the datasets, in addition to the Kruskal-Wallis test because (a) ANOVA is known to be quite robust to violations of the normality assumption when sample sizes are large, and (b) the Shapiro-Wilk statistic was at least 0.78 ($p < .001$), indicating a distribution close to normal (values closer to 1 indicate a more normal distribution). Both ANOVA and Kruskal-Wallis tests indicated a lack of statistically significant differences across the groups (weeks) for the CHIPS scores dataset. This means that based on the data and the tests performed, there isn't enough evidence to conclude that the scores differed significantly from bi-weekly period to another.

Figure 3 shows the distribution of responses across the 33 health symptoms ordered by the severity of the symptom. This was done by pooling the votes (%) from the last three categories "(2")", "(3)" and "extremely bothered (4)" and then ordering the symptoms in descending order. In other words, the symptoms that were most prevalent and bothersome within the sample appear on top of the plots. Across the study campaign, about 60% of the participants were bothered by any kind of symptoms, indicating generally high physical health, also reflected in the low CHIPS scores (Figure 2). What is more interesting to note, however, is that the list of the most prevalent physical symptoms remains fairly consistent across the four bi-weekly sampling periods albeit in slight changes in the order in which they appeared. The five most prevalent symptoms were "sleep problems", "feeling low in energy", "muscle tension or soreness", "back pain" and "constant fatigue". At least 18% of the study participants were bothered by these symptoms.

3.2 Sleep difficulty

The statistical summary in Figure 4 provides an insight into the AIS scores, representing the experience of sleep-related issues reported every four weeks. The median scores were consistent across the two sampling periods, indicating stable sleep problem severity over time. The 'Overall' column suggests a slightly higher median, pointing to an overall moderate insomnia level among participants. Outliers were present, particularly in the second month, suggesting that some participants experienced significantly higher insomnia severity. The interquartile range (IQR) was broad, indicating more variability in the central 50% of the data.

Figure 5 shows the distribution of responses across the eight sleep-related problems ordered by severity. This was done by pooling the votes (%) from the last two categories of "(2)" and "high difficulty (3)" and then ordering the problems in descending order. The prevalence of problems was slightly higher in the first month, with at least 10% of the participants reporting moderate difficulties with four or less issues. The most prevalent problems were "sleepiness during the day" (17%), "early final awakening" (15%), "sleep duration" (14%) and "sleep induction" (11%). These problems were also the most prevalent during the second month with at least 8% of the participants experiencing one or more of them. High difficulty levels were consistently low across both months, indicating that severe sleep problems were less common among the participants.

ANOVA and Kruskal-Wallis tests indicated a lack of statistically significant differences across the groups (weeks) for the AIS scores as well.

3.2 Correlations

The correlation matrix in Figure 6 provides insights into the relationships between different well-being metrics that have already been discussed earlier. In addition to those metrics, we have included three metrics of perceived performance, well-being and satisfaction while WFH, extracted from a bespoke IEQ questionnaire that was also administered as a part of the larger WFH study. A more detailed analysis of the outcomes from this questionnaire is presented in another paper [13]. The matrix values range from -1 to 1, where 1 indicates a perfect positive correlation, -1 indicates a perfect negative correlation, and 0 indicates no correlation.

Performance while working from home showed a moderate positive correlation with satisfaction at 0.63, suggesting that higher work performance is associated with increased satisfaction. The correlations between performance and well-being, and between well-being and satisfaction were positive but weaker, around 0.26 and 0.20, respectively.

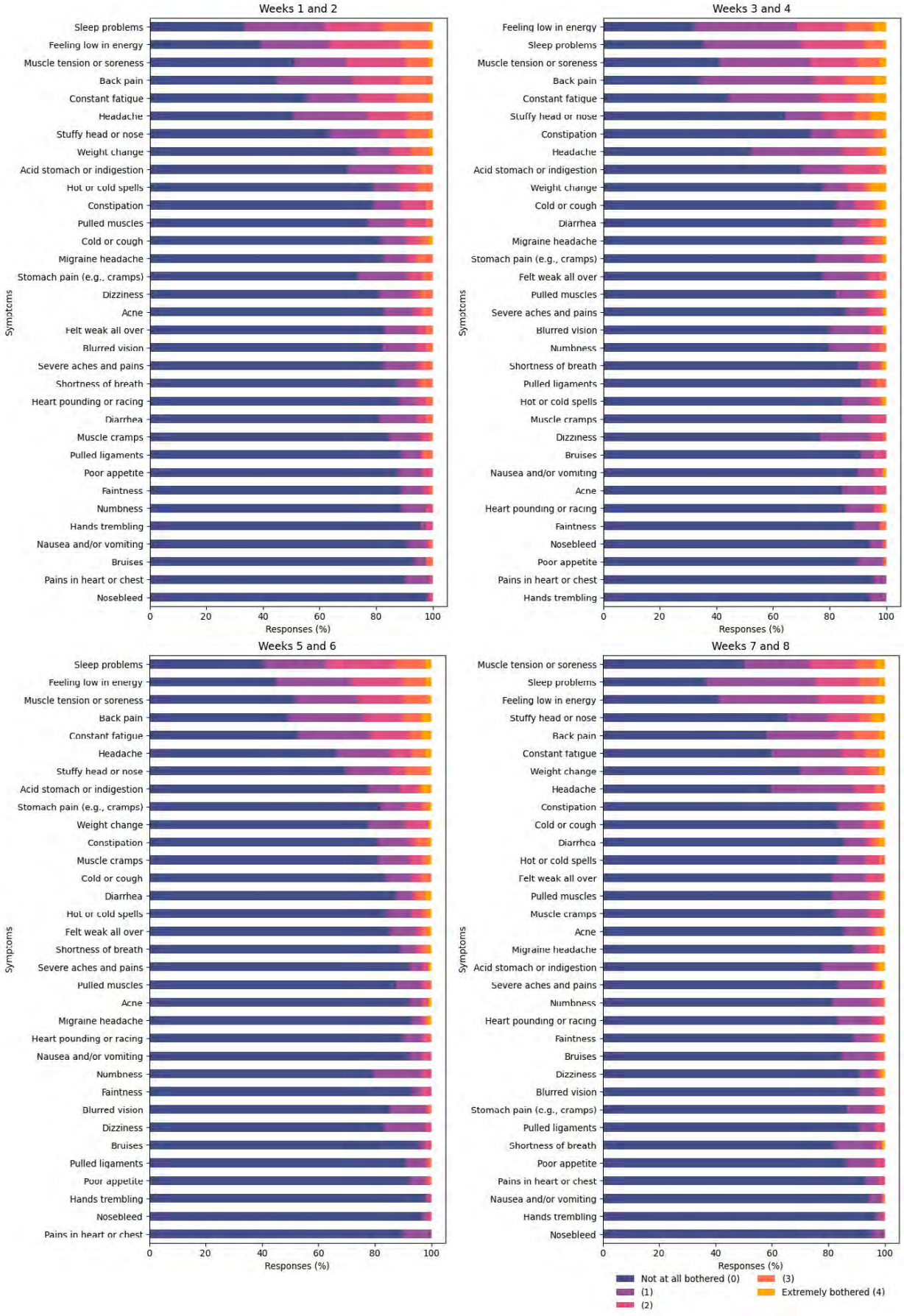

Figure 3: A bi-weekly distribution of responses across the 33 physical health symptoms from CHIPS

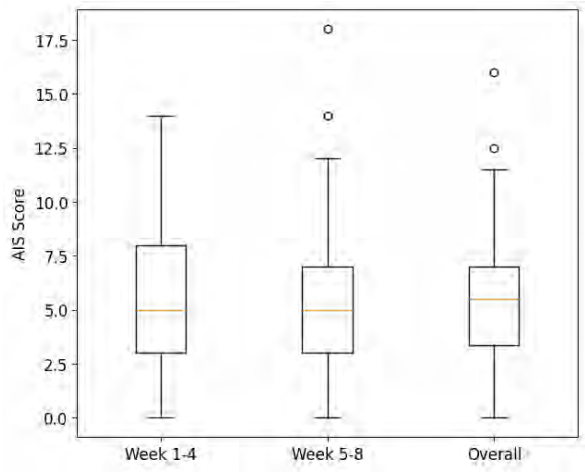

Figure 4: A monthly visual summary of the AIS scores

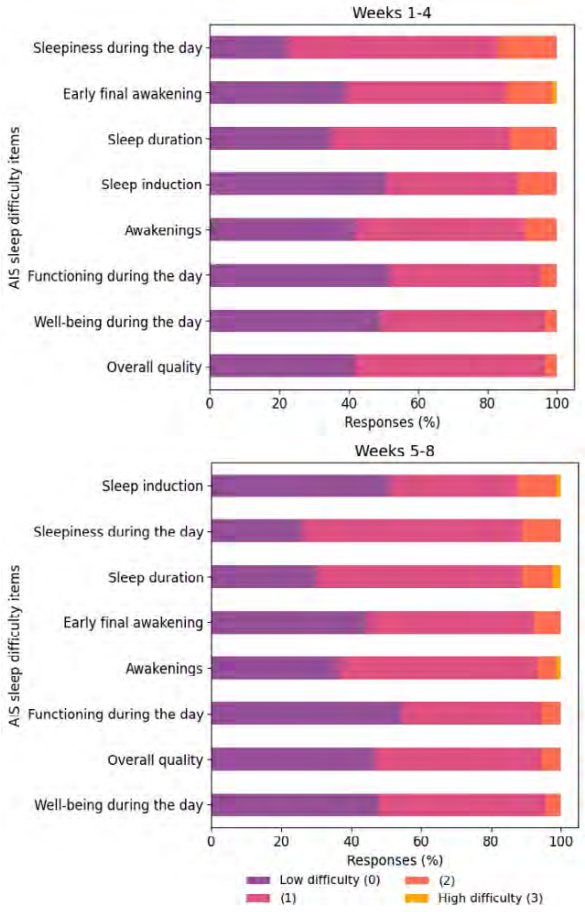

Figure 5: A monthly distribution of responses across the eight sleep difficulty items from AIS

The weekly activity scores generally showed moderate to strong positive correlations with each other, indicating that individuals who are more active in one week tended to maintain similar activity levels in other weeks. Notably, these scores showed no significant correlation or a very weak correlation with the WFH performance metrics. This suggests that the weekly activity levels do not strongly relate to how individuals rate their performance, well-being, or satisfaction with working from home.

Both average CHIPS and AIS scores showed significant positive correlation with each other (0.66), suggesting a strong relationship between these two assessments. However, these average scores showed generally weak or negative correlations with both the WFH performance metrics and the weekly activity scores. For instance, performance and average AIS score had a correlation of -0.20, indicating a slight tendency for higher performance ratings to associate with lower AIS scores.

In summary, while activity levels appeared consistently correlated week over week, they did not strongly correlate with how individuals perceive their work performance, wellness, or satisfaction. Additionally, the average scores from CHIPS and AIS assessments showed a strong relationship with each other but not with other metrics. This analysis highlights the complex and possibly independent nature of work-related self-assessments and physical activity patterns.

4. CONCLUSION

This paper presented an analysis of the subjective assessment of physical well-being in WFH settings, based on a field study conducted in the Pacific Northwest region with 94 participants during the summer of 2022. Physical well-being was assessed in terms of three broad metrics - the level of physical activity, the prevalence of physical symptoms and the occurrence of sleep-related problems.

At least 80% of the participants engaged in high and moderate levels of physical activity weekly, and the scores for these activities showed consistent correlations from week to week. The most prevalent physical symptoms included sleep problems, feeling low in energy, muscle tension or soreness, back pain, and constant fatigue, with at least 18% of participants being bothered by these issues. Sleep-related problems were predominantly characterized by sleepiness during the day, early-final awakening, sleep duration, and sleep induction issues. An overall assessment of the responses indicated a moderate to high level of physical well-being among the study participants while working from home. The CHIPS and AIS scores demonstrated a strong relationship with each other but not with other measured metrics. None of the physical well-being metrics showed significant correlations with participants' perceptions of their work performance, well-being, or satisfaction while working from home.

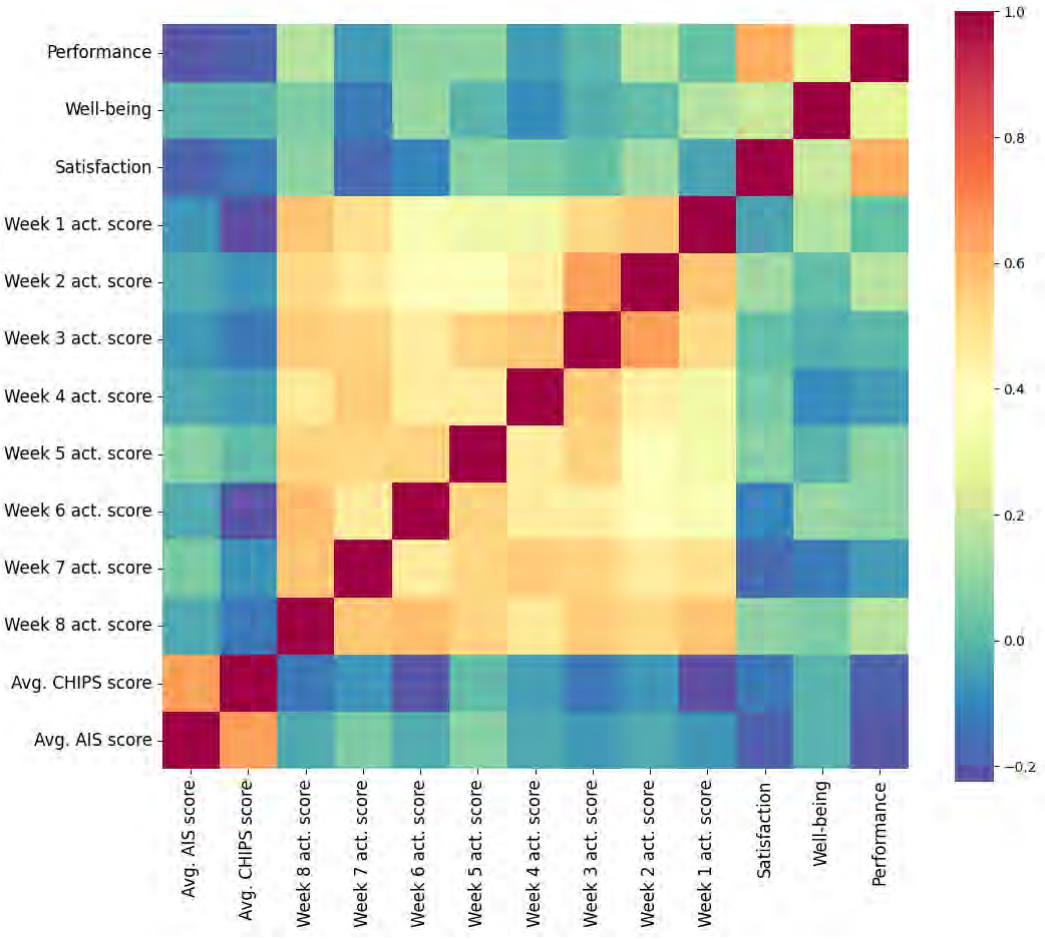

Figure 6: Spearman rank correlation matrix

REFERENCES

[1] Smith L, Jacob L, Trott M, Yakkundi A, Butler L, Barnett Y, et al. The association between screen time and mental health during COVID-19: A cross sectional study. Psychiatry Res 2020;292:113333. https://doi.org/10.1016/j.psychres.2020.113333.

[2] Gerding T, Syck M, Daniel D, Naylor J, Kotowski SE, Gillespie GL, et al. An assessment of ergonomic issues in the home offices of university employees sent home due to the COVID-19 pandemic. Work 2021;68:981–92. https://doi.org/10.3233/WOR-205294.

[3] Robertson MM, Ciriello VM, Garabet AM. Office ergonomics training and a sit-stand workstation: Effects on musculoskeletal and visual symptoms and performance of office workers. Applied Ergonomics 2013;44:73–85. https://doi.org/10.1016/j.apergo.2012.05.001.

[4] Mann S, Holdsworth L. The psychological impact of teleworking: stress, emotions and health. New Technology, Work and Employment 2003;18:196–211. https://doi.org/10.1111/1468-005X.00121.

[5] Ayyagari R, Grover V, Purvis R. Technostress: Technological Antecedents and Implications. MIS Quarterly 2011;35:831–58. https://doi.org/10.2307/41409963.

[6] Manu S, Rysanek A. An overview of indoor environmental conditions in work-from-home settings. The 11th International Conference on Indoor Air Quality, Ventilation & Energy Conservation in Buildings, Tokyo, Japan: 2023.

[7] Manu S, Rysanek A. A preliminary analysis of indoor air quality in work-from-home settings. The 18th Healthy Buildings Europe Conference, Aachen, Germany: 2023.

[8] International Physical Activity Questionnaire n.d. https://sites.google.com/site/theipaq/home (accessed November 6, 2021).

[9] Craig CL, Marshall AL, Sjöström M, Bauman AE, Booth ML, Ainsworth BE, et al. International physical activity questionnaire: 12-country reliability and validity. Med Sci Sports Exerc 2003;35:1381–95. https://doi.org/10.1249/01.MSS.0000078924.61453.FB.

[10] Carnegie Mellon University. CHIPS - Laboratory for the Study of Stress, Immunity, and Disease - Department of Psychology - Carnegie Mellon University n.d. https://www.cmu.edu/dietrich/psychology/stress-immunity-disease-lab/scales/html/chips.html (accessed November 6, 2021).

[11] Cohen S, Hoberman HM. Positive events and social supports as buffers of life change stress. Journal of Applied Social Psychology 1983;13:99–125. https://doi.org/10.1111/j.1559-1816.1983.tb02325.x.

[12] Soldatos CR, Dikeos DG, Paparrigopoulos TJ. Athens Insomnia Scale: validation of an instrument based on ICD-10 criteria. Journal of Psychosomatic Research 2000:6.

[13] Manu S, Rysanek A. Perceptions of IEQ, well-being and work performance in work-from-home settings, Ahmedabad, India: 2022.

PLEA 2024 WROCŁAW
(Re)thinking Resilience

Affordable housing in times of pandemic:
Investigations on thermal comfort and ergonomic conditions of two case studies in São Paulo

MONICA DOS SANTOS DOLCE UZUM[1, 2] BEATRIZ GOMES SENA[1] JOANA CARLA SOARES GONÇALVES[3]

[1] Paulista University (UNIP), São Paulo, Brazil
[2] Escola da Cidade, São Paulo, Brazil
[3] Architectural Association School of Architecture, London, UK

ABSTRACT: The study investigated the conditions of thermal and ergonomic comfort during the pandemic and periods of social distancing. To achieve this, two housing complexes involved in initiatives led by the Housing Department of the São Paulo Municipal Government within the Água Espraiada Joint Urban Operation were explored. The first is the Corruíras Housing Complex, and the second is the Jardim Edite Housing Complex. Consequently, the research sought answers regarding how socially-oriented housing accommodates thermal and ergonomic conditions during periods of social isolation. The methodology involved scrutinizing architectural projects to assess how they implemented bioclimatic strategies and addressed ergonomics for daily living activities. This was followed by the development and administration of a questionnaire to residents, considering functions relevant during periods of social isolation. The conclusion drawn was that these buildings, acknowledged for their significance in producing socially-oriented housing, accommodated both scheduled and unscheduled activities during periods of social distancing, thereby facilitating adaptations in living during these times.
KEYWORDS: Affordable Housing, Pandemic, Thermal Comfort, Ergonomic, Community.

1. INTRODUCTION

This study investigated the conditions of thermal and ergonomic comfort during the pandemic and social distancing periods. To do so, two residential complexes that are part of the social actions promoted by the Housing Department of the Municipal Government of São Paulo – SEHAB/PMSP were explored within the Água Espraiada Consortium Urban Operation: The Corruíras Housing Complex (Fig. 1 and 3) designed by Boldarini and Associates office between 2008 and 2012, it features 244 housing units among two different housing types[1] and, The Jardim Edite Housing Complex (Fig. 2 and 4) designed by MMBB + F+H offices in 2010, it features 252 housing units among seven different housing types, as well school restaurant, basic health unit and a nursery [2].

Figure 1: Site plan of The Corruíras Housing Complex.

The housing complexes are nationally recognized for their architectural potential in relation to accommodating both programmed and community activities of living.

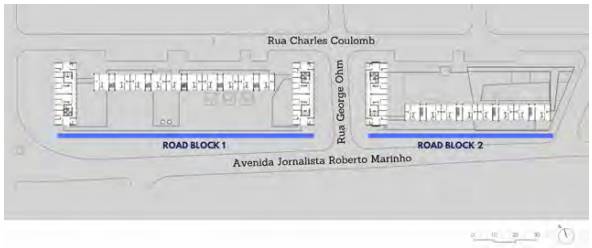

Figure 2: Site plan of The Jardim Edite Housing Complex.

Figures 3 and 4: External view of The Corruíras Housing Complex and The Jardim Edite Housing Complex.

Therefore, this research aimed to address its central question: how to ensure that social housing units consider thermal and ergonomic conditions

during periods of social isolation, and address issues where the user becomes vulnerable in an atypical scenario, understanding that one of the major impacts of the pandemic was the increased use of homes for work, education, and study purposes [3].

The secondary objectives of the research were the presentation of the simplified diagnosis of the conditions of thermal and ergonomic comfort in times of social isolation of the most representative housing units of the case studies. It is important to refine new projects to prepare homes for the living conditions imposed during the COVID-19 pandemic, considering the activities within the architectural program. As we have witnessed, the design of dwelling spaces has undergone transformations throughout history due to adaptations necessary to meet sanitary requirements [4].

Figures 5 and 6: Example of typical plan of the housing unit of Corruíras (unit type 1) and Jardim Edite (unit type 3).

2. METHOD

The research development was based on data collection regarding the historical background of case studies, followed by the creation of a photographic archive depicting the current situation of the complexes, and the collection of project graphic materials.

The next phase involved the development of São Paulo's climatic diagnosis. Simultaneously, insolation studies of the complexes were conducted to assess whether the recommended bioclimatic strategies had been incorporated into the projects.

To evaluate ergonomic comfort, habitual living activities were listed, encompassing non-habitual activities up to the onset of the pandemic, such as remote classes and work.

The compilation of these stages provided the foundation for creating a questionnaire subsequently administered to residents of the two complexes. Following the questionnaire's implementation, data tabulation, result analysis, and conclusions were drawn.

3. THERMAL COMFORT: CLIMATIC CONTEXT AND DESIGN STRATEGIES

The city of São Paulo (latitude 23.85°S; longitude 46.64°W; altitude 792m) is situated in a region with a humid subtropical climate (Cfa), according to Köppen [5], being characterized by warm-humid summer days with predominantly partially cloudy sky and cool and drier winter days with predominantly sunny sky. Prevailing wind directions are south and northeast during the summer months and southwest and north during the winter months. Air temperatures are moderate for most of the year with an annual average of approximately 19°C. Additionally, due to the subtropical conditions and the 60 percent annual frequency of overcast sky, diffuse radiation in São Paulo can reach approximately 50 percent of the total global radiation on the horizontal plan along the year, therefore, having a significant impact on buildings solar gains.

Lessons resulting from the climatic context, it was possible to confirm that the main bioclimatic strategies indicated for the city of São Paulo is the natural ventilation, shading of openings in hot periods and thermal mass for heating [6].

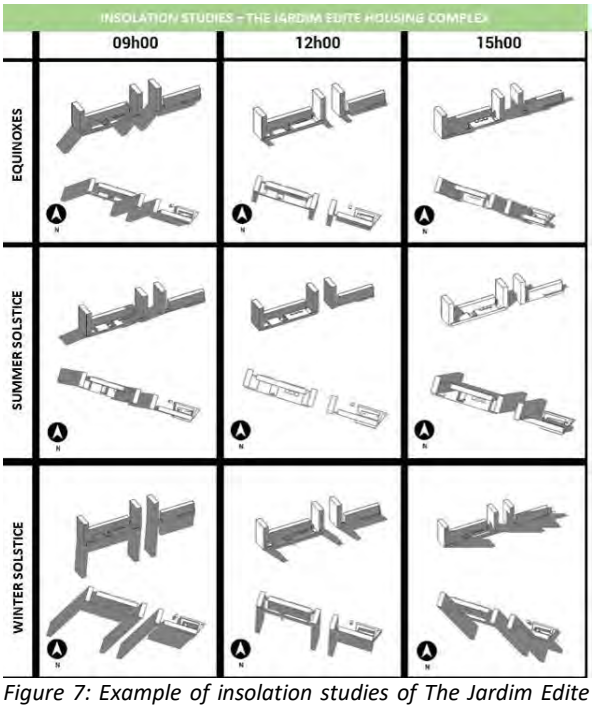

Figure 7: Example of insolation studies of The Jardim Edite Housing Complex.

The plots of the complexes feature their largest extensions facing the southwest orientation. Consequently, both implementations - aiming for the best solar relationship - directed the majority of the openings of the housing units towards the southwest and northeast directions. Considering that the northeast facade receives the most sunlight throughout the year and being aware of the impact of diffuse radiation on the southwest facades, the

projects incorporated architectural elements for solar protection, such as external blinds, cornices, and perforated elements (cobogós), to fulfill the strategy of shading the openings. (Fig. 7 to 11)

For the implementation of the natural ventilation strategy, the complexes opted for a set of openings with sufficient apertures positioned to facilitate the percolation of cross-ventilation. Consequently, all areas within the housing units, especially those intended for prolonged occupancy, can benefit from this strategy. (Fig. 12 and 13)

Figures 8 and 9: Architectural elements for shading and natural ventilation of The Corruíras Complex- View of the main facade featuring openings and perforated elements, and view of the common circulation area, emphasizing the use of perforated elements.

Figures 10 and 11: Architectural elements for shading and natural ventilation of The Jardim Edite Complex- View of the internal facade featuring openings and view of the common circulation area, emphasizing the use of perforated elements.

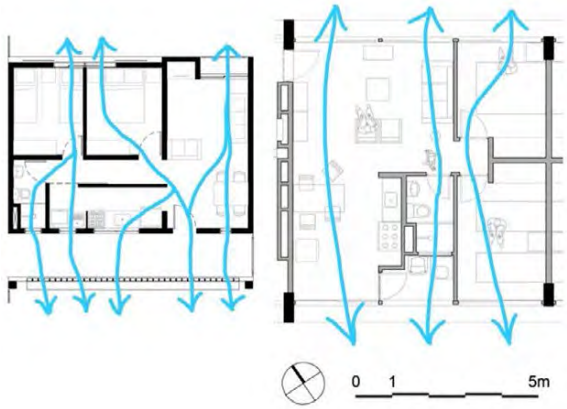

Figures 12 and 13: Architectural elements for natural ventilation of The Jardim Edite Complex- View of the internal facade featuring openings and view of the common circulation area, emphasizing the use of perforated elements.

These findings aided in formulating the questions posed to the condominium residents, operating on the premise that only the common uses of dwelling were considered in the design development of the complexes, without contemplating the simultaneous use of spaces by all residents - a factor that increases internal thermal load and may worsen discomfort conditions due to heat during hot periods but also improve thermal comfort during cold periods.

4. ERGONOMIC COMFORT

The autonomous housing units within the complexes encompass spaces intended for communal living: a living room, bedrooms, kitchen, dining area, a complete bathroom, and an internal service area within the autonomous unit equipped with space for a washing machine, sink, and clothes-drying area (clotheslines). In Brazil, where the demand for housing is about 5,9 million households [7], particularly for the target population, the complex projects aimed to include as many housing units as possible. This led to the autonomous spaces being designed with sufficient area for their intended use. (Fig. 13 and 14)

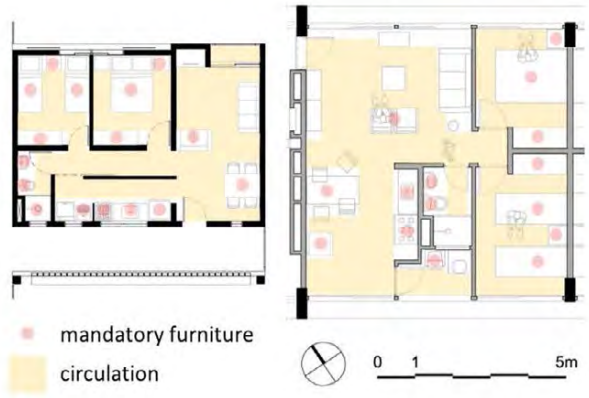

Figure 13 and 14: Internal layout of housing units.

However, during periods of social isolation, the use of these living spaces expanded to encompass activities not initially envisioned in the projects. This included simultaneous usage of spaces by all occupants for leisure, work, and remote learning.

In Brazil, concerning functionality and accessibility, there exists a set of laws and regulations for building performance and accessibility that ensure resident satisfaction during the use and performance of daily activities. These instruments provide indications regarding the size and shape of rooms, as well as minimum ceiling height, and criteria regulating the possibility of expanding ground-floor units and the functioning of plumbing installations considering the potential for simultaneous use, for example.

Regarding ceiling height, the minimum height cannot be less than 2.50 meters, except for

vestibules, halls, corridors, sanitary facilities, and pantries where a reduction to 2.30 meters is allowed.

There are also normative specifications regarding the minimum availability of spaces for the use and operation of housing, indicating environments, furniture, equipment, and minimum circulation.

Regarding suitability for people with reduced mobility, requirements are related to the necessary common and private areas such as: access and full use of facilities, limitation of slopes and spaces to traverse, use of ramps or elevators, minimum corridor and door width, height and position of sanitary fixtures, availability of handles and support bars, among others. It should also be ensured that the floor system for the private area is adapted for housing people with physical disabilities or reduced mobility.

The research evaluated housing complexes in terms of functionality and accessibility based on architectural designs, laws, and regulations, and both comply with the criteria and the compilation of data helped in the development of the quiz applied to residents.

5. SURVEY WITH THE RESIDENTS

Based on the observations made during the project surveys, fieldwork, and analyses, inputs emerged for formulating a questionnaire with questions intended for the residents. According to the Brazilian research code, whenever investigations involve human subjects, obtaining approval from the national ethics committee is essential. Thus, the research project underwent this stage and received approval to conduct the survey.

The questionnaire was developed to obtain empirical insights from the inhabitants of the studied complexes and to gain an understanding of their perception of space in everyday life and during the pandemic. Google Forms was used as the platform to structure the questionnaire, which consisted of 57 questions divided into four sections.

The first section gathered information about the users (residents), including questions about: age; gender; occupation; disability; place of residence in the complex; duration of residence in the complex; number of residents in the housing unit and their ages; residents' occupations; residents' work and study schedules; and residents' work and study locations.

The second section contained questions about the housing unit, focusing on the need for additional furniture during social isolation; satisfaction level regarding: the building (common areas), the housing unit (private areas), building location, size of the housing unit, room distribution, and size of windows and their openings.

The third section addressed apartment comfort with questions about natural ventilation in summer; use of blinds and curtains; use of cooling and/or heating equipment; frequency of window and door openings; artificial light usage patterns; and perceived amount of natural light.

The fourth section was dedicated to the use of equipment, appliances, and furniture, inquiring about their types, characteristics, and frequency of use in the apartment.

The responses were collected between January and February 2022, with 20 questionnaires administered per condominium, totaling 40 complete responses.

6. RESULTS

About the housing unit the residents who responded to the surveys in Corruíras Complex considered the overall project as good to excellent (70%), with good dimensions (50%), good to excellent conditions for layout disposition (95%), and good window opening sizes (70%). The residents who responded to the surveys in Jardim Edite Complex regarded the overall project as excellent (70%), with excellent dimensions (65%), good conditions for layout disposition (70%), and excellent window opening sizes (80%). (Fig. 15 and 16)

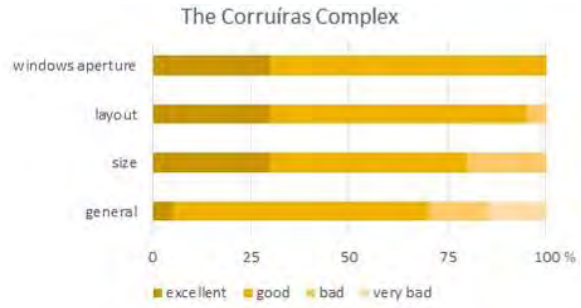

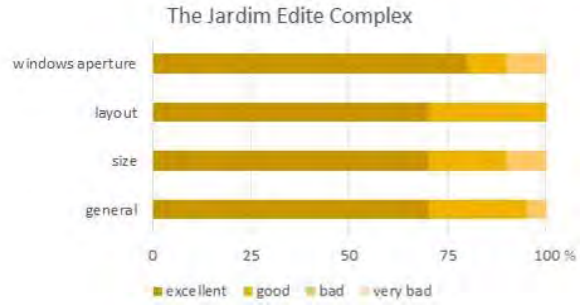

Figures 15 and 16: Perception of complex residents regarding the housing unit.

The results regarding thermal comfort in the warm period, pointed out that most respondents consider the temperatures great or good (Fig. 17), computing for the housing complex Jardim Edite and housing complex Corruíras, respectively 85.0% and

88.9% but a significant number of 15.0% and 11.2% describes the conditions as bad or very bad. (Fig. 18)

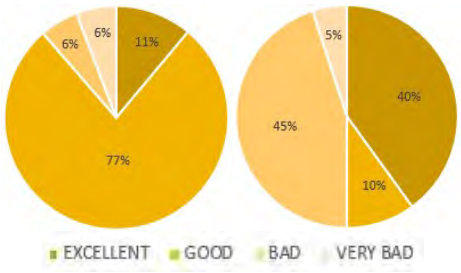

Figure 17: Corruíras and Jardim Edite perceptions of internal temperature in the warm period.

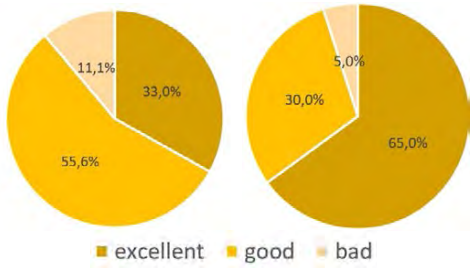

Figure 18: Corruíras and Jardim Edite perceptions about natural ventilation in the warm period.

During the warm season, in Corruíras complex, 90% of residents keep their windows fully open during the morning, and 15% do so during the night; 27.8% of residents reported solely relying on natural ventilation for cooling, 61.1% used artificial fans, and 11.1% used air conditioning. In contrast, at Jardim Edite complex, all residents keep their windows fully open during the morning, and 25% do so during the night; 20% of residents relied solely on natural ventilation, 65% used artificial fans, 15% used air conditioning, and 10% utilized air humidifiers. It is evident that although a majority of residents consider natural ventilation during the warm season as excellent to good, they predominantly employ various equipment for ambient cooling purposes.

Regarding thermal comfort during the cold season within the Corruíras complex, 27.8% of residents find indoor temperatures excellent, 55.6% consider them good, 5.6% find them poor, and 11.1% very poor. Window seals in this complex are rated excellent by 58.9% of residents, good by 44.4%, and poor by 16.7%. Concerning window management, 75% affirm opening them in the morning and 70% completely closing them at night. The majority of residents (94.1%) do not use air heating equipment during the cold season, while 5.9% use halogen heaters.

In Jardim Edite during the cold season, 15% consider indoor temperatures excellent, 70% deem them good, and 15% find them poor. Window seals in this complex are rated excellent by 50% of residents, good by 45%, and poor by 5%. Regarding window management, 75% stated opening them in the morning, while 90% completely close them at night. Most residents (64%) do not use air heating equipment during the cold season, 21% use halogen heaters, and 15% use other types of heating.

This research showed that during the period of social isolation caused by the COVID-19 pandemic, spatial changes were made in most of the housing units surveyed. The changes were made by the residents themselves to adapt the residential spaces to house activities not foreseen in the project.

Only 20% of respondents in both complexes indicated they had not made adjustments to their apartment furniture. The research demonstrated that concurrent use of spaces by all residents led to alterations in the majority of residents' internal layouts. Adjustments to existing furniture arrangements accounted for 57% in Corruíras and 35% in Jardim Edite. There was a need to remove furniture for adaptation during social isolation in 18% of Corruíras apartments and 10% of Jardim Edite apartments. The addition of furniture occurred in 5% of cases in Corruíras and 35% in Jardim Edite – in all these instances, residents reported no intention to remove the added furniture after the period of social isolation. (Fig.19)

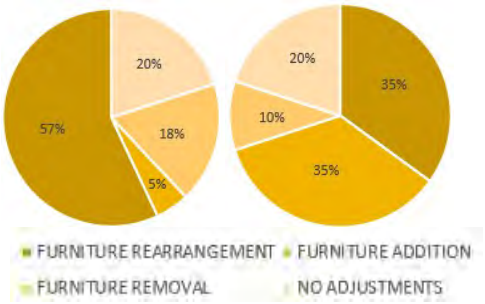

Figure 19: Corruíras and Jardim Edite furniture adjustments in the pandemic and social distancing periods.

The spaces utilized for remote learning and study activities, common during the studied period, were divided among the living room, bedroom, and kitchen, with the living room being the most frequently used in both complexes. This type of usage was not observed in 25% of Corruíras apartments and 50% of Jardim Edite apartments. (Fig. 20 and 21)

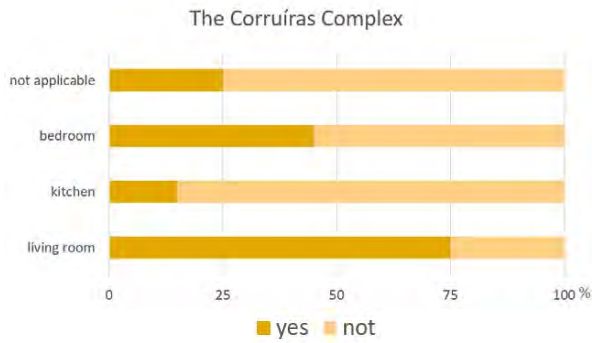

Figure 20: Corruíras spaces used for remote classes.

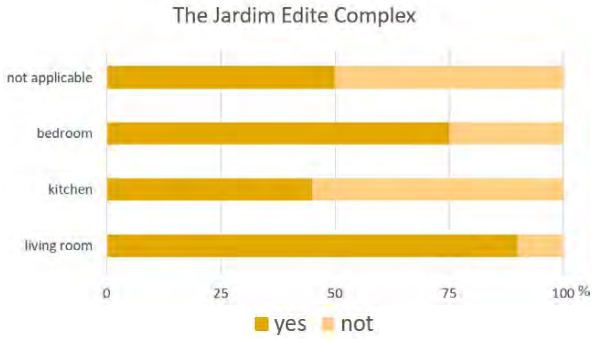

Figure 21: Jardim Edite spaces used for remote classes.

For remote work, the most preferred spaces were the bedrooms, followed by the kitchen and living room. It is important to note that all interviewees from the Corruíras complex expressed the need to conduct work activities within their apartments, while only 15% of those interviewed from the Jardim Edite complex did not engage in work activities during the period of social isolation. (Fig. 22 and 23)

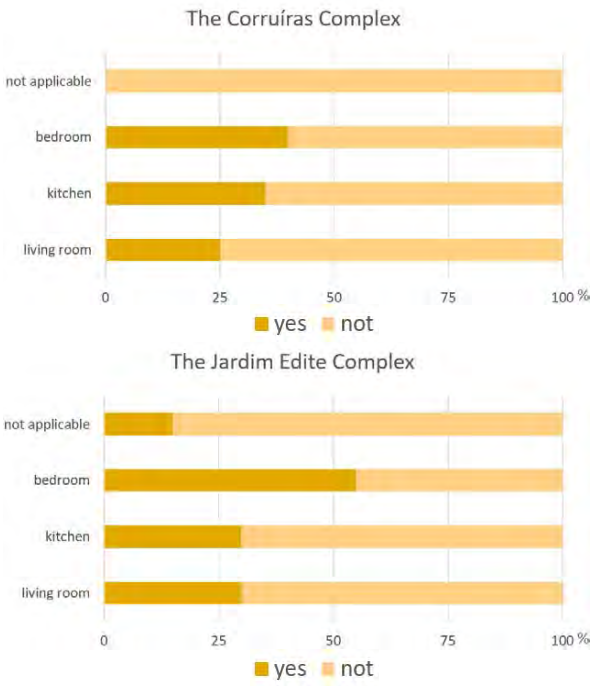

Figures 22 and 23: Corruíras and Jardim Edite spaces used for remote work.

7. CONCLUSION

The results point to the necessity of a more attentive approach to address demands for the development of a social housing program that encompasses discussions on spaces for remote work, study, and leisure activities, as well as interactions stemming from concurrent space usage. It was observed that dwellings requiring furniture removal were precisely those with a higher number of residents, including children who had a greater need for open spaces. Nevertheless, despite simultaneous use by all residents, significant issues of thermal discomfort were not reported. Even with intensified internal activity, perceptions of comfort during the warm period remained favorable.

Following an analysis of the field survey data, it was concluded that the buildings, recognized for their significance in social housing production in the city of São Paulo, were able to accommodate both planned and unplanned activities during periods of social distancing, facilitating adaptation in living experiences during these times.

ACKNOWLEDGEMENTS

We thank Paulista University (UNIP), its Ethics Committee, Bianca Alicia de Souza Silva and the residents of the housing complexes for their support in the development of the research.

REFERENCES

1. Lara, F. L., (2019). Boldarini Arquitetos Associados p. 129-139.
2. Vada, P., (2019). Conjunto Habitacional do Jardim Edite / MMBB + H+F Arquitetos, [Online], Available: <https://www.archdaily.com.br/br/01-134091/conjunto-habitacional-do-jardim-edite-slash-mmbb-arquitetos-plus-h-plus-f-arquitetos/ [28 Aug 2023].
3. Menezes, R. C. de; Jansen, A. C. The emergence and impacts of home office strategy during the pandemic scenario of COVID-19. In: International Journal of Advanced Engineering Research and Science (IJAERS). Vol-7, Issue-9, Sep- 2020. DOI: 10.22161/ijaers.79.6
4. Chang, V. The post-pandemic style. Slate, 19 de abril de 2020. Available: < https://slate.com/business/2020/04/coronavirus-architecture-1918-flu-cholera-modernism.html> [15 Nov 2023].
5. Peel, M. C., B. L. Finlayson, and T. A. Mcmahon. 2007. "Updated World map of the Köppen–Geiger Climate Classification." Hydrology and Earth System Sciences 11: 1633–1644.
6. Uzum. M. S. D. O desempenho térmico da habitação econômica em edifícios no período de 1930 a 1964 no centro da cidade de São Paulo: Estudos analíticos de simulação computacional para diretrizes de requalificação arquitetônica. [Online] Available: https://oasisbr.ibict.br/vufind/Record/BRCRIS_bf090334b8805cdefa137de507c662b0/ [28 Aug 2023].
7. Iter-american Development Bank (IAD). Habitação de Interesse Social no Brasil – Construindo novas oportunidades: Panorama 2020 e foco em desafios prioritários. [Online] Available: https://publications.iadb.org/pt [15 Nov 2023]

PLEA 2024 WROCŁAW
(Re)thinking Resilience

Environmental Conditions of the Brazilian Informal City:
Fieldwork in the Case of Community *Morro Azul*, Rio de Janeiro

JOANA C. S. GONÇALVES[1], PATRICIA PAIXÃO[2], EDUARDO PIZARRO[3]

[1]Architectural Association School of Architecture & Bartlett School of Architecture - UCL, London.
[2] Faculty of Architecture and Urbanism of the University of São Paulo (FAUUSP), São Paulo, Brazil.
[3]São Judas Tadeu University, Faculty of Architecture, São Paulo, Brazil.

ABSTRACT: In Brazil, the most populated country in Latin America, approximately 11 thousand favelas (local terminology for slums) are the home to around 16 million people (census 2022). The city of Rio de Janeiro (latitude 23°S) has the largest territory covered by slums in the country - approximately 19%. Given the warm and humid conditions of the local climate, natural ventilation and shading are key strategies for thermal comfort in buildings throughout the year. In this context, this paper presents a closer look to the reality of the environmental conditions in a favela in Rio de Janeiro - Community Morro Azul, focusing on qualitative and empirical evaluations, including a photographic record of the built environment, a survey with residents, and indoor measurements in loco. Exposed brick walls (without render), small windows and light-weight metal roofs were seen as usual features related to the risks of overheating. In the worst-case scenario, measurements in loco showed peak indoor temperatures reaching 38°C whilst outdoors was around 28°C. To cope with warm conditions, almost 90% of interviewed occupants use mechanical funs, and 37% declared the adoption of air-conditioning. The outcomes from fieldwork informed recommendations to improve the thermal resilience of slums residences in Rio de Janeiro, including the increase of thermal resistance and reflection of external walls and roofs.
KEYWORDS: Informal City, Self-Built, Thermal Conditions, Tropical Climate, Fieldwork

1. INTRODUCTION

Since the late 20th century, living in buildings in an informal city has become an act of social and environmental resilience, given the lack of infrastructure as well as the poor quality of the built environment. In Brazil, the most populated country in Latin America, there are approximately 11 thousand favelas, according to the 2022 Census (a 40% increase in the number of people living in slums in the country, since the last census in 2010), being the home to approximately 16 million people and 6.6 million households [3].

The city of Rio de Janeiro (latitude 23°S) has the largest territory covered by slums in the country, with the percentage of informal households in *favelas* (local terminology for slums) of approximately 19%, accounting for 763 *favelas* [3]. Given the predominant warm and humid conditions of the Rainy Tropical Climate (Aw - Savannah Climate, under the Koppen climate classification), constant natural ventilation accompanied by shading are key building design strategies for thermal comfort in Rio de Janeiro throughout the year [5].

In this context, this paper presents a closer look to the reality of the environmental conditions in a favela in Rio de Janeiro called *Community Morro Azul*, focusing on qualitative and empirical evaluations, including a photographic record of the built environment, a survey with residents, and indoor measurements *in loco*. This work is part of a series of papers about the environmental conditions of the informal city in Brazilian cities, published by the same research group in PLEA 2014, 2018 and 2022 [2, 4, 6].

2. CLIMATE

The city of Rio de Janeiro (latitude 22.91°S; at sea level) is in a region of tropical savanna climate (Aw) within proximity to an area of tropical monsoon climate (Am) [5]. This is essentially a warm and humid climate during the whole year round. The average annual temperature is 23.6°C. February is the hottest month with an average minimum temperature of 24°C and average maximum of 31°C.

The highest relative humidity occurs in March (82%) and the lowest in November (73%). The average hourly horizontal global solar irradiation in the summer is around 960 W/m^2, falling to 590 W/m^2, in the coolest month. Given the predominant warm and humid conditions, constant natural ventilation accompanied by shading are key design strategies for thermal comfort in Rio de Janeiro (RJ) during the whole year. Because of the significance of global radiation, attention should be put into the thermal resistance of the building envelope, particularly regarding solar gains from the roof. In addition, it is a hypothesis of this research that thermal mass can assist in moderating high temperatures, especially if coupled with night-time ventilation.

3. CASE STUDY: COMMUNITY *MORRO AZUL*

Located in the south zone of the city of Rio de Janeiro, among the neighborhoods *Flamengo,*

Botafogo and *Laranjeiras,* the *favela* of *Comunidade Morro Azul* (Community Morro Azul) – a reasonable small favela in Rio de Janeiro, housing a bit more than 5.000 people, is currently supported by public infrastructure, being close to a range of working opportunities for its residents (Fig. 1a and Fig. 1b), [3]. This urban area also offers connections by public transport to various parts of the city. The informal settlement is at the west side of the hill called *Morro Azul*, receiving the sea breeze from Guanabara Bay. The formation of this informal settlement began in the 1940s [7]. It follows the pattern of several favelas in Brazil of typical compact urban form and land-use, self-construction with bare brick, metallic roofs and restricted widow elements.

Figures 1a and 1b: Above - Aerial view of Community Morro Azul, Rio de Janeiro. Photo: Google Earth. Below – Map of the location of Morro Azul with its vicinities (in red – case-study residential building).

4. RESEARCH METHODS

Fieldwork in the case study of the Community Morro Azul included three complementary activities: technical assessment of photographic record of the built environment; survey with the residents; and measurements in loco of the thermal conditions in a typical residential building.

5. PHOTOGRAPHIC ASSESSMENT

5.1 Methodological approach

A technical assessment of more than 100 photographs taken between 2020 and 2023 was carried out, highlighting positive and negative building features for the indoor environmental conditions, following the experience of the precedent project for the UN Habitat [4]. This assessment created the basis for refurbishment guidelines of residential units, contemplating specific, but replicable and technically simple modifications of materials and building components, aiming for better internal thermal conditions. The existing positive environmental building features as well as the problematic ones were systematized as Adequate Existing Characteristics and In Need for Interventions. Both (positive and negative) features informed the formulation of an initial list of recommendations for the self-built refurbishment of those homes.

This initial critical assessment of the favela buildings was drawn from principles of environmental design, applicable to the local tropical climate and included mainly: 1. The thermal properties of the construction (meaning the insulation of the building fabric – U value); 2. General treatment of facades and roofs (color and shading); and 3. Apertures for ventilation (type, size and location). In this paper, two reference cases were selected to exemplify the applicability of such environmental technical assessment, covering a range of features and issues associated with the self-built practice, commonly found in the local built environment.

5.2 Reference Cases

Case-Study 1: Alley Buildings (Fig. 2):

Figure 2: Case-Study 1 – Alley Building. Typical narrow street in Community Morro Azul, RJ. Photo: P. Paixao.

Adequate Existing Features (circled in blue): (1) Windows of different sizes and aperture types, facilitating natural ventilation and occupants' control. The "maximum-air" aperture at the top level of the windows increments stack effect; (2) Lower floors are shaded by the front buildings, mainly, and by narrow horizontal elements.

In Need for Interventions (circled in red): (1) External walls rendered with cement and unpainted – at the top floors (unobstructed), these facilitate heat gains mainly from impinging solar radiation due to high U values and high solar absorption; (2) Narrow canyon - limits the view of the sky and daylight access, in addition to restricting air movement between buildings. However, it results in a significant shaded façade area, particularly on the lower floors; (3) Small overhang is not enough to shade the window below for most of the sun hours on the facade; (4) External bare solid brick or hollow ceramic block walls - these facilitate heat gains mainly from impinging solar radiation and temperature difference due to its high U Value (Heat Transfer Coefficient), besides reducing daylight in the space between buildings; (5) Small and unshaded windows hindering natural ventilation, whilst allowing direct solar gains.

Case-Study 2: Main Street Buildings (Fig. 3):

Figure 3: Case-Study 2 – Main Street Buildings. Typical main street in Community Morro Azul, Rio de Janeiro. Photo: P. Paixao.

Adequate Existing Features (circled in blue): (1) As in the previous case - windows of different sizes and aperture types, facilitating natural ventilation and occupants' control. The "maximum-air" aperture at the top level of the windows increments stack effect; (2) External walls rendered and painted in light colors – an effective strategy to reduce solar gains through the building fabric; (3) Shaded terraces - the suspended metal roofs reduce a portion of the direct solar gains onto the last floor slab; (4) Metal roofs painted in light colors reflect over 85% of the impinging horizontal solar radiation, approximately, protecting the terraces (occupable open spaces) and the slabs from direct solar gains.

In Need for Interventions (circled in red): (1) External walls rendered and unpainted - as in the previous case study; (2) External bare solid brick or hollow ceramic block walls: as in the previous case study; (3) Small overhang: as in the previous case study; (4) Metallic roof in natural grey color and without an internal slab, leading to significant amounts of solar gains to the room below, due to the high U value; (5) Unobstructed external façades in dark colors, increasing solar absorption into the rooms; (6) Terraces enclosed with unshaded large windows, transforming originally shaded open spaces (often exposed to wind) into indoor spaces with high concentrations of solar gains (also due to the thermally weak roof component) and limited exposure to air movement; (7) the use of air conditioning regardless the façade material.

5.3 Key findings

The completed sample of referential cases indicates a few common features that characterize the self-built environment of the *favela Comunidade Morro Azul* in Rio de Janeiro (known to be the same across other informal settlements in the city). In this context, the most common features that contribute to the risk of overheating are presented below alongside initial recommendations derived from this environmental critical assessment:

Lack of facade treatment: Hollow ceramic or concrete bricks and, occasionally, solid earth brick walls without external rendering or paint. This results in reasonably high U values and high absorption that facilitate solar gains through the fabric. *Recommendation*: External rendering acts reducing heat gains from impinging solar radiation and high temperatures (above 30 to 32^{0}C) through walls, whilst adding material protection against the typical intensive tropical sun and rain. Guidelines from local building standards say: External walls – light-weight and of reflective color, U Value ≤ 3,60 W/m^2.K; Roofs - light-weight and of external reflective color, U Value ≤ 2,30 W/m^2.K. The U value of bare solid bricks is 3,70 W/m^2.K (close to the local standards), whereas the perforated ceramic brick without render is 2.93 W/m^2.K, going down to 2,48 W/m^2.K with external render.

Small windows: insufficient window apertures for effective natural ventilation, particularly during the warm periods of the year. Often, the same standardized aluminum-based frame windows, generally used for social housing developments across the country, is commonly adopted here. Guidelines from local standards say: Window apertures > 40% of the room floor area; shading of all apertures and cross ventilation in all rooms for the whole year. Despite its general use across the country, technical studies have proved its inefficiency to provide the required air changes for natural cooling, according to the local standards [5]. In addition, windows are often without external proper shading. *Recommendation:* The

informality of the self-built practice also generates a range of window types, including those with wider apertures (although these are less common), which should be encouraged, with the addition of external shading, such as louvers and awnings (Figure 4).

Metal Roofs: When covering open terraces with single metal sheets, such thermally fragile roof component poses threat to thermal comfort due to the transmittance of long-wave heat irradiation. Furthermore, the geometry of such roofs still allows direct solar penetration in terraces, which are usually bare concrete slabs that transmit solar gains to the rooms below (Fig. 4). In the worse cases, rooms are covered directly with metal sheets, without the slabs, increasing solar gains. Guidelines from local standards say that roofs should have ventilated cavities. *Recommendations:* Metal roof sheets with external light-colored paint, increase thermal resistance of terrace slabs with the insertion of thermal insulation, for example.

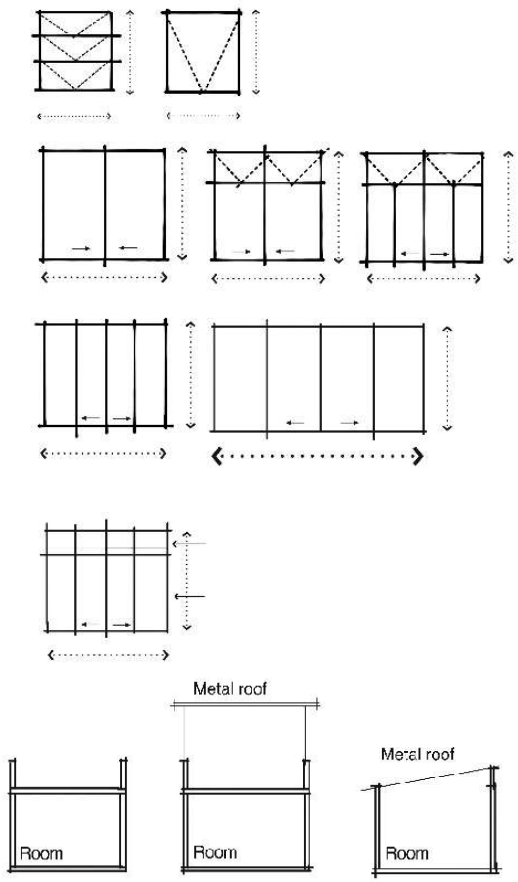

Figure 4: Range of window and roof types found in Community Morro Azul. Diagrammatic sketches drawn from the photographic record.

6. RESIDENTS' SURVEY

A questionnaire regarding the general perception of the built environment as well as the internal conditions was applied to over 100 residents, including topics of thermal, acoustic, and visual comfort and health conditions associated with solar access and fresh air. Despite the technical focus of this research on thermal conditions, the residents' survey was an opportunity to capture a more holistic perspective of the occupants, to improve the final recommendations for refurbishment. The responses to eight key questions are presented in Figure 5.

Initially, half of the interviewed people declared that their homes are generally warm during the year. This is related to incoming solar gains, due to a general lack of solar protection (96%) on windows and poor ventilation (65%). On the other hand, the majority (63%) finds their homes drafty in the cooler days, pointing out to leaky window frames. Regarding other cooling strategies, 52% of the residents interviewed have air-conditioning machines – a significant amount. In addition, the great majority declared to have mechanical funs - a low energy strategy to increase thermal comfort by increasing air movement. With respect to other qualities, according to the residents interviewed, the majority of the houses are not dark during the day but are noisy – an issue that imposes challenges to the improvement of natural ventilation.

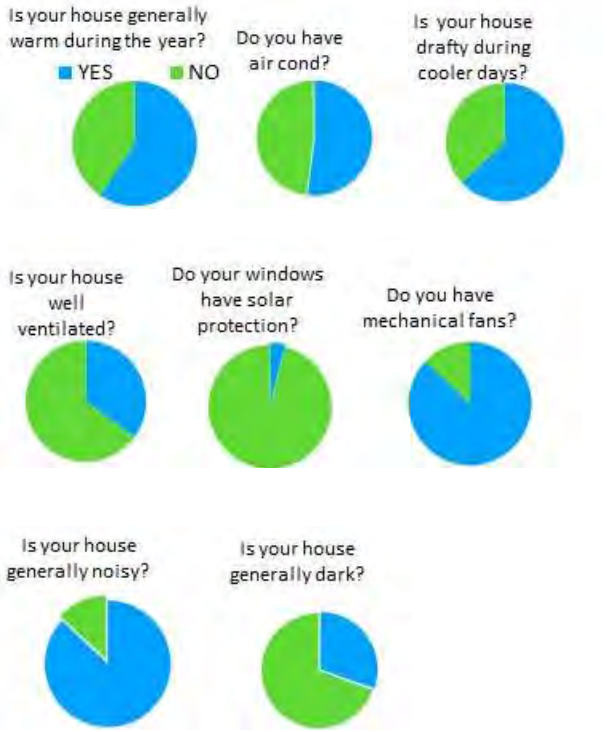

Figure 5: Results from 8 questions extracted from the questionnaire applied in the Community Morro Azul.

In parallel to that, more in-depth conversations with some residents gave insights into people's resilience and their ability to adapt to discomfort and challenging environmental conditions, following the *Story-telling* methodology [8]. On an individual level, the conversations revealed personal preferences and strategies to adapt to discomfort. For example, in the case of the resident (Fig. 6a) who feels rather thermally uncomfortable and declares the wish to live with the air conditioning on (if affordable), however,

only turns it on during very hot nights, because the other resident absolutely dislikes air conditioning.

Figures 6a and 6b: Left: External view of the house - Right: The alley houses Photos: P. Paixao.

On another situation, a resident that lives in an alley (Fig. 6b) complaint about mold in the internal walls all year round and the frequent health problems because of excessive humidity. In this case, high internal humidity levels can be associated with restricted air changes and lack of solar access. For another resident, his house is warm all year round, situation that became worse with a wall built by the neighbor, blocking the east breeze from Guanabara Bay (Fig. 7a and Fig. 7b).

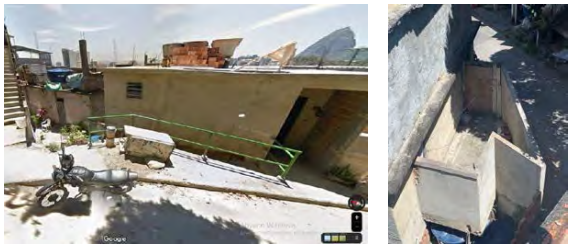

Figures 7a and 7b: Left: space between houses before the construction of the neighboring wall. Right: after the wall that blocks the east breeze.

7. MEASUREMENTS IN LOCO

A particular aspect of Morro Azul is the replicability of the housing typology - a 40 m² two-story building with two bedrooms, a living room, a kitchen and a bathroom, being different from other favelas that follow a slightly more random self-construction layout (Fig. 8 and Fig. 9). The case-study house is located at the top of the hill, without any major obstruction, with windows oriented towards North - capturing most of the annual solar radiation, and East. In this case, the external walls (U value = 2.37 W/m².K) were completely rendered and painted in light color, the terrace is covered with the typical metal sheet roof and windows follow the standardized aluminum frame model, with different sizes in different rooms, being the larger one in the living room (with four glass panels – two sliding, plus smaller top openings). A family of 5 people live in the house. One of them spend the week days out for work and comes back home at night. The others spend most of the time usually at home.

Figure 8: Floor plans of the case-study house

Figure 9: The case-study building. Photo: Google Maps.

Measurements *in loco* of the thermal conditions were taken during a summer and a winter period of three weeks, in three rooms, being the living room, facing west and one bedroom in the 1st floor, and another bedroom in the 2nd floor, both facing east. In this paper, the results of one day of measurements during the summer period, February 27th, 2023, were selected to illustrate the worse existing thermal conditions in the house (Fig. 10 and Table 1).

Whilst peak external temperatures stay around 28°C, all rooms surpass the higher limit of the comfort zone during most of the day. The top floor bedroom, with windows closed (due to no occupation), shows temperatures as high as 38°C. In the first floor, the bedroom, which is closed during the day, has peak temperatures around 34°C, whilst in the living room, in the same floor, peak temperatures stay around 31°C In the covered (metallic sheet) roof terrace, temperatures reach 33°C, showing that the microclimate in the favela is warmer than in the closest meteorological station. This is probably caused by the transmitted irradiation through the roof, coupled with limited air movement.

At night, the indoor temperatures drop to close or below the limit of the comfort zone (ASHRAE 55). The high temperatures in the bedrooms are associated with the absence of natural ventilation, coupled with excessive solar gains, which are even more significant on the terrace slab, despite the metal sheet roof. In the worst case (2nd floor bedroom) the peak temperature is 10°C higher than the outdoor. Indoor temperatures

drop at night due to windows open because of occupation, but still remain reasonably high, close to the top of the comfort zone, around 5°C higher than the outside and possibly being comfortable to sleep. In the nighttime situation, when indoor temperatures are around 28-29°C, the use of fans (a popular adaptive strategy identified in the residents' survey, is proved to be an effective means to improve the thermal conditions.

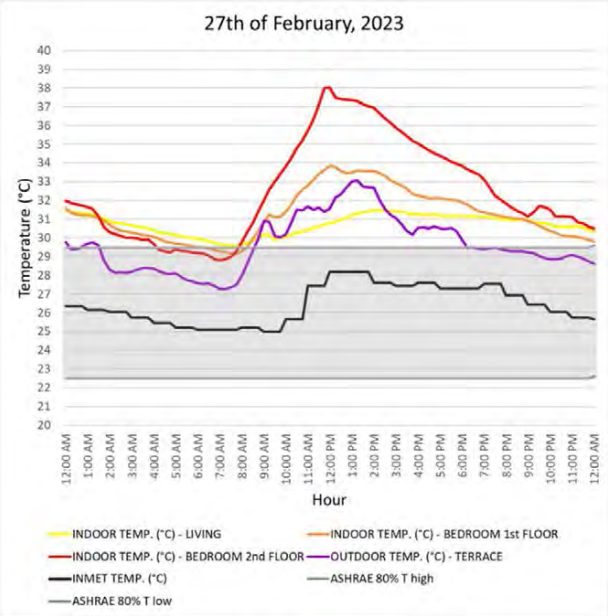

Figure 10: Indoor and outdoor temperatures in different rooms the case-study building, during the 27th of February - a summer day.

Table 1: Internal Temperatures of rooms in the residential case-study building, showing the maximum and minimum temperatures in three rooms, alongside the respective DT *of space room, in the hottest day of summer period of measurements, February 27th, 2023.*

	HOUR	MAX. TEMP. °C	HOUR	MIN. TEMP. °C	ΔT °C
Living Room	14:30	31,5	06:45	27,2	4,29
Bedroom 1st floor	12:15	33,8	07:00	27,5	6,30
Bedroom 2nd floor	12:00	38,0	06:45	27,2	10,7
Roof top terrace	13:15	33,1	02:15	25,1	7,49
INMET	12:00	28,2	01:00	22,5	5,70

8. FINAL CONSIDERATIONS

By bringing together a technical analysis of physical aspects of the built environment (by means of photographs), with views of the residents and measurements *in loco* of a typical unit, this research project identified specific aspects for improvement, whilst also considering the occupants' preferences and abilities to adapt and adjust their environmental conditions. A systematic compilation of the outcomes from all three phases of the fieldwork informed the elaboration of effective physical interventions to improve the thermal resilience of residential buildings in slums in the tropical city of Rio de Janeiro.

From the fieldwork, a few common features that dominate the self-built environment of Community Morro Azul (and most of the *favelas* in Rio de Janeiro) and contribute to the potential of overheating (identified in the case-study of the fieldwork, with internal temperatures up to 10º higher than the outside in the extreme case) are: 1. Lack of façade treatment, revealing ceramic or solid earth brick walls without external rendering and paint. External rendering is one of the main advisable strategies to reduce heat gains from impinging solar radiation on walls, whilst adding material protection against the typical tropical rain; 2. Predominance of reasonable small windows (the same standardized aluminum frames used for social housing developments across the country), with inefficient opening for the necessary ventilation; and 3. When covering open terraces with metallic sheets, the negative impact of such thermally fragile roof construction can still pose a threat to thermal comfort due to long-wave heat irradiation, if not painted in light color.

Looking forward, the outcomes from the fieldwork also informed the elaboration of analytical scenarios in which designed alterations of different features of the existing residential building were tested and compared, including alternatives for the treatment of external walls, roofs and different sizes and solar protection on windows. Such analytical studies are the subject of future publications.

ACKNOWLEDGEMENTS

Thanks to *Morro Azul* Housing Association and their residents for collaborating with this work.

REFERENCES

1. ASHRAE (2017). ASHRAE 55 - Thermal Environmental Conditions for Human Occupancy Atlanta, ASHRAE.
2.Gonçalves, J.C.S et al (2014). Examining the Environmental and Energy Challenges of Slums in São Paulo, Brazil. *In PLEA 2014*, Ahmedabad.
3. IBGE- [on-line]
4. Paixão, P.C.; et al (2022). Improving the environmental conditions of favela homes through a participatory process. *In PLEA 2022*, Santiago.
5. Peel, M.C.; Finlayson, B.L.; Mcmahon, T.A. (2007). Updated world map of the Köppen–Geiger climate classification. *Hydrol.Earth Syst.* 11: 1633–1644, 2007.
6. Pizarro, P. E.; et al (2014). Everyday House. *In PLEA 2018*, Hong Kong.
7. Santos, C.N.F. dos., (1981). Movimentos Urbanos no Rio de Janeiro. *Zahar Editores*, p. 95-149.
8. Valença. M.M. (2019). Storytelling as an active learning strategy. *Revista Carta International*. Vol.14 P.221-243 DOI: 10.21530/ci.v14n2.2019.917.

3.3. Re-thinking resilience through renovations and adaptations of buildings and spaces (including cultural and natural heritage retrofitting, methods to improve performance of existing buildings and spaces)

PLEA 2024 WROCŁAW
(Re)thinking Resilience

The European Union's Sustainable Energetic Policy Evaluation in the Aspect of Improving the Quality of Residents' Life

MARTA SKIBA,[1] NATALIA RZESZOWSKA,[1] ALICJA MACIEJKO,[1] MARIA MRÓWCZYŃSKA,[2] MAŁGORZATA SZTUBECKA,[3] JAN KAZAK,[4]

[1] University of Zielona Góra, Institute of Architecture and Urban Planning, Zielona Góra, Poland
[2] University of Zielona Góra, Institute of Civil Engineering, Zielona Góra, Poland
[3] Bydgoszcz University of Science and Technology, Faculty of Civil and Environmental Engineering and Architecture, Bygoszcz, Poland
[4] Wrocław University of Environmental and Life Sciences, Institute of Spatial Management, Wrocław, Poland

ABSTRACT: Energy policy has a significant impact on the state of the environment and, therefore, on residents' health and life expectancy, especially in highly urbanized areas. Reducing emissions is currently one of the necessary actions that must be taken at the scale of individual countries to ensure sustainable development. The article aims to indicate the best ways to develop energy policy by assessing development scenarios in terms of extending the life of city residents. This study proposes an advanced methodology for assessing development strategies by integrating the Technique for Order Preference by Similarity to Ideal Solution (TOPSIS) and incorporating them into a multicriteria decision-making (MCDM) support system. The TOPSIS model allowed for the illustration of the features of many criteria and the identification of relationships between ways, allowing for selecting the best way to develop energy policy.
KEYWORDS: public health, extending the life of residents, sustainable energy policy of countries

1. INTRODUCTION

Sustainable development of urban areas is a growth pattern that will meet residents' current and future needs while protecting the natural environment [1]. Therefore, the international community has undertaken several activities to assess the impact of emissions on the environment and the quality of life and health of residents while attempting to measure indicators and parameters enabling their implementation [2]. The sustainable development goals presented in the study [3] for the OECD in 2013–2018 and based on the report of the Stiglitz-Sen-Fitoussi Commission, including the measurement of economic and social performance [4], require an expansion of the set of parameters and indicators used to monitor progress while focusing on a small number of indicators appropriate for all countries. Development and progress must be considered holistically and in a long-term analysis of different types of capital by addressing the many interactions that shape sustainable development and sustain future prosperity (natural, human, social, and economic capital).

A factor that directly impacts residents' quality of life is the implementation of energy policy regarding energy certification and the modernization and renovation of energy-inefficient buildings in the construction and architecture sector. The success of the energy transformation, despite the top-down guidelines of the European directive, depends mainly on the individual actions of local authorities and property owners and the investment financing policy. The essential factor applies to almost all existing residential buildings that do not meet the increased requirements for new buildings, including emission-free standards [5]. An important factor in activities for sustainable development is energy, including new concepts of its development and the assessment of existing energy systems in terms of their compliance with the principles of sustainable energy development [6].

Access to clean energy positively impacts societies, and over-extraction of fossil fuels and population growth are accelerating climate change and environmental degradation. Implementing an energy policy that rationalizes energy consumption while increasing the share of renewable energy is a way to find a balance between energy's positive and negative impact on society [7, 8]. The consequences of the transition to sustainable and clean energy for energy security and its impact on society are issues that have not been sufficiently researched.

The energy sector can now be assigned two strategic functions [9, 10]. The first concerns the

stability and efficiency of the energy system. Its strength is necessary for the implementation of most economic processes, and any deficit reduces the population's level and quality of life and slows economic growth. The second function concerns environmental protection [9, 10, 11]. Improving the quality of the environment corresponds to the rational use of clean energy based on renewable energy sources. Sustainable consumption and resource-saving associated with clean energy improve the quality of life. The state's energy policy plays a key role here, promoting clean energy and reducing social inequalities, undoubtedly enhancing the quality of life [12, 13].

Research on the relationship between energy systems and society's quality of life is a fundamental element in creating a framework for the effective and efficient implementation of sustainable energy policy. Nadimi et al. [7] analyzed data on the quality of life index as a function of final energy consumption per capita, establishing a strategy of actions to reduce poverty, CO_2 emissions, and a sequence of increasing energy consumption for three types of countries: pre-development, developing and developed. In this research, the authors proposed energy consumption sequences and their priorities for individual groups of countries, which fulfills one of the key postulates related to the rationalization of energy consumption. Adeeb et al. [14] have created a model to support policymakers and relocation analysts in assessing the performance of smart cities and setting performance improvement targets to transform urban development towards a more sustainable, resilient, and livable pattern. Chen and Dagestani proved that the development of clean energy contributes to the low-carbon development of smart cities based on research on existing smart city pilot projects that significantly impact energy security and sustainable development [15].

Wang et al. [16] traced the direction of causality between CO_2 emissions, renewable energy consumption, the linear and circular economy, and globalization, revealing that economic growth and globalization increase CO_2 emissions intensity. On the other hand, using renewable energy sources helps to increase environmental integrity [17]. Renewable energy development in accordance with the concept of a circular economy should be based on the locality of energy production and consumption. Installations enabling energy recovery from waste require their transport, which also translates into an increased carbon footprint [18].

Implementing the energy transformation in practice requires coordinated actions, which should be included in the energy policy framework. Energy policy may concern various stakeholders depending on the scale of the investment and the type of activities undertaken. Based on the European Green Deal framework agreement, an energy policy at the European Union level was adopted in 2021 [19]. These issues are also managed within national policies and those adopted for smaller areas. These may be administrative units such as regions or provinces, but non-governmental organizations may also refer to the issue of local energy policy. As research shows, unfortunately, the level of stakeholder awareness of the need to consider activities supporting the energy transformation is still low in some communities. That applies to people representing both public administration and the social sector [20]. Other studies have shown that participants' level of awareness in the energy transformation process is crucial for their support of systemic activities in the field of renewable energy [21]. To convince these stakeholders to make an effort to transform the existing system, data-verified knowledge is needed about the extent to which a sustainable energy system is related to society's quality of life. Mainly since investments in the renovation and modernization of buildings will be individually financed, despite the systemic support from financial institutions, which, due to the very high costs of such projects, may be associated with a decline in the quality of life and even impoverishment and homelessness of a large part of the population. Global benefits are difficult to translate into individual benefits in the initial phase of transformation, requiring lifestyle changes and investments with an organizational dimension that exceeds the capabilities of many people. The problems that will arise in implementing the energy transformation are multi-threaded, as they concern technical, social, organizational, and legal issues related to, among others, property rights.

Integrating renewable energy into the conventional grid is another key development benefit. Blasi et al. [22] note that such integration increases the ability to implement emission reduction programs, ultimately allowing for achieving sustainable development and decarbonization goals. Including renewable energy sources in cities can also reduce electricity production costs [23].

Analyzing the available literature, it was noticed that there was a need to undertake research aimed at assessing policies based on various criteria, which would be focused on criteria related to the life and health of residents and the implementation of sustainable energy activities. Hence, the article aims to identify the development path based on the criteria that have the most significant impact on residents' health and life extension in the sustainable energy policy of countries.

2. MATERIALS AND METODS

In implementing the objectives of the European Union's sustainable energy policy, the level of implementation in individual countries should be

assessed, considering the use of RES, which affects residents' quality of life, particularly health and life expectancy. Such an assessment should also guide decision-makers on which actions are most effective and which actions in their countries may still have the potential to be exploited. To carry out such an assessment, the article used data for 27 EU countries available in [2], which were assessed using the TOPSIS method, known for its multi-criteria decision-making methods. The criteria that were adopted to analyze and evaluate the activities of individual countries are as follows:

- Climate related economic losses [Euro per inhabitant] – A1
- Share of renewable energy in gross final energy consumption by sector (Renewable energy sources in electricity) [%] – A2
- Share of renewable energy in gross final energy consumption by sector (Renewable energy sources in heating and cooling) [%] – A3
- Health impacts of air pollution [Years of life lost] – A4
- Premature deaths due to exposure to fine particulate matter (PM2.5) [Premature death – Rate] – A5
- Population change - Demographic balance and crude rates at national level [Number] – A6
- GDP per capita in purchasing power PPS [Volume indices of real expenditure per capita] – A7
- GDP and main components (output, expenditure, and income) [Current prices, million Euro] – A8.

The values of the criteria adopted for the analysis describing health effects, premature deaths, and demographic changes for selected EU countries are summarized in Table 1. Table 1 contains information for five countries for which the value of the A5 criterion was the lowest and five for which it was the highest.

In their research, the authors used the technique of order preference by similarity to ideal solutions, called TOPSIS (Technique for Order Preference by Similarity to Ideal Solution) [24, 25]. The TOPSIS method is a well-known multi-criteria decision support method that evaluates solution variants about the ideal solution [26, 27]. The main idea of this method is to calculate the distance of each solution from the optimal solution, then determine the similarity indices of individual solutions, and finally create a ranking of the evaluated solutions based on the ranking coefficient described in Equation (1):

$$R_i = \frac{d_i^-}{d_i^- - d_i^+} \quad (1)$$

The distance d_i^- was determined from Equation (2):

$$d_i^- = \sqrt{\sum_{j=1}^{n} \left(v_{i,j} - v_j^-\right)^2} \quad (2)$$

and the distance d_i^+ from Equation (3):

$$d_i^+ = \sqrt{\sum_{j=1}^{n} \left(v_{i,j} - v_j^+\right)^2} \quad (3)$$

The variables v_j^+ and v_j^- used in Equations (1) and (2) are values that describe the ideal and opposite solutions in the light of the *j* criteria adopted for the analysis. Typically, solutions are ranked in the order of decreasing values of the *R* coefficient assessment.

Table 1: Values of criteria describing health for selected EU countries.

Country	Criteria		
	A4 [Years of life lost]	A5 [Premature death – Rate]	A6 [Number]
FIN	1 862	3	5 517 919
SWE	5 254	5	10 230 185
EST	938	6	1 324 820
IRL	7 165	12	4 904 240
LUX	1 084	15	613 894
GRC	94 763	88	10 724 599
HUN	98 819	89	9 772 756
POL	452 460	94	37 972 812
ROU	217 526	95	19 414 458
BGR	106 671	142	7 000 039

3. RESULTS

An assessment of the EU's sustainable energy policy using the TOPSIS method was carried out for the research. The method required defining weights for individual criteria A1-A8, which were determined based on experts' opinions on sustainable development, energy policy, and human health. The weight values are presented in Table 2.

Table 2: Weight values for individual evaluation criteria.

Criteria A_i /Weight W_i			
A1/0.10	A2/0.20	A3/0.15	A4/0.15
A5/0.16	A6/0.08	A7/0.05	A8/0.06

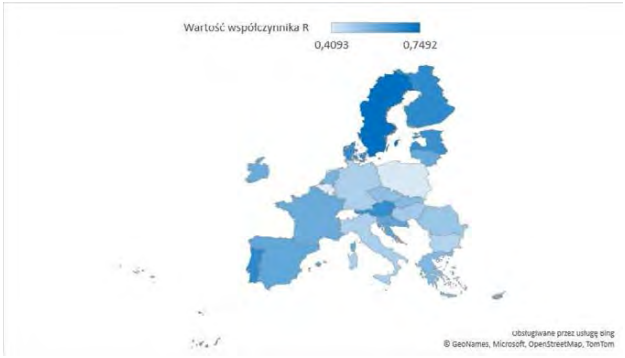

Figure 1: Assessment of energy policy based on the value of the ranking coefficient R.

Then, in accordance with the algorithm of the proposed method, the ideal and opposite solutions were identified. In the next step, the distances of individual EU countries from these two solutions were determined and the ranking coefficient *R* was calculated. The assessment of the activities of individual EU countries in the field of sustainable energy planning, with particular emphasis on health factors, was presented graphically in Figure 1. The results show that Finland, Sweden, and Estonia have the best energy policies in terms of the analyzed criteria. However, the countries with the worst results are Bulgaria, Poland and Belgium. This study provides valuable information to decision-makers and can contribute to their decision support systems; the proposed methodology can effectively evaluate and rank existing alternatives.

The TOPSIS method was used to assess the EU's sustainable energy policy in the context of residents' health and quality of life, supporting multi-criteria decision-making. The method is widely used in solving decision-making problems in the field of economics [28, 1], spatial management [29], sustainable development [27], planning energy and clean energy [30] and many others. Using this method allowed the definition of energy policy criteria that have the most significant impact on the quality of life of residents and the identification of those countries whose actions contribute to improving the quality of life.

4. DISCUSSION

Continuous investments and political actions are needed to guarantee sustainable development and constant improvement of residents' quality of life. In their study of pilot cities, Chen and Dagestani used clean energy generation as the dependent variable, measured by the weight of electricity consumption in cities and provinces and the number of installed clean energy generators at the provincial level [15]. In their article, Abu-Rayash and Dincer presented a comprehensive smart city model and an integrated system based on renewable energy to achieve carbon neutrality in the city. The results showed a strong correlation between the governance index and energy and environmental indicators [31].

There is limited research on how implementing smart city solutions may lead to additional benefits and/or trade-offs in achieving the SDGs [23].

The research results on the classification of individual countries can only be treated as an intermediate material for improving energy policies in other countries. The environmental conditions and, consequently, the energy potential for particular types of renewable energy differ significantly between European regions. Additionally, social differences, including the level of environmental awareness or attitudes and the level of acceptance of specific activities, vary between communities in the European Union. Identifying those countries that can be described as exemplary in implementing the energy transformation should be treated only as a place to look for good examples. Solutions proven in one Member State do not have to be adapted in precisely the same way in another country. It seems more reasonable to look for qualitative relationships linking the change in energy systems with the quality of life in society. Quantitative research answered the question of where it can obtain patterns to effectively link energy transformation with improving society's quality of life. The results of qualitative research may answer the question of how to carry out an effective transformation.

Multi-criteria analysis is successfully used to assess and solve a wide range of problems described by many criteria, which is constantly developing and expanding to include the use of, for example, a fuzzy criteria evaluation system, new approaches to weighting or determining the final hierarchy of proposed solutions [32, 33, 34]. Taking into account the use of the TOPSIS method to support decision-making processes related to sustainable energy policy, the following activities were carried out: research on identifying the most appropriate types of renewable energy sources depending on the analyzed regions [35], studies on the efficiency of various types of renewable sources [36], or identifying barriers related to the introduction of energy from renewable sources into the energy system [37].

5. CONCLUSION

As a result of the analyses, EU countries were identified where energy policy was implemented to improve the quality of life of residents and, at the same time, followed a sustainable development path. These countries include Finland, Sweden, and Estonia. However, the countries with the worst results are Bulgaria, Poland and Belgium. Based on the research results, it is possible to establish a new approach to ranking decision variants for a set of energy policy development arrangements supporting the decision-

making process that reflects concern for the health of residents.

Assessment methods based on variant ranking are easy to implement, and the potential of the TOPSIS method is noticeable, which is confirmed by the large number of applications of the approach to solving practical problems. It is worth emphasizing that the proposed method can be the basis for creating a hybrid approach combining, for example, a fuzzy method of assessing individual solutions and information entropy to determine the importance of weights.

REFERENCES

1. Ahmadi, Z., Dehaghi, M. R., Meybodi, M. E., Goodarzi, M., & Aghajani, M., (2014). Pollution Levels in Iranian Economy Sectors Using Input-output Analysis and TOPSIS Technique: An Approach to Sustainable Development. *Procedia - Social and Behavioral Sciences*, 141: p. 1363–1368.
2. Statistics | Eurostat, [Online], Availble: https://ec.europa.eu/eurostat/databrowser/explore/all/all_themes?lang=en&display=list&sort=category [12 november 2023].
3. Measurement of Economic Performance and Social Progress (HLEG), (2018). [on-line] https://www.oecd.org/wise/measurement-economic-social-progress.htm [2.12.2023].
4. Stiglitz J. E., A. Sen and J.-P. Fitoussi, (2009). "Commission on the Measurement of Economic Performance and Social Progress," [on-line], [2 november 2023].
5. Kertsmik K., Kuusk K., Lylykangas, K., Kalamees, T., (2023). Evaluation of renovation strategies: cost-optimal, CO_2e optimal, or total energy optimal? *Energy and Buildings*, 287: 112995.
6. Graczyk, A., (2017). Wskaźniki zrównoważonego rozwoju energetyki. *Optimum. Studia Ekonomiczne*, p. 53–68.
7. Nadimi, Reza, Koji, Tokimatsu, Kunio, Yoshikawa, (2017). Sustainable energy policy options in the presence of quality of life, poverty, and CO2 emission, *Energy Procedia*, 142: p. 2959-2964, https://doi.org/10.1016/j.egypro.2017.12.314.
8. Fouladvand, J., (2022). Behavioural attributes towards collective energy security in thermal energy communities: Environmental-friendly behaviour matters. *Energy* 261: 125353, https://doi.org/10.1016/j.energy.2022.125353.
9. Guzović, Z., Duic, N., Piacentino, A., Mathiesen, B. V., and Lund, H., (2022). Recent advances in methods, policies and technologies at sustainable energy systems development. *Energy* 245: 123276. doi:10.1016/j.energy.2022.123276.
10. Habeşoğlu, O., Samour, A., Tursoy, T., Abdullah, L., and Othman, M. (2022). A study of environmental degradation in Turkey and its relationship to oil prices and financial strategies: Novel findings in context of energy transition. *Front. Environ. Sci.* 10: 876809. doi:10.3389/fenvs.2022.876809.
11. Ligozat, A.-L., Lefevre, J., Bugeau, A., and Combaz, J., (2022). Unraveling the hidden environmental impacts of AI solutions for environment life cycle assessment of AI solutions. *Sustainability*, 14: 5172. doi:10.3390/su14095172.
12. Bernhard, O., Ishioro,, Ph.D. (2023). Electricity energy consumption and quality of life: evidence from an electricity energy-deficient economy. *International journal of applied research in social sciences*, doi: 10.51594/ijarss.v5i3.482
13. Nadimi Reza, Koji, Tokimatsu., (2019). Potential energy saving via overall efficiency relying on quality of life. *Applied Energy*, doi: 10.1016/j.apenergy.2018.10.039.
14. Adeeb A. Kutty, Murat Kucukvar, Nuri C. Onat, Berk Ayvaz, Galal M. Abdella, (2023). Measuring sustainability, resilience and livability performance of European smart cities: A novel fuzzy expert-based multi-criteria decision support model, *Cities*, 137: 104293, https://doi.org/10.1016/j.cities.2023.104293.
15. Chen, Pengyu, Dagestani, Abd, Alwahed, (2023). Urban planning policy and clean energy development Harmony-evidence from smart city pilot policy in China, *Renewable Energy*, 210: p. 251-257, https://doi.org/10.1016/j.renene.2023.04.063.
16. Wang, M., Hossain, M., Mohammed, K., Cifuentes-Faura, J., Cai, X., (2023). Heterogenous Effects of Circular Economy, Green energy and Globalization on CO2 emissions: Policy based analysis for sustainable development, *Renewable Energy*, 211:,p. 789-801, https://doi.org/10.1016/j.renene.2023.05.033.
17. Zhang J., Zheng, T., (2023). Can dual pilot policy of innovative city and low carbon city promote green lifestyle transformation of residents ？ , *Journal of Cleaner Production*, 405: 136711, https://doi.org/10.1016/j.jclepro.2023.136711.
18. Lubańska, A., Kazak, J.K., (2023). The Role of Biogas Production in Circular Economy Approach from the Perspective of Locality. *Energies*, 16: 3801. https://doi.org/10.3390/en16093801.
19. https://www.consilium.europa.eu/en/policies/green-deal/ [on-line] [1 november 2023].
20. Furmankiewicz, M., Hewitt, R.J., Kapusta, A., Solecka, I., (2021). Climate Change Challenges and Community-Led Development Strategies: Do They Fit Together in Fisheries Regions? *Energies*, 14 : 6614. https://doi-1org-1000010p607ae.han.bibl.up.wroc.pl/10.3390/en14206614.
21. Mustafa, S., Long, Y., Rana, S., (2024). Role of domestic renewable energy plants in combating energy deficiency in developing countries. End-user perspective, *Energy Reports*, 11: p. 692-705, https://doi.org/10.1016/j.egyr.2023.04.370.
22. Blasi, S., A. Ganzaroli, I., De Noni, (2022). Smartening sustainable development in cities: Strengthening the theoretical linkage between smart cities and SDGs, Sustainable *Cities and Society*, 80: 103793, https://doi.org/10.1016/j.scs.2022.103793.
23. Sharifi, Ayyoob, Allam, Zaheer, Bibri, Simon, Elias, Khavarian-Garmsir, Amir, Reza, (2024). Smart cities and sustainable development goals (SDGs): A systematic literature review of co-benefits and trade-offs, *Cities*, 146:, 104659, https://doi.org/10.1016/j.cities.2023.104659.
24. Haktanır, Elif, Kahraman, Cengiz, (2024). Integrated AHP & TOPSIS methodology using intuitionistic Z-numbers: An application on hydrogen storage technology selection, *Expert Systems with Applications*, 239: 122382, https://doi.org/10.1016/j.eswa.2023.122382.
25. Kaya, Tolga, Kahraman, Cengiz, (2011). Multi-criteria decision making in energy planning using a modified fuzzy TOPSIS methodology, *Expert Systems with Applications*, 38(6): p. 6577-6585, https://doi.org/10.1016/j.eswa.2010.11.081.
26. Lin, S.-S., Shen, S.-L., Zhang, N., Zhou, A., (2021). Comprehensive environmental impact evaluation for concrete mixing station (CMS) based on improved TOPSIS method. *Sustainable Cities and Society*, 69: 102838.

27. Vidal, R., & Sánchez-Pantoja, N., (2019). Method based on life cycle assessment and TOPSIS to integrate environmental award criteria into green public procurement. *Sustainable Cities and Society*, *44*: p. 465–474.
28. Sagnak, M., Berberoglu, Y., Memis, İ., Yazgan, O., (2021). Sustainable collection center location selection in emerging economy for electronic waste with fuzzy Best-Worst and fuzzy TOPSIS. *Waste Management*, 127: p. 37–47.
29. Rane, N. L., Achari, A., Saha, A., Poddar, I., Rane, J., Pande, C. B., & Roy, R., (2023). An integrated GIS, MIF, and TOPSIS approach for appraising electric vehicle charging station suitability zones in Mumbai, India. *Sustainable Cities and Society*, 97: 104717.
30. Le Roux D., Olivès R., Neveu P., (2023). Combining entropy weight and TOPSIS method for selection of tank geometry and filler material of a packed-bed thermal energy storage system, *Journal of Cleaner Production*, 414: 137588, https://doi.org/10.1016/j.jclepro.2023.137588.
31. Abu-Rayash, Azzam, Dincer, Ibrahim, (2023). Development of an integrated sustainability model for resilient cities featuring energy, environmental, social, governance and pandemic domains, *Sustainable Cities and Society*, 92: 104439, https://doi.org/10.1016/j.scs.2023.104439.
32. Dhumras, Himanshu, Rakesh, Kumar, Bajaj, (2024). On potential strategic framework for green supply chain management in the energy sector using q-rung picture fuzzy AHP & WASPAS decision-making model, *Expert Systems with Applications*, 237(Part B): 121550, https://doi.org/10.1016/j.eswa.2023.121550.
33. Lakshmi, K., Vasantha, K.N., Udaya, Kumara, (2024). A novel randomized weighted fuzzy AHP by using modified normalization with the TOPSIS for optimal stock portfolio selection model integrated with an effective sensitive analysis, *Expert Systems with Applications*, 243: 122770, https://doi.org/10.1016/j.eswa.2023.122770.
34. Islam Md., Rabiul, Aziz Md. Tareq, Mohammed Alauddin, Zarjes, Kader, Md. Rakibul, Islam, (2024). Site suitability assessment for solar power plants in Bangladesh: A GIS-based analytical hierarchy process (AHP) and multi-criteria decision analysis (MCDA) approach, *Renewable Energy*, 220: 119595, https://doi.org/10.1016/j.renene.2023.119595.
35. Saeidi, Reza, Younes Noorollahi, Javad Aghaz, Soowon Chang, (2023). FUZZY-TOPSIS method for defining optimal parameters and finding suitable sites for PV power plants, *Energy*, 282: 128556, https://doi.org/10.1016/j.energy.2023.128556.
36. Bilgili, Faik, Zarali Fulya, Miraç Fatih Ilgün, Cüneyt Dumrul, Yasemin Dumrul, (2022). The evaluation of renewable energy alternatives for sustainable development in Turkey using intuitionistic fuzzy-TOPSIS method, *Renewable Energy*, 189: p. 1443-1458, https://doi.org/10.1016/j.renene.2022.03.058.
37. Solangi Yasir Ahmed, Cheng Longsheng, Syed Ahsan Ali Shah, (2021). Assessing and overcoming the renewable energy barriers for sustainable development in Pakistan: An integrated AHP and fuzzy TOPSIS approach, *Renewable Energy*, 173: p. 209-222, https://doi.org/10.1016/j.renene.2021.03.141.

PLEA 2024 WROCŁAW
(Re)thinking Resilience

Climate-Change Adapted Natural and Built Urban Systems via a Grasshopper's GIS-workflow.

EMANUELE NABONI[1,2, 3]

[1]Royal Danish Academy, Copenhagen, Denmark [2]
University of Parma, Italy
[3]Norman Foster Institute, Madrid, Spain

ABSTRACT: Focusing on the urban area of Gothenburg, Sweden, we developed a workflow merging advanced thermal tools with GIS to predict micro-climate change adaptability for 2050. The aim is to devise digital workflows that sustain adaptive urban growth to climate change and harmoniously align buildings' design to the natural local capital based on thermodynamic projections.
We synergized GIS with Rhino/Grasshopper, using Morpho, a custom-made Grasshopper plugin (C#, Python - ShrimpGIS, Morpho) to integrate with ENVI-met's high-resolution microclimate maps. This visualizes future outdoor microclimates and future thermal building performances in a simple representation, indicating areas of synergy.
Our study carries significant practical implications for urban planning and building design. It has revealed microclimatic variations across its zones, with urban regions showing high thermal activity and forests acting as critical thermal buffers. The findings also highlight the need for more climate-responsive designs, particularly in the context of recent and hyper-insulated buildings showing thermal disconnection from site opportunities for passive cooling.
KEYWORDS: Urban Microclimate, Climate Change Adaptation, Geographic Information Systems (GIS), Parametric Modeling, Grasshopper, Morpho Plugin, Outdoor Thermal Comfort, Indoor Thermal Comfort

1. INTRODUCTION

In recent summers, Sweden has been grappling with a significant temperature rise, a trend that has led to many heat-related deaths. This urgent issue is particularly pressing for vulnerable towns like Stenungsund, an area by Gothenburg shaped by 1970s urban planning and facing real estate pressures for expansion. Our research addresses this pressing need by providing insights into how urban expansion can be matched with temperate urban microclimates, particularly during summers. This approach is a departure from traditional methods that often isolate the design of urban morphologies from natural eco-zones and architectural entities, overlooking their complex thermodynamic, fluid, and radiative interactions, especially in mesoscale meteorological phenomena driven by climate change.

Adapting expansive urban sectors to climate change remains uncommon, leaving urban planners, architects, and policymakers grappling with questions about climatic performance and the overarching adaptability of urban spaces, natural systems, and buildings. While the GIS-integrated approach is expanding, most of the urban sectors are still stuck with tools and methodologies that, although valuable, often fall short of providing the granularity required to assess vast urban sections and, more critically, in offer predictive insights into future climatic patterns and their impacts on our built environments. In this context, the need for precise, accessible, and innovative tools is paramount [2].

1.1 Research Questions

These tools should be seamlessly integrated into GIS and simulate and predict urban and building responses under various climatic scenarios, catering to stakeholders from decision-makers to citizens [3-4]. A set of critical questions arise naturally:

- *Can interactive GIS-rooted tools provide detailed thermal insights into urban spaces and their architectural components amid evolving climate patterns via semi-automated workflows?*
- *How can urban designs align with thermal comfort, both outdoors and indoors, under projected climate conditions?*

In response to these questions, the paper introduces a digital workflow that merges GIS with Rhino/Grasshopper ecosystems, supported by C# and Python-based plugins, via Morpho, a custom-made Grasshopper plugin developed by one of the authors [5-6-7]. The workflow leads from GIS to accurate microclimatic and building indoor data calculators via ENVI-met and customizable visualizations in Grasshopper.

This approach provides an example of reviewing the microclimatic behaviour of natural systems, urban settings, and building performance. We offer a sample of the practical design insights that could be provided by navigating the complexities of climate change with the GIS-based microclimatic workflow.

Using Stenungsund as a focal point, we aim to dissect these intricate relationships, elucidating the microscale thermodynamic exchanges and the macroscopic implications for urban planning and resilience strategies. Microclimate considerations, alongside building-specific simulations, form the crux of these requirements, driving the imperative to evaluate how spaces between buildings and the buildings interact with and are influenced by climatic factors.

Figure 1: The modelled area of Stenungsund refers to a specific portion of the city, which is in the Västra Götaland County of Sweden.

2. METHODS

2.1 Microclimatic Simulation of a Large and Complex Area

We selected an area of 1 km x 1km of dense vegetation and an irregular topography punctuated by small valleys. Urban development by the coast is replacing vegetation with asphalt and buildings. Cool, transpiring green surfaces are replaced with heat-absorbing dark surfaces such as extended parking lots and heat-storing massive surfaces such as concrete are used for buildings.

Coastal developments have often proposed very elongated buildings that could block the wind, create more friction, and reduce the ability of other buildings to lose heat to the night sky. This is added to climate change effects, which seem to cause a local heat effect in which summer temperatures are significantly hotter than in the surrounding countryside.

We sourced our data from two principal avenues: current microclimate observations from a locally established weather station and future climate projections based on the IPCC's scenario 8.5, zeroing in on the year 2050. The climate will significantly change in Stenungsund (Sweden) with a substantially hotter summer. The chart (fig. 2) shows variations in dry bulb temperature in 2050 compared to recorded data in a locally built weather station. The first chart displays a monthly analysis, and the second focuses on temperature recorded during a typical summer week.

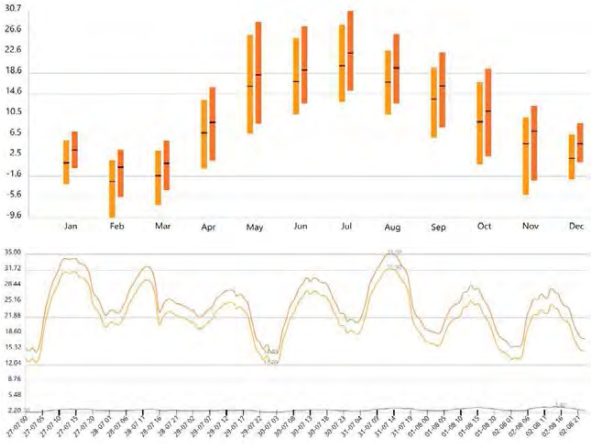

Figure 2: Temperature Chart (y axe), monthly and in the typical summer week. In red are projections for 2050, and in orange are current trends.

2.2 Grasshopper's GIS-Semiautomated Simulations

The first part of the work concerns creating and programming a digital workflow, primarily based on Morpho (a Grasshopper plugin that interfaces with ENVImet) (Table 1) and developed by one of the research collaborators, Antonello di Nunzio. The workflow leads from GIS to accurate microclimatic and building indoor data.

Morpho significantly enhances the digital workflow. It adeptly manages data layers extracted from Geographic Information Systems (GIS)—such as terrain, vegetation (fig.3), and urban structures—and converts them into a format usable within ENVImet. This functionality is pivotal for modelling and analyzing urban microclimatic factors like temperature distribution, airflow, and moisture levels.

The process starts with automated data collection, sourcing climate data from Standardforslag för Energibehov vid Byggnadsutformning (SVEBY) and the Swedish Meteorological and Hydrological Institute (SMHI). When this data is imported into Rhino, Morpho's toolkit allows for effectively sorting and refining the data based on ownership and type criteria. Using Rhino, with the aid of Morpho, the workflow proceeds to develop a three-dimensional model that accurately depicts the urban landscape, encompassing detailed building structures, vegetation, and landforms - components for precise microclimate simulation (fig.4).

The utility provided by Morpho allows for a direct interface with ENVImet, simplifying the complex process of setting up and running simulations. This direct connection eliminates the potential for inefficiencies from using intermediary formats or tools, ensuring a more streamlined and error-resistant workflow.

Table 1: A comprehensive roadmap from GIS to microclimatic results

Steps	Key Procedures & Tools
Automated Data Collection	Source climate data from SVEBY and SMHI. Acquire infrastructure and vegetation data from GIS portals and compensate for missing data using other digital maps.
Automated Model Settings	Rhino for data inspection after GIS data import. Segregate data based on ownership and types. Develop a 3D model with buildings, vegetation, and terrain attributes. Ensure compatibility with ENVI_MET using the custom-made tool Morpho.
Simulation	Microclimate simulation with ENVI_MET automatically sizes the resolution for optimized computational demands. Forecast future climate data in line with global projections like the IPCC's scenarios.
Visualisation:	Use Morpho and other plugins (Dragonfly KTTtool, MeshEdit to conduct comparative visual analyses.
Export	Convert data to universally accepted formats for GIS software using ShrimpGIS. Ensure compatibility with ArcGIS.

In the simulation phase, Morpho's role is expanded to configure the model's resolution to ensure computational efficiency while automatically tailoring the model to specific project needs. It facilitates the inclusion of future climate predictions based on global scenarios, such as those proposed by the Intergovernmental Panel on Climate Change (IPCC), into the simulations.

For visualization, plug-ins collaborate to create detailed visual representations of the microclimatic conditions, allowing for an extensive comparative analysis of different climate scenarios and their effects on external and internal building environments. The concluding step involves Morpho ensuring the simulated data is converted into widely accepted formats for Geographic Information Systems software, particularly ArcGIS, demonstrating its capability to prepare data for a broad spectrum of uses.

The innovation extends to the visualization capabilities inherent to Grasshopper, augmented by Morpho to support intricate microclimatic simulations. Grasshopper's intuitive visual programming interface enables users without in-depth coding knowledge to engage with microclimatic modelling.

Figure 3: shows Information on tree species extracted from the GIS model. Each species is modelled in ENVImet according to its specific evaporative transpiration model.

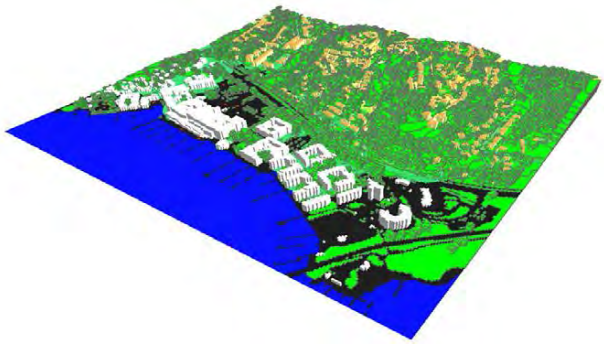

Figure 4: Automatically Generated ENVImet Model from GIS. This demonstrates the semi-automated import of textured topography from GIS and captures the intricate elevation details of Stenungsund's landscape for precise microclimate simulation.

3. COMMENTED RESULTS

3.1 Microclimatic Outcomes

The study presents a comprehensive temporal analysis, incorporating climatic parameters such as airflow patterns, surface and mean radiant temperatures, the Universal Thermal Climate Index, and localized Air Temperatures. These parameters are meticulously evaluated for the urban fabric, including the built environment and vegetative landscapes. A snapshot at 15:00 hours, representing peak afternoon conditions on a typical summer day, is selected to contextualize the discussion.

In the first visualization (Fig. 6), we observe a pronounced thermodynamic interplay between the urban built environment and its encompassing milieu. The simulation reveals that constructed zones, predominantly featuring materials with high thermal

mass and low permeability, exhibit elevated surface temperatures. This effect amplifies the urban heat island phenomenon and escalates the thermal load within buildings, posing challenges for indoor climate management and necessitating increased energy expenditure for cooling purposes.

Conversely, natural landscapes, including open spaces and forested areas, demonstrate remarkable cooling potential, exhibiting up to a 10°C reduction in temperatures compared to their urban counterparts. The simulations highlight the efficacy of vegetation in mitigating heat through natural processes such as transpiration and shade provision. This bioclimatic cooling is not limited to the outdoor environment; it also extends indoors, as evidenced by the lower internal temperatures of buildings proximate to vegetated zones, thus alleviating the cooling demands on these structures.

Fig. 7 offers a comparative analysis of delta temperatures, accentuating the variances between contemporary and projected future conditions. Here, the intensified green hues delineate areas experiencing the most substantial temperature increments—up to 2.5°C—especially in locales with sparse vegetative canopy. In stark contrast, the stability of temperatures beneath forested expanses is depicted, underscoring the resilience of these natural systems against climatic shifts anticipated by the year 2050.

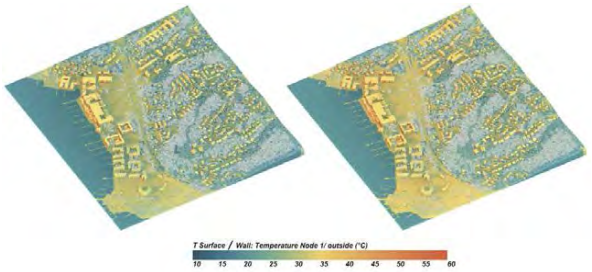

Figure 5: Comparing Surfaces Temperature simulation on a summer day: current and 2050 conditions at 3 PM. All surfaces are included. Buildings are modelled in their thermal interaction with the outside and based on their internal variable and dynamic temperature.

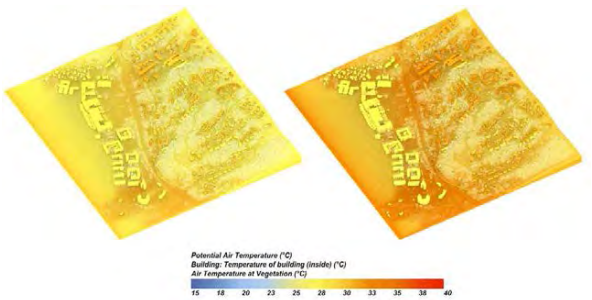

Figure 6: Temperature simulation on a summer day: current and 2050 conditions at 3 PM. It is noticeable how specific forest canopies keep an almost unvaried temperature despite increases in regional temperatures.

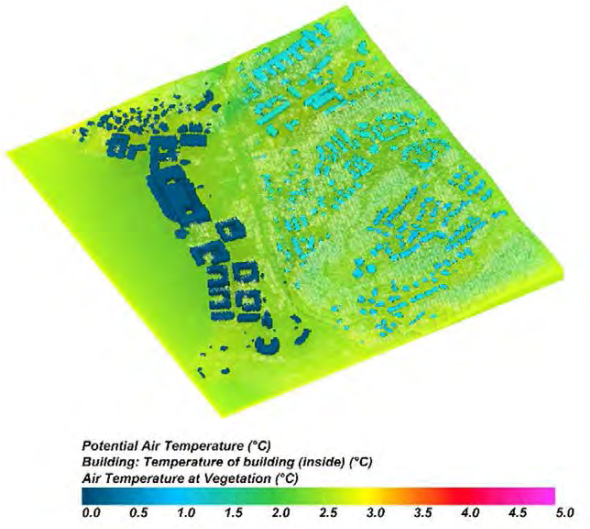

Figure 7: Delta Temperature simulation on a summer day: comparing current and 2050 conditions at 3 PM. It is noticeable how different constructions will feature different temperature increases when projected in a future climate.

3.2 Indoors: Influence of Construction Type and Context

In Fig. 8, the daily temperature profiles for various types of buildings are analyzed to understand the influence of construction era and insulation on indoor thermal behaviour. Traditional buildings, constructed in the 1960s and represented by the blue line, exhibit a pronounced diurnal temperature variation due to suboptimal insulation. Such structures experience peak indoor temperatures nearing 28°C when exterior conditions reach 30°C. Nevertheless, they offer notable nocturnal cooling, with internal temperatures descending to approximately 20°C, providing substantial nighttime comfort despite their less efficient insulation during the day.

Conversely, the modern residential units, indicated by the red line and situated proximate to coastal areas, demonstrate the capability to sustain uniform indoor temperatures, ranging from 27 to 28°C day and night. This temperature constancy is a result of advanced insulation techniques. However, this also implies that heat is retained during nighttime, which could adversely affect sleep quality due to the diminished nocturnal cooling.

The yellow line delineates the temperature profile for contemporary office buildings, which parallels the pattern observed in modern residential units but exhibits marginally higher peaks. The elevated temperatures can be attributed to the internal heat gains from office equipment and lighting. These structures may struggle to maintain comfort during peak afternoon temperatures without adequate cooling systems. The gradual decrease in nighttime temperature further indicates that these buildings

tend to retain heat, potentially compromising comfort for individuals working late or utilizing the space after hours.

Finally, the green line represents the newer family residences, constructed in the 1980s and 1990s and situated near forested areas. These buildings benefit from the thermal mass inherent in their construction and the mitigating effects of the adjacent forest. This combination not only tempers the increase in indoor temperatures during daylight hours but also promotes significant nocturnal cooling, capitalizing on the cooler ambient environment provided by the forest.

This comprehensive analysis, depicted in Fig. 8, underscores the significance of building insulation, thermal mass, and proximity to natural landscapes in shaping the indoor thermal environment, which is critical for developing climate-adaptive urban living spaces.

Figure 8: Daily temperature profiles across various building types showing the Influence of construction era and insulation. In red are new residential units, in yellow are new offices, in blue are older family houses built in the 60s, and in green are newer family houses built in the 80s and the 90s in the proximity of forests.

4. ARGUMENTED CONCLUSIONS

The conclusory remarks of this treatise revisit the interrogatives articulated at the paper's outset:

- *Can interactive GIS-rooted tools provide detailed thermal insights into urban spaces and their architectural components amid evolving climate patterns?*

In contemporary urban climate studies, the proposed workflow for Grasshopper significantly advances the incorporation of Geographic Information Systems (GIS) into microclimatic modelling. This advancement constitutes a methodological paradigm shift characterized by the semi-automated processing of GIS data. This fundamental enhancement streamlines the laborious and data-intensive tasks inherent in urban climatic analysis. The efficacy of this transformation lies in the detailed parsing, analysis, and interpretation of complex urban data sets, which are typically complicated to manage due to their size and complexity.

Since most plugins used in this process are free for download, the democratization of this advanced analytical process is another salient feature. Consequently, this fosters a collaborative and interdisciplinary approach to urban climate resilience studies, allowing for broader participation in decision-making processes.

Notwithstanding its potential, the workflow has some limitations. The fidelity of microclimate simulations is contingent upon the quality and resolution of the underlying GIS data. Additionally, the computational demand for high-resolution simulations across extensive urban areas can be significant, potentially constraining the scope of the studies based on the available computational resources.

Future work to improve this workflow involves refining data acquisition and processing techniques to mitigate GIS data gaps. Enhanced computational algorithms could be developed to optimize simulation run times without compromising the granularity of the outputs. Moreover, the integration of real-time data feeds could be explored to enhance the dynamism of the simulation model, enabling it to respond to live climatic conditions.

In conclusion, the proposed Grasshopper workflow substantially advances GIS-based microclimatic modelling, potentially significantly enhancing urban climate adaptation strategies. Its ongoing development is poised to address existing limitations and embrace future opportunities in urban environmental simulation.

The second question the paper aims to answer is:

- *How can urban designs align with comfort standards, both outdoors and indoors, under projected climate conditions?*

The research systematically investigates the alignment of urban design with interiors under evolving climate projections. It scrutinizes the thermodynamics of indoor and outdoor environments,

contingent on variables such as construction materials, architectural techniques, urban configuration, and natural elements. The graphical representations, particularly the temperature charts, elucidate the dynamic interactions between these factors.

The colour gradients in the image series from the current state to projections for 2050 highlight the exacerbating effect of urban heat islands on indoor thermal regulation. The delta temperature visualizations serve as a diagnostic tool, charting areas with significant anticipated temperature increments and assessing buildings' thermal adaptability to these changes.

This data suggests that future urban design must hybridise historical construction practices with modern techniques to ensure thermal comfort indoors. By utilizing the hyperlocal daily temperature fluctuations and leveraging location-specific advantages—such as the cooling effects of proximate forested areas—buildings can be designed to optimize thermal comfort effectively with a balanced level of insulation that considers. Considering the projected increase in summer temperatures due to anthropogenic climate change, the critical balance between the mitigation of daytime heat gain and the facilitation of nocturnal cooling is a vital design consideration.

The findings advocate for an integrated urban design strategy prioritising buildings' thermodynamic performance interacting with the environment. These strategies, rooted in scientific inquiry and evidence-based design, are essential for creating sustainable and livable urban environments in the face of climate change.

ACKNOWLEDGEMENTS

The Swedish National Agency FORMAS funded the project. The author thanks Antonello di Nunzio for contributing to the Workflow, Graziano Marchesini for performing some simulations, Thomas Amlov for managing the project, and Roberta Cocci Grifoni for advising.

REFERENCES

1 IPCC, 2023: Summary for Policymakers. In: Climate Change 2023: Synthesis Report. IPCC, Geneva, Switzerland, pp. 1-34,

2 Naboni, Emanuele, and Lisanne Havinga. 2019. 'Regenerative Design In Digital Practice. A Handbook for the Built Environment.

3 Mauree, D., Coccolo, S., Perera, A. T. D., Nik, V., Scartezzini, J.-L., & Naboni, E. (current). A New Framework to Evaluate Urban Design Using Urban Microclimatic Modeling in Future Climatic Conditions. Sustainability, 10(4), 1134. https://doi.org/10.3390/su10041134

4 Maiullari, D., Gherri, B., Finizza, C., Maretto, M., & Naboni, E. (2021). Climate change and indoor temperature variation in Venetian buildings: the role of density and urban form. Journal of Physics: Conference Series, 2042

5 Di Nunzio, A., Morpho: A plugin to create Envimet 2.5D and 3D models (INX), write configuration files (SIMX), and run simulations. GitHub. Retrieved from https://github.com/AntonelloDN/Morpho

6 Di Nunzio, A., 1. Grasshopper plugin - AntonelloDN/Morpho GitHub Wiki. Retrieved from https://github-wiki-see.page/m/AntonelloDN/Morpho/wiki/1.-Grasshopper-plugin

7 ENVI-met, Plugins: Enhance your model. ENVI-met. Retrieved from http://www.envi-met.com/plugins/

PLEA 2024 WROCŁAW
(Re)thinking Resilience

Remarks on Olgyay's quotes
about irradiation on curved roofs

THANOS N. STASINOPOULOS[1]

[1] Izmir University of Economics, Izmir, Turkey

ABSTRACT: This paper focuses on two quotes from Victor Olgyay's "Design with Climate" regarding the relationship between geometric properties and thermal performance in domes and vaults commonly used as roofs in warm regions. Specifically, the paper examines the statement that "the envelope of a hemispherical vault is roughly three times the surface of its base" and explores the assertion that "the radiation of high sun positions is diluted on a rounded surface". The study validates the first statement in geometric terms and then shifts attention to the latter, which has been extensively researched by various scholars. Building upon previous findings, the work confirms Olgyay's claim regarding insolation per unit surface area but challenges the assertion regarding total solar load. In fact, curved roofs receive more irradiation than horizontal roofs of the same footprint, depending on their Base to exposed Surface ratio. This correlation applies to all convex roof shapes, whether curved or not.
KEYWORDS: Olgyay, solar radiation, curved roofs, insolation and forms.

1 INTRODUCTION

"Design with Climate" [13] has been a seminal publication in the environmental design literature for decades, with a recent new edition [14]. This study is motivated by a paragraph on page 7 of the book's Introduction, where it is stated that *"the envelope of a hemispherical vault is roughly three times the surface of its base", "so the radiation of high sun positions is diluted on a rounded surface."*. Over the years, these statements have been echoed by numerous scholars. This paper addresses their validity in two aspects: geometric and solar. The first part examines the geometric terms and relationships mentioned by Olgyay, while the second part explores the quotation's implications for the difference in solar energy incidence between curved roofs (vaults and domes) and horizontal roofs.

2 GEOMETRIC ASPECTS

2.1 "Roughly three"

Olgyay's term "hemispherical vault" likely referred to a hemispherical dome. The surface F of such a dome with a radius R is $2\pi R^2$, and its base B is πR^2. Therefore, the ratio F/B is 2, not "roughly three" as stated by Olgyay. However, the ratio of around three can be applicable to elongated forms, such as the corbelled domes found in various parts of the world since ancient times, including Mesopotamia (Fig. 1), Turkey (Fig. 2), Ireland (Fig. 3), among others. Such forms were likely shaped by the construction requirements of the corbelled system rather than driven by thermal or solar considerations. With the appropriate height in such shapes, the ratio between the curved surface and its base can indeed be "roughly three" or even greater. Fig. 4 illustrates four variations of ellipsoid domes with the same base but different heights, where the F/B ratio of shape D is exactly three. Appendix 1 describes "dome" and "vault" in geometric terms.

Figure 1: Ancient domes, conical and hemispherical, depicted in an engraving by Assyriologist Austen Henry Layard based on a bas relief from Nimrud. Source Layard [10] plate 32.

Figure 2: Beehive-like roofs in Harran, Turkey made of limestone. Their profile is identical to the much earlier Assyrian conical domes, due to the same construction technique. Source Wikipedia.

Figure 3: A clochán (beehive hut) on the Dingle Peninsula, Kerry, Ireland. Source Wikipedia.

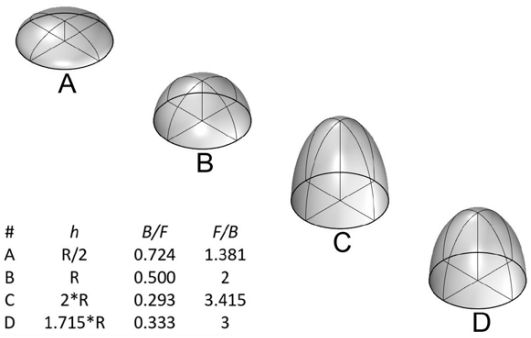

#	h	B/F	F/B
A	R/2	0.724	1.381
B	R	0.500	2
C	2*R	0.293	3.415
D	1.715*R	0.333	3

Figure 4: Ellipsoid domes with base radius R and various heights h. Option D matches Olgyay's assertion "roughly three times the surface of its base". By the author.

2.2 Vault instead of dome

The curved surface of a semicylindrical barrel vault spanning a rectangle of dimensions $p * q$ has an area $F = \pi pq/2$, and the ratio of surface area to base $F / B = \pi/2$ or roughly 1.57, which is not *"roughly three"* once again. However, this calculation does not consider the vertical end walls of the vault that complete the vaulted roof (shape 2 & 3 in Figure 5). If we include them too, then the vault F / B ratio can be equal to 3 when p / q = 1.82 (shape 3 in Figure 5) [see Appendix 2 for relevant calculations]. This proportion does not correspond to the usual types of vaults, as a typical vault bridges the shortest distance between walls and thus has a p / q ratio of less than 1.

Evidently, the specific statement of "roughly three" in "Design with Climate" is geometrically ambiguous. However, it is reiterated in the newer edition of the book [14] and has been mentioned in various other publications, such as Kilical [8] (p.112), Soflaei [17] (p.13), Mahyari [11] (p.29), Tavassoli [22] (p.116), among others.

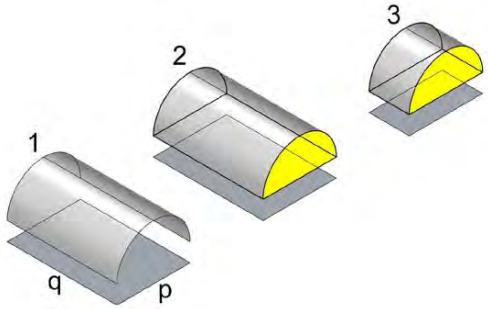

Figure 5: Variations of barrel vaults: (1) without vertical sides, (2) with vertical sides, (3) with vertical sides and an F/B ratio of 3 (see Appendix 2). By the author.

3 SOLAR ASPECTS

3.1 Curved versus flat roof

Another ambiguous statement in the same paragraph of "Design with Climate" is that *"the radiation of high sun positions is diluted on a rounded surface."* Perhaps Olgyay implies that when the solar beam is nearly vertical, a curved roof receives the same solar load as its base but at a lower intensity per square surface area. This may hold true momentarily when the sun is at its zenith, as both the roof and the base share the same vertical solar beam. However, this is not the case at lower positions of the sun when the profiles of the two surfaces, as seen from the sun, differ (Figure 6). Furthermore, the global irradiation includes a component reflected from the ground, which reaches the curved surface but not a horizontal one (Figure 7). While the total irradiation on the curved roof is higher, the average intensity may be lower compared to the horizontal roof due to their differences in size. The difference in irradiation between domed or vaulted roofs and their horizontal footprint (flat roof) requires further examination, as discussed below.

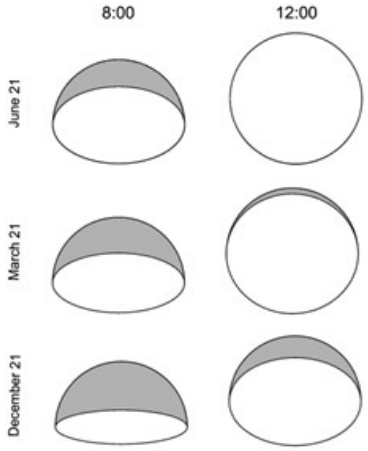

Figure 6: Views of a hemisphere in Riyadh as seen from the sun. The white part represents the horizontal base, while the grey part represents the portion of the curved surface outside the solar beam reaching the base. At noon, the flat base and the curved surface receive almost equal solar beam radiation. However, during the rest of the day, the curved surface receives more radiation than the base (grey part). In addition to the additional beam radiation, the three-dimensional surface receives radiation reflected from the surrounding ground.

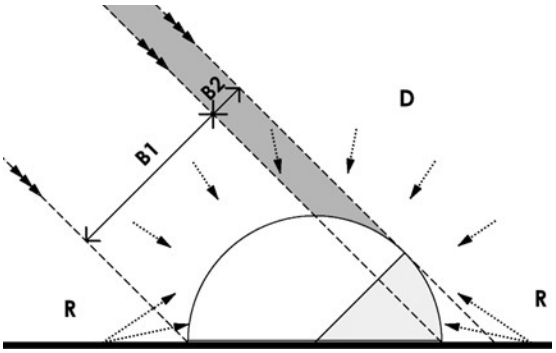

Figure 7: The 'solar profile' (perpendicular to the sun rays) of the base of the dome is B1. The curved surface has a larger profile, B1+B2, which means that it receives more beam radiation. The base and the curved surface receive the same amount of diffuse radiation D, but the dome receives also ground reflected radiation R. Even when the solar rays are vertical and B2≈0, the dome receives more global radiation than its base due to the reflected component.

3.2 Related research

The difference between the average and the total irradiation on a roof is highlighted by Pearlmutter [16]: *"A reduction in surface temperatures, or a reduction in the "average heat increase" of the roof surface, does not substantiate a reduction in overall heat transmission to the interior, since this reduced average heat increase is taking place over a larger total surface area."* In his quantitative experiment Pearlmutter found that *"the vaulted surface's cumulative daily global exposure is shown to be higher than the flat roof by 10% in the N-S orientation and by 15% when facing E-W"*.

Similar conclusions have been reached by Tang et al [21]: *"a domed roof with half dome angle of 90° absorbed daily about 20% more beam radiation and 30% more total radiation than a flat roof did during the summer months". Also "a domed or vaulted roof will absorb more solar radiation than its corresponding flat roof"*.

However, other researchers have interpreted Olgyay's citation as suggesting that curved forms receive less total radiation:

- *"Olgyay showed that the lower indoor air temperature of curved roof buildings is due to the lower absorbed solar radiation, compared to flat roofs. His findings were later confirmed by Konya"* by Elnokaly et al. [3].
- *"The hemispherical vault receives around 35% less energy than the flat roof between the equinoxes"* by Gomez et al. [6].
- *"domed-roof forms facilitate a significant decrease in the received average daily solar irradiance above their surface compared to flat surface, in both summer and winter…Thus, they reduce the required energy for cooling in hot climates"* Ayoub [1].

Such references indicate a confusion regarding the insolation on curved and flat roofs in the extensive research on the subject. Various aspects of the environmental performance of curved and flat roofs have been explored by researchers like the aforementioned, as well as by Konya [9], Soflaei et al. [17], Tavassoli [22] and others, with reviews of related work given by Ayoub [1] and Elnokaly [3]. In addition to insolation, some studies consider also heat transfer through the roof and the effects on indoor temperature, using theoretical models like Moustafa et al. [12] and Yildirim et al. [23], or actual monitoring like Başaran [2] and Pearlmutter [16].

Elseragy [4] established a theoretical basis and validated the thermal advantages of curved roof forms in hot-arid regions. He also identified the "self-shading" property as an advantage of curved roofs, which was agreed by Gómez-Muñoz et al. [6] and referred to as "auto shading."

3.3 A study on insolation and form

The present study contributes to the existing research on the comparison between curved and flat roofs, with a focus on quantitatively assessing the difference in insolation (solar radiation) between these two types. The analysis is based on previous research conducted by the author [18] & [19], which investigated the impact of geometric shape on the insolation of various convex forms, including domes and vaults. In this earlier work, the author compared the irradiation intensity (i) on various convex forms (Figure 8) to that on a horizontal surface (h). The author divided each 3D surface into planar facets and used the algorithm proposed by Page [15] to calculate the monthly solar energy incident on these facets, considering beam, diffuse, and ground-reflected irradiation on inclined surfaces exposed to solar rays. This process was repeated for a total of 71 forms (Figure 8) across three different locations (London, Athens, Riyadh) and for three values of ground albedo (0, 0.2, 1) under average sky conditions, resulting in a total of 639 cases. The monthly values were then aggregated to obtain annual insolation values, which are discussed in the present study.

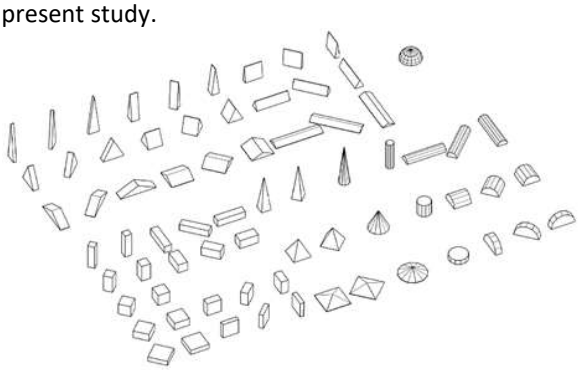

Figure 8: The convex shapes studied by the author in [18]. They consisting of 71 cases deriving from five generic types with varying dimension proportions and orientations. For each case, the monthly insolation under average sky conditions was calculated for three locations (London, Athens, Riyadh), including beam, diffuse, ground-reflected components for 3 values of ground albedo (0, 0.2, 1).

In the research conducted by the author, it was observed that the ratio of irradiation intensity (i) to horizontal irradiation (h) followed a linear percentage trend based on the proportion between the horizontal base of the form (B) and its exposed surface (F). This linear relationship was referred to as the "form insolation index" (m-index), which represented the effects of geometric shape on the incident energy per unit surface area. A similar concept was mentioned by Gomez in a later study [6]. The linear relationship between the m-index and the B/F ratio was further validated in a more recent study that utilized available radiation datasets for the same locations (London, Athens, Riyadh) as well as two

additional locations (Reykjavik and Lagos) at different latitudes [20].

A significant conclusion from that research was that high-profile forms exhibited a lower m-index compared to low-profile forms, indicating that the average insolation on any form was less than that on a horizontal surface throughout the year. This finding confirmed Olgyay's assertion that curved roofs receive less solar intensity compared to horizontal roofs. This observation applies to all forms, curved or not, and across all latitudes, not just in warm arid climates. In high latitudes, where the sun's path is lower, irradiation on upright surfaces is promoted over horizontal surfaces, resulting in higher m-index values, as depicted in Figure 9. The slope of the linear relationship could be influenced by highly reflective surroundings, such as snow or light-coloured sand, as shown in Figure 10 for 3 albedo values.

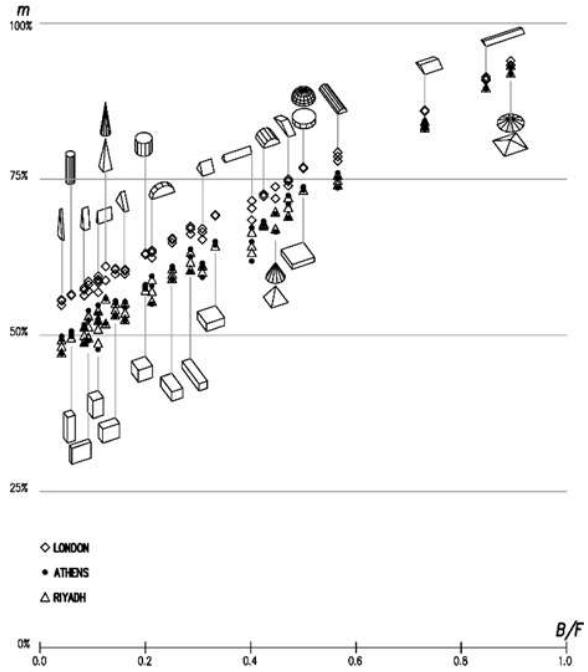

Figure 9: The insolation on a particular form per unit surface area exhibits a linear relation with its base-to-surface ratio B/F. This linearity is observed across all locations, with slight variations attributed to orientation. Higher latitudes promote higher insolation on upright surfaces compared to horizontal, which explains the higher values of m-index in London. From [18].

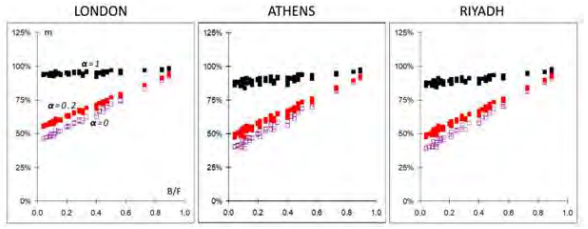

Figure 10: m-index in three locations for three different albedo values (0, 0.2, 1), demonstrating the impact of reflectivity on the relationship between the m-index and the B/F ratio. Image adapted from [18].

The findings of that study provide valuable insights into the quantitative disparities in insolation between curved and flat roof types, specifically examining the relationship between geometric shape, base-to-surface ratio, and insolation.

3.4 Average and total insolation on curved forms in warm arid climates

Moving on to the specific findings related to curved forms in warm arid climates, the research by the author included observations from Riyadh. Figure 11 provides an example of the linearity between the m-index and the B/F ratio in Riyadh. It shows that for a hemisphere with a B/F ratio of 0.5, the m-index is 72% of the incidence on a horizontal surface. Similarly, a barrel vault with a square base and a north-south axis, with a B/F ratio of 0.42, has an m-index of 68%. Both cases demonstrate that the average solar intensity on the curved surface is lower than that on a horizontal surface.

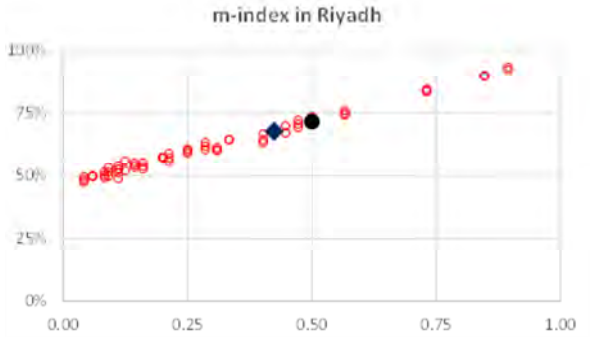

Figure 11: The graph shows the annual ratio $m=i/h$ between the unit irradiation i on the surface of a convex form In Riyadh, and the unit irradiation h on horizontal as a function of the B/F ratio. The hemisphere ● has B/F=0.5 and m=72%, while the vault ◆ values are 0.42 and 68% respectively. Radiation values are annual global under average sky for ground albedo 0.2. Similar linearity appears also for beam, diffuse, reflected radiation. Data from [18].

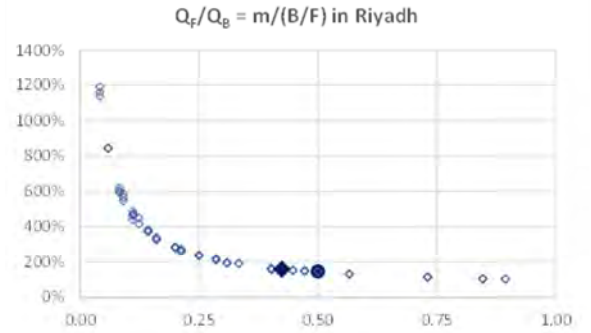

Figure 12: Comparison of the total irradiation Q_F on the surface F of a form in Riyadh to the irradiation Q_B on its base B as a function of the base-to-surface B/F ratio. Low x-values indicate upright shapes, while x=1.00 indicates a horizontal surface. All other forms receive more solar load than their horizontal base, especially the tall ones with low B/F ratio. The hemisphere ● has B/F=0.5 and its Q_F/Q_B ratio is 143%. The values of the vault ◆ are 0.42 and 159% respectively. Data from [18].

The previous information pertains to irradiation per unit surface area. However, it should be noted that a curved roof typically has a surface area larger than its horizontal base. The energy received by the entire surface area F of such a roof is $Q_F = F*i$, and by a horizontal surface equal to its base B is $Q_B = B*h$, where i and h represent the average irradiation values as explained earlier. Therefore, the ratio Q_F / Q_B can be expressed as $F*i / B*h$ or $(F/B)*(i/h)$ or $m/(B/F)$. Figure 12 illustrates that relation in Riyadh using data from [18]. The graph clearly demonstrates that all forms receive more total radiation than their horizontal base, with the amount increasing exponentially with the height of the form, as indicated by its B/F ratio. It is evident that the explanation presented in Figure 7 for a hemisphere applies to all three-dimensional forms as well.

4 DISCUSSION AND CONCLUSIONS

4.1 On geometry

Section 2 above highlights certain perplexing details in Olgyay's geometric statement. The surface-to-base ratio of an elongated dome could be *"roughly three,"* but it does not hold true for a hemispherical form, which has an exact ratio of two. On the other hand, if the statement was referring to a cylindrical vault, the associated geometric relations also do not seem to support it, except in the case of an unusual vault that spans the long dimension of a space instead of the more common short dimension. It would have been helpful if "Design with Climate" provided further explicit clarification on this topic.

4.2 On insolation

Even if Olgyay had been more precise in his use of geometrical terms and relations, his conclusions on insolation would not have been affected. The quantitative relations described in section 3 confirm his assertion about the lower average insolation on curved roofs compared to horizontal surfaces. This applies not only to roofs but also to any convex form, whether it is a roof or a building volume. However, it is important to note that the total amount of solar energy incident on the entire exposed surface is always higher than that on the footprint of the structure. In other words, a flat roof receives less total solar load than a three-dimensional roof, making the former option relatively "cooler" in comparison.

In addition to the insolation aspects, the geometry of the roof has implications for the thermal conditions within the internal space. As depicted in Figure 13, adding a flat roof to a given wall perimeter does not alter the internal volume. Assuming that the perimeter wall is of fixed height in all cases, a curved roof not only increases the total volume but also expands the exposed surface area of the building. The presence of a curved ceiling leads to air stratification, with warm air gathering at a higher distance from the living area, and facilitates its expulsion. This is a benefit not present in the case of flat ceilings. Furthermore, the heat emitted by the warm curved ceiling is positioned farther away from the occupants.

These effects of roof geometry are combined with the processes initiated by building materials, which are influenced by factors such as roof size, available resources and know-how, and the local climate. Several studies, as reviewed by Elnokaly et al. [3], have demonstrated the interaction between these factors. However, it is important to note that the focus of the present study is solely on the incident radiation on the roof types mentioned by Olgyay, with an extension to additional forms that are used as roofs or building volumes. The findings of this study apply to these additional forms as well. The main factor influencing the intensity and total amount of solar radiation received is the base-to-surface ratio (B/F) of any convex form. Energy per unit surface area is greater for forms with a high B/F ratio (i.e., low-profile forms), but the total energy received by the entire surface is less (Figure 14). •

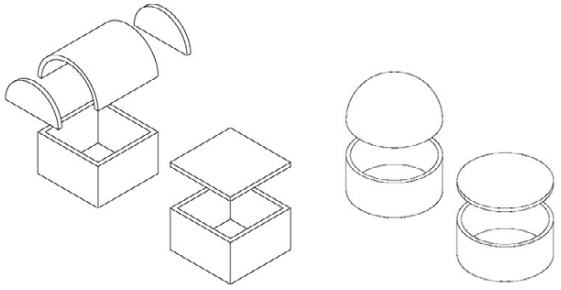

Figure 13: Adding a roof on a walled space changes its external surface and the internal volume according to the geometry of the roof, as observed by Fathy [5].

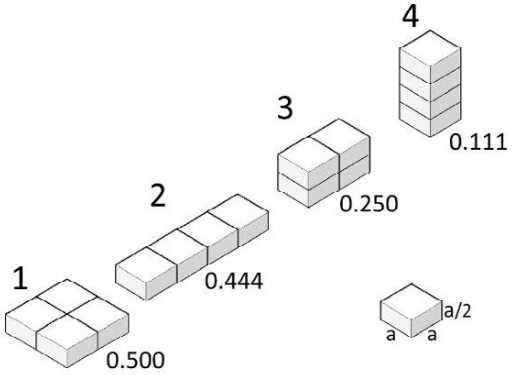

Figure 14: four groups of identical boxes with the same volume but different base-to-surface (B/F) ratios, as shown. These varying ratios result in different amounts of unit and total insolation, as demonstrated in Figure 12. For instance, the exposed surface of Box 1 receives less total solar energy compared to Box 4. One reason for this difference is that Box 1 has a lower height, which means it is less exposed to reflected radiation.

APPENDIX 1 - Terminology

In geometric terms, a typical 'vault' is a surface generated by the extrusion of a vertical arc along a non-coplanar path, the barrel vault being the most common type. A 'dome' is generated by revolving a vertical arc around a coplanar vertical axis (Figure 15). Therefore, a more accurate description would likely be either "hemicylindrical vault" or "hemispherical dome". There are only few publications using the ambiguous term "hemispherical vault", like Gomez [6] and Herraez [7].

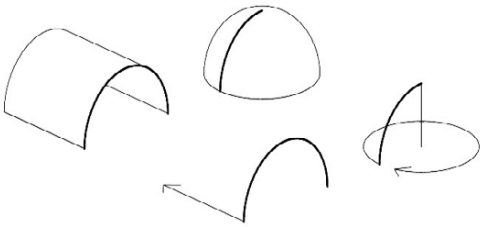

Figure 15: Generation of a typical vault and dome.

APPENDIX 2 – Barrel vault calculations

The total surface F of the barrel vault (2) in Figure 5 consists of the cylindrical top A and the two vertical ends V+V:

$$F = A + 2V \quad [1]$$

where $A = \pi pq/2$ [2]

and $2V = \pi p2/4$ [3]

therefore $F = \pi pq/2 + \pi p2/4$ [4]

and $F/B = (\pi pq/2 + \pi p2/4) / pq$

$= \pi/2 + \pi p/4q$ [5]

Based on [5], the ratio F/B can be equal to 3 if p / q = 1.82 (option 3 in Figure 5). But such proportion does not correspond to the usual types of vaults where the p / q ratio is typically less than 1.

If the vertical ends are excluded, then F / B = (πpq/2) / pq = π/2 = 1.57 for any p/q proportion.

REFERENCES

1. Ayoub M., Elseragy A., 2018. Parameterization of traditional domed-roofs insolation in hot-arid climates in Aswan, Egypt. Energy & Environment, Vol. 29(1) 109–130.
2. Başaran T., 2011. Thermal Analysis of the Domed Vernacular Houses of Harran, Turkey. Indoor and Built Environment 20(5):543-554.
3. Elnokaly A., Ayoub M., Elseragy A., 2019. Parametric investigation of traditional vaulted roofs in hot-arid climates. Renewable Energy, Volume 138, pp. 250-262, ISSN 0960-1481, DOI: 10.1016/j.renene.2019.01.061.
4. Elseragy A., 2003. Architectural and Solar Potential of Curved and Flat Roofs in Hot Arid Regions, with Reference to Egypt. PhD Thesis, University of Nottingham, Nottingham, UK.
5. Fathy, H., 1986. Natural Energy and Vernacular Architecture. University of Chicago Press, Chicago, p.50.
6. Gómez-Muñoz Victor M., Porta-Gándara M. Á., Heard C., 2003. Solar performance of hemispherical vault roofs. Building and Environment, Volume 38, Issue 12, pp. 1431-1438.
7. Herraez J., Denia J. L., Priego J. E., Rodriguez J., Navarro P., Martin M. T., 2021. Cultural Heritage Restoration of a Hemispherical Vault by 3D Modelling and Projection of Video Images with Unknown Parameters and from Unknown Locations, Applied Sciences 11(12):5323.
8. Kilical A. A., 1990. Vernacular Approach to Climatic Variables in Central Saudi Arabia, Journal of Architecture and Planning -King Saud University, vol. 2, pp. 99-118, Riyad.
9. Konya A., 1980. Design Primer for Hot Climates. Architectural Press.
10. Layard A. H., 1853. The monuments of Nineveh vol. 2, John Murray London.
11. Mahyari A, 1996. The Wind Catcher, A passive Cooling Device for Hot Arid Climate, PhD thesis, Department of Architectural and Design Science, The University of Sydney.
12. Moustafa W. S., Hegazy I., Eldabousy M., 2018. Roof geometry as a factor of thermal behavior: Simulation based study of using vaults and domes in the Middle East zone. International Journal of Low-Carbon Technologies 13(3).
13. Olgyay V., 1963. Design with Climate: Bioclimatic Approach to Architectural Regionalism. Princeton University Press.
14. Olgyay V., Lyndon D., Reynolds J., Yeang K., 2015. Design with Climate: Bioclimatic Approach to Architectural Regionalism - New and expanded Edition, Princeton University Press.
15. Page J. K. (edit.), 1986. Prediction of Solar Radiation on Inclined Surfaces' vol. 3. Reidel, for the Commission of the European Communities.
16. Perlmutter D., 1993. Roof Geometry as a Determinant of Thermal Behaviour: A Comparative Study of Vaulted and Flat Surfaces in a Hot-Arid Zone. Architectural Science Review, 36:2, 75-86.
17. Soflaei F., Shokouhian M., Zhu W., 2017. Socio-environmental sustainability in traditional courtyard houses of Iran and China. Renewable and Sustainable Energy Reviews, Volume 69, pp.1147-1169.
18. Stasinopoulos T. N., 1999. Geometric Forms & Insolation – An analytical study of the influence of shape on solar irradiation, PhD dissertation, NTUA School of Architecture, Athens 1999 (in Greek, w. English summary). DOI: 10.12681/eadd/11791.
19. Stasinopoulos T. N., 1998. Form Insolation Index. Proceedings of the 15th PLEA Conference 'Environmentally Friendly Cities', Lisbon. pp 563-566 (ISBN 1873936818).
20. Stasinopoulos T.N., 2020. Geometric forms and insolation II -- A reassessment of the relation between shape and solar irradiation. Proceedings of the 34th PLEA conference, A Coruna, Spain [online].
21. Tang R., Meir I.A., Etzion Y., 2003. An analysis of absorbed radiation by domed and vaulted roofs as compared with flat roofs. Energy and Buildings 35 pp.539–548.
22. Tavassoli M., 2016. Urban Structure in Hot Arid Environments: Strategies for Sustainable Development. The Urban Book Series, p.116, Springer International Publishing.
23. Yildirim E., Firatoğlu Z.A., Yeşilata B. 2017. Investigation of the effect of the roof geometry on building thermal behaviour. Uludağ University Journal of The Faculty of Engineering, Vol. 22, No. 3.

PLEA 2024 WROCŁAW
(Re)thinking Resilience

The Potential of Translucent Fabric Layers as Solar Protection

Assessing the Role of Indoor Curtains in Long-wave Radiation

MARC ROCA-MUSACH[1], ISABEL CRESPO CABILLO[1], HELENA COCH[1]

[1]Universitat Politècnica de Catalunya, Barcelona, Spain
Research group on Architecture, Energy and Environment (AiEM)

ABSTRACT: In response to the changing climate, effective building design is crucial for regulating indoor conditions while minimizing the energy consumption. This study addresses the impact of translucent fabric layers (indoor curtains) as solar protection devices, considering user-driven factors in their energy performance. We measure the indoor radiation in a residential case study in two phases: (i) a supervised phase over a day, with curtains rolled up and down by the investigators, and (ii) an unsupervised long-term phase (1.5 years) where curtains were controlled by the users. In the supervised phase, the curtains demonstrate an average filtering coefficient of 51.5%, which varies throughout the day: a minimum filtering coefficient of 40% occurs around solar noon, while raises up to 70% in the evening. In the unsupervised phase, curtains remain down for over 30% of the year, with users' choices possibly influenced by factors beyond thermal considerations. These results enhance our understanding of user interactions with movable passive systems and offer valuable insights for the design of energy-efficient buildings.
KEYWORDS: Translucent fabric layers, Indoor curtains, Solar protection, User interaction, Energy performance.

1. INTRODUCTION

The climate is changing, shifting to higher temperatures and longer heat-waves [1]. To adapt to this new scenario, building designers need to provide buildings with tools to regulate indoor conditions. While mechanical systems require an energy supply, passive strategies, such as solar protection, insulation and night ventilation, are good alternatives to guarantee adequate indoor conditions without increasing energy consumption [2, 3].

Fenestration systems are complex parts of buildings that regulate the relation between the indoors and the outdoors in multiple ways: some elements provide the ability to ventilate, modify thermal transmission, control privacy, regulate the received solar radiation, and many other functions. Due to the high impact of solar radiation on the energy performance of buildings [4], in this paper we focus on the role of solar protection devices.

Solar protections perform well when they are placed on the outside face of windows [4, 5]. However, some filters that have other main functions also contribute to reducing the received solar radiation indoors. Fabric layers, such as indoor curtains, can be used for privacy or lighting control, as well as for solar protection.

The objective of this paper is to quantify the filtering effect that an indoor fabric layer (*curtain*) has on the received solar radiation in an indoor space.

To fully assess the role of curtains, we cannot focus only on the physical properties, but we also have to consider that users will roll up and down this device manually. Due to the wide range of functions of a single device (solar shading, light control, privacy, ventilation control…), it is difficult to predict the reasons that lead people to activate some shading devices, thus it is also hard to estimate their energy performance [6].

2. METHOD

We achieved the aim of this paper by measuring the radiation received indoors in a residential case study. The dwelling accounted for a window with indoor, translucent, fabric curtains and We measured the received radiation with a pyranometer on the indoor face of the curtain, on a vertical plane. We also registered the outdoor horizontal solar radiation provided by a weather station located 1.1 km away. All the data was collected with a datalogger connected to a *RaspberryPi* for remote storage of the data. The indoor measurements were registered every minute, while the outdoor measurements were registered on irregular intervals as provided by the weather station (approximately every 20 minutes).

2.1 Measuring campaign

The measuring campaign was undertaken in two phases. The first phase was supervised by the investigators, in which the curtains were rolled up and down every 20 minutes under different solar radiation conditions (direct and indirect solar radiation). This first phase lasted for one day. The window was always closed, so the glass always

influenced the received radiation inside. Moreover, the inhabitants of the house were not present during this phase. Photos were taken before and after the curtains were raised or lowered as additional evidentiary support.

With the collected data, we focused on the values of radiation measured by the pyranometer just before and after the curtains were rolled up or down. For each pair of values, we calculated the variation between the first and the last value to determine the filtering effect of the curtains. The final filtering coefficient is the average of the partial values.

The second phase of measurements was unsupervised and lasted for one and a half year. The aim of this phase is to estimate the long-term effect of curtains when controlled manually by the inhabitants of the apartment. No instructions were given to them so that they could manipulate the curtains according to their preferences.

The data from the second phase was processed to identify periods when curtains were rolled down. This identification process was carried on by detecting sudden dropdowns on the received radiation indoor. If the variation value is close to the filtering coefficient calculated in the first phase, with an allowed margin of error of ±10%, the curtains are considered to be rolled down. However, this estimation needs to be corrected with the solar radiation outside. If there is also a sudden dropdown in the outdoor solar radiation, then the curtain is considered unchanged.

2.2 Case study

The case study analysed here is located in the city of Barcelona, Spain. It has a Mediterranean coastal climate, with hot summers and mild winters. The average annual rainfall is around 600mm, mainly distributed between autumn and spring. The driest season is summer [7]. Due to its climate, buildings in Barcelona require heating during the winter and cooling during the summer. However, an appropriate management of the natural energy resources (such as solar radiation) can reduce the energy need of buildings [8].

The studied dwelling is located in a singular neighbourhood called *Urbanització Meridiana*, built in the 1940's as a public housing neighbourhood [9]. Due to the low budget and the period when these buildings were constructed, they did not account for any solar protection devices integrated in the building. However, currently almost all the apartments remodelled their windows in order to have solar protections, either at the internal or the external face.

Specifically, the apartment analysed is located on the ground floor of a three-story building. The apartment has three external façades, one oriented to the north-east, one to the north-west, and the third one oriented to the south-east (Figs. 3 and 4).

Figure 1: General view of the window (left), and detail photo of the position of the pyranometer (right).

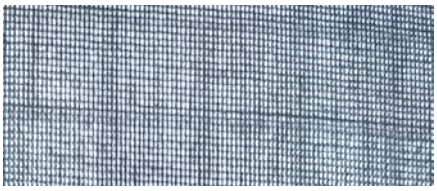

Figure 2: Detailed photo of the curtain's web.

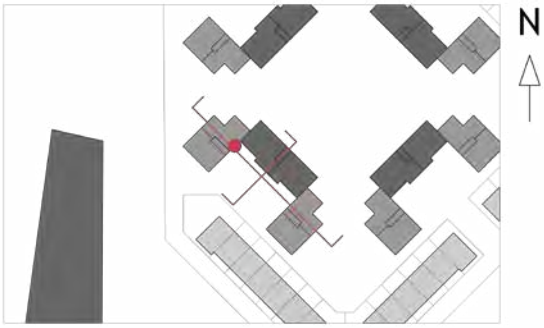

Figure 3: Plan view of the analysed neighbourhood.

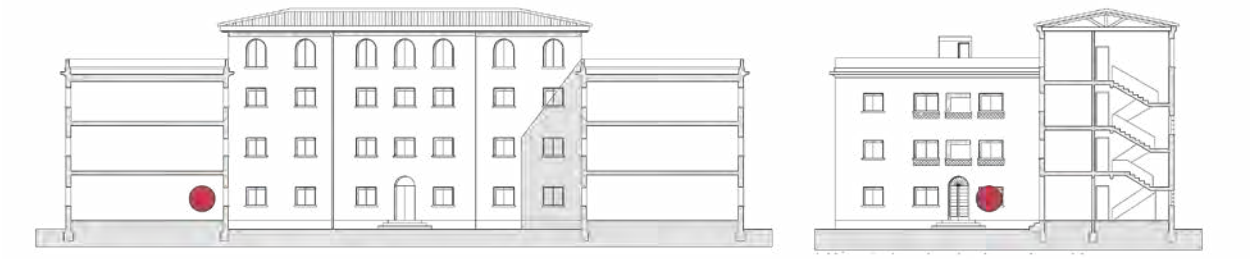

Figure 4: Section views of the measured window.

The window where the pyranometer was located is on the south-east façade. The size of the window is 1.45 m wide and 1.15 m high. The fenestration system is made of an aluminium window frame without thermal break, single pane glass, and a white fabric indoor curtain that is 0.4 mm thick (indoor curtain) (Fig. 1). The curtain's web density is 58% (Fig. 2). The indoor curtain must be rolled up and down manually. Due to the neighbouring buildings, this window is fully obstructed from the east and is partially obstructed from the south (Fig. 5).

The stereographic projection of the sun path in Figure 5 corresponds to the position of the pyranometer, and it shows the masked areas caused by the obstruction from other buildings. From Fig. 5 we calculated that the Sky View Factor of the pyranometer is 6.9%.

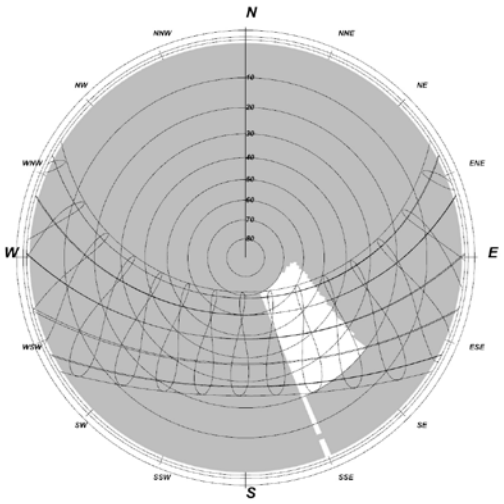

Figure 5: Stereographic projection of the sun path with indication of the shading mask produced by the obstructing buildings nearby.

Figure 6: Image of the sky during the supervised phase.

3. RESULTS

This section is divided into two parts: the first part describes the results from the supervised phase, and the second part describes the results obtained from the unsupervised phase.

3.1 Supervised phase

During the supervised phase, curtains were rolled up and down by the investigators every 20 minutes, from 8:00 h to 18:00 h solar time. The data before and after this period was irrelevant due to the lack of radiation on the window. We measured the received vertical radiation inside and the horizontal radiation outside. The weather conditions were sunny with some high clouds, as shown in Fig. 6.

Figure 7 shows the received radiation inside on the vertical plane, where the grey areas indicate periods when the curtains were rolled down. Figure 8 shows the measured outdoor horizontal radiation during the supervised phase. Table 1 is an extract of the data plotted in Fig. 7, where we registered the received radiation inside just before and after the curtains were rolled up or down. It also shows the calculated variation between the values before and after, which are used to estimate the filtering coefficient of the curtains.

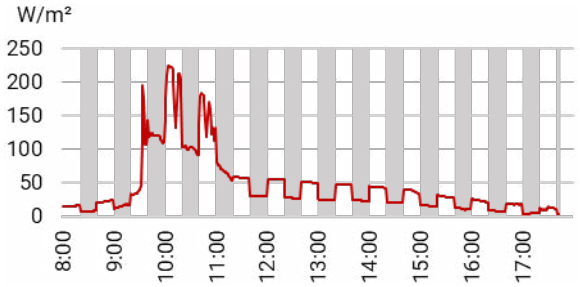

Figure 7: Measured radiation INSIDE on a vertical plane during the supervised phase (solar time). Grey areas indicate that the curtains were rolled down

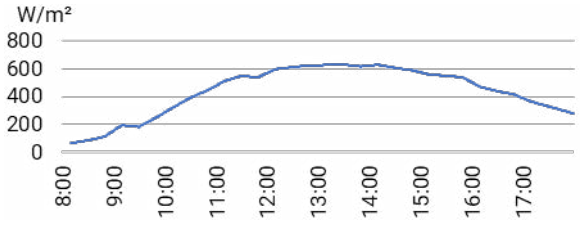

Figure 8: Measured radiation OUTSIDE on a horizontal plane during the supervised phase (solar time).

The average filtering coefficient of the analysed curtains is 51.5%. However, the average is a summarized value that hides the full effect of the curtains along the day. Figure 9 is a plot of the variation between each pair of measurements.

Table 1: Sample of the measurements of the received solar radiation inside before and after every action.

Solar time	Before (W/m²)	Action	After (W/m²)	Variation (%)
9:00	24.9	DOWN	12.0	-51.9%
9:20	17.12	UP	33.62	49.1%
9:40	174.24	DOWN	106.34	-39.0%
10:00	111.1	UP	211.5	47.5%
11:00	132.1	DOWN	81.9	-37.9%
12:00	30.3	UP	56.2	46.1%
13:00	50.0	DOWN	25.9	-48.2%
…	…	…	…	…
	Filtering coefficient (average):			51.5%

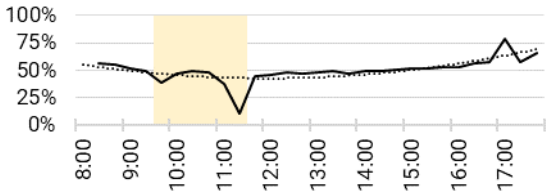

Figure 9: Graph of the calculated filtering coefficient. The yellow area indicates the period with direct solar radiation.

Figure 9 shows the variation of the filtering coefficient of the curtains along the day, under the different radiation conditions. The overall values can be approximated using a polynomic tendency curve of degree 2 (plotted as a dotted curve). The curve has a minimum filtering coefficient of 40% around the solar noon, and the filtering effect increases while the outside radiation decreases.

Nonetheless, there are some values that highly differ from the tendency curve. These peaks correspond to the measurements at 9:40, 11:40 and after 17:00. The first two peaks correspond to the time frame when the curtains were exposed to direct solar radiation. The values after 17:00 were measured under conditions of low outside radiation, so small variations produce a high impact on the calculation of the filtering coefficient. In the evening, the filtering coefficient raises up to 70%. To help understand these singular moments, Figure 10 shows the photos of the curtains just before and after the roll action.

Figure 10: Sample photos before (left) and after (right) the action of rolling down the curtains.

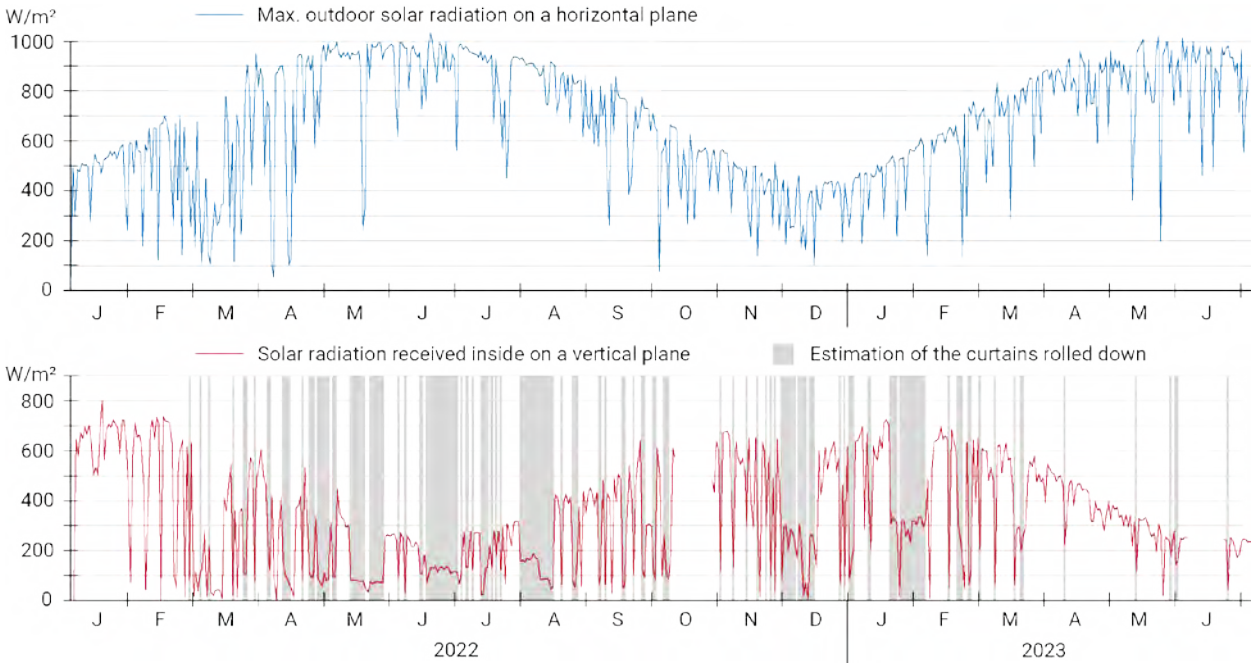

Figure 11: Measured radiation inside and outside, and estimation of the position of the curtains (grey area) during the unsupervised phase.

3.2 Unsupervised phase

During the unsupervised phase, the users of the apartment lived normally and managed the curtains according to their personal preferences. We registered the vertical radiation inside with the same pyranometer at the same position as in the supervised phase, as well as the horizontal radiation outside from the nearest weather station. This period lasted between January 10th 2022 and July 4th 2023, for a total amount of 540 days. However, there are two periods for which data is unavailable due to technical issues with the datalogger: from October 14th to 29th 2022, and from June 6th to 21st 2023. This provides a total of 508 valid days.

Figure 11 plots the data collected during this phase. The radiation outside (blue) and inside (red) are plotted separately because they were measured on different planes. This is evident by reading the date when the maximum radiation is received on each graph. The horizontal outside radiation had the maximum on the summer solstice (June 21st) of 1089 W/m². However, the maximum received vertical radiation inside happened between the winter solstice and January, which corresponds to a south-east façade with high obstruction on the east.

Figure 11 provides a general idea of the thermal effect of curtains. On the graph, it is possible to clearly identify sudden changes in the levels of inside radiation which deviate from the expected maximum for the time of the year. These sudden fluctuations could have been either by the change on the external weather conditions, or the roll down of the curtains. Combining both criteria, we highlighted the estimated days when curtains were rolled down, which corresponds to 31.2% of the days of the year. It is noticeable that these periods are spread along the year, and not concentrated on specific months or seasons. Combining the filtering effect of curtains (51.5%) and the action of people rolling up and down the curtain (31.2% of days rolled down), provided the interior space with a reduction on the received radiation of 16.1%.

To analyse in further detail the role of the curtain minute by minute, Figure 12 shows three sample days under three different weather conditions, all of which have the curtain rolled up. On the sunny day, the effect of direct solar radiation is clearly noticeable as radiation values arise up to 700 W/m² between 9:00 and 11:00. However, during the rest of the day, the window only receives indirect radiation, which remains constant around 100 W/m². On the cloudy and the rainy day, however, the received radiation is irregular, with values that hardly surpass 100 W/m².

Having understood Figure 12 helps to interpret a graph of a day when the curtains were rolled down between 9:15 and 14:30 (Fig. 13). This day was chosen as an example because it perfectly shows the filtering effect of curtains under direct and indirect conditions. The filtering coefficient on this day is around the previously calculated on the supervised phase (51.5%).

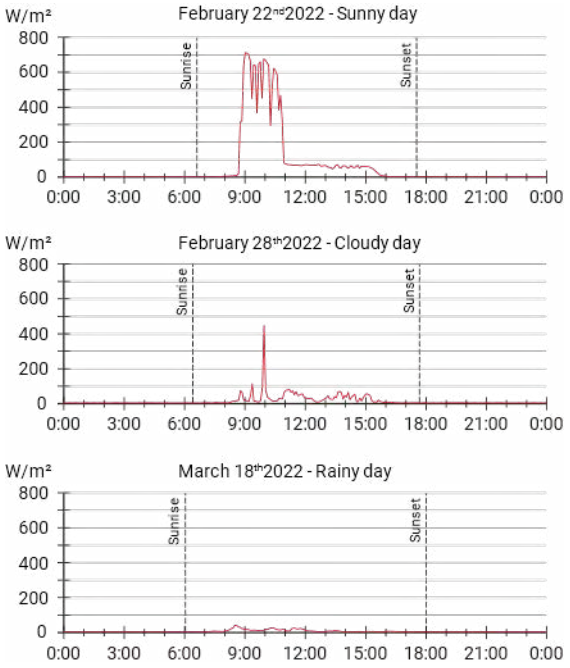

Figure 12: Detailed indoor radiation for three sample days under different weather conditions and no curtain.

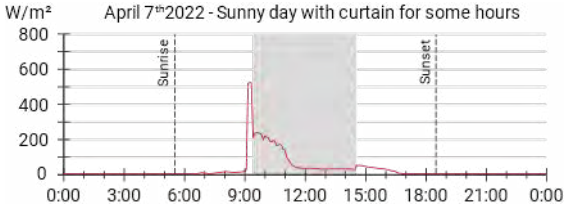

Figure 13: Detailed indoor radiation for a sunny day when the curtains were rolled down for some hours.

4. DISCUSSION

The results of this paper help to understand the role that fabric curtains have on the radiation received indoors. In this analysis we considered the physical properties of the curtain and the role that users have on controlling the curtains manually.

The results of the supervised phase of measurements showed that a white fabric curtain that is 0.4 mm thick placed at the indoor face of a window can reduce the indoor radiation by 51.5% on average. However, we noticed that the curtain's filtering effect is variable throughout the day. Their effect is due to the reflective capacity of the fabric layer (white colour), the density of the web and the lack of thermal inertia (thin fabric). In this paper we

did not measure other factors, such as the indoor illumination level or the curtain's temperature, that could help to understand its additional impacts in future works. Nonetheless, the filtering effect of the curtains on the received radiation indoors cannot be ignored.

In the analysis of the unsupervised phase, we identified an irregular pattern of rolling up and down the curtains. There are full days, even long periods of two or three weeks, when users kept their curtains rolled down (highlighted in Fig. 11). Apparently, these periods are not concentrated in warm seasons as would be expected according to an optimal control of solar radiation for thermal conditioning. This means that the users' decisions for rolling up and down the curtains are not directly related to thermal perceptions. This is comprehensible as curtains have more functions, such as light or privacy control. In this paper we do not interview or collect data from the users that took part of the unsupervised phase of measurements. The reasons leading people to make decisions on behalf of their living environment are diverse and varied. This study does not focus on the reasons why people act, but on the effects of their actions. We performed the unsupervised phase for a long period (1,5 years) to minimize the bias of people's choices. The data gathered in this study reinforces the multifunctionality of curtains and the fact that thermal optimisation is not always the priority for users.

5. CONCLUSION

This paper aimed to measure the filtering effect that indoor fabric layers (curtains) have on the received solar radiation in an indoor space. Our analysis included an understanding of their physical properties and the role of the manual operation by the users. The filtering effect was analysed in two phases: (1) a supervised phase when we measured the filtering effect in a case study under different radiation conditions, and (2) an unsupervised phase when we measured the long-term effect including the role of the manual control by the users.

In the supervised phase (1), the results showed that a white fabric curtain that is 0.4 mm thick placed at the indoor face of a window can filter the indoor received solar radiation by 51.5% on average. However, this value is not constant along the day.

In the unsupervised phase (2), we noted that curtains remain down for over 30% of the year, but not necessarily concentrated on warm periods. Users might not only utilize the curtains for thermal reasons, but also other functions, such as privacy, lighting and ventilation.

The outcomes of this paper hold great importance in enhancing our understanding on user interactions with movable passive systems, and they offer valuable insights for future advancements in user-centred control systems. Our findings are relevant given the uncommon opportunity to collect data from a user-involved case study spanning a 1.5-year duration. These findings furnish valuable insights for the design of energy-efficient buildings.

ACKNOWLEDGEMENTS

This research has been developed under the project PID2020-116036RB-I00, funded by the Spanish Ministry of Science and Innovation (MCIN), ref. number MCIN/AEI/10.13039/501100011033. It is also supported by the Secretariat of Research and Universities of the Generalitat de Catalunya and the European Social Fund.

REFERENCES

1. Intergovernmental Panel on Climate Change (2023) AR6 Synthesis Report: Climate Change 2023 — IPCC.
2. Frank Th (2005) Climate change impacts on building heating and cooling energy demand in Switzerland. Energy and Buildings 37:1175–1185
3. Suárez R, Escandón R, López-Pérez R, León-Rodríguez ÁL, Klein T, Silvester S (2018) Impact of Climate Change: Environmental Assessment of Passive Solutions in a Single-Family Home in Southern Spain. Sustainability 10:2914
4. Tzempelikos A, Athienitis AK (2007) The impact of shading design and control on building cooling and lighting demand. Solar Energy 81:369–382
5. Invidiata A, Ghisi E (2016) Life-cycle energy and cost analyses of window shading used to improve the thermal performance of houses. Journal of Cleaner Production 133:1371–1383
6. Chen G, Yao J, Zheng R (2021) Energy related performance of manual shading devices in private offices: An occupant behavior-based comparative study using modeling approaches. Case Studies in Thermal Engineering 27:101336
7. Ajuntament de Barcelona (2023) Barcelona climate. https://www.barcelona.cat/temps/en/climatologia/clima_barcelona. Accessed 18 Oct 2023
8. Roca-Musach M, Garcia-Nevado E, Alonso-Montolio C, Crespo Cabillo I, Coch Roura H (2023) Comparison of the Thermal Effect of Two Automatic Controls of Roller Shutters in an Academic Space. In: Littlewood J, Howlett RJ, Jain LC (eds) Sustainability in Energy and Buildings 2022. Springer Nature, Singapore, pp 261–270
9. Fernández Crespí B (2013) Estudi del teixit residencial de la Urbanització Meridiana de Barcelona.

Portable System for Monitoring Environmental Variables:
Application to Thermal Comfort in Urban Canyons in Curitiba (Brazil)

BIANCA MILANI DE QUADROS[1] EDUARDO LEITE KRÜGER[2] MARTIN GABRIEL ORDENES MIZGIER[1]
WALTER IHLENFELD[2] SOLANGE MARIA LEDER[3]

[1]Universidade Federal de Santa Catarina, Florianópolis, Brazil
[2]Universidade Tecnológica Federal do Paraná, Curitiba, Brazil
[3]Universidade Federal da Paraíba, João Pessoa, Brazil

ABSTRACT: Sky view factor (SVF) has been used in studies of microclimate, however its impact on different seasons is still unclear. The present study analyses the influence of urban morphology on outdoor thermal comfort (OTC) employing a Portable Low-cost Environmental Monitoring System (PLEMS) developed by the authors. For this, we developed and calibrated the PLEMS (1), performed the monitoring of the walking routes on summer and winter (2) and established the correlation analysis between urban morphology and the condition of comfort and thermal stress (3). The results found point to a low correlation without statistical significance ($p>0.05$) between SVF and UTCI for the sample of 12 points in both seasons, confirming that SVF is not a reliable predictor for accurately assessing thermal condition of an outdoor space. The localized variations in the values measured by PLEMS compared to the reference station demonstrated that it was able to correctly capture the urban signals during the thermal walks. Within the urban canyons of the routes, the temperature was 1.6℃ higher than that recorded by the reference station.
KEYWORDS: Thermal comfort, Open spaces, Urban morphology, Dynamic measurements, PLEMS.

1. INTRODUCTION

The increase in population and the densification of cities cause morphological and environmental transformations, which are reflected in problems related to human thermal comfort. The poor quality of the thermal environment influences life quality and public health. In addition, economic, commercial, social and leisure activities are impacted by outdoor thermal comfort (OTC) [1].

In computer-aided urban climate studies, stationary weather stations are frequently adopted to validate simulation models. In this context, several studies have used fixed meteorological stations to investigate thermal effects from urban variations [1-4]. A limitation is that, since in many cases meteorological stations are located at just one specific point within the urban canyon, or even further away (e.g., airports), measured data are not able to capture the diversity of existing spatial patterns and their thermal implications in urban settings. Thus, the application of a portable environmental monitoring system seeks to overcome such limitations [4].

Various urban morphology indicators were developed and employed to link urban spatial configuration to OTC. Among the studies, street aspect ratios (H/W), sky view factor (SVF) and street axis orientation are significant as the most influential parameters [5]. According Qaid et al. [6], mean radiation temperature is the main environmental parameter affected by urban morphology at street level. Furthermore, Lobaccaro et al. [7] showed that orientation and aspect ratio have a strong impact on the degree and amplitude of thermal peaks at the pedestrian level. The impact of SVF is more significant on east-west streets than on north-south streets. Additionally, the greenery arrangement implies in different impacts on the outdoor thermal comfort of streets with different orientations [8].

Several studies have examined the influence of urban morphology on OTC [5-8], however the impact of SVF on thermal comfort at the pedestrian level in both seasons (summer and winter) remains uncertain. The aim of this study is to analyze the influence of urban morphology on OTC employing a Portable Low-cost Environmental Monitoring System (PLEMS) [9] developed by the authors in two 4-day periods in summer and winter, respectively, in subtropical Curitiba, Brazil (Koeppen's Cfb).

2. METHODS

Pre-defined routes in a densified urban area were dynamically evaluated in terms of OTC, as follows:

- Initial step: development and calibration of the PLEMS;
- Monitoring: Definition of the study area and walking routes;
- Analytical step: Correlation analysis between urban morphology features and OTC data.

2.1 Development and calibration of the PLEMS

Figure 1 presents the construction details of the PLEMS. The data collected by the sensors are GPS locational data (1); air temperature and air humidity (2); globe temperature (3); wind speed (4); illuminance (5); sound pressure levels (6) and CO2 concentration (7). The collected data can be viewed in real time on

an LCD screen attached to the equipment and, within a 90-second cycle, data are stored as a ".csv" file.

The casing consists of an electric distribution enclosure to which two 0.80 meter and a 1.00-meter PVC tubes were fixed with plastic clamps (i) in the center, so that the globe thermometer is not shaded. To position all the sensors aligned, two switch plates (ii) were used. To protect the air temperature and humidity sensor, a solar shield (iii) (3D-printed via Thingiverse) was printed in PLA and varnished, with an aluminum foil film fitted to the cover, as recommended by Ham [10]. To allow people with different heights to use the equipment, there are adjustable bar and straps (iv). In the present study, the height of the sensors was adjusted to 1.90 meters in relation to the ground; and the globe at 2.10 meters.

Figure 1: PLEMS sensors and construction details.

Calibration of the sensors was carried out in a climate chamber with partial thermal control with reference equipment: the SENSU comfortmeter developed at LMPT/UFSC (Federal University of Santa Catarina) and a Kestrel 3000 propeller anemometer. The sensors were positioned at a height of 1.80 m in the center of the chamber and monitored under thermal conditions controlled by a 9,000 BTU split air-conditioning unit (Philco Eletrônicos®), for three hours, during which the setpoint temperature was maintained at 16°C for one hour, and, after that, the A/C was turned off. For the calibration procedure, minute-by-minute measurement data were considered.

After comparing the PLEMS sensors with reference equipment, each environmental quantity was assigned a regression statistic (R^2), a statistical method that allows examining the relationship between two or more variables, and Kruskal-Wallis non-parametric analysis (*p-value*), used in situations where you want to compare two or more independent groups, with a quantitative response variable. The mean absolute error (EMA) was the indicator used to determine the application of the regression equation with calibration bias.

The EMA represents the absolute average between the data collected and simulated in the calibration process between the measured data. According to [11], the smaller the results of the statistical equations, the closer the simulated values are to the actual measured values (Equation 1).

The obtained results of the regression statistics for the thermal variables (air temperature, air humidity, globe temperature and ventilation) are presented in Table 1. The null hypothesis test was rejected for all variables, therefore, for each dataset, the value measured with PLEMS was corrected based on the regression equations.

$$\mathbf{EMA} = \frac{\sum_{i=1}^{n} |P_i - O_i|}{N} \qquad (1)$$

Where Pi – predicted value;
Oi – observed value;
N – number of measurements (60 points).

Table 1: Summary of calibration results.

Var.	Kruskal-Wallis test (*p-value*)	Regression equation	R^2	EMA with validation
Ta	0.2144	N/A	0.97	0.24
RH	0.0001	RH'= 0.9535*RH +1.8994	0.99	0.55
Tg	0.0455	Tg'=1.0845*Tg -1.6575	0.99	0.13
Ws	0.2728	N/A	0.97	0.09

The mean absolute error was the indicator used to determine the application of the regression equation with calibration bias when it reduced the mean absolute error. Although the data collected by PLEMS are within the error range of reference equipment measurements, with the exception of what occurs in illuminance measurement, the non-parametric Kruskal-Wallis analysis indicated that there is a statistical difference (*p-value*<0, 05) among the measurements carried out on the equipment for the variable relative humidity, globe temperature for which a sensor calibration procedure was applied using linear regression analysis.

2.2 Definition of the study area and walking routes

Curitiba is located at 25°25'48'' S and 49°16'15'' W and at a mean altitude of 920 meters above sea level. According to the Köppen-Geiger classification, the city of Curitiba is *Cfb* (Temperate oceanic climate), characterized by a temperate climate with mild summers. While in the coldest month (July) the average temperature is 12°C, in the hottest month (February) the average is 23°C. The absolute minimum and maximum temperatures recorded in these months are -2°C and 32°C, respectively. Throughout the year, the eastern wind has a greater frequency of occurrence.

The study area was selected due to the heterogeneity in terms of morphological factors and urban greenery, also considering safety aspects for carrying out field measurements at given times of day. Thus, the study area comprises diverse aspect ratios (shallow, medium, and deep canyon), different solar orientations (north-south and east-west street axes), with and without vegetation. Additionally, in order to verify whether PLEMS was able to correctly capture urban-related signals during the thermal walks, a comparison was drawn to a reference weather station (Hobo T/RH logger) placed on the rooftop of a building within the study area (Figure 2).

The area was surveyed at 01 reference station and 12 monitoring points, spread over six routes, each formed by two blocks, which are analyzed and named according to their urban morphology and solar orientation condition, resulting in three north-south routes (RNS) and three east-west routes (REW): RNS1, RNS2, RNS3, REW1, REW2 and REW3. The routes are approximately 250 meters long each, resulting in a total distance of 1.5 km covered in one hour.

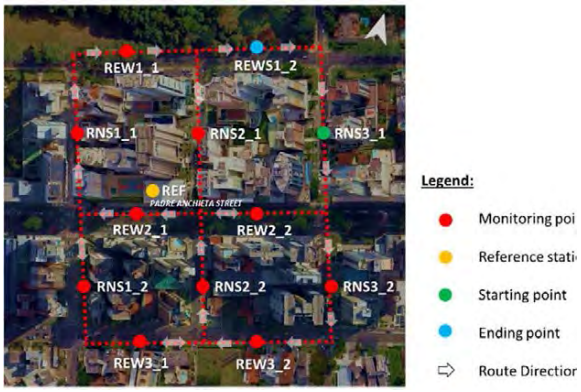

Figure 2: Urban area and measured points.

Four days with forecasts of clear sky were selected for the thermal walks at three-time stamps (0 UTC, 12 UTC, 18 UTC), in summer (from March 16th to 19th) and winter (from June 24th to 27th). Apart from measured variables, the Universal Thermal Climate Index (UTCI) was computed. The UTCI is defined as the air temperature of the reference condition causing the same thermophysiological model response as the actual condition. Such equivalence is based on the dynamic physiological response between both. A computed UTCI value is an equivalent temperature obtained from a set of air temperature, radiation, wind, and humidity data that corresponds to the air temperature in the reference condition of radiation, humidity, and wind speed, both producing the same thermal strain condition [10]. A thermal stress assessment scale comprises 10 different categories ranging from extreme cold stress to extreme heat stress.

To calculate the thermal comfort index, the UTCI Calculation application (http://www.utci.org/utcineu/utcineu.php) developed by the International Society of Biometeorology (ISB) was employed. It is necessary to convert wind speed values at a height of ten meters to the input data for calculating the thermal index, using the conversion factor proposed by Bröde et al. [12], according to Equation 2. The mean radiant temperature (Tmrt) was calculated in accordance with [13], considering forced convection, using Equation 3.

$$va = va_{xm} * \frac{log(\frac{10}{0,01})}{log(\frac{x}{0,01})} \qquad (2)$$

$$T_{mrt} = \left[(t_g+273)^4 + \frac{1,1*10^8*va^{0,6}}{\varepsilon_g*D^{0,4}}*(t_g-t_a)\right]^{1/4} - 273 \qquad (3)$$

Where va - wind speed at ten meters high (m/s);
va_{xm} – wind speed at x meters high (m/s);
Tmrt - mean radiant temperature (°C);
t_g – globe temperature (°C);
ε_g - emissivity of the globe thermometer material (dimensionless);
D – diameter of globe thermometer (m);
t_a – air temperature (°C).

Hemispherical photographs were taken to collect urban morphology data expressed by SVF which is determined by the distinction between the area covered by obstacles and the visible area of the sky. The equipment used was a Nikon D3100 model camera with a Sigma 8mm fisheye lens (with a total viewing angle of 180° in all directions), supported on a tripod 1.20 meters height from the ground.

The estimated value of magnetic declination, i.e., the angle of difference between true North and magnetic North, was calculated using the NOAA - National Oceanic and Atmospheric Administration online calculator (https://www.ngdc. noaa.gov/geomag/calculators/magcalc.shtml). As a result, a declination of 20°10'W ± 0°25' was obtained for the day of data collection, modifying 0°7'W per year. The calculation considers the latitude and longitude of Curitiba, the date of measurement and is based on the World Magnetic Model (WMM).

SVF values were obtained from the images' analysis and processing by the *RayManPro Version 3.1 Beta©* software, developed by the Human Biometeorology Research Center under the supervision of Prof. Dr Andreas Matzarakis.

2.3 Correlation analysis between urban morphology features and OTC data

Based on the SVF and microclimatic data collected *in situ*, the influence of urban morphology on thermal comfort conditions in open spaces was analyzed. This way, the input data were compared in terms of

calibrated values of Ta (°C), Trmt (°C), RH (%) and Ws (m/s) at each point measured in the study area.

For initial characterization of the thermal behavior of urban canyons, comparative graphs of microclimatic variables and UTCI calculated for the four days of collection were generated. This analysis allows the identification of behavior patterns between the measured points and the selection of the representative day for the analysis of the influence of urban morphology on the thermal environment. In addition, for the selected day, regression analyses of the UTCI against the SVF were established. From the graphs, it was possible to analyze the degree of correlation between the indicators studied.

3. RESULTS AND DISCUSSIONS

3.1 Thermal behavior of urban canyons

To select the representative day for analysing the influence of urban morphology on the thermal behaviour of canyons, a comparative analysis was carried out on nighttime data (0 UTC or 9 pm local time) aiming at conditions that best characterise the Urban Heat Island (UHI) (Figure 3).

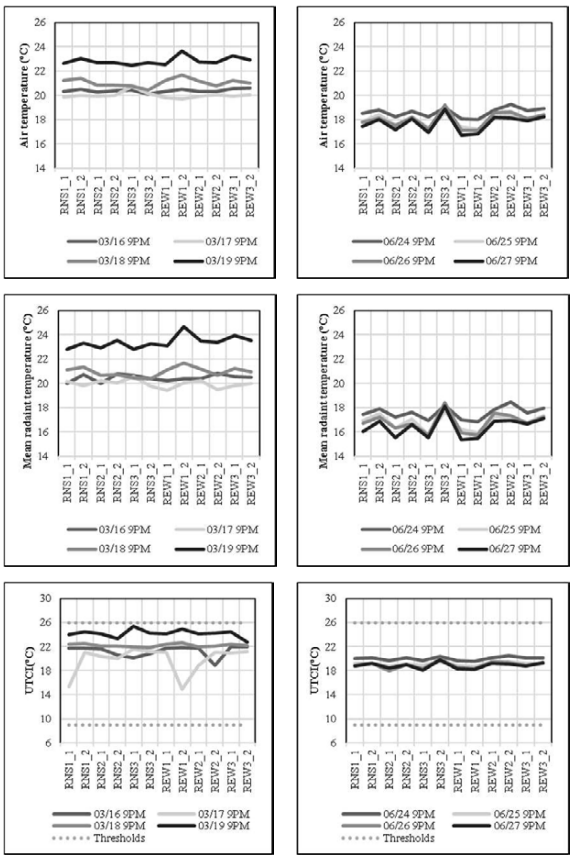

Figure 3: Ta, Tmrt and UTCI in summer (left) and winter (right) at 9pm, with comfort thresholds for the UTCI.

In summer, the two last monitoring days (March 18 and 19) present quite a similar point-by-point variation of the air and mean radiant temperature. The first two monitoring days (March 16 and 17) were partially clouded, with increased cloudiness at night. In winter, all monitoring days resulted in similar behaviour regarding the three variables, possibly due to clear-sky conditions during the thermal walks. Based on such preliminary visualization, March 19 and June 27 were selected for an in-depth analysis.

3.2 Sky view factor in the study area

Obtained SVF values in the study area vary from 0.04 to 0.43 (Figure 4). The hemispherical photos illustrate the 12 points monitored (3-min stops at each point). Points REW2_2 and REW1_1 represent places with greater urban density, with SVF of 0.04 and 0.08, respectively. In contrast, locations with low density occur at points RNS2_2 and REW3_2, with SVF of 0.28 and 0.43, respectively.

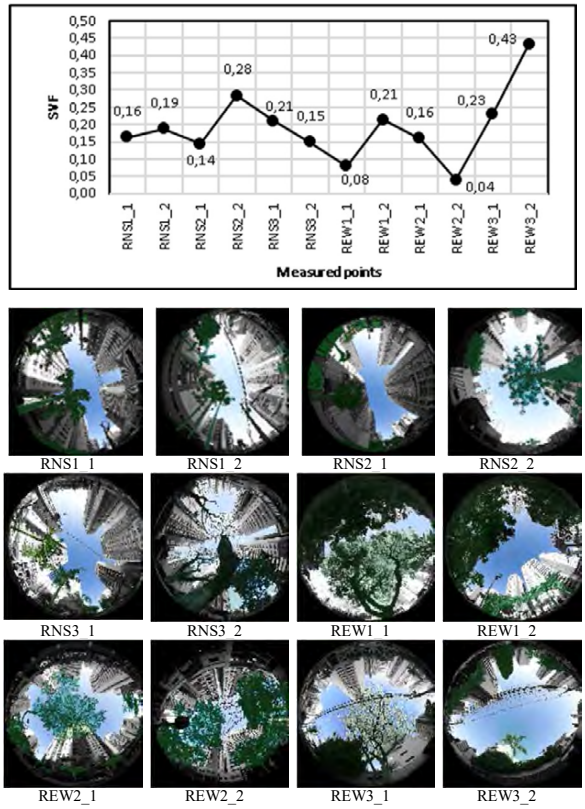

Figure 4: SVF of the monitoring points in the study area.

3.3 Comparison between PLEMS x reference station

The points measured on the urban routes had higher temperatures than the reference station. In fact, the difference between the average air temperature measured by PLEMS and the reference station was 1.6℃. On the other hand, the relative humidity showed a negligible difference, being very similar to the average between the measured points and the reference station. The point-by-point analysis shows that the minimum air temperature and the maximum relative humidity occur at point REW1_1, which is a point with the greatest canopy cover.

Similar trends of decreasing air temperature and increasing relative humidity are observed, with localized variations in the values measured by PLEMS, due to the urban signals (Figure 5). The results demonstrate that the PLEMS was able to correctly capture urban-related signals during thermal walks.

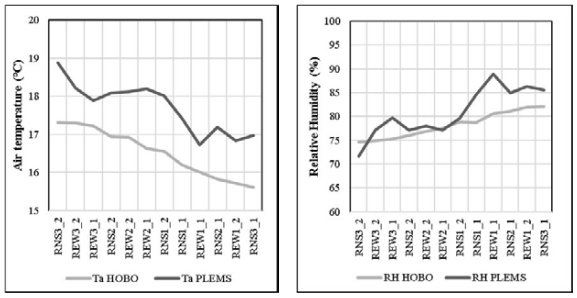

Figure 5: Ta and RH measured by PLEMS and the reference station on June 27 at 9 pm.

3.4 Discussion on the correlation between UTCI x SVF

This section summarizes the most relevant outcomes given by microclimate measurements, considering the thermal comfort index UTCI and the morphological aspect represented by SVF. As shown in Table 2, most points follow the same heating or cooling behavior in summer and winter. This analysis allows us to observe points that can be critical in an extreme heat situation or even in future climate change scenarios. Points RNS3_2, REW2_1, REW2_2 and REW3_2 result in higher temperatures in relation to the average for both seasons.

Based on urban morphology data and microclimatic data, a correlation was established between the SVF and the UTCI in the study area during the summer and winter days (Figure 6). To minimize the influence of urban vegetation, the correlation only includes points located in canyons without trees. Apart from the summer dataset for 9am (R^2=0.74), correlations were rather low and without statistical significance (p>0.05) for the sample of 12 points. Previous studies also suggest that SVF is not crucial for determining thermal comfort conditions due to the diversity of other climatic variables and urban aspects that together affect the local microclimate [14]. The non-directional nature of SVF may not be able to account for human thermal sensation [1]. When investigated as an isolated parameter, SVF is not able to accurately predict the thermal conditions of an outdoor space, especially because incoming solar radiation has a stronger effect on Tmrt [15].

Improvements in the degrees of association between SVF and UTCI were observed when points with trees were removed from the sample, with N=5. In this case, an R-squared of 0.30 was found for June 27 (with p>0.05) and 0.74 for March 19 (with p=0.06). The lack of statistical significance in observed associations and the lack of consistency between the relative relationship between SVF and UTCI outcomes for the 12 points indicates the need for considering other morphological factors. Possible explanatory variable may include the Gross Space Index (GSI), the Floor Space Index (FSI) and solar orientation of the canyon axis [16]. Additionally, thermal properties of buildings and trees are quite different, and the proportion will inevitably influence the effects of SVF on the thermal environment. Therefore, a single SVF cannot precisely quantify the urban geometry. According to Yan et al. [17] buildings and trees must also be considered with the use of building and tree view factors (BVF, and TVF, respectively).

Table 2: UTCI color rank for the 12 points (coldest points in blue to hottest in red) in the sequential order of the walking routes for March 19 (summer) and June 27 (winter).

Points	SVF	Summer UTCI 9PM 03/19	Winter UTCI 9PM 06/27
RNS1_1	0.16	21.8	18.8
RNS1_2	0.19	22.3	19.2
RNS2_1	0.14	23.0	18.4
RNS2_2	0.28	19.6	19.0
RNS3_1	0.21	22.9	18.1
RNS3_2	0.15	23.5	19.8
REW1_1	0.08	23.2	18.3
REW1_2	0.21	23.8	18.2
REW2_1	0.16	24.0	19.2
REW2_2	0.04	23.9	19.1
REW3_1	0.23	22.9	18.8
REW3_2	0.43	24.4	19.3

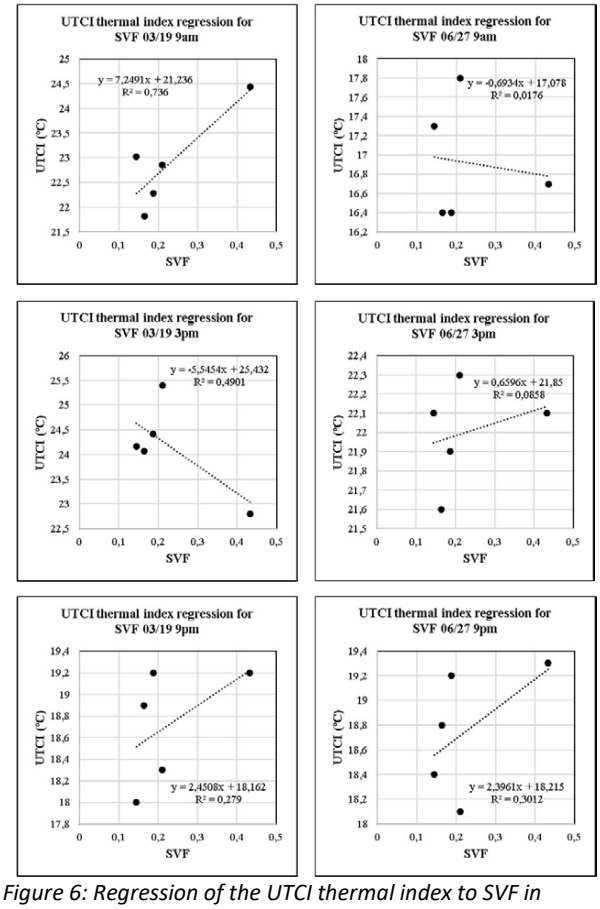

Figure 6: Regression of the UTCI thermal index to SVF in summer and winter at 9am, 3pm and 9pm.

4. CONCLUSION

This article aimed to analyse the influence of urban morphology on OTC employing a Portable Low-cost Environmental Monitoring System (PLEMS). The main contributions of this research are employing portable meteorological instrumentation as an alternative to traditional fixed measurement methods, identifying climate changes in urban canyons and analysing the condition of thermal comfort in open spaces. Localized variations in the values measured by PLEMS, compared to the reference station, demonstrated its ability to accurately capture signals related to urban conditions during the thermal walks. Within the urban canyons of the routes the temperature was 1.6℃ higher than that recorded by the reference station.

The results found point to a low correlation without statistical significance ($p>0.05$) between SVF and UTCI for the sample of 12 points in both seasons, confirming that SVF is not a reliable predictor for accurately assessing thermal condition of an outdoor space.

In general, the ranking of the coldest and hottest points shows a trend towards similar behavior for the same point in winter and summer, which demonstrates that morphological aspects influence local microclimate in both seasons. However, as demonstrated in the correlation graphs, urban morphology has a greater influence on human thermal comfort conditions in summer than in winter, especially during the day. Moreover, intra-urban canyon points with dense tree canopy reduces the correlation between UTCI and SVF which implies the conclusion that the presence of vegetation strongly affects human thermal comfort.

The study has shown us the validity of the PLEMS device to account for urban effects on the thermal field in dynamic assessments of OTC. Further studies could include the consideration of other morphological factors by means of multiple correlation for understanding associations between microclimate and urban features. In our research, future steps are to performance a temporal and spatial calibration of an urban climate simulation model of the studied area in ENVI-met with the data collected by the reference station and PLEMS in both seasons. This will result in an accurate urban simulation model for studying heat mitigation strategies.

ACKNOWLEDGEMENTS

The authors would like to thank CAPES (*Fundação Coordenação de Aperfeiçoamento de Pessoal de Nível Superior*) and CNPq (*Conselho Nacional de Desenvolvimento Científico e Tecnológico - Edital Universal*) for the financial support for the development of this research.

REFERENCES

1. Lau, K. K. L., Shi, Y., & Ng, E. Y. Y. (2019). Dynamic response of pedestrian thermal comfort under outdoor transient conditions. *International journal of biometeorology*, 63, 979-989.

2. Igawa, N. and H. Nakamura, (2001). All Sky Model as a standard sky for the simulation of daylight environment. *Building and Environment*, 36: p. 763-770.

3. Kittler, R., (1985). Luminance distribution characteristics of homogeneous skies: a measurement and prediction strategy. *Lighting Research and Technology*, 17(4): p. 183-8.

4. Perraudeau, M., (1988). Luminance models. In *National Lighting Conference*. Cambridge, UK, March 27-30.

5. Zhang, J., Li, Z., & Hu, D. (2022). Effects of urban morphology on thermal comfort at the micro-scale. *Sustainable Cities and Society*, *86*, 104150.

6. Qaid, A., & Ossen, D. R. (2015). Effect of asymmetrical street aspect ratios on microclimates in hot, humid regions. *International journal of biometeorology*, 59(6), 657-677.

7. Lobaccaro, G., Acero, J. A., Sanchez Martinez, G., Padro, A., Laburu, T., & Fernandez, G. (2019). Effects of orientations, aspect ratios, pavement materials and vegetation elements on thermal stress inside typical urban canyons. *International Journal of Environmental Research and Public Health*, 16(19), 3574.

8. Venhari, A. A., Tenpierik, M., & Taleghani, M. (2019). The role of sky view factor and urban street greenery in human thermal comfort and heat stress in a desert climate. *Journal of Arid Environments,* 166, 68-76

9. Krüger, E.; Ihlenfeld, W.; Leder, S.; Lima, L. (2023). Application of microcontroller-based systems in human biometeorology studies: a bibliometric analysis. INTERNATIONAL JOURNAL OF BIOMETEOROLOGY, v. 67, p. 1, 2023.

10. HAM, J. *Radiation Shield for Weather Station Temperature/Humidity*. [S. l.], 2015. [Online], Available: https://www.thingiverse.com/thing:1067700 [12 May 2023].

11. WILLMOTT, C. J. (1982) Some comments on the evaluation of model performance. *Bulletin of the American Meteorological Society*, Lancaster, 63, 11, 1309-1313.

12. Bröde, P., Fiala, D., Błażejczyk, K., Holmér, I., Jendritzky, G., Kampmann, B., ... & Havenith, G. (2012). Deriving the operational procedure for the Universal Thermal Climate Index (UTCI). *International journal of biometeorology*, 56, 481-494.

13. INTERNATIONAL ORGANIZATION FOR STANDARDIZATION. ISO 7726. *Ergonomics of the thermal environments – Instruments for measuring physical quantities*. Genève: ISO, 1998.

14. Jamei, E., Rajagopalan, P., Seyedmahmoudian, M., & Jamei, Y. (2016). Review on the impact of urban geometry and pedestrian level greening on outdoor thermal comfort. *Renewable and Sustainable Energy Reviews*, 54, 1002-1017.

15. Krüger, E. L., Minella, F. O., & Rasia, F. (2011). Impact of urban geometry on outdoor thermal comfort and air quality from field measurements in Curitiba, Brazil. *Building and Environment*, 46(3), 621-634.

16. Elzeni, M., Elmokadem, A., & Badawy, N. M. (2022). Classification of urban morphology indicators towards urban generation. *Port-Said Engineering Research Journal*, 26(1), 43-56.

17. Yan, H., Wu, F., Nan, X., Han, Q., Shao, F., & Bao, Z. (2022). Influence of view factors on intra-urban air temperature and thermal comfort variability in a temperate city. *Science of The Total Environment*, 841, 156720.

PLEA 2024 WROCŁAW
(Re)thinking Resilience

The lighting effects in Burgos Cathedral (Spain):

Virtual reconstruction, using software tools, of the hierophanies generated within the Conception Chapel in the 15th century.

EZEQUIEL USON[1] JOSE ANTONIO GARATE[2] VICTOR JORGENSEN[3] EVA ESPUNY[4]

[1]Ezequiel Uson, UPC Sénior, Barcelona, Spain
[2]José Antonio Garate, Historian, Burgos, Spain
[3]Victor Jorgensen, Architect, Burgos, Spain
[4]Eva Espuny, Architect, Barcelona, Spain

ABSTRACT: Special lighting effects, popularly known as "miracles of light" are generated at the solstices or equinoxes in three medieval churches located in the Spanish city of Burgos and its surroundings. These hierophanies can be observed in religious buildings which were designed and constructed by medieval architects associated with what is known as the "Taller de los Colonia" formed by Juan de Colonia, his son Simon and his grandson Francisco. The premise of this research is that the same lighting effects were also generated in the Capilla de la Concepción, Chapel of Burgos Cathedral (Figure 1), and were visible before the Capilla de Santa Tecla was built in the 18th century. The latter, which was built onto the southwest side of the existing chapel, blocked the oculus that had previously allowed the entry of the sunlight which had illuminated its interior altarpiece at the equinoxes. This paper virtually reproduces the lighting effects that would have been observed in the 15th century. It does so by using solar simulation software tools and, to provide a better understanding, describes the knowledge of geometry and astronomy that would have been required of the architects responsible for these works.
KEYWORDS: Lighting effects, Taller de los Colonia, Burgos Cathedral, Capilla de la Concepción, Solar simulation software.

1. INTRODUCTION

Burgos Cathedral is one of the most notable examples of religious architecture in Spain. It is located at the foot of the Cerro del Castillo (castle hill), on the Camino de Santiago (Way of Saint James), on a site on which a Romanesque cathedral had previously stood. It is the result of a long construction process that began in 1221 and lasted until the 18th century. Although the French-influenced Gothic architectural style predominates, the building combines other artistic trends with rather unique harmony. In 1984, the cathedral was declared a UNESCO World Heritage Site.

Juan de Colonia (c.1410-c.1479) played an important role in the late Gothic phase of the cathedral's construction. This master builder, who was of German origin, revolutionized the architectural panorama of Burgos in the mid-15th century. It is said that he arrived in Burgos in 1440, having been brought there by Bishop Alonso of Cartagena, on his return from the Council of Basel, and was commissioned to finish off the towers of the cathedral by adding two openwork spires based on Central European models. He built the spires (1442-1458) in the main building and also a spectacular dome to go with them (c.1470). However, the latter collapsed in 1539 and was subsequently replaced by the Renaissance dome that can be seen today. Juan de Colonia is also credited with the construction of the *Capilla de la Visitación* (Chapel of the Visitation) (c.1440-1442), the parapet of the triforium, and the design of the *Capilla de la Concepción* (Chapel of the Conception) (c.1477) [1].

His son, Simón de Colonia (c.1450-1511), is a key figure in late Gothic architecture in Burgos. His work is characterized by the introduction of innovative roofing systems and the significant role of sculptural decoration. He would have been trained in his father's workshop, succeeding him as master builder of the cathedral and being responsible for completing projects that his father had begun before his death, such as the Conception Chapel in Burgos Cathedral or the Miraflores Charterhouse chapel.

The workshop of Colonia particularly stands out for its ability to incorporate the phenomenology of light, which was something that had great importance in the medieval Christian imagination. They had bequeathed to posterity the hierophanies visible in the churches of San Juan de Ortega, Santa María de Miraflores and San Nicolás de Bari, all of which are located in the city of Burgos and its surrounding area. These lighting effects, which are popularly known as the "milagros de la luz" (miracles of light), had the purpose of emphasizing the stories represented by the sculptural groups found inside the respective buildings. These cannot have

been the product of accident or coincidence, as they are found in three different churches. They were therefore the result of deliberate interventions and always coincide with the solstices or equinoxes of the astronomical calendar.

2. LIGHTING EFFECTS IN THE CAPILLA DE LA CONCEPCION OF BURGOS CATHEDRAL

In the Capilla de la Concepción, or Capilla de Santa Ana, of Burgos Cathedral (1477-1488), visitors' attention is drawn to a blinded oculus located in the highest part of the southwest wall, just in front of the altarpiece, which was made by Gil de Siloe (1483-1486), on the northeast wall. Its function was probably not only to illuminate the chapel since this had already been achieved by the large Gothic stained-glass window in its northwest side and by another opening to the southeast. (Fig. 3).

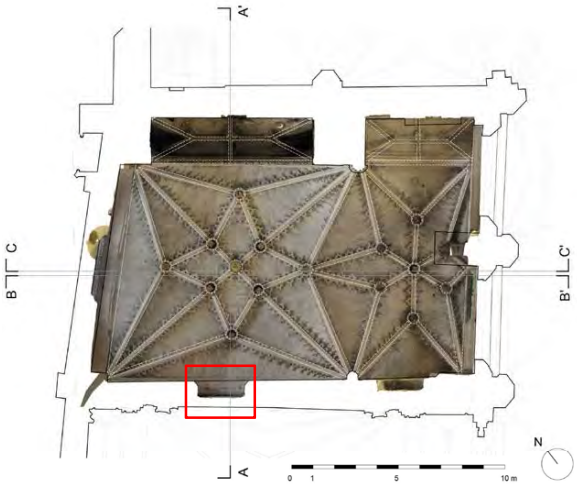

Figure 1: Plan of the Capilla de la Concepcion, obtained from a digital scan. On the south wall, it is possible to observe the blinded oculus, while the altarpiece is located in the north wall. Inside, the projection of the vaults is visible.

The construction of this chapel (Fig. 1) has traditionally been attributed to the architects of the Taller de los Colonia. Juan de Colonia started this work and his son Simón finished it. During the first half of the 18th century, the Capilla de Santa Tecla was built by demolishing four small Gothic chapels, of lower height, that had previously stood on this site (Fig.2). The new chapel was built onto the southwest side of the Capilla de la Concepción and - as a consequence - the oculus that had previously allowed the entry of sunlight was blocked (Fig.3).

Based upon this, the hypothesis that the oculus could have been specifically designed with the purpose of generating similar lighting effects to illuminate the interior altarpiece on certain special occasions (Fig. 4) would not seem unreasonable, particularly as this also occurs in the three others, previously mentioned, churches designed by the Taller de los Colonia. Based on this hypothesis, the current research was undertaken with the objective of demonstrating that what was initially a product of intuition could, in fact, constitute a reasonable premise. To demonstrate this, it was necessary to reconstruct the past by virtually recreating the lighting effects that would have been seen inside this chapel in the 15th century. This was possible using solar simulation software and applying an appropriate methodology [2].

Figure 2: Sequence of the construction of the Capilla de la Concepción in the15th *century and that of Santa Tecla, in the 18thcentury, starting from the transept*

Figure 3: Section AA'. The position of the blinded oculus of the Capilla de la Concepcion, in the central image, to the right of the Capilla de Santa Tecla and to the left of the north transept.

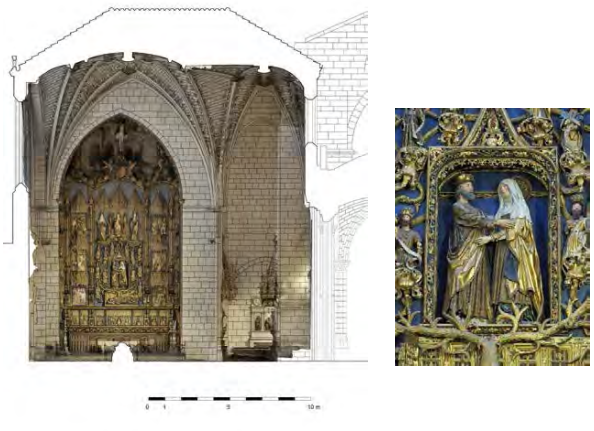

Figure 4: Section CC'. The Gil de Siloe altarpiece (1483-1486), located in front of the walled oculus. The image on the right shows a detail from the main sculptural group: the embrace between Saint Joachim and Saint Anne, the parents of the Virgin Mary.

3. THE CREATION OF LIGHTING EFFECTS IN MEDIEVAL CHURCHES.

The positioning of openings in the walls of religious buildings in order to generate lighting effects on specific dates of the astronomical calendar served a theological purpose: it demonstrated the importance that the "theology of light" had in the medieval Christian imagination. In medieval art and architecture, light acquired a transcendent significance, being used to symbolise what was sacred and as a manifestation, or expression of God [3]. As a result, in some medieval churches, on certain days of the astronomical calendar, which often corresponded to solstices or equinoxes, "light effects" were generated to accompany liturgical acts. The creation of these lighting effects was not the product of mere chance, but rather the result of the resolution of three different types of problems in the design and construction of the building [4].

- An astronomical problem: the alignment of the building with visible points on the horizon that coincided with the rising, or setting, of a certain celestial body (whether the sun, planets, stars or the moon) on certain specific dates of the liturgical calendar.
- A geometric problem: the positioning of the openings and their relationship with the floor plan and elevation of the building, so as to ensure that the entry of sunlight on specific dates illuminated certain sculptural groups inside the building.
- An ornamental problem: the design and positioning of the sculptural elements so that a specific image was illuminated by rays of sunlight on a specific day of the astronomical calendar.

It is evident that medieval architects had the knowledge of astronomy and geometry that was required to generate these lighting effects. Although we do not know exactly all the geometric canons they used, their training, which was acquired in monastic and cathedral environments, was organised into two blocks: the trivium (three ways) and the quadrivium (four ways) [5]. This knowledge dated back to ancient times. It was included in "the seven liberal arts" that had been taught in the classical world and was transmitted to the medieval world via successive translations and reproductions of ancient texts. This transmission of knowledge also occurred at Burgos Cathedral. Some of these liberal arts were represented on the archivolts of the Puerta del Sarmental (Sarmental Portal) (c.1235-1240), next to the cathedral school. In the Middle Ages, this school would have been housed in the old Episcopal palace [6]. References to geometry, music, grammar and rhetoric have been identified on these archivolts and it is known that in some cathedrals the great architects of the Gothic period were represented as geometers, with compasses and measuring rods in their hands (Fig.5).

Figure 5: A sculpture representing a geometer, which can be seen on the Puerta del Sarmental (c.1235-1240), of Burgos Cathedral. On it, two schoolchildren contemplate how their teacher draws figures using a measuring rod and a compass (which has since "disappeared") on a drawing board.

4. A HYPOTHESIS ABOUT THE GEOMETRIC TOOLS AND PROCEDURES USED BY MEDIEVAL ARCHITECTS TO ACHIEVE LIGHTING EFFECTS.

In order to determine the path followed by a ray of sunlight, Gothic architects used simple geometric operations and then transferred their results to real-scale layouts on the ground. They worked with tools such as the gnomon (Fig. 6a), the astrolabe, the analemma of Vitruvius, and Ptolemy's analemma. These tools enabled them to determine the azimuth at sunrise on any day of the year and also the celestial coordinates corresponding to different times during the day. With these instruments, a knowledge of Euclidean geometry [7], the help of scale models - including very basic, simplified graphs- and setting out two similar right-angled triangles, they were able to use Thales's theorem to measure any height by simply working with a gnomon (Fig.6b). A good architect could then choose the exact position of openings that, when placed at topologically significant points, would produce surprising lighting effects.

a) Image taken from Vilas-Estévez [8]

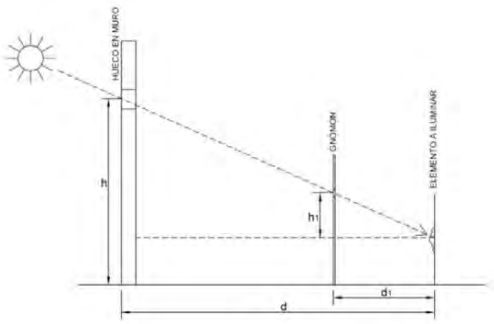

b)

Figure 6, a) and b): Determination of the height of the opening using Thales's theorem: the height of the opening in the exterior wall of the building is obtained by applying the formula h=dxh1/d1, in which d1 = the distance between the gnomon and the shadow cast, h1 = the height of the gnomon's perforation, and d = the distance between the shadow cast and the wall in which the opening must be made.

5. VIRTUAL RECREATION OF THE PAST USING SOLAR SIMULATION SOFTWARE.

A precise methodological process was applied to virtually recreate the lighting effects that were generated in the Capilla de la Concepción before the oculus located in the southwest wall was bricked up. The methodological process includes the following steps:

- The elevation of the *Capilla de la Concepción* was determined from a digital scan. A restitution was then obtained, using the SketchUp program, [9] based on a point cloud (Figure 1)
- The position of the chapel was then established by marking the azimuth of the main axis of Burgos Cathedral and by determining its geographical coordinates.

The geographical coordinates of the cathedral were obtained using Google Earth: 42º20'26''N 3º42'16W, as was the orientation of the main axis of the building: 221º, measured clockwise from the north.

- An EPW (Energy Plus Weather) file was then created with the software Meteonorm V8 [10], once the exact position of the Capilla de *la Concepción* chapel had been determined from its geographical coordinates.

- A first approximation of a stereographic solar diagram was then prepared using the Andrew March App (Fig. 7).

To determine the days and times on which the images would have been illuminated by the sun, we used Andrew Marsh's "Sun-path App" [11], applying it to a three-dimensional survey of the chapel (Fig. 8). Doing this, it was possible to obtain an initial approximation of the day and time on which the altarpiece would have been illuminated by sunlight. This then allowed us to determine the azimuth and solar height corresponding to the period studied. In this case, it turned out that the sculptural group that represents the embrace between Saint Joachim and Saint Anne would have been illuminated by the sun's rays at the spring and autumn equinoxes, when the sun had an azimuth of 222.58º and a height of 39º

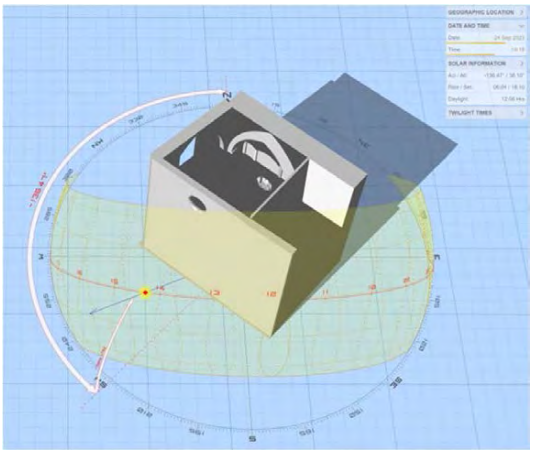

Figure 7: *The depiction of the sun path created using Andrew Marsh's App.*

- Previous determination of the days on which the sculptural group would have received direct sunlight.

In order to simulate the different times of the year, the 3D survey of the chapel and the climate file were imported into Archiwizard V8 software [12]. The spring equinox currently occurs in the northern hemisphere between March 20th and 21st, while the autumn equinox is between September 22nd and 23rd. According to the simulation of direct annual solar radiation run using the Archiwizard V8 software (Fig. 9), which included placing a solar receiver on the central sculptural group, this monument would have received direct sunlight for a few days in the second half of March and in the second half of September, coinciding with the two equinoxes.

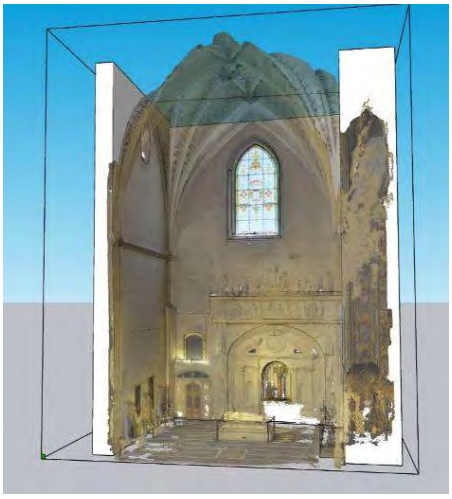

Figure 8: Three-dimensional survey of the Capilla de la Concepción, obtained from a digital scan.

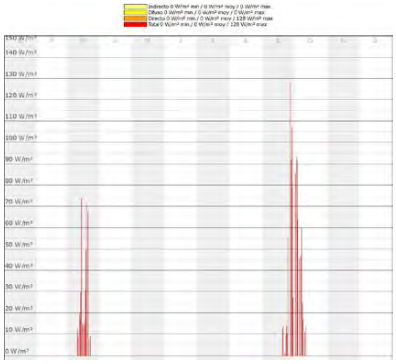

Figure 9: Mapping the reception of direct sunlight by the sculptural group representing "El abrazo de San Joaquín y Santa Ana".

- Reproduction of the lighting effect produced by the path of the sun for one hour.

The image shows that this sculptural group would have received its maximum amount of sunlight in March, at between 3 p.m. and 4 p.m. UTC (EU winter time), which would have corresponded to between 2 p.m. and 3 p.m. in solar time. Similarly, in September, it would have received the impact of direct sunlight at between 4 p.m. and 5 p.m. UTC (EU summer time), which would have corresponded to between 2 p.m. and 3 p.m. solar time (Fig.10 and Fig. 11).

Figure 10: Path of sunlight illuminating the sculptural group representing "El abrazo de San Joaquín y Santa Ana" between 2 p.m. and 3 p.m. on March 20th and September 22nd. Image obtained from a simulation run using Archiwizard V8 software.

Figure 11: Simulation of the impact of the sun's rays that the sculptural group representing "El abrazo de San Joaquín y Santa Ana" would have received at 2:34 p.m. (solar time) on March 20th and September 22nd.

a)

b)

Fig 12a) and b): Reproduction of the lighting effect that would have been generated by sunlight striking the sculptural group representing "El abrazo de San Joaquín y Santa Ana" on the altarpiece of the Capilla de la Concepción. This would have occurred at the equinoxes. These images were obtained from a textured digital scan on the Rhinoceros software under the same sun settings.

6. CONCLUSION

In medieval art, light takes on a transcendent meaning; it is used as a symbolic reference to the sacred, as a manifestation or expression of God. In reality, this idea has its origins in the early days of Christianity, in the numerous references found in the Gospels. It later passed through the Church Fathers and endured throughout the Middle Ages. In the case of the Capilla de la Concepción of Burgos Cathedral, which was the object of this investigation, the symbolic charge would be representing divine intervention in a miraculous conception.

When it comes to finding an image that effectively conveys the idea of the immaculate conception of Mary, in the Hispanic medieval context, the elegant theme of the embrace of her parents at the Golden Gate of Jerusalem ended up prevailing. After many years of marriage, Joachim and Anne had not been able to have children. One day, Joachim was reproached for this reason while presenting his offering in the temple of Jerusalem, after which, dejected, he retired to the desert. Then, they both received a visit from an angel, who announced to them that they were expecting a child and that she was going to be exceptional. Joachim and Anne then went to celebrate the good news together with a reunion that took place at the Golden Gate of Jerusalem. By focusing, therefore, the sunlight on the theme of the Embrace before the Golden Gate, the divine intervention in the immaculate conception of Mary would be staged.

If we manage to abstract ourselves from the excessive current electric lighting, very far from the lighting designed by the creators of the chapel, we can imagine the great expressiveness that the luminous phenomenon would achieve. The prevailing twilight in this cathedral space at sunset would intensify the beam of light that penetrated through the western oculus. This would make the polychrome and gilded elements of the illuminated altarpiece shine, making them stand out powerfully from the rest. In addition, the colourful vault, with the presumably azure-painted webbing and the gilded ribs that emerge from them, would further increase the visual impact of the phenomenon.

Considering its connection with the spring equinox (celebrated on March 25th), the phenomenon would coincide with the vespers service (around six in the evening). Contemplating the gradual illumination of the scenes of the capital during such significant dates and at such a liturgical moment had to constitute a very suggestive experience.

The architects of the Taller de los Colonia had to establish where the oculus generating the light source needed to be opened and the dimensions and shape required to project a circular image on the illuminated figures. They must also have calculated where and how the figures needed to be located at the altarpiece and how the sculptural elements had to be designed in order to achieve spectacular lighting effects on certain specific dates of the astronomical calendar. The apparent intentionality behind this phenomenon would seemingly imply that the configuration of the altarpiece was also determined by the desired lighting phenomenon. Organising this would have called for considerable rapport between the architect and the sculptor.

Finally, it should be underlined that the use of simulation methodology combined with solar software tools allowed us to demonstrate the validity of the hypothesis formulated for this research. The intentionality behind the lighting effects generated on the altarpiece of the Capilla de la Concepción on certain designated dates of the Julian astronomical calendar, which was then in use, has been clearly demonstrated. This was evident prior to 1734 when, as a consequence of the construction of the adjacent chapel of Santa Tecla, the light source was blocked.

ACKNOWLEDGEMENTS

I would like to give special thanks to the Chapter of Burgos Cathedral for facilitating access to the cathedral and for enabling us to obtain and process all of this information.

REFERENCES

1. Ibáñez, A. C. and Payo, R. J. (2008). *Del Gótico al Renacimiento. Artistas burgaleses entre 1450 y 1600*, Burgos: Caja Círculo (p. 65).

2. Uson,E. (2023). Deciphering the Greek Temple: Verification with Software Tools of the solar Design of the Parthenon in Athens and the Temple of Zeus in Olympia. in *European Journal of Architecture and urban Planning* London.UK, Vol2 , Issue 1, January, 2023 (pp 9-18). Available: http://dx.doi.org/10.24018/ejarch.2023.2.1.19 .

3. Nieto, V. (1989). *La luz, símbolo y sistema visual. El espacio y la luz en el arte gótico y del Renacimiento*, Madrid: Cuadernos Arte Cátedra (pp. 13-14).

4. Incerti, M. (2012). Astronomical Knowledge in the Sacred Architecture of the Middle Ages in italy in Nexus Ntw-Vol 15, nº3 ,2013 ,(pp.503-526) Kim William Books, Turin.

5. McClusley, S.C. (1993). Astronomies and rituals at the Dawn of the Middle Ages *in Astronomies and cultures.III Oxford International Symposium on Archeoastronomy* Colorado: University press of Colorado. Niwot. (pp.100-123).

6. Sánchez Ameijeiras R. (2001). La portada del Sarmental de la catedral de Burgos. Fuentes y fortuna, Barcelona: Matèria. Revista internacional d'Art, número 1, (pp. 171-181) Barcelona: Publicacions i Edicions de la Universitat de Barcelona.

7. Barnabas, H. (2008). (ed), Fibonacci's De Practica Geometrie, in *Sources and Studies in the History of Mathematics and Physical Sciences* . New York: Springer . . Available at I:https://doi.org/10:107/978-0387-72931-2

8. Vilas-Estevez, B. Varela R. Gonzalez –Garcia, AC (2018). Illumination effects at the Cathedral of Saint James. (Galicia) First results. in *Mediterranean Archaeology and Archaeometry*, vol.18, Nº4 (pp251-258), Greece.

9. SketchUp Software, available online at http://www.sketchup.com

10. Meteonorm software, available online at http://meteonorm.com/en

11. Andrew March Software, available online at https://andrewmarsh.com/software/

12. Graitec Archiwizard Software available online https://7Fr.Graitec.com/Archiwizard

PLEA 2024 WROCŁAW
(Re)thinking Resilience

A Comparative Analysis of the Effectiveness of Nature-Based Stormwater Management Solutions at the Neighbourhood Scale

YU CHEN[1]; JACOPO GASPARI[1]; LIA MARCHI[1]; ERNESTO ANTONINI[1]

[1]University of Bologna, Department of Architecture, Bologna, Italy

ABSTRACT: Water is a primary resource for humans to live; however, due to the high urbanization and the effects of Climate Change, impervious urban surfaces have largely increased, which easily leads to flood problems during intense rain events, threatening the resilience of the built environment and communities. Nature-Based solutions (NBSs) are deemed as effective means to address water-related hazards; furthermore, they can contribute to climate change adaptation and mitigation, thus improving urban resilience. However, their effective planning and implementation is still difficult because it lacks a comprehensive framework for their integration in existent environments. This paper aims to pave the ground for future studies on this gap and explore integrated hydrological contributions for designing resilient cities. To accomplish this, the authors compare the effectiveness of the most popular Nature-Based stormwater management solutions (green roofs, rain gardens and vegetated swales) at the neighbourhood scale according to two relevant hydrological performance indicators: runoff volume reduction and peak flow reduction. It also evaluates their contribution to urban resilience with relevant resilience indicators. In conclusion, these three solutions show high efficiency in managing stormwater but vary in contributing to resilience performance regarding their own characteristic.
KEYWORDS: Nature-Based Solutions, runoff volume reduction, peak flow reduction, stormwater management, urban resilience

1. INTRODUCTION

In recent years, many countries such as Italy, Germany, Belgium, the UK, and the US have suffered the effects of intense rain events as a consequence of Climate Change (CC). At the same time, developing countries such as China have also experienced severe floods because of the high demand for rapid development, which led to a sharp increase in urban impervious surfaces. This rise in the percentage of sealed soils has changed urban hydrological systems, accelerating the frequency and severity of water-related hazards [1]. Furthermore, the Intergovernmental Panel on Climate Change (IPCC) alerts that changes in precipitation will harshen with every degree of global warming, increasingly leading to flooding. This will pose great risks to both people and the built environment [2]. As a response, the resilience concept emerged to help cities adapt to climate disasters and improve their capacity to tackle hazards, among which flooding. Hence, cities are searching for new and effective solutions to move towards more resilient settings, and stormwater management emerges as a crucial field of action in this regard [3]. Among the most popular stormwater management strategies, Nature-Based Solutions (NBSs) have been proven to effectively address water-related challenges and simultaneously provide multiple environmental, economic and social benefits. However, effective planning and implementation of NBSs is still difficult because it lacks a comprehensive framework for their integration in existent environments [4].

This paper offers a comparative analysis of the effectiveness of the most popular NBSs based on common hydrological performance indicators that are suitable for measuring solutions at the roof level and also solutions at the ground level at the neighbourhood scale. The aim is to pave the ground for future studies on the potential integration of roof and ground level solutions to enhance stormwater management system for managing urban water-related challenges and, at the same time, improving to urban resilience.

2. NATURE-BASED SOLUTIONS FOR STORMWATER MANAGEMENT

Conventional stormwater management, also known as grey infrastructure, such as curbs, gutters, and pipes to collect, convey and treat stormwater, have been proven inadequate to changing environmental conditions [5]. So, cities have been exploring new ways, such as sustainable drainage system (SUDS), best management practice (BMP), low impact development (LID), water-sensitive urban design (WSUD), blue and green infrastructure (BGI) and the sponge city concept (SC) [6]. These terms

have been used to define similar concepts of NBSs in different parts of the world, which are “inspired by, supported by, or copied from nature”, and they use or mimic natural processes to control surface runoff volumes and timing, thereby mitigating the potential for flooding during intense rain events [7].

In recent decades, NBSs have received increased attention especially for their side-benefit on urban resilience. NBSs can indeed contribute to city resilience by leveraging on natural or ecological retention, detention, infiltration, and drainage potentials while improving outdoor microclimate thanks to the evapotranspiration capacity of natural elements. NBSs such as green roofs (GR), constructed wetlands (CW), rain gardens (RG), permeable pavements (PP) and vegetated swales (VS) have been widely implemented in cities for managing stormwater. Among them, green roofs, rain gardens and vegetated swales are the most recurrent solutions for water management at the neighbourhood scale. Green roofs are of high value because roof surfaces account for 40-50% of all impervious surface areas in developed urban areas [8]. Besides their hydrological performance, GRs can improve the thermal performance of buildings, contribute to mitigating the urban heat island, and improve air quality by capturing dust particles, etc. Rain gardens not only play a major role in rehabilitating the water cycle but also help promote well-being with nature; they work very well in addressing rainwater and enhancing biodiversity and ecosystem resilience. Vegetated swales are usually used to convey stormwater runoff, they can capture pollutants and attenuate runoff volumes, they simultaneously provide a variety of environmental benefits as well as improvement in biodiversity and amenity [6,9].

Their effectiveness has been largely studied in the literature, but mainly focusing on single solution at a time, while a systemic approach would allow their better integration and functioning. Many authors have indeed pointed out that these solutions have limits by their own [3]. For example, Ercolani et al. [10] illustrated that green roofs perform more effectively in smaller-magnitude frequent storms. Ishimatsu et al. [11] reported that rain gardens are more suitable to handle small discharges of rainwater. Ruangpan et al. [12] pointed out that vegetated swales could work much well during heavier and shorter rainfall events. However, these limits might be overcome if the solutions are synergically combined and connected with other urban features and requirements.

3. METHODOLOGY AND MATERIALS

The methodology of this study (Fig. 1) consists of three main phases. Phase 1 is to find the common hydrological performance indicators of green roofs, rain gardens and vegetated swales separately from the existing literature and select the two most relevant for the neighbourhood scale. Phase 2 is to retrieve data from the scientific literature and applicative case studies to quantify (or set feasible value ranges) the performance of these solutions according to the two indicators and make them comparable. Given additional benefits that the solutions bring in terms of resilience, phase 3 links the outcomes from phase 2 with a set of relevant resilience indicators. On this basis, intuitive radar charts are produced to help choose the best solution/combination of solutions case by case.

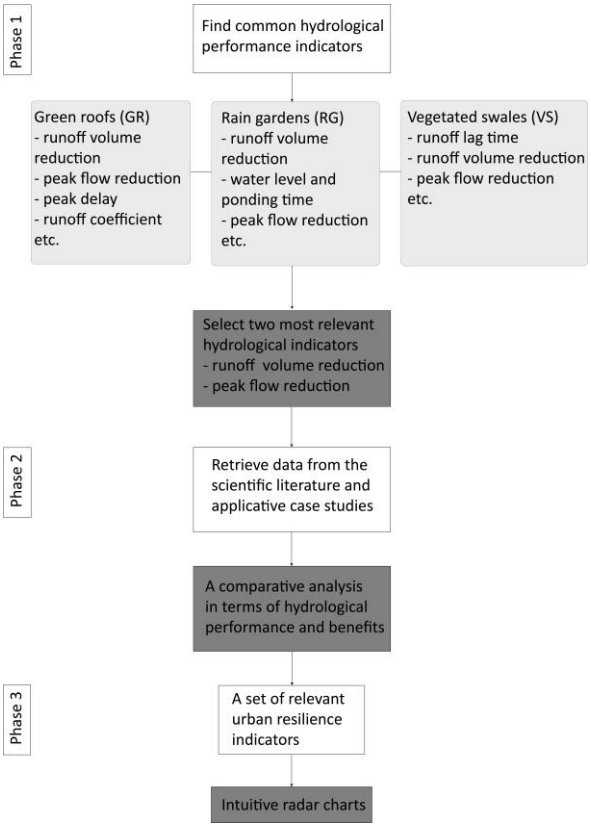

Figure 1: Methodological flow of this study. White rectangles represent phase and aim, light grey rectangles represent activity, and dark grey rectangles represent the output.

Regarding the first phase, several indicators from the existing literature can be used to assess the hydrological performance of these NBSs individually. For the study of the hydrological performance of green roofs, the indicators found in the literature were runoff volume reduction, peak flow reduction, peak delay, runoff coefficient and peak attenuation, etc. For rain gardens hydrological performance indicators, runoff volume reduction, water level and ponding time, peak flow reduction, infiltration rate, peak flow delay time, etc; indicators such as runoff lag time, runoff volume reduction, peak flow reduction, soil drainage capacity, etc, are used to evaluate the hydrological performance of vegetated

swales. Phase 1 lists: i) runoff volume reduction, ii) peak flow reduction, iii) peak delay, iv) runoff coefficient, v) water level and ponding time, vi) runoff lag time. Indicators i) and ii) have been especially investigated in recent years both in research projects and applicative case studies, runoff volume reduction refers to through implementing NBSs, how much stormwater runoff volume can be reduced compared to an impervious surface, and peak flow reduction is widely used measure of stormwater impact because it is associated with the maximum erosion damage [13]. These two indicators are selected because they are more direct and comprehensive for understanding their reduction rates before and after the implementation of NBSs, but significant variations in performances are detected depending on the study. That is why a systematic comparison would help extract proper performance range or values.

Despite pertaining to different levels (green roofs to the roof level and rain gardens and vegetated swales to the ground level) these solutions can be measured with common hydrological performance indicators – i) runoff volume reduction and ii) peak flow reduction. On this basis, the three solutions are further analysed assuming a comparative approach for the selected indicators i) and ii) (phase 2), the results are comprised of a reliable range of functioning (and average values) for each solution (Table 2).

Then, given that NBSs for water management are nowadays preferred to conventional grey infrastructure for their additional support to urban resilience, the solutions are analysed further by retrieving their benefits from the literature and linking them with a set of relevant resilience indicators for cities. The relevant resilience indicators are selected from the work by Feldmeyer et al. [14] and combined with Sharifi and Yamagata [15]. The indicators cover multiple dimensions of urban resilience, and they can be divided into five main categories and corresponding action fields, each action field refers to one resilience indicator, ranging from the water management category to biodiversity, air quality, maintenance, costs, and social issues (Table 1).

Table 1: Dimensions and action field of the resilience evaluation.

Dimension	**Action field**
Environment	Soil and green spaces
	Water management
	Biodiversity
	Reduction of environmental impacts (air, temperature, energy, etc)
Infrastructure	Robustness and redundancy of critical infrastructure
	Infrastructure efficiency
Economy	Economic structure
	Dynamism
Society	Research projects
	Knowledge and risk competence
	Community bonds, social support, and social institutions
	Safety and well-being
Governance	Participation and collaboration
	Management of resources
	Strategy, plans and environment
	Education and training

Resilience indicators related to the environmental dimension are mainly associated with availability, quality, accessibility, and conservation. NBSs can mitigate adverse environmental impacts (urban heat island, air pollution, etc), reduce flood hazards, and provide ecosystem services to enhance the resilience of the neighbourhood. NBSs related to infrastructure resilience are about the multi-functionality of spaces and facilities, regular monitoring, maintenance and upgrade. The economic dimension of urban resilience includes indicators of employment rate and job opportunities, while dynamism means investment in green jobs and the economy. Relevant resilience indicators in society refer to social attention to extreme rain events or flooding, experience, and available information. Furthermore, implementing NBSs can strengthen community bonds and improve safety and well-being, both physical and psychological health. With reference to governance, resilience related to NBSs is mainly about multi-stakeholder planning and decision making, cross-sector collaboration, investment, resources management, strategies planning for water-related challenges, and educational activities.

Results from phase 3 will be shown by means of intuitive radar charts. The rating for these five dimensions is from 1 to 5, where 1 shows poor performance and 5 shows excellent performance. For dimensions which have four action fields, each account for 25%, while for dimensions which have two action fields, each account for 50%. So taking the environmental dimension as an example, if sums up to 100%, it equals to 5.00 in radar charts; if sums up to 75%, it equals to 3.75; if sums up to 50%, it equals to 2.50 in radar charts; if sums up 25%, it equals to 1.25 in radar charts. Overall results are discussed basing on the outcomes of the comparison and detected limitations.

4. RESULTS AND DISCUSSION

4.1 Analysis of phase 1 and phase 2

Table 2 shows the comparative analysis of three selected solutions – GRs, RGs and VSs based on runoff

volume reduction and peak flow reduction – these two hydrological performance indicators for stormwater management.

Table 2: A comparative analysis of selected solutions (extract).

Solution	Runoff vol. red. (%)	Peak flow red. (%)	Reference or case study
1. GR	80	80	Residential area in Beijing (CHN) [16]
	68	89	University campus in Michigan (US) [17]
	…	…	Other case studies not included here
	70	86	Average value
2. RG	50	48	Joinville neighb. (BR) [18]
	53	-	Residential neighbourhood in Colorado (US) [19]
	…	…	Other case studies not included here
	52	45	Average value
3. VS	55	40	Luleå neighb. (SE) [20]
	64	74	Parking lot in Auckland (NZL) [21]
	…	…	Other case studies not included here
	58	55	Average value

From the above table, it emerges that green roofs are the most effective of the three solutions; the average value for runoff volume reduction and peak flow reduction is 70% and 86%, respectively, while much higher than the average value of rain gardens and vegetated swales. This result is also in correspondence to the average range from the existing literature review in general, green roofs can reduce stormwater runoff volume by 30-86%, reduce peak flow rate by 22 to 93% [13]; rain gardens can reduce surface runoff by 25-69% and peak runoff by 12-71% [6]; swales can reduce runoff volumes by 15%-82% and peak runoff rates by 4%-87% [22]. Carpenter and Kaluvakolanu [17] tested three full-scale roofs on the campus buildings and demonstrated the efficiency of green roofs compared with asphalt roofs and stone ballasted roofs; furthermore, different storm sizes also be monitored, and results indicated that green roof was highly efficient in capturing small storm events and was able to retain 68% of rainfall volume, while reduced peak discharge by an average of 89%. The rain garden built in a residential neighbourhood in Lakewood, Colorado, US, was monitored for three years and concluded that it can effectively reduce average runoff volume by 53% [19]. Fassman and Liao [21] monitored vegetated swales in New Zealand under 42 storm events and found that vegetated swales show effective control of stormwater runoff by reducing runoff volume by 64% and peak flow by 74%.

However, studies often use ideal state and boundary limitations which do not depict actual conditions. As in the case described by Yao et al. [16], who assume that rainwater can be drained from green roofs directly into the drainage system without infiltration losses. In real cases, rainwater flow from the roofs can pass over impervious surfaces (ground level), causing infiltration losses. Furthermore, the retention capacity of green roofs is limited when facing heavy storms; in this case, there is a high need to consider a combination of multiple solutions to make up for this deficiency.

Similar conclusions emerge for rain gardens. For instance, Goncalves et al. [18] tested and compared five different rain events for seven scenarios (single solution and combined solution) implementing decentralized stormwater controls and find that the scenario “Rain Garden_10 perc” (occupy 10% of the sub-catchment area) can work effectively as a single solution. However, the limitation of this study is it only considers single or two integrated solutions, and they are all at the ground level, while multiple choices (>2) or connect with green roofs may be much more effective.

Concerning vegetated swales, the same need to adopt a system approach stands out. Rujner et al. [20] performed a field experiment on a 30 meters section of an urban grassed swale in sandy soils by simulating 14 rainfall events of 30-minute duration. However, they did not consider the different soil types, which is instead a very important factor that affects the retention and infiltration of different rain events, not to mention the relevance of this choice to the range of possible urban functions that can be performed nearby.

The results, on the one hand, comprehensively demonstrate the effectiveness of the three considered solutions at the neighbourhood scale, and on the other hand, emphasize the necessity of implementing multiple solutions to compensate the inadequacies of a single NBS to deal with stormwater management and urban resilience effectively. Indeed, even if green roof shows the best average performance to water management and does not require extra urban land surface, compared to the other two solutions, it might be challenging to implement them in dense historical urban environments, where it might be easier to implement rain gardens or vegetated swales in public or private outdoor spaces (e.g., gardens).

4.2 Analysis of phase 3

Table 3 shows the urban resilience evaluation based on these three solutions with multiple benefits – environmental, social, and economic impacts.

Table 3: Assessment of three solutions for urban resilience indicators.

Action field	GR	RG	VS
Soil and green spaces (25%)	●	●	●
Water management (25%)	●	●	●
Biodiversity (25%)	●	●	○
Reduction of environmental impacts (air, temperature, energy, etc) (25%)	●	●	●
Mean score	3.75	3.75	2.50
Robustness and redundancy of critical infrastructure (50%)	●	●	●
Infrastructure efficiency (50%)	●	●	●
Mean score	5.00	3.75	3.75
Economic structure (50%)	●	●	●
Dynamism (50%)	●	●	●
Mean score	3.75	3.75	2.50
Research projects (25%)	●	●	○
Knowledge and risk competence (25%)	○	○	○
Community bonds, social support, and social institutions (25%)	●	●	○
Safety and well-being (25%)	●	●	●
Mean score	3.75	3.75	1.25
Participation and collaboration (25%)	●	●	●
Management of resources (25%)	○	●	●
Strategy, plans and environment (25%)	●	●	●
Education and training (25%)	●	●	○
Mean score	3.75	5.00	2.50

Note: ● – Likely valuable contribution to the criterion (>25%), ● – some potential contribution to the criterion (between 12.5% and 25%), ○ – very limited contribution to the criterion (< 12.5%).

The radar chart (Fig. 2) was created for the direct visual performance from the Table 3 results. The top of the polygon in Figure 2 represents Environment; the two wings of the polygon in the middle are Infrastructure and Governance; the two indices at the bottom reflect Economy and Society.

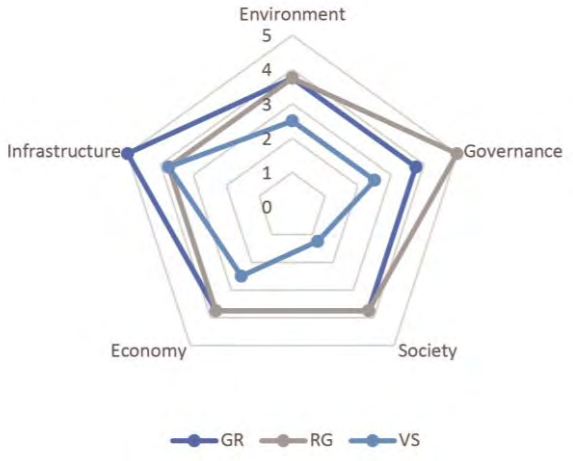

Figure 2. Intuitive radar charts for urban resilience evaluation.

From the intuitive radar charts, there are several important findings.

1) Green roofs and rain gardens show high value in the environmental dimension; green roofs can contribute to soil health, and intensive green roofs can be easily accessible with diverse plantings; besides water management benefits, they also help combat urban heat island and air purification, reduce noise and are biodiversity-friendly. Rain gardens are attractive landscapes and sustainable stormwater management solutions for residential areas serving various ecosystem functions. Vegetated swales act less compared to the other two.

2) For infrastructure dimensions, green roofs work best because they do not need extra space if implemented and can be applied in different urban density patterns; in addition, they perform well in thermal insulation and energy efficiency, thus contributing a lot to reducing the need for heating, cooling and electricity infrastructure. Rain gardens and vegetated swales can contribute to groundwater recharge, which is significant for maintaining groundwater levels and supporting local aquifers.

3) Implementing these stormwater solutions can create more green job opportunities because of the engineering and construction process, thus promoting economic development.

4) For the social dimension, all of these can strengthen the neighbourhood connection and promote safety and well-being. Still, citizens do not know much about these solutions, although scientific communities have devoted many research activities.

5) Rain gardens show the best performance in the governance dimension because they tend to get more willingness from the neighbourhood residents from the existing literature.

However, the limitation of the study is related to the subjectivity of selected resilience indicators and also the given scores.

5. CONCLUSION

Green roofs, rain gardens, and vegetated swales show high efficiency in managing stormwater based on runoff volume reduction and peak flow reduction but vary in hydrological performance regarding their design characteristics and facing different storm events. It is necessary to think about how to combine these solutions to find a balance between roof and ground levels based on the common hydrological performance indicators, thus maximizing the hydrological performance.

In addition, they also perform differently in terms of urban resilience evaluation. Current research focuses on linking its hydrological performance and urban resilience of each solution separately. While it could work much better to connect them together and increase the water retention and detention capacity, thus contributing to improving the cities' resilience in terms of climate change effects.

Therefore, if future studies can investigate how to integrate effectively green roofs with other stormwater solutions at the ground level based on the common hydrological performance indicators, both water retention capacity and urban resilience features can be significantly improved. To this regard, the study lays the foundation for developing a comprehensive framework capable of considering pros and cons of each solution and their optimal integration according to context conditions. Further steps are still under development to provide more precise outcomes.

REFERENCES

1. Senes, G., Ferrario, P. S., Cirone, G., Fumagalli, N., Frattini, P., Sacchi, G., & Valè, G. (2021). Nature-Based Solutions for Storm Water Management—Creation of a Green Infrastructure Suitability Map as a Tool for Land-Use Planning at the Municipal Level in the Province of Monza-Brianza (Italy). *Sustainability*, *13*(11), Article 11.

2. *IPCC — Intergovernmental Panel on Climate Change*. Retrieved 27 November 2023, from https://www.ipcc.ch/

3. Liu, W., Chen, W., & Peng, C. (2014). Assessing the effectiveness of green infrastructures on urban flooding reduction: A community scale study. *Ecological Modelling*, *291*, 6–14.

4. Nelson, D. R., Bledsoe, B. P., Ferreira, S., & Nibbelink, N. P. (2020). Challenges to realizing the potential of nature-based solutions. *Current Opinion in Environmental Sustainability*, *45*, 49–55.

5. Qiao, X.-J., Liu, L., Kristoffersson, A., & Randrup, T. B. (2019). Governance factors of sustainable stormwater management: A study of case cities in China and Sweden. *Journal of Environmental Management*, *248*, 109249.

6. Song, C. (2022). Application of nature-based measures in China's sponge city initiative: Current trends and perspectives. *Nature-Based Solutions*, *2*, 100010.

7. European Commission. (2015). https://data.europa.eu/doi/10.2777/765301

8. Mentens, J., Raes, D., & Hermy, M. (2006). Green roofs as a tool for solving the rainwater runoff problem in the urbanized 21st century? *Landscape and Urban Planning*, *77*(3), 217–226.

9. Sañudo-Fontaneda, L. A., Roces-García, J., Coupe, S. J., Barrios-Crespo, E., Rey-Mahía, C., Álvarez-Rabanal, F. P., & Lashford, C. (2020). Descriptive Analysis of the Performance of a Vegetated Swale through Long-Term Hydrological Monitoring: A Case Study from Coventry, UK. *Water*, *12*(10), Article 10.

10. Ercolani, G., Chiaradia, E. A., Gandolfi, C., Castelli, F., & Masseroni, D. (2018). Evaluating performances of green roofs for stormwater runoff mitigation in a high flood risk urban catchment. *Journal of Hydrology*, *566*, 830–845.

11. Ishimatsu, K., Ito, K., Mitani, Y., Tanaka, Y., Sugahara, T., & Naka, Y. (2017). Use of rain gardens for stormwater management in urban design and planning. *Landscape and Ecological Engineering*, *13*(1), 205–212.

12. Ruangpan, L., Vojinovic, Z., Di Sabatino, S., Leo, L. S., Capobianco, V., Oen, A. M. P., McClain, M. E., & Lopez-Gunn, E. (2020). Nature-based solutions for hydro-meteorological risk reduction: A state-of-the-art review of the research area. *Natural Hazards and Earth System Sciences*, *20*(1), 243–270.

13. Li, Y., & Babcock, R. W. (2014). Green roof hydrologic performance and modeling: A review. *Water Science and Technology*, *69*(4), 727–738.

14. Feldmeyer, D., Wilden, D., Kind, C., Kaiser, T., Goldschmidt, R., Diller, C., & Birkmann, J. (2019). Indicators for Monitoring Urban Climate Change Resilience and Adaptation. *Sustainability*, *11*(10), 2931.

15. Sharifi, A., & Yamagata, Y. (2016). Urban Resilience Assessment: Multiple Dimensions, Criteria, and Indicators. In Y. Yamagata & H. Maruyama (Eds.), *Urban Resilience* (pp. 259–276).

16. Yao, L., Wu, Z., Wang, Y., Sun, S., Wei, W., & Xu, Y. (2020). Does the spatial location of green roofs affects runoff mitigation in small urbanized catchments? *Journal of Environmental Management*, *268*, 110707.

17. Carpenter, D. D., & Kaluvakolanu, P. (2011). Effect of Roof Surface Type on Storm-Water Runoff from Full-Scale Roofs in a Temperate Climate. *Journal of Irrigation and Drainage Engineering*, *137*(3), 161–169.

18. Goncalves, M. L. R., Zischg, J., Rau, S., Sitzmann, M., Rauch, W., & Kleidorfer, M. (2018). Modeling the Effects of Introducing Low Impact Development in a Tropical City: A Case Study from Joinville, Brazil. *Sustainability*, *10*(3), Article 3.

19. Jiang, Y., Yuan, Y., & Piza, H. (2015). A Review of Applicability and Effectiveness of Low Impact Development/Green Infrastructure Practices in Arid/Semi-Arid United States. *Environments*, *2*(2), Article 2.

20. Rujner, H., & Leonhardt, G. (2016). *Advancing green infrastructure design: Field evaluation of grassed urban drainage swales*.

21. Fassman, E. A., & Liao, M. (2009). *MONITORING OF A SERIES OF SWALES WITHIN A STORMWATER TREATMENT TRAIN*.

22. Ekka, S. A., Rujner, H., Leonhardt, G., Blecken, G.-T., Viklander, M., & Hunt, W. F. (2021). Next generation swale design for stormwater runoff treatment: A comprehensive approach. *Journal of Environmental Management*, *279*, 111756.

PLEA 2024 WROCŁAW
(Re)thinking Resilience

Analysis of Air Velocity, Pressure Coefficient and Pollutant Dispersion in Generic Models of Urban Canyons with Computational Fluid Dynamics

CAROLINA GIROTTI[1], AMANDA SAYURI OIZUN[2], SAMUEL B. MELO NAZARETH[1], FERNANDO AKIRA KUROKAWA[2], ALESSANDRA R. PRATA SHIMOMURA[1]

[1] Faculty of Architecture and Urbanism of the University of São Paulo, São Paulo, Brazil
[2] Polytechnic School of the University of São Paulo, São Paulo, Brazil

ABSTRACT: In the urban environment, the urban form has a direct impact on the behavior of natural ventilation and the dispersion of atmospheric pollutants. The urban form and its interference in the behavior of natural ventilation and the dispersion of atmospheric pollutants is explored in this article through the simulation of four variations of urban canyon with H/W varying between 1.5 and 6. Thus, the objective of this work is to evaluate how the H/W influences the behavior of natural ventilation and atmospheric dispersion. The evaluation was carried out using the Computational Fluid Dynamics: OpenFOAM® software. The results indicate that H/W ratio the height of buildings and wind direction are the variables that most influence wind speed at pedestrian height, on the other hand, the distance between buildings and wind direction are the variables that most affect the pressure coefficient of facades and the dispersion of atmospheric pollutants.
KEYWORDS: Urban canyon, Computational Fluid Dynamics, Natural Ventilation, Pollutant dispersion

1. INTRODUCTION

Urban canyons are formed by buildings that create a canyon configuration between them, which affects the dynamics of natural ventilation in urban areas [1, 2].

Natural ventilation is important for renewing the air in dense urban spaces, as it helps to disperse air pollutants, reduce heat accumulation, and improve thermal comfort [3–5].

Among the factors that most influence natural ventilation in urban canyons is iterations in fluid dynamics induced by building predominantly manifest in the formation of recirculation zones in the lee of high-rise edifices, a phenomenon referred to as the wake effect. This effect extends beyond the immediate vicinity of the building, influencing not only the structural integrity of the building itself but also having significant implications for local health and air quality parameters [1, 3].

Others factors that influence natural ventilation can be considered: 1. stack effect, which occurs when the hot air inside the urban canyon is expelled upwards, while the colder air is drawn into the space, this vertical air movement promotes air circulation and renewal; 2. wind direction and speed, which play a crucial role in the natural ventilation of urban canyons; 3. urban form, which affects the pattern of natural ventilation, such that taller buildings can create more restrictions on airflow, while lower buildings allow more air intake; and 4. pressure facade coefficient (Cp), which measures the pressure difference between the windward and leeward sides of the buildings, affecting the cross airflow [1, 5, 6].

Numerous factors pertaining to urban morphology exert influence on the modification of flow zones within an urban locale. As per the research conducted by Azizi and Javanmardib (2017) and Guo et al. (2017), the primary determinants are the height and distance of buildings [7, 8].

Considering the relationship between urban canyons, natural ventilation and the dispersion of atmospheric pollutants, the authors Wang et. al. (2010) and Nazridoust & Ahmadi (2006) show that wind speed (Ws) plays a significant role in the dispersion of gaseous and particulate pollutants in street canyons, whereas higher Ws lead to reduced pollutant concentrations in canyons. Singh at. al. (2017) conducted a three-dimensional numerical simulation and observed higher concentrations of pollutants on the leeward side of the street canyon compared to the windward side [9–11].

Therefore, the objective of this article is to analyze Ws and Cp and an outline of the dispersion of atmospheric pollutants in urban canyons with different H/W ratios, with an ambient air velocity of 2 m/s, in three wind directions 0°, 45° and 90° for ventilation and in two directions 0° and 90° for dispersion of pollutants.

2. METHODOLOGY

The research methodology encompasses CAD modeling and Computational Fluid Dynamics (CFD) and is divided into six stages: 1. three-dimensional modeling, 2. mesh production, 3. definition of boundary conditions, 4. numerical calculation of the simulation, 5. simulation validation and 6. data analysis.

Within the ambit of this investigation, four distinct geometric scenarios representative of urban canyons were meticulously chosen. These scenarios incorporate height-to-width (H/W) ratios spanning 1.5, 3.0, and 6.0, as elucidated in Figure 1.

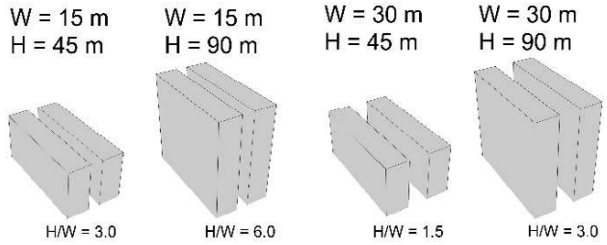

Figure 1: Urban canyons analyzed.

2.1. Computational Fluid Dynamics Simulation

To conduct the Computational Fluid Dynamics (CFD), the simulation domain was carried out with five times the height (h) of the buildings on the sides, top and outlet and fifteen times h in the inlet, with the objective of investigating only one wind direction, according to guidelines established by COST [12], as it shows in Figure 2.

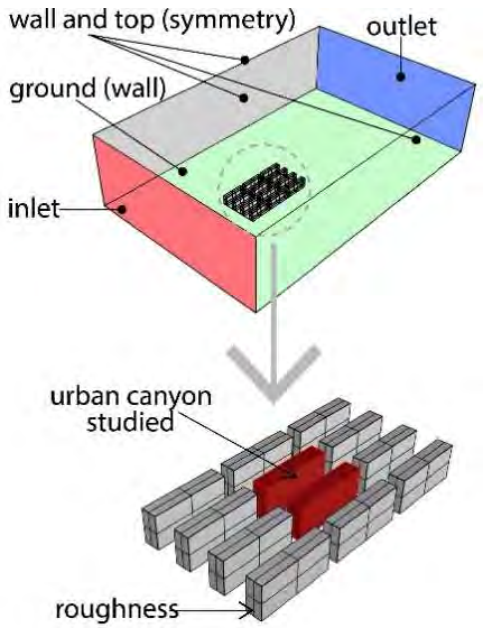

Figure 2: Simulation domain.

A mesh was made in Ansys using an unstructured methodology. The objective of this technique was to create prism-shaped elements in the vicinity of the terrain and structures, thereby enabling a more accurate analysis of the boundary layer's detachment properties. [13].

Five meshes were developed with the aim of validating the simulation through the mesh independence test and M3 was chosen for the development of the CFD simulation considering the best computational cost and stability in the results, as shown in Table 1 and Figure 3.

Table 1: Mesh independence test data

	M1	M2	**M3**	M4	M5
nodus	$3.5x10^4$	$8.4x10^4$	**$1.6\ x10^5$**	$2.8\ x10^5$	$5.3\ x10^5$
elements	$2.0x10^5$	$3.4x10^5$	**$5.5x10^5$**	$1.1x10^6$	$2.1x10^6$
min size	1,52	0,44	**0,33**	0,22	0,16
max size	304,00	89,00	**66,75**	44,50	32,30
average orthogonality	0,85	0,85	**0,87**	0,86	0,86
average skenews	0,24	0,25	**0,27**	0,24	0,23
max courant	0,88	0,86	**0,86**	0,86	0,86
residual value	$5,2x10^{-12}$	$1,7x10^{-12}$	**$1,0x10^{-12}$**	$2,6x10^{-14}$	$4,3x10^{-13}$
Δ t	0,15	0,10	**0,056**	0,052	0,05
Total time run (s)	$3.5x10^{10}$	$4.1\ x10^{10}$	**$2.1\ x10^{11}$**	$6.8\ x10^{11}$	$3.3\ x10^{13}$
U center point	0,51	0,20	**0,87**	0,88	0,87
P center point	5,78	-0,35	**-0,49**	-0,50	-0,51

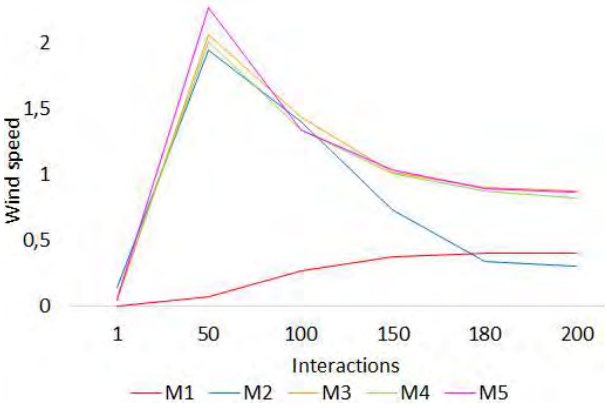

Figure 3: mesh independence test graph.

Employing a boundary condition for the delineation of the Atmospheric Boundary Layer (ABL) that is more representative of the ventilation characteristics within an urban environment (Figure 4 and equation 1), an ambient air velocity of 2 m/s was incorporated at the height of the pedestrian.

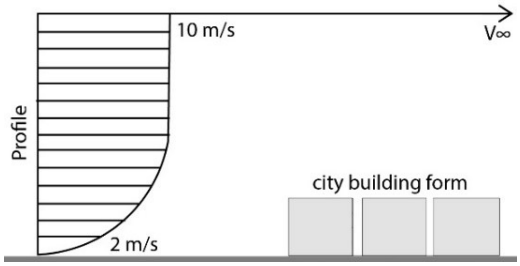

Figure 4: wind profile.

$$\frac{U}{U_{ref}} = \left(\frac{h}{h_{ref}}\right)^{\alpha} \quad (1)$$

Where: ∪ is the Ws at a specific height; ∪ ref is the reference Ws; h is the Height at which the Ws is measured; h ref is the reference height; and α is the exponent associated with the specific wind profile.

The simulation covered three different wind directions: 0°, 45° and 90°. The simulation was carried out using the OpenFOAM 9 software, taking advantage of the icoFOAM model, considering the air fluid, with viscosity 0.01, and the scalarTransportFOAM to simulate the dispersion of atmospheric pollutants.

IcoFOAM is a solver for incompressible laminar flow, which does not use any turbulence model. It solves the Navier-Stokes equations directly using the PISO algorithm, which is a pressure-velocity coupling scheme. The solver assumes that the flow is transient and requires an initial condition and boundary conditions for the velocity and pressure fields [14].

ScalarTransportFOAM is a solver that solves a transport equation for a passive scalar, which requires a specified stationary velocity field, which has been established through icoFOAM simulation. In scalaTransportFOAM, the atmospheric pollutant is applied through a setFields, which uses the Volume of Fluid Method (VOF), a computational technique for approximating free surfaces, categorized as Eulerian method, Eulerian methods are characterized by a grid system, which can be either static or dynamic (equation 2) [15].

$$\frac{\partial c}{\partial t} + v * \nabla C + \nabla * [C(1-C)U_r] = 0 \quad (2)$$

Where: C is the concentration; $\frac{\partial c}{\partial t}$ is the rate of temporal change of concentration; v is the fluid velocity vector; ∇C is the is the spatial gradient of concentration; and U_r is the radial component of velocity.

To ensure the accuracy of the simulation results, the only cases considered were those in which the residuals were less than 1x10^{11}, the Courant number was approximately 1 and there was less than 10% change in physical stability in the mesh independence test [12, 16]. Figure 4 presents a summary of the methodological process divided into 4 stages: pre-processing, validation, simulation and analysis.

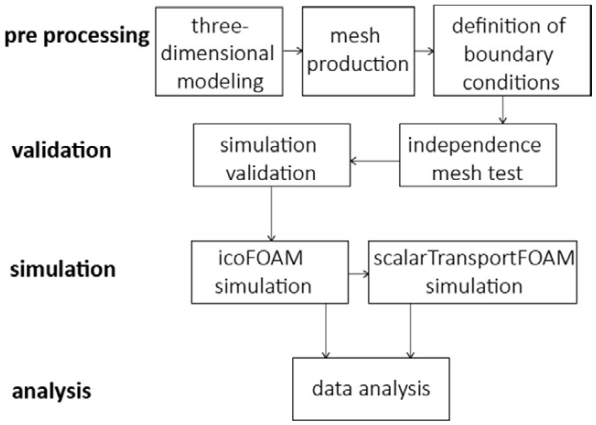

Figure 5: methodological process

As Figure 5 shows the paper's methodology is separated into 4 stages: 1. pre-processing, which encompasses the development of the three-dimensional model, the production of meshes and the definition of boundary conditions; 2. Validation, which involves testing independence with five meshes and numerical validation; 3. Numerical simulation, which was divided into icoFOAM to simulate natural ventilation and scalarTransportFOAM to simulate pollutant dispersion; and 4. Analysis, which involves analyzing the results.

3. RESULTS

To better visualize the results, a circular cut was made in the results with a top view of Ws and dispersion of atmospheric pollutants (Figure 6).

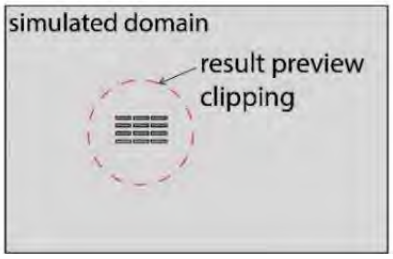

Figure 6: Result preview clipping

The findings were bifurcated into two segments: natural ventilation, encompassing Ws and Cp, and atmospheric pollutant dispersion (Figures 7 and 8).

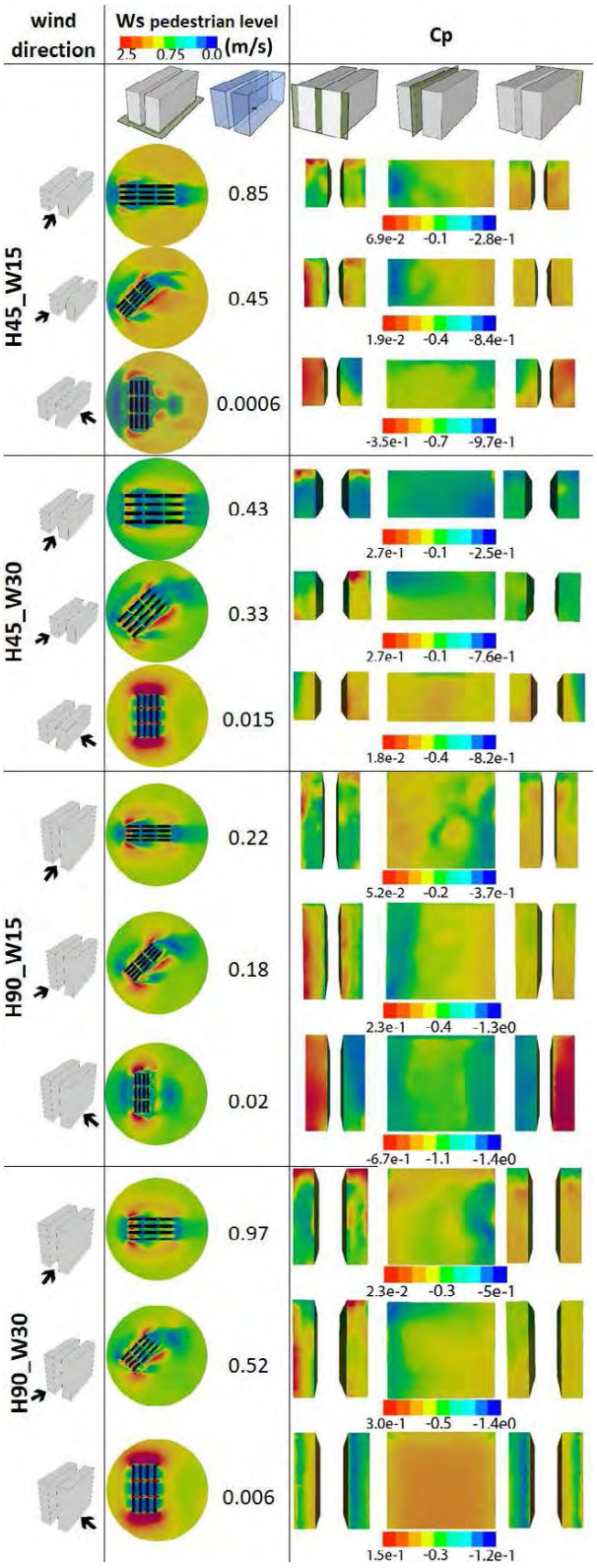

Figure 7: CFD simulation results (H45_W30 and H90) of Ws and Cp

The natural ventilation outcomes are scrutinized by evaluating the Ws at the pedestrian level (top view) and the Cp at wind directions of 0°, 45°, and 90°, as illustrated in Figures 7 and 8.

The results of Figure 7 show that the taller the building and the narrower the distance between the buildings, the lower the Ws at the height of the pedestrian, this result agrees with the authors with Haddid & Al-Obaidi (2022) and Ai & Mak (2018) [17, 18].

Regarding the Cp, the results show that the greater the distance between the buildings, the greater the Cp of the buildings [19, 20].

The results of the generic dispersion of pollutants in the top view (pedestrian height) were analyzed in wind directions with highest and lowest Ws 0° and 90° (Figure 8).

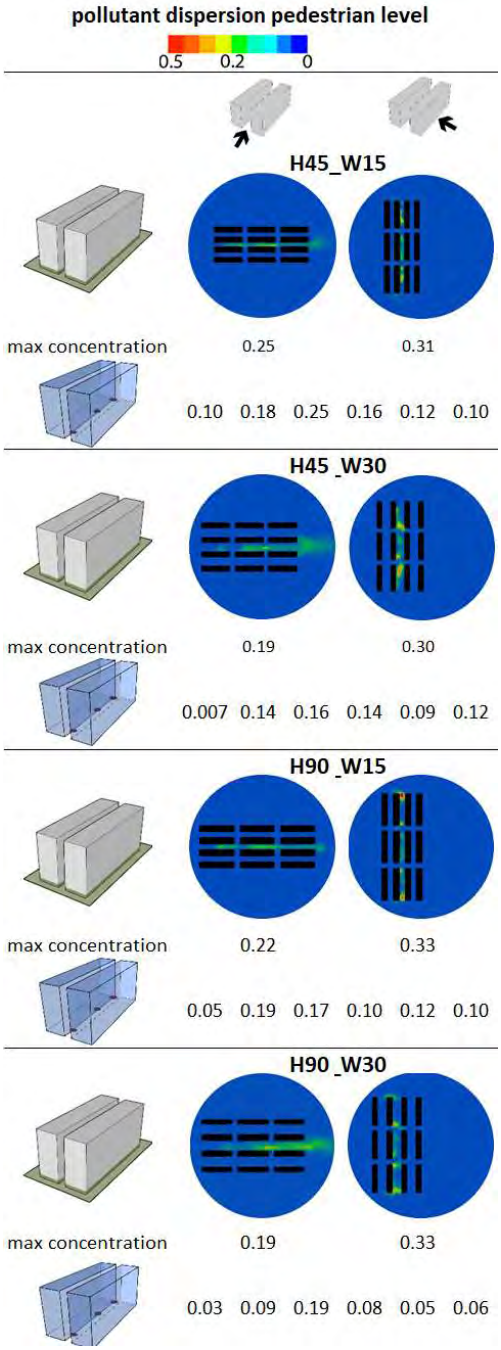

Figure 8: CFD simulation results of pollutants dispersion

Figure 8 presents the results of the dispersion of atmospheric pollutants in urban canyons investigated generically, that is, a type of pollutant was not

established in this simulation. The results showed that the dispersion of pollutants improved with increasing distance between buildings (H/W ratio).

Furthermore, the analysis of the results revealed that the concentration of pollutants at a specific point in the center of the urban canyon was lower with wind at 90°, or in the lee of pollutant emissions, however, it was considerably higher at the ends of the urban canyons, in that direction. wind.

In relation to the maximum contraction value, the highest concentration value is in the 90° wind direction and highest at the highest height analyzed (H = 90). The lowest concentration value is in the 0º wind direction with the lowest height of the buildings and the greatest distance between them (H45_W30).

The value of atmospheric pollutants did not vary as much as the Ws, however, when considering the entire extension of the canyon, the simulation with a wind direction of 90º showed a higher concentration of pollutants, due to the low Ws, a result that agrees with the authors [9–11, 21].

When comparing the results obtained for Ws and dispersion of atmospheric pollution, a relationship can be noted between low Ws and the highest concentration of atmospheric pollutants, as shown in Figure 9.

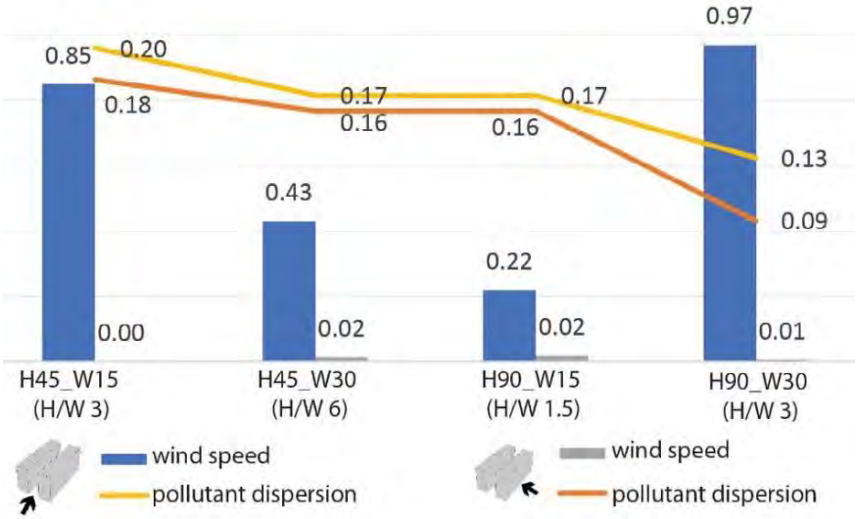

Figure 9: Results for Ws *and atmospheric pollution dispersion*

As illustrated in Figure 9, the H/W ratio, a crucial parameter in urban climatology studies, suggests that building height is the predominant factor influencing Ws at pedestrian level. On the other hand, the distance between buildings seems to be the most significant variable that affects the Cp.

The dispersion of air pollutants is impacted by the height of buildings and the distances between buildings. The height of buildings directly affects Ws, which in turn affects the dispersion patterns of air pollutants. Furthermore, greater distances between buildings can induce eddies formations, which have a significant impact on the dispersion of air pollution.

4. CONCLUSION

The results obtained from the analysis of urban canyon simulation results elucidate that the vertical height of buildings is the main parameter that impacts Ws at pedestrian level. On the other hand, the distance from the buildings was the predominant factor in modulating the Cp. It was also found that the dispersion pattern of airborne contaminants depends on both the height and spacing of structures.

Furthermore, it was observed that the concentration of atmospheric pollutants showed a consistent decrease with the increase in the distance between buildings at a ventilation angle of 0°. However, at the 90° ventilation angle, due to the formation of vortices, there was a higher concentration of atmospheric pollutants throughout the urban canyon under investigation.

This paper is a component of an ongoing doctoral investigation, which currently has preliminary findings to disclose. There remains a necessity for further comprehensive exploration concerning the dispersion of pollutants and the urban form. Additionally, enhancements in the simulation that encompasses the chemical composition of atmospheric pollutants are warranted.

ACKNOWLEDGEMENTS

Grant #2021/14533-7, São Paulo Research Foundation (FAPESP).

Grant #2023/01130-7, São Paulo Research Foundation (FAPESP).

Grant #2023/07771-4, São Paulo Research Foundation (FAPESP).

REFERENCES

1. Oke T.R. Street design and urban canopy layer climate. Energy Build 11: 103–113, 1988.
2. Georgakis C, Santamouris M. On the estimation of wind speed in urban canyons for ventilation purposes—Part 1: Coupling between the undisturbed wind speed and the canyon wind. Build Environ 43: 1404–1410, 2008.
3. Ratti C, Di Sabatino S, Britter R. Urban texture analysis with image processing techniques: winds and dispersion. Theor Appl Climatol 84: 77–90, 2006.
4. Girotti C, Nazareth S.B.M., Shimomura A.R.P. Aerodynamic analysis of urban blocks Case study in open, row and vertical blocks. PLEA 2021, 2021.
5. Grimmond C.S.B, Oke T.R. Aerodynamic Properties of Urban Areas Derived from Analysis of Surface Form. Journal of Applied Meteorology 38: 1262–1292, 1999.
6. Grimmond C.S.B, Roth M, Oke T.R, Au Y.C, Best M, Betts R, Carmichael G, Cleugh H, Dabberdt W, Emmanuel R, Freitas E, Fortuniak K, Hanna S, Klein P, Kalkstein LS, Liu CH, Nickson A, Pearlmutter D, Sailor D, Voogt J., Climate and More Sustainable Cities: Climate Information for Improved Planning and Management of Cities. Procedia Environ Sci 1: 247–274, 2010.
7. Azizi M.M, Javanmardi K. The Effects of Urban Block Forms on the Patterns of Wind and Natural Ventilation. Procedia Eng 180: 541–549, 2017.
8. Guo F, Zhu P, Wang S, Duan D, Jin Y. Improving Natural Ventilation Performance in a High-Density Urban District: A Building Morphology Method. Procedia Eng 205: 952–958, 2017.
9. Singh A.P, Bhatia P, Chaudhary K.K. 3-Dimensional Numerical Simulation of Pollution Dispersion in an Urban Street Canyon. International Journal of Advance Research and Innovation 5: 99–104, 2017.
10. Nazridoust K, Ahmadi G. Airflow and pollutant transport in street canyons. Journal of Wind Engineering and Industrial Aerodynamics 94: 491–522, 2006.
11. Wang P, Zhao D.Q, Cai G.T, Liao C.P. Numerical Simulation of Traffic Emissions in Urban Street Canyon. Adv Mat Res 168–170: 1548–1551, 2010.
12. Franke J, Hellsten A, Schlünzen H, Carissimo B. Best Practice Guideline for the CFD Simulation of Flows in the Urban Environment: COST Action 732 Quality Assurance and Improvement of Microscale Meteorological Models. Hamburg: 2007.
13. Brandão R.S, Alucci M.P. Thermal Behavior of Urban Canyons Using Numerical Modeling, Cfd Simulation and Gis Mapping. In: SimBuild 2010. 2010, p. 244–251.
14.OpenCFD. icoFOAM [Online]. 2018. https://www.openfoam.com/documentation/guides/latest/doc/guide-applications-solvers-incompressible-icoFoam.html [19 Oct. 2023].
15. OpenCFD. scalarTransportFOAM [Online]. 2018. https://www.openfoam.com/documentation/guides/latest/doc/guide-applications-solvers-basic-scalarTransportFoam.html [19 Oct. 2023].
16. NASA. Tutorial on CFD Verification and Validation [Online]. 2023. https://www.grc.nasa.gov/www/wind/valid/tutorial/iterconv.html [12 Sep. 2023].
17. Al Haddid H, Al-Obaidi K.M. Examining the impact of urban canyons morphology on outdoor environmental conditions in city centres with a temperate climate. Energy Nexus 8: 100159, 2022.
18. Ai Z.T, Mak CM. Wind-induced single-sided natural ventilation in buildings near a long street canyon: CFD evaluation of street configuration and envelope design. Journal of Wind Engineering and Industrial Aerodynamics 172: 96–106, 2018.
19. Gough H, King M-F, Nathan P, Grimmond C.S.B, Robins A, Noakes C.J, Luo Z, Barlow J.F. Influence of neighbouring structures on building façade pressures: Comparison between full-scale, wind-tunnel, CFD and practitioner guidelines. Journal of Wind Engineering and Industrial Aerodynamics 189: 22–33, 2019.
20. Kim Y.C, Tamura Y, Yoon S. Proximity effect on low-rise building surrounded by similar-sized buildings. Journal of Wind Engineering and Industrial Aerodynamics 146: 150–162, 2015.
21. Gallagher J, Lago C. How parked cars affect pollutant dispersion at street level in an urban street canyon? A CFD modelling exercise assessing geometrical detailing and pollutant decay rates. Science of The Total Environment 651: 2410–2418, 2019.

PLEA 2024 WROCŁAW
(Re)thinking Resilience

Identification of Positive Energy District (PED) transition scenarios through a methodology feasibility study

The case study of Alcorcón, Spain

MARTINA DELL'UNTO[1] LOUISE-NOUR SASSENOU[1,2] LORENZO OLIVIERI[1,2] FRANCESCA OLIVIERI[1]

[1]Department of Construction and Technology in Architecture, Escuela Técnica Superior de Arquitectura, Universidad Politécnica de Madrid, Av. de Juan de Herrera 4, 28040 Madrid, Spain
[2] Instituto de Energía Solar, Universidad Politécnica de Madrid, Av. Complutense 30, 28040 Madrid, Spain

ABSTRACT: Positive Energy Districts (PEDs) are a relevant tool that can be used to drive a sustainable and inclusive energy transition in cities. However, there is still a need to address the various challenges blocking these models, including administrative, economic, and energy system integration barriers. To this end, a methodology is proposed to explore the potential of different PED scenarios in an existing district to guide the implementation of a real transition. The proposed methodology first analyses the initial state of the district, considering the urban environment, climate, building orientation, and energy demand. Next, the methodology proposes scenarios using passive and active transition strategies identified in the previous step. Finally, the PED level that the district can achieve is determined. To validate this methodology, the flow has been applied to a case study located in the municipality of Alcorcón, Spain. Results show that the possible PED transition scenario for the selected district is Virtual with an annual energy surplus of 4 GWh.
KEYWORDS: Positive Energy District; PED levels; methodology feasibility; case study, Energy Transition

1. INTRODUCTION

Cities are responsible for 75% of primary energy consumption and generate 60% of global GHG emissions [1]. Therefore, in the current climate change scenario, it is necessary to act as soon as possible in urban environments to reduce their impact. In this sense, the European Commission (EU), through the development of the European Strategic Energy Technology Plan (SET Plan) [2], has proposed ten strategic actions to reduce costs and improve the performance of low-carbon energy technologies. Action 3, named "Creating smart home technologies and services to deliver smart solutions for energy consumers," is further divided into two sub-actions, where 3.2 "Smart cities and communities" focuses on initiatives that can promote the energy transition of cities. This sub-action proposes to promote the transition of 100 Positive Energy Districts in different cities that could be pilots and examples for the future deployment of these models. Despite the great potential of PEDs, there are currently several obstacles to their deployment, including legal, economic, and energy system integration barriers. Given these barriers, it is necessary to find tools that can overcome them. A first step in this direction can be to assess the potential of districts to be converted into PEDs.

In the literature on PEDs different levels are defined [3]:

- Autonomous PEDs (APEDs): this is the most ambitious scenario where the district itself can generate positive energy. It is positive net energy balance (NEB) within their geographical boundaries.
- Dynamic PEDs (DPED): this is the intermediate scenario between complete independence and flexibility of boundaries with the environment and the rest of the city. It is a positive annual NEB with energy exchange with the territory to compensate for energy deficits or surpluses.
- Virtual PEDs (VPEDs): this is the most flexible scenario, where part of the district's energy is generated in the virtual boundaries close to the district. It is a NEB within their virtual boundaries.

These PED levels represent different levels of ambition and potential for district transformation. In that sense, they could also constitute the milestones of a transition roadmap that a district would progressively follow until it reaches the most ambitious level. Therefore, by identifying different PED levels it will be possible to determine the scope of the selected district and improve its positive energy production.

This study proposes a methodology to assess the potential of a district to be transformed into a PED, according to the different levels of ambition. This work proposes a three-step methodology and is validated with a case study in Alcorcón, Spain.

2. MATERIALS AND METHODS

The main objective of this research is to develop a methodology leading to the identification of possible

PED scenarios and resulting PED level – APED, DPED, or VPED - that can be achieved in an existing district.

The methodology (Fig. 1) consists of three stages: First, conduct a study of the current morphological, climatic, and energy characteristics of the district (stage 1). Then, select the possible passive and active strategies that can improve the district (stage 2). Finally, identify the achievable PED ambition of the case study (stage 3).

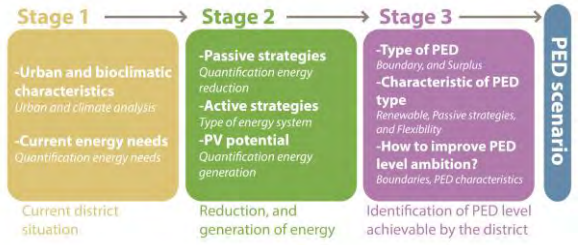

Figure 1: Workflow of the methodology to evaluate the PEDs ambition.

The case study in the district of Alcorcón validates the methodology (outlined in section 3).

Stages 1 and 2 are derived from a feasibility study published in September 2023 [4]. This work is a continuation of that study by refining the stages and integrating stage 3 for the identification of the PED ambition.

2.1 Stage 1 – Current district situation

The first phase aims to analyse the current energy and environmental situation of the district, studying its urban and bioclimatic characteristics and calculating its energy needs. To do this, the urban environment is first analysed, using urban monitoring tools of the city and the QGIS tool [5]. The main characteristics studied are the type of land use (residential, commercial, etc.), the age of construction of the buildings, the typology of the buildings (e.g., two-storey single-family house), and, finally, the roof surface of the buildings.

A bioclimatic analysis is then carried out with the Climate Consultant 6.0 tool [6]. This tool evaluates the needs of the buildings according to the climate in which they are located and identifies possible passive strategies.

Finally, the current energy demand of the district is analysed by selecting the sample buildings of the area (BT1, BT2, BTn…), which reflect the main characteristics of the constructions present in the neighbourhood.

For the calculation of energy demand, the different types of energy are estimated separately: heating, cooling, domestic hot water (DHW), and electricity.

The heating and cooling demand is calculated using an Energy Certification Tool (ECT) available in the territory of analysis. In the case study, the CE3X tool [7], recognised by the Spanish Ministry for Ecological Transition and the Demographic Challenge, has been used. Then, the results generated by the application according to the type of building will be added together to obtain the final result (TD_{Heat} and TD_{Cool}), following Equations (1,2):

$$TD_{Heat} = D_{Heat}BT1 + D_{Heat}BT2 + D_{Heat}BTn \quad (1)$$

$$TD_{Cool} = D_{Cool}BT1 + D_{Cool}BT2 + D_{Cool}BTn \quad (2)$$

where TD_{Heat} – Total demand of heating (GWh Year);
TD_{Cool} – Total demand of cooling (GWh Year);
D_{Heat}- Heating Demand (kWh/m^2 year);
D_{Cool}- Cooling Demand (kWh/m^2 year);
BT1, BT2, BTn…-m^2 of district's building type.

DHW demand is calculated using the reference standard of the country (TD_{DHW}), following Equation (3). In the case study, reference has been made to the IDAE Technical Guide on DHW [8].

$$TD_{DHW} = Cons_{DHW} \times SD \quad (3)$$

where TD_{DHW} – Total demand of DHW (GWh Year);
$Cons_{DHW}$- DHW consumption at 60 °C (Litres/day at 60 °C);
SD- Stocking Density (m^2/person).

The calculation of the district Electricity Demand (DED) uses data retrieved from different sources. First, Public Lighting Demand (PLD) is estimated using public data available in the reference municipality. Then, demand in residential buildings (DED_{Res}) is estimated using the methodology [9] ($DED_{light+vent}$) and with statistical data on the consumption of household appliances (DED_{Appl}), following Equation (4):

$$DED_{Res} = DED_{light+vent} + DED_{Appl} \quad (4)$$

where DED_{Res} – Residential district electricity demand (kWh Year);
$DED_{light+vent}$ - Residential district electricity demand of lighting and ventilation from MAKING-CITY methodology [9];
DED_{Appl}- m^2 of district's residential use for a total consumption of statistical household appliances (GWh Year).

Last, the electricity demand in non-residential buildings (DED_{Nres}) is again estimated using an ECT.

Given that this methodology will be used to identify the potential of the selected district in general. This estimate of current energy demand assumes the Equation (5):

$$Consumption \cong Demand \quad (5)$$

In cases where more details of the energy demand identification of a district are required, it is advised to use energy simulation tools and/or, if possible, real data of the building types.

2.2 Stage 2 – Energy demand reduction and generation.

In this stage, the reduction in energy demand in the district's buildings is quantified. This reduction is calculated thanks to the ECT, integrating the passive strategies identified in stage 1 into the different building types.

Once the reduction in energy demand is quantified (TDR_{Cool} and TDR_{Heat}), the renewable energy generation is estimated. This calculation considers only the most common systems: aerothermal and photovoltaic (PV) panels.

The aerothermal generation is estimated using the current value of the reduced energy demand for heating, cooling, and DHW, and the COP equivalent to 3. To simplify the calculations of the methodology, a conservative number equal to 3 has been considered for the COP, considering a standard aerothermal equipment. With this value, it is possible to calculate the electrical demand of the equipment using the following Equations (6,7):

using the following Equations (6,7):

$$EE_{Heat+DHW} = TD_{Heat+DHW}/3 \quad (6)$$

$$EE_{Cool} = TD_{Cool}/3 \quad (7)$$

where $EE_{Heat+DHW}$ – Heating and DHW electrical energy (GWh Year);
EE_{Cool} – Cooling electrical energy (GWh Year);
TD_{Heat} – Heating and DHW total demand (GWh Year);
TD_{Cool} – Cooling total demand (GWh Year);

Once the electricity demand of the aerothermal system is identified, the solar electricity required by the district is quantified using the PVGIS tool [10], the reference software for estimating the PV potential.

Having estimated the PV potential of the areas, the PV generation of the selected district is estimated using the following Equation (8):

$$PVG = (PV_{Energy\ Prod} \times CA)/TBDA \quad (8)$$

where PVG – PV district generation (kWh Year);
$PV_{Energy\ Prod}$ – Cooling electrical energy (GWh Year);
CA – Collector area (m^2);
$TBDA$ – Total m^2 of Build-up district (GWh Year).

Finally, the amount of electricity surplus that can be achieved with the scenario proposed in the stage is calculated using the following Equation (9):

$$ES = PVG_{tot} - DED_{tot} > 0 \quad (9)$$

where ES – Electric Surplus (GWh Year);
PVG_{tot} – Total PV district generation (GWh Year);
DED_{tot} – Total district Electric Demand (GWh Year).

This stage calculates the surplus energy of a district considering the standard renewable energy systems. If more types of renewable energy systems can be used in the district, in addition to the typical ones (PV and aerothermal), the formula would be transformed into Equation (10):

$$ES = REG - DED_{tot} > 0 \quad (10)$$

where ES – Electric Surplus (GWh Year);
REG– Total district Renewable Energy Generation (GWh Year);
DED_{tot} – Total District Electric Demand (GWh Year).

2.3 Stage 3 – Identification of PED levels achievable by the district

Based on the results of stages 1 and 2, stage 3 aims to define the PED level (APED, DPED, and VPED) of the possible scenario(s) for the selected district.

To identify this PED level, the methodology proposes an analysis of the main characteristics of the PED scenario identified in stages 1 and 2.

The analysis follows three steps. First, the level of PED achieved with the proposed scenario (Table 1) is identified by defining the types of boundaries considered and the type of energy surplus achieved.

Table 1: PED level of the scenario.

	APED	DPED	VPED
Boundary	Geographical	Geographical	Virtual
Surplus (ES=REG-DED > 0)	Inside and energy export	Inside and energy exchange with outside	Virtual, support from nearby area

In the following, the PED level and the characteristics of the scenario are defined (Table 2). This step creates an overview of the solutions applied in the scenario. The three main characteristics considered in this step are: 1) types of renewable energy systems that have been considered, 2) type of passive strategies and their goals (if they reach to transform buildings into NZEB or if only demand reduction is achieved) and 3) flexibility systems foreseen within the district. This last point is mandatory only in the case of reaching the APED goal.

Table 2: PED ambition, characteristics of the scenario.

	APED	DPED	VPED
Renewable energy	more systems better	various type of systems	1 system for thermal energy and 1 system for electricity
Passive strategies	NZEB level	NZEB or demand reduce	Demand reduces
In-district flexibility	Electric storage and thermal storage mandatory	Electrical and/or thermal storage may be available	Not mandatory

To conclude this stage, an assessment is made of how the PED level could be improved (Table 3). This analysis is used to assess the goal and consider next steps in order to raise the ambition level of the scenario.

Table 3: PED ambition, improve scenario level of ambition.

	APED	DPED	VPED
Boundary	x	x	-
Improve energy surplus	x	x	x
Renewable energy	x	x	Not mandatory
Passive strategies	x	x	Not mandatory
In-district flexibility	x	Not mandatory	Not mandatory

3. RESULTS

The methodology, for its validation, has been applied to an existing district of about 1 km^2, located in the south-western part of Alcorcón, Spain.

In accordance with stage 1, the urban environment is analysed first (Fig. 2). The district has a mixed use, the buildings have been constructed between 1990 and 2006, the predominant typologies are residential blocks of 5-6 floors and the roofs are predominantly pitched and 26% flat.

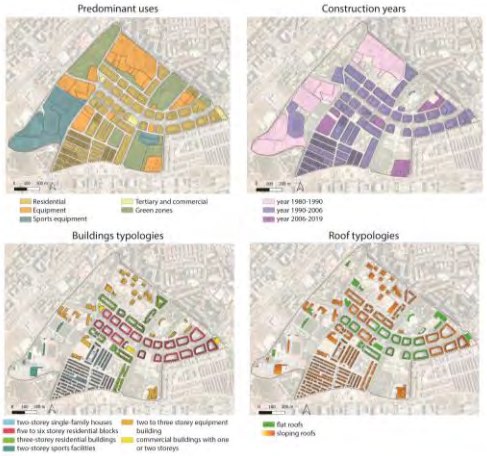

Figure 2: Urban Analysis from QGIS.

The district was then analysed at bioclimatic level, using the Climate Consultant 6.0 tool. The results of this analysis (Table 4) show that specific passive and active strategies are needed to achieve winter and summer comfort in the climate of Alcorcón.

Table 4: Results of bioclimatic analysis from Climate Consultant 6.0.

Strategy	Hour/year
Passive Solar Direct Gain High Mass	1507
Internal Heat Gain	1975
Sun Shading of Windows	842
High thermal mass night flushed	670
Heating, add humidification if needed	3226

Then, the initial demand of the selected district is estimated. For this calculation, first nine typical buildings representing the main building characteristics of the district have been identified. Subsequently, the heating and cooling demand of each building has been estimated thanks to the Spanish ECT CE3X. As a result, the total demand has been calculated using the formulas (1) and (2). The DHW demand for each building type was then estimated using the formula (3) of the Spanish guide [8] and finally, the total DHW demand was calculated.

Lastly, the electricity demand has been estimated in three steps, first the PLD has been calculated using a study carried out by the municipality, then the DED_{res} has been calculated using the formula (4) considering the equation (5), and finally the DED_{nres} has been calculated again thanks to CE3X (Table 5).

Table 5: Current Energy Demand Building Type (kWh/m^2 year)

Building type	D_{heat}	D_{cool}	D_{DHW}	ED_{Res} and N_{Res}
BT1 W-E	121.6	18.8	40.2	28.4
BT1 NE-SW	117	17.4	40.2	28.4
BT2-W-E	81.6	20.1	14	28.4
BT2-NE-SW	81.3	18.3	14	28.4
BT3-NE-SW	88.3	16	11.4	28.4
BT3-N-S	71	14.4	11.4	28.4
BT4	38.9	37.7	28.5	27.44
BT5	157	64.04	5.7	33.88
BT6	70.3	17.6	95.4	19.35

The results obtained are 52 GWh/year for heating, 10 GWh/year for cooling, 10 GWh/year for DHW, and 17 GWh/year for electricity.

Then, according to stage 2, passive solutions adapted to the neighbourhood have been identified to reduce its energy demand. The proposed solutions are derived from the bioclimatic analysis of stage 1. These passive strategies foresee improved façade insulation, replacement of windows and shading with

awnings in the west, east, south, and south-west directions, green roofs, and green walls. The total reduction was estimated using the CE3X tool and for the Natural Based Solution (NBS) interventions, the items [11-14] were used. Thanks to the application of these passive strategies, it was possible to reduce the demand by 25% in heating and 60% in cooling (Table 6).

Table 6: Reduced Energy Demand PED scenario.

Type of demand	Initial	PED Scenario	% Reduction
Heating	52	40	25
Cooling	10	3	60

Based on the reduced demand, the electricity consumption of an aerothermal system to balance the demand was calculated using the formulas (6), and (7). The result of this estimation is that 17 GWh of electricity per year is needed to cover the heating demand and 1 GWh per year for cooling.

Once the total electricity demand of the transition scenario was obtained, the potential electricity generation of a PV system was estimated. Using the PVGIS tool and the formula (8), the electricity generation to cover the electricity demand of the district was determined. To do so, equation (9) has been considered since a PED needs to generate a surplus of energy.

To cover this surplus, it is planned to install a PV system on the roofs of the buildings, on solar pergolas installed in various areas of the district's urban environment, and in an area outside but close to the district (Virtual area) (Table 7).

This system generates a surplus of 4 GWh per year of electricity.

Table 7: PV generation of PED scenario.

PVG	GWh year
Buildings roof	18
Urban area	2
Virtual area	19

Finally, stage 3 assesses the level of ambition of the PED scenario. The analysis (Fig. 4) shows that the APED and DPED in this scenario are not achievable. However, the VPED scenario is possible, since, thanks to the Virtual Power Generation Zone, a surplus can be generated.

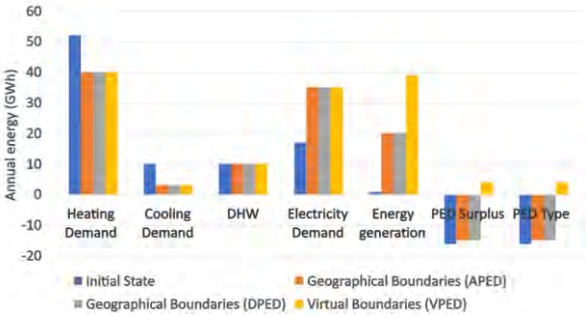

Figure 4: Level of ambition of the PED scenario.

Once the PED level is defined, the characteristics of the proposed PED scenario are analysed (Fig. 5). In this way, it is possible to identify strengths and weaknesses that could be improved by achieving a more ambitious PED scenario.

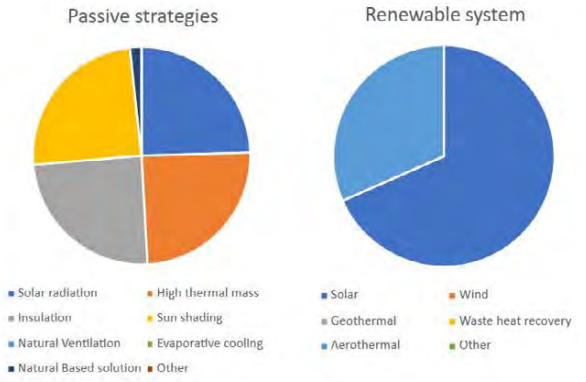

Figure 5: PED scenario characteristics.

Finally, future actions have been identified to achieve the different levels of PED ambition (Fig. 6).

In the case study, passive strategies could be increased with the ambition to achieve NZEB-level building renovations and increase NBS in the urban environment. Other renewable energy systems can also be integrated to achieve energy surplus within the district boundaries. In addition, to achieve the APED level of ambition it will be necessary to install systems that increase energy flexibility within the geographical boundaries of the district.

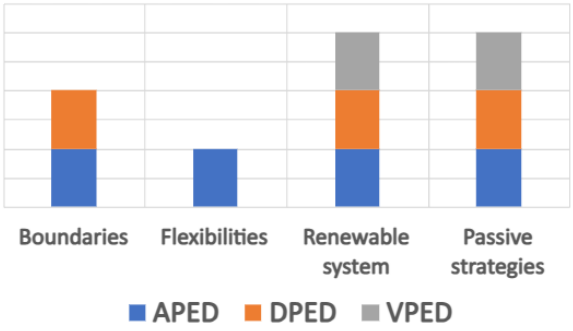

Figure 6: Future actions to improve PED level of ambition.

4. CONCLUSION

This paper introduced a three-step methodology to assess the potential of a district to become a PED according to the different possible levels (APED, DPED and VPED). To demonstrate the validity of the methodology, it has been applied to a case study in Alcorcón, Spain. This case study assessed the feasibility of transforming the existing district into a PED and the goal set by the proposed scenario. In the PED scenario identified (stage 1 and 2), it was not possible to achieve a level of APED and DPED. However, it is possible to achieve a VPED by including an area close to the district in the renewable electricity generation network. Future research could raise the level of the selected district following the guideline generated by stage 3. In more detail, other types of renewable energies such as geothermal, heat recovery or mini-wind or solutions such as building integrated photovoltaics (BIPV) could be included. Achieving a higher PED level will also require deep retrofitting of buildings with passive strategies and increasing the flexibility of the energy system through storage systems.

ACKNOWLEDGEMENTS

The research presented in this paper has received funding from the Spanish Ministry of Science, Innovation and Universities via a doctoral grant to the second author (FPU20/07591) and from the Comunidad de Madrid through the call Research Grants for Young Investigators from Universidad Politécnica de Madrid as part of the project APOYO-JOVENE S21-LI6SVQ-77-664ZUQ.

REFERENCES

1. Ritchie, H.; Roser, M.; Rosado, P. CO_2 and Greenhouse Gas Emissions. [Online], Available: https://ourworldindata.org/co2-and-greenhouse-gas-emissions [10 February 2023]
2. European Commission. (2018). SET-Plan ACTION n°3.2 Implementation Plan Europe to become a global role model in integrated, innovative solutions for the planning, deployment, and replication of Positive Energy Districts.
3. Albert-Seifried, V., Murauskaite, L., Massa, G., Aelenei, L., Baer, D., Krangsås, S. G., Alpagut, B., Mutule, A., Pokorny, N., & Vandevyvere, H., (2022). Definitions of Positive Energy Districts: A Review of the Status Quo and Challenges. *Smart Innovation, Systems and Technologies*, 263, 493–506. https://doi.org/10.1007/978-981-16-6269-0_41
4. Dell'Unto, M.; Sassenou, L.-N.; Olivieri, L.; Olivieri, F., (2023). Technical Feasibility for the Boosting of Positive Energy Districts (PEDs) in Existing Mediterranean Districts: A Methodology and Case Study in Alcorcón, Spain. *Sustainability*, 15, 14134. https://doi.org/10.3390/su151914134
5. QGIS Open Source Geographic Information System, [Online], Available: https://qgis.org/es/site/ [15 June 2023]
6. Climate Consultant 6.0, [Online], Available: https://www.sbse.org/resources/climate-consultant [15 June 2023]
7. Efinovatic CE3X Software, [Online], Available: https://efinova.es/CE3X [15 June 2023].
8. IDAE, Guía Técnica Agua Caliente Sanitaria Central, [Online], Available: https://www.idae.es/publicaciones/guia-tecnica-agua-caliente-sanitaria-central [20 January 2023].
9. Moreno, A. G., Vélez, F., Alpagut, B., Hernández, P., & Montalvillo, C. S. (2021). How to achieve positive energy districts for sustainable cities: A proposed calculation methodology. *Sustainability*, 13(2), 1–19. https://doi.org/10.3390/su13020710
10. European Commissions PVGIS, [Online], Available: https://joint-research-centre.ec.europa.eu/pvgis-online-tool_en [20 April 2023].
11. Banti, N.; Ciacci, C.; Di Naso, V.; Bazzocchi, F. (2023). Green Walls as Retrofitting Measure: Influence on Energy Performance of Existing Industrial Buildings in Central Italy. *Buildings*, 13, doi:10.3390/buildings13020369.
12. Coma, J.; Pérez, G.; de Gracia, A.; Burés, S.; Urrestarazu, M.; Cabeza, L.F. (2017). Vertical Greenery Systems for Energy Savings in Buildings: A Comparative Study between Green Walls and Green Facades. *Build Environ*, 111, 228–237, doi:10.1016/j.buildenv.2016.11.014.
13. Silva, C.M.; Gomes, M.G.; Silva, M. (2016) Green Roofs Energy Performance in Mediterranean Climate. *Energy Build*, 116, 318–325, doi:10.1016/j.enbuild.2016.01.012.
14. Al-Kayiem, H.H.; Koh, K.; Riyadi, T.W.B.; Effendy, M. (2020) A Comparative Review on Greenery Ecosystems and Their Impacts on Sustainability of Building Environment. Sustainability, 12, 1–26, doi:10.3390/su12208529.

PLEA 2024 WROCŁAW
(Re)thinking Resilience

Integration of BIM and BES in sustainable architecture design process: case study of a developing country

KIMNENH TAING[1,2], SIGRID REITER[1], VIRAK HAN[3] , PIERRE LECLERCQ[1]

[1]Faculty of Applied Science, University of Liege, Quartier Polytech - allée de la Découverte 9 - Bât B52, 4000, Liege, Belgium
[2] Research and Innovation Centre, Institute of Technology of Cambodia, Russian Federation Blvd., P.O. Box 86, Phnom Penh, Cambodia
[3] Faculty of Civil Engineering, Institute of Technology of Cambodia, Russian Federation Blvd., P.O. Box 86, Phnom Penh, Cambodia

ABSTRACT: The integration of Building Information Modeling and Building Energy Simulation in the architectural design process has been increasing rapidly and many discussions are produced regarding this topic in the western country. For developing countries where these technologies have started to be practiced recently, the research about utilization and how to implement them correctly in the design process is still limited. The aim of this paper is to study the current situation of BIM and BES application in the design process of a sustainable building in developing country. 10 architectural firms who practice sustainable design in Cambodia were interviewed using 7 rigorous research steps to get some insight on the current practice of these two methods in sustainable building design and how building designers would like to implement them in the future. A current design process integrating BIM and BES is identified. Certain issues concerning the mal-practice of BIM and BES in Cambodia to the purpose of sustainable principle are discussed. A 5-phases design process integrating BIM and BES since the early design phase is proposed to resolve these issues and to fit better with the context of developing countries.
KEYWORDS: Design process, Sustainable design, BIM, BES, Developing country

1. INTRODUCTION

Sustainable architecture is a key factor to a resilient society and its realization depends on architects to put this principle into practice in their projects. Of course, designing a sustainable building can add challenges to architects. Therefore, many methods and tools have been introduced into the design process to help designers achieve this goal.

Traditional tools such as sketching, computer aided design (CAD) are still strongly used by architects in their design process since decades. However, advanced digital aided design tools, such as parametric modelling and building simulations have started to be integrated more and more into the architectural design process [1].

Building Information Modeling (BIM) is a technology that can be applied in architectural design process to help optimizing and sharing green building information between architects and engineers, which facilitates collaboration and cooperation between stakeholders [2], [3]. The utilization of BIM linked with Building Energy Simulation (BES) has also been increasing for realization of building thermal performance analysis to help designers find the best design strategies to provide comfort in buildings with low energy consumption [4][5][6]. It has been strongly agreed that these two tools are increasingly promoting sustainable architecture [7]. For this purpose, these two methods have been practiced and studied widely in developed countries in terms of integration in the design process for achieving building sustainability [8][9]. However, research studies on their use in developing countries, such as Cambodia, are still very limited.

Therefore, some research questions arise: (1) Are BIM and BES used in the current design process of buildings in developing countries? (2) Do BIM and BES improve or facilitate the design process of a sustainable building in the context of a developing country? (3) If so, at which phase should BIM and BES be integrated in the design process?

In this paper, we will analyse the current utilizations of BIM and BES in the design process of a sustainable building in a developing country taking Cambodia as our case study. The impact of these tools on the design process, when they should be implemented and the perspective of architects that practice them in their projects in Cambodia are also discussed.

2. EXISTING DESIGN PROCESS

Generally, the architectural design process is divided into 4 phases starting from pre-design (programming, initial concept), schematic design (form and function, building envelope), design development (design detail, structure) and construction documentation. To enhance collaboration between stakeholders and for helping

architects to take into account aesthetic, functional and technical requirements in their design process, Integrated Design Process (IDP) has been introduced with 5 design phases from problem or idea, analysis, sketching, synthesis and presentation [10]. With BIM and BES started to be integrated in the design process, a 6-phases architectural design process for sustainability (DEPROSU) integrating BIM was created in the US by Farias Stipo in 2015 based on a literature review and interviews in architectural firms [8]. The proposed design process as shown in figure 1 is divided into (1) information gathering for design, (2) design, (3) construction documentation, (4) construction process, (5) commissioning and (6) operation. BIM is highly recommended to be practiced in phase 2, 3 and 6 as it is associated with improved communication, collaboration, and coordination. However, the link between BIM and BES in the design process was not clearly discussed and the aspects of sustainable design were not mentioned in each design phase.

3. METHODOLOGY

Our qualitative research method used in this study is based on semi-structured interviews, aiming to better understand the practice of using BIM and BES in the architectural design process in Cambodia. The applied method includes 7 rigorous research steps: (1) selection of the architectural firms to be interviewed, (2) development of an interview guide, (3) exploratory interview to correct and validate the interview guide, (4) realization and recording of the interviews, (5) complete transcription of the interviews and anonymization of the answers, (6) analysis of the content of the interviews, and finally (7) the interpretation of the results of the study and the development of its conclusions.

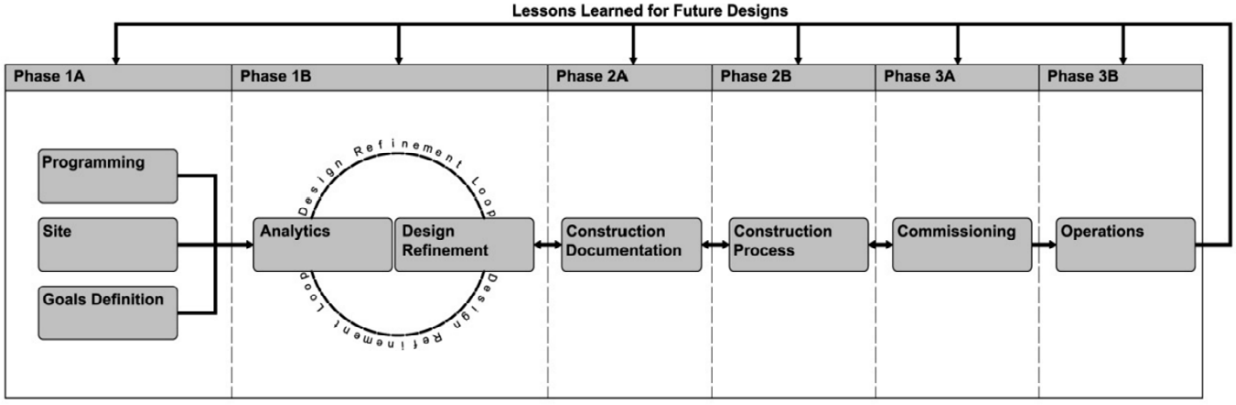

Figure 1: Simplified diagram of DESPROSU[8]

A guide for the interview was developed to keep the interview in line with our objectives. It consists of questions asking on the subjects below:

- Order of their design process (function, form, façade design, material choices, etc.….).
- Tools used in the conception phase (sketch, diagram, CAD 2D, CAD 3D, BIM, BES).
- Their focus on sustainable design.
- Implementation of BIM and BES in their project (at what stage, benefits, disadvantages, and limitations…).
- Evaluation method on performance of building (if BES isn't practiced in their company).
- Project with requirement of green building certification.
- An overall design timeline combining all the steps of design, tools used at each step, collaboration and decision making.

We interviewed 10 architectural firms located in Cambodia which take into account sustainable design into their projects. The characteristics and selection criteria of the architectural firms that we interviewed are: (1) practice of sustainable or bioclimatic design in their projects, (2) having at least 5 years of experience in the field of architecture in Cambodia, (3) having at least 5 architects working in their company, (4) having a company's head office located in Cambodia or working mainly for projects in Cambodia.

The semi-structured interviews were conducted with one or two architects simultaneously from each company to know in detail how they integrate BIM and BES in their design process. Two of them are also the founders of their firm that lead the team to practice BIM and BES in their company as well. As designers, they can understand and clearly describe the impact and utilization of these two methods to achieve sustainable projects and how they currently integrated them in their project and what they would like to change in the future.

4. DATA COLLECTION AND INTERPRETATION

We collected in total 8 hours and 17 minutes of audio, 64 pages of answer to the 18 questions and 10 pages of side note. From the interviews, architects answer to the question of design timeline and order of their design process allow us to identify a current

practice of design process in Cambodia as shown in Fig.2.

The traditional 4 stages of design process is still practiced following the steps of:

- Pre-design: site visit, programming, initial draft design for client.
- Schematic Design : function, space arrangement, form and façade design are more defined, size of the openings, sustainability aspect are integrated.
- Design Development : choice of materials, landscape design, detail of structural elements and integration of mechanical, electrical and plumbing systems (MEP).
- Documentation: final plan realization.

The discussion on different tools and methods used during the design process to create and execute conception ideas shows that basic tools such as sketch and CAD are still the main tools used for all steps of the design process for companies that design noncomplex projects such as residential villas. Three architects mention that "For now, we design and evaluate the performance of buildings based on our experiences and architectural knowledge that we already have where BIM isn't necessary yet. Moreover, the complexity of BIM could extend the duration of designing for simple projects''. One company whose most of their projects are residential buildings, use physical models to evaluate their design in terms of shading, natural light, and ventilation. However, there are 3 firms that have already integrated both BIM and BES in their design process for the last 5 years. While one of them use these two methods for all their projects, the other two companies use them only for large scale or complicated projects or when there is requirement from the client.

When talking about BIM, the architects mentioned that the use of it is more as 3D model instead of a protocol for coordination or collaboration. For non-regular practice company, the integration of BIM model occurs at the middle stage of design process such as the end of Schematic Design or Design Development for visualization of shading devices, to help facilitate the collaborations with structural and mechanical engineer and conducting BES in the following design stage. Whereas companies that regularly practice BIM models since the early design phase (start of Schematic Design) have the purpose of shorten the design period (generating both form and function at the same time) in addition to other purposes similar to those of companies that do not practice it regularly.

However, regarding to BES, all three companies integrate it in a similar way. As practice of BES requires an expert, energy consultant companies normally come in at the end of the Design Development stage. Hence, BES are used in Design Development to verify the design strategies or to see if the building energy consumption meets with the requirements of green building certificates or to convince their client to accept the design that they proposed. In terms of collaboration with structural and MEP engineers, it happens at the end of Design Development where all the main architectural design is completed which therefore could produce errors between technical and architectural design. As the important design choices are already made at this stage, they must go back to Schematic Design to solve all the errors which of course takes time and creates conflicts between actors involved in the project.

From the analysis of the answers, as there are no guidelines for BIM or BES practices in Cambodia yet,

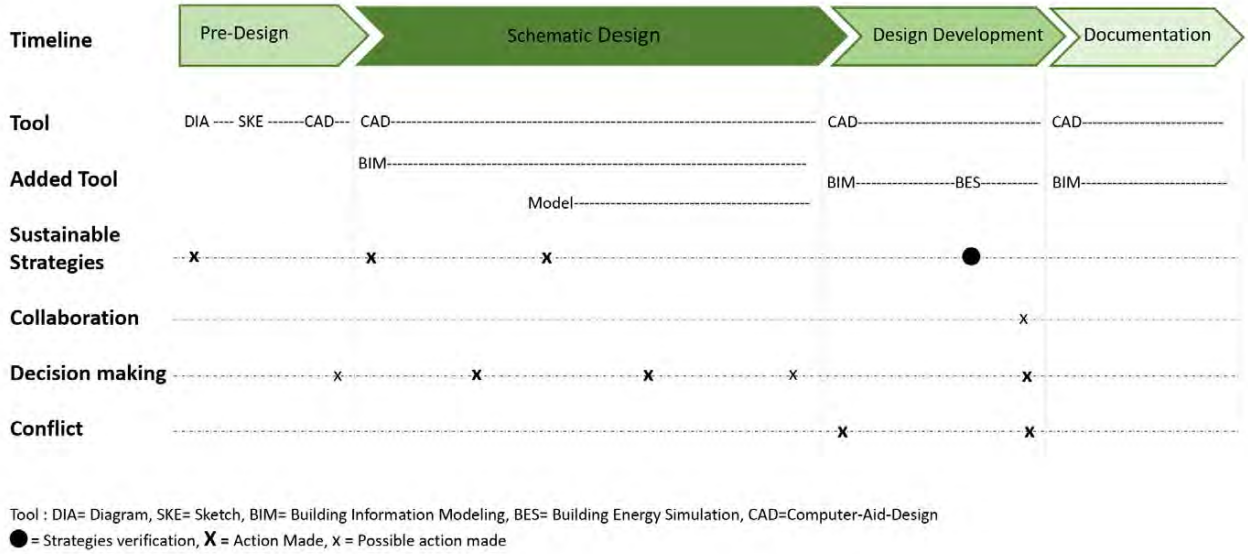

Figure 2: Current practices of the architectural design process integrating BIM and BES in Cambodia identify from the interviews.

the practice of these two methods can be varying from one company to another, depending on company protocol, available data sources, human resource, and client requirements. However, there are similar issues that we can identify from these interviews which are:

- Implementation of BIM start too late into the design process, when all the main design options are already decided.

- The delayed of collaboration with structural engineer in the process generates technical problems, impacts a lot of the design choices, and takes long time to modify the project.

- BES are not involved directly during the design process and are not used to help with sustainable strategies design choices but to verify the concept which doesn't benefit the architects during the design process to help them achieve green building goals. Moreover, if verification from BES show any problems, it is either too late to modify the project or it would take a lot of time to solve.

Overall, we can see that the use of BIM and BES currently bias towards the purpose of client or meets with green building certificate requirement rather than being used for the advantage of the architects and other actors involved in the project during the design phase. Integrating BIM and BES since the early stage of design process is what current practitioners and non-practitioners of these methods expect to do in the future.

5. PROPOSITION OF 5-PHASES DESIGN PROCESS

To address the current limitations encountered and issues indicated above, a 5-phases design process integrating BIM and BES for sustainable building in developing countries was proposed (Fig.2). The proposed design process divides the pre-design phase into 2 more phases where the implementation of BIM and BES can be added and can assist the architect to achieve sustainability in their buildings since the preliminary design.

The 5-phases design process includes:

- Site and Programming: collection of data, site visit, client requirements where basic tools can be applied

- Concept Design: initial concept is created: the form, the space and functionality of the building, and the sustainable performances to be achieved are defined, where BIM should be integrated as BIM model can generate both form and function of the building at the same time and can help sharing building information and selecting targeted performances and sustainable building strategies.

- Schematic Design: detail of design concept such as openings, space, façade, choice of material and overall design of building envelop, which is a critical design phase that needs an integration of BIM and BES for the reason that BIM model can help shorten the time of detail drawing, store all design data that can be used later to conduct BES to evaluate building performance according to different design choices that have been created. Here BES can help the architect directly in the design process for the purpose of obtaining a sustainable building.

- Design Development: focus on structural detail and MEP, the project is at the end of the design phase. BIM model plays an importance role for smooth communication between architects and engineers at this stage. Moreover, BIM and BES models that are already completed can help for last minute decision making and verification to the requirement of client or green building certificate.

- Documentation: final plan execution, preparation for construction phase where BIM model is a necessity as it stores all design data completed since the early design phase for project coordination to facilitate the construction phase.

As we can see, BIM is encouraged to be applied since the early design phase and be practiced throughout the design process until the documentation. The importance of practicing BIM and BES in early stage of design process is to help

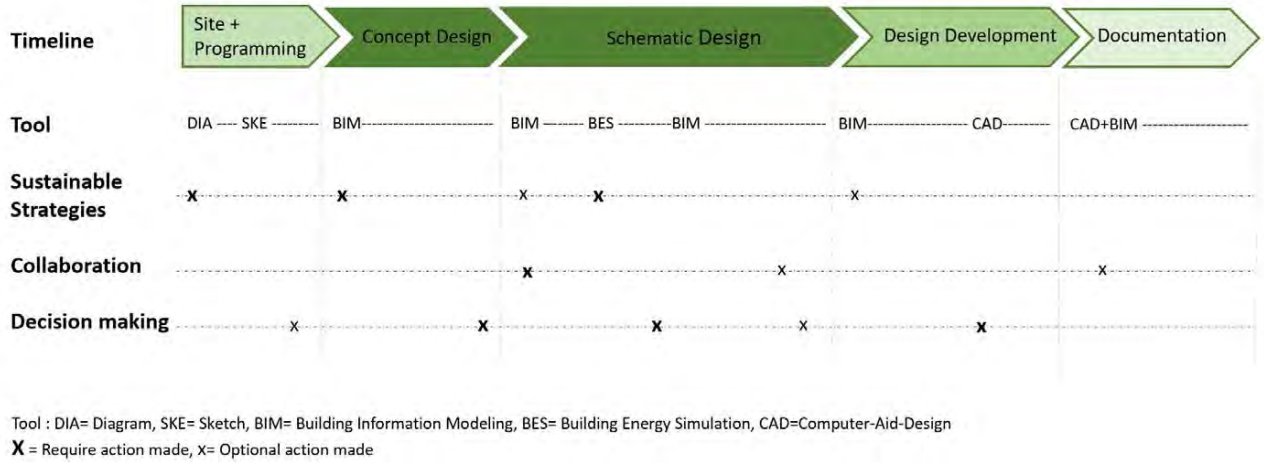

Figure 3: Proposed 5-phases design process integrating BIM and BES

with using these two methods in the correct way to achieve a sustainable building goal (design choices with sustainable principles, comfort in the building and low energy consumption) and to allow since the beginning of the design, collaborations between actors to avoid conflicts in the later design stages.

Regarding the interaction between BIM, BES and sustainable aspects, BIM model completed from Concept Design can be used to conduct BES in Schematic Design easily for decision making of sustainable design strategies such as shading devices to protect direct sun radiation, position and orientation of the openings to allow natural light and ventilation into the building, sustainable material choices, to achieve best possible performance for building.

Decision making can happen many times in the design process. However, the most important one for aspect of sustainable design is at the end of Concept Design where target is set and at the middle of Schematic Design where main sustainable strategies are applied, and the most sustainable concept can be easily chosen with the help from BES. Hence, BES should be integrated in Schematic Design. With the initial use of BIM in Concept Design, the BIM model can be exported to create a building energy model (BEM) for example in Revit software where both BIM and BEM model can be created or exported as a gbXML file for other energy software which facilitate the use of BES in this stage as well.

In terms of collaboration with structural and MEP engineer, it should start since Schematic Design where the concept begins to develop into more details. At this stage, any decision for architectural concept which answers to sustainable principle proposed by architect also gets an agreement from structural and MEP engineer to avoid technical problem. In consequence, integration of BIM in this stage is also critical for clash detection and smooth communication between stakeholders.

Comparing to 4 phases traditional or current design process, the phase added into the proposed design process allows the architect to have time to fully design an initial concept with BIM model which will easily be developed into a more detailed design later in Schematic Design and can be practiced directly later with BES to help evaluate building performance. Moreover, comparing to the 6-phases design process which includes both design and construction phase that was proposed by Farias Stipo [8], the 5-phases design process proposed in this study focus more on the implementation of BIM since the early design phase and its interaction with BES to help realizing the sustainable design integration in the design phase and collaboration with all stakeholders for avoiding numerous conflicts. The main purpose of the 5-phases design process is to help architects design a sustainable building thanks to utilization of BIM and BES.

For developing countries such as Cambodia, that don't have BIM guidelines and where there is no requirement for green building certificate yet, the 5-phase design process take into account the current issue facing with mal-implementation of BIM and BES in buildings design. This new design process would easily help architects to start and put in place the step of designing/practicing BIM and BES, as well as prepared designers and companies in the related field for when BIM and BES will become a necessity or a definite requirement later in the future.

6. CONCLUSION

The innovation of this study consists in collecting useful information for understanding the current use of BIM and BES for sustainable building design in a developing country and proposing a new architectural design process integrating them at an earlier design stage to improve the sustainability of buildings in this context.

The practice of BIM and BES in sustainable design process in developing countries has increased in the last decades but is still limited. The current design process integrating these two methods isn't clear yet and can be very complex for some companies. In Cambodia, the utilization of these two methods does not yet respond well to the purpose of sustainable building design in conception phase related to decision making to certain design aspects.

A 5-phases design process integrating BIM and BES is proposed where these two methods are highly recommended to practice since the early design phase as they could help with collaboration and decision making of concept choices since this stage. As BIM can facilitate the conducting of BES, they should be practiced together. As expertise is required for utilization of these two methods, the traditional design process can still be put into practice for noncomplex projects where experience, theory or physical model are applicable for collaboration and building thermal performance analysis.

The limited number of architectural firms in Cambodia that meet the selection criteria of this study is the main limitation of this research. Moreover, the data collected in this study concern the only case study of Cambodia. It would be interesting to study the same topic in other developing countries and comparing the results found in different developing countries would be interesting for future research.

ACKNOWLEDGEMENTS

Thank you to Académie de Recherche et d'Enseignement Supérieur (ARES) for funding this research.

REFERENCES

1. N. A. Megahed, (2015) “Digital Realm: Parametric enabled Paradigm in Architectural Design Process,” *Int. J. Archit. Eng. Constr.*, vol. 4, no. 3, doi: 10.7492/ijaec.2015.018.

2. L. Ji-Xiang, J. Tang-Ming, and L. Xing-Ye, (2020) “The Analysis of Green Building System Based on BIM,” *IOP Conf. Ser. Earth Environ. Sci.*, vol. 495, no. 1, doi: 10.1088/1755-1315/495/1/012054.

3. D. Utkucu and H. Sözer, (2020) “An evaluation process for natural ventilation using a scenario-based multi-criteria and multi-interaction analysis,” *Energy Reports*, vol. 6, pp. 644–661, doi: 10.1016/j.egyr.2020.02.001.

4.Y. Lu, Z. Wu, R. Chang, and Y. Li, (2017) “Building Information Modeling (BIM) for green buildings: A critical review and future directions,” *Autom. Constr.*, vol. 83, no. August, pp. 134–148, doi: 10.1016/j.autcon.2017.08.024.

5. O. Oduyemi and M. Okoroh, (2016) “Building performance modelling for sustainable building design,” *Int. J. Sustain. Built Environ.*, vol. 5, no. 2, pp. 461–469, doi: 10.1016/j.ijsbe.2016.05.004.

6. Y. T. Chang and S. H. Hsieh, (2020) “A review of building information modeling research for green building design through building performance analysis,” *J. Inf. Technol. Constr.*, vol. 25, pp. 1–40, doi: 10.36680/j.itcon.2020.001.

7. P. H. Lin, C. C. Chang, Y. H. Lin, and W. L. Lin, (2019) “Green BIM assessment applying for energy consumption and comfort in the traditional public market: A case study,” *Sustain.*, vol. 11, no. 17 doi: 10.3390/su11174636.

8. F. J. Farias Stipo, (2015) “A standard design process for sustainable design,” *Procedia Comput. Sci.*, vol. 52, no. 1, pp. 746–753, doi: 10.1016/j.procs.2015.05.121.

9. A. Farzaneh, D. Monfet, and D. Forgues, (2019) “Review of using Building Information Modeling for building energy modeling during the design process,” *J. Build. Eng.*, vol. 23, no. January, pp. 127–135, doi: 10.1016/j.jobe.2019.01.029.

10. N. Thuesen, P. H. Kirkegaard, and R. L. Jensen, (2019) “Evaluation of BIM and Ecotect for conceptual architectural design analysis,” *EG-ICE 2010 - 17th Int. Work. Intell. Comput. Eng.*

PLEA 2024 WROCŁAW
(Re)thinking Resilience

Passive cooling strategies for India:
Verification of the hygrothermal model of a naturally ventilated apartment in Bengaluru

SHANTI SRINIVAS[1] DAVID ALLINSON[1] ARASH BEIZAEE[1]

[1]Loughborough University, Loughborough, UK

ABSTRACT: Whole building hygrothermal simulations can help evaluate the effectiveness of passive measures in regulating temperature and RH to improve thermal comfort and reduce air conditioner use. This paper provides a method for the verification of the hygrothermal model of a naturally ventilated apartment in Bengaluru, India. The hygrothermal model is considered verified as the rooms monitored meet the criteria for Mean Absolute Error, Root Mean Square Error, R^2 and the Absolute Error in temperature and RH for temperature and RH predictions. This method can be used in other studies that include hygrothermal predictions of indoor air conditions during the cooling season and to evaluate the effectiveness of passive measures.
KEYWORDS: Hygrothermal model verification, passive measures, thermal comfort, naturally ventilated buildings

1. INTRODUCTION

Summers account for 60% of the total energy consumption in India's urban households (1). This is directly related to Air Conditioner (AC) use (2), and nearly 10% of India's total electricity consumption is due to space cooling requirements (3). Rapid increase in AC ownership and use is one of the key drivers of the increase in peak electricity demand in India (3). Air-conditioning accounted for 40% to 60% of summer peak load in large Indian cities and is estimated to be 30% of national peak demand by 2030 (4). However, a significant proportion of India's population (~60-70%) cannot afford air conditioners (5). The World Energy Outlook 2023 report by the International Energy Agency (IEA) estimates that there could be two ACs per household in India by 2050 leading to a ninefold rise in energy consumption due to their use (3).

Bengaluru, the fifth largest city and the IT capital of India, has a temperate climate (6). 46% of building permits issued in Bengaluru to date are for multiple family units, including high- and low-rise buildings (7). Thermal comfort depends on indoor temperature and Relative Humidity (RH). Retrofitting existing buildings with passive measures which effectively reduce and/or dissipate heat gains and regulate indoor temperature and RH without the use of electricity can reduce the uptake and use of ACs (8) and ensure thermal comfort for all (9).

Whole building hygrothermal simulations can help evaluate the effectiveness of passive measures such as natural ventilation, solar shading, window glazing, thermal mass and moisture buffering materials, in regulating both temperature and RH to improve thermal comfort (10). It is important to be able to verify the hygrothermal predictions. The ASHRAE Guideline 14–2014 suggests upper limits for the Coefficient of Variation of the Root-Mean-Square Error (CVRMSE) and the Normalised Mean Bias error (NMBE) for validation of hourly and monthly energy consumption predictions (11). However, the CVRMSE validation limit is too large for use with indoor air temperature and RH and NMBE are prone to error cancellation effect skewing results (12).

A recent review of hygrothermal simulations studies recommends the use of Mean Absolute Error (MAE), the mean of the absolute value (the non-negative magnitude of the real number) of the difference between the monitored and simulated values, and Root Mean Square Error (RMSE), the square root of the mean of the square of the difference between monitored and simulated values, as they avoid the error cancellation effect and normalisation effect inherent in NMBE and are therefore more reliable (12). Other studies have used a variety of different indices and criteria to verify the temperature and RH predictions for historical buildings (12, 13). This has resulted in varying recommendations for control parameters, statistical indices, thresholds and validation periods (12, 13). Standardised guidelines for verifying the predictions of hygrothermal building models are needed.

This paper provides a method for the verification of hygrothermal simulation for a naturally ventilated apartment located in a high-rise building in Bengaluru that would be suitable for assessing passive measures to reduce the use of air conditioning.

2. METHODOLOGY

The hygrothermal model was verified using data collected in a case-study apartment.

2.1 The case study apartment

A typical two bedroom naturally ventilated apartment on the sixth floor of a seven storey high rise building in urban Bengaluru was monitored over the summer of 2022 from mid-Feb to mid-May 2022. The building was occupied by 2 occupants. Indoor air temperature and RH were monitored using Onset HOBO U12-011 data loggers (accuracy ± 0.35°C from 0° to 50°C and ±2.5% from 10% to 90% RH (typical), to a maximum of ±3.5% including hysteresis, (14)) positioned in the two bedrooms and lounge. A building survey (Figure 1) and an occupant interview, to gather information required to create the occupancy, appliance use and window opening/closing schedules, were carried out during the monitoring period.

2.2 Creating the hygrothermal model

The model geometry was created in DesignBuilder v6.1.8.021 (15) based on the building survey and then imported into WUFI Plus v3.5.0.1 (16), a whole building Heat and Moisture Transfer (HAMT) energy simulation software. The thermal properties of construction materials were obtained from literature (17–19). The hygrothermal properties in the WUFI Plus software materials database that were the closest match in density to those identified from literature were used in the WUFI model (Table 1).

The external/party walls and the internal partitions were 0.23m and 0.135m thick respectively with cement plaster, brick and cement plaster layers. Intermediate roof and floor (assumed to be adiabatic as there were apartments above and below) were 0.12m thick with floor tile, reinforced cement concrete and cement plaster layers. A wall external shading factor of 0.4 was used (20). The typical daily occupancy and appliance use schedules required by WUFI Plus were created using data gathered during the building survey and occupant interview (Table 1).

Weather data was sourced from the Shiny Weather data website (21) in the .wac format required by the software. Shading due to neighbouring trees and buildings and furniture in the apartment were not modelled. Linear thermal bridges at building junctions were modelled as per BRE Appendix K for thermal bridges (22).

The air flow network model in WUFI Plus was used to model infiltration and ventilation. Pressurisation test to determine the infiltration rate of the apartment was not carried out. The infiltration rate of 20 ACH@50Pa was used as it was found to vary between 10 and 30 ACH@50Pa from a study on 30 Indian apartments in Ahmedabad, India (23). The flow coefficients for walls, door and windows were determined using the inbuilt pressurisation test in the WUFI Plus v3.5.0.1 software by specifying the flow exponents and discharge coefficients for leaky buildings (24). Based on the occupant interview, the Bedroom1, Bathroom and Ensuite windows were modelled as open all day; Bedroom2 and Kitchen windows open from 6 am to 10 pm; and Study window open from 6 -7 pm. Height and width of window opening areas are detailed in Table 1.

Figure 1: Case study building layout

2.3 Calibrating the hygrothermal model

A sensitivity analysis was performed to quantify the effect of uncertainty in various model input parameters (25). The critical parameters (Table 2) identified from literature were varied from their central estimate between an upper and lower limit, also identified from literature, one-at-a-time. An initial RH of 62.5%, the annual mean of the indoor RH and outdoor RH for Bengaluru, was assumed for all building components and multiple year simulations were run to determine the water content in the existing building component layers, once they reached dynamic equilibrium, to use in the parametric simulations (26). The resulting temperature and RH profiles were compared to understand their impact on the predictions. All predictions were compared with the monitored data using the MAE and RMSE determined using equations (1**)** and (2**)**. The results were used to identify the parameters which were most impactful in reducing both MAE and RMSE for both temperature and RH. To calibrate the model, the parameters identified by sensitivity analysis were varied in different combinations. The model was deemed to be calibrated when the results satisfied the verification criteria specified in Table 3 and Table 4.

$$\mathbf{MAE} = \frac{1}{n}\sum_{i=1}^{n}(\boldsymbol{am} - \boldsymbol{as}) \qquad \textbf{(1)}$$

where *MAE* – Mean Absolute Error;
n - number of datapoints;
am - absolute monitored value;
as - absolute simulated value;

$$\mathbf{RMSE} = \sqrt{\frac{1}{n}\sum_{i=1}^{n}(\boldsymbol{m} - \boldsymbol{s})^2} \qquad \textbf{(2)}$$

where *RMSE* – Root Mean Square Error
n - number of datapoint
m - monitored value
s - simulated value

Table 1: Basecase model data

Wall materials[1]	Thermal conductivity (W/mK)	Porosity (-)	Bulk Density, (kg/m³)	Specific heat capacity, (J/KgK)	Water vapour diffusion resistance factor (-)	Typical built-in moisture content (kg/m³)
Cement Plaster (18)	0.72	0.30	1762	840	25	280
Solid brick masonry (18)	0.90	0.24	1920	800	10	100
Reinforced Cement Concrete (18)	1.58	0.18	2258	880	248	147
Ceramic tiles (19)	1.60	0.17	2120	850	33	0
Oak old (WUFI Plus)	0.15	0.35	740	1400	223	104

Windows	Thickness (mm)	U-value (W/m²K)	SHGC (-)	VLT (-)
Single glazed (17)	0.3	5.88	0.86	0.8

Room data Source: Building survey and occupant interview	Floor area (m²)	% Occupancy (%)	Daily Convective heat gains (W)	Daily Radiant heat gains (W)	Daily Moisture gains (g/h)
Ensuite	4.19	14.6	412.80	194.45	360.50
Kitchen	8.06	25.0	11378.65	391.60	932.00
Study	12.65	16.6	437.20	211.80	331.50
Bedroom2	11.86	60.4 weekdays / 52.1 weekends	1968.50	456.50	495.25
Verandah	4.96	6.3	131.25	65.75	566.50
Bathroom	2.91	12.5	342.60	146.80	270.50
Bedroom1	13.22	39.6	1652.73	342.78	436.00
Lounge	34.04	35.4	2854.40	1165.50	808.50

Window and wall data	External door/window orientation and type	External Window/ Door area (m²)	Window Opening area (m²)	Flow exponent (-)/Flow coefficient (dm³/(sm²Pan)/Discharge coefficient (-)	External shading factor (-) (18)
Ensuite	E (louvre window)	0.28	0.06	0.6/0.036/0.5	0.64
Kitchen	N (sliding window with grill)	0.69	0.15	0.6/0.056/0.5	0.69
Study	N (turning plate window)	2.26	0.3	0.6/0.069/0.5	0.77
Bedroom2	E and N (turning plate windows)	2.26 E / 1.11 N	0.3, 0.3	0.6/0.069/0.5	0.72 E / 0.78 N
Verandah	N (sliding window no grill)	3.52	0.05	0.6/0.014/0.6	0.64
Bathroom	W (louvre window)	0.29	0.06	0.6/0.036/0.5	0.4
Bedroom1	E (turning plate window)	2.26	0.3	0.6/0.069/0.5	0.71
Lounge	Front door facing S	1.92	N/A	No windows	N/A
Walls	-	-	-	0.84/0.545	0.4

[1] where VLT – Visible Light Transmittance; SHGC – Solar Heat Gain Coefficient

Table 2: Sensitivity analysis parameters

Parameter[2]	Lower limit	Central estimate	Upper limit
Infiltration rate ACH@50 Pa (27)	10	20	30
External shading factor (20)	0.4	0.7	-
Internal heat gains	Halved	As surveyed	Doubled
Moisture gains	Halved	As surveyed	Doubled
Thermal properties of brick (28)	ρ -1807; λ - 0.5893; C - 934.8	ρ– 1920; λ - 0.9; C - 800	ρ– 1952; λ– 1.1; C - 863
Window U-value - (29, 30)	U-value -3.4; VLT - 0.39; SHGC - 0.42;	U-value -5.88; VLT - 0.8 SHGC - 0.86,	U-value – 7.1; VLT - 0.58 SHGC - 0.70,
Hygrothermal properties of brick (WUFI Plus)	Wvdrf – 4; RWC – 1.5; WAC – 0.25	Wvdrf – 45; RWC – 18 WAC – not specified	Wvdrf – 19; RWC – 1.2 WAC – 0.142
Solar absorption (-) (WUFI Plus)	0.2	0.3	0.4
Window opening area (m²)	Halved	As surveyed	Doubled

[2] where - ACH, Air Change per Hour; Pa, Pascal; U-value (W/m²K); SHGC, Solar Heat Gain Coefficient; VLT, Visual Light Transmittance; ρ, density (kg/m³); λ, thermal conductivity (W/m-K); C, specific heat capacity (J/kg-K); WVDRF, Water Vapour Diffusion Resistance Factor; RWC, Reference Water Content (kg/m³); WAC, Water Absorption Coefficient (kg/m²s$^{0.5}$)

The verification criteria for indoor air temperature, MAE and RMSE, were as recommended by Jain et al., (31) with the limits recommended by Huerto-Cardenos et al., (12) (Table 3). The verification criteria for indoor RH were based on the absolute error method used by Tariku et al., (32) with the limits recommended by Huerto-Cardenos et al., (12) (Table 4). The calibrated model was considered to be verified if it met the criteria as detailed in Table 3 and Table 4 achieving at least Level 2 of the absolute error between monitored and simulated temperature (AET) and RH (AERH).

Table 3: Temperature criteria for model verification

Statistical index	Temperature Criteria
Mean Absolute Error (MAE)	< 1˚C (31)
Root Mean Square Error (RMSE)	< 1˚C (31)
Absolute Error in Temperature (AET) (Level 2)	<2˚C for >95% of monitoring period
AET (Level 1)	<1˚C for >95% of monitoring period
Coefficient of Determination (R^2)	>0.75 (33)

Table 4: RH criteria for model verification

Statistical Index	RH Criteria
Mean Absolute Error (MAE)	<5%
Root Mean Square Error (RMSE)	<5%
Absolute Error in RH (AERH) (Level 2)	<10% for >95% of monitoring period
AERH (Level 1)	<5% for >95% of monitoring period
Coefficient of Determination (R^2)	>0.75 (33)

3. RESULTS

3.1 Sensitivity analysis and calibration

Results for each permutation of the sensitivity analysis were analysed. The bar chart, Figure 2, shows the parameters and how much they reduced the MAE and RMSE for the temperature and RH predictions for the lounge. Bar charts were also created and analysed for Bedroom1 and Bedroom2.

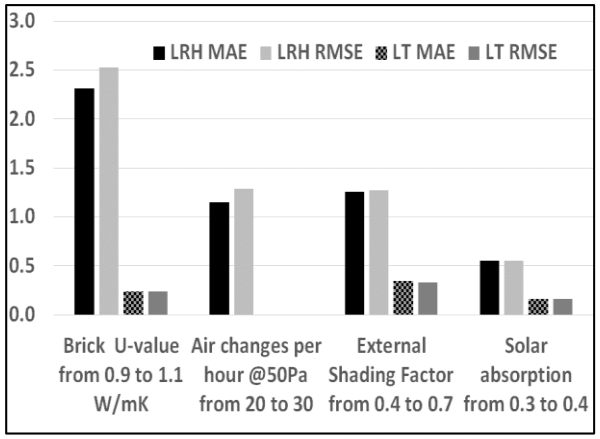

Figure 2: Reduction in MAE and RMSE for temperature and RH predictions due to changes in parametric values for the Lounge

The air infiltration rate, the external shading factor, the brick's thermal and hygrothermal properties, the window U-value, solar absorption and window opening area were found to be the parameters to have the most impact on the predictions for all three rooms. Further simulations were run for infiltration rates of 15 and 25 ACH@50Pa; external shading factor 0.2, 0.3, 0.5, 0.6, 0.8 and 0.9; brick thermal conductivity of 0.4, 0.5, 0.7, 0.8, and 1 W/mK; Window U-value of 5.1W/m^2K and surface absorptivity of 0.5 and 0.6.

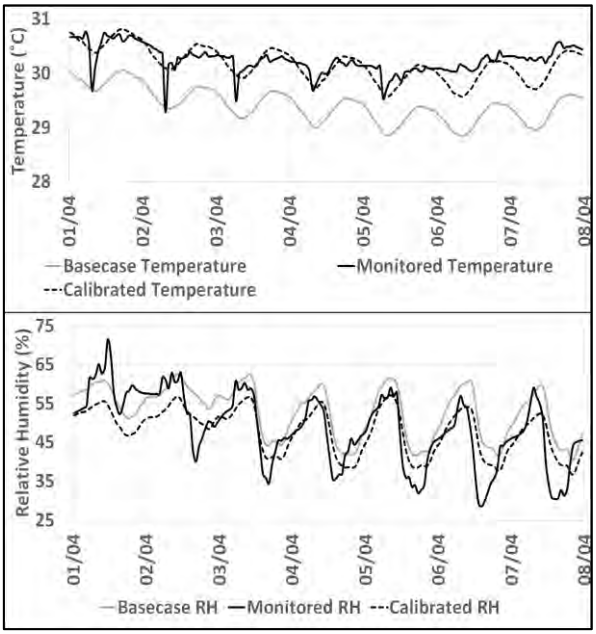

Figure 3: Comparing the temperature and RH profiles for basecase and calibrated models and measured data for the Lounge in 2022

Figure 3 shows the temperature and RH profiles from the basecase model, calibrated model and the measured data. The combination of parameters, which best reduced the MAE and RMSE of both indoor temperature and RH, to create the calibrated model is shown in Table 5.

3.2 Model verification

The results of the calibrated model are shown in Table 6 and Table 7. For more than 99% of the simulation period, AET was <2˚C and for 80-97% of the simulation period AET was <1˚C in all three rooms (Table 6). The MAE and RMSE of indoor RH predictions was <5% and R^2 was >0.75 for all three rooms. For 96% of the simulation period the AERH was <10% in all three rooms; for 72-76% of the simulation period the AERH was <5% (Table 7). Therefore, the calibrated model met the Level 2 criteria for AET and AERH. The MAE and RMSE of indoor temperature predictions for Bedroom2, Bedroom1 and Lounge were both <1˚C and R^2 was >0.75 meeting the rest of the verification criteria.

Table 5: Basecase and Calibrated model settings

	Basecase model	Calibrated model		
Parameters[3]	**All rooms**	**Bedroom1**	**Bedroom2**	**Lounge**
Infiltration rate ACH@50Pa	20	Same as basecase		
External shading factor	0.4	0.7	0.4	0.7
Internal heat gains	as in Table 1	Same as basecase		
Moisture gains	as in Table 1	Same as basecase		
Thermal properties of brick	ρ (kg/m3) – 1920; λ (W/m-K) – 0.9; C (J/kg-K) – 800	ρ (kg/m3) – 1952; λ (W/m-K) – 1.1; C (J/kg-K) – 863		
Hygrothermal properties of brick	WVDRF – 45; RWC – 18; WAC – not specified	WVDRF – 19; RWC – 1.2; WAC – 0.142		
Window U-value	U-value -5.88, SHGC – 0.86, VLT – 0.8	Same as basecase		
Solar absorption (-)	0.3	Same as basecase		
Window opening area (m^2)	as in Table 1	Same as basecase		

[3] where - ACH, Air Change per Hour; Pa, Pascal; ρ, density (kg/m3) ; λ, thermal conductivity (W/m-K); C, specific heat capacity (J/kg-K); WVDRF, Water Vapour Diffusion Resistance Factor; RWC, Reference Water Content (kg/m^3); WAC, Water Absorption Coefficient ($kg/m^2s^{0.5}$); U-value (W/m^2K); SHGC, Solar Heat Gain Coefficient; VLT, Visual Light Transmittance

Table 6: Temperature results for 15 Feb - 14 May 2022

Verification criteria (Level2)	AET <2℃ for >95% of simulation period	<1℃	<1℃	> 0.75
	% of simulation period when AET was <2℃	**MAE (℃)**	**RMSE (℃)**	**R^2 (-)**
Bedroom2	99.0	0.56	0.71	0.88
Bedroom1	99.8	0.79	0.90	0.86
Lounge	99.9	0.33	0.44	0.94

Table 7: RH results for 15 Feb - 14 May 2022

Verification criteria (Level2)	AERH <10% for >95% of simulation period	<5%	<5%	>0.75
	% of simulation period when AERH was <10%	**MAE (%)**	**RMSE (%)**	**R^2 (-)**
Bedroom2	95.6	3.79	4.83	0.85
Bedroom1	95.9	3.76	4.79	0.85
Lounge	95.7	3.60	4.73	0.81

4. DISCUSSION

The calibration of the model was considered acceptable as it met the verification criteria up to Level 2 criteria for AET and AERH (Table 6 and Table 7). The level 1 criteria was not achieved because of the uncertainties, assumptions and software limitations.

The hygrothermal properties of the building's construction materials are not known and so those from the WUFI Plus database that were the closest match in density were used. The daily typical occupancy and window/front door opening and closing schedules were reasonably well known, but occupant behaviour is stochastic and varies with climate, work commitments, illness and other personal reasons including going away on holiday and having guests to stay.

An older version of the software (WUFI Plus v3.2.0.1) had to be used to determine the flow coefficients because version v3.3.0.2 crashed repeatedly, a known issue. WUFI Plus v3.3.0.2 did not accept flow coefficient values >1 $dm^3/(sm^2Pan)$ (even though the built-in pressurisation test suggested them) and U-values greater than 5.88 W/m^2K for window glazing, including when that glazing is specified in the WUFI database. Therefore, it was not possible to model the upper limit of window glazing of 7.1 W/m^2K.

It was difficult to calibrate the model because of the interdependency between temperature and RH and how this varied between the different rooms. For example, Bedroom2 was the most difficult room in the model to calibrate because it had two external surfaces with windows and therefore more solar heat gains. Reducing the window U-value from 5.88 W/m^2K to 3.4 W/m^2K was effective in reducing MAE and RMSE of the predicted RH only for Bedroom2 but increased them in the Lounge and Bedroom1 because of the heat and moisture transfer between the rooms. The approach outlined here was time consuming but effective. However, this was one case study in a specific climate and further testing of this approach is required. Future work should develop simpler approaches for calibrating hygrothermal models.

5. CONCLUSION

This paper provided a method for the verification of hygrothermal simulation for a naturally ventilated apartment in urban Bengaluru with respect to both indoor temperature and RH. It is recommended that these verification criteria can be used in other studies that include hygrothermal predictions of indoor air conditions during the cooling season. The resulting model is deemed to be suitable for assessing passive measures which effectively reduce and/or dissipate

heat gains and regulate indoor relative humidity without the use of electricity This can reduce the uptake and use of ACs and ensure thermal comfort for all.

REFERENCES

1. Thapar, S. (2020). Energy consumption behavior: A data-based analysis of urban Indian households. Energy Policy, 143, 111571.
2. Singh, J., Mantha, S.S. and Phalle, V.M. (2018). Characterizing domestic electricity consumption in the Indian urban household sector. Energy Build, 170, 74–82.
3. - International Energy Agency, (2023). World Energy Outlook 2023. [Online], Available: https://iea.blob.core.windows.net/assets/66b8f989-971c-4a8d-82b0-4735834de594/WorldEnergyOutlook2023.pdf.
4. Abhyankar,N., Shah,N. and Park,W.Y. (2017). Accelerating Energy Efficiency Improvements in Room Air Conditioners in India: Potential, Costs-Benefits, and Policies. [Online], Available: https://escholarship.org/uc/item/8710154k
5. Kachhawa, S., Kumar, S. and Singh, M. (2019). Decoding India's residential building stock characteristics to enable effective energy efficiency policies and programs. In. ECEEE. [Online], Available: https://www.eceee.org/library/conference_proceedings/eceee_Summer_Studies/2019/7-make-buildings-policies-great-again/decoding-indias-residential-building-stock-characteristics-to-enable-effective-energy-efficiency-policies-and-programs/2019/7-252-19_Kachhawa.pdf/
6. Bureau of Indian Standards (2016). National Building Code of India 2016 Volume 1. [Online], Available: https://archive.org/details/NBC2016VOL.2.pdf
7. National Informatics Centre Building Related Information and Knowledge Systems. [Online], Available: http://briks.gov.in/Report/ReportHome.aspx
8. IEA (2018). The Future of Cooling: Opportunities for energy-efficient air conditioning. [Online], Available: https://doi.org/10.1787/9789264301993-en
9. Sustainable and Smart Space Cooling Coalition (2017). Thermal comfort for all. [Online], Available: https://shaktifoundation.in/wp-content/uploads/2017/09/Thermal-Comfort-for-All.pdf
10. Little, J., Ferraro, C. and Arregi, B. (2015). Assessing risks in insulation retrofits using hygrothermal software tools. [Online], Available: https://www.historicenvironment.scot/archives-and-research/publications/publication/?publicationId=8a2a7b9d-e3b2-4c7d-8c17-a59400a8387b
11. ASHRAE (2014). Guideline 14-2014 -- Measurement of Energy, Demand, and Water Savings.
12. Huerto-Cardenas, H.E., Leonforte, F., Aste, N., Del Pero, C., Evola, G., Costanzo, V. and Lucchi, E. (2020). Validation of dynamic hygrothermal simulation models for historical buildings: State of the art, research challenges and recommendations. Build Environ, 180, 107081.
13. Costa-Carrapiço, I., Croxford, B., Raslan, R. and Neila González, J. (2022). Hygrothermal calibration and validation of vernacular dwellings: A genetic algorithm-based optimisation methodology. Journal of Building Engineering, 55, 104717.
14. ONSET HOBO U12 Temp/RH Data Logger (U12-011) User's Manual | Onset's HOBO and InTemp Data Loggers. [Online], Available: here
15. DesignBuilder Software Ltd - Home. [Online], Available: https://designbuilder.co.uk//
16. WUFI Plus. [Online], Available: https://wufi.de/en/software/wufi-plus/
17. Shukla, Y., Rawal, R. and Shnapp, S. (2015). Residential buildings in India: Energy use projections and savings potentials. [Online], Available: https://www.eceee.org/library/conference_proceedings/eceee_Summer_Studies/2015/6-policies-and-programmes-towards-a-zero-energy-building-stock/residential-buildings-in-india-energy-use-projections-and-savings-potentials/
18. BEE (2018). Eco-Niwas Samhita 2018. [Online], Available: here.
19. Cook, M.J., Shukla, Y., Rawal, R., Angelopoulos, C., Caruggi-De-faria, L., Loveday, D., Spentzou, E. and Patel, J. (2022). Integrating low energy cooling and ventilation strategies in Indian residences. Buildings and Cities, 3, 279–296.
20. Matthews, R. (2018). More about PHPP - Part 2 of an Introduction to PHPP. [Online], Available: here.
21. Shiny weather data. [Online], Available: https://shinyweatherdata.com/
22. BRE (2006). Appendix K : Thermal bridging. [Online], Available: here.
23. Mathur, U. and Damle, R. (2021). Impact of air infiltration rate on the thermal transmittance value of building envelope. Journal of Building Engineering, 40, 102302.
24. Orme, M. and Leksmono, N. (2002). AIVC Guide 5 Ventilation Modelling Data Guide. [Online], Available: here.
25. Belleri, A., Lollini, R. and Dutton, S.M. (2014). Natural ventilation design: An analysis of predicted and measured performance. Build Environ, 81, 123–138.
26. Zirkelbach,D., Schmidt,T., Kehrer,M. and Künzel,H.M. WUFI ® Pro 5 Manual WUFI ® Pro-Manual 2 PREAMBLE. [Online], Available: here
27. Mathur, U. (2020). Estimating the effect of air infiltration rate on RETV values: on-site measurements and energy simulations. [Online], Available: here
28. Greentech Knowledge Solutions Pvt. Ltd., CEPT Research and Development Foundation and CEPT university (2020). Thermal Performance of Walling Material and Wall Technology. [Online], Available: here.
29. Kasamsetty, S. (2018). Projecting National Energy Saving Estimate from the Adoption of High Performance Windows Glazing in 2030. [Online], Available: here.
30. Gorantla, K., Shaik, S. and Setty, A.B.T.P. (2017). Effects of Single, Double, Triple and Quadruple Window Glazing of Various Glass Materials on Heat Gain in Green Energy Buildings. Materials, Energy and Environment Engineering, 10.1007/978-981-10-2675-1_5.
31. Jain, N., Burman, E., Mumovic, D. and Davies, M. (2020). Improving model calibration methods: a case study application of incorporating IEQ with energy. [Online], Available: here.
32.Tariku, F., Kumaran, K. and Fazio, P. (2011). Determination of indoor humidity profile using a whole-building hygrothermal model. 10.1007/s12273-011-0031-x. https://doi.org/10.1007/s12273-011-0031-x
33. Nouri, A., Frisch, J. and van Treeck, C. (2021). Statistical Methodologies for Verification of Building Energy Performance Simulation. [Online], Available: https://doi.org/10.26868/25222708.2021.30538

PLEA 2024 WROCŁAW
(Re)thinking Resilience

In-situ U-values of Traditional Solid Masonry and Early Mass Concrete Walls in Ireland:

Results from the FabTrads and Built to Last Projects

CAROLINE ENGEL PURCELL[1], JOSEPH LITTLE[2], ROSANNE WALKER[1], ANNA HOFHEINZ[1], OLIVER KINNANE[1]

[1]University College Dublin, Dublin, Ireland

[2]Technological University Dublin, Dublin, Ireland

ABSTRACT: This paper discusses in-situ U-value measurements of 27 uninsulated solid walls of traditional masonry and early mass concrete construction across Ireland as part of the FabTrads and Built to Last projects. As increasing attention is focused on upgrading the poorest performing building stock, it is imperative that a thermal efficiency baseline is set for commonly found types of solid wall construction that is based on both in-situ U-value measurements and laboratory-derived hygrothermal properties. As it stands, no large-scale publicly available dataset of in-situ U-values exists in Ireland and therefore assumptions of thermal efficiency are based on DEAP defaults. This paper discusses the validity of these U-value defaults, comparing them with in-situ U-value test results to date.

KEYWORDS: In-situ U-values, Traditional Buildings, Thermal Efficiency, Hygrothermal, WUFI

1. INTRODUCTION

The National Energy and Climate Plan for Ireland (2021-2030) commits to retrofitting 500,000 homes to B2 BER or cost optimal level by 2030. An estimated 1/6th of Ireland's building stock is traditional construction and it is anticipated that the performance of these buildings will come under increased scrutiny as more attention is placed on buildings with the lowest BERs [2]. However, there is widespread international evidence of inappropriate retrofit works causing long term damage to traditional building fabric [2-5]. Default U-values in the National Calculation Methodology are often used by Irish building professionals when designing thermal upgrades for traditional buildings as these are readily accepted by the local Building Control Office, however it has long been questioned how these defaults were derived and whether they are truly indicative of the thermal performance of traditional solid masonry construction.

The FabTrads project and Built to Last case studies were designed to bridge these knowledge gaps by providing accurate thermal performance data and specific case study based guidance on retrofit options. While the FabTrads project is ongoing, the U-value measurements of the Built to Last project were carried out in spring of 2014 and are published here for the first time.

Using in-situ U-value measurements from both projects, the team will work with the Sustainable Energy Authority of Ireland and the National Standards Authority of Ireland to revise the default U-values for a range of traditional solid masonry and early mass concrete walls to improve the accuracy of BER (EPC) assessments accordingly. By the end to the FabTrads project, it is anticipated we will have tested or collated in-situ U-value measurements for up to 50 traditional Irish buildings of varying construction types, thus creating the largest sample-set of in-situ U-value tests in Ireland to date.

Additionally, the FabTrads project is measuring the hygrothermal properties of a range of traditional construction materials in use in Ireland between 1700 and 1940 through a series of laboratory tests. The findings will be incorporated into a new dataset to support more accurate hygrothermal modelling in accordance with IS EN 15026:2007.

2. METHODOLOGY & SCOPE

The FabTrads project and Built to Last case studies followed the same principles, adhered to the same boundaries and used different but similar measurement equipment. The FabTrads project used the GreenTEG gSKIN U-value kits with one heat flux sensor, one indoor and one outdoor ambient temperature sensor and a data logger. Heat flux sensors were fixed to the walls using manufacturer-supplied double-sided tape and ambient temperature sensors were positioned to hang 5cm away from the wall surfaces as per manufacturer instructions. In the Built to Last project a bespoke set-up was used featuring three heat flow meters (located to take account of thermal stratification), five thermocouples to record surface and ambient temperature (°C) and a data logger. Thermal putty (coating the 'cold' face of heat flow meters) ensured undulations of wall surfaces

would not impact on the measurement of heat flow. Masking tape adhered the sensors to the wall surface finish, which was protected from the putty by a polythene membrane.

Figure 1. GreenTEG gSKIN U-value kit with ambient temperature sensors, heat flux sensor and data logger.

Figure 2. Built to Last heat flow meters, thermal couples data logger and set up.

The tests were conducted by two separate teams with no overlap, but all tests complied with the requirements of ISO 9869-1:2014. The set-up of each test conformed to the following guidelines:

- North facing walls were given preference to avoid results being skewed by solar irradiation.
- A relatively constant indoor temperature approximately 10˚ Celsius above outdoor temperatures was maintained throughout the duration of each test.
- All potential thermal bridge conditions were avoided (e.g. window, door and wall junctions) as much as possible. Ideally sensors should be placed at least 1.5m away from any potential thermal bridges.
- All tests were run longer than the 72-hour minimum as prescribed by ISO 9836-1:2014 to ensure that compliant data were collected.
- Both projects tested at least two locations on the same wall to measure differences due to construction and condition, and to derive an average U-value for the wall.

Due to the recommended 10˚ Celsius differential required to adequately measure heat flow through the walls, in-situ U-value tests must generally be done in the winter months between October and April in Ireland. This limits the number of tests that can be done in a single year so to maximise the testing opportunities while ensuring valid test results, the FabTrads tests were generally run for 6-7 days and moved from one building to the next each week.

The U-value measurements run by both projects were non-invasive so in most instances it was not possible to examine the exact build-up of each wall tested. Where works were being done in the building, measurements and photographs were taken of the opening up works. In other instances, historic building guides and conservation knowledge were relied upon to make professional assumptions about the wall build-up.

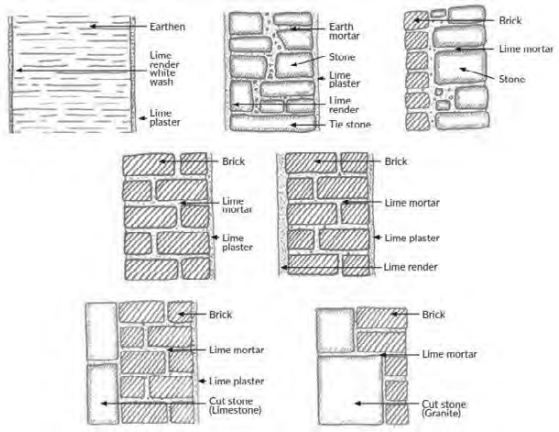

Figure 3. Illustrative example of traditional solid masonry walls in Ireland [6].

Where possible, wall samples (bricks, stone, mortar, etc.) were collected for hygrothermal laboratory testing with the FabTrads project to inform transient modelling (using WUFI Pro simulation software) at a later stage. No laboratory testing was done as part of the Built to Last case studies so default data from the WUFI database was used for calculations.

Built to Last was funded by Dublin City Council and was confined to buildings within Dublin, while FabTrads was funded by the Sustainable Energy Authority of Ireland with a remit to test materials and buildings over the breadth of the country. Buildings

were chosen to represent the variety of local masonry materials and traditional solid wall construction found in Ireland.

=

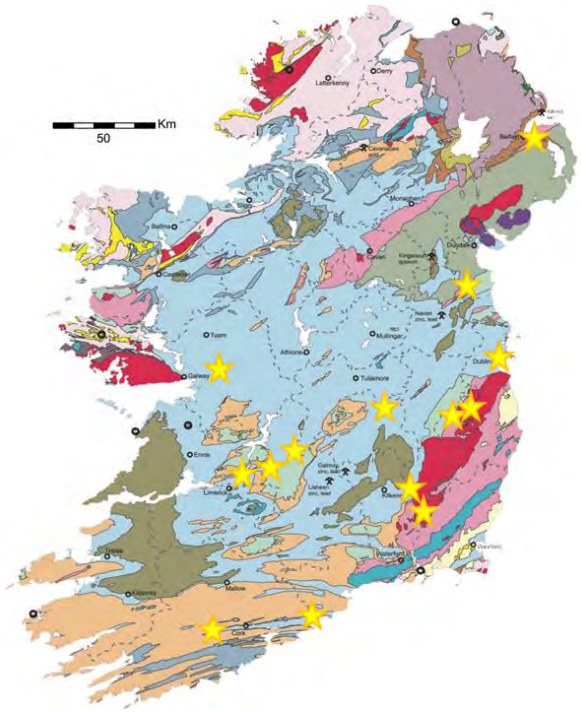

Figure 4. Locations of FabTrads and Built to Last U-value testing completed as of December 2023. Note: one star may represent multiple buildings tested.

3. RESULTS

This paper presents initial results from the first year and a half of FabTrads in-situ U-value testing of traditional (pre-1940) solid masonry and early mass concrete walls in Ireland alongside the results of in-situ U-value testing conducted as part of the Built to Last case studies.

Six buildings were tested as part of the Built to Last project and 21 buildings have been tested to date as part of the FabTrads project. The Built to Last project results include comparisons of in-situ U-values with calculated U-values according to BR 443 and ISO 6946:2017 using thermal conductivities from standards and guidance documents, however this will be done at a later date for the FabTrads project once the hygrothermal properties of the wall materials are ascertained through laboratory testing.

Where default U-values are referred to, this refers to the default U-values used in the Dwelling Energy Assessment Procedure (DEAP) used by Building Energy Rating (BER) assessors in Ireland [1]. The relevant default DEAP U-values by age band (Figure 5) and masonry type are shown in Figure 6.

Details and results of the six Built to Last buildings tested are shown in Table 1 and Figure 7.

Details and results of the 21 FabTrads buildings tested to date are shown in **Error! Reference source not found.**, Figure 8 and Figure 9.

Age band	Years of construction
A	before 1900
B	1900-1929
C	1930-1949
D	1950-1966
E	1967-1977
F	1978-1982
G	1983-1993
H	1994-1999
I	2000-2004
J	2005 -2009
K	2010 onwards

Figure 5. DEAP age bands for assigning default U-values and other data [1].

Wall type	Age band										
	A	B	C	D	E	F*	G*	H	I	J	K
Stone	2.1	2.1	2.1	2.1	2.1	1.1	0.6	0.55	0.55	0.37	0.27
225mm solid brick	2.1	2.1	2.1	2.1	2.1	1.1	0.6	0.55	0.55	0.37	0.27
325mm solid brick	1.64	1.64	1.64	1.64	1.64	1.1	0.6	0.55	0.55	0.37	0.27
300mm cavity	2.1	1.78	1.78	1.78	1.78	1.1	0.6	0.55	0.55	0.37	0.27
300mm filled cavity	0.6	0.6	0.6	0.6	0.6	0.6	0.6	0.55	0.55	0.37	0.27
solid mass concrete	2.2	2.2	2.2	2.2	2.2	1.1	0.6	0.55	0.55	0.37	0.27
concrete hollow block	2.4	2.4	2.4	2.4	2.4	1.1	0.6	0.55	0.55	0.37	0.27
timber frame	2.5	1.9	1.9	1.1	1.1	1.1	0.6	0.55	0.55	0.37	0.27
Unknown	2.1	2.1	2.1	2.1	2.1	1.1	0.6	0.55	0.55	0.37	0.27
425 mm Cavity Wall	1.73	1.51	1.51	1.51	1.51	1.1	0.6	0.55	0.55	0.37	0.27
425 mm filled cavity	0.6	0.6	0.6	0.6	0.6	0.6	0.6	0.55	0.55	0.37	0.27

Figure 6. DEAP default U-values for exposed walls based on wall type and age band [1].

Table 1. Built to Last: Comparison of default, calculated and measured U-values for the six walls studied.

1	2	3	4	5	6	7	8
No.	Address	Type of wall	Width (mm)	Default U-value (W/m²K)	Calculated U-value (W/m²K)	Measured U-value (W/m²K)	Uncertainty ± 28% (W/m²K)
1	Henrietta Street	stone wall (40 mm render & plaster)	750	2.1	1.03	1.03	24 %
2	Ailesbury Gardens	Fair-faced solid brick, plastered	400	1.64	1.21	1.13	31 %
3	Mountjoy Square	Fair-faced solid brick, plastered	365	1.64	1.34	1.18	62 %
4	Ashfield Avenue	Fair-faced solid brick, plastered	240	2.1	1.87	1.62	30 %
5	Niall Street	mass conc. wall, render & plaster	255	2.2	2.50	2.76	28 %
6	**Dingle Road**	**mass conc. wall, render & plaster**	**233**	**2.2**	**2.63**	**3.18**	**22 %**

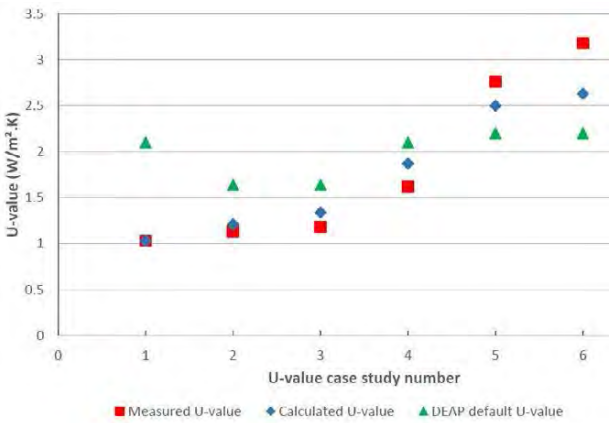

Figure 7. Built to Last: measured, calculated and DEAP default U-values.

Table 2. FabTrads building details and average in-situ U-value test results.

Address	Date Built	Wall Depth (mm)	Primary Masonry Material	Construction details	Average Internal Temp [C]	Average External Temp [C]	Average U-value (W/m2K)
Connolly Station Annex, Dublin	1891	480	Brick	Solid brick - exposed externally, internal lime plaster on the hard	25.3	13.1	1.52
South Circular Rd, Dublin	1860s	500	Limestone	Solid calp rubble - lime mortar and external cement render	12.0	8.4	2.79
St Kevin's Park, Dublin	1910	240	Brick	Solid brick - small cavity between internal and external leafs - internal lime plaster on the hard	11.7	7.8	1.58
Knockduff House, Co. Carlow	1740	480	Granite	Solid rubble granite walls - external NHL 3.5 render & internal lime skud	8.3	3.0	1.35
Parochial House, Co. Louth	1860	620	Limestone	Solid limestone rubble (tbc) - external concrete render & internal bonding plaster w/ wallpaper	21.7	3.4	2.72
Riverview House, Co. Cork	1800	660	Limestone	Solid limestone rubble - internal & external lime render	18.8	8.2	1.92
Crumlin Road, Dublin	1930s	400	Brick	Solid brick - exposed externally, internal lime plaster on the hard	20.6	9.3	2.18
Portarlington Station, Co Laois	1850	480	Limestone	Solid cut blue limestone - exposed externally, internal lath & lime plaster	25.7	4.2	1.91
Kent Station, Cork	1893	510	Brick	Solid brick (possible <100mm cavity) - exposed externally, internal lime plaster on the hard	24.3	10.6	1.34
Lighthouse Rd, Co Cork	1890s	400	Brick	Solid brick - external concrete render, internal lime plaster on the hard	24.0	8.8	2.00
Parochial House, Co. Louth	1860	440	Limestone	Solid limestone rubble (tbc) - external concrete render, internal lime plaster	22.8	11.1	2.96
Belle Isle House, Co. Clare	1778	700	Limestone	Solid limestone - external cement render, internal lime plaster on the hard	22.6	7.0	1.84
Chief Steward's House, Dublin	1865	600	Granite	Solid ashlar granite - exposed externally, internal lath and lime plaster	22.2	7.4	1.55
Cross St, Co. Galway	1900	580	Limestone	Solid limestone with brick inner leaf - exposed externally, internal lime plaster on the hard	17.8	5.9	2.50
Kings Rd, Belfast	1895	300	Brick	Solid brick - exposed externally, internal lime plaster on the hard w/ textured wallpaper	20.2	7.9	1.09
Woodlock Hall Library, Dublin	1853	600	Limestone	Solid cut calp limestone - exposed internally & externally	20.9	11.9	1.67
Directors House, Dublin 8	1870s	450	Granite	Solid granite - exposed externally, internal lime plaster on the hard	21.2	10.9	1.76
Connolly Gardens, Dublin 8	1930s	250	Mass concrete	Mass concrete - external cement pebbledash, internal plaster on the hard	17.9	11.8	3.31
Roscrea Railway Station	1875	540	Sandstone	Solid sandstone - exposed externally, internal lime plaster on the hard	17.1	9.3	1.86
Nenagh Railway Station	1865	500	Sandstone	Solid sandstone - external painted lime render, internal lime plaster on the hard	19.7	12.7	2.37
Eldred Terrace, Cork	1887	520	Limestone	Solid limestone - external cement render, internal lime plaster on the hard w/ wallpaper	17.9	8.4	2.50

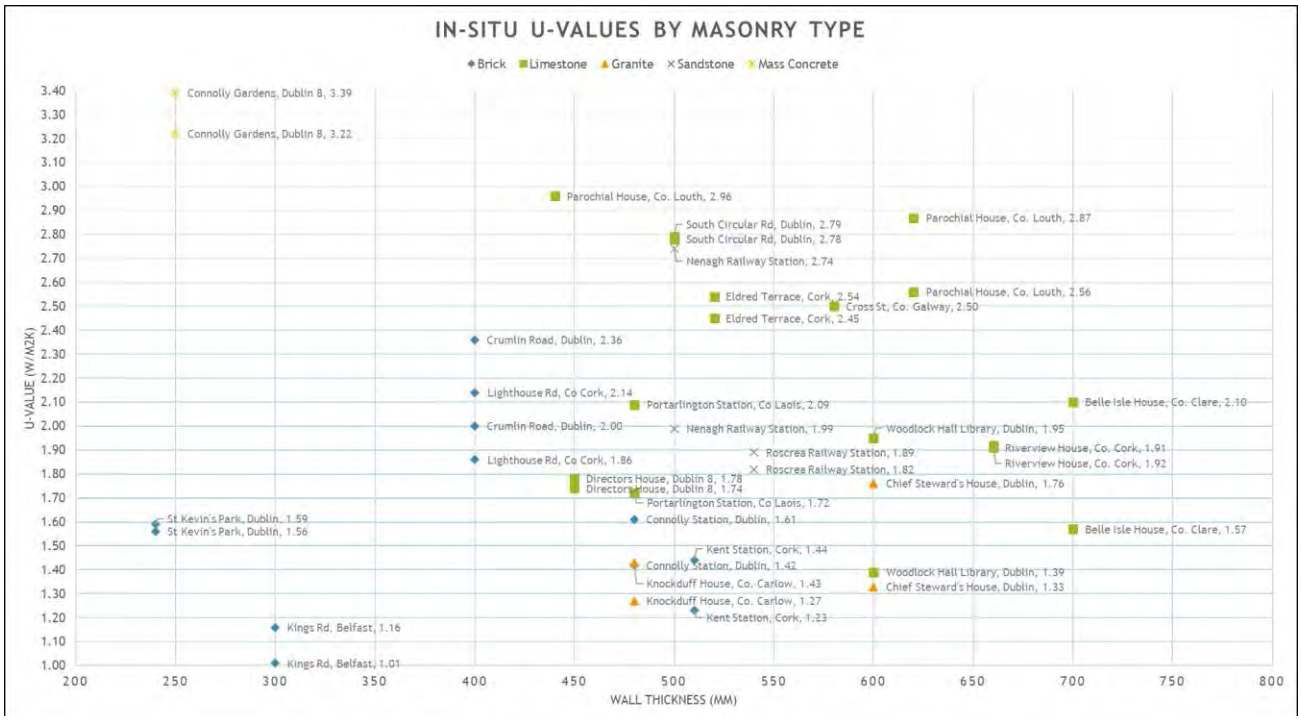

Figure 8. FabTrads in-situ U-values by masonry type and wall thickness.

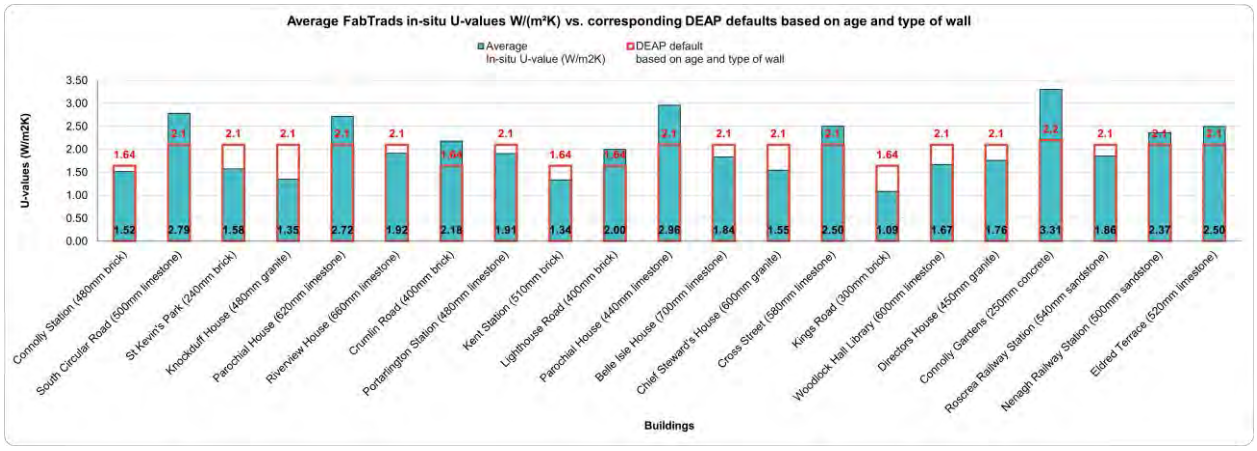

Figure 9. FabTrads average in-situ U-values versus corresponding DEAP default U-values [1].

4. DISCUSSION

In the 6-building sample of the Built to Last study, the default U-values in the DEAP methodology underestimate the thermal efficiency of the four solid brick and stone walls but overestimate the thermal efficiency of the two early mass concrete walls. The calculated U-values (using WUFI database defaults) are a closer fit to the measured performance, most likely due to the care taken to locate and size materials which have lower thermal conductivity, such as mortar joints and plaster. In contrast, nine of the 21 FabTrads in-situ U-values were found to exceed the corresponding DEAP default U-value by age and wall type. Of these, five are limestone walls, two are brick, one is sandstone and one is mass concrete.

Only three mass concrete walls have been tested to date across the two projects but of these the in-situ U-value is on average 33.1% higher than the DEAP default of 2.2 W/m^{2}K.

Of the six brick walls ≥325mm, two had in-situ U-values greater than the 1.64 W/m^{2}K default, with an average in-situ U-value across the six walls equal to 1.55 W/m^{2}K. Of the three brick walls ≤325mm, all had an in-situ U-value less than the DEAP default with an average in-situ U-value of 1.43 W/m^{2}K, which is nearly 38% lower than the default of 2.1 W/m2K. The average in-situ U-value across all 9 brick walls is 1.52 W/m^{2}K.

Ten limestone walls were tested across the two projects, with five exceeding the DEAP default. Overall, the average in-situ U-value of these ten walls is 2.18 W/m^{2}K, which is only slightly higher than the 2.1 W/m2K DEAP default for stone walls of any type and thickness.

All five of the limestone walls that exceeded the DEAP default clearly exhibited excess moisture retention. If the average in-situ U-values were calculated based on saturated versus dry walls, the average for saturated walls is 2.69 W/m^{2}K versus 1.67 W/m^{2}K for dry walls. This starts to give data to the long-accepted conservation adage that a dry wall is a warm wall.

Too few solid sandstone, granite and earthen walls have been tested at the time of writing to draw any definite conclusions.

5. LIMITATIONS

Since the objective of this research was to test as many different traditional walls as possible over the course of two winters, it was not an option to open up or core into most of the walls tested and therefore, in many cases, the exact build-up of the walls at the points tested is not known. The thermal efficiencies of traditional walls are expected to vary not only due to material thermal conductivities and thickness, but also due to the proportion of masonry to mortar, the presence of voids, the moisture content and repair condition of the wall.

To further understand the impact of the masonry to mortar build-up, unventilated voids and moisture on the in-situ U-value of solid walls, a follow-on study has begun that will use further destructive and non-destructive monitoring and measurement methods on a sample set of representative traditional wall types in Ireland to 1) confirm the exact wall build-up; 2) measure in-situ U-values over a longer period of time and 3) monitor the impact of moisture on the in-situ U-values. This on-site testing will again be done alongside lab-based material testing and validation of hygrothermal models using FabTrads material properties in accordance with IS EN 15026:2007.

6. CONCLUSION

Over the 36-month duration of the FabTrads project, in-situ U-value tests will be conducted on at least 36 traditional solid masonry walls. In addition to the data provided in this paper, further tests will include sandstone, granite and earthen walls to fill out the dataset.

As the in-situ U-values are the result of a complex assembly of the different properties and thicknesses of the masonry and mortar, plus the impact of voids and moisture content, further analysis will be done over summer 2024 based on the hygrothermal properties derived for a representative selection of traditional Irish masonries and mortars in the FabTrads laboratory. Thermal conductivity is being tested according to ASTM D5334 Transient Line Source method for stone and for bricks a different steady-state comparative method (Divided Bar apparatus) is being followed, which follows the principles of C177 and C518.

Where both in-situ testing was possible and masonry samples were obtained, a WUFI Pro model using FabTrads lab-derived hygrothermal properties will be created to compare the calculated versus in-situ U-values for each wall. These models can then be adjusted to analyse the impact of the proportion of stone to mortar, unventilated voids and moisture levels on the calculated U-value. Through modelling, we will 1) be able to determine how accurate the WUFI models are compared to the in-situ U-value tests, and 2) be able to determine a correlation between moisture retention and increased U-values.

Considering the impact of the aforementioned variables, we may find that a set of dry and saturated default U-values should be determined for typical masonry types based on the laboratory tested dry and saturated thermal conductivity values of each. We may also find that the DEAP defaults for solid masonry walls should be broken down further into different masonry types and wall thicknesses. This recommendation will be based on the laboratory derived dry and saturated thermal conductivities, in-situ U-value test results and WUFI models using FabTrads hygrothermal properties.

6. ACKNOWLEDGEMENTS

The in-situ U-value testing conducted as part of the FabTrads project is supported by the Sustainable Energy Authority of Ireland under Grant Agreement 21/RDD/R22947.

7. REFERENCES

1. Sustainable Energy Authority of Ireland, (2023). Domestic Energy Assessment Procedure (DEAP) Manual - Version 4.2.5. Sustainable Energy Authority of Ireland: Dublin.
2. Engel Purcell, C., (2018). Deep Energy Renovation of Traditional Buildings: Addressing Knowledge Gaps and Skills Training in Ireland. The Heritage Council: Dublin.
3. Gemmell, A. et. al., (2014). Solid wall heat losses and the potential for energy saving: Literature review. Building Research Establishment Ltd.: Watford, England.
4. Rhee-Duverne, S. and P. Baker, (2013). Research into the thermal performance of traditional brick walls. English Heritage: London.
5. May, N. and C. Rye, (2012). Responsible Retrofit of Traditional Buildings. Sustainable Traditional Building Alliance: London.
6. Department of Housing, Local Government and Heritage, (2023). Improving Energy Efficiency in Traditional Buildings: Guidance for Specifiers and Installers. Government of Ireland: Dublin.

PLEA 2024 WROCŁAW
(Re)thinking Resilience

Living Places: Healthy Homes for People & Planet

A simulation-based evaluation to ensure optimal indoor environment

JENS CHRISTOFFERSEN,[1] STEFFEN MAAGAARD,[2] KASPER REIMER,[3] SIOBHAN ROCKCASTLE,[4] AMBRA GUGLIETTI,[1] NICOLE DI SANTO,[1] LUCILE SARRAN[1]

[1] VELUX A/S, Hoersholm, Denmark
[2] Artelia A/S, Copenhagen, Denmark
[3] EFFEKT Arkitekter ApS, Copenhagen, Denmark
[4] OCULIGHT dynamics,

ABSTRACT: The architectural design of Living Places, the way it is formed, shaped and designed provides the interior with plenty of daylight all year round. The design incorporates window control with its accessories to effectively mitigate overheating and create a comfortable thermal environment. Openable windows with high attention on easy air passages throughout the building certify high indoor air quality. Living Places and its design provide us with an indoor experience over time and space, which is an experience we enjoy and that connects us to the outside, making the outdoor dynamics integrated with the interior. We have used the compass model and simulated the performance, a total of 60.000 indoor climate simulations, to identify the most significant design parameters and to see if it provides the desired result. In addition, we have built a full-scale model and we are collecting insights through simple measurements of the indoor environment. Overall, the simulation shows that Living Places satisfies all main parameters of the 'healthiness' criteria: daylight, thermal comfort, indoor air quality and acoustic quality. It is a building concept that allows abundant daylight and fresh air, enhancing indoor climate quality, and showing how to build sustainability for people and the planet.
KEYWORDS: Living Places, Compass, Indoor Environment, Health, Full-scale demonstration buildings

1. INTRODUCTION

Since spring 2020, nationwide lockdowns caused by the pandemic have forced many to work, learn and live at home. For some, this has renewed their appreciation of their home, for others, the living conditions and indoor environment have become an extra challenge. The role of our buildings is changing and there is an urgency to provide sustainable, healthy and affordable housing solutions. We spend 90% of our time indoors, and the healthiness of our indoor environment has received increasing attention over the last decades and has been the subject of publications and guidelines by governmental agencies and the World Health Organization (WHO). We know we can design homes that enable an indoor environment that is regenerative with a high focus on humans and how it affects our mental and physical health and well-being. Enabling an 'optimal' indoor climate is an essential aspect of house design and WHO has distinguished the following aspects of the 'healthiness' of the indoor environment:

- Thermal environment
- Air quality environment
- Noise environment
- Light environment.

The architectural design of Living Places, and the way it is formed, shaped and designed provide the interior with an abundance of daylight all year round. The design incorporates window control with its accessories to effectively mitigate overheating and create a comfortable thermal environment. Openable windows with high attention to easy air passages through the building certify high indoor air quality. Living Places and its design provide us with an indoor experience over time and space, which is an experience we enjoy and that connects us to the outside, making the outdoor dynamics integrated with the interior.

2. DESIGN AND PERFORMANCE DRIVERS

A home should be designed to enable an indoor environment that is regenerative and focused on humans, their mental and physical health, and well-being. How homes are designed and operated plays a crucial role in supporting physical and mental health. Enabling an optimal indoor climate is an essential aspect of house design.

The Compass model provides the foundation for Living Places and serves as a strategic tool which outlines seven points of relevancy to guide the building and development process. This paper focuses on healthy building principles and presents the outcome of the strategic design and performance drivers to ensure a healthy indoor environment.

The design drivers are; 1) visual, where building design typology ensures plenty of daylight to

eliminate the need for electric lighting during the day, 2) thermal environment, with drivers to design for year-round comfort, while ensuring temporal and spatial variations in the thermal environment, 3) indoor air quality, with focus on maximizing ventilation potential through stack effect and optimal positioning of windows, and 4) acoustics to ensure sound is transmitted and spread at optimal levels, through considerations in design, operation and construction.

Figure 1: Visualization of the timber-framed Living Places Concept House.

Table 1: Overview of Living Places

Concept House	Description
Size	144 m^2
Floors	3
Building principle	Timber frame construction
Foundation	Screw pile foundation
Room height	2.6 m
Heating application	Air to water heat pump
Heating source	Radiators
Ventilation	Natural or hybrid

The performance drivers implement the design drivers through the typology of Living Places. Within the 1) visual environment, the drivers are securing sufficient daylight [1] by optimizing the window design and utilising direct sunlight within the different spaces and use by the occupant, without creating high contrast and glare problems. The positioning of windows influences the distribution of daylight in a room. Combining windows in multiple facades/roofs determines the amount of 'useful' daylight throughout the day with the changing sun position. Strategic window position will take into account the relation between the view to the outside and occupants ability to supply information of orientation, give experience of weather changes and allow us to follow the passage of time and nature over the day and year. The thermal environment ensures temporal and spatial variations using sufficient ceiling height, careful building depth, and strategic location of openable windows supported by sensors to regulate the indoor climate [2]. Proper use of solar shading will reduce solar heat gain and potential overheating. Additional use of ventilation strategies (e.g. natural or mechanical) to cool indoor spaces via outdoor air, sometimes referred to as ventilative cooling, commonly uses increased ventilation airflow rates and night ventilation. From an energy-conscious perspective (e.g. minimize or eliminate cooling systems), using a natural ventilative cooling principle by opening windows is a very direct and fast method of influencing the thermal environment, either by increased air motion or by use of temperature difference between outdoor and indoor temperatures. Additionally, maximizing ventilation potential through the stack effect and optimal positioning of windows will safeguard high indoor air quality, as well. In addition, the use of low off-gassing labelled products and material, demand-controlled ventilation and zone subdivision of individual rooms with proper filtration support high performance. One important function of the building envelope is to protect the interior from unwanted outdoor noise. Ensuring sound is transmitted and spread at ideal low levels, through considerations in design, operation and construction will minimize noise disturbance that could affect our sleep and other negative effects.

2.1 Simulations

The Active House specifications [3] include the vision and knowledge needed to meet the technical requirements for achieving the design concept's performance levels and a holistic approach (biodiversity, local culture, and location). We use an Active House Radar according to the Active House specifications, together with a Multivariable Building Simulations tool to explore the solution space for each parameter to reach a target indoor climate level according to the Compass model and the healthy building principles.

With a Multivariable Building Simulations (MIBS) method, the project engineering partner has established a platform of tools, in which a design team can explore the entire solution spectrum when the 'optimal' design is to be found. The tools can inform the building design team which drivers can achieve the best possible basis for a healthy indoor environment (see example in figure 2).

Figure 2 shows an example of indoor climate simulations for a sleeping room to evaluate the thermal environment and indoor air quality. The upper chart shows the thermal environment, where

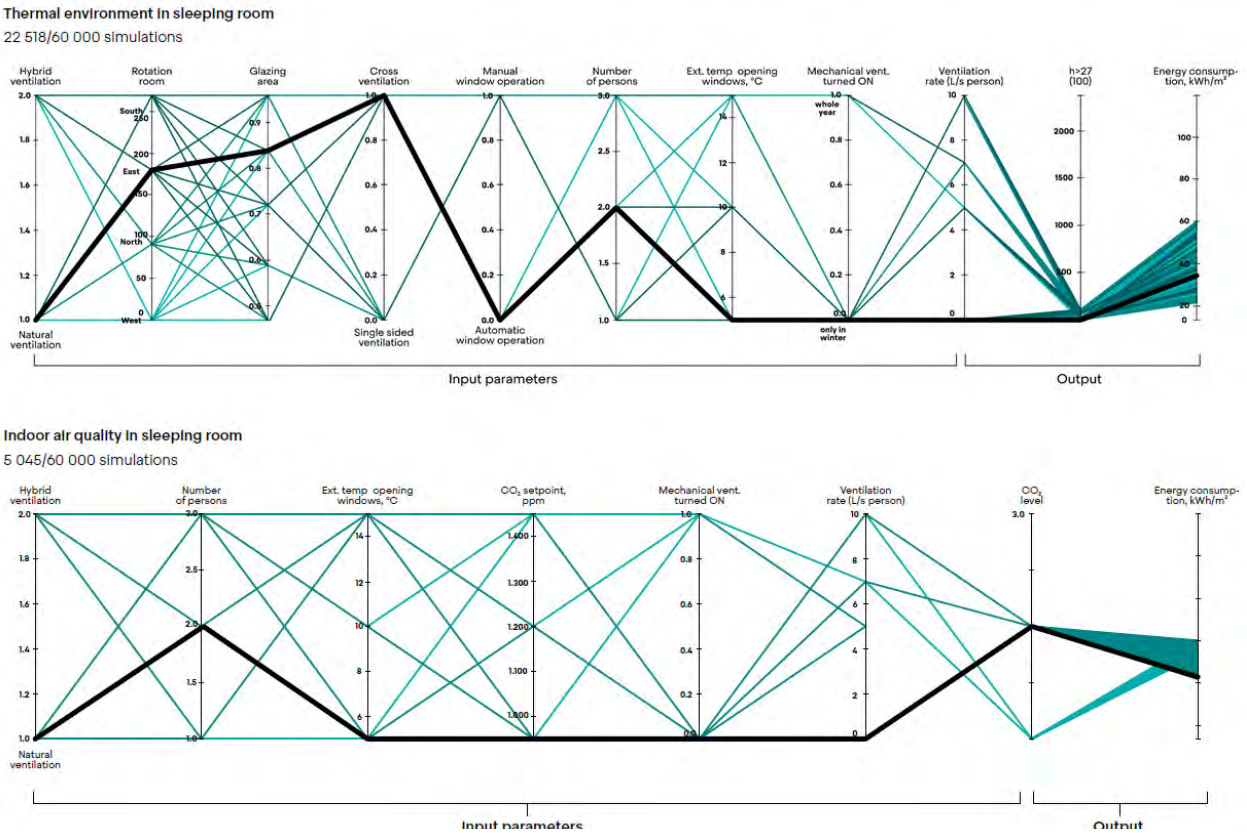

Figure 2: The charts shows the indoor climate simulations for a sleeping room, where one solution with natural ventilation have been selected to get the best possible trade-off between energy consumption, temperature, and indoor air quality. The charts show one of the possible scenarios for the project to ensure a good healthy indoor.

the black line illustrates one input parameter with natural ventilation (left starting point) that has been selected to get the best possible trade-off between output parameters of energy consumption and indoor temperature. The other key input parameters are: room orientation, glazing area, whether the room is single-sided or cross-ventilated, whether the windows open manually or automatically, number of people, outdoor temperature for automatic opening, time with mechanical ventilation, and the ventilation rate. The lower chart show the input parameters for the indoor air quality in the sleeping room. By setting key design and performance criteria, using these design tools will illustrate a possible solution space, and by taking different decision the solution space can either increase or decrease, and show immediately how an adjustment in the design will affect the other design parameters and what the impact will be on the selected output parameters.

3. RESULTS

As part of the Living Places project, and essential for the evaluation of the indoor environment, a total of 60.000 indoor climate simulations have been performed on a room basis to identify the most significant design parameters. We have essentially separated the analysis depending on ventilation principle, natural ventilation and hybrid ventilation, and performed 30.000 simulations for each scenario. Each scenario, as illustrated in figure 2 example, has a set of input parameter variations which is evaluated to an output criteria for the thermal and atmospheric indoor climate, as well as energy consumption (heating and fan). Based on these analyses, the most sensitive design parameters have been used to find the most resilient building design depending on ventilation principles.

Using a parallel coordinate plot a lot of different paths to the design “goal” have been showcased (see fig. 2), but also paths that cannot fulfil the ambitious requirements to the indoor environment. As an example, depending if the building use solely a natural ventilation solution or if it use a hybrid solution, the most influential parameters in relation to thermal comfort and air quality are different as well as similar. There are common parameters such as the number of people in the space for both natural and hybrid ventilation solutions, the specifics differ based on the approach. For natural ventilation, outdoor temperature where the window can be opened and CO_2 setpoint take precedence, while for a hybrid solution, factors like the activation time of mechanical systems ventilation system (winter / all year) and their usage during specific periods become critical.

Table 2: Values and KPI for a good indoor environment based on peer-reviewed research.

Component	Indicator	Parameter	Indoor Climate Class I
IAQ	Particles	Ventilation filtration	ePM1 55%
		Extractor hood efficiency, >75%, l/s	40
	CO_2	Bedrooms, ppm	≤1000
		Vent. rate build, l/s pr. m^2	≥0.5
	VOC	TVOC	300
	Radon	Bq	≤100
	Relative Humidity	RH 95% of time	≥30-≤50
	Temperature	Overheating, 100h > temp	<26.5°
Acoustic		Sound pressure level	<27
Visual	Daylight	$sDA_{300,50\%}$ floor area	≥50%

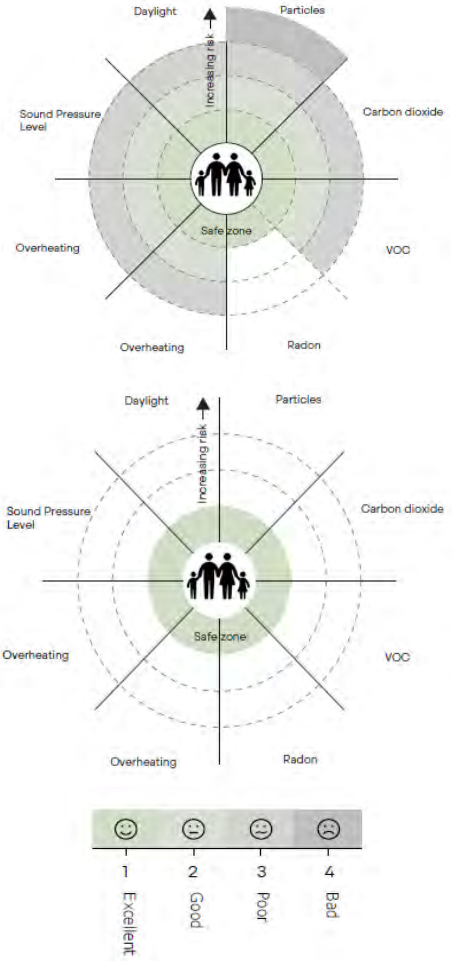

Figure 3: Using an Active House Radar shows that each parameter is described in table 1. The upper radar is a benchmark of a typical EU single-family house and the lower radar is Living Places (lower)

3.1 Overheating

The design incorporates window control effectively to mitigate overheating, regardless of the building's orientation. Versatility and flexibility are valuable attributes in creating a comfortable thermal environment and the simulation results demonstrate that all rooms at all three-floor levels consistently meet or exceed thermal comfort requirements as defined in the Danish Building legislation as hours above 27°C (e.g. 100h) and 28°C (e.g. 25h), which are commonly used indicators of potential thermal discomfort. The number of hours above 27°C and 28°C is well below the specified limits for thermal comfort. The simulation outcome indicates that the design successfully addresses overheating concerns, as the number of hours above 27° varies depending on building orientation, and floor level. In the living room/kitchen the number of hours above 27°, depending on orientation, varies from 40 to 70 hours (e.g. highest towards the West) to slightly above 50 hours in the top floor bedroom. A similar tendency can be observed with the number of hours above 28 which is less than 25h. The simulations also show how and when to use windows to boost the mechanical ventilation rate with natural ventilation, when the mechanical ventilation can be turned off to save energy and how large windows can be used in specific orientations. In general, the parametric sensitivity analysis indicates that in a naturally ventilated house, the key parameters to fulfil thermal comfort are the outdoor temperature, when windows can open, the number of people, and the air-flow rate when windows are open. In the hybrid solution, the key parameters are set-point and time for activation of mechanical ventilation, and ventilation airflow rate for the mechanical solution and airflow rate when naturally operated.

3.2 Ventilation and indoor air quality

Simulation of the Living Houses shows that the indoor CO_2 level according to [3] is within level 1 (e.g. < 400 ppm above outdoor CO_2 concentration). The parametric sensitivity analysis indicates that with a naturally ventilated house, the key parameters to reduce CO_2 concentration are the CO_2 set-point, air-flow rate (7-10 l/s per person) and outdoor temperature when windows open (> 5 °C) and number of people. Strategically opening windows to allow fresh air circulation, and diluting indoor CO_2 levels will maintain higher air quality. In the hybrid solution, the key parameters are; set-point and time for activation of the mechanical ventilation system (year-round or just in the winter months) and the air-flow rate when the mechanical and natural solution is active in operation during occupied hours. Overall, the hybrid solution and active use of strategic

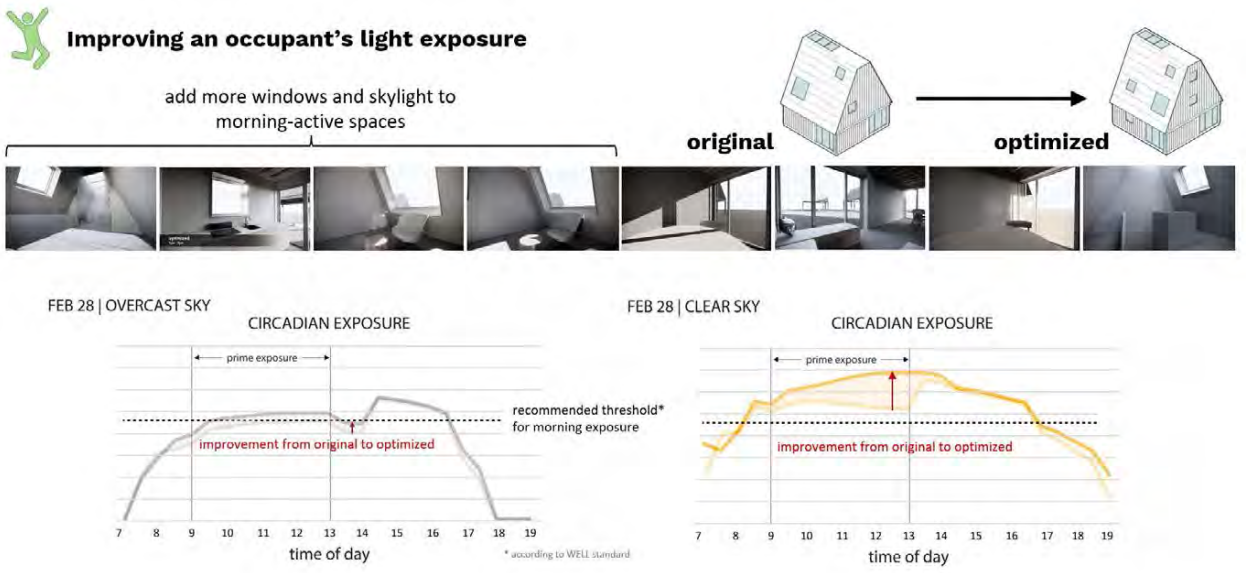

Figure 4: Illustration of daytime recommended threshold level and estimated level of circadian light exposure, February 28, for an overcast sky and a clear sunny sky. The two different lines illustrated with an upward arrow exemplify attention to optimize daylight-specific window openings arrangement to increase the circadian light exposure according to a "walk around" behaviour within the different type of spaces in Living Places.

window openings maintain an energy-efficient solution, adapting to seasonal variations, but winter months and limited window openings show an increase in CO_2 level, if the energy consumption should be maintained low.

3.3 Visual and non-visual effects of daylight

We also took the simulation of the visual environment a step further than just to comply with existing standards and guidelines. An external collaboration partner, OCULIGHT dynamics, simulated Living Places with complementary tools to allow evaluation of how light will affect the occupants, whether it is physiologically (e.g. vitality) or emotionally, or how comfortable a daylit environment will be perceived from an occupant's perspective. To evaluate our overall experience of daylight, we need to know how much light we receive at eye level over the day, across seasons over the year. If our indoor environment provides us with too little light, thereby making us light-deprived, it can have long-term negative consequences on our well-being, affecting our mood, melatonin production, immune system and many other essential aspects of our health and vitality. Whereas being exposed to enough light can be highly beneficial, like promoting higher alertness and better sleep. Within that framework, daylight should be evaluated from a viewpoint perspective as well – or rather, from a large number of viewpoints within the space to represent enough possible perspectives –, and not only based on light reaching a horizontal plane.

The daylight simulation results show that the design of the Living Places offers a very convincing way to utilize daylight, with sufficient daylight provision and good levels of vitality and comfort especially on sunny days over the year, as well as when the sky is overcast. According to the criteria for daylight provision stated in [1], a space is considered to provide adequate daylight if a target illuminance level [e.g. recommended 300 lx] is achieved across a fraction of the reference plane [e.g. recommended 50%] within a space for at least half of the daylight hours. The outcome of the simulation shows that the minimum recommended spatial daylight autonomy (sDA) target of 300 lux is achieved across almost 90% of the reference plane at all three-floor levels, and about 65% of the area reaches the highest level of 750 lux. Additional evaluation shows that a majority of positions and view directions within the space are visually comfortable, with only limited situations that can cause visual discomfort or glare. Figure 4 illustrates the evaluation of light exposure and its contribution to health potential from a human-centric perspective [4]. Attention to optimising daylight-specific window opening arrangements to increase the circadian light exposure according to a "walk around" behaviour could influence the way we recommend occupants to spend time in the brighter areas of the spaces, especially in the morning, when the light signal is essential to let our body know the day is up and make sure we receive the proper light exposure and the right time. Figure 4 shows a recommended threshold level and the estimated circadian exposure to promote sufficient light exposure over each hour depending on sky type, time of year and improvement of daylight-specific window opening arrangement. Even a worst-case scenario,

February 28, illustrates that the recommended light exposure when the sky is overcast is just fair, while a clear sunny sky provides sufficient exposure the whole day.

3.4 Indoor measurements

Indoor CO_2 measurements (spring) in each room of the two unoccupied Living Houses, indicate that the indoor CO_2 level is above the simulation levels. The house with a hybrid ventilation solution and maintained 'in-use' mechanical air flow (e.g., 10 l/s per person, bedrooms), shows measured IAQ score, according to [3], at level 2 (e.g. 550 ppm above outdoor CO2 concentration), while the naturally ventilated building solution is about level 3 (e.g. 800 ppm above). The thermal measurements also show a higher performance in the building with the hybrid solution (e.g. CLT house) than the natural ventilated solution (e.g. timber-frame). According to [2,3] these early spring measurements are merely to confirm the simulations, and an extended measurement protocol is expected next year.

4. DISCUSSION

Effectively window control strategies with its solar shading accessories are a crucial aspect, especially in regions or times where high outdoor temperatures can impact indoor comfort. A building design's ability to maintain a good thermal environment across various orientations underlines its adaptability. Although there is some variation in the number of hours above certain temperature thresholds, this information can be valuable for fine-tuning specific design elements but the number of hours to evaluate summer comfort is well below the specified limits and it indicates that the design successfully addresses overheating concerns.

Optimizing daylight-specific window openings for circadian light exposure based on a "walk around" behaviour within different types of spaces involves strategically considering the placement and characteristics of windows and the spectral composition of the glazing material used. The simulation shows that future evaluation should consider a spatial analysis of each area and view position within the building to understand the natural patterns of daylight. By incorporating a mix of direct and diffuse daylight, as well as, adopting the scientific recommendation for indoor light exposure, future design considerations will pay special attention to spaces that are frequently traversed or used for specific activities in terms of daylight optimization. As illustrated in Living Places, this aims to bring brighter, cooler light in the morning and during the day to promote wakefulness and alertness, and gradually transition to warmer, softer light in the evening to support relaxation and sleep. A higher emphasis on substantial daylight provision is essential for our visual perception and to minimize the use of electric light during daytime. A report by RAND Europe [5] shows that on average, 5% of European households are affected by self-reported perception that their dwelling is too dark, which could have an impact on the probability of switching on the electric lighting.

5. CONCLUSION

We have used the compass model and simulated the performance to see if it provides the desired result. In addition, we have built a full-scale model and we are collecting insights through simple measurements of the indoor environment. Overall, the simulation shows that Living Places satisfies all main parameters of the 'healthiness' criteria: daylight, thermal comfort, indoor air quality and acoustic quality. It is a building concept that allows abundant daylight and fresh air, enhancing indoor climate quality, and showing how to build sustainable for people and the planet.

ACKNOWLEDGEMENTS

The authors wish to acknowledge the invaluable contribution of the project partners – VELUX, EFFEKT Architects and Artelia Denmark. We would also like to thank our inspiring collaboration with OCULIGHT dynamics.

REFERENCES

1. EN 17037:2018+A1:2021. Daylight in Buildings.
2. EN 16798-1:2019. Energy performance of buildings - Ventilation for buildings - Part 1: Indoor environmental input parameters for design and assessment of energy performance of buildings addressing indoor air quality, thermal environment, lighting and acoustics-Module M1-6.
3. Active House 2020. The Active House Specifications 3rd edition.
4. Brown TM., Brainard GC., Cajochen C., et al. (2022) Recommendations for daytime, evening, and nighttime indoor light exposure to best support physiology, sleep, and wakefulness in healthy adults. *PLOS Biology 2022; 20(3): e3001571.*
5. RAND Europe. Poor indoor climate: Its impact on health and life satisfaction, as well as its wider socio-economic costs. RAND Corporation. Report no. RR-A1323-1. 2012.

PLEA 2024 WROCŁAW
(Re)thinking Resilience

Language of Movement for Building Assessment:
A Review of the Evaluation Methods of the Human Movement in the Built Space

MOSLEH AHMADI[1]
[1]Faculty of Architecture, Gdansk University of Technology, Gdansk, Poland

ABSTRACT: The purpose of this article is to provide a framework for the categorization of methods and techniques of human movement evaluation, measurement, and assessment in the built space. The reviewed methods have been put together in a framework by the consideration of the level of movement and the timescale. In doing so, the phenomenon of movement has been distinguished as a four-level of movement scale that are subject to eight timescales. These four levels are imbedded movement, dynamic posture, dynamic location, and dynamic agent. Finally, twenty selected techniques and methods are defined and the methodological procedures of each of them have been described. These methods are mainly derived from studies on daylighting and comfort.
KEYWORDS: Movement, Daylighting, Architecture, Comfort, Methodology

1. INTRODUCTION

A collection of choreographic postures has been employed to establish a distinctive movement vocabulary, governed by geometric rules specifically formulated for the human body. This codified grammar of movement, detailed in a set of rules, intricately shapes the dynamics of the human body, giving rise to a nuanced corporeal experience [1]. Consequently, the deliberate and coordinated movements originating from diverse parts and joints of the body can be meticulously observed and monitored, offering valuable insights into various variables associated with the psychophysiological conditions of individuals. This paper explores a selected set of architectural and urban studies to shape a comprehensive review of evaluation methods for human movement within built spaces, exploring the complex language of movement as a tool for building assessment.

The interdisciplinary nature of the research, drawing insights from neuroscience, biometrics, and psychology, further broadens the understanding of human movement. This expansion of scope highlights the multifaceted nature of movement and its profound impact on psychophysiological conditions. As a result, the research facilitates a structured approach to the analysis of human movement, enabling more informed, user-centric decisions in diverse contexts within the built environment.

2. METHODOLOGY

This paper reviews the diverse approaches employed for measuring, assessing, and evaluating movement within a selected group of studies in architecture and urbanism. The contexts of the studies selected to review are daylighting and comfort that evolved around the main keywords of 'movement', 'daylight', and 'architecture'. It explores the intricacies of the methodologies applied in these studies, shedding light on the tools, instruments, and techniques utilized to capture and analyze movement data. For classification of these methods, movement could be distinguished into three main scales (Fig. 1).

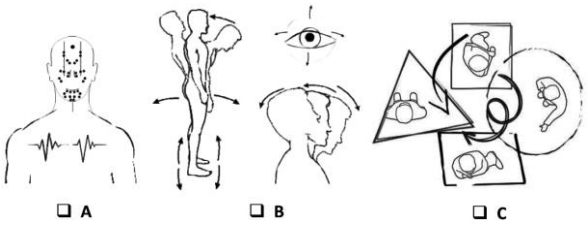

Figure 1: movement scales. Movement of the facial muscles and heart (A), Movement of the joints and eye (B), and Movement of the body through the space (C) (source: author).

By categorizing movement into distinct levels and timescales, the comprehensive framework provided here enriches the theoretical foundation of architectural and urban studies and empowers it with practical applications and examples for each movement level and timescale.

3. RESULTS

Based on the review on the selected studies a table could be created illustrating the methods of evaluating movement in the built space. The table provides a structured overview of movement levels categorized across various timescales, ranging from instant to annual intervals. It distinguishes movement in four scales of micro-scale (imbedded motion of organs), mid-scale (reposition, redirection, ocular movement, limb movement) (Table 1), macro-scale

(relocation, movement through space), and mega-scale (occupation cycle, migration, walking rate) (Table 2).

Table 1: Methods of evaluation of movement in the built space based on the scale and time of the movement for micro and mid scales.

Movement level / **Timescale**	**Micro-scale:** Imbedded motion / movement of organs	**Mid-scale:** Reposition / redirection / ocular movement / movement of the joints
Instant (a range of seconds)	* Biometric analysis (EEG, SGR, EMG, PPG) * Affectiva iMotions video analysis	* Eye Tracking, Motion sensing * Adaptive zone * Time-of-Flight sensing * Vision-based pose estimation
Momentary (minutely or a range of minutes)	* Biometric analysis (EEG, SGR, EMG, PPG) * Affectiva iMotions video analysis	* Eye Tracking * Adaptive zone * Time-of-Flight sensing * Vision-based pose estimation
Temporary (hourly or a range of hours)	* Smart bracelet recording	* Eye Tracking * Adaptive zone * Time-of-Flight sensing
Diurnal (daily)	* Smart bracelet recording	* Actigraphy

Table 2: Methods of evaluation of movement in the built space based on the scale and time of the movement for macro and mega scales.

Movement level / **Timescale**	**Macro-scale:** Relocation / movement pattern	**Mega-scale:** Occupation cycle / migration / walking rate / trajectory
Instant (a range of seconds)	* Timelapse footage with short intervals * Video recording analysis * Direct Observation * Time-of-Flight sensing * Behavioral mapping	* Long Short-Term Memory (LSTM) trajectory prediction
Momentary (minutely or a range of minutes)	* Timelapse footage with short intervals * Video recording analysis * Space syntax * Direct Observation * Time-of-Flight sensing * Vision-based motion tracking * Behavioral mapping	* Datalogging * Monitoring * Long Short-Term Memory (LSTM) trajectory prediction * Space syntax * Behavioral mapping
Temporary (hourly or a range of hours)	* Timelapse footage with intervals * Space syntax	* Datalogging * Monitoring * Space syntax * Behavioral mapping
	* Direct Observation * Time-of-Flight sensing * Vision-based motion tracking * Behavioral mapping	
Diurnal (daily)	* Timelapse footage with long intervals * Actigraphy * Space syntax * Time-of-Flight sensing	* Datalogging * Monitoring * Space syntax
Periodic (weekly)	* Actigraphy	* Actigraphy * Monitoring * Web-based observation
Cyclical (monthly)	* Actigraphy	* Actigraphy * Monitoring * Web-based observation
Quarterly (seasonally) / **Annual** (yearly)	-	* Observation * Web-based observation

4. DISCUSSION

The methods addressed in the tables (1, and 2) could be categorized in four movement types of imbedded motion, dynamic position, dynamic location, and dynamic agent each of which occur in different levels. Therefore, they require different approaches of analysis.

4.1. Small-scale Movement: Imbedded Motion

"The body expresses movement even when motionless" [2]. This notion stems from the physical and physiological facts that even in a static position, the same push and pull of the environmental and biological forces needed for motion occurs. This ongoing struggle is characterized by the constant interaction between the body and gravitational forces (refer to neutral body orientation as depicted by researchers [3]), as well as the dynamic interplay within the skeletal framework and musculature.

Heartbeat variability represents a form of motion generated by the cardiac muscle. This dynamic aspect was a pivotal factor in the mood-related analysis conducted by Peper et al. [4]. Consequently, in this study, posture, conceptualized as a distinct form of movement, was established as the independent variable, with heartbeat variability serving as the dependent variable (Fig. 3). In a separate investigation [5], the Photoplethysmogram (PPG) was employed to measure heartbeat variability, contributing to a deeper understanding of emotional responses and stress levels. Moreover, recognizing heartbeat variability resulting from physical activity, essentially movement within movement, presents an avenue for developing a thermal comfort model, as illustrated in the work by [6].

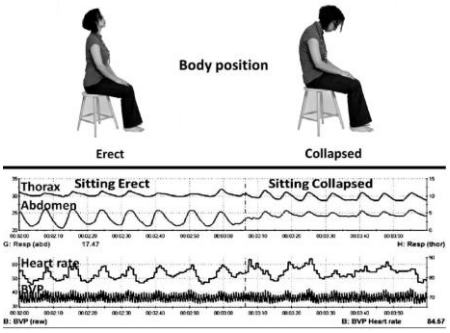

Figure 3: Effect of posture on respiratory breathing pattern and heart rate variability (source: [4]).

Beyond the motions orchestrated by the internal activities of human organs, studies investigating sleep have underscored the significance of readiness for movement and activity. Understanding this readiness holds particular importance in the realm of movement studies, as the body aligns its internal chronometer with environmental cues, leading to variations in activity-rest patterns across different environmental conditions [7]. These patterns can be intentionally manipulated to achieve specific timing for movement and activity. Consequently, in these scenarios, human activity patterns and schedules are established as independent variables, exerting influence on how the built space should be approached. Considering this, regression analysis has been employed to predict human movement [8].

Biometric tools to record and map human experience is one of the recent areas of research. Ergan et al. [5], in their research argue that to map the experience of human effected by the architectural design features, the use of body area sensor network concept proves to be useful. In doing so, they [5] integrated Electroencephalogram (EEG), facial- or vision-based Electromyography (EMG), Galvanic Skin Response (SGR), Photoplethysmogram (PPG), and Eye Tracking tools with virtual reality environment to analyze human experience in the virtual built space.

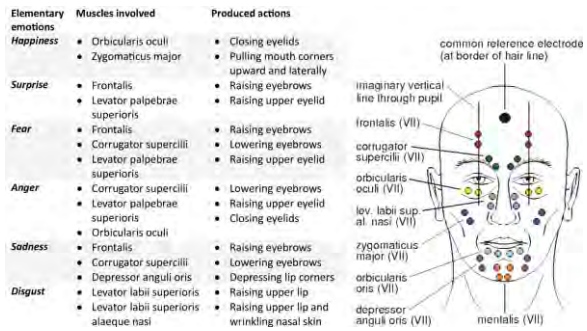

Figure 4: Connection of the emotional expressions with the produced facial actions (Source: [10]).

Deciphering the facial expressions would help to assess the affective impact of architectural features on the user. Each produced action is linked to an emotional state representing the condition of the built space (Fig. 4). Beside EMG tool, cutting edge software could have the ability of analyzing the affective impact of the architectural elements. For instance, Affectiva iMotions is a facial expression analysis software that evaluates the video recordings of the users to read the facial expressions [9]. This technology enhances the precision of evaluating the affective responses of individuals to various architectural features.

Eye tracking technologies play a pivotal role in advancing the assessment of dynamic visual attention, as demonstrated by the use of portable eye trackers [11]. These technologies excel not only in pinpointing areas of interest but also in generating insightful heatmaps [12]. Moreover, the analysis extends to factors such as the direction of gaze, the degree of eye opening, and pupil size, particularly valuable for investigations into daylighting [13].

4.2. Medium-scale Movement: Dynamic Posture and Position

Dynamic physical expressions and the activity of limbs and body parts shape the overall dynamic state of the human body in the space. The study of different postures and positions of the body in the space could determine valuable information for the researchers and designers collecting data on mood, sleep, and activity rates in the built space.

The dynamic portrayal of the body within an environment serves as a valuable tool for assessing human emotive states. Paterson's study [14] on the experiential aspects of architecture, focusing on vision and touch, demonstrates that user mood states can be discerned through the observation of postures and gestures. Building on this notion, researchers [4] conducted an experiment linking depression levels and emotional recall to varying postures, including both erect and collapsed conditions (refer to Fig. 3). Consequently, understanding the motivations and stimuli driving user movement within a building becomes feasible by gauging mood states, which can be deduced through posture and gesture observation.

The dynamic appearance of the body in space is not limited to visual observation; it extends to the use of motion sensors to monitor user activity, enabling strategic adaptations of the built environment to meet occupants' needs. Research in this realm includes the application of passive-infrared (PIR) motion sensors, notably enhancing adaptive lighting control through movement detection [15]. Additionally, ceiling-mounted Time-of-Flight sensors (ToF) provide opportunities for gesture recognition [16], extending their utility beyond mere recognition to applications like occupancy sensing, people counting, and activity monitoring. This multi-faceted

approach facilitates comprehensive analysis of movement and interaction patterns within a space.

Limb activities could be considered as the main parameter of shaping the dynamic position and posture in the space. A tool to measure physical activity at this level is Actigraph. This tool could be used for different purposes ranging from physical activity assessment such as speed, activity counts, activity intensity, and steps per a given time [17] to rest/activity or sleep/wake cycle [18] [19]. Actigraphy with the use of actiwatches was a method to study the level of activity of participants in a long-term survey to study well-being and sleep quality [20].

Activity of the joints is also noteworthy specially for studies related to healthcare, safety, and sports. This activity defines the grammar of human skeleton motion while performing certain tasks. Motion could be captured through vision-based human motion sensing for ergonomic and biomechanical analysis [21]. The motion data in Liu et al.'s [21] research is consisted of the angles at body joints and could be depicted in a 3D or 2D illustration (Fig. 6A).

Dynamic direction or position of view is an output of the movement of head or the rotation of body. In daylighting studies, this behavior is attributed to the concept of 'adaptive zone' in which the visual comfort of the observer would be evaluated [22]. Although the method known as adaptive zone is initially to assess visual comfort and not movement, however, the view angles introduced to run the analysis imply the existence of movement of the body in a fixed location. Therefore, it could be possible to use this method for the evaluation of other environmental effects.

4.3. Large-scale Movement: Dynamic Location

The dynamic interplay of the body with the space between points has been used to study the successfulness of the spatial design. The most basic form of movement analysis on the surface is space syntax methodology. While space syntax is taking into account factors such as movement patterns, cognition, and behavior [23], it could not cover all aspects of human movement varying from different timescales and levels explained previously in this article. In this method movement is a part of analysis based on the analysis of the spatial configurations integrated with social structures other than tracking and sensing movement [24]. Connectivity and integration are the two closely related factors when it comes into the study of movement as a link between different spatial units. These factors find application in generating heatmaps [25].

More direct approaches could be implemented to have a more accurate track of movement. Autographical shading and dotting on the map to locate the spatial appraised points [26], phenomenological writings and modeling [27], and autoethnography of the experience of movement [28] were three techniques to assess the experience of the space. They [28] understood atmospheres emerging according to the levels of activity and movement. With this approach each location is given an identity. Emotional representation of the locations in the space has been introduced as a variable dependent on the affective state of people in different locations besides spatial navigation [26]. Here movement described as spatial navigation plays an extraneous role for the independent variable. Chun and Towse [29] express that with auto-ethnographical approach researchers will narrate their 'own spatial experiences' to guide further design decisions.

Mapping of perceived daylight boundaries and best locations through survey and based on participants' drawing was a method of perceptional representation of the locations in the space [30]. This research aimed to understand the perception of users. In urban, researchers [31] have used timelapse photography with 1.5 minutes intervals to capture the use of resting areas in a square over time scale to assess each location.

Mapping human behavior to examine independent variables has captured the interest of many researchers. For example, in a study on the impact of the daylighting condition, the users' movements in a café have been mapped to understand whether the daylit areas are busiest or not [32]. Hong et al. [33] conducted a behavioral mapping using virtual agents. They used Dassault Systèmes' 3DVia Virtools which is a visual programming platform to create anthropomorphic goal-oriented agents mimicking human activities with four defined parameters defining and limiting the range of behaviors. Their goal was to find an optimal match between human activity and built environment in architectural design. In another context, aiming to classify behavior pattern, researchers [34] were able to model manual lighting control behavior patterns based on daylight illuminance and interior layout. To categorize, occupancy detectors were used to understand the change of occupancy and interaction pattern with the change in the layout and daylight conditions. Based on the data, a fuzzy logic model through MATLAB FIS editor was constructed.

Observation is the first method of data collection in studies related to behavior of people in a space regarding the use of space or the elements in the space [35]. More convenient methods such as, time-lapse photography has proven to be a good method for the analysis of occupation cycle and pattern to study the energy use [35]. However, for the study of occupancy, the use of computer vision sensors and cameras is a good method for data collection is a more advanced methodology [36].

The rate of corporeal and sensory engagement with the environment as a dependent variable has been studied through observation and monitoring in different studies [37]. The higher the level of environmental affordances, the higher the rate of corporeal and sensory engagement. Or in better terms, the richness of quality environmental

affordances directly contributes to an enhanced adaptive engagement experience.

4.4. Mega-scale Movement: Dynamic Agents

Some certain studies such as post occupancy evaluation that involve long duration measurements or studies on urban components that involve higher intensities and volumes of movement patterns require other methods of evaluation. In other words, movement could also be interpreted and studied as the change in occupant counts or occupancy duration in each location. For instance, Jens and Khoudi [38] have grouped these two parameters with seats and tables to understand which place shows lesser change in occupants count and duration before and after a planned intervention. Based on this knowledge, the impact of different conditions on the occupancy patterns could be deciphered.

Pedestrian motion is the most analyzed parameters in the urban studies. For example, in an early study, Burse [39] simulated the movement and route decision of virtual individuals in an open space through an online multi-agent system called BOTworld to analyze human thermal comfort in different microclimatic condition.

On the urban scale, there have been many other studies considering user movement as a dependent variable on the environmental conditions or morphology. For example, researchers [40] have tried to simulate user movement through the analysis of the relationship of movement with the urban components. de Montigny et al. [41] have visually inspected the volumes of walking to establish its correlation with the locally felt weather.

One of the most important problems when dealing with volumes of movement is safety issues. For this reason, predicting models such as image processing have been used to predict trajectories of the pedestrians (Fig. 6B). However, the improved method of trajectory prediction has been recently introduced [42].

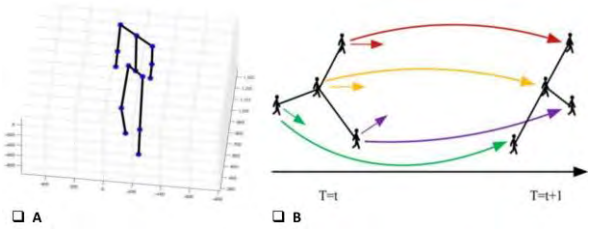

Figure 6: A 3D skeleton extraction for motion sensing and analysis (A) (Source: [21]). Prediction of the human movment (B) (Source: [42])

5. LIMITATIONS

While this research helps the understanding of human movement within built spaces, it is essential to acknowledge that the proposed framework is not comprehensive and can benefit from further refinement. The correlations between movement levels and timescales could be more robust, and to enhance the validity and generalizability of the framework, a systematic review encompassing a broader range of references beyond those primarily related to daylighting and comfort is recommended. The current review provides a valuable starting point, offering practical insights and applications, yet a more comprehensive analysis could strengthen the results and refine the framework.

6. CONCLUSION

Based on the framework presented in this article that classifies movement into 4 levels and 8 timescales, the diversity of movement evaluation has been shown. 20 methods have been introduced and explained here to measure, assess, or evaluate human movement inside the built space. These methods are: Biometric analysis (EEG, SGR, EMG, PPG), Affectiva iMotions video analysis, Eye Tracking, Motion sensing, Adaptive zone, Time-of-Flight sensing, Vision-based pose estimation, Timelapse footage with short intervals, Video recording analysis, Direct Observation, Long Short-Term Memory (LSTM) trajectory prediction, Space syntax, Vision-based motion tracking, Datalogging, Monitoring, Smart bracelet recording, Timelapse footage with intervals, Timelapse footage with long intervals, Actigraphy, and Web-based observation.

In addition, the classification introduced here does not consider methods as subject-specific. Therefore, depending on study they could be modified. It is important to note that this review is a contribution to the establishment of a framework to practically correlate human movement with architecture.

REFERENCES

1. Piedade Ferreira, M., Cabral, D., & Duarte, J. P. (2011). The Grammar of Movement: A Step Towards a Corporeal Architecture. Nexus Network Journal, 13(1), 131–149.

2. Macarthur, J. (2007). Movement and tactility: Benjamin and Wölfflin on imitation in architecture. The Journal of Architecture, 12(5), 477–487.

3. Hauplik-Meusburger, S. (2011). Architecture for astronauts: Activity-based approach. Springer Wien NewYork.

4. Peper, E., Lin, I.-M., Harvey, R., & Perez, J. (2017). How Posture Affects Memory Recall and Mood. Biofeedback, 45(2), 36–41.

5. Ergan, S., Radwan, A., Zou, Z., Tseng, H. A., & Han, X. (2019). Quantifying human experience in architectural spaces with integrated virtual reality and body sensor networks. Journal of Computing in Civil Engineering, 33(2), 04018062.

6. Zhang, Y., Liu, J., Zheng, Z., Fang, Z., Zhang, X., Gao, Y., & Xie, Y. (2020). Analysis of thermal comfort during movement in a semi-open transition space. Energy and Buildings, 225, 110312.

7. Ahmadi, M. (2020). The experience of movement in orbital space architecture: A narrative of weightlessness. Cogent Arts & Humanities, 7(1), 1787722.

8. Das, A., & Paul, S. K. (2015). Artificial illumination during daytime in residential buildings: Factors, energy implications and future predictions. Applied Energy, 158, 65–85.

9. Kulke, L., Feyerabend, D., & Schacht, A. (2020). A Comparison of the Affectiva iMotions Facial Expression Analysis Software with EMG for Identifying Facial Expressions of Emotion. Frontiers in Psychology, 11.
10. Boxtel, A. (2010). Facial EMG as a tool for inferring affective states. Proceedings of Measuring Behavior 2010 (Eindhoven, The Netherlands, August 24-27, 2010).
11. de la Fuente Suárez, L. A. (2020). Subjective experience and visual attention to a historic building: A real-world eye-tracking study. Frontiers of Architectural Research, 9(4), 774–804.
12. Rusnak, M. A., & Rabiega, M. (2021). The Potential of Using an Eye Tracker in Architectural Education: Three Perspectives for Ordinary Users, Students and Lecturers. Buildings, 11(6), 245.
13. Yamín Garretón, J. A., Rodriguez, R. G., & Pattini, A. E. (2016). Glare indicators: an analysis of ocular behaviour in an office equipped with venetian blinds. Indoor and Built Environment, 25(1), 69–80.
14. Paterson, M. (2011). More-than visual approaches to architecture. Vision, touch, technique. *Social & Cultural Geography*, *12*(3), 263–281.
15. Gunay, H. B., O'Brien, W., Beausoleil-Morrison, I., & Gilani, S. (2017). Development and implementation of an adaptive lighting and blinds control algorithm. Building and Environment, 113, 185-199.
16. Jia, L., Afshari, S., Mishra, S., & Radke, R. J. (2014). Simulation for pre-visualizing and tuning lighting controller behavior. Energy and Buildings, 70, 287–302.
17. Chomistek, A. K., Yuan, C., Matthews, C. E., Troiano, R. P., Bowles, H. R., Rood, J., Barnett, J. B., Willett, W. C., Rimm, E. B., & Bassett, D. R. (2017). Physical Activity Assessment with the ActiGraph GT3X and Doubly Labeled Water. Medicine & Science in Sports & Exercise, 49(9), 1935–1944.
18. Baker, F. C., & O'Brien, L. M. (2017). Sex Differences and Menstrual-Related Changes in Sleep and Circadian Rhythms. In Principles and Practice of Sleep Medicine (pp. 1516-1524.e5). Elsevier.
19. Manber, R., Bootzin, R. R., & Loewy, D. (1998). Sleep Disorders. In Comprehensive Clinical Psychology (pp. 505–527). Elsevier.
20. Lee, J., & Boubekri, M. (2020). Impact of daylight exposure on health, well-being and sleep of office workers based on actigraphy, surveys, and computer simulation. Journal of Green Building, 15(4), 19-42.
21. Liu, M., Han, S., & Lee, S. (2016). Tracking-based 3D human skeleton extraction from stereo video camera toward an on-site safety and ergonomic analysis. Construction Innovation, 16(3), 348–367.
22. Bian, Y., Leng, T., & Ma, Y. (2018). A proposed discomfort glare evaluation method based on the concept of 'adaptive zone'. Building and Environment, 143, 306-317.
23. Yamu, C., van Nes, A., & Garau, C. (2021). Bill Hillier's Legacy: Space Syntax—A Synopsis of Basic Concepts, Measures, and Empirical Application. Sustainability, 13(6), 3394.
24. Bafna, S. (2003). Space Syntax. Environment and Behavior, 35(1), 17–29.
25. Both, K., Heitor, T., & Medeiros, V. (2013). Assessing Academic Library Design: A Performance-Based Approach. 337–346.
26. Galvez-Pol, A., Nadal, M., & Kilner, J. M. (2021). Emotional representations of space vary as a function of peoples' affect and interoceptive sensibility. Scientific Reports, 11(1), 16150.
27. Bader, A. P. (2015). A model for everyday experience of the built environment: the embodied perception of architecture. The Journal of Architecture, 20(2), 244–267.
28. Sumartojo, S., Edensor, T., & Pink, S. (2019). Atmospheres in Urban Light. Ambiances, 5.
29. Chun, S., and Twose, S. (2019). On the effect of therapeutic spaces: a case for an autoethnographic study in architecture. In Proceedings of the Annual Design Research Conference 2019: 99-115. Melbourne, 2020.
30. Izmir Tunahan, G., Altamirano, H., Teji, J. U., & Ticleanu, C. (2022). Evaluation of Daylight Perception Assessment Methods. Frontiers in Psychology, 13.
31. Krüger, E. L., Piaskowy, N. A., Moro, J., & Minella, F. O. (2019). Identifying solar access effects on visitors' behavior in outdoor resting areas in a subtropical location: a case study in Japan Square in Curitiba, Brazil. International journal of biometeorology, 63, 301-313.
32. Dubois, C., Demers, C., & Potvin, A. (2009). Daylit spaces and comfortable occupants: A variety of luminous ambiences in support of a diversity of individuals. In Proceedings of the PLEA.
33. Hong, S. W., Schaumann, D., & Kalay, Y. E. (2016). Human behavior simulation in architectural design projects: An observational study in an academic course. Computers, Environment and Urban Systems, 60, 1–11.
34. Cılasun Kunduracı, A., & Kazanasmaz, Z. T. (2019). Fuzzy logic model for the categorization of manual lighting control behaviour patterns based on daylight illuminance and interior layout. Indoor and Built Environment, 28(5), 584–598.
35. Hunt, D. R. G. (1979). The use of artificial lighting in relation to daylight levels and occupancy. Building and environment, 14(1), 21-23.
36. Omar, O., García-Fernández, B., Fernandez-Balbuena, A. A., & Vázquez-Moliní, D. (2018). Optimization of daylight utilization in energy saving application on the library in faculty of architecture, design and built environment, Beirut Arab University. Alexandria engineering journal, 57(4), 3921-3930.
37. Atmodiwirjo, P. (2014). Space affordances, adaptive responses and sensory integration by autistic children. International Journal of Design, 8(3), 35-47.
38. Jens, K., & Khoudi, A. (2022). Using computer-vision sensors to study the impact of window views on occupancy and self-assessed productivity in flexible working environments: an intervention study. Intelligent Buildings International, 1-13.
39. Bruse, M. (2007). Simulating human thermal comfort and resulting usage patterns of urban open spaces with a multi-agent system. In Proceedings of PLEA (Vol. 24, pp. 699-706).
40. Yıldız, B., & Çağdaş, G. (2020). Fuzzy logic in agent-based modeling of user movement in urban space: Definition and application to a case study of a square. Building and Environment, 169, 106597.
41. de Montigny, L., Ling, R., & Zacharias, J. (2012). The Effects of Weather on Walking Rates in Nine Cities. Environment and Behavior, 44(6), 821–840.
42. Zeibo, J., Mishra, M. K., Panda, A. R., Mishra, B. S. P., & Mallick, P. K. (2021). Pedestrian Trajectory Prediction in Crowd Scene Using Deep Neural Networks (pp. 277–288).

PLEA 2024 WROCŁAW
(Re)thinking Resilience

Carbon flows at neighborhood scale

Case study in Geneva, Switzerland

ULRICH LIMAN, SOPHIE LUFKIN, EMMANUEL REY[1]

[1]Ecole polytechnique fédérale de Lausanne (EPFL), Lausanne, Switzerland

ABSTRACT: In a context of political commitment targeting net zero in 2050, controlling carbon flows is an essential operational imperative. The LOCUS methodology (Low carbon urban strategy) makes it possible to establish an exhaustive vision of carbon flows at neighborhood scale and to develop a strategy marking out the achievement of net zero in 2050. This unique approach, developed within the framework of the "Maillages Fertiles" research project, provides planners with information on: the carbon intensity of the neighborhood, the points of vigilance to consider during its development and the measures to prioritize to achieve net zero. Its application to the Praille-Acacias-Vernets (PAV) sector allows us to illustrate the structure of the method and to present the preliminary results obtained on this vast changing urban area.
KEYWORDS: Carbon neutrality, Sustainable neighborhood, Carbon footprint, Urban transition, Net zero.

1. INTRODUCTION

By ratifying the Paris Agreement in October 2017 [1], a legally binding instrument on climate change based on the work of the IPCC [2, 3], the Swiss Confederation has committed to reducing its emissions by half by 2030 and by 70 to 85% by 2050 (compared to 1990). Accepted by popular vote in June 2023, the Climate and Innovation Act [4] explicitly provides for the country to reduce its net greenhouse gas emissions to zero by 2050 [5]. These ambitious climate objectives are therefore part of the framework conditions guiding public policies, which should result in particular in significant developments for the built environment.

However, such an objective cannot be satisfied with the simple juxtaposition of isolated technical or behavioral solutions. This ecological limit encourages decision-makers and planners to be more transversal and to make public policies more consistent, to abandon a sectoral approach in favor of a systemic one. Territorial planning then rhymes with integrated design, so that all domains of emissions, often intertwined, are considered with a view to a massive and synergistic reduction of their footprint.

Planning new or transforming neighborhoods – real functional units of the urban fabric – represents a decisive opportunity to realize the ecological transition towards a more symbiotic and decarbonized society, ensuring that the basic needs of all are maintained. Only this scale allows us to grasp the major determinants of an eco-balance, namely the acts of building, living, working, consuming and moving.

Through the integration of several scales of analysis and multiple domains of greenhouse gas emissions, the LOCUS methodology aims precisely to take into account these issues at the neighborhood scale by answering extremely topical questions. Under what conditions is net zero achievable? Why is concerted and united action by all stakeholders, from decision-makers to users, required? What opportunities for synergies can be mobilized at this scale alone and what equalizations can be activated from a spatial (intra/inter neighborhood) or sectoral point of view (agriculture & food, economy & consumption, construction, operation and mobility)? Is the carbon investment made in favor of public spaces significant, relevant and offsetable in situ? What are the main carbon sinks in an urban neighborhood: vegetation or buildings? Finally, in 2050, what will be the most carbon-intensive areas: operation, construction or food?

2. METHODOLOGY

The LOCUS methodology, a real matrix analysis, uses the most recent knowledge and normative frameworks in terms of carbon footprint.

In order to establish a decarbonization strategy aligned with the Paris Agreement objectives, the LOCUS methodology is structured in four distinct stages:

- Setting the decarbonization ambition applicable to the programmatic diversity of the study perimeter;
- Designing a comprehensive 3D model of the neighborhood including public spaces, infrastructures and built volumes;
- Establishing all gross and net carbon flows according to current legal frameworks and behaviors;
- Identifying a viable path to net zero by testing scenarios mobilizing the various sources of savings and potential carbon sinks.

2.1 Decarbonization ambition

By declaring climate emergency [6], the Canton of Geneva intends to limit greenhouse gas (GHG) emissions to 1 tCO_{2eq}/inhab.year in 2050 – budget used here to qualify net zero. This carbon ceiling is relevant because it meets the objectives set in the Paris Agreement, the cantonal climate plan Geneva 2030 - 2nd generation [7, 8] and the exploratory study "Carbon neutrality in Geneva in 2050" [9], from which we extracted the impact of the Agriculture & Food, respectively Economy & Consumption domains.

To convert the objective of 1 tCO_{2eq}/inhab.year into targets per m^2 of Usable Floor Area (UFA), we considered the programmatic mix of the site and the human density for each use, as well as 50% of the targets relating to construction, operation and mobility described in [10]. Regarding the decarbonization remaining to be undertaken by the materials industry by 2050 [11] and the probable gains on this horizon [12], we have set two emission ceilings (Table 1):

- **Target A "Carbon neutrality"**: it corresponds to the impacts induced by ideal behaviors in terms of food and consumption according to [9], to which we add half of the targets relating to construction, operation and mobility described in [10], prejudging the reduction in carbon intensity of the materials available by 2050;
- **Target B "Towards carbon neutrality"**: applicable from 2022, it relaxes the target A requirement for the Construction domain, considering the carbon intensity of currently available materials.

Table 1: GWP targets [$kgCO_{2eq}/m^2_{UFA}.yr$] established for the 2030 (Target B) and respectively 2050 (Target A) deadlines.

Emission domains	Target B	Target A
Agriculture & food	6.5	6.5
Economy & consumption	1.5	1.5
Construction	9.0	4.5
Operation	2.1	2.1
Induced mobility	2.8	2.8
Total neighborhood target	**21.9**	**17.4**

2.2 Comprehensive numerical model

First, we build a detailed three-dimensional model of the program hosted within the study area (Fig. 1), characterizing each work (public spaces, infrastructures, networks and built volumes) and each type of population hosted (inhabitants, jobs, clients). All of the constituent elements of the neighborhood are then systematically quantified and characterized in terms of materiality and lifestyles.

Figure 1: 3D model of public spaces and buildings. White buildings are existing. Grey buildings have dimensions > 30 m and brown ones < 30 m (the latter can be built in wood without major additional investment).

In the presence of contaminated soils, LOCUS aims to:

- Limit earth movements by questioning the location choices for buildings and basements, networks and infrastructure;
- Decarbonize earth disposal according to the type of waste (A to E) and the mode of transport chosen.

The built volumes are characterized in detail in order to quantify four determinants of the eco-balance: human density, built density (habitable premises or not), compactness of volumes and orientation of facades (passive and active solar). For the sake of traceability, all of these quantities are established by construction element and by program.

2.3 Traceability of carbon flows

In order to guarantee the traceability of carbon flows, a crucial information when establishing decarbonization strategies, LOCUS adopts a matrix approach structured by intervention perimeters, macro/micro building elements and emission domains (Tables 2 and 3). After describing the composition of each microelement, all objects constituting the neighborhood are converted into carbon flows and assigned to an emission position. Finally, a synthetic representation of these flows (Fig. 2) reveals the major determinants of the eco-balance and governs the establishment of a decarbonization strategy for the neighborhood.

Table 2: Public spaces

Macroelements	Microelements	Emission domain
"Espaces rivières"	Preparatory works (clearing, demolition)	Construction
	River developments (including excavation and earth disposal)	Construction
	Crossings and (foot)bridges	Construction
	Soft mobility routes, lighting	Construction
	Networks and pipelines (rerouting)	Construction
Public domain	Preparatory works	Construction
	Development of the public domain, lighting	Construction
	Networks and pipelines (new)	Construction
	Excavation and earth disposal	Construction
Natural capture	Growth of arborization	Negative emissions

Table 3: Built spaces

Macroelements	Microelements	Emission domain
Construction	Above-ground premises (housing, activities, etc.)	Construction
	Underground premises (additional premises, car parks)	Construction
	Technical installations	Construction
	Excavation and earth disposal	Construction
Wood sequestration	Biogenic carbon of the wood material used	Negative emissions
Operating energy	Heating / Air Conditioning	Operation
	Domestic hot water	Operation
	Electricity	Operation
Mobility	Inhabitants	Induced mobility
	Jobs	Induced mobility
	Clients	Induced mobility

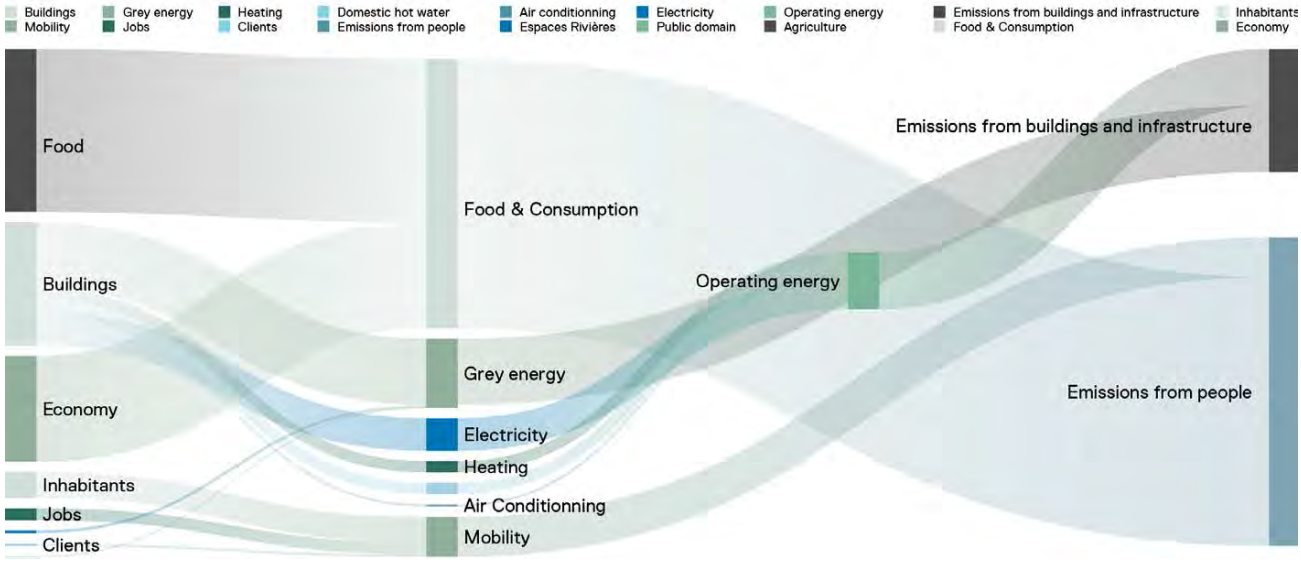

Figure 2: Sankey diagram of the neighborhood's carbon flows based on current gross emissions ($kgCO_{2eq}/m^2_{UFA}.year$).

2.4 A viable path towards net zero

During this last stage, we study carbon flows and their relationships, identify the main decarbonization sources, carbon sinks and possible spatial and/or sectoral equalizations that can be mobilized. Finally, to establish the path towards net zero in the scientific sense of the term [14], four scenarios of decreasing carbon intensity are developed (Table 4):

- Current: Geneva legal framework and lifestyles in 2022;
- Transition: 60% reduction in carbon emissions (2030 commitments of Paris Agreement);
- Capture: net zero with active CO_2 capture (2050 commitments of Paris Agreement);
- Sobriety: net zero without offsetting or capture (2050 commitments of Paris Agreement).

*Table 4: Summary of the main assumptions used for the four scenarios of decreasing carbon intensity down to net zero. Figures on the left represent the overall emissions for each scenario, expressed in tCO_{2eq}/pers.year. *THPE = Very High Energy Efficiency.*

		Agriculture & Food	Economy & Consumption	Grey Energy	Operating Energy	Daily Mobility
Current Current legal framework and lifestyles	12.0	**Agriculture**: status quo **Food**: wastage -5%, meat -30%, dairy products and exotic foods ; status quo	**+5% vs 2012 emissions** (1.30 tCO_2/inhab.year). Incentive measures, circular economy versus an all-digital and connected society	**Energy-intensive construction method** Additional premises in the basement Disposal of earth and waste (type ABCDE) by truck	**SIA 380/1** **Qh,li, single flow** Heating: remote (Swiss mix) / Cooling: refrigeration units / Electricity: 100% Swiss mix **Renewable: 31%**	**Daily distances and modal shift according to SIA 2039** **2015 fleet** GWP = 6.1 $kgCO_2/m^2.y$
Transition Paris Agreement 2030	4.9	**Agriculture**: status quo **Food**: wastage -10%, meat -50%, dairy products -25%, luxury food -50%, local and/or seasonal products ++	**+0% vs 2012 emissions** Support for low-carbon companies, planned obsolescence and advertising of carbon-intensive products prohibited	**Traditional construction method** Additional premises in the basement Disposal of earth and waste (type ABCD) by truck, type E by train	**THPE*** **70% Qh,li, double flow** Heating: interim / Cooling: refrigeration units / Electricity: 20% PV, 80% Swiss mix **Renewable: 85%**	**Daily distances and modal shift according to SIA 2039** **2030 fleet** GWP = 3.4 $kgCO_2/m^2.y$
Capture Paris Agreement 2050 with active capture	1.4	**Agriculture**: GWP -90% (urban farming / direct sale) **Food**: optimal diet for health and the environment, vegetables++, local, seasonal	**-88% vs 2012 emissions** Support for local companies active in the transition and the circular economy. Fewer possessions > pooling	**75% traditional construction method, 25% wood construction** 1 basement level only Disposal of earth and waste (type AB) by truck, type CDE by train	**THPE*** **70% Qh,li, double flow** Heating: Génilac and Géniterre / Cooling: Génilac and refrig. units / Elec: 7% PV, 93% vitale bleu **Renewable: 87%**	**Daily distances and modal shift according to SIA 2039** **2050 fleet (100% electric)** GWP = 2.5 $kgCO_2/m^2.y$
Sobriety Paris Agreement 2050 without active capture	1.0	**Agriculture**: GWP -92% **Food**: optimal diet for health and the environment, education on healthy and low carbon eating, quotas on animal products, 0 wastage	**-90% vs 2012 emissions** Development of the industrial, artisanal and commercial fabric linked to reuse and repair. Pooling at neighborhood scale	**50% traditional construction method, 50% wood construction** 1 basement level only Disposal of earth and waste (type ABCDE) by train	**THPE*** **70% Qh,li, double flow** Heating: Génilac and Géniterre / Cooling: Génilac and refrig. units / Elec: 7% PV, 93% vitale vert **Renewable: 95%**	**Daily distances: -20% and 2050 modal shift** (40% public transport, 28% soft mobility, 32% cars) **2050 fleet (100% electric)** GWP = 2 $kgCO_2/m^2.y$

Agriculture & Food, Economy & Consumption

These first two emission domains include the values from the study [9], itself based on the planetary health diet established by the EAT-Lancet commission [13]. To determine a carbon footprint according to the program, we applied the following distribution keys:

- Food: the activity rate of the Swiss population [15] allows us to define the number of meals taken as a resident (87%) and as an employee (13%);
- Consumption: the territorial carbon balance of the Canton of Geneva [16] specifies the share attributable to housing (68%) and companies (32%).

Grey energy

The impact of materials is established in accordance with SIA 2032 technical specifications [17] and the most recent KBOB database [18]. The impact of buildings and public spaces is amortized over 60 years, excluding the temporary developments of the Drize river, amortized over 10 years.

In order to study the elasticity of the carbon impact of materials, we have established three commonly used construction methods, then modulated their proportion according to the scenario.

The Current scenario exclusively uses the Energy-intensive construction method. The Transition scenario implements the Traditional method. Then, wood is introduced gradually: 25% for the Capture scenario, 50% for the Sobriety scenario (all buildings of less than 30 m).

Operating energy

The 3D model of the neighborhood allowed us to establish the energy reference surface as well as the form factor, deliberately degraded by 10% to allow for the architectural variety that still needs to be expressed at this stage. According to current standards, we have established the energy requirements for heating and domestic hot water production, cooling of premises as well as electricity. By considering the yields specific to each type of energy production, we calculated the final energy requested and then the neighborhood's carbon impact for each scenario, using a specific energy mix. Ultimately, the 3D model allowed us to estimate the solar potential, by quantifying, for each orientation, the activatable surfaces on roofs and facades – excluding shaded areas or areas reserved for other uses (ventilation installations, elevator shafts, glass surfaces, etc.). These calculations comply with the Geneva legal framework [19] and the Swiss normative corpus [20, 21, 22, 23, 24].

Mobility

First, the carbon impact of daily mobility is defined according to SIA 2039 [25]. This methodology makes it possible to assess the carbon impact of induced mobility based on Swiss reference values, corrected by factors depending on the quality of the site.

The carbon impact of mobility is established for each use and type of user according to the following equation (1):

$$GWP = F_{corr} \times GWP_{baseline} \quad (1)$$

with $GWP_{baseline}$ = baseline greenhouse gas emissions, depending on the current and future quality of the Swiss vehicle fleet ($kgCO_{2eq}$ / m^2_{UFA}.year).

Then, in addition to the two standardized fleets [25] reflecting the quality of the current and 2030 fleets, we have established a 2050 fleet, in line with the new political orientations and expected efficiency gains [26]. For the sake of completeness, the impact of the different means of transport includes the grey energy of vehicles and infrastructure.

Finally, the 2050 modal shift is established:

- Based on the current behavior of residents;
- Calculating the carbon impact for the 2050 fleet;
- Adapting the share of each mode of transport to achieve the target carbon budget.

3. RESULTS

Building the neighborhood according to current standards and behaviors would generate the emission of 66 $kgCO_{2eq}/m^2_{UFA}$.an, i.e. 3 times target B and 4 times target A. Currently, our eating or consumption habits each mobilize the entire 2050 carbon budget. The same observation applies to the construction sector (grey and operating energies, mobility), which exceeds target A by more than 45%.

In other words, a net zero neighborhood requires optimal decarbonization of all emission domains. Any impasse (Current scenario) or half-measure (Transition scenario) tends to weaken the achievement of carbon neutrality in 2050, requiring subsequent corrective measures whose feasibility appears unlikely within the time horizon of a single generation (Fig. 3). Only the Capture and Sobriety scenarios, which clearly differ from current practices, appear likely to achieve the ambitious climate objectives of the Paris Agreement for 2050. The Capture scenario adopts measures limiting emissions to target B and actively removes the excess CO_2 emitted for an annual additional cost estimated at 4.2 million CHF. The Sobriety scenario achieves target A by maximizing wood construction and promoting the decarbonization of materials expected by 2050.

The PAV, a changing urban sector, benefits from numerous pre-existing infrastructures (public transport, road, sewerage or electricity networks). This is why, despite the realization of major public developments (renaturation of two rivers, soft mobility routes and crossings, park, extension of heating networks, etc.), the impact of public spaces only represents 3.5% of the carbon budget (target A). These investments are relevant since they favor soft mobility and renewable energies, which contribute to the decarbonization of the operation and mobility domains. Finally, this impact is entirely compensable in situ by two carbon sinks, namely the growth of 2,130 new trees to be planted and the use of wood for approximately a quarter of the planned buildings.

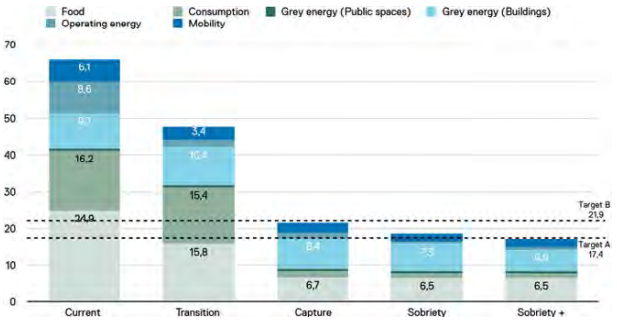

Figure 3: Net carbon emissions by domain and targets A-B applicable to the neighborhood. Target A = 17.4 $kgCO_{2eq}/m^2_{UFA}$.year. Target B = 21.9 $kgCO_{2eq}/m^2_{UFA}$.year. The Sobriety+ scenario mentioned here for information purposes takes up the hypotheses of the Sobriety scenario with 100% wood construction.

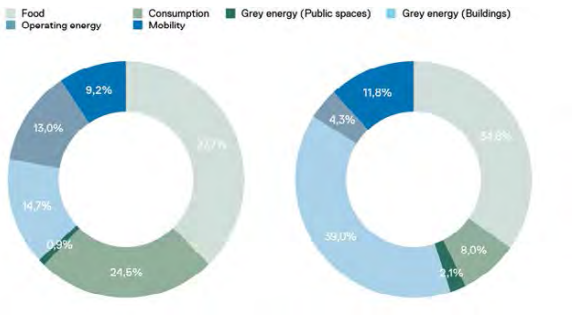

Figure 4: Distribution of the neighborhood's net carbon emissions. Left: Current scenario (2022). Right: Sobriety scenario (2050).

4. CONCLUSION

The preliminary results confirm the scale of the climate challenge, both on a global level and at neighborhood scale, and allow us to formulate some recommendations aiming for net zero by 2050:

- Reduce emissions by a factor of 4 compared to current standards, practices and behaviors;
- Opt for the measures described in the Sobriety scenario, encourage voluntary change in our lifestyles and strengthen the target dedicated to construction materials, whose carbon intensity must fall by half by 2050 [12];
- Abandon overly sectoral approaches in favor of a systemic vision and an operational partnership from political decision-makers to future residents;
- Anticipate the redistribution of the most carbon-intensive domains by 2050 (construction materials and food), in order to focus on the essential;
- Create generously vegetated and arborized public spaces, which have a proportionately low carbon footprint and promote soft mobility, well-being and climate adaptation.

In 2024, the PAV Project Management wishes to broaden the perimeter of the research in order to:

- Consolidate the neighborhood's carbon intensity by integrating new unique sectors, due to the functions they accommodate or their progress (under construction or even appropriation);
- Add a monitoring tool to the LOCUS methodology, making it possible to monitor the neighborhood's carbon impact over the course of the projects, define a budget for each of them and thus guarantee the achievement of net zero.

ACKNOWLEDGEMENTS

This study was conducted as part of the "Maillages fertiles" interdisciplinary research project, mandated by République et canton de Genève, Département du Territoire (DT), Direction Praille Acacias Vernets (DPAV).

REFERENCES

1. UN, United Nations et UNFCCC, (2015). Paris Agreement. Paris, France. Available: https://unfccc.int/files/essential_background/convention/application/pdf/english_paris_agreement.pdf
2. IPCC, (2018). Global Warming of 1.5°C. Cambridge University Press. Cambridge (UK and New York).
3. IPCC, (2023). Climate change - Synthesis Report.
4. Loi fédérale sur les objectifs en matière de protection du climat, sur l'innovation et sur le renforcement de la sécurité énergétique adoptée le 18 juin 2023.
5. Office fédéral de l'environnement, (2021). Stratégie climatique à long terme de la Suisse. Berne.
6. Conseil d'État, (2019). L'urgence climatique est déclarée. Communiqué de presse du Conseil d'État du 4 décembre 2019, rapport relatif à la motion intitulée "Une réponse politique à l'appel des jeunes pour sauver le climat". Available: https://www.ge.ch/document/communique-presse-du-conseil-etat-du-4-decembre-2019#extrait-18390.
7. République et Canton de Genève, (2021). Plan climat cantonal 2030 - 2e génération.
8. Conseil d'État, (2021). Objectif neutralité carbone: présentation du Plan climat cantonal renforcé. Available: https://www.ge.ch/document/objectif-neutralite-carbone-presentation-du-plan-climat-cantonal-renforce.
9. UNIL, (2020). Étude exploratoire "Neutralité carbone" à Genève en 2050. Proposition de 4 scénarios. Available: https://www.ge.ch/document/etude-exploratoire-neutralite-carbone-geneve-2050.
10. SIA, (2017). Cahier technique SIA 2040. La voie vers l'efficacité énergétique. SIA, Zurich.
11. Priore YD., G. Habert, T. Jusselme, (2023). Exploring the gap between carbon-budget-compatible buildings and existing solutions – A Swiss case study. *Energy and Buildings*, 278.
12. Treeze Ltd., M. Alig, R. Frischknecht, L. Krebs, L. Ramseier, P. Stolz, (2020). LCA of climate friendly construction materials - Final report V.2. Uster.
13. Willett, W., J. Rockström, B. Loken, M. Springmann, T. Lang, S. Vermeulen, (2019). Food in the Anthropocene: the EAT–Lancet Commission on healthy diets from sustainable food systems. *The Lancet Commissions* 393 (10170): 447-92.
14. Fragnière A., P. Thalmann, (2023). Pour une stratégie de décarbonation fondée sur la science. E4S.
15. OFS, (2021). Taux d'activité en EPT selon le sexe, la nationalité, les groupes d'âges, le type de famille.
16. République et Canton de Genève, (2015). Bilan Carbone® territorial du canton de Genève. Available: https://www.ge.ch/document/11701/telecharger.
17. SIA, (2010). Cahier technique SIA 2032. L'énergie grise des bâtiments. SIA, Zurich.
18. KBOB, (2022). Eco-building database 2009-1-2022. KBOB, Zurich.
19. République et Canton de Genève, (2022). Règlement d'application de la loi sur l'énergie (REn) L 2 30.1, révisée le 5 octobre 2022.
20. SIA, (2016). Norme SIA 380/1. Besoins de chaleur pour le chauffage. SIA, Zurich.
21. SIA, (2006). Norme SIA 380/4. L'énergie électrique dans le bâtiment. SIA : Zurich.
22. SIA, (2007). Norme SIA 382/1. Installations de ventilation et climatisation - Bases générales et performances requises. SIA : Zurich.
23. SIA, (2017). Norme SIA 387/4. Électricité dans les bâtiments – Éclairage : calcul et exigences. SIA, Zurich.
24. SIA, (2015). Cahier technique SIA 2024. Données d'utilisation des locaux pour l'énergie et les installations du bâtiment. SIA, Zurich.
25. SIA, (2016). Cahier technique, SIA 2039. Mobilité - Consommation énergétique des bâtiments en fonction de leur localisation. SIA, Zurich.
26. Mobitool, (2020). Facteurs mobitool v2.1. Association Mobitool et treeze Ltd.

PLEA 2024 WROCŁAW
(Re)thinking Resilience

Daylight metrics and requirements:
a review of reference documents for architectural practice

AMANDA MOURA PINHEIRO [1] CLÁUDIA NAVES DAVID AMORIM [1]
NATALIA SOKOL [2] JUSTYNA MARTYNIUK-PĘCZEK [2]

[1] University of Brasília, Brasília, Brazil
[2] Gdańsk University of Technology, Gdańsk, Poland

ABSTRACT: Daylight has always been part of the architectural practice, since architects always used it to define spaces and create complex structures. Daylighting is, nowadays, seen as key strategy for sustainability, energy efficiency and resilience in buildings. This article aims to investigate daylight requirements in reference documents for architectural practice, through the collection and qualitative analysis of documents. To the analysis, primary documents were collected through active searches and through the application of a survey to daylight specialists from different countries. Then, 130 reference documents were analysed, divided into standards, rating systems, building and urban codes, regulations and guidelines. Results show that static and dynamic metrics are common within standards and rating systems, while building and urban codes and regulations often use metrics based on building and urban geometry. Among standards and rating systems, Daylight Factor (DF) is still one of the most used metrics, even if dynamic metrics offer advanced analyses; building and urban codes and regulations are very specific from each location, with predominant use of geometric metrics; and guidelines can use both types of metrics.
KEYWORDS: Daylight requirements, Standards, Rating systems, Building and urban codes, Regulations, Guidelines.

1. INTRODUCTION

Daylight has always been essential to mankind's development: it allows visibility and influences health [1,2,3]. Due to that, it is a vital part of architectural practice: using daylight, architects define spaces and create high complexity structures, in order to provide comfortable and pleasant places [4,5]. Moreover, daylighting is one key strategy to increase energy efficiency and contributes to enhance buildings' resilience against failures of electricity [3,6].

Daylighting requires a wide comprehension of how it affects occupants and spaces, which is not always clear to architects [7,8,9]. In that context, daylight requirements, even though cannot ensure good design, may contribute to better guidance, avoiding poor design decisions and facilitating architectural practice [9,10,11].

The requirements concerning daylight in reference documents are composed by metrics — a combination of quantities and conditions — and parameters — values or boundaries that act as guidance to enable evaluations [10,11,12].

As there is a large number of possible international reference documents, in this article, the documents evaluated were: standards, rating systems, building and urban codes, regulations and guidelines, considered crucial for buildings' and cities' projects. Those documents are developed by international and national authorities, professional organizations or institutions [11].

Standards are official publications with technical recommendations about the quality, safety and other features of a product [13]. In the case of buildings, standards provide guidance about daylight, acoustic, thermal comfort, performance, etc [2].

Rating systems are schemes that measure levels of compliance or performance of buildings, according to specific criteria [14]. Today, rating systems are seen as key drivers of sustainability in architecture, and have a significant commercial appeal [2].

Building and urban codes are elaborated by local authorities, focused on development and construction, defining rules about buildings and urban fabric. Building and urban codes propose design, regulation and planning, with the aim to achieve higher quality spaces [15]. Also, the existing urban fabric can and should be enhanced by the rules defined by codes, as they are expected to assure sustainable strategies, social and ecofriendly development, nature-based solutions, and so on. Usually, codes are legally binding and seen as "models" for jurisdictions [15,16].

Regulations are documents to ensure buildings are secure for people in or around them. Elaborated by the state or local government, regulations contain a series of approved requirements and rules for urban spaces and buildings, covering the technical aspects of construction. Historically, their application is necessary to building construction activities and to compose a city's governance [17,18].

Guidelines are a set of policies, rules and procedures promulgated and/or amended by the developer or the local control authority, that act as a guide for architectural activities [18]. Guidelines also help to preserve the long-term vision and property value of a community, by outlining requirements for builders, regarding styles and exterior features, as well as provide a set of good design practices [19].

This article investigates daylight requirements on reference documents for architectural practice. The work is part of the *Commission Internationale de l'Eclairage* (CIE) Technical Committee 3-61 (TC 3-61), which aims to assess the feasibility of global harmonization of daylight requirements.

2. METHOD

The steps fulfilled during the research were:

- Collection of primary documents: sent by members of TC 3-61 and other specialists, or collected from associations and stakeholders' websites, from Dec/2022 to Feb/2024;
- Application of survey: sent to daylight specialists from research institutes and associations, to gather information from different countries;
- Elaboration of summary tables: according to document, requirements, countries, metrics;
- Analysis of data and conclusions: quantitative and qualitative analysis of the findings.

This article comprehended the analysis of 130 primary reference documents obtained, including standards (45), rating systems (26), building and urban codes and regulations (49) and guidelines (10).

3. RESULTS AND DISCUSSION

The reference documents were received in their original versions or in summaries elaborated by specialists. The documents include not only requirements specifically related with daylight, but also those related to lighting in general, energy efficiency, architecture, and urbanism. This article, though, focused on requirements that influence daylighting in buildings and in urban fabric.

3.1 Daylight requirements and metrics

Daylight requirements are basically composed by parameters and metrics. Those must be accurate enough to evaluate the project's features [9]. A "parameter" is a limit, or a boundary, that acts as a factor that enables judgement or evaluation of something — e.g., a numerical value. As for "metric", it is a way to measure or evaluate something, with the use of figures or statistics [2,12].

Requirements influence directly on building and urban design strategies, since those are crucial references for practitioners [9]. Yet, for their use to be effective in architectural practice, requirements have to be objective, simple, testable, replicable, and able to give robust and reliable results [20].

Daylight metrics are classified between static, dynamic and geometric. Static metrics, the first created, were initially calculated by tables and two-dimensional drawings, based on point-in-time illuminances under a single sky condition [9,21,22, 23]. As main example of static metrics, there is Daylight Factor (DF) and its variations. Dynamic metrics, introduced by year-round climate-based daylight modelling (CBDM) embodying 8,760h/year of climatic data, allowed the acceleration of calculations and provision of realistic and accurate results [9,22]. Therefore, dynamic metrics are based on what time of the year daylight is able to provide the light levels required. As examples of dynamic metrics, there are Daylight Autonomy (DA), Spatial Daylight Autonomy (sDA), Useful Daylight Illuminance (UDI), Annual Sunlight Exposure (ASE), Sunlight Exposure and Daylight Glare Probability (DGP) [2,21,22].

The geometric metrics are those related to areas, distances, angles, as well as building shape and material properties, such as Window-to-Floor Ratio (WFR), Window-to-Wall Ratio (WWR), Outside views, setbacks, lightwells, obstruction and shadowing angles, Visible Light Transmittance (VLT) [20]. Metrics and their definitions are found in Table 1.

Table 1: Definitions of found daylight metrics.

Metrics	Definitions
Daylight Factor (DF)	ratio of illuminance on a horizontal surface to the unobstructed overcast sky, considering reflections [2,21]
Average Daylight Factor (DF_{avg})	ratio of illuminance on a horizontal surface to the unobstructed overcast sky, considering reflections, across a grid of points [2,21]
Daylight Autonomy (DA)	ratio of occupied hours in a year in which a minimum illuminance range is attended only by daylight [23,24]
Spatial DA (sDA)	area of work plane that meets an ideal illuminance ($sDA_{lx/\%}$) [21]
Useful Daylight Illuminance (UDI)	range of illuminances values across the work plane along one year [24]
Annual Sunlight Exposure (ASE)	amount of sunlight reached in a part of occupied hours per year [25,27]
Target Illuminance (E_T)	illuminance achieved across 50% of the reference plane for at least half of the daylit hours [28]
Minimum Target Illuminance (E_{Tmin})	minimum illuminance achieved across 95% of the reference plane for at least half of daylit hours [28]
Sunlight Exposure	sum of the time (h) in which spaces are exposed to sunlight [28]
Outside views	visual contact with the surroundings through openings façades [28]
Daylight Glare Probability (DGP)	probability of discomfort by glare, based on vertical luminance and illuminance of source [7,21]

Daylight Glare Index (DGI)	the ratio of total window area to total floor area [21]
Window-to-Floor Ratio (WFR)	the ratio of total window area to total floor area [29]
Window-to-Wall Ratio (WWR)	the portion of an exterior wall that consists of windows [30]
Obstruction angles	the angle from the centre of the window to the top of the surrounding elements [31]
Shadowing angles	the angle from the centre of the window to the most external point of the solar protection [31]
Setback distances	the minimum distance required between a structure and the front, side, or rear plot boundaries [32]
Visible Light Transmittance (VLT)	the portion of visible light that passes through a glazing system [33]
Lightwell	internal spaces open to the air that allow light and air indoors [34]

3.2 Documents collected

Table 2 shows the distribution of documents in different geographical and climatic conditions, with predominance of European countries. All other continents were also represented.

Table 2: Reference documents received and origin countries.

Document	Country	Quantity
STANDARDS	Europe	2
	Italy	5
	Denmark	1
	Norway	1
	UK	2
	Germany	2
	Netherlands	2
	Slovenia	1
	Greece	2
	Czech Republic	1
	Austria	1
	Turkey	1
	Poland	3
	France	6
	Sweden	1
	Brazil	3
	Chile	1
	Colombia	2
	USA	3
	Canada	1
	China	1
	Russia	2
	South Africa	1
GUIDELINES	UK	2
	Netherlands	1
	Estonia	1
	Turkey	1
	Singapore	1
	Japan	1
	Chile	2
	Colombia	1
RATING SYSTEMS	UK	1
	Netherlands	1
	Italy	1
	Sweden	1
	Germany	1
	France	3
	USA	3
	Canada	3
	Australia	1
	Colombia	1
	Brazil	5
	Chile	2
	Japan	1
	China	1
	South Africa	1
BUILDING AND URBAN CODES/ REGULATIONS	Italy	9
	Netherlands	1
	Norway	1
	Poland	1
	Austria	1
	Belgium	1
	Croatia	1
	Hungary	1
	Denmark	1
	France	4
	Germany	1
	Slovenia	1
	Sweden	2
	Spain	1
	Ireland	1
	Turkey	1
	USA	3
	Canada	1
	Brazil	9
	Chile	1
	Bolivia	2
	New Zealand	3
	Japan	1
	China	1

The documents are applied differently, according to each country. For example: building and urban codes are the common mandatory documents to comply, while rating systems and guidelines are optional. Standards are mandatory when laws give them this status, as happens in Brazil [26].

Different metrics appear on these documents, and the simple analysis of quantities is important to understand which are the most used worldwide. Table 3 summarizes the occurrence of daylight metrics in the 117 documents analysed.

Table 3: Occurrence of daylight metrics in documents.

Type	Metrics	Standards	Rating Systems	Guidelines	Building and Urban Codes / Regulations
Static	DF	30	13	4	8
	DF_{avg}	1	2	3	8

	DGI	2	1	0	0
	Outside Views	18	14	3	10
Dynamic	E_T	16	3	0	1
	E_{Tmin}	16	2	0	3
	DA	2	5	1	1
	sDA	6	6	0	2
	UDI	2	6	1	0
	ASE	4	4	0	0
	Sunlight Exposure	17	2	3	2
	DGP	17	4	2	0
Geometric	WWR	1	5	2	2
	WFR	5	4	3	28
	Window sizes / areas / head heights	2	1	0	6
	Setback distances	3	1	2	12
	Shadowing angles	1	2	2	3
	Obstruction angles	0	1	2	4
	Lightwells	0	0	0	1
	VLT	4	4	0	4

Static metrics, mostly DF and variations, are mentioned 69 times. Nonetheless, dynamic metrics now are more common: together, those metrics (DA, sDA, UDI, E_T, E_{Tmin}, DGP, ASE) are found in 104 of all documents. Sunlight exposure, found 24 times, is especially important to countries with cold winters, in order to ensure natural heating, as other benefits. In sunny climates, excessive sunlight exposure can provoke glare occurrence or elevated heat gains, if not properly regulated.

Outside views are also a recurrent requirement in all documents — mentioned in 45 of them — and are important for all buildings. In several documents, especially those based on EN 17037, there are objective parameters to classify views out (angles, view composition, distance of view, etc), while in other documents this analysis is still very subjective.

WFR is mentioned 40 times; followed by the setback distances, found in 18 of them; WWR was found in 10, while obstruction and shadowing angles appeared in 8 and 7 documents, respectively.

3.3 Standards

Standards, usually, are not mandatory, except when a law or government decree refers to it, or specifically gives the standard that status [26].

The metrics and requirements found were: DF, appearing in 30 documents; Outside views, 18 times; DGP and Sunlight Exposure, 17 times; E_T and E_{Tmin} appeared in 16 documents each; sDA, with 6 mentions; ASE and VLT, mentioned in 4 standards; setback distances were mentioned 3 times, while DA, UDI, DGI, window sizes were mentioned 2 times; other metrics, such as DF_{avg}, WWR and shadowing angles were mentioned in 1 standard each.

EN 17037:2018 is one of the most influent standards, since it became a reference for European countries — which have their versions of EN 17037 — and also for others outside Europe, like the Brazilian standards ABNT NBR 15215:2023 and ABNT NBR 15575:2023. Metrics used are DF, sDA, DGP, views.

EN proposed a climatic adaptation of DF, based on different median external diffuse illuminances and consequently different parameters (values) of target DF, e.g. from 0.2% in Cyprus (for 100 lux) to 5.4% (for 750 lux) in Reykjavik. Despite that, for sunny climates, this could lead to overheating and glare if windows are enlarged to achieve the target DF.

LM 83:2023 is another significant standard, published by the Illumination Engineering Society of North America (IESNA). LM 83 consolidated sDA and ASE in its first version from 2012. In 2023, the revision maintained the ASE method, but unfolded sDA in two parameters: the usual $sDA_{300/50\%}$ in 75% or 55% of used area, and $sDA_{150/50\%}$ in 50% of used area in spaces with less critical visual tasks. sDA and ASE became very common also in other documents.

$sDA_{300lx/50\%}$ and $ASE_{1000lx/250h}$ are the most found parameters for these metrics, meaning that those became the target values independently of the climatic conditions. This may seem a problem at first, but considering that sDA and ASE are dynamic metrics, it is possible to design spaces towards those results through computer simulations.

3.4 Rating systems

Rating systems are non-mandatory [27] but have an important economic appeal for stakeholders. LEED (USA) and BREEAM (UK) are the most popular rating systems worldwide, as they are applied in numerous countries. In most cases, those systems are adopted with the same metrics and parameters as the original American and British versions.

Other Rating Systems analysed were WELL (USA), Protocollo ITACA (Italy), Selo Azul Caixa and INI-C (Brazil), HQE (France), CASA Colombia, DGBN (Germany), Living Building Challenge (USA/Canada), CASBEE (Japan), BCA Green Mark (Singapore), Green Star (Australia), Green Star Rating (South Africa), CES and CVS (Chile) and GB/T 50378-2019 (China).

The requirements found were: DF, with 13 mentions; Outside views were mentioned 14 times; UDI and sDA, 6 times; DA and WWR, 5 times; ASE, WFR and VLT, 4 times; E_T is mentioned 3 times. With 2 mentions each, DF_{avg}, E_{Tmin}, shadowing angles and Sunlight Exposure. Setbacks, window areas, obstruction angles and DGI were mentioned once.

Standards and Rating Systems improved along time in parallel with the evolution of metrics, from static to dynamic, using similar parameters. On one

hand, Rating Systems focus on higher performance and, even though not being mandatory, the sustainability aspect is vital in those schemes. As a way to set higher performance goals, there are more categories — i.e., $sDA_{300lx/50\%}$ in 55%, 75% or 90% of occupied area; outside views for 50% or 100% of spaces, among others. On the other hand, Standards are a reference for professionals, to guide an acceptable performance and avoid design mistakes. Standards and Rating Systems also have in common that both are influential in many countries.

3.3 Building and urban codes/Regulations

As Building and Urban Codes and Regulations are similar, they were analysed together in this article. Codes, as well as Regulations, are the main reference for practitioners during architectural practice, since both are mandatory and legally binding — implying that inconsistencies with the requirements might even withhold constructions.

The found requirements were: WFR, in 28 documents; Setback distances, mentioned 12 times; Views out, mentioned 10 times; DF and DF_{avg}, 8 times each; window areas were mentioned in 6 documents; VLT and obstruction angles, 4 times; E_{Tmin} and shadowing angles, 3 documents; Sunlight exposure, WWR and sDA were found 2 times. Lightwells, DA and E_T are mentioned in 1 document.

Codes and Regulations are focused on a particular area of application and provide orientations for a wide quantity of schemes, projects and situations in that specific place [16,17]. Parameters commonly found for WFR, for example, vary according to the typologies of buildings and needs of the project. For housing, WFR falls into the range of 1/10 to 1/12 and from 1/7 to 1/8; for offices, from 1/8 to 1/10; for schools, kindergartens and classrooms, WFR values above 1/7, sometimes reaching 1/4 to 1/5, are recommended. Static and dynamic metrics do not appear often on these documents.

3.4 Guidelines

In the international context, guidelines are not common in many countries. This may justify why only few documents were found — a low representativity that hinders a wider evaluation. The requirements found were: DF, found 4 times in guidelines; DF_{avg}, found 3 times, as were Sunlight Exposure, Views out and WFR; DGP, WWR, setbacks, shadowing and obstruction angles were mentioned 2 times each. DA and UDI were found once each.

In countries that have Guidelines as manuals, those are elaborated by professional organizations. Guidelines are mostly not mandatory: instead, they can be a reference for practitioners, whether to facilitate the comprehension and application of other documents — e.g. Codes, Regulations — or to guide better design practices. Hence, guidelines' requirements are in between those two groups: those keen to aid professionals to apply mandatory documents regarding building and urban geometry; and those focused on better practices apply static and dynamic metrics.

4. CONCLUSION

This article explored daylight requirements in reference documents, demonstrating the many ways that daylight is treated. Three groups were verified: one composed by standards and rating systems, since those tend to have similar requirements; other by building and urban codes and regulations, also with similar metrics; lastly, the guidelines, that in most cases depend on the focus of the document.

The most well represented were the European countries. North and South America, Asia and Oceania were also represented. Only a few documents from Africa were received, possibly due to the lack of access or few published information.

DF remains a widely used metric, especially in European countries. Even the parameters being different, considering each local condition of median external diffuse illuminances as proposed by EN 17037, it is still limited and performs better for overcast skies. The parameters, in general, are the same for many countries, which could lead to issues with excessive heating, when used in sunny climates.

Dynamic metrics provide more reliable results. The key to dynamic metrics is to have target parameters to comply that truly consider local climates. With a goal set, the strategies used by designers may differ, but the results meet the recommendations. The most used dynamic metrics for daylight provision is Target Illuminance and variations, along with Spatial Daylight Autonomy (sDA). For glare assessment, Daylight Glare Probability (DGP) is the most used, while Sunlight Exposure expresses the access to sunlight indoors.

Metrics based on geometry, instead, influence directly the architectural and urban projects, since they shape the buildings and intermediate their relation to the surroundings. The most used are WFR and setback distances. Similar parameters are used for different locations, which indicates the limitation of this metrics, as used presently. Their main advantage is to be familiar to architects and urban planners, but new parameters should be further developed, to adapt to different climates and sky conditions, providing solutions to control the same variables — i.e., in sunny climates determine a reduced WFR, while colder climates might require more window areas. Connecting geometric to dynamic metrics could clarify how both types of metrics impact each other during the design process, as well as building and urban spaces.

ACKNOWLEDGEMENTS

Authors would like to thank CIE TC 3-61 members and to Aurum Grant at Gdańsk Tech, for their rich contribution to this work. Also, authors thank financial support from Gdańsk University of Technology by the DEC-1/2022/IDUB/II.1a/Au Grant, under the AURUM "Excellence Initiative – Research University" program. Brazilian National Council of Scientific and Technological Development (CNPq) and Coordination of Improvement of Graduate Level (CAPES) are gratefully acknowledged as well.

REFERENCES

1. Knoop, M. et al. (2020). Daylight: What makes the difference? *Lighting Research and Technology:* 52, p. 423-442.

2. Tregenza, P.; Mardaljevic, J. (2018). Daylighting buildings: Standards and the needs of the designer. *Lighting Research and Technology*, 50: p. 63-79.

3. Boubekri, M. (2008). Daylighting legislation. In: *Daylighting, architecture and health building design strategies*. 1. ed. [s.l.] Elsevier, v. 1, pp 49-52.

4. Mardaljevic, J.; Andersen, M. (2012). Prescribing for daylight: can we account for the disparate measures within a unified modelling framework? *Proceedings of Experiencing Light 2012 Conference*. The Netherlands.

5. Rayham, P. (2015). *Daylighting standards: Do we have the correct metrics?* The UCL Institute of Environmental Design and Engineering, London, UK.

6. Turan, I. et al. (2020). The value of daylight in office spaces. *Building and Environment*, v. 168.

7. Kruisselbrink, T. et al. (2018). Photometric measurements of lighting quality: an overview. *Building and Environment*.

8. Verso, V. et al. (2021). A survey on daylighting education in Italian universities. *Journal of Daylighting*, p. 36-49.

9. Sokół, N. (2019). *Daylight evaluation for multi-family housing* (Thesis). Gdańsk University of Technology, Poland.

10. Pinheiro, A.; Amorim, C. (2023). Daylight requirements: an overview of definitions, progress and gaps. *Proceedings of the CIE 30th Session*, vol.1. Ljubljana, Slovenia. p. 380-390.

11. International Energy Agency (IEA) (2021). IEA SHC Task 61 / EBC Annex 77: Integrated Solutions for Daylighting and Electric Lighting. *Technical Report A1.2 – User Perspective and Requirements: Use Cases*. 102p.

12. Dictionary LLC. (2023). *Dictionary*. Available from: https://www.dictionary.com/ [11 Jun. 2023].

13. Griffith University Library Guides. (2023). *Standards and codes*. Available: https://libraryguides.griffith.edu.au/c.php?g=574592&p=3962487 [22 May 2023].

14. Designing Buildings. (2023). *Green rating systems*. Available: https://www.designingbuildings.co.uk/wiki/Green_rating_systems#:~:text=Rating%20systems%20measure%20relative%20levels,efficiently%20throughout%20the%20project%20lifecycle [22 May 2023].

15. Choy, N. (2023). *Why urban design codes? The role these technical instructions can play in generating positive social outcomes*. Available: https://www.alliesandmorrison.com/research/why-urban-design-codes [22 May 2023].

16. Commission for Architecture and the Built Environment (CABE). *Building sustainable communities: the use of urban design codes*. London, UK. Available: https://www.designcouncil.org.uk/fileadmin/uploads/dc/Documents/the-use-of-urban-design-codes.pdf [25 Apr. 2023].

17. Urbanist Architecture (UA). (2023). *The A-Z of building regulations drawings with building regs checklist*. Available: https://urbanistarchitecture.co.uk/building-regulations-drawings/#:~:text=Building%20Regulations%20are%20standards%20that,technical%20aspects%20of%20construction%20work. [4 Jun. 2023].

18. Imrie, R.; Street, E. (2009). Regulating design: The practices of architecture, governance and control. *Urban Studies*, v. 46, n. 12, p. 2507–2518.

19. Law Insider. (2023). *Architectural guidelines definition*. Available: https://www.lawinsider.com/dictionary/architectural-guidelines [22 May 2023].

20. Tregenza, P.; Wilson, M. (2011). *Daylighting: architecture and lighting design*. 1. ed. New York, NY: Routledge, v. 1.

21. Ayoub, M. (2019). 100 Years of daylighting: A chronological review of daylight prediction and calculation methods. *Solar Energy*.

22. Mardaljevic, J. (2021). The implementation of natural lighting for human health from a planning perspective. *Lighting Research and Technology*, v. 53, n. 5, p. 489–513.

23. Reinhart, C. F.; Mardaljevic, J.; Rogers, Z. (2006). Dynamic daylight performance metrics for sustainable building design. *LEUKOS – Journal of Illuminating Engineering Society of North America*, v. 3, p. 7–31.

24. Nabil, A.; Mardaljevic, J. (2005). Useful daylight illuminances: A replacement for daylight factors. *Energy and Buildings*, v. 38, p. 905–913.

25. Marcondes Cavaleri, M.P.; Cunha, G.R.M.; Gonçalves, J.C.S. (2018). Iluminação natural em edifícios de escritórios: avaliação dinâmica de desempenho para São Paulo. *PARC Pesquisa em Arquitetura e Construção*, v. 9, p. 19–34.

26. Battagin, I.L.S. (2014). *Norma não é lei, mas por força de lei é obrigatória*. Available: https://www.cimentoitambe.com.br/wp-content/uploads/2014/06/NORMAS-E-LEIS.pdf. [8 Dec. 2023].

27. Bellia, L. et al. (2017). Lighting role in green building rating systems: comparison between different assessment criteria in an Italian building. *Lux Europa*, pp. 51-55.

28. Comité Européen de Normalisation (CEN). (2018). *EN 17037:2018 – Daylight in Buildings*. ISBN 9780580944208.

29. Illustrated Dictionary of Architecture. (2012). *Window-to-floor ratio*. Available: https://encyclopedia2.thefreedictionary.com/Window-to-floor+ratio. [29 Dec. 2023]

30. Troup, L. et al. (2019). Effect of window-to-wall ratio on measured energy consumption in US office buildings. *Energy and Buildings*, 203.

31. Chung, W.J.; et al. (2019). Potential lighting and thermal demand reduction in office buildings using blind control considering surrounding buildings. *Journal of Asian Architecture and Building Engineering*, v. 18, p. 262–270.

32. Law Insider. (2023). *Setback distance definition*. Available: https://www.lawinsider.com/dictionary/setback-distance. [29 Dec. 2023].

33. Yeom, S. et al. (2023). Determining the optimal visible light transmittance of semi-transparent photovoltaic considering energy performance and occupants' satisfaction. *Building and Environment*, 231.

34. Designing Buildings. (2024). *Lightwell*. Available: https://www.designingbuildings.co.uk/wiki/Light_well [13 Mar. 2024].

PLEA 2024 WROCŁAW
(Re)thinking Resilience

Satellite Infrared Imagery Analysis for Urban Design

Understanding and predicting the impact of landcover on urban microclimate

ERIDA BENDO[1], MARJAN GHOBAD[1], JOSE QUESADA-ALLERHAND[2], NAVID HATEFNIA[1]

[1]Buro Happold, Berlin, Germany
[2] Technical University of Munich, Munich, Germany

ABSTRACT: To improve the urban or landscape design impact, this research explores the potential of using satellite data, to understand and predict the impact of future design on microclimate. Urban areas have always been the hub of economic, social, and cultural activities, contributing significantly to the growth and development of our world. However, in the past, the design choices made for urban areas have often faced challenges to consider the environmental consequences, resulting in negative impacts on the environment and human health. As climate change intensifies, adopting sustainable urban design is crucial to address these challenges. Two main components serve as the basis of this study, land surface temperature derived from satellite imagery and landcover. Based on extended research that outlies a clear relation between these two geospatial layers, a methodology for extracting land surface temperature is presented. Through a pix2pix machine learning model, this methodology is extended into predicting how changes in landcover can impact land surface temperature, thus improving or exacerbating the heat island effect in man-made environments.
KEYWORDS: land surface temperature, landcover, urban design, machine learning, data-driven decision-making,

1. INTRODUCTION

Significant advancements in satellite technology have revolutionized our ability to capture high-resolution imagery of the entire planet, thereby opening up opportunities to monitor and understand environmental changes like never before. One of the most significant technological leaps has been the ability to track land surface temperature (LST), a pivotal indicator in understanding climatic shifts. The use of infrared satellite systems has been instrumental in detecting LST by capturing the Earth's infrared radiation flux.

The complexity of LST is influenced by various factors inherent to different land types. For instance, grassy expanses, asphalt pavements, or rocky terrain can profoundly impact local microclimates [1]. Thus, understanding the intricate relationship between land cover characteristics and LST across diverse climatic zones is the key to deciphering the multifaceted interplay between environmental variables and temperature trends.

To address this intricate relationship, this paper explores the question, "Can LST be predicted based on land cover attributes across varying climatic zones?" The study methodically introduces an innovative approach that extracts and forecasts LST information using publicly available datasets and open-source libraries. This methodology harnesses the prowess of satellite image analysis coupled with machine learning algorithms, promising precise predictions of LST.

The implications of this research carry significant weight and extend to a broad range of domains. Architects, urban planners, and policymakers stand to benefit significantly from insights gleaned from satellite imagery analysis and machine learning models. These insights empower informed decision-making in devising sustainable design strategies aimed at mitigating detrimental environmental impacts. Moreover, the findings are a compass for crafting eco-friendly policies and practices that foster sustainable development while safeguarding precious natural resources. The results of this study have the potential to contribute significantly to the scientific literature, and further research in this area may pave the way for improving our understanding of the complex interplay between environmental variables and temperature trends.

2. BACKGROUND

In recent years, there has been a noticeable increase in the effort to extract and predict the Earth's land surface temperature (LST). This growing interest has led to numerous studies that share common characteristics. The primary reliance on Landsat thermal infrared bands to derive crucial LST data is one of these shared qualities. To obtain this information, researchers use various algorithms and freely available Landsat data, a valuable resource that drives much of this exploration. However, the journey continues after data extraction. When moving into the prediction realm, these studies consistently pivot towards a

critical element: integrating input parameters rooted in land use and land cover (LULC). These parameters serve as inputs to different machine learning workflows seeking to predict LST dynamics. This cohesive approach, combining Landsat-derived LST data with machine learning for forecasting future trends, driven by LULC parameters, is at the heart of contemporary investigations in this domain. Research conducted across various studies has investigated the correlation between Land Use Land Cover (LULC) and Land Surface Temperature (LST) parameters. [1] conducted a quantitative investigation to scrutinize the interrelationship between LST and various LULC indices. These indices encompassed the Normalized Difference Vegetation Index (NDVI), Normalized Difference Water Index (NDWI), Normalized Difference Bareness Index (NDBaI), and Normalized Difference Build-up Index (NDBI). The study findings revealed inverse correlations between NDVI, NDWI, NDBaI, and LST, while demonstrating positive correlations between NDBI and LST.

The study referenced in [1] adopted a similar methodology, examining the correlations between LST and various land cover variables (including NDVI, NDBI, NDBaI, Albedo, and NDWI) across diverse urban settings. The findings revealed intriguing patterns: During summer months, indices such as NDVI and NDBI emerged as primary influencers of LST, exerting substantial impacts. However, as winter sets in, this influence diminishes, yielding importance to factors like proximity to coastal regions and the NDBaI index, which assume greater significance in shaping LST dynamics.

[2] presented a thorough analysis of land surface temperature (LST) dynamics in the urban landscape of Toronto. Exploring various land use categories, including commercial, industrial, and recreational areas, it elucidated the average temperature profiles associated with each. Additionally, [3] articulated a nuanced perspective on the intricate relationship between LST and vegetation indices such as NDVI and built-up indices like NDBI within distinct LULC types. Contrary to a linear correlation, the relationship between these variables fluctuates across different LULC categories, influenced not only by geographic location but also by seasonal variations.

Considering this relationship between Land Surface Temperature (LST) and Land Use/Land Cover (LULC), several studies attempted to predict temperatures based on land use and cover characteristics. Many machine learning models have been explored for this purpose, spanning from traditional linear regression models to neural networks. These investigations underscore the diverse methodologies employed to capture the complex interactions between land use patterns and surface temperatures.

Furthermore, [4] applied a linear regression model to forecast forthcoming LST patterns in Vienna based on land use categories. Similarly, [5] utilized regression techniques to predict LST data for both 2025 and 2030 utilizing LULC data. Conversely, [6] adopted a Random Forest regression model, employing 20 variables associated with terrain attributes, vegetation indices, built-up areas, and bareness indices to predict LST. Impressively, [7] achieved notable success through the implementation of two distinct models: a Geographically Weighted Regression (GWR) model and a Long Short-Term Memory (LSTM) network. Furthermore, [8] and [9] contributed to this field by employing Artificial Neural Networks (ANNs) in their respective methodologies.

In addition, [10] conducted an extensive investigation, comparing the predictive capabilities of four distinct machine learning models—MARS, WNN, ANFIS, and DENFIS—in forecasting LST for the Beijing region in 2010. The study encompassed a comprehensive set of inputs, incorporating parameters such as latitude, longitude, and height, as well as spectral indices like NDVI, NDWI, and NDBI, along with temperature data spanning from 1995 to 2004. After rigorous analysis, the study concluded that ANFIS and DENFIS emerged as the top-performing models in accurately predicting LST dynamics. All these diverse approaches highlight the breadth of methodologies employed in modelling LST dynamics, highlighting the complex nature of urban thermal dynamics.

3. METHODOLOGY

The paper presents a comprehensive methodology to predict design impact using satellite imagery and machine learning techniques. The methodology is divided into two main sections. The first section explains how to extract LST (Land Surface Temperature) information from satellite infrared imagery. The second section of the methodology describes a machine learning approach that uses historical LST data and landcover information to predict design impact. The machine learning algorithm can identify patterns and make accurate predictions by analysing the LST data of different landcover types and their corresponding design impacts.

3.1 Data gathering and analysis

The process commences with acquiring infrared satellite images pivotal for subsequent analysis, a task seamlessly executed using Landsat data. The expansive initiative known as the Landsat program has been a cornerstone of Earth observation endeavours since its inception in 1972 under the auspices of the United States Geological Service (USGS). Spanning nine dedicated missions, each contributing to a comprehensive understanding of our planet's

dynamics, the most recent addition to this lineage, Landsat 9, took flight in 2021 [12].

The missions under the Landsat program are equipped with diverse instrumentation tailored for observing Earth. Specifically, this study concentrates on harnessing data derived from Landsat missions 8 and 9, pivotal components in this study's data acquisition. These satellites can capture imagery across the visual and near-infrared spectrum at a resolution of 30 meters, while their prowess extends to sensing the infrared spectrum at a slightly coarser resolution of 100 meters [13]. Within the scope of this investigation, the study zeroes in on the near-infrared and infrared sensors integrated into these satellites, crucial tools instrumental for data collection and analysis.

The data obtained from Landsat missions is conveniently accessible to the public through the USGS Earth Explorer website [14]. This user-friendly platform allows users to choose their preferred Landsat mission, pinpoint the specific image location, and specify the measurement's time. Moreover, users have the possibility to apply additional filters, such as defining the percentage of cloud coverage and tailoring the data retrieval process to suit their specific research or analysis needs.

Numerous techniques exist to convert the irradiance detected by the infrared sensors into surface temperatures. While Extensive research is dedicated to this area, delving into these methods lies beyond the scope of this paper. To comprehensively understand this process, [15] offers an in-depth exploration. Additionally, [5] and [7] are practical examples showcasing the application of the Mono-window algorithm using GIS data.

For the purpose of this work, the python library *geemap* [11] has been used for extracting Landsat satellite imagery, stored in the Earth Engine Data Catalog provided by Google [12]. From this dataset, different band information can be extracted by specifying the desired time-period of acquisition by the satellite. ST_B10 is a band generated by the Landsat Service that contains calculated surface temperature based on different thermal bands [13]. This band was extracted through the python library geemap, further on applying the specified multiplicative scale factor of 0.00341802 and an additive offset of 149. The last step consisted in removing areas that were covered by clouds and that could contain wrong information by analysing the QA_PIXEL (pixel quality) band.

This methodology empowers the extraction of land surface temperature data across the globe, covering any specific area and desired period within the timeframe of Landsat satellite observations. However, it is crucial to acknowledge an essential facet of Landsat's operational cycle—an inherent 16-day

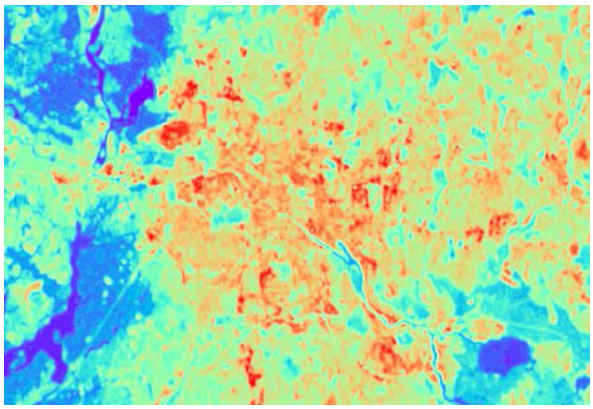

Figure 1: Surface temperature of the city of Berlin averaged over the summertime at 11 AM, with 30 degrees difference in temperature between 10 and 40 Celsius, which is notable due to urban densification, urban materials and lower vegetation.

repeat pattern with an equatorial crossing time at 10:00 AM. This temporal rhythm underscores a critical limitation: for any given location, data is available for just a single hour of the day, occurring once every 16 days [19]. This cyclic nature of data capture means that while Landsat provides comprehensive global coverage, its observations are time-restricted, capturing specific moments in the diurnal cycle at a 16-day interval. Understanding this temporal constraint is pivotal when utilizing Landsat data for precise temporal analyses or detailed assessments requiring specific time-of-day information.

3.2 Machine learning model

At this stage, the pix2pix machine learning model was chosen for the sake of accurate prediction. Initially proposed by [20], this model embodies a conditional adversarial network architecture specifically designed for the task of image-to-image translation. Functionally, the pix2pix model adeptly captures and comprehends the intricate correlations between an input image and its corresponding output. Through a meticulous training process, the model discerns and internalizes these relationships, thereby equipping itself with the proficiency to generate predictive outputs for any given input image. This capacity for predictive inference post-training stands as a potential to the model's acquired ability to extrapolate and generate probable output images, thereby exemplifying its utility in predictive tasks across diverse domains requiring image prediction and transformation.

For preparing the dataset, comprising imagery of land surface temperature and landcover attributes, the geemap python library was used [11]. The methodology for extracting land surface temperature has been explained in section 3.1. Simultaneously, the extraction of landcover information was derived from

the extensive repository of public datasets housed within the US National Land Cover Database [21]. Notably, this database encompasses a comprehensive array of landcover categories spanning the entirety of the United States. However, the scope of this study was somewhat constrained due to the dataset's geographic coverage, influencing the selection of the designated test location. It is worth highlighting that this procedural framework holds replicability potential for diverse global locales, contingent upon the accessibility of relevant landcover information. This potential underscores the adaptability and transferability of the outlined approach to different geographical contexts, paving the way for its widespread applicability beyond the confines of the study area.

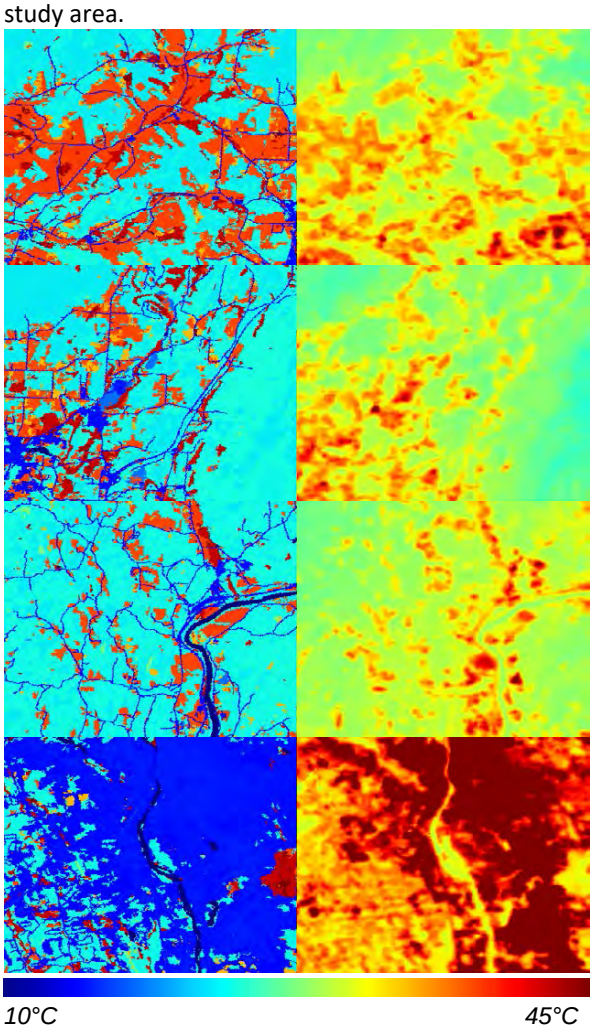

Figure 2: 4 samples from the dataset used for training the pix2pix model: on the left landcover categories (from NLCD 2019) and on the right the respective land surface temperature (June-August 2019). The samples were taken around the area of Boston.

3.3 Performance and evaluation

The pix2pix model was trained on a dataset of 1000 samples containing landcover and land surface temperature for the time span from June until August 2019 around the urban area of Boston. As already mentioned, the landcover was extracted from the US National Landcover Database for 2019 and the land surface temperature from the Landsat collection 8 infrared bands. Some of the results are presented in the figure below. The model can predict land surface temperatures that are visually similar to the ground truth.

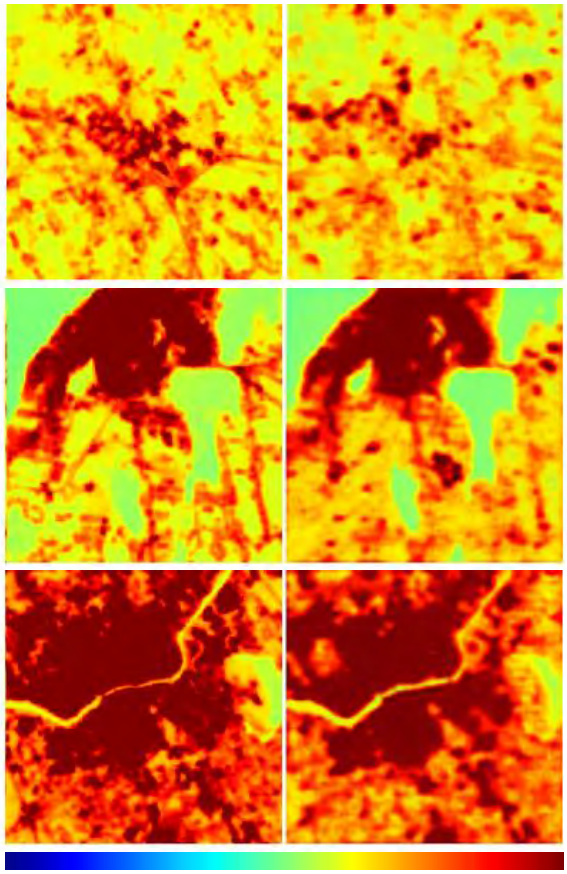

Figure 3: On the left, the current land surface temperature and on the right the generated land surface temperature by the trained model.

There are however some temporal and spatial limitations that come with this methodology. The first important factor causing these limitations, is the quality of the dataset at hand. The used land surface temperature data from Landsat has a coarse resolution of 30 meters captured at a single time during the day in a 16-day cycle. This means that based on this data, we can only predict land surface temperature at an urban scale and are not able to give any insights at what happens in a scale smaller than 30 meters. This is a limitation that can be overcome with access to proprietary datasets that provide increased temporal coverage with a bigger resolution.

The second factor is the machine learning model itself. The pix2pix model can predict on samples that have the same scale as the images it was trained on. Our model is trained on samples with a size of 256x256 pixels. Considering that the size of one pixel is 30 meters, the predicted sample has a bounding box with

a width and length of 7.68 km. In the case of studying bigger areas, they can be subdivided in patches, but the parts near the edge of the patch might not be accurate since the effect of the neighbouring patches is not considered while predicting the single patches.

Considering these two limitations and the achieved results from the test try we conclude that our methodology is successful in the study of land surface temperature trends only at an urban scale.

4. DISCUSSION

This section explores the simulation process's limitations and challenges, shedding light on the complexities encountered in its application. Many of the constraints encountered stem from the paucity of data available for training machine learning algorithms. The acquisition of satellite images through platforms like Landsat presents a substantial limitation as these images are captured for specific areas at singular time points, offering only a snapshot of the landscape at a particular hour. This temporal restriction severely curtails the comprehensive analysis of a given area, impeding the nuanced understanding of its dynamics. Notably, variations in surface temperature across different hours significantly influence the local microclimate, underscoring the importance of temporal intervals in satellite imagery for a more robust analysis. However, there is a promising trajectory toward mitigating these limitations. Foreseen advancements in satellite technology are anticipated to augment data accessibility, enabling the acquisition of images at diverse timeframes for a single location. This expanded access to multi-temporal can diminish these constraints, providing a richer dataset for enhanced analysis and insights into the complicated interactions of environmental factors affecting microclimates.

Another challenge concerns the meticulous selection of the data source employed in the machine learning training phase. This decision necessitates a thoughtful approach to identifying a region with climatic conditions closely resembling the target area. The rationale behind this discerning choice lies in recognizing that macroclimatic elements, such as proximal mountain ranges, rivers with significantly diverse water temperatures, and prevailing wind intensities, lead to considerable influence on local climatic nuances. The significance of these factors on the microclimate highlights the imperative for the chosen data source to mirror not solely air temperature and humidity but also to encompass broader regional attributes. Achieving this congruence in regional characteristics is crucial, ensuring a comprehensive representation of the environmental variables that shape and impact the microclimate. This strategic alignment between the data source and the target area's climatic intricacies forms the foundation for robust and accurate machine learning model development.

Despite these challenges, the proposed methodology has invaluable advantages, which, through continual refinement and development, reinforce its effectiveness and broaden its scope of applicability. The foremost advantage of the proposed methodology lies in its capacity to simulate prospective design scenarios by drawing upon past occurrences of similar phenomena. This departure from physics-based simulations causes a distinctive vantage point, enabling the anticipation of a design's impacts within conditions closely mirroring real-world occurrences. This alignment with real-world conditions offers invaluable insights into potential outcomes rooted in empirical occurrences within the natural environment. Moreover, the continual evolution of this method holds promise for unravelling the complexities inherent in conditions governed by the complex interactions of numerous environmental parameters. Future advancements can illuminate and decipher the complexities of multifaceted scenarios encompassing urban systems, morphologies, topographical features, and even the influences of underground water levels and precipitation patterns on the urban microclimate. This development underscores the method's potential to decipher and model the intricate web of interactions shaping urban microclimatic dynamics, heralding a more comprehensive understanding of environmental complexities.

5. CONCLUSION AND NEXT STEPS

The convergence of satellite infrared image analysis and artificial intelligence methodologies is a potent gateway to delve deeper into comprehending and predicting the impact of urban designs on the built environment. Through the assimilation of historical data and the cultivation of machine learning models geared toward predicting design impacts, there lies a profound opportunity to enrich our insights into the potential ramifications of urban and landscape development.

This paper underscores land surface temperature (LST) as a pivotal determinant within the urban microclimate. The results of the machine learning model done in the test locations confirm previous research that considers landcover a determining factor that affects LST. By acknowledging this relation, the presented study illuminates the direct influence of design decisions on the thermal dynamics of urban spaces.

It is important to state that the chosen methodology will have different accuracies in different test locations depending on the presence of other factors that might diminish the effect of landcover, such as altitude or proximity to water bodies.

Understanding and quantifying the effect of land use on LST in different climatic zones and geographic locations can be the object of study of further research. The introduction of other input factors to the prediction task and the examination of other machine learning models would further add to the robustness and accuracy of the prediction.

Ultimately, this paper serves as a valuable contribution to the collective endeavour to support sustainable architecture and foster best practices in urban design. They serve as guideposts, steering the discourse and actions toward a future where urban landscapes harmonize with nature, mitigating environmental impacts and nurturing sustainable, resilient communities.

ACKNOWLEDGEMENTS

Sincere gratitude is extended to Buro Happold for the invaluable support provided throughout this study. The team at Buro Happold facilitated the opportunity to implement the research within a practical implication in a real work context.

REFERENCES

1. M. Naserikia, M. Hart, N. Nazarian and B. Bechtel, "Background climate modulates the impact of land cover on urban surface temperature," *Scientific Reports,* 2022.
2. C. Rinner and M. Hussain, "Toronto's Urban Heat Island - Exploring the Relationship between Land Use and Surface Temperature," *Remote Sensing,* pp. 1251-1256, 2011.
3. D. Tran, F. Pla, P. Latorre-Carmona, S. Myint, M. Caetano and H. Kieu, "Characterizing the relationship between land use land cover change and land surface temperature," *ISPRS Journal of Photogrammetry and Remote Sensing,* pp. 119-132, 2017.
4. C. Walder, *Predicting Land Surface Temperatures in Urban Areas from Landsat 8 Images - A GIS Based Approach,* Vienna, 2021.
5. L. Tian, Y. Tao, M. Li, C. Qian, T. Li, Y. Wu and F. Ren, "Prediction of Land Surface Temperature Considering Future Land Use Change Effects under Climate Change Scenarios in Nanjing City, China," *Remote Sensing,* 2023.
6. N. Rengma and M. Yadav, "A generic machinge learning-based framework for predictive modeling of land surface temperature," in The International Archives of the Photogrammetry, Remote Sensing and Spatial Information Sciences, Tehran, 2022.
7. H. Jia, D. Yang, W. Deng, Q. Wei and W. Jiang, "Predicting land surface temperature with geographically weighed regression and deep learning," *Data mining and knowledge discovery,* 2020.
8. A. Castro, N. K, B. Vignesh, G. Kumar, R. Kumar, J. Antony and S. P, "Mapping and Forecasting the Land Surface Temperature in Response to the Land Use and Land Cover Changes Using Machine Learning over Southernmost Municipal Corporation of Tamil Nadu, India," *Research Square,* 2022.
9. A. K. Ranjan, A. Anand, P. S. Kumar, S. K. Verma and L. Murmu, "Prediction of Land Surface Temperature Using Artificial Neural Network in Conjunction with Geoinformatics Technology Within Sun City Jodhpur (Rajasthan), India," 2018.
10. E. K.Mustafa, Y. Co, G. Liu, M. Kaloop, A. Beshr, F. Zarzoura and M. Sadek, "Study for Predicting Land Surface Temperature (LST) Using Landsat Data: A Comparison of Four Algorithms," *Advances in Civil Engineering,* p. 16, 2020.
11. Q. Wu, "geemap: A Python package for interactive mapping with Google Earth Engine," *The Journal of Open Source Software,* 2020.
12. "Earth Engine Data Catalog, Landsat 8," [Online]. Available: https://developers.google.com/earth-engine/datasets/catalog/landsat-8. [Accessed 30 October 2023].
13. "Landsat Collection 2 Surface Temperature," [Online]. Available: https://www.usgs.gov/landsat-missions/landsat-collection-2-surface-temperature.
14. X.-L. C. Chen, H.-M. Zhao, P.-X. Li and Z.-Y. Yin, "Remote sensing image-based analysis of the relationship between urban heat island and land use/cover changes," *Remote Sensing of Environment,* pp. 133-146, 2006.
15. U. G. Survey, "Landsat Satellite Missions," [Online]. Available: https://www.usgs.gov/landsat-missions/landsat-satellite-missions. [Accessed 30 October 2023].
16. U. G. Survey, "Landsat 8-9, Collection 2 (C2) Level 2 Science Product (L2SP) Guide," 2023.
17. [Online]. Available: https://earthexplorer.usgs.gov/. [Accessed 10 October 2023].
18. M. T. Wubet, "Estimation of Absolute Surface Temperature by Satellite Remote Sensing," International Institute for Geoinformation Science and Earth Observation, 2003.
19. "Landsat 8," [Online]. Available: https://www.usgs.gov/landsat-missions/landsat-8.
20. P. Isola, J.-Y. Zhu, T. Zhou and A. A. Efros, "Image to Image Translation with Conditional Adversarial Networks," 2016.
21. "Multi-Resolution Land Characteristics (MRLC) Consortium," [Online]. Available: https://www.mrlc.gov/.

PLEA 2024 WROCŁAW
(Re)thinking Resilience

Exploring Energy Efficiency with Adaptive Temperature Ranges: Thermal Envelope Assessment in Tiny House Design

A case study in the hot and humid climate of San Antonio, Texas, USA

PANOS KARAISKOS[1] ANTONIO MARTINEZ-MOLINA[2] MILTIADIS ALAMANIOTIS[1]

[1]University of Texas at San Antonio, San Antonio, USA
[2] Drexel University, Philadelphia, USA

ABSTRACT: The 1970s energy crisis catalyzed a global shift towards energy conservation and sustainability, notably impacting building regulations. In the United States, the International Energy Conservation Code (IECC) played a pivotal role, in shaping standards. Simultaneously, the rising popularity of the Passive House standards reflected an increasing demand for energy-efficient buildings. The aim of the study is to investigate the relationship between energy efficiency and occupant behavior in a tiny house located in San Antonio, Texas, USA. Using DesignBuilder software powered by EnergyPlus, dynamic energy simulations informed the assessment process. The study encompassed IECC compliance, actual construction conditions, and adherence to the PHIUS standard building envelopes. Three temperature range scenarios, aligned with ASHRAE guidelines, were considered to address diverse comfort preferences. Results revealed that the PHIUS standard envelope outperforms, cutting annual heating and cooling energy by 74% compared to the IECC envelope. Tighter temperature settings increase annual heating and cooling loads by 72%-75% across all envelope types, despite the significant building envelope upgrades, underscoring user behavior's significant impact. This investigation bridges energy efficiency and occupant behavior, offering a holistic and practical approach to building performance assessment.

KEYWORDS: Tiny House, Energy Consumption, Thermal Comfort, PHIUS, Building Performance

1. INTRODUCTION

Buildings play a pivotal role in global energy consumption, accounting for approximately 40% of the total energy needs in various countries [1–3]. Similarly, in the United States, the building sector contributes to about 40% of the overall primary energy consumption and a significant 76% of electricity usage, thereby exerting a substantial influence on associated greenhouse gas (GHG) emissions. Among the key contributors to energy consumption within buildings, heating, ventilation, and air conditioning (HVAC) systems stand out, representing roughly 35% of the total energy utilized by buildings [4]. In the United States, the International Energy Conservation Code (IECC) played a crucial role in shaping building regulations and standards [5, 6]. Concurrently, an increase in the popularity of energy-efficient standards such as the Passive House standards can be attributed to this growing environmental consciousness and the demand for energy-efficient, sustainable, and cost-effective buildings [7]. Thicker and continuous insulation can significantly reduce the amount of energy required to maintain a comfortable temperature indoors [8]. However, as the thickness of insulation increases, the potential for energy savings diminishes [9].

Research has shown that the real energy consumption of buildings can be up to three times higher than initially estimated [10]. This performance gap is attributed to various factors, including the behavior of occupants, a parameter often overlooked in the energy simulation process [11, 12]. Analysis of the impact of occupant behavior has been fairly overlooked in building energy performance analysis [10].

Furthermore, there is a strong need to obtain appropriate occupant behavior data to develop strategies to close the energy performance gap as much as possible to achieve better energy efficiency in residential buildings [13].

Thus, the aim of this study is to explore how occupant behavior, specifically in terms of thermostat preferences, affects the energy performance of a tiny house in San Antonio, Texas. By incorporating a range of thermostat preferences, the study aims to investigate the relationship between energy efficiency and occupant temperature preferences. The estimation of energy consumption entailed performing dynamic energy simulations using the DesignBuilder software, powered by the Energy Plus calculation engine [14]. The systematic assessment process was conducted to study three thermal envelope types: (1) based on the International Energy Conservation Code (IECC), (2) considering the building's actual construction, and (3) adhering to the PHIUS standard. The assessment encompassed

thermal envelope elements such as insulation for walls, floors, and ceilings, along with window types and infiltration levels. Moreover, this research project also explores three different temperature range scenarios, all adhering to ASHRAE 55 guidelines [15] to incorporate occupant behavior in this investigation.

The analysis of different scenarios takes into consideration a range of individual comfort preferences and diverse situations, providing a more holistic assessment of thermal envelope performance in buildings. The findings reveal that the PHIUS standard stands out as the top-performing building envelope, demonstrating a significant 74% reduction in total annual heating and cooling energy consumption compared to the IECC model within a specified temperature range. Moreover, the results indicate that the adoption of more restrictive temperature settings leads to an increase in the annual total load for heating and cooling, ranging from 72% to 75% across all three building envelope types, highlighting a significant impact stemming from occupant behavior.

This investigation brings together two critical aspects of building design—energy efficiency and occupant preference for temperature variability. By considering both factors simultaneously, the study provides a more holistic and practical investigation methodology for building performance assessment.

2. METHODOLOGY

This study employed a quantitative research approach, employing both a tangible real-world case study (Figure 1) and a computational energy model (Figure 2). The building simulation model encompassed a varying degree of insulation within its envelope assembly. The investigative process unfolded across three sequential phases: initial conformity with the IECC code, existing *as-built* conditions, and alignment with the rigorous PHIUS standard. Additionally, the investigation incorporated three distinct indoor environmental scenarios, aimed at evaluating diverse indoor temperature thresholds.

Figure 1: Exterior views of the tiny-house building.

2.1 Building description

This case study is a one-story tiny-house residence, with a rectangular shape measuring 6m (20ft) (front and rear) by 3.6m (12ft) (sides) and a 3m(10ft) height a total area of 22.3 m^2 (240ft^2) and a volume of 66.9m^3 (2400ft^3). It features living and kitchen areas, in addition to one bathroom and one small storage room.

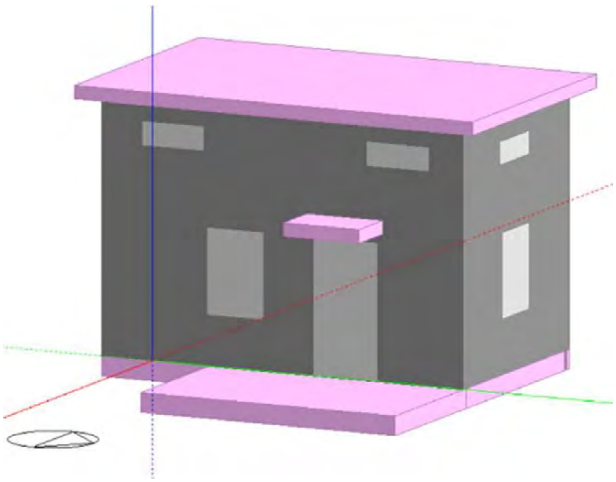

Figure 2: 3D view of the house in DesignBuilder software.

2.2 Data collection process

Information was collected from diverse sources, including the IECC, the PHIUS organization, and the owner of the featured tiny house under study. This data was utilized to develop and simulate the building models that accurately represented three specific building envelope types. The initial model was constructed in accordance with the current IECC code, adhering to the building code applicable to the location of the case study. The second model adheres to the building's *as-built* state and finally, the third model is aligned with the PHIUS standard.

2.2.1 IECC model

The IECC stands as the most widely recognized national model standard for energy-efficient residential construction. In this study, the initial examination of energy efficiency adheres to the IECC's minimum requirements concerning the envelope characteristics of the subject building (Table 1).

The case study site, San Antonio, Texas, USA, is situated in Bexar County, falling within climate zone 2 as defined by the IECC. For climate zone 2, the building envelope is required to be properly sealed, tested, and verified as having an air leakage rate no higher than 5 air changes per hour (ACH) at 50 Pascals. Furthermore, for climate zone 2, wood frame walls and floors require a minimum of R-13 insulation, windows must not exceed a U-0.4 value, and roofs require a minimum insulation of R-38. Notably, in zone 2, the foundation type—whether basement, slab, or crawlspace—does not mandate additional insulation.

Table 1: Table 1: IECC building envelope requirements for climate zone 2.

	Zone 2
Fenestration U-Value	0.4
Skylight U-Value	0.65
Glazed Fenestration SHGC	0.25
Ceiling R-Value	38
Wood Frame Wall R-Value	13
Mass Wall R-Value	4/6
Floor R-Value	13

2.2.2 As-built model

The as-built conditions of the tiny house have an improved insulation envelope over the IECC minimum requirements; however, they do not reach the PHIUS standard requirements. Specifically, the as-built conditions (Table 2) are as follows: 2x4 wood stud construction wall with R-19 batt insulation. Batt R-38 insulation on the roof and R-19 rigid EPS for the floor. The window type is a standard ply gem circa 2019 with a U-0.30 value and solar heat gain coefficient (SHGC) of 0.25.

Table 2: Building Envelope Characteristics for the three energy models.

	IECC	*As built*	PHIUS
Wall R-Value	13	19	32
Floor R-Value	13	19	32
Roof R-Value	38	38	60
Fenestration U-Value	0.4	0.3	0.22
SHGC	0.25	0.25	0.25
Airtightness	5	3	0.5

2.2.3 PHIUS model

PHIUS (Passive House Institute US) and Passivhaus (or Passive House) are both organizations that promote the Passive House standard, which is an energy-efficient building design approach. However, they operate in different regions and have some variations in their standards. PHIUS, based in the United States, has developed its climate-specific standards, in partnership with the U.S. Department of Energy (DOE) and Building Science Corporation, to suit the diverse climatic conditions across the country. On the other hand, Passivhaus, associated with the Passivhaus Institute in Germany, has a global presence and provides a more generalized standard that applies to all climates worldwide.

In the case study specific to the city of San Antonio, Texas, the PHIUS energy requirements for the tiny house building are detailed, considering an envelope area of 1,348 ft² (125.23 m²) and an interior conditioned floor area (iCFA) of 240 ft² (22.30 m²).

The PHIUS heating and cooling load criteria are established as follows: The annual heating demand is set at 10.1 kBtu/ft² (31.9 kWh/m²) per year, emphasizing the amount of energy required for heating purposes. Simultaneously, the annual cooling demand is specified as 42.5 kBtu/ft² (134.4 kWh/ m²) per year, indicating the energy needed for cooling within the given climate context [16, 17].

In conducting this study, the authors utilized the climate-specific requirements outlined by the Passive House Institute US (PHIUS) for energy performance modeling. The decision to employ these requirements was based on their attainability, as indicated by the outcomes of our energy modeling simulations. Additionally, the study considered the building envelope characteristics specified in the PHIUS passive building standard certification guidebook for zone 2 [16]. The resulting building envelope characteristics for the PHIUS model (Table 2) incorporated these recommendations and simultaneously ensured adherence to the energy requirements stipulated by PHIUS.

2.3 Experimental scenarios

Table 3 displays the array of experimental scenarios employed in this research. A comprehensive investigation encompassed a total of nine individual scenarios. As previously mentioned, the implementation of these scenarios was executed through DesignBuilder energy models which utilize the EnergyPlus simulation program. The parameters for these scenarios encompass the 3 differently designed thermal envelopes, and also 3 unique temperature setpoints.

The temperature ranges analyzed in this study adhered to the guidelines stipulated by ASHRAE 55[15], also being referenced by the Canadian Centre for Occupational Health and Safety (CCOHS)[18] for comfortable indoor temperatures. ASHRAE 55 provides a framework for defining a range of temperatures within which a substantial majority of occupants are anticipated to experience thermal comfort, typically referred to as an operative temperature range. The study adopted these specific recommendations of a temperature of 24.5°C with an acceptable range of 23-26°C for summer conditions, and an optimum temperature of 22°C with an acceptable range of 20-23.5°C for winter conditions[19]. Notably, the CCOHS specified that these conditions are grounded in Table 3 from ASHRAE Standard 55, taking into account 50% relative humidity and an average air speed of <0.15 m/s. Additionally, as of the latest ASHRAE 55, 2020 [15], no specific upper or lower humidity limit for thermal comfort is defined. Nevertheless, a humidity limit of 65% is recommended to address Indoor Air Quality (IAQ) concerns and mitigate the potential for conditions conducive to microbial growth. This 65% limit was uniformly applied across all scenarios by implementing dehumidification measures to counteract higher humidity percentages.

Various factors, including clothing insulation, activity levels, age, gender, and body mass index (BMI), are recognized as influential in shaping

individual preferences for thermal comfort [20]. This highlights the intricate and multifaceted aspects of indoor environmental quality concerning thermal comfort. In this study, three thermostat setting ranges were examined for the sake of experimental control. One conformed to the standard range established according to the ideal temperatures for winter and summer as per ASHRAE and CCOHS. A second range was intentionally less restrictive, while the third was set to be more restrictive, yet all fell within the broader ASHRAE range. The authors recognize that real-world conditions may vary and that alternative thermostat preferences based could have been employed.

Table 3 outlines the various simulation scenarios employed to investigate the relationship between energy efficiency and user behavior in the tiny house. The table presents three distinct building models: the IECC model, the as-built model, and the PHIUS model. Each model is subjected to three temperature scenarios, classified based on their restrictiveness.

Table 3: Different simulation scenarios used in this study.

	IECC	*As built*	PHIUS
Less restrictive 20-26°C, ± 5°C setback	Scenario 1	Scenario 4	Scenario 7
Standard range, 22-24.5-°C, ± 5°C setback	Scenario 2	Scenario 5	Scenario 8
More restrictive 23-23.5°C, ± 5°C setback	Scenario 3	Scenario 6	Scenario 9

The less restrictive temperature range (20-26°C) with a ±5°C setback is represented by Scenarios 1, 4, and 7 for the IECC, as-built, and PHIUS models, respectively. Scenarios 2, 5, and 8 depict the standard temperature range (22-24.5°C) with the same setback. Lastly, the more restrictive temperature range (23-23.5°C) with a ±5°C setback is illustrated by Scenarios 3, 6, and 9. These scenarios serve as a comprehensive set of conditions to assess how different temperature settings, in alignment with established standards, impact the energy performance of the tiny house under each thermal envelope model. The table thus provides a systematic framework for comparing and analyzing the energy consumption and efficiency outcomes across various simulation scenarios, offering a nuanced understanding of the interplay between thermal parameters, and building performance.

3. RESULTS

The following section showcases the outcomes of the study in three parts: the IECC model, the as-built model, and the PHIUS model. Each of these models adhered to the building envelope characteristics outlined in Table 2, and they were employed to scrutinize their energy efficiency under the three varying temperature setpoints for both heating and cooling, as delineated in Table 3.

3.1 IECC model

Upon initial examination of this investigation, it becomes evident that there is a consistent increase in both heating and cooling loads when evaluating the more restrictive settings within the International Energy Conservation Code (IECC) model for the tiny house. The higher the stringency of temperature settings, the greater the annual energy consumption required to maintain the indoor temperature at these specified setpoints (Figure 3).

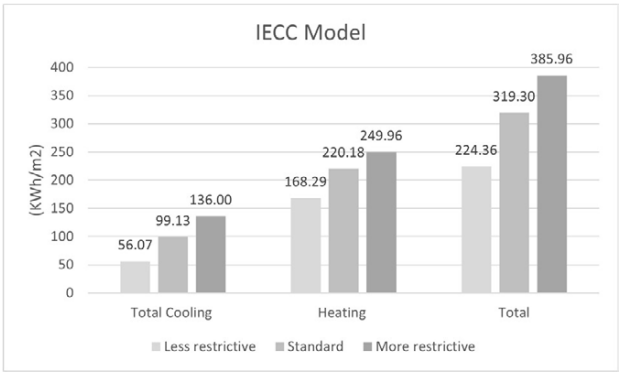

Figure 3: IECC model annual energy consumption in kWh/m².

Surprisingly, an unforeseen incongruity arises, as the heating loads starkly contrast the cooling loads, deviating from expectations given the prevalent hot and humid climate of the case study location. This divergence could potentially be attributed to the lenient IECC regulation for airtightness of the building, leading to a substantial increase in heating loads during winter months. The inclusion of the more restrictive temperature range results in a 72% increase in the total energy consumption for cooling and heating compared to the less restrictive temperature range.

3.2 As-built model

The as-built model demonstrates a notable enhancement in both cooling and heating loads for the tiny house (Figure 4). Similar to the IECC model, the heating load surpasses the cooling load, a deviation from the anticipated pattern in the hot climate under study. Additionally, the total energy consumption for cooling and heating experiences a 75% increase when the more restrictive temperature range is introduced compared to the less restrictive counterpart.

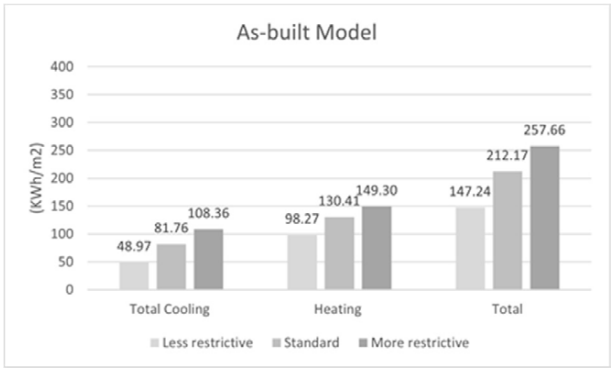

Figure 4: As-built model of annual energy consumption in kWh/m².

3.3 PHIUS model

The passive house model initially demonstrates a notable enhancement in the anticipated overall energy performance of the building, evident in improvements in both heating and total cooling demands. Notably, the cooling-to-heating load ratio aligns more logically with the hot climate conditions of this particular case study. An intriguing observation arises when considering the standard and less restrictive temperature setpoints, where both cooling and heating loads meet PHIUS requirements. However, upon testing more restrictive temperature settings, the annual heating load for the tiny house exceeds the 31.9 kWh/m² PHIUS criteria, reaching 32.28 kWh/m². Additionally, the total energy consumption for cooling and heating experiences a 72% increase when the more restrictive temperature range is introduced compared to the less restrictive counterpart, despite the highly improved thermal envelope.

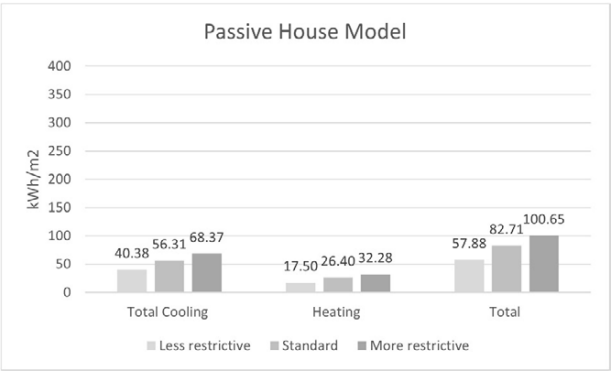

Figure 5: Passive House model annual energy consumption in kWh/m2 for the tree temperature range.

4. DISCUSSION/CONCLUSION

In conclusion, this study delved into the intricate dynamics between energy efficiency and occupant behavior within a tiny house case study in San Antonio,

Texas. The results unveil the impressive efficacy of the PHIUS standard envelope, showcasing a significant 74% reduction in annual heating and cooling energy compared to the IECC envelope. Noteworthy is the revelation that, despite substantial enhancements to the building envelope, the adoption of tighter temperature settings led to a significant 72%-75% surge in annual heating and cooling loads across all envelope types, underscoring the pivotal role of occupant behavior in shaping energy consumption patterns. The study accentuates the substantial impact of occupant preferences on energy usage, aligning with the PHIUS's commitment to advancing energy-efficient, climate-specific standards for passive buildings. Furthermore, the research sheds light on the significance of personal comfort preferences, potentially elucidating instances where buildings may fall short of meeting PHIUS standards based on comprehensive annual consumption for heating and cooling. By integrating critical aspects of building design—namely, energy efficiency and occupant temperature preferences—this investigation proposes a more holistic methodology for evaluating building performance, offering valuable insights for future sustainable architectural endeavors. The application of energy efficiency standards is crucial for mitigating environmental impact and reducing resource consumption. The choice of San Antonio, Texas, as the study location introduces a crucial geographical context. Notably by testing the Passive House standard, commonly associated with cold climates, this investigation challenges traditional assumptions by exploring the applicability of well-insulated envelopes in warmer climates like San Antonio. This highlights the potential broader implications of this study, suggesting that energy-efficient design strategies, traditionally employed in colder regions, might also yield great benefits in warmer climates.

Future work stemming from the presented academic work could involve conducting regional variations in the relationship between energy efficiency and occupant behavior, with a focus on different cities or climates. Comparative studies might extend the research to different residential building types, considering policy implications and potential updates to building codes. Examining social and cultural factors, exploring renewable energy integration, and studying resilience during extreme weather events are other avenues for further investigation.

ACKNOWLEDGEMENTS

The authors extend their sincere gratitude to David Komet for his contribution to this study.

REFERENCES

1. B. Farhanieh and S. Sattari, “Simulation of energy saving in Iranian buildings using integrative modelling for insulation,” *Renew Energy*, vol. 31, no. 4, pp. 417–425, Apr. 2006, doi: 10.1016/j.renene.2005.04.004.

2. T. Ogulata, R. Tug, and O. Ogˇulata, “Sectoral energy consumption in Turkey,” 2002. [Online]. Available: www.elsevier.com/locate/rser

3. E. L. Vine and E. Kazakevicius, “Residential energy use in Lithuania: the prospects for energy efficiency,” 1999. [Online]. Available: www.elsevier.com/locate/energy
4. U. Department of Energy, “AN ASSESSMENT OF ENERGY TECHNOLOGIES AND RESEARCH OPPORTUNITIES Chapter 5: Increasing Efficiency of Building Systems and Technologies,” 2015.
5. IECC, “IECC DIGITAL CODES SECTION R402 BUILDING THERMAL ENVELOPE,” IECC DIGITAL CODES. Accessed: Jul. 07, 2023. [Online]. Available: https://codes.iccsafe.org/s/IECC2015/chapter-4-re-residential-energy-efficiency/IECC2015-Pt02-Ch04-SecR402#:~:text=The%20building%20thermal%20envelope%20is,leakage)%20requirements%20of%20the%20code
6. ICC Digital Codes, “International Energy Conservation Code IECC.” Accessed: Aug. 20, 2023. [Online]. Available:https://codes.iccsafe.org/content/IECC2021P2/preface#:~:text=Introduction,and%20new%20energy%2Defficient%20designs.
7. https://passivehousenetwork.org, “Building codes are changing in big steps toward Passive House.” Accessed: Aug. 20, 2023. [Online]. Available: https://passivehousenetwork.org/codes/
8. U.S. Department of Energy, “Insulation.” Accessed: Aug. 20, 2023. [Online]. Available: https://www.energy.gov/energysaver/insulation
9. D. Pan, M. Chan, S. Deng, and Z. Lin, “The effects of external wall insulation thickness on annual cooling and heating energy uses under different climates,” *Appl Energy*, vol. 97, pp. 313–318, 2012, doi: 10.1016/j.apenergy.2011.12.009.
10. E. Delzendeh, S. Wu, A. Lee, and Y. Zhou, “The impact of occupants’ behaviours on building energy analysis: A research review,” *Renewable and Sustainable Energy Reviews*, vol. 80. Elsevier Ltd, pp. 1061–1071, 2017. doi: 10.1016/j.rser.2017.05.264.
11. S. Chen, W. Yang, H. Yoshino, M. D. Levine, K. Newhouse, and A. Hinge, “Definition of occupant behavior in residential buildings and its application to behavior analysis in case studies,” *Energy Build*, vol. 104, pp. 1–13, Jul. 2015, doi: 10.1016/j.enbuild.2015.06.075.
12. K. Schakib-Ekbatan, F. Z. Çakici, M. Schweiker, and A. Wagner, “Does the occupant behavior match the energy concept of the building? - Analysis of a German naturally ventilated office building,” *Build Environ*, vol. 84, pp. 142–150, Jan. 2015, doi: 10.1016/j.buildenv.2014.10.018.
13. C. Far, I. Ahmed, and J. Mackee, “Significance of Occupant Behaviour on the Energy Performance Gap in Residential Buildings,” *Architecture*, vol. 2, no. 2, pp. 424–433, Jun. 2022, doi: 10.3390/architecture2020023.
14. https://designbuilder.co.uk/, “Design Builder.” Accessed: Aug. 20, 2023. [Online]. Available: https://designbuilder.co.uk/
15. ASHRAE, “STANDARD 55 – THERMAL ENVIRONMENTAL CONDITIONS FOR HUMAN OCCUPANCY.” Accessed: Oct. 22, 2023. [Online]. Available: https://www.ashrae.org/technical-resources/bookstore/standard-55-thermal-environmental-conditions-for-human-occupancy
16. “Certification Guidebook,” 2021. [Online]. Available: www.Phius.org
17. “Phius 2021 Performance Criteria Calculator v3.1.” Accessed: Oct. 22, 2023. [Online]. Available: https://ssccust1.spreadsheethosting.com/1/bc/830791e0e82174/Phius%202021%20Criteria%20Calculator%20v3.1/Phius%202021%20Criteria%20Calculator%20v3.1.htm
18. “Canadian Centre for Occupational Health and Safety.” Accessed: Oct. 22, 2023. [Online]. Available: https://www.ccohs.ca/
19. CCOHS, “Thermal Comfort for Office Work - Recommendations provided by CSA Z412-17.” Accessed: Oct. 22, 2023. [Online]. Available: https://www.ccohs.ca/oshanswers/phys_agents/thermal_comfort.html
20. W. Yao, X. Li, W. Cao, G. Li, L. Ren, and W. Gao, “Research on the influence of indoor thermal environment and activity levels on thermal comfort in protective clothing,” *Energy Build*, vol. 279, Jan. 2023, doi: 10.1016/j.enbuild.2022.112681.

PLEA 2024 WROCŁAW
(Re)thinking Resilience

Investigating the Impact of Passive Cooling Strategies on Energy Consumption and Thermal Performance:
A Case Study of Courtyard Housing in a Hot Arid Climate

ABEER ALQAED[1,2] JOANNE PATTERSON[1]

[1] Cardiff University, Cardiff, the United Kingdom
[2] University of Bahrain, Manama, Bahrain

ABSTRACT: This research explores passive cooling strategies to enable sustainable and energy-efficient buildings in hot-arid climates. With Heating, Ventilation, and Air-Conditioning (HVAC) systems consuming a significant portion of global energy, accounting for around 50% of the global building energy demand, the potential of passive cooling in historic courtyard houses is studied. The impact of a selection of appropriate retrofitting scenarios is evaluated, including green roofs, green courtyards, and natural thermal insulation, using dynamic energy simulations. Results show notable energy savings and improved thermal performance, yet challenges persist in meeting thermal comfort benchmarks. The study recommends hybrid strategies and emphasizes the importance of avoiding increased moisture content in indoor air.
KEYWORDS: Energy Consumption, Thermal Performance, Passive Cooling, Historical Fabric, Hot-Arid.

1. INTRODUCTION

The pursuit of sustainable and energy-efficient building design has become increasingly crucial, especially in regions characterized by hot-arid climates. Heating, Ventilation, and Air-Conditioning (HVAC) systems currently consume around 50% of the global building energy demand [1]. A recent study conducted in Bahrain by the Electricity and Water Authority (EWA) statistics, revealed that more than 80% of energy in Bahrain is consumed by air conditioning. 2021 was one of the seven warmest years on record IEA (2022) and energy consumption for space cooling has more than tripled since 1990. Hence, a dramatic rise in associated carbon dioxide emissions in recent years [2], has resulted in a global look for alternative solutions to fossil-fuel resources for energy.

Given the increasing concern for energy conservation and sustainability, passive cooling strategies have gained significant attention in the design and construction of housing in hot arid climates [3]. Passive cooling refers to technologies or design features adopted to reduce the temperature of buildings without the need for power consumption, responding to local climate and site conditions to maximize the thermal comfort of building users while minimising energy use [4].

The effectiveness of passive cooling strategies in hot arid climates has been carried out. A study in Dubai showed that implementing passive cooling systems of shading devices, double glazing, and natural ventilation with green roofs in houses reduced the annual energy consumption by 23.6% [4]. The use of insulation materials has demonstrated an improved thermal performance, improving energy efficiency in hot-arid climates [5,6,7].

This research focusses on three courtyard houses (House A, House B, and House C) located within the historic core of Bahrain over 120 years old (Figure 1). These homes were selected as they are typical of the area, access could be gained to the homes to obtain relevant data and they were in acceptable living conditions. The gross floor areas for House A, House B, and House C are 100m², 206.3m², and 130.8m², respectively. The houses were originally designed to be dependent on natural ventilation strategies including the use of the courtyard as a climate modifier, and openings in walls that facilitated cross ventilation. The air allowed into the inner rooms was naturally cooled through various techniques such as Mashrabeya shading and *Liwan* (shaded corridor around the courtyard), along with the presence of vegetation. These elements collectively contributed to an evaporative cooling effect and solar control. However, due to changes in people's thermal expectations, climate change, and advancements in technology, active cooling systems are now being used.

House A *House B* *House C*

Figure 1: Pictures of the three case study houses - House A, House B, and House C.

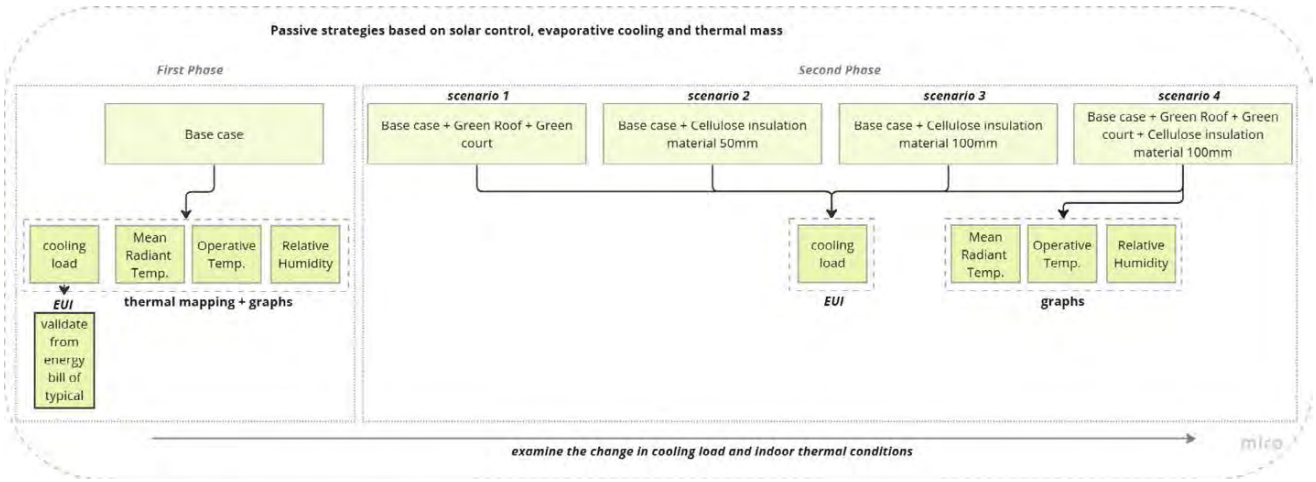

Figure 2: Research methodology

This paper conducts a comparative analysis, assessing energy consumption, internal temperature, and relative humidity across five scenarios for the three courtyard homes: a baseline case and four retrofit scenarios. The retrofit strategies incorporate a green roof, a green courtyard, and the application of natural wall insulation material in two different thicknesses on the internal faces of the wall. The fifth scenario combines all these strategies, as illustrated in Figure1. The research aims to provide meaningful insights into the effectiveness of these passive cooling strategies in enhancing the overall thermal performance and energy efficiency of the three case study courtyard houses. The research aligns with Bahrain's vision 2030 and its green building and sustainability objectives. The vision seeks to integrate eco-friendly practices into the design, construction, operation, and maintenance of buildings. Bahrain Vision 2030 aims to enhance resource efficiency, reduce environmental impact, and create resilient, energy-efficient structures aligned with global sustainability standards.

2. METHODOLOGY

Rhino and Grasshopper software are used as digital modelling and simulation tools, augmented with Ladybug and Honeybee plugins. This combination of software has been selected as it can handle complex parametric models, allowing for a thorough evaluation of multiple strategies. The energy simulations are run via OpenStudio-EnergyPlus engines. These tools provide a comprehensive platform for dynamic energy simulations and precise thermal performance analysis. Virtual models of three courtyard houses have been created and thermal performance is compared across all scenarios. Weather data for the location was obtained in the form of an EPW (EnergyPlus Weather) format file from the local meteorological centre in Muharraq city, Bahrain where the case study houses are located. The climate zone chosen was "very hot," as determined by the ASHRAE climate zone classification.

As illustrated in Figure 2, two phases were followed in this study. The first phase of the modelling includes simulating the average end-use intensity (EUI) for energy consumption and the cooling load of the three houses in kWh/m^2 as base cases. This is validated by the energy bill of a typical Bahraini family house that was obtained from Electricity and Water Authority (EWA) in Bahrain. Thermal mapping for the baseline indoor thermal conditions including the indoor temperatures, and indoor Relative Humidity are visualized and compared with the thermal comfort benchmark.

The second phase involves modelling and simulating the four retrofitting scenarios for three homes; Scenario 1-base case with a green roof and green courtyard; Scenario 2-base case with 50-millimetre thickness Cellulose wall insulation; Scenario 3-base case with 100-millimetre thickness Cellulose wall insulation; Scenario 4-base case with green roof, green courtyard and 100-millimetre thickness of Cellulose wall insulation. Studies indicate that cellulose is a highly efficient insulation material, particularly beneficial for hot-arid climates [8]. The average end-use intensity (EUI) for energy consumption for the cooling load of the three houses for the four scenarios was simulated and compared with the base case to examine the change in energy performance. Indoor thermal conditions including mean radiant temperature, operative temperature, and relative humidity were plotted in graphs for scenario 4 and compared with the base case.

In the context of thermal performance, Mean Radiant Temperature is the average temperature of surrounding surfaces, essential for assessing radiant heat exchange and understanding how building elements influence occupant comfort. Operative Temperature, on the other hand, serves as a comprehensive metric, incorporating air temperature, mean radiant temperature, airspeed, and humidity to evaluate the overall thermal

environment within a space. For the three case study houses, the modelling was set to classify the building program as a midrise apartment, and the three houses operate in a free-running mode. The selection of construction characteristics was based on the building vintage set to pre-1980. Table 1 illustrates the data input for the as-built construction materials and their thermal properties for the case study houses.

To simulate the courtyard houses effectively, different rooms were modeled as separate thermal zones. Since the focus of the study is on the courtyards and their passive impact on regulating internal temperatures, relevant parameters to the courtyards are chosen as fixed parameters during modelling and simulation. These parameters encompass the number of courtyards in each house, the courtyard width-to-height ratio, their different orientations among the three case studies and the building envelope materials considering the different wall thicknesses.

Table 1: Thermal properties of building materials in the three case study houses – input data in Grasshopper for baseline modelling.

Materials	***Thickness (m)***	***Thermal Conductivity (W/m.K)***	***Density (Kg/m³)***	***Specific Heat (J/kg.K)***
Wall layers				
Limestone plaster	0.03	0.45	1538	938
Coral stone	0.5	0.83	2000	790
Limestone plaster	0.03	0.45	1538	938
Roof and floor layers				
Clay mud	0.2	0.68	1840	1480
Limestone plaster	0.03	0.45	1538	938

The additional scenarios encompass two passive strategies. The first is the *evaporative cooling* and solar control through the incorporation of green roofs and green courts. The second is a *thermal mass* strategy through the use of Cellulose as natural thermal insulation material, modeled in two different thicknesses 50mm and 100mm. Cellulose enhances thermal mass through its phase change properties. With a thermal absorptance of 0.9, it absorbs 90% of incident thermal radiation. Its low thermal conductivity (0.04) slows heat transfer, while its high specific heat allows it to absorb and retain considerable heat energy before experiencing a significant temperature change. The following table illustrates the thermal properties of the passive strategies applied for green roofs and the natural insulation material (Table 2).

Table 2: Thermal properties for the evaporative cooling and thermal mass strategies.

Strategy 1 Evaporative cooling Green Roof and courtyard trees					
Height of the plant	*Leaf reflectivity*	*Leaf emissivity*	*Soil thickness*	*Density of soil*	*Specific heat of soil*
(m)			***(m)***	***(Kg/m³)***	***(J/kg.K)***
0.2	*0.22*	*0.95*	*0.2*	*1100*	*1200*
Strategy 2 – Thermal mass Cellulose insulation material in walls					
Conductivity	*density*	*Spec heat*	*Roughness*	*Thermal absorptanc*	*Solar absorptanc*
(W/m.K)	***(Kg/m³)***	***(J/kg.K)***			
0.048	*65*	*2020*	*Rough*	*0.9*	*0.7*

This approach facilitates the examination of the impacts of singular passive interventions on indoor thermal comfort and energy use. The goal is to conduct meaningful comparisons and evaluations among the three case studies and the four different strategies during the simulations.

The heating, ventilation, and air conditioning (HVAC) system must be capable of providing thermal comfort conditions as prescribed in (Table 3) which have been obtained from Bahrain's green building code [9].

Table 3: Thermal comfort benchmark set by Bahrain green building code.

95% of the Year	***Lower Limit***	***Upper Limit***
Dry Bulb Temperature	22.5˚C	25.5 ˚C
Relative Humidity	30%	60%

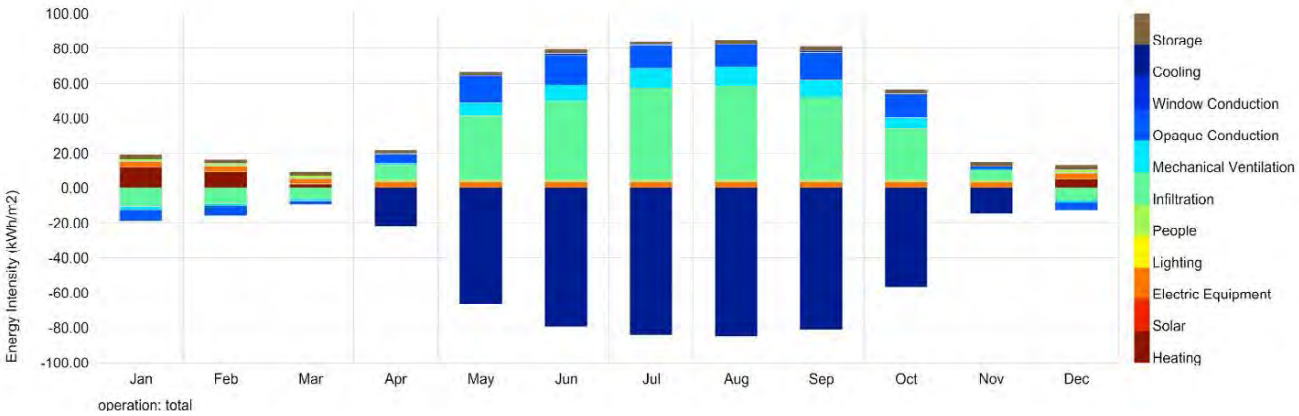

Figure 3: Baseline Modelling –Thermal load /energy Balance chart for Houses A, B, and C.

3. RESULTS AND DISCUSSIONS

The energy simulation and thermal performance of the first phase including the baseline houses are presented followed by the second phase including the baseline with the different passive cooling scenarios.

3.1 Baseline scenario: energy simulation results

In the first phase, an annual energy simulation was carried out to analyse the energy performance of the case study homes A, B, and C. Results indicate an average annual end-use intensity (EUI) for energy consumption for the base case for House A- 584.8 kWh/m^2, House B- 524.9 kWh/m^2, and House C- 496.6 kWh/m^2. A significant portion of the energy, approximately 83.5% of the total energy consumption, was consumed for cooling purposes (Table 4).

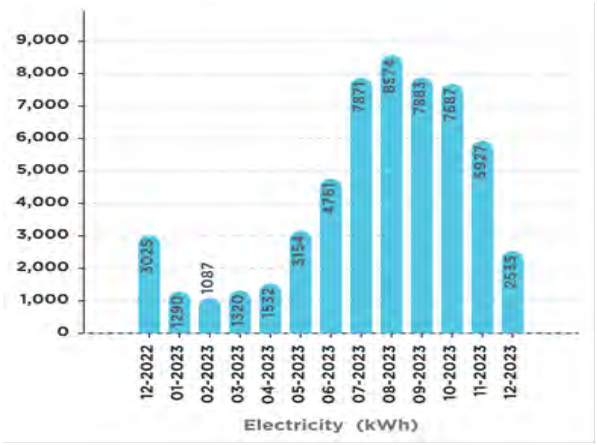

Figure 4: Energy bill for the annual energy consumption in kWh for a typical Bahraini family house obtained from Electricity and Water Authority (EWA).

The results of the energy simulation were calibrated by comparing the total annual simulation results and the energy consumption from an actual energy bill for a typical Bahraini family house that has a gross area of 110 m^2 (Figure 4). The average annual energy consumption for the typical house was 514.9 kWh/m^2, which is close average to the simulation results. This suggests that the simulation results are reasonably accurate in predicting energy consumption. Both the energy simulations and the energy bill confirm that the cooling load is the primary contributor to energy consumption, with the peak occurring in August.

The thermal load/energy balance chart as shown in Figure 3 presents the heat gain and heat loss throughout the year for the base case, which helps to understand the cause of the heat imbalance, hence informing the strategies that should be prioritised to address the energy balance in the building.

Figure 3 reveals a significant level of infiltration in the three case study houses, accounting for approximately 75% of the total heat gain. The infiltration is primarily attributed to the high surface area-to-volume ratio and the porous nature of coral stone walls. The second primary cause of the heat imbalance is the thermal conduction through the opaque fabric, contributing around 12.5% to the total heat gain.

The absence of any form of thermal insulation in the entire fabric exacerbates this issue. Consequently, retrofit scenarios become essential for effectively mitigating both infiltration and thermal conduction.

Enhancing thermal wall insulation and optimizing thermal mass will reduce air infiltration. As the three houses lack thermal insulation layers, a natural sustainable material single insulator has been added to the internal faces of the walls in the model. Two different thicknesses are tested. This strategy aims to improve the overall thermal performance of the building by minimizing heat transfer and maximizing the building's ability to store and release heat efficiently.

The strategy of evaporative cooling and solar control is also tested through the integration of green roofs and a green courtyard. Green roofs, with their insulating properties, can help mitigate thermal conduction through the building structure. The added layer of vegetation acts as a buffer, reducing the transmission of heat through the roof and into the interior spaces by creating a cooler surface. Similarly, green courtyards can provide shading and minimize heat transfer through exterior walls by reducing the direct impact of solar radiation on the building's envelope.

Table 4: EUI of the energy for House A, House B, and House C, for the baseline model and the three passive cooling scenarios; S1- Green roof retrofit and green court, S2- Cellulose insulation 50mm, S3- Cellulose insulation 100mm, S4- all strategies.

End Use (EUI) **kWh/m^2**	***House A***					***House B***					***House C***				
	Base case	**S1**	**S2**	**S3**	**S4**	Base case	**S1**	**S2**	**S3**	**S4**	Base case	**S1**	**S2**	**S3**	**S4**
Heating	29.6	24.6	24.2	23.8	23.1	19.9	16.0	16.7	16.5	15.0	15.9	14.8	15.8	15.5	13.2
Cooling	**488.0**	**429.2**	**411.4**	**387.9**	**322.0**	**437.7**	**387.7**	**385.9**	**370.6**	**314.4**	**415.0**	**364.6**	**359.3**	**343.4**	**287.8**
Interior Lighting	4.9	4.9	4.9	4.9	4.9	4.9	4.9	4.9	4.9	4.9	3.4	4.9	4.9	4.9	4.9
Electric Equipment	38.4	38.4	38.4	38.4	38.4	38.4	38.4	38.4	38.4	38.4	38.4	38.4	38.4	38.4	38.4
Water Systems	23.9	23.9	23.9	23.9	23.9	23.9	23.9	23.9	23.9	23.9	23.9	23.9	23.9	23.9	23.9
Total EUI	**584.8**	**521.0**	**502.8**	**479.0**	**412.4**	**524.9**	**471.0**	**469.9**	**454.4**	**396.7**	**496.6**	**446.7**	**442.3**	**426.1**	**368.2**

3.2 Baseline scenario: thermal performance results

Thermal mapping of operative temperatures and relative humidity is illustrated for House A during July and August (Figure 5 and Figure 6). Referring to Table 3, the analysis indicates that current indoor temperatures consistently exceed the benchmark for thermal comfort standards by almost 4 degrees. This raises concerns about potential discomfort and challenges for occupants during these months. Additionally, relative humidity levels, with a maximum reaching 59.2%, approach the upper limits of acceptable conditions.

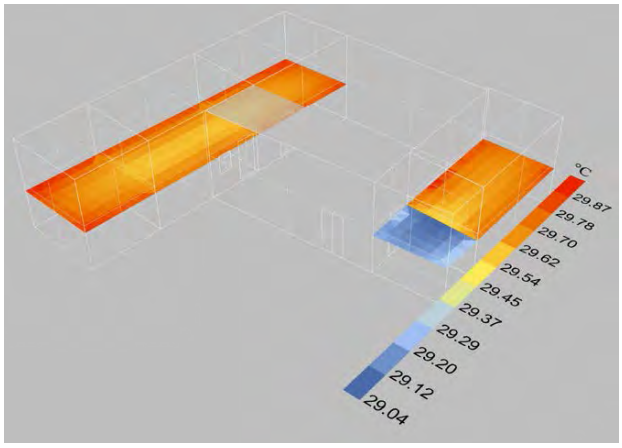

Figure 5: Thermal mapping of operative Temperatures (°C) in baseline modelling of House A during July and August months.

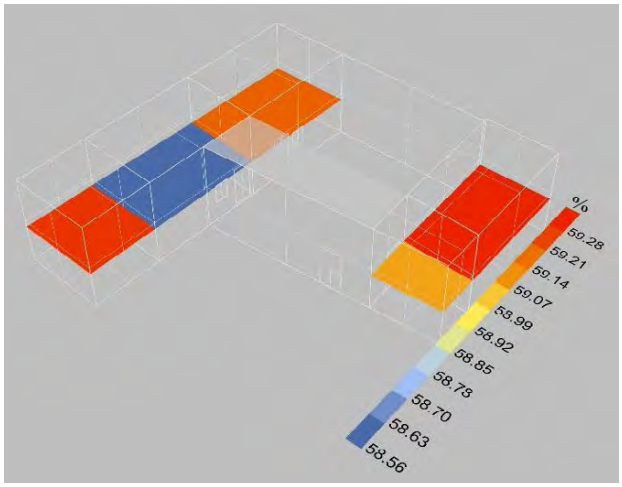

Figure 6: Thermal mapping of relative Humidity (%) in baseline modelling of House A during July and August months.

3.3 Passive cooling scenarios: energy simulation results.

In the second phase, modifications to the baseline were carried out to assess the impact of four different retrofit scenarios (Table 4). For scenario 1, the simulation results indicated energy consumption savings of approximately 10.9% in House A, 10.3% in House B, and 10.1% in House C. Scenario 2 achieved slightly higher energy savings, reaching 14% in House A, 10.5% in House B, and 11.1% in House C. The implementation of Scenario 3 resulted in higher energy savings of about 18.1% in House A, 13.4% in House B, and 14.2% in House C. As expected, the optimal solution was Scenario 4, demonstrating a significant total reduction in energy use of 29.5% in House A, 24.4% in House B, and 25.9% in House C (Table 4).

Table 4 and Figure 7 illustrate the influence of the four retrofit scenarios on the average cooling load reduction in the three houses. The results indicate a total reduction from 488 kWh/m² to 322 kWh/m² in House A, from 438 kWh/m² to 314 kWh/m² in House B, and from 415 kWh/m² to 287.7 kWh/m² in House C. This signifies an overall cooling load reduction of approximately 140 kWh/m² through combining the two strategies of evaporative cooling and improved thermal mass.

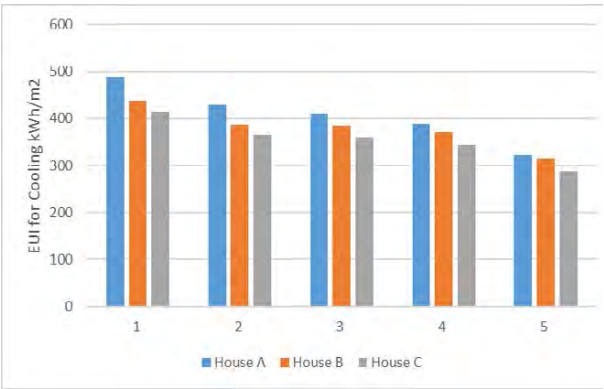

Figure 7: annual EUI for cooling load for the three case study houses, (1) base case, (2) retrofitting scenario 1, (3) retrofitting scenario 2, (4) retrofitting scenario 3, (5) retrofitting scenario 4.

3.4 Passive Cooling Scenarios: Thermal Performance Results

The thermal performance of the houses was examined by logging the annual environmental data from simulations. A comparative analysis was then conducted on the indoor mean radiant temperature, indoor operative temperature, and indoor relative humidity between the base case scenario and scenario 4, the optimum energy-saving scenario.

The results revealed that the highest drop in mean radiant temperature was in August, approximately 2.4 °C in house A, 2.1 °C in house B, and 1.96 °C in house C (Figure 8). However, the operative temperature demonstrated a less positive impact on thermal comfort conditions, with a maximum drop in indoor operative temperature in August of 1.2 °C in house A, 1 °C in house B, and 0.82 °C in house C (Figure 9).

The indoor relative humidity in the different zones of the three houses increased by 1-3%. This increase can be attributed to the enhanced evaporative cooling and the reduced air leakage, causing a rise in the moisture content in the air (Figure 10).

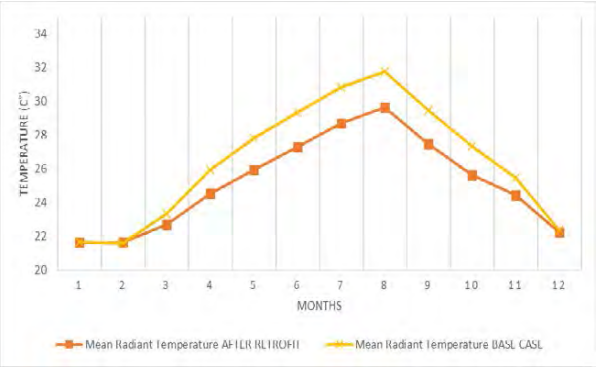

Figure 8: Annual mean radiant temperatures before and after retrofit -average across the three homes.

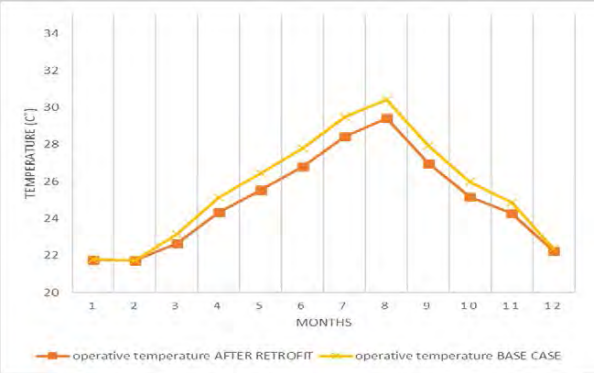

Figure 9: Annual operative temperatures before and after retrofit -average across the three homes.

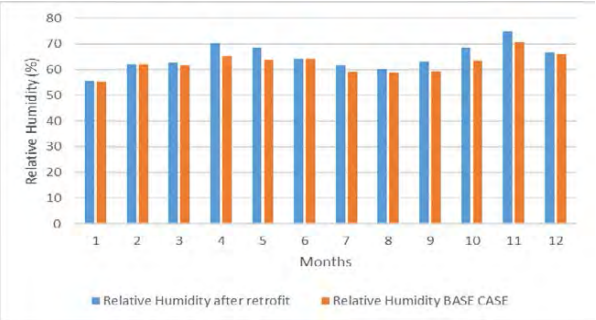

Figure 10: Annual Relative humidity before and after retrofit- average across the three homes.

4. CONCLUSION

The results indicate notable improvements in energy use when each strategy was implemented individually. The integration of natural insulation materials with the evaporative cooling strategies demonstrated a positive impact on the overall thermal performance of the building with energy savings, ranging between 24.4% and 29.5% compared to the single retrofit scenarios. Additionally, the study unveiled that an insulation material thickness of 100mm proved to be considerably more effective than the 50mm counterpart. This insight suggests that the incorporation of the thicker internal insulation material could offer an enhanced and more robust solution for optimizing thermal performance.

However, even with the implementation of the two strategies – evaporative cooling and the improvement of thermal mass, the average mean radiant temperature and operative temperatures in August and July remain 2 °C above the benchmark of the thermal comfort requirement. Further strategies need to be implemented as hybrid scenarios in the future to prevent the use of active HVAC systems. Evaporative cooling strategies have positively influenced the indoor air temperature, while they slightly increased the relative humidity, which will negatively affect the overall comfort levels, pushing levels into the zone of discomfort (Table 3). This also therefore suggests that additional strategies need to be implemented to reduce moisture content in the air.

In conclusion, this study highlights the potential of passive design strategies to reduce energy consumption whilst moving towards comfortable indoor environments, and provide guidance for sustainable adaptations, emphasizing the importance of preserving architectural integrity and meeting occupants' thermal comfort needs, especially in hot arid climates. The findings align with Bahrain Vision 2030's green building and sustainability objectives, emphasizing the need for sustainable solutions throughout the entire lifecycle of buildings.

REFERENCES

1. Elnaklah, R., et al., (2021). Thermal comfort standards in the Middle East: Current and future challenges. *Building and Environment, 200*, 107899.

2. International Energy Agency. (2022). Global Energy Review: CO2 Emissions in 2021, [online], Available: https://www.iea.org/reports/global-energy-review-co2-emissions-in-2021-2 [10 October 2023].

3. Mori, H., Kubota, T., Antaryama, I. G. N., & Ekasiwi, S. N. N., (2020). Analysis of window-opening patterns and air conditioning usage of urban residences in tropical southeast Asia. *Sustainability, 12*(24), 10650.

4. Taleb, H. M., (2014). Using passive cooling strategies to improve thermal performance and reduce energy consumption of residential buildings in U.A.E. buildings. *Frontiers of Architectural Research, 3*(2), p. 154–165.

5. Kumar, D., et al., (2020). Comparative analysis of building insulation material properties and performance. *Renewable and Sustainable Energy Reviews*.

6. Abu-Jdayil, B., Mourad, A. H., Hittini, W., Hassan, M., & Hameedi, S., (2019). Traditional, state-of-the-art and renewable thermal building insulation materials: An overview. *Construction and Building Materials,* p. 214, 709-735.

7. Alsaqabi, Y., Almhafdy, A., Haider, H., Ghaffarianhoseini, A., & Ali, A., (2023). Techno-Environmental Assessment of Insulation Materials in Saudi Arabia: Integrating Thermal Performance and LCA. *Buildings, 13*(2), 331.

8. Doğramacı, P. A., & Aydın, D., (2020). Comparative experimental investigation of novel organic materials for direct evaporative cooling applications in hot-dry climate. *Journal of Building Engineering, 30*, 101240.

9. Ministry of Works, Municipalities Affairs and Urban Planning, Kingdom of Bahrain, (2021). Bahrain Green Building Code (Version 1.0), [online], Available: https://benayat.app.gov.bh/Green_Building_Code_Eng_01.12.2021_PS_AG_v1.2_Master.pdf [16 October 2023].

PLEA 2024 WROCŁAW
(Re)thinking Resilience

Passive Cooling Calendars
the surprising variety of annual patterns in hot climates

ARAM YERETZIAN[1] MARK DEKAY[2]
[1]School of Architecture and Design, American University of Beirut, Lebanon
[2]College of Architecture + Design, University of Tennessee in Knoxville, USA

ABSTRACT: Passive cooling strategies are integral to vernacular typology patterns in Arabic-speaking countries, yet difficult to classify using existing IECC climate zones. This research addresses the efficacy of various passive/low-energy cooling strategies for housing and other buildings with low internal heat gains. The method employs a dynamic adaptive-comfort model in psychrometric analysis using methods from Givoni and others to assess applicability for monthly average and cooling design days in 29 Arabic-speaking cities. The results are presented graphically as Passive Cooling Calendars that map strategies' effectiveness during each month of the year. The calendars can help architects and design teams select strategy combinations best suited to a particular climate type. Results clearly illustrate the differences in strategies among similar desert climates (IECC zone 0B, 1B, etc.) having divergent humidity regimes, such that evaporative cooling is recommended for hot-dry-arid cities, like Kuwait City, yet comfort or cooling ventilation is recommended for several months in hot-dry-humid Muscat, Oman. Results show the diversity of climates that are often typed similarly, plus corresponding appropriate design responses. The hot season limits of strategies and their applicability in transitional and cooler months are revealed.
KEYWORDS: Climate types, cooling strategies, Arab-speaking cities, natural ventilation, adaptive comfort

1. INTRODUCTION

This paper outlines assessment of passive and low-energy cooling strategies using a dynamic adaptive-comfort-based model. The month-by-month method tests feasibility on both average days and hotter 2% cooling design-days. This evolution of pre-design analysis methodology became necessary, firstly, because of developments in the science of adaptive comfort and, secondly, from our analysis of passive cooling strategies in 29 major cities from the 22 countries of the Arabic-speaking world (ASW). The region has such extremely hot climates that passive/low-energy cooling is not feasible in all hot months, and in some climates works best in "winter".

Given the diversity of climates' character, a range of vernacular typologies can be found across the ASW regions. In addition to the various building materials (earth, stone, wood, etc.), the passive design strategies are different as they relate to and temper the outdoor environment. Figures 1 and 2 illustrate the diversity of vernacular building types that exist, for example, in the cities of Doha, Qatar, and Tunis, Tunisia. Strategies in Doha include thick mud brick wall and roof construction, enclosed courts, small openings and narrow streets. Types in milder Tunis, employ ventilated courtyards, covered arcades, larger openings and vegetation, as well as thick walls built with local stone. Such vernacular solutions improve thermal comfort for inhabitants both indoors and outdoors—this being achieved using low-tech materials and methods evolved across generations.

The larger context of this paper is a project to re-

Figure 1: Qatari Vernacular Domestic Architecture [1]

Figure 2: Dar Othman, Tunis [2]

commend design strategies for housing design in climates of the ASW, beginning by attempting to map vernacular passive/low-energy cooling approaches to the IECC climate zone system in an effort to correlate cooling strategies with the region's variations. We could observe a loose fit, but anomalies thwarted the effort, particularly with strategies that addressed humidity and evaporation. We first need to solve what appeared to be an issue with the IECC system itself.

2. NEED FOR THE NEW APPROACH

The authors' article, "Dry Versus Arid: a new approach to climate types in hot regions" (in review) found that IECC/ASHRAE climate zones [3] and the Köppen-Geiger (K-G) zoning [4], the two most common systems for classifying climates and associating potential passive heating and cooling design strategies, were quite ineffective in IECC Zones 0B to 3B because of their use of precipitation as a marker for humidity (Fig. 3). This fails to distinguish, for example, between hot-humid Jeddah and hot-arid Riyadh, both in Saudi Arabia, having low "desert" rainfall (zone 0B). In the IECC system, 0 is the hottest zone and 8 is the coldest. A are "moist" types, and B climates are "dry".

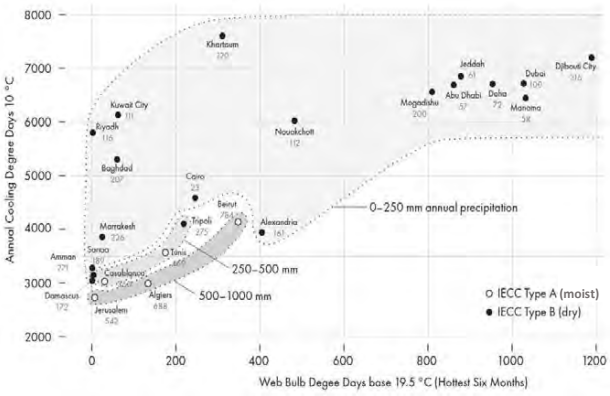

Figure 3: Failure of precipitation-based classification to distinguish humid vs arid conditions in hot ASW cities

CRTKL's online *ClimateScout* tool [5], for example, based on K-G, recommends the same cooling strategies for both arid Riyadh and humid Jeddah (same K-G and IECC zone). Clearly, we needed a better method. These systems' reliance on precipitation partially explained the misfit we were observing between vernacular cooling strategies and IECC zones.

For decades predesign determination of passive strategy feasibility has been based on climate analysis using bioclimatic overlays on Olgyay's bioclimatic chart [6] and on Givoni's psychrometric chart [7] by Watson and Labs [8] and applied in tools such as Climate Consultant (CC) [9]. Each of these used *a fixed comfort zone* with cooling strategy overlays defined relative to the boundary of that comfort zone. CC offers various comfort models from ASHRAE and California, with the resulting passive cooling zones sometimes quite different among the models.

Early manual methods were based on plotting for a particular location the average day highs and lows of Dry Bulb Temperature and coincident Relative Humidity for each month. Watson + Labs used hourly data to calculate the percentage of annual hours that fall into a cooling overlay zone. Milne offered in CC the option to define the period for which the hours are calculated. In practice, the authors have repeatedly observed first-hand from decades of teaching that both student and non-expert practitioners frequently misinterpret these percentile effectiveness results in several ways. Two examples: Givoni's rules for "High Mass" cooling exclude ventilation (windows are closed) and he assumes a relatively large diurnal range; however, counting hours within a zone does not necessarily associate high and low temperatures to yield a predicted indoor temperature. Secondly, Givoni's "Natural Ventilation" zone is actually a "Comfort Ventilation" zone in which increased air velocity cools a person with warm air to increase perspiratory evaporation. In contrast, "Cooling Ventilation" requires outside air cooler than inside. Outside air is therefore actually at conditions *within* the comfort zone. A common guideline is to stop cooling ventilation when the outside air is above the comfort zone. These thermal dynamics are all highly occluded in the conventional use of bioclimatic pre-design analysis. In our experience, few users of these tools make such distinctions.

3. UPDATING WITH ADAPTIVE COMFORT

More recently, Marsh [10] has used a monthly comfort zone that varies based on the monthly mean temperature, based on the Adaptive Comfort Model from ASHRAE [11], to modify the Milne/Givoni method. Like Milne, the passive cooling overlays are defined relative to this moving comfort zone. This approach significantly changes the feasibility of the various passive cooling strategies, relative to any fixed zone. A flexible zone is also more aligned with the more recent ASHRAE model of flexible comfort parameters rather than any zone. In many cases, this update is a game-changer for passive/low-energy cooling effectiveness.

4. METHODOLOGY

Our approach was, in each city, to assess for each of 12 months several strategies' effectiveness on the average day and the cooling design-day using Marsh's method for a moving adaptive comfort zone plotted on the psychrometric chart, combined with Givoni's overlay system, and employing rule-based thermal design guidelines for each strategy.

The process starts by obtaining each month's average daily high and low temperature and relative humidity values from TMY files in their EPW form using the Climate Consultant software's bult-in algorithms. On both average and cooling design-days, the starting

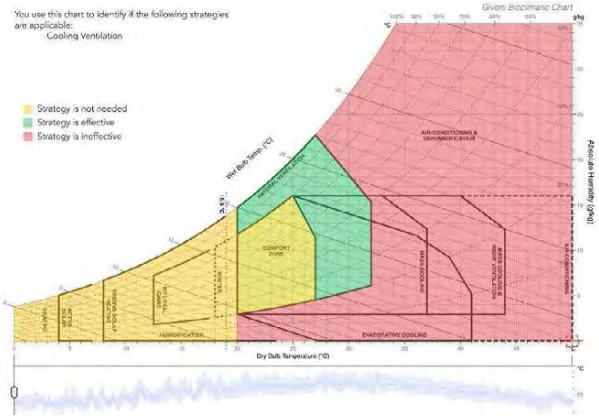

Figure 4: Assessing Comfort Ventilation

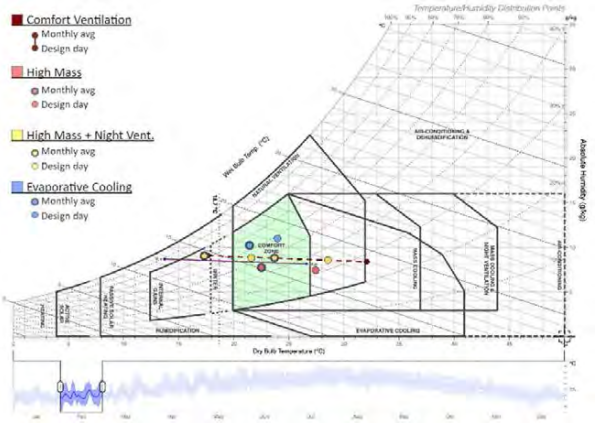

Figure 5: Example, Abu Dhabi in February. Comfort Ventilation is effective on the design day and not required on the average day.

point is the high Dry Bulb Temperature (DBT) and coincident Wet Bulb Temperature (WBT). We use ASHRAE's most recent 2% design-day DBT and coincident WBT for analyzing a hot day, paired with TMY data to find associated lows and paired WBT.

The percentage of hours meeting adaptive comfort criteria is calculated monthly using CC. *Comfort* vs. *cooling* ventilation types are distinguished. Givoni's guidelines for estimating indoor temperatures are applied to high mass without and with night ventilation. The subsequent sub-sections present the cooling strategies analysis methods. The following abbreviations are used:

Table 1 Abbreviations

Cf-V	Comfort Ventilation (by air movement)
Cl-V	Cooling Ventilation (by DBT difference)
TMY	Typical Meteorological Year
NV	Natural Ventilation
DBT	Dry Bulb Temperature
WBT	Wet Bulb Temperature
RH	Relative Humidity
T_{in} ave	Average indoor DBT
ADLT	Average Day Low DBT
ADHT	Average Day High DBT
Range	Outdoor DBT variation (low to high)
T_{in} swing	Indoor DBT variation (low to high)
T_{in} max	Indoor maximum DBT
DDLT	Design-Day Low DBT
DDHT	Design-Day High DBT
MDR	Mean Daily Range of DBT

4.1– Comfort Ventilation

Comfort Ventilation (Cf-V) admits outdoor air for physiological cooling and a psychological feeling of comfort and assumes (here) an indoor velocity of 2 m/s (3.2 mph), a light breeze. For a month's *average day*, plot on the psychrometric chart a line defined by the high DBT/coincident WBT and low DBT/coincident WBT (Fig. 5). Locate the average daily high (the top point on the line) on the graph. If the point is beyond the (adaptive) Comfort Zone and within the Natural Ventilation (NV) zone, Comfort Ventilation (Cf-V) is effective with adequate air movement (Fig. 4). If it lies within the comfort zone or below, Cf-V is not needed. If it is beyond (above) the NV zone, Cf-V is ineffective.

For the *design-day*, use the ASHRAE cooling 2% Design-Day High Temperature (DDHT) and subtract the published Mean Daily Range (MDR) of DBT from the DDHT to get the Design-Day Low Temperature (DDLT) [12]. Plot the DDHT/WBT point. Next, draw a line at same slope as the average day line to get the coincident WBT at the DDLT. This line represents the design-day (Fig. 5). The potential error in this quick, approximate method is that the hot design-day will typically have a greater daily DBT range than an average day (the MDR).

If the DDHT point is within the comfort zone or below, Comfort Ventilation (Cf-V) is not needed. If the point falls within the NV zone, Cf-V is effective. If DDHT is beyond the NV zone then Cf-V is ineffective.

The authors' current work is to automate the process so that analysis of strategies' effectiveness requires simply selecting a location. The automated method will find both average and design-day high and low DBT in a TMY file and will more accurately calculate for their coincident WBT than the approximate method described previously.

4.2 Cooling Ventilation

For Cooling Ventilation (Cl-V) assessment, plot on the psychrometric chart the same data as used in the Cf-V analysis. If the average day high temperature point falls in the yellow zone (Fig. 6), Cl-V is not needed; if it is in the green zone, Cl-V is effective; if in the red, Cl-V is ineffective. Note that the upper limit of the green zone is about 3.5 °C (6.3 ˚F) lower than the comfort zone high, which is a conservative value.

4.3 High Mass (without ventilation)

Givoni [7] gives approximate methods for determining the effectiveness of High Mass without ventilation (HM) by estimating resulting indoor temperatures. The method assumes good solar shading and insulation and light exterior colors. Grondzik + Kwok [13] de-

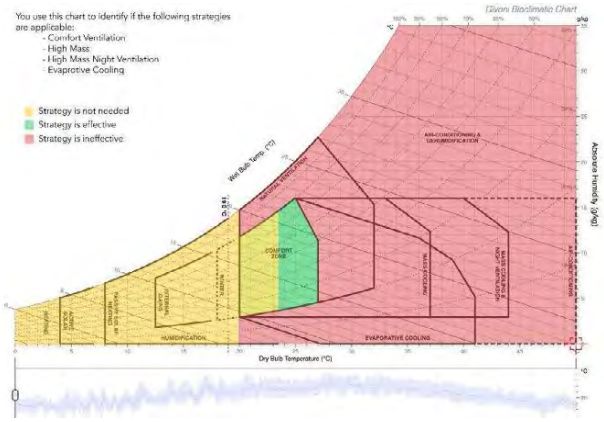

Figure 6: Assessing Cooling Ventilation

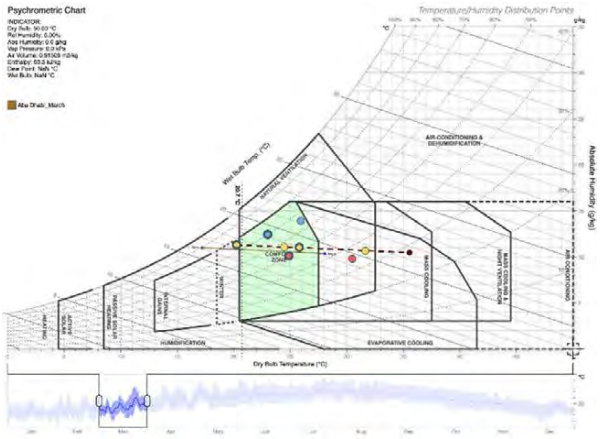

Figure 7: High Mass analysis, Abu Dhabi, March

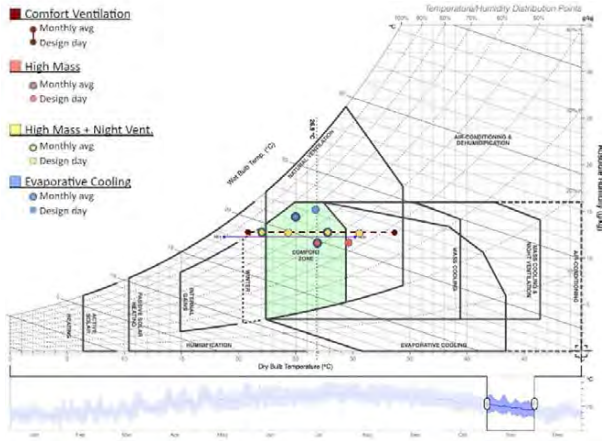

Figure 8: Night-Ventilated Mass, Abu Dhabi, November

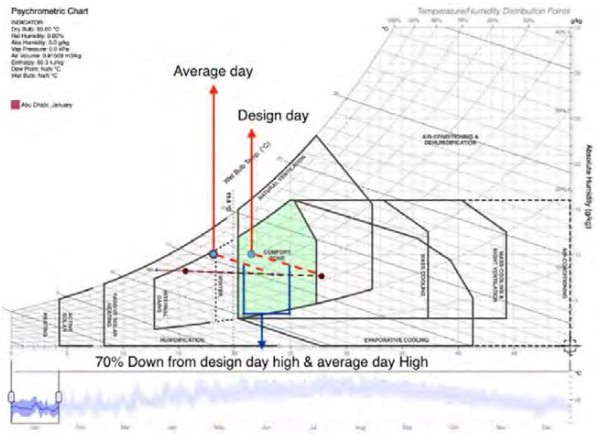

Figure 9: Direct Evaporative Cooling, Abu Dhabi, January: effective on design day and not required on average day.

fine a high mass budlings as having 2 m² of mass surface area per 1 m² of floor area with 3 in (7.6 cm) thickness of exposed ordinary weight concrete.

For an average day each month, we adapt Givoni's approach as follows (all temperatures in ˚C):

A—Calculate the indoor average DBT (T_{in} ave):

$$T_{in}ave = 1.5°C + \left(ADLT + \frac{Range}{2} \right) \quad (1)$$

B—Calculate the indoor DBT variation (T_{in} swing) for each month:

$$T_{in}swing = 0.15 \times Range \quad (2)$$

C—Calculate the indoor DBT maximum (T_{in} max) for each month:

$$T_{in}max = T_{in}ave + \left(\frac{T_{in}swing}{2} \right) \quad (3)$$

D—Calculate the indoor DBT minimum (T_{in} min) for each month:

$$T_{in}min = T_{in}ave - \left(\frac{T_{in}swing}{2} \right) \quad (4)$$

For the design day, the same method is used, substituting *DDLT* for *ADLT* in formula 1 and ASHRAE's *MDR* for the average day's *Range* in formulas 1 and 2. If the T_{in} *max* data point falls below the comfort zone (Fig. 7), then HM is not needed. If T_{in} *max* is within the comfort zone, HM will be effective, and if above the comfort limit, ineffective. The pink circles in Fig. 7 show that, in Abu Dhabi during March, HM is effective on the average day and ineffective on the hot day.

ilated Mass

methods for assessing High Mass *with* *n* by estimating resulting indoor temg the closed period. The strategy is var- to as night-cooled mass, nocturnal con-, or Night-Ventilated Mass (NVM), as per (Fig. 8). The building remains closed during the hot period of the day, absorbing heat gains in structural thermal mass, and is opened for ventilation during cooler night periods when heat stored in the mass can be removed. Natural ventilation air flow of 2–3 m/s or mechanical ventilation is typically required. In the calculations, T_{in} *min* and T_{in} *max* refer to indoor temperatures *without* ventilation on the day being evaluated (estimated previously for High Mass).

age day:

ne minimum indoor DBT (T_{min} vent):

$$T_{in}\,min - 0.5\,(T_{in}\,min - ADLT) \quad (5)$$

ne indoor high DBT (T_{max} vent):

$$T_{in}\,\max - 0.25\,(T_{in}\,\max - ADHT) \quad (6)$$

ign day, DDLT is substituted for *ADLT*. If the T_{max}*vent* data point falls below the comfort zone (Fig. 8), then the NVM strategy is not needed. If

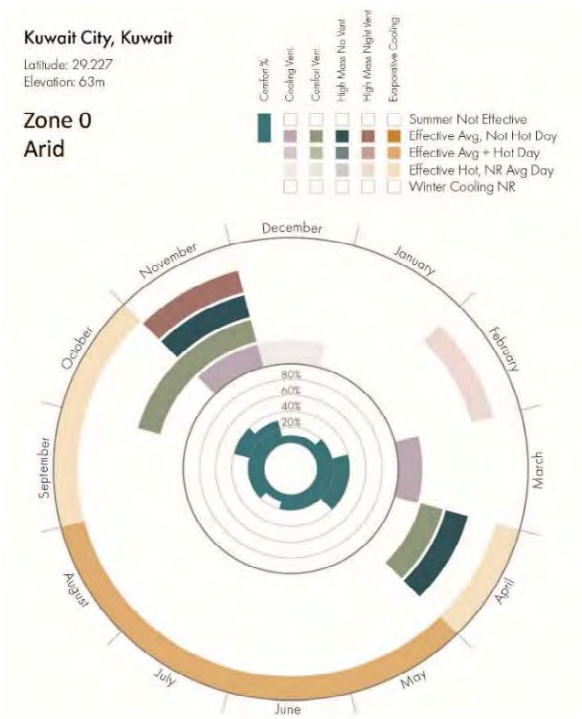

Figure 10: Passive Cooling Calendar for Kuwait City

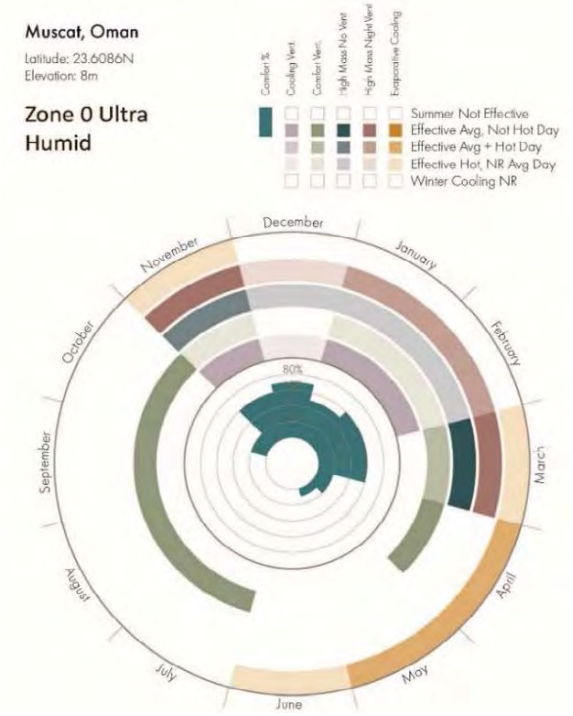

Figure 11: Passive Cooling Calendar for Muscat, Oman

T_{max}*vent* is within the comfort zone, NVM will be effective, and if above the comfort limit, ineffective. During November in Abu Dhabi, the strategy is effective on the average day and ineffective on the design day.

4.5 Direct evaporative cooling

Starting with the high temperature outdoor conditions that are above the comfort zone on the psychrometric chart, move down the wet bulb temperature line approximately 70% of the distance to saturation (Fig. 9). If the resulting point, which represents the supply air temperature, is within the comfort zone, then evaporative cooling will be effective; if outside the comfort zone, ineffective. This method assumes a 70% efficient direct evaporative cooler, which could be of either the mechanical (with fan) or passive downdraft type.

5. RESULTS

The analysis methodology allows the identification of effectiveness in each city for six strategies on both average and hot days across twelve months of the year (Fig. 10, 11). Results are potted on a radial calendar with rings indicating each strategy's feasibility in three colors. The NR designation means the strategy is Not Required. White on the calendar's winter/cool side means that cooling is not required. White on the summer/warm side months means that the climate is too hot for that strategy to be effective. The percentage of monthly hours meeting adaptive criteria without any applied strategy are plotted in the center.

Passive Cooling Calendars for 29 cities, covering the ASW countries, have been completed. An architect or a design team could consult this diagram at the initial pre-design climate analysis and concept design stages to understand the applicability of such strategies during the different months of the year. In most cases some combination of strategies is required to address cooling during different months.

The results show a surprising range of passive cooling feasibility, even within the same IECC zone (Figs. 10, 11). Evaporative cooling effectiveness is easily distinguished. Fig. 10 shows the Passive Cooling Calendar for Kuwait City. The city's harsh climate, categorized as IECC type 0-B (very hot/dry), is quite arid. Consequently, only the evaporative cooling (EC) strategy is effective on the hot day and is not required on the average day in April, September and October, while EC is effective on the average *and* hot day during May, June, July and August. Other strategies are ineffective for the five hottest months and are mostly applicable in November and April. Cooling ventilation applies on average March days and hot days in December.

In the hot and humid city of Muscat (also IECC zone 0-B and low rainfall), in contrast to Kuwait City, evaporative cooling is not effective on hot days between June and November (Fig. 11). Instead, most of the cooling strategies apply in the coolest months of November to March. For example, comfort ventilation is effective for the average day in April and during July to October; for the average and hot day in March; and on the hot day during November, January and February.

The radically different applicability of strategies in cities of the same IECC zone confirms our previous results (Fig. 3) and shows that the IECC system requires

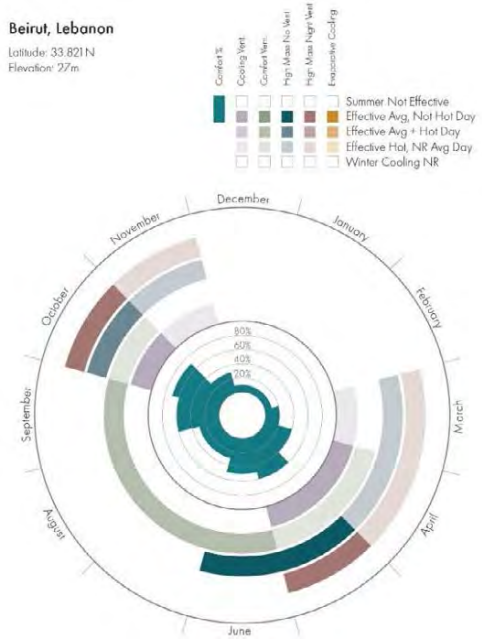

Figure 12: Passive Cooling Calendar for Beirut,

revision. As such, we are certain that neither all vernacular cooing types, nor all passive cooling strategies, can be associated with current IECC zones.

Fig. 12 illustrates the Passive Cooling Calendar for Beirut, Lebanon, which has a Mediterranean climate (IECC Zone 2A). Given the humid context, evaporative cooling is not effective at any time during the year. The other strategies, cooling ventilation, high mass and night-ventilated mass, are effective for the average day during October and May. They are effective for the hot day during March, April and November. The comfort ventilation strategy is effective on the average and hot day from June to September. The central circles in the calendars show the percent of adaptive comfort for outdoor conditions. In Kuwait City, the highest percent of comfort is 40 % in April and October; Muscat, 70 % in December; and Beirut, 70 % in October.

Although space does not allow illustration, the set of 29 Passive Cooling Calendars demonstrate that some strategies, such as adaptive comfort hours, cooling ventilation and comfort ventilation, align well with the IECC numerical zone types (0–3), which are based on annual cooling degree days, generally showing increasing effectiveness in the cooler zones.

6. LIMITS

Marsh's comfort zones used in the study assume still air, while boundaries can be extended upward with moving air, so results may be conservative relative to potential upper edges of comfort. Further extension of the comfort zone would also extend the feasibility period of some strategies. Similarly, comfort limits (and thus feasibility periods) during closed HM and NVM strategies can be extended with indoor fans. These effects have not been included and suggest further refinements and additions. Cooling ventilation estimates are conservative; increasing upper limits to nearer upper comfort zone boundary would expand feasibility. Only direct evaporative cooing effectiveness with moderate efficiency is estimated in this study. Higher efficiencies may be achieved with advanced passive strategies or indirect evaporative cooling, whether passive, roof spray, roof pond, or mechanical. Increased evaporative cooling efficacy would extend outdoor temperature limits and thus, the season.

7. CONCLUSION

The city-based Passive Cooling Calendars, as implemented, provide a useful picture of a place's strategic options in relation to its annual variability. The estimation methods are simple and approximate, but accurate enough for pre-design and concept selections. Additional cooling strategies—and passive heating strategies—could be added in future work.

The team is currently working on developing an online platform to automate the analysis process and generate the calendar graphics. The coding of automated calculations will allow both more precise performance estimates and the use of either historical or simulated future climate data files.

ACKNOWLEDGEMENTS

The work presented herewith was supported by a Fulbright Scholar Grant, University of Tennessee, Knoxville and the American University of Beirut. The research team also included Perto Michael, Munzir Mohamed and Zachary Dulin.

REFERENCES

1. Cultural Heritage Framework for Preserving Qatari Vernacular Domestic Architecture, AL-Mohannadi, R Furlan + M D Major
2. The Relevance of the Eco-Construction Twinning Project in Tunisia, Ghada JALLALI, Ministry of equipment, Tunis, Tunisia. World SB 14 Conference, Barcelona (2014).
3. International Code Council (2021). *2021 International Energy Conservation Code*. IECC: Country Club Hills, IL
4. University of Veterinary Medicine, Vienna (2010). Köppen-Geiger Climate Classification Map for Google Earth
5. CRTKL (2023). CLIMATESCOUT. CallisonRTKL, callisonRTKL.com
6. Brown, G Z (1984). *Sun, Wind + Light: architectural design strategies,* 1st ed. Wiley
7. Givoni, B (1992). Comfort, Climate Analysis and Building Design Guidelines, *Energy and Buildings* 18: 11–23
8. Watson, D + K Labs (1993). *Climatic Design: Energy-Efficient Building Principles and Practices*. McGraw-Hill
9. Milne, M (2021). Climate Consultant 6.0. Los Angeles: UCLA, sbse.org/resources/climate-consultant
10. Marsh, A (2018). Psychrometric Chart. andrewmarsh.com/software/psychro-chart-web/
11. ASHRAE (2020). Standard 55: Thermal Environmental Conditions for Human Occupancy. Atlanta: ASHRAE
12. ASHRAE (2009). Climatic Design Conditions. ashrae-meteo.info
13. Grondzik, W T + A G Kwok (2014). *Mechanical and Electrical Equipment for Buildings.* 12th ed. Wiley

PLEA 2024 WROCŁAW
(Re)thinking Resilience

Summer Energy Use and Comfort Analysis in Rural Chinese Dwellings: A Case Study of Low-income Older Populations in Shandong

DI YANG[1] NEVEEN HAMZA[1] ROSE GILROY[1]

[1] Newcastle University, Tyne and Wear, United Kingdom

ABSTRACT: This paper aims to understand indoor environmental conditions and occupant daily behaviour in the homes of older people in rural cold climates in China, focusing on the Shandong region. The study employs a mixed-methodological approach to explore correlations between environmental factors, the state of building fabric, and the energy use behaviour of older people in different familial settings. Qualitative questionnaire surveys, interviews, and observations on five types of older households are correlated to quantitatively monitored indoor environmental conditions. Results indicate a higher energy use intensity that however fails to provide comfortable indoor living environments. Economic affluence and a younger generation cohabiting the houses also affect the type of fuel use and duration of use to provide comfortable indoor conditions.
KEYWORDS: Energy Use Behaviour, Architectural Interventions, Rural China, Older people, Thermal Environment.

1. INTRODUCTION

In China, substantial national ongoing rural-to-urban migration leads to an escalating ageing population concentration in rural areas. In 2021, older people over-60s comprised 23.8% of the Chinese rural population, compared with 15.8% in cities [1]. This 8.0% gap is almost doubled when compared with the 4.3% recorded in 2015 [2].

The majority of older rural residents in China are characterized by below-average to low levels of per capita income [3]. Houses occupied by older rural people are poorly designed and maintained, with poor internal air quality, and high heating energy consumption, leading to major problems with thermal comfort [5,6]. Heavily relying on biomass and other solid fuels, these households have limited access to clean and efficient domestic heating systems [7].

Rural residential buildings consume 23.76% of China's total energy, with relatively low energy efficiency, particularly in the northern regions of China, known for their extreme seasonal temperature fluctuations between 41.1°C in summer while winter temperatures can plummet to as low as -53°C [6]. Yang et al. [7] recognize that northern rural houses are normally built without sufficient insulation. The energy-saving measures for passive design building envelopes are explored by Fan et al. [8] for northern rural houses in China. Through field studies on rural houses. According to Wang et al. [9], the thermal environment quality of traditional houses in cold climate zones is inferior. Given the unique demographic structure of rural areas in China, where more than 60% of the older population and children often remain in the villages while the young, working-age population migrates to urban centres for employment, leading to "elderly village," it becomes particularly important to understand this context [10].

Studies on energy usage patterns in rural households reveal that residents' electricity usage behaviour is influenced by income level, educational background, household size, and the number of electrical appliances owned [11]. Even during high temperatures, rural older people continue to rely on natural ventilation and electric fans to cool their living spaces in different climate zones [12]. Nonetheless, the findings of Cui et al., [13] present a contrasting scenario, revealing that rural residents in China's hot summer and cold winter climate regions tend to use air conditioning systems for heating without realizing that their behavioural patterns may lead to high energy consumption. Wu et al., [14] survey found that as high as 79% of rural households in northern China continue to use traditional low-efficiency self-constructed stoves. 17.1% and 58.6% of rural residents use coal and solid biomass as their main cooking fuel, respectively, while areas with lower per capita household incomes use more solid fuels [15].

Existing literature reveals a significant gap in understanding the energy use behaviour of older individuals in rural China, particularly in relation to the influence of family structures and member dynamics on their energy consumption habits.

This paper aims to understand the occupant energy use behaviour of the older population in China's cold climate zone and the impact of household characteristics and socio-economic variables on energy consumption in the home. The following objectives are:

- To understand indoor environmental conditions and occupant daily behaviour in the homes of older people in rural China.

- To establish quantitative relationships between specific environmental factors and the energy use behaviour of older occupants.
- To qualitatively study the impact of key socio-economic variables (like income levels, and educational background) on building energy consumption and the daily living needs of the older population.

2. METHODOLOGY

Table 1: 5 types of older respondents' information.

Household type	House ID	Personal characteristic				House information	
		Gender	Age	Income (Yuan per month)	Education	Building type	Monitoring location
Three generation living together	TGL-01	F	80+	Less than 1000	Illiterate	Brick-concrete structure	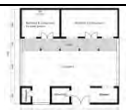
	TGL-02	F+M	60-65	Over 5000	Junior high school	Brick-concrete structure	
Older people living with grandchildren	OLG-03	M+F	60-65	4000-5000	Junior high school	Brick-concrete structure	
	OLG-04	F+M	60-65	2000-3000	Junior high school	Brick-concrete structure	
Older people living with children	OLC-05	M+F	60-65	Over 5000	Illiterate	Brick-concrete structure	
	OLC-06	F+M	60-65	3000-4000	Primary school	Brick-concrete structure	
Older couple living together	OCL-07	M+F	71-75	Less than 1000	Junior high school	Brick-concrete structure	
	OCL-08	F+M	71-75	2000-3000	Highschool	Masonry structure	
Older people living alone	OLA-09	M	71-75	1000-2000	Primary school	Brick-concrete structure	
	OLA-10	F	71-75	Less than 1000	Illiterate	Brick-concrete structure	

The case study is centred on a representative village situated in the cold climate zone of the southwestern region of Linyi City, Shandong Province. The village comprises 306 houses, with 278 occupied and 28 unoccupied, indicating about 90% occupancy. Older residents live in 118 houses, while other demographic groups occupy the remaining 160. Older couples represent 58% of the households, older adults living alone account for 25%, and three-generation households are relatively rare at 10%. The dominant living arrangements suggest a trend of independence post-marriage or urban migration, with notable social and economic support among older couples.

This study undertakes a mixed-mode inquiry method to address domestic energy consumption and fuel poverty for older people of low socioeconomic status in rural areas. Conducting monitoring indoor conditions, questionnaire surveys, interviews, and observations on five types of older households in rural areas in the summer to correlate their energy consumption behaviours with indoor environmental conditions.

A mixed-methods study was used to qualitatively look at how older people's behaviours affect energy use based on interviews and observation and to quantitatively assess the impact of the indoor environment on older residents based on questionnaires and on-site monitoring. In on-site monitoring, indoor temperature and relative humidity are recorded every 5 minutes using a HOBO UX100-003 data logger with accuracies of ±0.21°C and ±3.5% respectively, while outdoor environmental conditions are monitored hourly by the China Meteorological Administration. The collected data will be used to establish energy use behaviour patterns in indoor environments.

The study focuses on older participants, defined as individuals aged 60 years and above, who are capable of living independently and healthily. This criterion ensures that the data collected is representative of the active older population residing in the village. Two households of each type from 5 different types of older households, with a total of 10 households are selected as a research sample. Personal characteristics and housing details of respondents across 5 types of older households (a total of 10 households) are comprehensively presented in Table 1. In this table, each of the 10 surveyed households is assigned a unique identifier, which will be used for detailed analysis in the conclusions section.

Data collection is carried out in the summer of 2023, from August 1st to September 5th. Two data loggers are placed in the living rooms of two houses of the same type at a height of 1.8 meters. Each week, the data loggers are moved to a different household type, continuing for five weeks to cover all 5 types of older households.

Qualitative insights from interview responses support the quantitative data obtained from measurements and surveys. This combined analysis helps in identifying energy use behaviour and influencing factors specific to different types of older households. The intent is to draw correlations between the lived experiences of older people, as captured in interviews, and the empirical data from environmental monitoring and surveys.

3. RESULTS AND DISSCUSSION

Table 1 delineates the personal characteristics, architectural information, and locations monitored by data loggers for the 5 types of respondents.

As depicted in Fig. 1, TGL_01 and TGL_02 exhibited daily temperatures that fluctuated in tandem with the external environment. TGL_01's monitoring encompassed an 83-year-old woman's bedroom, serving as a combined space for living, dining, and sleeping, demarcated only by wardrobes. The occupant demonstrated consistent cooling behaviour, keeping doors and windows open all day without or seldom using an electric fan:

"I always keep the doors and windows open. I also have an electric fan and a cool mat, making for a comfortable living situation."

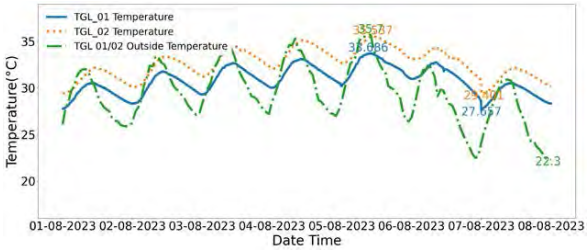

Figure 1: Indoor and outdoor thermal environment of Three generations living together (TGL) in two houses during 01~08/08/2023.

The dwelling is shaded by a 2-meter porch, and the architectural insulation is effective, though no window curtains are installed within. During times of excessive indoor heat, she relocates to an air-conditioned bedroom for cohabitation with their children. During the interview, TGL_01 emphasized her conservative energy use:

"Ever since my son and daughter-in-law returned from the city to live with me, the air conditioning has been on every day, I still cringe every time air conditioner is turned on."

TGL_02, observing a 60-year-old woman's living room, exhibited a longer thermal lag, slower to reach peak indoor temperatures following the peak outdoor temperatures, with indoor temperatures consistently around 2°C higher than TGL-01. The temperature curve was more volatile, despite both employing a combination of natural ventilation and electric fans for cooling. A 7.5m by 3m conservatory reduces direct solar gains but also retains more heat. The living room experienced more internal gains, with five family members frequently entering the living room after work and school to dine and watch television.

TGL_02 detailed a more comfortable financial situation, permitting the use of more electrical appliances and regular air conditioning in the bedroom:

"When I feel hot, I go back to my bedroom and turn on the air conditioning. If it's not too hot, I just use the fan. Compared to other villagers, my living conditions are better in many aspects."

TGL_01 quotes reflect a thrifty energy approach, discomfort with unnecessary expenditure, and reliance on family for cooler accommodations. TGL_02, a 60-year-old woman's living room, shows higher temperatures and a pronounced thermal lag, possibly due to a larger space and window area, increased internal gains, and family activities that generate heat. These narratives underscore how energy use, household dynamics, and personal

preferences shape the thermal environment in rural older individuals' homes.

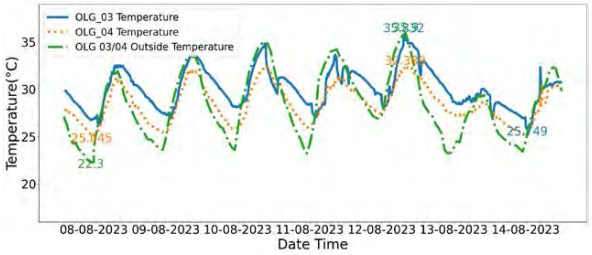

Figure 2: Indoor and outdoor thermal environment of older person living with grandchildren (OLG) during 08~14/08/2023.

Fig. 2 presents the environmental conditions within two residences of older couples living with their grandchildren only, OLG-03 and OLG-04.

OLG_03 is the home of a 65-year-old man and his wife, who share their space with their 2 teenage grandchildren. This multifunctional area, used for living, dining, and sleeping, is separated merely by a curtain. The presence of a multi-generational family in OLG_03 likely leads to more dynamic and diverse space usage, resulting in temperature and humidity fluctuations due to activities such as cooking, door usage, and other behaviours. The home lacks south-facing windows and relies on an open iron door for ventilation and sunlight. The energy-saving air conditioning is operated only when the grandchildren are present, underscoring the elderly couple's efforts to economize on energy expenses:

"On exceptionally hot days when we go out to do farm work, the kids turn on the energy-saving air conditioner, which has a lower electricity cost. But if they are at school, we don't use the air conditioner; just a fan is sufficient for us."

The couple also faces the challenge of energy poverty for cooking:

"We generally don't use the gas stove for cooking; we burn free firewood and straw on a traditional stove. We live frugally because there's no spare money at home."

OLG_04, monitored in the living room of a 61-year-old woman, reveals a consistent internal environment with no clear indication of air conditioning use, contrasting with the resident's admission of lifestyle habits:

"When it's above 30°C in the summer, whether during the day or night, I will turn on the air conditioning in the living room or bedroom."

As the energy costs are covered by her children who have moved to the city, she expresses a lack of awareness regarding the expenses, thus often resorting to air conditioning for cooling:

"The energy bills are certainly not minor, but all the expenses are paid by my children, and I'm not aware of the exact amount."

In OLG-03, the elderly couple's frugal lifestyle and energy-saving measures are a direct result of financial necessity, while in OLG-04, the financial freedom afforded by the children allows for a more liberal use of cooling appliances. These narratives illustrate the varying degrees of energy awareness and financial limitations that shape the living conditions and thermal comfort strategies in rural older households.

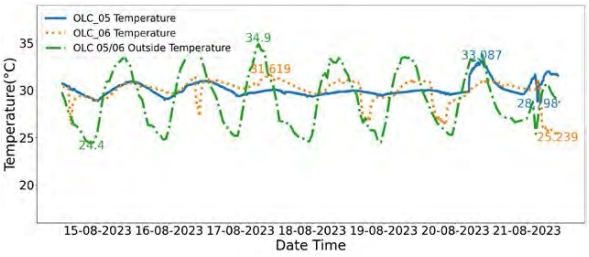

Figure 3: Indoor and outdoor thermal environment of older people living with children (OLC) during 15~21/08/2023.

Fig. 3 displays the environmental conditions within two cohabitation residences, OLC-05 and OLC-06, where elderly individuals reside with children.

OLC-05 is the abode of a 62-year-old male and his spouse, who share this newly constructed modern edifice, completed in 2022, with their second son. It is a three-story building featuring large, double-glazed fenestrations without draperies, which account for the observed minimal fluctuations in indoor temperature and humidity, with an interior temperature peak at a mere 33.08°C. The absence of air conditioning utilization in the dwelling implies a reliance on natural ventilation and possibly the building's thermal mass to maintain a comfortable indoor climate:

"I find it quite comfortable and have never felt it to be excessively hot. On particularly sweltering days, we use an electric fan in the living room."

Residing in the new home, the pleasant interior conditions do not necessitate frequent activation of air conditioning, signifying an enhancement in living standards and low energy consumption:

"My energy expenditure is low, but indeed higher than in previous years, owing to an improved quality of life and a larger dwelling space."

OLC-06, as a conventional single-story construction, typically exhibits more pronounced natural temperature variations due to less effective insulation. The conservatory and porch diminish direct solar ingress, thereby reducing heat accumulation during the daytime. The pronounced temperature dips in the chart indicate the occupant's resort to activating air conditioning to alleviate discomfort from overheating, substantially relying on active cooling for indoor comfort:

"Summers are certainly hot. We switch on the air conditioner in the living room."

The cost of energy consumption is deemed acceptable by the elderly residents of OLC-06, and despite not facing energy poverty and having access to gas stoves for cooking, cultural influences from the

village sometimes dictate a preference for traditional cooking methods:

"Ordinary life doesn't make me perceive energy costs as excessive; these are essential energies that must be used. Even though I possess a gas stove, there are times I opt to use the traditional stove to burn firewood and straw for cooking."

The modern infrastructure of OLC-05 offers a stable indoor environment, mitigating the need for air conditioning through efficient insulation and potentially improved natural ventilation. In contrast, OLC-06's reliance on air conditioning during certain periods signals a greater variation in indoor climate, influenced by the older construction of the building and possibly less efficient thermal properties. OLC-05 maintains comfort passively, whereas OLC-06 requires active cooling to compensate for a lack of modern insulation materials, achieving a similar level of comfort.

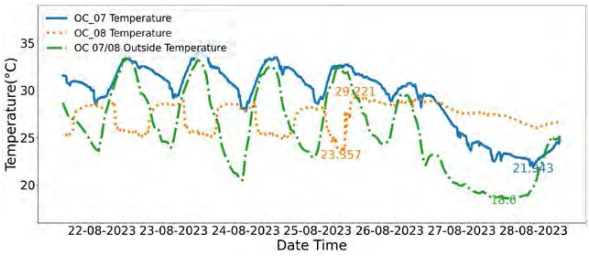

Figure 4: Indoor and outdoor thermal environment of older couples living together (OC) during 22~28/08/2023.

Fig. 4 presents the environmental conditions within and outside two residences, OC-07 and OC-08, inhabited by elderly couples.

Residence OC-07 is the abode of a 75-year-old male and his spouse, with a modest living space of merely 33 square meters, ranking as the smallest amongst the interviewees. The space, partitioned by wardrobes into a bedroom, living area, and dining space, lacks a ceiling and is equipped only with metal doors and windows without any sun-shading devices, yet remains relatively dim indoors. The graph depicts indoor temperatures consistently exceeding outdoor levels throughout the week, peaking at 34.1°C. The room, devoid of air conditioning, relies solely on natural ventilation:

"When it gets extremely hot, I turn on the electric fan and strip down to the waist. Although I have a handheld fan, I seldom use it due to laziness."

Energy consumption is minimal, with no financial assistance from children who have migrated to the city, leaving the older generation with a clear understanding of their energy expenses and facing energy poverty. Despite owning a gas stove, traditional free biomass-fueled stoves are the primary cooking method:

"My energy expenditure is quite modest. For cooking gas, I use only three canisters a year, as I predominantly cook with a traditional stove using free straw or firewood. Electricity costs me less than 20 yuan per month, and water is about 130 yuan annually."

OC-08, inhabited by a 72-year-old woman and her partner, is an over-two-decade-old traditional single-story masonry structure with a sloping roof and porch. The chart reveals a regular pattern of air conditioning use, activated during the day and turned off at night. After August 26, a cessation of air conditioning usage is noted, likely due to a significant decrease in outdoor temperatures affecting cooling behavior. This household has the longest duration of air conditioning use among the five categories of elderly residences:

"When it's hot outside, I don't feel the heat once inside, as the air conditioner is on."

Despite perceiving electricity as costly, the pursuit of a comfortable environment prevails, maintaining the use of air conditioning:

" Air conditioning is only used for about a month in the summer, with this month's electricity bill around 200 yuan and around 50 yuan in other months."

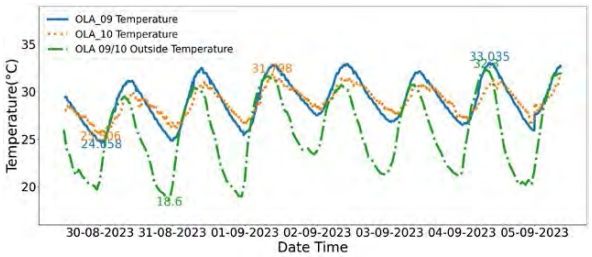

Figure 5: Indoor and outdoor thermal environment of older individual living alone (OLA) during 30/08/2023~05/09/2023.

Fig. 5 illustrates the internal and external environmental conditions of residences OLA-09 and OLA-10, occupied by solitary older individuals, serving as the base case studies for the five distinct types of elderly dwellings examined in this research. Both homes demonstrate diurnal cycles of temperature and humidity closely aligned with external environmental patterns, relying extensively on natural ventilation through open doors and windows combined with the use of electric fans for cooling.

Residence OLA-09 is inhabited by a 73-year-old solitary male, with the living space divided by wardrobes into a bedroom, living area, and dining space. The windows are sealed with oiled paper rather than glass. This dwelling experiences slightly larger fluctuations in indoor temperature than OLA-10 and maintains higher relative humidity levels. The resident prefers to keep doors and windows open throughout the day to cool down, while the presence of other visitors can influence this cooling behaviour:

"I generally keep the doors open all day for good air circulation."

The older individual, having lost his spouse, now shoulders the energy bills alone without financial support from his children. To economize, he resorts

to traditional free stoves, leaving the residence with minimal electrical appliances:

" Mostly, I cook with a traditional stove burning free straw and firewood. Annual electric bills might be around 200 yuan a year."

Residence OLA-10, occupied by a 73-year-old woman, exhibits an indoor thermal environment trend very similar to OLA-09 but with a slightly longer thermal lag, indicating better insulation properties of the building. Although financially supported by her children, who pay for her energy and communication expenses, she retains a habit of frugality, refraining from using air conditioning even when feeling hot:

"At night, if it's too hot to sleep, I turn on the electric fan."

The juxtaposition of the living experiences in OLA-09 and OLA-10 provides a poignant glimpse into the lives of the solitary older living. While OLA-09 exhibits a more hands-on and traditional approach to maintaining a suitable indoor climate, OLA-10, despite having financial support, shows a preference for passive cooling methods. Both instances underline a broader narrative of independence, with a propensity towards conserving energy and enduring higher temperatures without resorting to modern cooling technology. This behaviour is a testament to the resilience and adaptability of the older generation, who balance their physical comfort with financial considerations and personal habits shaped by a lifetime of experiences.

4. CONCLUSION

Research on the occupant behaviour of China's rural residents shows that, although rural buildings have the highest energy use intensity, they still fail to meet the thermal comfort requirements of occupants [16]. Through the implementation of surveys, interviews, and observations, this study evaluated five types of elderly households to understand their indoor environmental conditions and daily behaviours. Employing a mixed-method approach, both quantitative and qualitative, the research explored the environmental factors and socio-economic variables affecting the daily energy consumption behaviours of different types of elderly inhabitants in low-income rural areas of Shandong, China. This investigation provides insights for future rural housing designs that should be energy-efficient, cost-effective, and climate-adaptive, thereby improving the living conditions of the elderly. Additionally, it emphasizes the importance of considering household dynamics, individual habits, and architectural characteristics in the formulation of strategies for energy usage and thermal comfort. Such an approach has the potential to address the high energy consumption of rural residential buildings.

ACKNOWLEDGEMENTS

I extend my deepest gratitude to Dr. Neveen Hamza and Professor Rose Gilroy for their invaluable mentorship and unwavering support. My sincere thanks also go to Dr. Tailin Chen from Newcastle University, whose technical expertise in data processing was indispensable to my work.

REFERENCES

1. State Council (2021) 7th National Census Bulletin, [Online], Available: http://www.gov.cn/guoqing/202105/13/content_5606149.htm.
2. Bao J, Zhou L, Liu G, Tang J, Lu X, Cheng C, Jin Y, Bai J (2022) Current state of care for the elderly in China in the context of an aging population.
3. Hu Y, Wei H (2022) The income structure and income inequality of the elderly in rural China. J. Nanjing Agric. Univ. Soc. Sci. Ed. 45–57.
4. Yao S, Jiang Z, Yuan J, Wang Z, Huang L (2022) Multi-objective optimization of transparent building envelope of rural residences in cold climate zone, China. Case Stud Therm Eng 34:102052.
5. Jun Guo; (2022) A Preliminary Study on the Present Situation of Self-built Houses in Rural Areas and Thinking of House Safety. Eng Constr Des (03 vo No.473):22–25.
6. Zhou Z, Shi H, Fu Q, Li T, Gan TY, Liu S, Liu K (2020) Is the cold region in Northeast China still getting warmer under climate change impact? Atmospheric Res 237:104864.
7. Yang X, Jiang Y, Yang M, Shan M (2010) Energy and environment in Chinese rural housing: Current status and future perspective. Front Energy Power Eng China 4(1):35–46.
8. Fan X, Zhu Y, Sang G (2017) Optimization design of enclosure structure of solar energy building in Northwest China based on indoor zoning. Atlantis Press, pp 30–40.
9. Wang Y, Dong Q, Guo H, Yin L, Gao W, Yao W, Sun L (2023) Indoor thermal comfort evaluation of traditional dwellings in cold region of China: A case study in Guangfu Ancient City. Energy Build 288:113028.
10. National Bureau of Statistics of China. (2020) National Bureau of Statistics of China, [Online], Available: https://data.stats.gov.cn/easyquery.htm?cn=C01.
11. Shahi DK, Rijal HB, Shukuya M (2020) A study on household energy-use patterns in rural, semi-urban and urban areas of Nepal based on field survey. Energy Build 223:110095.
12. Wei D, Zhao G, Liu S, Yang L (2022) Indoor thermal comfort in a rural dwelling in southwest China. Front Public Health 10.
13. Cui Y, Yan D, Chen C (2017) Exploring the factors and motivations influencing heating behavioral patterns and future energy use intentions in the hot summer and cold winter climate zone of China. Energy Build 153:99–110.
14. Wu J, Hou B, Ke R-Y, Du Y-F, Wang C, Li X, Cai J, Chen T, Teng M, Liu J, Wang J-W, Liao H (2017) Residential Fuel Choice in Rural Areas: Field Research of Two Counties of North China. Sustainability 9(4):609.
15. Tang X, Liao H (2014) Energy poverty and solid fuels use in rural China: Analysis based on national population census. Energy Sustain Dev 23:122–129.
16. Yu S, Eom J, Evans M, Clarke L (2014) A long-term, integrated impact assessment of alternative building energy code scenarios in China. Energy Policy 67:626–639.

PLEA 2024 WROCŁAW
(Re)thinking Resilience

Coupling between detailed building energy models and a data driven urban canopy model

MIGUEL MARTIN[1] MARIO BERGES[2] JANTIEN STOTER[1]
CLARA GARCIA SANCHEZ[1]

[1] Delft University of Technology, Delft, The Netherlands
[2] Carnegie Mellon University, Pittsburgh, United States

ABSTRACT: This paper describes a data driven urban canopy model that can be coupled with detailed building energy models. The data driven model is used to assess the outdoor air temperature and humidity in a street canyon considering as inputs weather conditions at the atmospheric layer, the surface temperature of surrounding building facades and the street, and the heat released from the use of air-conditioning. Predictions made by the model were tested using measurements of the outdoor air temperature and humidity collected between April and August 2019 in Singapore. Results show that the model estimates the outdoor air temperature with a similar accuracy than others that were validated using the same input and test data, while providing estimates with a higher temporal resolution and considering urban morphology with a higher fidelity. They also demonstrate that the model can predict the impact of waste heat releases and cool pavement on the outdoor air temperature and building energy consumption. In the future, vegetation could be considered as an input of the model if the land surface temperature is measured using an infrared thermal camera. Another improvement would be to define weather conditions at the atmospheric layer from rooftop measurements or a climate model.
KEYWORDS: Urban heat island, Urban canopy modelling, Building energy modelling, Machine learning, Mitigation strategies

1. INTRODUCTION

For the last three centuries, most cities in the world have considerably expanded to accommodate their inhabitants. By 2050, it is expected that almost two thirds of the world's population will live in urban areas [1]. This trend in urbanization is the cause of several climatic hazards, including Urban Heat Islands (UHIs). UHIs primarily result from the heat accumulated in cities and the wind breeze obstructed by buildings. They provoke serious thermal discomfort in the outdoor environment and increases in the energy consumed in indoor spaces. The former consequence of UHIs has been declared a major threat to public health since the heat wave episodes of the summer 2023 in various parts of the world [2].

Given the influence of urbanization on UHIs, urban planning plays a major role to improve outdoor thermal comfort and minimize building energy consumption [3, 4]. To determine benefits of mitigations strategies to UHIs before their implementation, urban planners can now count on virtual replicates or digital twins of a city. City Digital Twins (CDTs) essentially consist of 3D city models to display the geometry of buildings, sensor data to monitor the indoor and outdoor built environment, and models to predict or prevent undesirable events that might occur in the city [5-7]. Whatever model is integrated into a CDT, it must meet certain requirements. One of them is to consider the urban morphology with the Level of Detail (LoD) expressed in the 3D city model [8]. Another one is that simulations using the model can be performed with low computational efforts. The latter requirement is particularly relevant for urban planners to make quick decisions on the strategies to adopt for mitigating UHIs.

To study UHIs through a CDT, it is necessary to include models that can perform simulations of interactions between buildings and their outdoor environment at the neighbourhood or city scale. The reason is the heat transferred from the envelope of buildings to the outdoor air is an important factor of UHIs [9]. In return, the outdoor air temperature and humidity strongly affect the energy consumed by buildings to maintain an appropriate level of thermal comfort [10]. Every increase in the energy consumed by buildings for cooling their respective indoor space is translated into an augmentation of waste heat releases, another important factor of UHIs.

Interactions between buildings and their outdoor environment are simulated using two coupled models: the Building Energy Model (BEM) and the Urban Microclimate Model (UMM) [11]. The former component assesses the energy consumed by a building, while the latter estimates outdoor conditions at the urban microscale, that is within a range of less than one kilometre. When the two components are coupled, the outputs obtained from one are iteratively used to define boundary conditions of the other until the end of simulations.

A first category of UMM, known as physically-based Urban Canopy Models (UCMs), predicts outdoor

temperature and humidity within a street canyon using a sensible and latent heat balance, respectively [12]. The heat balances describe time variations of the outdoor air temperature and humidity within the street canyon with respect to heat fluxes coming from surrounding surfaces and anthropogenic heat sources. The street canyon is either considered as a single air volume or a stack of multiple air volumes. In either case, physically-based UCMs assume that buildings are cubes with similar dimensions which are separated by streets of equal widths. It means they consider the urban morphology with a low level of detail, which is a major limitation to integrate them in a CDT.

To estimate outdoor conditions at the neighbourhood scale, while considering the urban morphology with a higher level of detail, studies have used computational fluid dynamics to approximate the wind flow and outdoor air temperature within a neighbourhood [13]. In addition to performing simulations using complex urban morphologies, this physically-based method provides estimates of outdoor conditions with a high spatial resolution. The temporal resolution, however, remains limited due to tremendous computational efforts that are required to perform simulations.

A recent review published by Wang et al. [14] demonstrates that the outdoor air temperature in the urban canopy layer can be assessed with a high temporal resolution using Data Driven Models (DDMs). These DDMs take as inputs land surface measurements collected by remote sensing and atmospheric weather conditions obtained by simulations. Both remote sensed data and weather simulated data are given at the mesoscale. In the majority of studies, these input data, together with measurements of the outdoor air temperature, are used to train and test two kinds of regression models, namely tree based models or artificial neural networks. The former type of DDMs usually fail in predicting the extreme values for the outdoor air temperature, while the latter model requires a large dataset and high computational efforts to be trained and tested. Whether a tree based model or artificial neural network is used as a DDM, it does not take into account how the outdoor air temperature at a specific point is affected by surrounding physical entities at the urban microscale, in particular buildings.

To consider buildings while predicting the outdoor air temperature at a specific location with a high temporal resolution, this paper describes a DDM that can be coupled with detailed BEMs. As most models shown in the literature, the DDM also considers as inputs atmospheric weather conditions and the land surface temperature. However, the land surface temperature is assumed to be obtained from a contact surface sensor or a thermal camera, which enable capturing the microscale effect of the street surface more accurately than a satellite.

Using the coupling between detailed BEMs and the DDM, the purpose of this study is to show that (1) outdoor air temperature and humidity in a street canyon can be predicted with a high temporal resolution and acceptable accuracy, (2) observations can be made on the impact of waste heat releases on the outdoor air temperature and the building energy use, and (3) it is possible to see how the outdoor environment and the building consumption are affected by cool pavement.

2. METHODOLOGY

2.1 The data-driven urban canopy model

The most important contribution of this work lies in a DMM that can predict outdoor air temperature and humidity in a street canyon with a high level of detail. The DDM is trained and tested using data collected by a series of weather stations in the street canyon. The weather stations should at least measure the outdoor air temperature, relative humidity, and pressure, so that the average outdoor air temperature ($\bar{T}_{can}$) and specific humidity ($\bar{q}_{can}$) at each time (t) in the street canyon can be observed and predicted.

Assuming the street canyon as a single layer, that is an air volume with uniform temperature and humidity, $\bar{T}_{can}$ and $\bar{q}_{can}$ are governed by sensible and latent heat balances, which can be expressed as:

$$V_{can} c_p \rho \frac{d\bar{T}_{can}}{dt} = \sum_{m=1}^{M} h_m A_m (\bar{T}_m - \bar{T}_{can}) + \sum_{n=1}^{N} H_n \qquad (1)$$

$$V_{can} c_p \rho \frac{d\bar{q}_{can}}{dt} = \sum_{p=1}^{P} h_p A_p (\bar{q}_p - \bar{q}_{can}) + \frac{c_p}{L} \sum_{q=1}^{Q} L E_q \qquad (2)$$

where V_{can} is the air volume of the street canyon (in m^3), c_p the specific heat capacity of dry air (in J/kg-K), ρ its density (in kg/m^3), L the latent heat of water vaporization (in J/kg), $\bar{T}_m$ the average temperature either of surrounding building facades, atmospheric layer, pavement, or vegetation (in °C), h_m or h_p their convective heat transfer coefficient (in W/m^2-K), A_m or A_p their surface area (in m^2), $\bar{q}_p$ their average specific humidity (in kg/kg), H_n the sensible heat released either from surrounding buildings or traffic (in W), E_q their rate of evaporation (in kg/s), m and p indices of thermal nodes, and n and q indices of sensible and latent heat sources. Equations (1) and (2) can be formulated as a linear state space model, such that:

$$\dot{\boldsymbol{x}} = \boldsymbol{A} \cdot \boldsymbol{x} + \boldsymbol{B} \cdot \boldsymbol{u} \qquad (3)$$

$$\boldsymbol{y} = \boldsymbol{C} \cdot \boldsymbol{x} + \boldsymbol{D} \cdot \boldsymbol{u} \qquad (4)$$

where $\boldsymbol{u} = \left[\bar{T}_1, \dots, \bar{T}_M, H_1, \dots, H_N, \bar{q}_1, \dots, \bar{q}_P, E_1, \dots, E_Q\right]^T$ and $\boldsymbol{x} = [\bar{T}_{can}, \bar{q}_{can}]^T$. From this formulation of sensible and latent heat balances, the DDM uses either a explicit or implicit time discretization scheme to predict state variables $\boldsymbol{x}_k$ at different time steps $t_k =$

$t_0 + k\Delta t$ as shown in Figure 1. Matrices $\boldsymbol{A_d}$, $\boldsymbol{B_d}$, $\boldsymbol{C_d}$, and $\boldsymbol{D_d}$ are derived from matrices $\boldsymbol{A}$, $\boldsymbol{B}$, $\boldsymbol{C}$, and $\boldsymbol{D}$, respectively, using a time discretization scheme.

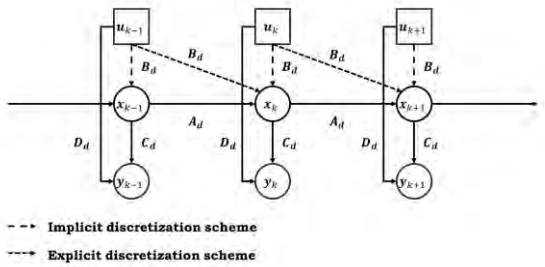

Figure 1. Discrete linear state space model used to predict outdoor air temperature and humidity in a street canyon.

Using the discrete linear state space model, the training phase of the DDM consists of finding the vector $\boldsymbol{h}$ of convective heat transfer coefficients that minimizes the discrepancy between estimates of $\overline{T}_{can}$ and $\overline{q}_{can}$ and their measurements. The training phase is thus expressed as a constrained multi-objective optimization so that:

$$\underset{\boldsymbol{h}}{\operatorname{argmin}}\, l^2\left(\overline{T}^{e}{}_{can} - \overline{T}^{m}{}_{can}\right), l^2\left(\overline{q}^{e}{}_{can} - \overline{q}^{m}{}_{can}\right) \qquad (5)$$
$$h_{lb} \le h_m \le h_{up}$$

where l^2 is the root mean square error with respect to the time discretization of the linear state space model, $\overline{T}^{e}{}_{can}$ and $\overline{q}^{e}{}_{can}$ estimates of the outdoor air temperature and humidity by the discrete linear state space model, respectively, $\overline{T}^{m}{}_{can}$ and $\overline{q}^{m}{}_{can}$ their measurements by weather stations in the street canyon, and h_{lb} and h_{up} the lower and upper bounds of convective heat transfer coefficients.

2.2 Coupling with detailed building energy models

The input vector ($\boldsymbol{u}_k$) of the discrete linear state space model is iteratively evaluated at each timestep (k) from different sources of information. Firstly, $\boldsymbol{u}_k$ consists of air temperature and humidity at the atmospheric level, which can be obtained either from measurements of a rural weather station or simulated data resulting from a climate model. Secondly, it consists of information measured or estimated at the street level. The surface temperature and humidity of pavement and vegetation, for instance, is assumed to be measured by a contact surface sensor or an infrared thermal camera. On the other hand, the sensible and latent heat released by traffic is usually assessed from an empirical model as in Grimmond [15]. Lastly, $\boldsymbol{u}_k$ is primarily composed of information that is simulated by detailed building energy models. It includes the surface temperature of surrounding facades and the waste heat releases.

Outputs ($\boldsymbol{y}_k$) provided by the discrete linear state space model after training and testing phases are used to specify boundary conditions of detailed BEMs. By default, boundary conditions of detailed BEMs are defined from typical meteorological data collected from a rural weather station. These meteorological data are iteratively replaced by $\boldsymbol{y}_k$ until a convergence criteria is achieved. The convergence criteria is established using the average sensible ($\overline{H}_{sys}$) and latent ($\overline{LE}_{sys}$) load of surrounding buildings so that:

$$l^2\left(\overline{H}_{sys}^{n+1} - \overline{H}_{sys}^{n}\right) \le \varepsilon_{\overline{H}_{sys}} \text{ and}$$
$$l^2\left(\overline{LE}_{sys}^{n+1} - \overline{LE}_{sys}^{n}\right) \le \varepsilon_{\overline{LE}_{sys}} \qquad (6)$$

where $\overline{H}_{sys}^{n}$ and $\overline{LE}_{sys}^{n}$ are the average sensible and latent loads estimated by detailed BEMs at the n-th iteration of the one-time-step dynamic coupling with the DDM. Figure 2 illustrates the coupled scheme between detailed BEMs and the DDM.

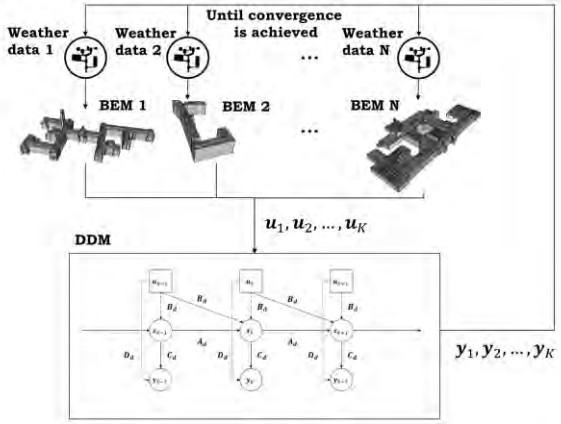

Figure 2. Coupling between detailed BEMs and the DDM.

2.3 Cool pavement

Cool pavement is a countermeasure to UHIs, whose effect on the outdoor air temperature and building energy consumption can be considered by the coupled scheme. The effect of cool pavement is assessed by modifying the surface temperature of the pavement ($\overline{T}_{pav}$), so that:

$$\overline{T}_{pav}^{cool} = \overline{T}_{pav} - \cos(\lambda_{sun}) \cdot \Delta T_{max} \qquad (7)$$

where $\overline{T}_{pav}^{cool}$ is the surface temperature of cool pavement, λ_{sun} the zenith angle of the sun (in Deg), and ΔT_{max} the maximum temperature decrease it can be achieved by the cool pavement.

3. CASE STUDY

3.1 Studied area

The coupled scheme was trained and tested using data collected by Miguel et al. [16] during a field experiment between April and August 2019 in a university campus of Singapore. The field experiment was primarily aimed at measuring weather conditions at four vertical heights of a single position within a street canyon. The street canyon is surrounded by four buildings and is only paved with asphalt.

3.2 Weather conditions and surface temperature

Measurements taken by Miguel et al. [16] at 3, 6, 9, and 12 meters on a flux tower were used to evaluate $\overline{T}^{m}{}_{can}$ and $\overline{q}^{m}{}_{can}$ in the street canyon. In contrast

with $\bar{T}^m{}_{can}$, $\bar{q}^m{}_{can}$ is not directly measured on the flux tower. It was assessed from the relative humidity measured at the four levels and the pressure at 3 meters. Both $\bar{T}^m{}_{can}$ and $\bar{q}^m{}_{can}$ were collected every 10 seconds. The mean over a 5-minute time frame was retained as measurement of $\bar{T}^m{}_{can}$ and $\bar{q}^m{}_{can}$. Measurements between June 6 and August 19 2019 were used to train and test the DDM. It means that the DDM was trained and tested on a dataset of 10368 samples of $\bar{T}^m{}_{can}$ and $\bar{q}^m{}_{can}$. The same amount of samples was used to specify $\bar{T}_{pav}$. $\bar{T}_{pav}$ was collected using a contact surface sensor.

3.3 Surrounding buildings

The street canyon where Miguel et al. [16] collected measurements of weather conditions is surrounded by four buildings: A, B, C, and D (see Figure 3). Their height varies from 15 to 24 meters, while the street canyon has a width of 10 meters.

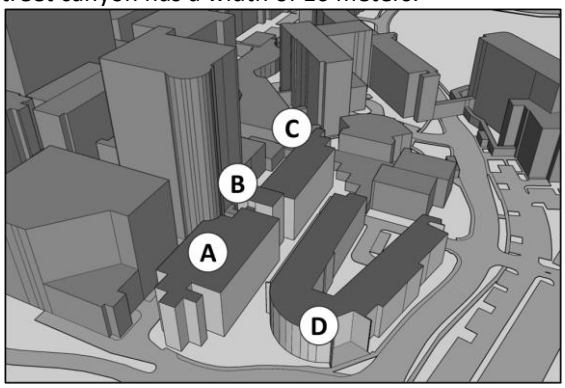

Figure 3. Buildings being modelled using EnergyPlus.

Buildings A, B, C, and D were modelled using EnergyPlus. Using this building energy simulation tool, it was possible to model buildings with LoD 1.2 as stated by Biljecki et al. [8]. Materials and internal heat gains were assigned from the Sketchup OpenStudio database (https://openstudio.net/) as those of typical office buildings in the tropics. An ideal load model was used to assess the amount of fresh air needed to keep the indoor temperature of buildings at 24 degrees Celsius and the relative humidity at 60%.

3.4 Baseline and scenarios

The baseline configuration refers to the original parameters of the coupled scheme that are used to evaluate increases or decreases in the outdoor air temperature or building energy demand caused by different scenarios. It was simulated using the Euler implicit method to discretize the linear state space model of the DDM. The multi-objective function stated in Equation (5) was optimized using the NSGA-2 method with h_{lb} equal to 0 Watts and h_{up} equal to 500 Watts. The convergence criteria was defined with $\varepsilon_{\bar{H}_{sys}}$ and $\varepsilon_{\overline{LE}_{sys}}$ equal to 0.01 Watts. The weather conditions at the atmospheric level were assumed to be equal to that recorded over a typical meteorological year in Singapore. In contrast with other scenarios, the baseline assumes that the outdoor conditions are not affected by waste heat releases and the surface temperature of the street is equal to measurements.

Therefore, scenarios aimed at estimating the impact of waste heat releases and cool pavement on the outdoor air temperature and building energy demand at the location where Miguel et al. [16] conducted their field experiment. Waste heat releases were assumed to be generated at a rate of 1.4 Watts per Watt of cooling consumed in buildings A, B, C, and D. It was also considered that 100% of them are sensible and go into the street canyon. In accordance with Anting et al. [17], it was supposed that cool pavement can achieve a decrease of 6.5 degrees Celsius at the highest exposure of the Sun.

4. RESULTS AND DISCUSSION

4.1 Simulations

In Figure 4, the hourly average outdoor air temperature as predicted by the DDM is shown in comparison to this assessed from measurements collected by Miguel et al. [16]. It is observed that the discrepancy between predictions and measurements is the lowest when the DDM is trained on 80% of measurements. It is usually expected that the accuracy of a DDM increases with respect to the size of its training set. Despite this observation, it is seen that the discrepancy between predictions and observations is higher at daytime than nighttime, that is when variations of the outdoor air temperature are the highest. This result certainly originates from the fact that $\boldsymbol{h}$ is assumed to be constant over time. From a physical point of view, its value is affected by wind speed and direction in the street canyon, and therefore, should vary over the day.

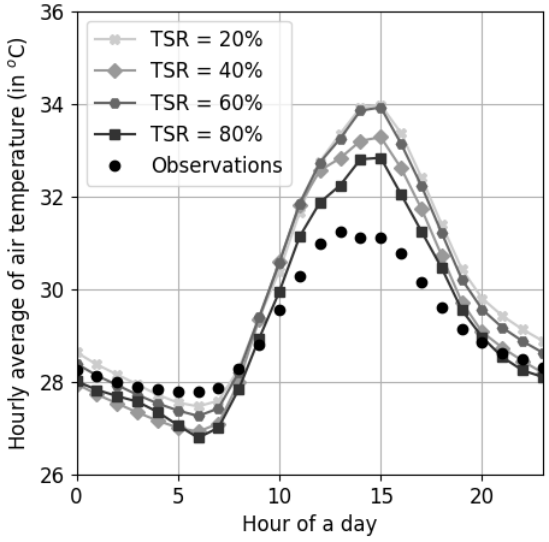

Figure 4. Average daily cycle of outdoor air temperature as measured by weather stations (dot) and as predicted by the DDM using different Training Split Ratios (TSR).

Although a time-constant $\boldsymbol{h}$ seems to limit the accuracy that can be achieved by the coupled scheme at daytime, results illustrated Table 1 show that the RMSE and MBE of the outdoor air temperature falls below 2.5 and 1.0 degrees Celsius, respectively, whichever split ratio is used to train the DDM. According to Miguel et al. [16], it is an acceptable accuracy when typical meteorological data are used to specify weather conditions at the atmospheric level. The accuracy of the coupled scheme could thus be improved if weather conditions at the atmospheric level were defined from measurements at the rooftop level or from simulations of a climate model.

Table 1. Root Mean Square Error (RMSE) and Mean Bias Error (MBE) between predictions and measurements of the outdoor air temperature and humidity using different Training Split Ratios (TSR).

TSR	Temperature		Humidity		Size test samples
	RMSE (K)	MBE (K)	RMSE (g/kg)	MAE (g/kg)	
20%	2.24	0.93	6.80	5.90	8291
40%	2.24	0.39	4.19	3.67	6219
60%	2.31	0.80	5.46	4.76	4146
80%	2.16	0.23	4.42	3.82	2074

4.2 Baseline-scenario analysis

From results shown in Figure 5, it seems that the outdoor air temperature would not be highly affected if waste heat was released in the street canyon connecting buildings A, B, C, and D. This result can be justified by the fact that buildings A, B, C, and D have a relatively small volume in comparison to other buildings that can be observed in the central business district of Singapore. However, it is important to note that the building consumption, as well as the waste heat releases, are certainly underestimated by the DDM in the case of Singapore. The main reason is that the 3D city model used to develop detailed BEMs was of a LoD 1.2, and thus, had no information about dimensions and positions of windows. As a consequence, buildings were assumed to be fully covered by walls, which neglects the impact of solar heat penetration on their cooling consumption.

Figure 6 illustrates the effect of cool pavement in the outdoor air temperature as predicted by the DDM. As expected, the highest decrease in the outdoor air temperature appears to be achieved between noon and 4pm. Although the effect of cool pavement on the outdoor air temperature can clearly be observed from predictions of the DDM, it should not be the only countermeasure to be considered by the coupled scheme. In addition to cool pavement, the coupled scheme should also be able to evaluate the impact of vegetation, another countermeasure to UHIs.

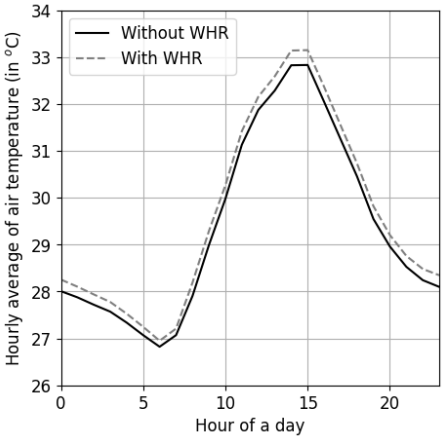

Figure 5. Average daily cycle of the outdoor air temperature predicted by the DDM with and without considering Waste Heat Releases (WHR) of buildings A, B, C, and D.

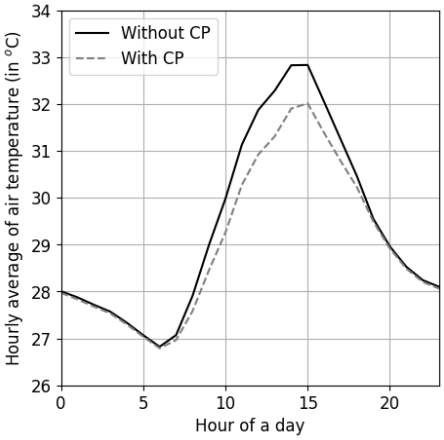

Figure 6. Average daily cycle of the outdoor air temperature predicted by the DDM with and without considering Cool Pavement (CP) in the street canyon.

Table 2 shows the average and highest impact of waste heat releases and cool pavement on the outdoor air temperature in the street canyon and the total sensible cooling load of buildings A, B, C, and D as assessed from the baseline. While waste heat releases appear to increase both the outdoor air temperature and the sensible cooling load, their magnitude looks to be reduced by cool pavement. Even though the result is consistent with expectation on the impact of waste heat releases and cool pavement, their accuracy could have been improved if detailed BEMs had been calibrated against measurements of the cooling load. Unfortunately, no metered data was collected during the experiment conducted by Miguel et al. [16].

Table 2. Average difference (Avg. diff.) and peak difference (Peak diff.) between the baseline and scenarios comprising Waste Heat Releases (WHR) and Cool Pavement (CP).

Scenario	Air Temperature		Sensible cooling load	
	Avg. diff. (K)	Peak diff. (K)	Avg. diff. (kW)	Peak diff. (kW)
WHR	0.25	0.67	1.78	4.69
CP	-0.34	-1.15	-3.90	-16.67

5. CONCLUSION

This study explained how interactions between buildings and their outdoor conditions can be simulated using a coupling between detailed BEMs and a data driven UCM. The DDM was trained and tested using measurements of outdoor air temperature and humidity collected in Singapore by Miguel et al. [16]. The DDM was also used to observe the impact of waste heat releases and cool pavement on the outdoor air temperature of the street canyon and the cooling consumption of buildings.

One result was that the DDM predicts the outdoor air temperature with a similar accuracy than the physically-based model validated by Miguel et al. [16] using the same input and test data. At the same time, it was shown that the DDM predicts the outdoor air temperature with a higher temporal resolution than the physically-based model while considering urban morphology with a higher level of detail. It means a DDM is certainly a more appropriate solution to predict outdoor conditions at the neighbourhood scale within a CDT than any physically-based UMM that can be coupled with detailed BEMs.

Another result was that the DDM is capable of predicting the impact of waste heat releases and cool pavement on outdoor conditions of a street canyon, which is a major improvement in comparison to other DDMs described in the literature [4]. This improvement was possible by defining a DDM that is still governed by fundamental principles of heat and mass transfer. Using the same principles, the DDM could easily consider additional sources of anthropogenic heat like traffic or countermeasures to UHIs like vegetation.

ACKNOWLEDGEMENTS

This research has received funding from the European Union's Horizon research and innovation programme under the Marie Sklodowska-Curie grant agreement No 101059484. The data were collected during the Virtual Campus project at the National University of Singapore, which was sponsored by the University Campus Infrastructure and the Office of the Deputy President.

REFERENCES

1. Srivastava, K. (2009). Urbanization and mental health. *Industrial psychiatry journal*, 18(2): p. 75.
2. Niranjan, A. *'Era of global boiling has arrived,' says UN chief as July set to be hottest month on record*. [Online] Available from: https://www.theguardian.com/science/2023/jul/27/scientists-july-world-hottest-month-record-climate-temperatures [27 July 2023].
3. Jamei, E., et al. (2016). Review on the impact of urban geometry and pedestrian level greening on outdoor thermal comfort. *Renewable and Sustainable Energy Reviews*, 54: p. 1002-1017.
4. Quan, S.J. and C. Li. (2021). Urban form and building energy use: A systematic review of measures, mechanisms, and methodologies. *Renewable and Sustainable Energy Reviews*, 139: p. 110662.
5. Schrotter, G. and C. Hürzeler. (2020). The Digital Twin of the City of Zurich for Urban Planning. *PFG – Journal of Photogrammetry, Remote Sensing and Geoinformation Science*, 88(1): p. 99-112.
6. Deng, T., K. Zhang, and Z.-J. Shen. (2021). A systematic review of a digital twin city: A new pattern of urban governance toward smart cities. *Journal of Management Science and Engineering*, 6(2): p. 125-134.
7. Li, X., et al. (2022). Big data analysis of the Internet of Things in the digital twins of smart city based on deep learning. *Future Generation Computer Systems*, 128: p. 167-177.
8. Biljecki, F., H. Ledoux, and J. Stoter. (2016). An improved LOD specification for 3D building models. *Computers, Environment and Urban Systems*, 59: p. 25-37.
9. Deilami, K., M. Kamruzzaman, and Y. Liu. (2018). Urban heat island effect: A systematic review of spatio-temporal factors, data, methods, and mitigation measures. *International Journal of Applied Earth Observation and Geoinformation*, 67: p. 30-42.
10. Li, X., et al. (2019). Urban heat island impacts on building energy consumption: A review of approaches and findings. *Energy*, 174: p. 407-419.
11. Sezer, N., et al. (2023). Urban microclimate and building energy models: A review of the latest progress in coupling strategies. *Renewable and Sustainable Energy Reviews*, 184: p. 113577.
12. Jandaghian, Z. and U. Berardi. (2020). Comparing urban canopy models for microclimate simulations in Weather Research and Forecasting Models. *Sustainable Cities and Society*, 55: p. 102025.
13. Toparlar, Y., et al. (2017). A review on the CFD analysis of urban microclimate. *Renewable and Sustainable Energy Reviews*, 80: p. 1613-1640.
14. Wang, H., et al. (2023). Machine learning applications on air temperature prediction in the urban canopy layer: A critical review of 2011–2022. *Urban Climate*, 49: p. 101499.
15. Grimmond, C.S.B. (2006). The suburban energy balance: Methodological considerations and results for a mid-latitude west coast city under winter and spring conditions. *International Journal of Climatology*, 12(5): p. 481-497.
16. Miguel, M., et al. (2021). A physically-based model of interactions between a building and its outdoor conditions at the urban microscale. *Energy and Buildings*, 237: p. 110788.
17. Anting, N., et al. (2017). Experimental evaluation of thermal performance of cool pavement material using waste tiles in tropical climate. *Energy and Buildings*, 142: p. 211-219.

PLEA 2024 WROCŁAW
(Re)thinking Resilience

Applying Visible Difference Prediction to View Visibility

STEPHEN WASILEWSKI[1] MARILYNE ANDERSEN[1]

[1]École polytechnique fédérale de Lausanne, Lausanne, Switzerland

ABSTRACT: This paper presents a preliminary model for relating the optical characteristics of different dynamic shading systems to the visibility of the view through these systems. View visibility is dependent on the optical properties of the façade, the incident lighting, and the view beyond which makes it challenging to measure and quantify how well a view can be seen through different façade layers. In turn, this makes it difficult to understand how the benefits of a view through a window are preserved or diminished by partially occluding façade layers. Instead of relying on human subjects to confirm the fundamental attributes of human visual perception across a large and diverse range of façade and view scenarios, existing vision models can be leveraged to synthetically analyze these scenarios. Such analysis, which is piloted in this paper, can help link the optical properties of façade systems to what will be visible through these systems. This study finds that one such model, the HDR-VDP-3, appears to correctly respond to the scenarios tested which should help guide future research into criteria for preserving the qualities of a view (whatever they may be) when viewed through façade shading systems.
KEYWORDS: Daylight, Views, Dynamic Facades, View Clarity

1. INTRODUCTION

The currently accepted framework for understanding view quality defines it as a function of content, access, and clarity [1]. View clarity is the property of the window/façade that determines how well an occupant has visual access to the view behind it. While this property is determined by the window/façade, it is dependent on how the view through the façade interacts with the content beyond. View clarity can also vary temporally with changing lighting conditions, both due to dynamic operation and how both the window and view content appear under a particular illumination.

To distinguish from this broad category of clarity that encompasses dynamic façade operation and complex interdependencies, the term *view visibility* is proposed here to refer specifically to *how well an occupant can see the available view*. This property is contingent on both the particular location of the occupant and the particular lighting conditions at the time of the observation. Of course, a solid wall will have no view visibility and a free opening (with no glass) will have perfect visibility, regardless of the view content and lighting conditions.

To refine the meaning of view visibility, we will start from the concept of view clarity, which is characterized by metrics that are typically based on optical properties of the material and are therefore specific to material assemblies. For instance, clarity of specular glazing is a function of transmission and specular reflection. For diffusing material, clarity is a function of near angle (clarity) and wide angle (haze) scattering. For fabric roller shades, the current state of the art is the View Clarity Index (VCI) [2], which depends, after an update, on normal-normal and normal-diffuse transmission [3]. Shading systems with larger scale openings, like venetian blind do not have a standard means of evaluating clarity.

While clear high-transmission glazing will naturally always afford a high-degree of view visibility (so long as the outside is significantly brighter than the inside), other performance and comfort requirements often lead to competing pressures on the transmission properties of a façade. Avoiding glare and heat gain from direct sun while also maintaining daylight and view is the central tension managed by dynamic façade systems including venetian blinds, roller shades, and electrochromic glazing. Each of these systems works to reduce the transmitted light in different ways and, consequently, the degree to which daylight and views are maintained while glare is mitigated vary considerably.

The visibility through electrochromic glazing can be degraded by changes in relative brightness across colors and the changing ratio between the transmitted view and the reflection of the interior (veiling reflections). These effects can be exacerbated if tinting leads to the use of electric lighting. Our ability to see through fabric depends on the openness of the weave (openness factor, OF), diffuse reflection and transmission, and whether an observer is close enough to the fabric relative to the size of the holes to perceive the surface as monolithic or as solid and void. Compared to shade fabric and glazing, exterior venetian blinds are much more angularly selective, capable of completely blocking views above (and below) a certain angle, while maintaining a high degree of openness in between. At typical dimensions, the view through venetian blinds is perceived as a combination of solid and void: beyond the open area, the view through venetian blinds is potentially degraded by “masking effects”, which describe the

A. Close Building | *B. Mixed Height Buildings* | *C. Buildings and Vegetation* | *D. Close Trees* | *E. Trees and Clouds* | *F. Distant Trees*

Figure 1: The six façade environment maps covering a range of view content, skylines, sun positions, and sky conditions.

way the pattern of the blinds interacts with the view content beyond.

This study investigates the suitability of an existing model of visual perception that accounts for these different modes of view degradation to relate view visibility to the physical characteristics of different dynamic façade systems. The objective is to offer a means of comparing systems reliably even when they cannot be concisely described by the same physical parameters, as is the case with the aforementioned façade materials.

2. METHODS

Both the task of and approach towards quantifying view visibility can be framed as a *visual difference prediction* (VDP). VDP models are used in image reproduction to compare the impacts of different artifacts, including those due to rendering, compression, and tone-mapping operators [4]. Such VDP models have the ability to account for low level eye-functions like eye adaptation and retinal receptor response, high-level processing functions like pattern masking and object identification, and combined or intermediate functions like contrast sensitivity, visual acuity, and color appearance. Most models that are referred to as VDP models focus on perceptible changes in achromatic contrast sensitivity, whereas models that account for color are called Color Appearance Models (CAM). CAMs can be used to predict color difference (which generally includes both brightness or lightness, hue and saturation) between two adjacent colors, but do not yet include the necessary spatial dimensions to assess color perception across a complex scene, so are left for future work to incorporate into assessing view visibility. With the growth of High Dynamic Range (HDR) imaging and display, achromatic VDP have been extended to large dynamic ranges and used to compare perception of images within the adaptive environment in which they are viewed, such as HDR-VDP-3 [5, 6]: this model is a "white-box" which means that the mechanisms of visual perception are directly applied (as opposed to "black-box" machine-learning algorithms) and uses a perceptually uniform encoding of luminance that has been validated up to 10,000 cd/m^2 [7]. Together, these features gives it high potential to extend to the novel application of the present study.

In this study, we used this promising HDR-VDP-3 model to compare the view from a room through a façade with different treatments to the identical unobstructed view through the façade openings. Images are generated with simulations using a range of high resolution HDR environment maps to both light the scene and provide highly detailed and realistic views. As shown in Figure 1, all six views include the direct sun incident on the façade, implying that some shading could be necessary. The process needed for capturing and preparing the HDR environment maps (with calibrated luminance, color, and accurate solar source without lens flare) is part of an ongoing study and will be published separately. These view images are used as the input for analysis, simulating a human observer in the space directly, rather than looking at the images.

In total, 11 different façade variants of three different systems are evaluated. The systems include clear and electrochromic glazing at three transmission levels, interior fabric roller shades at two openness levels and two fabric colors, and exterior venetian blinds at four tilt angles. Note that the material model for fabric roller shades used in this study required an ad hoc development, which will be described in a separate publication as well. The 11 systems are:

- *Clear*: Glass 80% VLT
- *EC6:* Electrochromic Glass 6% VLT
- *EC1:* 1% VLT
- *Dark 8%:* Fabric with 8% OF, 10% VLR, and 6.8% VLT
- *Dark 4%:* 4% OF, 10% VLR, and 4% VLT
- *Light 8%:* 8% OF, 35% VLR, and 9.8% VLT
- *Light 4%:* 4% OF, 35% VLR, and 7% VLT
- *Blinds 0°:* 10 cm flat blinds with 30% VLR
- *Blinds 15°:* rotated 15°
- *Blinds 30°:* rotated 30°
- *Blinds 45°:* rotated 45°

2.1 Simulation

The simulated model is a replica of a mock office test chamber with a south facing window, with a specific framing geometry (six window parts, one of which has a thicker frame). This model was selected to enable future studies validating the accuracy of the proposed simulation approach that would include physical measurements and human subject studies. In this approach, a color–and luminance–calibrated fisheye HDR image taken from the perspective of the façade is used as the view out and source of

illumination. Using *Radiance*, the HDR image represents sky and ground as seen from the façade. The direct sun is extracted from the HDR and modelled as a light source to accurately capture shadow rays. Figure 2 describes the components of the simulation model. Material reflectance for all interior surfaces were taken from previously collected measurements.

Along with the reference scenario, which is simulated with no glazing (or any other material) in the window openings, 11 different façade system variants were simulated for all six view environments shown in Figure 1 from a single point located 1.5 meters from the façade. The images were rendered at 6000 pixels wide and then filtered to 3000 pixels which preserves the maximum resolution of the environment maps and exceeds by 1.5 times the acuity of 6/6 (20/20) vision. This is important so that the visual difference prediction can account for these fine scale details. Each variant was also simulated with two electric lights within the room capable of providing a median 300 lux across a horizontal work plane at 1 meter above the floor (which was simulated for all sources as a 50 cm grid). For each image, whenever the daylight alone does not provide 300 lux illuminance in the back half of the room, the light from the rear electric light is added at the minimum of 25, 50, 75 or, if needed, 100% so as to provide 300 lux and maintain functional light levels across all variants. Then, if the rear light and daylight are not enough to provide at least 300 lux to the front half of the room as well, the front electric light is added too, again at the appropriate (minimal) dimming level to achieve 300 lux. This is to account for the fact that the less transmissive systems, like EC1, will realistically need supplemental electric lighting, which could contribute to veiling reflections on the façade and thus should be accounted for when evaluating a given system's *view visibility* potential.

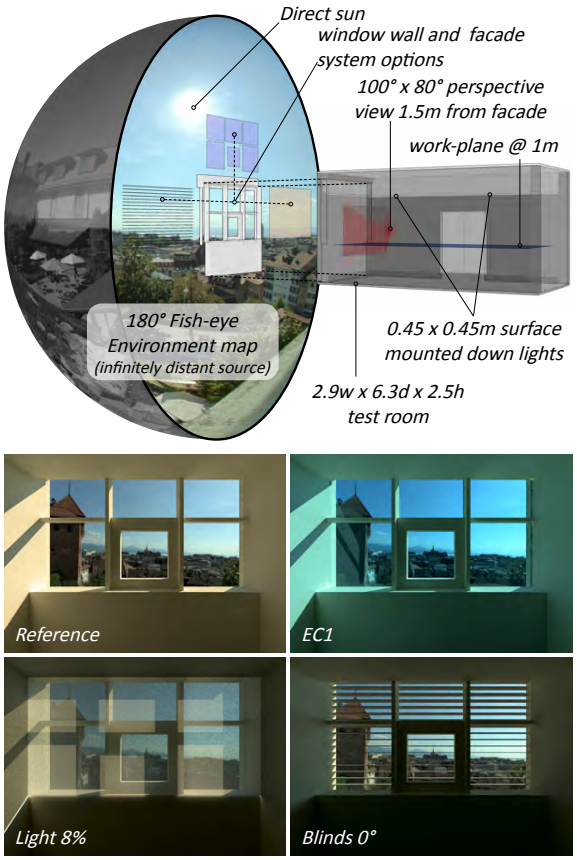

Figure 2: Exploded schematic of the simulated scene and example result renderings, one for each of the three system types tested and the reference.

2.2 Evaluation

Version 3.0.7 of HDR-VDP-3, implemented in *Matlab* was used to perform the contrast detection and visual difference prediction. The software performs several different "tasks". The "side-by-side" task, which is intended to compare two images next to each other, was chosen as the closest match to this application. The process by which the model is applied in this study is outlined in Figure 3. After simulating both the reference and test conditions within the same environment (1), a virtual observer is visually adapted to the visual environment present in each case (reference and test separately) and the detectable details across each scene are identified (2A,B). Here, "visually adapted" means that the range and sensitivity of the model eye (pupil, photoreceptors) is set to match the likely state of a human observer in that environment. Then, these contrast detection maps from the test and reference data can be compared (indicated with a star in the figure) to identify which visible details in the reference will be perceptible in the test image (3). Only considering the differences within the free view area, HDR-VDP-3 outputs the probability of detecting a difference: what is reported here is the complement (one minus the probability), which we intepret as the degree to which the images are the same. The visible details in the view are preserved so long as the relative contrast remains high, and visible details introduced by the facade (such as the lines of blinds, the patches of sun visible on shades, and the fabric weave), do not mask the perception of the reference view. This prediction of pixel by pixel view visibility (3) is multiplied by the reference contrast (2B), leading to a weighted prediction of view visibility (4), which can be summed into an single value for the scene, expressed as a proportion of perfect visibility. The idea behind this weighting, which is perhaps self-evident, is that the visible details in a view are those necessary to preserve, whereas areas of the view without visible contrast can be obscured without degrading the overall perception of the view content. In other words, hiding what is visible is more consequential than hiding that which already cannot be seen. To match

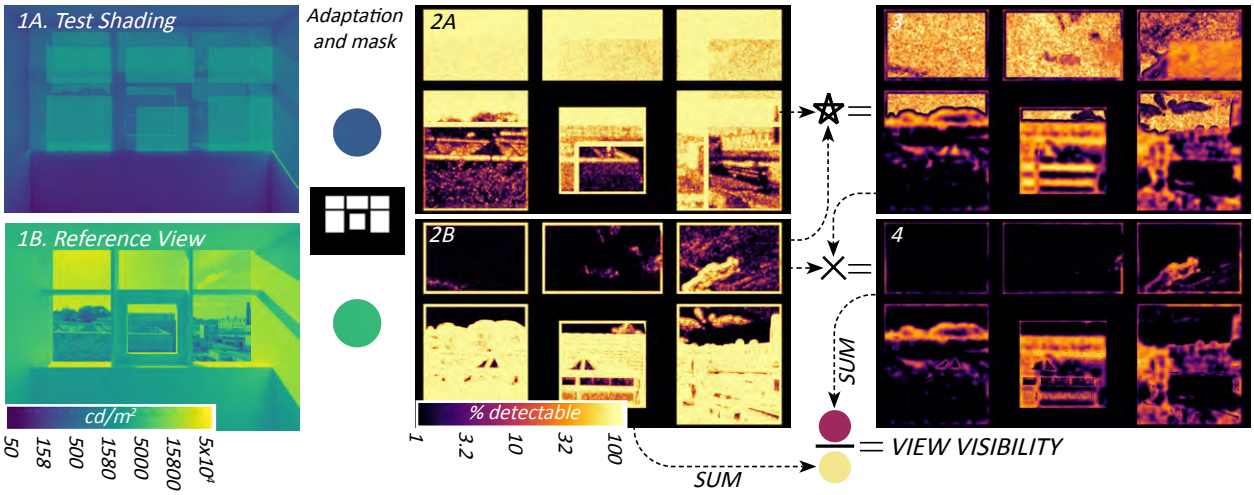

Figure 3: Overview of the visual difference prediction process. The Left images shows simulated luminance, the central detectable contrast, and the right the similarity between test and reference (see text). The final view visibility is the sum of the pixel values in image 4 divided by the sum of 2A, which yields the percentage of visible contrast in the reference view likely to be visible through the test façade.

this intuition to the model output, the *sensitivity_correction*, described in the model's documentation as the main adjustment parameter, was set to -1.0, meaning the contrast and difference sensitivity was reduced by a factor of 10. This value established the clearest hierarchy of the major scene details, where dominant elements in the scene, like the skyline, were highlighted much more than smaller scale details like leaves, or wispy clouds.

While Figure 3 shows the detectable contrast (2A,B) merged across frequency bands (how quickly the image is changing across pixels), the model operates on a range of frequencies independently. The HDR-VDP-3 model accounts for the different contrast sensitivities across these bands and includes the masking effects that interfering patterns can have on our ability to accurately reconstruct scene detail in the brain based on the signals received from the eye. Preliminary results were found to be far too sensitive to low frequency changes, with nearly identical images yielding vastly different results, so the *ignore_freqs_lower_than* option was used to stabiize the results.

3. RESULTS

Figure 4 shows the weighted contrast detection of some of the tested shaded systems for portions of a selection of the views to qualitatively evaluate the models responsiveness to the different ways the included scenarios reduce view visibility.

Scene A (see Figure 1) affords a close view across a narrow street to a building. The visible details are of a high contrast compared to the other scenes and are also predominantly rectilinear. The sun strikes the façade from a high incident angle and is filtered through light cloud cover. Because many of the detectable edges are horizontal lines, this scene is the worst performing for all the venetian blind scenarios. As seen in the contrast map for *Blinds 0°*, many of these horizontal details are occluded or masked by the horizontal blinds. Conversely, this is the best performing scene for both light shade scenarios. The relatively weak sun does not cause much veiling illumination, and the high contrast details of wall to window means that even with the contrast loss from the shade fabric, most detail is still readily visible. For shade fabric, greater openness matters more than color, with the *light 8%* outperforming the dark *4%*.

Scene C contains a mix of vegetation, buildings and sky. For this scene, *blinds 30°*, *dark 4%*, and *light 8%* all get similar overall view visibility scores, however the contrast maps in Figure 4 reveal that where and how the view is degraded vary considerably. The blinds preserve the views to the vegetation very well, even allowing for some reconstruction across the individual slats. The building elements are moderately well preserved, although similar to scene A, the horizontal details are lost. Because of the slat angle, the view to the sky is almost entirely blocked, and very little of the clouds remains visible. The *dark 4%* openness shades do not preserve the dark vegetation as well as the blinds but do a better job preserving the views of the buildings. While the *light 8%* fabric preserves the most detail of the cloud in the upper right and the view through the shades that are not directly illuminated by the sun, there is more severe contrast loss behind the directly illuminated fabric, especially in front of trees.

This veiling illumination is even a problem for the *dark 8%* fabric when the background is dark and the sun is strong, such as **scene D**. While the trees are mostly visible wherever the fabric is shaded by the mullions, almost nothing is visible through the directly illuminated fabric. Scene D is the only scene where the electrochromic glazing scenarios exhibited significant view visibility loss: because of the bright sun and dark view content, even at 6% VLT the sun illuminating the interior wall causes some veiling reflections that

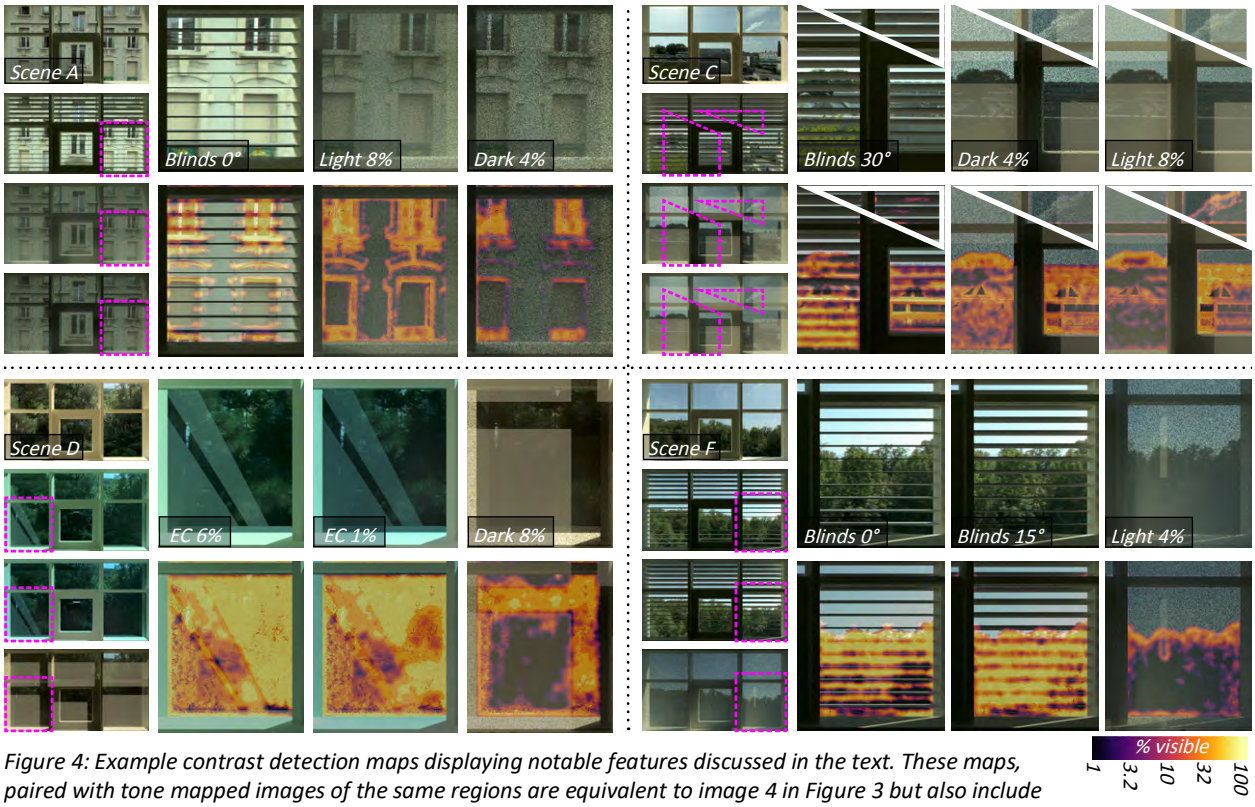

Figure 4: Example contrast detection maps displaying notable features discussed in the text. These maps, paired with tone mapped images of the same regions are equivalent to image 4 in Figure 3 but also include the tone-mapped pixels as background. The reference condition (no glass or other obstruction beyond the mullions on the façade) is shown above the three featured facades for each scene with callout box indicating the section(s) of the view shown.

reduce the contrast of the view to the trees (visible in the lower left of the *EC 6%* map in Figure 4). At *EC 1%*, these veiling reflections also include the other walls of the room, which, because of the low daylight levels through the 1% glazing, are illuminated with electric lights to maintain sufficient indoor lighting levels.

Scene F yields the highest view visibility for all but the light fabric shades and *EC 1%*. In both of these cases, there is too much loss of contrast due to veiling in front of the dark trees, even though the sun strikes the façade from a high angle. Interestingly, the *blinds 15°* outperform the *blinds 0°* for this scene, even though according to any geometry-based analysis, the horizontal blinds would have a higher view openness. This is driven by two things. First, most of the scene detail is below the horizon line where the two blind positions have nearly equivalent view factors. Second, at 0° the tops of the blinds are visible, creating high contrast edges with the dark trees behind that tends to introduce a stronger masking effect.

Figure 5 plots the view visibility for all 11 scenarios and six scenes. Three scenes, A, D and F, are overlayed as line plots to show where we can see a change in relative performance between the scenes for each scenario. Generally, the view visibility predicted from the HDR-VDP-3 model aligns with our experience. Clear glazing, even at low transmission, will afford by far the best view compared to fabric shades and blinds, but is still susceptible to contrast loss dues to veiling reflections. Shades with darker fabrics generally preserve views better than lighter fabrics, especially when lower angle, high-intensity sun is directly incident. Shades with higher openness factors always preserve view better when the fabric is the same. Venetian blinds that are more open to the view beyond are likewise going to afford better visibility, but the ideal angle will depend on where, in the field of the view, most of the relevant view content resides.

For comparison, Figure 5 also plots, as Xs, the geometric view visibility calculated as the percentage of direct view rays that will transmit through each façade system from the same view point. Clear glazing will always have 100% visibility for any transmission greater than zero. The fabric roller shades generally outperform their geometric openness, while venetian blinds underperform theirs. As blinds also provide a smaller cutoff angle, there is a greater reduction in free area visible in a real perspective view compared to a flat parallel accounting of view openness.

These comparisons, both within system and accounting for visual perception mechanisms, are already applicable as an image processing tool to complement other tone-mapping and qualitative rendering techniques.. However, calibration against human subject data will be important future work in order to develop robust numeric quantities to compare across façade system type. While we might expect intuitively that fabric roller shades and venetian blinds will perform similarly, the HDR-VDP model has only been calibrated to viewing images with certain types of introduced degradations, which may

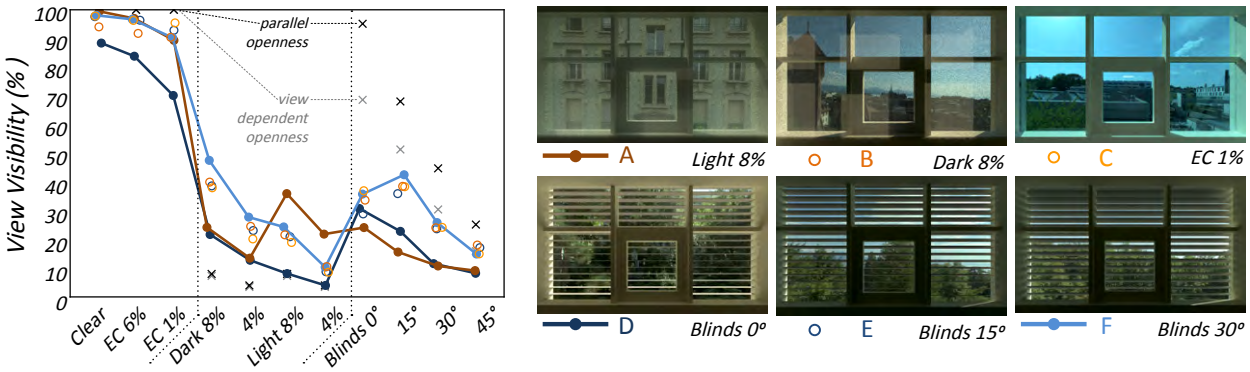

Figure 5: View visibility across the six tested environments for each of the 11 facades. Lines A, D, and F trace the visibility of these three scenes across the different facades revealing how different view content and lighting conditions lead to different relative performance between façade types and properties. The Xs indicate the geometric view visibility for each façade. Each view is shown with a relatively well performing façade.

not directly align with the degradations introduced by the subject and process used in this study.

4. CONCLUSION

This study explored an original application of an existing visual difference prediction model to evaluate the newly introduced concept of *view visibility*, i.e. the extent to which the main features of a view out may be preserved when filtered through a given façade system. Three different commonly used dynamic façade systems – venetian blinds, fabric shades and electrochromic glazing, for various configurations each – were tested on six different view environments for this purpose, leading to an interesting distribution of view visibility values, with general trends following intuition and a strong potential to robustly compare view preservation across scenarios. A visual analysis of the different output contrast detection maps also revealed that the model properly accounts for adaptation across visual environments, loss of contrast due to veiling, and masking due to pattern interference. With calibration through controlled human participant experiments, such a model shows promise to enable the direct comparison of view visibility across façade systems, thereby aiding in the development of a generalizable view visibility metric. In particular, the relative visibility loss due to the screened view through shades needs to be balanced with the loss due to masking effects from larger scale patterns like venetian blinds. Compared to a geometric approach to view visibility, the results of this study are more aligned with both our intuition and experience looking through these systems, suggesting that this approach warrants further investigation.

View visibility is a critical component in the chain connecting building occupants to the outside world and is the link that architects and other building industry practitioners often have the greatest control over. This preliminary study already suggests how different view content may imply different relative success of dynamic façade systems. For instance, that electrochromic glazing will not perform as well when the view is mostly not sky and/or mostly objects with low reflectance. Likewise, lighter fabrics with greater diffuse transmission may be a better choice when the view is mostly towards other buildings, but a darker fabric may better preserve views to trees and sky.

This research should help set up future studies to directly compare a given façade system's ability to maintain view while also investigating other key daylight performance criteria, such as glare, daylight availability, or potential to induce physiological effects and/or influence circadian rhythms.

ACKNOWLEDGEMENTS

This research was funded in whole or in part by the Swiss National Science Foundation (SNSF) 197178.

REFERENCES

1. Ko, W.H., M. Kent, S. Shiavon, B. Levitt, and G. Netti, (2021). A Window View Quality Assessment Framework. *LEUKOS*, 18: p. 268-293.
2. Konstantzos, I., Y-C. Chan, J.C. Seibold, A. Tzempelikos, R.W. Proctor, and J. B. Protzman, (2015). View clarity index: A new metric to evaluate clarity of view through window shades. *Building and Environment*. 90: p. 206-214.
3. Flamant, G., W. Bustamante, A. Tzempelikos, and S. Vera (2022) Evaluation of view clarity through solar shading fabrics. *Building and Environment*. 212: p. 108750.
4. Mantiuk, R., S.J. Daly, K. Myszkowski and H.P. Seidel, (2005). Predicting visible differences in high dynamic range images: model and its calibration. *Human Vision and Electronic Imaging X*. 5666: p. 204-214.
5. Mantiuk, R., K.J. Kim, A. Rempel and W. Heidrich (2011). HDR-VDP-2: a calibrated visual metric for visibility and quality predictions in all luminance conditions. In *ACM SIGGRAPH*.
6. Mantiuk, R., D. Hammou and P. Hanji (2023). HDR-VDP-3: A multi-metric for predicting image differences, quality and contrast distortions in high dynamic range and regular content. *Preprint.* DOI:10.48550/arXiv.2304.13625
7. Mantiuk, R. and M. Azimi, (2021) PU21: A novel perceptually uniform encoding for adapting existing quality metrics for HDR, *2021 Picture Coding Symposium (PCS)*, Bristol, United Kingdom.

PLEA 2024 WROCŁAW
(Re)thinking Resilience

Framework and validation of a new LCA tool for buildings in the Latin America region.

Case study: Screening LCA of a bioclimatic house in a hot-dry climate

VÍCTOR ALBERTO ARVIZU-PIÑA[1], ITZIA GABRIELA BARRERA ALARCÓN[2], MARIANA ABIGAIL CARMONA GUZMÁN[1], EDWIN ISRAEL TOVAR JIMÉNEZ[3], CARLOS J. ESPARZA-LÓPEZ[4], LUIS ARTURO VARGAS ROBLES[3]

[1]Universidad Iberoamericana Ciudad de México, Ciudad de México, México.
[2] Centro de Investigación en Ciencias e Información Geoespacial, Ciudad de México, México.
[3]Universidad Iberoamericana León, León, México.
[4]Universidad de Colima, Colima, México.

ABSTRACT: Several Life Cycle Assessment (LCA) tools have been generated seeking to facilitate its application in buildings. However, most of them are focused on Europe or the US, leaving aside the Latin American region. This paper presents part of the results published in the article 'An open access online tool for LCA in building's early design stage in the Latin American context. A screening LCA case study for a bioclimatic building', where a new LCA tool for buildings in Latin America is presented and validated. It is analyzed how this software (EVAMED) addresses the requirements established in the literature for LCA tools in early design phases. A screening LCA of a bioclimatic project is presented as a case study. A validation has been made by comparing the results obtained with those of a commercial software. The difference between both tools does not exceed an average of 40% considering various environmental impact categories. The results show EVAMED covers several of the requirements established for LCA tools for buildings early design stages, like the use of regional and international databases and the BIM-LCA integration. Bioclimatic strategies achieve a 30% reduction in the carbon footprint of the case study.
KEYWORDS: BIM, LCA, Early design stage, Screening LCA, Building assessment tool.

1. INTRODUCTION

Life Cycle Assessment (LCA) is a methodology that has been widely accepted to evaluate and, eventually, improve the energy and environmental performance of buildings. Its application is increasing into the normative and legislative schemes of various countries, mainly in the European region [1]. Although LCA in buildings entails certain methodological and practical application difficulties, various tools have been generated to facilitate its application [2]. However, most of these tools have been concentrated in the European and North American context, leaving aside the Latin American region [3].

This paper presents part of the results published in the article 'An open access online tool for LCA in building's early design stage in the Latin American context. A screening LCA case study for a bioclimatic building' [3], where a new LCA tool for buildings in Latin America, called EVAMED, is presented and validated. The main objective of this tool is to assist the building sector stakeholders, mainly in Mexico and the rest of Latin America, from the first design phases, to create buildings with a lower environmental impact throughout their whole life cycle. Some of the main features of this tool are the following:

- Friendly interface and oriented to a non-LCA expert user.
- Automation in the Bill of Quantities (BoQ) through a Revit model.
- Possibility of performing screening and simplified LCA from the early design phases.
- Suggestion of construction systems based on the geometry modelled in Revit (LOD 200).
- Building materials database, not just international, but from Mexico and Latin America.

Because the objective is that this tool can be useful from the first design phases, it contemplates a BIM-LCA integration. Although it considers the life cycle phases that an LCA screening requires (A1-A3, B6), it also contemplates other stages, such as construction (A3-A4), replacements (B4) and deconstruction (C1).

The first advances in the development of this tool were presented at PLEA 2022, where the usefulness of the tool to calculate the carbon footprint of building materials (stages A1-A3) during the design phase was

shown [4]. Now, this paper presents the validation of the software and a case study that includes the use phase of a bioclimatic building is presented (Screening LCA).

1.1 EVAMED framework

EVAMED is based on a series of algorithms that implement the calculation logic of the LCA methodology. It is based on the life cycle phases and the modules defined in the EN 15978 standard. The EVAMED framework can be divided into 4 general parts:

1. Design proposal. Revit is the program used to establish the link with the BIM environment. It is also possible to use other CAD modeling software, although without being linked to the tool.
2. Bill of Quantities (BoQ). For simplified 3D models (LOD 200) a plug-in developed in DYNAMO is used to calculate and propose different options for construction systems to the user. For detailed 3D models (+LOD 300) the plug-in reads the material information specified by the user. In case of not using Revit, the user can perform the BoQ manually using a predefined xlms spreadsheet. In all cases, an Excel file is generated and imported into the tool.
3. LCA calculation. The calculation algorithms of the EN 15978 standard are used, and the life cycle phases indicated in figure 3 are considered. The MEXICANIUH, EPDs and Ecoinvent databases are used.
4. The results are shown through different types of graphs. The user analyzes the results and assesses the need to make adjustments to the analyzed building (fig. 1).

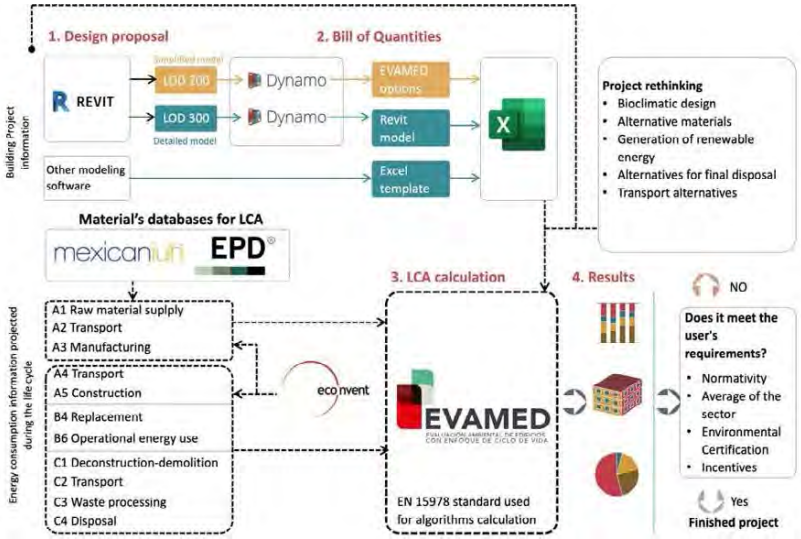

Figure 1: EVAMED framework

2. METHODS

The validation process of the tool was carried out in two ways: (1) validation of the functionalities as a useful tool during the first building design phases and (2) validation of the results of the calculations of potential environmental impacts. For the first validation, an analysis of the features proposed by Meex et.al. [2] for LCA tools useful for the first design phases was carried out, where a series of basic requirements that an LCA tool should meet to be useful from the early design phases are proposed. These requirements are divided into four axes: (1) data-input, (2) calculation, (3) output, and (4) usability in the design process. For the second validation, a comparative analysis of the results obtained from the case study, with EVAMED and a commercial software (One Click LCA) is made. Due to the complexity of the LCA methodology, this comparison focuses on the general results, without going into a detailed analysis of their causes, which is beyond the scope of this paper. The work of A. Kamari, B., et.al. [5] is also used as a reference, since they also use One Click LCA to compare results with a new LCA software developed by the authors.

A case study of a social housing prototype in a hot-dry climate of northern Mexico is presented. This housing project is part of a research carried out by Marincic Lovriha, Ochoa de la Torre, & Alpuche Cruz [6], in which bioclimatic strategies are implemented and analyzed. These strategies have a positive impact in the use phase by minimizing the energy requirements, but how do they influence their embodied carbon footprint? EVAMED tool is used to give an insight in this regard. A screening LCA is implemented, so just phases A1-A3 and

B6 are analyzed, and only the carbon footprint is considered. Thus, two houses are analyzed: the reference house with conventional design and materials, and the bioclimatic house with design strategies and alternative materials to minimize energy needs during its use phase. One square meter of construction is used as a functional unit. A thermal simulation was carried out by Marincic Lovriha, Ochoa de la Torre, & Alpuche Cruz [6] to obtain the energy demand during the use phase of both houses, established in 50 years. The TRNSYS Simulation software Studio version 16 was used.

3. RESULTS

3.1 Usefulness as a useful tool during the early design phases

Data-input

According to Meex et al. [2], data input should be fast, limited, and consistent with the design phase. For EVAMED, the data input could be divided into three parts: general information of the project, BoQ for the production phase (A1-A3), and life cycle configuration of the project. For the first one, general information of the project is defined: type of project (housing, business, office, etc.), location, construction area, habitable area, number of levels and useful lifetime. For the BoQ input EVAMED considers three options:

- *Manual*. Users can download a template file in xlsm format that can be filled selecting the construction materials that are preloaded in the EVAMED database. This file can be loaded into the tool.
- *Automated for LOD 200 Revit models*. When user has modeled just a basic geometry (like a box), without specifying materials or construction systems, an xlsm file can be generated with the quantification of different construction systems, calculated from that modeled basic geometry. Different options of construction systems are generated for each element of the envelope. To carry out this BoQ, a Plug-in has been developed with programming in Python and Dynamo. The calculation methods and formulas for the quantification of each construction system are based on the Complementary Technical Standards of the Construction Regulations for Mexico City.
- *Automated for LOD +300 Revit models*. When the user has specified construction materials in a Revit model, a file with an xlsm extension can be generated with the BoQ and BoM (Bill of Materials). This file can be uploaded to EVAMED.

Regarding the life cycle configuration, is carried out through a wizard-type process of four general stages: (1) production; where the user is shown the quantification of materials loaded with the xlsm file; (2) construction, (3) use and (3) end of life, where information on energy consumption is requested from the user. Figure 2 shows an example of the interface during project configuration (input data).

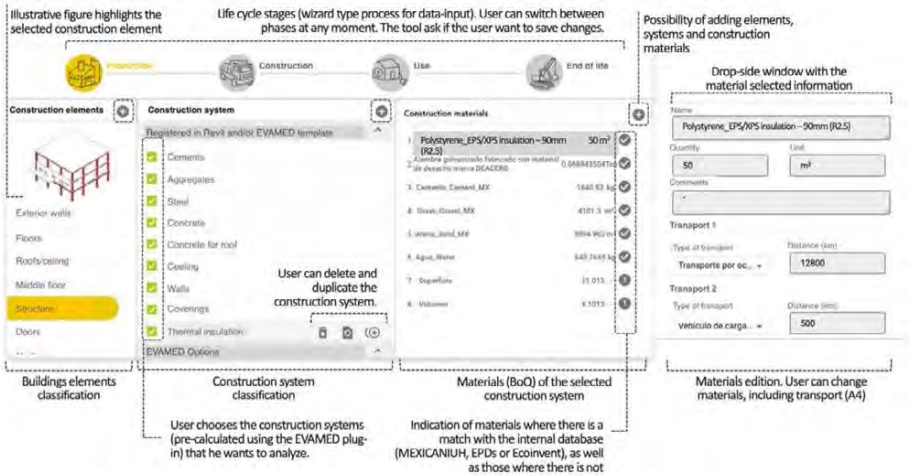

Figure 2. Project configuration view (wizard-type process)

Calculation

Meex, et.al. [2] divides the methodological framework into three sections:

- *Methodological and calculation choices*. All methodological decisions must be pre-programmed in the tool, ready to be used by the user, especially for the early design phases. For EVAMED, the environmental impact categories and the algorithms of the standard EN 15978:2011 are considered. The basic principle of the environmental impacts'

calculation consists of multiplying the total amount of each product or service with its respective unitary environmental impact.

- *Scope of the assessment*. A holistic approach that considers the environmental impact assessment of materials and the calculation of operational energy demand is desirable in an LCA tool for buildings. At this point in the EVAMED development, the analysis of energy demand must be carried out externally. However, the user can enter the energy consumption of the use phase manually.
- *Time-investment*. Because in the early design phases of a building the objective is to evaluate different design and materials options, the time invested must be kept as low as possible. Modifications can be made directly in the tool, either in the BoQ or at some stage of the life cycle. The results are displayed in real time, although it is necessary to switch between the configuration and the results view.

Output

It is necessary to present the results in a clear and easy way so the users can interpret them. Using charts is preferable to long and detailed reports [2]. Since in the early design phases of a building the objective is to evaluate different design and material options, the time invested should be as low as possible. It is also desirable to use reference values (benchmark) so that the user can easily assimilate the environmental impact of his project with respect to other similar buildings. However, not all countries have enough information to establish these benchmarks. EVAMED presents the results in three levels of detail: (1) by life cycle stages, (2) by construction elements and (3) by construction materials. All the graphs are interactive, so the user can explore different levels of detail.

Usability in the design process

This section can be divided into two parts:

- *Adaptability & flexibility*. All data should be adapted to the design stage, easy to review or change without loss of data and that alternative solutions should be easily created and tested in parallel within the application. A parametrized input of the data for calculation is desirable [2]. In EVAMED the user can make parametric modifications directly in the project configuration section, at any stage of its life cycle. In case of choosing to modify the geometry of the 3D model in Revit, it is necessary to generate a new Excel file with the BoQ and import it into EVAMED.
- *Comparison & feedback loops.* According to Meex et al. [2], a comparison with a reference point or a target value would be desirable, as well as to compare multiple variants of their own design project. Another requirement is that high impact elements of the building, should be clearly indicated, preferably in a visual way (e.g. by means of green-red color scales) so that users can see which building parts have the largest optimization potential. In EVAMED these suggestions are addressed. Comparisons can be made between the results of different projects and/or versions of the same project, for example, between a baseline and various modified options. Also, for the construction elements results, an illustrative figure of a building is used to show where the environmental impacts are concentrated.

3.2 Validation of the tool

To validate the calculations, two building houses have been modeled in EVAMED and One Click LCA: one with conventional design and materials (reference), and another with bioclimatic strategies and alternative materials (bioclimatic). Orientation, proportion, solar protection on doors and windows, and use of insulating materials are some of the design strategies considered for bioclimatic housing.

Table 1 shows the results of the reference building with both software. Although One Click LCA presents, on average, lower environmental impacts for the production (A1-A3) and use (B6) phases, with -40% and -15% respectively, none of the environmental impact categories exceeds +- 67% difference between both software. For the production phase, the smallest difference is in the Global Warming category (-12%), while for the use phase, the smallest difference is in the Abiotic Depletion Potential category (-4%). On the other hand, the work of Kamari et al. [5] reports that One Click LCA has an average of +31% more environmental impacts for the production phase, with the Ozone Depletion Potential category presenting the greatest difference with +224%.

Table 1: Comparison of the LCA results delivered by EVAMED and One Click LCA

Environmental Impact Category		EVAMED (1)			OneClick LCA (2)			Difference 2 to 1		Difference reported by [8] (A1-A3)
Impact category	Unit	A1-A3	B6	Total	A1-A3	B6	Total	A1-A3	B6	
ADPe	kg Sbe	3.09E+01	1.19E-01	3.10E+01	Not reported			-	-	Not reported
ADPf	MJ	7.35E+04	2.71E+06	2.78E+06	3.89E+04	2.61E+06	2.65E+06	-47%	-4%	-11.5%
GWP	kg CO2e	1.04E+04	1.37E+05	1.47E+05	9.10E+03	1.69E+05	1.78E+05	-12%	-23%	-30.1%
ODP	kg CFC11e	4.77E-04	2.03E-02	2.08E-02	2.17E-04	1.62E-02	1.64E-02	-55%	-20%	224%
AP	kg SO2e	3.90E+01	1.76E+03	1.80E+03	1.28E+01	6.57E+02	6.70E+02	-67%	-63%	-26.7%
EP	kg PO4e	2.84E+00	1.11E+02	1.14E+02	2.27E+00	9.77E+01	1.00E+02	-20%	-12%	0.2%
WSP	m^3	4.48E+01	-	4.48E+01	Not reported			-	-	Not reported
POCP	kg C2H4e	1.87E+00	9.79E+01	9.98E+01	Not reported			-	-	32.9%
Average								-40%	-15%	31%

ADPe: Abiotic depletion potential (ADP-elements) for non fossil resources, ADPf: Abiotic depletion potential (ADP-fossil fuels) for fossil resources, GWP: Global Warming Potentia, ODP: Ozone Depletion Potential, AP: Acidification Potential, EP: Eutrophication Potential, WSP: Water Scarcity Potential, POCP: Photochemical Oxidation Potential

The comparative analysis shows that EVAMED presents fewer differences with One Click LCA, compared to the software developed by Kamari et al. [5]. However, it is necessary to mention that in both cases, the differences may be due to the different databases considered in the respective software. Although the three-software use EPDs as the main source of information, the results can vary significantly due to the different EPDs considered and selected by users in each tool [5].

3.3 Screening LCA results

By life cycle stages

The results show that the bioclimatic house has a lower carbon footprint with 2.92E+03kg CO_2 eq/m^2 vs 4.15E+03 kg CO_2 eq/m^2 of the reference house. Not just the use phase of the bioclimatic house has a lower carbon footprint, but also the production phase (table 3).

Table 3: Global Warming Potential (kg CO2 eq/m^2)

	Reference	Bioclimatic
Production phase	2.92E+02	1.90E+02
Use phase	3.86E+03	2.73E+03
Total	**4.15E+03**	**2.92E+03**

By building elements

Exterior walls have the highest environmental impact in the reference house, while in the bioclimatic house there are the fourth position. The roof is the element that has the greatest carbon footprint in the bioclimatic house. The graphs shown by EVAMED are presented by percentage, with a color scale from dark-brown to yellow-green (although it is also possible to know the exact amount of emissions from each construction element). In addition, a representative figure of a building is shown where each element (foundation, exterior walls, interior walls, roof, etc.) is represented by the same color as the graph. The objective is that users be able to quickly visualize where the environmental impacts are concentrated, rather than knowing the exact emissions amount. The user can interact with the graph by clicking on the labels of the construction elements to highlight them in the graph and in the figures (fig. 3).

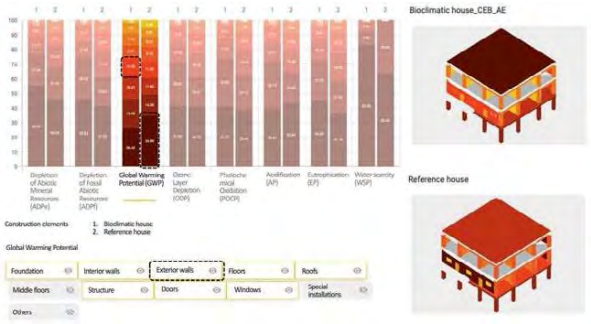

Figure 3: Environmental impacts by building elements

4. CONCLUSIONS

Numerous studies have been developed on the implementation of LCA in the building sector. The parametric approach and BIM-LCA integration are the main approaches suggested by studies to bring LCA closer to decision makers during the early phases of the design process. Most of the existing LCA tools have been focused on regions of Europe, Asia and the USA, leaving the Latin American region out of reach. EVAMED is a tool which main objective is to contribute to the paradigm shift of sustainable building in Mexico and Latin America.

Although the requirements established by Meex et al. [2] for LCA tools for buildings in the early design phases are mainly intended for European countries, EVAMED considers several of these requirements. The

validation analysis showed that One Click LCA presents an average of 40% more environmental impacts than EVAMED in the production phase. Regarding the Production phase in the Global Warming category, EVAMED presents an average of 15% more CO2 emissions, compared to the results of One Click LCA. This difference is less than the one presented by Kamari et al. [5], who shows a difference of +621% with One Click LCA. However, it should be noted that these differences between software depend a lot on the specific EPDs considered in each tool, as well as other input data considered for other the life cycle stages (transport, machinery, energy sources, etc.).

The case study results showed that the bioclimatic design strategies not just managed to reduce the carbon footprint of the use phase by 28%, but also the production phase by 25%. Most of the proposed bioclimatic strategies are related to design, rather than to the implementation of additional construction elements (for example, solar protections). The change from industrialized materials (hollow cement block) to handmade ones (Compact Earth Block) also helped not to increase the embodied carbon footprint.

4.1 Limitations and future work

Two main limitations of this first version of EVAMED can be detected compared to other LCA-BIM software, however, this does not prevent its operation:

- *Does not provide real-time feedback on environmental impacts due to design changes.* Because EVAMED is an external tool to any BIM software, design changes are not reflected in real time in environmental impacts. This could slow down the practitioner workflow. However, if there is a modification to the Revit 3D model, a new Excel file with the actualized BoQ can be generated and imported into EVAMED. The user can also manually modify the BoQ directly in the tool, and the new environmental impacts can be analyzed.
- *Does not offer suggestions/alternatives to improve environmental performance*. It does not use optimization algorithms to propose solutions, however, it is possible to visualize, in a building schematic figure, the construction elements with the greatest environmental impact in each category considered (global warming, eutrophication, etc.). This allows the user to quickly detect where to focus efforts to improve the environmental performance.

Beyond the aforementioned technical aspects, an important step for the development of EVAMED (and for any LCA tool for buildings), is its adoption by architects, builders and designers. For this, the incorporation of the life cycle approach within the normative and legislative scheme of the construction sector in countries like Mexico is essential. As the life cycle approach becomes a requirement for new construction and renovating existing buildings, tools like EVAMED may evolve and be incorporated into the workflow of building practitioners.

ACKNOWLEDGEMENTS

The authors thank the National Laboratory of Sustainable Housing and Communities for providing the information related to the case study presented, as well to CADIS for providing the MEXICANIUH database, and the students who have been involved at some point in the project. This project is funded by the Research Department (Dirección de Investigación) of the Universidad Iberoamericana Ciudad de México.

REFERENCES

1. Arvizu-Piña VA, Cuchí Burgos A. (2017). Promoting sustainability in Mexico's building sector via environmental product declarations. International Journal of Life Cycle Assessment. https://doi.org/10.1007/s11367-017-1269-z.
2. Meex E, Hollberg A, Knapen E, Hildebrand L, Verbeeck G. (2018). Requirements for applying lca-based environmental impact assessment tools in the early stages of building design. Build Environ. 2018;133 January:228–36.
3. Arvizu-Piña VA, Armendáriz López JF, García González AA, Barrera Alarcón IG. (2023). An open access online tool for LCA in building's early design stage in the Latin American context. A screening LCA case study for a bioclimatic building. Energy Build. 2023;295 September.
4. Arvizu-Piña VA, García González A, Tortolero Baena A, Arce Anguiano RR, Carmona Guzmán MA, Gazulla Santos C, et al. (2022). Calculating the carbon footprint of different construction options during the building design phase in the Latin American context. The EVAMED case study. In: PLEA STGO 2022. Will Cities Survive? The future of sustainable buildings and urbanism in the age of emergency. 2022. p. 929–33.
5. Kamari A, Kotula BM, Schultz CPL. (2022). A BIM-based LCA tool for sustainable building design during the early design stage. Smart and Sustainable Built Environment. 2022;11:217–44.
6. Marincic Lovriha I, Ochoa de la Torre JM, Alpuche Cruz MG. (2020). Propuesta de vivienda económica para clima cálido seco, en Hermosillo, Sonora. In: Romero Moreno RA, Ochoa de la Torre JM, editors. Universidad de Sonora Universidad Autónoma de Baja California. Primera. Universidad de Sonora, Universidad Autónoma de Baja California; 2020. p. 115–36.

PLEA 2024 WROCŁAW
(Re)thinking Resilience

Implementing High-Performance Building Codes:
A Hands-On Curriculum for Undergraduate Architecture Education

RANIA LABIB[1]

[1]Prairie View A&M University, a Texas A&M University, Prairie View, Texas, USA

ABSTRACT: This paper presents a novel approach to architectural education, focusing on the integration of hands-on building commissioning exercises within the curriculum to enhance undergraduate students' understanding of high-performance building codes and sustainable design practices. The course was structured into four modules: Indoor Air Quality, Thermal Comfort, Daylighting and Visual Comfort, and Building Envelope Efficiency. Each module combined theoretical lectures with practical applications, allowing students to engage directly with real-world environments. Observations indicated a significant improvement in students' comprehension and test scores compared to traditional lecture-based methods. This shift towards experiential learning not only deepened students' theoretical knowledge but also developed their practical skills in sustainable architecture. The approach demonstrates the effectiveness of hands-on learning in architectural education, preparing students to meet the challenges of sustainable design in their professional futures.
KEYWORDS: High Performance Buildings, Building Commissioning, Building Energy Codes, Energy-efficient Buildings Standards, Architectural Education

1. INTRODUCTION

A gap exists in conventional architectural education, which often emphasizes design and aesthetics while sidelining practical, sustainability-focused aspects like energy efficiency and environmental impact. This educational disconnect limits the ability of upcoming architects to effectively contribute to the sustainable development goals. To address this gap, there is a need for an integrated approach that combines theoretical knowledge with practical applications, particularly in the context of high-performance building codes.

This paper introduces an innovative educational framework developed for a net-zero energy class, which aims to bridge this gap. The framework emphasizes hands-on building commissioning tasks, drawing inspiration from the American Society of Heating, Refrigerating and Air-Conditioning Engineers (ASHRAE) Guideline 0.2-2015 [1]. The curriculum is structured to provide students with in-depth lectures on topics such as indoor air quality codes, thermal comfort, daylighting, and ASHRAE 90.1 standards [2]. Following each lecture, students engage in practical tasks, surveying a classroom environment to apply their newly acquired knowledge.

The hands-on tasks are carefully designed to integrate seamlessly into the curriculum. Students work in teams to examine various aspects of the building environment, including indoor air quality, thermal comfort, daylighting and glare, employing tools like thermal imaging to evaluate insulation and air filtration. This practical approach not only ensures the application of theoretical knowledge but also fosters collaborative learning and critical thinking.

The impact of this hands-on approach on student learning has been significant. It has not only improved student engagement but also enriched their understanding of high-performance building codes. By effectively elevating theoretical knowledge to practical application, students are better prepared to contribute to sustainable architectural practices. The findings from this approach suggest that such educational frameworks have the potential to transform architectural education, making it more relevant to contemporary challenges in sustainability.

Moreover, the implications of adopting such frameworks extend beyond the classroom. They signify a shift in architectural education towards a more holistic approach, where sustainability is not just an optional module but a core component of the curriculum. This shift is essential for preparing future architects to play a pivotal role in creating sustainable and resilient built environments.

In conclusion, the integration of hands-on commissioning tasks in architectural education, aligned with high-performance building codes, is not only innovative but necessary. It paves the way for a new generation of architects who are not only skilled in design but also adept in creating buildings that are environmentally responsible and sustainable.

2. METHODOLOGY

The objective of this research was to evaluate the effectiveness of hands-on building commissioning tasks similar to the tasks detailed in ASHRAE's Guideline 0.2-2015, in enhancing undergraduate architecture students' understanding of high-performance building codes. The study adopted a

multi-dimensional approach, involving both theoretical instruction and practical application. The curriculum was embedded within a net-zero energy class and aimed to transition students from a traditional lecture-based learning model to an interactive, hands-on approach.

Over the course of the semester, the class was divided into four modules, each focusing on a critical aspect of high-performance building codes: Indoor Air Quality, Thermal Comfort, Daylighting and Visual Comfort, and Building Envelope Efficiency. After a series of lectures in each module, students were tasked with commissioning activities, which involved surveying and evaluating one classroom environment. The parameters examined during these commissioning tasks were selected to align closely with the high-performance building codes and standards taught in the lectures.

Each module employed standardized instruments and research-grade equipment to ensure the consistency and reliability of the data gathered in commissioning one classroom within the school's building. The findings from these commissioning tasks were then compared to the high-performance building codes to assess compliance and identify areas for improvement.

One particularly engaging commissioning exercise for the students was the use of thermal photography through a drone, which captured their interest due to the innovative use of technology. This method was employed in the Building Envelope Efficiency module, where students utilized the drone to take thermal images of the building. The focus was on examining the thermal performance of the building envelope, specifically targeting walls and roofs. This hands-on approach not only provided a dynamic learning experience but also offered a practical perspective on assessing and understanding the thermal efficiency of architectural structures.

2.2 INDOOR AIR QUALITY MODULE

In the Indoor Air Quality module, students used Greywolf Sensing Advanced Sense meters, calibrated for precision by the manufacturer, to measure a range of air pollutants in a design studio over a 24-hour period. The instruments were calibrated to measure concentrations of Carbon Dioxide (CO2), Carbon Monoxide (CO), Sulfur Dioxide (SO2), Ethanol (EtoH), Total Volatile Organic Compounds (TVOC), Particulate Matter 2.5 (PM2.5), and Particulate Matter 10 (PM10). Please see table one for an example measurement by the students over a 24-hour period. See Figure 1.

Students were instructed to compare their findings with established codes such as Environmental Protection Agency (EPA) guidelines [3], Occupational Safety and Health Administration (OSHA) standards [4], and the Leadership in Energy and Environmental Design rating system (LEED) [5] . By aligning the collected data with these established codes and standards, students were able to assess the level of compliance of the classroom environment and identify areas requiring improvement. See Table 1.

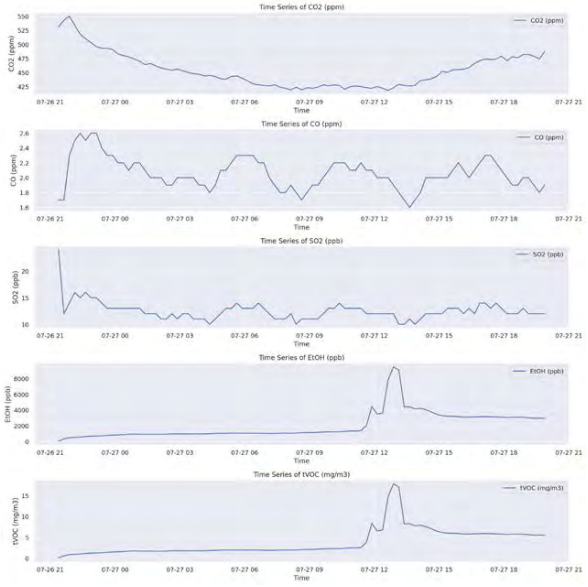

Figure 1: A graph of partial IAQ data collected by the students. The graphed data include CO2, CO, SO2, EoTH, and tVOC levels over 24-hour period.

Table 1: Partial list of the Measured pollutants by the students and comparison to the recommended limits by OSHA, EPA, and LEED. OSHA limits are based on 8-hour period.

Gas	AVG	OSHA	EPA	LEED
CO (ppm)	2	50	9	--
CO2 (ppm)	454	5,000	--	1,000
SO2 (ppm)	0.012	5	0.075	--
EtOH (ppm)	2	--	--	--
tVOC (mg/m3)	0.9	--	0.5	0.25

2.3 THERMAL COMFORT MODULE

In the Thermal Comfort module, students utilized research-grade instruments within a classroom to measure factors influencing human thermal comfort, consistent with their study in the Indoor Air Quality module. See Figure 2 for a list of the devices used to collect thermal comfort and IAQ data. They employed a heat index meter for data on air temperature and mean radiant temperature, while also assessing air speed and humidity. These parameters were carefully chosen to correspond with ASHRAE Standard 55, which outlines the thermal environmental conditions for human occupancy. Utilizing the Predicted Mean Vote (PMV) method outlined in ASHRAE 55 [6], students analyzed their findings, gaining a comprehensive understanding of how environmental

factors contribute to thermal comfort in architectural spaces.

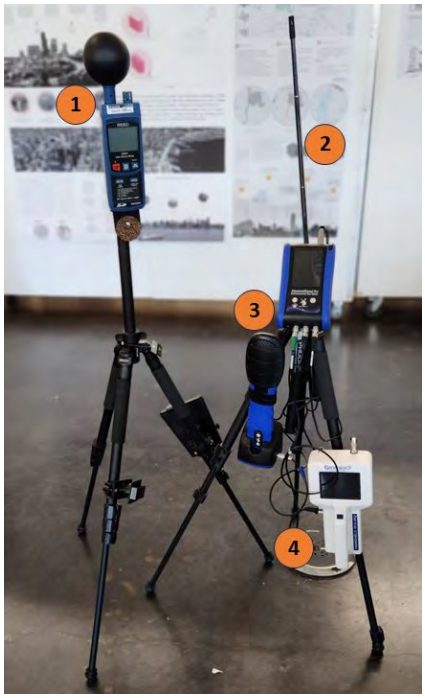

Figure 2: Equipment setup used by the students to collect data required for accessing thermal comfort and IAQ in the design studio. List of the devices: 1-Heat Index Meter, 2-Air Velocity Meter, 3-Gases Meter, 4- Particulate Matter Meter.

For their thermal comfort analysis, students measured conditions at three classroom points: adjacent to the window, centrally, and away from the window. Utilizing the Center for the Built Environment's Thermal Comfort Tool from the University of California [7], they applied the PMV method from ASHRAE Standard 55 (see Figure 3). Near the window, the air temperature and mean radiant temperature (MRT)—determined using a black globe thermometer—were both 20°C. The air speed was 0.1 m/s with a relative humidity of 37%. Accounting for a seated, quiet activity level (1 met) and typical classroom attire (0.61 clo), the PMV result was -1.96, suggesting a cooler than comfortable condition with a 75% probability of dissatisfaction (PPD). These conditions failed to meet ASHRAE Standard 55-2020's compliance, aligning with student feedback gathered through discussions and informal surveys indicating discomfort.

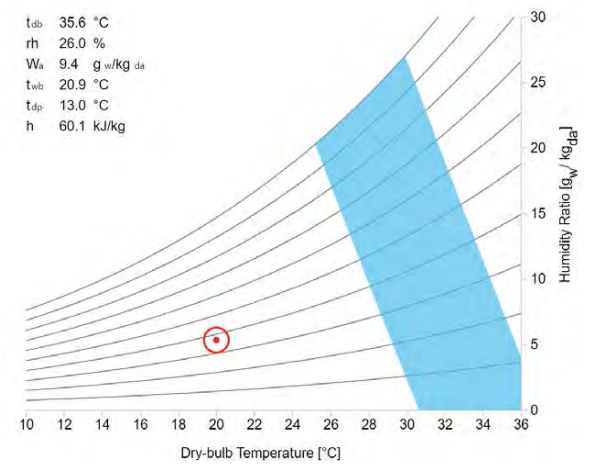

Figure 3: Psychrometric Chart utilizing PMV method showing cold sensation at the location next to the window.

2.4 DAYLIGHTING & VISUAL COMFORT MODULE

In the Daylighting and Visual Comfort module, an emphasis was placed on the pivotal role that daylighting and glare control play in creating comfortable and energy-efficient buildings. Understanding the balance between natural light benefits and the potential for visual discomfort is critical in architectural design. To this end, students engaged with research-grade equipment to evaluate the lighting conditions in the classroom, the consistent focus of the course's practical modules. They measured illuminance levels using a Konica Minolta Illuminance Meter to objectively assess the quality of daylight within the room (see Figure 4).To address glare and visual discomfort, students utilized both a luminance meter and a camera with a fisheye lens, capturing a wide view of the room's lighting scenario [8]. See Figures 5-7. The data obtained provided valuable insights into the interplay of light and space, which were then carefully compared to the guidelines provided by the Illuminating Engineering Society (IES) [9], integrating established standards with hands-on learning. Therefore, allowing the students to understand the practical implications of daylighting design and create strategies for balancing natural light benefits against the risk of visual discomfort.

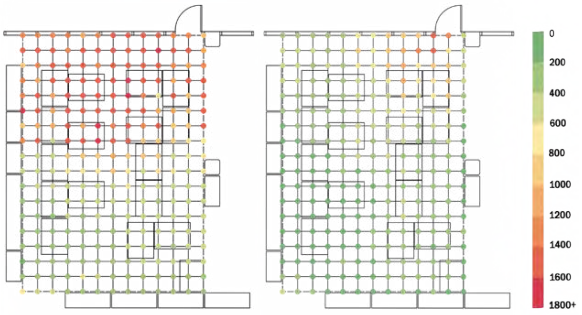

Figure 4: Daylight availability survey of the examined studio. The collected data show the daylighting availability in lux in the morning (left) and late afternoon (right).

Figure 5: A 180-degree fisheye view for glare analysis.

Figure 6: Glare analysis of the examined view. Glare sources are highlighted in green.

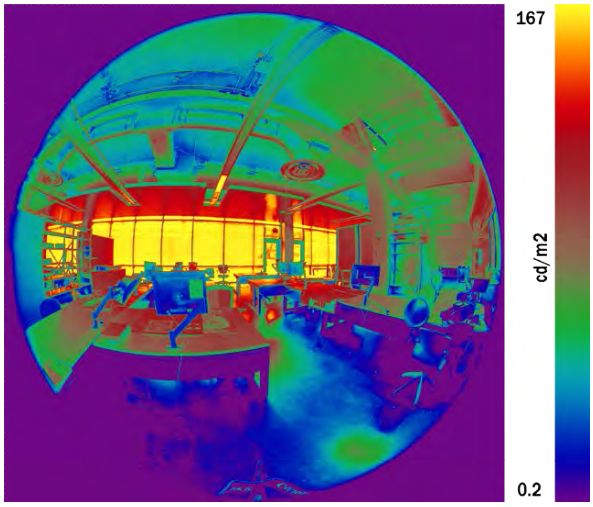

Figure 7: luminance map of the examined view.

2.5 BUILDING ENVELOP PERFORMANCE MODULE

In the Building Envelope Efficiency module, students utilized both a handheld FLIR thermal camera and a drone-equipped thermal imaging system to conduct an in-depth analysis of the design studio's thermal integrity. This dual approach allowed for a detailed examination of temperature variations on surfaces, pinpointing problems related to air infiltration, thermal bridging, and insulation deficiencies. By analyzing these thermal images alongside high-performance building standards, students were able to critically assess the envelope's efficiency. This practical experience not only reinforced their theoretical knowledge but also highlighted the importance of meticulous envelope design in achieving energy-efficient buildings. The outcomes of this module were visually documented.

students were tasked with creating 3D thermal models using photogrammetry, a method that involves taking overlapping photographs at various angles, including straight down shots. This technique requires a series of images taken around the object at a consistent flight altitude with significant overlap—usually 60-80%—between images. These overlapping images, when processed, allow for the reconstruction of a 3D space, giving detailed insights into the thermal characteristics of the building's envelope [10]. See Figure 8.

In the Building Envelope Thermal Analysis section, alongside photogrammetry for 3D thermal modeling, students also conducted detailed examinations of the envelope using a handheld FLIR thermal camera. This device complemented the drone's broad overview by allowing close-up inspections of areas suspected to have thermal inefficiencies. By juxtaposing the wide-ranging thermal perspectives from the drone with the precise, localized data from the handheld camera, students could obtain a holistic understanding of the building's thermal performance. This dual approach provided a comprehensive assessment of the envelope's insulation effectiveness, air leakage, and potential thermal bridges. See Figure 9.

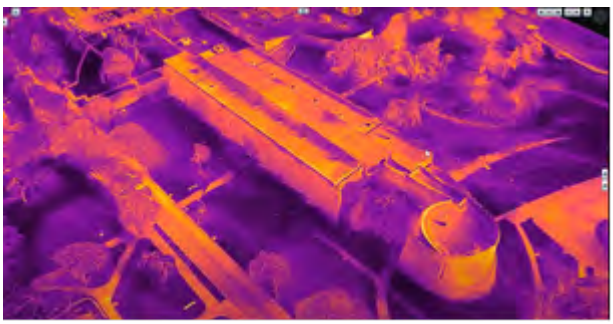

Figure 8: A thermal 3D model produced by the students to examine the thermal performance of the entire building envelope including the roof.

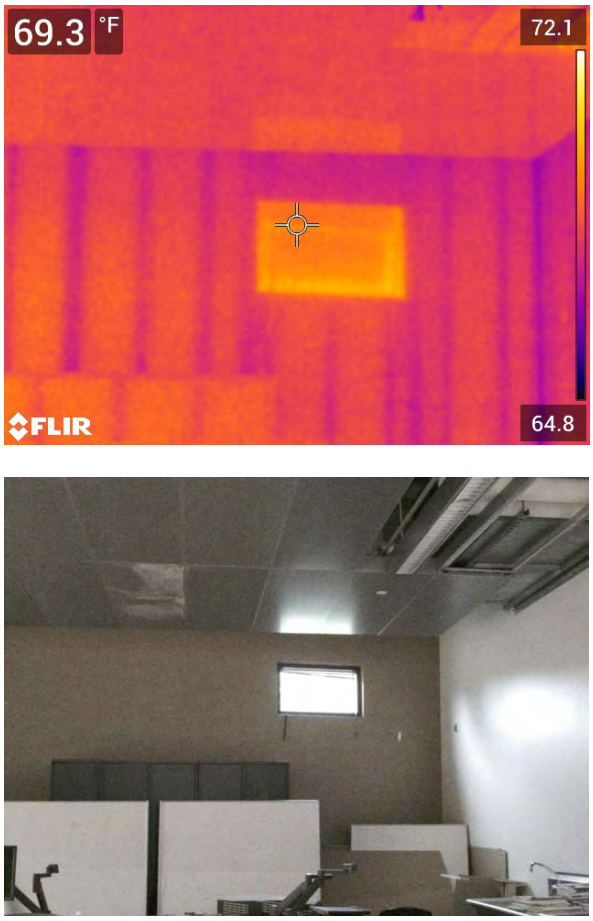

Figure 9: Top; A thermal picture taken with a handheld Flir Infrared camera. Bottom; a visible picture of the same scene. The thermal photo indicates some heat escape through the area right above the window located in the examined design studio.

3. FUTURE IMPLICATIONS AND RECOMMENDATIONS

This hands-on commissioning curriculum's success has significant implications for the future of architectural education. It suggests a shift towards more experiential learning models, which can be implemented in various architectural courses, enhancing student engagement and practical understanding of sustainable design principles. Recommendations for future courses include establishing partnerships with industry professionals and organizations for resource support, integrating newer technologies to keep pace with industry standards, and conducting formal studies to quantitatively measure the impact of such pedagogical approaches.

4. STUDENT FEEDBACK AND REFLECTIONS

Although formal data collection was not conducted, anecdotal observations and informal discussions indicated that students found the hands-on activities enriching and more engaging than traditional lecture-based learning. Many students expressed that the practical application of theoretical concepts greatly enhanced their understanding of high-performance building codes and sustainable design practices. The interactive nature of the exercises, particularly the use of innovative technologies like drones for thermal photography, was frequently cited as a highlight. This feedback underscores the value of experiential learning in architectural education, suggesting a positive reception and a deeper level of engagement from the students.

5. LIMITATIONS AND CHALLENGES

This section addresses the limitations and challenges encountered during the implementation of the hands-on commissioning curriculum. One of the primary challenges was the resource-intensive nature of the approach, requiring access to specialized equipment and tools, which may not be readily available in all educational settings. Additionally, the time required to conduct hands-on activities was significantly greater than traditional lecture-based methods, posing scheduling challenges. There was also a learning curve associated with the use of technology, such as drones and advanced sensing equipment, which required additional training for both students and instructors. These factors, while manageable, highlight the need for careful planning and resource allocation in adopting this experiential learning model in architectural education.

6. CONCLUSION

This study's exploration into hands-on commissioning exercises as a pedagogical tool in architectural education reveals a transformative impact on student learning. The integration of practical exercises in line with high-performance building codes has not only enriched students' theoretical understanding but also significantly improved their practical skills. This was evident in the notable enhancement of their test scores. It's important to note that this observation of improved scores is based on instructor assessments, as a formal analysis of the test results was not conducted. Nonetheless, this perceived enhancement in performance is a promising indicator when compared to the outcomes of past student groups who were primarily exposed to traditional lecture-based methods.

Crucially, the students' ability to apply complex theoretical concepts in real-world scenarios signifies a deeper level of learning. By participating in commissioning activities, students developed a nuanced understanding of sustainable design practices, a skillset indispensable in the modern architectural landscape. Their engagement in tasks like thermal imaging, air quality assessment, and

daylighting analysis provided them with hands-on experience that is often lacking in conventional architectural education.

Furthermore, the method fostered a collaborative learning environment, enhancing students' teamwork and problem-solving abilities. These are key competencies that will benefit them in their professional careers. The integration of innovative technologies, such as the use of drones for thermal photography, not only captivated the students' interest but also prepared them for the evolving technological advancements in the field of architecture.

The success of this educational approach advocates for a paradigm shift in architectural education, where experiential learning becomes a core element of the curriculum. By bridging the gap between theory and practice, this method prepares students to be not just designers but architects capable of contributing significantly to sustainable and resilient built environments.

This hands-on commissioning curriculum has proven to be a necessary and innovative approach in architectural education. It has paved the way for a new generation of architects, equipped with a robust understanding of high-performance building codes and a passion for sustainable design. This approach is integral for cultivating architects who are not only adept in design but are also champions of environmental responsibility and sustainability in their professional practices.

ACKNOWLEDGEMENTS

The author wishes to extend gratitude to the students who assisted with the preparation and setup of equipment for the fourth-year Net Zero Energy course at the School of Architecture. Special thanks go to Richard Wietkoswki, Carlos Manuel Vivero, and Jalen Stokes for their invaluable support in ensuring the equipment was ready for use.

REFERENCES

1. New ASHRAE Guideline Focuses On Optimum Facility And System Operation, (n.d.). https://www.ashrae.org/about/news/2015/new-ashrae-guideline-focuses-on-optimum-facility-and-system-operation (accessed August 26, 2023).
2. ASHRAE 90.1-2022 (I-P) | ASHRAE Store, (n.d.). https://www.techstreet.com/ashrae/standards/ashrae-90-1-2022-i-p?product_id=2522082 (accessed August 26, 2023).
3. O. US EPA, Creating Healthy Indoor Air Quality in Schools, (2014). https://www.epa.gov/iaq-schools (accessed August 26, 2023).
4. Indoor Air Quality in Commercial and Institutional Buildings, (n.d.).
5. S. Kubba, LEED v4 Practices, Certification, and Accreditation Handbook: Second Edition, 2015. https://doi.org/10.1016/C2015-0-00887-5.
6. Standard 55 – Thermal Environmental Conditions for Human Occupancy, (n.d.). https://www.ashrae.org/technical-resources/bookstore/standard-55-thermal-environmental-conditions-for-human-occupancy (accessed December 3, 2023).
7. CBE Thermal Comfort Tool, (n.d.). https://comfort.cbe.berkeley.edu (accessed December 3, 2023).
8. C. Pierson, C. Cauwerts, M. Bodart, J. Wienold, Tutorial: luminance maps for daylighting studies from high dynamic range photography, Leukos. 17 (2021) 140–169.
9. Home - Illuminating Engineering Society, (n.d.). https://www.ies.org/ (accessed August 26, 2023).
10. F. Remondino, L. Barazzetti, F. Nex, M. Scaioni, D. Sarazzi, UAV photogrammetry for mapping and 3d modeling–current status and future perspectives, Int. Arch. Photogramm. Remote Sens. Spat. Inf. Sci. 38 (2012) 25–31.

PLEA 2024 WROCŁAW
(Re)thinking Resilience

Effect of Night Ventilation on Thermal Comfort in Public University Office Rooms

LOUIS BOTHE[1], SEYED AZAD NABAVI[1], AND PHILIPP GEYER[1]

[1]Sustainable Building Systems Group, Institute for Design and Construction, Faculty of Architecture and Landscape, Leibniz University Hannover, Germany

ABSTRACT: According to a study conducted by the International Energy Agency (IEA), it was found that buildings account for approximately 40% of global energy consumption, with about 75% of that energy being used in the operational phase a significant portion of 50 % of a building's energy consumption is allocated to thermal comfort. One approach to positively impact the energy consumption of buildings in summer and counteracting overheating is night cooling, where building components with thermal capacity are cooled by air during night periods. This paper aims to investigate, if night cooling enhances thermal comfort in a university building in Hannover, Germany. The building experiences significant heating during summer. In this regard, we developed an experiment to measure the impacts of night cooling on thermal comfort. In this study, data was gathered from three rooms to analyse and discuss how various night ventilation methods impact thermal comfort by measuring actual performance data. The results of this research indicate that night cooling is not an effective method for improving the thermal comfort inside the building of the Faculty of Architecture at Leibniz University Hannover due to low thermal mass and below-average thermal properties of the building components.
KEYWORDS: Energy, Comfort, Night Cooling, Night Ventilation

1. INTRODUCTION

Thermal comfort plays the most significant role in the subjective perception of a building by its occupants, making it essential to allocate a substantial portion of a building's energy to maintain thermal comfort. Buildings account for approximately 40% of global energy consumption, with 75% dedicated to their operation and use [1]. Considering the diminishing fossil fuel resources and the relatively small share of renewable energy of final energy consumption for heating and cooling in Germany, positive impacts on the energy consumption for building operations represent a potential space for improvement [3]. According to studies by the International Energy Agency (IEA), the cooling energy consumption of buildings has a smaller share with around 1/6 of the share for heating [4]. However, when examining the trend in the energy end-users, such as space heating, space cooling, water heating, lighting, and cooking, it becomes evident that the energy demand for space cooling shows the highest growth rate. Between 2010 and 2018, the end energy demand for space cooling increased by 33%, and this trend is expected to continue due to global warming [4]. Referring to the examined location of Germany, it can be specified that the annual average daily mid-temperature has been steadily increasing, especially since 1980 [5]. These results show that not only the cooling load of buildings is continuously rising but also the duration of cooling periods is getting longer. Consequently, investigating building cooling methods, especially passive and regenerative techniques that counteract heat gain during summer, has become increasingly important. During this process, spaces are initially heated through solar radiation and heat absorption, particularly by opaque building elements in the facade [6]. Subsequently, the building structure absorbs this heat due to its thermal mass. Methods for cooling buildings are diverse, ranging from active cooling systems such as air conditioning to activated solid building components, depending on the building's characteristics [7]. Night cooling refers to the process of cooling thermally retentive volumes that have been heated during the daytime due to solar radiation and heat absorption, and subsequently cooling them during the colder night by ventilation, thus ensuring that the reheating of spaces due to the cooled thermal mass occurs at least time-shifted [2]. Previous studies about night cooling primarily investigate the effect of night cooling on solid buildings with simulation tools and without the effects of user behaviour. This study specifically examines the method of night cooling and whether its influence can improve thermal comfort in a university building during the summer period by measuring the actual performance of the building with sensors, while the daily operations in the building are taking place The examined building is a skeletal building with a concrete curtain wall and sliding windows. The studied rooms are on the top floor (third floor) and house the Institute of Building and Construction, Faculty for Architecture and Landscape, Leibniz University Hannover.

2. BACKGROUND

In the book "Building Services and Energy efficient Buildings" by Prof. Dirk Bohne, the fundamentals for understanding night cooling are explained. The book addresses both the ecological and technical advantages of night cooling, supported by reference projects. Furthermore, Bohne observes that night cooling has no significant impact on the daily temperature profile for buildings with low thermal storage mass [2]. Regarding the state of research on night cooling and night ventilation, authors Solgi et al. wrote an overview in their paper "A Literature Review of Night Ventilation Strategies in Buildings" [8]. They categorize papers on night ventilation based on research methods (measurements, simulations, long-term studies, operation/vacancy), building typology, climatic zone (humid, arid, moderate, cold), and geographic location. The literature can be broadly classified into simulation/numerical research, measurements/ monitoring, and a combination or comparison of simulation and measurements. Geographically, the studies are particularly concentrated in Europe [8]. Climatically, the focus of the analysed literature is on moderate zones. Notably, the research-density is higher in simulations of buildings without user behaviour, while the lowest research density is found in measurements / monitoring [8]. A recent study in the section of on-site measurements is one by PlanTeam Schwarz and GreenSpleen (InnoVision Group) from 2022, where an empty floor of a solid office building in Berlin was used for an experimental setup similar to our research [9]. The study found that night cooling achieved significantly cooler room temperatures both during the daytime and for a year. During the hot period, night cooling significantly improved thermal comfort [9]. After analysing the research methods of parts of the existing literature, the research findings are particularly relevant in terms of showing essential factors for the effectiveness of night cooling that are explained in the following paragraphs. It becomes evident that most of the existing literature is based on simulations. The research presented in this paper is addressing the niche of measured data analysis and the actual performance of a building in terms of night cooling and aims to fill this research gap.

2.1 Key Parameters for the effectiveness of night cooling

Air Change Rate:

Artmann's paper specifically examines the influence of indoor air change during night ventilation on thermal comfort [10], [11]. He concludes that particularly in the case of natural ventilation, wind conditions within the range of 0.2 to 4 air changes per hour are the relevant factor for thermal comfort [10].

Thermal Effective Mass:

Among other factors, the thermal mass of the building is mentioned as one of the main factors for the effectiveness of night cooling. Shaviv et al. found that in buildings with high thermal mass, the indoor maximum temperature can be reduced by 3-6°K [13]. Improvements are also observed in constructions with moderate thermal mass. However, buildings with light thermal mass led to worsened thermal comfort [13]. Finn et al. further specify that double the thermal effective mass area leads to a temperature difference of 3K, which emphasizes the relevance of thermal mass to the effectiveness of night cooling [14].

Building and Windows:

The application of natural ventilation assigns greater importance to the form and size of windows [12]. In one study, cross- or single-sided ventilation was found to have no significant impact on the cooling load in the building, as both variants achieved an 8 times air change per hour confirming Artman's findings. [12].

Temperature Difference and Duration:

The effectiveness of night cooling is maximized in regions such as deserts and arid zones with night temperatures below 20°C [15]. Givoni, therefore, examined the decrease in indoor temperature based on the temperature difference during the night, which supports the studies of Artmann and Geros [15]. Yang also identifies the duration of the cooling period as another factor. He simulated a cooling period of 400 hours, achieving a reduction of the cooling load by approximately 60% [16]. However, this simulation serves only as an illustration and cannot represent a real scenario.

Regarding the research methodology, it can be noted that a significant amount of research has focused on simulations. On-site measurements or experimental data collection for buildings in operation are particularly lacking. For this research, we subjectively assume that on-site measurements provide the most representative research results and the most reliable data due to the performance gap between simulated and measured scenarios based on assumptions that are made in the simulation climate-wise and building components-wise [17]. Also, simulations don't include user behavior such as opening windows.

2.2 Thermal comfort

While the term "comfort" initially pertains to subjective perception, various methods have been developed to quantify thermal comfort. Therefore, room temperatures are measured in relation to outdoor temperatures, incorporating an element of "acceptance" for people to render comfort a measurable value. Key scientific models for assessing thermal comfort in summer include the comfort fields

researched by Fanger, Frank, and Roedler [18]. Notably in Germany, normative standards like DIN 1944-2 specify permissible maximum temperatures for certain spaces. Internationally, ISO 7730 serves as an evaluation basis. This standard is also incorporated in the ASHRAE Standard 55 (USA)[18]. Figure 1 illustrates the comfort field for naturally ventilated spaces according to ASHRAE, which is referenced in this work due to its practical applicability and connection to ISO 7730. The comfort field includes two curves: one representing 80% and another showing the boundary for 90% user acceptance for room temperatures.

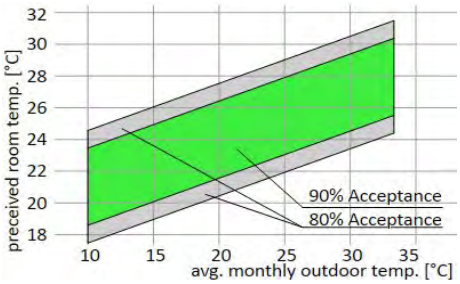

Figure 1: ASHRAE Standard 55 comfort field

3. METHODOLGY

The process of evaluating the impact of night cooling on the thermal comfort in the building in this paper includes four steps. We collected data from three separate rooms to measure the effects of different night ventilation methods on thermal comfort parallel. As a first step, we selected the rooms on the top floor to measure the data. The selection was based on several characteristics such as representative usage of the rooms, the exposure through the southern facade, the size of the windows in each room, thermal characteristics in the surrounding rooms, and the equal thermal mass in the components of the rooms.

As a second step, we set up the rooms with different night ventilation methods 1) naturally ventilated, 2) non-ventilated, 3) mechanically ventilated.

As a third step, we set up the three rooms with identical sensors in the same place to measure a data set with temperature, humidity, light intensity, and light color over 5 days in an interval of 15 minutes as a compact but less precise measurement period with Enviro sensors. In a second measurement period conducted under the same settings, we studied the temperature profiles of surface temperatures of different building components, to get an insight on the thermal characteristics of the rooms and materials. We collected and preprocessed the data from the sensors by using Python, and evaluated and compared the different night ventilation methods with their different room temperatures. As the last step, we pointed out the effects of the different night ventilation methods on the thermal comfort of the building. The night ventilation in the naturally ventilated room was achieved by simply opening the windows. In the mechanically assisted room, the night ventilation was increased by a standard fan. The data sets were supplemented with external data on outdoor temperature and then preprocessed. In the second measurement period, we studied the thermal characteristics of the building components in the studied rooms and their surface temperatures. Therefore, we installed Raspberry Pi sensors on the surfaces of building components and secured them from room temperature influences by using a polystyrene capsule with an open side to the surface of the building component. The night ventilation methods were evaluated and compared based on their room temperatures and outdoor temperatures.

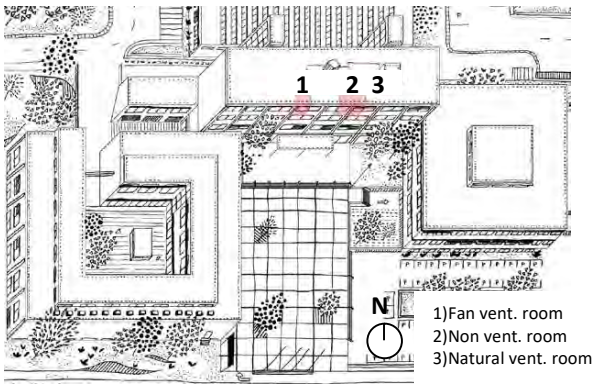

Figure 2: Axonometric Drawing of the Faculty of Architecture and Landscape, marked

3.1 Rooms and construction

For this study, three representative rooms on the top floor of the Faculty of Architecture and Landscape building were chosen. The selected rooms are used as office cells. The main structure of the building is made of beams, columns, and ceilings/floors that result in a skeleton structure with a curtain wall. The floor consists of 295 mm reinforced concrete, with a floor structure of 50mm screed and a linoleum covering. The ceiling serves as the flat roof and is made of 295 mm reinforced concrete, topped with 70mm of EPS insulation and waterproof membranes. The beams are made of 400x300mm reinforced concrete. The column behind the facade is the same dimension. The horizontal room closure is made by the curtain wall facade. The facade is a curtain facade made of concrete panels with core insulation and an interior balustrade made of concrete with radiator space. It has approximately 65% of horizontal sliding steel windows. The interior walls are constructed as drywalls with mineral wool core insulation.

4. RESULTS AND DISCUSSION

The results of this study show the temperature profiles of rooms with different ventilation methods during three measurement periods while the building

is used. Based on this study the impact of night cooling on thermal comfort in the specific rooms is analyzed. In Figure 3 the different temperature profiles are presented along with the outdoor temperature trend, the light intensity, and the light color. The main diagram (bottom) shows the temperature profiles, the relative humidity, and the outside temperature. The top diagram shows the light intensity and light color. In general, the relationships between the temporal daily courses and the resulting temperature trends can be observed over 5 days. Temperatures, indoor and outdoor, rise during the day with the progression of sunlight, and they cool down during the night. At the same time, it can be observed, that the relative humidity decreases with rising temperatures and increases with falling temperatures, as warmer air has a higher capacity for humidity. Following the three ventilation methods and comparing them to the outside temperature, it becomes evident that the temperature profiles have a larger spread in terms of night temperatures from the ventilated rooms in comparison to the non-ventilated rooms. The profiles align parallel to the outside temperature trend during the day. The ventilated rooms cool down significantly more during the night periods than the non-ventilated room. Furthermore, none of the methods result in room temperatures lower than the outdoor temperature.

Analyzing the charts chronologically, the peaks of light intensity on the first two days of measurement can be attributed to the appearance of the cleaning staff, who also closed the windows and turned off the fan. As a result, the increase in room temperature occurs with the peak of light intensity, while the outside temperature rises more slowly. On the second day of the measurement period, a rapid temperature drop in the non-ventilated room is noticeable, which cannot be explained by the measured data (Fig. 3a). This phenomenon suggests the influence of user behavior, likely opening the window. On the third day of the measurement period, a significant peak in the naturally ventilated room is evident, which is also attributed to user behavior, such as touching or approaching the sensor (Fig. 3b). On the fourth day, a rapid drop and subsequent rise in the outside temperature can be observed. This is reflected in all indoor temperature profiles, indicating the dynamic behavior of the rooms in terms of temperature. At the same time, the graph of light intensity also drops significantly, corresponding to cloud cover. Also, the humidity rises fast suggesting rainfall (Fig. 3c). On the last day of the measurement period, the temperature profiles of the rooms do align also during the night because the windows could not be opened due to bad weather (Fig. 3d). Furthermore, the maximum temperatures of the last three days in the naturally ventilated room are slightly higher than in the non-ventilated room, despite cooling down more during the night. This contradicts initial expectations and may be explained by different user behavior. To quantitively examine the ventilation methods and their impact on thermal comfort in the researched rooms, the temperatures are analyzed using the comfort field defined by the ASHRAE Standard 55[18]. In Figure 4, the three ventilation methods are presented alongside the curve representing the 80% Comfort field based on the ASHRAE Standard 55. Considering an average outdoor temperature of 20,75 °C during the measurement period, the 80% acceptance temperature is around 27°C. To compare the different ventilation methods, the areas out of the 80% acceptance are colorized and the integral areas of the graphs are pointed out to get a quantitative view of the effectiveness of each method. Analyzing the three figures by comparing the critical areas that are out of the thermal comfort field (ASHRAE), it becomes evident that the non-ventilated room has the most amount of critical area with 76,75 hours of temperatures above 27°C. The fan-ventilated room has 62 hours of temperatures above 27 °C, while the natural ventilated room has 59 hours of temperatures above 27 °C. To get an insight into the thermal characteristics of the studied rooms, in the second measurement period, we analyzed the surface temperatures of the building components during the day. Due to bad weather conditions, the windows had to stay closed and no ventilation happened. Figure 5 shows the temperature profiles of the concrete facade (interior surface), the drywall surface, and the surface of the floor. Overall, it can be said, that the studied room gains much heat compared to the moderate outdoor temperatures. Comparing the surface temperatures of the different building components shown in Figure 5, the phase shifts of heat gain become evident. The surface temperature of the drywall rises first, the floor and facade surface temperature follow with a phase shift of about half an hour. Also, the maximum surface temperature of the drywall is roughly one degree higher, compared to the surface temperature of the massive building components. Considering similar heat storage capacities and the significantly lower weight per area of the drywall (36 kg/m²) compared to the weight per area of the façade (384 kg/m²) combined with a much bigger share of drywall (36m² drywall, 4,3 m² façade) the aligning temperatures of both components becomes clear.

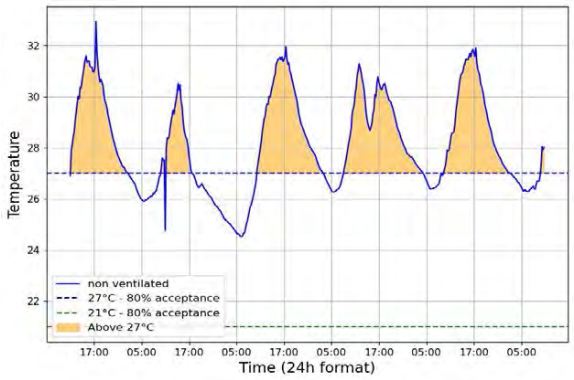

a)

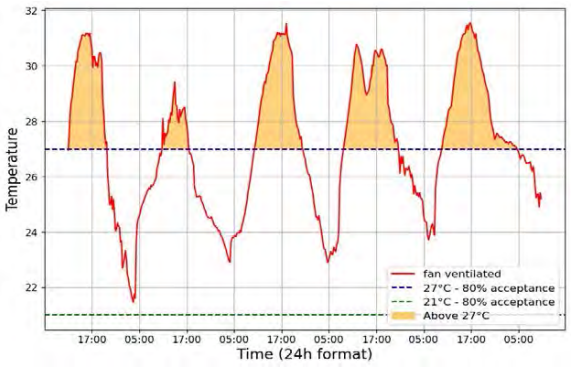

b)

Table 01: improvement result after night ventilation

Method	Orange area *[h*°C]*	Improvement *[%]*
Non ventilated	76,75	0
Natural ventilated	59,0	23,13
Fan ventilated	62,0	19,22

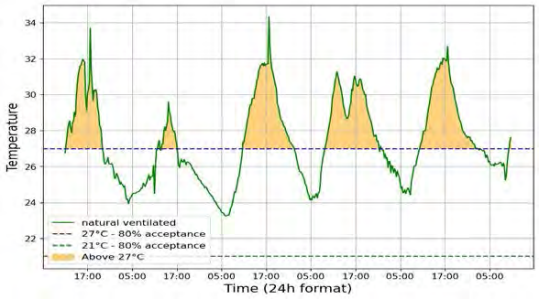

c)

Figure 4: Comparison of ventilation methods

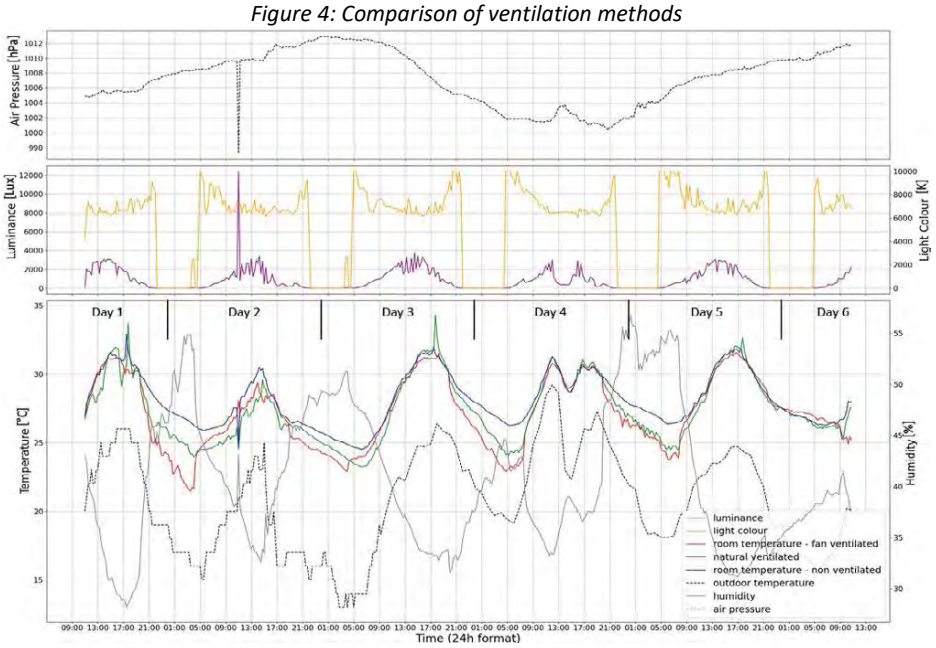

Figure 5: Quantitative analysis of the ventilation methods on thermal comfort.

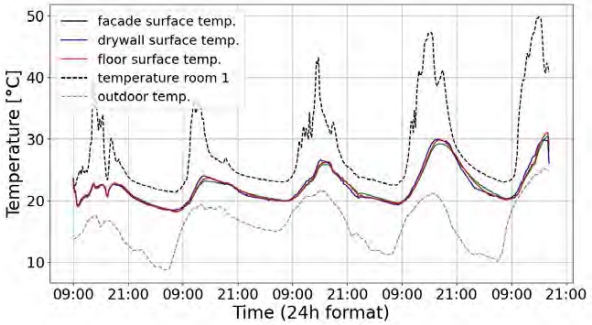

Figure 3: Surface temperatures of building components.

5. CONCLUSION

In this paper, we studied the effects of night cooling on thermal comfort in public university rooms with building components that have significantly below-average thermal characteristics. Considering the high temperatures in the rooms due to solar heat gain and heat transfer into the building in the summer, we set up three ventilation methods for comparable rooms and analyzed the effects of each ventilation method over two measurement periods of 5 days. While night

cooling through night ventilation is considered an effective method for thermal comfort in the literature, this study indicates that night cooling is not an effective method for improving thermal comfort inside the researched building. Although the rooms cool down significantly during the night, they rapidly heat up again when the windows are closed due to radiational heat gain through the façade and from the core of this story and so adopt the temperatures of the surrounding rooms. As the outdoor temperatures rise during the day, the rooms heat up through thermal gains also caused by radiation. The highest temperatures are reached in the rooms due to solar gains through south-facing windows. Due to the quantitative evaluation of comfort fields, improvements in thermal comfort through night ventilation can be observed. Through fan-assisted ventilation, thermal comfort is improved by 19.2% when considering the measurement period. Through natural ventilation, it is improved by 23.13%. Nevertheless, it should be emphasized that the building heats up quickly during the day and there are almost no differences in temperature profiles of the different ventilation methods. Especially during work hours, the temperatures in the building outside the assessed thermal comfort range are observed. To be precise, the unventilated room has around one hour of comfortable temperature (below 27°C) during the working hours (08:00 – 09:00) over the measurement period of 5 days. The mechanically and naturally ventilated rooms improve to 3 hours of comfortable temperatures during the working hours over 5 days. The reasons for the small impact of night ventilation on thermal comfort can be found in the building construction and the building components of the Faculty for Architecture and Landscape. On one hand, there are considerably below-average thermal properties of the facade. On the other hand, there is a low thermally effective mass in the skeletal construction of the building. In summary, none of the ventilation methods significantly influence the room temperature throughout the day or improve the thermal comfort in the rooms during the next day.

ACKNOWLEDGEMENTS

This research is part of a seminar at the Department of Sustainable Building Systems at the Institute for Design and Construction within the Leibniz University Hannover. First, I would like to express my gratitude to Prof. Dr.-Ing. Philipp Geyer and M.Sc. Seyed Azad Nabavi from the Institute of Design and Construction, Department of Sustainable Building Systems for initiating, supervising, and organizing the research project. Other thanks go to the Department of Building Construction and Design for providing the testing facilities and granting unrestricted access to the spaces.

REFERENCES

1. L. Ramseier and R. Frischknecht, “Umweltfußabdruck von Gebäuden in Deutschland,” Bundesinstitut für Bau-, Stadt- und Raumforschung (BBSR), 2020.
2. D. Bohne, Ökologische Gebäudetechnik. Vieweg+Teubner Verlag, 2004.
3. Working Group on Renewable Energy-Statistics, “Development of Renewable Energy Sources in Germany in the Year 2022,” Federal Ministry for Economic Affairs and Climate Action, 2023.
4. International Energy Agency. and Global Alliance for Buildings and Construction., 2019 global status report for buildings and construction. International Energy Agency, 2019.
5. “Trends der Lufttemperatur | Umweltbundesamt.” Accessed: Jul. 18, 2023. [Online]. Available: https://www.umweltbundesamt.de/daten/klima/trends-der-lufttemperatur#steigende-durchschnittstemperaturen-weltweit
6. D. H. W. Li and J. C. Lam, “Solar heat gain factors and the implications to building designs in subtropical regions,” Energy Build, vol. 32, no. 1, 2000.
7. A. Dentel and U. Dietrich, “DOKUMENTATION PRIMERO-KOMFORT. Thermische Behaglichkeit- Komfort in Gebäuden,” Rud. Otto Meyer-Umwelt-Stiftung, 2006.
8. E. Solgi, Z. Hamedani, R. Fernando, H. Skates, and N. E. Orji, “A literature review of night ventilation strategies in buildings,” Energy and Buildings, vol. 173, 2018.
9. InnoVisionGruppe, “Was bringt eine Nachtauskühlung?“ TGA + E, 2023.
10. N. Artmann, “Cooling of the Building Structure by Night-time Ventilation,” Aalborg University, 2009.
11. N. Artmann, H. Manz, and P. Heiselberg, “Climatic potential for passive cooling of buildings by night-time ventilation in Europe,” Appl Energy, vol. 84, no. 2, 2007.
12. E. Gratia, I. Bruyère, and A. De Herde, “How to use natural ventilation to cool narrow office buildings,” Build Environ, vol. 39, no. 10, pp. 1157–1170, Oct. 2004.
13. E. Shaviv, A. Yezioro, and I. G. Capeluto, “Thermal mass and night ventilation as passive cooling design strategy,” 2001. [Online]. Available: www.elsevier.nl/locate/renene
14. D. P. Finn, D. Connolly, and P. Kenny, “Sensitivity analysis of a maritime located night ventilated library building,” Solar Energy, vol. 81, 2007.
15. B. Givoni, “Performance and applicability of passive and low-energy cooling systems,” Energy and Buildings, 1991.
16. L. Yang and Y. Li, “Cooling load reduction by using thermal mass and night ventilation,” Energy Build, 2008.
17. E. Cuerda, O. Guerra-Santin, J. J. Sendra, and F. J. Neila, “Understanding the performance gap in energy retrofitting: Measured input data for adjusting building simulation models,” Energy Build, vol. 209, 2020.
18. A. Dentel and U. Dietrich, “DOKUMENTATION PRIMERO-KOMFORT Thermische Behaglichkeit-Komfort in Gebäuden,” Rud. Otto Meyer-Umwelt-Stiftung, 2006.
19. Archifachschaft Hannover, “Archifachschaft Hannover.” Accessed: Sep. 28, 2023. [Online]. Available: https://www.instagram.com/archifachschaft_hannover/?hl=de
20. Leibniz Universität Hannover, “Fakultät für Architektur und Landschaft.” Accessed: Sep. 28, 2023. [Online]. Available: https://www.archland.uni-hannover.de/de/

PLEA 2024 WROCŁAW
(Re)thinking Resilience

Natural Ventilation and Particulates Dispersion in Single-room Dwellings:

An investigation of retrofit vents in informal settlements in Nairobi

LEONIDAS TSICHRITZIS[1] FILBERT MUSAU[1]

[1]Glasgow School of Art, Glasgow, United Kingdom

ABSTRACT: Poor indoor air quality is associated with various ill-health conditions; and appropriate natural ventilation is recognized as an effective means to keep both buildings and occupants healthy. Natural ventilation is crucial where people spend most of their time in indoors with pollutants. The purpose of the work reported in this paper was to examine the potential impact of retrofitting options of vents on improving indoor air quality by removing particulates produced during cooking. It focused on single-room dwellings in informal settlements in Nairobi, Kenya. The dwellings are occupied by extremely low-income householders who typically live and sleep in the same room that they cook and dine. The majority of the dwellings are windowless. Where present, windows are rarely opened, either because they are occluded by crowded items, or due to insecurity, or to keep out mosquitoes. We used Computational Fluid Dynamics (CFD) to simulate air flow and particle dispersion, focusing on $PM_{2.5}$. The results show that retrofits for natural ventilation can effectively reduce indoor particulates. The effectiveness is highly related to the type, size and location of retrofit vents, and to the fresh air inlet velocity.
KEYWORDS: Informal housing, ventilation retrofit, indoor air quality, particulate dispersion.

1. INTRODUCTION

Natural ventilation of indoor spaces is important to reduce particulate matter with a diameter of 2.5µm ($PM_{2.5}$), or less, which are dangerous to human health [1, 2]. Exposure to ambient $PM_{2.5}$ is associated with various types of cancer [3], increasing the morbidity and mortality rates related to lung cancer and decreasing the survival time of patients [4]. It is also linked with respiratory and cardiovascular illnesses, increased blood pressure, and negative effects on the heart, the brain, and the placenta [1, 2, 5]. Particles produced during cooking are a common source of poor indoor air. They are directly related to biomass fuels, stove properties, cooking temperatures, and cooking styles [6]. The problem tends to be greater in developing countries, where higher indoor pollutants are generally observed [7], mainly due to the less clean fuels, and limited technology and mechanical methods available [6]. Therefore, sufficient natural ventilation during, and after cooking, is essential to maintain healthy indoor air quality.

Informal urban settlements in the global south experience challenges of overcrowding, poor ventilation and PM from biofuels. The research reported in the current paper studied informal dwellings occupied by extremely low-income people in Nairobi, Kenya. The dwellings are mostly single storey and single room. Less often they have two or three storeys (Fig. 1). The purpose was to assess the impact of natural ventilation interventions on effective PM dispersion. It evaluated innovative designs of vent options that are low cost, and easy to install and maintain. The designs addressed challenges that prevent occupants from achieving sufficient natural ventilation: (i) adverse weather conditions; (ii) lack of windows and/or vents; (iii) windows that are not opened enough due to privacy, insecurity etc.; (iv) interior overcrowding; (v) to keep mosquitoes out; and (vi) insufficient understanding of the importance of ventilation by the residents. The back-to-back layout of the dwellings allowed natural ventilation retrofit designs for only the front wall and roof fabrics. The effectiveness of natural ventilation is related to window opening behaviour, the penetration factor, and air exchange rate [8]; and the window surface area that is kept open for ventilation [9]. In general, small diameter particles tend to follow air flow more precisely, and their dispersion relies more on natural ventilation compared to larger particles [10].

2. THE CASE STUDY CONTEXT

The location of the informal settlement is in Nairobi, which has subtropical highland climate with dry and wet seasons. Temperature variations are small, generally within the human thermal comfort zone, and suitable for the opening of natural ventilation apertures throughout the year, except a short period in July. Existing spatial policies and unavailability of affordable land and housing have made Nairobi one of the most unequal cities in Africa – influencing housing quality, density and activity adjacencies. These, along with rapid urbanisation,

have resulted in numerous informal settlements [11, 12]. More than 4 million people in Nairobi live in crowded conditions in over 100 informal settlements, occupying only 5% of the total residential area [13]. Although studies in such settlements have revealed high exposures to PM [14, 15, 16, 17], such evidence has not translated into actions towards architectural interventions. Existing energy policies do not consider the harmful $PM_{2.5}$ produced by biomass fuels, or gas, and kerosene used in the settlements.

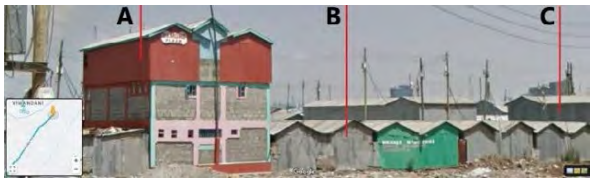

Figure 1. Typical morphology of dense informal single-room housing at Mukuru kwa Ruben, Nairobi. (A) Three storeys; (B) Two storeys; and (C) One storey. (source: Image - Google street view, annotated by authors).

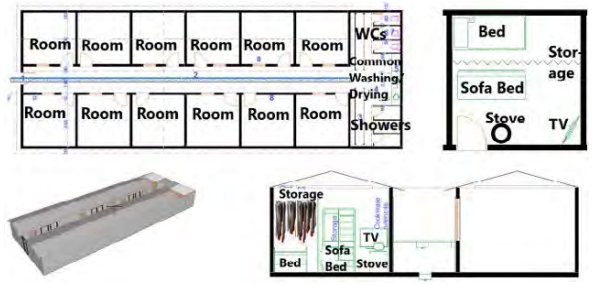

Figure 2. Block of informal one-storey single-room dwellings at Mukuru kwa Ruben informal settlement in plan, section and perspective view.

The dwelling construction is typically timber and corrugated iron sheets for walls and roofs. Natural stones or adobe are also often used for walling. Each plot of land typically contains two rows of single-room dwellings separated by a narrow access corridor (Fig. 2). Each row has five to ten dwellings depending on the plot length. Dwellings have a square plan of size 3.30m x 3.30m (L x W) internally; a 15° dual pitched roof with ceiling heights of 2.10m and 2.50m at eaves and ridge respectively; and a single entrance door of size 1.9m x 1m (H x W). Most are windowless. Some might have a window of size 0.90m x 0.65m (H x W), but not usually opened as it is occluded by crowded storage or due to insecurity, or to keep out mosquitoes. Dwellings are typically back-to-back with those of adjacent plots; and have one aspect, with the door and window (where present) facing the external corridor, allowing limited cross ventilation. The cooker or stove is slightly offset from the middle of the Front Wall facing the external corridor. Its height and diameter are 0.30m.

All cooking, relaxing, sleeping and other activities happen in the single room, increasing PM exposure to occupants. A large proportion of Kenya's urban population lives in such conditions. Over 60% of Kenya's population in informal settlements live in Nairobi [18], and nearly a third of them are poor – a much greater fraction compared to the 9% poor in formal settlements. So far, efforts to improve the living conditions in these settlements in Nairobi, such as the Kenya Informal Settlements Improvement Project (KISIP), focus on tenure security and infrastructure, but not on the quality of dwellings and indoor environments. Improvements of their indoor air quality would be of great value. The current project, therefore, aimed to study the potential of natural ventilation retrofits and build on the efforts by the KISIP and NGOs working on sanitation improvements.

3. METHODOLOGY

Natural ventilation retrofit options were designed and assessed quantitatively through Computational Fluid Dynamics (CFD); and through physical retrofits and PM measurements on selected dwellings. The CFD results are presented in the current paper – focussing on $PM_{2.5}$ dispersion in the room air during and after cooking. Numerical and the physical modelling errors need to be verified and validated by comparing them with high quality experimental data. The methodology, therefore, included validation of the CFD model. This examined the grid resolution and the turbulence model used.

3.1. Model validation

The CFD model validation was based on experimental data from a study with sufficient accuracy [19]. Grid independence studies were also obtained for the appropriate mesh selection. These data have been used to validate past studies [20, 21]. The validation room is 0.80m x 0.40m x 0.40m (Fig. 3). The inlet and outlet have a similar square size of 0.04m x 0.04m and are located centrally at the short walls of the room, opposite each other. The inlet is 0.20m below the ceiling, and the outlet is 0.20m above the floor. The inlet velocity is 0.225m/s resulting in around 10ACH. Particles with diameters between 2µm and 20µm are injected in through the inlet, continuously for 1,800s. The density of the particles is 1,400 kg/m^3.

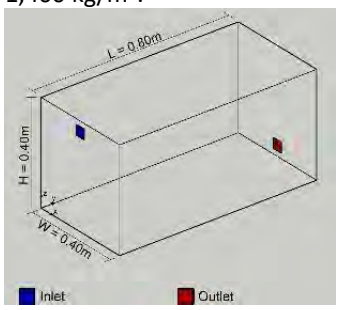

Figure 3. Axonometric representation of the room that was used for CFD model validation.

The non-commercial OpenFOAM software was used for the CFD simulations. The PIMPLE algorithm

was used for pressure-velocity coupling, along with steady Reynolds-averaged Navier-Stokes (RANS) equations for the creation of the flow and the k-omega SST turbulence model. For the lagrangian particles' cloud, the transient reacting ParcelFoam solver was used. The field flow and the particle trajectories were analysed in three-dimensions. The particles might stick at walls or escape through the outlets. However, they rebound back at the inlets of the domain. No slip boundary conditions were implemented for the vertical and the top boundaries of the computational domain and walls. Zero gradient conditions were implemented at the outlet.

To ensure that the courant number remains relatively constant throughout the simulation, the time step was determined based on the courant number [22]. For the present study, the time step is 0.025s. The accuracy of the CFD simulations and the computational cost strongly depends on the number of cells that the mesh employs. To allow grid independence, several meshes were tested. Velocity profiles were measured at three positions: y = 0.20m; y = 0.40m and y = 0.60m and compared with the experimental data [19]. As the grid resolution increased, the quality and accuracy of the mesh improved - with the results closer to the experimental data. However, after a certain grid resolution, finer meshes didn't necessarily improve the results (Fig. 4).

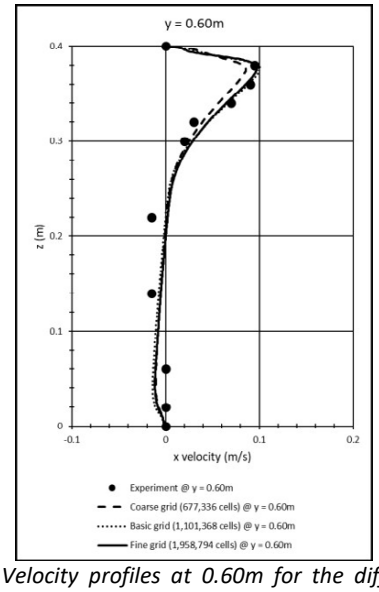

Figure 4: Velocity profiles at 0.60m for the different grid resolutions examined compared with experimental data.

3.2. CFD model setup

The dimensions for the one-room and cooker (source of pollutants) described in Section 2 and shown in Fig. 5 are used for the CFD model setup. The room volume is 25.27m3. The door is located 0.15m from the Left Wall. The effectiveness of natural ventilation during and after cooking was evaluated for four scenarios (Figs. 6): (i) **Scenario 0 (S0) - 'Base case'**: Gaps at the bottom and the top of the door (0.20m from eave height) as an inlet and outlet respectively. Each gap is 0.01m high and 1m long; (ii) **Scenario 1 (S1) - 'Middle Ceiling Outlet'**: Base case plus an outlet vent at the middle and along the room's ceiling that is 0.10m wide; (iii) **Scenario 2 (S2) - 'Front Wall Outlet'**: Base case plus an outlet vent of similar size as the one at S1 at the top and along the room's Front Wall; and (iv) **Scenario 3 (S3) - 'Front Wall Holes Inlet/Front Wall Holes Outlet'**: Base case plus six round holes of 0.15m diameter at the Front Wall of the room - three holes at 0.13m above the floor level serve as inlets, and three at 0.13m below the eaves serve as outlets.

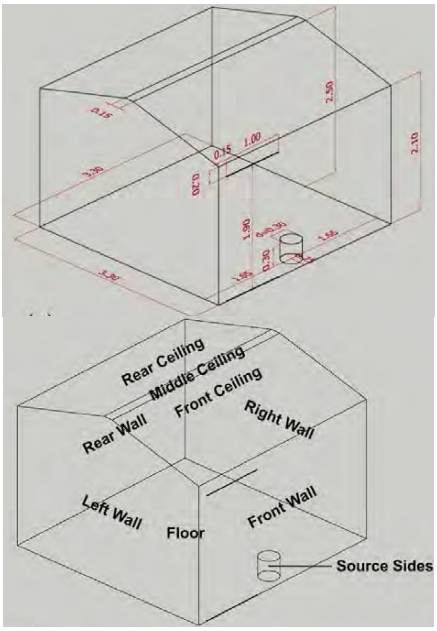

Figure 5: Dimensions of the room tested with CFD and boundary conditions of the CFD model setup.

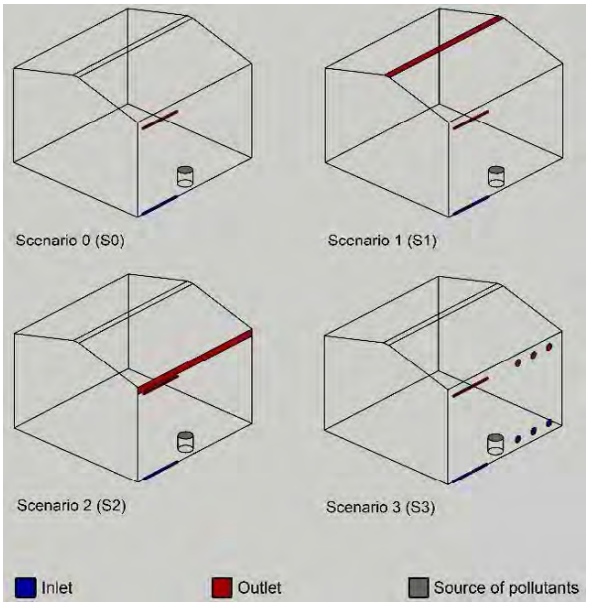

Figure 6: Axonometric view of the scenarios examined showing the inlets, outlets and the source of pollutants.

The computational grid is based on the resolution examined in Section 3.1 and has the same properties

and cells' size for all scenarios. Additional layers of cells have been added at the inlets and outlets of the computation domain for increased accuracy, which results in a slightly different total number of cells for the different scenarios. For simplicity, the CFD model does not include household items e.g. furniture. Fresh inlet air is constant and is not affected by outdoor temperature, pressure, humidity, and wind speed. Simulation times between 0s and 600s represent the cooking activity during which particles are injected in the room from the cooker with a constant rate, and 600s onwards represent the period after cooking. In all scenarios, the infiltration rate is 1 Air Change per Hour (ACH). As a result, the inlet air velocity at S0, S1 and S2 is 1m/s, while that at S3 is 0.12m/s to achieve 1ACH. The room is only naturally ventilated. The air flow is related to the air velocity at the inlets and is driven by buoyancy. Cooking (particle emission from the top surface of the cylinder) is performed at a constant rate for 10 minutes.

4. RESULTS AND DISCUSSION

The indoor dispersion and escape of particles for the four scenarios are discussed below. However, not all the particles escape in the first instance, as many remain stuck on surfaces. Results of stuck particles; dispersion at critical breathing levels in sitting, sleeping and standing positions; and results from two other scenarios will be reported in a separate paper.

4.1. Particle dispersion in the air

The results show that at the base case (S0), the particles ejected during cooking remain in the air for the longest (7,560s) followed by S3 (5,490s). The particles are fully dispersed after 1,230s and 1,260s for S1 and S2 respectively. Although particles at S0 require the longest time to disperse, the highest numbers are observed at S3 until time = 1,380s. There are 33% more particles in S3 compared to S0 at their peaks when cooking ends at time = 600s. As expected, particles start accumulating at the start of cooking (time = 0s) and increase during cooking. The highest numbers are observed around, or slightly before the end of cooking, and decrease after cooking. However, variations occur across scenarios. The highest are observed at S0 and S3 at time = 600s, with 32% and 42.7% of the total injected respectively. For S2 the highest are at time = 540s with 4.6%; and for S1 at time = 480s with 8%.

After cooking, they drop quickly at S0, but with a significantly slower pace compared to the other scenarios. The total injected drop below 10% at time = 1,020s for S0. This drops below 5% at time = 1,470s and time = 1,440s for S0 and S3 respectively. From time = 90s onwards, the percentage is higher at S3 compared to S0. However, the reduction rate between two subsequent measuring times is greater at S3. At S3, the particles decrease with an average rate of 7.5% from time = 600s to 1,500s and average rate of 6.3% from times = 1,500s to 3,000s. Afterwards, the reduction rate decreases further. At S0, the reduction rate is smaller with an average of 6.1% from times = 600s to 1,500s; and a relatively constant value of approximately 4% from times = 1,500s to 3,000s.

At the time with the highest percentage to the total injected (and compared to S0), S1 has 75.2% less particles, S2 has 85.7% less, and S3 has 33.3% more. Considering the highest percentage of particles that are dispersed in the room's air most of the time, S3 is the least effective design, mainly due to the inlet and outlet positions which restrict particle movement. At S1, the particles in the room's air range between 7% and 8% of the total injected from times = 120s to 600s, fluctuating for less than 5.35% between two consecutive measuring times during that period.

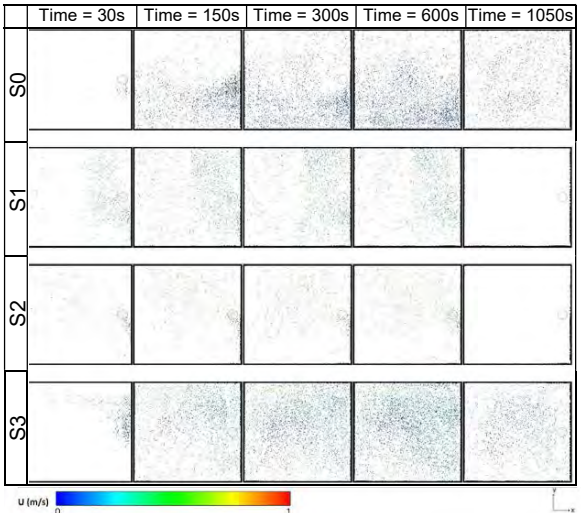

Figure 7. Top view of particle dispersion at between 1.5 and 2m above the floor for different scenarios and times.

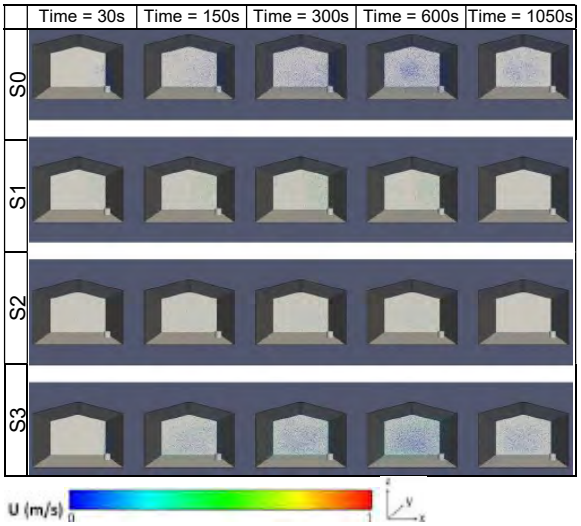

Figure 8: Perspective view of particle dispersion for different scenarios and times.

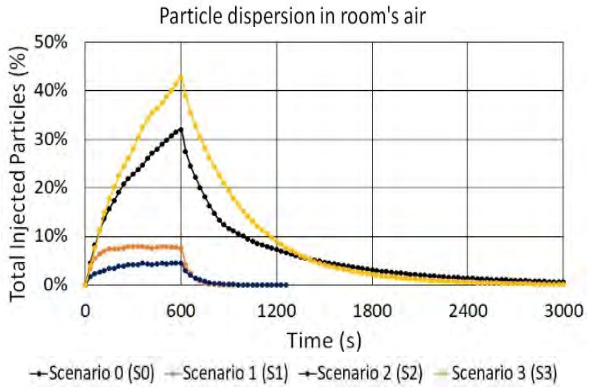

Figure 9. Percentage of total injected particles that are dispersed in the air till time = 3000s for different scenarios.

The particles are reduced rapidly when cooking ends and the dispersion drops below 5% of the total injected particles after time = 630s. This translates into an average reduction rate of 42.6% between times = 600s and 900s. For S2, the highest levels of particles in the room's air are 4.6% of the total injected, and apart from being lower compared to S1, they also appear slightly later while cooking, and between times = 210s and 600s. Between times = 600s and 1,200s, the average reduction rate of particles is 29.5% for S2. However, the deposition time at S2 is 30s longer than S1. At S2, less particles are dispersed in the air up to time = 660s compared to S1. Figures 7 to 9 show particle distribution at selected times for the scenarios examined.

4.2. Particles escape from the outlets

The percentage of injected particles that escape from the outlets, together with the time required for the particles to escape, determine the effectiveness of the natural ventilation intervention. The particles deposited at surfaces are considered as temporary depositions as they might suspend or circulate again within the room air due to an air draft or a change in their properties. S2 was the most effective intervention with 91.56% of the total ejected particles escaping the room. It was followed by S1 where 76.98% of the particles escaping the room. S0 is the least effective. Table 1 shows the percentages that escape the room via all the outlets of each scenario.

At S0 and S3, the particles start escaping from the door's outlet from time = 60s onwards, and for the other scenarios from time = 30s. From the total particles injected, only 15.53% escape from the door's outlet at S0, meaning that almost 85% remain in the room and end up on its surfaces. At S3, 20.79% escape from the Door's outlet, which is the highest percentage among the scenarios, despite having additional outlets. A further 23.82% escape from the Front Wall holes outlets, resulting in more than 55% remaining indoors. On the other hand, a significant percentage of the particles escape from the outlets at the rest of the scenarios. Most escape from the outlets either at the Middle Ceiling or Front Wall. The contribution of the Door's outlet is limited.

At S1, 69.25% escape from the Middle Ceiling outlet and 7.73% from the Door's outlet. As a result, only 23.02% end up at the room's surfaces at S1. The contribution of the Door's Outlet is further reduced at S2, despite this scenario allowing for the greatest percentage of particles to escape from all the outlets overall. Only 1.22% escape from the Door's outlet at S2. Its particle dispersion is mainly driven by the Front Wall outlet through which 90.34% escape, allowing only 9.66% to remain indoors - which is much less compared to S1.

Table 1. The percentage of particles that are deposited at the room's surfaces or escape from its outlets for the different scenarios examined.

		Scenario 0 (S0)	Scenario 1 (S1)	Scenario 2 (S2)	Scenario 3 (S3)
Surface	Floor	4.80%	3.76%	0.71%	5.74%
	Source Sides	1.80%	0.43%	0.18%	1.80%
	Front Ceiling	5.31%	3.88%	1.61%	6.35%
	Middle Ceiling	0.41%	*	0.04%	0.48%
	Rear Ceiling	3.27%	0.70%	0.11%	5.59%
	Front Wall	32.51%	9.02%	4.57%	21.28%
	Left Wall	30.96%	3.42%	1.12%	5.73%
	Rear Wall	4.80%	1.09%	0.08%	7.90%
	Right Wall	0.61%	0.71%	0.03%	0.53%
		84.47%	**23.02%**	**8.44%**	**55.40%**
Outlet	Door	15.53%	7.73%	1.22%	20.79%
	Middle Ceiling	**	69.25%	**	**
	Front Wall	**	**	90.34%	**
	Front Wall Holes	**	**	**	23.82%
		15.53%	**76.98%**	**91.56%**	**44.60%**
	Total	**100.00%**	**100.00%**	**100.00%**	**100.00%**

*In this scenario the surface is an outlet

** In this scenario the outlet is not applicable

4.3. Application of designed interventions

Cost-efficient retrofit solutions for improvement of natural ventilation of single-room dwellings were examined. They are easy to install and maintain and can work together with windows and/or doors, or as standalone. Natural ventilation can be provided by ensuring that vents will be kept open, especially during cooking, but also after cooking to ensure particle dispersion. Where cooking happens three or more times a day in scenarios which require more than two hours to fully disperse particles, the indoor air quality is expected to be low for extensive periods. Combining multiple measures is expected to increase natural ventilation. To overcome the security, privacy and noise issues that discourage window opening, the proposed locations of interventions are either on the low or high heights of walls or roofs. This also allows the hanging of belongings at walls. The proposed integrated gauzes for all scenarios will prevent mosquito entry. The ceiling outlet option requires a cap for rain protection.

5. CONCLUSIONS

The interventions examined show improved natural ventilation compared to the base case, resulting in quicker particle dispersion and less particle deposition at room surfaces. The designs consider the local climate and user thermal comfort, privacy, security, and protection from mosquitoes. Vents at the Middle of the Ceiling along the roof cap dispersed particles quicker than those at the Front Wall. However, the latter allow more particles to escape from them, resulting in less particle dispersion in the indoor air. The findings show that even with the use of limited technology and cost, appropriate design interventions can lead to significant improvements to indoor air quality conditions in single-room dwellings. This will be highly beneficial for many people in the wider global south, Sub-Saharan Africa and Kenya, where the estimated populations that live in slums are 24%, 55%, and 56% [23] respectively. For continuing effective performance of the interventions, it is important for occupants to have adequate understanding of the links between indoor air quality and health. This might require user education on the purpose of the design interventions. Although a fixed inlet velocity has been assumed for this study, in reality, there might be periods that the ACH are lower or higher due to varying wind speeds and the temperature and pressure differences between indoors and outdoors. Further work is required to evaluate a range of conditions; sizes, positions and number of vents installed across the room; as well as different combinations of them.

ACKNOWLEDGEMENTS

The study was funded by the British Academy.

REFERENCES

1. He, L.Y., Hu, M., Huang, X.F., Yu, B. De, Zhang, Y.H., Liu, D.Q., 2004. Measurement of emissions of fine particulate organic matter from Chinese cooking. Atmos. Environ. 38, 6557– 6564.

2. Zhai, S.R., Albritton, D., 2020. Airborne particles from cooking oils: Emission test and analysis on chemical and health implications. Sustain. Cities Soc. 52, 101845.

3. Poulsen, A. H. et al., 2023. Air pollution with NO2, $PM_{2.5}$, and elemental carbon in relation to risk of breast cancer– a nationwide case-control study from Denmark. Environmental Research, 216(2), p. 114740. doi: 10.1016/j.envres.2022.114740.

4. Yang, L. et al., 2023. The $PM_{2.5}$ concentration reduction improves 677 survival rate of lung cancer in Beijing. Science of the Total Environment. The Authors, 858(38), p. 159857. doi: 10.1016/j.scitotenv.2022.159857.

5. Kaur, K. et al., 2022. $PM_{2.5}$ exposure during pregnancy is associated with altered placental expression of lipid metabolic genes in a US birth cohort. Environmental Research. Elsevier Inc., 211(February), p. 113066. doi: 10.1016/j.envres.2022.113066.

6. Abdullahi, K.L., Delgado-Saborit, J.M., Harrison, R.M., 2013. Emissions and indoor concentrations of particulate matter and its specific chemical components from cooking: A review. Atmos. Environ. 71, 260–294.

7. Costanzo, V., Yao, R., Xu, T., Xiong, J., Zhang, Q., Li, B., 2019. Natural ventilation potential for residential buildings in a densely built-up and highly polluted environment. A case study. Renew. Energy 138, 340–353.

8. Mašková, L., Smolík, J., Ondráček, J., Ondráčková, L., Travnickova, T., Havlica, J., 2020. Air quality in archives housed in historic buildings: Assessment of concentration of indoor particles of outdoor origin. Build. Env. 180, 1–10.

9. Yang, F., Kang, Y., Gao, Y., Zhong, K., 2015. Numerical simulations of the effect of outdoor pollutants on indoor air quality of buildings next to a street canyon. Build. Env. 87, 10–22.

10. Rim, D., Novoselac, A., 2010. Ventilation effectiveness as an indicator of occupant exposure to particles from indoor sources. Build. Environ. 45, 1214–1224.

11. Pamoja Trust and SDI, 2008). An Inventory of the Slums in Nairobi. Pamoja Trust, Urban Poor Fund International and Shack/Slum Dwellers International. Nairobi, Kenya.

12. Amnesty International, 2009. Kenya, The Unseen Majority: Nairobi's Two Million Slum-Dwellers. Amnesty International Publications, London.

13. UN-Habitat, 2019. 'Kenya Habitat Country Programme Document (2018-2021) Nairobi, Kenya. https://shorturl.at/chzNY (last accessed 29.03.2023).

14. Egondi, T., Muindi, K., Kyobutungi, C., Gatari M., and Rocklöv, J., 2016. Measuring exposure levels of inhalableair-borne particles ($PM_{2.5}$) in two socially deprived areas of Nairobi, Kenya. Environmental Research 148:500–506.

15. Egondi, T., Ettarh, R., Kyobutungi, C. Ng, N. and Rocklöv, J., 2018. Exposure to Outdoor Particles ($PM_{2.5}$) and Associated Child Morbidity and Mortality in Socially Deprived Neighbourhoods of Nairobi, Kenya. Atmos. 9.

16. Ngo, N. S., Gatari, M., Yan, B. Z., Chillrud, S. N., Bouhamam, K., and Kinney, P. L., 2015. Occupational exposure to roadway emissions and inside informal settlements in sub-Saharan Africa: A pilot study in Nairobi, Kenya, Atmos. Environ., 111, 179–184, https://doi.org/10.1016/j.atmosenv.2015.04.008, 2015.

17. Muindi, K., Murage E.K., Egondi T., Rocklöv, J., Ng N., 2016. Household Air Pollution: Sources and Exposure Levels to Fine Particulate Matter in Nairobi Slums. Toxics, 4(3), 12.

18. World Bank. Kenya Informal Settlements Improvement Project 2 (P167814). 2019. https://shorturl.at/cmqJQ (last accessed 19.12.2023).

19. Chen, F., Yu, S.C.M., Lai, A.C.K., 2006. Modelling particle distribution 590 and deposition in indoor environments with a new drift-flux model. Atmos. Environ. 40, 357–367.

20. Zhang, T., Zhang, Y., Li, A., Gao, Y., Rao, Y., Zhao, Q., 2022c. Study on the kinetic characteristics of indoor air pollutants removal by ventilation. Build. Environ. 207.

21. Xu, G., Wang, J., 2017. CFD modelling of particle dispersion and deposition coupled with particle dynamical models in a ventilated room. Atmos. Environ. 166, 300–314.

22. Zhou, H. Y., Zhong, K., Jia, H. W., & Kang, Y. M., 2022. Analysis of the effects of dynamic mesh update method on simulating indoor airflow induced by moving objects. Build. Environ. 212, 108782.

23. UN-Habitat, 2016. Slum almanac 2015-2016: Tracking improvements in the lives of slum dwellers. Nairobi, Kenya: United Nations Human Settlements Programme.

PLEA 2024 WROCŁAW
(Re)thinking Resilience

Assessing View Clarity in Electrochromic Glazing: A Quantitative Approach

NASIM GOLI BAGHMAHYARI,[1] PEIMAN PILEHCHI HA,[2] FARHAD BARAHIMI,[3]

[1] Department of Architecture, Bu-Ali Sina University, Hamedan, Iran
[2] Healthy Living Spaces lab, Institute for Occupational, Social and Environmental Medicine, Medical Faculty, RWTH Aachen University, Aachen, Germany
[3] Department of Architectural Technology, Pars University, Tehran, Iran

ABSTRACT: The Quality of View (QV) through windows significantly impacts human well-being, with view clarity representing a crucial aspect within QV assessments. Electrochromic (EC) windows, capable of dynamically adjusting tint levels to manage light and heat penetration, offer varying degrees of view clarity. Evaluating this clarity is vital for a comprehensive understanding of how EC windows influence human comfort in architectural settings. This study introduces a unique quantitative approach to assess the clarity of views facilitated by EC windows. Employing advanced image processing techniques, a novel methodology tailored for this purpose was developed, generating 1152 images through the Radiance engine. These images considered multiple factors such as viewpoint, tint level, separate window zones, and time of day. Using the Landolt-C chart as a simulated view target under diverse EC window configurations, the study compared simulated images with a reference image, applying the Saliency Guided Enhanced Structural Similarity algorithm (SG-ESSIM) —an image quality assessment algorithm. The study's outcomes underscore the method's ability to identify optimal EC window configurations, effectively maximizing QV. Furthermore, this methodology holds promise for integration with other EC window control strategies, presenting opportunities for trade-off solutions in multi-objective simulation designs.
KEYWORDS: Visual Comfort, Window view, Image processing, Computer Vision, View quality

1. INTRODUCTION

One of the main functions of windows and shading devices is to let enough daylight in and to offer a view out [1]. Exposure to daylight and outside view can enhance workers' productivity, occupants' mood and satisfaction, lower stress levels and relax eye muscles [1–5]. While interesting views [6] may influence discomfort glare tolerance, the prevalence of glare poses challenges in sustaining a consistently clear view throughout the day. Consequently, solutions such as EC glazing have gained popularity as potential solutions.

EC glazing has been used as an architectural solution that can control the amount of radiation entering a building while providing the occupants with a view of the outside by utilising its “switchable” transmittance technology. The EC glazing system consists of multilayer coatings on the glass which on applying low voltage induces ion migration from the EC layer resulting in modulation of the optical properties seen as a colour change of the glazing [1].

A tri-zone EC, which is studied in this paper, is a type of multi-zone EC that has three independently controllable zones. This would be fitted to the tri-functional-zone concept of windows providing daylight, view, and balustrade [14]. Some studies focus on multi-zone EC but window split purposes and pane numbers are different [13, 15-17]. For instance [15] used a window with two independently controlled panes, top and bottom, and aimed at determining if EC can be controlled to provide lower lighting energy consumption while maintaining occupant visual comfort.

Previous studies into QV employed two assessment methodologies: quantitative [5, 7–9] and qualitative [2,4,10]. The predominantly qualitative nature of these studies makes them susceptible to errors stemming from a limited number of participants, view angles, and time.

One involved EC [4], but none of them applied an image-processing technique that mimics human vision and achieves the results based on simulation from beginning to end.

Utilizing such techniques helps to manipulate and test the view target, angle, and other factors across various hours and seasons with relative ease.

The authors are unaware of any reported implementation of a computer-based method for projecting or analyzing view images, despite the suggestion of such a technique in two studies, [2,4], as part of their future work or as an alternative approach to their chosen one.

One of the drawbacks of ECs is changing indoor colour perception depending on the tint level. It is mentioned in [5] that the shifted colour of the outdoor view may affect contrast sensitivity and colour perception.

Such shift colour in ECs is investigated in [4,11,12]. These studies did not aim to lower the colour shift or change it in any way, rather they investigated the effect of EC on how differently the colour of experiments will show under EC effect. Another study [13] investigated the possibility of achieving a neutral spectrum when using EC in buildings.

This study proposes using colour shift as a factor in decision-making. By allowing to choose the amount of colour shift, this paper considers colour shift in conjunction with view clarity assessment and offers a range of solutions. Therefore, the optimal solution will depend on the specific context in which EC will be used. This means that while the view clarity score may not change significantly, there is potential to choose between various levels of colour shift in the optimum solution which designers or users can choose from.

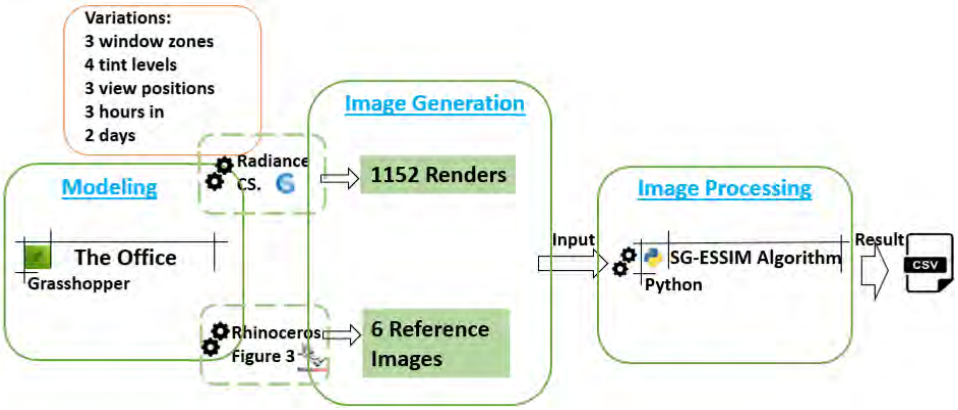

Figure 1: The view clarity assessment framework

2. METHODOLOGY

This study employs an advanced image processing technique, introducing a novel methodology tailored for assessing the view clarity (Fig.1)

A south-faced office with a three-horizontal-zone window with electrochromic glazing was modelled in Rhinoceros. Each zone potentially has four tint levels that can be independently changed. Three viewpoints in the room were considered to assess the view from different angles. Views were rendered on the 21st of March and June at 9:00, 12:00, and 15:00, with the Radiance engine in ClimateStudio (CS). Therefore, the window view database includes 1152 renders, 192 for each hour of each month. Renders were input to the Saliency Guided Enhanced Structural Similarity (SG-ESSIM) an image quality metric algorithm in Python to assess the clarity of the target seen through the window. The outcome was a CSV file with all renders' view clarity (SG-ESSIM) scores.

Aiming for the lowest colour shift, the sum of the tint levels of 3 zones was considered as the total tint level (TTL). The view clarity scores along with TTL were used to draw Pareto frontier lines for proposing optimum solutions (Fig.5 graph a to f). As the middle zone is the one responsible for providing a view outdoors [18], its tint level is reported in Table 2 for better comparison.

2.1 Model generation

The room model generated in Grasshopper is a south-facing room located in Isfahan, Iran, with a dimension of 6*5 meters with 3 meters height on the sixth floor at 15 meters above the ground. It has a window to the south with a window-to-wall ratio of 70%, (Fig. 2). The window has been split into three horizontal equal panes, top, middle, and bottom, as recommended by [14]. Three viewpoints were defined to render from different angles. The three view positions were 3 meters from the window, they were in the middle of the room, and their gaze directions were from the positions to the center of the window, (Fig. 2). The eye level was 1.17 meters.

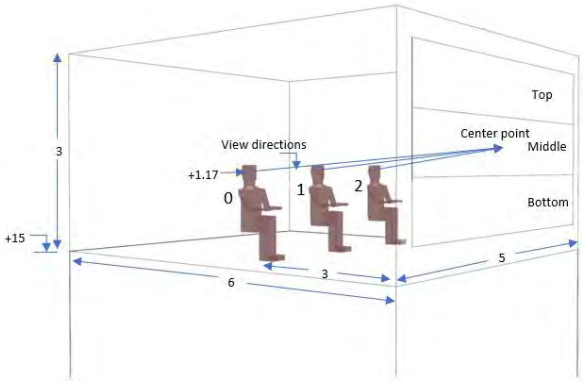

Figure 2: The model dimensions, three view positions, and the window's three zones (panes), (all dimensions are in meters)

Each pane can get one of the four existing tint levels at a time. Sage glass brand's tint levels were used (Table 1).

Table 1: The model materials' features and the EC glazing tint levels, Tvis: Visible transmittance (%), TL: The glazing's Tint level from 0 the clearest level to 3, Spec: Specularity, Ro: Roughness

Glazing	Tvis				
TL 0	59.7%				
TL 1	17.3%				
TL 2	5.5%				
TL 3	0.9%				
Material	Reflectance			Ro	Spec
	R	G	B		
Ceiling	0.86	0.85	0.78	0.20	0.35%
Walls	0.73	0.66	0.54	0.20	0.21%
Floor	0.36	0.37	0.36	0.2	1.07%

2.2 Window view target

The Landolt-C chart is used as a view target. The Landolt-C optotype is a standardized symbol for testing vision, developed by Swiss ophthalmologist Edmund Landolt [19]. It consists of a ring with a gap in different positions (left, right, bottom, top, and the 45° positions in between), resembling the letter C. The stroke width is 1⁄5 of the diameter, and the gap width is the same [20]. In [4], Landolt-C was used as a target for taking high dynamic range pictures from the inside to compare its clarity under different window layers. We chose this target because it has a common shape and a consistent number of edges that the algorithm can detect. Also, it makes comparing the renders' quality easier than any random targets. The target is assumed to be hung without any background at a 6-meter distance from the window. We rotated the chart by 90 degrees to have an equal series of C sizes in each window pane in all three views (Fig. 3). The material for this target was CS's black colour.

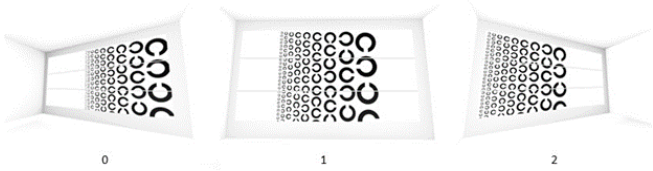

Figure 3:The Landolt-c chart is the view target from three view positions of 0, 1, and 2, looking toward east, south and west, respectively. These view images were simulated without any window pane as reference images.

2.3 SG-ESSIM algorithm

SG-ESSIM is an image quality assessment method that takes into account the human visual system's perception of salient regions in an image. It aims to provide a more accurate evaluation of image quality by focusing on the most visually important areas of an image [21]. The algorithm has been implemented in the Python environment with the help of Open-Source Computer Vision (OpenCV) and Numerical Python (NumPy) two Python libraries for computer vision and numerical operations, respectively.

2.4 Code description

Several functions were defined to prepare as well as process the score of images. The preprocess function converts the reference view images and 1152 sample images to grayscale.

Then the SG_ESSIM function as the main implementation of the SG-ESSIM algorithm preprocesses the reference and sample images, computes the directional gradients of the pre-processed images, retrieves the parameters for the computation, computes the gradient differences between the directional gradients of the reference and sample images, calculates an edge map based on the maximum gradient magnitudes, and computes the quality score using the SG-ESSIM formula and the edge map.

2.5 Process steps

In the first step, the sample images are resized to the same dimensions, and the pixels are perfectly aligned for accurate comparison. All the pixels of the photo, except for the ones in the window, are set to the same value, making them ineffective in the process. The output photos of the first stage are placed as the input of the SG-ESSIM algorithm.

The second part of the code implements the SG-ESSIM algorithm. The SG-ESSIM algorithm was used to measure the quality of the renders compared to the reference images. For the reference images, we used Rhino to render views while the glasses were eliminated. In this situation, the renders show all the elements (C shapes) of the target clearly, and we can use them as references to compare the clarity of other renders (Fig.3). The highest possible score represents the full similarity to the reference is 100% and the lowest is 0%. The result of the algorithm is a CSV file with all window combinations' SG-ESSIM scores and images of detected edges (Fig.4) for each render.

Figure 4: Left: A simulated view generated by CS for view position 0, tint levels of 0, 0, 2 top to bottom. Middle: The resized grayscale format. Right: The detected edges after running the SG-ESSIM algorithm

The example shown in Fig.4 is an image rendered on the 21st of March at 15:00 from view position 0, (Fig.3). The tint levels of the top, middle, and bottom panes are TL0, TL0, and TL2 (Table 1). The left image is the simulated view, and the middle and right images are produced while running the algorithm. The SG-ESSIM

score for this example was 90.9% and is the 25th best in the same time and position group.

The results of the SG-ESSIM score and the TTL in each time and position were applied to draw the Pareto frontier to see a range of the most optimum solutions in Fig.5.

3. RESULT AND DISCUSSION

The developed framework was evaluated by comparing the renders assessed with it. The results confirmed that it performed flawlessly. The algorithm correctly assigned higher SG-ESSIM scores to renders with higher clarity. Checking the results, the authors observed the SG-ESSIM algorithm correctly assigned higher scores to the clearer images with more detected edges.

The chart analysis shows the SG-ESSIM scores of March's renders are higher than the June at all studied hours. This can show the effect of the sun's position in a view's clarity seen through the window.

A significant finding from the analysis was that the optimal SG-ESSIM score occurred when the TTL was 4, across all six trials. This suggests a possible way to estimate the clarity of the image based on the tint level.

Regarding the view positions, the results show the following:

- At 9:00 and 12:00, human position 0, looking toward the east, has the highest SG-ESSIM for all TTLs, while at 15:00, position 1, looking toward the south, provides the most optimum clear view.
- None of the 6 times resulted in any combination achieving its highest SG-ESSIM at position 2, looking toward the west.

These findings indicate that in this case study, arranging the occupants' desks so that their directions are aligned with positions 1 and 0 will result in the highest SG-ESSIM. The results were consistent seasonally but varied throughout the day. It was observed that in the afternoon, position 1 provides more clear view than positions 0 and 2. This suggests flexible desk allocations, allowing workers in the morning and afternoon to change their locations. Even without such flexibility, positions 1 and 0 still provide the most optimum results.

The shape of the view target can affect the view seen by occupants, so using this method to help designers decide on desk positions should be individualized based on each case. Further investigation in the future may eliminate the target dependency for this aspect.

After choosing the position, the best combination of TTL and SG-ESSIM can now be selected for each time with an automatic control system.

Fig.5 charts show depending on the designer's preference, design goals, or function of the space, a trade-off that balances view quality and interior lighting colour can be selected from the Pareto optimal solutions.

The middle pane of a window has the most impact on the view quality, as explained in section 1. The selected option from the Pareto frontier chart and its corresponding middle pane tint level are displayed in Table *2*. Besides SG-ESSIM and the total tint level, the middle tint level is another factor that affects the choice of the combination.

The data in the table is sorted from the lowest total tint level to the highest.

One of the intended benefits of this method is enabling the use of view as a control strategy factor. This can be combined with other visual, and thermal comfort principles, and result in an optimized combination with a high-clarity view. Another application of this method in an earlier step is in making interior design decisions, as it demonstrates the benefits and drawbacks of each position.

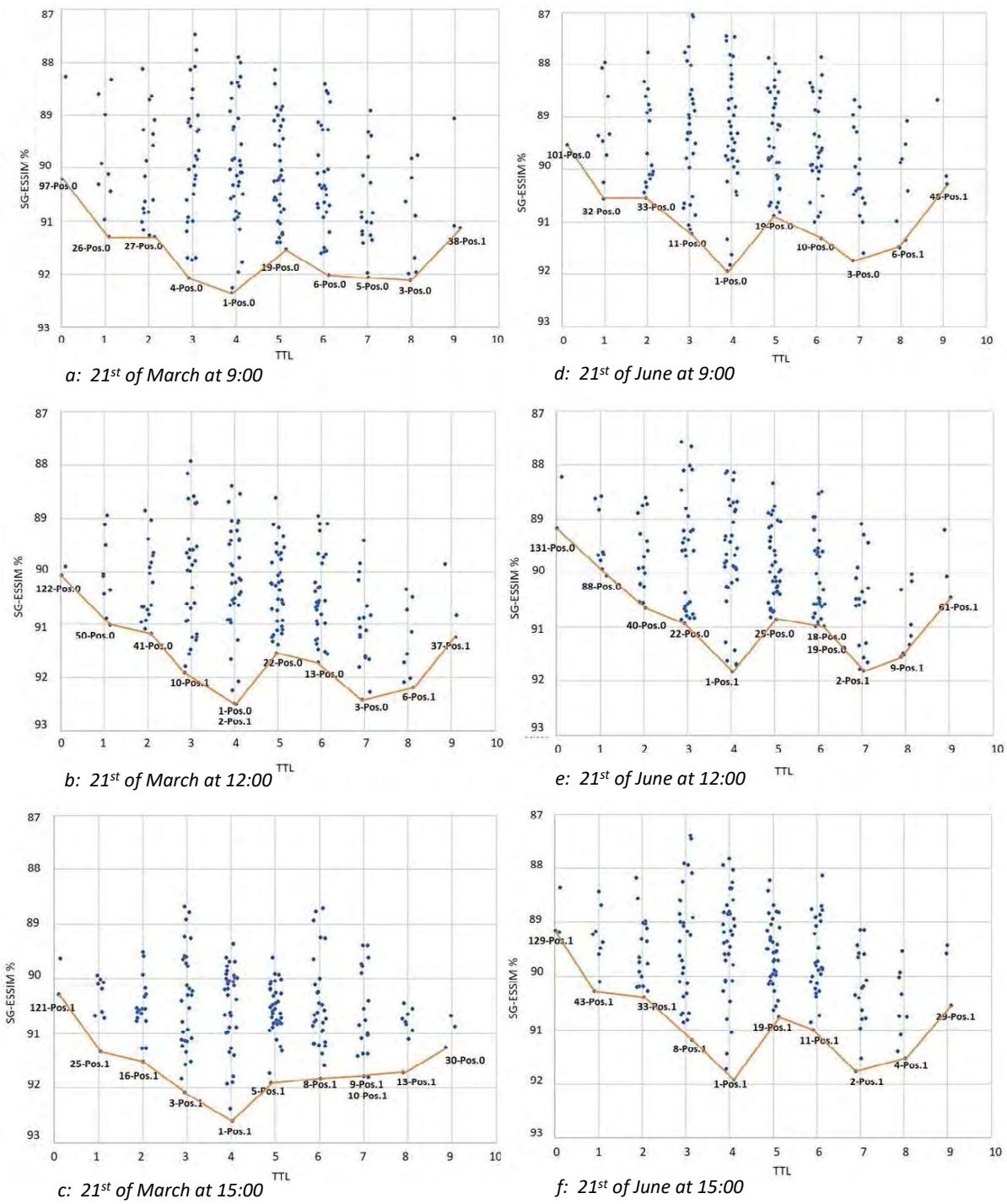

Figure 5: Graph a-f showing the SG-ESSIM (view clarity) scores and the sum of tit levels of 192 EC window combinations were calculated for different times and positions. The Pareto Frontier line is depicted in red and the model numbers corresponding to the most optimum clear views are indicated. TTL data on the Y-axis are presented with a jitter for enhanced visualization. The SG-ESSIM scores were multiplied by 100 for better comparison in the Pareto charts. The position of each combination on the Pareto line was written near each point number as: (Pos.). See Figure 3 for view positions.

4. CONCLUSION

This paper presents a method to evaluate the clarity of the scenes visible through the window. The method involves using a computer to analyze the view based on the rendering results from the Radiance engine. Then, an image quality assessment algorithm evaluates the clarity of the renders using the SG-ESSIM algorithm. The results indicate that the algorithm can identify the clearest image among the others and that the clarity score correlates with the number of edges and C shapes detected in the image. This method allows optimal view quality selection through EC windows and also has the potential to be combined with other control strategy factors such as thermal or visual comfort to achieve a balanced solution in multi-objective scenarios. In an initiative stage, this method

helps make interior design decisions by analyzing the benefits and drawbacks of each position where occupants sit.

Table 2: The selected solutions from the Pareto line on the 21st of March and June, their total tint level, their middle pane tint level (Mid TL), and their SG-ESSIM score. TTL: Total Tint Level is the sum of the three panes tint levels. TL: Tint Level defined from 0 (lightest) to 3(darkest)

21st March at 9:00				**21st June at 9:00**			
# Render	TTL	Mid TL	SG-ESSIM%	# Render	TTL	Mid TL	SG-ESSIM%
97	0	0	90.23	101	0	0	89.52
26	1	0	91.30	32	1	0	90.57
27	2	1	91.30	33	2	2	90.55
4	3	2	92.07	11	3	2	91.23
1	4	2	92.36	1	4	2	91.94
19	5	3	91.54	19	5	0	90.89
6	6	3	92.02	10	6	3	91.31
5	7	3	92.05	3	7	3	91.75
3	8	3	92.11	6	8	3	91.51
38	9	3	91.12	48	9	3	90.28

21st March at 12:00				**21st June at 12:00**			
# Render	TTL	Mid TL	SG-ESSIM%	# Render	TTL	Mid TL	SG-ESSIM%
122	0	0	90.07	131	0	0	89.45
50	1	0	91.01	88	1	0	90.05
41	2	2	91.17	40	2	0	90.65
10	3	2	91.91	22	3	2	90.93
1,2	4	2	92.49	1	4	2	91.83
22	5	0	91.53	25	5	0	90.86
13	6	3	91.71	18,19	6	3	90.99
3	7	3	92.42	2	7	3	91.81
6	8	3	92.19	9	8	3	91.55
37	9	3	91.23	61	9	3	90.45

21st March at 15:00				**21st June at 15:00**			
# Render	TTL	Mid TL	SG-ESSIM%	# Render	TTL	Mid TL	SG-ESSIM%
121	0	0	90.28	129	0	0	89.19
25	1	0	91.33	43	1	0	90.28
16	2	0	91.51	33	2	2	90.39
3	3	2	92.08	8	3	2	91.18
1	4	2	92.61	1	4	2	91.92
5	5	1	91.91	19	5	2	90.76
8	6	3	91.82	11	6	3	91.00
9,10	7	2-3	91.79	2	7	3	91.76
13	8	3	91.71	4	8	3	91.52
30	9	3	91.26	29	9	3	90.55

ACKNOWLEDGEMENTS

Peiman Pilehchi Ha was funded by a research grant (21055) by VILLUM FONDEN.

REFERENCES

1. Jain, S. Karmann, C. Wienold, J. (2022). Behind electrochromic glazing: Assessing user's perception of glare from the sun in a controlled environment. *Energy and Buildings*, 256.
2. Hellinga, H. Hordijk, T. (2014). The D&V analysis method: A method for the analysis of daylight access and view quality. *Building and Environment*, 79.
3. Lee, E. Matusiak, B. Geisler-Moroder, D. Selkowitz, S. Heschong, L. (2022). Advocating for view and daylight in buildings: Next steps. *Energy and Buildings*, 265.
4. Ko, WH. Brager, G. Schiavon, S. (2017). Building envelope impact on human performance and well-being: an experimental study on view clarity. [Online]. Available: https://escholarship.org/uc/item/0gj8h384
5. Ko, WH. Kent, MG. Schiavon S, Levitt B, Betti G. (2022). A Window View Quality Assessment Framework. *The Journal of the Illuminating Engineering Society*, 18.
6. Tuaycharoen, N. Tregenza, P. (2005). Discomfort glare from interesting images. *Lighting Research and Technology*, 37.
7. Chang CY. (2021). Window View Quality: Investigation of Measurement Method and Proposed View Attributes. PhD thesis, University of Sheffield. [Online]. Available: https://etheses.whiterose.ac.uk/29784/
8. Flamant, G. Bustamante, W. Tzempelikos, A. Vera, S. (2022). Evaluation of view clarity through solar shading fabrics. *Building and Environment*, 212.
9. Konstantzos, I. Chan, YC. Seibold, JC. Tzempelikos, A. Proctor, RW. Protzman, JB. (2015). View clarity index: A new metric to evaluate clarity of view through window shades. *Building and Environment*, 90:206–14.
10. Li, W. Samuelson, H. (2020). A new method for visualizing and evaluating views in architectural design. *Developments in the Built Environment*, 1.
11. Arbab, S. Matusiak, B. Martinsen, F. Hauback, BC. (2017) The impact of advanced glazing on color perception. *Journal of the International Colour Association*.
12. Matusiak, B. Nazari, M. Angelo, K. (2021). Colour shift due to Chromogenic dynamic glass [Internet]. Milano: *AIC 14th Congress.* Available: https://www.researchgate.net/publication/355427790
13. Mardaljevic, J. Kelly Waskett, R. Painter, B. (2015) Neutral daylight illumination with variable transmission glass: Theory and validation. *Lighting Research and Technology*, 48.
14. Reinhart C. (2012). 4.430 Daylighting. MIT Open Course Ware [Online], Available: http://ocw.mit.edu/
15. Fernandes, LL. Lee, ES. Ward, G. (2013) Lighting energy savings potential of split-pane electrochromic windows controlled for daylighting with visual comfort. *Energy and Buildings*, 61: 8–20.
16. Wu, Y. Wang, T. Lee, ES. Kämpf, JH. Scartezzini, JL. (2019). Split-pane electrochromic window control based on an embedded photometric device with real-time daylighting computing. *Building and Environment*, 161.
17. Ganji Kheybari, A. Steiner, T. Liu, S. Hoffmann, S. Controlling Switchable Electrochromic Glazing for Energy Savings, Visual Comfort and Thermal Comfort: A Model Predictive Control. *CivilEng*, 2.
18. Reinhart, C. (2014). Daylighting handbook I Fundamentals Designing with the sun.
19. Evans, J. (2006). Standards for visual acuity. [Online], Available: https://www.nist.gov/document/visualacuitystandards1pdf
20. Danilova, M. Bondarko, V. (2007) Foveal contour interactions and crowding effects at the resolution limit of the visual system. [Online], Available: https://www.ncbi.nlm.nih.gov/pmc/articles/PMC2652120/
21. Varga, D. (2022) Saliency-Guided Local Full-Reference Image Quality Assessment. *Signals*, 3.

PLEA 2024 WROCŁAW
(Re)thinking Resilience

Predicting annual hourly daylight performance of buildings using Conditional Generative Adversarial Network (cGAN)

ANIS MANAL[1] YOU-JEONG KIM[1] YUN KYU YI[1] YONGHYUN YU[2]

[1] University of Illinois at Urbana-Champaign, Champaign, USA
2 University of Ulsan, Ulsan, Korea (South)

ABSTRACT: With the current climate crisis, there has been a growing interest in understanding how building facades impact the indoor performance of the building. To this end, annual performance simulations are being conducted to improve building efficiency in terms of daylight, energy, ventilation etc. However, with complex building facades, such as dynamic shading systems, such annual performance evaluation come with heavy computation load and time. To overcome these limitations of annual performance simulation, many studies have looked toward machine learning which can predict building performance instantaneously with reasonable accuracy. This paper presents a novel methodology that uses conditional generative adversarial network (cGAN) to predict annual daylight in buildings instantaneously. Seven different kinds of building geometries are studied, each with different window locations, size, horizontal and vertical shading devices, and at different times of the day with varied sky conditions. Results indicate a prediction accuracy of 96% generated in less than a second. The main contribution of the research lies in the proposed methodology that demonstrates the suitability of the cGAN model called Pix2pix as a proxy model, generating fast and highly accurate results, for rapid annual daylight prediction and illustrating it on a contour plot during early design phase.
KEYWORDS: Daylight, Window shading, Machine learning, Data-driven design, Pix2pix

1. INTRODUCTION

Building performance simulations have recently allowed researchers to develop innovative facade strategies, ensuring indoor environmental quality, occupant health and wellbeing. Continuous developments in the field of daylight prediction have led to the introduction of Climate-based daylight modelling (CBDM). CBDM uses realistic sun and sky conditions derived from standard meteorological data for daylight prediction. However, this involves time-consuming ray tracing methods to capture the hourly climatic variations year-round. This is computationally expensive with a high simulation runtime, making rapid decision-making in the early design phase challenging.

This research proposes a model that predicts indoor illuminance in 20 milliseconds while maintaining a reliable prediction accuracy. While cGAN's reduced computation time make real-time simulations possible, its image-based predictions allow designers with no building-physics expertise to receive feedback on their design. Efficiency in runtime allows in-depth design exploration and bridges the gap between performance feedback and design decision-making in the early stages.

2. BACKGROUND

Recently, with easy accessibility to Machine Learning (ML) models such as Artificial Neural Network (ANN), Generative Adversarial Network (GAN), etc. rapid daylight prediction methods has become possible. However, ANN outputs one numerical value per ANN model, which restricts designers in visualizing a comprehensive daylight distribution [1]. On the other hand, GAN, which consists of a generator to generate fake images and a discriminator to identify them, can't control the image generation process in the absence of labelled inputs. To overcome this limitation, conditional GAN (cGAN) was developed [2], where an additional class label embedded with contextual information is used to control the image generation process.

While cGAN has been used in several image-to image translation tasks [3-4], its architecture application has been limited to space layout [5-7], and energy efficiency [8]. Using a smaller dataset of 575 cases, cGAN has been used in daylight prediction [9]. In a previous study, the authors used the pix2pix-based cGAN model to predict daylight for a simple box geometry and generate contour plots to graphically present the daylight distribution. However, the testing geometry consisted of oversimplified parameters with minimum complexity.

For this reason, this paper further investigates pix2pix as a proxy model to rapidly predict annual daylight performance with high accuracy, while adopting more complex and detailed variables.

3. METHODOLOGY

The overall methodology for rapid daylight prediction using cGAN consisted of the following four steps: 1) geometry modelling with variable parameters and dataset creation using twenty-three variables involving the building geometry, window, shading devices, time, and dynamic sky; 2) running daylight simulations to obtain daylight contour plots corresponding to each case in the dataset; 3) encoding the images of building geometry to train the cGAN model; and 4) daylight prediction of new test cases using the trained model.

These steps are discussed below.

3.1 Geometry modelling

To predict daylight for a range of possible window shading configurations located in different façade orientations, the study tested an L-shaped building geometry. The geometry has arms that can extend along both the x- and y-axes (x_1, x_2) (Fig. 1). It is 3 m tall and has a rectangular window of varying width and height on each of the south (x_3, x_4), east (x_5, x_6), and west (x_7, x_8) façade (Fig. 2). Since there is no direct daylight access through north facades, it was modelled as a solid wall.

Each window on the south (x_9, x_{10}; x_{15}, x_{16}), east (x_{11}, x_{12}; x_{17}, x_{18}), and west (x_{13}, x_{14}; x_{19}, x_{20}) façade consists of varying number and depth of vertical fins and horizontal overhangs as shading devices respectively (Fig. 2). However, on the same façade, the windows have the same shading device parameter values.

The time variable was represented through the hour-of-year (x_{21}), indicating changing sun position from 6:00 am to 6:00 pm, resulting in 4,380 hours for whole year. Sky condition was represented using sky cover, ranging from 0 (clear sky) to 10 (overcast) (x_{22}).

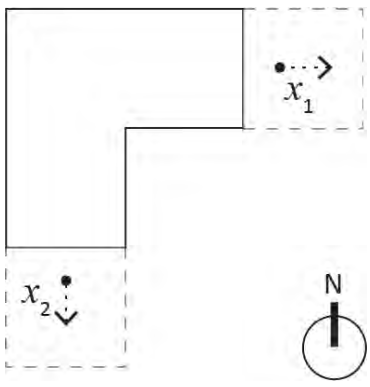

Figure 1: Types of building geometry cases studied.

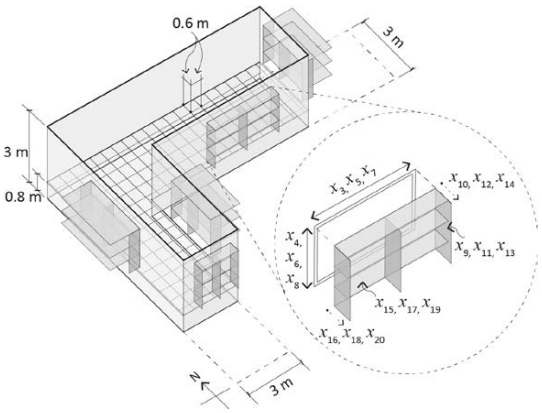

Figure 2: Variable parameters for the building geometry.

Table 1 shows the twenty-three variables used in the study, their value ranges, and the steps considered. These variable parameters were used to create the full dataset, which consisted of 2100 cases.

Table 1: Variable parameters for seven cases.

Variable label	Variable name	Value range	Step
X_1	*x*-axis extension	3.0 – 6.0 m	0.1
X_2	*y*-axis extension	3.0 – 6.0 m	0.1
X_3, X_5, X_7	Window width (South, East, West)	1.2 – 2.4 m	0.1
X_4, X_6, X_8	Window height (South, East, West)	1.2 – 1.8 m	0.1
X_9, X_{11}, X_{13}	Fin number (South, East, West)	0 - 4	1
X_{10}, X_{12}, X_{14}	Fin depth (South, East, West)	0 – 0.9 m	0.1
X_{15}, X_{17}, X_{19}	Overhang number (South, East, West)	0 - 4	1
X_{16}, X_{18}, X_{20}	Overhang depth (South, East, West)	0 – 0.9 m	0.1
X_{21}	Hour of year (HOY)	1 - 4380	1
X_{22}	Sky cover	0 - 10	1

2.2 Daylight simulation

The 2100 cases generated were used to run daylight simulations with the sensor grid located at a height of 0.8 m from the floor level.

The hypothetical building was assumed to be in New York City, NY. The weather data was obtained from the weather station located at LaGuardia Airport (TMY3).

The daylight model also requires accurate material characterizations in order to account for building surface reflections. Therefore, the ceiling and wall surfaces for the daylight model were modeled with a reflectance of 70%, while the floor surface was modeled with a reflectance of 20%. A double-Glazed Unit (DGU) was used as the glazing assembly, with a U-value of 1.62 W/ (m^2.K), a Solar Heat Gain Coefficient (SHGC) of 0.28, and a Visible

Transmittance (TVis) of 47.9%. The Radiance parameters used were -ab 6 –lw 0.01, as accuracy of results are typically increased with -ab values higher than 4 (Mardaljevic, 1995).

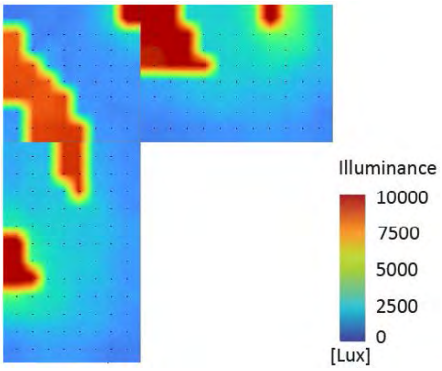

Figure 3: Daylight simulation contour plot.

The daylight contour plots were generated with illuminance levels between 0 lux to 10,000 lux represented by a color gradient from blue to red respectively. For instance, Figure 3 shows the contour plot of a representative case. This L-shaped geometry has arm extension along X- and Y-axis of 4.3 m and 4.9 m. The south window width and height are 1.6 m and 1.4 m, east window width and height are 1.8 m and 1.4 m, west window width and height are 1.6 m and 1.6 m. The south windows have 2 fins 0.3 m deep and one overhang on south 0.2 m deep. The east windows do not have any fins or overhangs. The west windows have one fin 0.2 m deep and two overhangs 0.5 m deep. The case was simulated on January 29, 10:00 am, which is the 681st hour of the year, with a cloud cover of 9.

In this way, 2100 daylight contour plots were collected from the daylight simulations. These contour plots serve as ground truth images for the cGAN model.

2.3 Image encoding and model training

To train cGAN, paired input images are required to be fed into the model. The paired images include a labelled image and a ground truth image.

In this paper, since each unique combination of the variables cast a unique shadow pattern on the floor, floor plan images with these shadow patterns were used to represent the twenty-three design variables and the time variable. The cloud cover corresponding to the specific hour-of-year was represented through shades of blue on the floor plan using Equation (1):

$$C_{(R, G, B)} = 255 - 255 \times (S/10) \quad (1)$$

where, $C_{(R, G, B)}$ - integer for R, G, and B value;

S - cloud cover, expressed in one-tenths.

Thus, the floor plans were encoded with the geometric and time-specific information (Fig. 4). The labelled image, paired with the corresponding daylight contour plot, of all the 2100 cases are then fed to the cGAN model to train it.

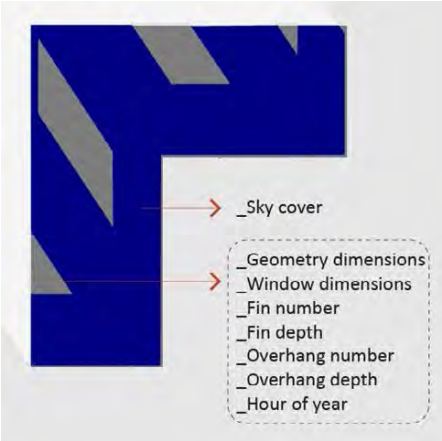

Figure 4: Example of labelled input image.

A cGAN model is trained by simultaneously training a Generative model (G) and a Discriminative model (D) [10]. The generator is provided with labeled input images (i.e., encoded images) to learn to generate fake output images (i.e., contour plots). The discriminator is provided with both the training data (real) and the generated data (fake) and is trained to classify the test data as real or fake. In this way, the discriminator and the generator undergo adversarial training.

The objective loss functions of the generator and the discriminator can be expressed as Equation (2-3):

$$L^{(G)}=\min [\log D(x|y) + \log (1-D(G(z|y)))] \quad (2)$$

$$L^{(D)}=\max [\log D(x|y) + \log (1-D(G(z|y)))] \quad (3)$$

The total value function can be stated as Equation (4):

$$\min_G \max_D V(D,G) = \mathbb{E}_{x\sim Pdata(x)}\left[\log D(x|y) + \mathbb{E}_{z\sim Pz(z)}\log\left(1 - D\left(G(z|y)\right)\right)\right] \quad (4)$$

where, G = the generator;

D = the discriminator;

x = input image;

y = ground truth image, and

z = random noise vector.

Adam optimizer with a learning rate of 0.0002 was used for training and the model was trained for 50 epochs.

2.4 Daylight prediction

Following model training with 2100 cases, the prediction performance of the model was tested with 50 new test cases, looking at windows on the south façade (Table 2). These cases were not part of the training dataset.

This test set consisted of 10 subsets with 5 pairs of input images in each subset. Each subset consisted of one variable parameter, while the other parameters remained fixed.

Table 2: Validation test parameters.

Subset	Case no.	X-axis extension	Y-axis extension	Window width	Window height	Fin no.	Fin depth	Overhang no.	Overhang depth	HOY	Cloud cover
A	1	1.6	1.7	8	6	2	1	2	1	4118	3
	2	1.7	1.6	8	6	2	1	2	1	4118	3
	3	1.8	1.5	8	6	2	1	2	1	4118	3
	4	1.9	1.6	8	6	2	1	2	1	4118	3
	5	1.8	1.8	8	6	2	1	2	1	4118	3
B	1	1	1	7.4	6	2	1	2	1	4118	3
	2	1	1	5.8	6	2	1	2	1	4118	3
	3	1	1	4.7	6	2	1	2	1	4118	3
	4	1	1	6.4	6	2	1	2	1	4118	3
	5	1	1	7.6	6	2	1	2	1	4118	3
C	1	1	1	8	5.5	2	1	2	1	4118	3
	2	1	1	8	5.7	2	1	2	1	4118	3
	3	1	1	8	5.8	2	1	2	1	4118	3
	4	1	1	8	4.6	2	1	2	1	4118	3
	5	1	1	8	5.9	2	1	2	1	4118	3
D	1	1	1	8	6	0	1	2	1	4118	3
	2	1	1	8	6	4	1	2	1	4118	3
	3	1	1	8	6	0	1	2	1	4118	3
	4	1	1	8	6	3	1	2	1	4118	3
	5	1	1	8	6	2	1	2	1	4118	3
E	1	1	1	8	6	2	2	2	1	4118	3
	2	1	1	8	6	2	2.2	2	1	4118	3
	3	1	1	8	6	2	2.1	2	1	4118	3
	4	1	1	8	6	2	2.1	2	1	4118	3
	5	1	1	8	6	2	0.5	2	1	4118	3
F	1	1	1	8	6	2	1	1	1	4118	3
	2	1	1	8	6	2	1	3	1	4118	3
	3	1	1	8	6	2	1	2	1	4118	3
	4	1	1	8	6	2	1	1	1	4118	3
	5	1	1	8	6	2	1	2	1	4118	3
G	1	1	1	8	6	2	1	2	0.7	4118	3
	2	1	1	8	6	2	1	2	1.6	4118	3
	3	1	1	8	6	2	1	2	2	4118	3
	4	1	1	8	6	2	1	2	1.8	4118	3
	5	1	1	8	6	2	1	2	0.5	4118	3
H	1	1	1	8	6	2	1	2	1	3640	3
	2	1	1	8	6	2	1	2	1	8509	3
	3	1	1	8	6	2	1	2	1	1882	3
	4	1	1	8	6	2	1	2	1	5106	3
	5	1	1	8	6	2	1	2	1	6902	3
I	1	1	1	8	6	2	1	2	1	4118	0
	2	1	1	8	6	2	1	2	1	4118	2
	3	1	1	8	6	2	1	2	1	4118	5
	4	1	1	8	6	2	1	2	1	4118	7
	5	1	1	8	6	2	1	2	1	4118	10
J	1	1.9	2	4.9	4.5	2	0.1	0	1.9	540	3
	2	1.3	1.7	7.8	5.2	1	0.3	3	2.4	1640	9
	3	1.6	1.8	6.4	4.6	2	2.2	2	0.7	3207	5
	4	1.2	1.7	6.7	4.4	4	1.5	1	2.3	6202	8
	5	1.4	1	4.1	5.4	2	0.6	3	1.7	302	0

For instance, subset A consisted of cases where the arm length for L-shaped building had varying extensions along X- and Y-axes, while all the other variables were kept unchanged. Similarly, subsets B and C has varying window widths and heights respectively. Subsets D and E tests varying fin numbers and depths, while subsets F and G looks at varying overhang numbers and depths.

Subset H tests varying hours of the year. The five hours of year (HOY) tested were 3640, 8509, 1882, 5106, and 6902 hrs, which correspond to June 1, 4pm; December 21, 12pm; March 20, 10am; August 1, 6pm; and October 15, 2pm respectively. The HOY for the reference case was 4118, which corresponds to June 21, 2pm. Subset I looks at varying cloud covers from 0 (clear sky) to 10 (cloudy).

The only exception is subset J, where all the parameters were assigned random values. Table 2 lists the values used in the 50 tests cases, categorized into 10 subsets.

Model performance was assessed using the Structural Similarity (SSIM) index, which measures the similarity between two images based on their pixel values (Wang et al., 2003). SSIM ranges between -1 and 1, indicating perfect similarity and anti-correlation respectively.

3. RESULTS AND DISCUSSION

To ascertain cGAN model performance, the predicted daylight contours are compared against those generated from simulation results (Fig. 5). Despite some inaccurate predictions, overall results indicate a close match between the predicted contour plots and the ground truth images obtained from simulation results. The resultant average SSIM was 0.96 which indicates a good prediction performance by the model.

The model performed the best in predicting the hour of year (Fig. 5 subset H) and cloud cover (Fig 5. subset I), both with an average SSIM of 0.976. Within subset H, it was seen that the lower the sun angle during a day the better the model performance. For example, H-1 i.e., June 1, 4 pm had the best prediction, followed by H-5 i.e., October 15, 2 pm and H-4 i.e., August 1, 6pm. H-2, December 21, 12pm; and H-3, March 20, 10am, performed the worst. Since more light can penetrate the interior of a space, it shows significant differences in the lit and the underlit areas, represented by high contrasting solar patch colors ranging from red to blue. This is perhaps why it is easier for the model to predict the image. On the contrary, H-3, being the only morning sun angle studied, showed the worst prediction result. As a high sun angle is mostly cut off from the room interior due to the presence of shading devices, the indoor daylight distribution has only subtle variations in blue color, which seems to make it harder for the model to predict.

As mentioned before, subset I shares the same SSIM of 0.976 as subset H. However, with subset I, the best performance was seen with the cloudiest sky (I-5) while the worst was seen during clear sky (I-1).

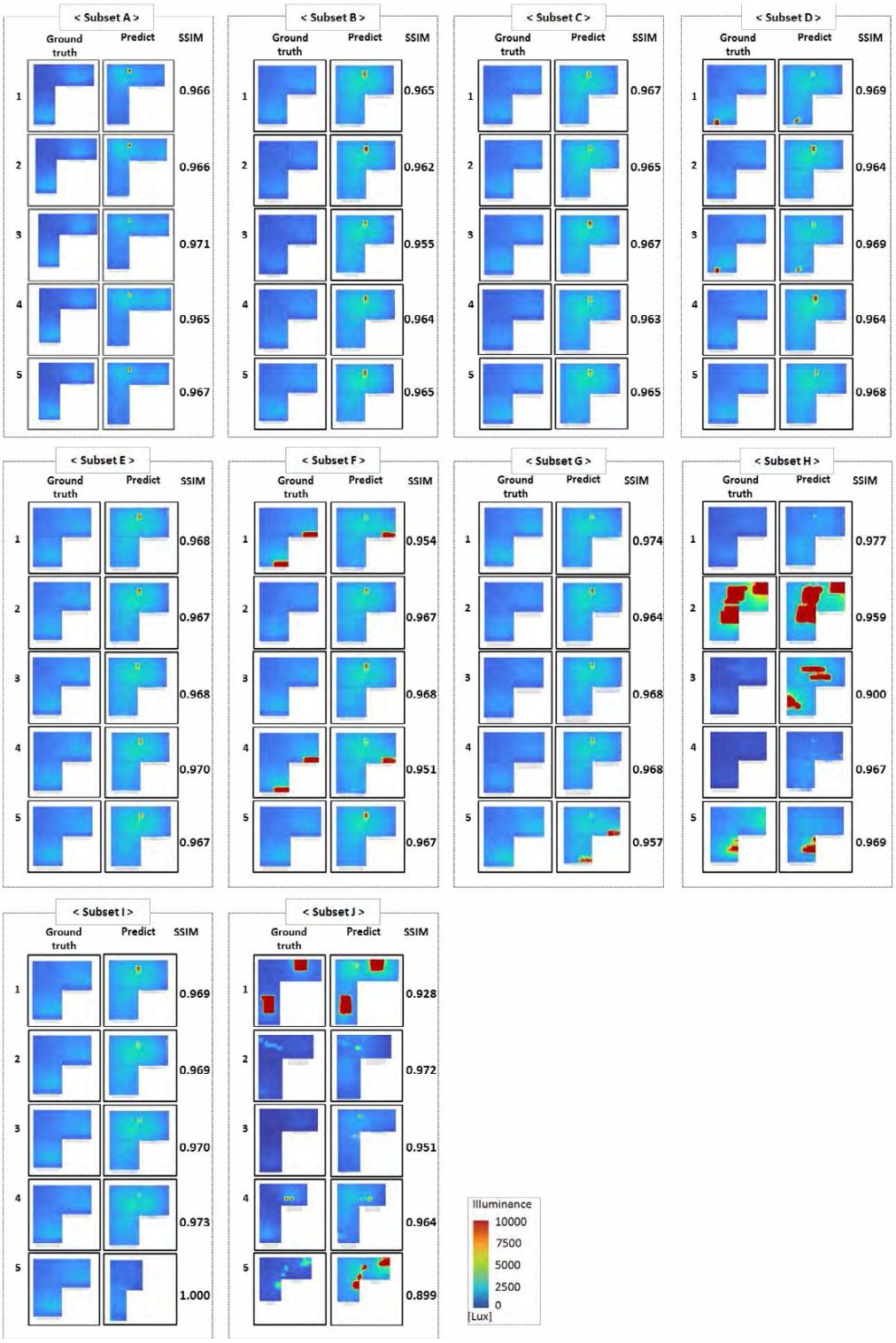

Figure 5: Model test results.

This contrasted with the performance of subset H since the clear sky will have strong daylight contrast and be relatively easier to predict while cloudy skies will create a gentler daylight distribution and be harder to predict for the model. But the model predicted daylight distribution under a cloudy sky relatively accurately.

The next best performance was seen with varying depth of vertical fins (subset E), with an average SSIM of 0.968. However, the prediction accuracy was found to be inconsistent, as two different cases (E-3 and E-4) both with the same fin depth of 2.1 m produced different SSIM (0.968 and 0.970 respectively). The SSIM between the highest possible fin depth of 2 m (E-1) and the lowest fin depth of 0.5 m (E-5) were also very close at 0.968 and 0.967 respectively, potentially falling within the margin of error.

This was closely followed by the prediction performance of the model looking at geometry dimensions (subset A) and fin number (subset D), both having an average SSIM of 0.967. In subset A, A-3 showed the best performance with SSIM 0.971. A-3 had one of the longer x-axis elongations in the study (18 m), which resulted in a larger south exposed window. This increased the daylight penetration in the interior, thereby making it easier for the model to predict the daylight distribution. In subset D, D-1 and D-3 produced more accurate results. However, these two cases had fin numbers of 0, meaning no vertical fins were modelled in the geometry. This suggests that in the particular test location of New York City, having fins can be detrimental to model prediction of building daylighting and shading.

Window height (subset C) and window width (subset B) show the next best performance with average SSIM of 0.965 and 0.962 respectively. Also, the maximum value for the window height was taken as 6 m, considering the fixed sill level, while those for the window width were taken as 8 m, considering typical column-to-column spaces.

The model prediction accuracy for overhang number (subset F) and depth (subset G) were slightly lower with SSIM of 0.961 and 0.954 respectively. This was surprising since a south facing window will have more daylight impact from a horizontal shading device like an overhang due to the sun's path than vertical shading devices.

The lowest prediction accuracy was seen when all the variables were randomized (subset J), having an average SSIM of 0.943. The second case, J-2, which had the longest x-axis elongation, and hence more space available to fit a south facing window, high window width and height, one very shallow fin, and three deep overhangs performed the best, with SSIM 0.972.

4. CONCLUSION

The paper proposes a novel application for cGAN as a proxy model in rapid annual daylight prediction. Using twenty-three variables, including two geometry dimensions, window dimensions, vertical fin number and depth, horizontal overhang number and depth, the hour-of- year, and sky cover, the proposed model predicted annual hourly illuminance with reasonable accuracy of 96%. The model was most able to predict daylight with changing hour of year and changing cloud cover.

However, the model has some limitations. The model training involved creating inputs and labels specific to the optimization task i.e., daylight performance of L-shaped buildings. For a different task, the model may need to be relabelled and retrained using a different input dataset. Also, while the model produced a visually close match when predicting direct daylight condition, it struggled to do so under diffused conditions, as seen by the red patches on the predicted plots that were not there in the ground truth plots. This may require a larger dataset training.

In future, the model testing will be expanded to other building geometries: variations of L-shapes, rectangular, square etc. The different geometries will investigate model accuracy with changing geometry complexity, building orientation, window orientation, and a larger dataset. The predicted outcome as contour plots can provide intuitive feedback to designers during the early design phase. The contour plots can help obtain the minimum and maximum illuminances, allowing designers to identify over-lit and under-lit zones. This fosters design and optimization of various complex shading systems.

REFERENCES

1. Han, Y., L. Shen, and C. Sun, (2021). Developing a parametric morphable annual daylight prediction model with improved generalization capability for the early stages of office building design. Building and Environment, 200: p. 107932.

2. Mirza, M., and S. Osindero, (2014). Conditional generative adversarial nets. arXiv:1411.1784.

3. Isola, P., J. Y. Zhu, T. Zhou, and A. A. Efros, (2017). Image-to-image translation with conditional adversarial networks. In Proceedings of the IEEE conference on computer vision and pattern recognition. Honolulu, Hawaii, July 21-26.

4. Ji, Y., H. Zhang, and Q. J. Wu, (2018). Saliency detection via conditional adversarial image-to-image network. Neurocomputing, 316: p. 357-368.

5. Huang, W., and H. Zheng, (2018). Architectural drawings recognition and generation through machine learning. In Proceedings of the 38th Annual Conference of the Association for Computer Aided Design in Architecture. Mexico City Mexico, October 18-20.

6. Rahbar, M., M. Mahdavinejad, M. Bemanian, A. H. Davaie Markazi, and L. Hovestadt, (2019). Generating synthetic space allocation probability layouts based on trained conditional-GANs. Applied Artificial Intelligence. 33(8): p. 689-705.

7. Chaillou, S. (2020). ArchiGAN: Artificial Intelligence x Architecture. In Architectural Intelligence: Selected Papers from the 1st International Conference on Computational Design and Robotic Fabrication (CDRF 2019). Singapore.

8. Wan, D., X. Zhao, W. Lu, P. Li, X. Shi, X., and H. Fukuda, (2022). A Deep Learning Approach toward Energy Effective Residential Building Floor Plan Generation. Sustainability. 14(13): p. 8074.

9. He Q. et al. (2021). Predictive models for daylight performance of general floorplans based on CNN and GAN: A proof-of-concept study. Building and Environment, 206: p. 108346.

10. Goodfellow, I., J. Pouget-Abadie, M. Mirza, B. Xu, D. Warde-Farley, S. Ozair, A. Courville, and Y. Bengio. (2020). Generative adversarial networks. Communications of the ACM. 63(11): p. 139- 144.

PLEA 2024 WROCŁAW
(Re)thinking Resilience

Application of Simple 2R2C Model on Large-Scale Smart Thermostat Data

YOU-JEONG KIM[1] ALEXANDER WAEGEL[2] MAX HAKKARAINEN[2] YUN KYU YI[1] WILLIAM BRAHAM[2]

[1] University of Illinois at Urbana-Champaign, Champaign, USA
[2] University of Pennsylvania, Philadelphia, USA

ABSTRACT: This study assesses the thermal properties of single-family homes during the heating season using a 2-Resistor, 2-Capacitor (2R2C) model applied to smart thermostat data from 2,958 U.S. houses. The model demonstrated satisfactory accuracy with an average Scatter Index (SI) of 5.8%, highlighting its potential for large-scale energy evaluations in existing buildings. Analysis revealed that the estimated time constants are significantly influenced by factors like climate zone, building age, and heating system stages, aligning with known thermal behavior principles and validating the model's effectiveness. However, challenges arose in accurately modeling warm, humid climates and in potentially overlooking key heat loss factors. As a conclusion, the limitations and possible future improvement were presented.
KEYWORDS: Dynamic Thermal Model, RC Model, Time Constant, Residential Building, Donate Your Data (DYD)

1. INTRODUCTION

Building energy modeling has been increasingly used to calculate complex and dynamic thermal behaviour of a building. However, when it is for existing buildings, it poses significant challenges because a real building contains uncertainties, such as occupants' behaviour, which cannot be modelled by traditional deterministic model. Moreover, collecting high-dimensional information and creating an accurate model for each building require too much time and cost [1].

To address these challenges, the Resistance-Capacitance (RC) model emerges as a valuable tool. The RC model represents building components with a limited number of resistances (R) and capacities (C), offering simplicity, interpretability, and computational efficiency [2]. It achieves a balance between physical and statistical approaches, making it well-suited for managing uncertainties in building energy modeling.

RC models have a wide range of applications within the building energy domain, encompassing tasks such as thermal load calculation, building control and optimization, and urban energy modeling [3]. Moreover, recent studies have utilized RC models to analyze extensive building stocks, thanks to the availability of large-scale, high-resolution datasets [4-6].

Recent studies have consistently adopted a 2-resistor, 2-capacitor model for a single-zone modeling, owing to their ability to accurately simulate thermal behavior while maintaining a level of simplicity [5, 7-10]. Additionally, when it is integrated with an inverse or data-driven method, the thermal properties of buildings (R and C terms) can be extracted even from sparse data sources [4, 11-14], providing valuable insights to guide decisions in building retrofitting.

Despite the numerous applications of RC models in various structures and purposes in previous research, there remains a gap in their application and validation with actual metered large-scale dataset. These RC models were barely tested for predicting the thermal properties of large amount of existing building stocks.

This paper aims to bridge this gap by applying an inverse 2R2C model to a smart thermostat dataset of heating season from single-family homes in the U.S. The specific objectives include developing an inverse 2R2C model to estimate the time constants of U.S. homes in heating season, evaluating its performance, and discussing the model's limitations and prospects for future improvement.

2. METHODOLOGY

2.1 Data description

The data used in this paper was obtained from smart thermostat users who agreed to anonymously share their thermostat usage the Donate Your Data (DYD) program administrated by ecobee Inc [15]. Each smart thermostat data contains operational data such as heating or cooling system runtimes, setpoints, indoor temperatures, and information on housing characteristics such as house type, floor area, location etc.

This study used the ecobee DYD data from 3,836 houses across the U.S. Since this study focuses on finding time constants in heating season, we used data between December 2020 and February 2021.

Table 1: Descriptions of data used in this study.

Attribute		Description
House Features	House ID	Anonymous unique ID of each house from ecobee DYD dataset
	State	State where the house is located from ecobee DYD dataset
	Climate zone	IECC climate zone where the house is located
	Floor area (ft^2)	Floor area of the house from ecobee DYD dataset
	House type	Structural type of the house from ecobee DYD dataset (detached, semi-detached, apartment, or unknown)
	Building age (yrs.)	Age of the house from ecobee DYD dataset
	Number of heat stages	Levels of heating output available from ecobee DYD dataset
Model Inputs	Heating runtime (sec)	System runtime for heating in 5-min interval from ecobee DYD dataset
	Indoor temperature (°C)	Indoor dry air temperature in 5-min interval from ecobee DYD dataset
	Outdoor temperature (°C)	Outdoor dry air temperature in 5-min interval from local weather data
	Solar irradiance (W/ m^2)	Global horizontal irradiance in 5-min interval from local weather data

Table 1 provides descriptions of dataset used in this study.

2.2 2R2C model

In this paper, a 2R2C structure, which was developed by [14], was used to explore the thermal characteristics of sample houses. The states of the model are given by the temperature T_e of the large heat accumulating envelope with the heat capacity C_e, and by the temperature T_i of the room air and possibly the inner part of the walls with the capacity C_i, R_e is the resistance against heat transfer between the room air and the large heat-accumulating envelope, while R_i is the resistance against heat transfer from the room air to the ambient air with the temperature T_i. The input energy, which is multiplication of system runtime fraction δ_{sys} and system power rate Φ_{sys} is supplied by heaters, and the solar radiation Φ_{solar} which penetrates through the windows with effective area A_e and A_i. The model structure is illustrated in Fig. 1.

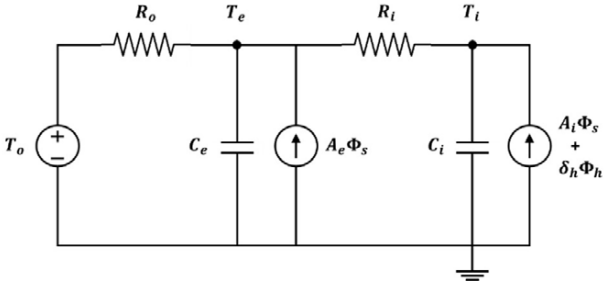

Figure 1: 2R2C model structure.

For simplification, we are not considering error terms to the differential equation for indoor temperature, assuming that the model is absolutely correct in reproducing the behavior of houses. Using an explicit discretization scheme, the indoor and envelope temperature at time t+1 can be calculated with all variables at time t as stated in Equation (1) and (2):

$$T_i^{(t+1)} = T_i^{(t)} + dt/C_i\,[1/R_i\,(T_e - T_i) + \delta_{sys}\Phi_{sys} + A_i\Phi_s]^{(t)} \quad (1)$$

$$T_e^{(t+1)} = T_e^{(t)} + dt/C_e\,[1/R_i\,(T_i - T_e) + 1/R_o\,(T_o - T_e) + A_e\Phi_{solar}]^{(t)} \quad (2)$$

where T_i – indoor temperature (°C);
T_e – envelope temperature (°C);
R_i – thermal resistance between the indoor air and the envelope (K/W);
R_o – thermal resistance between the envelope and the ambient air (K/W);
C_i – heat capacitances of the envelope (J/K);
C_e – heat capacitances of the interior (J/K);
A_i – effective solar gain area for interior (m^2);
A_e – effective solar gain area for envelope (m^2);
Φ_{sys}– power rate of heating system (W);
Φ_{sol} – global horizontal solar irradiance (W/ m^2);
δ_{sys} – runtime fraction of heating system (-).

2.3 Least squares optimization

The optimal values for the unknown parameters (R_i, R_o, C_i, C_e, A_i, A_e, and Φ_{sys}) for each building was estimated by the least squares optimization algorithm with given input variables (T_i, T_o, δ_{sys}, and Φ_{solar}). It finds the optimum values by minimizing the sum of squared residuals between the measured indoor temperature and the output of the function defined above.

3. RESULTS AND DISCUSSION

3.1 Model Performance and optimization results

To assess the model's performance, the dataset was split into training and test sets; 80% of the data from a 3-month period (72 days) served as the training set, while the remaining 20% (18 days) was used for testing, applied to each house.

Initially, the study involved 3,836 houses. However, this number was reduced due to several exclusion criteria: removal of houses lacking sufficient winter data, exclusion of homes in climate zone 1A without winter heating systems, and elimination of outliers with excessively high Root Mean Square Error (RMSE) to maintain analysis reliability. After applying these criteria, the number of houses eligible for optimization was reduced to 2,958. Table 2 provides a detailed summary of the optimization results for these 2,958 houses.

Table 2: Optimization and model test results for 2958 houses.

Attributes	Mean	Min.	Max.	Std.
R_i	4.1e-04	1.0e-04	2.0e-03	4.6e-04

Model Param-esters	R_o	1.4e-02	1.0e-04	3.9e-02	7.8e-03
	C_i	9.6e+06	6.6e+06	1.0e+07	7.9e+05
	C_e	8.9e+07	1.0e+05	1.0e+08	2.4e+07
	A_i	1.7e+00	2.8e-14	8.5e+00	2.1e+00
	A_e	1.6e+00	5.6e-12	1.0e+01	2.5e+00
	Φ_{sys}	5.0e+03	5.0e+03	5.0e+03	4.1e-02
RMSE		1.16	0.08	3.43	0.70
SI		5.8%	0.4%	34%	3.6%

Generally, the model demonstrated proficiency in accurately simulating the thermal dynamics of these houses. This is exemplified in Figure 2(a), which illustrates the test results from a house where the model's optimization was particularly effective. The average RMSE was 1.16, meaning that the average distance between the observed data values and the predicted data values is 1.16°C.

For more comprehensive view of model performance, we evaluated Scatter Index (SI) which is normalization of RMSE by the mean of observed value. The average SI value of the model was 5.8%. Based on rule of thumb, the model is acceptable when SI < 10%, and it is very good when SI < 5%. Based on this criterion, our model demonstrates a commendable level of predictive accuracy, although there is still room for further enhancement.

In evaluating the optimization of the model's parameters, we observed that most parameters fell within acceptable ranges and exhibited reasonable standard deviations. However, a notable exception was the system power rate (Φ_{sys}), which consistently gravitated towards its lower limit of 5 kW, indicating suboptimal optimization. Given that the capacity of a typical residential gas furnace is approximately 20 kW [16], this trend implies that the model may not be effectively capturing the operational dynamics of the heating system.

The 2R2C model is assuming that thermal output of the system is proportional to the runtime of the system. However, it might not be strictly proportional due to some reasons. First, for heating systems that can modulate their output (like modulating boilers or variable refrigerant flow systems), the heat production can be adjusted based on demand. This means longer runtimes don't necessarily equate to proportionally more heat, as the system may run longer but at a lower output. Second, even for systems that operate with a fixed output (on/off behavior), the relationship might not be strictly proportional due to startup and shutdown losses.

As shown in Fig. 2(b), for about 68% of the whole sample, the model overestimated the indoor temperature; the model prediction (red dashed line) was greater than the measured data (grey solid line). This implies that the model might not fully account for all the factors influencing heat loss, such as window opening.

Another possible reason could be the suboptimal optimization of the system power rate. It was previously noted that the model does not accurately capture the thermal dynamics of the heating system, leading to an unrealistically low estimation of the heating system's power rate. Such an underestimation could inadvertently result in an overestimation of the building envelope's thermal resistance and capacitance, as the model attempts to compensate for the heat gain and loss. Consequently, these overestimated values for resistance and capacitance might be driving the increase in the model's predicted indoor temperatures for the test dataset.

Figure 3 presents the performance of the model across different climate zones. It was observed that the model's RMSE is notably higher for houses located in warm and humid areas. In these areas, there is a frequent need for both heating and cooling within a single day during winter as shown in Fig 2(c). In addition, residents in such climates often use both natural and mechanical ventilation to regulate indoor temperatures and humidity.

Given these conditions, the 2R2C model, which is primarily designed for conditions where heating is the primary concern, may not be able handle such variability and complexity, leading to its reduced effectiveness in these specific climate zones.

3.2 Estimated time constant

Based on the optimization results, the time constant (τ), which represents how quickly the building envelope and the interior space respond to temperature changes, was calculated for each house using Equation (3):

$$\tau = (R_i + R_o) \times (C_i + C_e) \quad (3)$$

The identified time constants ranged widely between 2.4 – 487.5 hours with a median of 153.4 hours (Fig. 4). When comparing homes in different climates (Table 3), it was found that houses in warm and humid regions had a median time constant (75.0 - 113.7 hr) that was lower than the median for the entire U.S. (153.4 hr). This suggests that homes in warm and humid areas tend to adjust to temperature changes more quickly than the average US home.

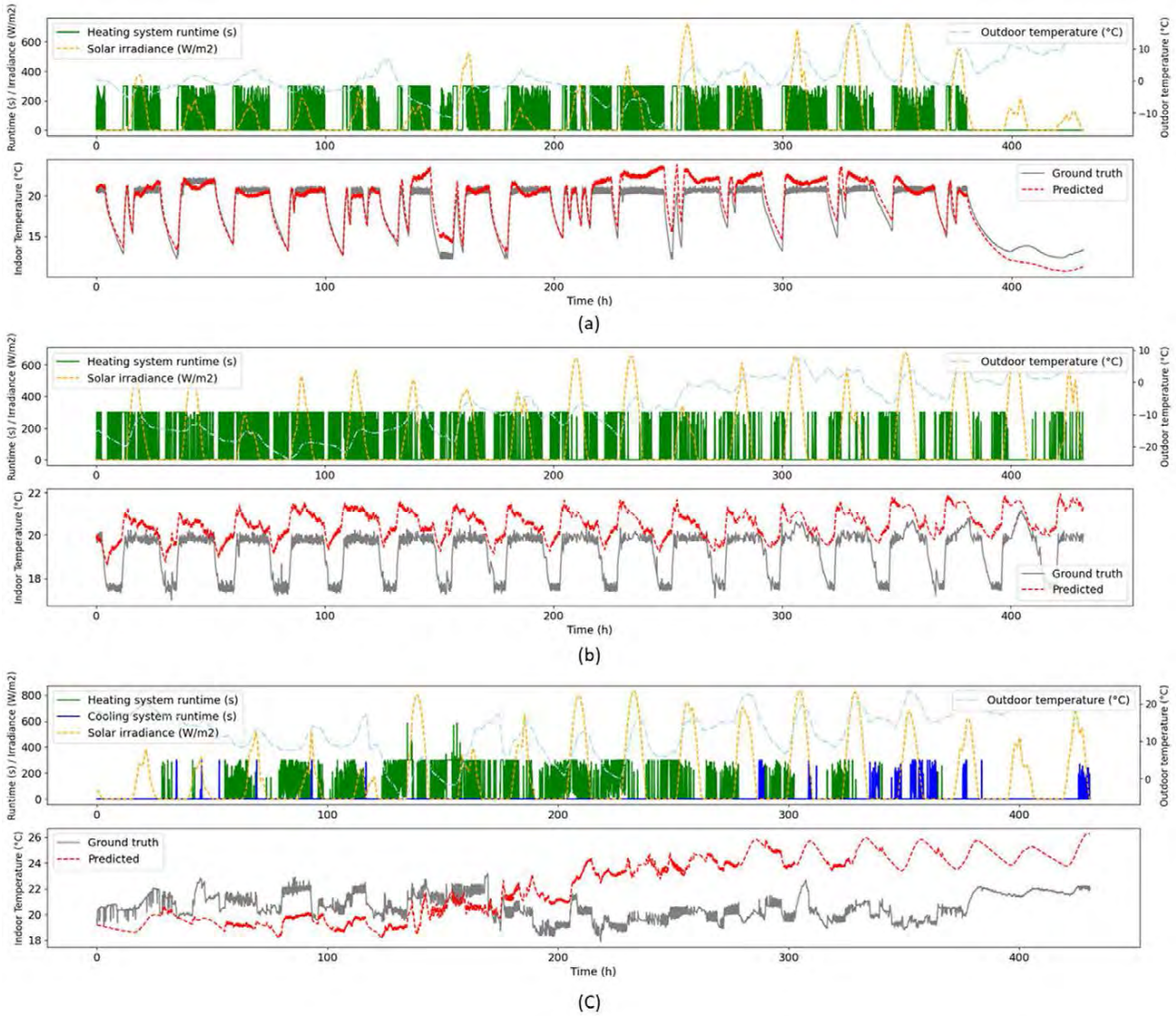

Figure 2: Model test results for: (a) a house with accurate predictions (RMSE = 0.4); (b) a house with overestimated indoor temperatures; and (c) a house in climate zone 2A with low accuracy (RMSE = 2.1).

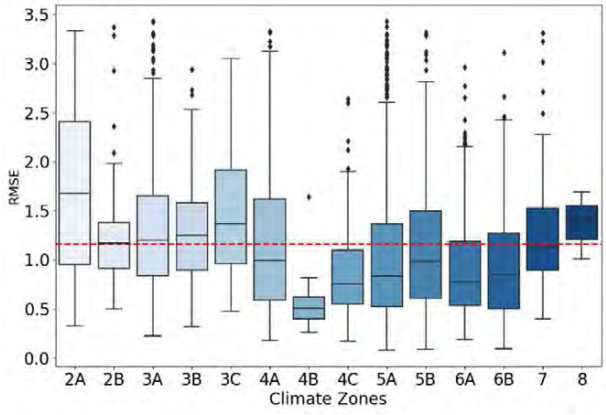

Figure 3: Model performance across different climate zones.

Considering that the model's RMSE in those climate zones were relatively higher than colder climate zones, this is likely because the model did not adequately account for the common practice in these regions of using both heating and cooling during winter and opening windows frequently to regulate temperature and humidity. As a result, the model may underestimate the true RC values for these houses, leading to less accurate predictions.

The median time constant was generally higher in colder climates compared to the U.S. average. This is consistent with the expectation that homes in colder areas are built with better insulation and more airtight designs to retain heat. Additionally, snow accumulation on roofs during winter can act as an extra layer of insulation, effectively increasing the thermal resistance and capacitance of these houses. This means that these homes are slower to lose heat and take longer to warm up.

Table 3: Estimated time constants for different climate zones.

	Count	Min.	Med.	Max.	Std.
2A	152	2.4	75.0	446.8	86.5
2B	60	30.2	273.6	472.6	115.6
3A	433	7.2	113.7	476.2	87.4
3B	108	10.6	180.8	484.6	121.9
3C	27	15.9	87.7	210.3	65.0
4A	637	12.7	133.4	447.2	88.1

4B	10	24.2	102.8	399.8	113.9
4C	139	5.9	153.8	481.4	99.9
5A	755	5.1	169.6	487.5	98.2
5B	213	25.6	183.9	451.2	96.7
6A	283	20.8	211.5	486.8	109.3
6B	84	17.0	216.3	426.5	101.2
7	53	25.2	230.6	486.6	104.8
8	4	151.9	241.7	399.1	125.1
All	2,958	2.4	153.4	487.5	101.9

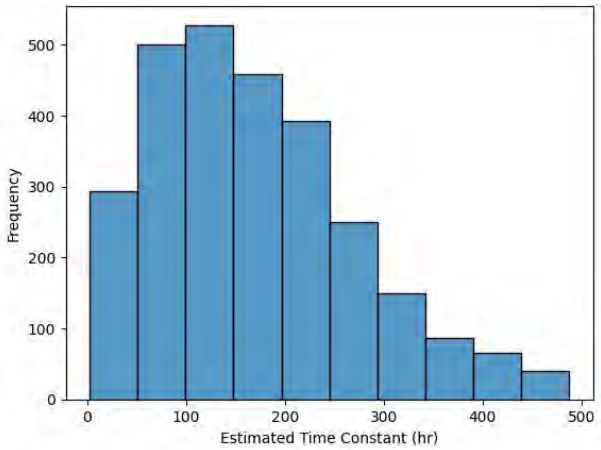

Figure 4: Histogram of estimated time constant (Median: 153.4 hours).

To investigate the correlation between the estimated time constants and various house features, we conducted multivariate linear regression. To compare the impact of each independent variable in a regression model on a common scale, we standardized your independent variables before fitting the model to get standardized coefficients. Standardized coefficients represent how many standard deviations the dependent variable will change, per standard deviation increase in the predictor variable. Therefore, by comparing the absolute value of the standardized coefficients, the impact of each house feature can be ranked.

Fig. 5 illustrates the ranking of seven house features based on their impact on time constants. Out of these, four features – location (climate zone), building's age, number of heating stages, and number of floors – demonstrate a statistically significant influence, as indicated by their p-values being less than 0.05.

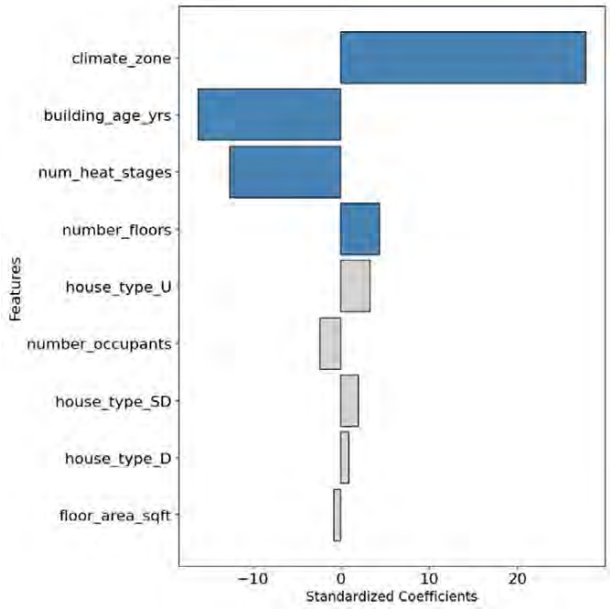

Figure 5: Ranking of house feature's impact on time constants

The house's location, specified by its climate zone, emerged as the most significant factor, showing the strongest positive impact on the time constant. Building age took the second rank, showing the strongest negative impact on the time constant. Newer buildings generally showed higher time constants, implying they are likely to be better insulated due to stricter building code. Conversely, older buildings tend to have lower time constants, which could be attributed to poorer insulation quality or deterioration over time.

The number of heating stages emerged as the third most impactful factor, showing a strong negative influence. This implies that homes with shorter time constants tend to be equipped with multi-stage heating systems. The negative correlation could suggest a reverse cause and effect: rather than multiple heating stages causing lower time constants, homes with faster temperature responses might require more complex system that can respond more quickly and closely to changes in demand. Furthermore, it's important to note that only 7% of the sample size (213 out of 2,958 homes) featured multi-stage heating systems. This relatively small proportion denotes that while the findings are notable, they may not be generalizable to all houses.

Among the two variables linked to the size of a house – the floor area and the number of floors – it was observed that the number of floors has the significant positive influence on the time constant. This means that houses with more floors tend to have higher time constants. This trend was expected as a result of the greater thermal mass of larger buildings.

It was initially expected that the detached houses to have lower time constants as the exposed surface area is larger for them. However, such relationship was not detected in this study.

The results from the correlation analysis further confirm the estimated time constants align with widely accepted knowledge. Specifically, it shows that these time constants are significantly influenced by key factors such as the house's location, age, and size. This finding supports the proposed model's potential applicability in large-scale building energy evaluations, as it captures essential characteristics that are known to impact building energy dynamics.

4. CONCLUSION

This study demonstrated the efficacy of applying a 2R2C model to smart thermostat data for evaluating the thermal properties of single-family homes, with a focus on heating season. The model was tested across a diverse sample of 2,958 houses. As a result, it showed acceptable accuracy with average SI of 5.8%. Moreover, the estimated time constants revealed significant dependencies on factors like climate zone, building age, and the number of heating system stages, validating the model's ability to accurately reflect key physical aspects of building thermal dynamics. These results highlight the model's potential in large-scale building energy evaluations, especially in existing buildings where capturing complex thermal dynamics is challenging due to sparce information and operational uncertainties.

However, the model faces challenges in warm, humid climates and may underestimate heat losses, such as through open windows, and inaccurately represent heating system dynamics. Future enhancements should focus on adapting to different climates, improving system behavior representation, and incorporating a stochastic approach to address uncertainties, especially human factors. Further validation with synthetic datasets from white-box model simulations is also suggested to ensure the model's parameters hold realistic physical interpretations.

With the proposed enhancements, the model will enable preliminary thermal dynamic assessments (such as time constants) for existing houses with limited building information. This will facilitate the identification of underperforming buildings compared to their peers and monitor them for deteriorating, providing crucial insights for retrofitting decisions.

ACKNOWLEDGEMENTS

The authors gratefully acknowledge the advice from Josiah Johnston at Daikin Open Innovation Lab Silicon Valley. Special thanks to ecobee, Inc. and its customers who participated in the Donate Your Data program, for their contribution of data. This research utilized the Delta advanced computing and data resource, supported by the National Science Foundation (award OAC-2005572) and the State of Illinois.

REFERENCES

1. Hong, T., Langevin, J., & Sun, K. (2018). Building simulation: Ten challenges. *Build. Simul.*, 11, 871-898.
2. Sonderegger, R. (1977). Diagnostic tests determining the thermal response of a house.
3. Li, Y., O'Neill, Z., Zhang, L., Chen, J., Im, P., & DeGraw, J. (2021). Grey-box modeling and application for building energy simulations-A critical review. *Renewable Sustainable Energy Rev.*, 146, 111174.
4. Doma, A., Ouf, M., Newsham, G., & Knudsen, H. (2021). Investigating the Thermal Performance of Canadian Houses Using Smart Thermostat Data. *ASHRAE Transactions*, (1).
5. Hossain, M. M., Zhang, T., & Ardakanian, O. (2021). Identifying grey-box thermal models with Bayesian neural networks. *Energy Build.*, 238, 110836.
6. Lauster, M., Teichmann, J., Fuchs, M., Streblow, R., & Mueller, D. (2014). Low order thermal network models for dynamic simulations of buildings on city district scale. *Build. Environ.*, 73, 223-231.
7. Kim, E. J., He, X., Roux, J. J., Johannes, K., & Kuznik, F. (2019). Fast and accurate district heating and cooling energy demand and load calculations using reduced-order modelling. *Appl. Energy*, 238, 963-971.
8. Rosin, S. (2018). Reduced Order Modeling for Virtual Building Commissioning.
9. Coffman, A. R., & Barooah, P. (2018). Simultaneous identification of dynamic model and occupant-induced disturbance for commercial buildings. *Build. Environ.*, 128, 153-160.
10. Zong, Y., Böning, G. M., Santos, R. M., You, S., Hu, J., & Han, X. (2017). Challenges of implementing economic model predictive control strategy for buildings interacting with smart energy systems. *Applied Thermal Engineering*, 114, 1476-1486.
11. Real, J. P., Rasmussen, C., Li, R., Leerbeck, K., Jensen, O. M., Wittchen, K. B., & Madsen, H. (2021). Characterisation of thermal energy dynamics of residential buildings with scarce data. *Energy Build.*, 230, 110530.
12. Belić, F., Hocenski, Ž., & Sliško vić, D. (2016, October). Thermal modeling of buildings with RC method and parameter estimation. *In 2016 Int. Conf. on Smart Systems and Technologies* (pp. 19-25). IEEE.
13. Zeifman, M., Lazrak, A., & Roth, K. (2020). Residential retrofits at scale: opportunity identification, saving estimation, and personalized messaging based on communicating thermostat data. *Energy Efficiency*, 13(3), 393-405.
14. Madsen, H., & Holst, J. (1995). Estimation of continuous-time models for the heat dynamics of a building. *Energy Build.*, 22(1), 67-79.
15. Ecobee Inc., "Donate Your Data," Ecobee, [Online], Available: https://www.ecobee.com/en-us/donate-your-data/ [Accessed: Mar 1, 2024].
16. Brand, L., & Rose, W. (2012). Measure Guideline: High Efficiency Natural Gas Furnaces (No. NREL/SR-5500-55493; DOE/GO-102012-3684). National Renewable Energy Lab.

PLEA 2024 WROCŁAW
(Re)thinking Resilience

Flooding in São Paulo:
A Call to Action for Resilient Infrastructure

SOLIMAR MENDES ISAAC[1], ANDRÉ EIJI SATO[1], GABRIELA KATIE SILVA MORITA[1]

[1] Faculty of Architecture and Urbanism of the University of São Paulo (FAUUSP), São Paulo, Brazil

ABSTRACT: This article investigates the impact of climate change in the city of São Paulo, specifically in the OD Zones Santa Marina, Barra Funda, Rudge and Bom Retiro. These areas are characterized by frequent and intense floods that affect urban mobility. Based on the application of the quantitative method of "Ergonomic Assessment of the Urban Environment", the article complements its methodology with a georeferenced analysis of pedestrian flows. The georeferenced analysis revealed that the study area, despite its importance for mobility, is very vulnerable to flooding. It is concluded that 95% of bus stops in the four OD zones are located in areas prone to flooding, indicating significant challenges in urban mobility. Regarding the displacements, crossing the Tietê River represents an obstacle for pedestrians and vehicles in the city, leading people to take risks in unsafe and inaccessible areas. The article also highlights the importance of microaccessibility as a crucial factor for the quality of urban life, emphasizing the need for a human-centered approach to urban design. Furthermore, the analysis points out the importance of accessibility during floods, calling attention to the urgency in developing strategies for more inclusive and resilient mobility.
KEYWORDS: Flood, Pedestrians, Accessibility, Resilience, São Paulo.

1. INTRODUCTION

Since the mid-1800s-1900s, human activities and the industrial revolution's effects have increased the frequency and intensity of various serious cataclysms, affecting different regions of the world, whether through unsustainable energy use, changes in lifestyle or new dynamics in consumption patterns [1].

According to the IPCC Sixth Assessment Report (AR6) [2], it is undeniable to affirm that climate change is human-caused and is changing the world by many extreme events such as heavy precipitations. Cities play an important part on humans since more than 56% of the world population live in urban settlements [3]. After COVID-19, many cities around the world had their own infrastructure and services compromised, especially on development cities. Although the city of São Paulo, Brazil, is the 33rd best in the world, the 17th richest city and the largest capital in Latin America [4], it still lacks many improvements in its urban infrastructure and, therefore, faces complex challenges related to the impact of climate change. The city has more than 11.451.999 inhabitants in 1.521,11 km², being not only the most populous, but also the most urbanised city in Brazil [5].

São Paulo has been suffering from heavy storms and consequently, floods. Data from the Inmet report (2022) [6] shows the frequency (in days) of extreme rainfall events in São Paulo (Fig. 1) - as can be seen when comparing the last three decades (2011-2020, 2001-2010 and 1991-2000) - and, although there has been a reduction in the number of days with rainfall above 50 mm, the number of days with rainfall above 80 mm and 100 mm has increased, respectively, from 9 to 16 days and from 2 to 7 days, a fact that goes hand in hand with the increase in extreme events in the metropolis - and in several other locations across the country.

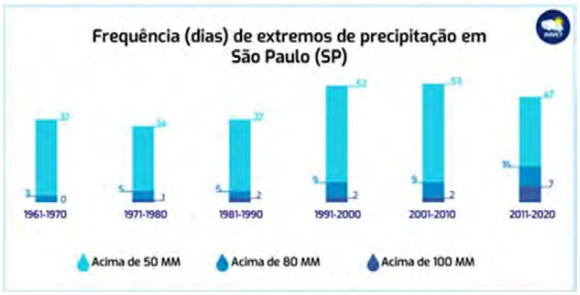

Figure 1: Frequency (days) of precipitation extremes in São Paulo (SP). INMET data.

In addition, from 2006 to 2023, the frequency and the intensity of heavy rainstorms have constantly increased over the years in São Paulo. In 2006, there were 13,121 registered floods. In 2023, that number jumped to 30,920 [7] and the annual average rainfall in the city was 1,400 millimetres, a 10% increase over the 10-year average [8]. The months with the highest number of floods is January, followed by February and March. Those months compose the summer period in the city. The increase in rainfall has caused a series of serious problems in the City of São Paulo, such as flooding and landslides. In 2023, the city recorded 1,200 flooding events, causing 223 deaths and leaving 23,600 people homeless.

Despite the fact that the municipality of São Paulo has adopted a series of actions to minimise the

problem of flooding over the last five years - such as the construction of new drainage channels to increase rainwater runoff capacity, public awareness campaigns on the importance of flood prevention and also the incorporation of innovative technologies for rainwater management, researches and studies point out that the city's infrastructure is still not prepared to deal with these events and, therefore, they have a serious negative impact on various services, especially urban mobility.

During floods, the majority of the transport modals literally stop and they all have to wait for the water to be drained. The city of São Paulo holds more than 15 million daily trips made by public transportation, being the second most used modal by its citizens [9]. From that, it is possible to affirm that public transportation and active means of transportation - which is the most widely used means of transport in the municipality - should have socioeconomic priority not only in public policies, but also in the management of a resilient city of São Paulo.

In this context, the objective of this article is based on the analysis of the complex interactions and intersections between the problems of public transport and flooding in the urban areas of São Paulo, aiming to analyse this type of urban morphology and to reflect on strategies that improve the citizens' quality of life and well-being. The case study for this analysis falls on the territory delimited by four Origin and Destination Zones [10]: Santa Marina, Barra Funda, Rudge and Bom Retiro. At the same time these regions are densely populated with great economic activity, they are also susceptible to flooding due to its own urban infrastructure, causing serious impacts on the citizens' travel routine.

2. METHODOLOGY

In order to achieve the objective of this article, this paper will highlight how climate changes trigger extreme events, such as flooding, which have become more frequent and intense throughout the years. This will be done through the analysis of the impact of these floods on urban mobility and how flooded roads hinder the flow of buses and pedestrians, leading to delays and interruptions in public transport routes. The paper also emphasises the importance of micro accessibility as a crucial facet of urban quality of life, highlighting how flooding compromises citizens' ability to access public transport points and the relevance of developing strategies to promote a more inclusive and resilient mobility.

On the issue of urban space and how pedestrians relate to it, it is important to highlight how Ergonomics, Walkability, Micro-accessibility and Intermodality are concepts and aspects that relate to and interfere with each other, simultaneously. Since Ergonomics can be understood as the relationship established between the urban space and its users (considering their perception) [11], Walkability brings the importance that micro-accessibility has as the ability to access a certain location on the micro scale of displacements on foot – which can be a place of public intermodality (bus stops, train and subway stations).

Having all that in mind, this article bases its own methodology on the application of the quantitative part of the "Ergonomic Assessment of the Urban Environment" method [11], along with a geoprocessing analysis of the case study area.

2.1 Case study area

The study area of this article is based on these four zones established by the Origin and Destination Survey [10] (a survey which investigates the pattern of trips that people make every day in a given region): Santa Marina (2,94 km²), Barra Funda (1,17 km²), Rudge (0,85 km²) and Bom Retiro (1,41 km²). They are located in the Central Area of the City of São Paulo and they add up to an area of more than 6,37 km², as seen in Figure 2.

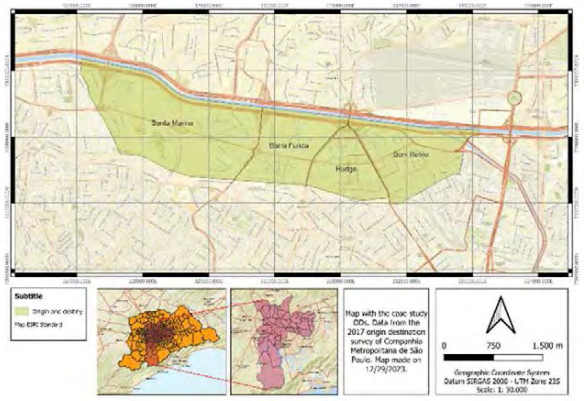

Figure 2: Localization map of the case study area (Santa Maria Zone, Barra Funda Zone, Rudge Zone and Bom Retiro Zone). Map prepared by the authors.

As mentioned above, these four zones are densely populated with great economic activity. Regarding the land use aspect, Santa Marina and Barra Funda have a predominance of Mixed Use Zones, while Rudge has the majority of Metropolitan Structural Zones and Bom Retiro has the Economic Development Zones.

The area is very important not only for São Paulo, but also for the citizens' mobility since it unites other centralities (North, West, South and East) and also is responsible for the Tietê River transposition. Over this way, it is in this section of the city that the main bridges that cross the Tietê River are located: Freguesia do Ó Bridge, Limão Bridge and Casa Verde Bridge. Alongside this aspect, since this case study area has the Tietê River in its proximity, it presents a lot of streams that go inside each zone. Thus, the four zones are very

vulnerable to flooding due to its own urban spatial conformity.

Just to have a notion, only in the Barra Funda Zone, the number of floods has increased from 10 (2006) to 44 (2023). In the past 10 years there have been 142 occasions when public transport has had to be interrupted, mostly due to above-average rainfall, such as in 2010, 2011 and 2022, with the latter year seeing the most affected stretches passing through lowland areas and in regions close to rivers and streams.

According to the study made by [12], this study area is a territory characterised by high walkability and low displacements on foot, showing low pedestrian diversity – which potentializes the lack of security.

2.2 Points of analysis

The first point of analysis focuses on recurrent flooding in these urban areas. Inadequate drainage infrastructure, combined with heavy rainfall, results in frequent flooding, which impairs not only mobility but also public and private infrastructure. The analysis will identify the main affected locations and their consequences on pedestrian mobility (Fig. 3).

Figure 3: Photo taken at the case study area, showing the dynamics of the section.

The second point of analysis explores the interaction between public transport systems and flooding. Delays, cancellations and route interruptions are common during adverse weather conditions. It will be evaluated how these events affect accessibility and passenger experience, as well as the operational efficiency of the system. In addition, areas of micro-accessibility will be highlighted, where flooding makes it difficult for passengers to access.

2.3 The Ergonomic Assessment of the Urban Environment - Qualitative measurement

The "Ergonomic Assessment of the Urban Environment" [11] is a method that uses Ergonomics as the guide of the measurement of the urban built environment qualities, aiming at the well-being of the pedestrians. This methodology has two types of assessment and for the matters of this article, we only focused on the quantitative category. This category takes into account the measurement of the physical and environmental factors that are classified as "urban kindness" (positive qualities) and "urban arrogances" (negative qualities).

It is important to note that this method is based on on-site observations and applied on the microscale level of walkability. In this analysis, 39 physical variables were evaluated and grouped into 9 topics, shown in the figure below (Fig. 4).

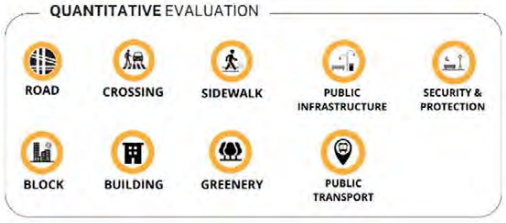

Figure 4: The ergonomic variables that are evaluated by the Qualitative Category of the Ergonomic Assessment of the Built Environment.

There are ergonomic assessment sheets to guide the process of the evaluation, as in Figure 5.

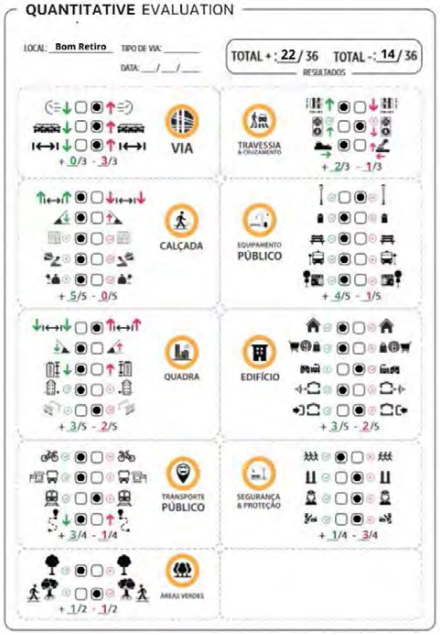

Figure 5: Quantitative evaluation sheet. Prepared by the authors.

The on-site visit took place on November 23rd, 2023 during business hours, between 2pm and 4:30pm. Besides that, this visit was taken walking by the Marquês de São Vicente Avenue, since this road links the four OD Zones.

2.4 The Geoprocessing analysis of the case study area

After defying the case study area and applying the Ergonomic Assessment of the Urban Environment, the methodology follows a comparative analysis between aspects of urban micro-accessibility (bus stops) and

the interference caused by flooding. This part was done through georeferenced analysis by the QGIS software (version 3.22.7) using São Paulo's open-sourced data by the GeoSampa platform.

3. RESULTS

3.1 On-site visit observations

In general, the visit was important to notice the main opportunities and challenges of the urban spaces towards a more resilient environment.

The major flux of pedestrians occurred nearby the intermodal station (buses, subways and trains) - located on the Barra Funda Zone. As we walked towards the Bom Retiro Zone, the presence of pedestrians was almost non-existent. It was observed that the urban spaces at this area were not pedestrian friendly (having lots of walls, fences and abandoned buildings). Thus, there were a lot of very vulnerable and unsafe spaces. The few pedestrians we saw were residents walking on the sidewalk of their own buildings without going much further than the setback space.

Another aspect that we noticed was that there were very few trash bins and a lot of solid waste spread across the sidewalks. At the same time there were just a few storm drains to collect rainwater. Over this way, it was possible to notice several rain puddles - from the rain that occurred on the same morning (Fig. 6). This indicates the insufficient urban infrastructure that could not drain the water correctly.

Figure 6: Photographic registers of the rain puddles from the on-site visit.

3.2 Ergonomics Assessment of the Urban Environment's results

The Quantitative Part of the Ergonomics Assessment of the Urban Environment was applied in the Marquês de São Vicente Avenue as this road links each of the four zones.

The zone rated most negatively is Santa Marina, while the zone with the most positive aspects is Barra Funda. It was interesting to notice that the road aspects - which take into account variables such as average road speed, vehicle flow and average road width - were rated negatively in all, as seen in the tables below. (Tables 1 and 2).

Aspects related to infrastructure (such as the existence or absence of garbage cans, seats, street lighting, signage and the proximity of bus stops), the block (length, slope, average height of buildings, existence or absence of an active façade and walls or railings) and safety (pedestrian flow, existence or absence of safety markers, police and traffic officers) are rated more negatively in Santa Marina and Rudge, being corroborated by the perception of the researchers during an on-site visit (Tables 1 and 2).

ZONES	ROAD	CROSSING	SIDEWALK	PUBLIC INFRASTRUC.	BLOCK
SANTA MARINA	100% Negative	66% Positive	60% Positive	60% Negative	60% Negative
BARRA FUNDA	100% Negative	66% Positive	100% Positive	80% Positive	100% Positive
RUDGE	100% Negative	100% Positive	80% Positive	60% Negative	60% Negative
BOM RETIRO	100% Negative	66% Positive	100% Positive	80% Positive	60% Positive

Table 1: Ergonomics physical variables. Prepared by the authors.

ZONES	BUILDING	PUBLIC TRANSPORT	SECURITY & PROTECTION	GREENERY
SANTA MARINA	100% Negative	75% Positive	100% Negative	100% Positive
BARRA FUNDA	80% Positive	75% Positive	50% 50%	50% 50%
RUDGE	60% Positive	75% Positive	100% Negative	100% Positive
BOM RETIRO	60% Positive	75% Positive	75% Negative	50% 50%

Table 2: Ergonomics physical variables. Prepared by the authors.

In the crossings, the best-rated area was the rudge, with all the physical variables positive. With regard to sidewalk aspects, the positive highlights are Barra funda and Bom Retiro, which may be influenced by the high pedestrian traffic and good flow of public transport in the vicinity.

The evaluation of the building aspect was more positive in Barra Funda, while the most wooded areas are located in Santa Maria and Rudge, even though this is not the biggest motivator for commuting in these areas. Public transport is well rated in all areas, with only train stations being further away.

From the results above, it is possible to point out that Barra Funda presented the best urban environmental features and Santa Marina and Rudge, the worst ones. Following this fact and during the visit, the pedestrians' flow was higher in the Barra Funda Zone and Rudge was the lowest.

3.3 Geoprocessing analysis' results

After analysing the area, it was found that from the totality of 123 bus stops, only 6 of them are outside the flooded areas. This means that more than 95% of bus stops in the area are subject to flooding.

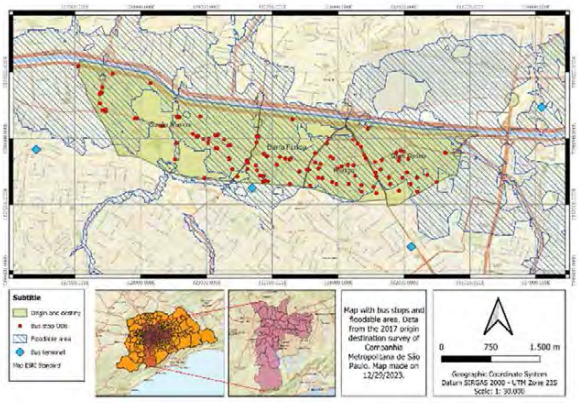

Figure 7: Situation of flooding points and proximity to bus stops. Map prepared by the authors.

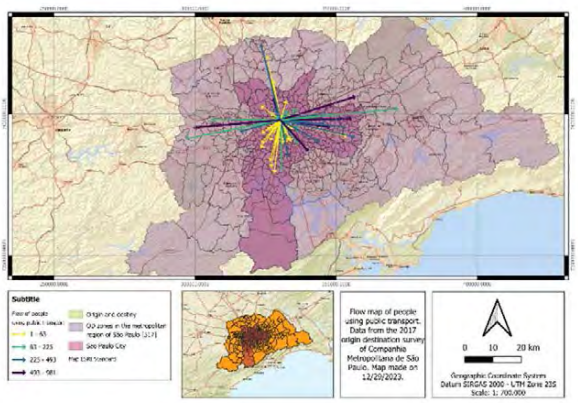

Figure 8: Map of flows of people using the public transport system in the metropolitan region of São Paulo. Map prepared by the authors.

With the analysis of pedestrian flows using public transport (Fig. 8), we were able to conclude that the movements with the largest number of people occur from the east-west of the Metropolitan Region to our study area. In second place, we have a higher movement of people coming from the extreme north zone of São Paulo when compared to the south zone.

The largest east-west flows can be attributed to the large population of residents in these regions and the movement of workers to the city's economic centers. As for the lower movement in the south, it may be influenced by the large job offer and diversity of public transport in the area.

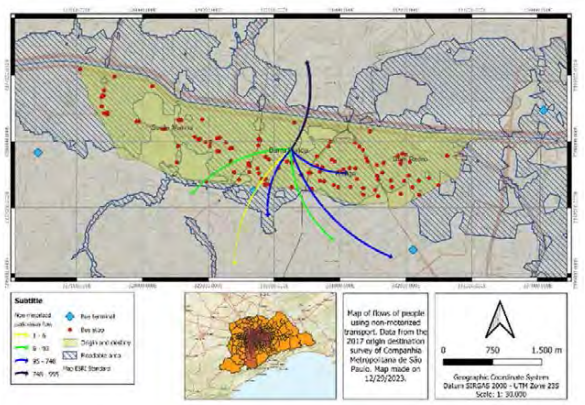

Figure 9: Map with the flows of non-motorized transports (bicycles and pedestrians) at the case study area. Map prepared by the authors.

In the analysis of non-motorized flows (Fig. 9), it was concluded that the largest number of people come from the Casa Verde neighbourhood. However, in order to do that, people need to cross the Tietê River to reach the study area and access the Barra Funda intermodal. This is done without accessibility and security, causing great discomfort to passers-by

The largest flows can be attributed to the difficulty of getting to the other side of the Tietê riverbank, considering that it is faster to get there on foot than by public transport at peak times. And also, the largest flows can be attributed to the reduced offers of public transport on this side of the river.

The second largest pedestrian flow comes from the central area of the city, from the neighbourhoods of Santa Cecília, Santa Efigênia and República. The lowest pedestrian flow is those in the Perdizes neighbourhood. This, in turn, is characterized by the commuting movement of university students. Characteristics of movement on the streets only at specific times.

4. CONCLUSION

This paper showed the importance of analyzing the urban environment based on the overlapping layers that make it up, having in mind the resilience for cities. In order to reduce flooding and besides the actions mentioned before, it is important to highlight that the City of São Paulo's government [13] has taken a series of actions to minimise the problem of flooding over the past five years. These actions include: building new drainage channels to increase rainwater runoff capacity, public awareness campaigns on the importance of preventing flooding and also the incorporation of innovative technologies for stormwater management. So, São Paulo City Hall has implemented green infrastructure initiatives such as rain gardens, green parking spaces, bioswales, landarte, green staircases, sidewalks with infiltration wells and conservation forests.

Specifically, in 2023, two new drainage channels were built in the Barra Funda neighbourhood (2 km) in addition to the implementation of two rain gardens, 10 sidewalks with infiltration wells and 50 green parking spaces [13].

These achievements, although preliminary, allow for preventive actions and can act as instruments that contribute to a more resilient city in the long term.

However, through the methodology followed by this article it was possible to see that at the same time the case study area is important for the mobility of São Paulo City, it is very vulnerable to floods too. Over the geoprocessing analysis' results, we can see that 95% of the bus stops of the four zones and the Marquês de São Vicente Avenue are located in a floodable area. That the largest movements of people by public transport are East-West, confirming the lack of employment and efficient transport in these areas.

As for non-motorized travel, we have the crossing of the Tietê River presenting itself as a latent obstacle for pedestrians and vehicles in the city of São Paulo. Making pedestrians take risks in unsafe and inaccessible areas.

Regarding the urban environment and the micro-accessibility aspect, it was interesting to notice that the results of this article strongly indicate that the urban environment has a major role in the pedestrians' presence at a microscale level. In the city of São Paulo, it is very common to find fences or walls surrounding the buildings as a way of individual protection. So, it is possible to find entire blocks filled with these elements that can act as urban arrogances for pedestrians. Thus, combining the understanding of environmental perception along with human - centered urban design can play a crucial point to make cities more attractive to people.

We also concluded the importance of microaccessibility as a crucial factor for the quality of urban life. Floods compromise citizens' access to public transport points, making it urgent to develop strategies for more inclusive and resilient mobility.

The analysis developed in this paper also contributes to the approximation of academics towards the municipal public management in favour of more resilient and sustainable cities.

The research was carried out through an open data platform (GeoSampa) using free and open-source software - an aspect that contributes to scientific research. A scenario like this can encourage better organization of civil society, promoting greater transparency and access to information, providing the population with the tools to communicate and claim their rights.

ACKNOWLEDGEMENTS

This study was financed in part by the Coordenação de Aperfeiçoamento de Pessoal de Nível Superior - Brasil (CAPES) – Finance Code 001.

REFERENCES

1. Climate Change 2023 Synthesis Report [Online], Available: https://www.ipcc.ch/report/ar6/syr/downloads/report/IPCC_AR6_SYR_LongerReport.pdf [18 December, 2023].
2. The Intergovernmental Panel on Climate, [Online], Available: https://www.ipcc.ch/report/ar6/syr/ [20 August, 2023].
3. The United Nations Human Settlements Programme, [Online], Available: https://unhabitat.org/wcr/ [20 August, 2023].
4. Best Cities, [Online], Available: https://www.worldsbestcities.com/rankings/worlds-best-cities/ [20 August, 2023].
5. Instituto Brasileiro de Geografia e Estatística (IBGE). Censo 2022 [Online], Available: https://cidades.ibge.gov.br/brasil/sp/sao-paulo/panorama [20 August, 2023].
6. Instituto Nacional de Meteorologia (INMET). Normais Climatológicas do Brasil 2022 [Online], Available: NORMAISCLIMATOLOGICAS.pdf (inmet.gov.br) [18 December, 2023].
7. Centro de Gerenciamento de Emergências Climáticas, [Online], Available: https://www.cgesp.org/v3/alagamentos.jsp [20 August, 2023].
8. Instituto de Pesquisa Econômica Aplicada, [Online], Available: https://www.ipea.gov.br [20 August, 2023].
9. Secretaria Municipal de Desenvolvimento Urbano (SMDU). Urban Report no. 40 (2019, p.6).
10. Metropolitano de São Paulo (METRÔ SP), Pesquisa Origem e Destino 2017 [Online], Available: http://www.metro.sp.gov.br/pesquisa-od/ [10 November. 2023].
11. Kronka Mülfarth, R. C., (2017). Methodological proposal for ergonomic evaluation in the urban environment: ergonomics too for the built environment. [Habilitation Thesis, University of São Paulo]. Digital Library of Theses and Dissertations of the University of São Paulo. https://teses.usp.br/teses/disponiveis/livredocencia/16/tde-07012019-141802/en.php
12. Albala, P. L. R. Pedestrian pathways: walkability, environmental comfort and strategic planning [Doctoral Thesis, University of São Paulo]. Digital Library of Theses and Dissertations of the University of São Paulo. https://www.teses.usp.br/teses/disponiveis/16/16132/tde-09032023-164035/en.php
13. Prefeitura Municipal de São Paulo, [Online], Available: https://www.capital.sp.gov.br/ [20 August, 2023].

PLEA 2024 WROCŁAW
(Re)thinking Resilience

Investigating View-out and Privacy Using Virtual Reality
The Effect of Graphical Realism on Subjective Votes

STEFFEN PETERSEN[,1] NIKOLAJ C. JACKSON[,1] MADS K. PEDERSEN[,1] MARKUS M. HUDERT[,1]

[1]Aarhus University Department of Civil and Architectural Engineering, Aarhus, Denmark

ABSTRACT: The mere objective of the built environment is to facilitate the well-being of the end user. The longevity of a solution thus depends on how well building designers understand what the end user wants. Longevity of solutions is important to obtain environmentally sustainable and resilient buildings, and continuous research in how the built environment affects humans is thus imperative to any sustainable development. Virtual Reality (VR) is used to generate data for the establishment of models that predict the impact of design variables on the human perception of visual aspect of the indoor environment during the design stage. However, there are still open questions on the expediency of VR as a tool for this purpose. This paper reports on an empirical study on how the graphical realism of VR affects the subjective assessment of view-out quality and privacy in a residential indoor environment. The results indicate that it is not likely that data are skewed by graphical realism of the interior representation. Furthermore, data also indicate that a larger window size reduces the notion of privacy more than it increased the view-out quality at the specific location featured in the experiment.
KEYWORDS: View-out quality, perception of privacy, virtual reality, building design

1. INTRODUCTION

The use of Virtual Reality (VR) as an empirical tool to study human perception in indoor environments has become increasingly popular as it enables researchers to scale up investigations of visual perception of indoor environments. An example is Petersen et al. [1] who used VR to study the impact of the different geometric configurations of kinetic facades on the psychological state and cognitive performance of building occupants. Another is Petersen et al. [2] who used VR to validate a proposal for predicting the mean vote on daytime view-out quality and privacy from dwellings from Purup and Petersen [3]. The visual aspect of indoor environments represented using VR has also been combined with the thermal aspect [4] as well as the auditive aspect [5] of the indoors in efforts to investigate their combined effect on human perception. The immediate advantage associated with using VR to investigate human perception of the visual aspects of indoor environments is that it enables quality assessment experiments involving several subjects evaluating a series of indoor environments without having to establish the indoor environments physically – let alone avoiding the time-consuming logistics in changing locations etc.

Several studies have been conducted on whether VR environments can substitute real environments for empirical research, e.g. Kuliga et al. [6], Chamilothori et al. [7], Saeidi et al. [8], and Heydarian et al. [9]. The findings indicate that it is possible to obtain reliable assessment of visual quality of indoor environments using VR. However – to the knowledge of the authors – there are currently no published studies on how the graphical quality of VR environments affects subjective votes on the indoor environmental quality. This aspect could be of importance as graphical quality may impact the experience of realism and thus the qualitative assessment of the represented environment.

This paper presents the results from an empirical study on how the graphical realism of VR affects the subjective assessment of indoor environments.

2. METHOD

The study reported in this paper took offset in a previous study by Petersen et al. [2] that conducted a VR-based experiment to validate proposed metrics for prediction of daytime view-out quality and privacy. In this validation study, an apartment was modelled in SketchUp and imported into Unity for VR assessment. The apartment was placed in external surroundings represented by 360˚ videos, and several subjects were then asked to assess the view-out quality and privacy from within the department. This modelling technique led to a somewhat "cartoonish" feel of the apartment interior, see Fig. 1. The question is whether this level of realism affected the subjective votes of the subjects.

To investigate this, a group of 54 subjects consisting of students in their early 20s volunteered for the experiment which was conducted during spring of 2023. The group was divided randomly into two groups of 27 subjects prior to the experiment.

Figure 1: The apartment used in the VR experiment of Petersen et al. [2].

The subjects in one of the groups were shown VR environments rendered in Unity, and the subjects in the other group were shown the same VR environment rendered in Unreal Engine. As seen in Fig. 2, the rendering in Unity has a somewhat "cartoonish" feel (left) whereas renderings in Unreal Engine are quite photo-realistic (right). Both renderings were embedded in surroundings represented by a 2D 360˚ movie.

Upon arrival at the experimental facility, the subject was instructed to remain still at a certain spot on the floor throughout the experiment, but they were permitted to turn around themselves and to reach forward. Next, the subject was introduced to the VR equipment and the features of the virtual environment. Once the subject was comfortable with the controls, the subject was teleported to the reference room shown in Fig. 2. Here the subject was initially asked to complete three exercises designed to encourage exploration of the virtual space with the intention to maximize the notion of immersion before the actual experiment began. The first exercise was counting the number of pillows in the apartment, the second exercise was to describe the colours of buildings visible through the window, and the third required the subjects to find two small bird sculptures within the apartment.

After completing the exercises, the subject was teleported to the single room apartment featured in the actual experiment and seated by the dining table from where the approximate view were as illustrated in Fig. 3 and 4. The subject was then orally asked two questions – originally in Danish – regarding their immediate perception of the view-out quality and privacy from this position:

- **Question 1:** To what extent do you feel private relative to your surroundings on a scale of 0-6 where 0 is 'not at all' and 6 is 'to a great extent'.
- **Question 2:** What do you think of the view-out on a scale of 0-6 where 0 is 'bad' and 6 is 'good'.

It was chosen to start the 7-point scale at zero instead of one since zero was believed to have a better association with 'not at all' and 'bad' in this experiment. The experiment was repeated for each subject so that they all were exposed to the same apartment twice but with two different window sizes: A medium glazing area (Fig. 3), and a large glazing area (Fig. 4). Both the order of window size and the questions were randomised between subjects of the experiment.

Figure 2: Renderings of the reference room used for immersion exercises prior to the actual experiment. Left: Rendering in Unity. Right: Rendering in Unreal Engine.

Figure 3: The apartment with large glazing areas used in the experiment. Left: Unity. Right: Unreal Engine.

Figure 4: The apartment with medium glazing areas used in the experiment. Left: Unity. Right: Unreal Engine.

This experimental design enabled the analysis of whether the graphical realism of renderings affects subjective assessment of view-out quality and privacy. Furthermore, it may also provide evidence on the effect of window size on the perception of view-out quality and privacy at the given surroundings.

The study can be categorised as a single-blind study as the underlying agenda of the experiment – to investigate the research question – was not revealed to the subjects and none of them were aware that the experimental design involved to different groups exposed to different levels of graphical realism.

3. RESULTS

A total of 27 subjects answered the two questions in each of the four apartment rooms in Fig. 3 and Fig. 4. The difference in votes for each of the two

questions in the two different renderings – Unity and Unreal, respectively – are compared and tested for statistical significance in the following.

All but one out of the eight groups of answers were normal distributed according to the Anderson-Darling test. The one group that was not normal distributed was the votes on privacy (Question 1) in the apartment with large windows rendered in the Unreal Engine (p=0.06). Consequently, a two-tailed students t-test was applied for testing whether any difference between answers can be ascribed the difference in scene rendering for all but Question 2 for the department with the large window; for this scenario, the Wilcoxon signed-ranks test was used.

Fig. 5 shows box plots of the votes on view-out quality and privacy for the medium glazing size. The difference in mean value for vote on view-out quality is 0.63 but it is not statistically significant (p=0.07). The difference in mean vote for privacy is 0.11 but not statistically significant (p=0.71).

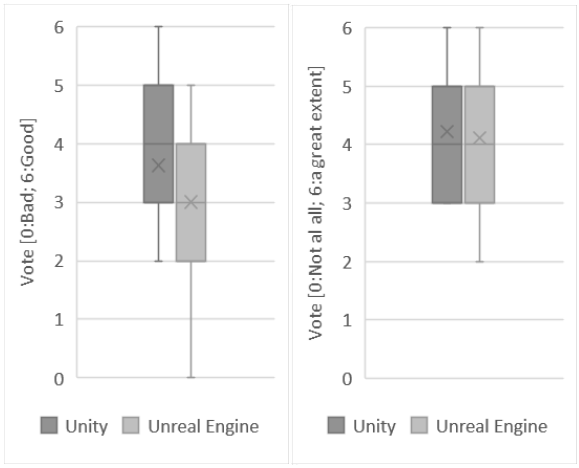

Figure 5: Votes on view-out quality (left) and privacy for medium glazing size (right)

Fig. 6 shows box plots of the votes on view-out quality and privacy for the large glazing size. The difference in mean value for vote on view-out quality is 0.37 but it is not statistically significant (p=0.38). The difference in mean vote for privacy is 0.2 but not statistically significant (p=0.72).

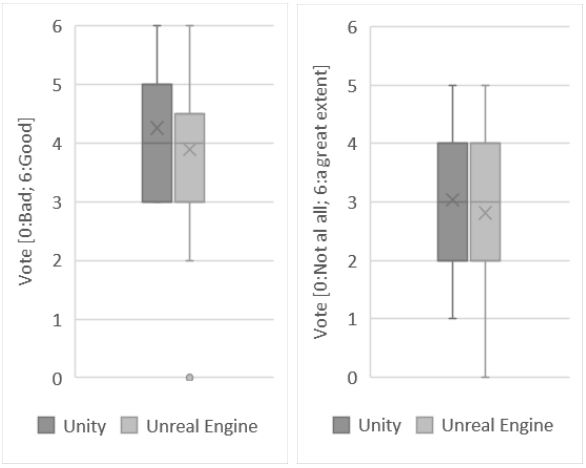

Figure 6: Votes on view-out quality (left) and privacy for large glazing size (right)

The mean vote of view-out quality for the large window apartment rendered in Unreal Engine is 0.9 higher than for the medium window apartment (p=0.02). The mean privacy vote was 1.3 lower for the large window (p=0.00007). The mean vote of view-out quality for the large window apartment rendered in Unity is 0.6 higher than for the medium window apartment (p=0.04). The mean privacy vote was 1.2 lower for the large window (p=0.0002).

4. CONCLUSION

The study reported in this paper indicate that the graphical realism of indoor environments in virtual reality (VR) has a minor but not statistically significant effect on subjective votes on view-out quality and notion of privacy in indoor environments. It is therefore not likely that research-based findings regarding view-out quality and privacy in indoor environments using VR are skewed by graphical realism of the interior. Future studies are needed to investigate whether the realism of the modelled exterior surroundings (in this study represented by a 2D 360˚ movie) could affect subjective votes. Furthermore, future studies may consider the effect of differences in brightness between the compared models. Lastly, the data from the experiments also indicate that a larger window size reduce the notion of privacy more than it increased the view-out quality at the specific location featured in the experiment.

Overall, VR seems to be an effective tool to accelerate research into the understanding of how human perceive visual aspects of the built environment. This knowledge may help building designers to obtain a longevity of solutions which is essential to the sustainable development of resilient buildings.

ACKNOWLEDGEMENTS

The authors would like to thank the voluntary participants of the VR experiments. A special thanks

to Helena Fraenkel and Patrick Olesen for their assistance during the data collection, and Louis Helledie for technical assistance with the modelling. No financial support was provided for the experiment.

REFERENCES

1. Petersen S., A. Szabo, K. Armoutaki, A. Kamari, and P.H. Kirkegaard, (2020). The impact of kinetic facades on building occupants: Psychological state and cognitive performance. *35th Passive Low-Energy Architecture (PLEA)*. A Coruna, Spain, 1-3 September.

2. Petersen S., D.L. Beck R. Lorck and P.B. Purup, (2020). Validation of Metrics for Prediction of Daytime View-Out Quality and Privacy: Human Subjects in Virtual Reality. *35th Passive Low-Energy Architecture (PLEA)*. A Coruna, Spain

3. Purup, P.B., S.H. Jensen, S. Petersen and P.H. Kirkegaard, (2017). Towards a Holistic Approach to Low-Energy Building Design: Consequences of Metrics for Evaluation of Spatial Quality on Design. *33rd Passive Low-Energy Architecture (PLEA). Edinburgh, Scotland*.

4. Rosenlund M., Y. Li, S. Petersen, (2019). Investigating Indoor Environmental Quality Using Virtual Reality in Climate Chambers. *REHVA World Student Competition Book of papers*. Bucharest, Romania.

5. Poulsen C. and E. G. Larsen, (2020). Investigation of the perceived acoustic environment in connection with the perceived view-out quality and privacy in residential buildings using virtual reality. *Master thesis*. Aarhus University, Denmark.

6. Kuliga S.F., T. Thrash, R.C. Dalton, C. Hölscher, (2015). Virtual reality as an empirical research tool — Exploring user experience in a real building and a corresponding virtual model. *Computers, Environment and Urban Systems*, 54: p. 363-375.

7. Chamilothori K., J. Wienold and M. Andersen, (2019). Adequacy of immersive virtual reality for the perception of daylit spaces: comparison of real and virtual environments. *Leukos* 15: p. 203-226

8. Saeidi S., C. Chokwitthaya, Y. Zhu and M. Sun, (2018). Spatial-temporal event-driven modeling for occupant behavior studies using immersive virtual environments. *Autom. ConStruct*., 94: p. 371-382

9. Heydarian A., J.P. Carneiro, D. Gerber, B. Becerik-Gerber, T. Hayes and W. Wood, (2015). Immersive virtual environments versus physical built environments: a benchmarking study for building design and user-built environment explorations. *Autom. ConStruct*., 54: p 116-126.

Evaluation of thermal comfort in library buildings in the tropical climate of Ghana:

(Case Study of the Balme Library in the University of Ghana, Accra, Ghana)

PARISA POURABRISHAMI[1] HANIYEH MOHAMMADPOURKARBASI[1] DANIEL NUKPEZAH[2] IAIN JACKSON[1] IRENE APPEANING ADDO[3] REXFORD ASSASIE OPPONG[4] STEVE SHARPLES[1]

[1] University of Liverpool, School of Architecture, 19-23 Abercromby Square, Liverpool, UK, L69 7ZG
[2] University of Ghana, Institute for Environment and Sanitation Studies, Legon, Accra, Ghana
[3] University of Ghana, Institute of African Studies, Legon, Accra, Ghana
[4] Kwame Nkrumah University of Science & Technology, College of Art and Built Environment, Kumasi, Ghana

ABSTRACT: Adaptive thermal comfort plays a crucial role in addressing climate change concerns, especially in Ghana. In this hot and humid region, air-conditioners are identified as one of the main culprits behind the rising trend in electricity demand and greenhouse gas emissions. Additionally, due to the limited prediction accuracy of Fanger's PMV model, there is a need to evaluate adaptive thermal comfort to develop a reliable model for tropical regions. This study evaluates the adaptive thermal comfort in the Balme Library in Accra, Ghana, in both naturally ventilated (NV) and air-conditioned (AC) modes. The presented adaptive model in this study is compared with the current international standards, such as ASHRAE-55 and CEN standards. Based on the linear regression of mean sensation votes (MTSV) and predicted mean votes (PMV) as a function of operative temperature, while the neutral temperature of PMV is 27.8 °C, the linear regression method in NV mode predicts a neutral temperature of 30.3 °C. Consequently, the PMV prediction is 2.5 °C lower than that of the linear regression method. Meanwhile, the current international standards underestimate the ranges of thermal preferences among building occupants, as this proposed model in this study reveals higher slopes in the linear regression model.
KEYWORDS: Adaptive comfort models, Hot and humid climate, Air-conditioned building, Naturally ventilated buildings

1. INTRODUCTION

Thermal comfort is one of the motivations to research climate change-related concerns which cause destructive effects on humans, the environment, and the quality of life. Climate change is a complex environmental issue and presents significant risks to ecological, infrastructure, and economic systems. In current conditions, human-induced climate change is causing dangerous and widespread disruption in nature and affecting the lives of billions of people worldwide, despite efforts to reduce the risks. People and ecosystems least able to cope are being hardest hit. Meanwhile, the potential effects of global climate change on buildings are a growing concern worldwide, as rising temperatures can significantly impact their energy performance and indoor thermal comfort conditions [1]. For instance, heat waves can cause large socioeconomic and environmental impacts. The observed increases in their frequency, intensity and duration are projected to continue with global warming [2].

Additionally, in sub-Saharan African countries, rapid growth of construction has led to the proliferation of low-quality buildings with high energy consumption. This trend has raised environmental concerns regarding their contribution to environmental threats [3,4]. As, buildings can have a great impact on the environment, because buildings are considered one of the most significant sources of energy use and greenhouse gas emissions [5]. Therefore, enhancing the sustainability of the building sector is crucial to combat climate change [6]. To achieve this crucial goal, architects and the other contributors involved in construction are responsible for addressing various concerns when designing buildings, with one of the most significant being ensuring compliance with building codes and standards to evaluate of thermal comfort. While designers and engineers commonly refer to international standards, such as ISO 7730, ASHRAE-55, CEN, and CIBSE for HVAC system sizing and temperature calculations. However, this approach fails to consider the satisfactory performance of buildings and occupants' tolerance levels.

Consequently, there is an increasing need in these countries to develop adaptive thermal comfort standards.

2. RESEARCH GAP

There are several justifications to evaluate the thermal comfort of Balme Library, located in Ghana's tropical climate. Increased urbanisation growth and the wasteful use of fossil fuels and non-renewable energy have led to climate change and the production of greenhouse gases. The depletion of fossil fuel resources, low efficiency, and high cost of their environmental impacts have made energy consumption optimisation and the use of renewable energy in construction inevitable [7]. On the other hand, by improving the standard of living, people expect a better level of comfort, which ultimately necessitates the use of heating, ventilation, and air conditioning (HVAC) [8]. Especially, in tropical, hot, and humid regions, such as Ghana, where the straightforward response to discomfort in this climate has been the adoption of air conditioners and mechanical cooling [9]. HVAC systems are crucial for maintaining a consistent temperature and humidity indoors all year long and making it possible to provide pleasant working and living conditions. However, it's important to recognise that the extensive use of HVAC systems can have adverse consequences. This includes an increased demand for electricity and consequently, a contribution to rising greenhouse gas emissions on a global scale [10]. Moreover, the rapid growth of construction in sub-Saharan African countries is characterised by low quality buildings and high energy consumption. This raises concerns about their contribution to environmental threats, especially climate change. This is a disquieting trend, and the initiatives taken to counteract it are few [11]. The progressive urbanisation has significantly impacted energy consumption, resource depletion and pollution and waste production [12]. African cities are outpacing the rest of the world in growth [13]. On the other hand, the comfort zone can differ in size and range within particular geographical areas [14,15] In addition, the necessities of adaptive thermal comfort research can be justified with the following reasons:

- Relying only on international HVAC standards neglects building performance and occupant comfort, causing energy inefficiencies, increased costs, and carbon emissions due to inadequate addressing of overheating and overcooling [16].
- International comfort standards may not be universally applicable to all climates due to variations in comfort preferences among people in different regions and climate zones [17].
- In hot and humid climates like Ghana, prioritise adaptive comfort and passive design over air-conditioning by implementing natural ventilation, shading, and insulation strategies to reduce energy consumption and environmental impact while meeting international standards like ASHRAE -55.
-

3. THERMAL COMFORT APPROACHES

Thermal comfort models can be used to gain insight into important building design variables and predict whether a given design will provide satisfactory thermal conditions [18]. Some popular thermal comfort models include the Predicted Mean Vote (PMV) model, Griffiths' method, and the adaptive model. The PMV model, introduced by Fanger in the late 1960s as a heat balance model, was developed from Fanger's laboratory and chambers studies [19]. International standards like ASHRAE 55 and CEN recommend using Fanger's model. The PMV model assesses human thermal comfort by considering six key factors: clothing thermal resistance, metabolic rate, air temperature, mean radiant temperature, air velocity, and relative humidity; and it predicts the mean thermal sensation vote of a large group of individuals based on the heat balance of the human body [20,21]. However, its limitations in accurately representing real-world conditions have raised doubts about its accuracy in predicting thermal comfort in actual buildings, including habituation, expectation, behavioural adjustments, and the availability of environmental control options [22,23,24,25]. And the adaptive thermal comfort model considers occupants' ability to adapt to different temperatures based on outdoor climate and seasonal variations, taking into account contextual factors such as access to environmental controls and past thermal experiences [26].

4. METHODOLOGY

4.1 CLIMATE

The climate of Ghana is characteristically tropical and was comparatively stable over recent years [27]. with rainy and dry seasons named Harmattan. According to Köppen & Geiger classification, this climate zone belongs to the Aw climate i.e., the tropical savanna climate characterised by very hot days and colder nights during the dry season [28].

4.2 SITE DESCRIPTION

There are different sections in the Balme library, including the Reference Hall, East Stack, West Stack, Ghana-Korea Information Access Centre on the ground floor, East Mezzanine (above East Stack), West Mezzanine (above West Stack), and Periodical Hall, The Students' Reference Library (SRL), African Library, and Reserved Collections on the first floor.

These sections have passive architectural features such as courtyards, outdoor corridors, and high ceilings indoors. Some rooms have been retrofitted with air-conditioning, while others remain naturally ventilated.

4.3 DATA ANALYSIS

To conduct the current research, two types of data analysis have been carried out, including analysing subjective and objective thermal comfort data in naturally ventilated and air-conditioned areas to establish an adaptive thermal comfort model for Ghana, utilising surveys and data loggers in comparison to the international standards, such as ASHRAE 55. To collect the indoor environmental variables, including air temperature (T_a), globe temperature (T_g), relative humidity (RH), and air velocity (V_a) during the surveys, wet-bulb globe temperature (WBGT) meter data loggers were used. The outdoor temperature and humidity were recorded over two years using Rotronic Instruments Temperature & Humidity data logger. The device was installed on the north-facing wall and a shaded area.

Regarding the subjective data, the questionnaires were distributed among the library users, and 664 individuals completed them, and 655 questionnaires were deemed acceptable for data analysis. This questionnaire involved specifying the location and orientations of the room to categorise the AC and NV modes. Another section collected demographic information of the participants, including gender and age. The third section included thermal comfort questions related to the subject's thermal sensation vote (TSV), thermal preference (TP), thermal acceptance (TA), humidity feeling (HF), airflow movement feeling (AF), and airflow preference (AP). The fourth section pertained to the activity level and clothing insulation, following the guidelines outlined in the standards [29,30].

It should be mentioned that the collected data has been analysed by using Python as the primary software. To conduct this survey, in addition to the aforementioned items, the mean radiant temperature (T_r), and the Operative temperature (T_{op}) were calculated via Equation (1) and (2):

$$Tr = [(T_g + 273)^4 + 1.1 \times 10^8 Va^{0.6} / \varepsilon D^{0.4} \times (T_g - Ta)]^{1/4} - 273 \quad (1)$$

Where D, is the diameter of the globe is 0.05 mm, and ε, the emissivity of the surface is considered 0.9. Air speed is ranging from 0.2 to 0.8 m/s for lightly clothed (0.5 – 0.7 clo) occupants in sedentary activities. And Va stands for air velocity. And also, to calculate the operative temperature the Equation (2) is used.

$$T_{op} = HT_a + (1 - H)\, T_r \quad (2)$$

Where, $H = h_c / (h_c + h_r)$, and Tr is the mean radiant temperature, hc is the convection heat transfer coefficient, and hr is the radiation heat transfer. The hr is defined as 4.7 W/m^2, and hc is considered for an air velocity of <0.2 m/s, according to the ASHRAE Standard 55. The neutral or comfort temperature (T_{comf}) or comfort zone is the operative temperature at which the average person will be thermally neutral, or the most significant proportion of a group of people will be comfortable [31]. While PMV depends on the six variables of T_a, T_r, RH, V_a, activity, and clothing level, however, it does not consider the expectations and adaptability of users.

4.4 ADAPTIVE MODEL

A regression analysis was carried out to estimate the mean T_{comf} over several days or weeks of the survey period. On the other hand, the Griffiths method suggests calculating the optimal temperature for individual comfort within a specific building and month. Based on the Griffiths method, the neutral temperature can be calculated by the following Equations (3,4) using the relationship from T_{op}, TSV, and G:

$$T_{comf} = T_{op} - (TSV - TSV_n)/G \quad (3)$$

Where the TSV is the thermal sensation vote, the TSV_n represents the neutral thermal feeling, and G is the Griffiths coefficient. For this case study and sensitivity analysis, G was at 0.25, 0.33, and 0.50. These equations mainly consider the weighted running mean temperature (T_{rm}) as an independent variable for outdoor temperature.

$$T_{rm} = \{T_{od-1} + \alpha T_{od-2} + \alpha^2 T_{od-3} \ldots\} / \{1 + \alpha + \alpha^2 \ldots\}, \quad (4)$$

Where:

T_{od-1} - daily mean outdoor temperature (°C) for the previous day;

T_{od-2} - daily mean outdoor temperature (°C) for the day before.

The constant α is a unitless constant that shows the time needed for thermal adaptation, and its rate is between 0 and 1. However, ASHRAE 55 recommended considering a range of 0.33 to 0.9 for α. The α = 0.8 is usually taken as a half-life of approximately 3.5 days [32]. The half-life (λ) calculation of an exponentially weighted Trm is given in the following Equation (5).

$$\lambda = 0.69/(1 - \alpha) \quad (5)$$

5. RESULT

5.1 Environmental conditions

Comparisons of the thermal comfort votes, such as subject sample size, indoor thermal conditions, and the PMV for air-conditioned (AC) and naturally ventilated (*NV*) rooms, are presented in Tables 1 and 2.

Table 1: Subject sample size and the survey results in AC rooms

Number of valid surveys	162		55% Male, 45% Female	
Variable	Mean	SD	Max	Min
Respondents age	23.8	6.5	60.0	16.0
Thermal sensation vote	-0.2	1.1	3.0	-3.0
Thermal Preference	-0.5	0.8	1.0	-2.0
Airflow Feeling	-0.4	0.8	2.0	-2.0
Airflow Preference	0.4	0.6	1.0	-1.0
Humidity Feeling	-0.2	0.8	3.0	-2.0
Humidity Preference	-0.5	0.7	1.0	-2.0
Clothing	0.4	0.1	1.1	0.3
PMV	-0.35	0.82	2.47	-2.24

Table 2: Subject sample size and the survey results in NV rooms

Number of valid surveys	429		60% Male, 40% Female	
Variable	Mean	SD	Max	Min
Respondents age	22.4	5.3	60.0	12.0
Thermal sensation vote	0.2	1.0	3.0	-3.0
Thermal Preference	-0.7	0.6	1.0	-2.0
Airflow Feeling	-0.4	0.8	3.0	-2.0
Airflow Preference	0.5	0.5	1.0	-1.0
Humidity Feeling	-0.2	0.8	3.0	-3.0
Humidity Preference	-0.3	0.7	1.0	-2.0
Clothing	0.4	0.2	1.4	0.3
PMVe, e= 0.5	0.48	0.24	0.99	-0.74

In terms of thermal sensation votes, the highest percentage (47.2%) of respondents experienced a comfortable feeling in the naturally-ventilated areas (Fig.1). As for thermal preference, approximately 52% of library users preferred a slightly cooler temperature in the NV mode, while 42.7% preferred the same in the AC spaces (Fig.2).

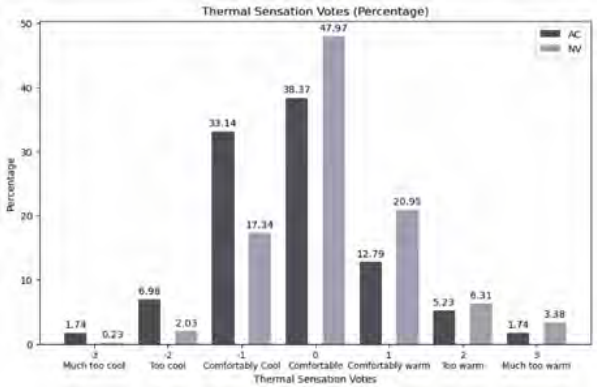

Figure 1: Thermal sensation votes (Percentage)

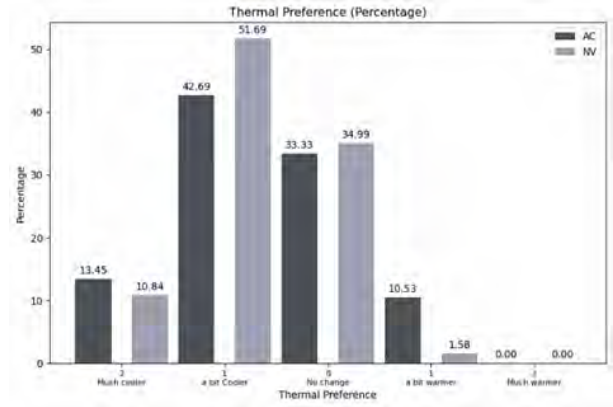

Figure 2: Thermal Preference votes (Percentage)

5.2 Outdoor environmental conditions

The outdoor data has been generated from the on-site data collected between January 2022 and September 2022. This dataset includes outdoor temperature and humidity, which are presented using box plot diagrams (Fig. 3).

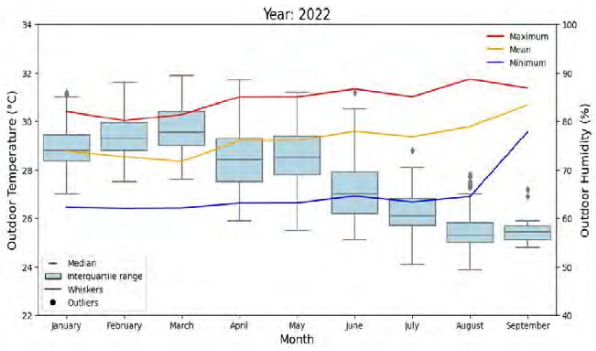

Figure 3: Outdoor weather conditions measured on-site.

Over the study period, the highest temperature belonged to May 2021, 32.95 °C, and the lowest one was in August 2022, 23.9 °C. The highest level of humidity was in September 2021, 90.60%, and the lowest was from January to May 2021, 62%.

5.3 Evaluation by Fanger's PMV

Figure 4 represents the linear regression of the mean sensation votes (MTSV) and predicted mean votes (PMV) as a function of operative temperature in both natural ventilated and air-conditioned modes. The Fanger and Toftum's [33] extended factor of 0.5 and the calculated factor (0.11) were used to compare the TSV with the MV and PMV_e.

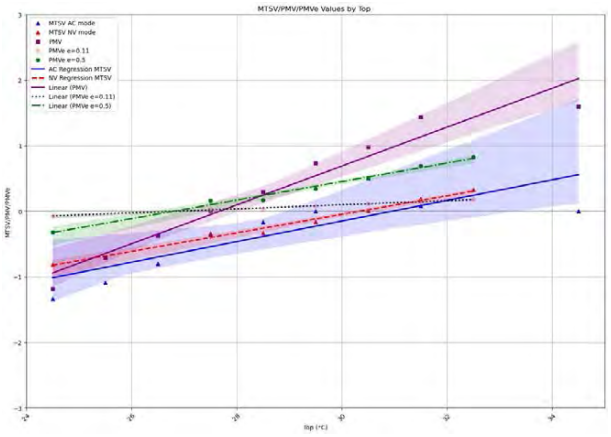

Figure 4: Linear regression of MTSV and the PMV as a function of operative temperature in NV and AC modes.

Based on this figure, the neutral temperature of PMV is 27.8°C, while the linear regression method in NV mode predicts a neutral temperature of 30.3°C. Consequently, the PMV prediction is 2.5°C lower than that of the linear regression method. Meanwhile, the

linear regression predicts a comfort temperature of 31°C in the AC mode. Therefore, the discrepancy increases in air-conditioned areas by approximately 3.2 °C. The increase in the slope in AC mode can be observed in the thermal sensation vote bar chart diagram, as 33.14 percent of subjects in the AC mode feeling "comfortably cool". Additionally, in the NV mode, while 47.97 percent of individuals voted for "comfortable" as a neutral feeling, representing half of the subjects, 20.95 percent of them voted for "comfortably warm", or 17.34 percent for "comfortably cool". Therefore, these factors might be the rational explanations for the lower-than-expected slope.

5.4 Comparison with the Standards

ASHRAE-55, as one of the most widely accepted international standards, for naturally-ventilated buildings, is primarily utilised to predict indoor comfort temperature by using the measured outdoor temperature. A comparison of the adaptive comfort temperature and the comfort zone is illustrated using the regression model with ASHRAE-55 (Fig.5).

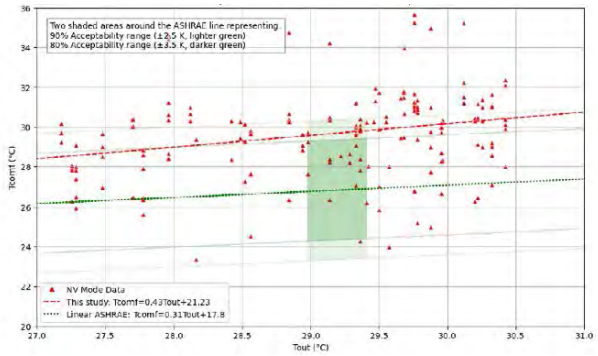

Figure 5: Comparison of the adaptive thermal comfort with the ASHRAE-55 standard

Figure 5 represents that the proposed adaptive model predicts a higher slope than the defined in the ASHRAE-55 standard. It means that this standard predicts a lower comfort range against the achieved results of the current study. And, in NV mode, the majority of the data points and their regression line reside above the standard. Additionally, in comparison with the CEN standard, while the slope of the CEN proposed model is 0.33 K^{-1} in the regression line, this study calculated higher ranges for thermal comfort with the slope of 0.43 K^{-1} for the linear regression as well.

6. CONCLUSION

The main aims of this research were to evaluate the thermal comfort in Balme Library, as a case study in Ghana, and to propose an adaptive thermal comfort model. The results of this research determine that the subjects whose origins were from Ghana, feel neutral or comfortable at different temperatures against the recommendations of the adaptive models of international standards, such as ASHRAE-55. For instance, in the case of NV, when compared to the ASHRAE-55 standard, which has a regression line slope of 0.31 K^{-1}, the slope of 0.43 K^{-1} for this case study suggests that Ghanaians can adapt to the climate faster than predicted by the standards. In AC mode, at the mean temperature of 28.60 °C, 38.37% of the subjects felt comfortable and 41.86% of them felt "comfortably cool", "too cool", and "much too cool". In NV mode, at the mean temperature of 30.24 °C, approximately half of the individuals (47.97%) voted for neutral feeling. Therefore, the current international standards and the HVAC building regulations underestimate the ranges of thermal preferences among the building's occupants.

REFERENCES

1. Kaitouni, S.I, Chahboun, R., Boushssine, Z., Cakan, M., brihui, J., & Ahachad, M. (2023). Simulation-based assessment of the climate change impact on future thermal energy load and indoor comfort of a light-weight ecological building across the six climates of Morocco. *Thermal Science and Engineering Progress*, 45-102137.

2. Barriopedro, D., García-Herrera, R., Ordóñez, C., Miralles, D.G.& Salcedo-Sanz, S. (2023). Heat waves: Physical understanding and scientific challenges. *Reviews of Geophysics. 61*. https://doi.org/10.1029/2022RG000780.

3. Lee J, McCuskey Shepley M. Benefits of solar photovoltaic systems for low-income families in social housing of Korea: renewable energy applications as solutions to energy poverty. Journal of Building Engineering March 2020; 28:101016. https://doi.org/10.1016/j.jobe.2019.101016.

4. Malinauskaite J., Jouhara H., Ahmad L., Milani M., Montorsi L., Venturelli M., Energy efficiency in industry: EU and national policies in Italy and the UK, Energy. 172, 255–269. doi:10.1016/j.energy.2019.01.130.

5. Zhou, X., Huang, Z., Scheuer, B., Wang, H., Zhou, G., & Liu, Y. (2023). High-resolution estimation of building energy consumption at the city level. *Energy*. 275, https://doi.org/10.1016/j.energy.2023.127476.

6. Wang, H. Yu, M., Lin, X.Y., Guo, H.J., Liu, H., Zhao, Y.R. et al. (2021). Prioritising urban planning factors on community energy performance based on GIS-informed building energy modelling. *Energy Build*, 249 Article 111191

7. Taher Tolou Del, M.S., Bayat, S., Zojaji, N. (2022). The effect of building plan form on the thermal comfort in the traditional residential patterns of the hot and dry climate of Qom. *Heritage Science*, https://doi.org/10.1186/s40494-022-00807-1

8. Rashdi& Embi, (2016). Analysing Optimum Building Form in Relation to Lower Cooling Load, *Procedia –Social and Behavioural Sciences*. 222. 782–790, https://doi.org/10.1016/j.sbspro.2016.05.161

9. Mohammadpourkarbasi, H., Jackson, I., Nukpezah, D., Apeeaning Addo, I., Assasie Oppong, R. (2022). Evaluation of thermal comfort in library buildings in the tropical climate of Kumasi, Ghana, *Energy and Buildings*, 268, https://doi.org/10.1016/j.enbuild.2022.112210.

10. Alam, Md.A, Kumar, R., Yadav, A.S., Arya, R.K & Singh, V.P. (2023). Recent developments trends in HVAC (heating, ventilation, and air-conditioning systems: A comprehensive

review. *Materials Today: Proceedings*, https://doi.org/10.1016/j.matpr.2023.01.357
11. Widera, B. (2021). Comparative analysis of user comfort and thermal performance of six types of vernacular dwellings as the first step towards climate resilient, sustainable and bioclimatic architecture in western sub-Saharan Africa. *Renewable and Sustainable Energy Reviews*.
12. Rodriguez, C.M., D' Alessandro, M. (2019). Indoor thermal comfort review: The tropics as the next frontier. *Urban Climate*.
13. Florio, P., Freire, S. & Melchiorri, M. (2023). Estimating geographic access to healthcare facilities in Sub-Saharan Africa by Degree of Urbanisation. *Applied Geography* 160, 103118. https://doi.org/10.1016/j.apgeog.2023.103118.
14. Chen, L. Kántor, N. & Nikolopoulou, M. (2022). Meta-analysis of outdoor thermal comfort surveys in different European cities using the RUROS database: The role of background climate and gender. *Energy & Buildings* 256, 111757.
15. Zhang, J., Khoshbakht, M., Liu, J., Gou, Z., Xiong, J. & Jiang, M. (2022). A clustering review of vegetation-indicating parameters in urban thermal environment studies towards various factors. *Journal of Thermal Biology*. 110, 103340.
16. T. Dwyer, (2017). Module 113: Determining thermal comfort in naturally conditioned buildings. [Online]. Available: https://www.cibsejournal.com/cpd/modules/2017-07-nat/. [Accessed 10 05 2022].
17. F. Nicol, M. A. Humphreys and S. Roaf, (2012). Adaptive Thermal Comfort. *Principles and Practice, 1st ed., New York: Routledge*.
18. Mamulova, E., Loomans, M., Loonen, R., Schweiker, M. & Kort, H. (2023). Let's talk scalability: The current status of multi-domain thermal comfort models as support tools for the design of office buildings. *Building and Environment*. 242, https://doi.org/10.1016/j.buildenv.2023.110502.
19. Fanger P. (1970). Thermal comfort, analysis and applications in environmental engineering. *Copenhagen: Danish Technical Press*.
20. Asif, A., Zeeshan, M., Raza Khan, S. & Sohail, N.F. (2022). Investigating the gender differences in indoor thermal comfort perception for summer and winter seasons and comparison of comfort temperature prediction methods. *Journal of Thermal Biology*. 110,103357. https://doi.org/10.1016/j.jtherbio.2022.103357.
21. Du, C., Lin, X., Yan, K., Liu, H., Yu, W., Zhang, Y. & Li, B. (2022). A model developed for predicting thermal comfort during sleep in response to appropriate air velocity in warm environments. *Building and Environment*. 223, 109478, https://doi.org/10.1016/j.buildenv.2022.109478.
22. J. VanHoof, (2008). Forty years of Fanger's model of thermal comfort: comfort for all? *Indoor Air.* 18.182–201, https://doi.org/10.1111/j.1600-0668.2007.00516.x
23. Y. Yang, B. Li, H. Liu, M.Tan, R.Yao, (2015). A study of adaptive thermal comfort in a well-controlled climate chamber. *Appl. Therm.Eng*. 76.283 291,https://doi.org/10.1016/j.applthermaleng.2014.11.004.
24. R. Maiti, (2014). PMV model is insufficient to capture subjective thermal response from Indians. *Int J. Ind Ergon*.44.349– 361, https://doi.org/10.1016/j.ergon.
25. L. Schellen, M.G.L.C.Loomans, M.H.deWit,B.W.Olesen, W.D.vanM.Lichtenbelt, (2012). The influence of local effects on thermal sensation under non-uniform environmental conditions, gender differences in thermophysiology, thermal comfort and productivity during convective and radiant cooling. *Physiol. Behav*. 107.252–261, https://doi.org/10.1016/j.physbeh.2012.07.008
26. de Dear R, Brager G. (1998). Developing an adaptive model of thermal comfort and preference. *ASHRAE Trans* ;104(1):145e67.
27. Dodoo, A. & Ayarkwa, J. (2019). Effect of climate change for thermal comfort and energy performance of residential buildings in a Sub-Saharan African, *Buildings*, 9(10).
28. Kottek M, Grieser J, Beck C, Rudolf B, Rubel F. World map of the Köppen-Geiger climate classification updated, (2006). *Meteorol Z*;15(3):259–63. https://doi.org/10.1127/0941 2948/2006/0130
29. ASHRAE, (2017). ANSI/ASHRAE Standard 55-2017: Thermal Environmental Conditions for Human Occupancy. *American National Standards Institute, Atlanta, GA*.
30.International Organization for Standardization, Ergonomics of the Thermal Environment-Analytical Determination and Interpretation of Thermal Comfort Using Calculation of the PMV and PPD Indices and Local Thermal Comfort Criteria, (2005) *International Organization for Standardization*.
31. F. Nicol, M. A. Humphreys and S. Roaf, Adaptive Thermal Comfort, (2012). *Principles and practice, 1st ed., New York: Routledge*.
32. M.A. Humphreys, H.B. Rijal, J.F. Nicol, (2013). Updating the adaptive relation between climate and comfort indoors; new insights and an extended database, *Building and Environment*, 63 40–55.
33. Fanger, P.O., Toftum, J. Extension of the PMV model to non-air-conditioned buildings in warm climates. (2002), *Energy and Building*, 34(6), 533-536.

PLEA 2024 WROCŁAW
(Re)thinking Resilience

Form-Sensitive Urban Building Energy Model:
A Simple Online Tool for Multi-Scale Analysis

JORGE RODRÍGUEZ-ÁLVAREZ[1], NATALIA ALVAREDO LÓPEZ[1]

[1]Universidade de A Coruña, A Coruña, Spain

ABSTRACT: This paper describes an Urban Building Energy Model that adapts thermodynamic and daylighting models to map the energy demand in large urban areas, displaying estimates of current or alternative planning scenarios. This online tool aims to support a wide range of users, from tenants to policymakers to identify the most effective energy conservation measures and policies based on the characteristics of the building stock and the urban fabric in each part of the city. The model incorporates the key variables that influence building energy use for heating, cooling and lighting, exploiting current datasets and open tools and libraries. The next stages of the research will test the application in different contexts (end-users, public administration…) to fine tune its features and usability.
KEYWORDS: Energy, Urban, Heating, Renovation, Maps

1. INTRODUCTION

The building sector is the main contributor to energy consumption in the European Union. It is responsible for nearly 40% of the total demand [1]. Despite improvements in construction technology and the strict requirements imposed by building regulations, the energy consumed by buildings has increased steadily at an average annual rate of 0.6% since 1990(Ibid). New tools are therefore required to tackle energy efficiency, not least assist on decision making processes.

The renovation of the building stock that is necessary to achieve climate neutrality is not advancing at the expected rate at the moment. This is partly due to the lack of tools to identify the spatial energy consumption patterns in cities. Although myriad energy models are now available to evaluate building energy performance, large-scale analysis has been constrained by the complexity and uncertainty of urban parameters [2].

This research leverages previous work and develop a new methodology to facilitate thermal and lighting demand calculations at the urban scale. The model applies original algorithms to take into account the specific urban morphology, building attributes and local climate and thus estimate the energy loads for heating, cooling and lighting. The energy model is deployed as an online interactive tool thus targeting a wide range of end users, from public administrations to individual households.

2. STATE OF THE ART IN URBAN BUILDING ENERGY MODELS

In the 2000s a first generation of Urban Building Energy Models (UBEM) emerged with projects such as CitySim [3], SunTool [4], Urban LT [2], ClimateLite [5], or Ursos [6]. In the following decade (2010-2020), the research focused on interoperability, which facilitated the use of well-established building-level thermodynamic models, such as the Urban Modelling Interface, UMI [7] or the most recent City Energy Analyst, CEA [8]. These two projects are mainly focused on new developments and are optimized for an intermediate scale (few urban blocks or a small district).

The latest trend in UBEM is to develop tools that can be accessed through the browser, without need for desktop installation. UBEM.IO [9] applies a web-based methodology to facilitate energy estimates for buildings on an urban scale. Other online platforms simply display pre-processed energy data, obtained from models or existing databases (e.g. London Heat Map [10] or London Building Stock Model [11]).

None of the existing tools currently combines the effect of urban morphology, with online access and interaction that enables the analysis of alternative scenarios.

3. METHODOLOGY

The UBEM developed in this research adapts a quasi-dynamic thermal model. The model deploys an analytical grid to adapt the resolution to the scale, thus generating rapid simulations for large urban areas. Then, the model exploits cadastral information to infer the key building properties. Finally, the energy calculation is undertaken using building archetypes for each cell of the grid. The model's structure (Fig. 1) takes advantage of cadastral datasets to obtain a basic cartography, with information of buildings' footprint and height.

The calculation of energy demand is carried out at two scales, at the mesh level and at the building level. The aim is for the calculation to be as automatic as possible, using open sources libraries and open data, scalable and generalizable to other areas. The process is fundamentally divided into two stages, the precalculation of the base layers, which is carried out using Geographic Information Systems, and the calculation of the energy demand using an ad hoc

design Python module, which receives as input the precalculated layers.

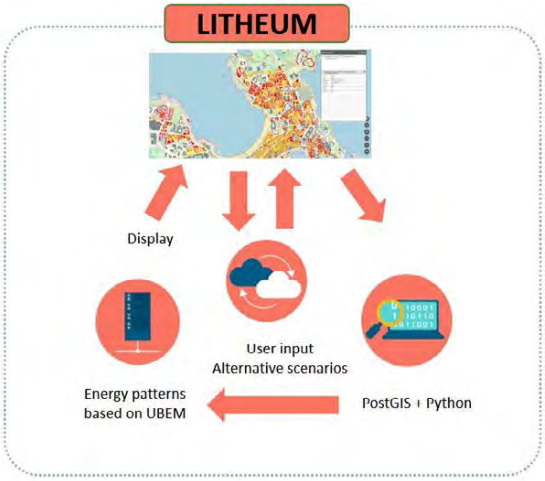

Figure 1: UBEM and online platform structure

Both the cartographic information, obtained from the plugin for QGIS Spanish Inspire Cadastral Downloader, and the alphanumeric information in CAT format, downloadable from the Cadastre Headquarters' own page (sedecatastro.gob.es). Only those buildings classified as residential use are taken into account.

3.1 Pre-processing stage: base layers

Two base layers need to be generated in order to store the necessary spatial and thermal information; one layer for the analytic grid and a second layer with the relevant parameters disaggregated at building level. The former will be used to facilitate large scale analysis and visualization while the latter enables detailed calculations for each building (*Fig*).

The methodology for the pre-calculation of these layers is similar for both grid and building level, except that at the grid level the results are aggregated according to the identifier of each grid cell and at the building level the data are directly related to the cadastral reference. In both cases, data derived from the urban morphology analysis itself and associated with it are used, included in the database of the source layer or linked through the cadastral reference from the CAT files.

The notional characteristic grid is derived using a model adapted from [12]. This model translates the actual urban fabric into a matrix composed of a number "n" of building blocks with the following attributes (Figure *)*:

-The area of the real urban sample and the notional characteristic grid are equal

-All building blocks of the grid are equal. Each block has the same Ground Floor Area (GFA) to Perimeter ratio than that calculated for the whole urban sample.

-Each block has the same proportion of its perimeter facing the Northern-Southern quadrant and the Easter-Western quadrant than for the whole urban sample

-The built-up area and the total perimeter of the grid is the same as for the urban sample

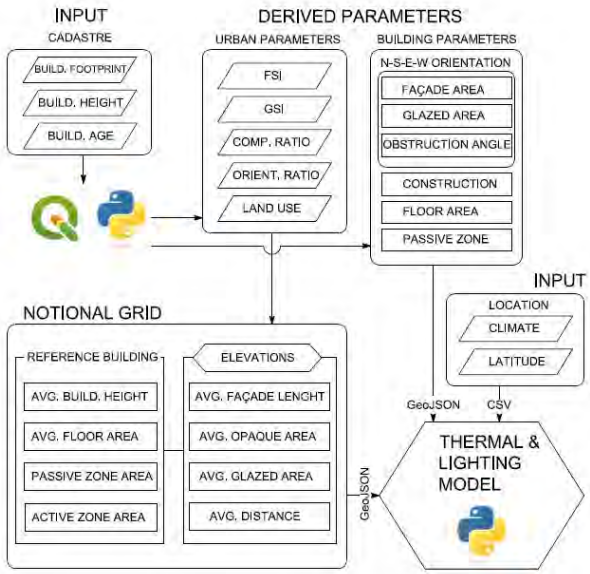

Figure 1. Flowchart of input and derived parameters to create the analytic grid and building data

The model will calculate the average value for all buildings within each cell. The formulation of the model enables filling the gaps in input variables (e.g. thermal insulation, glazing properties…) with typical default values, which can be verified and modified at any time.

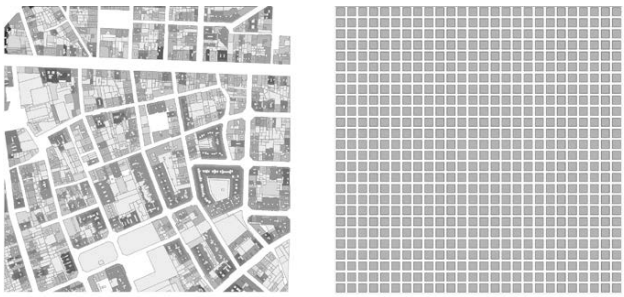

Figure 3 Notional grid (right) versus actual urban fabric (left) as derived from the model

In order to calculate the energy demand, data related to the geographical position, the proportion of windows, the construction systems, etc. are also added; as well as other data that will be displayed on the web.

The calculation of the attributes is carried out using Python, and specific libraries, such as PyQGIS, Pandas and Numpy. , requiring the introduction of the building layer downloaded from the cadastre into the script. The grid layer is created in GeoJSON format, and it contains the attributes listed in Table 1

Table 1 Grid Layer attributes

Identifier	Description	Source
id	Unique mesh identifier	
Env	Exposed Envelope	Data obtained from the cadastre layer
GFA	Ground Floor Index	
I	Height	
MOR	Main orientation	
Or	orientation ratio	
W_D	% domestic use	
W_ND	% non-domestic use	
GSI	Ground Space Index	Data derived from the cadastre layer, for web visualization
FSI	Floor Space Index	
comp	Compactness	
Lat	Latitude	Other data necessary to calculate demand
Gz	Glazing ratio	
tc	Thermal capacity	
Ct	Construction type mesh side	

For the building level pre-processing algorithms were developed and coded in Python to automatically calculate each building's exposed envelope area, the solar obstruction in each orientation, and to break down the uses in each floor.

To calculate the exposed envelope, we create a loop that computes the perimeter's length that touches other buildings and the length that is exposed in each floor. Then the code multiplies the length of the exposed perimeter by the floor height (assumed as 3m in domestic buildings). The exposed perimeters are classified according to their orientation (*Fig*) in order to assign glazing ratios (based on building age and typology) and calculate incoming solar radiation in the thermal model, using orientation and obstruction angles as derived in these steps.

To obtain solar obstruction we developed a tray tracing method. The code generates lines from the centre of each building with 12 different azimuths at 30-degrees intervals (*Fig*). Those lines are intersected with opposing buildings so that for each intersection we calculate the obstruction angle as the arctangent of the obstructing building's height by the distance between both buildings. A loop repeats the operation for all buildings along the intersecting line (we set a limit of 200m) to finally select the highest obstruction angle, which is assigned to the building. The process is repeated for 12 orientations and all buildings in the study area. It must be noted that this algorithm can take quite some time to process a medium size city. Initial tests carried out for Pontevedra (80.000 inhabitants) took five days. Subsequent optimization reduced the computing time to 12 hours. The reduction of the number of angles and length of the rays can further optimize the model.

Figure 4 Highlighted exposed perimeters are classified according to their orientation.

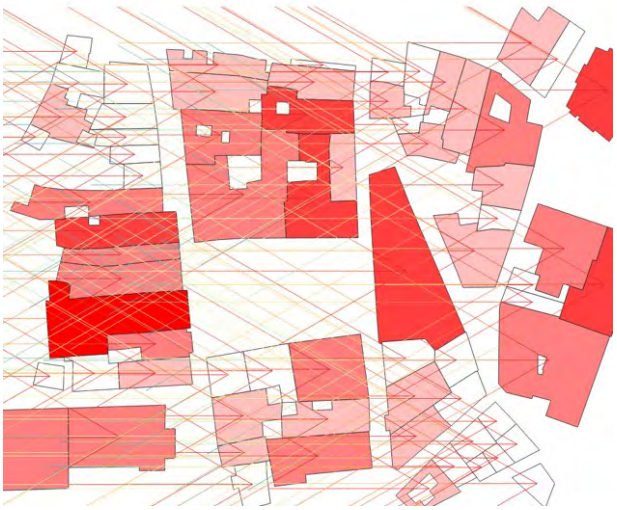

Figure 5 Raytracing to calculated solar obstruction. The image shows rays for azimuths 240, 270, 300

The buildings' geometry and their derived parameters, which are listed in *Table 2* are compiled in a GeoJSON file, which will be subsequently fed into the thermal and lighting calculations modules.

Table 2. Building Layer attributes

Identifier	Description	Source
RefCat	Unique building identifier	Data obtained from the cadastre layer
Env_N	Envelope Area North	
Env_E	Envelope Area East	
Env_S	Envelope Area South	
Env_O	Envelope Area West	
GFA	Floor Area	
I	Building Height	
MOR	Orientationi of the facades	
OBS_N	Obstruction angle north	
OBS_E	Obstruction angle east	
OBS_S	Obstruction angle south	
OBS_O	Obstruction angle west	
date	Construction date	
W_D	% domestic use	
W_ND	% non-domestic use	
Lat	Latitude	Other data necessary to calculate demand
Gz	Window ratio	
tc	Thermal capacity	
CT	Construction type	

3.2. Energy demand calculation

For the calculation, a Python module has been developed that follows the methodology developed in [12], in which, taking into account morphological, climatic, construction, and location-related parameters, a sequence of 7 steps is applied to obtain heating, cooling and lighting loads (Fig):

1- Calculation of heat losses through the exposed parts of buildings' envelope. Total conductive and convective losses are estimated and divided by the built-up area to obtain the Heat Loss Coefficient (HLC) in W/m²K.

2- Heat loss per hour. The hourly heat losses are calculated based on the difference between the indoor comfort temperature and the outdoor temperature, multiplied by the Heat Loss Coefficient ((Ti-Te) * HLC).

3- Internal heat gains. Internal casual heat gains are determined for each type of building according to predefined schedules derived from literature [13], [14]

4- Solar gains. Direct and diffuse solar gains are calculated using a multi-step procedure. First, the vertical solar radiation on each orientation is obtained from the climatological database. We use the sun's position and the obstruction angle (obtained as defined in 3.1) to infer the hourly direct solar gains on each façade. The resultant value is weighted by the window to wall ratio to obtain the indoor solar gains. Similarly, the diffuse solar gains are calculated based on weather data, obstruction angle, the glazed area, and the glazing solar transmission.

5- Utilization factor. The total solar gains are weighted by the utilization factor, which is the ratio between the useful solar gain and the total gains. We apply a function derived from correlations proposed by [15]

6- Space heating/ cooling demand. In the next step, we compare the heat gain to loss balance, together with the outdoor temperature, to obtain hourly estimates of the indoor temperature. If the resultant value is above or below the comfort range a heat/cooling load is added accordingly. The total annual loads are obtained by iterating this step.

7- Daylight Factor (DF). The model assumes that the living spaces are side lit, so the approximate estimation method proposed by the Building Research Establishment [29] is applied. We obtain the external illuminance from the climatic data. The need for additional artificial lighting is defined as 150 lux [30]. The internal spaces are divided into passive and active zones as in Baker and Steemers [31]. The indoor illuminance is found by combining DF and outdoor illuminance. When it is below the required levels artificial lighting will be added in the passive zone. The final load can be obtained by multiplying the assigned power of artificial light per square meter (assumed as 6w/m²) by the hours of operation of the artificial lights.

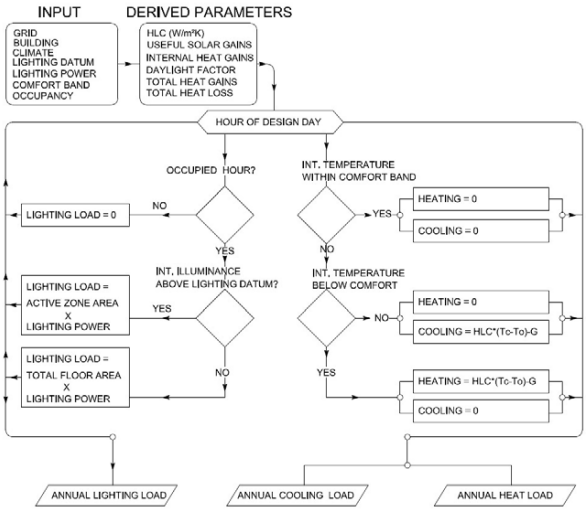

Figure 6 Flowchart of the thermal and lighting model

The results from these calculations will be added to the GeoJSON table of attributes as Heating, Cooling and Lighting loads in kWh/m² per year. The online interactive map will display a colour code to reflect the performance of each cell of the grid or for each building, depending on the chosen visualization mode. In addition, one a single element is selected (cell or building) the application will display a summary chart with the broken-down monthly loads (Fig)

3.3. Free running performance

Since the ultimate goal of the application is to promote energy savings and passive operation whenever possible it was considered convenient to provide a graphic display of indoor temperatures with no additional heating or cooling. We followed the same procedure described above instead of defining the indoor comfort band we calculated the heat to loss balance to determine the monthly average thermal difference in steady state conditions. Then, we assigned a decrement factor and time lag based on the thermal inertia input parameter and typical values. We calculated the hourly temperatures using a sinusoidal formula to distribute the average indoor temperature over the daily cycle in a way that reflects the thermal swing and time lag defined before:

$$Ti = (DecF \cdot TSo/2) \cdot \sin(((-1/12)*(hour-Tlag)-1/6)*pi)+TMo \quad [F.1]$$

Where:

Ti= hourly internal temperature (ºC)
DecF = Decrement Factor
Tso= Outdoor temperature
hour = time of the day
Tlag = Time lag
pi = Constant Pi
TMo= Average monthly indoor temperature

The above model was calibrated to generate meaningful results. The goal was to reflect the

patterns of performance in a simplified method that could be quickly processed in web browsers. The chart was initially generated using the python library Matplotlib *(Fig)* but in the online platform is translated into javascript using ChartJS.

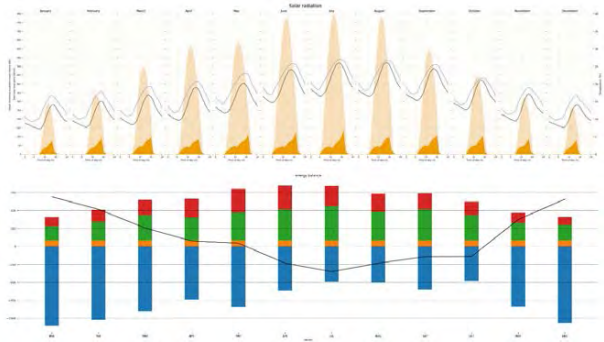

Figure 7 Snapshot of the summary charts produced by the application

3.4. Online interactive map.

The novelty of this application resides in the fact that it is hosted online, and it is connected to a map server, which allows user to interact with the input and output parameters. The basic structure of the platform consists of a GeoServer that hosts a PostGRE SQL database (Fig). The server fetches the base GeoJSON files with the initial parameters and heating, cooling and lighting values for grid and buildings. These data are interpreted and displayed in a map, adapting the visual styles and legend according to the range of results.

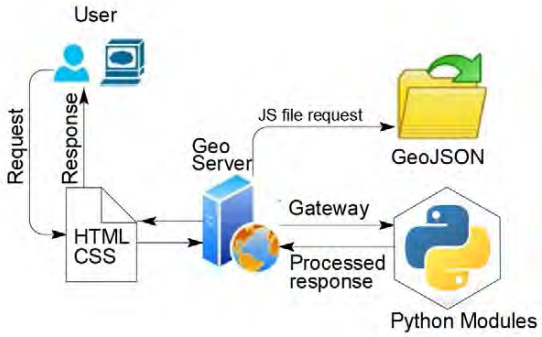

Figure 8 Architecture diagram of the online platform

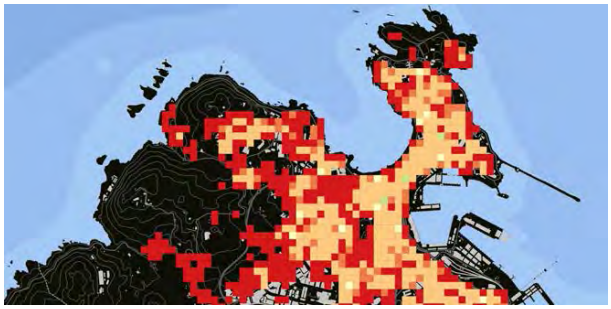

Figure 9 Example of simulated heating demand displayed in the grid for A Coruña city.

The user can access the featured elements and design custom requests. Single buildings or grid cells are accessed by clicking them on the map (*Fi*) . This action triggers the custom functions. Users can introduce or modify the key input parameters to override default values or evaluate energy conservation measures. The model takes the new requests to the python modules to recalculate thermal and lighting performance and fetches the processed response to display the new values in the map. In this way it is possible to visualize the effect of the selected measures in the energy demand (map and energy balance) or internal temperature (charts).

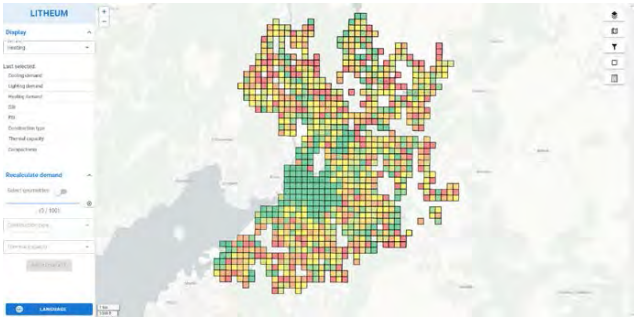

Figure 10 Urban energy portal for the city of Pontevedra. Grid view

Figure 111 Urban energy portal for the city of Pontevedra. Building level view, results of selected building are displayed on the left bar

The beta version of the application can be found at https://litheum.citic.udc.es/. Figures 9-11 show a series of snapshots of the interface and interactive features of the tool. Fig shows the initial heating loads for Pontevedra, which is a municipality of 80.000 inhabitants located in the northwest of Spain. The grid view is applied by the default to speed up the data loading process. When the user zooms in the disaggregated values by buildings appear automatically (*Figure 111).* A button allows users to switch between grid or building view at will, although there is a limit to which the latter can by displayed to prevent overloading.

The interactive options intend to be intuitive and simple. In this version, the user can select among several building typologies by simple names (retrofit, low carbon…). These names are connected to specific U-values, ventilation rates, etc…so they will be reflected in the resultant demand and temperature.

The following stages of the research include various trials, where the application will be tested with real users. We have also planned several focus

groups with relevant stakeholders to collect their feedback and continue improving the tool.

Figure 22 Detail of parameters and recalculation options

4. CONCLUSION

This paper explained the development of an online application that computes urban building energy demand, considering the urban form and building characteristics. The urban energy model has been designed to be hosted online and allow interaction. The main objective is to facilitate the exploration of energy demand patterns to all users regardless of their expertise but also to provide meaningful results without complex modelling. The model will be fine-tuned and adapted to the feedback provided in the trials to be undertaken in the next stages.

ACKNOWLEDGEMENTS

Grant TED2021-130779A-I00
Funded by MCIN/ AEI/10.13039/501100011033/ and by "European Union NextGenerationEU/PRTR

REFERENCES

1. DEA, «2018 Implementing the Energy Performance of Buildings Directive (EPBD). Country Reports», 2018.
2. C. Ratti, N. Baker, y K. Steemers, «Energy consumption and urban texture», *Energy and Buildings*, vol. 37, n.º 7, pp. 762-776, jul. 2005, doi: 10.1016/j.enbuild.2004.10.010.
3. D. Robinson, Ed., *Computer modelling for sustainable urban design: physical principles, methods and applications*. London ; Washington, DC: Earthscan, 2011.
4. D. Robinson *et al.*, «SUNtool – A new modelling paradigm for simulating and optimising urban sustainability», *Solar Energy*, vol. 81, n.º 9, pp. 1196-1211, sep. 2007, doi: 10.1016/j.solener.2007.06.002.
5. BRE, «ClimateLite . Designing Low Carbon Buildings», 2009. Accedido: 6 de junio de 2022. [En línea]. Disponible en:https://www.bre.co.uk/filelibrary/pdf/cap/Climate_Lite_Leaflet_Layout_1.pdf
6. J. Turégano y M. Hernández, «Urban design with sustainable energy criteria. Computer application for municipalities. The Ursos Project». 2008.
7. C. Reinhart, T. Dogan, A. Jakubiec, T. Rakha, y A. Sang, «Umi – An Urban Simulation Environment For Building Energy Use, Daylighting And Walkability», presentado en 2017 Building Simulation Conference, ago. 2013. doi: 10.26868/25222708.2013.1404.
8. J. A. Fonseca, T.-A. Nguyen, A. Schlueter, y F. Marechal, «City Energy Analyst (CEA): Integrated framework for analysis and optimization of building energy systems in neighborhoods and city districts», *Energy and Buildings*, vol. 113, pp. 202-226, feb. 2016, doi: 10.1016/j.enbuild.2015.11.055.
9. Y. Q. Ang, Z. M. Berzolla, S. Letellier-Duchesne, V. Jusiega, y C. Reinhart, «UBEM.io: A web-based framework to rapidly generate urban building energy models for carbon reduction technology pathways», *Sustainable Cities and Society*, vol. 77, p. 103534, feb. 2022, doi: 10.1016/j.scs.2021.103534.
10. Centre for Sustainable Energy, «London Heat Map». Accedido: 20 de junio de 2023. [En línea]. Disponible en: https://maps.london.gov.uk/heatmap
11. UCL Energy Institute, «London Building Stock Model». Accedido: 20 de junio de 2023. [En línea]. Disponible en: https://maps.london.gov.uk/lbsm-map/public.html
12. J. Rodríguez-Álvarez, «Urban Energy Index for Buildings (UEIB): A new method to evaluate the effect of urban form on buildings' energy demand», *Landscape and Urban Planning*, vol. 148, pp. 170-187, abr. 2016, doi: 10.1016/j.landurbplan.2016.01.001.
13. S. Chen, W. Yang, H. Yoshino, M. D. Levine, K. Newhouse, y A. Hinge, «Definition of occupant behavior in residential buildings and its application to behavior analysis in case studies», *Energy and Buildings*, vol. 104, pp. 1-13, oct. 2015, doi: 10.1016/j.enbuild.2015.06.075.
14. M. Jia, R. S. Srinivasan, y A. A. Raheem, «From occupancy to occupant behavior: An analytical survey of data acquisition technologies, modeling methodologies and simulation coupling mechanisms for building energy efficiency», *Renewable and Sustainable Energy Reviews*, vol. 68, pp. 525-540, feb. 2017, doi: 10.1016/j.rser.2016.10.011.
15. Y. G. Yohanis y B. Norton, «Utilization factor for building solar-heat gain for use in a simplified energy model», *Applied Energy*, vol. 63, n.º 4, pp. 227-239, ago. 1999, doi: 10.1016/S0306-2619(99)00032-X.

PLEA 2024 WROCŁAW
(Re)thinking Resilience

Structural Shape Optimization For The Reduction Of Embodied Carbon And Energy

Development of a workflow for the integration of optimization processes at the early stages of truss structure design

GINNIA MORONI[1,2] ERIC FORCAEL[1] CRISTIAN BERRIOS[2]

[1] College of Engineering, Architecture and Design, Universidad San Sebastián, Concepción, Chile
[2] College of Architecture, Construction and Design, Universidad del Bío Bío, Concepción, Chile

ABSTRACT: As the operation of buildings become more efficient, the carbon emissions generated by other phases of the building's life cycle should also be mitigated to fully address the climatic crisis. In this sense, structural systems have an important role in the total embedded carbon of a construction. This paper proposes a workflow to inform the conceptual design development of truss structures with data about material quantity and embedded carbon. For this, a multi-objective optimization process enables the integration of different criteria such as structural performance, shape complexity, utilization ratio and design rationalization. The procedure is implemented in Rhino/Grasshopper, using a parametric model that can be adjusted by the designer, according to the project requirements. The workflow is applied to a study case of a sports hall located in Chile. The results show that the mass and embedded carbon can be decreased by over 60%. It also allows assessing different rationalization levels of the design, to maintain a reduction of these variables, while enabling a more suitable truss for construction.
KEYWORDS: Structural conception, layout optimization, generative design, material quantity, embedded carbon

1. INTRODUCTION

The built environment is responsible for more than 40% of natural resources extraction and 30% of carbon emissions globally [1,2]. These carbon emissions include operational and embodied carbon. The former refers to greenhouse gas (GHG) emissions produced during the use phase of the building. The latter refers to embodied carbon or GHG emissions in the rest of the life cycle phases: material extraction, component production, transport, construction, maintenance, and demolition. Until now, important advances have been made concerning the operational emissions of buildings. However, as the built environment becomes more efficient in their operation, their energy and embodied carbon emissions become more relevant, representing 50% to 90% of total emissions in their life cycle [3]. The highest percentage of embodied carbon comes from the structural system, due to their high material mass and energy-intensive production [4].

The total material quantity of a structure is directly proportional to the total embodied carbon of the building. One of the main factors determining the material quantity is the shape of the structure. A structural shape optimized for the loads, will reduce the cross-sectional areas and the number of elements necessary for the structure, leading to material savings of up to 70% [2].

Another relevant aspect is the application of this optimization processes at an early stage of design, where decisions can have a greater influence on the reduction of the total material quantity and, consequentially, on the total embodied carbon [5]. For this, the integration of architectural, structural, and environmental variables is a key aspect [6]. Multi-objective optimization allows including different types of variables and objectives, admitting a multi-disciplinary optimization. However, this has not been largely studied in the literature [7].

Furthermore, the optimization of truss layouts has been widely studied. Nevertheless, while results can reduce the mass of the structure in large percentages, other aspects of design are rarely considered. One of these is the standardization of the truss elements. The optimized structures are usually composed of bars with different cross-sections, making them less suitable for construction, and demanding high manufacturing costs [8].

This paper aims to generate a workflow that allows evaluating different geometries for truss structures, its material quantity, and its carbon footprint, contributing to the reduction of the environmental impact of the structure at an early stage of design. This process would support and inform the decisions during the definition of the building's shape, decreasing the material quantity and, in consequence, the embedded emissions of the structure.

For this, a multi-objective optimization is put in place, considering criteria such as shape, displacements,

utilization ratio, design rationalization and material quantity. A case study is then analysed to test the proposed workflow.

2. METHODOLOGY

The research is based on a quantitative non-experimental methodology. The proposed optimization process considers architectural, structural and construction aspects intended to reduce the environmental impact of the structure, specifically, minimizing material quantity and embedded emissions. The workflow was executed in Rhino/Grasshopper, using the finite element analysis plug-in Karamba 3D and the multi-objective optimization plug-in Wallacei X. The embedded carbon emissions were estimated with a life cycle assessment of the results, considering phases A1 to A3 (material extraction, transport, and manufacturing), performed with the One Click LCA software. Finally, the tool Rhino.inside.Revit was used to transfer the final design to a Revit model.

2.1 Workflow

The process begins with the initial configuration, where the plan dimensions of the structure are defined, including the span. The designer can set the configuration to only symmetric results. They can also introduce the X coordinate for the ridge node on the elements and 2 other nodes on the top chord. These three nodes plus the extreme nodes of the top chord are control points for the design generation (Figure 1). The setup allows to work with 4 different types of load cases, as seen in Table 1, and 6 levels of design rationalization (Figure 2).

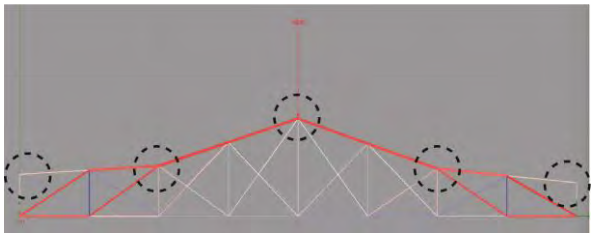

Figure 1: Truss showing the 5 control points of the design generation process. The three in the middle can have their X coordinate adjusted by the designer.

Table 1: Definition of the different load cases.

Name	Description
LC0	Concentrated permanent and live load on ridge node
LC1	Permanent and live loads on every top chord node
LC2	Permanent and earthquake loads on every top chord node
LC3	Wind loads on every top chord node

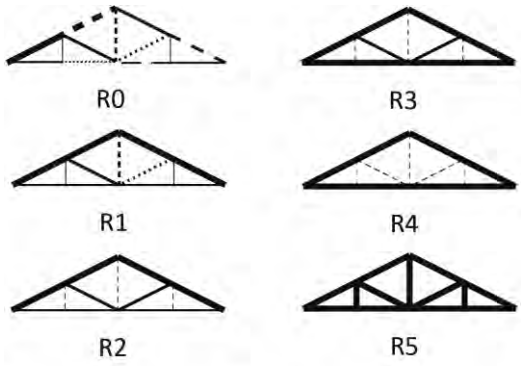

Figure 2: Representation of the different rationalization levels, R0 being the lowest, where all bars can have different cross-sections, and R5 the highest, where all bars have the same cross-section.

Then, the multi-objective optimization is carried out, the variables being the number of subdivisions on the truss, the Z coordinate of the 5 control points, the configuration of the truss' web and the number of trusses in the system. The optimization objectives are set to be the minimization of the structural mass and the nodes' displacements, and the maximization of the average utilization ratio of the truss' bars.

This process generates a total of 5000 design options, with different levels of optimization for each objective. These results are then filtered, leaving only those that reduce the mass of the structure by at least 50% of the original design, have a maximal displacement of L/700, according to Chilean regulations, and have an average utilization ratio of at least 50%. The qualified designs are then ranked by their mass and the embedded emissions are calculated for the top-ranked layouts.

The next step is verifying the top-ranked designs for the different load cases, optimizing the cross-sections on the bars and, in consequence, modifying the mass of the structure. For each bar, the largest cross-section is taken, reaching a maximum volume, which can withstand any of the load cases.

Subsequently, the designs are checked for each of the rationalization levels, where the mass increases from the lowest level, where there is no rationalization, to the highest level, where all the bars of the truss are the same, taking the most constrained cross-section. The embedded emissions are recalculated for the different rationalization levels, presenting this information to the designer, who can choose a design and a rationalization level that responds to the project's design requirements, considers a level of standardization for the structure, and takes into account the quantity of embedded emissions.

Finally, the process includes the standardization of the connections, which has shown almost no relevance in the final mass of the chosen design, since the cross-sections of the truss members remain

practically the same. The designer can choose to transfer this design directly to Revit, to continue the development of the project. A diagram of the full process is shown in (Figure 3).

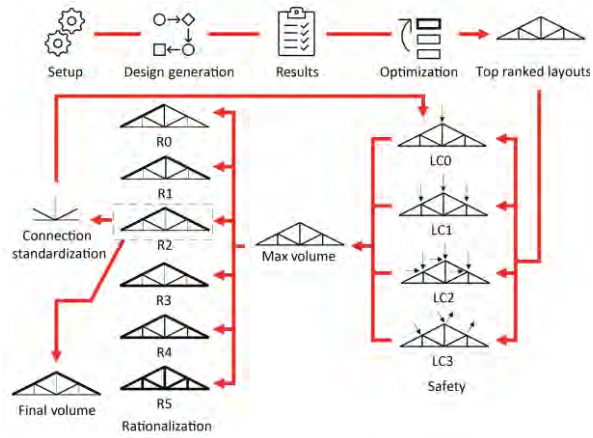

Figure 3: Workflow of the proposed process.

2.2 Case study

As a case study, we examine a sports hall of 20x30m in plan dimensions as seen in Figure 4. The original design considers steel frames with hollow structural sections of 550x225mm and 4mm thickness, and battens with C-shaped profiles of 120x50 and 3mm thickness. The steel quantity for the original structure is 23,094.4 kg, corresponding to 63,222.49 kgCO_2e, considering the whole frame. The roof structure represents 63.45% of the mass and 63.46% of the embedded carbon. This structural typology is commonly used for these types of projects in Chile.

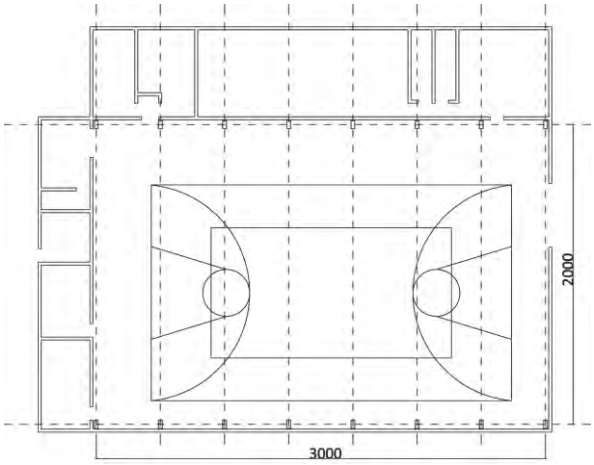

Figure 4: Plan of the case study, dimensions in cm.

The loads for the study were determined according to Chilean regulations. The NCh 1537 Chilean Standard [9] indicates how to determine dead and live loads. Accordingly, the roof was considered as a metal sheet of 5 mm thickness, an OSB board of 11,1 mm thickness, a layer of mineral wool insulation of 100 kg/m^3 and thickness of 100 mm, and plywood of 12 mm as the interior finish. This resulted in a distributed load of 0.377 kN/m^2. This was added to the structure's self-weight. The live loads on the structure established by this standard are 1 kN/m^2, for a roof with access only for maintenance.

The seismic loads were determined with NCh 433 Chilean Standard [10], considering a location in zone 3, which results in the highest acceleration values, a soil with compressive strength between 0.05 and 0.2 MPa, and occupation category considering buildings where there is frequently agglomeration of people. To consider the seismic loads, the equivalent static loads were applied, according to the static analysis method established in this standard. This resulted in a basal shear force of 135.65 kN.

For the wind loads, the NCh 432 Chilean Standard [11] establishes that for buildings of a maximum 4m height above ground, the basic pressure is 0.7 kN/m^2. The windward pressure is multiplied by a factor depending on the roof slope (Equation 1), while the leeward pressure must be multiplied by a factor of 0.4.

$$WP=(1.2\sin\alpha-0.4)q \qquad (1)$$

where WP - windward pressure (kN/m^2);
α - slope's angle (rad);
q - basic pressure (kN/m^2).

This resulted in a leeward pressure of 0.28 kN/m^2, while the windward pressure was recalculated in the optimization process, according to the geometry of the trusses. For the optimization, the truss elements were rectangular hollow sections ASTM A36.

3. RESULTS

The procedure results in support for decision-making at the early stages of design, favouring the reduction of the material quantity and embedded emissions in the structure. It also allows considering constructability issues, regarding the rationalization of the structural elements and shape complexity, and architectural aspects, such as volume shape and visual clarity.

The results are composed of around 100 admissible designs, which reduce the weight of the original roof structure by 50% or more, have a maximum displacement of L/700, according to Chilean regulations, and a utilization ratio average of at least 50%. These solutions have slightly different layouts, mostly regarding their height and web configuration. By changing adjustments in the optimization initial configuration, the process generates different resulting geometries. Thus, the designer can choose the most adequate for the project. Some examples can be seen in (Figure 5).

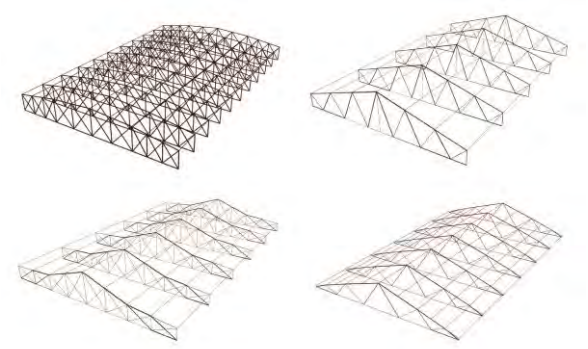

Figure 5: Different layouts resulting from different processes.

As stated before, the embedded carbon of a structure is directly related to its material quantity. The 3 best-ranked designs reduce the structural mass of the roof from 64.72% to 65.3%. Regarding the embedded carbon, the reduction represents the same percentages, in relation to the original roof structure (Figure 6). If we look at the entire structure, the reduction of embedded carbon is around 41% for each case. For the best-ranked layout, the roof structure represents 37.6% of the total embodied carbon from the structure, while on the original design, it represents 63.46%.

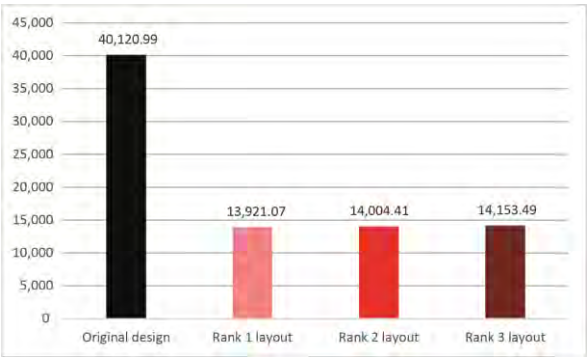

Figure 6: Embodied carbon ($kgCO_2e$) on the original design vs the 3 best-ranked layouts.

The verification of all load cases for the chosen designs allows getting the maximal cross-sections for each bar, ensuring that the truss layout can withstand different load scenarios. The maximum volume augments the structural mass by around 5% from the highest mass value corresponding to LC0, which still represents a reduction of 63.53% from the original frame design (Table 2).

Table 2: Mass (kg) variation of the 3 best ranked layouts, for the different load cases and the maximum volume.

	LC 0	LC1	LC2	LC3	Max. Volume
1	5,085.3	3,820.3	3,848.09	2,610.1	5,343.6
2	5,115.8	3,702.6	3,742.9	2,631.7	5,364.6
3	5,169.9	4,344.2	4,352.08	3,029.1	5,337.6

By augmenting the rationalization of the structure, the structural mass also increases. This part of the process allows the designer to compare different rationalization levels according to their structural mass and embedded carbon. The amount of embedded carbon in the maximum volume defined in the previous stage for the best-ranked layout is 14,628.41 $kgCO_2e$, compared to the original design, which is 40,120.99 $kgCO_2e$. The highest level of rationalization, where all the truss members have the same section, considering the most critical bar, has an embedded carbon of 37,408.46 $kgCO_2e$, representing a reduction of 6.76% from the original design. However, the different rationalization levels in between can represent a relevant reduction while still having a level of regularization of the cross-section sizes (Figures 7 and 8).

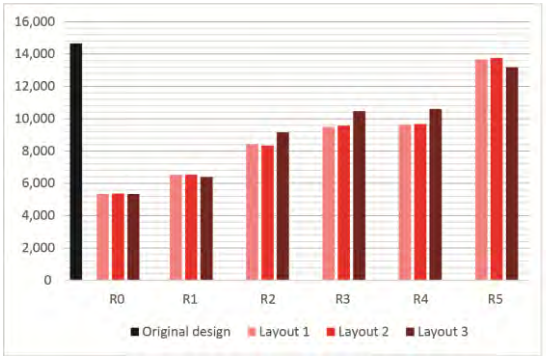

Figure 7: Mass (kg) variation for the 3 best-ranked layouts on each rationalization level.

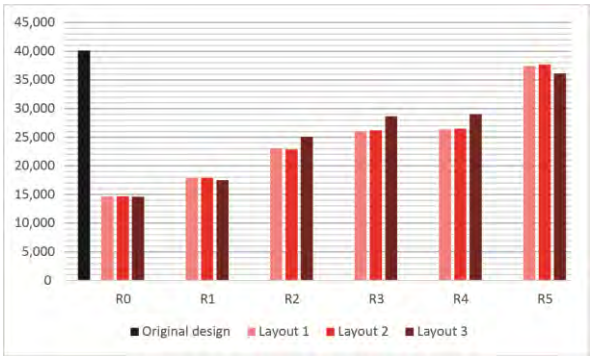

Figure 8: Embodied carbon ($kgCO_2e$) variation for the 3 best-ranked layouts on each rationalization level.

Regarding the shape of the results, the admissible designs present low shape complexity, which makes them more suitable for construction and can be architecturally desirable. By adjusting the process for symmetry or asymmetry and the position of the control points, the designer can adapt the results according to the project requirements and architectural expression.

4. CONCLUSION

This article presents a design generation procedure for truss structures that can support

decision-making during the early stages of design, facilitating the comparison between different truss layouts, regarding their material quantities and embedded emissions. The process allows the consideration of constructability issues and architectural aspects concerning the shape and rationalization of the structure.

The results show that a reduction of material quantity of 65.3% is possible, with a reduction of the same percentage of the embedded carbon value. The procedure generates around 100 admissible solutions, with at least 50% material quantity reduction, while maintaining an average utilization ratio of 50% on the truss members. This gives the designer the possibility to choose the most appropriate for the project, while considering its carbon footprint. It also generates non-complex shapes that benefit constructability.

The process also assists in the evaluation of different rationalization levels, which is an important factor for construction efficiency. This can increase the structural mass, affecting the embedded carbon, and reduce the utilization ratio, but can also be desirable for feasibility. The information given to the designer allows for the assessment of different levels of rationalization, comparing its material quantity and embedded carbon, thus making it possible to choose a medium-level rationalization, adequate for the construction requirements, and with a relevant reduction of the structural mass and carbon footprint.

The presented workflow will help to integrate all these variables in the early stages of design to make informed decisions. Consequently, generating efficient and sustainable results, that are also feasible and visually consistent with the design intentions. Future work will address the relation between some of the geometrical characteristics of the results and their influence on the reduction of material quantity and embedded emissions, and its relationship with the utilization ratio of structural members.

ACKNOWLEDGEMENTS

This work was funded by the National Agency of Research and Development, ANID – Subdirección de Capital Humano / Doctorado Nacional / 2021-21211651.

REFERENCES

1. United Nations Environment Programme, 2021 Global Status Report for Buildings and Construction: Towards a Zero emission, Efficient and Resilient Buildings and Construction Sector, Nairobi, 2021. https://globalabc.org/resources/publications/2021-global-status-report-buildings-and-construction (accessed September 22, 2022).

2. P. Block, T. Van Mele, M. Rippmann, F. Ranaudo, C. Calvo Barentin, N. Paulson, (2020). Redefining structural art: Strategies, necessities and opportunities, Structural Engineer, 98(1).

3. D. Fang, N. Brown, C. De Wolf, C. Mueller, (2023). Reducing embodied carbon in structural systems: A review of early-stage design strategies, Journal of Building Engineering. 76, 107054. https://doi.org/10.1016/J.JOBE.2023.107054.

4. C. De Wolf, J. Brütting, C. Fivet, (2018). Embodied Carbon Benefits of Reusing Structural Components in the Built Environment: A Medium-rise Office Building Case Study. In Smart and Healthy Within the Two-Degree Limit Proceedings of the 34th International Conference on Passive and Low Energy Architecture, The Chinese University of Hong Kong, Sha Tin New Town, Hong Kong, December 10-12.

5. B. D'Amico, F. Pomponi, (2018). Accuracy and reliability: A computational tool to minimise steel mass and carbon emissions at early-stage structural design, Energy and Buildings, 168, p. 236–250. https://doi.org/10.1016/J.ENBUILD.2018.03.031.

6. Forcael, E., Puentes, C., García-Alvarado, R., Opazo-Vega, A., Soto-Muñoz, J., & Moroni, G. (2022). Profile Characterization of Building Information Modeling Users, Buildings, 13(1). https://doi.org/10.3390/BUILDINGS13010060

7. D. Yang, S. Ren, M. Turrin, S. Sariyildiz, Y. Sun, (2018). Multi-disciplinary and multi-objective optimization problem re-formulation in computational design exploration: A case of conceptual sports building design, Automation in Construction, 92, p. 242–269. https://doi.org/10.1016/J.AUTCON.2018.03.023.

8. H. Lu, Y. Xie, (2023). Reducing the number of different members in truss layout optimization, Structural and Multidisciplinary Optimization, 66(3), p. 1-16. https://doi.org/10.1007/S00158-023-03514-Y/FIGURES/20.

9. Instituto nacional de normalización. (2009). Diseño estructural – Cargas permanentes y cargas de uso (INN Norma Chilena nº 1537). Santiago, Chile.

10. Instituto nacional de normalización. (2012). Diseño sísmico de edificios (INN Norma Chilena nº 433). Santiago, Chile.

11. Instituto nacional de normalización. (2010). Cálculo de la acción del viento sobre las construcciones (INN Norma Chilena nº 432). Santiago, Chile.

PLEA 2024 WROCŁAW
(Re)thinking Resilience

Leveraging Google reviews to explore users' dissatisfaction with student accommodation in Melbourne

DORSA FATOUREHCHI[1] CHRISTHINA CANDIDO[1] KATIE SKILLINGTON[1] HEMANTA DOLOI[1]

[1] Faculty of Architecture, Building and Planning, The University of Melbourne, Melbourne, Australia

ABSTRACT: Amid increasing demand for investment in student accommodation in Australia, ensuring high-quality lodgings has become vital for sustaining a positive student experience. To achieve this, accommodations should provide an environment where students feel comfortable, healthy, and well. This research aims to identify key design and performance gaps in current purpose-built student accommodation (PBSA) in Melbourne. Through a text-mining approach, nearly 2000 online reviews from 16 PBSA in Melbourne were analysed and compared, concentrating on students' perceptions regarding comfort and dissatisfaction. Sentiment, thematic, and probability analysis were implemented to reveal performance-related issues. This research found that students' dissatisfaction often centred on the Indoor Environmental Quality (IEQ) of their rooms. Interestingly, students' dissatisfaction with their physical surroundings was not strongly influenced by the quality or availability of communal spaces. Probability analysis revealed that students who were dissatisfied with IEQ were 85% more likely to be dissatisfied with the interior design features of their rooms. The same cohort was also more than 50% likely to make negative comments about lack of controllability and adaptive opportunities within their rooms, demonstrating the importance of autonomy for students in their private spaces. Through the consideration of occupants' dissatisfaction, the findings indicate the importance of addressing interior design and IEQ performance as potential solutions to enhancing the performance of PBSA in Melbourne.
KEYWORDS: Comfort, student accommodation, IEQ performance, Interior design

1. INTRODUCTION

Purpose-built student accommodation (PBSA) is a fast-growing building portfolio in Australia because of the strong demand from international students which accounts for the third-largest export item for the country [1]. Despite pandemic constraints, Melbourne has seen an increase in the number of PBSAs, from 70 in 2018 to 110 in 2023 [2]. Combined, these buildings host a total of 20,000 students in Melbourne alone – this is 38% of total resident population in the Central Business District (CBD) [3].

This recent boom has prompted the release of new guidelines for establishing a baseline for building performance in the sector, such as the Student and Shared Accommodation Guidelines [4], which makes recommendations about private indoor space sizes, communal spaces, neighbourhood characteristics, sustainability, and waste management. However, as part of IEQ criteria, these guidelines highlighted issues regarding temperature in student accommodation that had been designed based on the existing Environmentally Sustainability Design (ESD) requirements. For instance, a report regarding student accommodation in Victoria pointed out several IEQ-related issues mentioned by some housing providers and Council officers, such as temperature and acoustic control within buildings [4]. Despite these efforts to establish building and IEQ performance, research studies are yet to follow suit – at the time this paper was written, only four peer-reviewed papers were found on Scopus reporting findings from IEQ-related research in student accommodation in Australia [5-8]. This is at odds with the increasing demand to build PBSAs around the country over the last decade. This is potentially a critical issue considering the documented effect of IEQ on students' health, dissatisfaction, and academic performance [9-11]. Studies have also shown the impact of biophilic design on psychological restoration of the students and higher academic scores [9, 12]. More recently, interior design has emerged as an important dimension, due to its significant effect on students' dissatisfaction [6-7, 13]. Accordingly, the International Education Association of Australia [14], the quality of student accommodation – in terms of interior design and IEQ performance – requires improvement [13, 8].

This paper contributes to the research gap in Australia by reporting findings about user dissatisfaction observed in PBSAs from data harvested from Google Reviews (GRs).

2. METHODS

This study analysed a total of 2,000 comments voluntarily posted on Google from 2013 to 2023, focusing on 16 student accommodation buildings in Melbourne. NVivo and Leximancer were used to analyse text database.

Sentiment analysis was used to identify reviews that were negative in nature. For this step, machine learning was utilised since such methods are indicated to be more accurate than other approaches [15]. Specifically, this research used an Azure machine learning algorithm as it has been shown that it can build effective sentiment analysis models to perform data analytics [16]. The sentiment scoring range was 0 to 1, with scores close to 1 being identified as positive [17]. This research purposefully selected reviews that scored close to 0 to extract the negative sentiments. As each review might contain positive and negative statement(s), this study implemented sentence-level sentiment analysis for higher accuracy [18]. Further, to develop insights regarding the most and least mentioned aspects in negative comments, exploratory content analysis was deployed to identify concepts that could aid the coding of the text-based data. This approach enabled themes to be defined as the coding process was completed. Finally, conditional probability analysis was conducted to understand the likeliness of different negative sentiments co-occurring with one or more identified themes.

3. RESULTS AND DISCUSSION

3.1 Prevalence of IEQ issues based on negative sentiments

Through analysing the content of data with negative sentiments, high-level concepts were identified. These concepts were room, experience, student activities, and social activities.

In the word frequency analysis (Fig. 1), it was demonstrated that the term “room” emerged as the most frequently used term in negative reviews with 1 to 3-star ratings. In terms of frequency, “room” was followed by “place”, “service”, “cleaning”, and “temperature (hot)”. This highlights the importance of private room amenity, services, and IEQ, such as thermal environment. More detailed concepts are shown in Fig. 2.

Sentiment scores of the negative reviews were also computed and the breakdowns are reported in Table 1.

Figure 1: Content and word frequency analysis of the scraped textual data.

The negative sentiment scores showed that thermal and IAQ aspects of private rooms were closer to zero, which suggests more negativity around those themes among dissatisfied users.

The thematic and sentiment analysis revealed interesting results regarding users’ dissatisfaction. As shown in Fig. 3, the negative sentiments were mostly centred around physical aspects of their private space and quality aspects of their communal spaces. This implies that when occupants were very dissatisfied, their priority concern was their private room’s thermal, visual, and acoustic comfort, architectural characteristics (e.g., size, layout, etc.), adaptive opportunities and systems (e.g., passive and active building system and controllability). In terms of communal spaces, quality aspects related to safety and security, utility, services, and facilities were the main issue among dissatisfied students.

Results suggest the critical role of student accommodation providers in maintaining the basic standards for IEQ. Without this maintenance or basic provision, students could experience significant dissatisfaction, especially if indoor environmental quality needs are not met in the private spaces. Interestingly, students’ IEQ complaints increased when they realised they had no control over temperature and noise, or even the unavailability of opportunities to retrieve their comfort. These factors – such as students’ autonomy, controllability, and privacy – underscored the criticality of these features for students to avoid discomfort and unhealthy situations in their private room.

It can also be concluded from the sentiment analysis that the mentioned features were negatively affecting students’ health. The high room temperature resulted in frustrated students, reducing their sentiment score (higher negativity) with their private spaces. The lack of controllability in these PBSA compounded these negative sentiments. Since this type of accommodation is considered an all-inclusive building (e.g., utility and housing costs in one bill), it is of utmost importance to address such existing problems in PBSA.

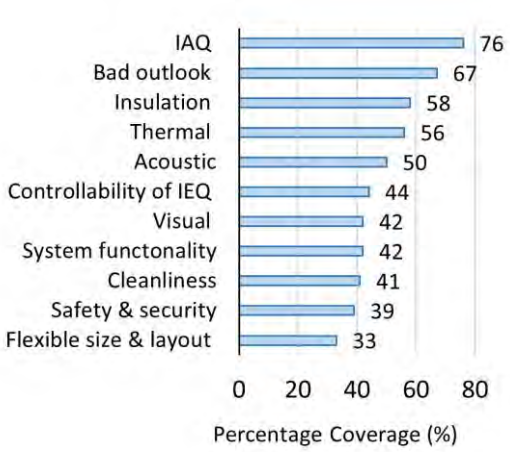

(a)

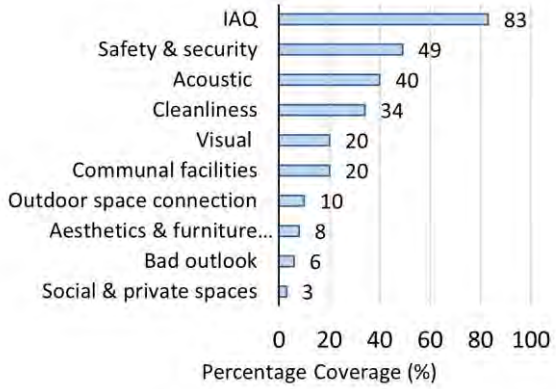

(b)

Figure 2: Percentage coverage of the themes among dissatisfied students with: (a) private rooms and (b) communal areas for IEQ and design aspects.

Table 1: Sentiment scores of negative reviews.

Space Type	Private Room		Communal Spaces	
Themes	Negative score average	SD	Negative score average	SD
Cleanliness	0.13	0.13	0.11	0.12
IAQ	0.11	0.14	0.15	0.13
Thermal	0.11	0.12	NA	NA
Visual	0.12	0.14	0.19	0.21
Acoustic	0.14	0.13	0.15	0.14
Aesthetics & quality of furniture	0.14	0.14	0.11	0.097
Bad outlook	0.16	0.20	0.21	0.12
Connection with natural light	0.15	0.16	0.36	0.095
Nature connection	0.20	0.12	NA	NA
Outdoor space connection	0.19	0.12	0.18	0.14
Insulation	0.17	0.16	NA	NA
IEQ controllability	0.1906	0.13	NA	NA
Functional active & passive systems	0.15	0.13	NA	NA
Flexible size, layout and storge	0.16	0.14	0.12	0.10
Safety and Security	0.17	0.15	0.13	0.13

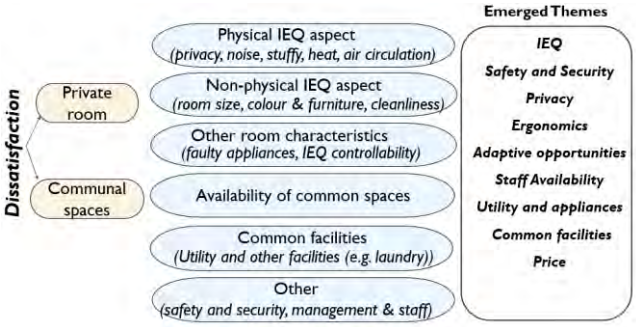

Figure 3: Emerged themes from the negative sentiments of online review.

Furthermore, among the students who showed dissatisfaction with their room, they would rather pay less and live in a lower-quality private housing than reside in a PBSA that was not prioritising their basic needs above other opportunities, such as social and recreational spaces. This finding emphasises how the availability of certain features in their room should be of paramount concern in interior design before providing additional communal features in any PBSA.

For the communal areas, the complaints were mostly about the availability or the adequacy of spaces for a particular purpose. Some of the students mentioned the low capacity of library areas and study spaces. There were also complaints regarding the availability of communal spaces to use during their free times (e.g., gym, cinema room, etc.). Other factors such as cleanliness, safety, and security aspects were also mentioned in the negative reviews. For instance, there were complaints regarding broken windows, safety and security in hallways, and stolen objects from communal areas, all of which negatively affected their perception of communal areas.

3.2 Emerged themes based on the negative reviews

3.2.1 IEQ

As previously discussed, IEQ was one of the most important features when it came to increasing dissatisfaction with private indoor environments. In some comments, students mentioned high temperatures and less natural ventilation as contributors to their negative feelings (e.g., frustration) and physical health (e.g., headache). For example, one user noted that "*when it's 25°C outside it's near 40-50°C inside, it feels unsafe …*".

Previous studies have highlighted the negative impact of thermal conditions and ventilation on

students' satisfaction levels and work efficiency [6-7]. Another study also pointed out that student dissatisfaction with IEQ may result in poor sleep quality and health symptoms [19].

The negative reviews for IEQ were mostly related to private spaces, but there were also some complaints associated with communal areas. For example, some students mentioned that due to safety reasons, users were unable to open their doors to take advantage of crossflow ventilation from the hallway.

3.2.2 Controllability, autonomy and affordance

As previously mentioned, another negative factor cited by the students was the lack of opportunity to change their indoor environment when users felt thermally uncomfortable. According to [20], the human-building interaction with respect to the thermal environment becomes crucial, as occupants can be comfortable in a wider range of temperatures than what is defined by standards. Therefore, controllability in the room can play a vital role in creating more comfortable environments by giving the users the autonomy to instantly change their indoor environment (e.g., operable windows). In one comment, a student mentioned that "*Ventilation in the room is noisy as hell and you can't do anything about it because windows are sealed.*" Users also indicated that no alternatives were provided to reduce indoor temperature. In line with this study, research conducted by [21] highlighted that controllable windows are necessary for sustainable student housing facilities. Many studies demonstrate that a constant thermal environment might not lead to more satisfaction among occupants. Therefore, the controllability feature in the indoor environment not only can create a more dynamic environment but could also result in perceptions of control and thus, higher satisfaction of occupants [22].

3.2.3 Inclusivity and adaptability in use

In terms of physical features, dissatisfied students mentioned both private and communal spaces in terms of adaptive opportunities. Students mainly complained about their room's size and layout. Some students referred to their room as a "*shoebox*", noting that it might not be worthy of the rent they are paying. In contrast, some students were satisfied with their room's layout, mentioning that "*Rooms are well lit with natural light and sizable*". This demonstrates the importance of interior design on students' satisfaction. In line with this finding, studies have shown the importance of interior design as a predictor of student satisfaction with their accommodation [23-24].

Reviews also mentioned available active and passive systems to control IEQ in their room when discomfort occurs. In one comment, a student criticised the unavailability of windows: "*the rooms open a tiny 2-3 inch's provided no ventilation*…".

The results from this study also aligned with [22], which regarded room size and flexibility as important facilities to be considered in sustainable housing. In a study by [25], room layout design was also shown to create spatial adaptation opportunities for the occupants in the context of residential buildings. Moreover, [26-27] pointed out the important role of room layout in balancing thermal comfort and energy savings in residential buildings.

For the communal spaces, reviews mostly complained about the inadequacy of most communal and private spaces to accommodate activities such as socialising, studying, or cooking. This outcome aligns with [28], which noted that a lack of adequate private and communal spaces has been identified as problematic in the Post Occupancy Evaluation (POE) of some student accommodation. In addition, the morphological configuration of communal spaces was indicated to predict students' satisfaction [23]. This might be due to the extent to which it can facilitate social interaction. Another study also highlighted the importance ratio of public spaces to private spaces, which could negatively affect their living, learning, and social experiences [29].

3.2.4 Connectivity and interaction

In terms of negative aspects, users criticised the view of the room *"… its location near cemetery, especially in rooms in which windows point at it looks terrifying*". In terms of light and colour, some students complained about the aesthetics of their private room "*I feel like I'm stuck in a dark grey box. It's aesthetically pleasing but at the same time it's very depressing and the lighting I feel is not enough too*". This aligns with other research that has highlighted the importance of bright colours to boost pleasure in students [30] and the efficacy of interior lighting on well-being [22].

In line with the results of this study, biophilic features and nature views appear to play an important role in increasing occupants' satisfaction and improving their attention [31-32].

3.2.5 Functionality and accessibility

This theme emerged? from comments focusing on the functionality of building systems, accessible facilities and amenities, proximity to campus, and efficient storage and space utilisation. Among the negative comments, building systems were mentioned to be useless to achieve thermal comfort during winter or summer, such as: "*Heater is not hot, it's completely useless in winter*". After a POE of student accommodation, a study [33] found that amenities related to IEQ (e.g., ventilation, lighting, and sound) were important elements in student accommodation facilities. Another study showed building facilities influenced students' comfort and

satisfaction, affecting their academic performance [34].

In terms of functionality of communal spaces, some users expressed complaints about the accessibility of some areas, such as their courtyard. In this instance, users mentioned being unable to use the courtyard, and considered it as being there solely for appearances.

3.3 Relationship between IEQ experiences and dissatisfaction in student accommodation

The probability analysis revealed that users dissatisfied with the IEQ of their private room were around 88% more likely to also report dissatisfaction with design-related issues of their room. Among the users dissatisfied with IEQ, it was 50% more likely that they criticise thermal issues (private and communal spaces), insulation, and controllability and adaptive opportunities in their room. Therefore, the room's thermal characteristics were the most important aspect of their comfort. It was interesting that thermally dissatisfied students were more inclined to negatively mention their rooms' poor outlook, insulation, controllability, connection with the outdoors, layout, and lack of adaptive opportunities. In terms of controllability of windows and thermal discomfort, users noted the lack of ventilation due to fixed windows in their private room. In terms of interior design and IEQ issues, users pointed out insulation and design-related issues of their floor plan. Results suggest that the uncontrollability and design-related issues (e.g., layout) exacerbated their thermal perception, contributing to lower health outcomes and compromised satisfaction.

Interactive effects were also seen between different IEQ aspects (e.g., thermal, visual, acoustic). Among the users dissatisfied with thermal comfort, it was 53% probable that they negatively mentioned noise and air quality. Among thermally dissatisfied users, it was also 54% more likely that they would express negative sentiments about health and design-related issues. The analysis showed that users dissatisfied with IEQ in their private space were 50% more likely to negatively talk about the indoor-outdoor connection of their space and the capacity of the communal spaces. As mentioned in the previous section, when users felt thermally uncomfortable in their private space, they also realised the lack of adaptable space in the communal spaces, which negatively affected their satisfaction. Some users mentioned that "*rooms no ventilation …and common study area has noisy students as it not a quiet library*". The probability analysis also showed that among users complaining about accessible communal spaces, it was 50% more probable that they were thermally dissatisfied with their private room. The result was in line with a study [35] that suggested users would feel uncomfortable if there were a lack of opportunities in their space to change IEQ.

4. CONCLUSION

This research demonstrated the important aspects to be investigated for re-establishing high-performance student accommodation based on users' longitudinal experiences from their spaces. For this purpose, a diagnostic approach was implemented to first identify the important factors affecting users' negative sentiments of their living environment, specifically examining health and dissatisfaction. It was found that dissatisfied users mostly highlighted the poor quality of their IEQ in their private room, paying less attention to the facilities provided by the communal spaces. Other negative aspects were the lack of adaptive opportunities in their private space, the available adaptive opportunities to maintain their comfort, and the flexibility of their room layout.

After analysing the users' sentiments form the reviews, the important themes were extracted for further analysis to explore whether these themes have contributing effects on users' health and dissatisfaction. This phase revealed that users' dissatisfaction was concurrently affected by multiple themes. Therefore, the assumption of a single cause and effect might not be a best approach to studying students' IEQ-related health and satisfaction, as there were design-related aspects that alleviated or worsened their experience with their built environment.

ACKNOWLEDGEMENTS

The authors would like to express their sincere gratitude to Sustainable and Healthy Environments (SHE Lab) and the Faculty of Architecture, Building and Planning and The University of Melbourne, for providing access to the facilities required for this research activity as well as a full PhD scholarship given to the first author of this paper.

REFERENCES

1. Deloitte Access Economics. (2015). The value of international education to Australia. A report by Australian Government Department of Education and Training.
2. City of Melbourne. (2021-2022). Annual Report 2021-2022.
3. Australian Bureau of Statistics. (2020) accessed 30 December, https://explore.data.abs.gov.au/
4. SGS Economics and Planning. (2022). Draft Student and Shared Accommodation Guideline. Monash City Council.
5. Almeida, L. M., Tam, V. W., Le, K. N., Huang, Z., & Forbes, S. (2022). Survey of energy-related occupant perceptions in a green-rated and in a non-rated building. *Advances in Building Energy Research*, *16*(1), 36-63.
6. Xu, L., Hu, Y., & Liang, W. (2022). Subjective and objective sensory assessments of indoor air quality in college

dormitories in Nanjing. *Building and Environment*, *212*, 108802.
7. Xu, X., Sunindijo, R. Y., & Mussi, E. (2020). Comparing user satisfaction of older and newer on-campus accommodation buildings in Australia. *Facilities*.
8. Kang, Y., Chang, V. W., Chen, D., Graham, V., & Zhou, J. (2021). Performance gap in a multi-storey student accommodation complex built to Passivhaus standard. *Building and Environment*, *194*, 107704.
9. Brown, J., Volk, F., & Spratto, E. M. (2019). The hidden structure: The influence of residence hall design on academic outcomes. *Journal of Student Affairs Research and Practice*, *56*(3), 267-283.
10. McCartney, S., & Rosenvasser, X. (2023). Not your parents' dorm room: Changes in universities' residential housing privacy levels and impacts on student success. *SAGE Open*, *13*(2), 21582440231178540.
11. Worsley, J. D., Harrison, P., & Corcoran, R. (2021). The role of accommodation environments in student mental health and wellbeing. *BMC Public Health*, *21*(1), 1-15.
12. Asim, F., & Shree, V. (2019). The impact of Biophilic Built Environment on Psychological Restoration within student hostels. *Visions for Sustainability*.
13. Ziguras, C., Alves, T., & Miles, S. (2020). Enhancing the design quality of purpose-built student accommodation. Melbourne, Australia: Australian Housing and Urban Research Institute Limited.
14. Burke, T. (2015). Does Australia have a competitive disadvantage in student accommodation? International Education Association of Australia.
15. Hartmann, J., Heitmann, M., Siebert, C., & Schamp, C. (2023). More than a feeling: Accuracy and application of sentiment analysis. *International Journal of Research in Marketing*, *40*(1), 75-87.
16. Harfoushi, O., Hasan, D., & Obiedat, R. (2018). Sentiment analysis algorithms through azure machine learning: Analysis and comparison. *Modern Applied Science*, *12*(7), 49.
17. Manjula, P., Kumar, N., & Al-Absi, A. A. (2021). Customer Sentiment Analysis Using Cloud App and Machine Learning Model. *In Proceedings of International Conference on Smart Computing and Cyber Security: Strategic Foresight, Security Challenges and Innovation* (SMARTCYBER 2020) (pp. 325-336). Springer Singapore.
18. Wankhade, M., Rao, A. C. S., & Kulkarni, C. (2022). A survey on sentiment analysis methods, applications, and challenges. *Artificial Intelligence Review*, *55*(7), 5731-5780.
19. Miao, D., Cao, X., & Zuo, W. (2022). Associations of Indoor Environmental Quality Parameters with Students' Perceptions in Undergraduate Dormitories: A Field Study in Beijing during a Transition Season. *International journal of environmental research and public health*, 19(24), 16997.
20. Nicol, J. F., & Roaf, S. (2017). Rethinking thermal comfort. *Building Research & Information*, *45*(7), 711-716.
21. Hassanain, M. A. (2008). On the performance evaluation of sustainable student housing facilities. *Journal of Facilities Management*.
22. Rohde, L., Larsen, T. S., Jensen, R. L., & Larsen, O. K. (2020). Framing holistic indoor environment: Definitions of comfort, health and well-being. *Indoor and Built Environment*, *29*(8), 1118-1136.
23. Amole, D. (2009). Residential satisfaction in students' housing. *Journal of Environmental Psychology*, *29*(1), 76-85.
24. Mustafa, F. A. (2017). Performance assessment of buildings via post-occupancy evaluation: A case study of the building of the architecture and software engineering departments in Salahaddin University-Erbil, Iraq. *Frontiers of Architectural Research*, *6*(3), 412-429.
25. Tadepalli, S., Jayasree, T., Visakha, V. L., & Chelliah, S. (2021). Influence of ceiling fan induced non-uniform thermal environment on thermal comfort and spatial adaptation in living room seat layout. *Building and Environment*, *205*, 108232.
26. Anand, P., Deb, C., & Alur, R. (2017). A simplified tool for building layout design based on thermal comfort simulations. *Frontiers of Architectural Research*, *6*(2), 218-230.
27. Horikiri, K., Yao, Y., & Yao, J. (2015). Numerical optimisation of thermal comfort improvement for indoor environment with occupants and furniture. *Energy and Buildings*, *88*, 303-315.
28. Khajehzadeh, I., & Vale, B. (2016). Shared student residential space: a post occupancy evaluation. *Journal of Facilities Management*, *14*(2), 102-124.
29. Oppewal, H., Poria, Y., Ravenscroft, N., & Speller, G. (2017). Student preferences for university accommodation: An application of the stated preference approach. *Housing, space and quality of life*, 113-124.
30. Ning, Y., & Chen, J. (2016). Improving residential satisfaction of university dormitories through post-occupancy evaluation in China: A socio-technical system approach. *Sustainability*, *8*(10), 1050.
31. Kamaruzzaman, S. N., Egbu, C. O., Mahyuddin, N., Ahmad Zawawi, E. M., Chua, S. J. L., & Azmi, N. F. (2018). The impact of IEQ on occupants' satisfaction in Malaysian buildings. *Indoor and Built Environment*, *27*(5), 715-725.
32. DeLauer, V., McGill-O'Rourke, A., Hayes, T., Haluch, A., Gordon, C., Crane, J., Kossakowski, D., Dillon, C., Thibeault, N., & Schofield, D. (2022). The impact of natural environments and biophilic design as supportive and nurturing spaces on a residential college campus. *Cogent social sciences*, *8*(1), 2000570.
33. Sanni-Anibire, M. O., & Hassanain, M. A. (2016). Quality assessment of student housing facilities through post-occupancy evaluation. *Architectural Engineering and Design Management*, *12*(5), 367-380.
34. Kumar, P. (2015). Optimizing building performance by experiential thermal comfort in student accommodation. *14th Conference of International Building Performance Simulation Association*.
35. Shin, J.-h. (2016). Toward a theory of environmental satisfaction and human comfort: A process-oriented and contextually sensitive theoretical framework. *Journal of Environmental Psychology*, *45*, 11-21.

PLEA 2024 WROCŁAW
(Re)thinking Resilience

Exploring Virtual-Real Interaction in Atrium Design through Mixed Reality and Generative AI: A Methodological Approach

XINXING CHEN[1] YINGNAN CHU[1] SHUANG LIANG[1] YEHAO SONG[*,1]

[1]Tsinghua University, Beijing, China

ABSTRACT: This paper presents a novel approach for integrating Mixed Reality (MR) and Generative Artificial Intelligence (AI) in the atrium renovation design process. We establish a workflow by developing a MR application, which enables user-centered behavioural observation and intelligent design. Using the showroom atrium as a case study, spatial interfaces are iteratively and instantaneously modified through the Generative AI method. Concurrently, MR facilitates rapid comparison and experiential analysis of the space in tandem with the actual showroom atrium, delivering a unique spatial feedback experience. This paper reports preliminary results from the practical implementation of this workflow, showcasing the method's potential in atrium renovation design research and future experiential architectural design. Consequently, this study introduces a new pathway for computational design and built environment experimentation.
KEYWORDS: Mixed Reality , Generative AI , User behaviour , Computational design

1. INTRODUCTION

As sustainable building continues to evolve, the atrium space has become an important research object with the complexity of the interior building forms. The atrium space helps organize the internal space and enhances indoor comfort using natural regulation, and their spatial interfaces and dimensions significantly shape users' visual experiences and spatial perceptions. Despite its importance, several challenges persist during the design process of atrium spaces, affecting the predictability of user experiences in the early design stages. Current spatial presentation methods limit designers' ability to rapidly and accurately understand the impact of atrium spaces on users and their preferences for different environments.

The rapid advancement of intelligent design presents potential solutions to these challenges, particularly through the emergence of MR and generative artificial intelligence (AI)-based designs. In architectural design education and construction, the use of Virtual Reality (VR) technology, exemplified by head-mounted glasses (Zhang et al. 2020; Fathy et al. 2023), and Augmented Reality (AR) technology, represented by devices such as the Hololens (Wang et al. 2013; Russo and Michele 2021), has been extensively researched and debated. Meanwhile, the exploration of Mixed Reality (MR) applications is gaining momentum (Alizadehsalehi et al. 2020).MR is a technology that seamlessly merges the real and virtual worlds by presenting images to users (Zhao et al. 2022). This not only enhances immersion but also enables real time interaction between users and MR spaces. In parallel, generative AI leverages various machine learning algorithms to swiftly generate images based on textual descriptions or existing visuals.

MR technology utilizes a display method similar to that of VR technology, presenting images on an opaque binocular display. The key distinction lies in its capacity to capture the environment through an integrated camera and reconstruct digital images of the real environment in real-time on the opaque binocular display, as exemplified by the Meta Quest Pro head-mounted display device. In contrast to optical display-based AR technology, this approach considerably expands the field of view (FOV) and enhances the imaging quality of virtual objects (Tan et al. 2022). However, a limitation of this method is that, unlike optical AR glasses, it does not permit direct transmission of ambient light, leading to reduced clarity and tolerance of the real environment (Emo et al. 2021).

As immersive environment technology matures, an increasing number of studies apply VR technology to assist architectural design and facilitate experiments in the built environment. In the realm of VR experiments, Latini et al. (2023) developed a comprehensive VR experimental framework, showcasing a high level of immersion and effectiveness in VR scenarios while assessing the impact of thermal environments within VR spaces. In the context of VR-assisted design, Liang et al. (2019) collected individual behavioural data while utilizing a workspace in VR, constructing and optimizing a cost function to achieve the optimal layout for spatial scenarios.

Meanwhile, MR is gradually gaining traction, benefiting from its ability to respond to real-world environments. In the domain of MR experiments, Chen et al. (2022) employed MR technology to overcome

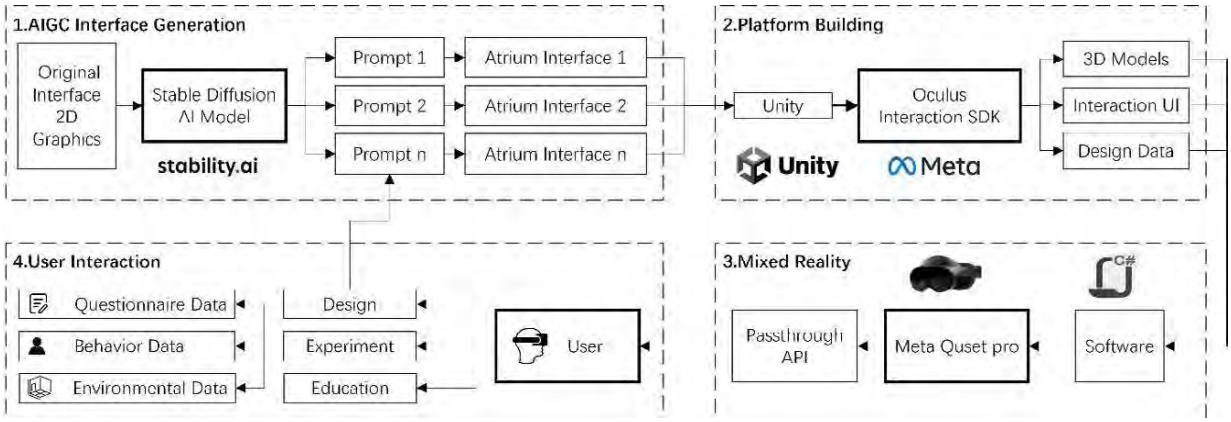

Figure 1. Platform workflow diagram.

the limitations of differing pedestrian performance in real-world and simulated environments. A MR space, encompassing both real and virtual pedestrians, was established in an actual architectural environment to study evacuation behaviour within the building.

In MR-aided design, Zhao et al. (2023) compared the applicability of three Extended Reality (XR) technologies, including AR, MR, and VR, for performance-based architectural design. They developed a program featuring interactive visualization of façade window geometries and indoor illuminance simulation, enlisting 120 students and young architects for evaluation. The results indicated that MR, compared to AR and VR, is the most suitable XR technology to achieve this goal. These studies demonstrate that while VR technology eliminates the need to construct a space for each experiment and enables cost-effective experimentation with multiple architectural spaces, MR technology enhances user interaction, mobility, and immersion within real spaces.

However, there are still several limitations to the current research. For instance, users cannot interact with the space swiftly and effectively, and the elements within the space must be predetermined, restricting quick iteration and modification. To address this issue, efficient generation of content is crucial, and generative AI presents a promising solution.

Consequently, this study aims to develop a software platform based on MR and generative AI that rapidly provides realistic and highly interactive MR environments for design or experimental needs. The experiment primarily investigates the following questions:

- Does MR provide satisfactory visual comfort and immersion, simulating the realism of an actual atrium?
- Compared to VR, does MR deliver a heightened level of immersion that facilitates the manifestation of interface changes?
- Can this experimental method effectively aid designers in refining the design of spatial interfaces and dimensions?

2. METHODS

As depicted in Figure 1, we employed the Unity 3D game engine as the development platform for the MR design system, tailored for Meta Quest Pro hardware. Throughout the development process, we utilized the Oculus Integration SDK along with several prefabricated components from Unity-Movement. In particular, we implemented the Passthrough API to present real space images captured by the front-facing camera of the headset, excluding areas designated for interface display. Additionally, we integrated features such as controller input, 3D model adjustment controls, and various other functionalities. These components were developed using the C# language within Unity 3D. The resulting MR application encompassed four primary functional sections: real-time capture and display of the actual space, presentation and adjustment of virtual interfaces, interactive and visual interfaces, and documentation of design and experimental data.

In this process, the transmission of design and experimental data is delineated as follows:

2.1 Spatial interface data

As illustrated in Figure 2, various design space interfaces are captured using a camera, perspective-corrected in Photoshop software, and the original spatial interfaces are imported into the Stable Diffusion integration package. Depth information is extracted from each interface utilizing the MiDas Depth estimation model within the Control Net plugin. By inputting different keywords, interface images with identical structural configurations but entirely distinct materials and visual effects are rapidly generated. The Euler A sampler is employed, and 20 iterations are performed. To achieve enhanced image effects, each generation incorporates a set of basic prompts. For each atrium exhibiting a unique style, several corresponding prompts are input, and interfaces with superior display effects are selected through multiple generations. Ultimately, the aforementioned images and model data are imported into the software application via Unity 3D.

Figure 2. Diagram of space interface generation

2.2 Interface operation data

Users can make real-time adjustments and experience the interface. By controlling the opening and closing of the virtual space interface with controller buttons, the current scene's actual effect is directly displayed when the interface is not visible, augmenting users' spatial perception and scene immersion. This approach is beneficial for studying a single interface while maintaining some interfaces unchanged in the real world. The 3D model adjustment component modifies the spatial dimensions of the atrium, adjusting length, width, and height to examine and investigate the impact of spatial dimensions on design and behaviour.

Figure 3. Experimental interface UI.

2.3 Behaviour and interaction data

When users wear MR glasses for real-time interaction, data collection encompasses UI operation data, eye-tracking data, real-time action trajectory data, and question and answer data.

3. EXPERIMENT

To evaluate the effectiveness of the application, we selected a typical atrium space as the experimental case study. This space serves as the side hall of an architecture school building, primarily functioning as an exhibition service and resting/discussion area. A total of 10 participants, all students in the field of architecture, were involved in the experiment.

The experimental protocol requires participants to undergo the following processes, engaging primarily with real-time atrium spaces in MR, hybrid virtual and real spaces under various spatial interface material elements, and the adjustment of spatial dimensions in three distinct scenarios:

First scenario: During the real-time atrium space experience, participants undertake two modes: standing and observing their surroundings, and walking freely. These modes aim to compare the influence of walking actions on immersion and comfort in the MR space.

Second scenario: Each spatial interface material appears in a random order to eliminate any sequence bias that could potentially affect participant choices. Additionally, each material space offers two modes: a MR interface (partially displaying real-time images and partially virtual interfaces) and a VR interface (completely VR interface). This comparison is intended to elucidate the impact of MR on participants' spatial experience.

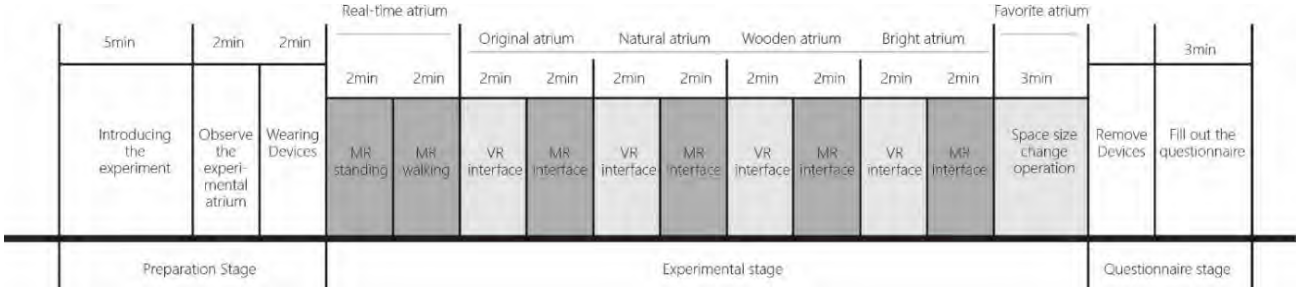

Figure 4. Flow chart of the experimental stage.

Third scenario: Participants manipulate sliders representing the length, width, and height of the space through a controller, adjusting the dimensions of the current space in real-time until they reach a level deemed most comfortable. Upon completion of the experimental scenario experience, participants complete a questionnaire.

The questionnaire consists of two sections: The first section entails basic statistical information (such as gender, age, height, visual impairments, education level, and previous experiences with VR or MR). The second section is completed after the MR cognitive task and includes questions regarding comfort and interactive intention (such as immersion, visual comfort, interactive intention, spatial presence, graphical satisfaction, scale perception ability, and preference).

4. RESULTS

After conducting the experiments described earlier, we can draw the following conclusions based on the collected data:

4.1 Good visual comfort and display performance in the MR atrium

MR offers good visual comfort and fewer discomfort situations. The questionnaire primarily inquired about participants' visual discomforts, such as eye fatigue, difficulty concentrating vision, lack of focus, and dizziness. 52% of participants reported no discomfort and 38% had mild effects, while only 10% showed moderate symptoms that did not interfere with normal observation. In evaluating the display of the mixed reality atrium, five metrics were used, including immersion, clarity, distortion-free, adaptability, and consistency, and their scores are shown in the box plot in Figure 5.

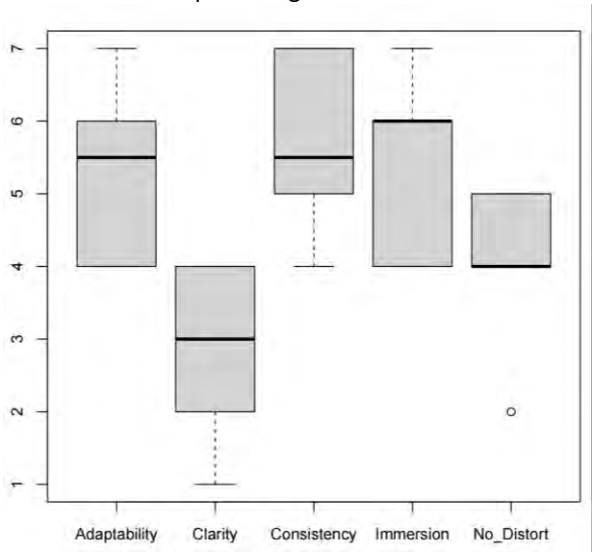

Figure 5. MR visual comfort and display performance.

The box plot illustrates the five key summary statistics, including the minimum, first quartile, median (second quartile), third quartile, and maximum. The data demonstrates a good performance in all metrics except for the lower clarity, especially the consistency score of the mixed reality and real atrium, which received the highest rating. However, the consistency of clarity and brightness between the virtual interface and the real interface needs improvement.

4.2 Higher Immersion in MR Compared to VR

Compared to VR, the immersion of the atrium in MR is higher, influenced by different atrium interfaces. Figure 6 presents a graphical comparison of immersion levels in VR and MR across various atrium environments. The white and gray segments in the graph represent the immersion scores for VR and MR, respectively. The findings indicate that MR technology provides an enhanced sense of presence compared to VR, though the observed difference is moderate. The average immersion scores for VR technology in the four atrium spaces were 4.6, 4.7, 5.0, and 5.4, respectively. In contrast, MR technology exhibited a wider distribution of participants' evaluations, with average immersion scores of 5.3, 5.6, 5.0, and 5.6 for the same atrium spaces. The primary factor contributing to this difference is the disparity in screen performance between the real and virtual interfaces, which influences the sense of immersion for some individuals.

In the study, we observed considerable individual variability in the level of comfort experienced when interacting with spatial interfaces. These differences were particularly evident when comparing various aspects of the interfaces, such as material realism, light comfort, richness of detail, and sense of scale realism. Notably, the level of comfort was found to be the highest for material realism, followed by light comfort, richness of detail, and finally, sense of scale realism.

To evaluate the participants' sense of immersion, we employed a seven-point Likert scale question, which asked, "Do you think the sense of immersion is better when you move in the scene than when you are stationary?" The average score for this query was 4.6, indicating a moderate preference for enhanced immersion when the participant was in motion within the scene.

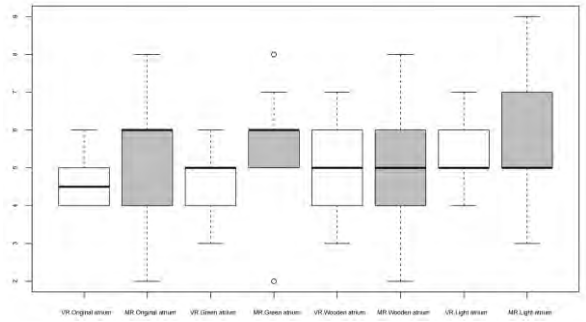

Figure 6. Immersion in different atrium.

4.3 Enhanced Support for Designers in Interface and Scale Design

In this study, we employed a seven-point Likert scale to evaluate participants' perceptions of the effectiveness of the experimental approach in assisting with design refinement and spatial experience. The scale ranged from "Not helpful at all" to "Very helpful." The mean score for this question was 6, suggesting that the approach can effectively support designers in their work.

Furthermore, during the scale adjustment experiment, the mean value of the modified height data was 105%, with 80% of the data falling within the 80% to 120% range. In terms of depth data, all data points were situated between 90% and 145%, yielding a mean value of 114.5%. For width data, 80% of the data points exceeded 100%, with an average value of 117.1%. These results demonstrate that experienced individuals generally increase width and depth data while maintaining height data, ultimately achieving a spatial scale that they perceive as comfortable. The space size adjustment function effectively aids designers in experiencing the space, revealing a relatively consistent preference for spatial scale comfort among participants. This consistency is beneficial for pre-design experience evaluation, optimizing atrium space scale satisfaction.

5. DISCUSSION

This methodology exhibits considerable potential for applications in other architectural domains, such as spatial transformation and interactive architecture. In spaces where human behaviour and experience serve as the foundation, this approach can address unforeseen issues at an early stage, minimize problems arising from human-environment interactions, and substantially reduce time and resources expended during the design phase. Notably, in areas where VR is predominantly employed, such as solving evacuation problems, teaching architecture and engineering, and conducting behavioural simulation testing, MR technology can deliver a more precise sense of spatial interaction, thereby enhancing the accuracy of tests and simulations.

Despite the numerous advantages of the proposed approach, certain limitations remain. Visually, there is room for improvement in the images provided by MR technology, such as enhancing resolution and tolerance, which could offer a visual effect akin to that of virtual objects and elevate the sense of immersion in space. In terms of interaction, the Generative AI generation currently employed requires pre-generation on the computer side before being imported into the MR platform, resulting in relative inefficiency. Moving forward, we aim to refine the method and achieve intelligent real-time modification of each spatial interface and element by directly inputting keywords into the platform, ultimately facilitating the integration of the virtual and real worlds.

6. CONCLUSION

In this study, we devised a novel method that combines MR and generative AI to assist in designing atrium spaces. This approach significantly enhances the ability to rapidly modify and experience atrium space interfaces by streamlining the process of measuring, modeling, altering materials, incorporating spatial elements, and rendering in conventional design methods. Furthermore, it generates spatial interfaces with varying design tendencies directly from real interface screenshots, enabling swift comparison of target solutions during the renovation and design process. The application of MR technology promptly reflects the generated spatial interfaces within the actual atrium space. The immersive nature and effectiveness of this method are convincingly demonstrated through experiments conducted in the atrium of an architectural college exhibition hall. Compared to traditional atrium space transformations, the integration of these two techniques substantially improves efficiency in both generation and representation stages. This method holds considerable promise and significance, with the potential to facilitate real-time design and alteration of virtual and real spaces in the future, ultimately blurring the boundaries between them.

ACKNOWLEDGEMENTS

This research was funded by the National Natural Science Foundation of China (Project No. 52078264), and the Nanning Scientific Research and Technology Development Programme (Project No. 20233041)

REFERENCES

1. Zhang, Y., Liu, H., Kang, S.C. and Al-Hussein, M., (2020). Virtual reality applications for the built environment: Research trends and opportunities. Automation in Construction, 118: p.103311.
2. Alizadehsalehi, S., Hadavi, A. and Huang, J.C., (2020). From BIM to extended reality in AEC industry. Automation in Construction, 116: p.103254.
3. Zhao, S., Pan, Q., Gao, D. and Cheng, J., (2022). Integrating internet of things and mixed reality to teach performance-based architectural design: a case study of shading devices. Education and Information Technologies, 27(7): p.9125-9143.
4. Latini, A., Di Giuseppe, E. and D'Orazio, M., (2023). Development and application of an experimental framework for the use of virtual reality to assess building users' productivity, comfort, and adaptive-behaviour. Journal of Building Engineering, 70: p.106280.
5. Chen, M., Yang, R., Tao, Z. and Zhang, P., (2022). Mixed reality LVC simulation: A new approach to study pedestrian behaviour. Building and Environment, 207: p.108404.
6. Wang, X., Kim, M.J., Love, P.E. and Kang, S.C., (2013). Augmented Reality in built environment: Classification and implications for future research. Automation in construction, 32 : p.1-13.

Exploratory Methodology for Evaluating Indoor Environments
From the Perspective of Adolescents

CECILIA PALARINO-VICO[1] BEATRIZ PIDERIT-MORENO[2]

[1]Ph.D. candidate in Architecture and Urbanism, Faculty of Architecture, Construction and Design, University of Bio-Bio, Concepción, Chile
[2] Faculty of Engineering, Architecture and Design, University of San Sebastian, Concepción, Chile

ABSTRACT: Indoor environments play a pivotal role in shaping the experiences, performance, and overall well-being of students within educational spaces. While some research has explored how classroom architectural attributes influence students' subjective perceptions and ways to enhance these environments, there's a notable gap in studies involving adolescents in the design stages. This knowledge would allow the adaptation of the spaces where they spend a large part of their day to their specific preferences and promote well-being. This study aims to assess the effectiveness of using virtual reality (VR) experiences for evaluating indoor spaces with adolescents. Adopting an experimental approach, it employs an interactive VR navigation system and a questionnaire to capture students' subjective perceptions of classroom lighting and qualitative stimuli affecting their experience. The 15 minutes experience with 10 students, each of 13-year-old, was successful, the questionnaire integrated within the virtual environment facilitated the immediate assessment of the space. This study provides a valuable methodological framework for optimizing learning environments from a subjective perspective with VR in the early stages, offering added value compared to conventional approaches, aligning with occupant-centered paradigms.
KEYWORDS: Indoor environments, virtual reality, subjective perception, classroom environment, learning spaces.

1. INTRODUCTION

The quality of indoor spaces significantly impacts the performance and well-being of occupants in learning environments [1–4]. The impact of physical factors on educational quality is extensively documented in research that has conducted post-occupancy evaluations in school contexts with young populations [5, 6]. However, few studies focus on how the architectural characteristics of the classroom influence students' subjective perception and satisfaction [7, 8]. In Chile, it is known that adolescents in public education tend to have low satisfaction with their classrooms. This is based on the response of 452 students with an average age of 13.5 years, collected during 2022 within the framework of the Fondecyt Regular research project 1210701. This fact is significant because these are the spaces where students spend most of their time.

This research approach is key to designing learning spaces that promote well-being from the students' perspective, rather than expecting students to adapt to spaces that do not fully satisfy their needs. Exploring the subjective perceptions of occupants from the initial design stages would allow the adaptation of buildings to the specific preferences of individuals. Furthermore, focusing research on adolescents fills a significant gap to obtain empirical data from a specific group, as studies on perception are usually conducted with adults. It is essential to address the well-being and experiences of adolescents at a stage of life where emotional indices begin to decline [9].

Virtual reality (VR) techniques offer the possibility to examine environmental stimuli from the initial design phases, avoiding reliance on significant investments of resources and time to conduct post-occupancy evaluations. VR allows individuals to have an immersive experience in spaces that have not yet been built and to get an initial impression of the stimuli that create a more pleasant experience for occupants. This approach aligns with new paradigms that define occupant-centred analysis models, to generate architecture that is resilient to the user experience.

Previous research has highlighted the potential of virtual reality for examining indoor environments previous studies [10–13], yet its widespread adoption for such studies remains limited and has been conducted primarily with adults. However, VR is recognized as a safe technique for adolescents, as as supported by reference [14].

In this context, this study aimed to investigate the potential use of virtual reality (VR) tools with adolescents to evaluate indoor environments and capture the impact on subjective perception, analyzing the lighting stimuli in educational environments. We present a pilot experience with adolescents, taking the Future Edu Space classroom as a case study. It was a virtual design for innovative pedagogy practices in mind. Therefore, the design proposes variety of configurations, and alternatives of light environments.

2. METHODOLOGY

The methodological approach of this study employed VR techniques to examine indoor environments from the perspective of the occupants. We employed a questionnaire to collect subjective impressions from students regarding the classroom's lighting atmosphere and the qualitative stimuli affecting their experience.

2.1 Experimental Design

The study was conducted at a public educational institution located in Concepción, Chile. The experiment took place in the library, as we required a dedicated room to set up the experiment. Three workstations were organized in a 16m² area, avoiding any possible distortion within the participants' visual fields. The introduction phase began with participants reading an information sheet and signing a consent form upon arrival. They completed a baseline survey while researchers prepared the virtual scenes.

Participants experienced the VR environment using an Oculus Rift 1 headset, which offers an image resolution of 1080 x 1200 pixels per eye, a refresh rate of 90Hz, and a field of view of 110°. Based on the manufacturer's guidelines, this device is considered suitable for people over 13. The researcher assisted participants in wearing the headset correctly and receiving full instructions on headset application, control operation, and navigational procedures within the virtual space designed for the experiment. They were positioned on a 1.50-meter diameter carpet at location 4, which demarcated the physical boundary for virtual navigation, centred on a fixed point with 360° visibility.

The VR experience consisted of viewing three immersive scenes, each presenting an alternative lighting environment, as outlined in Figure 1. But involved two stages:

Stage 1, participants observed three VR scenes to familiarize themselves with the proposed spaces. The order of scene presentation was alternated between participants to control for selection bias based on the amount of light perceived in the scenes. The viewing time for each scene was free but lasted between 2 and 3 minutes. This stage culminated selecting the space they perceived as the most pleasant to learn.

Stage 2, participants re-entered their selected scene further to characterize the perceived atmosphere through a detailed questionnaire. The questionnaire with descriptive attributes of the space, based on their subjective perception of the environment, is detailed in section 2.2 "Instrument". Before answering the questionnaire, they were encouraged to take their time to observe each scene, ensuring that their choices accurately reflected their experience at that moment. The headset allowed participants to interact with the space and take the survey interactively on a virtual whiteboard using a remote control. At the same time, a researcher verbally asked the questions, eliciting voice responses from the participants as well. When the first assessment was completed, they repeated the process in the other two scenes to complete the characterization of the three atmospheres.

Participants entered the study individually, adhering to a standardized protocol outlined in Figure 2. The experimental session lasted approximately 10 to 15 minutes, involving an introduction and a virtual experience.

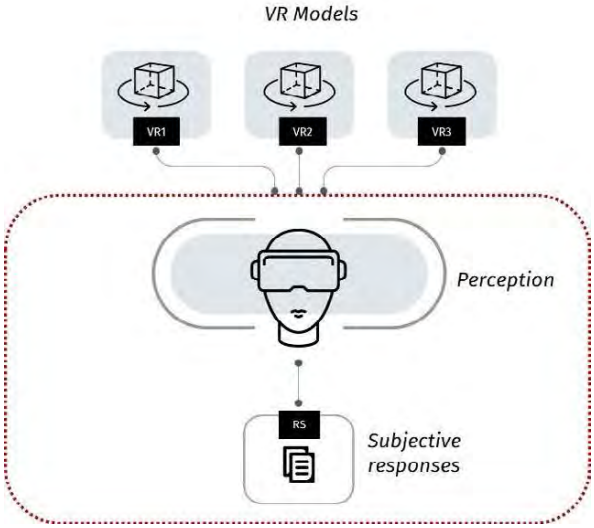

Figure 1: Experimental design scheme.

			VR EXPERIENCE		
Phase	**Introduction**		**Stage 1**		**Stage 2**
Researcher	Background	Set VR headset	VR Induction	Break	Background concepts
Participant	Consent		3 scenes visualization		3 scenes valoration
Instrument	Baseline Survey		Scene Selection		Atributtes Survey
Duration	3 min	1 min	3 min	1 min	4 min
	≈12 minutes				

Figure 2: Experimental protocol study.

2.2 Instrument

The rating survey aimed to capture participants' subjective impressions of the atmosphere, based on specific attributes. It employed a semantic differential scale, utilizing adjective pairs to delineate attributes of space and light. The selection of adjectives drew upon methodologies for quantifying perceived visual environments, as applied in studies by Vogels [15, 16] and reviewed in the context of indoor lighting effects by Kong [17].

Although these studies proposed a wide array of terms, this survey narrowed the list down to six pairs of adjectives carefully chosen to balance attributes of physical space and perceived lighting impressions. The

word pairs included narrow/wide, colorless/colorful, monotoned/varied, dark/luminous, gloomy/bright, and cold/cozy. Participants rated their impressions on a scale from 1 to 6 for each pair of opposing adjectives, choosing the score that best aligned with their perceptions. They were encouraged to thoroughly observe each environment before responding, ensuring their answers reflected their most genuine and subjective perceptions of each scene.

2.3 Participants

The experiment was conducted at the school where the students were enrolled on August 2, 2023, between 08:00 and 13:00. The study recruited 10 students, comprising an equal gender distribution of 5 males and 5 females, all of whom were enrolled in the same grade. All participants were over 13 years, with a mean age of 13.7 years and a standard deviation of 1.05 years ($\mu = 13.7$, $\sigma = 1.05$). While not a prerequisite for participation, 60% of the students reported having previous experience with virtual reality, and 80% were experienced with video games—factors that could potentially influence their interaction with the VR setup.

Ethical approval for the experiment was granted by the Bioethics and Biosafety Advisory Committee of the Research Department at the University of Bío-Bío. Our adherence to ethical research protocols mandated the obtaining of informed consent from all participants, ensuring voluntary participation and compliance with ethical standards. Given the challenges associated with obtaining school permits, we conducted a pilot study with 10 students. Insights from this preliminary study will inform the conduct of subsequent experiments with larger samples, aiming to explore indoor environments across diverse educational settings.

Figure 3: Participants in immersive experience

2.4 Case study environment

The study utilized a virtual environment, the Future Edu Space (FES). Occupying an area of 70m², FES features a flexible design that accommodates a variety of learning modalities. Furthermore, FES adheres to Chilean norms and standards for lighting, acoustics, air quality, and thermal comfort [18–20].

The design of FES strategically integrates learning spaces with the educational context and the outdoor environment, emphasizing different modes of interaction. Distinctive variations in the proportion and orientation of openings define the environments within FES, each yielding unique lighting effects. While materials and textures are consistent across all settings, it is the manipulation of lighting that alters the perception of light, thus delineating three distinct atmospheres: unilateral, bilateral, or multilateral.

These atmospheres comply with daylighting standards for educational spaces, verified through the Useful Illuminance indicator to achieve at least 50% UDI compliance [18–20]. Daylighting is suitable for visual comfort, proposing possible scenarios in which we want to evaluate only how the occupants perceive the lighting environment. Simulations utilized the Climate Studio plug-in for Rhino software [21], with virtual scenes rendered in Unity to realistically simulate light interaction with various materials and textures. The reflectance properties of the material in the simulation were 20% on floors, 50% on walls, and 70% on ceilings. These simulations were performed annually for the assumed orientation of the north and south windows, using climate data from Concepción, the location of our pilot study. Table 3 details the characteristics of the atmospheres.

Table 1. Daylight performance of 3 atmospheres

Code	Daylight Provision	Openings (%)	$UDI_{100\text{-}2000lx}$ (%)
VR1	Unilateral	18	53
VR2	Bilateral	22	70
VR3	Multilateral	40	80

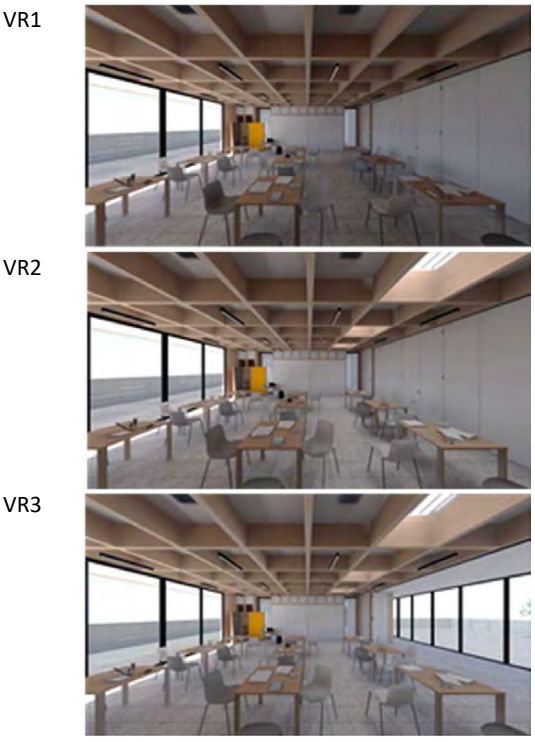

Figure 4: FES atmospheres

360° images of the interior space were generated from a central viewpoint, facilitating horizontal and vertical head movements. The observation height, set at 1.40 meters, aligns with the average anthropometry of a standing 13-year-old adolescent, ensuring an age-appropriate viewing perspective.

Using FES case study provided continuity to the research project and fed the integrated design process from its initial phases through to the occupants' experience of the environment.

3. RESULTS

The results of the experimental study are presented in three sections: the effect of using the VR headset to assess indoor spaces with adolescents (Subsection 3.1), the application of the instrument for rating the scenes (Subsection 3.2), and the perceptual impressions of the environment on subjective assessments (subsection 3.3).

3.1 VR with adolescents

The pilot study was designed to determine a virtual reality navigation workflow for assessing indoor spaces and the experiences of 13-year-old students. Participants demonstrated good command of the tool. Those with prior virtual reality experience demonstrated greater skill in interacting within the immersive space. However, inexperienced participants were also able to complete the activity, requiring a longer induction time.

The planned duration of the experiment was sufficient to develop the full experience, allowing for proper visualization and evaluation of the three scenes. Although research suggests that VR is safe for children to use for up to 30 minutes daily [14], participants began showing pressure marks on their skin from the headset and experienced fatigue after 15 minutes. It is estimated that inexperienced VR participants might experience visual fatigue if the experiment is extended.

Participants engaged effectively with the questionnaire within the virtual environment. They had the ability to vote within the immersive space using the Oculus Rift remote control, which provided them with autonomy in responding and the flexibility to change their vote if uncertain. This aspect introduced innovation into the experiment, as environmental research involving virtual reality typically relies on verbal responses for survey evaluations [5, 17]. Moreover, similar studies involving adolescents are not previously documented.

3.2 Subjective assessments

The terms used in the instrument and the implemented rating system were satisfactory in this study. Participants understood the terms describing physical attributes, evaluating all items without leaving any question unanswered. Regarding the rating scale, the proposed semantic differential scale allowed participants to assign ratings from 1 to 6, grading their approximation to each term. However, the placement of the questionnaire within the immersive environment had a positive impact, as participants had a visual reference to the rating scale in the space to be rated, thereby simplifying their responses.

The assessments aimed to determine response patterns of subjective experience in an environment, through a frequency analysis of responses. In paired-pair scales, there is uncertainty regarding the equidistance between scale items among participants, attributable to subjective interpretation and assessment of responses. However, the analysis of this study assumed that each participant applied a consistent rating on the scale. Therefore, it was possible to identify a general tendency (or pattern) of the visual stimulus perceived by the participant.

Figure 5 shows different response patterns in each environment, indicating that participants perceived differences with respect to the visual stimulus of light. For example, the brighter VR3 scene exhibited a trend towards higher ratings on attributes interpreted as highly stimulating. In contrast, the atmospheres with less illumination (VR1 and VR2) received medium stimulus ratings, with more scattered and homogeneous responses.

	scale	1	2	3	4	5	6	
VR1	narrow	1	0	4	3	1	1	wide
	colorless	0	1	4	1	2	1	colorful
	monotone	1	1	3	2	1	2	varied
	dark	1	4	2	2	1	0	luminous
	shady	1	3	2	4	0	0	bright
	cool	0	3	2	2	1	2	cozy
VR2	narrow	0	1	1	5	0	3	wide
	colorless	1	2	4	1	1	1	colorful
	monotone	0	1	4	3	1	1	varied
	dark	0	2	1	4	1	2	luminous
	shady	2	1	3	2	1	1	bright
	cool	0	0	4	2	1	3	cozy
VR3	narrow	0	0	0	1	4	5	wide
	colorless	0	2	0	3	2	3	colorful
	monotone	0	0	1	4	3	2	varied
	dark	0	0	0	2	3	5	luminous
	shady	1	0	3	2	2	2	bright
	cool	1	0	0	3	1	5	cozy

Figure 5: Frequency distribution of subjective evaluations of virtual environments

3.3 Perceptual impressions

Although the goal of this study was to explore the tool rather than draw conclusive results about the space, the experience served as a continuation of the research on the educational prototype FES, integrating the subjective experience of occupants in the space. The sample size was too small to have definitive conclusions about the environmental alternatives.

However, there was a very evident and unanimous trend of students' preference for the brighter alternative, VR3, as the space of greatest satisfaction. Furthermore, no order effect was detected in the visualization of lighting scenes, whether from brighter to less bright or vice versa.

For further analysis of the perceptual impressions of the atmospheres, an analysis method was adopted that divides the evaluation scale into three distinct stimulus ranges. This division enables clear differentiation between a neutral stimulus and the two extremes of the scale, representing opposite perceptions. The extremes of the scale can be interpreted as representing positive and negative perceptions, with a neutral perception in the middle, as illustrated in Figure 6. This analytical approach simplifies the presentation and analysis of results in percentages, offering an accurate depiction of the predominant perceptual trends for each atmosphere.

scale	1	2	3	4	5	6
	low/negative stimuli		medium stimuli		high/active stimuli	
scene	spatial impression values					
VR1	13%		57%		27%	
VR2	17%		60%		23%	
VR3	7%		30%		63%	
scene	lighting impression values					
VR1	40%		47%		13%	
VR2	17%		53%		30%	
VR3	7%		33%		60%	

Figure 6: Impression of the spatial and light stimulation of virtual environments.

Regarding descriptive attributes, the lighting dimension exhibited a more pronounced distinction of characteristics across the three scenes compared to the spatial dimension. For instance, the brightest classroom received higher ratings for brightness and lightness adjectives (60%), in contrast to the other two scenes, which were rated as intermediate (53%) and intermediate to low (47%) in terms of stimuli. Within spatial concepts, the notion of amplitude was more prominent than others. This can be attributed to lighting being the direct variable under investigation in the experiment, without any modification to materials or textures.

4. DISCUSION

The article describes a pilot experiment that explores the immersive experience of adolescents in educational spaces. The chosen methodology, combining VR with questionnaires, offers significant added value over more conventional approaches. Virtual reality (VR) provides an experience very close to that of the physical environment and was well received by the study participants. Exploring this technology with adolescents is relevant to tailor the workflow and the questionnaire to their cognitive abilities. The experiment was satisfactory in terms of technology use and the application of the instrument with 13-year-olds. Even with students from lower socioeconomic school contexts, who presumably have less access to new technologies.

Further studies with a larger sample are needed to obtain significant results regarding environmental qualities. However, this work contributes to an ongoing study on environmental attributes, suggesting the need for methodological improvements in future research. This includes enhancing navigation to facilitate entry and exit from scenes, and the display options for survey rate.

The study presented some limitations in experimental aspects that were intentionally not addressed in the project. For example, how we constructed the scenes that presented the lighting atmospheres, but this should be considered in future works. The methodology applied can be used with different groups of participants to evaluate interior spaces with specific objectives to promote environments that best support their preferences and promote the well-being.

5. CONCLUSION

This study emphasizes the importance of using innovative tools to explore occupant-centered design paradigms and create interior environments that are resilient to the expectations of the people who will inhabit the spaces more closely. The application of virtual reality in the design process offers the opportunity to understand and respond to the specific preferences of occupants. Especially by integrating into the research the preferences and needs of adolescents who may have a different subjectivity from other groups of people; ensuring that educational spaces are truly inclusive and adaptive.

ACKNOWLEDGEMENTS

This work received funding from the National Agency for Research and Development (ANID) through the Scholarship Program DOCTORADO NACIONAL 2022-21221821, as part of the FONDECYT research project number 1210701. We would like to thank the Future Edu Space Project, financed by the Innovation Fund for Competitiveness (FIC-R), Code BIP 40011072-0, for providing the information utilized in this study.

REFERENCES

1. Barrett P, Davies F, Zhang Y, Barrett L (2017) The Holistic Impact of Classroom Spaces on Learning in Specific Subjects. Environ Behav 49:425–451. https://doi.org/10.1177/0013916516648735

2. Barrett P, Zhang Y, Davies F, Barrett L (2015) Clever Classrooms - Summary Report of the HEAD Project

3. Nair P, Fielding R, Lackney J (2009) Design Pattern 21:

Lighting, Learning and Color. In: The Language of School Design: Design Patterns for 21st Century Schools., Reprinted. Education Design Architects, pp 156–161
4. Nair P (2016) Redesigning School for Student Centered Learning. Harvard Education Press
5. Fisher K (2001) Schooling Issues Digest Building Better Outcomes : The Impact of School Infrastructure on Student Outcomes and Behaviour. Aust Dept Employment, Educ Train Youth Aff Canberra
6. Cleveland B, Fisher K (2014) The evaluation of physical learning environments: A critical review of the literature. Learn Environ Res 17:1–28. https://doi.org/10.1007/s10984-013-9149-3
7. Nair P (2014) Blueprint for Redesigning Schools for Student-Centered Learning
8. Medhat Assem H, Mohamed Khodeir L, Fathy F (2023) Designing for human wellbeing: The integration of neuroarchitecture in design – A systematic review. Ain Shams Eng J 14:102102. https://doi.org/10.1016/j.asej.2022.102102
9. Bisquerra R, PUnset E, Mora F, et al (2012) ¿Cómo educar las emociones? La inteligencia emocional en la infancia y la adolescencia
10. Chamilothori K, Wienold J, Andersen M (2019) Adequacy of Immersive Virtual Reality for the Perception of Daylit Spaces: Comparison of Real and Virtual Environments. LEUKOS - J Illum Eng Soc North Am 15:203–226. https://doi.org/10.1080/15502724.2017.1404918
11. Rockcastle S, Chamilothori K, Andersen M (2017) An Experiment in Virtual Reality to Measure Daylight-Driven Interest in Rendered Architectural Scenes. In: Building Simulation 2017
12. Kaimara P, Oikonomou A, Deliyannis I (2022) Could virtual reality applications pose real risks to children and adolescents? A systematic review of ethical issues and concerns. Springer London
13. Kreutzberg A, Naboni E (2019) 360° VR for Qualifying Daylight Design. SHS Web Conf 64:02015. https://doi.org/10.1051/shsconf/20196402015
14. Rauschenberger R, Barakat B (2020) Health and Safety of VR Use by Children in an Educational Use Case. 878–884. https://doi.org/10.1109/vr46266.2020.00010
15. Vogels I (2008) Development of a Tool to Quantify Experienced Atmosphere. 25–41
16. Vogels I (2008) Atmosphere Metrics: a tool to quantify perceived atmosphere. Int Symp Creat an Atmos. https://doi.org/10.1007/978-1-4020-6593-4
17. Kong Z, Liu Q, Li X, et al (2022) Indoor lighting effects on subjective impressions and mood states: A critical review. Build Environ 224:. https://doi.org/10.1016/j.buildenv.2022.109591
18. CES (2022) Certificación Edificio Sustentable. Manual de Evaluación y Calificación 1.1. Santiago
19. Mineduc (2018) Creando nuevos espacios educativos: Guía de criterios de diseño para proyectos de ampliación, reposición y construcción nueva
20. TDRe MOP M de OP de C (2016) Terminos De Referencia estandarizados (TDRe). Guia Tec Apoyo N°10 83
21. Solemma LLC (2023) Climate Studio v1.9.8389.22035. https://www.solemma.com/ClimateStudio
22. Chinazzo G, Wienold J, Andersen M (2019) Daylight affects human thermal perception. Sci Rep 9:1–16. https://doi.org/10.1038/s41598-019-48963-y
23. Castilla N, Llinares C, Bravo JM, Blanca V (2017) Subjective assessment of university classroom environment. Build Environ 122:72–81. https://doi.org/10.1016/j.buildenv.2017.06.004

PLEA 2024 WROCŁAW
(Re)thinking Resilience

Multimodal Testing and Upgrading the Urban Microclimate

A case study in a Mediterranean warm climate neighbourhood

CARLOS ALBERTO RIVERA GOMEZ[,1] JULIA HIRUELO PÉREZ[,1] VICTORIA LÓPEZ-CABEZA[,1]

CARMEN GALÁN-MARÍN[1]

[1]School of Architecture. University of Seville (Spain)

ABSTRACT: The Urban Heat Island phenomenon, exacerbated by global warming, poses a public health risk during periods of heat stress, particularly for elderly individuals with low purchasing power. This is especially relevant in Seville's social neighbourhoods, constructed between the 1950s and 1980s, which are characterized by low-quality construction. The challenge lies in adapting these aging urban spaces as a passive measure to enhance comfort within these residences. This study proposes the validation of three complementary methodological approaches: remote sensing, in-situ monitoring, and microclimatic simulations. The focus is on public and transitional spaces in a Sevillian neighbourhood, with the aim of improving comfort and thermal resilience. The results will be utilized to analyse the impact of climatic and morphological parameters on the comfort of urban spaces. Furthermore, it will assess how the application of new technologies can evaluate the climatic efficiency of new designs from both an environmental and socioeconomic perspective.
KEYWORDS: Urban Heat Island, Thermal Comfort, Remote Sensing, Monitoring, Simulation, ENVI-met, Crop Monitoring.

1. INTRODUCTION

The effective and environmentally conscious management of the urban environment has become a leading focal point within the primary challenges of the urban agenda aimed at sustainable development [1]. The research imperatives of the 21st century require heightened endeavours in generating novel research that shows innovative protocols for comprehensive inspection, diagnostic mechanisms, and decision-making models, all directed toward a more holistic urban resilient paradigm. This research seeks to determine the most pragmatic and optimized renovation strategies to counteract the ongoing climatic obsolescence of the current layout of cities. Moreover, the repercussions of global climate change have precipitated an accelerated implementation of strategies focused on bioclimatic and passive renovation actions. These strategies are designed to enhance the environmental performance of outdated public spaces conceived decades ago, which currently exist beyond the boundaries of established comfort parameters. In addition to these factors, the susceptibility of individuals inhabiting urban environments, which is projected to encompass 68% of the global population by 2050 according to United Nations [2] will experience an increase due to the Urban Heat Island (UHI) effect. This effect is currently a prevalent global issue, posing a significant threat to the functionality and liveability of cities and their associated ecosystems, in addition to implications for public health. According to a study conducted in the Mediterranean and Middle East regions [3], elevated temperatures contribute to a heightened incidence of myocardial infarctions and heat strokes among adults. In the case of children, they contribute to an increase in the risk of respiratory and renal disorders. As for the elderly population, which is projected to be 16% of the global population by 2050, they may experience even bigger heat-related risks, an elevated prevalence of chronic health issues and a further reduction in both cognitive and physiological capabilities.

This research aims to propose a multimodal assessment model on urban environmental ergonomics for the identification of feasible and passive measures that improve comfort conditions in residential neighbourhoods. The innovation of this method lies in a cross-analysis based on a combination of modelling and monitoring methods of the microclimatic framework conditions of urban spaces. The model is applied and tested in urban areas of a residential area designed under the guidelines of the modern movement. This typology of neighbourhoods, built in Europe between the 1960s and 1980s, is characterised by broad public spaces of its urban layout. The main goal focus on the methodological insights and implications from an integral diagnosis and proposal for improving the climatic resilience of these areas, thereby serving as a decision-support procedure in order to identify optimal interventions that would ensure a more appropriate thermal comfort performance.

2. MATERIALS AND METHODS

2.1 Case study

The selected case study corresponds to a neighbourhood built in the 1960s in the city of Seville (Spain). This city is subjected to a Mediterranean mild and warm climate, considered Csa according to the Köppen-Geiger climate classification. The average annual temperature of 18.6 ^{o}C, places it as one of the warmest cities in Europe. The neighbourhood is defined by a double grid of buildings. On the one hand, a network of low-rise single-family houses. The size of the urban spaces between them and the profuse vegetation mean that these places are significant for microclimatic analysis. On the other hand, high-rise multi-family buildings are integrated into the urban fabric, creating wider urban canyons. The scarce vegetation, the morphological variability of the canyons and their prolonged exposure to solar radiation, wind, air temperature and relative humidity changes present these as an interesting counterpoint to the previous ones. In the following image (Figure 1), a plan of the layout of the slum used as a case study is shown. Three microclimatic typologies are distinguished due to the distribution of buildings: microclimates between groups of low-rise buildings, microclimates on the ground floor under high-rise buildings and microclimates of the public space.

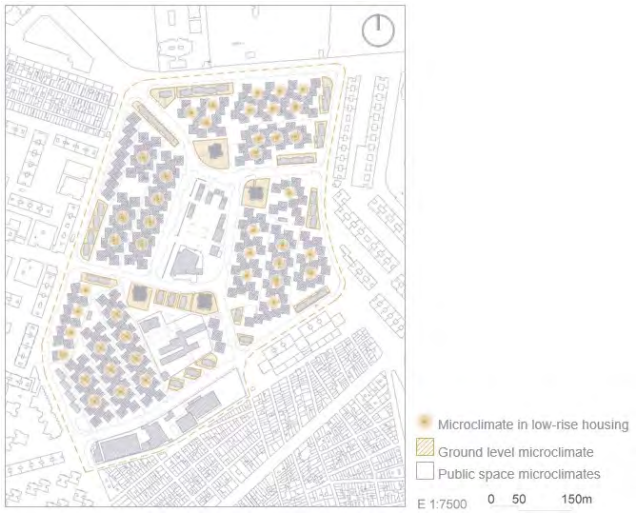

Figure 1: Case study microclimatic typology distribution.

2.2 Methodology

The methodology used was based on both monitoring tools and microclimatic modelling software. The monitoring campaigns were performed at two scales using complementary methods. On the one hand, satellite remote sensing, and, on the other, through field monitoring campaigns.

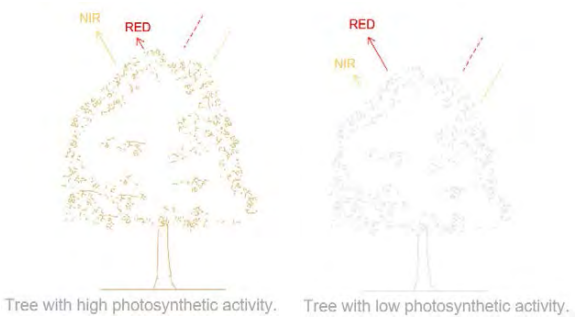

a b

Figure 2: NDVI analysis of vegetation: a) High and b) Low photosynthetic activity.

For the first one, satellite remote sensing, Crop Monitoring software was applied. This tool is based on a satellite monitoring system for field supervision created by EOS Data Analytics (EOSDA), a provider of satellite image analysis such as EOS, Sentinel 2, and Landsat 8. NDVI (Normalised Difference Vegetation Index) [4] can be determined by Crop Monitoring. It measures the state of the vegetation according to the amount of radiation absorbed or reflected by the chlorophyll in the leaves, it also provides an estimate of the vegetation density, with values between -1.0 and 1.0. Figure 2 shows an NDVI analysis of vegetation: a) High and b) Low photosynthetic activity. Trees with higher chlorophyll will have a higher NVDI index, which will graphically reflect in yellowish or greenish tones. However, trees with low chlorophyll will absorb infrared and reflect more red radiation. It will be indicated in reddish and orange tones. This directly impacts on the microclimate because vegetation, especially large vegetation masses such as trees, have a greater or lesser influence on the microclimate of the environment through evapotranspiration and radiation depending on their photosynthetic activity.

On the other hand, in the field monitoring campaign, several instruments were used for the acquisition of the basic parameters: air temperature, relative humidity, and black globe temperature (by a thermo-hygrometer TC100, TROTEC), wind speed (by an anemometer TA300, TROTEC) and pavement surface temperature (by an infrared thermometer Raytek Raynger). Figure 3 shows the distribution of the microclimatic monitoring points from the field campaign.

Figure 3: Microclimatic monitoring points distribution in the case study analysis from the field campaign.

With regards to the urban microclimatic modelling, ENVI-met tool was used, which consists in a simulation software for three-dimensional microclimatic models. ENVI-met simulates climatological interactions between surfaces, vegetation, and the atmosphere, generating accurate high-resolution microclimate calculations.

Figure 4: NDVI analysis of relevant case study areas using Crop Monitoring software.

The program makes it possible to analyse the effects of planning strategies according to the urban climate, which is a major advance over other programs. This is a significant advantage when compared to other programs. This software was also used to calculate the UTCI (Universal Thermal Climate Index) of the current state and a proposal for microclimatic improvement applied on the analysed case study.

3. RESULTS AND DISCUSSION

The microclimate study based on the Crop Monitoring software determined areas with lower photosynthetic activity which resulted in a variation of NDVI index. Figure 4 shows NDVI analysis of relevant case study areas using Crop Monitoring software.

The microclimate study based on the field monitoring campaign allowed the identification of hot spots and areas with a higher incidence of UHI. Figure 5 shows the thermal values along the route of the different monitoring points, as well as the difference between the temperatures monitored in situ and the corresponding temperatures measured at the airport located outside the city. This can therefore be considered the resulting UHI in these location points for the monitoring period considered.

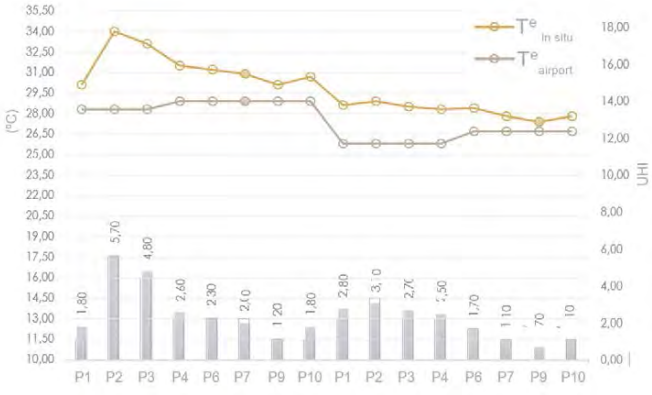

Figure 5: Thermal values and UHI for the different monitoring points.

The analysis performed using the Crop Monitoring software and the field monitoring campaign allowed categorising the efficiency of the urban morphology from the point of view of its relative microclimatic efficiency. Figure 6 shows this categorisation at the measurement points.

Figure 6 Categorisation of the relative microclimatic efficiency of the case study at measurement points.

For the modelling with ENVI-met software, two different models were generated corresponding to one of the areas of the case study with the worst microclimatic resilience characteristics according to previous remote sensing and field monitoring analyses. One of these models corresponded to the current state of the area. The other model incorporated changes consisting of replacing hard paving with more permeable ones and introducing a vegetated pergola that covered a central area of the modelled area. Figure 7 shows the ENVI-met view of both models.

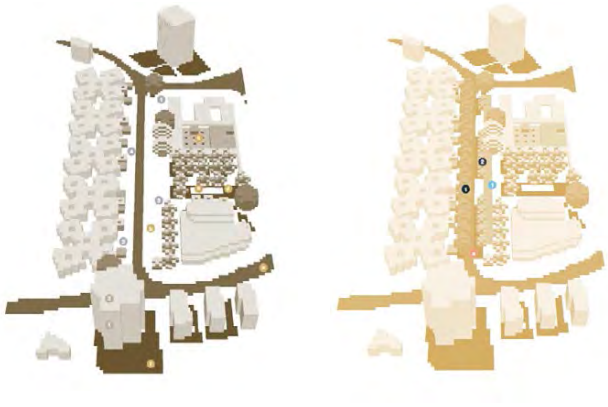

a b

Figure 7: ENVI-met view of previous (a) and proposed (b) models showing measuring points and pavement changes.

After a detailed analysis of the calculation models of the current state and the proposal, a series of conclusions were drawn: At 17:00 h the intervention manages to produce a drop in the thermal sensation up to 6 ºC. However, at 22:00 h, in the absence of direct solar radiation, there is a very slight increase in the wind chill of 1 ºC compared to the current state. thermal sensation 1 ºC with respect to the current state. The variation can be up to 2 ºC higher in places with hard pavements and dense vegetation (Figure 8). Soft pavement and shading elements, greatly affects the reduction of the thermal sensation in the hottest hours of the day. To ensure that the tree canopy does not hinder the rapid heat exchange of the pavement with the night air, the tree layout should be modified.

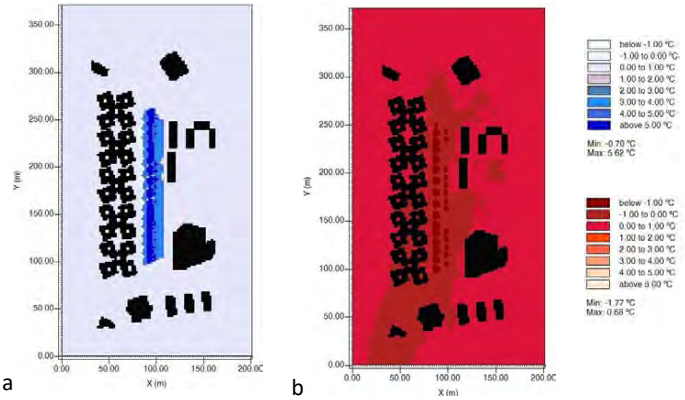

a b

Figure 8: Difference in UTCI values between the models: (current state and proposed) a) at 17:00 and b) at 22:00.

Analysing the air temperature and UTCI data in the proposed adaptation of the case study, generalized temperature drops are observed, which means that during the hottest hours of the day the temperature is up to 4 ºC lower than in the previous state. As a future line of research, it would be convenient to study the microclimatic performance if pavements, shading, and vegetation strategies were extended in the southeast orientation of the case study.

If the air temperature, pavement temperature and UTCI variables of the previous and proposed models are analysed for a central point of the model, changes in pavement surface temperature and UTCI values can be seen. Moreover, these changes increase during the hottest hours of the day. Figure 9 shows a graph comparing the values of air temperature, pavement temperature and UTCI for a central point of the study area considering both models.

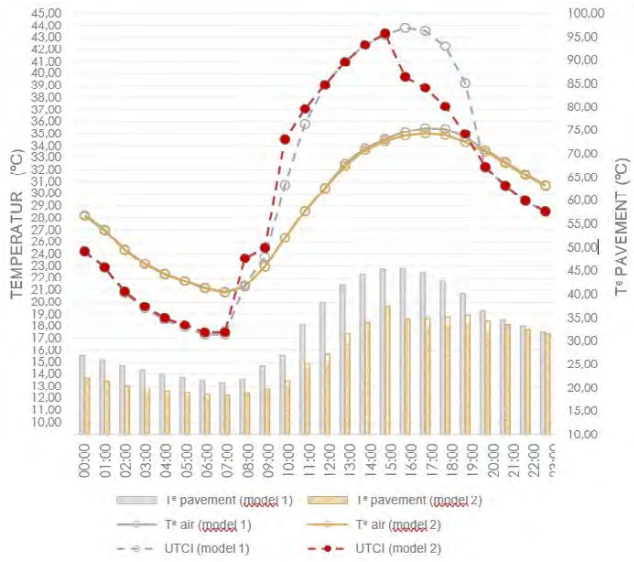

Figure 9: Comparison of air temperature, pavement temperature and UTCI for a central point of the study area considering both models.

4. CONCLUSIONS

A methodology based on the implementation of tools for microclimatic measurement and modelling has led to the following conclusions.

Firstly, remote sensing software has provided information on the spatial distribution of microclimates and their associated parameters based on vegetation. This technique has allowed the identification, at the neighbourhood scale, UHI due to lack of vegetation or excessive exposure to solar radiation and harmful gases, causing vegetation to become sick. The immediacy and ease of data collection, as well as the generation of highly intuitive technical graphics, are notable aspects of this technique. Its main disadvantages are its specialization in rural environments and its lack of connection with geographic information systems.

Secondly, in-situ monitoring has allowed for the collection of detailed data on temperature, humidity, and wind speed conditions during hours with and without direct radiation, on a day of intense heat. This has enabled the analysis of the morphology of public spaces (selected squares and streets) and their thermal variations, evaluating the parameters of air temperature and thermal sensation, in order to study their effectiveness in mitigating heat. The most effective stops have proven to be those with high vegetation density; with mainly shaded spaces; preferably with north-south orientation and pedestrian use.

And, lastly, microclimatic simulations have allowed the prediction of the thermal behaviour of one of the most vulnerable spaces in different scenarios (analysed through monitoring) and the evaluation of the effectiveness of possible adaptation strategies. These simulations have also allowed the exploration of solutions such as the implementation of new vegetation, pavements, and shade elements. The proposal implies a significant improvement in the hottest hours with up to 6ºC difference in thermal sensation, compared to the current state. In other time slots, less effective results are collected, so it is inferred that a change in the general pavement throughout the route, the closure of the vegetable pergola on its southeast side, or the introduction of environment humidification elements, could improve the microclimate. It would be of interest to evaluate new project simulations with this change of parameters, to guarantee the effectiveness of the final design.

The steps of the proposed methodology could, therefore, be applied to different case studies for the identification and possible mitigation of urban hotspots. However, the present study can be completed with the development of new lines of research. Among others: To extend, the monitoring periods, to heat waves episodes, including, in the modelling, the IPCC's climate forecasts for the middle and end of the century. And, also, to raise new design proposals simulating days with different climatic conditions. This will allow the analysis of the resilience of the parameters introduced in the new design.

ACKNOWLEDGEMENTS

This work has been supported by the project PID 2021-124539OBI00 funded by MCIN/AEI/10.13039/501100011033 and by "ERDF A way of making Europe"; project TED 2021-129347 B–C21 funded by MCIN/AEI/10.13039/501100011033 and by the "European Union NextGenerationEU/PRTR "; grant US.22-07 funded by Junta de Andalucía (Consejería de Fomento, Articulación del Territorio y Vivienda). The authors gratefully acknowledge AEMET (State Meteorological Agency) for the data supplied.

REFERENCES

1. United Nations. (2021). Transforming our world: The 2030 agenda for sustainable development. In A/RES/70/1. https://doi.org/10.1201/b20466-7.

2. United Nations. (2022). Habitat Core Team. Envisaging the Future of Cities. https://unhabitat.org/world-cities-report-2022-envisaging-the-future-of-cities.

3. Neira, M., Erguler, K., and Ahmady-Birgani. (2023) Climate change and human health in the Eastern Mediterranean and Middle East: Literature review, research priorities and policy suggestions. Environ Res; 216: 114537. https://doi.org/10.1016/j.envres.2022.114537.

3. EOS Data Analytics I. (2023) NDVI: Vegetation Index Formula and Use in Agriculture. https://eos.com/es/make-an-analysis/ndvi/

PLEA 2024 WROCŁAW
(Re)thinking Resilience

Pop-up Urban Furniture in Bamboo:
an Environmental Parametric Design

LAÍS DE GUSMÃO COUTINHO[1,2], EDUARDO GASPARELO LIMA[1], CAMILA CALEGARI MARQUES[3], JOANA CARLA SOARES GONÇALVES[4]

[1] School of Architecture and Urbanism of USP, São Paulo, Brazil
[2] National Council for Scientific and Technological Development scholarship holder, São Paulo, Brazil
[3] Polytechnic University of Catalonia, Catalonia, Spain
[4] Architectural Association School of Architecture, London, United Kingdom

ABSTRACT: The history and heritage value of the Elevado Presidente João Goulart, located in downtown São Paulo and popularly known as Minhocão, drew the attention of the Architectural Association (AA) to conduct one of its visiting schools. Minhocão, configured as an elevated roadway, is closed to vehicular traffic on weekends, allowing the city centre's population to occupy and make use of the space. The workshop's proposal was the development of a temporary bamboo structures for this area. The objective of this article is to present the methodological procedure used for the development of one of the structures within the workshop. The theoretical stages were conducted to understand the material to be worked with, including its bending capacity. Additionally, participants learned how to create self-supporting structures with paper strips and utilized specific software with environmental and structural assessment plugins. Upon obtaining the necessary knowledge, the design process for the structure commenced. Despite the division of teams, participants consistently exchanged information to attain an outcome in which bamboo could endure and enhance conditions for pedestrians. In the end, the structure was transported and assembled on Minhocão (1:1), where it spent an entire day, allowing for the evaluation of the public's interaction with it.
KEYWORDS: Environmental Comfort, Integrated Design Process, Linear Park, Temporary Architecture, Bamboo

1. INTRODUCTION

The *Elevado Presidente João Goulart*, commonly referred to as *Minhocão* (which translates to "great earthworm" in Portuguese), is an elevated roadway constructed in 1971 to address connectivity issues between the eastern and western zones with the central area of São Paulo [1] (Fig. 1). Machado [2] elucidates that this approximately 3.5 km long road is situated within the context of the Brazilian Military Dictatorship, adhering to the prevailing road planning principles of the era, which prioritized vehicular circulation.

The substantial impact on the landscape of the region resulted in significant urban transformations in the vicinity, influencing the dynamics of the neighbourhoods [2]. Consequently, since its inception, the *Minhocão* has been a subject of numerous controversies and discussions regarding its future [3]. In 2013, a coalition of architects, professors, activists, and artists established the *Parque Minhocão Association*, headquartered in an apartment with windows directly facing the elevated highway [4]. According to Veja [4], the group's aim is to advocate for the permanent closure of the road to vehicular traffic, envisioning its transformation into a linear park through organized events and discussions.

Nowadays, the thoroughfare serves as a park during weekends and holidays, being closed to motor vehicles. Nevertheless, on weekdays, it continues to accommodate thousands of vehicles from 7 a.m. to 8 p.m. [5], thereby assuming a dual functionality (Fig. 2).

Figure 1: On the left, Minhocão being built in the 70s. In the centre, Minhocão recently opened. On the right, current image of Minhocão. Photos: Author unknown.

Figure 2: On the left, Minhocão during weekdays, and, on the right, Minhocão closed as a park. Photos: Author unknown.

It is worth mentioning that Avenida Perimetral, which connected the main road junctions in Rio de Janeiro, was also focus of discussions like those

highlighted above. However, between 2013 and 2014, almost five kilometres of the elevated road were imploded to make way for works to revitalize the city's port area - Porto Maravilha Project [6]. In contrast to the example provided, instances such as the High Line in New York and the Promenade Plantée in Paris employed portions of the pre-existing infrastructure to establish linear parks within the urban environment.

The conversion of *Minhocão* into a park entails additional considerations, notably the need to incorporate urban furniture and vegetation. This is because the redevelopment project devised by Curitiba architect Jaime Lerner [7], commissioned by the *Sindicato da Habitação* in 2017, has been in abeyance since 2019. This necessity is intended to create a more comfortable environment for users and to encourage the sustained use and appropriation of urban spaces.

The prospect of converting the elevated roadway into an urban linear park, along with the imperative to furnish the space either permanently or temporarily, motivated the Architectural Association to conceive an AA Visiting School specifically centred on *Minhocão* [8]. The scope of this initiative involved the development of 1:1 prototype for shading structures utilizing parametric weaving techniques with bamboo and other locally sourced materials.

In recent years, the proliferation of projects focused on short-term and dynamic spaces has been on the rise, emerging as a novel solution. Referred to by various names such as temporary architecture, ephemeral architecture, and pop-up architecture, this design approach involves interventions, structures, displays, enclosures, or interactive spaces that are characterized by their temporary, flexibility, collaborative, and adaptable nature for diverse people, uses, and durations [9]. Then, temporary urbanism can also play a significant role in revitalizing urban spaces and facilitating the transition toward future resilient and sustainable cities.

In this context, this paper demonstrates the development of a temporary woven structure rooted in the principles of environmental design for the *Minhocão*, informed by analytical and practical procedures. This paper also presents the methodology used during the 10 days of workshop, as outlined in Section 2, leading to the proposed design.

The design exercise presented is one of the projects generated during the AA Visiting School São Paulo 2019, hosted by *Escola da Cidade*, an architecture school in the centre of São Paulo, close to the elevated road. The event brought together students and professionals from various countries, and the workshop resulted in three projects developed by the students. The workshop and its results were the focus of an article published in The New York Times at the time [10].

2. METHODOLOGY

It is important to note that the methodology employed followed the workshop's predefined flow, which had been previously established by the organizers and was divided into three stages: (I) preparation; (II) execution; and (III) assembly.

2.1 Preparatory stage

The preparation stage encompassed lectures on *Minhocão*, bamboo, and design process. The objective was to comprehend the various dimensions of the site, material, and processes involved, spanning physical, spatial, environmental, cultural, and heritage considerations. These lectures were immensely significant in fostering an understanding and appreciation of all aspects relevant to the design process, such as the attachment that the downtown population has to the elevated roadway and their desire to occupy this space.

Within the preparation stage, several small workshops were conducted. The first, led by Alison Martin, focused on self-supporting structures created with strips of paper in reduced scale, aiming to test different shapes (Fig. 3). The second, led by Samuel Bertrand and Henrique Lattes, covered the fundamental functions of Rhinoceros software and Grasshopper, along with the utilization of Ladybug, an environmental comfort plugin. With Ladybug, it is possible to perform climatic diagnostics by visualizing and analysing weather data, such as psychrometric charts, sun paths, wind roses, among other functionalities. Additionally, the plugin allows for geometric studies, such as incident radiation and shading.

Figure 3: Students working with tutors Alison Martin and James Solly during the preparatory stage.

In the third workshop, conducted by James Solly, the team continued with Rhinoceros/Grasshopper, but this time incorporating the Kangaroo and K2Engineering plugins. Kangaroo allows the simulation of physical behaviours, including structural forces, tension, compression, bending, and gravity effects on complex geometries. Simultaneously, the K2Engineering plugin enhances the capabilities of Kangaroo by providing a specialized toolkit for structural calibration, accurately simulating, and fine-

tuning structural properties, such as analysing the bamboo's loads and bending capacity. Therefore, with these two plugins, it was possible to assess in each structure whether the material would withstand the loads and curvature imposed by the evaluated urban furniture design. Additionally, a two-day practical activity took place at a bamboo-producing property to provide hands-on experience with different types of materials, their flexibility, and the optimal methods for cutting and attaching them.

2.2 Execution stage

In the execution stage, the class was divided into three teams to develop one urban furniture each. All teams had the same steps to follow. First, it was necessary to conduct studies on paper strips, considering factors such as the ability to protect people from direct radiation, the ease of transportation and assembly, and the possibility for residents to appropriate the urban furniture for their preferred use. Thus, various volumetric options were explored using a reduced paper model until a definitive proposal emerged. All shapes were analysed in software and the presented plugins, and then executed in a 1:1 bamboo prototype – the studies developed for the proposed project elucidated here will be presented in the results section.

In this manner, the group underwent division due to the substantial workload and the restricted time frame. One faction undertook the task of load and flexibility analyses utilizing the Kangaroo plugin, while another focused on environmental analyses employing the Ladybug plugin. A third segment assumed responsibility for the graphical presentation of the project. Despite these distinct roles, all three fronts operated within the same workspace, facilitating communication, information exchange, and file sharing. Upon the completion of the project, the group proceeded with the cutting and assembly of bamboo on the ground floor of the *Escola da Cidade* building, where ample space and the possibility of removing the structure after assembly were available (Fig. 4).

Given that the workshop spanned only 10 consecutive days, the 3-day execution stage demanded an exploration of each member's strengths and a robust connection among team members. This connection was of greatest importance to facilitate an integrated design process, which was crucial not only due to the limited time but also because of the scarcity of available materials.

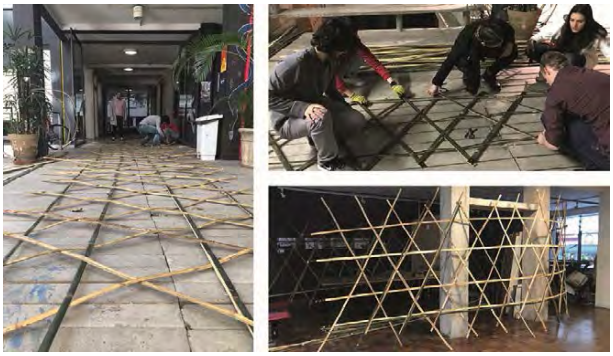

Figure 4: Group executing the proposed project (1:1 scale) in the entrance hall of Escola da Cidade.

2.3 Assembly stage

Sunday was selected as the concluding day of the workshop, during which *Minhocão* would be inaccessible to vehicular traffic throughout the entire day, and, in addition, it is the day that São Paulo downtown residents use the space the most. Thus, in the stage referred to here as "Assembly stage", the structure was transported to the elevated roadway. A specific location for installation was chosen based on the environmental variables that had been previously studied – explained in the following session.

From this juncture, close observation was directed towards the interactions of the site users with the structure. It is important to underscore that designing such an unconventional piece of urban furniture holds limited value unless there is an opportunity to witness how the intended audience will adopt and utilize the structure (Fig. 5).

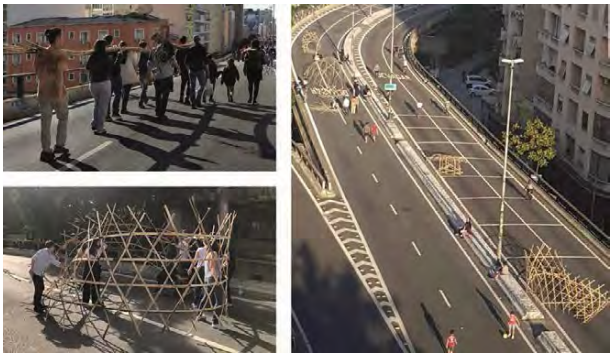

Figure 5: Students taking the parts to the assembly location and building the prototype. On the right, projects produced during the AA Visiting School São Paulo 2019 in Minhocão.

3. RESULTS

As previously mentioned, the final structure evolved as a culmination of systematically progressing through all stages of the workshop flow, adhering to the employed methodology. Initially, a critical idea was generated about the significance of the location for the population and the importance of gradually transforming *Minhocão* into a linear park, starting with temporary structures for weekends, with the goal of a complete transformation and adaptation of the area.

The initial designs of the pop-up urban furniture were created and tested on paper, in a reduced scale, following Alison's teachings. The entire team participated in this stage, exchanging information, and offering input during the production. After several proposals and discussions regarding the shading capacity of some of the developed forms, the team decided to conduct studies on a Möbius strip, a known shape with some symbology, bringing a poetic dimension of temporary infinity to the project (Fig. 6).

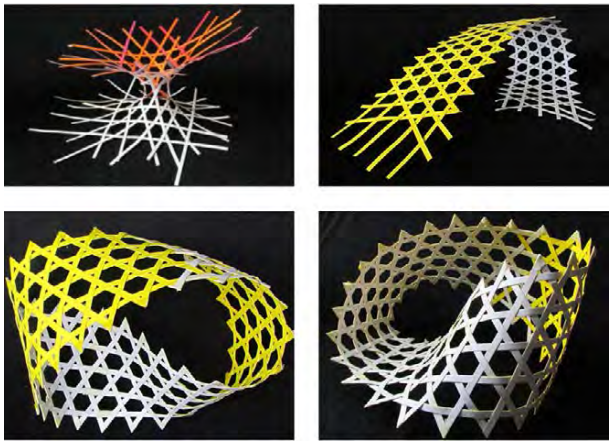

Figure 6: At the top of the image, two proposals made on paper strips are presented; at the bottom, the proposed form (Möbius strip) is shown from two different angles.

The selection of the Möbius strip was also influenced by the shape it assumes when supported on a horizontal surface. This consideration stems from the fact that, depending on the scale and rigidity of the material, it becomes feasible to generate spaces – either shaded or sunny – where users can recline on the structure or simply remain within it, thereby providing various options for the user.

With the final form determined, the bamboo strips began to be cut into uniform width of 25 mm. Additionally, the shape was transposed to Rhinoceros through parameterization executed in Grasshopper, utilizing the Kangaroo plugin, which also simulated the intricacies of the manufacturing process (Fig. 7A). In conjunction, based on the dimensions and flexibility of bamboo, the K2Engineering plugin was used to create load and bending moment diagrams. Each outcome achieved through this plugin was verified by means of physical testing.

These studies defined the bamboo length to prevent the material from breaking. In some simulated lengths, such as 18 and 15 meters (Fig. 7B and 7C), it was observed that the material would not withstand the bending (yellow and red arrows). Therefore, the length of 10 meters (Fig. 7D) was established as the feasible option (all arrows in shades of blue).

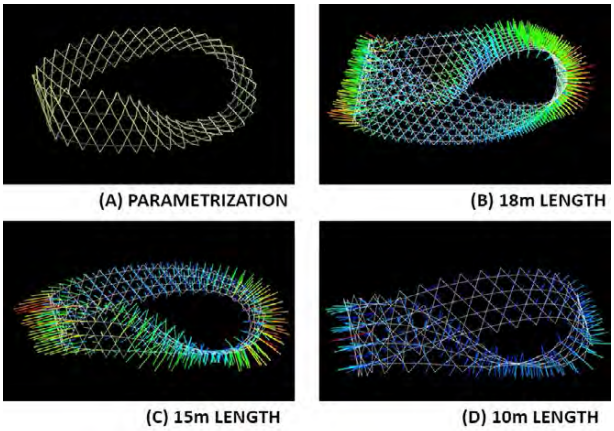

Figure 7: (A) Shape parametrization; (B) Bamboo slats placed longitudinally with a length of 18 meters, (C) 15 meters and (D) 10 meters.

Subsequently, a climatic diagnosis for the city of São Paulo was developed, along with studies on shading and radiation using the Ladybug plugin.

Regarding the climate, the city of São Paulo (Latitude 23.85° S; Longitude 46.64° W; Altitude 792 meters above sea level) is situated in a subtropical region, and its Köppen-Geiger climate classification is temperate with no dry season and hot summers (Cfa). Solar radiation plays a significant role in elevating temperatures, particularly on sunny days. On typical warm days with clear skies, for example, temperatures can easily surpass 30 °C in the early afternoon.

Initially, the environmental studies were conducted on *Minhocão* without furniture to comprehend the optimal location for deploying the structure, considering the dense surroundings of the highway (Fig. 8A and 8B). Following that, a radiation study of the object itself was undertaken to understand the best configuration and orientation (Fig. 8C). Finally, the studies were conducted with the structure already positioned in the defined location (Fig. 8D).

In accordance with these analyses, a 1:1 scale prototype of a Möbius strip made of bamboo was executed in the entrance hall of *Escola da Cidade*. Bending and torsion tests were conducted in this setting to achieve the desired shape. Nevertheless, the model was kept open for ease of transportation to *Minhocão*. Consequently, on the final day of the workshop, the bamboo structure was transported to the elevated road and finalized on-site, where bends, twists, fittings, and lashings were executed.

Several points need to be highlighted. The first pertains to solar radiation incidence. As anticipated, the incorporation of a film at strategic points in the bamboo weave to reduce direct solar radiation without impeding the airflow is desirable. This is particularly crucial given that the bamboo weave was crafted with considerable spacing. In the scenario where this developed urban furniture is not

temporary, intended for use only on weekends, but rather permanent, as in the creation of a definitive linear park, various local plant species were studied. These species vary in density and can be strategically placed for shading according to different times of the year (Fig. 9), in addition to contributing to the local microclimate.

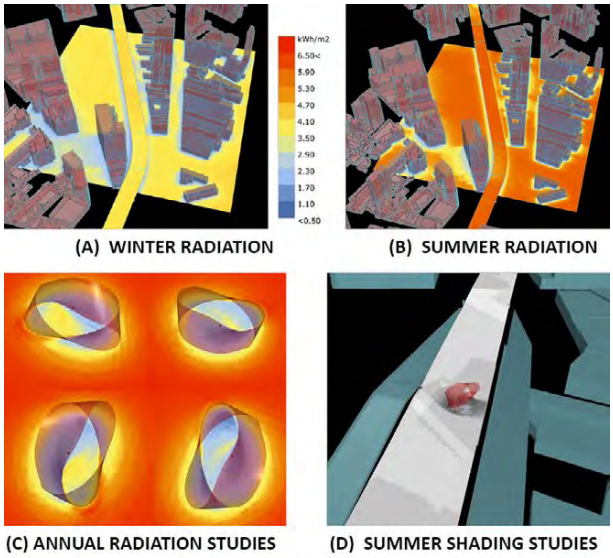

Figure 8: (A) Studies of radiation on the winter solstice; (B) Studies of radiation on the summer solstice; (C) Annual radiation studies of the urban furniture proposed; (D) Summer shading studies.

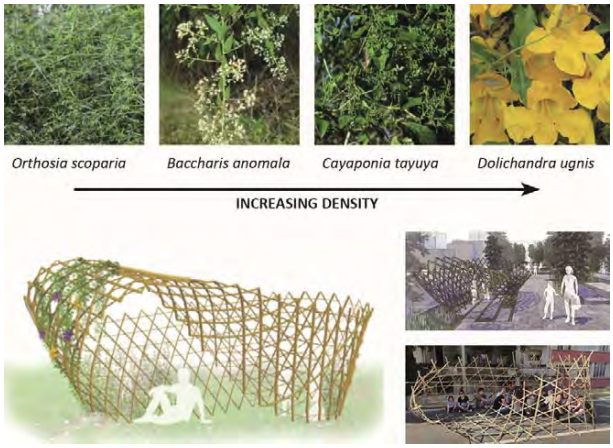

Figure 9: Local vegetation species studied according to their density and shading capacity, urban furniture proposed with the studied vegetation and implementation imagens.

The second point concerns the structure of the urban furniture. To ensure that it retains the intended design and studied configuration, it is imperative to incorporate a fitting and supporting structure. This entails having less ground contact area and more coverage area. Additionally, as a third point, it should be noted that the work was carried out manually and craft-wise, without the use of tools or personal protective equipment. This approach resulted in limited standardization of components and rendered it impossible to execute a more tightly woven bamboo pattern. However, it is understood that the final product was merely a prototype, and the intention is to assess and enhance this structure for ultimate use.

Afterwards, and throughout the remainder of the day, the interaction of site users with the structure was observed. In addition, the experience also provided constructive conversations with the surrounding residents, who began to reflect on the space use and the importance of furniture in places of this type for the users' comfort and permanence.

4. CONCLUSION

This article has outlined the development of a prototype of temporary urban furniture for one of Brazil's main elevated roadways. The methodological procedure followed the stages of a workshop conducted by the Architectural Association. Nevertheless, it is understood that these same stages can be replicated for the fabrication of other prototypes, whether using bamboo or other easily accessible and manageable materials. These prototypes can then be analysed and evaluated using the mentioned plugins.

The integration of parametric design into an integrated design process was indispensable for a ten-day workshop, allowing for a rapid understanding of the project and testing of possibilities within minutes. Consequently, when executing the physical model, all dimensions and formats were already defined. It is understood that both the use of parametric tools and the integrated design process are essential strategies to enhance sustainable and resilient architecture. However, when these procedures are applied to larger teams and projects, maintaining such a seamless flow becomes more challenging. Brazil is still progressing at a slow pace in transitioning from traditional design processes, which employ tools that generate significant rework and foster limited communication among professionals. It is imperative to expand the use of these strategies in Brazilian design processes, beginning by incorporating them into design studios within universities to facilitate broader adoption.

Furthermore, it is worth highlighting that initiatives of this nature are highly significant as they have the capacity to foster a sense of belonging and improve the environmental comfort of places such as *Minhocão*, which during the week may not be very inviting to pedestrians. These initiatives can originate from governmental bodies, a renowned British architecture school, a collective of artists and architects, or even through small individual actions. They can be implemented in the central areas of large metropolises like São Paulo or in more secluded neighbourhoods of smaller cities.

The demand for urban furniture in *Minhocão* is significant, to the extent that, two years after the AA Visiting School, the Municipal Department of Urban

Planning and Licensing initiated the installation of benches and platforms on Elevado Presidente João Goulart during weekends (Fig. 10). While most of the tactical furniture provided comprises dynamic seating to accommodate users, the issue of intensified solar radiation on clear-sky days remains a challenge yet to be addressed.

Figure 10: Tactical urban furniture made available by São Paulo City Hall in Minhocão during weekends. Photos: Edson Lopes.

Other noteworthy aspect is the utilization of bamboo as the chosen material for the furniture. This material grows rapidly in various climatic conditions, establishing itself as a resilient alternative. Not only is it renewable, but it also reduces costs and travel footprints. Moreover, it is both sturdy and lightweight, making it easy to transport. Due to all these advantages, it is evident that the use and promotion of this material need to be expanded, with a greater focus on skilled labour and investment in research.

This workshop elucidated the remarkable importance of developing an innovative design for temporary structure adapted to an urban context, considering the environmental comfort concepts together with technological design tools. The parametric design becomes an ally in the design process, accelerating the progress in design, positioning, and assembly, saving rework, and reducing material loss. In addition, the workshop was an integrative and an exchanging experience, with people from different places, with different climatic, social, cultural conditions, and knowledge, which enriched the teamwork development. Moreover, certain open spaces with exclusive use need to be rethought so that people can take advantage of the city in its broadest sense and, for that, mechanisms that provide comfort to the user are a necessity.

ACKNOWLEDGEMENTS

Thanks to AA for the scholarships granted, to tutors that advised the work – James Solly, Alison Martin, Samuel Bertrand and Henrique Lattes –, as well as the colleagues who contributed to this concept design – Claudia Carunchio, Julia Getscho, Kristian Whittaker, Maria Eduarda Rahal, Pedro Herman and Pohan Chu.

REFERENCES

1. Câmara Municipal de São Paulo. *Especial Minhocão*, [Online], Available: https://www.saopaulo.sp.leg.br/especiaiscmsp/especial- minhocao/ [22 August 2023].
2. Machado, A. C. P. *Para além de um viaduto: uma análise de usos e discursos sobre o Parque Minhocão.* Dissertação (Mestrado em Ciências). Universidade de São Paulo, 2019.
3. Moura, L. B. *Minhocão: ressignificação do espaço por meio de intervenções culturais.* TCC (Especialização). Gestão de Projetos Culturais. Universidade de São Paulo, 2017.
4. Veja São Paulo. 2016. *Associação é criada para transformar Minhocão em parque*. [Online]. Available: https://vejasp.abril.com.br/cidades/associacao-quer-transformar-minhocao-em-parque [22 August 2023].
5. CET. Companhia de Engenharia de Tráfego. *Elevado Presidente João Goulart (Minhocão)*, [Online], Available: http://www.cetsp.com.br/consultas/seguranca-e-mobilidade/elevado-presidente-joao-goulart-(minhocao).aspx [22 August 2023].
6. Monié, F. Silva, V. S. da. 2015. *O projeto Porto Maravilha de revitalização da área portuária do Rio de Janeiro entre inovações e retrocessos na produção do espaço urbano.* Revista Transporte y Territorio, Buenos Aires, Argentina, [Online], Available: chrome-extension://efaidnbmnnnibpcajpcglclefindmkaj/https://www.redalyc.org/pdf/3330/333039205007.pdf [27 December 2023].
7. Gazeta do Povo. 2017. Jaime Lerner comandará transformação do Minhocão em parque suspenso, [Online], Available: www.gazetadopovo.com.br/haus/urbanismo/minhocao-sao-paulo-jaime-lerner-parque-linear-pedestres/ [27 December 2023].
8. AA. *AA São Paulo Visiting School*, [Online], Available: https:/ /saopaulo.aaschool.ac.uk/2019-high-line-paulista/ [27 December 2023].
9. VECTORWORKS. 2019. *The rise of temporary and pop-up architecture,* [Online], Available: https://di-a.de/wp-content/uploads/2018/07/dittelarchitekten_architect_magazine-pop-up-box.pdf [27 December 2023].
10. NY Times. *In Brazil, Mending an Urban Fabric with Geometry and Bamboo*, [Online], Available: https://www.nyti mes.com/2019/07/29/science/math-weaving-bamboo.html [20 Augst 2023].

PLEA 2024 WROCŁAW
(Re)thinking Resilience

Cooling Energy Consumption Estimation in Residential Buildings: Utilising Statistical Models for Benchmarking

AMIRA ELNOKALY[1] SHIREEN ALQADI[2]

[1]School of Architecture and the Built Environment, University of Lincoln, Lincoln, United Kingdom

[2] Architecture Engineering Department, Birzeit University, West Bank, Palestine

ABSTRACT: This study delves into the complex impacts of climate change on the built environment, focusing on the shift in internal conditions within structures due to extreme climates. The consequent rise in energy consumption to optimize indoor comfort becomes a pressing concern. Specifically, this research meticulously estimates cooling energy usage within Palestinian housing, critically relevant in a global climate of rising temperatures. Employing a comprehensive multi-mode survey, data was collected from 320 households in Hebron, situated in the West Bank. Analysis revealed the intricate interplay of various factors, including building characteristics, adopted cooling methods, socioeconomic aspects, and adaptive comfort behaviour, significantly affecting cooling energy expenditure. A robust regression model was developed, precisely estimating cooling energy consumption in Palestinian households. Beyond estimation, this model serves as a vital benchmarking tool, enabling stakeholders like households, policy makers, and professionals to accurately assess cooling consumption. Moreover, it facilitates insightful comparisons with anticipated future consumption patterns under evolving climatic conditions. This proactive approach equips stakeholders to adapt and mitigate climate change impacts within the built environment. Consequently, this research enhances comprehension of the nuanced relationship between climate change and energy usage in the built environment, offering a practical tool empowering informed decisions and climate-resilient housing policies in Palestine.
KEYWORDS: Cooling Energy; Comfort; Consumption Estimation

1. INTRODUCTION

The energy sector in Palestine faces significant and complex challenges, including energy insecurity, economic constraints, and unsustainable consumption [1]. Except for fuel wood, a substantial proportion of Palestine's energy resources and electricity are sourced from Israel, playing a crucial role in the energy landscape [1]. Moreover, the political situation in the region has a notable impact on the supply of energy resources [1]. The housing sector, a major consumer of energy within Palestine, lacks submeters to accurately measure energy usage for heating, cooling, and cooking, revealing a significant gap [2].

Recently the design of low, zero and positive energy buildings has become an important topic on the global level. Green buildings in Palestine have started to be considered recently. In the Palestinian case, green buildings are not only important to minimise the environmental harm, but also to be able to provide comfortable indoor spaces with the limited available energy. However, moving towards these models should be coupled by suitable behaviour to ensure the proper performance of the green buildings. Encouraging action such as energy conservation based on information alone has proven ineffective and could not lead to a sustained change in environmental behaviour [3]. Hence, establishing benchmarking tools to define an energy performance baseline at both building and city levels is critical [4,5]. On the building level it helps the users to compare their energy consumption with similar buildings and analyse their behaviour versus the performance of the building, then define potential behavioural or physical changes (retrofitting strategies) needed to minimise the energy consumed [6]. On the city level, energy benchmarking an important guiding value for building energy-saving work and can help in forming of suitable city level policy measures and programs to improve energy efficiency of buildings.

Climate change is imposing an unprecedent challenge for policy makers, designers, and users. The anticipated increase of temperature will potentially affect the users' health, wellbeing and even mood and mental health [7]. On the other hand, the COVID-19 pandemic has highlighted the importance of healthy and sustainable buildings, thereby magnifying the need of action to provide sustainable built environments [8]. Hence, understanding the impact of climate change on the building performance is critical to mitigate the undesirable impact on the buildings' users who would consume additional amount of energy to reach the comfort level.

Future energy demand is likely to increase because of climate change, but the extent of this

demand depends on many interacting sources of uncertainty [9]. In accordance with the trends of warming, the heating demand is predicted to decrease in many domains whereas the opposite is the case for the cooling demand [10]. The amount of change in demand depends on the location and the climatic zone [11]. The use of tailored passive design strategies may reduce the future annual cooling and heating energy demand in buildings [12]. Conventional passive strategies that focus on heating such as internal wall insulation, roof insulation, reflective foil, thermally reflective roofs and thermally heavy floor coverings should be use carefully and more attention should be given to passive strategies that promotes cooling such as shading and ventilation [13,14].

This study focuses on evaluating cooling energy consumption due to its direct impact on residents' thermal comfort, especially considering the expected increase during extreme summer climatic conditions. It also aims to create an actual baseline to be compared with predicted future cooling demand as anticipations of future climatic conditions suggest a shift in building energy performance [15]. By assessing cooling energy consumption, this study aims to identify potential alterations in consumption patterns attributed to climate change, positioning itself as a valuable benchmarking tool for the future [15].

Data was collected from 320 households in Hebron using a multimode survey method. The primary contribution of this study lies in formulating three regression models to estimate cooling energy consumption within the Palestinian housing sector. Statistical models, like regression, provide a reliable means to estimate energy consumption in buildings [16]. The developed regression model accurately predicts the total annual energy consumed for cooling, incorporating physical and socioeconomic parameters. Additionally, it considers usage patterns of cooling systems, household thermal comfort levels during summer, and initial adaptive comfort strategies employed to enhance thermal comfort. This model serves as a simplified benchmarking tool, empowering professionals, policymakers, and households to assess and quantify cooling energy usage within the housing sector in Hebron [16].

2. RESEARCH METHOD

In examining the intricate relationship between climate change and the built environment, particularly focusing on the impact of extreme climates on internal conditions in structures, this study addresses the escalating energy consumption challenges associated with optimizing indoor comfort. The specific focus is on cooling energy usage within Palestinian housing, a context particularly relevant in the face of global temperature increases. The research methodology employed a comprehensive multi-mode survey, collecting data from 320 households in Hebron, situated in the West Bank [17].

2.1 Factors contributing to the cooling energy consumption and the statistical models.

The study acknowledges the diverse factors influencing cooling energy expenditure, encompassing building characteristics, adopted cooling methods, socioeconomic aspects, and adaptive comfort behaviour [18, 19]. To navigate this complexity, a robust regression model was meticulously developed to precisely estimate cooling energy consumption in Palestinian households [20] [20, 21]. Beyond its estimation function, the model emerges as a critical benchmarking tool. Stakeholders, including households, policymakers, and professionals, can utilize this tool for accurate assessments of cooling consumption [22, 23]. Importantly, the model facilitates insightful comparisons with anticipated future consumption patterns under evolving climatic conditions [20].

This proactive approach equips stakeholders to adapt and mitigate climate change impacts within the built environment. By enhancing comprehension of the nuanced relationship between climate change and energy usage, this research offers a practical tool for informed decisions and climate-resilient housing policies in Palestine.

Although the climate in Hebron is considered a Mediterranean climate in general, there is an impact of the microclimatic parameters of the study area of the examined case in which the investigated building unit is located [24]. The discrepancy between the meso-climate the different areas is mainly due to the greenery and the Urban Heat Island (UHI) effect. Studies have shown that loss of greenery in urban areas elevated urban night-time temperatures which will increase summer cooling loads compared to the reference rural site [25, 26]. 'Urban Heat Island' phenomenon (UHI) or "Urban Warming" refers to a distinct urban climate that is mainly attributed to the urban–rural variation of several factors commonly connected to urbanisation. These factors include the thermal properties of surfaces and material used, the urban morphology, and air pollution [27]. (UHI) has many implications including thermal discomfort and increased cooling energy demand [28].

Due to limited available land in the city of Hebron and the surrounding refugee camps, the amount of vegetation is very limited compared to the villages. In investigating the local climate's impact on residential buildings, the study considered three types of settlements: city, surrounding villages, and refugee camps [29]. Each settlement type exhibits

distinct urban forms, building densities, and amounts of vegetation.

There is also a tremendous effect of the building design on the cooling energy consumed. The design of buildings' shape and orientation [30,31]. More parameters have been carried out in several studies previously such as the building shape, volume to surface ratio (VSR), and compactness are usually chosen as the influencing parameters during the optimum design of a building [31]. The building envelope and level of insulation which usually includes the insulation of the wall, roof, window, and ground, Window Wall Ratio (WWR), and infiltration also play an important role in building energy performance [32]. In addition, thermal mass insulation and reflective insulation are the two main technologies used for controlling the thermal performance of the building [33]. However, of climate change since the climate has recently been changing and is anticipated to continue the buildings should be carefully designed to prevent overheating in summer through climate proof design depending on the previously mentioned strategies [34].

In this paper, the physical characteristics of housing units, including typology, age, size, shape, orientation, window parameters, surface-to-volume ratio, and grouping of buildings, significantly influence cooling energy consumption.

The study also recognizes the crucial role of construction materials and envelope characteristics, such as heat transfer coefficient, insulation thickness, thermal mass, and glazing solar heat gain coefficient, in affecting building performance and energy consumption. Additionally, strategies such as increasing housing albedo, implementing green roofs, and incorporating passive design measures like external shading can limit cooling energy demand [35, 36].

Given the survey method used for data collection, the research focused on simple and non-technical parameters to enhance the response rate and data validity [37]. Housing typology was classified based on a socio-physical perspective, considering household type, number of users, and occupancy type. Respondents were also queried about adaptive comfort behavior, further enriching the study's insights [37].

2.2 Regression Models in Estimating Cooling Energy Consumption

Regression methods play a pivotal role in establishing mathematical relationships between the dependent variable, in this case, energy consumed for cooling, and explanatory variables (predictors) [38]. Previous research has successfully employed regression methods to predict total energy consumption in the residential sector [39] and estimate cooling energy usage in households [40]. In this study, a comprehensive regression model was developed for the entire sample, encompassing households employing various cooling methods, including air conditioning units and fans.

To address the potential multicollinearity issue inherent in regression models, a Ridge regression model was employed. This technique enhances the stability and accuracy of the regression model, particularly when dealing with highly correlated predictors. The use of Ridge regression ensures a robust analysis, contributing to the reliability of the findings and the overall quality of the regression model.

In the context of multiple linear regression, all available predictors are incorporated simultaneously, each assigned an appropriate slope to quantify its individual impact [41]. The coefficient of determination, denoted as R^2, plays a pivotal role in evaluating the model's quality. Acting as a key indicator, R^2 measures the goodness of fit of the linear model. Essentially, it signifies the proportion of the dependent variable's variation explained by the regression equation [42].

The R^2 value ranges from 0 to 1, with a higher preference for models approaching an R^2 value close to 1 [43]. This metric becomes crucial in assessing the model's effectiveness in capturing the variation in cooling energy consumption, providing stakeholders with a clear understanding of the model's predictive power.

2.3 Data Collection: A Multimode Survey in Hebron

To gather comprehensive insights into cooling energy consumption, an independent multimode survey was meticulously conducted in Hebron, located 30 km south of Jerusalem. Hebron experiences an average temperature ranging from 9 to 32°C, with a mean temperature of 21°C [26]. The survey spanned from December 2016 to January 2017, ensuring a representation of seasonal variations.

The research questions were purposefully designed to align with the local context, addressing the unique factors influencing cooling energy consumption. Eighteen distinct factors were investigated for their impact, as detailed in Table 1. The survey elicited responses from 322 households, achieving a response rate of 63% through direct interactions and 259 responses through an internet survey.

This multimodal approach enhances the robustness and comprehensiveness of the dataset, allowing for a nuanced analysis of the myriad factors influencing cooling energy consumption in the specific context of Hebron. This paper is among a series of papers in which the results of this questionnaire is analysed into different topics and lessons learnt [44], [45].

Table 1: Parameters Examined for Modelling Cooling Energy Consumption

NO	PARAMETER	NO	PARAMETER	NO	PARAMETER
1	Type of settlement	8	Total monthly income	14	Number of fans used
2	Building typology	9	Level of thermal insulation of walls	15	Number of air conditioning systems used
3	Household size	10	Number of months in which cooling systems are used	16	Using other cooling system (desert AC, etc.)
4	Occupancy rate	11	Duration of occupancy	17	Level of thermal comfort in summer
5	Building age	12	Using fans	18	First adaptive comfort measurement taken when feeling hot
6	Total area	13	Using air conditioning units		
7	Main building materials				

2.4 Cooling Energy Consumption Calculations

The determination of cooling energy consumption involved a meticulous process, starting with inquiries about the usage of cooling systems such as fans or air conditioning units within households.

For those utilizing fans, the calculation of annual energy consumption from electrical systems (AEC) for cooling (in kilowatt-hour, kWh/year) employed the formula:

$$AEC=110\times Q\times H\times 30/1000 \quad (1)$$

where *AEC* (Electricity): The annual energy consumption from electrical systems for cooling in kilowatt-hour (kWh)/year

110 - Average Wattage of fans in the local market

Q - the number of fans used in the house

H - Average number of hours in which the fan is used per day

N - Number of cooling months

For households relying on air conditioning systems, respondents specified the wattage, quantity of units, and average usage duration during the cooling season. Utilizing data from producer catalogues, average wattages for common air conditioning systems in the Palestinian market were considered, as presented in Table 2.

Table 2: Average Wattages of Common Air Conditioning Systems for Cooling in the Palestinian Market (Researcher, 2017, based on data from producers' catalogues)

Product	*Model*	*Wattage for cooling*
Media Air conditioning system	Platinum-18GIQ	0.96
Media Air conditioning system	Platinum-23GFI	1.54
Media Air conditioning system	Platinum-32GIQ	1.86

The annual energy consumption by the air conditioning systems for cooling was calculated using the following formula:

$$AEC\ (electricity) = W*Q*H*N*30/1000 \quad (Eq.\ 2)$$

where AEC (Electricity): The annual energy consumption from electrical systems for heating or cooling in Kilowatt-hour (kWh)/year

W- Wattage (gained from the producer catalogue for each system shown in table 2)

Q - Number of Air conditioning systems used by the household

H - Average number of hours in which the system used per day

N - Number of cooling months

3 RESULTS AND DISCUSSION

The analysis of the datasets led to the derivation of the Fitted Regression Equation (M) for evaluating annual heating energy consumption (Y):

$$Y(M) = -3400.88 + \sum_{i=1}^{15} F \quad (3)$$

The coefficient of determination $\mathbf{R^2}$ for the models (M) is calculated as 0.73. This indicates that the developed model can elucidate approximately 72.8% of the annual cooling energy usage it was designed to predict. Figure 1 visually compares the fitted values from the regression analysis with the calculated values based on the survey responses, providing an insightful depiction of the model's performance.

While various methods exist for estimating cooling energy, employing building energy simulation models proves intricate due to its time-consuming nature and the need for detailed data, often unavailable in the Palestinian context [45,46,47]. Furthermore, simulations tend to overlook socio-economic factors. In contrast, the cooling degree days method efficiently calculates cooling energy needs, but it falls short in estimating actual household consumption. This research emphasizes the practicality and reliability of the developed regression model in capturing nuanced factors, including socio-economic aspects, contributing to a more accurate assessment of cooling energy consumption in Palestinian

households.

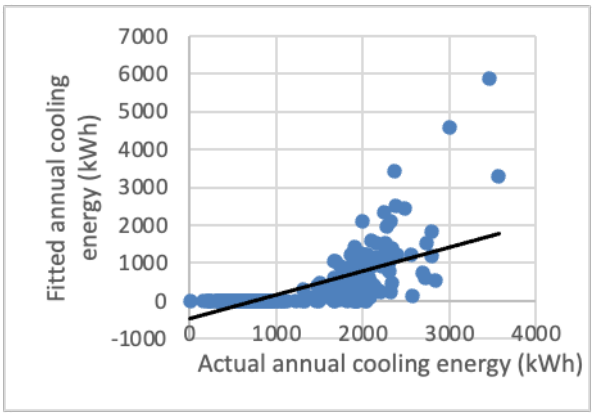

Figure 1: The actual vs. the fitted energy used for cooling (M)

4. CONCLUSION

Advancing energy quantification and future climate preparedness

Efficiently quantifying energy consumption in buildings is pivotal for optimising energy use and transitioning towards self-sustaining, eco-friendly energy technologies in Palestine. This study undertakes the critical task of delineating current cooling energy utilization in households, providing insights into potential trends influenced by climate change.

The paramount contribution of this paper lies in the development of a robust regression model employing Ridge Regression Analysis. This model precisely estimates cooling energy consumption in Hebron's residential sector, leveraging empirical data gathered through a comprehensive multimode survey.

The derived model (M) exhibits an impressive R2R^2*R*2 of 73%, offering a nuanced understanding of the factors influencing total annual cooling energy. Key determinants include housing typology, age, construction materials, insulation, total area, cooling systems employed, number of cooling months, household income, occupancy period, thermal comfort during summer, and thermal behavior. Beyond estimation, this model emerges as a valuable benchmarking tool for assessing residential cooling energy, facilitating future comparisons and anticipating shifts in global climatic conditions.

The findings presented herein hold significance not only for Hebron but also offer a robust methodology applicable globally. As climate change becomes an escalating concern worldwide, the developed regression model stands as a rigorous, transferable framework for assessing and benchmarking residential cooling energy consumption, aiding policymakers, researchers, and practitioners in fostering sustainable practices and resilient housing policies globally.

Understanding the present time energy consumption trends can provide a baseline for the professional and policy makers to quantify the impact of providing tailored fit solution and adaptation strategies to increase the thermal comfort of users under the shadow of climate change. These adaptation strategies can be proposed on several scales such as increasing the vegetation and green roofs on the city scale, or through rational use of materials and other passive design solutions on the building level.

REFERENCES

1. Junaidi, A., Anayah, F.M., Assaf, R., Hasan, A.A., Monna, S., Herzallah, L., Abdallah, R., Dutournié, P., & Jeguirim, M. (2022). An overview of renewable energy strategies and policies in Palestine: Strengths and challenges. Energy for Sustainable Development.
2. Al Qadi, S., Behzad, S. and Amira, E. (2017). Predicting the Energy Performance of Buildings Under Present and Future Climate Scenarios– Lessons Learnt. In: FIRST INTERNATIONAL CONFERENCE ON CLIMATE CHANGE IPCCC 2017. Ramallah-Palestine: Engineers Association - Jerusalem Center.
3. Xie, X., Lu, Y., & Gou, Z. (2017). Green building pro-environment behaviors: Are green users also green buyers? Sustainability, 9(10), 1703. https://doi.org/10.3390/su9101703
4. Sokratis Papadopoulos, Constantine E. Kontokosta, (2019), Grading buildings on energy performance using city benchmarking data, Applied Energy, Volumes 233–234, Pages 244-253, ISSN 0306-2619
5. Mutschler, R., Rüdisüli, M., Heer, P., & Eggimann, S. (2021). Benchmarking cooling and heating energy demands considering climate change, population growth and cooling device uptake. Applied Energy, 288, 116636.
6. Al Qadi, S.B.; Elnokaly, A.; Sodagar, B. Predicting the energy performance of buildings under present and future climate scenarios: Lessons learnt. In Proceedings of the First International Conference on Climate Change (ICCCP), Albireh, Palestine, 8–9 May 2017.
7. Berry, H., Bowen, K., & Kjellström, T. (2009). Climate change and mental health: a causal pathways framework. International Journal of Public Health, 55(2), 123–132. https://doi.org/10.1007/s00038-009-0112-0
8. Sarmas, E., Forouli, A., Marinakis, V., & Doukas, H. (2024). Baseline Energy Modeling for Improved Measurement and Verification through the Use of Ensemble Artificial Intelligence Models. Information Sciences, 654, 119879. https://doi.org/10.1016/j.ins.2023.119879
9. Van Ruijven, B., De Cian, E., & Wing, I. S. (2019). Amplification of future energy demand growth due to climate change. Nature Communications, 10(1). https://doi.org/10.1038/s41467-019-10399-3
10. Larsen, M. A. D., Petrović, S., Radoszynski, A. M., McKenna, R., & Balyk, O. (2020). Climate change impacts on trends and extremes in future heating and cooling demands over Europe. Energy and Buildings, 226, 110397. https://doi.org/10.1016/j.enbuild.2020.110397
11. Wan, K. K., Li, D. H., Pan, W., & Lam, J. C. (2012). Impact of climate change on building energy use in different climate zones and mitigation and adaptation implications. Applied Energy, 97, 274–282. https://doi.org/10.1016/j.apenergy.2011.11.048
12. Invidiata, A. (2016). Impact of climate change on heating and cooling energy demand in houses in Brazil. Energy and

Buildings, 130, 20–32. https://doi.org/10.1016/j.enbuild.2016.07.067
13. Karimpour, M., Belusko, M., Xing, K., Boland, J., & Bruno, F. (2015). Impact of climate change on the design of energy efficient residential building envelopes. Energy and Buildings, 87, 142–154. https://doi.org/10.1016/j.enbuild.2014.10.064
14. Liu, S., Kwok, Y. T., Lau, K. K., Ouyang, W., & Ng, E. (2020). Effectiveness of passive design strategies in responding to future climate change for residential buildings in hot and humid Hong Kong. Energy and Buildings, 228, 110469. https://doi.org/10.1016/j.enbuild.2020.110469
15. Deroubaix, A., Labuhn, I., Camredon, M., Gaubert, B., Monerie, P. A., Popp, M., ... & Siour, G. (2021), Large uncertainties in trends of energy demand for heating and cooling under climate change. Nature communications, 12(1), 1-8.
16. Martín Rojo, D. (2022). Statistical analysis of energy performance certificates of maltese offices.
17. Misni, A. (2015). The Effect of Building Construction and Human Factors in Cooling Energy Use. Procedia - Social and Behavioral Sciences, 202, pp.373-381.
18. Huang, K. and Hwang, R. (2016). Future trends of residential building cooling energy and passive adaptation measures to counteract climate change: The case of Taiwan. Applied Energy, 184, pp.1230-1240.
19. Ballarini, I., Corrado, V., Madonna, F., Paduos, S. and Ravasio, F. (2017). Energy refurbishment of the Italian residential building stock: energy and cost analysis through the application of the building typology. Energy Policy, 105, pp.148-160.
20. Quan, S. J., & Li, C. (2021). Urban form and building energy use: A systematic review of measures, mechanisms, and methodologies. Renewable and Sustainable Energy Reviews, 139, 110662
21. Pflug, T., Kuhn, T., Nörenberg, R., Glück, A., Nestle, N. and Maurer, C. (2015). Closed translucent façade elements with switchable U -value—A novel option for energy management via the facade. Energy and Buildings, 86, pp.66-73.
22. Reilly, A. and Kinnane, O. (2017). The impact of thermal mass on building energy consumption. Applied Energy, 198, pp.108-121.
23. Santamouris, M. (2014). On the energy impact of urban heat island and global warming on buildings. Energy and Buildings, 82, pp.100-113
24. Τσόκα, Σ., Velikou, K., Τολίκα, K., & Tsikaloudaki, K. (2021). Evaluating the combined effect of climate change and urban microclimate on buildings' heating and cooling energy demand in a Mediterranean city. Energies, 14(18), 5799. https://doi.org/10.3390/en14185799
25. Erell, E., & Zhou, B. (2022). The effect of increasing surface cover vegetation on urban microclimate and energy demand for building heating and cooling. Building and Environment, 213, 108867.
26. Bowler, D. E., Buyung-Ali, L. M., Knight, T. A., & Pullin, A. S. (2010). Urban greening to cool towns and cities: A systematic review of the empirical evidence. Landscape and Urban Planning, 97(3), 147–155. https://doi.org/10.1016/j.landurbplan.2010.05.006
27. Oke, T. R. (1995). The Heat Island of the Urban Boundary Layer: Characteristics, causes and effects. In Springer eBooks (pp. 81–107). https://doi.org/10.1007/978-94-017-3686-2_5
28. Nuruzzaman, M. (2015). Urban Heat Island: Causes, Effects and mitigation measures - a review. International Journal of Environmental Monitoring and Analysis, 3(2), 67. https://doi.org/10.11648/j.ijema.20150302.15
29. Santamouris, M. (2014). On the energy impact of urban heat island and global warming on buildings. Energy and Buildings, 82, pp.100-113
30. Andersson, B., Place, W., Kammerud, R., & Scofield, M. P. (1985). The impact of building orientation on residential heating and cooling. Energy and Buildings, 8(3), 205–224. https://doi.org/10.1016/0378-7788(85)90005-2
31. Mahmoud, A. A. (2022). The influence of buildings proportions and orientations on energy demand for cooling in hot arid climate. SVU-International Journal of Engineering Sciences and Applications (Online), 3(1), 8–20. https://doi.org/10.21608/svusrc.2022.119125.1028
32. Pan, D., Chan, M. Y. J., Deng, S., & Lin, Z. (2012). The effects of external wall insulation thickness on annual cooling and heating energy uses under different climates. Applied Energy, 97, 313–318. https://doi.org/10.1016/j.apenergy.2011.12.009
33. Axaopoulos, I., Axaopoulos, P. J., & Gelegenis, J. (2014). Optimum insulation thickness for external walls on different orientations considering the speed and direction of the wind. Applied Energy, 117, 167–175. https://doi.org/10.1016/j.apenergy.2013.12.008
34. Fosas, D., Coley, D., Natarajan, S., Herrera, M., De Pando, M. F., & Ramallo-González, A. P. (2018). Mitigation versus adaptation: Does insulating dwellings increase overheating risk? Building and Environment, 143, 740–759. https://doi.org/10.1016/j.buildenv.2018.07.033
35. Santamouris, M. (2014). On the energy impact of urban heat island and global warming on buildings. Energy and Buildings, 82, pp.100-113
36. Yıldız, Y. and Arsan, Z. (2011). Identification of the building parameters that influence heating and cooling energy loads for apartment buildings in hot-humid climates. Energy, 36(7), pp.4287-4296
37. Baniassadi, A., Heusinger, J. and Sailor, D. (2018). Building energy savings potential of a hybrid roofing system involving high albedo, moisture retaining foam materials. Energy and Buildings, 169, pp.283-294.
38. van Hooff, T., Blocken, B., Timmermans, H. and Hensen, J. (2016). Analysis of the predicted effect of passive climate adaptation measures on energy demand for cooling and heating in a residential building. Energy, 94, pp.811-820.
39. Kontokosta, C. and Tull, C. (2017). A data-driven predictive model of city-scale energy use in buildings. Applied Energy, 197, pp.303-317.
40. Lü, X., Lu, T., Kibert, C. and Viljanen, M. (2015). Modeling and forecasting energy consumption for heterogeneous buildings using a physical–statistical approach. Applied Energy, 144, pp.261-275.
41. Bozdogan, H. (2004). Statistical data mining and knowledge discovery. Boca Raton, FL [etc.]: Chapman & Hall/CRC, p.233.
42. Kavgic, M., Mavrogianni, A., Mumovic, D., Summerfield, A., Stevanovic, Z. and Djurovic-Petrovic, M. (2010). A review of bottom-up building stock models for energy consumption in the residential sector. Building and Environment, 45(7), pp.1683-1697.
43. Halawa, E., & van Hoof, J. (2012). The adaptive approach to thermal comfort: A critical overview. Energy and Buildings, 51, 101–110. https://doi.org/10.1016/J.ENBUILD.2012.04.01113
44. Al Qadi, S Elnokaly, A. and Sodagar, B. (2019). The role of the benchmarking tools in increasing the collective awareness of energy consumption at the domestic sector, 2nd International Conference on Civil Engineering – Palestine, Engineers Association, Jersalem Center
45. Al Qadi, S., Sodagar, B. and Elnokaly, A. (2018). Estimating the heating energy consumption of the residential buildings in Hebron, Palestine. Journal of Cleaner Production, 196, pp.1292-1305
46. Timeanddate.com. (2018). Climate & Weather Averages in Hebron, West Bank, Palestinian Territories. [online] Available at: https://www.timeanddate.com/weather/palestine/hebron/climate [Accessed 5 Aug. 2018].
47. Fumo, N. and Rafe Biswas, M. (2015). Regression analysis for prediction of residential energy consumption. Renewable and Sustainable Energy Reviews, 47, pp.332-343

PLEA 2024 WROCŁAW
(Re)thinking Resilience

Improved Workflows for Environmental Building Certification
An investigation in Sweden

JI ONN TAN[1] JONAS GREMMELSPACHER[2] AGNIESZKA CZACHURA[1] LUIS RICARDO BERNARDO[1]

[1]Lund University, Energy and Building Design, Lund, Sweden
[2] Solenco AB, Malmö, Sweden

ABSTRACT: Environmental Building Certification (EBC) assessments, involving modelling, simulation, and grading calculation, are often time-consuming, prompting a need for streamlining. This investigation assesses existing Building Energy Modelling (BEM) workflows for Swedish context of EBC, focusing on extracting building geometry from Autodesk Revit with minimal information losses, and considering both low learning curve and automation. The methodology involves a comparative study, a review of BEM workflows and resources, and evaluation of strengths and weaknesses of the developed workflow. Results show that none of the analysed BEM tools fully meet the criteria of good Building Information Modelling to Building Energy Modelling (BIM-BEM) interoperability, compatibility for Swedish EBC, and high post-simulation automation. Challenges include thermal comfort assessments, limited alternatives for BEM tools in Swedish EBC assessments, and scarce reliable BIM-BEM interoperability approaches from Revit. The developed BEM workflow using Grasshopper for Rhinoceros demonstrates high potential but still not entirely unsuitable for Swedish EBC assessments.

KEYWORDS: Building Information Modelling (BIM), Building Energy Modelling (BEM), Interoperability, Scripting, Environmental Building Certification.

1. INTRODUCTION

The European Union has set an ambitious target to become the first climate-neutral continent by 2050 [1]. Sweden is aiming to achieve this goal by 2045 [2], with 23 Swedish cities committing to reaching climate neutrality by 2030 through binding agreements [3]. Despite these initiatives, buildings and the construction sector still account for 34% of global energy demand and 37% of CO2 emissions [4].

The ongoing energy crisis, influenced by global natural gas supply fluctuations, has strongly impacted electricity prices in Sweden and the northern electricity market Nordpool. Considering these challenges, sustainable building design that promotes efficient use of resources becomes imperative. In this context, Environmental Building Certifications (EBCs), commonly known as green building rating systems, play a crucial role as tools to evaluate the environmental performance of buildings.

EBCs such as *Miljöbyggnad*, *BREEAM-SE*, *LEED*, *NollCO2*, and *GreenBuilding* objectively assess a building's environmental performance based on specific criteria [5]. However, the assessment process involves time-consuming steps such as building modelling, simulation, credit calculation for grading, and report writing. Sustainability consultants conduct energy calculations in Building Energy Modelling (BEM) tools, often requiring information from Building Information Modelling (BIM) created by others. Poor interoperability between BIM and BEM poses challenges [6-9], with consultants having to recreate 3D geometry models, leading to time wastage and data loss. Moreover, not all available BEM tools align with Environmental Building Certifications assessments, and few are tailored to meet Swedish regulations.

Automating credit calculation for Environmental Building Certification assessments can streamline processes, enabling consultants to focus instead on design innovation and energy efficiency improvements. This study investigates existing workflows and further develops the most promising one.

2. METHOD

Several BEM tools (accessed date: prior May 2023), including *IDA ICE* [10], *ClimateStudio* [11], *Honeybee* (*Grasshopper*) [12], *IESVE* [13], *DesignBuilder* [14], and *TasEngineering* [15], underwent analysis based on three performance criteria: C1) BIM-BEM Interoperability; C2) Compatibility for Swedish Environmental Building Certifications; and C3) Post-Simulation Automation Feasibility (Figure 1).

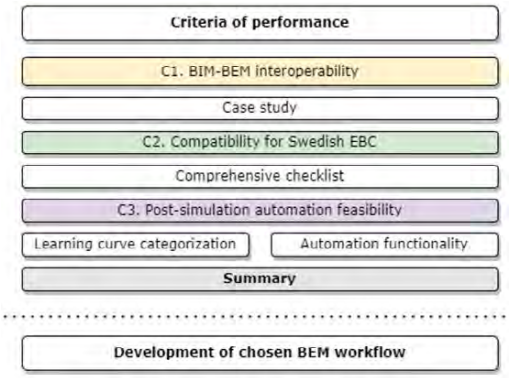

Figure 1: Illustration of the overall method

2.1 Performance Criteria

C1) BIM-BEM Interoperability:

As previous research shows [9, 16-19], many current BIM-BEM interoperability methods exhibit challenges in geometrical transformation consistency. In recent years, there is a novel BIM-BEM interoperability approach named *Pollination* which allow users to export energy and daylight analytical models using the architectural model (*Autodesk Revit*) into exchanged format including *gbXML*, *IESVE GEM*, *IDF*, *OSM*, *hbjson*, etc. Different from the automatic and semi-automatic *gbXML* (default *gbXML*), this tool enables the users to methodically visualize and validate the model floor by floor before exporting into the respective format.

A comparative study of the energy analytical model in both BIM (Figure 2) and BEM environments was conducted for *Honeybee* (*Grasshopper*), *IESVE*, *DesignBuilder*, and *TasEngineering* using a building case study. Qualitative evaluation encompassed the number of thermal zones, appearance of shadings, and external construction elements (e.g., walls, roofs, floors, and windows). *IDA ICE* and *ClimateStudio* were excluded from further investigation as they lacked exchangeable formats from *Pollination*.

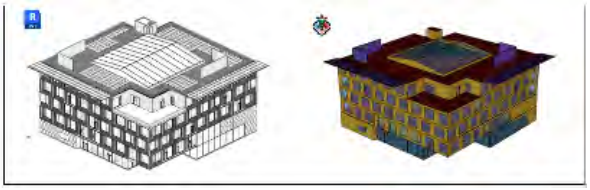

Figure 2: Revit model and Pollination export

C2) Compatibility for Swedish Environmental Building Certifications:

In this phase of the study, all selected Building Energy Modelling (BEM) tools were subjected to a thorough examination of their compatibility with the specific requirements outlined by Swedish Environmental Building Certifications, namely *Miljöbyggnad* and *BREEAM-SE*. The assessment aimed to ensure that each tool possesses the essential simulation characteristics and input-output capabilities necessary for a comprehensive evaluation under these certifications. These encompass simulation characteristics, including dynamic and multi-zone simulations, as well as an extensive array of input parameters. Ranging from user-input weather files to detailed specifications of external construction materials, such as thermal conductivity and thickness, the tool addresses considerations like external glazing materials, thermal bridges, and internal gains. This encompasses factors like appliances, lighting, occupancy density, and metabolic rates. Moreover, the BEM tool should adeptly manage elements related to domestic and service hot water, total air infiltration rates (air leakage), and ventilation systems, covering requirements, schedules, and control mechanisms. Additionally, integral specifications for heating and cooling systems, like Coefficient of Performance (COP) for heating and Energy Efficient Ratio (EER) for cooling, must be included. The tool also factors in thermal comfort considerations, such as air velocity, clothing levels, and specific details like design winter temperature. In terms of output capabilities, the BEM tool is designed to address annual energy consumption, encompassing heating, ventilation, comfort cooling, and domestic/service hot water energy. It also considers property electricity, including lighting, fans, pumps, and appliances. Notably, the BEM tool's proficiency in producing thermal comfort outputs, such as operative temperature at an arbitrary point and zone operative temperature, is crucial for conducting comprehensive assessments under certifications like *Miljöbyggnad*.

Computational fluid dynamics (CFD) in the context of buildings provides a deeper insight into air flow and heat transfer processes within and around building spaces. CFD workflows were excluded from this study as it is not a standard workflow for sustainability consultants in Sweden due to its labour intensive and time-consuming characteristics.

C3) Post-Simulation Automation Feasibility:

The functionality and learning curve of post-simulation automation for *Miljöbyggnad* and *BREEAM-SE* certifications were evaluated. The desired functionalities included simple arithmetic operations, conditional statements, simulation input and output retrieval, user input, and data export to Excel. Sub-criteria such as community support, documentation, tutorials, support teams, downloadable plug-ins, scripting templates, testing, and troubleshooting efficiency, built-in scripting, and visual scripting were considered to assess ease of development. *IDA ICE* is excluded from the study due to its pre-existing developer-made automatic calculation tool [20-21] for *Miljöbyggnad* and the Swedish Building Regulation (BBR) [22], hence, it is automatically assumed to feature high post-simulation automation feasibility.

The threshold boundary for categorizing a low learning curve is assumed to be at least 70% score of

"ease of development" (Table 2), while the threshold boundary for distinguishing between an intermediate learning curve and a steep learning curve is assumed to be 40%.

2.2 Developed BEM Workflow

After evaluation, one suitable BEM workflow was identified among the selected tools. This workflow was chosen for further development to improve and streamline the process for Environmental Building Certifications assessments.

3. RESULTS

3.1 Performance Criteria

C1) BIM-BEM Interoperability:

The *hbjson* file seamlessly integrated into *Honeybee* (*Grasshopper* for *Rhinoceros*), ensuring the accurate transfer of all 47 thermal zones, alongside external constructions like walls, floors, roofs, glazing areas, and shadings.

Similarly, the *gbXML* file smoothly imported into *DesignBuilder*, guaranteeing the transfer of all 47 thermal zones and accurately capturing external construction elements, including walls, floors, roofs, glazing areas, and shadings. This successful import was replicated in *IESVE* as well.

In contrast, the *gbXML* file faced challenges during import into *TasEngineering*, where the boundary condition of external walls was altered and registered as an external floor. Despite this anomaly, all 47 zones and other external construction elements, such as floors, roofs, glazing areas, and shadings, were correctly imported.

In summary, illustrated in Figure 3, *TasEngineering* faced challenges in accurately receiving the geometry file from the *Pollination* export. On the positive side, *Honeybee*, *DesignBuilder*, and *IESVE* seamlessly received their respective data exchange schemas without encountering any issues related to thermal zones, external construction elements, or shadings.

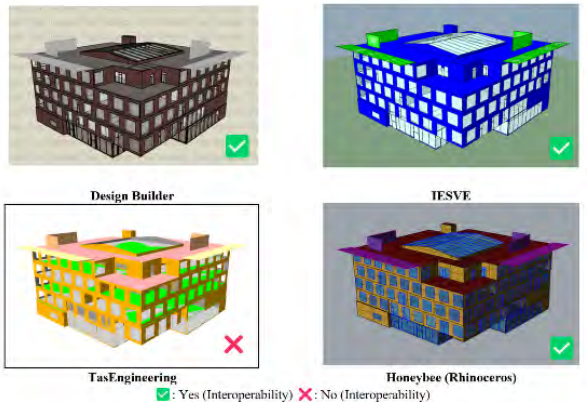

Figure 3: Analytical model visualization

C2) Compatibility for Swedish Environmental Building Certifications:

Table 1 illustrates a concise overview of the Environmental Building Certification (EBC) comprehensiveness assessment and compatibility of each Building Energy Modelling (BEM) tool with various simulations. The table outlines each tool's adherence to EBC requirements, building codes, and standards, as well as its suitability for different simulation types.

Table 1: Comprehensive checklist summary

		DesignBuilder	Honeybee	IESVE	ClimateStudio	IDA ICE	Tas Engineering
	Dynamic simulation	☑	☑	☑	☑	☑	☑
	Multizone simulation	☑	☑	☑	☑	☑	☑
Input	User-input climate file	☑	☑	☑	☑	☑	☑
	External construction opaque material	☑	☑	☑	☑	☑	☑
	External glazing material	☑	☑	☑	☑	☑	☑
	Thermal bridges	☑	◐	☑	☑	☑	☑
	Internal gain & schedule	☑	☑	☑	✗	☑	☑
	Service/domestic hot water	☑	☑	☑	✗	☑	☑
	Total infiltration rate (Leakage)	☑	☑	☑	☑	☑	☑
	Ventilation	☑	☑	☑	✗	☑	☑
	Heating and cooling	◐	◐	☑	✗	☑	☑
	Thermal comfort simulation (BREEAM)	☑	☑	☑	☑	☑	☑
	Thermal comfort simulation (Miljöbygnnad)	✗	✗	✗	✗	☑	✗
Output	Energy simulation	☑	☑	☑	✗	☑	☑
	Thermal comfort simulation (BREEAM)	☑	☑	☑	☑	☑	☑
	Thermal comfort simulation (Miljöbygnnad)	✗	✗	✗	✗	☑	✗
	Solar radiation	☑	☑	☑	☑	☑	☑
	Comprehensiveness	✗	✗	✗	✗	☑	✗

☑:Yes ✗: No ◐: Required workaround

DesignBuilder, in conjunction with *EnergyPlus*, excels in *HVAC* modelling but lacks the input capability for heating and cooling system distribution losses. Nevertheless, a workaround involves separately calculating distribution losses outside the simulation. *DesignBuilder* faces limitations in thermal comfort simulation, as it does not allow specifying the location and physical size of room heating units. Additionally, it cannot provide operative temperature output at an arbitrary room location.

Honeybee, utilizing the *EnergyPlus* simulation engine, lacks input capability for thermal bridging. However, users can manually calculate adjusted U-values considering thermal bridging effects. Like *DesignBuilder*, *Honeybee* lacks specific input capabilities for heating distribution losses, room heating unit location and size, and operative temperature output at an arbitrary location within a room. Customizability for HVAC systems is limited by default, but when combined with the plugin *Ironbug*, a component of *Ladybug Tools*, users can tailor the HVAC system according to *OpenStudio* HVAC options.

IESVE, with *ApacheSim*, excels in comprehensive construction specification input, detailed internal heat gain input, and in-depth HVAC modelling. However, it lacks input functionality for specifying the location and physical size of room heating units and operative temperature output at arbitrary locations without utilizing computational fluid dynamics (CFD) simulation.

IDA ICE, a Swedish Building Performance Simulation (BPS) tool, fulfils all simulation characteristics and input-output capabilities. It allows for easy entry of distribution losses for heating, cooling, and domestic hot water in one dialogue box, with additional input options through the *Miljöbyggnad* extension.

On the other hand, *ClimateStudio* offers basic HVAC schemes with limitations. Users cannot specify the type of heating or cooling system, and the heating system cannot distinguish between air systems and hydronic systems. It lacks input capability for heating distribution losses, domestic/service hot water distribution losses, and fan total efficiency. Due to limitations in setting HVAC schemes, *ClimateStudio* is not considered suitable for energy simulations in both *BREEAM-SE* and *Miljöbyggnad* assessments.

TasEngineering stands out with comprehensive HVAC modelling and the flexibility to create custom HVAC schemes. It allows input for thermal bridging data and efficiency parameters but lacks input and output capabilities for room heating unit location, size, and operative temperature at specific locations within a room.

C3) Post-Simulation Automation Feasibility:

DesignBuilder, incorporating EMS runtime scripting, C# Scripting, and Python Scripting, offers comprehensive HVAC modelling capabilities. Although it lacks detailed descriptions for Model Attributes in its database, users can view them directly from the interface. Troubleshooting script issues may pose a challenge as it requires running a simulation. *DesignBuilder*'s text-based scripting, while extensive, may be challenging for sustainability consultants lacking prior programming training.

Honeybee, within the *Grasshopper* interface, leverages scripting tools like GhPython and C#. As an open-source application with strong community support, it provides comprehensive documentation for simulation parameters. Users benefit from tutorials and documentation, and downloadable plug-ins like *TT-toolbox* enhance capabilities, allowing direct data export to Excel. Graphical input components enhance usability and prevent errors.

IESVE's Python scripting through its API, VEScripts, provides systematic documentation of simulation parameters, although lacking detailed parameter descriptions. The Content Store offers scripting packages, including those for extracting and exporting simulation results. It provides a variety of scripting templates, but like DesignBuilder, it employs text-based scripting.

ClimateStudio, hosted in the *Grasshopper* interface, utilizes GhPython and C#. While lacking open-source status, it offers the benefits of Grasshopper's interface, enabling visual scripting and downloadable plug-ins. However, it lacks community support, clear documentation for simulation parameters, and the ability to access source code.

TasEngineering supports various scripting languages and automation tasks. It provides capabilities for inputting simulation data from Excel, extracting results, and exporting data to Excel. Coding tutorials are available, but they focus on Tas3D specifically. Like *DesignBuilder* and *IESVE*, *TasEngineering* relies on text-based scripting.

Table 2: Functionality and ease of development

	DesignBuilder	Honeybee	IESVE	ClimateStudio	Tas Engineering
Functionality	☑	☑	☑	☑	☑
Community and forum	0	1	0	0	0
Documentation for simulation parameters	1	1	1	0	0
Tutorial on scripting	1	1	1	1	1
Support Team	1	1	1	1	1
Downloadable plug-in	1	1	1	1	0
Official scripting templates	1	1	1	1	0
Efficient testing and troubleshooting	0	1	1	1	1
Build-in scripting	1	1	1	1	0
Visual scripting	0	1	0	1	0
Ease of development score (%)	67%	100%	78%	78%	33%

As shown in Table 2, all investigated BEM tools meet the required functionality for post-simulation automation. In terms of ease of development, *Honeybee*, *ClimateStudio*, and *IESVE* score above 70%, indicating a low learning curve. *DesignBuilder*'s scripting tool falls into the intermediate learning curve category, while *TasEngineering*'s approach is deemed steep.

3.2 Developed BEM workflow

None of the evaluated BEM tools (Figure 5) managed to meet all three performance criteria—good BIM-BEM interoperability, complete compatibility for Swedish EBC, and high post-simulation automation feasibility. However, excluding thermal comfort assessment for *Miljöbyggnad*, both *Honeybee* and *IESVE* display significant potential for the development of a streamlined BEM workflow. Ultimately, the Honeybee workflow was chosen for further development due to its superior post-simulation feasibility compared to *IESVE*. Additionally,

the shared origin of *Pollination* and *Honeybee* under *Ladybug Tools* ensures a high level of cohesiveness between the extracted building geometry and simulations.

The streamlined *Honeybee* workflow incorporates multiple plug-ins, including *Pollination*, *Ironbug*, *Ghpython*, and *TT-toolbox*. Figures 4 illustrates this streamlined energy simulation workflow.

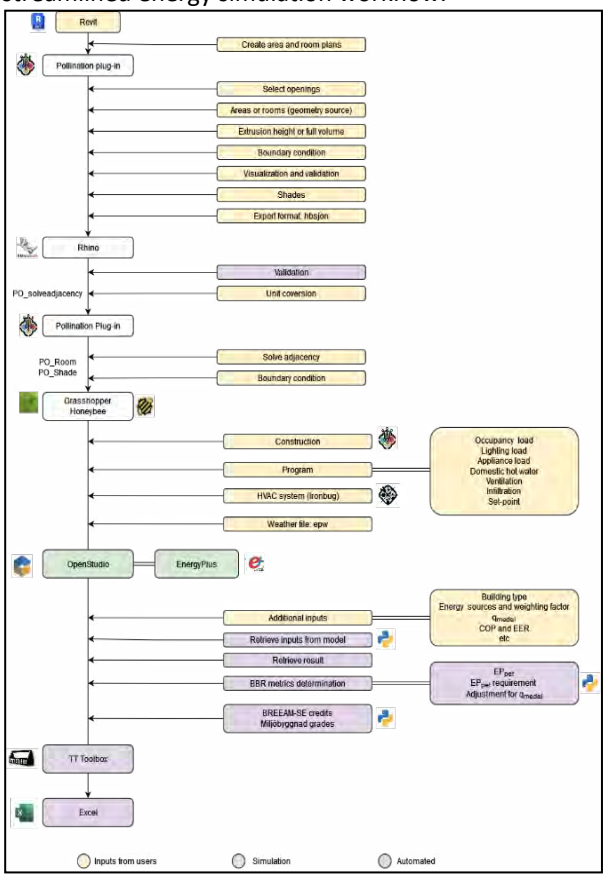

Figure 4: Developed workflow (Honeybee)

4. DISCUSSION

A notable observation arises regarding the limited availability of tools specifically designed for compliance with Swedish building codes. Out of the six tools analysed, only *IDA ICE* originates from Sweden and therefore emerges as the sole option tailored for Swedish Building Code compliance. A similar observation applies to the analysis of BIM-BEM interoperability approaches. The selected tools lack reliable interoperability options. Previous studies have shown inconsistencies with default *IFC* and *gbXML* formats during the BIM to BEM translation.

Architectural models and energy analytical models inherently differ, requiring processing to transform the former into the latter. The creation of energy analytical models typically involves some level of manual intervention, posing challenges for fully automatic or semi-automatic approaches.

In the BIM-BEM interoperability study, *DesignBuilder*, *Honeybee*, and *IESVE* demonstrated compatibility with *Revit Pollination*. *TasEngineering* encountered issues with correctly receiving the *gbXML* export through Pollination. *IDA ICE* and *ClimateStudio* showed limitations in reliable BIM-BEM interoperability approaches.

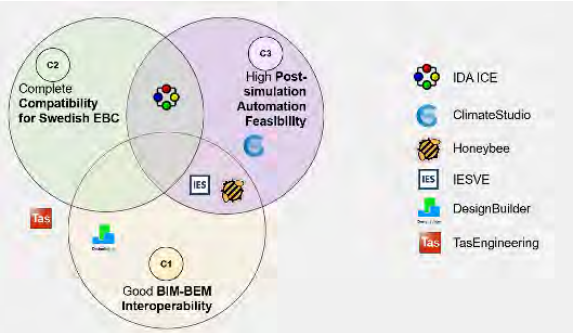

Figure 5: Summary of performance criteria

From the compatibility for Swedish EBC study, *IDA ICE* fulfils all necessary requirements. *DesignBuilder*, *Honeybee*, *IESVE*, and *TasEngineering* lack the ability to accommodate inputs for room heating unit location and physical size and lack capability for thermal comfort metrics without CFD. *ClimateStudio* falls short in HVAC modelling.

Achieving *Miljöbyggnad* thermal comfort assessment may be challenging without CFD simulations in alternatives to *IDA ICE*. *DesignBuilder*, *Honeybee*, *ClimateStudio*, and *IESVE* follow assumptions unsuitable for such assessments. *IDA ICE*'s *Miljöbyggnad* extension enables input of radiator details and person placement for thermal comfort.

Regarding post-simulation automation feasibility, *IDA ICE* offers developer made Swedish EBC calculation tools. *Honeybee*, *IESVE*, and *ClimateStudio* have a low learning curve, suitable for users for automating tasks. *DesignBuilder* has an intermediate curve, while *TasEngineering* requires a steeper learning curve.

This study did not exhaustively cover all BEM tools and BIM-BEM interoperability approaches worldwide. Future research could expand the analysis, incorporating user testing for learning curve analysis and evaluating Pollination's interoperability with complex façade shapes. Comparative studies on input and simulation times for different BEM workflows and exploration of EBC schemes beyond Swedish standards are potential avenues for future research.

Lastly, it's crucial to note that since the studies were conducted before May 2023, the conclusions of this study may need to be updated due to the rapid evolution of software.

5. CONCLUSION

Conducting environmental building certification (EBC) assessments poses significant challenges, primarily due to poor interoperability between Building Information Modelling (BIM) and Building Energy Modelling (BEM) tools. Sustainability

consultants often face time-consuming tasks recreating 3D energy models, and while some tools offer good BIM-BEM interoperability, they often lack the necessary detail for accurate thermal performance evaluation. Post-simulation tasks, compounded by the complexity of assessments and buildings, are prone to errors and labour-intensive efforts. This study identified and further developed a BEM workflow that extracts *Revit* building geometry with minimal losses, provides adequate detail for Swedish EBC assessments, and offers a low learning curve for automation development.

In essence, no single BEM tool met all three performance criteria: good BIM-BEM interoperability, complete compatibility for Swedish EBC, and high post-simulation automation feasibility. *IDA ICE* excels in Swedish EBC assessments and provides developer-made automation tools but falls short in BIM-BEM interoperability. *IESVE* and *Honeybee* show potential in importing *Revit* geometry with low learning curve for automation but lack complete Swedish EBC compatibility without a CFD workflow. *DesignBuilder* excels in BIM-BEM interoperability, *ClimateStudio* in post-simulation automation, while *TasEngineering* falls short in all criteria.

This study highlights a scarcity of BEM tools designed for Swedish EBC compliance and reliable BIM-BEM interoperability from *Revit* in the current market. No *IDA ICE* alternative fully meets the input and output requirements for Swedish EBC, emphasizing the challenge of conducting thermal comfort simulations for *Miljöbyggnad* assessments. The *Revit Pollination* plug-in proves valuable for achieving good BIM-BEM interoperability by enabling users to refine and validate the analytic model before export. The developed *Honeybee* workflow, incorporating multiple plug-ins, demonstrates significant efficiency but is still not fully suitable for Swedish EBC assessments.

REFERENCES

1. European Commission (2019, December 11). The European Green Deal. Retrieved from https://ec.europa.eu/info/sites/default/files/european-green-deal-communication_en.pdf.
2. The Ministry of Infrastructure. (2020). Sweden's Integrated National Energy and Climate Plan. Government of Sweden. Retrieved from https://energy.ec.europa.eu/system/files/2020-03/se_final_necp_main_en_0.pdf.
3. Viable Cities (2021, December 8). Climate-neutral cities 2030. Retrieved from Viable Cities: https://en.viablecities.se/klimatneutrala-stader-2030.
4. United Nations Environmental Programme, "2021 GLOBAL STATUS REPORT FOR BUILDINGS AND CONSTRUCTION" 2021. [Online]. Available: www.globalabc.org.4. International Daylight Monitoring Programme, [Online], Available: http://idmp.entpe.fr/ [16 June 2008].
5. Certifiering – Sweden Green Building Council, [Online], Available: https://www.sgbc.se/certifiering/
6. Gerrish T, Ruikar K, Cook M, Johnson M, Phillip M (2017, March 20). Using BIM capabilities to improve existing building energy modelling practices.
7. Hijazi M, Kensek K, Konis K (2015). Bridging the gap: Supporting data transparency from BIM to BEM.
8. Sanhudo L, Ramos NMM, Poças Martins J, Almeida RMSF, Barreira E, Simões ML, et al (2018, June). Building information modeling for energy retrofitting – A review. Renewable and Sustainable Energy Reviews, 89: p. 249-260
9. Porsani GB, de Lersundi KDV, Gutiérrez ASO, Bandera CF (2021, March). Interoperability between Building Information Modelling (BIM) and Building Energy Model (BEM). Applied Sciences, 2021, 2167.
10. IDA ICE, [Online], Available: https://www.equa.se/en/ida-ice
11. ClimateStudio — Solemma, [Online]. Available: https://www.solemma.com/climatestudio
12. Ladybug Tools | Honeybee, [Online], Available: https://www.ladybug.tools/honeybee.html
13. IES Virtual Environment , [Online], Available: https://www.iesve.com/software/virtual-environment
14. DesignBuilder Software Ltd, [Online], Available: https://designbuilder.co.uk/software/product-overview
15. Tas Engineering – EDSL, [Online]. Available: https://www.edsl.net/tas-engineering/
16. Farzaneh A, Monfet D, Forgues D (2019, May). Review of using Building Information Modeling for building energy modeling during the design process. Journal of Building Engineering, 23: p. 127–135.
17. Gourlis G, Kovacic I (2017, February). Building Information Modelling for analysis of energy efficient industrial buildings – A case study. Renewable and Sustainable Energy Reviews, 68: p. 953–963.
18. Bracht, M.K., Melo, A.P., & Lamberts, R. (2021). A metamodel for building information modeling-building energy modeling integration in early design stage. Automation in Construction, 121, 103422.
19. Kovacic, Iva & oberwinter, lars & müller, christoph & Achammer, Christoph (2013). The "BIM-sustain" experiment - simulation of BIM-supported multi-disciplinary design". Visualization in Engineering. 40327. 10.1186/2213-7459-1-13.
20. EQUA Simulation AB (2022). Guide – Anpassning Sverige
21. EQUA Simulation AB (2022). Guide – Miljöbyggnad i IDA ICE
22. Boverket´s mandatory provisions and general recommendations, BBR, BFS 2011:6 with amendments up to BFS 2018:4.

PLEA 2024 WROCŁAW
(Re)thinking Resilience

Photobiological Parameter Evaluation:
Work environment simulation impacted by obstructed daylight

RODRIGO GALON[1] LEONARDO MARQUES MONTEIRO[1]

[1]University of Sao Paulo, Sao Paulo, Brazil

ABSTRACT: Shading due to proximity between buildings can reduce or compromise the quality of natural lighting in work environments and, consequently, impact the quality of lighting throughout the day. The objective of the research is to evaluate the photobiological parameter equivalent melanopic lux (EML) in prolonged daytime work environments, shaded by adjacent buildings. The methodology of this study foresees: simulations of the work environment and the possible impact of shading from adjacent buildings on the level of EML; and environment simulations with Integrative Lighting guidelines. Through gradual simulations, the aim is to verify the possibility of reestablishing minimum EML levels through compensatory electrical lighting configurations for a healthy photobiological day for individuals in this environment. The research foresees as a concrete object of study a working environment with prolonged stay during the day. In relation to simulations, the research will provide verification of the impact of shading on the quality of environments in terms of Lighting for a healthy photobiological day and proposing a methodology for compensating obstructed natural lighting. The research aims therefore to contribute to the current debates on sustainability and resilience in cities, regarding daylight and electric lighting solutions for healthier environments.
KEYWORDS: Lighting, EML, Obstruction, Well-being

1. INTRODUCTION

This research focuses on evaluating the lighting of work environments daylights impacted by the shading of adjacent buildings, regarding the photobiological well-being of the occupants possibly caused to the occupants of these environments, what may lead to a decrease in quality of life and consequent decrease of productivity. Even with luminous parameters according to the regulation standards dealing with technical lighting, there can be harmful light configurations to the physiological and psychological well-being. The objective is to evaluate the photobiological parameter *Equivalent Melanopic Lux* (EML) in environments of prolonged daytime work, shaded by adjacent buildings. The methodology of this study provides: simulations of the work environment and the possible impact of shading from adjacent buildings on the EML level; and simulations of the environment with Integrative Lighting guidelines. Through gradual simulations, the aim is to verify the possibility of restoration of minimum EML levels through electrical lighting settings compensation for a healthy photobiological day for the occupants and resiliently adapt and maintain or regain functionality after a daylight interruption. The concrete object of study is a work environment of prolonged stay in daytime.

2. LITERATURE REVIEW

2.1 Light and non-visual perception

On the relevant physiological issue for this study, we highlight the spectral neurophysiological sensitivity of the human Circadian System, with the discovery of a new class of photoreceptors known as intrinsically photosensitive retinal ganglion cells (ipRGCs), sensitive to the blue portion of the visible spectrum that directly impacts the suppression of melatonin produced in the pineal gland [1], with consequent synchronization of daily physiological rhythms with the light/dark cycle.

The human photobiological system is considered as a planning basis for the lighting system, imprinting itself on the development of projects such as, for example, those carried out with Human Centric Lighting (HCL) practices [2]. Currently, Integrative Lighting is defined by the CIE (International Commission on Illumination) as grounded lighting in the study of interactions between the human neurophysiological system and the psychic apparatus to the stimulus of light.

2.2 Equivalent Melanopic Lux and WELL

For scientific research investigating "light and health", we can make use of metrics consolidated by International WELL Building Institute, which uses the *Equivalent Melanopic Lux* (EML) as a measurement unit. The biological effects of light in humans can be measured in EML, and this proposed alternative metric is weighted for the ipRGCs and not for the cones, as is the case with conventional lux [3]. Regarding lighting, natural light is placed as the protagonist and main agent for improving the quality

of the environment, mainly due to its full spectrum and variance throughout the day, and electric lighting is its complement to the integrative project.

The EML depends on the intensity of the photopic light stimulus in lux, and the spectral power density of the light at the measurement point (user height). Given a spectrum of light, each of the five equivalent α-opic illuminances are related each other in a proportion called Melanopic Ratio (R), where for each unit of measurement (Eα), the rhodopic illuminance values are calculated, melanopic, cyanopic, chloropic and erytropic, according to the equation (1). For a specific spectrum, the equivalent "α-opical" Lux for each of the five photoreceptors in the eye (three cones, rods and the ipRGCs) is derived.

$$E_{\alpha} = 72\,983.25 \int E_{e\lambda}(\lambda)\, N_{\alpha}(\lambda)\, d\lambda \qquad (1)$$

The EML metric is the result of the product of photopic illuminance (E) and melanopic proportion (R), according to the equation (2):

$$EML = (E) \times (R) \qquad (2)$$

Where *EML* – Equivalent Melanopic Lux
E – photopic illuminance (Lux)
R – melanopic ratio

2.2 Access to the Sun

However, given the increase in the level of obstruction of natural light due to the proximity between buildings resulting from real estate densification, or other possible causes of obstruction or enclosure situations caused by density in urban cities, there may be a decrease or impairment of the urban environmental quality itself [4]. The greater the density of the urban built space, the less exposure to daylight and views to nature will typically occur.

In these cases, as access to sky lighting and insolation will be through the spaces between buildings, we can verify the possibility of compensation for electric lighting in the absence of natural light, through Integrative Lighting guidelines, thus offering the ideal light composition for a healthier photobiological day.

Daylight and view versus solar and glare control pose a challenge when trying to prioritize health and well-being as a fundamental human requirement, thus possibly affecting variations in energy efficiency of buildings [6].

Access to the sun is not replaceable: we are exposed to natural light sources like solar energy since the beginning of human existence, but we have been exposed to electric lighting for a few centuries only, and to LED sources, specifically, for few decades. Even with the consolidation of LED as a light source and its wide usability, electric lighting is unable to reproduce the high variability of natural sunlight nor its benefits.

3. METHODOLOGY

The method is analytical, through computational simulation of the concrete object of study: daytime office type work environment. For this, a hypothetical work environment was modelled (Figure 1) in the Rhinoceros® 3D 7 software, with the dimensions: length 8.0m; width 6.0m, ceiling height 3.00m. The environment has a glazing opening facing the south façade, with dimensions: length 4.50m; height 1.50m; guardrail height 1.00m.

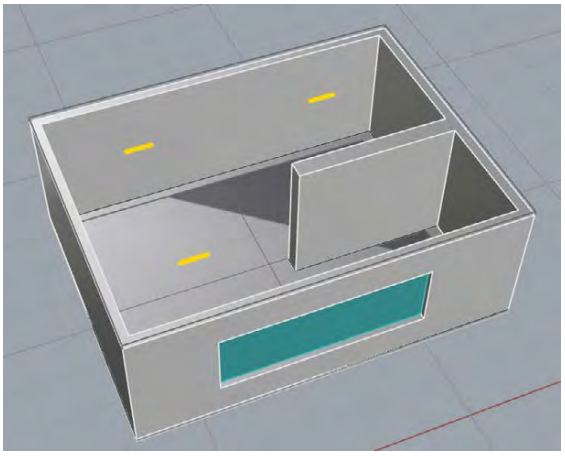

Figure 1: office environment 3D model.

The WELL feature L03 characteristic certification is adopted for this research, and the minimum level EML 275, as well as other guidelines, are contained in this feature. For the simulation, the ALFA (Adaptive Lighting For Alertness) Solemma® software was chosen because it returns the EML as well the photopic Lux levels calculations directly through the simulation, by incorporating the spectral characteristics of both the light sources and the materials and return better fidelity of simulation results for evaluating non-visual effects by vertical illuminances [5], installed as a plugin in the modelling software of Rhinoceros® 3D 7.

The inputs for the simulation in ALFA include:

- Modelled object;
- Location set to: São Paulo (coordinates -23.55 °N; -46.64 °E; 769m elevation sea level);
- Sky condition set to: CLEAR;
- Environment materials (Table 1);
- Electric light source: linear luminaire (2450 lumens) with diffuse lens applied to the ceiling with respective IES photometric (Figure 2) specifications and SPD - spectral power distribution (Figure 3);
- EML reference level set to 275 (according to WELL).

The calculation grid planes were configured with 1.25m spacing between calculation planes, in 6 directions of the observer's view each one, with heights of 1.20m for the offset view plane and 0.75m for the offset work plane.

Element	Material	Especularity
WALLS	white painted	0.40%
FLOOR	light brown wooden	2.00%
CEILING	white painted	0.40%
OBSTRUCTION	grey painted	1.50%
Element	**Material**	**Transmitance**
GLAZING	single plane clear 6mm	tvis = 88% SGHC= 0,82

Table 1: characteristics of the materials used in the model.

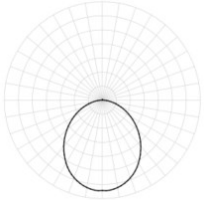

Figure 2: Luminaire photometric distribution curve.

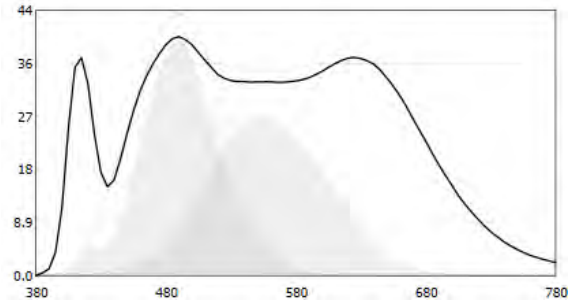

Figure 3: spectral curve of the SPD light source (LED 1.00).

The simulation scenario is completed with the definition of the calculation plans to be evaluated in the simulations, so that they are representative of a supposed layout in which 4 tables are positioned with 2 interlocutors facing each other, forming 8 calculation points (Figure 4).

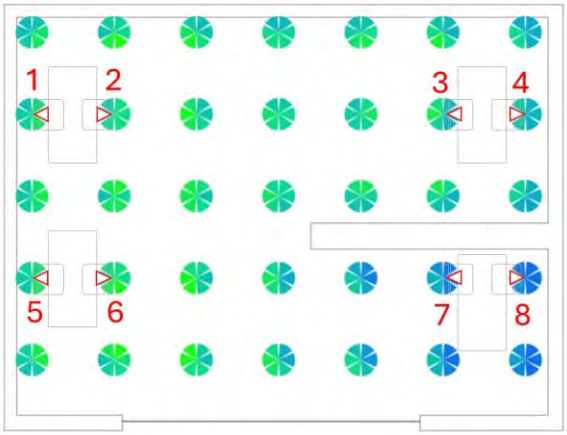

Figure 4: The 8 grid calculation points, according to hypothetical interlocutors facing each other.

4. Results Analysis and Discussion

The methodology was developed in two moments, presenting the following results: In the first battery of simulations for the modelled environment, gradual configurations of obstructions by figurative barriers that simulate buildings adjacent to the simulated environment must be simulated, until the EML levels are below the defined by WELL guidelines for this research. These figurative barriers represent situations where the urban constructive densification can form around the object of study, when, for example, the minimum distance designated by law at the edge of the land is not respected.

The first shot of simulations has realized the influence of natural light with the distribution of higher EML levels at points close to the window Figure (5).

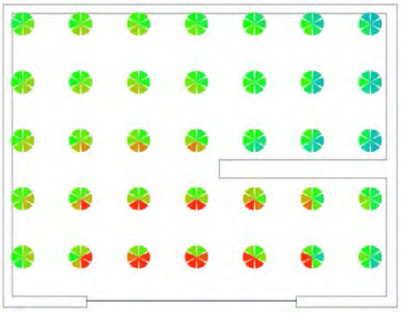

Figure 5: higher EML levels at the points close to the window, with no barriers.

After 3 steps of gradual increase obstruction, EML levels drop drastically, approaching zero at some calculation points. These gradual obstruction configurations were:

- A – a 10,00 meters high frontal barrier, positioned 1,50m away from de window facade;
- B – a 20,00 meters high frontal barrier, positioned 1,50m away from de window façade;
- C – 3 20,00 meters high barriers, positioned 1,50m away from de window façade, and two lateral façades (Figure 6).

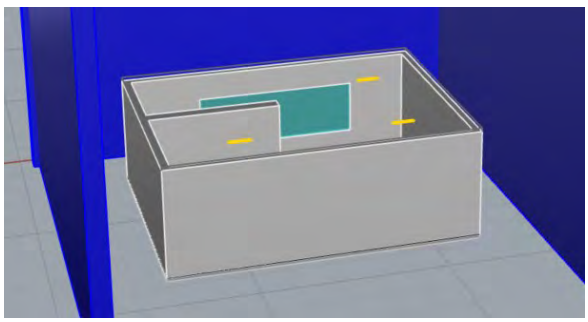

Figure 6: The C configuration with three barriers involving three facades of the study object.

It was observed that the increase in height tested between configurations A and B does not influence the drop in EML levels as much as configuration C, which involves the object of study through the south facade and side facades, reducing the possibility of non-frontal natural light entering, making this the simulation with critical configuration (Figure 7), in relation to the EML level, to be the starting point for the second moment of this methodology.

For this second moment of the methodology, it was necessary to establish the period of the year and the period of the day in which the next simulations would take place with an increase in electrical lighting using LED luminaires. The winter solstice was adopted as the appropriate date because it is the period with the lowest solar incidence in the southern hemisphere, June 21st. The time of day for the simulations was adopted with reference to WELL requirement L03, which establishes that level 275 EML must be reached in at least 4 hours per day, starting by noon. It was then necessary to simulate the hourly bands of June 21st to visualize this panorama of variation in the EML level throughout the day (Table 2).

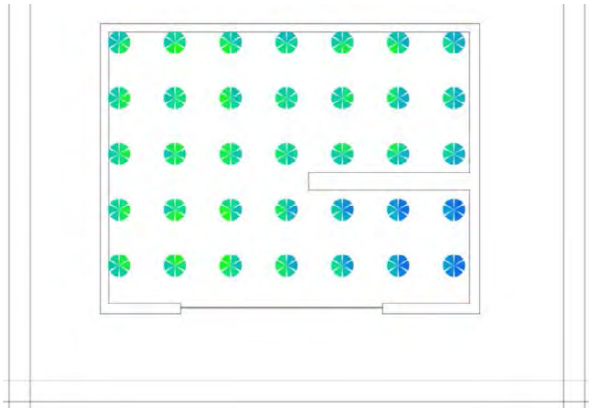

Figure 7: Enclosure in three façades, EML levels drop drastically reaching close to zero in some points.

According to Table 2, we perceive the critical hour with EML levels below 275 at 16:00, with the average EML (Melanopic Lux) result of 167, with only 3.3% of calculation points above 275 (Figure 8).

	EML levels								
1	220	249	318	534	631	602	343	262	**218**
2	149	172	214	362	448	386	229	162	**138**
3	91	97	108	156	165	147	112	98	**95**
4	168	183	203	284	319	277	211	182	**170**
5	229	296	369	781	944	880	487	312	**244**
6	154	205	245	399	535	490	280	188	**153**
7	70	118	211	473	566	462	197	130	**79**
8	115	195	346	817	944	789	291	192	**132**
	08:00	*09:00*	*10:00*	*11:00*	*12:00*	*13:00*	*14:00*	*15:00*	*16:00*

Table 2: EML levels at 8 grid calculation points along the day 21st june hour by hour.

The time 16:00 was defined as the point to start the increments of LED technology light luminaires, since reestablishing the minimum EML levels for this time, will consequently imply minimum levels reached for the other times.

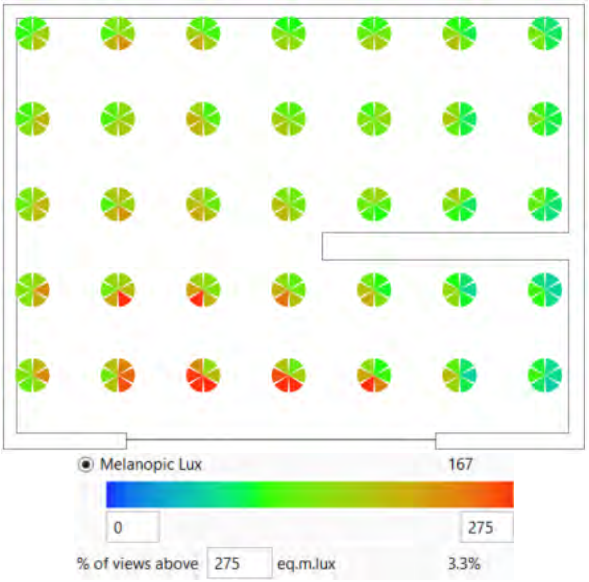

Figure 8: the simulated configuration with 3 luminaires returns only 3.3% of calculation points with EML levels above 275.

The first simulation with the modelling of the critical time regarding the EML level, were tested with an increment of a 2x3 grid luminaires (Figure 9) in the place of the three luminaires original concept.

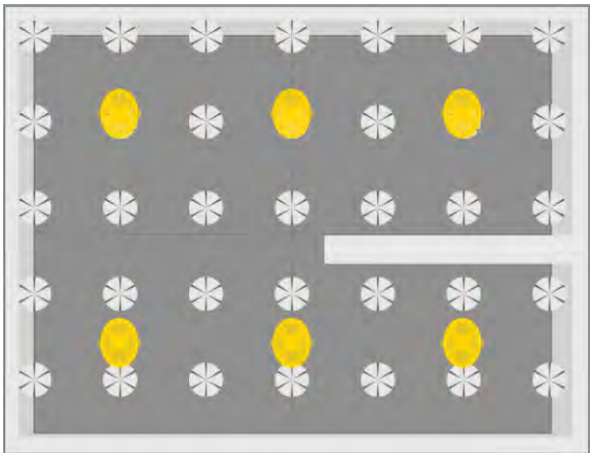

Figure 9: luminaires grid configuration 2x3.

An increase in EML levels above 275 can be seen between the result of the simulation with just 3 luminaires (Figure 8) and the result of this first increase (Figure 10), with 38.1% of calculation points above 275.

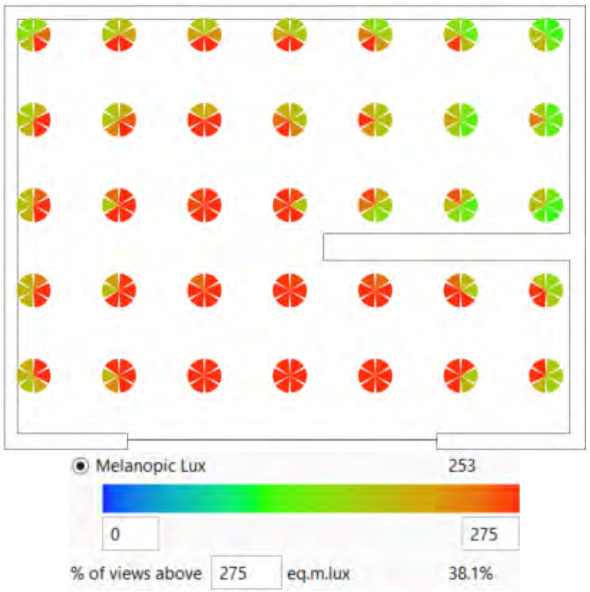

Figure 10: The simulated configuration with a 2x3 luminaires grid returns 38.1% of calculation points with EML levels above 275.

The second simulation with the modelling of the critical time regarding the EML level, were tested with an increment of a 4x3 grid luminaires (Figure 11) in the place of the previous grid.

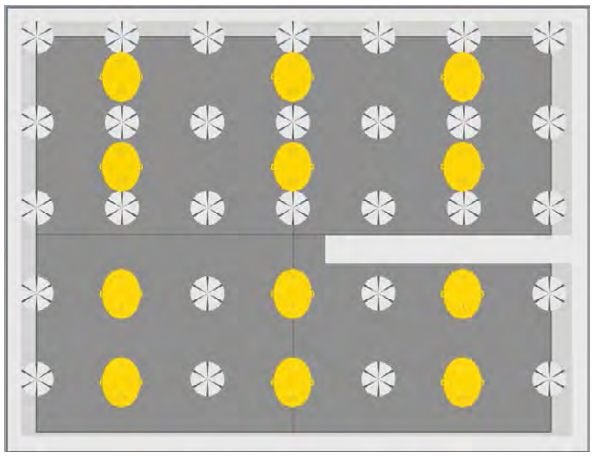

Figure 11: luminaires grid configuration 4x3.

In this last simulation, we can see the scope of the increase in the grid of 4x3 luminaires (Figure 12) with 92.2% of the calculation points above 275.

The comparison (Table 3) with the original configuration and the compensated electric lighting configurations for EML (melanopic lux) and for the respective conventional lux (photopic lux) of the 8 points calculated shows the methodology effectiveness.

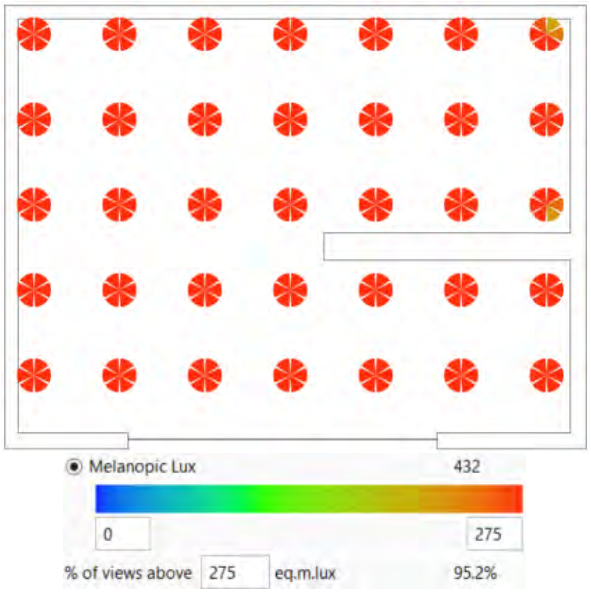

Figure 12 The simulated configuration with a 4x3 luminaires grid returns 95.2% of calculation points with EML levels above 275.

It is important to mention that standards dealing with illuminance only consider visual issues, do not consider non-visual effects of light in human physiology, and illuminance alone does not guarantee quality of lighting. While the illuminance level in the horizontal plane (lux) deals quantitatively with the intensity of lighting on the work plane, the EML deals with a qualitative issue of illuminance in the vertical plane, depending fundamentally on the SPD of the light source.

	EML	Lux	EML	Lux	EML	Lux
1	218	240	306	340	535	596
2	138	161	201	235	349	409
3	95	114	147	175	272	325
4	170	191	248	280	452	510
5	244	264	329	361	574	633
6	153	177	218	253	369	431
7	79	91	199	231	324	379
8	132	145	309	341	503	558
	original		*2x3*		*4x3*	

Table 3: evolution of the increase in EML level, and comparison of EML (melanopic lux) and conventional lux levels.

In the second battery of simulations for the modelled environment, gradual luminaires distribution configurations were simulated until the minimum EML levels are reached validating the hypothesis of possible restoration of EML levels with the compensation of electric lighting for the environment studied in the situation of critical obstruction barriers.

The amount of light is often related only to carrying out tasks. However, quantity and quality of light can be associated in the project, even in the case of projects in which meeting quantitative recommendations is the main objective, since, depending on the task performed, the level of lighting becomes a normative requirement.

5. CONCLUSIONS

The process of this research highlights the fact that the evaluation of environments by melanopic metric or by circadian stimulus in the design process is still under development. Even with the manifestation of the CIE in proposing a standard metric for melanopic lux, to be adopted by the International System of measurements, there is no approval for such metrics so far.

The knowledge we currently have about ways to measure specificities of non-visual light stimuli due to their spectral distribution is initial. We do not know if there are other interactions between different wavelengths of light with neurophysiological, psychological, or behavioural aspects, to the point of definitively depositing in the supposed compensation with electric light the solution to the problem of natural light obstruction in work environments.

In addition to the qualitative characteristics of lighting and considering sustainable design, the successive increase of luminaires to compensate EML levels with electric lighting also highlights the energy impact that urban density indirectly causes on the environment and the importance of preserving the daylighting for a sustainable design in built spaces.

An environment with greater autonomy in relation to electric lighting can be considered more resilient, as it offers adequate conditions of use even under circumstances in which there is no adequate energy supply. In terms of "sustainability", the reduced dependence on electrical energy also points to a more sustainable lighting solution.

The ability to adapt the built space to environmental changing conditions through electric compensation (like restoring healthier EML levels after some daylight interruption) does not eliminate the value of using natural resources wherever and whenever possible.

We think that, given the current scenario of urban densification, it becomes important to combine lighting, well-being and circadian hygiene in contemporary architectural projects and research.

It is necessary to continue to advance research in neurophysiology and neuropsychology to understand stimuli and responses still unknown. Thus, research based on consolidated concepts and available tools contribute to fostering the improvement of simulation methodologies and tools.

ACKNOWLEDGEMENTS

I am extremely grateful so far, to my academic advisor and my partner for their guidance, and to Solemma for the availability of the ALFA software student license.

REFERENCES

1. LUCAS, R., PEIRSON, S., BERSON, D., BROWN, T., COOPER, H., CZEISLER, C., FIGUEIRO, M., GAMLIN, P., LOCKLEY, S., O'HAGAN, J., PRICE, L., PROVENCIO, I., SKENE, D., BRAINARD, G. Measuring and using light in the melanopsin age. Trends in Neurosciences. 37. 2013.

2. HOUSER K.W.a and ESPOSITO T. Human-Centric Lighting: Foundational Considerations and a Five-Step Design Process. Front. Neurol. 12:630553. 2021. doi: 10.3389/fneur.2021.630553.

3. WELL Building Standard, LIGHT. Feature L03 circadian lighting design. https://v2.wellcertified.com/en/wellv2/light/feature/3. (acessed: 15 july, 2023).

4. MELLO, M. R. de A. F. Adensamento Construído e o Desempenho Térmico e Luminoso das Edificações: *A relação entre Orientação, Obstrução e Área Envidraçada*. Tese de Doutorado – Faculdade de Arquitetura e Urbanismo da Universidade de São Paulo – São Paulo SP, 2020.

5. BELLIA L., BŁASZCZAK U., DIGLIO F., e FRAGLIASSO F. Assessment of melanopsin-based quantities: Comparison of selected design tools and validation against on-field measurements, Building and Environment, vol. 232, pp. 1–15, 2023, doi: 10.1016/j.buildenv.110037.

6. LEE, Eleanor S.; MATUSIAK, Barbara Szybinska; GEISLER-MORODER, David; SELKOWITZ, Stephen E., HESCHONG, Lisa. Advocating for view and daylight in buildings: Next steps, Energy and Buildings, Volume 265, 2022, 112079, ISSN 0378-7788, https://doi.org/10.1016/j.enbuild.2022.112079.

PLEA 2024 WROCŁAW
(Re)thinking Resilience

Procedure for Assessing Urban Glare on Building Façades

Analysis and methods for resilience and sustainability

RAQUEL SANCHES

PhD, Postgraduation in Architecture and Urbanism, University of São Paulo (FAUUSP), São Paulo, Brazil

ABSTRACT: The complexity of lighting studies necessitates the evaluation of lighting levels and spatial quality to ensure user comfort. Architects demonstrate a commitment to designing environments that prioritize internal visual performance, integration with the external surroundings and energy efficiency. However, there is a neglect of the urban context in relation to internal performance expectations. Buildings are conceived using glazed or reflective and emissive surfaces that redirect visible and thermal incident radiation back to the city, thereby reducing internal heat gains. Daylight radiation at high intensity causes glare phenomena, which refers to visual discomfort experienced by pedestrians and has an impact on the local microclimate by increasing the surrounding temperature. It is understood that the urban environmental quality can be ensured through an assessment and classification procedure that considers the probability of glare occurrence during the project design, specifically focusing on façade performance. The rating scale will be built based from the results of parametric ray-tracing simulations involving different geometric shapes and façade surfaces, resulting in heat maps. The final evaluation will be by mean of a combined classification approach, taking into account the probability of glare occurrence as determined by the geometric shape and surface materiality of the building envelope.
KEYWORDS: daylighting, glare, urban, building evaluation, microclimate

1. INTRODUCTION

As a representation of modern and corporate architecture, in the city of São Paulo in the early 1970s, on Brigadeiro Faria Lima avenue and later on Eng. Luís Carlos Berrini avenue, the appearance of tall buildings made up of glass façades without any type of solar protection was observed. An architectural style that has been reproduced to this day, it has benefits in countries with temperate climates as it contributes to greater permeability of natural light, visible sky, heat insulation and optimizes the artificial conditioning system (10). However, in cities with tropical climates, glass curtain walls without solar protection have implications such as excess light in the areas perimeter to the façades, which results in the use of internal solar protection and an increase in the thermal load due to the use of artificial lighting and air conditioning systems to achieve internal comfort.

However, in order to reduce the impact of heat gain and excess light, glass façades have become envelopes made up of surfaces with high solar reflection indices. Envelopes with a high external reflection index have a high capacity to return thermal radiation (long waves) to the urban environment and consequently lower the temperature of the building envelope (15).

The benefits to individuals of the presence of natural light and visibility to the external environment have been confirmed by studies that show lower rates of insomnia and depression, as well as greater productivity and better receptivity to high levels of luminosity due to visual accommodation (1); (9).

However, the condition of the internal environment cannot override the comfort of users in the urban context, because reflective envelopes also cause the reflection of short waves, or visible radiation, which at high intensity leads to the occurrence of glare.

The phenomenon of glare is given by the difficulty of visual accommodation to extreme conditions of light or brightness, causing momentary blindness, distraction or visual annoyance. IESNA(6). Glare can be perceived by people in urban environments from the direct and indirect reflection of sunlight that impacts the building envelope, affecting pedestrians on sidewalks, occupants of neighboring buildings and drivers. The damage to visual capacity can be so intense that the distinction between objects and people is compromised by a "veil of illuminance" that strips scene of contrast, known as disabling glare.

In addition to the high specularity of the envelope surfaces, which has an impact on the intensity of sunlight reflection, architectural geometry, such as convex and concave shapes, directs the reflection of the sun's rays, which can distribute or concentrate them, known as "solar convergence". (11);(5).

Cases of important buildings such as the Vdara hotel in Las Vegas, the Walt Disney Concert Hall in Los Angeles and the MaterDei hospital in Salvador (23), demonstrate how envelope designed without reflectivity and emissivity criteria, combined with

geometry that favor the high concentration of solar rays, cause direct and indirect visual glare in neighboring buildings. In addition, the reflection of long-wave radiation can deform and deteriorate the incident surfaces or affect the local microclimate by raising the temperature, which we call "thermal glare".
(7)

Studying the process from conception to execution of buildings, it can be said that the tool with the greatest control over the occurrence of glare is the architectural design process. It is during the design phase that architects and designers must evaluate and consider the definition of elements and materials for façade surfaces.

In this context, in an attempt to fill the gap in the design process, the author proposes a method for evaluating and classifying the behavior of curtain walls in relation to the probability of glare occurring, which is user-friendly and highly applicable based on a combination of 2 criteria: visual and thermal (surface heating), resulting in final performance.

The designer's assessment is based on the identification of the characteristics proposed in the project in terms of the type of materials specified on the façade and the form relative to the architectural design, compared to a scale that represents the capacity of the architectural ensemble to cause urban glare.

To define the impact scale about visual glare discomfort, computer simulations will be carried out to determine the vertical illuminance (Ev) levels, through Annual Daylight Glare Probability (DGP) levels, obtaining the evaluation scale between imperceptible glare and intolerable glare. (12);(13),

In order to build the impact scale about solar reflection heat up, parametric computer simulations will be developed using Rhinoceros 3D software and the Grasshopper plugin + Ladybug and Honeybee, using forward raytracing analysis, in different typologies, generating Heatmaps (3). It provides a graphical projection of the density of intersection reflected rays, in terms of the greater or lesser density of points representing the concentration or diffusion of reflected solar rays, that impacts the pedestrian urban layer.

The procedure classification levels will be constructed from the results of the qualitative and quantitative analysis of Heat maps and DGP and Ev correlation, done individually, giving to the respective classification scales and the final score.

2. OBJECTIVE

The aim of this paper is to demonstrate the methodology for assessing the performance of façades on high-rise buildings based on the geometry and materiality of the envelopes for the climatic conditions of the city of São Paulo, in order to mitigate and avoid the occurrence of visual and thermal urban glare.

3. METHOD

The proposed evaluation procedure was based on the descriptive method for energy evaluation of commercial and residential buildings, Procel Edifica (4), a Brazilian energy efficiency label like U.S. Environmental Protection Agency label, Energy Star. Procel proposes the partial and systematic analysis and classification of criteria. These criteria are then combined and weighted based on the level of impact on the building in terms of energy efficiency, resulting in the building's final rating.

It is understood that by defining the criteria and carrying out computer simulations, it will be possible to create relationships and identify the impact of different shapes, emissivity and surface reflectivity on solar reflection in the area surrounding the buildings.
The simulations will be carried out considering a critical sky condition, i.e. the type of clear sky defined by the CIE (International Commission on Illumination), with little or no obstruction of sunlight by clouds (9).

Therefore, the methodological procedures for constructing the evaluation procedure first sought to survey and characterize the geometric types of tall buildings that have been repeatedly reproduced in the city of São Paulo, in order to define the simulation models. Subsequently, there developed a database of transparent and opaque support materials for architects to consult when evaluating their buildings.

Preliminary simulations were carried out to validate the **2-stage** building assessment methodology; the first to evaluate the impact of geometry on solar reflection in terms of geometric shape and materiality, and the second assessing the likelihood of visual glare. Finally, the results were processed, quantitative and qualitative analysis of the data obtained and determination of the weighting indices for different façade orientations, in order to obtain the final classification of the envelope.

3.1 Data collection: Geometry and material data

The definition of geometries and materials that best reproduce the current architectural language being developed by architects for new buildings means that the envelope models available in the procedure will be reproduced in new buildings in the city, ensuring the validity and applicability of the updated, efficient and perennial evaluation method.

For the purpose to define the geometric shapes that best reproduce the architecture of tall buildings in the city of São Paulo, the photographic survey area was established as the axis along Cidade Jardim avenue to Dr. Chucri Zaidan avenue in the Morumbi district. At the axis of the study, it is possible to observe a sample of the most recognizable high-rise

corporate buildings built since the year 2000, including environmental certifications ones.

A photographic survey was carried out of around 20 buildings (fig. 1), according to the criteria of greatest architectural expression and repeatedly reproduced geometry. Subsequently, 6 predominant geometries were selected for evaluation and as a reference model for applying the procedure: prism (right angle), angular shape (obtuse and acute) and curves (concave and convex), deriving, depending on the refinement of architectural proposals, into 22 base geometries, as shown in fig. 2.

Figure 1 - Photographic survey of geometries: acute and obtuse angular, convex, prism and concave (AUTHOR,2023)

Figure 2 - Reference shapes for study, acute and obtuse angular shapes, convex, concave, prism and folding. (AUTHOR, 2023)

The survey of surface materials was based on bibliographical references and technical data sheets. Once the data had been compiled and listed in a range of emissivity and reflectivity every 0.20 points (0.01;0.20;0.40;...;0.90 and 0.98), 11 variations of reflection indices were defined for the study.

3.2 Envelope Evaluation: Computer simulations results

The assessment of the impact of the envelope to determine the classification in terms of impact levels, as a function of the overall shape and materiality will be carried out using computer simulations of accumulative DGP analysis during the year and forward ray-tracing simulations, obtaining Heat Maps.

The geometric models for assessing the impact through computer simulations was developed using Rhinoceros+Grasshopper plugin (fig.3) taking into account that the building is made up of 4 equal faces, in order to explore the behaviour of 360º solar reflection in all facade orientations, at different solar positions. It will consider the building in isolation, i.e. without any interference or obstruction from neighbouring buildings.

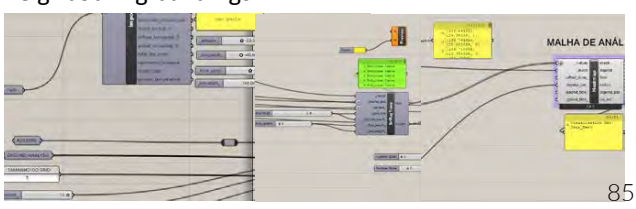

Figure 3: Raytracing Simulations and neighbourhood impact. (author,2023)

These preliminary evaluations have been made considering the most critical façade material reflection property, the specular surface (2 bounces), comprising the critical capacity of the number of reflections that reach the ground, resulting in a reflection pattern presented on a horizontal plane.fig.4

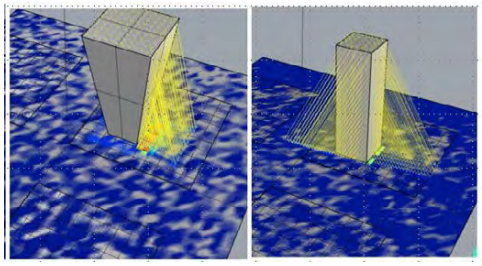

Figure 4: Solar reflection (rays) neighbourhood impact_ Angular65º (left), prisma 90º (right). (author,2023)

Simulation parameters
Weather data: São Paulo (Energyplus Weather data- TMY-2007-2021)
Bounces: 2 and **Grid size:** 5
Intersection density (ID) = **N** (number of intersections in one mesh surface/ **A** (mesh area)

Although, the first analyses considered only specular surfaces to validate the methodology, the results of 11 variations of reflective materials will be included in the total data package of the proposed procedure.

The simulations were developed considering the climate data for the city of São Paulo and the solar positions with the highest impact of radiation surfaces (13), 20º (7h-17h), 30º (7h30-16h30pm), 40º (8h30-15h30), 50º (9h-15h00), and 60º (10h-14h), fig. 5, all over the year, in summer, in equinox and in winter.

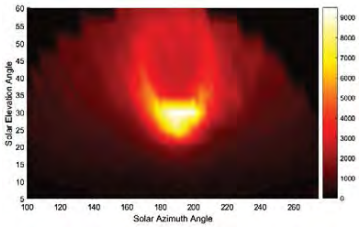

Figure 5 - Falsecolor map of peak radiation flux under various solar positions (13)

In the first stage, the building envelope and the neighbourhood area impact are assessed through forward raytracing simulations, in order to obtain, the area of influence of solar reflection and as well as

diffuse inter-reflections (radiosity), from facades and heat maps at pedestrian urban layer (PUL). Fig.6

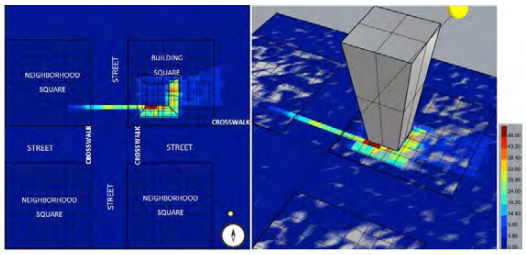

Figure 6: Angula65º - Raytracing Simulations Heatmaps – Intersections rays and neighbourhood impact. (author,2023)

The evaluation matrix was built based on raytracing analysis results.

Through simulations it was possible to qualify possible to quantify and classify the impact on the concentration or diffusion of solar rays (visible radiation, short waves and invisible, long waves) and area of influence, indicating high levels of luminance will be demonstrated through a heatmaps scale of high (3 points), medium (2 points) and low (1 point) impact, as well as, solar orientation facade impact coefficient on each building geometry, projected by the envelopes determining the scope of sunlight reflection, fig 7 (4)

ANGULAR65								
DECEMBER 21		CONCENTRATION	DENSITY		AREA OF INFLUENCE			
SUMMER		3	2	1	3	2	1	IMPACT LEVEL
SOLAR ANGLE	TIME	HIGH	MEDIUM	LOW	HIGH	MEDIUM	LOW	
20º	7h00	3			3			6
30	7h30		2		3			5
40	8h30	3				2		5
50	9h00		2			2		4
60	10h00	3					1	4
60	14h00		2				1	3
50	15h00		2			2		4
40	15h30	3				2		5
30	16h30	3			3			6
20	17h00	3			3			6

Figure 7: Hourly Envelope evaluation results matrix (author,2023)

The global impact level of each geometry identified was based on the sum of the hourly impact level, while the weighting coefficient for each façade was determined by qualitatively assessing the surface area of solar reflection on the PUL.

Table 1: Overall Impact level Envelope evaluation results matrix and Façade coefficient (author,2023)

PRISMA90												
DECEMBER 21		CONCENTRATION	DENSITY		AREA OF INFLUENCE				FACADE S.ORIENTATION COEFFICENT			
SUMMER		3	2	1	3	2	1	IMPACT LEVEL	0	1	2	0
SOLAR ANGLE	TIME	HIGH	MEDIUM	LOW	HIGH	MEDIUM	LOW		NORTH	SOUTH	EAST	WEST
20º	7h00			1	3			4	0	1	2	0
30	7h30			1	3			4	0	1	2	0
40	8h30			1	3			4	0	1	2	0
50	9h00			1		2		3	0	1	0	0
60	10h00		2			2		4	0	1	0	0
60	14h00		2			2		4	0	0	0	0
50	15h00		2		3			5	0	0	0	0
40	15h30			1		2		3	0	1	0	0
30	16h30			1	3			4	0	2	0	1
20	17h00			1	3			4	0	2	0	1
All Day		Overall building impact level						39		1.2	2	1

Based on the results of the solar reflection of the facades regarding the intersection density of the reflective solar rays (ID) and their coverage, it is possible to predict the possibility of impact on the surroundings or on neighboring buildings in the urban context. Therefore, it was determined critical positions regarding the use of streets, sidewalks, crosswalks and neighboring buildings. as shown in the studies by J.ZHU (12), fig.8

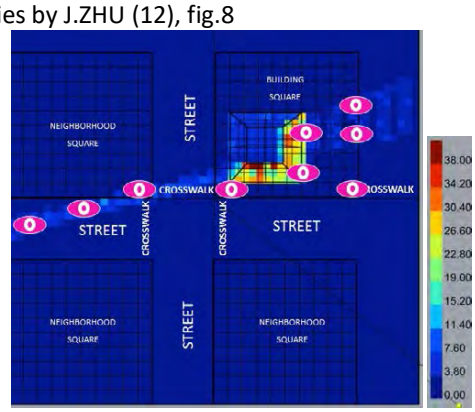

Figure 8: Heat Maps and Critical position definition. (author,2023)

In the second stage, the intensity of the solar rays reflected at the critical points will be quantified, qualifying the level of discomfort experienced by users, using the DGP metric (13).

The critical positions identified will be used as the observer's points of view for the hourly assessment of the level of vertical illuminance in the eye (Ev-lux) and, obtaining the correlation of the vertical illuminance with the level of discomfort proposed by the DGP, as well as the level of limit luminance of 10,000cd/m2 emitted by facades. (14)

4. EVALUATION PROCEDURE APPLICATON

4.1: Identification of the impact

The evaluation procedure will consist of matrices of results obtained from computer simulations for each geometry assessed. table2.

[-0po8he process will be applied by architects and designers in a linear fashion, starting with the definition of the geometry similar to the architectural design and the reflection indices of the façade materials specified in the project.

Based on the combination of the building's 2 variables, the level of impact will be demonstrated (C.), built on the diagnosis and evaluation of the results of DGP and heat maps the computer simulations.

where:

A1= building geometry _ **B1** = reflectivity

C = heatmaps Impact Level

Table 2: Façade evaluation matrix (Author, 2023).

	A1	B1	C	Facade Weighing coefficient			
	Geometry	Reflectivity Suface	Density+Influence area (HeatMaps)	North	South	East	West
SUMMER		Specular	39	0	1.2	2	1
		0.01 - 0,10	15	0	1.2	2	1
		0,10 - 0,20	20	0	1.2	2	1
	Prisma	0,20 - 0,40	22	0	1.2	2	1
		0,40 - 0,60	26	0	1.2	2	1
		0,60 - 0,80	30	0	1.2	2	1
		0,80 - 0,99	34	0	1.2	2	1

Façade orientation will be simplified considering only 4 cardinal points, using this graph below. fig.9

Figure 9: Axis Simplification building solar orientation. (5)

4.2 Facade solar orientation: Weighting Coefficient.

The building must be analysed by façade, and a correction index will be applied according to its solar orientation, due to altitude and the angle of direct solar incidence, reducing or increasing the score that will characterize the degree of likelihood of glare occurring.

4.3 General Building Classification

The procedure is a user-friendly application and can be applied to the any building form, even in its complex envelope geometries, because its individual analysis.

As final result of applying the procedure, the overall rating of the building will be obtained from the evaluation in 2 phases.

First analysis phase, through evaluation per facade in the 3 seasons of the year, obtaining a partial score, table 3. The second phase is based on the evaluation of the highest levels of vertical illuminance/DGP at the critical points evaluated. The final classification of the building will be based on the simple sum of the scores obtained in phases 1 and 2, using table 4.

The solar density evaluation, for each façade and season, will be based on the application of equation 1, and their respective solar orientations.

Equation 1:

A1 ⇨B1 = C x D = Score per façade (PP)

where: C = heatmaps Impact Level _ ***PP***: is Final Score per façade _ ***FWC-*** is weighting according to solar radiation impact

Table 3 – *One Season Building evaluation table* (Author, 2023)

		A1	B1	C	Facade Weighing coefficient				PP
		Geometry	Reflectivity Suface	Density+Influence area (HeatMaps)	North	South	East	West	
SUMMER	Facade 1	prisma	specular	39	0	1,2	2	1	39
	Facade 2	prisma	0,10 - 0,20	20	0	1,2	2	1	24
	Facade 3	prisma	0,10 - 0,20	20	0	1,2	2	1	40
	Facade 4	angular	0,10 - 0,20	20	0	1,2	2	1	0
	Partial building classification								103

Afterwards the total building classification to analysis 1, will be obtained through the sum of summer, equinox and winter building assessed, equation 2.

Equation 2:

$PP_{(SUMMER)}$+$PP_{(EQUINOX)}$+$PP_{(WINTER)}$=TotalBuildingClassificatio 1

Table 4 – Analysis Phase 1- Building Classification - Glare assessment table by façade all season year (Author, 2023)

		A1	B1	C	Facade Weighing coefficient				PP
		Geometry	Reflectivity Suface	Density+Influence area (HeatMaps)	North	South	East	West	
SUMMER	Facade 1	prisma	specular	39	0	1,2	2	1	39
	Facade 2	prisma	0,10 - 0,20	20	0	1,2	2	1	24
	Facade 3	prisma	0,10 - 0,20	20	0	1,2	2	1	40
	Facade 4	angular	0,10 - 0,20	20	0	1,2	2	1	0
	Partial building classification								103
		A1	B1	C	Facade Weighing coefficient				PP
		Geometry	Reflectivity Suface	Density+Influence area (HeatMaps)	North	South	East	West	
EQUINOX	Facade 1	prisma	specular	34	0	1,2	2	1	34
	Facade 2	prisma	0,10 - 0,20	15	0	1,2	2	1	18
	Facade 3	prisma	0,10 - 0,20	15	0	1,2	2	1	30
	Facade 4	angular	0,10 - 0,20	15	0	1,2	2	1	0
	Partial building classification								82
		A1	B1	C	Facade Weighing coefficient				PP
		Geometry	Reflectivity Suface	Density+Influence area (HeatMaps)	North	South	East	West	
WINTER	Facade 1	prisma	specular	30	1,2	0	1	2	60
	Facade 2	prisma	0,10 - 0,20	11	1,2	0	1	2	0
	Facade 3	prisma	0,10 - 0,20	11	1,2	0	1	2	11
	Facade 4	angular	0,10 - 0,20	11	1,2	0	1	2	0
	Partial building classification								71
Analysis 1 - Total Buiding Classification									256

For the evaluation of stage 2, a matrix of results obtained from the DGP simulations at the critical positions defined in the forward raytracing simulations will be used. table 5.

Table 5 – Phase 2- Façade evaluation matrix (Author, 2023)

DGP ANALYSIS MATRIX - (Critical Positions)							
Season	Geometry	Reflectivity Suface	Vertical Illuminance Level (Ev)	North	South	East	West
SUMMER	Prisma	0.01 - 0,10	<1000 lux	0 - 0,15 (1point)	0 - 0,15 (1point)	0 - 0,15 (1point)	0 - 0,15 (1point)
		0,10 - 0,20	1000 - 2000	0 - 0,15 (1point)	0,15-0,30 (2points)	0,15-0,30 (2points)	0 - 0,15 (1point)
		0,20 - 0,40	2000 - 2500	0 - 0,15 (1point)	0,15-0,30 (2points)	0,15-0,30 (2points)	0 - 0,15 (1point)
		0,40 - 0,60	2500 - 3000	0 - 0,15 (1point)	0,30 - 0,35 (3points)	0,15-0,30 (2points)	0 - 0,15 (1point)
		0,60 - 0,80	3000 lux - 4.000lux	0 - 0,15 (1point)	0,30 - 0,35 (3points)	0,15-0,30 (2points)	0 - 0,15 (1point)
		0,80 - 0,99	> 4000 lux	0 - 0,15 (1point)	0,35 - 0,40 (4points)	0,30 - 0,35 (3points)	0 - 0,15 (1point)
		Specular	> 4000 lux	0 - 0,15 (1point)	0,35 - 0,40 (4points)	0,30 - 0,35 (3points)	0 - 0,15 (1point)

Through this matrix of results, the illuminance and DGP levels can be observed as a function of the solar orientation of the façade studied.

Following the same methodology applied in phase 1, table 6, the evaluation carried out for each period of the year and individually for each façade can be quantified to obtain the final PG score.

Table 6 – One Season Building evaluation table (Author, 2023)

	PHASE 2 - DGP						PG
	Geometry	Reflectivity Suface	North	South	East	West	
SUMMER	Facade 1	prisma	specular			0 0,15 (1point)	1
	Facade 2	prisma	0,10 - 0,20		0 - 0,15 (1point)		1
	Facade 3	prisma	0,10 - 0,20			0,15-0,30 (2points)	2
	Facade 4	angular	0,10 - 0,20	0 - 0,15 (1point)			1
	Analysis 2 - Partial Building Classification						5

Therefore, the total PG score is obtained from the sum of the PG in summer, equinox and winter, equation 3.

Equation 3:

$PG_{(SUMMER)}$+$PG_{(EQUINOX)}$+$PG_{(WINTER)}$=TotalBuildingClassification 2

The Final Score (FP) and the Probability Glare building Classification will result from summing up de Total Building Classification of stage 1 (Heatmaps) and Stage 2(DGP analysis), through the table 7.

Table 7 - Score for the final classification of the likelihood of glare occurring in the building (Author, 2023).

FINAL PONTUATION	BUILDING GLARE CLASSIFICATION
<120	No glare probability
120 - 200	Low glare probability
201 - 249	Likelihood Glare probability
250 - 279	Glare probability
>280	Hight Glare probability

5. CONCLUSION

In order to meet the proposal of creating an evaluation procedure, parametric simulations will be carried out, making it possible to define criteria and the classification of the impact of glare in urban environment, mainly in urban pedestrian layer.

Finally**,** the procedure is an early design tool, to predict problematic glare, and to assess as part of development proposals at planning stage mitigation until the building performance.

In Brazil there is no kind of Municipality building facades glare regulation, so, this is in keeping with the greater goal to have this procedure as part of best practice guideline city code.

The study also contributes to the creation of a database with more than 300 compositions of glass and opaque materials for façade cladding, compiled from manufacturers and suppliers data sheets and informations.

This evaluation procedure research paper is part of the ongoing PhD thesis. The first stage matrix evaluation has been development, while the second stage, DGP simulations, area under validation. However, the full procedure structure, methodology application and initial values of classification scale can already be observed at the present paper.

REFERENCES

1. Boyce,P.R. Human factors in lighting. Lighting research Center. 2 ed. NY: ed. Taylor and Francis. 2003.
2. Correio 24horas. The Second Sun Has Arrived: Salvador's New Hospital "Blinds" and Annoys Neighbours. By Moyses Suzart. 10 oct 21
3. Deng.L;Schiler.M; Noble.D; Kyle.K. Exterior Glare Simulation: Understanding Solar Convergence From Concave Facades using heat Maps. USC School of Architecture. L.A. USA. PLEA Los Angeles: Cities, buildings and people: For the regeneration of the environment.2016.8p.
4. Procel. National Program for the Conservation of Electric Energy. According INMETRO Law n° 372/2010 and Law nº 17 de Jan 16,2021. University of Santa Catarina. Florianópolis. April. 2013a
5. Suk.J. Y; Schiler.M; Kensek.K Post-treatment analysis of glare correction of Walt Disney concert hall. American Solar Energy Society Conference. 2007
6. Suk.J. Y; Schiler.M; Kensek.K Development of a new daylight glare analysis methodology using the absolute glare factor and the relative glare factor. Energy and Buildings. Elsevier. 2013. p.113-122.
7. Suk.J. Y; Schiler.M; Kensek.K Reflective and specularity of building envelopes: how materiality in architecture affects human and visual comfort. Architecture and Science Review. 2017
8. Zhu, J; Wolfram J; Rein, G. Computer simulation of sunlight concentration due to façade form: application to the 2013 Death Ray in Fenchurch Street, London. Journal of Building Performance Simulation,12:4. nov.2018. p.378-387.
9. Edwards, L; Torcellini, P. A literature Review of the effects of natural light on building occupants. NREL, Colorado. EUA. 2002. p.54.
10. Laranja, A.C. Urban parameters and the availability of indoors Daylight. 2010. 242 p. Thesis PhD Architecture and Urbanism Faculty of Architecture and Urbanism, Federal University of RJ, 2010.
11. Schiler.M; Valmont.E. Microclimatic Impact: Glare Around the Wall Disney Concert Hall. School of Architecture. University of Southern California. USC. Los Angeles. 2005.p.6. Available at <www.sbse.org/awards/docs/2005/1187.pdf> Accessed on July 21, 2017.
12. Wienold, J.; Christoffersen, J. Towards a New Daylight Glare Rating, Lux Europa, Berlin. 2005. p157-161.
13. Wienold,J; Christoffersen,J. Evaluation and development of a new glare prediction model for daylight environment with the use of CCD cameras. Energy and building. 38.2006.p.743-757
14.Yang, X; Globe, L; Stephen, W. Simulation of Reflected Daylight from Building Envelopes. 13th IBPSA Conference France. Aug.2013. p.26-28

PLEA 2024 WROCŁAW
(Re)thinking Resilience

Enhancing Urban Walkability in Extreme Heat

Climate Adjusted Walkability Metrics

ERIN HEIDELBERGER[1] HONEYKSHA WAGHELA[2] ERIC PIETRASZKIEWICZ [1]
CARLOS CEREZO DAVILA[1]

[1]Kohn Pederson Fox, New York, USA
[2] Kohn Pederson Fox, London, UK

ABSTRACT: In areas of the world that face extreme heat, and in increasingly more areas around the globe facing increased heat events under climate change, walkability is limited by climatic conditions. This paper summarizes existing literature on pedestrian behaviours in extreme heat and introduces a comprehensive design workflow aimed at mapping and enhancing urban walkability in extreme heat. Focused on improving pedestrian comfort and walkability, the workflow models the correlation between outdoor thermal conditions and pedestrian behaviour, adjusting walking speeds and total walk times based on perceived temperatures. The results of this workflow, climate adjusted walkability metrics, are demonstrated on a sample project in the Middle East. This case study emphasizes the critical role of designing for comfort and demonstrates the use of the workflow as a design tool.
KEYWORDS: Walkability Metric, Microclimate Design, Pedestrian Outdoor Comfort, Extreme Heat

1. INTRODUCTION

A vital role of urban design is to promote walkability and connectivity. The term 'walkability' can be defined as the level of friendliness that the built environment offers to pedestrians [1]. In the past, the focus to achieve walkability has been on properly distributing program and building pedestrian oriented infrastructure. However, in extreme climates this can fall short as microclimate intricacies are overlooked, rendering streets uncomfortable for pedestrians due to limited solar control and wind flow. July 2023 marked the hottest month in recorded global temperatures since 1880 [2], and with the trend of more cities globally experiencing extreme heat designing for pedestrian thermal comfort is becoming increasingly more important.

This paper proposes a new simulation metric and representation method to assess and design for climate adjusted walkability metrics, crucial for site-specific walkability and creating resilient urban designs in extreme climates and changing climate scenarios. Unlike conventional walksheds relying solely on travel distance, this approach modifies pedestrian behaviours based on perceived temperatures, accounting for willingness to walk, walking speed, and walking time in extreme heat. A case study then demonstrates how this metric was applied as a design tool on a sample master plan project in the Middle East, where extreme climates significantly challenge walkability. The case study looks at pedestrian comfort and walkability across the master plan and along a key pedestrian path.

2. LITERATURE REVIEW

Although lot of literature is available regarding the methods and experiments for measuring how outdoor thermal conditions affect human comfort and walking patterns at a given time, limited work has focused on understanding the issue dynamically.

A cross-national analysis involving 31 countries found that ambient temperature strongly influenced pedestrian walking speed [3]. Cooler cities consistently showed higher pedestrian speeds compared to warmer counterparts. Another study revealed a fourfold increase in perceived travel time when transitioning from a comfortable thermal environment to a stressful one [4]. Investigations into walkability in Dubai linked outdoor thermal comfort and tolerable walk time to dynamic thermal comfort. These studies showed decreased willingness to walk when outdoor temperatures exceeded 33°C [5]. Research also suggested that shade and appropriate wind could alleviate heat-related discomfort during pedestrian activities in arid desert climates [6].

Table 1: Pedestrian behaviour patterns under different degrees of heat stress

	No Thermal Stress	Moderate Heat Stress	Strong Heat Stress	Very Strong Heat Stress
Temp. (°C)	<26°	26° - 32°	32° - 38°	38-46°
Walk Time (mins)	Up to 20	Under 14	Under 8	Under 2
Walk Speed (m/s)	1.4	1.2	1	0.8

2.1 Summary of Findings

Table 1 summarizes the findings of pedestrian behaviour in high-temperature environments, defining walking time and speeds by temperature range and thermal perception. This summary provides a basis for understanding pedestrian patterns in extreme heat under uniform conditions, but do not account for the dynamic conditions a pedestrian would experience moving through the built environment.

2.2 Impact of Design Interventions

In addition to understanding how perceived conditions impact pedestrian behaviours, it is also important to understand what factors in an environment impact perceived temperature and what design intervention measures can be used to reduce thermal stress in hot climates. Pedestrian thermal stress is influenced by meteorological factors (including dry bulb temperature, solar radiation, relative humidity, and wind speed) and non-meteorological factors (including metabolic rate and clothing thermal resistance) [7]. The importance of meteorological parameters' impact on thermal perceptions varies by location: air temperature dominates in shaded areas, solar radiation in continuous sunlight, and wind speed in wind-amplified locations [8].

Research into improving thermal comfort in hot climates has identified several design interventions to improve pedestrian experience and therefore walkability. Shading, whether from trees or canopies, significantly mitigates pedestrian thermal stress during mid-day hours, especially when combined with vegetative ground cover. Overhead shading, coupled with grass, yields a modest reduction in thermal stress, creating a 'comfortable' thermal state throughout the day [9]. In fully vegetated courtyards, peak daytime temperatures are up to 2.5 °C lower, demonstrating the crucial role of shading in enhancing outdoor comfort and walkability in a hot, arid climate [10].

Shading through urban design is another measure to optimize outdoor comfort in hot climates. Kariminia et al. [11] studied Isfahan, Iran, finding that increasing the height-to-width ratio from 0.1 to 0.3 in a historic square decreased the Physiological Equivalent Temperature (PET) by 1.6°C, reducing discomfort over 3 hours. In Ghardaia, Algeria, Ali-Toudert and Mayer [12] studied the impact of street grid orientation on comfort, revealing better thermal performance in northeast–southwest and northwest–southeast streets. A 12.5% sky view factor decrease can reduce UTCI by 1° [13].

In hot and arid climates, air movement provides natural cooling, dissipating heat through enhanced evaporation and reducing perceived temperatures. This cooling effect is crucial for mitigating the impact of intense solar radiation, making outdoor environments more comfortable. Additionally, improved ventilation through air movement prevents heat pockets, ensuring a more pleasant experience in urban settings. Research indicates that a wind speed of 1 m/s to 1.5 m/s has the potential to reduce air temperature by up to 2 °C [14].

Water bodies are an additional strategy to improve thermal comfort in outdoor environments due to their ability to increase humidity and reduce air temperature in urban areas. Evapotranspiration from wet grass can reduce the ground surface temperature by 6-8°C below the average surface temperature of the bare soil [15].

Barakat et al. [16] assessed 3 different microclimates in Alexandria, Egypt, a hot and dry climate. They found that thermal conditions can be improved by combining mitigation strategies, specifically reducing the pavement areas, and increasing greenery surfaces, water bodies, and the number of trees. It is documented that these changes reduce air temperature and average radiation temperature while increasing humidity and comfort.

3. METHODOLOGY

While the literature clearly establishes a link between perceived temperature and pedestrian behaviour, no design-applicable method is available to correlate the two as a function of modelled thermal conditions. This paper therefore proposes a potential function to be evaluated based on perceived temperatures.

3.1 Perceived Temperature Modelling

The Universal Thermal Comfort Index (UTCI) is one of the most comprehensive indices for calculating heat stress in outdoor spaces [17] taking into consideration the dry bulb temperature, relative humidity, solar radiation, wind speed, and personal factors including clothing thermal resistance and metabolic rates [7]. For this workflow, UTCI is simulated and mapped across the project area using Rhinoceros 3D (Rhino) and Grasshopper, including the Ladybug Tools plug-ins. The calculation follows the workflow developed by Kessling et. al. [18].

Meteorological data is sourced from the Abu Dhabi International Weather for Energy Calculation (IWEC) weather file, available from the Department of Energy EnergyPlus Weather Data database [19]. This meteorological data is representative of typical conditions in the area, based on historical data collection. Modified weather files based on future climate projections can also be used in the simulation to test the long-term walkability in a design against the impacts of climate change [20].

3D geometry of the design and surrounding context, modelled in Rhino, is also included in the simulation. The output of the UTCI modelling is a mesh of perceived temperatures along the designated analysis plane for the chosen analysis period.

3.2 Climate Adjusted Walkability Modelling

A typical walkshed analysis, regardless of pedestrian comfort, defines all areas that a pedestrian can reach from a set origin point(s) in a determined amount of time, i.e. 5 minutes. This modeling requires the origin point(s) and a complete pedestrian network to be included in the Rhino model as inputs. Then, paths from the origin point to every unique location in the network are generated. The length of these paths is determined by the distance that can be traveled in the set amount of time, assuming a constant speed of 1.4 m/s in a climate-agnostic scenario. Using the example of 5 minutes, this means the paths would be no longer than 420 meters.

When generating these paths, all potential paths from the origin point along the pedestrian network are tested at a set interval, i.e. 5 meters, building up until the maximum path length is reached or the branch of the pedestrian network ends. Then all shorter, coincident paths that were generated in the process of identifying the longest unique path are removed, leaving only unique paths for the analysis. While this step of removing coincident paths is not critical in a climate-agnostic walkshed, it is important for the proposed function to reduce simulation time.

In the climate adjusted walkshed, the walking speed and length of path are adjusted down from the ideal, climate-agnostic walkshed. The closest point from the UTCI mesh along all paths included in the ideal walkshed are pulled to get the perceived temperatures along the walking paths. Then, a sliding average of these values over the past 30 seconds is calculated to account for the impact of the pedestrian's thermal history. This sliding average sets the walking speed based on the values in Table 1, and it is also used to test against the end condition.

The sliding average of the perceived temperatures along the paths are compared against an end condition to determine when the walk is terminated. To account for the increased fatigue as people walk in high heat scenarios, as shown in the decreased walking times at higher levels of thermal stress established in the literature review, this cut off temperature decreases as the walk progresses. While in the beginning of the walk there is an initial 34° cut off temperature, to approximate pedestrians decreased likelihood to start a walk-in strong heat stress, it linearly decreases to 31° over the course of the first 2 minutes, where it stays for the duration of the walk. If the end condition is never met, the walk ends after the pre-determined amount of time for the walkshed.

3.4 Results and Visualization

Results are visualized over the key paths or across the entire design. The function can be used to test or highlight the effectiveness of microclimate design measures and design for true walkability, even in extreme heat. Select microclimate measures, with an impact on UTCI and therefore walkability, that can be assessed with this workflow include shading strategies including vegetation, wind flow, and water features.

4. CASE STUDY

This function is demonstrated through a case study project developed by the architecture office Kohn Pedersen Fox (KPF) in the Middle East. The project is a coastal master plan in Abu Dhabi, with housing, commercial, and cultural spaces. The project aims to establish a connected district activated by pedestrians throughout the day and night. The harsh climate of Abu Dhabi, with average daytime highs ranging between 26°-49° throughout the year, necessitates careful consideration of pedestrian thermal comfort to achieve these goals. The case study reflects a representative April day from 8 am to 8 pm with up to 32° dry bulb and 40° perceived temperatures. The case study compares climate-agnostic walkability modelling, a base case without added microclimate design measures, and a design case with carefully placed pedestrian canopies, increased air movement, and water features to reduce the perceived temperatures.

4.1 Walkshed Application

The function was used to compare 5-minute walksheds around the masterplan in the climate-adjusted base case and design case. Figure 1 showcases pedestrian connectivity around the development with walksheds originating at all bus rapid transit stops. The stops were positioned to match major programmatic hubs in the development, with the climate-agnostic walking distances in mind. The base case, shown in orange and accounting for the impact of perceived temperature and without specific microclimate measures, demonstrates that these stops are not connected and that pedestrians have limited mobility around the development. In the design case, shown in blue, the lower perceived temperatures have greater connectivity between the rapid transit stops. The total area covered in the

walksheds increases by 228% in the design case over the base case.

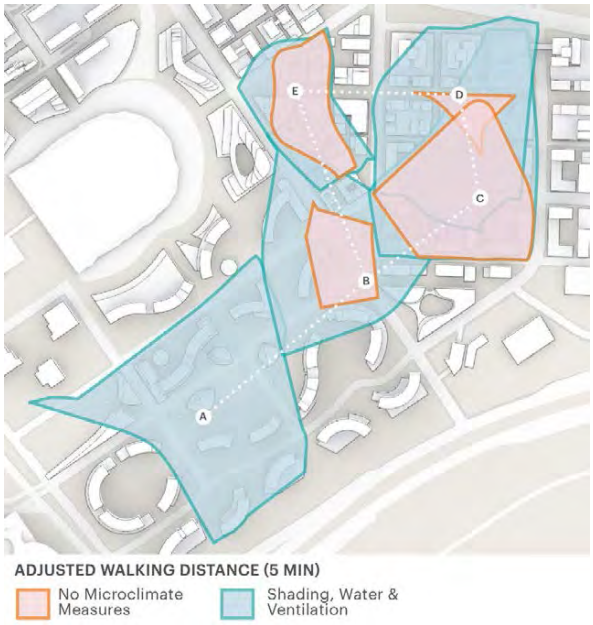

Figure 1: Climate adjusted walksheds

Figure 2: Key pedestrian path overlaid on UTCI map

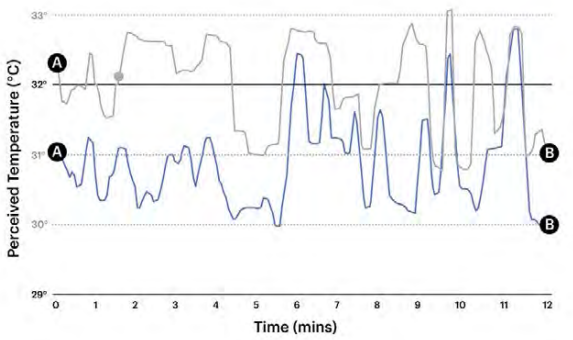

Figure 3: Perceived temperature along key pedestrian path

4.2 Key Path Application

In addition to looking at walkability metrics across a larger area of the masterplan, this workflow can also be used for a more detailed look at specific, key pedestrian paths through the design. Figure 2 highlights a pedestrian path from the residential neighbourhood through some cultural programming to the main retail hub, overlaid on the design case UTCI map. Figure 3 showcases the pedestrian experience over a 12 min, 1,000 m path in the masterplan. The grey line shows perceived temperatures across the path without specific microclimate measures in the base case. This walk ends after 86 m and lasts less than 1.5 minutes, indicated by the dot on the graph. The blue line shows the perceived temperatures in the design case, with added mitigation measures, which lasts the full 12 mins, 1,000 m.

5. DISCUSSION

The proposed function aims to combine typical pedestrian behaviours under different perceived temperatures and apply them to walkability modelling to introduce new climate adjusted walkability metrics in extreme heat scenarios.

5.1 Results

For this case study, the walkability metrics were applied to the base case and design case after they were prepared and not throughout the design process. In an ideal case, they would be used throughout the process first when designing the urban geometry and then to identify where microclimate measures are needed and what measures will be most effective.

The impacts of the urban geometry are obvious in both the walkshed and key path applications of this tool. In the walkshed application, the difference in urban shading can be observed by looking at Point A, which is in the least dense area of the master plan and has no walks started in the base case. The opposite can be seen in points C and E, which are in more dense areas of the design. These points have the least difference between the base case and design case since the built environment itself

provides solar protection and lowers the perceived temperature. Along the key path there is the biggest difference between the base case and design case in the first half of the walk where there is less context. As the path moves into the denser areas of the masterplan the perceived temperatures in the base case drop.

Intervention measures can be tested both at an individual, key path application and at the full master plan scale in the walkshed application. Knowing where the base case fails, specific design intervention measures can be placed along the route to increase comfort and extend the walk. Along this key pedestrian path that meant adding more concentrated mitigation measures in the first half of the walk and using mitigation measures to supplement in the second half of the walk.

5.2 Assumptions in Modelling

Both the UTCI modelling and results as well as the function to correlate perceived temperature and pedestrian behaviours have assumptions baked in that can impact the results of the metric.

The UTCI modelling has default assumptions about the meteorological and non-meteorological factors that make up the perceived temperature. This includes the temperature difference between the air temperature and surface temperature, the ground surface reflectivity, and a modifier to the wind speeds from the typical weather data based on surrounding context and analysis plane height, as well as the initial skin temperature and clothing thermal resistance of the hypothetical pedestrian. While all the values used are industry standard, they can vary by location and cultural practices that are not accounted for in the model.

UTCI modelling also assumes a pedestrian that is static in space and not moving between different conditions, as is the case with a pedestrian moving throughout the proposed design. While this function adds in a 30 second sliding average to account for thermal history the modelling does not fully account for the previous experiences of the pedestrian and how moving between lower and higher degrees of heat stress can impact thermal comfort.

In addition to these inputs, the UTCI results are also impacted by the date and timeframe chosen for the analysis. In this case study a date in mid-April was chosen based on local cultural practices. This period of the shoulder season typically has more common pedestrian activity during the day in Abu Dhabi. Later, in the heat of the summer, pedestrians are more common after sundown as temperatures drop. By choosing a different timeframe of the year or a different subsection of hours in the day, both the UTCI and pedestrian behaviours can vary widely.

Similarly, the cut off temperatures used in the end conditions of the walk have been selected to match the time of the year and approximate pedestrian decision making. In the absence of a full pedestrian behaviour study specific to the location of the case study, general assumptions were used from the literature review. Both the end conditions and walking speeds could be adjusted with more locally and culturally specific data to refine the analysis as such data is available.

5.4 Future Work

This initial proof of concept of a climate adjusted walkability metric and case study application are meant to introduce climatic considerations into walkability analyses. There are many areas where this work can and should be expanded.

Future work includes converting the metric from a series of walksheds starting at discrete points to a heat map showing climate adjusted walkability from all points on a map, expanding the workflow to account for cold stress as well as heat stress, and adjusting the metric based on cultural behaviours of different communities around the world.

To address some of the potential impact of the assumptions in the UTCI modelling and function, CFD wind flow data for the design can be substituted for the wind speed information included in the typical weather data. This will better account for surrounding conditions as well as differentiate areas across the proposed design. In place of just the UTCI mesh, with no thermal history, a dynamic thermal comfort model, like the one presented by Fiala et. al [21], can be used to better account for how thermal stress builds overtime and how that impacts thermal comfort.

In addition to more local and culturally specific data, an additional layer of pedestrian decision making can enhance the function. For instance, the walkshed application is always assuming that a pedestrian will take the shortest path to a unique location, but this misses cases where a slightly longer, but more comfortable path is available to the pedestrian.

6. CONCLUSION

This key metric and representation method are essential to designing resilient, connected, and healthy urban spaces in extreme heat conditions. This method combines outdoor thermal comfort with walking speed and distance to create climate adjusted walksheds. These can be used: As a design tool when planning new urban areas or interventions to help determine the form of the built environment and positioning of canopies, awnings, and trees; As a tool to test how resilient urban area are to the increase in extreme heat events with changing

weather; To argue in favour of investing in pedestrian thermal comfort strategies; And, to promote design for walkability.

ACKNOWLEDGEMENTS

The authors would like to thank the KPFep and KPFui teams for their support in completing this work.

REFERENCES

1. Abley, S. (2005) Walkability Scoping Paper. P 2, New Zealand.
2. O'Shea, C.A. (2023). NASA Clocks July 2023 as Hottest Month on Record Ever Since 1880. *NASA.* [Online], Available: https://www.nasa.gov/news-release/nasa-clocks-july-2023-as-hottest-month-on-record-ever-since-1880/#:~:text=Temperature%20%E2%80%9Cnormals%E2%80%9D%20are%20defined%20by,the%20hottest%20month%20on%20record.
3. Levine, R. V., and Norenzayan, A. (1999). The pace of life in 31 countries. *J. Cross Cult. Psychol.* 30: p 178–205.
4. Rakha, T. (2015). Towards comfortable and walkable cities : spatially resolved outdoor thermal comfort analysis linked to travel survey-based human activity schedules [Thesis, Massachusetts Institute of Technology].
5. Al Sabbagh, Nihal (2019). Walkability in Dubai: Improving Thermal Comfort. [PhD Thesis, The Open University].
6. Balakrishnan, P. (2012). Cool spots in hot climates: A means to achieve pedestrian comfort in Sharjah, U.A.E., [MArch, AA School of Architecture].
7. Zare, S., et. al. (2018). Comparing Universal Thermal Climate Index (UTCI) with selected thermal indices/environmental parameters during 12 months of the year. *Weather and Climate Extremes*, 19: p 49-57.
8. Xie, Y. et al. (2022) Experimental study and theoretical discussion of dynamic outdoor thermal comfort in walking spaces: Effect of short-term thermal history. *Building and Environment*, 216: p. 109039.
9. Shashua-Bar, L., Pearlmutter, D., and Erell, E. (2011). The influence of trees and grass on outdoor thermal comfort in a hot-arid environment. *International Journal of Climatology*, 31(10), 1498–1506.
10. Shashua-Bar L, Erell E, and Pearlmutter D. (2009). The cooling efficiency of urban landscape strategies in a hot dry climate. *Landscape and Urban Planning* 92: p. 179–186.
11. Kariminia, S., Sabarinah, S.A., and Ahmadreza, S. (2015). Microclimatic conditions of an urban square: Role of built environment and geometry. *Procedia-Soc. Behav. Sci.* 170: p. 718–727.
12. Ali-Toudert, F., and Helmut, M. (2006). Numerical study on the effects of aspect ratio and orientation of an urban street canyon on outdoor thermal comfort in hot and dry climate. *Build. Environ,* 41(2): p. 94–108.
13. Balakrishnan, P. (2014). Cool spots in hot climates: a means to achieve pedestrian comfort in hot climates. In *PLEA (Passive Low Energy Architecture).* Ahemdabad, India.
14. Erell, E., Pearlmutter, D., an Williamson, T. (2012). Urban microclimate: Designing the spaces between buildings. In *City Weathers: Meteorology and Urban Design.* Manchester.
15. Evaporative cooling (2023) NZEB. Available at: https://nzeb.in/knowledge-centre/passive-design/evaporative-cooling/ (Accessed: 15 November 2023).
16. Barakat, A., Hany, A., and Zeyad, E.S. (2017) Urban design in favor of human thermal comfort for hot arid climate using advanced simulation methods. *Alex. Eng. J.*, 9: p. 533–543.
17. Blazejczyk, K., and Krawczyk, B. (1994) New climatological-and-physiological model of the human heat balance outdoor (MENEX) and its applications in bioclimatological studies in different scales. *Polish Academy of Sciences Institute of Geography and Spatial Organization.*
18. Kessling, W., Engelhardt, M., and Kiehlmann, D. (2013). The Human Bio-Meteorological Chart – A design tool for outdoor thermal comfort. In *PLEA2013 – 29th Conference, Sustainable Architecture for a Renewable Future*. Munich, Germany, September 2013.
19. Weather Data, [Online], Available: https://energyplus.net/weather
20. Moazami, A., Nik V.M., Carlucci, S., and Geving, S. (2019). Impacts of future weather data typology on building energy performance – Investigating long-term patterns of climate change and extreme weather conditions. *Applied Energy,* 238: p 696-720.
21. Fiala, D., K. Lomas, and M. Stohrer. (2003). First Principles Modelling of Thermal Sensation Responses in Steady State and Transient Boundary Conditions. *ASHRAE Transactions,* 109(1): p. 179–186.

PLEA 2024 WROCŁAW
(Re)thinking Resilience

Rethinking Materials for Buildings:
Exploration of plastic bottles as construction material

SOO JEONG JO[1]

[1]Louisiana State University School of Architecture, Baton Rouge, Louisiana, USA

ABSTRACT: The present study aims to explore the potential of plastic bottles as construction material focusing on the structural systems of the construction. This research was motivated by the increasing concern for plastic waste and pollution, that threatens human health and ecosystems, and seeks a solution to this plastic waste problem by identifying the feasible construction methods utilizing plastic bottles. To achieve this research goal, a systematic review of literature and projects was conducted, and an educational activity was developed based on the review. In the educational activity, eleven teams of two students worked on a plastic bottle chair project utilizing various construction methods and complementary materials. The project outcome showed the good potential of plastic bottles as construction materials and the bottles may be used without infilling materials if a proper system for structural connection and support can be developed. The significance of this study is the effort to introduce plastic bottles and the supporting systems as general construction materials, and the methodology that reviews multiple cases rather than a single project. The contribution of this study is promoting circular material cycle and affordable construction utilizing this "low tech - high impact" process.
KEYWORDS: Recycle, Plastic bottle, PET, Chair, Construction

1. INTRODUCTION

Increasing plastic waste and pollution have become a major concern recently, threatening human health and ecosystems. According to UNESCO, about 80% of marine pollution is plastic waste (Figure 1), which affects around 17% of marine species [16]. Although the production of plastic in the last ten years outweighs the production in the previous century, which may triple the amount of plastic waste in oceans by 2040, only 10% of the current plastic waste is being recycled [15-16]. The negative impacts of plastic waste have been widely known, such as the contamination of the environment, air pollution from uncontrolled incineration, and food contamination for wildlife and human beings [18].

Figure 1: About 80% of marine pollution is plastic waste (source: Science Photo Library, CC BY-NC).

Responding to these issues, Fischer and Kowalski (1998) stated that the material cycle loop should be closed by utilizing wastes as material resources [3]. Also, Braungart and McDonough (2022) mentioned that the zero-waste design with a circular approach should be part of green city planning [7]. One of the effective ways of participating in these zero-waste efforts in the building industry would be increasing recycled materials for construction, which may reduce the need for new materials and processing [11].

This paper particularly focuses on plastic bottles, one of the most used items in the world, exploring their potential as construction materials through a literature review and educational activities under the following research question: how plastic bottles can be assembled while gaining the required structural capacity for construction? The effort to identify the prototypes and generalize the findings based on multiple projects rather than focusing on a single project as a one-time event may be the significance of this study, which would help further dissemination of the construction using plastic bottles.

2. BACKGROUND

As the problem of plastic waste and pollution has been exacerbated, researchers and educators have tried to find a solution by utilizing plastic bottles for design and building material studies. Lalzarliana, Lalngaihawmaa, and Sainia (2018) emphasized the growing concerns about the demolition wastes of concrete constructions and plastic wastes and proposed a combination of these two materials, plastic bottles filled with crushed concrete aggregates, as construction materials. By testing different mixing

ratios, they found that 5% was the optimal water content for compressive strength.

Nováková, Šepsb, and Achtena (2017) developed a recycled product, PET(b)rick, focusing on the stacking feature and blow-molding technology of the recycled plastic material. By testing the structural performance of the materials, they found that the proposed material has sufficient resistance to stress, pressure, heat, and freezing to be a fill-in material if an appropriate medium can be filled with an appropriate amount. They also claimed that exhibiting designs made of recycled materials, such as PET(b)rick, may have a social impact appealing to others to think further about plastic waste problems and actions they can do [11].

Mansour and Ali (2015) also conducted experiments focusing on the infill materials to investigate and compare the structural and thermal performance of plastic bottles filled with different materials. Their study results indicated that plastic bottle blocks have a good structural capacity for partition walls or bearing walls for one roof slab. The study also found that the thermal capacity of air-filled bottles was higher compared to dry or saturated sand-filled bottles or conventional block construction, which shows the potential of plastic bottles as thermal insulation material [6].

Haque and Islam (2021) focused on the application of the plastic bottle brick that they developed in the Rohingya displacement camps in Bangladesh, which is the largest refugee camp in the world. The current shelters in the camps are not resistant enough to natural disasters in the region, thus, the refugees in the camps suffer from unstable and unhygienic living conditions. The authors developed a plastic brick system utilizing plastic bottle wastes to provide an affordable solution to this problem. In this system, the bottles were filled with sand and placed at the center of the cardboard-framed brick. The space between the bottle and frame was filled with hand-blended mortar, which helped gain the structural capacity to resist extreme weather conditions [5].

In addition to the aforementioned research, artistic installations and projects have been also performed by various designers and artists. For example, Archtech S.r.l. built Two-O-Four Chair in Trento, Italy [13]. This chair design emphasizes the transparency of the chair by using transparent plastic bottles and lighting. Similarly, Pawel Grunert exhibited the SIE43 Chair in Milan, Italy [17]. This project uses a metal frame to support plastic bottles and create the wave shape of the chair. Also, Varnai Gyula displayed an installation artwork, Giant Armchair, in Budapest, Hungary utilizing 2,500 plastic bottles stacked with packing tapes [9]. Different from other projects, the Human-Computer Interaction Lab at the Hasso Plattner Institute in Potsdam, Germany, focused on the connector design of plastic-bottle truss structures [2].

While the reviewed research achieved the structural strength of plastic bottles for construction by studying the performance of infill materials and filling the bottles with the materials, the reviewed artworks used various connectors and framing systems for stability and strength. Although many similar studies and projects are found in the literature, most studies tend to focus on one project rather than comparing multiple projects and identifying prototypes. Also, not many studies on stacking and connecting systems for plastic bottles are available. The present study aims to fill this knowledge gap and identify stack and connection prototypes for construction with plastic bottles.

3. METHODOLOGY

The present study employed a qualitative case study approach that allows an empirical, holistic, and multifaceted investigation in a real-world setting [41014]. To perform the study, relevant literature and existing projects were first reviewed, then, a design-build project for an architecture course was developed based on the review. The course was an elective for 4th and 5th year undergraduate students and graduate students about sustainability. In the proposed design-build project, each group had two students to design and build a one-to-one scale chair made of recycled plastic bottles. Although students could choose the materials for stacking and connecting the bottles, only recycled or biodegradable material options were allowed. The project poster had to describe the material selection process, design concept, and construction process, such as sketches, diagrams, and photos of the testing and making processes. For example, a group presented a photo of an experiment to compare the structural capacity of different plastic bottles to explain their material selection processes (Figure 2). Another group presented their construction process and explained how a truss structure could become a support for the seat (Figure 3).

The evaluation criteria of the project were *Material selection, Structural stability, Efficiency, Comfort*, and *Creativity*. In the *Material selection* criterion, the primary material should be plastic bottles or jars, while other recycled or biodegradable materials should be complementary for structural support. In the *Structural stability* criterion, the load-bearing capacity of the chair should be a minimum of 200 lb (91 kg). In the *Efficiency* criterion, the making process should be short and simple enough to easily assemble and disassemble the chair. In the *Comfort* criterion, the ergonomics of the chair were evaluated, such as the chair dimensions, including the height, compared to average human body sizes. In the *Creativity* criterion, creative and innovative design that experiments with

a unique and novel chair form and structure received additional points.

Figure 2: Material selection process of a project – comparing the structural capacity of a water bottle and a sports drink bottle to explain the team's material finding process (source: Gabe DeLiberty, Leah LeBlanc).

Figure 3: Construction process of a project – utilizing truss structure for the support (source: Omid Elhami, Maryam Sinejani).

After the evaluation of the projects, the structural materials and design approach of each team were analyzed and compared to categorize the information. This result was compared to the referenced projects and literature. Figure 4 summarizes the process of this study.

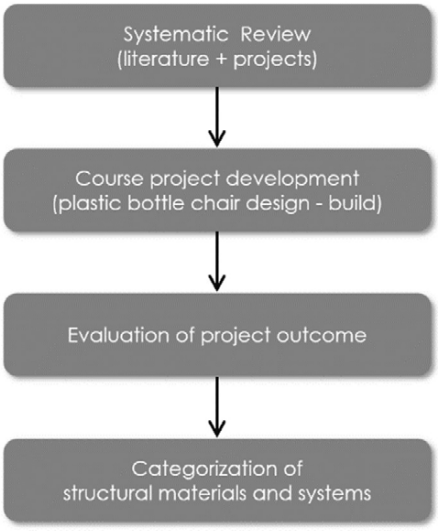

Figure 4: Process of the present study.

4. RESULTS AND DISCUSSIONS

A total of eleven chairs were designed and built as an outcome of this project. Plastic bottles of different types and sizes were used for the project, such as water bottles and jars, other drink bottles, and milk jars. Some projects actively utilized the colors of the bottles to achieve the color scheme of the team's design (Figure 5).

Figure 5: Made of sports drink bottles, biodegradable tapes, and packaging boxes. The colors of the bottles were actively utilized to achieve the color scheme of the design (source: Gabe DeLiberty, Leah LeBlanc).

For structural connections and supports, wrapping, framing, filling, and weaving were the primary methods. Employed materials for the project were as follows: boxes, edge protectors for packaging, twine, soil and gravel, plastic wraps, and plastic bags. Some projects added non-structural materials, including newspapers and plants, to improve the comfort and sitting experience for the users. Table 1 shows the various construction strategies of the chairs completed in this project. It should be noted that some materials minimally used in the project were not counted in this categorization. Also, the total number of teams in the table exceeds 11 due to the teams employing multiple methods and materials.

Table 1: Construction and material strategies of the plastic bottle chair projects.

Projects	Primary material	Supporting material	Construction methodology
1	Milk jar	Plastic wrap	Wrapping
2	Water bottles and jars	Twine	Weaving
3	Water bottles	Edge protectors, screws	Framing
4	Sports drink bottles	Boxes, tapes	Framing
5	Water bottles	Plastic bags, newspapers	Weaving
6	Water bottles and large drink bottles	Yarn, plastic wrap	Weaving and wrapping
7	Water bottles	Plastic wrap, boxes, newspapers	Wrapping and framing
8	Water bottles	Wood bars, tapes	Wrapping and framing
9	Water bottles	Twine, plants, boxes, water, clothes	Weaving, framing, filling
10	Water bottles and jars, large drink bottles	Plastic wrap, boxes	Wrapping and filling
11	Water bottles	Twine, boxes	Weaving and wrapping

The distribution of structural approach in this project was as follows:

- Wrapping – 6 teams
- Framing – 5 teams
- Weaving – 5 teams
- Filling – 2 teams

The distribution of structural framing and connection materials in this project was as follows:

- Boxes – 5 teams
- Plastic wrap – 4 teams
- Twine – 3 teams
- Tapes – 2 teams
- Edge protectors – 1 team
- Plastic bags – 1 team

Figures 6 - 8 show the example projects that employed wrapping, framing, and weaving methods respectively.

Figure 6: Made of milk jars and used plastic wraps. Primary construction method is wrapping (source: Adeyinka Ariwajoye, Nicole Jacobo).

Figure 7: Made of water bottles and used edge protectors. Primary construction method is framing with edge protectors and screws (source: Omid Elhami, Maryam Sinejani).

Figure 8: Made of twine, water bottles and jars. Primary construction method is weaving (source: Jiahui Li, Sanaz Salajegheh).

The result of this study showed that plastic bottle chairs could gain the required structural strength without filling the bottle with additional materials other than air if a proper support or stacking system can be developed. This may be the reason that not many students chose to use filling compared to wrapping, framing, and weaving. The most preferred material for structural support was boxes due to the easy access to the material. Plastic wraps were also used by four teams claiming that those materials were recycled or biodegradable. Twines and tapes were purchased materials, but biodegradable products. Not many groups chose to use edge protectors for their structural materials, but many noted them as promising materials since they are often used for packaging. Plastic bags were all recycled and easy to access, however, the processing time for using the bags as connectors was longer than other methods.

The most challenging part of the project was supporting the seat at an appropriate height. Except for specific design concepts that require a low height, a comfortable height, which is around 16 – 18" (400 – 450mm), had to be provided for the seat. Students who did not use a framing system for the support had to find plastic bottles with the right size and structural strength, and a good assembly method that could achieve the required height and support the required structural load. Another challenge that the project teams faced was the controversy about the sustainability of the connection and support materials. Although plastic and metal products for structural connections, such as plastic wraps, plastic bags, and edge protectors, were recycled materials from other packages, they are not biodegradable, and their availability may be discontinuous. These issues can make the sustainability of structural materials questionable. Despite the challenges, the completed chair project showed the potential of plastic bottles as construction materials for indoor environments and identified various feasible construction approaches.

5. CONCLUSION

The present study was motivated by the increasing concern about plastic waste and pollution and tried to find a solution to this problem by exploring the potential of plastic bottles as a construction material. Questioning the structural connection and stability of the construction using plastic bottles, existing research and some design-build projects were reviewed. Based on the review, a plastic bottle chair project was developed in an elective course for upper-level undergraduate and graduate students in an architecture program. In this project, eleven teams of two students designed and built one-to-one scale chairs made of plastic bottles experimenting with various assembly methods. The project outcomes showed that providing a framing system to stack and support plastic bottles was the most preferred structural solution by the designers, and the boxes were the most popular material for the support. The small sample size would be the limitation of this study; thus, further studies are necessary to generalize these findings.

The present study may contribute to minimizing plastic waste by reclaiming plastic bottles as construction material that may help create a circular material cycle loop. In addition to this environmental contribution, the present study may promote more affordable design using plastic bottles that do not require specialized knowledge to build, in other words, a low-tech, but bringing a high impact [12]. The case study and comparative analysis approach of this research investigating multiple projects may be helpful in generalizing the findings and identifying the prototypes of the construction with plastic bottles. Finally, introducing further studies on recycled materials in architectural education may contribute to the dissemination of recycled materials in the building industry. Inviting students, who are future professionals, to the ongoing discussions on plastic waste and pollution and how to collaborate with others to solve these issues, may lead to a broader impact of the study. Future research can be continued to further projects and courses for expanding the sample size. Also, the scale of the design-build projects can be enlarged to walls or pavilions to expand the structural challenges and discussions.

REFERENCES

1 . Cook, C. R., & Halden, R. U. (2020). Ecological and health issues of plastic waste *Plastic waste and recycling* (p. 513-527): Elsevier.

2 . District, M. (2017). TRUSSFAB: CREATING LARGE-SCALE STRUCTURES FROM PET BOTTLES. from https://materialdistrict.com/article/trussfab-structures-pet-bottles/

3 . Fischer-Kowalski, M. (1998). Society's metabolism: the intellectual history of materials flow analysis, Part I, 1860–1970. *Journal of industrial ecology, 2*(1), p. 61-78.

4 . Groat, L. N., & Wang, D. (2013). *Architectural research methods*: John Wiley & Sons.

5 . Haque, M. S., & Islam, S. (2021). Effectiveness of waste plastic bottles as construction material in Rohingya displacement camps. *Cleaner Engineering and Technology, 3*, p. 100110.

6 . Mansour, A. M. H., & Ali, S. A. (2015). Reusing waste plastic bottles as an alternative sustainable building material. *Energy for sustainable development, 24*, p. 79-85.

7 . McDonough, W., & Braungart, M. (2010). *Cradle to cradle: Remaking the way we make things*: North point press.

8 . Miandad, R., Barakat, M., Aburiazaiza, A. S., Rehan, M., Ismail, I., & Nizami, A. (2017). Effect of plastic waste types on pyrolysis liquid oil. *International biodeterioration & biodegradation, 119*, p. 239-252.

9 . Morgan, H. (2012). Giant Armchair Constructed From 2,500 Salvaged Plastic Bottles by Várnai Gyula. from https://inhabitat.com/giant-armchair-constructed-from-2500-salvaged-plastic-bottles-by-varnai-gyula/

10 . Noor, K. B. M. (2008). Case study: A strategic research methodology. *American journal of applied sciences, 5*(11), p. 1602-1604.

11 . Nováková, K., Šeps, K., & Achten, H. (2017). Experimental development of a plastic bottle usable as a construction building block created out of polyethylene terephthalate: Testing PET (b) rick 1.0. *Journal of Building Engineering, 12*, p. 239-247.

12 . Paihte, P. L., Lalngaihawma, A. C., & Saini, G. (2019). Recycled Aggregate filled waste plastic bottles as a replacement of bricks. *Materials Today: Proceedings, 15*, p. 663-668.

13 . S.r.l., A. (2014). Two-O-Four Chair. from https://architizer.com/projects/two-o-four-chair/

14 . Silverman, R. M., & Patterson, K. (2021). *Qualitative research methods for community development*: Routledge.

15 . UNEP. (2023). UN Environment Programme. from https://www.unep.org/interactives/beat-plastic-pollution/

16 . UNESCO. (2023). Ocean Literacy Portal. from https://oceanliteracy.unesco.org/plastic-pollution-ocean/

17 . Yoneda, Y. (2012). Pawel Grunert's SIE43 Chair is Made from a Cascade of Clear Blue Plastic Bottles. from https://inhabitat.com/pawel-grunerts-sie43-chair-is-made-from-a-cascade-of-clear-blue-plastic-bottles/

PLEA 2024 WROCŁAW
(Re)thinking Resilience

Plot Vs Block Developments

Thermal Comfort in Planned Urban Residential Neighbourhoods for Dhaka

AFEEFA ADEEBA RAHMAN[1,2], ATIQUR RAHMAN[1]

[1]Bangladesh University of Engineering and Technology, Dhaka, Bangladesh

[2] Military Institute of Science and Technology, Dhaka, Bangladesh

ABSTRACT: Urban microclimates play an important role in the comfort sensation of the urban residents for their productivity and well-being and impact energy consumption and sustainability. Various building and planning regulations in the case of plot distribution are responsible for creating a varying urban microclimate that affects the comfort parameters of the residents. The recent update of the DAP (Detailed Area Plan 2022-2035 for Dhaka) has introduced the block concept with the prevailing plot-based development policy. The variation of the building block and plot-based development policy will influence the urban microclimate and eventually control the environmental parameters affecting the comfort of the residents. This paper aims to measure the environmental impact of neighborhoods with block and plot developments to compare them to identify the development with better thermal performance for a residential neighborhood. The methodology includes a literature review, selection of sample sites, simulation and analysis, and comparison of the results. The lack of existing real cases of block development for a physical survey is considered the limitation of the study. The paper concludes with the block-based development having better thermal performance with the scope of further exploration of the block morphology to give guidelines for future residential neighborhoods.
KEYWORDS: Sustainability, Energy Efficiency, Thermal Comfort, Simulation.

1. INTRODUCTION

According to the ASHRAE standards, thermal comfort is a sensation or psychological state of mind to feel the impact of the surrounding environment [1]. The environmental factors of Air temperature, Radiant temperature, Airspeed, and Humidity affect the thermal feeling. Urban morphology is important in thermal sensation by affecting the urban microclimate [2].

The arrangement of the buildings in the urban area creates a unique microclimate and regulates thermal comfort. From the bioclimatic chart of Olgay, in a tropical area like Bangladesh, to ensure thermal comfort, it needs wind flow (to ensure evaporative cooling) and to minimize heat gain by solar radiation [3]. Considering the effectiveness of block development, a new proposal is made in the Detailed Area Plan 2022-2035 keeping the provision for plot unification and developing building blocks with the criteria of the unified plot following the Floor Area Ratio (FAR) and Maximum Ground Coverage (MGC) following the building regulations [4].

This paper aims to study the microclimate of the urban neighborhood with existing plot development and future block-based development to analyze the environmental parameters of outdoor temperature, wind flow, solar radiation, relative humidity, etc., and compare the aspects of thermal comfort based on the comfort parameters in the context of Dhaka City to suggest probable scope for a resilient neighborhood.

2. METHODOLOGY

The research approach is a mixed method that includes experimental and simulation studies. The literature review and microclimatic study identify the parameters for the thermal comfort of Dhaka city. The literature review also helps to identify the research gap in the specific field in the context of Dhaka. The research concludes by analyzing and comparing the microclimatic simulations of the existing plot-based and future hypothetical block development in ENVI-MET (demo version 5.0.1) [5].

2.1 Literature Review

Various studies have addressed the impact on urban geometry and morphology to identify the impact on human thermal comfort in Dhaka City. One study concludes that the small plot-based development hampers thermal comfort by reducing airflow and trapping more solar radiation. Shifting and going to blocks can increase airflow and keep space for urban communities [6]. Another study identifies the urban geometry of Dhaka city as the guiding element for outdoor thermal comfort in the summer PET range (Physiological Equivalent Temperature) [7]. Studies have also addressed the comparison of urban microclimate and comfort situations following different updates of building regulations of Dhaka City [8, 9].

The government of Bangladesh has proposed a block-based development system rather than plot-based

development in the new Detailed Area Plan (DAP) to ensure sustainable development goals [4]. To ensure Dhaka city's future livability and sustainability, the DAP proposes to keep greater open space by allowing greater heights for the new buildings by merging the small plots for block-based design [10].

2.2 Dhaka City Comfort and Microclimate Study

The exposure to uncomfortable outdoors makes the indoors uncomfortable [11, 12]. From the existing comfort studies of Dhaka city, the thermal comfort temperatures vary from (23.1-32.5)^{0}C[12, 13].

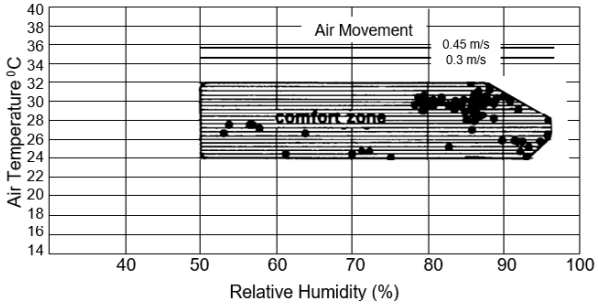

Figure 1: Outdoor comfort zone, summer [13].

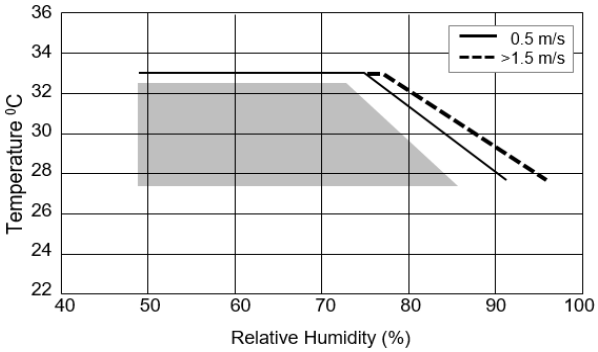

Figure 2: Outdoor comfort zone, summer [12].

The Average temperature of cooling months (March to October) is higher than 30 ^{0}C and the Maximum temperature of summer months is higher than 35 ^{0}C indicating a need for higher energy need for cooling to ensure comfort [14]. Feeling conditions in ladybug grasshopper from the three available EPW files (Shahjalal International Airport, Tejgaon AB, and Tejgaon MIL) of Dhaka City, in all three cases, above 60%-time people feel hot considering hot, neutral, and cold that needs strategies to maintain neutral condition to ensure thermal comfort.

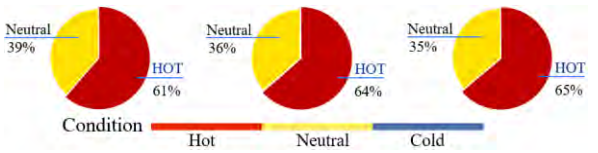

Figure 3: Hot and neutral feelings Percentage (EPW analysis in Grasshopper) [15, 16].

Olgyay's bioclimatic chart for thermal comfort shows that the comfort zone can be extended upwards to a higher temperature and downwards to a lower temperature using air movement and radiation respectively. But, from Figure 4, since the upper limit needs to be addressed to ensure comfort in Dhaka city, Air movement should be increased decreasing solar Radiation [3].

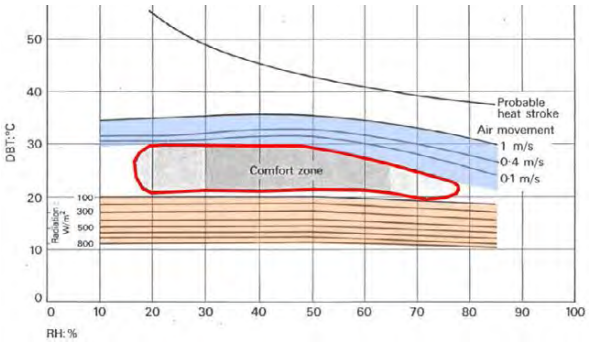

Figure 4: Bioclimatic Chart for tropical region [3].

2.3 Selecting the sample site

The sample site is a small area of Purbachal, primarily developed based on Plot layout but has the flexibility to Block development according to the new gazette of DAP 2022-2035.

In the plot-based development, the total area for 13 plots in sqm is 7438, and considering the FAR rules from Imarot Nirman Bidhimala 2008 (Building construction rules, 2008), the total floor area is 36,419.24 sqm with FAR 4.52 and the total ground coverage is 4276.35 sqm with MGC 57.5 and minimum stories for each building is 8-stories.

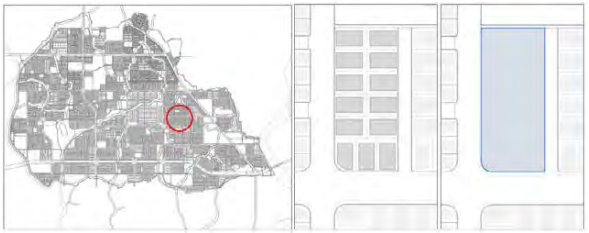

Figure 5: From left to right, Selected site in Purbachal Masterplan, Plot-based Development, Scope for Block-based Development.

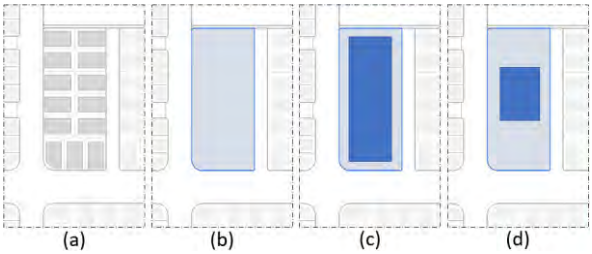

Figure 6: (a) Plot Layout, (b) Site for Block Layout, (c) Footprint with summation of plot development, (d) Footprint with height flexibility for the block.

In the block-based development, the total area by merging 13 plots in sqm is 7438, and considering the FAR rules from Imarot Nirman Bidhimala 2008 and maintaining the density and keeping the total floor area to be 36,419.24 sqm.

Considering the extendable height provision from DAP 2022, the ground coverage is kept at 2,276.2025 sqm with 16 stories. The total floor area is kept the same, to accommodate the same number of people considering the density concern. The development is such that it has a scope for urban community space enhancing environmental quality where trees can be planted that can further reduce air temperature by evapotranspirational cooling.

3. ANALYSIS AND COMPARISON

For the analysis of environmental parameters in plot-based and block-based development, the cases are simulated in ENVI-MET (demo version 5.0.1) after setting up the same criteria for each case. Both the developments are modeled with ENVI-MET spaces with Dhaka for location considerations. The Block-based model since it has a large open space has the provision for green incorporation, and so, 3d trees are added in this model. In the set-back area of all the buildings in each case, simple grass is added. No additional tree is added in the plot-based development due to the lack of available space [5].

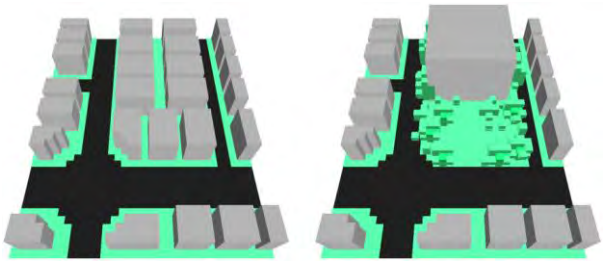

Figure 7: Plot-based (left) and block-based (right) development models of an area of Purbachal, Dhaka in ENVI-MET [5].

The simulation file is prepared with simple forcing on the hot day of the summer equinox of 21 June 2023. Considering the weather from the historical climatic database of Dhaka City based on the weather station, temperature, and humidity are set with maximum and minimum temperatures of 33 ^{0}C and 28 ^{0}C with the time of maximum and minimum temperatures at 1600 o'clock and 0400 o'clock, and with maximum and minimum relative humidity of 66% at 0400 o'clock and 91% at 1300 o'clock respectively with wind direction of 180 (direct south). The simulation is run for 48 hours starting at 0300 o'clock having the first 24 hours for model stabilization and the rest to get the full-day profile of microclimatic analysis. The simulation results are analyzed, compared, and visualized in ENVI-MET Leonardo [5, 17]. For analysis, the hours considered are the hottest hours (after stabilizing the model) of 1200 o'clock to 1700 o'clock on June 22, 2023.

3.1 Analysis of Wind Speed

The wind speed of both plot and block-based developments are analyzed in the hottest hour of the day (1600-1700 o'clock), in all the axes. The accumulated result of each hot hour starting from 1200 o'clock to 1700 o'clock shows that the average wind speed at that time in plot-based development and block-based development are respectively 1.23 and 1.37 m/s. This indicates that, in block-based development, due to better wind aperture and larger open space in front of the building, there is a better provision for wind flow that can be accessed in this case with no additional building barrier. The building height also gives better access to wind in the facades.

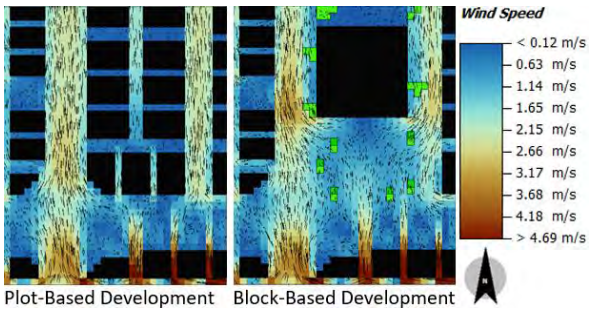

Figure 8: The visualized data layers of wind speed in the XY-axis on Leonardo, ENVI-MET [5].

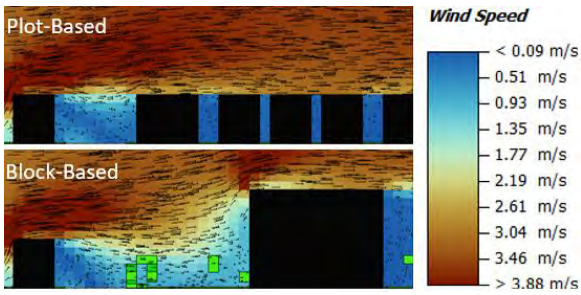

Figure 9: The visualized data layers of wind speed (m/s) in the YZ-axis on Leonardo, ENVI-MET [5].

In plot-based development, all the buildings have similar heights having very less set-backs as open space. So the buildings act as a single building with a large area footprint and the wind flows above the buildings (Figure 9) allowing very little to no wind penetration inside the buildings except for the ones in the south. In this case, most of the buildings fall under the wind-shadow zone having no wind movement in the rest of the buildings. Whereas in block-based development due to having larger open space, wind can penetrate better inside the open space.

3.2 Analysis of Solar Radiation

According to the bioclimatic chart, in the context of Dhaka city having a warm-humid climate, the solar radiation needs to be reduced to minimize heat gain to ensure thermal comfort in the summer period. The simulation results from ENVI-MET Leonardo for direct, diffused, and reflective solar radiations in the plot-based model are higher than the block-based model, indicating an improvement in solar heat gain.

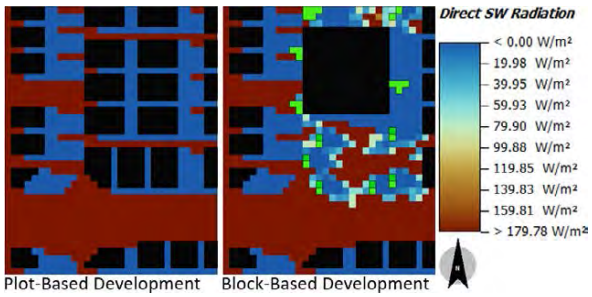

Figure 10: Visualization of Direct solar radiation in Leonardo, ENVI-MET [5].

Considering the additional open space in the block-based development that can be utilized in incorporating landscape features of vegetation or waterbody can help reduce the solar radiation gain in this case. The vegetation helps reduce solar gain by creating shadow and both trees and water can help in evaporative cooling.

For the plot-based model, the three types of solar radiation values (direct, diffused, and reflected) are respectively, 229.17 W/m^2, 205.54 W/m^2, 116.64 W/m2, and for the block-based, the reduced radiations are 203.17 W/m^2, 197.37 W/m^2, 107.82 W/m2 respectively. The comparisons are visualized in Figure 10-12 and analyzed in Table 1, showing an individual and overall reduction in heat gain by solar radiation in the block-based development.

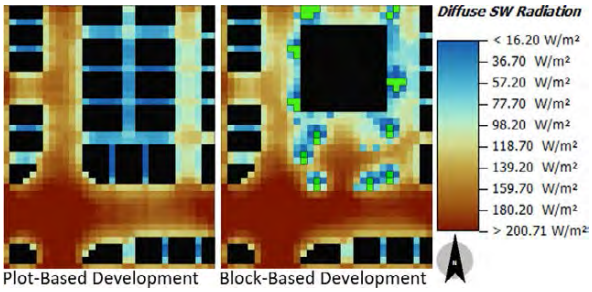

Figure 11: Visualization of Diffused Solar Radiation in Leonardo, ENVI-MET [5].

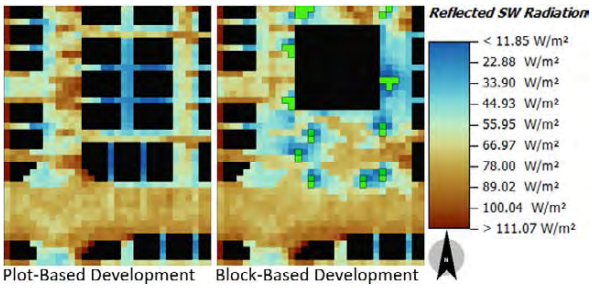

Figure 12: Visualization of Reflected Solar Radiation in Leonardo, ENVI-MET [5].

3.3 Analysis of Relative Humidity

Considering the hot and humid climate of Dhaka, the humidity remains higher in the hottest months creating additional discomfort [3]. A minimization of relative humidity will facilitate better evaporative cooling for thermal comfort. In the sample sites, the incorporation of the trees in the open space of the block model might have increased the humidity level to a very low percentage of 0.49% which is from 56.22% to 56.71% that can be neutralized by the higher wind flow as seen from the data analysis of wind velocity comparison from 3.1.

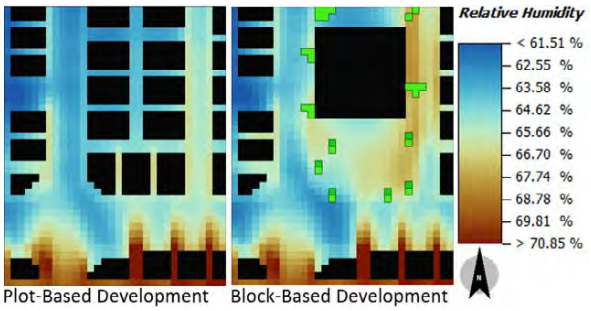

Figure 13: Visualization of Relative Humidity in Leonardo, ENVI-MET [5].

3.4 Analysis of Potential Air Temperature

To ensure thermal comfort in the hot summer day of a tropical climate like Dhaka, the potential air temperature needs to be reduced as the maximum feeling condition is hot (Figure 3).

Analyzing the results, the Potential Air Temperature (PAT) in plot-based development is 34.24 ^{0}C and in block-based development, it could be reduced to 33.09 ^{0}C due to the incorporation of green and open space and also due to the reduction in footprint and roof surface area. The decrease in potential air temperature leads the overall environmental quality towards comfort range to ensure the thermal comfort of the residents.

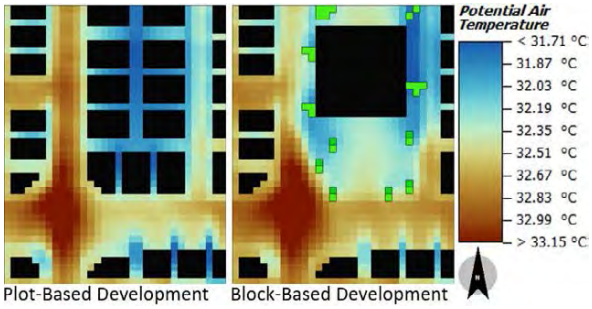

Figure 14: Visualization of Potential Air Temperature in Leonardo, ENVI-MET [5].

3.5 Analysis of Mean Radiant Temperature

Analysis of the Mean Radiant Temperature (MRT) in the sample models shows that the block model has a lesser value for the MRT that is 54.97 ^{0}C which is 1.79 ^{0}C lower than the plot-based model of 56.76 ^{0}C indicating betterment in environmental character for user comfort.

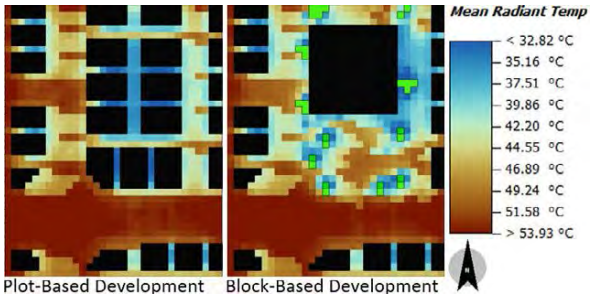

Figure 15: Visualization of Mean Radiant Temperature in Leonardo, ENVI-MET [5].

4. FINDINGS AND RESULT

The analysis of environmental data for each model (plot and block-based) in Table 1 shows that the block model except for the Relative Humidity, performs better for criteria of thermal comfort. The humidity although higher in the block-based model, can be further channelled by wind flow with further research in block model variation as mentioned in section 6.

Table 1: Environmental parameters for plot-based, block-based situations and comparison of change.

Environmental Parameters	Plot-based development	Block-based development
Wind speed m/s	1.23	**1.37**
Direct Solar Radiation (W/m^2)	229.17	**203.17**
Diffused Solar Radiation (W/m^2)	205.54	**197.37**
Reflected Solar Radiation (W/m^2)	116.64	**107.82**
Relative Humidity %	56.22	**56.71**
Potential Air Temperature ^0C	34.24	**33.09**
Mean Radiant Temperature ^0C	56.76	**54.97**

The simulation analysis conducted in ENVI-MET (demo version 5.0.1) shows that:

- The wind speed is increased from 1.23 m/s to 1.37 m/s which is an overall increase of 11.4% approximately.
- The mean radiant temperature and potential air temperature have decreased in block development which positively affects the thermal comfort in the context of Dhaka [5]. The decreases are respectively 1.79 ^0C and 1.15 ^0C.
- The decrease in direct, diffused, and reflected solar radiations are respectively 26 (W/m^2), 8.17 (W/m^2), and 8.82 (W/m^2). So the overall decrease in heat gain by solar radiation is 42.99 (W/m^2).
- The increase in relative humidity is 0.29%, which can be minimized again by the existing increased wind flow in the block-based development.

5. LIMITATIONS OF THE RESEARCH

Due to the absence of existing real cases of plot-based development (under construction) which has the option of block-based development, the physical survey of the case is yet to be carried out.

6. FUTURE SCOPE OF THE RESEARCH

The development of guidelines for future block-based growth of Dhaka City is the main future possibility of the research.

- Analysis of environmental parameters in different sites with variation in orientation and wind access and analyzing the sites with block-based developments can be a future research focus.
- Using various aspects of the block layout like single buildings or multiple buildings, their orientation, façade treatment, solid void relationship, etc.
- Analyzing different entry routes to the site to further explore the feasibility of various block layouts.

7. CONCLUSION

The paper gives insights into the probable positive change in the environmental parameters in the future Block-based development to lead towards thermal comfort. Various morphological changes in the building mass and layout can be attained with the block concept that can address environmental considerations. The block development not only has scope for additional community space but also facilitates better airflow and reduces potential and mean radiant temperature showing better thermal comfort. So the block development can be further studied and worked to explore the possibilities of block-based development to implement a block-based layout for ensuring the future livability of Dhaka city based on thermal comfort.

The paper concludes with recommendations for developing the block concept in not only the residential sector but also in other sectors of the city let alone the country to incorporate the environmental aspects to attain user comfort for the resilient living of the future.

ACKNOWLEDGEMENTS

The authors express their gratitude to the Department of Architecture, of their affiliated Institutions.

REFERENCES

1. ASHRAE, (2021). 2021 ASHRAE Handbook—Fundamentals. ASHRAE.
2. Tumini, I., Higueras García, E., and Baereswyl Rada, S., (2016). Urban microclimate and thermal comfort modelling: Strategies for urban renovation. International Journal of Sustainable Building Technology and Urban Development, 7(1): p. 22–37, [Online], Available: https://doi.org/10.1080/2093761X.2016.1152204
3. Koenigsberger, O., Ingersoll, T., Mayhew, A., & Szokolay, S. (1975). Manual of tropical housing. y Orient Blackswan Private Limited, [Online], Available: https://www.academia.edu/30105808/Manualoftropicalhousing_koenigsberger_150824122547_lva1_app
4. রাজধানী উন্নয়ন কর্তৃপক্ষ (রাজউক), Government of Bangladesh GOB, and গৃহায়ন ও গণপূর্ত মন্ত্রণালয়, (2022). DAP Vol-I.
5. ENVI-met, (2022). ENVI-met Decoding Urban Nature (5.0.1) [Computer software].
6. Ahmed, Z. N., (2015). Small Plots or Blocks? Planning for the future. Energy & Power; Fortnightly Magazine, Ed. M.M.A. Hossain: p. 123-129.
7. Sharmin, T., Steemers, K., and Humphreys, M., (2019). Outdoor thermal comfort and summer PET range: A field study in tropical city Dhaka. Energy and Buildings: p. 198, 149–159, [Online], Available: https://doi.org/10.1016/j.enbuild.2019.05.064
8. Iftekhar R., (2015). Study on the impact of building regulation on street morphology and ensuing microclimate in planned residential area of Dhaka City. Department of Architecture.
9. Sharmin, T., and Rahaman, M., (2023). A new workflow of urban scale 3D modelling and simulations to test the implications of the latest area-based FAR regulations on microclimate in the megacity Dhaka.
10. Islam, M. J., (2022) No more plot housing scheme for Dhaka as gazette issued finalising DAP. The Business Standard, August 23, [Online], Available: https://www.tbsnews.net/bangladesh/gazette-issued-finalising-1528-sq-km-dap-area-dhaka-city-482462.
11. Lee, K., & Lee, D., (2015). The Relationship Between Indoor and Outdoor Temperature in Two Types Of Residence. Energy Procedia: p. 78, 2851–2856, [Online], Available: https://doi.org/10.1016/j.egypro.2015.11.647.
12. Ahmed, K. S., (2003). Comfort in urban spaces: Defining the boundaries of outdoor thermal comfort for the tropical urban environments. Energy and Buildings, 35(1): p. 103–110 August 23). https://doi.org/10.1016/S0378-7788(02)00085-3.
13. Mallick, F. H., (1996). Thermal comfort and building design in the tropical climates. Energy and Buildings, 23(3): p. 161–167, [Online], Available: https://doi.org/10.1016/0378-7788(95)00940-X
14. Climaplus Mit., (n.d.). [Online], Available: from http://climaplusbeta.com/.
15. Ladybug Tools (1.6), (2022). [Computer software], [Online], Available: https://www.ladybug.tools/
16. Rhinoceros 3D (7.13), (2021). [Computer software] , [Online], Available: https://www.rhino3d.com/.
17. Weather Spark, (n.d.). Dhaka 2022 Past Weather (Bangladesh). Weather Spark, [Online], Available: https://weatherspark.com/h/y/111858/2022/Historical-Weather-during-2022-in-Dhaka-Bangladesh#Figures-Summary.

PLEA 2024 WROCŁAW
(Re)thinking Resilience

Combining Transfer Learning and Synthetic Time-Series Data to Predict Building Energy Consumption

PHILIP LAY[1], SEYED AZAD NABAVI[1], PHILIPP GEYER[1]

[1]Institute for Design and Construction, Leibniz University Hannover, Hannover, Germany

ABSTRACT: This study explores the usability of pretrained & fine-tuned data-driven building energy models to enhance model transferability across buildings. Using this transfer learning approach, four models were pretrained on synthetic data and tested on real building data. Two models were applied directly to the test data, and two models were previously fine-tuned. Fine-tuning involved adjusting the pretrained models by using the initial parameters for further optimization. Utilised algorithms were Multiple Linear Regression (MLR) and Random Forest Regression (RFR). The synthetic data were generated by simulating 804 variants of physical building energy models, using EnergyPlus. The MLR model applied directly to the target data performed with a mean CV-RMSE of 25.3 % and the RFR model with a mean CV-RMSE of 31.2 %, which decreased to 26.1 % after fine-tuning. Although these results show lower accuracy compared to models developed in similar studies, the models offer improved generalization and lower computational cost. The enhanced generalization potential enables these models to be versatile in various building types and scenarios. This is especially relevant for applications in data-scarce environments, where historical building data are inaccessible. Additionally, their lower computational cost enables more frequent usage in resource-limited settings, such as optimization.
KEYWORDS: Building Energy Modelling, Building Energy Prediction, Data-Driven Model, Transfer Learning, Data Scarcity

1. INTRODUCTION

Buildings accounted for 34 % of the global final energy consumption in 2022 and the energy demand in buildings is continuously trending upwards with a 1 % growth rate over the last decade [1]. Directly and indirectly, this energy consumption is negatively impacting the environment. 33.5 % of global carbon dioxide emissions were related to building operations and construction in 2022 [1]. Reduced energy consumption enhances the environmental performance of a building. To analyse the situation of a particular building in this regard, Building Energy Modelling (BEM) and Building Performance Simulation (BPS) allow to simulate the energetic behaviour of a building [2]. BEM and BPS provide a means to approximate the influence of chosen parameters on a building's energy consumption. This allows for sound decision-making during the design phase, in building control, or planning retrofit measures.

Building energy models are abstractions of reality, simplified descriptions of complex systems and processes regarding energy in buildings [2]. In the literature, building energy models are commonly classified as physical models ('white box models'), hybrid models ('grey box models') or data-driven models ('black box models') [3]. Physical models use specific building characteristics and mathematical equations to model and simulate thermodynamic processes within the building and between building and environment. Data-driven models do not rely on specific building characteristics and thermodynamic equations, but on high-quality datasets and data mining algorithms [4]. Hybrid models are a combination of physical and data-driven models.

During the last decade, the number of scientific publications on data-driven models has increased significantly [4]. With the expansion of sensor installations and advancement in building energy management, more and higher quality data become available. These high-quality datasets bring forward the advantages of the data-driven approach. In particular, well-trained data-driven models promise a reduction of performance gap and a significantly reduced simulation time. The term 'performance gap' refers to the difference between predicted energy performance and actual measured energy performance [5].

Two constraints limiting the application of data-driven methods in building energy prediction are: (1) the need for large amounts of training data, and (2) customised, building-specific model development [6]. Usually, models are not simply transferable from one building to another. To overcome these challenges, transfer learning is a promising approach that aims to improve model performance on a target domain by transferring knowledge gained from a source domain. Transfer learning was applied, for example, by Fan et al. (2020), Ribeiro et al. (2018), and Gao et al. (2020) [6–8]. These studies used data from similar buildings to train a data-driven model and applied that model to their particular target building. Another way to address data scarcity offer hybrid models, specifically

using simulation results from a physical model as training data for a data-driven model. Oh et al. (2020) and Li et al. (2021) used this approach to train data-driven models [9, 10]. These hybrid approaches use physical models of the corresponding target buildings as a source for the training dataset. They still rely on building information for the physical model, a commonly mentioned weak point of physical models [9, 11]. Furthermore, this method limits the trained data-driven model to a specific building with the risk of overfitting. Applying instead a pretrain & fine-tune strategy, leveraging knowledge derived from a diverse synthetic dataset, offers independence from target building data and improved model transferability.

This study aims to investigate the usability of data-driven building energy models pretrained with simulation results from variants of a physical model. Special attention is given to model transferability to overcome challenges of data scarcity and leverage advantages of big data. The models are trained with daily time-series data and tested on a dataset of a real building. The target quantity to be predicted by the building energy models is the building's daily heating energy consumption in GJ.

2. METHODOLOGY

The approach applied in this study is divided into four parts: Generation of the synthetic data and preparation of the metering data of the real building, data preprocessing, training and fine-tuning, and evaluation of the machine learning models. The development of the data-driven models was conducted by means of the programming language Python [12] and the machine learning library scikit-learn [13].

2.1 Source and target datasets

To construct the source dataset used for pretraining, 804 variations of a physical building energy model were created. To generate the different variants, the parameters of the physical model were changed systematically. For each of the 804 models, an energy simulation was carried out using the building energy simulation program EnergyPlus version 22.2.0 [14]. The following parameters were considered before feature selection: Volume, floor area, external gross wall area, external net wall area, external window area, wall-to-window ratio, average temperature setpoint at peak heat demand. For all simulations, weather data from the International Weather for Energy Calculation (IWEC) for Munich, Germany (weather station identification: 108660) were used and provided through an EnergyPlus Weather (EPW) file. To obtain daily time-series data, the hourly data from the EPW file were used to calculate the daily average, minimal, and maximal values. Before feature selection, the following daily weather data aspects were considered: Average dry bulb temperature, minimal dry bulb temperature, maximal dry bulb temperature, precipitation, speed of wind, direction of wind, atmospheric pressure. Of this generated dataset, 80 % was used for training and hyperparameter tuning, and 20 % for testing. Considering the time-series nature of the data, the split was conducted without shuffling.

Basis for the target dataset is a three-story educational and research building located on the Mechanical Engineering Campus of the Leibniz University Hannover in Germany. The room types are mainly offices, seminar, and class rooms, as well as laboratories. Building characteristics were derived from construction documentation. The considered features are the same as in the source dataset above. For the weather features, a dataset was created using weather data from the closest weather stations to the location of the building. That are the weather station Hannover-Herrenhausen (identification: D2011) and Hannover (identification: 10338). The data were received by means of the meteostat API. To account for seasonal relevance, the available building's heating energy consumption time-series data (27/11/2022 – 26/11/2023) was trimmed to the actual heating period. Thus, data from 01/05/2023 to 15/10/2023 were excluded, resulting in a sample size of 197.

2.2 Data preprocessing

The two datasets described above were preprocessed before being passed to the machine learning models. For all models, that data were processed the same way. To handle missing data in features and targets, the values were interpolated in a linear way. The features are divided into static features and time-series features. Static features remain the same during a simulation (e.g. volume), while time-series features change their values (e.g. dry bulb temperature). For both algorithms, one-day time lags of the time-series features were created. The data were standardised by means of scikit-learns StandardScaler.

Feature engineering was conducted to improve the quality of the trained models. Considering collinearity, linear relationships between the input features, is crucial when applying linear models [15]. The Variance Inflation Factor (VIF) of each feature was calculated and the number of input features was reduced until all considered features had a VIF below 10. The following six input features were used to train the models: Floor area, wall-to-window ratio, one-day time lag of average dry bulb temperature, of average wind direction, of average wind speed, and of daily heating energy consumption.

2.3 The data-driven models

Random Forest Regression (RFR) and Multiple Linear Regression (MLR) are two frequently used machine learning algorithms in building energy

prediction [11]. For each algorithm, models were developed using two approaches: pretraining with fine-tuning, and direct transfer without fine-tuning. Furthermore, each algorithm was used to train a benchmark model directly on the target data. In total, six models were developed.

In linear regression, the class of linear functions is the hypothesis space to find the best-fit model from [16]. The simplest case is univariate linear regression, where a straight line is fitted to the input data. To consider multiple input features, multivariable linear regression is applied. Scikit-learn's Lasso Regressor was applied, using the *warm_start* parameter for fine-tuning. The penalty term was minimised by setting *alpha* = 10e-14. This way, the loss function closely resembles squared error.

Random forest regression is categorized under ensemble learning [16]. It involves combining multiple decision trees to make predictions. These trees use nodes to classify instances. Starting at the root and ending at the leaves, each node tests an attribute and the leaf's output classifies the instance. If the output is a set of finite values, the learning problem is termed classification; if it is numerical, it is called regression. The trees' results are combined using a certain type of bagging (also called bootstrap aggregating). From the training set, *k* subsets are generated by randomly selecting *n* examples from the training set. For each of those *k* subsets, the attributes (input features) are randomly picked. This reduces the over-representation of highly predictive attributes and decreases correlation among subset functions. For each subset, the machine learning algorithm chooses the accordingly best-fit function. To receive predictions, the results of these *k* functions are aggregated, with the output in regression being their average.

For the RFR models, two hyperparameters of scikit-learn's RandomForestRegressor were tuned: The considered number of features when looking for the best split (*max_features* = 0.7), and the maximum tree depth (*max_depth* = None). These hyperparameter settings were chosen based on 5-fold time-series cross-validation, using the synthetic (source) dataset. The parameter grid of *max_features* contained the following values: None, 'sqrt', 'log2', 0.7, 0.5, 0.3, 0.1. The grid of *max_depth* contained the values None, 5, 10, 15, 20, 25, and 30.

To fine-tune the linear model, parameters from a prior fit on the source dataset (pretraining) were used as the initialisation parameters for a subsequent fit (fine-tuning). In case of the RandomForestRegressor, 200 additional trees were added to the 100 pretrained trees.

2.4 Evaluation of the data-driven models

To account for the limited amount of available target building data, 5-fold time-series cross-validation (growing-window forward-validation) was carried out on the target dataset. The training set was used to fine-tune the transfer learning models, and train the benchmark models. All models made predictions on the test set of each fold. The models were evaluated using Mean Absolute Error (MAE), Root Mean Squared Error (RMSE), Coefficient of Variation of the RMSE (CV-RMSE), and Weighted Mean Absolute Percentage Error (WMAPE). From the 5 folds, the metric's mean values were calculated. Figure 1 shows the entire target building's heating energy consumption, together with a visualisation of the growing-window forward-validation.

3. RESULTS

An overview of the results is given in Table 1, which shows the mean values of the performance metrics derived from the time-series cross-validation. Figure 2 provides the RMSEs on each of the 5 folds.

3.1 Linear regression models

The MLR Direct Transfer Model, outperformed the other models across all metrics, with an MAE of 1.43 GJ, and a CV-RMSE of 25.27 %. Both the MLR Benchmark Model and the MLR Fine-Tuned Model showed identical performance, with an MAE of 1.61 GJ, and a CV-RMSE of 26.3 %. The MLR Benchmark Model needed on average 180 iterations to converge in training, and the MLR Fine-Tuned Model needed on average 84 iterations to converge in the fine-tuning process. Figure 3 gives an example of MLR model performance on target data.

Table 1: Evaluation metrics (mean values)

Model	MAE	RMSE	CV-RMSE	WMAPE
MLR – Benchmark	1,61	2,09	26,30 %	19,89 %
MLR – Direct Transfer	1,43	1,90	25,27 %	18,60 %
MLR – Fine-Tuned	1,61	2,09	26,30 %	19,89 %
RFR – Benchmark	1,64	2,12	27,44 %	20,79 %
RFR – Direct Transfer	1,81	2,41	31,23 %	23,00 %
RFR – Fine-Tuned	1,49	1,98	26,10 %	19,40 %

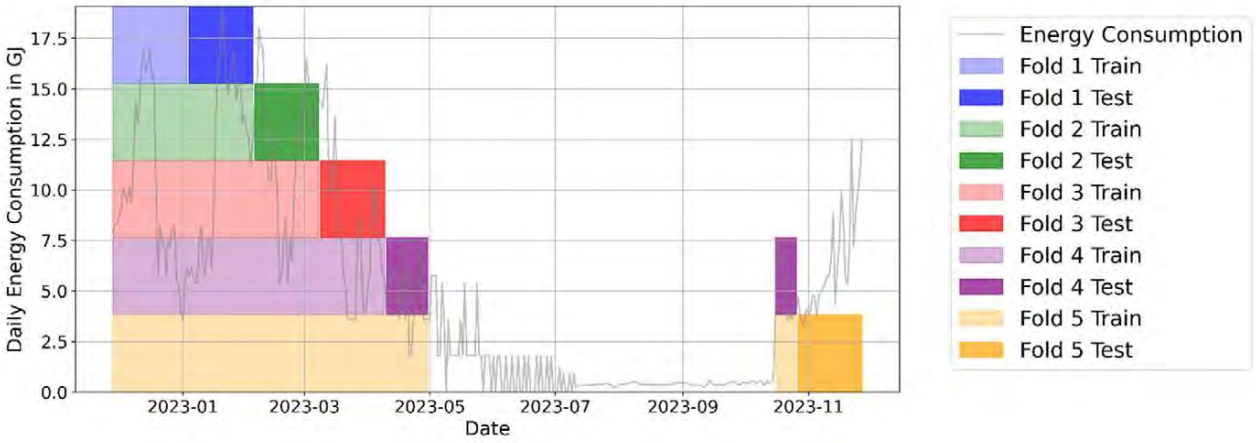

Figure 1: Daily heating energy consumption in GJ of the target building and the train-test splits of the 5 folds in the growing-window forward-validation. Data between 01/05/2023 till 15/10/2023 were not considered.

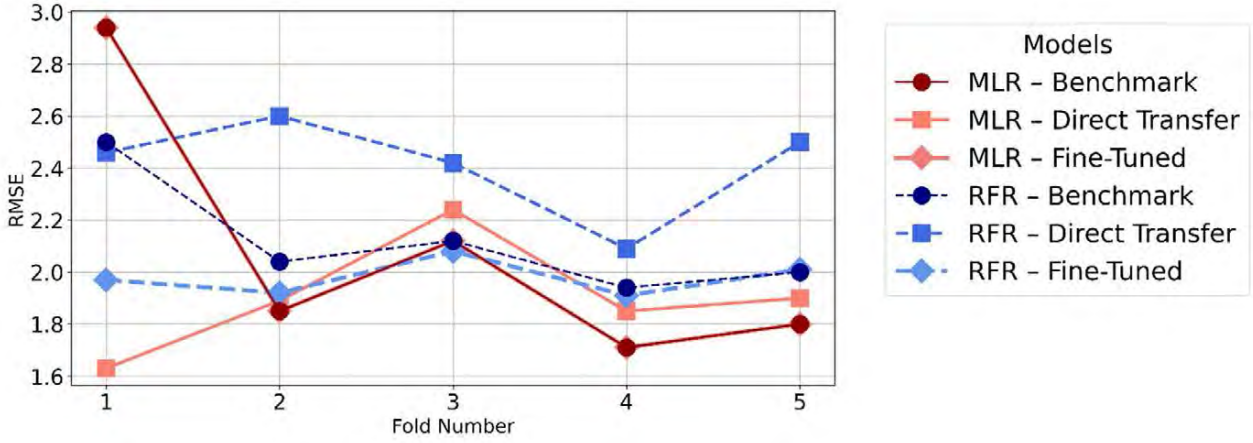

Figure 2: Root Mean Squared Error (RMSE) of the models calculated for each of the 5 cross-validation folds.

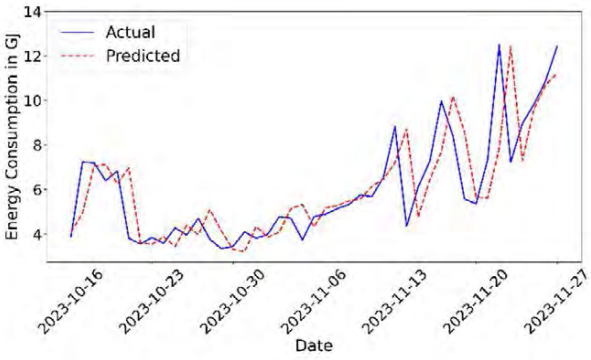

Figure 3: Visual evaluation of the MLR Fine-Tuned Model. The pretrained model was fine-tuned on heating period 1 and tested on heating period 2 (starting from 16/10/2023).

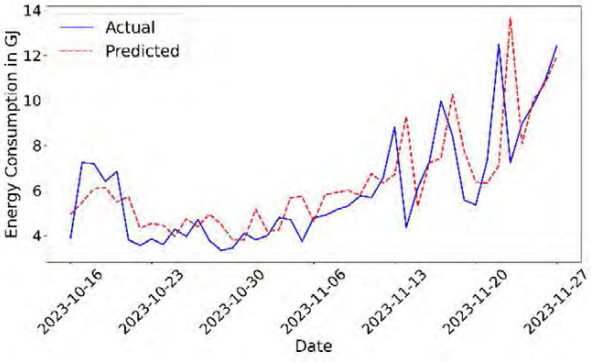

Figure 4: Visual evaluation of the RFR Fine-Tuned Model. The pretrained model was fine-tuned on heating period 1 and tested on heating period 2 (starting from 16/10/2023).

3.2 Random forest regression models

The RFR Fine-Tuned Model outperformed the other RFR models, ranking second-best overall with an average MAE, and CV-RMSE of 1.49 GJ, and 26.1 %, respectively. The RFR Direct Transfer Model showed the highest errors of all models and, in contrast to the fine-tuned variant, could not outperform the RFR Benchmark Model. In Figure 4 predictions of the RFR Fine-Tuned Model are plotted.

4. DISCUSSION

The MLR Benchmark Model and the MLR Fine-Tuned Model were both fitted on the train sets of each fold. However, the MLR Fine-Tuned Model was pretrained on synthetic data, which led to different initialisation values of the model parameters. Both models delivered equivalent performance metrics, with an average MAE of 1.61 GJ and an average CV-RMSE of 26,3 %. This observation suggests that the optimization algorithm (coordinate descent) arrived at a similar optimum in both scenarios. However, the MLR Fine-Tuned Model achieved this with fewer iterations. This implies a more efficient optimization path, owing to a better initialisation provided by the pretraining. Directly applied to the test data, the pretrained MLR model's performance exceeds the other models. This indicates good generalization of the pretrained MLR model.

The Random Forest Regression (RFR) Direct Transfer Model performed the least effective among the models developed. This indicates poorer generalization derived from the pretraining than the pretrained MLR model could achieve. Thus, the pretrained RFR model may be overfitted to the training data. Furthermore, the feature selection methodology, based on the reduction of collinearity, works in favour of the MLR models.

However, the Direct Transfer Models in general show good generalization, with an average CV-RMSE of 25.3 % (MLR), and 31.2 % (RFR). The fine-tuning of pretrained RFR model improved the model's performance substantially, reducing the mean CV-RMSE to 26,1 %. This demonstrates the potential of the pretrain & fine-tune approach for this model type. On the other hand, for the MLR model, fine-tuning led to a slight reduction in performance, increasing the mean CV-RMSE of 25.3 % (direct transfer) to 26,3 % (fine-tuned). This ambiguity shows the complexity of deciding when to apply which method. In comparison to the MLR Benchmark Model, the MLR Fine-Tuned Model provides the advantage of higher efficiency, indicated by fewer iterations to convergence. Furthermore, as Figure 2 shows, both Benchmark Models perform worse than all other models on the first fold, which contained the fewest training samples. This illustrates the strength of pretrained models in data-scarce environments.

Feature engineering boosted the performance of the MLR models, and testing more feature combinations might lead to further improvements. The application of regularization, e.g. through Ridge or Lasso regression is expected to further enhance model performance. To improve the performance of the RFR models, special attention should be given to possible overfitting to synthetic (source) data and better generalization. Generalization might be improved through further tuning of more hyperparameters. Also, a finer parameter grid for cross-validation with the already considered hyperparameters *max_features* and *max_depth* could improve the performance. Additionally, different feature selections for the RFR models might lead to better performance and generalization.

It is insightful to compare the results with those of similar studies in the field. Oh et al. trained a data-driven model with simulation results of a physical model of their particular test building [9]. The applied machine learning algorithm was a Long Short-Term Memory (LSTM) model, a form of a Recurrent Neural Network (RNN) model. From varying training and testing periods, four cases were created, yielding CV-RMSE values between 17.9 % and 26.1 %. In this study, the CV-RMSE values are between 25,3 % (MLR Direct Transfer) and 31.2 % (RFR Direct Transfer), which indicates that a slightly lower accuracy was reached. This discrepancy in accuracy might be attributed to the building-specific approach adopted by Oh et al., as opposed to the broader, synthetic data-driven methodology used here. The generalization, transferability, and thus applicability to a variety of buildings is likely higher than in [9], since the models here were pretrained on synthetic data derived from 804 different physical building energy models. Another benefit of the here presented approach is the lower complexity and thus lower run-time of MLR and RFR models compared to LSTM models.

Despite the apparent disparity in accuracy, the approach adopted in this study is notable for its broader applicability and reduced computational demands. This is particularly pertinent in scenarios where specific building data are not readily available and when computational costs are a critical factor. Example use cases would be early design stage buildings energy prediction, optimization scenarios with a variety of conducted simulations or prediction of heating energy consumption in existing buildings with no detailed historical data available.

Even though the models show solid performance metrics models could likely be further refined, particularly with respect to accuracy and generalization from synthetic to real-world data. A crucial role plays the synthetic training data and its ability to accurately reflect real building environments. Thus, a promising direction of future research is further investigation of the generation of diverse and

representative synthetic data. Furthermore, using a mix of synthetic and real building data of a plurality of buildings as training data will diversify the training dataset and will likely support the model generalization. To exploit further the idea of transfer learning, different approaches, such as domain adaption might be explored. Regarding the pretrain & fine-tune approach of this study, additional hyperparameter tuning on the target dataset could further improve the performance. This could be carried out, e.g., by applying nested cross-validation. Testing the models on longer time periods of real building data will improve the validity of the performance metrics. Applying different machine learning algorithms to the here introduced approach of transfer learning might lead to interesting insights.

5. CONCLUSION

This study presents investigations on the usability of data-driven building energy models pretrained using synthetic data and fine-tuned to predict energy demand of a target building. The synthetic data were generated through 804 variants of physical building energy models, simulated with EnergyPlus. These physical models were not specifically adapted to the target building. The machine learning methods linear regression and random forest regression were applied and the corresponding models tested on real building heating energy consumption data. An evaluation of the models performances showed their potential in real-world scenarios, with CV-RMSEs ranging from 25.3 % to 31.2 %.

Compared to results from studies such as that by Oh et al. [9], which utilised LSTM models, achieving CV-RMSE values between 17.9 % and 26.1 %, the current approach exhibits a slightly greater error margin. Nonetheless, the here introduced methodology is expected to offer benefits in generalization, transferability, and lower computational complexity, especially when compared to more complex models such as LSTMs. Combining synthetic data with transfer learning appears as an efficient alternative for assessing building energy consumption in scenarios characterised by data scarcity. It works with lower computational costs than physical building energy models and improved generalization compared to conventional data-driven models. This reduces the need for specific historical energy consumption data from a building. Promising paths of future research are the exploration of more diverse synthetic training data, application of a wider range of data-driven models, using more diverse test data, and the application of a pretrained model in a real use-case scenario. Overall, the combination of transfer learning and synthetic data to predict building energy consumption emerges as a promising strategy to handle data scarcity and enhance model transferability.

ACKNOWLEDGEMENTS

The authors appreciate the support of Stephan Kabelac, and the Faculty of Mechanical Engineering of the Leibniz University Hannover, and thank the German Research Foundation (DFG) for funding this research.

REFERENCES

1. International Energy Agency (IEA), [Online], Available: https://www.iea.org/reports/tracking-clean-energy-progress-2023 [15 August 2023].
2. Beausoleil-Morrison, I., (2021). Fundamentals of building performance simulation. New York, London, Routledge Taylor and Francis Group.
3. Sun, Y., Haghighat, F. and Fung, B. C., (2020). A review of the-state-of-the-art in data-driven approaches for building energy prediction. *Energy and Buildings,* 221.
4. Liu, H., Liang, J., Liu, Y. and Wu, H., (2023). A Review of Data-Driven Building Energy Prediction. *Buildings,* 13(2).
5. de Wilde, P., (2014). The gap between predicted and measured energy performance of buildings: A framework for investigation. *Automation in Construction,* 41: p. 40–49.
6. Fan, C., Sun, Y., Xiao, F., Ma, J., Lee, D., Wang, J. and Tseng, Y. C., (2020). Statistical investigations of transfer learning-based methodology for short-term building energy predictions. *Applied Energy,* 262.
7. Ribeiro, M., Grolinger, K., ElYamany, H. F., Higashino, W. A. and Capretz, M. A., (2018). Transfer learning with seasonal and trend adjustment for cross-building energy forecasting. *Energy and Buildings,* 165: p. 352–363.
8. Gao, Y., Ruan, Y., Fang, C. and Yin, S., (2020). Deep learning and transfer learning models of energy consumption forecasting for a building with poor information data. *Energy and Buildings,* 223.
9. Oh, K., Kim, E.-J. and Park, C.-Y., (2022). A Physical Model-Based Data-Driven Approach to Overcome Data Scarcity and Predict Building Energy Consumption. *Sustainability,* 14(15).
10. Li, X. and Yao, R., (2021). Modelling heating and cooling energy demand for building stock using a hybrid approach. *Energy and Buildings,* 235.
11. Chen, Y., Guo, M., Chen, Z., Chen, Z. and Ji, Y., (2022). Physical energy and data-driven models in building energy prediction: A review. *Energy Reports,* 8: p. 2656–2671.
12. Python Software Foundation, (08/06/2022). Python 3.10.6 Documentation.
13. Pedregosa, F., Varoquaux, G., Gramfort, A., Michel, V., Thirion, B., Grisel, O., Blondel, M., Prettenhofer, P., Weiss, R., Dubourg, V., Vanderplas, J., Passos, A., Cournapeau, D., Brucher, M., Perrot, M. and Duchesnay, E., (2011). Scikit-learn: Machine learning in Python. *Journal of Machine Learning Research,* 12: p. 2825–2830.
14. U.S. Department of Energy, (28/09/2022). EnergyPlus Version 22.2.0 Documentation. Engineering Reference.
15. Kutner, M. H., (2005). Applied linear statistical models. Boston, McGraw-Hill Irwin.
16. Russell, S. J. and Norvig, P., (2021). Artificial Intelligence. A Modern Approach. Hoboken, NJ, Pearson.

From National to District: Evaluating the Applicability of National-Scale Energy Models to District-Level Building Stock in Barcelona's Besòs River Area

MARIA KARATSIOMPANI[1] MARIANA PALUMBO[1] OLGA ALCARAZ SENDRA[2] PABLO BUENESTADO[3]

[1]Department of Architecture and Technology, Vallès School of Architecture (ETSAV), Universitat Politècnica de Catalunya - BarcelonaTech (UPC), Barcelona, Spain
[2] Research Group on Science and Technology of Sustainability (CITES), Barcelona East School of Engineering (EEBE), Universitat Politècnica de Catalunya - BarcelonaTech (UPC), Barcelona, Spain
[3]Department of Mathematics, Barcelona East School of Engineering (EEBE), Universitat Politècnica de Catalunya - BarcelonaTech (UPC), Barcelona, Spain

ABSTRACT: The building sector holds immense potential for reducing greenhouse gas emissions. To achieve the necessary decarbonisation and enhance energy efficiency, a detailed understanding of the building stock and its energy behaviour at various scales is crucial. In Spain, national strategies, that use archetype approaches to assess and prioritize interventions, are recently applied at the district scale. However, this study proposes that methodologies designed for the national scale may not be applicable at the district level. The primary objective is to test national-scale energy models on an intermediate district scale, specifically the western coast of Besòs River in Barcelona. The study compares U-values of residential building archetypes from national models with those calculated from the energy performance certificate database (EPC) at the dwelling level. The results confirm the hypothesis that national segmentation criteria inadequately explain the building stock variability at the district level. Significant deviations between EPC-derived U-values and those predicted by national models were observed across various building segments. Clustering classification did not reveal a straightforward relationship between the produced clusters and the variables used in national models. This emphasizes the need for more tailored approaches to understand and address energy efficiency at different scales in the building sector.
KEYWORDS: energy renovation, building stock segmentation, district-level analysis, uncertainty, thermal transmittance

1. INTRODUCTION

The building sector is the biggest energy consumer in the European Union, with high environmental impacts associated. Currently, 75% of the European building stock is energy inefficient, while only about 1% of it undergoes energy renovation annually [1]. The European Union current policy highlights the necessity of energy retrofitting of the European existing building stock. In October 2020, the “Renovation Wave” initiative was launched, aiming to at least double renovation rates over the next decade and prioritize building renovations according to greater energy and resource efficiency.

To guarantee investments on energy renovations, it is necessary to accurately forecast the potential of the improvements to be implemented. This calls for in-depth studies of current and future energy use of building stock, in different scales, from individual buildings to urban and national models, allowing a deep understanding of the building stock.

In Spain, the Long-Term Strategy for Energy Renovation in the Building Sector (ERESEE) is developed on the basis of national housing stock characterisation that follows a deterministic, archetype approach. This means that the building stock is divided into groups of similar buildings according to qualitative variables (segmentation). Then, geometrical and thermal properties are assigned (characterization), creating archetypes of buildings that are exemplary. The energy demand is calculated for each group´s archetype, scaling up by multiplying the results by the number of houses of each archetype. This approach is useful on a national scale; however, it has been criticized for oversimplifying the diversity of the building stock, particularly when applied on a smaller scale [2]. As the execution of national plans is usually carried out at the urban or district scale it is crucial to bridge the gap between national models and the complexities of local building stocks.

In this sense, district level models are a recently developed research field and has gained great importance for two main reasons: informing neighbourhood regeneration projects and designing district-level energy supply systems incorporating renewable sources and community involvement. The absence of a standardized framework at the district

level often leads to the application of nationally established models by local decision makers.

The goal of this research is to evaluate the reliability of Spanish national archetype approaches at a district level, focusing on the thermal transmittance (U-value) of facades and openings in residential buildings, through a case study. The case study, located on the western coast of Besòs River in Barcelona, targets neighbourhoods undergoing urban renewal with high vulnerability levels.

2. METHODOLOGY

To reach the goals of this study, a methodology has been developed that compares the facade and openings U-values of the building stock segments, as defined in the methodologies at a national scale with the U-values, as calculated from the Energy Efficiency Performance Certificate (EPC) database at the dwelling scale. The different steps of the methodology are shown in Figure 1.

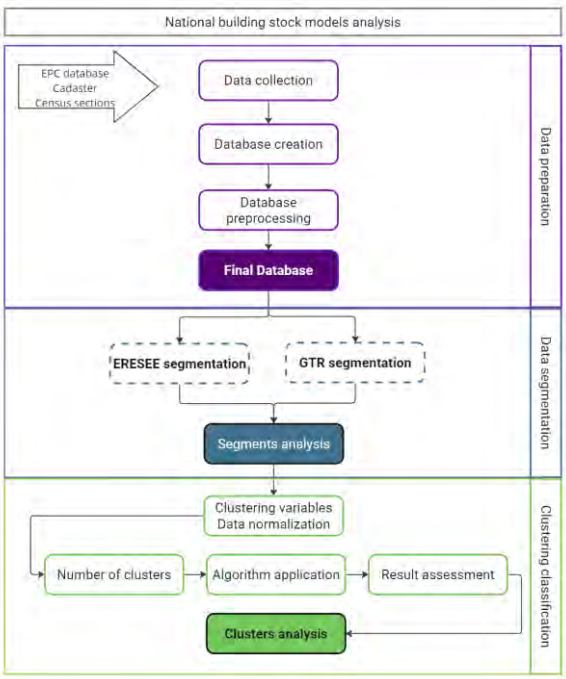

Figure 1: Methodology overview

The selection of the two U-values for the comparison is based on their role in determining envelope thermal properties, impacting thermal balance, and subsequently, energy demand. Literature supports their significant influence on heating and cooling energy consumption [3]. At the same time, they present a grade of uncertainty and can be altered with renovations—an aspect not considered by archetype models.

2.1 National building stock models analysis

From the existing national building stock segmentation methodologies, three of them were deeply analysed and two of them were chosen for the comparison with the EPC database; The Working Group for Rehabilitation (GTR) and the ERESEE. These two methodologies serve as the foundation for energy retrofitting policies in the Spanish residential building sector. Both GTR and ERESEE use common segmentation variables, such as *year of construction, building typology, and number of floors*.

2.2 Data preparation

Overall, the databases used in the present study are the Energy Performance Certificate database (EPC), provided by Generalitat de Catalunya, Department of Climatic Action, Food and Rural Agenda, the Spanish Cadastre and the census sections, provided by Cartographic and Geologic Institute of Catalonia (ICGC).

The EPC database, mandatory for new constructions, property sales or rentals, and relevant renovations, contains 1.44 million lines, each representing an energy performance certificate. With 71 columns providing detailed information, it serves as a crucial link between known segmentation variables and unknown archetype data during the characterization step.

However, it is important to underline the limitations and data quality of the EPC database. Accuracy relies on technician expertise and inspection detail, posing challenges for existing buildings with unknown construction layers. Default values are often applied, based on technician knowledge or software-provided estimates, leading to an approximation rather than a precise representation of the building stock reality.

The three databases, combined using QGIS software, resulted in a total of 11.150 certifications. After exporting to RStudio, atypical values were identified, corrected, or deleted, according to the case, prior to a general analysis of quantitative variables, as well as observing histograms and boxplots.

2.3 Data Segmentation

The next step was the segmentation of the database according to the selected methodologies, as shown in Table 1. Two additional variables, GTR and ERESEE, were incorporated. The segment names were assigned through database filtering according to the defined segmentation criteria. The wall and openings U-values for each segment, as indicated in the ERESEE and the GTR methodologies, were compared against the values in the EPC database, using graphs created in RStudio.

Furthermore, to evaluate the difference of the predetermined values of both methodologies and the EPC results, the deviation percentage is calculated for each segment, using Equation (1):

U-value deviation (%) = 100 x (EPC U-value – Methodology U-value) / Methodology U-value (1)

where EPC U-value (W/m^{2}K) is the median for each segment and Methodology U-value is the value given by the ERESEE and GTR for the corresponding segment.

Table 1: Building segments definition for GTR (up) and ERESEE (down)

Building Segments **GTR**			
	Single-family	Multi-family	
N. of floors		< = 3	> 3
inhabitans	< 10.000	< 10.000	> 100.000
< = 1940	(A)	NA1	B
1941 – 1960			
1961 – 1980	(C)	NA2	F
1981 – 2001	(G)	(H)	J
2002 – 2007			
2008 - 2020			

Building Segments **ERESEE**			
	Single-family	Multi-family	
N. of floors		< = 3	> 3
inhabitans	< 10.000	< 10.000	> 100.000
< = 1940	Uu < 40	Cc < 40	Bb < 40
1941 – 1960	Uu 40-60	Cc 40-60	Bb 40-60
1961 – 1980	Uu 60-80	Cc 60-80	Bb 60-80
1981 – 2001	Uu 80-07	Cc 80-07	Bb 80-07
2002 – 2007			
2008 - 2020	Uu 08-20	Cc 08-20	Bb 08-20

2.4 Clustering classification

Clustering is an unsupervised machine learning technique that involves separating a data set into subgroups of related data [4] and has recently been applied in the building sector for various purposes, such as identifying representative buildings [5]. In this study, clustering is applied to test the relationship between algorithm-produced clusters and the segmentation parameters.

K-means clustering with the Hartigan-Wong algorithm [6] was chosen for its simplicity and computational efficiency, using facade and openings U-values as clustering variables. The optimal number of clusters was determined by two widely used indexes: The Silhouette [7] and the Elbow index.

3. RESULTS

3.1 Segments creation and mapping

The GTR and ERESEE segments were developed and mapped as outlined in the methodology. In Figure 2 the distribution of the ERESEE segments in the case study is shown. Since the chronological segmentation of GTR methodology is less detailed than ERESEE, bigger groups of same-coloured buildings are visible, making it possible to recognize the construction period of the neighbourhoods.

There is a substantial variance in the number of dwellings across the segments, ranging from as few as 14 to almost 6.000 dwellings. As expected, multi-family buildings of more than 3 floors constituting 91.1% of the residential building stock, while more than half of them (52.3%) were built during the period 1960 – 1980.

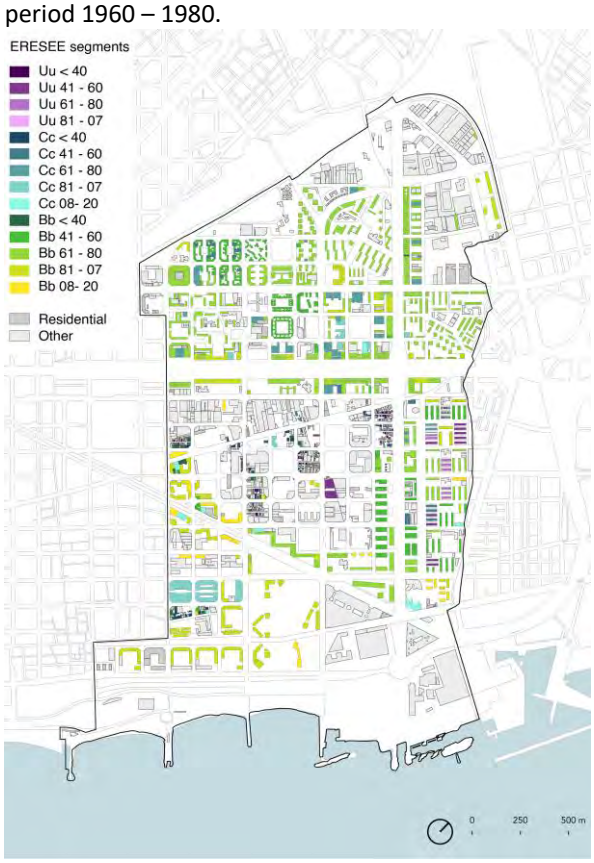

Figure 2: ERESEE segments in the case study.

3.2 U-Values overview

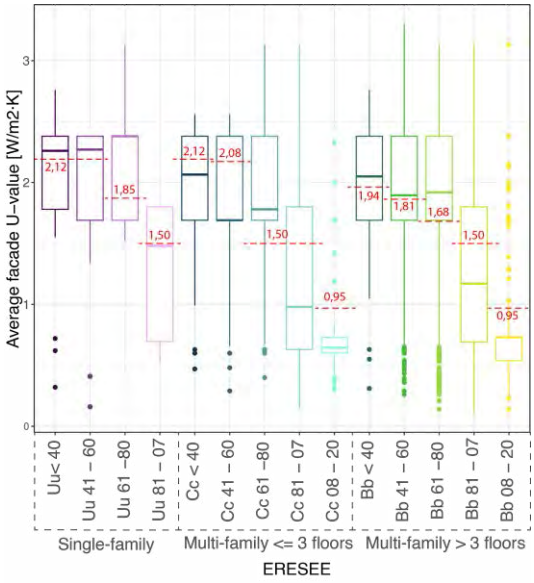

Figure 3: Facade U-values overview boxplot per ERESEE segment. With red lines, the determined from ERESEE methodology values.

In Figure 3 the facade U-values boxplots for each ERESEE segment are displayed. They are ordered by housing typology (single-family, multi-family up to 3 floors and multi-family higher than 3 floors) and from older to more recent construction period. The red horizontal lines on the plot indicate the values given by the ERESEE, for the corresponding archetype.

Figure 3 depicts similar overlapping boxes of the walls U-values across all building typologies and construction periods until 1980 of walls U-vales. This implies that half of the data points are in the same range. The same behaviour can be observed for both methodologies in the boxplots of walls and openings´ U-values across all segments. The similarity in the size and the overlap creates doubts about how well the segments are divided.

However, a notable shift emerges in the period 1981 - 2007, where the boxes are much bigger compared to all the rest of the construction periods, across all building typologies. This means that half of the values in these groups are spread out over a wider range, with more variability across all building typologies in this period. In this case, the segments could be further divided. Towards this explanation contribute their distributions, plotted in histograms, where two peaks can be observed. Conversely, after 1980, openings U-values tend to have more compact boxplots, with less variation in the values. This could possibly be explained by either a more limited and regulated use of windows in the territorial context or the compliance with thermal regulations established after the 80s.

3.3 Deviation assessment

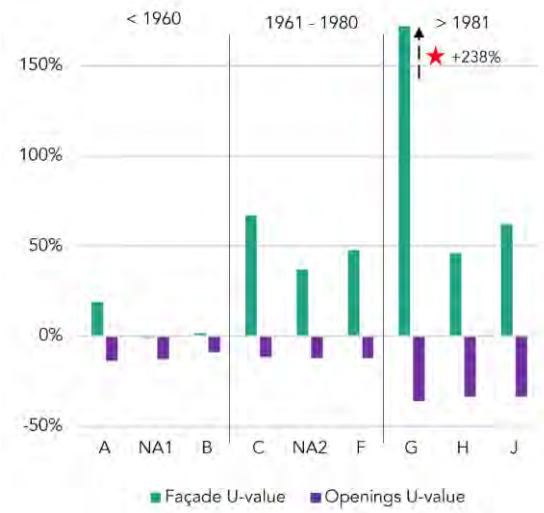

Figure 4: Facade and openings´ U-values deviation percentage, per GTR segment.

Furthermore, high deviation percentages are observed between the predicted by the GTR and ERESEE U-values and the median values in the EPC database for each segment. Negative percentage indicates that the thermal performance of the building stock is overestimated, meaning that it is better than predicted. Positive percentage indicates that the thermal performance of the building stock is underestimated, meaning that it is worse than predicted.

GTR shows higher deviations than ERESEE of up to 238% in segment G (Figure 4). The facade U-values have been underestimated, while the openings U-values have been overestimated. In the case of ERESEE, both facade and walls U-values of buildings after 1980 have generally been overestimated, since they have negative percentages of around -20% to -30%, with maximum deviation of -38%. U-values of building built before 1980 have generally been underestimated, since most segments have positive percentages of deviation.

In both cases, the greatest deviations take place in the most recently constructed building stock.

3.4 Clustering classification

The clustering classification algorithm detected ten optimal clusters. They are named from better to worse combination of U-values, from 1 to 10.

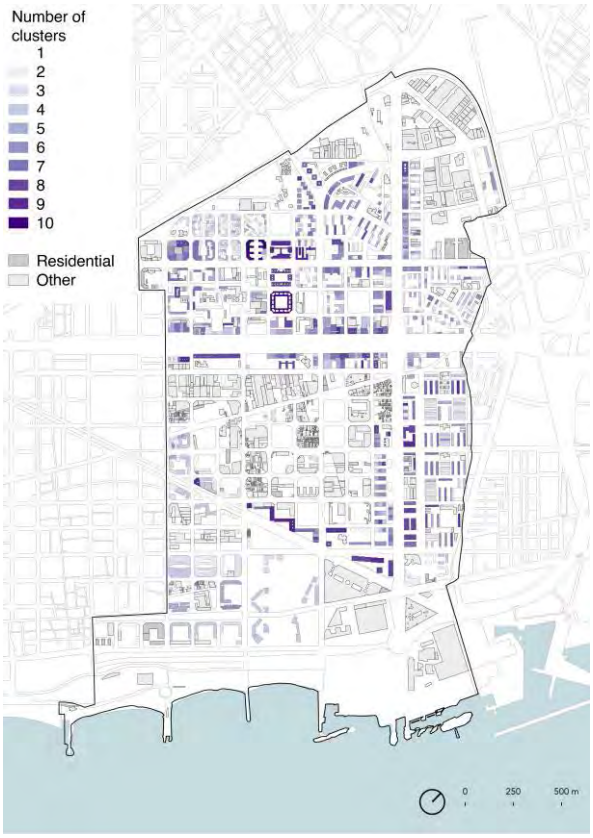

Figure 5: Number of clusters per building.

The clusters´ mapping showed less patterns of same clusters in neighbouring buildings, although they were built in the same period and probably with the same technique. The clusters are spread in the neighbourhood with more variability. In addition, a

big number of buildings contain flats belonging to different clusters. Figure 5 shows the number of clusters per building, showcasing a range from 1 to 10 clusters, with a considerable number falling within intermediate values.

In the scatterplot of Figure 6, the facade U-values are in the x axis and the openings U-values are in the y axis, with the clustering result in different colours and the shapes of the limits of the clusters. The resulting clusters are compact and separated from each other without overlapping, indicating distinct patterns within the dataset.

From the same figure, it can be observed that the points in the plot don't follow a linear pattern, meaning that one U-value does not grow linearly with the other U-value. This underlies the fact that higher thermal performance of the facade (low facade U-values) is not necessarily combined with high performance of the openings (low openings U-values), and vice versa. Thus, buildings that perform well in one part of the building don't necessarily perform well in other parts of the building as well. Moreover, the scatterplot distinctly reveals the existence of predetermined values, evident along both the horizontal and vertical axes.

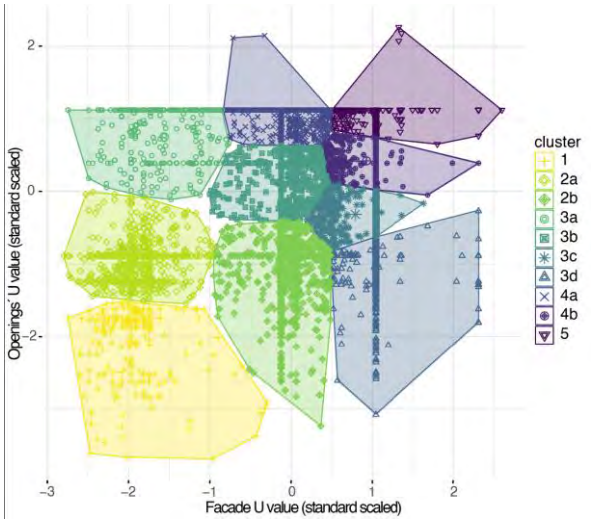

Figure 6: K-means clusters result on Facade (x axis) and openings (y axis) U-values (W/m²K). The values are normalized with standard scaling (mean value of zero and a unit variance value).

In examining the segmentation variables *(housing typology and number of floors)* no apparent pattern or direct relationship emerged within the algorithm-produced clusters. Notably, there is no cluster exclusively associated with higher or lower constructions, nor is there a cluster exclusive to single-family or multi-family buildings.

To illuminate the construction period aspect, Figure 7 presents pie charts illustrating the distribution of clusters within each construction period. It is evident that no cluster is solely representative of a specific construction period; rather, clusters comprise buildings constructed across various time frames.

Nevertheless, the clusters exhibiting superior performance, particularly clusters 1 and 2a, distinguished by a predominant green colour, predominantly feature dwellings built after 1980. Conversely, the periods preceding 1980 exhibit a more evenly distributed representation across clusters, with varying shades of blue and purple, indicative of comparatively poorer performance.

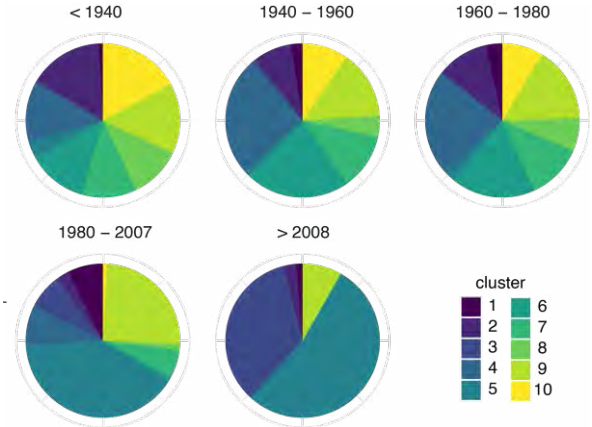

Figure 7: Distribution of clusters per period of construction

4. CONCLUSIONS

The study of EPC U-values per segment yielded interesting findings. Multiple overlapping boxplots were found, suggesting similar range of U values across different segments. In addition, segments with boxplots with large boxes and whiskers, as well as two subgroups within their histograms were found, especially in facade U values in the period 1980 – 2007. This suggests diverse construction techniques during this period due to an explosion of technological solutions and materials in the building sector. Those observations raise questions about both the significance of the difference in the thermal transmittance of the segments in the first case, and the insufficiency of the segmentation to explain the variability of the thermal transmittance in the second case.

Comparing the U-values assigned by methodologies with the EPC database medians per segment revealed significant deviations, impacting thermal performance assessment. For instance, GTR methodology underestimates facade U values, up to 238% for certain buildings.

The k-means algorithm produced 10 optimal clusters, revealing no clear relation to housing typology, number of floors or construction period. Clusters with higher facade U-values don't necessarily have higher opening U-values, suggesting window replacements without comprehensive energy renovations. This supports the hypothesis that

traditional segmentation criteria alone may not fully explain U-value variation at a district level, where territory specific data are needed.

An important contribution of this study is the dwelling-scale analysis of the heterogeneity of the building stock, unlike the applied block-scale methodologies. Most buildings (85%), as shown in Figure 8, incorporate dwellings from up to 6 different clusters, while only 13% of the buildings are represented by only one cluster, highlighting the relevance of scale in heterogeneity of the building stock. The intra-building variety of clusters suggests diverse thermal properties due to renovations, like the installation of thermal insulation in parts of the facade, the creation of new volumes with materials of poorer or better thermal properties than the general facade, or the openings renovation and alteration of the original openings' dimensions.

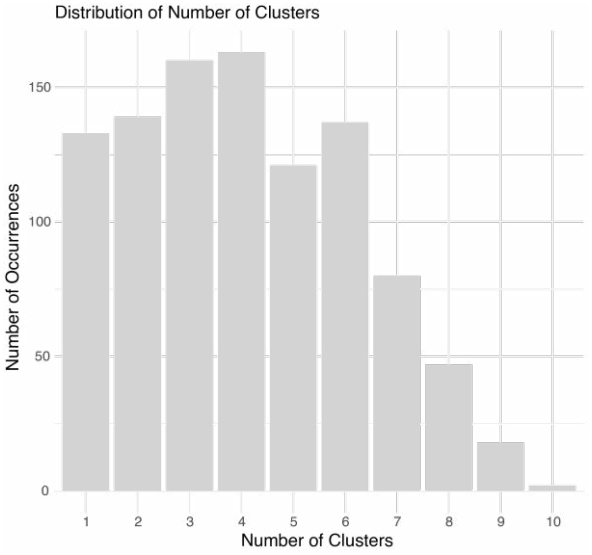

Figure 8: Number of clusters per building.

A major aspect of this study is data quality at the district level. The EPC database, while weekly updated, contains default values due to the certificate acquisition procedure, although in Spain a physical visit by a technician is mandatory. Determining stricter procedures to acquire the energy performance certificate could improve the accuracy of the EPC database and should be considered by the European and national standards.

As the default values in the EPC database may potentially influence the outcome of k-means clustering, future work could consider assessing their impact. This can be achieved by specifically incorporating the calculated values and excluding the default ones. While the necessary information is present in the EPC database, it requires pre-processing before its utilization in statistical analyses.

In future studies, an incorporation of additional thermal characteristics related to the building stock into the clustering algorithm could be explored. Including other properties such as the solar factor of the openings and infiltrations, could improve the overall understanding of the thermal state of the building stock. This exploration could potentially lead to more adequate clusters that better reflect the diversity within the building stock. Furthermore, an investigation into methods for predicting cluster membership could be considered. In this way, the clusters could be expanded using predictive classification methods, such us random forests that have already been applied with successful results [4].

Through this study it has become evident that the natural variability of the existing building stock is underestimated at district level, since the to-date segmentation criteria (housing typology, year of construction and number of floors), have been proven to be unable to explain the variation in U-values. The deterministic archetype methodologies, which have been the foundation of current Spanish energy retrofitting policies, may not fully capture the natural variability present in the existing building stock. The failure of the existing segmentation criteria to explain the variation in U-values highlights the need for more nuanced and district data-driven approaches in policy formulation.

REFERENCES

1. European Commission. (2020a). A Renovation Wave for Europe - greening our buildings, creating jobs, improving lives.

2. Reinhart, C. F., & Cerezo Davila, C. (2016). Urban building energy modeling - A review of a nascent field. In Building and Environment (Vol. 97, pp. 196–202). Elsevier Ltd. https://doi.org/10.1016/j.buildenv.2015.12.001

3. Silva, A. S., & Ghisi, E. (2020). Estimating the sensitivity of design variables in the thermal and energy performance of buildings through a systematic procedure. Journal of Cleaner Production, 244. https://doi.org/10.1016/j.jclepro.2019.118753

4. Jain, A. K., Murty, M. N., & Flynn, P. J. (2000). Data Clustering: A Review.

5. Tardioli, G., Kerrigan, R., Oates, M., O'Donnell, J., & Finn, D. P. (2018). Identification of representative buildings and building groups in urban datasets using a novel pre-processing, classification, clustering and predictive modelling approach. Building and Environment, 140, 90–106. https://doi.org/10.1016/j.buildenv.2018.05.035.

6. Hartigan, J. A., & Wong, M. A. (1979). Algorithm AS 136: A K-Means Clustering Algorithm. In Source: Journal of the Royal Statistical Society. Series C (Applied Statistics) (Vol. 28, Issue 1).

7. Petrovi´c, S. P. (n.d.). A Comparison Between the Silhouette Index and the Davies-Bouldin Index in Labelling IDS Clusters.

PLEA 2024 WROCŁAW
(Re)thinking Resilience

Rethinking Jute as a Biomaterial for Tensile Architecture in a Hot-humid Climate

GOLAM MORSALIN CHOUDHURY RANA[1], KHANDAKAR SHABBIR AHMED[1]

[1]Dept. of Architecture, Bangladesh University of Engineering & Technology (BUET), Dhaka, Bangladesh

ABSTRACT: This paper explores the opportunity to use the jute fabric as biomaterial for tensile membrane architecture in hot-humid climate of Bangladesh. Jute is very beneficial to the environment. Jute has a high tensile strength, is harmless, and biodegradable. Using products based on jute is environmentally friendly, sustainable, and lowers carbon emissions. Since ancient times, jute has been used to make twine, ropes, and bags; Bangladesh is the natural home of the best jute. The world's top exporter of jute is Bangladesh. Jute is used to make a wide range of items. Engineered textiles, such as Jute Geo Textiles (JGT) derived from Jute, find use in filtration, riverbank erosion management, and road building. In this study Jute yarn is weaved with different pattern and quantity of polyester and cotton yarn to achieve optimum tensile strength and then coated with PVC to make it durable and increase its strength. The Jute fabric yarn was collected from Bangladesh Jute Research Institute (BJRI), weaved with Polyester and Cotton in Bangladesh University of Textiles (BUTEX) lab and tested in Bangladesh University of Engineering & Technology (BUET) lab facilities. A simulation software ixcube Forten was used for simulation. It is found that 2Jute-1Polyester fabric has optimum has optimum tensile strength to be used as Tensile Membrane.
KEYWORDS: Jute, Jute fabric, Tensile membrane structures, Lightweight structures, Environment friendly material

1. INTRODUCTION

Jute is an excellent example of eco-friendliness and sustainability. Jute is biodegradable and compostable. The carbon footprint of Jute is very low. Jute grows quick. Bangladesh is the natural home of the best quality Jute in the world. Jute is positioned second after Cotton in terms of production, consumption, and availability worldwide [1]. One study shows that chemical treatment of jute fabric increases its longevity [2]. Jute geo textiles are used for soil erosion protection [3]. Specially treated Jute geo textile has higher durability [4]. Therefore, Jute has the opportunity to be used as a technical textile in the field of Tensile Architecture, but its strength upgradation through fiber mixing and coating are necessary for better sustainability and longevity.

Tensile Architecture is a lightweight structure system with a membrane or fabric held in tension. It can be a permanent, semi-permanent or temporary structure. Tensile architecture is evolved from the concept of Nomadic Tent, which was used for centuries by Arab Bedouins, Mongols. "The Shamiana" tents are introduced in the Indian subcontinent by the Mughals [5]. Tensile Architecture has many uses, from large span structures like airports and stadiums to small structures like shade shelters. The construction fabric market is currently worth 1.47 billion USD and is expected to grow to 2.26 billion USD by 2023 [6].

The global drive for bio-based and sustainable developments guided by Kyoto protocols on greenhouse gas reduction and CO2 neutral production provides a higher perspective on the natural fiber market [7]. As there are fewer alternatives to synthetic fabric, jute fabric can be a good material for Tensile Architecture in hot-humid Bangladesh due to its strength, eco-friendliness, availability, and affordability. But jute fabric needs to improve its strength and environmental performance for its durability. The combination of Jute fabric, polyester and cotton with coating has been studied for better understanding their performances under tension load.

2. OBJECTIVE

This paper investigates the potential use of Jute fabric to be used as an alternative biomaterial in Tensile Architecture in hot-humid climate of Bangladesh. It will enhance the applicability of the Jute fabric and lead the way to a sustainable and green future uses as a membrane material.

3. METHODOLOGY

This study is mainly focused on constructing a jute fabric made of through the combination of jute, cotton, and polyester yarn. Based on the literature survey, a target fabric weight is set for construction. Jute reinforced membrane samples were made by combining different amounts of jute, cotton, and polyester yarn. These Test samples are the applied surface coating to increase fabric cohesion and bonding. The lab tests are done at BUET and BJRI

where following tests are performed the strength of the samples for weight, elongation, and tensile strength for comparative study.

3.1 Literature Review

Bangladesh is the natural home of the best quality Jute in the world and it is one the major exporter of raw Jute in the world [8]. Jute is now being used in diversified fields such as technical textiles for civil engineering, automotive application, electrical and leather industries, medical, environmental protection, etc. Jute textiles are now used for making automotive parts, medical textiles for implants, Agro textiles for crop protection and protective clothing for heat and radiation protection for firefighters and metal welders.

Jute fabric and polymer-based Natural Fiber Composite (NFC) corrugated sheet termed as 'Jutin' has been invented by Bangladesh Atomic Energy Commission (BAEC) led by Dr. Mubarak Ahmad Khan in 2010. Jute based packaging bag "Sonali bag" has recently been developed by Dr. Mubarak Ahmad Khan and his team in 2018 [9], which is comparable to the common polybag, but it is biodegradable and friendly to the environment. The Jute-cotton or other synthetic fiber blended yarn is well studied. Sulphonated Jute-Cotton blended yarn and fabric have almost equivalent properties of 100% Cotton fabric [10]. Jute-Polyester blend is studied by [11] and Jute-Acrylic blend is studied by [12].

Synthetic fabric or technical textiles are used in Tensile Architecture. The most used technical textiles in Tensile Architecture are such as PVC (Polyvinyl chloride) coated PES (Polyester) or PVDF (polyvinylidene bifluoride) coated PES material, etc. [13]. Unfortunately, these materials are not biodegradable and can increase environmental pollution [14]. So, there is a potential need for natural fabric in this field and jute fabric can fill that role.

3.2 Jute and its properties

There are two Jute types of trade: white (Chorchorus capsularis) and Tossa (Chorchorus olitorius). Tossa Jute is softer, silkier, and stronger than white Jute. It is also known as Paat in Bangladesh. Jute fiber is collected from the best or skin of the Jute plant. That's why Jute fiber falls into the bast fiber category. Jute plant grows in hot humid rainy alluvial lands. Jute plant is photo reactive; it harvests within 120 days. It grows up to six to ten feet high. Matured Jute plants are cut, tied in a bundle, and put into slow flowing water for several weeks for fermentation. Jute fibers are pulled off from the bark, washed carefully and dried in the sun.

(*Shahnewaz Karim, Auyon , 2011)*

Figure 1: Preparation of Jute fibre from jute bark

Jute is a cellulose-based material. It is stiff and yellowish because of hemicellulose and lignin. Each Jute fiber is composed of smaller units known as fibrils. They are arranged in right-handed spirals and make closely held molecular chains which known as micells.

The chemical composition of jute is as follows—

Alpha Cellulose	58-63%
Hemicellulose	21-24%
Lignin	12-14%
Pectin	0.2-0.5%
Fat & Wax	0.8-1.5%
Mineral Materials	0.6-1.1% [14]

5. TENSILE MEMBRANE

Tensile membrane structures use lightweight fabric or membrane that is loaded only in tension and supported by a primary structure. Tensile membrane structures are lightweight, flexible and more stable than conventional structures. The membrane material used in Tensile Architecture are regarded as construction fabric or technical textiles. Based on material strength five different types of fabric are proposed by Messe Frankfurt [15], where type I fabric has tensile strength of 60kN/m in warp and weft. And type II fabric has tensile strength of 88kN/m. Most commonly used materials are PVC coated Polyester fabric. The PVC compound is added to the fabric directly via floating knife method where a fabric is stretched flat and PVC compound is then even spread over fabric via a knife [16].

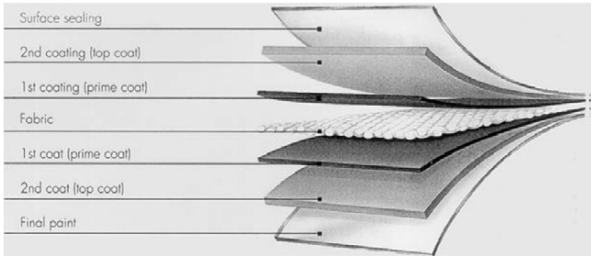

Figure 2: Coated Tensile Membrane layers

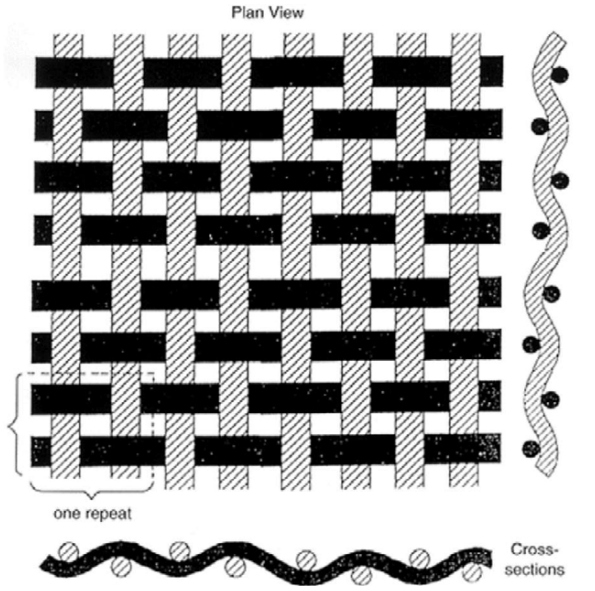

Figure 3: Plain weave composition of a tensile membrane fabric

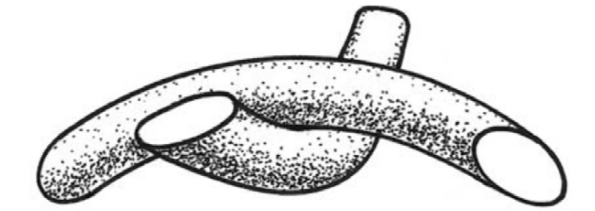

Figure 4: Yarn overlapping in a plain weave

5.1 Fabric Composition

The proposed Jute membrane aims to achieve Type I membrane as proposed by the Messe Frankfurt.

Proposed Tensile Membrane Fabric Construction 01
Jute yarn (2 ply) as warp, Yarn Count = 13 lb/spydle (Ne 1.32 Nec) Available at BJRI
Polyester filament as weft = 600 denier (66.66 tex = 8.85 Nec)
Warp/inch= 30, Weft/inch=40
Warp (Jute) weigh in gm/m2 = (30×39.37×1.0936×453.6)/(840×1.32) =528.40 gm
Weft (Polyester) weigh in gm/m2 = (40×39.37×1.0936×453.6)/(840×8.85) =105.08 gm
Total Fabric weight (calculated) = (528.40+105.08) = 633.48 gm/m2

5.2 Sample Preparation

For testing purposes, seven the samples of various composition have been developed in BUTEX CCI Lab using 13lb/spindle Jute yarn, 600denier Polyester yarn, and Ne 3 Cotton yarn. Sample description given below in the following table.

Table 1: Jute/Polyester/Cotton weaved samples

Sl. No.	Sample ID	EPI/PPI	Coating
1.	1 Jute-1Cotton	15/15	Uncoated sample
			Coated sample
2.	1 Jute-1Cotton in Warp, 1 Jute-1Polyester in Weft	15/15	Uncoated sample
			Coated sample
3.	1 Jute-1Polyester	15/15	Uncoated sample
			Coated sample
4.	1 Jute-2Polyester	15/15	Uncoated sample
			Coated sample
5.	1 Jute-3Polyester	15/15	Uncoated sample
6.	2 Jute-1Polyester	15/15	Uncoated sample
			Coated sample
7.	3 Jute-1Polyester	15/15	Uncoated sample
			Coated sample
8.	1/1 Jute Fabric	15/15	Uncoated sample
			Coated sample
9.	1/1 Polyester	15/15	Uncoated sample
			Coated sample

5.3 Sample testing

Sample weight, tensile strength, thickness, and elongation are tested in Geotech Lab of Dept. of Civil Engineering, Bangladesh University of Engineering & Technology. Strip tensile strength was done according to ASTM D4595. Coated fabric was done in old Dhaka coating factory through direct application method.

Figure 5: Uncoated Jute-Polyester fabric samples

Figure 6: Sample preparation for testing.

Figure 7: Coated Jute-Polyester fabric on left and coated jute fabric on right.

Figure 8: Strip tensile strength testing at Geotech lab, BUET.

6. TEST RESULTS & DISCUSSION

From the strength test we can see that uncoated jute-jute fabric has the highest strength due to its thicker jute yarn which breaks under heavy load early due to its less strain, compared to the polyester yarn (table 02). However, 1/1 Polyester, 3jute-1Poly, 2Jute-1Poly fabric exhibited similar tensile strength due to their similar fabric weight.

Table 2: Uncoated fabric strip tensile strength

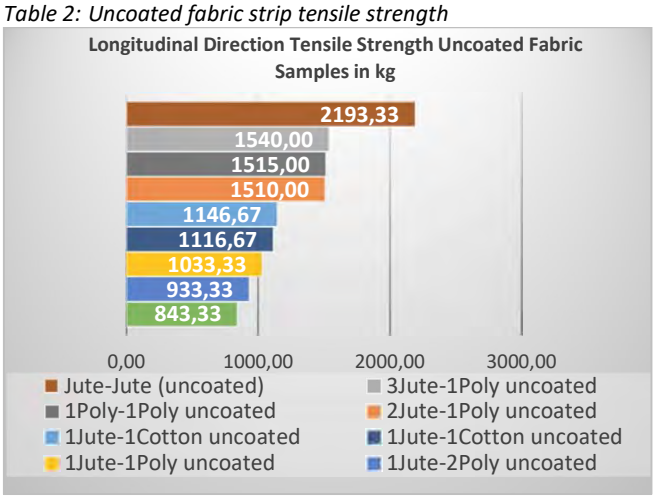

Table 3: Coated fabric strip tensile strength

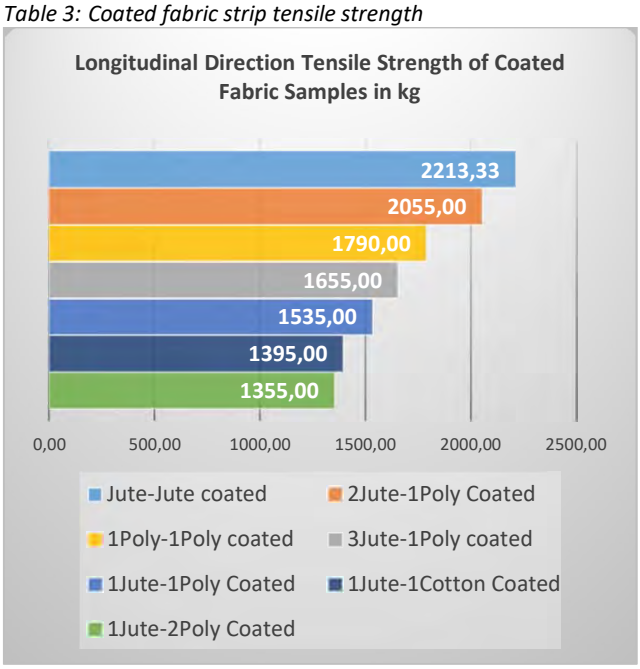

PVC surface coating helps in tensile strength increment. As we can see that there is significant increase of tensile strength in longitudinal or warp direction. However, in case of Jute-Polyester samples, the tensile strength of 2Jute-1Polyester has increased the most (table 02), it is around 36% increase from 1510 kg/m to 2055kg/m. the strength of jute-jute coated fabric has slightly increased from 2193kg/m to 2213.33kg/m though it is the highest strength

among other samples. Which indicate that PVC coating has less impact on jute yarns strength, compared to the polyester yarn. However, the highest tensile strength is gained by 1/1 coated Polyester sample which is around 73% (table 4). The coated Jute-Cotton combination fabrics have less tensile strength gain than other samples.

Table 4: Coated fabric weight

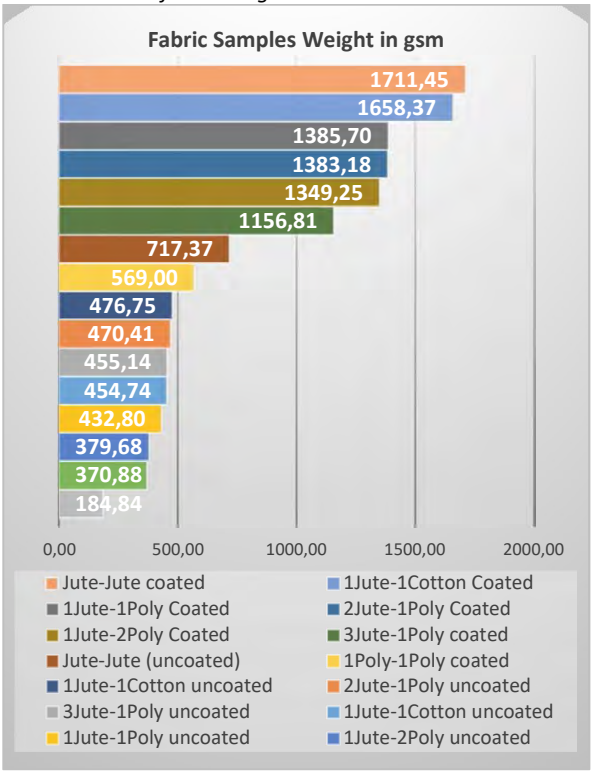

Table 4: Sample fabric Thichkness

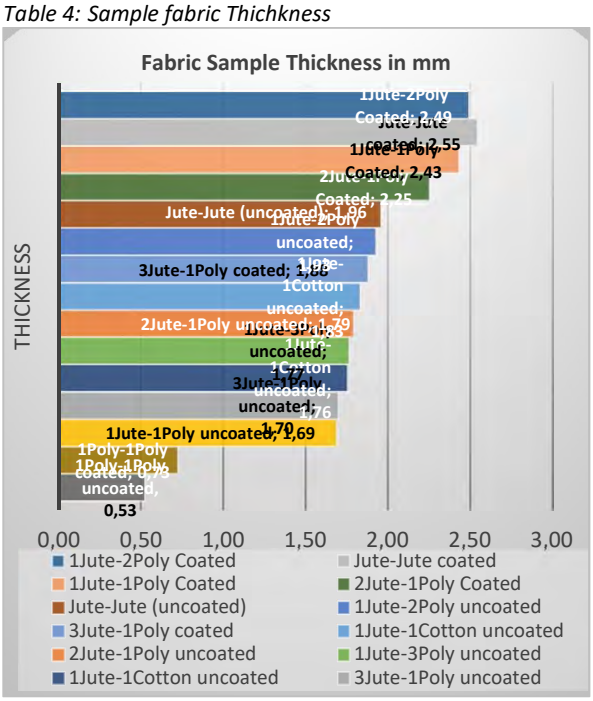

The PVC coating has added extra weight to fabric samples. Jute-jute coated fabric is the heaviest of all, followed by jute-cotton fabric and other samples. If we adjust the gsm of Jute-jute fabric to match with jute-polyester fabrics which is around 1373gsm then we find that jute-jute fabric strength is lower than 2jute-1poly coated fabric.

9. SURFACE STRESS SIMULATION

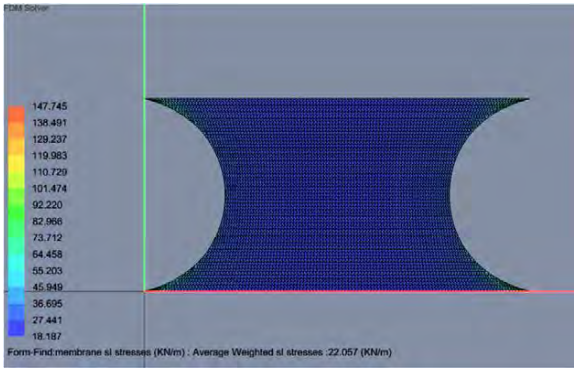

Figure 9: sI stress simulation of 2Jute-1polyester fabric using ixcube forten software.

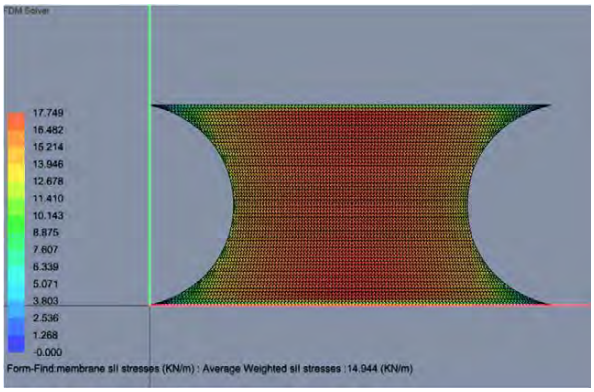

Figure 10: sI stress simulation of 2Jute-1polyester fabric using ixcube forten software.

The membrane surface stress simulation was done via ixcube forten tensile membrane software to observe the surface stress of 2Jute-1polyester fabric. It is found that sI stress is about 22.067 kN/m (figure 09) and sII stress is 14.944kN/m (figure 10) which is ok to withstand seasonal storms in Dhaka [17].

8. CONCLUSION

Coating enhances the tensile strength of jute fabric, particularly in Jute-Polyester composite fabric. 2Jute-1polyester fabric has better tensile strength among the samples studied. So coated 2Jute-polyester weaved fabric can be used as tensile membrane in small to medium sized projects. As climate of Bangladesh is hot humid coated jute-polyester fabric will improve its longevity and sustainability. So jute weaved with polyester with coating can be a biomaterial for tensile membrane projects in hot humid climate like Bangladesh. This research has paved the way for future development of jute based

biomaterial for lightweight, cost effective tensile architecture.

REFERENCES

1. Jahan, A. The environmental and economic prospects of jute with a connection to social factors for achieving Sustainable Development. Master thesis in Sustainable Development, Department of Earth Sciences, Uppsala University (2019)
2. Ghosh, S. K., Ray Gupta, K., Bhattacharyya, R., Sahu, R. B., & Mandol, S. (2014). Improvement of Life Expectancy of Jute Based Needlepunched Geotextiles Through Bitumen Treatment. *Journal of The Institution of Engineers (India): Series E*, *95*(2), 111–121. https://doi.org/10.1007/s40034-014-0036-y
3. Islam, M. S., Khan, A. J., & Siddique, A. (2016). *Effectiveness of Treated Jute Geo-textiles (JGT) in River Bank Protection*. *June*.
4. Saha, P., Roy, D., Manna, S., Adhikari, B., Sen, R., & Roy, S. (2012). Durability of transesterified jute geotextiles. *Geotextiles and Geomembranes*. https://doi.org/10.1016/j.geotexmem.2012.07.003
5. Chowdhury, Z. (2015). An imperial Mughal tent and mobile sovereignty in eighteenth-century Jodhpur. Art History, 38(4), 669–681. https://doi.org/10.1111/1467-8365.12174
6. Construction Fabrics Market by Type (PVC, PTFE, ETFE), Application (Tensile Architecture, Awnings & Canopies, Facades), and Region (Europe, North America, APAC, Middle East & Africa and South America) - Global Forecast to 2023, ID: 4655527, Market Research Report, (October 2008)
7. Jan, E. G. (2009). Environmental benefits of natural fibre production and use. *Proceedings of the Symposium on Natural Fibres*, 3–17. ftp://ftp.fao.org/docrep/fao/011/i0709e/i0709e03.pdf
8. Niloy, A. C. (2021). Jute: Solution to Global Challenges and Opportunities of Bangladesh. *SEISENSE Business Review*, *1*(2), 59–75. https://doi.org/10.33215/sbr.v1i2.633
9. Kabir, D. M., Razzaque, D. M. A., & Rabi, M. R. I. (2019). *Reviving Exports of Jute Products from Bangladesh A study prepared as part of the BEI project on Trade and Investment*.
10. Salam, M., Farouqui, F., & Mondal, M. I. (1970). A Study on Sulphonated Jute-cotton Blended Yarn and Fabrics and their Characteristics. *Bangladesh Journal of Scientific and Industrial Research*, *42*(3), 281–286. https://doi.org/10.3329/bjsir.v42i3.666
11. Dip, T. M., Begum, Prof. Dr. H. A., Hossain, Md. A. al, Uddin, Md. M., & Faruque, Md. O. (2018). Analysis of Physico-Mechanical Properties of Jute and Polyester Blended Yarn. *International Journal of Scientific Research and Management*, *6*(09). https://doi.org/10.18535/ijsrm/v6i9.ec02
12. Sinha, A. K., & Basu, G. (2001). Studies on physical properties of jute-acrylic blended bulked yarns. *Indian Journal of Fibre and Textile Research*, *26*(3), 268–272.
13. Berger, H. (2005). Materials for Tensile Structures. In *Light Structures - Structures of light* (Second Edi). Author House.
14. Thornton, J. (2002). Enviromental impacts of polyvinyl chloride building materials. Washington, D.C.: A Healthy Building Network Report. 110pp
15. Forster, Brian., & Mollaert, Marijke. (2004). *The European design guide for tensile surface structures*. Tensinet.
16. Singha, K. (2012). A Review on Coating & Lamination in Textiles: Processes and Applications. *American Journal of Polymer Science*, *2*(3), 39–49. https://doi.org/10.5923/j.ajps.20120203.04
17. Golam Morsalin, A., & Rana, C. (n.d.). Exploring "Golden Fiber" Jute as Tensile Membrane Architecture in Dhaka.

PLEA 2024 WROCŁAW
(Re)thinking Resilience

The Effect of Rivers on Energy Balance at the Neighborhood Scale

A comparative analysis of four Rhodanian sites in France and Switzerland

SERGI AGUACIL MORENO[1] SARA FORMERY[2] MARTINE LAPRISE[2] EMMANUEL REY[2]

[1] Building2050 group (BUILD), EPFL Fribourg, Smart Living Lab, Switzerland
[2] Laboratory of Architecture and Sustainable Technologies (LAST), EPFL Lausanne, Switzerland

ABSTRACT: This research aims to compare the greenhouse gas (GHG) emissions of new neighbourhood projects near the Rhône River in France and Switzerland. The study considers the influence of the river on energy demand and resilience to climate change of 12 project-based visions across four locations, based on three design scenarios developed for each site in architectural workshops at the Ecole polytechnique fédérale de Lausanne (EPFL). Artificial weather files account for the river's effect, facilitating a comparison between scenarios with and without the river's influence. Methodologically, 3D digital models are used to calculate environmental impacts, integrating data from the Swiss material database and following the SIA 2032 Swiss standard. Findings suggest the Rhône River significantly affects building energy demand, showing a 3-6% fluctuation in demand, depending on water presence or not and 1-2% fluctuation for the global environmental impact. The study underlines the importance of considering climate conditions and water presence in urban planning and building regulations.
KEYWORDS: Environmental impact, low carbon neighbourhood design, multi-criteria assessment, project-based visions

1. INTRODUCTION

The objective of this research is to compare the environmental impact – greenhouse gas (GHG) emissions – of new neighbourhood projects located on four study sites in France and Switzerland near the Rhône River. For each site, three neighbourhood design scenarios (project-based visions) were elaborated during specific architectural workshops at EPFL [1].

The study offers a comparison of the environmental impact of the different urban typologies. By analysing the energy demand for building operation, we are able to explore the level of resilience of different urban typologies in relation to climate change and whether the presence of the river helps or worsens the situation.

The influence of the river has been taken into account by generating artificial climate files where the presence of water (Rhône River) and the effect of the buildings (urban form) are taken into account using open-source tools that are based on low computational cost methods (as opposed to full high-resolution computational fluid dynamics (CFD) simulations).

In order to be able to assess the influence of the river, two types of files have been obtained - for each site and urban design - one without the effect of the river and the urban form and the other with these effects. These files serve as input for the energy simulation by means of the calculation engine. In addition to the operating energy, the grey energy due to the construction has been integrated into the analysis, taking as a reference a type of construction that corresponds to the usual practice for contemporary buildings of the Minergie type [2] with wood-based construction typology.

2. METHODOLOGY

The approach uses as input data the 3D digital models of the project-based visions, in order to automatically obtain the surfaces and material quantities of the different construction components (e.g. glazed surface or opaque façade).

At the same time, the available roof and façade surfaces are automatically detected in order to evaluate the solar and electricity production potential on site.

Then, using the visual programming language Grasshopper [3], the reference environmental impact values of the KBOB building material database [4] and the guidelines of the SIA 2032 standard [5] are applied to calculate the environmental impact of each scenario expressed in terms of greenhouse gas (GHG) emissions.

The set of urban design variants is generated from the three different visions per each of the four locations: Sion (CH), Geneve (CH), Givors (FR) and

Avignon (FR). In total, we analyse 12 different project-based visions (Figure 1).

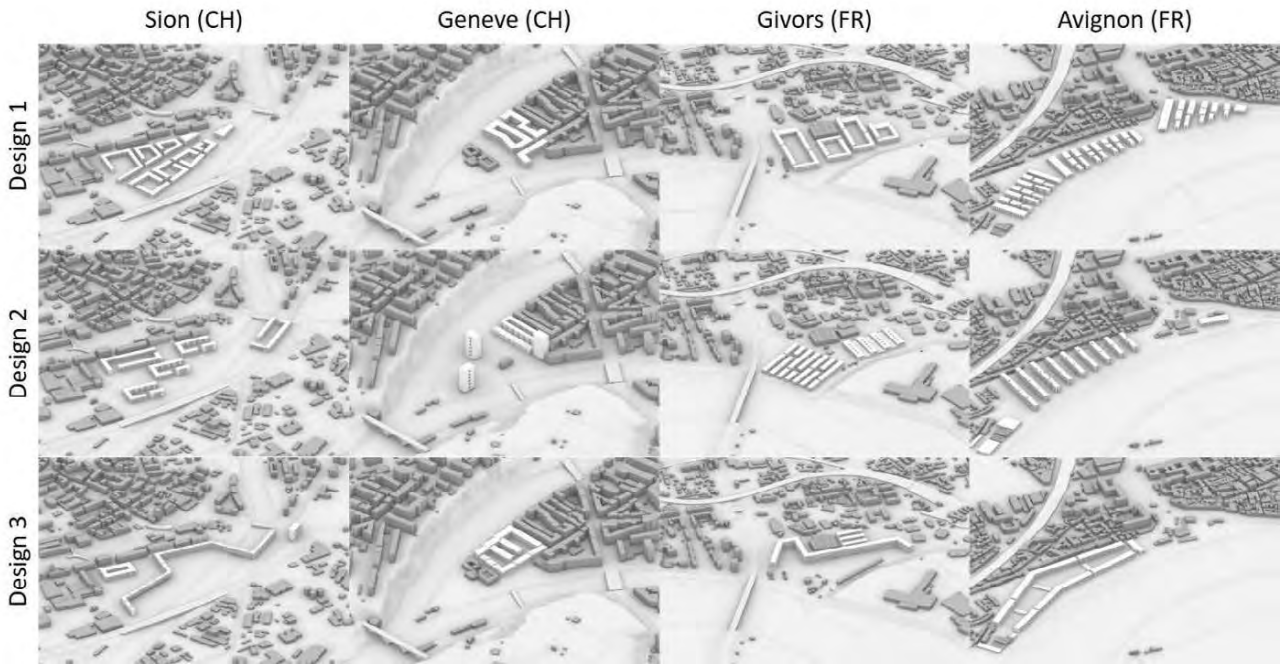

Figure 1: Overview of the twelve studied neighbourhood designs (project-based visions).

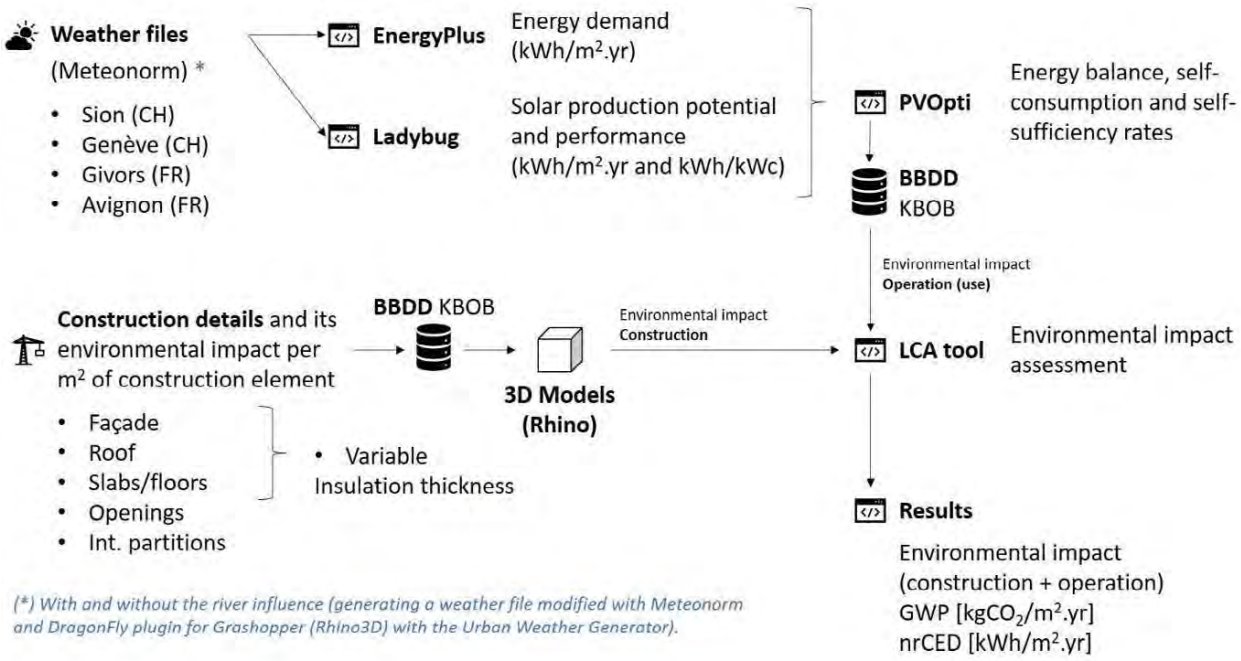

Figure 2: Overview of the workflow for the global analysis. GWP: global warming potential. nrCED: non-renewable cumulative energy demand.

This project has been developed following a five-phase methodology:

1) Analysis of the different study sites (two in France and two in Switzerland) and obtaining the different climate files with contemporary

data (last 10 years). The files that take into account the presence of cold water (Rhône river) have also been generated.

2) For each site, 3 different project-based visions have been analysed based on a series of architectural workshops conducted at EPFL Lausanne (Switzerland).
3) From the 3D models, simulations of the energy potential and renewable energy production have been carried out to obtain the operating energy for each study site, vision and climatic situation.
4) Parametric definition of the building materials to be used, in order to perform the complete life cycle analysis, including the grey energy of the building materials.
5) Comparison of the results. In terms of resilience to climate change, it is based on the evolution of energy demand (heating and cooling) depending on the urban design and the weather file used (with or without influence of the urban context and river).

The workflow to be applied in this research is summarized in Figure 2.

3. RESULTS

We here present some results showing that the presence of the Rhône River has a non-negligible effect on the energy demand of the buildings. Both in summer, with a reduced need for cooling the buildings, and in winter with an increased need for heating in some cases.

3.1 Analysis of the different study sites and climatic conditions

We have generated climate files for each of the sites using Meteonorm software [6] and modified files have been generated that take into account the built environment and the presence of water.

For each of them, psychrometric charts – generated using Climate Consultant tool [7] – have been analysed to see the differences in terms of comfort zones combining temperature and humidity according to ASHRAE 55.

As an example, in Figure 3 the analysis done for the first site, Sion in Switzerland, is presented.

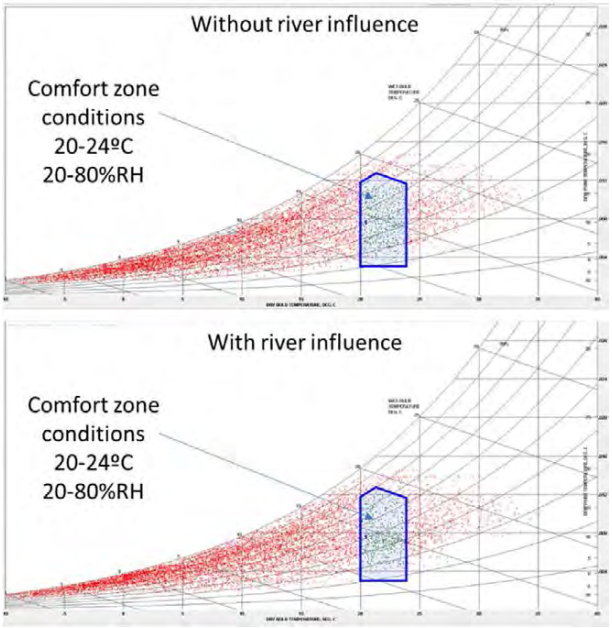

Figure 3: Psychrometric chart for the Sion site, with and without the influence of the water (river).

Table 1: Total of comfort hours per year for the 4 sites (Sion, Geneve, Givors and Avignon), with and without the influence of the water (river).

Scenarios/Site	**Without river**	**With river**
	Comfort hours	
Sion (CH)	708	699
Geneve (CH)	621	637
Givors (FR)	874	804
Avignon (FR)	983	883

The analysis of the climatic data with hourly data on the psychrometric charts shows that the presence of the river decreases the hours of comfort, mainly due to the cooling effect (in winter) and the increase of the ambient humidity (winter and summer).

3.2 Project-based visions analysis

For each site and project vision (scenarios), we have measured the different parameters that will serve as input data in the next phase, where solar, energy and environmental impact simulations are carried out.

Table 2 shows a summary of the data collected in terms of total floor, ground floor, roof, exterior wall and glazing area.

For each scenario a number of square meters of activity (or type of use) have been identified (residential, commercial and school/cultural), calculated according to the SIA 416. The different uses carry a series of simulation hypotheses that are defined in the SIA 2024:2015 [8] with use schedules for occupancy, lighting, heating/cooling, ventilation and domestic hot water (DHW).

Table 2: Surface dimensions in each design scenario.

Scenarios	Floor	Ground	Roof	Ext.Wall	Glazing
	m²				
SI1	166,740	29,578	20,591	50,397	28,936
SI2	151,563	20,198	18,081	50,781	29,056
SI3	134,910	16,540	14,469	31,101	32,269
GE1	78,266	10,456	7,642	19,536	15,254
GE2	84,704	11,186	6,484	22,131	26,636
GE3	85,158	19,996	8,596	9,273	16,738
GI1	150,377	19,407	19,344	44,270	26,637
GI2	154,596	42,037	28,061	31,209	18,517
GI3	113,724	15,350	12,212	18,081	24,754
AV1	123,219	22,437	21,009	69,685	24,876
AV2	76,455	5,704	13,799	21,751	18,228
AV3	91,146	17,007	14,869	10,464	20,004

With this data, standardized simulations have been performed to allow comparison of the results. Table 3 defines the square meters for each type of use.

Table 3: Floor area per usage.

Scenarios	Residential	Commercial	School/cultural
	m²		
SI1	99,218	14,366	23,578
SI2	93,813	19,497	18,055
SI3	88,142	8,052	20,550
GE1	50,293	13,229	4,288
GE2	54,688	12,272	6,558
GE3	44,355	14,893	4,288
GI1	82,185	38,539	10,246
GI2	68,074	30,521	13,964
GI3	61,212	26,916	10,246
AV1	63,979	10,054	26,749
AV2	37,313	13,478	11,865
AV3	52,664	19,185	2,290

3.3 Operational energy balance analysis

For each scenario and site, hourly energy simulations have been performed with the EnergyPlus engine and Designbuilder [9,10] calculation engine to obtain the total energy demand for lighting, heating/cooling, ventilation and DHW.

For all case studies, an all-electric HVAC system based on an air-to-water heat pump with a COP of 3.5 for heating/cooling and a COP of 3 for domestic hot water has been considered.

The definition of the heating energy demand limit is based on the SIA380/1:2016 [11], so we have been able to adjust for each case study in its specific context the insulation thickness that allows to respect this energy demand limit for heating. In this way, the case studies (two in Switzerland and two in France) have been contextualized. This limit value, which helps to define the efficiency of the thermal envelope, depends on the floor area, the envelope surface in contact with the outside and the average temperature of the building site.

Table 4 summarizes the limit values to be respected per indoor floor area.

Table 4: Heating energy demand limit according to SIA380/1.

Scenarios/Site	1	2	3
	kWh/m².year		
Sion (CH)	30.34	29.66	28.31
Geneve (CH)	25.87	27.60	27.34
Givors (FR)	24.10	26.98	22.56
Avignon (FR)	24.48	21.56	19.17

Regarding the photovoltaic solar energy production potential, the assumption for the calculation is the use of 80% of the available roof surface with standard east/west oriented solar panels and an overall efficiency of 20%. The solar energy calculation was done using the 3D model (Rhino 3D) for each case study and the Ladybug tool [12].

Table 5: Electricity balance (without river influence).

Scenarios	Demand	Production	SC	SS
	kWh/m².year		%	
SI1	35.7	47.1	22.30%	29.50%
SI2	36.7	46.7	23.60%	30.00%
SI3	35.2	36.4	26.80%	27.80%
GE1	38.7	30.7	34.70%	27.50%
GE2	38	28.4	36.00%	26.90%
GE3	39.2	25.3	41.70%	26.90%
GI1	38.9	40	30.20%	31.00%
GI2	38	19.6	52.50%	27.00%
GI3	38.3	27.4	40.10%	28.70%
AV1	32.9	79.5	14.30%	34.60%
AV2	35.5	57.4	20.80%	33.70%
AV3	38.1	40.1	29.30%	30.80%

Table 6: Electricity balance (with river influence).

Scenarios	Demand	Production	SC	SS
	kWh/m².year		%	
SI1	36.2	47.1	22.40%	29.20%
SI2	37.2	46.7	23.70%	29.70%
SI3	35.7	36.4	27.00%	27.50%
GE1	39.3	30.7	34.90%	27.30%
GE2	38.6	28.4	36.20%	26.70%
GE3	39.7	25.3	41.90%	26.70%
GI1	39.6	40	30.40%	30.70%
GI2	38.7	19.6	52.90%	26.80%
GI3	39	27.4	40.40%	28.40%
AV1	33.7	79.5	14.50%	34.20%
AV2	36.2	57.4	21.00%	33.30%
AV3	38.9	40.1	29.50%	30.50%

The results of the final energy balance, without taking into account the presence of water and the

urban context (using the different weather files generated in phase 1), are summarized in Tables 5 and 6, respectively, in terms of energy demand, electricity production, self-consumption (SC) and self-sufficiency (SS).

As expected, the overall electrical energy to meet the different types of consumption (heating/cooling, etc.) varies depending on the climatic conditions (with and without the influence of the river). In general, the demand is higher with the presence of the river, mainly due to the increase in heating demand and the higher humidity in summer which affects the efficiency and consumption of electricity for cooling.

3.4 Constructions elements and embodied energy balance analysis

In order to be able to calculate the environmental impact of building materials, the type of construction and the layers of different materials for the thermal envelope have been defined (Tables 7 to 11). For each material, the environmental impact has been taken into account according to the KBOB2022 database defined from Ecoinvent data [4].

Table 7: Definition of façade layers and their thickness.

	Layer	Th. (cm)
1	Wood (spruce)	1.5
2	PE vapour barrier	0.02
3	OSB-type chipboard	2.7
4	Expanded polystyrene (λ: 0.04 W/mK)	22 (*)
5	Wooden beam 12cm each 60 cm (Spruce)	12
6	Hard particleboard	2.7
7	Wooden batten 50mm each 60 cm (Spruce)	5
8	Wood (spruce)	2.4
** Varies according to the energy demand limit of each site*		

Table 8: Definition of roof layers and their thickness.

	Layer	Th. (cm)
1	Round gravel	5
2	Bituminous waterproofing sheet	0.8
3	Expanded polystyrene (λ: 0.04 W/mK)	22 (*)
4	Bituminous vapour barrier	0.3
5	Wood (spruce)	2.4
6	Wooden batten 50mm each 60 cm (Spruce)	12
** Varies according to the energy demand limit of each site*		

Table 9: Definition of internal floor layers and their thickness.

	Layer	Th. (cm)
1	Particleboard	2.4
2	PE vapour barrier	0.02
3	Wooden beam 12cm each 60 cm (Spruce)	12
4	Wooden beam 12cm each 60 cm (Spruce)	5
5	Stone wool, ρ:30kg/m3	8
6	Wood (spruce)	1.3

Table 10: Definition of ground floor layers and their thickness.

	Layer	Th. (cm)
1	Cement screed, 85 mm	8.5
2	Acrylonitrile-butadiene-styrene (ABS)	0.001
3	PE vapour barrier	0.02
4	Expanded polystyrene (λ: 0.04 W/mK)	22
5	Bituminous waterproofing membrane	0.4
6	Concrete foundation slab	25
7	Reinforc. (2%) of the concrete beam slab	2%
8	Lean concrete	8
** Varies according to the energy demand limit of each site*		

Table 11: Definition of internal floor layers and their thickness.

	Layer	Th. (cm)
1	Hard particleboard	1.25
2	Stone wool, ρ:30kg/m3	5
3	Wood frame 5cm each 60 cm (Spruce)	5
4	Hard particleboard	1.25

3.5 Global environmental impact (operational and embodied) comparison

Compiling the data and the calculations made during all the preceding phases, the global environmental impact (Life Cycle Analysis) is obtained for each of the scenarios without taking into account and taking into account the presence of the river.

Firstly, table 12 presents the environmental impact for the operational (use) part (due to energy consumption) expressed in terms of GHG emissions. For this operational part, the differences between taking into account or not the water presence (Rhône River) near the urban area is about 3-6% increase/decrease in demand.

Table 12: Environmental impact results for operation (use) of the buildings, with and without water presence.

	Without river	**With river**
Scenarios	$kgCO_2/m^2.year$	
SI1	1.80	1.86
SI2	1.90	1.96
SI3	2.20	2.26
GE1	2.77	2.84
GE2	2.80	2.87
GE3	3.04	3.10
GI1	2.33	2.41
GI2	3.12	3.20
GI3	2.81	2.89
AV1	0.18	0.27
AV2	1.27	1.35
AV3	2.25	2.34

Secondly, table 13 presents the global environmental impact for the operational (use) and

construction (embodied) part expressed in terms of GHG emissions. For the global impact, the differences between taking into account or not the river is about 1-2% increase/decrease in demand.

Table 13: Global environmental impact results for operation (use) and embodied (construction) of the buildings, with and without water presence.

	Without river	**With river**
Scenarios	$kgCO_2/m^2.year$	
SI1	4.76	4.82
SI2	4.85	4.90
SI3	4.96	5.01
GE1	5.46	5.53
GE2	5.79	5.86
GE3	5.71	5.76
GI1	5.13	5.22
GI2	6.08	6.16
GI3	5.35	5.43
AV1	4.02	4.10
AV2	4.29	4.36
AV3	4.94	5.04

These results should be considered as preliminary as the project continues and a more complete analysis is planned integrating a CFD study using Envi-met [13] for the creation of modified climate files taking into account the urban form and the presence of water and vegetation. Likewise, we will integrate climate files that take into account the different horizons (2030 to 2100) and various RCP (Representative Concentration Pathway) climate change scenarios.

4. CONCLUSION

For the moment, our efforts have been concentrated on the analysis using modified climate files through a simplified workflow and low computational cost open-source tools (namely Ladybug and Dragonfly). It is observed that it is in the operational part (use) that the river has the greatest impact.

However, our intention for the research project is to show how climate change (through RCP files), the presence of water (river) and vegetation can have an impact on the results, having for example a higher/lower need for insulation, better/worse outdoor temperature/humidity conditions that would allow passive strategies, or making the overall environmental impact higher or lower.

Considering global warming, a first hypothesis to investigate is whether the river could have a strong positive influence, in particular against the urban heat island effect. Future work will also deepen the study of the interactions with urban form and environmental parameters (vegetation including its type, wind, etc.). The methodology already developed and presented in this paper provides a solid framework for these upcoming steps.

ACKNOWLEDGEMENTS

The authors thank the team of Laboratory of Architecture and Sustainable Technologies (LAST) involved in this research, the Building2050 group and the Ecole polytechnique fédérale de Lausanne (EPFL) for its support.

REFERENCES

1. EPFL, Design studio projects of Prof. Emmanuel REY, “Rhodanie Urbaine” (2018-2022), EPFL, Lausanne.
2. Minergie, Minergie certification label, 2023.
3. Robert McNeel & Associates. Rhinoceros 3D Software. Seattle, Washington, Etats-Unis, 2020.
4. KBOB, « Données des écobilans dans la construction 2009/1 :2016 ». Berne, 2016.
5. Société Suisse des Ingénieurs et des Architectes. SIA 2032 :2010 « L’énergie grise des bâtiments ». Zurich, 2010.
6. Meteotest, Meteonorm software, 2018.
7. UCLA, Climate Consultant, 2020.
8. Société Suisse des Ingénieurs et des Architectes (SIA), SIA 2024:2015 - Donées d’utilisation des locaux pour l’énergie et les installations du bâtiment, (2015).
9. US Department of Energy (DOE), EnergyPlus, 2020.
10. DesignBuilder, DesignBuilder software v.7, 2023.
11. Société Suisse des Ingénieurs et des Architectes, SIA 380/1:2016 Besoins de chaleur pour le chauffage, Zurich, 2016.
12. Ladybug tool LLCC, Ladybug, 2023. https://www.ladybug.tools/.
13. ENVI-met GmbH, Envi-met software, 2023. https://www.envi-met.com/.

PLEA 2024 WROCŁAW
(Re)thinking Resilience

Design Recommendations for Office Building Facades Based on Visual Comfort and Minimum Energy Consumption Criteria: The case of Chile

WALDO BUSTAMANTE[1,2], DANIEL URIBE[3], GILLES FLAMANT[2], SERGIO VERA[2,3,4], GERMAN MOLINA[3]

[1]School of Architecture, Pontificia Universidad Católica de Chile, Santiago, Chile
[2] Centre for Sustainable Urban Development (CEDEUS), Pontificia Universidad Católica de Chile, Santiago, Chile
[3] Department of Construction Engineering and Management, School of Engineering, Pontificia Universidad Católica de Chile, Santiago, Chile
[4] UC Energy Research Center, Santiago, Chile

ABSTRACT: Recently, highly glazed facades in office buildings have become widespread worldwide, including in Chile, impacting their occupants' thermal and visual comfort. This study is conducted to propose design strategies for the glass facades of office buildings in Chile, aiming to achieve thermal and visual comfort for office occupants with minimal energy consumption. Multiple simulations are performed to analyse thermal and visual comfort for office occupants while simultaneously determining energy consumption for heating, cooling, and artificial lighting. The Oficity calculation engine is used to determine the mentioned energy consumptions and estimate visual comfort indicators like sDA and ASE. Nocturnal and daytime ventilation for cooling was also evaluated. The simulations consider an office space (3.6 x 5.4 x 2.7 m) with an adiabatic envelope, except for the glass facade exposed to the exterior. Six cities have been considered, from Arica (18.5 S) to Punta Arenas (53.2 S). The conclusions indicate that the size of the glazed facade area should be limited to a 50% window-to-wall ratio, using selective glass. Nocturnal ventilation is recommended in inland cities like Santiago and Calama, while daytime ventilation could be beneficial in coastal cities (Arica and Concepción), as well as in Temuco.

1. INTRODUCTION

In recent decades, around the world, office buildings have been designed with highly glazed facades, resulting in high energy consumption for thermal conditioning and severe issues related to thermal and lighting comfort for their users. Very similar typologies of office buildings, with extensive glass facades, are found in different latitudes around the world, as if the type of climate in these areas does not influence their energy and environmental performance.

Indeed, the impact on energy consumption and the thermal and visual comfort of occupants in office buildings has been extensively studied in various cities worldwide, including Chile [1,2,3, 4, 5]. In the case of Santiago, Chile, facades of office buildings in over 100 structures built during the first decade of this century have been analyzed. It was determined that more than 50% of the office buildings constructed in this city exhibit a window-to-wall ratio (WWR) between 75 and 100% [4]. In another more recent study, 6 out of 9 buildings analyzed in Santiago, Chile, have a WWR equal to or greater than 70% [6]. Moreover, other research has demonstrated that reducing the WWR of facades implies a significant decrease in energy consumption for cooling [7].

Chile shows a high climatic diversity from north to south, stretching between the cities of Arica (18.5° S) and Punta Arenas (53.2° S). This variability is also evident among coastal cities and urban centers situated between the Coastal Range and the Andes Mountains, where thermal oscillation and solar radiation are typically higher than those observed on the coast at the same latitude [8]. Furthermore, in Chile, there has been a growing trend in extreme weather events in recent decades [9], highlighting the importance of enhancing the thermal and environmental performance of buildings.

This is crucial to effectively confront these extreme climatic phenomena and safeguard their occupants. On the other hand, the country has committed to achieving carbon neutrality by 2050, with commitments related to energy transition. However, weak progress can be observed in Chile regarding energy efficiency policies for buildings. The construction sector in Chile consumes 25% of the total energy, with 6% corresponding to public

buildings. Currently, Chile lacks mandatory standards related to thermal performance and visual comfort in office buildings. In this regard, the Ministry of Public Works in the country has a set of recommendations outlined in the Environmental Comfort and Energy Efficiency Terms of Reference (TDRs), which applies to public buildings under the ministry's responsibility [6, 10]. The criteria in these Terms of Reference are primarily based on the thermal performance of these buildings.

Additionally, the country has the Sustainable Building Certification System (CES) [11], which is voluntary for public-use buildings and based on international standards, such as ASHRAE55. However, from this system, it's not possible to clearly deduce architectural design recommendations for office buildings, as some certified buildings under this system have fully glazed facades. Finally, it's worth noting that there are still no studies defining these standards and design recommendations for office buildings based on criteria for minimal energy consumption while simultaneously meeting criteria for visual and thermal comfort for their occupants.

Considering the aforementioned, the objective of this study is to establish a set of design recommendations for office buildings in different climates across the country, based on criteria aimed at achieving a minimum total energy consumption for their thermal conditioning and artificial lighting, while simultaneously ensuring the visual and thermal comfort of their occupants.

2. METHODOLOGY

The methodology of this study involves a parametric analysis of a series of variables related to glazed facades and solar protection in office buildings in different cities of the country. From this analysis, design recommendations are established to reduce energy consumption and meet minimum visual and thermal comfort requirements.

The parametric analysis was conducted through simulations in an office space. This space corresponds to an office in a standard building defined in the IEA-SHC TASK 27 A1 [12]. This building consists of a central corridor with offices for approximately 2 people on each side along the length of the building.

The selected office space is an intermediate office on a middle floor; therefore, all its surfaces are considered adiabatic, except for the glazed façade exposed to the outside.

The internal dimensions of the office are 3.6 m x 5.4 m x 2.7 m, as shown in Figure 1. The reflectance of the interior surfaces is 0.1 for the floor, 0.5 for the wall, and 0.8 for the ceiling.

The space considers three types of internal loads: Equipment: 15 W/m^2. People: 2 persons. Lighting: 8 W/m^2. All internal loads are active during the working period between 09:00 and 18:00 on weekdays, during which energy consumption for thermal and visual comfort is determined. Ventilation rates were determined with ASHRAE 62.1 standard [13].

2.1 Thresholds and performance indicators

As a minimum lighting requirement, 400 lux in the workplace is considered, which aligns with the Chilean Sustainable Building Certification System (CES) [11]. Artificial lighting is defined to provide at least the mentioned 400 lux on the work plane in the absence of natural lighting.

To assess energy performance, sufficiency of natural lighting, and visual comfort of the evaluated cases, the following parameters are considered: Total annual energy consumption (kWh/m2 year), which includes artificial lighting, cooling, and heating.

Visual comfort was assessed using the metrics Spatial Daylight Autonomy sDA300/50% and Annual Sunlight Exposure ASE2000/400h.

To evaluate the energy performance, adequacy of natural lighting, and visual comfort of the evaluated cases, the following parameters are considered:

- Total energy consumption (kWh/m2year): It corresponds to the sum of the annual energy consumption from lighting, heating, and air conditioning in the office
- Spatial Daylight Autonomy sDA300/50%: Corresponds to the percentage of the office area that meets a minimum illuminance of 300 lux by natural light for 50% of the working time. The percentage should exceed 55%.
- Annual Sunlight Exposure ASE2000/400h: Corresponds to the percentage of the office area that exceeds an illuminance of 2000 lux for more than 400 hours of work per year. It should be less than.

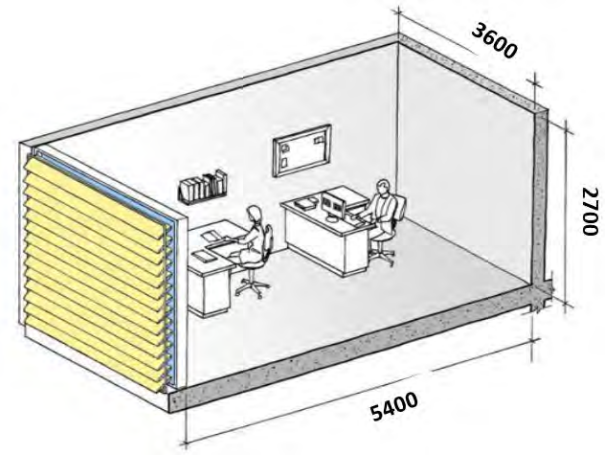

Figure 1: Dimensions of the simulated office

2.2 Simulation parameters

Since this study is conducted in the southern hemisphere, the following three orientations of the office space glazed façade have been studied: North, East, and West. Regarding the size of the glazed surface of the facade, percentages (or window to wall ratio; WWR) of 30, 50, 70, and 90% were considered.

2.3 Characteristics of glazed systems

The characteristics of the glasses assumed in the simulations range from single-pane to double-pane glass with a certain level of selectivity. In one of the double-glazed systems, argon gas was considered. The rest have air between the two panes of the façade system.

The following table shows the U-value (thermal transmittance), Solar Heat Gain Coefficient (SHGC), and Visible Transmission (Tv) of the glass types used in the simulations

Table 1: Type of glazing considered in the study

Type of Glazing	U W/m2 K	SHGC	Tv
Simple (SG)	5.8	0.86	0.86
Double (air) (DG-air)	2.9	0.77	0.81
Double Low e (air) DG Lowe-air	1.9	0.69	0.77
Double Low e (argon) DG Lowe-argon	1.3	0.62	0.80
Double Selective (air) Sel 1	1.8	0.27	0.37
Double Selective (air) Sel 2	1.5	0.35	0.70
Double Selective (air) Sel 3	1.5	0.26	0.50

2.4 Solar protection systems

With the purpose of controlling the incident solar radiation on the facade to prevent overheating indoors and for natural lighting control, the use of a solar shading system has been considered, consisting of vertical louvers. The louvers have a width C of 5 cm and a spacing B of 5 cm between them. The slat's reflectance is 60%.

The following figure displays the parameters characterizing the exterior vertical solar shading louvers, where A represents the slat's opening angle Figure 2). For this study, opening angles of 30°, 45°, and 60° have been considered. Additionally, the facade without exterior solar shading has been considered. An interior curtain has also been assumed with solar transmittance (Ts) of 20% and visible transmittance (Tv) of 18%, as well as luminous transmittance characteristics.

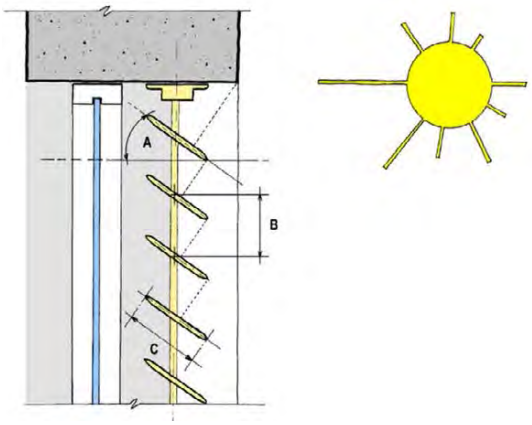

Figure 2: External vertical louvers

2.5 Ventilation strategies

In order to try to decrease cooling energy consumption, the application of nighttime ventilation and daytime ventilation strategies was assumed from October to March each year. Regarding nighttime ventilation in the hours preceding the workday (from 22:00 of the previous day until 7:00), hourly air exchanges of 1.0 air changes per hour (ach), 3.0 ach, and 6.6 ach were considered. As for daytime ventilation, it was assumed to be 1.0 ach and 3.0 ach. These air exchanges are in addition to air infiltrations and the ventilation set for the two occupants of the office space, which amounts to a value of 0.74 ach. Air infiltration was assumed to be at 0.4 ach.

2.6 Cities

In this study, cities from the northernmost point of Chile (Arica) to Punta Arenas, located in the Patagonia region at the extreme south of the country, have been considered. Undoubtedly, it is expected that as one goes from the north to the south of the country, the climate will become progressively colder. However, in addition to the variation in latitude, one must consider the influence of the ocean and the fact that inland cities are situated between two mountain ranges for much of the country (up to approximately latitude 41.5 S). Indeed, the coastal mountain range acts as a barrier preventing the ocean's effect from penetrating inland. This implies that the temperature fluctuations in coastal cities are lower than those in the interior. This can be observed, for instance, in Figure 3, which displays the temperatures of Santiago and Concepción (the latter having higher minimum temperatures than Santiago, despite being located farther south). Generally, inland cities also experience less cloud cover, resulting in higher solar radiation compared to coastal cities. (Note the cities of Arica and Calama as examples).

Table 2: Cities considered in the study

City	Latitude South °	Köppen Climate Classification	Solar Radiation (kWh/m2 year)
Arica	18.5	BWk	1546
Calama	22.5	BWk	2414
Santiago	33.5	BSk	1910
Concepción	36.8	Csb	1493
Temuco	38.7	Csb	1354
Pta. Arenas	53.2	Csc	899

2.7 Simulation process

The simulations were carried out using the code of the online software Oficity (www.oficity.cl), which performs dynamic simulations of natural lighting and energy consumption in an office building. Oficity utilizes the calculation engines Radiance and EnergyPlus, two validated and widely used tools in scientific research. Two simulations are conducted per hour over a complete year. These simulations encompass all possible combinations among the mentioned parameters (orientation, type of glazing, glazing area, type of solar protection including louver angle, and variations in ventilation), for which the energy consumption for heating, cooling, and artificial lighting to reach corresponding thresholds is determined. Simultaneously, the respective visual comfort indicators (sDA and ASE) are calculated.

To estimate the heating and cooling energy consumption, it is assumed that the office has a heat pump for air conditioning with a coefficient of performance (COP) of 3.0 for both heating and cooling. The cooling thermostat is set at 25°C, while the heating thermostat is set at 20°C.

To estimate artificial lighting consumption, Oficity considers dimmable luminaires capable of adjusting power according to lighting needs.

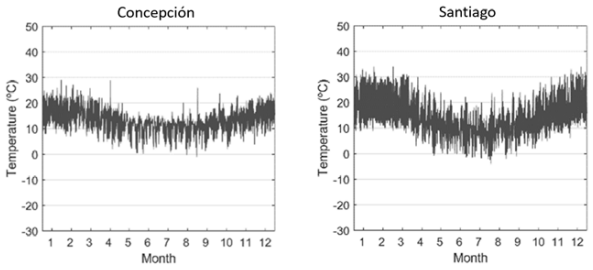

Figure 3: Annual variation of temperature in Concepción and Santiago

3. RESULTS

For each city, the minimum energy consumption values obtained in the north orientation are shown in Table 3. The same type of information is presented in Tables 4 and 5 for west and east orientations. It is noticeable that the prevailing window size in almost all cases corresponds to a WWR (window-to-wall ratio) of 50%. The exception is the case of Punta Arenas, where for east and west orientations, the minimum energy consumption corresponds to WWR cases of 30%. This could be explained by the fact that heating energy consumption prevails in this city. It can also be observed that total energy consumptions tend to decrease in cities further south in the country. This is explained by the general trend where the highest total energy consumption tends to be significantly higher for cooling compared to heating consumption.

Table 3: Summary of Results for North-Facing Office

	WWR %	Type of window	SDA %	ASE %	Total Energy kWh/m^2 year
Arica	50	Sel 3	63	0	27.9
Calama	50	Sel 3	60	0	37.1
Santiago	50	Sel 3	77	0	27.7
Concep.	50	Sel 3	70	0	20.1
Temuco	50	Sel 3	63	0	16.1
P. Aren.	50	Sel 3	60	0	14.1

Table 4: Summary of Results for West-Facing Office

	WWR %	Type of window	SDA %	ASE %	Total Energy kWh/m 2 year
Arica	50	Sel 2	77	0	45.5
Calama	50	Sel 2	60	0	49.7
Santiago	50	Sel 2	73	0	43.4
Concep.	50	Sel 2	70	0	28.3
Temuco	50	Sel 2	67	0	26.2
P. Aren.	30	Sel 2	57	0	17.4

Table 5: Summary of Results for East-Facing Office

	WWR %	Type of window	SDA %	ASE %	Total Energy kWh/m 2 year
Arica	50	Sel 3	60	0	37.3
Calama	50	Sel 2	70	0	29.3
Santiago	50	Sel 3	57	0	28.3
Concep.	50	Sel 2	80	0	20.6
Temuco	50	Sel 2	70	0	16.4
P. Aren.	30	Sel 2	57	0	16.6

As an example, in the case of Arica (with predominantly hot climate) and for the north orientation, the office space has artificial lighting consumption of 3.9 kWh/m2 year and cooling consumption of 24.0 kWh/m2 year, with zero heating

consumption. In the case of Punta Arenas, with a predominantly cold climate, under the same orientation, the lighting consumption is 6.4 kWh/m2 year, cooling is 4.4 kWh/m2 year, while heating reaches 3.3 kWh/m2 year. Comparing these values with the case of Santiago, it is observed that for this city, the office space oriented to the north has an artificial lighting energy consumption of 3.2 kWh/m2 per year, no heating consumption, and a cooling consumption of 24.1 kWh/m2 per year.

Regarding the angle of the louvers, in general, it ranged between 0° and 30°, including east and west orientations

On the other hand, it is interesting to observe the results obtained when applying daytime and nighttime ventilation strategies for cooling the office space during the spring and summer periods in the respective cities.

In the case of the city of Arica, the effect on energy consumption (where cooling consumption prevails) of daytime ventilation is similar to that of nighttime ventilation. This could be explained by the fact that daytime temperatures in this coastal city are not extremely high during summer, due to the influence of the ocean. See figure 4. The figures 4 through 8 show simulations of all cases by city (from most to least energy-efficient) in which daytime and nighttime ventilation are applied

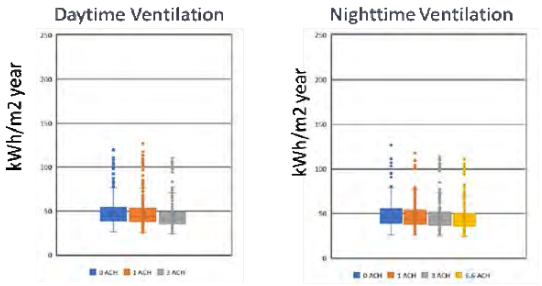

Figure 4: Arica: Impact of daytime and nocturnal ventilation on energy consumption

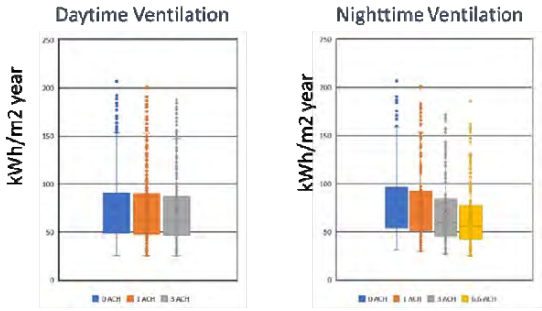

Figure 5: Calama: Impact of daytime and nocturnal ventilation on energy consumption

In the case of Calama, as shown in figure 5, a significant difference is observed in the effect on energy consumption for indoor air conditioning between daytime and night-time ventilation. This is explained by the high thermal oscillation between day and night throughout the year in this city, including the summer season. Therefore, it is advisable to use night-time ventilation to reduce cooling energy consumption in office buildings in this city.

In the case of Santiago, it's possible to observe a greater impact on the decrease of night-time ventilation than daytime ventilation (See figure 6). This could be explained by the lower temperatures in this city during summer periods compared to daytime.

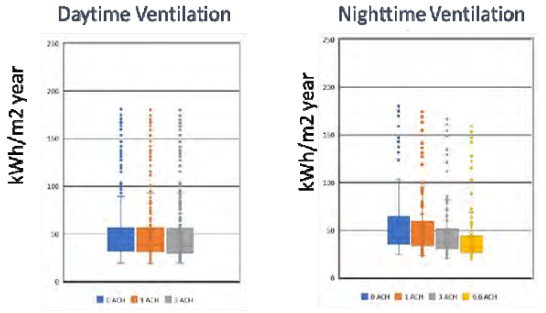

Figure 6: Santiago: Impact of daytime and nocturnal ventilation on energy consumption

In the case of Concepción, nighttime ventilation shows a significant impact on reducing energy consumption for interior conditioning, but daytime ventilation might be sufficient, as seen in Figure 6. It's worth noting that Concepción is a coastal city.

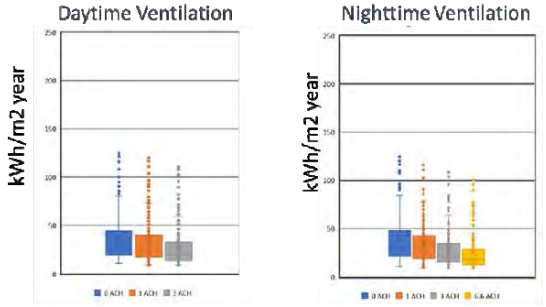

Figure 7: Concepción: Impact of daytime and nocturnal ventilation on energy consumption

In the case of Temuco, nocturnal ventilation also shows a significant impact. However, due to the lower temperatures in this city during the day, daytime ventilation could also be applied for cooling the indoor environment in summer. See figure 8.

In the case of cities like Punta Arenas, located at the southernmost tip of the country, it doesn't make sense to apply additional cooling strategies such as daytime and nighttime ventilation since the cooling demands are not high in this city

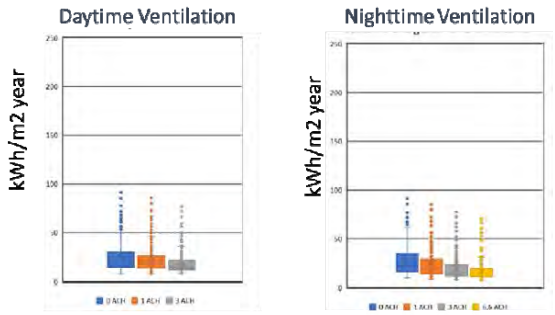

Figure 8: Temuco: Impact of daytime and nocturnal ventilation on energy consumption

4. CONCLUSION

Based on this study, recommendations have been established for the design of glazed facades for office buildings located in various cities with different climates in Chile. These recommendations consider criteria to achieve a minimum total energy consumption (summing up heating, cooling, and artificial lighting) while simultaneously achieving thermal and visual comfort for the occupants of the office space.

For the development of this study, a parametric analysis was conducted involving various variables that influence the energy performance and lighting in office buildings. The study involved simulations where energy consumption for heating, cooling, and artificial lighting necessary to achieve the considered thresholds of thermal and visual comfort were simultaneously determined.

In this study, representative climatic data from the involved cities have been considered; however, these data do not necessarily encompass the heatwaves observed in these cities in recent years. In the future, it is advisable to conduct these studies using climate databases that account for these heatwaves to assess the scope of the problem and find solutions to adapt the buildings that will face these extreme climatic phenomena. In this regard, other cities in the country should also be considered in future studies. At the same time, other types of solar protection systems could also be considered, such as the vertical louvers analyzed in this study but with different dimensions and spacing between louvers, as well as perforated systems and lighter options like exterior solar shading fabrics

ACKNOWLEDGEMENTS

This work was funded by the National Agency for Research and Development (ANID), Chile, under research grant FONDECYT 1181686. The authors also gratefully acknowledge the research support provided by CEDEUS under the research grant ANID/FONDAP1523A0004.

REFERENCES

1. Uribe, D., Vera, S., Bustamante, W., McNeil, A., Flamant, G. (2019). Impact of different control strategies of perforated curved louvers on the visual comfort and energy consumption of office buildings in different climates. *Solar Energy.* Volume 190, 15, 495-510.

2. Lam, T. C., Ge, H., Fazio, P. 2015). Impact of Curtain Wall Configurations on Building Energy Performance in the Perimeter Zone. for a Cold Climate. *Energy Procedia.* Volume 78, 352-357.

3. Chan, Y-C., Tzempelikos. A. (2013). Efficient venetian blind control strategies considering daylight utilization and glare protection. *Solar Energy.* Volume 98, Part C, 241-254.

4. Bustamante, W., Vera, S., Prieto, A. and Vasquez, C. (2014) "Solar and Lighting Transmission through Complex Fenestration Systems of Office Buildings in a Warm and Dry Climate of Chile". *Sustainability,* Vol. 6, No 5, 2786-2801.

5. Uribe, D., Bustamante, W., Vera, S. (2017). "Seasonal optimization of a fixed exterior complex fenestration system considering visual comfort and energy performance criteria". *Energy Procedia*. Volume 132, 490-495.

6. Trebilcock, M., Soto-Muñoz, J., Piggot-Navarrete, J. (2020) Evaluation of thermal comfort standards in office buildings of Chile: Thermal sensation and preference assessment. *Building and Environment*. 183, 197158.

7. Pino A., Bustamante, W., Escobar, R., y Encinas F. (2012). "Thermal and Lighting Behavior of Office Buildings in Santiago of Chile". *Energy and Buildings*. 47(1):441-449.

8. Instituto Nacional de Normalización. (2019). NCh 1079. Arquitectura y Construcción. Zonificación climática y térmica para el diseño de edificaciones. Instituto Nacional de Normalización. Santiago, Chile

9. González-Reyes, A., Jacques-Coper, M., Bravo, C., Rojas, M., Garreaud, R. (2023). Evolution of heatwaves in Chile since 1980. *Weather and Climate Extremes*. Volume 41, 100588.

10. CITEC UBB TDRe, T´erminos de Referencia Estandarizados con Parámetros de Eficiencia Energética y Confort Ambiental, para Licitaciones de Diseño y Obra de la Dirección de Arquitectura, Según Zonas Geográficas del País y Según Tipología de Edificios, 2012.

11. Instituto de la Construcción (2014). Manual de Operación Sistema de Certificación de Edificación Sustentable. [Online] Available: www.certificacionsustentable.cl/documentos/.

12. van Dijk, D. (nd), Thermal and solar modelling and characterisation; the role of IEA SHC Task 27. [Online]. *Available in: https://task27.iea-shc.org/publications*.

13. ASHRAE ANSI/ASHRAE Standard 62.1-2019. Ventilation for Acceptable Indoor Air Quality- ASHRAE 2019.

PLEA 2024 WROCŁAW
(Re)thinking Resilience

Defining a common set of Key Performance Indicators for Positive Energy Districts

MELINDA OROVA[1,2], ANDRÁS REITH[1,2]

[1]ABUD Ltd., Budapest, Hungary
[2] Marcel Breuer Doctoral School of Architecture, University of Pécs, Pécs, Hungary

ABSTRACT: The concept of Positive Energy Districts (PEDs) is one of the central pillars for driving the urban energy transition, but a common definition has not been established yet. PED Key Performance Indicators (KPIs) are not yet consolidated either and cover a diverse field of sustainability aspects. The investigation of PED definitions can support the establishment of a common set of KPIs for projects with PED ambitions. The definitions of five prominent EU programmes and six PED-relevant projects across Europe were investigated to determine their commonalities. The results showed that only Energy related aspects were considered at least in 7 of the 11 definitions (Energy generation, Energy balance, Energy efficiency, and Active management). Additionally, five definitions also consider GHG emissions and Energy flexibility aspects and 4 of them include Participatory approaches. The associated KPIs of these aspects form the common KPI list of the investigated definitions, which can support the further development of a base PED definition and also to establish a common ground for performance assessment for projects with PED ambitions.

KEYWORDS: Positive Energy Districts; Key Performance Indicators; neighbourhood sustainability

1.INTRODUCTION

The concept of Positive Energy Districts (PEDs), one of the central pillars for driving the urban energy transition, has been developed through EU initiatives and research programmes, but a common definition has not been established yet [1]. Mayor organisations, programmes, research projects and individual PED projects have their own interpretation of how energy balance is calculated, what are the scale and boundaries of projects and what key concepts are needed to be covered by a PED [2]. It is clear the PED concept originates from the energy balance assessment, but the existing PED definitions show that the scope of PEDs go beyond the energy aspect and cover challenges related to social, economic or environmental sustainability as well.

Indicators are needed to measure the performance of PED projects, which have also started to be developed in relation to individual PED projects [3] and EU H2020 projects with pilot cases [1, 4, 5, 6, 7, 8]. These build upon widely researched building and neighbourhood level sustainability indicators developed for research, governmental or commercial purposes [9] and smart city indicators [6].

Systemic reviews of PED related KPIs collect indicator sets based on sustainable neighbourhood concept definitions [10] and state that their methodological approaches are based on KPIs supported by decision making criteria analyses, Life Cycle Thinking methods or their mixture [11] and that PED KPIs mainly categorised by and cover the three pillars, i.e., environmental, economic, and social of sustainability [12].

Similarly to the PED definition, Key Performance Indicators (KPIs) are not yet consolidated either and cover a diverse field of sustainability aspects [12]. This means that projects with PED ambitions can get lost in the wide vision of the different initiatives and the related target metrics is not supporting to determine where to focus their efforts. Therefore, a standard set of PED KPIs could help on one hand to develop a base PED definition [10] and also to establish a common ground for performance assessment.

The aim of the research is to define a common indicator set for PEDs by assessing the commonalities in existing PED definitions.

2. METHODOLOGY

To define a common set of PED indicators, first the different PED definitions were collected from literature focusing on prominent EU programmes and PED-relevant projects across Europe. The SET-Plan Action 3.2 [13], Horizon 2020 Framework Programme – Smart Cities and Communities calls [14], EC Joint Research Centre, JPI UE [15] and the European Energy Research Alliance [16] programmes and initiatives establish the EU level decarbonisation goals and research areas for Positive Energy Districts, while ATELIER [4], MAKING-CITY [5], POCITYF [6], SPARCS [7], +CityxChange [17] and syn.ikia [1] are lighthouse

projects of the H2020 programme with their own interpretation of PEDs.

The definitions from the above listed sources are collected and detailed in [2], which were then extracted and reviewed for this research. All sources were also assessed based on their availability of developed KPI sets (no EU initiatives defined KPIs, all H2020 projects developed KPI sets), which were then collected along with additional sources from literature to establish a pool of indicators used on this field.

To determine the commonalities in potential indicators based on the PED definitions, the following steps were taken:

1. the text of the definitions was split according to which part of the PED performance characteristic/attribute each sentence part relates to;
2. the main sustainability categories and sub-categories a definition section relates to were identified;
3. the KPIs that can measure the performance of PEDs for each category and sub-category were identified and selected from the collected pool of indicators;
4. the following characteristics of the identified common indicators were analysed: dimension of sustainability coverage, assessed life-cycle, assessment scale, relevant stakeholders, type of the calculation;
5. the results of the deconstruction of definitions and related KPI assignations were compared, the cutoff point between Core and Optional indicators was defined to establish the most common PED themes and KPIs.

For example: the syn.ikia definition can be dissected (Step 1) to seven statements, one of them is “90% Renewable energy generation off-site”, which can be categorized (Step 2) into the Energy topic and Energy generation subtopic. From the indicator pool, the renewable or non-renewable thermal or electrical energy generation on- or off-site KPIs can be identified (Step 3) to measure the success of complying with the definition section. These indicators are in the Environmental sustainability domain, relate to the Design and Operation life-cycle of the project and can be measured on building and neighbourhood scale (Step 4). Compared to the others, energy generation indicators can be considered as Core KPIs in PED developments (Step 5).

3. RESULTS OF DEFINITION INVESTIGATION AND CORE KPI SET ESTABLISHMENT

The categories and sub-categories of the indicators are defined based on common neighbourhood sustainability topics (Buildings, Community, Ecology, Economy, Energy, Infrastructure, Location, Resources, Mobility [19]) and the categorisation of newer PED indicators (additional topics: ICT, Governance, Residents). After the review and combination of the topics in the different sources, the list of categories was defined to be used in this research: Energy, Environmental Performance, Economic performance, Society and Residents, Mobility, Materials and Resources and Governance (Table 1).

Table 1: KPI Categories and Subcategories considered in at least one of the PED definitions

Main category	Subcategory
Energy	Energy generation
	Usage factors
	Energy balance
	Energy efficiency
	Energy savings
	Active management
	Flexibility
Environmental Performance	Emission
	Emission reduction
	Resilience
Economic performance	Cost
	Cost reduction
Society and Residents	Participatory approach
	Life quality of users
	Inclusiveness
	Affordability
Mobility	Mobility
Materials and Resources	Materials
Governance	Scalability
	Local context

3.1 Energy

The Energy category is represented in all the investigated definitions with clear performance targets (Table 2). The results also show that the energy KPIs cover the three most important functions of districts in the context of their urban energy system [18]: all of the eleven definitions consider energy production and seven of them consider energy efficiency and energy flexibility topics. Additionally, seven consider active energy management which includes the use of integrated Building Management Systems, peak-load reduction strategies and smart metering and 5 definitions mention the flexibility topic.

3.2 Environmental Performance

The results show that emissions reduction is a quantified target of seven of the definitions, but they

differ in their considered emissions type. The syn.ikia and JPI UE definitions consider the overall greenhouse gas emissions of the district and target their 100% reduction, while the SET-Plan Action 3.2, EERA JPSC, ATELIER, SPARCS and +CityxChange definitions target net zero CO_2 emissions.

The deeper investigation of the available indicators of the considered initiatives shows that both CO_2 and GHG emissions only take into account the operational energy related emissions and embodied carbon emissions is not considered yet.

From other environmental indicators only JPI UE mentions Resilience aspect, focused on the resilience of the energy supply.

Table 2: Energy targets of the 11 investigated PED definitions

	Energy efficiency	Energy generation	Energy balance
SET Plan Action 3.2.	-	local surplus RES	net zero import
Horizon 2020	-	-	+
JPI UE	-	local surplus RES	+
EC Joint Research Centre	near zero energy demand	demand covered to a very significant extent by RES	+
EERA JPSC	-	local surplus RES	+
ATELIER	-	surplus RES	+
MAKING-CITY	-	-	+
POCITYF	-	-	+
SPARCS	-	local surplus RES	+
syn.ikia	-	90% RES generation	+
+CityxChange	-	local surplus RES	net zero import

-: no target defined; +: positive energy balance

3.3 Economic performance

Only the syn.ikia project mentions in its PED definition that PEDs should target "10% life cycle costs reduction compared to the level of 2020 nearly zero-energy buildings". As operation energy costs clearly connected to the energy reduction targets, all other definitions imply a certain degree of cost reduction by complying with PED requirements.

When considering the available indicator pool for economic performance all PED Horizon projects define the Payback Period KPI and three of them (syn.ikia, POCITYF and ATELIER) also considers Investment cost and Operation Cost indicators. Other financial indicators that are mentioned in the KPI pool: Debt Service Coverage Ratio, Economic Value Added, Local Job Creation, Energy Poverty, Average CO2 abatement costs etc.

3.4 Society and Residents

The category Society and Residents includes both the aspects related to participation and engagement and the social impact of PED developments as well.

As the participation of all stakeholders in the PED development process can improve the predictability of project outcomes, ensure more just and knowledgeable operations, facilitate community cohesion and improve communications to bring a system-wide energy transformation through collective action [20], some of the PED definitions (4 of 11) target the use of Participatory approaches in their definition as well. EC Joint Research Centre indicates the open and voluntary qualifications for the participation requirement.

The indicator pool from the investigated projects also includes metrics to measure the quality (e.g.: Degree of satisfaction, Degree of local community involvement in the implementation and planning phase) and quantity (e.g.: Percentage of citizens' participation in online decision-making) of participatory actions.

Different aspects of the social impact of PED developments are mentioned by 1-1 PED definition:

- Life quality of users (JPI UE)
- Inclusiveness (JPI UE)
- Affordability: (SET-Plan Action 3.2.)

3.5 Mobility, Materials and Resources and Governance

There is a discrepancy in the mention of mobility targets in the PED definitions and the number of developed project mobility related KPIs: only JPI UE mentions mobility in its definition, but SPARCS, POCITYF, MAKING-CITY and ATELIER projects all define several relevant KPIs.

Only the Horizon 2020 and POCITYF definitions mention materials and resource management, highlighting on circularity principles. Also, these consider governance related aspects such as the scalability of the PED development (to encourage better replication of the innovative concept), specific requirements of ICT technologies and the consideration of the local context.

3.6 Missing topics

The investigation of the relevant PED aspects coverage by the PED definitions compared with the available indicator pool shows that all main categories are covered by at least one definition.

This definition-based approach for KPI development ignores some aspects commonly considered in sustainability projects, such as: water, indoor and outdoor comfort, safety, investment-related indicators. This may be a result of several definitions only mentioning that PED projects should be in line with environmental, economic and social

sustainability principles without specifying any particularities.

3.7 Core KPI list and optional indicators

The results of the PED definition assessment shows that only the Energy generation, Energy balance, Energy efficiency, and Active management aspects were considered at least in 7 of the 11 definitions. Additionally, five definitions also consider GHG emissions and Energy flexibility aspects and 4 of them Participatory approaches. All the other PED aspects only included in one definition. Based on these results the cutoff point for Core indicators is at least 4 mentions. Table 3 shows the Core categories and the associated KPIs that can measure the PED performance of the requirement.

Table 3: Common KPIs identified by assessing the selected definitions

Category	KPI
Energy generation	Renewable thermal energy generation off-site
	Renewable electrical energy generation off-site
	Non-renewable thermal energy generation off-site
	Non-renewable electric energy generation off-site
	Renewable thermal energy generation on-site
	Renewable electrical energy generation on-site
	Non-renewable thermal energy generation on-site
	Non-renewable electric energy generation on-site
	Ratio of generated renewable energy used within the PED boundaries
Energy balance	Energy imported from outside the PED
	Energy exported from the PED
	Renewable energy imported from outside PED
	Renewable energy exported from the PED
Energy efficiency	Total primary energy demand
	Total annual saved primary energy
Active management	Integrated Building Management Systems
	Percentage of systems with smart energy meters,
	Percentage of peak load reduction
Flexibility	Flexibility index
	Energy storage capacity installed
GHG emissions	CO2 emission
	non-CO2 GHG emission
	GHG emission
	CO2 emission reduction
	non-CO2 GHG emission reduction
	GHG emission reduction
Participatory approaches	Local community involvement in the implementation and planning phase
	Energy citizenship

The common indicator set mainly consist of energy related KPIs, from the non-energy aspects of sustainability only indicators measuring GHG emissions are commonly considered. This means that currently only the Environmental dimension of sustainability is covered in the common indicator set and Social and Economic dimensions are ignored.

In addition to the common indicators, other, less frequently appearing KPIs were identified as well covering the rest of environmental (Resilience, Mobility, Materials and Resources, Local context) and the economic (Cost reduction, Scalability), and social (Life quality of users, Inclusiveness, Affordability) dimensions of sustainability. These indicators can be considered as optional indicators, where their usage could depend on the individual ambition of PED developments.

District characteristics are also established in the definitions. They focus on defining the geographical boundaries (mainly as districts with several connected buildings within a defined area), usage type (mixed use), building type (new or renovation) and included components (buildings and energy systems). These characteristics are quantifiable but differ from the indicators as they are not related to the performance of a PED district. However, they are useful for outlining the scope of the PED concept, as in establishing what kind of districts can target PED ambitions and use the developed concepts and methodologies.

Table 4: Number of PED aspects considered in the different definitions

	Number of aspects
SET Plan Action 3.2.	10
Horizon 2020	10
JPI UE	13
EC Joint Research Centre	7
EERA JPSC	6
ATELIER	11
MAKING-CITY	8
POCITYF	10
SPARCS	3
syn.ikia	6
+CityxChange	11

4. CONCLUSION

The study investigated five prominent EU programmes and six PED-relevant projects across Europe to determine the commonalities between their PED definitions. The research demonstrates that energy, carbon emissions and participatory approaches can be considered as the core targets for any PED project.

Additionally, there are several optional aspects that individual projects can target, but are not clearly mentioned and quantified in the existing PED definitions. As theoretical research on the Positive Energy District concept is still ongoing, new PED definitions (or updates of the existing ones) can emerge. With the application of the methodology outlined in this paper on them can result in adding new entries to the common aspect list.

Currently less research is available on non-energy ambitions of PEDs [10] which is reflected in the

existing PED definitions. However, the identification of what is needed on the non-energy related aspects should be considered as integral parts of PEDs. Therefore, without creating overly broad scope that can risk diluting the core ambitions of PEDs, it is necessary to improve existing PED definitions to better reflect all PED ambitions.

After establishing the core PED aspects, relevant indicators were selected to establish a Core PED KPI set. This common indicator set to evaluate PED performance is needed to bridge the gap between the wide-ranging PED research in academia and the practice where projects with PED ambitions need clear targets to achieve.

The comparison of the common KPI list with the indicators developed within some of the assessed projects or initiatives also shows that the initiatives consider more sustainability aspects or categories than what can be identified from their definitions. For example, the POCITYF project developed 8 of its 63 KPIs to cover the topic of Mobility, however the goal of providing sustainable transport modes and infrastructure for electric vehicles does not appear in the PED definition of the project (adopted from the Horizon 2020 Framework Programme) [6].

Finally, the core KPIs can also be used to finetune current PED definitions of to establish new ones with defining the focus areas where they intend to measure the performance of districts. This research can provide the following recommendations:

- PED scope: a PED definition should clearly set what kind of boundaries, functions, components PED districts should include
- New definitions should at least include quantified goals for energy efficiency, flexibility and production and GHG emissions
- It is recommended to adapt life-cycle thinking in setting targets for carbon emissions to also consider the embodied carbon impacts
- The targets for mobility within a Positive Energy District is recommended to be included in the definition
- It is recommended to add targets for social and economic sustainability
- PED definitions could define the recommended range of topics for customization, to provide space for individual circumstances and ambitions

ACKNOWLEDGEMENTS

This article is based upon work from COST Action 19126 Positive Energy Districts European Network PED-EU-NET, supported by COST (European Cooperation in Science and Technology, www.cost.eu).

The authors acknowledge the support by the KDP-2021 program of the Ministry for Innovation and Technology of Hungary from the source of the National Research, Development and Innovation Fund.

REFERENCES

1. Salom, J., Tamm, M., Andresen, I., Cali, D., Magyari, Á., Bukovszki, V., Balázs, R., Dorizas, P. V., Toth, Z., Zuhaib, S., Mafé, C., Cheng, C., Reith, A., Civiero, P., Pascual, J., & Gaitani, N. (2022). An Evaluation Framework for Sustainable Plus Energy Neighbourhoods: Moving beyond the Traditional Building Energy Assessment (Energies, (2021), 14, 4314, 10.3390/en14144314). *Energies*, *15*(15), 1–25.

2. Albert-Seifried, V., Murauskaite, L., Massa, G., Aelenei, L., Baer, D., Krangsås, S. G., Alpagut, B., Mutule, A., Pokorny, N., & Vandevyvere, H. (2022). Definitions of Positive Energy Districts: A Review of the Status Quo and Challenges. *Smart Innovation, Systems and Technologies*, 263, 493–506.

3. Leibold, J.; Schneider, S.; Tabakovic, M.; Zelger, T.; Bell, D.; Schöfmann, P.; Bartlmä, N. (2020) 'Zukunftsquartier'—On the Path to Plus Energy Neighbourhoods in Vienna. *Sustainability in Energy and Buildings, Singapore, 2020; Springer Singapore: Singapore, 2020*; 199–209, ISBN 978-981-32-9868-2.

4. University of Deusto, Amsterdam University of Applied Science, & Paul Scherrer Institute. (2020). ATELIER Deliverable 9.1: Repository of definitions of terms, key characteristics archetypes, and a set of KPIs.

5. Rönty, J., Känsälä, K., Kiljander, J., Rehu, J., Rinne, S., Sanz-Montalvillo, C., Vasallo, A., Nauta, J., & Tonen, J. (2020). Making City D5.2 – Project Level Indicators.

6. Angelakoglou, K., Kourtzanidis, K., Giourka, P., Apostolopoulos, V., Nikolopoulos, N., & Kantorovitch, J. (2020). From a comprehensive pool to a project-specific list of key performance indicators for monitoring the positive energy transition of smart cities—An experience-based approach. *Smart Cities*, 3(3), 705–735.

7. Ntafalias, A., Papadopoulos, Panagiotis Menyktas, K., Tountas, I., Papadopoulos, G., Kousouris, S., & Tsitsani, A. (2021). SPARCS D2.2 Definition of SPARCS Holistic Impact Assessment Methodology and Key Performance Indicators.

8. Caballero, N., Bottecchia, L., Galanakis, K., & Ackrill, R. (2019). Smart-BEEjS D5.2 Development of a Standardised Method for Impact Evaluation of Positive Energy Districts.

9. Orova, M., & Reith, A. (2021). How Rating Systems Support Regenerative Change in the Built Environment (M. B. Andreucci, A. Marvuglia, M. Baltov, & P. Hansen (eds.); pp. 131–144). *Springer*. https://doi.org/10.1007/978-3-030-71819-0_7

10. Brozovsky, J., Gustavsen, A., & Gaitani, N. (2021). Zero emission neighbourhoods and positive energy districts – A state-of-the-art review. *Sustainable Cities and Society*, *72*(May), 103013.

11. Marotta, I., Guarino, F., Longo, S., & Cellura, M. (2021). Environmental sustainability approaches and positive energy districts: A literature review. In *Sustainability* (Vol. 13, Issue 23). MDPI.

12. Guarino, F., Bisello, A., Frieden, D., Bastos, J., Brunetti, A., Cellura, M., Ferraro, M., Fichera, A., Giancola, E., Haase, M., Kantorovitch, J., Neumann, C., Mankaa, R., Segura, I. L., Traverso, M., Tumminia, G., Volpe, R., Zhang, X. (2022). State of the Art on Sustainability Assessment of Positive

Energy Districts: Methodologies, Indicators and Future Perspectives. *Smart Innovation, Systems and Technologies*, 263, 479–492.
13. SET-Plan Working Group. (2018). SET-Plan Action n°3.2 Implementation Plan.
14. European Commission. (2017) Horizon 2020 Work Programme 2018-2020: 10. Secure, clean and efficient energy.
15. JPI UE Positive Energy District definition [Online] Available: https://jpi-urbaneurope.eu/ped/ [31 December 2023].
16. Wyckmans, A. Strategic Research Agenda of the EERA Joint Programme Smart Cities. [Online] Available: https://www.iqs.se/library/4893/eera-jpsc-ped-sra_wyckmans.pdf [31 December 2023].
17. Hynes; Sweeney; Lynch; Rood; Chiddaarwar. (2020). +CityxChange D7.1 Approach and Methodology for Monitoring and Evaluation.
18. JPI Urban Europe (2020) Europe Towards Positive Energy Districts. *Austrian Research Promotion Agency*, Vienna.
19. Reith, A., & Orova, M. (2015). Do green neighbourhood ratings cover sustainability? *Ecological Indicators*, 48, 660–672.
20. Steemers, K., Krangsås, S. G., Ashrafian, T., Giancola, E., Konstantinou, T., Liu, M., Maas, N., Murauskaitė, L., Prebreza, B., & Soutullo, S. (2022). Challenges for a Positive Energy District Framework. *Sustainability in Energy and Buildings: Research Advances*, 8, 10–19.

PLEA 2024 WROCŁAW
(Re)thinking Resilience

Sensitivity analysis of the built stock in Spain

Full factorial experiment and Yates analysis

ALFONSO GODOY,[1] ANNA PAGES-RAMON,[1] PAU FONSECA I CASAS,[1] ALBERTO CUCHI[1]

[1]**Universitat Politecnica de Catalunya Barcelona Tech, Barcelona, Spain**

ABSTRACT: The European Union aims to reduce emissions and achieve net decarbonisation by 2050. To support this goal, the Renovation Wave strategy aims to increase the rate of energy renovation of buildings. However, current assessment tools for energy renovation projects may not be accurate or consistent, leading to discrepancies between simulation results and actual building performance. A new energy study methodology using statistical methods to treat input and result data is necessary. This methodology simplifies the energy performance assessment process and the evaluation of energy refurbishment results. This article contains part of the first phase of this methodology which involves sensitivity analysis, which was conducted using three case studies from Spanish residential housing. Two types of analysis were performed: individual parameter sensitivity and Yates analysis considering parameter interactions. The results indicate that the methodology can effectively assess the sensitivity of buildings to various parameters and their combined effect.

KEYWORDS: Energy, thermal simulation tools, retrofitting, Sensitivity Analysis.

1. INTRODUCTION

The European Union is committed to reducing emissions and to achieve net decarbonisation by 2050. To this end, the "Renovation Wave" strategy has been developed, aiming at significantly increasing the rate of energy renovation of buildings. To achieve this goal, it is also necessary to provide technicians with simple and reliable assessment tools. The most widely used calculation engines for dynamic thermal simulation, while being contrasted, continue to present robustness concerns mainly due to the lack of accuracy and consistency of the input data. This is generally the case for infiltrations, or when the thermal characteristics of the building envelope are to be determined for existing buildings, and may lead to important discrepancies between the results obtained from the simulation and the actual performance of buildings[1].

The MAREnE research project in which this work is framed proposes an energy study methodology using a statistical approach in the treatment of input and result data, implementing sensitivity and uncertainty quantification methods, which simplifies the energy performance assessment process and the evaluation of the results obtained in energy refurbishment.

In the present work the results of the first steps in the development of the above-mentioned methodology, are presented, which correspond to the sensitivity analysis.

This analysis has been carried out using three of the typologies resulting from a previous nationwide study conducted by the authors. This study concludes with the definition of 3 typologies, each one representative of a cluster of buildings, for each of the 5 regions into which the national territory has been divided according to climatology. Each typology differs from the others in according to the following indicators: (1) the ratio between the surface area of the building and the surface area of the thermal envelope and (2) the ratio between the length and the width of the building.

In this paper, the results obtained for the "Mediterranean" climate zone, represented by the climate of Barcelona, are shown. The three typologies studied are depicted in Table 1 and Figure 1.

Table 1. Reference buildings for each of the clusters in the North Atlantic climate.

Cluster	name	W (m)	L (m)	h (m)	area (m^2)
1	BA_09_15_12	9	15	12	540
2	BA_03_27_06	3	27	6	162
3	BA_15_03_06	15	3	6	90

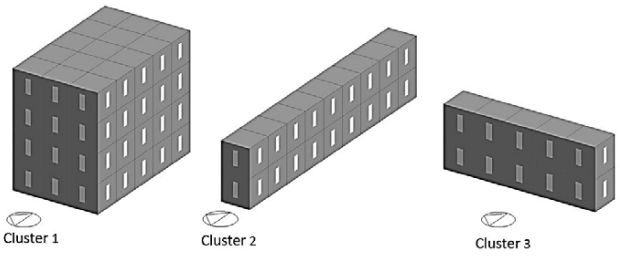

Figure 1. Image of the thermal models of each of the clusters used for the energy simulation

2. METHODOLOGY

Five study variables were chosen for the sensitivity analysis on the basis of their relevance in the energy performance of a building. These are presented in

Table 2. Initially, we considered to include two other parameters: orientation and ground floor transmittance. However, these were later discarded with the aim of limiting the number of simulations to be carried out. The first, because it was already included as a variable in the typological study performed previously. The second, due to its minor influence on the overall building performance.

Table 2. Study variables with the value of the two levels.

Variable	*type*	*(+)*	*(-)*
1. Infiltration (ach)	Continuous	0,13[(1)]	3,75[(5)]
2. Façade transmittance	Discrete	0,23[(2)]	3,00[(3)]
3. Roof transmittance	Discrete	0,19[(2)]	2,50[3)]
5. Window to Wall %	Continuous	10[(4)]	60[(4)]
7. Glass transmittance	Discrete	1,50[(2)]	5,70[(4)]

(1) limit Passivhaus [2] *(4) Energy Certificate database* [3]
(2) Annex E DBHE CTE [4] *(5) INFILES project* [5]
(3) Rvalues for the energy certification of existing buildings [6]

A 2^K factorial experiment was conducted, with K=5. The main effects and interactions between the factors (previously referred to as variables) and their values were analysed for a total of 160 cases. In order to carry out the experiment, a minimum and a maximum value was defined for each of the parameters. For example, in the case of infiltration, a ratio of 0.13 ach was defined as the minimum value (most favourable) and a ratio of 3.75 ach as the maximum value (most unfavourable). No intermediate values were studied to enable a 2^k factorial analysis to be applied. The maximum and minimum values of the parameters analysed were defined according to literature and are presented in Table 2.

The DesignBuilder, E+ and JPlus tools were used to make the experiment. The output data used as indicators were the annual heating and cooling demand.

Once the results of the simulations were obtained, two types of analysis were performed. The first focused on the absolute differences that each of the parameters yielded individually, for which the difference in demand was calculated and pooled for all cases where only one parameter changed. Each of the parameters studied therefore generated 16 demand variation values that were grouped together for further analysis.

The second used the Yates analysis to observe the sensitivity considering the combination of the parameters according to their degree of interaction.

The results obtained were arranged according to the "Yates order" to obtain the "estimated effect" between the factors.

2.1. **Thermal demand difference analysis**

For the analysis of the variation in heating and cooling demand, the demand results were normalised by dividing them by the surface area of the building under study. Subsequently, the cases were grouped according to the factor modified and the results of the cases differing by only one factor were compared. For example, the case where the roof and façade are improved was compared with the case where the roof, façade and infiltrations are improved. This allows us to see the effect of the improvement of infiltrations interacting with other factors. Once the demand change values were obtained for each of the cases, the cases were plotted using a box plot chart. Studying the data using a box plot chart provides valuable information about the distribution of the data, as it provides the chance to examine whether the data are evenly distributed or, on the contrary, outliers exist. It also makes it possible to observe whether the data are skewed towards a certain value, or how sensitive the results are to the variation of the factors' values.

2.2. **Yates algorithm**

The effect calculation in Yates' algorithm is a useful tool for understanding the interaction between factors in a factorial design [7]. It helps to identify whether the interaction between two factors is significant and its kind, that is, the effect that one factor on the other, which can be:

Positive effect: indicates that the two factors interact to increase the effect of the first factor. For example, if the effect in Yates' algorithm for factors A and B is positive, it means that increasing the level of factor B will increase the effect of factor A as well.

Negative effect: indicates that the two factors interact to decrease the effect of the first factor. For example, if the effect in the Yates algorithm for factors A and B is negative, it means that increasing the level of factor B will decrease the effect of factor A.

Null effect: indicates that the two factors do not interact. For example, if the effect in Yates' algorithm for factors A and B is null, it means that increasing the level of factor B has no effect on the effect of factor A.

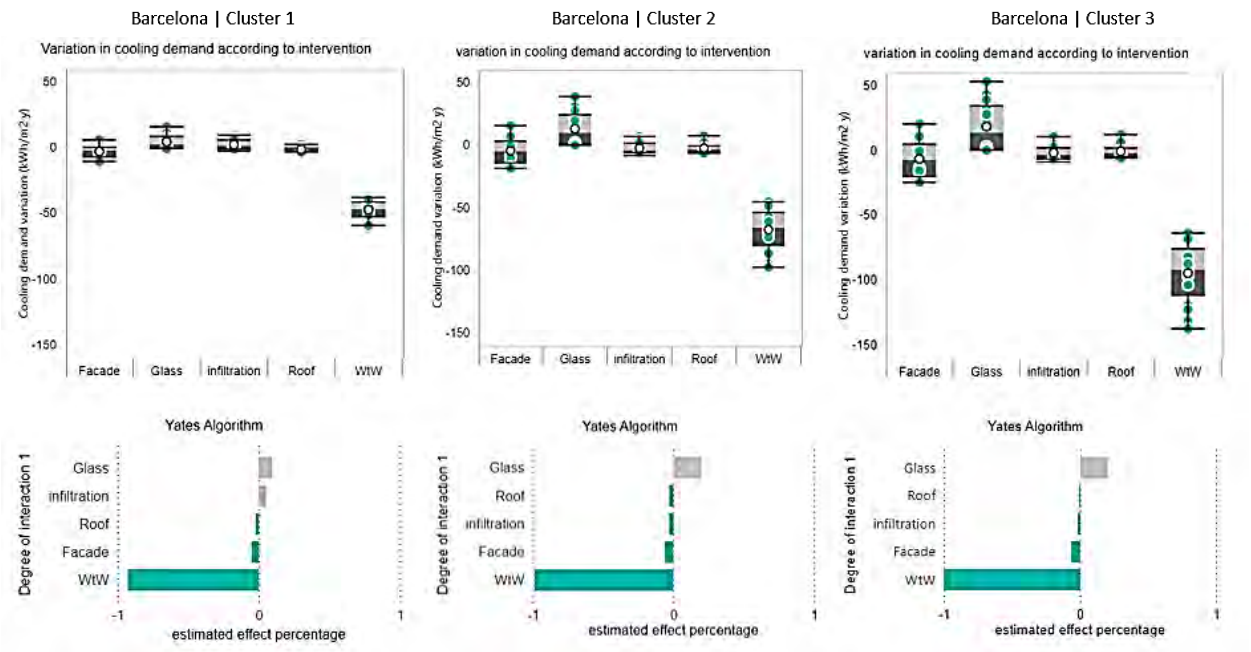

Figure 2. Box plot with demand variations (top charts) and estimated percentage effect for Yates cooling (graphs below) for each of the clusters studied.

3. RESULTS

The sensitivity of the three models (representative of each of the three clusters analysed) has been studied for both heating and cooling.

The analysis of the results of each parameter individually unveils the potential influence on the energy demand of each parameter, as well as its variability depending on the value of the other parameters. The sensitivity and dispersion of the results are depicted in Figure 2 and Figure 4.

3.1. Analysis of the influence of independent factors

Cooling demand

In terms of cooling, when the factors are analysed individually, the behaviour of the 3 clusters have a similar pattern, which it can be observed in Figure 2, both in the box plot and the bar chart.

Among the five factors analysed, the window to wall rate (WtW) is the one that presents the greatest estimated effect on cooling demand. The value of such effect is negative, which means that reducing WtW entails a reduction in the cooling energy demand.

Glazing transmittance is the factor with the second highest estimated effect in general terms, but in this case, its effect is positive and thus, increasing its value results in an increased demand. In turn, the thermal transmittance of the façade has a much more moderate effect, being the transmittance of the roof and infiltrations the two factors with lower estimated effect. In the case of the latter, some differences in trends can be observed between the clusters: in cluster 1, the reduction of air infiltration (improvement of airtightness) leads to an overall increase in demand.

However, in clusters 2 and 3, improved airtightness leads to a reduction in cooling demand, even slightly more than reducing the roof transmittance.

It is noticeable that the variation in demand in absolute terms (kWh/m2 y) when the value of one of the factors is changed is lower in cluster 1 than in the other two clusters. However, when analysed in percentage terms, the variations are very similar in the 3 clusters.

These results indicate that, in the case of an energy retrofitting, the most effective intervention action would be the reduction of the window surface, followed by the reduction of the glass transmittance. Reducing the transmittance of the façade, which is the most common intervention, would have a much more moderate effect, while acting the air tightness or the roof transmittance would have little impact on the overall cooling demand.

Figure 3 shows how the variations of improvement in percentage terms, with respect to the initial demand, are much more similar between the three clusters than what is observed if the variation of demand in absolute terms is analysed in Figure 2.

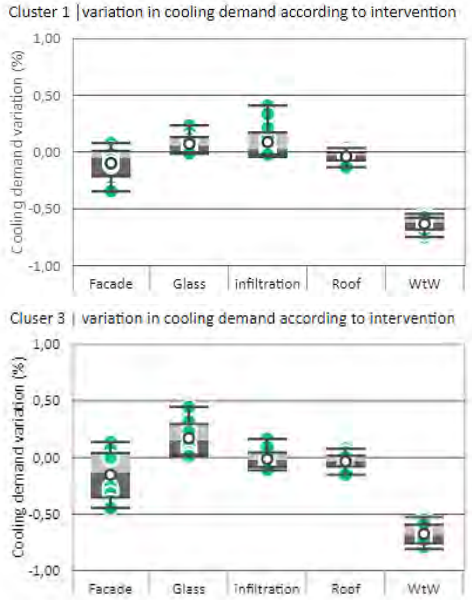

Figure 3: Percentual cooling demand variability of clusters 1 and 3 for each of the factors.

Heating demand

The results obtained for heating demand are presented in Figure 4.

Again, the trends are similar in the three cases, being air tightness, façade transmittance, glass transmittance and roof transmittance the factors with higher estimated effect in this order.

The data from the box plot indicate that the WtW factor can have both a positive and a negative estimated effect. However, the Yates algorithm gives only a positive effect.

In clusters 2 and 3 the sensitivity of the model to the value of the façade transmittance and the infiltrations is similar. This is somehow an expected result as these two clusters represent building where the façade surface with respect to the built area is higher than in cluster 1.

3.2. Analysis of the interaction between factors

When analysing the interaction between factors, some may be expected and known results, while others present more uncertainty. For instance, one of the interactions that are interesting to investigate is the one between WtW rate and glass transmittance and their combined effect on heat demand. This is presented in Figure 4. This figure shows how in some combinations the reduction of the WtW rate results in a reduction of the demand, while in other cases it entails an increase in demand.

A further observation of the results shows that all the cases in which reducing the WtW rate (from 60% of openings to 10%) results in a reduction in the heating demand (negative improvement), correspond to cases where the glass transmittance is 5.7 (highest value).

Table 3. Cases where a reduction in WtW means a reduction in demand.

ID_Comp	ID_Yates	Descriptive name	Heating	Cooling
A8	ABDE	WW_10 | ach_0,13 | G_U5,7 FS0,7 | F_U0,23 | C_U0,48	3,39	25,96
A8	BDE	WW_64 | ach_0,13 | G_U5,7 FS0,7 | F_U0,23 | C_U0,48	17,87	69,60
A7	ABD	WW_10 | ach_0,13 | G_U5,7 FS0,7 | F_U0,23 | C_U2,8	17,98	27,17
A7	BD	WW_64 | ach_0,13 | G_U5,7 FS0,7 | F_U0,23 | C_U2,8	30,88	69,24
A15	ADE	WW_10 | ach_3,73 | G_U5,7 FS0,7 | F_U0,23 | C_U0,48	106,51	19,45
A15	DE	WW_64 | ach_3,73 | G_U5,7 FS0,7 | F_U0,23 | C_U0,48	108,78	68,20
A14	AD	WW_10 | ach_3,73 | G_U5,7 FS0,7 | F_U0,23 | C_U2,8	124,71	22,40
A14	D	WW_64 | ach_3,73 | G_U5,7 FS0,7 | F_U0,23 | C_U2,8	125,51	69,21

In turn, all the cases in which demand increase is more noticeable (more than 30 kWh/m2) present a low glass transmittance.

Table 4. Cases where the reduction in WTW results in an increase in demand greater than 30kWh/m2.

ID_Comp	ID_Yates	Descriptive name	Heating	Cooling
A6	ABCE	WW_10 | ach_0,13 | G_U1,5 FS0,7 | F_U3 | C_U0,48	50,35	29,04
A6	BCE	WW_64 | ach_0,13 | G_U1,5 FS0,7 | F_U3 | C_U0,48	8,49	79,64
A3	ABC	WW_10 | ach_0,13 | G_U1,5 FS0,7 | F_U3 | C_U2,8	65,54	31,01
A3	BC	WW_64 | ach_0,13 | G_U1,5 FS0,7 | F_U3 | C_U2,8	19,97	78,55
A13	ACE	WW_10 | ach_3,73 | G_U1,5 FS0,7 | F_U3 | C_U0,48	171,40	29,31
A13	CE	WW_64 | ach_3,73 | G_U1,5 FS0,7 | F_U3 | C_U0,48	99,33	75,33
A12	ACDE	WW_10 | ach_3,73 | G_U1,5 FS0,7 | F_U0,23 | C_U0,48	99,48	19,15
A12	CDE	WW_64 | ach_3,73 | G_U1,5 FS0,7 | F_U0,23 | C_U0,48	60,97	76,02
A11	ACD	WW_10 | ach_3,73 | G_U1,5 FS0,7 | F_U0,23 | C_U2,8	118,06	22,10
A11	CD	WW_64 | ach_3,73 | G_U1,5 FS0,7 | F_U0,23 | C_U2,8	79,11	76,01
A10	AC	WW_10 | ach_3,73 | G_U1,5 FS0,7 | F_U3 | C_U2,8	187,08	32,01
A10	C	WW_64 | ach_3,73 | G_U1,5 FS0,7 | F_U3 | C_U2,8	116,66	76,07

The rest of the cases in which reducing the WtW rate results in a moderate increase in the heating demand (lower than 30 kWh/m2) include cases with both the high and the low glass transmittance. In these cases, other factors, such as the wall transmittance, roof transmittance or infiltrations, are playing a role in the energy behaviour of the building.

Table 5. Cases where a reduction in WTW means a slight increase in demand.

ID_Comp	ID_Yates	Descriptive name	Heating	Cooling
A9	ABE	WW_10 | ach_0,13 | G_U5,7 FS0,7 | F_U3 | C_U0,48	55,81	28,93
A9	BE	WW_64 | ach_0,13 | G_U5,7 FS0,7 | F_U3 | C_U0,48	39,40	68,24
A5	ABCDE	WW_10 | ach_0,13 | G_U1,5 FS0,7 | F_U0,23 | C_U0,48	0,64	26,96
A5	BCDE	WW_64 | ach_0,13 | G_U1,5 FS0,7 | F_U0,23 | C_U0,48	0,10	85,83
A4	ABCD	WW_10 | ach_0,13 | G_U1,5 FS0,7 | F_U0,23 | C_U2,8	13,38	27,93
A4	BCD	WW_64 | ach_0,13 | G_U1,5 FS0,7 | F_U0,23 | C_U2,8	5,55	83,00
A2	AB	WW_10 | ach_0,13 | G_U5,7 FS0,7 | F_U3 | C_U2,8	70,85	30,92
A2	B	WW_64 | ach_0,13 | G_U5,7 FS0,7 | F_U3 | C_U2,8	53,04	68,57
A16	AE	WW_10 | ach_3,73 | G_U5,7 FS0,7 | F_U3 | C_U0,48	177,47	29,65
A16	E	WW_64 | ach_3,73 | G_U5,7 FS0,7 | F_U3 | C_U0,48	146,79	69,60
A1	A	WW_10 | ach_3,73 | G_U5,7 FS0,7 | F_U3 | C_U2,8	192,91	32,32
A1	base	WW_64 | ach_3,73 | G_U5,7 FS0,7 | F_U3 | C_U2,8	162,56	70,95

The relationship between the WtW rate and the glass transmittance is reflected and directly quantified in the results yield through the Yates analysis, which are shown in Figure 5.

The 4 strongest relationships are: (1) AC, window to wall rate with glass thermal transmittance; (2) BD, air infiltration with façade thermal transmittance; (3) AB, window to wall rate with air infiltration; and (4) AD, window to wall rate with façade thermal transmittance.

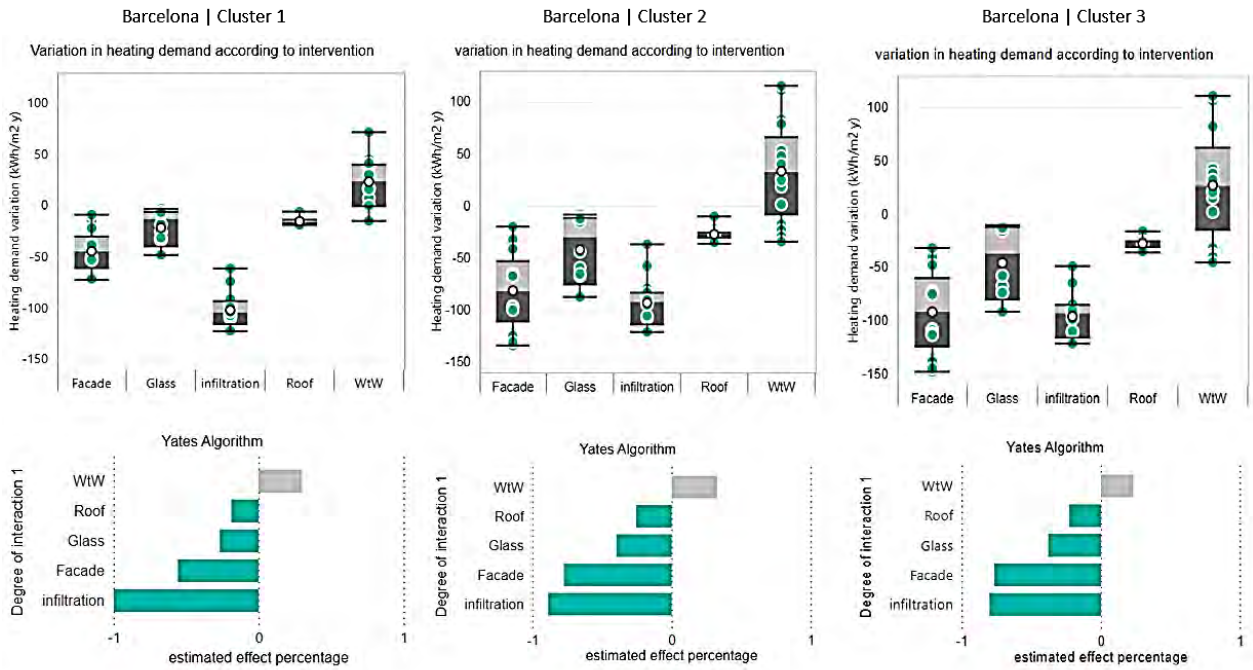

Figure 4. Box plot with demand variations (top charts) and estimated percentage effect for Yates heating (graphs below) for each of the clusters studied.

It is noticeable that two of the strongest relationships involve air infiltrations (factor B). Considering how the infiltration parameters are introduced in the simulation, the relationship of the infiltrations with the transmittance of the façade and with the percentage of glazing is not consistent. This is probably due to the weight of the infiltration alone.

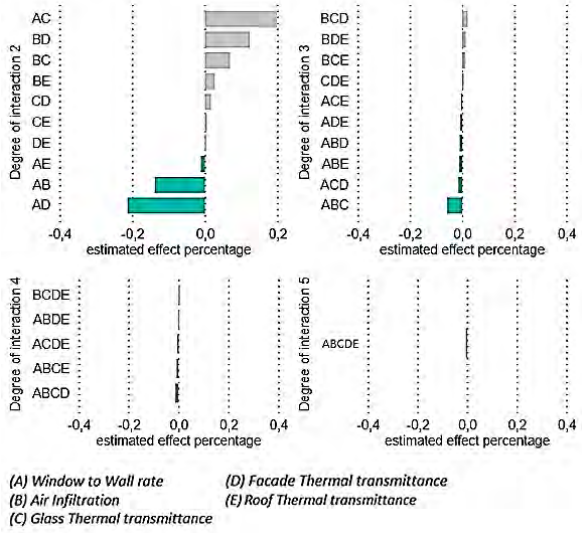

Figure 5. Estimated percentage effect between factors for interaction degrees 2, 3, 4 and 5.

4. CONCLUSION

The individual parameter sensitivity analysis, in combination with the study of their aggregate effect using the Yates Analysis, is presented as an appropriate methodology to obtain high quality information on the energy performance of buildings.

Individually, regarding heating demand, infiltrations are presented as the most sensitive variable, followed by the thermal transmittance of the façade, the thermal transmittance of the glass and the percentage of openings in the façade. The window to wall ratio has a particular behaviour, with a reduction in some cases and an increase in others.

The Yates analysis shows a clear relationship between the window to wall ratio and the thermal transmittance of the openings. This is an expected result but demonstrates that the methodology is capable of quantitatively assessing this type of relationship.

The Yates algorithm also gives either a positive or negative estimated effect per factor, even if in some cases the effect can be in one sense or the other.

Further analysis is needed in order to examinate some interactions between factors that were yielded by the Yates' algorithm, and which in a first glance do not seem to correspond to what would be expected. conform to reality.

It should be noted that the study is limited to quantifying the sensitivity of the cooling and heating demand to the different parameters analysed, without making a qualitative or quantitative assessment of what would be an optimal design solution. For the latter, it would be necessary to take into consideration

other aspects such as natural lighting, the relationship with the exterior or cost.

ACKNOWLEDGEMENTS

This research is part of the project TED2021-132187B-I00 funded by MCIN / AEI/ 10.13039 /5 01100011033 and by the European Union NextGenerationEU/PRTR.

4. REFERENCES

1. P. De Wilde, The gap between predicted and measured energy performance of buildings: A framework for investigation, Autom. Constr. 41 (2014).
2. Wolfang Schnieders, Passive Houses in South West Europe, Passiv. Inst. (2009).
3. ICAEN, Certificats d'eficiència energètica d'edificis: tancaments | Dades obertes de Catalunya, (n.d.).
4. Ministerio de Vivienda, Código Técnico de la Edificación (CTE), Real Decreto 314/2006 17 Marzo. BOE 74 (2006).
5. F.M. Jesús, P.C. Irene, G.L.R. Alonso, P. Cristina, E. Víctor, A. De Larriva Rafael, F.A. Jesica, D.V.M. Jesús, D.C.D.V. José, M.C. Manuel, P.M.M. Ángel, M. Alberto, Methodology for the study of the envelope airtightness of residential buildings in Spain: A case study, Energies. 11 (2018).
6. MIYABI, Centro Nacional de Energías Renovables (CENER), Instituto para la Diversificación y Ahorro de la Energía (IDAE), Manual defundamentostécnicos decalificaciónenergéticade edificiosexistentes CE3X | 004 (2), 2012.
7. D.C. Montgomery, Design and Analysis of Experiments, in: Transl. Radiat. Oncol., 9th ed., Elsevier, 2023: pp. 527–530.

Mapping the Exposure to Extreme High Temperatures in Elderly Population Based on Local Climate Zones:
A Case Study of Guangzhou City

MENGYAN YANG[1] AIXIN ZHENG[2]

[1] LAY-OUT Planning Consultants Co., Ltd, Shenzhen, The People's Republic of China
[2] Harbin Institute of Technology, Harbin, The People's Republic of China

ABSTRACT: The Local Climate Zone (LCZ) method, relying on surface cover characteristics, addresses the limitations of the traditional urban-rural dichotomy and is increasingly applied in climate research. While existing LCZ studies mainly focus on regional surface features and urban heat island intensity, few address the living conditions of residents, particularly during extreme heat. Given the global aging population trend and physiological characteristics of the elderly, their safety in extreme heat environments is a pressing concern. This study, based on remote sensing, meteorological, and population data, investigates high-temperature exposure risks for the elderly in Guangzhou. By mapping the LCZ, analyzing heat risks for each type, studying elderly residential preferences, and exploring the relationship between preferred LCZ types and frequent heat risks, we identify significant heat exposure risks in areas favored by the elderly. This underscores an unnoticed vulnerability, demanding urgent attention to improve living environments for this vulnerable demographic in the face of heat risks.
KEYWORDS: heat risk, heat exposure, local climate zone, extreme high temperatures, elderly population

1. INTRODUCTION

As the impact of global warming intensifies, extreme high-temperature events are becoming increasingly frequent [1]. One of the main reasons for urban heat is the rapid development of urbanization, which replaces natural surfaces with impermeable surfaces such as asphalt, resulting in significantly higher urban temperatures compared to rural areas, known as the Urban Heat Island (UHI) [2]. UHI not only affects the urban environment, causing problems such as rapid energy consumption and deteriorating air quality [3] but also has a significant impact on human health [4], particularly threatening larger populations in urban areas.

Simultaneously, against the backdrop of global aging, the elderly, as a numerous yet vulnerable group, are one of the populations most likely to be adversely affected by high temperatures [5]. The elderly have a high incidence of cardiovascular and respiratory diseases, which are the main health hazards caused by high temperatures. Existing research indicates that the elderly are more susceptible to the impact of high temperatures [6], with higher mortality rates in regions with a high UHI effect compared to those with a low UHI effect [7]. Detailed research indicates that the risk of mortality associated with temperature in European cities tends to rise as temperatures approach the extreme limits of each city's typical temperature range, particularly affecting older age groups, their mortality rate exhibits exponential growth, starting from 1% [8]. Therefore, more attention should be paid to research on the elderly and heat risks.

Local Climate Zones (LCZ) refer to regions spanning from hundreds of meters to several kilometers in horizontal scale, where surface cover, structure, materials, and human activities are uniformly distributed [9]. The LCZ theory provides researchers with a standardized classification method based on surface cover characteristics. Due to its ability to overcome the limitations of the traditional "urban-rural dichotomy," LCZ has gained prominence in climate research. Existing studies on LCZ primarily focus on regional surface characteristics and urban heat island intensity, showing the potential to analyze exposure to high temperatures of the urban residents [10]. However, few LCZ-related studies have focused on vulnerable residents during extreme high-temperature events, especially the elderly. In fact, the vulnerability of the cardiovascular and respiratory systems of the elderly implies that their living environment safety is a critical issue in the context of extreme high temperatures. Therefore, studying the extreme heat exposure of the elderly using the LCZ framework is crucial.

Guangzhou city is one of China's important metropolises with a rich history and culture, boasting a population of 19.73 million. Although it is in the early stages of population aging, the large population base and rapid aging make the elderly population in Guangzhou numerous and continuously increasing. As a city with a high level of urbanization, Guangzhou

suffers from a severe UHI effect, forming a regional UHI cluster with other cities in the Pearl River Delta, such as Shenzhen and Foshan. Guangzhou primarily focuses on urban renewal as a means of urban development, requiring more attention to resident needs and direct improvement of living environments. Therefore, studying the heat risks faced by the elderly in Guangzhou is of great significance for maintaining the local elderly population's life and health and improving their living environment.

This study explicitly targets Guangzhou, which is experiencing rapid population aging, to explore the extreme heat exposure of the elderly population. The main objectives of the study include: (1) mapping Guangzhou's LCZs and analyzing surface cover characteristics, (2) mapping the distribution of the elderly population and studying their living patterns, (3) identifying heat risk areas in Guangzhou and assessing the exposure of the elderly population in these areas, and (4) integrating maps of low-latitude regions, elderly population distribution, and heat risk to study the relationship between the living environment of the elderly and heat exposure.

2. MATERIALS & METHODS

2.1 Data

Remote sensing image data from Google Earth in 2020 and population data from WorldPop in 2020, providing age and structure data based on the global population census database, were used. The population data predict the population quantity per 100m x 100m grid, including males and females, focusing on restricted areas in China. Temperature data for June to August 2020 with cloud cover less than 20% were obtained from the MODIS product MOD11A1.006, released by NASA.

2.2 Methods

2.2.1 Preprocessing

Using ArcGIS tools, the geographic coordinate system was standardized to GCS WGS 1984, and the projected coordinate system was standardized to WGS 1984 UTM Zone 49N, with a resolution of 100 meters x 100 meters. Specifically, the temperature data needed to be transformed using the MRT tool.

2.2.2 Mapping Local Climate Zones

Using the World Urban Database and Access Portal Tools [11] method based on the LCZ theory. The main steps were as follows:

(1) Create training files in Google Earth containing 17 subfolders named according to the LCZ classification framework. Each subfolder includes 5-15 training area shapes with simple rules, with the shortest side greater than 200 meters. Export the training files in “kmz” format.

(2) Submit the training application, including basic information and training files, to https://LCZ-generator.rub.de/. After receiving the result files, including LCZ maps and evaluation files, optimize the training files until the overall accuracy reaches 0.75 or higher, based on report prompts and Google Earth image map comparisons.

2.2.3 Mapping elderly population distribution

According to WHO standards, people aged 65 and above were defined as the elderly. ArcGIS tools were used to overlay the downloaded eight population data layers to obtain the elderly population layer. To ensure calculation accuracy, the background value of the population data was adjusted from “Nodata” to “0”, and then the population data layers were added using the raster calculator.

2.2.4 Mapping extreme high temperatures

Based on the minimum lethal temperature from relevant studies [12], 38.3°C was chosen as the threshold for extreme high temperature in this study. When loading temperature data in ArcGIS, the "LST-Day" band was selected. The "Raster Calculator" was used to convert temperature data to Celsius, were used as follows:

$$T = N * 0.02 - 273.15 \quad (1)$$

where T - Celsius temperature (◦C);

N - original data.

Subsequently, the "Raster Calculator" was employed to filter data greater than or equal to 38.3°C. Finally, the "Mosaic Tool" was used to merge the various filtered datasets, generating the map of extreme high temperatures, with the calculation method using "average."

2.2.5 Data analysis

(1) Use the "Raster to Polygon" tool in ArcGIS to convert extreme high temperatures data into vector data format as the heat risk area layer. Use the "Extract by Mask" tool to extract the elderly population in the heat risk area.

(2) Use the "Zonal Statistics as Table" tool in ArcGIS, with LCZ data as input data, to statistically analyze the distribution of the elderly in each LCZ, the distribution of heat risk areas, and the distribution of the elderly in risk areas.

3. RESULTS

3.1 Mapping local climate zones in Guangzhou

In Guangzhou City, there are 15 LCZ types (Fig. 1), with built types accounting for 23.91% of the total area. This percentage is quite high in the context of a mega-city and is twice the proportion in Beijing, the capital of China (11%). Built types mainly include LCZ6 (open low-rise), LCZ4 (open high-rise), and LCZ2 (compact mid-high-rise). LCZ6 is mainly distributed in urban villa areas and suburban villages, revealing the existence of a large number of low-density living spaces in Guangzhou. LCZ4 represents modern high-rise residential areas in urban districts, typical

residential areas in modern Chinese cities. LCZ2 mainly covers self-built houses and old neighborhoods due to the unique land ownership relationship in Guangzhou. Some land belongs to community residents, and to increase land value, they tend to build dense and tall residential buildings on their own land. LCZ2 is often adjacent to LCZ8 (large low-rise) because community residents usually build both residences and factories on their own land, forming a unique "urban village" within the city. Land cover types account for 76.09% of the total area, with LCZA (dense trees) and LCZB (scattered trees), characterized by dense and scattered trees, mainly distributed in the north and east of the city, being critical components of the urban ecosystem. LCZG (water) are distributed in the city, mainly the Pearl River, playing a crucial role in Guangzhou's economic development.

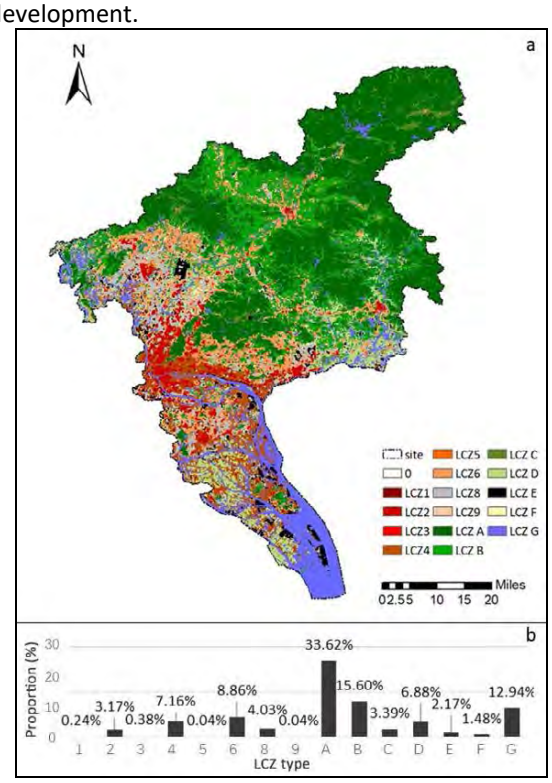

Figure 1: The spatial distribution of LCZs in Guangzhou (a. the map of LCZs in Guangzhou; b. the proportion of LCZs)

3.2 Mapping elderly population in different LCZs

The total elderly population in Guangzhou is approximately 1.12 million, but there are significant differences in different regions (Fig. 2). About 79.4% of the elderly population is distributed in built types, mainly concentrated in LCZ4 (25.16%) and LCZ2 (22.22%). The old city area is the main part of LCZ2, while LCZ4 has a large green area and good lighting, with both areas having generally higher population densities. LCZ6 and LCZ8 are also major residential areas for the elderly, accounting for 17.3% and 12.3% of the elderly population, respectively, mainly located on the urban outskirts with low-rise housing and factories. In contrast, very few elderly people are distributed in LCZ1 (compact high-rise) and LCZ3 (compact low-rise), accounting for less than 3%, totaling approximately 26,000 people. About 20.6% of the elderly population is distributed in areas with scattered trees, totaling around 63,000 people, mainly in LCZB, an area consisting of orchards and plantations, while the elderly population in other LCZs is below 4%. Considering that the majority of the elderly population is distributed in built types, subsequent research will focus on the heat risk situation faced by the elderly in this large category of areas.

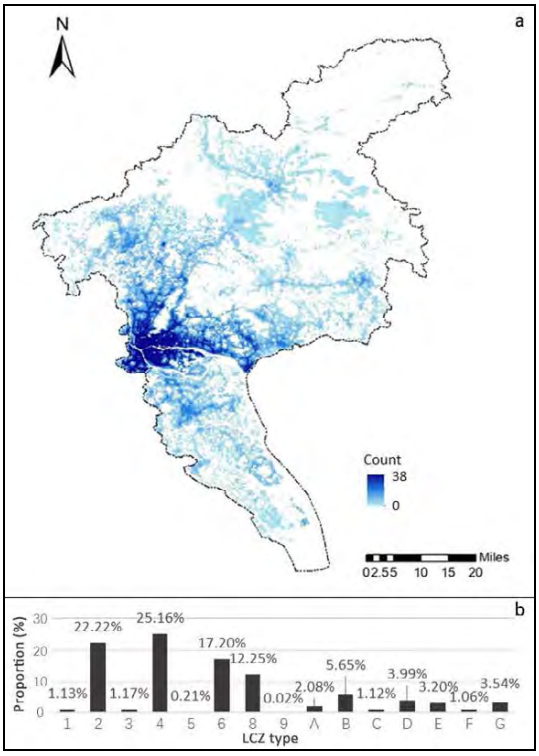

Figure 2: The spatial distribution of elderly population in Guangzhou (a. the elderly population distribution in Guangzhou; b. the proportion of elderly population in different LCZs)

3.3 Extreme high temperatures of different LCZs

The total area of heat risk areas in Guangzhou is approximately 468.4 square kilometers, accounting for 6.30% of the total area of Guangzhou (Fig. 3). They are mainly distributed in the central urban area, Huadu District, and the central area of Zengcheng District, with built types LCZ8, LCZ2, and LCZ4 being dominant. These three LCZ types together account for 67% of the total heat risk area. The results indicate that the heat risk areas in Guangzhou are mainly located in areas where these three LCZ types are mixed. Among them, LCZ8 is mainly industrial land with surfaces covered by cement and hard paving and almost no greenery. LCZ2 and LCZ4 are the main residential areas, forming a compact distribution with LCZ8. In this situation, the heat released from industrial land diffuses to surrounding residential land, being a significant factor leading to the concentrated

formation of heat risk areas. At the same time, LCZ2 and LCZ8 are the two types of areas with the highest probability of risk occurrence, far exceeding other built types. (Fig. 4) LCZ2, due to its high and dense buildings, has difficulty dissipating heat, making it prone to forming heat risk areas. LCZ8, on the other hand, releases a large amount of heat due to its industrial land characteristics, thereby forming risk areas. Among land cover types, LCZE (rock and hard) has the highest probability of risk occurrence, highlighting the significant impact of greenery on the formation of heat risk areas.

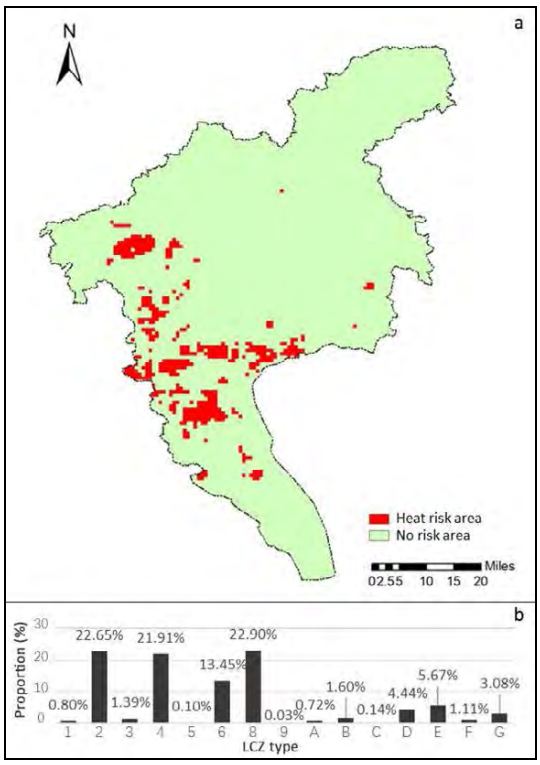

Figure 3: The spatial distribution of heat risk areas in Guangzhou (a. the heat risk area distribution in Guangzhou; b. the proportion of heat risk area in different LCZs)

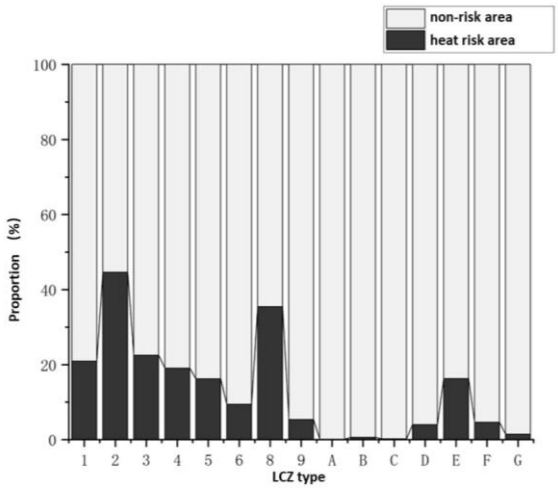

Figure 4: The heat risk proportion of different LCZs

3.4 Heat exposure in the elderly population

Approximately 327,000 elderly people in Guangzhou are in high-temperature risk areas, accounting for 29.1% of the total elderly population (Fig. 5). Of the elderly people at risk, 92.8% are distributed in built types, mainly in LCZ2, LCZ4, and LCZ8, totaling around 303,000 people. This is consistent with the fact that these three LCZ types have the highest distribution of heat risk areas in Guangzhou. Among them, LCZ2 and LCZ4 are not only the regions with the most elderly people at risk but also the regions with the highest distribution of the elderly population. This indicates that the heat risk faced by the elderly has been overlooked, as no one subjectively wants to live in areas with the highest risk. It is noteworthy that LCZ8, besides LCZ2 and LCZ4, has the highest distribution of elderly people at risk, accounting for nearly 20%, significantly higher than LCZ6. However, in the statistics of the distribution of the elderly population, LCZ6 contains a significantly higher number of elderly people than LCZ8. Combining the differences in land cover characteristics between LCZ6 and LCZ8, we conclude that the spacing between buildings and the green space coverage are closely related to the exposure of the elderly to heat risk.

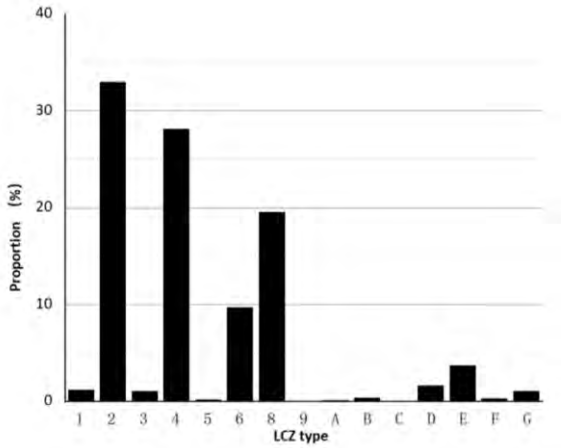

Figure 5: Heat exposure in the elderly population of different LCZs

4. DISCUSSION

4.1 Correlation between elderly distribution and extreme high temperatures

Observing the significant overlap between the LCZ types where the elderly population is most concentrated and those with the highest frequency of heat risk area, we further explored the correlation between the elderly population and heat risk area. We established a coordinate system with the elderly population as the x-axis and the count of heat risk zones as the y-axis. Each LCZ's position was marked on the coordinate system based on the respective elderly population and heat risk area count (Fig. 6). Overall, LCZs with a higher elderly population tended to have more heat risk areas, indicating a strong

positive correlation between the elderly population's distribution and the number of heat risk areas. Notably, LCZ8 stood out as a deviation, surpassing the expected number of risk zones, aligning with the characteristic of higher risk occurrence in this LCZ type. Optimizing the living environment for the elderly to reduce heat risk involves contrasting the compositional elements between no risk areas and heat risk areas, such as supplementing the lacking blue-green spaces in high-risk areas.

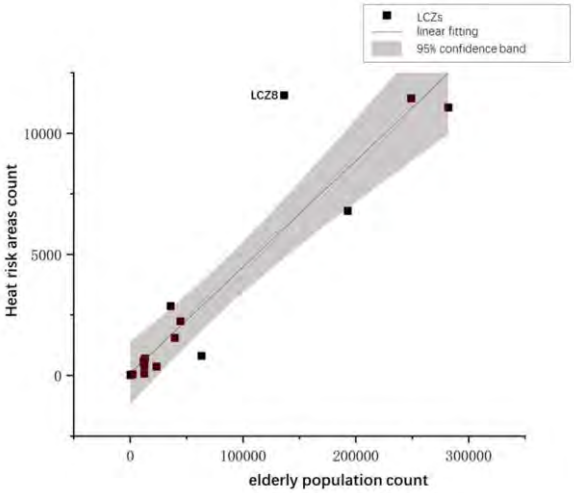

Figure 6: The linear fitting of elderly distribution and heat risk

4.2 Comparison of residential preferences between the elderly population and the general population

To emphasize the focus on the elderly population, we compared the distribution patterns of the elderly with those of the general population. In different LCZs, the elderly and the general population in Guangzhou exhibited a high degree of consistency. The top four LCZs for both groups, in terms of their respective total proportions, were LCZ4, LCZ2, LCZ6, and LCZ8, in descending order (Fig.7). This suggests that the elderly in Guangzhou typically reside in mixed areas with the general population. This phenomenon aligns with China's policy promoting aging in place and is influenced by local customs and family cultural beliefs. A slight difference is observed in the proportions of LCZ4 and LCZ2, where the elderly population exceeds that of the general population, while LCZ6 and LCZ8 exhibit the opposite trend. Consequently, it can be inferred that the elderly prefer residing in high-rise buildings, reflecting their inclination towards modern high-rise communities, while the general population may be more associated with industrial areas due to work-related factors. In future urban development, attention should be paid to improving the ecological environment in old urban areas and industrial office areas to enhance the quality of living.

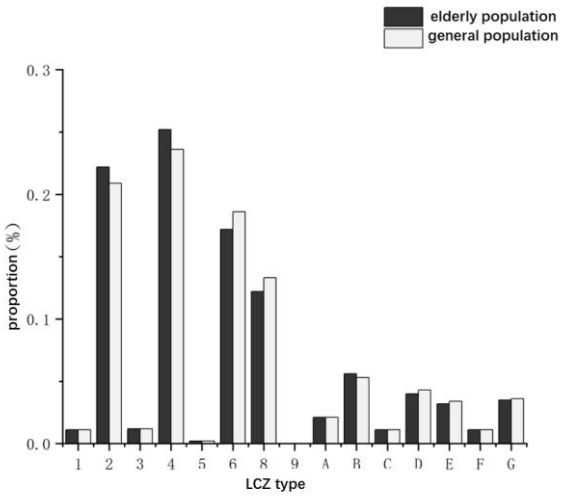

Figure 7: Comparison of residential preferences between the elderly population and the general population

5. CONCLUSION

The distribution of LCZs in Guangzhou is predominantly characterized by the land cover types (76.09%). However, nearly 80% of the elderly population inhabits areas classified by built types, with LCZ2, LCZ4, and LCZ6 being the primary types. These zones are correlated with the spatial characteristics of Guangzhou's urban structure and the layout of urban villages. Simultaneously, these three types are the main distribution areas for the elderly population. Guided by policies promoting aging in place and the urban context, the elderly in Guangzhou cohabitate with the general population, primarily in high-rise and mid-high-rise residential buildings. The primary heat risk areas in the city are found in LCZ2, LCZ4, and LCZ8, showing a substantial overlap with the distribution areas of the elderly population. The analysis of the correlation between the elderly population distribution and heat risk area indicates a significant positive correlation. Future research could explore the differences in elements among different LCZs and discover effective approaches to reduce heat risks for the elderly.

Approximately 29.1% of the elderly population in Guangzhou is exposed to heat risks, indicating a severe threat to the current health of the elderly. Considering the overlap between the regions where the elderly prefer to live and areas with a higher concentration of heat risk area, it is evident that this threat has been overlooked for an extended period. We recommend that Guangzhou further refine its urban renewal policy guidelines. While the city has initiated urban renewal activities early on and has focused on improving the quality of life for the elderly through services and activity spaces, future urban development should consider the transformation of outdoor spaces commonly used by the elderly to alleviate their exposure to heat risks. Special

attention is needed for LCZ2 and LCZ8, where heat risk area has a disproportionately high prevalence, to genuinely improve the living environment for residents.

REFERENCES

1. Climate Change 2021: The Physical Science Basis, [Online], Available: https://www.ipcc.ch/report/ar6/wg1/ [9 August 2021]

2.Chen L, Frauenfeld O W. Impacts of urbanization on future climate in China [J]. *Climate Dynamics*, 2016, 47 (1): 345-357.

3.Liao W L, Li D, Liu X P, et al. Examination and projection of urbanization effect on summertime hot extremes in China [R]. Online: EGU General Assembly Conference Abstracts, 2020.

4.HEAVISIDE C, MACINTYRE H, VARDOULAKIS S. The urban heat island: Implications for health in a changing environment[J]. *Current Environmental Health Reports*, 2017, 4(3): 296–305.

5.Ho J Y, Shi Y, Lau K K L, et al. Urban heat island effect-related mortality under extreme heat and non-extreme heat scenarios: A 2010–2019 case study in Hong Kong[J]. *Science of the Total Environment*, 2023, 858: 159791.

6.Bunker, A., Wildenhain, J., Vandenbergh, A., Henschke, N., Rocklov, J., Hajat, S., Sauerborn, R., (2016). Effects of air temperature on climate-sensitive mortality and morbidity outcomes in the elderly; a systematic review and meta-analysis of epidemiolog

7.Ho J Y, Shi Y, Lau K K L, et al. Urban heat island effect-related mortality under extreme heat and non-extreme heat scenarios: A 2010–2019 case study in Hong Kong[J]. *Science of the Total Environment*, 2023, 858: 159791.

8. Economic valuation of temperature-related mortality attributed to urban heat islands in European cities, [Online], Available: https://doi.org/10.1038/s41467-023-43135-z [17 November 2023]

9.Stewart, Ian D., and Tim R. Oke. Local climate zones for urban temperature studies. *Bulletin of the American Meteorological Society* 93.12 (2012): 1879-1900.

10.Zhou Yi, Zhang Guoliang, Jiang Li, Chen Xin, Xie Tianqi, Wei Yukai... & Lun Fei. (2021). Mapping local climate zones and their associated heat risk issues in Beijing: Based on open data. *Sustainable Cities and Society*, 74.

11.Demuzere, M., Kittner, J., & Bechtel, B. (2021). LCZ Generator: A Web Application to Create Local Climate Zone Maps. *Frontiers in Environmental Science*, 9: 637455.

12.Estoque, R. C., Ooba, M., Seposo, X. T., Togawa, T., Hijioka, Y., Takahashi, K., et al. (2020). Heat health risk assessment in Philippine cities using remotely sensed data and social-ecological indicators. *Nature communications*, 11(1), 1581.

PLEA 2024 WROCŁAW
(Re)thinking Resilience

Physiological indicators in IEQ-cognitive performance research in offices: A review of literature

FUZHI MU [1]

[1] School of Architecture, Design and Planning, The University of Sydney, NSW 2006, Australia.

ABSTRACT: This paper summarizes the literature review on some broadly used physiological indicators in IEQ-cognitive performance discipline. Several physiological indicators, including HR/HRV, EEG, CBF and skin temperature, are presented and compared by explaining their pros and cons via literature research. Skin temperature is more sensitive to thermal environment rather than cognitive performance. Correlation between HR/HRV and cognitive performance is only observed related to indoor thermal and lighting environment rather than noise condition. And higher HR/HRV can cause faster task response and lower task accuracy. EEG is an effective method to detect level of brain activity affected by thermal and acoustic stimuli. Strong correlation is observed when testing problem-solving and decision-making tasks. Lack of evidence is found from literature to study the correlation between noise condition and CBF in indoor offices. Further research on enhancing current knowledge on existing physiological indicators in recommended. The gap on how lighting/noise impact physiological measurements and cognitive performance is bigger than thermal environment. And looking for a new indicator that can better connect IEQ stimuli and different cognitive task performance maybe another option.
KEYWORDS: heart rate/heart rate variability, skin temperature, EEG, cerebral blood flow, cognitive load.

1. INTRODUCTION

With the global warming and the intensification of greenhouse gas emissions over the past 100 years, coupled with the increase in time people spend indoors in recent decades, IEQ (Indoor Environmental Quality) now has become one of the essential research topics because its significant impact on occupants' well-being and behaviour, as well as cognition. Previous research categories IEQ into four parts: IAQ (Indoor Air Quality), thermal comfort, Acoustic and Visual Environment. Furthermore, each element of IEQ stimuli have corresponding potential impact on cognitive performance of indoor workers. Over the past few decades, multiple disciplines have placed emphasis on cognitive performance and conducted in-depth research on it. And in the research related to IEQ and cognitive performance, various physiological measurement has been used as indicators to quantify relevant metrics of cognitive performance and cognitive load. Those physiological parameters play a role in jointing IEQ discipline and cognition discipline. However, the current findings on the correlation between cognitive performance and IEQ factors is still not completely solved. It is hard to measure actual cognitive performance because of the complexity of both cognition and IEQ system. Parsons defined "performance" as "the extent to which activities have been carried out to achieve a goal". (1) This definition indicates that there are two potential ways to evaluate the performance: intensity of activity or achievement of the goal. Zhang et al summarized three primary methods to evaluate cognitive load: 1) primary task performance, 2) subjective perceptions of cognitive load, 3) physiological responses. (2) Task performance can normally be measured according to task score and completion time, but it is hard to directly measure cognitive load. Therefore, in current cognitive performance study, scientists use multiple "activities" to indicate cognitive load, which involves different psychological and physiological factors. Psychological factors including mental fatigue and workload are normally measured using s set of questionnaires, and most of physiological factors can be directly measured by instruments during the experiments. Applied physiological measurements includes heart rate or heart rate variability, EEG, pupillometry, blood pressure, oxygen saturation, body and skin temperature, respiratory rate, eye movement, ECG, EDA, and cerebral blood flow, etc. The experimental results for those responses are still ambiguous and sometimes conflicting. Also, the results may vary across different adopted cognitive tasks and selected indoor environmental variables.

Cognitive functions are divided into six categories by Wang et al.: attention, perception, memory, language function, higher order skills and social cognition, with their respective sub-categories. (3) Each cognitive function is associated with corresponding brain activity at specific brain region. Because of those biological diversity, it is necessary to understand the interaction among each IEQ stimuli and cognitive performance by adopting various physiological measurements to indicate cognitive load or performance. However, the diversity of definition of

cognitive performance in different research and the feeling of invasion on physiological measurement tools gives additional difficulty on filling the gap in this research field. (4,5)

For maintaining health and meeting safety requirements, also increasing productivity and reducing labour cost, office environments start to obtain great attention in this discipline as a complex psycho-physical system. (6) Previous research does not address enough focus on the function of indoor office environments. In indoor offices, some cognitive functions including attention, memory and higher order tasks such as problem-solving and decision-making are highlighted. This review paper is to summarize some popularly applied physiological measurement sin published literature relevant to cognitive performance and IEQ stimuli in office environments, with consideration on various cognitive tasks, to make it easier to understand the the correlation among those variables and help researchers to fill the gap in further studies.

2. Methodology

This research mainly based on survey of the literature contains all the following aspects: Cognitive performance/Cognitive load, at least one IEQ stimuli, office environment, applied physiological measurements in the experiment. Physiological indicators such as attention, memory, problem-solving and decision-making will be highlighted during the review because of the office environment. Indoor Air Quality will not be discussed in this literature research. Reviewed literature including journal articles, conference papers, books are collected across multiple platforms. All the selected experimental studies are implemented in real offices or simulated office environments.

3. Findings

3.1 Skin temperatures

Previous research found that skin temperature is an effective physiological indicator to reflect the occupants' response to thermal environment. Compared with all other reviewed physiological measurements, skin temperature is the best one to indicate occupants' sensation and comfort, especially in hot environments. (7) In moderate condition, skin temperature can also be used as indicator to thermal sensation. (8) And in the last few years, scholars suggest there is a correlation between skin temperature and cognitive performance. General evidence suggests higher skin temperature comes with lower cognitive performance. Yeom and Delogu found that participants' cognitive performance in response time and working memory is negatively correlated with air temperature between 18◦C and 28◦C, and relatively high skin temperature of specific local body part is correlated negatively with cognitive performance. (9) And in a climate chamber that meets requirements of the office environment, Hao's team suggests only skin temperature at wrist can be used as indicator in hot environments, and skin temperature at 34.5◦C is recommended for optimal performance to six cognitive texts. (8) Instead of using skin temperature only, Tsutsumi et al. chose to study the correlation between skin wittedness and cognitive performance with two simple tasks under different relative humidity levels, but it is found that cognitive performance is relatively stable with change in relative humidity even skin wittedness obviously decreased (10).

Skin temperature is normally considered highly related to thermal environment and the effect of lighting conditions and noise levels on skin temperature is hard to be observed. Fanger's previous study showed that noise is not significantly correlated with thermal sensation and skin temperature. (11) And Luo et al. studied the effect of CCT (correlated colour temperature) and found that, even cognitive performance changed under different CCT level, change on skin temperature is not observed during the experiment. (12) Relationship between office noise and skin temperature is very poor in moderate temperature environment. (13)

3.2 Heart rate/Heart rate variability

Heart rate is a high-quality physiological indicator to cognitive performance in moderate temperature environments, because it is highly relevant to thermal stress and can be real-time monitored. Also, it can be measured using small devices in a non-invasive way. But there is still doubt whether heart rate can be used as a physiological indicator in environments with high thermal stress. Chen et al. found that, in hot environments, when heart rate is raised up to 90bpm, the speed and accuracy of Stroop test and d2 test decline significantly, and when this number reach 100bpm, the accuracy of visual learning, addition, multiplication and typing also dropped. (14) And there is an inverted U-shaped relationship is observed between the accuracy and heart rate in his research. In moderate thermal environments, when thermal comfort is maintained by adjusting air velocity, heart rate also increases significantly with elevated air temperature and pNN50 decreased. (15) But the cognitive performance decreases with elevated air temperature. Therefore, in both moderate and high thermal environments, HR/HRV can be used as an indicator to predict cognitive performance for indoor workers.

Apart from the effect of thermal environment on HR/HRV, Smolders observed the level of illumination at eye can also cause response at heart rate. Heart rate

Table 1. Correlation between skin temperature and cognitive performance under different cognitive tasks and IEQ variables in office environments

Cognitive function	Response time, working memory	Emotion, learning and memory, perception, thinking, psychomotor and attention	Answering speed, accuracy	Planning ability, verbal ability, working memory, mental spatial manipulation
Cognitive tasks	OSPAN (Operation span task), vigilance task	Stroop test, calculations, digit span task, visual learning, grammatical reasoning and visual reasoning time	Addition task, text typing	Hamsphire tree task, grammatical reasoning task, digital span task, spatial rotation task
IEQ variables	Temperature at 6 scales between 18◦C to 28◦C	Hot environments with 3 air temperature levels: 26◦C, 30◦C and 34◦C	Relative humidity at 4 levels: 40%, 50%, 60% and 70% SET* constantly at 25.2◦C	2 levels of CCT (2700K and 5700K) with illuminance at 500 lux at eye
Skin temperature and cognitive performance	Specific body parts (arm, wrist (back), wrist (in), neck) generally negatively correlated with cognitive performance	Forehead and wrist skin temperature are highly related to thermal sensation, but only skin significantly relevant to cognitive performance	No significant difference on cognitive performance is observed during the experiments. Skin wittedness significantly decreased with exposure time especially in lower RH environment	Skin temperature is not affected by different CCT level. CCT at 5700K benefits more to cognitive performance than 2700K
	Yeom and Delogu (9)	Hao et al. (8)	Tsutsumi et al. (10)	Luo et al. (12)

and rise over the baseline in a high illuminance condition and drop below the baseline in a low illuminance condition. (16) And participants' performance on reaction time is better when heart rate is higher. However, this research only addressed lighting condition without mentioning other IEQ factors. Different types of noise in office can affect cognitive performance is observed by Brocolini et al. without significance. (17) But this correlation currently is not found by observing occupants' HR/HRV. There lacks enough evidence on the correlation among heart rate, cognitive performance, and noise condition in office environment. (18) The combined effect of both air temperature and noise level is higher than individuals on working memory, sustained attention and reaction time. (18) And this pattern can be also observed in Abbasi's research. The combined effect of noise and air temperature is more obvious than each individual. (19) they also found the impact on heart rate by air temperature is more significant when noise level is relatively high, And mean heart rate is lower at different air temperature when noise level is low. (19) Which means heart rate is more sensitive when air temperature or noise level is higher.

3.3 Electroencephalogram (EEG)

EEG is an instrumental test that can measure the level of brain activity and pattern to observe wearer's cognitive load in real-time. It is a newly applied technology in IEQ-cognitive performance discipline. However, compared with devices used to measure skin temperature and heart rate, devices used in EEG measurement is much larger and more invasive during the test which is always a potential influential factor on subjects' perception and comfort. But skin temperature and HR/HRV cannot directly measure brain activity like EEG.

An experimental study using EEG to measure cognitive load by Wang et al. suggests that, in moderate environment, higher cognitive load can be caused by higher air temperature with increase of theta band activity of frontal lobe and decrease of alpha band activity of parietal lobe, and generally better performance is observed in relative cooler environment. (20) Another study on cognitive performance by Oh et al. also applied EEG to investigate the effect of noise level and illuminance in a simulated office. (21) In his study, significant correlation between relative theta activity level and average reaction time is observed under dimmer lights and lower noise level, and he also noticed lighting intensity alone cannot have a significant impact on EEG measurements but noise and combined effect of noise and lighting both can correlate with EEG level. A more detailed research on how noise interact with brain activity and cognitive performance by Astuti et al. They noticed not only noise level, but type of noise also significantly correlated with cognitive performance. (22) And participants' attention condition is best when they are exposed to noise level at 65dBA in both continuous and intermittent types. And when noise level reach 70dBA in both types, mental workload start to play a role in impacting participants' cognitive performance. Literature listed above found no effect of illuminance and CCT on EEG

Table 2. Correlation between HR/HRV and cognitive performance under different cognitive tasks and IEQ variables in office environments.

Cognitive functions	Perception, attention, working memory, etc	Sustained attention, working memory, visual research, capacity to direct attention	Spatial orientation, logical reasoning, working memory, sustained attention.	Response accuracy, response time, working memory
Cognitive tasks	Stroop test, d2 test, visual learning, addition, multiplication, typing	Psychomotor Vigilance test, Necker Cube Pattern Control test, Letter digit substitution test	5 typical office work tasks and 7 neurobehavioral tests	N-back test
IEQ variables	Air temperature: 26◦C, 30◦C, 33◦C, 37◦C, 39◦C. Relative humidity: 50% and 70%.	Illuminance at eye level: 200lx, 1000lx and 4000lx	Air temperature: 24◦C, 26◦C and 28◦C with maintained comfort by changing air velocity and clothing value	4 air temperature levels: 18◦C, 22◦C, 26◦C and 30◦C 2 noise levels: 55dBA and 75dBA
HR/HRV and cognitive performance	A generally inverted-U relationship is observed between accuracy of test and heart rate.	Increased subjective alertness and vitality, better sustained attention at higher illuminance, higher HR/HRV at higher illuminance, shorter reaction time and increased arousal at higher illuminance	Elevated air temperature caused lower cognitive performance when comfort is maintained, heart rate increased with air temperature but pNN50 decreased with elevated air temperature	Combined effect of air temperature and noise is more significant than individuals, Heart rate is more sensitive in higher noise level environment and higher temperature environment
	Chen et al. (14)	Smolders et al. (16)	Lan et al. (15)	Abbasi et al. (19)

signal. No literature about the effect of daylight factor on EEG and cognitive performance is found.

3.4 Cerebral blood flow (CBF)

Functional Near-Infrared Spectroscopy (fNIRS) is commonly applied in neuroscience and biology to measure patterns of cerebral blood flow. Compared with the popularity of fNIRS in other discipline, it is not commonly applied in IEQ discipline. Similar with EEG device, fNIRS test devices also have a non-negligible volume which may be invasive during cognitive test. The application of fNIRS and cerebral blood flow in IEQ discipline is first introduced by Tanabe and Nishihara as an indicator to cognitive load (4). It can measure the concentration of chromophores oxygenated hemoglobin (ΔO_2Hb) and deoxyhemoglobin (ΔHHb) with specific algorithm which can be significantly influenced by the level of mental workload/cognitive load. In Tanabe and Nishihara's research, when operative temperature varies between 25◦C and 33◦C, the increase rate of both ΔO_2Hb and total hemoglobin in frontal lobe significantly increased with temperature in three cognitive tasks. But only task performance in this experiment did not change with higher physiological measurements. Another experiment by Nishihara et al. investigated the correlation between thermal environment and cognitive performance. (23) And performance in accuracy and response rate has no signiticant difference even the change rate of cerebral blood flow is different. Second experiment by Tanabe and Nishihara tested effect of lighting condition. They observed difference on cerebral blood flow under different tasks at 3 lux levels but no obvious different is observed on CBF. No enough evidence was found to prove correlation between noise and CBF in indoor offices.

4. CONCLUSION

The effect of indoor environmental factors, cognitive performance, cognitive load and relevant physiological measurements need further investigation. Among all those physiological measurements above, skin temperature is the best one to predict thermal stress. Therefore, in both moderate and stressful thermal environments, the difference on skin temperature is obvious. But only the wrist skin temperature is significantly relevant to cognitive performance. Skin temperature is not sensitive to change of surrounding CCT. When CCT largely increases, cognitive performance is affected but no change on skin temperature is observed, which means skin temperature is highly correlated with cognitive load and thermal stress only, and it is not a high-quality indicator to cognitive performance. Further research on the effect of different noise

conditions and other lighting characteristics on skin temperature in offices is recommended.

Compared with heart rate variability (HRV), heart rate can better reflect cognitive performance after reach a certain level. When heart rate is high enough, performance to task under multiple functions will lose accuracy in both moderate and stressful thermal environments. Same as skin temperature, heart rate is also highly relevant to thermal stress. When thermal comfort is maintained with elevated air temperature, heart rate could increase when cognitive performance is declining. But cognitive performance could increase with heart rate under different illuminance condition. Therefore, the application of heart rate as cognitive performance indicator depends on the independent variable. Further research on the correlation between heart rate and noise on cognitive performance in offices is suggested.

EEG and fNIRS are two technologies that can measure level of brain activity. Compared with other physiological parameters, brain activity level can better predict cognitive load. The results of EEG measurements are dependent on cognitive task type and measured part of brain. There are obvious individual difference using EEG to measure cognitive load and stronger EEG signal can successfully predict lower cognitive performance in moderate thermal environments. Using EEG technology can help researchers to observe the direct impact of thermal condition and noise level on cognitive load, but it fails to analyze the correlation between illuminance level and cognitive load. Same patterns can be observed using cerebral blood flow. Compared with change in indoor environmental factors, differences on cognitive task difficulty cause stronger brain activity difference.

From the review and analysis of some broadly applied physiological parameters, the selection of applied physiological indicators in IEQ discipline should be determined based on the purpose of research. To observe the difficulty level of cognitive task and cognitive performance, brain activity is possible to be a good indicator. And for experiment on the correlation between thermal environment and cognitive performance, heart rate and skin temperature are probably helpful. EEG and cerebral blood flow patterns are also affected by different noise levels which makes them good method to observe the cross-modal effect or combined effect between thermal condition and noise level. However, there is no credible physiological indicator that can connect indoor lighting condition and cognitive performance. To better understand how the complex IEQ system affect cognitive performance in office work, further study on looking for another physiological indicator is required. Further research on other existing physiological measurements also need to be enhanced.

REFERENCES

1. Parsons, K. (2004). Human Thermal environments: The Effects of Hot, Moderate, and Cold Environments on Human Health, Comfort, and Performance. Third Edition (3rd ed.). CRC Press.
2. Zhang, F., de Dear, R. and Hancock, R. (2019). Effects of moderate thermal environments on cognitive performance: A multidisciplinary review. *Applied Energy*, 236: p. 760-777. http://doi.org/10.1016/j.apenergy.2018.12.005.
3. Wang, C., Zhang, F., Wang, J., Doyle, J.K., Hancock, P.A., Mak, C.M. and Liu, S. (2021). How indoor environmental quality affects occupants' cognitive functions: A systematic review. *Building and Environment*, 193: 107647. http://doi.org/10.1016/j.buildenv.2021.107647.
4. Tanabe, S. and Nishihara, N. (2004). Productivity and fatigue. Indoor Air, 14(7): p. 126-133. http://doi.org/10.1111/j.1600-0668.2004.00281.x.
5. De Dear, R., Nathwani, A., Candido, C. and Cabrera, D. (2013). The next generation of experimentally realistic lab-based research: the University of Sydney's indoor environmental quality laboratory. Architectural Science Review, 56(1): p. 83-92. http://doi.org/10.1080/00038628.2012.745807.
6. Zhang, X., Du, J. and Chow, D. (2023). Association between perceived indoor environmental characteristics and occupants' mental well-being, cognitive performance, productivity, satisfaction in workplaces: A systematic review. Building and Environment, 246: 110985. http://doi.org/10.1016/j.buildenv.2023.110985.
7. Song, W., Zhong, F., Calautit, J.K. and Li, J. (2024). Exploring the role of skin temperature in thermal sensation and thermal comfort: A comprehensive review. Energy and Built Environment, http://doi.org/10.1016/j.enbenv.2024.03.002.
8. Hao, S., Wang, F., Guan, J., Tang, K. and Wang, X. (2023). Skin temperature indexes to evaluate thermal sensation and cognitive performance in hot environments. Building and Environments. 242: 110540. http://doi.org/10.1016/j.buildenv.2023.110540.
9. Yeom, D.J. and Delogu, F. (2021). Local body skin temperature-driven thermal sensation predictive model for the occupants' optimum productivity. Building and Environment, 204: 108196. http://doi.org/10.1016/j.buildenv.2021.108196.
10. Tsutsumi, H., Tanabe, S., Harigaya, J., Iguchi, Y. and Nakamura, G. (2007), Effect of humidity on human comfort and productivity after step changes from warm and humid environment. Building and Environment, 42(12): p. 4034-4042. http://doi.org/19.1016/j.buildenv.2006.06.037.
11. Fanger, P.O., Breum, N.O., Jerking, E. (1977). Can colour and noise influence man's thermal comfort? Ergonomics, 20: p. 11-18. http://doi.org/10.1080/00140137708931596.
12. Luo, W., Kramer, R., Kompier, M., Smolders, K., de Kort, Y. and Lichtenbelt, W.V.M. (2023). Effects of correlated color temperature of light on thermal comfort, thermophysiology and cognitive performance. Building and Environment, 231: 109944. http://doi.org/10.1016/j.buildenv.2022.109944.
13. Witterseh, T., Wyon, D.P. and Clausen, G. (2004). The effects of moderate heat stress and open-plan office noise distraction on office work. Indoor Air Proceedings.
14. Chen, Y., Wang, Z., Tian, X. and Liu, W. (2023). Evaluation of cognitive performance in high temperature with heart rate: A pilot study. Building and Environment, 228: 109801. http://doi.org/10.1016/j.buildenv.109801.

15. Lan, L., Tang, J., Wargocki, P., Wyon, D.P. and Lian, Z. (2021). Cognitive performance was reduced by higher air temperature even when thermal comfort was maintained over the 24-28◦C range. Indoor Air, 32: e12916. http://doi.org/10.1111/ina.12916.
16. Smolders, K.C.H.J., de Kort, Y.A.W. and Cluitmans, P.J.M. (2012). A higher illuminance induces alertness even during office hours: Findings on subjective measures, task performance and heart rate measures. Physiology & Behavior, 107: p. 7-16. http://doi.org/10.1016/j.physbeh.2012.04.028.
17. Brocolini, L., Parizet, E., Chevret, P. (2016). Effect of masking noise on cognitive performance and annoyance in open plan offices. Applied Acoustics, 114: p. 44-55. http://doi.org/10.1016/j.apacoust.2016.07.012.
18. Sepehri, S., Aliabadi, M., Golmohammadi, R. and Babamiri, M. (2019). The effects of noise on human cognitive performance and thermal perception under different air temperatures. JRHS, 19(4): e00464.
19. Abbasi, A.M., Motamedzade, M., Aliabadi, M., Golmohammadi, R. and Tapak, L. (2020). Combined effects of noise and air temperature on human neurophysiological responses in a simulated indoor environment. Applied Ergonomics, 88: 103189. http://doi.org/10.1016/j.apergo.2020.103189.
20. Wang, X., Li, D., Menassa, C.C. and Kamat, V.R. (2019). Investigating the effect of indoor thermal environment on occupants' mental workload and task performance using electroencephalogram. Building and Environment, 158: p. 120-132. http://doi.org/10.1016/j.buildenv.2019.05.012.
21. Oh, D., Kim, J., Kim, H., Jang, H., Hong, T. and An, J. (2023). Analyzing the impact of indoor environmental quality on physiological responses and work performance: Implications for IEQ control strategies. Building and Environment, 244: 110845. http://doi.org/10.1016/j.buildenv.2023.110845.
22. Astuti, R.D., Suhardi, B., Laksono, P.W. and Susanto, N. (2024). Investigating the relationship between noise exposure and human cognitive performance: Attention, stress, and mental workload based on EEG signals using power spectrum density. Applied Sciences, 14: 2699. http://doi.org/10.3390/app14072699.
23. Nishihara, N., Xiong, J., Kim, J., Zhu, H. and de Dear, R. (2022). Effect of adaptive opportunity on cognitive performance in warm environments. Science of Total Environments, 823: 153698. http://doi.org/10.1016/j.scitotenv.2022.153698.

County-Level Assessment of Building Stock Thermal Resilience During Heat Waves and Power Outages

MOHAMED A. BELYAMANI[1] KRITIKA KHARBANDA[2] NAN MA[1,] HOLLY SAMUELSON[2] [1]

Worcester Polytechnic Institute, Worcester, United States of America

[2] Harvard Graduate School of Design, Cambridge, United States of America

ABSTRACT: This paper demonstrates how building stock models, such as ResStock in the US, can be useful for resilience testing. We examined the thermal resilience of residential buildings in Illinois during simulated extreme weather events and power outages using ResStock models. Our results reported significant vulnerability, with the median dry bulb temperature (DBT) peaking at 32.5°C within 41 hours during the heatwave with power outage, and the 85th percentile DBT reaching 38.4°C in 42 hours. The Heat Index (HI) exceeds the danger level, with a median of 36.14 °C within 21 hours on the first day indicating extreme caution for 11 consecutive hours, and the 85th percentile DBT reaching 51.3 °C in the same timeframe indicating danger level for 11 hours. Analysis of building characteristics highlights the crucial role of building design, emphasizing the importance of thermal regulation in building infrastructure, particularly in those with finished attics or concrete masonry units (CMU). A geospatial vulnerability assessment identified the most thermally vulnerable and resilient counties and further investigated these counties' socioeconomic status based on the federal poverty level (FPL). We found that low-income households are often in buildings with less thermal resilience and are at a greater risk during extreme temperature events.

KEYWORDS: Passive Survivability, Heatwave Events, Residential Energy Modelling, Indoor Heat Vulnerability, Geospatial Vulnerability Assessment

1. INTRODUCTION

1.1. Background

The impacts of climate change have been felt across the globe, exposing populations to more frequent and more severe weather events [1-2]. As global temperatures rise due to the accumulation of greenhouse gases in the atmosphere, various regions are experiencing changes in weather patterns and an increase in extreme weather phenomena. Between 2020 and 2022, the U.S. experienced 60 separate weather and climate disasters, each exceeding a billion dollars in damages [3]. Notable occurrences among these included unprecedented heatwaves and wildfires in California, Oregon, and Washington during the fall of 2020 [4], a historic winter storm/cold wave event focused on the Deep South and Texas in February 2021 [5], and a drought and heatwave in the Western and Southern Plains states in the summer of 2022 [6]. Extreme weather occurrences, along with power outages, present a specific threat to energy infrastructure and fundamental services reliant on electricity. This situation jeopardizes the effective functioning of buildings in maintaining safe indoor environments. However, buildings should play a fundamental role in enhancing resilience against climate change events such as heatwaves to safeguard the safety and well-being of occupants. Therefore, a research question arises: which segments of our residential building stock are most at risk of overheating with the increasing frequency and severity of extreme weather events and power outages? Thus, the objective of this paper is to 1) investigate the thermal resilience of existing residential building infrastructure, with a focus on the efficacy of homes in mitigating heatwave challenges with power outages and 2) create a replicable framework for such analysis.

1.2. Previous studies

Previous studies on thermal resilience emphasize its role in providing human comfort and safety during extreme climate events. Sheng et al. [7] delved into an assisted living facility's response to heatwaves and power outages, emphasizing the significance of passive envelope strategies and natural ventilation. White et al. [8] explored resilient, sustainable design approaches, demonstrating how passive building techniques bolster resistance to outages. Sengupta et al. [9] explored the resiliency and passive survivability of an office building, sustainable design approaches, demonstrating that implementation of cooling systems active or passive as well as sun blinds are important to combat overheating risks during heatwaves. Another Sengupta et al.'s [10] study focused on overheating risks in educational buildings during heatwaves and outages, shedding light on the vital role of resilient cooling strategies.

Prior work primarily explored thermal resilience in a specific building. However, our research aims to

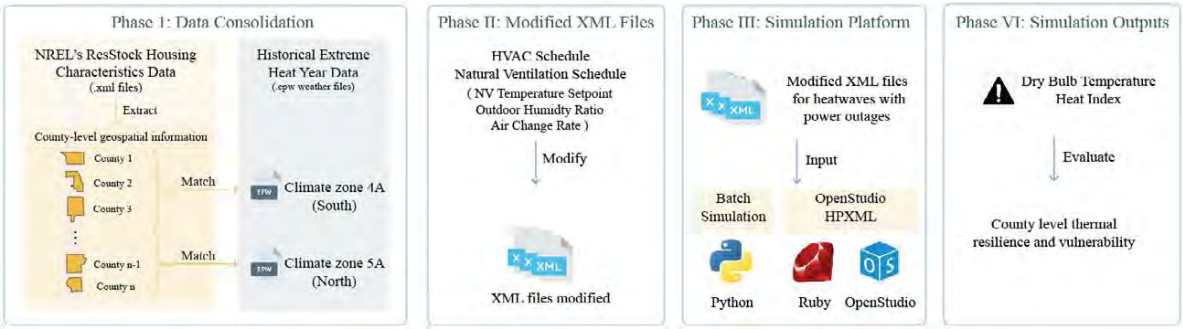

Figure 1: Methodological framework for building thermal resilience simulation.

extend this scope by geo-spatially evaluating the thermal resilience of a diverse set of residential buildings. This expansion allows us to conduct a comprehensive analysis of the thermal resilience of existing residential infrastructure in the face of heatwave challenges and power outages, with the ultimate goal of establishing a replicable methodology for such investigations.

2. METHODS

In this study, we investigate thermal resilience in the US housing stock using ResStock [11]. Built on the OpenStudio / EnergyPlus building energy simulation engine, the ResStock database has an extremely rich documentation of US residential building characteristics across various geographical resolutions ranging from national to county level. ranging from national to county level. Detailed information on the characteristics of the housing stock and how to access their metadata is provided in Ref [11]. To our knowledge, this is the first published study using the ResStock database for resilience testing. We randomly selected a 20% sample of ResStock buildings (n=4,374) in Illinois to create a meaningful subset of housing and achieve a county-level assessment of building thermal resilience. We focused on Illinois for two primary reasons: 1) Diversity: e.g., dense urban, suburban, and rural areas with multiple climate zones. 2) Notable changes in weather patterns: an increasing frequency of extreme weather events in recent years [12,14].

2.1 Methodological framework for building thermal resilience

To assess thermal resilience, we selected July 2012's peak heat period in Chicago as a representative extreme heat scenario. Two metrics such as Dry Bulb Temperature (DBT) and Heat Index (HI) [15] are used to measure occupant heat exposure and vulnerability. As illustrated in Figure 1, our methodological framework involves the following four-phase process. The first phase gathers representative samples from the 2023 ResStock database, with each building model having an XML file and a CSV file for annual schedules (i.e., window, HVAC operations). For Illinois' two climate zones (4A and 5A), we coupled each building model with appropriate weather files, using Chicago and Springfield as reference cities for zones 5A and 4A, respectively. The second phase modifies XML files to simulate power outages and window opening schedules during heatwaves which includes disabling HVAC systems, then setting higher thresholds for the natural ventilation temperature setpoints, maximum air exchange rates, and outdoor humidity ratios (to enable window opening to avoid indoor overheating). The third phase focuses on configuring the simulation platform using the OpenStudio-HPXML workflow framework. This framework integrates the OpenStudio software suite with the Home Performance XML (HPXML) data standard, which is especially useful for large-scale computation as it simplifies managing and automating multiple building simulations and data handling. Along with this framework, a batch simulation can be launched for a representative sample of buildings (in our study, n=4,374). The final phase involves extracting and analyzing the time series data to assess thermal resilience based on the simulation outputs.

Our methodological framework, built in Python 3.7, automates the majority of the simulation process, offering a pipeline for future research in assessing building thermal resilience. Our developed framework is applicable to buildings that rely on HVAC for cooling during heatwaves. The framework incorporates a pre-outage (normal operation), phase of three days, followed by a simulated three-day power outage, resulting in a total evaluation period of six days.

3. RESULTS AND DISCUSSION

3.1 Building thermal resilience analysis during heatwaves and power outage

Figure 2 presents our simulated results of the hourly DBT before and during the blackouts. On the first day of the outage, the median DBT value reached 31.5°C within an 18-hour period from the outage onset. The 85th percentile DBT peaked at 37.4°C in the same timeframe. The highest peak in the three-day outage scenario occurred on the second day, with the median DBT hitting 32.5°C at 41 hours post-outage, and the 85th percentile of residential buildings reached a maximum of 38.4°C at 42 hours. These results demonstrate the risk for significantly elevated indoor temperatures in residences without

interventions, posing risks of discomfort, as well as health and safety concerns. These findings are consistent with prior research [7], where our results are reported with the 85th percentile instead of the 95th percentile to mitigate the influence of potential outliers and extreme values.

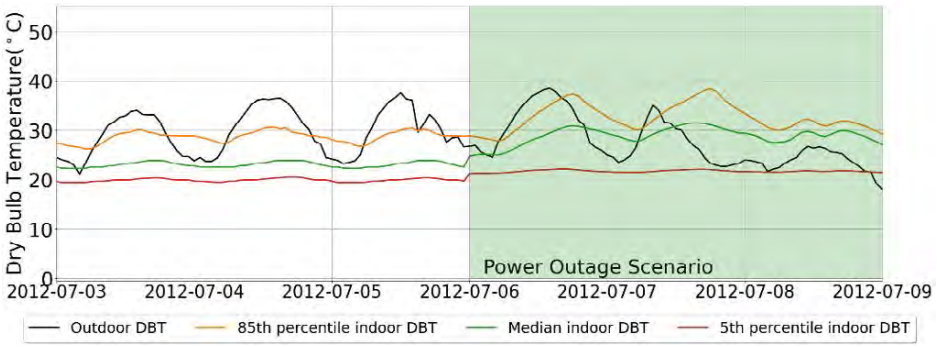

Figure 2: Hourly DBT distribution among the 4,374 residences and outdoor air temperature during the 2012 heatwave.

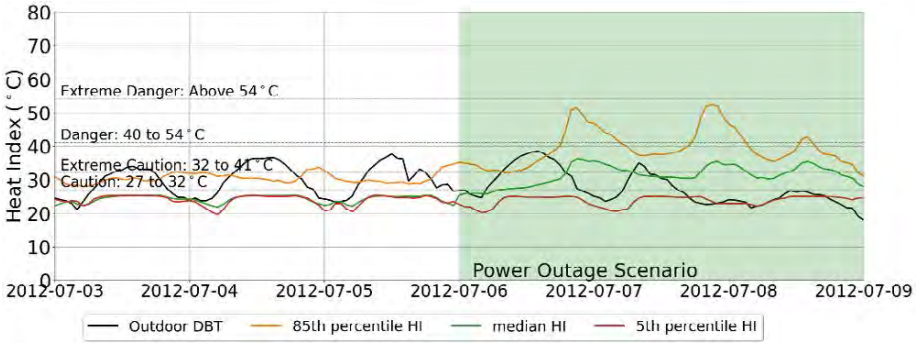

Figure 3: Hourly HI distribution among the 4,374 residences and outdoor air temperature during the 2012 heatwave.

temperatures reached 30°C within a 20-hour period. However, our study reveals an oscillating pattern in line with outdoor temperature fluctuations, differing from previous study.

In examining HI performance, Figure 3 shows the HI variation during a three-day power outage. On the first day, the median HI hits 36.14 °C in a 21-hour period from the start of the outage, indicating extreme caution for 11 consecutive hours. The 85th percentile HI peaked at 51.35 °C in the same timeframe reaching the danger zone and persisting for 11 hours. By the second day, the maximum HI across all simulated buildings in Illinois reached a median of 35.5 °C at 47 hours post-outage and persisted for 9 consecutive hours. The 85th percentile HI peaked at 52 °C at 46 hours post-outage. This temperature, indicative of the danger zone, persisted for 11 hours at the state-level. These observations in the simulated data set highlight a potential need for better preparedness in the majority of Illinois buildings to sustain safe conditions during simultaneous power outages and heatwaves, posing a significant threat to occupants' safety. Our findings align with those in Ref [5], which also identified an extreme caution level within an 8-hour period, indicating similar building performance. Notably, even short periods of power outages, such as a one-day blackout, can lead to reaching the extreme caution level within the first day. This highlights the urgent need for mitigation and adaptation strategies to promote resilient building practices in Illinois. Here,

3.2 Thermal resilience profiles across different climate zones

The comparison of simulated building resilience results across the two different Illinois climate zones, as shown in Figure 4, demonstrates the variation in DBT, Relative Humidity (RH), and the HI. There is a marked difference between the overall state conditions and climate zone 4A, where 4A consistently shows higher temperatures and median thermal performance for both DBT and HI compared to the state average. These findings prompt further investigation into how different building characteristics contribute to resilience during power outages and heatwaves.

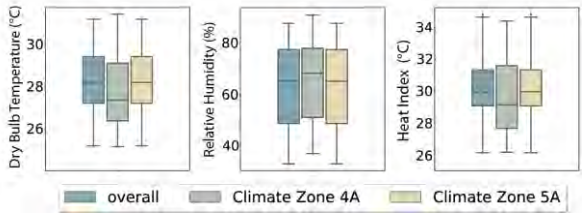

Figure 4: Boxplot of indoor DBT, RH, and HI for the 4,374 residences across two Illinois climate zones during the 2012 heatwaves on the three-day power outage.

3.3 Influence of building characteristics

In general, buildings are designed based on a group of fixed assumptions and conditions in the design or renovation phases. However, the actual performance of buildings during occupancy often diverges from these architect-intended initial conditions. In this

section, we investigate a range of building characteristics to determine which are correlated with overheating, particularly by analyzing mean and maximum DBT temperatures. Examined design variables include attic types, wall insulation levels, and air changes per hour (ACH).

The ridgeline plots in Figure 5 show the probability distribution of the mean and maximum temperatures across different attic types during heatwaves and blackouts. As can be seen, residences featuring finished attics or cathedral ceilings demonstrate a noteworthy reduction in mean temperature compared to other types with an average mean of 27 °C. It also shows less variability in temperature, suggesting a more regulated and consistent indoor climate. This pattern may highlight the critical role of attic construction in moderating indoor thermal environments, pointing to the potential benefits of strategic attic design for improved thermal resilience.

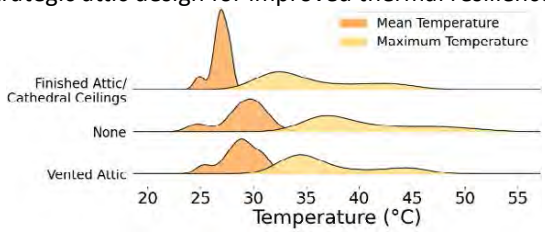

Figure 5: Ridgeline plot illustrating the distribution of mean and maximum temperatures across various attic types on the first day of heatwaves without power.

Figure 6 reveals significant variations in the thermal resilience of different wall types. Concrete masonry units (CMU) with a 6-inch hollow and uninsulated structure are correlated with better thermal performance than brick and wood stud walls, possibly due to CMU's high thermal mass and efficient thermal behavior [16]. CMU-walled dwellings are typically correlated with stable indoor temperatures, averaging around 27°C and peaking at 32°C. Brick walls are correlated with slightly less resilience than CMU, but their peak temperature probability is substantially higher, reaching the extreme caution level as defined by the HI. Wood stud walls are correlated with the least thermal resilience, with a 10-15% likelihood that peak temperatures could exceed 42°C, entering the danger level per HI standards.

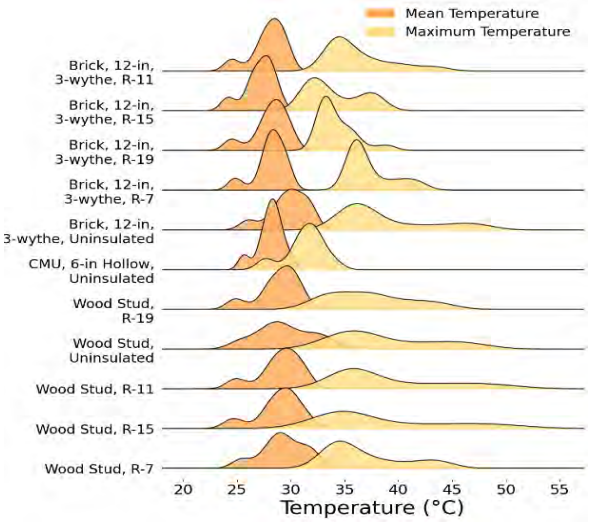

Figure 6: Ridgeline plot illustrating the distribution of mean and maximum temperatures across various wall insulation levels on the first day of heatwaves without power.

The ACH in a building is commonly used as an indicator of air infiltration. Evaluating the degree of infiltration helps in assessing the potential for mitigating indoor heat by exchanging it with outdoor air or preventing the loss of cooler indoor air. Figure 1 illustrates the ACH values and their corresponding average and peak temperatures as computed by the HI. Notably, airtight dwellings (1 ACH and 2 ACH) show reduced temperature variability and lowest mean temperature profiles. However, there is still a notable probability of these dwellings reaching peak temperatures in the extreme caution zone as defined by the HI. This suggests that while airtightness contributes to resilience, it could also lead to overheating concerns during certain periods. Conversely, buildings with higher ACH (e.g., 3 ACH, 5 ACH and higher) often experience wider and more elevated temperature ranges. As can be seen from Figure 7, on average there is a 20-30% likelihood of these dwellings reaching the extreme caution level. We are not suggesting here that the ACH should be indiscriminately increased or decreased to improve resilience. Instead, we aim to highlight what could be "good" versus "poor" design based on overheating risk assessment.

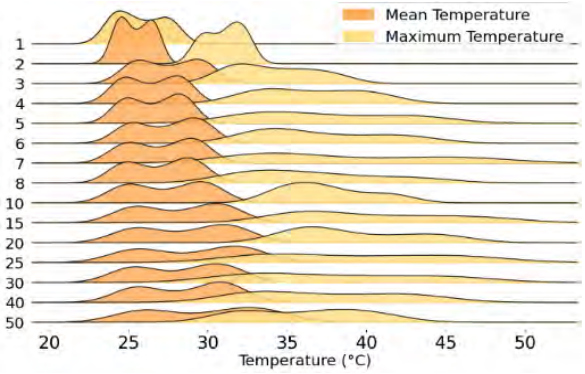

Figure 7: Ridgeline plot illustrating the distribution of mean and maximum temperatures across ACH variations on the first day of heatwaves without power.

3.4 Geospatial vulnerability and resilience assessment

Exploring thermal resilience at the county level is critical due to the distinct climatic and architectural variations that exist within different regions. Such a granular approach allows us to tailor resilience strategies more effectively, addressing specific local challenges and enhancing the overall safety and comfort of residents in varying geographic and climatic conditions. We employed a geographical information

system (GIS) approach to visually convey the regional disparities in thermal vulnerability and resilience. Figure 8 presents the results, which averaged the peak HI of each residential building in a county, aggregating the data for all residential buildings in that county on the first day of a heatwave coincided with a power outage. The color gradient represents the severity of heat exposure measured by the HI. This county-level analysis reveals significant spatial disparities in thermal resilience. Counties in blue display relatively lower HI values, which suggests that residences in these areas maintained cooler conditions and their dwellings are indicative of better thermal resilience. The red-shaded counties, on the other hand, show higher HI values, signifying areas where the indoor conditions are likely more stressful and potentially hazardous, thus highlighting a greater need for effective cooling solutions and thermal design improvements in these counties. This breakdown can guide the state resource allocation for enhancing thermal safety.

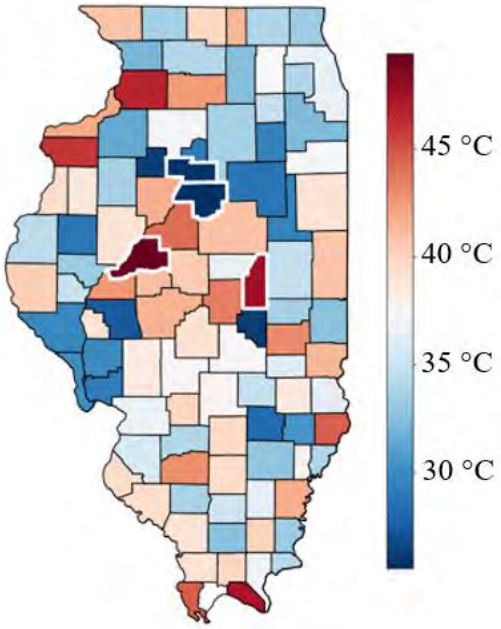

Figure 8: County level spatial distributions of HI.

Additional analysis was conducted for the most resilient and vulnerable counties in Illinois, outlined in white, in Figure 8. The most vulnerable counties, i.e. those with the highest HI are Piatt County with a mean HI of 47.7°C, and mean DBT of 35.6°C, and Mason County with a mean HI of 49.5°C, and a mean DBT of 35.5 °C. The most resilient counties in terms of HI are Woodford County, with a HI of 25.5°C and a mean DBT of 24.7°C, and Marshall County, with a HI temperature of 25.8 °C and a mean DBT of 25.5°C. We further correlated these counties with their socioeconomic status according to the federal poverty level (FPL). The FPL, an economic measure, uses a percentage to compare household income against the poverty threshold. Lower FPL percentages indicate incomes closer to the poverty line. Figure 9 shows that households with annual incomes below 100% of the FPL experience a wide range of HI values, suggesting these buildings are more prone to inadequate thermal control, elevating health risks during heatwaves and power outages. A similar pattern was observed in households with 150-200%, 200-300%, and 300-400% of the FPL. This suggests a correlation where lower-income households, which are often in buildings with less investment in thermal resilience measures, are at a greater risk during extreme temperature events. Our findings emphasize the need for targeted interventions in building design and energy assistance programs to protect vulnerable populations from extreme heat.

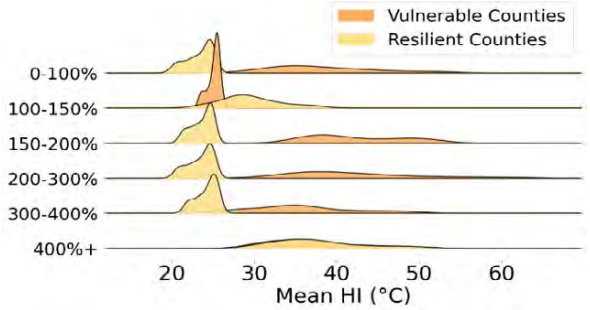

Figure 9: Heat disparities and socioeconomic status in the most resilient and vulnerable counties.

These findings not only illuminate the varying degrees of vulnerability across Illinois counties but also provide essential context for enhancing preparedness and resilience in the face of extreme temperatures and power outages. This analysis also allows us to delve deeper into understanding the building characteristics associated with vulnerability to overheating. This type of analysis can equip decision-makers with the knowledge needed to implement targeted strategies for improving the overall resilience of buildings and communities in the region.

4. LIMITATIONS AND FUTURE WORK

In this study, we used the ResStock energy models, which do not represent individual existing buildings but are based on building stock statistics and, in aggregate, have been validated to match measured energy data [17]. These models have not been validated in terms of indoor thermal conditions, and, therefore, their accuracy for these outcomes is unknown. Furthermore, we only used a 20% sample of Illinois residential buildings from the ResStock database for thermal resilience evaluation due to computational cost constraints. For more comprehensive analysis, future research could expand the dataset size, possibly using the full database to explore wider patterns and characteristics for building resilience evaluation across construction years and varying degrees of retrofitting. This would provide a more detailed understanding of the factors that contribute to thermal resilience in residential

buildings. In addition, nationwide thermal resilience evaluation also would benefit from identifying the vulnerable state and/or the most vulnerable counties across the nation, which is possible with this dataset and high-performance computing clusters.

Future research on building thermal resilience could incorporate more demographic data. National surveys like the U.S. Census can supplement ResStock models by providing detailed demographic information. This would allow users to quantify resilience measures through computing metrics like physiologically equivalent temperature (PET) and perceived temperature (PE). Additionally, our study assumed that occupants would open windows when outdoor temperatures are lower than indoor temperatures, but this may not always be true without empirical evidence or measurements of window-opening behavior during power outages. Therefore, there is a need to collect more data on such behaviors.

5. CONCLUSION

Our study developed a methodological framework which can investigate the vulnerability of residential buildings to extreme temperatures during power outages, a consequence of climate change-induced weather events. Through the use of ResStock models, our research demonstrates a means to understand the risks posed to indoor thermal conditions and delves into the factors influencing resilience. Building characteristics such as attic type, wall material, insulation, and infiltration are correlated with an infrastructure's ability to withstand extreme conditions. Our analysis shows that the HI reached critical levels indicating extreme caution and danger zones during blackouts, with the 85th percentile HI peaking at 52°C. This highlights the acute threat to occupant safety during simultaneous power outages and heatwaves. Moreover, our geospatial vulnerability assessment reveals regional disparities in thermal resilience across Illinois counties, correlating socioeconomic status with overheating vulnerability. This approach equips stakeholders with knowledge to develop targeted strategies for enhancing the overall resilience of residential infrastructure in the face of escalating climate challenges. Our research contributes not only to the understanding of building thermal dynamics but also offers a replicable methodology for future studies, guiding efforts to create thermally safe and climate-resilient communities.

REFERENCES

1. Anderson, G., & Bell, M. (2011). Heat waves in the United States: mortality risk during heat waves and effect modification by heat wave characteristics in 43 U.S. communities. Environmental Health Perspectives, 119(2), 210–218. DOI: 10.1289/ehp.1002313

2. Hondula, D., Balling, R., & Vanos, J. E. (2015). Rising temperatures, human health, and the role of adaptation. Current Climate Change Reports, 1, 144–154. DOI: 10.1007/s40641-015-0016-4

3. Smith, A. B. (2020). U.S. Billion-dollar Weather and Climate Disasters, 1980 - present (NCEI Accession 0209268), [Online], DOI: 10.25921/STKW-7W73 [05 June 2023].

4. National Oceanic and Atmospheric Administration (2021). 2020 U.S. billion-dollar weather and climate disasters in historical context, [Online], Available: https://climate.gov/disasters2020 [05 June 2023].

5. National Oceanic and Atmospheric Administration (2022). 2021 U.S. billion-dollar weather and climate disasters in historical context, [Online], Available https://climate.gov/news-features/blogs/beyond-data/2021-us-billion-dollar-weather-and-climate-disasters-historical [05 June 2023].

6. National Oceanic and Atmospheric Administration (2023). 2022 U.S. billion-dollar weather and climate disasters in historical context, [Online], Available: https://climate.gov/news-features/blogs/beyond data/2021-us-billion-dollar-weather-and-climate-disasters-historical [05 June 2023].

7. Sheng, M., Reiner M., Sun K., Hong T. (2023). Assessing thermal resilience of an assisted living facility during heat waves and cold snaps with power outages. Building and Environment, 230, 110001. DOI: 10.1016/j.buildenv.2023.110001.

8. White LM (2020). ASSESSING RESILIENCY AND PASSIVE SURVIVABILITY IN MULTIFAMILY BUILDINGS. *ASHRAE Top Conference Proceedings*. p. 144–155.

9. Sengupta, A., Deleu, J., Lucidarme, B., Breesch, H., & Steeman, M. (2023). Assessing Thermal Resilience To Overheating In An Office Building.

10. Sengupta, A., Breesch, H., Al Assaad, D., & Steeman, M. (2023). Evaluation of thermal resilience to overheating for an educational building in future heatwave scenarios. *International Journal of Ventilation*, 22 (4): p. 366–376. DOI: 10.1080/14733315.2023.2218424 10. Sengupta A.

11. ResStock, [Online], Available: https://resstock.nrel.gov [10 June 2023].

12. CLIMATE CHANGE IN ILLINOIS, [Online], Available: https://stateclimatologist.web.illinois.edu/climate-change-in-illinois [10 June 2023].

13. Chen K, Newman AJ, Huang M, Coon C, Darrow LA, Strickland MJ, et al (2022). Estimating Heat-Related Exposures and Urban Heat Island Impacts: A Case Study for the 2012 Chicago Heatwave. *GeoHealth*, 6(1), e2021GH000535. DOI: 10.1029/2021GH000535.

14. Chicago, IL Temperature Records, [Online], Available: https://www.weather.gov/lot/Chicago_Temperature_Records [10 June 2023].

15. NOAA. Heat Index, [Online], Available: https://www.noaa.gov/jetstream/global/heat-index [15 June 2023].

16. Ben-Alon L, Rempel AR. Thermal comfort and passive survivability in earthen buildings (2023). Building and Environment, 230, 110339.

17. Wilson E, Christensen C, Horowitz S, Horsey H (2016). A High Granularity Approach to Modeling Energy Consumption and Savings Potential in the U.S. Residential Building Stock. No. NREL/CP-5500-83077. National Renewable Energy Lab.

PLEA 2024 WROCŁAW
(Re)thinking Resilience

Modern Methods of Construction: Do we need them for a resilient net zero future for UK housing?

A performance comparison of MMC and traditional Masonry Housing

HARRY SUMNER[1,2], ESFANDIAR BURMAN[1]

[1]University College London, London, United Kingdom
[2] Bennetts Associates, London, United Kingdom

ABSTRACT: Against the backdrop of a global climate crisis and recent pandemic, the need for affordable, sustainable and future-resilient housing has never been greater. Despite having some widely acknowledged benefits in terms of quality and scalability, Modern Methods of Construction (MMC) are still relatively misunderstood and underutilised in the housing industry, with only 6 to 10% of new homes being built using MMC. Whilst the government is committed to increasing the number of new MMC homes, current literature lacks rounded analytic comparisons to support or reject the use of MMC for future UK housing stock. Using a building performance model, a RIBA Stage 4 MMC housing case study is assessed against a traditionally-built masonry counterpart. Three Key Performance Indicators (KPIs) are identified to provide a holistic view of performance: Operational Energy, Embodied Carbon and Summertime Overheating (CIBSE TM59). The results suggest that whilst there is an opportunity for high quality factory-led methods to reduce heating demand significantly by reducing linear thermal bridging, the challenge of reducing future climate resilience in lightweight MMC homes needs critical consideration. The need for more careful consideration of materials for whole life performance is highlighted, particularly when balancing opposing objectives such as reducing material weight and transportation costs, reducing upfront carbon, and improving passive cooling performance.
KEYWORDS: MMC; Modular Housing; Net zero; Upfront Carbon; Future Resilience.

1. INTRODUCTION

Against the backdrop of a global climate crisis and period of economic recession, the need for healthy, affordable and sustainable housing has never been greater. Despite having some widely acknowledged benefits in terms of quality and scalability, Modern Methods of Construction (MMC) are still relatively misunderstood and underutilised in the UK housing sector, less than 10% of new homes being built using MMC [1]. As the most accepted description in the UK to date, the MMC Definition Framework describes 7 categories of MMC covering a spectrum of building approaches from 2D and volumetric factory-led pre-manufacturing approaches through to site-led process improvements and innovations, each having different use cases and efficacies.

Whilst research has been conducted into the perceived drivers and barriers to wider MMC uptake generally, current literature lacks holistic numerical comparisons to support or reject these perceptions to allow them to be addressed. This paper offers a rounded, quantitative and qualitative assessment using a case study approach, comparing a RIBA Stage 4 MMC housing case study with a notional traditional masonry counterpart.

2. PREPARING THE MANUSCRIPT

As a nation, the United Kingdom (UK) has a history with MMC which links back to the post-war era and the associated national housing shortage. The Housing Act (1944) saw the Ministry of Works begin a government-led campaign to tackle the crisis, with the ambitious target of producing 500,000 'Emergency Factory Made' homes across the nation through a combination of military direction and private sector execution [2]. Such an immense undertaking required fast production, whilst minimising human and material resources, to avoid disrupting the existing supply chains. As such, prefabrication methods were adopted to produce a range of housing typologies, one of the most recognisable post-war 'pre-fabs' being the 'A' house semi-detached steel-framed structure (Fig. 1). Similar

Figure 1: Post-war prefabricated semi-detached houses, Harrow [3]

approaches were seen in the United States and Australia [4]. International procurement of pre-manufactured housing as early as the 1940s marked the beginnings of the global MMC market which exists today.

The magnitude of the housing shortfall in the UK at present is not dissimilar to that of the post-war shortage. From 2021, the Department for Levelling Up, Housing & Communities (DLUHC) is faced with supplying 345,000 homes annually to meet current demand for housing in the UK [5]. Whilst The Climate Change Act 2008 commits the UK Government to achieving 'net zero Carbon' by 2050, current projections show the nation falling short of the 2025 and 2030 carbon targets, with the likelihood of more challenging measures becoming a reality [6].

Considering the compounding demands and challenges the industry faces from: net zero 2050 targets; a UK Construction workforce that has decreased considerably in the last two decades [7]; and increased demand for healthy affordable homes to limit the housing crisis, it is crucial to investigate the net zero challenges and opportunities available through MMC for future housing in the UK. To date, qualitative research has identified various drivers for MMC housing uptake in the UK such as improved quality and improved sustainability [8,9,10], but few studies have numerically assessed MMC building performance.

3. LONG-TERM THINKING: BALANCING QUALITY AND QUALITY IN HOUSING DELIVERY

Buildings, in particular houses, are inherently designed to meet our fundamental human needs: providing shelter, security and comfort [11]. In recent years there has been growing concern over the quality, value and longevity of new housing stock in the UK. Beyond the usual on-site construction errors and defects which contribute to the operational performance gap [12] there are also particular concerns around the suitability of lightweight off-site construction for the future climate.

Whilst limited research has been conducted into the overheating of domestic modular construction, it is acknowledged to be a growing issue across UK housing with around 20% of homes already experiencing overheating even in relatively mild summers [13]. Despite the increasing climate challenge, when designing net zero housing comfort, wellbeing, and overall indoor environmental quality (IEQ) in buildings are still a priority to be achieved alongside low carbon design to avoid impacts on human health and unnecessary future remedial works.

4. METHODOLOGY

4.1 Comparative Case Studies

This paper aims to investigate whether there are benefits or disadvantages to the use Modern Methods of Construction in achieving net zero resilient housing in the UK, using a case study approach. Two case studies were chosen:

- **MMC Detached House Case Study**
  A 4-bedroom House which uses lightweight Linear Modular MMC construction. The case study was at RIBA Stage 4 at the time of the study and was a typology being repeated across a large housing development in the North West of England.
- **Traditional Masonry Counterpart**
  A 4-bedroom House which uses traditional methods of construction for UK housing. The geometry was all derived from the 'real' case study but uses a typical masonry construction as defined by Building Control approved build-ups and junctions.

The geometry (Fig. 2) was defined by the architects' drawings and was kept the same in both studies to provide a focus on the materials and construction method and to avoid a commentary on the specifics of this design.

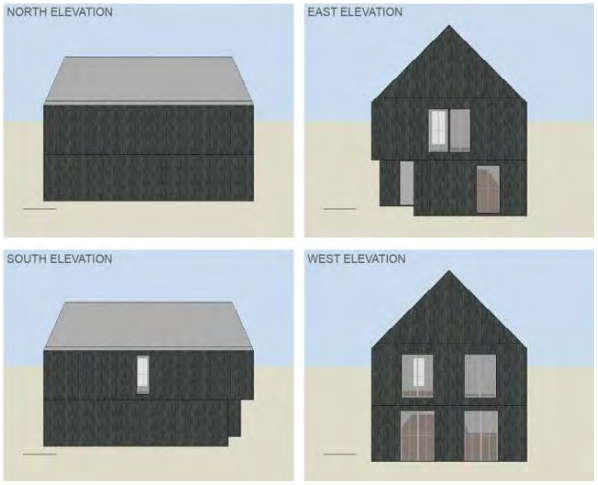

Figure 2: Building Performance Model Geometry

4.2 KPIs and Modelling Approach

This research aims to investigate whether there are benefits to the use Modern Methods of Construction in achieving net zero housing in the UK, using a case study approach. Three core KPIs were chosen to give an assessment of total performance: Cradle-to-gate Embodied Carbon (A1-A3) and Annual Operational Energy Use Intensity (EUI) to cover Net Zero performance criteria, and TM59 methodology assessing comfort and resilience against overheating (Table 1). All three metrics were assessed in the same building performance model using DesignBuilder (v6.1.8.21). Embodied Carbon was calculated using

the software's inbuilt tool, making hand calculation alterations where necessary (e.g. substructure and frame elements excluded from the thermal model). Information for the MMC Case Study was taken from RIBA Stage 4 documents whilst the comparative masonry case information was gathered from Local Authority Building Control approved junctions.

Table 1: Key Performance Indicators and relevant criterion.

KPI	Target Criterion	Period/ Scope
Operational Energy [14]	≤35 kWh/m²·yr	Annual
Embodied Carbon [14]	≤400 $kgCO_2e/m^2$	A1 - A3
Summertime Overheating (CIBSE TM59) [15]	(A) ΔT ≥1°K for ≤3% of occupied hours (B) bedrooms not >26°C from 22:00 -07:00 for > 1% of those hrs annually	(A) May to September (B) Annual

5. RESULTS AND DISCUSSION

5.1 Operational Energy

Operational Energy showed marginal variance between the cases with the central estimate being 41.0 kWh/m²·yr (Masonry) and 41.8 kWh/m²·yr (MMC) (Table 2). The primary difference observed was the level of heat loss at the roof where the MMC case has a reduced insulation specification versus the traditional case. In both cases the EUI is greater than the targeted value of 35 kWh/m²·yr, with the central estimate exceeding by 17.1% for the MMC case. The case study uses a relatively moderately performing Air Source Heat pump with nominal COP of 2.6 meaning heating consumption is significantly lower than if a traditional boiler were used.

Table 2: Summary of Operational Energy predictive results for the Central Estimate (applying 50% SAP 10.2 Ψ-values)

Operational Energy Breakdown and Total (kWh/m²·yr)					
	Heating	DHW	Lighting	UELs	**Total**
MMC	10.6	8.0	3.7	19.6	**41.8**
Masonry	9.7	8.0	3.7	19.6	**41.0**

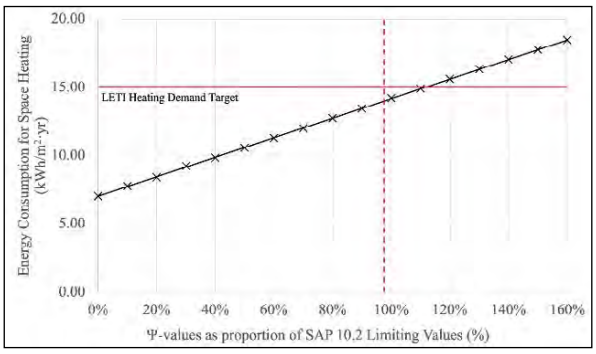

Figure 4: Impact of Linear Thermal Bridging upon Annual Energy Consumption for Space Heating

By using high quality factory-led construction it is believed improved thermal bridging can be a potential beneficial attribute for MMC housing over traditional methods. For the Central Estimate, 50% of SAP 10.2 Values [16] were assumed across all junctions. In the MMC case study, three junctions (Lintels, Wall-ground floor, Roof-wall) accounted for 70% of heat losses across all junctions. A sensitivity analysis showed that linear thermal bridging has a significant impact on Heating Demand, which could be reduced by 50% if bridges were eliminated in the case study through factory-led methods, versus a design with policy limiting ψ-values (Fig. 4). If a thermal bridge-free design were achieved for the MMC case, the EUI would reduce to 38.3 kWh/m²·yr, however it could be argued relatively negligible for the overall net zero balance as heat sources and the grid decarbonise further.

5.2 Embodied Carbon (A1-A3)

The main body of the analysis considers the 'cradle to gate' life cycle stages A1-A3 as defined in BS EN 15978 [17] which includes the emissions relating to material extraction, transport, and manufacturing but not the transport to site and construction emissions. On average this accounts for 80% of embodied carbon for small residential buildings in the UK, meaning that the target can be estimated to 400 kgCO2/m2 for stages A1-A3 based on LETI guidance [14].

The margins between the two cases are negligible, and both fell below 350 $kgCO_2e/m^2$ showing reasonable performance (Fig. 5). A comparison of the two cases shows the Traditional Masonry case outperforming the MMC case study by 2.1% with the key differences occurring in the building fabric, superstructure, and substructure. The relative impact of the superstructure is greater in the MMC case. The Masonry and Concrete blockwork act as a load-bearing compression system and façade in the traditional case, whilst for the MMC Case study, there is a requirement for additional glue-laminated timber framing elements (columns and beams) to provide vertical and lateral support to the perimeter of prefabricated SIPs panels.

Despite this additional structure, the highest contribution related to the building fabric which

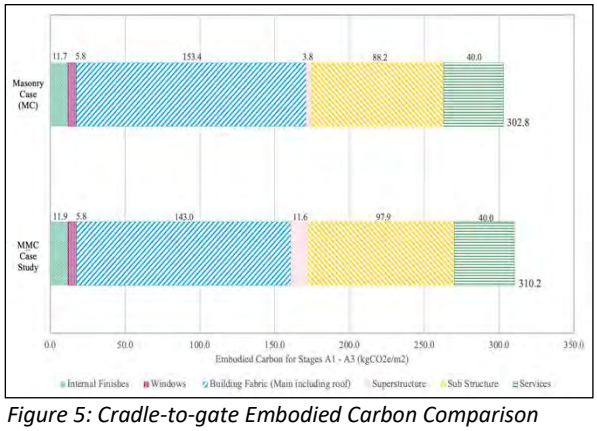

Figure 5: Cradle-to-gate Embodied Carbon Comparison for both cases

accounted for 46.1% of A1-A3 emissions in the MMC case. This indicates there is a need for greater focus on comparing upfront embodied carbon savings within the building fabric against the operational impacts upon heating and cooling demand across the building life to better inform decision-making.

5.3 Summertime Overheating

Both case studies were assessed against a series of weather files from the PROMETHEUS database of future weather data [18]. The weather files align to a series of scenarios: a baseline; 2030 central estimate, and stress tests for each case study (Table 3). The weather files increase in severity when moving from the medium emissions to the high emissions scenarios, and from the 50th to 90th percentile scenarios (Fig. 6).

Table 3: Weather files and Test Cases for Overheating Study

Period	Emissions Scenario	Test Scenario
Current	Current	Baseline
2030	Medium 50th Percentile	Central Estimate
2030	Medium 90th Percentile	Stress Test
2030	High 50th Percentile	Central Estimate
2030	High 90th Percentile	Stress Test

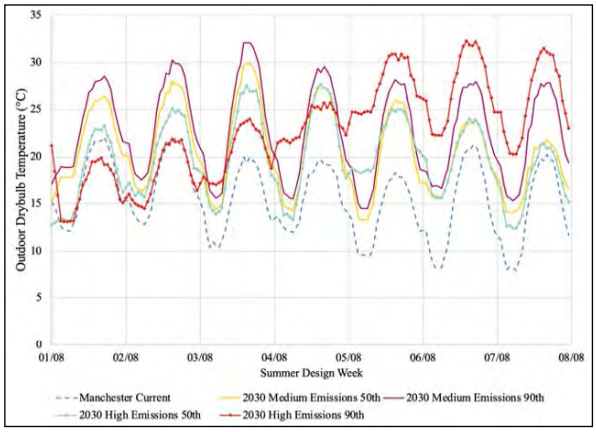

Figure 6: Comparison of Outdoor Dry-bulb Temperature for August 01 – 07 for 5 current and future weather files

Focusing primarily on the CIBSE TM59 Criterion A (% Overheating hrs), the Masonry case significantly outperforms the MMC case across all zones and test scenarios. When analysing just the zones at high-risk for overheating (kitchen-diner, southern bedroom) the results suggest that the traditional masonry housing is more resilient to future overheating than MMC-led housing which prioritise lightweight construction (Fig. 7). In the High Emissions Stress test 4 out of 6 zones failed across either TM59 Criterion A or B for the MMC case whilst only 1 failed in the Traditional Masonry case.

Analysing the internal temperature during a reference summer week for the two high risk areas suggests two potential issues for the MMC case study in the stress test scenario:

(i) *Highly Airtight and Insulated walls* - During the design summer week (01 - 08 Aug) the operative temperature in the kitchen-diner stayed notably higher during the night in the MMC case (up to 2°C). This suggests insufficient background ventilation and highly insulated walls retain heat gains from equipment during the unoccupied night-time hours.

(ii) *Lack of thermal mass* - During the design summer week (01 - 08 Aug) the operative temperature in Bedroom 2 closely follows outdoor air temperature whilst the masonry shows a clear thermal lag between zone and external air temperatures, benefitting from exposed thermal mass to delay temperature peaks (Fig. 8).

Whilst it is acknowledged that the results relate to a specific case study, the factors contributing to a more significant overheating risk in the MMC case (i.e. high airtightness, well insulated and low thermal mass) are factors typical in MMC housing due to a

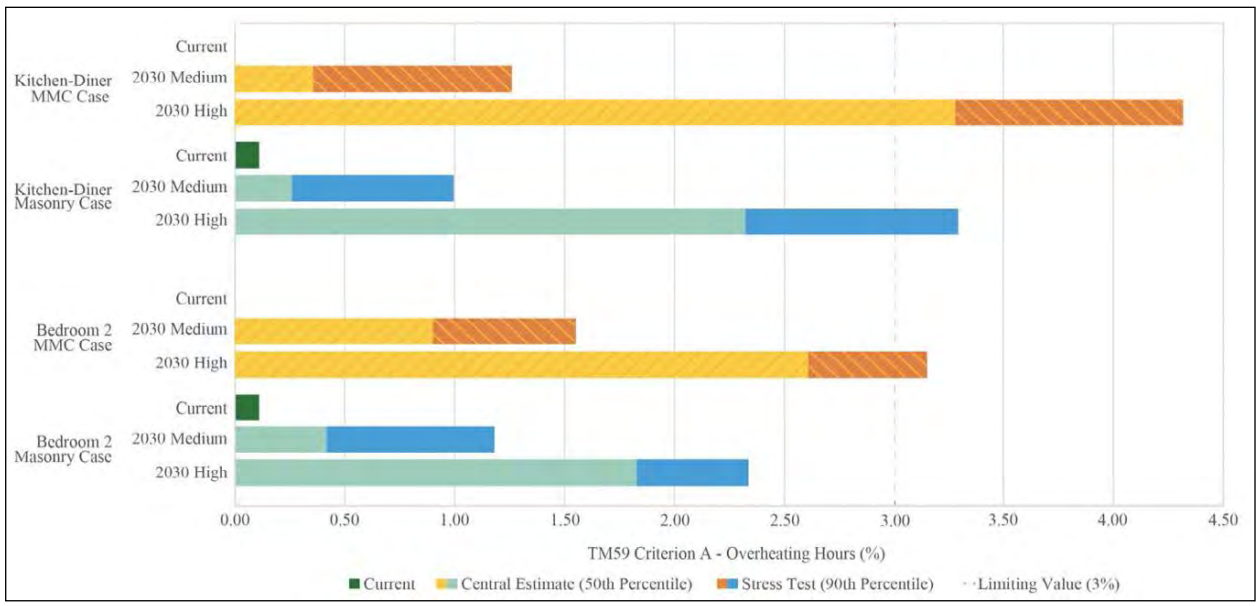

Figure 7: Comparison of TM59 Criterion A Overheating Hours for MMC and Masonry Case by Zone

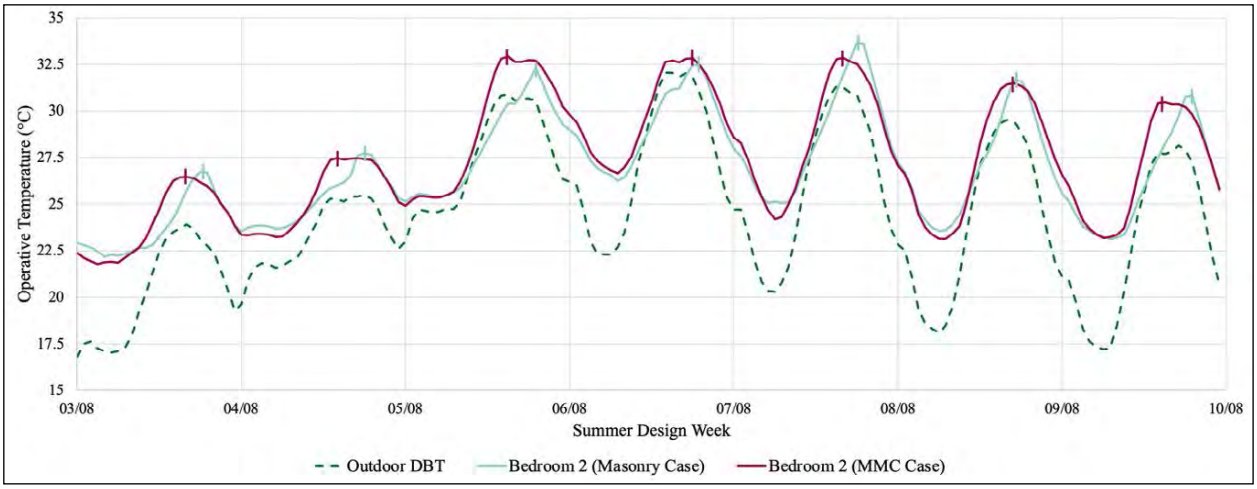

Figure 8: Comparison of Bedroom 2 Overheating for MMC and Masonry Cases for August 03 – 09, 2030 High Emissions 90th Percentile (Stress test)

focus on high quality factory-led manufacture and the need to reduce loading for transportation and site safety. In the move to future resilience housing thermal mass needs to be considered a priority for its passive cooling potential. Whilst the net operational carbon savings may be low [19] or net-neutral for housing (due to relatively low cooling loads), thermal mass is anticipated to have high efficacy in terms of comfort in the Northern European context over the lifespan of new buildings [20] limiting reliance on mechanical cooling (and the grid) and improving life preservation in the case of extreme climate events.

6. CONCLUSION

MMC offers some clear benefits in the context of achieving net zero in terms of quality control, thermal continuity, and heating demand reduction. The studies demonstrated relatively comparable results for the MMC and traditional masonry case for operational energy and A1-A3 embodied carbon, however it was identified that with adequate detailing, factory-led MMC methods have the potential to reduce heating demand by 50% by eliminating thermal bridging.

In the TM59 assessments the Masonry Case significantly outperformed due to its higher thermal mass, with the MMC case failing Criterion A in the 2030 Medium and High stress tests (90th Percentile). Whilst assessment against future climate data is not yet a regulatory requirement in the UK, it is evident that not considering this at design stage will result in inadequate future performance. The results highlights the need for more rigorous analysis of overheating in the context of new MMC housing, in particular lightweight timber prefabricated systems, balancing the upfront and whole life carbon impacts of opting for materials with higher thermal mass. The term 'MMC' encompasses a wide range of building techniques but does not define material selection; as such, despite trends towards lightweight construction, thermal mass and MMC do not have to be mutually exclusive qualities.

Critically, if overheating resilience is not addressed in new building stock, there will be significant future impacts both on carbon and occupant wellbeing. Carbon savings achieved through pre-manufacture are likely to be lost through the need for retrofit measures and active cooling over the life cycle of the building. Thus, further understanding of material specification and its impacts upon overheating resilience and whole life carbon is needed to avoid new housing stock becoming prematurely obsolete, in turn resulting in further embodied carbon impacts for rectifying or replacing.

ACKNOWLEDGEMENTS

Sincere thanks to Dr Joe Jack Williams and FeildenCleggBradley Studios for their support in executing this research, and to the Institute for Environmental Design and Engineering (UCL) for facilitating this conference submission.

REFERENCES

1. Savills (2020) Modern Methods Of Construction UK Cross Sector-Spring 2020: What can MMC offer the housebuilding industry in the UK?. Available from: https://pdf.euro.savills.co.uk/uk/spotlight-on/spotlight-modern-methods-of-construction-spring-2020.pdf
2. Hashemi, A. (2013). Review of the UK housing history in relation to system building.
3. Abbott, J. (n.d.). Prefabricated Houses, Harrow Weald – Modernism in Metroland. [Online]
Modernism in Metro-land. Available from : https:// www.modernism- inmetroland.co.uk/prefabricated-houses-harrow-weald.html [Accessed 28/11/21].
4. Hearn, J. (2018). A short history of prefabrication | History, Design | Prefab Museum. [Online]
Available from: https://www.prefabmuseum.uk/content/history/short-history-prefabrication [Accessed 28/11/21].
5. Wilson, W. and Barton, C., (2021). Tackling the under-supply of housing in England housing in England. Available: https://researchbriefings.files.parliament.uk/documents/CBP-7671/CBP-7671.pdf

6. Climate change targets: the road to net zero?. [Online] Available: https://lordslibrary.parliament.uk/climate-change-targetsthe-road-to-net-zero/.
7. Employment by industry - Office for National Statistics, [Online], Available: https://www.ons.gov.uk /employmentandlabourmarket/peopleinwork/employment andemployeetypes/datasets/employmentbyindustryemp13
8. Goodier, C. and Gibb, A. (2007). Future opportunities for offsite in the UK. Construction Management and Economics, 25(6), pp. 585–595.
9. Nadim, W. and Goulding, J.S. (2010). Offsite production in the UK: The way forward? A UK construction industry perspective. Construction Innovation, 10(2), pp. 181–202.
10. Elnaas, H., Didado, K. and Ashton, P. (2014). Factors and Drivers Effecting the Decision of Using Off-Site Manufacturing (OSM) Systems in House Building Industry. Journal of Engineering, Project, and Production Management, 4(1), pp. 51–58.
11. Race, G.L. (2006) KS6: Comfort. 1st ed. London: CIBSE.
12. van Dronkelaar, C. et al. (2016) A Review of the Regulatory Energy Performance Gap and Its
Underlying Causes in Non-domestic Buildings. Frontiers in Mechanical Engineering, 1, p. 17.
13. Potton, E. and Hinson, S. (2020) Housing and Net Zero. [Online]. Available from: www.parliament.uk/ commons-library|intranet.parliament.uk/commons library. [Accessed 24/12/2021].
14. Low Energy Transformation Initiative, (2020). LETI Climate Emergency Design Guide. *LETI.* London.
15. CIBSE, (2017) TM59 Design methodology for the assessment of overheating risk in homes. *Chartered Institution of Building Services Engineers.* London.
16. DfBEIS, (2022). The Government's Standard Assessment Procedure for Energy Rating of Dwellings - Version 10.2. *BRE Garston for DfBEIS.* Watford.
17. British Standards Institute (2011) BS EN 15978:2011 Sustainability of construction works.
18. Eames, M., Kershaw, T. and Coley, D. (2011). On the creation of future probabilistic design weather years from UKCP09. *Building ser. Eng. Res. Technol.* London. Sage Publications UK, pp 127-142.
19. Sansom, M. and Pope, R.J. (2012). A comparative embodied carbon assessment of commercial buildings. The Structural Engineer, pp. 38–48
20. de Toldi, T., Craig, S. and Sushama, L. (2022). Internal thermal mass for passive cooling and ventilation: adaptive comfort limits, ideal quantities, embodied carbon. Buildings and Cities, 3(1), p.42–67.

PLEA 2024 WROCŁAW
(Re)thinking Resilience

Optimizing Daylighting:
Exploring Visual and Non-Visual Effects through Weather, Orientation, and Location

LILIANA O. BELTRÁN[1], LUMING XIAO[1]

[1]Texas A&M University, Department of Architecture, College Station, USA

ABSTRACT: This paper presents a comprehensive analysis of daylight performance in a standard office across twelve different locations. The assessment covers both the visual and non-visual impacts of daylight, taking into account aspects such as vision, glare, view quality, and circadian rhythms. Evaluation criteria are based on the prerequisites for daylight and view credits outlined in LEED v.4 [1], in conjunction with the WELL 2.0 Building Standard [2] for daylighting evaluations. The assessed space is outfitted with sidelight windows, representing a typical section of an office within a multi-story building. The study's findings shed light on how daylight performance is influenced by geographical location, prevailing weather conditions, window dimensions, shading devices, glass transmittance, and floor plate depth. Notably, the study demonstrates the feasibility of designing spaces that meet the daylight and view credit criteria of LEED v.4 while complying with the circadian lighting requirements of WELL 2.0 in diverse locations. Achieving this goal relies on implementing window systems that provide ample bright light while employing minimal window size and shading devices to control glare at occupants' eye level.
KEYWORDS: Daylighting, Equivalent Melanopic Lux, LEED, WELL Standard, Healthy Buildings

1. INTRODUCTION

The benefits of daylighting have been widely documented by numerous researchers. Daylighting serves as an effective strategy to reduce reliance on electric lighting, diminish cooling and heating loads, and enhance human comfort, well-being, and productivity [3]. This paper analyses the application of the daylight metrics developed by the Illuminating Engineering Society (IES) LM-83-12 Standard [4] adopted by LEED v.4 [3], and the WELL 2.0 Q4 2023 [2] Building Standard, across twelve diverse locations. Even though the latest LM-83-23 [5] release, an updated version of the LM-83-12 Standard includes changes such as a reduced illuminance threshold value of 150 lux for spaces with minimal visual tasks, a dirt depreciation factor, and a higher Annual Sun Exposure of up to 20%.

The latest WELL 2.0 Standard mandates an Equivalent Melanopic Lux (EML) exceeding 150 EML (1 point) or 275 EML (3 points) at vertical viewing positions. Moreover, the WELL standard offers an alternative provision for projects with enhanced daylighting, providing 3 points for Circadian Lighting attainment when a project achieves 180 EML and a spatial daylight autonomy (sDA300,50%) of more than 75% and annual sunlight exposure (ASE) less than 10% of occupied floor area, between 8:00 and 18:00 hours.

This paper explores the feasibility of achieving both the LEED v.4 (sDA300,50%> 75%, ASE <10%) and the WELL 2.0 (EML>200, EML>275) points concurrently in regularly occupied spaces.

2. METHODOLOGY

Twelve locations were chosen, ranging from latitudes 0° to 65° in the Northern Hemisphere (refer to Table 1). These locations represent a variety of climates, featuring distinct sky conditions that vary from predominantly clear skies (e.g., Phoenix) to consistently overcast skies (e.g., Caracas and Anchorage). Moreover, they experience varying durations of daylight throughout the year, with shorter daylight hours in winter days (around 7.5 hours) and longer summer days (up to 18 hours). In Fig. 1 three sky types (clear, partly cloudy and cloudy) are depicted across three locations (Quito, Phoenix and Anchorage) showcasing their respective monthly percentages (displayed in the left column) and the fluctuating monthly hours (presented in the right column).

A typical south-facing office space was modeled in Rhino, featuring windows on a single façade that represents a section of a deep open-plan office measuring 3.0 m high, 6 m wide, and 9.1 m long. The space includes a window spanning from 4.5 m to 5.7 m wide and 1.5 m to 2 m high, with a visible transmittance (Tvis) ranging from 60% to 70%. Additionally, the window wall ratio (WWR) varies from 40% to 70%. The interior surface reflectances are 0.7 for the ceiling, walls, and shading and 0.2 for the floor. No blinds were used in the simulations.

Table 1: Locations, latitude, and annual sky types (%).

Location	Latitude	Clear Sky	Partly Cloudy	Cloudy
Quito	0.1	9	87	4
Caracas	10.6	10	34	56
Puerto Rico	18.4	13	64	22
Miami	25.8	18	61	21
Houston	30.0	26	41	33
Phoenix	33.4	69	21	10
San Francisco	37.6	29	48	23
New York	40.7	14	54	32
Boston	42.3	26	39	35
Seattle	47.4	16	30	53
Edmonton	53.6	34	33	33
Anchorage	61.1	14	28	58

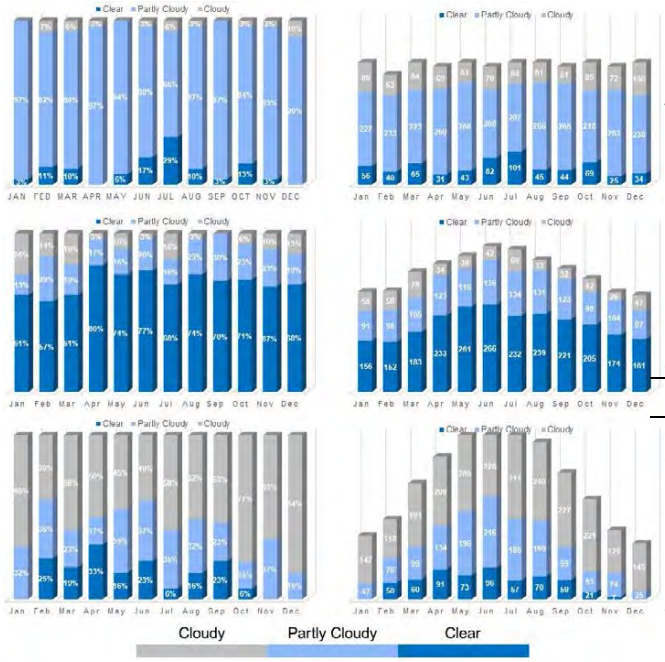

Figure 1: Sky types of Quito (top), Phoenix (center) and Anchorage (bottom); monthly percentages (left column) and monthly hours (right column).

The Rhino office model was linked to the RADIANCE-based ClimateStudio 1.9 [6] plugin in Grasshopper to generate climate-based annual hourly illuminance data for 150 sensors within the space. Each location underwent over 1,000 iterations (see Table 2). Simulations meeting the criteria to attain 4 points of LEED v.4 daylight credits were chosen. These selected simulations were compared against WELL's EML circadian metrics, in addition to the mean autonomous UDI (Useful Daylight Illuminance), the disturbing glare across regularly occupied floor area sDG (Spatial Disturbing Glare) and LEED VF (View Factor) 3 or above. For simulating the non-visual effects of light, the Multispectral Lighting Simulation Grasshopper plugin (Lark v.3.0) [7, 8] was utilized. Lark specifically simulated the EML values (over the 150 locations at 1.2 m high of 8 vertical view directions, totaling 1,200) exceeding 200 and 275 EML, in more than 75% of floor area, in spaces that met the criteria for 4 points of LEED v.4 (sDA>75%, ASE>10%, and VF>3) around noon during the solstices (March, September) and equinoxes (June, December).

3. RESULTS

The outcomes from the parametric runs of LEED v.4 and WELL 2.0 metrics across the 12 locations are depicted in Fig. 2 and Table 2. A higher number of cases meeting the LEED v.4 criteria were observed in regions with lower latitudes, specifically between 0° and 30°. However, at latitudes above 30°, the number of iterations decreased due to the meticulous selection of windows and shading devices tailored to diverse sky conditions and solar geometry. Notably, Quito demonstrated the highest count of LEED v.4 compliant cases among the locations studied, consistently maintaining partly cloudy sky conditions throughout the year. Surprisingly, despite Phoenix, receiving the highest annual incident daylight (138 lux-hours x 106 [9], positioned at an intermediate latitude with more clear days annually, it only met 1/9 and 1/5 of the LEED v.4 metrics criteria achieved by Quito and Caracas, respectively.

Table 2: Iterations, LEED v.4, and EML>200 cases over 75% of floor area in June.

Location	Iterations	LEED v.4	75% EML>200
Quito	972	962	145
Caracas	972	554	7
Puerto Rico	972	285	35
Miami	972	138	20
Houston	972	104	90
Phoenix	128	103	0
San Francisco	128	81	0
New York	128	56	0
Boston	128	50	0
Seattle	128	47	0
Edmonton	128	29	0
Anchorage	128	10	8

3.1 sDA, ASE, UDI and sDG

Table 3 presents a summary of four visual metrics for the 12 south-facing locations. Overall, all locations achieved high sDA values. The highest $sDA_{300,50\%}$ of 100% occurred in latitudes 30° and below, with a similar ASE of 7%. Higher latitudes achieved a slightly lower sDA (ranging from 91% to 99%), except for Anchorage, which achieved 85% (refer to Figure 2). Notably, at these latitudes, the sDA is lower at the rear of the space. This decrease in sDA is attributed to extensive shading used to control sunlight.

The average autonomous UDI in low latitudes (0° to 33°) exceeds 80%. However, in higher latitudes (above 37°), UDI declines due to lux values dropping below 100 lux at the back and center of the space, coupled with excessive UDI exceeding 3,000 lux at the front. Overall, the percentage of sDG throughout the

floor area remains relatively consistent, ranging from 19% to 28%. Nonetheless, Anchorage showed the highest sDG, reaching 33% of the floor area. This higher sDG in Anchorage is likely attributed to lower sun angles, causing shading devices to obstruct most of the year's sunlight from entering the occupant's eyes (at 1.2 m) and back wall without reaching the work plane.

Table 3: Summary of visual metrics (%) of the 12 South-facing locations.

Location	sDA	ASE	UDI	sDG
Quito	100	7	77	26
Caracas	100	7	81	19
Puerto Rico	100	7	82	28
Miami	100	7	80	19
Houston	100	7	80	20
Phoenix	99	10	80	26
San Francisco	100	5	77	21
New York	98	5	71	21
Boston	95	1	71	23
Seattle	97	0	68	22
Edmonton	91	7	64	25
Anchorage	85	4	57	33

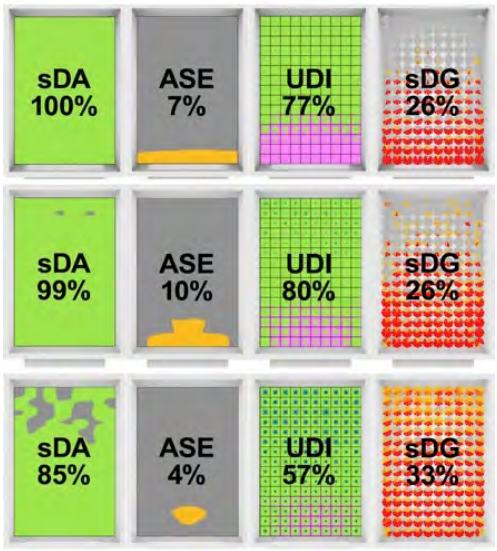

Figure 2: sDA, ASE, UDI, and sDG of the South-facing room in Quito (top), Phoenix (center), and Anchorage (bottom).

3.2 Circadian Lighting and Views

The recommendations set forth by the International WELL Building Institute for office spaces require vertical light levels at the occupant eye level that surpass the horizontal task plane illuminance metrics established in LEED v.4 [10].

Table 4 provides a summary of the results derived from parametric simulations, focusing on EML values exceeding 200 and 275 during March, June, September, and December across the twelve locations. June consistently exhibits the lowest EMLs across all locations, while December records the highest. It is evident that none of the locations achieved EML values exceeding 275 over 100% of the floor area throughout the year. In this study, specific workstation locations, as defined by the WELL 2.0 standard, were not determined. Instead, the aim was to attain EML values exceeding 275 (WELL 2023) and 200 (WELL 2029) across 75% of the floor area during the solstices and equinoxes. Observations reveal that EML values exceeding 200 are consistently met throughout the year in lower latitudes (below 30°) from Quito to Houston. Even in Caracas, characterized by predominantly cloudy conditions, EML values exceeding 200 covers over 76% of the floor area in June. The exception among higher latitudes in Anchorage, where over 81% of the floor area meets EML values exceeding 200. In latitudes above 33°, however, EML values surpassing 200 covers less than 72% of the floor areas in June.

None of the 12 locations achieved EML values exceeding 275 across 75% of the floor area in June, with Quito reaching just over 72%. Yet, in other months like December, all locations successfully achieved EML values exceeding 275, ranging between 82% and 100% of the floor area, as illustrated in Table 4 and Fig. 3's right column.

Table 4: Percentage of the floor area of EML>200 (upper) and EML>275 (lower) at noon.

Location	Mar.	Jun.	Sep.	Dec.
Quito	88	83	85	99
	76	72	69	83
Caracas	85	76	84	99
	75	66	74	90
Puerto Rico	88	80	91	100
	76	69	77	85
Miami	83	81	90	100
	72	70	77	85
Houston	95	81	90	100
	80	69	78	89
Phoenix	80	66	80	96
	66	57	69	82
San Francisco	76	68	78	89
	65	56	67	80
New York	75	70	77	100
	64	59	68	92
Boston	81	71	75	100
	70	59	64	97
Seattle	87	72	89	100
	74	61	76	100
Edmonton	72	70	77	100
	61	58	65	99
Anchorage	97	81	99	97
	88	69	92	90

Fig. 3 depicts the distribution of EML by vertical view directions across the space in Quito, Phoenix, and Anchorage. As expected, areas adjacent to the window plane consistently register the highest EML values across eight vertical view directions

throughout the year. These areas, covering approximately one-third to half of the floor area, consistently register high EMLs. Next to this region is an intermediate area, where view directions facing the windows achieve EML values exceeding 275, whereas those facing the back wall fall below 200 EML. Moreover, areas closer to the back wall show EML values exceeding 200 but below 275 EML. The distribution of EML values heavily relies on daylight that reflects off the side and rear walls.

Fig. 4 illustrates the illumination perceived by occupants in December in Quito, Phoenix, and Anchorage. The floating spheres in the space indicate potential workstation locations at the occupant's eye level (1.2 m). In low latitudes, the brightest area (>2,500 lux) is concentrated around the front of the room, creating an overall bright space. However, in Anchorage, due to the low sun position, the side and back wall receive a substantial amount of light. Occupants facing the window also experience bright light, which results in EMLs above 90% of floor area, while the sDG in Fig. 3 confirms the prevalence of disturbing glare mainly in directions facing the window.

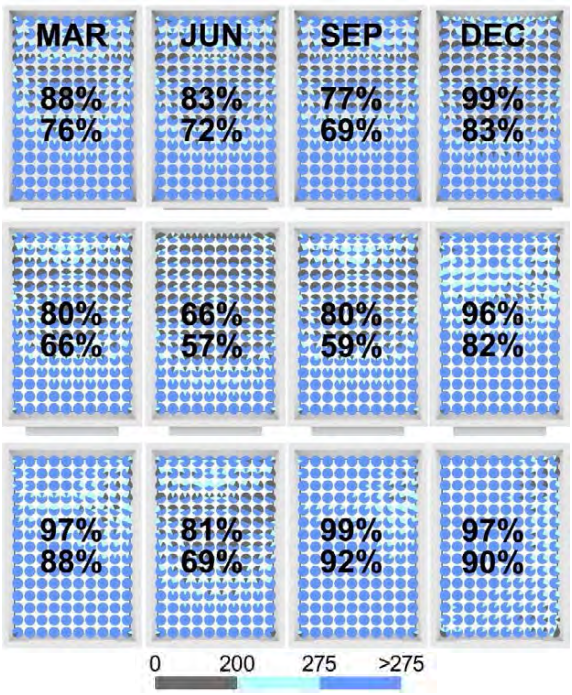

Figure 3: EML>200 (top number) and EML>275 (bottom number) of Quito (top row), Phoenix (center row), and Anchorage (bottom row) in solstices and equinoxes.

3.3 Views and Projection Factors

The parametric simulations included the selection of shading devices intended to intercept direct sunlight while preserving occupants' external views. The Projection factor (PF) denotes the degree to which daylight penetration through a window is obstructed by external shading. Consequently, higher PF values correspond to lower sDA, ASE, and EMLs. Fig. 5 illustrates the noticeable increase in PFs corresponding to latitudinal changes from 0° to 62°. Specifically, south-facing facades in low latitudes (0°–20 °) necessitate minimal shading devices (PF Horizontal, PFH 0.2 to 0.6; PF Vertical, PFV 0 to 0.1) to align with LEED and WELL metrics. In intermediate latitudes (25°–50°), extended shading is required (PFH 0.8-1.4; PFV 0-0.1), while higher latitudes (>50°) mandate extensive shading that substantially obstructs the window glass (PFH 1.3-2, PFV 0.2).

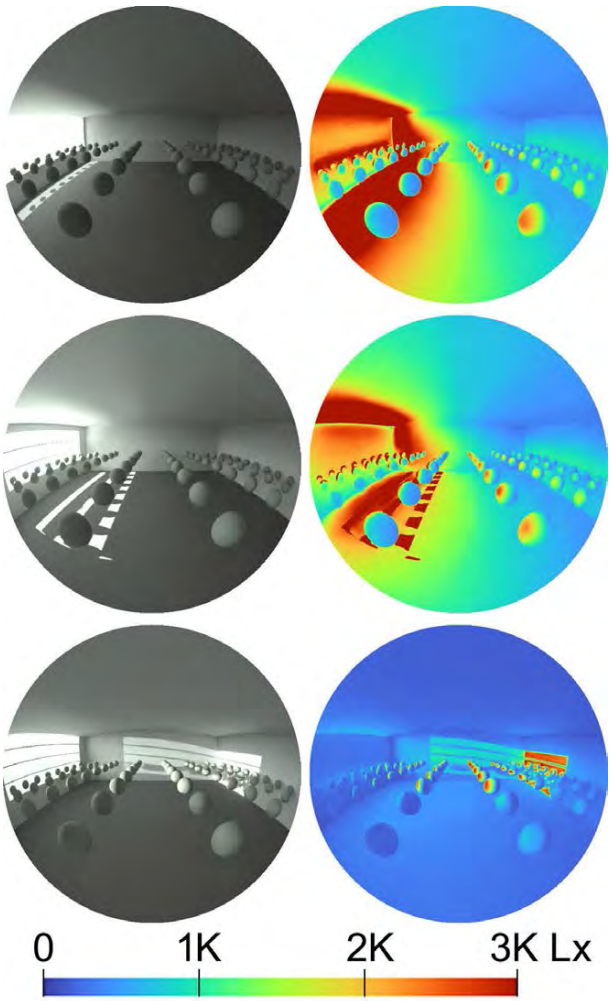

Figure 4: Renderings and False Colors (illuminance) of Quito, Phoenix, and Anchorage in December.

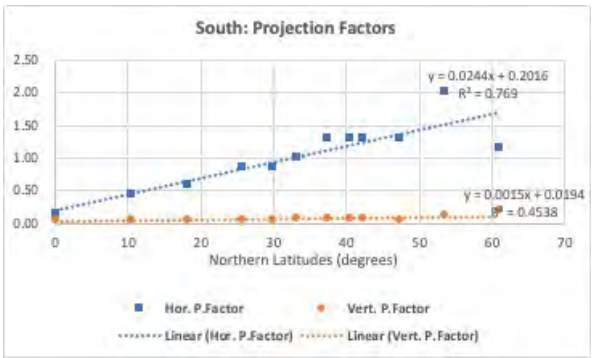

Figure 5: Horizontal and Vertical Projection Factors.

All EML cases met the LEED's v.4 View Factor requirement of 3, allowing for vertical and horizontal view angles (hVAs and vVAs) exceeding 40°. Fig. 6 showcases the view angles observed across the twelve locations. As anticipated, the trend lines of view angles contrast with those of the PFs (Fig. 5). The hVAs decreased from 81° to 29° from low to high latitudes, attributed to lower sun angles and the use of deeper shading devices. Conversely, vVAs consistently ranged between 90° and 80°.

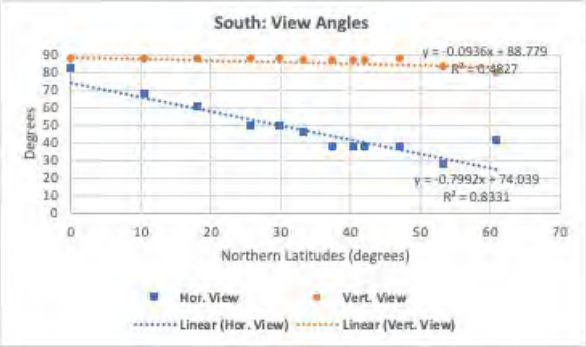

Figure 6: Horizontal and vertical view angles.

Table 5 provides a summary of WWR, Tvis, and the overall area of shading devices. Low latitudes exhibited larger window areas, approximately 67% of wall area, with fewer shading devices. This trend was attributed to predominantly cloudy and partly cloudy skies from Quito to Houston. Intermediate latitudes showed a reduced WWR, approximately 30%, compared to low latitudes, with larger shading areas. Higher latitudes (above 47°) displayed a slightly large WWR in comparison to intermediate latitudes, along with extensive shading, such as in Edmonton (Table 5). The Tvis of glass remained consistent across all locations.

Table 5: WWR, Tvis, and Total Shading Area (m^2).

Location	WWR	Tvis	Shading Area
Quito	0.67	70%	3.1
Caracas	0.67	70%	6.6
Puerto Rico	0.67	70%	8.4
Miami	0.67	70%	11.9
Houston	0.67	70%	11.9
Phoenix	0.48	70%	10
San Francisco	0.48	70%	13
New York	0.48	70%	13
Boston	0.48	70%	13
Seattle	0.54	70%	14.5
Edmonton	0.51	70%	21.2
Anchorage	0.56	70%	15.8

4. DISCUSSION

- Despite meeting current LEED v.4 requirements, none of the 12 locations achieved the existing EML>275 recommendations at 100% in all workstations. Achieving higher EML values at 100% of workstations may require narrower or less deep spaces. Additionally, EML values were highest for view directions facing the windows and lowest for those facing the back wall, suggesting that sidelight windows alone may not be the most effective daylighting system. Employing other systems such as additional windows, top lighting (clerestory or skylights), horizontal solar light pipes, supplementary electric lighting, blue-tinted glass, or interior wall colors tinted in blue could augment daylighting. Solar light pipe studies [11] have shown that they can be effectively used in facades oriented toward the East, South, and West. Moreover, increasing window sizes with high thermal performance, like triple-pane low U-value (or high R-value) and low SHGC, could be beneficial. Otherwise, energy-efficient LED lighting can be designed for workstations to achieve the required 275 EML values. An evaluation by researchers at PNNL on an existing building in Chicago, IL revealed challenges in meeting the EML levels of WELL v2 2019 at 100% of workstations in an open office space, even with supplementary electric lighting.
- The control of sunlight beyond ASE metrics is crucial to prevent direct glare in workstations facing southern directions, particularly in high latitudes. Maintaining at least a view factor of 3, in combination with LEED and WELL metrics, can ensure visually comfortable spaces, providing various health benefits to occupants.
- Our parametric lighting simulation, including renderings and false-color images, effectively highlighted interior spaces' responses to glare and high EML values at occupants' view directions. These visual representations provide valuable insights for designers to address lighting issues. However, there is currently a lack of metrics or parametric tools that report outcomes in three dimensions.
- Studies have demonstrated the positive effects of visual connections to the outdoors on occupants' health, well-being, cognitive performance, and stress recovery [12]. Combining LEED and WELL metrics with at least a view factor of 3 can ensure occupants' visual comfort and promote their health. All the cases of this study achieved a view factor of 3.

5. CONCLUSION

The results demonstrate the feasibility of meeting the LEED v.4 lighting and view requirements across all 12 locations while managing thermal loads through relatively smaller Window-to-Wall Ratios (WWRs) and minimal shading. In most locations, the WELL 2.0

EML>200 values were consistently achieved throughout the year, except for five high-latitude areas. To improve EML values in these high-latitude regions, larger WWRs and shorter shading devices might be necessary. However, these modifications could potentially impact cooling and lighting loads [13]. It is notable that Spatial Disturbing Glare (sDG) tends to increase with larger WWRs and sun exposure.

Designing for circadian lighting demands a meticulous approach to window system design, aiming to provide bright light, preferably from reflected sunlight bouncing off shading devices and interior reflectors towards the ceiling. Balancing the control of sunlight without compromising outdoor views poses a challenge for architects and lighting designers worldwide. Leveraging daylight has the potential to significantly enhance the quality of life and the overall health of building occupants.

ACKNOWLEDGEMENTS

The authors would like to thank the Texas A&M University Triads for Transformation, T3 Grant (ID #1729) for funding this research project.

REFERENCES

1. U.S. Green Building Council, (2013). LEED v.4 Reference Guide for Building Design and Construction**.**
2. WELL Building Standard v2, (2023). [Online], Available: https://devwellv2.wellcertified.com/wellv2/en/overview**.**
3. Heschong Mahone Group, (2012). Daylight metrics—PIER Daylighting Plus Research Program. [Online], Available: http://www.h-m-g.com/DaylightPlus/Daylight_Metrics.htm
4. Illuminating Engineering Society of North America, (2012). LM-83-12 Approved Method: IES Spatial Daylight Autonomy (sDA) and Annual Sunlight Exposure (ASE), New York: IES.
5. Illuminating Engineering Society of North America, (2023). LM-83-23 Approved Method: IES Spatial Daylight Autonomy (sDA) and Annual Sunlight Exposure (ASE), New York: IES.
6. Solemma, (2023). ClimateStudio, [Online], Available: https://www.solemma.com/climatestudio.
7. Inanici, M., (2023). LARK 3.0. [Online], Available: http://faculty.washington.edu/inanici/MI-RESEARCH.html#Lark.
8. Inanici, M., et al (2023). Evaluation of sky spectra and sky models in daylighting simulations. Lighting Res. Technol. 2023; 55: 502–529.
9. Beltrán, L, et al (2020). Evaluation of Dynamic Daylight Metrics, Based on Weather, Location, Orientation and Daylight Availability, [Online], Available: https://oaktrust.library.tamu.edu/handle/1969.1/188889.
10. Safranek, S., et al (2023). Lighting for Health and Wellness Recommendations in Offices, [Online], Available: https://www.osti.gov/servlets/purl/1971618
11. Beltrán, L., (2020). Assessing the Lighting Performance of an Innovative Core Sunlighting System, [Online], Available: https://link.springer.com/chapter/10.1007/978-3-030-37635-2_43.
12. Won Hee Ko., et al (2022). Window view quality: why it matters and what we should do
13. Safranek, S., et al (2020). Energy impact of human health and wellness lighting recommendations for office and classroom applications. Energy and Buildings, 226, 110365.

PLEA 2024 WROCŁAW
(Re)thinking Resilience

Passive Climate Change Adaptation through Facade Design:
A Case Study in Railway Station Application.

MARCELLO TURRINI[1] BARBARA GHERRI[1] EMANUELE NABONI[1,2, 3]

[1]University of Parma, Parma, Italy
[2]Royal Danish Academy, Copenhagen, Denmark
[3]Norman Foster Institute, Madrid, Spain

ABSTRACT: This research paper addresses the urgent need for a methodological approach to develop energy-independent transportation stations tailored for the climatic challenges anticipated by 2050 due to climate change. Highlighting the increasing implications of global warming, the study examines the potential of the building envelope to ensure thermal comfort within transit hubs, aiming to reduce dependence on high-energy mechanical cooling systems via passive options.
Through a thorough analysis of current design shortcomings, this paper presents a novel framework that aligns with climate change standards and anticipates urban development needs in a warmer world. Using state-of-the-art simulation tools and a practical case study—a bridge station in Southern Italy—the research evaluates the performance of various passive options for the projected summer conditions of 2050 involving the building envelope. The results emphasise the significance of enhanced natural ventilation in improving indoor thermal comfort. In conclusion, this study paves the way for informed, sustainable, and user-focused transportation station designs that are prepared for the challenges of a changing climate.

KEYWORDS: Climate change, Passive cooling, Façade Design, Natural ventilation, Railway station, Grasshopper.

1. INTRODUCTION

One of the most tangible effects of climate change is the increased demand for building cooling, a concern underscored by the Intergovernmental Panel on Climate Change (IPCC) [1]. The primary global strategy to combat warming is to limit temperature rise to 2.0°C, ideally to 1.5°C above pre-industrial levels. This seemingly minor difference of 0.5°C leads to a roughly 13% increase in cooling degree days in Italy [2]. Consequently, it is imperative for nations to foster initiatives that curb greenhouse gas emissions and adapt their infrastructures, a point strongly highlighted by UNEP in 2022, noting the limited progress made by institutions in this direction to date [3].

In this scenario, a critical challenge is to balance energy efficiency with maintaining consistent summer thermal comfort. Infrastructure spaces, which must provide thermal comfort for numerous users while minimizing greenhouse gas outputs, present a particularly complex aspect of this challenge. With traditional energy-intensive systems becoming less viable due to their environmental impact, there is a pressing need for low-emission alternatives.

This challenge brings railway stations into focus. Effective climate adaptation can significantly reduce reliance on energy-intensive systems [4], thereby playing a crucial role in mitigating the climate crisis. This leads to a crucial question:

How can passive design, which leverages natural energy sources and reduces mechanical cooling, be the cornerstone for climate-adapted, resilient railway stations?

However, conceptualizing these solutions alone is not enough. Their practical application and effectiveness depend on thorough, data-driven evaluations of climate change impacts [5, 6]. This introduces another vital question:

Given our changing climate and the current shortcomings in our design approaches, how can we effectively utilize simulation tools in climate change scenarios?

This study seeks to answer these questions by detailing a specific adaptation process for a railway station currently under construction, examining various options for its envelope, and establishing a methodological framework to evaluate its climate responsiveness.

2. CASE STUDY

This case study examines a project initiated by the Italian railway operating company aimed at implementing energy-saving and decarbonization technologies in its newly constructed stations, with a particular focus on climate change adaptation. The ultimate goal of this project is to achieve indoor comfort both for contemporary operations and for 2050 without relying on HVAC systems, leveraging instead a building façade designed to moderate and interact dynamically with solar radiation and wind.

The railway station in Xirbi, Italy, coordinates 37.536238, 14.057025, exemplifies this approach with its bridge-like structure over railway tracks, oriented north-south as shown in Figure 1. The design incorporates a floor made of reinforced concrete with a 40% open floor area, which significantly increases thermal interaction between the station's interior and the external environment. The east and west facades, along with the roof, are equipped with a continuous skin of photovoltaic cells that optimize energy efficiency by harnessing solar energy. Continuous glazing at the north and south ends enhances natural light and contributes to passive solar gain, which further influences the building's thermal dynamics. This results in a unique hybrid interior-exterior space that challenges conventional climate control solutions. The design challenge is to create a façade system that not only responds to solar radiation to maximize energy efficiency but also manipulates natural air flows to maintain comfort throughout the year, particularly during the peak summer months. This requires a sophisticated understanding of the interplay between climate, climate in 2050 and air openings.

The study was conducted, using weather data projected for the year 2050, obtained from Meteonorm 8.0 software and adjusted according to the IPCC 8.5 scenario. Analysis centered around the hottest week of the year, from August 17 to August 2. Due to inconsistencies in cloudiness on August 19 between the years 2022 and 2050, August 18 was selected for a detailed analysis as it presented consistent cloud coverage of zero tenths in both years. On this selected day, the peak temperature is expected to reach 34.8 °C in contemporary wearther and 37.9°C at 3:00 pm in 2050. Prevailing winds during August typically come from the northern quadrant.

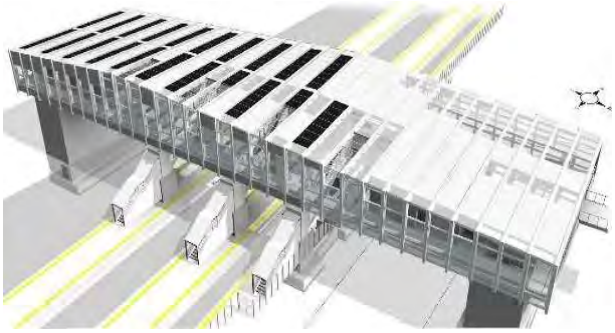

Figure 1. Reference building. Railway station of Xirbi, Italy.

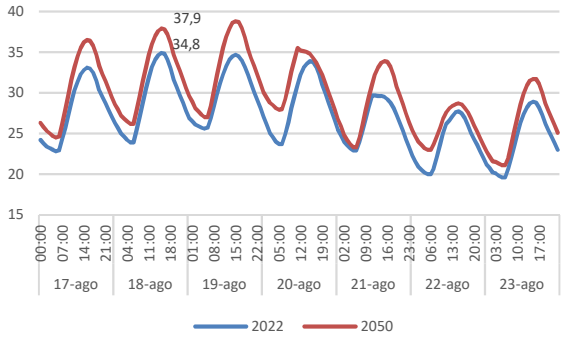

Figure 2. Air temperature (°C) in the hottest week of 2022 and 2050

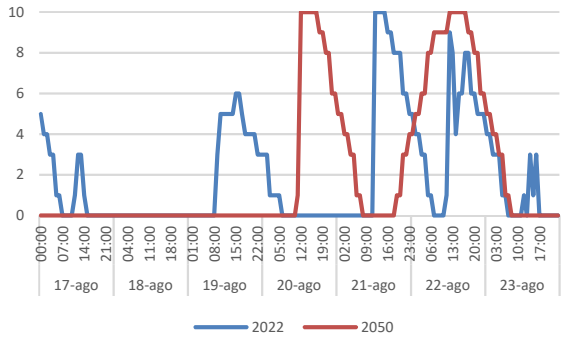

Figure 3.Cloudiness index, measured in tenths, during the hottest thermal week of 2022 and 2050.

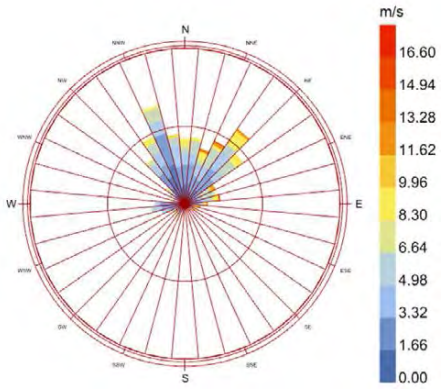

Figure 4. The wind rose for August 2050. Notably, the northern quadrant is the primary origin of prevalent wind patterns, with a modal speed registered at 4 meters per second.

3. ALIGNMENT TO CLIMATE CHANGE WITH PASSIVE OPTIONS

The design of the façade was conceptualized to be adaptive to escalating temperatures and evolving climatic conditions, with projections extending to the year 2050. The thermodynamic interaction between the building's external and internal environments is facilitated by openings at north and southern facades, fostering a dynamically varied range of indoor conditions. As the project aims to assess thermal comfort in spaces devoid of HVAC cooling systems. This necessitates the exclusion of conventional comfort indices typically applied to air-conditioned interiors, directing the selection towards alternative

parameters such as the Universal Thermal Climate Index (UTCI), which is pertinent for evaluating open and semi-open spaces.

The building was conceptualized as a wind tunnel to harness the prevailing northern summer breezes effectively. The building's longitudinal orientation is strategically aligned with these winds, forming the foundation of a passive ventilation strategy. This strategy utilizes the north and south façades as architectural conduits, serving as the inlet and outlet for wind flow, eaxh of which is characterized by varying degrees of façade porosity. These variations are the primary scope of this investigation as they are the modulator of the air flows and consequently they impact UTCI values. Table 1 underscores the variation in facade treatments, effectively grading the building's adaptive capacity to modulate internal air velocities through natural ventilation alone:

Table 1. Variation of openings in north and south facades.

Option		Description	Opening
1	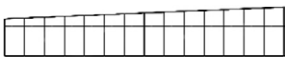	The north and south facades are completely closed.	0%
2		The upper part of the facades is completely opened	31%
3	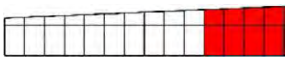	In both facades, one-third is opened vertically	31%
4		Vertical full-height openings in both facades	35%
5		Both facades are completely opened.	100%

Closed Facade (0% Open): This baseline scenario entails a non-porous envelope, precluding the ingress of natural ventilation, thereby simulating a controlled thermal environment.

Upper Openings (31.1% Open): Introducing upper-level openings capitalizes on the stack effect, facilitating warm air exhaust and inducing lower-level cooler air inflow.

Vertical Side Openings (30.8% Open): This approach focuses on creating unidirectional wind ingress, thereby inducing a singular vector of airflow.

Alternating Vertical Openings (35.2% Open): Alternating openings across the facade encourage a more distributed and turbulent airflow, potentially improving indoor air mixing.

Fully Open Facade (100% Open): This maximizes natural ventilation, allowing for full wind penetration.

4. OUTDOOR SCRIPTS FOR INDOOR SPACES

The diagrammatic workflow in figure 5 and 6 presents a sophisticated strategy to inform design for 2050 through the integration of simulations for radiative transfer and airflow dynamics, employing tools like Radiance, Eddy 3D, and Ladybug Tools. Together, these tools facilitate a comprehensive assessment of thermal comfort within semi-exterior spaces as it relates to the Universal Thermal Climate Index (UTCI).

Radiative Heat Transfer Modeling with Radiance: This component of the methodology harnesses Radiance for its nuanced modeling of radiative heat transfer, quantifying the percentages of solar radiation interacting with the building's envelope and materials. By capturing the specific wavelengths of solar energy, Radiance provides essential input on how radiant heat influences surface temperatures, directly impacting local microclimatic conditions and, by extension, the UTCI.

Airflow Dynamics with Eddy 3D: In parallel, Eddy 3D simulations, empowered by OpenFoam technology, provide an analysis of airflow within and around the structure. This analysis informs the UTCI by modeling how air movement, induced by natural ventilation and the different facades porosities, can regulate thermal conditions through convective heat transfer.

Ladybug Tools Integration: Ladybug Tools steps in as the critical integrator, enabling the synthesis of the radiative and airflow simulations. Ladybug Tools acts as a computational platform that interprets the output from Radiance and Eddy 3D to produce UTCI comfort maps. These maps are generated by placing virtual sensors within the 3D environment, capturing the interactive effects of radiation and airflow to predict thermal comfort levels across different areas and scenarios.

By leveraging the synergistic potential of these advanced modeling tools, the methodology extends to evaluating five design options, each assessed through the UTCI lens provided by Ladybug Tools. This process ensures that each design proposal is scrutinized for its potential to sustain occupant comfort, given the anticipated climatic shifts by 2050.

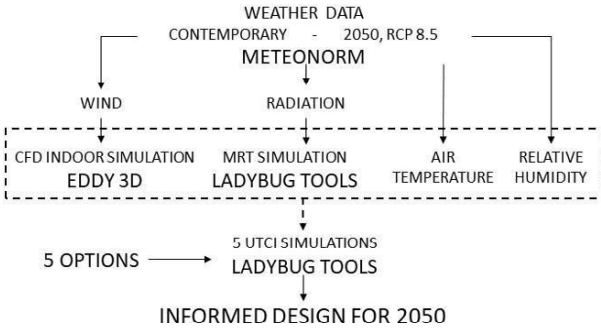

Figure 5. Combining Indoor Environmental Simulation with Outdoor Climate Data for Enhanced UTCI Comfort Mapping

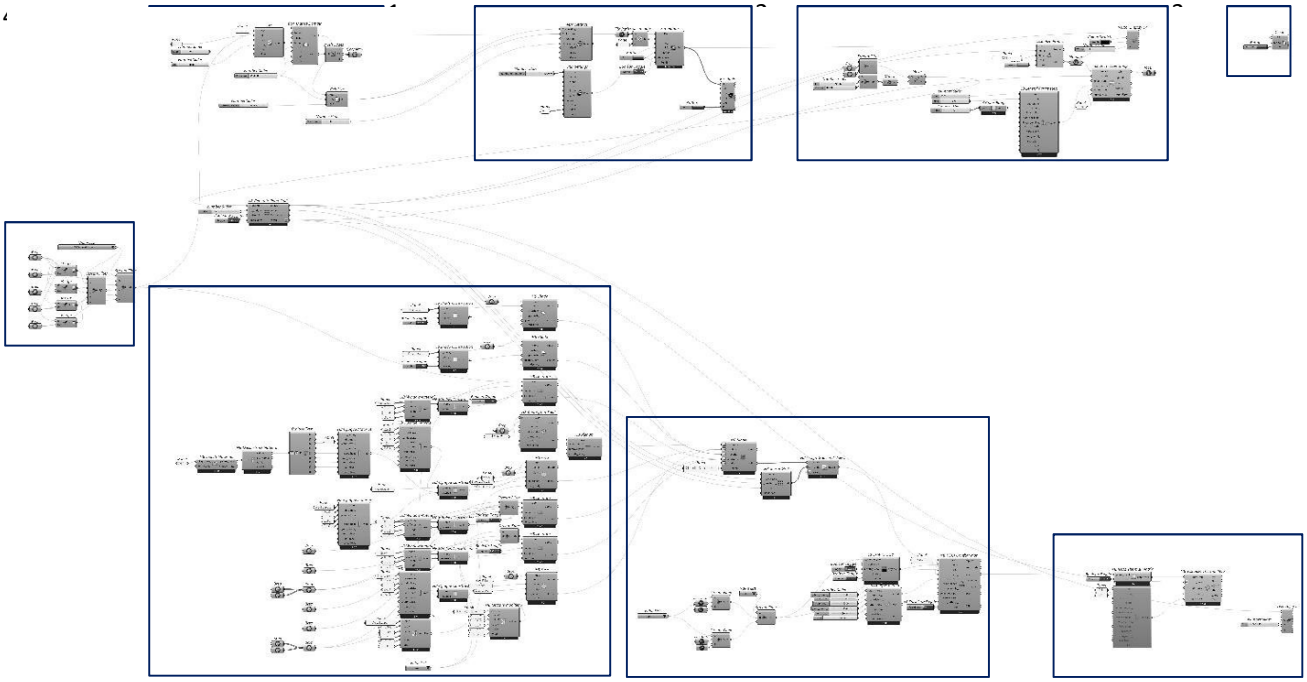

Figure 6. GRASSHOPPER workflow. 1. CFD, simulation domain; 2. CFD, mesh & simulation; 3. CFD, visualization; 4. CFD, clean data; 5. CFD + UTCI, sensor grid; 6 options; 7. UTCI, model; 8. UTCI, simulation; 9. UTCI, visualization.

5. RESULTS

This study presents a streamlined, data-driven analysis for future climate-adaptive design, yielding numerical and visual results to evaluate thermal comfort. The numerical results reveal a correlation between the façade openness and the average UTCI—key in predicting thermal comfort levels for 2022 and 2050. This is captured in Tab. 2, highlighting the resilience of Option 5, which significantly mitigates the rise in UTCI compared to the more sealed Option 1.

Visual results, shown in Figures 8, 9, and 10, depict the spatial distribution of the Mean Radiant Temperature (MRT) and thus the internal surface temperatures that are crucial for comfort, ventilation, and UTCI, respectively. These figures demonstrate the effectiveness of facade options in distributing natural ventilation and controlling MRT, thereby influencing the UTCI values within the building. The comparative analysis of these options reveals how passive design considerations can significantly reduce thermal stress, showcasing the potential for architecture to adapt to the warming climate. Option 5, with open north and south façades, performs best in current conditions and emerges as the most effective in responding to the predicted climate change scenario, suggesting its viability as a long-term passive cooling strategy. This architectural decision, focusing solely on the passive manipulation of the built environment, could nearly nullify the impact of climate change on the station's thermal comfort by 2050, as per the worst-case scenario projected by the IPCC.

Table 2. Average UTCI values (°C) inside the building on 8 August at 3:00 pm.

Option	2022 (°C)	2050 (°C)	Delta (°C)
1	34.72	36.65	1.93
2	34.25	35.92	1.66
3	34.18	36.26	2.08
4	33.80	35.73	1.93
5	33.34	35.27	1.93

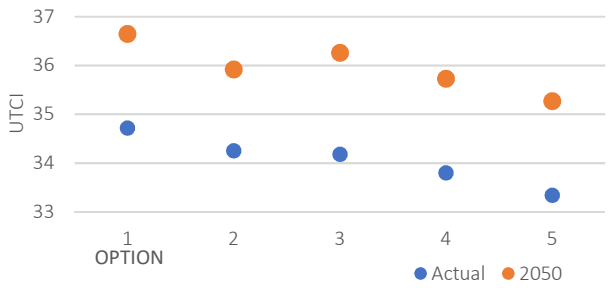

Figure 7 Comparison of the options. Option 5 is the most resilient, and it is on 8 August 2050 at 3:00 pm.

The visual analyses further support the selection of Option 5, with the MRT results indicating cooler interior conditions and the ventilation maps showing enhanced airflow, essential for maintaining comfort without relying on mechanical systems. The UTCI mappings confirm that this option provides a consistent thermal environment conducive to passenger comfort in the face of rising future temperatures.

Reading the maps leads to assessing the spatial distribution of microclimate parameters and the influence of geometry on comfort factors.

MRT (Fig. 8). Due to the varying levels of transparency of the roof and the east and west facades, there is an uneven distribution of MRT within the building. Among the three lifts, the central part is the one with the lowest MRT, about 35°C. This is due to a lower transparency of the infill panels in the roof. Along the perimeter of the building, the MRT is higher due to the increased penetration of the sun's rays from the west at 3:00 pm and the radiation reflected from the external floors to the north and south, with a variation contained in a range between 36.5°C and 39°C. In the outdoor areas, the MRT reaches values above 41°C.

Ventilation (Fig. 9). Option 1, where the two glazed walls to the north and south are all closed, is compared with option 5, which numerically gives the best results in UTCI. In option 1, weak air movements can be seen at the large central opening on the floor and the small openings on the west façade. Generally between 0 m/s and 1.8 m/s. The wind speed increases significantly in option 5, where the two glass walls to the north and south are completely open. There is a constant level of 2.5 m/s, which is equivalent to a light breeze according to the Beaufort scale, with accelerations of up to 5 m/s in the part near the inlet, which corresponds to a gentle breeze according to the Beaufort scale, and a deceleration of up to 0.5 m/s in the central space between the ascents, equivalent to light air in the Beaufort scale.

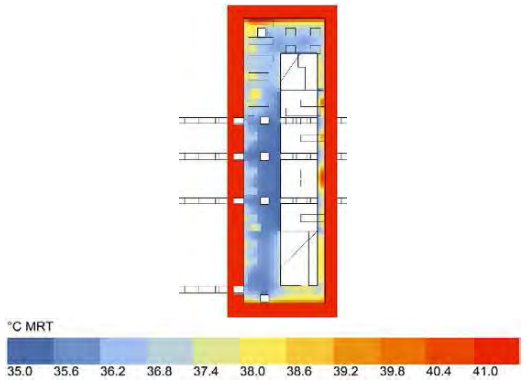

Figure 8. MRT in 2050. The lowest value of about 35°C is in the core of the building.

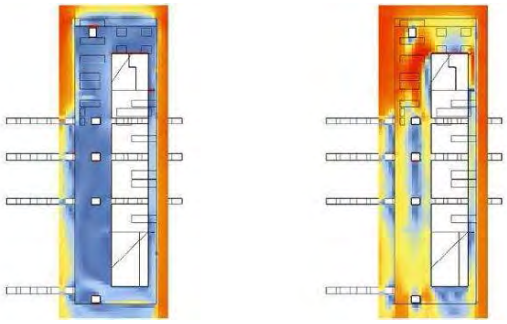

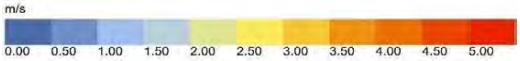

Figure 9. Ventilation at 3:00 pm. Option 1 is on the left, and Option 5 is on the right. Opening the north and south facades leads to air velocity of up to 5 m/s on the northern side of the building.

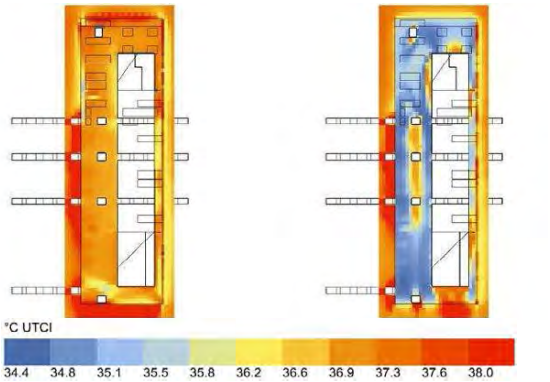

Figure 10. UTCI in 2050. Option 1 is on the left, and option 5 is is on the right. The drop in UTCI in option 5 reaches 2.5°C almost uniformly in the building.

UTCI (Fig. 10). Considering 8 August at 3:00 pm, we are in one of the absolute hottest hours of the year 2050. It is therefore not surprising that the UTCI values are very high and always in the 'Strong Heat Stress' range of the UTCI scale, i.e. between 32°C and 38°C. However, when comparing option 1, where there is an almost constant UTCI of approximately 37 °C throughout the building, in option 5, significant temperature drops are noted with a consequent attenuation of thermal discomfort. In particular, the UTCI drops almost uniformly by about 2.5 °C to 34.5 °C. In the areas where the wind speed is lower, there are higher UTCI values, up to 36.8 °C, which indicates the role of wind as a carrier of thermal comfort in this geographical area. Furthermore, where wind speeds are higher, in option 5, the UTCI value is not the absolute lowest but is around 35.3 °C.

6. ARGUMENTED CONCLUSIONS

Addressing Passive Design in Climate-Adapted Railway Stations.

How can passive design, which leverages natural energy sources and reduces mechanical cooling, be the cornerstone for climate-adapted, resilient railway stations?

Passive design's potential as a foundational element for climate-adapted, resilient railway stations becomes evident when considering the necessity for indoor spaces that respond to outdoor climate variations. In the study spanning the present and projections for 2050, simulation tools such as outdoor modules have been paramount in assessing the impact of a porous and discontinuous building envelope on semi-indoor comfort levels. Such assessments demonstrate the critical role of passive design in balancing indoor comfort with minimized mechanical

cooling. However, our understanding of comfort levels and their external climatic influences has deepened, revealing that different design options perform variably across time. Option 1, which relies on closed facades, may suffice under current climatic conditions but falls short when considering the year 2050's scenarios. In contrast, Option 5, characterized by open facades, aligns with the future's expected increase in temperatures, emphasizing the need for designs that can maintain thermal comfort over time. Thus, passive design becomes not only a matter of energy efficiency but also of future-proofing buildings against the evolving demands of climate change.

Utilization of Simulation Tools in Climate Change Scenarios

Given our changing climate and the current shortcomings in our design approaches, how can we effectively utilize simulation tools in climate change scenarios?

When harnessing simulation tools for climate change scenarios, it becomes apparent that relying solely on present-day weather data is inadequate. This research shows a clear divergence between design options when current and future climatic conditions are considered. While Option 1 might be suitable for today's climate, Option 5's open facade design emerges as the superior approach for 2050, highlighting the importance of incorporating long-term climate projections into passive design strategies. The application of these tools provides a scientific basis for forecasting and validating architectural responses to future climate challenges, advocating for an anticipatory design ethos. This forward-thinking mindset allows designs to adapt to and evolve with the predicted changes in climate, ensuring long-term resilience and sustainability of infrastructures like railway stations. Thus, the role of simulation tools extends beyond simple prediction to become integral in informing an adaptive architectural strategy that proactively responds to the anticipated extremes of future climate conditions.

ACKNOWLEDGEMENTS

Our thanks go to Italferr S.p.A. for their support and cooperation in this study, and to Raffaele Marino and Marco Capobianchi for their contributions that were instrumental in the direction and outcome of our work.

REFERENCES

1 IPCC, 2023: Summary for Policymakers. In: Climate Change 2023: Synthesis Report. IPCC, Geneva, Switzerland, pp. 1-34,

2. Miranda, N.D., J. Lizana, S.N. Sparrow, M. Zachau-Walker, P.A.G. Watson, D.C.H. Wallom, R. Khosla, and M. McCulloch. 2023. 'Change in Cooling Degree Days with Global Mean Temperature Rise Increasing from 1.5 °C to 2.0 °C'. Nature Sustainability 6 (11): 1326–30. https://doi.org/10.1038/s41893-023-01155-z.
https://doi.org/10.21203/rs.3.rs-2401990/v1.

3 UNEP. 2022. 'Emissions Gap Report (EGR) 2022: The Closing Window – Climate Crisis Calls for Rapid Transformation of Societies'.

4. Han, X., H. Zhang, T. Zhu, and L. Wang. 2020. 'Analysis of Natural Ventilation Design in Large Space of Railway Station'. In. Vol. 508.

5. Naboni, Emanuele, and Lisanne Havinga. 2019. 'Regenerative Design In Digital Practice. A Handbook for the Built Environment.

6. Naboni, E., R. Siani, M. Turrini, E. Touloupaki, B. Gherri, and F.D. Luca. 2023. 'Experiments on Microclimatically Adapt a Courtyard to Climate Change'. In IOP Conference Series: Earth and Environmental Science Vol. 1196.https://doi.org/10.1088/1755-1315/1196/1/012032.

Assessment of Acoustical Parameters in Refurbishment of Classrooms

CRISTIAN DIPPEL,[1] BEATRIZ PIDERIT-MORENO,[2]

[1]Universidad del Bío-Bío, Concepción, Chile
[2] Universidad San Sebastián, Concepción, Chile

ABSTRACT: Acoustic parameter as reverberation time (RT), background noise (L_{Aeq}) and Speech intelligibility STI are related to the well-being of its occupants and to the suitability of a space to be a learning environment. In Chile, public education classrooms have been refurbished as a strategy to provide better welfare conditions reducing the costs and environmental impact of generating new buildings. The objective of this research is to evaluate the outcome of an acoustic refurbishment project by evaluating its physical characteristics and in-situ measurements of RT, L_{Aeq} and STI. The results indicated that the reverberation times and background noise do not meet the regulatory objectives; no airborne noise transmission strategies have been applied and no minimum absorbing material surfaces have been considered. Yet, the STI can be achieved with the applied strategies. This difference calls for a review of the limit values and the conditions under which measurements are performed: the STI assessment in unoccupied classrooms may not relate to the situation in actual teaching practices.
KEYWORDS: Indoor Environmental Quality; Classroom Acoustics; Speech Transmission Index; Speech Intelligibility; Reverberation Time

1. INTRODUCTION

The acoustic quality of educational spaces can directly affect the performance and concentration of the students who spend their time in them. Classrooms can be reverberant and noisy places, affecting the learning process. [1, 2]. Some studies position noise as one of the annoying factors identified by most children in school classrooms [2]. Noise, above certain levels, is a factor that increases physical stress [3]. In general, the field study of indoor environmental quality shows an urgent need for acoustic measures in school classrooms [4]. Other studies show that the acoustic quality of the educational facilities built in Chile is often deficient [5, 6].

The Speech Transmission Index (STI), introduced by Steeneken and Houtgast, is a crucial metric for assessing speech clarity. It considers factors like reverberation time (RT), background noise (L_{Aeq}), signal-to-noise ratio (SNR), and the positions of the speaker and listener. The result is a numerical value from 0 to 1, with a label indicating one of five ratings (refer to Table 1). For school classrooms, the accepted STI value is usually above 0.6, indicating good intelligibility.

Table 1: STI Value and Speech Intelligibility Evaluation.

Category	Excellent	Good	Fair	Bad	Poor
STI	>0,75	0,6-0,75	0,45-0,60	0,30-0,45	<0,30

The RT and SNR variables relate to design aspects that could be improved in an existing classroom refurbishment: surface absorption and external noise insulation. On the other hand, the distance between speakers, speech levels and overall noise levels are diverse depending on different teaching scenarios. Traditional in-situ measurement methods consider teacher-centred teaching while contemporary methods consider student-centred teaching [7].

SNR is measured as the difference between the teacher's voice and the background noise measured in the empty classroom. If the background noise values are high, the speakers voice must be raised. The background noise value can be elevated by the presence of external or internal noise. High vocal effort for extended periods of time can affect the vocal health of teachers.

A higher reverberation time (RT) can reduce speech transmission index (STI) due to prolonged sound reflections masking the signal. Higher signal-to-noise ratio (SNR) can improve STI by minimizing background noise influence. While international standards suggest an RT of less than 0.6 s, some studies propose ranges of 0.3 to 0.9 s for optimal speech intelligibility (STI) [8].

Acoustical guidelines, as described in various sources [9-11], focus primarily on traditional instructional classrooms. For these environments, the speech transmission index (STI) should register a value equal to or greater than 0.6 throughout the space. This criterion is crucial to ensure that the teacher's message remains audible throughout the classroom.

In the current landscape, enhanced acoustic standards are imperative for school infrastructures, even those initially designed without them. The refurbishment of classrooms emerges as a viable

solution to meet these standards by optimizing interventions and circumventing the environmental impacts associated with new construction. This study is focused on evaluating the effectiveness of acoustic rehabilitation being applied in educational facilities in Chile, to understand if these interventions meet the necessary requirements to ensure adequate acoustic quality.

2. MATERIALS AND METHODS

To achieve this objective, an architectural characterization is carried out in a first stage to compare the acoustic performance of the classrooms and to identify the gaps. In a second stage, a room without acoustic rehabilitation and two with acoustic rehabilitation are evaluated to assess the effectiveness of the interventions and evaluate their suitability.

The case study took place in the city of Concepción, Chile. Measurements in existing buildings are taken to align classroom acoustics with established standards. Reverberation time and background noise were measured to determine the STI in simulation software.

2.1 Characterization of acoustic quality in classrooms.

The acoustic strategies of the case studies have been evaluated with the criteria applied by Piderit-Moreno et al. (2023) [12] using an analysis matrix of their design characteristics in relation to indoor environment quality (IEQ) factors.

In acoustics the matrix looks at space design and interior conditioning. These aspects have been constructed based on the consultation of different design guides or regulations and identify features that are observable in classrooms to rate with an index from 0 to 2: where 0 is inadequate, 1 is adequate and 2 is effective. The 5 rating criteria are shown in Table 2. The application of the matrix provides a percentage of compliance with the architectural parameters that influence the acoustic quality, for this descriptive analysis based on those proposed by Piderit-Moreno [12] below the thresholds:

- Excellent (85% to 100%): outstanding compliance with architectural acoustic parameters, almost all aspects are present and well implemented.
- Satisfactory (71% to 85%): effectively comply with most of the architectural acoustic parameters, there is room for minor improvements.
- Acceptable (41% to 70%): show basic compliance with acoustic parameters, could be significantly improved.
- Unacceptable (26% to 40%): have significant deficiencies in several architectural acoustic parameters, requiring major improvements.
- Poor (0% to 25%): show widespread and severe non-compliance with architectural acoustic parameters. Indicates the absence or inadequate implementation of most parameters.

Table 2: Factors for acoustic evaluation of classrooms.

Parameter	2- Effective	1- Adequate	0- Inadequate
AC01 - Room Height	≤ 2.4 m	>2.4-≤3.5 m	> 3.5 m
AC02 - Window Frame Material and Glass Quality	DVH w/o thermal bridges	DVH w/ thermal bridges	Single Glass
AC03 - % Glazed Surface	< 10% of total surface	11%-16% of total surface	> 16% of total surface
AC04 - % Ceiling with Absorbent Material	> 40% Absorbent Surface	20% - 40% Absorbent Surface	< 20% Absorbent Surface
AC05 - % Wall with Absorbent Material	> 20% of surface w/ absorbent material	< 20% of surface w/ absorbent material	No absorbent material on walls

2.2 Evaluation of acoustic refurbishment

Three elementary school classrooms were selected in three different buildings. Two classrooms, namely “A Classroom” (Figure 1) and “B Classroom” (Figure 2), have undergone recent acoustical enhancements. Meanwhile, one classroom, “C Classroom” (Figure 3), remains in its original state. In structural terms, all classrooms have a seismic-resistant reinforced concrete structure based on load-bearing walls. The physical characteristics of the classroom were captured using a high-resolution 3D scanner. This recorded data allows for extraction of information, including interior measurements, surface materiality, furniture presence, and the number of occupants. Table 2 presents an overview of the physical characteristics of the classrooms. Generally, none of them surpasses 54 m² and 177 m³.

Table 2: Comparison of classroom physical characteristics.

Name	A classroom	B classroom	C classroom
Acoustic Treatment	Yes	Yes	No
Depth (m)	6.90	7.60	7.00
Width (m)	7.40	5.70	7.80
Height (m)	3.23	3.20	3.20
Area (m²)	50.86	42.43	53.75
Volume (m³)	157.69	129.89	176.85

Figure 1: A Classroom 360° scan.

Figure 2: B Classroom 360° scan.

Figure 3: C Classroom 360° scan.

The unoccupied background noise level, measured as A-weighted 5-minute equivalent noise levels ($L_{Aeq(300s)}$), employed a B&K-4942 microphone at 1.2m height in the room's centre. RT measurement, following UNE ISO 3382-2:2008 standard, used a B&K-4295 omnidirectional loudspeaker at 1.5m height in three points: teacher's front position and two student positions. B&K-4942 microphones at 1.2m height were placed in three student positions, all with distances exceeding 1m from reflecting surfaces. SAMURAI software for SINUS Noise & vibration analysis obtained both parameters. Measurements occurred after hours, with furnished and unoccupied classrooms. Figure 2 shows the floor plan of the case study, which illustrates the criteria for the placement of omnidirectional loudspeakers and microphones.

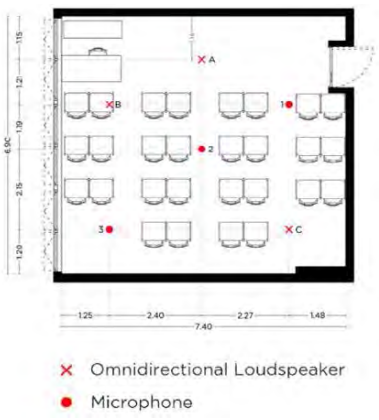

Figure 4: Loudspeakers and microphones location criteria.

2.3 STI measurement through computer simulation

Using EASE v4.3 software, the simulation for STI employed a tool predicting and analysing sound propagation in built spaces. This software models and evaluates space response to sound sources, predicting RT and obtaining Sound Pressure Level (SPL) and STI distribution. Calculation follows the IEC 60268-16 standard. The absorption and scattering characteristics of the internal surfaces were tabulated according to the 3D scans and calibrated according to the RT measurements.

The STI Simulation was made on an instructional class scenario, a replica of the number of students observed in each classroom was used: 28, 25 and 26 for classrooms A, B and C respectively. In this scenario, all sources were located at 1.65m height and all receivers at 1.00m height.

Vocal effort level values were defined according to ANSI 3.5:1997 standard. In the instructional situation the high vocal effort level was used.

3. RESULTS

Classroom observations reveal an acoustic refurbishment strategy involving acoustically absorbent gypsum plasterboard on part of the ceiling and top walls. Ducts for air renewal are lined with standard gypsum plasterboard. Refurbished classrooms have PVC window frames, airtight double glazing, and EIFS system exterior coating. However, there are no interventions on corridor-facing glass, nor is there insulation treatment for corridor or other room walls; these consist only of concrete with a plastered and painted finish in all classrooms.

3.1 Classroom Characterization

The application of the evaluation matrix for the characterization of acoustic quality in classrooms was carried out within the framework of the research [CISBAT]. It was applied to 30 classrooms that represent the quality of the built environment in Chile and among which are the cases studied.

In the analysis of the acoustic quality of the classrooms based on architectural parameters, it was found that 57% (17 classrooms) were classified in the 'Poor' category, indicating serious acoustic deficiencies. In addition, 27% (8 classrooms) were classified as 'Unacceptable', suggesting the presence of significant acoustic problems. On the other hand, 10% (3 classrooms) achieved a 'Satisfactory' rating, and 6% (2 classrooms) were evaluated as 'Acceptable'. Notably, no classrooms were rated in the 'Excellent' category. These results underscore the need for attention and improvements in classroom acoustics to create optimal educational environments.

As shown in Figure 5, the results of the acoustic parameters show that most of the classrooms have an adequate height (AC01) and most of them do not have

adequate or efficient materials in their windows (AC02). The ratio of glazed area to classroom area is in most cases higher than 11% (AC03). But, the most notorious aspect is related to the amount of absorbent material included in classrooms: most of them do not have an adequate amount in ceilings and none of them have an adequate amount in walls (AC04 and AC05).

These last parameters are the only ones that are directly related to the will to include an acoustic treatment and are not a consequence of other decisions in the architectural design.

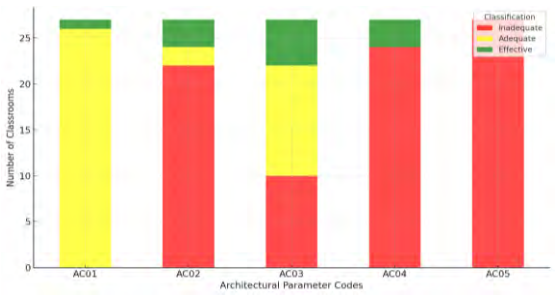

Figure 5: Distribution of Acoustical Parameters in Classrooms Rated as Poor

Table 3 focuses on the parameters described in the 3 classrooms studied. Classrooms A and B, which were refurbished, both obtained 80% in the acoustic aspect. In their overall weighted performance (which includes all environmental aspects) they obtained 79% and 78% respectively, rated as "satisfactory". Classroom C, which was not refurbished, obtained 20% compliance in the acoustic aspect and 27% in its overall weighted performance, rated as "unacceptable".

The interior conditioning strategies observed in the classrooms: improvements in the quality of the windows, inclusion of acoustic absorption, thermal insulation, and mechanical air renewal systems, make a noticeable difference in the rating of the classrooms studied.

Table 3: Evaluation of acoustic parameters in the studied cases.

	A classroom	B classroom	C classroom
AC01	1	1	1
AC02	2	2	0
AC03	0	0	1
AC04	1	1	0
AC05	1	1	0

3.2 Reverberation Time and Background Noise results

The RT20 and background noise results show the differences between the cases. The case that does not have acoustic enhancements has, as expected, a higher RT20. The increase of absorbing surfaces in the upper positions substantially improves the RT as shown in Figure 6 which compares the RT results in octave bands between 250 Hz and 4KHz. The RT difference in the octaves from 500Hz to 1000Hz is more noticeable than in the higher (4000Hz) and lower (250Hz) frequencies. The difference recognized in classrooms affects the frequencies corresponding to speech. The RT obtained is directly related to the existence of absorbent material and to the volume of the enclosure. Regarding the absorption of the surfaces, Classroom A (0.82 s.) and Classroom C (1.20 s.), which have a more similar surface and volume, differ significantly due to the existence of absorbent material in the first one. Among the two rooms with acoustic treatment, the smaller one Classroom B has a notoriously lower average reverberation (0.65 s.) time with respect to the classroom with treatment and larger volume.

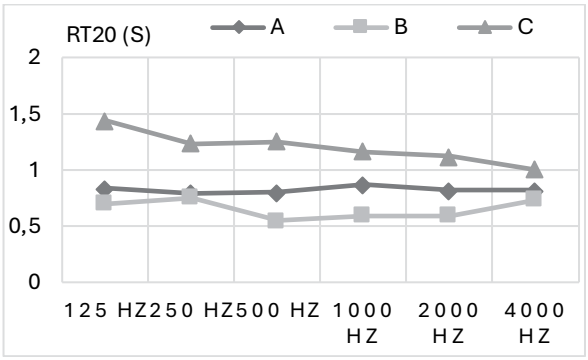

Figure 6: RT20 results in seconds and octave bands

The $L_{Aeq(300s)}$ background noise measurement gave the results shown in Figure 7. Refurbished classrooms show similar noise levels that according to Nch 352 local standard [29] can be called "moderately quiet" environment. On the other hand, the non-remodeled classroom shows a higher noise level reaching 50.4 dB(A), a level qualified as "noisy environment" according to the same standard.

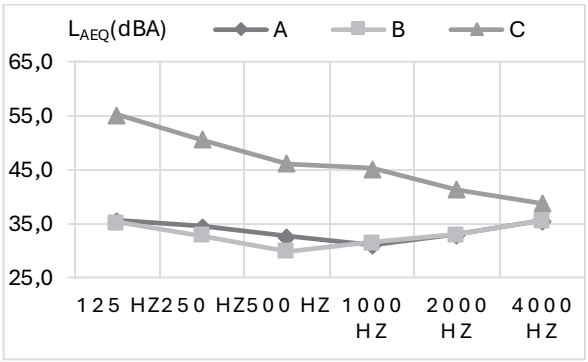

Figure 7: Background noise results expressed in dB(A).

3.3 Calculated STI

The STI calculation was obtained using the software's "Area Mapping" module. Values were

obtained for each receiver position, and, in addition, an image of the audience area was extracted and superimposed with the classroom plan in figure 8 to know the behaviour of the index in the space; in these images, the black dots indicate the position of the receivers. Finally, the averages of the values delivered in each classroom are compiled in Table 4.

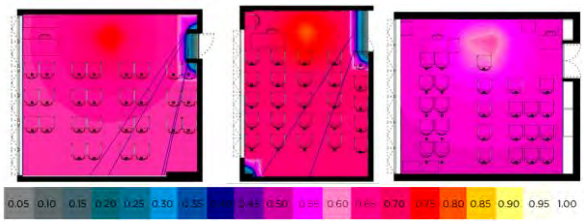

Figure 8: STI in classroom plan.

Table 4: STI for instructional class

	A classroom	B classroom	C classroom
STI	0.63	0.70	0.52

Classrooms A and B achieve an STI value above 0.6 and meet the requirements of the revised standards. Although the acoustic treatment is similar in both, Classroom B has a lower volume, which influences a lower reverberation and a higher STI decay distance. Classroom B obtained a performance STI of 0.52 considered "fair".

4. DISCUSSION

The average of the central bands (500, 1000 and 2000 Hz) was used to compare the RT values with the standards consulted. The average of the central bands is 0.82 s. for classroom A, 0.58 s. for classroom B and 1.18 s. for classroom C. According to ANSI and the Chilean standard, the established value should be ≤0.6 s. [9,11] for classrooms of smaller volume (≤283 m3). Classroom B complies with the standard. Despite having a similar treatment, classroom A does not reach the recommended value. Anyway, the acoustic treatment led classroom A to a shorter RT than classroom C, whose volume and surfaces are very similar to those of classroom A before being refurbished.

The revised standards, setting an RT value of 0.6 s. for unoccupied classrooms, align with studies associating this value with good intelligibility performance. Optimal intelligibility, particularly in the presence of moderate background noise (below 25 dB), can be ensured with values less than 0.4-0.5 s. [14]. In all these scenarios, only the classroom B has met these RT values. Therefore, the acoustic treatment criteria applied were effective only in a classroom with a volume below 130 m3.

Some studies find higher RT values acceptable, noting that the support provided by RT to sound transmission can reduce the vocal effort required by teachers. In the study conducted by Puglisi et al., they identify an optimal value of 0.7 s. for this purpose.

The consulted standards specify maximum background noise levels of around 35 dB(A), mostly ranging from 30 to 40 dB(A). However, all measured classrooms exceeded these values. Both classrooms A and B recorded similar values of 42.5 and 42.4 dB(A) respectively, surpassing the recommended levels. Classroom C had a notably high value of 50.4 dB(A), surpassing the consulted standards and studies. Despite this, the noise levels in classrooms A and B align with those reported in other studies[9].

The proposed maximum "ideal" and "acceptable" noise levels are 25 dB and 20 dB below the speech level at 1m from the speaker, respectively [14]. This criterion provides precision in assessing classroom noise, indicating that refurbished classrooms maintain an acceptable noise level for instructional situations with elevated teacher voice levels.

Classroom A and B underwent refurbishments, addressing thermal, ventilation, and acoustic aspects, yet failed to meet RT and L_{Aeq} standards. The design emphasis on thermal and ventilation, without insulation improvements, may explain this shortfall, lacking compliance with national educational facility requirements. While there's a significant enhancement compared to the original Classroom C, assessing the renovation costs in relation to the achieved improvements becomes crucial for a comprehensive evaluation.

Refurbished classrooms achieve mean STI values above 0.6 for the instructional situation, this value being recommended for classrooms in the consulted standards [9-11]. Some criteria suggest that for students under 12 years of age a higher STI is needed, and the best performance of this group can be obtained with an STI above 0.7 [13]. Classroom C only reaches an STI of 0.55 for the instructional classroom, considered outside the desirable range for a classroom, since regular intelligibility is achieved with a high vocal effort.

Better acoustic insulation to the exterior would be a contribution to the instructional activity. Although it has not been a condition for obtaining a good STI, it could provide better results in future refurbishment projects.

The strategies included in the classrooms: increasing the absorbing surfaces in the ceiling and walls and improving the insulation of the windows contributed to obtain the desired STI values and to achieve an improvement in the RT and Background Noise values when compared to a baseline state and to the school enclosures present in the context.

These interventions, in a general characterization, have led the classrooms to stand out among their peers with satisfactory levels in an environment that

presents many cases of infrastructure with unacceptable interior conditioning.

5. CONCLUSIONS

This study has compared the performance of representative cases of educational buildings in the local context. A broad comparison has been made on their architectural design and interior fit-out characteristics and then the performance of acoustical improvements being implemented in these types of facilities has been evaluated.

The rating of the educational facilities in the context revealed major deficiencies and significant gaps in most of the facilities evaluated. This situation underlines the urgent need to review and improve architectural aspects related to acoustics, such as sound insulation, reverberation control and acoustic absorption, to create more effective and comfortable learning environments.

In conclusion, the proposed reforms have had a notable impact on the studied acoustic parameters, significantly reducing reverberation time (RT) and equivalent continuous noise level (L_{Aeq}). However, they have not met all expected standards. The use of acoustic absorbers has helped lower the RT, but only to 0.6 s. in classrooms under 130m³. Background noise levels have exceeded the recommended 30-40 dB(A) range in both refurbished and original state classrooms. Nevertheless, 42 dB(A) is deemed acceptable if speakers project loudly. The refurbished classrooms have achieved STI values exceeding 0.6 for instructional settings.

The observed refurbishment works constitute a significant investment, unavailability time of the classrooms and environmental impact associated with the construction. It is to be expected that works involving this deployment of resources will take a more extensive view of the importance of acoustics in school environments. Future renovations should consider more demanding parameters that allow classrooms with teaching practices different from traditional classes, the use of less vocal effort by teachers and the inclusion of students with learning disabilities. These considerations are necessary to think of more inclusive, efficient, and prepared spaces for future educational challenges.

Future studies may address the type of strategies needed to reform classrooms by providing acoustical conditions that consider contemporary educational challenges, e.g., flexibility and integration of students with learning disabilities.

ACKNOWLEDGEMENTS

This work has been funded by Fondecyt 1210701, "Characterization of physical learning environments in school classrooms that promote academic self-esteem and school motivation."

REFERENCES

1. Klatte, M., Bergström, K., & Lachmann, T. (2023). Does noise affect learning? A short review on noise effects on cognitive performance in children. Frontiers in Psychology.
2. Bluyssen, P. M., Zhang, D., Kurvers, S., Overtoom, M., & Ortiz-Sanchez, M. (2018). Self-reported health and comfort of school children in 54 classrooms of 21 Dutch school buildings. Building and Environment, 138, 106–123. https://doi.org/10.1016/j.buildenv.2018.04.032
3. Hamida, A., Zhang, D., Ortiz, M. A., & Bluyssen, P. M. (2023). Indicators and methods for assessing acoustical preferences and needs of students in educational buildings: A review. Applied Acoustics, 202, 109187. https://doi.org/10.1016/j.apacoust.2022.109187
4. Bluyssen, P. M., Zhang, D., Kim, D. H., Eijkelenboom, A. M., & Ortiz-Sanchez, M. (2021). First SenseLab studies with primary school children: exposure to different environmental configurations in the experience room. Intelligent Buildings International, 13(4), 275–292. https://doi.org/10.1080/17508975.2019.1661220
5. Arroyo, G., & Wegertseder, P. (2018). Evaluación de la calidad acústica de aulas escolares en establecimentos educacionales municipales (IBPSA 2018).
6. Aguilar, J. R. (2019). Una mirada a los criterios de diseño acústico de la infraestructura educacional en Chile. Revista Ingeniería de Construcción, 34(2), 115–123. https://doi.org/10.4067/S0718-50732019000200115
7. Dovey, K., & Fisher, K. (2014). Designing for adaptation: the school as socio-spatial assemblage. The Journal of Architecture, 19(1), 43–63. https://doi.org/10.1080/13602365.2014.882376
8. Astolfi, A., Bottalico, P., & Barbato, G. (2012). Subjective and objective speech intelligibility investigations in primary school classrooms. The Journal of the Acoustical Society of America, 131(1), 247–257. https://doi.org/10.1121/1.3662060
9. Association of Noise Consultants, & Institute of Acoustics. (2015). Acoustics of Schools: a design guide.
10. MINEDUC. (2016). Criterios de diseño para los nuevos espacios educativos. https://bibliotecadigital.mineduc.cl/handle/20.500.12365/4638
11. ANSI/ASA. (2022). ANSI S12.60-2002 Acoustical performance criteria, design requirements, and guidelines for schools.
12. Piderit-Moreno, M. B., Leighton, J., Chandia, V., & Perez-Fargallo, A. (2023). Method to assess the integration of personalization, stimulus and environmental design principles in school classrooms. Journal of Physics: Conference Series, 2600(14), 142010. https://doi.org/10.1088/1742-6596/2600/14/142010
13. Minelli, G., Puglisi, G. E., & Astolfi, A. (2022). Acoustical parameters for learning in classroom: A review. In Building and Environment (Vol. 208). Elsevier Ltd. https://doi.org/10.1016/j.buildenv.2021.108582
14. Bistafa, S. R. (1999). A comparative study of speech intelligibility metrics and the derivation of optimum reverberation time and maximum background-noise level for classrooms. https://doi.org/10.4224/20331303

3.4. Analysis and methods for resilience and sustainability (e.g., new design and simulation tools, evaluation methods)

Exploring the Nexus between the New European Bauhaus and Military Barracks Regeneration:

A Synergistic Approach for Sustainable Urban Development

MARTA RUDNICKA-BOGUSZ[1]

[1]Wroclaw University of Science and Technology, Faculty of Architecture
Wroclaw, Poland

ABSTRACT: The New European Bauhaus Compass emerges as a comprehensive framework aiming to combine aesthetics with sustainability and inclusivity. Across Europe, numerous decommissioned military barracks, reminiscent of past conflicts or strategies, lie under-utilized or abandoned. They present an opportunity for regeneration under this NEB Compass framework. These complexes, with their robust structures and vast landscapes, pose a significant opportunity for redevelopment benefitting historic cities they are a part of, in accordance with the current golden standards. With proper regeneration, they can serve a multitude of purposes, combining cultural centres, housing and green public spaces. This article explores the possibilities of integrating the principles of the New European Bauhaus into military barracks regeneration, drawing from relevant real life case studies. They emphasize the importance of considering environmental sustainability, community engagement and historical context in urban development.
KEYWORDS: military barracks, sustainable regeneration, The New European Bauhaus Compass

1. INTRODUCTION

Historic military barracks across Europe stand as an embodiment of state's policies, pride and ambitions of localities, and vestiges of past conflicts. They constitute a cultural capital in the cityscape of historic garrison towns [1]. Built in strategic locations, they often occupy prime urban or peri-urban land. As a result of developments in warfare, military barracks suffer obsolescence and become brownfields. Considering, that the societies transition towards sustainable and circular practices, the regeneration of military barracks presents a unique opportunity to repurpose underutilized spaces for the betterment of communities [2].

The New European Bauhaus (NEB) initiative represents the European Union's vision of combining aesthetics, sustainable development, functionality and inclusivity in architectural design and urban planning to foster harmonious urban living in accordance with the motto: "beautiful, sustainable, together" [3]. Military complexes comprise of buildings varying in scale and function. Most often constructed for maximum functionality, they now serve as excellent opportunities for regeneration projects that align with NEB's tenets. The regeneration of military barracks presents an opportunity to revitalize historic urban spaces while addressing the challenges of repurposing obsolete structures.

This article explores the significance of military barracks regeneration in the context of achieving circular societies, focusing on environmental, social, and economic aspects. Through case studies and analysis, it demonstrates how adaptive reuse of barracks contributes to resource efficiency, community cohesion and economic revitalization. It demonstrates the synergies between NEB and barracks regeneration, drawing on real-life examples. Integrating these two areas offers the potential for innovative urban regeneration that assures aesthetic appeal, sustainability, and community well-being. This paper strives to prove, that by applying the principles of NEB, the challenges of military barracks transformation can be turned into opportunities, leading to a novel approach that could serve as a model for adaptive and holistic urban redevelopment.

2. RESEARCH METHOD

The New European Bauhaus Compass (NEB Compass) was adopted as a research activity scheme, and its guidelines were used as the basis for further analysis. The NEB Compass was chosen, taking into account that historic barracks complexes are part of a cultural heritage rooted in the local cultural landscape, most of them not being legally protected monuments. The use of this tool as a reference frame helped quantify the diagnosis of revitalization potential and indicate appropriate directions of adaptation.

The Compass is a reference framework. For each value and for each working principle, it presents three levels of ambition. They may be used to guide the design of a project from its first stages. On the other

hand, it can be also used to verify the already completed designs for the accordance with the NEB principles.

The method sets three levels of advancement for each competency. The first ambition level sets the boundary conditions. Only design fulfilling the requirements of these basic features can be analysed further. The second and third levels build on the starting definitions, expanding them with growing aspirations. The ambitions for a beautiful project are: to (re)activate (BI), to connect (BII) and to integrate (BIII). The goals in sustainability are: to repurpose (SI), to close the loop (SII) and to regenerate (SIII). The objectives in inclusivity are: to include (TI), to consolidate (TII) and to transform (TIII).

The presented case studies were chosen based on a broader research, to present all the aspects of the discussed issue. The research method begins with a combination of literature review, visual analysis, and contextual studies to form a comprehensive understanding of the chosen case studies and verify their overall success. Then NEB framework is applied to identify if the regeneration fulfils all the requirements. Ultimate comparison of these two checks if they overlap.

3. CASE STUDIES

3.1 Tempelhof Airport in Berlin

The Tempelhof Feld was originally a community meadow occasionally used as parade ground by the military, before becoming an airport in the 1920s. Expanded by new barracks buildings, in 1933 the airport was turned into concentration camp Columbia House [4], a fact commemorated in 1994 with a sculpture by Georg Seibert at the corner of Columbiadamm [5]. After the clearing of the camp, the airport served as one of the focal points in the plans of Albert Speer to create Germania. After the war the airport was used to overcome the Berlin Blockade imposed by the Soviets. The facility was closed in 2008 and a year later, the city held a limited competition for the redevelopment of the site. The results of the competition sparked a wide public debate and motivated bottom up initiatives for preservation of the historic shape of the area. In 2015 the authorities established a refugee camp in the airport's buildings. Today the facility evokes manifold associations. It simultaneously acts as an international symbol of totalitarianism, war trauma, cold war resistance and humanitarianism [6].

The tarmac strips at Tempelhof Field are used on a daily basis for social activities, including sports and leisure (BII), providing much needed relaxation space in the heart of the city. Since its decommissioning the site hosted numerous public events and artistic activities, like music festivals or fashion shows, sporting events (e.g. marathons) and community engaging undertakings like fairs (BI). All the development activities, e.g. concerning the refugee camp assume a reversible form due to the fact that the building is a protected historic monument (BIII).

The project mainly repurposes historic structures and is based on existing urban plan (SI). The 2,5 by 2 km space of the aerodrome remains an open meadow for outdoor activities, contributing to absorption of rainwater (SII). The meadow is lined with high elderly trees and in parts assigned to allotment gardens, contributing to bigger biodiversity in the area (SIII), as many shortlisted birds and insects dwell and use the area as their feeding grounds.

The project grants widest possible public accessibility of Tempelhof Park's green area (TI). Due to the area's unchanged morphology, it remains the evidence of all the historic events that have transpired there (TIII) becoming a medium of social conscience. The area's transformation is under constant social consultation and no activity or investment can be undertaken without grassroots participation (TII).

The transformation of Tempelhof Airport in Berlin into a public park and community space demonstrates an urban renewal, which is sustainable and participatory. The airport's adaptive reuse aligns with NEB ideals, merging functional design with historical preservation influencing the beautification of the neighbourhood and the betterment of life.

Figure 1: Chassé Military Compound in Breda after regeneration: we can see the co-dependency between buildings, kept historic edifices (red), the vistas (blue) and the unifying park. (elaborated by author on the basis of [8])

3.2 Chassé Military Compound in Breda

Chassékazerne is the signature 19th-c. building in barracks complex occupying a site neighbouring the city centre in Breda with a military tradition dating back to the 17th-c. An elongated main building was built at the roll call square. Furthermore, an exercise hall, an officers' canteen and an infirmary were built in a similar, but simplified style along the access road to the roll call site [7]. The barracks went out of

service in 1993. Since then the Breda local authorities sought a function for the complex. The city decided to put out a closed design competition for the masterplan [8]. Several proposed projects were deemed unsatisfactory, before OMA were commissioned to prepare the masterplan, teaming up with West 8 for landscaping.

The masterplan assumed the form of a "campus" with the prevalence of park space, providing a green enclave within the neighbourhood. On the site and in its vicinity were situated mostly solitary buildings: the 1970s town hall, the 1980s Chassé Theater, the barracks themselves, Breda's Museum in the renovated Kloosterkazerne (SI), the new Holland Casino and the Mezz Muziekcentrum. The 13 ha district was densified with 8 new build structures to host 700 housing units (luxury apartments, rental housing, subsidized housing, and residences for seniors and the disabled); 30,000 sq m. of office space; 2,000 sq m. of retail space; 1,500 sq m. underground parking spaces and 8 ha of public parkland.

The new and old buildings were paired. The new build was developed in relation with its counterpart vis a vis to ascertain consistency (BI). To establish spatial relations with the city, special attention was given to a network of paths for pedestrians and cyclists and sightlines, such as the vista to the old town (BII) [7]. They determine the position and volume of several new-build forms. The campus model, unites buildings that are different from each other because of special architectural and typological characteristics. It allows for unification of different dwelling styles (BIII).

In the Chassé regeneration project, the landscape is the element providing cohesion to the plan [7]. The site was designed as one large park-like space. Along with Wilhelmina Park the site constitutes a part of a green corridor wedged between the city centre and the southeast edge of the city. Multiple oak trees were planted, contributing to enhancing biodiversity and improving the amount of greenery in the city (SIII), at the same time enhancing rainwater retention (SII). Although the site provides much needed parking space for the nearby area, all parking takes place underground (SIII).

With the regeneration design, the area once secluded and clandestine because of its military use was opened and included in the city. The area is designed as overtly accessible to diverse social groups given the varied accommodation it offers, including social housing and lodgings for the elderly (TI). Thus, the design aims to build a community where different groups can peacefully live alongside each other and interact (TIII). Moreover, in the case of Chasse Park the municipality is the owner of public space, and management is divided in "basis management" (by the municipality) and "additional management" (executed by residents and entrepreneurs) [9].

The regeneration embodies innovative ways of thinking about the city in the best NEB sense. Instead of a square or a street, it is the park, which organizes the space of the site. It sets the tone for spatial and social relations. Freeing the pedestrians from the constraints of the traffic it allows for parking underground, catering to the needs of all. As a result, the central city not only acquires a new mix-use area, but a park as well, additionally preserving its architectural heritage (Fig. 1).

3.3 The Arsenal in Venice

The goal of the regeneration of the Arsenal in Venice was the reintegration of the city's largest and historically most significant military site. The Arsenal was a huge construction site for ships, developed between the 12th and the 20th -c. Since WWI it was being gradually abandoned. In 1980 the Arsenal became an exhibition site for the Biennale on the occasion of the 1st International Architecture Exhibition. Since 1999, consecutive parts of the site have been included in a program for the regeneration of the area. About 50.000 sq m. (25.000 sq m. indoor space) of the Southeast area of the Arsenal have become a permanent site of the Biennale activities. In addition to the central international exhibitions of the Art and the Architecture sections, select countries rent spaces in the complex for their national pavilions, in exchange for contributions to the building's renovation costs. The regeneration project was an attempt to interweave sustainable development with history and architectural value of this exceptional place (SI). The buildings were not altered but enhanced inside with modern construction trusses and refurbished, e.g. fitted with sustainable heating (SII). The process leaves the structure and the outer shell intact and is reversible [10].

Although part of the huge compound is still used as a military base by the Italian Navy, the complex is freely accessible during the Biennale or the rest of the year upon request. Visiting the site is a fascinating way to discover the secrets of the military power of the Venetian Republic, a bit of the recent history of the city, and a collection of world-famous contemporary art exhibitions (BI).

The Arsenal of Venice complex was once the largest industrial establishment in Venice. Even after shedding its military function, it remained a symbol of a former economic, political and naval power of the city. It occupies an area of approximately 32 ha. Considering the size of Venice, which is 670 ha, the possibilities this compound may grant the city become apparent. It accommodates the largest open area in Venice - a potential site for public institutions

that Venice needs urgently. A grassroots organization, The Forum Futuro Arsenale, is protesting plans to expand the influence of the Biennale in the Arsenal. The activists argue that too much attention is paid to mass tourism and that the city depopulates due to the tourist monoculture supported by the municipality [11]. The association proposes nine projects for the site to benefit the local community and create a place for traditional crafts in the city, such as shipbuilding. Still, it seems the authorities support the plan to adapt a subsequent portion of the complex for the use by the Biennale and its inclusion in the tourist structure of the city [12].

The revitalization of the Arsenal complex in Venice displays the harmonious integration of historical heritage with contemporary design and function. This case demonstrates how historical structures can be transformed into modern, functional spaces while preserving their identity [13]. However, it does not reinforce a sense of belonging or include citizen participation and is not an inclusive space for social interaction. Thus, it fails to meet the NEB goals: BII, BIII, SIII, AII and AIII.

3.4 The Royal Arsenal in London

Regenerating military barracks invigorates local economies by generating employment opportunities and creating new neighbourhoods. The Royal Arsenal Riverside turned a 31-ha area of derelict industrial land into a successful, sustainable mixed-use development. This revitalization led to an influx of residents and businesses, propelling economic growth while preserving selected historical heritage.

The Royal Arsenal's importance is in the act that it was once the driving force of the neighborhoods' economy – at its height employing more than 80,000 people. It begun its history in 1671 when the site was purchased by the Crown and was used for the maintenance and storage of cannons. An industrial workshop was constructed on the site in the 17th-c. From this nucleus the Arsenal grew through the 18th-c. to accommodate the barracks, a military academy, the Royal Brass Foundry, the New Carriage Square and the Officers' Quarters. The decommissioning of the Arsenal begun in the 1930s. Because in the 1950 military production was in decline, 40 ha of the site were sold for use as a trading estate. The final winding-down of the site commenced in 1964 and the ordnance factories were closed in 1967.

A commercial competition led to the selection of a masterplanning, design and management team led by Llewelyn Davies Yeang. An underlying aim of the regeneration strategy was delivering economic and social regeneration while keeping unique architectural heritage. The masterplan set out the strategy to ensure a high degree of flexibility for economic viability. The commercial success of the regeneration was based on promoting a wider range of uses and ensuring active street frontages within the layout. Two strong axes run along cardinal direction's through the masterplan, No. 1 Street (N-S) from the Thames towards town center is a grand pedestrian avenue with rows of trees. Wellington Avenue (E-S) distributes traffic across the complex.

The site was arranged around five overlapping activity areas: housing on the waterfront and running back to Wellington Avenue; business and services in the eastern part, at the main road; museums and heritage attractions in the vicinity of No. 1 Street and the river pier; commercial leisure activity in the south-western part (BIII). The site also establishes strong links with the River Thames through the riverboat pier – a part of Blue Ribbon Network, which promotes the use of the waterways for leisure, passenger traffic and transport (SII). The masterplan strategy aimed to retain and bring back into use the maximum number of historic buildings, both statutory Listed Buildings and those of local historic interest (SI). New construction, encompassed ca. 80,000 sq m., taking up the place of removed historic buildings and spaces. Other elements such as track plates have been re-sited in thresholds, and salvaged artefacts have been used as public art (BI). The masterplan included a series of linked civic spaces, to provide a sense of place for local people and employees, which could also be enjoyed by visitors (BII). The public-realm design also included public open space alongside the Thames and its riverside walkway, and a small local park in the center of the site (SIII).

The public were consulted when the planning application was made and again in the second stage of the project (TII) [14]. The Royal Arsenal was an inaccessible military industrial site, hidden behind high walls. The regeneration opened it, granting the wider public access to the River Thames and historic monuments it encompassed. The regeneration strategy established community benefits, such as arts and culture facilities, equal opportunities promotion, public open space and social services, e.g. local employment training initiatives designed to help young people and the unemployed (TII).

The regeneration aligns with NEB by: reconnecting a secluded site into the city; establishing wide public consultation and training programs; improving the amount of green sites in the city; improving green transport-related schemes, e.g. a connection to the Waterfront Transit system.

4. DISCUSSION

Cities are neither *tabula rasa* nor *palimpsest*. The many layers of development accumulated through time make each city unique and foster local identity. Even so, living, resilient cities must be susceptible to

change, to become fit for the 21st-c. An initiative to reconcile progressiveness with historical identity is the New European Bauhaus. The NEB emphasizes several core principles, including sustainability, circular economy, inclusivity and aesthetic quality. These principles lay the foundation for creating transformative urban spaces that resonate with both historical context and contemporary needs. This aligns with the goals of revitalizing decommissioned historic military barracks into vibrant, functional and sustainable urban spaces, which reflect local history and tradition.

Military barracks, once focal points of local economy and development, symbols of local pride [15], should now find new purpose in a circular society. These expansive estates encompass multiple historic buildings and many open spaces, like the roll call areas and paddocks. The manifold benefits of military barracks regeneration include reduced environmental impact, enhanced social integration and economic and ecologic sustainability. Barracks repurposing also means retaining culturally viable spaces for the cohesion of cultural landscape [16] and the continuity of its narrative.

The regeneration of military barracks poses multifaceted challenges, including structural adaptation, historical preservation and community integration, especially in places where they were linked to ethnic disputes. However, these challenges are accompanied by opportunities: to redevelop vast brownfields in centres of the cities in ways that address current urban growth, environmental concerns, and social well-being. Cities can reimagine military complexes in a way that reflect both their historical significance and contemporary needs. This synergistic approach has the potential to set a precedent for holistic and adaptive urban regeneration across Europe and beyond, fostering resilient, vibrant, and socially cohesive communities.

Decommissioned military complexes pose a challenge in urban development. Many of these sites have faded from the public consciousness. The reason is that while people are familiar with the history and significance of the barracks site – and the history revolving around them - the sites were inaccessible to the public for decades or even centuries. Societies lived alongside them, but they remained unmarked spots on mental maps of the city. The core task of conversions is therefore to overcome the separation of these areas. However, it should be done not only to develop new uses and a new identity, but also in a way preserving all the key sentimental values and their material representations present at the site. The regeneration should preserve both the architectural fabric and the artefacts.

While usually the architect is impatient with what he finds on the site that hampers him, these *objet trouvé* extend the architectural potential of both the architect and the site. They introduce complexity that would be artificial otherwise [17], as exemplified by the Chassé complex. The historic urban layout and the historic barracks architecture constitute these "found objects" – the ready made solution to two of the three boundary conditions of the NEB Compass – the beautiful and the together.

Regenerating a large historic site for mixed-use is a complex process. Main challenge is posed by the need to find uses for multiple historic buildings. These new uses must be resilient to fluctuating economy and property market conditions. In particular, the new facilities have to be able to survive the challenging early stages of redevelopment when their expense will probably exceed income. A strategy has to ensure a high degree of flexibility for economic viability. The masterplan should provide the intent and respect for the heritage, while allowing the private-sector developers to advance the elements of the masterplan in their own way. A proper strategy should illustrate possibilities instead being a precise specification for every use in every building, and the experience of the Royal Arsenal proves that. For this to happen, all the actors in the regeneration process must be confident that the commitment to quality and respect for heritage would remain, even as plans change in detail over time. This can be ascertained by public-private partnership and social participation in the process. Without it, as illustrated by the Venetian Arsenal example, even potentially socially beneficial initiatives can be viewed as hostile. The key missing factor seems to be the greater involvement of non-institutional initiatives. The planning phase of regeneration needs to include participation practices, e.g. surveys. Second approach should include reversible adaptation strategies for temporary use and greater flexibility. This can be illustrated by the 2014 referendum when Berliners decided not to use the gigantic site of the former Tempelhof airport and barracks for increased density through new construction. The grassroots-fostered regeneration effort resulted in a reuse model in which the unchanged site serves modern society. On the other hand, concerns for its economic sustainability arise, while many of its historic structures remain unused, but need to be economically supported.

A sustainable regeneration strategy is reached when the combined achievements start to outweigh the contribution of the individual stakeholders. The conditions for this to happen have to be engineered through masterplan. This will never be possible unless all the stakeholders involved in the project have a shared vision of the site's potential and a clear idea of what makes it special and important to local people and investors alike. Its sustainability then becomes a

function of what the site can offer and the potential that stakeholders can see in it – not just for themselves but also as something that deserves to be passed on to the care of the next generation.

5. CONCLUSION

The research proves that there exist multiple common denominators between barracks regeneration and sustainable city development as envisioned by NEB. First is the beautification of city by integrating more historic and sentimentally charged architecture into the cityscape. Second is the concept of a circular economy, emphasizing *inter alia* the continuous use of resources through repurposing and regeneration of historic architecture. Moreover, the morphology of barracks allows, during their regeneration, for creating many new parks and green areas within the inner city. Third by opening to the public the historic areas of town, which were inaccessible due to their military function, granting the wider public more communal space for social interaction.

The research also revealed issues hindering the regeneration potential of military sites. One of the most pressing problems is the monocultural approach to the regeneration masterplanning, with single-function design or an inflexible approach, constraining the regeneration within only one strategy of regeneration. Such approach does not guarantee long term beneficial effects of regeneration. It may also lead to alienation of local populace, if a new neighborhood on a reclaimed post-military land is dedicated solely to benefit its developers. Therefore, the biggest issue is the right amount and quality of social participation. Effective regeneration should be measured not only quantitatively, but mostly by taking into account the human experience and impact on the urban biodiversity.

The research illustrates that even if NEB Compass was not the basis for the revalorization project, but the design was executed in such a way that the NEB Compass conditions are met, it will be a more successful endeavor than those not adhering to NEB. It also proves that the regeneration efforts executed with the greatest sensitivity to the barracks typology and their *genius loci* tend to check all the boxes with the NEB. Consequently, the method of choice for planning of extended program of barracks regeneration should be the NEB Compass. The NEB Compass is a multilevel framework suitable for not only design but also programming of regeneration efforts. It enables effective addressing of the formal, ecologic and societal challenges faced by the contemporary city.

ACKNOWLEDGEMENTS

The research was financed by the National Science Center: 2018/31/D/HS2/03383.

REFERENCES

1. Rudnicka-Bogusz, M., (2021). Legnica's Grenadier Barracks as a cultural capital in the urban space. Architectus, 1(65): p. 21-30.
2. Jarczewski, W. and Kuryło, M., (2010). Regeneration of post-military areas in Poland. Europa XXI, 21: p. 117-133.
3. European Commission. "The New European Bauhaus." 2021 [Online], Available: https://new-european-bauhaus.europa.eu/index_en
4. Bijak, A., and Racoń-Leja, K., (2018). Political aspects of Tempelhof Field. Technical Transactions, 2: p. 27-44
5. KZ Columbia House [Online], Available: https://www.thf-berlin.de/en/history-of-location/national-socialism/kz-columbia-house [10 December 2023]
6. Parsloe T., Berlin's Tempelhof: The camp too controversial to customize, [Online], Avilable: https://deeply.thenewhumanitarian.org/refugees/articles/2017/06/22/berlins-tempelhof-the-camp-too-controversial-to-customize [10 November 2023]
7. Monumenten in Nederland. Noord-Brabant [Online], Available: https://www.dbnl.org/tekst/sten009monu02_01/sten009monu02_01_0030.php [21 November 2023]
8. Beliën J, Looman B, (2011). Chassé Park, a masterplan misunderstood?, .docs, 1: p. 33
9. van der Putt, P., (2011). Chassé Park Breda. DASH | Delft Architectural Studies on Housing: The Urban Enclave, 5: p. 148-155.
10. Venice – regeneration of the Arsenal [Online], Available: http://ekologiakonstruktywnie.mazovia.edu.pl/venice-regeneration-of-the-arsenal [21 November 2023]
11. Clark, C., Pinder, D., 1999 Naval heritage and the revitalisation challenge: lessons from the Venetian Arsenale, Ocean & Coastal Management, vol. 42, Issues 10–11, p.933-956,
12. Goldstein, C., A Venice Coalition Is Protesting Plans to Permanently House a Biennale Archive in the Arsenale, artnet, [Online], Available: https://news.artnet.com/news/venice-arsenale-protests-2070942 [27 November 2023]
13. Germen, M.S., (1992). The Arsenal of Venice: A Study on the Degree of Context-Conscious Architecture. Master Thesis, Massachusetts Institute of Technology.
14. Thomas Street Masterplan Spd [Online], Available: https://consultations.royalgreenwich.gov.uk/UploadedFiles/Second%20Draft%20Thomas%20Street_SPD.pdf [11 November 2023]
15. Rudnicka-Bogusz, M., (2022). The Genius loci Issue in the Revalorization of Post-Military Complexes: Selected Case Studies in Legnica (Poland). Buildings, 2 (12): p. 1-33.
16. Gyurkovich, M., (2013). Hybrydowe przestrzenie kultury we współczesnym mieście europejskim, WPK, Kraków.
17. Chaslin, F., (1992). Un rationalisme paradoxal, Entretien avec Rem Koolhaas, l'Architecture d'aujourd'hui, 280: p.162-169

PLEA 2024 WROCŁAW
(Re)thinking Resilience

Evaluating Energy Efficient Retrofit Measures for a Pre-1930 UK Home

PRAVEENA POCHAMPALLI[1], RENATA TUBELO[2], LUCELIA RODRIGUES[2], MARK GILLOTT[2], ROBERT NASH[3]

[1] Buildings, Energy and Environment Research Group, Faculty of Engineering, University of Nottingham, Nottingham, United Kingdom
[2] Department of Architecture and Built Environment, University of Nottingham, Nottingham, United Kingdom
[3] Active Building Centre Research Programme, Swansea University, Swansea, United Kingdom

ABSTRACT: In the United Kingdom, buildings account for 49% of the total greenhouse gas emissions, and domestic buildings around 22%. In this paper, the authors present a study of energy efficient retrofit measures applied to a pre-1930s mid-terrace dwelling located in Nottingham, UK. Firstly, a series of building envelope improvements aiming to reduce heating demand were evaluated sequentially using dynamic building simulations. Secondly, low-carbon heating systems were introduced and their impact evaluated considering a varying coefficient of performance, aligned with the fabric improvements. The findings suggested possible 50% reduction in heating demand through typical fabric optimisation measures. The adoption of low carbon heating systems led to a 50% decrease in carbon emissions compared to the emissions produced by a typical gas heating system. The results also indicated the relevance of coordinating the fabric optimisation with the installation of air source heat pump to optimise carbon savings.

KEYWORDS: Energy performance, Carbon emissions, Building fabric, Retrofit, Low-carbon heating system

1. INTRODUCTION

Buildings account for 49% of the total United Kingdom (UK) greenhouse gas emissions, and the residential sector for circa 22%, primarily carbon dioxide emissions from energy use for heating [1]. The UK government has set a greenhouse gases net zero emissions target by 2050, and is debating whether to set a target to improve the energy efficiency of homes [2]. The UK has one of the oldest and least energy-efficient housing stock in Europe [3]. Approximately 80% of the buildings that will form the UK's housing stock in 2050 have already been built, with most built before 1990, when building energy standards were not yet established. This accounts for 28 million residential buildings that will require retrofit, which poses a significant challenge to the housing sector [3].

In Nottingham, within the East Midlands region, 62.2% of the residential buildings are houses, 29.9% are flats, 5.6% are bungalows and 2.3% are maisonettes [4]. As a proportion of Nottingham's total housing stock, the most common house type is mid-terrace houses, which account for 22.4% of all residential buildings [5,6].

The Energy Performance Certificate (EPC) assesses a building's energy efficiency and assigns an A to G band scale with band A, indicating the highest efficiency and lowest operating costs and band G, indicating the least efficient and highest operating costs [5]. The UK Government's EPC database contains EPC records for 164,460 residential buildings in Nottingham. Among these, 61.2% of the EPC's, comprising the majority of residential buildings built before or during the first half of the 20th Century, fall below band C. Furthermore, 75% of the mid-terrace houses are classified within EPC bands D to G [6].

In order to improve building energy performance and reduce carbon dependency, it is important to retrofit the fabric, adopt low carbon heating systems and integrate renewable energy technology [1].

In this paper, the authors adopted a representative case study of pre-1930s mid-terrace dwellings in Nottingham as a vehicle to examine retrofit measures through a sequential approach using dynamic building simulation. The main aim of the study was to understand the impact of each fabric measure alongside the integration of an air-source heat pump on the performance of the building.

2.CASE STUDY

The case study selected was a 3-storey, 3-bedroom, mid-terrace house with a total floor area of 67m² (Figure 1). The house is part of the Nottingham City Homes tenancy scheme, within the umbrella of Nottingham City Council. The house was constructed out of 215mm solid brick walls, solid ground floor,

and cold roof with reduced levels of insulation. Internal partitions were made out of lath and plaster internal studs and internal floors were assumed as a typical 19mm timber flooring on 100 mm joists and 12.5 mm plasterboard ceiling based on Chartered Institution of Building Services Engineers (CIBSE) guidelines [7]. The existing windows were double-glazed. The air permeability of the building envelope was assumed as 15 m3/hm2 @ 50Pa based on the old Part L 2013 regulations, a typical value for a house of this age in the UK [8].

Figure 1: Mid-terrace house (Top) from Google Map data (2023) and simulation model (Bottom)

3. CLIMATE

Nottingham is classified as a cool-temperate climate according to the Köppen-Geiger climate classification. The Climate Consultant 6.0 EPW format climatic data indicates a steady range of dry bulb temperatures from 2°C to 21°C throughout the year, with long winters, short summers, and abundant rainfall year-round. The relative humidity reaches its highest point at 87.5% between November and January, then decreases to approximately 74% in July and August. Nottingham typically experiences four distinct seasons: summer (June-August), winter (December-February), spring (March-May), and autumn (September-November). The climate analysis show that the energy demands for buildings in this region are mostly influenced by heating requirements due to the much longer heating period compared to cooling period. Design strategies must prioritise airtightness and efficient insulation to prevent heat loss from the building in colder seasons.

The Committee on Climate Change (2019) indicated that the housing stock in the UK is inadequately prepared for both the present and future climate conditions. It has also been pointed out that the way existing homes are retrofitted often falls short of design standards and proposed that existing homes around the UK should be transformed to be low carbon, low-energy by adopting measures such as loft insulation, wall insulation, double or triple glazing, as well as utilising low-carbon heating sources like heat pumps and heat networks [9]. This climate study informed the overall investigations and decisions made.

4. METHODOLOGY

This study investigated housing retrofit through two different stages. Stage 1 considered building fabric optimisation using typical retrofit measures, while stage 2 adopted low-carbon heating systems and renewable energy generation.

Retrofit stage 1: Fabric optimisation

Building fabric as-built was first examined to establish current heating demand. Next, a series of simulations were carried out to measure the energy reduction achieved by adopting selected cumulative changes on the fabric up to Part L 2021 notional levels [10].

The sequential approach considered the likelihood of the measures and consisted of a method developed for evaluating retrofit fabric measures (Figure 2). This method was developed as part of a much larger study that looked at retrofit across different UK housing typologies of varied periods. For this case study, some of the retrofit measures were not considered (marked with X) as they would be costly and disruptive then, not deemed representative of a typical retrofit. Scenarios 3 and 5 were not tested due to the fact that replacing solid ground floor would be an unlikely measure carried out and the windows were already double glazing.

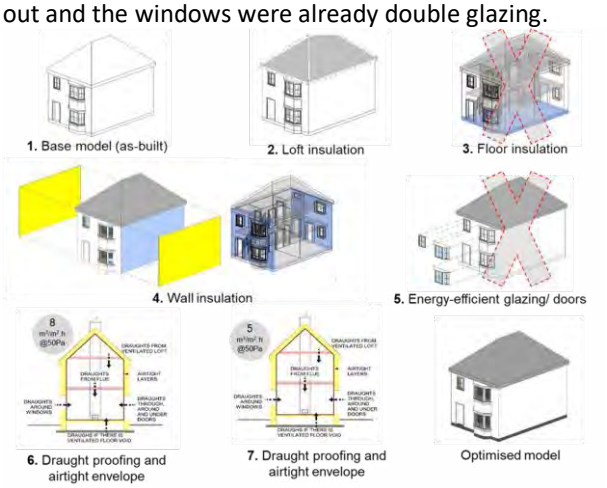

Figure 2: Typical retrofit stage 1 scenarios for simulation

The method considers a total of seven simulation scenarios (base model plus six levels of building fabric improvements) (Table 1). In this investigation, the key scenarios considered for simulation were:

- Loft insulation, measured in W/m^{2}K
- Wall insulation, measured in W/m^{2}K
- Varied Airtightness levels (Draught Proofing), measured in m^3/hm^2 @ 50Pa

Table 1: Building fabric optimisation simulation scenarios

Scenario	Retrofit measure
1 (As-built)	Highly infiltrated (15 m^3/m^{2}h), poorly or non-insulated building envelope.
2	Added loft Insulation to scenario 1 (FHS target)
3	Added loft insulation + floor insulation (considered as-built and not optimised)
4	Added loft insulation + floor insulation + external insulation on the walls (FHS target)
5	Added loft insulation + floor insulation + wall insulation + energy-efficient glazing and doors (considered as-built and not optimised)
6	Added loft insulation + suspended floor insulation + wall insulation + energy-efficient glazing and doors + draught-proofing and airtight layer (8 m^3/m^{2}h)
7	Additional draught-proofing and airtight layer to scenario 6

Table 2 summarises the U-values for the as-built and optimised scenarios. Building fabric optimisation included 200mm of rock wool insulation applied to solid walls and replacement of 230mm existing roof insulation by 450mm of rock wool insulation. Existing double-glazing windows and solid floors were not altered.

In scenario 6, the draught-proofing was upgraded to improve the airtightness of the building to 8m^3/m^{2}h @50Pa as per Part L 2021 maximum permitted target [10]. In scenario 7, the fabric energy efficiency of the whole building envelope was optimised by further reducing the airtightness level to 5m^3/m^{2}h @50Pa as per Part L 2021 notional levels [10].

Table 2: Summary of existing and proposed values for building envelope thermal transmittance (U-values) and air permeability

Mid-terrace 3-storey 3-bedroom	Existing U- value	Proposed Target U- value: Part L 2021 notional building
External Wall	2.02 W/m^{2}K	≤ 0.18W/m^{2}K
Roof	0.3W/m^{2}K	≤ 0.10W/m^{2}K
Party walls	1.48 W/m^{2}K	as existing
Internal partitions	1.30 W/m^{2}K	as existing
Ground floor	1.47W/m^{2}K	as existing
Intermediate floors	1.57 W/m^{2}K	as existing
Air permeability	15 m^3/hm^2@50 Pa	5 m^3/hm^2@50 Pa

Retrofit stage 2: Consideration of Low-carbon heating systems & renewable energy generation

The main aim was to comparatively evaluate the impact of passive measures when combined with low-carbon heating systems. An air source heat pump (ASHP) and solar photovoltaics panels (PV) were integrated in the model (Figure 3). The simulations were carried out to measure energy consumption and carbon emissions comparing ASHP and a typical gas boiler heating system. One of the main aims was to gain an insight into which stage of building fabric optimisation, ASHP is better installed, i.e. when its performance is not diminished by a leaky fabric.

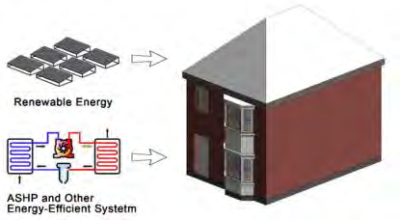

Figure 3: Retrofit stage 2 scenarios for simulation

Typical gas boiler and ASHP heating systems were adopted for space heating and domestic hot water (DHW). Heating inputs were considered as mentioned in Table 3 and DHW mean consumption was adopted as 75 litres/day [11-12].

For the gas boiler, the seasonal efficiency was 0.89; the seasonal coefficient of performance (SCOP), which identifies how many kW of heat a system can generate for every kW of electricity, was 0.8; there was no ventilation heat recovery effectiveness. The ASHP was considered as the central heating system working with radiators. The ASHP SCOP was varied from 1.8 to 2.8 for space heating and 1.5 to 2 for domestic hot water based on [13-15]. This means, for a well-insulated house with a well installed ASHP a typical SCOP for space heating would be 2.8 and SCOP for water heating would be 2. This is because water heating requires a higher temperature to be achieved, upwards of a 45°C gain, and the ASHP is less efficient when delivering these higher temperatures (works at maximum 50-55°C); whereas space heating can be operated with lower temperature gains, typically 30-35°C, ideal for under floor heating.

For renewable energy generation, 8 solar PV panels were considered based on the usable roof area of a mid-terrace archetype. The panel type was monocrystalline silicon and the other specifications include panel size of 2m², with module nominal efficiency 0.20, Nominal cell temperature (NOCT) as 42°C and temperature coefficient for module efficiency Pmax as -0.36%/°C [16]. The panels were inclined at 43° and oriented towards the West, as per case study orientation.

The total energy demand was calculated considering the energy needed to run the house over a period of a year. It considered space heating, electricity (lighting and appliances) and hot water inputs.

Total carbon emissions of the heating were calculated using the Standard Assessment Procedure (SAP) 10.2. Natural gas and electricity were assumed to have carbon emission factors equivalent to 0.21 (kgCO2e/kWh) and 0.136 (kgCO2e/kWh), respectively [17].

Simulation assumptions

The assumptions adopted in the simulation model are described in *Table 3*. Heating setpoints were based on CIBSE guidelines [7]. No cooling systems and active design improvements were considered.

Table 3: Assumptions adopted in the simulation model

Parameter	Description	Assumption	Profile
Weather	Nottingham	Typical weather year	Nottingham_ CIBSE-DSY
Air permeability	Base model	15 m^3/hm^2 @ 50Pa	
	Test model	8 m^3/hm^2 @ 50Pa	Part L 2021 maximum permitted
	Improved model	5 m^3/hm^2 @ 50Pa	Part L 2021 notional
Heating profile	Base model heating setpoint	Lower thermal comfort temperature limits in dwellings according to CIBSE (2019b, p. 1-10): Bathrooms: 20°C Bedroom: 17°C Circulation: 19°C Kitchen: 17°C Living:22°C	Extended from October to March
Internal gains, based on TM59 [18]	Bedroom Occupancy	Sensible 75 W/person, Latent 55 W/person, Density 2; 70% during sleep activity	As per schedule
	Bedroom Lighting	2 W/m^2, Radiant Fraction 0.45,	18-23 hour
	Bedroom Equipment	Sensible 80 Watts, Radiant Fraction 0.22	As per schedule
	Living Room Occupancy	Sensible 75 W/person, Latent 55 W/person, Density 2	As per schedule
	Living Room Lighting	2 W/m^2, Radiant Fraction 0.45	18-23 hour
	Living Room - Equipment	Sensible 150 Watts, Radiant Fraction 0.22	As per schedule
	Kitchen - Occupancy	Sensible 75 W/person, Laten 55 W/person, Density 2	As per schedule
	Kitchen - Lighting	2 W/m^2, Radiant Fraction 0.45	18-23 hour
	Kitchen - Equipment	Sensible 300 Watts, Radiant Fraction 0.22	As per schedule
	Circulation area and bathroom - Lighting -	2 W/m^2, Radiant Fraction 0.45	18-23 hour
	Bedroom Equipment	Sensible 1.75 W/m^2, Radiant Fraction 0.22	18-23 hour
Heating system	Base model / Improved Model (gas boiler)	Seasonal efficiency: 0.89. SCoP (kW/kW): 0.8. No ventilation heat recovery No CH(C)P.	Normal natural gas metre
	Test model for ASHP	Central heating system through radiators. ASHP SCoP for Space heating – 1.8 for base case and increased to 2.8 at later scenarios ASHP SCoP for Domestic hot water - 1.5 for base case and increased to 2 at later scenarios	Air source heat pump (Electricity)

5. RESULTS AND DISCUSSION

Results are shown in terms of heating energy demand for fabric optimisation. For low-carbon heating systems and renewable generation consideration, the results are analysed in terms of energy demand and carbon emissions.

Retrofit stage 1: Fabric optimisation

The results are shown in Figure 4 and indicated that loft insulation reduced the heating demand by 3% in scenario 2, when compared to the base model (scenario 1). Floor was not optimised in scenario 3 and remained same as scenario 2. External wall insulation showed to be the most significant optimisation measure thereby reducing the heating demand by 29% in scenario 4 in comparison to scenario 3. Windows and doors optimisation was not considered in scenario 5. Draught-proofing and airtight layer reduced heating demand by 20% in scenario 6. A further reduction in airtightness level in scenario 7 delivered 2% improvement in relation to scenario 6.

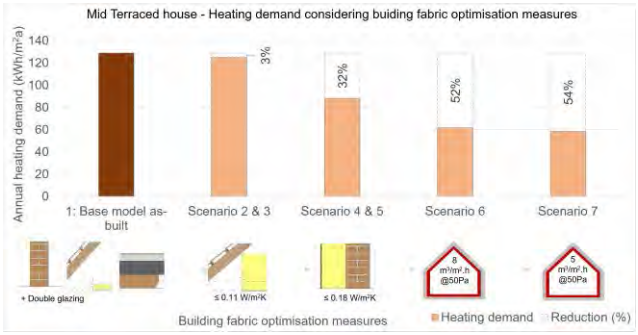

Figure 4: Typical retrofit fabric measures

The mid-terrace house initial heating demand was estimated to be 130 kWh/m^2. The combination of sequential retrofit measures allowed the heating demand to be reduced to 59 kWh/m^2, this represented a reduction of 54% in the demand.

Roof insulation showed one of the least impacts in terms of reducing heating demand, but this is also one of the easiest strategies to be implemented. Roof insulation showed a reduction of 3% in the heating demand, equivalent to 4kWh/m^2. The most impactful insulation measure to reduce heating demand was the consideration of wall insulation. It reduced the energy demand by 29%, equivalent to 41 kWh/m^2.

Airtightness improvement from 15 to 5 m^3/m^{2}h @50 Pa reduced the overall heating demand by 54%, resulting to 59 kWh/m^2.

Retrofit stage 2: Consideration of Low-carbon heating systems & renewable energy generation

Figure 5 displays comparatively the simulation results in terms of energy consumption and carbon emissions for ASHP and a conventional gas heating system.

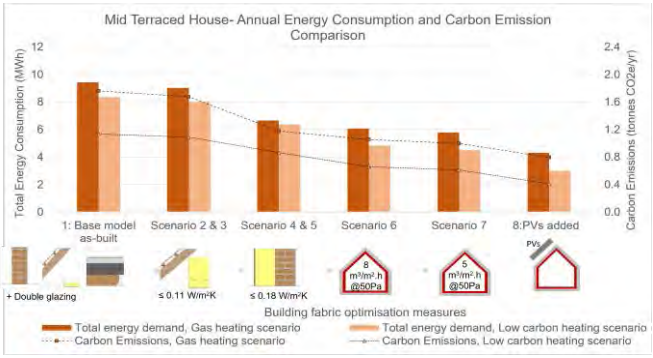

Figure 5: Typical retrofit – heating systems annual energy consumption & carbon emissions

The total energy consumption from using a gas boiler for heating was significantly higher in leaky, non-insulated buildings and was significantly reduced when fabric optimisation measures were considered. The total annual energy demand represented 9 MWh for the as-built scenario (including DHW) and with the addition of the fabric optimisation measures, the overall energy demand was reduced by 39%, which corresponded to 5.7 MWh. The contribution of renewable energy further reduced the energy demand to 4 MWh.

The total energy consumption when adopting ASHP was slightly lower in comparison to the gas boiler heating system. This was due to the efficiency of the system and inputs adopted. For the simulations, ASHP Seasonal coefficient of performance (SCOP) value varied between 1.8 to 2.8 across the scenarios for space heating and between 1.5 to 2 for hot water. A noticeable reduction in the demand could be noticed by the sequential improvement in the fabric. The total annual energy demand was higher in the uninsulated, leaky envelope, which corresponded to 8MWh. Once the fabric optimisation measures were considered, the energy demand was reduced by 46%, reaching nearly 4.5MWh. Renewable energy further reduced the total annual energy demand to 3 MWh.

In terms of carbon emissions, a considerable difference was observed when considering a traditional gas boiler as heating system in comparison to ASHP. As expected, the carbon emissions with gas boiler system were higher in comparison to the low-carbon heating system. For a mid-terrace house with a typical 1930 building fabric and a gas boiler system, the carbon emission levels nearly corresponded to 1.7 tonnes CO_2/yr in comparison to nearly 1 tonne CO_2/yr when typical retrofit fabric measures were considered. Comparatively, when adopting ASHP as the heating system, the carbon emissions corresponded to 1 tonne CO_2/yr and were reduced to half when the fabric optimisation measures were considered, respectively. Renewable energy further reduced the total carbon emissions to 0.4 tonnes CO_2/yr, resulting in an overall reduction of carbon emissions by 64%. It is noteworthy that the external wall insulation of the fabric optimisation measures has contributed significantly to reducing energy consumption and carbon emissions.

The energy and carbon simulation results indicated that implementing fabric optimisation strategies can lead to a 50% reduction in both energy consumption and carbon emissions. Furthermore, it was noted that implementing low-carbon heating system led to an additional 50% decrease in carbon emissions compared to the emissions produced by gas heating systems (Figure 5).

However, it is important to note that the energy costs are dictated by the price of the kWh of energy source. In the UK, still gas has a lower price when compared to electricity, what might discourage the take on of low-carbon heating systems. More research is needed to understand which stage of building fabric optimisation, ASHP should be installed without negatively impacting on household energy bills.

6. CONCLUSION

In this paper, the authors assessed at a typical retrofit of a pre-1930 mid-terrace house in Nottingham, UK, considering fabric measures, low-carbon heating systems and renewable energy.

The wall insulation was one of the most impactful fabric measures, resulting in a considerable 29% reduction compared to the previous strategy. This is due to its larger exposed envelope area in comparison to the other fabric elements.

The research also highlighted that the replacement of gas boilers by low-carbon heating systems should only be considered when a certain degree of improvement was carried out on the fabric. ASHP are most suited to installation in better insulated quality-built homes that demand lower heat output due to the characteristic of its operation at lower temperatures. Its adoption in leaky homes means that ASHP runs continuously and are likely to impact negatively on the thermal comfort of the occupants, assuming radiators are kept at the typical sizes.

Through this research, the authors have demonstrated that in order to retrofit an existing dwelling within the context of climate emergency, it is imperative to consider a holistic approach that considers building fabric improvements, the integration of renewables and the consideration of low-carbon heating systems.

ACKNOWLEDGEMENTS

This work was funded by the UK Government through the UK Community Renewal Fund 2021/22. The authors would like to acknowledge the project partners Focus Consultants, Active Building Centre Research Programme, and Nottingham Energy Partnership as well as Nottingham City Council for their valuable help and assistance in facilitating this work.

REFERENCES

1. LETI 2020. LETI Climate Emergency Design Guide. Jan 2020 ed. London: London Energy Transformation Initiative (LETI).
2. Government, H.M., 2017. Clean Growth Strategy.
3. PASSIVHAUS TRUST 2022. Passivhaus retrofit in the UK. v.2.
4. Nottingham facts and figures (2021) ONS. Available at: https://www.ons.gov.uk/visualisations/areas/E06000018/ (Accessed: 02 March 2024).
5. OFFICE FOR NATIONAL STATISTICS 2023. Energy efficiency of housing in England and Wales: 2023
6. UK GOVERNMENT 2021a. Energy Performance of Buildings Data England and Wales.
7. CIBSE 2019a. CIBSE Guide A: Environmental Design. Incorporating corrections as of May 2019. London, United Kingdom: The Chartered Institution of Building Services Engineers (CIBSE).
8. HM GOVERNMENT 2010. The Building Regulations 2010: approved document, L1B: Conservation of fuel and power in existing buildings. 2013 edition.
9. UK housing: Fit for the future? (2019) Climate Change Committee. Available at: https://www.theccc.org.uk/publication/uk-housing-fit-for-the-future/ (Accessed: 27 September 2022).
10. HM GOVERNMENT 2021b. The Building Regulations 2010. Part L: Conservation of fuel and power. Volume 1: Dwellings. 2021 edition.
11. ENERGY SAVING TRUST 2008. Measurement of Domestic Hot Water Consumption in Dwellings.
12. BRE. 2019. Domestic Annual Heat Pump System Efficiency (DAHPSE) [Online]. Building Research Establishment Ltd (BRE). Available: https://tools.bregroup.com/heatpumpefficiency/hot-water-consumption.
13. Carroll, P. et al. (2020) *Air Source Heat pumps field studies: A Systematic Literature Review, Renewable and Sustainable Energy Reviews.* Available at: https://www.sciencedirect.com/science/article/pii/S1364032120305621 (Accessed: 19 March 2024).
14. Interim heat pump performance data analysis report (2023). Available at: https://es.catapult.org.uk/wp-content/uploads/2023/03/EoH-Interim-Heat-Pump-Performance-Data-Analysis-Report-1.pdf (Accessed: 05 March 2024).
15. Meek, C. (2021) Heat pumps and UK's decarbonisation. Available at: https://www.recc.org.uk/pdf/performance-data-research-focused.pdf (Accessed: 07 March 2024).
16. Jinko Solar (2020). Available at: https://www.jinkosolar.com/en/site/dwparametern (Accessed: 27 September 2022).
17. BRE 2022. SAP 10.2: The Government's Standard Assessment Procedure for Energy Rating of Dwellings.
18. CIBSE 2017. CIBSE TM59: Design methodology for the assessment of overheating risk in homes. London, United Kingdom: Chartered Institution of Building Services Engineers (CIBSE).

PLEA 2024 WROCŁAW
(Re)thinking Resilience

A case study of the multi-objectives optimisation of an office energy retrofit in Indonesia's hot-humid climate

NISSA AULIA ARDIANI[1], STEPHEN SHARPLES[1], HANIYEH MOHAMMADPOURKARBASI[1]

[1]University of Liverpool, Liverpool, United Kingdom

ABSTRACT: It has been estimated that buildings account for more than 40% of global energy consumption, and this demand will continue to grow in line with increasing population and urbanisation. Therefore, there is a growing demand to develop retrofit systems in existing buildings to improve their energy performance, especially in developing countries such as Indonesia. The aims of this research were to use a multi-objective optimisation framework to investigate the most optimum solutions for the energy retrofit of an actual office building located in a hot-humid climate based on environmental criteria (minimise cooling energy) and social criteria (reduce discomfort hours) and to provide recommendations for energy retrofit projects for similar office buildings in Indonesia. The variables used in this optimisation were window-to-wall ratio, glazing type, window blind type, and shading type.
KEYWORDS: Multi-objective optimisation, Optimum solution, Building retrofit, Energy efficiency

1. INTRODUCTION

Building retrofit refers to upgrading existing buildings to improve their energy efficiency, comfort, and overall performance. Retrofitting existing buildings reduces energy consumption and greenhouse gas emissions worldwide, enhances energy efficiency, boosts occupants' productivity, decreases maintenance costs, and contributes to better thermal comfort [1]. However, choosing an optimal retrofit strategy usually involves considering many different approaches. Attia et al. [2] concluded that multi-objective optimisation (MOO) is one of the most vigorous forms of optimisation because it generates sets of solutions from trade-offs between two or more conflicting design objectives. The MOO concept relies on identifying all feasible solutions (building design or retrofit options), which are Pareto-optimal or non-dominated. Being non-dominated implies that no solution within it can improve an objective without being disadvantageous to at least another one. Those solutions constitute the Pareto front, representing the optimal trade-off between the objectives considered in the analysis [3].

Several retrofit case studies using genetic algorithms through MOO have been investigated. An active archive non-dominated sorting genetic algorithm (NSGA-II) has been applied by Rosso et al. [4] to attain the optimum solution for retrofitting residential buildings in Rome, Italy. Their method reduced computational time and identified a MOO solution that decreased annual energy demand by 49.2%, yearly energy costs by 48.8%, and CO2 emissions by 45.2% while achieving 60% lower investment costs than other criterion-optimal solutions. Lu et al. [5] found that occupants-oriented retrofit options, such as utilising lighting sensors based on occupancy, setting higher temperature setpoints, and reducing plug loads, could significantly exceed technological retrofits like replacing chillers and installing a green roof. Seghier et al. [6] proposed an optimisation method for retrofitting building information modelling (RBIM) to find the building envelope for an office building in Malaysia with two objectives: minimising the overall thermal transfer value (OTTV) and minimising retrofit costs. The method utilised three different software: Autodesk Revit for BIM authoring tools, Dynamo for visual scripting, and MATLAB to customise (NSGA-II) optimisation.

A review study from Hashempour et al. [7] revealed that most MOO retrofit studies were from developed countries. There have been very few retrofit studies for buildings located in hot-humid climates. Tavakolan et al. [8] recommended future studies in a different type of building and a different climate, i.e. a hot-humid climate. Hence, this study aimed to investigate and test a multi-objective optimisation energy retrofit of an office building in a hot-humid climate using environmental and social criteria (reduce discomfort hours) to apply the most optimum retrofit strategies.

2. METHODOLOGY

2.1 Case study, digital twins, and validation

The selected case study areas were the 4th, 9th, and 17th floors of the Ministry of Public Works and Housing, Republic of Indonesia (Pekerjaan Umum dan Perumahan Rakyat - PUPR)'s Office Building, as seen in Figure 1. The building's form and orientation had been designed to prevent direct solar radiation and to enhance thermal comfort. The floors were chosen to demonstrate the performance of the building's lower,

middle, and top floors. Three loggers were installed for a month's continuous monitoring of indoor air temperatures and relative humidity in three rooms on each designated floor in October 2022 (Figure 2). The 4th and 9th floors represent the typical office layout in the PUPR building, while the 17th floor consists of a hall and a large dining area for occasional events. Based on the as-built drawings and building surveys, the existing building was digitally modelled in the DesignBuilder (DB) dynamic thermal simulation software (https://designbuilder.co.uk/). Figures 3 and 4 show the typical floor plans of the PUPR building. The digital twins of the three different floors were developed in DesignBuilder (DB) in separate files to avoid complicated simulations and computer crashes.

The building uses thermal-resistant glass for windows, a super silver dark blue 8 mm glass with a U-value of 5.739 W/m^{2}K. An opaque curtain wall consists of 8mm glass, plasterboard 12mm, glass wool 145mm, and plasterboard 12mm with a U-value of 0.225 W/m^{2}K. The cladding aluminium façade consists of 5mm thick metal aluminium, an air gap of 19mm, and cast concrete of 475mm, giving a U-value of 0.402 W/m^{2}K. The tiled wall at the front façade, from the ground floor until the 4th floor, consists of 15mm thick ceramic tiles, 10mm thick cement plaster, 100mm concrete block, and a 10mm thick cement plaster, with a U-value of 1.348 W/m^{2}K. The office spaces in the PUPR building utilise a central air conditioning system and a VAV dual duct water-cooled chiller with refrigerant R-134a. The seventeen-storey building also uses natural ventilation in its circulation areas, including corridors, lift lobbies, staircases, and toilets.

Figure 1: Pictures of the PUPR building and office interior

Figure 2: Loggers in 4th, 9th, and 17th floor

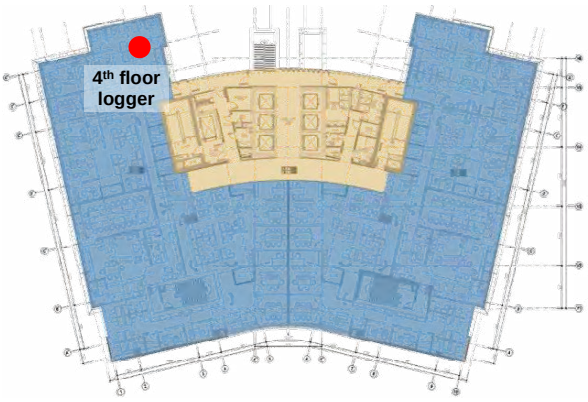

Figure 3: Typical 2nd, 3rd, 4th, 15th, 16th floor plans

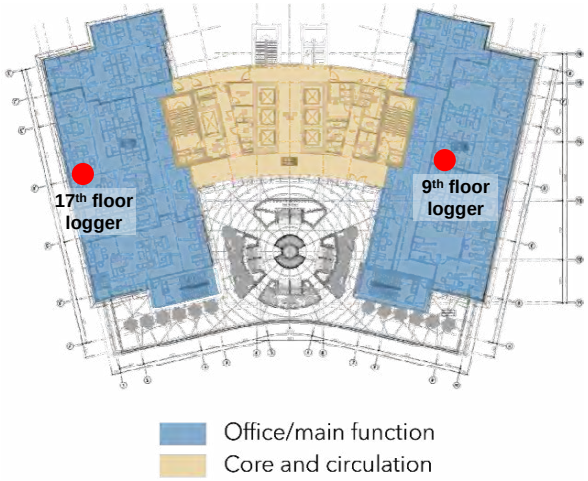

Figure 4:Typical 5th-14th & 17th floor plans

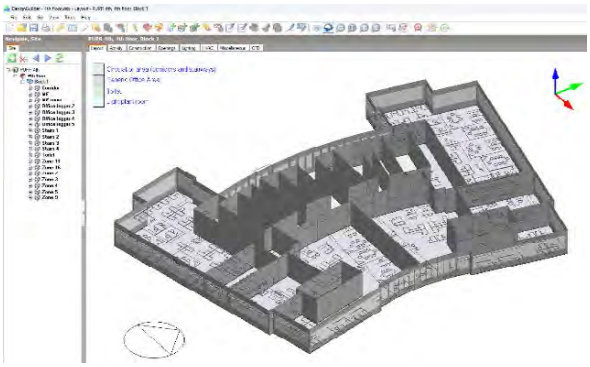

Figure 5: Digital twins of the 4th floor in DesignBuilder

Figure 6: Digital twins of the 9th floor in DesignBuilder

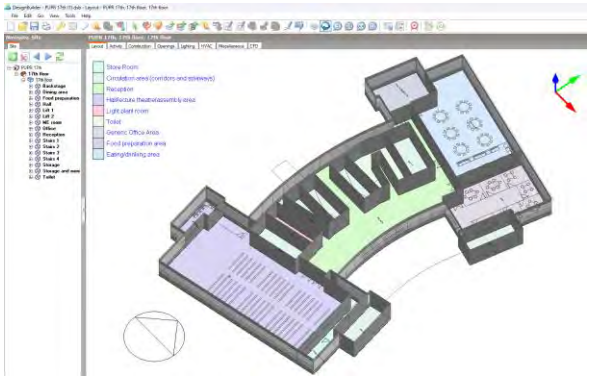

Figure 7: Digital twins of the 17th floor in DesignBuilder

The baseline models were built in DB by importing the DXF files of each floor. Thermal properties and construction materials in all zones were customised according to the on-site measurements and data provided by the building manager. Figures 5, 6, and 7 show the digital twins on the 4th, 9th, and 17th floors of the PUPR building, respectively.

Weather data used in Design Builder were derived from the commercial software Meteonorm (https://meteonorm.com/en/), which calculates hourly values of weather parameters (station, interpolated, or imported data) using a stochastic model. Thus, the weather data of the office's location could be generated as EPW files and utilised in DesignBuilder. The outdoor temperature data from Meteonorm were then compared to the measured outdoor temperature and validated using the ASHRAE procedure [9]. Figure 8 reveals the comparison of outdoor temperature between the measured and Meteonorm data. The outdoor logger for measurement was located on an outdoor terrace shaded by the overhang on the ground floor. From this chart, the Meteonorm weather data shows more extreme lows and highs because of the average temperature from nearby weather stations.

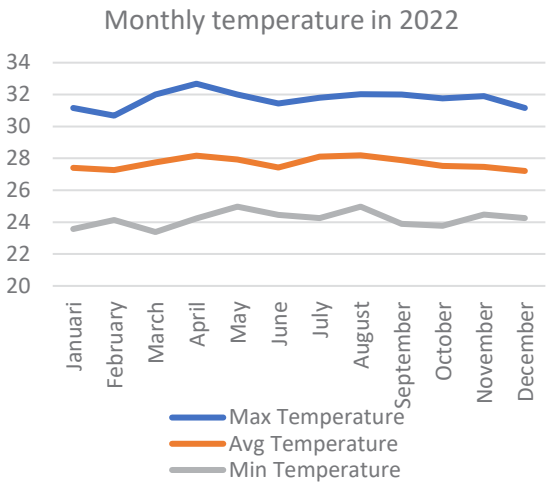

Figure 9: Average monthly air temperatures from Jakarta International Airport (CGK)

Figure 9 shows the monthly temperature of Jakarta city measured at the Jakarta International Airport in 2022. The average monthly air temperatures are very similar throughout the year due to Jakarta's location near to the Equator and its hot humid climate or tropical climate. This is in contrast to the monthly average air temperatures in subtropical climates, which have four seasons with marked temperature differences between summer and winter.

Energy simulations were then performed to calculate current energy performance during October 2022. The air temperatures in the selected zones (DB models) where the loggers were installed were then compared and validated against the measured data using the procedure given by ASHRAE using the formulae for Mean Bias Error (MBE) and Coefficient of the Variation of the Root Mean Square Error (CVRMSE). According to ASHRAE 14 (Section 6.3.3.4.2.2) [9], if using hourly data, the validation accuracy of the model should be +/- 10% for MBE and

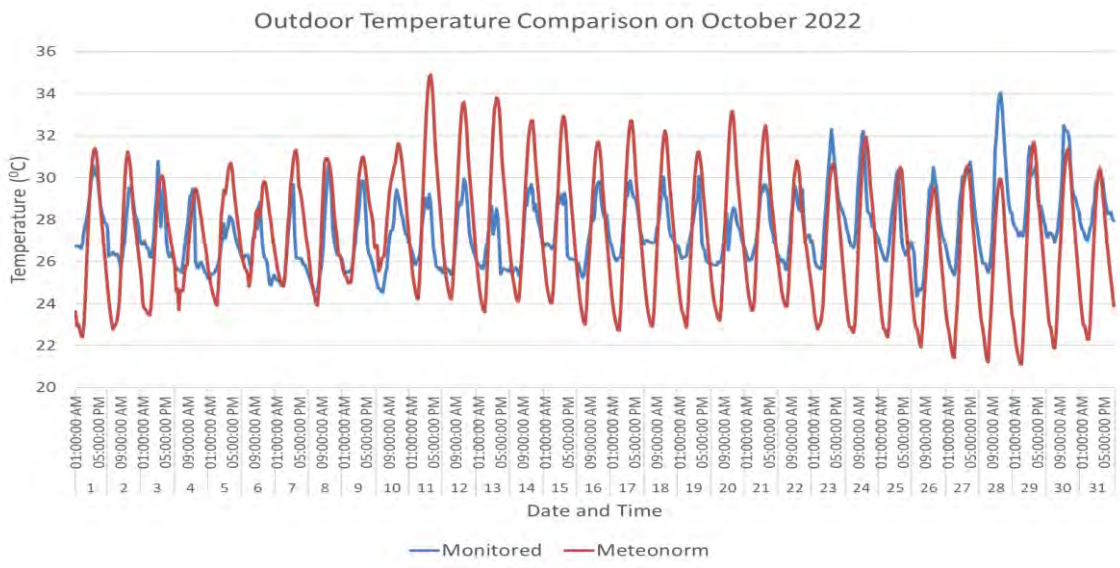

Figure 8: Measured and Meteonorm outdoor temperature comparison

<30% for CV(RMSE). The validation result for all three model floors and the outdoor temperature can be seen in Table 1. The results indicate that all models were within the ASHRAE standard and could be used for the next step, i.e. optimisation.

Table 1: Model validation result

Validation Result (Hourly Data)				
Model	MBE (%)	N_MBE (%)	RMSE (%)	CV(RMSE) (%)
4th floor	0.16	0.66	1.80	7.28
9th floor	-0.73	-3.02	2.11	8.71
17th floor	0.04	0.14	2.77	10.46
Outdoor temperature	-0.28	-1.03	2.40	8.75

2.2 Optimisation process

Table 2. Objectives and variables for the optimisation

Objectives		Variables				
1	2	Glazing type	Cooling setpoint temperature (°C)	Window Wall Ratio (WWR)	Window blind type	Local shading type
Discomfort (All Clothing) (hr)	Cooling energy (kWh)	Double Clear 6mm/13mm Air (U-value=2.665 W/m²K)	Min 22, Max 28 Step (parametric) 2, Step (optimisation) 0.2	Min 20, Max 80 Step (parametric) 20, Step (optimisation) 2	none	0.5m projection Louvre
		Double Clear 6mm/13mm Argon (U-value=2.511 W/m²K)			Blind with high reflectivity slats	1.0m projection Louvre
		Double LoE (e2=.1) Clear 6mm/13mm Air (U-value=1.761 W/m²K)			Blind with low reflectivity slats	1.5m projection Louvre
		Double LoE (e2=.1) Clear 6mm/13mm Argon (U-value=1.493 W/m²K)			Blind with medium reflectivity slats	0.5m Overhang
		Double LoE (e2=.1) Clear 6mm/6mm Air (U-value=2.429 W/m²K)			Micro Louvre	1.0m Overhang
		Double LoE (e2=.2) Clear 6mm/6mm Air (U-value=2.552 W/m²K)			Mid-pane blind with medium reflectivity slats	1.5m Overhang
		Project BIPV Window (U-value=1.960 W/m²K)			Venetian blinds – light diffuse	2.0m Overhang
		Single LoE (e2=.2) Clear 6mm (U-value=3.779 W/m²K)			Venetian blinds – medium diffuse	No Shading

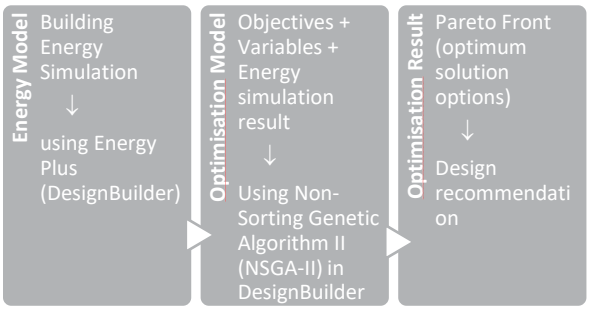

Figure 10: Multi-objective optimisation process

This study's optimisation objectives were to increase thermal comfort (minimise discomfort hours) and minimise the cooling energy. Additionally, six variables were added to the optimisation: glazing type, cooling set point temperature (°C), local shading type, window wall ratio (WWR), and window blind type. Table 2 shows the selected objectives and variables chosen as the parameters for the optimum retrofit strategies. After developing and simulating the energy model in DesignBuilder, as well as validating it, the next step was to create the multi-objective optimisation using Non-Sorting Genetic Algorithm II (NSGA-II) directly in DesignBuilder to get the optimum solutions (Pareto Front) for retrofit recommendation (Figure 10).

3. RESULT AND DISCUSSION

From the energy simulation in DesignBuilder, the total site energy usage during October 2022 for the 4th, 9th, and 17th floors were 55,078.07 kWh, 39,887.86kWh, and 40,851.67kWh, respectively (Table 3). The 4th floor consumed more energy than the other floors, which might be due to the geometry and building area being larger than the other floors. Table 3 also shows that the district cooling intensity on each floor was more than 85% of the total site energy demand. This result confirmed that air conditioning took up most of the energy consumption of the PUPR building.

Table 3: Current energy performance of DB models

Model	Total Site Energy (kWh)	District Cooling (kWh)	Energy Per Total Building Area [kWh/m²]	District Cooling Intensity [kWh/m²]
4th floor	55,078.07	47,790.17	32.50	28.20
9th floor	39,887.86	34,235.64	32.62	28.00
17th floor	40,851.67	37,599.33	31.39	28.89

After obtaining the energy simulation results, an optimisation to generate retrofit solutions in each floor model was simulated directly in DesignBuilder using the selected objectives and variables shown in Table 2. The optimisation options or settings are a maximum generation of 200, a generation for convergence, and an initial population of 20 each.

The results of the simulations and optimisations in DesignBuilder showed that there were 35 sets of optimal retrofit design solutions for the 4th floor (Figure 12—top), 14 sets for the 9th floor (Figure 12—middle), and 55 sets for the 17th floor (Figure 12—bottom). Table 4 recommends configurations with the most optimum solution based on the Pareto front result for all three models.

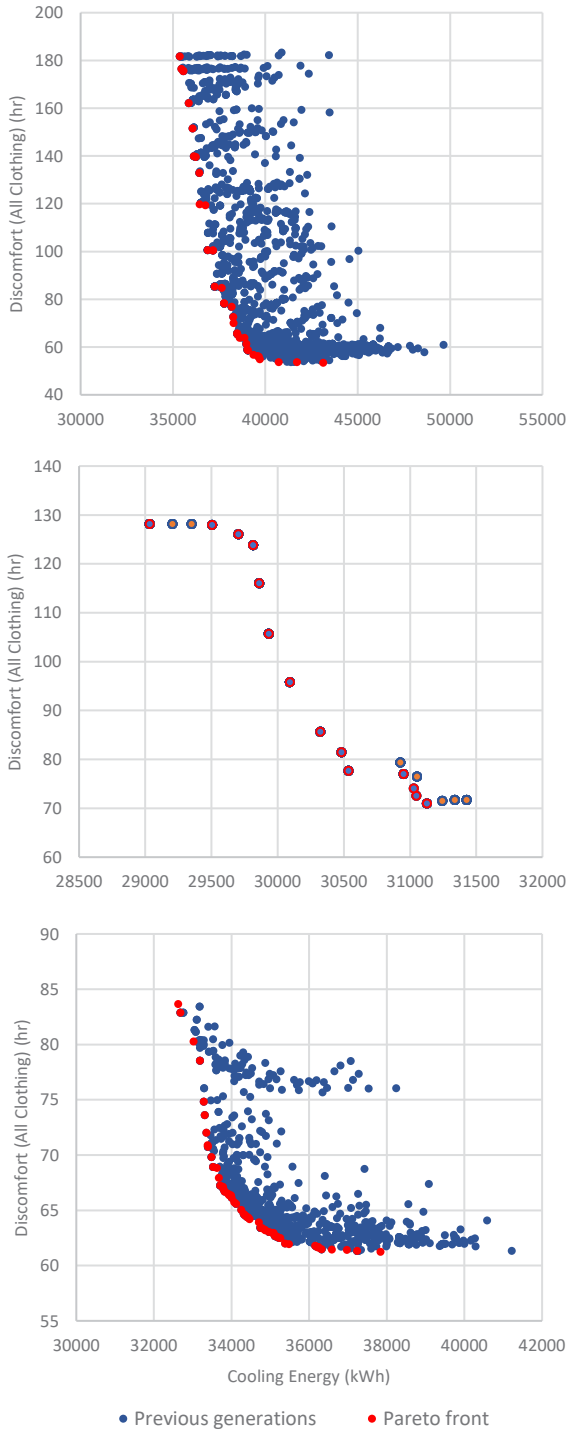

Figure 11: Optimisation results (discomfort hours v cooling energy) of the 4th floor (top), 9th floor (middle), and 17th floor (bottom)

The optimum option for the 4th-floor model, which would have a cooling energy demand of 37,785.30 kWh and 78.17 discomfort hours, using double LoE clear glass 6mm/13mm with air cavity (e2=1) + 1.5 m projection louvre + light-diffusing Venetian blinds + cooling setpoint temperature of 24.6 ^{0}C + 50% WWR. This option will reduce the cooling energy demand by 25.94% compared to the current building performance. The most optimum option for the 9th-floor model would have a cooling energy demand of 30,323.58 kWh and 85.6 discomfort hours using double clear 6mm/13mm with air cavity + 1.5m overhang blind with low reflectivity slats + cooling setpoint temperature of 26^{0}C + 64% WWR. This option can reduce the cooling energy on the 9th floor by 11.42%. The most optimum option for the 17th-floor model would have a cooling energy demand of 34,368.4 kWh using BIPV (Building Integrated Photovoltaic) + 1.5m projection louvre + blind with high reflectivity slats + cooling setpoint temperature of 23.4^{0}C + 46% WWR. This option will decrease the cooling energy on the 17th floor by 8.59%.

Based on all Pareto front solutions for the three models, the glazing type of double LoE clear glass 6mm/13mm with argon cavity (e2=1) and Double LoE clear glass 6mm/6mm with air cavity (e2=1) appeared the most beneficial compared to the other selected glazings in the optimisation. A 1.5 m projection louvre and a 2 m overhang occurred most frequently in the optimisation results for local shading type. Lastly, for the window blind type, light-diffusing Venetian blinds were shown to be the most optimum options.

4. CONCLUSION

This study applied MOO to retrofit an office building in the hot-humid climate of Indonesia. Three validated Design Builder digital twins of the office building were developed for the MOO analysis. The optimal trade-offs between the objectives considered in the study to minimise cooling load and minimise discomfort hours were also identified.

Based on the Pareto Front result in the optimisation calculations in Design Builder, the recommendation for the most optimum retrofit strategies is using:

(1) Double LoE clear glass 6mm/13mm with air cavity (e2=1) + 1.5 m projection louvre + light-diffusing Venetian blinds + cooling setpoint temperature of 24.6 ^{0}C + 50% WWR,

(2) Double clear glass 6mm/13mm with air cavity + 1.5m overhang + blinds with low reflectivity slats + cooling setpoint temperature of 24.2^{0}C + 60% WWR, or

(3) Project BIPV (Building Integrated Photovoltaic) Window + 1.5 projection louvre + blinds with high reflectivity slats + cooling setpoint temperature of 23.4^{0}C + 46% WWR.

Table 4: Recommendation of optimum sets of solutions

Floors	Objective		Variable				
	Cooling energy (kWh)	Discomfort (All Clothing) (hr)	Cooling setpoint temperature (°C)	Window to Wall %	Glazing type	Local shading type	Window blind type
4th	35,389.75	181.59	26	34	Dbl LoE (e2=.1) Clr 6mm/13mm Air	1.5 m projection Louvre	Venetian blinds - light (modelled as diffusing)
	37,785.3	78.17	24.6	50	Dbl LoE (e2=.1) Clr 6mm/13mm Air	1.5 m projection Louvre	Venetian blinds - light (modelled as diffusing)
	43,138.76	53.25	22	64	Dbl Clr 6mm/13mm Air	1.5m Overhang	<None>
9th	29,035.21	128.13	26	64	Dbl LoE (e2=.2) Clr 6mm/6mm Air	1.0m Overhang	Blind with medium reflectivity slats
	30,323.58	85.60	24.2	60	Dbl Clr 6mm/13mm Air	1.5m Overhang	Blind with low reflectivity slats
	29,035.21	128.13	26	64	Dbl LoE (e2=.2) Clr 6mm/6mm Air	1.0m Overhang	Blind with medium reflectivity slats
17th	32,630.07	83.64	26	74	Dbl LoE (e2=.1) Clr 6mm/13mm Arg	1.5 m projection Louvre	<None>
	34,368.4	64.45	23.4	46	Project BIPV Window	1.5 m projection Louvre	Blind with high reflectivity slats
	37,846.89	61.22	22.4	30	Dbl Clr 6mm/13mm Arg	1.0m Overhang	Blind with low reflectivity slats

However, detailed information on the building's materials' thermal properties was limited, so default materials similar to the current building were applied in the DesignBuilder models. The occupancy schedules were also not available. Hence, in DesignBuilder, the general office schedule from 9.00 to 17.00 was chosen for weekday activity.

For future studies, investigating the impact of the geometry of the building on the optimisation results and the cost-benefit analysis would be important. Furthermore, utilising multi-criteria decision-making could be beneficial for selecting the most optimum solution to retrofit the building in a hot-humid climate. This approach could ask the stakeholders, such as building users, architects, engineers, and academics, to be involved in analysing retrofit recommendations. Then, further research will apply the exact solutions to different types of buildings in hot-humid climates.

ACKNOWLEDGEMENTS

This study was part of the lead author's PhD projects at the University of Liverpool, United Kingdom. All authors gratefully acknowledge the research funding from the Centre for Education Funding Services of the Ministry of Education, Culture, Research, and Technology and the Endowment Fund for Education of the Ministry of Finance, Republic of Indonesia.

REFERENCES

1. Ma, Z., et al., Existing building retrofits: Methodology and state-of-the-art. Energy and Buildings, 2012. 55: p. 889-902.
2. Attia, S., et al., Assessing gaps and needs for integrating building performance optimization tools in net zero energy buildings design. Energy and Buildings, 2013. 60: p. 110-124.
3. Costa-Carrapiço, I., R. Raslan, and J.N. González, A systematic review of genetic algorithm-based multi-objective optimisation for building retrofitting strategies towards energy efficiency. Energy and Buildings, 2020. 210.
4. Rosso, F., et al., Multi-objective optimization of building retrofit in the Mediterranean climate by means of genetic algorithm application. Energy and Buildings, 2020. 216.
5. Lu, Y., et al., An integrated decision-making framework for existing building retrofits based on energy simulation and cost-benefit analysis. Journal of Building Engineering, 2021. 43.
6. Seghier, T.E., et al., BIM-based retrofit method (RBIM) for building envelope thermal performance optimization. Energy and Buildings, 2022. 256.
7. Hashempour, N., R. Taherkhani, and M. Mahdikhani, Energy performance optimization of existing buildings: A literature review. Sustainable Cities and Society, 2020. 54.
8. Tavakolan, M., et al., A parallel computing simulation-based multi-objective optimization framework for economic analysis of building energy retrofit: A case study in Iran. Journal of Building Engineering, 2022. 45.
9. American Society of Heating, Refrigerating and Air Conditioning Engineers, ASHRAE Guidelines: Measurement of Energy and Demand Savings. 2002: Atlanta, GA, p. 15.

PLEA 2024 WROCŁAW
(Re)thinking Resilience.

Fabric energy efficiency in housing retrofit:
the role of whole-life operational and embodied carbon emissions

MAY ZUNE[1] HADI ARBABI[1], DANIELLE DENSLEY TINGLEY[1]

[1] Department of Civil and Structural Engineering, University of Sheffield, United Kingdom.

ABSTRACT: UK housing decarbonisation through retrofit faces massive challenges to be consistent with 2050 Zero Carbon targets, considering the large proportion of inefficient building stock. As the design for fabric-energy-efficiency and the demand for energy consumption from modern lifestyle increases, its trade-off with the embodied carbon investment and the unintended consequences from a high-performance building envelope becomes increasingly important. We developed a model which considered both building performance metrics and existing UK Energy Performance Certificates (EPCs) metrics to investigate long-term quality and acceptability of retrofits, i.e., overheating mitigation and ventilation improvement, considering a 20- and 50-year building lifespan. The model combines energy demand assessment, indoor environmental assessment, the Future Homes Standard and EPC's cost-energy-carbon metric. A dynamic simulation study for seven predominant built forms in the South Yorkshire housing stock was designed to investigate deep retrofit results under predicted future climate conditions in the 2030s, 2050s and 2080s. The study focused on whole-life emissions from operational and embodied carbon over different timescales whilst considering a healthy indoor environment in buildings. The findings present an efficient way of combining building performance metrics and EPC metrics in a housing retrofit model that aids decision-making for homeowners, stakeholders and policymakers.
KEYWORDS: Domestic retrofit; Housing stock; Energy Performance Certificate; Retrofit metrics; Energy efficiency.

1. INTRODUCTION

In the context of the UK government's legally binding 2050 Zero Carbon targets, rapid mass retrofit is imperative, given the age and inefficiency of homes across the UK [1]. This mass retrofit is a significant multifaceted challenge to address fabric energy efficiency, fuel poverty, cold home-related health problems and associated embodied carbon from refurbishments.

The Energy Performance Certificate (EPC) is a policy instrument aiming to improve the operational energy performance of buildings through its cost-energy-carbon index from A to G in rating [2]. It acts as a primary source of data in reviewing potential domestic retrofits. The EPC's cost-energy-carbon metric, however, may not be fit for the UK's whole-life-carbon roadmap due to assumptions in the way energy consumption is estimated and the lack of consideration for thermal comfort and indoor air quality [3]. Studies have suggested ways of combining the existing EPC cost-energy-carbon index with performance assessment metrics such as comfort and indoor air quality are worthwhile to extend assessments beyond immediate retrofit delivery to improve their fitness for purpose [3].

The robustness of retrofit measures relies on how the various facets of building performance are balanced against one another. The Future Homes Standard (FHS) and Approved Document L (AD-L) recommend limiting the maximum U-values for the fabric energy efficiency of homes to avoid heat losses and air leakages [4]. However, increased insulation can increase overheating in poorly designed buildings with airtight buildings because they often rely on the careful use of natural and mechanical ventilation to achieve acceptable indoor air quality.

Prior to a retrofit, if a household has an under-consumption of energy services, or the pre-retrofit construction of a dwelling is better than its EPC record, the pre-bound effect occurs and the energy savings gap between pre- and post-retrofit could be smaller than the expected [5]. Post retrofit, if a household's daily rhythm of heating and ventilation needs are changed or a technology failure is found in construction, the rebound effect occurs, and an energy efficiency increase may also lead to an increase in the final energy consumption [5]. These effects could lead to inaccuracies in calculating the retrofit payback period and the subsequent national retrofit and decarbonisation policy.

Our exploratory case study investigates whole-life emissions from operational and embodied carbon whilst considering a healthy indoor environment in buildings. We present fabric retrofit measures for seven archetype-based models by incorporating the current SAP metrics, FHS and AD-L guidance, and additional lifetime metrics, e.g. overheating mitigation and indoor environmental conditions, over different timescales. This study aims to understand how these metrics affect the long-term quality and

acceptability of retrofits, and how the rebound and prebound effects influence pre- and post-retrofit comparisons.

2. METHODOLOGY

The South Yorkshire (SY) housing stock, which houses 1.8% of the UK's residential stock, was selected for a case study. Most properties were constructed between the early 1900s to 1970, with semi-detached and terraced houses being the predominant built forms (Figure 1). Seven archetypes were selected for a deep retrofit investigation of the SY housing stock (Figure 3). Besides the 1930s semis, all other houses have heated attic rooms. The architectural drawings of the archetypes were traced from local property advertisements whilst their applicability and generalisability were further assessed. The relationship between the treated floor areas (TFA) to heat loss form factors (HLFF) and the window area (WA) to window-to-floor area (WWR) of the selected archetypes are shown in Figure 2.

Cavity walls or solid brick walls, an uninsulated ground floor, an uninsulated suspended wooden floor, a pitched roof with insulation at joints, and double-glazing are found in most of the SY housing [2]. Solid brick walls were considered in Victorian houses whereas cavity walls were considered in other houses. The U-values of the building envelopes were derived from the RdSAP 2012, as shown in Table 1. The post-retrofit U-values were derived from the FHS and the latest AD-L.

For the pre-bound scenario (Table 4) with better insulation than the base model, the U-value of walls was considered as 0.8 W/m2K, and the U-value of windows was considered as 2.5 W/m2K. For the rebound scenario (Table 4) with technical failures in retrofit construction, the U-value of walls as 0.228 W/m2K and air permeability 10m3/h.m2@50Pa were considered.

To consider the impacts of future worst-case climatic conditions on retrofit scenarios, three scenarios, the medium emissions (RCP 6.0, A1B) for 2030 and high emissions (RCP 8.5, A1FI) for 2050 and 2080, were chosen for this work [6].

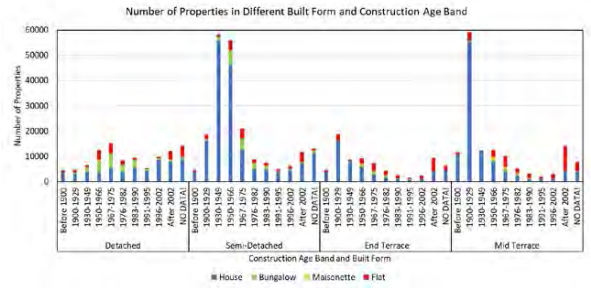

Figure 1. Construction ages and built forms of the South Yorkshire housing stock.

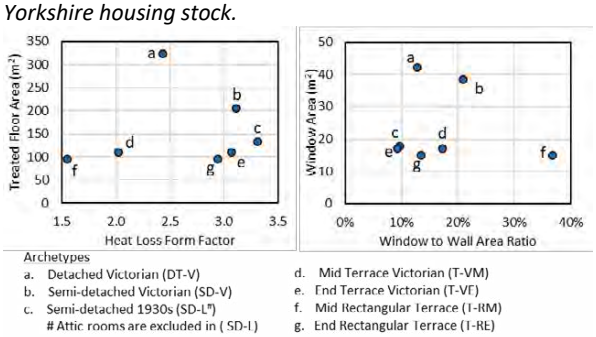

Figure 2. Archetype information used in the study.

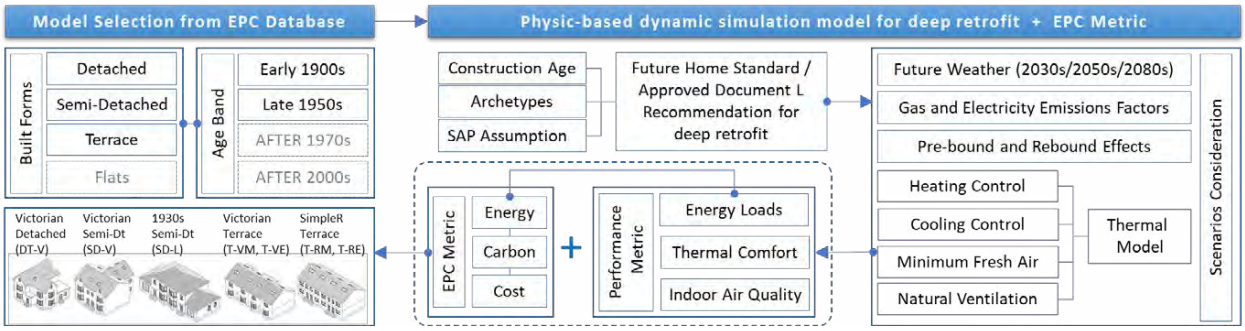

Figure 3. Overview of deep retrofit investigation using the archetype-based models for the South Yorkshire housing stock.

Table 2 presents the operational settings used in pre-retrofit and post-retrofit models. Table 3 presents the heating scenarios under both rebound (RB) and pre-bound (PB) effects.

Electricity marginal greenhouse gas (GHG) emissions factors from 2023 to 2100 were taken from BEIS [7], which is an optimistic prediction for grid decarbonisation. For instance, the GHG emissions from the UK electricity generation in 2023 is 0.207 kgCO2e per kWh whilst the BEIS prediction (published in November 2023) is 0.133 kgCO2e per kWh for 2023 and 0.120 kgCO2e per kWh for 2025 and decreased down to 0.002 kgCO2e per kWh in 2050. Emission factor changes from 2025 to 2080 were considered to calculate accumulated carbon emissions from heat pumps and gas boilers. Regarding the standard variable tariff for electricity and gas prices, the current energy price per unit from 1 October to 31

December 2023 [8] was considered in this study to compare energy costs for pre-retrofit and post-retrofit scenarios. These were £0.27 and £0.07 for electricity and gas respectively for 1kWh.

The retrofit embodied carbon emissions were calculated from the cradle-to-gate (A1-A3) and construction (A4-A5) stages. This included (i) different insulation materials such as EPS, PIR, PUR, XPS, glass wool, stone wool and wood fibre, (ii) material finishes, vapour control membrane, airtight membrane and paints, (iii) window and door replacements, and (iv) upgrading service systems such as heat pumps and gas boilers. For this work, we chose the EPS insulation for comparison. Factors used for global warming potential (GWP) and embodied carbon calculation for individual houses were taken from [9].

Table 1. U-values used in the study.

U-value (W/m^{2}K)	Reference model (SAP)	Deep retrofit model (AD-L)
Roof	0.68	0.15
External Wall (Solid)	2.10	0.18
External Wall (Cavity)	1.60	0.18
Ground Floor	1.60	0.18
Internal Partition	2.25 (assumption)	
Window	3.10	1.4
Door	3.00	1.4
Air permeability	15	8 m^3/hm^2@50Pa

Table 2. Operational settings used in the simulation models.

Parameters	Values	Ref.
Indoor operative temperature		
Heating (Category II)	on if T > 20°C	[10]
Cooling (Category II)	on if T > 26°C	[10]
Natural ventilation (windows)	22°C < T < 26°C	
Fresh air and (continuous) mechanical ventilation		
Min fresh air (other rooms)	0.49 l/s/m^2	[10]
Bathroom extract ventilation	8 L/s	[11]
Kitchen extract ventilation	13 L/s	[11]
CO2 generation rate	0.005 L/s	[11]
Building usage and schedules		
Occupancy (Bedroom)	Single bedroom	[12]
Occupancy (Others)	Follow rooms	[12]
Equipment and lighting	Follow rooms	[12]
HVAC Systems		
Boiler CoP	0.85 (assume)	-
Heat Pump CoP for heating	2.8 (assume)	[13]
Heat Pump CoP for cooling	3.5 (assume)	[13]
Heat recovery	Enthalpy	-
Internal heat gain	2.1 W/m^2	[14]
Shading (assumption): Apply if solar radiation > 120 W/m^2 in the daytime and apply it during the night		
Orientation: South-facing rear garden, north-facing entrance, east and west sides for party walls.		
Suburbs terrains with no adjoining buildings.		

The operational carbon emissions from different archetypes were calculated from the results of physics-based dynamic simulation models. The energy cost and carbon emissions were calculated following EPC metric and grid decarbonisation scenarios based on modelled energy loads. Finally, the results of both metrics were reviewed for whole-life operational and embodied carbon emissions to understand energy, cost and carbon emissions versus acceptable indoor conditions for thermal comfort and indoor air quality in different timescales. The simulation results were calculated using dynamic energy and thermal simulation programs (EnergyPlus / Design Builder) considering variations in fabric-energy efficiency, thermal models and weather files for the studied houses.

Table 3. Pre-bound and rebound scenarios in heating.

Case	Heating scenarios
Base	The heating is on at all times if T < 20°C.
PB-1	The heating is on if T < 20°C and is off during sleeping hours.
PB-2	The heating is on if T < 20°C and is off during sleeping hours + daytime.
PB-3	The heating is on if T < 20°and is off in some spare/unoccupied rooms.
PB-4	If building insulation is slightly better than the based model while the heating is on if T < 20°C.
PB-5	The heating is on if T < 18°C.
RB-1	The heating is on if indoor T < 21°C.
RB-2	If retrofit construction has technical failures; the heating is on if indoor T < 20°C.
PB: Pre-bound effects. RB: Rebound effects	

3. RESULTS

3.1 Operational carbon emission for heating

The accumulated operational carbon emissions in seven studied archetypes from 2025 to 2080 are presented in Figure 4 and Figure 5. The operational carbon emissions could be reduced by a factor of 7.5 by deep-retrofit construction while the same gas boilers were used in Figure 4. As the detached Victorian house has a larger floor area, its operational energy consumption was the highest among the seven houses whereas the rectangular plan mid-terrace had the lowest demand.

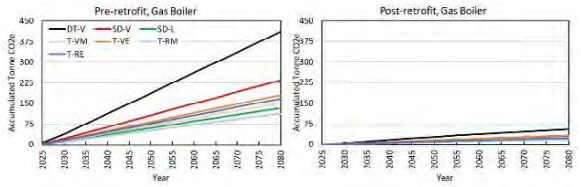

*Figure **4**. Accumulated operational carbon emissions for heating in seven houses from 2025 to 2080, considering the same consumption-based emission factor for natural gas.*

By switching the gas boiler to a heat pump, as shown in Figure 5, if the energy consumption for cooling and ventilation is also added, the operational carbon could be reduced by a factor of 10 using current national grid emission factors or reduced by a factor of 113 using grid decarbonisation scenarios.

3.2 Indoor environmental conditions

The consequence of the deep-retrofit scenario, which intended to reduce heating energy consumption from highly insulated and airtight construction, was a higher median indoor air temperature and a greater summer overheating risk than in less insulated homes. Figure 6 presents a comparison of annual hourly indoor temperatures and indoor carbon dioxide (CO_2) concentrations in three houses for five scenarios (a-e), considering 3.5m^2 differences in areas in the main bedrooms of the houses, with south-facing windows. Mechanical ventilation (MV) has an important role to play in removing indoor pollutants in retrofitted buildings. When the MV was applied in scenarios (d) and (e), the annual mean temperatures and indoor CO_2 concentrations were also reduced. The smaller the room the higher CO_2 concentration.

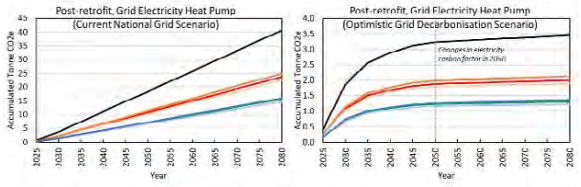

Figure 5. Accumulated operational carbon emissions for heating, cooling and mechanical ventilation in seven houses from 2025 to 2080, based on current national grid and future decarbonised grid for electricity.

Figure 7 shows the annual distribution of indoor operative temperature and indoor air CO_2 concentration, yielding a total of 8760 hours a year, for a bedroom in a 1930s semi-detached house. As shading was applied in the rooms, summer overheating did not exceed 25°C for more than 10% (876 hours) of the year, as the Passivhaus suggested [14], f the house is considered fully occupied. However, higher annual median temperatures were found if the post-retrofit construction had no MV. A high frequency of temperature distributions was found near ±2°C of the heating set point, and small distributions of temperatures above 25°C were found in Figure 7. If shading is excluded in the pre-defined scenarios, overheating could be expected as the unintended consequence of highly insulated, airtight buildings. Variations in hourly occupancy patterns affect the indoor CO_2 generation rate while temperature and air pressure differences between indoors and outdoors affect the air change rate of a room. If the room had no MV, high air CO_2 concentrations above 900ppm were observed as the windows were closed. One could argue that daily window opening could remove indoor pollutant concentrations, instead of following the pre-defined input from Table 2. When the MV was added in the post-retrofit model, the indoor air CO_2 concentration was lower than 1000ppm, as [10] suggested, despite inconsistent distributions in its frequency.

3.3 Cost saving

A deep-retrofit could reduce annual heating demand up to 5 to 6.8 times whereas the coefficient of performance (COP) of the heat pump is 3.29 times more efficient than the gas boiler. However, the tariff for electricity is nearly 4 times higher than gas for 1kWh. As a result, energy cost-saving was not directly proportional to reducing energy demand if a gas boiler was switched to a heat pump. Figure 8 presents energy-cost savings from seven houses.

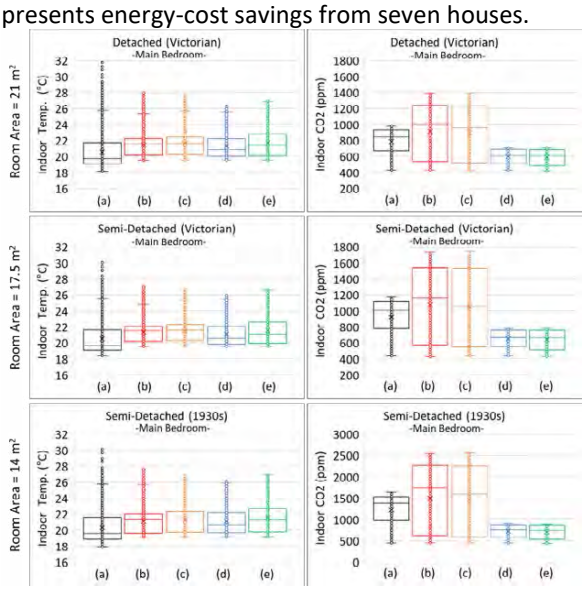

Figure 6. Annual indoor temperature and air CO2 concentration for south-facing bedrooms in three houses. [(a) Pre-retrofit in 2030 (b) post-retrofit in 2030 (c) post-retrofit in 2050 (d) post-retrofit in 2050 and MV added (e) post-retrofit in 2080 and MV added.]

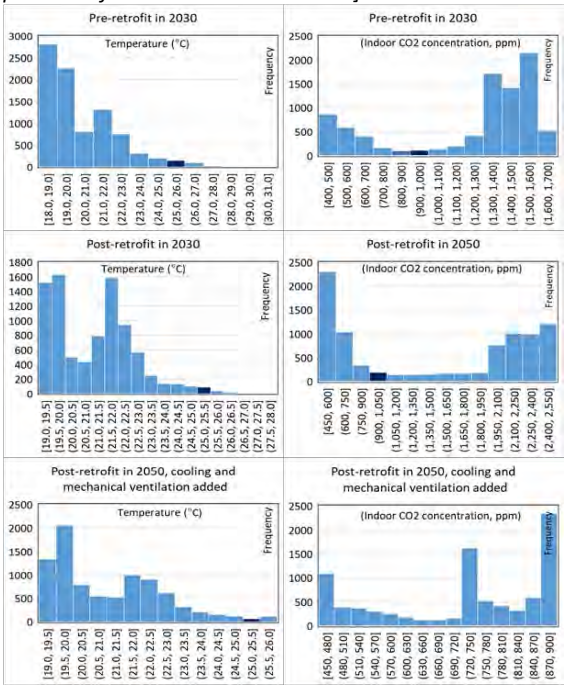

Figure 7. The frequency of annual hour distribution in indoor temperature and indoor air CO2 concentration, an example of a bedroom room in a 1930s semi-detached house.

3.4 Pre-bound and rebound effects

Figure 9 presents a comparison of pre-bound (PBE) and rebound (RBE) effects considering scenarios described in Table 3 that result in energy-saving before a pre-retrofit (-value) and overconsumption after a retrofit (+value).

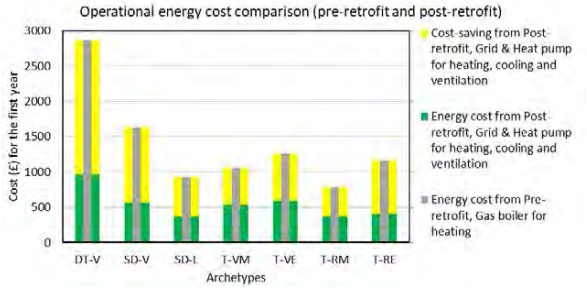

Figure 8. Annual energy cost saving in seven houses.

Reducing heating hours (PB-1) could save more energy in a pre-retrofit model than in a post-retrofit model. The length of heating hours is not a direct measure of heating energy-saving as the temperature differences between indoors and outdoors contribute to the variation of heating demand that causes different results of pre-bound scenarios. Reducing heating set points to 18°C (PB-5) could save more energy in a post-retrofit model than in a pre-retrofit model; however, this may not be realistic as energy efficiency in a post-retrofit condition can lead to an increase in the consumption of energy services due to the rebound effects [5].

Increasing heating set points to 21°C (RB-1) could bring more overconsumption in a post-retrofit model than in a pre-retrofit model; however, the personal preference of the individual could affect variation in heating set point temperatures. The most uncertain overconsumption for heating is unknown technical failures from a post-retrofit model. In this work, the RB-2 resulted in the highest overconsumption of heating. Due to differences in the number of rooms, TFA, HLFF and WWR between the DT-V and SD-V, their pre-bound and re-bound results were different.

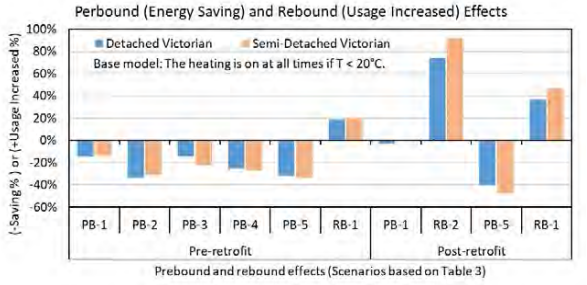

Figure 9. Pre-bound and rebound effects according to the scenarios shown in Table 3.

3.5 Carbon reduction

Figure 10 presents accumulated whole-life operational and embodied carbon emissions over different timescales for the SY housing stock. Significant carbon reduction was found by adding a deep retrofit construction to the current housing stock which has domestic heating from gas boilers. It needs to be highlighted that the results of whole-life carbon emissions from heat pump scenarios contained the energy demand for cooling and ventilation whereas the whole-life carbon emissions from gas boilers scenarios were considered for heating energy demand only. Nonetheless, switching to a heat pump from a gas boiler has benefits in carbon reduction and maintaining necessary indoor environmental conditions. The projected amount of CO_2e emissions is indicative only, as it is based on average energy consumption requirements from seven archetypes. The approximate projections from operational and embodied CO2e emissions, however, showed evidence of a promising decarbonisation path from retrofit and electrification of heating systems using heat pumps.

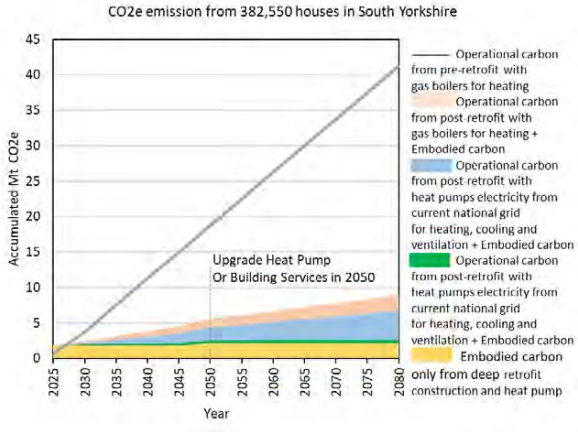

Figure 10. Operational carbon emissions and embodied carbon emissions over time, presented from 2025-2080.

4. DISCUSSION

This study aimed to address reducing domestic operational carbon emissions originating from gas boilers, and an inefficient building fabric. The method was structured to combine EPC metrics, FHS and AD-L guidance and carbon factors from a decarbonised electricity grid, considering the impacts of future weather years, lifespan of deep-retrofit construction, related embodied carbon emissions, maintenance and replacement of MEP over different timescales. Deep-retrofit fabric-first approach, heat pumps for heating, cooling and ventilation and current energy prices for pre-and-post-retrofit scenarios compared to seven archetypes.

The thermal efficiency and airtightness of the building fabric influence the indoor air temperature and air CO2 concentration, which can be improved in the post-retrofit models; however, unintended consequences of an over-heating risk and a lack of fresh air demand a potential need for cooling in extreme summer temperatures and mechanical ventilation. In the results, a higher annual median

temperature in the post-retrofit scenario revealed that the end users need an adaption for changes in indoor thermal comfort. Overheating was not reported in the results shown in scenarios (d) and (e) of Figure 6 and Figure 7 due to the use of shading in the simulation models. Further studies on the effects of external and internal insulations together with thermal mass and the end user's behaviour in using shading are needed to understand potential overheating in retrofitted homes to ensure they can adapt to changing climate conditions. Whilst the energy demand for cooling and ventilation is expected in a post-retrofit scenario to maintain necessary ventilation for indoor air quality, the annual energy cost-saving figure showed a promising result from deep retrofit and switching a gas boiler to a heat pump. The monetary payback time for an energy-saving retrofit can vary by several factors; therefore, further studies are necessary to understand how different archetypes affect retrofit ROI (return on investment).

The use of static occupancy schedules and equipment schedules is common in building energy and thermal simulation models whereas the drawback of a "typical" schedule needs to be acknowledged as a problematic limitation in the results. Physiological, psychological and random factors of the end users are not "typical" while the energy usage behaviour of a household could be varied according to the environmental factors, time-related factors, and contextual factors. Further studies are necessary to investigate how those factors found in the prebound and rebound effects of energy consumption as their consequences influence indoor environmental conditions and carbon reduction. Further studies will explore the impact of these factors on energy use by conducting post-occupancy evaluation surveys for a sample of the SY housing stock and integrating these findings into the modelling.

5. CONCLUSION

The exploratory case study focused on whole-life operational and embodied carbon emissions over different timescales for the SY housing stock whilst considering a healthy indoor environment in post-retrofit scenarios. Whilst the EPC database can be undoubtedly used as a primary source in reviewing potential domestic retrofits, additional performance-related metrics and carbon emissions-related factors are necessary to consider ensuring the long-term quality and acceptability of retrofit project delivery, to tackle fuel poverty, health inequalities, and achieve wider societal benefits in cost-saving and decarbonisation. The findings present how the resilience of housing can be achieved by integrating careful ventilation mechanisms and necessary shading in housing retrofit, as well as adapting the transition between heat balance modes (the use of heating and cooling) to free-running modes for adaptive thermal comfort.

The comparison of the projected amount of CO_2e emissions could vary as the rebound effects arise from the improvement of energy efficiency while carbon factors for grid electricity and fuels change over time. For policymakers, this work also can be used to understand deep retrofit of homes at scale, the need for an in-depth cost-benefit analysis for retrofit, the need for deployment in low-and-zero energy HVAC systems for UK homes and relevant solutions and to understand making mass retrofit a reality.

ACKNOWLEDGEMENTS

This project was supported by Research England funding to the South Yorkshire Sustainability Centre.

REFERENCES

1. BEIS (2021) *Net Zero strategy: Build back greener*, Department for Business, Energy and Industrial Strategy.
2. BRE (2023) *SAP 10. The Government's Standard Assessment Procedure used in the Energy Performance Certificates (EPC).* Building Research Establishment: UK.
3. T. Fawcett and M. Topouzi (2020) *Residential retrofit in the climate emergency: the role of metrics.* Buildings and Cities. 1(1): p. 475–490.
4. DLUHC (2021) *The Future Buildings Standard: 2021 Consultation on changes to Part L and Part F (published in December)*.
5. R. Galvin, (2016) *The Rebound Effect in Home Heating: A guide for policy-makers and practitioners*. UK and USA: Earthscan.
6. PROMETHEUS (2010) *Future weather files,* University of Exeter.
7. BEIS (2022) *Electricity emissions factors to 2100 and conversion factors for final energy demand, published in November.*, Department for Business, Energy & Industrial Strategy.
8. OFGEM (2023) *Energy price cap* Current energy price per unit: 1 October to 31 December 2023.
9. D. Abbey, H. Arbabi, C. Gillott, W. Ward, and D.D. Tingley (2022) *Demolish or reuse? – The balance between operational and embodied emissions in the retrofit of commercial buildings* in *Sustainable Built Environment D-A-CH Conference (SBE22)*. Berlin: IOP Conference Series: Earth and Environmental Science.
10. BSI (2019) *BS EN 16798-1 Energy performance of buildings. Ventilation for buildings*, The British Standards Institution: UK.
11. CIBSE (2011) *Indoor air quality and ventilation*, The Chartered Institution of Building Services Engineers: UK.
12. CIBSE (2017) *Design methodology for the assessment of overheating risk in homes*. The UK.
13. S.D. Watson, J. Crawley, K.J. Lomas, and R.A. Buswell (2023) *Predicting future GB heat pump electricity demand.* Energy and Buildings. 286.
14. C. Hopfe and R. McLeod, (2015) *The Passivhaus Designer's Manual: A technical guide to low and zero energy buildings*. London: Routledge.

PLEA 2024 WROCŁAW
(Re)thinking Resilience

Environmental optimum in the retrofitting of existing buildings

A case study in the Mediterranean climate

MARTA GALISTEO-GARRIDO[1,3], ANNA PAGES-RAMON[1,2], JOAQUIM ARCAS-ABELLA[3]

[1] School of Architecture, Universitat Politècnica de Catalunya (UPC), Barcelona, Spain
[2] Architecture, Energy and Environment (AiEM), School of Architecture (UPC), Barcelona, Spain
[3] Cíclica Arquitectura SCCL, Sant Cugat del Vallès, Spain

ABSTRACT: Facing the climate emergency from the building sector, it is necessary to apply climate change mitigation and adaptation measures in the built environment. Among the areas that can be worked on, the research focuses on energy retrofitting of existing buildings, addressing carbon dioxide emissions associated with energy consumption in the building operational phase (Operational Carbon, OC) and embodied energy in building materials (Embodied Carbon, EC). Currently the main focus is on reducing the OC of inefficient buildings and the EC of building materials is still rarely considered. The question is whether it makes sense to consider an energy retrofit that emits more carbon dioxide with the intervention materials than the carbon dioxide that can be saved at the operational level, during the lifecycle of the building. The research aims to explore if there is an optimal energy renovation, which reduces the maximum OC using the minimum EC for the intervention materials. The study attempts to define the environmental optimal retrofitting of existing buildings for a limited number of intervention options, applying a specific methodology and using the optimization tool integrated in the Design Builder software (Energy Plus).
KEYWORDS: Housing retrofitting, embodied carbon, building life cycle, decarbonisation, Pareto Front.

1. INTRODUCTION

In the European Union (EU), the building sector is responsible for approximately 40% of the total energy consumption and 36% of the associated greenhouse gas emissions. [1]. In the Spanish level, the building sector consumes 30.1% of the total energy and emits 25.1% of the associated greenhouse gas emissions [2], a little less in proportion than the EU. Facing the climate emergency, mitigation and adaptation measures must be applied in the built environment, to move towards adequate, accessible habitability without exceeding the limit of resources that the planet can regenerate.

Half of the current main dwellings in Spain were built before 1980 [3]. That year, energy efficiency criteria was starting to be applied in the regulation *Normas Básicas de la Edificación* (NBE-CT-79) [4]. This means that the Spanish building stock has become old and is energy inefficient.

According to the EU objectives, the European countries must reduce energy consumption by 40% and the associated emissions by 55% by 2030 compared to 1990, reaching climate neutrality by 2050 [5]. In this context, building rehabilitation and urban regeneration can and must become the driving force in the building sector. The built environment faces three challenges that require a transformation process to meet society's demands: habitability, efficiency and equity [6].

At EU level, a minimum annual rehabilitation rate of 3% is proposed for existing buildings [5], a measure that has been considered and extended in the Spanish strategy for energetic renovation [7].

Currently, the main focus of mitigation measures for existing buildings is on reducing the operational energy of inefficient buildings. An example is the Minimum Energy Performance Standards (MEPS), which will lead to progressively abandon the lowest energy qualifications until the "A" qualification is reached by 2050 [1], although it is not yet fully defined. The environmental impact of building materials, even though they are beginning to be taken into account [5], in practice they still are rarely considered. But the impact represents, on average, 1/3 of the total emissions in a building's life cycle [8].

The aim of this paper is to determine the retrofitting option which represent the highest operational carbon (OC) reduction through the lowest embodied carbon (EC) in the intervention materials. This is applied for a limited number of possible interventions and in a case study. Based on the best options results, the question to be discussed is to analyse if the best resulting energy retrofits emit more carbon dioxide with the materials of the intervention than the carbon dioxide that can be saved during the building's life cycle.

2. METHODOLOGY

The methodology relates the EC of the renovation's materials and the OC associated to a building's heating and cooling energy consumption.

It is applied to an existing building case study, which current state data is collected. A limited

number of interventions is determined for each building element, according to the technical and physical possibilities that the current state offers and to the most common interventions applied in Spain.

Using the optimisation tool (Genetic Algorithm NSGA2), which is integrated in the Design Builder program (Energy Plus) [9], two optimisation objectives are set: reducing total OC and reducing EC of the intervention. The optimisation combines all the intervention options and determines, although with some level of uncertainty, the least carbon-emitting combinations of interventions by drawing a Pareto Front curve [9].

2.1 Calculation data

The EC ($kgCO_2/m^2$, kgCO2/kg) data for the construction materials were obtained from the iTec – BEDEC database [10], which is applied in Catalonia (Spain). New materials were created in Design Builder with this EC information so that the software could calculate with the Catalan territory's data, which is where the case study is located.

The OC ($kgCO_2$/year) data were obtained from simulations with Design Builder software and the calculation tool used by it, Energy Plus. The input data were obtained from the Spanish *Código Técnico de la Edificación* (CTE) [11] reference values.

Therefore, the data affecting the OC calculation and results has been extracted from the CTE regulations, such as climatic data, occupancy standards and reference values for lighting, domestic hot water, appliances and systems, ventilation and infiltration. Conversion factors for calculating CO_2 emissions from each type of energy are obtained from Catalan territory data [12].

Note that the varying values due to the different renovations are the infiltrations and the physical characteristics of the building envelope.

2.2 Constructive definition

The construction systems of the building's current state were defined according to the reference constructive characterization considered in the Spanish level [13], based on the building typology and the year of construction [14].

Considering the current status (CS) characteristics, interventions for each building element are proposed and can be seen in section 3. The CS of each building element is also taken into account in input data and calculation, leaving the possibility of no-intervention.

For each building element (building envelope: facades, windows, roof, ground floor; interior elements: interior partition walls, floor slabs), intervention options are determined, to test the following parameters:

- Thermal insulation thicknesses.
- Thermal insulation materials: expanded polystyrene, rock wool, cork.
- Intervention positions: interior, within, replacement, exterior.
- Addition of thermal inertia on the inside.
- Window replacement.

2.3 Results presentation

The results are shown graphically as point clouds: the EC is placed on the vertical axis and the OC on the horizontal axis. Each point on the graph represents a different combination of interventions. The combinations that are closest to 0.0 and dominate over the others form the Pareto Front curve. Therefore, the graph shows the relationship between the rehabilitation EC and the OC reduction compared to the current state.

To determine an environmental optimum, the building's years life cycle variable (t) is added. It is represented in the graph as straight lines and determine which Pareto Front intervention will emit the least carbon at the end of a building's useful life, by combining EC and OC. The straight lines are obtained using Equation (1):

$$TC = EC + OC \times t \qquad (1)$$

where TC – Total carbon emitted ($kgCO_2$)
EC – Embodied carbon intervention ($kgCO_2$)
OC – Operational carbon ($kgCO_2$/year)
t – Building's life cycle (years)

In a similar approach, one previous and relevant example [15] is the "embodied energy factor", which was defined as the amount of embodied energy required to reduce one unit of operational energy for 60 years of a new construction building's life cycle, set by regulation. But in case of renovations, the starting point is a specific current state from which to work, in terms of OC and building characteristics.

In order to facilitate the interpretation of results shown as point clouds, other straight lines are added in the graphs indicating the EC amortization years according to OC reductions.

3. CASE STUDY

The methodology was applied to an existing multi-family residential building (GF+4), with dominant orientation NNW (337,5º) - SSE (157,5º), in a Mediterranean coastal town (Catalonia), in the C2 climate zone according to CTE. It was built in 1995 and has a certain level of thermal insulation.

In order to carry out a more complete analysis, the same 3D model (Figure 1) has been used to create a second case study applying the construction systems of 1970. That decade, energy regulations for buildings weren't applied yet in Spain, so building envelopes didn't have any thermal insulation.

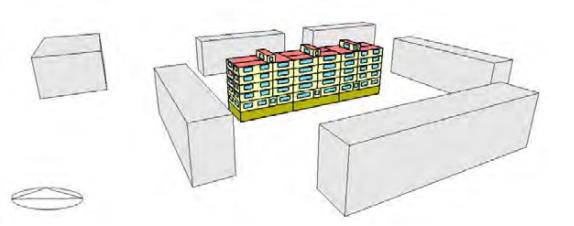

Figure 1: 3D model created in Design Builder

In summary, the method is tested on two case studies, different only at a constructive level in their current status (CS), as shown in Tables 1 and 2.

Table 1: Current status enclosures case study 1, 1970

Building element	**Composition ext - int** (thickness in cm)	**U** (W/m2·K)
Façade	Cement mortar (2) + hollow brick (14) + air gap (9) + brick (4) + gypsum (1)	1.32
Windows	Aluminium frames (no thermal break) + double glazing	3.58
Flat roof	Ceramic tiles (1) + cement mortar (1) + impermeable layer (0.3) + concrete (10) + unidirectional concrete slab (25) + gypsum (2)	1.44
Ground floor	Ceramic tiles (2.5) + cement mortar (2.5) + unidirectional concrete slab (25)	2.07
Interior partitions	Gypsum (2) + hollow brick (4) + gypsum (2)	2.60
Interior slabs	Ceramic tiles (2.5) + cement mortar (1) + unidirectional concrete slab (25) + cement mortar (2)	2.06

Table 2: Current status enclosures case study 2, 1995

Building element	**Composition ext - int** (thickness in cm)	**U** (W/m2·K)
Façade	Hollow brick (14) + expanded polystyrene (3) + air gap (7) + brick (4) + gypsum (1)	0.75
Windows	Aluminium frames (no thermal break) + double glazing	3.58
Pitched roof	Ceramic roof tiles (2) + partially ventilated air gap (25) + extruded polystyrene (6) + unidirectional concrete slab (25) + gypsum (2)	0.41
Ground floor	Ceramic tiles (2.5) + cement mortar (2.5) + unidirectional concrete slab (25)	2.07
Interior partitions	Gypsum (2) + hollow brick (4) + gypsum (2)	2.60
Interior slabs	Ceramic tiles (2.5) + cement mortar (2.5) + waffle slab (30) + gypsum (2)	2.06

Following the objectives and methodology explained, intervention possibilities for each building element are determined:

1. Façade interventions (16 possibilities + CS):
   - Exterior thermal insulation polystyrene (6, 8, 10 and 12 cm).
   - Exterior thermal insulation rock wool (6, 8, 10 and 12 cm).
   - Exterior thermal insulation cork (6, 8, 10 and 12 cm).
   - Cellulose fiber insufflation in air gap.
   - Cellulose fiber in air gap + 6 cm exterior thermal insulation (polystyrene, rock wool, cork).

2. Openings (8 possibilities + CS):
   - Replacement to wood frames and double glazing (with no solar protection, with 50 cm wood overhang, with 100 cm wood overhang and with programmable blinds).
   - Replacement to aluminium with thermal break and double glazing (with no solar protection, with 50 cm wood overhang, with 100 cm wood overhang and with programmable blinds).

3. Flat roof (15 possibilities + CS):
   - Exterior thermal insulation polystyrene (10, 12, 14 and 16 cm) + concrete pavement.
   - Exterior thermal insulation rock wool (10, 12, 14 and 16 cm) + ceramic flooring.
   - Exterior thermal insulation cork (10, 12, 14 and 16 cm) + concrete pavement.
   - Exterior thermal insulation 10 cm (polystyrene, rock wool, cork) + growth substrate and vegetation.

4. Pitched roof (12 possibilities + CS):
   - Interior thermal insulation polystyrene (10, 12, 14 and 16 cm).
   - Interior thermal insulation rock wool (10, 12, 14 and 16 cm).
   - Interior thermal insulation cork (10, 12, 14 and 16 cm).

5. Ground floor (8 possibilities + CS):
   - Interior thermal insulation polystyrene (6 and 8 cm) + concrete pavement.
   - Interior thermal insulation cork (6 and 8 cm) + (wooden floor or ceramic flooring).
   - Addition of concrete pavement.
   - Addition of ceramic flooring.

6. Interior partitions (2 possibilities + CS):
   - Addition of sand-lime brick (one and both sides).

7. Interior slab (3 possibilities + CS):
   - Addition of new pavement (concrete, ceramic flooring, wooden floor).

The combination between all variables, for 1970 case would be 264,384 possible combinations; for 1995 case would be 214,812.

Without optimization methods, as in this case is the algorithm, the calculation of each possibility and the subsequent comparison between them would be too time-consuming.

4. RESULTS

Note that the OC reductions obtained for each combination of interventions have a partial effect on the total carbon dioxide emissions of the building, since only passive strategies affecting heating and cooling energy consumption are used and showed in the graphs (Figures 2 and 3).

The different variables of years of building's life cycle (t) draw the lines that can be seen in Figures 2 and 3, identifying the optimal intervention for each case. Consequently, in case a point closer to (0, 0) is found in relation to any of these lines through new simulations with new variables, it would be a new optimal point. For example, the point (5, 300) in Figure 2 would be a new best option for 50 and 100 years life cycle but not for 25 years life cycle.

On the other hand, the optimal choices found show that as the variable (t) is higher, the EC has less influence, because there is more time for amortisation. Instead, the lower the variable (t), the more weight the EC has in the total emissions, which is why the optimal intervention is located at lower values of EC in the Pareto Front.

In absolute values, the 1970 building reduces more OC because it was, initially, more inefficient and has more improvement potential than the 1995 case.

Tables 3 and 4 show the optimal combination of interventions for each case and 50-year life cycle. It has been prioritised to expose 50-year results because they are the years of a building's useful life established by CTE regulations.

They show how the algorithm has prioritised materials with low EC, such as cork or wood, compared to polystyrene or aluminium; the prioritization of wood frame windows replacement and 50 cm overhang placement is observed; higher thermal insulation thicknesses appear among the options introduced; for interior elements, a tendency towards non-intervention is observed, although in the case of 1995 a certain amount of thermal inertia is added.

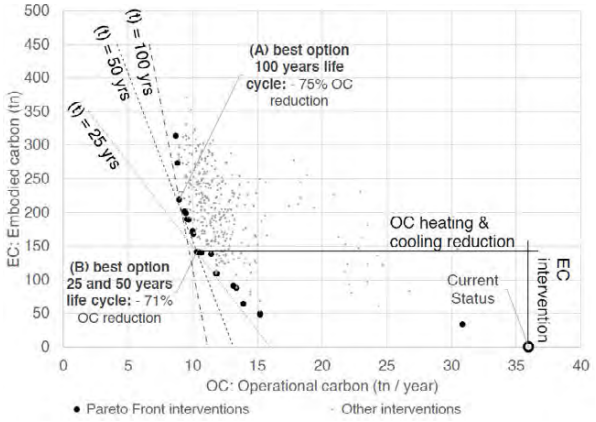

Figure 2: Optimisation for 1970 existing building.

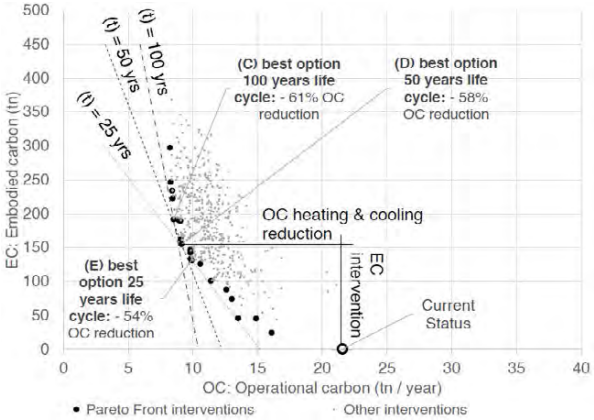

Figure 3: Optimisation for 1995 existing building.

Table 3: Optimal renovation, 50 years life cycle, 1970 case.

Enclosure	Variable	EC (kgCO2/ m2)
Façade	Exterior thermal insulation, 12 cm cork	45
Openings	Wood frames and double glazing + 50 cm overhang	268
Flat roof	Exterior thermal insulation, 10 cm cork	19
Ground floor	Interior thermal insulation, 8 cm cork + ceramic flooring	15
Interior partitions	Current state (no intervention)	0
Interior slab	Current state (no intervention)	0

Table 4: Optimal renovation, 50 years life cycle, 1995 case.

Enclosure	Variable	EC (kgCO2/ m2)
Façade	Exterior thermal insulation, 12 cm cork	45
Openings	Wood frames and double glazing + 50 cm overhang	268
Flat roof	Exterior thermal insulation, 14 cm cork	20
Ground floor	Current state (no intervention)	0
Interior partitions	Addition of sand-lime brick (one side)	20
Interior slab	Current state (no intervention)	0

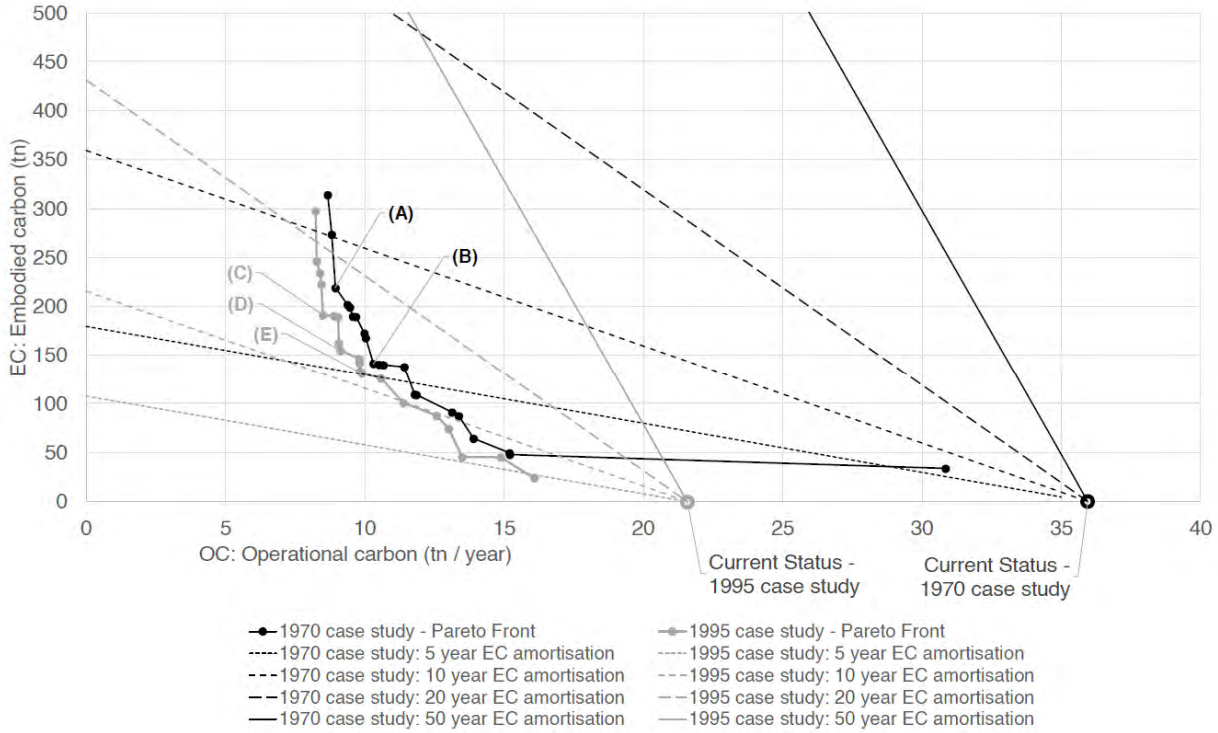

Figure 4: Comparison between the case studies: 1970 and 1995. Current states, Pareto Front curves, optimal combinations for 25, 50 and 100 years of useful life and EC amortisation years.

More extensive results indicate that there are certain variables that are better than others. For each building element, tendencies for intervention choices can be noticed. In the development of this research, the input data will be further refined to check the variation in results. Here follows a general observation in Pareto Front results:

- Thermal insulation thicknesses: higher thermal insulation thicknesses predominate among the variables introduced
- Thermal insulation materials: low EC materials such as cork or wood predominate.
- Intervention positions: external interventions predominate when different options are available.
- Addition of thermal inertia on the inside: a gradient from more inertia at the top of the graph to less inertia at the bottom is observed. Non-intervention predominates for interior slabs and inertia addition predominates for internal partitions.
- Window replacement: wood frame and double glazing window replacement with 50 cm overhang predominates.

Overall, Figure 4 shows how the algorithm works by searching for the potential between the minimum EC and the minimum OC. Comparing the case studies' Pareto Front curves, although with different starting points, it is observed how both reach similar post-intervention OC values.

On the other hand, also in Figure 4, the amortisation years of the EC are shown in relation to the OC savings obtained with each intervention. This is done to check whether the interventions prioritised in Pareto Front are counterproductive in relation to the years of buildings' lifespan or whether they quickly compensate the EC of the energy retrofit.

Regarding this, Figure 4 shows graphically how the current state OC efficiency level directly influences the years of EC compensation.

For example, the best option at 50 years life cycle, the intervention's EC for 1970 building is amortised after 5,5 years, with its OC reduced by 71%; on the other hand, for 1995 building, the EC is amortised after 12,5 years, with its OC reduced by 58%.

5. CONCLUSION

In the Pareto front curve of the analysed cases, considering that the EC analysis has been taken into account, no counterproductive interventions have been found. Nonetheless, the EC has a significant impact on the total carbon emissions of the building's life cycle.

With the analysed buildings, it can be seen that the EC amortisation time is higher for the 1995 case than for the 1970 case, as the first one is more efficient than the second one in their current status.

For newer, supposedly more efficient buildings, it becomes even more necessary to use decarbonised materials for their energy retrofitting, because the improvement potential is not as high as less efficient buildings. Consequently, it becomes more difficult to

amortise the intervention's EC in the lifespan of the building.

Therefore, the study shows that it is important to consider the EC of building materials and should be included in the calculations to reduce it, as occurs with OC. Depending on the design, the material choices and the current status of the building, just having the objective of an OC reduction for energetic renovations may be counterproductive in terms of environmental costs.

For each specific building, this analysis could be very different considering that the physical characteristics, geometry, orientation, occupancy, environment and/or interventions considered are specific to local conditions. Therefore, it is recommended to study the specific cases in order to reach more realistic results.

As it has been seen, both case studies reach similar OC values after the interventions. Firstly, it is considered that the reduction could be increased with the introduction of new, more refined variables based on the analysed results. For example, by introducing interventions with thicker thermal insulation. Secondly, note that the interventions are based on passive strategies, but it is considered that if the active systems (performance of air conditioning systems and energy sources) were changed, an improvement in OC would be observed. However, then the EC of the new appliances or systems replacing the old ones should be considered.

It is emphasised that the methodology proposed is very time-consuming, considering the preparation of data for each specific case, the long duration of calculations and the subsequent data processing. Ways to automate the methodology and reduce the time involved in the study could be explored.

On the other hand, it is also important to have accurate data available, both for embodied energy and emissions, and for case-specific characteristics of each case study.

Finally, research possibilities in architectural and energetic fields derived from this study are listed: variation in results. Here follows a general observation in Pareto Front results:

- The effect of adding thermal inertia.
- Tests with a wider variety of materials.
- Introduction of other types of interventions such as galleries or shading.
- Tests with more future-oriented climate files when the climate is expected to be warmer. The climate files used come from the CTE data, based on the past.
- "Business as usual" and/or real cases energy retrofitting EC and OC calculation to analyse whether they are counterproductive interventions.

ACKNOWLEDGEMENTS

This research is carried out within the context of an Industrial Doctorate (project code 2023 DI 00031), a collaboration between the company Cíclica Arquitectura, the PhD programme Architecture, Energy and Environment (AiEM), Universitat Politècnica de Catalunya (UPC), and the PhD student. We would like to thank the financial support of the Industrial Doctorates Plan, an initiative of the Research Department and Universities of Generalitat de Catalunya, managed by Agència de Gestió d'Ajuts Universitaris i de Recerca (AGAUR), Consorci de Serveis Universitaris de Catalunya (CSUC), and the collaboration of Fundació Catalana per a la Recerca i la Innovació (FCRI).

REFERENCES

1. European Parliament and Council (2018). Directive (EU) 2018/844 on the energy performance of buildings (EPBD).
2. Bellver, J., Cossent, R., Linares, P., Romero, J., Pérez, M., y Rodríguez Matas, A. (2020). Observatorio de Energía y Sostenibilidad en España. Universidad Pontificia de Comillas.
3. Cíclica i GBCe, from Instituto Nacional de Estadística (INE) (2018). Enquesta Contínua de Llars ECH.
4. Consejo General de la Arquitectura Técnica de España (CGATE) y Mutua de propietarios (2020). Informe rehabilitación energética en España: Una oportunidad de mejorar el parque edificado en España. Madrid.
5. European Comission (2020). Renovation Wave: Aiming to improve energy efficiency, boost the economy and deliver better living-standards for Europeans. Brussels.
6. Cíclica i GBCe, (2020). PAS-E, Passaporte del edificio, Instrument for staged deep rehabilitation.
7. Secretaría de Estado de Transportes, Movilidad y Agenda Urbana, Secretaría General de Agenda Urbana y Vivienda (2020). Actualización 2020 de la Estrategia a Largo Plazo para la Rehabilitación Energética en el Sector de la Edificación en España (ERESEE).
8. Aslanides, A., Kuczera, A., and Caffi, M. (2020). Built4People| People-centric sustainable built environment (Draft). European Commission.
9. Design Builder Manual [Online] – http://designbuilder.co.uk/helpv7.0/
10. Database iTeC, Banc BEDEC Construcció (2021), [Online] - https://itec.cat/
11. Ministerio de Transportes, Movilidad y Agenda Urbana (MITMA) (2022), Código Técnico de la Edificación en España, Documento Básico HE Ahorro de energía (CTE-DB HE)
12. Oficina Catalana del Canvi Climàtic (2019), Guia pràctica per al càlcul d'emissions de gasos amb efecte hivernacle (GEH).
13. Ministerio de Transportes, Movilidad y Agenda Urbana (MITMA), from Instituto Nacional de Estadística (INE) (2018), Encuesta Contínua de Hogares (ECH).
14. Ministerio de hacienda y función pública, secretaría de estado de hacienda y dirección general del catastro: Sede Electrónica del Catastro, Spain. https://www.sedecatastro.gob.es/
15. Venkatraj, V., Kumar Dixit, M., Yan, W., Lavy, S. (2020): Evaluating the impact of operating energy reduction measures on embodied energy.

PLEA 2024 WROCŁAW
(Re)thinking Resilience

Exploring The Potential of Energy Savings Through Retrofitting Traditional Heritage Buildings

A Case Study of Abu Jaber House in Al Salt, Jordan

KAMAL HADDAD[*,1] SIMON LANNON[,1] ESHRAR LATIF[,1]

[1]Welsh School of Architecture, Bute Building, Cardiff University, King Edward VII Ave, Cardiff CF10 3NB

ABSTRACT: Reducing energy demands in buildings has become a key interest to achieve net-zero goals. Jordan, as a country, imports over 95% of its energy from neighbouring countries, initiating the need to find strategies to reduce energy consumption. This research investigates the feasibility of achieving energy savings by retrofitting heritage buildings with preservation conditions. Specifically, the study assesses the effects of building's fabric interventions and systems interventions on heating, cooling, and lighting loads using Ladybug tools in Grasshopper3D as a modelling method. Retrofit measures encompass changes in glazing type, incorporation of shading devices for existing windows, reduction in infiltration rates, addition of thermal insulation, enhancement of sensible heat recovery efficiency, and interventions in the lighting system by lowering lighting power density and introducing a daylight control system. Additionally, the study explores the potential of integrating renewable energy sources, such as photovoltaic panels for sustainable energy production. Results indicate that fabric interventions, like adding a 30 mm aerogel layer for thermal insulation, yield over 10% energy savings. Similarly, introducing a daylight control system can reduce the demands by 11%. The study establishes a systematic framework for energy modelling applicable to buildings with similar conditions, providing valuable insights for sustainable retrofitting strategies.
KEYWORDS: Energy consumption, heritage buildings, retrofit, daylight control, renewable energy.

1. INTRODUCTION

Significant efforts are being made globally to mitigate the environmental impacts resulted from the climate change crisis [1]. Various strategies are proposed to address this issue, including the debate between promoting energy efficiency in new builds or retrofitting existing buildings [2]. Energy retrofit is an effective method for reducing energy consumption [2], but it requires assessing the compatibility of the building fabric with the retrofit plan.

In Jordan, to reach net zero targets, governmental and non-governmental initiatives have made great strides in decarbonising the built environment and lowering operational energy [3]. Such policies are being implemented since Jordan is a country that imports over 95% of its energy from neighbouring countries [3]. Therefore, conducting energy simulations to evaluate a building's energy performance is a critical factor in resolving the energy crisis in the country.

This research works on presenting an overview of the energy performance in one of the most significant buildings in the heart of the UNESCO protected city of Al-Salt, Jordan. The research is carried out a thorough simulation-based analysis of the original function of the building, in addition to its newly adopted function, which was changed recently, to compare the energy performance and the impact of the transformation. Additionally, several retrofit solutions that range from fabric adjustments to systems interventions are studied to understand the anticipated performance.

2. RESEARCH BACKGROUND

Jordan's population has increased drastically in the past few decades, resulting in a huge impact on the residential sector, and increasing demand for energy [3, 4].

This section presents the current energy circumstances in Jordan, shedding light on the importance of undertaking such research in the country. Additionally, the climatic conditions of Al-Salt city are discussed to highlight the energy demands required for operating the building's services. Furthermore, the selected building for the study is introduced with an emphasis on its heritage significance in the city as well as its current fabric conditions which will be used as a base to model and simulate the overall loads.

2.1 Energy in Jordan

The residential sector in Jordan is thought to account for 43% of the country's overall power usage [3]. The heating and cooling of residential structures in Jordan account for almost 38% of total energy consumption, according to a 2016 assessment of rising zero-emission building sector objectives in the Middle East and North Africa (MENA) region [3].

Jordan faces two primary issues in its energy landscape: a rising demand for energy and a severe shortage of domestic resources to meet this demand [5]. In 2019, the peak load of Jordan's electrical system peaked at 3,380 MW in January, surpassing the January 2018 figure of 3,205 MW by approximately 5.5% [6]. The average annual growth rate from 2010 to 2019 stood at around 2.7%, but the load has consistently grown at a rate of approximately 3 to 5% each year. This steady increase poses an additional challenge for the adaptation of the systems in Jordan [4]. However, the Renewable Energy Law of 2012 set a goal for 10% of the nation's energy composition to be sourced from renewables by 2020, equivalent to a capacity of 1,800 MW, primarily derived from wind (1,200 MW) and solar (600 MW). Jordan has since increased its target for the proportion of renewables in the power mix, which has increased from an initial 31 to 50% by 2030 [6].

2.2 The climate in Al Salt City

Al Salt experiences long, warm, and dry summers, as well as cold and generally clear winters. The temperature typically ranges from 4°C to 31°C throughout the year, with rare occurrences of it falling below 0°C or rising above 34°C. The hot season typically lasts for 4.4 months, from May to October, with the daily high temperature averaging above 27°C. July is the hottest month in Al Salt, with an average high of 30°C and low of 19°C. On the other hand, the cool season spans 3.2 months, starting from December to March, and has an average daily high temperature below 15°C. January is the coldest month, with an average low of 4°C and high of 11°C [7].

In Jordan's mid-region, there are approximately 3290 annual sunlight hours on average. This abundant sunlight creates an efficient opportunity for using photovoltaic systems to generate electricity, offering a potential to reduce energy costs through renewable resources. Additionally, the solar radiation in Jordan is high where it varies between 4 and 8 kWh/m^2, which implies a potential of 1400-2300 GWh per year annually [8].

Throughout the year, Al Salt experiences varying amounts of rain days. From November to March, which is the start of the wetter season, there is a larger than 13% probability that any given day will be rainy. With an average of 7.2 days with at least 1 mm of precipitation, January has As Salt's wettest days. From March to November, there are 8.0 months during which it is drier. With an average of 0.1 days with at least 1 mm of precipitation, July has the fewest rain days in As Salt [7].

2.3 Abu Jaber house

One of the unique heritage buildings and currently most visited attraction in the city centre of Al Salt City is Abu Jaber House. The building was built in multiple phases between 1896 and 1905, which can be noticed from the colour of the stone which differs between floors and sections. The ground floor level has stone walls 60 – 100 cm thick and is currently used as shops in addition to including the entrance to the upper levels. The first floor, however, is arranged around a vaulted courtyard that is used to distribute the different zones and rooms. The second floor also consists of three courtyards that are connected to the different rooms and spaces [9].

Figure 1: A street view of Abu Jaber house.

3. RESEARCH METHODS

Due to its cultural and architectural significance, Abu Jaber house was selected as a case study aiming to communicate to the industry, the benefits of energy modelling and retrofitting similar buildings. The study works on building an energy model that is a simplified representation of the building's geometry, considering the materials used and the adopted construction systems.

The research uses Grasshopper3D [10] as a computational environment for modelling along with Ladybug tools [11] to simulate the energy performance with special focus on the building's thermal loads and lighting loads as they have the largest contribution to overall demands. Initially, the energy model will be studied to understand the original state of the building as a residential building. However, currently the buildings functionality has been transformed into a museum and show case of the city and its culture. Hence, a simulation of the building with its new adopted program is required to understand the impact on the change of energy consumption and to build a baseline model to assess potential energy retrofit interventions.

Nonetheless, this research explores different retrofit measures that can be adopted to mitigate the energy crises in the country. Even though some of the proposed measures can be difficult to implement due

to its listing and UNESCO protection status, the study of such scenarios can be potentially reflected on other similar buildings in the city or beyond that may not share the same listing status.

In this study, the modelled floor area of the building is 632 m2. It is also critical to mention that the ground floor of the building was not considered in the energy model as its functionality remained the same as shops.

The study works on simulating different shallow and deep retrofit solution to understand the impact of each case on the overall energy performance as follows; (i) examining the impact of the glazing system by testing various types of glazing; (ii) adding a horizontal shading device with different depths to the existing windows, (iii) improving the airtightness of the building by exploring reductions of the infiltration intensity rates by 5%, 10%, 25%, 40%, and 60%; (iv) enhancing the fabric's insulation by adding an internal layer of aerogel (u value = 2.1 W/m2 k) with thicknesses of 10mm, 20mm, 30mm, 40mm, 50mm ; (v) enhancing the sensible heat efficiency factor of the used HVAC system (Ideal air) by testing a factor of 0.6, 0.7, 0.8, 0.9, and 1; (vi) Optimising the used lighting systems by exploring lighting power densities between 9 and 5.

Additionally, this paper investigates the implications of introducing a daylight control sensor system that works on dimming the lights when natural daylighting is satisfied. For exploring the impact of applying such system, the sensors were defined at the centre of each room's floor area. The illuminance setpoint was set to 300 lux while the lowest power and lowest lighting output the lighting system can dim to, are set to 0.3 and 0.2 respectively.

Besides, this research works on performing a multi variant optimisation using Galapagos solver in Grasshopper3D, to find the most optimised values for the investigated parameters to reach the lowest EUI.

Furthermore, a comparative analysis of the potential savings when installing photovoltaic (PV) panels using PVGIS-SARAH2 dataset within PVGIS tool [12] to estimate the electricity production of the PV panels, where the azimuth and slope of the panels was optimised to 16° and 27°.

Table 1 below demonstrates the setup of the activity program for the residential case (intended use), and the museum case (current use). The used values for the used parameters were retrieved from archival documents [9] or from Ladybug Tool's dataset [11] when not available.

Table 1: The activity and HVAC programs for the residential and the museum cases [9.11]

Parameter	Residential	Museum
Heating setpoint (°C)	21.7	21
Cooling setpoint (°C)	24.4	24
Occupancy density (people/m^2)	0.0196	0.1497
Equipment power density (W/m2)	0	3.5
Lighting power density (W/m2)	6.4	10.7
Air Changes per Hour (ach per hour)	2.88	5.76
HVAC sensible heat recovery factor	0.6	0.5

Currently, the fabric's exact construction details are not fully documented, however, the researchers have worked on approximating the tectonics of the different fabric elements using available archives and site visits. As discussed, the external walls are primarily made of an average of 600 mm hard limestone, while the internal walls were made of soft limestone with an averaged thickness of 400mm. The floor of the first level is 650 mm of dense concrete, while the second level and the external floors are 300 mm and 400 mm respectively made of concrete.

For examining the impact of glazing type on the building's performance, the specifications of the tested glazing types which includes the u value, SHGC factor, and the visible transmittance factor were retrieved from the standard assessment procedure (SAP 10.2) [13] as listed in table 2 below.

Table 2: The activity and HVAC programs for the residential and the museum cases

Scenario	U-value (W/m^2 K)	SHGC	Transmittance factor
Single glazing (Original)	4.80	0.70	0.85
Double glazing (Air filled)	2.20	0.77	0.76
Double glazing (Low emissivity)	0.90	0.77	0.76
Double glazing (Argon filled)	2.60	0.54	0.76
Triple glazing	1.60	0.35	0.64

4. RESULTS

4.1 Exploring the impact of changing the building's activity on the energy performances

As discussed, the original building design was residential, necessitating a simulation under those conditions. Results showed normalized annual heating and cooling loads of 103 kWh/m2 and 58.3 kWh/m2, respectively, with an annual lighting load of 3.4 kWh. Simulations of the current conditions, serving as a benchmark for retrofit measures, revealed changes due to the building's transformation into a gallery and showcase. New parameters, such as equipment loads, people's density, and lighting power density (see Table 1),

were considered. The simulation indicated a 6.7% increase in Energy Use Intensity (EUI) post-activity change. Internal heat gains led to reduced annual heating loads (78 kWh/m2) but increased cooling demand (80 kWh/m2), with lighting demands rising to 36 kWh/m2.

Based on the simulation of the current conditions, it was demonstrated that the loads from, cooling, heating, infiltration, lighting, window conduction, and fabric conduction, have fluctuated throughout the year, therefore, the measures discussed in the upcoming sections were proposed in attempt to reduce the demands.

4.2 Exploring the impact of glazing type

The glazing percentage for Abu Jaber house is approximately 15%, therefore, studying the performance of different glazing types is crucial. Hence, five distinct types of glazing were explored; (a) the existing original single layered glazing as a benchmark (BM), (b) air filled double glazing, (c) low-e air-filled double glazing, (d) argon-filled double glazing, and (e) air filled triple glazing. The results of the investigation are demonstrated in table 3 below.

Table 3: The thermal loads and overall saving in implementing different glazing types.

Scenario	Heating (kWh/m^2)	Cooling Deman(kWh/m^2)	Potential savings
a (BM)	78.45	79.53	-
b	71.74	81.27	2.40%
c	67.72	82.71	3.80%
d	79.66	72.72	2.90%
e	83.11	66.71	4.30%

Based on the previous simulations, it is noticed that the change of glazing type helps in reducing the overall EUI of the building and therefore reducing the energy costs.

4.3 Exploring the impact of using shading devices on the widows

In this exploration, different depths of horizontal shading devices were tested that varied between 10 cm and 50 cm. Adding a shading device contributed with an increase in the annual heating and lighting demands and a similar decrease in the cooling loads. Overall, this behaviour has maintained the building's EUI at around 208 kWh/m^2. Therefore, adding shading devices is proven to be an insufficient solution for this building which is contributed to having the largest area of glazing on the northern façade, therefore, the heating and lighting demands would increase.

4.4 Exploring the impact of reducing infiltration rates

According to the simulations of Abu Jaber house, it was noticed that airtightness of a building and the increase in infiltration heat losses through the building's age can greatly increase the annual energy demands. Therefore, controlling the air tightness of the building can reduce both heating and cooling loads of the building as presented in figure 2.

The infiltration intensity rates of the building relate to the fabric's efficiency. Therefore, increasing the air tightness of the building can be performed by reducing the cracks and gaps in the fabric and any potential thermal bridging zones. In addition, replacing the old windows frames with newer ones would contribute to reducing the infiltration rates.

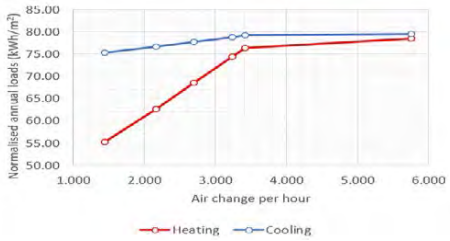

Figure 2: Explored thermal demands at different air changes per hour.

4.5 Exploring the impact of thermal insulation

As no records imply the presence of any type of thermal insulation layers, it is critical to understand the impact of adding a single layer of thermal insulation to the internal faces of the walls. Due to the impracticality of adding the insulation within the fabric, the simulation was based on experimenting adding an insulation layer with different thicknesses that varied between 10 mm and 50 mm. Figure 3 demonstrates that adding a 30 mm layer of aerogel had the largest difference in minimising the heating loads. However, adding thicker layers had smaller impact. The impact of adding insulation had insignificant impact on the cooling loads.

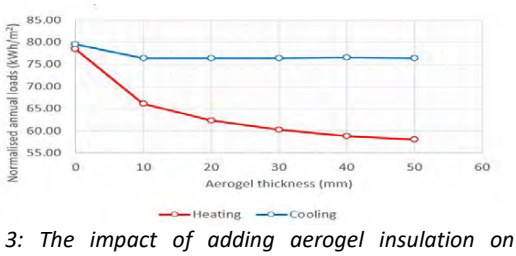

Figure 3: The impact of adding aerogel insulation on thermal demands.

4.6 Exploring the impact of enhancing HVAC system efficiency

Currently, the building's heating is primarily dependant on portable heating units. Therefore, an ideal air HVAC system (non-mechanical) was used in

the energy modelling of the building. To test the impact of improving the efficiency of the heat recovery and heat preservation within the building, the sensible heat recovery factor was changed between 0.6 and 1, where 1 represents a 100% heat recovery efficiency.

Figure 4 illustrates that the increase of the heat recovery efficiency would have significant positive implications on reducing the heating and cooling loads. Such improvements can be assured by performing other measures like adjusting the glazing type as well as reducing the infiltration intensity rates.

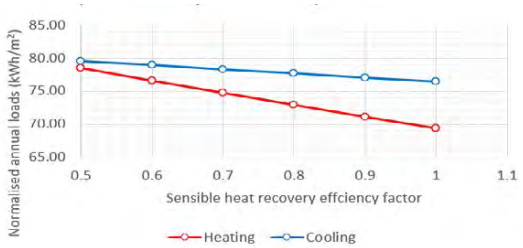

Figure 4: The normalised annual thermal demands with different HVAC system efficiency factors

4.7 Exploring the impact of optimising installed lighting systems

Based on initial comparative simulations between the building's lighting loads, it is noticed that a massive increase in the lighting loads have occurred. Hence, studying the impact of optimising the lighting system is needed. The lighting power density (LPD) which is controlled by the lighting type and illuminance was used to test the implications on the thermal loads as well as the lighting loads. The graph in figure 5, presents the impact of the reduction of lighting power densities on the thermal loads. It is observed that lower LPD increases the heating demands since the lighting system emits less heat, which consecutively reduces the cooling loads.

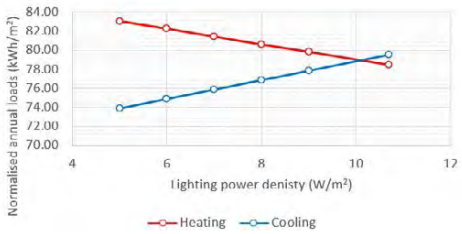

Figure 5: The impact of adjust lighting power densities on heating and cooling demands.

Nonetheless, the simulation highlights the significant role of optimising the lighting system in reducing the lighting loads of the building which can be reduced up to 53% if LPD is reduced to 5 W/m^2. This solution can be one of the most effective, where reducing LPD to 6 W/m^2 can reduce the overall energy consumption by 9%.

4.8 Exploring the impact of introducing a daylight control sensor system

This measure introduces coupling the building with a daylight control system that involves dimming the lights and turning it off if the senor reading reaches the illuminance set point of 300 lux. Such measure was performed on all the individual measures discussed in this paper. All results have presented a significant reduction on the EUI in total and its breakdown of thermal loads and lighting loads. The EUI of the baseline model was reduced by 10.58%. The highest reduction was noticed when changing the glazing type to low emissivity double glazing with total reduction of 11%.

4.9 Performing Multi Variant optimisation to reduce EUI

After running the optimisation using Galapagos solver in Grasshopper 3D, it was demonstrated that applying the suitable measures results in a drastic reduction of the energy use intensity and its breakdowns. EUI was reduced by 50.5% when compared to its current situation with a reduction in heating, colling and lighting demands of 48%, 16% and 69% respectively. The simulation was run for around 112 hours after it has been terminated due to reaching 50 stagnant without improving the optimisation objective as defined in the optimisation setup. Table 4 presents the measures and their associated values in addition to the reduction percentage in energy consumption compared to the current conditions.

Table 4: The measures and values that were concluded based on the multi variant optimisation.

Measure	Value	Reduction (%)
Glazing type	Low e	14.4
Air changes per hour	2.7 ach	16.4
Insulation thickness	3 cm	21.6
Sensible heat efficiency	0.8	14.4
Lighting power density	7 W/m^2	13.5
Shading Device	0.0 m	-

The simulation has demonstrated that applying the different measures results in a drastic reduction of the energy use intensity and its breakdowns. EUI was reduced by 50.5% when compared to its current situation with a reduction in heating, colling and lighting demands of 48%, 16% and 69% respectively.

4.10 Exploring the impact of installing PVs

Considering the total floor area of the building and its current EUI of 208 kWh/m^2 and using Crystalline silicon PV panels with 19% efficiency, the PV peak capacity was approximated to 46 kWp.

According to the simulation, the normalised annual production of energy is estimated to reach 121 kWh/m^2. Furthermore, the calculations have taken into consideration that the total loss of production is around 23.16% considering 14% system loss, 2.28% losses caused by the angle of incidence, 0.6% loss due to spectral effects, and 8.02% of losses that may be caused by the temperature and low irradiance.

Figure 6 illustrates the energy balance, comparing estimated PV production to the heating, cooling, and lighting loads of the most effective measures discussed in section 4.9 throughout the year. PV panel production peaks in July, with the lowest output occurring in January. Simultaneously, the highest energy demand coincides with hot months, causing a shortfall in PV energy to meet demands. However, considering the cumulative net production over the year, the system generates an export of 1.8 kWh/m^2 after satisfying heating, cooling, and lighting needs. These findings underscore the necessity of implementing an energy storage system to supply the building with renewable energy during periods of lower electricity production.

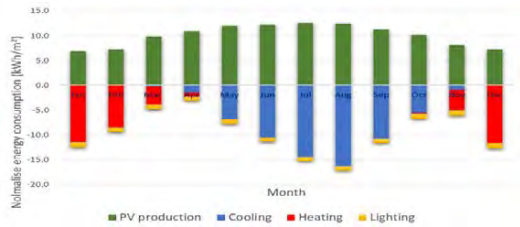

Figure 6: Energy balance of fix-angle PV production compared to the thermal and lighting demands.

It is critical to mention that this study was considering the thermal and lighting loads due to clear consequence on the energy consumption of the building. However, other loads in the building contribute to the overall energy consumption such as the infiltration loads, hot water supply and the electric equipment used in the building urging the need to apply such measures.

5. CONCLUSION

The study systematically analyses a UNESCO-protected heritage building, assessing thermal and lighting loads, energy demands, and potential retrofit solutions. Accordingly, the developed system is encouraged to be used for buildings with similar conditions. This energy modelling approach is advised before any intervention to anticipate potential consequences, understand implications of changes on the building's heritage value, and suggest precautions and measures to minimise negative results.

The study demonstrated that interventions on the fabric had the highest impact on reducing the annual energy consumption. For instance, independent interventions such as adding 30 mm layer of aerogel as a thermal insulation can result in over 10% of energy savings, in parallel, reducing the infiltration intensity rates by 40 % can result in over 13.5% of energy savings. Additionally, interventions on the used lighting system have promising impact when reducing the lighting power density from 10.7 W/m^2 to 7 W/m^2 can contribute to over 8% of savings. In parallel, implementing effective measures coupled with a daylight control sensor system can further reduce energy consumption by 50.5%. Based on the discussed results, the following points can be highlighted:

- Changing a building's program and functionality without proper consideration can greatly increase energy demands.
- Introducing daylight control sensors to high-lighting-demand buildings like museums significantly reduces overall energy use and its breakdowns.
- Integrating PV panels have proven to be sufficient in satisfying the building's major demands after applying retrofit measures with a production of 121 kWh/m^2 making an electricity export of 1.8 kWh/m^2.
- While implementing different can significantly reduce energy consumption, the heritage value of the building must be taken into consideration.

REFERENCES

1. Lelieveld, J., et al., *Climate change and impacts in the Eastern Mediterranean and the Middle East.* Climatic change, 2012. 114: p. 667-687.
2. Coyne, B. and E. Denny, *Retrofit effectiveness: Evidence from a nationwide residential energy efficiency programme.* Energy Policy, 2021. 159: p. 112576.
3. Schimschar, S., et al., *Accelerating zero-emission building sector ambitions in the MENA region (BUILD_ME).* no. April. Available:https://www.buildings-mena. com/files/BUILD_MECountryReport-Egypt_. pdf, 2020.
4. Alrwashdeh, S.S., *Energy sources assessment in Jordan.* Results in Engineering, 2022. 13: p. 100329.
5. Energypedia, *Jordan Energy Situation*. 2014.
6. Enerdata, *Jordan Energy Information*. 2022.
7. weatherspark, *Climate and Average Weather Year Round in Amman, Jordan*. 2023.
8. Alrwashdeh, S.S., F.M. Alsaraireh, and M.A. Saraireh, *Solar radiation map of Jordan governorates.* International Journal of Engineering & Technology, 2018. 7(3): p. 1664-1667.
9. RSS, *The architectural heritage in the Hashimite Kingdom of Jordan - Al Salt City*. Vol. 1. 2011, Amman: Royal Scientific Society.
10. McNeel, R., *Grasshopper 3D.* URL: https://www. grasshopper3d. com/3, 2014.
11. Roudsari, M.S. and M. Pak, *Ladybug: a parametric environmental plugin for grasshopper to help designers create an environmentally-conscious design.* 2013.
12. Huld, T., R. Müller, and A. Gambardella, *A new solar radiation database for estimating PV performance in Europe and Africa.* Solar energy, 2012. 86(6): p. 1803-1815.
13. *Standard Assessment Procedure (SAP 10)*. 2023, BRW.

PLEA 2024 WROCŁAW
(Re)thinking Resilience

Balancing Energy-Efficiency and Health in Retrofitted Dwellings to the EnerPHit Standard

Achieving Optimal Indoor Environmental Quality

ALEJANDRO MORENO-RANGEL[1], TIM SHARPE[1]

[1]University of Strathclyde, Glasgow, UK

ABSTRACT: It is widely known that the UK has the least energy-efficient building stock in Europe, which contributes to over 30% of total greenhouse gas emissions. To improve the energy performance of both new and existing buildings, the UK is implementing policies to improve performance. One of the retrofit solutions, EnerPHit, has been applied in a tradiational stone tenement building in Glasgow as a test of this approach.
The findings to date indicated that the project has been effective in providing comfortable, healthy dwellings with low energy usage and high levels of occupant satisfaction. but some individual dwellings are exceeding targeted consumption levels. Despite this, the dwellings maintain good indoor temperatures, generally within the EnerPHit performance targets, without sacrificing thermal comfort. The indoor air quality and ventilation targets were met with CO2 levels below 1,000ppm throughout the monitoring period, and there was no evidence to suggest that the MVHR systems were switched off or malfunctioning. Currently, there are no apparent concerns regarding interstitial moisture in the construction.
There are valuable lessons to be learned from this retrofit program, particularly the significance of occupant behaviour, expectations, and their engagement with building systems, but the project has also highlighted the need for construction skills to enable delivery and proper maintenance and operation of new building systems.
KEYWORDS: Energy, Comfort, EnerPHit, net zero retrofit, indoor environment.

1. INTRODUCTION

In order to tackle Climate Change, new net zero targets have been implemented by several countries. When considering the complete life of a building, the built environment is responsible for over 50% of the carbon emissions [1]. Many countries have started looking at the Passivhaus Standard to meet these commitments [2], for instance, Scotland.

The UK has Europe's worst energy-efficient building stock, contributing over 30% of total greenhouse gas emissions [3]. In a determined push towards net zero, the UK government introduced the Future Homes Standard in England, while Scotland established the Domestic Building Environmental Standards (2025) Bill, akin to the renowned Passivhaus standard. These policies represent significant milestones, but at present, a substantial number of existing buildings still heavily rely on natural gas for heating, hot water, and cooking. Thus, retrofitting existing buildings emerges as the foremost challenge. While evidence of the performance of new builds to the Passivhaus in Scotland is available [4], little is available about retrofits.

Approaches to retrofit pose different challenges; without holistic measures to ensure that both energy and environmental measures are improved, unintended consequences may occur.

While the Passivhaus principles are still applicable for EnerPHit [5], there are some key differences in terms of heating and cooling demand, 25kWh/m2/year instead of the 15kWh/m2/year for Passivhaus Classic, as well as the airtightness level (n50) of 1.0 h-1 @ 50 Pa compared to the 0.6 h-1 @ 50 Pa for new builds. These considerations recognise the changes associated with working with existing buildings. Beyond the operational carbon emissions, EnerPHit buildings have other benefits, such as adequate ventilation and indoor air quality (IAQ), improved thermal comfort and a low risk of internal condensation [6]. However, challenges related to limitations associated with the refurbishment of existing buildings still exist [7]. Some of these challenges are related to the building occupants' behaviours; others may be related to the refurbishment process and skills in the construction sector. While the key driver for retrofitting is the reduction of carbon emissions, we should also consider other aspects of the indoor environment that can impact occupants' health and energy use. Hence, the risk of overheating, mould and condensation, should be considered alongside IAQ and ventilation, particularly in Passivhaus dwellings [8].

This work presents the energy monitoring and indoor environmental conditions (thermal comfort and indoor air quality) of one of the largest deep energy residential retrofits to the EnerPHit Standard in a historic tenement building in Scotland.

2. METHOD

The building's energy retrofit design and construction happened between 2020 and 2022, with the first occupants moving in November 2022. This paper presents the indoor environmental (temperature, relative humidity and carbon dioxide) analysis between the 9th of February and the 26th of June 2023 of 6 of the 8 one-bedroom flats. Energy reading were taken directly from the electricity and gas meters during the installation of the sensors and a further visit was scheduled in August 2023 to collect the second readings. The retrofitted building is a traditional pre-1919 4-storey red sandstone tenement consisting of eight one-bedroom social housing flats and a communal close and backcourt (see Figure 1).

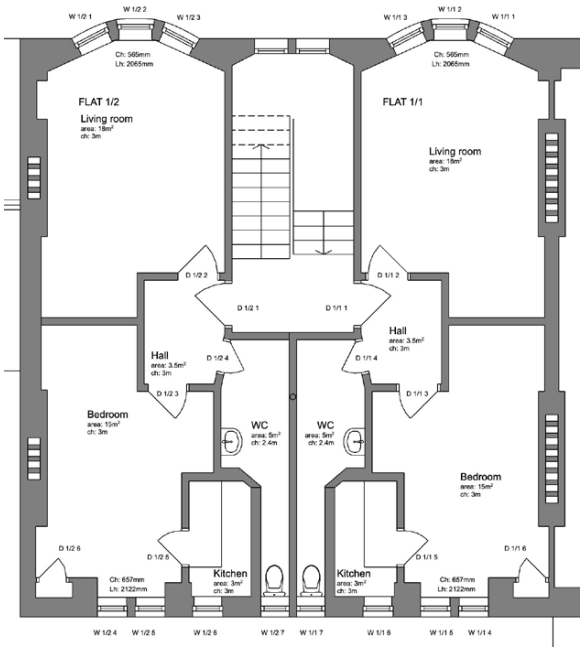

Figure 1: Floor plan of the building. Source: John Gilberts Architects.

The data was collected using a commercial monitoring kit (Gateway - AICO Ei1000G SmartLINK, sensors - AICO Ei1025 SmartLINK). The sensors were installed in each of the flats' living room, kitchen and bedroom. Data were collected at 15-minute intervals for each of the parameters [Temp -10 to 40; Relative humidity 15-95%RH; Carbon dioxide 0-5000ppm]. Energy consumption was collected through manual meter readings.

Stone tenements have a unique structure and appearance that makes installing external wall insulation (EWI) on stone facades difficult. Although in this case EWI could be placed on the brick elevations on the sides and rear, improving U-values on the stone facade requires internal insulation. However, adding internal insulation may make the stonework colder and wetter, which can pose a risk to timber elements such as floor joists that protrude into the stonework. To investigate this interstitial moisture sensors were installed in beams during construction to assess this risk. These sensors use an OmniSense G-4-NBIOT-EU Gateway with 4G Cellular Data, which wirelessly connects with temperature and moisture sensors embedded in the construction. The wireless-powered gateway is located in the loft space, and the sensors for interstitial condensation were placed during construction at the bottom front side and top back of the building.

Individual air source heat pumps (ASHP) are used to heat four of the flats (ground and first floor flats), extracting heat from the external air to provide hot water for radiators and domestic use. Modern and efficient combi gas boilers heat the remaining four upper flats. Each of the eight flats is equipped with a mechanical ventilation heat recovery unit (MVHR) located above the bathroom ceiling. These units remove moist and stale air from the kitchens and bathrooms while simultaneously bringing in fresh air from the outside. By utilising a heat exchanger, the MVHR system transfers heat from the stale air to the fresh air, minimising heat loss and reducing the overall heating demand. The six upper flats also have wastewater heat recovery units installed in the bath/shower systems. This allows the captured heat from the wastewater to be recirculated back into the hot water system, effectively reducing the demand for water heating.

3. RESULTS

3.1 Energy use

To date energy use has been collected through meter readings. During the periods – February 2023 to August 2023. The readings collected were used to determine the annual electricity demand of each flat and the building as a whole. The annual estimation was based on a simple extrapolation between the days when meter readings were taken, the estimation of the space heating demand for the electric heating flats (second and third floors) was also extrapolated based on the heating demand for those using gas.

The average electricity demand for the six flats was 23.94 kWh/m². However, there was a variation in this figure when comparing the flats that used electricity as a source of heating via the heat pump versus those that used gas. For the flats that used electric heating, their electricity consumption between February and August 2023 was 29.62 kWh/m², while for those that used gas for space and water heating, it was 18.26 kWh/m². Additionally, for the flats using gas heating, the average consumption during this period was 33.20 kWh/m².

the average estimated annual electricity demand for all the flats is 39.81 kWh/m²year, which is lower than the average home in Scotland, estimated at 43.4 kWh/m²year by Ofgem. By comparing the electricity

consumed by the gas and heat pump flats, we can estimate the energy required for space and water heating for flats that use electricity as a source of heating via the heat pump. This indicates an estimated annual demand of 19.89 kWh/m²year for heat pump flats. Assuming a figure of 15 kWh/m²year for water heating, this would indicate a space heating demand of 4.89 kWh/m²year, which is below the EnerPHit target of 25 kWh/m²year.

However, the annual space and water heating consumption for flats with gas heating is estimated to be 51.91 kWh/m²year. Taking into account an assumed 15 kWh/m²year for water heating gives a space heating load of 36.91 kWh/m²year, which is higher than the EnerPHit target of 25 kWh/m²/year. Based on these numbers, the estimated average annual heating demand for the building is 20.90 kWh/m²year.

The readings collected were used to determine the annual electricity demand of each flat and the building as a whole. The estimation was based on a simple extrapolation from days when meter readings were taken. The average estimated annual electricity demand for all the flats is 39.81 kWh/m²year, which is lower than the average home in Scotland, estimated at 43.4 kWh/m²year by Ofgem. By comparing the electricity consumed by the gas and heat pump flats, we can estimate the energy required for space and water heating for flats that use electricity as a source of heating via the heat pump. This indicates an estimated annual demand of 19.89 kWh/m²year for heat pump flats. Assuming a figure of 15 kWh/m²year for water heating, this would indicate a space heating demand of 4.89 kWh/m²year, which is below the EnerPHit target of 25 kWh/m²year.

However, the annual space and water heating consumption for flats with gas heating is estimated to be 51.91 kWh/m²year. Taking into account an assumed 15 kWh/m²year for water heating gives a space heating load of 36.91 kWh/m²year, which is higher than the EnerPHit target of 25 kWh/m²/year. Based on these numbers, the estimated average annual heating demand for the building is 20.90 kWh/m²year (Figure 2).

Based on the annual estimations, the flats that use electricity as a source of heating via the heat pump would meet the EnerPHit target. However, these figures do not include any measurement of the effectiveness of the WWHR system, so caution is required. If effective, it may reduce hot water energy consumption, which would then impact the space heating loads. Based on the data to date, this would appear to be less impactful on the heat pump flats.

The EnerPHit standard for space heating in cold temperate climates, like the UK, is to be below 25 kWh/m²year, and the total annual energy demand should not exceed 60 kWh/m²year. The former standard is being met, but the latter is at an aggregate figure of 65.77 kWh/m²year. However, this number appears to be inflated by gas consumption and higher electrical use in one of the heat pump flats. There are several possible explanations for these variances, including incomplete data, patterns of use and consumption, the ability of a gas system to oversupply, and a relatively cool spring that increased demand. Clearly, some flats are using significantly more energy than others, and further investigation is necessary to understand this. Several potential issues are raised later in the report, such as a lack of information about system usage, extended occupancy periods, varying expectations for thermal comfort, and control issues. Additionally, the two missing flats may affect averages once their figures are known. All these figures are estimated, and once complete data is available, there is a need for further verification. However, based on the evidence so far, the flats appear to be on target to meet the EnerPHit standards, suggesting a successful retrofit.

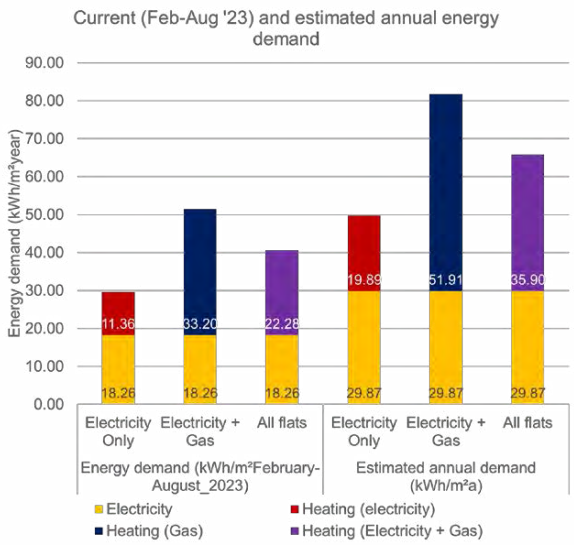

Figure 2: Mean annual energy demand for different flats (estimated from consumption between 28/January to 23 of August 2023). Source Authors.

3.2 Indoor temperatures

During the monitoring period, the indoor temperature in all flats remained within the acceptable range according to the EnerPHit standard, which is between 20°C to 25°C. However, the H2 flat had indoor temperatures above 25°C for more than 10% of the time. The rest of the flats had an acceptable level of overheating according to the Passivhaus standard, which allows for temperatures above 25°C for 10% of the time. The overheating temperatures, as defined by the Passivhaus standard, were mostly observed during the heat waves in June. The temperature ranges are shown in Table 1.

The upper flats had lower indoor temperatures compared to the lower flats – a potential explanation

could be the type of heating. However, during the 2022 heating season, the H2 flat experienced some temperature problems. Despite this, the occupant reported that the flat was easy to heat to a desired temperature and were comfortable with the warm temperatures.

Typical daily average indoor temperature levels in the different rooms of the flats were [daily average mean (daily average min - daily average max)]:

- Bedroom: 21.8°C (18.0 – 26.4°C)
- Kitchen: 21.8°C (15.2 – 30.8°C)
- Living room: 20.7°C (17.0 – 25.9°C)

Table 1: Temperature ranges in the different households between 27/01/2023 and 26/06/2023. Source: Authors.

Home		<20°C (%)	20°C-25°C (%)	>25°C (%)
H1	Bedroom	1%	96%	3%
	Kitchen		Data lost	
	Living	51%	48%	1%
H2	Bedroom	4%	67%	30%
	Kitchen	3%	53%	44%
	Living	2%	61%	37%
H3	Bedroom	0%	90%	10%
	Kitchen	5%	89%	6%
	Living	21%	74%	5%
H4	Bedroom	34%	66%	0%
	Kitchen	38%	62%	1%
	Living	38%	62%	1%
H5	Bedroom	22%	70%	9%
	Kitchen	13%	85%	2%
	Living	59%	38%	3%
H6	Bedroom	20%	78%	2%
	Kitchen	33%	60%	8%
	Living	62%	35%	3%

3.3 Relative humidity

The indoor relative humidity levels in the building were mostly within the recommended range of 40%RH to 60%RH, which was confirmed by occupant satisfaction surveys. This indicates that the occupants were generally satisfied with the levels, and there were low levels of mould problems. However, it is worth noting that there were frequent occurrences of levels below 40%RH, particularly in March and April, with the H2 flat having significantly higher occurrences of humidity levels below 40%RH, driven by the higher temperatures. Extended periods of time with humidity levels below 40%RH can cause dry skin, itchy skin, and dry eyes. Despite this, the H2 occupants reported feeling comfortable as they were used to these levels.

The indoor relative humidity levels were lower in the lower flats compared to the upper flats. This could potentially be explained by the fact that temperature levels could mask the real humidity levels, as warmer air can hold a higher moisture level. Warmer temperatures were more frequent on the lower floors.

Typical daily average indoor relative humidity levels in the different rooms of the flats were [daily average mean (daily average min - daily average max)]:

- Bedroom: 43.61%RH (29.4 – 62.5%RH)
- Kitchen: 44.4%RH (25.4 – 50.8%RH)
- Living room: 46.5%RH (33.1 – 61.4%RH)

3.3 Carbon dioxide

Carbon dioxide (CO_2) is a commonly used indicator of ventilation in environmental monitoring. CO_2 levels are an effective indicator of occupancy and/or ventilation levels . Generally, keeping CO_2 levels below 1000 ppm is considered a good measure of ventilation, as it is broadly equivalent to a ventilation rate of 10 l/s/person. It is worth noting that there are significant associations between ventilation and health, and some energy efficiency measures in retrofitting may potentially reduce ventilation levels.

However, it should be noted that the flats in question are relatively small and have low occupancy rates, so it is unlikely that CO_2 levels would be excessive under normal conditions. The flats are equipped with a Mechanical Ventilation with Heat Recovery (MVHR) system, which mechanically extracts air from kitchens and bathrooms and supplies air with recovered heat into the occupied space. Therefore, if CO_2 levels are elevated, it may indicate that the system is disabled or not functioning properly.

The monitoring carried out showed that indoor carbon dioxide levels remained below 1,000 ppm most of the time. This indicates good ventilation and indoor air quality levels, which was corroborated by the occupant satisfaction surveys.

Typical daily indoor carbon dioxide levels in the different rooms of the flats were [daily average mean (daily average min - daily average max)]:

- Bedroom: 527 ppm (418 - 1,013 ppm)
- Kitchen: 515 ppm (356 - 899 ppm)
- Living room: 506 ppm (419 - 992 ppm)

3.4 Interstitial condensation

Moisture issues can arise when interstitial condensation occurs within an enclosed wall, roof or floor cavity structure. This type of condensation happens when moisture-laden air vapour permeates through a building's fabric elements, encountering temperature variations along the way, and condenses within the building rather than on the surface. Wood moisture equivalent (WME) is a measurement of the (theoretical) percentage of moisture content that would be attained by a piece of wood in contact with, or in close proximity to, a moisture equilibrium across a host of materials. We can use the %WME to determine how fast a wall is drying and the risk for

the occurrence of rot and fungus. Based on the WME levels, the wall was drying up between February and mid-March and then stayed relatively stable until June, when it started to get some moisture. However, the levels remain below recommended for dry rot, cellar fungus, white pore or mini fungus (>25 %WME). The recommended WME levels are below 15%WME. Measured WME levels are constantly below 15%WME – the recommended levels to avoid any risk of rot, although common furniture beetle may proliferate above 12%WME. There was a high variability on one of the internal sensors, however it is likely that the variability here is due to proximity to central heating pipes.

4. DISCUSSION

It should be noted that these are early findings, without complete data, and with a number of estimations. While this energy and indoor environment monitoring demonstrate a good performance of the building, there were some issues with the operation and maintenance of the building which indicate that there are still lessons to be learned in retrofitting buildings.

One of the main issues with the flats was related to the heat pumps. During winter, one of the occupants was left without heating for about 1.5 weeks due to a broken heat pump. The engineers had to visit three times to diagnose the problem, and then once more to fix it. They searched for the problem next to the system or inside the building, but the outdoor pipes were frozen, causing further issues. This occurred on some of the coldest days in December, leaving the occupants very disappointed. It suggests that there may be a skills gap related to the proper maintenance and operation of heat pumps, which must be addressed as the uptake in the region develops. Unfortunately, there is no monitored data during this period to identify the effect on internal temperatures.

Another issue was occupant behaviour. For example, some occupants did not turn off heating, possibly due to higher comfort expectations and low energy prices. One instance of this was when the heating was left on for a couple of days during winter, causing discomfort to the surrounding flats as it was too hot. Although this may be expected in such cases, and in other buildings, this 'free' heat may be beneficial, the external fabric is designed to keep the heat inside but there is little thermal barrier between adjacent flats. The occupants suggested that there should be a safety feature to prevent such mishaps in the future. The only solution they had was to reach the housing association to mediate.

3. SUBMISSION INSTRUCTION

Log in to the paper submission site which is at http://www.conftool.org/plea2024/ and go to "Your Submissions" – "Final Upload".

You can then upload the doc, pdf files. Additionally, you can upload a recorded 7 minutes presentation in mp4 file (regular papers) or a 2-minutes presentation in which you present the 'pitch elevator', i.e. a brief speech that outlines an idea of your research to encourage other participants to read your long paper and to start the dialogue with you. This form of presentation will be used at PLEA 2024 to fully eliminate printing posters while unlocking the paper potential for discussion and interaction with PLEA Participants (both on-site and on-line). Consequently, there will be NO POSTERS this year and we will do our best to have sustainable, 'no printout' conference. We will grow new trees instead of cutting them.

Make sure to load the correct manuscript, if you have more than one. You may not upload any other files then the ones listed in this section. Note that it is possible to repeat the editing/uploading process and overwrite your file with a newer one until the submission deadline. Please only do this if absolutely necessary.

Thank you very much!

5. CONCLUSION

This paper presents the energy and indoor environmental quality of a deep energy retrofit to the EnerPHit standard carried in a sandstone tenement in Glasgow. The following are the key lessons learned from the monitoring of this building:

Energy Consumption and targets. From an energy perspective, the dwellings appear to be performing well above the targeted levels of consumption, with an estimated annual consumption for space of 33.20 kWh/m² year for the gas flats and 11.36 kWh/m² year for the heat pump flats. The estimated annual consumption for the whole block is 35.90 kWh/m² year.

Good thermal environmental performance. During the monitored period, the low energy consumption did not seem to compromise the thermal comfort of the dwelling. The average indoor temperatures were within the Enerphit performance targets. Additionally, the house did not seem to be negatively affected by a period of hot weather during early summer. However, one dwelling was an exception, but it was confirmed that the occupant had a preference for a different level of comfort.

Good IAQ/Ventilation. The dwellings remained below 1,000 ppm CO_2 throughout the monitoring period, and there was no evidence of the MVHR systems being switched off or failing.

Interstitial condensation risks in timber. There are no obvious concerns regarding the presence of interstitial moisture at this stage. However, ongoing monitoring is necessary due to changing conditions and potential adverse weather.

Overall performance. From a technical perspective, based on the data available to date, the retrofit appeared to be very successful in providing very low energy, comfortable, healthy dwellings with high degrees of occupant satisfaction.

ACKNOWLEDGEMENTS

The authors would like to thank the building occupants, John Gilbert Architects and Southside Housing Association for their support in this project.

REFERENCES

1. IPCC, Chapter 9: Buildings, in *Climate Change 2022: Mitigation of Climate Change*, 2022, pp. 9–1 to 9–168. [Online]. Available: https://www.ipcc.ch/report/ar6/wg3/
2. A. Moreno-Rangel, E. Tsekleves, P. Young, M. Huenchunir, and J. M. Vazquez, Design research role on supporting net-zero buildings, in *PLEA 2022 Will cities survice?*, Santiago, Chile: PLEA, Nov. 2022.
3. ONS, *Greenhouse gas emissions, UK: provisional estimates: 2021,* Nov. 2022.
4. A. Moreno-Rangel, Passivhaus, *Encyclopedia*, vol. 1, pp. 20–29, 2021, doi: 10.3390/encyclopedia1010005.
5. A. Moreno-Rangel, T. Sharpe, G. McGill, and F. Musau, Indoor Air Quality and Thermal Environment Assessment of Scottish Homes with Different Building Fabrics, *Buildings*, vol. 13, no. 6, p. 1518, Jun. 2023, doi: 10.3390/buildings13061518.
6. P. Leardini and M. Manfredini, Modern housing retrofit: Assessment of upgrade packages to enerphit standard for 1940-1960 state houses in Auckland, *Buildings*, vol. 5, no. 1, pp. 229–251, 2015, doi: 10.3390/buildings5010229.
7. B. Dorota Hrynyszyn and L. Cornelia Felius, Upgrading of a Typical Norwegian Existing Wooden House According to the EnerPHit Standard, in *Cold climate HVAC 2018 Sustainable Buildings in Cold Climates*, D. Johansson, H. Bagge, and A. Wahlström, Eds., Kiruna, Sweeden: Sringler, Mar. 2018, pp. 183–193. doi: https://doi.org/10.1007/978-3-030-00662-4_16.
8. A. Moreno-Rangel, T. Sharpe, G. McGill, and F. Musau, Indoor air quality in passivhaus dwellings: A literature review, *Int J Environ Res Public Health*, vol. 17, no. 13, pp. 1–16, 2020, doi: 10.3390/ijerph17134749.

PLEA 2024 WROCŁAW
(Re)thinking Resilience

Climate change as a challenge in the protection of historical architecture.

Case study on revitalization and adaptation to climate changes of traditional rural objects.

BARTOSZ FELSKI[1]

[1]Sopot University of Applied Sciences, Sopot, Poland

ABSTRACT: Regardless of the problems with climate change mitigation, the urgent need for adaptation measures cannot be overlooked; Not all negative elements of anthropogenic pressure will be eliminated in the future. In such a complicated matter as spatial development, it is quite a challenge. It should be realized that due to the specificity of the construction industry, the architectural substance, as a rule, is implemented for many decades. The article is a case study of a historical, vernacular building from the 19th century in the West Pomeranian Voivodeship in Poland. On the one hand, the applied solutions to save historical buildings protected by law as heritage are a response to the social needs of the local community, and on the other hand, they are a way of adapting historical architecture to the progressing climate change, which makes it possible to extend its life cycle and thus minimize the carbon footprint of the investment. The presented solutions use circular design activities and can be easily scaled up to other similar historical objects, so they can become an effective tool for adapting to climate change, and due to the use of recycled materials – also a tool for mitigating climate change.
KEYWORDS: Circular designing, climate adaptation, carbon neutral, clay building, heritage

1. INTRODUCTION

In August 2021, the first of three parts of the IPCC Sixth Assessment Report, on the physical basis of climate change, was published, which is a kind of summary of the current state, projected scenarios of its changes and the related adaptive possibilities of modern societies. According to the report, it is clear that "*human activity has led to global warming at a rate not seen in at least the last 2,000 years*." All signatories to the Paris Agreement [1] agree in principle that the observed increase in greenhouse gas concentrations since about 1750 is indisputably caused by human activity. Although published in 2011 Fifth Report required each party to reduce emissions, these concentrations continued to rise, reaching an annual average of 410 ppm in 2019. Currently, the CO2 concentration at NOAA's Mauna Loa observatory is already around 422.14 ppm [2], which means that with the climate sensitivity currently established, the safe warming threshold of 1.5°C would be exceeded by mid-2029 [3]; It would have been, if it were not for the fact that the global distribution of temperatures is influenced by many factors, both natural and anthropogenic. The complexity of these processes and a number of climate couplings resulted in the warming level of 1.5°C already being exceeded by the end of 2023 [4]. In the author's opinion, this is undoubtedly the greatest failure from the point of view of contemporary post-industrial civilization, which cannot be ignored without comment. Regardless of the state of climate imbalances and projected SSP [5] scenarios, it is necessary to expect the need for urgent action to slow down the discussed changes in every area of human activity, including construction.

In addition to the climate change mitigation problems mentioned in the report, the urgent need for adaptation cannot be overlooked, which is a natural consequence of exceeding the target of a safe level of global warming a decade earlier than forecast. Not all negative elements of anthropogenic pressure will be eliminated soon. In such a complicated and complex matter as spatial planning, this is quite a challenge, as confirmed by The World Heritage Committee at its 29th session in 2005 [6]. It should be realized that due to the specificity of the construction industry, the architectural substance is usually implemented over many decades. In this context, it is important to note that the historical architecture that is of interest to the author was created at a time when climate change was out of the question [7] and in no way corresponds to the dynamically developing adaptation needs in this area. What is more, historical buildings are very often objects of high cultural and aesthetic value, bound by specific legal regulations and conservation protection. Such a situation narrows the repertoire of possible adaptation measures.

2. AGEING MODERNITY – ARCHITECTURE AS A FUNCTION OF TIME

Historical architecture is valuable for many reasons, but it is also burdened with the rigor of heritage conservation, where it is often difficult to achieve adequacy in terms of adaptation requirements. According to the author, the current state of climate imbalance, which is a consequence of progressing climate change, shows that the problem of adaptation of traditional vernacular architecture to the "new, greenhouse" reality is an important topic, although it is rarely discussed in science in a comprehensive way [8,9]. In addition to the collection of "iconic" buildings that create a context in the historical substance of the city, whose cultural values are indisputable, there are still old buildings that are not under strict protection. Their modernization is not so strictly regulated by the conditions of conservation protection. These buildings also create a context, although the lack of strict legal protection means that the quality of the renovations carried out and the set of solutions used can leave much to be desired, thus reducing their cultural and aesthetic attractiveness. The author deliberately narrows down the issues to vernacular architecture, without dealing with the entire spectrum of adaptations of historical buildings. Regional and vernacular architecture protected only within the framework of the municipal (local) heritage register is a large part of protected objects, although their value is often underestimated, and the possibilities of increasing their value, including modernization activities, fall on the shoulders of private investors. This can result in the risk of losing authenticity and, so, cultural values. In the discussed area of Poland (West Pomeranian Voivodeship), rural buildings are often the legacy of many years of not investing in this region of the country, which builds the image of the voivodeship as a problem area in systemic terms. Underinvestment in local communities and a deep social and economic crisis of local communities in small West Pomeranian villages are among the main causes of the collapse in the context of spatial investment in the area.

Adaptation to potential climate changes projected in the next few decades will therefore require not only the construction of a new (ecological) architectural substance, but also the largely renewal of existing, often historic architecture built with the use of traditional technology.

Only architecture that is adequate to the expected functional parameters, aesthetic, but also energy-efficient and safe in terms of construction will be able to be considered socially attractive and will have a chance to exist in the structure of villages and cities. This, in turn, is a real tool for extending its life cycle, which is an important aspect from the point of view of reducing emissions of the construction industry. In the case of their modernization and adaptation to new conditions (including climatic conditions), it is natural that greenhouse gas emissions will appear because of investment activities. It`s also important to note that embodied carbon emissions are already neutralised after 100 years; not demolishing that historical architecture means, in fact, the possibility of omitting a new investment and it`s new carbon footprint.

In conclusion, according to the author, the aging of architecture is a complex function of many factors. Time as a variable in architecture and its impact on the environmental balance of a project is a well-known problem, but very rarely addressed in the context of traditional architecture. Historically, time was a "transparent" architectural element (its impact was not noticeable until the object was old enough to collapse). Nowadays, the time factor is consciously considered as a decisive element for the profitability of an investment. In order to properly carry out the revitalization of the historical architectural substance, it is necessary to realize that historical buildings were under the influence of the same laws of physics, this is due to their use, construction processes, previously completed renovations and reconstructions, and the specificity of the technologies used. Now they need an individual approach each time. After all, there are many examples where poorly applied modern technologies have led to the destruction of a historic building, and the matter is further complicated by two factors: the first is the passage of time, which can affect the durability of individual elements of the building, and the second is the modularity of "layers" expressed in their technical reliability [10].

3. SUBJECT MATTER AND SCOPE OF RESEARCH

The article is a case study of a historic, vernacular building, where the applied solutions to save the historic buildings could then be scaled up to other similar objects. In the area of the West Pomeranian Voivodeship and in areas with a similar construction tradition, there are a lot of analogous buildings that will be destroyed and replaced with a new architectural substance generating an added burden on the carbon dioxide budget, if they are not renovated. If their social attractiveness is increased, life cycle will be extended. The applied solutions are aimed at extending the life cycle of the building by giving it a new function, new technical and economic values, and thus making it an attractive object. This will mean cutting the demolition phase of life cycle and replacing the building with a new structure. In this way, the carbon footprint of the investment process is minimized while keeping the spatial context of the village and its aesthetic and cultural values. CO_2 stays in the atmosphere for about 100 years, so leaving a historic building minimizes the carbon footprint.

In addition, the solutions applied and described in this article are also aimed at adapting the facility to new threats caused by climate change, such as reduced snow cover in winter and the resulting increased risk of ground freezing and destruction of historical foundations. Some of the solutions are based on the "*Natural Based Infrastructure*" principle [11], promoted by UNEP as solutions with a high potential for mitigating climate change. The preservation of vernacular architecture and thus the preservation of its cultural values as an element of heritage is quite a challenge in the face of dynamically changing expectations in terms of adequacy of functions and utility values. The challenge will be to preserve historical values while optimizing the functional layout to contemporary expectations and additionally protecting the existing spatial structure against the potential impact of climate change, minimizing the carbon footprint of the investment. Taken together, all these challenges appear to be complex and fraught with a high risk of uncertainty. Szymanowska-Gwiżdż et al. rightly point out [12] that the modification of historic buildings must consider the postulates of preserving historical and cultural values. In the author's opinion, the changing reality due to the ongoing climate processes also requires considering these new aspects in architecture – including the revitalized one.

The described building was built in the second half of the 19th century, around the years 1850-1870. In this case, due to the period of construction and the fact that it has not been renovated practically since 1911. This gives grounds to assume that in the case of this investment, it will be necessary to modernize not only the basic elements of the installation equipment of the facility or the external structure (sheathing, window and door joinery, roof sheathing), but also to verify the condition of the main supporting structure [fig. 2].

As mentioned earlier, in the author's opinion, each building should be considered in a time module corresponding to the usability of the individual layers of the building described below [13], while taking into account contemporary conditions (including climatic conditions).

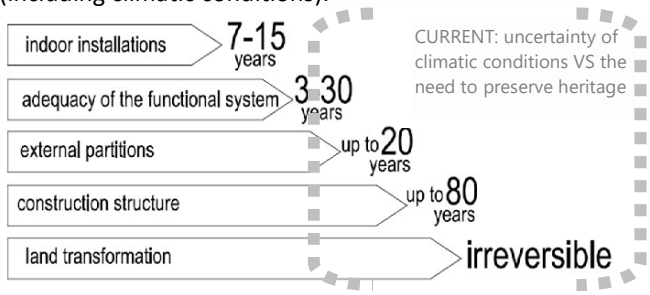

Figure 1: Diagram of time periods in architecture vs climate changes.

Figure 2: Building before renovation, source: M. Okła

To understand the extent of interference in the existing structure of featured building, it is necessary to look at the specifics of the frame structure and understand its operation. The mullion and transom structures (half- timbered) are one of the frame structures that use wood as a material for making load-bearing elements. The base here are vertical load-bearing columns always made of a single element, embedded in the sockets of the foundation laid horizontally on the foundation and fastened with a horizontal cap at the height of the ceiling with glazing.[1] Between the vertical elements there are horizontal transom elements, fixed in sockets made in wooden posts.[2] In the corners of the walls, there are additionally braces stiffening the structure and protecting the entire structural system against horizontal forces, m.in. from the wind (gable facades).

The loads from the roof, ceiling and walls were fully transferred to the foundation in half-timbered structure through a continuous ground beam.

This is quite an important structural assumption, taking into account the fact that in many cases (including the one discussed) these foundations were made of stones, without the use of a cement-based binder, and after such a long time of using the building, the wooden structure of the half-timbered wall is in poor technical condition [fig.3]. Two important conclusions can be drawn from the analyses of the existing structure of the building carried out in the years 2017-2021.

[1] A slab is a ceiling filling consisting of a mixture of clay and ash, sometimes vegetable additives as an insulating material; Despite its original function, which was to fill and stiffen the ceiling, it is also worth mentioning the additional role of the glazing as a kind of heat accumulator, which stored the surplus heat from the unused attic in the summer and gave it back in the transitional period. The ash in the glaze had an antiseptic function.

Figure 3: Building before renovation, source: author

1. More than 150 years of use of the building led to damage (deformation) of the foundation [see fig.2]; In addition, a foundation that was too shallow caused it to undergo displacements related to soil comparison and freezing processes. After all, the technical knowledge of that time did not focus on the depth of the foundation, but rather on counteracting the capillary rising of moisture through the walls [14], which, according to the currently available knowledge, was one of the biggest problems of the construction industry at that time [15].
2. The conclusion from the conducted analyses was the urgent need to carry out renovation works aimed at strengthening or possible replacement of the timber frame structure while protecting the foundation against freezing [fig.6]. In addition, these works should respond in advance to the projected climate changes while maximizing the authenticity of the building and minimizing the carbon footprint of the renovation phase. What is more, in order for these activities to be scalable to other investments in the future, the renovation must also be financially rational. The redevelopment process must therefore take all these guidelines into account and not be a mere compromise.

4. CHALLENGES

As Colette pointed out [16] *"Climate change is primarily a threat that has physical impacts. But, in turn, these effects have societal and cultural consequences. When it comes to cultural 'dynamic' heritage – i.e. buildings and landscapes where people live, work, worship, and socialize – it is important to underline the cultural consequences. These consequences can be derived from the degradation of the property under consideration."*

When talking about contemporary climate challenges, we have in mind a whole set of potential threats [17], although in general we should pay attention to three basic aspects – adaptation to climate change, mitigation of climate change and development of the circular economy – all three elements have been regulated for several years by the European Union regulations [18]. In the context of historical buildings, the threat associated with changing climate parameters may undoubtedly be the inadequacy of the foundation level of the building to the changing specific properties of winter periods.

4.1. FREEZING OF THE BASEMENT OF THE BUILDING

The visible constant trend of climate change was the basis for the EU directive M/515 [19], which, as Godlewski points out [20], indicates the need to "*build and maintain more climate-resilient infrastructure by changing and adapting the provisions of the standards used in the construction industry*". Paradoxically, this is not due to a decrease in average temperatures, but to the progressing warming of the climate, i.e., an increase in global temperatures and the disappearance of snow cover. Ground covered by a layer of snow freezes to a much lower depth due to the insulating properties of snow. The values of the maximum position of the zero isotherm in the ground not covered by snow are more than twice as deep as in the case of the ground covered by snow cover, which is confirmed by research conducted over the years by Gródecki [21] and Ickiewicz [22]. This is quite significant, because with the warming of winters, the number of days with snow cover in Poland is decreasing; according to IMGW data, in the period 1961-2020 the number of days with snow cover decreased on average from 63.9 to 39.5 [23]. The negative impact of changing climate parameters during winter on architectural heritage has also been highlighted as an important aspect by UNESCO [24] and United Nations Environment Programme in *Climate Leadership* programme [25].

In the analysed historical building, a decision was made to adapt to the changing reality in two ways: to protect the foundations against both freezing and heat energy losses, and to relieve the existing half-timbered structure of the walls. The first one is aimed at protecting the foundation against the destructive effects of frost and increasing the energy efficiency of the building, thus increasing the attractiveness of the building in the economic aspect. The second is to relieve the external wall and transfer the loads from the roof to the new wooden columns. The stone foundations are too shallow, and there is no rational way to sink them without losing the authenticity of the building; It is also impossible to pick up ground level around a building (covering foundations) without losing its aesthetic and historical value. For this reason, it was decided to use wooden columns and make them an added, independent structure inside the building to relieve the external walls. The columns were placed on new foundations inside the building (fig.6), at a depth that considers the increased impact of frost. These poles were made of wood obtained from the demolition of a barn from the same time, so that the newly created structure does not stand out from the original

substance. In addition, this measure significantly reduced the carbon footprint of direct emissions. The construction works were analysed following the ISO 14064 standard, and obtaining material from the demolition of another facility is a conscious action in the field of circular economy [26], influencing the improvement of the MRP factor[3]. The problem of freezing foundations has not been noticed for years. In old buildings, heat losses were enormous, although the cost (financial and environmental) of heating was low at that time. Large heat losses through the lower part of the walls and through the stone strip footing caused the ground to heat up and move the frozen zone away from the structure (fig.4).

The problem of freezing appeared at the time of making a concrete band "combined" with a stone bench, which was to stabilize the structure of the building (XXth century) and when the floor and external wall were insulated (fig.5).

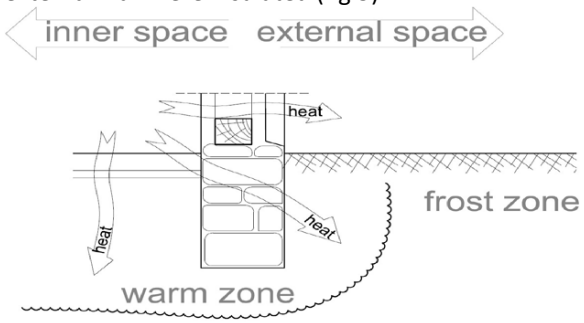

Figure 4: Diagram of the existing foundation – original layout from the 19th century, source: author

Actions aimed at increasing energy efficiency resulted in a reduction in heat losses to the ground, and thus increased the risk of freezing of the foundations. Previously, excessive heat emission *de facto* moved the "cold" zone further away from the foundation. Bearing in mind the fact that the disappearing snow layer due to climate change may result in increased freezing, it was decided to intervene in the form of horizontal insulation of the concrete band. This will keep the frost away from the shallow stone bench (fig. 6).

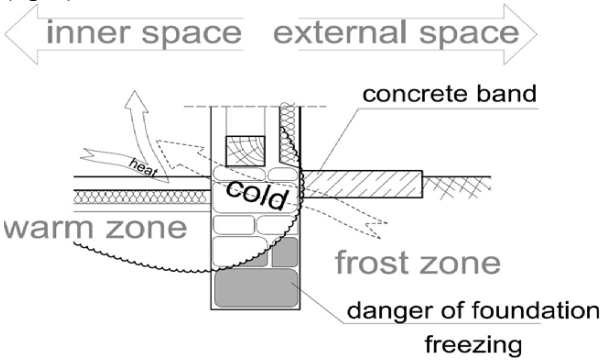

Figure 5: Diagram of the foundation after modernization; 1960, source: author

[3] MRP – Materials Reusability Potential indicator – one of the factors of circularity of architecture.

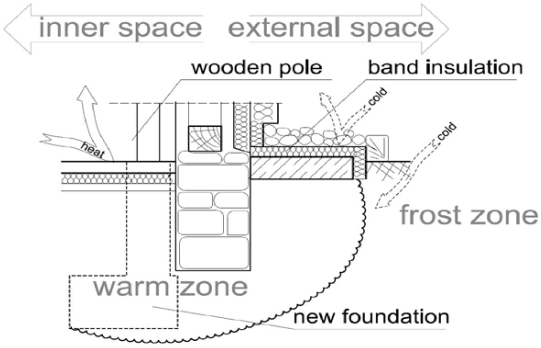

Figure 6: Diagram of the foundation after modernization; 2020, source: author

The described activities were carried out after analysing various environmental scenarios of the renovation and assessing the CO2 budget. In addition, both the materials for the construction of the columns, the edge elements and the insulation of the foundations come from recycling (see MRP indicator), and the stone covering of the thermal insulation was made of local stones, minimizing ADP factor[4] of the investment.

5. CONCLUSION

In the author's opinion, the activities in the field of renovation and reconstruction of historic nineteenth-century residential buildings described in the case study show that with precise and appropriate use of techniques and knowledge of traditional methods of building construction, it is possible to carry out investments in a way that is sensitive to the issues of respect for cultural heritage and aspects of beauty in rural space. At the same time, in a manner adequate to the modern needs of adaptation to climate change, considering the entire life cycle of the building to minimize the carbon footprint of the investment.

Figure 8, 9: Insulation of the foundation following the schemes (after/during work); Condition approx. 2020, source: author

According to the author, such a comprehensive approach to the problem would allow to scale up that way of operation for future investments of a similar nature, so that the adaptation of traditional

[4] ADP – Abiotic Depletion Potential.

architecture to new climatic conditions could become a specific tool for mitigating climate change.

Figure 10: The building after rebuilding, source: author

(Carbon footprint of article: 0,835kg CO2e)

REFERENCES

1 Adoption of The Paris Agreement, *Framework Convention on Climate Change*, (2015). Paris: p. 4-6.

2 https://www.co2.earth/ [Online], [30 August 2023].

3 https://www.mcc-berlin.net/en/research/co2-budget.html?fbclid=IwAR1owltwJ5ZpugQbffHKmDxeF5zjengaJYsgNIexTPhXDX4Pooy2LrKIrd4, [Online], [30 August 2023]

4 https://berkeleyearth.org/august-2023-temperature-update/?fbclid=IwAR3dPmPoWQncujRiPBTeOT5a6GfPpm3YO7bMbmscB_v1rP6dQy3aS1wzJPg, [Online], [16 December 2023].

5 Masson-Delmotte, V., P. Zhai, A. Pirani, S. Connors, C. Péan, S. Berger, N. Caud, Y. Chen, L. Goldfarb, M.Gomis, M. Huang, K. Leitzell, E. Lonnoy, J. Matthews, T. Maycock, T. Waterfield, O. Yelekçi, R. Yu, and B. Zhou (2021). IPCC: Climate Change 2021: *The Physical Science Basis. Contribution of Working Group I to the Sixth Assessment Report of the Intergovernmental Panel on Climate Change,* Cambridge University Press, Cambridge, United Kingdom and New York, NY, USA, 2391 pp. doi:10.1017/9781009157896: p. 571.

6 Colette A., (2007). *Case studies on climate change and world heritage*, UNESCO World Heritage Centre, Paris: p.7

7 *Ibid*. p. 64.

8 *Op. cit*. Colette A.

9 Jeliński T., Konarzewski Ł., Czemplik C., Zaręba A., Wójcik R., Kosiński P., Pękała E., Czachowska A., (2022). Restoration and modernization of historical buildings in the era of climate crisis, ISBN 978-83-62168-25-5, Sendzimir Foundation, Croatia Green Building Council.

10 Mancaster A., Symons K., (2013). A method and tool for 'cradle to grave' embodied energy and carbon impacts of UK buildings in compliance with the new TC350 standards, *Energy and Buildings,* 66(11).

11 https://wedocs.unep.org/20.500.11822/44022, [Online], [29 November 2023].

12 Szymanowska-Gwiżdż A., Orlik-Kożdżoń B., Krause P., Steidl T., (2016). Change in dampness of partitions of historical buildings under given conditions of external climate*, Journal of Civil Engineering, Environment and Architecture*, Issue 63: p. 590.

13 Felski B., Architecture as a tool for mitigating climate change. Case study on the example of selected projects*,* DOI:10.13140/RG.2.2.13224.60161, the study was a part of a research project *"Architecture as a mitigation tool in climate change".*

14 Niewierowicz M, (1930). Wznoszenie budynków z gliny. Poradnik według metody M. Niewierowicza z 44 szczegółowemi tablicami*,* Vilnius, (reprint: Wydawnictwo GÓRNOLESIE, 2014), ISBN 978-83-61085-04-1: p. 5-12.

15 Felski B, (2021). Selected issues of revitalization and adaptation to climate change of traditional rural architecture, *19/I/2021 Space Economics Society*, ISSN 2353-0987, DOI: 10.5281/zenodo.7020398, Sopot: p.9-36

16 *Op. Cit*. Colette A.: p.64,65.

17 Hunnisett Snow J., Curtis R., (2016). Climate change adaptation for traditional buildings, *Historic Environment Scotland*, Edinburg: p.6.

18 Op. Cit. Regulation EU 2020/852.

19 European Commision: M/515 EN 2012 Mandate for amending existing Eurocodes and extending the scope of structural eurocodes, Brussels 2012.

20 https://inzynierbudownictwa.pl/przemarzanie-gruntu-a-projektowanie-fundamentow/ [Online], [10 May 2022].

21 Gródecki W., (1971). Analiza niektórych czynników przemarzania gruntów w warunkach rzeczywistych, doctoral dissertation, Warsaw University of Technology, Warsaw.

22 Ickiewicz I., (2010). Foundations of direct foundations in the function of soil freezing*,* Bialystok University of Technology, Scientific Dissertations, Bialystok.

23 https://naukaoklimacie.pl/aktualnosci/zmiana-klimatu-w-polsce-na-mapkach-468/ [Online], [10 May 2022].

24 *Op. Cit*. Colette A.: p.64.

25 Felski B., (2024). Architecture of the new reality. Adapting cities to climate change. *Biznes na rzecz zmian 2023*, UPEP/GRID-Warszwa, Warsaw,: p.44-51.

26 Regulation EU 2020/852 of the European Parliament and of the council of 18 june 2020 on the establishment of a framework to facilitate sustainable investment, and amending regulation eu 2019/2088, [Online], Available: https://eur-lex.europa.eu/legal-content/PL/TXT/?uri=CELEX%3A32020R0852 [29 September 2023].

PLEA 2024 WROCŁAW
(Re)thinking Resilience

Can We Avoid Overheating Through Passive Adaptation Strategies?

A performance assessment of a residential building on a temperate climate

ANE VILLAVERDE[1], LEIRE GARMENDIA[1], LAURA QUESADA-GANUZA[1], ZIORTZA EGILUZ[1], EDUARDO ROJÍ[1]

[1]University of the Basque Country UPV/EHU, Plaza Ingeniero Torres Quevedo, 48013 Bilbao, Spain

ABSTRACT: As climate change intensifies, even temperate regions will confront building overheating and rising cooling energy demands. Therefore, promoting passive adaptation strategies to protect inhabitants from extreme heat and avoid air conditioning use is essential. Focusing on a residential building in northern Spain, this work assesses the effectiveness of hard and soft adaptation in reducing indoor overheating. The strategies assessed include natural ventilation, sun protection, envelope insulation, window improvement, envelope albedo increase, and balcony installation. The building is simulated using the plug-in Ladybug Tools, and the simulation period is 2022 summer. Using the Spanish Building Code standard, the results show that even if the adaptation strategies significantly improve thermal comfort, they are not able to keep discomfort hours under the acceptable limit.
KEYWORDS: Adaptation Solutions, Building Adaptation, Occupant Behaviour, CTE, Thermal Comfort

1. INTRODUCTION

The year 2022 set unprecedented heat records in various areas, including the temperate climate region of the Basque Country in Spain. That year also registered the second warmest summer in the Basque region since the existence of records, only preceded by the summer of 2003 and followed by the summer of 2023 [1,2]. Experts predict that this trend will continue as climate change will increase the frequency and intensity of heat waves [3]. According to scientific evidence, this threat is not limited to locations with warm climates. Researchers argue that extreme heat will be an increasing problem in temperate climates in the following years, where overheating in buildings and the associated energy consumption for cooling are expected to increase [4,5].

Therefore, adapting dwellings to the new climatic trend is crucial to ensure people's wellbeing and safety, especially the most vulnerable individuals, such as the younger and older population. Building-level passive adaptation strategies, which do not need an active energy source to be effective, have been proven to reduce building overheating and cooling energy demand [6,7].

These building-level adaptation strategies can be divided into soft and hard adaptation[8,9]. Soft adaptation strategies do not significantly alter building physical elements, such as natural ventilation, using existing sun protection or reducing interior heat gains. Natural ventilation has been identified as one of the most effective strategies to reduce indoor overheating [8,10,11]. Natural ventilation when the outdoor temperature is lower than the interior diffuses the heat accumulated indoors during the warmer hours of the day, and it is crucial to avoid heat accumulation during heat waves. Sun protection, especially using exterior elements [10], is crucial to avoid sun radiation indoors and its consecutive temperature rise. Shading could be understood as a hard adaptation when new shading elements are installed. However, existing curtains or blinds designed for sleep comfort can also be easily used as sun protection. Besides, reducing interior heat gains is also effective in reducing indoor temperatures, for instance, by replacing light bulbs emit heat [12].

Hard adaptation includes those strategies that significantly alter building physical elements. Hard adaptation includes improving envelope insulation, adding shading elements or changing envelope coating. Adding insulation to the envelope is a controversial strategy, as several studies have highlighted that highly insulated dwellings are more prone to overheating than those less insulated [13]. However, other studies have argued that insulation is only linked to overheating when other factors are at play, such as lack of natural ventilation or sun protection [14]. Moreover, researchers have proved that increasing envelope insulation lowers cooling energy consumption [7,15].

Adding external shading elements such as rollers, overhangs, or shutters is very effective when the existing building does not have shading elements [10,12]. Interior curtains can also be installed, but exterior shading is more effective than interior. Finally,

changing the envelope coating to a higher albedo material reduces overheating indoors [12], as it increases the percentage of sun radiation reflected, reducing heat transmitted through the envelope.

2. METHOD AND OBJECTIVE

This research implements and simulates different adaptation strategies to test their effectiveness in reducing overheating without active cooling. The study's objective is to evaluate the potential of passive adaptation strategies to avoid overheating in a residential building. This study applies the Spanish Building Code overheating assessment criteria to evaluate whether the case study building is within acceptable thermal comfort limits under different adaptation scenarios.

The strategies assessed include soft and hard adaptation strategies. As soft adaptation, natural ventilation and the use of existing sun protection are assessed. As hard adaptation, envelope insulation, window improvement, envelope albedo increase, and balcony installation are evaluated.

The strategies are simulated using the building performance simulation Ladybug Tools package linked to the EnergyPlus simulation engine. For 3D modelling purposes, Rhinoceros software is used. Data analysis is conducted using MATLAB.

2.1 Case Study

The study focuses on a case study building in Bilbao, a city in the Basque Country (Spain), which is characterised by a temperate oceanic climate. The building was constructed in 1960 and represents a typical example of Spanish social housing built between 1960 and 1970 [16]. This housing design is recognised for not having insulation in the envelope and therefor does not ensure indoor thermal comfort in winter; making it suitable for overheating assessment. The building is replicated several times along the neighbourhood in which it is located, presenting in 11 different orientations. Aiming to observe the impact of orientation on strategy effectiveness, simulations are done for the orientations north-south and east-west. The study presents the results for two locations (the living room and one bedroom) of the central apartment on the last floor of the building (see Figure 1), as they represent a favourable double sided room (the living room), and an unfavourable single sided room (the bedroom).

2.2 Overheating assessment criteria

The Spanish Building Code sets the regulatory standard that limits overheating in residential buildings in Spain [17]. According to this standard, during the summer months spanning June to September, only 4% of occupied hours can surpass a defined thermal comfort threshold [18]. This threshold varies depending on the time of day: between 15:00 and 22:59, the limit is set at 25ºC, while from 23:00 to 6:59, it is 27ºC. However, no specific temperature threshold is established between 7:00 and 15:00. To calculate the standard, the day-time threshold was applied for the living room operative temperature and the night-time threshold for the monitored bedroom operative temperature. Regarding the occupation hours, to represent a worst-case scenario, it was assumed that the dwelling is always occupied during the hours when a temperature threshold is established, from 3 pm to 7 am. To compare the results with a less unfavourable occupation schedule, an additional assessment is conducted for, assuming that occupants are out every day from 6 pm to 8 pm.

In addition to this, to understand the performance of the building in case of an extreme event, the research examines the reduction of the maximum operative temperatures during a severe heatwave.

2.3 Simulations

The period chosen for the simulation is the 2022 summer, from June 1st to September 31st. Special attention is drawn to the heat wave that occurred between July 12th and July 18th to monitor interior operative maximum temperatures during this extreme heat event. Spanning six days, the recorded maximum temperature during this heatwave reached 40.4ºC [19]. The primary meteorological data is obtained from Zorrotza weather station, situated in the heart of Bilbao city, and supplemented by additional information from the Bilbao airport station, providing data on insolation and atmospheric pressure.

Figure 1: floorplan and photo of the building simulated.

Table 1: scenarios with adaptation strategies

Scenario	Natural ventilation	External roller blinds	Insulation increase and infiltration reduction	Albedo increase	Balcony and louvres
Baseline WORST	✗	✗	✗	✗	✗
Baseline SUB	9 pm to 8 am 0.3 opening	✓	✗	✗	✗
Baseline OP	1ºC difference 0.9 opening	✓	✗	✗	✗
Retrofit 1 SUB	9 pm to 8 am 0.3 opening	✓	✓	✗	✗
Retrofit 1 OP	1ºC difference 0.9 opening	✓	✓	✗	✗
Retrofit 2 SUB	9 pm to 8 am 0.3 opening	✓	✓	✓	✗
Retrofit 2 OP	1ºC difference 0.9 opening	✓	✓	✓	✗
Retrofit 3 SUB	9 pm to 8 am 0.3 opening	✓	✓	✓	✓
Retrofit 3 OP	1ºC difference 0.9 opening	✓	✓	✓	✓

Adaptation strategies are combined to create different adaptation scenarios, and each is simulated for both building orientations. Every scenario simulated is summarised in Table 1. First, soft adaptation strategies are combined to emulate two occupant behaviour patterns. The behaviour pattern Optimal (OP) represents an ideal occupant behaviour. In this behaviour pattern, existing sun protection is used during the daytime and windows are closed only when the outdoor temperature is 1ºC higher than the indoor temperature. The fraction of the window that is assumed to open is 0.9, representing a window with two mobile slides fully open. Interior doors are opened simultaneously with the windows to allow indirect cross-ventilation. The existing sun protection consists of external opaque roller blinds simulated as opaque planes covering the window area completely.

A Suboptimal behaviour pattern (SUB) is created to represent a realistic occupant behaviour. In this behaviour pattern, existing sun protection is used as in the Optimal pattern and natural ventilation occurs only between 9 pm and 8 am. The fraction of the window that is assumed to open is 0.3, representing a semi-open window. This behaviour pattern is considered to be more realistic because natural ventilation does not require continued temperature motorisation and because the smaller window opening implies a more conservative behavioural assumption. As in the Optimal pattern, interior doors are opened simultaneously with the windows to allow indirect cross-ventilation.

Hard adaptation strategies are organised according to the level of ambition of the strategy in relation to climate change adaptation goals and cost of intervention. First, a retrofit scenario is simulated, emulating a traditional energy-saving intervention. In this retrofit option (Retrofit 1), adjustments are made to the U-values of the façade, roof, and windows and the enclosure infiltration rate to align with the specifications outlined in the Spanish Building Code. External insulation is implemented in the exterior for both the roof and façades, a strategic choice supported by studies indicating its superior benefits compared to internal insulation [10,20].

In the second retrofit option (Retrofit 2), in addition to the changes of Retrofit 1, a coating with a higher albedo value is applied to the façade and roof. In the third retrofit scenario (Retrofit 3), in addition to strategies from Retrofit 1 and 2, a balcony with louvres that completely shades the original façade is added.

Then, each retrofit option is combined with the two occupant behaviour patterns, the optimal and the suboptimal. Additionally, three baseline simulations are conducted without any retrofit intervention, two with the Optimal and Suboptimal patterns, and one with a worst-case occupant behaviour pattern where sun protection and natural ventilation are not used. The assessment with reduced occupancy is only conducted in the most favourable scenario, Retrofit 3 Optimal. The rest will be assessed with full time occupancy.

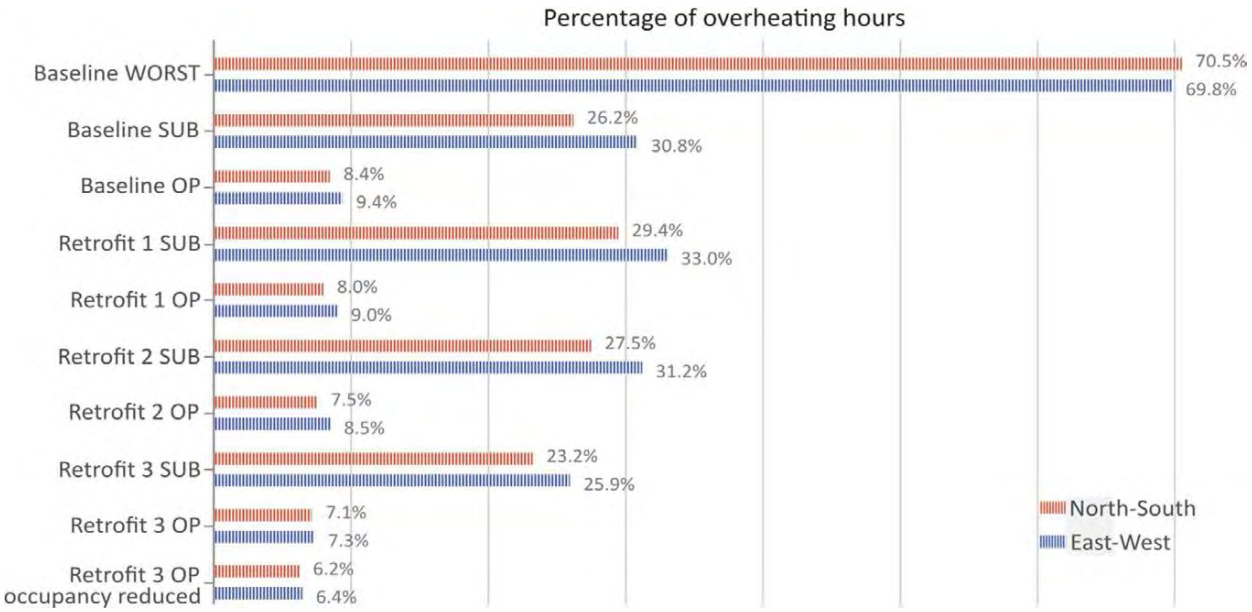

Figure 2: percentage of overheating hours for the different adaptation scenarios according to the Spanish Building Code standard

3. RESULTS

The results of the Retrofit 1 scenario show that optimal ventilation is needed to ensure the insulation and infiltration rate reduction effectiveness. This is in line with previous studies on the topic [14,22,23]. When the Retrofit 1 scenario is simulated with the Suboptimal pattern, discomfort hours are higher than the same occupant pattern in the Baseline scenario, 29.4 % (north-south) and 33.0% (east-west). When the Optimal pattern is introduced, discomfort hours are reduced compared to the Baseline scenario with the Optimal pattern, with discomfort hours of 8.0 % (north-south) and 9% (east-west). Regarding maximum temperatures, there is no worsening of the results in the Suboptimal combination. For instance, while the maximum temperature in the East-West living room during the Baseline Suboptimal scenario is 32.9ºC, during the Retrofit 1 Suboptimal scenario, it is 32.3ºC, 0.6ºC lower. This could indicate that the increase of thermal insulation and infiltration reduction is especially effective at reducing peak temperatures.

Retrofit 2 Suboptimal scenario results show a worsening of discomfort hours compared to Baseline Suboptimal, highlighting again the importance of adequate ventilation. The percentage of discomfort hours at the Retrofit 2 Suboptimal scenarios are 27.5 % (north-south) and 31.2% (east-west). When the Optimal occupant pattern is introduced, discomfort hours are slightly reduced compared to the Baseline Optimal scenario, with discomfort hours of 7.5 % (north-south) and 8.5% (east-west). Regarding maximum temperatures, a slight improvement is observed from Retrofit 1 scenarios in both rooms and orientations. This tendency is also observed in the Retrofit 3 scenario.

In Retrofit 3, where balconies and shading louvres are added in the perimeter of the building, a reduction of the discomfort hours for both Optimal and Suboptimal patterns is achieved. The discomfort hours in the Retrofit 3 Suboptimal scenario are 23.2 % (north-south) and 25.9% (east-west), and in the Retrofit 3 Optimal scenario, 7.1 % (north-south) and 7.3% (east-west). This reduction shows the benefits of blocking sun radiation not only in windows but also in the opaque areas of the façade.

When occupation time is decreased at Retrofit 3 Optimal scenario, assuming that the dwelling is not occupied from 6 pm to 8 pm, discomfort hours are reduced to 6.2 % (north-south) and 6.4 % (east-west). Compared to Retrofit 3 Optimal, the reduction is almost one point for both orientations, more significant than the reduction achieved from Retrofit 2 Optimal to Retrofit 3 Optimal. This shows that the comfort standard is susceptible to occupation hours and raises the question of the suitability of assuming the occupation hours in this type of study.

4. DISCUSSION

In this study, nine different adaptation scenarios (table 1) are simulated for the 2022 summer in Bilbao. These scenarios are then assessed using the Spanish Building Code to determine the discomfort hours during summer and the maximum indoor temperature during a severe heatwave.

The results of the different occupant behaviour patterns in the Baseline scenario show that indoor thermal comfort can be substantially improved with

Figure 3: maximum operative temperature during July heat wave

the efficient use of sun protection and natural ventilation. This finding aligns with the results of previous studies on the topic [12,21,22]. When the Baseline Worst scenario is simulated, discomfort hours are 70.5% (north-south) and 69.8% (east-west). When combined with the Suboptimal pattern, discomfort hours are reduced to 26.2 % (north-south) and 30.8% (east-west). When the Optimal pattern is introduced, discomfort hours are reduced to 8.4 % (north-south) and 9.4% (east-west).

Regarding maximum temperatures, a considerable gap is observed between the Baseline Worst and the Optimal and Suboptimal combinations (see Figure 3). The greatest gap is observed in the east-west apartment living room, with a difference of 11.7ºC between the Baseline Worst and Baseline Optimal scenarios. Interestingly, regarding maximum temperatures, the difference between Baseline Suboptimal and Baseline Optimal is less pronounced than the percentage of discomfort hours. This may indicate that natural ventilation, while helpful at improving overall summer thermal comfort, is less successful at keeping extreme temperatures at bay.

5. CONCLUSION

This study assesses the effectiveness of passive adaptation strategies in enhancing thermal comfort within a case study apartment located in a temperate region. The evaluation, based on the warm summer of 2022, reveals the challenge of maintaining indoor temperature within an acceptable range.

The study shows a notable impact of ventilation patterns on thermal comfort, even influencing the effectiveness of retrofitting measures like façade insulation and infiltration reduction. In Retrofit 1, where façade insulation and infiltration reduction were applied, the difference in the percentage of discomfort hours between optimal ventilation and suboptimal ventilation was up to 34 points. This underscores the significance of encouraging natural

ventilation, and finding means to promote these practices among occupants. The current understanding of summer habits among inhabitants of temperate cities, as well as the limits constraining the adoption of soft adaptation strategies, remains an area yet to be explored.

On the other hand, hard adaptation strategies also proved effective, however, to a lesser extent than soft adaptation. The combination façade insulation, infiltration reduction, albedo increase and balcony installation reduced the percentage of discomfort hours up to 5 points. Nevertheless, the combination of the Optimal pattern and Retrofit 3, which included every hard adaptation strategy tested, could not keep overheating hours below 4 %, the maximum allowed by the Spanish Building Code. According to these results, more than the passive strategies tested in this study is needed to assure an acceptable thermal comfort range in a summer like 2022.

Keeping houses comfortable and safe during future summers is likely to be done through more than just a single measure but by combining different approaches. This highlights the need to explore further the combination of different low-carbon adaptation strategies, such as low-energy mechanical ventilation or cooling, Urban Heat Island reduction strategies or other building-scale passive cooling strategies.

ACKNOWLEDGEMENTS

This work was funded by UPV/EHU (PIF 2020 contract), SAREN research group (IT1619-22, Basque Government) and the MCIN/ AEI / 10.13039/501100011033 / FEDER, UE through Oladapt (PID2022- 138284OB-C31) project.

REFERENCES

1. Basque Government, Euskalmet defines the year 2022 as the warmest, [Online], Available: https://www.euskadi.eus/noticia/2023/euskalmet-califica-el-ano-2022-como-el-mas-calido-de-las-series-historicas [11 December 2023].
2. Basque Government, Euskalmet defines this summer as the third warmest, [Online], Available: https://www.euskadi.eus/noticia/2023/euskalmet-califica-este-verano-como-el-tercero-mas-caluroso-desde-que-existen-series-historicas [11 December 2023].
3. IPCC, *Climate Change 2022: Impacts, Adaptation and Vulnerability Contribution of Working Group II to the Sixth Assessment Report of the Intergovernmental Panel on Climate Change*, *Cambridge University Press*, Cambridge University Press, Cambridge, UK and New York, NY, USA, (2022).
4. R. Gupta and M. Gregg, Using UK climate change projections to adapt existing English homes for a warming climate, *Building and Environment* 55 (2012) 20–42.
5. M. Taleghani, M. Tenpierik, and A. van den Dobbelsteen, Energy performance and thermal comfort of courtyard/atrium dwellings in the Netherlands in the light of climate change, *Renewable Energy* 63 (2014) 486–497.
6. J. Zuo et al., Impacts of heat waves and corresponding measures: a review, *Journal of Cleaner Production* 92 (2015) 1–12.
7. M.W. Anwar et al., Analysis of the effect of passive measures on the energy consumption and zero-energy prospects of residential buildings in Pakistan, *Build. Simul.* 14 (4) (2021) 1325–1342.
8. D. Coley, T. Kershaw, and M. Eames, A comparison of structural and behavioural adaptations to future proofing buildings against higher temperatures, *Building and Environment* 55 (2012) 159–166.
9. E. Oikonomou et al., Modelling the relative importance of the urban heat island and the thermal quality of dwellings for overheating in London, *Building and Environment* 57 (2012) 223–238.
10. S.M. Porritt et al., Ranking of interventions to reduce dwelling overheating during heat waves, *Energy and Buildings* 55 (2012) 16–27.
11. F. Barbolini, P. Cappellacci, and L. Guardigli, A Design Strategy to Reach nZEB Standards Integrating Energy Efficiency Measures and Passive Energy Use, *Energy Procedia* 111 (2017) 205–214.
12. E. Oikonomou et al., Assessing heat vulnerability in London care settings: case studies of adaptation to climate change, *in* Proceedings of BSO-V 2020, *International Building performance Simulation Association England*, Loughborough, UK, (2020).
13. S.M. Tabatabaei Sameni et al., Overheating investigation in UK social housing flats built to the Passivhaus standard, *Building and Environment* 92 (2015) 222–235.
14. D. Fosas et al., Mitigation versus adaptation: Does insulating dwellings increase overheating risk?, *Building and Environment* 143 (2018) 740–759.
15. M. Kharseh, M. Al-Khawaja, and F. Hassani, Comparison between different measures to reduce cooling requirements of residential building in cooling-dominated environment, *Energy and Buildings* 88 (2015) 409–412.
16. M. Varela Alonso, Ocharcoaga El polígono de las flores amarillas, Universidad del País Vasco/Euskal Herriko Unibertsitatea, 2017.
17. S. Attia et al., Overheating calculation methods, criteria, and indicators in European regulation for residential buildings, *Energy and Buildings* 292 (2023) 113170.
18. Ministry of Transport, Mobility, and Urban Agenda, *CTE HE Energy saving*, *Spanish Government.*, (2022).
19. L. Quesada-Ganuza, Heat Waves Risk Assessment of Historic Urban Areas: Historic Buildings and their Urban Environment, Universidad del País Vasco/Euskal Herriko Unibertsitatea, 2022.
20. A. Mavrogianni et al., Building characteristics as determinants of propensity to high indoor summer temperatures in London dwellings, *Building and Environment* 55 (2012) 117–130.
21. C. Schünemann et al., Mitigation and adaptation in multifamily housing: overheating and climate justice, *Buildings and Cities* 1 (1) (2020) 36–55.
22. A. Mavrogianni et al., The impact of occupancy patterns, occupant-controlled ventilation and shading on indoor overheating risk in domestic environments, *Building and Environment* 78 (2014) 183–198.
23. M. Mulville and S. Stravoravdis, The impact of regulations on overheating risk in dwellings, *Building Research & Information* 44 (5–6) (2016) 520–534.

PLEA 2024 WROCŁAW
(Re)thinking Resilience

A Lost Opportunity:
Shedding light on the conservatory and the Irish bungalow

SARAH CREMIN[1] SHANE COLCLOUGH[1] OLIVER KINNANE[1] PHILIP CROWE[1]

[1] UCD School of Architecture, Planning & Environmental Policy, Dublin, Ireland

ABSTRACT: Freestanding bungalows proliferated in rural Ireland from the 1970s. Many were subsequently extended with the addition of conservatories, which often disappoint, being uncomfortably hot in summer and cold in winter. In the aftermath of World War 2, the availability of cheap oil stymied development of solar architecture [22]. The basic principles of passive solar design were largely forgotten or ignored. This paper hypothesizes that Irish conservatories from recent decades underperform for this reason. An attached conservatory can potentially provide heat to the adjoining rooms and protect those rooms from heat loss in winter and heat gain in summer as well as enhancing health and well-being of the homeowner. When this potential is not fulfilled, the attached conservatory represents a lost opportunity. In the context of the climate emergency and the housing shortage in Ireland, the attached conservatory merits study, as a part of the existing housing stock which must be retained and adapted where possible to achieve its potential.
KEYWORDS: Attached conservatory, Bungalow, Sunspace, Passive solar

1. INTRODUCTION

The Irish countryside is dotted with thousands of one-off houses, many self-built with designs from a best-selling pattern book called 'Bungalow Bliss', first published in 1971 [1]. These homes were a 'direct expression of the dreams and aspirations of their owners' [2]. They combined aspects of the vernacular cottage with the classical forms of the Irish 'Big House' and, importantly, raised living standards [3].

The proliferation of one-off houses in scenic locations radically altered the landscape and drew criticism from environmentalists and architects. The word 'bungalow', which originated in India [4], became tainted in Ireland. In India it had evolved to define a single storey dwelling on a raised plinth with pitched roof and protruding porch, surrounded by a veranda. The bungalow typology was popular with colonial communities who transported it worldwide [4], to places like Southern California where it has positive connotations [5]. In recent years the negative perception of the bungalow in Ireland has shifted, partly due to its reappraisal in exhibitions and books.

'Bungalow Bliss' was the brainchild of Jack Fitzsimons, who designed the houses and conceived the books as manuals for those who had neither the culture nor the financial resources to hire an architect [1]. A front elevation and plan were provided for each design as well as key information such as floor area, room dimensions and estimated cost (Figs.1, 5). Advice about services focused on oil-fired central heating systems and provision of hot water with an electric immersion heater.

Irish bungalows were improved and extended over time. The conservatory was a popular addition from the 1990s. The front cover of the tenth edition of 'Bungalow Bliss', published in 1993 [6], illustrates the largest house in the book, Plan No. 225, and it boasts a conservatory in a prominent position, commanding a view to the front and back of the home (Fig. 1). Three other designs in Edition 10 also included conservatories. The conservatory, once the preserve of the rich, was now within reach of every homeowner.

Figure 1: Bungalow Bliss, Edition 10, 1993.

While enjoyed for their light and views, twentieth century Irish conservatories are often uncomfortably hot or cold. Their underperformance has given rise to an industry which specialises in replacing glass roofs with solid roof tiles. This paper hypothesizes that Irish conservatories from recent decades underperform

because they ignore the fundamental requirements of passive solar design and thus represent a lost opportunity.

2. SOLAR ARCHITECTURE

Solar architecture has existed since time immemorial. 2,500 years ago, the houses of ancient Greece were designed to trap warmth from the sun in winter and to block out sunlight in summer to avoid overheating [7].

2.1 The glasshouse and the conservatory

Glasshouses were first built in the Netherlands in the sixteenth century [8]. Their precise purpose, for example as peach house, fernery, or orangery dictated their aspect, humidity, temperature, and ventilation requirements. Most also collected and stored rainwater [7].

From the 1790s, glass conservatories were attached to country houses, where they occupied a key position 'directly accessible from adjacent polite rooms… serving as both social and botanical spaces' [8]. They changed the relationship between the house and garden and by extension between humans and nature. Many Irish country houses of the period feature attached conservatories. The conservatory at Bellevue in Co. Wicklow (Fig. 2) is thought to be the first and was the largest in Europe when completed in 1793 [9].

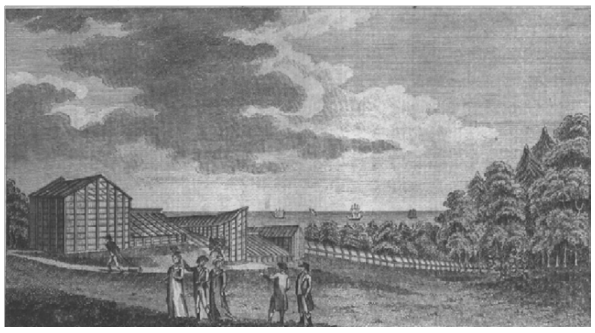

Figure 2: Bellevue, Co. Wicklow, Ireland.

2.2 Sunspaces: how they work

The attached conservatory can be described as a 'sunspace', a glazed, unheated space, typically constructed as an extension to an existing building, adjacent to a heated room, and thermally separated from it with an opening [10]. There is a tradition of attaching glazed rooms to housing in Europe such as gallerias in Northern Spain, and wintergardens in middle Europe.

The air in the sunspace is heated by direct sunlight. This warm air can be distributed into the adjoining rooms by simply opening doors or windows or via a heating system. When warm air stays within the sunspace, it acts as a thermal buffer, reducing the amount of heat escaping from the adjoining rooms in winter and at night-time, and reducing the amount of heat entering those rooms from outside in summer [11]. The sunspace must be thermally separated from the adjoining rooms to act as a thermal buffer.

Factors which affect the performance of a sunspace include climate, orientation, presence of nearby buildings or trees and occupant behaviour. South-facing is best in Northern Europe. A south-facing sunspace can significantly reduce the heating load in winter in Dublin, which experiences a temperate oceanic climate [12].

Temperatures in Europe are rising at twice the global average over the past 30 years [13]. A west facing sunspace risks overheating [12]. External shading to block direct sunlight and adequate ventilation at the highest point to release accumulated heat can mitigate the risk. Regulating a sunspace is more complex than opening or closing windows and its effectiveness is determined by how well the homeowner understands and controls it [12].

Characteristics of the sunspace itself such as its form, proportions, dimensions, glass type, quantity of glass, ventilation, shading, thermal mass, and the type of separation between the sunspace and adjoining rooms also impact its performance. Materials with thermal mass such as exposed brick can absorb and store heat which is then released slowly when the temperature cools.

3. 'BUNGALOW BLISS' ORIENTATION

'Bungalow Bliss' houses were sited parallel to the road, and accordingly a 'frontage' dimension was provided for each design (Fig. 5). A drawing titled 'Aspect' in Edition 5 shows a road that runs in a north-south direction, giving the rooms a west or east-facing orientation (Fig. 3). Edition 10 was the first to dedicate a section to siting and location. The emphasis is on landscaping, prospect and how to avoid an 'obtrusive siting' [6]. Only two sentences are dedicated to orientation. The 'front of the house facing south benefits from the sunshine' while an east-facing window is recommended for the kitchen, the most important room 'for the housewife' (Fig. 4), [6].

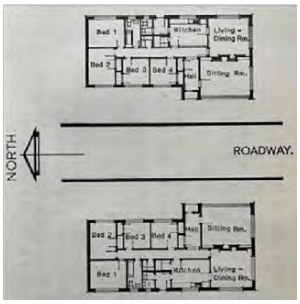

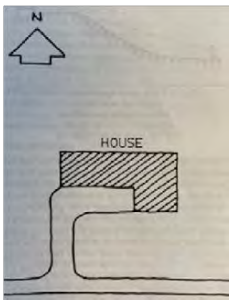

Figure 3: 'Aspect' Edition 5, 1975. Figure 4: Edition 10, 1993.

If the front of the house shown in Plan 225 faces south, the conservatory then faces due west and risks overheating (Fig. 5). The conservatory forms a

symmetrical composition in elevation and plan, its orientation a function of the house layout rather than location of the sun. Whereas Irish vernacular buildings 'were carefully integrated into their environment' [24], this innate knowledge of place and climate was ignored in the latter half of the twentieth century . The availability of cheap fossil fuels for heating allowed the homeowner to locate their house facing the road, 'to emphasise the design' [6], regardless of orientation.

Figure 5: Plan 225, Bungalow Bliss, Tenth Edition.

4. METHODOLOGY

4.1 Case Studies 1 and 2

A filtered search for 'houses on sale with a conservatory' was conducted on property website www.myhome.ie on 18 December 2023. Two 1970s bungalows with conservatories were selected, located within an hour's drive of Dublin. Their orientation was obtained via aerial views on *Google Maps*. Building Energy Rating (BER) certificates were accessed online. Description of the bungalows is based primarily on visual observation.

4.2 Case Study 3, Indoor Environmental Quality (IEQ)

Case Study 3 is the home of co-author Shane Colclough. The author interviewed Shane and Yvonne Colclough on 8/3/2024.

Five-minute IEQ data was collected, using the commercially available Netatmo monitoring equipment [15]. The data collected is presented in Figure 16.

The two sensors were shaded from direct sunlight (Fig. 14). The Netatmo's inbuilt optical CO^2 sensor automatically calibrates once per week, baselining at 400 ppm and has a stated accuracy of ±50 ppm or ± 5%. While the actual range was found to be wider in reality in some individual units (possibly up to ± 250ppm) the CO^2 sensor here is being used as an indicator for occupancy and is sufficiently accurate in this regard.

Table 1: Specifications of monitoring equipment

Metric	Range	Accuracy
indoor temp	0°C to 50°C	± 0.3°C
indoor RH	0 to 100%	± 3 %
indoor CO^2 conc.	0 to 5000 ppm	± 50ppm / ± 5%
noise level	35 to 120 dB	n/a
outdoor temp	-40°C to 65°C	
outdoor RH	0 to 100%	± 3 %

5. ATTACHED CONSERVATORY CASE STUDIES

5.1 Case Study 1

This charming two-bedroom bungalow sits on a steeply sloping site in a village an hour's drive south of Dublin. The bungalow is located parallel to the road with a front garden facing the public realm and a more private rear garden (Fig. 6). This location required substantial build-up at the southwest end of the bungalow to raise it above garden level (Fig. 7).

Figure 6. Aerial view of Case Study 1, Google Maps.

The conservatory protrudes beyond the compact form of the bungalow giving it a panoramic view over the garden and wooded landscape (Figs. 6, 7). Its form echoes that of a Victorian conservatory, the cast iron of old replaced with double-glazed, uPVC sections.

Figure 7. Back garden with steep slope

The kitchen connects to the dining room conservatory through a wide opening framed by an exposed steel beam overhead, which suggests that the opening was enlarged and the conservatory added after the house was originally built (Fig. 9). There is a

long, low radiator on the north wall and a bare light bulb hangs over a solid, wooden table with six chairs.

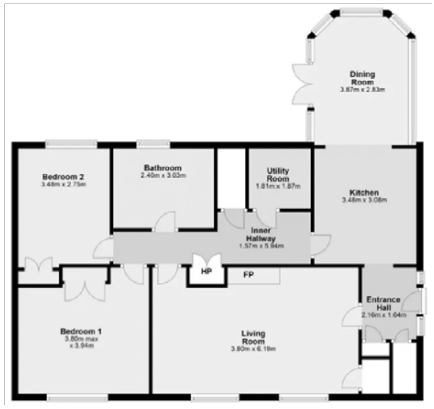

Figure 8: Floor plan of Case Study 1.

Figure 9: Kitchen & dining room conservatory, Case study 1.

Although the photographs show a home that was well maintained, no care was taken with its orientation. The conservatory faces northwest and will experience direct sunlight only from the west and southwest. The house itself blocks sunlight from the south (Fig. 6). In winter, there will be little direct sunlight and inconsequential passive solar heat gain. In fact, heat from the bungalow may escape through the dining room conservatory because it is fully open to the kitchen. To work effectively as a thermal buffer would require thermal separation between the two rooms. The ceramic floor tiles will store a little heat.

This dining room must be delightful on a sunny spring or summer's evening. However, it must be very uncomfortable when it's dark and cold outside and the surface temperature of the glass is lower than the air, causing the occupants to lose heat rapidly.

It is possible to speculate, without measurements or simulation, that this conservatory will not provide free heat from the sun for the adjoining kitchen. Rather, it is likely to be a significant contributor to the bungalow's low Building Energy Rating (BER) of F, given that the significant heat loss from the glazing is within the thermal envelope. BER ratings, calculated by the national energy rating software DEAP, range from a high of A to a low of G. Heating this house will require considerable energy.

5.2 Case Study 2

This neat, rural bungalow, constructed in the late 1970s, sits at the back of a mature garden (Fig. 10). The attached conservatory was added in 1998.

Figure 10: Aerial view of Case Study 2, Google Maps.

The conservatory is entered through sliding doors from the sitting room (Figs. 11, 12). Although it looks pleasant and is furnished for relaxation, it faces north and is surrounded by trees, which will block sunlight from east and west when they are in leaf. A plug-in electric heater suggests that the room must be heated when in use (Fig. 12).

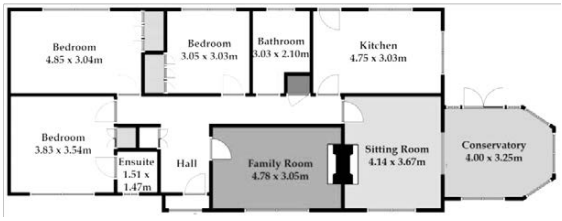

Figure 11: Floor plan of Case Study 2.

The conservatory is unlikely to gain passive solar heat at any time of year. Doors separate the conservatory from the sitting room, thereby minimizing heat loss from the latter. While this home has a relatively poor BER of D1, the conservatory is outside the thermal envelope, and the heat loss from the large areas of glazing are not further reducing the BER rating.

Figure 12: Sitting room and conservatory, Case Study 2.

5.3 Case Study 3

This two-storey, C1 rated house is located 37kms from Dublin. It was constructed in 1999, its attached conservatory a feature that set it apart. In 2023 the owners undertook a renovation, adapting their home to better suit their needs after their adult children had moved out. They considered replacing the conservatory with a larger extension but decided to retain it due to its frequent use year round.

It was noted during the renovation planning stage that the overall heat loss from the building would be

reduced by 12% by excluding the conservatory from the thermal envelope.

Figure 13: Aerial view showing Case Study 3, Google Maps.

The conservatory, which faces due south and west, is double-glazed with double doors to the kitchen and garden and a radiator against the kitchen wall (Fig. 14). Although small at 5.9m^2, it accommodates a round table, two wicker chairs and an armchair. A beech hedge alongside is just high enough to afford privacy (Fig. 15).

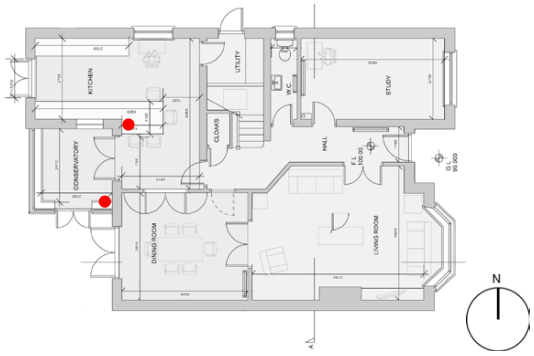

Figure 14: Ground floor plan, Case Study 3, with location of sensors shown in red

Figure 15: The conservatory, Case Study 3.

The owners work from home and like to meet in the conservatory for coffee breaks and lunch. It's a place to escape when the house is busy. They love sitting in the conservatory on a Sunday morning, and when it's raining outside. A folded clothes rack is often used to dry clothes. Seedlings are grown and potatoes chitted. The conservatory is used most in the shoulder seasons. On sunny days the doors into the kitchen are opened to allow transfer of heat. The owners perceive it to be a 'very useful and pleasant' space, even on the coldest winter days.

Between 27 January and 11 February, the temperature in the conservatory was consistently higher than the outdoor temperature and the owners sat in it on six occasions, as evidenced by peaks in CO^2 levels (Fig. 16). The conservatory was too cool on 30 January, February 1 and 11 and on those days the temperature was raised with a 2kW fan heater.

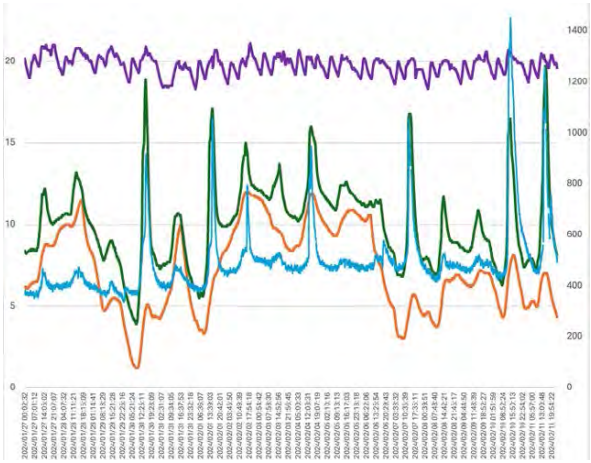

Figure 16: Temperature {°C} & Conservatory CO^2 concentration {ppm}, 27 January - 11 February 2024.

6. HEALTH AND HOME

The glasshouse was invented to make an artificial climate for exotic plants, and with its development 'the triumph of science over nature was put on full display' [16]. Health reformers soon made links between architecture, climate, and human health [16]. In 1860 Florence Nightingale wrote that darkened rooms were harmful, and that sunlight was necessary for speedy recovery from illness. This idea led to the design of hospital wards that were filled with sunlight. In the twentieth-century tuberculosis sanatoria focussed on provision of fresh air and sunlight [17].

The Covid-19 pandemic obliged people to stay at home for extended periods and has placed renewed attention on the connection between our homes and our health and well-being [18]. Many continue to work from home while those who are vulnerable in any way have always spent considerable time at home.

The conservatory can potentially enhance the health and well-being of homeowners by providing plentiful daylight, sunlight and views to the outdoors and nature. The idea that nature promotes healing can be traced to ancient Greece and is confirmed by recent studies in neuroscience [17].

7. CONCLUSION

Adding a conservatory to an existing house is a relatively straightforward and affordable way to gain an extra room. There is no need to engage an architect or engineer or their fees. Instead, a conservatory supplier takes charge of the design and installation. An extension under 40m^2 can be added to the rear of an Irish house without securing planning permission, saving time and money. This partly explains why so many were built in Ireland from the 1990s, divorced

from their original purpose as a glazed room heated by the sun. The absence of professionals may also explain why many are incorrectly oriented.

The attached conservatories featured in 'Bungalow Bliss' Edition 10 and case studies 1 & 2 exhibit fundamental shortcomings that adversely affect their performance. Case study 3 provides evidence that a well oriented conservatory improves thermal comfort and connects the homeowner to daylight and nature, even in the depths of winter, with all the associated health benefits. Perhaps the attached conservatory is more appropriate as flexible space for occasional use rather than for the intense daily use required of the dining room in Case Study 1.

Housing in Ireland is amongst the most inefficient in Europe [19]. The Irish government has set itself the objective of retrofitting 500,000 homes by 2030. Although the goal is deep retrofit with a target BER of B2 or better, most retrofits do not reach B2 [23]. Grants are available for partial or whole house upgrades but none cater for measures that would improve the performance of an existing conservatory. Is it time to promote and fund smaller scale, shallow retrofitting strategies, that would improve parts of the home and consume less embodied carbon than deep retrofits?

According to historian and theorist, Daniel A. Barber, we must embrace discomfort to significantly reduce carbon consumption [20]. Experiencing a range of temperatures makes us feel more alive while a constant temperature is dull and forgettable [21]. The conservatory can play a role by providing inhabitable, in-between space whose temperature follows the seasons. Even when its passive solar performance is suboptimal, it benefits human health by providing natural light and views to nature.

The question is whether it is possible to adapt and improve underperforming conservatories. The answer will differ in each case but it is clear that intelligent adaptive reuse must begin to take precedence over the tendency to demolish and replace existing conservatories and building stock, given the local housing shortage and global climate emergency. In some cases thermal separation could be achieved by installing doors between the conservatory and adjoining house. Realigning the attached conservatory with its historical origins as an unheated, thermally separated sunspace would capitalise on its inherent advantages as a potential source of heat and thermal buffer, as well as reducing energy consumption and giving a higher BER rating to a cohort of underperforming houses, in line with national objectives. The attached conservatory merits further study and adaptation to realise its potential.

ACKNOWLEDGEMENTS

Thank you to Dr. Samantha L. Martin for her advice.

REFERENCES

1. Duncan, A., (2022). *Little Republics: The Story of Bungalow Bliss*. Dublin, The Lilliput Press.
2. O'Toole, F. & Kelly, A. (2021). *We Don't Know Ourselves: A Personal History of Ireland Since 1958*. London, Head of Zeus.
3. Rowley, E., (2017). Housing in Ireland. 1740-2016. *The Cambridge Social History of Modern Ireland*, 212.
4. Gupta, S., (1996). The Colonial Bungalow. *Architecture Plus Design*, 13, 87.
5. Mattson, R., (1981). The Bungalow Spirit. *Journal of Cultural Geography*, 1, p. 75.
6. Fitzsimons, J., (1993). *Bungalow Bliss*, Kells (Co. Meath), Kells Art Studios.
7. Butti, K. & Perlin, J., (1981). Reprinted 2009. *A Golden Thread*, London, Marion Boyars Publishers Ltd.
8. Tropp, R., (2021). 'The most original and interesting part of the design': The attached quadrant conservatory at the dawn of the nineteenth century. *Studies in the history of gardens & designed landscapes,* 41: p. 234-256.
9. O'Kane, F. & O'Byrne, R., (2022). *Digging New Ground: The Irish Country House Garden, 1650-1900*, Dublin, Ireland, Irish Georgian Society: p.70, 134.
10. Bugenings, L. A. & Kamari, A., (2022). Bioclimatic Architecture Strategies in Denmark: A Review of Current and Future Directions. In *Buildings*, 12, 224.
11. Ulpiani, G., Giuliani, D., Romagnoli, A. & Di Perna, C., (2017). Experimental Monitoring of a Sunspace Applied to a NZAB Mock-Up: Assessing and Comparing the Energy Benefits of Different Configurations. In *Energy and Buildings*, 152, 194.
12. Monge-Barrio, A. & Sánchez-Ostiz, A., (2015). Energy Efficiency and Thermal Behaviour of Attached Sunspaces, in the Residential Architecture in Spain. Summer Conditions. In *Energy and Buildings*, 108, 244.
13. Press Release from the *World Meteorological Organization*, 2/11/2022 [Online]. https://wmo.int/news/mediacentre/temperatures-europe-increase-more-twice-globalaverage
14. Mihalakakou, G., (2002). On the Use of Sunspace for Space Heating/Cooling in Europe. In *Renewable Energy*, 26, 415.
15. Netatmo Weather Station specifications. Netatmo n.d. https://www.netatmo.com/enus/weather/weatherstation/specifications [Online].
16. Valen, D., (2016). On the Horticultural Origins of Victorian Glasshouse Culture. In *Journal of the Society of Architectural Historians*, 75, 403.
17. Sternberg, E.M., (2010). *Healing Spaces: The Science of Place and Well-being*, London; Cambridge, Mass; Belknap Press of Harvard University Press.
18. Peters, T. & Halleran, A., (2021). How Our Homes Impact Our Health: Using a Covid-19 Informed Approach to Examine Urban Apartment Housing. In *ArchNet-IJAR,* 15, p.10-27.
19. Kinnane, O., Grey, T. & Dyer, M., (2017). Adaptable Housing Design for Climate Change Adaptation. *Proceedings of the Institution of Civil Engineers. Engineering sustainability*: p. 170-249.
20. Barber, D.A., (2019). After Comfort*,* In *Log* (New York, N.Y. 2003), 45.
21. Heschong, L., (1979). *Thermal Delight in Architecture*, London; Cambridge, Mass; MIT Press.
22. Barber, D.A., (2016). *A House in the Sun: Modern Architecture and Solar Energy in the Cold War*, New York, NY, Oxford University Press.
23. Research by Orlaith McGinley, University of Galway, indicates that less than 10,000 from a total of 50,000 retrofits reached B2 in 2022. Construct Innovate webinar 23/9/2023 [Online].
24. Aalen, F. H. A., Whelan, K. & Stout, M., (2011). *Atlas of the Irish Rural Landscape*, Cork, Cork University Press.

PLEA 2024 WROCŁAW
(Re)thinking Resilience

Potential and Challenges of Vertical Farming on Building Facades in Practice

XI ZHANG[1] AYSU KURU[1] ARIANNA BRAMBILLA[1] EUGENIA GASPARRI[1]

[1] School of Architecture, Design, and Planning, The University of Sydney, Sydney, NSW, Australia

ABSTRACT: Feeding a rising global population through the conventional agriculture paradigm is becoming a significant challenge under the pressure of noticeable climate change, depleting valuable resources, and demands for high-quality food. Vertical farming (VF) combined with facades is able to improve the sustainability of urban food supply chains by shortening transportation distance and increasing food production while reducing land use, water consumption, and chemical inputs. However, there are very few tangible applications in practice, which means there is a need to comprehend the benefits and potential challenges in further exploring this technology. Therefore, this research aims to emphasise the benefits and challenges of the combination of VF and facades via case study analysis and literature research. The results show that combining farming systems and facades has positive impacts on the sustainability of environmental, social, and economic aspects. Food supply resilience improvement is the core of VF on façade projects. However, the potential adverse environmental impacts, user concerns, and high investment costs are the main challenges to its widespread adoption. Policy support and technological advancements can help address these difficulties, leading to realising the full benefits.
KEYWORDS: Vertical Farming, Facades, Food, Energy

1. INTRODUCTION

With increasing population growth, it is projected that by 2050, an additional 2.5 billion residents will inhabit urban areas [1]. Combined with urban sprawl, climate change, and the occurrence of environmental and social disasters like the COVID-19 pandemic[2, 3], these situations present a huge challenge to increasing food yield in limited agricultural land for the rising food requirements.

Recent research highlights that there would be a rise of nearly 1℃ to global mean surface air temperature by 2100 without revolutionary changes in food production and consumption [4]. In response to this challenge, there has been a growing focus on vertical farming (VF), which is the implementation of stacked food growing systems on rooftops, facades, and multi-story buildings' interiors rather than on the ground to increase food production, reduce land requirements, and shorten the supply chain [5, 6]. Together with technological developments, including soilless cultivation technologies, light-emitting diodes (LED), Internet of Things (IoT), robotics, artificial intelligence (AI), and smart devices, there is great potential for integrating food production systems within and on buildings [7, 8]. However, it is important to note that technologies driven by external energy, especially lighting systems, can result in high energy demands and increased greenhouse gas emissions when applied indoors [9]. Therefore, using natural light sources, especially those attached to or integrated into building envelopes, shows promise [10].

With an increasing urban density since more high-rise buildings were constructed, the proportion of vertical to horizontal surfaces is rising. Vertical greenery systems provide opportunities for growing plants on facades, but edible plants are still scarce. In this sense, understanding the benefits and challenges of VF in empirical practice is crucial to developing appropriate guidelines for the future implementation of VF on facades.

This study analyses eleven selected case studies worldwide with the following aims:

- To gain a better understanding of the extent of VF on facades could benefit the resilience of urban areas.
- To identify and discuss the challenges that hinder the uptake of VF on building facades.

2. MATERIALS AND METHODS

The methodology of this study is summarised into four steps, from the selection and identification of the case studies to the explanation of the data extracted and analysed.

2.1 Case studies search

Case studies were identified through searches of publications and online search engines like Google. Keywords including "vertical farming on facades", "edible walls", "farming walls", "building-integrated agriculture", and "food production on buildings" were used in the search for relevant case studies.

2.2 Case studies selection

This research focuses on the realised projects that have been implemented and used and designed projects that are in the initial design stage. The following eligibility criteria were established for the selection and analysis of the developmental projects: (1) prototypes were not included, (2) projects mainly focusing on indoor plant factories or greenhouses with stacked growing systems were excluded, as their fundamental purpose is to develop indoor vertical farming, whereas the focus of this study is farming systems installed on building facades, and (3) projects with limited available information about farming systems and functions were excluded.

2.3 Data collection

The concept of VF has existed since 1915, when Gilbert Ellis Bailey invented the term "vertical farming" [5, 6]. However, there are relatively few projects that integrate agriculture with facades, and there is little research on applied case studies. The needed data were mainly collected via developers' official websites, dedicated websites including archdaily.com and dezeen.com, and the relevant literature. Data for projects situated in Sydney—The Jungle House—were collected through on-site visits and email interaction with designers to gain an in-depth understanding of the main purpose, the encountered challenges, and users' attitudes during the residence. Figure 1, Figure 2, and Table 1 show the images and a total list of the selected case studies and references used for each case study.

2.4 Data analysis

The benefits focus on the function performance of VF on facades to identify and discuss its benefits and challenges for improving the sustainability of environmental, social, and economic. Considering that some selected projects are in the initial conceptualisation stage and the absence of direct site visits of built projects, these benefits were gathered from the information provided by projects, whereas the challenges were mainly inferred from existing research on VF on facades. Finally, future prospects related to policy support and technology advancements were discussed.

The analysis of selected case studies mainly focuses on four key aspects (shown in Table 1 and Table 2):

- Basic information (name, location, architects/designers, project status, building type). Project status refers to the current state of a project, like in the design stages and has been built and used in practice, and the building type means the primary application of projects, like residential (accommodation), commercial (office or/and market), pavilion (showcase), and research.
- Farming information (crop location, crop species, and cultivation technologies used).
- Main functions. These refer to the main purpose of projects, like promotional (concept presentation and publicising), commercial (trade activities), educational (learning knowledge), and research (exploring and developing knowledge).
- Other major functions.

Table 1: Basic information of the selected case studies.

ID	Name/Location	Architects/Designers	Dates	Project Status	Building Types	Refs.
D01	Jian Mu Tower - Shenzhen (CHIN)	Carlo Ratti	2021	D	Co	[11, 12]
D02	Vertically Integrated Greenhouse (VIG) - Abu Dhabi	Kiss + Cathcart	2009	D	Co	[13, 14]
D03	GreenBelly	AVL Studio	N/A	D	N/A	[15, 16]
D04	The Farmhouse	Precht	2019	D	Mix	[17, 18]
D05	Urban Vertical Farm of Brightfood - Shanghai (CHIN)	Stefano Boeri Architetti	2021	D	Co	[19]
D06	Homefarm - Singapore	Spark	2014	D	R	[20, 21]
B01	The Jungle House - Sydney (AU)	CplusC	2019	B	R	[22]
B02	The USA Pavilion - Milan (IT)	James Biber	2015	B	P	[23-25]
B03	Urban Farming Office - Ho Chi Minh City (VNM)	VTN	2022	B	Co	[26, 27]
B04	Greenhost Boutique Hotel - Indonesia	Paulus Mintarga	N/A	B	Co	[28-30]
B05	Tampines Blk 146 Vertical Farm - Singapore	Netatech Company	2021	B	R	[31, 32]

* List of acronyms – D: Design Stage, B: Built; R: Residential, P: Pavilion, Co: Commercial, Mix: Mixed; N/A: Not Available

Figure 1.Images of the selected case studies (D01-D05).

Table 2: Farming information and functions of the selected case studies.

ID	Farming Information			Main Functions	Other Major Functions			
	CL	CS	CT		IITC	RBEC	WC	JO
D01	BDS	V, He, F	H	Promotional	✓	✓	✓	N/A
D02	BDS	V, F	H	Promotional	✓	✓	✓	N/A
D03	BLF	V, F	S, H, Ae	Commercial	✓	✓	✓	✓
D04	BDS	N/A	N/A	Promotional	N/A	N/A	N/A	N/A
D05	EF, TF	V, F	N/A	Promotional	N/A	N/A	N/A	N/A
D06	CF	V, He	S, Aq	Promotional	N/A	N/A	✓	✓
B01	BDS	SP	FT	Educational	N/A	N/A	✓	N/A
B02	BLF	V, He, G	H	Promotional	N/A	N/A	✓	✓
B03	WF	V, He, F	N/A	Promotional	✓	✓	✓	N/A
B04	BF	He	H	Promotional	N/A	N/A	✓	N/A
B05	BLF	V, R	H	Research	N/A	N/A	✓	✓

* List of acronyms – CL: Crop Location, CS: Crop Species, CT: Cultivation Technologies; BDS: Between Double Skin, BLF: Blind Facades, WF: Window Facades, BF: Balcony Facades, TF: Terrace Facades, CF: Corridor Facades; SP: Silver Perch, V: Vegetables, He: Herbs, G: Grains, F: Fruits, R: Rice; H: Hydroponic, FT: Fish Tank, S: Soil, Ae: Aeroponic, Aq: Aquaponic; IITC: Improve Indoor Thermal Comfort, RBEC: Reduce Building Energy Consumption, WC: Water Conservation, JO: Job Opportunity; N/A: Not Available

Figure 2. Images of the selected case studies (D06-B05).

3. RESULTS AND DISCUSSION

3.1 Environmental sustainability

3.1.1 Food miles reduction

The formation and expansion of cities rely highly on the large amount of food transported from distant regions worldwide [33], leading to adverse environmental effects. Shortening food production-consumption distance can reduce greenhouse gas (GHG) emissions along urban food supply chains and minimize food waste caused by transport spoilage because of variance cooling practices and perturbation damage like rainfall [34]. Only B01 – The Jungle House did the life cycle assessment (LCA) and showed an obvious reduction in the total carbon dioxide equivalent of the project [22].

However, existing research has proven that the carbon footprint of building-integrated agriculture is higher than that of conventional land farms due to artificial lighting requirements[9]. Sunlight accessibility for VF on facades and photovoltaic utilisation (e.g., D03 – GreenBelly [15, 16]) provide opportunities to reduce the net energy consumption for lighting. Hence, further assessment is needed to determine the effectiveness of short transport distances in reducing GHG emissions, as transportation in most food supply chains has a relatively limited effect on emissions.

3.1.2 Water saving

Hydroponic, aeroponic and aquaponic systems (e.g., D03 – GreenBelly [15, 16] and D06 – Homefarm [20, 21]), precipitation collection (e.g., D01 – Jian Mu Tower [11, 12] and B05 – Tampines Blk 146 Vertical Farm [31, 32]), and wastewater filtrating and recycling (e.g., B01 – The Jungle House [22]) lead to the reduction of water usage for VF on facades. Integrating aeroponic methods displays a more significant opportunity for water consumption, plant growth rate and quality, fertiliser usage, and crop yield than hydroponics [7]. Recirculating aquaponics can reduce the frequency of water changes[36]. Water volume utilised for irrigation can be reduced through such water management and conservation, thereby withdrawing freshwater used by farming to satisfy the additional resident demands.

3.1.3 Indoor and outdoor thermal comfort

VF on facades can adjust indoor thermal comfort by providing solar shading and cooling through evaporation in summer and acting as solar capture devices to warm and insulate facades in winter, such as D02 – VIG [11, 12] and B03 – Urban Farming Office [26, 27], resulting in energy demand reduction for space conditioning in buildings. If VF on facades can be widely used around the cities, the urban heat island (UHI) effect will likely be mitigated [26, 27].

3.1.4 Biodiversity

For vegetation, biodiversity refers to cultivated species by humans and developed species naturally [38]. It is not the primary purpose of the development of integrating farming into facades. B03

– Urban Farming Office [26, 27] generally pointed out that the increase of green ratio in site areas and growing various crop species benefit the region's biodiversity without further explanations. In terms of planted crops, in B02 – The USA Pavilion, up to 42 crops were successfully cultivated in unclosed environmental conditions [23-25]. If plants are grown in the gap between the double skin with managed growing conditions, the impacts of changing environmental conditions can be minimized, which contributes to introducing novel crops and re-introducing forgotten crops [34]. Research exhibited that although people are interested in biodiversity in agricultural environments, the study of the hosted animals and plants in the following faming management remains scarce [38].

3.2 Social sustainability

3.2.1 Food security improvement

The unique feature of VF on facades is the capability to produce food by occupying minimal or no land compared to other types of agriculture like community agriculture, indoor farming, and rooftop farms. High-rise buildings in metropolises offer total available vertical surfaces that are significantly larger than horizontally vacant surfaces [35]. Hence, most cases aimed to promote combining farming and facades.

The façades in D06 – Homefarm, including corridor facades, were expected to offer around 30 tons of food per month [20, 21]. B04 – Greenhost Boutique Hotel (growing crops on balcony facades) and B05 – Tampines Blk 146 Vertical Farm (VF adjacent to the blind facades) aimed to provide food in Sleman and Singapore with limited arable lands in cities [28-32]. The designer of D04 – Farmhouse intended to strengthen the connection between residents living in urban towers and agriculture by growing food on the outside layer of facades to help them easily access food [17, 18].

In fact, the availability of light, water, nutrients, temperature, relative humidity, airflow, and carbon dioxide (CO_2) concentration impacts crop growth rate and productivity [34]. D01 – Jian Mu Tower combined hydroponic systems and AI management on these environmental variables and was estimated to have the capacity to produce approximately 270,000 kg of food per year in a 218-meter-high building [11, 12].
However, it should be noted that unclosed VF on facades is easily influenced by unpredictable and instantly changing climate conditions. In B01 – The Jungle House, the designer and the owner showed that the fish ready to harvest died since the fine ash settled on the pond's water surface during the January 2020 bushfire disaster. Growing crops in enclosed environments, including between double skins (e.g. D02 – VIG [13, 14]) and using ETFE membrane materials for covering (e.g. D05 – Urban Vertical Farm of Brightfood [19]), is able to mitigate the effects of seasonal changes, animals and pest damage on yield. However, there will be non-uniform growth conditions in a fully enclosed environment because of inappropriate planning, environmental control measures, and maintenance [34].

3.2.2 Job opportunity

B02 – The USA Pavilion had dedicated workers responsible for harvesting and managing crops during the Milan Expo 2015 [23-25]. D06 – Homefarm could offer full-time and part-time job opportunities for residents of retirement homes [20, 21]. Hiring staff becomes necessary when harvested food is sold at its place of production (e.g., D03 – GreenBelly [15, 16]). Apart from these jobs related to direct interaction with plants, VF on facades also provides indirect occupations such as constructing farm structures and developing advanced planting technologies [7].

3.2.3 Education

One of the projects is geared towards educational goals. B01 – The Jungle House highlighted that the primary aim is to educate the owners' children, inner-city individuals with no farming knowledge. Hence, this project allows children to directly access gardening to understand how to grow, maintain, and harvest food, rainwater collection, and solar power operation. In fact, lacking relevant gardening knowledge may not be limited to the next generation.

3.2.4 User perceptions

Existing research has shown that not only the lack of knowledge of gardening but also the accessibility of crops, the protection from human and biological damage, invested efforts, costs, and crop yield are users' main concerns, and residents have various preferences [35]. Some consumers prefer personally involved cultivation management as enclosed crop production may increase the risk of pathogen development and negatively impact the nutritional value of food, whereas automatically controlled systems are preferred by others as needless to invest too much time [34, 39]. Hence, user mistrust and unmet preferences can both become barriers to the promotion of VF on facades.

3.3 Economic sustainability

Some of the chosen projects highlighted that bringing food production closer to consumers could reduce transportation costs and food prices (e.g., D03 – GreenBelly [15, 16]), while others believed that the total building energy cost could be reduced by adjusting indoor thermal comfort (e.g., D02 – VIG [13, 14]). However, there is scarcely credible literature on the economic feasibility from the start of investment and operating costs to disposal at the end of the life

cycle. After all, to successfully cultivate crops on facades, the plant light requirement, like suitable light quantity and spectrum, should be satisfied as a critical factor, which is very costly when plants need supplementary energy, especially in a fully controlled growing environment [9, 34]. Besides, the construction and maintenance may also incur significant costs. For instance, B02 – The USA Pavilion faced significant debts after the Milan Expo 2015, which may be partly because of the farming facades.

Therefore, advancing novel, appropriate and optimised farming system designs and a circular systems approach can mitigate economic risks [34]. For example, optimising the natural inputs, including solar radiation, precipitation, and organic waste (see Section 3.1), may improve the economic feasibility of VF on facades.

4. FUTURE PROSPECTS

4.1 Policy support

Currently, agricultural policymaking versus urban/building planning and construction are institutional separation, which hinders the acceptance and success of the novel farming paradigm [34, 37]. It is still challenging to find suitable farming places in city buildings, considering zoning laws, technical feasibility, and other potential social issues [37]. This may be one of the reasons why only a few projects were built. However, it is crucial to have a supportive policy environment to draw public attention and take action. Such support will facilitate the practical implementation of VF on facades.

Simple initiatives are inefficient in helping VF on facades diffuse over a territory. The holistic circularity strategy, which connects cultivation systems and buildings to reduce waste and GHG emissions efficiently, has been proposed and emphasised to aid the future upscaling of VF on facades [37]. D'Ostuni et al. specified that this strategy includes three main aspects: renewable energies, sustainable water management in the cultivation systems, and waste recovery in treating buildings' wastewater for nutrient extraction [37]. More than half of the selected projects claim rainwater collection as an alternative water source for irrigation in the production system. Besides, renewable energies, like solar (e.g., B05 – Tampines Blk 146 Vertical Farm [31, 32] and D03 – GreenBelly [15, 16]), are used to power buildings and farms.

4.2 Technology advancements

The integration of advanced technologies, including cultivation and management systems in VF on facades, is crucial to improving vertical surface suitability for farming to achieve a higher yield and quality of food while minimising resource investments and environmental impacts. Only D01 – Jian Mu Tower used AI-supported management to monitor and automatically manage irrigation, nutrients, and other matters in the growing areas to take care of crops day by day [11, 12]. The D01 project featured moveable farming systems on its facades, allowing workers to customise their movement via a mobile app to adjust the indoor micro-climate conditions, positively affecting their productivity.

In the future, it can be vital to explore how advancements in digital technologies, such as IoT, AI, drones, and blockchain, can support VF on facades market acceptance and uptake.

5. CONCLUSION

In conclusion, this paper has highlighted that VF on facades is a potential new solution to meet food requirements. It is crucial to understand the benefits and challenges of the development of this technology.

In terms of environmental sustainability, the reduction of GHG emissions by shortening food miles is the main benefit of VF on facades, which is followed by saving water and improving indoor and outdoor thermal comfort. It still lacks a comprehensive analysis of the environmental impacts from food production to disposal stages. Meanwhile, a focus on the ability to shelter biodiversity within the façade farming is important since it benefits urban nature conservation as a supplementary form of green spaces.

VF on facades also has the potential to benefit social sustainability by improving food security, offering job opportunities, and strengthening people's gardening knowledge, whereas people's concerns and their various preferences are obstacles to the new type of implementation.

The biggest problem is cost. Although it is possible to reduce family food expenditures by reducing food transportation distances, the costs of constructing and maintaining farming facade systems may easily offset the savings from reduced transportation expenses.

Policymaking and technological advancements in cultivation should be taken into account when approaching VF on facades since they might help overcome these challenges, thereby improving VF's wide promotion and successful implementation on facades. Besides, the benefits and challenges are currently theoretical and will require further quantitative and qualitative research in the future.

ACKNOWLEDGEMENTS

Some information about the B01 was provided by its designer and owner, Clinton Cole. We would like to express our appreciation for his support and help.

REFERENCES

1. United Nations. World Urbanization Prospects: the 2018 Revision. [Online], Available: https://population.un.org/wup/Publications/ [1 December 2023].
2. Kim, C.G., (2012). The impact of climate change on the agricultural sector: implications of the agro-industry for low carbon, green growth strategy and roadmap for the East Asian Region.
3. Lal, R., (2020). Home gardening and urban agriculture for advancing food and nutritional security in response to the COVID-19 pandemic. *Food security*, 2020. 12(4): p. 871-876.
4. Ivanovich, C.C., et al., (2023). Future warming from global food consumption. *Nature Climate Change*, 13(3): p. 297-302.
5. Al-Kodmany, K., (2018). The vertical farm: A review of developments and implications for the vertical city. *Buildings*, 8(2): p. 24.
6. Despommier, D., (2010). The vertical farm: feeding the world in the 21st century. Macmillan.
7. Sharma, S., N. Dhanda, and R. Verma. (2023). Urban Vertical Farming: A Review. in *2023 13th International Conference on Cloud Computing, Data Science & Engineering (Confluence)*. IEEE.
8. Kalantari, F., et al. (2017). A review of vertical farming technology: A guide for implementation of building integrated agriculture in cities. in *Advanced engineering forum*. Trans Tech Publ.
9. Beacham, A., L. Vickers, and J. Monaghan, (2019). Vertical farming: a summary of approaches to growing skywards. *The Journal of Horticultural Science and Biotechnology*, 94: p. 1-7.
10. Tablada, A. and V. Kosorić, (2022). Vertical farming on facades: transforming building skins for urban food security, in *Rethinking Building Skins*. p. 285-311.
11. Jian Mu Tower, [Online], Available: https://carloratti.com/project/jian-mu-tower/ [1 December 2023].
12. Jian Mu Tower: A Project by CRA-Carlo Ratti Associati. [Online], Available: https://www.youtube.com/watch?v=xABtQ2l6Npw/ [1 December 2023].
13. Kisscathcart. Vertically Integrated Greenhouse, [Online], Available: https://kisscathcart.com/integrated_agriculture.html#/ [1 December 2023].
14. Gould, D. and T. Caplow, (2012). 8 - Building-integrated agriculture: a new approach to food production,in Metropolitan Sustainability, *Woodhead Publishing*. p. 147-170.
15. Vertical Urban Garden, [Online], Available: http://www.greenbelly.org/ [1 December 2023].
16. Blind Building Facades Become Urban Farms with Scalable Scaffolding System. Available:https://weburbanist.com/2018/09/17/blind-building-facades-become-urban-farms-with-scalable-scaffolding-system/ [18 March 2024].
17. Precht's the Farmhouse concept combines modular homes with vertical farms, [Online], Available: https://www.dezeen.com/2019/02/22/precht-farmhouse-modular-vertical-farms/ [18 March 2024].
18. The Farmhouse, [Online], Available: https://www.precht.at/project/001-the-farmhouse/?index=0/ [18 March 2024]
19. Stefano Boeri Architetti Combines Architecture, Agriculture, and Aesthetics in Newly Unveiled Project. [Online], Available: https://www.archdaily.com/968665/stefano-boeri-architetti-combines-architecture-agriculture-and-aesthetics-in-newly-unveiled-project?ad_campaign=normal-tag/ [18 March 2024].
20. Homefarm, [Online], Available: https://archello.com/project/homefarm/ [18 March 2024].
21. Homefarm, [Online], Available : https://www.instagram.com/sparkarchitects/reel/CyNffDhr3Eq/ [18 March 2024].
22. The Jungle House, [Online], Available: https://cplusc.com.au/project/welcome-to-the-jungle-house/ [1 December 2023].
23. USA Pavilion, [Online], Available: https://www.archdaily.com/628092/usa-pavilion-milan-expo-2015-biber-architects/ [1 December 2023].
24. EXPO Milano 2015, USA Pavilion, [Online], Available: https://www.biber.co/architecture/expo-milano-2015-usa-pavilion-1/ [1 December 2023].
25. Nowysz, A., (2022). Urban Vertical Farm–Introduction to the Subject and Discussion of Selected Examples.*Acta Scientiarum Polonorum Architectura*, 20(4): p. 93-100.
26. Urban Farming Office, [Online], Available: https://vtnarchitects.net/en/ [1 December 2023].
27. Urban Farming Office / VTN Architects, [Online], Available: https://www.archdaily.com/995655/urban-farming-office-vtn-architects/ [1 December 2023].
28. Suparwoko and B. Taufani, (2017). Urban Farming Construction Model on the Vertical Building Envelope to Support the Green Buildings Development in Sleman, Indonesia. *Procedia Engineering*, 171: p. 258-264.
29. Greenhost Eco-Friendly Boutique Hotel. [Online], Available: https://aim2flourish.com/innovations/greenhost-eco-friendly-boutique-hotel/ [1 December 2023].
30. Greenhost Boutique Hotel, Available: https://www.youtube.com/watch?v=8Is2fMKkCJA/ [1 December 2023]
31. Tampines Blk 146 Vertical Farm Successfully Grows & Harvests Made-in-S'pore Rice, [Online], Available: https://mothership.sg/2022/02/tampines-vertical-farm-rice/ [1 December 2023].
32. Urban Farming on Building Walls, [Online], Available: https://www.temasekfoundation.org.sg/programmes-r/urban-farming-on-building-walls/ [1 December 2023].
33. Steel, C., (2013). Hungry city: How food shapes our lives. *Random house*.
34. van Delden, S.H., et al., (2021). Current status and future challenges in implementing and upscaling vertical farming systems. *Nature Food*, 2(12): p. 944-956.
35. Kosorić, V., et al., (2019). Survey on the social acceptance of the productive façade concept integrating photovoltaic and farming systems in high-rise public housing blocks in Singapore. *Renewable and Sustainable Energy Reviews*, 111: p. 197-214.
36. Kumar, R., A. Fayaz, and M. Kaundal, (2023). Vertical Farming: The Future of Controlled-environment Agriculture and Food-production System. *Current Journal of Applied Science and Technology*, 42(48): p. 74-86.
37. D'Ostuni, M., et al., (2024). Understanding the complexities of Building-Integrated Agriculture. Can food shape the future built environment? Futures, 144: p. 103061.
38. Royer, H., Yengue, J. L., & Bech, N. (2023). Urban agriculture and its biodiversity: What is it and what lives in it? *Agriculture, Ecosystems & Environment,* 346, 108342.
39. Tablada, A., et al., (2020) Architectural quality of the productive façades integrating photovoltaic and vertical farming systems: Survey among experts in Singapore. Frontiers of Architectural Research, 9(2): p. 301-318.

PLEA 2024 WROCŁAW
(Re)thinking Resilience

Retrofit and Preservation of Modern Architectural Facades:
A simplified approach to sustainable transformation

BARBARA KELLY SILVA DE SOUTO [1] CLÁUDIA NAVES DAVID AMORIM [1]
JOSÉ MANOEL MORALES SÁNCHEZ [1]

[1] University of Brasília, Brasília, Brazil

ABSTRACT: Historic buildings without due official recognition of their cultural significance are likely to lose their original characteristics. This phenomenon leads to an increasing loss of the original characteristics of historic facades, especially in modern architectural structures. In the case of these buildings, it becomes even more challenging to associate renovations with sustainable strategies. In this sense, the article aims to present a simplified approach that guides energy retrofit interventions compatible with heritage preservation. In general terms, the entire evaluation process considers the influence of structural forms on facades, both on natural lighting and solar control, aiming for energy efficiency and more sustainable transformations. The obtained results are grounded in the classification of buildings using the quantitative-qualitative variable Visible Facade Value (VFV). This measure is defined as the sum of visible attributes of the facade, considering both the outlook of cultural significance attributes (CA), which identifies if the building has a relevant historical origin, and the outlook of the building's structure attributes (SA), which identifies systems and typologies of structural forms. Combined with energy efficiency variables like Window Wall Ratio (WWR), glazing type and solar control elements, this approach assists in classifying the rigor of preservation, promoting more effective approaches for interventions aimed at sustainability, energy efficiency and the conservation of architectural heritage.
KEYWORDS: Modern Architecture, Heritage Preservation, Energy Retrofit, Structural Forms, Cultural Significance

1. INTRODUCTION

The issue of sustainability in the built environment is indispensable when considering architectural preservation, given that energy and materials were expended in the construction of a building, and these resources continue to be necessary for its maintenance and lifespan. Consequently, there is a need to link preservation parameters with strategies that enhance energy efficiency, considering a range of systems that constitute the structure. This relationship implies, for instance, understanding the visible structure of a building's facade along with the systems that comprise it. Concerning the aspect of heritage preservation, historical buildings should be prioritized in the discussion, as they represent a significant part of the urban fabric in major cities worldwide, although there may be variations in urban configurations from one country to another.

Historic buildings lacking official recognition of their heritage value are vulnerable to losing their original characteristics. Unfortunately, this situation is frequently observed in the context of modern architecture [1]. In face of the increasing demands for energy efficiency and environmental quality, the concept of energy retrofit emerges as a viable solution for these structures. This process allows for the structure's system renewal, extending its lifespan and ensuring compliance with normative performance standards, becoming even more crucial when dealing with historically and culturally significant constructions. To this, it is crucial to harmonize preservation criteria with energy retrofit practices. Thus, it also requires a thorough analysis of the various systems that compose a building, considering, for example, the interconnection between the facade structure and the underlying systems. In this context, the research conducted by [3] provided a consistent case study by selecting Brasília, a city where the modernist movement is prominently consolidated [2]. Over the years, this city has witnessed a notable increase in the number of buildings that have deviated from the canonical standards of modernist architecture (Fig. 1).

Figure 1: Intervention on the facade of a building in Brasília

The direct result of this phenomenon is the proliferation of facades that have lost their distinctive characteristics. Therefore, the objective of this article is to present an approach that guide energy retrofit interventions compatible with the preservation of modern non-residential buildings, mainly considering the influence of the structural shapes of the facades. This study was part of a postgraduate dissertation that evaluated a set of methods aimed at assisting in

project decisions, particularly for addressing buildings that, despite having cultural value, are unknown and susceptible to the disfigurement of their facades [3, 4, 5]. The research adopts a qualitative-quantitative approach, precisely to interpret and analyze data from modern non-residential buildings, identifying the impact of strategies and considering attributes that can be incorporated into heritage valuation.

The main concepts addressed encompass three major research cores: (1) Heritage preservation, aiming at understanding values of significance; (2) Structure, seeking to establish common characteristics of modern architectural buildings and their facade typologies defined by visible structure; and, finally, (3) Energy retrofit, studying the impact of energy efficiency variables for envelope treatment.

Therefore, to validate this approach guiding energy retrofit interventions compatible with the preservation of modern non-residential buildings, this article presents the evaluation of four buildings located in the central zone of Brasília (Fig. 2), selected based on criteria such as the number of floors, year of construction, and the variety of structural forms of facade typologies, such as fine grid, open grid, boxed, and curtain wall [3-4].

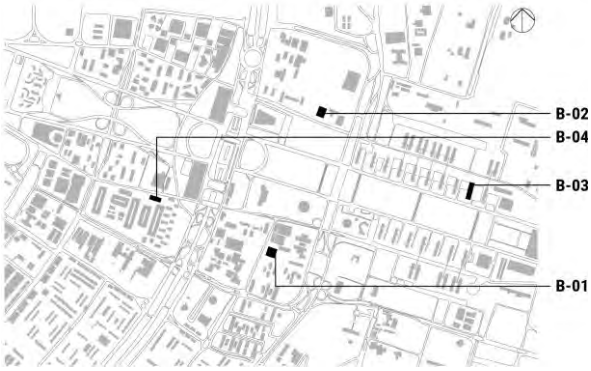

Figure 2: Map of the center of Brasília highlighting the location of the buildings selected for application of the method

2. METHOD

2.1 The proposed approach for evaluating retrofit compatible with the heritage preservation

The four-step process, outlined in Fig. 3, is described below.

Figure 3: Steps of the asset valuation method

Step 1. This involves a diverse data collection, including information such as location and layout, authorship, and year of construction, along with photographs. Geometric characteristics of the envelope and variables related to energy efficiency are also examined. Among the parameters considered are the Window Wall Ratio (WWR), solar shading elements for each facade orientation, as well as the influence of shading angles. Optical properties of glass, such as Solar Heat Gain Coefficient (SHGC), Visible Light Transmission (VLT), and Solar Absorptance (α) are also considered. Thus, the descriptions provided align with the prerequisites for calculations outlined in the INI-C manual, which considers indices tailored to the climate in Brazil [5]. It is important to mention that the method can be further adapted to other climates, including parameters according to the best energy efficiency practices for each climate.

Step 2. The evaluation of facade attributes is conducted by identifying the visible values of the building analysed from two distinct perspectives. In the first perspective, the Cultural Significance Attribute (CA) is determined through a qualitative-quantitative examination of observed parameters, such as "Origin and Authorship," by scrutinizing information like the year of construction, architectural influence, and the reputation of the design team. The second attribute, "Representativeness," considers the key features relevant to the historical, technical, or authorial context. The third parameter, "Rarity," assesses the category or typology representative of the building's generation. Finally, the fourth parameter, "Completeness," verifies the integrity of the structure. The objective of this phase is to provide "indications and probabilities" for weighing factors capable of deducing parameters of cultural significance in modern architectural buildings, based on observed characteristics on the facade, in addition to concise historical information and technical drawings [1, 7, 8, 9, 10].

The second analysis determines the Structural Attributes (SA) from the perspective of the structural forms of modern architectural facade typologies, such as structural thin grid, structural open grid, boxed, and curtain wall, as showed in Table 01 and Fig.4 [11, 4, 3, 5]. Additionally, the SA attributes encompass values for the facade system structure, where the expression of planning in the composition of facades considers the structural forms and the volumetric shape in which the volumetry and construction components of the building are analysed.

Table 1: Description of visible structural forms outlined by Siegel (1966)

Structural Form		Description
THIN GRID STRUCTURAL		The facade has only one window module between the structural supports
OPEN GRID STRUCTURAL		The facade has two or more window modules between the structural supports.
BOXED BUILDING	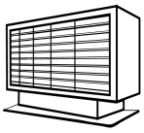	The structure is placed in front and the construction elements are equalized with a uniform external appearance. Thus, it is architecture with the demarcation of facades with a fine sense of scale.
CURTAIN WALL		These are buildings that have lower structural value, according to Siegel, but that also have strategies that highlight the building structurally.

In Fig. 4, it is noteworthy to highlight the pattern established through the study of the 32 forms identified in Siegel's definitions [3, 4, 5, and 11]. This pattern allowed for the correlation between the Window Wall Ratio (WWR) and the heritage valuation scale, which prioritizes the level of preservation of modern architectural facades [4-5].

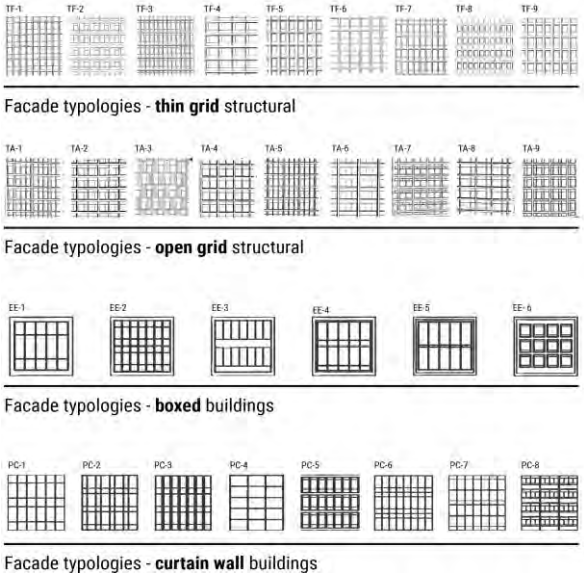

Figure 4: Facade typologies and structural forms [11]

From this parameter, according to [4], the forms with the most value to be preserved are, in decrescent order: Thin and Open Grid Structural (very high preservation rigor), Boxed (high preservation rigor) and Curtain wall (medium preservation rigor). Besides these, also the typology of glass skin was added, since is a very common one in Brasilia. This one is classified as low preservation rigor.

Step 3. The Preservation Values Declaration stage essentially involves combining the heritage valuation scale with the result of the summation of variables investigated in phases 2, CA, and SA. This is done to determine the qualitative-quantitative variable Visible Facade Value – VFV, both for the total quantity of attributes (VFV_t) and the average of the attribute summation (VFV_{avg}), as presented in Table 2 [5].

Table 2: Parameters comprising the qualitative-quantitative variable (VFV) Visible Facade Value

Variable	Parameters	Total
CA	Origin;Representativeness; Rarity; Compleness	4
SA	Clear reading; Expresses lightness; Floating plans; Floor plan defined by linear layout; concept related to the design of the structural grid; Reveals nature; Use of pilotis; Predominant openings; Brises; Ground floor; Side; Roof	12
VFV_t	SA+CA	16
VFV_{avg}	[SA+CA]/2	8

In order to balance the different number of parameters of CA and SA presented on table 2, the value of $VFV_{avg}=8$ was adopted as a boundary for the classification of the facades.

For the evaluation scale, the 09 combinations of facade forms, based on tables 1 and 2 are as follows:

- Thin grid: 25% ≤WWR≤54% and $VFV_t \geq 8$
- Open grid: 59%≤WWR≤79% and $VFV_t \geq 8$
- Boxed: 45%≤WWR≤83% and $VFV_t \geq 8$
- Curtain wall: 67%≤WWR≤84% and $VFV_t \geq 8$
- Thin grid: 25% ≤WWR≤54% and $VFV_t \leq 8$
- Open grid: 59%≤WWR≤79% and $VFV_t \leq 8$
- Curtain wall: 67%≤WWR≤84% and $VFV_t \leq 8$
- Glass skin: WWR≥80%

In figure 5, the resulting scale is showed. The level of preservation rigor is determined based on the classification of Siegel [4] and "VFV_t" result, which is relevant for prioritization when the quantity of attributes is equal to or greater than 8. This criterion is indicated by the chromatic indicator, as shows the figure 5. The color red will be assigned for very high rigor, yellow for high rigor, green for medium rigor, and blue for low rigor, depending on the obtained

result. The ranges of WWR are not constant or crescent, but they indicate the kind of interventions are necessary: very high WWR % (above 50%) without any solar protection elements (curtain wall, glass skin façades) indicates a potential low energy efficiency and comfort, asking for solar protection, glazing changes and even WWR reduction.

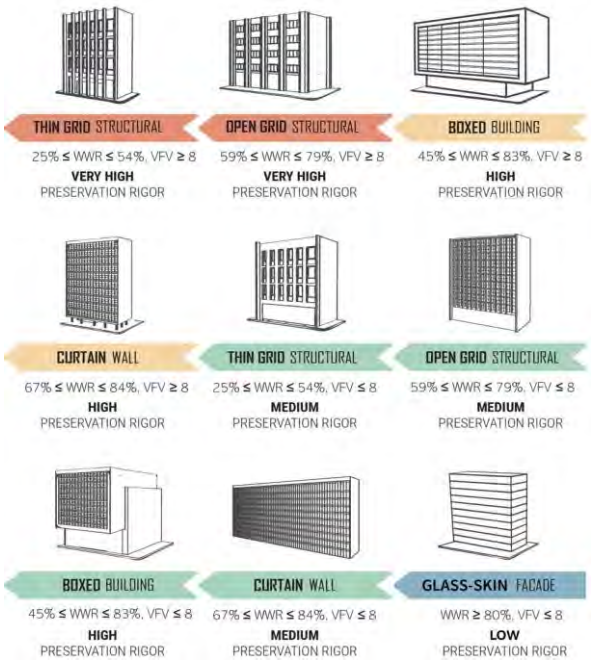

Figure 5: Scale of Valuation of Built Heritage with WWR and VFV, the last one resulting from the application of attributes of cultural significance (CA) and structure (SA)

Step 4. The project decision, representing the final phase, links the values declared in step 3 to a catalogue containing Guidelines for energy retrofit interventions. These guidelines are specifically tailored to the 9 typologies of structural forms [5], aligning with heritage preservation. In broad terms, the synthesis of the main strategies proposed in the mentioned catalogue is presented in Table 3, highlighting guidelines that vary according to the level of rigor in the intervention, encompassing both cultural and structural preservation as well as energy efficiency improvement.

Table 3: Summary of the main requirements that support retrofit and heritage preservation guidelines.

Guidelines	Main recommended requirements
Heritage preservation	a) Indication of the degree of modernization of the historical and cultural elements of the facades; b) Suggestions for replacing or restoring the construction components of the facade system
Energy Retrofit	a) Recommendation for changing the glass according to the indicated SHGC (%) b) Suggestion on combining envelope retrofit strategies c) WWR recommendation (%) for improving energy efficiency

This integrated approach aims to strike a balance between the historical value of the building and the implementation of sustainable solutions to enhance its energy efficiency.

3. RESULTS AND DISCUSSION

For the application of the proposed method, four buildings located in the central zone of Brasília's Pilot Plan were selected (Fig. 2), with data illustrated in Fig. 6, including: the building's name, image, project author, year of construction, and type of public or private use.

Figure 6: Location and data of the 4 selected buildings

The synthesis of key geometric characterization and energy efficiency variables, depicted in Fig. 7, highlights information such as the number of floors, and facade areas considering total surface and opening surface, contributing to the determination of WWR (%). In addition to these parameters, data on solar orientation, shading mask, and optical properties of the glass are included.

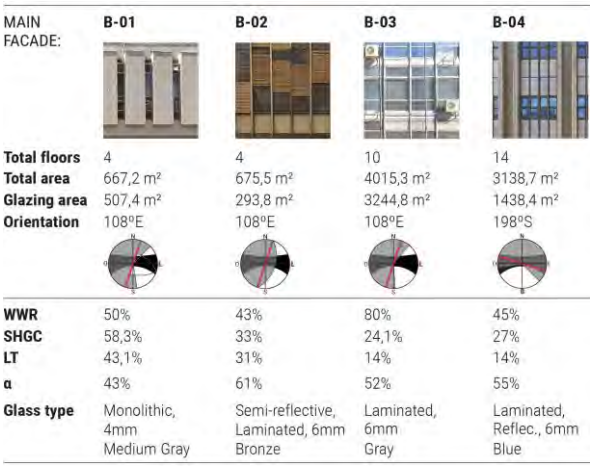

Figure 7: Summary of geometric characterization and energy efficiency variables.

3.1 Identification of Values

This section aims to present the results obtained from the representative sample, as depicted in Figure 8, allowing for the categorization of buildings into different levels on the heritage valuation scale based on the assigned weight of the Visible Façade Value (VFV). VFV_t, as showed in table 2, was calculated summing the number of attributes related to Cultural and structural Significances (CA + SA). This number is compared with the average of 8 (VFV_{avg}) to define the category of preservation.

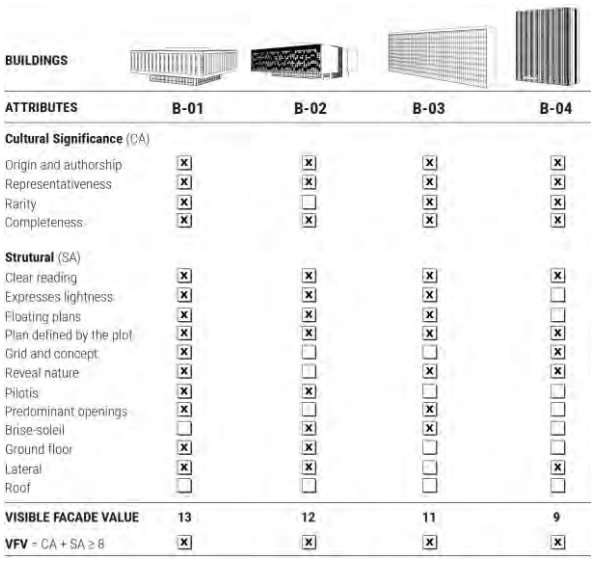

BUILDINGS	B-01	B-02	B-03	B-04
ATTRIBUTES				
Cultural Significance (CA)				
Origin and authorship	☒	☒	☒	☒
Representativeness	☒	☒	☒	☒
Rarity	☒	☐	☒	☒
Completeness	☒	☒	☒	☒
Strutural (SA)				
Clear reading	☒	☒	☒	☒
Expresses lightness	☒	☒	☒	☐
Floating plans	☒	☒	☒	☐
Plan defined by the plot	☒	☒	☒	☒
Grid and concept	☒	☐	☐	☒
Reveal nature	☒	☐	☒	☒
Pilotis	☒	☒	☐	☐
Predominant openings	☒	☐	☒	☐
Brise-soleil	☐	☒	☒	☐
Ground floor	☒	☒	☐	☐
Lateral	☒	☒	☐	☒
Roof	☐	☐	☐	☐
VISIBLE FACADE VALUE	13	12	11	9
VFV = CA + SA ≥ 8	☒	☒	☒	☒

Figure 8: Qualitative-quantitative evaluation of attributes and Visible Façade Value

Based on the conducted assessment, it is possible to determine the hierarchy of structural forms on the heritage valuation scale and emphasize the preservation rigor [4,5,11], as indicated in Figure 9.

Figure 9: Result of buildings on the heritage valuation scale

3.2 General Guidelines for Heritage-Compatible Retrofit Intervention

In the context of the general guidelines for heritage-compatible retrofit intervention, this section outlines the conclusive analysis of the last stage of the proposed method.

This phase focuses on identifying potential modifications to facades, adopting the heritage valuation method. Essentially, this segment serves as a simplified guide for decision-making, providing discernible strategies for both retrofit and preservation in a concise evaluation. Thus, the results gathered in the stage of identification of values will be integrated into the strategies outlined in the catalogue of general guidelines applicable to the nine typologies. This catalogue has been consolidated in Table 3, highlighting the key criteria to be considered.

In Fig. 10, the approach presented aims to offer a clear and cohesive view of possible interventions in buildings, aligning comprehensively with the principles of heritage preservation and energy efficiency.

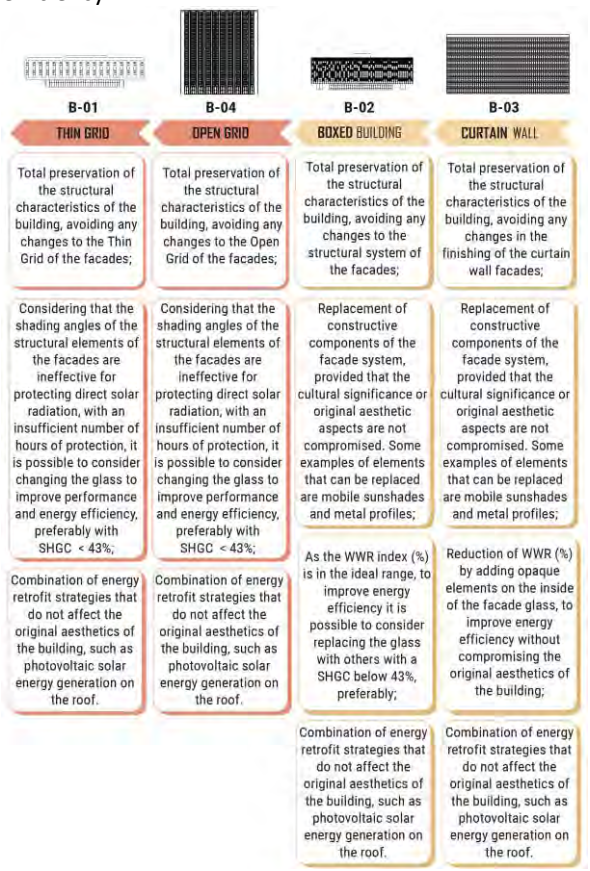

Figure 10: Result of the general intervention guidelines for buildings B-01, B-02, B-03 and B-04.

The results of this case studies show the indicated intervention guidelines, considering the preservation rigor and the best combination of energy efficiency strategies, considering the WWR, presence or absence of solar protection elements and glazing characteristics.

4. CONCLUSION

The article's findings underscore the significant influence that the building facades hold concerning the pursuit of energy efficiency. The analysis and comparison of buildings become relevant to evaluate the recommended design guidelines for facade interventions aiming to improve energy and comfort issues, but respecting the building attributes that characterize them. The combination of Structural Atributes (SA), Cultural Significance Attributes (CA), defined Visible Façade Value (VFV) that merged with energy efficiency parameter Window Wall Ratio

(WWR) resulted in a new method to define general intervention guidelines for retrofits. That is especially applicable to modern legacy buildings that do not have a specific entity to preserve their historical and cultural values. The proposed method showed to be applicable as a guide to decide the best interventions for each building model, respecting building characteristics and allowing the improvement of energy issues, leading to a more sustainable retrofit approach.

ACKNOWLEDGEMENTS

Acknowledgements for the Research Support Foundation of the Distrito Federal (FAPDF), to the National Council of Scientific and Technological Development (CNPq) and the team from the Environmental Control and Energy Efficiency Laboratory (LACAM) of the University of Brasilia.

REFERENCES

1. PRUDON, T. Preservation of modern architecture. Hoboken, N.J.: Wiley, 2008. Publications Office of the European Union, Luxembourg.

2. FICHER, S.; ACAYABA, M. M. Arquitetura moderna brasileira. São Paulo: Projeto Editores Associados Ltda., 1982.

3. AMORIM, C.N.D. (Org.); SÁNCHEZ, J.M.M; CRONEMBERGER. J.; et.al. Iluminação natural e eficiência energética: critérios para intervenção em edifícios não residenciais modernos do Plano Piloto de Brasília. Relatório Final Projeto de Pesquisa. Fundação de Apoio à Pesquisa do Distrito Federal (FAP/DF), p. 81, 2020.

4. SÁNCHEZ, J.M.M; AMORIM, C.N.D. Valuation of Modernist Envelope as Criteria for Architectural Intervention Aiming Energy Efficiency. In: Structures and Architecture, International Conference on Structures and Architecture (ICSA), Dinamarca, ISBN: 978-0-367-90281-0, ch086, p.723-730, 2022.

5. SOUTO, B.K.S. Arquitetura moderna, retrofit energético e preservação: estudo de caso em Brasília. 2023. Dissertação (Mestrado em Arquitetura e Urbanismo da Universidade) – Universidade de Brasília, Brasília, 2023.

6. INMETRO. INSTITUTO NACIONAL DE METROLOGIA, QUALIDADE E TECNOLOGIA. Portaria nº 42, de 24 de fevereiro de 2021. Instrução Normativa Inmetro para a Classificação de Eficiência Energética de Edificações Comerciais, de Serviços e Públicas (INI-C) [...]. Diário Oficial da União: seção 1, ano 159, n. 45, p. 44, junho de 2021. < https://pbeedifica.com.br/sites/default/files/INI-C_Portaria%20309%20de%202022.pdf > Acesso em: 26 dez. 2022

7. IPHAN. INSTITUTO DO PATRIMÔNIO HISTÓRICO E ARTÍSTICO NACIONAL. (2005). Manual de elaboração de projetos de preservação do patrimônio cultural. Ministério da Cultura, Instituto do Programa Monumenta. Cadernos Técnicos, Brasília. 2005.

8. SILVA, P. M. Conservar, uma questão de decisão: o julgamento na conservação da arquitetura moderna. 2012. 236 f. Tese (Doutorado em Arquitetura). Universidade Federal de Pernambuco, Recife, PE. 2012.

9. ZANCHETI, S. M.; HIDAKA, L.T.F. A Declaração de Significância de exemplares da Arquitetura Moderna. Centro de Estudos Avançados da Conservação Integrada. Textos para Discussão no. 57. Olinda, 2014.

10. RUSSELL, R.; WINKWORTH, K. Significance: a Guide to Assessing the Significance of Cultural Heritage Objects and Collections. Heritage Collections Council Australia LTD. 2º Ed. Canberra, 84 p., 2009. Disponível em: < https://dms-cf-06.dimu.org/file/022wazTV2z6e >. Acesso em 14 nov. 2022

11. SIEGEL, Curt. Formas estructurales en la arquitectura moderna. México: Continental, 1966.

PLEA 2024 WROCŁAW
(Re)thinking Resilience

The lack of green and the lack of space:
Urban redesign proposal for a consolidated area in the city of São Paulo

LUIZA SOBHIE MUÑOZ[1] DANIEL FELIPE OUTA YOSHIDA[1] BARBARA GARCIA FERREIRA[1] DENISE HELENA SILVA DUARTE[1]

[1]University of São Paulo, São Paulo, Brazil

ABSTRACT: Climate change will get worse if GHG emissions and land surface changes to make place for impervious surfaces are not controlled. Through its shading effect and evapotranspiration mechanisms, the vegetation, especially trees, can promote climate adaptation and, therefore, should be part of the entire urban fabric. However, if vegetation in new urban planning processes represents a challenge, increasing it throughout the consolidated areas is even harder. Thus, innovative strategies focus beyond those traditional places, such as parks and squares, are needed. Several cities worldwide have developed and implemented innovative policies focused on redesigning their public spaces to ensure and increase the vegetation within their urban fabrics. Thus, this work aims to develop an urban redesign proposal for a consolidated area of the city of São Paulo and asses its impacts on microclimate, at the pedestrian level. The results showed that increasing the green in a consolidated area through an urban redesign proposal is feasible, even representing a challenge for the urban design and urban planning. Moreover, for the microclimate impacts, reductions up to 1,3 °C, 21,4 °C, 25,1 °C and 11,3°C were simulated for air, surface and mean radiant temperatures and PET Index, respectively, in the proposed scenario for specific points at the pedestrian level.
KEYWORDS: Green Infrastructure, Climate Adaptation, Nature-Based Solutions, Urban Design, Climate Change

1. INTRODUCTION

Climate change is the most serious environmental challenge cities face nowadays. In the global scale, greenhouse-gases emissions are the main driver but, in the local one, anthropogenic actions like the suppression of urban greening and changings in land cover amplify climate change effects [1]. This overlap is responsible to cause the urban energy imbalance [2], the urban heating and for aggravating extreme events like flooding, landslides, droughts, and modifying precipitation patterns [3]. This is mainly because, the more impervious surfaces, the more emissions of longwave radiation are released [4] and less latent heat is available in the atmosphere [5]. The urban energy imbalance, especially, is related to some urban characteristics, such as generated heat, lack of evaporative cooling, low surface reflectivity and reabsorption of reflected radiation [6].

Therefore, vegetation, especially trees, is essential to tackle these problems, to promote climate adaptation and mitigation [7, 8], to improve thermal comfort [9, 10], and to encourage social interactions in public spaces [11]. Regarding thermal comfort, the shading and evapotranspiration effects of trees can reduce both air and surface temperatures [12] and, consequently, the mean radiant one [13]. However, the thermal performance is deeply related to tree's geometry and species [14], leaf area index and density (LAI and LAD), trees spacing [15, 9] and, mainly, the interaction between the green and the urban morphology [16, 9].

Thus, green infrastructure (GI) should integrate urban planning policies as a planning tool to make the increase and implementation of the vegetation feasible, even in densely built areas. This can be a step towards developing a green network able to fight drainage problems, temperature rise and loss of biodiversity [17, 18]. Also, ecosystem services delivered by GI help decreasing heat-related mortality and increasing the liveability in cities [10, 19]. Finally, applying GI as a planning tool means taking urban growth and built infrastructure planning into account [20].

However, increasing vegetation within consolidated areas, where generally there is a lack of space to do it, represents a challenge. To do so, innovative strategies, focusing beyond those traditional places, such as parks and squares, are needed. Remaining areas, idle ones within the blocks and parking lots represent new opportunities of land use for GI. Cities like New York [21], Hong Kong [22], Chicago [23] Glasgow [24] (Fig. 1) and Madrid [25] have developed and applied innovative strategies to redesign the consolidated urban space and increase the vegetation wherever is possible like, among other possibilities, on sidewalks, streets, idle areas, school patios and open spaces.

Thus, this work aims to develop an urban redesign proposal using innovative spatial strategies, beyond

traditional places, that enables GI in a consolidated area in the city of São Paulo, also assessing the microclimate effects in the existent and proposed situation with numerical simulation.

Figure 1: Current situation of Argyle Street, in Glasgow, and the redesign proposal. Source: Glasgow City Council, n.d.

2. MATERIAL AND METHODS

To achieve the goals, a segment of the Jornalista Roberto Marinho Avenue and its surroundings were selected (Fig. 2). This avenue is an important arterial road, close to the Sao Paulo expanded downtown presents an intense and heavy traffic of vehicles during most part of the day and large areas are covered by asphalt and concrete. Also, the selection is due to urban obstacles, such as a new elevated monorail system and an open channelled stream by this avenue.

Figure 2: The selected study area. Retrieved from Google.

Due to the monorail, new users came to the area, bringing an intense flux of pedestrians and cyclists, deserving climate amenities, currently inexistent. Regarding its surroundings, the area is mainly residential.

2.1 The redesign proposal

To develop the redesign, a wide range of strategies were applied. These strategies result from a systematization of urban instruments and public policies focused on increasing the vegetation within consolidated public areas. For this, the proposal considered the dimension of sidewalks, streets, pre-existent cycle lanes, existent vegetation, although scarce, road fluxes and patterns of use of the spaces, supported by current standards of the city of São Paulo [26, 27].

The current situation and the proposed urban design were developed on AutoCAD®. To do so, a satellite image of the area from Google Maps, and a DWG of the blocks from GEOSAMPA[1] were used as a base layer for the drawings. After that, images representing the urban interventions were post-processed on Adobe Photoshop®.

[1] GEOSAMPA, the São Paulo GIS database. Available at: https://geosampa.prefeitura.sp.gov.br/PaginasPublicas/_SBC.aspx#

2.2 Modelling the scenarios and vegetation data

The modelling phase was developed on Monde, for both scenarios, as part of ENVI-met model. Thus, it was possible to define the area, to model the volumes and surfaces and to apply the surface materials. For both current and proposed scenarios, concrete and asphalt were specified, specifically for the city of São Paulo as well as the most common building components for facades and roofs in the city [28]. The soil profile, a sandy clay loam one, was based on a previous work [29], as well as the street trees [30], both developed in the same research group.

These trees were modelled on Albero, the editable database on ENVI-met model, according to a very common tree species, Sibipiruna, following the Technical Manual of Urban Arborization, published by the São Paulo Department of Green and Environment (SVMA) of the city of São Paulo. In this context, the trees presented 15m high, a crown with 9m of diameter and 1 m^2/m^3 of leaf area density (LAD), which is equivalent to an adult and large typical tree in São Paulo [31].

2.3 Climate data, general properties, and the Thermal Comfort Index: PET (Physiological Equivalent Temperature)

Full forcing climate data were used for current and proposed situations. This data was developed

based on a previous work which registered on-site microclimate data in April 2016 and 2018, during hot periods [32]. The thermal comfort index PET [33] can be calculated on ENVI-met through the BIO-met plug-in by defining some parameters. In this work, the parameters were set as follows on Table 1. It is important to highlight that a light clothing value was considered for the static clothing parameter and an activity such as walking was considered for the metabolism one. The main details and input configuration can be seen on Table 1.

Table 1: Input parameters on ENVI-met

General Inputs	
Start day	03/04/2016
Wind speed in 10m above ground	1m/s
Specific humidity in 2500m (g water/kg air)	8
Simulation duration	24 hrs
Start hour	05:00
Ending hour	04:59
Telescoping	7%
Simulation Resolution	3m
Soil humidity (upper layer 0-20 cm)	65
Soil humidity (middle layer 20-50 cm)	70
Soil humidity (lower layer 50-200 cm)	75
Soil humidity (bedrock layer below 200 cm)	75
Soil initial temp. (upper layer 0-20 cm)	20 °C
Soil initial temp. (middle layer 20-50 cm)	20 °C
Soil initial temp. (lower layer 50-200 cm)	19 °C
Soil init. temp. (bedrock layer below 200 cm)	18 °C
BIO-met inputs	
Age	35
Weight	70 kg
Height	170 cm
Gender	Male
Static clothing Insulation	0.5
Sum metabolic work	130 W

3. RESULTS AND DISCUSSION

3.1 The redesign proposal

The main concern of this proposal was to redesign the urban space of the study area and its elements to increase the vegetation. Without spatial possibilities for green squares and pocket parks, this proposal was based on reorganizing the space, mainly focused on unveiling urban design possibilities to find space for vegetation in a consolidated urban area. To do so, some strategies were applied, which can be classified into four main categories: (i) depaving, when impervious surfaces were replaced by vegetated ones; (ii) reorganization of the street, which involved replacing, moving and modifying its elements; (iii) reactivation of idle areas, bringing life and social interaction possibilities to these places; (iv) planting trees wherever it was possible. A summary of the proposal can be seen in Figure 3.

The urban design interventions were made by understanding the pedestrian fluxes and the cycle lane routes. Currently, there are cycle lanes on both sides of the avenue, which are not protected from the vehicles. Regarding the pedestrian paths, they are shaded in some areas and completely exposed in others. For microclimate and drainage purposes, depaving strategies were considered a priority, therefore most of impervious surfaces were converted into vegetated ones, especially some sidewalk segments. These changes included implementing rain gardens and other permeable surfaces. For the latter case, those surfaces were combined with trees, implemented at every 9 meters, to ensure a shaded path for the pedestrians.

As identified by numbers 1 and 2 (Fig. 3), the existent cycle lanes were removed and a new and bidirectional one was proposed. Also, a garden bed, identified by number 3 in the same figure, was added as part of the depaving strategy. This garden bed could not only create space for increasing the vegetation and improve the landscape but also increase the security for the cyclists. More details about all these elements implemented – rain gardens, cycle lanes, and permeable surfaces – can be found in the schematic drawing available on Figure 4. Also, an image representing the current situation can be seen (Fig. 4), for comparison between the current situation and the proposed one.

Reorganizing the street elements was carried out mainly through extending the width of elements such as garden beds, and sidewalks. For the first case, both garden beds located at the centre of the avenue and at some edges of sidewalks, as shown in numbers 5 and 7, respectively, were extended over the road, therefore, trees and lawns could be proposed. To make this redesign possible in this avenue, a car lane was supressed, action identified by number 4 (Fig. 3). For the sidewalks, some of them were also extended in width over roads, therefore, rain gardens and permeable surfaces were included, as represented by number 6 (Fig. 3).

The extension of the width of some sidewalks in crossing areas was also proposed in number 8, but more focused on creating bicycle parking areas and paths for the pedestrians. For the latter, this strategy was associated with the implementation of permeable paving. Number 9 (Fig. 3) shows the raised crosswalks, proposed to improve the pedestrians' security.

Finally, some shared streets – one within the block and the other parallel to the avenue – were proposed. These areas are currently idle and paved with asphalt, being used only as parking spaces. Thus, to improve its role under the environmental and social perspectives within the urban fabric, permeable pavements were proposed as well as trees. Urban furniture and other elements that support social use could be also implemented in these areas, and cars could circulate in a lower speed, only to access the households. Some wooden decks

could be implemented in areas that are currently green, but in which there is a lack of urban elements that support social life and gathering providing a more comfortable outdoor experience.

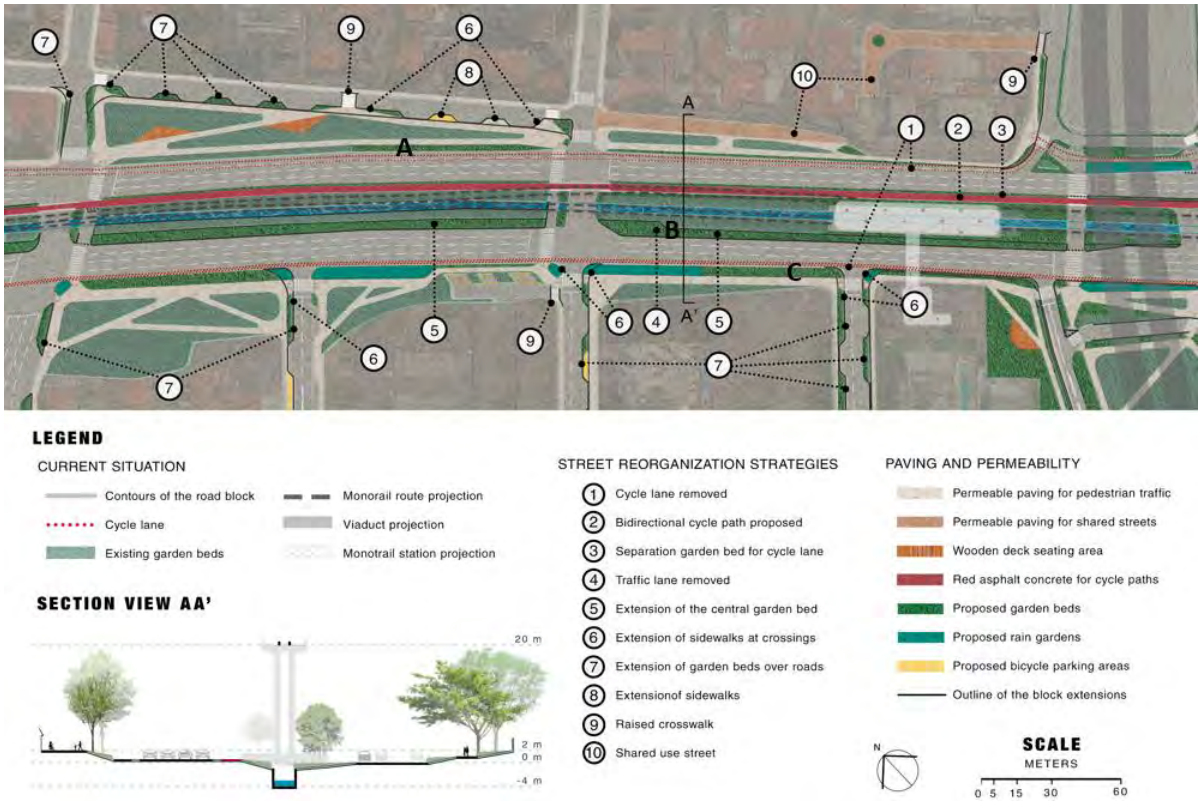

Figure 3: The general redesign proposal and the strategies applied.

Figure 4: Details of the proposal in Section A-A'and the current situation. Image retrieved from Google Maps.

3.2 The impacts on microclimate

The microclimate impact of these proposals for the users of the avenue and its surroundings was assessed quantifying the cooling effect. The hottest period of the day was registered at 2 p.m. for all the variables – air, mean radiant and surface temperatures for both current and proposed situations. The maximum difference between these situations for surface temperature and PET Index

were registered at 2 p.m., while for the others it happened at 3 p.m.

The effects of vegetation on the amelioration of the microclimate and comfort variables analysed are clear. In Fig. 5 is possible to observe the maximum difference between both situations for all the variables and PET Index, which highlights the effects of evapotranspiration and shading. To better understand these impacts at the pedestrian level, some targeted points in the scenarios were analysed (Fig. 3).

Points A and C are placed on sidewalks where, originally, there were no trees and lawns, while point B is placed on a proposed vegetated surface, originally paved with asphalt. In the hottest period, the points A, B and C showed a reduction up to 1,2 °C, 1,1 °C and 1,3 °C for the air temperature in the proposed situation, respectively. For the mean radiant temperature, also during the hottest period of the day, these points showed a reduction up to 22,7 °C, 17,7 °C and 25,1 °C, respectively, in the proposed scenario. For surface temperature, these reductions were up to 19,2 °C, 21,4 °C and 20,8 °C. Finally, for the PET Index, reductions up to 10,1 °C, 10,7 °C and 11,3 °C were registered for the same points, respectively. Although the reductions are notably, the thermal perception rating remained very hot, which means extreme heat stress.

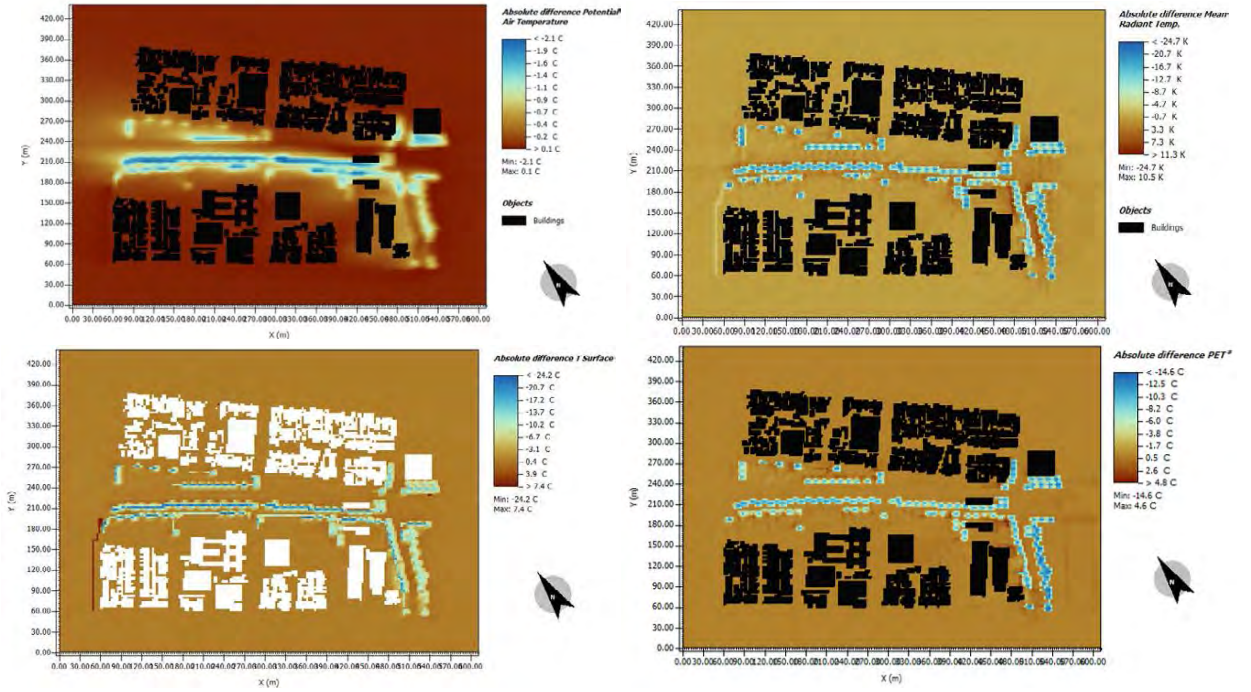

Figure 5: The difference between the situations for all the microclimate variables and PET Index at the hottest period of the day (2p.m. for surface temperature and PET Index and 3p.m. for the others.

4. CONCLUSION

Vegetation is essential to ameliorate the urban microclimate, reducing the land surface temperature, mitigating urban heating, and allowing the rainwater infiltration. In this sense, GI must be included in urban planning and design, even in consolidated areas, either along the streets or within the blocks, taking advantage of small and less conventional spaces for green areas. Thus, innovative urban design strategies are important and were proposed as a showcase for a consolidated area in the city of São Paulo, in which new users were attracted by the monorail, pedestrians and cyclists mainly, currently experiencing a hostile environment, without any microclimate amenity. More than this, proposals like this can be replicated to other similar areas throughout the city. The results showed that these interventions are challenging, but feasible, and that they can improve thermal comfort at the pedestrian level, given the reductions of up to 1,3 °C, 21,4 °C, 25,1 °C and 11,3 °C in air, surface and mean radiant temperatures and PET Index registered in the simulations, respectively, for specific points at the pedestrian level.

ACKNOWLEDGEMENTS

This research was supported by São Paulo Research Foundation (FAPESP) - grants #2021/04751-7, #2023/03279-8, # 2022/08401-3 and #2021/11762-5 and by the National Council for Scientific and Technological Development (CNPq) - grant #312592/2021-3 and PIBIC #2022-1178.

REFERENCES

1. IPCC (INTERGOVERNMENTAL PAINEL ON CLIMATE CHANGE), (2021). Climate Change 2021: The Physical Science Basis. *IPCC Working Group I Contribution to AR6,*

[Online], Available: < https://www.ipcc.ch/report/ar6/wg1/>, [10 set, 2021].
2. OKE, T. et al. (2017). *Urban Climates*. Cambridge: University Press.
3. Un Environment Programme (UNEP), (2020). Adaptation Gap Report 2020. *United Nations Environment Programme*, [Online], Available: https://www.unep.org/adaptation-gap-report-2020, [13, Mar, 2021].
4. Stone, B. Jr. (2012). *The City and the Coming Climate: Climate Change in the Places We Live*. Cambridge University Press.
5. Erell, E., Pearlmutter, D. & Williamson, T. (2011). *Urban microclimate - designing the spaces between buildings*. Earthscan.
6. Duarte, D. H. S. (2016). Vegetation and climate-sensitive public places. In: Emmanuel, R (Ed.). *Urban Climate Challenges in the Tropics: Rethinking Planning and Design Opportunities* (p. 111-162). Imperial College Press.
7. Barreira, A. P. et al. (2023). Perceptions and preferences of urban residents for green infrastructure to help cities adapt to climate change threats. *Cities*, 141.
8. Yu, Z. et al. (2017). How can urban green spaces be planned for climate adaptation in subtropical cities? *Ecological Indicators*, 82, 152–162.
9. Ouyang, W. et al. (2023). How to quantify the cooling effects of green infrastructure strategies from a spatio-temporal perspective: Experience from a parametric study. *Landscape and Urban Planning,* 237: p. 104808.
10. Santamouris, M. and Osmond, P. (2020). Increasing Green Infrastructure in Cities: Impact on Ambient Temperature, Air Quality and Heat-Related Mortality and Morbidity. *Buildings,* 10: p. 1-34.
11. NG, E. et al. (2012). A study on the cooling effects of greening in a high-density city: An experience from Hong Kong. *Building and Environment*, 47: p. 256 – 271.
12. Coutts, A., and Tapper, N. (2017). Trees for a Cool City: Guidelines for optimised tree placement. *Cooperative Research Centre for Water Sensitive Cities*, 25.
13. Erell, E. (2017). *Urban Greening and Microclimate Modification*. In: Tan, P., Jim, C. (Eds) Greening Cities. Advances in 21st Century Human Settlements (p. 73-93). Springer, Singapore.
14. Morakinyo, T. E. et al. (2018). Performance of Hong Kong's common trees species for outdoor temperature regulation, thermal comfort and energy saving. *Building and Environment*, 137, 157–170.
15. Lai, D. et al. (2023). Effects of different tree layouts on outdoor thermal comfort of green space in summer Shanghai. *Urban Climate*, 47.
16. Lau, K. et al. (2022). Urban Greening Strategies for Enhancing Outdoor Thermal Comfort. In *Outdoor Thermal Comfort in Urban Environment: Assessments and Applications in Urban Planning and Design* (pp. 85–100). Springer.
17. Intergovernmental Panel on Climate Change, I. (2022). *Climate Change 2022: Impacts, Adaptation and Vulnerability.*
18. UK GBC, U. G. B. C. (2022). *The Value of Urban Nature-Based Solutions.*
19. Norton, B. A. et al. (2015). Planning for cooler cities: A framework to prioritise green infrastructure to mitigate high temperatures in urban landscapes. *Landscape and Urban Planning*, 134, 127–138.
20. Benedict, M., A. and McMahon, E. (2002). Green Infrastructure: Smart Conservation for the 21st Century. *Renewable Resources Journal,* 20: p. 12-17.
21. City of New York, (2021). NYC Plaza Program: application guidelines. *New York City Department of Transportation,* [Online], Available: https://www.nyc.gov/html/dot/downloads/pdf/nyc-plaza-program-guidelines.pdf, [20 Dez, 2021].
22. Civil Engineering and Development Department (CEDD), (2019). Greening Master Plan. *Topics in Focus,* [Online], Available: https://www.cedd.gov.hk/eng/topics-in-focus/index-id-2.html, [10 ago, 2020].
23. Center for Neighborhood Technology. (2016). *RainReady Midlothian: Plan*, [Online], Available: https://cnt.org/publications/rainready-midlothian-plan
24. Glasgow City Council. (n.d.). Avenues. Overview. Retrieved August 1, 2023, from https://www.glasgow.gov.uk/avenues.
25. Ayuntamiento de Madrid. (2023). *Manual de Soluciones Basadas en la Naturaleza: Fomento de Biodiversidad en la Ciudad de Madrid.* Ayuntamiento de Madrid and ARUP. (2019). *Madrid + Natural.*
26. São Paulo, (2020). Decreto Nº 59.671, de 7 de agosto de 2020. *Diário Oficial da Cidade de São Paulo, 08 de agosto de 2020, p.3,* [Online], Available: https://legislacao.prefeitura.sp.gov.br/leis/decreto-59671-de-7-de-agosto-de-2020, [10, Aug, 2023].
27. São Paulo, (2021). Manual de Desenho Urbano e Obras Viárias. *Prefeitura Municipal de São Paulo,* [Online], Available: https://manualurbano.prefeitura.sp.gov.br/manual, [17, Aug, 2023].
28. Gusson, C. S. et al. (2020). Impact of Built Density and Surface Materials on Urban Microclimate for Sao Paulo, Brazil: Simulation of Different Scenarios Using ENVI-met Full Forcing Tool. Planning Post Carbon Cities: 35th PLEA Conference on Passive and Low Energy Architecture, A Coruña, 1st-3rd September 2020: Proceedings, Vol. 1, 2020 (Technical Articles), ISBN 978-84-9749-794-7, p. 818-823.
29. Shinzato, P. (2014). *Impacto da vegetação nos microclimas urbanos em função das interações solo-vegetação-atmosfera*. São Paulo: FAUUSP, 2014. Tese (Doutorado em Arquitetura e Urbanismo) Faculdade de Arquitetura e Urbanismo, Universidade de São Paulo.
30. Yoshida, D. F. O. et al, (2022). The microclimate effects of urban green infrastructure under RCP 8.5 projection and plant vitality. Will plants be enough? Will Cities Survive?: 36th PLEA Conference on Passive and Low Energy Architecture, Santiago 22nd-25th November 2022 Proceedings, Vol. 1, 2022, p. 308-313.
31. Yoshida, D., F. O., and Muñoz, L., S. (2023). Plant's health and microclimate in a warming world, [Online], Available: https://www.researchgate.net/publication/376186115_Plant's_health_and_microclimate_in_a_warming_world
32. Shinzato, P. et al, (2019). Calibration process and parametrization of tropical plants using ENVI-met V4 – Sao Paulo case study, *Architectural Science Review*, 62, 112-125.
33. HÖPPE, P. The physiological equivalent temperature – A universal index for the biometeorological assessment of the thermal environment. International *Journal of Biometeorology*, 43, p. 71–75, 1999.

PLEA 2024 WROCŁAW
(Re)thinking Resilience

Assessment of Indicators for Resilience of Heritage Structures:

Case Study of Havelis in Lucknow

ANAM AMJAD[1] AMANJEET KAUR[1]

[1]National Institute of Technology, Hamirpur, India

ABSTRACT: Resilience in the context of heritage structures is a crucial and multifaceted concept. Heritage sites around the world face numerous challenges, such as natural disasters, urbanization, and climate change. Preserving these sites is essential for cultural continuity, socio-economic development, and sustainable urban planning. While previous research has made progress in understanding heritage resilience, there's a need for a comprehensive understanding of the various indicators and their impact on resilience. This study aims to fill this research gap by exploring how different factors can enhance the resilience of heritage structures. The main goal is to create a holistic framework that incorporates all identified indicators and test the framework in the heritage havelis of Lucknow. The analysis assesses the influence of different indicators on heritage structure resilience and suggests practical preservation and development strategies. This not only promotes the preservation of these invaluable heritage sites but also supports the development of effective policies and strategies, contributing to a more sustainable urban landscape.

KEYWORDS: Heritage Resilience, Indicators, Literature Review, PRISMA, Qualitative Content Analysis

1. INTRODUCTION

Heritage, for any country, embodies its history, traditions, culture, and artistic impression acting as a thread that connects past, present, and future generations. “Historic buildings keep collective memories alive, strengthening collective solidarity to achieve enduring goals related to the three classic pillars of sustainability in society, economy, and environment”. Besides preserving the identity of a place, it acts as a magnet for tourists - encouraging economic opportunities, providing educational resources, promoting social cohesion, and supporting sustainable urban development. Due to its inherent sustainability, the cultural heritage sector requires comprehensive frameworks and perspectives to address its challenges effectively during any intervention in historical buildings, which involves various actions like preservation, conservation, maintenance, repair, refurbishment, rehabilitation, renovation, and restoration, and is, therefore, crucial to develop tangible strategies and approaches [1].

The resilience of heritage structures refers to their ability to withstand challenges while preserving their cultural, historical, and physical integrity. According to Folke et al. 2010, “Resilience may be defined as the capability of a system or process to absorb disturbance” [2].

The significance of preserving cultural heritage and passing it on as a means to create inclusive, secure, resilient, and sustainable cities and human settlements is an integral component of both the UN Agenda 2030 and the international policy on Disaster Risk Reduction for the year 2015-2030. Nonetheless, the role of culture in addressing these crucial challenges remains an aspect that has not received adequate attention in the current scientific literature on resilience [3].

This research aims to delve into the various factors that contribute to the resilience of heritage places. By examining these indicators, one can gain insights into how communities, institutions, and economic activities impact the ability of heritage places to thrive amidst changing circumstances. The suggested framework is then further tested in the heritage homes of Lucknow.

2. LITERATURE REVIEW

The literature review undertaken reveals that diverse studies emphasize various parameters and indicators when assessing the resilience of heritage buildings, underscoring the necessity for a comprehensive framework that integrates these diverse factors. This will allow for a holistic understanding of their collective impact across different situations.

2.1 Previous Research

A significant body of literature has emerged, aiming not only to understand vulnerabilities in cultural heritage but also to propose strategies for enhancing resilience against various disturbances [4].

The concepts of risk and resilience have become increasingly relevant to cultural heritage, especially archaeological sites and monuments, which are

perceived as vulnerable to various risks, including deliberate destruction in armed conflicts. Simultaneously, there is a growing consensus on the need to conserve cultural heritage as a resource for fostering cultural resilience, reducing disaster risk, and promoting peace and reconciliation [2].

As the concept of Community Resilience has evolved, scholars have noted significant advancements in urban planning. According to Mulligan, this evolution effectively merges community dynamics and resilience within the intricate social-ecological system, particularly in the context of urban environments [3]. This understanding delves deeper into socio-ecological systems and the cultural and political aspects of the community.

Recognizing the importance of sustainable tourism development, a separate investigation presents an evaluation system to assess the resilience of cultural heritage sites. This system comprises three primary sub-systems: socio-cultural, economic, and ecological aspects [5].

Efforts to preserve built heritage can boost local identity and recognition and act as catalysts for economic benefits from adaptive reuse projects. These economic incentives can also influence socio-cultural aspects and public relationships [6].

In a distinct research endeavour, a best practice research methodology is applied to investigate cultural heritage resilience in historical areas, based on the codification and analysis of good practices collected from EU-funded projects [7].

Another examination introduces a comprehensive approach to managing energy retrofit transformations and preservation efforts in historical districts, using the principles of "resilience thinking" [8].

Similar studies, such as the one in New Zealand [9], examine existing policies and practices related to retrofitting historic buildings to identify current obstacles, difficulties, and potential energy retrofitting strategies, including seismic upgrading.

Another investigation contributes to the discussion of the role of knowledge and practices in preventing and recovering from risks in heritage preservation and community-based disaster management [10].

2.2 Methodology for Review

To accomplish the specified objective, the study encompasses a review of relevant documents, journal papers, and websites that explore various indicators. After searching the literature, Qualitative Content Analysis (QCA) is employed to identify various indicators with various dimensions, that impact heritage resilience, as shown in Fig. 2.

A systematic review using the PRISMA guidelines (Preferred Reporting Items for Systematic Reviews and Meta-Analyses) was conducted. The literature selection process began with a search on Google Scholar and then expanding the sources to include Web of Science and The Lens. This initial search yielded a total of 7829 total records. After removing 57 duplicate records, the research was focused on full-text, peer-reviewed articles within a time frame of 2013-2023, resulting in 460 articles for a more in-depth systematic review. From these, studies with a similar field of study were considered eligible, leading to the inclusion of 139 references in the QCA.

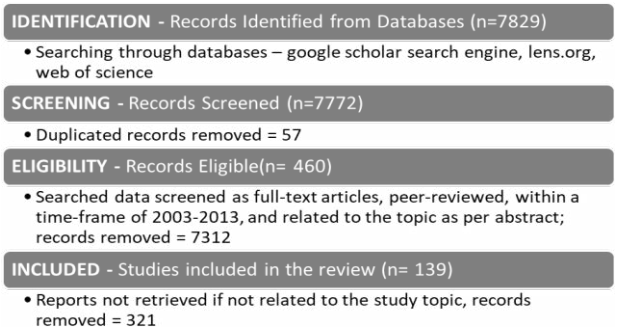

Figure 1: PRISMA flow diagram of systematic literature search

2.3 Analysis of the Literature

From the literature, 12 key indicators were identified and grouped into four resilience themes based on a study of cultural heritage and community resilience in volcanic disaster regions [4] for Qualitative Content Analysis (QCA). The framework encompasses four fundamental themes: social, economic, institutional, and infrastructure (Fig. 3).

INDICATORS IMPACTING RESILIENCE OF HERITAGE BUILDINGS		
THEMES	**INDICATORS**	**COUNT IN PAPERS REVIEWED**
SOCIAL	Cultural Vulnerability	39
	Community Resilience	30
ECONOMIC	Economic - Funding and Resources	14
INSTITUTION	Political	1
	Policy and Legal Frameworks	22
	Stakeholders	11
	Tourism	15
INFRA-STRUCTURE	Adaptive Capacity	28
	Hazard Exposure	40
	Energy and Resource Efficiency	5
	Urban Regeneration	9
	Climate Change	38

Figure 2: Indicators identified in the literature review

Figure 3: Indicators Explained

Analysis reveals that natural risks and climate change-induced structural degradation are prime factors impacting resilience. Cultural practices, community roles, and stakeholder involvement also influence survival. Adaptive capacity through facade change, function alteration, and retrofitting extends building life and utility. These indicators interact differently across heritage sites, demanding context-aware policies for balanced city development while preserving heritage.

3. STUDY AREA

Lucknow, situated along the river Gomti, is the capital and largest city of Uttar Pradesh, India. It has been a multicultural city, going through different rulers like the Hindus, Mughals, Nawabs, and then the British, leaving an overall impact on the city's architecture, characterized by monuments, old neighbourhoods, and commercial markets.

Due to its rich history, the city is adorned with magnificent structures and has influenced its lifestyle, cuisine, art, and craft traditions. While many monuments are protected by National and State initiatives, there are also forgotten places that hold significance in the city's narrative. Preserving these places and making them resilient against the test of time is equally important.

3.1 Old Houses of Lucknow

They can be split into two kinds based on the socio-economic status of the inhabitants. The first kind consists of kothis, havelis, and palaces, which were built by the Nawabs and their courtiers showcasing impressive architecture. The second type of house was owned by middle-income folks [11].

Spatial Layout - Houses were designed with inward-facing layouts, featuring one or multiple square courtyards. The larger courtyard, accessible from outside streets, was designated for men's quarters (Mardana), while the smaller courtyard, accessed through the men's courtyard, served as the women's quarters (Zenana). These courtyards facilitated natural ventilation, provided private spaces conforming to social norms, and were central to family activities [12].

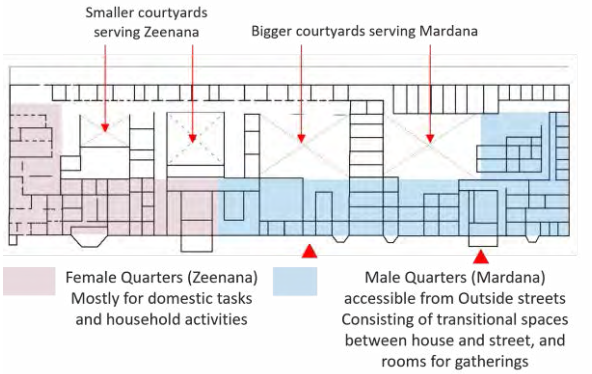

Figure 4: General Layout of the Havelis

Structural Details and Building Materials – The havelis were generally cuboidal in shape with varying lengths and widths and spanning two to three floors in height. Commonly used materials were lakhauri bricks and lime, with roofs made of timber joists or jack arches. The thick load-bearing masonry walls (45-90 cm) had a rough or lime and stucco plaster finish. Doors and windows were made of wood and dressed with lime mortar mouldings [11] [13].

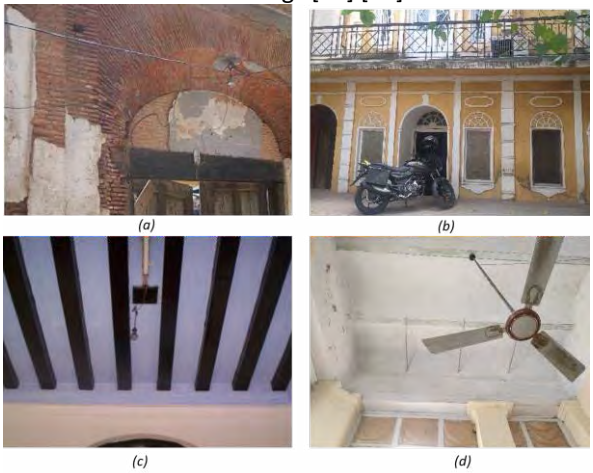

Figure 5: (a- Masonry wall of Lakhauri Bricks [11], b- Windows with lime mortar mouldings, c- Roof made of Timber Beams [11], d – Vaulted Ceiling Roof)

Common Architectural Elements – These houses showcased a distinctive architectural style characterized by stucco work (showcasing motifs and floral patterns), columns embedded on walls, timber doors with semicircular fanlights, semicircular arches, multiple entrances on facades, and decorative cornices.

Figure 6:(a- Timber door with semi-circular fanlights, b- Semi-circular arches and multiple entrances on the façade, c- Columns embedded on walls, d – Stucco work)

4. CASE STUDY

For the understanding three havelis have been discussed in this study, taking into consideration that the design and the basic layout of all Nawabi havelis are similar, but their current uses can be different, depending on the size or the status of the inhabitants.

4.1 Salempur House, Qaiserbagh

This ancient haveli is a part of the Qaiserbagh Complex, built during the reign of the last ruler of Awadh, Nawab Wajid Ali Shah. Constructed in 1847, it was once the residence of the Nawab's wife, later awarded to Raja Nawab Ali Khan, the taluqdar of Salempur.

Planning and Spaces - The ground floor consists of guest bedrooms with en-suite bathrooms, while the first floor consists of various rooms in front meant for gatherings. One spacious chamber, panelled in Burma teak, served as a dining room where lavish banquets were hosted. A particular room, initially a billiard room, remains unchanged, showcasing cusped arches adorned with columns and intricate floral, leaf, and vine motifs painted in pink, green, and white and a Dhani roof crowned with a skylight [14]. The rear section houses capacious rooms, now used as bedrooms with expansive terraces.

Present Use - The haveli is not commercially active to ensure privacy. Instead, some rooms along with the lawn serve as a venue for cultural activities and literary festivals, lectures, and competitions, promoting Awadh culture.

Figure 7: Salempur House (a- Outer Facade, b- Meeting room panelled in Burma Teak, c- Corridors on the first floor, d – Unchanged Billiard room)

4.2 Iqbal Lari Manzil, Mashakganj

Situated close to Lucknow's City Railway Station, this house constructed in 1928 boasts a large, old gate adorned in white and green paint.

With two gates, one leading to the upper floor mardana section and the other to the ground floor zenana, the latter now serves as the main entry to the house, adorned with intricate stucco decorations. The zenana provides direct access to the family's private ground floor imambara. Within the zenana, a stairway ascends to the upper floors unveiling a vast terrace. A corridor connects the terrace to the mardana living quarters, where the verandah, once a traditional space has transformed into a dining room, adapting to the family's changing needs.

Present Use - The owner rents out a part of the palace for film shoots and plans to offer some rooms to tourists curious about Lucknow's history. A school occupies the downstairs to maintain the property. The garden once used for gatherings is now a commercial parking area.

Figure 8: Iqbal Lari Manzil (a- Main Gate with the school board, b- Imambara, c- Verandah converted into Dining Room, d – Garden converted into commercial parking)

4.3 Mahmudabad House, Qaiserbagh

This house in the Qaiserbagh Complex was assigned to Raja Mahmudabad after the revolt of 1857, and his family still lives there, maintaining its original appearance.

This house features spacious courtyards which were the main centres of activity. The larger front rooms served as gathering spaces during both the Nawabi and British eras, hosting social events. In the contemporary context, these rooms maintain their hospitality function. Meanwhile, the upper floor now accommodates the family, whereas servant quarters at the rear persist in their historical role. The Haveli has lots of open spaces, in the form of multiple courtyards as well as large gardens out in front.

Present Use - The primary emphasis of the owner lies in preserving the authentic features of the house. The distinct yellow walls and green doors of Qaiserbagh are diligently maintained to uphold their original aesthetic. Furthermore, significant attention is dedicated to the conservation of fixtures such as the boiler, Victorian-era basin, shower, and bathtub, with concerted efforts aimed at their preservation, including the retention of vintage electrical switches and regulators. Although public activities are not a regular occurrence, certain spaces are sometimes utilized for film screenings, thereby ensuring the continual vibrancy and vitality of the place.

Figure 9: Mahmudabad House (a- Outer Facade, b- Drawing room on the Ground Floor, c- Vintage electric fixtures and Boiler, d – Courtyard)

5. ANALYSIS

Through comprehensive site visits and interviews conducted with owners and relevant stakeholders, a thorough analysis of the data collected was done. The objective was to gain insights into the initiatives taken to ensure the utilization of these structures. This helped in further analysis within the proposed framework, providing an understanding of how various indicators contributed to their continued use. The findings offered insights to suggest further interventions that can be implemented to increase the resilience of these structures.

Based on inputs from owners and stakeholders, various challenges hindering heritage resilience were identified. These ranged from multiple ownership, where not all owners might prioritize preservation, to private ownership with reduced government interventions, financial constraints due to high preservation costs, and sometimes a lack of pride in heritage. Identifying these hurdles and suggesting interventions tailored to them could increase resilience.

The previously discussed framework outlines indicators influencing the resilience of heritage structures to varying degrees. Analysis of Lucknow's havelis revealed how these factors interact, drawing insights from 30 experts and stakeholders involved with these buildings, and ranking factors accordingly.

INDICATORS IMPACTING RESILIENCE OF HAVELIS IN LUCKNOW		
THEMES	**INDICATORS**	**RANKING**
SOCIAL	Cultural Vulnerability	7
	Community Resilience	5
ECONOMIC	Economic - Funding and Resources	4
INSTITUTION	Political	9
	Policy and Legal Frameworks	11
	Stakeholders	8
	Tourism	3
INFRA-STRUCTURE	Adaptive Capacity	1
	Hazard Exposure	2
	Energy and Resource Efficiency	10
	Urban Regeneration	6
	Climate Change	12

Figure 10: Ranking of different indicators in the Case Study

The ranking highlights key factors in creating resilience: Adaptive capacity, Hazard Exposure, Tourism, Funding and resources, and Community resilience. Adaptive capacity ensures different and new uses for the old buildings; hazard exposure expresses the need to preserve buildings from natural hazards and decay, while tourism enhances relevance and resource generation, which also increases the value of the place for the people. The analysis reveals working on these five indicators would have the most impact on resilience. These indicators also exhibit interconnectedness. For example, tourism impacts funding and resource allocation, policy and legal frameworks can alter stakeholder involvement, and

the adaptive reuse of old houses contributes to urban regeneration.

Although policy and legal frameworks appear inconsequential for heritage resilience in the case of expert opinion, case studies revealed their potential significance. Tailoring policies such as offering restoration subsidies, and government agreements with owners for unused spaces will incentivize owners to preserve these houses. In the absence of government support, owners of historic houses strive to preserve them, doing the best they can. Initiatives like cultural activities at Salempur House foster community engagement, sharing the legacy and promoting Awadh culture. Allowing filmmaking in certain spaces helps maintain the houses' original glory, serving as tangible links to the past and offering insight into bygone eras. However, with nuclear families and individuals relocating, these houses face challenges due to few occupants. Establishing a school in Lari Manzil aids in upkeep and benefits the community. Support from the government as well as from the surrounding community would encourage the owners for better repurposing of these houses, ensuring a more sustainable future.

6. CONCLUSION AND FURTHER RECOMMENDATIONS

Despite the commendable efforts of owners, the condition of these historical houses remains far from optimal. Addressing these challenges requires the development of policies aimed at generating income, potentially through tourism. Owners should be granted flexibility in utilizing the space, with the funds generated reinvested into much-needed renovations. Creating resilience demands collective efforts, including the formation of groups comprised of like-minded individuals, especially when governmental support is lacking. Actions such as sensitizing the public, fundraising initiatives, adaptive reuse of spaces, and policy generation are integral components of a comprehensive solution. Moreover, initiatives supporting craftsmen and investing in research and development of construction techniques are also important for preserving architectural details.

Exploring potential uses for these houses, given Lucknow's rich cultural heritage, reveals opportunities to breathe new life into these structures. From hosting workshops and training centres that showcase Lucknow's traditional handicrafts, such as the intricate chicken work and zardozi, to establishing cafes or eateries that serve Lucknow cuisine, these endeavours not only revive the historic houses but also contribute to the promotion of Lucknow's vibrant culture. Through thoughtful planning and community involvement, these historic houses can be repurposed, ensuring their relevance and vitality for generations to come.

REFERENCES

1. Karimi, F., Valibeig, N., Memarian, G., & Kamari, A. (2022). Sustainability Rating Systems for Historic Buildings: A Systematic Review. *Sustainability*, *14*(19), Article 19. https://doi.org/10.3390/su141912448

2. Holtorf, C. (2018). Embracing change: How cultural resilience is increased through cultural heritage. *World Archaeology*, *50*(4), 639–650. https://doi.org/10.1080/00438243.2018.1510340

3. Fabbricatti, K., Boissenin, L., & Citoni, M. (2020). Heritage Community Resilience: Towards new approaches for urban resilience and sustainability. *City, Territory and Architecture*, *7*(1), 1–20. https://doi.org/10.1186/s40410-020-00126-7

4. Wardekker, A., Nath, S., & Handayaningsih, T. (2023). The interaction between cultural heritage and community resilience in disaster-affected volcanic regions. *Environmental Science & Policy*, *145*, 116–128. https://doi.org/10.1016/j.envsci.2023.04.008

5. Hu, H., Qiao, X., Yang, Y., & Zhang, L. (2021). Developing a resilience evaluation index for cultural heritage site: Case study of Jiangwan Town in China. *Asia Pacific Journal of Tourism Research*, *26*(1), 15–29. https://doi.org/10.1080/10941665.2020.1805476

6. Aigwi, I., Egbelakin, T., Ingham, J., Phipps, R., Rotimi, J., & Filippova, O. (2019). A performance-based framework to prioritize underutilized historical buildings for adaptive reuse interventions in New Zealand. *Sustainable Cities and Society*, *48*. https://doi.org/10.1016/j.scs.2019.101547

7. Santangelo, A., Melandri, E., Marzani, G., Tondelli, S., & Ugolini, A. (2022). Enhancing Resilience of Cultural Heritage in Historical Areas: A Collection of Good Practices. *Sustainability*, *14*(9). https://doi.org/10.3390/su14095171

8. Cantatore, E., & Fatiguso, F. (2021). An Energy-Resilient Retrofit Methodology to Climate Change for Historic Districts. Application in the Mediterranean Area. *Sustainability*, 13(3). https://doi.org/10.3390/su13031422

9. Besen, P., Boarin, P., & Haarhoff, E. (2020). Energy and Seismic Retrofit of Historic Buildings in New Zealand: Reflections on Current Policies and Practice. *Historic Environment-Policy & Practice*, *11*(1), 91–117. https://doi.org/10.1080/17567505.2020.1715597

10. Ibabao, R. A., Balinas, V., Camena, J., Trance, R., Defiesta, G., Grio, M. E., Oreta, A. W., & Penaredondo, S. (2022). Heritage Community Resilience: The Experience of Stakeholders in Calle Real, Iloilo City, Philippines. IOP Conference Series: Earth and Environmental Science, 1091(1), 12011. https://doi.org/10.1088/1755-1315/1091/1/012011

11. Aligarh Muslim University, & Kamal, M. A. (2021). Assessment of Traditional Architecture of Lucknow with reference to Climatic Responsiveness. *Architecture and Engineering*, *6*(1), 19–31. https://doi.org/10.23968/2500-0055-2021-6-1-19-31

12. Srivastava, M. (n.d.). Architecture and Development as Instruments for Political Control and Marginalization in Lucknow, India.

13. Gulati, R., & Pandya, Y. (2014). Comparative Thermal Performance of Vernacular Houses at Lucknow: A Quantitative Assessment & Dominant Multiple Strategies. *Proc of PLEA 2014, 30th Conf. on Passive and Low Energy Architecture, Ahmedabad, India, 16-18 December 2014.*

14. Chakravarti, A. (2017). Rehaish At Home in Lucknow. *Sanatkada Publications.*

PLEA 2024 WROCŁAW
(Re)thinking Resilience

Retrofitting Schools in Chile
Integration Resilience Criteria

BEATRIZ PIDERIT-MORENO[1] CHARLOTTE BERTINO[2] VÉRONIQUE FELDHEIM[2]

[1] Faculty of Engineering, Architecture and Design, University of San Sebastian, Concepción, Chile
[2] Faculté Polytechnique de l'Université de Mons, Belgique

ABSTRACT: This article investigates the design of resilient and sustainable schools in Chile, a country frequently affected by natural disasters. It focuses on adapting existing schools to serve not only as comfortable educational spaces, but also as safe havens during emergencies. Using the MC-401-F school of mass typology as a case study. A rehabilitation plan is proposed that addresses challenges such as earthquakes and climate change. The methodology includes the selection of resilience and sustainability criteria based on literature and adapted to local realities. A detailed analysis of the climate and types of recurrent disasters in the region was carried out, integrating passive and active design strategies to guarantee indoor environmental comfort, verifying natural lighting, air quality, and thermal comfort evaluated by TRNSYS software in normal and emergency conditions, in case of catastrophe. The results show that, in normal operation, passive design strategies are not sufficient to achieve comfort temperatures, necessitating active heating. In emergency mode, effective thermal control is achieved with low rates of discomfort, although some areas such as the gym and library require improvements in ventilation and shading. This study highlights the importance of an integrated approach to school rehabilitation, balancing energy efficiency, comfort, and resilience. The findings suggest that although resilience criteria are met, there are opportunities for improvement in ventilation optimization and solar management to address specific thermal challenges.
KEYWORDS: Resilience, Sustainability, Architectural Design, School Retrofitting, Climate Adaptability.

1. INTRODUCTION

This article explores the academic experience of designing schools under a resilience approach, integrating criteria of sustainability and adaptability in the face of crises resulting from natural disasters. It focuses on integrating design guidelines into existing schools, which ensure comfortable educational spaces, and at the same time in a disaster situation, can function as safe havens in emergency situations.

We focus on Chile, a country that is frequently subject to increasingly frequent natural disasters as a result of climate change. Earthquakes, tsunamis, volcanic eruptions, and extreme variations in weather are constant challenges that significantly impact the infrastructure and safety of its inhabitants. Rehabilitation considering resilience criteria is proposed for a school located in the town of Concepción, which in recent years has faced severe natural disasters, including devastating earthquakes such as the one in 2010, and frequent forest fires, exacerbated by climate change. These events have challenged the community and its resilience.

This reality makes the integration of resilience and sustainability criteria into school design not only a necessity, but an urgent priority. The increasing frequency and severity of these natural events demand an architectural response that not only mitigates the risks, but also ensures the continuity of education and the well-being of school communities in adverse situations. In this sense, the retrofitting of existing schools and the careful design of new constructions must contemplate not only educational needs, but also the ability to adapt and respond efficiently to these natural emergencies [1]. Capacity to manage disaster risks needs to be increased in order to reduce the vulnerability of the built environment. Several authors indicate that it is possible through the incorporation of resilience criteria [2–4].

Chilean schools serve as a refuge for the population in case of natural disasters to which the country is highly exposed: fires, volcanic eruptions, tsunamis, earthquakes and floods [1]. In Chile, the concept of resilience has often been applied to constructions because, backed by a strong regulatory framework, they have withstood various natural disasters. However, this interpretation of resilience focuses solely on the structural resilience of buildings and the moment in which disaster occurs, ignoring other temporal dimensions and the relationship with sustainability [3, 5]. During the 2010 earthquake in Chile, schools were used as crucial shelters for affected communities, providing safe space and essential resources for thousands of people displaced by the disaster. That is why certain schools, in key geographical areas, need to have the technical capacity to withstand a disaster, in order to then house and provide assistance to communities [5].

2. METHODOLOGY

The methodology developed in this study focuses on the application of specifically selected design criteria to rehabilitate Chilean schools, with particular emphasis on adaptability to natural disasters and environmental sustainability. Apart from achieving the adaptation of educational spaces, the improvement of the indoor environment (IEQ) for students is proposed. It is recognized that in many Chilean schools, IEQ conditions are deficient due to what I do not consider important environmental criteria, such as adequate ventilation, natural lighting and thermal comfort.

Therefore, the criteria of resilience and sustainability were selected, based on the existing literature and adapted to local realities [5]. Subsequently, a massive Chilean school typologies were selected as a representative case study. The specific location of the case study was determined, taking into account factors such as the prevalence of natural disasters and regional climatic particularities. A comprehensive study of the local climate and the most recurrent types of disasters was conducted, providing a framework for assessing the vulnerability and adaptive capacity of educational infrastructures.

The rehabilitation process was based on the previously defined criteria of resilience and sustainability, culminating in an architectural proposal that integrates these considerations. In addition, a detailed energy analysis was conducted, which included the evaluation of daylighting using VELUX Daylight Visualizer 2, indoor air quality based Sustainable Building Certification (CES) [6] and indoor thermal comfort through building modelling using TRNSYS softwar. The latter was carried out under two distinct operational scenarios: normal conditions and emergency conditions, thus providing a holistic approach to the understanding and design of resilient and sustainable schools in environments prone to natural disasters.

2.1 Rehabilitation of typology of mass schools.

In our analysis of the Chilean education system, we highlight the typology of MC-401-F schools, born out of a massive government construction program between 1965 and 1985, a period in which more than 2,500 of these schools were built. Despite their number, these schools, still operational, have become obsolete and do not meet the current expectations of the Ministry of Education in terms of educational quality and indoor environmental conditions [6].

The MC-401-F model, part of the Chilean System of Standard Schools (SCEE), is characterized by its technical design for rapid and participatory construction. It consists of steel frames and interconnected prefabricated elements, complemented by metal anchors, concrete foundations, and exterior brick and wood walls [6]. This study proposes a rehabilitation plan for these schools, highlighting their preformed steel structure and a 3-meter grid, brick exterior walls with casement upper windows and a wooden roof with a metal roof (Figure 1).

This prefabricated method was crucial for the rapid expansion of education and represents an important cultural and social legacy in Chile, symbolizing the popular power and community autonomy of the 1960s, reinforcing the importance of its rehabilitation.

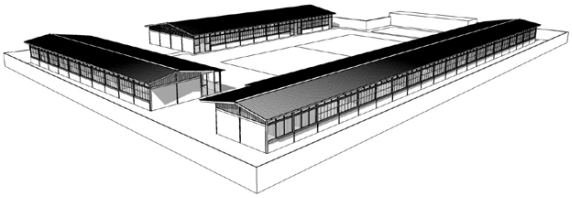

Figure 1 - 3D modeling of an MC School Typologie.

3. DEVELOPMENT OF A RETROFITTING PLAN

In this study, the ten resilience and sustainability criteria for the construction of public buildings, developed in response to the natural hazards faced by different regions in Chile [1], have been reviewed. It is observed that these criteria do not consider anthropological risks due to their lower predictability. In the process of adapting these criteria to the rehabilitation of buildings, those that are not relevant have been discarded, particularly the first five that focus on site selection.

It has been established as a premise that schools must be able to maintain uninterrupted living conditions, even when disconnected from water and electricity networks, and must house first aid supplies for 90 days.

The focus will be on the thermal comfort aspects under two modes of operation: as an educational space and as an emergency shelter, through a dynamic thermal analysis. In addition, the guidelines for the design of new educational spaces established by the Chilean Ministry of Education have been consulted and applied [7], which are aimed at improving the quality of education through the improvement of living conditions and comfort in schools, aimed specifically at architects. To support integrated passive design, the manual "Passive Design and Energy Efficiency in Public Buildings" has been used [8], which provides constructive and architectural solutions adapted to each climate in Chile. In addition, certain resilience and sustainability criteria require compliance with CES standards. [9].

For the rehabilitation of schools in Concepción, a set of key criteria has been established, focused on improving both the resilience and sustainability of buildings. These criteria have been carefully selected to ensure that the structures not only comply with current regulations, but also align with the goals of a

more environmentally friendly architecture tailored to the needs of the community.

The following are the specific criteria incorporated into the rehabilitation process:

- Resilient Landscape: Sport ground as an evacuation zone for 850 people. 880 m² area as a natural retention basin for floods. Raised structure for protection and improved access.
- Mixed Community Use: Outdoor areas and community garden. Facilities such as the infirmary and gym accessible to the community.
- Building Shape Adaptation: Seismic design, regular structures, and uniform distribution of structural elements. Ductile metal structure for seismic load absorption.
- Repairable and Adaptable: Use of wood to facilitate repairs and adaptations by occupants.
- Low Impact Materials: Priority to responsible and local materials like wood. Reuse of existing materials.
- Evolving Spaces: Design to accommodate refugees, emergency capacity for 327 people. Storage of emergency supplies and communications.
- Provision Storage: Safe storage of flammable materials. Underground water tanks for 327 people for 30 days.
- Safety Zones and Escape Routes: Wide evacuation corridors and well-planned exterior accesses. Compliance with fire resistance regulations in construction materials.
- Integration of Passive Design Strategies: Bioclimatic design for natural lighting and air renewal. Compliance with green building certification requirements.
- Indoor Thermal Comfort: Ensuring that the indoor temperature is within a comfortable range during occupancy.

3. DEVELOPMENT OF STRATEGIES

The preliminary analysis of the climate in Concepción was fundamental for architectural rehabilitation, particularly in schools. Concepción, Chile, is classified in the Köppen climate classification as Csb, warm temperate with winter rains and warm summer. Table 1 below summarizes the climatic characteristics.

It was chosen to orient the living spaces towards the north to maximize free solar gains during the winter. The heat captured is conserved by of a high-performance envelope with suitable insulation and an air infiltration prevention. To protect the building against the risk of overheating, solar protections have been put in west and north side to block the sun's rays during the hottest months. Only the concrete floor slab provides inertia which generates beneficial direct heat return in winter (Figure 3). Since rainfall is frequent in Concepcion, rainwater collected from roofs is stored in underground tanks to be filtered for drinking.

Table 1: Summary of the climate of Concepción.

Aspect	Characteristics
General Climate	Template
Average Temperature in Warmest Months	17°C - 18°C
Average Temperature in Coldest Months	9°C - 10°C
Summer Description	Comfortable, dry and mostly uncluttered
Winter Description	Long, cold, wet and partly cloudy
Average Humidity	Medium: 78%, Low: 67% in January, High: 86% in June
Wind Direction (Summer/Spring)	Southwest
Wind Direction (Autumn/Winter)	North
Pp total annual	1.110 mm

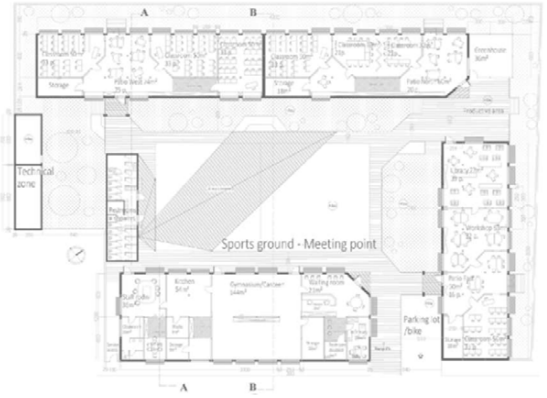

Figure 2: 3D Sketchup model of the Concepcion's prototype (own realization)

Figure 3 - Concepcion's school retrofitted cross section (own realization).

It was assumed that the building can be easily dismantled to reuse the existing steel structure to build a new light envelope. Thus, the flood risk is managed by raising the building by 1m with a steel structure extension and the large open land acts as rainwater collection and infiltration. The central outdoor space is also elevated to be used as a safe evacuation place for the population and is sized to gather 850 people. Excepted the kitchen and the infirmary, all rooms should be able to be converted

into emergency accommodation for 330 refugees in total. The whole construction system has been chosen to be simple, such as the initial MC-school was, to be easily repaired by the occupants (see Figure 2).

Given that the building has a ductile metallic structure, it is necessary to lower the center of gravity in case of seismic. That's why the floor is a concrete slab that acts as a rigid diaphragm to distribute the lateral loads on the columns while higher building elements are lighter, made with wood frame. Finally, the volumes have been designing as regular as possible to avoid torsion in case of horizontal loads.

Against the risks of spreading forest fire flames, the buildings are surrounded by a safety zone free of vegetation, buildings or other flammable materials.

4. RESULTS

4.1 Daylight Analysis

The daylighting requirement from CES is that 75% of regularly occupied spaces must achieve at best a Daylight Factor between 5% and 10%, and otherwise between 2% and 5% [9]. We observe in Figure 4 a homogeneous distribution of natural light in the regularly occupied premises, with a daylight factor average higher than 3%, which is consistent.

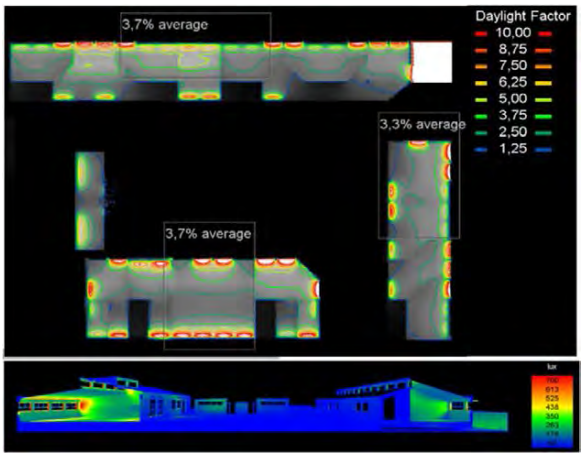

Figure 4: Isolux diagram of the Daylight Factor (DF) calculation and cut-off with illuminance values (Lux).

The lighting cross-section in Figure 4 confirms that the size and position of the windows, especially the high windows, allow for a more uniform distribution of natural light around a target illuminance value for classrooms of 300lux.

In addition, a second requirement for visual comfort is to ensure visual access to the outdoors [9]. To comply with this, at least one window per room was introduced with a threshold 40 cm from the floor, thus ensuring that the view is allowed even in a seated position.

4.2 Ventilation Analysis

The requirement of the air quality is that the hygienic ventilation rates must be provided by natural ventilation for at least 75% of the regularly occupied premises [9] Different calculation methods are systematically proposed by this guide to evaluate the performances of the envelope or the systems.

The one we have chosen for the calculation of the natural cross ventilation rate by opening the high windows is the following:

$$Qav = 1800 \cdot Av \cdot V0{,}5 \quad \text{with}$$
$$V = Ct + Cw \cdot Vm2 + Cst \cdot Hv \,|(Ti - Te)| \qquad (1)$$

Qav = Renewal air flow rate (m3/h)

Av = Window opening area (m2)

V = Wind velocity (m/h)

Ct = 0,01 coefficient that takes into account wind turbulence (-);

Cw = 0,001 coefficient that takes into account the wind speed (-);

Vm = Average meteorological wind speed at 10m altitude (-);

Cst = 0,0035 coefficient taking into account the chimney effect (-);

Hv = Window height (m)

Ti = Average annual T° inside the facility (ºC);

Te = Average annual outdoor weather T° of the locality (ºC)

We used this formula to size the number of openings to be placed, given that for security and practical reasons, we wanted only the high windows 60cm-height to be fully opened. As the windows are 2.5m wide and the upper part is split in 3, we worked with opening units of 60cm by 80cm. We used the data available through the TRNSYS weather file for the locality of Concepcion to derive the average annual wind speed of 3.5m/s, the average annual outdoor temperature of 12,5°C although the indoor temperature is set at 20°C for all regularly occupied premises.

For both emergency and normal operation, we verified that the number of openings provided per room was sufficient to ensure the minimum renewal of air. In fact, these hygienic air change rates differ according to the use of the spaces so most of the rooms must ensure two different natural ventilation rates: one for the normal use as educational space and another for emergency accommodation in case of the premises are converted in emergency. The certification provides rates to be considered by use, which we used for the calculation of the air renewal of each space, in both modes of operation [9].

4.3 Dynamic Thermal Simulation

A dynamic thermal assessment was carried out to analyze the temperatures in each room from hour to hour, contrasting them with the pre-established comfort temperatures. In the normal mode of

operation, it was established that the indoor temperature should be maintained between 18 and 20 °C in all facilities, and a minimum temperature of 18 °C and a maximum of 25 °C were set in the gymnasium. In emergency situations, a minimum temperature of 15 °C and a maximum of 25 °C were defined.

The school was thermally zoned based on its orientation, capacity, and occupancy schedules, as illustrated in Figure 5. Sanitary blocks and storage areas, marked in gray on the plans, were not modeled. Since the building has two distinct modes of operation, normal and emergency, two different models were developed using the same envelope. Occupancy schedules and internal loads were based on both our own assumptions and the data required by the Certification [9].

Figure 5: School floor plan with thermal zoning (own calculations).

During normal operation, it was determined that it was not possible to achieve comfort temperatures completely passively, due to insufficient solar gains and internal gains in the early hours and on colder days. This led to the installation of an active heating system to meet thermal needs. For cooling, natural cross ventilation proved sufficient, eliminating the need for an active air conditioning system. The number of operable windows was slightly increased to ensure proper air renewal and facilitate cooling during the hottest months.

After optimizing the building envelope and functional distribution, Table 2 shows the results of a year of normal operation of the main venues.

Table 2: Discomfort rate in normal operation (own calculations)

Room	Cold discomfort (%)	Hot discomfort (%)
Classrooms 1	21.26	0.58
Classrooms 2	19.76	-
Classrooms 3	22.17	9.49
Patio interior West	15.29	-
Patio interior North	18.98	-
Patio interior East	23.61	3.15
Staff Room	32.61	-
Library	24.47	3.09
Gymnasium	16.58	-

Heat discomfort rates were low, thanks to passive cooling and effective sun protection. The rate of cold discomfort was higher, due to the limitation of heating to 18.2 °C to reduce consumption. However, the average seasonal temperatures in each area during the periods of occupation indicate that the envelope and regulation ensure adequate temperatures inside, limiting heating consumption to 11.5 kWh/year.m².

In our analysis of the emergency mode, it was assumed that, for practical reasons and due to the connection with the rainwater reserves, only the main sanitary block remains operational, and the wet rooms are out of use. We also consider that electronic appliances and kitchen equipment are not used regularly, reducing the corresponding internal loads to zero.

During an emergency, the building must be able to operate completely passively, ruling out active heating, ventilation, or air conditioning systems. Regulatory ventilation and passive cooling are ensured by natural cross ventilation, and air renewal is effected by opening the windows. We base our strategy on the fact that the opening surface of the window's during occupancy is sufficient to ensure the necessary hygienic airflow.

The results of the rate of discomfort during the emergency operation, presented in Table 3, reveal that the classrooms experienced low rates of discomfort due to both cold and heat, with percentages ranging between 3.96% and 4.87% for cold, and between 1.64% and 1.95% for heat. Notably, the Staff Lounge and Library saw higher rates of heat discomfort, reaching as high as 5.07%. Only the gym presents a higher risk of overheating, reaching 12.17%, due to its large glass surfaces, which could be improved with the following optimization which would consist of considering the opening of the doors for overventilation.

Table 3: Discomfort rate in emergency operation (own calculations)

Room	**Cold discomfort (%)**	**Hot discomfort (%)**
Classrooms 1	4.23	1.76
Classrooms 2	-	1.95
Classrooms 3	3.96	1.64
Patio interior West	-	3.17
Patio interior North	-	1.76
Patio interior East	-	2.0
Staff Room	4.87	3.82
Library	-	5.07
Gymnasium	-	12.17

5. CONCLUSION

The simulations and analyses carried out in this study on the rehabilitation of school buildings in

Concepción, considering resilience criteria, have provided valuable insights. In terms of normal operation, it was evident that passive design strategies were not sufficient to achieve the desired comfort temperatures, especially in the morning hours and on the coldest days. The implementation of an active heating system proved crucial to maintain the right conditions, while passive cooling using natural cross ventilation was effective, eliminating the need for an active air conditioning system.

In the emergency scenario, the results indicate effective thermal control in most areas, with generally low rates of heat and cold discomfort in classrooms. However, certain areas, such as the Gymnasium and Library, showed higher rates of heat discomfort, suggesting the need to review and optimize the ventilation and shading strategy in these specific spaces.

The conclusions suggest that, although the resilience criteria have been widely met, there are opportunities for improvement, especially in the optimization of ventilation and solar management for spaces with greater thermal challenges. This highlights the importance of a comprehensive and tailored approach to the rehabilitation of school buildings, where energy efficiency and indoor comfort are balanced with the needs of resilience and sustainability.

ACKNOWLEDGEMENTS

This research arises from the international collaboration between the University of Mons and the University of Bío-Bío. It is part of the final thesis of Charlotte Bertino, who obtained her master's degree in civil engineering architecture. The principal author was the tutor, while Professor Feldheim from the University of Mons acted as co-tutor. This research received funding from Fondecyt, 1210701.

REFERENCES

1. Ministerio de Educación Gobierno de Chile. (2010). La reconstrucción en Educación.
2. Islam H., El-adaway, & M.ASCE. (2017). Sustainable Disaster Recovery: Multiagent-Based Model for Integrating Environmental Vulnerability into Decision-Making Processes of the Associated Stakeholders. Journal of Urban Planning and Development, 143(1), 04016022. https://doi.org/10.1061/(ASCE)UP.1943-5444.0000349
3. Saunders, W. S. A., & Becker, J. S. (2015). A discussion of resilience and sustainability: Land use planning recovery from the Canterbury earthquake sequence, New Zealand. International Journal of Disaster Risk Reduction, 14, 73–81. https://doi.org/https://doi.org/10.1016/j.ijdrr.2015.01.013
4. Naser, M. Z., & Kodur, V. K. R. (2018). Cognitive infrastructure - a modern concept for resilient performance under extreme events. Automation in Construction, 90, 253–264. https://doi.org/https://doi.org/10.1016/j.autcon.2018.03.004
5. Tapia, M., & Piderit-Moreno, B. (2018). Integración de criterios de Resiliencia y Sustentabilidad para el diseño de edificios educacionales en Chile. In E. Arq & E. de A. P. U. C. De (Eds.), III Congreso Interdisciplinario de Investigación en Arquitectura, Diseño, Ciudad y Territorio. Retrieved from https://www.plataformaarquitectura.cl/cl/923720/criterios-de-resiliencia-para-el-diseno-de-edificios-educacionales-en-chile
6. Schwartz Lau, C. (2020). Utopía y realidad: las escuelas MC.
7. MINEDUC. (2016). Criterios de diseño para los nuevos espacios educativos.
8. Piderit, M. B. (2012). Manual de Diseño Pasivo y Eficiencia Energética de Edificios Públicos.
9. Edificios de uso público versión 1.1 diciembre de 2022 sistema nacional de certificación de calidad ambiental y eficiencia energética para edificios de usos públicos Manual de Evaluación y Calificación. (n.d.).

Renovation Of Typological Clusters with Building-Integrated Photovoltaic Systems

Analysis of the characteristics of each typological cluster in Spain and proposals for renovation using BIPV systems

IRENE DEL HIERRO[1] LORENZO OLIVIERI[1,2] FRANCESCA OLIVIERI[1] ESTEFANÍA CAAMAÑO-MARTÍN[1,2] CESAR BEDOYA[1] NURIA MARTÍN[3] JESÚS POLO[3] CARLOS SANZ[3] MIGUEL ALONSO-ABELLA[3] JOSÉ CUENCA[3] ANA MARCOS[1,3] MARINA DE LA CRUZ[3]

[1]Department of Construction and Technology in Architecture, Escuela Técnica Superior de Arquitectura, Universidad Politécnica de Madrid, Av. de Juan de Herrera 4, 28040 Madrid, Spain
[2]Instituto de Energía Solar, Universidad Politécnica de Madrid, Av. Complutense 30, 28040 Madrid, Spain
[3]Photovoltaic Solar Energy Unit (Energy Department CIEMAT), Avda. Complutense 40, 28040, Madrid, Spain

ABSTRACT: Building renovation represents a minimal percentage in the construction sector in Spain and in Europe as a whole. This scenario provides an ideal opportunity to propose measures that promote such interventions. To enhance energy generation and address this issue from a distributed energy perspective, one of the most suitable solutions is the implementation of building-integrated photovoltaic systems (BIPV). Thus, this research delves into the use of these systems in residential building renovations to promote their installation. For this purpose, a classification in typological clusters comprising groups of buildings with the same characteristics is carried out with the aim of establishing standard BIPV interventions for each of them, with the purpose of addressing all types of buildings. Therefore, an exhaustive analysis of each group and cluster is carried out, studying their characteristics, and proposing different possible interventions that benefit both the integrated photovoltaic system and the building.
KEYWORDS: Building-Integrated Photovoltaic (BIPV), typological clusters, renovation, photovoltaic, refurbishment

1. INTRODUCTION

Official statistics on building renovation in Spain show that renovation rates are too low (less than 1% of the potential identified in 2014), as are the annual growth rates to make Spain climate neutral by 2050 [1]. The European scenario is very similar: about 75% of the building stock was built without any energy performance requirements but only 1 % of buildings are renovated for energy efficiency each year [2]. Effective action is needed to accelerate the rate of energy renovation, as demonstrated by the European initiative A Renovation Wave for Europe [3]. Along with it, the need to increase the share of renewable energies in our cities makes building integrated photovoltaics (BIPV) an attractive solution which combines local and renewable generation of electricity with the use of photovoltaic architectural qualities unattainable with conventional photovoltaic modules, both in new and retrofit projects.

1.1 Photovoltaic systems in buildings

Before continuing, it is necessary to define some basic aspects related to BIPV installations [4]. When it is decided to install this type of photovoltaic systems in buildings, there are two internationally known and defined ways of proceeding:

·Additive photovoltaic systems, which are commonly identified by the acronym BAPV which stands for Building Added/Applied/Attached Photovoltaics. These systems use conventional PV modules, whose sole design purpose is to convert solar radiation into electricity, which can be fixed to the roof and facade thanks to a metal or wooden structure that is, in turn, anchored to the structural support. When we find a BAPV installation, it is a photovoltaic system additional to the building itself and without any relationship or cladding function, being two independent elements. In this way, this type of installation will function as one more of the set, as well as the ventilation, lighting, and heating system, among others.

·Integrated photovoltaic systems, referred to as Building-Integrated Photovoltaics (BIPV). The elements of this photovoltaic system are designed to integrate and replace components of the building envelope itself, playing a central role in the functionality and architectural quality of the building. In this way, the components of the BIPV system belong to the external layer of the building and, apart

from generating electricity, can fulfil one or more functions such as protection against climatic agents, fire, and noise, generate shade that will reduce solar gains, provide thermal insulation, and allow natural lighting, among others. For all these reasons, by performing all these functions apart from energy production, these types of BIPV installations are also known as multifunctional elements.

Within BIPV, the installation of PV elements is a prerequisite for sustaining the building's operational capacity. This means that, if at some point in the life of the building it is necessary to remove the PV system, it will be mandatory to replace it with another envelope element, since it would remove a part of the structure that has basic functions to ensure habitability. Therefore, a BIPV element is both a photovoltaic and a building element. More precisely, a BIPV element constitutes the smallest indivisible PV unit within a BIPV system, maintaining functionality directly related to the building structure [5]. For instance, a solar tile exemplifies the BIPV element encompassing a solar rooftop (BIPV system). Therefore, a BIPV system is a photovoltaic system that is formed by modules that fulfil the function of the previously stated. The BIPV products contain the different electrical components necessary for the electrical installation, and, in addition, they have the structural mechanical assembly system that guarantees the fixing to the support structure, which in this case is the building itself. The fasteners employed are typically like those used in traditional building construction for anchoring conventional construction elements. However, they are designed with the specific characteristics of the BIPV system in mind. This is crucial because in a BIPV installation, the objective is not only to ensure reliable mechanical fastening but also to establish effective electrical interconnection between its components. The growth of BIPV has boosted the development of a wide range of products covering solutions for flat and sloped roofs, facades and exterior elements that enable the integration of photovoltaics into the building [6,7].

1.2 BIPV market

As for the BIPV systems market, the current outlook is positive after the difficulties that have arisen since the beginning of this sector. Today these systems have reached a great technical development, both the modules themselves and the installation, with a growth of use in construction that is enhanced by a constant reduction in costs. The price of these installations is one of the characteristics that has fluctuated the most over time, being initially a relevant barrier. There are different policy initiatives to encourage their expansion, depending on the country, focused on reducing carbon emissions and improving energy efficiency.

Despite all this, the BIPV market still has a long way to go, both in terms of dissemination and application. This is due to different limitations, such as a lack of training of professionals in the sector in this type of solutions and a lack of personnel with practice in the combination of construction and photovoltaic installations. BIPV is therefore a niche market, and this situation is not expected to change radically in the short term, especially due to competition from traditional PV and building solutions. Progressive growth of BIPV is expected to be driven by its unique characteristics that allow it to provide solutions that other systems cannot address, such as meeting the requirements of positive energy buildings in urban and architectural contexts where BAPV solutions are not viable. When addressing the state of the BIPV market, it is complex to cover as it is directly dependent on different incentives, applications, and business models, encompassing various infrastructures and sectors, such as residential and commercial. This system provides technical solutions as varied as photovoltaic shingles for a single-family home to a photovoltaic glass façade for an office building. Bearing in mind that it depends on the specific definition applied, the European BIPV market varied between 300 MW and 500 MW per year in 2022, and it is believed that globally it could reach 2 GW [8]. These data are estimates, as they are affected by custom solutions whose data vary compared to glass-to-glass BIPV systems. Even so, simplified BIPV solutions, i.e. with conventional PV modules with anchoring structures, tend to be the most widely used. Although these installations are the most widely used, the BIPV market provides a wide range of solutions that can be adapted to each case, with customized modules in terms of size, shape, and colour, which is driving their use in the market. In addition, a participation by China and the entry of prestigious international manufacturing companies show the important growth of BIPV [8].

This research aims to encourage and promote the use of BIPV technology in renovation projects by establishing a refurbishment intervention model that includes these systems for each typological set considering the unique characteristics of each of them. This study is based on the previous classification carried out by the Ministry of Development of the Spanish Government of the different types of clusters in the Spanish housing stock [9]. The classification groups buildings into different typological clusters, and these clusters include buildings with common characteristics. An analysis of these clusters is developed according to their potential for integrating BIPV solutions and renovation interventions are proposed using these

systems adapted to their morphological characteristics.

The focus of this research aligns with the overarching theme of "Building resilience with innovation and technology" proposed for PLEA 2024. The aim is to drive innovation and enhance awareness regarding the application of integrated photovoltaic systems in building interventions.

2. METHODOLOGY

The first step of the research was a review of the different types of clusters that can be identified in Spain. The clusters were then analyzed to propose a photovoltaic intervention that enhances and benefits from its own morphology. Finally, for each cluster the most appropriate BIPV retrofit measures were proposed based on in-depth studies of real buildings and a specific BIPV retrofit design.

The two main parameters used in the study [9] to create a classification that fairly represents each building model are the number of floors above ground and the year of construction. Three groups are presented: single-family houses with 1 and 2 storeys, multi-family dwellings with 3 or fewer floors and multi-family dwellings with 4 or more storeys.

The construction periods are as follows: before 1940, 1941-1960, 1961-1980, 1981-2007 and 2008-2011. With this classification, it is possible to group buildings according to similar construction, structural and aesthetic characteristics, as well as their energy efficiency. These data make it possible to propose renovations that meet current needs. The combination of these parameters results in 15 different typologies. To facilitate the identification of each cluster, a letter is defined for the three main building types: letter U for single-family houses; letter C for multi-family buildings with 3 or less floors; and letter D for multi-family houses with more than 3 floors (Table 1).

Therefore, considering the singularities of each cluster, both architectural and constructive, and the present problems to be solved, in most cases derived from their year of construction (mainly thermal and insulation problems), this study proposes measures that provide the building with a constructive envelope that solves problems related to the low energy performance of the building from a passive point of view, and at the same time can convert solar energy into electricity to be used in the building. The most suitable areas for the integration of these systems, with high solar irradiation, little shading, and suitable construction characteristics for BIPV, are analyzed and prioritized. The ideal areas for photovoltaic systems are those with the highest solar gain, such as roofs and facades, which are the two target areas for the implementation of these systems in the renovation of buildings.

Each of the typological clusters shown in the table presents buildings with their own unique characteristics, but common within the group of buildings they represent. This makes it possible to establish standardized renovations that can be carried out for this group, with the possibility of adapting them to each case. These solutions will be the most appropriate by taking advantage of its qualities and discarding those implementations that do not benefit the operation of the photovoltaic systems. In this way, the intervention procedure to include BIPV systems will be different in each of them, so in-depth research is necessary to take full advantage of their characteristics.

3. RESULTS

Within the three main types of buildings that structure the classification, renovation proposals with BIPV systems can be common for typological clusters belonging to the same group, since their formal characteristics are similar, but with some differences, which will be considered and addressed in this analysis.

Before starting to analyze the results, several premises must be taken into account. On the one hand, one aspect to take into account is the visibility of the intervention itself, since if the surface where

Table 1: Classification of the different typology clusters.

	<1940	1941-1960	1961-1980	1981-2007	2008-2011
U					
C	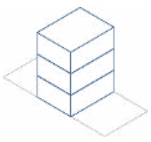	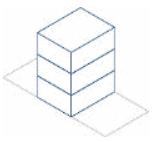	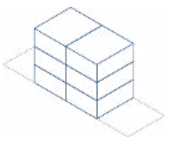	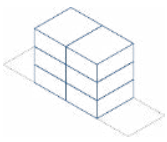	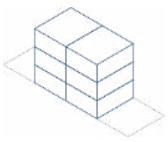
D	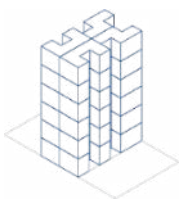	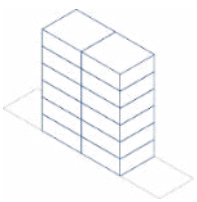	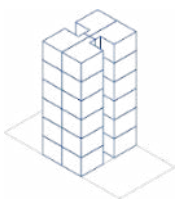	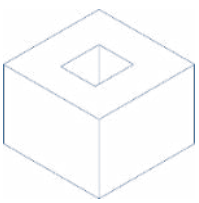	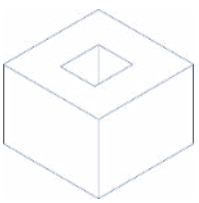

the intervention is to be carried out is not visible and does not add any architectural value to the building (the roofs present in type D clusters are the perfect example due to the high heights), a BAPV solution could be chosen, which is more economically profitable. In the same way, this study prioritizes and promotes the use of BIPV systems, and in the case mentioned above, with the objective of both energy production and a search for improved thermal performance. With this, another aspect to take into consideration is that the facades will always be visible, therefore, whenever there is a solar resource BIPV installation is prioritized, and in the case that there is not, it is urged to perform a passive rehabilitation, with the premise of caring for the aesthetic quality of the intervention and the building itself.

3.1 Clusters U

The main characteristics that will mark the possible renovation using BIPV systems in clusters U <1940, U 1941-1960, U 1961-1980, U 1981-2007, and U 2008-2011 are the conditions of their facades and roofs. In addition, the average number of floors in these clusters, which range from one to two, with an average height of 6 meters, must be considered. As they are single-family dwellings, usually semi-detached, there are only two facades available for action. The main facade would be the appropriate space for the location of the photovoltaic modules and the rear facade, usually delimiting the inner courtyard area, as a possible space after a study of shadows to determine whether the performance of the modules is adequate. It should be taken into account that this building typology of single-family housing can also be commonly found isolated on a plot, which implies that the possible performance of the facade can be extended to the full four available. However, the most suitable for intervention will be those facing south, east and west, with the possibility of the north side if, after the study of shadows, it is shown that its installation is profitable. Finally, as long as the shadows cast by the adjoining dwellings as well as the overhangs and urban elements allow it, the entire available height of the facade should be intervened.

As for the roofs, this type of construction has gable roofs and in the most current constructions flat roofs can be found. In the first case, it will be necessary to study the orientation of the gables, with the south, southeast and southwest to obtain the best values of uptake per square meter, discarding those oriented to the north if their performance is not adequate. In the case of flat roofs, it will be necessary to create an auxiliary structure with the appropriate orientation and inclination to allow the correct installation. When this occurs, it should be integrated as much as possible away from the common BAPV structures.

3.2 Clusters C

Buildings classified within clusters C<1940, C 1941-1960, C 1961-1980, C 1981-2007, and C 2008-2011 share most of their characteristics, differing in the year of construction and the number of free facades. They are a type of cluster that is commonly located in the interior of cities, with an average of three floors and with one or two dwellings on each floor, leaving a height of 9-10 meters. In addition, they are often located in an urban fabric with narrow streets and, when combined with the high height of the buildings, direct light does not usually penetrate the interior of these roads and they are areas of constant shadows. On the other hand, the predominant type of roof is the sloping gable roof with only one facade to the exterior, because it is adjacent to other buildings on the other three sides or because it has an interior facade facing a small courtyard used only for ventilation and lighting.

Thus, the priority space for the intervention is the sloping roofs, as they are the usual ones in this complex and are ideal for capturing solar radiation, with a lower risk of cast shadows. Despite this, it is necessary to take into consideration the differences in height of the adjoining buildings, as well as the protruding elements that may obstruct the passage of sunlight, such as mansard roofs. Actions on facades are more limited. The existence of small interior courtyards means that the only facade on which radiation can be captured and, therefore, the BIPV systems can be used is the one that faces the exterior, since the other two are adjacent to buildings. As one of the main objectives is to improve the habitability inside the house, the facades to interior courtyards are also a target of intervention but with an ETICS solution (External Thermal Insulation Composite System) [10]. On the main front, problems are also observed due to the urban fabric where they are usually located, i.e., the historic centers and city centers, with narrow street widths and different heights of nearby buildings, causing constant shadows on most of the height of the facade. Whenever possible, priority should be given to acting on the entire facade, and when the situation is not favorable, a viable intervention is to act on the surface of the upper floor, as this is one of the areas with the lowest risk of shadows and the highest solar incidence.

When these scenarios arise, where one part of the façade has a BIPV installation and another part of the surface without a photovoltaic intervention, it is necessary to define very precisely the BIPV rehabilitation to be carried out so that the integration with both the remaining façade and the whole is adequate. Performing this type of action is a

challenge, but it is possible thanks to the wide range of BIPV elements on the market, with different sizes, shapes, colours, and textures, and to the professional experts who are trained in the fields of architecture, photovoltaics, and energy, who will make the best possible design for each case.

3.3 Clusters D

The morphology of the buildings of the clusters included in group D are diverse but share common characteristics. The building typology of cluster D 1941-1960 is the linear block, of cluster D 1961-1980 the H-block, and clusters D 1981-2007 and 2008-2011, the modern block. These types of buildings are usually found in areas of urban expansion and growth, with wider roads that allow light to enter the interior, with the sole exception of the D<1940 cluster, which is frequently built in the inner areas of cities. Regarding their formal characteristics, they are buildings with an average of six floors with two or four dwellings per floor, so they range from 18-19 meters in height. The predominant roofs are flat, with the presence of sloping roofs, but in a lower percentage. They have two exterior facades and adjoin two buildings on each of their sides, except for the modern blocks, which have four exterior facades and large interior courtyards.

In this group, the ideal areas for intervention are both roofs and facades, the latter with more restrictions. If the building has a sloping roof, which is the least common in this group, this scenario will be used for the installation of a photovoltaic roof after the removal of the existing one. When the roofs are flat, it is recommended to install a second photovoltaic roof with a suitable slope for the performance created with self-supporting concrete blocks. When the roofs are flat and not passable, the design should prioritize and focus on the optimization of the energy performance, both in terms of reduction of the building's energy demand and energy generation. This will be possible thanks to an external thermal insulation that is integrated into the self-supporting structure of the modules. When roofs are passable, in addition to everything related to energy performance, the needs of the inhabitants of the building itself must be taken into consideration and the use of the roof space must be made possible. In these cases, priority is given to solutions such as photovoltaic pergolas, which make energy generation compatible with the use of the roof.

Compared to the previous cases, there are more intervention possibilities in the facade as at least two of them have outside views, which can be used for the installation of BIPV modules. It would be necessary to study the urban structure and the width of the street to see if it is profitable to act on the entire free height of the facade. When it is suitable, it will be the priority action to be carried out. As for modern blocks, the number of available facades increases as four of them are bordering the exterior and it will be possible to act on their entire surface, provided that the performance is adequate due to the risk of shadows. In the same way, the facades of the inner courtyard of these blocks could also be considered suitable surfaces for the installation of photovoltaic modules, with the prior study of shadows cast by the building itself to determine which faces are suitable for action.

In addition, there are two possible actions in all clusters. These are interventions on terrace parapets and skylights. If residential buildings have these elements, they are ideal spaces for their performance, with the possibility of installing modules with transparency that allow sunlight into the interior and, at the same time, capture solar radiation.

4. CASE STUDY

A real building corresponding to one of the defined clusters is selected as an example to show the application of the methodology established in the research. The residential building selected for the proposed rehabilitation is in the Villaverde district of Madrid, Spain. The typology of this building is a five-storeys linear block with two dwellings of 74 m^2 each, built in 1970 and classified in the cluster D 1961-1980. As for its exterior characteristics, it has a gable roof with a pitch of 20° and a north-south orientation, so it falls within the range of inclination between 20° and 40° [11], a classification that will help when studying the complete urban fabric in which it is located. This building has only two façades where intervention is possible, as there are blocks on the east and west sides. For all these aspects, this construction presents an opportunity for renovation with BIPV systems (Fig. 1).

Figure 1: External view and urban floor plant of the building.

After the corresponding study of irradiation and shadows to determine the available solar resource, these are the annual irradiation values on the roof and façade surfaces, with north-south orientation, obtained by the PVGIS program [12]:

- ·North roof slope with 20°: 1380 kWh/m^2.
- ·South roof slope with 20°: 2021 kWh/m^2.
- ·North façade with 90°: 320 kWh/m^2.
- ·South façade with 90°: 1395 kWh/m^2.

As can be seen and as expected, these data are higher on the south side of the roof and on the facade of the same side, so these will be the main areas of intervention, but not the only ones. For the north-facing surfaces, the façade is not a target for intervention due to the low values collected, but the north roof slope presents data that are sufficient to evaluate the BIPV installation in this area.

The proposed BIPV solutions for the target surfaces are a BIPV ventilated roof and a BIPV ventilated façade, consisting of a layer of thermal insulation bonded to the existing structure, a system of primary metal guides anchored to this same support which, in turn, supports the structure of secondary guides placed transversally and longitudinally along the facade to which the photovoltaic modules are attached. In relation to the thickness and material of the thermal insulation, the CTE DB-HE establishes maximum values for Madrid, located in zone D [13]. To satisfy the requirements of transmittance values lower than 0.41 $Wm^{-2}K^{-1}$ in the façade and 0.35 $Wm^{-2}K^{-1}$ in the roof a minimum thickness of about 10 centimeters is required with an insulating material with a thermal conductivity of 0.04 $Wm^{-2}K^{-1}$. The metallic support structures for the panels create a space for ventilation of the rear faces of the photovoltaic modules, which prevents them from heating up and ensures better performance. In addition, the panels used can be aesthetically treated to ensure integration with the urban environment by hiding the photovoltaic cells and in any color required.

5. CONCLUSION

There is an urgent need to increase the rate of renovation of the existing housing stock using BIPV systems, not only to reduce the energy consumption of buildings, which can be achieved through traditional renovation, but also to contribute to the promotion of decentralized electricity generation based on local renewable energies, with the consequent effect of decarbonizing the electricity generation mix and democratizing energy. In this sense, it should be noted that any energy refurbishment that does not integrate local renewable electricity generation is a missed opportunity to move faster towards zero-emission buildings, districts, and cities. This study aims to promote the inclusion of BIPV systems in refurbishment projects by providing standard intervention models that simplify the decision-making process for the designer.

ACKNOWLEDGEMENTS

Participation in PLEA 2024 is possible thanks to the research project Renovation Innovative Global Solutions with Building Integrated Photovoltaics (RINGS-BIPV) [14], consisting of projects PID2021-124910OB-C31, which coordinator is CIEMAT, and PID2021-124910OB-C32 in charge of the Technical University of Madrid, funded by Ministry of Science and Innovation, State Research (AEI) and the European Regional Development Fund.

REFERENCES

1. 2020 update of the long-term strategy for energy renovation in the building sector in Spain (ERESEE), (2020). ERESEE 2020. Ministry of Transport, Mobility and Urban Agenda.

2. Energy efficiency in buildings, [Online], Available: https://commission.europa.eu/news/focus-energy-efficiency-buildings-2020-02-17_en [01 December 2023].

3. A renovation wave for Europe, [Online], Available: https://energy.ec.europa.eu/topics/energy-efficiency/energy-efficient-buildings/renovation-wave_en [21 December 2023].

4. Berger, K., Cueli, A. B., Boddaert, S., Del Buono, M., Delisle, V., Fedorova, A., Frontini, F., Hendrick, P., Inoue, S., Ishii, H., Kapsis, C., Kim, J., Kovacs, P., Martín-Chivelet, N., Maturi, L., Machado, M., Schneider, A. and H. Rose Wilson, (2018). International definitions of "BIPV". Report IEA PVPS T1-04: 2018. International Energy Agency.

5. Martín-Chivelet, N., Kapsis, K., Wilson, H. R., Delisle, V., Yang, R., Olivieri, L., Polo, J., Eisenlohr, J., Roy, B., Maturi, L., Otnes, G., Dallapiccola, M. and W. M. P. Upalakshi Wijeratne, (2022). Building-Integrated Photovoltaic (BIPV) products and systems: A review of energy-related behavior. *Energy and Buildings*, 262, 111998.

6. Reijenga, T., et al. Successful Building Integration of Photovoltaics- A Collection of International Projects. IEA-PVPS Task 15, 2020.

7. Kumar Shukla, A., Sudhakar, K. and P. Bareder, (2017). Recent Advancement in BIPV product technologies: A review. *Energy and Buildings*, 140: p. 188-195.

8. IEA PVPS Trends in Photovoltaic Applications 2023. IEA-PVPS, 2023.

9. De Santiago, E., Arcas-Abella, J., Pagès-Ramón, A., Larrumbide, E. and D. Huerta, (2019). Segmentación del parque residencial de viviendas en España en clústeres tipológicos. ERESEE 2020. Ministerio de Fomento.

10. About ETICS, [Online], Available: https://www.ea-etics.com/etics/about-etics/ [21 December 2023].

11. De Santiago, E., Román López, E., Caamaño Martín, E., Romadillos Arroyo, G. and C. Sánchez-Guevara, (2019). Estudio sobre el potencial de generación de energía solar térmica y fotovoltaica en los edificios residenciales españoles en su contexto urbano. ERESEE 2020. Ministerio de Fomento.

12. 12. Huld, T., Müller, R. and A. Gambardella, (2012). A new solar radiation database for estimating PV performance in Europe and Africa. *Solar Energy*, 86 (6): p. 1803-1815.

13. CTE DB-HE, [Online], Available: https://www.codigotecnico.org/pdf/Documentos/HE/DBHE.pdf [21 December 2023].

14. RINGS-BIPV website. https://rings-bipv.com/ [04 December 2023].

PLEA 2024 WROCŁAW
(Re)thinking Resilience

Strategies to Improve Landscape in Designing for Rural Sustainable Environment:

Analysis of villages in Yunnan, Southwest China

YUN GAO[,1] Adrian PITTS[,1] WEN JIANG[,2] LING ZHOU[,1]

[1]University of Huddersfield, Huddersfield, UK
[2]Southwest Forestry University, Kunming, P.R.China

ABSTRACT: This study analyses rural development in relation to the landscape in four villages in Yunnan, Southwest China. Three cases are in remote mountainous areas with unique natural environment and special fauna and flora species, and one case is adjacent to developed urban area. The research project demonstrates that farmland and natural environment features around rural and urban areas cannot be considered as separate areas, independent of design considerations for the built environment. The cultivation of the landscape, protection of biodiversity, energy saving measures and villagers' daily activities are closely linked to each other. The design and planning policies suitable for each village should be discussed with the participation of local villagers through a process of research into its characteristics and identities. Furthermore, the relationships between the rural economy, lifestyles and the landscape have significantly changed. Boundaries of natural environment and farming land are constantly shifting. In Yunnan, development of the local economy goes hand in hand with protection of biodiversity, encouragement for energy efficiency and long-term heritage protection. To encourage the participation by local communities, associated local policies need to consider improving commercial services, promoting economic development, and building local capacity for employment.
KEYWORDS: landscape, biodiversity, energy saving, rural development, Southwest China

1. INTRODUCTION

This paper describes a project that explores innovative strategies for designing buildings and public spaces in rural areas in Southwest China. In particular, it emphasises use of landscape design in order to promote sustainable living and biodiversity. Landscape here refers to both natural and artificial landscape in and around surrounding villages. Southwest China is famous for the region's diverse geographical features and natural environment which combines mountains and rivers. Historically the occupants of settlements in these contexts have developed various skills and methods for harmoniously co-existing with the landscape. However, rapid changes arising from urbanization, together with impacts of climate change have brought new problems; there are now needs to develop new methods to include the landscape within sustainable design of the built environment.

Landscape changes have had influences on people's lives, for example rapid urbanization in China has led to large areas of agricultural land being acquired for non-agricultural purposes such as commercial or residential [1]. Many rural populations have changed from agricultural or natural capital-based livelihoods to those requiring a wider range of resources to sustain them. At the same time, "Grain for Green" government policies (for converting farmland that is susceptible to soil erosion back to natural vegetation since 1999) have also had impacts on the rural environment. Economic development such as the rapid expansion of road systems changed the landscape in rural areas which also saw rural areas integrated further within nearby urban areas. Therefore, farmland and natural environment features such as water bodies and green areas around rural and urban areas can no longer be considered as separate areas, independent of design considerations for the built environment. The landscape and settlements overlap. Carraneo and Lotto's study [2] of projects in Europe proposed to use intensification as a strategy to create sustainable density of activities and spaces for citizens in which the natural environment and the rural-urban environment co-exist harmoniously. Yan et. al.'s study [3] examines how the Chinese concept of *fengmao* (wind and appearance, a term that has been developed to denote the local and context-specific features of a place including landscape). This has been widely used in evaluating, maintaining and preserving cultural heritage. UNESCO's draft mid-term strategy for 2022 to 2029 states as one of its aims "to raise awareness of climate change's impact on biodiversity and on the diversity of the world's natural, geological and cultural heritage" [4]. The assessments used in rural areas and many guidelines provides a broad framework to emphasise building of beautiful cities where humans and nature coexist in

harmony, and in a beautiful countryside which is green, ecologically rich, and liveable. However, more detailed strategies for different areas that include landscape in design are needed.

In this project, by analysing four case studies in Southwest China, the authors explore how landscape is closely related to local communities' lifestyles and provides the design strategies impacting relationships between the landscape and settlements.

2. STRATEGIES FOR CONSIDERING LANDSCAPE

This study develops strategies for considering landscape in design interventions. The strategies are aimed to protect biodiversity of the area, develop sustainable living, improve the competitiveness of local agriculture and crafts, and develop local business capability and diversification. This includes the following key themes:

2.1 Cultivation of the landscape:

To protect biodiversity and improve the quality and the economic value of natural environment and valuable crops (such as local products from bamboo).

To promote new uses of local agricultural and forestry products.

To improve infrastructure facilities for sustainable use of water resources and soil protection.

2.2 Energy saving activities:

To encourage use of clean energy, for example: biomass, production of pellets, photovoltaic or solar panel systems, wind power etc.

To support the creation of local micro-businesses and services in the field of environmental management.

To upgrade existing rural buildings by converting them to be used for diverse services such as hostels or local community centres.

2.3 Cultural, social life and daily activities:

To recover aspects of architectural heritage, especially those of historical and cultural value, and to create places of culture and nature.

To consider landscape as part of the local history and identity.

To create commercial and tourist services, production and distribution of food products and local crafts, craft course, educational farm, biological research etc.

3. CASE STUDIES IN YUNNAN PROVINCE

The project explores design in Zhangjiaping, Yinshan, and Huodi, all villages in the Yuwan village administration area of Daguan town in Zhaotong county; and Damoyu village on the outskirts of Kunming city in Yunnan Province. Yunnan sits on a plateau that adjoins the Himalaya Mountain range, and is well known for its geographical diversity, biodiversity and number of ethnic groups living in the area. Historically those characteristics have played significant roles in the formation of human settlements in the region.

The villages were chosen as case studies because of their shared characteristics. For example, in those villages, many young villagers now inhabit and work in cities in order to enhance income. This has led to an aging population remaining in the settlements. In some cases, remaining villagers have been relocated away from their original homes to different counties in the province.

None of the villages studied in the project have been classified as a "Traditional Village", a title awarded to villages with historical importance for their cultural heritage in rural China. Therefore, support funding from the local government does not help with the protection of traditional cultural heritage. Villagers' incomes are therefore also less supported by tourism.

Existing research conducted in the villages shows that there is a lack of formal procedures that can be used to provide guidelines or to assess results and promote three aspects listed above [5, 6]. This study therefore focuses on the means to include landscape in the design strategies for sustainable living.

3.1 Villages in Yuwan Village District in Zhaotong

The three villages studied in Yuwan Village District are located in the northeast of Yunnan Province in the transition zone from the Sichuan Basin to the Yunnan-Guizhou Plateau. As of 2022, the jurisdiction covers one district, nine counties, and one county-level city, which include many ethnic groups all within a mountainous area.

Daguan County in Zhaotong historically acted as the main transportation hub between Yunnan and Sichuan Provinces. The forest coverage rate of Daguan is 45.8%, including 22 varieties of trees for producing timber products, and 133 types of precious Chinese medicinal materials such as *Gastrodia* and *Eucommia*. Daguan County is also known as the Town of Qiongzhu (*qiongzhuea tumidinoda*), with 100,000 mu (66.67km^2) of production accounting for 43% of that in southwest China, and a major production area in the world.

Yuwan Town is located in the south of Daguan County. There is a total of 20 village groups in the administration area, of which Huodi village group is located in cold highland climate zone, and the rest are within a combination climate of river valleys and alpine mountainous areas. The villagers mainly grow maize, potato, flue-cured tobacco, tea, bamboo etc. Three representative village groups within Yuwan Village, namely Zhangjiaping, Yinshan and Huodi were studied and are discussed below.

3.1.1 Zhangjiaping village in Yuwan District

Zhangjiaping Village (Fig. 1) is situated in a mountainous area at an altitude of 1720m and covers an area of 2.41km^2, (annual average temperature is 11℃, and annual precipitation 1500mm). The farmland is suitable for planting corn and other crops; the area is also well known for its bamboo products. The village has 72 families and a rural population of 313. Many local traditional houses were constructed using stone.

Figure 1: Zhangjiaping village. (insource: authors 2023)

Zhangjiaping is about 5 km away from the town centre. The road is well constructed with convenient transportation systems compared to other villages in the area. The overall architectural configuration and texture of the countryside are well preserved, and most of the architectural forms and materials have retained certain regional characteristics (Fig. 2). Young people from the village are now mainly migrant workers who have shifted to larger cities over many years. Village families who have improved their income level have built new houses closer to the town centre; and 4 households have moved to the Jingan New District (a new settlement which was constructed to accommodate families relocated from poverty-stricken and inhospitable areas). As a result, there are many empty houses in the village.

Figure 2: Zhangjiaping village. (Source: authors 2023)

Villagers' houses are distributed in the mountainous area, where there is little flat farmland and most of what there is, is located on the hillside adjacent to villagers' houses.

3.1.2 Yinshan village in Yuwan District

Yinshan is located about 15 km from the town centre. The concrete road to it was completed in 2020, but road transport is still very difficult due to the steep slope on some hillsides. Before 2020, Yinshan's residential buildings were all of stone and the village had its own dedicated stone masons with the skills to build local houses. During the authors' field study by in the village, the residents proudly introduced the place where they grew up, which they named a "Stone Forest". Due to the inconvenience of transportation, the village and the beautiful surrounding natural environment is little known to outsiders, although it is well-known locally. The Yinshan "Stone Forest" area has dense stone distributions, yet villagers graze cows and horses in the area and the "cow lane" is carved out among stones (Fig. 3). The area of Yinshan stone forest is rich in vegetation species. The survey team frequently found national second level protection plant species in the area. Yinshan with its remote location, and intact natural environment and landscape, provides an exemplary natural environment for human settlement.

Figure 3: Roads for cows and horses. (insource: authors 2023)

3.1.3 Huodi village in Yuwan District

Huodi village, about 40 km away from the town centre, is the most remote village in Yuwan Village district (Fig. 4). There are transportation difficulties and income generation is lower than other villages; as a result, most of Huodi's villagers responded to the local government call and opted to move to Jingan New District. Huodi is the water source of Yuwan Town, and spring water passes through Yuwan Town, Daguan County and then Zhaotong City. The natural ecological environment of Huodi Village is considered to be excellent, and the largest local bamboo forest is nearby and is a source from which to earn income and produce food.

At present, Huodi Village also plans to build a bamboo shoot processing factory and create certified organic bamboo shoot products (such as exquisite furniture and other crafts with "artistic appearance") to be sold around the country. These each create

more opportunities for local villagers to enhance their income.

Figure 4: Bamboo forest in Huodi village. (Source: authors 2023)

3.1.4 Discussions about three villages in Yuwan

The unique natural environment in Yuwan has provided the means for many generations to make a living. It provided local people with many special natural products such as the bamboo and herbs that only grow in the high-altitude environment such as in Yuwan. On the other hand, the mountainous areas also restrict the development of local economy because of the difficulties in transportation. Due to the remote location with consequently less impact from the rapid urbanization processes that influenced other places in China, the local biodiversity is well protected. However, there is a need to promote new uses of local forestry products to raise local incomes and attract young villagers to return.

Technical improvements in production and training in new systems are needed to achieve aspirations: currently bamboo products are hand made by complicated traditional methods which limits the number of products. The local government policy is to provide training programmes to improve and optimize the procedure and create new innovative design, which can potentially attract young people to engage with the creation of local micro-business and services.

There are many empty stone houses in all three villages built by masons using local materials. They are mostly terraced houses with narrow fronts and deep depths. The walls of the stone house are around 60cm in thickness with small openings. Those features are adapted to the local climate characteristics of cold winter and hot summer. Empty properties are currently in danger of dereliction and being demolished. The locals converted some of them into drying rooms for agricultural products which also provided essential winter food for villagers when the transportation becomes much more difficult in certain seasons. The authors have been developing proposals following the field study to convert some empty houses into a community centre and canteen that will serve the remaining population (mostly children and aged villagers) and provide training on using computers and AV to encourage communication among villagers and with the outside world.

Overall, Huodi as the water source for Yuwan town and Zhaotong district, together with the beautiful natural environment of the mountains provides good attractions for tourists. However, it is important to improve the infrastructure and to create commercial and tourist services, such as craft course, educational farms, and biological research for the plan to attract more visitors.

The case studies in Yuwan district demonstrated that in the remote mountainous area in Yunnan, the protection of the natural environment, encouragement and maintenance for the use of clean energy, protection of the local heritage and the raising villagers' living standards are closely linked to the landscape (which is important part of the local history and identity). The planning policy for each village needs to take into account the landscapes as an essential part of the local development.

3.2 Damoyu village

Damoyu Village (Fig. 5) on the outskirts of Kunming is different from the remote villages in Yuwan, in that it has benefited from the close relationships with the adjacent urban area. Historically it is a Yi ethnic village established in the 18th century. Damoyu means "black bamboo forest" in Yi language. It sits adjacent to Qipanshan National Forest Park and a large reservoir. The village is located 15 km west of Kunming, at an altitude of 2200m with an annual average temperature of 13.2°C, and an annual precipitation of 920mm.

Although agriculture is still an important source of income for villagers, in Damoyu it only accounts for 18% of income. The main product are vegetables, and in the past many villagers' incomes were generated from mining and transportation. The town is rich in mineral resources; its quartz sand reserves ranked first in China. Many villagers who had good income from the mining industry constructed buildings of four to five stories height along the entrance road; many with courtyard for cars and vans (Fig. 6). Since 2015, hotels and restaurants have become increasingly popular because increasing visitors from Kunming, some even rented houses to stay. The village has thus undergone a radical change with one-fifth of its inhabitants coming from nearby cities and renting houses in the village.

3.2.1 Agricultural impacts on the landscape

While mining development has brought huge economic value, the original vegetation has been severely damaged; years of mineral mining have left the mountains full of caves with safety risks such as landslides; village roads have also been damaged by transport vehicles. After meetings between

government management departments, village committee members and villager representatives, it was decided to close mining, restore the ecology and explore new ecological industries at the same time. Since 2018, the local government has closed all the private mining in the area in order to protect the natural environment. Villagers who were engaged in mining and transportation generally returned to agriculture. Many empty land areas have been reclaimed for agriculture again. However, the agricultural products have changed fundamentally. Previously, villagers primarily grew rice, wheat and corn. During the field study in 2023, the authors found that those crops did not grow well due to long periods of frost and other local climate problems. Therefore, villagers have shifted to grow vegetables and fruits which are easier to cultivate and can also be sold to tourists coming to the village (Fig. 7).

Figure 5: Damoyu Village (Source: authors 2018)

Figure 6: Damoyu Village (Source: authors 2023)

The local government has set up policies to support and encourage villagers to move to agriculture mechanization. However, the authors field study showed that the majority villagers are still using traditional farming methods. The reasons could be that the governmental support focused on the subsidy for purchasing machinery rather than training on the knowledge and skills for using machinery. Therefore, the movement to improve the new technology adaptation need further consideration.

Although many tourists visit the village because of its reputation for producing good apples, trading of the fruits only occurred between villagers and tourists. The number of visitors can be affected by weather and other factors, which in turn will influence the sale and a long-term plan and multiple system of diverse types of fruits are needed.

Figure 7. Market in Damoyu (Source: authors 2023)

The authors' research projects propose to consider the following aspects to protect the biodiversity and raise the living standards:

1) Develop distinctive brands of agricultural and forestry products. For example, the success of the apple production and trading in villages can be used for other products.

2) Promote new ways of using local agricultural and forestry products. For example, training sessions for promoting knowledge of planting fruit trees, sustainable ways for controlling insects, and for retaining product freshness after picking.

3) Introduce new technologies and equipment, which are linked to necessary training programmes.

4) Introduce sustainable agriculture such as organic agriculture, green agriculture etc. This will improve the sustainable use of water resources and soil protection.

5) Design and plan the landscape and road system to shorten the distance between the farm and consumers. Allow public space for apple trading in the village and set up space for resting, washing and storing fresh fruits and vegetables before they are transported to trading centres.

3.2.2 Human impacts on the landscape

The living activities of the villagers have affected two aspects significantly. The first concerns problems related to toilets, waste disposal, and sewage treatment. The villagers use particular kinds of "dry toilets" which do not use water flush, which is common in rural areas where water resources are scarce. Some toilets are well equipped with designs to solve the smell and hygiene issues, such as using chemicals or to cover excreta after use with materials such as wood, sawdust or lime. Some toilets are very basic with open sewage, and the period to empty the dry toilet also affect the smell and hygienic problems, especially in summertime. Based on the authors' survey of the visitors' views about the village, the cleanliness of the toilets had a significant impact on the overall environment of the village and the perception of tourists. Due to local beliefs and customs, villagers in Damoyu Village use dry toilets detached from their houses. Similar to some other

rural areas of Yunnan, villagers rarely allow toilets to be built inside the buildings. According to the villagers of Damoyu Village, they believe that the toilet is an unclean place and placing it inside the house will violate the areas for gods in the house. Therefore, most people's toilets can only be placed in the courtyard outside the house. Some even built those on the side of the streets outside the courtyards. Therefore, dry toilets located in various locations in the village are an urgent problem that needs to be solved in the environmental sanitation improvement of Damoyu Village.

Secondly, other human activities that may affect environment relate to energy use. These include: installing solar water heaters; promoting the use of firewood-saving stoves to replace traditional old stoves; promoting clean energy and energy-saving and environmentally friendly technologies in rural areas; and use of biogas digesters for village households. Those aspects also need to be successful in their implementation.

4. CONCLUSION

The case study locations discussed in this paper are not those 'Traditional Villages' listed by government which would include high levels of traditional heritages and thus have funding support to protect tradition and promote development. The case studies are similar to many other 'normal villages' and still have various opportunities for developments. The case studies discussed in the paper demonstrate that the relationships between the rural economy, lifestyles and the landscape are closely related in particular regions and locations. In the Yuwan villages, the movement of people following the local government policies, and the mixture of the function for rural and urban population in Damoyu village shows that new strategies are needed for such multi-function villages and their more mobile populations. In this increasingly changing context, the identified issues to be addressed are: the cultivation of the landscape, such as to protect biodiversity and improve the quality and the economic value of natural environment and valuable crops (such as local products from bamboo); and the promotion of new uses of local agricultural and forestry products, which have to be considered together with economy development.

Various evaluation and identification index systems for traditional villages in China generally emphasise the protection of traditional buildings, revitalization, development of economy, tourism, transportation and resource management. There are fewer policies on rural development that include "landscape" as a special catalogue for consideration. This is important due to changed lifestyles and the opportunities for income enhancement as elements in evaluation and planning.

The relationships between the rural economy and lifestyles with the landscape have changed significantly in recent years. Boundaries of natural environment and farming land are constantly shifting. Sustainable design and planning principles suitable for each village should be discussed with the participation of local villagers through a process of research of its characteristics and identities with the consideration of long-term benefits.

In summary, this study analyses rural development in relation to the landscape in two village areas in Yunnan, Southwest China. It is argued that historical heritage and geographical features in the region are important factors affecting rural development. The case studies demonstrate that to promote sustainable living and protect the biodiversity in rural areas in Southwest China, it is important to combine the measures with those that can protect biodiversity, promote economic development and build local capacity for employment. It is also beneficial to promote tourist flows into the area by developing relationship with the outside world and to raise the architectural quality and environmental sustainability.

ACKNOWLEDGEMENTS

Special thanks due to villagers in the studied villages that helped us in the field works. This research was funded by the research fund from the Sustainable living Research Centre at the University of Huddersfield

REFERENCES

1. Liu, Y. F. Fang, and Y. Li, (2014) Key issues of land use in China and implications for policy making. *Land Use Policy*. 40: p.6-12.

2. Cattaneo, T. and R.D, Lotto, (2014). *Rural-Urbanism-Architecture: Design strategies for small towns development*, Alinea Editrice s.r.i.

3. Yan, Y., D. Lossifova, and Y. Ren, (2021). More than 'urban character': an introduction to the concept of fengmao and fengmao-led planning and design in China. *Uran Design International,* 26:p. 211–9

4. UNESCO. (2021). Draft medium-term plan, 2022–2029: Paris: UNESCO, [Online]. Available: https://unesdoc.unesco.org/ark:/48223/pf0000375755_eng [12 October 2023]

5. Gao, Y., A. Pitts, and W. Jiang, 2023. Peri-urban villages in Kunming, Southwest China: history of change with dual urban–rural characteristics. *The Journal of Architecture*. 27, p. 7-8.

6. Pitts, A., Y. Gao, Q. Wen., LL. Dong (eds.), (2020). *Collection of Design Projects from Southwest China Rural Innovation and Sustainable Development Research Alliance*, Huazhong University of Science and Technology Press, Wuhan, China.

PLEA 2024 WROCŁAW
(Re)thinking Resilience

Evaluation of Retrofit Design Impacts on Carbon Emissions:
A Case Study of Cullinan Studio's Foundry Project

NOEMIE LANG[1], ELSA MENDOZA[1], JIHO OH[1],
LUCELIA RODRIGUES[1], RENATA TUBELO[1], LORNA KIAMBA[1]

[1]Department of Architecture and Built Environment, University of Nottingham, United Kingdom

ABSTRACT: Around 80% of 2050's building stock already exists. To achieve UK's net zero target, the energy performance of this stock needs to be addressed. In this paper, the authors looked at a retrofit project of an office building in London. The aim of the research was to assess the impact of the retrofit by looking at the Whole Life Carbon (WLC) emissions. The WLC was evaluated by calculating the operational and embodied carbon for 60 years' lifetime, using LETI methodology. Simulations were carried out to compare the previous office performance, the current performance and additional design improvements for increasing energy efficiency. These iterations considered double insulation, changing windows' properties and adopting Mechanical Ventilation with Heat Recovery system (MVHR). The results indicated that the retrofit measures reduced more than 50% of the embodied carbon when compared to a new construction. In terms of operational carbon, the retrofitted project reduced emissions by 34% from the previous office. The MVHR had the greatest benefits of the tested strategies, reducing heat demand by 39% and only increasing embodied carbon by less than 3% compared to the retrofitted scenario. Retrofitting the building stock was found to be crucial for meeting the 2050 Net Zero target.
KEYWORDS: Retrofit, Embodied Carbon, Operational Carbon, Whole Life Carbon Assessment, Energy Efficiency

1. INTRODUCTION

The UK's built environment is currently responsible for 25% of total UK greenhouse gas emissions [1]. Around 80% of the buildings that will form the 2050 housing stock already exists and these are inefficient and underperform [2]. To achieve UK's net zero target by 2050, the energy performance of this stock needs to be addressed.

Existing buildings provide a unique opportunity to positively exploit the potential use of these spaces while allowing adaptation, resiliency and reducing embodied carbon emissions from demolition and new buildings. With this in mind, the Foundry by Cullinan Studio was explored to determine the impact of the retrofit strategies on the Whole Life Carbon (WLC) emissions. The building was evaluated at three different stages: before retrofit, retrofitted and with the consideration of additional design strategies for improved energy efficiency.

2. CLIMATE

The case study is situated in Greater London. According to Atkinson's Climate Classification from 1953 [3], London is classified under temperate climate, and experiences warm mild summers and mild to cool winters with abundant precipitation throughout the year.

In accordance with these climate conditions, the main comfort strategies for buildings should consider increasing the heat gains in winter. Passive design strategies are relevant to design for solar heating. Some of these main strategies are 1) orienting the majority of the glass area south to maximize winter sun exposure, and designing overhangs to fully shade in summer, 2) providing double or triple pane high performance glazing (Low-E) on west, north, and cast, but clear on south for maximum passive solar gain, 3) reducing heating needs through heat gain from lights, occupants and equipment, 4) using High Efficiency heaters or boilers, 5) keeping the building right sized to reduce excessive floor area and excessive heating, cooling and lightning energy and 6) using extra insulation that will improve indoor temperature and be cost effective [4].

3. CASE STUDY

The Foundry is a retrofit project on a Victorian 19th century warehouse building, in which the south-east facade and roof's wooden truss are listed [5]. The retrofit proposal by Cullinan Studio aimed for design studio spaces to have the daylight and the views to the canal enhanced while retaining as much as possible of the existing building to reduce the embodied carbon emissions and the project cost. The only demolished element was a 45m^2 brick wall from the north-west facade towards the street entrance. A fabric-first approach was used for the rest of the walls by adding more insulation inside as well as on the floors and roof.

Figure 1: North façade of Cullinan Studio's Foundry Project.

4. METHODOLOGY

London Energy Transformation Initiative (LETI) is a network of professionals established in 2017 that aims to support the transition of the built environment to net zero carbon, through a series of guidelines [6]. LETI developed a methodology for assessing the carbon emissions of buildings throughout their lifecycle and published it in the Opinion Piece on Operational Carbon in Whole Life Carbon (WLC) Assessments [7]. They proposed a methodology for the conversion of operational energy into operational carbon, to be added to the embodied carbon and to get the WLC impact of the building.

It consists of a split carbon factor calculation to separate the emissions between decarbonised electricity and the non-decarbonised sources [7]. The carbon factor takes into consideration an estimate of the UK's amount of renewable energy production and the future possible projection of its decarbonisation [7]. The limit for decarbonised factor is the LETI Energy Use Intensity (EUI) target, depending on the building use. The EUI target for offices was 55 kWh/yr/m^2. When a building consumption surpasses this target, the carbonised factor is applied to the additional energy used (Equation 1).

Equation 1: LETI Whole Life Carbon.

The methodology to calculate the current operational energy use was by performance simulations using Passive House Planning Package (PHPP) [8]. PHPP is a design tool that runs in Excel and considers steady state. Two different scenarios were considered in the investigation: the building before and after retrofit.

As per fabric first approach, only external building components were considered during the simulations and calculations and these were the external walls, the roof, and the floors. The assumptions considered for the original building were based on existing drawings, which consisted of brick walls of 500mm with a U-value of 1.24 W/m^{2}K and single-glazed windows. For the retrofit simulation, the additional layers were considered with final U-values of 0.11 W/m^{2}K for the south-east facade and 0.21 W/m^{2}K for the north-west facade, as well as the windows improvement to double-glazing (0.44 W/m^{2}K).

For embodied carbon (EC) emission calculations, EC factors were assigned to each different material depending on the source, density and transportation distances using OneClick Life Cycle Assessment (LCA) tool [8]. OneClick is a software with a large construction LCA database for automated life-cycle assessments. The materials chosen from the OneClick database were assumptions as close as possible to the building components described in the available plans.

To improve the current heating demand (retrofitted building) from 45 to 25 kWh/yr/m^2 (Passive House EnerPHit target for retrofit projects) [9], four iterations were tested. The first iteration was to add more insulation to the fabric, although limited by the possibilities of the internal space. The second was to change the windows to reduce the heat losses and the third one was to adopt the Mechanical Ventilation with Heat Recovery (MHRV) system's use to the whole building. The last proposal considered the three iterations together to comprehend the whole potential. The operational carbon (OC) and embodied carbon (EC) for these iterations were calculated by the same methodology using PHPP and OneClick LCA. As for the EC, the criteria assessed was the total carbon emissions of the materials of the retrofit added to the estimated emissions from each of the proposed iterations.

5. RETROFIT RESULTS

The results of the retrofit here are presented and discussed in terms of operational energy, embodied carbon and whole life carbon.

5.1 Operational Energy

Based on the real consumption, Cullinan Studio had a previous energy use intensity of 133 kWh/yr/m^2 in its former office (Cullinan Studio, 2023). The retrofit design performance simulation had a 55 kWh/yr/m^2 target in Max Fordham's Energy Strategy Assessment design retrofit proposal (information given by Cullinan Studio), but the current resultant energy use corresponds to 88 kWh/yr/m^2 (Cullinan Studio, 2023). The performance gap between the design simulation and the real building performance is 33 kWh/yr/m^2 (Figure 2). The retrofit achieved a 34% reduction of the operational energy. The analysis using PHPP tool showed a 199 kWh/yr/m^2 heating demand before the retrofit and a 45 kWh/yr/m^2 for a retrofit scenario. This indicates a 77% improvement through fabric first approach for heating demand. As the Passive House heating demand target was 25 kWh/yr/m^2, the proposal iterations aim to improve the heating demand further than 55% in comparison a to a non-retrofitted scenario.

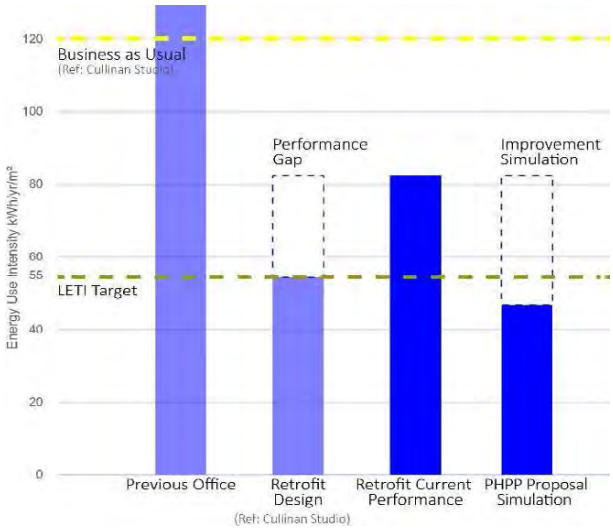

Figure 2: Operational Energy Comparison.

5.2 Embodied Carbon and Whole Life Carbon

Compared to the EC impact of new built offices with average emissions equivalent to 1200 kgCO_2e/m^2, the Foundry retrofit approach demonstrated how the emissions could be highly reduced by reusing the existing building (261 kgCO_2e/m^2). The retrofit materials and transportation stages EC represented 65% of the lifecycle of the upfront carbon. The total EC represented 17% of the WLC of the building. For one year, the total predicted emissions were 23,050 kgCO_2e. The total WLC assessment for 60 years added up to 1,383 tonnes of carbon emissions (Figure 3).

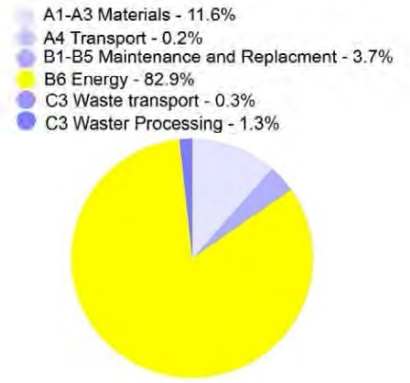

Figure 3: WLC 60 years of Cullinan retrofit, 1383 tonnesCO_2e projection.

5.3 Discussion

The retrofit demonstrated to have improved the building's operational performance by 34% in comparison to a non-retrofitted scenario, with a performance gap of 33% from the retrofit simulation. This implies the effect of assumptions and limitations of performance simulations, supporting the importance of a Post-Occupancy Evaluation (POE) to understand the impacts of decision making.

In terms of EC, the superstructure represented the highest impact with 72% of the total EC emissions, mostly because of the attributed high emissions of the use of steel and glass materials. Concrete's emissions are generally high, but in the project, concrete was used only in the foundation reinforcement and so, equivalent to 18% of the total EC emissions. There was an expected significant increase on EC for the components that were not included, as internal partitions, PV panels and MEP systems. Nevertheless, the EC represents a small percentage on the WLC compared to operational carbon (OC) from stage B6, hence, reducing energy use was the focus in the improvements proposed. The retrofit being limited by the buildings conditions and orientation could not use many sustainable passive strategies and could only be improved by insulating the fabric, improving the glazing quality, and improving the natural ventilation strategies.

6. FURTHER IMPROVEMENT RESULTS

The analyses of potential improvements were carried out using PHPP tool and consisted of improving fabric insulation, glazing efficiency and mechanical ventilation strategies. The heating demand of the retrofit was calculated to be 45 kWh/yr/m^2, and the improvement aimed for the Passive House EnerPHit target of 25 kWh/yr/m^2.

6.1 Operational Carbon

In the first iteration, insulation was increased from 145mm to 290mm for the north wall, from 80mm to 160mm for the east wall, from 150mm to 300mm for the west wall and from 100mm to 200mm for the roof. As the south wall was already highly insulated, adding

double insulation was not feasible. These changes led to a 15% reduction with a resultant heating demand of 38.4 kWh/yr/m^2. It is noted that the implications of these interventions might be too disruptive for the building's daily use. Also, the additional work needed to achieve this (removal of plasterboard, frames and finishes) would increase the cost of the iteration.

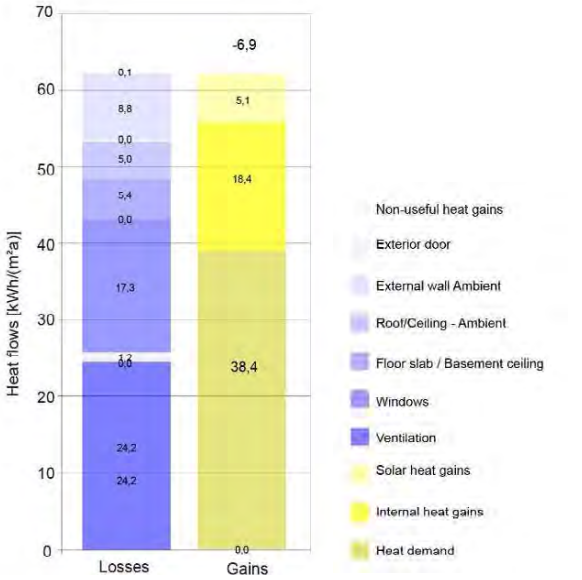

Figure 4: Proposal 1 double insulation PH heat demand balance

The second proposal consisted of replacing the double-glazed windows by a more energy efficient windows. The specifications for the existing windows were assumed to be a double glazing 4/16/4mm (argon filled, g-value=0.62, g-value, U-value=1.26W/m^{2}K). The proposed windows were considered to be triple glazing 4/12/4/12/4 (Krypton filled, g-value=0.42, U-value = 0.44 W/m^{2}K and 0.74 W/m^{2}K for the frames). Improving the window quality made a 16% reduction with a resultant heating demand of 37.8 kWh/yr/m^2. Whereas this strategy might be the most expensive, there is the least complicated change in comparison to the addition of insulation.

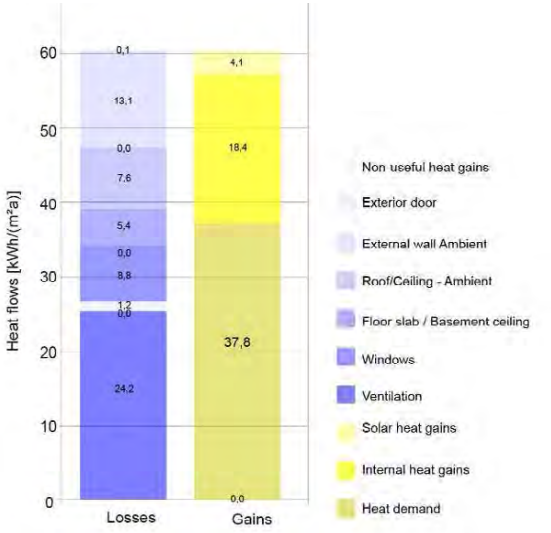

Figure 5: Proposal 2 windows quality PH heat demand balance

The third iteration considered was implementing Mechanical Ventilation with Heat Recovery for the whole building. A standard MHRV unit was considered with a 75% heat recovery efficiency inside the thermal envelope during the working hours. The air requirements were estimated for 75 occupants with a supply air 30 m^3/p*h. This results indicated that this was the most effective improvement. It represented a 39% reduction of heating demand, equivalent to 27.3 kWh/yr/m^2, almost achieving the Passive House EnerPHit target. The implication of this change requires change in equipment and ducting for the operation of the system.

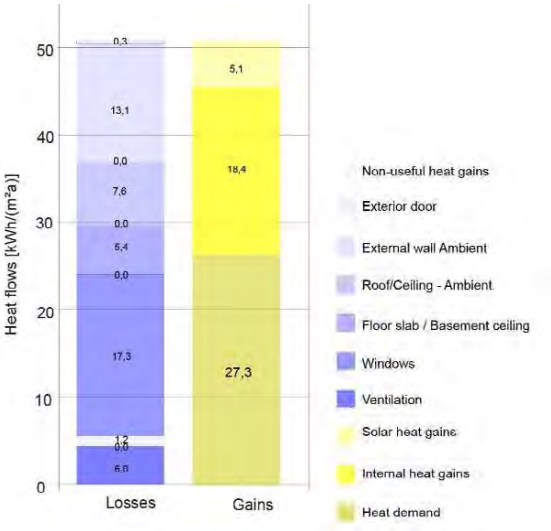

Figure 6: Proposal 2 MHRV, PH heat demand balance

The last iteration considered the three iterations combined. Whereas it is the most expensive and disruptive solution, it goes beyond the EnerPHit target and achieves the Passive House standards for new built with a 12.6 kWh/yr/m^2 heating demand, which represents a 72% reduction from the current

retrofitted scenario (Figure 8). Considering 60 years of building lifetime, this proposal's OC results in 682 $kgCO_2e/m^2$, which represents 40% of the whole life projection of the building as it is now (1138 $kgCO_2e/m^2$).

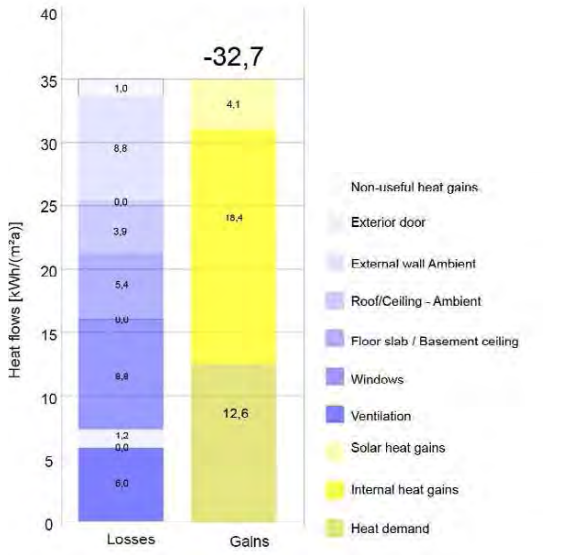

Figure 7: Proposal 4 all iterations, PH heat demand balance.

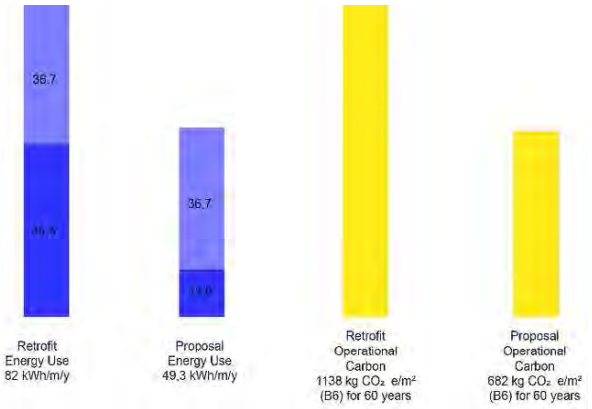

Figure 8: Operational Carbon Proposal Impact.

6.2 Embodied Carbon

As adding more insulation, replacing windows, implementing the ventilation system's pipes, all represent increasing the amount of new materials, construction processes and waste management, all the iterations will have a negative impact on the EC. Considering the last proposal with all the strategies together, the emissions' impact through OneClick tool, was an increment of 24 $kgCO_2e/m^2$ corresponding to a 9% increase from the current retrofit EC. Nevertheless, the assumptions made for the EC calculations did not include the emissions from the interior components and the Mechanical, Electrical and Plumbing (MEP) systems because of the lack of data available. Therefore, emissions would be greater in reality. Even so, these percentages still prove a low impact on EC emissions in contrast to the benefits of reducing the operational carbon.

6.3 Whole Life Carbon

The total carbon emissions in a 60-year assessment showed the importance of focusing on reducing energy use. Considering the current building's operational and embodied carbon, the WLC emissions would represent 1383 tonnes of CO_2. In comparison, the modifications to achieve Passive House standard sums up to a total of 947 tonnes of CO_2 emissions, representing a 31% reduction when compared to the retrofitted scenario. This reduction only considered the heating demand, if new occupancy patterns or equipment's efficiency are improved in the future, then this reduction of emissions could be greater.

With the LETI split carbon factors methodology and considering a 1200 $kgCO_2e/m^2$ for EC and 120 $kWh/yr/m^2$ for operational energy for an average new office building (Cullinan Studio), we can surmise that the WLC emissions might be approximately 2920 tonnes of CO_2. This proves that the retrofit as it is, has already reduced its emissions by more than half. For the proposed second stage retrofit (including the increased insulation, optimised glazing and MVHR combined), the projected emissions are three times less than the new usual building scenario and 31% less than the current Foundry retrofit design (Figure 9).

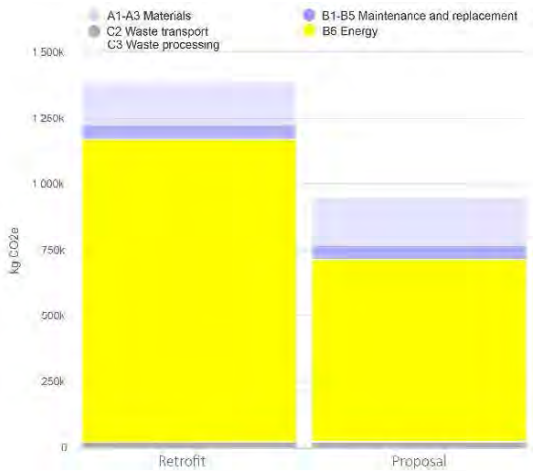

Figure 9: WLC Retrofit and Proposal Comparison.

7. CONCLUSION

The LETI methodology allowed for an integral framework to assess the research of WLC emissions. Although the retrofit project of Cullinan Studio was designed to achieve the energy use intensity LETI target of 55 $kWh/yr/m^2$, they attained an energy use of 88 $kWh/yr/m^2$ which still corresponds to a great reduction of 34% from their previous office (prior to retrofit).

Considering the pros and cons of each proposed iterations, the most efficient was the third proposal,

MVHR system, reducing the most heating demand. Additionally, compared to the embodied carbon impact of new built offices average emissions of 1200 $kgCO_2e/m^2$ (Cullinan Studio), the Foundry retrofit approach demonstrated how the emissions could be highly reduced by reusing the existing building (261 $kgCO_2e/m^2$).

It is noted that although this research provided a wider picture of the impact of retrofit on carbon emissions, the assumptions made during the various calculations because of the missing data, for both OC and EC reduced the reliability of the results. To understand the impact of each material choice, it is important to consider the carbon factor through all the design process. The WLC assessment proved the importance of a retrofit approach for the built environment. The most important design strategy must be to reduce the energy consumption as it had the greatest impact on the long term. Although the reuse approach reduced the carbon footprint by half, the percentage it represents is only 17% of the WLC emissions (Figure 10).

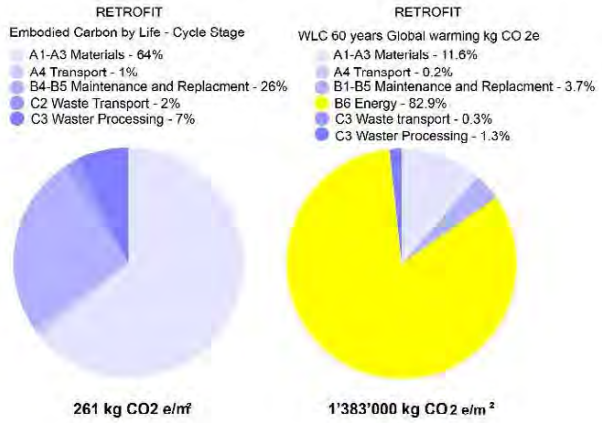

Figure 10: Embodied Carbon and WLC One Click.

If built environment professionals understand the impact of reusing and retrofitting the current available building stock, a great positive effect on the Net Zero roadmap would be possible. As a start, benchmarks, policies and regulations should be considering LETI targets as a reference for enhancing the built environment footprint.

ACKNOWLEDGEMENTS

We would like to express our sincere gratitude to the individuals who have played a significant role in the successful completion of this paper. First and foremost, we extend our heartfelt appreciation to our supervisors, Prof. Lucelia Rodrigues, Dr. Renata Tubelo and Dr. Lorna Kiamba for their guidance, invaluable insights, and continuous support throughout this research journey.

We extend our heartfelt appreciation to Cullian Studio, to Samuel Crow, the responsive architectural assistant, and architects Carol Costello and Johnny Winter for their support for this research. Their invaluable contributions, from organizing our interactions to sharing expert insights during the site visit, greatly enhanced the quality of this research.

REFERENCES

1. UKGBC, (2021). Net Zero Whole Life Carbon Roadmap. London: UKGBC. A Pathway to Net Zero for the UK Built Environment. UKGBC, 11.21 [viewed 12.05.23]. Available at: <https://ukgbc.org/wp-content/uploads/2021/11/UKGBC-Whole-Life-Carbon-Roadmap-A-Pathway-to-Net-Zero.pdf>

2. PRASAD, S., (2014). 'Chapter 1: Retrofit in Practice', in PENOYRE, G. and PRASAD, S., (2014). Retrofit for Purpose, Low Energy Renewal of Non-Domestic Buildings. London: RIBA Publishing.

3. Szokolay, S. (2014). Introduction to Architectural Science: The Basis of Sustainable Design, Taylor & Francis Group, London. P. 33

4. Climate consultant 6.0, (2023) Society of Building Science Educators. [viewed 29.12.23]. Available at: < https://www.sbse.org/resources/climate-consultant>

5. Heritage Gateway, (2012). HER [102420] Baldwin Terrace (Post Medieval Engineering Works & Bell Foundry). [viewed 22.12.23]. Available at: <https://www.heritagegateway.org.uk/Gateway/Results_Single.aspx?uid=22712837-b7e2-4a50-8d6e-746fd8cb7ea2&resourceID=191993>

6. London Energy Transformation Initiative (LETI), (2021). Climate Emergency Retrofit Guide. LETI, 01.10.21 [viewed 08.05.23] [Online] Available at: <https://www.leti.uk/retrofit>

7. London Energy Transformation Initiative (LETI), (2023). Operational Carbon in Whole Life Carbon Assessments. LETI, 20.02.23 [viewed 23.10.23]. Available at: < https://www.leti.uk/opinionpieces>

8. Passive House, (2021). Passive House Planning Package. 2021 [viewed 23.19.23]. Available at: <https://passivehouse.com/04_phpp/04_phpp.htm>

9. OneClick LCA, (2021). Passive House Planning Package. 07.21 [viewed 23.19.23]. Available at: < https://www.oneclicklca.com/construction/life-cycle-assessment-software/>

10. Passipedia, (2023). Criteria for the Passive House, EnerPHit and PHI Low Energy Building Standard. [viewed 22.12.23]. Available at: <https://passipedia.org/_media/picopen/9f_160815_phi_building_criteria_en.pdf>

PLEA 2024 WROCŁAW
(Re)thinking Resilience

Acoustic Performance of the Double C-Block:
The Tune of Sustainable Design

ALEXIA BONELLO GHIO [1], LUCA CARUSO[1], VINCENT BUHAGIAR[1]

[1]Department of Environmental Design, Faculty for the Built Environment, University of Malta, Msida, Malta

ABSTRACT: Hollow Concrete Blocks (HCB) greatly under-perform, from an acoustical point of view, due to loss of solid mass negatively impacting the wall's acoustic and thermal performance. An innovative Double C-Block (DCB) aims to offer a competitive technology able to replace the HCB, with a design that inhibits noise transmission, by virtue of its unique geometry and embedded triple layered, S-shaped polyurethane foam. Acoustic performance of the two blocks was compared by in-situ testing of two identical test cells, as well as a laboratory testing of two comparative elements in a hermetically insulated 'hot-box', and calculating their respective sound reduction indices (SRI), all in line with established ISO standards. For the DCB, a maximum value of 30dB was estimated using the Mass Law theory. Although there is scope for improvement, the results are highly promising, with the DCB already exceeding in acoustic (and thermal) performance over the HCB. This should augur well for the use of the DCB in facades to mitigating traffic noise as well as domestic noise between third party walls. The purpose of this article is to disseminate scientific evidence in favour of the DCB's acoustic performance, with a potential upgrade from technology readiness level TRL4, as laboratory-grade prototype testing, to TRL6, lined up ready for full-scale production.
KEYWORDS: Acoustic comfort, Well-Being, Sound Reduction Index (SRI), building acoustics.

1. INTRODUCTION

A steady increase in urbanization worldwide [1] is obliging more people to live in densely populated areas, predominantly apartments. Malta is no exception to urban sprawl. In addition, the built environment has increased levels of airborne sound such as traffic, construction noise, and internally, private conversations, loud music, all transmitted through slender party walls. All this contributes to the depletion of occupant's overall wellbeing. Noise can impact the quality of life of inhabitants of any age. Studies have shown that daily exposure to a persistently high noise level is harmful to a person's mental health and wellbeing because this can cause loss of hearing, sleep disturbances, and accentuate other mental or physical illnesses [2].

In Malta and elsewhere, both façades and internal third-party walls have become slenderer, for want of indoor space and speed of construction, replacing the double leaf globigerina 460mm limestone by the mass produced 230mm HCB (hollow concrete block). It is an established fact that loss of mass means loss of acoustic isolation.

The DCB as an innovative building element, is a major improvement over the HCB, in that it is a fully insulated, with enhanced thermal and sound insulation, yet still a load-bearing block. Moreover, it is even more a space saver, as it is now reduced to 190mm wide. This paper delves into its noise reduction properties, chiefly its sound reduction index (SRI).

2. LITERATURE REVIEW

Sound is a mechanical progression of particles that occurs in a medium, such as air, after which the eardrum then interprets as sound. When sound exceeds safe threshold can become a nuisance to people's wellbeing. Through the scientific study of acoustics, the expert is able to understand what are the characteristics that inhibit transmission of sound waves and exploit it to its advantage to create an engineered soundproof building block. Such characteristics include namely, bending stiffness, wall resonance, damping control, coincidence regions (resonance), and ultimately wall thickness (mass). All of these influence the sound transmission loss in relation to each frequency band perceived by the human beings [3].

Noise can be considered a nuisance when the levels are above 30dBA [4]. A typical load-bearing single leaf masonry wall is constructed from blocks (or bricks) of various material with a thin layer of mortar in-filling the area of contact to affectively transfer the loads of the structure onto the ground. The use of HCB blocks is not always ideal for specific purposes such as high-performing building facades because the internal void creates a lower solid-void ratio, and according to Mass Law, results in a decreased sound absorption capacity. Thus, its ability to reduce sound waves passing through it is highly dependent on the material characteristics that govern its bending stiffness control and damping

coefficients [5]. Subsequently, the location of its critical frequency is an important parameter which is controlled by the thickness of the element, as stated by Mass Law. However, when looking at the relationship for the transmission loss, frequency and thickness, the critical frequency is also influenced by the choice of material because it is dependent on the ratio of the materials density to the Young's Modulus [6]. This highlights the importance of material characteristics and wall thickness used.

The Double C Block (DCB) was designed with the intention of increasing the sound reduction index (SRI) of a single leaf sandwich wall. A DCB unit has a total thickness of 200mm with the concrete layer of 40 mm each and with an embedded 8 mm 'S-shaped' Polyurethane (PUR) industry-grade spray-on foam insulation, as shown in Fig. 1. The aim is to create a prefabricated insulated masonry block with sound absorbing materials so as to achieve a boundary wall that is also readily soundproof as soon as it is installed, that reduces time and labour costs, while ensuring higher quality production control [7].

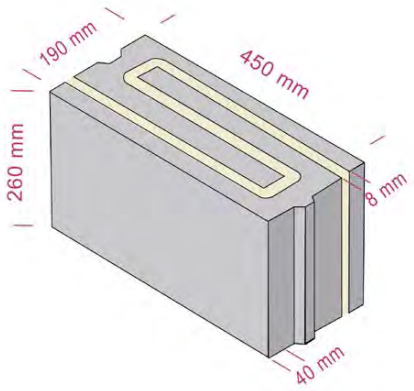

Figure 1: Illustration of DCB unit and dimensions.

It is important to note that recent literature shows several options to build single-leaf load-bearing masonry blocks achieving a theoretical transmission loss rating from 42 [8] to 53 dB [9] (the latter obtained in field tests). This range will be taken as the goal to reach for the innovative DCB block.

3. METHODOLOGY

In this research paper, ISO 10140-2 [10] was used as a reliable methodology to obtain the laboratory measurement of sound insulation of the block. The said methodology allows to calculate the standardised sound reduction index (R_w), also known as sound transmission loss (TL). This R_w rating represents the highest performance of the block in ideal conditions and controlled variables and it can only be measured under laboratory investigations. The measurement is standardised to allow for comparison with other competing masonry blocks earlier discussed in literature review.

ISO 16283-3 [12], on the other hand, discusses the procedures to carry out field experiments of sound insulation of building facades and façade elements. From this standard the $D_{nt,w}$ is obtained and it takes into consideration the combination with other structural elements in a building that may cause flanking pathways and sound leakages. Whilst R_w denotes the highest, and often theoretical, acoustic rating of an assembly, $D_{nt,w}$ reveals the performance that may be experience in an urban context.

3.1 Laboratory experiment of the DCB wall

An un-plastered single leaf wall made up of DCB block was built inside an hot box apparatus with particular care in minimizing the defects due to labour that may influence the results [11]. IN accordance with ISO 10140-2 it is assumed that ideally all of the sound energy travels directly through the test specimen only and the containment of sound within the room would render it to be highly reverberant. The left side of the wall was designated as the source room and the right side of the wall was the receiving room, as in Fig. 2 a and b.

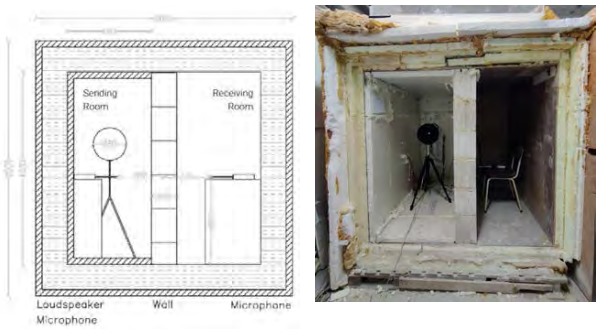

a) b)

Figure 2: Laboratory set-up of DCB wall in room. a) dimensions b) experimental set up with white noise generator.

A sound level meter (SLM) was placed in each room to record the average sound pressure levels in order to measure the changes in sound levels across the DCB wall. White noise was generated by a loudspeaker which was positioned inside the source room, i.e. the left side of the wall. All readings were recorded and uploaded to the computer to calculate the sound reduction index (R).

3.2 Field experiment of DCB and HCB rooms

The field experiment was then carried out to study both the innovative DCB block and commonly used HCB block, in the outdoors unpredictable environment. This test consisted of constructing two identical single leaf rooms at University of Malta campus that is highly exposed to traffic and construction noise. The SLMs were installed to test both mock up rooms, one built with the DCB as load bearing wall and the other with HCB, and another SLM placed 2m away from both facades.

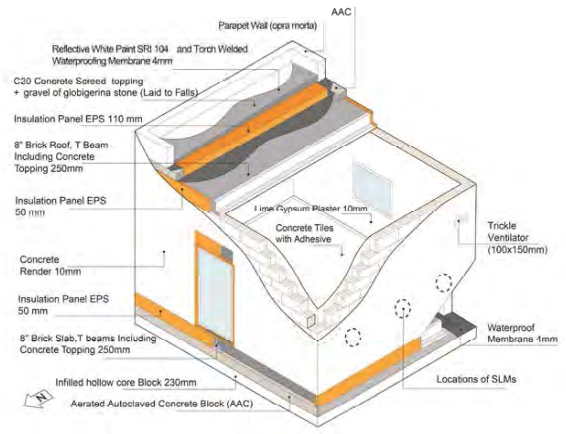

Figure 3: The full-scale test cell adapted from [7].

An overview of the construction of the test cell is available in Fig. 3 and 4.

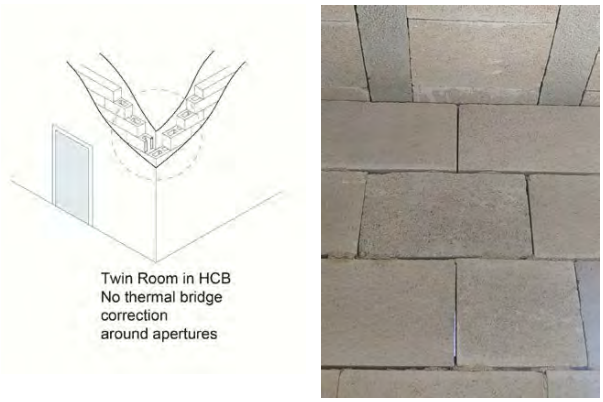

a) b)

Figure 4: The full-scale test cell reproduced from [7]. a) DCB and b) the wall to roof junction showing the evident absence of homogenous mortar joint in vertical and horizontal directions.

The experimental set up consisting of the SLM is show in Fig, 5.

a) b)

Figure 5: The ISO 10140-2:2021 Element Method.
a) SLM measuring the outdoor noise. b) SLM on the wall.

Figure 6: The ISO 10140-2:2021 Global Method with the equipment and furniture present inside the mock up room.

It is important to note that both test cells were built including two200x100mm bare ventilation openings that were not sealed during the experiment (as typical in local construction practice). According to ISO 16283-3 [12], two methods can be performed to test the external noise insulation of a facade: the *element building method* and the *global facade method*. Both use traffic and construction noise as the outdoor source sound. They measure the sound levels originating from the nearby traffic and construction noise over a specified period of time and is expressed in decibels (dB) to obtain the average sound pressure level (L_2) as per equation below.

$$L_2 = 10 \log (1/n \times \Sigma_i 10 \,\hat{}\,(L_{p,i}/10))$$

Once all the necessary data was collected they were then retrieved and analysed. The equivalent sound levels per one-third octave were extracted from the files and inputted into the sound level difference equations to find the standardised level difference ($D_{tr,2m}$). Since it is dependent on frequency, ISO 717-1 [13] was then consulted to calculate the weighted standardised sound level difference in traffic ($D_{2m,nt,w}$)

- $D_{n,e}$ = L1 - L2 + 10 log (A_0/A) for laboratory rating
- $D_{tr,2m}$ = -10 log (1/n x Σ10^(-$D_{2m,i}$/10)) for field rating
- weighted apparent sound reduction index (R'_w)
- R = L1 - L2 + 10 log (S/A) for laboratory rating
- $R_{,tr,s}$ = L1,s - L2 + 10 log (S/A) – 3 for field rating

Where $L_{1,s}$ and L_2 are the average outdoor and indoor sound pressure level on the test surface respectively.

Also, the adsorption factors to consider the presence of furniture and other bulky elements inside the room.

4. RESULTS

The three results mentioned in the methodology were obtained and plotted in the graph as shown in Fig. 7 below:

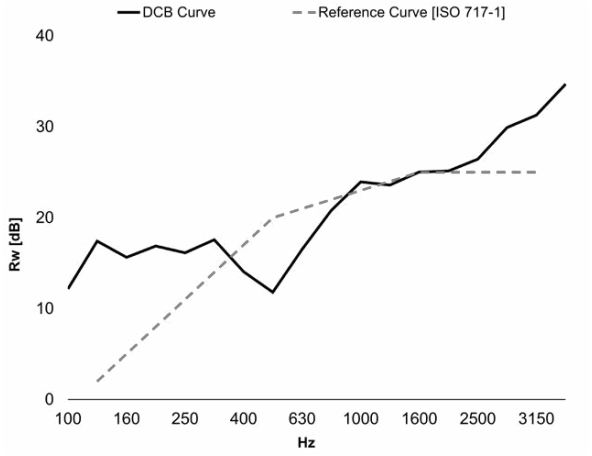

Figure 7: Laboratory acoustic results of DCB wall.

When it comes to in-situ tests the results were then listed in Table 1 :

Table 1: Tabulated results for HCB and DCB acoustic performance in laboratory and field conditions.

Metric	DCB (lab)	DCB (field)	HCB (field)
R_w (C;Ctr) dB	24 (0,-2)		
D_w (C;Ctr) dB	31 (-1,-3)		
$R'_{tr,s,w}$ (C;Ctr) dB		17 (-1,-2)	15 (0,-1)
$D_{tr,2m,w}$ (C;Ctr) dB		26 (-2'-3)	21 (0,-2)

It was immediately observed that the measurements obtained are less than those found in literature with an average of 48dB.

5. DISCUSSION

The results obtained allow for a comparison between the laboratory and field results of the DCB walls as well as the field results of the DCB and HCB walls, both of which are discussed in detail below.

5.1 Laboratory and field results of the DCB wall

The obtained results indicate that the DCB wall has a good acoustic performance when assessed under ideal laboratory conditions as opposed to its in-situ measurements. The comparisons between these two types of experiments highlighted a measured difference that was found to be greater by an increase of 7 dB and 5 dB for the sound reduction index and sound level difference ratings respectively. In fact, the literature studied denotes that these variations are within a tolerable range because *'It is generally accepted that even with ideal site conditions the minimum loss of performance between dB (R_w) and dB ($D_{tr,2m,w}$) will be between 4 and 6 dB'* [14]. Since the measured difference of the results of the field and in-situ experiments satisfy what was expected in theory, it suggests that both practical experiments were conducted properly.

To further understand what causes these different ratings between both experiments and the reasons for them, an assessment based on the differences was carried out. This investigation clearly highlighted that the variations are mostly the result of the different environments and construction techniques used. Even though the same masonry block was tested, its change in environment caused an increase in several uncontrollable variables that were responsible for the increase in pathways for the sound waves to travel through. Such uncontrollable variables that were encountered in the field experiments include, but are not limited to, the following:

- Flanking sound transmission pathways
- Direct sound leakages;
- Unsteady/unpredictable source sound levels;
- Inadequate diffusion of sound.

All of these variables were eliminated in order to obtain the best possible outcome in the controlled laboratory experiment, whereby the indirect sound passageways were minimised by enclosing the entire envelope of the laboratory set-up with insulating material. Ideally, the laboratory results represent the ideal and perfect performance of the wall. However, the dimension of the insulated box may have had an influence for reflection of sound. Having this threshold in mind allows for a reliable comparison of the wall acoustic rating in an outdoor setting.

One of the noticeable differences in the field experiments occurred due to the different experimental set up that was required on site and in the laboratory. While the laboratory method only required a single leaf wall sample to be installed, the field method required that the size of room typically found in an apartment had to be constructed. All of the additional structural elements combined to erect the testing rooms may have contributed to transmit vibration with the result that a higher-than-expected sound intensity was measured in the receiving room. This means that the overall structure did not sufficiently abate the sound waves and hence the hypothesis of sound travelling directly through the wall specimen only is not valid. Consequently, the measured transmission loss of the wall in question, was way less than the theoretical R_w.

Since the testing rooms were also used to carry out other types of experiments, such as the in-situ measurement of the U-value, some perforation had to be done on the walls of both the HCB and DCB rooms alike. Another macroscopic difference with laboratory set up was the presence of air vents on the

facade, which allowed for sound energy to enter directly, although this is deemed to be of marginal influence. However, the advantage of these 'flaws' being identical in both rooms was that in the comparison between the two rooms cancels out. In future, to achieve optimum results, it is imperative that the construction of such test cells avoids thes passive vents (yet they are typical of habitable rooms). Otherwise, unnecessary holes and cracks and in the walls should be properly sealed to ensure that an airtight envelope is attained. Other preferential sound leakage paths could be associated to the local practice of not putting enough mortar along the horizontal and vertical masonry joints, typically relying only on the finishes (pointing and render layers). Thus, the acoustic performance of the wall is diminished not due to the type of masonry block used, but due to bad workmanship.

5.2 Field results of DCB and HCB rooms

The equivalent sound level for outdoor road traffic was measured as having an average value of 60 dB. This sound level is so high that the surrounding noise would cause annoyance to the inhabitant, according to [14]. The wall's single unit rating was then subtracted from the outdoor sound level to calculate the amount of sound that was expected to be experienced inside a dwelling. A value between 29-34 dB was calculated for the DCB wall and 40 dB for the HCB wall. This conveyed that the transmitted background noise in the DCB structure reached sound levels that were very faint, which is comfortable for the average person.

Compared to other ratings of different types of masonry walls that were found in the literature earlier mentioned, the airborne sound insulation of the DCB block as well as the HCB block greatly underperformed. The average ratings from the literature compared to the DCB results are as follows;

- Single leaf wall; R_w = 49 dB > DCB; R_w = 24 dB
- Double leaf wall; $D_{nt,w}$ + Ctr = 50 dB > DCB; $D_{tr,nt,w} + C_{tr}$ = 23 dB

The weighted sound reduction index (R_w) and weighted standardised level difference ($D_{nt,w} + C_{tr}$) values of the DCB unit are also lower than the required minimum values, in accordance with legal notice introducing the Italian standard UNI 11367 (residential buildings) [15].

- Rw = 40 dB > DCB; Rw = 24 dB
- $D_{nt,w} + C_{tr}$ = 45 dB > DCB; $D_{tr,nt,w} + C_{tr}$ = 23 dB

One explanation for such low results is that during the laboratory experiments, even though the apparatus and layout were positioned and installed in accordance to the ISO standards, the heavily insulated door panel did not completely seal the opening well enough, and so sound waves may have penetrated through. This could have increased the sound levels inside the receiving room which would have been picked by the SLM, thus giving higher sound transmission values. A similar effect was also noticeable during the field experiments. Small holes were made through the façade and openings were not sealed properly. Evidently, even the slightest void reduces the sound transmission loss through the wall in question. Even though such defects impaired the true results of the wall's performance, they were apparent in both experiments, rendering the comparison and contrasts of the experiments to be relatable to the other, since effects were cancelled.

6. CONCLUSION

Overall, the results prove that the innovative DCB wall performs better than the typical HCB wall when measured under the field experiments. The comparison between the two types of masonry blocks studied achieved a difference of 2 dB and 5 dB for the apparent sound reduction index and the traffic sound level difference ratings respectively. Therefore, the innovative DCB, can effectively replace it because it is specifically developed to provide a more resource-efficient design that inhibits noise transmission, by virtue of its unique geometry and S-shaped acoustic insulation polyurethane foam embedded within the prefabricated unit. This design also does not compromise the load bearing capacity that a structural wall requires. The DCB aims to utilise sound absorbing materials within the production of the building block so as to achieve a boundary wall that is also readily soundproof instantly, as soon as it is installed. This demonstrates that by deploying technically advanced masonry block, the user can achieve both an improved acoustic and thermal performance, and possibly inhibit moisture transfer.

However, the absence of mandatory building codes (in Malta) prescribing sound-proof building elements is certainly not promoting the implementation of such innovations. Also, professionals must make more informed decisions in every step of the design process. Continuous professional development is a paramount in this respect because all professionals involved in the design of today's buildings should have the necessary knowledge of acoustics and materials science to better understand the immediate and long-term consequences of design decisions made at the planning stage so as to opt for better quality ones.

Ultimately the aim is to design resilient buildings that will withstand the unfavourable outdoor environment, while necessarily consider all the safety and well-being parameters of their occupants.

Promising case studies like the DCB, notwithstanding the limitations of the methodologies

and further research needed, have the advantage of providing evidence to the professional, researcher and end-user to strive for better performing alternative and competitive construction technology that are necessary to make this leap towards a higher quality in design in the built built environment.

ACKNOWLEDGEMENTS

This research is an outcome of the Double C-Block project, a three-year research project, for which funding was provided by the Malta Council for Science and Technology (MCST) under the Technology Development Programme (TDP) grant reference R&I_2019_010T (DCB Double C Block). This research was also funded under MCST TDP lite grant R&I-2022-003L (RESCIU Re-Engineered Stone and Concrete Insulated Unit).

The authors acknowledge the work on the data logging setup and noise monitoring sampling, supported by Inġ. Noella Cassar and Mr. Nicholas Azzopardi.

REFERENCES

1. Envisaging the Future of Cities, [Online], Available: https://unhabitat.org/sites/default/files/2022/06/wcr_2022.pdf (20 December 2023).
2. Hänninen, O. et al (2014). Environmental Burden of Disease in Europe: Assessing Nine Risk Factors in Six Countries, *Environmental Health Perspectives*: pp. 439 - 446.
3. Low Frequency Sound Insulation Dwelling, [Online], Available: https://shura.shu.ac.uk/20009/2/Maluski%20208854.pdf (20 December 2023).
4. Noise fact sheets, [Online], Available: https://www.who.int/europe/news-room/fact-sheets/item/noise (20 December 2023).
5. Santoni, A.; Fausti, P.; Bonfiglio, P. (2019). Building materials: Influence of physical, mechanical and acoustic properties in sound prediction models, *Building Acoustics*: pp. 3-20.
6. Gösele & E. Schröder, K. (2013). Handbook of Engineering Acoustics.
7. Caruso, L.; Buhagiar, V.M.; Borg, S.P (2023). The Double C Block Project: Thermal Performance of an Innovative Concrete Masonry Unit with Embedded Insulation. *Sustainability*, 15, 5262.
8. New Zealand Concrete Masonry Manual, [Online], Available: https://concretenz.org.nz/page/masonry_manual (20 December 2023).
9. Block HDIII 44/20 Graphite BASF-NEOPOR®, [Online], Available: https://en.blocchiisotex.com/wp-content/uploads//2021/07/Technical-Sheet-HDIII-44-20-graphite-ING.pdf (20 December 2023).
10. ISO 10140-2, (2021).
11. Measurements in Building Acoustics, [Online], Available: https://www.bksv.com/media/ doc/br0178.pdf (20 December 2023).
12. ISO 16283-3, (2016).
13. ISO 717-1, (2013).
14. Acoustics In Buildings, [Online], Available: https://www.acoustic-products.co.uk/faq/acoustics-in-buildings/ (20 December 2023).
15. UNI 11367, (2023).

PLEA 2024 WROCŁAW
(Re)thinking Resilience

Sustainable Adaptation of Historic Industrial Buildings

Study of key building elements and their impact on occupant comfort in Gleichrichtwerk Tegel

KATARZYNA BACZYNSKA[1], PAULA CADIMA[1]

[1]Architectural Association School of Architecture, London, United Kingdom

ABSTRACT: Historic industrial buildings provide a unique typology, characterized by high thermal mass and large internal volumes. Despite industrial retrofit projects gaining popularity in recent years, few structures are repurposed for residential use. A rectifier plant Gleichrichtwerk Tegel in Berlin, Germany, was selected as an example of an industrial building to be adapted for apartments. A site visit and computer simulations were conducted to better understand thermal and daylighting performance of the structure. Manipulation of key factors such as external wall insulation, window size, glazing type and room volume allowed to explore strengths and weaknesses of the building. The study aimed at providing a framework to inform future retrofit projects.
KEYWORDS: Retrofit, Adaptive reuse, Historic industrial building

1. INTRODUCTION

Between the 1880s and 1945 multiple complexes dedicated to electrical energy production and distribution were constructed in Berlin, Germany, earning the city the title of European 'Electropolis' [5]. According to the VDE (Verband der Elektrotechnik Elektronik und Informationstechnik e.V) database, there are still more than 200 hundred buildings of this type remaining in Berlin [7]. Despite retrofit projects drawing a lot of attention in the recent years, only a small percent of post-industrial objects in Berlin are converted for residential use. Considering their unique characteristics and potential for sustainable retrofit, this is a missed opportunity.

This paper is based on a broader dissertation project aimed at investigating the adaptation of historic industrial building for residential purposes [10]. Environmental simulations conducted at a 1920s rectifier plant *Gleichrichtwerk Tegel* in Berlin, Germany, aimed at examining the impact of the envelope characteristics on the building's thermal and daylighting performance. Key factors such as insulation levels, window proportions and room volumes were assessed. Results of the study aim at providing guidelines for further conversion for residential use.

2. CLIMATE CONSIDERATIONS

Germany is split into two distinct climates under the Köppen-Geiger classification: the temperate, no dry season, warm summer (Cfb) and the cold, no dry season, warm summer (Dfb) [1]. The data from the Berlin Tegel weather station (52˚31' N, 13˚17' E), shows the coldest month of the year is January, with the minimum/maximum daily average dry bulb temperature of -7.2˚C/9.4˚C, and an average relative humidity of 80%. The warmest month is August, with the minimum/maximum daily average dry bulb temperature of 14.8˚C/27.6˚C, and an average relative humidity of 66% [2]. The climate is strongly heating-oriented and experiences four distinct seasons with large temperature variations. For this reason, dealing with the heating demand is the primary issue in converting an uninsulated industrial building for a residential use.

3. CASE STUDY: RECTIFIER PLANT

Rectifier plant *Gleichrichtwerk Tegel* (Fig.1) was chosen as a typical example of an industrial building for a proposed adaptation project for residential purposes. It was designed between 1925 and 1927 by Richard Brademann as a part of electrical infrastructure supplying power to Berlin's S-Bahn rail and continues to serve its purpose today.

Figure 1: Gleichrichtwerk Tegel in spring 2023.

The building is oriented along the northwest-southeast axis. The ground floor is divided into smaller rooms storing electrical equipment, while the upper floor serves as two large open volumes with auxiliary

rooms on the northwest and southeast sides of the building (Fig. 2, Fig. 3). The structure is 38 m long and 14.6 m deep, with its two stories having floor-to-ceiling heights of 4.7 and 5.8 m respectively (Fig. 4). Walls are uniformly constructed with brick: external ones are approximately 50 cm thick and partitions are between 15 to 25 cm thick. Ceiling structure is made of cast concrete with supporting steel beams. Similarly, the roof structure is made of two uninsulated concrete layers 10 to 15 cm thick, with a 30 cm airspace in between and a bituminous layer on top. The building has original single-glazed windows with steel frames. It has been equipped with a system of vents running along the main elevation which allows for natural stack ventilation. The building is listed by the Berlin State Monuments Office (*Landesdenkmalamt Berlin*) and protected [8].

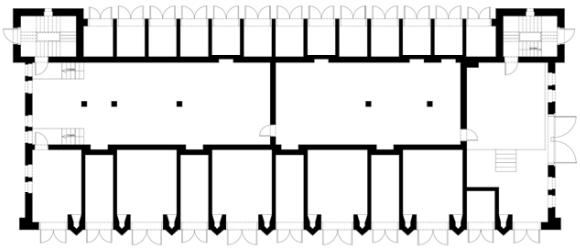

Figure 2: Existing ground floor.

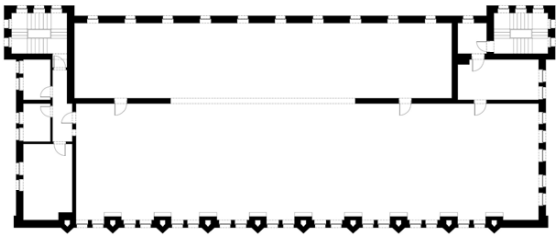

Figure 3: Existing first floor.

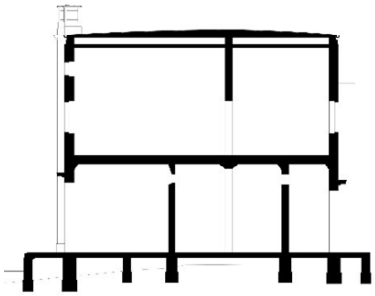

Figure 4: Existing section.

A site visit conducted in July 2023 allowed to confirm the layout of the building was mostly preserved as compared to the original 1920s construction documentation. Additional assumptions regarding the properties of the building fabric were made based on existing literature.

4. ANALYTIC STUDIES OF THE RECTIFIER PLANT

4.1 Methodology

The goal of this research paper was to examine how the building's fabric, window proportions, and room volumes impact the internal conditions as well as the potential for residential retrofit. One of the key questions was to find out the performance difference between a single-aspect unit and a double-aspect one. Another investigation was to find out the effect of adding new floors on top of the original structure. To do so, the thermal performance of a unit on a theoretical intermittent floor was compared with a unit on a an existing first (top) floor. The study recognizes that the existing German regulations regarding the retrofit of protected buildings would significantly limit the number and scale of changes which could be introduced in a real-life retrofit project. However, striving to arrive at most environmentally sound and well-performing solutions, it suggests exploring changes to the existing fabric, limited to the northeast (back) elevation.

Computer simulations were carried out to assess the thermal performance of the structure and daylighting levels inside. A simplified model of the building was created in *Rhino 7*, and *Grasshopper*. Daylighting studies of Daylight Autonomy were conducted using *Ladybug, Honeybee,* and *Radiance*. Thermal simulations were conducted using *Energy Plus*. The weather file for Berlin for the period 1991-2010 was extracted from Meteonorm 7.3.

4.2 General assumptions

Based on the original design of the façade, window spacing, and building depth, a 13.6 m by 4.6 m unit was laid out as a basis for all simulations. The model unit was placed on the first floor, which has good adaptability potential due to its open layout. The heating setpoint was set at 18˚C for the winter period, and the cooling setpoint was set at 28˚C for the summer period, based on the EN16798 adaptive comfort standard [4]. Due to the building being retrofitted for residential use, lighting loads of 4 W/m2 and electrical equipment loads of 15 W/m2 were assumed, and the occupancy pattern was set as two people occupying the space between 0:00 to 8:00 and 17:00 to 23:00 on a weekday, and all day on a weekend. In addition to supplying 30 m3 of fresh air required for each occupant, the model allowed natural ventilation following the occupancy schedule. The natural ventilation was limited to times when the outside temperature fell between 21 and 28˚C.

4.3 Base case

In the base case scenario of environmental simulations, the original building envelope parameters were input into the software. The u-values and boundary conditions for each component can be seen in Table 1. An infiltration rate of 0.5 ACH was assumed.

	U-value [W/m2*K]	Boundary condition
Roof	0.80	Exposed
External wall	1.20	Exposed
Partition wall	2.32	Adiabatic
Floor	0.88	Adiabatic
Windows	5.00	-

Table 1: Envelope properties – base case scenario.

Three simulations were carried out to compare the performance of a northeast facing unit, a southwest facing unit, and a dual-aspect one (Fig. 5). The internal loads used are outlined in section 4.2. Simulations assumed the original height of the first floor (5.8 m) and existing spacing and size of the windows. As a result, the glazing-to-floor ratio was 13.5% for the NE single-aspect unit, 21.6% for the SW single-aspect unit, and 13.5% for the double-aspect unit.

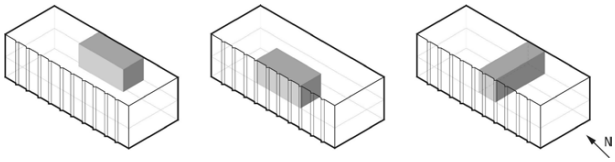

Figure 5: Single-and-dual aspect unit orientation.

Results show a big discrepancy in heating loads between the three cases (Figure 6). For the single-aspect northeast unit, the heating and cooling loads were 229 and 0.5 kWh/m2, respectively. For the single-aspect southwest unit, the heating and cooling loads were 214 and 1 kWh/m2. The dual -aspect unit performed the best, with a heating load of 176 kWh/m2 and a cooling load of 0.5 kWh/m2.

The same round of simulations was repeated assuming the units to be on an intermittent floor instead of the top one. The single-aspect northeast unit had the simulated heating load of 137 kWh/m2 and the cooling load of 0.5 kWh/m2. The single-aspect southwest unit had a simulated heating load of 124 kWh/m2 and a cooling load of 1 kWh/m2. The dual-aspect unit had a simulated heating load of 83 kWh/m2 and a cooling load of 0.5 kWh/m2. The improvement in the thermal performance of each unit is not surprising, and can be attributed to the changed boundary condition of the roof plane. However, results indicate a potential benefit of adding floors constructed with materials with better insulating properties, on the top of the existing structure. Materials such as CLT could be considered in the further design phases.

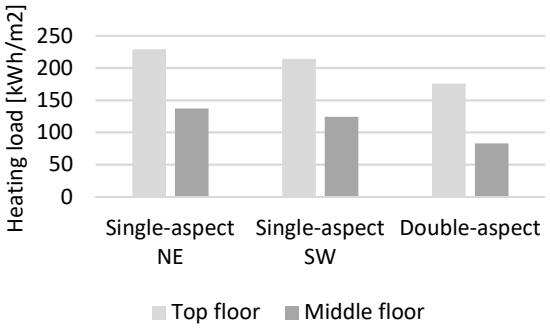

Figure 6: Comparison of the heating loads between single and double-aspect units depending on unit placement and orientation, under base case fabric scenario.

4.4 Improved fabric properties

Based on preliminary simulations, the dual-aspect unit on an intermittent floor was selected for further experimentation. The infiltration rate was changed to 0.25 ACH, more appropriate for a retrofitted building. The U-values of the external wall and windows were improved, while all other parameters assumed in the base case were preserved. In this round of simulations, two scenarios were considered: one adhering to the u-values recommended by the German regulation [5], and the one assuming the best-case scenario. In the German regulations' scenario, u-values of 0.28 W/m2*K for the external wall, and 1.3 W/m2*K for windows were assumed. For the best case, the u-values were improved up to 0.16 W/m2*K for the external wall, and 0.9 W/m2*K for the window.

Adhering to the existing German regulation allowed lowering the heating load of the unit to 20 kWh/m2, as compared to 83 kWh/m2 simulated in section 4.3 (base case), resulting in a 76% decrease. The best case simulated resulted in a heating load of 13 kWh/m2, a 84% decrease from the base case. The cooling loads in both scenarios remained unaffected, with values below 0.5 kWh/m2.

4.5 Proposed floor plan

Simulations described in sections 4.3 and 4.4 show the dual-aspect unit to have a great environmental potential. Due to its thermal performance and design allowing for cross-ventilation, it was chosen as a key model guiding the design of a residential floor plan. A floor layout was created, including seven units of varying sizes. The existing staircases were preserved, and an additional core was added in the middle of the structure. The resulting design features four double-aspect units with floor areas ranging from 62 to 70 m2, and three single-aspect southwest facing units, ranging from 36 to 48 m2 (Fig 7).

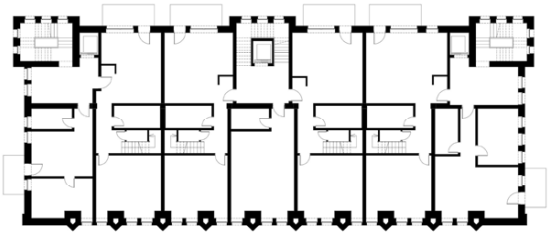

Figure 7: Proposed residential floor layout.

Due to the unique character of the front (southwest) elevation, its windows sizes and spacing were kept as original. The back (northeast) elevation had to be redesigned with more windows, in order to make the layout viable. In the double-aspect apartments, the bedrooms are oriented southwest, and the living rooms are oriented northeast. While this setup contradicts typical room placement in a residential building, it creates a possibility for opening the back (northeast) elevation and adding balconies to the communal spaces. Bathrooms and corridors were placed in the middle of the structure because they have lower daylighting requirements than other rooms.

This proposed space layout was used as a basis for further simulations which manipulated window size and height of the rooms inside a unit. While simulations conducted in sections 4.3 and 4.4 assumed the unit to be a one large volume, the significant height of the first floor of the building (5.8 m) opens possibilities for breaking up the space into two floors with lower ceilings. Four different volumetric layouts were considered and are illustrated in Figure 8. They are arranged as separate one bedroom and living room apartments (layouts A and B), or two-level apartments with two or three bedrooms (layouts C and D). Subsequent simulations assumed a simplified layout of apartment units and omitted bathrooms and corridor spaces.

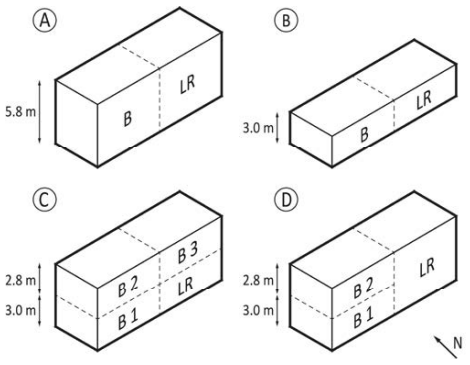

Figure 8: Different room layouts tested.

4.6 Daylighting performance

Due to the residential character of the retrofit, the Daylight Autonomy (DA) was selected as the performance metric to assess the daylighting inside the units. It is often considered more accurate than other metrics as it factors in the actual geographical location of the building, as well as the changeable sky conditions throughout the year. It calculates the percentage of occupied hours over the year, during which a task can be performed while relying solely on daylighting [9]. The subsequent metric, Spatial Daylight Autonomy calculates the percentage of the area which achieves the assumed Daylight Autonomy goal. A threshold of 50% of area reaching the DA 50% of the occupied time is usually considered as sufficient for the space to be considered daylit [6]. According to the CIBSE Guide A, the recommended lighting levels for occupant comfort are 100 lux in bedrooms, 50-300 lux in living rooms, and 150-300 lux in kitchens [4]. In the four proposed floor layouts, kitchens and living rooms are joined into one space. For this reason, 100 lux for bedrooms and 150 lux for living rooms were used as thresholds in the DA simulations.

The DA simulations were carried out in order to compare the performance of the four layouts proposed in section 4.5. The rooms in the middle of the double-aspect units receive no direct daylight, and thus rely solely on artificial lighting. For the first round of simulations, the original size and spacing of windows were preserved. In this case, the layout scenario C would not be viable due to the lack of clerestory windows on the northeast elevation.

In the layout scenarios A and B, the entire areas of the southwest facing bedrooms reached the 100 lux threshold during at least 90% of the occupied hours. The northeast facing living rooms performed slightly worse, although both would still be considered daylit. In layout scenario A, about 60% of the area reached the 150 lux threshold for more than 70% of the occupied hours. In layout scenario B, the entire area reached the threshold for at least 60% of the occupied hours, with most of the area reaching the threshold for at least 70% of the occupied hours. In layout scenario D, the entire area of the lower level bedroom reached the threshold for 90% of the occupied hours, while the entire area of the upper level bedroom reached the threshold for 70% of the occupied hours. The living room reached the threshold for at least 50% of the occupied hours.

Changes to the northeastern (back) elevation were suggested in order to improve the daylighting levels in northeast facing rooms, making layout scenario C viable. The first step was to add clerestory windows, matching those on the front elevation. Next, one balcony door was added per unit. The window spacing was altered to fit the suggested floor layout. Newly added windows followed the proportions of the original windows in the building. The comparison between the original and proposed back elevation can be seen in Figures 9 and 10.

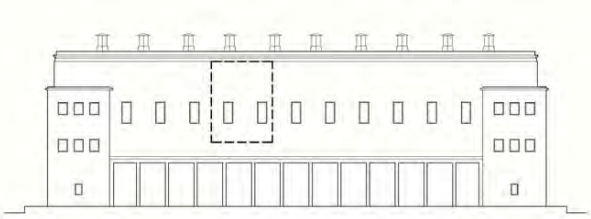

Figure 9: Existing back elevation with simulated unit outlined.

Figure 10: Proposed back elevation with simulated unit outlined.

As a result of increasing the window-to-floor ratio, the results of daylight autonomy simulations in the northeast facing rooms were significantly higher. In layout scenarios A, B, and D all of the living rooms area reached the 150 lux threshold at least 70% of the time. Introduction of the clerestory windows allowed for exploring layout scenario C, and placing a bedroom on the upper level of the unit, on the northeast side. The DA results for this scenario showed the living room area reached the 150 lux threshold for over 70% of the occupied hours, however about 60% of the bedroom area reached the 100 lux threshold for only 40-50% of the occupied hours. Based on the results, layout scenario D (Fig. 11, Fig. 12) was deemed particularly promising for further development.

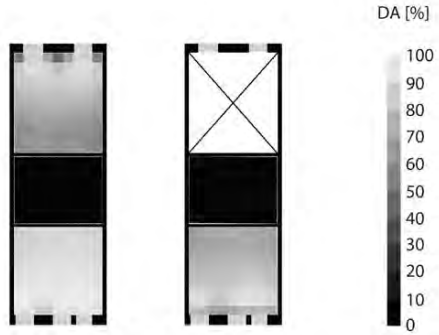

Figure 11: DA simulation results for layout D: lower level (left) and upper level (right) under original window placement.

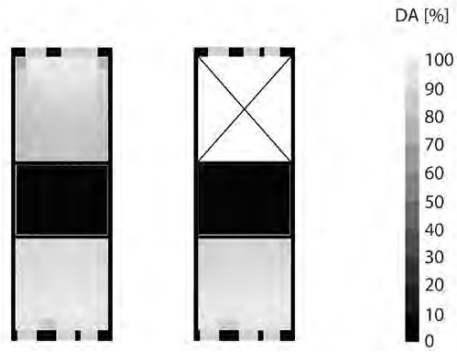

Figure 12: DA simulation results for layout D: lower level (left) and upper level (right) under suggested window placement.

4.7 Combined effects of key factors manipulation

Based on the proposed floor plan and four unit layout scenarios, another series of thermal simulations were carried out. This time, the unit was simulated in a multi-zone system, with heating loads of individual rooms combined. The changes to window number introduced in section 4.6 were factored in the model. The occupancy was increased, depending on the number of bedrooms, and the schedule was adjusted to reflect different room use throughout the day. The rest of simulation parameters remained unchanged. Two fabric versions were tested: one following the German regulations (external wall u-value = 0.28 W/m2*K, window u-value = 1.30 W/m2*K), and one considered the best case (external wall u-value = 0.16 W/m2*K, window u-value = 0.90 W/m2*K). The results of the simulations can be seen in Table 2 below.

Layout scenario	Regulation heating load [kWh/m2]	Best case heating load [kWh/m2]
A	24	15
B	10	8
C	19	12
D	20	13

Table 2: Simulated heating load for the four layout scenarios, under two different envelope specifications.

In all thermal simulations conducted on the 4.6m by 13.6m sample unit, the cooling load did not exceed 0.5 kWh/m2. Nonetheless, in this round of simulations the summer period was analysed in addition to the winter period, to assess the severity of a potential overheating issue. The smallest proposed apartment was modelled, under the assumption it would perform the worst due to its size (36 m2) and single-aspect southwest orientation. Results indicate the heating loads to be 0.15 kWh/m2 and the cooling loads to be 1 kWh/m2, for both envelope scenarios. With improved nighttime ventilation, application of external horizontal shading, and application of blinds, the cooling load can be decreased to 0.57 kWh/m2. A detailed analysis revealed the internal operative temperature only exceeds the upper threshold of the comfort band (28˚C) for 32 hours in a year, all of them during a heat wave week in July. As per the assumed occupancy schedule, 13 of the 32 overheating hours would occur during the unoccupied time. The highest simulated hourly temperature reached just above 30˚C. While undesirably high, the temperature could be mitigated by adaptive occupant measures, such as the use of a table fan. Simulations show air movement of 0.6 m/s to be enough to make the internal conditions comfortable for the occupant.

6. CONCLUSIONS

The purpose of this research paper was to explore possible layouts for residential adaptation of a historical building and study how changes to the building envelope could impact the thermal and daylighting performance of planned residential units. A site visit confirmed few changes were introduced to the building and its fabric and original materials were preserved. Due to its large open volumes, especially in the first floor, the structure offers good flexibility for different residential layouts.

In order to study the difference between single- and dual-aspect units, three layouts were tested: a single-aspect NE facing unit, a single-aspect SW facing unit, and a double-aspect (SW-NE) unit. Simulations showed the double-aspect unit to have 23% lower heating loads than the single-aspect northeast facing unit, and 18% lower heating loads than the single-aspect southwest facing unit. Additionally, units placed on an intermittent floor had 40-50% lower heating loads than units placed on a top floor. This shows a potential benefit in adding new floors on top of the original structure.

Improving the insulation levels and windows had the biggest impact on thermal performance. Complying with u-values of 0.28 W/m2*K for external wall and 1.30 W/m2*K for windows, as regulated by the German building code, decreased the heating load of the double-aspect unit to 20 kWh/m2 (76% improvement as compared to the uninsulated base case). With application of more stringent and costly measures, with u-values of 0.16 W/m2*K for external wall and 0.90 W/m2*K for windows, it was possible to lower the heating loads to 13 kWh/m2 (84% improvement).

Daylight autonomy simulations revealed the current window sizes and placement result in suboptimal daylight levels, especially once unit is divided into individual rooms. Adding windows to the northeast (back) elevation leads to improved daylighting performance in all rooms in the four layout scenarios tested. The 100/150 lux threshold was reached at least 60% of the time. However, increasing the window sizes has an adverse effect on both heating and cooling loads. Under the u-values required by the German regulations, the heating loads ranged between 10 and 24 kWh/m2, depending on the room layout. For the best-case envelope scenario, the heating loads ranged from 8 to 15 kWh/m2.

The rectifier plant *Gleichrichtwerk Tegel* shows a great potential for residential retrofit. The dual-aspect unit arrangement is the preferred layout version for residential adaptation due to its thermal performance and a potential for cross-ventilation. The original height of the first floor of the building allows for introduction of two-level units and rooms with varying heights. As a next step, additional insulating devices, such as nighttime shutters, can be considered to further decrease the heating loads. External shading devices can also be applied to tackle the potential issue of overheating during the summer period. Finally, transom windows can be applied to improve daylighting levels in rooms in the middle of the units. All in all, strategies outlined here are applicable to other historic industrial buildings of a similar size and could be useful in other retrofits for a residential use.

REFERENCES

1. Beck, H. et al., (2018) Present and future Köppen-Geiger climate classification maps at 1-km resolution. *Scientific Data*, (5(1):180214).
2. Berlin Tegel - Weather Station. *Berlin Tegel Weather Data (1991-2010)*. Retrieved: 9.04.2023
3. Bundesministerium für Wohnen, Stadtentwicklung und Bauwesen (2020). Gesetz zur Vereinheitlichung des Energieeinsparrechts für Gebäude und zur Änderung weiterer Gesetze. Vom 8. August 2020, [Online], Available: https://www.bgbl.de Retrieved: 26.05.2023.
4. CIBSE (2008) Concise Handbook. London, Chartered Institution of Building Services Engineers.
5. Dame, T. (2014). Elektropolis Berlin: Architektur- und Denkmalführer. Berlin: Michael Imhof Verlag.
6. Dogan, T., Park, Y. C., (2018) A critical review of daylighting metrics for residential architecture and a new metric for cold and temperate climates. *Lighting Research and Technology*, 51(2).
7. Historische Orte der Elektrotechnik, [Online], Available: https://www.vde.com/de/geschichte/karte
Retrieved: 26.05.2023
8. Landesdenkmalamt Berlin (2023). Denkmaldatenbank, [Online]. Available: https://denkmaldatenbank.berlin.de/ [14 June 2023].
9. Reinhart CF, Mardaljevic J, Rogers Z., (2006). Dynamic daylight performance metrics for sustainable building design. *Leukos* 2006; 3: 7–31
10. (Author) (2024) Retrofitting for climate change. Adapting historic industrial buildings for residential use. MArch Dissertation.

PLEA 2024 WROCŁAW
(Re)thinking Resilience

Towards Lower Temperature Heating:
A framework to support decision-making for energy renovations of existing Dutch dwellings

PRATEEK WAHI, THALEIA KONSTANTINOU, MARTIN TENPIERIK, HENK VISSCHER

Faculty of Architecture and the Built Environment, Delft University of Technology, Delft, The Netherlands

ABSTRACT: This study introduces a systematic framework to facilitate decision-making in selecting renovation options for preparing existing Dutch dwellings for utilising lower temperature heat (LTH) supplied by district heating (DH) systems. The framework was applied to an archetype terraced intermediate house built between 1945 and 1975 to identify the renovation options required for transitioning from existing High-Temperature (90/70℃) supply from gas-boilers to Medium Temperature (70/50℃) supply from DH systems. The framework's effectiveness was demonstrated by systematically assessing the readiness of the archetype dwelling for LTH use, reducing the number of viable renovation options, evaluating the financial feasibility using a life cycle costing approach and generating decision support insights through comparative analysis. The framework identified an optimised solution involving cavity wall insulation, exhaust ventilation and switching to low-temperature radiators. This solution incurs low initial investment and global costs while significantly reducing space heating and underheated hours. As a result, the framework provides tangible solutions for the specific use case and can serve as a valuable tool for dialogue among stakeholders during the decision-making process.
KEYWORDS: Energy Transition, Thermal Comfort, Heating Demands, Cost-Benefits, District Heating

1. INTRODUCTION

Lower temperature district heating systems offer a natural gas-free alternative for heating our dwellings. Compared to traditional district heating (DH), these systems supply heat at temperature below 75℃ [1]. This allows for integrating sustainable heating sources [2], reduces network heat losses and improves distribution efficiencies [2]. For dwellings, heating with lower temperature heat (LTH) can improve thermal comfort and indoor air quality [3,4].

Currently, only 6.4% of households in the Netherlands are connected to a DH system, although by 2050, it is expected that 50% of the sustainable heat will be supplied through them [5]. Consequently, the DH system with a lower temperature supply will be crucial in decarbonising the residential heating sector. However, with LTH, existing dwellings with higher heating demands may encounter thermal discomfort due to the reduced heating capacity of original heat distribution systems (e.g., radiators) and high heat losses [6,7]. Moreover, higher peak loads from these dwellings can create bottlenecks for reducing the supply temperature at the district level and designing future networks with sustainable heating sources [8]. As a result, existing dwellings might require energy renovations before connecting them to a DH system with a lower temperature supply.

In this study, energy renovations refer to modifications at the building level to decrease heating needs, making it suitable for LTH with sustainable heat sources [9,10]. However, stakeholders, including municipalities, private individuals and professional parties such as developers or housing associations, encounter decision-making challenges in selecting the appropriate renovation options specific to their context [10]. The heterogeneity of the existing dwelling stock, with variations in types and characteristics [11], makes it difficult for stakeholders with extensive portfolios to identify and prioritise dwellings that require renovations to enable using LTH. Additionally, the availability of numerous renovation options [11–13] and limited decision support further hinder the selection of suitable renovation options [10], impeding the renovation rates in the Netherlands. Therefore, a systematic approach is needed to support the stakeholders in preparing the existing dwellings for LTH from DH systems.

This paper introduces a comprehensive framework that aids decision-making in selecting renovation options for existing dwellings in the Netherlands to enable using LTH from DH systems. Through its application to archetype dwelling, the study aims to illustrate its advantage in 1) assessing the readiness of the dwelling for LTH use, 2) reducing the number of viable renovation options, 3) evaluating the financial feasibility of these options using a life cycle costing approach, and 4) preparing decision support insights through comparative analysis. The findings from the framework's application have the potential to impact the decision-making process and mitigate challenges for the stakeholders involved.

2. MATERIALS AND METHODS

A systematic framework is crucial when choosing appropriate renovation options for LTH supplied by DH systems. Figure 1 presents a concise six-stage decision support framework that can be adapted to various dwelling types. It addresses both the preliminary investigation and actual decision-making aspects.

2.1 Identification and Diagnosis

The initial stage of the framework focuses on identifying the target dwellings and establishing the benchmark performance metrics to assess their readiness for LTH. For this study, an archetype representing a terraced intermediate house built between 1946-1975 is selected. The terraced house constitutes around 42% of the entire dwelling stock of the Netherlands. Of these, 40-50% were constructed between 1945-1985 [14]. A calibrated parametric model developed in Rhino Grasshopper, with Ladybug and Honeybee plugins for energy analysis, is employed to establish the benchmark performance of the archetype in the existing high-temperature (HT) supply.

2.2 Evaluate suitability for LTH

In this study, a dwelling case is deemed ready for LTH if it either maintains or improves the space heating demand and reduces underheated hours in lower temperatures compared to the benchmark performance in HT supply [15]. Key performance indicators (KPIs) encompass annual space heating demand (kWh/m^2) and occupied hours below the threshold of 20% PPD or percentage of people dissatisfied [16].

This stage first involves establishing the transition goals for lowering the supply temperature, such as reducing the existing supply temperature from HT(90/70℃) to medium temperature (MT) level of 70/50℃ as accepted in the Netherlands [15] but may vary internationally. Once defined, the dwelling's performance at lower temperatures is compared to HT benchmark performance through KPIs to evaluate its LTH readiness. If the dwelling is not ready, the next step involves developing a solution space of potential renovation options to prepare the dwelling for the lower supply temperature transition goal defined earlier.

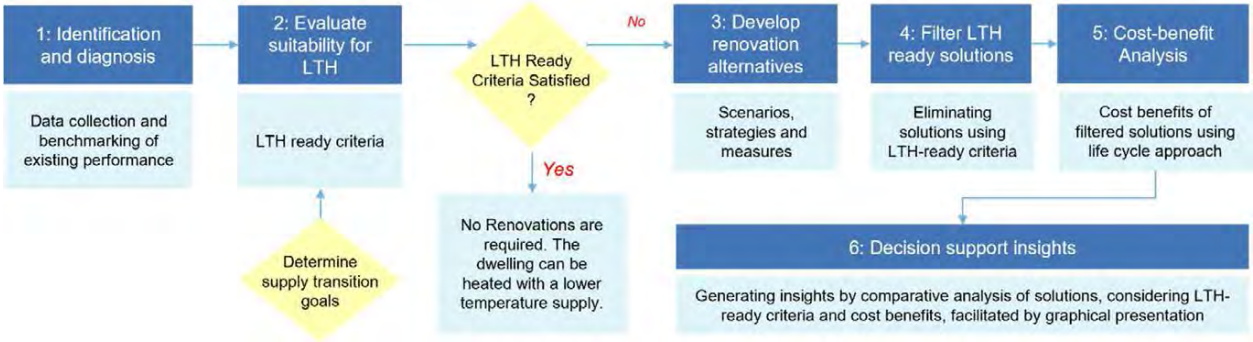

Figure 1: Proposed framework to support decision-making in selecting renovation solutions for using LTH from DH systems.

2.3 Develop Renovation Alternatives

Given the availability of various renovation options often leading to decision paralysis, this stage utilises a sub-framework designed to systematically identify and organise the available renovation options into scenarios, strategies and measures. Scenarios represent the diverse situations to achieve the renovation objectives. In this study, the renovation objective is to prepare the dwelling for heating with lower supply temperature transition goals set in stage 2 of the framework. Three different levels of renovation interventions—basic, moderate and deep—are considered to achieve the objective. Once scenarios are established, various strategies, or application-level alternatives, are identified to address each renovation scenario. Finally, product-level measures are outlined for implementing the renovation strategies. For a detailed explanation of the sub-framework, readers are referred to the study by Wahi et al., 2023 [15].

2.4 Filter LTH-ready solutions

The renovation options identified in Stage 3 undergo an evaluation to filter out the solutions that can prepare the dwelling for the transition goals identified in Stage 2. For the same, the solutions are dynamically simulated using the parametric model, and their performance is compared against the benchmark performance of the dwelling in the HT supply. Solutions that fail to improve space heating demand or reduce underheated hours are excluded. This results in a filtered set of desirable solutions that can prepare the dwelling for LTH.

2.5 Cost-Benefit Analysis

Assessing costs and benefits is paramount for stakeholders in decision-making. Given the importance of evaluating the trade-offs between initial renovation investments and the ensuing benefits, such as operational cost savings or improved thermal comfort, this stage focuses on conducting a cost-benefit analysis for the desirable LTH-ready

solutions. A life cycle costing methodology is adopted for calculating global costs over a 30-year time frame. The global costs (GC) are calculated as the sum of initial investment costs for renovation and the net future costs of operation, maintenance and replacement discounted to present value or Net present value (NPV). This study uses a real interest rate of 2.8% and an inflation rate of 2 % for calculating NPV.

2.6 Decision-support insights

The purpose of the framework is to provide support for decision-making and facilitate the selection of appropriate solutions. Consequently, it becomes imperative to consolidate and communicate the results clearly and insightfully. As a result, a graphical representation is generated to depict the performance evaluation outcomes of LTH-ready solutions and their cost-benefit analyses. This graph serves as a vital tool for communicating the performance of various solutions, enabling stakeholders to navigate trade-offs effectively and gain insights into selecting the appropriate solutions tailored to their specific contexts.

3. RESULTS

The study aims to demonstrate the application of the framework on existing dwellings in the Netherlands. It showcases its utilisation in addressing decision-making challenges associated with transitioning from HT supply to LTH. The framework is applied to an archetype terraced intermediate dwelling constructed between 1945-1975 to demonstrate the same. Table 1 outlines the typical characteristics of the archetype dwelling.

These characteristics were used to establish the benchmark performance of the archetype dwelling under the existing HT supply. Annual simulations, following the Test reference year (TRY) specified by NEN 5060 [17], were conducted to determine the KPIs, including space heating demand (kWh/m^2) and underheated hours, acting as benchmarks in the HT supply context. The underheated hours were only evaluated for the living room, as it can be used as a proxy for evaluating the thermal comfort of the entire dwelling [15].

Subsequently, the readiness of the archetype dwelling for a lower temperature supply goal was evaluated, focusing on the transition towards MT supply (70/50 ℃). Table 2 illustrates the performance of the dwelling in HT and MT supply. The space heating demand in MT decreases as the radiator capacity also decreases with the reduction in supply temperature. Consequently, the space heating system's reduced capacity (radiators) is insufficient to compensate for the heat losses, thus resulting in a higher number of underheated hours. Therefore, the archetype dwelling in its existing condition is not ready to be heated with an MT supply and requires renovation before being connected to the DH system with an MT supply.

Table 1: Typical characteristics and assumptions of selected archetype terraced house from 1945-1975 [18]

	Properties	Units
Compactness Ratio	1.22	-
Usable floor area	142	m^2
Window-Wall Ratio of facades	0.38	-
Ground floor, *U*	1.75	W/m^{2}K
External Wall, *U*	1.19	W/m^{2}K
Roof, *U*	0.82	W/m^{2}K
Windows, *U*	2.73	W/m^{2}K
Doors, *U*	3.31	W/m^{2}K
Infiltration rate	3	dm^3/s.m^2
Ventilation System	System A: Natural supply and exhaust	-
Temperature Setpoint	Living Room and Kitchen: 20 Other spaces: 16	℃
Number of occupants	3	-
Lighting and Equipment density	4	W/m^2

Table 2: Benchmark performance of the archetype dwelling in HT supply compared to the MT supply.

Supply Temperature	Annual space heating demand [kWh/m^2]	Occupied underheated hours[1]
HT Supply (90/70)	163	1630
MT supply (70/50)	130	2123

[1]*Out of 5840 occupied hours in a year.*

Three scenarios based on the level of renovation intervention—basic, moderate, and deep—were employed to achieve the renovation objective of preparing the dwelling for MT supply. The basic intervention level, entailing no changes to the building envelope, involves strategies such as increasing the capacity of the heating system to compensate for increased underheated hours or lowering the setpoint temperature to reduce the space heating demand. The moderate intervention level focuses on selected improvements to the building envelope, such as changing windows, cavity insulation or improving the ventilation system. In contrast, deep renovation encompasses holistic changes to the dwelling to exploit the combined effect of improvements at the building envelope, system, and control levels. Table 3 provides an overview of the renovation scenarios indicating the intervention level required for MT supply along with corresponding strategies. The measures aligned with each strategy are derived from the RVO platform, indicating energy-efficient renovation measures at the product level, including investment costs [19].

Table 3: Organisation of the solution space in the form of renovation scenarios, strategies and measures [15,19].

Scenario	Strategy	Measure
Basic	Increasing heating capacity	Existing HT Radiators[1], Radiators with extra convectors
	Reducing setpoint temperature	20[1], 19 [°C]
Moderate	Improving ventilation system	System A: Natural Ventilation[1], System C: Mechanical exhaust ventilation
	Cavity wall insulation *(U)* + infiltration rate	1.19[1], 0.63, 0.56, 0.48 [W/m²K]
	Improving window insulation *(U)* + infiltration rate	2.73[1], 1.6, 1.5, 1.2 [W/m²K]
	Infiltration rate due to improvement in envelope	3[1], 2 [dm³/s.m²]
	Basic + Moderate combinations	-
Deep	Replacing existing radiators	Radiators with extra convectors
	Reducing setpoint temperature	20[1], 19 [°C]
	Replacing ventilation system	System D: Balanced mechanical ventilation with heat recovery (MVHR)
	Airtight envelope	0.4 dm³/s.m²
	External Wall insulation *(U)*	0.26, 0.21, 0.17 [W/m²K]
	Replacing windows *(U)*	1 [W/m²K]
	Internal roof insulation *(U)*	0.27, 0.15, 0.14 [W/m²K]
	Underneath ground floor insulation *(U)*	0.48, 0.27, 0.24 [W/m²K]
	Replacing external door *(U)*	1.4 [W/m²K]

[1] *Existing condition of the dwelling.*

As indicated in Table 3, the basic intervention level leads to three measures, excluding the base case involving the existing radiators and setpoint temperature. On the other hand, the moderate intervention level includes individual as well as combinations of strategies, leading to 124 combinations of measures. The deep intervention level involves 54 measures combining explicitly fixed measures while varying four strategies. Consequently, these 182 measures are simulated parametrically in MT supply, and their performances were assessed against the benchmark performance of the dwelling in HT supply to identify solutions suitable for MT supply.

In addition, Figure 2 illustrates the solutions that do not meet the LTH-ready criteria for improving space heating demand and reducing the underheated hours compared to benchmark performance in HT supply. Notably, it is observed that the basic intervention level cannot prepare the dwelling, whereas only 46 moderate measures prove effective in preparing the dwelling for MT supply. In contrast, all the deep renovation solutions demonstrate the capability of preparing the dwelling for MT supply.

The subsequent step involves a comprehensive cost-benefit analysis of the filtered solutions. As outlined in section 2.5, GC was calculated using the NPV for each measure combination over a 30-year timeframe. The investment costs were sourced from the RVO platform [19], including components, labour, and installation costs for the filtered measures. Operating costs were based on the fixed and variable rates for gas, electricity and DH as of 2022. A baseline for comparison of GC was established using a base case scenario with no renovation while only considering gas boiler maintenance and replacement through its lifetime. Once the GC was calculated for all desirable LTH-ready options, it was plotted against the thermal comfort benefits of LTH-ready solutions, forming the graphical representation to support decision-making.

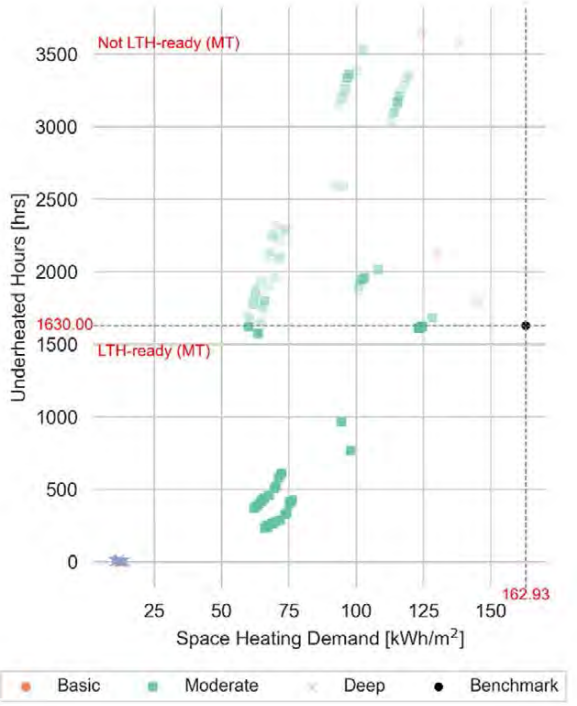

Figure 2 Filtered solutions for LTH-readiness. Out of 182 measures, only 100 can prepare the dwelling for MT supply.

Figure 3 shows the life cycle costs, as GC (includes investments, maintenance, and operation costs) and the associated benefits stemming from the reduction of underheated hours (thermal discomfort) due to the

renovations. The graph visually depicts the range of space heating demand for each measure, with the base case (no renovation, existing condition with HT supply with gas-boiler) serving as the benchmark for visual comparison of the performance of LTH-ready measures.

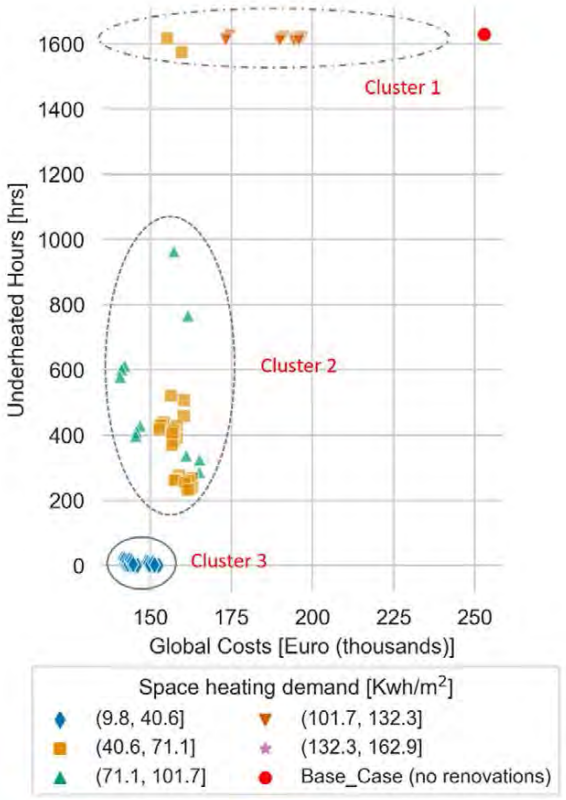

Figure 3 Decision Support Insights: Evaluating the cost-benefits of the LTH-ready solutions.

Upon observing Figure 3, the measures can be categorised into three clusters. Cluster 1 comprises 14 renovation measures that are on the cusp concerning the LTH-ready criteria compared to the base case scenario. These solutions can improve the space heating demand by 20-60% and reduce GC by 22-38% from the base case. However, thermal comfort improvements are marginal, with an average reduction in discomfort hours of only 1%. As a result, it can be argued that the measures within cluster 1 can correspond to the minimum renovation intervention required for heating the dwelling with MT supply. Given the limited impact of these measures on improving thermal comfort, it is imperative to analyse the trade-offs only between initial investment and global costs.

The options with the lowest investment costs are the measures with cavity wall insulation of 0.56, 0.48, or 0.63 W/m^{2}K with LT radiators (refer to Table 3). These solutions incur initial investment costs ranging from 2.3k to 2.8k euros, with an average 24% reduction in space heating demand and a 31% reduction in global costs. In contrast, the solution with a cavity wall insulation of 0.48 W/m^{2}K, glazing insulation of 1.2 W/m^{2}K, mechanical exhaust ventilation (type C) and a temperature setpoint of 19°C achieves a 38% reduction in the GC. Even though this measure can reduce the space heating demand by 63%, it entails a higher initial cost of 26k euros. Consequently, if the preference is to minimise renovation intervention and changes to the dwelling, thus reducing overall hassle, the option for cavity wall insulation with a switch to LT radiators can be considered the minimal renovation solution required by the archetype dwelling for heating with MT supply from DH systems.

Cluster 2 encompasses 32 moderate-level measures that can reduce the space heating demand and the number of underheated hours by 40-60% and 40-85%, respectively, compared to the base case. Simultaneously, these measures can reduce GC within the 35-45 % range. Among these, the solution with minimal investment costs (3k euros) involves only replacing the ventilation system with type C (mechanical exhaust , natural supply), which leads to a 42%, 41% and 37% reduction in the space heating demand, the number of discomfort hours, and GC, respectively. Moreover, the solution with the lowest GC at 140k euros achieves a 44% reduction in GC from the base case. This is attained by replacing the ventilation system with type C and adding cavity wall insulation of 0.48 W/m^{2}K. With an investment of only 3.5k euros, this solution reduces the space heating by 56% and the number of discomfort hours by 64%. Finally, the solution with the highest thermal comfort, providing an 85% reduction in discomfort hours, integrates a ventilation system type C with cavity wall insulation of 0.48 W/m^{2}K, glazing with a U-value of 1.2 W/m^{2}K and LT radiators. While this measure results in a 60% reduction in space heating demand and a 36% reduction in global costs, it does require a higher initial investment of 28k euros.

Finally, the third cluster comprises deep renovation solutions that can reduce the number of discomfort hours with considerable energy savings by around 90%. Furthermore, these solutions exhibit a reduction in global costs by around 44%. Even though these measures can have the highest benefits, they also account for the highest initial investment, between 40-55k euros.

Examining Figure 3 and the insights it provides, the measure incorporating the cavity wall insulation of 0.48 W/m^{2}K for the archetype dwelling, paired with exhaust ventilation system type C and a switch to LT radiators, emerges as the optimised solution for preparing the dwelling for MT supply. This measure requires a comparatively lower investment of 3.5k euros, just a thousand euros more than the minimum suggested in cluster 1, and substantially reduces discomfort hours and space heating demand. However, an additional factor of future readiness

could be considered: whether the solution remains effective in satisfying LTH-ready criteria if the supply temperature is further reduced to a Low-Temperature (LT) supply of 55/35℃ while contributing to the lowest GC.

4. CONCLUSION

This study presents a systematic framework to facilitate decision-making in selecting renovation options to prepare existing Dutch dwellings for heating with LTH supplied through DH systems. By applying the framework to a typical terraced intermediate dwelling from 1945-1975, the study showcases its effectiveness in evaluating its readiness for LTH in its existing condition and identifying necessary renovations for a transition to MT supply. The framework organises the available renovation options and aids in effectively filtering out the solutions that cannot prepare the dwelling for LTH. Thus, it offers a curated solution space tailored to the specific context of the dwelling. Moreover, the study employs a life cycle costing approach and conducts a cost-benefit analysis to assess the financial feasibility of the filtered solutions. The results are presented graphically to provide insights on prioritising measures based on their impact on LTH readiness and global costs. Through the framework's application, an optimised solution with a cavity wall insulation of 0.48 W/m^{2}K, mechanical exhaust ventilation type C and a switch to LT radiators is identified for MT supply. This solution leads to the lowest investment and global costs while substantially reducing space heating demand and underheating hours. However, due to space limitations, this study only describes renovations required for transitioning to MT supply. Future studies will explore Low-Temperature (LT) supply scenarios, particularly at 55/35℃, to identify solutions satisfying LTH-ready criteria while contributing to the lowest GC. In conclusion, the framework provides tangible solutions for a specific use case and serves as a valuable tool for dialogue among stakeholders in the decision-making process. Nevertheless, validating the framework through real cases and associated stakeholders is vital to refining its utilisation in the decision-making process.

ACKNOWLEDGEMENTS

This study was carried out with the support from the MMIP 3&4 scheme of the Dutch Ministry of Economic Affairs & Climate Change and the Ministry of the Interior & Kingdom Relations.

REFERENCES

1. DNE Research National Warmtenet Trendarapport 2021; 2020.
2. Dahl, M.; Brun, A.; Andresen, G.B. (2017). Using Ensemble Weather Predictions in District Heating Operation and Load Forecasting. *Applied Energy* 193: p. 455–465.
3. Ovchinnikov, P., Borodinecs, A., Millers, R. (2017). Utilisation Potential of Low Temperature Hydronic Space Heating Systems in Russia. *Journal of Building Engineering*, 13: p. 1–10.
4. Wang, Q., Ploskic, A., Song, X., Holmberg, S. (2016). Ventilation Heat Recovery Jointed Low-Temperature Heating in Retrofitting—An Investigation of Energy Conservation, Environmental Impacts and Indoor Air Quality in Swedish Multifamily Houses. *Energy and Buildings*, 121: p. 250–264.
5. Beckman, K., van den Beukel, J. (2019). The Great Dutch Gas Transition. Vol. 54.
6. Ovchinnikov, P., Borodiņecs, A., Strelets, K. (2017). Utilisation Potential of Low Temperature Hydronic Space Heating Systems: A Comparative Review. *Building and Environment*, 112: p. 88–98.
7. Tunzi, M., Østergaard, D.S., Svendsen, S., Boukhanouf, R., Cooper, E. (2016). Method to Investigate and Plan the Application of Low Temperature District Heating to Existing Hydraulic Radiator Systems in Existing Buildings. *Energy*, 113: p. 413–421
8. Harrestrup, M., Svendsen, S. (2015). Changes in Heat Load Profile of Typical Danish Multi-Storey Buildings When Energy-Renovated and Supplied with Low-Temperature District Heating. *International Journal of Sustainable Energy*, 34: p. 232–247.
9. Asdrubali, F., Desideri, U. (2018). Chapter 9 - Energy Efficiency in Building Renovation. In *Handbook of Energy Efficiency in Buildings: A Life Cycle Approach*. Butterworth-Heinemann: p. 675–810.
10. TKI Urban energy. (2019). Versnelling van Energierenovaties in de Gebouwde Omgeving (MMIP 3) Inhoudsopgave.
11. Taillandier, F., Mora, L., Breysse, D. (2016). Decision Support to Choose Renovation Actions in Order to Reduce House Energy Consumption e An Applied Approach. *Building and Environment*, 109: p. 121–134.
12. Jafari, A., Valentin, V. (2017). An Optimization Framework for Building Energy Retrofits Decision-Making. *Building and Environment*, 115: p. 118–129.
13. Amorocho, J.A.P., Hartmann, T. (2022). A Multi-Criteria Decision-Making Framework for Residential Building Renovation Using Pairwise Comparison and TOPSIS Methods. *Journal of Building Engineering*, 53.
14. Centraal Bureau voor de Stastiek. (2023). 42 Procent van Alle Woningen Is Een Rijtjeshuis. [Online], Available: https://www.cbs.nl/nl-nl/nieuws/2022/31/42-procent-van-alle-woningen-is-een-rijtjeshuis [17 July 2023]
15. Wahi, P., Konstantinou, T., Tenpierik, M.J., Visscher, H. (2023). Lower-Temperature-Ready Renovation: An Approach to Identify the Extent of Renovation Interventions for Lower-Temperature District Heating in Existing Dutch Homes. *Buildings*, 13.
16. Peeters, L., de Dear, R., Hensen, J., D'haeseleer, W. (2009). Thermal Comfort in Residential Buildings: Comfort Values and Scales for Building Energy Simulation. *Applied Energy*, 86: p. 772–780.
17. Stichting Koninklijk Nederlands Normalisatie Instituut. (2021). Nederlandse Norm 5060 + A1. Vol. 1.
18. Cornelisse, M., Kruithof, A.F., Valk, H.J.J. (2021). Rapport Standaard En Streefwaardes Bestaande Woningbouw.
19. RVO. (2023). Kostenkentallen. [Online], Available: https://digipesis.com/ [30 December 2023].

PLEA 2024 WROCŁAW
(Re)thinking Resilience

Overlooked? Supporting Sustainable Renovation for People who are Blind or have Low Vision

ALINA BOYUKLIEVA,[1] STELLA BOESS,[1] TOMASZ JAŚKIEWICZ,[1]

[1]Delft University of Technology, Delft, The Netherlands

ABSTRACT: This paper addresses designing for accessibility of renovated housing. The investigated case evaluates interfaces of heating and ventilation systems in a demonstration apartment for an intended renovation of high-rise social housing in Amsterdam, the Netherlands. We selected a focus on people who are blind or have low vision (PBLV). We conducted two qualitative studies with different target groups, (expert) users and building domain experts, to answer two research questions: First, what are the accessibility limitations of the currently installed HVAC systems in social housing, using the example of the demo apartment? Second, in what way can we enable stakeholders aiming to commission a renovation to make decisions that improve accessibility? We argue based on interviews and remote observations that PBLV face many issues. For example, home control interfaces commonly lack features such as a voice control option or tactile buttons, making them inaccessible for this group and less accessible for everyone else. To tackle this challenge, we propose a guidebook supporting decision-makers in assessing and implementing accessibility in renovation projects of social housing. The final evaluation confirmed that such an intervention fills a gap for human-centred tools in zero-energy renovations.
KEYWORDS: accessibility, low vision, zero-energy, renovation, guidelines

1. INTRODUCTION

Currently, many older buildings are being transformed into more sustainable zero-energy housing. However, while these buildings may be equipped with technology needed for zero-energy operation, there are still many challenges preventing them from achieving that. One such challenge is the mismatch between residents' abilities, habits and knowledge and the home systems' functioning. A common example of such a mismatch is that residents do not know about or do not trust ventilation systems and maintain habits of long duration window-opening, reducing the energetic performance of the building [1]. Another example is that residents may struggle to understand and interact with the set of new interfaces they encounter in newly renovated homes. Such interfaces may be part of home energy management systems, system controls or home-control apps [e.g., 2, 3]. Often, these are new designs associated with new sustainable technologies. Usability issues with them can affect building's energy performance too. Usability issues can also have cross effects with residents' well-being in their daily home life [4, 5].

This paper addresses designing for accessibility of renovated housing. While accessibility encompasses a wide range of people and issues, in this paper we particularly focus on people who are blind or have low vision (PBLV). Based on interviews and remote observations in a newly realised demonstration apartment, we argue that PBLV face many issues, for example with dealing with home control interfaces. The demonstration apartment serves as a case for us to enquire: how could the decision-makers who commissioned this apartment be supported in commissioning technology that works better for PBLV?

To this end, we addressed the needs of the professional stakeholders/decision-makers in fulfilling the needs of PBLV. We produced a document that synthesises accessibility advice and evaluated it with two decision makers and four experts in accessibility for visually impaired. Based on this evaluation, we argue that guidelines support stakeholders in assessing and implementing accessibility in renovation projects of social housing.

The paper gives an overview of the context studied and explains the relevance and challenge of designing for PBLV. We then present two studies: first, a brief evaluation study of the demo apartment supported by interviews with a group of PBLV. A 'PBLV home energy guidebook' is developed based on this evaluation study. The second study is an evaluation of the guidebook with professional stakeholders. The paper concludes with a discussion of the implications of the intervention for PBLV and other possible target groups.

1.2 Accessibility in social housing

In 2023, WHO stated that 'at least 2.2 billion people have near or distance vision impairment' [6]. Anyone wearing glasses experiences

the effects of visual impairment when being without them. While visual impairment itself is already associated with reduced sense of well-being, being or feeling excluded from the use of one's own home environment is likely to exacerbate this further. Since an important goal of a renovation is to improve residents' comfort and well-being, especially while in the safe space of their home, such exclusion should be avoided [7, 8].

Hence, the decision-making process in housing renovations should be driven also by the aspect of accessibility. In one of the European standards 'NEN 17210: Accessibility and usability of the built environment – Functional requirements' it is explicitly stated that it must be ensured that '*ventilation and heating equipment are operational*' for all kinds of diverse users [9]. That makes designing inclusively not just an option but a requirement. While we have chosen to focus on residents with visual impairments here due to limited scope, overlapping or contrasting needs of other user groups, for example older people, or ones unfamiliar with such technology, should also be considered in the design process. A recent study argues that even though modern home appliances bring benefits to our everyday lives, '*due to the lack of accessibility support from the manufacturers and designers, a considerable number of people in need of accessibility support have been ignored*'. [8]

1.3 Issues for PBLV

While the experience of each person with a disability is very specific and a one-size-fits-all approach is implausible [10], we identified some common problems that PBLV face on a daily basis and the ways they tackle them. For example, products that provide only one control option might be limiting access. From user testimonials that PBLV have published on the internet, it can be gleaned that: among the most essential features in an accessible product for users with low or no vision are high contrast colours, buttons with high tactility, loud enough speakers, audio feedback, offline voice dictation, high compatibility with visual aids, add-ons and customizability [11]. Affordability and sturdiness were found to be as important [12].

1.4 Context

This paper takes as its case the evaluation of interfaces of heating and ventilation systems in a demonstration apartment (demo apartment) (Figure 1) for an intended renovation of high-rise social housing in the Netherlands. The demo apartment was realised as a fully functioning full-scale prototype of the intended technology within a housing block planned for renovation. It was made available to the residents and the housing association to decide on the renovation. We were given the opportunity to engage this context in our research.

Figure 1: Floorplan of the demo apartment

1.5 Research questions

We defined two main research questions:

1. *What are the accessibility limitations of currently installed sustainable HVAC systems in social housing, using the example of the demo apartment?*
2. *In what way can we enable stakeholders aiming to commission a renovation to make decisions that improve accessibility?*

1.6 Method

We conducted two user studies. The first study addressed the first research question through gathering testimonials and conducting user interviews and observation (section 2) with PBLV including experts in visual impairment. We used this data to define the design space and propose an intervention (section 3) that contributes to answering the second research question. This intervention was qualitatively evaluated both with the initially interviewed users and an additional number of professional decision makers (section 4).

2. INTERVIEWS AND OBSERVATIONS WITH PBLV

2.1 Method

To expand and evaluate the findings from the desk research, we conducted six qualitative open-ended interviews with users with visual impairments. To obtain more diverse insights, the recruited participants had different nationalities and cultural backgrounds. Three were Bulgarian and three were Dutch. Expert user 1 was completely blind as a result of losing his vision 20 years ago. He was an expert in accessibility and coaches other visually impaired people how to use digital applications. Expert users 2 and 3 had a similar occupation but still had low remaining vision. The other three participants were regular users, one of which was fully blind (Regular user 2), one able to slightly distinguish light and bright colours (Regular user 3) and one with overall blurred vision and night blindness (Regular user 1). Each interview lasted approximately an hour and was semi-structured. Three of the interviews took place in real life and three were led online because of the

corona virus restrictions. One of the real-life interviews was combined with a field study where various accessibility products were evaluated in the context of use at a centre equipped with smart technologies, supporting PBLV in The Netherlands.
To assess the accessibility during the interviews, we sought to understand to what extent '*agents can convert a resource ... into a functioning*' [13]. This means, we studied whether the participants were able use the resources provided – the sustainable technologies – for something of benefit to them. We used storytelling to elicit responses from the participants. We explained the systems in the demo apartment, including their interfaces in terms of functionalities and controls. We then asked the participants to talk us through how they would perform specific tasks such as changing the temperature setting. That approach helped identify the possible accessibility limitations of the systems while also uncovering additional accessibility requirements. To discover the latent needs of the users, we asked them to talk about their habits, the products they liked using in their everyday life and the obstacles they meet. The focus of the discussion was on indoor climate and interaction controls.

2.2 Results

Some of the main usability and accessibility issues identified within the demo-apartment are similar to other zero-energy housing, for example the slow response to big changes in temperature of the low-temperature heating system [14]. Another example is the uncomfortable location of some controllers [15]. All the interviewed PBLV said that they will be unable to use them because of the lack of voice control option or truly tactile buttons. While the bathroom radiator and the ventilation units were equipped with buttons, the fact that they were not embossed, were too small and did not provide any kind of audio feedback made them not accessible. The position of the controller of the bathroom radiator increased the complexity of interaction further: it was positioned low behind the bathroom sink (Figure 2). There was an app to control those systems, but it was not accessible. Another problem was that a part of the system (the bathroom radiator) was not communicating with its other parts, which caused both confusion and inefficiency and as a result, also lack of trust.

Figure 2: Video still of access to the heating control. Link to video: https://openresearch.amsterdam/media/attachment/2022/9/5/video1_alina_boyuklieva_master_thesis-471954357.mp4

We discovered that the systems were missing basic accessibility controls, such as voice control option, tactile control option such as clear buttons, vibration, or quick temperature feedback. The visual accessibility, meaning possibility to zoom in, good contrast, etc. was also very low.

In discussions with the client stakeholders of the demo apartment, we sought to define what would be the most useful result from this research for them. In a complex context such as this one, various kinds of interventions could help stakeholders [16]. In this case, it was agreed that a useful result would be to not just present an evaluation of the existing solution, but to provide advice for the clients of the renovation solution (a housing association). This advice should support their decision process on the next iteration of the renovation solution. Clients could then use the advice to decide on and ask for more accessible products and solutions, some of which are available on the market.

Such products were discussed during the interviews. Two of the interviewees who were coaching PBLV (Expert users 1 and 2) shared valuable insights about common user behaviours observed in their practice. Expert user 2 mentioned that most people with whom he works prefer a combination of automated and regular devices. He also notices that youngsters pick up smart technology faster while the older generations still prefer physical interactions when available.

Overall, the systems that these people use in their everyday life to control their homes are mostly smart systems like Apple Home Kit, Google Home, and other similar devices that they control mostly by voice [14].

We categorised the main advantages and disadvantages of smart systems. App support seemed to serve as a great means of interaction and control when designed with accessibility in mind. Nonetheless, some users mentioned that they do not completely trust the privacy policies and would rather not use it. Voice control was another functionality,

which was met with mixed opinions. While adding an accessibility layer to each device, it could be frustrating and confusing when the user cannot guess the exact command. That suggests that combining several control options (audible, tactile, and visual) will result in higher accessibility.

While some smart devices are misleadingly considered accessible, others positively contribute to the users' well-being by bringing them independence and empowerment. The interviewees, as well as the literature review, confirmed that the one-size-fits-all approach is implausible for users with disabilities [10]. Every person's disability is different, everyone has learned to tackle it in their own way. Therefore, a personal approach is one of the most important things to keep in mind when designing for this target group.

We found that accessible smart thermostats and electric heater controllers already exist. Some of those are not only more suitable for people with visual impairments but also for all residents because of their broad functionality and compatibility. However, they were not implemented in the current renovation. This indicates that there is an unaddressed need for connecting the right systems to the right scenarios. That could be achieved, for example, through careful investigation of systems available on the market and connecting them to users' needs. A method to evaluate a specific user scenario in terms of the accessibility of applied devices would be of use for the stakeholders responsible for the renovation.

3. INTERVENTION

In the consultation with the experts on the renovation client stakeholder side, the most desirable intervention turned out to be to develop clear and concrete guidelines, requirements, and recommendations. We produced a set of guidelines for the clients of the renovation on how to look for accessibility of proposed solutions. The clients should be able to apply them fast, leading to immediate results. The guidelines needed to be simple, straightforward, easily comprehensible, and accessible. This way, the barrier to using them would be lower and the likelihood of people applying them would increase. The guidelines also needed to be motivating and reveal their value. As Expert user 2 mentioned: *'I am stunned that such information exists but is not being spread and applied.'* The set of guidelines was built in the form of a booklet with design guidelines (guidebook) (Figure 3) that provides concise, actionable steps towards accessibility in the easiest and least time-consuming way possible.

Figure 3: The cover of the guidebook, available for download under the title 'Booklet' at: https://openresearch.amsterdam/en/page/88258/msc-thesis---designing-for-a-more-accessible-zero-energy-system

An AR app connected to the guidebook provides access to interactive models and videos introduced earlier (Figure 1) that show a first-person view.

For transferability, the set of guidelines took the specific apartment as a starting point, but it was designed to be as independent as possible of the conditions of a specific refurbishment project. The content of the guidebook is tailored so that non-designers can follow it. It is based on European standards such as EN 17210:2021 [9]. While those standards provide rules, the guidebook provides steps such as how to perform basic user studies and evaluations to fulfil the rules. Furthermore, it summarises the basic accessibility requirements in a comprehensible manner and supports this with visual material underlining their importance.

In addition, the guidebook provides a tool which could further improve the product selection process, namely the 'Design Fundamentals' evaluation matrix. It incorporates six general requirements – accessibility, trust, simplicity, adaptability, low-maintenance, and robustness that a product should fulfil to be likely to succeed in the context.

4. INTERVENTION EVALUATION

4.1 Method

The guidebook was evaluated through six open-ended interviews. However, it could not be assessed in the projected use scenario, again due to covid restrictions. Four of the interviews were with the PBLV who also participated in the first study described in section 2 – they evaluated the content in terms of completeness, quality, and clarity. The other two interviews were with decision-makers on the client stakeholder side: a project manager for the renovation project to which the demo apartment belonged and an ICT specialist from a Dutch Sustainability Hub – they evaluated the tool in terms of usability, accessibility, and impact.

To provide the information to the PBLV, we created an accessible format of the guidebook by transferring only the text into Word so that they could access it through screen readers. We sent the

document a few days before our meeting so that they could take as much time as they need to explore it.

4.2 Results

Both PBLV expert user interviewees were pleased with the guidelines and recommendation sections which they described as '*practical, implementable, understandable, good quality and elaborate'*. Expert user 2 even mentioned: '*Such guidelines are very much needed. I hope that they will use them!*' Expert user 2 and Expert user 3 suggested some ways to motivate people to use the guidelines by evoking empathy [17]. For example, by adding a link to an app that simulates different types and stages of visual impairments in real time. This approach could help project managers to take on a new perspective and make better informed decisions when it comes to selecting systems.

During the guidebook interview with Regular users 2 and 3, we summarised the information orally at our real-life meeting as the guidebook was only in English. They thought that it covered the basic principles of accessibility and did not have any other remarks.

The evaluation with the client-side decision makers was conducted in a combined interview. The project manager said that the guidebook is '*very needed*' and valuable. He gave some advice on how to improve it in terms of comprehensiveness. For example, he advised us to add a clear explanation about the target reader. He also proposed a flowchart on the steps that the user is expected to undertake so they do not get lost in the process. The ICT expert confirmed that the AR app makes it more appealing to read. He added that it complements the current form of the guidebook and opens room for future development. In the short term, he suggested that the interactions with the systems installed in the demo-apartment could be integrated in the app so that some tests could be performed remotely. Then, those could turn into a VR version allowing more thorough experience, more accurate conclusions, and boost inclusivity. Current rendering software such as Enscape already provide the opportunity to experience a 3D model in VR.

5. DISCUSSION

This paper addresses a significant gap in the current discourse on sustainable housing, particularly in the context of accessibility for PBLV. The transformation of older housing to zero-energy is a necessary goal. However, it brings to light the crucial issue of the interface between residents and home systems, in terms of accessibility —a gap that if not addressed, can undermine the energy-saving objectives and the quality of life of residents, especially those with visual impairments.

This study's findings illuminate the importance of integrating accessibility into the sustainable renovation of social housing, in this case with a focus on the experiences of PBLV. The development of a guidebook from these insights serves as a cornerstone for stakeholders, outlining essential steps to embed inclusive design principles in line with European standards such as EN 17210:2021 [9]. The research underlines the potential of smart home technologies to significantly improve the living environments for PBLV conditional on a design process that is deeply rooted in user feedback and iterative development. Our findings align with previous research [15] suggesting that more, easy to adopt, tools are needed for the planning and then decision-making phase. Only doing an evaluation post-occupancy is too late.

Feedback from PBLV and professional stakeholders during the guidebook evaluation underscores its usefulness and points towards a critical gap in current renovation practices. One of the most important takeaways is that when striving to develop an accessible product, the best strategy is to apply a participatory approach where you involve PBLV in the process. Yet, despite its advantages, the adoption of the guidebook is not without challenges. It is possible that the introduction of tools like these will meet systemic barriers such as resistance to costs and to changes in established practices.

Based on the study, we argue that the broader usability benefits of accessible design extend to all residents, not just PBLV, thereby enhancing the overall living experience. While the guidebook originated from a single case study, the principles it champions are scalable and adaptable, suggesting a model for inclusive design that could be replicated in diverse housing renovation projects.

Limitations of this research are the small sample size and the specific socio-cultural and building context of the case study. They may limit the generalizability of the results. Future research should include a more extensive and varied demographic. It should also cover different building projects to validate the guidebook's applicability across different contexts. Additionally, the long-term efficacy and impact of the implemented guidelines on energy consumption and resident well-being remain to be empirically tested.

6. CONCLUSION

In conclusion, the study contributes a practical, evidence-based resource aimed at reconciling the objectives of energy efficiency and accessibility. These are often perceived as disparate but may also often align. Our study calls for a shift in renovation practices towards an inclusive paradigm where sustainability is not at odds with accessibility, and

where the living needs of all residents, especially those with visual impairments, are met with dignity and foresight.

ACKNOWLEDGEMENTS

We thank the Municipality of Amsterdam and Stiching Woon! for supporting this research. We also thank Koninklijke Visio and the participants of the research for providing their expertise and time.

REFERENCES

1. Spiekman, M. E., Boess, S. U., Santin, O. G., Rovers, T. J. H., & Nelis, N. (2022, September). Effects of energy-efficient renovation concepts on occupant behaviour and hence building performance. In IOP Conference Series: *Earth and Environmental Science* (Vol. 1085, No. 1, p. 012023). IOP Publishing. https://doi.org/10.1088/1755-1315/1085/1/012023

2. Van Dam, S. S., Bakker, C. A., & Van Hal, J. D. M. (2012). Insights into the design, use and implementation of home energy management systems. *Journal of Design Research* 14, 10(1-2), 86-101. https://doi.org/10.1504/jdr.2012.046141

3. van Beek, E., Giaccardi, E., Boess, S., & Bozzon, A. (2023). The everyday enactment of interfaces: a study of crises and conflicts in the more-than-human home. *Human–Computer Interaction*, 1-28. https://doi.org/10.1080/07370024.2023.2283536

4. Fabbri, M., De Groote, M., & Rapf, O. (2016). *Building Renovation Passports: Customised roadmaps towards deep renovation and better homes.* BPIE documents https://www.bpie.eu/wp-content/uploads/2017/01/Building-Passport-Report_2nd-edition.pdf.

5. Chappells, H. (2010). Comfort, well-being and the socio-technical dynamics of everyday life. *Intelligent Buildings International*, 2(4), 286-298. https://www.tandfonline.com/doi/epdf/10.3763/inbi.2010.0003

6. WHO, 2023, Blindness and vision impairment, https://www.who.int/news-room/fact-sheets/detail/blindness-and-visual-impairment

7. Gatt, D., Caruana, C., & Yousif, C. (2020). Building energy renovation and smart integration of renewables in a social housing block toward nearly-zero energy status. *Frontiers in Energy Research*, 8, 560892. https://doi.org/10.3389/fenrg.2020.560892

8. Lee, J. H., Kim, Y. M., Rhiu, I., & Yun, M. H. (2021). A persona-based approach for identifying accessibility issues in elderly and disabled users' interaction with home appliances. *Applied Sciences*, 11(1), 368. https://doi.org/10.3390/app11010368

9. EN 17210:2021: *Accessibility and usability of the built environment – Functional requirements*, January 2021, ICS 91.040.01. https://accessible-eu-centre.ec.europa.eu/content-corner/digital-library/en-172102021-accessibility-and-usability-built-environment-functional-requirements_en

10. Bichard, J. A., Coleman, R., & Langdon, P. (2007). Does my stigma look big in this? Considering acceptability and desirability in the inclusive design of technology products. In *Universal Access in Human Computer Interaction. Coping with Diversity: 4th International Conference on Universal Access in Human-Computer Interaction*, UAHCI 2007, Held as Part of HCI International 2007, Beijing, China, July 22-27, 2007, Proceedings, Part I 4 (pp. 622-631). Springer Berlin Heidelberg. https://doi.org/10.1007/978-3-540-73279-2_69

11. The Blind Life (2021). *BlindShell Classic 2 – The Most Accessible Phone Just Got Better!*, [Video] YouTube https://www.youtube.com/watch?v=5r9V_UsJ6ng

12. The Blind life (2018). *Why Is Assistive Technology So Expensive?,* [Video] YouTube https://www.youtube.com/watch?v=zNvzVJIQix4

13. Bianchin, M., & Heylighen, A. (2018). Just design. *Design Studies*, 54, 1-22. https://doi.org/10.1016/j.destud.2017.10.001

14. Leporini, B., & Buzzi, M. (2018, April). Home automation for an independent living: investigating the needs of visually impaired people. In *Proceedings of the 15th International Web for All Conference* (pp. 1-9). https://doi.org/10.1145/3192714.3192823

15. Rooney, C., Hadjri, K., Faith, V., Rooney, M., McAllister, K., & Craig, C. (2018). Living independently: Exploring the experiences of visually impaired people living in age-related and lifetime housing through qualitative synthesis. *HERD: Health Environments Research & Design Journal*, 11(2), 56-71. https://doi.org/10.1177/1937586717696699

16. Rijn, H., Sleeswijk Visser, F., Stappers, P. J., & Özakar, A. D. (2011). Achieving empathy with users: the effects of different sources of information. *CoDesign*, 7(2), 65-77. https://doi.org/10.1080/15710882.2011.609889

17. Groeneveld, B. S., Boess, S. U., & Freudenthal, A. (2013). Community-based co-design for informal care: bridging the gap between technology and context. *IFAC Proceedings Volumes*, 46(15), 266-273. https://doi.org/10.3182/20130811-5-US-2037.00043

PLEA 2024 WROCŁAW
(Re)thinking Resilience

Adaptation and reuse of buildings

The role of radiant temperatures distribution as a resilience factor

JUDIT LOPEZ-BESORA[1], ANTONIO ISALGUE[1], HELENA COCH[1]

[1]Universitat Politècnica de Catalunya, Barcelona, Spain
Research Group on Architecture, Energy and Environment (AiEM)

ABSTRACT: Enhancing resilience in construction practices necessitates a thoughtful consideration of repurposing existing structures to meet contemporary needs. Traditional buildings, however, pose challenges in acquiring construction and thermal data due to variables beyond technicians' control. This study underscores the significance of obtaining such data for advancing the adaptation and reuse of traditional buildings over their demolition. The research compares two spaces of similar dimensions constructed with different systems by monitoring air temperatures and employing thermography. Analysing temperature distribution in both a traditional and a contemporary house during a winter and a summer week reveals noteworthy findings. In winter, the traditional house exhibits more consistent temperatures across surfaces and air, with generally cooler surfaces compared to the contemporary one. In summer, the traditional house maintains a cooler profile in both air and radiant temperatures. These results contribute valuable insights for furthering research on preserving and repurposing traditional buildings, enhancing our understanding of their thermal responses. Such knowledge can serve as a strategic approach for adapting buildings to climate change and future scenarios.
KEYWORDS: Traditional house, Monitoring, Thermal performance, Radiant temperature, Building preservation

1. INTRODUCTION

The renovation and reuse of existing buildings is an important issue from the perspective of urban resilience, especially in Europe [1]. Historical and old buildings are scattered in small towns, villages, and the countryside, as most of them were built before the exodus of the population to cities in the mid-twentieth century. Historical buildings and traditional housing configure many European old city centres since they were originated much before urban expansion.

Lacking heritage value, many of these housing are demolished rather than adapted and reused. Its preservation is important to maintain historical memory [2-4], to manage resources rationally, and to avoid abandonment and depopulation of the territory and historical city centres. Traditional housing buildings could extend their lifespan if they were in good condition and the necessary changes were made through retrofit actions.

The construction typology of historical buildings is traditional, with heavy load-bearing walls and small openings. In the Mediterranean climate, with mild winters and hot summers, this configuration has worked quite well for years [5]. This architecture, combined with passive strategies such as the management of ventilation and sun exposition by occupants, has proven to be sufficient to achieve thermal satisfaction. However, their thermal performance today is often considered poor because buildings can take a long time to heat up or cool down, and because they are considered non-sufficiently insulated [6-8]. For this reason, many retrofit actions consist of increasing thermal insulation through the addition of an insulation layer or other similar solutions [9,10]. This layer has an impact on air temperature, but also on radiant temperature, which plays an important role in thermal sensation. This behaviour is expected to be different in traditional buildings compared to contemporary ones because of their different construction typology, especially what refers to mass and insulation. Many studies analyse the thermal performance of traditional buildings with prototypes and simulations that replicate reality. However, historical constructions are difficult to parametrize and simulate because they were built without accurate control of materials and techniques. For this reason, it is important to advance in their thermal performance by collecting feasible data from the functioning of existing buildings [11-15].

In this work, we compare two spaces in two houses placed side-by-side by monitoring their thermal performance. One of them (House 1) is a traditional house and the other one (House 2) is a contemporary one. In a previous work [16], we evaluated the effect of mass and insulation on air temperature in the same case of study, in a winter and a summer week under free-running thermal operation. We concluded that the air temperature alone does not justify the addition of a layer of thermal insulation. In this study, we incorporate one variable, the temperature of the interior surfaces (walls, ceiling, and floor). The objective is to have a

better approximation of the thermal functioning of the space by approximating the temperature of sensation in existing buildings so as to contribute to their adaptation and reuse in a building resilience scenario.

2. METHODOLOGY

2.1 Case of study

The spaces subject of this study are two living rooms in two terraced houses (Fig. 1). They are in a small Spanish village in the Catalan pre-coastal mountain range (40°17'N), 750 m above sea level. This area has a warm-summer Mediterranean climate (Csb), according to Köppen's climate classification. The average annual temperature is 13,3°C with a fluctuation of 17,9°C. The daily oscillation is 10°C. The average humidity is 70,3% and the annual precipitation is 535 mm/year.

Figure 1: House 1 (left) and House 2 (right), west façade.

Both houses have a ground floor with the living room preceded by an entrance hall (Fig. 2). They have three floors above ground and two semi-basement floors. They have a heating system with an oil boiling and radiators, and no cooling. The orientation of the façades is east and west, with the living room facing west. Their composition, window area, surface area and volume are equivalent. The traditional house (House 1) was built about 100 years ago. The façade walls are 60 cm thick in one sheet of stone masonry. The windows have single glazing and wooden frames. The contemporary house (House 2) was built in 2015 under thermal regulations. It has a façade composed of two ceramic sheets (14+7 cm) and 5 cm of polystyrene thermal insulation (U=0,45 W/m^{2}K). The windows are high-performance, with thermal breaks and double glazing.

The study spaces have an area of 36,4 m^2 (House 1) and 34,5 m^2 (House 2). Their volume is 92,2 m^3 and 91,7 m^3, respectively. The characteristics of the building envelope in the study spaces are detailed in Table 1 and Table 2. For each element, there are four defining parameters: surface S (m^2), U-value (W/m^{2}K), total mass of the element M (kg), and effective mass M' (kg). M' refers to the mass from the insulation inwards or half of the width if there is no thermal insulation. The listed elements are façades (F), windows (W), partition walls (PW), partitions (P), doors (D), floors (FL), and ceilings (C), identified in Figure 3. The U-value of partition walls, partitions, doors, floors, and ceilings are not listed since they are considered adiabatic surfaces.

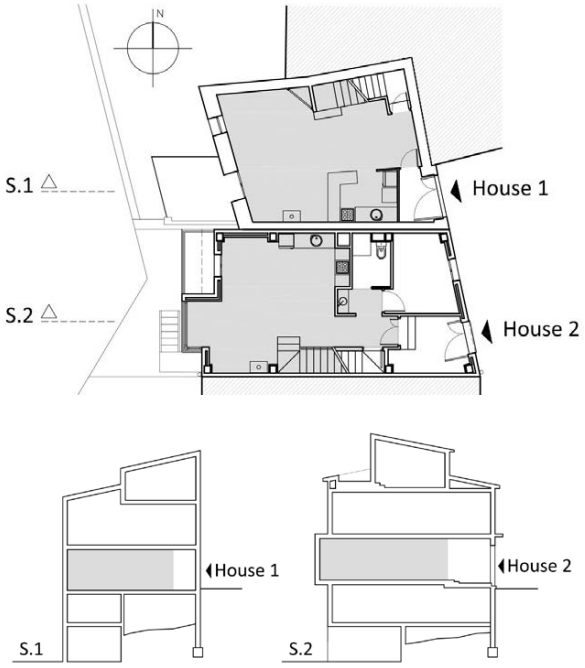

Figure 2: Floor plan and section of the houses (in grey, the studied area, the living room).

Table 1: Characteristics of the building envelope, House 1.

Code	S (m²)	U-value (W/m²K)	M (kg)	M' (kg)
F1	10,5	1,91	13192	6596
W1	3,1	4,30	77	77
PW1	7,2	-	6057	3028
PW2	14,8	-	14322	12454
P1	11,2	-	558	279
D1	2,8	-	-	-
FL1	8,3	-	2543	1271
FL2	28,1	-	8605	1652
C1	36,4	-	11148	5574
TOTAL	**122,4**	**-**	**56500**	**33581**

Table 2: Characteristics of the building envelope, House 2.

Code	S (m²)	U-value (W/m²K)	M (kg)	M' (kg)
F2	13,0	0,45	2493	849
W2	8,2	2,70	286	286
PW2	10,2	-	9830	1282
PW3	12,8	-	6438	1609
P2	14,2	-	926	463
D1	6,8	-	-	-
FL3	34,6	-	10585	5292
C2	34,6	-	10585	5292
TOTAL	**134,4**	**-**	**41142**	**15075**

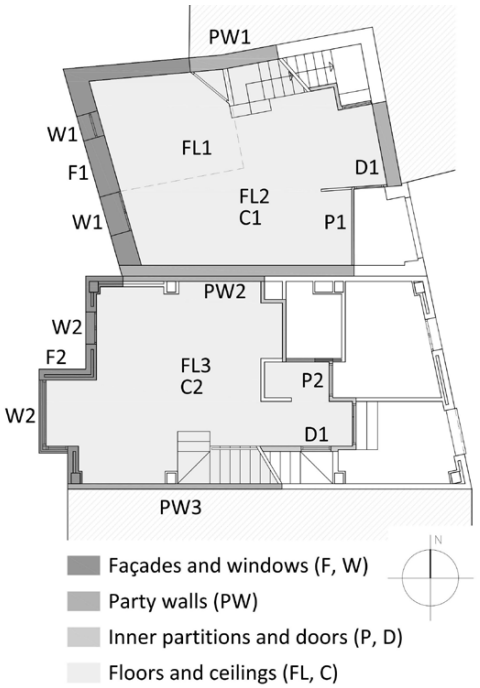

Figure 3: Floor plan with identification codes of the building elements.

2.2 Materials and methods

The houses were monitored for more than three years (2019-2023), during which they were in operation as a second residence. This document shows the results of one winter weekend (10-12 February 2023) and one summer weekend (30 June – 2 July 2023). The houses were unoccupied on the previous days and had normal activity during the weekend. In winter, the heating system was turned on when arriving home (at 10:20 on 10 February in House 1 and 13:00 on 11 February in House 2) and turned off just before leaving.

A TESTO 175 H1 data logger was placed in each living room to measure air temperature and relative humidity every 20 minutes, starting at the o'clock. Sensors T_H1 (House 1) and T_H2 (House 2), were placed in an equivalent position at the northwest corner of the living room at 1,5 m height (Fig. 4). Infrared pictures were taken during the weekend with a FLIR TG267 thermal imaging camera at five points in the interior (Fig. 4): on the walls (TS1_N, TS1_W, TS1_S / TS2_N, TS2_W, TS2_W'), on the ceiling (TS1_ce / TS2_ce) and on the floor (TS1_fl / TS2_fl).

Weather data were gathered from a station located 50 m away from the houses, managed by *meteoprades.net* (764 m altitude, UTM coordinates E 334739, N 4573418). Data obtained from this source were air temperature (°C), relative humidity (%), and solar radiation (W/m²). The timing of weather data registers was synchronized with the sensors.

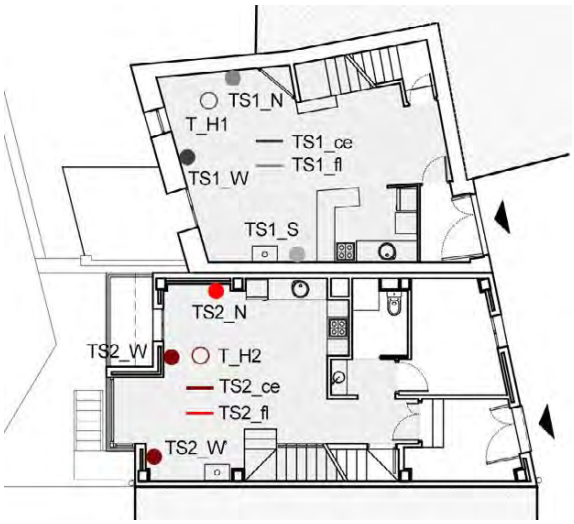

Figure 4: Floor plan with identification codes of the measurement points.

3. RESULTS AND DISCUSSION

The results show the air and radiant temperatures in each living room, together with the outdoor temperature (Figs. 5 and 6). The data for the winter period were influenced by occupancy and the start of heating, while the summer data were influenced only by occupancy.

The winter results show that House 1 needs more time than House 2 to raise its air temperature when turning on the heating (Fig. 5). This result is influenced by the time when people arrived in each house. In House 1 it was on Friday evening while in House 2 it started on Saturday early afternoon. The preferred operating temperature is higher in House 2 than in House 1, as shown in the graph.

Focusing on radiant temperatures (Figs. 5 and 7), all surfaces in House 1 keep cooler than the air until Saturday 11 in the afternoon. After this moment, some temperatures reach higher values than the air temperature, especially on the ceiling. The lowest values in the traditional house correspond to vertical surfaces, especially the west façade (TS1_W) and the north façade (TS1_N).

In House 2, the results show a different trend. Before turning on the heating, the air and radiant temperatures are similar. After a few hours after turning on the heating, the façade and the ceiling

reach higher temperatures than the air in the interior. The day after, the results are similar. The façade and the ceiling are the warmer surfaces, with values over the air temperature.

If we compare the radiant temperature of both spaces, House 2 reach higher values than House 1, especially the west façade and the ceiling. Just before and after noon, the difference between the façades is around 7°C. The ceiling shows a lower difference, around 4°C. Consequently, the façade of the old house remains much cooler than the façade of the contemporary one.

The graph also shows that the radiant temperatures in the contemporary house have a greater amplitude compared to the traditional one. The temperature difference between walls, floor and ceiling measured in House 1 (ΔT) ranges from 1,5 to 5,1°C. In House 2, ΔT ranged from 0,5 to 9,4°C (Fig. 9). Consequently, the distribution of radiant temperatures in winter is more balanced in the traditional house than in the contemporary one.

In general terms, House 1 shows more thermal inertia than House 2 if we consider all the temperatures involved.

The summer results show less amplitude in air temperature and radiant temperature in both houses (Fig. 6). As for air temperature, House 1 air temperature is 1°C below House 2. The evolution of temperatures is very similar along the weekend in both cases. The thermal oscillation is low, around 2°C and 3°C between day and night in Houses 1 and 2, respectively.

The radiant temperatures in House 1 and House 2 are very similar to air temperature (Fig. 8). Looking more in detail, radiant temperatures remain slightly above the air temperature in both cases. The lowest value of radiant temperature in House 1 corresponds to the west façade, which remains under the air temperature much of the time. On the opposite, the highest value is the ceiling. In House 2, the trend is similar. The temperature of the ceiling remains always over the air temperature, while the façade is cooler than the air much of the time and sometimes warmer, but next to the air temperature value. As for the difference in temperature between walls, floor and ceiling, the radiant temperature is similar in both cases. In House 1 it ranged (ΔT) from 0,3 to 1,6°C and in House 2, it ranged from 0,7 to 2,2°C (Fig. 10).

Consequently, the air and the radiant temperatures in the traditional house are lower than in the contemporary one, which means that in this summer period, the traditional house remained cooler than the contemporary one.

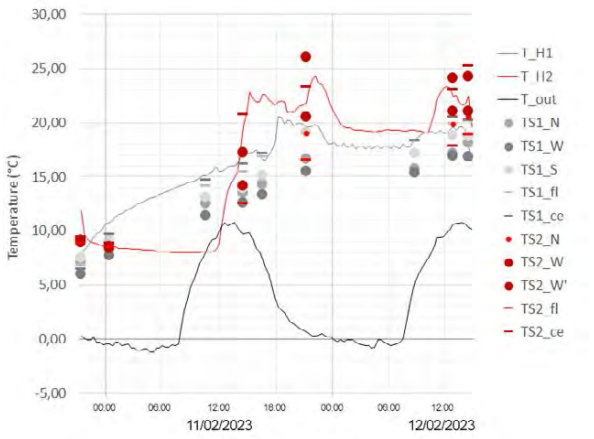

Figure 5: Air and radiant temperature in House 1 and House 2 (10/02/2023 to 12/02/2023).

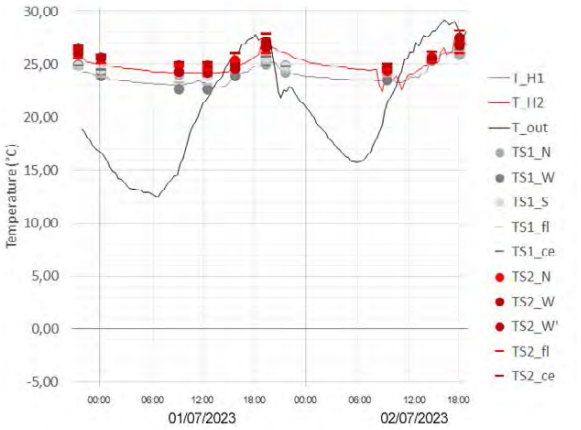

Figure 6: Air and radiant temperature in House 1 and House 2 (30/06/2023 to 02/07/2023).

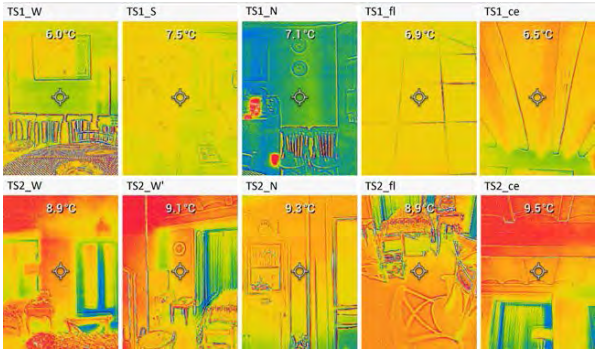

Figure 7a: Infrared pictures with radiant temperature (10/02/2023 - 23:30 UTC+1).

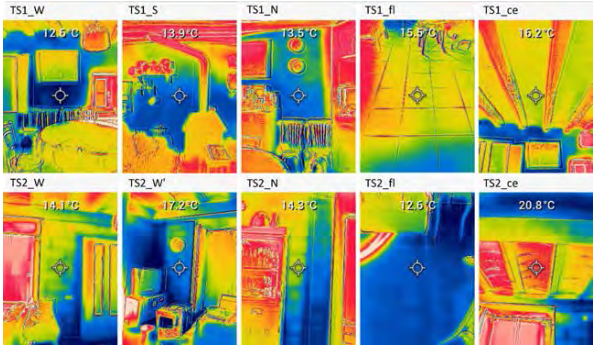

Figure 7b: Infrared pictures with radiant temperature (11/02/2023 – 15:30 UTC+1).

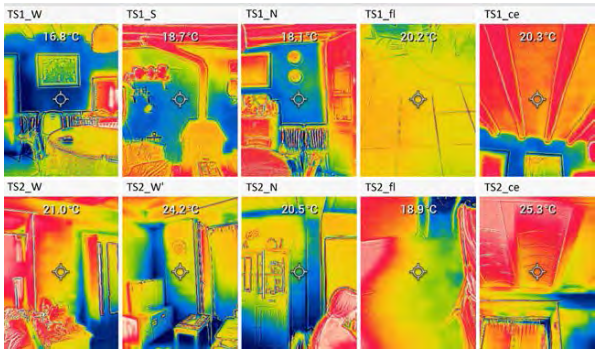

Figure 7c: Infrared pictures with radiant temperature (12/02/2023 – 16:00 UTC+1).

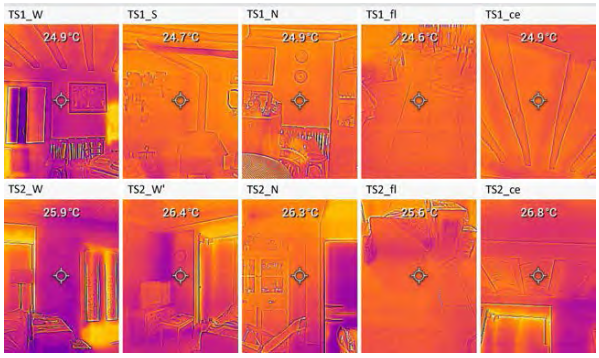

Figure 8a: Infrared pictures with radiant temperature (30/06/2023 – 21:00 UTC+2).

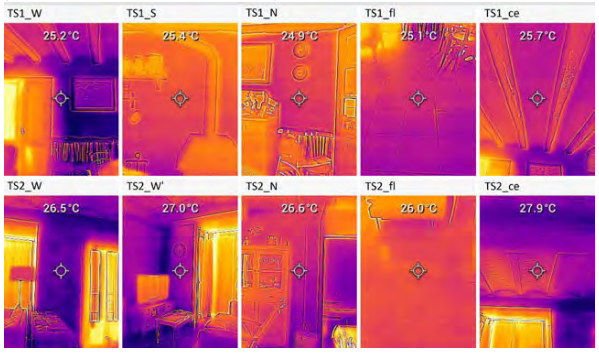

Figure 8b: Infrared pictures with radiant temperature (01/07/2023 – 20:30 UTC+2).

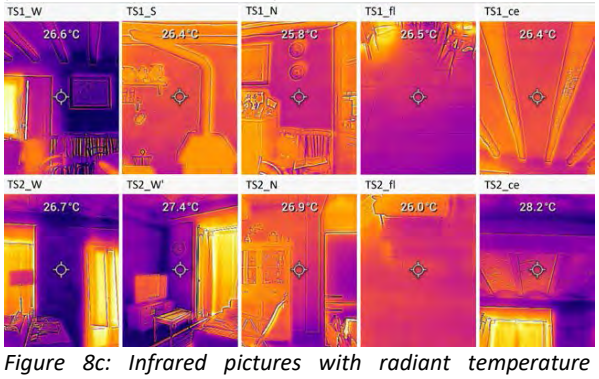

Figure 8c: Infrared pictures with radiant temperature (02/07/2023 – 19:20 UTC+2).

Figure 5 and Figure 6 show an asymmetry and a large amplitude of radiant temperatures with respect to air temperature in House 2, which is not the case of House 1. However, this difference is not noticeable in summer. Another visible result is the temperature difference between horizontal and vertical surfaces. In general terms, the ceiling and floor reached higher temperatures than the walls, so the temperature distribution was not homogeneous in the space in the studied periods.

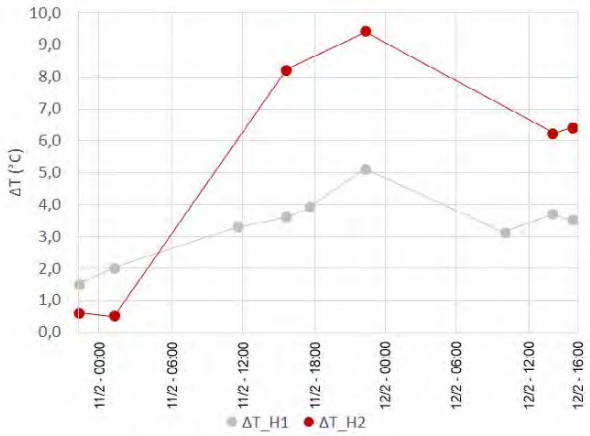

Figure 9: temperature difference (ΔT) of interior surfaces in winter (10/02/2023 to 12/02/2023).

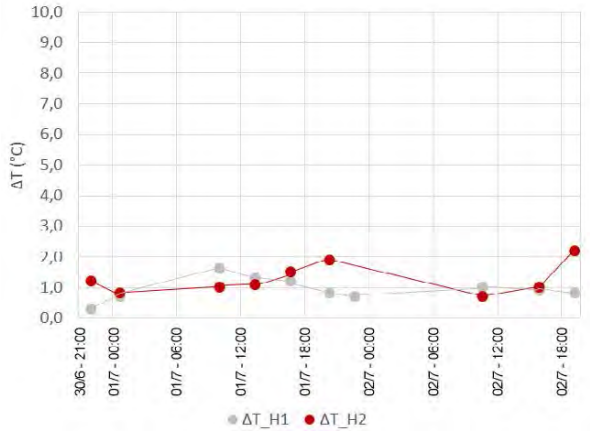

Figure 10: temperature difference (ΔT) of interior surfaces in summer (30/06/2023 to 02/07/2023).

4. CONCLUSION

The thermal performance in summer and winter leads to different conclusions. In winter, the radiant temperature of the walls remains the lowest of all temperatures in the traditional house, even though this house shows a more balanced distribution of radiant temperatures than the contemporary one. It can be interpreted as a higher thermal inertia in the house built with a traditional system. The contemporary one is less balanced in terms of radiant temperature distribution, but the ceiling and the façade reach higher temperatures than the air. The situation in winter indicates that more emphasis should be placed on vertical surfaces than on horizontal ones if a balanced distribution of temperatures and thermal sensation is the objective. This situation is especially important in winter and less so in summer, according to the results obtained.

In summer, the traditional house remains cooler than the contemporary one. The lower air

temperature together with lower radiant temperatures suggest that this typology may be more adapted than a contemporary house to heatwaves, which will become increasingly frequent in a future climate change scenario.

One of the main contributions of this work is the assessment of real buildings under real conditions based on more than three years of data recording. The case study represents two existing typologies of buildings which bring us the opportunity to compare opposite construction systems. Studying the thermal performance of buildings under laboratory conditions has precious value, but it represents a reality somewhat far from what happens in buildings with occupants, building imperfections and other uncertainties. The results obtained here contribute to further research on the reuse of traditional buildings to make them resilient to future scenarios of various kinds.

ACKNOWLEDGEMENTS

This research is part of the project PID2020-116036RB-I00, funded by MCIN/ AEI/ 10.13039/ 501100011033.

We acknowledge Meteoprades organization (meteoprades.cat) for providing weather data.

REFERENCES

1. Hao, L., Herrera-Avellanosa, D., Del Pero, C. and Troi, A., (2020). What are the implications of climate change for retrofitted historic buildings? A literature review. *Sustainability*, 12, 7557.

2. Mariani, S., Rosso, F. and Ferrero, M., (2018). Building in historical areas: identity values and energy performance of innovative massive stone envelopes with reference to traditional building solutions. *Buildings*, 8, 17.

3. Martinez-Molina, A., Tort-Ausina, I., Cho, S. And Vivancos, J.L., (2016). Energy efficiency and thermal comfort in historic buildings: A review. *Renewable and Sustainable Energy Reviews*, 61: p. 70-85.

4. Ding, G., (2013). Demolish or refurbish – Environmental benefits of housing conservation. *Australasian Journal of Construction Economics and Building*, 13 (2): p. 18-34.

5. Gagliano, A., Patania, F., Nocera, F. and Signorello, C., (2014). Assessment of the dynamic thermal performance of massive buildings. *Energy and Buildings*, 72: p. 361-370.

6. Stéphan, E., Cantin, R., Caucheteux, A., Tasca-Guernouti, S. and Michel, P., (2014). Experimental assessment of thermal inertia in insulated and non-insulated old limestone buildings. *Building and Environment*, 80: p. 241-248.

7. Costa-Carrapiço, I., Neila-Gonzalez, J., Raslan, R. and Sanchez-Guevara, C., (2022). Understanding the challenges of determining thermal comfort in vernacular dwellings: A meta-analysis. *Journal of Cultural Heritage*, 58: p. 57-73.

8. Galatioto, A., Ciulla, G. and Ricciu, R., (2017). An overview of energy retrofit actions feasibility on Italian historical buildings. *Energy*, 137: p. 991-1000.

9. Webb, A.L., (2017). Energy retrofits in historic and traditional buildings: A review of problems and methods. *Renewable and sustainable Energy Reviews*, 77: p. 748-759.

10. Yang, W., Xu, J., Lu, Z., Yan, J. and Li, F., (2022). A systematic review of indoor thermal environment of the vernacular dwelling climate responsiveness. *Journal of Building Engineering*, 53, 104514.

11. Giuliani, M., Henze, G.P. and Florita, A.R., (2016). Modelling and calibration of a high-mass historic building for reducing the prebound effect in energy assessment. *Energy and Buildings*, 116: p. 434-448.

12. Cardinale, N., Rospi, G. and Stefanizzi, P., (2013). Energy and microclimatic performance of Mediterranean vernacular buildings: The Sassi of Matera and the Trulli district of Alberobello. *Building and Environment*, 59: p. 590-598.

13. Timur, B.A., Basaran, T. and Ipekoglu, B., (2022). Thermal retrofitting for sustainable use of traditional dwellings in Mediterranean climate of southwestern Anatolia. *Energy and Buildings*, 256, 111712.

14. Cantin, R., Burgholzer, J. Guarracino, G. Moujalled, B., Tamelikecht, S. and Royet, B.G., (2010). Field assessment of thermal behaviour of historical dwellings in France. *Building and Environment*, 45: p. 473-484.

15. Caro, R. and Sendra, J.J., (2020). Evaluation of indoor environment and energy performance of dwellings in heritage buildings. The case of hot summers in historic cities in Mediterranean Europe. *Sustainable Cities and Society*, 52, 101798.

16. Lopez-Besora, J., Isalgue, A., Coch, H. and Crespo, I., (2023). Influence of mass and insulation in building retrofitting. *PLEA 2022 conference Book of proceedings, Volume 1*, p. 135-140.

Rethinking Social Resilience Through Refurbishment and Adaptions:

A Comprehensive Review of a Transformed Residential Dwelling in Dhaka, Bangladesh.

SHAFIQUE RAHMAN[1], NABILAH NARGIS[2]

[1] Ph.D. Candidate at Faculty of Built Environment & Surveying, Universiti Teknologi Malaysia.
[2] B. Arch, Rajshahi University of Engineering & Technology, Rajshahi, Bangladesh.

ABSTRACT: This research delves into the refurbishment of 'Mirza Bari,' a century-old building tailored to accommodate second generations of the owner's three children's families, preserving its historical essence while nurturing familial bonds within shared living spaces. The study explores the social resilience instilled through this unique approach, emphasizing sustainability and low-energy aspects. Instead of demolishing the house into a multi-storeyed building, the old house has been refurbished and extended while preserving its originality. A social participatory framework has been adopted, incorporating interviews, focus groups, and observations to assess their shared living experiences and refurbishment impacts. Also, the refurbishment process has evaluated the design parameters that help address low energy use and better indoor environment quality (IEQ) within the building. The design has harmoniously integrated the extended part with its existing part in such a way that it was able to reconnect and share common spaces, also ensuring the distinct privacy of three households, meeting modern needs. Findings revealed that the refurbishment process balanced architectural preservation with contemporary enhancements, fostering modern functionality. This study underscores the significance of shared spaces in revitalizing communal connections, designing solutions that help sustainability, and evolving family dynamics into shared living environments like 'Mirza Bari.'
KEYWORDS: Refurbishment, Adaptive reuse, Social Resilience, Cultural Heritage.

1. INTRODUCTION

Rapid urbanization and housing development are posing a threat to various social and cultural issues, including the loss of cultural heritage, social isolation, fragmentation, and the disappearance of green spaces [1]. The conflict between heritage preservation and redevelopment is a constant unresolved matter, and this has prompted reevaluating the need to preserve heritage, culture, social engagement, and connectivity through Architectural semiotics.

Narayanganj, a part of Dhaka and established as a municipality in 1876, has become the country's 6th largest city [2]. However, it is facing challenges due to rapid industrialization and urbanization. Like many other cities, Narayanganj has seen the unrestrained rise of industries, commercial centres, and residences without adequate urban planning, resulting in a heavily crowded and disordered urban environment [3]. The construction of megastructures destroyed the city's cultural urban fabric and heritage, leading to an imbalance between density and liveability, which appeals to the need for revitalizing old traditions and culture. However, the impact and significance of refurbishing old heritage buildings amid this urban chaos still lack an evaluation framework. Hence, this study aims to identify the social impact of refurbishing a residential building on community well-being. A residential renovation project has been chosen as an example of how maintaining cultural heritage through design can promote social resilience in this urban instability. The research focuses on "Mirza Bari," a 128-year-old abandoned abode. Instead of demolishing it to construct a multi-storied building, the old house was renovated and extended while maintaining its originality.

Through this project, the significance of architecture and adaptive reuse in promoting social resilience by preserving cultural heritage and traditions has been studied. By retaining the essence of the past, the case study building successfully captured the essence of bringing the family together through refurbishment, contributing to social cohesion and resilience.

2. LITERATURE REVIEW

The 'heritage building' concept encompasses structures listed as monuments of national or international importance and includes buildings intertwined with cherished local landscapes within the community [4]. Heritage building' can connect to the entire society's meaningful social values and protect social connections and a sense of identity [5]. The

buildings not only have architectural value, but they also embrace many collective memories and stories. Therefore, heritage buildings are pivotal in passing down the cultural identity to further generations. Where they can no longer serve their original function, proposing new functions and purposes is inevitable to ensure the perseverance of the value of the heritage buildings [6]. Also, architectural refurbishment projects have the ability to bring economic, environmental, and social advantages to urban communities and address the low energy consumption aspects [7].

However, refurbishment is an intricate undertaking that requires participants in the process to have a clear understanding of how to perceive the most suitable prospects for a building's future at a given location and time [8] and its Influence on societal aspects. Thus, this research aims to compile a list of key aspects that must be considered while evaluating the social implications of restoring a building with historic value in the urban context. To illustrate this, the study examines a residential dwelling in Dhaka, chosen as a representative case of a densely populated urban area struggling with substantial redevelopment pressures.

Therefore, this research aims to understand the design and renovation process, evaluating the design parameters undertaken for the renovation of the case study, which contributes to retaining the cultural spatial organization and enhancing functional connectivity. It also depicts how refurbishing an old building rather than demolishing it can promote social resiliency and preserve heritage.

3. RESEARCH OBJECTIVES

The main objectives of this research are,

a) To evaluate the design parameters of the refurbishment process and its impact on sustainability, energy efficiency, and social resiliency within 'Mirza Bari.'
b) To analyse how integrating historical preservation and modern functionality through refurbishment can retain cultural heritage and tradition.

4. METHODOLOGY

Step 1: A literature review of existing literature on social resilience, sustainable refurbishment, community engagement, and participatory approaches in architectural projects.

Step 2: Identifying and studying the chosen 128-year-old residential building that has been refurbished with its original form, analysing its history, spatial characteristics, and significance.

Step 3: Review the refurbishment process and how it retained the old essence of the structure.

Step 4: Social participatory framework.

- Conducting interviews and surveys with the focus group (members of the family) to gather experiences and preferences related to shared living,
- refurbishment involvement
- the impact of shared spaces on family bonds.
- observing interactions within shared spaces and participating in communal activities.

Step 5: Analysing the social impact of the building on family relationships and how the refurbishment process has influenced social resilience, considering both tangible (physical changes to the building) and intangible outcomes (community perceptions and interactions).

Step 6: Evaluating the building's energy efficiency and IEQ (indoor environment quality).

5. DESIGN APPROACH

The design concept aimed to reunify the entire family within a single household, reminiscent of its previous arrangement. Its core objective was to restore family unity within shared living space and transmit the culture to future generations while conserving the intrinsic structure and essence of the residence, as delineated in Figure 1.

Expanding the original dwelling while conserving its authentic characteristics catered to housing three separate households for the three children. Consequently, the design harmoniously articulated and integrated the extended portion with the existing structure. This integration facilitated the sharing of communal spaces, such as a courtyard and shared terrace, enabling collaboration while preserving privacy for the three distinct families concurrently.

The design approach encompassed two primary facets: the refurbishment of the original residence and the construction of an extension to accommodate new functionalities, all while ensuring the preservation of the cultural courtyard.

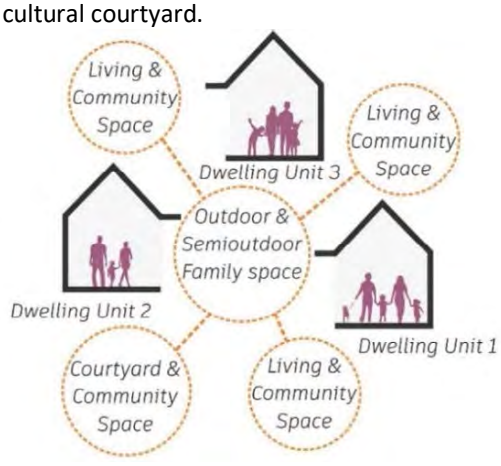

Figure 1: Concept of collaborating three separate dwellings.

The extension on the upper floor was connected with an 'L' shaped staircase, creating a double-height space with enhanced light, ventilation, and connectivity to the courtyard. Figure 2 shows the spatial connectivity and transformation of the functional zoning within the refurbished design.

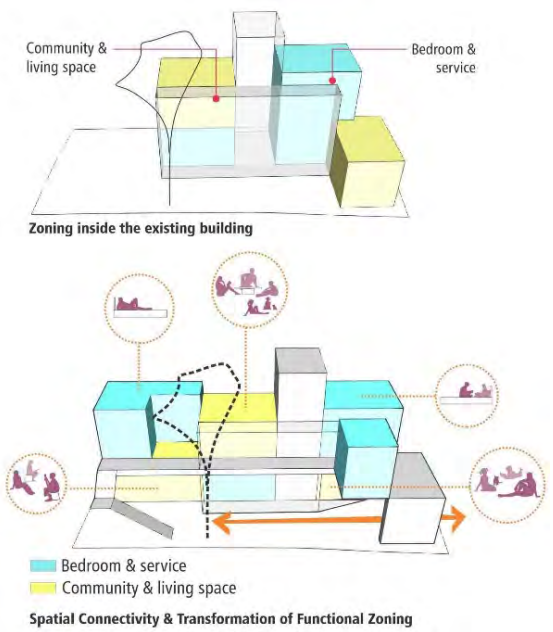

Figure 2: Functional placement of the refurbished design.

6. REFURBISHMENT PROCESS

The refurbishment process starts with strengthening the old masonry structure and retaining the walls. A mixed masonry and steel frame was adopted to strengthen the old structure, framing the main masonry structure with steel beams and columns for added rigidity. The spatial distribution of new and old functions was adjusted to improve living conditions for the occupants.

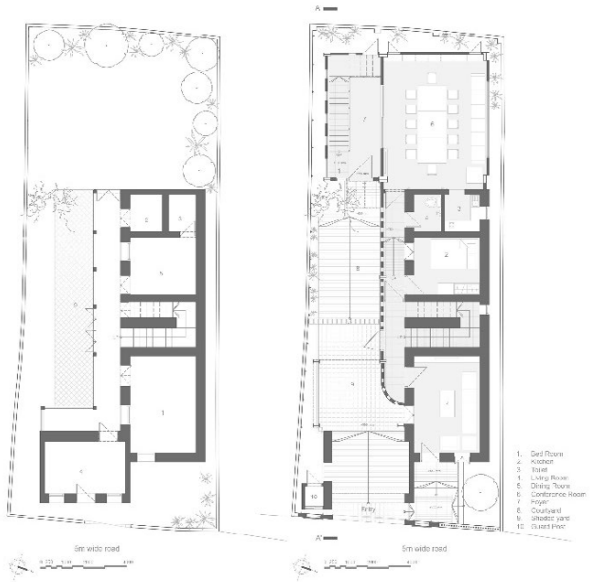

Figure 3: Existing (left) and proposed (right) ground floor plan.

Perforated screen façades built of concrete brick blocks have been constructed to separate distinct zones, providing private space while maintaining ventilation, which is necessary for this tropical environment.

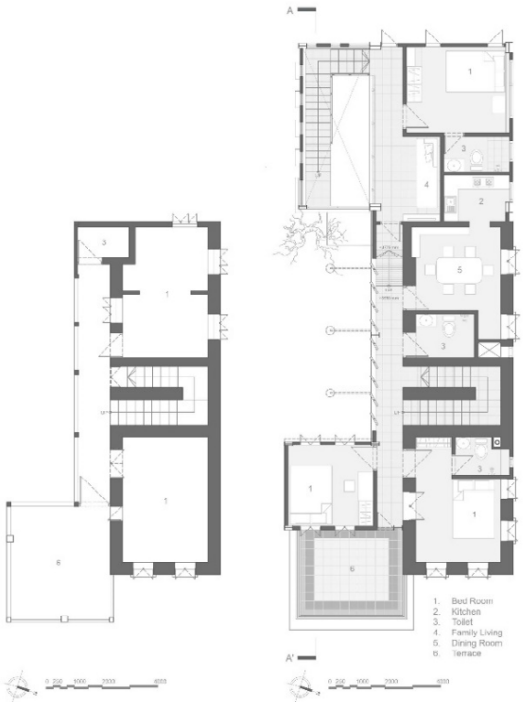

Figure 4: Existing (left) and proposed (right) first-floor plan.

Wooden textured floor finish and furniture reflect the character of vernacular culture. The ceiling adorned with 'sitalpati' (a mat made from murta plants) enhances the space decoratively.

Figure 5: Existing (above) and proposed (below) east elevation.

The double-height space at the staircase, enclosed with exposed brick and glass windows, exudes grandness. The connected corridor between existing and extended parts features an iron cast railing and pivoted screen windows, echoing the atmosphere of an old loggia space.

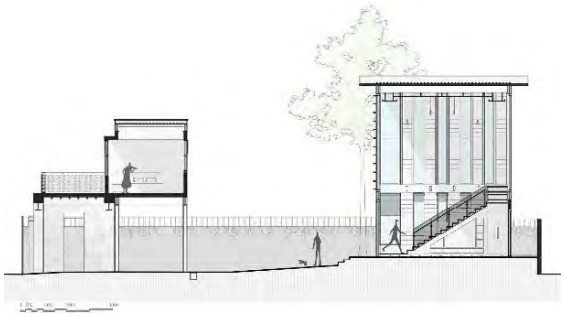

Figure 6: Proposed section AA'

Figures 6 and 7 showcase the refurbished project, highlighting its emphasis on visual aesthetics and connectivity.

Figure 7: Proposed south elevation

7. SOCIAL PARTICIPATION AND FINDINGS

The data analysis obtained from social participation with a focus group comprising 6 family members (2 from each child's family) revealed multifaceted insights into the experiences and perceptions concerning shared living spaces and the refurbishment process.

7.1 Shared Living Experiences

The data revealed diverse feelings towards shared living experiences after the refurbishment. Most participants sincerely appreciated the heightened social connections facilitated by communal areas like the cultural courtyard and terrace. Their enthusiasm was evident in statements such as "Our time in the courtyard has truly strengthened our family bond; we cherish it." Within this positive sentiment, a few individuals highlighted occasional challenges in ensuring personal space in these shared zones. Despite this, their feedback emphasized the overall success of the shared spaces in fostering family togetherness.

7.2 Refurbishment Involvement:

Insights into refurbishment involvement highlighted varying levels of engagement among family members. Approximately two individuals actively participated in the design decisions, while others assumed more passive roles but expressed contentment with the outcome. The children shared their nostalgic connections to the house, courtyard, and terraces, expressing a desire to revitalize these spaces to recapture cherished memories. Their input significantly influenced the refurbishment process, contributing to the elegant recreation of these memory-laden areas. Furthermore, their remarkable assistance and cooperation provided invaluable support to designers and workers, enhancing the overall project execution.

7.3 Impact of Shared Spaces on Family Bonds:

The unanimous appreciation for shared spaces like the courtyard and terrace in strengthening family bonds was remarkable. Some members expressed an interest in boosting family togetherness through increased organized activities. Statements such as "Our family reunion in the courtyard was fantastic" were coupled with a desire for more activities on the terrace, showcasing the positive impact of shared spaces on family connections.

7.4 Perceptions of Privacy and Connectivity:

The analysis highlighted the collective recognition of the need for privacy and connectivity within shared spaces. Family members acknowledged and appreciated features that balanced the two aspects. Illustratively, remarks such as "We have partitions in shared spaces for privacy, but it still feels connected" and "We've adjusted seating in the terrace without isolating anyone" showcased the desire to harmonize privacy with communal connections.

7.5 Importance of the preservation of the building to the community:

The building embodies traditional values within the community. As the esteemed owner, Dr. Mirza was a highly respected figure, and the building served as a symbol of honour, prestige, and a trustworthy place within the community. Therefore, restoring the building to its former state brings joy and satisfaction to the community, particularly among the elderly population.

Collected data from interviews and observations underscored the building's significant influence in fostering stronger family relationships within the shared living environment that can help social resiliency. The findings also accentuated the need for a delicate balance between privacy and connectivity within communal areas. Additionally, insights into family expectations highlighted opportunities and significance of refurbishment and adaptive reuse for retaining culture and tradition. The entire process also conveys a message from the designers and investors that this refurbished project reflects a contrast within urban development and demonstrates the possibility of integrating old traditions with new necessities, fostering social harmony and resilience.

8. EVALUATING SUSTAINABILITY

A meticulous evaluation encompassing material choices, preservation techniques, and structural

adaptations has been done aiming to understand sustainability while preserving the historical significance of 'Mirza Bari.' The refurbishment focused on maintaining the building's original form and structure, respecting heritage conservation. There was a deliberate effort to retain historical elements to uphold the building's cultural identity and architectural legacy. A purposeful selection of sustainable materials aligned with environmental objectives. Through strategic choices emphasizing durability, environmental friendliness, and resource efficiency, the refurbishment aimed to minimize environmental impacts.

Integrating intricate 'jali' work into the screen walls improved air circulation in the tropical climate and showcased a fusion of tradition and sustainability in the design. Extending and enlarging windows also maximized natural light penetration, reducing reliance on artificial lighting. This transformation significantly enhanced daylight quality, air circulation, ventilation, and spatial quality, thereby augmenting the Indoor Environment Quality (IEQ). These adaptations enhanced the building's environmental performance and notably improved occupants' well-being by providing a more comfortable and healthier indoor environment. Table 1 outlines the design elements and work process that contributed to enhancing sustainability and reducing energy consumption.

Table 1: Sustainability and energy evaluation through Preservation, transformation, and evaluation.

Architectural Style		Work process	Work style
Fenestration	Window & Openings	Previous Style: Hybrid colonial style, semicircular arch with keystone, elevated crown [5][6]. Preserved in original form. Enlarged windows for increased daylight and better cross ventilation. Incorporated new semi-circular arch windows in the extension, aligned with the original style.	Preservation, Transformation, and adaptation
	Screen wall	Transformed existing facades using screen walls to improve air circulation. Integrated traditional 'Jali work' into the screen walls, establishing semi-private spaces that ensure adequate light and ventilation.	Transformation and adaptation
Facade	Materials	Considering the old expression, new materials have been chosen, creating a raw, amiable, and homey environment. Enhanced space aesthetics by integrating locally sourced 'sitalpati' (also known as 'nakshipati') as decorative elements on the ceiling, utilizing traditional materials skilfully.	Transformation and adaptation
	Texture & Color	Using con-mix and concrete finish outside creates a raw texture, while indoors, refined colored textures foster a cozy atmosphere. Neutral exterior colors embody traditional style, while vibrant interior hues balance the rawness and signify family unity.	Transformation and adaptation
Structure	Roofing Style	Style: Rafter-purlin structural system. Preserved and reinforced with additional steel frames to strengthen the old structure.	Preservation
	Retrofitting system	Steel columns and beams have been introduced to reinforce the old structure. Steel columns and beams have been used in the extended part to gain structural flexibility and lightweight construction.	Transformation and adaptation
Functional Arrangement	Accessibility & Circulation	Preserved the linear corridor linking the outdoor courtyard to the indoor terrace and spaces. Efficiently designed circulation flow connects the three households while ensuring separation when required. The extended linear corridor maintains spatial connectivity. A new staircase has been added for easy access and a playful connection between the extension and existing parts.	Preservation, Transformation, and adaptation
Open spaces	Courtyard & Terraces	The old Mahogany tree within the courtyard has been preserved. The easy flow of movement within the space has been created by connecting the courtyard and the new double-height staircase zone. The transformed railing has preserved and reconnected the old memory terrace with other spaces. The terraces have been transformed by improving connectivity and have been adapted for family gatherings and celebrations.	Preservation, Transformation, and adaptation
Detailing	Railing	Iron cast railing transformed that resemble the traditional ornamented iron cast railing.	Transformation
	Wall preservation	Initially, the old plaster was removed to address poor wall conditions. Chemical treatment strengthened the walls, followed by replastering and painting to restore their integrity.	Preservation
Climatic consideration	IEQ Updating	The building now enjoys increased natural daylight through considerate updates to the old openings, significantly improving the indoor environment. The refurbishment process remarkably enhanced daylight quality, ventilation, and circulation, improving the Indoor Environment Quality (IEQ) through additional openings, screen walls, and functional organization.	Preservation, Transformation,
Intangible quality	Spatial quality	Revitalizing traditional spaces evokes cherished family memories, enhancing spatial experience. Careful adjustments to space quality and functional flow greatly enhance the overall spatial experience. The preserved old staircase, adorned with warm, bright colors, creates an ambient environment. Maintaining the architectural style, both in the extended part and new elements, ensures the preservation of the original aesthetic.	Preservation, Transformation, and adaptation

Therefore, the refurbishment's strategic blend of preservation, transformation, and adaptation strategies reflects a holistic approach toward sustainability. By retaining historical elements, utilizing sustainable materials, and integrating innovative adaptations, 'Mirza Bari' achieves a harmonious balance between heritage preservation and enhancement of environmental performance, contributing to its longevity and relevance in a modern context.

9. RESULT AND DISCUSSION

The project's refurbishment effectively integrated the old and new sections, seamlessly linking communal areas like hallways, staircases, a courtyard, and shared terraces. This thoughtful architectural design now accommodates the families of the owners' three children together, providing each with private space and offering shared areas such as the courtyard for communal gatherings. The design allows for controlled separations when necessary but encourages reconnection, fostering a strong sense of communal living. Every detail of the original structure has been meticulously preserved and enhanced through retrofitting, ensuring functional connectivity and accessibility to the extended portions. Figure 1 illustrates the condition of the building before and after the refurbishment, offering insight into the transformation process.

Figure 8: Existing (left) and proposed (right) conditions.

The case study's refurbishment process has successfully helped preserve heritage, reduce energy consumption, and retain tradition and social resilience. Retaining the building's originality upheld its historical significance, nurturing a shared sense of heritage, tradition, and culture. Sustainable materials and design integration, like 'jali' work, bridged tradition and sustainability, enhancing community identity.

Strategic alterations like window modifications enhanced indoor environmental quality and occupants' well-being. Findings from the social participatory model confirmed occupants' appreciation for communal areas, enhancing familial ties and community engagement. This initiative showcases refurbishment design solutions that rejuvenate heritage, reinforce family bonds, and foster social resilience within architectural settings.

10. CONCLUSION

Successful adaptive reuse and refurbished projects can introduce a modern dimension that provides value for the future and also respects and retains a building's heritage significance [11]. In summary, Mirza Bari exemplifies the harmonious union of heritage and modernity, showcasing that architecture can breathe life back into cultural treasures while adapting to the ever-changing demands of a dynamic city through design. This transformative project not only retained cultural identity but also fostered community connectivity. Therefore, the refurbishment of 'Mirza Bari' serves as a model showcasing the potential of architectural endeavours to preserve heritage, promote sustainability, and strengthen social resilience.

ACKNOWLEDGEMENTS

Our heartfelt gratitude to the design team of the reviewed project: Shafique Rahman (Lead Architect), Shanila Saifullah (Project Architect), Rakib Patwary (3D Visualizer), and Mashkura Chowdhury (Documentation) for their collaboration and contribution.

REFERENCES

1. M. Ahmed, "Urbanization and Environmental Problem: An Empirical Study In Sylhet City,Bangladesh," Research on humanities and social sciences, vol. 4, pp. 161–172, 2014.
2. "Narayanganj City Corporation." Accessed: Jul. 29, 2023.
3. A. H. M. Noman et al., "City profile: Narayanganj, Bangladesh," Cities, vol. 59, pp. 8–19, Nov. 2016, doi: 10.1016/j.cities.2016.05.020.
4. S. Lamei, "Insights into Current Conservation Practices,"
5. UNESCO UIS, "Cultural heritage | UNESCO UIS," UNESCO UIS.
6. D. MIsIrIIsoy and K. Günçe, "Adaptive reuse strategies for heritage buildings: A holistic approach," Sustain Cities Soc, vol. 26, pp. 91–98, Oct. 2016, doi: 10.1016/j.scs.2016.05.017.
7. A. Power, "Does demolition or refurbishment of old and inefficient homes help to increase our environmental, social and economic viability?," Energy Policy, vol. 36, no. 12, pp. 4487–4501, Dec. 2008, doi: 10.1016/j.enpol.2008.09.022.
8. "Adapting Buildings for Changing Uses: Guidelines for Change of Use Refurbishment - David Kincaid - Google Books."
9. "Development Of Hybrid Colonial Architecture - 2190 Words | Bartleby."
10. N. Utaberta et al., "Sumarni Ismail, Nangkula Utaberta, Mohd Yazid Mohd Yunos, Nor Atiah Ismail, Noor Fazamimah Mohd Arifin., A Review on the Architectural Styles of Colonial Buildings Bangladesh" 2015.
11. D. of the E. and H. Australian Government, "Adaptive Reuse Preserving our past, building our future," 2004.

PLEA 2024 WROCŁAW
(Re)thinking Resilience

Exploring the Building Forms and Passive Performance of Bioclimatic Stilted Granary of Tujia Ethnic Group

YONGJIE PAN [1,2], HAN XU [1], TONG ZHANG[1,*]

[1] School of Architecture, Southeast University, Nanjing, China
[2] Department of Built Environment, National University of Singapore, Singapore, Singapore

ABSTRACT: The bioclimatic design strategies implemented in traditional productive buildings, including granaries, have historically received minimal attention. This paper concentrates on the Tujia stilted granaries in Enshi Prefecture, aiming to explore how environmental requirements for grain storage and regional construction traditions influence the building forms of these vernacular granaries. The research employs a combination of field investigations, environmental data measurement, and Computational Fluid Dynamics (CFD) simulations to assess the efficacy of passive design strategies against external factors such as wind and solar radiation. The comprehensive analysis, both qualitative and quantitative, reveals that the architectural features of the Tujia stilted granaries, including their layout, spatial organization, and interfaces, are strategically adapted to the regional climate. These findings offer valuable insights and approaches for the development of regional green building forms that comply with similar requirements for environment control.
KEYWORDS: Vernacular architecture, stilt house, granary, bioclimatic design, passive performance

1. INTRODUCTION

As the final stage of food production, grain storage has garnered significant attention across history. In the pre-industrial era, confronted with adverse regional climate factors encompassing solar radiation, wind, and precipitation, humans predominantly employed passive strategies to regulate the temperature and humidity within grain storage facilities. These factors, combined with regional resources and culture, have led to the development of various types of granaries, each with distinct form characteristics. While the climate adaptability of vernacular dwellings has been extensively discussed and developed over the past century, the bioclimatic strategies of productive buildings, such as granaries, have received little attention [1]. Some studies have been conducted to address this gap, encompassing research objects from Spain [2-6], Turkey [7], India [8], Mexico [9], and China [10], and primarily focusing on the typical form [9,10] of granaries and their construction strategies [7,11] to meet the grain storage requirements. This study takes the stilted granary of Tujia ethnic group as the research object. It aims to investigate the impact of environmental requirements for grain storage and regional construction traditions on the formation of vernacular granaries and to assess the performance of passive strategies subjected to external energies such as wind and solar radiation.

2. MATERIALS AND METHODS

2.1 Regional characteristics

Enshi Tujia and Miao Autonomous Prefecture (Enshi Prefecture) is located in the mountainous southwestern corner of Hubei province, China. According to the Köppen climate classification, this region is categorized as Cfa. Due to the complex topography and significant elevation differences, the area exhibits a pronounced vertical climatic variation, characterized by the phenomenon that 'one mountain can display all four seasons and the weather changes every ten miles'.

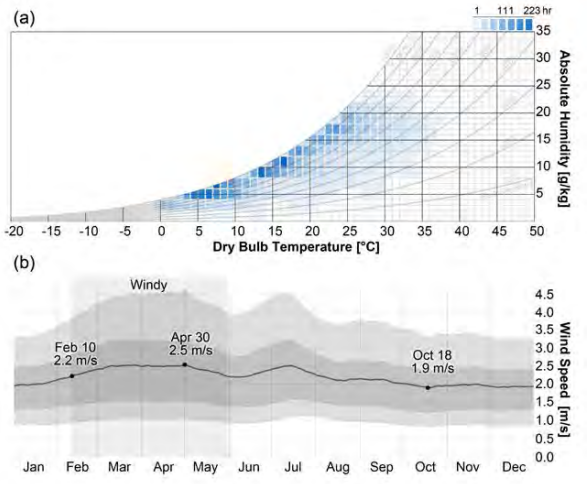

Figure 1: Climate and average weather year round in Enshi, (a) enthalpy diagram, (b) wind frequency.

Figure 1 illustrates the region's climate, showing both the enthalpy diagram and wind frequency data, highlighting the environmental conditions for grain storage. The region's dry bulb temperature varies from a minimum of -1°C to a maximum of 37.7°C annually, with an average of 17°C. The region is

characterized by consistently high humidity year-round, reflected in an average relative humidity of 77.4%. Regarding the wind environment, the prevailing direction is from the southwest, with the windy season lasting from March to June. Despite the obstruction posed by mountainous terrain, the area maintains an annual average wind speed of 2.2 m/s. Overall, the primary challenges for grain storage in the Tujia agglomeration area arise from the region's sultry summer climate and persistent high humidity throughout the year. Conversely, the region's favourable wind conditions present a valuable opportunity to enhance granary ventilation, cooling, and dehumidification strategies.

Under the factors with mountainous terrain, dense forests, a hot and humid climate, the most apparent feature of vernacular architecture of this region is the stilt housing form [12]. The stilt housing approach (Figure 2) involves elevating the living floor on the rugged topography, which not only facilitates the creation of vertically layered living spaces, but also effectively avoids ground-level insects, animals, and humidity. The wooden wall enclosures and roofs of these stilt houses are designed with vents to enhance natural convection, effectively facilitating the removal of indoor heat and humid air. The sloping roof of the stilt house features extended eaves, which provide effective shading. The attic, situated beneath the roof, serves a dual purpose: it is utilized for grain storage and also acts as an air layer above the living space, significantly diminishing heat radiation during summer. Additionally, the region's frequent precipitation has influenced the roof's design, which includes upward-curved eaves to facilitate far-reaching rainwater drainage, thereby minimizing moisture accumulation.

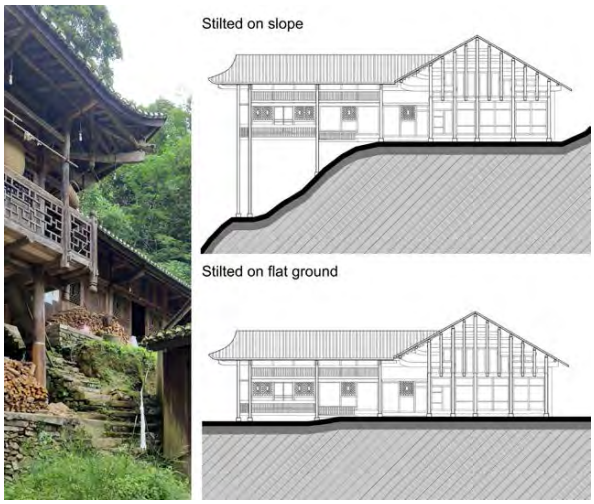

Figure 2: The exterior view and schematic diagram of Tujia stilt house.

2.2 Studied case and methods

In typical Tujia villages, houses exclusively used as granaries for grain storage are uncommon. The Tujia people, whose agricultural production is primarily family-based, usually store grain in the upper semi-open storey or hang them on the external corridors of their *Qianzi* homes. Following the establishment of the People's Republic of China, the traditional methods of grain storage proved no longer inadequate to meet the capacity and technical requirements demanded by the new collective grain storage policy.

Confronted with the challenges of preserving grain in the local hot and humid climate, the Tujia people drew inspiration from the stilt house, and created the unique type of stilted granary that embodied the context of climate adaptation and regional construction techniques. The stilted granary adopts the "stilted on flat ground" construction technique characteristic of Tujia stilt houses, with the column-and-tie framework, known as *Paishan*, forming the core of its construction system. The interior space is partitioned into distinct storage compartments (called *Ao*) using wooden partitions situated between the columns. Supporting these timber columns are half-meter-high stone pillars. This tectonic design elevates the grain storage plane above the ground, efficiently mitigating issues related to regional humidity and rodent infestation.

Figure 3: The exterior view of Xuanen No. 1 granary.

The field investigations in Enshi Prefecture have identified three primary sites remaining stilted granaries. This paper focuses on the Xuanen No. 1 granary, notable for its early construction date (1951) and its current state of preservation (Figure 3).

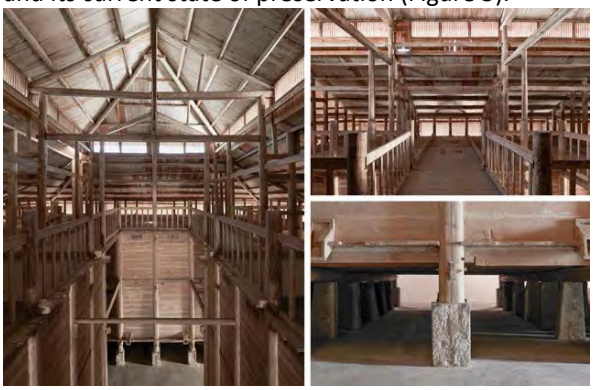

Figure 4: The interior views of Xuanen No. 1 granary.

This granary features an external stone wall enclosing interior wooden silos, which are organized into three groups, each comprising four units known as '*Ao*'. Uniquely, the silos' bases are elevated from the ground by an overhead floor, facilitating grain storage and maintenance. The silos are topped with a platform designed for the efficient loading and unloading of grain (Figure 4). Additionally, the granary's roof incorporates a "clerestory," a distinctive architectural feature prevalent in traditional "palace-style" granaries.

Through on-site surveying and mapping, architectural drawings such as plans and sections, along with photographs highlighting construction details, were obtained. The research then delves into a qualitative exploration of the bioclimatic characteristics of the building form, including layout, shape, space, interface, and material, to discern their impact on the granary's passive environmental performance.

To supplement this qualitative analysis with quantitative data, the research team conducted an extensive three-day environmental data measurement at the Xuanen No. 1 granary from August 20 to August 22, 2022. Utilizing low-power sensors and IoT technology [13], the team gathered critical data under hot and humid conditions to evaluate the thermal and ventilation performance of the granary (Figure 5). Given the limitations in sensor coverage and the variable nature of the wind environment, the study also employed CFD simulations. These CFD simulations helped predict how air moves through the granary under various conditions, providing a clear picture of its ability to ventilate naturally without using energy.

Figure 5: The environment measurement scheme based on low-power sensors and IoT technology.

3. THE BIOCLIMATIC CHARACTERISTICS OF BUILDING FORM

3.1 Layout and morphology

Reasonable layout and morphology facilitate the initial selection of external climatic conditions, thereby enabling the acquisition of appropriate external energy. The granary, characterized by a regular rectangular volume encompassed by towering walls, employs a small shape coefficient to effectively hinder the intrusion of external heat. Additionally, the pitch of the granary's roof and the depth of its eaves are key morphology features that further demonstrate the building's resistance to solar radiation.

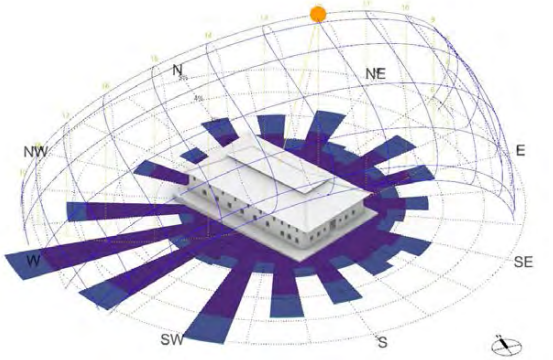

Figure 6: The Layout of granary in relation to wind direction and sun path.

In terms of orientation, the structure's longer side is strategically oriented to align with prevailing winds, enhancing ventilation through the majority of its openings, as illustrated in Figure 6. Moreover, the granary's long side at a 64.6° angle perpendicular to the south is a deliberate design decision aimed at optimizing radiative heat gain in the summer. This approach is based on the principle that south-facing walls generally receive more solar heat gain compared to east- and west-facing walls. However, for grain silos, excessive solar heat gain in the summer is not desirable.

3.2 Space and interface

The granary employs a space gradient strategy tailored to the distinct requirements of wind, light, thermal, and humidity conditions in varying spaces, a concept akin to "Thermal Onion". In this framework, the grain storage space is situated at the innermost part, while the surrounding corridors and foyer serve not only as circulation routes but also as buffer zones to mitigate the impact of unfavourable climatic conditions (Figure 7).

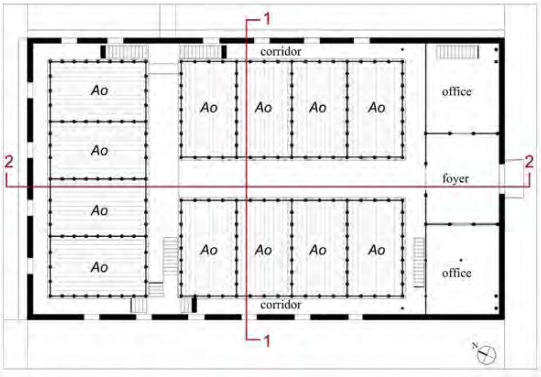

Figure 7: The ground plan of granary.

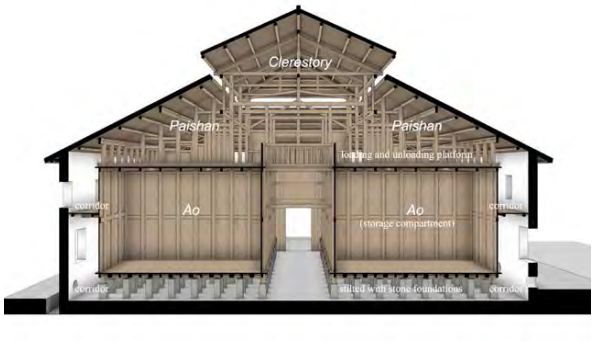

Figure 8: The section 1 perspective view.

The granary's multistage roof design, in conjunction with the vertical void, function as an atrium in regulating the indoor environment. The openings on the granary's envelope act as channels for the exchange of energy between the interior and exterior environments; the dimensions, location, and angle of these openings are strategically designed to direct the building's energy exchange process via convection and radiation. From the sectional view (Figure 8), it's observable that the circular openings located at the bottom of the granary's exterior walls act as air inlets within the buoyancy-driven ventilation system. The alignment of these openings with the stilted space, combined with the vertical distance between them and the top "clerestory" outlet, is strategically positioned to maximize the ventilation effect under this mechanism.

3.3 Material and construction

Approaches to lower summer grain storage temperature and humidity through material choices and construction techniques can generally be divided into two main categories: the reduction of heat conduction and the improvement of heat convection. These strategies are primarily focused on the three key enclosing elements of the structure: the walls, floors, and roofs.

In the Xuanen No. 1 granary, masonry, a material characterized by high density and thermal mass, is utilized in the outermost enclosure wall to create a barrier and buffer for heat and moisture transmission between the interior and exterior. The enclosure of the storage space (*Ao*) consists of horizontally spliced planks, each measuring 30mm in thickness. These planks harness not only the tensile and compressive strength of timber but also the low thermal conductivity of wood fibers, thus effectively mitigating external periodic temperature fluctuations. At the floor level, the *Ao* are raised above the ground on stone pillars, more than one meter high, providing a safeguard against heat and moisture transfer from the ground. Additionally, the airflow channels beneath the *Ao* facilitate natural ventilation within the indoor spaces. The granary's composite roof, which includes tiles, felt, sarking, and rafters, further contributes to an efficient thermal envelope, ensuring a stable internal climate suitable for grain storage.

4. THE MONITORING AND SIMULATION OF PASSIVE PERFORMANCE

4.1 Monitoring of thermal performance

Figure 9 presents a box plot illustrating the temperature measurements at various points within section 1-1 of the granary, recorded from August 20 to August 22. This data clearly demonstrates the gradient mechanism in the spatial organization of the granary, which plays a crucial role in thermal environment conditioning. In this setup, the surrounding corridors and atrium act as regulating spaces, providing a climate buffer for the storage space (*Ao*). The granary's temperature gradients are characterized by distinct variations, both vertically (top to bottom) and horizontally (from exterior to interior). Moreover, the *Ao* displays exceptional temperature stability, maintaining daily temperature fluctuations within a 3℃ range. Remarkably, during periods of peak summer heat, the temperature differential between the *Ao* and the external environment remains consistently within 6-8℃. The synergistic nature of temperature and relative humidity makes the wet environment of the granary shows similar gradient differences as well.

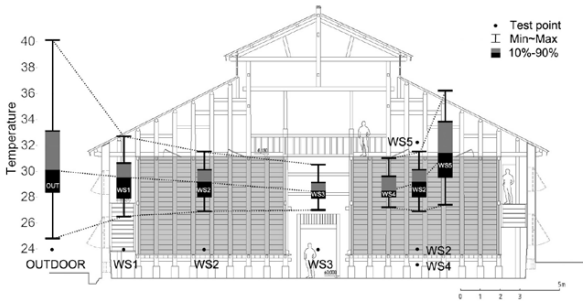

Figure 9: Spatial temperature difference of Section1.

Figure 10 illustrates the spatial temperature variations among different test points in Section 2-2 of the granary. During high temperature periods, indoor test points on the granary's south side register higher temperatures compared to those on the north side. This observation corroborates the effectiveness of the office space on the south side acting as a heat flow barrier. When integrated with the data presented in Figure 9, it becomes evident that the northern *Ao* exhibits superior thermal performance compared to the southern *Ao*. This is indicated by a temperature difference of 0.7°C during high-temperature periods, along with greater thermal stability characterized by smaller daily temperature fluctuations. Additionally, Figure 10 highlights the atrium space's potential in fostering a comfortable thermal environment under hot climatic conditions. The atrium not only functions as a climatic buffer

zone, but also provides a conducive operational environment for grain handling activities.

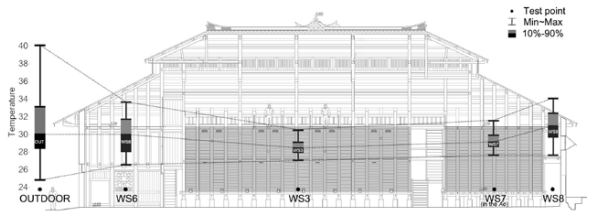

Figure 10: Spatial temperature difference of Section2.

4.2 Simulation of ventilation performance

Figure 11 illustrates the air flow paths within the granary under two distinct scenarios: wind-driven and buoyancy-driven ventilation. In the buoyancy-driven scenario, prevalent when outdoor wind speeds are low, the vertical temperature gradient in the atrium space drives the inflow of outdoor air through a circular opening at the bottom of the façade, exiting through the skylight at the top. Conversely, in the wind-driven scenario, which occurs when outdoor wind speeds are high, the granary's numerous openings facilitate this ventilation pattern. The openings on the windward and leeward sides of the structure are aligned directly opposite each other, thereby effectively minimizing the resistance and deviation in the airflow path.

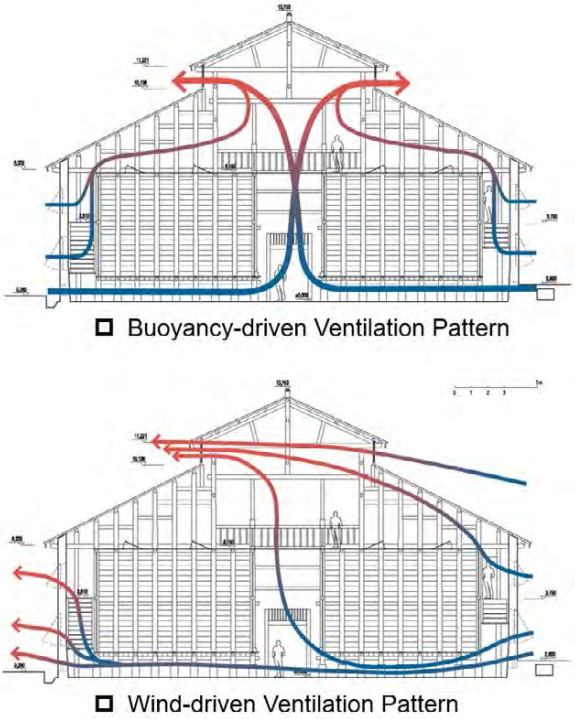

Figure 11: Diagram of airflow organization under buoyancy-driven and wind-driven ventilation pattern.

Figure 12 displays the variation curves of wind speed data collected from each test point in Section 1-1 of the granary during the field measurement period. These curves reveal that, even under conditions of low outdoor wind speed, a considerable airflow is still present within the granary.

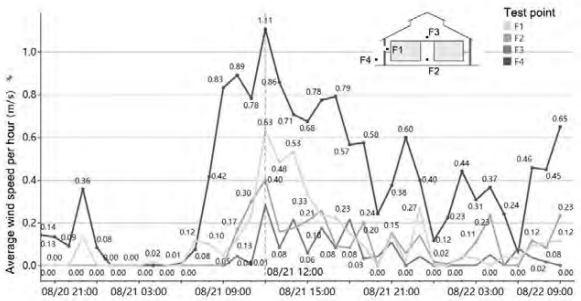

Figure 12: Statistics of wind speed at each test point of section 1-1.

Figure 13 presents the simulated wind environment of the granary under meteorological conditions analogous to those during the field measurement period (an outdoor air temperature of 32°C and a wind speed of 1 m/s), assuming an unstacked interior within the granary. The CFD software PHOENICS, with its advantage of obtaining enough resolution to assess the flow field of air, is used to simulate natural ventilation in the granary. The simulation results exhibit a high correlation with the measured data, particularly in the gradient of wind speed observed from the outdoor environment to the outer side window, and then sequentially to the lower and upper atrium.

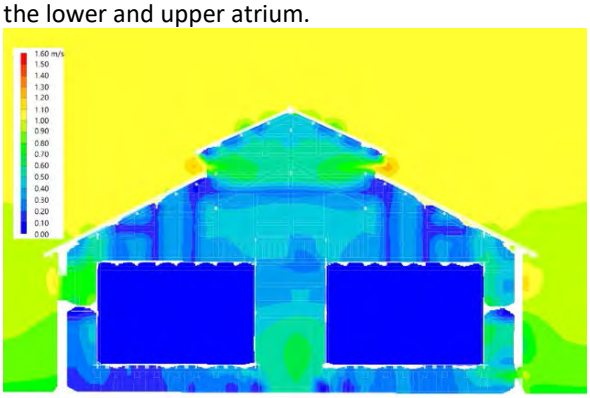

Figure 13: Simulation result of wind environment in the state of buoyancy-driven ventilation pattern.

Figure 14 displays the simulation results for the granary's wind environment under conditions of high outdoor wind speed (3m/s). In this wind-driven ventilation scenario, natural wind enters through the opening on the windward side, moves across the elevated floor and upper space of the granary, and exits through the opening on the leeward side. Notably, the air velocity in the upper space of the granary is higher, even leading to the formation of a minor vortex. Within the granary, a hierarchy of wind speeds is observed, with the sequence being windward side aisle > leeward side aisle > overhead floor > atrium. The overall wind speed within these areas is generally maintained at about 1.5m/s.

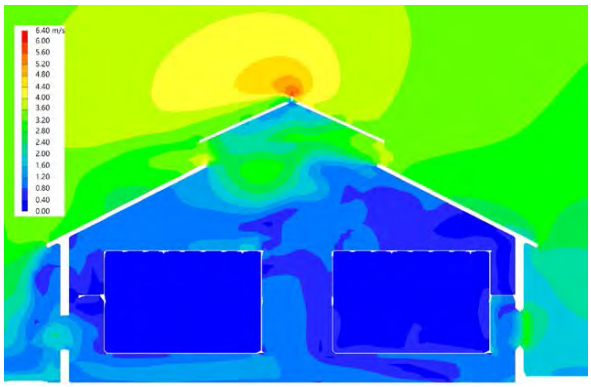

Figure 14: Simulation result of wind environment in the state of wind-driven ventilation pattern.

5. CONCLUSION

This study delves into the relationship between "building form" and "passive performance" in Tujia stilted granaries, encompassing a comprehensive approach that merges qualitative strategic considerations with quantitative analysis based on collected and simulated data. The analysis investigates multiple aspects such as layout, shape, space, interface, and material, aiming to discern how these architectural features impact the passive environmental performance of the granaries. The finds demonstrate efficient passive strategies of stilted granaries for temperature regulation and ventilation, adapted to local climatic conditions. Our findings highlight the crucial role of traditional construction methods in achieving sustainable architecture. The bioclimatic design principles evident in Tujia stilted granaries offer valuable insights for developing environmentally responsive buildings in similar climates. Future research could extend this analysis to other vernacular productive architectures, further enriching our understanding of sustainable building practices.

ACKNOWLEDGEMENTS

This research was supported by the National Natural Science Foundation of China (No. 52178007), and the Graduate Research and Practice Innovation Program of Jiangsu Province (KYCX21_0109); Financially supported by China Scholarship Council (No. 202206090269).

REFERENCES

1. Pan Y., Zhong W., Zheng X., Xu H., & Zhang T. (2024). Natural ventilation in vernacular architecture: A systematic review of bioclimatic ventilation design and its performance evaluation. *Building and Environment*, 253, 111317.

2. Saá, C., Míguez, J. L., Morán, J. C., Vilán, J. A., Lago, M. L., & Comesaña, R. (2011). The influence of slotted floors on the bioclimatic traditional Galician agricultural dry-store structure (hórreo). *Energy and buildings*, 43(12): p. 3491-3496.

3. Orszt, M., & Raszeja, E. (2022). Historical rural architecture of North Portugal and Spanish Galicia: Local vernacular forms and concept of adaptation, case study of Porreiras. *VITRUVIO - International Journal of Architectural Technology and Sustainability*, 7(2), 46–59.

4. Valls, A., García, F., Ramírez, M., & Benlloch, J. (2015). Understanding subterranean grain storage heritage in the Mediterranean region: The Valencian silos (Spain). *Tunnelling and Underground Space Technology*, 50, 178–188.

5. Saá, C., Míguez, J. L., Morán, J. C., Vilán, J. A., Lago, M. L., & Comesaña, R. (2012). A study of the influence of solar radiation and humidity in a bioclimatic traditional Galician agricultural dry storage structure (horreo). *Energy and Buildings*, 55, 109–117.

6. Perez-Garcia, O. A., Carreira, X. C., Carral, E., Fernandez, M. E., & Marino, R. A. (2010). Evaluation of traditional grain store buildings (horreos) in Galicia (NW Spain): Analysis of outdoor/indoor temperature and humidity relationships. *Spanish Journal of Agricultural Research*, 8(4), 925–935.

7. Erarslan, A. (2021). An example of traditional timber building techniques from Anatolia. Granary structures in the region of the Eastern Black Sea, Turkey; serender. *International Wood Products Journal*, 12(1): p. 58-70.

8. Mobolade, A. J., Bunindro, N., Sahoo, D., & Rajashekar, Y. (2019). Traditional methods of food grains preservation and storage in Nigeria and India. *Annals of Agricultural Sciences*, 64(2), 196–205.

9. Guerrero, L. (2013). Vernacular earthen granaries in Mexico. In *Vernacular Heritage and Earthen Architecture*, 17-22.

10. Wang, Y., Yi, Y., Zhang, N., & Du, J. (2018). A study of the forms and technology of traditional Granary buildings in the middle and lower reaches of the Fu River. *Journal of Asian Architecture and Building Engineering*, 17(2): p. 175-182.

11. Xu, H., Pan, Y., Zhang, T., & Yang, Y. (2023). Study on methodology of repair by disassembly: the case of Buyi ethnic construction techniques of a timber granary in Guizhou province, China. *International Journal of Architectural Heritage*, 0(0): 1-21.

12. Zhang, T., Xu, H., & Wang, C. (2022). Self-adaptability and topological deformation of Ganlan architectural heritage: Conservation and regeneration of Lianghekou Tujia village in Western Hubei, China. *Frontiers of Architectural Research*, 11(5), 865–876.

13. Pan, Y., & Zhang, T. (2022). Research on vernacular architecture environment measurement scheme based on low-power sensors and IoT technology. *Architecture Technique*, 28(10), 44–47.

PLEA 2024 WROCŁAW
(Re)thinking Resilience

Retrofitting Non-Domestic Historic Buildings:
The Douglas Primary School Case Study

ELSA MENDOZA[1], LUCELIA RODRIGUES[1]

[1] Department of Architecture and Built Environment, University of Nottingham, United Kingdom

ABSTRACT: In order to reduce the carbon emissions from the built environment, retrofitting the existing building stock is crucial. Circa 25% of UK buildings were built before 1950 and are considerably over the average building 60-years lifespan. Retrofitting to reduce energy use and operational emissions, would also provide an opportunity for increased building longevity. Historic buildings are particularly hard to treat as any applied strategies need to work around the need to preserve their historically significant features. In the UK, structures of particular architectural and/or historic interest are placed on statutory lists that indicates the need for special protection, and are subject to stringent regulations, which mean they cannot be demolished, extended, or altered without special permission. The aim of this work was to identify strategies for energy efficient retrofit of a selected case study: a former listed Victorian school currently occupied as a community centre with a number of functions. The methodology included a comparative analysis of existing approaches, in-situ assessment with data monitoring and assessment of operational carbon. The results demonstrated the benefits of retrofitting listed buildings with a fabric first approach, that resulted in 83% reduction of operational carbon emissions, even though ideal retrofit heating demand targets were not met.
KEYWORDS: Retrofit, Historic Buildings, Heritage, Energy Efficiency, Operational Carbon Emissions

1. INTRODUCTION

The increasing greenhouse gas (GHG) emissions caused by people are the fundamental contributors to climate change [1]. The built environment sector is accountable for 25% of these emissions [2]. In the UK, around 80% of the building stock that will be occupied in 2050 already exists today [4]. From this existing building stock, over 25% was built before 1950 [5].

In order to preserve the historic building stock, in the UK, structures of particular architectural and/or historic interest are placed on statutory lists that indicates the need for special protection, and are subject to stringent regulations, which mean they cannot be demolished, extended, or altered without special permission. The National Heritage List for England, originated in 1882, consist of over 400,000 entries and over 10,000 conservation areas [7] with heritage value. The values assessed for determining the significance of a building are the aesthetic value, communal value (i.e. the meaning of a place for the people related to it), evidential value (i.e. the potential of a place to demonstrate an historic aspect of the past) and the historical value [8]. However, specific characteristics and construction components of these buildings imply specific performance challenges and retrofit limitations, in addition to the listed restrictions they may have.

2. METHODOLOGY

The aim of this work was to explore retrofit strategies on a listed Victorian non-domestic building, while understanding its constraints and limitations, for improving the performance efficiency.

The selected case study was the former Douglas Primary School, a grade II listed building from 1885 in Nottingham, UK, in a cool temperate climate zone, with a Treated Floor Area (TFA) of 1,343.50 m^2 (Figure 1). Afterwards, its use changed to a mixed-used building, as it was purchased and adapted by Primary, an arts organisation with a large community involvement, providing studio spaces for artists, two galleries, a book shop, a bakery and a courtyard for community participation.

Figure 1: Primary from Ilkeston Rd. Source: Author 20.06.2023

The building had two storeys plus a basement, traditional Victorian red brick facades with terracotta dressings and hipped plain tile roofs. The significance value of the building relied on its aesthetic exterior Victorian features and communal values, as it was considered an educational landmark outside the city centre. The intense use of the former school left few interior historic features, some of them rescued by the artists in their private studios, nevertheless, damp, finishes in poor condition and previous not-sensible

interventions were detected. Hence, interior interventions were more feasible to consider for the retrofit approach, as no conservation limitations were found, on the contrary, some Victorian features were considered for potential restoration.

The methodology proposed for this research was divided in three stages: (1) the comparative analysis of strategies and approaches, (2) the case study analysis and baseline through an in-situ assessment and (3) the operational carbon modelling. Initially, a critical assessment of existing literature on traditional historic buildings provided a qualitative approach of their architectural value, function and construction. Moreover, two best-practice precedent studies were compared to understand the benchmarks and former used designed strategies that were proved to have a good operational performance.

Then, for the quantitative assessment, the in-situ assessment included gathered performance data from four different rooms, representing the different occupancy uses around the building. The baseline operational carbon and heat demand were assessed by Passive House Planning Package (PHPP). The resulted energy use per year was used for operational Whole Life Carbon (WLC) calculation, i.e. the projected calculation of carbon emissions for all the building lifespan, in this case considered for 60 years. Operational WLC was calculated following LETI (London Energy Transformation Initiative) methodology of a split carbon factor that takes into consideration an estimate of the UK's amount of renewable energy production and the future possible projection of its decarbonisation [10].

Once the areas of improvement for the fixed geometry were identified, in line with the significance assessment, a series of design iterations were tested in PHPP, to improve performance towards the studied targets and standards. The research limitations were the time availability for data gathering and the weather conditions of the summer period when the research was developed. Moreover, a limitation of the research scope was the lack of information available about the construction materials to develop a trustable embodied carbon assessment to complement the operational energy Whole Life Carbon (WLC) calculation.

3. COMPARATIVE ANALYSIS OF STRATEGIES AND APPROACHES

The comparative analysis included the available retrofit standards and regulations, mostly focused on housing, as it has the highest impact on carbon emissions (69% of the operational emissions from buildings) [11], the analysis of the main Victorian buildings' envelope characteristics, and two best-practice precedent studies.

3.1 Victorian Buildings

The most common traditional construction system for historic building's fabric was the solid wall. Construction could vary from single-skin brickwork to stone walls, as narrow as 100 mm thick up to rubble-filled walls of a metre or more thickness [12]. Each material would have a different thermal conductivity and moisture permeability, although most of them were breathable, i.e the moisture was able to be absorbed in the exterior and then evaporate when the wall dries, resulting in moisture equilibrium. Materials used in retrofit, repair and maintenance must be selected with care to preserve this permeability and moreover, its historic character.

Furthermore, the first experimentations with cavity wall constructions were from early Victorian Period, with the aim of providing a better protection from driving rain, preventing damp from passing through, enhancing stability and economy of the materials [13]. It consisted of two brickwork layers tied together, but separated at least by a 2" cavity. By the end of the 19th century, there was a consensus between builders that the cavity walls required a small amount of ventilation [13]. Construction details showed that they provided bottom ventilation through airbricks or grilles [14].

3.2 Precedent Studies: Foundry Project Cullinan Studio

The Foundry was the retrofit project of Cullinan Studio's headquarters office in London in 2012. Originally, the building was a Victorian 19th century foundry warehouse with the southeast facade and roof timber truss locally listed. The building had a gross internal area of 785 m^2 distributed in three storeys.

The construction was of solid brick wall with an early use of steel structure, timber flooring and a timber truss roof. The retrofit approach implemented was a fabric-first approach with internal and external insulation. The chosen material to keep wall breathability was natural recycled newspaper cellulose insulation, blown-applied in a timber battens frame, finished with a plasterboard. The roof was kept and insulated under the existing battens. The building was certified with BREEAM 'Excellent' rating. The total retained elements of the building represented 80% of the fabric that reduced the embodied carbon impact by 50% when compared to a new construction. The retrofit achieved a 34% improvement in operational energy use with 88 $kWh/m^2/yr$.

3.3 Precedent Studies: Zetland Houses

A pair of semi-detached housing retrofit project in Zetland Road was developed by Ecospheric and Guy Taylor in Chorlton, Manchester in 2018. Originally, the houses were built in 1894, but underwent several modifications through the years. Each house had 187 m^2 for a total gross internal area of 374 m^2 distributed

in three storeys and a cellar floor. The project was the first Passive House EnerPHit Plus certification in the UK [15]. They aimed to retain the most of the existing fabric, avoided the use of any petrochemicals and implemented a fabric first approach with high levels of internal natural recycled newspaper cellulose insulation for the front facade and external insulation for the rest. The interior details as plaster cornices and ceiling roses, some lost through time, were reinstated to recover the Victorian character.

The project simulated a heating demand of 12kWh/m^2/yr. To offset the houses' orientation, the designers implemented a passive strategy for the rear northwest facade, of rotating the window towards the south to increase 15% the solar gains and have the windows staged from the bottom to the upper floor to reduce stratification from the natural rising of heat within the envelope. The retrofit was very successful, as it reduced 95% the operational energy demand, and estimated a 7-fold carbon emissions reduction [16].

3.4 Retrofit Strategies, Approaches and Limitations

The different strategies and targets were compiled and compared with five scenarios (i) target value for constrained domestic buildings, (ii) the average semi-detached house in Nottingham, (iii) Zetland Houses, (iv) Foundry Office, and (v) the Primary baseline (current use) (Table 1).

All the approaches aimed for deep retrofitting, with at least 70% energy consumption reduction. The heating demand target for cool temperate climates of Passive House EnerPHit was 25 kWh/m^2/yr, nevertheless, LETI suggested 60 kWh/m^2/yr for constrained (hard-to-treat) buildings. Although it was a target value for domestic buildings per m^2, non-domestic uses, areas and space volume differ in occupancy patterns, internal gains and scale. This was shown in the baseline Primary building (v) that had a 10 times higher heating demand. The EnerPHit certification of case (iii) achieved the highest energy reduction. The feasibility strategies for breathability, moisture balance and condensation risk (i.e. water vapour condensation when warm, humid internal air meets a sufficiently cold surface within the wall construction [7] are crucial when assessing traditional constructions. The U-value to reduce condensation risk on traditional solid walls was 0.32 W/m2.K [7]. However, best-practice precedent studies demonstrated potential to surpass those and aimed for new building Passive House standards by adopting complementary strategies.

The baseline analysis through the in-situ assessment would provide information of the current performance, repair and maintenance issues and improvement potential.

Table 1: Retrofitting Approaches for Constrained Buildings (abstract version).

Strategies	Energy Reduction	Heating Demand	Overheating Risk	Wall U-Val	Roof U-Val	Floor U-Val	Airtightness
	%	kWh/m^2/yr	%		W/m^2.K		ach @50Pa
(i) LETI Target	70%	60	10%	0.32	0.22	0.20	3.0
(ii) Av. House	-	168	*a	1.35	0.25	1.04	11.50
(iii) Zetland	98%	12	0%	0.17	0.14	0.16	0.9
(iv) Foundry	40%	45	8.6%	0.20	0.19	0.45	5.0
(v) Primary	-	512	0%	1.35	2.94	2.70	12.0

*a: 20% of homes in the UK are in overheating risk [7].

4. IN-SITU ASSESSMENT

The site visits provided the baseline information about the building construction typology and condition. The fabric characteristics were analysed and there were two possible scenarios following Victorian construction typologies: (a) traditional breathable brick and a half thick solid masonry wall, in an English Bond for 338mm (Figure 2); and (b) early cavity wall, breathable and ventilated, with bonding bricks, for 374mm, which justifies the use of air grilles in the facades, although their location did not correspond with bottom wall traditional air bricks (Figure 3). Both walls presented a similar U-value, (a) 1.35 W/(m2K) and (b) 1.51 W/(m2K), respectively. Therefore, the following dynamic performance simulations were assessed assuming solid wall fabric, as it was the most common construction type for the period and would broaden the scope of the research impact.

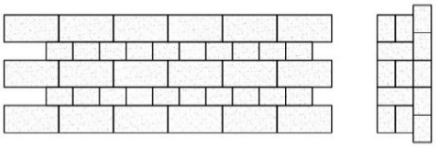

Figure 2: English or old English Bond Façade, solid wall. Author, based on Adams, 1907, Fig. 127, p.59

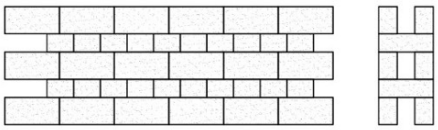

Figure 3: Dearne's Hollow Wall Façade. Author, based on Adams, 1907, Fig. 205-206, p.74

Four rooms were analysed to represent the main different uses of the building: (a) studio, (b) bakery, (c) book shop and (d) office (Figure 4).

Figure 4: Primary Building, Ground Floor. Plans provided by Primary, Edited by Author

Data monitoring for air temperature was gathered by Tinytag Ultra2 data loggers, one in each assessed room, for three summer weeks. A parallel register of Nottingham's weather temperature at 13:00 was gathered throughout the period for comparison. Results were compiled and extrapolated to current Design Summer Year (DSY) climate data for 2020 with a medium high emissions scenario.

The thermal assessment showed a delay of one day between the Weather Channel peak temperatures and the Tinytag room air temperature highest measurement, both for the lowest and highest peaks (Figure 5), demonstrated the thermal storage capacity of the walls' thermal mass. If the walls would be insulated on the inside, the thermal mass capacity would be significantly reduced. The external insulation could help increase the building's weather resistance and the effect of thermal mass, but it goes against conservation of the building. Therefore, interior insulation may be the more feasible if the breathability of the wall is kept and if it's performance surpasses the thermal mass benefits of the previous wall.

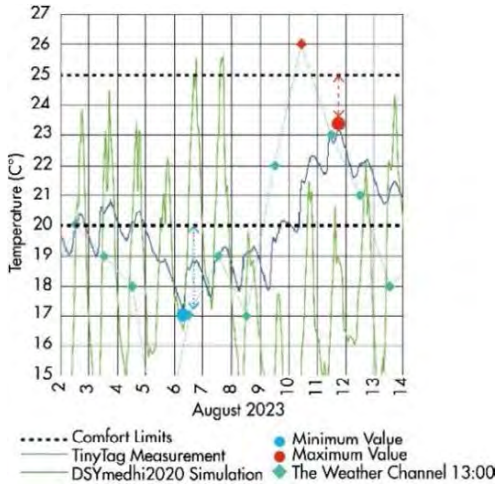

Figure 5: Room (a) Studio thermal measurements compared to exterior temperature

The indication of a general low interior temperatures was proved in the PHPP assessment with a high heating demand, where the highest energy losses were through the roof, unintentional ventilation, external walls, and windows. Based on the simulated electricity use of 36 kWh/m^2/yr and heat demand of 512.8 kWh/m^2/yr, the Whole Life Carbon for the resulting operational energy of 736,865 kWh/yr was calculated following LETI methodology of split carbon calculation (Equation 1).

Equation 1: Split Carbon Calculation [17]

$$WLC_{OC} = (EUI\ Target\ x\ dcf) + (Re\ x\ cf)\ x\ 60y$$

$$WLC_{OC} = (4{,}586.45) + (173{,}014.29)\ x\ 60$$

$$= \mathbf{10,656,044\ kgCO_2}$$

Where:

WLC_{OC} = Whole Life Carbon for Operational Carbon

$EUI\ Target$= LETI Energy Use Intensity for Office typology 55 kWh/m^2/yr x 1,345 m^2 = 73,975 kWh [18] as the closest available for the occupancy typology.

dcf = decarbonised factor 0.062 kgCO$_2$/kWh

cf = carbonised factor 0.261 kgCO$_2$/kWh

60y = 60-years building's lifespan

The WLC calculation for the operational energy resulted in 10,656 tonCO2e, over 60 times higher than the LETI target for housing of 160 tonCO2e [7] and without taking into account the embodied carbon of the existing building. However, compared to the retrofit project of the Foundry (1,383 tonCO2e), Primary's WLC OC is over 7 times higher, without embodied carbon included. This demonstrated how non-domestic buildings need to be assessed and compared to specific standards and targets that anticipate the typology's limitations and characteristics, as the housing benchmarks are far away from the non-domestic performance.

5. MODELLING

The baseline evaluation provided an insight of the building's requirements for a holistic retrofit resilience approach. The main cause for the high WLC emissions for operational energy was the building's heating demand. The orientation resulted in a lack of solar gains and high heat loss through the building's envelope. Hence, based on the in-situ assessment, a bespoke fabric-first approach was tested with PHPP by a series of retrofit interventions by element. The methodology was additive, where each iteration was tested from the former iteration result.

The first iteration was the (1) replacement of the damaged roof, followed by (2) interior wall insulation to preserve the historic facades and restore the breathability and moisture balance, (3) replacing the single-glazed windows with a traditional timber frame with double glazing, (4) improving airtightness level, (5) introducing MVHR system and (6) insulating the ventilated ground floors between joists (Figure 6).

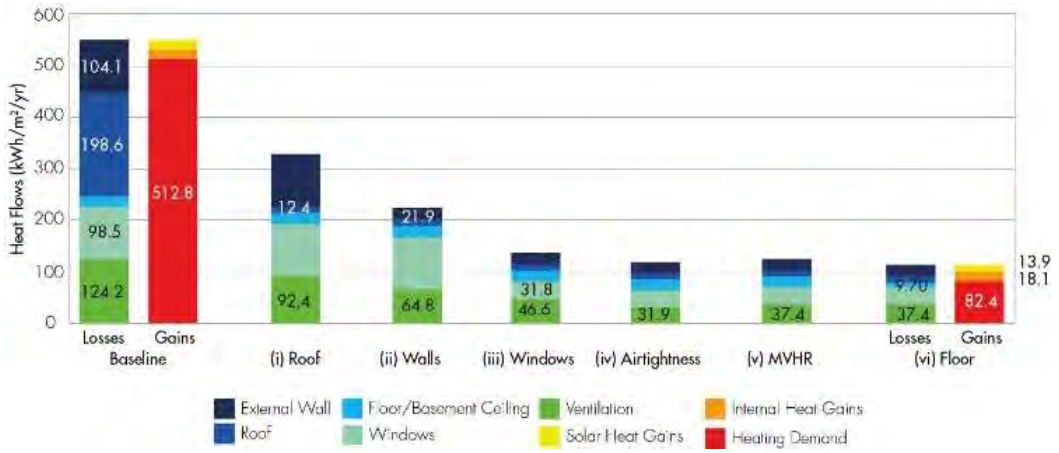

Figure 6: Proposal iterations PHPP Energy Balance Heating, Annual Method

Further resilience strategies such as form factor reduction, increased solar gains through windows and exterior insulation to retain thermal mass were not feasible given the listed conditions of the building.

The predicted condensation in the exterior walls was assessed and compared to the baseline solid wall performance that presented a mostly evenly slope of vapour pressure through the wall thickness. In contrast, the proposed interior wall insulation presented a significant temperature drop after the insulation limit, presenting a condensation risk point (Figure 6).

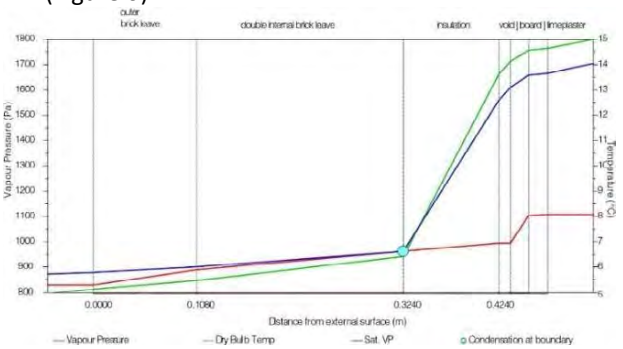

Figure 6: Design Proposal Wall Condensation Prediction

The improved proposal had an energy demand of 42 kWh/m^2/yr and a heating demand of 82 kWh/m^2/yr, resulting in a total operational energy use of 166,955 kWh/yr. The heating demand was still far from achieving the LETI domestic constrained target of 60 kWh/m^2/yr and the Passive House EnerPhit target of 25 kWh/m^2/yr. The Whole Life Carbon of operational energy, by LETI split carbon calculation, for the retrofit proposal on the fixed geometry resulted in 1,731 tonCO_2e, 83% less than the current emissions projection of 10,656 tonCO2e.

The improved thermal efficiency of the roof (1) was proved to be the best, under the resilience fabric first approach, with a 93% improvement. Although the insulated walls U-value calculation did not comply with the condensation risk targets, best-practice precedent studies demonstrated that with breathable moisture control membranes and natural materials, an improved U-value could be achieved. However, the interior wall insulation proposed for the second iteration (2) presented condensation risk. Further research on insulation variations (such as thickness and reduced thermal performance) should be tested to reduce condensation risk without compromising the thermal improvement achieved, the second highest by building element, of 79%.

The low internal heat gains indicated a low occupancy density for the available area, in line with the possible adaptable strategies for a layout improvement. The solar heat gains were restricted by the significance value of the exterior walls, impeding increasing size or additional windows.

8. CONCLUSION

The research aimed to explore, compile and extrapolate the existing standards and precedent approaches to be applicable for a listed Victorian non-domestic building, to improve the performance

efficiency. The methodology was divided into three stages: (1) the comparative analysis of strategies and approaches, (2) the case study analysis and baseline through an in-situ assessment and (3) the operational carbon for the fixed geometry.

The key outcomes of the research included the understanding of the performance limitations for complex retrofits, taking Primary as a vehicle. (1) The comparative analysis of strategies highlighted the importance of a constrained U-value for reducing the condensation risk in traditional solid walls, and failing to achieving so, was proved to have risks. So, further assessment on different interior insulation strategies or retaining the walls' thermal mass without insulation should be tested to find a balance between the best performance without hazards. (2) The in-situ assessment showed the heating demand was still the most important challenge to assess for the cool temperate climate of Nottingham, as it represented the highest energy demand and the highest thermal discomfort. (3) The modelling of the design proposal achieved a heating demand reduction of 84%, although the rooms presented a comfort gap between 25-70% of the hours still under the comfort limit.

The listed building's limitations to modifying the exterior facades limit the possible passive strategies to increase heat gains. The chosen resilient fabric-first approach was proved to improve the building's performance and longevity, however it felt short to achieve the existing standards for heating demand from LETI and Passive House EnerPhit.

ACKNOWLEDGEMENTS

I would like to express my deepest appreciation to my supervisor Prof Lucelia Rodrigues, for all her advice, support and for the inspiration through this journey. I also want to recognise the support from the University of Nottingham Faculty of Engineering that sponsored me with the Excellence Award Scholarship and from the Mexican Conacyt-SACPC-FINBA 2022 scholarship. I would like to extend my heartfelt appreciation to Primary for their support for this research.

REFERENCES

1. INTERGOVERNMENTAL PANEL ON CLIMATE CHANGE (IPCC), 2007. *Fourth Assessment Report: Climate Change 2007*. Available at <www.ipcc.ch>

2. UK Green Building Council (UKGBC), 2021. Net zero Whole Life Carbon Roadmap. London: UKGBC. *A Pathway to Net zero for the UK Built Environment.* UKGBC, Nov, 2021 [viewed 12.05.23] [Online] Available at <https://ukgbc.org/wp-content/uploads/2021/11/UKGBC-Whole-Life-Carbon-Roadmap-A-Pathway-to-Net-Zero.pdf>

4. PENOYRE, G. and PRASAD, S. (2014) Retrofit for Purpose, Low Energy Renewal of Non-Domestic Buildings. London: RIBA Publishing (p. 3-4)

5. BUILDINGS PERFORMANCE INSTITUTE EUROPE (BPIE) (2011) *Europe's Buildings under the Microscope.* [Online] Available at <http://www.bpie.eu/publication/europes-buildings-under-the-microscope/>

7. LETI (2021). Climate Emergency Retrofit Guide. LETI, 01.10.21 [viewed 08.05.23]. Available at: <https://www.leti.uk/retrofit> (p.23, 193, 72, 22)

8. BRITISH STANDARDS INSTITUTION (BSI) (2013) 'BS 7913:2013 Guide to the conservation of historic buildings'. BSI Standards Publication, 2013. [viewed 26.07.23]. [Online] Available at:<https://bsol.bsigroup.com/Bibliographic/BibliographicInfoData/000000000030248522> (p.7)

10. LETI (2023b) LETI Opinion Piece: Operational Carbon in Whole Life Carbon Assessments. LETI, 20.02.23 [viewed 25.02.23] [Online] Available at:<https://www.leti.uk/_files/ugd/252d09_5911f23632d54b4cbac0cca740c6aa93.pdf> (p.1)

11. UK Climate Change Committee (UKCCC) (2019) Net zero – Technical Report V, 02.05.2019, CCC [Online] Available at: <https://www.theccc.org.uk/publication/net-zero-technical-report/> cited in LETI (2021) Climate Emergency Retrofit Guide. LETI, 01.10.21 [viewed 08.05.23] [Online] Available at: <https://www.leti.uk/retrofit> (p.18)

12. HISTORIC ENGLAND (2016a). Energy Efficiency and Historic Buildings. Insulating Solid Walls. Edition v.1.1. 29.04.16 [viewed 09.08.23] [Online] Available at: <https://historicengland.org.uk/images-books/publications/eehb-insulating-solid-walls/> (p.3)

13. HISTORIC ENGLAND (2016b). Energy Efficiency and Historic Buildings. Insulating Early Cavity Walls. Edition v.1.1. 29.04.16 [viewed 09.08.23] [Online] Available at: <https://historicengland.org.uk/images-books/publications/eehb-early-cavity-walls/heag083-early-cavity-walls/> (p. iii, 9)

14. ADAMS, H. (1907). Building construction: comprising notes on materials, processes, principles, and practice, including about 2,300 engravings and twelve plates. London: Cassell&Co.

15. PASSIVHAUS TRUST (2018) Zetland Road [viewed 20.07.2023]. [Online] Available at: <https://www.passivhaustrust.org.uk/projects/detail/?cId=91

16. ECOSPHERIC (2021) Zetland Road: 2021 UK Passivhaus Awards [viewed 20.07.2023]. [Online] Available at: <https://www.passivhaustrust.org.uk/UserFiles/File/UK%20PH%20Awards/2021/PHTawarads2021_Zetland%20Road_sensitive%20info%20removed.pdf> (p.4)

17.LETI (2023a) Improving Consistency in Whole Life Carbon Assessment and Reporting: Carbon Definitions for the Built Environment, Buildings & Infrastructure. LETI, 01.01.23 [viewed 08.05.23] [Online] Available at: < https://www.leti.uk/carbondefinitions> (p.1)

18. LETI (2020) LETI Climate Emergency Design Guide. LETI, 01.01.20 [viewed 08.05.23] [Online] Available at: <https://www.leti.uk/cedg> (p.36)

PLEA 2024 WROCŁAW
(Re)thinking Resilience

Air Cooling Concepts for Post-War Residential and Office Buildings in Germany based on Historical Models

ALEXANDER KADER

German University of Technology, Muscat, Oman

ABSTRACT: This paper explores innovative air cooling concepts for post-war residential and office buildings in Germany by drawing inspiration from historical models. In the context of contemporary construction practices emphasizing energy-intensive cooling systems, the study aims to bridge the gap between past architectural wisdom and present needs. The challenges faced by post-war buildings due to rising urban temperatures and inadequate insulation are demonstrated. The research proposes the integration of forgotten cooling strategies from pre-modern builders, emphasizing the importance of passive approaches that respect historical contexts. The objective is to synthesize historical knowledge and innovative ideas, offering a comprehensive framework for enhancing air conditioning systems in post-war structures. The conclusion highlights the potential of integrating air cooling strategies from historical structures with modern technologies to achieve comfortable indoor environments while reducing energy consumption. The findings contribute to sustainable building practices, offering implications for the revitalization of existing buildings and the development of energy-efficient cooling approaches. The discussion delves into the feasibility of transforming post-war buildings with passive cooling systems, emphasizing the preservation of architectural aesthetics during energetic retrofits.
KEYWORDS: ecological retrofitting, natural ventilation, climate change adaptation, low energy cooling systems, applying vernacular techniques

1. INTRODUCTION – WHY WE URGENTLY NEED TO IMPLEMENT COOLING CONCEPTS FOR POST-WAR BUILDINGS IN GERMANY

Rising urban temperatures pose an increasing challenge to existing structures, a consequence of shifting climate zones. This predicament is acutely felt by post-war residential and office buildings, which suffer from inadequate insulation and construction standards. Addressing this issue demands the redevelopment of innovative passive strategies that counteract overheating while focusing on historical contexts.

Such approaches not only enhance comfort and reduce energy consumption but also safeguard our architectural heritage. It is imperative to usher in a new era of climate-responsive design, where the lessons of the past harmonize with the needs of the present and the aspirations of the future. Many historical structures have been crafted with proficient air cooling systems which can serve as case studies. Given the impending shift in climate zones over the coming decades, there exists an opportunity to glean insights from these existing cooling systems that have effectively operated in warmer climatic regions.

1.1 Aim of the study

In the wake of the post-war era, residential and office buildings underwent significant transformations to accommodate evolving societal needs and technological advancements. However, as contemporary construction practices prioritized modern amenities and energy-intensive cooling systems, there is a growing urgency to revisit and harness the wisdom embedded in historical architectural approaches.

This research endeavors to bridge the gap between past and present by investigating the feasibility of integrating cooling techniques from vernacular contexts into post-war buildings.

By drawing inspiration from traditional designs that once adeptly navigated climatic challenges without the reliance on electricity-intensive cooling, this study seeks to reimagine air cooling methods that harmonize comfort, sustainability, and heritage.

Against the backdrop of mounting concerns over energy consumption and environmental impact, this research holds a twofold promise.

Firstly, it aims to uncover the forgotten cooling strategies employed by pre-modern builders and architects, decoding their principles for application in contemporary contexts.

Secondly, it aspires to propose innovative, eco-conscious adaptations that can potentially reshape the landscape of air conditioning in post-war residential and office spaces. Through this exploration, a renewed synergy between historical ingenuity and modern demands could pave the way for more balanced and efficient cooling solutions, benefiting both occupants and the planet.

1.2 Objective and Rationale

The research of this paper aims to provide passive air cooling solutions to reduce the excess heat income of post-war buildings. It has the goal to find ways how the re-application of vernacular air cooling strategies can be implemented as an essential part of sustainable retrofits of post-war residential and office buildings, also as an adaptation measure for a hotter climate in the future. It poses the question how to conceptionally and technically integrate passive ventilation based cooling systems into existing buildings of the post war era.

Through the sequential steps presented during the chapters of this paper, this study seeks to synthesize historical knowledge, innovative ideas, and practical solutions, culminating in a conceptual framework for enhancing the sustainability of post-war structures with air cooling systems. Aligned with future climatic demands, by analyzing the thermal comfort strategies employed in these historical structures and integrating them with modern technologies, this research provides a set of suggestions for achieving comfortable indoor environments while reducing energy consumption and environmental impact.

The findings hold significant implications for the revitalization of existing buildings and the development of new, energy-efficient cooling approaches, contributing to the overall advancement of sustainable building practices of the modern era.

The following part contains an evaluation about the feasibility of transforming postwar buildings with passive cooling systems. Additionally, a special focus is set on how an energetical retrofit can be realized in a way that the esthetics of post-war buildings (which often have a high architectural value) can be maintained.

1.3 Heat-related mortality problem in Germany

Due to the increasing number of heat-related death incidents which occurred during heat periods in recent years, it becomes more and more obvious that the problem will be dramatically multiplied within the upcoming decades of this century, if no measures will be taken against it.

For example, according to [3], in Germany during the summer of 2022 there have been an estimated 8,173 heat related death cases and – in regard to the entire Europe – the authors pledge for an urgent reaction by the governing authorities: "The high heat-related mortality that Europe experienced during the summer of 2022 calls for national governments and relevant agencies in the European Union and continental levels to increase the ambition and effectiveness of heat prevention and adaptation plans with urgency" [3]. One of the reasons for this is that the living conditions in many flats in Germany are inappropriate due to a lack of cooling possibilities. Therefore, there is a grand responsibility to find ways to avoid solar overheating of residential buildings to reduce the number of people affected and dying due to heat stress generated by summerly heat periods and lack of cooling options of their apartments.

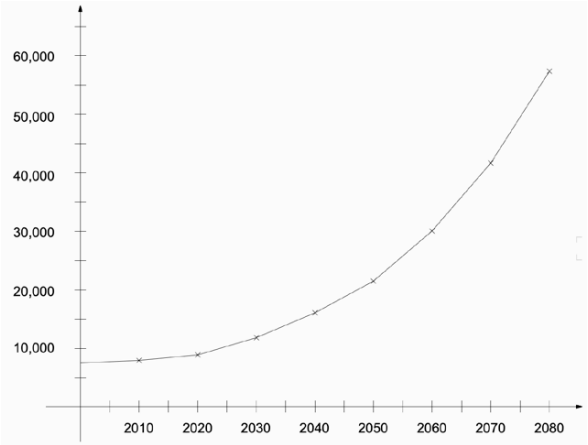

Figure 1: Estimation of predicted annual average heat related death cases (y-axis) in Germany for the next decades (x-axis) in case that no interventions against overheating of interior spaces would be done (estimation by author still vague, based on numbers until 2022 [3])

1.4 Air cooling strategies

Focusing on vernacular architecture from different climate zones, the following air cooling strategies have been selected to be analyzed in regard to a possible application on post-war buildings: cross ventilation as wind-induced air movement; single sided ventilation as wind-induced air movement (with relatively low efficiency); stack ventilation as temperature-induced air movement; wind- and temperature-induced ventilation through courtyards; solar chimneys as a variation of stack ventilation; wind catcher ventilation; natural ventilation through air channels. In addition, air cooling systems with help of fans (fan assisted natural ventilation) have been considered as well.

2. EXISTING BUILDING STOCK IN GERMAN INNER CITY AREAS – BURDEN OR POTENTIAL?

2.1 Challenges of post-war buildings

Subsequently, an exploration of post-war residential and office buildings is conducted. This step involves a depiction and assessment of the architectural and structural characteristics of these buildings. Post-war buildings, often constructed between the 1940's and 1980's, face several challenges in terms of energy efficiency. These issues arise from the construction methods, materials used, and design standards prevalent during that era. Some common deficits are as described in the following points. Many post-war buildings were constructed with minimal consideration for insulation. This lack of

insulation can result in increased heat loss during the winter and heat gain during the summer, leading to higher energy consumption. Older buildings often feature single- or double-pane windows, which are much less energy-efficient and which have much lower u-values than the glazing and framing standards we have today. Often the entire building skin (walls, ceiling, foundation plate) has a too low insulation and low u-values. Many post-war buildings may have outdated heating, ventilation, and sometimes air conditioning systems (HVAC) that are less energy-efficient compared to contemporary systems. Inefficient HVAC systems contribute to higher energy consumption and costs. Most residential buildings of the post-war era do not have air conditioning systems for cooling. In terms of sustainability, the lack of air condition systems on a large scale can be seen as an advantage (in many Southern European cities, the use of AC's constitutes a large amount of CO_2-emissions. Poor sealing around doors and windows can lead to drafts and air leakage, reducing the effectiveness of heating and cooling systems. Proper air sealing is crucial for maintaining a comfortable indoor environment and minimizing energy waste.

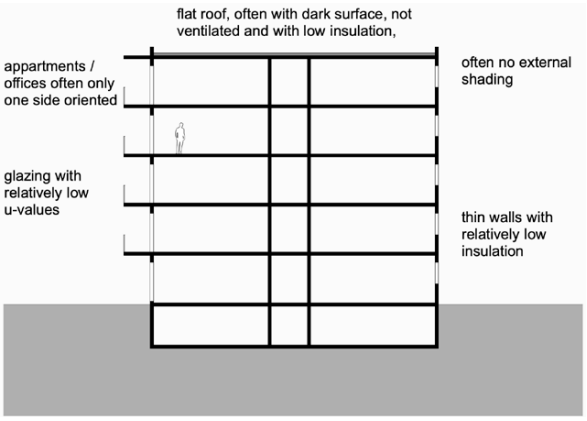

Figure 2: Schematic section with some typical characteristics of post war buildings

Many post-war buildings were constructed before modern energy efficiency standards and building codes were established. Furthermore, many buildings contain structural challenges such as thermal bridges. Often the buildings do not contain enough thermal mass for heat or cold storage to passively improve interior comfort. In many cases, there is direct sun exposure and lack of external sun screens. Many post-war buildings lack opening mechanisms or ventilation openings to enable cross ventilation through the building façades (windows and walls) and also through elements within the building which block cross ventilation (walls/doors). It is not seldom that floor plans are oriented only towards one direction, thus with the disadvantage of preventing natural air flow across the building.

With all these flaws, are post-war buildings a burden which is hindering sustainable urban development? With a focus on air cooling strategies, it is the thesis or argument of this paper, that for the majority of post-war buildings, it is feasible and reasonable to energetically retrofit these buildings instead of demolishing them.

2.2 Application of air cooling systems in vernacular architecture

Historical vernacular strategies and air cooling systems are analyzed and taken as role models. Since due to climate change and according to respective scientific studies, a shift in climate zones for Germany is predicted, vernacular cooling systems of other, more hotter climate zones are analyzed and evaluated as well (e.g. Mediterranean climate). The floor plans of many pre-war buildings in Germany have been designed in a way that cross ventilation is possible. Some buildings, for example the town hall of Hamburg (built at the end of the 19th century), are equipped with a complex set of ventilation channels in order to naturally ventilate spaces in a more refined and effective way.

From studies of pre-war buildings in hotter climates a variety of air cooling principles can be extracted [1, 9]. Due to climate change, for the first time in history, these strategies can be applied in Northern Europe as well and safeguard a part of our building stock from solar overheating in summer.

For their buildings in hotter climate zones, in times of Modernism before World War II, some architects successfully integrated passive air cooling techniques into their buildings in order to keep them comfortable with natural ventilation. Casa Giuliani in Como / Italy by Giuseppe Terragni from 1939 constitutes an example for the integration of natural ventilation [9]. In 1927 and 1928 Le Corbusier developed a refined air flow based ventilation concept, called "Respiration System for Buildings", which constitutes an example for ventilation through air channels and shafts [15]. Architects like Alfonso Reidy or MM Roberto applied and further developed ventilation techniques in Brazil. Focusing on contemporary architecture, within hotter climate zones one can find many examples of naturally ventilated constructions, e.g. buildings from Balkrishna Doshi in India.

3. ELABORATION AND DISCUSSION OF AIR COOLING STRATEGIES

This stage encompasses the conceptualization and development of case studies, ideas and sketches for application/integration of historical air cooling systems. The concepts focus on the effective application and integration of air cooling systems for post-war buildings. A key element of this stage is the

formulation of air flow pathways to optimize system efficiency. Vernacular techniques applied in historical buildings often serve as role models.

All following strategies may be applied if they are reasonable and esthetically possible in the individual case. However, for each building the feasibility of each strategy hast to be checked before choosing which strategy would be installed. Before applying an air cooling strategy, it should be evaluated if the strategy can be combined with another sustainable design strategy, for example in regard to cold protection in winter.

In relation to the implementation of air cooling systems, there can be differentiated between three categories: a) buildings which are suitable for creating cross ventilation through the façades; b) multistorey buildings in which additional ventilation shafts or channels need to be installed in order to generate passive air flows for cooling; c) buildings which contain atriums or other types of vertically oriented open spaces.

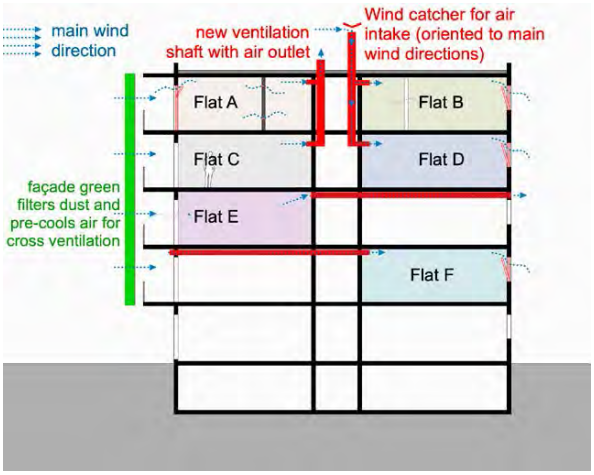

Figure 3: Enabling cross ventilation for apartments or offices with window orientation only to one direction (schematic section)

• Add new openable facade elements to enable natural air flow: In many cases the existing windows are not suitable for cross ventilation so that adequate openable windows or façade integrated ventilation openings could be installed in addition. In case of an extensive retrofit, existing windows might be replaced with windows which are more adequate not only for cross ventilation but also for thermal optimizations and other factors. Windows with tilt function often are suitable for cross ventilation. Before the advent of air conditioning systems and controlled ventilation, the majority of buildings could be cross ventilated, especially in buildings from hotter climate zones, e.g. southern Europe, this has been an essential design feature [11]. The architect Hassan Fathy has applied and further developed vernacular cross ventilation techniques from previous centuries and applied in his project for hot and arid climates in Egypt, dated from the 1940's to the 1980's [12].

• Create adequate openings for cross ventilation in interior walls, doors or ceilings inside the building: The air flow needs to pass from building side to another side to enable cross ventilation. Many apartments or office spaces are not built for these kinds of natural air flows. To make them utilizable, new ventilation openings might be implemented accordingly within interior walls, doors or ceilings.

• Implement ventilation channels if necessary: As shown in figure 3, ventilation shafts and air channels might be installed to create air flows for apartments or office spaces which are oriented only to one direction. Many buildings dated from before the second world war contain refined cooling channels. Besides buildings in hot climates, these techniques sometimes have been applied as well in cooler regions. The natural air cooling systems of the town hall in Hamburg from 1897 is such an example.

• Benefit from ground cooling of incoming air: Build channels and shafts for air flow to pre-cool incoming fresh air through ground cooling. (Especially to avoid heat loss of outgoing air in winter, this strategy could be combined with the use of an air to air heat exchanger. Thus, incoming winterly air would be warmed by outgoing air.) Examples of historical models for ground cooling can be found in many old palace buildings, e.g. Topkapi Palace in Istanbul or Red Fort building in New Delhi, among many others.

• Build wind catching towers: If the specific situation is favorable, wind catchers for air intake might facilitate and increase the air flow within a building. They can be oriented towards the main wind directions. Historical models for wind catching towers can be found for example in Yazd, Iran where these cooling techniques have been used for many centuries.

• Make use of stack ventilation: Existing atriums or other adequate vertically oriented spaces might be transformed in a way that air flows are generated by the stack ventilation effect generated by rising air. The building has to be equipped with adequate openings for outgoing air, e. g. on the upper side of an atrium, and for the incoming air, e. g. through the windows of the offices or residential spaces.

• Increase thermal mass: Massive building material can absorb and store the cold brought by ventilation with cool air. Thus, during the hottest hours of the day, the wall can keep the interior spaces cool. Heat peaks can be significantly buffered.

• Enable night cooling: Since external temperatures are significantly lower at night than during the day, during heat periods it can be much more efficient to ventilate and cool interior spaces during night times only, and avoid an intake of hot air during the day. In combination with thermal mass, in

this way, the cold of the night can be stored and keep interior spaces cool during the day. Office spaces may be equipped with automated opening mechanisms which enable an activation of cross ventilation during the night, when usually the users are not present.

• Install ceiling fans to generate air movement: With relatively low electricity consumption, a cooling effect can be generated by ceiling fans. Even though moving air is not cooler than non moving air, it feels accordingly and the maximum temperature in which we still feel comfortable can be a few degrees higher.

• Reducing air humidity for better comfort: With lower humidity, heat feels less hot. If on hot days natural ventilation is active only during the cooler nights, indoor comfort can be improved during the day by air dehumidifiers. Since all dehumidifiers consume significant amounts of energy, their use cannot be seen as passive system. They should possibly be avoided and other, more sustainable strategies might be applied. However, if the other strategies cannot be applied, or in combination with other strategies , air dehumidifiers might be necessary to achieve the comfort required. In that case the more sustainable thermally driven systems should be selected [19].

• Erect a new exterior façade layer around the building to create a thermal buffer zone: Due to the high effort, relatively high amount of grey energy, rather high costs and the change of the original appearance of a building, this strategy might be applied only if multiple benefits are achieved, such as a thermal improvement for winter and summer as well as an additional living space in form newly created balconies or terraces which are positioned within the buffer zone. In regard to passive air cooling there are several benefits since the air flow can be directed in various modes according to the best performance under the different climatic conditions. For example, to avoid overheating, the space between the old and new façade can serve as a climatic buffer, hot summerly air can rise and be led out of the building, thus preventing the interior space from overheat. Many buildings in Southern Europe with arcades, pergolas and other cantilevering building parts are historical examples. Additionally, there are contemporary retrofits in which with added 'climate mediator zones' generate an improved building performance. An example for this is the retrofit of a residential building block from the 1960's called in Bordeaux 'Transformation of 530 Dwellings' by Lacaton Vassalle in which also passive air cooling plays a major role.

• Apply façade green for cooling: During summer, the leaves of climbing plants can shade the façades and also cool air by transpiration from their leaves (air used for ventilation).

• Activate evaporative cooling: Spaces are cooled with the principle of the adiabatic cooling in which heat is absorbed by the evaporation process of the water and thus reducing the indoor air temperature. As applied for centuries in vernacular architecture of hot regions, evaporative cooling can be applied with water bodies, e.g. in courtyard houses or in porous clay vessels which are filled with water [12].

• Integrate solar chimneys: Buildings can efficiently be ventilated by the hot air draft generated by solar chimneys. However the implementation of solar chimneys requires a relatively high effort and often is not compatible with the esthetic appearance of the building [18].

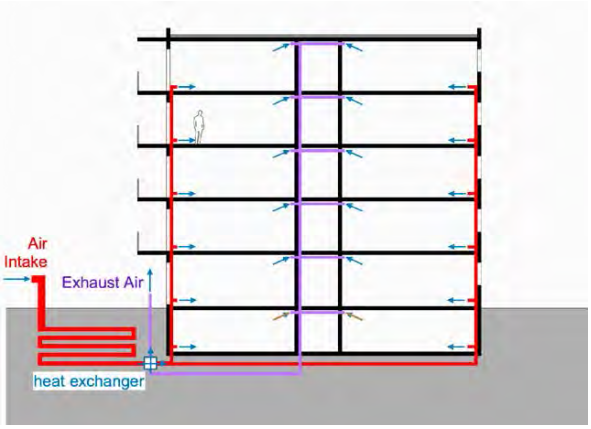

Figure 4: Ventilation strategy with pre-cooling of air through the ground, fan assisted (optional with heat/cold recovery by heat exchanger)

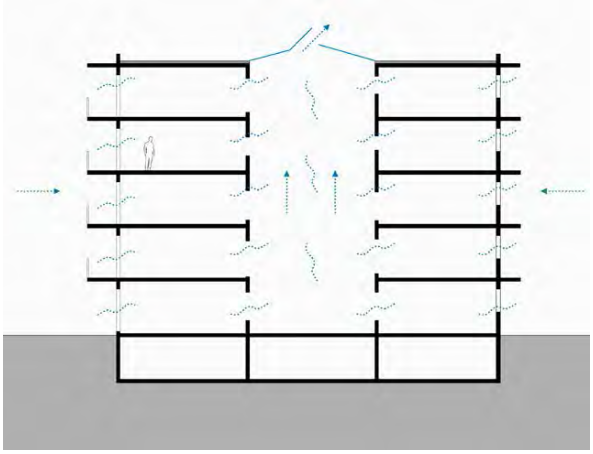

Figure 5: Stack ventilation generated by rising hot air

4. CONCLUSION – AIR COOLING SYSTEMS CAN SERVE AS A VIABLE TOOL IN THE TRANSFORMATION PROCESS OF MAKING POST WAR BUILDINGS MORE ENERGY EFFICIENT

We can see that many historical examples are placed in climate zones with hotter climates. Due to the climate change, the air cooling techniques of these buildings become applicable also in Northern European buildings.

During the evaluation process and the selection of the options (before choosing the air cooling strategies to implement with a project), also other factors have to be considered holistically. For example the building's insulation, sun protection, daylight use, embodied energy of new construction material as well as esthetic aspects. The different factors are to be combined in a way that they support each other and create synergies. Thus the building's initial energy consumption should be significantly reduced while the qualities towards a better sustainability, comfort and esthetics are significantly improved.

Since most post-war buildings are different in their settings, the selection which air cooling strategies should be applied, can not be generalized. Individual considerations are necessary for each specific situation.

From the range of the single intervention options explained in chapter 4.2, the most adequate strategies have to be chosen during a careful selection process. Besides a thorough analysis of the building's individual characteristics, also software based building performance simulations could be conducted to facilitate the selection process and possibly verify the intervention's outcomes (e.g. computational fluid dynamics analysis).

In conclusion we can summarize that air cooling systems can serve as a viable tool in the transformation process of making post war buildings more energy efficient. Before choosing the strategies, they have to be evaluated individually regarding a) energy efficiency, b) installation and maintenance costs, c) embodied energy of the new retrofit interventions and technical installations**.** If the prioritization process of choosing the most effective combinations of intervention strategies is executed precisely, also from an economic point of view, the retrofit options appear reasonable and cost efficient.

REFERENCES

1. Cook, M. J., Shukla, Y., Rawal, R., Angelopoulos, C., Caruggi-De-Faria, L., Loveday, D., Spentzou, E., & Patel, J. (2022). Integrating low energy cooling and ventilation strategies in Indian residences. Buildings and Cities, 3(1), pp. 279–296. DOI: https://doi.org/10.5334/bc.197.
2. Böhnig, J. (2005). Altbaumodernisierung im Detail. Rudolf Müller Verlag.
3. Ballester, J., Quijal-Zamorano, M., Méndez Turrubiates, R.F. et al. (2023). Heat-related mortality in Europe during the summer of 2022. *Nat Med* 29, pp.1857–1866. https://doi.org/10.1038/s41591-023-02419-z.
4. Vázquez-Ramos, C. I., & Marvuglia, A. (2021). Enhancing energy efficiency and sustainability in historical buildings through retrofitting strategies. *Journal of Building Engineering*, 42, 103091.
5. Attia, S., Hamdy, M., & Carlucci, S. (2020). Passive cooling design strategies for retrofitting existing buildings: A literature review. *Journal of Building Engineering*, 27, 101003.
6. Attia, S., & Belkhouane, H. (2019). Strategies for the integration of passive cooling techniques in existing office buildings: A case study in Switzerland. *Energy Procedia*, 158, 1622-1627.
7. Chahal, R., & Choudhury, D. (2019). Passive cooling techniques for energy-efficient buildings: A review. *Energy and Buildings*, 196, 288-306.
8. Kader, A. (2022). Towards climate change adapted built environments – Retrofitting the existing building stock of multistorey residential buildings from the 19th and early 20th century in urban areas in Germany". IOP Conference Series. *Materials Science and Engineering*.
9. Passe, U., & Battaglia, F. (2015). Designing spaces for natural ventilation – An architects guide. Routledge.
10. Kohler, N., & Rattalino, F. (2019). Assessing retrofitting strategies to enhance passive cooling potential of low-rise housing in mild climates. *Energy and Buildings*, 187, 1-14.
11. Frey, P. (2010). Learning from Vernacular. Towards a new Vernacular Architecture, Actes Sud, Arles.
12. Fathy, H. (1986). Natural Energy and Vernacular Architecture. Principles and Examples with Reference to Hot and Arid Climates, University of Chicago Press.
13. Sodikov, I., Santamouris, M., & Georgakis, C. (2017). A review of building retrofitting strategies for energy efficiency in different climatic zones. *Energy and Buildings*, 148, 511-522.
14. Roaf, S., Fuentes, M., Thomas, S. (2014). Ecohouse 3: A design guide. Routledge.
15. Barber, D. A. (2020). Modern Architecture and Climate: Design before Air Conditioning. Princeton University Press.
16. Roaf, S. (2017). The solar house: Passive heating and cooling. Routledge.
17. Roaf, S., & Nicol, F. (2008). Adaptive thermal comfort: Principles and practice. Routledge.
18. Charvat, P., Jicha, M., Stetina, J. (2004). Solar Chimneys for Residential Ventilation. 25th AIVC Conference on Ventilation and retrofitting.
19. Akhtar, M. U. S., Fadlallah, S. O., Khan, M. I., Asfand, F., Al-Ghamdi, S. G., Mishra, R. (2023). Sustainable humidity control in the built environment: recent research and technological advancements in thermal driven dehumidification systems. *Energy and Buildings*, ENB 113846
20. Wong, N. H., & Sia, A. (2019). Passive cooling technologies for buildings: A review of principles and options. *Renewable and Sustainable Energy Reviews*, 107, 91-105.

PLEA 2024 WROCŁAW
(Re)thinking Resilience

Retrofitting our Way to a Fossil-Fuel-Free Future

How can urban gas stations be mobilized for climate resilience and sustainable urban environments?

SHAHD ALY[1], HAGAR IBRAHIM[1], SHERIF GOUBRAN[1], ISLAM MASHALY[1], AMAL HAMDY[1], KHALED TARABIEH[1]

[1]The Department of Architecture, School of Sciences and Engineering (SSE) The American University in Cairo (AUC), Cairo, Egypt

ABSTRACT: This paper tackles the urgent global climate change crisis, focusing on its pivotal role in countries' to mitigate its impacts. Specifically, it examines their endeavours to curb dependence on fossil fuels for transportation and energy. This dependence, exacerbated by rapid urban growth, has driven resource depletion and environmental instability, fueling climate change. Therefore, transforming fossil fuel-based urban infrastructure becomes crucial for future cities' sustainability and resilience. The world urgently needs a transition to resilient cities that address interconnected human, economic, energy, and environmental concerns. This paper delves into global initiatives promoting green development, reducing carbon emissions, and adopting clean technologies to lessen dependence on fossil fuels. To explore this transformation, the paper employs a studio-based approach that reimagines existing fossil fuel infrastructure—in this case, urban gas stations—through retrofit strategies. Students envision these stations in 2050, no longer fueling vehicles but functioning as strategic hubs fostering neighbourhood resilience and contributing to sustainable development. The design brief challenged the students to create a compelling vision for a specific gas station, incorporating socioeconomic, cultural, and resilience functions. By analysing these student projects, the research aims to provide valuable insights for implementing retrofit strategies, ultimately propelling the transition towards a resilient urban environment.
KEYWORDS: fossil fuel, retrofitting, urban gas stations, resilience, and design strategies

1. INTRODUCTION

The role of rapidly emerging nations in reducing and mitigating climate change is garnering increasing attention, particularly in reducing their reliance on fossil fuels for transportation and energy production. Through renovating and adapting buildings and spaces, the efficiency and performance of communities in these countries are enhanced. This paper aims to delve into the critical issue of fossil fuel-based urban infrastructure within the context of future cities. The sustainability and resilience of urban infrastructure are essential as cities evolve and adapt. Throughout history, urban growth has been heavily dependent on fossil fuels used to power heating, energy production, transportation, etc.[1]. Nevertheless, the consequences of this dependency, ranging from resource depletion to environmental degradation and climate change, are becoming increasingly apparent.

The paper focuses on urban fossil fuel infrastructures and the transition to resilient cities that tackle the various human, economic, energy, and environmental issues resulting from fossil fuel consumption. There is a trajectory for many countries to invest in green development, specifically in electrification and public transport, which can significantly reduce carbon emissions and dependence on fossil fuels [2]. For instance, urban areas are adopting electric transport and replacing private vehicles with public options. In addition, some countries offer free public transportation. There is an expectation that, as the technology for clean energy continues to develop, the demand for fossil fuels will drop. Moreover, increased regulations will reduce access to fossil fuels, resulting in an overall decrease in consumption.

In this forthcoming era, significant climate change will likely occur even with substantial environmental measures taken. This may manifest as extreme heat events, floods, droughts, shortages of clean water, etc. This paper utilises a studio-based design-research methodology to explore and study how the existing urban fossil fuel infrastructure can be mobilised through retrofitting to serve climate resilience and sustainable development in urban environments.

2. BACKGROUND

2.1 Retrofitting for Resilience:

It is important to understand and explore the transformation of industrial cities and their shift away from being the core and the potential obsolescence of gas stations in their current form. Therefore,

examining the historical development of industrial cities and identifying the reasons for their decline can aid in predicting future trends and the impact of technological advancements on urban infrastructure as they become obsolete. Thus, the question arises of how populations will repurpose and reuse the abundant sites and urban infrastructures that will become obsolete.

America's older industrial cities that flourished throughout the industrial era are now abandoned and plagued by serious decay issues [3]. Their predicament is connected to economic developments and changing trends. Today's industrial cities face numerous challenges, including rising unemployment and poverty rates, social isolation and segregation, physical building abandonment and obsolescence, affecting the city's urban life [4]. In light of this, it is more crucial than ever to design different futures for these collapsing cities, deriving from and developing each city's existing potential [4].

It is crucial to retrofit structures on the verge of obsolescence due to their detrimental effects on our country's environment and urban life. The projects demonstrate varied strategies for retrofitting existing gas station structures. Some projects opted for a complete repurposing of the structures, while others retained the existing frameworks with alterations, whereas some only preserved specific portions of the original structures.

2.2 Design driver related to climate change:

Emissions regulations will certainly impact future building developments. Therefore, the reliance on technology and legislative measures can be combined to reduce the load on energy demand and consumption by 2050. According to new research from the International Energy Agency (IEA) [5], buildings account for almost one-third of the world's primary energy consumption, as well as one-third of all greenhouse gas emissions connected to direct and indirect energy usage [8]. The disparity between accomplishments for climate change reductions and the necessary benchmarks continues to expand annually. The energy transition indicators presented in Figure 1 by the International Renewable Energy Agency (IRENA) underscore the urgent need for accelerated progress across various energy sectors and technologies [6].

Hence, students formulated assumptions either envisioning a highly severe environmental condition influenced by escalated climate change by 2050, or a scenario involving less extreme climate change. The selected scenario significantly influenced the diversity in building responses, resulting in distinct projects featuring unique solutions and approaches to energy consumption, energy generation, and climate-related issues. The variations in the solutions and architectural interventions implemented by each project extended to the chosen locations, further emphasising the tailored nature of the solutions implemented in each project.

2.3 The importance of the socioeconomic- strategy:

A global focus has been on addressing the exceptional socioeconomic catastrophe resulting from the COVID-19 pandemic while aiming to "recover greener" or "build back better." Emphasising the significance of socioeconomic strategy in urban infrastructures for a fossil fuel-free future, many countries and organisations have aligned their activities with the United Nations' Sustainable Development Goals (SDGs). Buildings are envisioned to function as community-centric entities, adapting to future needs and demographics [7]. Most human activity occurs within buildings, accounting for around one-third of all global direct and indirect energy-related carbon emissions [8]. Consequently, it is anticipated that future building design and functionality will be influenced by environmental, demographic, and resource factors that are yet to be determined. Disruptive breakthroughs, societal changes, and new issues like resource scarcity, inequality, and climate change will impact future building construction. Thus, it is crucial to create a forward-looking vision that considers the substantial impact that buildings have on the environment and the energy consumption, well-being, and health of their occupants [8].

As each student tackles a different theme or issue in their repurposing of the gas station, the approach to the typology differs. For instance, various important factors affect building design philosophy and guide the choice of functions, including resource scarcity, population, inequality, well-being and mental health, flooding and rainwater, pollution, water scarcity, global warming and heat waves, climate crisis, and awareness.

Consequently, the transformation of spatial functionality from current uses to more inventive functions in the future within the socioeconomic spectrum relies on the scenarios envisioned by individual students and the themes they address.

2.4 Mobility at the Urban Scale:

Mobility in cities is an integral factor that will experience rapid change in the future due to the behavioral shifts of the population and advancements in technology. The convergence of various transportation modes under the umbrella of mobility is expected to gradually shift towards public transport and other sustainable methods, aiming to diminish the environmental footprint in the future.

Moreover, it is becoming increasingly evident that the energy transition has already begun, with

renewable energy sources taking the place of fossil fuels. Reliance on renewable energy for transportation is increasing [9]. According to Lovins, the transformation in the mobility sector will witness a shift from "personal internal-combustion gasoline steel-dominated vehicles" to a future dominated by "shareable electrified, autonomous lightweight service vehicles" [10].

3. APPROACH

Thirty years from today, it is safe to assume that private gas-fueled cars will no longer occupy the roads of the numerous countries navigating toward a transformative era. Instead, citizens will commute primarily via clean public transit or electric vehicles. However, even with the realisation of this future scenario, and even if significant environmental action were to be implemented, there would nevertheless be inevitable and long-lasting impacts from climate change.

Envisioning this post-fossil fuel transition encourages the exploration of a future wherein people choose to embrace cleaner, more sustainable, and environmentally friendly modes of transportation. This transition addresses the urgent need to mitigate the environmental impact of fossil fuel dependency. Such conversions encompass a spectrum of environmental challenges. These challenges include extreme heat events, floods, torrential rain, droughts, and an increased risk of clean water shortages. The post-fossil fuel era presents an opportunity for greener and more efficient transportation and creative and innovative solutions and adaptive measures to resist the complex climate-related challenges that will persist for years.

3.1 Pedagogical Studios as Exploration Spaces:

As a case study to explore the potentials of this project, undergraduate third-year architecture engineering students at the American University in Cairo (AUC) were all given the same brief to consider how urban gas stations can be reimagined as resilience hubs for the neighbourhoods they serve. The students were placed in a dynamic environment and exposed to a transitional learning experience that defies conventional learning methods. Thus, the studio became a place that welcomed new and innovative pedagogical strategies. As a result, this gave the students freedom to tackle the issues and themes mentioned above from different perspectives.

4. METHODOLOGY

4.1 Problem Setup

The students were expected to develop design strategies wherein they would imagine and create a future scenario, then respond with a design that utilises the strategic location of one urban gas station of their choice to provide socioeconomic, cultural, and resilience functions while utilising the existing structures within the station. Additionally, the designs were required to be energy-optimised.

The students were briefed that their designs should promote architecture that adapts to the dynamic changes in the environment and energy sources. Their design plan must, therefore, strongly emphasise cutting emissions and moving away from fossil fuel-centric design thinking by proposing a pathway to a completely sustainable energy supply. Each student's design was expected to present a new form of sustainable repurposing of gas stations, which, as a result, created a design response based on the strategy adapted to address:

1. Changes in mobility and the need to accommodate these changes
2. Socioeconomic changes lead to the emergence of new functions
3. The retrofit strategy to reuse the existing structure
4. The climate change scenarios that can influence the design and functional program.
5.

4.2 Studio Setup

After introducing all students to the project brief, the studio aimed to further foster their ideas and provide useful feedback on their work. The project was split into phases, each aiming to tackle a specific goal. The first was the site choice and ideation, where students had to choose their locations, conduct site analysis, and identify the existing structures. They were then asked to propose a concept for the program with regard to these existing structures. Subsequently, the design phase began by schematically proposing the retrofit strategy of the structures, then doing so technically, whereby solutions were implemented. The projects then shifted to the energy optimization phase, where the design was altered based on environmental and energy analysis to reach its full potential.

4.3 Thematic Analysis

The students' proposals provided spaces serving social and/or economic (socioeconomic) functions. These could include commerce, community gardening, town halls, sports spaces, family support services (nurseries, playgrounds, etc.), or library-like spaces. The proposals were also required to defend the community against the localised risks from climate change (resilience functions). This could include flood or rain shelters, water reservoirs for drought situations, food reserve spaces, or passively cooled spaces for extreme heat waves. Furthermore, their project required technology and passive techniques to generate and conserve energy to reach near zero-energy buildings (energy functions). Given the

program and function change added to repurposing the urban infrastructure, a cultural function was added. This added function aims to raise awareness about climate change and sustainability through a museological component that supports a vision of a healthy, sustainable, and resilient city. Such projects included galleries, permanent collections, workshop spaces, and digital, augmented, and virtual reality spaces.

The students' design proposals provided examples of this future reliance architecture, addressing the human, economic, energy, and environmental concerns expected in Egypt by 2050. Their proposals represent the possibility of a more sustainable future. A series of themes emerged as a result of the students' approaches. These can be categorised under three major themes:

- Human
  - Resource Scarcity and Population
  - Inequality
  - Well-being and Mental Health
- Environmental
  - Flooding and Rainwater
  - Pollution
  - Water Scarcity
- Climate
  - Global Warming and Heat Waves
  - Climate Crisis and Awareness
  - Waste
  -

4.4 Design Drivers for Future Climate Resilience:

All projects addressed socioeconomics, climate change, retrofitting, and mobility concerns. These multifaceted issues provided the context for the design strategies employed by the students. Each challenge established a spectrum ranging from highly extreme to less extreme conditions, showcasing the diverse approaches taken by the students in tackling these complexities. The concept was to illustrate that the design approaches for social resilience structures were addressed by either directly confronting extreme events or formulating adaptive strategies, thus developing the notion that buildings do not need to take extreme measures to tackle the problem. Each project was analysed on a score from 1 to 5, (1 being the least extreme and 5 being the most extreme) about the following drivers.

The spectrum for each strategy will be as follows:

- Socioeconomics
  - Scale 1 (less extreme): augmentation of existing functions.
  - Scale 5 (more extreme): new functions in the future.
- Climate Change
  - Scale 1 (less extreme): adapting to climate change.
  - Scale 5 (more extreme): future uncertain events.
- Retrofitting
  - Scale 1 (less extreme): traditional adaptive reuse; utilising existing structures.
  - Scale 5 (more extreme): reconfiguring existing structures
- Mobility
  - Scale 1 (less extreme): continuation of private modes.
  - Scale 5 (more extreme): transitions in mobility concepts.

5. RESULTS & DISCUSSION

5.1 Studio Outcome

The brief was run in the studio at AUC for two consecutive semesters. For this study, 28 projects were selected based on their completion and comprehensive outcome. The projects spanned various locations within Egypt. Figure 1 shows this variation:

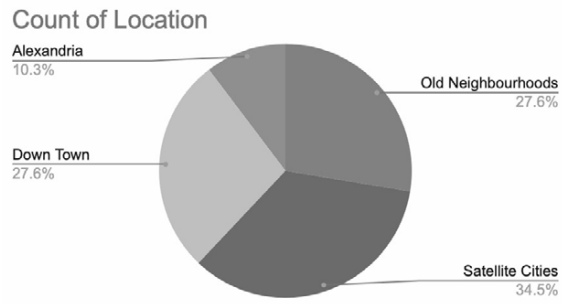

Figure 1: Distribution of Project by Location

5.2 Analysing the Outcomes

Based on the categorization and thematic analysis of the emerged themes (human-related, environment-related, and climate-related), the first theme focused on human issues like population growth and inequality, addressed through retrofitting strategies. The second theme covered general environmental concerns, while the third centred on climate-driven issues like heat waves. Each project addressed a specific 2050 scenario in Egypt within these themes, employing design strategies such as socioeconomic considerations, climate change adaptation, retrofitting techniques, and mobility enhancements. The graphs below illustrate varying degrees of adherence to the design strategy across all projects. Some adopted an extreme perspective in addressing the issues, while others opted for a more moderate approach. This shows diversity in the proposed solutions.

Figure 2: Example of a project by Hagar Ibrahim showing the integration and addition of existing and new structures

5.3 Thematic Analysis Outcome

The thematic analysis indicates that the large array of challenges facing Egypt in the future scenarios that the students examined mainly consider resources and awareness. Figure 3 below shows the distribution of the projects across the nine themes.

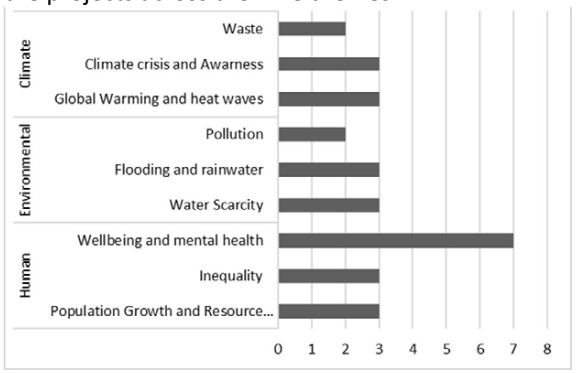

Figure 3: Distribution of number of projects per subtheme

5.4 Design Drivers for Future Climate Resilience:

Overall, the retrofitting strategies tended to fully optimise the existing structures without demolishing any of it. However, the majority implemented additions to the existing structures. For example, many students added walls or partitions to utilise the space under the shed structure that exists. Figure 4 shows the retrofitting design approaches observed in the projects. Figure 5 shows an example of the typical approach, where the gas station shed is repurposed and changed to house new functions.

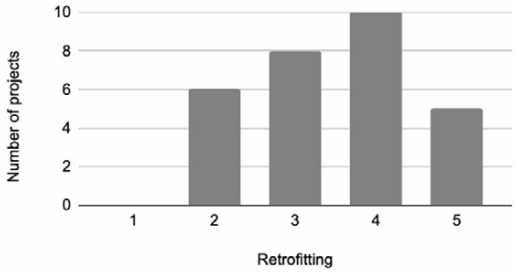

Figure 4: Distribution of projects's retrofitting approach (1 = less extreme and 5 = more extreme).

Figure 5: Example from a project by Amira Maamoun that shows the retrofitting approach used.

The mobility strategies indicated that most students considered the future scenario to be a continuation of current mobility trends. Figure 6 shows the mobility design approaches observed in the projects.

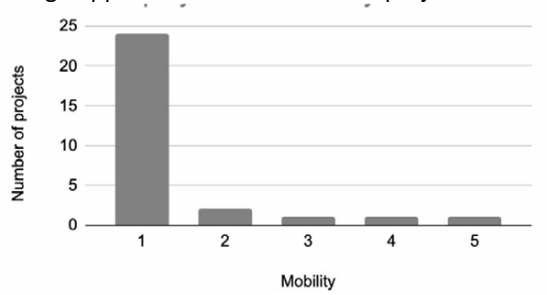

Figure 6: Distribution of project's mobility approach (1 = less extreme and 5 = more extreme).

The socioeconomic function decisions varied, showing a range of interpretations of the future scenarios impacting the structures' program. Figure 7 shows the socioeconomic design approaches observed in the projects and figure 8 shows the climate change approaches.

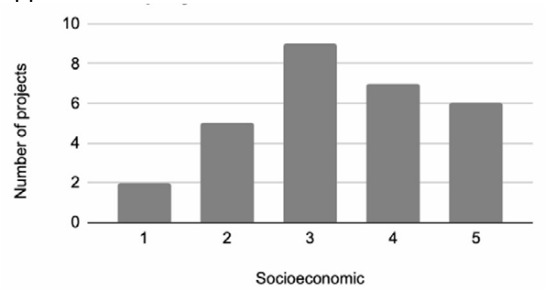

Figure 7: Distribution of project's socioeconomic approach (1 = less extreme and 5 = more extreme).

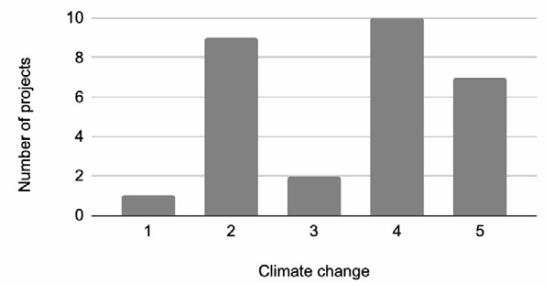

Figure 8: Distribution of project's climate change approach (1 = less extreme and 5 = more extreme).

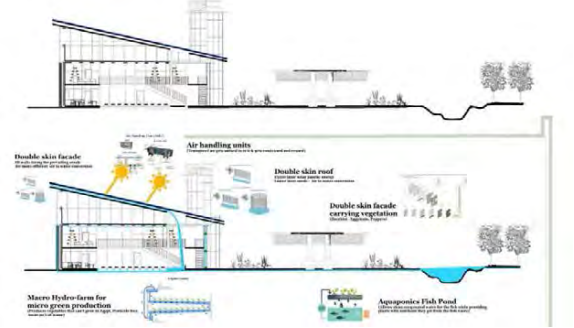

Figure 9: *Example from a project by Salma Hamoud that shows the climate change approach used.*

6. CONCLUSION

The idea of a city free of fossil fuels has been a topic of interest for many researchers. In a paper by Mutter [11] analysing the possibility of a complete transition to electric vehicles in Sweden, many points were found to align with the students' directions, such as general human awareness roles. However, the studio exploration offered new perspectives complementing technical research outcomes with visual and design outputs that can help future cities on different levels.

Solutions could potentially be achieved through strategies such as retrofitting and readaptation. This study has used the architecture studio to explore new viewpoints, opportunities, and future solutions for mainstreaming the adaptation of the soon-to-be-obsolete infrastructures in the urban context.

Although this studio exercise allowed students to explore the problem and potential reuse strategies, it is possible that the studio setup could have been a constraint within the thinking framework for the future of the structures. Furthermore, since all students were at similar educational levels and backgrounds, it is possible that this resulted in the generation of similar ideas influenced by pre-existing knowledge. A future investigation to explore the problem further could present the brief to a more diversified sample of students and architects, which can generate further proposals.

7. REFERENCES

1. *Rutter, P. D., & Keirstead, J. (2012). A brief history and the possible future of urban energy systems. Energy Policy, 50, 72–80. https://doi.org/10.1016/j.enpol.2012.03.072*

2. Abubakar, I. R., & Dano, U. L. (2019). Sustainable urban planning strategies for mitigating climate change in Saudi Arabia. Environment, Development and Sustainability, 22(6), 5129–5152. https://doi*.org/10.1007/s10668-019-00417-1*

3. *Murray, C., & Berube, A. (2018). Brookings - quality. independence. impact. https://www.brookings.edu/wp-content/uploads/2018/04/2018-04_brookings-metro_older-industrial-cities_full-report-berube_murray_-final-version_af4-18.pdf*

4. *Fernandez, B. (2010) shaping the future for industrial cities decay: urban planning and memory retrieval. Archivo Digital UPM. https://oa.upm.es/5978/1/FernandezAgueda_ponencia_2010_02.pdf*

5. *Transition to sustainable buildings – analysis - IEA. (2013). IEA. https://www.iea.org/reports/transition-to-sustainable-buildings*

6. *Harichandan , S., Kar, S. K., Bansal, R., Mishra, S. K., Balathanigaimani, M. S., & Dash, M. (2022). Energy transition research: A bibliometric mapping of current findings and direction for future research. Cleaner Production Letters. https://www.sciencedirect.com/science/article/pii/S2666791622000240*

7. *Õunmaa, L. (2021). What are the socio-economic impacts of an energy transition?. UNDP. https://www.undp.org/eurasia/blog/what-are-socio-economic-impacts-energy-transition*

8. *Wang, N., Phelan, P. E., Harris, C., Langevin, J., Nelson, B., & Sawyer, K. (2018). Past visions, current trends, and future context: A review of building energy, carbon, and sustainability. Renewable and Sustainable Energy Reviews, 82, 976–993. https://doi.org/10.1016/J.RSER.2017.04.114*

9. *Majewski, W. A. (2023). Fossil Fuels and Future Mobilityhttps://dieselnet.com/tech/energy_mobility.php*

10. *Camilla Bausch, Lovins, A. B., & Töpfer, h. c. mult. K. (2016). World energy transitions outlook. IRENA. https://www.irena.org/Digital-Report/World-Energy-Transitions-Outlook-2023*

11. *Mutter, A. (2021). Embedding imaginaries- electric vehicles in Sweden's fossil fuel-free future. Futures, 129, 102742. https://doi.org/10.1016/j.futures.2021.102742*

PLEA 2024 WROCŁAW
(Re)thinking Resilience

Retrofitting classrooms

Diagnostic and improvement for lighting and energy efficiency in Chilean public schools

ANDREA MARTÍNEZ[1], VALENTINA GONZALEZ[1], ISAAC SOTO, & MARÍA ISABEL RIVERA[1-2]

[1] Departamento de Arquitectura, Facultad de Arquitectura, Urbanismo y Geografía, Universidad de Concepción, Chile
[2] Centre for Sustainable Urban Development (CEDEUS), Chile

ABSTRACT: Retrofitting existing schools has become an urgent task in an increasingly changing climate and with the slow rate of the construction of new schools. Built several decades ago, many existing schools keep operating below current standards or recommendations for good indoor environmental quality. As we face an increasingly changing climate, those stressed learning spaces require solutions that could be simple and affordable to implement. This study uses measured data to document existing lighting conditions for predominant prototypical classrooms in a mild-temperate climate in Chile and predicts the effects of simple envelope retrofits. Those measurements were taken in the solstices, and curtains were open (lights on and off) and closed (light on) conditions; luminance evaluation was assessed through high dynamic range images. As the classroom does not comply with the reference thresholds, a series of simple envelope passive retrofits were evaluated through simulation. The study reveals the value of envelope retrofits being tested, revealing the potential for improvements through simple and affordable solutions for tight school budgets. This study shows that simple retrofitting could be implemented with little disruption, improving lighting and energy performance in buildings that will remain operative in the coming decades.
KEYWORDS: Existing buildings, Daylight, Retrofit, Measurements, Simulation

1. INTRODUCTION

Children deserve to spend most of their childhood in healthy and comfortable spaces. In particular, exposure to daylight and views are essential to their growth, as is the case for all human life. [1, 2], visual health, production of Vitamin D and circadian regulation, and creating a positive environment for learning [3, 4]. Regarding lighting and energy performance, many schools do not feature envelopes that could harvest daylight and improve comfort and energy efficiency. In the case of Chilean schools, previous research has reported a lack of indoor environmental quality in schools [5-7]. Some of these schools were built several decades ago and did not necessarily fulfill current standards or achieve current recommendations. Therefore, retrofitting existing schools has become urgent to reach indoor spaces that restore well-being and health.

2. METHODOLOGY

This study applied a set of data collection for diagnostic and prediction tools for evaluating retrofits for classrooms of a prototypical public school in Chile used as a study case. This typological classroom is still predominant in public schools in the country, built massively to one of the country's reforms in education in the 1960s. At the time, a government-private initiative (Sociedad Constructora de Establecimientos Educacionales in Spanish) created systematic modular, prototypical, fast-built schools nationwide. These schools are now recognized for their historical significance because of their industrialized methods, but they must improve their performance to meet current standards [8].

Figure 1: View of the classroom used as a case study for a predominant prefabricated school from the 1960s.

The school is located in an urban area of Concepción, a coastal city (altitude 15mts) in the central-southern region of Chile (Lat 36°49', Long 73°2'). It corresponds to a Mediterranean climate with winter rains and coastal influence Csb (i) [9]. Average hourly Global Horizontal and Direct Normal illumination reaches 55 Klux and 49 Klux in summer (February), while 17 Klux and 11 Klux in winter (June), respectively. [10]

This study reports on a west-oriented classroom (Figure 1) with openings on two sides. The main

windows to the façade provide the classroom with daylight. In contrast, the other side, with smaller windows at the top of the interior wall, adjoins an interior corridor lit only by artificial light. Windows are single clear glass in an aluminum frame. Commonly, the classroom is used with cloth curtains in afternoons due to the intense western sun, as featured in Figure 1. At those times, six fluorescent light fixtures provide artificial light. Student desks are typically organized facing the front of the classroom; for that reason, measurements were taken on a grid of around a 2-meter distance determined during the pandemic.

Schools in Chile, as all non-residential buildings, lack updated indoor environmental quality (IEQ) standards and visual comfort requirements such as the international standards by IESNA [11]. The only code for schools dates from the 1980s [12] When illuminance levels were defined as lower than the current standards described in Table 1.

Table 1: Reference threshold based on national codes and international standards

Metric	Value	Ref.
Illuminance	180 lux*[a]	DS548 [1]
	300 lux (min)*[b]	IES [2]
Luminance ratio	3:1 task-adjacent surface 1:10 task to non-adjacent surface	IES [2]
DF	2% to 5% mínimum	LEED[4]
sDA	>90%	CHPS[3]
ASE$_{1000,250}$	<10%	LEED[4]

[1]Chilean code for school buildings, Decreto 548-1989, [13]
[2] IESNA recommendations for educational facilities [11]
[3] CHPS Criteria [14]
[4] LEED v4.1 Daylight exemplary performance. Option 1. Daylight Factor DF [15]. *[a] In less favourable desks can be complemented by artificial light. * [b] minimum in area

This school is an excellent example of most schools in the country. It features single-glass windows and fluorescent light fixtures. The set of retrofits this study proposes are simple strategies that respond to limited educational investment capital, particularly in public schools.

2.1 Diagnostic of illuminance and luminance

The criteria for evaluating daylight and artificial light quality in the classroom interior focused on assessing illuminance and luminance. The first challenge was defining the dates intended to be as close to the solstices as possible. Still, the measurements had to be scheduled close to these dates, considering the school year and the occupancy, to avoid disruptions or shades. Additionally, sky conditions at this location fluctuate in all seasons, so several days of measurements were taken. We finally report measurements in clear-sky conditions for the school year's beginning (March 1-summer) and middle (June 27-winter).

Measurements were taken in three iterations:

1) curtains (open), artificial lights (on);
2) curtains (open), artificial lights (off), and
3) curtains (closed), artificial lights (on)

The availability of light and its distribution was assessed through illuminance -the amount of luminous flux (measured in lux) that a surface receives per unit area ($1m^2$)- with high-precision equipment: a Li-cor 250-A photometer with an LI-210R photo sensor, in 10-second average measurements at the desk plane approximately 0.70m above the ground, as recommended in [11, 16, 17]. Before each iteration, outdoor illuminance levels were taken at the same height in a shaded

For visual comfort, the High Dynamic Range (HDR) imaging technique was used to identify glare areas and evaluate the luminance distribution according to various studies in the literature [18, 19] Using Photosphere software version 1.8.6U (2010). This technique captures several images at different shutter speeds while maintaining the same aperture (F-11). A full-frame, mirrorless Nikon Z5 camera and an 8mm (fisheye) lens were used. Four views were taken, representing students' and teachers' contexts.

2.2 Evaluation of retrofits

Retrofit strategies are evaluated throughout the Climate Studio plugin for Rhinoceros. The model represented the existing geometry and materiality as closely as possible to the current conditions of the classroom, both inside and outside. Albedo was considered a 0.2 A baseline, modeled with the current cloth curtains to be compared to the measurements. Once the closest representation was achieved, a new baseline eliminated curtains for the best analysis of the strategies to increase daylight while controlling discomfort due to glare.

Table 2: Passive Retrofit Strategies

#		Description
R1	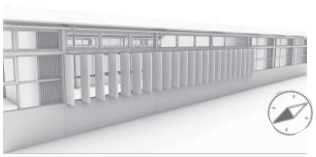	Exterior Vertical lamellas (40cms width @ 40cms) white aluminum
R2		Exterior Vertical lamellas (30cms width @ 30cms) white aluminum
R3		R2 + Skylights (30x60cms) insulated clear glass

Credits: authors' images from the Rhinoceros model

Three Retrofits were tested that could represent affordable and modular prefabricated solutions that could be built fast and with minor disruptions. Two of these (R1, R2) aiming to create external sun

protection, consisted of vertical lamellas in a perpendicular array to the façade. Skylights have been added (R3) to the best resulting from the previous ones, to increase daylight availability in identified inner areas of the classroom.

3. RESULTS FROM FIELD MEASUREMENTS

The measurements indicate that illuminance levels, distribution, and visual comfort due to glare are not achieved on summer and winter days.

3.1 Diagnostic for illuminance performance

Regarding illuminance levels and distributions (Table 2), the classroom had insufficient levels considering the Chilean code requirements. 180lux is not achieved in the interior desks only with daylight, which could be achieved by turning lights on as a complement. Nevertheless, 180lux is not achieved in winter when curtains are closed. As per international standards, the classroom reaches 300-750lux of its area in 45% (summer) and 22% (winter). Complemented with artificial light, those areas can increase to 63% (summer) and 39% (winter). However, areas following the façade are overlit by daylit or complemented with artificial light, reaching up to 43% in winter. On the other side, areas far from the façade are underlit with values <300 lux, which, in winter, corresponds to 20% of the area (lights on), reaching 43% of the area (lights off).

Table 3: Illuminance levels of the west-oriented classroom for (March 1st) and winter (June 27th).

Curtains	Open	Open	Closed
Light fixtures	On	Off	On
Summer March 1th , 14:25-15:09 hrs	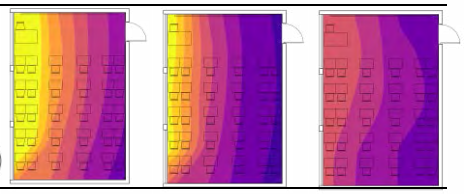		
Mean	634 lux	450 lux	388 lux
Median	542 lux	338 lux	371 lux
Exterior shaded	4.890 lux	4.870 lux	4.114 lux
<300 lux	3%	38%	26%
300-750 lux	63%	45%	74%
>750 lux	34%	17%	0%
Winter June 27th, 14:01-14:51 hrs	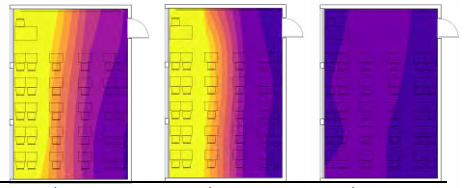		
Mean	1.485 lux	1.117 lux	195 lux
Median	1.180 lux	641 lux	202 lux
Exterior shaded	3.400 lux	2.906 lux	2.906 lux
<300 lux	18%	35%	100%
300-750 lux	39%	22%	0%
>750 lux	43%	43%	0%

Isocurves are represented using Plotly [20].

3.2 Diagnostic for luminance performance

The study of luminance reveals higher luminance median values in summer than winter. However, several sources of high-contrast are identified either season. High contrasts are revealed due to direct or reflected sun or the brightness of light fixtures, whether on a task-to-adjacent or task-to-non-adjacent surface.

As shown in Table 4, four views are illustrated (open curtains, lights on) with the corresponding ratios for winter and summer. Position of the occupant, either a child seated at the back of the room or a teacher in front are affected by high contrast due to direct and reflected sun in surfaces. Those ratios overpass the maximum recommended values of 3:1 (task : adjacent surface) and 1:10 (task : non-adjacent surface) referenced in Table 1.

In view a) a student is affected by the reflected light in the floor (1:22 in winter) and the light fixtures (ratio 1:140 in winter, 1:100 in summer).

In view b), high contrasts exist at the teacher's desk regarding to closer surfaces in the wall (14:1 in winter), and from the outside light (4.2:1 in summer). light fixtures are one of the sources of high contrast as measured to one of the student's desks (ratio 1:106).

In view c), high contrast are present from the windows to the students desks (12:1 in winter and 13.5:1 in summer), and among surfaces in the view scope in light fixtures and the ceiling (218:1 winter) or with the whiteboard (50:1 in summer).

In view d, representing the teacher's workplace, ratios over 1,000:1 are given in planes close to the desk or from the exterior light to the screen.

4. RESULTS FROM SIMULATIONS

The retrofit strategies are compared to the baseline condition and addressed in field measurements for the sample winter day. A single strategy combination showed that illuminance levels improved in the classroom, allowing every desk at least the minimum 180lux required by the Chilean code. Table 5 illustrates the metric as retrofit options are performed. The solution, including the skylight (R3), allowed this classroom to fulfill performance metrics for international references. Incorporating these retrofit solutions, the classroom can achieve a median illuminance level of 314 lux (winter) y 627 lux (summer), achieving the minimum level recommended by IES for educational spaces. Also, the Daylight Factor resulting from R3 is the highest among the explored options, with a higher uniformity coefficient of 0.64. Despite the skylights, there are no significant changes in the Glare performance, showing few points for disturbing or intolerable glare. Combining strategies (for sun protection and top daylight) leads to better distribution to the inner part of the classroom. Regarding annual metrics, the classroom would perform a yearly average lux of 2.285lux, maintaining Daylighting autonomy of 100% while having an ASE of less than 10%.

Table 4: High Dynamic Range images processed with ratio information for four different views (iteration with open curtains and lights on). In circles, luminance values expressed in cd/m2

#	Winter	June 27th,14:30 hrs – 15:30hrs	Summer	March 1th , 14:30-15:30 hrs
a	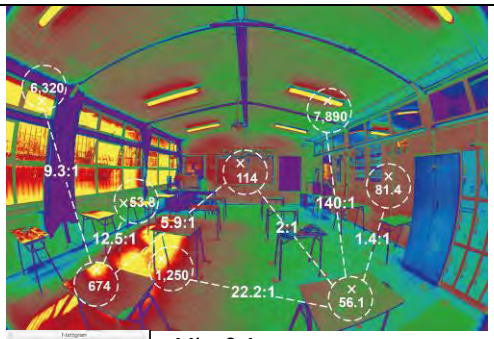	 Min. 0.4 Max. 27.700 Median: 53	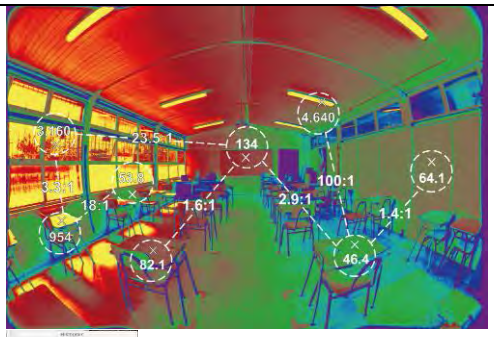	 Min. 0.148 Max. 26.000 Median: 63.5
b	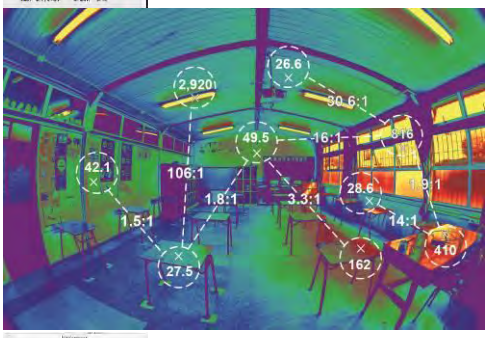	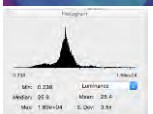 Min. 0.23 Max. 16.900 Median: 25.9	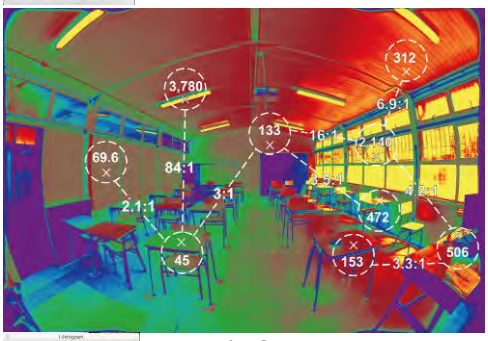	 Min. 0.17 Max. 22.800 Median: 66.7
c	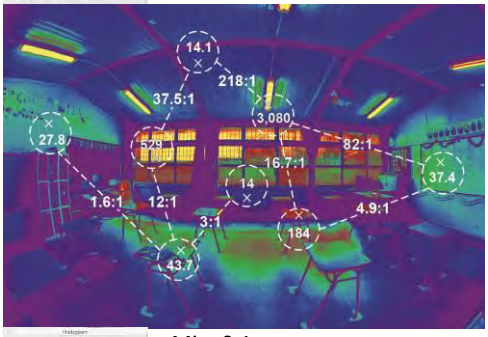	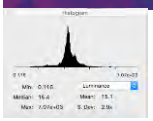 Min. 0.1 Max. 7.070 Median: 15.4	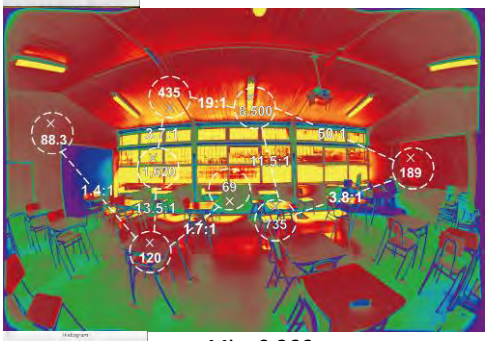	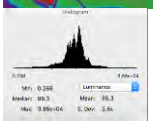 Min. 0.266 Max. 38.800 Median: 99.3
d	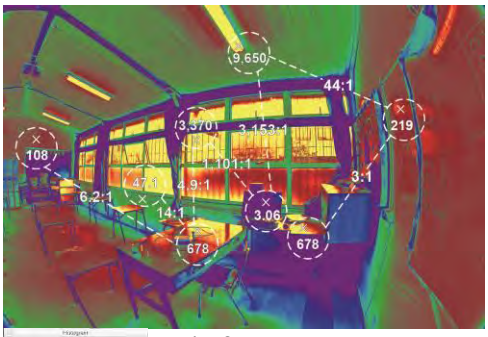	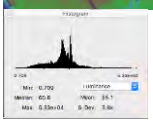 Min. 0.7 Max. 53.330 Median: 60.8	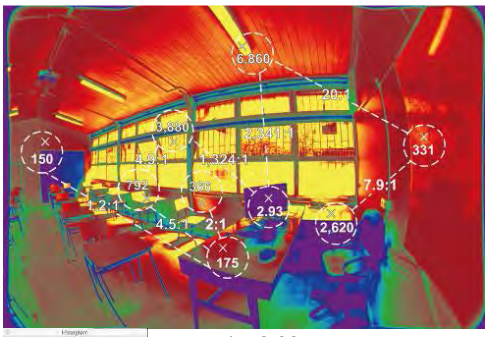	 Min. 0.225 Max. 45.400 Median: 144

Table 5: Results of lighting and energy metrics of retrofit strategies. Illuminance (levels and distribution) and glare performance

Annual Performance Metrics	**Summer illuminance** June 27th, 14:00 hrs	**Winter illuminance** March 1st 14:00 hrs	**Summer Glare**	**Winter Glare**
BASELINE Aver. lux: 3.342 Mean DF 6.13% Min DF 2.61% Median DF 4.51% Uniformity 0.43 sDA 100% ASE 30.3% sDG 98.13%	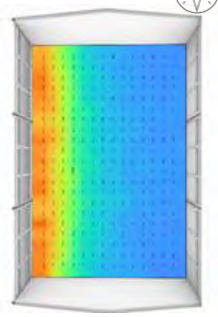 Mean 922 lux Median 681 lux	 Mean 546 lux Median 400 lux		
R1 Aver. lux: 2.071 Mean DF 3.6% Min DF 1.64% Median DF 2.89% Uniformity 0.46 sDA 100% ASE 15.3% sDG 77.21%	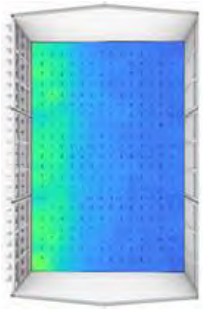 Mean 543 lux Median 445 lux	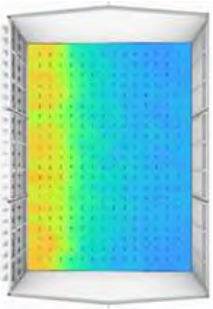 Mean 321 lux Median 258 ux		
R2 Aver. lux: 1.938 Mean DF 3.35% Min DF 1.45% Median DF 2.74% Uniformity 0.43 sDA 100% ASE 5.1% sDG 79%	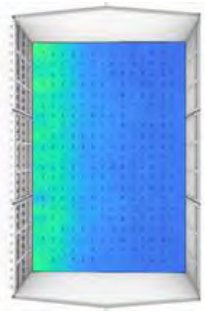 Mean 504 lux Median 407 lux	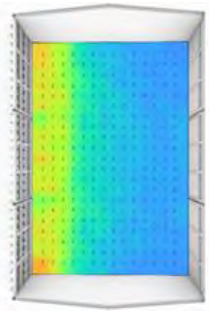 Mean 299 lux Median 238 lux		
R3 Aver. lux: 2285 Mean DF 4.11% Min DF 2.63% Median DF 3.47% Uniformity 0.64 sDA 100% ASE 9.2% sDG 89.41%	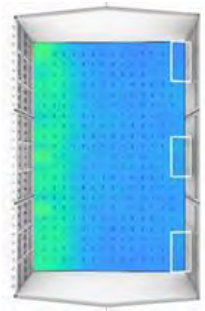 Mean 617 lux Median 627 lux	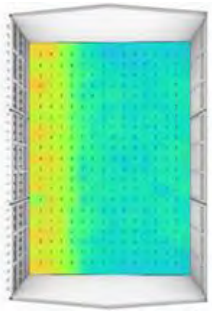 Mean 367 lux Median 314 lux		

5. DISCUSSION

The case study classroom currently does not comply with the minimum lighting requirements for a less stringent Chilean code. 180 lux are not achieved in winter when curtains are closed, which is a typical school setting due to the direct sun and low-performance envelopes (draft). Therefore, at those times, children are learning under deficient light conditions. The simple retrofits studied indicate that overlit could effectively be reduced by façade control. As a complement, upper light (skylights) effectively increases daylight availability to the underlit portion of the classroom.

Further exploration is needed for retrofits that improve the glare control. The study would also be complemented with solutions for improving the thermal envelope. The affordable effects of the studied retrofits must be explored further to understand decreased solar heat gains due to the sunshade proposed in this study. Considering that this school typology is still predominant in the country, the results of this study could be applied to schools with identically oriented pavilions. They could also be informative for east-oriented classrooms.

6. CONCLUSION

This paper evaluates retrofit strategies after addressing a diagnostic of an existing typological classroom. The classroom does not comply with the minimum lighting requirements by national code or international standards. The field data showed that illuminance levels were unevenly distributed, too high on student desks next to the façade and too low at the desks in the classroom's interior. With the intent of revealing the value of envelope retrofit to replace cloth curtains, the tested strategies fulfilled the performance metric used as reference thresholds. Measurement provides complex data for standard practices in classrooms in the country. One of these practices is operating the classroom with closed curtains and artificial light turned on despite the abundance of daylight. As observed, with little or no sun control, illuminance levels are highly high next to the window. It is important to note that illuminance levels measured for winter were performed earlier than those for summer. Therefore, the reported values in the diagnostic could be worse later in the afternoon, considering the regular school operation could be later in the afternoons. Further exploration is needed to simulate illuminance and luminance for summer conditions. Likewise, annual glare studies would be informative in predicting possible problems coming from the skylights. Nevertheless, retrofitting existing buildings contributes to achieving energy reduction goals in buildings that remain operative in the coming decades.

ACKNOWLEDGEMENTS

Thanks to Mrs. Marlene Muñoz, the school's Principal, and its community for gently facilitating our measurements. This study has been supported by the ANID grants PAI-77180057 and FONDECYT-11240683; FONDECYT 11221255, and FONDAP 1523A0004.

REFERENCES

1. Heschong, L., *Visual Delight in Architecture. Daylight, Vision, and View*. 1st Edition ed. 2021, London: Routledge.
2. Ludlow, A.M., *The functions of windows in buildings.* Lighting Research & Technology, 1976. 8(2): p. 57-68.
3. Hobday, R., *Myopia and daylight in schools: a neglected aspect of public health?* Perspectives in Public Health, 2015. 136(1): p. 50-55.
4. Barrett, P., et al., *The impact of classroom design on pupils' learning: Final results of a holistic, multi-level analysis.* Building and Environment, 2015. 89: p. 118-133.
5. Armijo, G., C.J. Whitman, and R. Casals, *Post-occupancy evaluation of state schools in 5 climatic zones of Chile.* Gazi University Journal of Science, 2011. 24(2): p. 265-374.
6. Rivera, M.I. and A. Kwok, *Thermal comfort and air quality in Chilean schools, perceptions of students and teachers*, in *Future of Praxis: Applied Research as a Bridge Between Theory and Practice. ARCC*, ARCC, Editor. 2019.
7. Trebilcock, M., et al., *The right to comfort: A field study on adaptive thermal comfort in free-running primary schools in Chile.*Building and Environment 2016. 114: p. 455-469.
8. Martinez, A., M.I. Rivera, and P. Arriagada, *Informing Early-Stage Building Energy Retrofit for Prototypical Public Schools in Chile*, in *RESILIENT CITY: Physical, Social, and Economic Perspectives. ARCC-EAAE 2022*. 2022, Architectural Research Centers Consortium: Miami, US.
9. Sarricolea, P., M. Herrera-Ossandon, and Ó. Meseguer-Ruiz, *Climatic regionalisation of continental Chile.* Journal of Maps, 2017. 13(2): p. 66-73.
10. Liggett, R. and M. Milne, *Climate Consultant 6.0*. 2017.
11. Illuminating Engineering Society, *Recommended Practice: Lighting Educational Facilities.* . 2020, IES: New York.
12. Ministerio de Educación, *Decreto 548*. 1989.
14. Collaborative for High Performance Schools, *National CHPS Criteria. Version 2.0. Criteria & Implementation Guide for New Construction & Major Renovation of School Buildings*. 2020.
15. The US Green Building Council. *LEED rating system*. 2023 [cited 2023 2023 august 14]; Available from: https://www.usgbc.org/leed.
16. Instituto de Salud Pública de Chile, *Instructivo para la evaluación de la luminancia e iluminancia en los lugares de trabajo*, D.d.S. Ocupacional, Editor. 2021: Santiago.
17. ASHRAE, *Performance Measurement Protocols for Commercial Buildings*. 2010.
18. Pierson, C., et al., *Tutorial: Luminance Maps for Daylighting Studies from High Dynamic Range Photography.* LEUKOS, 2021. 17(2): p. 140-169.
19. Jakubiec, J., et al., *Accurate Measurement of Daylit Interior Scenes Using High Dynamic Range Photography*. 2016.
20. Plotly. *Plotly Chart Studio*. 2023; Available from: https://chart-studio.plotly.com/create/?fid=RGate:140#/.

PLEA 2024 WROCŁAW
(Re)thinking Resilience

Exploring the Impact of Pavement Materials on Surface and Air Temperatures in Arid Climates

MOHAMED H ELNABAWI [1]; NEVEEN HAMZA [2]; TAREK AHMED[3]

[1]Architectural engineering, College of Engineering, United Arab Emirates;
[2]School of Architecture, Planning and Landscape, Newcastle University, Newcastle Upon Tyne, UK;
[3]Department: Architecture and Built Environment, Northumbria University, UK

ABSTRACT: The paper investigates the impact of retrofitting pavements in a neighborhood setting, with a specific focus on mitigating the urban heat island (UHI) effect during the summer. The study aims to predict improvements to surface and air temperature at pedestrians' level using urban modelling, utilizing ENVI-met software. The research observes key environmental parameters such as ambient air temperature and mean radiant temperature for validation. By comparing different scenarios to a base case, the study evaluates the overall efficiency of proposed interventions, such as white topping and permeable interlocking. The results indicate that both the white topping and permeable sidewalk showed surface temperatures close to the ambient air temperature, with the permeable interlocking sidewalk having the lowest average surface temperature throughout the day. Additionally, the permeable interlocking sidewalk exhibited lower air temperatures compared to the base case during the daytime, and after 19:00, it slightly outperformed the white topping in reducing air temperature. This research contributes to our understanding of how pavement retrofit technologies can be evaluated on a neighborhood scale, providing valuable insights for making strategic decisions regarding the implementation of sustainable pavement technologies in cities.

KEYWORDS: Cool pavement, ENVI-met, Air temperature, Urban Heat Island

1. INTRODUCTION

Accelerated urbanisation, being strongly linked to global warming, has sparked several well-known environmental threats which are difficult to tackle, such as the degrading of the urban microclimate and increased ambient urban air temperatures, known as the urban heat island (UHI) effect [1,2]. A UHI takes place when temperatures increase in the built-up urban spaces compared to the adjacent rural areas, mainly as a result of the comparatively larger amount of incident solar energy absorbed and stored by man-made materials. UHIs have a substantial effect on day and night-time temperatures, but also indirectly raise air conditioning loads, deteriorate air and water quality, lower pavement lifespans, and worsen heatwaves. According to the 2021 United Nations Climate Change Conference (COP26) [3], climate change continues to be perceived as the gravest threat to humanity, and with the current status of the 'climate action failure', there is a high risk that over the next decade there will be accelerated environmental damage than ever seen at a global scale [3]. As the COP28 President aptly stated, 'The impacts of climate change are already at our doorstep, posing one of the greatest threats to human health in the 21st century'' [4]

In response, recent research has made it possible to create technological solutions to mitigate the effects of UHIs [5-7]. By improving thermal losses and lowering equivalent benefits, mitigation strategies seek to balance the thermal budgets in cities. Among the top proposed techniques are those aiming to include green infrastructure (e.g., trees and grass) [8,9], cool roofs [10,11], pavement-related strategies [12], water-related strategies (irrigation and blue infrastructure such as lakes and ponds) [13], and designs of urban morphology and building geometry [14].

These techniques have proven effective in mitigating UHIs, enhancing urban thermal comfort, and reducing UHI stress [15-17]. However, it is essential to identify strategies that allow for interventions at the local level, to mitigate for climate and anthropogenic changes. Therefore, the study examined the effect of replacing paving materials at a neigbouhhood level on the microclimate, in terms of surface temperature, air temperature and mean radiant temperature.

As pavements cover much of urban surfaces and contribute to the development of heat island [18], appropriate surface material choices are considered one of the most effective techniques to mitigate heat island and reduce surface temperature in urban areas [19, 10]. As previous studies indicated that pavement materials contributed to high urban surface temperatures in dry and hot climate. In hot arid areas pavement materials will increase surface temperatures, and subsequently air temperatures by 2–3 ◦C higher than surroundings. In the tropical climate, paving surfaces with low reflective man-made surfaces such as concrete, bricks, and asphalts can bring air temperature to as high as 40◦C [18]. In

another study for 4500 square meters of reflective pavements in the Mediterranean climate of Athens, cool pavements successfully reduced the ambient temperature by 1.9°C and surface temperature by 12 °C during a typical summer day [22]. However, cool pavements are still an evolving technology and much still unknown about their applications, features and design strategies [23]. In the Middle East, and in hot arid climates, limited performance data of reflective pavement technologies, their applications [24] and their impacts on UHI are available [22]. In addition, little attention has been paid to the resulting effect of cool materials on outdoor thermal comfort [25]. In the context of urban planning, it is essential to determine how cool pavement can create a better-quality urban environment and improve thermal comfort conditions. Thus, to promote knowledge of the advantages of a cool pavement, the research aims to quantify the potential of cool pavement materials on cooling the surface temperature and ambient air temperature when applied at the micro-urban level in the hot arid climate of Al Ain city in UAE.

2. METHODOLGY

The relationship between the different pavement applications, mitigating the UHI and improve urban microclimate at pedestrian levels, can be detected either through observational approaches [22,25] or by predictive environmental simulation [27,28], with the latter enabling the comparative assessment of microclimatic parameters before and after the morphological intervention, under similar boundary conditions [29]. The research framework was designed based on the following four steps;

1. Identification of a typical neighbourhood morphological and physical features via a literature review;
2. In situ field measurements, to determine climatic conditions, collecting meteorological data as stated by ASHRAE [30] including air temperature (Ta), solar radiation (W/m2), relative humidity (RH), and air velocity (va).
3. Creation of an urban microclimate modelling for validating the base case by comparing the modelling outcomes with the field measurements;
4. Development of a parametric urban microclimate analysis to compare different cool pavement retrofit technologies in terms of air and surface temperatures.

2.1 The study context (base model and location)

The field study was conducted in Al Ain city (Abu Dhabi), UAE, positioned between 24.1302° N, 55.8023° E. Al Ain has wide diurnal temperature fluctuations and scarce rain fall (group B Koppen classification); as such, it is placed in sub group BWh as arid/desert with a hot climate [31]. The city's air temperature fluctuates between a maximum of 35.8–43.3°C and a minimum of 21.7–28.9°C in summer, and in winter between a maximum of 23.9–26.5°C and a minimum of 11.3–17.1°C.

The case study neighbourhood is located in the west of the city centre (Figure 1). With a total area of 131,300 m^2. The urban characteristics of the site are summarised in Table 1. There is a lack of green spaces or water bodies to reduce heat gain and improve the microclimate.

2.2 In Situ Field Measurements

Micro-climatic data monitoring was conducted in summer 2022 between 15–22 August. The Vantage Pro 2 weather station, with an integrated solar radiation sensor, was used to collect the main microclimatic data parameters, following the ASHRAE Standard [30]. The parameters were: air temperature, relative humidity, solar radiation and wind speed (Table 2). The weather station was mounted externally and set up to collect identical measurements as would a standard 150 mm globe at 1.1 m above ground. This corresponds to the typical height of the centre of gravity for an adult [32] (Figure 2). The average value of each measured variable was used for subsequent analysis.

Figure 2. Site plan of the case study compound in Al Ain city (495m x 260m) 250 x 130 x 30 (125 x 65 x 30)

Table 1. Characteristics of the case study urban site

Land use	Residential
Buildings	2 floors
Building %	37.5%
Shaded areas	3.6%
Green %	4%
Streets and pavements	53.7%

Figure 3. the portable weather station used for the micro-climatic data monitoring

2.3 Urban Microclimate Modelling: The Base Model

The urban microclimate was simulated using the three-dimensional, non-hydrostatic climate model, ENVI-met 5 [33,34]. ENVI-met utilizes the principles of thermodynamics and fluid dynamics to simulate interactions between buildings and the atmosphere. The model area was represented by a grid of dimensions 250 x 130 x 40, with a resolution of 2 m x 2 m x 4 m in the X, Y, and Z directions, respectively (Figure 4). The model area was rotated 18 degrees eastward from the grid's north. Surrounding the main area, nesting grids were set at 0. Different soil profiles were assigned, with [SD] representing a sandy soil, [PD] representing a dark concrete pavement for soil A and B, respectively, [ST] representing asphalt for streets, and [PG] representing grey concrete tiles for pavements. To capture microclimatic variables, six receptors were strategically placed around the buildings, providing snapshots of data every hour. The model's boundary conditions and simulation parameters, detailed in Table 2, remained consistent across all scenarios. Full forcing boundary conditions were enabled using the EnergyPlus weather file. The simulations were conducted on 16-17 August, which were considered average summer days, starting at 05:00. However, only the results from day two were utilized for subsequent analysis, as day one was used for the spin-up period to ensure greater consistency and numerical stability in the model's physics and dynamics.

Table 2. Main ENVI-met variables in each tested scenario

Date (local)	17 August 2022 at 05.00
Duration	48 h
Dimension	250 x 130 x 40 (grid cell)
Resolution (X, Y, Z)	2 m x 2 m x 4 m
Boundary conditions	Full forcing
Indexed view sphere (IVS) module	Activated
Lowest grid cell split	Yes

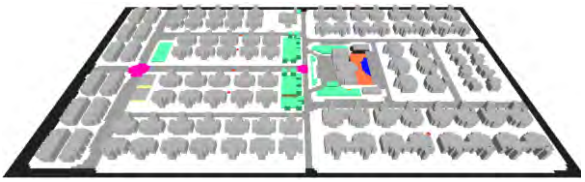

Figure 4. The ENVI-met 3D model of the neighbourhood

2.4 Database preparation for examined cool pavement scenarios

The construction properties of the buildings and site remained consistent across the various pavement scenarios. The only modifications made were to the paving materials, as outlined in table 3. These adjustments included changes to albedo, emissivity, and heat conductivity. Based on these criteria, the materials considered most suitable for selection were white-topping for road surfaces. This material offers high resistance to heavy vehicular traffic, good skid resistance, and a non-glare albedo for drivers [35]. Additionally, permeable interlocking concrete blocks were identified as appropriate for car parking plots and sidewalks, as they contribute to a larger proportion of permeable surface area on the site.

Table 3. The physical properties of the tested paving materials

	ALBEDO	EMISSIVITY	HEAT CONDUCTIVITY (W/M K)
WHITETOPPING	40	0.91	1.63
PERMEABLE INTERLOCKING	0.50	0.90	2.0

3. RESULTS AND DISCUSSION

3.1 Validation of the Base Model by Measurements

To assess the accuracy of the ENVI-met outputs, the simulated values were compared to the on-site monitored data. Hourly measurements of air temperature and mean radiant temperature (MRT) were recorded using a portable weather station at a height of 1.1 m on 17 August. Figure 5 illustrates that the simulated and monitored values for air temperature and MRT exhibit similar patterns, with a slight variation of 2-4.7°C in air temperature and an average difference of 4.8°C for MRT. The maximum difference of 9°C occurred at 15:00. These results indicate that the simulated model accurately captures the existing patterns in air temperature and MRT.

Furthermore, using the root mean square error (RMSE) on an hourly basis (Equation 1). The values for air temperature and MRT were found to be 3.03% and 5.19%, respectively. These values fall within the tolerance criteria for RMSE set by ASHRAE 14 (±20%) [36, 37]. This provides confidence in the model's ability to capture the main microclimatic characteristics of the urban site and supports the application of the same adjustments to other modeling scenarios for assessing proposed roof scenarios.

$$\text{RMSE} = \sqrt{\frac{\sum_{i=1}^{N}(x_i - \hat{x}_i)^2}{N}} \qquad (1)$$

where *RMSE*- root mean square error;
i- variable i;
N - number of non-missing data points;
xi - actual observations time series
X- estimated time series

3.2. Comparative Results

Using the same validation modelling settings for the cool pavement scenario. By comparing the amended scenario with the base case, the analysis focused on the surface temperatures of urban pavement and air temperatures. The ENVI-met LEONARDO module was utilized to visualize and quantify the results in a graphical format.

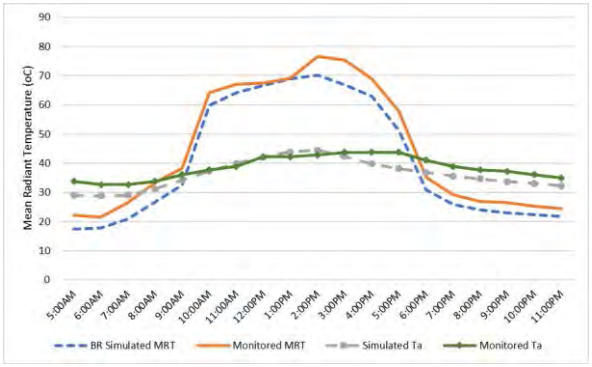

Figure 5. The monitored and ENVI-met Ta and MRT calculated using the globe thermometer [Equation 1].

3.2.1 Analysis of surface temperatures

Overall, the variation in surface temperature was influenced by the pattern of shortwave radiation, with a time lag. Table 4 compares the surface temperatures before and after the pavement change at two receptor locations. Receptor 1 had the Concrete pavement grey replaced with Permeable interlocking, while receptor 2 had the Concrete pavement dark replaced with white topping surface. The white topping surface demonstrated the greatest temperature reduction at 12 pm, with a decrease of 5.5°C compared to the base case temperature of 52.6°C, resulting in a temperature difference of 5.5°C. At 5 pm, the temperature difference was 1.58°C. After sunset, the surface temperatures dropped rapidly due to the absence of direct solar radiation and the cooling effect of radiative exchange with the sky. However, the base case took longer to cool down and thus maintained a higher surface temperature compared to the ambient air temperature.

In terms of performance, the permeable interlocking surface outperformed the concrete pavement grey. It achieved a surface temperature reduction of 3.65°C at 12 pm, compared to the base case temperature of 44.5°C, resulting in a difference of 3.65°C. The difference between the white topping and permeable surface may also be influenced by their locations. The white topping is further away from the buildings and is more exposed to direct sunlight (as shown in Figure 6), while the permeable surface is used as sidewalks around the buildings and is less exposed to direct solar radiation. Additionally, the two surface materials employ different mechanisms to deal with solar radiation. The high albedo of the white topping reduces the amount of energy stored during the day, while the vegetation on the permeable surface utilizes evapotranspiration. After sunset, photosynthesis ceases, resulting in a lower latent heat flux, with only evaporation from the substrate layer occurring. Figure 6 displays the surface temperature results at 12 pm for the base case configuration.

Table 4. the simulation outcomes for the base case and the cool pavement scenario

	Average Surface Temperature (°C)			
Timing	9	12	17	19
Concrete pavement dark (Base Case)	33.7	52.6	45.9	38.3
White topping	32.6	47.1	44.32	37.63
Concrete pavement grey (Base Case)	26.8	44.5	41.57	36.85
Permeable interlocking	24	40.85	39.84	35.98

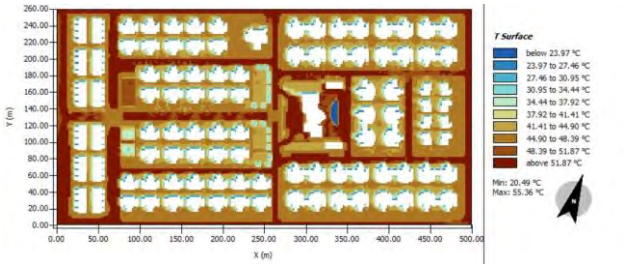

Figure 6. The ENVI-met simulated surface temperature for the base case at 12pm.

3.2.2 Cooling impact on air temperature at the pedestrian scale

The reduction in surface temperatures involves various factors, including the decrease in convective motions between the soil and air, resulting in a different heat load at the pedestrian level. To gain a comprehensive understanding of both scenarios, analyses were conducted to assess the air temperature recorded by the same receptors used for validation and surface temperature analysis.

According to the findings presented in table 5, both scenarios exhibited a cooling impact during the day. In the case of the white topping, the reduction in air temperature seemed to be linked to its albedo value. A higher albedo resulted in more shortwave radiation being reflected, leading to a lower air temperature [38]. On the other hand, the permeable surface, with its vegetation space, allowed for evapotranspiration and the conversion of solar radiation into latent heat, resulting in a cooling effect on the air. However, it is worth noting that this may contribute to increased air temperatures at night in city centres [39]. Nevertheless, a cooling effect was noticed for the proposed scenario at night compared to the base case, possibly because the base case lower albedo values caused more heat absorption during the day, leading in turn to a higher surface temperature, as seen in table 4. This heat takes more time to be let into the night-time atmosphere, creating a small increase in air temperature. As seen in table 5, the white topping achieved the maximum reduction in air temperature at 12pm, with a maximum reduction of -1.56°C, followed by a reduction of -0.82°C and -

0.71°C, at 5pm and 9am respectively. This reduction decreases till it reaches -0.63°C after sunset at 7pm.
For the permeable sidewalk, it recorded relatively lower air temperature compared to the white topping, again due to its location and limited sun exposure duration compared to the white topping. The maximum value for air temperature was 40.87°C compared to 42.1°C for the base case, with difference of 1.23°C, after the sunset both the permeable and white topping reached a close value of 37.41 and 37.47 respectively. All these results were also highlighted by previous studies, reporting a reduction in air temperature caused by the reflectance of pavements, in the range of 0.15 to 3.0°C [40,41].

Table 4. the simulation outcomes for the base case and the cool pavement scenario

	Average potential Temperature (°C)			
Timing	9	12	17	19
Concrete pavement dark (Base Case)	34.3	42.6	43.4	38.1
White topping	33.59	41.04	42.58	37.47
Concrete pavement grey (Base Case)	34.1	42.1	43.2	38
Permeable interlocking	33.58	40.87	42.39	37.41

Figure 6. The ENVI-met simulated Air Temperature for the Base case at 12pm

4. CONCLUSION

The study evaluated a combination of two types of cool pavements with different mechanisms, using ENVI-met microclimate modelling accompanied by in-situ field measurements that could be applicable on a large scale and replicable in other contexts. These data sets enabled validation. Results showed that both the white topping and permeable sidewalk had surface temperatures similar to ambient air, with the permeable interlocking exhibiting the lowest surface temperature throughout the day. The permeable sidewalk also had the lowest ambient air temperature on the pedestrian scale during the day and outperformed the white topping in air temperature reduction after 19:00. High albedo values in cool materials allowed air temperature to dominate over solar radiation by heating the surface during the day. Finally, this study highlights the need to consider the accretion of dirt and dust on pavements as this adversely affects the capacity of the reflective materials to reflect sunlight, and in turn will increase solar heat gain. Further, future research can be directed toward combination of more mitigation strategies such as green roofs and the installed PV panels.

ACKNOWLEDGEMENTS

The manuscript is a part of a funded research by the United Arab Emirates University, Grant Code 12N102.

REFERENCES

1. Oke, T. R. 1982. “The Energetic Basis of the Urban Heat Island.” Quarterly Journal of the Royal Meteorological Society. Royal Meteorological Society (great Britain) 108 (455): 1e24.
2. Li, H., et al. 2018. “A new Method to Quantify Surface Urban Heat Island Intensity.” Science of the Total Environment 624: 262e72
3. The Global Risks Report 2022, 17th Edition Published by the World Economic Forum. Available online: https://www3.weforum.org/docs/WEF_The_Global_Risks_Report_2022.pdf (accessed on 15 July 2022). ISBN: 978-2-940631-09-4.
4. COP 28 THE PRESS RELEASE. avilable online on 231202_COP28 WCAS Health PRL_Release.pdf (accessed on 2nd of March 2024)
5. H. Akbari, M. Pomerantz, H. Taha, Cool surfaces and shade trees to reduce energy use and improve air quality in urban areas, Sol. Energy 70 (3) (2001) 295e310.
6. D. Mauree, E. Naboni, S. Coccolo, A.T.D. Perea, V.M. Nik, J.L. Scartezzini, A review of assessment methods for the urban environment and its energy sustainability to guarantee climate adaptation of future cities, Renew. Sustain. Energy Rev. 112 (2019) 733–746, https://doi.org/10.1016/j.rser.2019.06.005.
7. M. Varentsov, T. Samsonov, M. Demuzere, Impact of urban canopy parameters on a megacity’s modelled thermal environment, Atmosphere 11 (2020) 1349, https://doi.org/10.3390/atmos11121349.
8. Razzaghmanesha, M., and M. Razzaghmanesha. 2017. “Thermal Performance Investigation of a Living Wall in a dry Climate of Australia.” Building and Environment 112: 45–62.
9. Sharma, A., P. Conry, H. J. S. Fernando, F. H. Alan, J. J. Hellmann, and F. Chen. 2016. “Green and Cool Roofs to Mitigate Urban Heat Island Effects in the Chicago Metropolitan Area: Evalua tion with a Regional Climate Model.” Environmental Research Letters 11 (6): 064004.
10. Morini, E., G. Touchaei A, F. Rossi, F. Cotana, and H. Akbari. 2018. “Evaluation of Albedo Enhancement to Mitigate Impacts of Urban Heat Island in Rome (Italy) Using WRF Meteorological Model.” Urban Climate 24: 551–566. doi:10.1016/j.uclim.2017. 08.001
11. Touchaei, A. G., H. Akbari, and C. W. Tessum. 2016. “Effect of Increasing Urban Albedo on Meteorology and air

Quality of Montreal (Canada) - Episodic Simulation of Heat Wave in 2005." Atmospheric Environment 132: 188–206.
12. Giorio, M.; Paparella, R. Climate Mitigation Strategies: The Use of Cool Pavements. Sustainability 2023, 15, 7641. https://doi.org/ 10.3390/su15097641
13. Santamouris, M. Cooling the cities—A review of reflective and green roof mitigation technologies to fight heat island and improvecomfort in urban environments. Sol. Energy 2012, 103, 682–703.
14. Sari, D. P. 2021. "A Review of How Building Mitigates the Urban Heat Island in Indonesia and Tropical Cities." Earth 2(3): 653–666. doi:10.3390/earth2030038.
15. Fintikakis, N.; Gaitani, N.; Santamouris, M.; Assimakopoulos, M.; Assimakopoulos, D.; Fintikaki, M.; Albanis, G.; Papadimitriou, K.; Chryssochoides, E.; Katopodi, K.; et al. Bioclimatic design of open public spaces in the historic cen tre of Tirana, Albania. Sustain. Cities Soc. 2011, 1, 54–62. [
16. Santamouris, M.; Synnefa, A.; Karlessi, T. Using advanced cool materials in the urban built environment to mitigate heat islands and improve thermal comfort conditions. Sol. Energy 2011, 85, 3085–3102.
17. Santamouris, M. Cooling the cities—A review of reflective and green roof mitigation technologies to fight heat island and improve comfort in urban environments. Sol. Energy 2014, 103, 682–703.
18. Benrazavi RS, Dola KB, Ujang N, Benrazavi NS 2016 Effect of pavement materials on surface temperatures in tropical environment Sustainable Cities and Society 22 94-103
19. Dimoudi, A.; Zoras, S.; Kantzioura, A.; Stogiannou, X.; Kosmopoulos, P.; Pallas, C. Use of cool materials and other bioclimatic interventions in outdoor places in order to mitigate the urban heat island in a medium size city in Greece. Sustain. Cities Soc. 2014, 13, 89–96.
20. Santamouris, M. (2013). Using cool pavements as a mitigation strategy to fighturban heat island – A review of the actual developments. Renewable andSustainable Energy Reviews, 26, 224–240. http://dx.doi.org/10.1016/j.rser.2013.05.047Santamouris
21. Rosenfeld, A., Akbari, H., & Bretz, S. (1995). Mitigation of urban heat islands:Materials, utility programs, updates. Energy and Buildings, 22(3), 255–265.
22. Santamouris, M.; Gaitani, N.; Spanou, A.; Saliari, M.; Giannopoulou, K.; Vasilakopoulou, K.; Kardomateas, T. Using cool paving materials to improve microclimate of urban areas—Design realization and results of the flisvos project. Build Environ. 2012, 53, 128–136
23. U.S. Environmental Protection Agency. 2012. "Cool Pavements." In: Reducing Urban Heat Islands: Compendium of Strategies. Draft. https://www.epa.gov/heat-islands/heat-island-compendium.
24. Algarni, S. 2019. "Potential for Cooling Load Reduction in Res idential Buildings Using Cool Roofs in the Harsh Climate of Saudi Arabia." Energy & Environment 30 (2): 235–253. doi:10.1177/0958305X18787340
25. Wang, X.; Li, H.; Sodoudi, S. The effectiveness of cool and green roofs in mitigating urban heat island and improving human thermal comfort. Build. Environ. 2022, 217, 109082
26. Kyriakodis GE, Santamouris M (2018). Using reflective pavements to mitigate urban heat island in warm climates—Results from a large scale urban mitigation project. Urban Climate, 24: 326–339.
27. Taleghani, M., Berardi, U., 2018. The effect of pavement characteristics on pedestrians' thermal comfort in Toronto. Urban Clim. 24, 449–459.
28. Tsoka, S.; Tsikaloudaki, K.; Theodosiou, T. Coupling a Building Energy Simulation Tool with a Microclimate Model to Assess the Impact of Cool Pavements on the Building's Energy Performance Application in a Dense Residential Area. Sustainability 2019, 11, 2519. https://doi.org/10.3390/su11092519
29. Zhai, Z. 2003. Developing an Integrated Building Design Tool by Coupling Building Energy Simulation and Computational Fluid Dynamics Programs (Doctoral thesis), Massachusetts institute of Technology.
30. ANSI/ASHRAE. Standard 55: 2017, Thermal Environmental Conditions for Human Occupancy; ASHRAE: Atlanta, GA, USA, 2017
31. M.C. Peel, B.L. Finlayson, T.A. McMahon, Updated World map of the k¨oppen-geiger climate classification, Hydrol. Earth Syst. Sci. 11 (2007) 1633–1644.
32. H. Mayer, P. H¨oppe, Thermal comfort of man in different urban environments, Theor. Appl. Climatol. 38 (1) (1987) 43–49.
33. M. Bruse, Simulating surface plant air interactions inside urban environments with a three-dimensional numerical model, Environ. Model. Softw. 13 (1998) 373–384, https://doi.org/10.1016/S1364-8152(98)00042-5.
34. H. Simon, Modeling Urban Microclimate: Development, Implementation and Evaluation of New and Improved Calculation Methods for the Urban Microclimate Model ENVI-Met (PhD Thesis), Universit¨atsbibliothek Mainz, Mainz, 2016 [Online], https://www.ipcc.ch/site/assets/uploads/sites/2/201F9/06/SR 15_Summary_Volume_Low_Res.pdf. (Accessed 17 October 2022)
35. Xie, J.; Zhou, Z. Numerical Analysis on the Optimization of Evaporative Cooling Performance for Permeable Pavements. Sustainability 2022, 14, 4915.
36. T. Hong, J. Kim, J. Jeong, M. Lee, C. Ji, Automatic calibration model of a building energy simulation using optimization algorithm, Energy Procedia 2017 (105) (2017) 3698–3704.
37. J. Cipriano, G. Mor, D. Chemisana, D. P´erez, G. Gamboa, Evaluation of a multi-stage guided search approach for the calibration of building energy simulation models, Energ Build 87 (2015) 370–385.
38. Elnabawi, M.H.; Hamza, N.; Raveendran, R (2023) 'Super cool roofs': Mitigating the UHI effect and enhancing urban thermal comfort with high albedo-coated roofs. Results in Engineering 19 (2023) 101269https://doi.org/10.1016/j.rineng.2023.101269
39. Sinsel, T., H. Simon, A. M. Broadbent, M. Bruse, and J. Heusinger. 2021B. "Modeling Impacts of Super Cool Roofs on air Temperature at Pedestrian Level in Mesoscale and Microscale Climate Models." Urban Climate 40: 101001. doi:10.1016/j.uclim.2021. 101001
40. N.H. Wong, Y. Chen, C.L. Ong, Sia, A. Investigation of thermal benefits of rooftop garden in the tropical environment, Build. Environ. 38 (2) (2003) 261–270, 2003.
41. Qin, Y. A review on the development of cool pavements to mitigate urban heat island effect. Renew. Sustain. Energy Rev. 2015, 52, 445–459.

PLEA 2024 WROCŁAW
(Re)thinking Resilience

Reimagining School Building

Comparison of Typologies for the Rural Ethiopia

ALPHA YACOB ARSANO[1], FISIHA I. LIKKE[1,2], HANNAH CHUNG[1], JOSEPH QUAN[1]

[1]Northeastern University, Boston, USA
[2]Lesley University, Cambridge, USA

ABSTRACT: This manuscript forms part of a pivotal series that rethinks the design of educational facilities in Ethiopia due to the impacts caused by internal conflict on educational infrastructure. The study places a special emphasis on sustainable, bio-climatic vernacular architecture for a contemporary school building. It explores the integration of local knowledge and cultural norms into both the architectural design and educational curricula of schools in Ethiopia. Through a comparative study of existing rural school typologies, the manuscript advocates for a transformative approach to school environments that enhance learning while being in harmony with the local climate and cultural heritage. The analysis presented herein serves as a call to action for design and construction professionals, investors, and policymakers to promote regionally adapted, sustainable educational spaces throughout Ethiopia and beyond. The goal is to develop school prototypes that are not only environmentally responsive but also culturally resonant, thereby supporting the infrastructure for quality education at the critical juncture of children's lives and the broader aspirations of the nation and beyond for a competent and sustainable future.
KEYWORDS: Contemporary vernacular, school performance, bio-climatic, sustainable

Figure 1: Conceptual sketch of memorial gathering space for contemporary vernacular school design, which serves as a hub for students as well as the local community.

1. INTRODUCTION: THE URGENCY TO RE-DESIGN SCHOOLS

Designing sustainable schools in Africa is crucial to address the educational needs of children and to promote environmental consciousness and resilience within communities. The biggest challenges of early education in Africa, especially in the rural area, include lack of physical infrastructure, limited access to exiting schools and learning resources, low quality of curriculum, and lack of stability due to war. Ethiopia, the second populous country in the continent, has been affected by internal conflict in the past three years that resulted in the destruction of thousands of schools, completely or partially, leaving millions of children without access to education (*Impact of the Northern Ethiopian War on Education - Link : Link*, n.d.).

Furthermore, according to the Ministry of Education of Ethiopia, most of the existing rural school infrastructure does not meet the basic requirements of a school facility. This manuscript presents design proposals for pre-K to middle schools in Ethiopia, particularly for areas that have been affected by recent conflicts. Moreover, the manuscript strives to compare different school typologies through the lens of environmental and contextual analysis. The overarching goal of the project is to make a larger call to design and construction professionals, investors, and policy makers where sustainable school designs are promoted not just nationally, but regionally across the African Continent.

2. BACKGROUND: EXISITING SCHOOL PROTOYPES AND RELEVANT PRECEDENTS

The most common examples of schools in rural Ethiopia fall in either of two categories**:** The first is a traditional *vernacular* style constructed using locally available materials like mud, thatch, or local stones featuring simple structures with pitched roofs, small windows, and open courtyards. The second category features a *standardized bar-typology* with classroom blocks that are easily replicated. Each block has multiple classrooms arranged in a linear or L-shaped layout with shared circulations and are designed primarily for standard-scalability but not customized.

Recent school constructions in the rural parts of Ethiopia are highly dominated by these standardized school designs as the vernacular styles which used to be typical of villages are becoming obsolete.

The third category of schools, rare in their existence, are the bio-climatic protypes that are designed for current needs and are called *contemporary vernacular*, by implementing sustainable building design strategies that are customized to local climatic and cultural context. The authors identified the following precedents of contemporary vernacular schools in Africa: the Green School in South Africa which utilizes passive design strategies, solar power, rainwater harvesting (*Green School South Africa / GASS Architecture Studios | ArchDaily*, n.d.); the Ilima Primary School in the DRC, which features sustainable materials with 99% of materials sourced from within ten kilometres of the site (*Ilima Primary School | MASS Design Group*, n.d.); the Gando Primary School designed by Francis kare Architects in Burkina Faso , which implemented improved low-tech and sustainable techniques so that villagers could participate in the process of construction, and the project became a landmark of community pride(Kéré Architecture & Archdaily.com, n.d.).

Additional examples are found in Asia where the climate presents a different challenge. For example, the Toongnatapin School Library by Arch SU Youth Architect Volunteer for Rural Development Camp in Danchang District, Thailand was constructed in just two weeks by architecture students in a remote area that has only small villages and sugarcane field (*Library Toongnatapin School / Student Committee, Faculty of Architecture, Silpakorn University | ArchDaily*, n.d.). The goal of the project is to improve infrastructure for rural societies.

However, having just a few of such projects is not sufficient. There is a need to expansively promote sustainable school design features by making viable school prototypes available to be adapted based on local contexts. The *sustainable, contemporary vernacular prototypes* shall further be integrated into school design guidelines and education policies across the continent.

3. COMPARISON OF PERFORMANCE

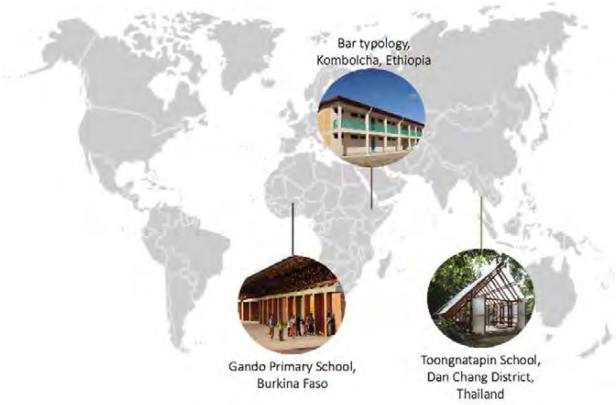

Figure 3: Three locations used for comparative performance analysis of the standardized bar-typology against the contemporary vernacular typology.

In this section we compare the construction and performance of a standardized bar typology hypothetically placed in Kombolcha (Ethiopia), Ouagadougou (Burkina Faso), and Bangkok (Thailand), against selected examples from the contemporary vernacular – Gando primary school, and Toongnatapin school.

Climate

We compare climatic conditions in Kombolcha, Gando, and Danchang Districts. Due to the absence of EPW weather files on *Building.OneClimate.org* for Gando, and Danchang District, the following closest cities are used for the analysis respectively: Ouagadougou and Bangkok.

Figure 4 shows false color map of annual solar radiation and we can read the direction where the largest annual solar radiation is received is about 10° due south. The three cities are located close to the equator (Kombolcha at 11° N, Ouagadougou at 12° N, Bangkok at 13° N). To reduce solar heat gain and glare through opening, roof overhangs and shading strategies are critical.

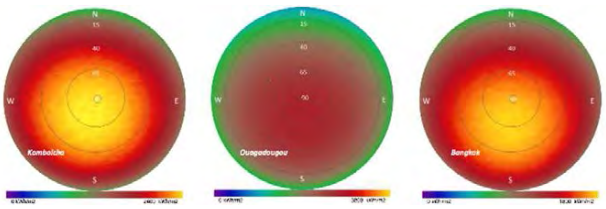

Figure 4: False color map of annual solar radiation levels for different surface orientations, using an upward-facing hemisphere.

Figure 5 shows that Kombolcha is a temperate climate, while Bangkok is a hot and humid climate. Ouagadougu has a hot and humid season as well as a hot and dry season.

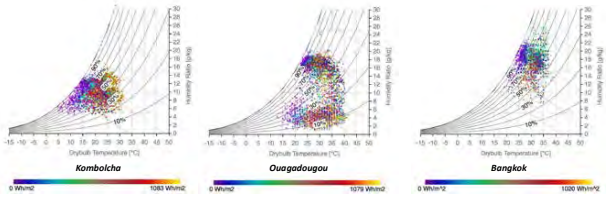

Figure 5: Psychometric chart showing school hours between 7am and 6pm. The false color represents solar radiation and the maximum value on the legend is adjusted for each location.

Kombolcha and Ouagadougu receive wind from multiple orientation in comparison to Bangkok, providing better opportunity for wind ventilation when cooling is needed, as shown in Figure 6.

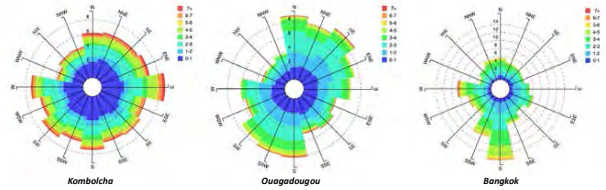

Figure 6: Wind chart showing the prevailing wind direction and speed hour hours between 7am and 6pm.

Construction

Unlike the traditional vernacular typologies, the *standard bar-typology* is a school design constructed in different locations using hollow concrete blocks construction materials and building form. It uses typical dimensions and design typologies across regions or the country.

On the contrary, the Gando school building construction centred around tying the structure to its community through the use of vernacular/locally abundant materials. It makes use of a clay/cement mix alongside corrugated metal roofs for environmental and economic efficiency. With this, the school is able to also provide adequate ventilation alongside suitable shading from the sun. Materials chosen are also able to endure the harsh rains of Burkina Faso's rainy seasons.

The Toongnatapin school library project, also supposed to be a waiting area, use natural features such as light and ventilation to draw the pleasant environment into the pavilion. Wood is the main structure material. The building walls and roofs are glazed by SCG Translucent Roof Sheet Panels which filter 90% of UV. The advantages of these panels are its lightweight and convenience to install. CONWOOD, wood-like concrete flooring is used for the interior floor. Finally, bricks are used on the exterior pavement and steps (*Library Toongnatapin School / Student Committee, Faculty of Architecture, Silpakorn University | ArchDaily*, n.d.).

Both projects, Gando Primary School and Toongnatapin School Library, use materials that are best adapted to their climatic context. The cement-clay bricks of Gando keep spaces cool in the hot and dry days while the open design, with light wooden structures of Toongnatapin provides shading and allows movement of air to keep spaces comfortable.

Natural daylight

The different typologies have different opening layout, determining the amount of daylight and ventilation getting into learning spaces.

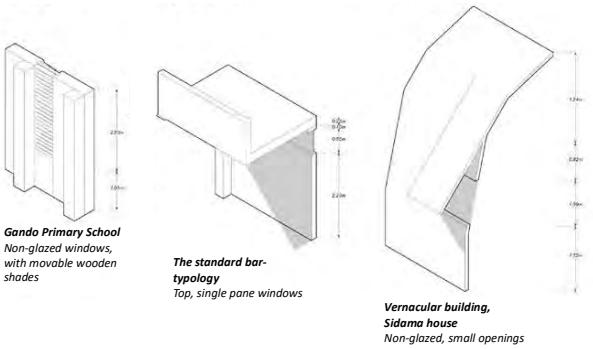

Figure 7: Window openings in the Gando Primary School, the standard bar-typology and a vernacular building in Ethiopia.

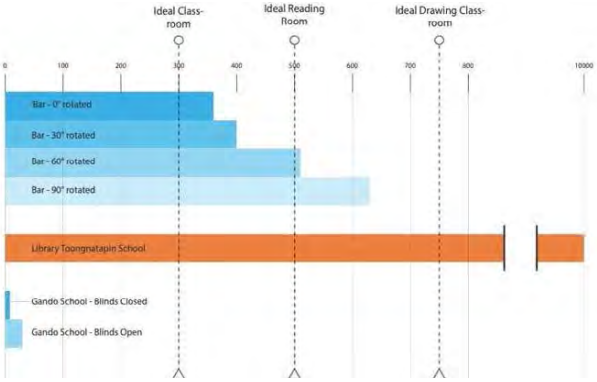

Figure 8: Comparison of availability of natural daylight using average lux values.

The standard bar-typology located in Kombolcha, Ethiopia receives sufficient daylight that is within the required range for an ideal reading room. However, looking at the annual solar exposure index (ASE) as a measure of potential glare, orientation of the building is very critical in maintaining indoor visual comfort. It is found that when the building is oriented 60° to 90° from the horizontal east-west axis, there is high risk for glare discomfort – 35% and 75% respectively.

The analysis shows that the amount of daylight in the Gando Primary School is lower than the standard requirement for an ideal classroom, primarily due to the small openings and the way the external shading is operated. As the contemporary vernacular school typologies are being optimized for better thermal

performance (as discussed in the following two sub-sections), it is important to pay attention to daylight availability and visual comfort.

Potential for natural ventilation

Cooling degree days (CDDs) are a measure of how hot the temperature is on a given day or during a period of days. And the discomfort hours due to high temperature (DisHigh) indicates the number of hours during occupancy when the indoor temperature is above 26°C. This upper comfort threshold can be adjusted based on the concepts of adaptive thermal comfort and the role of air movement for physiological cooling. For example, in the case of Bangkok/Danchang District, a hot and humid climate, enhanced air movement will play a very crucial role and the extended adaptive method with a 1.2m/s air movement suggests that indoor operative temperature of up to 32°C is acceptable for an outdoor prevailing temperature of 28°C.

Gando Primary School, Ilima Primary School and the Toongnatapin Library are acknowledged for being thermally comfortable by leveraging local climate, construction techniques and materials. On the other hand, the main limitation of the standard bar-typology is the absence of customized bio-climatic design strategies.

Thermal comfort requirements

When the standard bar-typology, with a low performance building envelope, as discussed in the construction section above, is analyzed for Kombolcha, Ouagadougu and Bangkok, the performance of the building varies (see Table 1). In comparison, the performance of the contemporary vernacular buildings for the three locations improved two to four times indicated by the reduction of discomfort hours due to high temperature.

Table 1: Comparison of bar-typology and contemporary vernacular for the three locations.

	CDD (18°C)	DisHigh Bar-typology	DisHigh Contemporary
Kombolcha	658	1545	743
Ouagadougu*	3862	2527	900
Bangkok*	4208	2700	700

**Comfort is predicted based on adaptive model and physiological cooling from elevated air movement is considered.*

Thermal mass

The diurnal temperature change in Kombolcha goes as high as 30 degrees. The minimum average in the hottest season is about 10 °C and the maximum average about 33 °C. The diurnal temperature change in Ouagadougu goes as high as 20 degrees. The minimum average in the coldest season is about 5 °C and the maximum during the hottest is about 43 °C. Bangkok has a humid and hot climate with only an average of 10 degrees diurnal temperature change. The primary building strategy used in Kombolcha is the use of high thermal mass given the high diurnal temperature difference. Night ventilation will be an effective strategy in Ouagadougu where night temperature goes down to about 20 °C when day temperate goes as high as 43 °C.

4. TOWARDS *CONTEMPORARY VERNACULAR*: DESIGN GUIDELINES FOR *SUSTAINABLE PROTOTYPES*

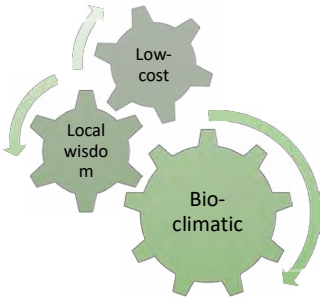

Figure 9: Proposed sustainable school design pillars: Low-cost - materials are sourced from the local area; local wisdom - combining local technology with new knowledge; bio-climatic – sustainable and healthy environment.

The proposed design approach for early education schools aims to provide viable prototypes that can be adapted to various locations based on environmental contexts, local community needs and cultural context. In the context of this project, contemporary vernacular is composed of three pillars, as shown in Figure 9.

The promoted *contemporary vernacular* prototypes incorporate variations in the physical space both indoors and outdoors to deliver engaging and interactive learning experiences. These strategies highly promote critical thinking skills, and social and emotional learning. The authors propose a combination of such programs with the space requirements shown in *Figure 10*. An example site plan and a representative building section are presented in *Figures 11* and *12*.

PROGRAM OVERVIEW	8944 6604 2340	GROSS M² INDOOR M² OUTDOOR M²
MEMORIAL + GATHERING 467 m²	467 m² of sheltered exterior space that serves as a gathering area to memorialize and create community.[1]	
LEARNING 2412 m²	200 m² 100 m² 200 m² 200 m² 600 m² 600 m² 50 m² 20 m² 20 m² 20 m² 372 m²	Library [2] Craft + Workshop Space MPR Study/Play Pre-K Classrooms (x2) [4] 1-3 Classrooms (x2 of each grade) [4] 4-6 Classrooms (x2 of each grade) [4] Health + Wellness Room Pre-K Bathroom [3] 1-3 Bathroom [3] 4-6 Bathroom [3] Circulation [7]
OUTDOOR ACTIVITY 374 m²	90 m² 56 m² 168 m² 50 m² 10 m²	Main Entrance Soccer Field Volleyball Court [7] Multipurpose Outdoor Area Outdoor Washroom
FOOD PREP + FARMING 4490 m²	500 m² 500 m² 490 m² 2500 m² 500 m²	Garden [8] Orchard [8] Chicken Coop [9] Kitchen + Dining Area [3] Circulation [5]
RESIDENTIAL 1062 m²	735 m² 70 m² 60 m² 20 m² 177 m²	Student Boarding (165 Students) [10] Teacher Boarding (14 Teachers) [11] Private Student Bathroom [5] Private Teacher Bathroom [5] Circulation [5]
MANAGEMENT + AMENITIES 130 m²	60 m² 30 m² 20 m² 20 m²	Teacher Offices + Workspace Break Room Main Storage Water Wells (x10)

Figure 10: An example of programs and their corresponding space requirements proposed for the pre-K to middle schools. This combination of programs can be adjusted for different locations based on the urgent needs of communities.

Minimizing environmental impact, promoting resource efficiency, and creating healthy learning environments is the second design parameter for the school prototypes. Passive design is a primary strategy where buildings are designed to maximize natural ventilation, daylighting, and passive cooling techniques. This helps minimize energy consumption and create comfortable learning spaces. The use of sustainable and locally sourced materials helps to reduce the carbon footprint and support the local economy.

Figure 11: Proposed site plan, showing how the proposed programs in Figure 10 can be organized for a given site.

The proposed sustainable design approach puts the local context and specific environmental challenges in each community at the centre of the design process. It harbors the national agenda of unity and the curriculum that incorporates learning-by-doing practices and provide the opportunity for students to hone specific technical skills while the output products support the students and the community to bring economic sustainability: orchards and chicken coops are designed as part of the school ecosystem; workshop spaces are hubs to craft creative projects, and innovate new products.

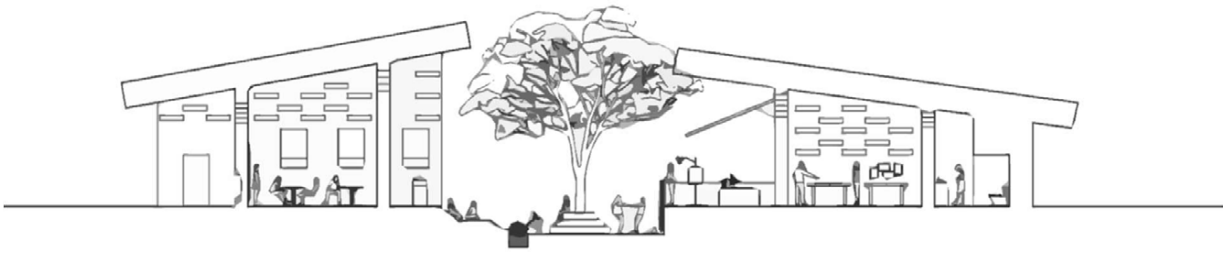

Figure 12: Representative section – illustration of the proposed indoor-outdoor learning spaces shown in a representative section. The indoor learning spaces are connected by an inner courtyard that has trees for shading, seating spaces, and small play/activity grounds. The classrooms and workshops spaces are buffered by semi-outdoor spaces. Large sport fields and community gathering spaces continue outward from these semi-outdoor spaces.

5. DISCUSSION AND FUTURE WORK

By integrating the principles of sustainability, local knowledge, and cultural norms in the educational themes both regionally and nationally in the design of the schools, we can create an educational environment that empowers students while fostering commitment to environment stewardship, resilience, and long-lasting sustainability.

In Ethiopia today, designing a physical space that fosters quality of education is crucial. These spaces aim to cultivate unity and peaceful thinking among students, guided by curricula that deliver a well-rounded educational experience. Such curricula are increasingly inclusive, offering differentiated instruction to meet the diverse learning needs and aptitudes of all students.

Participatory design through action research and design probs

In future work, thinking about the implementation of contemporary vernacular school prototypes, the following methods will be used as a tool to further reimagine and elaborate the design approaches.

Participatory Action research: Engaging stakeholders and the community, including future users, in the research and design process to co-create design that reflects their needs and insight.

Design & cultural probs: materials designed to provoke inspirational responses from diverse communities. The probes are part of the design strategy of pursuing experimental design in a responsive way. They address a common dilemma in developing projects for unfamiliar groups.

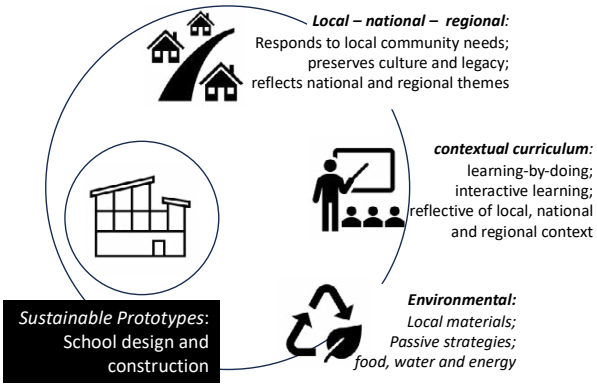

Figure 13: Envisioned comprehensive design approach that integrates sustainable design goals with community engagement and national themes.

This proposed project is not the first of its kind. There have been some attempts by design professionals and architecture students that start from community-based design and culminate in the construction of schools in different parts of Ethiopia. One example is the Shebraber School, which is a collaborative project designed by EthiopiaStudio2.0, a second-generation team of eleven Arizona State University M.Arch graduate students, led by practicing local architect Jack DeBartolo 3 (Shebraber School / EthiopiaStudio2.0 | ArchDaily, n.d.). Students travelled to a remote village community 120 miles southwest of Addis Ababa, the capital city of Ethiopia, to research, develop, and design new classrooms and administration buildings for a school serving children within a 10km radius, many of whom walk hours for the chance to attend.

In future work, the authors will propose school design prototypes that can be adapted for different rural villages. The goal of this project is to present a different kind of alternative, that combines improved concepts of sustainability featured in the vernacular style with the flexibility and scalability of standardized design approach in a form of adaptable sustainable prototypes for early education schools.

ACKNOWLEDGEMENTS

We would like to thank Northeastern University and the College of Arts, Media and Design for the generous support.

REFERENCES

1. *Green School South Africa / GASS Architecture Studios | ArchDaily*. (n.d.). Retrieved August 30, 2023, from https://www.archdaily.com/978637/green-school-south-africa-gass-architecture-studios?ad_source=search&ad_medium=projects_tab
2. *Ilima Primary School | MASS Design Group*. (n.d.). Retrieved December 25, 2023, from https://massdesigngroup.org/work/design/ilima-primary-school
3. *Impact of the Northern Ethiopian War on Education - Link : Link*. (n.d.). Retrieved December 30, 2023, from https://linkeducation.org.uk/impact-of-the-northern-ethiopian-war-on-education/#:~:text=Conflict%20has%20led%20to%20the,totally%20closed%20since%20January%202022
4. Kéré Architecture, & Archdaily.com. (n.d.). *Gando Primary School / Kéré Architecture | ArchDaily*.
5. *Library Toongnatapin School / Student Committee, Faculty of Architecture, Silpakorn University | ArchDaily*. (n.d.). Retrieved December 25, 2023, from https://www.archdaily.com/940797/library-toongnatapin-school-student-committee-faculty-of-architecture-silpakorn-university
6. *Shebraber School / EthiopiaStudio2.0 | ArchDaily*. (n.d.). Retrieved December 28, 2023, from https://www.archdaily.com/197694/shebraber-school-ethiopiastudio2-0

PLEA 2024 WROCŁAW
(Re)thinking Resilience

The potential of using mobile, vertical urban farms in the context of designing cities resistant to climate change.

ANNA BERBESZ[1] , KAJETAN SADOWSKI[1] , JAKUB ONYSZKIEWICZ[1]

[1] Wroclaw University of Science and Technology, Wroclaw, Poland

ABSTRACT: The article presents case studies on the MoFa modular vertical urban farm MoFa. As part of the preliminary research, the leading design solutions appearing in the architectural and urban space in the conceptual and implementation phase were analyzed. In addition, important patent applications on a global scale were presented. The article presents an original case study of the potential resulting from the installation of mobile vertical urban farms on the gable elevations of buildings made in large panel technologies (here: WWP and Wk-70). A detailed analysis of the façade structure was carried out and the scope of the study covered buildings located within the administrative borders of the city of Wroclaw in Poland. A quantitative analysis of buildings of different heights was carried out along with determining the surface and orientation of the gable walls. A proposal for a vertical greenhouse system with a rotational cultivation system was presented, and its production potential was calculated in relation to typical greenhouse crops for two selected species. Additional indirect, measurable profits resulting from the installation of the system were indicated, such as the reduction of heat loss through penetration for the gable facades of buildings, the use of rainwater, and the reduction of the carbon footprint of food transport.

KEYWORDS: urban farming, vertical farm, local food production

1. INTRODUCTION

Urban farming in connection with the postulate of sustainable urban development in building resilience to climate change has been the subject of scientific research in recent decades. The design of urban farms and especially their integration into the existing urban structure is an important step toward reducing the carbon footprint and shortening the path between the point of organic food production and the consumer. The system of a vertical, modular and mobile façade farm that can be mounted on the gable walls of residential buildings presented in this article is a complete architectural response to the above-described postulate of reducing the carbon footprint of food production and transport. This system also has additional, indirect, and measurable benefits resulting from its installation, such as reducing heat losses through the penetration of gable building facades, using and storing rainwater, sequestering carbon dioxide and oxygen production, and activating local communities.

2. RESEARCH METHODOLOGY AND DATA ANALISYS

Preliminary research was conducted on three parallel paths. The first one concerned the development of the concept of a modular mobile urban farm, MoFa. This concept has been modeled, described, and submitted for patent protection. The second path concerned the analysis of source materials and literature in integrated urban farms. This allowed us to determine the current state of knowledge and obtain data in agriculture. The third one included the analysis of data regarding a case study - gable walls of buildings made using industrialized technologies and within the administrative boundaries of Wrocław. The combination of research and analyzes allowed to show the potential of vertical crops on the facades of existing buildings in cities with medium-density buildings. This is an important aspect of using climate change (net increase in global temperature extending the growing season in temperate climates) to ensure healthy, locally produced food while shortening supply chains with high carbon footprints. The obtained data was related to demographic data within the presented research field - the city of Wrocław.

2.1. MoFa – MOBILE URBAN FARM CONCEPT

A modular and mobile vertical farm allows for local production of healthy and organic food. The creators intended it to be a product dedicated to the gable elevations of buildings constructed using technologies industrialized in the second half of the 20th century (mainly WWP and Wk-70), although installation possibilities of the farm is limited only by architectural conditions, and it can be installed on any gable elevation. The production and harvesting of leafy vegetables (because this is the expected main product of the crop) is supervised by the residents of the buildings on the facades of which the farm will be installed. This allows for the elimination of the supply chain between the manufacturer and the customer (in this case, it is the same person), which directly translates into the carbon footprint associated with the transport of products. The farm enables ground and hydroponic production. It can be expanded with

an aeroponics cultivation system. An important element is social activation and participation, which has a positive impact on neighborly relations. The system is modular, which allows you to multiply elements both horizontally (at intervals of up to 1.00 m) and in height (adapting the farm to the height of the building's facade). Installing a vertical mobile farm (Fig. 1) on the facade has a positive effect on both the acoustics of the building and the thermal insulation of the partition in the installation zone (by increasing the temperature in the gable elevation zone, heat losses through penetration are eliminated).

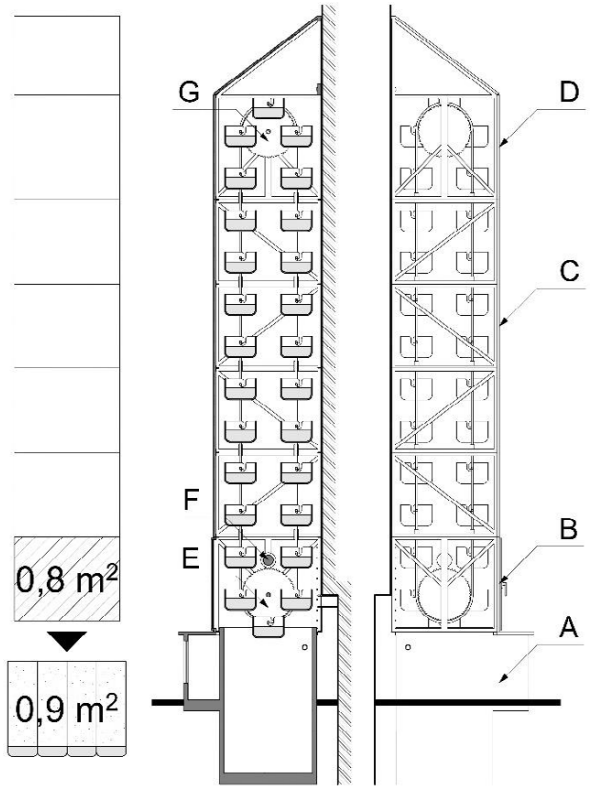

Figure 1: MoFa vertical farm schematic: A-rainwater tank, B-revision module, C-middle module, D-upper module, E-lower rotating wheel, F-tube engine, G-upper rotating wheel.

Thanks to the element of mobility, the entire facade of the building is used, which has a positive impact on both the illumination of crops (pots in constant rotation obtain the sunlight necessary for the photosynthesis process) and the aesthetic values of the facade (unused spaces are functionally developed). The farm is operated at ground level, which does not require specialized pre-training of users. Because of the above-mentioned photosynthesis process (carbon dioxide sequestration and oxygen production), the air quality in the farm assembly zone improves. Air humidity also improves because of evaporation processes accompanying crops. The farm is equipped with a water tank and a bypass system to connect rainwater drains collected from the roofs of buildings, which allows its management in the event of rainfall and use in the event of drought. Thanks to a system of photovoltaic cells and LED diodes, the system produces the energy necessary to rotate the pots during the day and illuminate the crops at night. The expected growing season in the mobile vertical farm is from March to November (10 months). The estimate of the vegetation area for each of the MoFa mobile farm modules is 0.9 m2 for each of the farm modules (with a façade area of 0.8 m2). Relative to 1 m2 of façade area, the vegetation area is 1,125 m2. The vegetation area was rounded to 1.0 m2 per 1.0 m2 of the facade area (100%) because of the installation of the farm on a plinth, which constitutes the lower rainwater tank, and the need to build a roof in the upper module.

2.2. Literature review

The literature analyzes on crops in urban environments show that since around 2015, there has been a significant increase in interest in this topic. The reasons for this phenomenon are multifaceted, ranging from the implementation of sustainable development tools, drawing attention to the circular economy, as well as technological development enabling the implementation of urban farms as free-standing or additive structures that enable the reuse of flat roofs or existing gable walls. Moreover, the development of technologies in urban cultivation has influenced the search for alternative directions of soil and soilless cultivation, for example, hydroponic [1]. Currently, keywords such as urban and peri-urban agriculture, food security, local food systems, community gardens, sustainable agriculture, climate change and vertical farming are increasingly appearing in the literature. The literature analyzes show that the integration of innovative technologies enables agriculture to save water, protect soil, reduce carbon dioxide emissions, and increase production efficiency. In the era of the Agriculture 4.0, industrialized agriculture and supply chains can become a central element of food production [2]. The development of modern agricultural technologies results from the search for new energy sources and innovative cultivation methods. Faced with the growing population of cities, it is necessary to look for new cultivation methods that would allow the transfer of traditional agriculture to urbanized areas. However, there is no single universal technological solution that would fully respond to the challenges related to increasing food production. The synergy of many different techniques seems to be the key to achieving a green revolution in the 21st century. One of the interesting solutions in this area is vertical farming. It is believed to be able to significantly contribute to the sustainable development of food production in cities. Vertical farming is one of the new methods that deserves detailed research in the next two decades,

especially if we want to live in harmony with nature. The ideal vertical farming should be affordable, sustainable, and safe to operate, while not requiring financial subsidies or external support. If these conditions are met, urban agriculture has the opportunity to provide food to 60% of city residents by 2030 [3]. Several patents are also appearing around the world related to the development of cultivation technology in the form of vertical farms. One solution is patent US11778956B2 by John G. Lert, Jr., William J. Fosnight, and Jeffrey C. Laba regarding an automated vertical farming system using mobile robots. The system consists of a storage structure equipped with a series of racks with shelves filled with plants. Additionally, autonomous mobile robots are used that move between shelves to move containers of plants to and from storage. Under the supervision of a control system, robots can transport a container with plants from the storage place to a dedicated service station. It is then possible to perform care treatments, including watering and providing the necessary nutrients, as well as collecting feedback about the plants, e.g. in the form of photos.

2.3. Case study data analisys

The data used for the assessment were downloaded from a 3D model based on metadata from the Spatial Information System of the city of Wrocław [4]. The background map and elevation centroids were imported into QGIS and exported to a vector file (Figure 2).

Figure 2: Partial plan of the City of Wrocław. Buildings made of prefabricated panels had been marked with 4 types of shading - author's elaboration..

In the first step, all buildings constructed using industrialized technologies in the second half of the 20th century (within the city's administrative boundaries) were marked. In the next step, the marked objects were "raised" from a flat plan to a height consistent with the height and number of floors in the buildings. The height of all objects was checked based on diagonal photo plans of Wrocław from 2015 available in SIP [5].

During the inspection, the buildings were divided into 4 categories according to the possibility of using the façade area:

- gable elevation without decorations (100% use of the area),
- façade with windows (75% of space utilization),
- façade with loggias/balconies (50% of space utilization),
- façade with loggias/balconies and windows (25% of space utilization).

Each facility and each elevation has been marked numerically. The areas of flat roofs of buildings were calculated, which directly translated into the indication of the rainwater collection potential, and the surfaces of facades were used to simulate the potential of vertical crops. Because of the plant lighting system implemented as part of the MoFa farm to simulate crop potential, the façade orientation was omitted in this variant. However, it was marked for each facade of each building. The facilities were grouped according to the district boundaries of the city of Wrocław (Old Town, Śródmieście, Krzyki, Fabryczna, Psie Pole) and summarized in a tabular form with demographic data regarding the number of inhabitants. These data are publicly available in the Wrocław Spatial Information System [5].

3. RESEARCH RESULTS

Modeling of buildings selected according to the methodology described in point 2.3 showed the possibility of using MoFa vertical farms on a total elevation area of 36.46 ha. Indicators showing the ratio between the development area in the horizontal projection of MoFa vertical farms (A_B) and the area of analogous farming on land equal to the crop area in a vertical farm (A_{MoFa}) were also calculated, showing that in the scale of the entire city, the vertical crop area is on average 3.15% of the farming area of soil-ground. Calculations were also performed for each district of Wrocław (Table 1).

Table 1 Vertical crop area (A_{MoFa}), building area (A_B), roof area (A_R) and A_B/A_{MoFa} ratio.

District	A_{MoFa} (ha)	A_B (ha)	(A_B/A_{Mofa}) (%)	A_R (ha)
Stare Miasto	6.05	0.23	3.79	12.97
Śródmieście	2.66	0.08	2.84	4.72
Krzyki	8.54	0.28	3.29	21.17
Fabryczna	14.48	0.42	2.90	32.72
Psie Pole	4.74	0.14	3.04	11.23
TOTAL:	36.46	1.15	3.15	82.82

The efficiency of vegetable production in urban farming depends on various factors, including plant species, production technology and location, and the results often differ significantly [6], although it is widely argued that Urban Agriculture (UA) is a resource-efficient form of sustainable agriculture that

can contribute to mitigate climate change [7]. A review of the proposed and used solutions shows the great advantage of production technology based on hydroponics, especially in the vertical system [8, 9]. In this study, a Vertical Farm MoFa was proposed, mounted on the gable facades of existing buildings in which hydroponic cultivation of tomatoes and lettuce was used. Production efficiency was determined based on literature research [6] and, after considering the available area of the vertical farm, the annual production was calculated in three variants: tomatoes only (18.585t), lettuce only (23.887t) and in the ratio of 50% to 50% (9.292t and 11.943t t). The results were compared with the average productivity of soil crops determined based on data from the Central Statistical Office [10], FAOSTAT [11] and literature [6, 12, 13, 14] showing that tomato production increased by 885% and lettuce by 1752%. This allowed for the calculation of the percentage of annual coverage of the demand for vegetable consumption (400 g day-1) according to WHO guidelines [10] for each resident by the production of tomatoes (PT.WHO) and lettuce (PL.WHO) (Table 2) and the percentage of annual covering the actual consumption of tomatoes (PT.AV, assumed 10 kg·y-1person-1) and lettuce (PL.AV, assumed 1.56 kg·y-1person-1) [11] (Table 3).

Table 2: Covering the annual demand for vegetables according to WHO by the production of tomatoes ($P_{T.WHO}$) or lettuce ($P_{L.WHO}$).

District	Residents	$P_{T.WHO}$ (%)	$P_{L.WHO}$ (%)
Stare Miasto	40,642	51.94	66.75
Śródmieście	96,361	9.63	12.38
Krzyki	130,349	22.87	29.39
Fabryczna	169,367	29.85	38.36
Psie Pole	72,530	22.81	29.32
TOTAL:	509,249	25.00	32.13

Table 3: Covering the annual demand for tomatoes or lettuce according to annual consumption through the production of tomatoes ($P_{T.AV}$) or lettuce ($P_{L.AV}$).

District	Residents	$P_{T.AV}$ (%)	$P_{L.AV}$ (%)
Stare Miasto	40,642	758.20	6247.46
Śródmieście	96,361	140.59	1158.32
Krzyki	130,349	333.91	2751.03
Fabryczna	169,367	435.77	3590.29
Psie Pole	72,530	33.07	2744.15
TOTAL:	509,249	364.96	3006.84

One of the advantages of hydroponic cultivation highlighted in research is the reduced water consumption compared to soil-ground cultivation. Based on data available in the literature [6, 12, 14] specifying the annual water demand per 1 m2 for hydroponic crops of tomatoes (24 dm3m-2) and lettuce (62 dm3m-2) and taking into account the possibility of collecting rainwater (WR) from the roof surfaces (it was assumed that 25% of the roof surface was used for each elevation, assuming an annual rainfall of 588 mm for the city of Wrocław), the annual rainwater coverage of the demand for growing tomatoes and lettuce was calculated in the ratio of 50% to 50% (WT+L). The results show that hydroponic agriculture can be based entirely on rainwater and on the scale of the entire city, only 12.87 % of collected water covers the demand for vertical agriculture (WEX) (Table 4).

Table 4: Annual rain water harvest (W_R), annual water demand at the MoFa farm (W_{T+L}) and percentage of rain water harvest use (W_{EX}).

District	W_R (m^3)	W_{T+L} (m^3)	W_{EX} (%)
Stare Miasto	19,067.00	2,598.00	13.63
Śródmieście	6,942.00	1,142.00	16.45
Krzyki	31,122.00	3,670.00	11.79
Fabryczna	48,103.00	6,222.00	12.94
Psie Pole	16,504.00	2,037.00	12.34
TOTAL:	121,738.00	15,669.00	12.87

In order to comprehensively evaluaate the impact of the Vertical Farm MoFa on the environment, it was decided to use Consequential Life Cycle Analysis (CLCA) which can be defined as a method that aims to describe how environmentally relevant physical flows would have been or would be changed in response to possible decisions that would have been or would be made [13]. In the analyzed case, the modules that differed most significantly between soil-ground cultivation and vertical hydroponic cultivation were selected. Due to the production method and its location, it was decided to analyze in module B6 in the processes characterized by the greatest differences, i.e.:

- electricity consumption due to additional lighting for hydroponic production,
- electricity consumption due to the operation of water pumping devices in a vertical system,
- electricity consumption due to the operation of engines ensuring constant rotation of plants on facade,
- production of electricity from photovoltaic modules located on roofs adjacent to the facade,
- reduction of heat losses through facade walls thanks to the vertical farm providing a thermal buffer,
- reduced fuel consumption due to shortening of the supply chain.

Proper lighting is crucial to achieve appropriate production efficiency [14] and is also one of the main consumers of electricity and a source of greenhouse gas emissions. Calculations based on the average demand for photosynthetic photon flux (PPF) in photosynthetic active radiation (PAR: 400 to 700 nm) for lettuce amounting to 65.39 µmol m-2s-1 [15] assuming exposure to 10 h day-1 showed the demand for electricity equal to 82.61 kWh m-2year-1 and

greenhouse gases (GHG) emission equal to 56.59 CO2eq m-2year-1 for the intensity of electricity emission equal to 685 kgCO2eq MWh-1. Additional consumers of electricity and sources of GHG emissions for the operation of pumps supplying water to the farm (940 W for a 12 m2 farm module, operation 4 hours a day) and the engine ensuring rotation (200 W, operation 12 hours a day) have shown electricity demand equal to 94.00 and 60.00 kWh m-2year-1, respectively, and GHG emissions equal to 64.39 and 41.10 CO2eq m-2year-1, respectively. After taking into account the potential size of Vertical Farms MoFa for the entire city, this means electricity demand (QD) equal to 86.267 MWh year-1 and GHG emissions (EQ) equal to 59,093 tCO2eq year-1. The electricity demand is covered by photovoltaic modules placed on the roofs directly adjacent to the facades on which the vertical farms are located. Assuming coverage of 70% of the available roof area (AR), annual PV energy production (PVP) calculated using the "Photovoltaic Geographical Information System" tool of the European Commission [16], amounting to 235 kWh m-2year-1, annual electricity production was calculated equal to 136,231 MWh year-1 and GHG emission savings equal to 93,318 tCO2eq year-1. The obtained shows the possibility of completely covering the needs for electricity on a city scale (157.92%), assuming the possibility of storing excess energy in the power grid (Table 5).

Table 5: Electricity demand (Q_D), electricity production by PV modules (PV_P) and the percentage of demand covered by production.

District	Energy needs (Q_D) (MWh)	Energy production (PV_P) (MWh)	Covering energy demand (%)
Stare Miasto	14,305.00	21,337.00	149.16
Śródmieście	6,288.00	7,768.00	123.54
Krzyki	20,203.00	34,827.00	172.39
Fabryczna	34,258.00	53,829.00	157.13
Psie Pole	11,213.00	18,469.00	164.72
TOTAL:	86,267.00	136,231.00	157.92

Another important aspect from the point of view of potentially reducing the negative impact on the environment and adapting the city to climate change is the shortening of the supply chain resulting from local food production. Many researchers report that local production in vertical farms reduces the carbon footprint of production, although many studies indicate an inverse relationship resulting from the high energy consumption of the production system in vertical farms [17, 18]. The Vertical Farm MoFa study took into account the avoided transport of tomatoes and lettuce, whose amount and the ratio of domestic transport to imports were determined based on statistical data [10]. To sum up, 46 % of tomatoes consumed in Poland are imported from a distance of approximately 1,946 km (the Netherlands, Turkey, Spain, Morocco, Germany, France) and 54 % come from a distance of approximately 150 km. 80 % of lettuce is imported from a distance of approximately 2,066 km (Spain, Germany, Italy) and 20 % comes from the country from a distance of approximately 150 km. The kgCO2eq emission factors per tonne of vegetables over these distances were also calculated, resulting from the assumed intensity of emission of truck transport with a capacity of 8t (Table 6).

Table 6: Average distance of vegetable transport (D_T), GHG emissions during one transport (E_{TR}) and GHG emissions per 1 transported tonne of vegetables ($E_{RT.1t}$).

Vegetable	(D_T) km	(E_{TR}) $kgCO_2\ km^{-1}$	($E_{TR.1t}$) $kgCO_2\ km^{-1}$
Imported tomatoes	1946	1251	156.42
Domestic tomatoes	150	96	12.06
Imported lettuce	2066	1328	166.05
Domestic lettuce	150	96	12.06

Summarizing the additional GHG emissions resulting from the demand for electricity, an additional carbon footprint (E_Q) in the B6 module of the vertical farm was calculated, amounting to 59,093 tCO_2eq on a city scale, as well as a negative carbon footprint (E_P) from avoided transport ($E_{TR.tot}$) amounting to -2,353.12 tCO_2eq, negative carbon footprint resulting from the production of electricity in PV modules (E_{PV}) of -93,318 tCO_2eq and a negative carbon footprint resulting from saved energy for heating (E_B) of -870 tCO_2eq (Table 7). The total carbon footprint calculated under CLCA ($E_{tot} = E_Q + E_{TR.tot} + E_{PV} + E_B$) is -37.448 tCO_2eq.

Table 7: Positive carbon footprint from electricity demand (E_Q), negative carbon footprint from energy gains (E_P) and total carbon footprint (E_{tot}).

District	E_Q tCO_2eq	E_P tCO_2eq	E_{tot} tCO_2eq
Stare Miasto	9,798.75	-15,150.54	-5,351.79
Śródmieście	4,307.48	-5,556.32	-1,248.84
Krzyki	13,838.73	-24,611.06	-10,772.33
Fabryczna	23,466.61	-38,152.87	-14,686.26
Psie Pole	7,681.02	-13,070.39	-5,389.37
TOTAL:	59,092.59	-96,541.18	-37,448.59

On the scale of the entire city, this means that there is no impact on the environment in the form of GHG emissions and the possibility of returning part of the produced energy to the power grid. However, a necessary requirement is the implementation of a photovoltaic installation, which is responsible for 96.66 % of the reduction in the carbon footprint of the vertical farm compared to 2.44 % resulting from the reduction of transport and 0.90 % from the reduction of heat losses through the thermal buffer.

5. CONCLUSION

As has been shown, the mobile modular MoFa vertical farm allows you to meet the demand for some

vegetables according to WHO standards and radically reduce water consumption compared to land crops. It is an energy self-sufficient unit where excess electricity production can be distributed in the on-grid system. The analysis of the operational carbon footprint shows negative values of 38,000. t CO2eq and local production emits <10% GHG due to short-haul transport. Future farm research should focus on confirming the potential for on-site production, examining the need to implement and operate a plant lighting system, and conducting a complete LCA analysis considering the built-in carbon footprint of the MoFa farm.

REFERENCES

1. Andre Fussy, Jutta Papenbrock, An Overview of Soil and Soilless Cultivation Techniques—Chances, Challenges and the Neglected Question of Sustainability, [in:] Plants 2022, 11(9).
2. Kumar Srinivasan, Vineet Kumar Yadav, An integrated literature review on Urban and peri-urban farming: Exploring research themes and future directions, [in:] Sustainable Cities and Society 99 (2023).
3. Fatemeh Kalantari, Osman Mohd Tahir, Ahmad Mahmoudi Lahijani, Shahaboddin Kalantari, A Review of Vertical Farming Technology: A Guide for Implementation of Building Integrated Agriculture in Cities, [in:] Advanced Engineering Forum, 2017.
4. internet source: https://geoportal.wroclaw.pl/en/ - accessed 14.07.2023
5. internet source: https://gis.um.wroc.pl/imap/?gpmap=demografia - accessed 17.11.2023
6. Dorr E., Goldstein B., Horvath A., Aubry C., Gabrielle B., Environmental impacts and resource use of urban agriculture: a systematic review and meta-analysis. Environmental Research Letters, 16 (9). Retrieved from https://par.nsf.gov/biblio/10333141 https://doi.org/10.1088/1748-9326/ac1a39
7. Artmann, M.; Sartison, K. The Role of Urban Agriculture as a Nature-Based Solution: A Review for Developing a Systemic Assessment Framework. Sustainability 2018, 10, 1937. https://doi.org/10.3390/su10061937
8. Kalantari, F., Mohd Tahir, O., Mahmoudi Lahijani, A., & Kalantari, S. (2017). A Review of Vertical Farming Technology: A Guide for Implementation of Building Integrated Agriculture in Cities. Advanced Engineering Forum, 24, 76–91. https://doi.org/10.4028/www.scientific.net/aef.24.76
9. Touliatos D., Dodd I.C., Mcainsh M., (2016), Vertical farming increases lettuce yield per unit area compared to conventional horizontal hydroponics, Food and Energy Security, 5,DOI 10.1002/fes3.83.
10. Statistics Poland, [Online], https://stat.gov.pl [29 November 2023].
11. Food and Agriculture Organization of the United Nations, [Online], Available: https://www.fao.org [29 November 2023].
12. Swain A.,Roy A., Biswas A., Chatterjee S., Viswanath M., (2021), Hydroponics in vegetable crops: A review, The Pharma Innovation Journal, 10(6): 629-634.
13. T. Blom, A. Jenkins, R.M. Pulselli, A.A.J.F. van den Dobbelsteen, The embodied carbon emissions of lettuce production in vertical farming, greenhouse horticulture, and open-field farming in the Netherlands, Journal of Cleaner Production, Volume 377, 2022, 134443, ISSN 0959-6526, https://doi.org/10.1016/j.jclepro.2022.134443.
14. Barbosa, G.L.; Gadelha, F.D.A.; Kublik, N.; Proctor, A.; Reichelm, L.; Weissinger, E.; Wohlleb, G.M.; Halden, R.U. Comparison of Land, Water, and Energy Requirements of Lettuce Grown Using Hydroponic vs. Conventional Agricultural Methods. Int. J. Environ. Res. Public Health 2015, 12, 6879-6891. https://doi.org/10.3390/ijerph120606879
15. World Health Organization, [Online], Available: https://www.who.int/tools/elena/interventions/fruit-vegetables-ncds [30 November 2023].
16. Całyniuk, B., Bucka, I., Karpe, J., Bucki, B. (2020). Study of consumption preferences and frequency of selected vegetables among female students of dietetics. Annales Academiae Medicae Silesiensis, 74, 60-67. https://doi.org/10.18794/aams/113631
17. Resh, H.M. (2004) Hydroponic Food Production: A Definitive Guidebook for the Advanced Home Gardener and the Commercial Hydroponic Grower. CRC Press, New Jersey.
18. Curran M.A., Mann M., Norris G.,The international workshop on electricity data for life cycle inventories, Journal of Cleaner Production, 2005, 8, 853–862.
19. Xydis G.A., Liaros S., Botsis K., Energy demand analysis via small scale hydroponic systems in suburban areas – An integrated energy-food nexus solution, Science of The Total Environment, Volumes 593–594, 2017, Pages 610-617, ISSN 0048-9697, https://doi.org/10.1016/j.scitotenv.2017.03.170.
20. Paz, M., Fisher, P.R. and Gómez, C. (2019), Minimum Light Requirements for Indoor Gardening of Lettuce. Urban Agriculture & Regional Food Systems, 4: 1-10 190001. https://doi.org/10.2134/urbanag2019.03.0001
21. Photovoltaic Geographical Information System, [Online], Available: https://re.jrc.ec.europa.eu/pvg_tools/en/tools.html#PVP [05 December 2023].
22. Jones, A., 2002. An environmental assessment of food supply chains: a case study on dessert apples. Environ. Manag. 30 (4), 560e576. http://dx.doi.org/10.1007/s00267-002-2383-6
23. Benis K., Ferrão P., Commercial farming within the urban built environment – Taking stock of an evolving field in northern countries, Global Food Security, Volume 17, 2018, pages 30-37, ISSN 2211-9124, https://doi.org/10.1016/j.gfs.2018.03.005.

PLEA 2024 WROCŁAW
(Re)thinking Resilience

Environmental Value in Historical Heritage Buildings in Mexico:

Case Study: Jesuit Ex-colegio de Tepotzotlán

ANIBAL FIGUEROA[1] GLORIA MARIA CASTORENA[2]

[1]Universidad Autonoma Metropolitana, Mexico City
[2]Universidad Autonoma Metropolitana, Mexico

ABSTRACT: The historic buildings analyzed were built in Tepotzotlán, forty kilometers away from Mexico City. They were designed as schools and seminars from the XVI to the XVIII centuries, initially by Franciscans (XVI century) and completed by the Jesuits (XVII and XVIII centuries). Its current state of preservation as a national museum allows us to review and evaluate different passive design strategies and technologies that permit them to operate as a self-contained autonomous and sustainable unit.
KEYWORDS: Tepotzotlan, rational use of natural resources, XVII Century buildings, sustainability, energy efficiency

1. INTRODUCTION

The architectural complex of the old school of *Tepotzotlán*, is located 40 km from Mexico City, in the municipality of *Tepotzotlán* in the State of Mexico. The buildings currently house the National Museum of the Viceroyalty, preserving over time an environmental legacy implicit in the design of its spaces and in the environmental technologies that allowed it to operate autonomously and sustainably at the time.

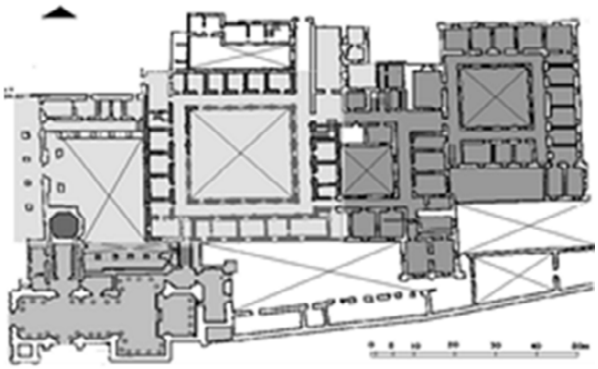

Figure 1: Architectural plan of the monastic complex

The complex is located in the original urban outline of the pre-Hispanic settlement in the form of a checkerboard coinciding with the cardinal points to take advantage of the sunlight in a cold climate and store the thermal energy in the building envelope. Located on the slopes of the Sierra de *Tepotzotlán*, in the highest elevation of the plain, the complex dominates the landscape and manages the acoustics of the town with the call of the bells, also enjoying a privileged position for the availability of water from natural runoff.

Architecturally, the function and design strategy for each environment is particular; the lighting, the acoustic response of the premises, the visuals and the aromatization and ventilation of the spaces are intentionally managed for each cloister with a central courtyard scheme creating a microclimate; while the design strategies and concepts for natural climatization are applied in a general way to the entire complex, such as direct solar use through the east orientation of the openings and indirect gains through the walls to the west where the openings are reduced to a minimum and the mass of the blind walls dominates. The materials used have been analyzed for their thermal properties and the response to humidity in the environment, from the foundations, walls, ceilings, insulation of the openings such as doors and windows, as well as the finishes and ornamental elements made on site.

2. METHODOLOGY FOR THE ENVIRONMENTAL ANALYSIS OF HISTORIC BUILDINGS

Based on the Bioclimatic Design Methodology (Fuentes, 2002.); we propose the adaptation of the following methodology in which some of the components are the same, but with a retrospective analysis of the design. An important addition to the Bioclimatic Design Methodology are the oral sources of chronists, historians and settlers; to support the design conclusions.

This methodology considers aspects of the natural environment that determine the accessibility of natural resources, such as topography, hydrology, pedology an geology to determinate the existing

materials in the region that was used in the historical heritage buildings. Climatic elements (temperature, humidity, wind, radiation and dominant natural phenomena) in their historical regression comparatively with the current climate, that allows determining the building´s response to human well-being. And socio-cultural aspects such as clothing and lifestyle (Clo), which define the methabolic activities (MET) developed in the buildings and their operation.

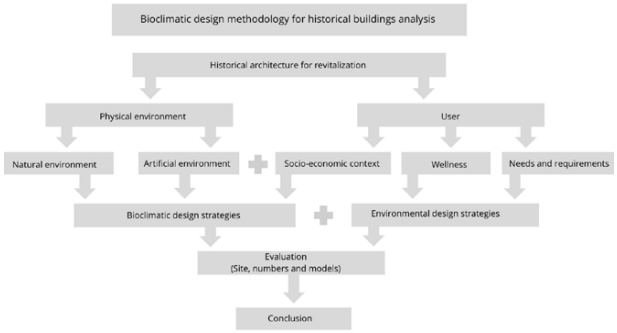

Figure 2: Bioclimatic Design Methodology for the Analysis of Historic Buildings

The bioclimatic design strategies synthesize the analysis of the climate and the hygrothermal comfort requirements: heating/cooling, humidification/ dehumidification, thermal inertia, massiveness/ lightness; as well as ventilation/air renewal. Added to these are the lighting, acoustic, aromatic perceptions, electromagnetic and psychological strategies applied in the architectural indoor design and management of outdoor areas.

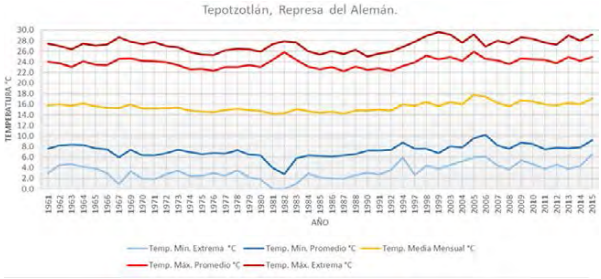

Figure 3: Regressive behavior of the average temperature in Tepotzotlán 1961-2015. (Castorena 2020).

The application of design strategies and concepts was evaluated on site (monitoring of physical and meteorological conditions) and through simulations (numerical and physical models) to quantitatively verify the behavior of its physical variables.

Back in the sixteenth and seventeenth centuries, self-sufficiency in food, energy and indoor comfort were vital, as well as the efficiency and awareness in the use of natural resources for the operation of the buildings and their exterior areas. Principles of sustainable urban design as well as passive and low energy architecture were desperately needed, when adapting European religious models to the New Spain climate.

The outcome of the environmental assessment of a locality´s historical build heritage provides an opportunity to revitalize old buildings in their sustainable operation; as well as providing answers to the environmental changes of modern architecture an urbanism in a specific place.

The main technologies and design concepts that were used on the Jesuit´s Colleges of Tepotzotlan are described below.

3. ENVIRONMENTAL TECHNOLOGIES

The environmental technologies used in the case study have been analyzed from the urban point of view and under the design principles of architecture linked to the climate, the materials and the construction systems used in the buildings.

On a urban scale, the complex of buildings is located in the lower part of the Sierra de Tepotzotlán, leaving the low lands in the valley for agricultural production. The orientation of the complex was based on the indigenous layout which followed the cardinal axes. The Spaniards respected this layout, designing cloisters with central *patios* whose dimensions and shapes respond to the amount of energy coming from the sun and the effects of the wind in a semi-cold bioclimate.

3.1 Passive air cooling or heating system

The orientation and shape of the buildings is determined by the thermal axis, in the route to the east, south and west; for direct and indirect heating and interior daylighting.

They used wood plates as insulation in doors and windows, to avoid losses at night due to convection and preserve the gains generated inside living spaces.

In the architecture of the monastic complex natural climate control, sunshade and daylighting is achieved by manual control of the operating parts of the wooden insulation in internal doors and windows. When combined with the use of massive walls for practical, constructive and thermal reasons, it provides a very stable indirect heat storage system.

In Tepotzotlán, warming is required in 68% of a year in nights year around and winter months; while the temperatures in the comfort zone correspond to 26.7% of the annual hourly values.

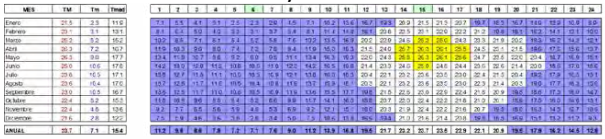

Figure 4: Hourly temperatures considering adaptive thermal comfort. Fuentes-Freixanet (2014).

Cooling is required only 4.6% of the year, so none of the cooling design strategies are applicable in the design of interior spaces; however, if the temperature data is analyzed against the relative humidity data, it is observed that shading and humidification are

required in most afternoon hours, particularly in spring. Therefore, controlled humidification through fountains and vegetation is a possible strategy for outdoor areas.

Figure 5: Hourly Relative humidity table considering hygrothermal comfort. Fuentes (2014).

The analysis of the ambient temperature was compared with the behavior of the temperature inside the exhibition rooms. The maximum outdoor thermal difference corresponds to the winter period with a value of 20 °C; in the same period, the indoor temperature in the Colleges has a variation of only 3 °C approximately, proving that the high mass and controlled ventilation produce a comfortable and stable indoor temperature

Hourly records of dry bulb temperature and relative humidity were used, through a cylindrical thermo-hygrograph, located inside the Marfiles Room.

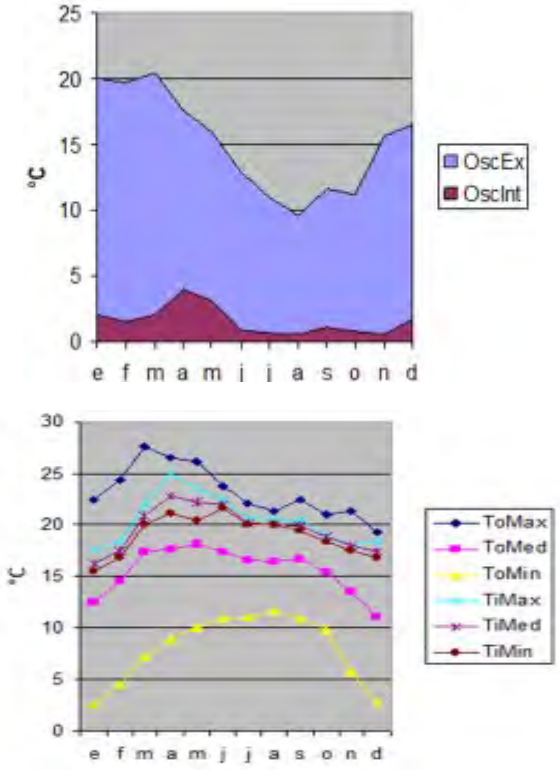

Figure 6: Thermal Oscillation and Indoor and Outdoor Temperatures in Marfiles Room. (Records control for preservation of art objects, property of the Museo Nacional del Virreinato).

As it is a semi-cold climate, the critical period corresponds to winter, so the thermal behaviour of a stone wall facing south and one facing west was analysed considering the thermal properties of the materials used; as can be noticed in the digital model (Ener-habitat program simulation)

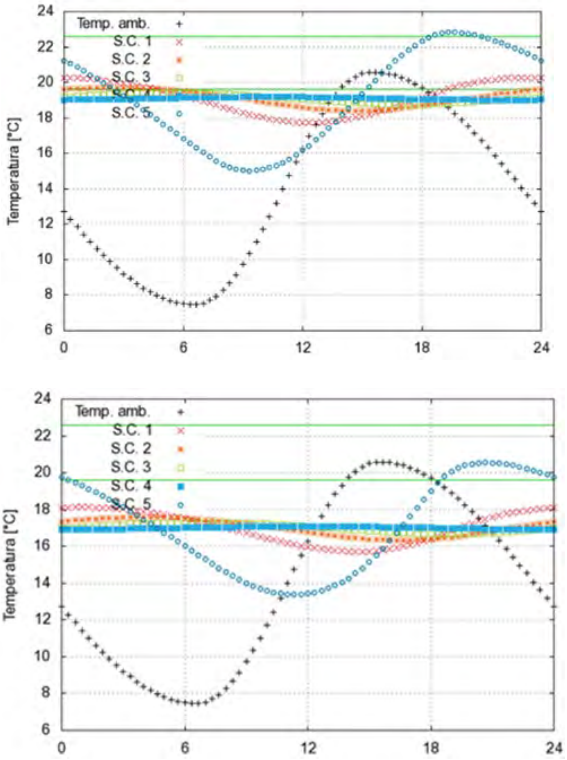

Figure 7: Interior temperature of the walls facing south and west during December. UNAM, et. Al. Ener-habitat, 2009.

In the rainy season humidity increase stabilizes the outside ambient temperature. Inside the premises there is thermal stability, with a reduction of 8°C on the temperature swing. Solar radiation was also used constantly to dry food (met and vegetables) for its preservation to be used year around. This is demonstrated by the large solar dryer located in the orchard.

As a bioclimatic strategy for temperature, humidity, wind and daylighting control, five different *patios* provide a microclimate. Each one of them is different in size, proportion, vegetation and finishes to provide specific conditions and uses. As a complement large open spaces, like the wooden atrium or the bare front plaza of the church, complement the distribution of buildings.

3.2 Solar Dryer

In the orchard the fruits and vegetables were produced as part of the regular diet. These products were preserved for the winter and spring dry seasons by sun drying them. The solar dryer originally had two large masonry columns that supported wooden beams to put plates and meshes with the products to be dried. A radiant clear polished stone floor around this devise reflected sun radiance and increased temperature. A water tank at the base of the columns was part of the system to prevent crawling insects and rodents from accessing the food.

3.3 Natural lighting systems

The intense sun direct radiation in central Mexico is a constant source of heat and light year around. Therefore, it was used by the Jesuits in many different ways to daylight spaces and also to produce remarkable lighting effects, using stucco, golden plated altars and even mirrors to reflect the light.

In the case study, the following systems were found to introduce natural light into the spaces:

- The central courtyard (indirect lighting).
- Vertical openings (windows).
- Horizontal openings (zenithal lighting through skylights and lanterns).
- Multiple reflections (mirrors and shiny surfaces).

Illuminance measurements were made with two Lutron model LX-1108 lux meters at noon in two east facing windows of the second floor of the novice's patio.

Table 1: Instantaneous illuminance at noon in a receded window with sitting bench in two different cells.

Point	Klux	Position of Measure
1	12.4	base of window
2	11.5	base of window

The amount of incident light inside the spaces is abundant and uniform, determined by the shape and location of the opening, the transmittance of glass and the multiple reflections produced in the deeply recessed angular frame of the window and the rest of the interior space.

Protection from the cold night wind on the north side of the buildings was achieved with only small windows in this orientation for lighting. On special spaces, like the library located on the upper floor of the orange trees cloister, there is a single high window that receives the diffuse light from the North.

The thickness of walls and roofs, allowed flared frames to reflect and modulate the entrance of light onto spaces increasing illuminance. This strategy has been particularly designed in each opening, with shapes adapted to the location, orientation and use.

They also considered the selection of materials used indoors for the reflection of daylight such as mirrors or burnished and shiny surfaces, which make lighting systems more efficient inside architectural spaces and produce surprising effects.

3.4 Sundials

The measurement of time was by the solar path, as evidenced by the two clocks located in the kitchen *patio*, one of which is not in operation because it lost its stylus, but the second is currently operating with precision.

The sun was also used to measure time in hours of sunshine for the development of all activities in the complex. The sundials are located on the top of the south facing wall in the kitchen *patio.* From there, all meals, religious services and activities were regulated with sundials and bells. The functioning cycle depended on the use of solar time.

3.5 Water cycle

Water has been and will be the element that determines the possibility of urbanizing a site. For that reason, the Jesuits developed two supply systems.

One of them came from the rainfall on rooftops. The water was captured, conducted, filtered and stored in the two cisterns of the *patio de los aljives*. Then it was carefully used in the services, kitchens and sinks in the kitchen cloister. Finally it was treated through a system located based in the south side of the orchard to finally irrigate vegetables and fruit trees.

Figure 8: Sun dial at the Kitchen Patio

Water —an essential resource for life, food production, personal hygiene and living spaces— was included as part of the design of the slopes of the

roofs as rainfall collecting elements, in the vertices and gargoyles as conduction systems and in the *patios* as filtering and storage mechanisms for rainwater. As mentioned, it was used in kitchens and production areas, but also in cleaning areas such as laundry, sinks and bathrooms.

Once the water was used, it was treated through anaerobic tanks, while an aerobic system was implemented through oxidation fields located in the orchard where the fruit trees underwent the final purification treatment before finally being discharged as runoff into absorption wells located in the low points of the lot.

3.6 Ventilation as Eco-Technology

In the Jesuit school of Tepotzotlán, the wind is used to cool the frigorific for the preservation of food and also at the wine cellar, to keep the wine in optimal conditions.

These spaces are built with massive stone walls and consists of two chambers separated by an arched wall constantly humidified by the water supply system of the kitchens that circulated in an open gutter on top of the wall, humidifying its mass by capillarity and therefore cooling down the spaces.

Table 2: Surface temperature measurements at 15 hrs. in March 21st in La cava (wine cellar) and the Frigorífico (frigorific).

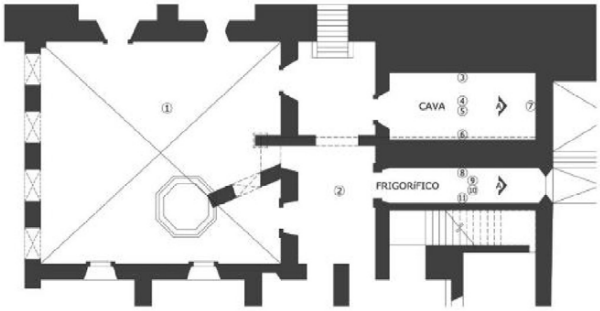

Point	Temperature	Location
1	27	1.2
2	27	1.2
3	16.2	wall
4	15.6	floor
5	16.8	ceiling
6	16.4	wall
7	15	wall
8	16	wall
9	15	floor
10	16	ceiling
11	17	wall

It can be noticed by the measurements taken on a hot spring day (27°C at 15hrs), that the cave and frigorific remain almost 12°C under the outdoor temperature. On average, the cave was at 16.2° and the frigorific was at 15.5°C. Surface temperature measurements were taken with a digital Infrared Thermometer IR; while the ambient temperature was recorded with a climate meter Kestrel 5500.

The design of the frigorific demonstrates the practical application of the scientific knowledge of the time (XVI and XVII centuries) to meet the cooling needs determined by climatic conditions.

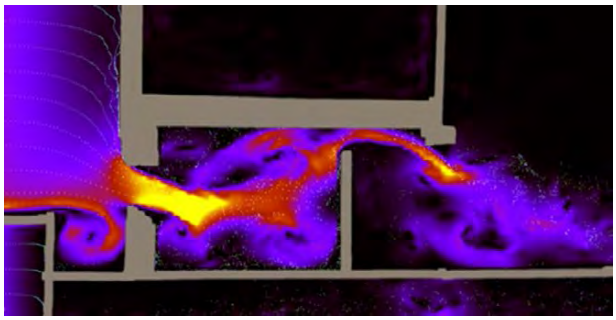

Figure 9: Simulation of wind movements at the frigorific. (WindTunnel Simulator)

Orientation and location of the spaces and the construction of wind-conducting elements, in addition to the massiveness and humidification of the walls generate a remarkable passive cooling effect for the preservation of food and wine.

CONCLUSION

It is remarkable to notice, the variety of strategies, materials and design elements used in the religious architecture of the XVII and XVIII centuries, of which there are abundant samples in different climates and sites of Mexico, that have not been analyzed from a bioclimatic point of view.

Revitalizing the bioclimatic and sustainable behavior of historical building complexes allows us to understand and evaluate the applied design concepts and strategies used to make spaces comfortable, efficient and sustainable.

Through monitoring and digital simulations, we can comprehend their thermal, lighting, and acoustic behavior, in reference to contemporary human well-being parameters.

At the same time, it allows us to think about the work of urban planners and architects of the past and the knowledge that we can implement, modernize and apply in the present for the immediate future in the face of the problems of water pollution, climate change, the use of clean energy, food production and the health of living spaces.

We all need to obtain the ancient knowledge to link the historical constructions with the response that present and future buildings face in the challenges of climate change, waste energy, the use of clean and natural resources, the conscious and responsible use of water, the cycle and disposition of

residues, as well as the well-being and health of the user.

ACKNOWLEDGEMENTS

Research studies for Tepotzotlán have been financed by numerous institutions and individuals, among them the Universidad Autonoma Metropolitana, Unidad Azcapotzalco; the H. Ayuntamiento de Tepotzotlán, the National Museum for the Viceroy Period and the Mexican National Institute of Antropology and History.

REFERENCES

1. UNAM et al. (2009). *Ener-Habitat. Evaluación térmica de la envolvente arquitectónica.* [Online], Available: www.enerhabitat.unam.mx

2. Rahlves, F. (1969). *Catedrales y monasterios de España*. Editorial Juventud, S.A. España.

3. Neri, G. (2015). *Monografía Municipal, Estado de México. H. Ayuntamiento Constitucional de Tepotzotlán.* [Online], Available at: http://www.inafed.gob.mx/work/enciclopedia/EMM15mexico/municipios/15095a.html

4. Meli, R. (2011). *Los conventos mexicanos del siglo XVI: construcción, ingeniería estructural y conservación.* Instituto de Ingeniería, UNAM/Porrúa: Ciudad de México, México.

5. Castorena, G. (2021). *Sustentabilidad en los edificios religiosos del siglo XVII y XVIII en México. Análisis comparativo por bioclima en tres casos de estudio.* UAM: Ciudad de México, México. [Online], Available at: http://zaloamati.azc.uam.mx/handle/11191/7538?show=full

Cultural Continuity and Resilient design: A case of Ainemane, Kodagu, India

VIVEK GOPALAKRISHNA CUCKEMANE, [1] ARULMALAR RAMARAJ, [1]

[1]Sathyabama institute of science and technology, Chennai, India

ABSTRACT: This research paper explores the relationship between cultural continuity and resilient design by examining the case of "Ainemane" as heritage dwellings. Ainemane traditional houses are found in the region of Kodagu in the state of Karnataka, India. As an important cultural heritage, it embodies the past generation's knowledge in design and construction. Amidst climate change, urbanization, and modernization challenges, preserving these heritage dwellings is crucial for their continued existence. This study investigates the inherent resilient features embedded within Ainemane and explores how they can be utilised and adapted to address contemporary challenges. This research aims to uncover the design principles and strategies that make Ainemane resilient through a literature review, field observations, and community interviews. Its findings will underscore the importance of cultural continuity in resilient design and showcase Ainemane dwelling's adaptive qualities. Moreover, the research will investigate the potential integration of modern technologies, materials, and approaches to enhance the resilience of Ainemane without compromising its cultural integrity. The inference of this research will be to enhance understanding of traditional architectural practices and their resilience against modern challenges. It provides architects, planners, and conservationists with insights to incorporate resilient design into Ainemane's preservation for cultural continuity.
KEYWORDS: Cultural heritage, Resilience, Heritage Dwellings, Conservation, Adaptation

1. INTRODUCTION

Resilience in vernacular architecture is a concept that highlights the remarkable adaptability and durability of traditional, locally rooted building designs in the face of various challenges. It is deeply intertwined with a natural understanding of the local environment and climate, resulting in structures that effectively withstand the challenges posed by of their surroundings [1]. These architectural solutions are often crafted from locally available materials and employ construction techniques that have evolved to respond to specific environmental conditions, whether it be extreme heat, heavy rainfall, or seismic activity. This sustainable use of resources not only lessens the environmental impact but also makes vernacular architecture more economically viable for local communities, as it relies on readily available materials and labour.

Beyond environmental considerations, resilience in vernacular architecture extends to cultural and social dimensions [1]. These buildings can adapt to shifting social and cultural needs, allowing them to remain functional and relevant within their communities. This adaptability fosters a strong sense of cultural identity and continuity, reinforcing a community's shared heritage and traditions. Furthermore, vernacular architecture often demonstrates a degree of disaster resistance, as it incorporates proven construction techniques that can minimize damage in the face of natural calamities.

In essence, the resilience of vernacular architecture embodies a holistic approach that values local knowledge, resources, and skills. It allows these buildings to withstand environmental challenges, provide for economic independence, and maintain cultural identity, all while offering a tangible connection to the past and a sustainable path forward for local communities [2].

Cultural continuity in architecture embodies the preservation and expression of a community's cultural heritage through building design. It entails using traditional design elements, materials, and construction techniques while adapting to modern needs, all to maintain a strong link with cultural traditions. Architectural spaces, such as temples and community centres, serve as venues for cultural rituals and events, reinforcing a sense of identity and belonging [2]. This practice ensures that a community's cultural values and architectural heritage continue to thrive in an ever-changing world. In essence, resilient design in vernacular architecture ensures that architectural traditions remain relevant and practical in the face of contemporary challenges while safeguarding cultural continuity by preserving and promoting cultural heritage. Both concepts work hand in hand to create architecture that is not only resilient but also deeply rooted in and reflective of the culture it serves.

The conservation and adaptation of heritage dwellings in the face of contemporary challenges

have become increasingly important. This research paper explores the complex relationship between cultural continuity and resilient design, with a specific focus on Ainemane as heritage dwellings. Ainemane, traditional houses found in the region of Kodagu in the state of Karnataka, India, not only hold architectural significance but also embody cultural heritage and knowledge. However, these invaluable dwellings face climate change, urbanization, and modernisation threats. This study aims to investigate the inherent resilient features of Ainemane and explore their potential adaptation to address current challenges.

1.1 Ainemane: Harmonizing Architecture and Culture in Traditional Dwellings

Ainmane (Fig. 1), a term specific to the Kodava people of the Kodagu district in Karnataka, India, is more than just a traditional architectural style; it is a living embodiment of the Kodava culture and heritage [3]. These houses are distinctive in their construction, reflecting indigenous wisdom and the Kodava way of life. The architectural features are not just functional but also deeply rooted in the community's cultural practices [3].

Figure 1: View of mukkatira ainemane

One of the key architectural aspects of Ainmane is the central courtyard. This courtyard serves as the heart of the house and is surrounded by various rooms and chambers. The thatched roofs, typically made from bamboo, grass, or palm leaves, offer both practicality and symbolism. They regulate indoor temperatures, making the house comfortable, and protecting it from heavy rainfall. The verandas, supported by wooden pillars, contribute to the house's aesthetics and functionality [3].

The cultural significance of Ainmane houses is multi-faceted. Firstly, they are a hub for religious and ancestral rituals. The central courtyard is where offerings and prayers are made to ancestors and deities, strengthening the connection between the house and Kodava spirituality. Additionally, Ainmane houses play a vital role in social and community life. They serve as the focal point for various cultural events and festivals, where the Kodava people come together to celebrate their traditions, exchange stories, and reinforce their sense of community. Ainmane houses also represent an important part of architectural heritage [3]. They reflect indigenous knowledge and craftsmanship, preserving the traditional building techniques and materials specific to the region. The design, layout, and rituals associated with these houses are instrumental in reinforcing the cultural identity of the Kodava community. Owning and maintaining an Ainmane signifies the continuation of a family's heritage, with these houses often passed down through generations. Moreover, Ainmane houses align with the cultural values of economic and environmental adaptability. They make efficient use of locally available materials and traditional construction methods, demonstrating a harmonious coexistence with nature.

In recent years, Ainmane houses have gained recognition as cultural heritage sites and have attracted tourists interested in learning about the Kodava way of life and traditions [4]. This tourism not only contributes to the preservation and promotion of Kodava culture but also highlights the broader importance of Ainmane in the context of India's rich and diverse cultural tapestry [4].

In essence, Ainmane houses are an embodiment of Kodava culture, spirituality, and architectural heritage. They are not just structures; they are symbols of continuity, identity, and resilience, connecting past, present, and future generations of the Kodava community.

1.2 Broader Context

Resilient design and cultural continuity in vernacular architecture are integral components of the broader global discourse on heritage preservation, sustainability, and cultural resilience [5-6]. Acknowledging comparative case studies, theoretical frameworks in anthropology and architecture, and socio-political and economic contexts enriches the understanding of traditional dwellings like Ainemane. Comparative analyses not only illuminate common patterns and unique adaptations but also provide a nuanced understanding of the dynamic relationship between culture, design, and resilience across diverse cultural contexts [6]. Theoretical frameworks, such as cultural ecology and socio-technical systems theory, offer deeper insights into how cultural practices evolve in response to ecological challenges and the socio-cultural dimensions of resilience. Additionally, examining the socio-political and economic context reveals the influence of globalization, tourism, urbanization, and government policies on heritage preservation and adaptation.

2. RESEARCH OBJECTIVES

The objective of this study is to examine the interaction between cultural continuity and resilient design, focusing on Ainemane as heritage dwellings. The specific research objectives are as follows:

a. To explore the architectural design strategies adopted in Ainemane that promote resilience, taking into account the community's cultural heritage and adapting to changing environmental conditions.

b. To identify the challenges and opportunities faced by the community in their efforts to maintain cultural continuity while embracing resilience in today's context.

3. METHODOLOGY

A single-case study methodology in architecture involves a comprehensive analysis of a specific building or public space [7]. The research delves deeply into the chosen case, through triangulation of data. The data collected are through architectural drawings, interviews, site visits, and archival research. The study considers contextual factors, including cultural and environmental influences, and aims to achieve various research goals, from understanding design processes to evaluating a building's impact. This qualitative research approach provides a detailed and holistic exploration of a singular architectural endeavour. In this research methodology, a single case research approach is adopted to achieve a specific set of objectives centred on the comprehensive understanding and documentation of Ainemane, a cultural and architectural heritage site situated in Kodagu. The methodology consists of four phases that are intricately linked, allowing for a thorough investigation.

First, the secondary data collection phase serves as the foundational step, where researchers delve into a wealth of existing knowledge within the domains of architecture and culture. This extensive literature review helps establish the historical context of Ainemane, unravel its cultural significance, and identify elements that have contributed to its resilience over time. This secondary data serves as a crucial backdrop against which subsequent research activities are framed.

Mukkatira Ainemane was chosen as a case example for the study. Visit to Ainemane in Kodagu provides first-hand exposure to the heritage site. During these visits, meticulous observations are made regarding various aspects of Ainemane, including its architectural features, construction techniques, spatial organization, and dynamic interaction with the surrounding environment. This immersive approach allows us to gain deeper insights into the physical aspects and historical elements of the heritage site.

Community engagement is the next vital component of the methodology. This phase involves direct interactions with local communities near Ainemane, heritage practitioners, and subject experts. Through questionnaires, interviews and discussions, the aim is to capture the perspectives and experiences of these stakeholders. The detailed questionnaire was prepared and it covered demographic information, cultural understanding, Ainemane awareness, challenges faced, integration of modern elements, community perspectives, architectural and cultural preservation, and the future outlook. Respondents' opinions on the importance of preserving Ainemane and suggestions for enhancing its resilience were recorded. Additionally, the questionnaire delved into community initiatives, architectural design principles, and the potential role of research in contributing to heritage preservation. A total of 8 respondents (7 male and 1 female) belonging to the Ainemane itself and 6 respondents (4 male and 2 female) from the neighbourhood helped in providing the data through questionnaires. The goal was to obtain a comprehensive understanding of stakeholders' perspectives on Ainemane's cultural and architectural significance in the face of contemporary challenges. The research seeks to understand how Ainemane has remained resilient and culturally significant from the viewpoint of the local community. Moreover, these interactions serve as an opportunity to explore and document the traditional knowledge and practices that have been handed down through generations and have played a role in the continuity.

Finally, the analysis phase brings together all the gathered information and data. The findings from the literature review, on-site observations, and community engagement are integrated, allowing us to identify key principles contributing to Ainemane's resilience. These principles often encompass architectural design, cultural preservation, and sustainable practices. The analysis also explores potential modern interventions that can be introduced to ensure the preservation and promotion of Ainemane while respecting its cultural heritage and historical significance. In addition, this phase underscores the ongoing importance of cultural continuity, emphasizing how the heritage site remains relevant and meaningful in the contemporary context.

Overall, this single case research methodology provides a comprehensive and holistic approach to the study of Ainemane, bridging the realms of history, architecture, culture, and adaptability. By thoughtfully combining secondary data, on-site observations, community engagement, and rigorous analysis, the aim is to make a meaningful contribution to the understanding and preservation of this unique cultural and architectural heritage site in Kodagu.

4. RESEARCH FINDINGS

The research findings offer a comprehensive exploration of the resilient design features inherent in Ainemane dwellings of Kodagu, shedding light on various architectural and construction aspects that contribute to their durability.

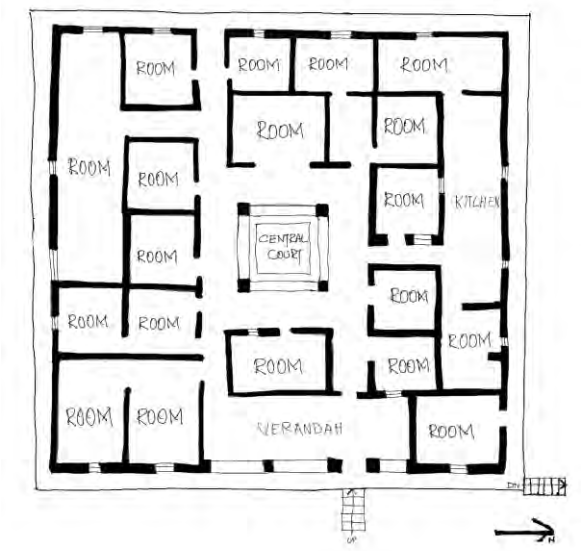

Figure 2: spatial layout sketch of Mukkatira Ainemane

One key aspect is the deliberate use of vernacular materials, such as locally sourced wood and mud, which aligns with vernacular practices and also provides insulation against extreme temperatures, ensuring structural stability over time. The incorporation of climate-responsive architectural features, including sloping roofs with overhangs, manages heavy rainfall efficiently and also prevents water damage, further enhancing the dwellings' resilience against environmental challenges.

The spatial layout (Fig. 2) within Ainemane is highlighted as a crucial component of their resilient design. The central courtyard, serving as a multifunctional space, promotes natural airflow and light, creating a harmonious living environment. Additionally, elevated structures mitigate flood risks, demonstrating an adaptability to the local climate that contributes to both longevity and durability. The study recognizes the role of traditional construction techniques, such as intricately carved wooden pillars and beams, as integral elements that not only reinforce the structural integrity of Ainemane but also carry cultural significance, reflecting the rich heritage of the Kodava community [8].

The research extends its focus beyond the physical attributes of Ainemane to underscore the broader implications of cultural continuity. It emphasizes the importance of preserving the authentic cultural elements of Ainemane, not only for their intrinsic value but also for their role in fostering community identity. The communal aspects of Ainemane, as spaces for cultural activities and rituals, are considered essential for passing down traditions to future generations, thus ensuring the continuity of the Kodava cultural legacy. This consideration becomes crucial in the context of Kodagu, known for its distinct cultural identity encapsulated in unique traditions, language, and customs. Cultural continuity in Kodagu involves not just the physical preservation of structures like Ainemane but also the meticulous continuation of traditional ceremonies, rituals, and social practices, emphasizing the living, emphasizing nature of Kodava culture [2-8].

Figure 3: View of central courtyard of mukkatira ainemane

The architectural features of Ainemane are elucidated, providing a detailed description of their layout, materials, and distinctive elements. Including traditional features like Kanni Kombare (dedicated dwelling space for the spirit of ancestors) and Nellakki Nadubade(central hall) (Fig. 3) adds layers to the architectural significance, reflecting the deep-rooted cultural practices embedded in the design of Ainemane houses. The intricate carvings, depicting cultural motifs such as elephants, horses, and geometric patterns, further emphasize the unique identity of these traditional Kodava houses.

The research transitions seamlessly into a captivating case study of Mukkatira Ainemane, illustrating how these resilient design principles and cultural continuity manifest in a specific historical context. Mukkatira ainemane serves as a living testament to Kodava heritage, with approximately 400 members rooted in the village of Kunjalageri. The meticulous record of the family's cultural continuity, as evidenced by the "Annayya, 1718 - 2000" book and a ten-generation family tree, provides a tangible record of the Mukkatira family's enduring legacy.

The architectural heritage of Mukkatira's Ainemane, built in 1718, is detailed with a focus on its distinctive features, including coiled elephant trunk carvings and lotuses adorning wooden pillars. The recent renovations, aimed at preserving the original structure while adapting to contemporary needs, exemplify the community's commitment to cultural resilience. The spiritual connections and rituals centred on Mukkatira's family deity, Mavishnu, add a spiritual dimension to the discussion, highlighting the intertwining of cultural and religious practices within the architectural framework of Ainemane [2-8].

The adaptive measures undertaken by the Mukkatira family, such as the construction of a

temple and the integration of electricity, showcase the community's proactive approach to modern challenges while maintaining the authenticity of their cultural practices. This adaptive resilience is further demonstrated through the flexibility in cultural practices, as seen in the shift of festival dates to align with practical considerations, emphasizing the community's ability to adapt without compromising core cultural values.

Overall, Mukkatira Ainemane emerges not merely as a physical structure but as a living chronicle of Kodava heritage. Through a nuanced exploration of resilient design, cultural continuity, and adaptive practices, the research underscores the enduring legacy of Kodava identity preserved in the foundations of Ainemane houses laid nearly three centuries ago. The study provides a rich and multifaceted understanding of how these traditional dwellings encapsulate the essence of Kodava culture, transcending time and preserving the cultural practices for generations to come [2-8].

5. DISCUSSIONS AND CONCLUSIONS

In the face of contemporary challenges posed by climate change, urbanization, and modernization, the research on the relationship between cultural continuity and resilient design, with a specific focus on the heritage dwellings of Ainemane in Kodagu, unfolds a narrative of profound significance. The findings of this study illuminate the intricate balance between preserving cultural heritage and embracing resilience, exemplified by the resilient design features inherent in Ainemane.

The architectural and cultural richness of Ainemane, as seen through the lens of the Kodava community, transcends mere physical structures. These traditional houses serve as living embodiments of Kodava culture, spirituality, and architectural heritage. The central courtyard, thatched roofs, wooden pillars, and intricate carvings are not just functional elements; they are symbols of continuity, identity, and resilience, connecting past, present, and future generations of the Kodava community [2-8].

The study's methodology, employing a Single Case Research approach, allowed for a comprehensive exploration of Ainemane. Through a combination of literature review, on-site observations, and community engagement, the research delved deep into the historical, architectural, and cultural dimensions of these heritage dwellings. The methodology facilitated the identification of key design principles and strategies that contribute to the resilience of Ainemane, offering valuable insights for responsible conservation. The findings underscore the importance of cultural continuity in the preservation and adaptation of heritage dwellings. Ainemane houses not only withstand environmental challenges and natural disasters but also foster cultural identity and community resilience [9]. The integration of modern technologies, without compromising cultural integrity, emerges as a potential avenue to enhance the resilience of Ainemane in the face of evolving challenges.

In essence, the research contributes to a holistic understanding of traditional architectural practices and their resilience. It provides a roadmap for the integration of resilient design principles into the preservation of cultural heritage, offering a bridge between the past and the future. The case study of Mukkatira further amplifies these themes, showcasing how a thriving okka (Family) in Kunjalageri has preserved its cultural identity through architectural heritage, spiritual connections, adaptive practices, and a commitment to continuity.

As heritage dwellings like Ainemane face the dual challenges of preservation and adaptation, this research serves as a road guiding the way forward. By recognizing the symbiotic relationship between cultural continuity and resilient design, architects, planners, and communities can work collaboratively to ensure the continued existence, adaptability, and relevance of these invaluable cultural treasures. In doing so, it not only honours the past but also creates a resilient path toward a culturally rich and sustainable future.

REFERENCES

1. Marilena Vecco. (2010). a definition of cultural heritage: From the tangible to the intangible. Journal of Cultural Heritage, 11(3), 321–324.

2. Saha, K., & Chowdhury, S. J. (2021). A Study of Vernacular Architecture and Settlement of Diaspora 'Manipuri' Community In Bangladesh (2021010243). Preprints.

4. Owsanecki, P. F. (1985). "Kanni-Mangala": A Microcosm of Coorg Identity. Sociological Bulletin, 34(1–2), 95–147.

5. Jeleński, T. (2018). Practices of Built Heritage Post-Disaster Reconstruction for Resilient Cities. Buildings, 8(4), 53. https://doi.org/10.3390/buildings8040053

6. Wu, J.-Y., & Chen, L.-C. (2023). Traditional Indigenous Ecological Knowledge to Enhance Community-Based Disaster Resilience: Taiwan Mountain Area. Natural Hazards Review, 24(1), 05022014. https://doi.org/10.1061/NHREFO.NHENG-1673

7. Lazar, J., Feng, J. H., & Hochheiser, H. (2017). Case studies. In Research Methods in Human Computer Interaction (pp. 153–185). Elsevier. https://doi.org/10.1016/B978-0-12-805390-4.00007-8

8. Somaya, B., Mascarenhas, P. V., Premnath, K. G., & Dyan Belliappa, N. N. (2005). *Silent sentinels: Traditional architecture of Coorg*. Hecar Foundation.

9. Sujatha, D. N. C. (2017). Archaeology on Coorg with Special Reference to Megaliths. 23.

10. Madhusoodhanan, S., Nair, A. S., Azmal, M., Rani, N., & Jain, R. (n.d.). Disaster Analysis of Kodagu District using Geomatics Technology. International Journal of Engineering Research, 8(06).

11. Li, Z., Diao, J., Lu, S., Tao, C., & Krauth, J. (2022). Exploring a Sustainable Approach to Vernacular Dwelling Spaces with a Multiple Evidence Base Method: A Case Study of the Bai People's Courtyard Houses in China. Sustainability, 14(7), 3856.

12. Vakha, M. (2016). Land use land cover mapping using Geo-informatics of Kodagu District, Karnataka. 7(1).

13. Alavi, S. F., & Tanaka, T. (2023). Analyzing the Role of Identity Elements and Features of Housing in Historical and Modern Architecture in Shaping Architectural Identity: The Case of Herat City. Architecture, 3(3), 548–577. https://doi.org/10.3390/architecture3030030
14. Chen, T.-L., & Cheng, H.-W. (2020). Applying traditional knowledge to resilience in coastal rural villages. International Journal of Disaster Risk Reduction, 47, 101564. https://doi.org/10.1016/j.ijdrr.2020.101564
15. Choudhary, P. (2016). Vernacular Built Environments in India. In Urban Disasters and Resilience in Asia (pp. 269–286). Elsevier. https://doi.org/10.1016/B978-0-12-802169-9.00017-3
16. Christians, C. G. (2007). Cultural Continuity as an Ethical Imperative. Qualitative Inquiry, 13(3), 437–444. https://doi.org/10.1177/1077800406297664
17. Dostoğlu, N. (2021). Re-viewing the role of culture in architecture for sustainable development. Journal of Design for Resilience in Architecture and Planning, 2(2), 157–169. https://doi.org/10.47818/DRArch.2021.v2i2017
18. Ekhaese, E. N., Evbuoma, I. K., & George, T. O. (2021). Socio-Cultural Resilience to Domestic Space Change, the Benin Traditional City Experience, Nigeria. IOP Conference Series: Earth and Environmental Science, 665(1), 012016. https://doi.org/10.1088/1755-1315/665/1/012016
19. Fatiguso, F., De Fino, M., Cantatore, E., & Caponio, V. (2017). Resilience of Historic Built Environments: Inherent Qualities and Potential Strategies. Procedia Engineering, 180, 1024–1033. https://doi.org/10.1016/j.proeng.2017.04.262
20. Ghorbani, M., Eskandari-Damaneh, H., Cotton, M., Ghoochani, O. M., & Borji, M. (2021). Harnessing indigenous knowledge for climate change-resilient water management – lessons from an ethnographic case study in Iran. Climate and Development, 13(9), 766–779. https://doi.org/10.1080/17565529.2020.1841601
21. Lahoud, A. L. (2008). The role of cultural (architecture) factors in forging identity. National Identities, 10(4), 389–398. https://doi.org/10.1080/14608940802518963
22. Mahgoub, Y. (2007). Architecture and the expression of cultural identity in Kuwait. The Journal of Architecture, 12(2), 165–182. https://doi.org/10.1080/13602360701363486
23. Utami, L. A., Lechner, A. M., Permanasari, E., Purwandaru, P., & Ardianto, D. T. (2022). Participatory Learning and Co-Design for Sustainable Rural Living, Supporting the Revival of Indigenous Values and Community Resiliency in Sabrang Village, Indonesia. Land, 11(9), 1597. https://doi.org/10.3390/land11091597
24. Zhang, H., & Nakagawa, H. (2018). Validation of indigenous knowledge for disaster resilience against river flooding and bank erosion. In Science and Technology in Disaster Risk Reduction in Asia (pp. 57–76). Elsevier. https://doi.org/10.1016/B978-0-12-812711-7.00005-5

PLEA 2024 WROCŁAW
(Re)thinking Resilience

The Environmental Conditions of the FAUUSP Building:
A case-study from the Brazilian Modernism in the city of São Paulo

JOANA C. S. GONÇALVES[1]; ROBERTA C. KRONKA MULFARTH[2]; RANNY X. L. MICHALSKI[2]; ANDRE SATO[2]; CRISTIANE SATO[2]

[1] Architectural Association School of Architecture & Bartlett School of Architecture - UCL, London.
[2] Faculty of Architecture and Urbanism of the University of São Paulo (FAUUSP), São Paulo, Brazil.

ABSTRACT: The Vilanova Artigas Building, the main building of the Faculty of Architecture and Urbanism of the University of São Paulo, FAUUSP, was opened in 1969 in the University City. The purity of the geometry and the strong presence of the concrete structure made this building a landmark of the Paulista School of Architecture, a branch of the Brazilian Modern Movement that followed the principles of Brutalism. An inward-looking aspect was created by three features: the multi-story central void named Salão Caramelo, the blind facades of the suspended concrete block and the continuous single roof of skylights. Studios and classrooms are located at the top floors, in the blind concrete rectangular box. The reasonably large illuminating roof area, and the consequent penetration of solar radiation, placed in the context of the subtropical climate of São Paulo, raises a question about the efficiency of the ventilation strategy involving the skylights and the atrium. The replacement of the skylights was part of the roof renovation completed in 2014. This paper presents the outcomes of empirical studies in the FAUUSP building that examined its current environmental conditions, post the roof refurbishment. The main outcome of the roof refurbishment was a pleasant daylight environment, cutting down the glare, however, thermal discomfort was improved but not eliminated.
KEY WORDS: Bioclimatic Modernism; Sub-Tropical Climate; Thermal Comfort; Daylight; Fieldwork.

1. INTRODUCTION

The building of the Faculty of Architecture and Urbanism of the University of São Paulo, FAUUSP – named Vilanova Artigas building (1969), located in the campus of the São Paulo University, is an expression of the geometric purity and the strong presence of the concrete structure that marked the Paulista School of Architecture, formed after the principles of Brutalism [7], (Fig.1). The building was listed as cultural heritage in 1982. The architectural concept highlights an inward-looking building, created by three features: the multi-story central void named Salão Caramelo, the blind facades of the suspended concrete block and the continuous roof of skylights, which together with the central void, distribute daylight and ventilation in the interior and enhance internal visual communication (Fig.2). In the words of Vilanova Artigas: "*The FAU building is a fluid, integrated, somatic space. The person does not know if s/he is on the first, second or third floor*", reinforcing the building's visual and spatial integration as one of the main design premises [7].

The approximately 40% illuminating roof area, and the consequent exposure to solar radiation, placed in the context of the subtropical climate of São Paulo, immediately raises question about the efficiency of the ventilation strategy (involving the central atrium and openings of the skylights), in the warmer days of the year, as well as about the risk of glare, particularly problematic in the studios and classrooms.

Over the years, the remaining spaces directly under the roof suffered a significant loss of daylight because of the natural degradation of the fiberglass. The replacement of the original skylights was part of the roof renovation completed in 2014, respecting the restrictions of the listed building [6]. For this reason, the area of transparency was maintained, but the material and the transmittance of the skylights were changed, as well as the distance between them and the roof structure, to increment airflow rates. Aiming to improve thermal and visual comfort across the various spaces under the roof, the objective was that the incident global solar radiation on the roof was admitted in the interior as diffused light only, without the direct component of sun rays [8].

Figures 1: External view of the FAUUSP building in the University City – the Faculty of Architecture and Urbanism of the University of Sao Paulo. Figure 2: View of the atrium and the surrounding internal spaces.

Despite the significant transparency roof area, were the changes in the design and specification of the skylights sufficient to create the acceptable environmental conditions, not achieved in the original project? This paper presents the outcomes of empirical studies of the FAUUSP building that examined its current environmental conditions, post the roof refurbishment, including measurements in loco and a detailed survey with the occupants. This

environmental assessment is part of a case-study series, of buildings from the Brazilian Modern Architecture in Sao Paulo (between 1930a and 1960s), which have been published in the previous PLEA Conferences (2018, 2020 and 2022) [5, 7 & 8].

2. ARCHITECTURE AND ENVIRONMENT

The overarching roof is made of a concrete waffled structure of 960 squared skylights of 2.75 by 2.75 metres base, originally made of transparent fibreglass components, that brings the studios, classrooms, circulation areas, and the central atrium under one single horizontal plan (Figs.3 & 4). Measuring 36 metres long, 19 metres wide and 15 metres high, the atrium named Salão Caramelo (Caramel Room, because of the colour of the epoxy floor) was conceived as an internal square, a multipurpose area integrated with the exterior and animated by the surrounding internal activities, and a place from where anyone can walk straight into the building (Fig. 5). This multistorey space plays a central role in the spatial experience through the building, providing the opportunity to contemplate the large illuminating roof, a kind of "delight of natural light from within," whilst making visible all the main spaces.

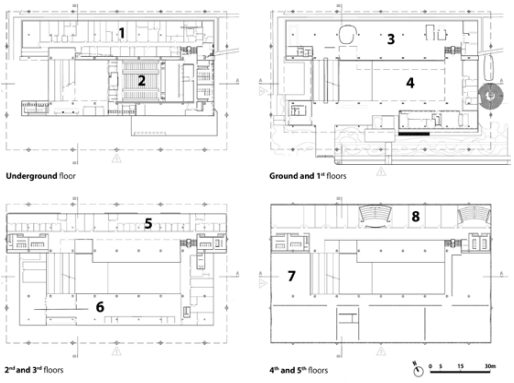

Figure 3: Floor plans of the Vilanova Artigas building, with the six half-levels in four plans: Underground level (1) workshop/laboratory spaces and (2) auditorium; Ground and 1st floor with (3) "museum" and (4) Salão Caramelo; 2nd and 3rd floors with (5) departments, interdepartmental studio and (6) library; 4th and 5th floors with (7) studios and (8) classrooms.

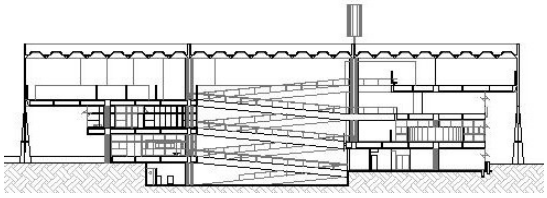

Figure 4: Cross section of the FAUUSP building showing at the top-level studio space on the left and classroom on the right.

Studios and classrooms are located at the top floors, in the blind concrete rectangular box (Figs. 6 & 7). The three different size classrooms (59, 87,5 and 174 m^2, approximately) are positioned on the last floor along the northeast side of the building, and the five studios (varying between 483 and 563 m^2, approximately) are half a level below, along the southwest side. With no side fenestrations, daylight in the studios and classrooms is obtained exclusively through the skylights, originally of transparent fibreglass, detached from the structure to allow air to flow out. The high ceilings in both the classrooms (3.65 metres) and studios (5 metres), combined with the homogeneous distribution of modular skylights, were idealised to offer an even distribution of top natural light. The trapezoidal prismatic form of the skylight has a key role in the distribution of daylight, by reflecting the incoming diffuse radiation from the horizontal square openings. As a result, despite the 16% horizontal transparency area, the internal visual perception of the roof is one of an entire illuminating surface.

Figure 5: Overview of Salão Caramelo, showing the overarching roof with the field of skylights and the vision communication among the internal spaces below it, qualified by daylight.

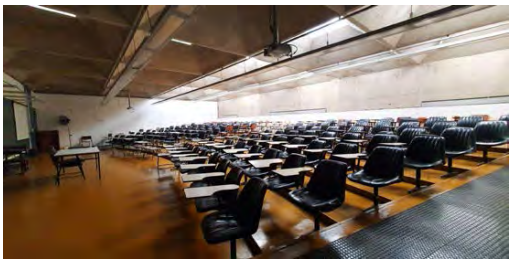

Figure 6: Classroom with daylight reintroduced in 2015.

Figure 7: Studio spaces with daylight reintroduced in 2015.

3. FIELDWORK

A set of measurements in situ of daylight, thermal and acoustic conditions targeted the classrooms and studios (the key learning spaces of the building) and the floor level of the atrium, in order to assess its role as a transitional environmental zone. The measurements of daylight and thermal conditions were taken in studio located in the middle of the plan (Studio 3) with the objective of seeing mainly the

environmental influence of the roof, whilst for the classroom, the choice was the northeast room, which receives the highest amount of impinging solar radiation from walls during the peak occupancy times (from early morning to mid-day), in addition to solar gains from the roof. In the classroom, daylight measurements were taken in two points, to capture the two daylighting zones created by the different transmittance of the skylights (20% under the seating area and 7% alongside the drawing wall). For the acoustic's assessment, the interest was in the most populated spaces, being the areas occupied by the first-year students (Classroom 801 and Studio 1) and the Salão Caramelo (Fig. 8). Sound levels were measured simultaneously in the three environments over two different days: during the school term and during the students' holidays. Reverberation time measurements were also carried out in Classroom 801. All measurements were taken during the summer period of 2020. In addition, a survey about the occupants' perception of the buildings' environmental condition was also conducted.

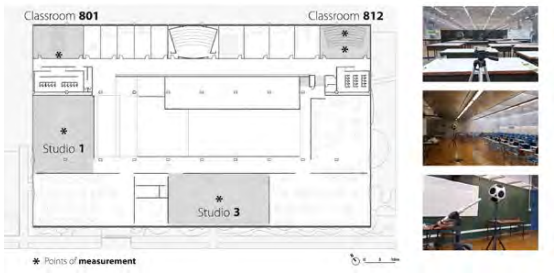

Figure 8: Floorplan of the two half levels of the studios and the classrooms in the FAUUSP building, with the indication of the points of measurement in the classrooms (801 and 812), studios (1 and 3) and atrium.

3.1. Thermal response

The measurements in the three spaces showed a trend of air temperatures with oscillations similar to the external environment, with the conditions in the classroom being the closest to the outdoors during the day, followed by the studio a bit below. On a clear day, the maximum air temperature in the classroom was almost 30 °C, approximately 1.5 °C below the peak outdoor temperature, still above the limit of the adopted comfort zone, ASHRAE 55 [3], by almost 2 °C. At the same time, temperatures in the studio remained around 29 °C. In the Salão Caramelo, the conditions were significantly milder with figures around 27 °C at peak, 4 °C below the external and well within the comfort zone. The significantly cooler conditions in the lower level of the atrium (at useful height, 1.2 metres near the ground) are related to the volume of the space in which the incoming solar radiation is dissipated, coupled with the proximity of the measurement position to permanently shaded concrete surfaces (floor and walls), away from the skylights and the solar radiation.

The comparative higher temperatures in the classroom and the studio reflect the impact of the solar radiation coming from the roof, coupled with the limited efficacy of natural ventilation. Between classroom and studio, the slightly better response of the latter during daytime is explained by the higher volume and the fact that this space is opened to the central void. During night-time, the pattern among spaces is inverted and the temperatures in the atrium are closer to the outside (1 °C higher), posing a notorious influence on the studio space, where the temperatures oscillate around 2 °C higher than the outside. In the classroom, the temperatures rise to 6 °C above the outside. Both the Salão Caramelo and the studio are more coupled to the outside (given the mixture of air volumes) and, therefore, they cool down quickly during the night, but the classroom does not.

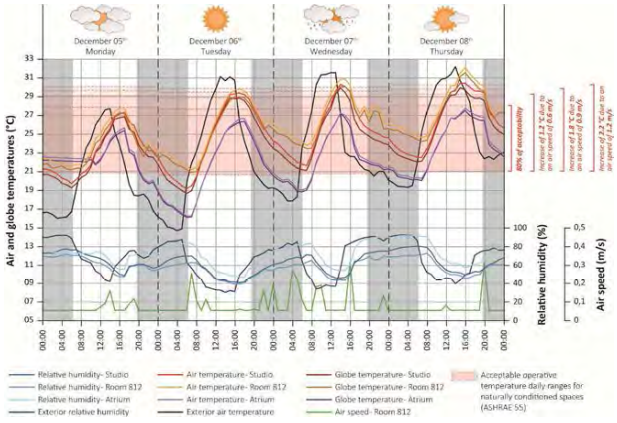

Figure 9: Thermal variables measured in Classroom 812, Studio 3 and Salão Caramelo, compared against external temperatures, between the 5th and 8th December of 2018. The upper limits of the comfort zone correspond to different average air-speeds (standard/up to 0.3 m/s resulting in approximately 28 °C of operative temperature for this week; 0.6 m/s - increase of 1.2 °C, reaching 29.2 °C; 0.9 m/s - increase of 1.8 °C, reaching 29.8 °C and 1.2 m/s - increase of 2.2 °C, reaching 30.2 °C), according to the thermal comfort model proposed by ASHRAE 55.

Despite the weight of the concrete structure and panels exposed to the interior, the relationship between the high thermal capacity of the materiality and the volume of the internal spaces resulted in low thermal inertia across the building, meaning not enough thermal inertia to create a heat sink and a consequent better thermal stability, in other words, less oscillation between minimum and maximum temperatures. Comparing the classroom and the studio, the thermal inertia is even lower in the latter because of the significantly higher volume, coupled with the opening to the atrium, keeping temperatures closer to the outside. On the other hand, in the classrooms, the air changes seemed not to be enough to remove the heat gains from solar radiation and occupation to keep the temperatures at or below the outdoor figures.

As shown in Figure 9, if higher levels of air movement were achieved, the upper limit of the comfort zone could be increased just above the mark of 30 °C, moving from approximately 28 °C to 29.2 °C (when air movement is at 0.6 m/s), getting as high as 30.2 °C (when at air movement is at 1.2 m/s). This means that, for the period of the measurements, discomfort because of high temperatures would only happen for a few hours in the afternoon of the warmest day, when external temperatures are above 31 °C. According to the adopted thermal comfort model, also known as *adaptive model*, an increase of up to 31 °C in the comfort band is possible with a reduction of the insulation resultant from clothing, known as clo level, from the standard 1.0 to 0.5, the equivalent to light clothes appropriate for warm conditions. In this case, the conditions in the studio would be within the comfort zone during the period of the measurements, and the classroom would remain uncomfortable in the afternoon. It should be noted that light clothes are a common practice among the occupants of many of the buildings in the University of São Paulo, but the reality is that the low records of airspeed aggravate the thermal sensation.

3.2. Daylight

The lighting conditions in the studios and classrooms were assessed through measurements in situ in two week and two weekend days, being one day of partially cloudy and another day of clear sky conditions (Fig. 10).

During the weekend days (March 16th and 17th), illuminance levels were slightly higher in the studios than in the classrooms. Although the skylights in the classrooms are closer to the work plan height, daylight in the studios is affected by a proportionally broader roof area, given the spatial openness of this part of the building. On the partially overcast day (March 16th), illuminance levels in the studio varied approximately between 870 lux at 8 am and 1,200 lux at 12 am (peak of sky illuminance), whilst in the classroom (under the sitting area of clear skylights), the values vary between 700 and 1.000 lux, when external availability was between 15.500 lux and 39.000 lux at the same times.

On the predominantly clear sky day (March 17th), the morning was overcast (with 6.800 lux outside), resulting in 270 lux in the studio and 230 lux in the classroom. At 12 am, daylight in the studio rose to almost 3.000 lux and in the classroom to 2.500 lux (when outside illuminance levels superseded 85.000 lux). During these two days, the levels under the darker area of the classroom, close to the drawing board, oscillated between 10 and 40 lux only, keeping the necessary low levels for the functioning of the room.

These measurements of the contribution of daylight, without the use of artificial light, proved that both the studios and the classrooms have sufficient daylight conditions on the work plan, not only under clear, but also potentially under overcast conditions, confirming the positive impact of the translucent skylights.

Overall, the contribution of daylight is significant in the main study spaces and exceeds the contribution of artificial lighting by a large margin, particularly in periods of clear sky, resulting in a range between 250 and 3.000 lux. Looking beyond the quantitative performance indicators, the measurements of luminosity depicted a clear trend of variations in internal lighting levels in the classroom and studio spaces, following the variability of external illuminance levels. Such variations are helpful to establish a positive sensorial experience, in which the occupants perceive the changes in the climate and feel connected with the outdoor environment, experiencing a psychological sense of time.

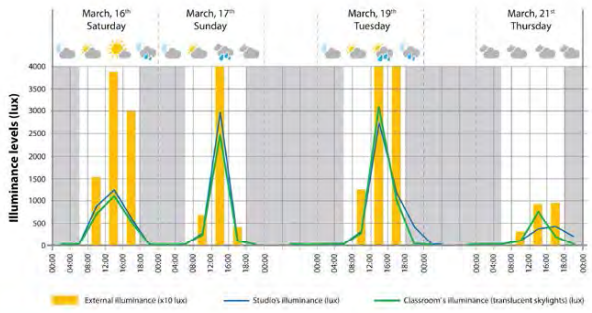

Figure 10: Illuminance levels (lux) measured in the Classroom 812 and Studio 3 on four days in March 2019: upper left corner, March 16th (Saturday); upper right corner, March 17th (Sunday); bottom left, March 19th (Tuesday); and lower right, March 21st (Thursday).

In the morning of the weekdays (March 19th and 21st), the difference between studio and classroom is inverted and slightly higher levels are found in the classroom, given the use of artificial light when the same is occupied. During the week, on the partially clear day (March 19th), it is interesting to see the consistent increase and decrease of lighting levels because of the sum of daylight and artificial light in both spaces, varying from approximately 500 lux around 8am (when artificial lights are switched on) to around 3.000 lux between 12am and 1pm, surpassing by a great margin the recommendations (when external levels exceeded 75.000 lux). After 6pm, the single contribution of artificial light becomes evident. On the totally overcast day (March 21st), the sum of daylight and artificial light result in levels between 500 and 1.000 lux in the morning period, once more showing the excessive and unnecessary addition of artificial light, which becomes useful in the afternoon, when total levels drop to or below 500 lux in both spaces. Hence, the use of artificial light increases the illuminance levels unnecessarily for most of the time.

3.3. Acoustic

Sound pressure levels were measured simultaneously in the three spaces throughout one entire typical academic weekday. As expected, in the *Salão Caramelo* and in the studio similar the acoustic behaviour was similar, both reaching 59dB, showing that these areas are acoustically connected. In the classroom, during occupied hours, LAeq was 59 dB. In addition, the reverberation were significantly higher than the recommended, given the significantly large volume of the room and its finishing surface materials of poor sound absorption. The measured sound levels were compared with the reference values for sound assessment of indoor environments in buildings, for different purposes of use, established by the Brazilian ABNT 10152 standard [1]. According to the standard, the L_{Aeq} reference value recommended for classrooms is 35 dB and for circulation spaces, 50 dB. Despite its multifunctional aspect, Salão Caramelo can be considered a circulation space, and the studios can be considered classrooms, for the purpose of this performance assessment. As a result, sound levels found in the three spaces were proved to be above national recommended values. In reality, the sound levels in the studios are more appropriate for a circulation space than a teaching environment.

It can be said the Vilanova Artigas thought about sound when positioning the classrooms and studios far from the outside, on the top level of the building, as if protected from the social sphere, with the classrooms separated from the rest of the building by walls with doors. However, the conception of the large atrium connecting all the environments, together with large volumes and materials that reflect the sound, ended up affecting the acoustic quality of the building as a whole.

In addition to adequate sound levels, teaching spaces need isolation from external noise and adequate reverberation, being this the key parameter for describing speech intelligibility. For this reason, the reverberation time of the classroom 801 was also measured and values are presented in octave frequency bands from 125 Hz to 8 kHz (Fig. 11). The revealed reverberation times were significantly higher than those recommended (from 0.6 to 1 second for the room volume), [2]. This poor result was expected, considering the significantly large volume of the room and its finishing surface materials, in panels of bare fibre cement and concrete floors (common in the brutalist architecture), of little sound absorption. The combination of high volume and low sound absorption is responsible for sound reverberation, allowing the sound energy of the speech to reverberate for a long time in the environment.

In summary, the evaluation in situ showed that both sound levels and reverberation times exceeded the recommended limits, revealing a delicate condition of acoustic comfort in the classrooms and studios of the building. High sound levels, when combined with high reverberation times, have a worse impact on the acoustic quality of the environments. In other words, neither of the spaces are acoustically suitable for their intended activities. Classroom 801 had the lowest sound levels, because it is a closed space, however, the levels found in situ were still not ideal for study tasks. Furthermore, its high reverberation time leads to difficulties in comprehending speech, and, consequently, hindering the learning process. This also compromises the vocal health of speakers in general, who need to raise their voice intensity to be understood.

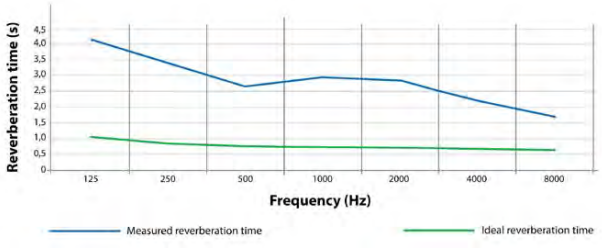

Figure 11: Reverberation time measured in Classroom 801 compared against ideal values for its use and volume, in octave frequency bands.

3.4. Occupants' perception

The study of the perception of the environmental conditions in the Vilanova Artigas building was carried out by means of a survey with students, focused on the studios and classrooms, complemented by an initial general view of the building as a whole. The responses convey a rather positive satisfaction of the occupants with the building, as approximately 70% of those interviewed classified it as "excellent", "satisfactory", which can be mainly related to the strong visual communication among the internal spaces (Fig. 12). Looking at the questions regarding the comfort conditions, more specifically, a remarkably positive satisfaction followed with the size of the spaces (100% positive) and the lighting conditions. On the other hand, thermal and acoustic comfort were taken more critically.

Regarding the studios, the good evaluation of the lighting conditions surpasses that of general satisfaction. Visual comfort is rated "satisfactory" and "excellent" by almost 90% of those who have good overall satisfaction with the building, being at the positive side of the qualitative assessment by more than 60% of those who do not have a good general rating. On the other hand, concerning thermal, the percentage of great dissatisfaction rises from 20% to more than 70% for those who do not appreciate the building. Even among those who give a good assessment of the building, thermal comfort is "not satisfactory" for almost 75% of respondents. The perception about the acoustic environment is very similar to that of the thermal. Approximately 70% of those who give a good assessment of the building still

rate it as “not satisfactory” or “poor”. From those who are not satisfied with the building in general, more than 80% rated the acoustic comfort negatively, in a studio or in a classroom.

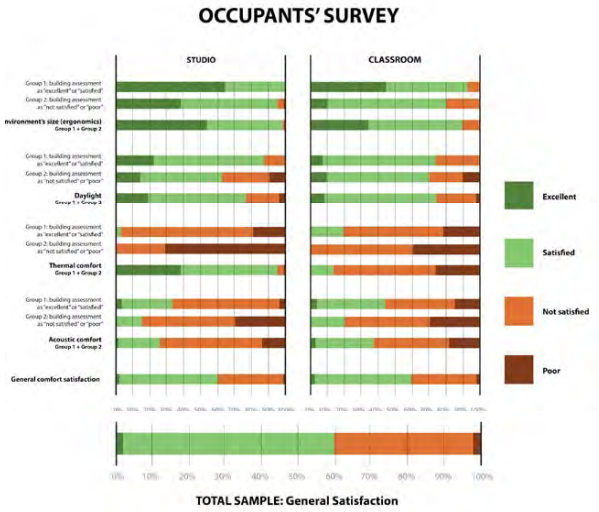

Figure 12: Results from the occupants’ survey about their general perception of the FAUUSP building and its specific environmental conditions in the studios and classrooms.

The perception about the classrooms are slightly better in terms of thermal and acoustic comfort, as well as lighting conditions than in the studios. The assessment of visual comfort is positive for approximately 75% of respondents. Regarding thermal, even for those who give a satisfactory assessment of the building, comfort is rated as “not satisfied” or “poor” for 80% of them. This negative assessment of thermal comfort rises to 100% for those who do not have a good general opinion of the building. Moving on to acoustics, the result is better, but still 55% of those who appreciate the building evaluate acoustic comfort as rather dissatisfactory. This percentage rises to 80% among those who do not appreciate the building in general.

4. CONCLUSION

The decision of opening the roof of the Vilanova Artigas building (with 16% of top transparency area) challenged the principles of environmental design applicable to the subtropical climate of São Paulo, where shading is key for good thermal and daylight conditions. Through the measurements in situ and the analytical work it was seen that roof exposure to solar radiation results in a direct and close relationship between external and internal environmental conditions. Such exposure proved to work for the daylight environment, with the translucent skylights brought in by the refurbishment of 2015, but still imposes clear limitations to thermal comfort, despite the predicted stack effect, mainly in the warmer days of the year.

The main outcome of the roof refurbishment was a pleasant daylight environment, cutting down the glare caused by the original transparent roof. By creating diffused daylight, the thermal discomfort caused by the occupants’ exposure to direct solar radiation was also eliminated. Even with the occurrence of hours of thermal discomfort in the most extreme periods, the renovation of the roof led to a significant improvement in the lighting and thermal conditions in the spaces of the FAUUSP Building and the rediscovery of the look of the remarkable roof structure.

ACKNOWLEDGEMENTS

Thanks to FAPESP, CNPq and CAPES for supporting this research. Thanks to the Directorships of FAUUSP for the support to the empirical studies in the building.

REFERENCES

1. ABNT (2017). ABNT NBR 10152: Acústica: Níveis de pressão sonora em ambientes internos a edificações. RJ.
2. ABNT (1992). ABNT NBR 12179: Tratamento acústico em recintos fechados. RJ.
3. ASHRAE (2017). ASHRAE 55-2017: Thermal Environmental Conditions for Human Occupancy.
4. Barossi, A. C. (2016). O edifício da FAU-USP de Vilanova Artigas. Editora da Cidade.
5. Gonçalves, J. C. S.; *et* al (2018). The Thermal Environment in High-Density Tall Building from the Brazilian Bioclimatic Modernism. *PLEA 2018*. Hong Kong.
6. Pinheiro, B. et al (2017). Keeping It Modern. Gety Institute.
7. Michalski, R. N. *et* al (2022). The case-study of the Sul American Bank building (1966). In: PLEA 2022, Santiago.
8. Mulfarth, R. C. K. *et* al (2020). The Potential of Passive Design for Offices in the City of São Paulo (1963). *PLEA 2020*, A Coruna.
9. Romero, M. de A. (2022). Edifício da FAUUSP: o restauro da arquitetura moderna. EDUSP.

3.5. Building resilience with innovation and technology (e.g., innovative materials and sustainable technologies)

PLEA 2024 WROCŁAW
(Re)thinking Resilience

Developing Coloured Photonic Material To Counteract Urban Overheating

HASSAN SAEED KHAN[1,2], MAT SANTAMOURIS[2], RICCARDO PAOLINI[2], OLIVIA JULIA[3], CAMILA CORREIA TELES[2], SHAMILA HADDAD[2], JIANXIU WEN[2], SAMIRA GARSHASBI[2], DJORDJE KRAJCIC[4], GIANLUCA RANZI[4], ALEX SOERIYADI[5], JAMES WEBB[5]

[1]School of Engineering and Technology, Central Queensland University, Sydney, Australia
[2]School of Built Environment, University of New South Wales, Sydney, Australia
[3]Solar Energy and Building Physics Laboratory, School of Architecture, Civil and Environmental Engineering, EPFL, Lausanne, Switzerland
[4]School of Civil Engineering, The University of Sydney, Sydney, Australia
[5]Lleaf Pty Ltd, Eveleigh, NSW, 2015, Australia

ABSTRACT: Urban overheating is a severe environmental concern. Highly absorbent construction materials, such as asphalt and concrete, are one of the primary contributors to urban overheating. The existing urban heat mitigation materials are insufficient to tackle the anticipated intensity of urban overheating. Consequently, developing advanced heat mitigation technologies with superior cooling is critical. Further, modern heat mitigation technologies (based on daytime radiative cooling) rely primarily on highly reflecting and emissive surfaces to limit solar radiation absorption. However, the highly reflective surfaces cause glare, preventing their use on roads and building facades. In addition, applying such non-colored coating in urban settlements is another concern. The research aims to develop colored daytime radiative cooling materials and reduce glare by decreasing surface reflection and compensating it with fluorescent cooling. The empirical investigation tested the performance of green perovskite polymer films with existing daytime radiative coolers (DRC). The outdoor thermal performance was evaluated by combining fluorescent and photonic materials in two different arrangements. The cooling benefits of colored Fluorescent daytime radiative coolers (CFDRC) were evaluated by comparing their surface temperature with that of photonic and nonfluorescent samples. The CFDRC was around 1°C higher than the highly reflective photonic material, and the nonfluorescent – CFDRC maximum surface temperature difference was around 3.5°C.
KEYWORDS: heat mitigation technologies, fluorescent materials, radiative coolers, quantum dots.

1. INTRODUCTION

Extreme climate change is occurring globally, and cities are growing warmer. Urbanization has significantly impacted local, regional, and global climatic conditions [1]. The frequency and intensity of extreme heat conditions have increased drastically [2]. Human-caused climate change has promoted the weather types that cause fires, increasing the danger of fire season in Australian cities by at least 30% [3]. These local, regional, and global climate shifts severely affect human health, energy, the economy, infrastructure, and the environment [4,5].

Urban greenery, evaporative cooling techniques, and cool materials could alleviate the effects of urban overheating and climate change. A simulation-based study revealed that cool materials could potentially minimize the impact of urban overheating in Sydney by up to 41%, while vegetation can decrease it by up to 29% [6]. Passive daytime radiative cooling (DRC) materials, which are highly reflective and emissive, may keep the surface temperature below the ambient temperature during the day. According to an empirical investigation, DRC materials reached a sub-ambient temperature of approximately 12.5°C in Alice Springs [7]. Due to the increased reflectivity, the DRC surfaces function as mirrors and cause glare. Therefore, such highly reflecting materials are unsuitable for building facades and pavements. Secondly, due to aesthetic concerns, such colorless surfaces are unwelcome in an urban setting. Colored fluorescent-based passive daylight radiative cooling (CFDRC) materials are proposed to mitigate overheating impact while addressing the challenges of glare and aesthetics.

A few studies have already investigated the impact of fluorescent materials with/ without photonic materials. However, further research is required to improve the cooling performance of such materials and fabricate scalable materials in the entire spectral range. [8] tested $CuInS_2$ (CIS)/ZnS, CdSe/ZnS, and PbS/CdS quantum dots (QDs) (with different band gap energies) coupled with silver-coated PET film to comprehend the heat-rejecting potential of QDs. On a typical sunny day, the surface temperature reduction potential of CdSe/ZnS QDs film by fluorescence cooling mechanism was around

2.5°C (QD surface vs. corresponding nonfluorescent sample without photonic), which raised to 8.1 °C with a highly near-infrared reflecting base layer (QD vs. QD+near infrared reflective layer). High-temperature reduction from the near-IR reflective layer illustrates the high penetrability of QDs. In another study, phosphor (fluorescent material) thermal performance was compared with QDs (green-emitting InP/ZnSe/ZnS quantum dots with a shell–core-core, quantum yield (Qy)= 95%, Outer diameter= 7.3 nm + 1.2 (PDMS as an emitter with this) [9]. A covering of metallic nanoparticles outperformed phosphors in terms of thermal performance. This was attributed to i) the acute absorption peak of metallic NPs being controlled by adjusting their size, whereas the phosphor absorbs widely, and ii) the phosphor has a low Q_Y and a larger Stokes shift. [10] utilized Cu-based quantum dots (QDs) coated on a white DRC film. The white film fabrication involved using colloidal inks containing hollow silica nanoparticles (H–SiO2), polymeric binders, and spray coating. The White films demonstrated average reflectivity and emissivity values of 97.2% and 94.3%, respectively. Furthermore, their temperature was 6.12°C lower than the surrounding ambient temperature when observed throughout the day. The fabrication of yellow, red, and brown CFDRC may reemit powers of 14.06, 28.36, and 43.92 W/m², preventing heat. Outdoor measurements demonstrated that the yellow and red DRC films had temperatures 3.25°C and 0.51°C lower than the ambient temperature.

Combining fluorescent and photonic materials aims to develop colored daytime radiative coolers with lower reflectance. The fluorescent cooling mechanism will offset the cooling loss caused by the composite material's reduced reflectance. Fluorescent material embedded in the emitter, such as Polymethyl methacrylate (PMMA), polyacrylate, or polycarbonate (PC), will absorb solar radiation in a high-intensity solar range (UV to absorption-edge wavelength) and reemit in a low-intensity solar region. The higher the peak emission wavelength, the greater the cooling benefits are.

2. FLUORESCENT DAYTIME RADIATIVE COOLING (FDRC) COMPOSITION

This research aims to combine reflecting and emitting layers with fluorescent materials to build superior single, double, or triple-layered colored fluorescent daytime radiative coolers (CFDRC). The fluorescent effect is the non-thermal/radiative relaxation of stimulated electrons. The fluorescent cooling effect happens when the energy level of the incident light is equal to or greater (shorter wavelength) than the bandgap energy of the fluorescent material. All photons with lower energy (higher wavelength) than the bandgap are transmitted through the fluorescent material because they lack the necessary energy to attain a higher energy level [11]. Three types of CFDRC arrangements were proposed by [12]. 1) three layered-structure- i) standalone emitter layer on the top, ii) Photoluminescence (PL) colorant in the middle, iii) solar reflector at the bottom, 2) emitter embedded with other particles, including PL colorant, ii) solar reflector, 3) emitters embedded in PL colorant, and solar scatterers (reflector).

The present study combined two photonic and fluorescent materials in two different arrangements to produce CFDRC. The first arrangement (arrangement-I) proposed a three-layer structure consisting of an emitter on the top with high thermal emission (8-13 µm) and high solar transmission (300-2500 nm) to allow incident solar-range light to pass through. A fluorescent film in the middle with fluorescence in 300 nm to absorption-edge wavelength (λ_{AE}), high light transmission (ranged λ_{AE} to 2500 nm), and a reflector at the bottom to reflect from λ_{AE} to 2500 nm. This arrangement used a 3M Enhanced Specular Reflector (ESR) silver Film with black coating on the reverse side as a reflector. It was combined with DuPont™ Tedlar® polyvinyl fluoride (PVF) film (Product series: TAP 15BM3), which is highly emissive. The combination of ESR and PVF as a photonic material was also proposed and tested by [7]. In the second arrangement (arrangement-II), Radi-cool- a single-layered photonic material (with high reflectance and emittance in the atmospheric window- https://www.gemar.com.ph/radicool) was used as a bottom layer, and the fluorescent film was placed on top of it (two-layered structure).

A 1mm thick polycarbonate (without any fluorescence) with identical optical and thermal properties as the fluorescent film was also paired with photonic materials in the same configurations to comprehend the fluorescence cooling potential.

3. GREEN FLUORESCENT FILM AND CHARACTERIZATION

The green perovskite ($CsPbBr_3$) quantum dots polymer films (5*5 cm) were fabricated by Quantum Solutions (https://quantum-solutions.com/product/qdot-lcd-sharpgreen-perovskite-film/). The perovskite quantum dots were embedded in the polyacrylate, with a total thickness of the film 320um. Both sides of the fluorescent films have barrier layers of 50um thickness. More details on the composition of the fluorescent film can be found in Figure 1.

Absorption edge wavelength (AE), PL quantum yield (PLQY), Stokes shift (SS), PL peak wavelength, and solar absorption are the key fluorescent and optical factors that contribute to the fluorescent cooling potential [11]. The higher the PL

peak wavelength, the higher the cooling potential of fluorescent material is [13]. The peak emission wavelength of the green perovskite fluorescent film was around 518nm. The quantum yield, the ratio of photons reemitted by the fluorescent material to the number of photons absorbed, was measured using Fluorescent Spectrophotometer FS5, and was around 95%. The higher the PLQY of fluorescent material, the better the cooling performance is. Stokes shift (SS), which is the energy difference between absorption edge (λ_{AE}) and PL peak wavelength (λ_{PL}), was around 33nm. Smaller Stokes shifts are needed to limit the heat loss caused by the Stokes shift. The PL spectra and the absorbance (1-Transmittance-Reflectance) of the fluorescent film are shown in Figure 2.

QDot™ LCD SharpGreen Perovskite Film, 10cm×10cm×300µm, 0.5 wt%, 2 pcs

Perovskite Quantum Dots polymer film, 520 nm emission peak, 0.5 wt%, total thickness 300 µm (active layer thickness 200 µm), size 10*10 cm, laminated by barrier layer (50 µm thickness)

Barrier layer: 50 µm thickness, VWTR < 0.001 g/m²-day @ 20 °C
Active layer: QDot™ SharpGreen Perovskite Quantum Dot in resin

Parameter	Actual Data	Specification	Method of Analysis
Appearance	Green- yellowish non-transparent	Film with colors from yellow to green	Visually
Appearance (UV Light)	Bright green	Film with green color	Visually w/UV Lamp
Thickness	320 µm	300 ± 30 µm	Digital Caliper, Mitutoyo
Emission peak	518 nm	520 ± 3 nm	Fluorescent spectrometer FS5, Edinburgh Instruments
FWHM	20 nm	≤ 25 nm	
PLQY	95%	> 85 %	

Figure 1. Composition of green perovskite quantum dots polymer films.

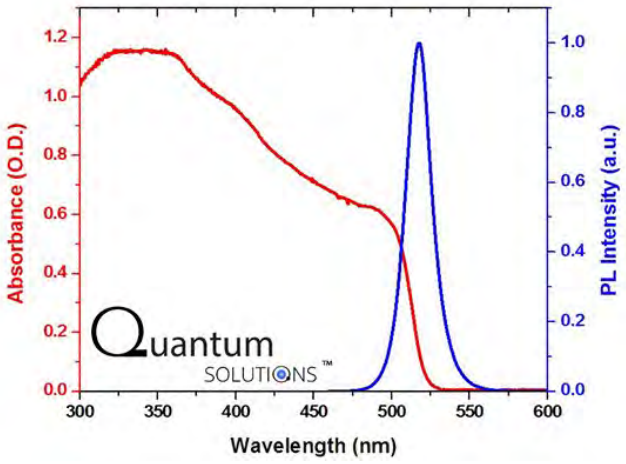

Figure 2. PL spectra and Absorbance of Green Fluorescent film

4. THERMAL CHARACTERISTICS

Fourier-transform Infrared Spectroscopy (FTIR Bruker INVENIO R) was used to measure the reflectance and transmittance of the samples in the infrared range with diffused gold integrating sphere attachment and diffused gold standard. In thermodynamic equilibrium, the emissivity (e) is equal to the absorptivity (a), as per Kirchhoff's law; therefore, emissivity was calculated as (e = i-t-r). The broadband emissivity was calculated using ASTM E408. The emissivity of the ESR was 57% in the atmospheric window (8-13 um) and 36% in the entire IR spectrum (4-40 um) (Figure 3B). The ESR was coupled with PVF, which has an emissivity of 87% in the atmospheric window and 62% in the IR spectrum (Figure 3C). Radi-cool has an outstanding emissivity of 92% in the atmospheric window and 88% in the IR band (Figure 3A). In the atmospheric window and the entire IR spectrum, the emissivity of both the green fluorescent film and the transparent polycarbonate was quite high, at around 93% and 96%, respectively (Figures 3D and 3E).

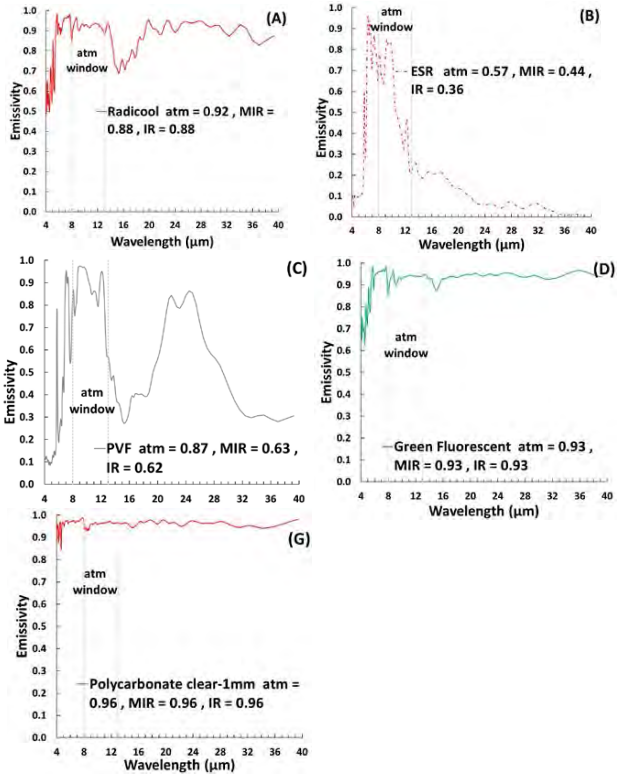

Figure 3. Thermal properties (Emissivity) of photonic, fluorescent, and nonfluorescent samples. A) Radicool, B) ESR, C) PVF, D) Green Fluorescent, E) Polycarbonate. (atm= atmospheric window (8-13um), MIR= Mid infrared range (4-20um), IR= Infrared range (4-40um)).

5. OPTICAL CHARACTERISTICS IN THE SOLAR RANGE

PerkinElmer Lambda 1050 UV–Vis-NIR Spectrometer with integrating sphere was used to measure the optical properties of the materials in the solar range. At three distinct locations, the optical characteristics of every material within the solar spectrum were measured, and the average was calculated. The broadband values were calculated using AM1.0GH - Normalized relative spectral

distribution of global solar radiation. The optical properties of the materials in the solar range are shown in Figure 4.

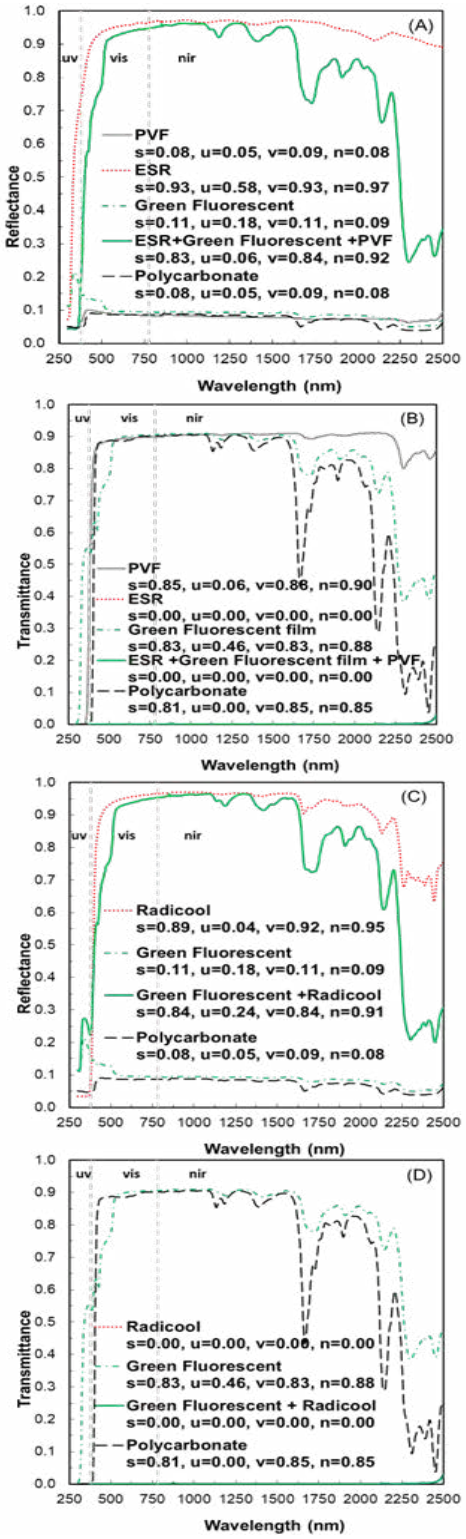

Figure 4. Optical properties of photonic, fluorescent, and nonfluorescent samples. A) Reflectance of materials in arrangement-I, B) Transmittance of materials in arrangement-I, C) Reflectance of materials in arrangement-II, D) Transmittance of materials in arrangement-II. (s= solar range, u= UV range, v= visible range, n= NIR range)

ESR has around 93% reflectance in the solar range (s), reduced to 83% when combined with green fluorescent film and PVF (Figure 4A). In the visible spectrum (v), the reflectance of the composite (ESR+Green fluorescent+PVF) decreased from 93% to 84%, considerably lowering the photonic material's glare (Figure 4A). The green fluorescent film absorbs until the absorption edge wavelength and then begins to transmit till the NIR spectrum, which the reflector will reflect (Figure 4B).

The PVF transmittance in the solr range is 85%, which is required for fluorescence (Figure 4B). This transparent PVF sheet also shields the underlying layers from ultraviolet (u) light, moisture, rain, and chemical erosion. Clear polycarbonate also has similar optical properties to green fluorescent film, with slightly lower transmittance in the NIR (n) range (Figure 4B). The Radi-Cool reflects around 89% in the solar range (Figure 4C). Combining the Radicool with green fluorescent film reduced the reflectance in the solar range to 84% (Figure 4C).

6. EXPERIMENTAL SETUP

The field measurements were performed from sunrise to sunset on 28th January 2023 during the summer. The experimental study was conducted on a basketball court at the University of New South Wales (UNSW), Sydney, Australia (-33.918632, 151.227132). According to the Koppen-Geiger climate classification, Sydney has a humid subtropical climate, warm in the summer and cold in the winter, with consistent yearly precipitation [14]. Meteorological parameters, including ambient temperature, dewpoint temperature, wind speed, wind direction, and atmospheric pressure, were recorded using two Gill MetPak Pro Weather Stations, and the average meteorological variables were computed. The relative humidity (RH) and absolute humidity (AH) were computed from ambient and dew point temperatures.

Two Huxseflux NR01 4-component and 2-component net radiometers were used to measure the shortwave and longwave radiations. The surface temperature was monitored using 3-wire Omega SA1-RTD-B surface mount RTD 100 Ω (±0.12 Ohms, ±0.30°C at 0°C), adhered on the backside of the sample. Data was recorded every 30 seconds using the Lontek datalogger DataTaker DT85, DT80, and CEM20. The 2.5-minute simple moving averages were calculated to smoothen the meteorological and surface temperature data. Six 5*5 cm samples- (i) PVF+green fluorescent+ESR, ii) Green fluorescent+Radi-cool, iii) PVF+ESR, iv) Radicool, v) PVF+polycarbonate+ESR, and vi) Polycarbonate+Radi-cool- were placed on the polystyrene board having dimensions (56*40*10 cm). The polystyrene board was covered with reinforced insulation tape from all

sides to minimize the parasitic heat transfer. Figure 5 depicts the sample boards and experimental setup.

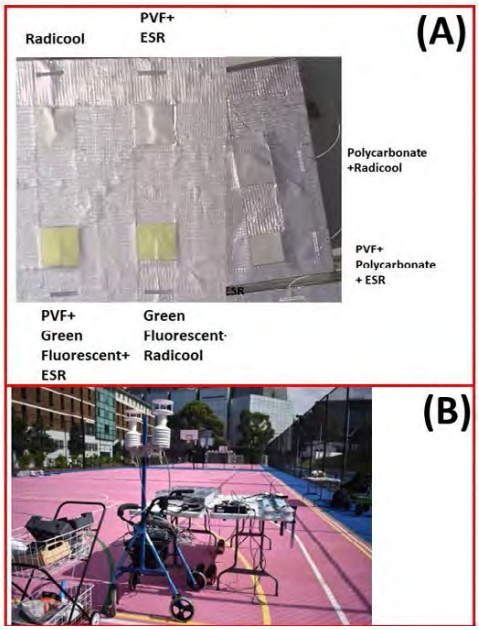

Figure 5. Experimental setup and samples A) Samples on polystyrene board, B) experimental setup

7. METEOROLOGICAL PARAMETERS

Figure 6 depicts the meteorological parameters during the field measurements. The peak shortwave radiation was 1032 W/m² (Figure 6A). The sky was partly cloudy until 11:00 a.m. but became clear for the rest of the day. 440 W/m² was the highest longwave radiation intensity (Figure 6B). At 1300, the maximum ambient temperature was 30.9°C (Figure 6C). The maximum wind speed was monitored at around 6.8m/s (Figure 6D). The humidity levels were very high throughout the day, and the maximum absolute humidity (AH) was around 20.2 g/m³ (Figure 6F). At such a high absolute humidity level, the atmospheric window is nearly closed, and materials cannot emit at their maximum capacity.

8. FIELD MEASUREMENT RESULTS

The field measurement results are presented in Figure 7. Due to the high humidity level, none of the photonic or CFDRC could attain the daytime sub-ambient temperature. The combination of ESR and PVF, which attained up to 7.4°C sub-ambient [15] at the peak Ambient time (Tambient) in the dry climatic conditions of Alice Springs, was around 7°C higher than ambient temperature (37.2°C) (Figure 7A). At the same time, the CFDRC (in arrangement-I) was about 1°C higher than the corresponding photonic material. This shows the potential of attaining sub-ambient temperature under dry-climatic conditions with the colored radiative cooling materials. The difference in surface temperature between the photonic and CFDRC remained consistent throughout the daytime (Figure 7A). The clear polycarbonate composite in arrangement-I was around 1.3°C higher than the CFDRC at the peak Tambient, and the maximum difference between CFDRC and polycarbonate composite in arrangement-I was up to 3.5°C in the afternoon. It illustrates the cooling potential due to the fluorescence mechanism, although clear polycarbonate composite was comparatively more emissive and slightly more reflective. At 1830, almost all samples, including photonic, CFDRC, and polycarbonate composite in both arrangements (arrangement-I and II), went sub-ambient. The daytime cooling performance of CFDRC in arrangement-II wasn't as good as in arrangement-I. It might be attributed to the comparatively higher reflectance of ESR in visible and in the NIR range compared to Radi-Cool.

Based on the findings, further fluorescent materials can be created that could reemit with a higher peak emission wavelength to maximize the cooling benefits of the fluorescence cooling process. To further reduce glare, these fluorescent materials can be used with reflectors that have reduced reflectivity.

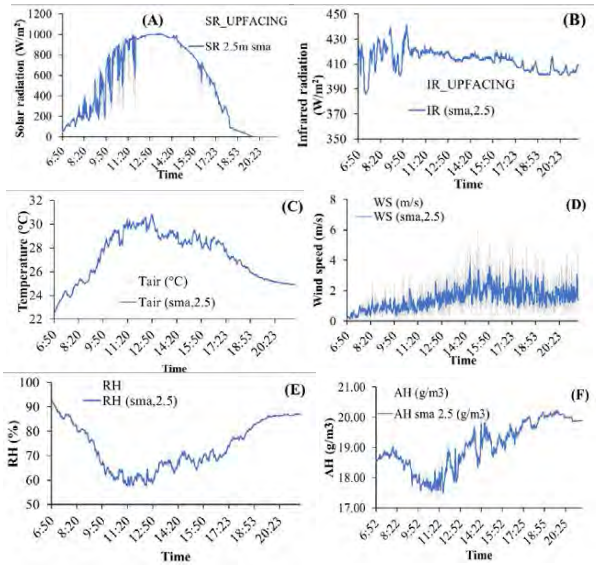

Figure 6. Meteorological conditions during experiment A) Shortwave radiations, B) Longwave radiation, C) Ambient temperature, D) Wind speed, E) Relative humidity, F) Absolute humidity (sma 2.5= 2.5 minutes simple moving average.

9. CONCLUSION

The colored Fluorescent daytime radiative coolers (CFDRC) were fabricated and compared against nonfluorescent and photonic materials. CFDRC surface temperature was around 1°C higher than the highly reflective photonic material, and the nonfluorescent–CFDRC maximum surface temperature difference was around 3.5°C.

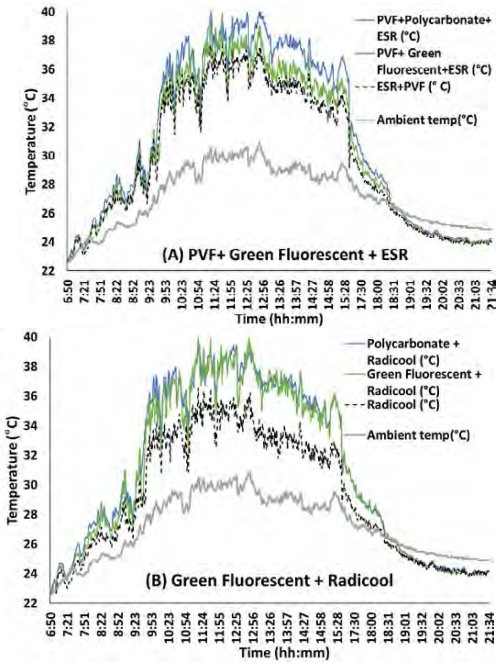

Figure 7. Surface temperature comparison with ambient temperature A) CFDRC and photonic materials in arrangement-I, B) CFDRC and photonic materials in arrangement-II

ACKNOWLEDGMENTS

This project has been supported by the Australian Research Council with the Discovery Project DP220100318, "Fluorescent daytime radiative cooling for urban heat mitigation". The authors acknowledge the facilities and technical assistance of the Spectroscopy Laboratory within the Mark Wainwright Analytical Centre (MWAC) at UNSW Sydney. We also thank the UNSW Design Futures Lab for the custom accessories for the scientific equipment.

REFERENCES

1. Khan, H.S. On the climatic synergies at the local, regional, and global scales. The impact on the built environment., UNSW Sydney, 2022.
2. Khan, H.S.; Santamouris, M.; Paolini, R.; Caccetta, P.; Kassomenos, P. Analyzing the local and climatic conditions affecting the urban overheating magnitude during the Heatwaves (HWs) in a coastal city: A case study of the greater Sydney region. Sci. Total Environ. 2021, 755, 142515.
3. Phillips, N. Climate change made Australia's devastating fire season 30% more likely. *Nature* 2020.
4. Santamouris, M. Recent progress on urban overheating and heat island research. Integrated assessment of the energy, environmental, vulnerability and health impact. Synergies with the global climate change. *Energy Build.* 2020, *207*, 109482.
5. Khan, H.S.; Paolini, R.; Caccetta, P.; Santamouris, M. On the combined impact of local, regional, and global climatic changes on the urban energy performance and indoor thermal comfort—The energy potential of adaptation measures. *Energy Build.* 2022, 112152.
6. Sydney Water, UNSW, CLCL *Cooling Western Sydney*; 2017;
7. Feng, J.; Gao, K.; Jiang, Y.; Ulpiani, G.; Krajcic, D.; Paolini, R.; Ranzi, G.; Santamouris, M. Optimization of random silica-polymethylpentene (TPX) radiative coolers towards substantial cooling capacity. *Sol. Energy Mater. Sol. Cells* 2022, *234*, 111419.
8. Garshasbi, S.; Huang, S.; Valenta, J.; Santamouris, M. On the combination of quantum dots with near-infrared reflective base coats to maximize their urban overheating mitigation potential. *Sol. Energy* 2020, *211*, 111–116.
9. Yalçın, R.A.; Blandre, E.; Joulain, K.; Drévillon, J. Colored radiative cooling coatings with fluorescence. *J. Photonics Energy* 2021, *11*, 1–16.
10. Yoon, T.Y.; Son, S.; Min, S.; Chae, D.; Woo, H.Y.; Chae, J.-Y.; Lim, H.; Shin, J.; Paik, T.; Lee, H. Colloidal deposition of colored daytime radiative cooling films using nanoparticle-based inks. *Mater. Today Phys.* 2021, *21*, 100510.
11. Garshasbi, S. Development and testing of advanced nano-scale fluorescent materials for urban heat mitigation, The University of New South Wales, Australia, 2021.
12. Min, S.; Jeon, S.; Yun, K.; Shin, J. All-Color Sub-ambient Radiative Cooling Based on Photoluminescence. *ACS Photonics* 2022, *9*, 1196–1205.
13. Garshasbi, S.; Huang, S.; Valenta, J.; Santamouris, M. Can quantum dots help to mitigate urban overheating? An experimental and modelling study. *Sol. Energy* 2020, *206*, 308–316.
14. Australian Bureau of Statistics (ABS) Climate and the Sydney 2000 Olympic Games Available online: https://www.abs.gov.au/AUSSTATS/abs@.nsf/Previousproducts/1301.0Feature Article32000 (accessed on 10th February, 2020).
15. Feng, J.; Khan, A.; Doan, Q.-V.; Gao, K.; Santamouris, M. The heat mitigation potential and climatic impact of super-cool broadband radiative coolers on a city scale. *Cell Reports Phys. Sci.* 2021, *2*, 100485.

Research on the Relationship between Urban Expansion and Surface Temperature in China's Capital Economic Circle

XU ZHANG[1] JOSEP ROCA CLADERA[1] BLANCA ARELLANO RAMOS[1]

[1]Centre for Land Policy and Valuations, Barcelona, Spain

ABSTRACT: This article analyzes the urban land expansion and the evolution of the thermal environment in the Beijing-Tianjin-Hebei region from 2001 to 2020, and calculates and draws the hierarchical distribution map of the urban heat island effect. In addition, the surface temperature of different circles and the inverse S function were fitted by dividing concentric buffer zones. The study found that the expansion of urban construction land in the Beijing-Tianjin-Hebei region showed radial development with Beijing as the center. There is an obvious positive correlation between the surface temperature of the Beijing-Tianjin-Hebei region and urban land. The spatial distribution of urban heat islands and urban land is also roughly the same. Moreover, the surface temperature in most periods of time conforms to the change pattern of the inverse S function curve, and each fitting parameter can reasonably describe the thermal environment of Beijing-Tianjin-Hebei and the evolution characteristics of urban areas.
KEYWORDS: Urban Expansion, Urban Thermal Environment, Surface Temperature, Urban Heat Island Effect, Inverse S Function

1. INTRODUCTION

The urban heat island effect is one of the typical characteristics of the urban thermal environment (Singh et al., 2017). It is an important result of changes in the urban thermal environment caused by urbanization and human activities, and is a direct example of environmental degradation (Chapman et al., 2017). In addition, the expansion of urban construction land is one of the main factors causing changes in the urban surface thermal environment (Ding Yue, 2020). Therefore, studying the intrinsic relationship between the expansion of construction land and changes in urban spatial thermal environment is helpful to analyze the spatiotemporal distribution and change patterns of urban surface thermal environment, as well as the synergistic effects of changes in urban spatial structure and thermal environment. While maintaining urban construction and economic development, and steadily improving scientific and technological levels, we must focus on solving ecological and environmental problems (Xu et al., 2022).

Based on this, this paper will take the Beijing-Tianjin-Hebei urban agglomeration, which is the fastest growing among the five urban agglomerations in China, as the research object. It is directly planned and guided by the central government and is the most dynamic development area centered on China's capital. It is also the development direction of China's large cities and conducts research on the relationship between urban thermal environment changes and construction land expansion. This study hypothesizes that urban territorial expansion contributes to the enhancement of urban thermal environment, but the intensity of the impact may be different in different seasons (winter and summer). In addition, the region also contains three major cities: Beijing, the capital, municipality and first city of China; Tianjin, the municipality; and Shijiazhuang, the capital of Hebei Province. They are interrelated and form the golden triangle of urban development and economic development (Figure 1).

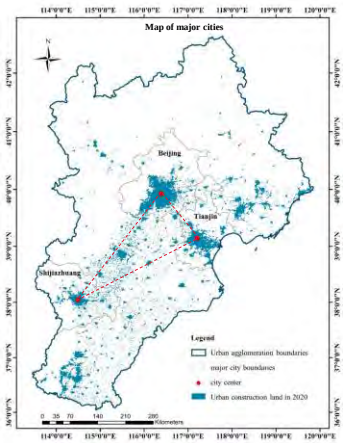

Figure 1: Map of major cities in Beijing, Tianjin and Hebei.

2. OBJECTIVE

The main objective of this study is to use MODIS remote sensing images to analyze the urban territorial expansion of the Beijing-Tianjin-Hebei urban agglomeration from 2001 to 2020, and the changing laws of surface temperature and heat island effect with the change of construction land. Finally, it is necessary to verify whether the surface

temperature of major cities in the economic circle follows the change pattern of a certain function curve as the distance from the city center increases.

3. METHODOLOGY

According to the specific objectives, this article will be divided into three main parts: expansion of urban construction land, urban thermal environment analysis, and concentric inverse S-curve verification analysis.

3.1 Expansion of urban construction land

3.1.1 MODIS land use classification

MCD12Q1(06) provides 500-meter resolution global land cover classification data (https://lpdaac.usgs.gov/products/mcd12q1v006/), and its classification is shown in Table 1. This study selects the band-IGBP classification, and the urban land number is 13. Since most of the data provided by MODIS starts in 2000, and the MCD12Q1 data starts in 2001 and ends in 2020, the research range we chose is 2001-2020.

Table 1: MCD12Q1(06) land cover remote sensing image classification.

Classification	IGBT (Type 1)	UMD (Type 2)	LAI/fPAR (Type 3)	NPP (Type 4)	FT (Type 5)
0	water	water	water	water	water
1	evergreen coniferous forest	evergreen coniferous forest	Cereals and Herbs	evergreen coniferous forest	evergreen coniferous forest
2	Evergreen broad-leaved forest	Evergreen broad-leaved forest	shrub	Evergreen broad-leaved forest	Evergreen broad-leaved forest
3	deciduous coniferous forest	deciduous coniferous forest	broadleaf crops	deciduous coniferous forest	deciduous coniferous forest
4	Deciduous broad-leaved forest	Deciduous broad-leaved forest	savanna	Deciduous broad-leaved forest	Deciduous broad-leaved forest
5	mixed forest	mixed forest	broadleaf forest	annual broadleaf vegetation	shrub
6	canopy thickets	canopy thickets	Coniferous forest	annual herbaceous vegetation	grassland
7	open bush	open bush	no vegetation cover	no vegetation cover	cereal crops
8	treey grassland	treey grassland	City	City	broadleaf crops
9	savanna	savanna			Cities and built-up areas
10	grassland	grassland			snow, ice
11	permanent wetland				Barren and sparse vegetation areas
12	crop	crop			
13	Cities and built-up areas	Cities and built-up areas			
14	Mosaic of crops and natural vegetation				
15	snow, ice				
16	Bare or low vegetation cover	Bare or low vegetation cover			
254	Unclassified area	Unclassified area	Unclassified area	Unclassified area	Unclassified area
255	fill value	fill value	fill value	fill value	fill value

3.2 Thermal environment analysis

3.2.1 Studying time selection for land surface temperature

MOD11A2 provides 1-km resolution diurnal surface temperature image data every 8 days (https://lpdaac.usgs.gov/products/mod11a2v006/). In order to study more representative surface temperatures in different time periods, we selected diurnal surface temperature data in winter (January and February) and summer (July and August) in 2001 and 2020. The data for each season is the average of all the data for the two months.

3.2.2 The relationship between LST and the proportion of construction land

After extracting and calculating the surface temperature for each period, we need to extract the image data of each surface temperature into the grid established in the previous step. A model is then established to analyze the intrinsic relationship between the proportion of urban construction land in the grid and surface temperature.

3.2.3 Analysis on the intensity of urban heat island effect and the scale of urban land use

In this step we will calculate the urban heat island effect and analyze its impact on built-up land. First, we classify cities and suburbs based on the density of built-up land. A threshold of 50% is used to distinguish high-density construction land and low-density construction land within the grid. High-density construction land is aggregated to form the central boundary, and the area below 25% is classified as urban outskirts (Feng et al., 2019; Lu et al., 2014).

At present, the urban heat island effect is generally defined as the temperature difference between urban and rural areas. Therefore, we use formula (2) to calculate the heat island intensity.

$$\Delta T = LST_{urban} - LST_{rural} \qquad (2)$$

Where:

ΔT is the heat island intensity;

LST_{urban} is the urban average surface temperature;

and LST_{rural} is the rural average surface temperature.

According to the heat island intensity classification rules, the standard deviation method is used to divide the intensity levels I to IV as shown in Table 3 (Wei, 2018).

Table 3: Urban heat island intensity classification.

Classification	Ranges
I	$LST_{rural} \leq LST < (LST_{rural} + 0.5\Delta T)$
II	$(LST_{rural} + 0.5\Delta T) \leq LST < (LST_{rural} + \Delta T)$
III	$(LST_{rural} + \Delta T) \leq LST < (LST_{rural} + 1.5\Delta T)$
IV	$LST \geq (LST_{rural} + 1.5\Delta T)$

3.3 Concentric circle inverse S-curve verification analysis

First, we need to find the urban centers of the three cities based on their construction land forms and main road networks. Then, using the circle-level gradient analysis method, concentric circles with an interval of 1km are used to construct multi-change buffer zones at the center of the city, and the average value of LST in each circle is counted to analyze the spatial variation of LST. The found city center points and the constructed concentric buffer zone are shown in the figure 2.

In order to make the numerical distribution of surface temperature in each city and time more standardized and uniform, so as to facilitate the fitting analysis with the inverse S function, we need to perform dimensionless processing on the LST of

each circle (Formula 3). At the same time, in order to be able to compare the differences between the LSTs of 2001 and 2020, we performed grouping before dimensionless processing. We divide the same season and time of the two years into a total of 4 groups for each city, namely summer daytime in 2001 and 2020; summer nighttime in 2001 and 2020; winter daytime in 2001 and 2020; winter nighttime in 2001 and 2020.

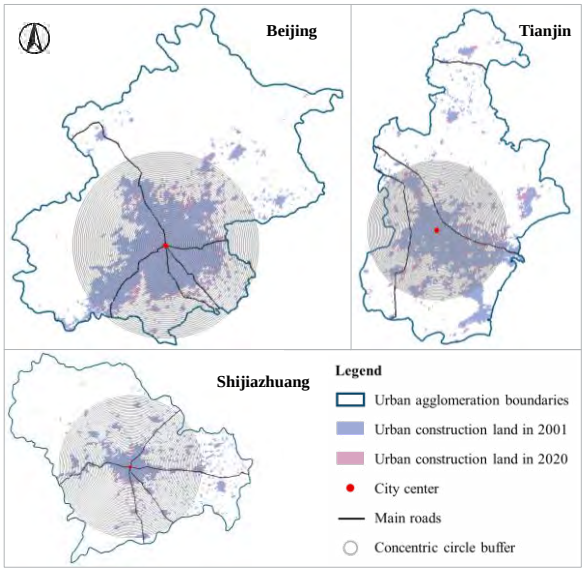

Figure 2: Urban centers and concentric buffer zones of the three major cities in Beijing, Tianjin and Hebei.

$$LST_d = \frac{LSTx_0 - LSTxmin}{LSTx_{max} - LSTxmin} \quad (3)$$

Where:
LST_d is the LST after dimensionless processing;
$LSTx_0$ is the average LST value of a certain circle;
$LSTx_{max}$ is the maximum value of the LST average value of each circle layer;
$LSTx_{min}$ is the minimum value of the LST average value of each circle layer.

Finally, all LST data are fitted with an inverse S-function model, the expression of the inverse S function is as follows. Combined with the characteristics of LST, the fitting parameters in the function are given the following meanings:

$$f(r) = \frac{1 - c}{1 + e^{a\left(\frac{2r}{D} - 1\right)}} + c \quad (4)$$

Where:
f(r) is the mean value of LST (◦C);
r is the radius from the circle to the city center; *e* is a natural constant (km);
a, c and D are all fitting parameters:
a controls the slope of the curve, and the larger a is, the faster the curve decays, indicating that the shape of the urban thermal environment is more compact;
c is the average value of LST at the edge of the city (◦C);
D reflects the radius of the urban thermal environment (km).

4. RESULTS

4.1 Thermal environment analysis

4.1.1 The relationship between LST and the proportion of construction land

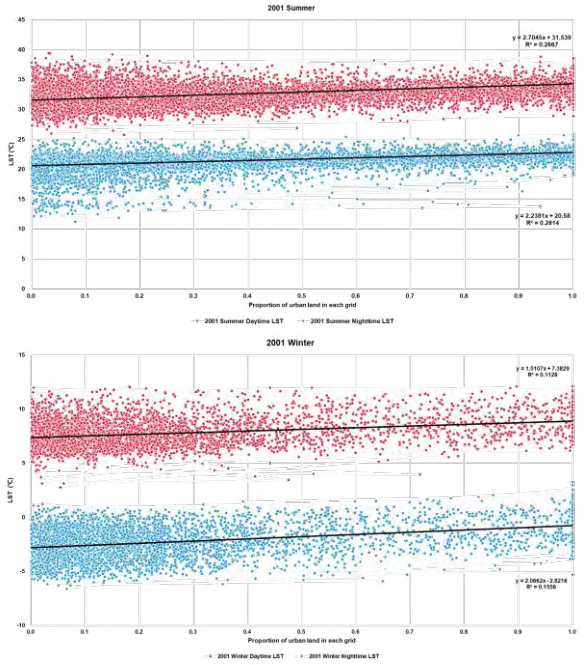

Figure 3: Scatter plot of the relationship between surface temperature and urban land proportion in Beijing, Tianjin and Hebei in 2001.

Figure 3 analyzes the relationship between surface temperature and the proportion of urban construction land in Beijing, Tianjin and Hebei in 2001 within each grid. The day and night temperatures in winter and summer in 2001 both tended to increase with the increase of the urban construction land ratio, but the linear relationship is weak.The dispersion degree of the relationship between the surface temperature and the proportion of construction land in winter is higher than that in summer. The model slope is highest in summer daytime (2.7), meaning the fastest ascent; winter daytime has the lowest slope (1.5). The temperature difference between day and night in summer is greater than that in winter.

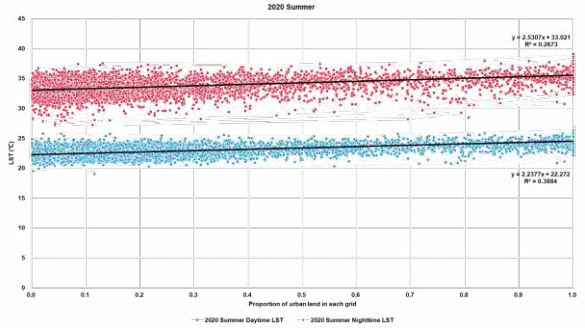

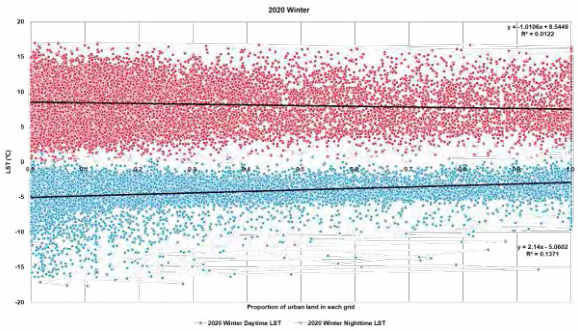

Figure 4: Scatter plot of the relationship between surface temperature and urban land proportion in Beijing, Tianjin and Hebei in 2020.

Analyzing the relationship between surface temperature and the proportion of urban construction land in 2020 (Figure 4), unexpectedly, the daytime surface temperature in the winter of 2020 was abnormal, and it decreased with the increase of urban land density. Compared to two decades ago, winters are very discrete and summers are more concentrated. In the 2020 model, the steepest slope is during the summer day (0.25). Overall, in the summer of 2020, daytime temperatures were about 1-2℃ warmer than in 2001, while nighttime temperatures were about 2℃ cooler. And the same is true in winter. The temperature difference between day and night in winter is further reduced.

4.1.2 Analysis of heat island effect

Figure 5 shows the statistics of the temperature difference between urban and rural areas in Beijing, Tianjin and Hebei during various periods, which is the urban heat island effect. It is very clear that the UHI in 2020 is higher than the UHI in 2001 under various scenarios, and the heat island effect becomes more intense. Especially during the daytime in summer, the UHI increased by 2.1℃ in 20 years. UHI did not exceed 1 in other periods, and only increased by 0.26℃ at night in 2020. UHI increased faster during the day than at night.

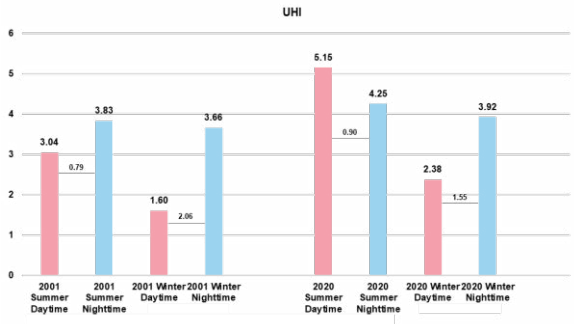

Figure 5: Statistics on urban heat island effect in Beijing-Tianjin-Hebei region.

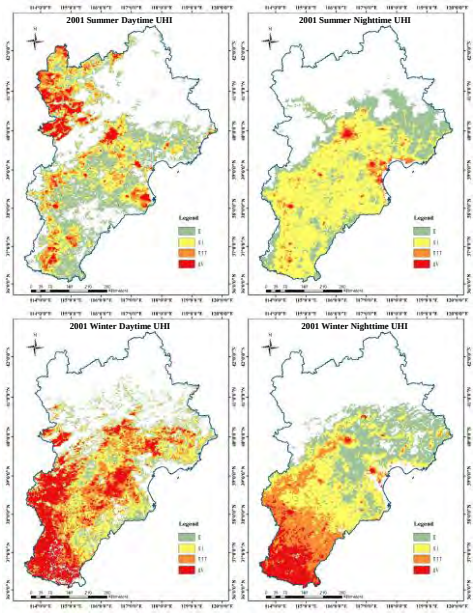

Figure 6: Graded distribution map of urban heat island effect intensity in Beijing, Tianjin and Hebei in 2001.

We drew the hierarchical distribution map of the urban heat island effect in Beijing, Tianjin and Hebei in 2001 and 2020 based on the urban heat island effect at different stages (Figure 6, Figure 7). The spatial distribution of UHI and urban land in the Beijing-Tianjin-Hebei region is roughly the same, and it is more concentrated and severe in the central and eastern parts of the region. However, in the summer of 2001, there was an abnormality during the day. Continuous UHI appeared in a large area in the northwest corner, and it was very serious, with high temperature above grade IV.

Although the analysis in the previous step shows that the UHI at night in 2001 was stronger than that during the day. However, in terms of spatial distribution, UHI above grade III is more widely distributed during the day than at night. Likewise, the UHI in summer 2001 was more severe than in winter, but the distribution of high-grade UHI in winter was wider. This just shows that in summer, the temperature difference between the central city and the peripheral areas is more obvious, which has a greater impact on residents living in different areas.

In summer, UHI at the southern end is not as good as in winter. The high-grade UHI in summer is mainly distributed in the high-density urban land range, and it is also densely distributed in the southern end at night in winter. In winter, most areas are affected by high-intensity UHI during the daytime.

In 2020, the UHI index is the largest, but from a spatial point of view, its level IV UHI is the least, with only a few small patches.

Similar to 2001, no matter summer or winter, day or night, the lower-level UHI is more widely distributed in space when the temperature difference between urban and rural areas is larger. At the same

time, UHI is more severe in southern regions in winter. The southern regions are almost entirely red during the winter day.

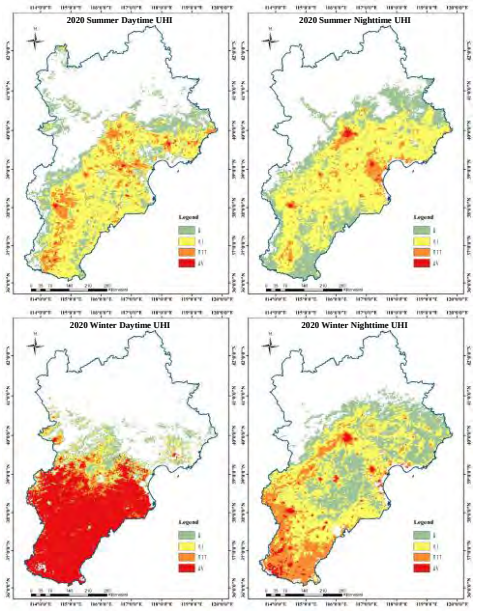

Figure 7: Graded distribution map of urban heat island effect intensity in Beijing, Tianjin and Hebei in 2020.

4.2 Concentric circle inverse S-curve verification analysis

We use the nonlinear least squares method to fit the mean LST to the inverse S function curve model to try to explore the distance relationship between the concentric layer LST to the center point of each city and the inverse S function fitting curve. The fitting parameter results and determination coefficient R^2 are summarized in Table 4.

Analyzing the results of fitting parameters, the LST in most cases conforms to the law of the reverse S-curve model.

- We only keep the fitting results with R^2 greater than 0.9, and consider their results qualified. We found that almost all of the three cities have anomalies during the daytime in winter. The daytime LST of Tianjin and Shijiazhuang cannot fit the model, and although the results of Beijing in 2020 are barely applicable, its R^2 is the smallest among all the results, only 0.91.
- The summer daytime LST of Tianjin in 2020 cannot be fitted either.
- Since the LST in other periods can be simulated by the inverse S model, it proves that their changing law is that they first decrease slowly as the radius of the concentric circle increases, then decrease rapidly, and finally decelerate and tend to 0. The key points of Beijing are 8km and 30km, Tianjin is 3km and 20km, and Shijiazhuang is 3km and 15km.

Table 4: Fitting parameters and R^2 for all time periods in each city.

		a	c	D (km)	R^2
Beijing	2001 Summer Daytime	3.03	0.20	40.78	0.957698
	2020 Summer Daytime	1.88	0.00	45.17	0.963909
	2001 Summer Nighttime	1.37	0.03	28.30	0.980452
	2020 Summer Nighttime	2.92	0.26	40.37	0.987387
	2001 Winter Daytime	2.22	0.00	168.40	0.753269
	2020 Winter Daytime	0.79	0.03	20.06	0.913274
	2001 Winter Nighttime	1.76	0.03	19.27	0.981148
	2020 Winter Nighttime	3.78	0.23	30.56	0.989
Tianjin	2001 Summer Daytime	3.18	0.04	20.59	0.994442
	2020 Summer Daytime	0.00	0.52	35.83	0.77159
	2001 Summer Nighttime	1.42	0.06	16.91	0.978466
	2020 Summer Nighttime	4.19	0.53	26.65	0.996531
	2001 Winter Daytime	0.52	0.14	7.54	0.80966
	2020 Winter Daytime	1.71	0.40	28.38	0.853856
	2001 Winter Nighttime	2.44	0.06	22.66	0.988365
	2020 Winter Nighttime	3.29	0.17	22.67	0.992731
Shijiazhuang	2001 Summer Daytime	3.28	0.04	15.37	0.990587
	2020 Summer Daytime	2.64	0.20	21.11	0.956413
	2001 Summer Nighttime	2.53	0.04	13.04	0.985649
	2020 Summer Nighttime	2.68	0.27	23.92	0.973656
	2001 Winter Daytime	37.12	0.15	0.00	No Data
	2020 Winter Daytime	0.00	0.69	0.17	0.505294
	2001 Winter Nighttime	2.84	0.14	13.02	0.983154
	2020 Winter Nighttime	3.83	0.07	18.21	0.98135

The fitting parameter “a” controls the slope of the curve. The larger “a” is, the faster the curve decays, indicating that the urban thermal environment is more compact.

- The "a" of each city's summer day in 2001 and winter night in 2020 is more than 3, and the "a" in winter is greater than that in summer. This shows that the shape of the high-temperature thermal environment in these two periods is relatively compact, and the high-temperature areas are more concentrated. Tianjin's 2020 summer night's "a" exceeded 4, the largest of all results.
- Except for Beijing's 2020 winter night with the smallest "a", all other cities had the smallest "a" during the summer day in 2001, and Beijing's "a" during this period was only greater than the 2020 winter night. The distribution of urban thermal environment during this period is the most scattered.
- The "a" results for Beijing and Tianjin are similar at each time, but Beijing has a wider value range. Tianjin's "a" value is overall larger than them.

The fitting parameter "c" is the mean value of LST at the city edge.

- All cities have "c" values between 0 and 0.69, but most are distributed between 0 and 0.2.
- Most of the "c" values of all cities are distributed between 0 and 0.2, and only the summer night in Tianjin in 2020 reached 0.53. It shows that the peripheral temperature in Tianjin during this period is relatively high.

The fitting parameter "D" reflects the radius of the urban thermal environment, and the analysis of "D" can judge the urban sprawl.

- The "D" of each city sample has increased to varying degrees, indicating that the urban high-temperature thermal environment has

also expanded. According to the previous analysis results, LST is positively correlated with the proportion of construction land, so we can think that each city has experienced different degrees of expansion in the past two decades.

- The thermal environment radius of Beijing and Shijiazhuang is the daytime in summer, but Tianjin is the largest at night in winter.
- The thermal environment radii of Beijing and Shijiazhuang are smallest at night in winter, while those in Tianjin are at night in summer.
- The fastest growth rate is in the summer night, and each city has increased by more than 10km.
- The slowest growth rate in Beijing is in summer daytime, Tianjin is in winter night, with an increase of only 0.1km, and Shijiazhuang is also in winter night.

5. CONCLUSION

Through analysis, this article finds that the expansion of urban construction land in Beijing, Tianjin and Hebei shows a radial development centered on Beijing. In the past 20 years, the outlines of large cities have increased significantly, and more land in the periphery of southern cities has been converted to urban land. At the same time, after urban expansion, urban land becomes more fragmented and disordered.

REFERENCES

1. Sun Yi, (2016). Research on the impact of urban expansion on urban climate - Taking Wuhan as an example. *Hubei University of Technology, School of Architecture and Civil Engineering.*

2. Xu Z, Blanca A, (2022). Urban sprawl and warming - Research on the evolution of the urban sprawl of Chinese municipalities and its relationship with climate warming in the past three decades. *The International Archives of the Photogrammetry, Remote Sensing and Spatial Information Sciences,* XLIII-B4-2022:209-2015.

3. Pandey P, Kumar D, Prakash A, et al., (2012). A study of urban heat island and its associationwith particulate matter during winter months over Delhi. *Science of the Total Environment,*414:494-507

4. Blanca A., Josep R, (2015). Urban Planning and Climate Change. *International Conference on Regional Science: Innovation and Geographical Spillovers: new approach and evidence.*

5. Lin Songliang, (2006). The impact of urbanization and environmental problems on regional economic development. *Chinese market,* 000 (040): 70.

6. Son N T. Thanh B X, (2018). Decadal assessment of urban sprawl and its effects on localtemperature using Landsat data in Cantho city, Vietnam. *Sustainable Cities and Society,* 36.81-91

7. Xu Zhang, Josep Roca, Blanca Arellano, (2022). Evolution of ecological patterns of land use changes in European metropolitan areas. *Proc. SPIE 12269, Remote Sensing Technologies and Applications in Urban Environments VII,* 1226906.

8. Singh P,Kikon N,Vernia P,(2017). Impact of land use change and urbanization on urban heat island in Lucknow city,Central lindia. A remote sensing based estimate. *Sustainable Cities and Society,* 32:100-114.

9. Chapman S, Watson J E M,Salazar A, (2017). The impact of urbanization and climatechange on urban temperatures: a systematic reviewJ. *Landscape Ecology,* 32: 1921-1935.

10. Ding Yue, (2020). Study on the spatial and temporal changes of construction land expansion and surface temperature in Hotan City. *Master's thesis of Xinjiang University.*

11. Masek J G, Lindsay F E, Goward S N, (2000). Dynamics of urban growth in the Washington DC metropolitan area, 1973-1996, from Landsat observations. *International Journal of Remote Sensing,* 21(18):3473-3486.

12. Rao P K, (1972). Remote sensing of urban heat islands from an environmental satellite. *Bulletin of the American Meteorological Society,* 53: 647-648

13. Howard L, (1833). Climate of London deduced from metrological observations. *London: Harvey and Dorton Press (3rd edition),* 1: 348.

14. Tran H, Uchihama D, Ochi S, (2006), Assessment with satellite data of the urban heat island effects in Asian mega cities. *International Journal of Applied Earth Observation and Geoinformation,* 8(1):0-48.

15. Zhao Anzhou, Pei Tao, Cao Sen, Zhang Anbing, Fan Qianqian, Wang Jinjie, (2020). Impact of urban expansion in Beijing, Tianjin and Hebei on vegetation and surface urban heat islands. *Chinese Environmental Science,* 40(4): 1825~1833.

16. Limin Yang, (2020). Effects of urban spatial structure change on urban thermal environment of Changchun. *Master's thesis, School of Earth Sciences, Jilin University.*

17. Feng Y J, Gao C T, Tong X H, (2019). Spatial Patterns of Land Surface Temperature andTheir Influencing Factors: A Case Study in Suzhou, China. *Remote Sensing,* 11(2): 182

18. Lu B B, Charlton M, Harris P, (2014). Geographically weighted regression with anon-Euclidean distance metric: a case study using hedonic house price data. *International Journal of Geographical Information Science,* 28(4): 660-681.

19. Wei Z, Feng C, (2018). Impacts of Grading Rule on Urban Thermal Landscape Pattern Research. *Sustainability,* 10(7): 2514.

20. Jiao L M, (2015). Urban land density function: A new method to characterize urban expansion. *Landscape and Urban Planning,* 139: 26-39.

21. Jiao Limin, Li Zehui, Xu Gang, (2017). The characteristics and patterns of spatially aggregated elements in urban areas of Wuhan. *Acta Geographica Sinica,* 72 (8): 1432-1443.

22. Bonafoni S, Keeratikasikorn C, (2018). Land surface temperature and urban density: Multiyear modeling and relationship analysis using MODIS and landsat data. *Remote Sensing,* 10(9): 1471.

23. Govind N R, Ramesh H, (2020). Exploring the relationship between LST and land cover of Bengaluru by concentric ring approach. *Environmental Monitoring and Assessment,* 192: 650.

PLEA 2024 WROCŁAW
(Re)thinking Resilience

The Earth Construction Fallacy
Hassan Fathy's New Gourna Revisited

SHADY ATTIA [1]

[1]Sustainable Building Design Lab, Dept. UEE, Faculty of Applied Science, Liege University, 4000 Liège, Belgium

ABSTRACT: The problems of earth construction uptake as a building technology in the Global South have long been recognized. The classic response to the low uptake has been newer compositions of construction earth blocks and biobased materials in one form or another. Nevertheless, the profession's modern origins of earth construction stem from responses to the destructive impact of concrete and fired brick. Relieving the destructive environmental impact using biobased and earthen materials led to many earthen construction products with low uptake. This paradox remains unresolved despite recent advances in the fabrication of earthen construction technologies using agro and non-agro-waste materials or the creation of new earth-building construction standards and new building materials engineers' efforts. This article reevaluates New Gourna in Luxor, Egypt, after 70 years of its creation, as a sustainable earth-based community in Luxor, Egypt, and whether earthen construction buildings and communities are socially and environmentally sustainable. Based on a field visit and interviews with local experts and users' current debates on the uptake of earthen construction and its sustainability, it outlines the intellectual origins of sustainability and analyses whether its theory supports the earthen construction hypothesis: earthen construction is more economically and socially sustainable than concrete construction. It concludes that conceiving buildings using earth and biobased resources in terms of materials with low environmental impact is neither necessary nor sufficient to achieve the goals ascribed to social acceptance, climate resilience, and economically viable communities. Instead, conceiving the buildings in terms of a long-term and participatory process holds more promise in attaining the elusive goal of a sustainable built environment. The study provides recommendations to inform funding and development aid agencies like the World Bank and the EU on the importance of adopting a holistic and multicriteria approach.
KEYWORDS: sustainable; building; design, environmental impact, bricks, materials, architecture

1. INTRODUCTION

The urbanization of the global south is accelerating fast. Urbanization in the Global South: where the world's 33 megacities, 27 are in the Global South [1]. In comparison, some scholars note the significance of concrete and reinforcing steel constructions to assure structural stability and extend buildings' service life as the result of modernization and advancements of materials science [2] - represented through multi-story buildings- other thinkers point to the continuing, if not increasing, Green House Gas (GHG) emissions associated with the use of those materials and the need to replace them with earthen and biobased construction materials [3]. Between these two poles, massive funding occurs from foreign development and cooperation agencies or national governments to build green communities using earthen construction in rural areas of the non-industrial world, or in other words, the Global South [4].

Earthen construction technologies, including adobe, compressed earth blocks (CEB), and rammed earth, confers environmental and socio-economic advantages [5]. For example, between 2000 and 2023, more than hundreds of studies have been published to promote different mixes and combinations of the earth with biobased fiber materials, including okra, cocos, banana, hemp, fonio, Bambusa vulgaris, invasive seaweed, jute, date palms, kenaf, rice husk, sugar cane and shea butter next to industrial waste fiber including plastic [6]. Despite the proliferation of research on CEB mainly led by civil engineers, there is a very low uptake of CEB in the housing market in the Global South. All continents possess a rich heritage of earthen architecture. It is estimated that about 1.7 billion people worldwide live in earthen houses [7]. About 50 % of the population is in developing [8] populations [7] (Fig. 1).

Figure 1: Earth construction areas of the world [7].

More importantly, most of those earthen and biobased constructions are not socially accepted. The Global South is a focus of world politics with significant energy and resource reserves and histories

of colonialism and imperialism. It is also the site of potentially immense green energy and material resources but is held back by resource-grabbing and neocolonial agendas [9].

New Gourna is a living example of using local materials and techniques and building a new community. New Gourna was designed by a pioneer of sustainable architecture, Hassan Fathy, in Luxor and was commissioned by the Egyptian Government in 1945. The project incorporated traditional techniques and materials, such as adobe-baked mud bricks, to build a community of affordable houses and services based on vernacular and bioclimatic design principles. Fathy borrowed from Nubian and Gourna architecture to create representative enclosed courtyards and vaulted roofing and chose to build in mud brick. Unfortunately, the project failed as most residents refused to move to the new village [10].

Hassan Fathy had a true vision of sustainable architecture, but the project failed after half a century of social rejection and faced serious degradation [11]. New Gourna Village's main characteristics include its reinterpretation of a traditional urban and architectural setting, its appropriate use of local materials and techniques [9], and its extraordinary sensitivity to climatic problems. Following concerns on the serious state of degradation of the village by both the World Heritage Committee and the academic world of experts on Hassan Fathy's architectural work who submitted an international petition, UNESCO initiated a project in 2009 to safeguard this important site. This was agreed to in consultation with the Ministry of Culture of Egypt and the Governorate of Luxor [10].

One theme of this paper is the paradox between using earthen and biobased materials for construction and those buildings' low uptake and acceptability by their potential occupants. Despite the great efforts over the generations to promote earthen construction, this paradox has yet to be adequately resolved. The perception that earthen and biobased construction is an 'architecture for the poor' remains one of the main reasons for their low uptake. On the other hand, architects and aid organizations in industrial countries strongly promote earthen construction in the Global South as a sort of eco-construction neo-orientalism [12]. Therefore, this research reinvestigates the case of New Gourna and inquires on how effective earthen and biobased materials as an option is attaining a deep-seated shift in green architecture in the Global South toward truly socio-economic viable communities and not only sustainable communities.

2. METHODOLOGY

This article assesses answers to the research question through a literature review and case study research. By examining factual evidence and intellectual foundations regarding New Gourna's failure, we can better judge whether earthen construction and biobased architecture are more sustainable than high-rise - concrete and reinforced steel constructions – and modern architecture.

The methodology uses both qualitative and quantitative methods of data collection and analysis. The methodology involved intensive observations of the state of the New Gourna community in 2023, 78 years after its construction. Two field visits took place in 2023. The purpose is to characterize the current buildings' state and distill learned lessons to understand the occupant's experience and the reasons behind the low uptake of earthen constructions in Egypt since then. Firstly, empirical evidence from the literature surrounds whether earthen and biobased architecture are sustainable and acceptable solutions in the Global South. This section remedies the first deficiency with a preliminary characterization of earthen constructions' low uptake and usability across several projects. It weighs the factual evidence on their socio-economic sustainability. Second, open interviews with some house occupants and users are conducted. During a field visit in February 2023, twelve stakeholders were interviewed, including the manager of the public buildings such as the Khan and the market.

Thirdly, a field study includes observations, photography, written documentation, and thermal comfort measurements of air temperature and humidity during July 2023. Two HOBO U12-012 (measuring temperature, relative humidity, and light data loggers were used to characterize thermal comfort in a dwelling based on outdoor and indoor temperatures. The dwelling in Figure 2 is the original Hassan Fathy house, where he spent most of his time in New Gourna.

Figure 2. After a major renovation, Hassan Fathy's residence stands alone, surrounded by high-rise concrete buildings.

Fourthly, open interviews, which took place, in some cases retrospectively, between 2013-2023, with architects and designers focused on the reasons for the low uptake of earth constructions in Egypt. Several architects were interviewed, including

Abdelhalim Ibrahim Gamal Abdel Amer, Adel Fahmy, Ahmed Hamid, Mohammed Hassanein, and Tarek Labib. The interviews focused on several criteria: standardization, durability, cost, social acceptance, and urban planning.

3. RESULTS

Adobe, compressed earth blocks, rammed earth, and bamboo are at the forefront of green and sustainable building materials for underprivileged societies in the Global South. However, the sustainability of using earth construction and biobased materials and their uptake by the local population in the Global South have fostered spirited debates. One strand of the debate is between housing durability and sustainability, and another is between free market land use and population uptake [13]. Based on the literature review findings [14] and our analysis, we can summarize the reasons for the failure of Hassan Fathy's New Gourna under four themes:

Firstly, the project did not ensure the use of durable earth blocks that last long and overcome water problems. The unfired adobe blocks could not resist the underground rising water levels, and the foundations were built using calcareous stones (limestone), which degraded over time. Moreover, the frequent flash rains eroded the mortar and bricks over time. The stability and durability of the buildings degraded significantly due to walls buckling and the structural cracks of domes and Nubian vaults. Without continuous maintenance, at least a major renovation every ten to fifteen years, there was no chance for such buildings to survive. Without the UNESCO support for renovation, the project would not have existed anymore.

Secondly, the project was not integrated into a comprehensive urban master plan that addresses infrastructure, sewage, and mobility issues. The dependence on septic tanks for sewage resulted in overflows and a constant increase in groundwater levels. With the population increase and the need for vertical expansion, the population abandoned the low-rise archetypes and opted for post and columns concrete buildings to reach 6-story buildings, as shown in Figure 2. Thus, the architect failed to anticipate the future need for densification.

Thirdly, the project was promoted as an architecture for the poor. The old Islamic and Arabic identity was emphasized in the architectural language. The residents strongly rejected sleeping under the Nubian vaults and domes. Residents associated the vaults and domes with tombs. Hassan Fathy was accused of being orientalist by imposing a certain style on the population influenced by personal heritage revival notions. Both messages were rejected by the local population aspiring for modern architecture under the influence of Westernisation and globalization. The occupants' social acceptance and involvement through a participatory design approach were missing during the design process. This was another key reason for the rejection of the project by the local community.

Fourthly, the construction technology did not improve thermal comfort as expected. Figure 3 illustrates the ambient temperature difference between outdoors and indoors during the summer of 2023. Despite the 40 cm thick walls in Figure 3, the lower temperature bounds remain above 30°C at night, making the house uncomfortable from the thermal point of view. Our observations and interviews indicate that occupants sleep outdoors during the night or on the roofs to avoid the overheating effects (see Figure 4). Also, air conditioning units were observed in the neighborhood for humification or cooling. Finally, the lessons learned from New Gourna are crucial for any future development that seeks to use earthen construction techniques in the Global South.

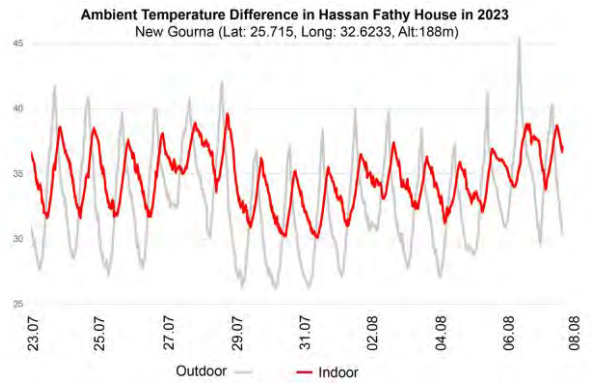

Figure 3. Ambient temperature in Hassan Fathy House between Jul. 23 and Aug. 08, 2023.

Figure 4. Residents sleep during hot summers outdoors under the portico of the Khan.

4. DISCUSSION

To put this finding in a contemporary and larger perspective, we must reflect on the importance of standardization of earth and biobased construction materials. Comparing the earth construction of Hassan Fathy (1945) in Egypt [15] and more recent

ones such as the projects of Francis Kere (2016) in Burkina Faso [16], [17] or the projects of Anna Heringer (2019) in Bangladesh [18], we can observe the same problems summarized in Figure 5.

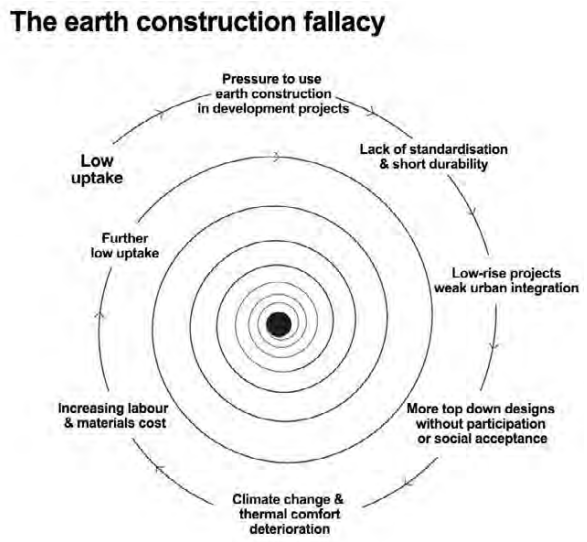

Figure 5. Earth-construction projects development process and its key shortcomings

Firstly, the Global South lacks a legal ecosystem of policies and standards that promotes using earthen and biobased materials for high-quality and sustainable architecture [19]. Future projects will fail without standardization of the mechanical, physical, and chemical properties of earth blocks, biobased components, agriculture bio waste, and their integrity as part of building structures. Earth construction reuires a learning process to build experience, transfer knowledge and assure its realization quality. On one extreme, earth and bio-based materials should not require constant maintenance. On the other extreme, the mechanical and structural performance of earthen and bio-based construction materials should not always be compared to reinforced concrete materials [20]. Municipalities and building codes worldwide require architects and engineers –for building permits- to achieve the same performance thresholds of reinforced concrete structures, which disqualifies earthen and bio-based construction projects and legally hinders their uptake as durable and robust construction materials. Without assuring the durability of eco-construction materials and avoiding their deterioration and intensive maintenance, any biobased or earthen construction will fail from a functional and structural durability point of view.

At the same time, adding chemical binders, such as cement [21], to any earth block will disqualify it environmentally as an ecological and low GHG emissions construction material [22]. The use of cement (8-12%) in stabilized CEB will make it unable to compete with concrete blocks and firebricks economically [23] and environmentally [22], especially when we calculate the total cost of technical training, marketing of earth construction products, maintenance, finishing and raising public awareness of sustainability nationally. The thickness of the walls of earth construction and their finishing quality are additional influential parameters.

Secondly, the Global South population is increasing rapidly, and the poor land use management and governance in many cities, next to capitalistic speculations, make access to land for new construction not affordable. Real estate speculation and political power structures in most countries of the Global South impede low-rise urbanization and land ownership. The lack of modern road infrastructure and difficulty funding water, sewer, and road infrastructure are other barriers to mobility. Consequently, low-rise urban development and spacious bioclimatic architecture – with large volumes and high ceilings- are not an option in many developing cities and countries. Thus, post-and-column structures are the most suitable building technology in densely populated communities.

Failing to address the urban density problem and suggesting only low-rise archetypes and projects located in remote areas and built by Western-educated architects using earthen and biobased materials [24] is naïve. In many cases, the efforts of many world organizations -including UN-Habitat and many European development organizations- to stimulate affordable housing in the Global South are counterproductive and lead to jeopardizing the sustainability of urban development in the long term. Therefore, the solution should be to promote high-rise bearing wall archetypes [25].

Thirdly, the social acceptance of earthen construction remains a challenge. The use of earth construction and biobased materials to build shelters in the Global South is a kind of green colonialism [9]. Many architectural schools and architects practice green colonialism, which does not lead to high-quality, climate-proof and healthy architecture. Therefore, participatory design process and communal collaboration are key for earth construction and urban development projects [13]. Earthen construction must be developed as a modern and high-quality architecture and not just a Western utopian projection of the use of ecological materials in the Global South driven by aid programs [26]. Aid-based earth construction is a political tool promoted by donors. As a consequence, during the last 30 years, there has been a strong movement of orientalism [15] in many North American and European architecture schools and research institutions that promote using ecological materials in Latin America, Africa [27], and Asia. Unfortunately, most of those designers fail to build earth

constructions in their permanent residence countries (Global North) because of the high-quality construction regulations that go beyond structural stability and require a building to be more than just a shelter.

However, within African and Asian countries, most earth and biobased construction projects are believed to target lower-income users [28], [29] or extremely rich users. The stigma of associating earth construction with poverty remains prevailing. Therefore, using earth construction for middle-income people should be the first step to promoting this technology. The finishing quality is the key. Housing authorities should prioritize promoting earthen construction for its architectural and life quality attributes [30], not environmental qualities. There is a need to show the beauty and capacity of earth and biobased materials and bring out the best of it. The right message is to promote earth materials as a high-end product and excellent architecture with different finishing qualities and varied fiber content.

Fourthly, the association of earthen and biobased architecture with unlimited acclimatization [30] must be broken. The overestimation of the role of hygrothermal properties of earthen construction to enhance indoor thermal comfort needs to be moderated and supported with evidence. A modern earthen construction must provide thermal comfort, and in hot and humid regions [31], this cannot be achieved without active systems, including electric fans, air conditioners and evaporative coolers. Earthen construction should not be only associated with naturally ventilated buildings or wide-limits adaptive thermal comfort models with extreme indoor thermal comfort conditions unless CFD and thermal simulation proves their performance.

Despite the perception of the improved thermal comfort effects of earthen architecture, it remains unsatisfactory in modern buildings in the Global South. The air acceleration of velocity, humidification or dehumidification strategies in indoor spaces are not a proxy for tolerating overheating, dust from sand storms, mosquitoes and overall discomfort. With climate change and the increasing intensity of heat waves, the Global South cities, towns, and villages' earthen construction must be associated with air quality and thermal comfort. People living in hot climates are striving for thermally comfortable houses. They aspire to live in better conditions than the older generations. Failing to equip earth construction projects with active cooling systems is unacceptable because it emphasizes the stigma of poverty and low-quality life, work and learning lifestyles. Also, the claims that people living in the Global South have an endless thermal adaptation ability are false.

Finally, the four shortcomings in Hassan Fathy's New Gourna and the wider global context are the most common themes in the literature [17], [30-32]. All four common problems, shown in Figure 5, are behind the Earth Construction Fallacy. They are closely interconnected and influence the uptake of earth construction technologies and materials. The key question to stand up against this fallacy is that architects and development organizations ask themselves a question: Does the earth and biobased architecture address this paper's four common sustainability problems? This is a question of self-critique.

5. CONCLUSION

This paper presented an important reflection on the earth construction practice through the investigation of New Gourna's Village in Egypt. The investigation attempts to overcome previous limitations of orientalism and romantic attitude in transforming earth and biobased materials into shelters and not architecture. By choosing the example of Hassan Fathy village, a UNESCO-recognized heritage, and tracking its evolution over 75 years, we raise the awareness of future designers about the earth construction fallacy. Also, we propose practical recommendations to cross the current barriers of earth construction uptake.

We must take care not to extend this critique too far. The attempts to use stabilized or unstabilized earth construction and biobased materials are encouraged, and we can envision high-density communities that mainly use earth construction. By reversing the barriers indicated in this study through a co-evolutionary process, the use of earth construction as a form of sustainable architecture is a viable one that we can strive to reach.

One of the main limitations of this study is that we did not address the cost and environmental impact of earth construction using a quantitative modeling approach for the investigated case study. There is a need to perform a full life cycle analysis, including cost based on environmental product declarations of earth construction projects, to quantify their impact. Several interviewed experts pointed out that construction labor cost is increasingly more important than the material sourcing cost. In most countries, the ratio between total material cost and the total construction labor cost tends to lean toward higher labor costs. In the Global South, the labor cost in the construction sector is becoming high [33]. Therefore, future work should focus on performing environmental and cost analysis with long building life scenarios and maintenance cycles to evaluate the durability of earth construction in comparison to concrete-based construction techniques.

ACKNOWLEDGEMENTS

The author thanks Abdelhalim Ibrahim Gamal Abdel Amer, Adel Fahmy, Ahmed Hamid, Mohammed Hassanein, and Tarek Labib for participating in the interviews over the last 20 years. Peace upon Abdelhalim Ibrahim and Tarek Labib, who left our world. Special thanks to the anonymous interviewees and volunteers who helped with the New Gourna, Egypt field study. This research has benefited from visits to new earth construction developments across Asia, Africa, and Latin America and analyzing their environmental impact and social acceptance.

REFERENCES

1. Myers, G. (2021) Urbanisation in the Global South, in Urban Ecology in the Global South, C. M. Shackleton, S. S. Cilliers, E. Davoren, and M. J. Du Toit, Eds., in Cities and Nature, Cham: Springer International Publishing, pp. 27–49.
2. Slak T. and Kilar V. (2005), Developments in the architecture of earthquake resistant high-rise buildings in the period from the end of the 18th to the beginning of the 20th century, vol. 81. WIT Press, London, UK.
3. Yadav, M. and M. Agarwal, (2021) Biobased building materials for sustainable future: An overview, Mater. Today Proc., vol. 43, pp. 2895–2902.
4. Vyncke, J., Kupers, L. and Denies, N. (2023) Earth as Building Material–an overview of RILEM activities and recent Innovations in Geotechnics, in MATEC Web of Conferences, EDP Sciences, 2018. Accessed: Dec. 02, 2023. [Online]. Available at: https://tinyurl.com/4jab3uxn
5. Hafez, H., El-Mahdy, D., Marsh, A. (2023) Barriers and enablers for scaled-up adoption of compressed earth blocks in Egypt," Build. Res. Inf., vol. 51, no. 7, pp. 783–797.
6. Valenzuela, M., Ciudad, G., Cárdenas, J.P., Medina, C., Salas, A., Attia, S., Tuninetti, V. (2024) Towards the development of performance-efficient compressed earth blocks from industrial and agro-industrial by-products: a review, Construction and Building Materials, Renewable and Sustainable Energy Reviews, vol. 194. 114323.
7. AVEI (2023) Earth construction areas of the world." Auroville Earth Institute, Auroville, India.
8. Fathy, H. (2010) Architecture for the poor: an experiment in rural Egypt. University of Chicago Press, Chicago, USA.
9. Hamouchene, H. (2023). Dismantling Green Colonialism: Energy and Climate Justice in the Arab Regio. Pluto Press, London, UK, ISBN: 9780745349213.
10. Ahmed, K. G. and Elgizawi, L. (2009) Two versions of 'New Gourna' and the dilemma of sustainability in new urban communities in Egypt," WIT Trans. Ecol. Environ., vol. 120, pp. 691–701.
11. UNESCO (2011) Safeguarding project of Hassan Fathy's New Gourna Village, UNESCO, Cairo, Egypt.
12. Said, E. (2023) Introduction to orientalism in imperialism, Routledge, London, UK.
13. Depraz, S., Cornec, U. and Grabski-Kieron, U. (2016) Acceptation sociale et développement des territoires. ENS éditions, Lyon, France.
14. Vasáros, Z. (2020) The Beginning. The Hassan Fathy Survey Mission: 2015-2017, Accessed: Dec. 02, 2023. [Online]. Available: http://real.mtak.hu/115428/
15. Steele, J. M. (2002) Orientalism and the other: The case of Hassan Fathy. Uni. of Southern California, USA.
16. Baker-Brown, D. (2019) School buildings and others in Burkina Faso, by Francis Kéré, in The Re-Use Atlas, RIBA Publishing, pp. 114–117, London, UK.
17. Zoungrana, O., Bologo Traoré, M., Pirotte, G., and Messan, A. (2018) Influence de la politique de valorisation sur l'usage des blocs en terre comprimée dans la ville de Ouagadougou," in NoMAD, Liege, Belgique, pp. 1–10.
18. Heringer, A., Howe, L., Rauch, M. (2022) Upscaling Earth: Material, Process, Catalyst,GTA Verlag. Zurich, Suisse.
19. Wyss, U. (2005) La construction en matériaux locaux, Etat d'un secteur à potentiel multiple, Ouagadougou, Bukina Faso.
20. Dahy, H. (2024) Bio-based Bridge Design and Construction, Video, Deutsche Welle, Stuttgart, Germany.
21. Sore, S. O., Messan, A., Prud'Homme, E., Escadeillas, G. and Tsobnang, F. (2018) Stabilization of compressed earth blocks (CEBs) by geopolymer binder based on local materials from Burkina Faso," Constr. Build. Mater., vol. 165, pp. 333–345.
22. Fernandes, J., Peixoto, M., Mateus, R. and Gervásio, H. (2019) LCA of environmental impacts of earthen materials in the Portuguese context: Rammed earth and compressed earth blocks, J. Clean. Prod., vol. 241, p. 118286.
23. Zami, M. S. and Lee, A. (2010) Economic benefits of contemporary earth construction in low-cost urban housing – State-of-the-art review, J. Build. Apprais., vol. 5, no. 3, pp. 259–271, Jan. 2010, doi: 10.1057/jba.2009.32.
24. Rincón, L., Carrobé, A., Martorell, I., & Medrano, M. (2019). Improving thermal comfort of earthen dwellings in sub-Saharan Africa with passive design. Journal of Building Engineering, 24, 100732.
25. Boukari, M., Mboup, N. B., Van Moeseke, G. and Thielemans, B. (2022) Un autre modèle d'habitat entre Ville et Bidonville: Proposition de logements abordables et durables pour le bidonville de Taiba à Dakar, Accessed: Dec. 03, 2023. [Online]. Available: http://tinyurl.com/2zedavrk
26. Nauta, H. (2023) Deze vondst van TNO zet de bouwsector in Malawi op z'n kop, Trouw News Paper, PCM Uitgevers, Amsterdam, the Netherlands.
27. Miles, M. (2006) Utopias of Mud? Hassan Fathy and Alternative Modernisms, Space Cult., vol. 9.2, pp. 115–139.
28. Bredenoord, J. and Kulshreshtha, Y. (2023) Compressed Stabilized Earthen Blocks and Their Use in Low-Cost Social Housing, Sustainability, vol. 15, no. 6, p. 5295.
29. Hafez, H., El-Mahdy, and Marsh, A. T. M. (2023) Barriers and enablers for scaled-up adoption of compressed earth blocks in Egypt," Build. Res. Inf., vol. 51, no. 7, pp. 783–797.
30. Pallubinsky, H., Kramer, R., & van Marken Lichtenbelt, W. (2023). Establishing resilience in times of climate change—a perspective on humans and buildings. Climatic Change, 176(10), 135.
31. Zoungrana, O., Messan, A. Nshimiyimana, P. and Pirotte, G. (2021) The paradox around the social Representations of Compressed Earth Block Building Material in Burkina Faso: the Material for the Poor or the luxury Material?, Open J. Soc. Sci., 9, 50-65.
32. Beccali, M., Strazzeri, V., Germanà, M. L., Melluso, V., & Galatioto, A. (2018). Vernacular and bioclimatic architecture and indoor thermal comfort implications in hot-humid climates: An overview. Renewable and Sustainable Energy Reviews, 82, 1726-1736.
33. Rahim, F., Yusoff, N. S. M., Chen, W., Zainon, N., Yusoff, S., & Deraman, R. (2016). The challenge of labour shortage for sustainable construction. Planning Malaysia Journal, (5).

PLEA 2024 WROCŁAW
(Re)thinking Resilience

Occupant behaviour in dwellings:
Lessons to achieve wellbeing and sustainability in social housing

OLIVIA GUERRA-SANTIN[1] MARLEEN SPIEKMAN[2]

[1]Department of the Built Environment, Eindhoven University of Technology, Eindhoven, The Netherlands
[2] TNO, Delft, The Netherlands

ABSTRACT: This study explores the critical role of building renovation in achieving energy transition goals, emphasizing the importance of not only enhancing energy performance but also addressing occupants' influence on indoor performance. While the trend in the industry involves making buildings 'user-proofed' through automation, limited user control options may lead to dissatisfaction and negative consequences for energy performance. The research investigates comfort preferences and behaviour in renovated and non-renovated homes in the Netherlands, aiming to design buildings supporting energy transition while ensuring occupant comfort. Findings reveal that occupants desire control over home systems, necessitating more information and feedback from new systems. Flexible systems that align with thermal comfort preferences are crucial. Noise issues from ventilation systems persist in both renovated and non-renovated homes, impacting air quality. Mental models play a role, with renovated homes requiring new models, especially for ventilation systems. The study underscores the need for occupants to modify their indoor environment and advocates for user-friendly interfaces, improved guidelines, comprehensive inductions, and better support to empower users and potentially decrease energy use while enhancing comfort in new and renovated buildings.
KEYWORDS: Occupant's behaviour, Energy-efficient homes, Thermal Comfort, Indoor Air Quality

1. INTRODUCTION

Building renovation is key in the efforts to achieve the energy transition goals. Currently, housing renovation projects aim at increasing the energy performance, but not enough attention is yet paid to the indoor performance of the buildings, and the effect that the occupants may have on this performance [1].

Previous research showed that occupants' behaviour can influence greatly the energy performance of buildings [2], however, most studies have focused on decreasing this influence on the energy performance. As consequence, we can see in the building industry efforts towards making buildings 'user proofed', e.g. by automating buildings, or decreasing the options for user control (e.g. non-openable windows, ventilation systems that cannot be turned off). However, previous experiences have shown that decreasing user control not only can increase user dissatisfaction but can also have negative consequences for energy performance and indoor environment quality [3]. And the focus on energy performance alone can even pose a risk to healthy and comfortable living [4].

In this paper, we investigate the differences in comfort preferences and occupants' behaviour in a number of monitored renovated and non-renovated case studies in the Netherlands, as well as the reasons behind the different comfort preferences and occupants behaviour. The goal of the study is to determine what possibilities exist in terms of looking into occupants diversity to design buildings that can support the energy transition, while maintaining the comfort, satisfaction and indoor air quality of the occupants.

2. METHODS

2.1 Data collection

For this study, we focused on three monitoring case studies in the Netherlands. One case with homes recently renovated with a total of 12 dwellings, and a case study with homes in which some renovation measures have been applied in the past (before 2007) with a total of 7 dwellings. Each monitoring case study consisted on a number of dwellings, in which a full monitoring campaign was carried out. Table 1 and 2 show the main characteristics of the case study dwellings.

The research questions in this research were as follows: 1) What is the energy-related occupants' behaviour in their homes?, and 2) what are the causes and consequences on environmental quality and energy use? In each case, different data collection methods were selected, given the differences in the characteristics of the dwellings and building systems.

The monitoring campaigns consisted of both quantitative and qualitative data collection methods, according to the particular objective of each case study.

Throughout the investigation, six distinct assessment methods were implemented, encompassing a technical inventory, an intake questionnaire, sensor-based monitoring, a reflective booklet, distribution of diaries, and an walkthrough-interviews.

- **Technical inventory:** A comprehensive technical inventory was conducted to gather essential technical details concerning the dwellings, including floor plans, installation types, construction year and renovation measures already carried out.
- **Intake questionnaire:** The intake questionnaire, administered face to face or via telephone, focused on background information regarding the household and home, complementing the technical data acquired.

Table 1: Dwelling characteristics (part 1)

Home code	A 1	A 2	A 3	A 4	B 1	B 2	1 b	2 b	3 b	4 b
Apartment	X	X	X	X						
Single family house					X	X	X	X	X	X
<1945							X	X	X	X
1946-1980	X	X	X	X	X					
>1980						X				
Energy neutral	X	X	X	X						
Label A					X	X	X	X	X	X
Label B to G										
Number of adults	2	1	2	1	1	2	1	2	2	2
Number of children	2				1	2	1		1	
Insulation: Average										
Insulation: Good					X	X	X	X	X	X
Insulation: Very good	X	X	X	X						
(Hybrid) heat pump	X	X	X	X						
Boiler					X	X	X	X	X	X
Radiators					X	X	X	X	X	X
Low temperature radiators	X	X	X	X						
Mechanical vent. exhaust										
Balanced vent. heat recovery	X	X	X	X	X	X	X	X	X	X
CO_2 central exhaust canal							X	X	X	X
Decentral mixing fans per room based on CO_2					X	X				

- **Indoor environment monitoring:** All dwellings were equipped with sensors to measure indoor temperature, CO2 levels, and relative humidity across all rooms. Additionally, temperature sensors on each radiator/convector (to measure when the radiator was on or off), measurement of ventilation settings (low, medium, high) via the power consumption of the mechanical ventilation system were implemented and where possible measurement of the thermostat settings. The sensors operated continuously for a minimum of two weeks during the winter, capturing data at 10-minute intervals to objectively portray heating usage and indoor air quality.
- **Reflection booklet and diaries**: Residents were tasked with completing a reflection booklet and filling in diaries for a minimum of four days. These instruments allowed residents to gather information on their comfort, clothing preferences, and insights into the use of the climate systems, including the thermostat, radiator valves, mechanical ventilation system, windows, cooker hood and vents.
- **Walkthrough-interviews –** In one of the visits, the researcher posed various questions, addressing the residents' heating and ventilation practices with their homes. This involved tracing the residents' daily routine on at least one moment in the day, elucidating the reasoning behind their behaviours and routines.

Table 2: Dwelling characteristics (part 2)

Home code	C 1	C 2	D 1	D 2	D 3	D 4	E 1	E 2	E 3
Apartment									
Single family house	X	X	X	X	X	X	X	X	X
<1945							X	X	X
1946-1980		X	X	X	X	X			
>1980	X								
Energy neutral									
Label A	X	X							
Label B to G			X	X	X	X	X	X	X
Number of adults	2	2	1	1	2	1			
Number of children	2	1			2				
Insulation: Average			X	X	X	X	X	X	X
Insulation: Good	X	X							
Insulation: Very good									
(Hybrid) heat pump	X	X							
Boiler			X	X	X	X	X	X	X
Radiators			X	X	X	X	X	X	X
Low temperature radiators	X	X							
Mechanical vent. exhaust			X	X	X	X	X	X	X
Balanced vent. heat recovery	X	X							
CO_2 central exhaust canal									
Decentral mixing fans per room based on CO_2	X	X							

2.2 Methods

For this research, we focused on the analysis of the walkthrough interviews. During the walkthrough interviews, participants (adults) were asked about the use of the home systems, as well as their satisfaction and daily practices in relation to energy related activities during the winter.

Thematic analysis was applied for the examination of data derived from the walkthrough. Coding procedures were established drawing upon existing literature and previous monitoring studies concerning occupants' behaviour. Additionally, recurrent themes explaining the rationale behind occupants' behaviour were considered. In the subsequent phase, codes were categorized into pre-established groups aligning with existing behavioural models and theories.

Supplementary labels were created to accommodate codes that did not align with any of the theoretical models.

3. RESULTS

Results have shown that households have very different comfort preferences and behaviours, which are related to occupants background and life situation, as well as to the characteristics of the home systems and the understanding that the users have of the systems. In the following section focus on the most important behaviours: use of mechanical ventilation system, natural ventilation (opening windows), and use of the heating system.

3.1 Ventilation behaviour

In the study, the seven not recently renovated homes have a mechanical ventilation exhaust system, while the 12 recently renovated homes have a balanced ventilation system with heat recovery, from which eight of them have automatic CO_2 control. In the 11 dwellings with ventilation systems without CO_2 sensors, the control consisted of three settings: 1) unoccupied home, 2) occupied home, and 3) setting for higher occupancy, showering or cooking. In eight of these 11 houses, the system was usually on the lowest ventilation setting almost at all times, with exception of cooking and showering, when the system was set to the highest level. The homes with CO_2 sensors worked based on CO_2 measurements.

Different reasons were reported for the low ventilation setting. In the not recently renovated homes (D and E), these reasons were the noise of the system, the draft created, and saving energy. These homes still had a mechanical exhaust ventilation system, thus occupants are used to employ windows and vents as the main way to provide fresh air into their homes and to remove humidity and odours, although most occupants make use of the mechanical ventilation as well.

In the recently renovated homes B and C (provided with balanced heat recovery ventilation with CO_2 sensors), the reasons related to turning (partially) off or adjusting the sensors of the system were also noise, drafts, and saving energy. However distrust on the system and the understanding of the residents about their new ventilation system were the mayor reasons to adjust manually the system or to open windows and vents for extra ventilation (vent were provided in four of the six homes).

In the A homes, renovated to zero-energy level, balance heat recovery ventilation was provided. In these homes, we see that the main reason to keep the ventilation setting in the lowest level is the noise, mistrust in the system (caused by the system not providing feedback to the users, but also due to problems with the systems), and due to lack of understanding on how the system works (e.g. occupant not being aware that the system also brings in fresh air).

In 15 of the 19 dwellings, the residents used additional ventilation by opening windows or vents (ventilation grids). This happens especially in bedrooms, where in 12 out of the 19 houses, windows were often opened at night. The reasons reported for this behaviour were: to cool the bedroom before or during sleeping, to remove dust, to provide extra fresh air, because they were advised to do so, and due to lack of trust in the system. The residents who kept their bedroom windows closed during the winter, reported the following reasons: trust in the ventilation system, following the instructions of the installers, or the house being otherwise too cold.

In eight houses, the ventilation system had some form of CO2-control. The interviews showed that residents in general do not trust or understand enough the system and so they modify it, for example they turned the system into a manual one or disabled it. Their reasons were related to draughts and noise caused by the system. In five of these homes, residents had to compensate by opening windows, while high CO_2 levels were found in the homes where windows where not open.

Table 3 shows the summary of the ventilation behaviours found in the case study, and the reasons for the behaviour abbreviated: noise caused by the ventilation system (Noise), trust or distrust in the system, linked to the understanding or lack of knowledge of the ventilation system (Trust/K), drafts caused by the system (Drafts), and efforts to save energy (Save energy).

Table 3: Ventilation behaviour and reasons

Home code	Cases	Day setting	Showering Cooking	Windows and vents	Reason
A1, 3-4	3	1	3	Bedroom open window (at night)	Noise Trust/K
A2	1	2	3		Trust/K
B1	1	Off at night	Window open		Drafts Noise
B2	1	Auto but adjusted	Auto	None	Noise
1b	1	Off	None	Vents in bathroom	Draft Save energy
2b	1	Auto but off if cold	Manually higher	All vents and windows bedroom always	Draft
b	2	Auto	Window/ vent in kitchen		Trust/K
C1	1	Auto (bedroom sensor off)	Window in kitchen	Windows bedroom at night	Noise Draft
C2	1	Auto	3	Closed	Trust/K
D4	1	3	Windows	Vent	Trust/K

				open	
D1-3, E1-3	6	1	3 and windows	Vent open	Draft Save energy

3.2 Heating behaviour

The heating behaviour also varied a lot among similar dwellings. More importantly, we can see how the type of heating and ventilation system, the type of control of the heating system, and the thermal properties of the building also have a large influence on the heating behaviour of the occupants. Tables 4, 5 and 6 show the heating-related occupant behaviour, colour coded according to the main reason for the behaviour. The tables are presented per type of heating system: heat pump and low temperature radiators/convectors, boiler and high temperature radiators in homes with heat recovery balanced ventilation, and boiler and high temperature radiators in homes with mechanical exhaust ventilation.

We observed, in all homes, that thermostat settings, which range from 18 to 24°C. Slightly lower settings (18-20°C) are seen in dwellings where saving energy is an important factor (either for environmental or financial concerns), while slightly higher settings (22-24°C) are seen in homes where thermal comfort is an important driver for behaviour. The reasons mentioned by the occupants in relation to the desired indoor temperature depended on factors such as lifestyle (working and studying schedules), caring for others (pets and visitors), sleeping preferences, level of activity (e.g. cleaning, exercising), and background (e.g. having lived previously in a warmer country).

The influence of the preferences for thermal comfort and fresh air, and the desire to save energy, on the use of the heating system is more evident in the setback of the thermostat (setting at night and when occupants are away). In the case studies, we found that in the (better insulated) houses with heat pumps, setbacks were rarely applied because of the slowness of the system to heat again the dwelling. On the other hand, residents of less insulated homes reported to setback the thermostat at nights and when nobody was home to save energy. For example, in dwellings with a boiler, households desiring to save energy and those having a preference for fresh air, tend to set the thermostat lower (10-17°C) than households focusing more on their own thermal comfort (14-18°C).

Table 4: Heating behaviour – heat pump

Home code	**A1, A3, C1**	**A2, A4**	**C2**
Heating System		Heat pump	
Level of Insulation		Very good insulation	
Thermostat setting	21-24	18-22	20
Thermostat Setback		None	
Use of Radiators	Based on use of spaces	Based on use of spaces	Bedrooms half open
Heating while windows open	No / yes	Yes, low heating	No, she was told.
Electric heater	Yes	No	No
Main reason for behaviour	Thermal comfort	Fresh air Health	Save energy

The use of radiators in different rooms are also related to both, personal preferences of the occupants for thermal comfort. These preferences are closely linked to a preference for fresh air in the bedroom during the night, and so the use of radiators is very much linked to the opening of windows during the winter. Households that want to save energy, never open windows when the heating is on, and tend to limit the amount if radiators open in bedrooms and other spaces. Households that prefer to live or sleep in cooler, fresh environments, tend to not heat bedrooms and keep the radiators off. An exception is a household with a heat pump (type A) where the convectors cannot be shut down in bedrooms. Last, in homes where thermal comfort is the most important driver, heating while windows are open, opening all radiators, and having extra heaters are more common practices.

Table 5: Heating behaviour – boiler and heat-recovery ventilation

Home code	B1, 1b, 2b	B2, 3b	4b
Heating System		Boiler	
Level of Insulation		Good insulation	
Thermostat setting	19-21	19-21	18.5
Thermostat Setback	14-18	15-17	16
Use of Radiators	Few rooms	All open	Few rooms
Heating while windows open	No	3b only in bedroom	No
Electric heater		No	
Main reason for behaviour	Thermal comfort	Thermal comfort	Save energy

Table 6: Heating behaviour – boiler and mechanical ventilation

Home code	D1, D3	D2, D4, E38	E37, E39
Heating		Boiler	

System			
Level of Insulation	Average insulation		
Thermostat setting	19-21	18-22	18-21
Thermostat Setback	15-17	18	10-16
Use of Radiators	Mostly on, off in bedrooms		
Heating while windows open	No	yes	No
Electric heater	No/Yes/No	No	No
Main reason for behaviour	Fresh air Health	Thermal comfort	Thermal comfort
Secondary reason for behaviour	Save energy	Habit or easiness	Save energy

The case study A, shows how the technical capabilities of the systems can also affect the occupants behaviour. In these home, no setback is used (or recommended) because of the installation of a low temperature heating system. This system reacts more slowly to changes, and thus the residents prefer to not open windows (for example at night for fresh air in bedrooms).

Furthermore, in this case study, the convectors in the different rooms had a booster option to dissipate faster the heated air, but the temperature of the different rooms could not be regulated separately from the living room. In two of these homes, residents reported dissatisfaction with this system, since they would prefer their bedrooms cooler.

4. DISCUSSION AND CONCLUSION

In this study, we investigated how occupants experience their homes in terms of indoor environmental quality and interaction with the building systems in a number of recently renovated and non-renovated homes. The study showed that occupants' behaviour depend both, on the preferences and needs of the residents, as well as on the characteristics of the dwellings and their systems. Common reasons for behaviour are the need for fresh air, temperature control, noise from installations, draughts produced by the ventilation system or by the quality of the building envelope, saving energy, and noise from others and from the outside. In this section we summarise the conclusion of this research, and we discuss the main aspects of this investigation.

- *Occupants like to keep control of their home, even in the presence of automated systems.*

Due to lack of information or lack of understanding on how the systems function, occupants feel the need to intervene in automated systems, for example automatic thermostats and CO2-based ventilation, to ensure their own comfort and well-being.

- *Occupants need more information and feedback from the system, especially in new systems which workings might seem 'against' common knowledge and old habits and practices.*

Building occupants seem to struggle to know if and when the ventilation or (low temperature) heating systems are working. Historically people relied on touching the radiator surfaces or through the noise emitted by the ventilation systems to determine whether the systems are working. However, these methods might not work with newer technologies.

- *People need flexible systems.*

Building users should be able to choose temperature settings, amount of fresh air, etc.) to match with their thermal comfort preferences, lifestyle and needs.

- *Noise from the ventilation system is a problem in both renovated and non-renovated homes.*

A noisy ventilation system does not only produce acoustic discomfort, for example at night time, but as a consequence of the noise, occupants will in most cases try to adjust, or lower the ventilation system, creating both moisture and air quality problems.

- *Users need support to create mental models of renovated homes.*

Occupants of buildings create models in their own minds regarding the way their home and home's systems function. Mental models come from daily interaction with the building, but can also be created based on experiences in previous homes.

In non-renovated homes, occupants seem to have clear mental models regarding the functioning of the heating system and the building thermal envelope, specifically regarding ways to avoid drafts, and ways to achieve thermal comfort, often in combination with efforts to save energy. On the other hand, occupants seem to make less efforts to have a clear mental model of the ventilation system, simply relying on vents and windows to provide fresh air and dissipate moisture.

In renovated homes, occupants need to create a new mental model of their home after the renovation or introduction of a new system. In the cases included in this study, these focus on the functioning of the ventilation system. In the homes of cases B and b, the ventilation system was the main renovation measure, while in the homes in case A, the heating system allowed very little interaction between the system and the user. However, the focus on the ventilation mental model could be caused by the fact that thermal comfort in winter has improved, while air

quality could deteriorate due to the increased air tightness of the dwellings if the ventilation systems are not optimally operated. However, how well the residents understand the effect of increase air-tightness of their homes is still an open question.

In general, in the renovated dwellings, systems that increase energy efficiency might create new problems for residents, for example overheating in the summer, lack of 'fresh' air, or less flexibility to control indoor temperatures (e.g. low temperature heating). Thus, occupants of renovated buildings have to experiment and learn from their new homes. For this, the above-mentioned information and feedback from the system to the users is crucial.

- *We need to Improve renovation processes and inductions to new/renovated homes.*

Previous studies have shown the need for more participation from residents during the design phase of renovation processes [5]. However, considering the actual needs and preferences of residents in the selection of the technologies in social housing might not be feasible. Therefore, a good induction to their renovated home, well developed (and tested) guidelines, and customer support for the heating and ventilation systems could help to avoid some current common problems causing dissatisfaction among tenants. Further research should be aimed at what is the most suitable and effective way to provide feedback to different types of users (e.g. older people, younger people), in different types of housing and living situations (e.g. social housing), and for different types of building systems and interfaces.

These study indicates the need for systems that allow occupants to modify their indoor environment according to their needs. Thus, in the design of new and renovated buildings, we should give (back) control to the users, or at least provide more information and better instructions on how the newly installed systems function, and how to use them. This can be achieved through better user-building interfaces, improve guidelines and manuals, better inductions of the occupants to their new homes, and better support from installers (via housing associations in the case of rental homes).

Designing systems that are more flexible, and improving the interaction of people with the building systems could potentially decrease energy use and increase the comfort of people.

ACKNOWLEDGEMENTS

This project is executed with the support of the MMIP 3 & 4 grant from the Netherlands Ministry of Economic Affairs & Climate Policy as well as the Ministry of the Interior and Kingdom Relations.

REFERENCES

1. Guerra-Santin, O., Rovers, T., and L. Itard, (2022). Monitoring (N)ZEB dwellings in the Netherlands Lessons learned from current practices. CLIMA 2022 Conference.
2. Hong, T., Yan, D., D'Oca, S., and Ch. Chen, (2017). Ten questions concerning occupant behavior in buildings: the big picture. *Building and Environment* 114 518-30.
3. Wolff, A., Weber, I., Gill, B., Schubert, J. and M. Schneider, (2017). Tackling the interplay of occupants' heating practices and building physics: Insights from a German mixed methods study. *Energy Research & Social Science* 32 65-75.
4. Ortiz, M., Itard, L., & Bluyssen, P.M. (2020). Indoor environmental quality related risk factors with energy-efficient retrofitting of housing: a literature review. *Energy and Building* 221, 1-10.
5. Wagner, A., O'Brien, W. and B. Dong, (2018). Exploring occupant behavior in buildings. Methods and Challenges ed Wagner A et al. (Cham: Springer) chapter 12 pp 307-10.

PLEA 2024 WROCŁAW
(Re)thinking Resilience

Renaturation of urban rivers as a climate adaptation strategy
Case study in Geneva, Switzerland

SOPHIE LUFKIN[1], EMMANUEL REY[1]

[1]Ecole polytechnique fédérale de Lausanne (EPFL), Lausanne, Switzerland

ABSTRACT: In a global context marked by the urgency of climate change, tangible actions towards the ecological transition are top priorities for the built environment. This paper presents the results of the "Maillages fertiles" research project, which seizes the opportunity of the reopening and renaturation of two urban rivers in Geneva, Switzerland, to explore the potential of innovative green open spaces as a climate adaptation strategy aiming at making the urban environment viable, desirable and resilient. The methodology is based on two comparative studies: 1) the literature review, identifying six relevant indicators; 2) the analysis of best practice neighborhoods, providing average values. The results show that all avenues must be combined to achieve climate resilience, linking all actors and placing climate transition issues at the center of decision-making processes and daily practices.
KEYWORDS: Urban transition, Climate adaptation, Green spaces, Sustainable urban design, Climate resilience.

1. INTRODUCTION

In a global context marked by the urgency of climate change, tangible actions towards the ecological transition are top priorities for the built environment. This means not only drastically reducing our carbon emissions, but also (re)designing our urban spaces to prepare for, and adapt to the inevitable impacts of climate disruption. In this perspective, the challenges faced by (semi-)public open spaces are highly complex and closely intertwined. Beyond urban densification strategies – which clearly remain vital [1-3] –, the issues include the creation of green spaces for the relaxation and well-being of urban dwellers, the reintroduction of biodiversity, the ecological and sustainable management of rainwater and floods, the integration of productive surfaces for urban agriculture, the fight against heat islands, as well as the reclaiming of public sphere to the benefit of inhabitants, so as to create gathering and living spaces enhancing neighborhoods' conviviality.

This paper presents parts of the results of a vast research project entitled "Maillages fertiles" [4]. Conducted by an interdisciplinary team of architects, urban planners, sociologists and climate engineers, the research seizes the opportunity of the reopening and renaturation of two urban rivers in Geneva, Switzerland, to explore the potential of innovative green open spaces as polyfunctional interfaces and sustainability activators [5] at the heart of neighborhoods in transition.

2. PRESENTATION OF THE CASE STUDY

The Canton of Geneva, with its small, densely built-up territory, is one of the locations most affected by global warming worldwide. Hence, public authorities have been committed for several years to climate change mitigation and adaptation strategies, such as the Cantonal climate plan, which sets the ambitious targets of a 60% reduction in CO_2 emissions by 2030 and carbon neutrality by 2050 [6]. Representing the greatest potential for housing and activities in Geneva, the Praille Acacias Vernets (PAV) urban project falls within this context (Fig. 1). It aims to transform a 230-hectare industrial and artisanal area – located in the heart of the city and well connected to the public transport network – into a mixed and dense urban neighborhood.

Figure 1: The PAV sector in Geneva (Photo: N. Sedlatchek).

Figure 2: The PAV perimeter and "Espaces Rivières" project.

The PAV project includes “Espaces Rivières”, which involves the creation of a major public space around the re-opening and renaturation of two urban rivers, the Aire and the Drize (Fig. 2). This long-term regeneration process appears as an ideal laboratory for the study of strategies aiming at making the urban environment viable, desirable and climate resilient.

3. OBJECTIVES AND METHODOLOGY

Conducted in close collaboration with the cantonal urban planning department, the research aims at assessing the urban morphology and green spaces of “Espaces Rivières” to highlight the strengths and weaknesses of the project. Recommendations are then formulated to identify avenues for improving its ability to contribute as a climate adaptation strategy.

The methodology is based on the combination of two comparative studies: 1) the literature review identifies six relevant indicators as well as a series of reference values (RV); 2) the analysis of a benchmark of best practice neighborhoods in Switzerland and Europe (Table 1) provides average values (AV) to enrich and nuance data from the literature review.

Table 1: List of best practice neighborhoods.

Name	Location	Area [ha]
Eaux-Vives	Geneva (CH)	256
Jonction	Geneva (CH)	85
Meyrin	Geneva (CH)	282
Lancy	Geneva (CH)	148
Opfikon	Zurich (CH)	97
Seebach	Zurich (CH)	85
Västra Hamnen	Malmö (SE)	166
Vesterbro	Copenhaguen (DK)	108
Île de Nantes	Nantes (FR)	374
Poblenou	Barcelona (ES)	155

The six indicators (1. Arborization, 2. Density of green spaces, 3. Proximity to green spaces, 4. Human density, 5. Functional mix, 6. Density of attenuating spaces) are then grouped in a radar-shaped diagram, which allows to visually compare the results of this multi-criteria analysis (Fig. 3).

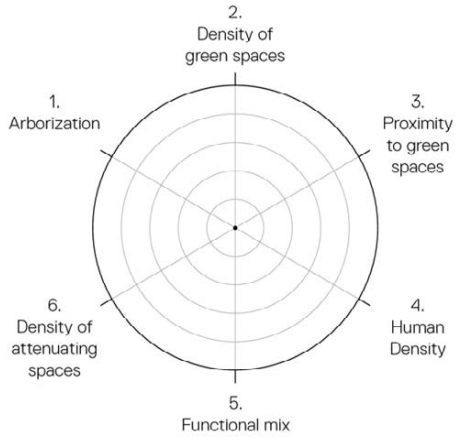

Figure 3: Radar-shaped diagram of the six indicators.

For each of the six indicators, the data are normalized on the sample of best practice neighborhoods. The center of the radar corresponds to the minimum value, while the end of the axis corresponds to the maximum value. Only the functional mix indicator escapes this rule: its scale is reversed.

Let us note here that the first three indicators (urbanization, density of green spaces, proximity to green spaces) characterize the presence of nature in the city, while the last three indicators (human density, functional mix and density of attenuating spaces), for their part, relate to urban morphology and demography. This series of indicators thus underlines a certain tension between urban densification strategies and the desire for quality public and green spaces, which are favorable to biodiversity and necessary for the well-being of urban residents. This tension, which seems quite fundamental, is actually at the heart of the concept of urban intensity. We formulate the hypothesis that, in an approach of optimized consideration of the different components, the main challenge is to achieve a trade-off between conflicting uses, in other words to establish a new balance between built parts and free spaces.

4. RESULTS

4.1 Results by indicator

To illustrate our approach, we present here results for each of the six indicators.

4.1.1 Arborization

There are several approaches to characterize urban forestry. We can cite, for example, the 3-30-300 rule, which requires that every citizen should be able to see at least three trees from their home, have 30 percent tree canopy cover in their neighborhood and not live more than 300 meters away from the nearest park or green space [7], or the calculation of the percentage of shaded area [8]. Considering these approaches difficult to implement, we retained the number of trees per hundred users of public space (inhabitants and jobs), which can be considered as an indicator of urban well-being. The reference value (RV) for this indicator is 11 trees per hundred users [9], which also corresponds to the average value (AV) of our benchmark neighborhoods (Fig. 4).

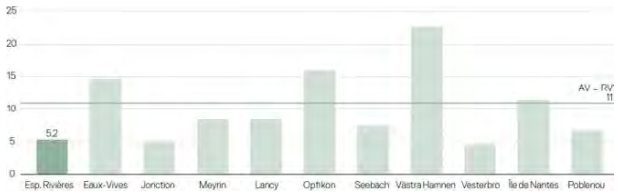

Figure 4: Arborization [trees/100·(inhabitants+jobs)].

These results highlight the scale of the challenge represented by the presence of trees within the

"Espaces Rivières" perimeter. Its score (5.2 trees per 100 users of public space) is more than two times lower than the average and the reference values. If the new trees planned by the project present certain arguments in favor of biodiversity and urban climate quality, they fail to compensate for the massive increase in human density in the sector (418 [inhabitants+jobs/ha]). Considering the performances of our benchmark neighborhoods, RV may certainly seem relatively ambitious, but not impossible to achieve and justified in the current context of climate adaptation. To approach RV, the number of trees planned for the project would have to be more than doubled, which represents a real challenge.

4.1.2 Density of green spaces

The density of green spaces is defined as the total surface area of green spaces in relation to the number of users of public space (inhabitants and jobs). As the concept of green spaces tends to vary quite a bit depending on the sources, it is necessary to clarify what it encompasses. As part of this study, we used the definition proposed by the European Urban Atlas, which includes public green spaces used mainly for recreational purposes (gardens, zoos, parks, natural areas and suburban forests) [10]. This definition remains relatively conservative, in the sense that it does not include private gardens, cemeteries, or non-public agricultural areas. The reference value RV for this indicator is 10 [m^2/inhabitant+job] [11], while the average value of the benchmark neighborhoods AV is 9,3 [m^2/inhabitant+job].

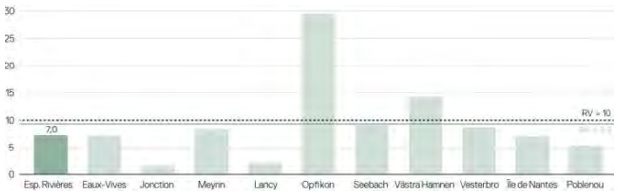

Figure 5: Density of green spaces [m^2/inhabitant+job].

Results clearly show that "Espaces Rivières", with 7 m^2 of green spaces per inhabitant and job, is clearly below the reference and average values (Fig. 5). However, it is interesting to note that only two benchmark neighborhoods reach RV: Opfikon, a peri-urban neighborhood located in the periphery of Zurich, Switzerland, and Västra Hamnen, an industrial brownfield converted into an eco-district in Malmö, Sweden. This illustrates not only that RV is ambitious, but also that target values calculated at city-scale – such as the RV provided by WHO [11] – may exceed those that we were able to measure on our benchmark at neighborhood-scale.

As a second analysis, we would like to confront the results of the density of green spaces indicator to the absolute area of green spaces. When we relate the surface of green spaces not to users of public space, but to the area of the neighborhood, "Espaces Rivières" appears to be one of the best rated neighborhoods in our sample. It totals 28% green spaces, while the average for our best practice neighborhoods is 18%. Nevertheless, as for the arborization indicator, this seems insufficient given the high human density expected in the neighborhood.

4.1.3 Proximity to green spaces

The density of green spaces represents important quantitative data, but it is not sufficient: their location and distribution are equally crucial parameters. It is fundamental to create small green spaces located close to living spaces, in addition to large, extensive and equipped green spaces – but sometimes far away. Hence the necessity to integrate an assessment of the proximity to green spaces.

Most sources tend to agree on the idea that city dwellers should have access to a public green space of at least 0.5 to 1 hectare within a linear distance of less than 300 meters from their place of residence, which approximately corresponds to a five-minute walking distance [12]. Complementing the information provided by the density of green spaces, the proximity to green spaces indicator thus calculates the percentage of inhabitants located within 300 linear meters of a green space of at least 0.5 hectares. Our reference value (RV) aligns with the WHO, which recommends that every resident has access to a green space within 300 meters of their home. Therefore, RV is 100%, while the average value AV of our benchmark neighborhoods is 92%.

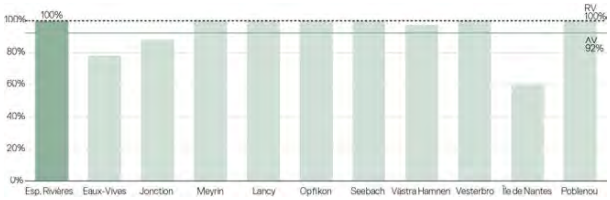

Figure 6: Proximity to green spaces [%].

For this indicator, "Espaces Rivières" obtains a completely satisfactory result, since all residents are located less than 300 meters from a green space (Fig. 6). Unlike the two previous indicators, almost all neighborhoods reach RV, which suggests that the target for proximity to green spaces may be a little bit less demanding. The distribution of green public spaces within "Espaces Rivières" therefore seems well adapted, mainly thanks to the judicious decision to locate a Grand Parc in the center of the sequence (Fig. 2), guaranteeing that residents have access to a major green space in less than five minutes on foot.

4.1.4 Human density

Human density is defined as the number of inhabitants and jobs per hectare. Let us clarify here

that the goal is in no way to maximize human density. The challenge is rather to seek a balanced situation, pursuing a qualitative approach to urban densification [13]. Indeed, too diffuse occupation tends to generate unsustainable structures, while too high a density is synonymous with promiscuity. Appropriate density brings together a critical mass of people and activities, allowing for efficient public transport service and guaranteeing the provision of socio-cultural amenities in a local structure while preserving the quality of life and the possibilities of harnessing the solar potential [14]. According to different sources, the optimal human density level would be around 120 inhabitants and jobs per hectare – which also corresponds to around 40 to 50 housing units per hectare. This level of density theoretically makes it possible to operate sustainable and viable mobility, while offering the possibility of tapping solar energy and giving a significant place to greeneries.

The average value AV calculated for our benchmark neighborhoods, which is almost 250 inhabitants and jobs per hectare, is significantly higher than the reference value RV (Fig. 7).

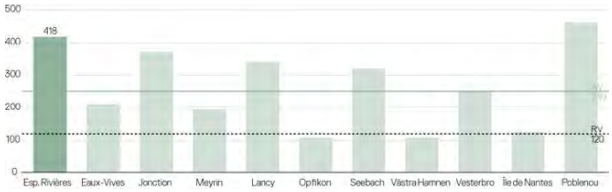

Figure 7: Human density [inhabitants+jobs/hectare].

As already mentioned above, “Espaces Rivières” stands out for its particularly high human density (418 inhabitants and jobs per hectare). Not only is the neighborhood 3.5 times denser than the reference value (RV = 120), it is also the second densest neighborhood in our benchmark, and more than 1.5 times denser than the average value (AV = 249).

A closer observation of the results allows us to somewhat nuance this observation. All the Swiss neighborhoods exceed the reference value RV (except for Opfikon, in the periphery of the Zurich urban region, which confirms its suburban character). Switzerland being a densely populated country, we can argue that it has a certain form of cultural acceptance towards rather dense urban situations.

Moreover, the example of Poblenou in Barcelona allows us to put into perspective negative and anxious perceptions of density. With more than 460 inhabitants and jobs per hectare, it is the densest benchmark neighborhood. A former industrial district having undergone a successful urban rehabilitation process, Poblenou is today renowned for its quality of life, at the heart of Barcelona's artistic culture. Therefore, provided that it is accompanied by architectural and landscape quality, density can be synonymous with urban intensity and richness of uses.

4.1.5 Functional mix

Functional mix, which is defined as the ratio between the number of jobs and the number of inhabitants, is intrinsically linked to the concepts of urbanity or urban intensity. It is a vector of values such as diversity, proximity or liveliness [13]. As with human density, the goal is not to maximize the number of jobs or residents, but rather to define, according to a coherent and balanced scenario, a qualitative functional mix, relevant and adapted to the context, which aims to integrate a wide enough range of activities to avoid forced mobility. Functional mix is an objective to be defined and negotiated on a case-by-case basis, according to a multitude of parameters such as the territorial, cultural or political context. Thus, no empirical reference value is available, nor otherwise desirable. We have therefore chosen to use the Swiss national average, which is slightly below 0.5 jobs per inhabitant. The benchmark average value reflects a significantly higher proportion of jobs (AV = 1,2), mainly due to Seebach, a neighborhood largely dedicated to activities located in the city of Zurich, Switzerland.

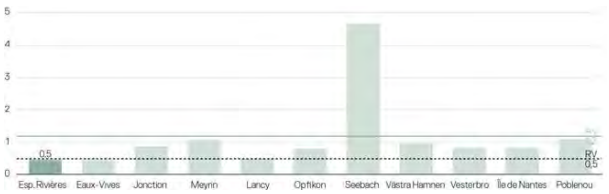

Figure 8: Functional mix [jobs/inhabitants].

The results (Fig. 8) confirm the rather residential vocation of “Espaces Rivières” (0,5 jobs/inhabitants), in comparison with the benchmark average (AV = 1,2). It is at the same level as the Swiss reference value, just like the mixed urban neighborhoods of Eaux-Vives and Lancy, both located in the Geneva urban region. Given the extreme tensions experienced by the Geneva housing sector, this evolution towards a neighborhood whose character will be largely residential seems desirable.

4.1.6 Density of attenuating spaces

This last indicator calculates the surface area of attenuating spaces in relation to the number of inhabitants and jobs. Attenuating spaces include all accessible or appropriable public spaces, that is to say mineral public spaces such as squares and pedestrian streets, but also green spaces, bodies of water and the banks of rivers, lakes or seas [15]. This indicator, which aims to enrich the data provided by the density of green spaces, provides information on the spaces available for different appropriations or use values.

The literature recommends an upper reference value of 12 m^2 of attenuating spaces per inhabitant and job [16]. This value would have the capacity to mitigate a high built density, that is to say, it would

balance the pressures exerted by built spaces on unbuilt public spaces, considered as decompression factors. Our benchmark average is estimated just below 14 m^2 of attenuating spaces per inhabitant and job (AV = 13,8 [m^2/inhabitant+job]).

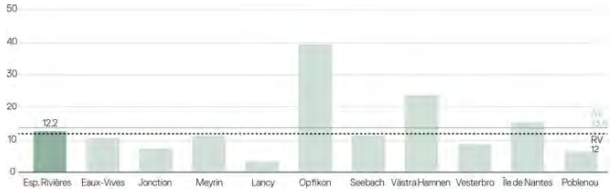

Figure 9: Density of attenuating spaces [m²/inhabitant+job].

"Espaces Rivières", with 12.2 m^2 of attenuating spaces per inhabitant and job, is just above the reference value and just below the average for our benchmark of Geneva, Swiss and European neighborhoods (Fig. 9). We can therefore estimate that the results of this indicator can be considered completely satisfactory.

Here, it is interesting to note that "Espaces Rivières" is truly exemplary in terms of the surface area of attenuating spaces compared to the surface area of its perimeter. With approximately 50% of attenuating spaces, it is clearly the neighborhood presenting the highest score among our benchmark. In contrast, our benchmark average is 26%, or almost half as many accessible public spaces. Contrary to what has been said for the density of green spaces, the extremely generous layout of "Espaces Rivières" seems to be sufficient to compensate for the arrival of the relatively high number of future users of public space.

4.2 Morphological profile of the neighborhoods

The morphological profile offers a synthetic vision of the six indicators calculated for this study. This synoptic representation provides an in-depth understanding as well as an effective means of communication of the strengths and weaknesses of "Espaces Rivières" in relation to our benchmark of neighborhoods (Fig. 10).

Far from a normative perspective, we aim here to characterize the atmosphere within the neighborhood, seeking a balance between built density, quality of public spaces, presence of nature and adaptation to climate change. The issue at the heart of the process is evaluating the extent to which the neighborhood manages to reconcile urban development and quality of life for the future inhabitants.

"Espaces Rivières" stands out for its high human density and its rather residential character, as well as for the proximity to green spaces that it offers to its inhabitants. As previously mentioned, the density of green spaces, as well as the arborization, appear as two more fragile elements.

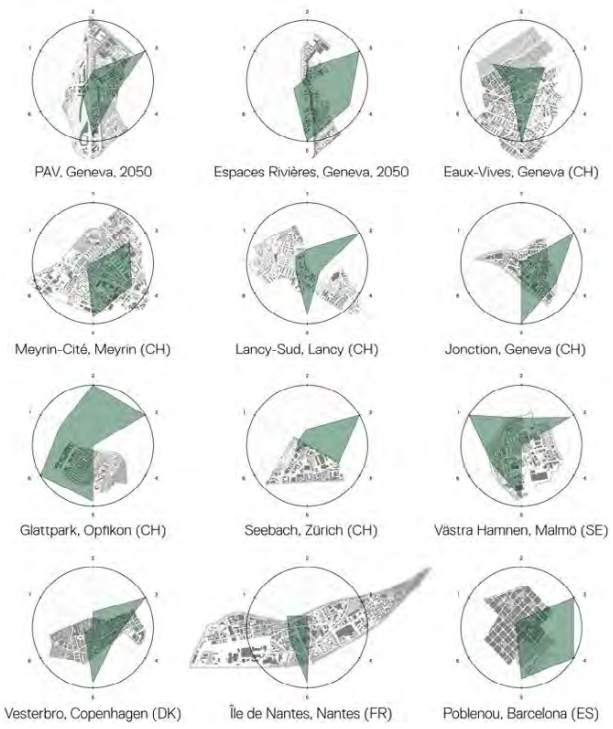

Figure 10: Morphological profiles of the "Espaces Rivières" case study and benchmark neighborhoods.

5. CONCLUSION

First of all, the comparative study confirms that "Espaces Rivières" is very ambitious in terms of human density. If we take into consideration the future users of the neighborhood – and not just the absolute surface area, which tends to be rather generous –, this high human density has a negative impact on two indicators, namely Arborization and Density of green spaces.

In order for green spaces to fully assume their essential climatic function – but also health-related, ecological, recreational and sociocultural –, we recommend respecting the reference value RV of 10 m^2 of green spaces per inhabitant and job (against 7 m^2 of green spaces per inhabitant and job in the project as currently planned). This target could be achieved through the combination of several strategies: activation of roofs (vegetable gardens or shared green spaces), creation of an additional park of 1 hectare and slight reduction in human density (around 9 to 10%, i.e. 378 [inhabitants+jobs/ha] instead of 418 [inhabitants+jobs/ha] in the current project).

Another more qualitative line of approach would consist of strengthening the public spaces and mobility networks meshing towards the green lungs surrounding "Espaces Rivières", by creating new soft mobility connections, such as bridges (Fig. 11). As demonstrated by other studies conducted in the framework of the "Maillages fertiles" research project, this additional carbon investment will quickly pay for itself if the connections are planned consistently.

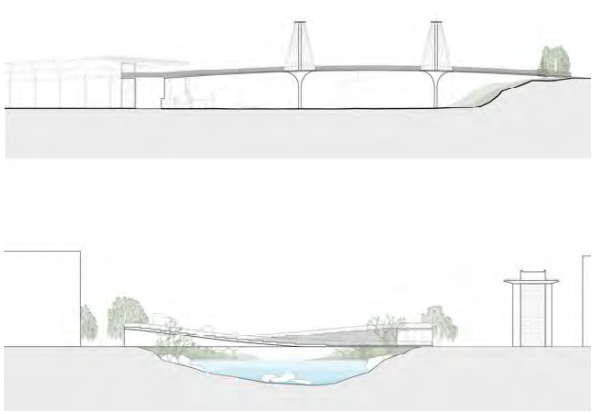

Figure 11: Two propositions of new soft mobility connections developed in the framework of the "Maillages fertiles" research project.

Given the scale of the climate adaptation challenges, these results highlight that we cannot ignore any strategy: all avenues must be combined to achieve the ambitious objectives of the urban transition. At the end of the research, "Espaces Rivières" appears more essential than ever to ensure the attractiveness and resilience of the future PAV neighborhood and, more broadly, of the entire Geneva urban region. Ultimately, only an exceptional dynamic – linking all actors and placing climate transition issues at the center of decision-making processes and tangible daily practices – will turn "Espaces Rivières" into an exemplary project for the canton of Geneva.

ACKNOWLEDGEMENTS

This study was conducted as part of the "Maillages fertiles" interdisciplinary research project, mandated by République et canton de Genève, Département du Territoire (DT), Direction Praille Acacias Vernets (DPAV).

REFERENCES

1. Lufkin, S., E. Rey (2016). Green Density. Interdisciplinary education and research project for the design of sustainable neighborhoods. In *PLEA 2016*, Los Angeles, USA, July 11-13.
2. Lufkin, S., E. Rey (2017). Neighbourhood-scale Evaluation to Benchmark the Integration of Urban Sustainability (NEBIUS). In *PLEA 2017*, Edinburgh, UK, July 2-5.
3. Rey, E., M. Laprise, S. Lufkin (2022). Neighbourhoods in Transition. Cham : Springer.
4. Rey, E., S. Lufkin (2023). Maillages fertiles. Lausanne: EPFL.
5. Dind, A., S. Lufkin, E. Rey (2018). Vers des activateurs de durabilité. In *Bâtir pour la mobilité durable*. Lausanne: EPFL.
6. République et Canton de Genève (2021). Plan climat cantonal 2030 - 2e génération.
7. Nieuwenhuijsen, M., P. Dadvand, S. Márquez et al. (2022). The evaluation of the 3-30-300 green space rule and mental health. *Environmental Research*, 215(2).
8. Schlaepfer, M., E. Amos, R. Olivier (2018). Projet NOS-ARBRES. Synthèse pour les instances de décision. Genève.
9. Observatoire des villes vertes (2020). Les villes les plus vertes de France. Palmarès 2020.
10. European Union (2011). Mapping Guide for a European Urban Atlas. Copenhagen: European Environment Agency, EEA.
11. World Health Organization. *Health Indicators of Sustainable Cities in the Context of the Rio+20 UN Conference on Sustainable Development*. WHO; Geneva, Switzerland: 2012.
12. World Health Organization. Regional Office for Europe. 2017. *Urban green spaces: a brief for action*. Copenhagen: World Health Organization. Regional Office for Europe.
13. Lufkin, S., E. Rey (2022). Influence de la texture périurbaine sur la durabilité d'un quartier. In *Living Periphery*. Lausanne: EPFL Press.
14. Pouchain, F., R. Ménard (2017). Analyse du potentiel solaire des toitures du Grand Paris. In *Vers la ville symbiotique ? Valoriser les ressources cachées*. Neuchâtel: Tracés.
15. Mazurek, H., D. Pereira (2015). Indicateurs Pays - Villes - Développement urbain durable. MC3 2015.
16. Agencia de Ecologia Urbana de Barcelona (2008). *Plan Especial de Indicadores de Sostenibilidad Ambiental de la Actividad Urbanística de Sevilla*. Barcelone: Gerencia de Urbanismo.

PLEA 2024 WROCŁAW
(Re)thinking Resilience

Impact of the urban modified albedo on the energy performance of buildings. The case of Rome, Italy

SERENA FALASCA[1], ANNA MARIA SIANI[1], STEFANO AGNOLI[2], MICHELE ZINZI[2]

[1] Department of Physics, "Sapienza" University of Rome, Piazzale Aldo Moro 5, 00185 Rome, Italy
[2] ENEA Italian National Agency for New Technologies, Energy and Sustainable Economic Development, Rome, Italy

ABSTRACT: The urban overheating is a well-documented phenomenon due to the local (Urban Heat Island) and global warming. Several adaption and mitigation strategies are available to counter such hazard and include the use of green and blue technologies, as well as the use of cool materials, able to reflect most of the incident solar irradiation and keep cool the urban structures and the surrounding air. This paper intends exploring the impact of cool materials for roof, urban pavements and roads in mitigating the urban climate in a Mediterranean metropolis like Rome, Italy. This task is carried out by meso-scale ground measurements' validated simulations, using the WRF model. Simulating the current conditions and modified urban albedo scenarios, it is found that the peak air temperature might be lowered by up 1.4°C, using the July 2020 period as reference. The local climate datasets are then inputted to TRNSYS17 software to assess the impact on the energy performance of residential buildings. It is found out that cooling energy needs can be reduced by up to 14% and 24% in insulated and not insulated buildings, respectively. It is also quantified the impact of the urban modified albedo with respect to the application at the single building level.

1. INTRODUCTION

Urban heat island, with the associated urban overheating, is a well-documented phenomenon, which demonstrates the hazard related to local climate change and the related negative impacts at environment, economic, social and public health level, with heavier consequences on the low income and more fragile segment of the population. The phenomenon takes origin by the positive thermal balance in the urban built environment mainly, depending on the synergic effect of different causes: absorption and storage of solar irradiation by the construction surfaces, the anthropogenic heat, the reduced evapotranspiration and surface permeability due to the lack green and natural areas, change and reduction of urban ventilation [0]. It is also associated with a typical atmospheric circulation, playing a significant role in local dispersion processes [0]. The interaction of local and global climate change exacerbates the thermal quality of cities, with more frequent and more intense extreme events, being the heat waves the most relevant [0].

Several solutions exist to counter urban overheating, and three main categories are identified: blue (water), green (vegetation) and white (materials) technologies [0]. The latter solution gained interest in the past three decades with the development of the cool materials, characterised by high albedo (or solar reflectance) and thermal emissivity, which minimise the solar irradiation absorbed by the construction surface and easily dissipate the residual stored heat by radiation [0]. Cool roofs use white or selective cool coloured materials, being the latter characterised by a very high reflectance in the near-infrared range while keeping the design colour in the visible range. The benefit of the technology are well documented by numerical analyses and field studies [0]. Mesoscale simulations have been recently introduced to predict the mitigation impact of higher albedo materials in cities, trying to understand potentials and risks of the technology application at large scale [0].

Objective of this paper is to quantify the improvement of the cooling energy performance of a residential building in the City of Rome (Italy), by dynamic analyses carried out at mesoscale and building level for different urban albedo scenarios. The original contribution of this work regard: i) extended monitoring period combined to a small observation grid, ii) the application of an innovative configuration of the Weather Research and Forecasting (WRF) model specifically implemented for the city of Rome as described in Section 3.1.

2. METHODOLOGY

The method consist of the following phases. Initially, the land and atmospheric models of the city are implemented in a meso-scale climatic model, which is validated against the near surface air temperature and wind speed and ground measurements (the detailed analysis is currently submitted for publication in a scientific journal). Next, a number of modified albedo scenario is defined and climatic simulations are run for

the month of July to generate the modified climatic data (namely: the air temperature and relative humidity, global solar irradiation on the horizontal and wind speed). There are finally used as input to simulate the energy performance of a typical residential Italian buildings, whose cooling energy performance is calculated modifying the albedo of the building roof under the reference climate as well. This double track allows quantifying the benefit of cool roofs when applied either, at single building and city scale levels.

The key performance indicator for the energy performance analysis is net cooling energy use, defined as the thermal energy required to keep the building at the desired set-point without introducing the efficiency of the cooling energy system.

2.1 Study area and period

Rome is the capital of Italy and is positioned in the middle of the Mediterranean basin, recognised as a hotspot for climate change [0]. The city belongs to the Csa class, Mediterranean climate, according to the Köppen-Geiger climate classification.

Rome has 2.85 million inhabitants, peaking 4.6 million if all the metropolitan area is considered. The municipality extension is about 1290 km² and a density of about 2200 inhab/km². Rome has extensive green areas but essentially located in the extreme periphery of the municipality territory; in fact, the urban green areas account for the 3.1% of the city surface only. The urban texture and the characteristics of the building stock are complex and stratified, consequence of a history lasting close to three millennia.

Table 1: Average and peak values of the main weather variables recorded at the Boncompagni station during July 2020.

Parameter	Unit	Average	Maximum
Air temperature	°C	27.0	37.4
Air relative humidity	%	52.3	88.4
Wind speed	m/s	1.6	3.9

The present study is based on the weather data of July 2020, whose main characteristics are reported in Table 1. The analysis is focused these 31 days to balance the huge calculation effort needed to carry out meso-scale with a period long enough to assess the impact on the building energy performance.

2.2 The reference building

The building consists of three floors, with two apartments per floor. It is one of the reference buildings studies for the energy performance analyses in the framework of the Italian national implementation of the EPBD [9]. This building was already used for energy and thermal performance analysed in previous works [10].

Each apartment has net floor area and volume of 89m^2 and 242m^3, respectively; the total windows area is 13.6m^2, distributed across three different orientations for each apartment. The height of each floor is three meters (including 30cm of masonry). The layout of the typical floor of the building is presented in Figure 1.

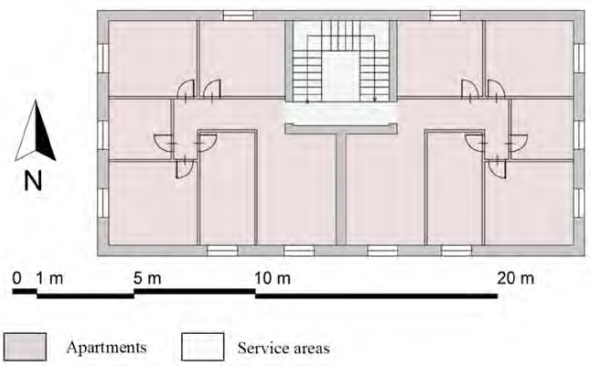

Figure 1. Plan of the typical floor of the reference building

Table 2: Main thermal properties of the building envelope components.

Envelope component	Insulation Y/N	U W/m^{2}K	R m^{2}K/W	CT kJ/K
Vertical wall	Y	0.29	2.98	330
Roof	Y	0.26	3.13	221
Ground floor	Y	0.29	2.98	635
Window	Y	1.85	0.37	---
Vertical wall	N	0.96	0.87	302
Roof	N	0.99	0.84	289
Ground floor	N	1.14	0.71	264
Window	N	5.60	0.01	---

Two building configurations are considered: with and without thermal insulation, representative of new and renovated buildings, and existing one, respectively. This choice allows to evaluate how the climatic conditions affect the performance buildings constructed and managed according to different standards and construction period. The main thermo-physical parameters (thermal transmittance U, resistance R and heat capacity CT) of the two building configurations are reported in Table 2.

In accordance with the requirements of the Italian building code for the assessment of the energy performance of buildings [11, 12], the following settings are defined for the building operation:

- Internal sensible heat gains equal to 5 W/m2 and
- Internal latent heat gains equal to 2.5 W/m2;
- Windows g-value equal to 0.89 and 0.60 for the single glazed unit of the uninsulated building and for

the low-e double glazing unit of the insulated building;

- 0.75 shading coefficient for external solar protection devices activated during daytime in summer.
- Set points for the net cooling energy need: 26°C for air temperature and 60% for air relative humidity, with the system always switched on.
- Natural ventilation 0.5 h^{-1} Air Change per Hour (ACH).

2.3 Definition of the "what-if" scenarios

The set of runs carried out for the meso-scale and building analyses includes a control case and three "what-if" scenarios simulating the application of cool materials on different types of urban surfaces, namely roads, urban pavements and roofs. In detail, the three scenarios have been implemented by assigning increasing albedo values to these surfaces with respect to the control case, from 0.15 to 0.5 for roads and pavements and from 0.2 to 0.8 for roofs (Table 3). The building energy performance calculations are carried out using the weather data obtained by the meso-scale simulations, as well as by changing the roof albedo values as defined in Table 1 in the control case weather conditions. It is here reminded that albedo is a synonym of solar reflectance, being the former used in urban studies and the latter in building elements characteristics. This modelling approach based on the execution of UHI mitigation scenarios performed with WRF presents numerous recent examples also regarding the application of cool materials [0,0].

Table 3: Control case and "what-if" scenarios form meso-scale simulations and for roof albedo variants in the control case.

Scenario	Road/Pavement	Roof
Control case	0.15	0.2
S1	0.3	0.4
S2	0.4	0.6
S3	0.5	0.8

3. CALCULATION

This section in split in two sub-sections; the first one describes in detail the city model carried out with the meso-scale software, whose outputs are used as inputs for the energy calculation carried out at building scale.

3.1 The city model

The Weather Research and Forecasting (WRF) model [0] is used here to simulate the atmospheric dynamics over the urban area of Rome. The model setup consists of four two-way nested domains covering most of the peninsular Italy (d01), central Italy (d02), Lazio region (d03) and the metropolitan area of Rome (d04); the scheme is graphically presented in Figure 2. Such domains have a horizontal grid size decreasing from 13.5km of the outermost domain to 0.5 km of the innermost domain and a vertical grid of 33 levels with the maximum resolution of about 12m near the ground. The physical configuration includes: the revised MM5 surface layer scheme, the Noah Land Surface Model, the Bougeault-Lacarrère Planetary Boundary Layer scheme coupled with the Building Effect Parameterization scheme, the Single-Moment 6-class microphysics scheme, the RRTM and the Dudhia schemes for long and short wave respectively [0]. Final operational global analysis data of the National Center for Environmental Prediction (0.25°× 0.25°, every 6 hours) are the initial and boundary conditions [0].

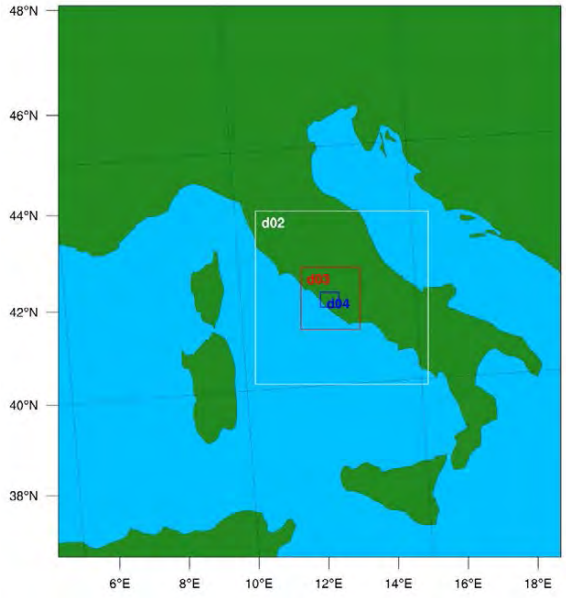

Figure 2: Geographical areas covered by the WRF computational domains.

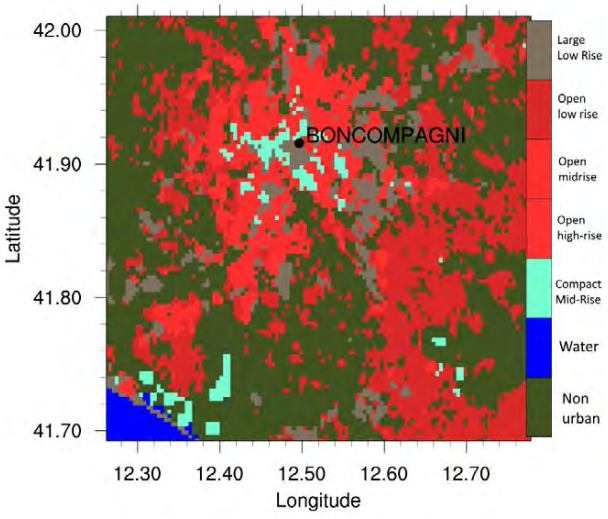

Figure 3: Urban land use categories in the domain over Rome according to the LCZ classification. The black dot identifies the

Boncompagni weather station whose acquisitions are used to validate the numerical results.

The land use dataset is derived from MODIS for non-urban cells, while it is derived from the World Urban Database and Access Portal Tools project (https://www.wudapt.org/) [0] based on the Local Climate Zones - LCZ [0,0] for the urban cells. Figure 3 shows the urban land use map embedded in the innermost domain over Rome.

3.2 The building model

The simulations are run using TRNSYS 17, a widely used and calibrated tool for thermal analyses in transient regime [0]. Each TRNSYS project consists of several routines linked together, each with a specific calculation task.

This project includes the following routines: a) the data reader for Generic Data Files, used to input the weather data; b) the radiation processor to calculate the solar irradiation; c) the psychometrics used to calculate moist air properties; d) the effective sky temperature for long-wave radiation exchange, v) the Multi-Zone building model; e) the slab on grade, to model the heat transfer to soil below.

14 simulations are run, considering the different building configurations, climatic data set and roof albedo variants. The simulations are run for 38 days; the first week is used to thermally charge the building according to the season conditions, next the 31 days of July are simulated. Simulation are sun in transient regime with one hour resolution step. The total net cooling energy need is the sum of the sensible and the latent heat to be removed from each apartment at the given set-points during the calculation period.

4. RESULTS

4.1 Evaluation of the model performances

The reliability of the WRF model in reproducing the thermal and dynamical fields over Rome in the control case is tested through the comparison of the timeseries of near-surface temperature and wind speed simulated (T2 and WS10) and that recorded by the Boncompagni downtown weather station of the network belonging to the regional environmental protection agency (ARPA Lazio). Such network includes fixed micro-meteorological stations with instrumental equipment compliant with the indications of the WMO (https://www.arpalazio.it/, in Italian). Figure 4 displays the average daily cycles of these variables and Table 4 summarizes some statistical parameters used for the quantification of the model performances. Specifically, the bias, the Pierson correlation coefficient (R) and the fraction of predictions within a factor of two of observations (FAC2). A perfect model would have bias equal to 0 and R and FAC2 to 1. The WRF performances in simulating the temperature are very satisfactory, while wind speed still has margins for improvement. Such discrepancy between the two quantities is a well-known feature of the WRF model.

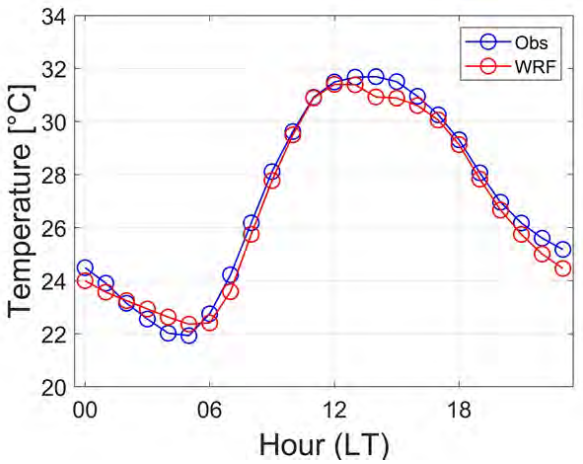

Figure 4: Average daily cycles of the observed and simulated air near-surface temperature for July 2020.

Table 4: Statistical parameters in the comparison between observed and simulated of near-surface temperature and wind speed at Boncompagni weather station.

Parameter	Temperature	Wind Speed
Bias	-0.24	0.39
R	0.96	0.77
FAC2	0.98	0.78

4.2 Near-surface temperature and wind speed

This conference paper is focused on the energy performances of buildings, therefore only an overview of the effect of the increased albedo on the urban climate will be provided here, referring the reader to another work (currently in preparation) specifically on the urban climate for such insights. Figure 5 show the average daily cycles of T2 for the control case (CTRL, in black) and the "what-if" scenarios. These cycles are averaged both in time over the month of July 2020 and in space across all cells characterized by urban land use categories. In the control case T2 ranges from about 22.5°C in the early morning to almost 30°C at 1pm. The maximum difference value is at 12pm in the scenarios. These values amount to 1.41°C, 0.93°C and 0.4°C for S3, S2 and S1 respectively. Concerning the wind speed, it found that WS10 is between approximately 1m/s at night and 3.3m/s at 4pm in the control case. The increase in albedo in “what-if” scenarios lead to a progressive decrease in WS10 in the central hours of the day. The maximum difference is observed at 2 pm

and is equal to 0.2 °C, 0.34 °C, 0.48 °C for scenarios S1, S2 and S3.

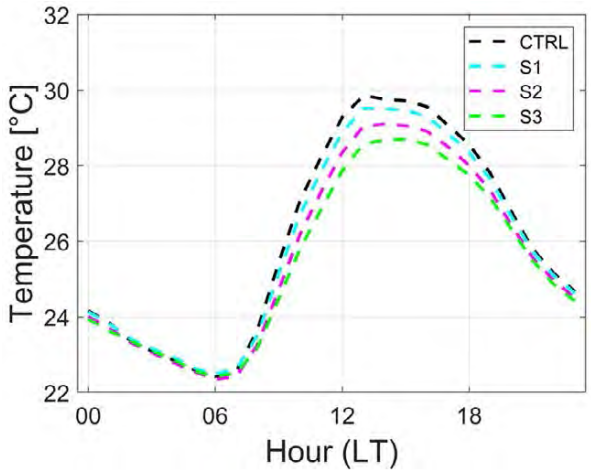

Figure 5: Average daily cycles of T2 in the control case and "what-if" scenarios.

4.3 The building energy performance

Tables 5 and 6 report the energy performance of the reference building in the insulated and not insulated configurations; the former presents the results in case of the modified albedo at urban scale; the latter 6 refers to the solar reflectance change at the single building scale. The quantity expressed in megawatt hour refers to the all building for easiness of comparison. It can be observed that the net cooling energy is about 15% for the not insulated building configuration, depending on the higher solar and thermal gains through the low thermal resistance of the building envelope. Such differences diminish with the increase of the albedo in both cases, due to the increase of the albedo of the roof.

Table 5: Energy Performance (EP) of the building with the urban modified abled.

Albedo scenario	EP_insulated [MWh]	EP_not_insulated [MWh]
Control case	16.6	19.7
S1	16.0	18.5
S2	14.9	16.5
S3	14.3	15.0

Table 6: Energy Performance (EP) of the building with difference solar reflectance of the roof

Albedo values	EP_insulated [MWh]	EP_not_insulated [MWh]
0.2	16.6	19.7
0.4	16.2	18.7
0.6	15.8	17.6
0.8	15.3	16.5

The impact of the albedo on the energy performance can be observed in relative terms in Figure 6. The energy saving achievable for the insulated building is about 8% increasing the albedo from the initial 0.2 up to 0.8 with linear tendency; the cooling saving raises up to 14% when the increase of the albedo is applied at city scale. It can be observed in this case that the trend is not linear, as the slope of the line in the 0.4-0.6 albedo variations is higher than those calculated in the other ranges. Beside this aspect, the high impact of the urban modified albedo can be easily inferred. The trend is similar, but the savings are more relevant for the not-insulated configuration. The cooling energy performance decrease peaks about 16% for the single building and savings are close to 24% for the urban-modified albedo case. Albedo values of 0.8 can be basically achieved with white materials, which often have several architectural and policy constraints in towns and cities. Interestingly, the building cooling energy performance achieved with the scenario 2 equals or improves those calculated for the 0.8 albedo in the single building case. This is a significant achievement as 0.6 albedo can be reached by several construction materials, as well by cool coloured materials, whose high near-infrared reflectance ensure adequate albedo values also for non-white colours.

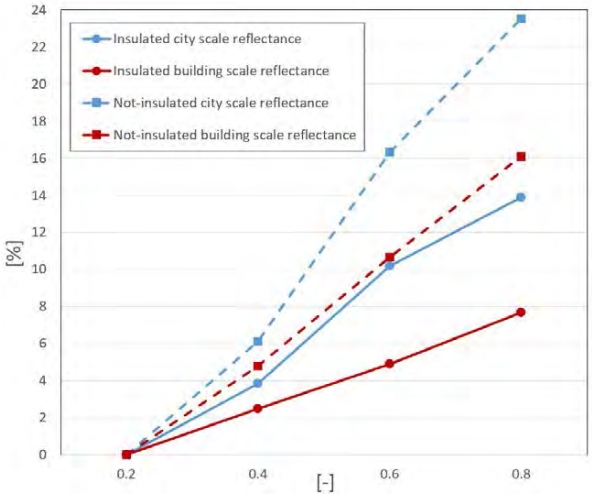

Figure 9: Energy performance of the building in the insulated and not insulated configuration. The roof reflectance refers to reference case, S1, S2, and S3 scenario for the city scale case.

5. CONCLUSION

This study presents the impact of the urban modified albedo on the energy performance of residential buildings in a Mediterranean metropolis. The urban model of Rome is implemented in WRF, and validated against ground measurements of the air temperature and the wind speed. The current configuration and three modified albedo scenarios are

modelled. The peak air temperature in the city can be lowered up to 1.41°C. The energy performance analysis of a reference building, carried out in transient regime, shows that energy savings up to 14% and 24% can be reached for insulated and not insulated buildings, respectively. These results outperform the savings achievable increasing the roof albedo of the single building, peaking 8% and 16%, respectively. The role of the modified urban albedo is thus crucial in a framework aimed at the decarbonisation of the building stock, threatened by the increase of the cooling energy in overheated cities in an overheated planet.

ACKNOWLEDGMENTS

Research funded by Project 1.7 "Technologies for the efficient penetration of the electric vector in the final uses" within the "Electrical System Research" Programme Agreements 22-24 between ENEA and the Ministry of Environment (PTR 22-24). Serena Falasca gratefully acknowledges fellowship funding from MUR (Ministero dell'Università e della Ricerca) under PON "Ricerca e Innovazione" 2014-2020 (D.M. 1062/2021). The computing resources and the related technical support used for this work have been provided also by CRESCO/ENEAGRID High Performance Computing infrastructure and its staff [0]. CRESCO/ENEAGRID High Performance Computing infrastructure is funded by ENEA and by Italian and European research programmes, see http://www.cresco.enea.it/english. The authors acknowledge ARPA Lazio for providing weather data.

REFERENCES

1. Oke, T.R., Johnson, G.T., Steyn, D.G. and I.D. Watson, (1991). Simulation of Surface Urban Heat Islands under 'Ideal' Conditions at Night - Part 2: Diagnosis and Causation, *Boundary Layer Meteorology*, 56: p. 339–358.

2.Falasca, S., Moroni, M. and A. Cenedese, (2013). Laboratory simulations of an urban heat island in a stratified atmospheric boundary layer. *Journal of Visualization*, 16: p. 39–45.

3.Perkins, E. S., (2015). A review on the scientific understanding of heat-waves —Their measurement, driving mechanisms, and changes at the global scale, *Atmospheric Research,* 164-164: p. 242-267.

4.Akbari, H., et al. (2015). Local climate change and urban heat island mitigation techniques – the state of the art. *Journal of Civil Engineering and Management*, 22: p. 1-16.

5.Santamouris, M., Ding, L., Fiorito, F., Oldfield, P., Osmond, P., Paolini, R., Prasad, D. and A. Synnefa, (2017). Passive and active cooling for the outdoor built environment – Analysis and assessment of the cooling potential of mitigation technologies using performance data from 220 large scale projects. *Solar Energy*, 154: p. 14-33.

6.Testa, J. and M. Krarti, (2017). A review of benefits and limitations of static and switchable cool roof systems. *Renewable and Sustainable Energy Reviews*, 77: p. 451-460.

7.Falasca, S., Ciancio, V., Salata, F., Golasi, I., Rosso, F. and G. Curci, (2019). High albedo materials to counteract heat waves in cities: An assessment of meteorology, buildings energy needs and pedestrian thermal comfort. *Building and Environment*, 163: p. 106242.

8.Lionello, P. and L. Scarascia, (2018). The relation between climate change in the Mediterranean region and global warming. *Regional Environmental Change*, 18: p. 1481–1493.

9.European Parliament. Directive 2010/31/EC of the European Parliament and of the Council of 19 May 2010 on the energy performance of buildings (EPBD recast). Official Journal of the downloaded at: eur-lex.europa.eu/legalcontent/EN/TXT/PDF/?uri=CELEX:32010L0031&from=EN.

10.Zinzi, M., Agnoli, S., Burattini, C. and B. Mattoni, (2020). On the thermal response of buildings under the synergic effect of heat waves and urban heat island. *Solar Energy*, 211: p. 1270-1282.

11.Decreto del Ministero dello Sviluppo Economico del 26 giugno 2015. Applicazione delle metodologie di calcolo delle prestazioni energetiche e definizione delle prescrizioni e dei requisiti minimi degli edifici.

12.UNI/TS 11300-1:2014 -Prestazioni energetiche degli edifici - Parte 1: Determinazione del fabbisogno di energia termica dell'edificio per la climatizzazione estiva ed invernale.

13.Falasca, S., Zinzi, M., Ding, L., Curci, G. and M. Santamouris, (2022). On the mitigation potential of higher urban albedo in a temperate oceanic metropolis. *Sustainable Cities and Society*, 81: p. 103850.

14.Jandaghian, Z. and U. Berardi, (2020). Analysis of the cooling effects of higher albedo surfaces during heat waves coupling the Weather Research and Forecasting model with building energy models. *Energy and Buildings*, 207: p. 109627.

15.Skamarock, W. C., et al. (2019). A description of the advanced research wrf model version 4. UCAR/NCAR. https://doi.org/10.5065/1DFH-6P97

16.National Centers For Environmental Prediction/National Weather Service/NOAA/U.S. Department Of Commerce. (2015). Ncep gdas/fnl 0.25 degree global tropospheric analyses and forecast grids [dataset]. https://doi.org/10.5065/D65Q4T4Z

17.Ching, J., et al. (2018). Wudapt: An urban weather, climate, and environmental modeling infrastructure for the anthropocene. *Bulletin of the American Meteorological Society*, 99: p. 1907–1924.

18.Stewart, I. D. and T.R. Oke, (2012). Local climate zones for urban temperature studies. *Bulletin of the American Meteorological Society*, 93: p. 1879–1900.

19.Demuzere, M., Argüeso, D., Zonato, A. and J. Kittner, (2022). W2w: A python package that injects wudapt's local climate zone information in wrf. *Journal of Open Source Software*, 7: p. 4432.

20.TRNSYS 17. www.trnsys.com

21.Iannone F. et al., (2019). "CRESCO ENEA HPC clusters: a working example of a multifabric GPFS Spectrum Scale layout," 2019 International Conference on High Performance Computing & Simulation (HPCS), Dublin, Ireland.

PLEA 2024 WROCŁAW
(Re)thinking Resilience

Circularity potential of building products

Material Flow Analysis of façade building components

MAGDALENA ZABEK[1] THALEIA KONSTANTINOU[1], JOSE-LUIS GALVEZ-MARTOS[2]

[1] Department of Architectural Engineering & Technology TU Delft University, Delft, The Netherlands
[2] TECNALIA, Basque Research and Technology Alliance (BRTA), Astondo Bidea, Derio, Spain

ABSTRACT: The construction industry, accounting for a significant portion of energy consumption and greenhouse gas emissions, is pivotal in achieving Europe's ambitious climate neutrality goal by 2050. Circular Economy (CE) principles and the renovation of existing buildings are identified as promising strategies to reduce raw material and energy consumption. However, the lack of knowledge and guidelines for effective CE design and construction in the built environment, along with heterogeneous metrics and standards, pose challenges. The research outlines an investigation study aimed at developing Key Performance Indicators (KPIs) for evaluating building products based on CE principles, focusing on façade renovation. The study emphasizes the need for a holistic approach, considering both material input and output flows, and introduces qualitative and quantitative KPIs addressing aspects such as recyclability, modularity, and local materials. The research proposes established frameworks like Life Cycle Assessment (LCA), Material Flow Analysis (MFA), and the Level(s) framework, but recognizes their limitations in assessing circularity comprehensively. The methodology involves a comprehensive analysis of material streams and circularity potential for nine components crucial to achieving a net-zero façade renovation. Results from the material flow analysis demonstrate the environmental impact of selected building products, such as insulation panels and photovoltaic panels. The research underscores the importance of informed design choices, leveraging adaptable KPIs, and visualizing resource flows to enhance decision-making for sustainable construction practices aligned with CE principles.
KEYWORDS: Circularity, Material Flow Analysis (MFA), Façade Renovation, Life Cycle Assessment (LCA), Key Performance Indicators (KPI)

1. INTRODUCTION

The construction industry plays a key role in influencing responsible and sustainable production and consumption of resources as it significantly contributes to energy use and greenhouse gas emissions, accounting for approximately 40% of the EU's energy usage and 36% of its greenhouse gas emissions. The built environment is also major consumer of extracted materials (50% by mass) and is responsible for generating 37% of the total waste in Europe [1].

Europe's ambitious goal is to achieve climate neutrality by 2050 requires significant decarbonization efforts and a reduction in raw materials and energy consumption. In this context, a calculation of life-cycle Global Warming Potential (GWP) will be obligatory [2] from 2027 on. Adopting Circular Economy (CE) principles and renovating existing buildings is a promising approach to meet this target. The mandatory inclusion of Life Cycle Assessment (LCA) and a recycling quota for building products has the potential to drive a significant influence toward the conservation and maintenance of the current building inventory [3].

Today, over 85% of Europe's existing buildings lacks energy efficiency standards [4]. Achieving net-zero energy buildings involves on-site generation of energy from clean, renewable resources, equaling the total energy consumed on-site. This necessitates deep renovation, capable of reducing energy consumption by 60% to 90%.[5]. However, the annual rate of deep building renovations in the EU falls far short of the recommended target. To address this, the European Commission initiated the Renovation Wave in 2020, aiming to double the annual rate of energy-based building renovations by 2030 [4]. In the context of upscaling facade renovation that incorporates various technologies, higher amounts of material will be required. This demand for resources makes it imperative that the early design phases for the renovation products and systems incorporate CE design objectives, considering end-of-life scenarios, as these activities significantly affect resource utilization, environmental impact [6] and embodied energy demand.

Up to now, the focus of sustainable development has been directed towards the energy consumption

incurred during the operational phase of buildings [7] leading to missing knowledge and guidelines supporting effective design and construction for a CE [8]. Moreover, assessing the impact of the design decision on the environmental impact is currently hindered by heterogeneity in metrics and standards [9] and missing user friendly guidelines. Besides, existing methods like LCA, Material Flow Analysis (MFA) or the European Commission's Level(s) framework [10] have limitations in evaluating circularity.

1.1 Objectives

This research belongs to the Horizon Europe project "Digital and physical incremental renovation packages/systems enhancing environmental and energetic behavior and use of resources", AEGIR [11], which focuses on implementing CE practices in the built environment by strategically selecting building materials and components during the early stages of the renovation process. The aim is to establish a closed-loop system throughout the façade renovation value chain. To this end, the first step is to develop Key Performance Indicators (KPIs) for supporting the design process in line with CE principles. This involves defining a comprehensive CE concept, reviewing common circularity measurement approaches, and presenting a practical method for validating building products in terms of material flows and use of secondary raw materials. KPIs shall be derived from methodologies assessing the environmental impact of materials and construction methods, contributing to a more sustainable decision-making process in façade renovation solutions. The overarching aim is to provide KPIs that function as a structured framework for directing decision-making procedures during the design phase. This process is complemented by the application of a standardized methodology at the product level to assess environmental impact and raw material utilization. The application of a standardized methodology during product selection, coupled with the integration of a comprehensive framework throughout the entire design process, is anticipated to generate a solution in line CE.

The research specifically applies this concept to a net-zero façade renovation solution, representing an innovative, modular, renewable, and industrialized building envelope for low-energy renovation. The research supports decision-making in product selection process of four façade renovation solutions by analyzing five building product groups specialized for achieving net-zero solutions. The objective is to comprehensively grasp the composition of two representative products of two selected groups and identify the associated material flows. This analysis is crucial for formulating strategies to establish closed-loop re-use systems for products that aim to achieve a net-zero façade renovation, such as PV panels, insulation, ventilation, windows, and energy storage batteries.

2. METHODS

This research focuses on implementing CE strategies by supporting the development of an industrialized building envelope solution for low-energy renovation by a holistic analysis of the material streams and circularity potential of construction products. To achieve this, KPIs based on the CE concept will be developed in section 3. In section 3.1 a review on the most common methods to assess circularity will be presented supporting the development of the KPIs. In section 3.2, the level of functionality to assess material streams will be defined, enabling the selection of an appropriate method for evaluating each product and its environmental impact in part 4. In this part results from the MFA will be presented and conclusions will be presented in part 5.

2.1 Review of sustainability frameworks

Standardized methods that measure the resource consumption and future waste streams of building products have been developed in the past such as LCA (ISO 14040:2006/14044:2006 and EN 15804) or Level(s) methodology [12], supported by programs and guidelines, such as the EU Action Plan for a Circular Economy [13] or the Green Taxonomy [14].

The definition of indicators within Level(s) remains adaptable, particularly in terms of methodology. An example of this is evident in the use of Level(s) 2.4, focusing on design for deconstruction. While Level(s) outlines a calculation workflow for the circularity score, certain aspects, such as the circularity coefficient assigned to specific building components, are left open, based on the "best possible outcome" of the component. Determining such characteristics involves expert judgment and additional considerations.

Material Flow Analysis (MFA) is another key method for quantifying the movement of materials within defined systems, including flows and stocks. It is essential in understanding the bio-physical aspects of human activities at various scales. Initially introduced in 1969 [15], MFA is now commonly used to track national material flows and plan waste management and recycling systems [16]. It complements other industrial ecology methodologies like LCA and input-output models [17], although they differ in objectives, level of functionality, and data requirements.

The LCA and MFA represent the most frequently used methodologies. However, there are many more circularity metrics that have been developed by companies, governments, and academics in the recent past. However, these metrics frequently exhibit contradictions in both their form and content, leading to confusion and misunderstandings regarding the CE concept. Additionally, there is a growing number of

frameworks, creating an excess of indicators aimed at measuring resource efficiency and assessing circularity performance [18].

2.2 Material Flow Analysis

To determine the raw material composition of a building component, the product substance is categorized into two main types i) primary and ii) secondary raw material. Primary raw material includes renewable and non-renewable materials. Secondary material includes reused and recycled material.

Furthermore, material streams are categorized into material in- and output streams. Material Input refers to the resources used to produce a component. Material output refers to resources being available after the End-of-Life (EoL) phase of products and can be categorized into three categories: i) transformation into other products, ii) disposal in landfills and iii) returning to the product's own material cycle as secondary material.

Material flows can be quantified by measuring mass or other indicators such as GWP. In this research GWP is utilized to assess the environmental impact of components during their production phase (LCA module A1-A3 as per EN 15804 definitions) in terms of CO2 equivalent. Data is sourced from the German Ökobaudat.de or available EPDs. The proportions of primary and secondary resources within the product are determined based on mass (kg) in percentage. The system is visually presented within a Sankey diagram.

This research concentrates on existing recycling methods and does not predict future material output flows. Uncertainty arises from the unknown connecting joint to the façade module. Further specific details can be evaluated through an assembly-level analysis.

3. RESULTS

LCA incorporates various indicators quantifying the potential environmental impact of a product or a service during different life cycle stages (module A-C in EN 15804). Within the Level(s) framework, several indicators correspond to the ones developed in the LCA such as:

- Global Warming Potential (GWP)
- Construction & demolition waste and materials (Hazardous substances)
- Durability.

Besides, indicators within the scope of EN 15804-based LCA that directly contribute to a CE are:

- Use of renewable resources
- Use of recycled material
- Use of reused material
- Materials for recycling or reuse.

The Level(s) methodology, introduced by the EU, goes far beyond those circularity evaluation practices. It can be used to report on and improve the performance of new-build and major renovation projects [12]. This framework comprises an extra range of indicators and standardized metrics to assess the sustainability performance of buildings in addition to LCA, of which we chose:

- Bill of quantities
- Design for adaptability and deconstruction.

While existing methods like LCA and the Level(s) framework are valuable for assessing the environmental impact of building products, there is a need for additional indicators that align with the holistic approach of the CE. The following aspects take a broader perspective and draw inspiration from two core concepts of the CE: the R-Strategies (Reduce, Reuse, Recycle) embedded in the Waste Directive [19] and the Cradle-to-Cradle concept [20]:

- Financial concept for multiple life circles [21].
- Modularity [22]
- Local Material [19]
- Low-Tech [20]
- Purity [20]
- Compostability [20].

Many of the above present KPIs are widely employed in the environmental assessment of specific objectives within various policies and regulatory frameworks. Such as the Environmental Product Declaration (EPD) by EN 15804 (CEN, 2012), providing a consistent and recognized methodology for evaluating the environmental performance of construction materials.

Similarly, aspects such as the bill of quantities, the ease of demountability, and other indicators pertaining to end-of-life (EoL) stages of construction products are integrated into the technical criteria of the Green Taxonomy, especially within the "Transition to a Circular Economy" aspect. Compliance with specific threshold values related to these indicators is typically required to access green financing instruments.

A comprehensive perspective on CE considers both the EoL phase and the manufacturing/extraction phase. Nevertheless, indicators that focus on future material output at the EoL are predominantly quantitative, making them challenging to benchmark, particularly in terms of disassembly or durability.

The presented KPIs are organized according to their qualitative or quantitative characteristics and their emphasis on either the material in- or output flow. These are outlined in table 1, which also includes their respective sources. This approach aims to provide a more comprehensive and nuanced guideline for the building product selection process.

Table 1: Qualitative (Ql) and quantitative (Qn) KPIs addressing material in- and output flows based on (1) LCA, (2) Level(s) or (3) CE definition

Input	Output
GWP (1,2) Ql	Demountability (2,3) Qn
Renewable resources (1) Ql	Durability (1) Qn
Recycled material (1) Ql	Modularity (3) Qn
Reused material (1) Ql	Low-Tec (3) Qn
Local material (3) Qn	Bill of quantities (2) Qn

	Financial concept (3) Qn
	Hazardous substances (1,3) Ql
	Materials for reuse/recycling (2,3) Qn
	Purity (3) Qn
	Compostability (3) Qn

3.1 Assessing Circularity Across Multiple Scales

Each of the mentioned methodologies has its limitations when it comes to assessing circular performance characteristics on various scales. It is recognized that sustainable manufacturing is comprised of three core levels: [23] "building, assembly, component". Each of these levels has its own distinct characteristics and limitations. As the selection of an appropriate component assumes to have a critical role in the environmental impact of a building [24], a common method specifically tailored for assessing the circularity of components will be selected. Table 2 shows instruments that assess circularity in relation to the level of functionality.

Table 2: directly (x) and indirectly (/) related frameworks to assess different level of functionalities

Instrument	Component	Assembly	Building
LCA	x	x	x
EPD	x	-	-
Level(s)	-	/	x
MFA	x	x	x

While LCA and EPDs are primarily utilized as an assessment tool at the component level, it has the flexibility to transition to a macro-level perspective when facilitating decisions on a larger scale. This includes supporting macro-level considerations concerning national policies or sector strategies related to technologies, services, or a collection of products. Nevertheless, it's crucial to note that LCA is not suitable for evaluating the overall performance of the global economy. In such cases, alternative tools like MFA would be more fitting and effective as it even goes beyond building level [18].

When considering priorities for circularity assessment, whether from a regulatory or strategic perspective, it is essential to emphasize that the analysis should always include a holistic view on all represented level of functionalities. In addition, qualitative KPIs, as for now, lack translation into quantitative analysis, introducing uncertainties. The choice of the circularity assessment framework should align with business, commercial, reputational, or regulatory priorities. For instance, if a construction product's commercialization strategy is to demonstrate compliance with specific indicators within Level(s) under the green taxonomy, the assessment should be conducted within the Level(s) methodological framework. However, if the emphasis lies on the utilization of secondary materials and the visualization of material streams, opting for a MFA proves to be the more fitting choice.

The MFA applied in this research assesses the material input (KPI Recycled/reused material) using GWP as an indicator at component level and will be used to critically evaluate the circularity of nine building products that are essential for the achievement of a circular facade renovation solution. The term component is defined as part of an assembly that is required for functionality, performs a unique and necessary function in the operation of the assembly, is removed in one piece and is indivisible for the use of the overall assembly [25].

3.2 Material Flow Analysis of insulation

Displayed are the outcomes of four selected components, encompassing both active (such as PV panels) and passive (like insulation) characteristics (figure 1).

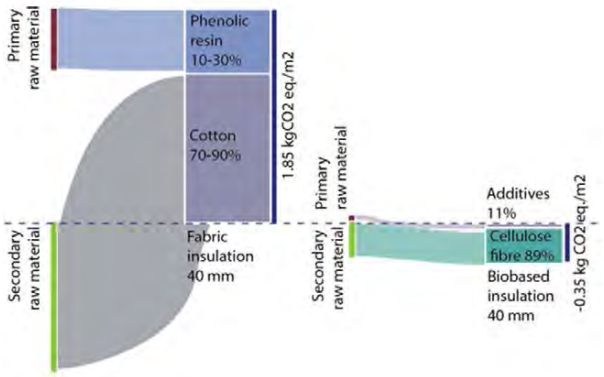

Figure 1: Material Flow Analysis of fabric (Product A) and biobased insulation (Product B)

The insulation panels are characterized using secondary materials (Product A: recycled cotton) and renewable materials (Product B: cellulose). Both products exhibit similar characteristics in terms of thermal conductivity (A 0.034 W/mK and B 0.041 W/mK) density (A 50/60 kg/m^3 and B 45 kg/m^3) and thickness (A/B 40 mm). Over a life span of 50 years Product A emits CO_2 emissions (1.85 kg CO_2/m^2) during product phase whereas Product B captures carbon emissions (-0.35 kg CO_2/m^2) due to the use of renewable material. Both have a high amount of secondary material, as 89% of Product B uses waste from paper production and Product A up to 90 % waste from textile production and 10 % of primary material (phenolic resin). Reuse and recycling options are restricted by the presence of fire-retardant substances like boron salt, which poses health risks. Consequently, owing to the absence of recycling systems, insulation is primarily disposed of in landfills or incinerated.

3.3 Photovoltaic (PV) Panels

The analyzed PV panels (**Error! Reference source not found.**) are a standard PV panel (PV1) and a flexible thin film PV panel (PV2) which are specialized

for façade application. PV1 is a standardized roof panel that has been adapted for use as a façade module in the case study, eliminating the need for a specialized and typically more expensive module. Both products encompass a series of production stages which result in high amount of CO2 emission for PV1 (68.9 kgCO2eq./m^2), PV2 emits up to 80 % less CO2 emissions (14 kg CO2eq./m^2) over a lifespan of 30 years. However, its power rate is 7 times less (63,1 Wp/m2 compared to a standard PV1 (212,8Wp/m^2). Both mainly consists of glass (up to 76-88%) and aluminum (7-8%) which accounts mostly for the CO2 emissions. According to manufacturer data, PV2 is composed of nanoscale carbon-based (organic) molecules that facilitate the production of thin products. Compared to a standard PV which typically has a thickness of between 200 and 300 µm, PV2 typically has a thickness of anywhere from a few nanometers to tens of micrometers which results in lower energy efficiency [26].

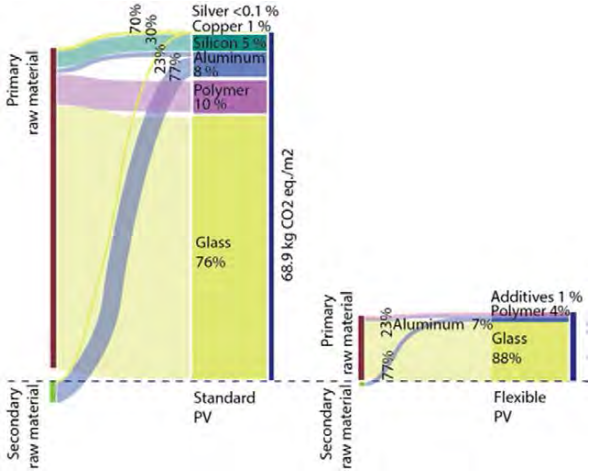

Figure 2: Material Flow Analysis of standard (PV1) and flexible (PV2) PV panels

Thin film technologies require less material overall compared to crystalline silicon. Flexible PV panels contain about 88-89% glass, 7% aluminum, 4% polymer with less than 1% semiconductor material (indium, gallium, selenium) and other metals (e.g. copper) [27]. Approximately 80 percent of a solar panel's weight comprises energy-intensive materials like aluminum and glass, posing recycling challenges due to the difficulty of separating glass from silicon, and the remaining 20 percent can be challenging to recover. However, materials like copper, plastics (including cables and junction boxes), and silver can be efficiently repurposed with careful separation, necessitating time and expertise to prevent contamination and safely dismantle the panels into raw components [28].

4. CONCLUSION

Currently, the use of methodologies that assess the use of secondary resources in the built environment is a novel area in architectural discourse. Yet, a comprehensive, user-friendly method that holistically assesses the circularity potential of products is lacking. This necessitates architects and manufacturers to make informed design choices during early stages based on holistic KPIs. The presented KPIs act as a guide during the design phase of a façade renovation project. Nevertheless, a comprehensive method to assess the circularity of products is necessarily which also includes additional information about parameter such as costs.

A pivotal element for comprehending circularity involves the visualization of resource flows. Displaying the utilization of primary and secondary material flows, alongside CO_2 emissions, using MFA as a standardized method supports the decision-making process and contributes to the preservation of natural resources for future generations. However, characterization of MFA requires expertise and further deliberation. In addition, the decision-making process needs further support by a variety of more indicators, especially focusing on the future material output. For example, flexible photovoltaic (PV) panels, in addition to the implemented MFA demonstrating low embodied carbon emissions, it is crucial to consider indicators like health related KPIs (hazardous substances) and other KPIs such as recyclability and reusability that provide insights into future material output flows. Therefore, this study introduced holistic KPIs that can guide the design process towards a circular solution. Future research could focus on the development of a tool that incorporates all presented KPI's and facilitates comparisons between products and includes additional parameters, such as cost.

Thus far, a combination of analytical assessments using standardized methods like MFA, alongside qualitative approaches represented by the KPIs identified in this research, is recommended for achieving a solution of a circular building component. This integrated approach enables a more thorough evaluation, considering both quantitative and qualitative aspects, leading to informed decision-making in sustainable construction practices.

ACKNOWLEDGEMENT

The authors acknowledge the funding received from the European Union's Horizon Europe research and innovation program under grant agreement No 101079961 (AEGIR project).

REFERENCES

1. EUROSTAT, Generation of waste by economic activity. https://ec.europa.eu/eurostat/statistics-explained/index.php?title=Waste_statistics#Total_waste_generation, 2023.

2. Commission, E., Proposal for a DIRECTIVE OF THE EUROPEAN PARLIAMENT AND OF THE COUNCIL on the energy performance of buildings (recast). Directorate-General for Energy, 2021(52021PC0802).

3. Dorn-Pfahler, S. and T. Lützkendorf, Ökobilanzielle Bewertung im Ordnungsrecht: Grundlagen und erste

Ansätze zur vereinfachten Bewertung von Gebäuden mit angewandten Ökobilanzen. Bundesinstitut für Bau-, Stadt- und Raumforschung (BBSR) im Bundesamt für Bauwesen und Raumordnung (BBR), 2023(44).
4. Commission, E., A Renovation Wave for Europe - greening our buildings, creating jobs, improving lives. 2020. 2020/662.
5. Thaleia Konstantinou and Charlotte Heesbeen, Industrialized renovation of the building envelope: realizing the potential to decarbonize the European building stock. Woodhead Publishing Series in Civil and Structural Engineering,
Rethinking Building Skins,, 2022: p. 257-283.
6. Vieira, P.S. and A. Horvath, Assessing the end-of-life impacts of buildings. 2008, ACS Publications.
7. Hildebrand, L. and U. Knaack, Embodied Energy in the Façade,. Sustainability, 2009. 1/2009.
8. Eberhardt, L.C.M., M. Birkved, and H. Birgisdottir, Building design and construction strategies for a circular economy. Architectural Engineering and Design Management, 2022. 18(2): p. 93-113.
9. Mirzaie, S., M. Thuring, and K. Allacker, End-of-life modelling of buildings to support more informed decisions towards achieving circular economy targets. International Journal of Life Cycle Assessment, 2020. 25(11) p. 2122–2139.
10. Commission, E., Level(s): Taking Action on the TOTAL Impact of the Construction Sector. Luxembourg Publications Office of the European Union, 2019.
11. https://aegirproject.eu, 2023.
12. Dodd, N., S. Donatello, and M. Cordella, Level(s) – A common EU framework of core sustainability indicators for office and residential buildings. JRC Scientific and Technical Reports, Issue. Office for Official Publications of the European Communitie., 2020.
13. Commission, E., Circular Economy Action Plan - For a cleaner and more competitive Europe. 2020.
14. Braune, A., et al., EU Taxonomy Study - Evaluating the marketreadiness of the EU taxonomy criteria for buildings. 2021.
15. Ayres, R.U. and A.V. Kneese, Production, consumption, and externalities. The American economic review, 1969. 59(3): p. 282-297.
16. Gao, J. and F. You, Dynamic Material Flow Analysis-Based Life Cycle Optimization Framework and Application to Sustainable Design of Shale Gas Energy Systems. ACS Sustainable Chemistry & Engineering, 2018. 6 (9): p. 11734–11752.
17. Moriguchi, Y. and S. Hashimoto, Material Flow Analysis and Waste Management. In R. Clift & A. Druckman (Eds.), Taking Stock of Industrial Ecology 2016(Cham: Springer International Publishing): p. 247-262.
18. Blanca Corona, et al., Towards sustainable development through the circular economy—A review and critical assessment on current circularity metrics. Resources, Conservation and Recycling,, 2019. 151.
19. Commission, E., Directive 2008/98/EC on waste (Waste Framework Directive), in European Parliament and the Council of the European Union. 2013, Official Journal of the European Union: Brussels.
20. Antonini, E., et al., Reversibility and Durability as Potential Indicators for Circular Building Technologies. Sustainability, 2020. 12(18): p. 7659.
21. Azcarate-Aguerre, J.F., A. Den Heijer, and T. Klein, Integrated Facades as a Product-Service System: Business process innovation to accelerate integral product implementation. Journal of Facade Design and Engineering, 2017. 6(1): p. 41-56.
22. Machado, N. and S.N. Morioka, Contributions of modularity to the circular economy: A systematic review of literature,. Journal of Building Engineering,, 2021. 44.
23. Luscuere, L. and D. Mulhall, Designing for the Circular Economy, Edited by Charter, M. Designing for the Circular Economy. Routledge, Routledge, Abingdon, Oxon; New York, NY, , 2018.
24. Akadiri, P.O., P.O. Olomolaiye, and E.A. Chinyio, Multi-criteria evaluation model for the selection of sustainable materials for building projects. Automation in Construction, 2013. 30: p. 113-125.
25. Commission, E., Circular Economy Principles for Building Design. 2020.
26. Aarsh Patel, Iradat Hussain Mafat, and Rajat Saxena, Passive thermal management of PV panels for enhanced performance using PCM. Handbook of Thermal Management Systems, 2023: p. 605-622.
27. Dominish, E., N. Florin, and S. Teske, Responsible Minerals Sourcing for Renewable Energy
. Report prepared for Earthworks by the Institute for Sustainable Futures, University of Technology Sydney, 2019.
28. ERI, PV Management / Solar Panel Recycling. 2023.

PLEA 2024 WROCŁAW
(Re)thinking Resilience

Passive Ventilation for Healthy Classrooms:
Comparative analysis of natural and hybrid ventilation systems to provide fresh air in temperate climates.

MATHIEU ARNAUD NACCARATO[1,2], ROSA SCHIANO-PHAN[1]

[1] University of Westminster, London, United Kingdom
[2] Savills Earth, London, United Kingdom

ABSTRACT: As we approach 2050 and the net zero carbon target, architecture is reimagined to reduce GHG emissions. Public projects are given particular attention. However, little effort is shown to reduce MEP systems. While passive cooling is well known, more studies are needed on minimizing carbon emissions from fresh air supply. This paper provides a comparative analysis of passive, hybrid and active systems providing fresh air to classrooms in temperate climates. Four case studies with heat recovery and CO_2 sensors are investigated through interviews and site visits. A life-cycle embodied carbon assessment found that the selected hybrid system leads to a reduction in carbon emissions. The paper outlines recommendations to prioritise passive strategies whilst maintaining adequate levels of IAQ. KEYWORDS: Ventilation, Passive, Hybrid, Air quality, Embodied Carbon

1. INTRODUCTION

1.1 Context

While the built environment directly or indirectly emits almost 40% of global greenhouse gases (GHG)[1], the way we design our cities is being questioned. Mitigating the effects of climate change requires an immediate paradigm shift to reduce anthropogenic emissions [2]. However, a long-term view is also essential to find solutions for adaptation, to inform projects and to avoid greenwashing.

To be climate resilient, architecture must not only enable people to adapt to climate change by providing them with comfortable places to thrive, but also offer concrete solutions to permanently reduce the carbon emissions associated with construction.

Public projects, such as school buildings, are presented as examples and are given special attention from architects and engineers. With millions of schools worldwide, the classroom is undoubtedly one of the most common type of space in these buildings. It also has a very high occupancy density, with an average of up to 31 students per classroom in some countries [3].

Ventilation is one of the key elements in the indoor-outdoor relationship, ensuring a healthy environment and the ability to adapt to changing thermal conditions. While extensive research promotes passive cooling against overheating, less is known about passive strategies to provide fresh air in non-domestic buildings to further reduce emissions associated with heating, ventilation and air conditioning (HVAC). Case studies show the potential to return to the basic principles of passive ventilation to reduce operational and embodied carbon emissions while improving indoor air quality (IAQ) and wellbeing.

1.2 Objectives

The objectives are to investigate the drivers and barriers to the implementation of passive ventilation strategies in classrooms, to identify the characteristics of four ventilation systems and their implementation in the design process, and to assess the embodied carbon emissions associated with three systems.

1.3 Structure and Methodology

Following a literature review highlighting the technical and cultural aspects of air quality, ventilation systems and carbon reporting, the paper is divided into both fieldwork and analytical work.

The fieldwork was carried out through a qualitative analysis involving the selection of four educational case studies with the following criteria: temperate climate, fresh air system, heat recovery and carbon dioxide (CO_2) sensors, delivered less than five years ago, variety of educational stage. Twenty participants were selected on the basis of their experience in the design of the selected buildings. Four semi-structured interviews with engineer or architect were conducted, organised in a general-to-specific order so as not to influence the interviewee and get representative data for all typologies. In addition, internal and external site visits and five unstructured interviews took place.

The analytical work consisted of an assessment of the life cycle embodied carbon emissions of three selected ventilation systems. This was done through a quantitative analysis involving data collection, 3D modelling and measurement. The CIBSE Technical Memoranda 65 (TM65) was used in the absence of environmental product declarations (EPDs).

2. BACKGROUND

2.1 Air Quality and Well-being

Air pollution is a major environmental risks to health [4]. Five major pollutants cause cardiovascular and respiratory chronic conditions in urban areas: carbon monoxide (CO), sulphur dioxide (SO_2), nitrogen dioxide (NO_2), ground level ozone (O_3), and particulate matters ($PM_{2.5}$, PM_{10}) [5]. Recent studies show that the surroundings of 2,000 schools and nurseries in the UK have dangerous levels of air pollution [6]. To bring in fresh air, the outdoor air should be of good quality.

Europeans spend 90% of their time inside buildings [7] and pollutants reduce attendance and affect pupils' performance [8]. IAQ should be maintained to both reducing contaminants from the building products (e.g., formaldehyde, volatile organic compound) and from the occupants [9]. Confined spaces require the removal of CO_2 produced by occupants. Oxygen concentrations below 12%, or CO_2 above 5% are hazardous [10]. CO_2 levels are used as an indicator to adjust ventilation rates to the occupancy (Fig. 1).

Simple manual controls are valuable in limiting the performance gap and avoiding frustration for building occupants [11]. Furthermore, as wellbeing is a state influenced by human multisensory perceptions [12], building design should facilitate flexibility and diversity of indoor environments, in connection to the outdoor.

Figure 1: CO_2 sensor with traffic light display in a classroom (Site visit A, 2023)

2.2 Ventilation Systems and Carbon Emissions

Developed to create a more comfortable indoor environment, active ventilation systems have reached an extreme. The "exclusive mode" theory relies on technology to overcome climatic variations and to provide a constant indoor environment [13]. However, the huge amount of energy required to 'neutralise' the external environment is no longer ethical nor aligned with the net zero targets, even with a decarbonised grid. On the other hand, passive systems remind us of the potential offered by the fundamental principles of wind and buoyancy. Used for centuries, they provide fresh air and cooling [14] without active energy.

Besides operational energy, embodied carbon emissions are being examined over the whole lifecycle of the building [15]. The lack of EPDs suggests that the assessments of MEPs are underexamined [16].

3. FIELDWORK: FOUR CASE STUDIES

3.1 Climates and Typologies

The four case studies are located within 50 km of London or Paris and share a comparable sun path, with a significant contrast between the summer and winter solstices. Falling in the KöppenGeiger classification "Temperate, No Dry Season, Warm Summer", their climate may evolve if the representative concentration pathway 8.5 is followed [17]. This is essential to keep in mind as the applicability of the study, which looks at specific ventilation systems, depends on the climate in which the buildings are located. Heat recovery systems are useful where there is a great difference between indoor and outdoor air temperatures during winter. This is the case in both cities, with a heating period over several months, the coldest months being January and February. However, temperatures in Paris are more extreme in both winter and summer. Overheating during warm seasons is a growing concern as temperature records are being broken frequently (e.g., 46.0 °C in June 2019 in France [18] and 40.3°C in July 2022 in the UK [19]). Paris has warmer summers than London, but school breaks start at the beginning of July whereas at the end of the month in the UK. The evaluated systems include summer strategies, with heat exchanger bypass and operable windows to allow night-time purge ventilation.

The four buildings represent the range of educational stages in the region: nursery (A), primary (B), secondary (C) and high school (D). The annual occupancy pattern is largely in the heating period, making the use of heat recovery systems relevant.

3.2 Components and Indoor Air Quality

Building Bulletin (BB) 101 reminds us that there is a large variety of systems, between mechanical and natural ventilation [20]. The selected sample includes passive (A, C) and hybrid modes (B, D).

The system in building A is made of a horizontal supply duct and a vertical exhaust chimney. Each classroom is served by two branches. Each consists of an inlet located on the facade and an outlet on the roof, to benefit from both buoyancy and wind forces.

The system in building C only uses vertical ducts, connected to a wind-driven roof mounted cowl unit. Four vertical ducts reach the classroom: two supply ducts deliver fresh air at a low level, and two return diffusers are located in the ceiling.

The system in building B is made of a facade unit. This hybrid ventilation system runs with a fan in winter. Louvres integrated on the facade allow a passive ventilation in summer via buoyancy effect.

The system in building D is an evolution of the one described above in building C, as it includes a roof mounted fan on top of the exhaust stack which runs on windless days. With an L-shape duct supply, this system needs only one branch per classroom.

In a post-pandemic context, IAQ became an essential topic, especially in high-density classrooms. CO_2 concentration is monitored in the selected buildings via sensors to meet local targets (e.g., a naturally ventilated space in the UK, daily average <1,500 ppm, >2,000 ppm for <20 consecutive minutes, <1200 ppm for the majority of the time [20]). This shift from a minimum air flow rate to a maximum CO_2 concentration promotes natural or hybrid ventilation systems and the use of demand-controlled ventilation (DCV). Precedent studies demonstrate that CO_2 levels remain below local thresholds in cases A and C [21, 22]. Other investigations show that airflow rates are more delicate to achieve due to the poor system airtightness or the diversity of monitoring tools [23].

Hybrid systems can do both. Based on the occupancy derived from CO_2 concentration, they provide sufficient outdoor air via fans when passive strategies alone are not effective enough. However, analysis of tender documents for the hybrid case studies reveals that the transition from passive to hybrid mode needs to be taken very carefully. While system B is integrated into the project as part of passive ventilation strategies, the fully passive mode of operation is limited to only part of the year in warmer months. In addition, drawings from system D indicate that the roof-mounted fan reduces the operative aperture area of the chimney and limits in the same way the potential for stack effect. While mechanical ventilation components are beneficial in developing innovative hybrid systems, it is critical to ensure that the fundamental principles of natural ventilation are applied and prioritised.

3.3 Space Implications of Systems

"*The whole building is designed around natural ventilation!*" mentioned an interviewee. The large duct size required for natural ventilation imposes considerable constraints on the design, especially when an air-to-air heat exchanger means that the supply and return flows must meet at the same point. However, these systems are often well integrated into the architectural design, with constraints varying for each case study.

The volume used by the distribution system is one of the first constraints. While a mechanical system with heat recovery would require dual ducts in the corridor, system D allows a generous floor-to-ceiling height and potentially inhabited circulations. However, the use of large ducts requires higher storey heights to limit the impact on the volume of the classrooms (D), at the risk of having to duplicate the system to reduce the size of ducts and, at the same time, duplicating the quantity of raw materials used (C). In some cases, the clear height under the false ceiling is a constraint imposed by the client, where it is considered that low elements could be excessively damaged (C), or used to hide objects without the knowledge of the school's supervisors (D).

The aesthetic aspect is related, even though the industrial look is sometimes deliberately pursued in projects, with visible ducts and a minimal amount of false ceiling (D). This aesthetic challenge applies both to the interior, where it can be very delicate to hide a hybrid box mounted on the facade (B), and to the exterior, with these facade units that imposes a window pattern (B), or with impressive chimneys that architects often choose to magnify (A).

Finally, the analysis of the drawings also revealed some crucial technical aspects. Mechanical ventilation systems are criticised by interviewees for the amount of floor space taken up by plant rooms. This must be considered when carrying out a full analysis, especially when these systems are not on the fifth facade but installed indoors, in place of useful space. It should be noted, however, that some passive ventilation systems require a very large number of service risers (A, C, D), taking up usable space on several floors, and involving additional costs and materials for structural reinforcements.

Figure 2: Assumed air quality in front of a park, England (Site visit C, 2023)

3.4 Barriers and Drivers of Natural Ventilation

The first two questions in the semi-structured interviews aimed to identify the barriers and drivers to passive strategies, before exploring in more detail the design specificities of the system and typology of the project in which the interviewee was involved.

The drawback of heat loss in the exhaust air and lack of control of IAQ were not relevant with heat exchangers and CO_2 sensors and, therefore, have not been mentioned. The irregularity and unpredictability of passive ventilation was the most frequently identified obstacle. While the buoyancy effect can be simulated, it is true that the wind is not a constant parameter. In addition, acoustic and air pollution from the surroundings of the building were often mentioned by interviewees. Finally, the lack of precedents and the client's reluctance was another point of difficulty mentioned.

All these points were largely outweighed by positive arguments in favour of passive strategies.

In response to energy losses, all interviewees mentioned the potential for operational energy savings: *"Indoor air quality is an important element in any ventilation system, not using electricity to do it is by far the best way if we can"*. Surprisingly, efforts into the reduction of embodied carbon linked to building services were only mentioned once, which suggests that this topic has yet to be fully explored.

In response to the unpredictability, stakeholders were keen to share the potential for greater user control, even if this can lead to performance gaps and higher energy consumption than predicted in some cases (A). The "*psychological benefit*" is also mentioned as referring to wellbeing: "*Seeing through an openable window, feeling the breeze*".

In response to the microclimate constraints, the architects and engineers cited cases where favourable conditions were a driver to passive strategies: long distance from main roads, proximity to natural areas considered beneficial to the project (Fig. 2).

Finally, in response to the lack of precedents or lack of involvement from stakeholders, examples of collaboration between architect, mechanical engineer, sustainability specialist and contractor were shown. In one case (A), the project was made possible by the creation of an independent entity (including the client, architects and engineers) to push the boundaries of sustainable design and multidisciplinary work. It is interesting to note that in half of the cases, the passive and hybrid strategies were initiated by the architect. In the other two cases, it was motivated by the sustainability expert, via a certification scheme.

4. ANALYTICAL WORK: EMBODIED CARBON

4.1 Objective

The objective of the analytical work is to assess the life cycle embodied carbon emissions (LCEC) over 60 years of the systems used in building C (passive) and in building D (hybrid), in comparison to a conventional "reference" system (balanced mechanical ventilation with heat recovery) (Fig. 3).

4.2 Precedents and Methods

Previous research estimated the carbon footprint of a UK educational building [24], but it did not include MEP systems and did not evaluate the impact per floor area unit. Benchmarks such as the London Plan Guidance suggest that the LCEC of schools should be below 1,000 kgCO_2e/m² Gross Internal Area (GIA), with 15% attributed to MEP services [25].

The assessment of the LCEC emissions, which includes modules A1-C4 and excludes B6-B7, is carried out over a 60-year period. The calculation covers at least 95% of the components using the CIBSE TM65 basic calculation when EPDs are missing.

A hypothetical school building is designed according to BB 103, with 16 classrooms of 30 people (8.6 x 7.2 x 3.0 m), arranged over two storeys of eight rooms with a central corridor [26]. The sizing is based on a common airflow rate of 8 l/s/p. 3D modelling with the software Rhino made it possible to list and measure all components. Three lifespan scenarios are considered. Two new parameters are proposed: the service risers' structural reinforcement (steel profile 31 kg/m), and the wasted floor area taken up by service risers and plant rooms (461 kg CO_2e/m²). The results are normalised in kg CO_2e/m² GIA.

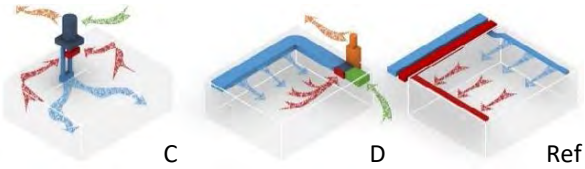

Figure 3: Axonometry of the passive (C), hybrid (D) and active (Ref) ventilation systems in a classroom

4.3 Results

Overall, the hybrid system D had the lowest LCEC values in all scenarios, between 30% and 43% lower than the reference active system, while the passive system C was in second place in the conventional and optimistic component life expectancy scenarios. This study demonstrates that the lifetime of the unit considered in the assessment had a significant impact on the results over a 60-year period (Fig.4). The assessment also reveals the variable impact of other components: the hybrid system D wasted 11 times less floor area, and used glass wool ducts that were half as carbon-intensive as the galvanised steel ones in the reference active system (Table 1).

Table 1: Life Cycle Embodied Carbon of the passive (C), hybrid (D) and active systems (Ref) over 60 years (kgCO_2e/m² GIA)

Part	C	D	Ref
DUCTS	5.72	28.40	30.72
UNITS	76.68	41.07	63.05
RISERS	4.58	5.63	0.95
WASTED AREA	6.09	1.29	14.65
TOTAL	**93.05**	**76.40**	**109.37**

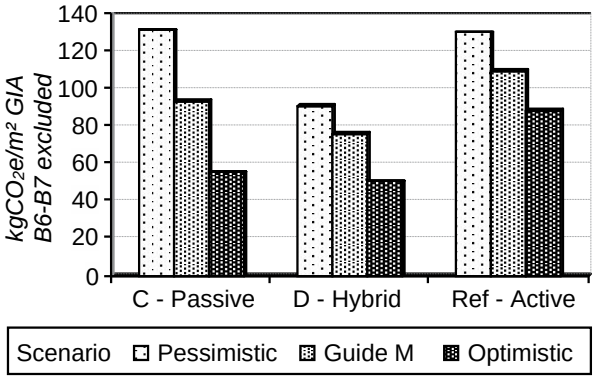

Figure 4: *Life Cycle Embodied Carbon assessment over 60 years according to three lifespan scenarios (kgCO_2e/m² GIA)*

4.4 Limitations

It is important to note that this study considers only three specific systems, and the results cannot be generalised as typical values for types of ventilation strategies. The main limitation is the lack of available data in MEPs. More information could be obtained from manufacturers but this is a resource intensive task outside the scope of this study. This study does not include operational energy, and therefore excludes refrigerants. Beyond fresh air, this would have required heating and cooling strategies to be considered with a thermal analysis throughout the year, which was outside the scope of the study. In addition, schools are protected and difficult to visit. Continuous monitoring and post-occupancy evaluation could not take place.

5. DISCUSSION

Interpretation of the assessment should consider the additional operational energy emissions. While the passive system does not require energy, the hybrid one runs fans when natural ventilation is insufficient and the reference active system always consumes electricity when it runs. We also draw lessons from the intersection of fieldwork and analytical work.

The passive system C is mainly wind-driven. Its localised fresh air supply may be heterogeneous and cause discomfort during winter. The component life expectancy impacts the emissions associated with the system. Ducts and chimneys could be integrated as building elements with high upfront carbon emissions that become viable over time. However, the impact of this vertical system on the space would worsen, further limiting layout evolution. Consideration of operational energy emissions could highlight more benefits, as this system is also effective for passive cooling with a heat exchanger bypass.

In the hybrid system D, the weak link is the roof fan, as it reduces the area of the exhaust chimney and therefore, the potential for stack effect. Fans ensure IAQ continuity even on windless days. They are likely to determine the life expectancy of the system if not maintained. A larger fan to facilitate natural ventilation or a photovoltaic panel for a self-generated system could be explored, but both solutions will increase the embodied carbon. Another solution to reduce emissions would be to combine fresh air and cooling strategies.

The reference active system offers a homogeneous airflow, but the unit is only used for fresh air, as radiators are considered in parallel. Its combined use for heating, cooling and fresh air would increase its efficiency and reduce the carbon impact associated with HVAC, but would also require the use of carbon-intensive refrigerants and an increase in the dimension of the ducts. Other strategies could involve several lighter units made of more plastic than metal.

Overall, this study reminds us of the potential of passive strategies (Fig.4) to limit the embodied carbon emissions related to MEPs (Fig.5).

The applicability of this research is not limited by its scope. Although it focuses only on ventilation to provide fresh air in London and Paris, it informs other projects in similar temperate climates where heat recovery is appropriate. It is essential to note that if the external temperatures when the rooms are occupied do not justify the use of a heat exchanger, then other strategies should be considered.

Moreover, the study only considers general classrooms in new build, with good airtightness and a localised system. Other typologies, with a different occupancy density, larger spaces or multiple storeys, could require longer lengths of ductwork which would increase pressure loss in passive ventilation systems.

Figure 4: Photo of a passive chimney seen through an operable window, France (Site visit C, 2023)

Figure 5: Mechanical, Electrical and Public health components in a construction site, France (Site visit E, 2023)

6. CONCLUSION

This paper illustrates that mechanical ventilation systems are not the only solution, at a time when natural-based solutions are coming back on the agenda to improve wellbeing and limit emissions associated with the built environment. Designers working on public educational building projects are uniquely placed to offer innovative solutions which are exemplars in preserving the health of future generations and implementing climate-resilient architecture.

Based on both fieldwork and analytical work, this research contributes to expanding the knowledge on ventilation systems to provide fresh air in classrooms. The authors recommend the following hierarchy. Firstly, natural ventilation should be facilitated as early as possible in the design process, with simple solutions that do not require active energy. The passive system C is an effective option for small classrooms if made to last, and CO_2 sensors are an interesting way to monitor indoor air quality. Secondly, heat recovery and other controls are implemented only when required by the climate and the occupancy. Indeed, they lead to air being ducted. The exchanger is made of carbon-intensive materials but reduces the heating loads. Thirdly, hybrid systems, which combine strategies rather than multiplying them, are used to support passive principles. The hybrid system D offers an interesting balance between embodied and operational carbon, but the mechanical component should not reduce the passive potential. Lastly, mechanical ventilation should be used when specific requirements must be met, with appropriate sizing and a decentralised system where it is more efficient. The reference system considered is heavy in both operational and embodied carbon emissions, even if it provides a homogeneous and controlled air flow.

In future investigations, it might be possible to also explore operational carbon emissions, cost analysis, maintenance and circular economy.

ACKNOWLEDGEMENTS

The authors gratefully acknowledge the assistance of Patrick Mauger, Ludovic Le Bras, Kartikeya Rajput, Dr Juan Vallejo, Vera Sarioglu, Amedeo Scofone, Mary-Joe Daccache, Ben Abel, Davor Stojnic, Giampiero Ripanti, Mathieu Le Bourhis, Charlotte Picard, Jonathan Purcell, Helen James and Jennifer Juritz.

REFERENCES

1. International Energy Agency, [Online], Available: www.iea.org/data-and-statistics/charts/co2-emissions-from-the-operation-of-buildings-in-the-net-zero-scenario-2010-2030 [02 January 2023]
2. IPCC Climate Change 2023, [Online], Available: www.ipcc.ch/report/ar6/syr/ [30 March 2023]
3. OECD / UIS / Eurostat, [Online], Available: www.oecd.org/education/education-at-a-glance/EAG2021_Annex3_ChapterD.pdf [03 December 2023]
4. World Meteorological Organization, [Online], Available: library.wmo.int/doc_num.php?explnum_id=11629 [9 August 2023].
5. UK Government, [Online], Available: www.gov.uk/government/publications/health-matters-air-pollution/health-matters-air-pollution [30 October 2022].
6. Mohamed, S. et al. (2021). Overheating and indoor air quality in primary schools in the UK. *Energy and Buildings,* 250: 111291.
7. VELUX, [Online], Available: www.velux.com/what-we-do/healthy-buildings-focus/healthy-homes-barometer [17 December 2022].
8. Mendell, M.J. and Heath, G.A. (2005). Do indoor pollutants and thermal conditions in schools influence student performance? A critical review of the literature. *Indoor Air*, 15: 27-52
9. BREEAM, [Online], Available: files.bregroup.com/breeam/technicalmanuals/sd/international-new-construction-version-6/content/05_health/hea_02.htm [Accessed 9 January 2023].
10. Bradshaw, V. (2006). The building environment: Active and passive control systems, Third edition. Hoboken: John Wiley & Sons Inc.
11. Tuohy, P. and Murphy, G.B. (2012). Why advanced buildings don't work. *Proceedings Windsor Conference: The Changing Context of Comfort in an Unpredictable World.*
12. Russo, F. (2022). MSc Architecture & Environmental Design, Health and Wellbeing. 7AEVD004W.1: Post Carbon Culture. University Of Westminster. *Unpublished*.
13. Hawkes, D. (2002). Essay 8 -The Selective environment. London: *The Spon Press*.
14. Ford, B., Schiano-Phan, R. and Vallejo, J.A. (2020). Chapter 1. The Architecture of Natural Cooling. Second Edition. London: Taylor and Francis, 1–22.
15. RICS et al. (2023). Whole life carbon assessment for the built environment. *Royal Institution of Chartered Surveyors.* 2nd edition.
16. CIBSE. (2021). TM65 Embodied carbon in building services: a calculation methodology. *Chartered Institution of Building Services Engineers.*
17. Beck, H. et al. (2018). Present and future Köppen-Geiger climate classification maps at 1-km resolution. *Scientific Data*, (180214).
18. Met Office, [Online], Available: www.metoffice.gov.uk/about-us/press-office/news/weather-and-climate/2022/record-high-temperatures-verified [10 December 2023].
19. Météo France, [Online], Available: meteofrance.com/magazine/meteo-questions/quelle-est-la-temperature-la-plus-elevee-enregistree-en-france [10 December 2023].
20. Building Bulletin. (2018). BB 101. *United Kingdom Government.* Version 1.
21. Lipinski, T. et al. (2017). Passive Ventilation with Heat Recovery in an Urban School. *CIBSE Technical Symposium.*
22. Switch. (2022). Retour d'expérience Ventilation naturelle avec récupération de chaleur (VNRC). *Unpublished*.
23. Ekopolis, [Online], Available: www.ekopolis.fr/ressources/batresp-vnrc [17 May 2023].
24. Keyhani, M. (2023). Mitigating Embodied Carbon in Educational buildings. *Engineering Future Sustainability 1(2).*
25. GLA, [Online], Available: www.london.gov.uk/sites/default/files/lpg_-_wlca_guidance.pdf [19 July 2023].
26. Building Bulletin. (2014). BB 103. *United Kingdom Government.*

PLEA 2024 WROCŁAW
(Re)thinking Resilience

Energy performance evaluation of affordable residential prototypes with different construction types

Three case studies in a hot and humid climate

LAYLA ISKANDAR[1], CARLOS FAUBEL[2], ANTONIO MARTINEZ-MOLINA[2,3], SAADET BEESON[1]

[1]School or Architecture and Planning, Klesse College of Engineering and Integrated Design, The University of Texas at San Antonio UTSA, 501 W. César E. Chávez Blvd, San Antonio, TX 78207, USA.
[2]Department of Architecture, Design & Urbanism, Antoinette Westphal College of Media Arts and Design, Drexel University, 3501 Market St., Philadelphia, PA 19104, USA.
[3]Department of Civil, Architectural, & Environmental Engineering, College of Engineering, Drexel University, 3141 Chesnut St., Philadelphia, PA 19104, USA.

ABSTRACT: The demand for housing that is both affordable and sustainable is a prevalent global phenomenon. Despite the multiple challenges, there is room for realizing advancements through innovative design methods, building materials, and technologies. This study delves into analyzing the energy performance and optimization strategies for three distinct housing prototypes in San Antonio, Texas, USA, as part of the "Single-Family Prototype Pilot Project" initiated by San Antonio Affordable Housing Inc. (SAAH). The three prototypes include a conventional wood-frame construction (control prototype), an optimized wood-frame construction, and a rammed-earth construction. Using DesignBuilder simulation software, the study evaluates and compares their energy performance, considering factors including cooling and heating loads, solar heat gains, indoor temperatures, and annual cooling costs. The results highlight significant energy savings achieved through optimization in the wood-frame prototype and prove the energy efficiency of natural construction typologies such as rammed earth. These findings demonstrate the feasibility of constructing energy-efficient and affordable housing in a hot and humid climate and contribute valuable insights for future sustainable housing practices.
KEYWORDS: Energy efficiency, Affordable housing, Sustainable construction, Energy optimization.

1. INTRODUCTION

It is well proven that research on constructing highly performing buildings and retrofitting existing ones is fundamental for decreasing global greenhouse emissions, curbing energy consumption, and enhancing the health and wellbeing of occupants [1]. As cities grow, the need for sustainable living solutions becomes a crucial necessity. In particular, San Antonio, Texas, USA, ranks among the fastest-growing cities in the United States [2] and is actively pursuing strategies to improve the environmental performance across multiple sectors, including housing. Addressing the pressing need for deeply affordable homeownership in San Antonio, specifically for families at or below 80% of the Area Median Income (AMI), the nonprofit organization San Antonio Affordable Housing Inc. (SAAH) [3] has launched "The Single-Family Prototype Pilot Project" (Pilot Project). This initiative involves collaborations with multiple entities to develop housing prototypes that are both sustainable and affordable, utilizing diverse materials and construction methods. SAAH is committed to providing affordable, quality housing to all citizens, regardless of their income levels, while ensuring the safety of the public. The authors of this paper served as the partners responsible for conducting an analysis of the energy performance and optimization of different housing prototypes which is crucial for the success of the Pilot Project.

The literature on energy optimization and affordability in housing underscores a critical intersection between sustainability and social equity in the built environment [4]. As the demand for energy-efficient housing grows, researchers are increasingly investigating strategies to optimize energy consumption without compromising affordability. Successful energy optimization in affordable housing requires a holistic approach, considering factors such as building materials, construction methods, and the unique local socio-economic context [5].

The study outlined in this paper focuses on the outcomes of phase 1 of the Pilot Project, encompassing the analysis of energy efficiency and design optimization of three prototypes chosen by the organization. One existing residential unit was selected as the control prototype for comparison purposes, while the other two houses are in the construction stage (phase 2), with on-site energy performance assessment planned for phase 3. Furthermore, post-occupancy evaluations are planned for phase 4 to validate the study's results on-site.

2. MATERIALS AND METHODS

The primary objective of this investigation is to evaluate, compare, and optimize the energy performance of the three specified prototypes before construction, using the energy simulation tool DesignBuilder [6], with EnergyPlus as calculation engine. Following the development of the energy models, a series of sensitivity analyses, including model calibration, were carried out. The outcomes for each prototype were analyzed with regard to cooling and heating loads, solar heat gains, temperatures, and annual cost of cooling (both sensible and latent).

2.1 Location and climate

The studied housing prototypes in this Pilot Project are located in San Antonio, Texas, USA. The area is characterized by a hot and humid climate, aligning with climate zone 2A as per The American Society of Heating, Refrigerating and Air-Conditioning Engineers (ASHRAE) Standard 169 [7]. Figure 1 illustrates the monthly distribution of air dry-bulb temperature and relative humidity based on the Typical Meteorological Year TMY3 data obtained from the San Antonio International Airport weather station [8]. The annual mean temperature in San Antonio, which suffers from hot summers, ranges between 16.1°C and 26.3°C, whereas the average relative humidity is 67.5%, with drier conditions during July and August.

The primary concern in this climate zone revolves around managing cooling and dehumidifying loads within indoor spaces. Passive design strategies, on their own, can only achieve a minimal percentage of comfortable hours inside buildings in this climate area. Therefore, additional solutions are required to ensure the thermal comfort of occupants, necessitating the incorporation of adequate active systems.

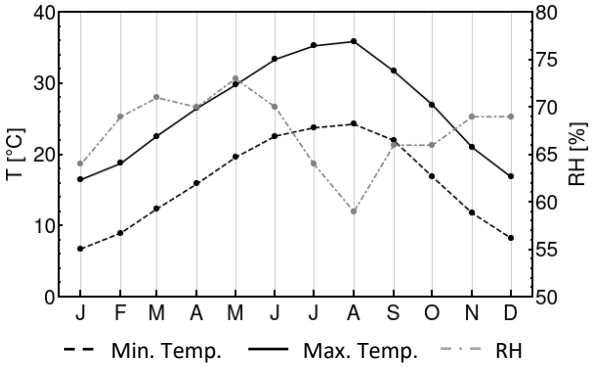

Figure 1: Monthly averages of air dry-bulb temperature and relative humidity from the TMY3 weather data for San Antonio, Texas, USA.

2.2 The housing prototypes

The three housing prototypes examined in this study are equivalent single-family houses designed and constructed by SAAH (except prototype A) as illustrative models for achieving affordable housing with improved energy performance. The prototypes are delineated in what follows.

2.2.1 The control prototype (Prototype A)

This prototype is an existing one-story residence featuring conventional American wood framing construction. Its shape is rectangular, measuring 11.6 m in both the front and rear dimensions, and 11.3 m on the sides, resulting in a total area of 131.1 m^2. The walls and roof are constructed with wood framing, and batt insulation is placed between the flat ceiling joists. The floor is a slab-on-grade, and the windows are single-hung, featuring a white vinyl frame and double-pane glazing. The house includes a living room, a kitchen, and a dining space designed with an open layout, along with a utility closet, three bedrooms and two bathrooms. Additionally, it is shaded with two porches, one at the front (3 m x 1.8 m) and one at the back (2.7 m x 1.8 m) of the house.

2.2.2 The wood-frame prototype with optimized energy efficiency (Prototype B)

This building is a one-story residence designed with a simple rectangular shape, measuring 14.5 m in both the front and rear dimensions, and 7.2 m on the sides, resulting in a total area of 104.4 m^2. The construction materials and methods are identical to those in the control prototype. This house includes a living room, a kitchen, and a dining space designed with an open layout, along with a utility closet, two bedrooms, and one bathroom. Additionally, it features a porch situated at the west entrance of the house (7.6 m x 2.4 m). The layout is designed to accommodate a potential building extension in the future, if deemed necessary.

2.2.3 The rammed earth prototype (Prototype C)

This prototype is a one-story residence designed with a simple rectangular shape, measuring 15.1 m in both the front and rear dimensions, and 7.5 m on the sides, resulting in a total area of 113.3 m^2. The construction of this house involves rammed earth walls, a slab-on-grade floor slab, and a roof structure composed of structural insulated panels. The windows are single-hung, featuring a vinyl frame and double-pane glazing. Moreover, the building includes a porch at the west entrance (7.6 m x 2.4 m). The layout closely resembles that of Prototype B.

The envelope characteristics of the housing prototypes are outlined in Table 1. The designations A, B1, B2, and C correspond to the control prototype, the wood-frame prototype before the energy optimization analysis, the wood-frame prototype after the energy optimization analysis, and the rammed-earth building, respectively.

Table 1: Envelope characteristics of the different prototypes. U-factor units are in W/(m² K).

Element	A	B1	B2	C
Walls	U-0.37	U-0.37	U-0.24	U-0.32
Roof	U-0.14	U-0.14	U-0. 14	U-0.14
Floor	U-0.53	U-0.53	U-0.53	U-0.53
Infiltration (ACH)	8.50	4.00	0.60	0.60
Windows	U-1.42 SHGC-0.25	U-2.16 SHGC-0.25	U-1.42 SHGC-0.25	U-2.27 SHGC-0.25

2.3 Building energy modelling

Detailed energy models for the three prototypes were developed using DesignBuilder software [6], as depicted in Figure 2. To facilitate comparison, some parameters were fixed across all the models. For instance, the occupancy density was set at 0.02 people/m², and the heating and cooling setpoint/setback were established at 20°C/17.8°C and 22.2°C/25.6°C, respectively. On the other hand, various characteristics, including materials, activity, construction typology, and mechanical systems, were varied to align with the unique design of each structure, as specified by the architectural, structural, and mechanical designs and drawings.

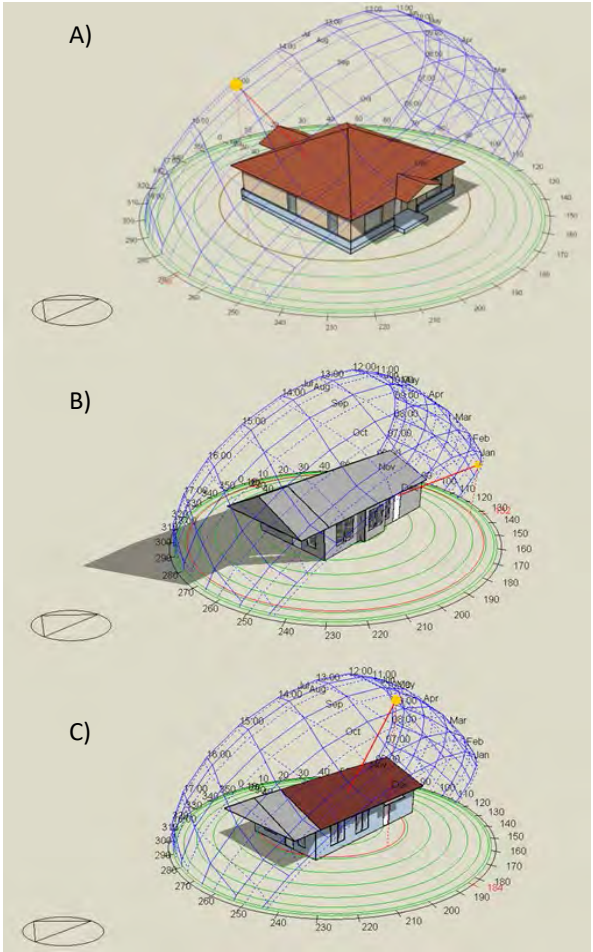

Figure 2: Three-dimensional rendering of the buildings in DesignBuilder: A) control prototype, B) wood-frame prototype with optimized energy efficiency, and C) rammed-earth prototype.

Prototype B has both cases—before (B1) and after (B2) the energy efficiency optimization—included in the analysis. As per the provided designs, prototypes A and B1 are equipped with a standard air conditioning and electric resistance heating system without mechanical ventilation as they represent conventional building typologies. In contrast, prototypes B2 and C feature a ducted mini-split air conditioning and electric resistance heating system with an energy recovery ventilator and dehumidifier.

2.4 Optimization of Prototype B

Multiple simulations were carried out on Prototype B with the objective of assessing and selecting optimizing strategies to enhance the energy efficiency of a conventional building assembly, all while considering affordability. The considered components included walls, roof, and floor insulation, airtightness, window glazing type, and roof overhang for shading. Through simulations and discussions with partners responsible for addressing affordability, it was determined that the best-balanced upgrades for Prototype B include the following (thermal transmittance, U-values, in W/(m² K)):

- An increase in wall insulation thermal transmittance beyond the code requirement of U-0.44 to U-0.25. Further increases in the U-value results in modest energy savings but escalated costs, leading to their exclusion.
- No additional increase in roof insulation thermal transmittance beyond the code requirement of U-0.15. Further enhancements in the U-value result in modest energy savings but escalated costs, leading to their exclusion.
- Reduction in the air infiltration rate from 4 ACH to 0.6 ACH by ensuring the building is airtight using house wrap with tape sealing and limiting openings for mechanical systems.
- Improvement in glazing conductivity from U-2.157 to U-1.420. Further reductions in the U-factor yield modest energy savings while increasing costs, resulting in their exclusion.
- Extension of the roof overhang on the south façade from 30 cm to 60 cm to decrease solar heat gain through the windows.

3. RESULTS AND DISCUSSION

This section delineates the outcomes of the comparative analysis of the different prototypes. The parameters subjected to comparison encompass loads, heat gains, indoor temperatures, and the annual cost of cooling.

3.1 Cooling and heating loads

To enhance energy efficiency, employing predictive control based on cooling and heating load prediction proves effective for demand and load reduction [9]. Figure 3 presents a comparative analysis of the annual cooling (sensible and total) and heating loads from building energy simulations across the different prototypes.

Prototypes A and B1 exhibit the highest loads due to the inefficient construction materials and methods. Notably, Prototype A's elevated infiltration rate, namely 8.5 ACH, contributes to significantly higher loads compared to Prototype B1, with an infiltration equal to 4 ACH. Optimization efforts on Prototype B, which corresponds to B2, demonstrate a remarkable reduction in cooling and heating loads by around 80% and 40% when compared to B1. Compared to the control Prototype A, these loads were also decreased by around 93% and 88%, respectively. Moreover, Prototype C proves to be exceptionally energy-efficient, displaying loads comparable to optimized Prototype B. In contrast to the control Prototype A, Prototype C exhibits approximately 95% lower sensible and total cooling loads and an 88% reduction in heating loads.

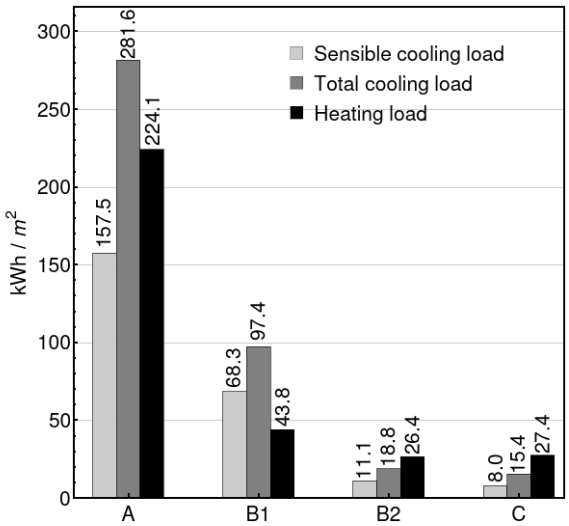

Figure 3: Annual cooling and heating loads for the different prototypes.

3.2 Solar heat gains

Reducing solar heat gain through the building fabric is a key strategy for decreasing energy demand in a building [10]. Therefore, this study also compared annual solar heat gains through the windows, exterior walls, and ground floor across the various prototypes, as depicted in Figure 4.

Prototype B pre-optimization, B1, experiences the highest solar gains through the windows, closely followed by Prototype C. The optimization process further decreases gains in Prototype B by 53%. Conversely, due to its efficient windows (Table 1), Prototype A records lower gains.

On the other hand, Prototype C registers the highest heat gains through walls, namely 5.5 times the ones for control Prototype A. This increase could be attributed to the characteristics of the wall material (rammed earth) and its thermal inertia, that absorbs solar radiation through the day and releases it at night when outdoor temperature drops. Additionally, these earthy walls do not have any insulation materials installed avoiding thermal absorption. The heat gains through walls were also higher in prototype B post-optimization (B2) compared to pre-optimization, B1.

Finally, all prototypes with a slab-on-grade experience heat dissipation through the ground floor. In particular, Prototype C has the most substantial losses, namely 5.4 times the ones in Prototype A, which positively impacts the reduction of cooling loads.

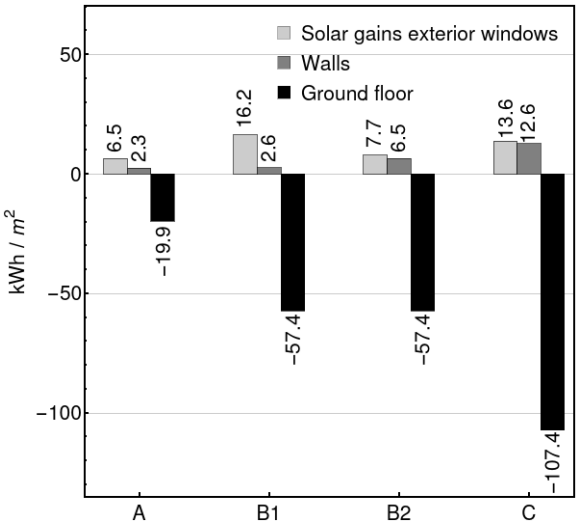

Figure 4: Comparison of the annual heat gains among the different prototypes.

3.3 Indoor operative temperatures

The indoor operative temperature is a critical indicator of human thermal comfort within air-conditioned spaces, making it an essential consideration [11]. The indoor operative temperatures for the different prototypes are presented in Figure 5.

Simulation findings for the annual average indoor operative temperature depicted in Figure 5 indicate that, prior to optimization, Prototype B exhibits the highest indoor operative temperature, with an annual average of 22.7°C. Through the optimization process, the average indoor temperature is reduced by over 1°C, bringing it in close alignment with that observed in Prototype A. Remarkably, Prototype C records the lowest temperature, boasting an annual average of 20.3°C, underscoring the efficiency of this construction type.

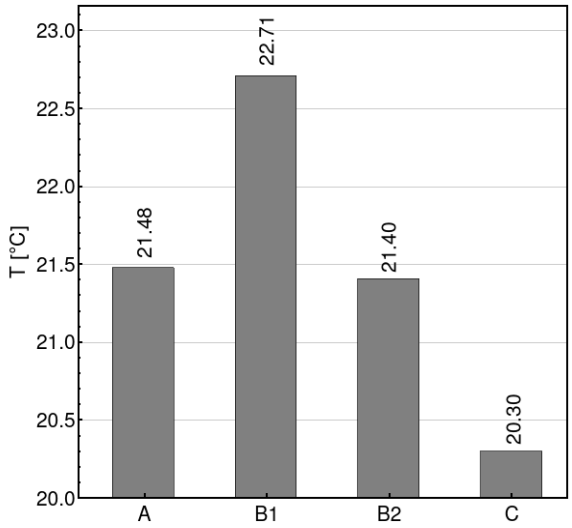

Figure 5: Annual average indoor operative temperature for the different prototypes.

3.4 Cooling cost analysis

Given the predominant concern for cooling in hot and humid climates, the annual electricity cost for cooling the prototypes was scrutinized to underscore the project's affordability aspect, as depicted in Figure 6. The results reveal that Prototype A accrues an approximate cost of $794 per year. In contrast, Prototype B, before optimization, incurs a 42% lower cost than Prototype A, due to reduced cooling loads associated with the infiltration rate. Following optimization, the annual cost for Prototype B significantly decreases to approximately $86 (81% reduction compared to B1). Prototype C exhibits the most economical scenario, boasting the lowest annual electricity bill in simulations, approximately $73 (91% decrease compared to Prototype A).

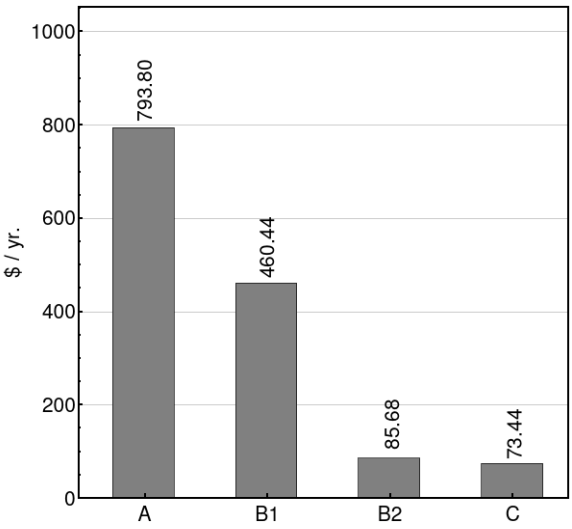

Figure 6: Annual average electricity cost for cooling the different prototypes.

4. SUMMARY AND CONCLUSIONS

This study analyzed and compared the energy performance of three distinct housing prototypes in San Antonio, Texas, USA. The research was commissioned by the San Antonio Affordable Housing Inc. (SAAH), a non-profit organization, as part of "The Single-Family Prototype Pilot Project". The first prototype features an existing conventional wood-frame construction type (control prototype), the second incorporates a conventional wood-frame construction type with optimized energy performance, and the third utilizes a rammed-earth construction type. The following conclusions can be deduced from the findings of this study:

- As expected, the control prototype (Prototype A) exhibits the least energy efficiency, primarily due to an elevated infiltration rate. However, the existing efficient windows result in lower heat gains in this prototype.
- Optimizing the wood-frame prototype (Prototype B) results in substantial energy savings, reduces heat gains, and indoor operative temperatures, leading to significant decrease in the annual cost of cooling.
- The rammed-earth prototype (Prototype C) demonstrates energy performance comparable to the optimized wood-frame prototype, achieving notable savings in cooling and heating loads, as well as the annual electricity cost for cooling when compared to the control prototype.

These results provide valuable insights into best practices for constructing family housing that is both energy-efficient and affordable. The next steps of this project involve completing the construction of the wood-frame prototype with optimized energy efficiency and the rammed earth prototype. This will be followed by an on-site energy efficiency evaluation to confirm the results of the simulations. Finally, post-occupancy evaluations are planned to monitor the performance of these prototypes.

ACKNOWLEDGEMENTS

This research has been supported by San Antonio Affordable Housing (SAAH).

REFERENCES

1. Martinez-Molina A., Tort-Ausina I., Vivancos J.L., and Cho S. (2016). Energy efficiency and thermal comfort in historic buildings: A review. *Renewable and Sustainable Energy Reviews,* 61: p. 70-85.
2. United States Census Bureau, (2023). Large Southern Cities Lead Nation in Population Growth. [Online], Available: https://www.census.gov/newsroom/press-releases/2023/subcounty-metro-micro-estimates.html
3. San Antonio Affordable Housing Inc., [Online], Available: https://www.sanantonio.gov/DSD/Constructing/Affordable-Housing-Team

4. Copiello, S. (2015). Achieving affordable housing through energy efficiency strategy. *Energy Policy*, 85: p. 288-298.
5. Moghayedi, A., Phiri, C., & Ellmann, A. (2023). Improving sustainability of affordable housing using innovative technologies: Case study of SIAH-Livable. *Scientific African,* 21, e01819.
6. DesignBuilder v.7, Available: https://designbuilder.co.uk
7. ASHRAE (2021). ASHRAE Standard 169 Climatic Data for Building Design Standards, Available: https://www.techstreet.com/ashrae/standards/ashrae-169-2021?gateway_code=ashrae&product_id=2238548
8. San Antonio International Airport Climate, weather by month, Average temperature (Texas, United States) - Weather Spark, [Online], Available: https://weatherspark.com/y/145850/Average-Weather-at-San-Antonio-International-Airport-Texas-United-States-Year-Round/ [n.a.].
9. Ma, J., Qin, S. J., & Salsbury, T. (2014). Application of economic MPC to the energy and demand minimization of a commercial building. *Journal of Process Control*, 24(8): p. 1282-1291.
10. Kandar, M. Z., Nimlyat, P. S., Abdullahi, M. G., & Dodo, Y. A. (2019). Influence of inclined wall self-shading strategy on office building heat gain and energy performance in hot humid climate of Malaysia. *Heliyon,* 5(7), e02077.
11. Hao, X., Xing, Q., Long, P., Lin, Y., Hu, J., & Tan, H. (2020). Influence of vertical greenery systems and green roofs on the indoor operative temperature of air-conditioned rooms. *Journal of Building Engineering,* 31, 101373.

PLEA 2024 WROCŁAW
(Re)thinking Resilience

Thermodynamic coupling to determine microclimate impact of avenue trees on building cooling energy

BRYON FLOWERS[1] KUO-TSANG HUANG[2]

[1]Ph.D. Candidate, Department of Bioenvironmental Systems Engineering, National Taiwan University, Taipei, Taiwan
[2] Professor, Department of Bioenvironmental Systems Engineering, National Taiwan University, Taipei, Taiwan

ABSTRACT: A current problem in sustainable design is establishing microclimate boundary conditions for building energy simulations. To overcome this limitation, this study presents a method that links building energy simulation and urban microclimate via a coupling platform called the Building Control Virtual Test Bed, or BCVTB; the case study being a typical office building surrounded by vegetation. The research begins with the modification of an EnergyPlus weather file using the Urban Weather Generator which has the advantage of accounting for local geometry and anthropogenic heat. The air temperature results of the UWG-generated weather file were on average higher than the rural TMY3. Microclimate data from ENVI-met simulations varied largely from the weather files. Coupling this microclimate data with EnergyPlus through the BCVTB generated results for variables that influenced cooling energy consumption. The results of these variables such as CHTC, surface temperature, and air temperature, were put through a pairwise correlation matrix which revealed a strong statistical relationship of 0.97 between surface temperature and air temperatures. It also showed CHTC to be inversely proportional to surface temperature, consistent with other studies. The BCVTB-coupling showed that vegetation accounted for 17% EUI reduction potential. Using only EnergyPlus underestimated energy consumption by 9%.
KEYWORDS: sustainable design, building energy, CHTC, ENVI-met, convective coefficient, surface temperature

1. INTRODUCTION

Over the last decades, detailed individual building energy modelling has become an established mode of analysis for building designers. But since buildings cannot be assumed standing-alone in an urban context, meteorological loads cannot be estimated generically as they are particular for each building. In order to consider the microclimate in building energy simulation studies, urban climate modelling (UCM) and BES have to be chained or linked together.

The Building Control Virtual Test Bed (BCVTB) is a software environment that allows users to couple difference simulation programs for simulation [1]. A general schematic of a coupling of 2 clients, x_1 and x_2, is shown in Figure 1. A fortified example of the application of the BCVTB is that of Ramesh [2] upon which this research methodology builds upon. As such, this research aims to develop and test a coupling method between EnergyPlus and ENVI-met and evaluate its performance in terms of cooling energy consumption. The objectives of this research are:

- To generate a modified weather file using the Urban Weather Generator (UWG)
- Create a coupling model between EnergyPlus and ENVI-met using the BCVTB.
- Evaluate the performance of the coupling method
- Evaluate the impact of avenue trees on the buildings cooling energy demand.

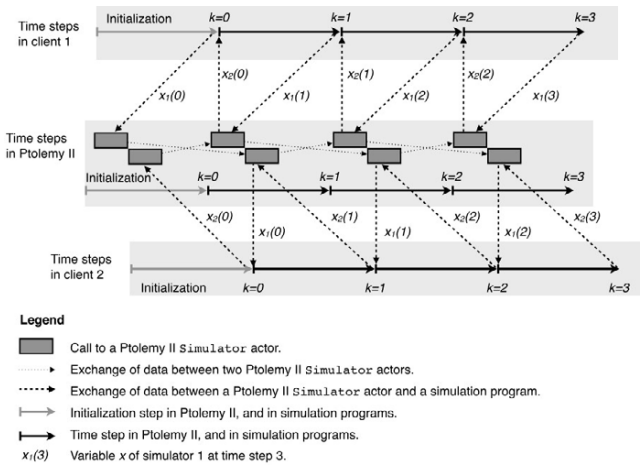

Figure 1 Data synchronization and function calls between Ptolemy II middleware and two simulation actors

2. MATERIALS AND METHODS

This research method involves 3 main sections that involve 4 simulators in order to complete the objectives.

2.1 Case Study

The location of the building model is Taipei, Taiwan, R.O.C. and is represented as a typical office building with 5 floors (Figure 2) with a total floor area of 2000 m^2. These floors are divided into 5 zones. Since the building is considered to be in a relatively dense urban environment, adjacent buildings were placed on all sides of the building, which is typical of Taipei's urban structure.

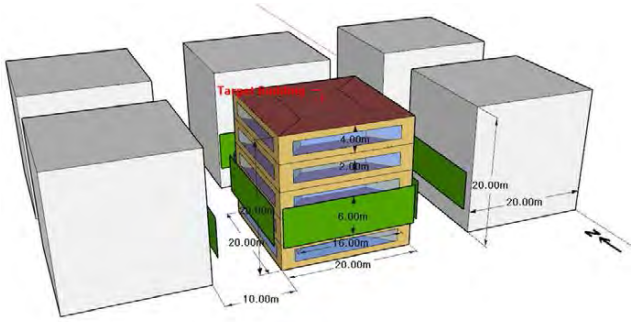

Figure 2 Case study building specifications.

2.2 Urban Weather Generator (weather file modification)

A crucial part of this study was modifying the typical meteorological weather file (Taipei TMY3.epw) used by the building energy simulation model so that it reflected the urban environment. The UWG was developed by Bruno Bueno [3] and has since been improved by Aiko Nakano [4], and Joseph Yang [5]. The type of building, road material, albedo and other properties had to be defined. An important advantage of the UWG to other weather file modifies was that it can account for anthropogenic heat flux from. The anthropogenic heat from traffic was taken from estimations of anthropogenic heat flux (AHF) in urban Taiwan from [6].

2.3 Microclimate Domain (ENVI-met)

To establish accurate boundary conditions for the study area, we employed ENVI-met, a widely-used dynamic simulation tool for microclimate analysis [7]. ENVI-met accounts for exchanges of energy and mass between vegetation and its surroundings. The domain of this simulation was modelled and is presented in Figure 3. The configuration of the simulation domain in ENVI-met was such that it closely approximated the scenario in EnergyPlus. As such, the location was the same. Trees being defined differently in ENVI-met were made to have a general cylindrical structure with an albedo of 0.12 and a leaf area index of 2.3 m^2m^2. The trees had a transmittance of 0.1. Simulations were carried out for the coldest and the hottest day of each month, totally 24 simulations for a typical year. A python script was coded to extract and map important microclimate data into text files for recovery and exchange.

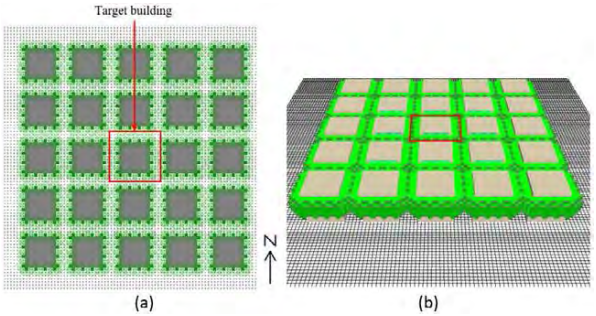

Figure 3 ENVI-met domain: (a) top-view of study target building model; (a) 3D view of the domain

2.4 Energy Domain

EnergyPlus is one of the most robust and used energy simulation tools available both at academic and commercial levels [8]. An disadvantage with EnergyPlus is that it simplifies the parameters like ground reflectance and tree transmittance [9]. Specifically, EnergyPlus represents tree transmittance as static obstructions with a constant transmittance value, a recognized limitation inherent in the tool. In an effort to surmount this constraint, a proposition for overcoming this limitation is presented in 2.5 which is generally based on an external interface in EnergyPlus that allows users to link it with other programs. The geometry of the EnergyPlus building model was presented in Figure 2. The EnergyPlus simulation was located in Taipei city. The building model represents a typical office building in the downtown area of the city, having an area of 2000m^2. The window-to-wall ratio is 0.4 and the zones are equipped with variable-air-volume type HVAC systems with chiller coefficient of performance of 5.0. Instead of running standard EnergyPlus simulations, a BCVTB framework was developed that coupled variables from both EnergyPlus and ENVI-met at synchronized time intervals.

2.5 Correspondence between ENVI-met and EnergyPlus

The coupling strategy that is employed by this research follows the method developed by Ramesh, S [2]. The BCVTB is the platform where this coordinated solution is built and simulated. To properly account for the microclimate in the energy simulation of the building was the EnergyPlus calculation of its internal load for zones which follows Equation (1):

$$Q_{internal\ loads} = q_{ihg} + q_c + q_{in} + \Delta E_{air} \quad (1)$$

where

$Q_{internal\ loads}$ – Building's cooling or heating loads
q_{ihg} – Internal heat gain
q_c – Convective heat transfer (W)
q_{in} – Heat transfer due to infiltration
ΔE_{air} – Energy change of air in the zone

The balance equation for the outside face of a building is calculated by Equation **(2)**:

$$q_{\alpha sol} + q_{LWR} + q_c - q_{ko} = 0 \qquad (2)$$

where

$q_{\alpha sol}$ − Absorbed direct and diffuse solar radiation heat flux
q_{LWR} − Net longwave radiation heat exchange
q_c − Convective heat transfer (W)
q_{ko} − Conduction heat flux (q/A)

The coupling method was developed based on Equation (1) and Equation (2). The variables in both equations were used selectively in the coupling platform where the nature of their calculation determined whether they were used or improved by a more accurate procedure. The variables calculated in the coupling platform and their input source are organized under 3 main sections: the direct and diffuse radiation section, a surface boundary conditions section, and an infiltration section. The incident radiation was attained from EnergyPlus as well as shadowing effects. For the surface boundary conditions, the surface temperature was calculated by EnergyPlus, however, the variables air temperature and wind speed were provided by ENVI-met. For the infiltration sections, the indoor zone-air temperatures were calculated by EnergyPlus, whilst the outdoor dry-bulb temperatures and the wind speed were given by ENVI-met.

The EnergyPlus calculation for convective heat flux (q_c) of building exterior surfaces can be defined by Equation (3):

$$q_c = h_c A\,(T_{surf} - T_{air}) \qquad (3)$$

where

q_c − Convective heat transfer (W)
h_c − Convective heat transfer coefficient ($W/m^2 \cdot K$)
A − Surface area (m^2)
T_{surf} − Temperature of building surface (°C)
T_{air} − Temperature of outside air (°C)

The convective heat transfer coefficient (CHTC) calculation developed by the international standard ISO 6946 [10] was used due to its suitability in a wind speed range of 1-10 m/s [9]. The calculation for the CHTC is given by Equation (4):

$$h_c = 4 + 4v \qquad (4)$$

where

h_c − Convective heat transfer coefficient ($W/m^2 \cdot K$)
v − Wind speed (m/s)

Equation (4) is a linear law and its accuracy heavily depends on the wind speed value at the building surface. Using wind speed data from ENVI-met is essential for determining CHTC due to its inherent consideration of the flow field around the building, presenting a more practical approach as oppose to utilize the CHTC correlations provided in EnergyPlus. To overwrite the CHTC calculated by EnergyPlus, it was necessary to employ the `ExternalInterface` object in EnergyPlus which allows EnergyPlus to couple with BCVTB at each time step. The radiative heat transfer coefficient (RHTC) was also considered in determining the surface boundary conditions and thus was implemented in the coupling solution. In EnergyPlus, the calculation for the RHTC is governed by Equation (5):

$$h_r = \frac{\varepsilon \cdot \sigma \cdot F_{sky}\left({T_{surf}}^4 - {T_{air}}^4\right)}{T_{surf} - T_{air}} \qquad (5)$$

where

h_r − Radiative heat transfer coefficient ($W/m^2 \cdot K$)
ε − emissivity
σ − Stefan – Boltzmann Constant ($W/m^2 \cdot K^4$)
F_{sky} − Sky temperature (°C)

3. RESULTS AND DISCUSSION

3.1 UWG generated weather results

The ambient temperature results of both the a standard Taipei TMY3 and the UWG modified TMY3 are presented in Figure 4. Observing the figure, it is evident that air temperature differed between both, with the UWG generated air temperatures (red curve) having a higher lower bound than the standard TMY3 (blue curve), especially for the warmer months of June to September.

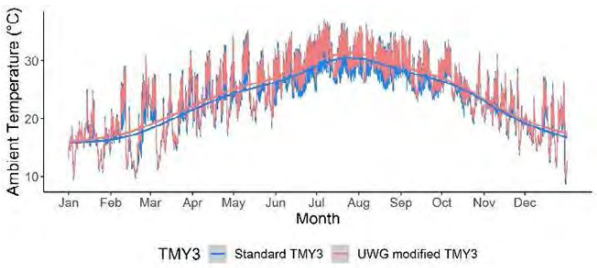

Figure 4 Ambient temperature comparisons between standard TMY3 data and UWG-generated TMY3 data.

3.2 ENVI-met microclimate results

Figure *5* compares the ENVI-met and TMY3 wind speed results for the warmest months of the year; the months between April and September. Notably, TMY3 exhibited significantly higher wind speeds than ENVI-met throughout all months, with TMY3's average wind speed at 2.66 m/s, demonstrating that wind speed is over-exaggerated. In August, both TMY3 and ENVI-met recorded their highest wind speeds, with TMY3 values being nearly 3.5 times larger than ENVI-met. This difference is possibly influenced by the obstructive

impact of 15-meter trees surrounding the target building in the ENVI-met simulation scenarios.

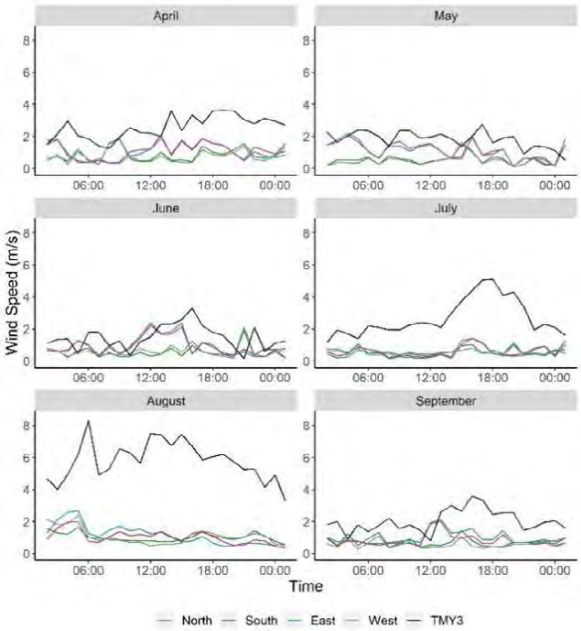

Figure 5 ENVI-met average wind speed results for north, south, east, and west façades of building model and the wind speed results of the standard TMY3 for Taipei.

3.3 BCVTB-coupling microclimate variable matrices

A Pearson's correlation matrix with pairwise scatterplots was created to assess the statistical significance of the BCVTB-coupling simulation variables, presented in Figure 6. Collinear variable pairings such as CHTC and wind speed were expected due to Equation (4). The plots Reveal a high significant positive correlation between air temperature and surface temperature, with an *r* value of 0.97. The figure also presents a negative CHTC and air temperature, supported by r values of 0.5 for both pairings. Such values express that as the convection coefficient which governs heat transfer increases, air temperature and surface temperature decreases. This may be due to the wind tunnel effect which removes hot air from the canyon subsequently lowering air temperatures. Correlations were strongly positive between RHTC, surface temperature, and air temperatures. A basic sensitivity analysis of sky temperature and surface temperature on RHTC indicated that when surface temperature is lower than sky temperature, $\mathbf{h_r}$ increases, particularly on very cold days.

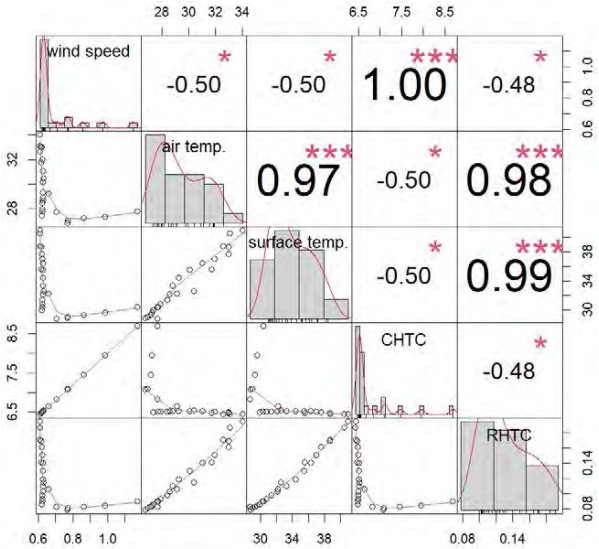

Figure 6 A correlation matrix of variables that were a part of the BCVTB-coupling simulation for the east façade of July 31st

3.4 BCVTB-coupling simulations surface temperature with Trees vs surface temperature results without trees

To show the effect of trees on microclimate, all the vegetation from the model was removed and the BCVTB-coupling simulations were re-run. The differences between the results from these simulations are summarized in Figure 7. The figure shows the months that are typically energy intensive. The difference was attained from subtracting the values of BCVTB-coupling simulations with Trees from BCVTB-coupling simulations without trees. These values are shown as ΔT. Positive ΔT values indicate that simulations without trees have higher surface temperatures than those simulations where vegetation was present. In contrast, negative ΔT values indicate that surface temperature values from simulations with trees are higher than those without trees. As such, the results generally show that surface temperatures were higher when vegetation was removed. The results also indicate that heat mitigation by trees varies depending of the time of year and time of day. From Figure 7, it is evident that the summer months of July to September have larger surface temperature differences compared to the months of May and June. With the transitions from summer to cooler months, the impact of trees on surface temperatures diminishes which coincides with a reduction of incoming solar radiation and subsequently cooler temperatures. A particular phenomenon can be observed during night time and early morning hours for all months. This is that the ΔT indicates that surface temperatures are higher for simulations with trees at nighttime or early morning hours. This coincides with the results presented in 3.3. Similar observations have been documented by [9]. The

results suggest that trees contribute to daytime cooling but retain nocturnal warmth. This warming effect is as a result of their canopy blocking heat elevation towards the cooler sky.

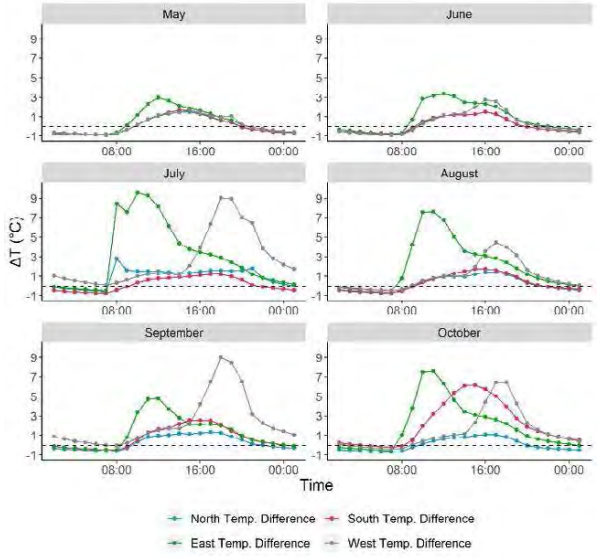

Figure 7 Surface temperature differences between BCVTB simulations with trees and without trees.

3.5 Impact of trees on Energy Use Intensity (EUI) and contributions of the proposed coupling method

The EUI of 3 simulation scenarios are presented in Table 1; BCVTB-coupling simulations with trees, BCVTB simulations without trees, and EnergyPlus-only simulations with trees. The represent the monthly EUI. An analysis of the performance of the co-simulation system in terms of its EUI output revealed that vegetation plays a huge impact on the cooling load of a building. July being the hottest month, showed a reduction potential of over 23% if trees are present. The simulations with trees and the simulations without trees in in the BCVTB cases showed differences close to 17%. Comparing BCVTB simulations with trees against EnergyPlus-only simulations with trees represented as reflective surfaces showed that EnergyPlus underestimated EUI by more than 9%. Such differences are attributed to the sophistication of the algorithms in the coupling strategy that exchange vital microclimate factors at synchronized time-steps. This enables provides a more accurate thermophysical boundary condition for enabling better building energy simulations.

4. CONCLUSION

This paper presented a methodology that bridges the existing gap between building energy simulation and urban climate modelling. This was achieved by devising a coupling strategy using the BCVTB Several conclusions were made from this study. Some of the primary findings of this research are as follows:

- A modification of the weather file corrected the air temperature, with average air temperatures being 23.96°C which is was higher than the standard TMY3 weather files showing the latter does not capture urban weather conditions.
- ENVI-met simulation microclimate data showed vast deviations from standard weather files especially for wind speed, where values were less than 3 times what the weather file suggested.
- A Pearson's r correlation matrix of variables from the BCVTB-coupling simulation results showed a strong positive statistical relationship between air temperature and surface temperature with an R of 0.97. The pairwise scatterplots also showed CHTC negatively correlated with surface temperatures which coincides with the findings of other studies.
- A modification of the CHTC and surface temperature using the BCVTB-coupling strategy improved the resolution of the microclimate impact of avenue trees on buildings. The removal of vegetation vastly increased surface temperatures up to 9% for some surfaces, especially during summer months. At nighttime however, trees canopies blocked the ascension of heat thereby increasing surface temperatures beyond the temperature of surfaces where vegetation was not present.
- Trees accounted for a EUI reduction of about 17%, on average for energy intensive months. Only utilizing EnergyPlus to make these determinations lead to the underestimation of the cooling effects of trees of up to 9% which shows that properly accounting for the microclimate improves building energy simulation accuracy.

Table 1 Total EUI comparison between BCVTB-coupling simulations with trees, BCVTB-coupling simulations without trees, and EnergyPlus-only simulations

Month	Total Energy Use Intensity (Wh/m^2·month)		
	BCVTB simulations with Trees	BCVTB simulations without Trees	EnergyPlus simulations with Trees
May	412.1	464.1	408.8
June	282.0	340.5	215.1
July	571.5	746.0	670.0
August	518.6	592.9	521.9
September	358.9	442.0	273.8
October	524.5	632.9	482.9

REFERENCES

1. Hyl, C.; Lee, E.; Liu, J.; Neuendorffer, S.; Cheong, E.; H, J.; Tsay, J.; Vogel, B.; Williams, W.; Xiong, Y., et al. Ptolemy II: Heterogeneous Concurrent Modeling And Design In Java. **2002**.
2. Ramesh, S. Urban Energy Information Modeling: A Framework To Quantify The Thermodynamic Interactions Between The Natural And The Built Environment That Affect Building Energy Consumption. Carnegie Mellon University, 2018.
3. Bueno, B.; Norford, L.; Hidalgo, J.; Pigeon, G. The urban weather generator. *Journal of Building Performance Simulation* **2013**, *6*, 269-281, doi:10.1080/19401493.2012.718797.
4. Bueno, B.; Nakano, A.; Norford, L.; Reinhart, C. Urban Weather Generator - a Novel Workflow for Integrating Urban Heat Island Effect within Urban Design Process. **2015**.
5. Yang, J.H. The Curious Case of Urban Heat Island: A Systems Analysis. Massachusetts Institute of Technology, 2016.
6. Koralegedara, S.B.; Lin, C.-Y.; Sheng, Y.-F.; Kuo, C.-H. Estimation of anthropogenic heat emissions in urban Taiwan and their spatial patterns. *Environmental Pollution* **2016**, *215*, 84-95.
7. Toparlar, Y.; Blocken, B.; Maiheu, B.; van Heijst, G.J.F. A review on the CFD analysis of urban microclimate. *Renewable and Sustainable Energy Reviews* **2017**, *80*, 1613-1640.
8. Corrado, V.; Fabrizio, E. Chapter 5 - Steady-State and Dynamic Codes, Critical Review, Advantages and Disadvantages, Accuracy, and Reliability. In *Handbook of Energy Efficiency in Buildings*, Asdrubali, F., Desideri, U., Eds. Butterworth-Heinemann: 2019. 263-294.
9. Yang, X.; Zhao, L.; Bruse, M.; Meng, Q. An integrated simulation method for building energy performance assessment in urban environments. *Energy and Buildings* **2012**, *54*, 243-251,
10. Standardization, I.O.f. Building Components and Building Elements - Thermal Resistance and Thermal Transmittance - Calculation Method (ISO 6946: 2007). **2007**.

PLEA 2024 WROCŁAW
(Re)thinking Resilience

Optimization of Energy Generation for PV:
Integrating parametric PV design with solar radiation simulation

SHAOBO YANG[1] PABLO LA ROCHE[1,2] ARIANNE PONCE[1]

[1]Arcadis, Los Angeles, USA
[2] Cal Poly Pomona University, USA

ABSTRACT: This study delves into the optimization of rooftop and façade photovoltaic (PV) design for building integration, aiming to maximize energy generation and reduce building carbon footprints. Providing renewable energy on-site and integrated into the design is the final step in the design process to minimize building emissions. The research proposes a method that combines parametric PV design with solar radiation simulation and optimization, which proves to be a useful tool for maximizing rooftop and façade PV energy generation. This method introduces a methodology, utilizing Grasshopper in Rhino, Ladybug package, and Python code, to optimize parametric PV panel placement on building facades and rooftops by considering azimuth, tilt angle, panel size, count, spacing, integrating solar radiation simulation and optimization for increased energy generation. The study also explores the daylight performance for optimized façade PV. The adaptability of the methodology revealed through different weather files highlights its versatility for application in different geographic locations. Results indicate that the optimized designs outperform baseline configurations, emphasizing the importance of precise PV panel placement. This study not only advances the effectiveness of PV integration and improves the potential of PV systems to improve energy efficiency and performance significantly.
KEYWORDS: Photovoltaic, Solar Energy, Optimization, Simulation, Radiation

1. INTRODUCTION

With increasing concerns about global warming, industries are investing heavily in environmental solutions. To combat climate change, it is important to reduce energy consumption and non-renewable energy consumption in buildings. Photovoltaic (PV) solar energy substitutes traditional electricity sources [1] and provides clean energy on-site.

On-site PV systems have the potential to reduce electricity losses that occur during the conventional transmission process utilized by central power plants for distributing electricity through long and complex power lines. When the photovoltaic system is installed in buildings, it is common practice to install PV modules on rooftops and facades. This approach minimizes the need for extensive mounting structures and reduces land requirements [2]. Integrating solar photovoltaic (PV) systems into building design has become an essential approach for achieving net-zero energy consumption by harnessing solar energy to generate electricity. The design of PV systems for building integration has become a critical research area that involves optimizing PV systems on building facades and rooftops.

However, implementing an inefficient design can significantly reduce the performance of the PV system. This paper proposes a PV design approach that optimizes the size and placement of PV panels to maximize energy generation by integrating parametric PV design with solar radiation simulation. The proposed method is expected to contribute to the wide-scale implementation of efficient and sustainable building design strategies that integrate PV systems, which is essential for creating energy-efficient buildings while reducing carbon footprints.

2. BACKGROUND AND LITERATURE REVIEW

Solar energy is a renewable power source derived from harnessing direct sunlight and converting it into electricity. It is clean and sustainable energy because it produces no harmful emissions compared to conventional fossil fuel-based electricity generation. Solar energy holds the highest potential for global popularization, especially when compared to other sources like biomass, which isn't entirely clean or readily replenished, and geothermal energy, which are constrained by location feasibility [3].

The site assessment is one of the most important tasks during the predesign phase of a photovoltaic (PV) system, serving to ascertain the suitability and value of both the site and building for PV installation. Environmental factors such as solar insolation, shading throughout the year, and cloud cover play a crucial role and necessitate thorough evaluation in this assessment [4]. In this context, the primary environmental assessment is the solar analysis, which measures the amount of solar irradiance, representing the sun's radiant energy received at a specific site on Earth. This solar analysis considers the impact of surrounding shading elements and the presence of diffuse and direct solar radiation and cloudiness to provide a more precise assessment of feasibility [5].

The design of photovoltaic (PV) solar collectors involves relationships between field and collector parameters and solar radiation data. The impact of shading and masking, expressed through the view

factor to the sky by adjacent collector rows, can significantly impact the energy output of the PV field by diminishing the incident radiation on the collector surfaces. The use of numerous rows of collectors, closely spaced together, can improve the overall energy generated. However, if they are too close together, they can also reduce direct beam incident radiation on the collectors due to shading and a decrease in the diffuse incident radiation as the view factor between the collectors and the sky diminishes. As a result, an optimal arrangement exists for collectors in a field, which can be designed to achieve varying optimal objectives, whether focused on energy output or economic considerations [6]. Previous studies delved into theoretical and practical optimizations for photovoltaic fields, focusing on four objective functions: maximizing annual incident energy, minimizing field area, reducing overall cost, and minimizing the cost of unit energy. The theoretical optimization results highlighted that the optimal designs are achieved when adhering to the minimal allowed distance between collector rows, employing the maximum allowable collector width, and fully utilizing the entire field length [6]. However, this study specifically focuses on maximizing the annual incident energy for solar panels. The variables under consideration include the number of modules, module spacing, tilt angles, and azimuth orientation.

3. METHODOLOGY

Integrating parametric PV design with solar radiation simulation and optimization could significantly increase energy generation for rooftop and facade PV systems. The research objective was to propose a method for optimizing the placement and configuration of PV panels on building facades and rooftops using Grasshopper in Rhino, Ladybug package, and Python code (Figure 1).

The proposed method consists of four main steps illustrated in Figure 1. The first step involves creating a parametric PV model in Grasshopper and Rhino, which enables the generation of thousands of iterations with different input variables, including azimuth, tilt angle, panel size, panel count, spacing, and PV panel type. The generated iterations represent various PV panel designs that optimize the energy generation of the building.

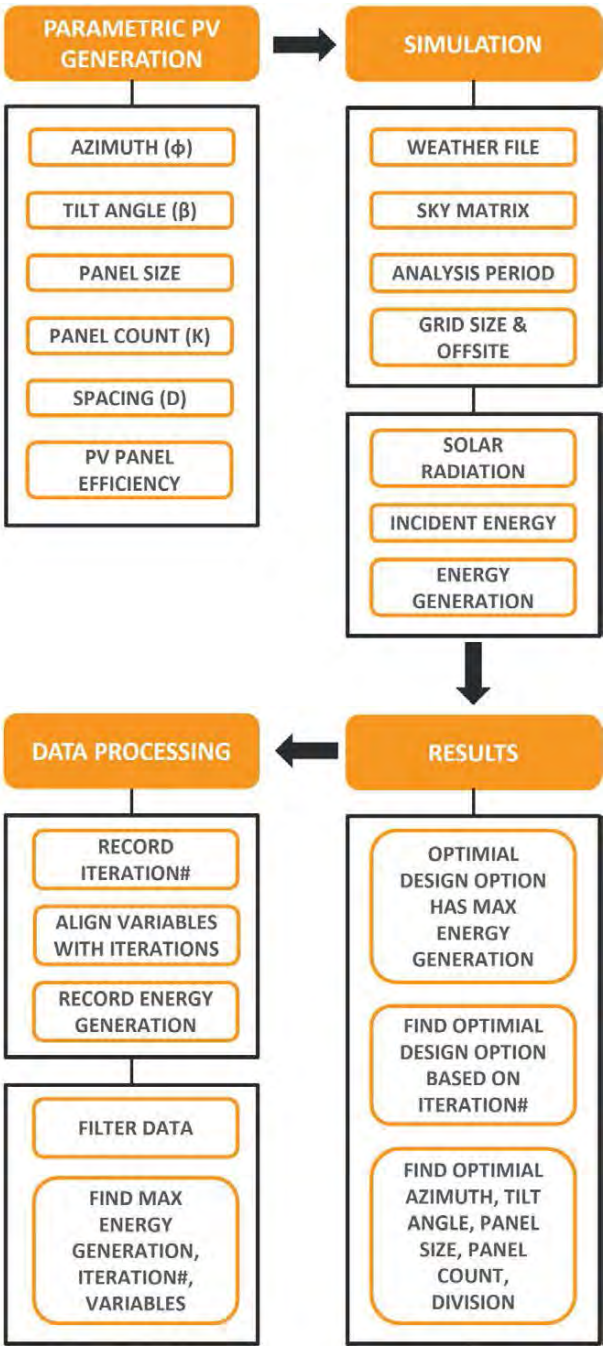

Figure 1 Methodology flow chart for PV optimization

The second step involves simulating the solar radiation incident on the PV panels for each generated iteration using the Ladybug package in Grasshopper. The inputs for the simulation include the EPW weather file, sky matrix, analysis period, grid size, and offset. The solar radiation simulation calculates the incident solar energy for each iteration, providing a measure of the energy generation potential of each PV panel design.

The third step involves recording the iteration number, aligning the input variables with the iteration number, and recording the corresponding energy generation for each PV panel design. The data is then filtered to find the iteration with the highest energy generation and its corresponding input variables. The

incident solar radiation can be calculated using the solar radiation simulation in the second step, and the PV panel efficiency and system losses are determined based on the characteristics of the PV panel and the system. The study assumed 20% efficiency for façade PV and 22% efficiency for rooftop PV energy generation.

3.1 Parametric PV variables

The tilt angle (β) is the angle between the panel and the horizontal plane. Solar azimuth angle (ϕ) is the angle between the direction of the panel and true south. Usually, panels with a shallow tilt generate greater energy output during the summer, while steeper angles are more efficient in the winter. The optimal fixed angle falls between these two extremes, resulting in the highest annual energy yield [7], usually close to latitude. The spacing between modules (D) significantly influences energy production. In PV arrays, row-to-row shading is a common issue that can diminish system efficiency. Increasing the number of collector rows (K) is likely to result in a net gain in incident energy, even when accounting for the shading losses that may occur from bringing the rows closer together [6]. The parametric PV field (Figure 2) comprises variables, including the number of panel rows (K), spacing between modules (D), tilt angles (β), and azimuth angle (ϕ). Other parameters contain panel length (L), width (H), and field width (W) (Table 1).

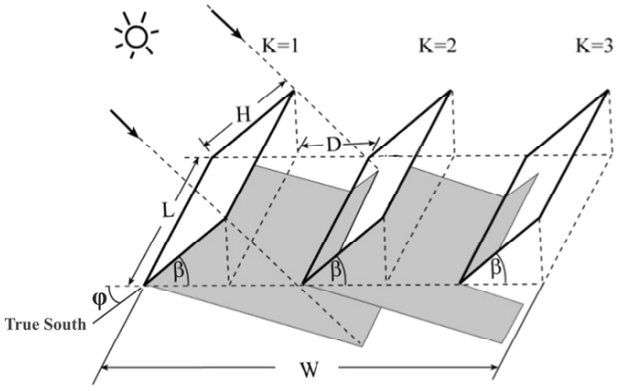

Figure 2 The variables of the parametric PV filed [6]

3.2 Simulation and optimization

TMYx format data is typical meteorological data derived from hourly weather data through 2021, available from US NOAA's Integrated Surface Database [8], which includes the local solar insolation in three ways: beam solar insolation (I_b) sometimes called the direct normal (I_{DN}), diffused solar insolation (I_d), and reflected insolation (I_r) [9]. The global insolation (I) is the sum of the three types of insolation. The following equations can calculate all three types of insolation on the receiving surface [10] [11]. See below Equation (1) (2) (3):

$$\boldsymbol{I_{bc}} = \boldsymbol{I_b}\left[\cos\boldsymbol{\alpha}\sin\boldsymbol{\beta}\cos\left(\boldsymbol{\varphi_s}-\boldsymbol{\varphi_p}\right) + \sin\boldsymbol{\alpha}\cos\boldsymbol{\beta}\right] \quad (1)$$

Where I_{bc} is the insolation on a specific surface;
α - solar altitude angle
β - tilt angle of panels
ϕ_s - solar azimuth angle in the winter solstice
ϕ_p - azimuth angle of the solar panel

$$\boldsymbol{I_{dc}} = \boldsymbol{I_d}\left(\frac{\mathbf{1}+\cos\boldsymbol{\beta}}{\mathbf{2}}\right) \quad (2)$$

Where I_{dc} is the diffused insolation on surfaces;

$$\boldsymbol{I_{rc}} = \boldsymbol{I_r}\left[\frac{\mathbf{1}-\cos\boldsymbol{\beta}}{\mathbf{2}}\right] \quad (3)$$

Where I_{rc} is the reflected insolation from surrounding surfaces;

The total insolation harvested by the system is the sum of the three types of insolation times the total area of the PV module. Defining the objective function as maximum annual incident energy (E_i) on the parametric PV field, the optimization problem is formulated as following Equation (4):

$$\textbf{Maximize energy}: \mathbf{C}\left(\overline{\mathbf{X}}\right) \textbf{ with respect to } \overline{\mathbf{X}}\left(\mathbf{D}, \boldsymbol{\beta}, \boldsymbol{\varphi}_{\mathbf{p}}, \boldsymbol{K}\right) \quad (4)$$

This study calculated annual PV solar system output using the simplified function of the following Equation (5):

$$\mathbf{E} = \boldsymbol{E_i} * \boldsymbol{r} \quad (5)$$

Where E is the energy generation from PV;
E_i - Maximum annual incident energy (kWh)
r - Solar panel efficiency (%)

The method involves creating a parametric PV model and inputting it into a solar radiation simulation to calculate the incident energy. The optimal rooftop PV design options are then determined based on the iteration with the highest energy generation. Because the facade PV is also in front of windows and works as a shading device, the optimal facade PV design options aim to achieve lower summer solar gain on glazing and higher solar radiation on each PV panel by finding the optimal spacing of panels. This ensures that the building's interior is not impacted by solar radiation while maximizing energy production. Daylight was also

measured with and without the PV shade. This method provides an efficient way to optimize the placement of PV panels on building facades and rooftops.

4. CASE STUDIES AND RESULTS

The first case study is a project for an office building in Malaga, Spain, focusing on optimizing photovoltaic (PV) systems on both the rooftop and facade. The second case study is the same building but now using a Seattle weather file for rooftop PV optimization. The parameter for simulations is shown in Table 1.

Table 1 Simulation Parameters

Simulation Parameters	
Timestep	Hourly
Analysis period	Annual
Sky matrix	Cumulative sky matrix
Grid Offsite	0.001m
Gird size	0.4 m
EPW weather file	ESP_AN_Malaga.AP.084820_TMYx.2007-2021 USA_WA_Seattle-King.County.Intl.AP-Boeing.Field.727935_TMYx.2007-2021

4.1 Facades PV optimization

This study conducted 140 iterations to optimize the height and spacing of south-facing façade photovoltaic (PV) panels. The parameters and variables for the parametric façade PV are shown in Table 2.

Table 2 The parameters and variables for the parametric façade PV

Parametric PV filed variables - Façade	
Azimuth angle (ϕ)	0°
Modules spacing (D)	2.65m, 1.98m, 1.59m, 1.32m, 1.13m, 0.99m
Number of PV rows (K)	1 - 7
Panel length (L)	1 m
Panel Width (H)	6.25 m
Field width (W)	2.65m, 3.96m, 4.77m, 5.28m, 5.65m, 5.94m
PV efficiency	20%

The objective was to maximize solar radiation received by the PV panels while minimizing radiation on the glazing that would enter the space and increase the cooling load. The optimized design achieved lower annual solar radiation on the glazing surface and higher solar radiation on each PV panel, indicating improved energy harvesting. The findings highlight the potential for enhancing solar energy systems by carefully optimizing PV panel parameters (Figure 3 and Figure 4).

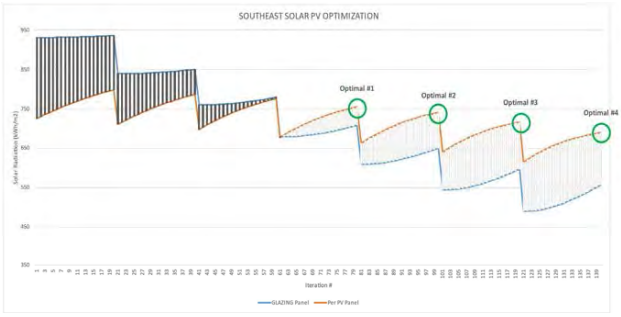

Figure 3 Iteration results for facade PV optimization

Figure 3 illustrates the iterations of facade PV optimization, highlighting the optimal design with lower annual solar radiation on the glazing surface (depicted by the blue line) and higher solar radiation on each PV panel (represented by the orange line), revealing the identification of four optimal designs.

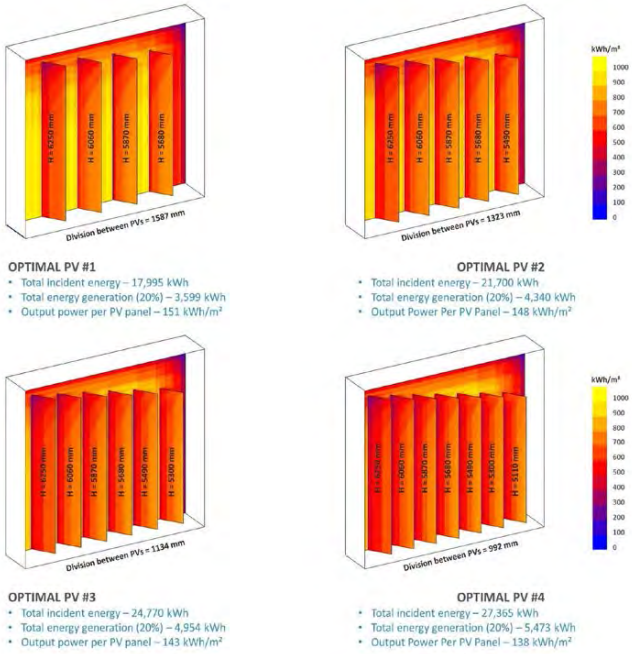

Figure 4 Proposed optimal design options for facade PV

The daylight study for optimal design option 1 was conducted to explore daylight penetration for transparent photovoltaic (PV) facades. The results of the daylight study show that the percentage of floor area that surpasses 300 lux during 50 percent of regularly occupied hours is 70%, which is considered "Nominally Acceptable" daylighting conditions based on IES LM-83-12 criteria (Figure 5).

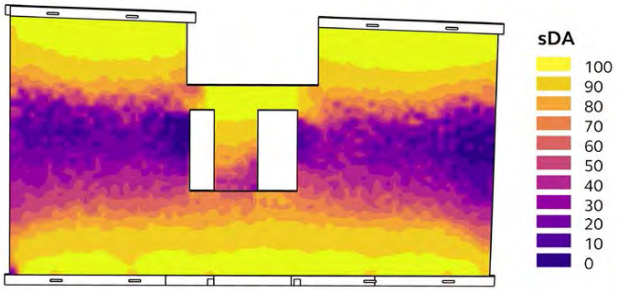

Figure 5 Daylight study for Optimal design option 1 - sDA =70%

Indeed, Optimal Design Option 1 represents a solution that not only maximizes photovoltaic (PV) energy generation but also effectively reduces excessive solar radiation on the glazing, simultaneously achieving the goal of providing ample and high-quality daylight within the building.

4.1 Rooftop PV Optimization

Another study on the rooftop focused on comparing various configurations of PV panel tilt angle, azimuth (orientation), and division (spacing between panels) to identify the best-performing combination of these parameters (Table 3).

Table 3 The parameters and variables for the parametric rooftop PV

Parametric PV filed variables - Rooftop	
Tilt angle (β)	0° - 55.0°
Azimuth angle (ϕ)	28.7° - 36.2°
Modules spacing (D)	Not less than 0.1016 m
Number of PV rows (K)	11 - 16
Panel length (L)	18 m
Panel Width (H)	3.49 m
Field width (W)	44 m
PV efficiency	22%

In a comprehensive simulation-based study, 6,090 iterations were performed to determine a PV panel system's optimal tilt angle, azimuth, and division to maximize energy generation (Figure 6) (Figure 7).

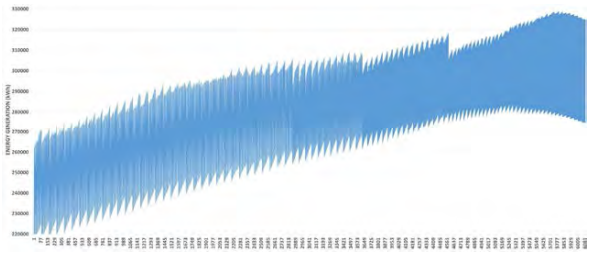

Figure 6 Iteration results for rooftop PV optimization (Malaga)

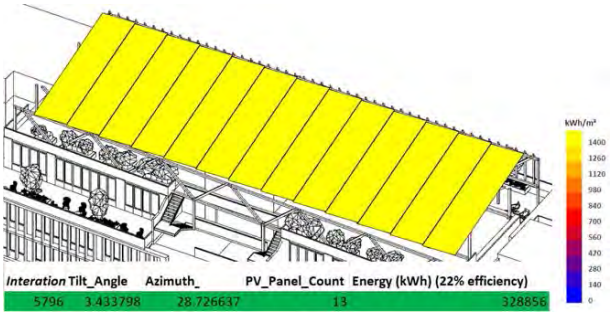

Figure 7 Proposed optimal design option for rooftop PV (Malaga)

By applying the same roof model with different weather files, this study highlights its potential for application across these two geographical locations, Malaga and Seattle. This study observes improvements in energy generation with the optimized designs. In Malaga, the optimized design, featuring a tilt angle of 3.43 degrees, an azimuth angle of 28.73 degrees, and 13 PV panels, produced 328,856 kWh of energy, outperforming the baseline design's 271,304 kWh, which has a 21.2% improvement.

The optimal rooftop PV using both Malaga and Seattle weather files is shown in Figure 8 and Figure 9.

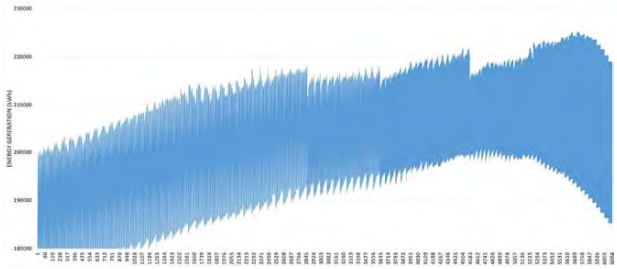

Figure 8 Iteration results for rooftop PV optimization (Seattle)

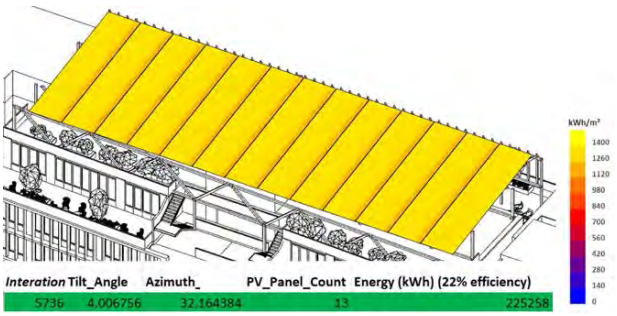

Figure 9 Proposed optimal design option for rooftop PV (Seattle)

While, in Seattle, the optimized design, with a tilt angle of 4.01 degrees, an azimuth angle of 32.16 degrees, and 13 PV panels, generated 225,258 kWh, surpassing the baseline design's 191,178 kWh, which has a 17.8% improvement (Table 4).

Table 4 The summary and comparison of rooftop PV results

Location	Design Option	Tilt Angle	Azimuth Angle	PV Panel	Energy (kWh)
Malaga	Baseline	36.67	28.73	12	271,304
	Optimal	3.43	28.73	13	328,856
Seattle	Baseline	47.55	28.73	12	191,178
	Optimal	4.01	32.16	13	225,258

These findings indicate the potential for this adaptable methodology to improve rooftop PV design, aligning configurations with specific geographical conditions.

5. CONCLUSION

The integration of parametric PV design and solar radiation simulation have been combined in a method to optimize energy generation for PV. Results indicate that the optimized designs outperform baseline configurations, improving the design through a more precise PV panel placement. The case study with façade PV design accomplishes several key objectives. It reduces annual solar heat gain on the glazing, increases energy production from the PV panels, and ensures effective daylighting. The results of optimizations from simulation demonstrate the importance of optimizing PV panel placement to maximize solar energy generation and improve the performance of solar panels.

While the optimal PV design shows the most energy generation, it's crucial to weigh the associated costs. The design option may require more PV panels, impacting project expenses. Achieving a balance between enhanced energy production and cost-effectiveness is essential for practical and economically viable solutions. A thorough evaluation, considering both energy performance and economic aspects, is necessary to ensure the selected PV design aligns with budget constraints.

Further research in this field could explore additional factors, such as cost, type and efficiency of PV panels, temperature, inverter efficiency, wiring and electrical losses, battery storage, and load profile, to refine the optimization process and achieve even higher levels of energy generation. The outcomes of such research will advance the feasibility and viability of solar energy as a major contributor to renewable energy needs and reduction of building carbon footprint.

REFERENCES

1. Salimzadeh, N, F Vahdatikhaki, and A Hammad. n.d. "BIM-Based Surface-Specific Solar Simulation of Buildings." Accessed August 28, 2019. http://www.iaarc.org/publications/fulltext/ISARC2018-Paper188.pdf.

2. Gong, X., & Kulkarni, M. (2005). Design optimization of a large scale rooftop photovoltaic system. *Solar Energy, 78(3), 362-374.*

3. Kabir, Ehsanul, Pawan Kumar, Sandeep Kumar, Adedeji A Adelodun, and Ki-Hyun Kim. 2017. "*Solar Energy: Potential and Future Prospects*." https://doi.org/10.1016/j.rser.2017.09.094.

4. Solar radiation basics. *Energy.gov.* (n.d.-b). https://www.energy.gov/eere/solar/solar-radiation-basics

5. Parida, Bhubaneswari, S Iniyan, and Ranko Goic. 2011. "A Review of Solar Photovoltaic Technologies." *Renewable and Sustainable Energy Reviews* 15: 1625–36. https://doi.org/10.1016/j.rser.2010.11.032.

6. Aronescu, A., & Appelbaum, J. (2017). Design optimization of photovoltaic solar fields-insight and methodology. *Renewable and Sustainable Energy Reviews*, 76, 882-893.

7. Gregg, A., T. Parker, and R. Swenson. 2005. "A "Real World" Examination of PV System Design and Performance." In Conference Record of the *Thirty-First IEEE Photovoltaic Specialists Conference, 2005., 1587*–92. IEEE. https://doi.org/10.1109/PVSC.2005.1488448.

8. *Global hourly - integrated surface database (ISD).* National Centers for Environmental Information (NCEI). (2023, August 11). https://www.ncei.noaa.gov/products/land-based-station/integrated-surface-database

9. Okoye, Chiemeka Onyeka, Onur Taylan, and Derek K Baker. 2015. "Solar Energy Potentials in Strategically Located Cities in Nigeria: Review, Resource Assessment and PV System Design." https://doi.org/10.1016/j.rser.2015.10.154.

10. Ning, Gui, He Kan, Qiu Zhifeng, Gui Weihua, and Deconinck Geert. 2018. "E-BIM: A BIM-Centric Design and Analysis Software for Building Integrated Photovoltaics." *Automation in Construction 87* (March): 127–37. https://doi.org/10.1016/J.AUTCON.2017.10.020.

11. Ibrahim, A, A. A El-Sebaii, M. R.I Ramadan, and S. M El-Broullesy. 2013. "Estimation of Solar Irradiance on Tilted Surfaces Facing South for Tanta, Egypt." *International Journal of Sustainable Energy 32* (2): 111–120. https://doi.org/10.1080/14786451.2011.601814

APPENDIX

As a service to the community, the link below includes the Grasshopper scripts:
https://drive.google.com/drive/folders/1iORsbMuL1jPJJV1ml-qtJhV7-Ns5JKzG?usp=drive_link

PLEA 2024 WROCŁAW
(Re)thinking Resilience

The Double C Block project: Hot Box studies

Deploying Heat Flux Method inside the Hot box apparatus to enhance the measurement of the block's thermal transmittance.

LUCA CARUSO[1] VINCENT BUHAGIAR[1]

[1]Department of Environmental Design, Faculty for the Built Environment, University of Malta, Msida, Malta

ABSTRACT: The Double C-Block (DCB) is an innovative Concrete Masonry Unit (CMU) with embedded insulation developed to provide, through its geometry, both thermal and acoustic performance, apart from its established load bearing capacity. The DCB is a proven faster construction process as it eliminates the need for external/internal insulation cladding. The first load-bearing prototype developed at the University of Malta was made of two concrete C-shaped skins bonded with sprayed polyurethane foam (PUF) as the insulation layer. Earlier studies through full-scale in-situ test cells reported thermal transmittance value U_{DCB} of 1.47 W/m^{2}K, already outperforming the local building energy code. When running steady-state simulations Finite Element Method (FEM), results persistently showed a difference in U-values, when compared to field studies. The methodology was therefore revisited to combine these field studies with hot-box apparatus as well as performing a new set of steady-state FEM simulations by using experimental values of concrete and PUF's thermal conductivity (TC). The latest U-value is now proven to be 1.40 W/(m^{2}K) thanks to the use of Heat Flux Method (HFM) inside a hot box apparatus. This brings the performance gap down from 51% to a more precise 11%. This establishes the DCB as an alternative to the standard hollow core blocks plus insulation cladding. These results now push it up the technology readiness levels scale(TRL), from TRL4 to TRL6, thus lined up for commercial production.
KEYWORDS: Energy Efficiency, Thermal Conductivity, Heat Flux Method (HFM), Hot Box, Finite Element Method (FEM).

1. INTRODUCTION

The International Energy Agency (IEA) has demonstrated that the use of more efficient building envelopes is a technical solution to improve the energy efficiency of buildings [1], and as a consequence the energy-related CO_2 emission of the building industry [2]. Mandatory and demanding building energy codes for new and retrofitted buildings are now requiring high performing building materials. The development of new technical solutions like the DCB must undergo a thorough testing phase, through different robust scientific methodologies, especially for the steady state heat transfer performance of the wall.

2. LITERATURE REVIEW

2.1 Hot Box and thermal conductivity assessment

Hot boxes are well-known standardized laboratory-graded tests that assess the steady-state thermal transmittance (U-value) of external walls according to ISO 8994:1994 [3]. The U-value is obtained by measuring the heat transferred from a hot to a cold chamber, both divided by a mock up wall. Heat flux is a temperature gradient difference. The hot box apparatus is essentially a temperature-controlled space with minimum flanking heat losses to make sure there is an effective one directional heat transfer within the wall. For example, in 2015, Pavlík et al. [4] performed an experiment on a 500 mm width fired clay masonry units filled with hydrophobic mineral wool. The blocks were neither plastered nor rendered. The blocks were successfully tested against different hygro-thermal climatic conditions inside a climatic chamber, an enhanced version of hot-boxes, capable of replicating not only the dry bulb temperature (DBT) but also the variation of indoor and outdoor relative humidity (RH).

Heat flux meters (HFM) are a well-established non-destructive technique aimed at measuring in-situ thermal transmittance of existing walls. The scientific set is well described by ISO 9869-1 [5] and include a heat-flux meter that passively measures the density of heat flux (expressed in W/m^2) through the wall and thermocouples (e.g. type T), to obtain the thermal conductance, or via ambient thermometers to establish the thermal transmittance. The whole set up is usually to dataloggers to record the practically instant recorded values to accumulate a dataset of not less than 72 hours.

The HFM measurement is typically known for being particularly sensitive to the variation of outdoor and indoor temperature conditions, thus influencing the speed at which the measurement reaches the convergence towards a stable U-value as emphasized

by Desogus et al. [6]. This is why Meng et al. [7] installed a small hot box to surround the HFM and thermocouples to their advantage: a temperature-controlled set-up guaranteed the conditions to have faster and more reliable measurements.

Asdrubali et al. [8] investigated the methodology described by all the international standard available on this topic, including the GOST standard that recommends the use of HFM apparatus. They deployed 12 heat fluxes and 142 thermocouples to precisely measure the thermal transmittance of a window inside a hotbox.

Caruso et al. [9] measured the in-situ U_{DCB} and compared to a theoretical threshold calculated using steady-state FEM based on handbook data of the thermal conductivity (TC) for concrete and PUF. Results pointed to a performance gap of 51% between in-situ U_{DCB} of 1.47 W/(m^{2}K) versus a U_{DCB} of 0.71 W/(m^{2}K) obtained via FEM.

It is important to point out that, TC (also denoted as k or λ) is one of the main thermophysical property of building materials. The concrete typically used in CMUs can be compared to the value listed in EN 1745 [10]: TC of the concrete block is reported to be between 0.82 and 1.11 W/(mK) in the range of density from 1800 to 2100 kg/m^3. ISO 10456 [11] is instead a valid reference to compare the TC of commercial PUF, and it was found that tabulated design value of the PU foam's TC is 0.05 W/(mK) with a density of 70 kg/m^3.

3. METHODOLOGY

3.1 Materials' mix design

The concrete used for the DCB is a typical no slump mix design with a declared net density of concrete of 2047 kg/m^3. For the DCB insulation layer a conventional PU soft foam commercially branded as Pattex PF100 with a declared density of circa 16-20 Kg/m^3. Fig. 1 gives an idea of the prototype under study.

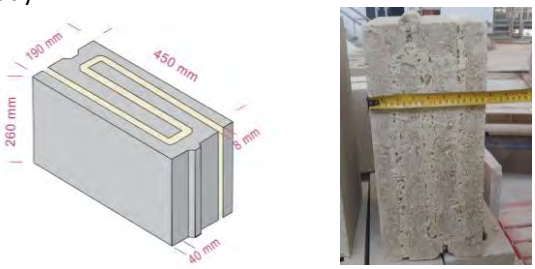

Figure 1: a) The DCB geometry: overall dimension of the multi-layered block; b) the manufactured DCB prototype.

3.1 Dry materials' density and thermal conductivity

The procedure to obtain the dry thermal conductivity and density, valid for both concrete and PU samples, was structured as follows. Samples were randomly extracted directly from the block and cut to the dimensions recommended by the manufacturer of the thermal conductivity analyser. For the concrete the sample was 10x10x4 cm and PUF was 10x10x1 cm, with the latter then stacked with other PUF samples to reach at least 5 cm thickness. During the measurement of the dry mass it was necessary to keep the sample in the oven at 40°C for cycles of 24 hours until the mass variation was stable around ±0.1% compared to previous readings. Once ready the samples were stored in desiccator filled with silica salt (< 3% of RH) to cool down to laboratory conditions 23±1°C before starting the TC measurements.

A TC apparatus, commercially known as ISOMET 2114, was used and it is based on a dynamic and transient measurement method where the sample is subjected to heat flow impulses and the relative temperature response is analysed. The apparatus has two type of sensor: a needle probe, used for the soft PUF, and a disk sensor for concrete. During the measurement both samples were kept in a sealed box with silica salts to maintain the RH < 3% at room temperature, 23±1°C, hence to guarantee dry TC conditions. The calculation of the extended uncertainty related to TC measurements was calculated as per [12] also include the limitations of the TC.

3.3 FEM Steady State thermal analysis

The DCB's complex geometry and the association of different materials requires an advanced calculation – according to the detailed method described in ISO 6946:2017 [13]. The dimensions of the simulated block are shown in Fig. 1.a).

A steady-state FEM software *Therm v.7.8* © was used to numerically resolves the steady state two-dimensional heat radiation–conduction problem. The numerical solutions are provided under the assumption of (i) constant physical material properties for isotropic medium; (ii)no heat is stored in the cross-section, and so all energy that enters the cross section on the interior surface leaves through the exterior surface. The boundary conditions — corresponding to the notional winter conditions ISO 6946 — are listed in Table 1 as follows:

Table 1: FEM winter boundary conditions as per ISO 6946.

Boundary Condition Name	DBT [°C]	Surface Resistance [m^{2}K/W]	h_{se}/h_{si} [W/(m^{2}K)]
Adiabatic	0	0	0
Exterior Surface Resistance— (Horizontal)	10	0.04	25
Indoor Surface Resistance— (Horizontal)	20	0.13	7.69

The solution provided by FEM software is associated to a mesh, and this must be adapted to the geometry inputted through several iterations, up to the desired accuracy. According to ISO 10211 [14]: 10 iterations and 5% max error were the criteria to accept results.

3.4 Description of the hot box apparatus

The experiment was carried out with a setup consisting of a 20 cm thick XPS insulated volume with a frontal aperture of circa 2.56 m^2. The data acquisition comprised two HFMs, and eight surface thermocouples type T (installed on either side of the specimen DCB wall). These thermocouples were evenly distributed across the wall as per Fig. 2. All sensors were attached the bare wall (without plastering) in order to (i) ensure direct measurements through the bare DCB only, (ii), to avoid anomalous heat flux variations, such as fixing sensors in close proximity to mortar joints, because of their different TC. (iii) to eliminate any inconsistency in plastering thickness. Without such precautions, data acquisition may have been jeopardised. The distance between the two HFMs was 10 cm (centre to centre).

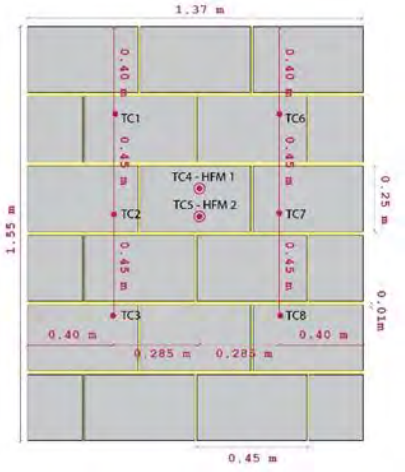

Figure 2: The set of thermocouples and heat flux sensors applied in the mock up wall inside the hotbox apparatus.

The power supply was provided to ceramic heaters via voltage and amperage meters and the cooling unit was a portable air conditioner with a fixed setpoint of 16°C to stabilize DBT inside the cold chamber.

Figure 3: the hot side of the hot box with the sensors installed.

Computer fans were also used to ensure a homogeneous temperature distribution inside the chamber and avoid air stratification when the heaters were on, in order to get steady-state conditions in every point of the wall. The data logging system is the same described in [9] compliant with ISO 9869. Portable stand-alone thermo-hygrometers measured the ambient conditions inside the hot and cold chamber to facilitate the calculation of overall wall thermal transmittance.

Some thermal images were taken to identify heat-losses through the hot box perimeter, and to facilitate the interpretation of the final results. It can be observed that the central part of the hotbox is thermally homogenous, Fig. 4.

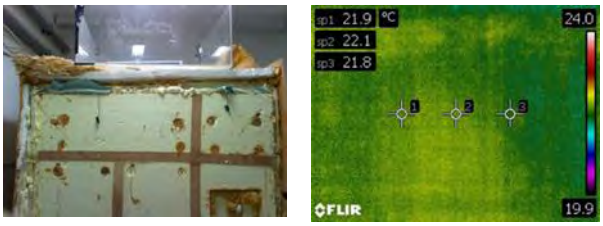

Figure 4: Central part of hotbox and infrared (IR) picture.

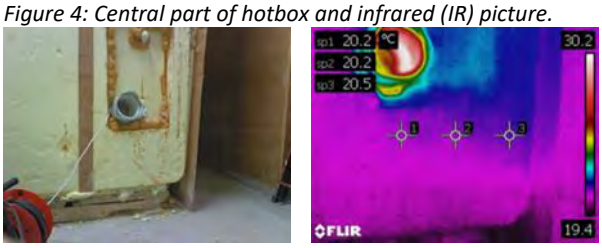

Figure 5: bottom right part of the hotbox and IR picture .

The major effort was to improve the sealing of the corners of the enclosure. While on the right-hand side there were no evident leaks besides the common geometrical thermal bridge, Fig. 5. Instead, the top and bottom part of the left side of the aperture when in operation showed few thermal leaks, Fig. 5.

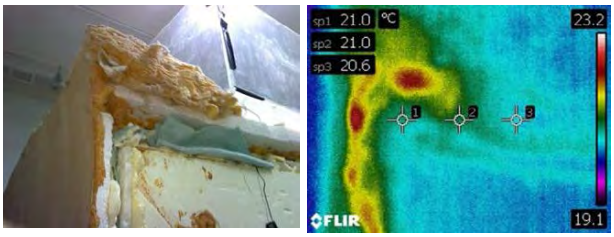

Figure 6: Top left part of the hotbox door with IR image.

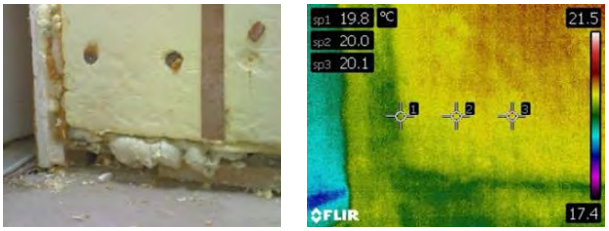

Figure 7: Bottom left part of the hotbox door with IR image.

4. RESULTS

4.1 Thermal conductivity assessment

The materials measured in this research are quite different from each other and all of them have their own specificities to be considered. All the samples were visually inspected to identify any potential defects that could influence the measurement, e.g. Fig. 8 for concrete.

Figure 8: The concrete being tested with disk sensor.

The full list of the measured TC for the concrete is included in Table 2. The concrete samples did not have an even surface and small pockets of air, due to the superficial aggregates, may have influenced the contact with the sensor (RC 11, highest TC and lowest TC for RC 12 and 16). The measured dry density is 1837 kg/m^3 circa 11% less than declared value. Also, RC 12 and 16 had also the lowest density of concrete thus confirming the association between low density and low TC.

Table 2: Measured dry TC on concrete sample at DBT 23±1°C and RH <3%.

Sample	ρ [kg/m3]	λ [W/(m K)]
UM-RC-10	1838	0.883
UM-RC-11	1949	1.014
UM-RC-12	1725	0.724
UM-RC-13	1795	0.869
UM-RC-14	1802	0.799
UM-RC-15	1934	0.950
UM-RC-16	1757	0.716
UM-RC-17	1820	0.863
UM-RC-18	1876	0.923
UM-RC-19	1879	0.854
Average	1837.522	0.86
Ext. Uncertainty k=2		0.13

The concrete TC has an average value of 0.86±0.13 W/(mK) with a dry density of 1838 kg/m^3. This value is in line with the standard EN 1745 [10] for CMUs.

The measuring set up for the PUF samples' TC is shown in Fig.9. A rather uniform conductivity is observed for the PUF notwithstanding the high porosity of the surface texture, as reported in Table 3.

Figure 9. The PUF being tested with needle probe.

Compared to literature value the λ_{foam} is very close to the design value of thermal conductivity of polyurethane foams, 0.05 W/(mK) with densitiy of 70 kg/m^3.

Table 3: Measured thermal conductivity on Foam and concrete sample at DBT 23±1°C and RH <3%.

Sample	ρ [kg/m3]	λ_{foam} [W/(m K)]
UM-PU-00	109.10	0.040
UM-PU-01	100.52	0.039
UM-PU-02	110.43	0.039
UM-PU-03	116.49	0.038
UM-PU-04	110.38	0.040
UM-PU-05	125.92	0.040
UM-PU-06	94.21	0.040
UM-PU-07	104.11	0.038
UM-PU-08	96.23	0.040
UM-PU-09	103.69	0.039
Average	107.11	0.039
Ext. Unc. k=2		0.006

The PUF manufacturer did not declare the λ_{foam} so the only meaningful comparison can be made with dataset from handbooks or international standards. Moreover, the evident change in density may be associated to peculiar boundary conditions of the foaming process, characterized by the s-shaped cavity of the DCB, with 10 mm thickness, an evident restriction to the free-foaming process. Also, this may have caused the creation of smaller pores, hence the low TC notwithstanding the density, where the solid part developed more than the gaseous phase. Indeed, the higher the density, smaller the foam pores are, hence the higher the thermal conductivity.

4.2 FEM steady state results

The experimental values of PUF and concrete's TC, as per Table 4, were included as input data in the numerical solution to Fourier's equations; this steady-state FEM analysis also included the impact of mortars. Since concrete has a noticeable extended uncertainty and the PU thickness may vary inside the cavity (via visual inspection sometimes the thickness was less than 5 mm), the simulations needed to be repeated using maximum and minimum thermal conductivity values.

Table 4: List of material properties used in steady state FEM analysis.

Material Name	Thickness [mm]	λd [W/(mK)]	e [-]	Source
Cement Mortar	10	0.72	0.93	[12]
Lime and Cement Render (Fassa Bortolo KC1)	10	0.55	0.91	Product Datasheet
Gypsum Plaster (Alcitek Gold)	10	0.43	0.91	Product Datasheet
PU foam	8	0.039 ±0.01	0.93	Experimental value
Concrete (Load Bearing)	40	0.86 ±0.13	0.93	Experimental value

The complex geometry of the DCB indicate that three heat transfer paths are possible, hence three different U_{DCB}. This can be observed by repeating the simulations for all the most representative sections involved in the heat transfer process as per Fig. 10.

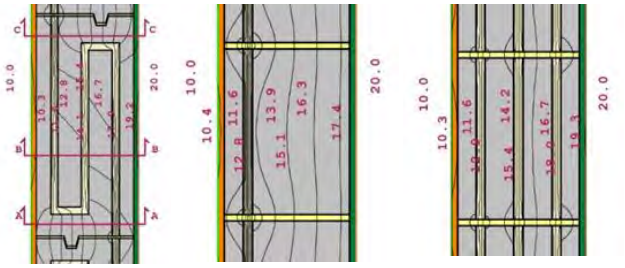

Figure 10. DCB wall: the three sections used to calculate the U_{DCB}; a) plan section; b and c) vertical section. All units in °C. Winter condition: Outdoor 10°C, indoor 20°C.

For this reason a weighted average was applied in vertical section Fig. 9(c,b) using the lenght of the block, 45 cm, as weight reference: section AA and CC are 5 cm long and the one related to section BB is 35 cm. Then an arithmetic average was performed to combine heat flux on plan and on vertical section.

Table 4 presents the overall outcomes for the U_{DCB} based on the FEM study. Three simulation were launched: one with maximum TC values, the second at minimum TC and the last with average values.

Table 4: U_{DCB} calculated via FEM according to ISO 6946's "detailed method" using maximum and minimum TC values.

Iteration	U_{DCB} [W/(m²K)]
Average TC	1.238
Max TC	1.404
Min TC	1.050

The scope is to have the widest theoretical range of the theoretical U_{DCB} to define the performance gap and also account for the limitation of HFM in-situ. Despite the different TCs, it can be observed that overall, the DCB isotherms exhibit a change in the heat flux that is caused by the presence of materials with different thermal conductivities (concrete, foam, and cement mortar). Near the insulating layer's change of direction, the fluctuations are also more pronounced, Fig. 10 a,b and c).

4.3 Hot Box measurements

The eight surface temperature gradients were averaged in a way to obtain three equivalent ΔTs representative of the temperature gradient observed across the hot and cold chamber. The hourly average of the temperature shows a step like variation of temperature after 24 and 48 hours, Fig. 11. This can be explained because of the incremental power given to the ceramic heaters from an initial value of 101.90 W to 143.77 W over the first 48 hours, and then kept until completion of the test.

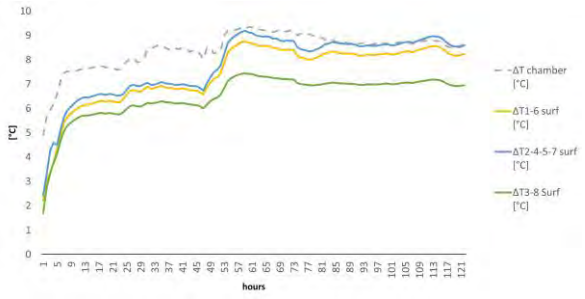

Figure 11: Temperature gradients across the hot and cold sides recorded during the first 5 days of the campaign.

It can be observed that after 48 hours the temperature gradient was more than 9°C between the hot and cold chamber while the lowest surface temperature gradient circa 7°C. The daily averages of the total R-value and hence the U-value is obtained with "average method" described in ISO 9869-1 [5] in different ways as plotted in Fig. 12.

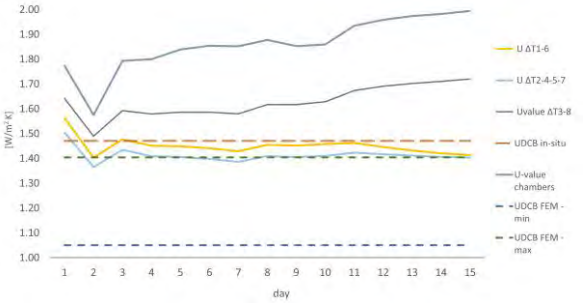

Figure 12. The daily U-value measurements compared to insitu value and FEM.

The $U_{\Delta T\ chamber}$ was obtained from the total resistance using ambient temperature of the hot and cold rooms. The U-values, associated to the different surface temperatures, were obtained by summing the measured R-value (related to the wall's conductance), and by adding the notional ISO 6946 surface

resistances. In both cases since the hot box measurements were done on a non-plastered wall it was thus necessary to add the thermophysical parameters of the plaster and render in order to make a meaningful comparison with FEM simulations. The list of convergence value of the U_{DCB} plotted in Fig. 12, were obtained after 5 days compared to the 12 days needed for the in-situ measurements, are listed in Table 5.

Table 5: U_{DCB} at which hotbox measurement converged.

Measurement point	U_{DCB} [W/(m^{2}K)]
$\Delta T_{1,6}$	1.41
$\Delta T_{2,4,5,7}$	1.40
$\Delta T_{3,8}$	1.72
$\Delta T_{chamber}$	1.99
In situ [9]	1.47

5. DISCUSSION

From figure 9 it can be observed that the upper part of the theoretical range obtained by FEM is much closer to the u-values calculated through $\Delta T_{2,4,5,7}$ and $\Delta T_{3,8}$ while $\Delta T_{1,6}$ is well outside this theoretical threshold. The first two are matching with the highest thermal conductivity values and hence the two methodologies are comparable. Hence $U_{\Delta T2,4,5,7}$ can be considered the most appropriate measuring point to calculate the thermal transmittance value of hotbox apparatus.

6. CONCLUSIONS

The declared in situ value 1.47 W/(m^{2}K) is now much closer to the most accurate U-value, and the performance gap is reduced from 51% to 11% using $U_{DCB\text{-}FEM}$ 1.24 W/(m^{2}K) and $U_{\Delta T2,4,5,7}$ 1.40 W/(m^{2}K). This performance gap also include the accumulation of errors related to different methodologies used. These results confirm that in-situ measurements are giving acceptable U-values, given that previously [9], theoretical PUF and concrete TC values were assumed being taken from manufacturer's specification, website and handbooks — often taken for granted.

The experimental set-up may therefore be established as a rigorously tested methodology, and robust enough to use for alternative geometry configurations, also with different re-engineered materials or building elements. Equally there are plans to test this further in a real building, namely the SLC (Sustainable Living Complex) at the University of Malta Campus, due for completion by end of 2025.

ACKNOWLEDGEMENTS

This research is an outcome of the Double C-Block project, a three-year research project, for which funding was provided by the Malta Council for Science and Technology (MCST) under the Technology Development Programme (TDP) grant reference R&I_2019_010T (DCB Double C Block). This research was also funded under MCST TDP lite grant R&I-2022-003L (RESCIU Re-Engineered Stone and Concrete Insulated Unit) .

The authors acknowledge the work on the data logging setup and samples preparation for TC tests to Mr. Nicholas Azzopardi and Mr. Alex Falzon, respectively, Assistant Laboratory Manager and Laboratory Officer at the University of Malta. The authors are also grateful to EURAC team, in particular Dr. Marco Larcher and Mr. Stefano Donzelli, for their support in the thermal conductivity measurements. The authors are also grateful to Cementstone Mfg. Co. Ltd. as the commercial partner producing on the MCST awarded grant.

REFERENCES

1. Building Envelopes, [Online], Available: https://www.iea.org/reports/building-envelopes (20 December 2023).
2. Global Status Report for Buildings and Construction: Towards a Zero-Emission, Efficient and Resilient Buildings and Construction Sector 2021, [Online], Available: https://www.unep.org/resources/report/2021-global-status-report-buildings-and-construction (20 December 2023).
3. ISO 8994, (1994).
4. Pavlík, Z.; Fort, J.; Pavlíková, M.; Erný, R, (2015). Laboratory Critical Experiment Simulating Long-Term Exposure to External Environment: A Hollow Block with Mineral-Wool-Fiber Cavity Filler, 2nd International Conference on Civil, Materials and Environmental Sciences: pp. 40-42.
5. ISO 9869-1, (2014).
6. Desogus, G.; Mura, S. and Ricciu, R., (2011). Comparing different approaches to in situ measurement of building components thermal resistance. *Energy and Buildings*, 43: p. 2613-2620.
7. Meng, X.; Luo, T.; Gao, Y.; Zhang, L.; Shen, Q. and Long, E (2017). A new simple method to measure wall thermal transmittance in situ and its adaptability analysis. *Applied Thermal Engineering*, 122: p. 747-757.
8. Asdrubali, F.; Baldinelli, G. (2010). Thermal transmittance measurements with the hot box method: Calibration, experimental procedures, and uncertainty analyses of three different approaches. *Energy and Buildings,* 43: p. 1618-1626.
9. Caruso, L.; Buhagiar, V.M.; Borg, S.P (2023). The Double C Block Project: Thermal Performance of an Innovative Concrete Masonry Unit with Embedded Insulation. *Sustainability*, 15, 5262.
10. BS EN 1745, (2012).
11. ISO 10456, (2007).
12. JCGM, (2008). Evaluation of measurement data – Guide to the expression of uncertainty in measurement.
13. ISO 6946, (2017).
14. ISO 10211, (2017).

PLEA 2024 WROCŁAW
(Re)thinking Resilience

Streamlining Renovation Workflow through Process Digitalization

Enhancing Information Flow, Accelerating Decision-Making, and Reducing Costs in the early stages of the renovation process

TATIANA ARMIJOS-MOYA[1], THALEIA KONSTANTINOU[1], BEÑAT ARREGI-GOIKOLEA[2]

[1] Delft University of Technology, Delft, Netherlands
[2] Tecnalia, Parque Tecnológico de Bizkaia, Basque Country, Spain

ABSTRACT: In typical practice of building renovation design, distributed teams communicate through technical drawings, but the construction industry lags in digitalization. This study addresses this gap by proposing a methodological framework integrated into digital tools for early-stage renovation processes. The framework, implemented as a web-based tool, gathers user inputs related to building details and preferences to generate alternative renovation scenarios. It utilizes databases for building characteristics, technologies, and life cycle assessment (LCA)/life cycle cost (LCC) calculations. The information flow involves user inputs, database storage, and processing layers, enabling simulations and scenario evaluations. The framework facilitates quick, cost-effective, and customized decision-making in the early design phases, aiming for energy-efficient retrofits. Results highlight the importance of databases, such as building characteristics and LCA/LCC, while emphasizing a clear communication protocol among stakeholders. Overall, the study seeks to accelerate and streamline the renovation process, promoting efficient collaboration and reducing time and costs.
KEYWORDS: Information flow, Renovation, Digitalization, Scenario generation, Decision-making process

1. INTRODUCTION

Current building design practice involves distributed teams, given the specialization of different professions and their inclination to form independent companies. These teams communicate product design details through technical drawings and specifications. In any discipline with distributed design teams, the timely exchange of information among the involved stakeholders is vital for the progress of the project [1-4]. Several studies on product and design development highlight sources of waste in the process. This includes inefficiencies stemming from subpar engineering leading to inadequate product or process performance, as well as waste within the development process. These studies advocate that emphasizing flow and value generation serves as a crucial complement for comprehending the process. In fact, it forms the foundation for analysis and subsequent improvement efforts in the process development [4, 5].

Furthermore, the process of digitalization is offering fresh possibilities and streamlining the overall construction process by generating intangible assets, which in turn enable more cost-effective and rapid design and production. Despite the progressive transformation of traditional design practices and communication methods through advancements in computer-aided design (CAD) software and building information modeling (BIM), several studies have indicated that the architecture, engineering, and construction sector is relatively slow in embracing digitalization, particularly concerning the creation of digital assets, the expansion of digital utilization, and the development of a highly digital workforce, when compared to many other manufacturing industries [6-8]. In fact, both researchers and practitioners have recognized the imperative need for a swifter pace of digitalization in the construction sector. It's worth noting that, in contrast to the extensive research and implementation efforts in the design and construction phases, there is a notable lack of attention in the area of renovation, retrofitting, and refurbishment, which are integral components of facility management [9-11].

Digitalization is revolutionizing the construction industry, speeding up design and production while reducing costs. However, the sector lags behind other industries in adopting digital technologies [9-11]. Embracing these technologies can boost innovation, enable local firms to access global advancements, and enhance productivity. To facilitate digitalization, the industry needs digital tools that provide common services and data for all stakeholders throughout the construction value chain [12].

Furthermore, several studies have shown that early-stage decisions have a significant impact on the overall duration and cost of the renovation project. A well-implemented framework in the early stages streamlines processes, reducing the time required for decision-making and minimizing unnecessary delays[13-15].

The development and implementation of a structure workflow will facilitate a systematic and efficient flow of information among stakeholders, ensuring that the right data is collected, processed, and utilized in a timely manner. This optimization will help preventing bottlenecks and communication gaps [16]. Therefore, the aim of this study is to develop a workflow framework that supports and expedites early-stage renovation process through the analysis and enhancing of the information flow. This framework aims to be integrated in digital tools that will support the renovation process by providing the different users with tailored solution packages combining the technologies that are best suited to the specific case considered.

2. METHOD

With the goal of assisting early-design choices in renovation processes, this paper determines the key parameters and the information flow of the renovation process among the different stakeholders and with the objective to accelerate and facilitate the decision-making process in the early stages of the design. This workflow framework is based on a process of analysing the key parameters required in the early stages from the design team and delivered by the client, and the outputs of the information processing. In essence, this outline requires comprehensive data gathering on the existing building to establish the most plausible current scenario and generate diverse renovation scenarios. These scenarios align with the goal of achieving energy savings while accommodating or enhancing user preferences. Evaluations, including energy performance simulation, Life Cycle Assessment (LCA), and Life Cycle Cost (LCC), discern environmentally and economically viable options, thereby elucidating key parameters influencing decisions in the early project stages. This approach allows for preliminary estimations of the intervention's viability. Consequently, three main steps were executed: (1) definition of information flow and KPIs, (2) creation of input databases, and (3) implementation in a digital tool.

2.1. Information Flow and KPIs Definition:

The first step is to define the key parameters that the renovation process requires to start the (re) design with obtaining the data from the building in a first iteration, maximizing the reduction of time and costs of the decision-making process and optimizing the information to be provided to the potential client, aiming to achieve a contract with that client.

The outputs obtained by the data processing are used to generate retrofitting scenarios that will be alternative solutions to renovate the building with the main goal to upgrade the building up to a highly energy efficient concept considering a life cycle perspective, calculating KPIs for embodied and operational energy, associated greenhouse gas emissions, comfort impacts, and economic viability.

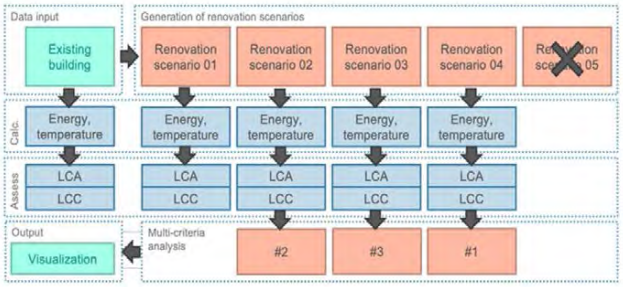

2.2. Implementation of Databases:

To establish the scenario generation framework, it was essential to define and implement different databases. In the previous step key parameters were defined and it was established that there will be inputs provided by the client directly and some inputs will be a set of standard values that will support the estimation of the buildings' construction technical parameters when little or no information about the building is available.

2.3. Implementation in a Digital Tool

Once the steps of the information flow and the required databases are defined, the aim is to implement this framework in a tool that will be a web-based tool that, by means of simplified calculations, simulates energy, cost, comfort, and environmental indicators. Besides the integration of databases, a communication protocol needs to be integrated to ensure data consistency and stakeholder collaboration throughout the project.

3. RESULTS

To create a systematic workflow for generating renovation scenarios (Figure 1), it was crucial to delineate and integrate various databases. Consequently, it became imperative to identify essential parameters and establish a set of standard values. These values enable the estimation of technical parameters related to the construction of buildings, particularly in cases where limited or no information about the building is accessible (Table 1). Besides the building characteristics' database, a library of technologies was defined that includes technical information about the different technologies that will be considered for the generation of renovation scenarios. Finally, an LCA/LCC database and framework was established to execute calculations related to the environmental impact and cost analysis of the different scenarios. The evaluation of the scenarios also pointed towards the direction of the renovation technologies that provide the best performance over the life cycle of the renovated building.

Figure 1. Information flow scheme

3.1 Implementation of Databases:

It is important to establish some key parameters or static information that is necessary for the calculations performed by the different tools: (1) a Building characteristic database setting standard values that help the system make an estimation of the buildings' construction technical parameters when no information about the building is available; (2) a Library of technologies database including technical information about the different technologies that will be considered for the generation of renovation scenarios; (3) an LCA/LCC database with the data necessary for the calculations related to the environmental impact and economic analysis of the technologies.

3.2 Information flow framework description:

Initially, the user inputs fundamental building parameters like shape, age, and location. These details are utilized by the designated database system (Table 1) to estimate probable values for various inputs, such as construction features or existing heating systems. Users can either accept these default values or provide more precise information if available. A preliminary simulation is conducted using these parameters and presented to the user/client for validating their comfort and energy consumption experience. Users can then make adjustments, which calibrate the baseline model. This functionality offers greater accuracy compared to more intricate building modeling software that lacks such feedback. The calibrated model undergoes another simulation, and the results are used to automatically generate proposed renovation scenarios involving a mix of renovation technologies. These suggestions are presented to the user before simulation, allowing them to discard options based on personal preferences or unforeseen constraints. Accepted renovation scenarios are simulated for energy and comfort performance, with an additional assessment of their life cycle's economic and environmental aspects. Lastly, a multi-criteria assessment is conducted to rank these renovation options according to the user's anticipated preferences regarding comfort, financial cost, and environmental performance. Alongside results presentation, users can adjust their preferences and observe the impact on the ranking of renovation scenarios. Notably, users only interact with the web frontend, while the web backend sequentially triggers the calculation modules without requiring user intervention.

3.3 Implementation of the methodological framework in a digital tool:

The integration of this information flow is incorporated into a methodological framework (Figure 2), executed through a digital tool. The comprehensive structure of this framework has been arranged using a layer model, illustrated in Figure 2. Each layer represents a specific set of tools and modules with varying purposes: User information layer, Data layer, and Processing layer.

Figure 2 presents the workflow and the communication among the layers. Communication between layers is provided through REST web services, providing a standard interface that ensures the correct communication between the different modules of the platform.

USER INFORMATION LAYER

The User Information Layer is the direct connection between the technical user and the digital tool. It is composed of the different user interfaces (or alternatively, front-end) that enable end users to interact with the platform and includes the interfaces of the platform and the tools developed. It allows the communication of:

- Inputs from the user regarding the building
- Outputs from the digital tool regarding the renovation process

All the inputs introduced by the users are stored in the databases.

DATA LAYER

The data layer corresponds to the common databases that store all the information necessary for the correct functioning of the platform and is used to share the information among the different modules and platform components.

Table 1. Information flow parameters considered for the scenario generation in the early phases of the renovation process.

<table>
<tr><th></th><th>INPUTS</th><th>FORMAT</th><th>PROCESS

How the information is processed</th><th>DATABASE

Information from a database</th><th>OUTPUTS

Scenarios Generation</th></tr>
<tr><td>DESCRIPTION</td><td>The user enters simple information about the building into the tool to obtain an initial estimation without having expert knowledge of the construction sector.</td><td colspan="3">• Fill-in basic information: location and building type information.
• Obtain initial building geometry information.
• Obtain default technical information of the building.
• Fill-in building use and current building services.
• Obtain baseline energy simulation.
• Fill-in information on current performance.
• Calibrate baseline energy simulation.</td><td>• The user can select from several renovation scenarios created by the framework/tool.
• The user can assess the results of the scenarios and decide which technologies to install in the building.</td></tr>
<tr><td>GEOMETRY</td><td>Floor area

Number of floors</td><td>Upload: Pictures of the building

Upload Pictures of the surroundings

Upload (if applicable) DWG files</td><td rowspan="2">+ open street maps = Initial geometry

Analysis of the surroundings for e.g. shading

Zoning of the façade + height of building</td><td rowspan="2">Climate zone

Weather data file</td><td rowspan="4">Scenarios Generation based on:
• Window-wall ratio
• Wall area
• Floor area
•
• Envelope opening area
• Room height
• Orientation
• Longitude
• Latitude
• Weather data file
• Envelope U-value
• Set point schedule
• Environmental outputs: kg CO2e/m2/a
• Economic outputs: €/m2/a</td></tr>
<tr><td>LOCATION</td><td>Location / address</td><td>Value field or select in map</td></tr>
<tr><td>BUILDING CHARACTERISTICS</td><td>Typology

Year of construction

Information related with the building energy consumption and performance</td><td>Drop-down menu

Value field

Value field (kWh/m2 year)/ Energy bills; Drop-down menu energy source</td><td>Filtering the building characteristics database

Type of construcion/ constrcution system + Location</td><td>Default/standard values: Thermal properties</td></tr>
<tr><td>USER</td><td>User goal and prefenrence

Building function</td><td>Drop-down menu: User ambitions

Drop-down: schedules / operational information</td><td>Define based on scenario generation

Database of standard operation schedules</td><td>Library of technologies, including information about energy savings

set_point_schedule</td></tr>
</table>

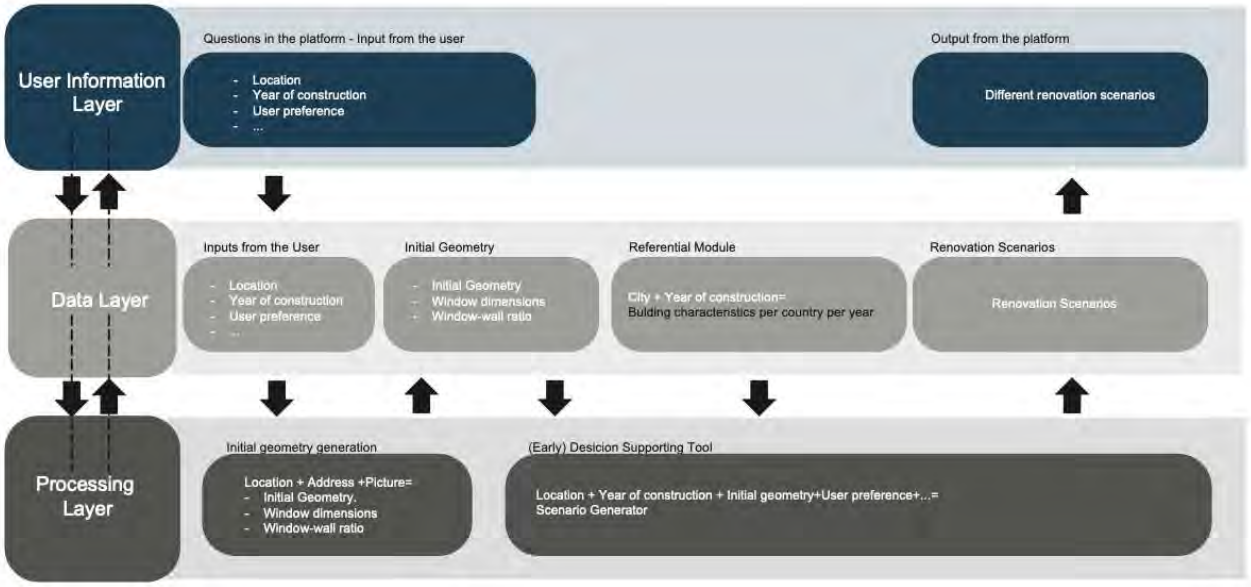

Figure 2. Workflow and the communication among the layers and how the different databases exchange information where the user introduces the firsts inputs of the building and how this information is generating different renovation scenarios.

The data layer is defined to store all the information necessary for the correct functioning and for the calculations that need to be executed by the different processes, including information about the users and their projects (inputs, calculation results, project information related to each phase in the renovation process, etc.). Within this data layer, there is a database of building characteristics [17, 18] of residential buildings that includes a set of standard values that help the framework to make an estimation of the buildings' construction technical parameters when no information about the building is available, including also static information that is necessary for the calculations performed by the different processes in the scenario generation. Furthermore, this data layer contains a 'Library of technologies' which is a catalogue that includes technical information about all technologies considered for the generation of renovation scenarios. Finally, there is an LCA/LCC database which includes the data necessary for the calculations related to the environmental impact and cost analysis of the technologies and the generated scenarios.

LCA calculations require the following data to be stored in the database:

- Material information of façade panels and systems
- Environmental impacts of materials for the various life cycle stages and other material properties
- Maintenance impacts of different panel types
- Carbon emission factors of electricity grids across Europe.

Environmental impacts of materials are sourced from EPDs, or average of EPDs or other generic databases in compliance with EN 15804. Carbon emission factors of electricity grids are sourced from the International Energy Association database or other national or international databases in Europe.

The LCC calculation will require the following additional data to be stored in a database:

- Procurement and installation cost of materials and façade panels.
- Cost of operational energy
- Cost of maintenance of façade panels

PROCESSING LAYER

The processing layer refers to the software modules that perform the main system processing and calculations and includes the digital tools that will generate different renovation scenarios with that will support the decision-making process in the early stages of the renovation. With very few inputs (e.g., location, age of building, simplified geometry, number of floors, use, etc.), this outline would suggest default options (Figure 1) that are most likely to be representative of the building, to perform simplified simulations (i.e., energy simulations, LCA, LCC) that might not be precise but are representative. At a later stage, if a design team gets involved, they could make a more accurate use of the tool for assessing design alternatives. Besides, it is essential that this framework is being implemented as a user-friendly tool that can be used without any specific expertise in building renovation or the construction process.

3.2 Communication and Coordination Protocol:

Another important finding is the establishment of a clear communication protocol among all the stakeholders in the renovation process to facilitate the coordination of the project. This protocol is an informative tool where critical aspects are shown and they must be approved by all the stakeholders to be

able to access the new phase or stage of the renovation process, generating agreement files and backup. It also helps the decision-making process by helping the design team or the project manager in providing a continuous overview of the process to guarantee that every decision made has been approved and accepted from all the parties, thus, avoiding future disagreements. It also provides all the information of the project, including logistics, technical responsibilities, changes in the budget/costs, timings on production, deliveries, regulations, etc. Additionally, it can show different levels of information to different stakeholders which will be assigned by the project manager (design team).

4. CONCLUSION

The main objective of this study is to support the renovation project in its early design phases and to facilitate the communication and coordination of the different stakeholders. Overall, this framework involves gathering data on the existing building to establish the most likely current scenario and to generate different renovation scenarios based on predefined databases and constraints. The scenarios are formulated based on the objective of achieving energy savings while maintaining or improving users' preferences, and they are evaluated through energy performance simulation, Life Cycle Assessment (LCA) and Life Cycle Cost (LCC). By examining these scenarios, the study identifies feasible environmental and economic options and determines the key parameters influencing early-stage decisions.

It was found out that it is necessary to develop and integrate different databases to facilitate the decision-making process in the earlier stages of the renovation process and to incorporate a clear communication and coordination protocol that will help managing the project. The framework aims to provide meaningful reductions in cost and time.

ACKNOWLEDGEMENTS

The study presented in this paper it part of the development of a digital platform, as part of ENSNARE (ENvelope meSh aNd digitAl framework for building Renovation). The authors would like to thank the project participants and the questionnaire respondents. This project has received funding from the European Union's Horizon 2020 research and innovation programme under grant agreement No 958445

REFERENCES

1. Eckert, C., P.J. Clarkson, and M. Stacey, *Information flow in engineering companies: problems and their causes.* Design Management: Process and Information Issues, 2001. 28: p. 43.
2. Gray, C. and W. Hughes, *Building design management*. 2007: Routledge.
3. Moreau, K.A. and W.E. Back, *Improving the design process with information management.* Automation in construction, 2000. 10(1): p. 127-140.
4. Tribelsky, E. and R. Sacks, *Measuring information flow in the detailed design of construction projects.* Research in engineering design, 2010. 21: p. 189-206.
5. Morgan, J. and J.K. Liker, *The Toyota product development system: integrating people, process, and technology*. 2020: CRC Press.
6. Gandhi, P., S. Khanna, and S. Ramaswamy, *Which industries are the most digital (and why).* Harvard business review, 2016. 1: p. 45-48.
7. Manyika, J., et al., *Digital America: A tale of the haves and have-mores.* McKinsey Global Institute, 2015: p. 1-120.
8. Wong, J.K.W., J. Ge, and S.X. He, *Digitisation in facilities management: A literature review and future research directions.* Automation in Construction, 2018. 92: p. 312-326.
9. Construction, M.H., *The business value of BIM for construction in major global markets: How contractors around the world are driving innovation with building information modeling.* Smart MarketReport, 2014: p. 1-60.
10. Lu, Y., et al., *Information and communication technology applications in architecture, engineering, and construction organizations: A 15-year review.* Journal of Management in Engineering, 2015. 31(1): p. A4014010.
11. Rezgui, Y. and A. Zarli, *Paving the way to the vision of digital construction: a strategic roadmap.* Journal of construction engineering and management, 2006. 132(7): p. 767-776.
12. David, A., et al., *DigiPLACE: Towards a reference architecture framework for digital platforms in the EU construction sector*, in *ECPPM 2021–eWork and eBusiness in Architecture, Engineering and Construction*. 2021, CRC Press. p. 511-518.
13. Attia, S., et al., *Simulation-based decision support tool for early stages of zero-energy building design.* Energy and buildings, 2012. 49: p. 2-15.
14. Hygh, J.S., et al., *Multivariate regression as an energy assessment tool in early building design.* Building and environment, 2012. 57: p. 165-175.
15. Østergård, T., R.L. Jensen, and S.E. Maagaard, *Building simulations supporting decision making in early design–A review.* Renewable and Sustainable Energy Reviews, 2016. 61: p. 187-201.
16. Prieto, A., T. Armijos-Moya, and T. Konstantinou, *Renovation process challenges and barriers: addressing the communication and coordination bottlenecks in the zero-energy building renovation workflow in European residential buildings.* Architectural Science Review, 2023: p. 1-13.
17. EPISCOPE. *EPISCOPE and TABULA European projects website*. 2016; Available from: https://episcope.eu/welcome/.
18. TABULA. *TABULA Webtool*. 2017; Available from: https://webtool.building-typology.eu/#bm.

PLEA 2024 WROCŁAW
(Re)thinking Resilience

Switchable Glazing in a Mediterranean Climate

Preliminary Investigation of a Novel Switchable Glazing Assembly

ETIENNE MAGRI[1], VINCENT BUHAGIAR[1], MAURO OVEREND[2]

[1] Department of Environmental Design, Faculty for the Built Environment, University of Malta, Malta.
[2] Department of Architectural Engineering & Technology, Faculty of Architecture & Built Environment, TU Delft, Netherlands.

ABSTRACT: The control of glare in office environments is often retrospectively improvised using shading devices, typically internal blinds. Despite the leap towards energy efficiency goals, visual comfort is still being compromised in climates with high solar insolation resulting in intolerable glare. This paper discusses the visual performance of a novel glazing assembly comprising of two, independently switchable (solar Polymer Dispersed Liquid Crystal and Suspended Particle Device) interlayers intended to control the visible light transmittance into an indoor space. Readings of DGP in a full-scale test cell are presented together with an analysis of the visual appearance of the glass.
KEYWORDS: Switchable Glazing, Adaptive Facades, Glare, Occupant well-being, DGP.

1. BACKGROUND

Excessive levels of daylighting in buildings having high glazing ratios in climates with high insolation levels is a matter that is frequently overlooked. The control of glare is often retrospectively improvised using shading devices, typically internal blinds. This means also blinding the view, with an unwarranted artificial lighting load during broad daylight. To address overheating issues, glazing technology of an insulated glazing unit (IGU) has evolved particularly through the use of static selective coatings on glass, thus delivering much of the expected performance in terms of low U-values, g-values, and visible light transmittance (VLT). However, despite the leap towards energy efficiency goals, visual comfort has often been compromised with lower daylight levels and partial blockage of external views. Internal shading devices, typically louvres or roller blinds are considered as cheap, quick-fix solutions for glare control and solar rejection of a façade. External shading devices are typically fixed and sometimes moveable to allow for their adjustment according to the external day-to-day climatic conditions.

1.2 The Research Gap: Problem defined.

In a cooling-oriented central Mediterranean climate, the main thrust in design trends is verging towards fully fletched glazed façades with a design 'overkill' in terms of daylighting requirements, while generating unwarranted cooling gains. Although yearning for unobstructed distant views, occupants often experience glare, distracting them from their daily tasks, while also impacting their overall health, well-being, and productivity.

This research has established gaps in the body of knowledge in that independent of how energy efficient they may be, static facades still have a limited degree of adaptability and tend to provide limited performance in adverse daytime conditions. The daylight and visual performance of a static façade is limited to basic control by blinds, often limiting views. This points to the need to reduce glare and the associated discomfort, without compromising the views which often come at a premium in real estate terms. This may be achieved by optimizing daylight levels and provide for appropriate shading while decreasing the need for daytime artificial lighting. The restrictions of conventional static facades therefore need to be overcome to avoid discomfort glare, protect views, and encourage productivity to prop up overall occupant well-being.

Figure 1: Buildings with a high glazing ratio in Malta, relying on indoor blinds for the control of glare.

2 ADAPTIVE GLAZING FOR VISUAL COMFORT

Buildings are naturally subjected to diurnal and seasonal changes. The concept of a responsive, adaptive building façade as opposed to spaces

protected only by static enclosures, relying on active, climate-controlling systems for the attainment of comfort, makes more sense now than ever. Glazing appears to be following the trend and need, of adaptability as technology seeks to address the need to bridge the gap between transparency and opaqueness.

Chromogenic glass is a generic term that refers to glass that can change its optical properties. The main functions of chromogenic glass when applied to architectural glazing is to control the flow of light and heat into and out of a glazing, according to the requirements of building occupants. The change of optical properties in chromogenic glazing can be in the form of absorptance, reflectance or scattering. Thermotropic materials allow for a change in state of the polymeric material, which affects its refractive index turning it from a solar transmitting material to a solar absorbing one, thus from transparent to translucent (Compagno, 1999), whereas thermochromic materials are based on the features of transition metal oxides which transforms the material from a solar transmitting to a solar reflective one (Granqvist, 2007). Photochromic materials alter their properties through the UV radiation in the solar spectrum, whereas electrochromic materials can alter their optical properties when triggered by an electric current. The most common of the electrically activated types are phase dispersed liquid crystals (PDLC), dispersed particle system (DPS) and electrochromics.

The UV-resistant PDLC privacy film (solar-PDLC) and SPD tinting technologies are two of the most established, commercially available products on the market today. These have the added advantage of being assembled in conventional glass-assembly factories without the need of any specialized equipment. Switchable dynamic glass appears to have a great potential at achieving privacy and daylight control, where besides having the ability to be manually controlled by building occupants, can in turn be pre-set on the basis of an automated control strategy.

3. AN INNOVATIVE GLAZING ASSEMBLY

The diverse properties of both solar PDLC and SPD technologies has prompted the author with an idea of possibly an *innovative combination of technologies within a single laminate*. Having a glass laminate with both solar-PDLC and SPD interlayers potentially allows for the external laminated sheet of glass in an IGU to offer both privacy and tinting properties according to the requirements of the building occupants. The solar PDLC film can be maintained in two states (**ON** [transparent] and **OFF** [translucent]), whereas the SPD can retain a *variable* tint by means of its electronic controllers. Different applications of how this glazing assembly can be set within an external façade are substantial and is believed that this combination of technologies, if proven to be effective at reducing overheating and glare for facades in a cooling-dominated climate, may push away conventional indoor blinds and shades, and given time, may possibly render them obsolete. In addition, having this technology capable of being connected to smart systems of buildings and the IoT, the possibilities of integration and control of this form of switchable glass assembly are practically endless.

3.1 Experimental Setup

For the scope of this study, two twin full-scale test cells were set up within the grounds of the University of Malta to carry out a series of comparative experiments between the prototype switchable glazing assembly and other forms of conventional, static facades (Figure 2).

The test cells were installed on precast concrete foundations laid out to permit the rotation of the test cells to face different orientations as required. A comparative testing approach as described by (Cattarin et.al., 2015) is being adopted, wherein the performance of a component, in this case the prototype glazing assembly, is assessed in relative terms to a reference element being tested at the same time.

For the assessment of the visual suitability of the indoor environment, the Daylight Glare Probability (DGP) metric developed by (Wienold & Christoffersen, 2006) will be measured using a state-of-the-art, calibrated luminance photometer, TechnoTeam© LMK Mobile 6 equipped with a SIGMA fish-eye lens, coupled with the proprietary LMK Labsoft© glare analysis suite.

Figure 2: Photos the full-scale, twin test cells installed at the University of Malta grounds.

4. METHODOLOGY

For the scope of this research, two pairs of films, each having dimensions of approximately 1.0m x 2.0m were cut to fit an overall glazed area of approximately 2.0 x 2.0m, both laminated in between an 8mm glass with a low emissivity coating on surface two and a 6mm extra clear glass with EVA interlayers in between the films. This glass laminate intends to combine both solar-PDLC and SPD films into a single laminate, and since the scope of this study focused solely on the visual performance of these films, their assembly into an insulated glass unit (IGU) for the assessment of their thermal performance, fall beyond the scope of this study. (Figure 3).

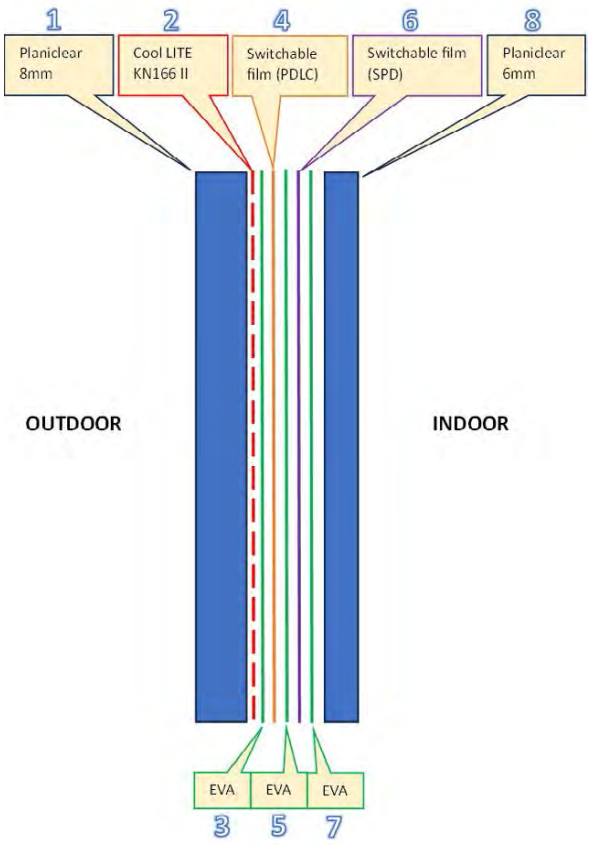

Figure 3: Schematic section of the novel switchable laminate.

Prior to lamination, both switchable films were prepared for the installation of the copper busbars through an edge deletion process, wherein the protective polyethylene terephthalate (PET) coating of the films and the actual formulation were carefully removed at two specific locations to expose the underlying conductive indium tin oxide (ITO). This allowed for the required space to attach the copper busbars to permit electric current to power-up the films. (Figure 4). Following the adhesion of the busbars with the ITO of the switchable films, two copper contact points for each film, of sufficient length to protrude from the edges of the laminate, were then soldered to the busbars themselves to provide for connecting the necessary wiring from the films to their proprietary electronic controllers (Figure 5). Two different controllers were required, one for each film, thus allowing for the control of each film independently.

Figure 4: Preparing films for busbar installation.

Figure 5: Preparing films for busbar installation.

Figure 6: Placement of films in between the interlayers prior to lamination.

5. PILOT STUDY: PRELIMINARY RESULTS

5.1 Suitability of the Testing Setup.

An initial DGP pilot study was conducted on a partly cloudy day in March 2023 to collect preliminary DGP readings inside the test cells without any glazing installed, this to assess the geometry and finishes of the test cells (Figure 7). The objective was to familiarize with the operation of the TechnoTeam© LMK mobile luminance photometer and its software for the analysis of the luminance maps generated by the camera itself and to obtain a preliminary indication of the DGP without any filtering provided by any of the glazing assemblies. The luminance photometer was mounted on a secure tripod and readings taken at three different positions within the cells: **1.5m**, **3.0m** and **4.5m** away from the opening. The luminance maps generated for the two extreme distances showed a *remarkable* difference in both the DGP readings and the number of light sources detected by the software. As expected, the closer the distance of the building occupant to the opening, the greater is the DGP (**79.38** at 1.5m; **34.39** at 4.5m) with a value in region of 30, being the threshold beyond which an occupant tends to perceive a scene as being too bright. It was also noted that the distance of a building occupant from the opening of the test cell had a substantial effect on the number of light sources in the field of view, perceived as being too bright (**115 light sources** at 1.5m; **5 light sources** at 4.5m). Figure 8 refers.

Figure 7: Placement of the luminance photometer within one of the test cells (no glazing installed)

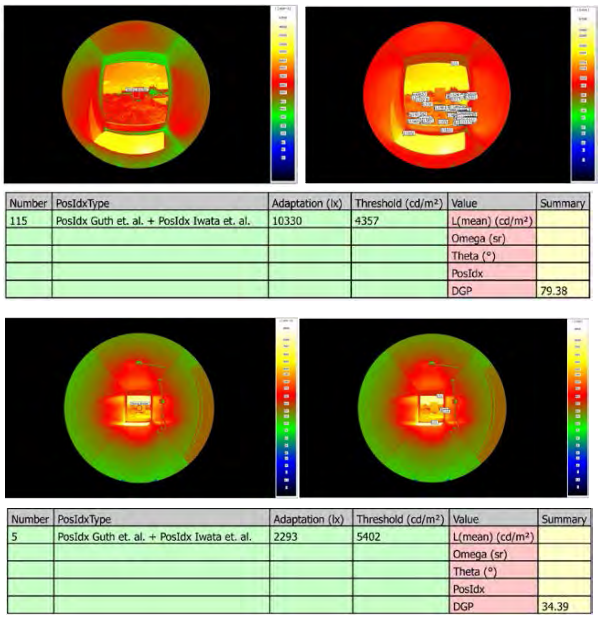

Number	PosIdxType	Adaptation (lx)	Threshold (cd/m²)	Value	Summary
115	PosIdx Guth et. al. + PosIdx Iwata et. al.	10330	4357	L(mean) (cd/m²)	
				Omega (sr)	
				Theta (°)	
				PosIdx	
				DGP	79.38

Number	PosIdxType	Adaptation (lx)	Threshold (cd/m²)	Value	Summary
5	PosIdx Guth et. al. + PosIdx Iwata et. al.	2293	5402	L(mean) (cd/m²)	
				Omega (sr)	
				Theta (°)	
				PosIdx	
				DGP	34.39

5.2 DGP Measurements for the switchable laminate.

Following the installation of the switchable laminate within one of the test cells (Figure 9), readings were taken on a clear, sunny day in November 2023, with the position of the sun perpendicular to the laminate. The scope of these field tests was to measure take readings of the DGP under different states of the films and to assess the visual quality of the test façade and that of the indoor environment within the cell itself. The luminance photometer was mounted on a secure tripod and readings taken at the centre of the test cell - 3.0m away from the opening. The luminance maps generated for two switching states (solar-PDLC OFF; SPD OFF) and (solar-PDLC ON; SPD OFF) are as shown in Figure 10.

Figure 9: The prototype switchable laminate installed within a test cell.

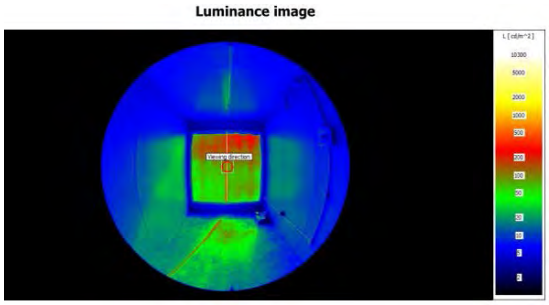

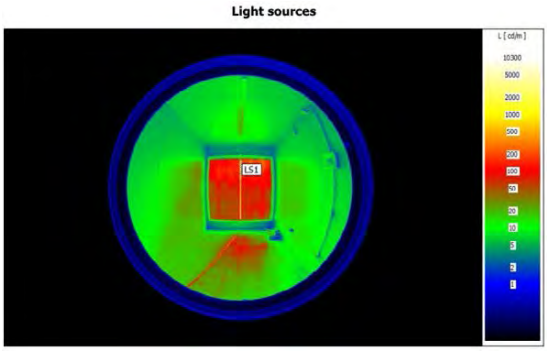

DGP table

Number	PosIdxType	Adaptation (lx)	Threshold (cd/m²)	Value	Summary
1	PosIdx Guth et. al. + PosIdx Iwata et. al.	88.73	4357	L(mean) (cd/m²)	
				Omega (sr)	
				Theta (°)	
				PosIdx	
				DGP	22.74

*Figure 10: Readings for (solar-PDLC **OFF**; SPD **OFF**).*

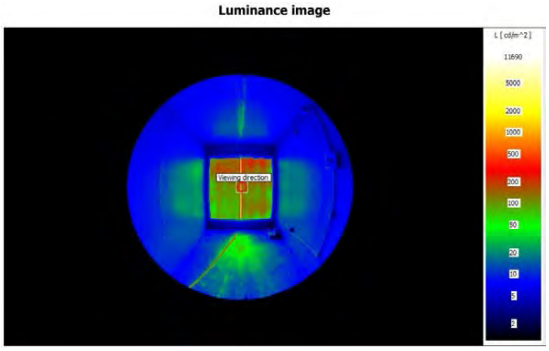

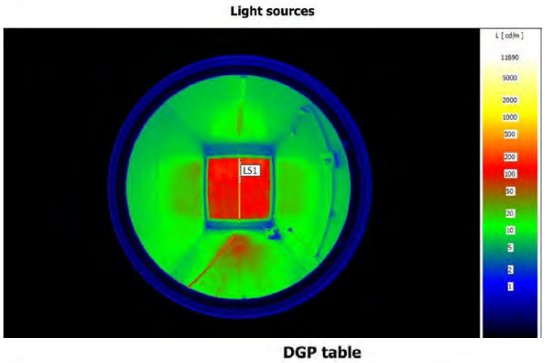

DGP table

Number	PosIdxType	Adaptation (lx)	Threshold (cd/m²)	Value	Summary
1	PosIdx Guth et. al. + PosIdx Iwata et. al.	96.8	4357	L(mean) (cd/m²)	
				Omega (sr)	
				Theta (°)	
				PosIdx	
				DGP	22.84

*Figure 11: Readings for (solar-PDLC **ON**; SPD **OFF**).*

When both films were switched off, the darkest state of the glazing was achieved. Measurements of the VLT through the laminate showed that in this state, the laminate blocked up to 99% of the visible light. The DGP reading of the scene taken from the viewing angle under consideration was 22.74, hence less than the recommended threshold of 30. The opacity of the glazing and its effectiveness at blocking visible light resulted in the photometer detecting the entire glazing areas as one light source (Figure 10). When the solar-PDLC was switched on to omit translucency of the file, the DGP reading showed a slight increase to read 22.84, with the glazing area still read as one light source by the luminance photometer (Figure 11).

*Figure 12: V*iew from the test cell (solar-PDLC **OFF**; SPD **OFF**).

*Figure 13: View from the test cell (solar-PDLC **ON**; SPD **OFF**).*

*Figure 14: Solar disc as seen with the naked eye. **LEFT**: solar-PDLC **OFF** - SPD **OFF**. **RIGHT**: solar-PDLC **ON** - SPD **OFF**.*

*Figure 15: View from the test cell (solar-PDLC **OFF**; SPD **ON**).*

*Figure 16: View from the test cell (solar-PDLC **ON**; SPD **ON**).*

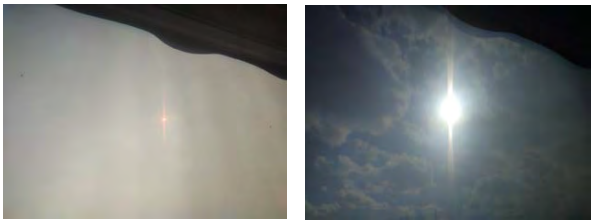

*Figure 17: Solar disc as seen with the naked eye. **LEFT**: solar-PDLC - **OFF**; SPD - **ON**. **RIGHT**: solar-PDLC - **ON**; SPD - **ON**.*

6. DISCUSSION

When both films were switched off (State-1), a complete visual disconnection could be noted within the test cell to the outside (Figure 12). A feeling of complete enclosure was observed, resulting in a sense of total privacy. The solar disc could be comfortably looked at directly with the naked eye (Figure 14 - left). In a state where the solar-PDLC film was switched on (State-2), only a marginal visual connection to the outside could be achieved. Results show that the blue SPD film in its OFF state tends to visually overpower the solar-PDLC privacy film in its ON state (Figure 13). In this state, the solar disc could also be comfortably observed with the naked eye (Figure 14 – right).

When the solar-PDLC film was switched OFF and the SPD film switched on (State-3), the blue tint of the SPD film was noted to disappear completely, save for a slight tint along the edges of the films. The translucency provided by the solar-PDLC film again provided for a complete visual disconnection from the outside, hence providing privacy (Figure 53). When observed with the naked eye under this state, the solar disc could also be comfortably looked at directly with the naked eye (Figure 17 – left). With both films switched on (State-4), bright and direct sunlight penetrated the test cell allowing for direct internal illumination of the internal space.

A visual connection to the outside was now noted, albeit with a degree of visual haze comparable to that provided by a transparent sheer curtain behind a conventional glass pane. This visual effect is likely to be caused by internal reflection of incident light onto the formulation particles of the solar-PDLC film itself when oriented horizontally (film switched ON). Under this state, the solar disc was visually unbearable to be directly looked at. (Figure 17–right).

7. CONCLUSIONS

Switchable solar-PDLC and SPD films have the potential of being integrated for the control of daylight. A prototype glazing assembly comprising both solar-PDLC and a tinting SPD within a single laminate was assembled and installed within a full-scale test cell.

Measurements of the DGP showed promising results in achieving a value within acceptable limits with both films allowing for a high degree of protection from the adverse effects of the solar disc causing disability glare when falling within the field of view.

This study has shown that in its bleached (quasi-clear) state, the switchable laminate did not offer full clarity of the view normally associated with clear glazing, potentially creating a degree of human dissatisfaction. This merits further investigation by conducting occupant satisfaction studies on a select number of participants working from the test cell itself.

REFERENCES

1. Cattarin G., Causone F., Kindinis A., Pahliano L., (2015), Outdoor test cells for building envelope experimental characterisation – A literature review. *Renewable & Sustainable Energy Reviews, Volume 54, 606-625, Elsevier.*

2. Compagno, A., (1999); Intelligent glass facades: material, practice, design, Birkhäuser Verlag.

3. Granqvist C.G., (2007), Transparent conductors as solar energy materials: a panoramic review, Solar Energy Materials and Solar Cells 91, 1529-1598.

4. Wienold, J., & Christoffersen J., (2006). Evaluation methods and development of a new glare prediction model for daylight environments with the use of CCD cameras. Energy and Buildings, 38(7), 743–757.

PLEA 2024 WROCŁAW
(Re)thinking Resilience

LuminLab: An AI-Powered Building Retrofit and Energy Modelling Platform

KEVIN CREDIT,[1] QIAN XIAO,[2] JACK LEHANE,[1] JUAN VAZQUEZ,[2] DAN LIU,[2] LEO DE FIGUEIREDO[2]

[1]Maynooth University, Maynooth, Ireland
[2]Trinity College Dublin, Dublin, Ireland

ABSTRACT: This paper describes the technical and conceptual development of the 'LuminLab' platform, an online tool that integrates a purpose-fit human-centric AI chatbot and predictive energy model into a streamlined front-end that can rapidly produce and discuss building retrofit plans in natural language. The platform provides users with the ability to engage with a range of possible retrofit pathways tailored to their individual budget and building needs on-demand. Given the complicated and costly nature of building retrofit projects, which rely on a variety of stakeholder groups with differing goals and incentives, we feel that AI-powered tools such as this have the potential to pragmatically de-silo knowledge, improve communication, and empower individual homeowners to undertake incremental retrofit projects that might not happen otherwise.
KEYWORDS: Energy efficiency, Building retrofit, AI, Machine learning, Pragmatism

1. INTRODUCTION

Energy use in buildings represents a significant proportion of both household expenses and carbon emissions. European electricity prices have been steadily rising over the past 15 years, hitting an all-time high of €28.4 per 100 kWh in 2022 [1]. According to the International Energy Agency (IEA), operational building use amounts to almost 30% of global energy consumption [2]. To reach the IEA's 2030 net zero emissions target, buildings' operational energy use must be reduced by about 25%, requiring significant retrofit investment for existing building stock.

Unfortunately, the pursuit of net zero emissions targets and operational energy use in Ireland, and globally, is often restricted by the pressure of practical considerations and the misalignment of incentives and behaviours in policy creation. The expected benefit of retrofit packages for policy-makers often does not match with householders' thermal comfort demands [3] or the widespread availability (and cost) of conventional materials [4].

In addition, the building retrofit process in Ireland is complicated and costly for individual homeowners. As Figure 1(A) shows, required knowledge is often siloed in stakeholder groups and, despite the perceived linearity of retrofit processes diagrammed, phased service provision can further compound information incompatibility between stakeholders, further fragmenting information flow across time [5].

In most cases, even basic energy assessments can entail specialised design professionals and in-person energy audits that can cost in the range of €600-€800. Should a homeowner decide to proceed, they can spend significant time and effort pursuing individual quotes, planning and managing the project, not to mention temporary loss of use of their home.

Crucially, the options design professionals and home contractors offer often focus on deep retrofit solutions that may lack significant investment return for individual homeowners, even in the current high energy cost environment. Amid the availability of a broad range of technologies and major efforts to promote and accelerate retrofit activities, identifying the most effective retrofit strategies that meet investment criteria remains a significant challenge for homeowners [6]. There is very little information provided on smaller-scale solutions and simple fixes that could result in energy efficiency increases [7].

The development of new artificial intelligence (AI) technologies, such as large language models (LLM) like ChatGPT, provides a significant opportunity to improve this building retrofit process. By informing retrofit decisions across domains, AI can potentially help identify effective retrofit strategies [8], which could also support the shared creation of statistical models and cost-benefit estimation [9] for energy and economic efficiency [10] alike.

However, given the very recent development of many of these AI technologies, from a theoretical perspective there has been relatively little work contextualising the use of AI for building retrofit in general or understanding the extent to which AI-driven decision support systems can improve energy efficiency and stakeholder engagement in home retrofit projects. Here we conceptualise AI's use for building retrofit as a pragmatic solution to the communication and knowledge barriers that arise in these projects. As posited by Hillier [11], in order "to understand building, then, we must understand it both as a product and as a process". Pragmatism, as a knowledge claim based on "practical problem solving and real-world research" [12] offers considerable

utility in addressing such measures as it is not committed to any specific school of thought, enabling researchers and designers to adopt the methods that best improve outcomes. Extending from this open and pluralistic epistemology, we envision AI tools as a part of a pluralistic methodology that can be used to help overcome the gaps in knowledge for individual homeowners, as well as the qualitative complexities of coordinating between stakeholder groups involved in retrofit projects. This offers particular significance in the multifaceted context within which energy retrofit research is nested, allowing for integration of practical action with the physical properties of retrofit packages — emphasising interconnectedness of buildings, systems, technologies and, critically, the stakeholder diversity required in retrofit solutions' design, production and eventual sustainment.

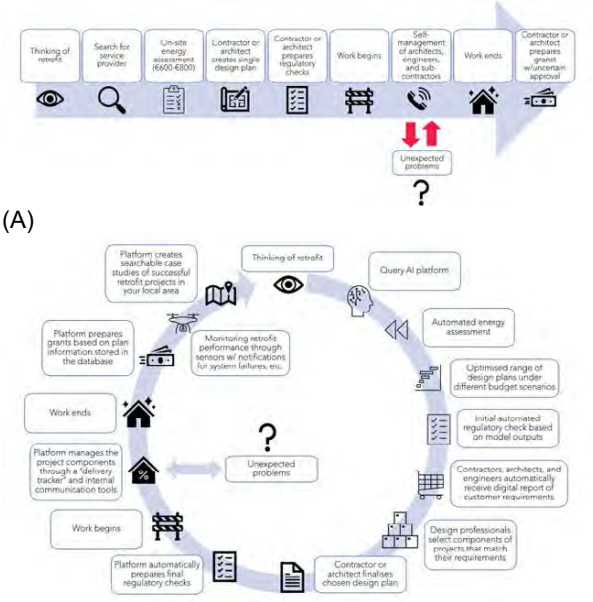

Figure 1(A)-(B): Current vs. proposed homeowner retrofit management process.

Given this pragmatic conceptual underpinning, the purpose of this paper is to describe the technical development of the 'LuminLab' AI-powered building retrofit platform created by the authors. This online tool integrates a purpose-fit human-centric AI chatbot and predictive energy model into a streamlined front-end that can rapidly produce and discuss building retrofit plans in natural language. As shown in Figure 1(B), the focus is on streamlining the end-to-end retrofit process by recognising its inherently recursive nature and eventually incorporating AI communication, modelling, and coordination tools at every stage, from project conception through planning, design, contractor assignment, coordination, and even monitoring. Providing an 'intelligent' chatbot agent that the user can interrogate helps to de-silo stakeholder knowledge and enable users to better understand the cost trade-offs inherent in the retrofit process. Currently (as described below) the platform engages users with a range of possible retrofit pathways tailored to their individual building needs on-demand.

We finish the paper with reflections on the process and our ongoing engagements with relevant stakeholders in Ireland. While the tool is not yet widely implemented, our pragmatic, stakeholder-driven development approach provides useful lessons and a roadmap for future AI-driven support systems in the design professions within Ireland, and beyond.

2. METHODS

The LuminLab platform is an online application to streamline the home retrofit process, primarily for homeowners in Ireland. In Section 2.1 we describe the platform's front-end design and its integration with the LLM chatbot and back-end databases and processing. Then, in Section 2.2 we describe specifics of the energy model used to optimise retrofit configurations under a range of budget conditions.

2.1 Platform and LLM

At its core, the LuminLab platform uses a fine-tuned LLM as an intelligent interface to offer contextualised guidance for the entire retrofit process. The application is designed with a user-friendly front-end; upon accessing the platform, users encounter a dashboard which encompasses four primary components:

1. **Chat Assistant:** the LLM interface is the cornerstone of the LuminLab application, which acts as a central gateway to its various features and functionalities. Its integration with advanced models and technologies positions it as a dynamic and intelligent assistant, guiding users through every aspect of their home retrofitting journey.
2. **Reports and Plans:** this section aggregates all documents and plans generated during the user-chatbot interaction. It acts as an organised repository of platform-generated user-specific retrofit plans, analytical reports of the analysis of user-provided data (e.g. from their home's BER certificate), and tailored recommendations from the Chatbot based on respective user questions.
3. **My City in 3D:** this module (under development) allows users to explore their home's urban context in a dynamic 3D visualisation. In the future it will integrate geospatial data with LLM-aided analysis, presenting crucial information in an immersive and informative manner. Other planned future extensions include 3D modelling software integration to create detailed renderings of individual buildings using only homemade videos of the premises, a novel approach to significantly enhance visualisation and support the planning process. The underlying technology based on Neuralangelo, developed by NVIDIA, can be tailored to architecture modelling applications.

4. **Useful Resources:** to allow users to explore the information underpinning the LLM's responses, the platform also provides an extensive library of resources, including regulatory frameworks, retrofitting guidelines, and environmental data. This data is actively referenced by the LLM.

The front-end interface, crafted using React and Material-UI (MUI), is specifically designed to cater to a diverse user base. MUI's versatile component library allows rapid iteration of interface designs, ensuring an intuitive and accessible user experience. This adaptability is crucial in addressing users' varied technological comfort levels. To accommodate different user preferences, the application offers two modes of interaction: a structured multiple-choice form and a text-based chatbot. The multiple-choice form provides a clear, guided experience, asking specific questions with defined options for ease of data entry. The chatbot allows users to input data conversationally, capturing detailed retrofit information, also complementing data from the form. Users can utilise both modes concurrently, ensuring a comprehensive and tailored data submission process for various technological comfort levels. The specifics and methodologies employed in the multiple-choice form are further elaborated in Section 2.2 below.

The back-end of the platform, implemented using Flask, handles data processing and API interactions. The integration of the LLM, using the Langchain library, with vector databases hosted on Pinecone, enables access to a wide range of information sources which can include generated reports, government retrofit and building regulations, as well as previous conversations. At the time of writing, all development and testing has been carried out using the GPT-3.5 model, while also exploring open-source alternatives such as Llama2 13B and Mistral 7B. This facilitates the delivery of personalised and accurate retrofitting advice via a single unified communication system.

The chatbot is enhanced with access to an energy modelling machine learning model, capable of leveraging user-provided information to generate personalised home retrofit plans. Once the energy model generates the plans, they are initially structured JSON files, comprised of key-value pairs representing distinct plan components. To ensure compatibility and seamless integration with the LLM, these JSON files are transformed into a text-based format, where additional context is provided for each feature. This modified plan is incorporated into the LLM knowledge base, utilising a methodology consistent with the integration of user messages and additional input data. Following this process, the model is equipped to interpret these plans and provide the user with detailed explanations and responses to their queries. The LLM reads and interprets these plans, responding to users' queries with detailed explanations. This seamless interaction between the deep learning model and LLM allows for a comprehensive and user-friendly advisory system.

To improve user interaction and response nuances, a secondary LLM instance is trained on a large database of questions and corresponding follow-up queries, employing a vector similarity search approach to generate contextually appropriate and relevant follow-up questions shown in Figure 2.

Figure 2: Chatbot interface showing an example of an initial query, data visualisations, and follow-up questions.

This feature is crucial in facilitating more meaningful interactions with users, ensuring their queries are comprehensively addressed by providing conversation paths they may not be aware of.

2.2 Energy Model

The energy model is used to help select appropriate retrofit components, generate detailed retrofit plans, and predict resulting energy ratings using deep learning methods. To do this, we use a classification model to predict the building features most related to increasing the building's energy performance rating, along with data on associated prices. This allows the user to select retrofit packages that correspond to their budget requirements.

The classification model is trained on the Energy Performance Certificates (EPC) dataset from the Sustainable Energy Authority of Ireland (SEAI) [13]. This contains over 1 million entries, categorised into 15 classes that correspond to different energy rating levels ('A1' being the best and 'G' being the worst). To build the predictive model we form 80%/10%/10% train/validation/test splits, where a different split is generated for each trial and all methods use the same splits. From the original 211-feature set that describe the individual building, we selected 41 features with both engineering and data-driven methods [14,15], ensuring the most relevant chosen features for our study. These 41 features are categorised into distinct groups based on different building aspects, including building envelope features like area of wall, roof, and door; building fabric features such as U-values for wall, roof, and door; heating system characteristics, notably main heating system efficiency; hot water-related attributes, including water storage volume; and spatial features such as the county code [14].

This project employs four deep learning algorithms to devise the classification model, namely multi-layer perceptron (MLP), self-supervised contrastive learning using random feature corruption (SCARF) [16], and coarse-to-fine-grained versions of MLP and SCARF. The MLP classifier is designed to determine the energy rating from selected building features. As Figure 3 shows, it consists of four hidden layers, with the input layer handling 41 feature dimensions. The data is passed through these hidden layers, with the class label predicted at output layer.

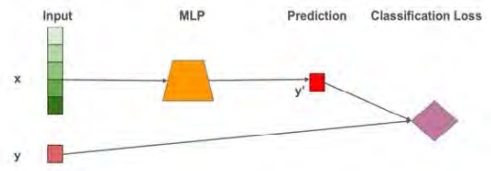

Figure 3: Diagram showing multi-layer perceptron (MLP).

We use the cross-entropy loss function to measure and minimise the difference between predicted and actual labels, aiding in the model's weight optimization. The subsequent stage involves fine-tuning, similar to the MLP classification process but with the initial phase's encoder translating input data into representations before MLP processing.

Meanwhile, SCARF operates in two stages, as shown in Figure 4. The initial unsupervised stage involves altering a randomly selected and replaced portion of the features — 30% in our case — based on a distribution derived from the training data [16]. Both the original and modified inputs are processed through an MLP-based encoder, generating respective representations. Here, the InfoNCE loss function is used, ensuring similarity between both corrupted and original inputs' representations [17].

(A)

(B)

Figure 4(A)-(B): Diagram showing unsupervised SCARF pre-training (A) and subsequent supervised finetuning (B). During pre-training, the encoder f *is trained to learn a good representation for the input data. After pre-training, classification head* g *is applied on the top of* f*, and both* g *and* f *are subsequently fine-tuned for classification.*

The complexity in distinguishing between, e.g., classes A1, A2, and A3 in the EPC data led us to adopt a coarse-to-fine approach. Initially, we consolidated several classes into broader categories, reducing the original 15 classes to 5. This process involved two stages: first, training a coarse-grained classifier on the merged classes, followed by the development of five fine-grained classifiers for the subdivided classes, as depicted in Table 1. These coarse categories were then used in both the MLP and SCARF models.

To assess the highest performing method for use in the platform, we compare the MLP and SCARF deep learning approaches against three other popular machine learning algorithms used for classification problems, namely decision tree, gradient boosted tree and random forest. The performance results for each model are given in Table 2 (for macro F1 score and accuracy), demonstrating deep learning methods' outperformance of traditional machine learning methods when applied to the EPC dataset. MLP achieves the highest accuracy overall.

However, it is important to note that MLP shows limited accuracy in predicting certain classes, such as A1 in Table 3. This discrepancy can be attributed to the highly imbalanced nature of the EPC dataset, as there are very few A1 observations. In such datasets, accuracy may not be the most effective metric for assessing the model's performance on minority classes. Interestingly, SCARF and coarse-to-fine-grained classification significantly enhanced the model's performance on challenging classes like A1.

Table 1: Mapping of original energy ratings (A1, A2, ..., G) to coarse categories (A, B, C, CD, EFG).

Original	A1	A2	A3	B1	B2	B3	C1	C2	C3	D1	D2	E1	E2	F	G
Transformed	A	A	A	B	B	B	C	C	CD	CD	CD	EFG	EFG	EFG	EFG

Despite these advancements, our models' overall performance is still not optimal. This limitation is largely due to the presence of missing fields and noise within the EPC dataset. For instance, we observed anomalies in the data, such as 10% of the floor area and floor U-values being recorded as zero. These missing observations are problematic, especially for U-values, where zero is not a plausible measurement.

Table 2: Macro F1 scores and accuracies on the EPC test set. All results are averaged over 5 runs with different seeds.

	Macro F1	Accuracy
Decision Tree	51.7%	51.2%
Gradient Boosted Tree	47.1%	49.5%
Random Forest	63.1%	62.8%
MLP	63.9%	69.5%
SCARF	65.8%	68.7%
coarse-to-fine grained MLP	66.8%	68.3%
coarse-to-fine grained SCARF	67.1%	68.6%

Table 3: Accuracies on the EPC test set for class A1, A2 and A3. All results are averaged over 5 runs with different seeds.

	A1	A2	A3
MLP	0%	90.6%	78.4%
SCARF	17.5%	86.1%	83.4%
coarse-to-fine grained MLP	36.8%	90.2%	79.6%
coarse-to-fine grained SCARF	29.6%	89.7%	82.1%

Substantively, our analysis revealed that building insulation features, particularly the U-values of walls and floors, have the most impact on these models. Note that model explanation tools such as LIME [18] and SHAP [19] are less reliable and effectively applied to deep learning models compared to linear or tree-based models. Therefore, we used the decision tree model's results to determine feature importance.

On the front-end, the LuminLab platform connects to the energy model; enabling users to retrofit homes by choosing from four key components: insulation (encompassing wall, roof, floor, window, door, and attic), boiler heating controls for temperature regulation, Mechanical Ventilation with Heat Recovery (MVHR) systems for air circulation, and solar panels (varying in number and power output)[1].

Within each component category, a variety of items are available for selection, each with associated characteristics and costs. For instance, in the category of door insulation, users can choose a door with specific properties, such as one made of aluminium with a U-value of 1.7, offered at a price of €1099. The system assumes a default comprehensive retrofitting approach, encompassing all components from wall insulation to the installation of solar panels. This default setting, however, may not align with users' actual requirements or preferences. Therefore, we empower users to customise retrofit components based on their unique needs and circumstances.

For each combination of items within different retrofit components, the model calculates a predicted energy rating. Each item in the combination influences specific home features. For example, selecting a roof with a U-value of 1.3 will adjust the home's original roof U-value to this new figure. Consequently, the model reflects such changes in home features which recalculates the energy rating accordingly. In addition, each item combination's cost is calculated, summing prices of all items in the plan. For each distinct energy rating obtained, we retain the combination with the lowest cost. Consequently, this determines the most cost-effective retrofit plan corresponding to each potential new energy rating. Moreover, any applicable grants from SEAI are also shown, aggregating item price minus potential grants. Figure 5 shows this general energy modelling process.

[1] Note: User inputs to the energy model are restricted to the information collected in the BER assessment, because the energy model uses only those features in the BER dataset to predict the best combination of elements (under the budget constraint) to improve BER. This means the information provided by the user is limited in terms of the level of detail (e.g., door jamb, glazed openings, etc.) to what is collected by BER assessors. However, future extensions of this project seek to be able to collect and incorporate finer levels of detailed information on the retrofit/configuration characteristics of homes.

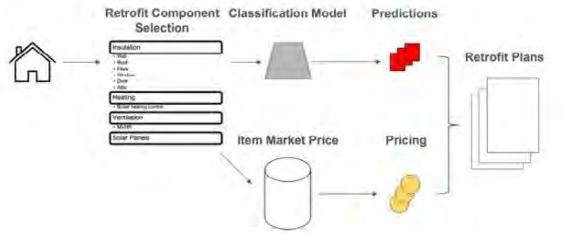

Figure 5: Schematic of the energy modelling process.

Ultimately, this system provides users with both energy rating post-retrofit and associated cost estimates for each proposed plan, enabling better-informed decisions for energy-efficient upgrades, particularly for fine-grained cost/efficiency trade-offs which are not always easy to estimate (even for knowledgeable homeowners) within the Irish market.

3. INITIAL FINDINGS AND CONCLUSIONS

While we have not yet widely tested the usage of the LuminLab platform in practice, initial findings and conclusions are presented from the development that may benefit retrofit scholars and practitioners.

First, from a global perspective: the platform's development – including everything from overall problem delineation to specific front-end design choices in the online tool – has been informed by conversations with a range of retrofit stakeholders in Ireland. These include government agencies and non-profit organisations such as the Sustainable Energy Authority of Ireland (SEAI), Dublin City Council (DCC), and Irish Green Buildings Council (IGBC), as well as individual homeowners, contractors, and architects.

Broadly, our stakeholder engagement attests to the lack of alignment between policy and practice. Given the technical nature of retrofit and decarbonisation policy, different groups perceive and engage with retrofit practice and measures of success differently. Despite each stakeholder group's perceived solutions to retrofit, each is often unaware of their disconnect with others' needs, priority areas, and lived experiences [20], attesting to the information fragmentation mentioned, compounded by the perceived linearity of the process in Figure 1(A) and 'phased' approach to service provision. For instance, policymakers create goals and standards that may have unintended consequences for contractors performing the work; homeowners may have alternate project goals (e.g., comfort) than what grants incentivise; and some specialised design knowledge may not be accessible in a small-scale project. This disconnection means that knowledge, resources, policies, and actions are siloed within stakeholder groups, making it difficult for individual homeowners to make sense of the complicated landscape that any retrofit project must traverse.

As for the specific technical components of the platform itself, we have found that enhancing LLMs with government data and regulations, carefully

refined from web and document sources, is key to ensuring accurate and relevant responses in regulatory contexts. In addition, creating user-friendly default prompts for LLM-integrated websites is crucial, considering that most users might not be familiar with advanced prompting techniques. This approach aims to optimise tool performance and effectiveness for typical user interactions. For the energy model, we found that data irregularities from provided 'real-world' sources highlight the need for robust data pre-processing and model development to accommodate or correct data inconsistencies. While in this context the coarse-to-fine-grained SCARF model performs best, future work may focus on improving data quality and exploring models that are more resilient to data imperfections, thereby enhancing the reliability and applicability of our system in commercial settings. Substantively, our analysis also shows that the U-values of walls and floors have the most significant impact on improving the energy performance rating of a given building

Collectively, these learnings offer a critical path for de-siloing retrofit and AI's role in achieving this. Moreover, the pragmatist framework's conceptual distinctions underscoring our approach could better position further research inquiry, freeing researchers and participants to engage in a pluralism of approaches and methods to best serve the research question; the same pluralism underscoring the misalignment between technology and policy, and qualitative complexities of stakeholders involved. If properly channelled, an AI-informed and sufficiently multi-stakeholder-engaged retrofit can offer an alternative to extant policy and practice. This would enable reciprocal learning not otherwise possible for stakeholder groups individually for extended retrofit sustainment at both national and international levels.

REFERENCES

1. Eurostat. (2022), Electricity & gas hit record prices in 2022 [Online], Available: https://ec.europa.eu/eurostat/web/products-eurostat-news/w/DDN-20230426-2

2. International Energy Agency (IEA). (2022), Energy consumption in buildings by fuel in the Net Zero Scenario, 2010-2030, [Online], Available: https://iea.org/data-and-statistics/charts/energy-consumption-in-buildings-by-fuel-in-the-net-zero-scenario-2010-2030-2.

3. Feijter, F. d. and Vliet, B. v. (2020). Housing retrofit as an intervention in thermal comfort practices: chinese and dutch householder perspectives. Energy Efficiency, 14(1).

4. Jankovic, L., Bharadwaj, P., & Carta, S. (2021). How can uk housing projects be brought in line with net-zero carbon emission targets?. Frontiers in Built Environment, 7.

5. Jallow, A. K., Lee, S., Castronovo, F., Zhang, Y., Chunduri, S., & Messner, J. (2013). Process-based information exchanges mapping for energy-efficient retrofit projects. Computing in Civil Engineering.

6. Hong, T., Piette, M. A., Chen, Y., Lee, S. H., Taylor-Lange, S. C., Zhang, R., … & Price, P. N. (2015). Commercial building energy saver: an energy retrofit analysis toolkit. Applied Energy, 159, 298-309.

7. Torres, J., Jauregui, O., and Urra, S. (2020). D3.1. Conclusions of the identification of local needs and actors in place. Turnkey Retrofit Horizon 2020 Project Report. Available: https://turnkey-retrofit.eu/wp-content/uploads/TR_D3.1_TEC_30_11_2020_Final.pdf.

8. Walter, T. and Sohn, M. D. (2016). A regression-based approach to estimating retrofit savings using the building performance database. *Applied Energy*, 179, 996-1005.

9. Noris, F., Delp, W. W., Vermeer, K., Adamkiewicz, G., Singer, B. C., & Fisk, W. J. (2013). Protocol for maximizing energy savings and indoor environmental quality improvements when retrofitting apartments. Energy and Buildings, 61, 378-386.

10. Ananwattanaporn, S., Patcharoen, T., Bunjongjit, S., & Ngaopitakkul, A. (2021). Retrofitted existing residential building design in energy and economic aspect according to thailand building energy code. Applied Sciences, 11(4), 1398.

11. Hillier, B. (1996). Space is the Machine; A Configurational Theory of Architecture. 1st ed. Cambridge, UK: Cambridge University Press Ltd. p.32.

12. Morgan, D. L. (2007). 'Paradigms Lost and Pragmatism Regained: Methodological Implications of Combining Qualitative and Quantitative Methods' In: Journal of Mixed Methods Research, 1(1), pp.48-76.

13. Sustainable Energy Authority of Ireland (SEAI). 2024. National BER Research Tool, [Online], https://ndber.seai.ie/BERResearchTool/ber/search.aspx.

14. Ali, Usman, et al. (2020). "A data-driven approach for multi-scale GIS-based building energy modeling for analysis, planning and support decision making." Applied Energy 279: 115834.

15. Ali U, Shamsi MH, Bohacek M, Hoare C, Purcell K, Mangina E, et al. (2020). A data-driven approach to optimize urban scale energy retrofit decisions for residential buildings. Appl Energy;267:114861.

16. Bahri, Dara, et al. "Scarf: Self-supervised contrastive learning using random feature corruption." arXiv preprint arXiv:2106.15147 (2021).

17. Aaron van den Oord, Yazhe Li, and Oriol Vinyals. Representation learning with contrastive predictive coding. arXiv preprint arXiv:1807.03748, 2018.

18. Ribeiro, Marco Tulio, Sameer Singh, and Carlos Guestrin. ""Why should i trust you?" Explaining the predictions of any classifier." Proceedings of the 22nd ACM SIGKDD international conference on knowledge discovery and data mining. 2016.

19. Lundberg, Scott M., and Su-In Lee. (2017). "A unified approach to interpreting model predictions." Advances in neural information processing systems 30.

20. Soliman-Junior, J; Awwal, S; Ayo-Adejuyigbe, M; Tzortzopoulos, P; and Kagioglou, M. (2022). Stakeholders' Perception in Early Stages of a Social Housing Retrofit Living Lab. IOP Conference Series Earth and Environmental Science, 1101(5), 052025.

PLEA 2024 WROCŁAW
(Re)thinking Resilience

Digital Wicker

Interdisciplinary and Research-Informed Teaching Concepts Exemplified Through Textile Fabrication Processes for Willow Structures

SASKIA NEHR[1], MICHELLE MONTNACHER[1], MICHAEL HOSCH[1], JAVIER FUENTES[2], ERIK ZANETTI[2], MORITZ DÖRSTELMANN[2]

[1] Karlsruhe Institute of Technology (KIT), Karlsruhe, Germany
[2] Professorship for Digital Design and Fabrication (DDF), Karlsruhe Institute of Technology (KIT), Karlsruhe, Germany

ABSTRACT: This paper presents a research-informed teaching (RIT) and learning approach that fosters interdisciplinary collaboration and hands-on experimentation for a dynamic advancement of academic research in the field of sustainable architecture. Additionally, transdisciplinary collaborations with various research partners and funding bodies within academic education underline the relevance of the teaching results and the importance of building and testing the developed concepts at architectural scale. This paper presents the example of interdisciplinary teaching courses that are part of a strategy for rapid innovation at the intersection of research and teaching at the Professorship for Digital Design and Fabrication (DDF) at the Karlsruhe Institute of Technology (KIT). They enable students to gain transformative knowledge in interdisciplinary teamwork focused on the intertwined topics of architecture, digital construction technology and sustainability. Here presented is one case study of the resulting student work, which addresses challenges in the construction sector through the exploration of low-emissions processing for circular materials such as willow, highlighting its rapid regrowth and adaptability of digital fabrication processes. The knowledge gained through these research-informed teaching methods is applied through the production of experimental prototypes that are used to visualize construction innovation for public discussion.
Keywords: research-informed teaching, design-through-making, digital fabrication, interdisciplinarity teaching, sustainable architecture

1. INTRODUCTION

In the context of architecture, digital design and sustainability the Professorship for Digital Design and Fabrication (DDF) at the Karlsruhe Institute of Technology (KIT) promotes the development and implementation of practical solutions and concepts for a resilient future of the construction sector.

The linear approach of today's construction sector results in significant waste generation and is responsible for over a third of global resource demands [1]. Consequently, the sector stands at the forefront of the global shift towards a circular economy, for example through natural and regenerative materials based on local sourcing and processing of rapidly renewable materials. Digital design and fabrication methods emerge as key enablers for the industrialization of such natural materials, addressing their scalability in construction. Digital methods contribute to a shift from standardized serial production to individualized mass production of resource and climate-adapted building components. With a research-informed teaching concept, DDF's research-informed teaching can empower future generations with the knowledge and skills necessary to address these challenges.

2. RESEARCH AND TEACHING

The teaching concept focuses on developing individual competencies within interdisciplinary teams at the intersection of research and teaching. In the context of the dynamic field of digital design and fabrication, this means not only mastering current tools but further contributing to the development of novel approaches. Digital technologies in architecture enable the exploration of the broad spectrum of possibilities within the entire design, planning and construction process. The inclusion of research into teaching underlines the importance of maintaining flexibility and curiosity to adapt to upcoming changes through constantly evolving technologies.

The integration of digital technologies, tools and methods into architectural studies enables and is enabled through interdisciplinary collaboration with other departments, which is ensured by forming multidisciplinary teaching, research and student teams within the courses.

2.1 Research-informed teaching

Research-informed teaching (RIT) describes different approaches in which research is integrated into teaching in higher education [2,3]. It encompasses the concepts of research-led, -tutored, -based and -oriented, which reflect different levels of practice and theory involvement and further vary by the student's participation (Fig.1). All these practices play a significant role in the teaching of DDF, focusing especially on the active participation of students in the research projects and their development, through research-oriented and research-based teaching. Research-oriented teaching emphasizes constructing knowledge through research and inquiry skills [4]. Based on this idea, the students are guided through a series of specific research questions to understand the existing state of art regarding materials, construction systems and digital fabrication processes. In addition, research-based teaching highlights the opportunity that students can independently generate scientific knowledge, by going through the entire research process [5].

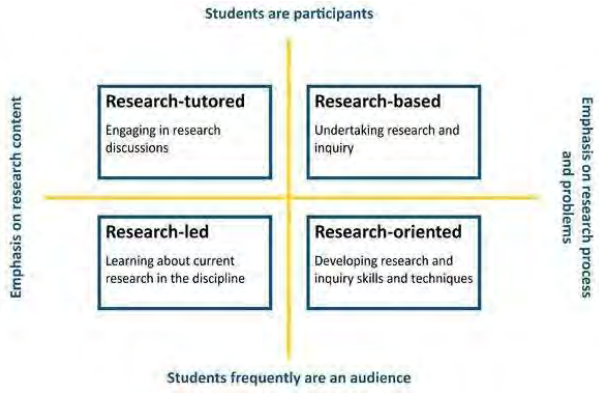

Figure 1: Healey, M., Jenkins, A., Developing undergraduate research and inquiry, The Higher Education Academy, Heslington (2009).

DDF offers the opportunity for students to participate in all phases of the research and project development within one semester, by developing a clear aim and framework for each class, while also ensuring knowledge transfer for the students of the consecutive semester projects. These learning styles encourage curiosity, problem-oriented, critical thinking and creativity to enhance subject comprehension. The autonomy of the students is supported by the opportunity to develop their own concepts and inform them through hands-on experiments, explorative prototyping [see paragraph 4.2] and individual research. Based on a widespread exploration of the emerging novel architectural design and construction repertoire through individual design work, resources are subsequently focused on the development of the most promising concepts in interdisciplinary group work.

In conclusion, research-informed teaching involves students actively participating in the research process - bridging the gap between teaching and research by combining theory and hands-on experimentation.

The interdisciplinary teaching and student teams actively merge architecture, engineering, mechanical engineering and automation, while further including experts in materials, structures and circularity.

2.2 Teaching methods

Within the course structure, students are guided through various "development phases". These phases encompass investigations on state of the art, architectural and structural design, concept exploration (Fig. 2), rigorous testing, the construction of customized machinery, hands-on digital fabrication and the construction of 1:1 scale research demonstrators (Fig. 3). Throughout the semester, skill-building tutorials introduce the students to computational design and digital fabrication tools, without requiring any prior knowledge.

In an initial investigation phase, students individually dive into specific topics related to the context and the state of the art concerning the aspects of the course. They then form groups to focus on advancing the state of the art in various development areas, applying a research-oriented and design-through-making approach. These groups also explore the architectural potential and possible further research tracks. Finally, students collaborate closely as one large group, merging knowledge from previous phases, to work on the final developments for a research demonstrator. This includes producing 1:1 scale building components through digital fabrication, conducting structural and assembly tests, as well as planning for exhibiting the final results. By following all these stages of the process, the students gain hands-on knowledge about research, digital design, fabrication and construction methods and at the same time generate valuable research questions for follow-up projects.

In this research-informed teaching approach, both group work and individual work hold relevance. Multiple individual investigations are gradually combined to form strong ideas through discussions, testing and refinement. These ideas then branch out into various research paths that lead to further concepts resulting in iterative research and learning loops. These loops involve distinct work phases, punctuated by meetings and discussions with all participants, followed by further work phases, which foster knowledge refinement and ensure continuous improvement. This research-informed teaching approach actively promotes a wide range of interdisciplinary and collaborative groups, cultivating

effective communication, diverse perspectives and collective problem-solving. These groups benefit not only from the diverse focus areas and expertise but also from the processes, approaches and soft skills contributed by the various backgrounds of the individuals within the group.

Figure 2: Exhibition of conceptual student work.

Figure 3: Transfer into 1:1 scale utilizing research facilities.

3. CASE STUDY: CIRCULARITY THROUGH DIGITAL DESIGN AND FABRICATION

The built environment is currently experiencing a growing awareness of the overdue digital transformation towards a circular economy. This momentum has been triggered by initiatives such as the European Green Deal and circular economy plans developed by governments at various levels, including national, regional and local actors. According to the World Economic Forum, the built environment is one of the sectors with the greatest opportunities for making a circular economy a reality. However, to accelerate the adoption of circular practices in the built environment, scalable innovation and the development of more ambitious regulations need to be at the forefront.

The principle of circularity focuses on the minimization of waste and the reduction of the environmental impact of products and systems. Circularity requires the material, the process and the product to be understood as a unit. By considering environmental impacts from the earliest design stages, the use of rapidly regrowing materials such as willow is an excellent foundation to facilitate long-term circularity in construction and enable short-term emission reductions through scalable but energy-efficient processing. This commitment to environmental responsibility aligns seamlessly with the deployment of digital design tools. By incorporating circularity into digital design processes, designers can create products that are more sustainable from the outset. Digital tools allow for the exploration of alternative design options, optimization of material usage and evaluation of environmental impacts, enabling the development of products that are environmentally responsible throughout their lifecycle. These tools empower designers to optimize their creations and make well-informed decisions throughout the design process. In this context, willow is well suited to both criteria, as it meets sustainability requirements and has great flexibility to be processed with various digital methods.

It is crucial to acquaint students with digitally enabled circularity concepts within architectural design studios to emphasize their grasp of innovative prospects. Connecting consecutive courses and utilizing results from previous courses fosters a complex and comprehensive perspective. Courses thereby do not only have educational value but generate relevant research results as a base for future students' work. This research-informed teaching approach also reinforces a pragmatic mindset towards repurposing existing resources, including existing knowledge and encourages students to think creatively about materials and processes, transcending their originally intended use.

3.1 Materiality

As an example of such digitally-enabled sustainable material choices, willow is a rapidly-renewable material that is widely available in Europe. It is thereby a great option to substitute conventional building materials. Willow regenerates quickly, allowing for multiple harvests within a short period of time. This fast regrowth makes it a highly efficient and renewable source for various applications with reduced ecologic impact, lessening the need for more finite building materials.

Wetland environments, commonly categorized as swamp areas, traditionally deemed unsuitable for standard agricultural or forestry practices due to their waterlogged nature, offer a promising opportunity for cultivating willow. The utilization of these specific terrains presents a distinctive prospect to optimize land-use efficiency in a way that diverges from conventional practices. It serves as a pioneering solution to effectively cater to the escalating need for renewable materials without engendering competition with established realms such as traditional food production or forestry operations. The unique ecosystem of swamp areas, with their inherent characteristics as carbon storage in combination with the high carbon sequestration potential of willow plantations could provide ecologically favorable material streams on multiple levels. The cultivation of willow typically involves fewer chemical inputs and less energy compared to the production of more conventional building materials. It has a lower carbon footprint, contributing to sustainability goals.

Additionally, willow is highly flexible, which makes it suitable for various digital and textile construction techniques, such as weaving and braiding (Fig. 4.). Weaving with willow involves using individual willow branches or twigs to create various woven objects, typically baskets and other small structures. Willow's flexibility further allows for the creation of curved and intricate structures, making it a versatile choice for certain designs. Untreated, the material is biodegradable, meaning it can decompose naturally over time, reducing the environmental impact when structures reach the end of their lifespan.

Figure 4: Bending of braided willow branches.

3.2 Digital fabrication

Digital fabrication offers numerous advantages, such as increased precision, customization and efficiency. Natural materials often have variations in their properties, composition and dimensions, which can pose challenges in industrialized fabrication processes, as the machines and software are typically optimized for standardized materials. In an initial design studio of DDF, students tried to rethink established digital methods and transfer them for the use of willow. For this purpose, tests were carried out with individual and combined willow branches to see what behavior they show. The advantages of digital fabrication were tested for dealing with willow in order to understand how this natural material behaves, especially its irregularities (Fig. 5). For example, individual willow branches were braided by raspberry pi controlled robots or pulled through a self-made splicing machine to connect them and create an infinite filament. Over the following semesters, the machines underwent refinements and adjustments, gradually evolving and enabling novel design and construction concepts (Fig. 6).

Digital weaving, also known as computer-controlled weaving, involves the use of computer technology to control weaving looms and create woven textiles with precise and intricate patterns. However, weaving a larger structure from willow with digital machines is unusual and therefore requires research and testing.

In weaving, there are typically two sets of threads: the warp threads (vertical threads) and the weft threads (horizontal threads). The warp threads are mounted on the loom and are attached to a warp beam, while the weft threads are inserted by the weaving mechanism. The weaving process as well as the mechanized weaving process must be adapted and optimized for working with willow and material-specific irregularities.

During the test phases in the courses, students took a close look at how the material can be processed more efficiently and the scalability of the process.

Figure 5: Digital fabrication concept from interdisciplinary student work.

Figure 6: Digital prefabrication of willow structures as scalable construction technology based on initial student work and subsequent development within interdisciplinary research.

3.3. Prototyping, evaluation and research transfer

The obtained knowledge about circular material systems and digital fabrication methods are directly integrated into the production and construction of experimental prototypes. Thus, direct discoveries and references are taken up and tested in small-scale models and experiments. Individual findings from smaller prototypes are subsequently combined into circular digital construction concepts by the students and the feasibility of the envisioned digital design and fabrication process as well as the technical performance are tested at a larger scale. Testing of building components at a 1:1 scale allows not only to evaluate the technical performance of novel construction methods but also to assess their architectural design qualities. The resulting research

questions can form the base for third-party funding proposals and the teaching-based concept development serves as a base for interdisciplinary research projects in larger consortia. Integrating the expertise of these research partners into ongoing teaching activities closes the loop of an intertwined research and teaching strategy.

Exploring novel architectural design and construction concepts and testing their application relevance can be massively accelerated through quick prototype iterations at various scales. This approach requires careful evaluation of the potential and limitations of the concept and an iterative framework in which concept development and hands-on prototyping alternate. Choices regarding fabrication and construction strategies can thus emerge through immersive, experiential learning as well as research- and experience-based decision making. During this process the validation of a concept is as valuable as unveiling of further relevant research questions. Within the first design studio initial questions about structure, circularity and digital fabrication methods were explored, which thereby raised further questions for the following semester on actual applications, integrating earth as the load-bearing component and optimizing the digital and circular production processes. Exploratory prototypes serve as concise experiments to gain insights into these questions and test important assumptions and concept properties. Initial explorations and prototypes on a smaller scale (Fig. 7) act as an immediate testing of basic theories and concept ideas, such as the general structure or processing options. They further give valuable insights and conclusions to inform further exploration on a larger scale, which then act as a holistic proof-of-concept validating design, material and fabrication choices. (Fig. 8).

The development process of the prototypes considers reciprocal relationships of several topics such as material streams, production technology, structural design, construction detailing, building physics and architectural design on different scales, ranging from the hybrid material system to the detailed tailored arrangement in tailored and fully recyclable building components and their reversible assembly into a construction system [6]. This involves structural design and structural tests of plant-based building components through digital simulations and executing small-scale qualitative tests [7]. Material investigations concentrate on exploring the behavior of earth- and plant-based materials, conducting initial tests to identify effective combinations. Machine construction aims to design, test and operate custom machinery for the digital fabrication of demonstrator components.

4 INNOVATION STRATEGY

To ensure a societally relevant impact of our work we employ an innovation and research strategy at the interdisciplinary interface of research and teaching that rapidly turns speculative and future-oriented explorations into real-scale application-oriented prototypes through the following six steps:

- Widespread concept exploration: rapid testing of speculative concepts in teaching formats.
- Focused 1:1 prototyping: funneling resources towards promising concepts emerging from step 1.
- Fundamental research: third party funded investigation of research questions emerging from step 2.
- Applied research: evaluate technological and architectural potential in full-scale demonstrators.
- Architectural building projects under the academic umbrella: evaluate economic and ecologic application potential under market conditions and provide a visible full-scale proof of concept implementation.
- Technology transfer to industry partner or university spin-off.

We are currently following and implementing these steps with two of our research endeavors: willow-earth hybrid structures and digital wood upcycling. While our digital wood research is currently within the earlier stages 2-3, our research into willow-earth composite structures yielded rapid success: Within only two years we successfully passed steps 1 – 4 starting with the master design studios “DigitalWicker” in winter term 2021/22 exploring digitally enabled concepts for design and fabrication of willow structures and “Digital Wicker 2.0” testing its combination with earth as hybrid material system in the 1:1 demonstrator “InterTwig” in summer term 2022. In-depth research of the digital design and fabrication methods for willow/earth hybrid construction was subsequently funded through the research projects “ReGrow” and “WillowWeave” and successfully tested at the Bundesgartenschau Mannheim 2023 in the demonstrator project “ReGrow Willow”. The follow-up research grant “ReSidence” is focused on applied research and development of a ceiling construction component including structural, fire and sound certification. In parallel, we receive numerous requests for applications in architectural projects and are currently preparing step 5 as an architectural application of fully certified willow/earth/wood hybrid ceiling components and anticipate the exploration of its market potential in 2025.

Figure 7: Exploratory prototype in teaching context

Figure 8: 1:1 scale research demonstrator "ReGrow Willow" at the Bundesgartenschau 2023 in Mannheim

5. CONCLUSION

Universities can play a pivotal role in shaping a sustainable future for the construction sector by challenging the linear approach in today's industry and advocating for low-emission and circular material cycles through the exploration of digital design and fabrication processes. The emphasis on materiality, exemplified by the case study of natural willow-earth composite, showcases the importance of environmental responsibility from the earliest design stages. The circularity of willow as a rapidly renewable construction material, particularly if grown in denaturalized former wetlands, holds enormous ecological potential. The development of bespoke digital fabrication processes enables a local low-emissions processing of such harvested materials by addressing challenges posed by inhomogeneous non-standardized grown building materials. In combination with digital design strategies, innovative circular construction concepts are enabled, simultaneously focussing on precision and efficiency while also incorporating concepts of redundancy and robustness in the design process.

The integration of research into teaching, with a focus on interdisciplinary collaboration, proves instrumental in developing individual competencies and fostering a dynamic exchange between academia and practical application. The structured innovation pipeline, from knowledge discovery to 1:1 prototypes and large-scale demonstration objects, showcases the transformative potential of such teaching methods. Furthermore, the collaborative and explorative prototyping efforts demonstrate the practical application of sustainable design principles, by efficiently visualizing construction innovation in a public discourse.

The presented research-informed teaching approach generates societally relevant innovations as a base for a digital transformation of the construction sector towards circular material streams and low-emissions construction. At the same time, it enables students to gain first-hand learning experience for creative problem-solving in interdisciplinary and internationally diverse teams as key transformative competencies to foster a culture of innovation and sustainability in practice and research.

ACKNOWLEDGEMENTS

The presented work is based on interdisciplinary student contributions at the Karlsruhe Institute of Technology (KIT) and research projects funded by the Sustainable Bioeconomy Strategy Baden Württemberg through the Ministry for Food, Rural Areas and Consumer Protection Baden-Württemberg (MLR).

REFERENCES

1. Çetin, S., De Wolf, C. and Bocken, N. (2021). Circular Digital Built Environment: An Emerging Framework. Sustainability, 13(11).
2. Healey, M., Jenkins, A., and Lea, J. (2014). Developing research-based curricula in college-based higher education. Higher Education Academy
3. Annie, L.C. and Shemim, F.K.S. (2019) 'Research Informed Teaching: A Brief Orientation', in 2019 Advances in Science and Engineering Technology International Conferences (ASET). 2019 Advances in Science and Engineering Technology International Conferences (ASET), Dubai, United Arab Emirates: IEEE, pp. 1–6.
4. Selje-Aßmann, N. (2020). Forschendes Lehren und Lernen – Ein Mehrdimensionales Modell für die lehrpraxis aus perspektive der Empirischen Wissenschaften. Forschendes Lernen, 71–86. https://doi.org/10.1007/978-3-658-31489-7_6
5. Didion, D.; Wiemer, M. (2009). Forschendes Lernen als interdisziplinäres Element des Studium Fundamentale. Journal Hochschuldidaktik, (20).
6. Zanetti, E., Olah, E., Haußer, T., Casalnuovo, G., La Magna, R., & Dörstelmann, M. (2023). InterTwig—Willow and Earth Composites for Digital Circular Construction. In M. R. Thomsen, C. Ratti, & M. Tamke (Eds.), Design for Rethinking Resources (pp. 491–511). Springer International Publishing.
7. Casalnuovo, G., Zanetti, E., Haußer, T., La Magna, R., & Dörstelmann, M. (2023). Digital Structural Design for Natural Composites: A Case Study of Willow-Earth Hybrid Construction. In A. Crawford, N. Diniz, R. Beckett, J. Vanucchi, & M. Swackhamer (Eds.), Habits of the Anthropocene: Scarcity and Abundance in a Post-material Economy. Proceedings of the 43rd Annual Conference of the Association for Computer Aided Design in Architecture: Vol. II (pp. 282–292). Association for Computer-Aided Design in Architecture (ACADIA).

PLEA 2024 WROCŁAW
(Re)thinking Resilience

Bio-HNV: Bio-based Humidity-responsive Night Ventilation for climate resilience

A new generation of responsive building skin for passive cooling

NATALIA PYNIRTZI[1,2], KUMAR BISWAJIT DEBNATH [1], JANE SCOTT [1], COLIN DAVIE [2], BEN BRIDGENS [1]

[1] HBBE, School of Architecture, Planning and Landscape, Newcastle University, UK
[2] School of Engineering, Newcastle University, UK

ABSTRACT: Moisture-responsive bio-based materials, such as wood veneers, are abundant and have great potential to perform as breathable building systems due to their reversible shape change through continuous deflection under different wetting and drying conditions, enabling the building envelope to passively respond to the environment while avoiding the need for mechanical ventilation resulting in operational energy reduction. Wood has been used in buildings globally for centuries; however, it has not been used in its thin monolayer form, acting as a humidity-responsive structure within a passive night ventilation system. This study evaluates the moisture responsiveness and functionality of wood veneer structures as responsive systems with potential use in external building facades of South Asian megacities. Weather data from New Delhi, India, were collected and analysed to give the operational requirements for the material systems. The woven veneer structures were exposed between low (20%) and moderately high (70%) relative humidity in a climate chamber at a constant temperature 25℃. The results showed that larch woven veneers present significant, rapid, and reversible changes in deflection (6mm opening after 1 hour at 50% humidity). The outputs of this study will inform the development and integration of wood veneer systems within breathable wall constructions for night ventilation.
KEYWORDS: Wood veneer, Moisture-Responsiveness, Climate-responsive, Night ventilation, Adaptive façade

1. INTRODUCTION

Extreme heat waves are becoming frequent and severe due to global climate change [1] with South Asian megacities among the most severely affected [DOI: 10.1126/science.1098704 2]. Night ventilation is known to be an effective passive cooling strategy in the South Asian context [3], with night vents traditionally incorporated in the building skin in South Asian buildings. However, passive night ventilation is less common in modern buildings, particularly in air-conditioned spaces requiring airtightness. Furthermore, traditional night ventilation requires manual control to achieve ventilation at the correct times.

Previous studies have shown that adaptive strategies can minimise the discomfort of indoor overheating through natural ventilation, which is offered by the effect of passive cooling [4]. In this study, the potential of a new generation of humidity-responsive night ventilation systems using bio-based materials, which can be retrofitted to existing buildings in the context of India's capital and megacity, New Delhi, is developed and explored.

Responsive façade systems typically utilise complex control and actuation systems (which are expensive to install and require energy for operation), or materials such as shape memory alloys with high embodied energy and other negative environmental impacts [5] [6]. Using bio-based humidity-responsive materials has potential to provide a ventilation system which autonomously responds to the external environment, whilst minimising the cost and environmental impact of the retrofit intervention.

Wood is an abundant, low-cost, bio-based material used extensively in construction. Wood also exhibits moisture-induced dimensional changes. The moisture content of wood changes in response to changes in ambient relative humidity (RH), expanding when wet and shrinking when dry. In a static building structure, any expansion or contraction of materials is seen as a problem, and carpenters and engineers have developed methods to minimise the impact of these dimensional changes on timber structures. However, the responsive nature of wood can be utilised to create facade elements which continuously respond to changing environmental conditions. Wood is anisotropic, with the greatest moisture-induced movement in the weak cross-grain direction:

typically, 8-10% expansion from oven dry to fully saturated, depending on species. The expansion along the grain is typically an order of magnitude lower [7]. The speed of response to moisture content changes depends on the wood's dimensions. A wooden board (e.g., 20mm thick) will take days to achieve equilibrium with the ambient RH, but a thin piece of wood veneer (e.g., 0.6-1.0mm thick) will start to respond in minutes and achieve equilibrium in hours.

Previous research has explored the potential for using wood veneer as a responsive building element [8][9]. To amplify the 8-10% cross-grain expansion and contraction into a larger movement, researchers create a bilayer material consisting of a wood veneer bonded to a non-responsive material such as plastic or fibreglass [10]. This works well and gives very large deflections but increases the negative environmental impacts of these systems by using non-bio-based materials and creating a composite material that cannot be recycled at the end of life. In this study, a novel single-layer responsive wood veneer system has been designed and tested. Cyclic tests were conducted in a climate chamber based on operational requirements for a night ventilation system in New Delhi.

2. MATERIALS AND METHODS

2.1 Materials

Wood bilayer systems have been developed in previous studies, and their hygroexpansion features are well explained [8]. A novel concept is presented here, involving a single-layer system of wood veneers. In this system, individual wood veneer strips, anchored at both ends, exhibit deflection under RH conditions higher than those at which they were initially secured, as shown in Fig. 1 (Up). Such veneer strips were placed in a woven pattern to create a woven veneer screen, which employs the dimensional response of wood to changes in RH to provide night ventilation.

Different wood species, grain orientations, weave patterns and fabrication conditions were explored to achieve the correct air permeability levels at specified RH levels. Scottish larch, a softwood and a coniferous tree is more prone to moisture absorption and release presenting a tangential and radial expansion coefficient of 9.1% and 4.5% respectively. This characteristic makes it responsive to changes in ambient humidity, leading to observable effects such as swelling and shrinking [11]. Scottish larch, a durable softwood primarily utilized in external cladding, is locally sourced in the UK, making it an ideal choice for this project. For future large-scale applications, indigenous Indian wood species will be employed.

Initially, this work involved a small-scale prototype made from a 6 mm thick, $180\,mm^2$ square plywood panel and a 0.6 mm thick, rotary-cut, Scottish larch veneer sheet. Nine rectangular strips, each measuring 160 mm in length and 30 mm in width, were laser-cut with the grain orientation perpendicular to the direction of the cut to achieve maximum deflection at high RH. These veneer strips were bolted to a 6 mm thick plywood panel measuring 180 mm x 180 mm using bolts with a diameter of 2mm and 20mm spacing. The panel included an aperture opening measuring 150 mm x 150 mm (Fig. 1: Down).

Consequently, a large-scale prototype was created to evaluate the performance of the small-scale one; 1 mm thick Scottish larch strips, 8.2 mm wide, and 44 mm long were fastened onto a 6 mm thick, $600\,mm^2$ square plywood panel. The attachment was achieved by bolting the larch strips onto the plywood. This plywood panel also included a 500 mm x 500 mm aperture opening. Both experimental setups were placed in a climate chamber with a constant temperature of 25^{o}C. During the small-scale tests, the RH was changed between four levels: 20%, 50%, 70% and 90%. These settings were chosen to investigate the moisture responsivity magnitude of the larch veneer strips and to help understand the behaviour of the woven veneer system. For the large-scale test, the RH range was reduced to 20% - 70% to fit with the climatic conditions in New Delhi (see 2.4). Previous tests on the effect of temperature on the wood panels gave negligible results, meaning focusing on the actual RH changes rather than the temperatures expected in New Delhi is useful.

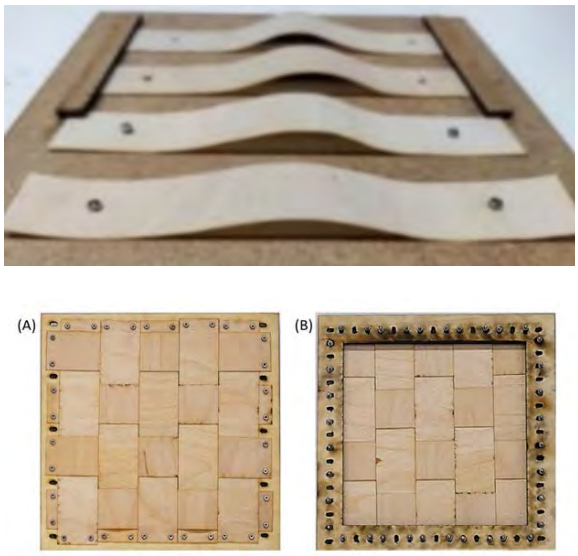

Figure 1: Up: Single layer system of larch veneer strips, fixed at both ends deflecting at RH = 90%. Down: Bio-HNV small-scale prototype (A) front, (B) back of the panel. Overall panel size= 180 mm x 180 mm, window size= 150 mm x 150 mm, Strip width= 30 mm, Strip length= 160 mm, Strip thickness= 0.6 mm.

2.2 Deflection measurements

The out-of-plane deflection of the larch veneers was measured manually using an RS PRO Digital Calliper with an accuracy of 0.1 mm. The maximum deflection was observed at the centre of the panel. The deflection from the panel surface to the highest deflection point was measured to ensure accuracy. Three deflection measurements were taken at different locations surrounding the centre of the panel. The same locations were measured each time, and the results were reported as the mean of these three measurements.

2.3 Cyclic tests

The small-scale cyclic tests lasted 5 consecutive days, and each cycle lasted 4 hours. The first cycle started at a r RH of 20%, where the woven structure remained for 1 hour. During the wetting process, the RH was set at 50% for an hour and was again increased to 70% for another hour. The drying followed the exact pattern until the RH settings were back to 20%.

Adjusting the RH settings in the climate chamber requires approximately 10 minutes for the system to reach a state of equilibrium at the desired RH level. Deflection measurements of the Bio-HNV were taken every 10 minutes until 30 minutes had passed, and then the Bio-HNV would be measured again at 1 hour. The next cycle would start when the Bio-HNV remained for 1 hour at RH=20%. The first two cycles are shown in Fig. 3A.

2.4 Dynamic Building Simulation Analysis for Night Ventilation

In parallel with the experimental work, the operation and practicalities of retrofitting the Bio-HNV systems were tested in the dynamic building simulation software DesignBuilder and EnergyPlus to evaluate their performance on indoor operative temperature and cooling energy demand on a building scale retrofit [12].

For the Base case, a single zone indoor office space (with 100 m^2 area) was modelled (A) with 10m length, 10m width and 3.5m height in Designbuilder with constructions and materials described in Table 1. A window (2.7m X 1.2m) with single-layer clear glass and a shading horizontal lentil on the South façade. There was an air-conditioning (AC) unit — Fan coil unit (4-Pipe) and air-cooled chiller— operating at 100% capacity (in summer) in the office, which operates during office hours from 9 am to 5 pm. The AC unit started to work at 25% capacity at 7-8 am and 50% by 9 am. The AC unit operated at 75% capacity during lunch from 12 noon to 2 pm. Also, the AC unit started to work at 50% capacity between 5 and 6 pm and 25% by 6 pm. The AC unit was not operating outside of office hours, weekends, and holidays. The set point temperature for the AC unit was 26°C and cooling set back was 28°C. There was no night ventilation under the Base case. We used the 'Generic office template' and 0.1110 people/m^2 for the activity template. Also, we used office equipment with a power density of 11.77 W/m^2. While simulating, we created an adiabatic component around the simulation zone's east, north and west sides to expose only the south wall to the outdoors.

The base case has only the window on the South façade, whereas there are Bio-HNV panels above the window in Scenario 1 (B&C). Under Scenario 1, the AC unit and Bio-HNV operated in three schedules: 7 am, 8 am and 9 am. At 7 am, the AC operated like the base case, but the Bio-HNV was operational from 7 pm-7 am. Under the 8 am schedule, the A/C unit started to work at 25% capacity up to 9 am and 50% by 10 am. The AC unit operated at 75% capacity during lunch from 12 noon to 2 pm. Also, the AC unit started to work at 50% capacity between 5 and 6 pm. The Bio-HNV was operational after office hours (6 pm-8 am) at 100% capacity. Under the 9 am schedule, the A/C unit started to work at 25% capacity up to 10 am and 50% by 11 am. During lunch, the AC unit operated at 75% capacity from 12 noon to 2 p.m. Also, the AC unit started to work at 50% capacity between 5 and 6 pm. The Bio-HNV was operational after office hours (6 pm-9 am) at 100% capacity. Bio-HNV scenario 2 had Bio-HNV panels above and under the window on the south façade and maintained the schedules of 7 am, 8 am and 9 am. Expanding of wood was not possible to be simulated directly into the model. We translated the opening of panel wood veneers into the percentage opening of the glazing area under the 'free aperture' option in the simulation model.

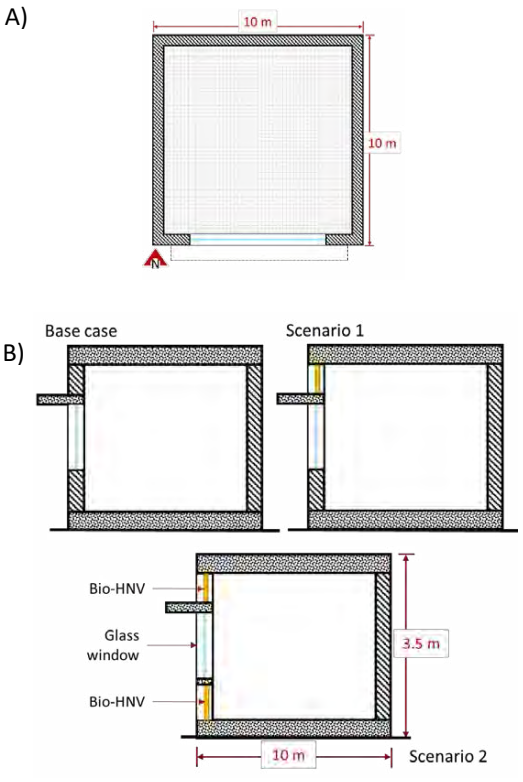

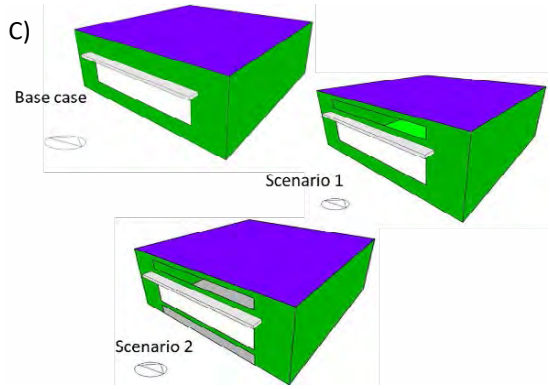

Figure 2: A) Plan of the simulation space, B) Section and C) Designbuilder model of Base case, Scenario 1 and 2. The drawings are not drawn to scale.

Table 1: Construction name, thickness, and materials; for the material properties, we used a software database.

Name	Thickness (m)	Materials	U-Value (W/m^2-K)
Exterior walls	0.280	Brick wall with cement plaster on both sides	1.977
Ground floor	0.925	Solid basement ground floor, uninsulated	1.066
Flat roof	0.200	Concrete slab	2.422
Glass window	0.003	Single-layer Glass windows	5.894

Two temporal analyses were conducted to evaluate the impact of the Bio-HNV on the indoor operative temperature and cooling energy demand. First, we selected three dates in summer (1 April, 1 July, and 2 September) to evaluate the impact on hourly indoor operative temperatures. Secondly, we analysed the effect of Bio-HNV on total summer (April 1-September 30) cooling energy demand.

3. RESULTS AND DISCUSSION

The initial results from the wood veneer experiments showed a significant out-of-plane displacement in response to RH changes. When RH increased from 20% to 50%, the centre of the panel deflected 6 mm out-of-plane within 1 hour. When RH increased from 50% to 70%, the deflection increased to 9.5 mm within 1 hour (Fig. 3A). The Bio-HNV structure deflects out-of-plane, generating spaces between the larch veneers (Fig. 3C), allowing air circulation through the screen at high RH.

The deformation is reversible; when RH is reduced, the woven veneer screen returns to its original position. However, the drying process is slower than wetting. Additionally, in the second cycle, both the sorption and desorption periods are prolonged, indicating that the larch veneers might experience reduced responsiveness after prolonged cyclic changes.

The aim was to illustrate that the woven wood veneer screen opens to allow air circulation when the RH exceeds 50%, reaching its maximum expansion at 70%. To validate this scenario, an extra RH step was introduced during the third cycle, extending its duration to 6 hours from the original 4 hours, with the upper limit of RH set at 90%. After 1 hour at RH = 90%, the Bio-HNV exhibits a greater deflection, measuring approximately 15 mm, as shown in Fig. 3B. The hysteresis curve depicted in Fig. 3B illustrates that, while drying, the wood retains a higher moisture content at a specific RH compared to wetting, a phenomenon attributed to sorption hysteresis [13].

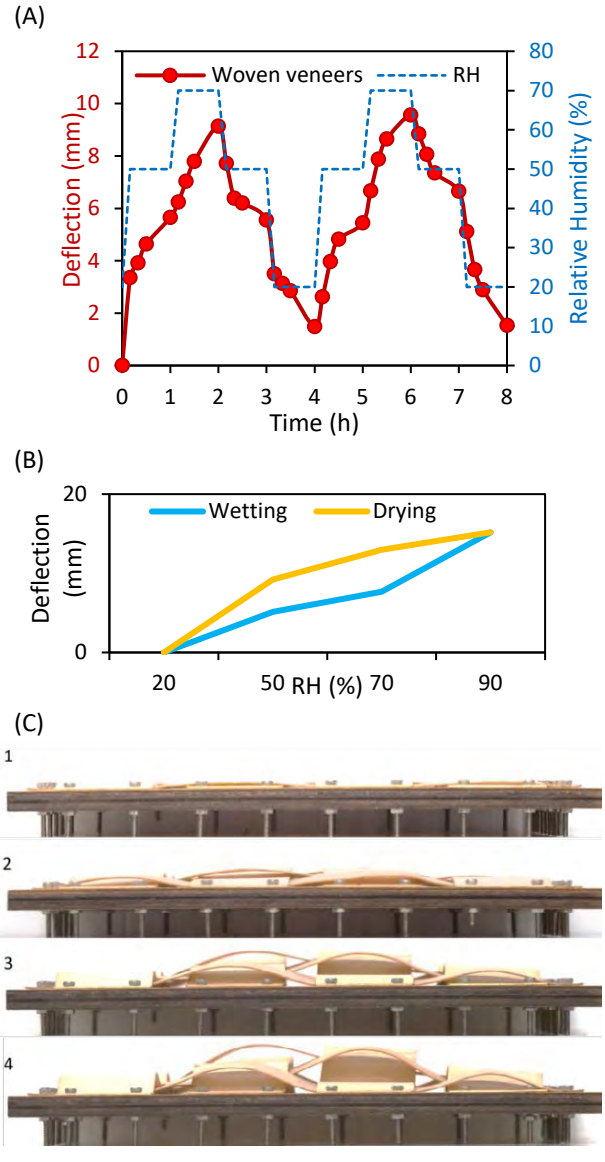

Figure 3: A) Bio-HNV small-scale prototype - Cyclic behaviour between RH = 20%, 50%, 70%. B) Hysteresis Curve of wood veneer swelling during one cyclic test at a constant temperature of 25 C and different RH levels: 20%, 50%, 70% and 90%. C) Humidity responsiveness of the Bio-HNV under different RH levels: (1) 20%, (2) 50%, (3) 70%, (4) 90%.

Upon completion of the small-scale tests, the goal was to upscale the concept to form a bigger structure that would benefit the research by ensuring that the design and functionality of the large-scale prototype would offer similar outputs to the small-scale one. A large-scale prototype was created, as described in section 2.2, and the results illustrated in Fig. 4 reveal that the thick larch strips follow a similar trend to the small-scale, thin larch strips. However, there is a distinction in that the thicker larch strips exhibit a higher deflection, approximately 12 mm, which can be attributed to the expanded span associated with the increased size of the upscaled larch veneer strips.

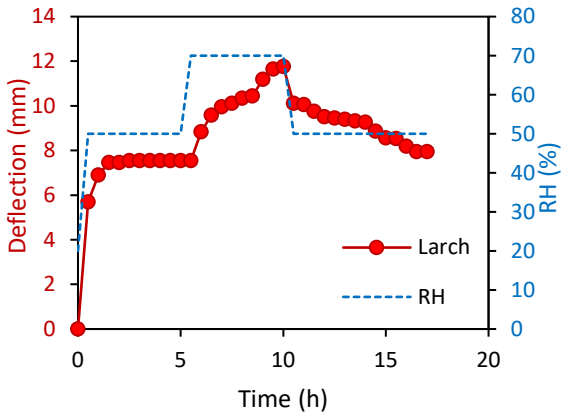

Figure 4: Bio-HNV large-scale prototype - Cyclic behaviour between RH = 20%, 50%, 70%.

This humidity-responsive character of the woven veneer structure was quantified and utilised to design different HNV solutions modelled in DesignBuilder and simulated in Energy Plus to assess the impact on indoor operative temperature, mechanical ventilation, and cooling demand in summer in New Delhi. Considering the Base case, Scenario 1 and 2 with different operational schedules (7 am, 8 am and 9 am), three selected dates in summer: April 1 (starting for summer), July 1 (peak summer), and September 2 (end of summer), the initial simulation results showed a smaller change in average operative temperature. The average operative temperature was 28°C (April 1), 30.8°C (July 1) and 30.7°C (September 2) under the Base case, which flatulated between -1°C to 0.6°C difference under Scenario 1 (Fig. 5A) and 2 compared to Base case, when the outdoor average temperature was 28.9°C (April 1), 32.9°C (July 1) and 32.8°C (September 2).

However, the significant impact of Bio-HNV-induced night ventilation was observed on the total cooling energy demand in summer (April 1-September 30). The total summer cooling energy demand was 9513.87kWh. If the Bio-HNV was operational up to 7 am, it could reduce the total cooling energy demand by 0.64% and 1.46% under Scenarios 1 and 2, respectively, compared to the Base case. However, when the Bio-HNV was operational up to 8 am, the total cooling energy demand was reduced by 6.00% and 6.67% under Scenarios 1 and 2 (Fig. 5B). The total cooling energy demand was reduced by 10.38% and 10.97% under Scenarios 1 and 2 compared to the base case when Bio-HNV was operational up to 9 am.

Therefore, the initial simulation results showed a smaller change in average daily operative temperature due to the application of Bio-HNV units for night ventilation but a significant (more than 10%) reduction in the cooling energy demand in the climatic context of New Delhi, India. Bio-HNV's operation significantly impacted the cooling energy demand with a non-optimal ventilation system (south-facing façade, small openings, no cross ventilation, and no insulation). Fig. 5A showed that the timing of the night ventilation closing was critical, and tuning Bio-HNV's humidity responsiveness for the opening/closing of the woven screen to specific humidity levels would be vital. Studies have shown that in India's hot-humid climatic context, cross-ventilation might increase the effectiveness of night ventilation with greater air circulation, ventilation strategies, building orientation and shape, wind speed, and wind direction [14, 15]. To improve the effectiveness of Bio-HNV, further studies on cross ventilation, room proportions, internal insulation, outdoor shading, opening sizes, and wind to induce air movement need to be explored with fluid dynamics simulation and physical prototype testing to develop a functional and high-performance bio-based responsive night vent for climate resilience to extreme heat in New Delhi [1].

A)

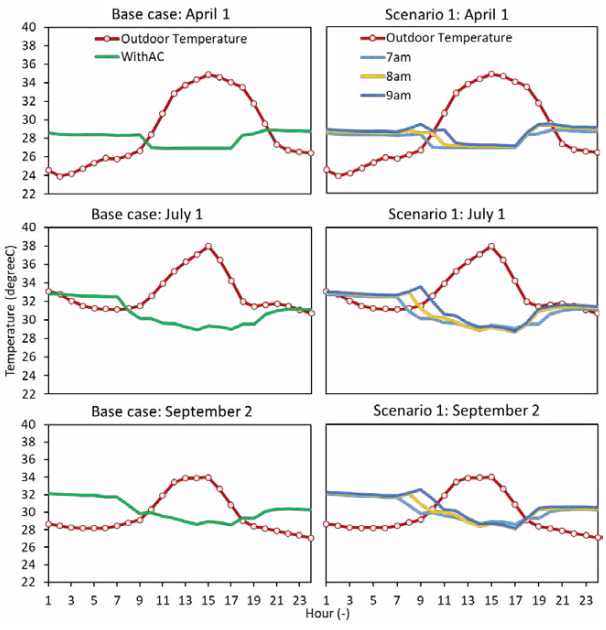

B)

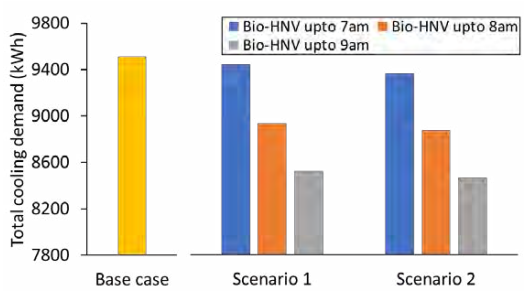

Figure 5: A) Hourly indoor operative temperature on April 1, July 1 and September 2 under the Base case and Scenario 1. Furthermore, we presented only the base case and Scenario 1 as the small differences between Scenarios 1 and 2; B) Total summer cooling energy demand.

4. CONCLUSION

This study assessed the humidity responsiveness and cyclic behaviour of a woven structure composed of larch wood veneers. The primary goal was to develop a naturally moisture-responsive system with the potential for application as a bio-based responsive night vent in buildings in New Delhi. The study aimed to explore the optimal design and functionality of this smart system within the specific climatic conditions of New Delhi.

The cyclic tests were conducted within a climate chamber at a consistent temperature of 25℃, varying between four specific RH levels: 20%, 50%, 70%, and 90%. The tests aimed to explore the degree and duration the Bio-HNV system undergoes expansion and contraction in response to diverse RH conditions. Results obtained from the cyclic tests on both the small-scale and large-scale Bio-HNV prototypes exhibited promising humidity-responsive characteristics in larch woven veneer strips across four distinct RH levels: 20%, 50%, 70%, and 90%. Significant deformation was observed at elevated RH in both small-scale and large-scale prototypes, with an average deflection of 9.5 mm and 12 mm, respectively, indicating the robust responsiveness of the system.

Initial simulation results showed a smaller impact on the average operative temperature due to the application of Bio-HNV units for night ventilation but a significant (more than 10%) reduction in the summer cooling energy demand in the climatic context of New Delhi, India. This study was the first step towards a functional and high-performance bio-based responsive night vent for climate resilience to extreme heat in New Delhi. With further development, Bio-HNV, a passive design solution, could reduce the active cooling and mechanical ventilation energy demand and create a circular, lightweight, modular wall component to be retrofitted on existing building skins.

ACKNOWLEDGEMENTS

This research was funded by the Leverhulme Trust as part of the 'RESPIRE: Passive, Responsive, Variable Porosity Building Skins' Research Project Grant (RPG-2021-023). We would like to thank Meteoblue (www.meteoblue.com) for the climate data collaboration.

REFERENCES

1. Debnath, K. B., Jenkins, D., Patidar, S., Peacock, A. D., & Bridgens, B. (2023). Climate change, extreme heat, and South Asian megacities: Impact of heat stress on inhabitants and their productivity. ASME Journal of Engineering for Sustainable Buildings and Cities, 4(4).
2. Meehl, G.A., Tebaldi, C., (2004). More Intense More Frequent and Longer Lasting Heat Waves in the 21st Century. Science DOI: 10.1126/science.1098704
3. Sadineni, S.B., Madala, S., Boehm, R.F., (2011). Passive building energy savings: A review of building envelope components. Renewable and Sustainable Energy Reviews 15:3617–3631
4. Lamberti, G., Contrada, F., Kindinis, A., (2023). Exploring adaptive strategies to cope with climate change: The case study of Le Corbusier's Modern Architecture retrofitting. Energy Build 113756.
5. Sommese, F., Badarnah, L., Ausiello, G., (2023). Smart materials for biomimetic building envelopes: current trends and potential applications. Renewable and Sustainable Energy Reviews 188
6. Yi, H., Kim, Y., (2021). Self-shaping building skin: Comparative environmental performance investigation of shape-memory-alloy (SMA) response and artificial-intelligence (AI) kinetic control. Journal of Building Engineering 35.
7. Hoadley, R.B., (2000). Understanding wood. Taunton Press Inc, ISBN: 9781561583584
8. Holstov, A., Bridgens, B., Farmer, G., (2015). Hygromorphic materials for sustainable responsive architecture. Construction Build Mater 98:570–582.
9. Menges, A., Reichert, S., (2012). Material capacity: Embedded responsiveness. Architectural Design 82:52–59.
10. Reyssat, E., Mahadevan, L., (2009). Hygromorphs: From pine cones to biomimetic bilayers. Journal of the Royal Society Interface. https://doi.org/10.1098/rsif.2009.0184
11. Ross, R.J., (2010). Wood Handbook : wood as an engineering material. Forest Products Laboratory, Centennial Edition. https://doi.org/10.2737/FPL-GTR-190
12. Debnath, K.B., Pynirtzi, N., Scott, J., Debnath, K.B., Davie, C., Bridgens, B., (2023). Potential of relative humidity as a proxy of air temperature in developing passive and adaptive building façades with bio-based responsive material. CEES 2023
13. García, E. L., Gril, J., De Palacios, P., Guindeo, C. A., (2005). Reduction of wood hygroscopicity and associated dimensional response by repeated humidity cycles. Annals of Forest Science 62(3), DOI: 10.1051/forest:2005020
14. Stasi, R., Ruggiero, F., Berardi, U., (2024). Influence of cross-ventilation cooling potential on thermal comfort in high-rise buildings in a hot and humid climate. Build Environ 248: 111096
15. Prabhakar, M., Saffari, M., de Gracia,. A, Cabeza, L.F., (2020). Improving the energy efficiency of passive PCM system using controlled natural ventilation. Energy Build 228: 110483.

PLEA 2024 WROCŁAW
(Re)thinking Resilience

Urban Heat Island Visualization and Analysis Platform.

The case of the 100 most populated Mexican cities.

ITZIA GABRIELA BARRERA-ALARCÓN[1], RODRIGO TAPIA MCCLUNG[1], CAMILO ALBERTO CAUDILLO COS[1], JORGE ALBERTO MONTEJANO ESCAMILLA[1] , VÍCTOR ALBERTO ARVIZU-PIÑA[2]

[1] Centro de Investigación en Ciencias e Información Geoespacial, Ciudad de México
[2] Iberoamericana Ciudad de México, Ciudad de México, México.

The urbanization process based on the artificialization of the natural coverage of the environment, as well as the various anthropogenic activities and the urban structure, are the main reasons that give rise to the phenomenon of the Urban Heat Island, which is identified from the thermal differences existing between urban areas and their surroundings. Identifying these areas within cities is of utmost importance because it allows us to locate areas where there is greater thermal vulnerability associated with high temperatures and that may be related to socioeconomic deficiencies, characteristics of precarious housing and age of the local population. This work presents a visualization and analysis tool of the Urban Heat Island in the 100 most populated Mexican cities, based on the presentation of day and night Land Surface Temperature cartography and urban land use.
KEYWORDS: Urban Heat Island, Visualisation Platform, Urban land use.

1. INTRODUCTION

Over the past seven decades, Mexico has experienced a rise of roughly 0.71 °C in average temperatures above the long-term climatic average [1]. This temperature increase is aligned with the global trend highlighted by the Intergovernmental Group of Experts on Climate Change (IPCC) [2]. Both minimum and maximum temperatures indicate a shift towards more warm and fewer cold nights across the nation. Projections suggest that between 2015 and 2039, the average annual temperature in Mexico will have increased by 1.5 °C, with the northern regions experiencing an even more significant increase of 2 °C.

Nonetheless, the way vulnerability and risk are distributed within urban areas is shaped by various individual and household factors, including income, the range of assets owned, health status, age, and gender. It is also influenced by their ability to anticipate, withstand, respond to, recover from, adapt to, and capitalize on hazards and stresses [3].

The Urban Heat Island (UHI) phenomenon has been studied extensively in various cities around the world. In Mexico, however, it is a topic of recent interest that has only been studied for some cities in the country. Most have focused on the analysis of the atmospheric UHI, its relationship with the urban environment, and the proposal mitigation strategies [4].

We study the phenomenon of surface UHI in the 100 most populated cities in the country – including metropolitan areas, conurbations, and urban centers with a population greater than 2,500 inhabitants – (Fig 1). This study focused on establishing the relationship between the intensity of thermal differences, urban form, functional structure, and climate.

Figure 1. The 100 most populated Mexican cities from the 2015 National Urban System definition.

Based on the obtained results, a visualization platform of the heat island phenomenon was developed based on the analysis of daytime and nighttime land surface temperatures and urban land use determined for the 100 cities under study. On the one hand, this will allow decision makers to support the generation of public policies regarding prevention, mitigation, and adaptation to high-risk urban thermal effects, and, on the other, aims at opening new research and collaboration niches in this area.

2. METHODS

Study location and period

As previously mentioned, the study analyzes the 100 most populated cities in Mexico according to the 2015 National Urban System, which includes 59

metropolitan areas, 16 conurbations, and 25 urban centers [5].

Land use data

Census data for 2020 from the National Institute of Statistics and Geography [6] were used, expressed through the Basic Geostatistical Areas (AGEB). The National Geostatistical Framework was used at the block level to identify housing use and define density. To identify the destinations of the land (equipment, various facilities and infrastructure), the specific geographic data contained in the Census Information Query System (particularly the Public Infrastructure System) is used and is complemented with points derived from the National Statistical Directory of Economic Units (DENUE) [7].

The primary land use classification for this study comprises ten categories that are commonly employed in Mexican urban planning (Table 1) and are adapted from [8].

Table 1. Land use categories

Land Use Classification	Code
High Density Housing	H-a
Medium Density Housing	H-m
Low Density Housing	H-b
High Density Mixed Housing	HM-a
Mixed Medium Density Housing	HM-m
Specialized Mixed	M
Equipment	E
Commerce and Services	CS
Industry	I
Sports, Recreation and Green Areas	AV

Remote sensing information extraction and processing

The methodology used for remote sensing was developed in four stages: download high (Landsat 8) and low resolution (MODIS) satellite imagery; calibrate Landsat bands; compute Land Surface Temperature (LST); and integrate results from different scales.

For the 100 cities, 117 Landsat 8 scenes were downloaded from the United States Geological Survey (USGS) [9]. Daytime images were downloaded for dates between January and December, 2018 with processing levels generated by the USGS.

Subsequently, the calibration of Landsat bands at reflectance levels was carried out, the calculation of the NDVI (Normalized Difference Vegetation Index) and the emissivity of the Earth's surface, from which the Land Surface Temperature was obtained.

Land surface temperature (LST) for the Modis sensor was downloaded as products MOD11A2 v006 and MYD11A2 v006, provided as an average of 8 days per pixel with a spatial resolution of 1 kilometer.

Daytime LST data were obtained from Landsat imagery at 30 m resolution and nighttime LST from MODIS at 1 km resolution. Therefore, spatial thermal sharpening needs to be applied to Modis to achieve a finer spatial resolution. This is done using the TsHARP algorithm [10], a technique based on the assumed relationship between NDVI and LST within a sensor scene. However, the slope of this relationship varies with land cover and climate [11].

Results of the thermal sharpening technique were compared with the original LST result of the corresponding MOD11A2 v006 and MYD11A2 v006 products. Agam [10] proposed the evaluation of the recovery precision by measuring the level of agreement between the reference temperature fields ($T_{R\,ref}$) and the temperature with the applied technique ($\widehat{T_{R\,high}}$). They are evaluated using the Root Mean Square and the Mean Absolute Errors (RMSE and MAE, respectively) and are calculated using the following formulas:

$$RMSE = \sqrt{\frac{1}{n}\sum_{i=1}^{n} \left(\widehat{T_{R\,high}} - T_{R\,ref}\right)^2} \quad (1)$$

$$MAE = \frac{1}{n}\sum_{i=1}^{n} \left|\widehat{T_{R\,high}} - T_{R\,ref}\right| \quad (2)$$

Isotherms

Isotherms are imaginary lines that connect points with the same temperature on a map. The regions between these lines represent areas where the temperature remains constant. In this case, they are used to visualize and understand patterns of rise and fall of temperature in cities.

Calculating contour polygons for LST rasters varying by 1 °C yields isotherm regions for each city, for both day- and nighttime.

After obtaining both day- and nighttime LST values for each pixel at 30m resolution, pixel values within each AGEB were averaged to enable direct comparisons with different land uses.

Using the centroid of each AGEB, a continuous surface was interpolated using the inverse distance weighting method with a cell resolution of 100 m and an exponent of 2. From there, isotherms were obtained for every degree Celsius and vectorized to represent areas with a specific range of temperature.

Platform development

The platform is developed using JavaScript, both on the server and the client. NodeJS is used on the server to query vector tiles. On the client, Mapbox GL JS is used to render interactive maps and layers, allowing users to pan and zoom, as well as change the bearing and tilt the user's horizontal orientation.

Users can scroll through the available cities or use the search box to limit the options. Whenever the user selects a city, the map is moved to the corresponding area of the country and displays the Landsat LST contours. Users can switch between Landsat and Modis to compare and explore the UHI phenomenon. Users can select from a list of predefined or draw their own transects to slice the city and populate a temperature-land use profile graph. This allows for quick identification of possible trends in land use and higher or lower temperatures. While hovering the mouse pointer over dots on the graph it is possible to locate where that point corresponds to the map. Users can also adjust transects' distances to obtain a finer or coarser profile graph, ranging from 300 m to 2,500 m. Depending on the urban structure of the city and the transect used, the profile graph may not show a continuous curve, as it is populated using urban blocks only. Charts are created using amCharts and spatial operations are performed with Turf.js.

Apart from using the land use categories from Table 1, depending on the extent of the selected transects, data from the European Space Agency's WorldCover project [12] are also queried to populate the profile chart. However, because isotherms are available only for urban AGEBs, the chart may contain a discontinuous line. Land use categories on the x-axis, however, are complete.

3. RESULTS

The main goal of this platform is to serve as a resource for examining and analyzing the occurrence of UHI phenomena in the 100 most populated cities within the Mexican National Urban System. Potential users include researchers, students, urban planners, and policymakers.

It allows for comparative analyses between daytime and nighttime LST and their relationship with land use. Furthermore, work is currently underway to incorporate a vulnerability index, together with a thermal well-being risk index, and accessibility to the nearest health infrastructure for early care and/or heat stroke emergencies. Another short-term goal is to enable automatic monthly imagery processing and isotherm extraction for the platform to stay up-to-date with relevant isotherms and allow the study and visualization of their spatio-temporal evolution.

At its current development stage, it enables users to visualize and compare day and nighttime temperatures for the 100 cities assessed in 2018, specifically during their respective warmest months (Fig. 2).

The platform allows users to observe the temperature distribution within the city, together with temperature ranges spanning from the highest to the lowest, both during the day and at night (Fig. 3).

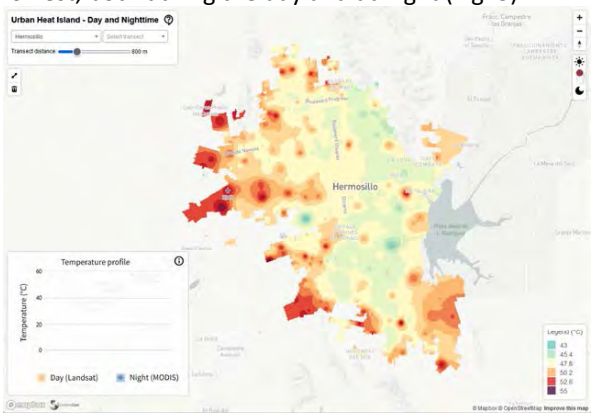

Figure 2: Diurnal Urban Heat Island Platform visualization. Example for the city of Hermosillo.

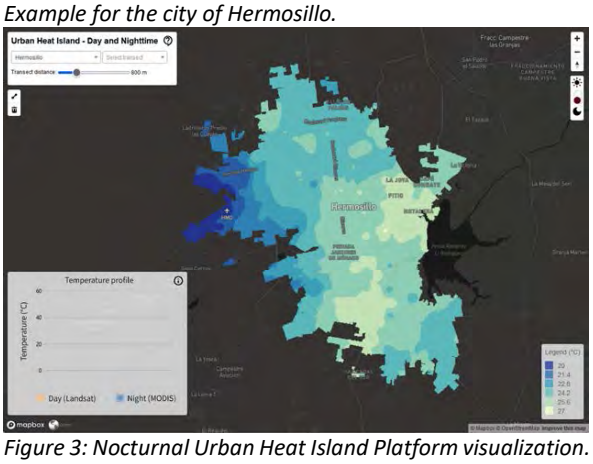

Figure 3: Nocturnal Urban Heat Island Platform visualization. Example for the city of Hermosillo.

3.1 Thermal profiles

As part of the analyses that can be performed on the platform, thermal profiles allow for graphical representations of temperature variations in a specific geographical area of the cities, both during day and night. These profiles can illustrate how temperatures change along predefined or user-drawn transects. The spacing between each measurement point can be adjusted by the user (ranging from 300 to 2,500 meters apart), or preloaded options can be used. Furthermore, the thermal profile, in its graphs, displays both daytime and nighttime temperatures along with their corresponding land use.

Figure 4 shows examples for the city of Hermosillo, located in the State of Sonora, in the northern part of the country. It is characterized by an extreme hot-dry climate, with an average annual temperature of 24.82 °C, a maximum annual average temperature of 32.2 °C, June is the warmest month of the year with an average monthly temperature of 39.6 °C, July has the highest average temperature of 32.6 °C, January registers the lowest average temperature of 16.6 °C, and, with respect to the average minimum monthly

temperature, August has the highest with 25.9 °C and January the lowest with 8.9 °C [13].

When tracing the thermal profile in the northern area of the city, it can be observed that the highest LST during the day occurs in mixed residential urban land use of medium intensity with 51 °C, but during the night it drops to 23 °C. Using the same profile, it is possible to identify the area with the lowest LST, which corresponds to equipment, with a daytime temperature of 47 °C and a nighttime temperature of 25 °C.

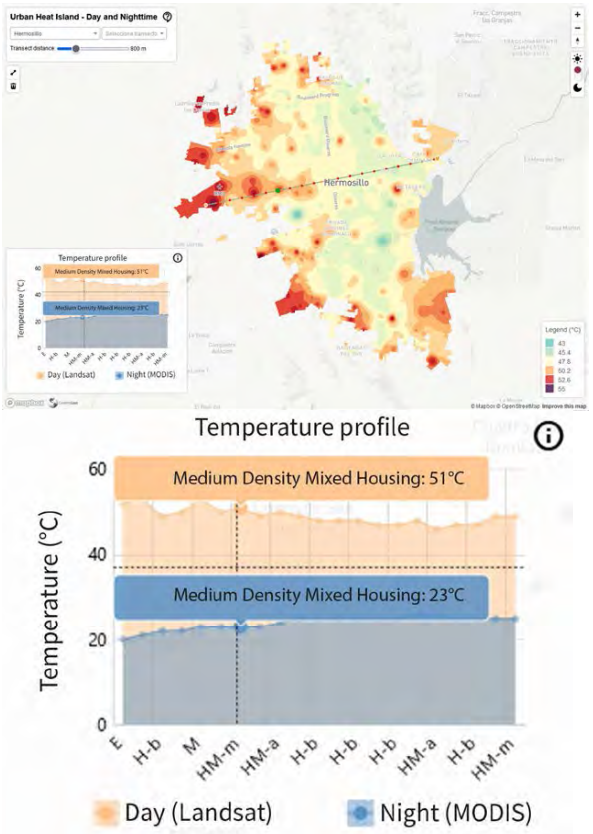

Figure 4: Thermal profile example for the city of Hermosillo.

4. CONCLUSION

This platform raises the possibility of socializing the results and information generated in different research projects related to Urban Heat Island, urban form, structure, and climate. The use of this platform and its associated results are helpful in developing mitigation strategies related to urban heat island and land use. When social, economic, and health indicators are incorporated into the platform, it becomes even more relevant to study the impact of where the most vulnerable population is located and their relationship with how they access public health services and infrastructure. With this, it is possible to make better decisions in terms of planning and designing more resilient cities that, in turn, are better prepared to face climate change and its associated consequences.

ACKNOWLEDGMENTS

The authors thank the Research Department of the Universidad Iberoamericana Ciudad de México for financing the presentation of this work.

REFERENCES

1.Murray-Tortarolo, G. N. (2021). Seven decades of climate change across Mexico. Atmosfera, 34(2), 217–226. https://doi.org/10.20937/ATM.52803

2. IPCC. (2023). Summary for Policymakers: Synthesis Report. Climate Change 2023: Synthesis Report. Contribution of Working Groups I, II and III to the Sixth Assessment Report of the Intergovernmental Panel on Climate Change, 1–34.

3. J. Hardoy and P. Romero Lankao, “Latin American cities and climate change: Challenges and options to mitigation and adaptation responses,” Curr. Opin. Environ. Sustain., vol. 3, no. 3, pp. 158–163, 2011.

4. Barrera-Alarcón, I. G., Camilo, C. cos, Sandra, M. F., Gerardo, Á. J., & Jorge, M. E. (2022). La isla de calor urbano superficial y su manifestación en la estructura urbana de la Ciudad de México. Revista de Ciencias Tecnológicas RECIT, 5(3), 312–330.

5. Consejo Nacional de Población. (2018). Sistema Urbano Nacional y zonas metropolitanas 2015, [Online], Available at: https://www.gob.mx/conapo/documentos/delimitacion-de-las-zonas-metropolitanas-de-mexico-2015

6. INEGI. Instituto Nacional de Estadística y Geografía. (2020). México en cifras, [Online], Available: https://www.inegi.org.mx/app/areasgeograficas/?ag=09#collapse-Resumen.

7. INEGI. Instituto Nacional de Estadística y Geografía. (2016). Directorio Estadístico Nacional de Unidades Económicas, [Online], Available: https://www.inegi.org.mx/app/mapa/denue/

8. R. Tapia-McClung, G. Ávila-Jiménez, J. Montejano-Escamilla, C. Caudillo-Cos, and I. G. Barrera-Alarcón, “Estimación de uso de suelo del Sistema Urbano Nacional en nivel manzana 2020”, 2022, [Online], Available: https://zenodo.org/records/7626566

9. USGS. (2020). United States Geological Survey., [Online], Available: https://www.usgs.gov

10. N. Agam, W. P. Kustas, M. C. Anderson, F. Li, and C. M. U. Neale, “A vegetation index based technique for spatial sharpening of thermal imagery,” Remote Sens. Environ., vol. 107, no. 4, pp. 545–558, 2007.

11. A. Karnieli, M. Bayasgalan, Y. Bayarjargal, N. Agam, S. Khudulmur, and C. J. Tucker, “Comments on the use of the Vegetation Health Index over Mongolia,” Int. J. Remote Sens., vol. 27, no. 10, pp. 2017–2024, 2006.

12. Zanaga, D., Van De Kerchove, R., De Keersmaecker, W., Souverijns, N., Brockmann, C., Quast, R., Wevers, J., Grosu, A., Paccini, A., Vergnaud, S., Cartus, O., Santoro, M., Fritz, S., Georgieva, I., Lesiv, M., Carter, S., Herold, M., Li, Linlin, Tsendbazar, N.E., Ramoino, F., Arino, O., 2021. *ESA WorldCover 10 m 2020 v100.* [Online] Available: https://zenodo.org/records/5571936

13. Servicio Nacional de Meteorología. (2010). Normales Climatológicas, Hermosillo, [Online], Available: https://smn.conagua.gob.mx/tools/RESOURCES/Normales8110/NORMAL26139.TXT

PLEA 2024 WROCŁAW
(Re)thinking Resilience

Strategies for Enhancing Non-visual Effects in Indoor Environments with Daylight

ADRIANA ALICE SEKEFF CASTRO[1] CLÁUDIA NAVES DAVID AMORIM[1]

[1] University of Brasília, Brasília, Brazil.

ABSTRACT: Natural light in architecture brings numerous benefits to human health, as well as playing a critical role in synchronizing the circadian rhythm due to the 24-hour light/dark cycle, impacting health and performance in activities that require concentration and learning. This article aims to explore architectural strategies to increase the quality of non-visual effects in the classroom using natural light. This article comprises two phases: a systematic literature review and a computer simulation of a real classroom located at a university in the tropical climate of the Southern Hemisphere. As a result, material reflectance, window to wall ratio - WWR and user orientation impacted non-visual effects. Regarding the layout of the classroom, it is recommended that the user is positioned to the side of the window. As a conclusion: pay attention to the reflectance used and the layout used in the environment. It is suggested that new standards could include target values and a protocol for measuring non-visual effects.
KEYWORDS: Non-visual effects, Daylight, Comfort, Classroom.

1. INTRODUCTION

Daylight in architecture has numerous benefits, encompassing aspects related to human health, reduced energy consumption, and environmental resilience [1-3]. Studies [4], emphasize that daylight can provide the optimal combination of light at specific times, making it a crucial primary source of human biological lighting. This perspective aligns with the stance of the *Commission Internationale de l'Eclairage* - CIE concerning the biological effects of light [5].

Many studies have focused on lighting within interior spaces, concentrating its visual and/or energy performance [6-10]. However, the incorporation of new standards for assessing lighting began following the discovery of intrinsically photosensitive retinal ganglion cells (ipRGCs) in 2001 [11-14]. The discovery sparked various multidisciplinary investigations into the non-visual effects [5,15]. These effects, which are accessed via the retina of the eye, have diverse influences, including neuroendocrine responses, alertness levels, mood, circadian rhythm and performance in activities that require concentration and learning [16]. Daylight plays a critical role in synchronizing the circadian rhythm due to the 24-hour light/dark cycle of the local environment. Through architectural strategies, how to increase the quality of the non-visual effect of light with daylight? Benefiting the health of the user and increasing the resilience of the environment (lower energy consumption).

This article aims to explore architectural strategies for increasing the quality of non-visual effects in the classroom (place of high permanence during the user's routine) with the use of daylight.

This article is part of an ongoing doctoral thesis.

2. METHOD

This article comprises two phases: a systematic review of the literature and a computer simulation of a real classroom located at a university in the tropical climate of the southern hemisphere. This classroom is the basis of subsequent computer simulations with the application of the best architectural strategies.

2.1 Systematic literature review

The systematic literature review is the first phase of the study. Its objective is to identify architectural strategies and ways of evaluating non-visual effects.

Articles published in the last five years were researched, coming from two databases, Scopus and Web of Science. Several keywords were used: metric, 'non-visual effect*', 'non-image-forming', NIF, 'circadian light*', monitoring, measurement, simulation, 'field evaluation', assessment, evaluation, 'human centric lighting', 'integrative lighting', 'circadian lighting', 'circadian stimulus', 'lighting projects', daylight*, classroom.

The selected article search type on the platforms was 'title, abstract, keyword' on Scopus and 'topics' on Web of Science. After the search, filters were applied: document type - article and review article; only in English language; published in journals.

2.2 Simulation

For the simulation, a real classroom located in a building with high bioclimatic and energy potential on

the university campus was used. Applied software: modeling, Rhinoceros; visual effects, ClimateStudio; non-visual effects, Adaptive Lighting for Alert (ALFA). The metrics applied in the study: visual effect of light - Spatial Autonomy of Daylight (sDA), Useful Illuminance of Daylight (UDI), Annual Exposure to Sunlight (ASE); and, non-visual effect of light, Equivalent Melanopic Lux (EML). Although the study focuses on non-visual effects, visual effects should not be discarded and will be evaluated according to current regulations in the country. Simulated times will be 9am, 11am, 3pm, 5pm.

The definitions of the number of simulations will be defined after the first stage, the systematic literature review, which may provide information on architectural strategies observed in the articles researched.

2.3 Case study - real classroom

The existing classroom used in the case study of this article measures 9.60 meters (width - window facade) by 13.60 meters (depth), with a ceiling height of 3.48 meters. Located on the campus of the University of Brasília - UnB, situated in the city of Brasília, in the Federal District - the capital of Brazil (15° 46′ 48″ South, 47° 55′ 45″ West). It is situated in a building known as the Bloco de Sala de Aula Norte - BSAN, constructed in 2015.

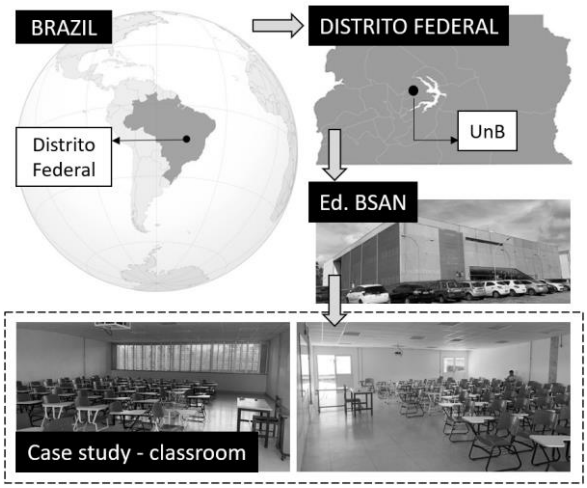

Figure 1: Geographic location of the classroom.

3. RESULTS

The initial outcome stemmed from the systematic literature review, followed by a selection of perspectives to evaluate the non-visual effects on lighting within the environment to identify the best design strategies.

3.1 Systematic literature review

The systematic review resulted in the selection of 41 articles. It was possible to identify various methods of evaluating non-visual effects, with the use of computer simulation being one of the most popular.

However, there is no consensus on the best way to conduct computer simulations to assess non-visual effects in the environment. This article utilized the basis of various papers as evaluation strategies, such as: variations in the internal reflectance of the environment [17,18,19], window dimension - Window-to-Wall Ratio (WWR) [18,20,21], layout of the space [15,16,22,23], impact of natural lighting throughout the year [2,15,22,23], and the impact of natural light at different times of use in the environment [2,15,22,23].

Among the software used for assessing non-visual effects, ALFA stood out as one of the most recommended [24,25]. Its outputs are measured in Equivalent Melanopic Lux – EML [25], one of the most used metrics for evaluation.

There is no consensus on the recommended dosage; however, this article will adopt the proposal of researcher T. Brown (275 EML), as it is part of important research groups in the field and serves as a reference for various other researchers. This dosage has also been adopted by the WELL Building Standard building certification [26,27,28].

3.2 Simulation method definition

Three distinct types of panoramas were conducted, culminating in 12 diverse simulation scenarios within the ClimateStudio software. Yet, to employ ALFA, which replicates the environment at precise moments (9am, 11am, 3pm, 5pm), 48 simulations became imperative. The proposed panoramas in this study, were:

- Panorama 1 - WWR = 61.45% (existing room with brises), and:
  - Scenario 1a: Reflectance - 90% (ceiling), 80% (wall), 40% (floor); December 21st (summer solstice); Scenario 1b: Reflectance same as scenario 1a, and June 21st (winter solstice);
  - Scenario 2a: Reflectance - 70% (ceiling), 50% (wall), 20% (floor); December 21st (summer solstice); Scenario 2b: Reflectance same as scenario 2a, and June 21st (winter solstice).
- Panorama 2 - WWR = 33,52% (with brises), and:
  - Scenario 3a: Reflectance - 90% (ceiling), 80% (wall), 40% (floor); December 21st (summer solstice); Scenario 3b: Reflectance same as scenario 3a, and June 21st (winter solstice);
  - Scenario 4a: Reflectance - 70% (ceiling), 50% (wall), 20% (floor); December 21st (summer solstice); Scenario 4b: Reflectance same as scenario 4a, and June 21st (winter solstice).
- Panorama 3 - WWR = 83,80% (with brises), and:

- Scenario 5a: Reflectance - 90% (ceiling), 80% (wall), 40% (floor); December 21st (summer solstice); Scenario 5b: Reflectance same as scenario 5a, and June 21st (winter solstice);
- Scenario 6a: Reflectance - 70% (ceiling), 50% (wall), 20% (floor); December 21st (summer solstice); Scenario 6b: Reflectance same as scenario 6a, and June 21st (winter solstice).

Simulations were carried out considering the real size of the classroom window (Panorama 1), as well as simulations considering the decrease (Panorama 2) and increase (Panorama 3) in the existing WWR.

The reflectance percentages used in the study fall within the acceptable range according to the Brazilian standard [29,30]. Tables 1 and 2 contain the materials inputted into the ClimateStudio and ALFA programs. No special material was created; only existing materials within the software were used. The material choices are associated with the specified reflectance percentage in each simulation proposal. Table 1 shows the highest reflectance percentages that can be used within the indoor environment - ceiling, wall, and floor [29,30].

Table 1: Layers and their respective material configurations in the ClimateStudio and ALFA software - employing the highest reflectance (%). Scenario 1a, 1b, 3a,3b, 5a, 5b

Layer	Material (standard in ClimateStudio)
Glass	Clear
Ceilling	Acoustic Ceilling Tile
Walls	Matte White wall
Floor	Grey Concrete Exterior Floor
Shading (brises)	Aluminium Grey Exterior Clading
Doors	Aluminium Door
Frames	Aluminium Window Mullion
Layer	**Material (standard in ALFA)**
Glass	Single Plane Clear 6mm Tvis 88%
Ceilling	Bristol Board
Walls	White Painted Corridor Walls
Floor	Wheat Bread
Shading (brises)	Aluminium White Cladding
Doors	Aluminium White Cladding
Frames	Aluminium White Cladding

Table 2 presents the lowest permissible reflectance percentages according to the Brazilian standard, considering their use in the indoor environment - ceiling, wall, and floor.

Table 2: Layers and their respective material configurations in the ClimateStudio and ALFA software - employing the lowest reflectance (%). Scenario 2a, 2b, 4a,4b, 6a, 6b.

Layer	Material (standard in ClimateStudio)
Glass	Clear
Ceilling	Ceilling LM83
Walls	Wall LM83
Floor	Floor LM83
Shading (brises)	Aluminium Grey Exterior Clading
Doors	Aluminium Door
Frames	Aluminium Window Mullion
Layer	**Material (standard in ALFA)**
Glass	Single Plane Clear 6mm Tvis 88%
Ceilling	White Sport Shirt
Walls	Light Grey Eletrical Chase
Floor	Dark Grey Floor Tiles
Shading (brises)	Aluminium White Cladding
Doors	Aluminium White Cladding
Frames	Aluminium White Cladding

The materials of the layers - doors, windows, shading (brises), and glass - remained unchanged for all simulations.

The simulations began with ClimateStudio to assess visual effects, as a lighting design proves useful only if it meets minimum quality standards regarding the visual impact of light. Parameters for acceptable natural light in the environment on the horizontal plane, at 0.75m from the floor, include Spatial Daylight Autonomy (sDA) - 300 lux for 50% of the area for 50% of daylight hours; Useful Daylight Illuminance (UDI) - 300 < useful illuminance for the user > 3000 lux [31,32]. In ALFA, 240 sensors were placed at 1.60m intervals (Figure 2), at a height of 1.20m on the vertical plane, to evaluate non-visual effects. Its parameter considers sensors with EML>275 as positive indicators for the non-visual effects of light (Figure 2)[26,27].

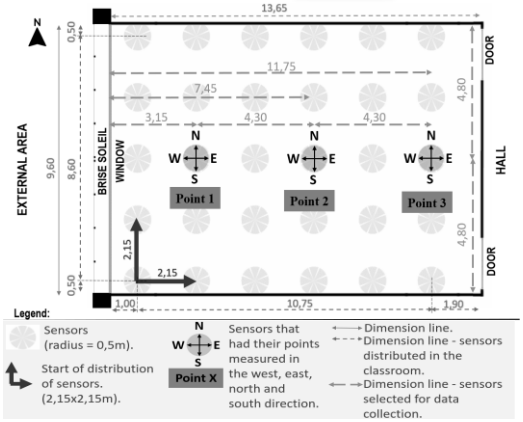

Figure 2: Classroom floor plan indicating the EML measurement sensors in the ALFA software and marking the EML survey points in the four orientations (north, east, south, and west). Sizing in meters (m).

The points (1,2,3) were intentionally selected to be in the middle, reducing interference from walls regarding light reflection, and their distance from the window was analyzed to better represent the impact of window distance on natural light entry. These points aim to analyze the optimal orientations (room layout) and window distance to achieve results greater than 275 EML.

3.3 Results of simulations and analisys

The results are compiled from various simulations and tabulations. For the presentation of results, we

will first display the outcomes for visual effects and subsequently those obtained for non-visual effects. Figure 3 displays the results obtained for sDA and UDI for all combinations.

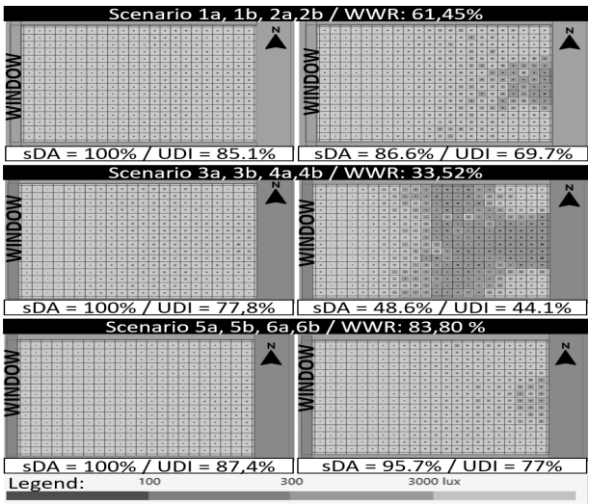

Figure 3: ClimateStudio result - sDA and UDI.

In general, despite the modification of the WWR, the greatest impact was observed in the change in the reflectances of the materials in the environment. Worst results in Scenario 2a,2b,4a,4b,6a,6b - 70% (ceiling), 50% (wall), 20% (floor).

The simulations for non-visual effects generated a greater number of data, there were 48 simulations, and for each simulation data was collected from the 3 central points in the four directions (north, east, south, west) (Table 3). In Figure 3, the analysis of the best to worst orientation regarding non-visual effects within the study environment. In this analysis, possible obfuscations are not taken into account, as the aim was only to understand which orientations received the most stimuli in EML.

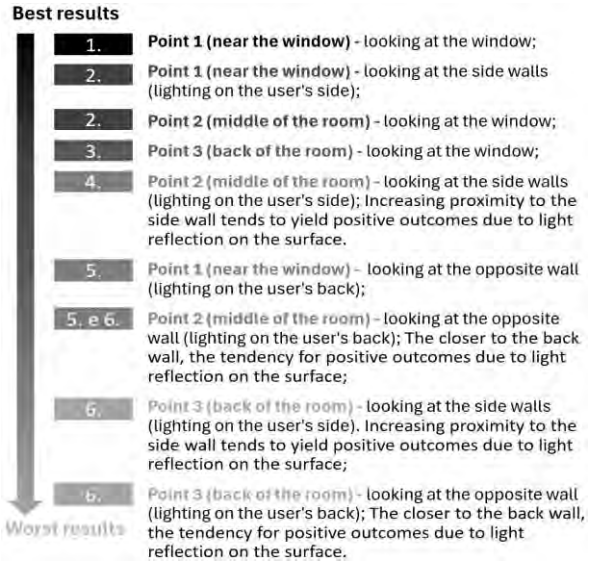

Figure 4: Analysis of points 1, 2 and 3 and their best guidelines for the non-visual effects of light.

Table 3: General results in non-visual effects in ALFA software.

Scenario	WWR (%)	Surface reflect.	Period of the year	Hour (point-in-time)	EML	% of views above 275 EML
1a	61.5	Ceiling: 90% Wall: 80% Floor: 40%	Summer Solstice (dec 21)	9am	678	100%
				11am	838	100%
				3pm	1.348	100%
				5pm	1.408	100%
1b	61.5	Ceiling: 90% Wall: 80% Floor: 40%	Winter Solstice (jun 21)	9am	470	100%
				11am	690	100%
				3pm	1.122	100%
				5pm	304	24%
2a	61.5	Ceiling: 70% Wall: 50%, Floor: 20%	Summer Solstice (dec 21)	9am	550	97.5%
				11am	665	99.2%
				3pm	1.050	100%
				5pm	1.020	94.2%
2b	61.5	Ceiling: 70% Wall: 50%, Floor: 20%	Winter Solstice (jun 21)	9am	376	63.8%
				11am	532	96.7%
				3pm	86.8%	98.3%
				5pm	237	31.7%
3a	33.52	Ceiling: 90% Wall: 80% Floor: 40%	Summer Solstice (dec 21)	9am	586	100%
				11am	671	100%
				3pm	1000	100%
				5pm	796	100%
3b	33.52	Ceiling: 90% Wall: 80% Floor: 40%	Winter Solstice (jun 21)	9am	374	78.8%
				11am	548	100%
				3pm	832	100%
				5pm	212	25.4%
4a	33.52	Ceiling: 70% Wall: 50%, Floor: 20%	Summer Solstice (dec 21)	9am	452	92.1%
				11am	527	95.8%
				3pm	726	71.3%
				5pm	603	55.8%
4b	33.52	Ceiling: 70% Wall: 50%, Floor: 20%	Winter Solstice (jun 21)	9am	290	41.3%
				11am	414	78.8%
				3pm	633	59.2%
				5pm	180	15.8%
5a	83.80%	Ceiling: 90% Wall: 80% Floor: 40%	Summer Solstice (dec 21)	9am	931	100%
				11am	1.212	100%
				3pm	1.809	100%
				5pm	1.360	100%
5b	83.80%	Ceiling: 90% Wall: 80% Floor: 40%	Winter Solstice (jun 21)	9am	645	100%
				11am	996	100%
				3pm	1.487	100%
				5pm	386	60.4%
6a	83.80%	Ceiling: 70% Wall: 50%, Floor: 20%	Summer Solstice (dec 21)	9am	715	99.6%
				11am	934	100%
				3pm	1.440	100%
				5pm	1.317	98.8%
6b	83.80%	Ceiling: 70% Wall: 50%, Floor: 20%	Winter Solstice (jun 21)	9am	503	75%
				11am	749	99.2%
				3pm	1.156	100%
				5pm	282	38.3%

Observing the results in Table 3 and Figure 3, reflectance had a significant impact on the classroom. It was observed that the times of 9am and 5pm have a certain deficiency in obtaining quantitative in EML. Regarding the period of the year, it is possible to

notice that the winter solstices have a low percentage of EML above 275, especially in scenarios 2b and 4b.

Therefore, even in environments with the percentages of reflectance allowed by the standard, in certain conditions such as winter and times around 9am and 5pm, non-visual effects will not be widely met.

Considering all the tests carried out, scenario 4b does not cover both visual and non-visual effects. Therefore, the worst combination formed was low reflectance, WWR 33.52%, winter solstice.

Regarding proper orientation in the environment, the logic follows that the closer one is to the window, the better the benefits. However, it's essential to consider whether there might be any disturbance due to glare. Keeping the gaze away from the window's direction can still yield non-visual effects within about 4 meters of the window. Yet, to maximize non-visual benefits, the optimal orientation involves directing oneself laterally to the window, essentially parallel to it. This approach allows for favorable results for both visual and non-visual effects. Nevertheless, it's important to highlight the need for further studies on environmental glare, as this data is not within the scope of this article.

4. CONCLUSION

Reflectance causes a considerable impact on non-visual effects, as observed in the presented results. Even if the variations in reflectance in the environment comply with the required standards in Brazil, it was noticeable that depending on other factors such as the time of year and the WWR (window-to-wall ratio), the classroom - the subject of study - could yield negative outcomes in both visual and non-visual effects.

In this particular case study, the classroom demonstrated favorable outcomes for both visual and non-visual effects, attributed to the specified reflectances and Window-to-Wall Ratio (WWR). Reflectance values adhered to Brazilian standards (90% for ceiling, 80% for walls, and 40% for the floor), while the WWR ranged between 61.45% and 83.80%, showcasing positive results.

Considering the original data from the environment, scenarios 1a and 1b, it can be observed that both visual and non-visual effects were met. However, there is a need for a more thorough evaluation regarding glare, given that it's a west-facing facade, a situation where visual discomfort due to excessive light commonly occurs. Avoiding glare is crucial, as closing the window causes early use of artificial light supplementation and obstructs access of natural light to the retina, the main source of the non-visual effects of light. Diffusion of light can help.

Based on the simulations, the positioning the students preferably laterally to the windows, as the student located with his back to the window, about 4 meters away from the window, have poor levels of stimulation of the non-visual effects.

Based on the simulations, the positioning of students is preferable to be lateral to the windows, since the student located with their back to the window, approximately 4 meters away from the window, presents low levels of stimulation from non-visual effects. The classroom is 13.6 meters deep, so in several simulated situations, students who have their backs to the window would have levels below 275 EML.

This research highlights gaps and suggestions. The absence of regulations (guidelines and certifications are not standards) makes progress in the scope of non-visual effects difficult.

It is expected that in the near future, there will be a standard of international relevance, which can provide data such as target values and protocols for monitoring and measuring data in internal environments. The lack of this documentation represents a challenge in reaching a definitive diagnosis.

Future standards incorporating non-visual effects in environments could guide the optimal design of spaces catering to both visual and non-visual effects. Drawing from examples such as this study, these standards could provide insights into utilizing optimal reflectances, Window-to-Wall Ratios (WWR), and appropriate layout designs tailored to their duration of use. Additionally, there are other variables not explored in this material, such as the type of glass and its colors, which involve further complexities in their utilization and could be addressed in future research.

As a suggestion, deepen the study regarding the student's orientation in relation to the window, given the current need to attend to visual and non-visual effects. Natural light is the best provider of spectrums that benefit non-visual effects, therefore, during sunny hours in a classroom, it would be ideal for all classrooms in Tropical climates to adopt the layout - student positioned sideways to window? Another suggestion is to identify more appropriate classroom measures with quality visual and non-visual effects with better use of natural light, thus providing a health benefit, greater savings and increased sustainability of future projects.

ACKNOWLEDGEMENTS

This study was financed in part by the Coordination for the Improvement of Higher Education Personnel – Brazil (CAPES) – Financial Code 001 and by the Fundação de Apoio à Pesquisa do Distrito Federal (FAP-DF).

REFERENCES

1. Boyce, P. R., (2022). Light, lighting and human health. Lighting Research and Technology, v. 54, n. 2, p. 101–144 *Building and Environment*, 36: p. 763-770.

2. Knoop, M. et al., (2020). Daylight: What makes the difference? *Lighting Research and Technology*, v. 52, p. 423–442.

3. Mardaljevic, J., (2021). The implementation of natural lighting for human health from a planning perspective. *Lighting Research and Technology*, v. 53, n. 5, p. 489–513

4. Amirazar, A. et al., (2021). A low-cost and portable device for measuring spectrum of light source as a stimulus for the human's circadian system. *Energy and Buildings*, v. 252, p. 111386, 1 dez.

5. CIE, (2029). Position Statement on Non-Visual Effects of Light - Recommending Proper Light at The Proper Time, 2nd Edition, [Online], Available: https://cie.co.at/publications/position-statement-non-visual-effects-light-recommending-proper-light-proper-time-2nd [3 october 2019].

6. Boyce, P. R., (1996). Illuminance Selection Based on Visual Performance—and other Fairy Stories. *Journal of the Illuminating Engineering Society*, v. 25, n. 2.

7. Li, D. H. W.; Cheung, G. H. W.; Lau, C. C. S., (2006). A simplified procedure for determining indoor daylight illuminance using daylight coefficient concept. *Building and Environment*, v. 41, n. 5, p. 578–589.

8. Mardaljevic, J., (2020). Simulation of annual daylighting profiles for internal illuminance. *Lighting Research and Technology*. 32, n. 3, p. 111–118.

9. Kwong, Q. J., (2020). Light level, visual comfort and lighting energy savings potential in a green-certified high-rise building. *Journal of Building Engineering*, v. 29.

10. Peña-García, A.; Salata, F., (2021). Indoor lighting customization based on effective reflectance coefficients: A methodology to optimize visual performance and decrease consumption in educative workplaces. *Sustainability (Switzerland)*, v. 13, n. 1, p. 1–13.

11. Berson, D. M.; Dunn, F. A.; Takao, M., (2002). Phototransduction by retinal ganglion cells that set the circadian clock. *Science*, v. 295, n. 5557, p. 1070–1073.

12. Brainard, G. C. et al., (2001). Action spectrum for melatonin regulation in humans: Evidence for a novel circadian photoreceptor. *Journal of Neuroscience*, v. 21, n. 16, p. 6405–6412.

13. Hattar, S. et al., (2002). Melanopsin-containing retinal ganglion cells: Architecture, projections, and intrinsic photosensitivity. *Science*, v. 295, n. 5557, p. 1065–1070.

14. Thapan, K.; Arendt, J.; Skene, D. J., (2001). An action spectrum for melatonin suppression: Evidence for a novel non-rod, non-cone photoreceptor system in humans. *Journal of Physiology*, v. 535, n. 1, p. 261–267, 2001.

15. Zeng, Y.; Sun, H.; Lin, B., (2021). Optimized lighting energy consumption for non-visual effects: A case study in office spaces based on field test and simulation. *Building and Environment*, v. 205.

16. Bellia, L.; Fragliasso, F., (2021). Good Places to Live and Sleep Well: A Literature Review about the Role of Architecture in Determining Non-Visual Effects of Light. *International Journal of Environmental Research and Public Health*, v. 18, n. 3, p. 1002, 23 jan.

17. Busatto, N. *et al*. (2020). Application of Different Circadian Lighting Metrics in a Health Residence. *Journal of Daylighting*, v. 7, p. 13–24.

18. Cai, W. et al., (2018). The impact of room surface reflectance on corneal illuminance and rule-of-thumb equations for circadian lighting design. *Building and Environment*, v. 141, p. 288–297, 15 ago.

19. Knoop, M. *et al*., (2019). Methods to Describe and Measure Lighting Conditions in Experiments on Non-Image-Forming Aspects. *LEUKOS - Journal of Illuminating Engineering Society of North America*. v.15, n.2–3, p.163–179.

20. Altenberg Vaz, N.; Inanici, M., (2021). Syncing with the Sky: Daylight-Driven Circadian Lighting Design. *LEUKOS - Journal of Illuminating Engineering Society of North America*, v. 17, n. 3, p. 291–309.

21. Yao, Q. *et al*., (2020). Efficient circadian daylighting: A proposed equation, experimental validation, and the consequent importance of room surface reflectance. *Energy and Buildings*, v. 210, p. 109784.

22. Konis, K., (2017). A novel circadian daylight metric for building design and evaluation. *Building and Environment*, v. 113, p. 22–38.

23. Ezpeleta, S. et al., (2021). Analysis of photopic and melanopic lighting in teaching environments. *Buildings*, v. 11, n. 10.

24. Bellia, L. *et al*., (2023). Assessment of melanopsin-based quantities: Comparison of selected design tools and validation against on-field measurements. Building and Environment, v. 232.

25. Alkhatatbeh, B. J.; Asadi, S., (2021). Role of architectural design in creating circadian-effective interior settings. Energies, v. 14, n. 20.

26. Brown, T. M., (2020). Melanopic illuminance defines the magnitude of human circadian light responses under a wide range of conditions. Journal of Pineal Research, v. 69.

27. Brown, T. M. et al., (2022). Recommendations for daytime, evening, and nighttime indoor light exposure to best support physiology, sleep, and wakefulness in healthy adults. PLoS Biology, v. 20, n. 3.

28. WELL. WELL v2, Q1-Q2 2023. [Online], Available: https://v2.wellcertified.com/en/wellv2/light/feature/3.

29. ABNT. NBR ISO/CIE 8995 - 1 ILUMINAÇÃO EM AMBIENTES DE TRABALHO. Rio de Janeiro: 2013. [Online], Available: https://www.normas.com.br/produto/normas-brasileiras-e-mercosul/pesquisar/nbriso-cie8995-1.

30. ABNT. CONSULTA PÚBLICA - Projeto de Revisão ABNT NBR 15215-4 Iluminação natural Parte 4: Verificação experimental das condições de iluminação natural interna. [Online], Available: https://www.abntonline.com.br/consultanacional/projetat.aspx.

31. IES, (2023). LM 83:23 - Approved Method: IES Spatial Daylight Autonomy (sDA) and Annual Sunlight Exposure (ASE). New York, USA.

32. CEN - EUROPEAN COMMITTEE FOR STANDARDIZATION. EN 17037: Daylight in buildings. Brussels.

PLEA 2024 WROCŁAW
(Re)thinking Resilience

Living Roofs for Cooling in Hot and Dry Climates:
Performance of insulated, uninsulated, and air-gap living roofs

LAURA RODRIGUEZ[1], PABLO LA ROCHE[2]

[1]La Universidad del Zulia, Maracaibo, Venezuela
[2] Cal Poly Pomona University & Arcadis, Los Angeles, USA

ABSTRACT: This paper discusses the cooling potential of three types of green roofs: insulated, uninsulated, and air gap. Different rules and schedules were tested for irrigation, water movement through the radiant pipes, fan operation, and cooling with outside air. A total of three monitoring series are discussed in this paper between November of 2017 and June and July of 2018. Results indicate the uninsulated living roof works best on warm days with lower daily swings, the insulated living roof works best on hot days with lower daily swings, and the air gap living roof works best on hot days with high daily swings. Temperature and relative humidity ranges that define the optimum performance of the different types of green roofs are plotted on the Building Bioclimatic Chart, and a chart with daily swing and temperature defining the conditions under which they are most effective.
KEYWORDS: Living Roofs, Passive Cooling, Green roofs, test cells, low carbon strategies.

1. INTRODUCTION

Following Anderson and Gough's classification [1], living or green roofs are a type of green infrastructure. Green infrastructure provides nature-based solutions that address climate change mitigation and adaptation interventions and reduce the impact of atmospheric warming.

A living roof is substantially covered with vegetation. They have been proven to have positive effects on buildings by reducing the stress on the roof surface, improving thermal comfort, reducing noise transmission into the building, reducing the urban heat island effect by reducing “hot” surfaces facing the sky, reducing stormwater runoff, reoxygenating the air and removing airborne toxins, and recycling nutrients and providing habitat for living organisms, supporting biodiversity and pollinators, all of this while creating peaceful environments.

Comparative research on the thermal performance of green roofs with other types of roofs has been conducted and has shown contrasting results [2-3].

This paper discusses the cooling potential of different living roof configurations during summer and fall: A) An insulated living roof with insulation under the planting material. B) An uninsulated living roof with the planting material thermally coupled to the internal space via a metal plate; and C) An air gap living roof with an air space of 38mm in addition to the insulation layer and the planting material.

These three configurations were tested over several months through different series to establish the most effective type of green roof for different temperature ranges during the testing period. The authors developed all configurations from previous prototypes [4-5] and tested them during the warm season in Pomona during the fall of 2017 and the summer of 2018. This work constitutes a line of research presented in previous PLEA conferences [6,8].

2. METHODOLOGY

2.1. Experimental setup

The test cells are located at the Lyle Center for Regenerative Studies at Cal Poly Pomona University, 30 km east of Los Angeles, California. The climate is hot and dry, with an average high August temperature of 31.5˚C and an average low of 5.3 ˚C in January. (Fig. 1)

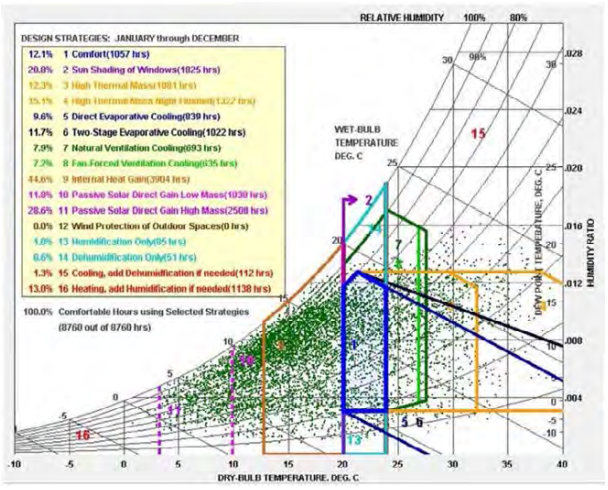

Figure 1: Climate zone 9, location of the tests

All modules are 1.35 m. × 1.35 m. × 1.35 m. with south-facing windows and similar envelope characteristics. (Fig 2). The test cell walls are 178 mm

thick, with drywall inside and 50.8 mm x 101.6 mm studs with glass wool insulation, OSB board, XPS insulation board, and plywood on the outside. The floor of the cell is OSB board and XPS insulation board. The U-value of the wall is 0.308 W/m2K, and the U-value of the floor is 0.299 W/m2K. The walls are painted white to reduce heat gain. A double-glazed window 610 mm wide x 610 mm high was installed in the south wall and was tested with and without shade. (Fig 3). The design of the roof is the only difference between the cells. All series in this paper had night ventilation and shade.

Figure 2: View of the Test Cells with Shade

2.1 Monitoring System and Schedule

Data were collected using HOBO-type data loggers by Onset computer (Model: U12-012, UX 120-006 M, TMC6-HD). These sensors were installed inside the cells in the middle of the space to monitor dry bulb temperature. Outdoor Dry Bulb Temperature and Relative Humidity were also collected on site. This paper discusses three monitoring series between November 2017 and June and July 2018.

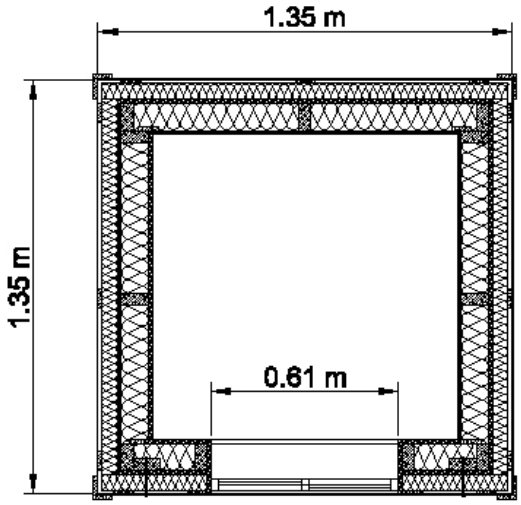

Figure 3: Horizontal section plan of the test cells

3. LIVING ROOF SYSTEMS

3.1. Insulated living roof.

This living roof had insulation underneath the planting material (See Fig. 4). With this type of roof, the aim is to evaluate the overall performance of the traditional thermal insulation available in any building and the substrate and layers necessary to build a green roof. The U-value of the insulated green roof, including the wood structure, was 0.282 W/m^2 K (See Table: 1).

Table 1: Insulated Living Roof U- Value

Material	mm	W / mK	U-Value (W / m^{2}K)
Soil	130	0.610	
Gravel	20	2.000	
Water Proofing Liner	1	0.210	
Metal Pan	2	44.000	0.282
OSB	11	0.130	
Glass Wool	21	0.044	
XPS	127	0.043	
Dry Wall	11	0.180	

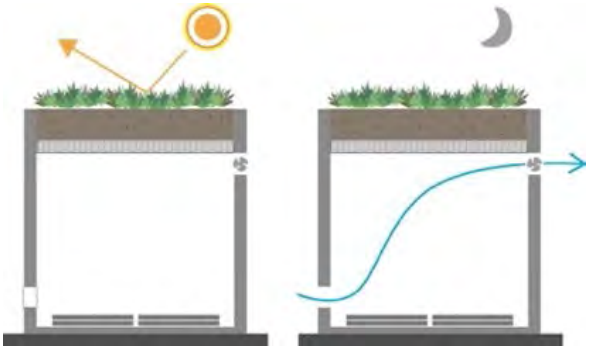

Figure 4: Insulated Living Roof

3.2 Uninsulated Living Roof

In the uninsulated living roof, the planting material is thermally coupled with the space's interior via a metal plate under the green roof. There is no insulation between the living roof and the space below (See Fig: 5). With this type of roof, the goal is to evaluate the influence that the substrate and the vegetated layer on a green roof have on the temperature inside a building. The U-value of the uninsulated living roof was 2.534 W/m^2 K (See Table 2).

Table 2: Uninsulated Living Roof U- Value

Material	mm	W / mK	U-Value (W / m^{2}K)
Soil	130	0.610	
Gravel	20	2.000	
Water Proofing Liner	1	0.210	2.534
Metal Pan	1	44.000	

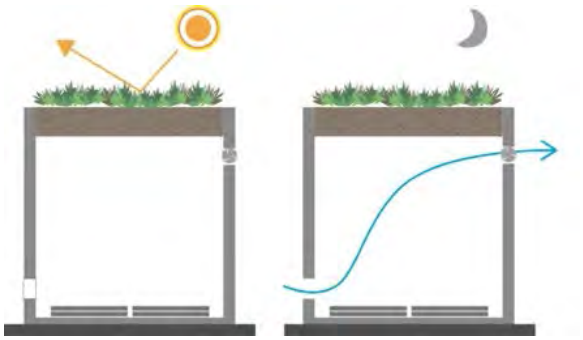

Figure 5: Uninsulated Living Roof

3.2 Air gap living roof.

The air gap living roof had insulation underneath the planting material with a 100mm air space separating the planting material from the insulation. With this type of roof, the goal is to evaluate the influence of the substrate and the vegetal layer, with the addition of an air space. (See Fig: 6). The U-value of the air gap living roof was 0.270 W/m^2 K (See table: 3).

Table 3: Air Gap Living Roof U- Value

Material	mm	W / mK	U-Value (W / m^{2}K)
Soil	130	0.610	
Gravel	20	2.000	
Water Proofing Liner	1	0.210	
Metal Pan	2	44.000	0.270
Air Space	100	0.20	
OSB	11	0.130	
Glass Wool	21	0.044	
XPS	127	0.043	
Dry Wall	11	0.180	

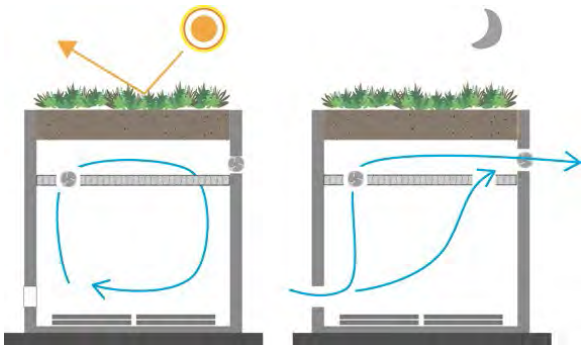

Figure 6: Air Gap Living Roof

4. RESULTS AND DISCUSSION

The three series tested had different conditions of outside temperature and swing. The results indicate that the three types of living roofs performed best under different conditions. Figure 7 shows the outdoor maximum and minimum temperature values, the swing, and the best performance of each type of living roof (overlaid in color rectangles).

The insulated living roof performs best when the outdoor swing is between 4˚C and 28˚C, and outdoor maximum temperatures are between 22˚C and 47˚C, with indoor maximum temperatures between 19˚C and 36˚C.

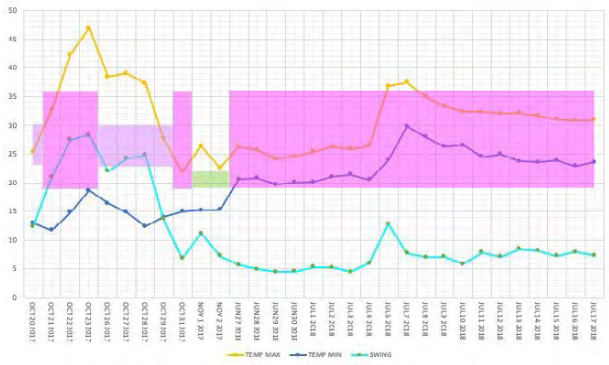

Figure 7: Outdoor maximum and minimum temperature and swing with the best-performing living roof

The uninsulated living roof performs best when the outdoor swing is lower, between 7˚C and 11˚C, with the outdoor maximum temperature below 26˚C (23˚C to 26˚C), with indoor maximum temperatures between 19˚C and 22˚C. In this series of tests, there are not enough values to verify the behavior of the uninsulated living roof. However, previous research by La Roche demonstrated that the uninsulated green roof performs better in a warm or mild climate with cool nights [9]. When combined with night ventilation, coupling the soil layer with the interior of the building stores heat in the green roof during the day that is then dissipated at night. Furthermore, the vegetation in the canopy layer improves the system's performance by blocking solar gains.

The air gap living roof performs best when the outdoor swing is between 12˚C and 25˚C and outdoor maximum temperatures are between 25˚C and 39˚C, with indoor maximum temperatures between 23˚C and 30˚C.

5. APPLICABILITY OF LIVING ROOF SYSTEMS UNDER DIFFERENT OUTSIDE TEMPERATURE AND SWING VALUES

To better understand the performance of the systems, daily recorded outdoor and indoor maximum temperature and relative humidity were plotted on the Building Bioclimatic Chart superimposed on the psychrometric diagram.

Since no mechanical cooling is used, comparing indoor and outdoor temperatures allows us to understand the system's performance. A lower indoor maximum temperature than the exterior temperature indicates a better cooling performance. Thus, the applicable range of outdoor values for optimum performance for each system is determined by the relationship between the indoor temperature and the comfort zone for a given exterior maximum

temperature. If the indoor conditions are inside the comfort zone for a given outdoor value, then the strategy is assumed to be effective for exterior temperature and relative humidity [6,8].

Another goal of analyzing this data was determining the applicability of the different living roof strategies under various conditions of outside temperature and swing. Colors were used to represent each option (pink for the insulated living roof (Fig.8), green for the uninsulated living roof, and purple for the air gap living roof (Fig.9). If the indoor temperature was inside the comfort zone (up to 27 °C) when the outdoor temperature was above the comfort zone, the strategy was considered to be effective in achieving thermal comfort. If the maximum temperature inside the cell was inside the comfort zone, the strategy was considered effective in achieving thermal comfort. If the values were between 27 °C and 31 °C, the strategy was "somewhat effective in achieving thermal comfort." [6,8]

The maximum temperature and minimum relative humidity outside were then plotted on the psychometric chart and compared with the interior data. For 31 selected days, 31 usable data points were plotted and tested under different conditions, considering the outside temperature and swing.

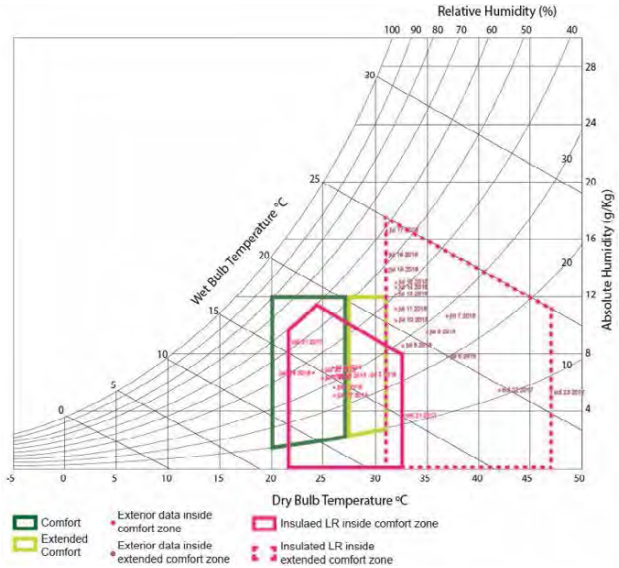

Figure 8: Psychrometric Chart for insulated living roof

5.1 Insulated Living Roof

Fig. 8 shows the Building Bioclimatic Chart with the data for the cell with the insulated living roof. The area in which the insulated living roof effectively achieves thermal comfort is indicated by a pink line, between 22 °C and 33°C Dry Bulb Temperature, and below 19g/ Kg of Absolute Humidity and approximately below 60% Relative Humidity. The pink dotted line defines the period during which this design strategy is somewhat effective, between 35 °C and 47 °C Dry Bulb Temperature, and below 25g/ Kg of Absolute Humidity, and below approximately 60% Relative Humidity.

5.2 Uninsulated Living Roof

The uninsulated green roof performs better in a warm or mild climate with cool nights. According to previous research, the uninsulated living roof effectively achieves thermal comfort between 23°C and 26°C Dry Bulb Temperature.

5.3 Air Gap Living Roof

Fig. 9 shows the Building Bioclimatic Chart with the data for the cell with the air gap living roof. The area where the air gap living roof effectively achieves thermal comfort is indicated by a purple line, between 25 °C and 37°C Dry Bulb Temperature, and below 21g/Kg of Absolute Humidity and below 50% Relative Humidity. The pink dotted line defines the period during which this design strategy is somewhat effective, between 37 °C and 39°C Dry Bulb Temperature, below 21g/Kg of Absolute Humidity, and below 50% Relative Humidity.

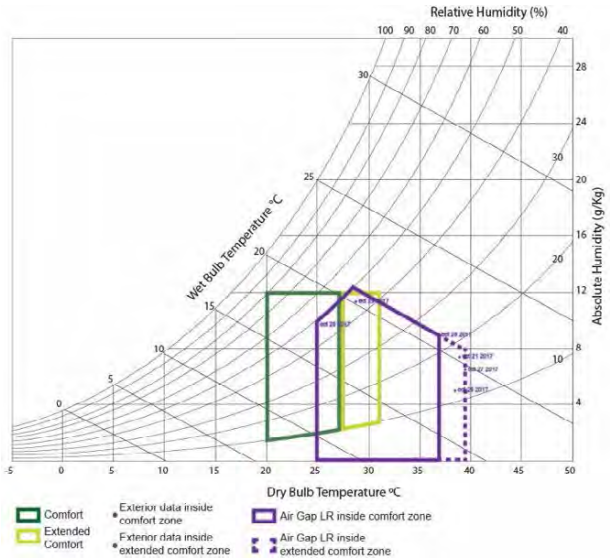

Figure 9: Psychrometric Chart for air gap living roof

6. CONCLUSION

Some experiments have been done to establish which configuration is the most appropriate for each temperature range during the analysis period, with night ventilation. Figure 10 shows the combination of maximum temperatures and daily swings under which the different types of living roofs perform best. The maximum and minimum values of the outside temperature with the best performance of each cell are plotted in the Y axis, drawing the average outside temperature with a line. The swing values are plotted on the X-axis with the best performance of each cell, drawing the swing average with a dotted line.

Results indicate that no living roof configuration works best under all outdoor conditions tested. The

performance of the different living roofs varies as a function of temperature and daily swing, which is affected by relative humidity. The uninsulated living roof works best on warm days with enough daily swing to cool the living roof at night (9 ˚C or higher). It works best with temperatures up to 26 ˚C but will still work with temperatures up to 32˚C. Because the green roof is not insulated, it acts as a thermal mass that improves the performance with night cooling. Good leaf coverage is important since the lack of insulation makes the roof more susceptible to solar radiation and heat transfer by conduction if not sufficiently shaded by the vegetation. After 32˚C, insulation is needed to reduce the heat gain during the day because the living roof does not have enough thermal capacity to store and dissipate energy gains. Providing air exchange with the exterior is always beneficial when it is cooler outside than inside.

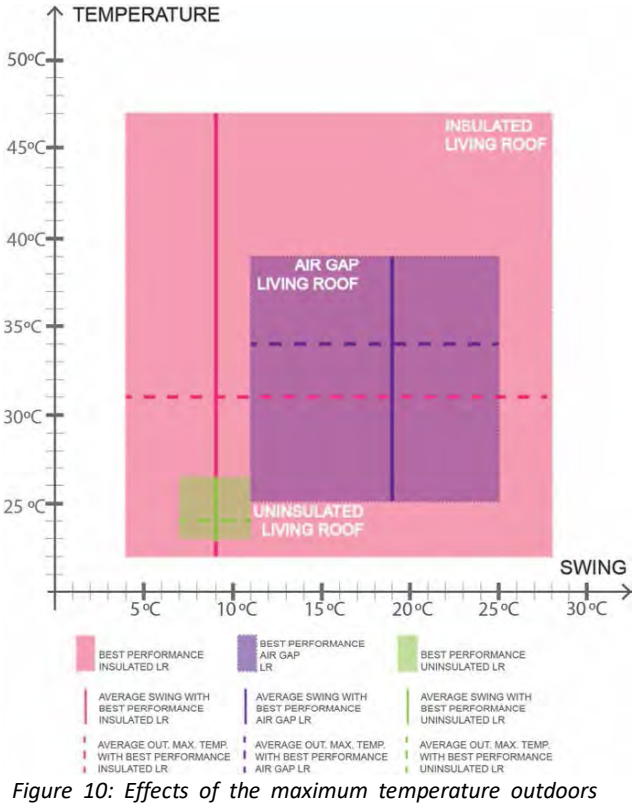

Figure 10: Effects of the maximum temperature outdoors and the average swing in the performance for each evaluated living roof

The insulated living roof works best on hot days (31˚C average) with lower daily swings (9 ˚C average) and is more effective than the uninsulated green roof during warmer temperatures. It works best with additional thermal mass inside the building space for night ventilation to be effective since the mass of the green roof is decoupled from the interior. It can work better than the uninsulated green roof with lower temperature swings.

The air gap living roof works best on hot days (34˚C average) with high daily swings (19 ˚C average) but also works well with lower temperature swings. The green roof mass works as thermal storage, which can be insulated when helpful to reduce heat gains from the exterior in the summer and heat losses in the winter. The thermal mass of the green roof can be coupled or decoupled from the interior as needed. There is potential to improve thermal comfort by lowering ceiling temperature, affecting Mean Radiant Temperature. It must provide air exchange when it is cooler outside than inside. It can recirculate air through its plenum when not collecting cool air from the exterior.

Generally, the insulated green roof works well with a wide range of temperatures and swings representing temperate, hot, humid, and hot and dry climates. The uninsulated living roof works best with mild climates and moderate to high swings. The air gap living roof works in more conditions than the uninsulated living roof.

Figure 11 shows the psychometric chart describing the conditions under which these three living roofs are most effective. This is a useful design guide for selecting the most effective living roof for cooling, considering the outside maximum temperatures and daily swings.

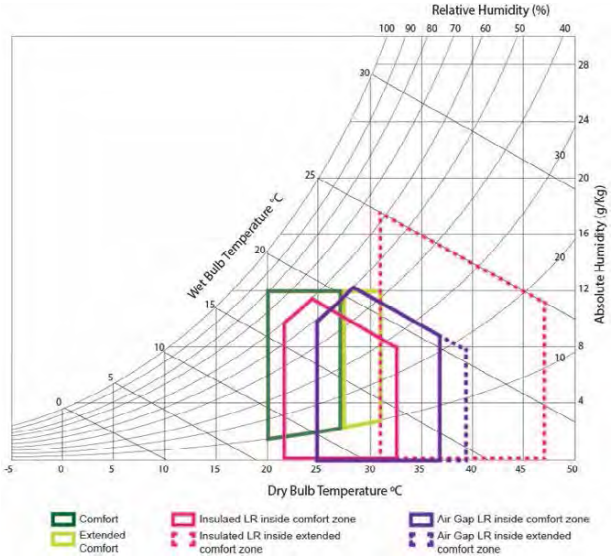

Figure 11: Psychrometric Chart for each evaluated living roof

The "insulated living roof" (Fig. 11) works best between 22 °C and 33°C DBT, below 19g/ Kg of Absolute Humidity and below 60% Relative Humidity. The reduced effectiveness area is from 35°C to 47 °C DBT, below 25g/ Kg of Absolute Humidity, and below 60% Relative Humidity.

The "living roof with air gap cooling" (Fig. 11) works best between 25°C and 37°C DBT, below 21 g/ Kg of Absolute Humidity and 50% Relative Humidity. The reduced effectiveness area is between 37 °C and 39 °C DBT, below 21 g/ Kg of absolute humidity and 50% Relative Humidity.

The "uninsulated living roof" works best between 23°C and 26 °C DBT, below the 60% Relative Humidity. However, there are only two data days to support this performance. More research needs to be done to amplify and verify the behavior of the uninsulated living roof.

Living roofs can augment indoor and outdoor cooling in buildings and outdoor spaces in warm climates. As with traditional passive cooling strategies, they work better in some climates with different conditions of temperature, relative humidity and solar radiation. In climates where most outdoor conditions are inside the applicability area, green roofs, when combined with night ventilation, can lead to more comfortable building conditions and increased energy efficiency. This should give them added value, thus increasing their applicability.

The living roofs tested and discussed in this paper are a type of green infrastructure that provides multiple benefits. They create green space, mitigate the urban heat island effect, cool the environment, and remove air pollutants. They also help cool the buildings underneath, reducing their carbon footprint.

Lastly, it is also important to integrate living roofs into the design process so they are not simply accessories attached to the project. They should be integral to the architectural design intent, as in Arcadis's Xylem designed for a project in a hot and humid climate (Fig 12) or in the Kaunas concert hall competition also by Arcadis, with an air gap green roof (Fig 13).

Figure 12: The Xylem, a living roof system developed at CRTKL/Arcadis for outdoor cooling.

Figure 13: Kaunas concert hall competition proposal by Arcadis that includes an air gap green roof.

REFERENCES

1. Vidya Anderson, V., Gough W. (2022) Nature-based cooling potential: a multi-type green infrastructure evaluation in Toronto, Ontario, Canada. International Journal of Biometeorology 66:397–410
2. H. Takebayashi, M. Moriyama, (2007) Surface heat budget on green roof and high reflection roof for mitigation of urban heat island, Build. Environ. 42 (8) 2971–2979.
3. M. Santamouris, (2014) Cooling the cities – a review of reflective and green roof mitigation technologies to fight heat island and improve comfort in urban environments, Sol. Energy 103 (2014) 682–703.
4. D. Yeom, P. La Roche, (2017). Investigation of the cooling performance of a green roof with a radiant cooling system. *Energy and Buildings,* 149: p. 26–37.
5. La Roche, P., Yeom, D., Ponce, A., (2020). Passive Cooling with a Hybrid green roof for Extreme Climates. *Energy and Buildings*, 224. 110243
6. Rodríguez L., La Roche P., (2018). Green Roofs for Cooling: Tests in a Hot and Dry Climate. *Passive Low Energy Architecture Conference PLEA.* Hong Kong, December 10-12.vol 1 80-85.
7. Rodríguez L., La Roche P., (2020). Living Roofs for Cooling: Impact of thermal Mass, Night Ventilation and Radiant Evaporative Cooling. *Passive Low Energy Architecture Conference PLEA.* A Coruña, September 1-3. vol. 1 109-114.
8. Rodríguez L., La Roche P., (2022). Living Roofs for Cooling in a Hot and Dry Climates: Effects of Temperatures and Swing. *Passive Low Energy Architecture Conference PLEA.* Santiago, Chile. November 10-12. 10th Parallel Session/ online. 427-432.
9. La Roche P., (2009). Low Cost Green Roofs for Cooling: Experimental Series in a Hot and Dry Climate. *Passive Low Energy Conference, PLEA 2009, Quebec Canada.*

PLEA 2024 WROCŁAW
(Re)thinking Resilience

Digital Toolmaking for Earth Building Components

The use of low-cost extruder and 3D printing to develop new fabrication approaches for cob and light earth bricks

TAVS JORGENSEN[1], SONNY LIGHTFOOT[1]

[1]Centre for Print Research, School of the Arts, UWE, Bristol, UK

ABSTRACT: This paper reports on ongoing research into innovative methods for extruding cob and light earth building components, aiming to establish a cost-effective fabrication system. The paper provides a brief contextual overview of related work and outlines the research's vision to create a low-cost fabrication system for experimenting with earthen-based composites in low-carbon construction. Various components of the fabrication system are presented, including a piston-based extrusion machine developed by the researchers. The use of low-cost filament 3D printers to create the extrusion profiles (known as dies) is also outlined, with details of printing parameters and die construction approaches. The paper reports on preliminary results of the characterisation of extruded samples in both dense cob and light earth composites, including shrinkage rates and compressive strength. Additionally, the paper presents experiments involving innovative interlocking brick designs and the production of earth bricks with cavities to illustrate the capabilities of the fabrication concept.
KEYWORDS: Extrusion, Toolmaking, Earth Bricks, Cob, 3D Printing

1. INTRODUCTION

Earth-based materials have been used for house building for centuries across in many cultures around the world [1]. Such materials, which is utilised cob buildings and adobe bricks manufacture, is typically a basic mixture of subsoil and fibre. In western culture the use of earthen based building materials almost disappeared in the 20th century, however the emerging climate crisis has spurred a re-evaluation due to their exceptionally low environmental impact [2]. Equally, new digital fabrication technologies are delivering disruptive impact across numerous sectors. This research seeks to combine these developments into innovation opportunities with earth-based building materials to contribute to low-carbon and sustainable construction practices. Specifically, this paper convers ongoing research focussed on developing novel approaches of using 3D printing technology in a toolmaking situation to fabricate extrusion dies to manufacture cob and adobe building components. This approach is tested in combination with a concept for a low-cost hydraulic ram extruder, thus presenting a competitive earth brick manufacturing system.

1.2 Context

Several recent research projects have explored new approaches with cob, focussing on both composition and construction methods. The CobBauge project [2]–[5] has established cob compositions that meet contemporary building performance standards. Notably, the CobBauge team has introduced a dual-composition approach for constructing cob walls. One layer serves as a 'structural layer', meeting loadbearing requirements using a dense earth composite (cob). The other layer, described as a 'thermal layer', is designed to provide insulation and is constructed with a light earth composite. In combination this hybrid cob/light earth wall concept has the capacity to perform to current building regulations standards [2].

The results from the CobBauge team present an exciting potential for re-evaluating the use of cob in contemporary constructions. However, conventional methods of constructing cob buildings remain a time-consuming affair, posing a potential limitation in adopting these new cob compounds. Typically, cob buildings are constructed by stacking cob in layers, known as 'lifts' [6], each 30–60 cm high. The construction process involves gradually building up the structure while tamping and shaping the cob walls to the desired form. Formwork can also be employed to enhance control over the dimensions of the cob wall and increase the speed of construction.

Several projects have explored the integration of digital fabrication and robotic technology earthen constructions. These initiatives encompass investigations into additive layer manufacturing (ALM) using customised Cartesian 3D printing systems [7], [8] or delivery facilitated by multi-axis robotic arms [9], [10].

This research takes a different approach from previous projects seeking to use new digital fabrication technologies, particularly 3D printing, in a *toolmaking* scenario, with profile extrusion as the production approach.

Extrusion is an extremely efficient manufacturing process that is used extensively to produce *fired* ceramic architectural components, such as bricks and tiles. However, in terms of *unfired* earth bricks, the use of extrusion as the manufacturing process appears to be significantly under-researched and underutilised [11], [12]. The underutilisation of extrusion to produce earthen building components could be due to difficulties in processing fibrous composites through extrusion machinery. Additionally, extrusion profiles (*dies*) typically require fabrication in steel by specialised engineering companies, making experimentation with the extrusion process expensive and with limitations to geometries that is achievable through convectional toolmaking technologies. Another potential contributing factor to the limited exploration of extruded earth composites is that industrial extrusion machines (such as those used in the ceramic industry) are costly and typically based on the *auger* principle (see Figure 1). While the auger extrusion approach provides a continuous extrusion flow that is advantageous for mass production, this approach is likely to be susceptible to jamming when exploring fibrous earth composites. An alternative extrusion method, based on the *piston* concept [13], illustrated in Figure 1, offers a simpler principle at significantly lower construction costs. Although the piston approach requires pausing the extrusion process for barrel refilling, it is very useful for experimentation in smaller and less standardised production situations, including trials with earth composite materials.

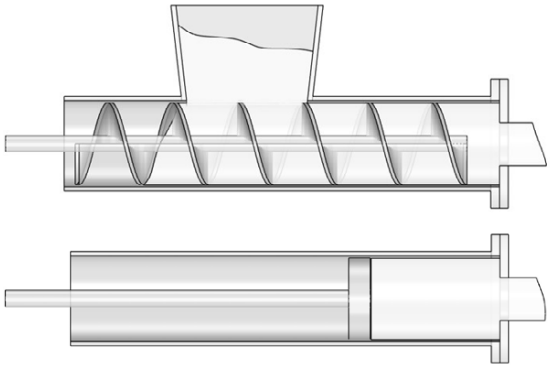

Figure 1: Auger extrusion principle illustrated at the top, with piston extruder illustrated below.

2. RESEARCH AIM, QUESTION AND OBJECTIVES

This research aims to contribute to low-carbon construction by presenting a low-cost production system that enables researchers, architects and builders to utilise digital tools to design and prototype new cob and adobe brick components. The research question could therefore be articulated as: How can 3D printing technologies help facilitate the exploration of new earth-based construction units based on the extrusion production method?

The objectives for addressing this research question/aim include the following:

- To test the use of a low-cost extrusion machine for use with earth composites.
- To develop a new toolmaking workflow using low-cost 3D printers to fabricate extrusion dies for earth composites.
- To undertake practical tests of the complete workflow system, including exploration of innovative designs with earth bricks.
- To undertake quantitative studies of the performance of the units produced by the system.

3. RESEARCH EQUIPMENT AND PROCESSES

This research is centred on the use of low-cost equipment with the aim of establishing a workflow that can be relatively easily replicated by other users who wish to explore extrusion of earth composites. The equipment pool consists of standard, consumer level, Fused Filament Fabrication (FFF) 3D printers, a forced action mixer and a piston-based extrusion machine constructed by the researchers.

3.1 Low-cost, piston-based extrusion machine

The extrusion machine utilised in this research has been constructed by the researchers primarily using off-the-shelf components, including a frame made from the Unistrut system [14] and extrusion barrels constructed from standard stainless-steel pipes. While the extruder design incorporated bespoke parts like pipe flanges and plunger brackets, these were fabricated locally by a metal fabricator via laser cutting. The piston's movement is facilitated by a hydraulic power unit capable of supplying the piston cylinder with up to 230 bar of system pressure. Hydraulic systems are ubiquitous for powering all kinds of plant and heavy machinery, and consequently basic hydraulic power systems are widely available at relatively low cost. The parts for the entire extruding machine used in this study come at a cost of around €3000.

Figure 2: Low-cost, piston-based extrusion machine with hydraulic power unit. Photo: T. Jorgensen, 2020.

3.2 3D printing technology and parameters

As a part of the complete design and production workflow developed in this research, low-cost FFF 3D printers play a central role in fabricating the extrusion dies. These dies have been developed a two-part construction approach: the core die body, known as the *pressure plate*, and the second part, the *nozzle,* which is attached with screws. Two different FFF 3D printers were utilised to optimise print quality and speed. For the pressure plates, a Creality CR10 S4 3D printer was used with a 0.8-mm nozzle to facilitate faster printing times. The commonly used Polylactic Acetate (PLA) biopolymer was used as the filament medium, with print settings including 0.6-mm layer heights, 3-layer perimeters, 3-layer top and base and a 20% infill. For the die nozzles, a Bambu X1 Carbon printer with a 0.4-mm print nozzle was used. 'Tough PLA' was selected for printing the extrusion nozzles due to its enhanced durability, particularly as the nozzle was identified as the most susceptible part to fracturing. The print settings for the nozzles included 0.2-mm layer heights, 4-layer perimeters, 4-layer top and base and a 30% infill density. These settings were chosen to ensure a finer surface quality, as any visible layering resulting from the 3D printing process would likely have the most significant impact on this part of the die. The decision to use these specific print settings for the nozzle is informed by the literature on paste extrusion, which highlights the potential impact of die surface texture on extrusion rheology [15].

Figure 3: 3D printing of extrusion dies. Photos: T. Jorgensen, 2023.

4. TEST SET-UP AND INITIAL FEASIBITITY RESULTS

Initial feasibility experiments were carried out to test whether the cob recipes established by the CobBauge team [3] could be extruded using the set-up. Initial tests focused on experiments with the light earth mixture. This composite was prepared with a commercial terracotta clay body (Valentine VC1D), which was mixed with additional water to create a clay slip with a consistency of 14 cm in diameter using a clay slip puddle test approach [2]. Using a forced action pan mixer, this slip was then mixed with hemp shiv with a ratio of 3 to 1 (hemp to clay slip by volume). The extruder was set up with a 250-mm pipe and a die with a square profile of 100 mm by 100 mm. The pressure plate section was initially designed to have a relatively short depth of 100 mm with sides tapering from the 100-mm square profile out to a round profile matching the extrusion barrel wall.

4.1 Establishing extrudability of light earth mixture

The initial tests utilised the CobBauge team's recipe for a light earth mixture. However, this 3:1 hemp-to-clay slip ratio was found to be too fibrous and would jam in the extrusion die. Experiments with extrusion die geometry were undertaken to remedy the issue. The depth of the pressure plate was extended to 150 mm and 200 mm to provide a more gradual taper. However, these alterations still failed to solve the issue of the mixture's extrudability. The slightly layered texture, which is characteristic of 3D printing, was also hypothesised to inhibit the flow of the earth composite but smoothing the surface of extrusion die with filler and subsequent sanding still failed to remedy the problem. Addressing the extrudability of the light earth composite was concluded to be unattainable through changes to extrusion die geometry or by improving the die surface. Altering the recipe of the composite appeared to be the only viable option to achieve extrudability. Several tests were undertaken in which the clay slip content of the mixture was gradually increased. Through these experiments, it was found that a ratio of 4 hemp shiv to 3 clay slip (57.4%–42.4% by volume) achieved a mixture that would extrude well. It was observed that adjusting the consistency of the clay slip had a positive impact on extrudability. Adjustment to the consistency of the clay slip was also found to aid the extrudability with a 'wetter' slip (determined by 14cm in the puddle test) found to separate from the hemp shiv in the extrusion situation. A 'drier' slip (8-10cm puddle test) was found to create a more extrudable composite. The initial tests in this investigation were carried out using a standard hemp shiv grade with pieces of up to 22 mm. However, a finer hemp shiv of 3.5 mm pieces was explored and found to improve the extrudability even further. This finer hemp shiv allowed for an even greater ratio, achieving 60% hemp shiv to 40% clay slip.

4.2 Extrusion of the standard cob mixture

Initial extrusion experiments focused on the use of light earth composite with adjustments to the hemp-to-clay slip ratio having to be implemented to ensure extrudability. Challenges in terms of extruding the denser cob mixture were expected, but the standard recipe used by the CobBauge team was found to extrude very well without any adjustment to the recipe. This recipe consists of clay (47.5%), sharp sand (51.7%) and 2.5% straw (barley) – all dry weights. The clay utilised was a commercial stoneware body (Sibelco HZ 3215) with the 'cigar test'

[16] used to determine the suitable addition of sand. Water was added for the mix to achieve a consistency that adhered to the 'drop ball test' [17]. This test requires achieving a 21-cm diameter when a 2-kg cob ball was dropped from a height of 1 m.

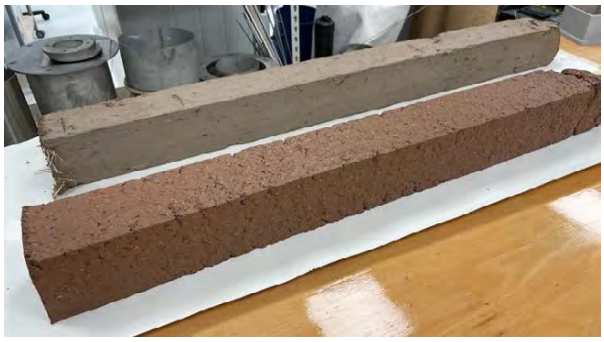

Figure 4: Extrusion tests with both standard cob mixture as well as light earth mixture. Photo: T. Jorgensen, 2020.

4.3 Effect of die geometry on surface resolution

After establishing the parameter of an extrudable light earth recipe and testing the extrudability of the cob mixture, tests on the effect of the extrusion die geometry on the surface fidelity of the extruded cob units were carried out. In particular, the impact of the length of the extrusion nozzle was investigated. Tests with 50-mm, 100-mm and 150-mm nozzles were undertaken, and it was found that there was clear visual evidence of improved surface fidelity with longer nozzles. The impact of the geometry of the pressure plate (the taper ratio in particular) was found to be less clear, and further testing is required to determine how this may affect the extrude parts.

Figure 5: Tests with various extrusion nozzle lengths to improve surface fidelity. Photos: T. Jorgensen, 2023.

5. CHARACTERISATION OF SAMPLES

A full range of characterisation tests of extruded samples are now underway to determine the effects of the extrusion process on the earth brick units produced. These tests include compressive strength, flexural strength, shear strength, dry density and thermal conductivity. While some of these tests are still in process, some preliminary results concerning shrinkage and compressive strength can be reported, which have some noteworthy results.

5.1 Shrinkage ratio of extruded earth brick units

One of the most surprising test results is the shrinkage rate in earth bricks produced by the extrusion process. Measurements were taken at the wet forming stage and compared with measurements of the units in a completely dry state. The tests were carried out by making marks 1000 mm apart on extruded test bars with a square cross section of 100 mm by 100 mm. Measurements of both light earth and cob mixtures showed surprisingly different shrinkage ratios in relation to the extrusion direction. For the cob mix, the shrinkage along the length of the extruded forms was under 1% (992 mm = 0.8%). In contrast, the cross section had an average of 7% shrinkage (93 mm). For the light earth composite, the shrinkage along the length of the extruded bars was recorded at 1.5% (985 mm). Measurements of the cross section recorded an average of 92 mm, indicating an 8% shrinkage. In conventional use of earth composites for in-situ construction (cob) or manufacture of adobe bricks, shrinkage rates of 1–4% have been reported [18]. The high level of shrinkage in measurements taken *across* the direction of extrusion and the difference in this rate compared with the shrinkage rate along the *length* of the extruded parts is significant and surprising. Additional tests on other extrude samples have been undertaken to validate these readings, with similar findings being recorded. The reason for this difference is not immediately clear, and further research is required.

5.2 Compression strength tests

Assessments of the structural performance of the extruded earth bricks produced in this research are not fully complete, but some recordings have been undertaken with results of potential significance. Samples for both the cob mix and the light earth mix were subjected to compression strength tests. Samples were produced with a 100 x 100 mm square profile extrusion die and then dried and cut into 100 mm lengths. The samples were tested for compressive strength in both the vertical and horizontal orientations in relation to the extrusion direction. The cob mix performed best, with the samples being oriented horizontally in relation to the extrusion direction, with a maximum of 19.68-kN load recorded. With the samples placed in a vertical orientation, the performance was slightly lower at 19.13 kN. The light earth mix recorded a maximum of 12.01-kN load in the horizontal orientation and 11.62 kN in the vertical orientation. All figures are based on an average of recordings from 3 test samples.

Both the performance of the cob and the light earth mixtures are far better than commercial earth brick products manufactured by pressing or moulding in frames [19], [20]. The structural performance of

the extruded samples also far exceeds that reported from in-situ cob building [5].

Similar to the results of the shrinkage tests, the findings from the compressive strength tests are surprising and potentially significant. The inherent alignment of clay particles and fibres in the extrusion process is hypothesised to be the core reason for this high level of performance.

6. EXPLORATION OF INNOVATIVE BRICK DESIGN APPROACHES

The extrusion process presents the potential for fast design exploration of geometries not easily achieved with traditional earth brick shaping methods, which typically utilise wooden frames or moulds [1]. To provide an initial exemplar of the new design possibilities using 3D printed dies in earth brick production via extrusion, initial design concepts explored interlocking bricks to facilitate rapid construction of earth buildings (see Figure 6).

Figure 6: Experiments with interlocking earth brick designs. Photo: T. Jorgensen, 2023.

This approach is proposed with either wet or dry brick units. Employing consumer-level 3D printing technology for die creation allows for the rapid exploration of a broad range of geometries at an exceptionally low cost. with material cost of a die approximately €15. This presents the potential of exploring innovative constructions approaches utilising different earth composites there, building on the hybrid wall layer approach established by the CobBauge team (design concept example illustrated in Figure 7).

Figure 7: Extruded earth brick design concept, Photo: Simon Regan, 2023.

6.1 Exploration of extruded earth bricks with cavities

Using extrusion to create earth composite bricks presents a good opportunity for creating units with hollow sections. These cavities are created using cores suspended in the extrusion dies. This is a method that is widely used for conventional ceramic bricks, as this approach presents several advantages, including reduction in material use, quicker dying times, increased thermal performance and easier transport and handling. To create hollow sections in extruded parts, die cores must be suspended by a frame/bar commonly known as a *bridge.* The principle of crating hollow sections in extruded parts relies on the ability of the extrusion medium to be separated by a bridge and then forced together again through pressure so seamless walls can be achieved. To ensure thorough reunification of the extrusion medium, the bridge is typically designed to be positioned as far as possible from the extrusion orifice. For ceramic extrusion, significant structural integrity is required by the bridge element, and the polymer used for standard 3D filament printing does not have anywhere near structural performance of the tool steel, which is normally used for the bridge element. To overcome this issue, a hybrid approach was taken in this research with the 3D printed dies designed to incorporate a stainless-steel metal bar on which 3D printed cores could be suspended. This die design is illustrated in Figure 8.

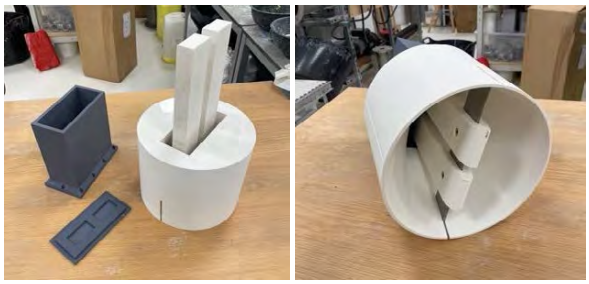

Figure 8: 3D printed extrusion dies with cores fitted to create earth bricks with cavities. Photo: T. Jorgensen, 2023.

Several experiments with the light earth mixture were undertaken with dies that incorporated cores, all with a good level of success.

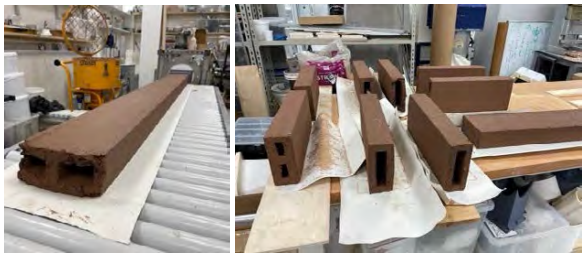

Figure 9: Experiments with cavities in extruded earth bricks. Photos: T. Jorgensen, 2023.

7. PRELIMINARY CONCLUSIONS AND DISCUSSION

The research has successfully demonstrated a solid proof-of-concept that low-cost 3D printers can be used effectively in a toolmaking scenario for the extrusion of earthen-based brick units. A key aspect of the manufacturing concept developed in this research is the low cost. A complete extrusion set-up, like the one utilised in this research, can be acquired for less than €5000. Based on the low cost the authors argue that the using 3D printing for creating earth brick extrusion dies presents innovation opportunities for the design of cob and adobe buildings. The research also seems to indicate that the extrusion process delivers unexpected material characteristics in the resulting earth bricks. Some of these characteristics may pose challenges, such as high shrinkage rates across the width of the extruded parts. Other characteristics, such as high compressive strength, present significant advantages. The remaining characterisation tests should provide a clearer picture of the overall potential of the extrusion process to deliver innovation in the quest to deliver low-carbon and more sustainable construction approaches.

ACKNOWLEDGEMENTS

The research has been facilitated via funding from the Arts and Humanities Research Council (UK) and Research England. Many thanks to Atul Vadgama, Max Tillotson and Hazel Luff for their valuable contribution to the testing and characterisation of the samples.

REFERENCES

1. G. Minke, 'Building with Earth: Design and Technology of a Sustainable Architecture', in *Building with Earth*, Birkhäuser, 2012. doi: 10.1007/978-3-7643-7873-8.

2. S. Goodhew, M. Boutouil, F. Streiff, M. Le Guern, J. Carfrae, and M. Fox, 'Improving the thermal performance of earthen walls to satisfy current building regulations', *Energy and Buildings*, vol. 240, p. 110873, Jun. 2021. doi: 10.1016/j.enbuild.2021.110873.

3. F. Streiff *et al.*, 'CobBauge – A hybrid walling technique combining mechanical and thermal performance'. doi: https://pearl.plymouth.ac.uk/handle/10026.1/16827

4. S. Goodhew and R. Griffiths, 'Sustainable earth walls to meet the building regulations', *Energy and Buildings*, vol. 37, no. 5, pp. 451–459, May 2005.
doi: 10.1016/j.enbuild.2004.08.005.

5. A. Azil *et al.*, 'Earth construction: Field variabilities and laboratory reproducibility', *Construction and Building Materials*, vol. 314, p. 125591, Jan. 2022. doi: 10.1016/j.conbuildmat.2021.125591.

6. A. Weismann and K. Bryce, *Building with Cob: A Step-by-step Guide: 1*, First Edition. Cambridge: Green Books, 2006.

7. V. San Fratello and R. Rael, 'Mud Frontiers', *Fabricate 2020*, pp. 22–27, 2020.

8. WASP, 'The first 3D printed House with earth | Gaia | 3D Printers | WASP'. Accessed: Jun. 19, 2023. [Online]. Available: https://www.3dwasp.com/en/3d-printed-house-gaia/

9. A. Veliz Reyes, W. Jabi, M. Gomaa, A. Chatzivasileiadi, L. Ahmad, and N. M. Wardhana, 'Negotiated matter: A robotic exploration of craft-driven innovation', *Architectural Science Review*, vol. 62, no. 5, pp. 398–408, Sep. 2019. doi: 10.1080/00038628.2019.1651688.

10. M. Gomaa, J. Carfrae, S. Goodhew, W. Jabi, and A. Veliz Reyes, 'Thermal performance exploration of 3D printed cob', *Architectural Science Review*, vol. 62, no. 3, pp. 230–237, May 2019. doi: 10.1080/00038628.2019.1606776.

11. A. Laborel-Préneron, J.E. Aubert, C. Magniont, C. Tribout, and A. Bertron, 'Plant aggregates and fibers in earth construction materials: A review', *Construction and Building Materials*, vol. 111, pp. 719–734, May 2016. doi: 10.1016/j.conbuildmat.2016.02.119.

12. F. Stazi, M. Serpilli, G. Chiappini, M. Pergolini, E. Fratalocchi, and S. Lenci, 'Experimental study of the mechanical behaviour of a new extruded earth block masonry', *Construction and Building Materials*, vol. 244, p. 118368, May 2020.
doi: 10.1016/j.conbuildmat.2020.118368.

13. F. Händle, *Extrusion in Ceramics*. Springer Science & Business Media, 2007.

14. 'Unistrut U.K. | Unistrut'. Accessed: Dec. 03, 2023. [Online]. Available: https://www.unistrut.co.uk/

15. J. Benbow and J. Bridgwater, *Paste Flow and Extrusion*. Oxford: Clarendon Press, 1993.

16. 'CobBauge Film 4: Cigar Test - YouTube'. Accessed: Dec. 10, 2023. [Online].
Available:https://www.youtube.com/watch?v=DvOl4Hu9nX8&list=PLi4U6xTEsJyrcssfyDe8JcB-ESEemSE6r&index=4

17. 'CobBauge Film 10: Ball Drop Test for Mix - YouTube'. Accessed: Dec. 10, 2023. [Online]. Available: https://www.youtube.com/watch?v=eN37WWICPDk&list=PLi4U6xTEsJyrcssfyDe8JcB-ESEemSE6r&index=10

18. K. Touati *et al.*, 'Earthen-based building: In-situ drying kinetics and shrinkage', *Construction and Building Materials*, vol. 369, p. 130544, Mar. 2023. doi: 10.1016/j.conbuildmat.2023.130544.

19. 'Strocks', H.G Matthews Limited. Accessed: Dec. 27, 2023. [Online].
Available:https://www.hgmatthews.com/lime-and-cob/natural-building-blocks/strocks/

20. 'Earth Blocks UK'. Accessed: Dec. 22, 2023. [Online]. Available: https://earthblocks.co.uk/

PLEA 2024 WROCŁAW
(Re)thinking Resilience

Nature-based solutions performance versus man-made hazards:
a literature review for enhancing the resilience of critical infrastructure.

LICIA FELICIONI[1,2], BARBORA RYBOVÁ[1], MICHAL SNĚHOTA[1,2]

[1]Czech Technical University in Prague, University Centre for Energy Efficient Buildings, Třinecká 1024, 273 43 Buštěhrad, Czechia
[2] Czech Technical University in Prague, Faculty of Civil Engineering, Thákurova 2077/7, 166 29 Prague, Czechia

ABSTRACT: Policymakers in Europe and beyond prioritize nature-based solutions (NBS) as a crucial strategy to tackle societal challenges, including mitigating the impact of climate change and contributing to the achievement of international goals. Risk management and resilience can be improved over conventional approaches, which is of utmost importance today, as Europe is not only confronted with several natural hazards but also with man-made threats. Therefore, to ensure the maximum effectivity of NBS, it is crucial to comprehend and enhance their capacity for preventing and enduring malicious attacks. Specifically, this paper lays the foundation for the Horizon Europe project titled "City nature-based solutions integration to local urban infrastructure protection for a climate-resilient society" (NBSINFRA). The paper explores the role of NBS in safeguarding infrastructure against man-made hazards while simultaneously being susceptible to such threats. Results revealed NBS interventions that effectively mitigate such threats and other NBS more vulnerable to man-made hazards, jeopardizing public safety and contributing to criminal activities if inadequately designed. Based on this review of the literature, landscape architecture and NBS implementation seem to already exploring how the integration of nature and urban environments can safeguard cities and their inhabitants not only from natural hazards but also potential human-made risks.
KEYWORDS: Nature-based Solutions; NBS; Man-made Hazards; Literature Review; Infrastructure.

1. INTRODUCTION

Critical infrastructure consists of assets or systems that are vital to the maintenance of certain societal functions. Natural disasters, criminal activity, or malicious behaviour may damage infrastructure, resulting in its destruction or disruption, which may severely impact the safety and well-being of citizens [1]. The protection of critical infrastructure as well as the mitigation of disaster impact are both dependent on constant innovation. The international community recognizes the imperative to diminish the risk posed by both natural and man-made hazards, a core principle underscored in the Sendai Framework for Disaster Risk Reduction [2].

In fact, policymakers in Europe and beyond prioritize nature-based solutions (NBS) as a crucial strategy to tackle various societal challenges, including addressing natural hazards, mitigating the impact of climate change, advancing sustainability goals, and contributing to the achievement of the United Nations' Sustainable Development Goals (SDGs) [3,4]. NBS are a cost-effective way to build infrastructure that is resilient to climate change-induced hazards while benefiting humans and biodiversity [5,6]. By combining NBS with local knowledge, critical infrastructure can be protected from natural and man-made disasters.

With solutions such as these, risk management and resilience can be improved over conventional approaches [7], which is of utmost importance today, as Europe is not only confronted with a number of natural hazards, including pandemics, droughts, heat waves, storms, floods, and wildfires but also with man-made hazards [8].

Nevertheless, disaster risk management and adaptation concentrate on minimizing exposure and vulnerability while enhancing resilience to the potential adverse effects of both natural and man-made hazards. Although it is acknowledged that risks cannot be entirely eradicated, these efforts enable assets to better withstand and cope with such challenges [9].

2. NBSINFRA HORIZON EUROPE PROJECT

The protection of infrastructures against hazards and, in particular, man-made ones, such as terrorism, cyber-attacks, or malicious behaviour, has been a priority of the European Commission with the European Programme for Critical Infrastructure Protection (EPCIP) [10]. Although much effort is being expended in re-naturalizing the infrastructure with NBS (e.g., Langemeyer and Baró [11]), man-made threats, along with natural disasters, pose a potential danger to the operating and monitoring systems of the infrastructure.

Therefore, to ensure the maximum effectiveness of NBS, its capability for preventing malicious attacks and sustaining them must be understood and further developed.

Specifically, this paper lays the foundation for the new Horizon Europe project titled "City nature-based solutions integration to local urban infrastructure protection for a climate-resilient society" (NBSINFRA) that just began in September 2023 (4-year project).

There is indeed a focus on improving resilience in vulnerable infrastructure, and the project's main objective is to enhance the local urban infrastructure protection against natural and man-made hazards through NBS co-design and co-creation for a sustainable and resilient society developing a methodology and toolkit that could serve as a best practice guide.

Existing and new approaches will be tested in five different locations, respectively, Aveiro (PT), Fingal (IE), Prague (CZ), Cologne (DE) and Ruse (BG), in the so-called City Labs.

In particular, a comparison of infrastructure vulnerabilities with and without NBS will be conducted via impact simulations and conditions comparisons. In addition to natural hazards, physical and cyber-physical attacks will be considered threats to the infrastructure and the NBS. For instance, NBS monitoring systems, which would reveal their wider benefits and impacts, may be potential targets of cybercrime and other man-made hazards.

2.1 Scope of the paper

The paper explores the role of NBS in safeguarding specific infrastructure against potential manmade hazards while simultaneously being susceptible to such threats. The purpose of this study is to determine whether NBS for infrastructure is at risk from man-made hazards or if NBS might offer protection from them by examining the available literature on the topic (Fig. 1).

3. METHODOLOGY

A manual review was conducted using three of the most widely used search engines, Web of Science, Google Scholar and Scopus. Keywords utilized in this search included 'Nature-based solution or NBS', ‘landscape design’, 'man-made or man-made hazards', 'cyber-attack* or cyber threat* or cybersecurity', 'terrorism', 'war*', ‘crime’ 'infrastructure', 'monitor* OR sensor*', ‘risk management’. At the same time, information was collected from online newspapers which reported case studies of real attacks on such infrastructure. Information was collected and clustered into two options. From this operation, the results highlight the successful implementation of NBS in mitigating different manmade hazards and at the same time, the most recurrent human threats they may face.

Two distinct clusters concerning NBS and manmade hazards are delineated: the first cluster pertains to potential attacks on critical infrastructure, which could be mitigated through the deployment of NBS (for instance, the use of wetlands to ram a vehicle); the second cluster addresses the vulnerability of NBS, often monitored through measurements and sensors to counteract natural hazards like floods and heat waves, or disruptions to the functionality of NBS itself (such as cases where hackers may interfere with the operation of valves in an irrigation system supporting a green wall, resulting in the demise of plants).

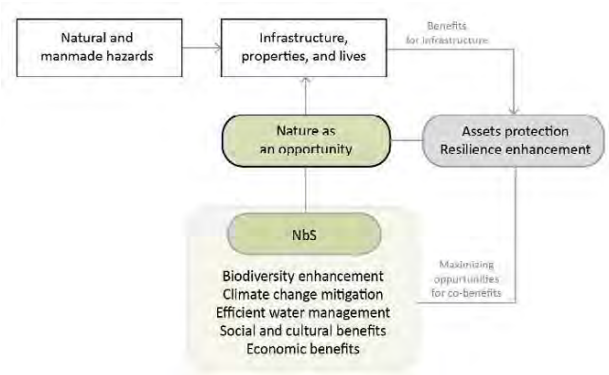

Figure 1: Benefits of NBS employed in infrastructure protection.

3. RESULTS AND DISCUSSION

The literature review delineated two primary clusters concerning the correlation between NBS and anthropogenic hazards. The first encompasses publications and instances of successful implementation of design solutions, illustrating how NBS can effectively mitigate manmade threats. The second cluster comprises records detailing the potential susceptibility of NBS to anthropogenic hazards.

3.1 Cluster 1 - NBS for manmade threats mitigation

Through the examination of existing literature, the primary challenges discerned within this cluster revolve around Crime and Terrorism, as evidenced by the findings presented in Table 1. The identified threats, specifically in terms of criminal activities and acts of terrorism, underscore the imperative for a nuanced understanding of how NBS may be influenced by, or conversely, impact these security-related issues. This further emphasizes the need for targeted strategies and adaptive measures to address and mitigate the associated risks effectively.

Table 1: Cluster 1 regarding NBS employed to mitigate and reduce the vulnerability of infrastructure and open spaces to manmade threats.

Manmade threat	Focus	References
Crime	Water security	[12,13]

	Properties and people	[14–17]
	Induced fire	[18]
Terrorism	Vehicle-ramming	[16,19–21]
	Explosive attack	[22,23]

Concerning Cluster 1, specifically within the "Crime" category, a thorough examination has been conducted on three principal issues. Cioffi [13] and Everard et al. [12] underscore the potential endangerment of water infrastructure, emphasizing its impact on water security. Additionally, they advocate for the integration of NBS and efficient water harvesting as viable measures to alleviate and diminish this vulnerability.

An expanding body of literature is investigating the correlation between urban greenspaces and crime, producing contrasted findings [17]. Notably, Venter et al. [15] observed that a greater prevalence of greenery in the vicinity of a building correlates with a decrease in reported crimes, including both violent and property offences; the same outcome resulted from the study of Wolfe and Mennis [14]. A significant correlation was found between the abundance of vegetation and a reduction in assaults, robberies, and burglaries, but not thefts. Urban planning policies could be influenced by this, especially as cities adopt green growth plans, emphasizing the importance of integrating sustainable crime prevention strategies into city planning.

Conversely, Koskela & Pain [24] and Sonti et al. [25] emphasize the potential influence of perceptions or fear of crime stemming from vegetation in neighbourhoods, attributing it to issues such as blind spots and excessive density of vegetation.

Furthermore, Regos [18] has underscored the potential of NBS as a preventive measure to mitigate wildfires increasingly instigated by human activities.

In the context of acts of terrorism within urban environments, particularly in open spaces and pedestrian zones, numerous publications and examples of best practices incorporate NBS.

Notably, Felix et al. [19] or the book of the Center for the Protection of National Infrastructure [20] exemplify how landscape design elements, such as trees and flower boxes, can function as defensive systems to enhance building security. They advocate for the incorporation of elements like elevated planters, trees, and benches or other street furniture as substitutes for bollards to offer perimeter protection for designated structures. These features may possess crash-resistant capabilities, providing the security benefits of crash-rated bollards without overtly signalling their protective function. Anti-terrorism barriers of this nature have been deployed in numerous European cities. Fig. 2 illustrates an example wherein plants are positioned within weathering steel cylinders, striking a balance between accommodating security for critical buildings and their occupants, and preserving the vibrancy of the public space.

Figure 2: Example of Nature-based solutions installed as anti-terrorism barriers in the city centre of Rimini, Italy. This was an initiative made in 2020 called "Incontro alle barriere" which means "meeting at the barriers". Photo: Felicioni L.

The relevance of landscaping in crime prevention is underscored by the RIBA report [21], providing another illustrative example. As an example, clearing or maintaining vegetation around parking lots may be necessary to ensure clear sightlines, create unobstructed camera views along perimeter fencing, provide patrol space for security guards, and eliminate potential shelter for intruders. Additionally, the addition of water features to the landscape enhances the site not only aesthetically, but also serves as both a habitat for wildlife and a physical barrier against intruders.

Moreover, NBS can serve as effective impediments to establishing blast-resistant infrastructure or buildings, as demonstrated by Koccaz et al. [22]. The judicious selection of suitable vegetative species becomes crucial, particularly when employed as a perimeter barrier in the guise of thorny hedges and dense hedgerows. Considerations for the ultimate size and maintenance requirements are necessary to prevent the obstruction of critical sight lines or the creation of potential hiding places. In a broader context, the strategic placement of taller vegetation near buildings is recommended to ensure the preservation of open sight lines [16].

In fact, the use of water and greenery for safeguarding against man-made hazards is not a recent concept in landscape architecture; people have employed this strategy for centuries, evident in structures like citadels or castles. The contemporary challenge lies in embracing an interdisciplinary

approach to adapt this traditional concept to the demands and knowledge of modern urban areas, considering the dynamics of current public spaces. Indeed, Fig. 3 exemplifies an ancient case showcasing the multifaceted application of NBS, extending beyond the mitigation of natural hazards, such as coastal flooding. Notably, the Citadel of Copenhagen in 1807 serves as a historical testament to the dual purpose of NBS, both in defence against military conflicts – exemplified during the Battle of Copenhagen against the United Kingdom – and contemporary employment for flood hazard mitigation. Presently, the terrain depression serves a primary function in addressing flood-related risks.

A contemporary example of NBS deployed for protective purposes is evident in the design of the US embassy in London, United Kingdom. The building is surrounded by a bioswale, primarily implemented for environmental considerations. However, the design is meticulously calibrated to effectively impede any moving vehicle attempting to breach the premises by strategically incorporating features capable of thwarting such attempts across the expanse of meadow grasses.

Figure 3: Close-up detail of the terrain depression and the water moat that surrounds the Citadel of Copenhagen, Denmark. Photo: Rybova B.

3.2 Cluster 2 - NBS threatened by manmade hazards

The primary challenges identified within this second cluster revolve around Crime and Cyber Attacks, as illustrated in Table 2.

Table 2 Cluster 2 regarding NBS potentially threatened by manmade hazards.

Manmade threat	Focus	References
Crime	People	[24,26,27]
Cyber attack	Monitoring systems	[28,29]
	Poisoning	[30]

Concerning the "Crime" category, prominent themes consistently circled around the integration of vegetation characteristics, such as density and height, with factors including illumination, legibility of pedestrian routes, and maintenance practices. These factors, coupled with the absence of signs of incivilities, collectively contribute to a positive perception of space. It is crucial to note that an inadequately designed environment may engender a fear of potential attacks by strangers, as exposed by Koskela & Pain [24] and Hosseinalizadeh [26].

In the "Cyber attack" category, the use of Earth Observation (EO) tools, including satellites and drones, for monitoring distant spots may be susceptible to cyber threats and hacking. Notably, Chrysoulakis et al. [29] underscores that EO presents unexploited possibilities, supplying essential data for evaluating the influence of NBS on urban dynamics, particularly in relation to energy, water, and carbon balances. In the event of a technological breach, there exists the potential for malicious use to disrupt disaster management and relief operations, subsequently amplifying the extent of damage and casualties. Another example is the water infrastructure, which is susceptible to direct targeting or contamination through the introduction of toxic substances or disease-causing agents [30]. Instances of such malicious activities are exemplified by hacker attacks on blue infrastructures, particularly irrigation systems, resulting in the introduction of hazardous amounts of chemicals. A notable episode occurred in Florida in 2021, and this was not an isolated occurrence, with several other incidents documented in Israel [31].

Noteworthy studies, such as those conducted by Koskela & Pain [24] and Ogletree et al. [17], explore public perceptions of greenery in urban environments and its capacity to mitigate criminality and other threats. For a considerable number of respondents, the presence of greenery contributes to a more pleasant and secure environment since the number of crimes reduced after the implementation of new green areas.

Furthermore, proper maintenance of NBS is essential. For instance, inadequate planting of a tree barrier can lead to weakened roots, resulting in reduced shading benefits and a compromised wind-barrier effect. Similarly, the use of low-quality substrate can impede rainwater retention, hindering effective evaporation and diminishing the cooling impact on the city during summer. Additionally, it may compromise trees' ability to provide sufficient protection to pedestrians in the event of a vehicle attack. This principle can be extended analogously to swales and rain gardens.

4. CONCLUSION

This study investigates the dual aspects of NBS in relation to their potential mitigation of, or

susceptibility to, man-made hazards. The literature review reveals two primary clusters: the first emphasizes NBS interventions that effectively mitigate such threats, while the second cluster consists of publications and examples highlighting the vulnerabilities of NBS to man-made hazards, which could pose risks to public safety and contribute to criminal activities if inadequately designed—such as in cases concerning dense vegetation that obscures blind spots.

Based on this review of literature, it is evident that landscape architecture has begun exploring how the integration of nature and urban environments can safeguard cities and their inhabitants not only from natural hazards but also potential human-made risks. Nevertheless, there are relatively few concrete examples of NBS being employed to mitigate manmade hazards.

The insights gathered from this study serve as foundational knowledge for the Horizon Europe NBSINFRA project, designed to enhance infrastructure resilience against both natural and man-made hazards. These findings will be instrumental in guiding the implementation of new NBS within the City Labs' locations but will also steer additional studies and applications of NBS for mitigating man-made hazards in various European contexts.

Future work will delve into the specific probabilities of encountering man-made hazards within the City Labs.

ACKNOWLEDGEMENTS

This research was supported by Project No. 101121210 “City Nature-Based Solutions Integration to Local Urban Infrastructure Protection for a Climate Resilient Society” (NBSINFRA). Funded by the European Union. Views and opinions expressed are, however, those of the author(s) only and do not necessarily reflect those of the European Research Executive Agency (REA). Neither the European Union nor the granting authority can be held responsible for them.

Funded by the European Union

REFERENCES

1. European Commission Critical infrastructure, [Online] Available: https://home-affairs.ec.europa.eu/pages/page/critical-infrastructure_en [20 June 2023].
2. UNISDR, The Sendai Framework for Disaster Risk Reduction 2015 - 2030.
3. United Nations, (2015). The Sustainable Development Goals; New York City;
4. Faivre, N.; Fritz, M.; Freitas, T.; de Boissezon, B.; Vandewoestijne, S., (2017). Nature-Based Solutions in the EU: Innovating with nature to address social, economic and environmental challenges. *Environmental Research*, 159, p.509–518, doi:10.1016/j.envres.2017.08.032.
5. EU-funded OPERANDUM project, [Online], Available https://www.operandum-project.eu/ (8 July 2023).
6. Dabbeek, J.; Silva, V.; Galasso, C.; Smith, A., (2020). Probabilistic earthquake and flood loss assessment in the Middle East. *International Journal of Disaster Risk Reduction*, 49, 101662, doi:10.1016/j.ijdrr.2020.101662.
7. Debele, S.E.; Leo, L.S.; Kumar, P.; Sahani, J.; Ommer, J.; Bucchignani, E.; Vranić, S.; Kalas, M.; Amirzada, Z.; Pavlova, I.; et al., (2023). Nature-based solutions can help reduce the impact of natural hazards: A global analysis of NBS case studies.
Science of The Total Environment, 902, doi:10.1016/j.scitotenv.2023.165824.
8. European Commission Directorate-General for European Civil Protection and Humanitarian Aid Operations (ECHO), (2021). Overview of natural and man-made disaster risks the European Union may face; ISBN 9789276293040.
9. Badina, S.; Babkin, R.; Bereznyatsky, A.; Bobrovskiy, R., (2022). Spatial aspects of urban population vulnerability to natural and man-made hazards. *City and Environment Interactions*. 15, 100082, doi:10.1016/j.cacint.2022.100082.
10. European Commission Critical Infrastructure Protection, [Online], Available https://joint-research-centre.ec.europa.eu/scientific-activities-z/critical-infrastructure-protection_en (30 July 2023).
11. Langemeyer, J.; Baró, F., (2021). Nature-Based Solutions Nature-based solutions as nodes of green-blue infrastructure networks: A cross-scale, co-creation approach. *Nature-Based Solutions*. 1, 100006, doi:10.1016/j.nbsj.2021.100006.
12. Everard, M.; Ahmed, S.; Gagnon, A.S.; Kumar, P.; Thomas, T.; Sinha, S.; Dixon, H.; Sarkar, S., (2020). Can nature-based solutions contribute to water security in Bhopal? *Science of The Total Environment*. 723, 138061, doi:10.1016/j.scitotenv.2020.138061.
13. Cioffi, G., (2015). The Terror Risk to Current Water Infrastructure System, York University.
14. Wolfe, M.K. and J. Mennis, (2012). Does vegetation encourage or suppress urban crime? Evidence from Philadelphia, PA. *Landscape and Urban Planning*. 108, p. 112–122, doi:10.1016/j.landurbplan.2012.08.006.
15. Venter, Z.S.; Shackleton, C.; Faull, A.; Lancaster, L.; Breetzke, G.; Edelstein, I., (2022). Is green space associated with reduced crime? A national-scale study from the Global South. *Science of The Total Environment*. 825, 154005, doi:10.1016/j.scitotenv.2022.154005.
16. Arnold, C. and M.A. Lasch, (2007). Site and Urban Design for Security Guidance Against Potential Terrorist Attacks FEMA 430;
17. Ogletree, S.S.; Larson, L.R.; Powell, R.B.; White, D.L.; Brownlee, M.T.J., (2022). Urban greenspace linked to lower crime risk across 301 major U.S. cities. *Cities.* 131, 103949, doi:10.1016/j.cities.2022.103949.
18. Regos, A., (2022). Nature-based solutions in an era of mega-fires; *Nature*. 607, 7919: 449-449.
19. Felix, M. and M. Elhefnawi, (2020). Landscape design elements as a defensive tool for building security. In Advances in Science, Technology and Innovation; Springer International Publishing: p. 227–238 ISBN 9783030173081.
20. Home Office; Center for the Protection of National Infrastructure; National Counter-Terrorism Security Office, (2012). Protecting Crowded Places: Design and Technical Issues; ISBN 978-1-84987-393-2.
21. RIBA, (2010). RIBA guidance counter-terrorism; London, England;

22. Koccaz, Z.; Sutcu, F.; Torunbalci, N., (2008). Architectural and Structural Design for Blast Resistant Buildings. In Proceedings of the The 14th World Conference on Earthquake Engineering: p. 8.
23. Landscape Architecture Aotearoa Designing to deter attackes - The Sandy Hook case study, [Online], Available https://www.landscapearchitecture.nz/landscape-architecture-aotearoa/2018/2/27/designing-to-deter-attacks-the-sandy-hook-case-study.
24. Koskela, H. and R. Pain, (2000). Revisiting fear and place: Women's fear of attack and the built environment. *Geoforum*, 3: 269–280, doi:10.1016/S0016-7185(99)00033-0.
25. Sonti, N.F.; Campbell, L.K.; Svendsen, E.S.; Johnson, M.L.; Novem Auyeung, D.S., (2020). Fear and fascination: Use and perceptions of New York City's forests, wetlands, and landscaped park areas. *Urban Forestry & Urban Greening*. 49, 126601, doi:10.1016/j.ufug.2020.126601.
26. Hosseinalizadeh, S., (2020). Safer Green Cities - A Study about Vegetation Impacts on Perception of Safety in Green Spaces Case Study, Politecnico di Milano.
27. Lis, A. and P. Iwankowski, (2021). Why is dense vegetation in city parks unpopular? The mediative role of sense of privacy and safety. *Urban Forestry & Urban Greening*. 59, doi:10.1016/j.ufug.2021.126988.
28. Kumar, P.; Debele, S.E.; Sahani, J.; Rawat, N.; Marti-cardona, B.; Maria, S.; Basu, B.; Sarkar, A.; Bowyer, P.; Charizopoulos, N.; et al., (2021). Earth-Science Reviews An overview of monitoring methods for assessing the performance of nature-based solutions against natural hazards. *Earth-Science Reviews*. 217, doi:10.1016/j.earscirev.2021.103603.
29. Chrysoulakis, N.; Somarakis, G.; Stagakis, S.; Mitraka, Z.; Wong, M., (2021). Monitoring and Evaluating Nature-Based Solutions Implementation in Urban Areas by Means of Earth Observation. Remote Sensing. 13, doi:10.3390/rs13081503.
30. BBC, Hacker tries to poison water supply of Florida city [Online], Available https://www.bbc.com/news/world-us-canada-55989843.
31. Kovacs, E. Irrigation Systems in Israel Disrupted by Hacker Attacks on ICS [Online], Available https://www.securityweek.com/irrigation-systems-in-israel-disrupted-by-hacker-attacks-on-ics/.

PLEA 2024 WROCŁAW
(Re)thinking Resilience

Structural Diversity of Full-Culm Bamboo Architecture in the State of São Paulo

Six Case Studies

BRIANNA CATHARINA BUSSINGER[1] CLAUDIA TEREZINHA DE ANDRADE OLIVEIRA[1]

[1]University of São Paulo, São Paulo, Brazil

ABSTRACT: This research explores the use of bamboo as a sustainable construction material in Brazil, particularly in the state of São Paulo. It systematically categorizes architectural typologies and design detailing of six case studies using full-culm bamboo as a structural primary element. The research employs a descriptive methodology, analysing bamboo structures in existing literature and through firsthand data gathered by the author via site visits and interviews. The paper highlights bamboo's versatility, demonstrating its use in various architectural types, from orthogonal to curvilinear, and connections ranging from low to high technological complexity. The case studies include an art gallery, residential and commercial spaces, and a cultural venue, which, when analysed under the proposed theoretical framework, reveal insights into the architectural characteristics and practical implementation of bamboo in the Brazilian scenario. This research underscores bamboo's potential as a key material for future environmentally-conscious architectural design in Brazil, while acknowledging current challenges in design processes and execution, due to its nascent status in the civil construction sector as a conventional material.

KEYWORDS: Bamboo Architecture, Full-Culm Bamboo, Sustainable Construction, Brazilian Architecture, Building Techniques

1. INTRODUCTION

Bamboo exhibits inherent sustainability evidenced by its global occurrence, rapid growth, and efficient carbon sequestration. Advancements in affordable treatment methods make bamboo both durable and accessible for construction [1]. The resilience of this bio-based material can be perceived from both an ecological and a social vantage point. In architecture, the use of bamboo is particularly advantageous for countries in the Global South, where its natural abundance and minimal processing requirements make it a viable building material [2].

Bamboo's versatility spans from advanced products like plyboards to its natural cylindrical shape, termed full-culm bamboo. Even unprocessed, it has properties that make it suitable for a variety of structural applications. Countries like Indonesia have integrated bamboo into their recent architectural fabric by merging traditional construction techniques with contemporary design strategies [3]. In contrast, Brazil is at the early stages of exploring bamboo's architectural potential and lacks a foundational bamboo-centric culture.

The main objective of this study is to systematically categorize the structural systems and joint techniques in six case studies in the state of São Paulo that use full-culm bamboo as a main structural element. This aims to provide a comprehensive perspective on bamboo's role in Brazil's sustainable construction trends and to aid in interpreting these structures' contribution to the evolution of bamboo architecture in Brazil.

2. MATERIALS AND METHODS

This study utilizes a descriptive approach, collecting technical information from existing literature on architectural projects and direct data acquisition by the author through site visits and interviews with architects responsible for the projects. Six case studies, built from 2016 onward, were selected based on their primary use of full-culm bamboo as a permanent structural element, their alignment with species recognized by the INBAR special economic interest list [4], and architectural significance. Professional architectural teams designed each case study, and they were built with supervised construction. The investigation excluded buildings created using algorithmic design approach, as they predominantly use forms of bamboo other than full-culm, such as splits, for construction purposes [5].

The analysis initiates by applying classification systems from three doctoral theses to categorize bamboo structures [6-8]. These systems, determined by recent studies, provide a comprehensive framework for understanding bamboo structures and connections, covering both broad structural concepts and a detailed overview of connections. Within this

framework, the case studies are examined to draw insights on characteristics of Brazilian bamboo architecture.

The six architectural projects selected to illustrate the varied use of full-culm bamboo architecture in Brazil and to be analysed under the proposed theoretical framework by this research are:

1. Galeria de Arte Catuçaba (2016) at São Luiz do Paraitinga by CRU! Architects: 110m² art gallery.

2. Casa de Hóspedes Picinguaba (2017) at Picinguaba by CRU! Architects: 60m² guest house.

3. Casa das Birutas (2019) at Piracaia by Gera Brasil: 212m² single-family residence.

4. Loja FARM Moema (2021) in São Paulo city by Rosenbaum: 247m² clothing store.

5. Casa da Música, Vitor Lotufo (2021): Botucatu - 100m² cultural music venue.

6. Unidade de Alimentação e Nutrição (UAN) at Fazenda Painal in Cravinhos by Niner Arquitetura: 200m² support facility.

3. CATEGORIES: STRUCTURE AND DETAIL

Recognized in building design since the early 2000s, and due to pioneering structures like the ZERI Pavilion built at the Expo Hannover by Simon Vélez [9], bamboo architecture merges bio-based materials with contemporary sustainable development needs. Despite its growing relevance, it remains largely absent from standard architectural education. However, the field's experts have been able to explore bamboo's versatile building potential, often through practical experience [6]. This section introduces categorizations for understanding the complexities of full-culm bamboo design and construction, offering a structured approach to this innovative architectural domain.

3.1 Structural grouping system

The first classification system, as outlined by Mouton (2021) [6], groups bamboo structures based on their level of orthogonality (Fig. 1). The study in question presented five structural groups as follows. The "organically woven freeform architecture" predominantly uses bamboo strips instead of full-culm bamboo, incorporates algorithmic design, and most structures under this category are temporary; this classification is not applicable for this study. The "curvilinear architecture" is form-active, deriving stability from its shape, capable of bearing axial forces in tension or compression but not bending moments. Arch-based structures are under this category. The "truss architecture" employs plain geometrical triangulation systems for efficient force transfer. "Geometric structures" are grounded in mathematical principles, resulting in distinct geometries such as space frames and grid shells. Grid shells can further be of hyperbolic paraboloid, pantograph grid shell, diagrid, or geodesic dome types. Lastly, "orthogonal bamboo architecture" involves the use of bamboo either horizontally or vertically, typically serving as beams and columns without any diagonal or curved application.

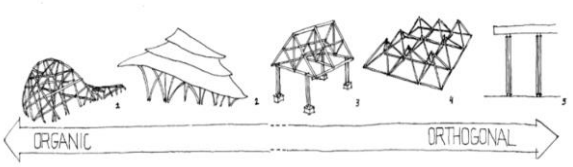

Figure 1: Bamboo structure typology progression [6].

The initial step for bamboo design may involve selecting a structural system based on project requirements and local resources. For example, different bamboo species suit specific structural types and force transfer requirements, besides presenting distinct aesthetic characteristics. The next phase in design focuses on the detailing of joints, where bamboo culms intersect and connect with other materials. Connectors are crucial for ensuring effective force transfer and the research conducted by Widyowijatnoko (2012) [7], proposes a classification system to guide these considerations.

3.2 Connection Classification

The second classification system discussed in this study addresses the connections of bamboo structures. As proposed by Widyowijatnoko (2012), connections are grouped based on the mechanisms of force transfer and the positioning of the connector (Fig. 2).

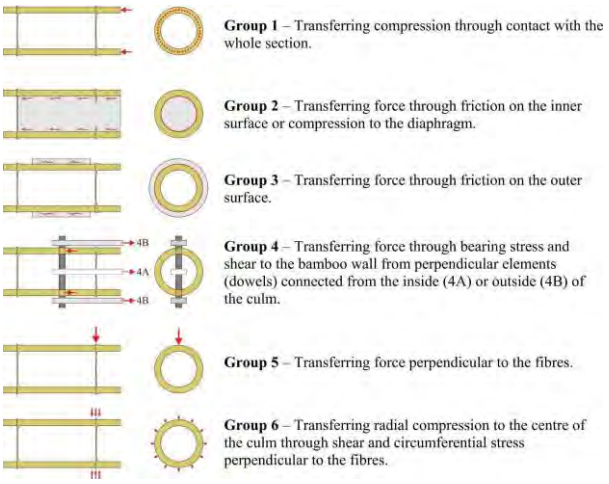

Figure 2: Illustration of force transfer in the six groups of bamboo connectors [7].

The 'Group 6' connectors, a specific connection type developed for a particular thesis, is not considered in this paper.

Bamboo structures often incorporate one or more connection groups. For instance, the widely used fish-

mouth connector combines elements of 'Group 1 and 4A', and sometimes includes a mortar filling from 'Group 2'. The proposed systematization is essential for designing connectors and the execution of these can range from traditional manual labour to a more advanced technological fabrication.

3.3 Technological Classification of connectors

Furthermore, Larrinaga (2022) [8] classifies connections based on their technological complexity:

- Low-tech connections: Embody traditional and vernacular techniques that rely predominantly on local resources and skills.
- Medium-tech connections: Employ standardized materials, commonly supplied by the civil construction sector. These materials interface with bamboo but aren't necessarily bamboo-specific.
- High-tech connections: Require specialized fabrication and demand specialized labour that are not bamboo-related.

The choice of connector technology affects the labour intensity and modernity of the fabrication process. Successful bamboo structures depend on a thoughtful process encompassing structural typology, force transfer at connection points, and effective fabrication methods of these connectors. The case studies are analysed across these categories.

3.4. Case studies analysis

The analysis categorized the gathered data based on structural systems [6], connection types [7], and connection technology levels [8], and resulted in the subsequent systematization shown in Table 1.

Table 1: Systematic Classification of Case Study Attributes.

Project	Architecture	Joints	Tech
1	Orthogonal + Curvilinear	2	High
2	Truss	2 and 4	High
3	Geometric + Curvilinear	3 and 5	Low and Medium
4	Truss	1 and 4	Medium
5	Geometric	3 and 5	Low and Medium
6	Truss	4	High

Table 1 reveals a diverse application of full-culm bamboo in Brazilian architecture, including all typologies proposed by Mouton (2021) – from orthogonal to curvilinear. The joint types used vary, and also incorporate all joint types classified in study [7]. Some projects employ a single type of connector, while others use a combination of two types of connectors, mixing and matching types in order to ensure correct force transfer throughout the structure. Technologically, the connections range from low to high complexity, indicating a mix of traditional and advanced construction techniques in these bamboo connections, however with a clear inclination to a more technological approach. None of the structures rely solely on low technological connectors.

4. ARCHITECTURAL FRAMEWORK EVALUATION

This section delves into how the categorization systems from three doctoral theses apply to the six case studies. The process begins with a broad overview of each structure, gradually narrowing down to focus on finer details and fabrication techniques. This approach offers a comprehensive understanding of each case study, linking theoretical concepts to their practical implementation in bamboo architecture. It provides a structured analysis, from general structural elements to specific joint types and technological methods used in construction.

4.1. Galeria de Arte Catuçaba

In the art gallery, the orthogonal structure is enhanced by curvilinear arches that form a pathway (Fig. 3), guiding visitors through the exhibit. The 'Group 2' violin connectors (Fig. 3), crafted from locally sourced hardwood, visually and functionally illustrate force distribution, creating a sense of suspension and lightness. This material and design fusion mirrors the estate's natural setting, offering an immersive experience akin to walking through bamboo portals.

Figure 3: Art gallery architecture and violin connector. Source: Author, 2023.

4.2. Casa de Hóspedes Picinguaba

The guesthouse is designed in between a rammed earth wall and an opposite glass curtain wall, and features two distinct bamboo truss formations. The first, outside the rammed earth wall, bridges the main and guest houses, using 'Group 2' connectors (Fig. 4) for both structural support and decorative purposes. Inside, the minimalistic trusses (Fig. 4) maximize the 60m² space and pair a bamboo culm with a steel rod in a 'Group 4' connection forming an inverted truss, exemplifying bamboo's strength. This structure supports a green roof and offers unobstructed garden views, providing a comfortable and spacious guest shelter.

Figure 4: Guest house architecture and 'Group 2' connector. Source: Author, 2023.

4.3. Casa das Birutas

This residence combines a geometric structural typology with curvilinear forms, resulting in a pantographic grid shell (Fig. 5) supported by bamboo arches for wide spans. The 100m² space, with an open floor plan, omits a traditional ceiling, integrating the bamboo structure into its interior design. Bamboo curving at the arches is achieved mechanically through V-section cuts. The assembly of the arches with the pantographic structure utilizes synthetic rope lashings typical of 'Group 3' and screws from 'Group 5' (Fig. 5) for securing connections. This rustic design, blending complexity with traditional methods, creates a sustainable home that offers panoramic views into the ecovillage's natural environment.

Figure 5: House architecture and 'Group 3+5' connector. Source: Gera Brasil, n.d.

4.4. Loja FARM Moema

At the clothing store in São Paulo, the renovation design concept introduced a new bamboo roof, enhancing the store's eco-conscious image. The roof's single plane trusses (Fig. 6), coupled with cross-braced beams, offer slenderness – which is the main structural concept developed by the architect. Bamboo's natural colour contributes to the store's airy, well-lit ambiance. Structural integrity is ensured through 'Group 1 + 4' connectors (Fig. 6), commonly denominated as fish mouths, blending strength with the sleek design ethos of the brand.

Figure 6: Store architecture and 'Group 1+4' connector. Source: Author, 2023.

4.5. Casa da Música

This music venue's structure, a geometric hyperboloid paraboloid (Fig. 7), is designed for optimal acoustics, utilizing bamboo's flexibility, specifically bending and torsion capacity. The use of 'Group 3' and 'Group 5' connectors (Fig. 7), combining steel rods and cable lashings, enhancing the structure's rigidity. This approach, initially focused on lashings, evolved to integrate steel for practicality. The venue's design stands out for its double-curved surfaces in the roof and walls, showcasing a fusion of function and architectural form exploration with bamboo as the main structural element.

Figure 7: Music venue and 'Group 3+5' connector. Source: Author, 2023.

4.6. Unidade de Alimentação e Nutrição (UAN) at Fazenda Painal

In the UAN project, the truss design, utilizing bamboo and steel, optimizes ceiling height (Fig. 8). Instead of bamboo, the lower chord of the truss is made out of steel and extends in one piece, circumventing eventual bamboo transportation issues and avoiding horizontal connections in bamboo culms. Bamboo, used for the triangular and upper chords, connects to the steel via gusset plates in 'Group 4' joints (Fig. 8). This arrangement distributes stress, preventing damage in bamboo culms. The trusses are inclined, achieved by adjusting cross-bracing dimensions, complementing to the design requirements of an inclined roof. The truss was assembled on-site and hoisted into place, facilitated by pre-perforated holes in the bamboo culms for steel rod fittings.

Figure 8: UAN cafeteria and 'Group 4' connector. Source: Author, 2023.

5. RESULTS

The case studies include a variety of functions such as an art gallery, residential and commercial

spaces, a cultural venue, and a support facility, spanning a wide range of dimensions from 60-247m². Central to their design is the use of bamboo, chosen for its sustainability and versatility. These buildings are located in diverse settings, from beaches and mountains to urban areas in São Paulo, showcasing bamboo's adaptability to different climates and environments.

5.1. Structural typology analysis

The case studies mainly feature orthogonal and truss structures, with trusses being the dominant typology. In contrast, curvilinear architecture, which is positioned in the opposite spectrum of the orthogonal style, is incorporated into two projects. However, it primarily serves to complement the main structural forms rather than being a central feature. These cases display unique bamboo curving techniques, but the presence of curvilinear elements in the overall designs is relatively minimal.

The case studies reflect a preference for using bamboo as a linear element, likely due to labour constraints and the availability of skilled builders. Despite these constraints, the use of linear bamboo elements leads to innovative designs, such as the hyperbolic paraboloid structure in the music venue. This example demonstrates that linear bamboo can be used to create complex, double-curved surfaces, proving that labour limitations do not necessarily restrict the potential for architecturally interesting and innovative structures.

Bamboo's versatility in different architectural styles highlights the complexity of designing and executing force-transferring connectors, yet such challenges are surmountable. The rise in connector sophistication indicates a shift in focus towards detailed design over general structural form. This variety in connector designs, from simple to complex, showcases Brazilian bamboo construction's adaptability and evolving nature.

5.2. Connectors analysis

In these bamboo structures, connectors are crucial yet challenging elements, revealing design and execution complexities. The study shows a prevalence of orthogonal and truss-architecture typologies and medium and high-tech joints in permanent constructions. In contrast, structurally complex designs often employ low to medium-tech methods. The use of diverse materials, other than bamboo in connections, demonstrates the varied adaptation strategies to local resources in the construction of these connectors, underscoring the challenges of specialized bamboo labour availability.

The case studies generally show an avoidance of the 'fish-mouth' connector, likely due to execution challenges and potential issues if not properly done. Instead, customized solutions involving metal plates, wood, and steel for external connections are preferred, reflecting a trend towards less specialized and advanced bamboo-specific construction techniques. Illustrating the evolution of bamboo construction in Brazil and a shift away from traditional, less technologically developed bamboo connector fabrication.

The varied structural uses of bamboo not only highlight its adaptability but also yield significant insights under systematic analysis.

6. DISCUSSION AND FINAL REMARKS

The study reveals that the design process in bamboo construction often necessitates creative solutions, especially during the execution phase. Given the lack of an established bamboo construction culture in Brazil, a wide range of strategies emerges to tackle contextual challenges. This diversity hinders the standardization and mass production of bamboo architectural typologies. While the findings highlight creativity, this aspect could limit the scalability of such projects. Overall, the study underscores bamboo's growing significance in Brazil's contemporary architectural landscape.

In these bamboo projects, architects embraced an experimental approach, mindful of potential challenges and durability issues. The construction phase involved various obstacles, including sourcing quality bamboo and integrating it with other construction methods. Nonetheless, the innovative solutions highlight Brazil's potential in mainstreaming bamboo construction. These projects, led by renowned architects, mark a pioneering phase for bamboo in Brazilian architecture, combining creativity with practical technology application. However, the study's insights are limited due to its focus on São Paulo and the small number of case studies.

The study concludes that full-culm bamboo in São Paulo demonstrates significant potential as a sustainable and adaptable construction material. Despite construction challenges and sourcing difficulties, innovative solutions and technological progress indicate a promising future for bamboo in both urban and rural architectural contexts. This research highlights the necessity for further exploration and development in bamboo construction, advocating for its broader integration into mainstream architecture. Bamboo's role in sustainable innovation positions it as a key material for the future of environmentally-conscious architectural design.

ACKNOWLEDGEMENTS

This research was made possible through the financial support of the Edital CAPES PROAP CCP-AU nº 01/2023, which facilitated essential site visits.

Special thanks are extended to the architects, builders, and other professionals who graciously dedicated their time for interviews, contributing significantly to the advancement of this research. Their insights and expertise have been invaluable in shaping the study's outcomes.

REFERENCES

1. Pereira, M. A. dos R., Beraldo, A. L., & Feffer, B., (2010). Bambu de corpo e alma (3a reimpre). Canal6.

2. IBC 2022 - Professor Kent Harries - Standardisation of full-culm bamboo structures, (2023, March 24). BambUSP. [Online], Available: https://www.youtube.com/watch?v=-SAq3d9VbZM&t=342s.

3. Elora Hardy: Magical houses, made of bamboo | TED Talk, (2015). [Online], Available: https://www.ted.com/talks/elora_hardy_magical_houses_made_of_bamboo [30 August 2023].

4. Maviton, M., & Sankar, V. R., (2023). Global Priority Species of Economically Important Bamboo (T. T. Long, L. Yanxia, & D. Jayaraman, Eds.). INBAR.

5. Naylor, J. O., Stamm, J., & Vahanvati, M. (2022). Applying Design Tools for Full-Culm Bamboo. In K. Harries & C. Papadopoulos (Eds.), *International Conference on Non-conventional Materials and Technologies*.

6. Mouton, S., (2021). Evaluation Framework for Sustainable, Innovative, Low-Cost Building Prototypes with Bamboo with Case Studies in Brazil [PhD]. Katholieke Universiteit Leuven.

7. Widyowijatnoko, A., (2012). Traditional and innovative joints in bamboo construction [PhD dissertation]. RWTH Aachen University.

8. Larrinaga, R. A., (2022). Uniones y Elementos de Conexión para Estructuras con Bambú: Clasificación y Desarollo de un Prototipo de Conexión [Doctorado]. Universitat Politècnica de Catalunya.

9. Dethier, Jean; Liese, Walter; Velez, Simon (2013). Grow your own house: Simón Vélez and bamboo architecture. 1. ed. Vitra Design Museum Zeri C.I.R.E.C.A.

PLEA 2024 WROCŁAW
(Re)thinking Resilience

A radiant-capacitive heating and cooling system (RC-HCS):
Performance analysis in full scale

EDUARDO GONZÁLEZ[1], EDUARDO KRÜGER[2], GABRIEL MORAES DE BEM[2], FABRICIO CARRARO[2], GLORIA PÉREZ[1], BORJA FRUTOS[1], CARMEN ALONSO[1], FERNANDO MARTIN-CONSUEGRA[1]

[1]Eduardo Torroja Institute of Construction Sciences (IETCC-CSIC), Madrid, Spain
[2] Federal University of Technology of Paraná (UTFPR), Curitiba, Brazil

ABSTRACT: The aim of this study is to present the initial results of the evaluation of a radiant- capacitive heating and cooling system with low energy consumption applied to a climate chamber. It is based on the use of radiant-capacitive modules that, through a hydronic circuit, take advantage of sky-radiative cooling at night and solar heating. Each of the components of the system is detailed and the results of the operation of the system in cooling and heating modes activated by the control system are analysed. Average daily cooling potential between 45 W/m² and 71 W/m² and an average heating power between 120-140 W/m² were found that allow maintaining thermal comfort conditions most of the time.
KEYWORDS: Radiant-capacitive system. Night-time radiative cooling. Low-energy system. Solar heating. Experimental study

1. INTRODUCTION

The development of technologies that contribute to reducing energy consumption, especially non-renewable primary energy, and that minimize greenhouse gas emissions became an increasingly pressing need. As up to 40% of the final electricity use in buildings is used for heating, ventilation and air conditioning (HVAC) systems, it is essential to reduce this consumption [1]. In this context, buildings that combine bioclimatic strategies with the application of passive heating and cooling techniques are promising. Radiant heating and cooling (RHC) systems have gained much popularity in recent decades due to their potential to provide thermal comfort with low energy consumption combined with silent operation and space savings [2].

Literature review of research on radiant heating and cooling systems points to possibilities of direct and indirect use of renewable energy as a heat source or for heat dissipation in these systems [3]. Among the advantages, environments provided with radiant conditioning systems promote thermal comfort with lower primary energy demand compared to systems that operate with conventional air conditioning [4]. The passive system analysed in the present study involves the cooling/heating of a fluid (water) coupled to the radiant cooling/heating of the interior space. In this case, the use of effective thermal mass leads to a greater energy efficiency and thermal stability as in Thermally Activated Building Systems, TABS [5].

The purpose of this paper is to describe and discuss results regarding the thermal behaviour of a low-energy radiant-capacitive heating and cooling system. The system is based on the use of radiative cooling at night and solar heating applied to a full-scale test cell, a Cost-effective Bioclimatic Chamber, CBBC. This article presents a synthesis of the system and some relevant results related to the cooling and heating potentials of the system, as well as its performance to ensure indoor comfort conditions.

2. METHODOLOGY

This is an experimental project where the system was conceived, dimensioned and applied in one of the two test cells [6] (Figure 1), intended for studies on environmental comfort and passive thermal conditioning systems. The test cells (Figure 1) are located in Curitiba, Brazil, at 25°26’33.6”S and 49°21’14.14”W, at an approximate altitude of 953 meters above sea level. The local climate is predominantly mesothermal with cool summer (Cfb), according to the Köppen-Geiger’s classification.

Figure 1: test cell used in experiments (CB1) and reference cell (CB2).

2.1 The RC-HCS

The basic concept of the system, termed "Radiant-Capacitive Heating and Cooling System" (RC-HCS), is based on passive radiant conditioning with very low energy consumption, basically relying on the use of renewable energy sources. The indoor radiant conditioning is based on the use of modular ceiling elements of high thermal capacity ("Radiant-Capacity Module" or RCM) through which the externally cooled or heated fluid (water) circulates, which thermally activates these elements [7].

Externally, the system uses panels facing the sky, which promote nocturnal radiative cooling or solar heating to the closed-circuit, hydronic system ("Sky Radiator/Solar Collector" or SR/SC).

A small pump warrants water circulation between the SR/SC, through the indoor radiant-capacitive modules (RCM) and to a 1,000 l water tank used for energy storage ("Thermal Energy Storage" or TES).

The implemented system comprises five groups of components (Figure 2): a) four Radiant-Capacitive Modules (RCM) indoors; b) five Sky Radiator/Solar Collector panels (SR/SC); c) a water tank for Thermal Energy Storage (TES); d) a Smart Control System (SCS) and e) a hydropneumatic pumping system with a set of pipes, hoses, valve switches, solenoid valves, connections and devices to measure water flow and volume.

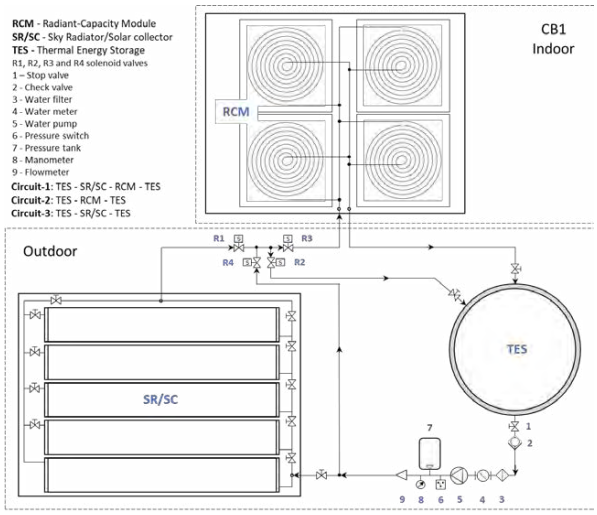

Figure 2: Scheme of RC-HCS components and water flow circuits.

2.2 The Radiant-Capacity Modules (RCM)

The RCMs, due to the enclosed water, offer thermal energy storage capacity to the environment, also increasing its overall thermal inertia, thus reducing indoor thermal fluctuation.

Each of the four RCMs was manufactured with 0.9 mm thick galvanized steel sheet and painted white, as shown in Figure 3. Their dimensions are 0.9 m x 0.9 m (radiant surface = 0.81 m^2) with a height of 0.07 m. They are filled with water up to 0.065 m and covered with a galvanized steel sheet of the same thickness. Inside, the RCM has an aluminium coil ¾" in diameter and 13.5 m long as a heat exchanger (Figure 3). The total area occupied by the four RCMs is 3.24 m^2. Considering the internal surface of the test room of 5.33 m^2, the RCM surface represents 60.7% of it. The volume of water in each RCM is 52.65 l, with a total of 210.6 l (0.2106 m^3).

Figure 3: RCMs as ceiling elements and the ¾" diameter aluminium coil inside the RCM as a heat exchanger.

2.3 Sky Radiator/Solar Collector (SR/SC)

The SR/SC is made up of five radiators measuring 3.0 m x 0.49 m (1.47 m^2), each made up of five extruded aluminium profiles measuring 3.0 m x 0.095 m x 8.3 mm, painted in black, and supplied with water by interconnecting hoses (Figure 4). The SR/SC was placed on a 50 mm thick polystyrene thermal insulation layer, which sits on a supporting platform with a 10% slope. The total area of the five radiators/collectors (SR/SC) is 7.35 m^2.

Figure 4: Extruded aluminium profile used in the manufacture of the SR/SC and SR/SC on the supporting platform.

2.4 Thermal Energy Storage (TES)

As Thermal Energy Storage (TES), a polyethylene water tank with a nominal capacity of 1,000 l is used. This tank sits on top of a 50 mm thick polystyrene sheet that isolates it from a concrete slab. It is covered by a 50 mm thick layer of expanded polyurethane.

The hydropneumatic system installed for pumping water consists of a 35 l pressure tank, with 1/4 hp (0.186 kW) water pump, pressure switch, pressure

gauge, flow meter, hydrometer and water filter. In addition to these components, the system has four solenoid valves, driven by the Smart Control System (SCS) and registration switches to facilitate different operating modes and experimental tests.

2.5 Smart Control System (SCS)

The RC-HCS is controlled by a Raspberry Pi 3 microprocessor, connected to 12 DS18B20 waterproof sensors, a four-channel relay and four Normally Closed (NC) solenoid valves. The installation architecture as well as the positioning of the sensors (Tw1, Tw2, Tw3, Tw4, Tw5, Tw6, Tw7, Ts, Tin, Tg, Tout and Tr) is illustrated in Figure 5.

The temperature sensors are connected in parallel to a prototyping board powered by the Raspberry Pi (3.3V), which has the installation of a 1 kOhm pullup resistor. The DS18B20 sensors have a 1wire communication protocol with temperature recording directly in degrees Celsius. To recognize the sensors, it was necessary to install the adafruit-circuitpython-ads1x15 library, created by the manufacturer of the ADC ADS1115 converter.

From data collected by all sensors, the Neutral Temperature (Tn) based on the ASHRAE adaptive thermal comfort model [8], the Mean Radiant Temperature (Trm) based on [9] and the Temperature Operative (To) based on [8] were determined, which, combined, govern the SCS, as well as the tolerance, fault and data storage mechanisms. Such routine was implemented in Python programming language version 3.9.5. The system developed is responsible for reading and storing data both locally (SD card connected to the Raspberry Pi) and in the cloud, via the open-source library gspread. This independent and redundant mechanism increases security in storing information in addition to allowing real-time monitoring of measurements and system behavior remotely.

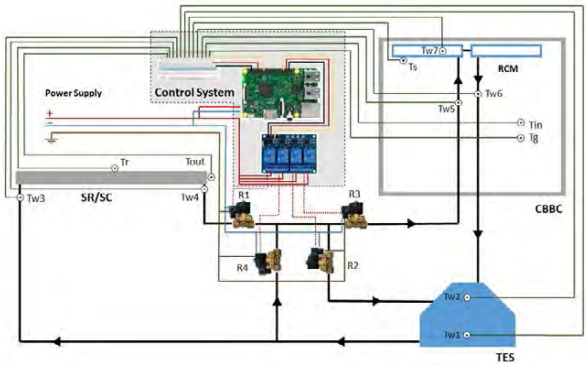

Figure 5: Layout of SCS components.

The system is programmed to perform checks every 5 minutes, which are responsible for activating the solenoid valves contingent on the operating rules established. At each time interval, the operating conditions are checked and the system generates a log (local and in the cloud) with recording of procedures, both for checking and operating circuits. This way, it is possible to monitor the functioning of the system as a whole.

3. RESULTS AND DISCUSSION

As a basis for further analyses, monitoring data for the reference test cell (CB2), identical to the experimental test cell (CB1), but without the passive system, are first discussed. The results of monitoring the RC-HCS in both cooling and heating modes are presented next.

3.1 Thermal performance of the reference (CB2) and experimental (CB1, with RC-HCS) cells

The thermal performance of CB1 is analysed in relation to CB2 in a free-running mode, without any cooling or heating by the RC-HCS. The test cells present two differences in their physical characteristics that need to be considered in the analysis. Regarding the type of window, CB2 has a doubled window, which provides double-glazing, against a single window with single glazing in CB1, which has the four ceiling-mounted RCMs. With the aim of comparing the thermal behaviour of the test cells in two periods (hot and cold), six days were selected as a sample, three in February and three in May.

Table 1 shows similar behaviour during the different days analysed. There is a difference between indoor averages, which are 0.4 °C higher in CB1, possibly due to differences of the window characteristics. The temperature offset is relatively small and consistent.

Table 1: Indoor temperatures in CB2 and CB1 on three hot days and three cold days.

	Indoor Temperatures CB2				Indoor Temperatures CB1					
Date	Tmax	Tmin	Tavg	FD_{CB2}	Tmax	Tmin	Tavg	FD_{CB1}	ΔT_{avg}	$\Delta T_{CB1}/\Delta T_{CB2}$
feb-01	28.4	22.0	25.0	0.46	27.6	23.2	25.2	0.32	-0.26	0.69
feb-02	28.8	23.6	26.2	0.51	28.3	24.8	26.6	0.34	-0.39	0.67
feb-03	28.1	23.2	25.7	0.45	27.9	24.7	26.4	0.29	-0.69	0.65
Average	28.4	22.9	25.6	0.47	27.9	24.2	26.1	0.32	-0.45	0.67
may-06	21.9	16.4	19.0	0.66	21.5	17.4	19.4	0.49	-0.37	0.75
may-07	20.7	15.6	18.3	0.55	20.6	16.8	18.7	0.41	-0.40	0.74
may-08	19.7	14.8	17.5	0.54	19.3	15.9	17.9	0.37	-0.44	0.70
Average	20.8	15.6	18.2	0.58	20.5	16.7	18.6	0.42	-0.40	0.73

The positive difference in the daily average temperature in the two test cells relative to outdoors is relevant and must be considered in performance analyses. Indoor temperatures are, on average, 3.7°C and 3.2°C higher than outdoors, in CB1 and CB2, respectively, with a consistent offset of 0.5°C between test rooms. The Decrement Factor (DF) (ratio between indoor and outdoor daily thermal fluctuations), in the case of CB1, is on average 0.37 and in CB2, 0.53, due to the added thermal mass (water contained in the RCMs).

3.2 Thermal performance of RC-HCS in cooling mode

Between March 26 and 29, 2022, the RC-HCS was evaluated under the following conditions: a) use of three of the five SR/SC radiators (4.41 m² of surface); b) average water flow of approximately 170 l/h; c) operation with control system in Circuit-1 (TES - SR/SC – RCM – TES) between 8:00 pm and 6:00 am. The average ambient temperature lied around 21°C, with maximum temperatures up to 29.7°C (Table 1), on days with relatively cloudy skies with daily values of global solar radiation between 3.6 and 5.2 kWh/m² and peak solar irradiance between 955 and 1075 W/m². The average wind speed over the four days was 1.4 m/s with maximum values reaching 5.4 m/s.

The nighttime radiative cooling potential of the SR/SC per unit area (CP) was calculated based on the difference in water temperature at the inlet and outlet of the radiator and the water flow through it, according to Erell and Etzion, [10], as follows:

$$CP_{SR/SC} = \dot{m} \times cp \times \Delta T / A \qquad (1)$$

Where $CP_{SR/SC}$ (W/m²) is the instantaneous cooling power of the radiator per unit area, $\dot{m}$ (kg/s) is the mass flow rate of water, cp (J/kg.K) is the specific heat of the water, ΔT (K) is the difference in water temperature between the inlet and outlet of the SR/SC and A (m²) is the surface area of the radiator. The results of these calculations are presented in Table 2. $CP_{SR/SC}$ values between 45 W/m² and 71 W/m² can be observed, with maximum instantaneous values of up to 114 W/m².

This cooling potential depends fundamentally on cloudiness, air temperature and humidity, and wind speed. In our study, the temperature of a metal plate (Tr) exposed to the sky was measured, and the difference between ambient temperature and that of the metal plate (DTr) was used as an indicator of nocturnal radiative cooling potential [11].

During the four days of the series, this potential was low. Only the night of 26-27/03 had DTr slightly higher than the others, with an average of 3.2 K and maximum values of up to 4.9 K. As expected, a high correlation was observed between DTr and $CP_{SR/SC}$ (with R^2 of 0.80).

Another way to evaluate the thermoenergetic performance of the system is by analyzing the amount of energy that the RC-HCS is capable to remove from the RCM (Q_{RCM}) during nighttime, and compare it with the average cooling potential of the RCM (CP_{RCM}). The heat dissipated in the RCMs was calculated for these four days, as follows:

$$Q_{RCM} = m \times cp \times \Delta T \qquad (2)$$

where Q_{RCM} (Wh) is the thermal energy removed, m (kg) is the mass of water contained in the RCM (210.6 l), cp (kJ/kg.K) is the specific heat of the water, ΔT (K) the difference of water temperature in the RCM between the beginning and end of the thermal exchange period (20:00 – 06:00). Table 3 presents the results of these calculations.

Table 2: Temperature reduction in the RCM, energy extracted from the RCM and average cooling capacity during the night period in the RCM and SR/SC.

Date	DTw7	Q_{RCM}	CP_{RCM}	$CP_{SR/SC}$
	K	Wh	W	W/m²
March 26	2.13	520	52	44.8
March 27	3.85	942	94.2	62.6
March 28	3.62	884	88.4	45.1
March 29	4.21	1029	102.9	71.2
Average	3.45	714	71.4	55.9

Figure 6 shows that, in CB1, the air temperature and the operating temperature are within the comfort range when outdoor temperature exceeds Tn, and even the upper limit of adaptive thermal comfort, with the exception of some moments when indoor temperature is below the lower comfort limit. In this case, this does not represent a problem, as it shows the system's ability to reduce the average indoor temperature relative to CB2 and outdoors. While CB1, in free-running mode, had indoor temperatures, on average, 3.7°C above outdoors, with the RC-HCS in cooling mode this offset was reduced to 0.9°C, even with climatic conditions not entirely favorable for nighttime radiative cooling. The difference between indoor temperatures in CB2 and CB1 on these days was 1.5°C, with cooling taking place only in CB1.

Note that the system's ability to reduce the maximum indoor temperature relative to outdoors (ΔTmax), is on average 4.2 K, varying from 3.1 K to 5.3 K (Table 2).

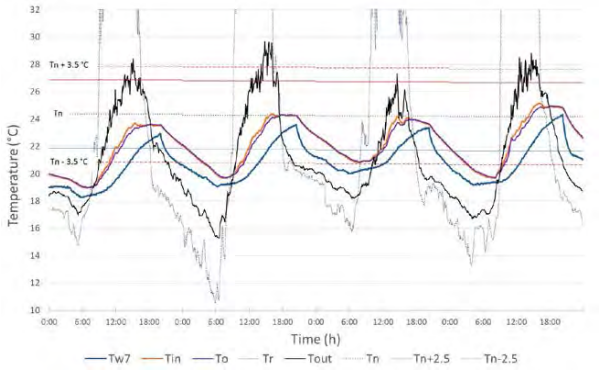

Figure 6: Indoor (Tin), outdoor (Tout), metal plate (Tr) temperatures, water temperatures in TES (Tw1) and in the RCMs (Tw7), neutral temperature (Tn) and adaptive comfort ranges, in cooling mode, between March 26th and 29th, 2022.

Table 3: Indoor and outdoor temperatures and thermal performance indicators of the system in cooling mode.

	Outdoor Temperatures			Indoor Temperatures			ΔT_{avg}	ΔT_{max}	FD
Date	Max	Min	Avg	Max	Min	Avg			
March 26	28,4	17,0	21,5	23,7	18,9	21,4	0,1	4,7	0,42
March 27	29,7	15,3	21,3	24,4	19,7	22,2	-0,9	5,3	0,33
March 28	27,3	18,2	20,8	24,2	20,8	22,4	-1,7	3,1	0,37
March 29	28,8	16,7	21,4	25,1	19,7	22,5	-1,2	3,7	0,45
Average	28,5	16,8	21,2	24,3	19,8	22,1	-0,9	4,2	0,39

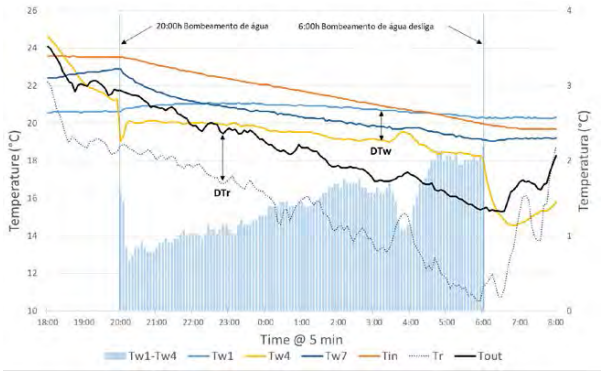

Figure 7: Indoor (Tin) and outdoor (Tout) temperatures, metal plate temperature (Tr), water temperatures in TES (Tw1), at the SR/SC exit (Tw4) and RCM (Tw7), in mode cooling, between March 26 and 27, 2022, with water circulation in Circuit-1.

3.3 Thermal performance of RC-HCS in heating mode

Between May 20 and 23, 2022, tests were carried out in heating mode, on days characterized by the entry of a cold front with daily minima between 4 and 5 °C and maxima between 19 and 21 °C (Figure 8 and Table 4). The first three days had relatively clear skies, with total global radiation in the horizontal plane between 3.3 and 3.4 kWh/m², and maximum irradiance values between 610 W/m² and 620 W/m². The fourth day was a partly cloudy day, with 2.6 kWh/m² of total irradiance and maximum values reaching 689 W/m². There were days without rain and wind with average speeds of around 0.8 m/s and maximum speeds of up to 3.3 m/s.

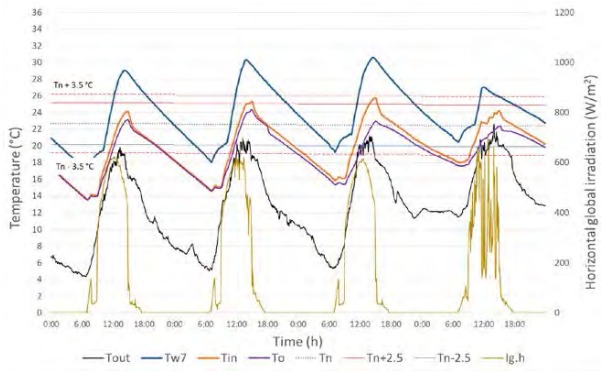

Figure 8: Indoor (Tin), outdoor (Tout) temperatures, and temperature of the metal plate (Tr), water temperatures in TES (Tw1) and in the RCMs (Tw7), neutral temperature (Tn) and adaptive comfort ranges and solar radiation, in heating mode , between May 20 and 23, 2022.

The RC-HCS worked on these four days driven by the automatic control system. During the four days, between 7:00 am and 10:00 am, heating Circuit-2 was activated (TES-RCM-TES, cf. Figure 2). Subsequently, Circuit-1 (TES-SR/SC-RCM-TES, cf. Figure 2) was automatically activated, with heated water from solar gains in the SR/SC to the through the RCMs following the guiding rules of the SCS.

Compared to outdoor averages of 10-15°C, in CB1 average temperatures varied between 18.5 and 22°C, that is, around 8°C above external temperatures. The heating observed in CB1 is mainly due to the solar heat supplied by the SR/SC to the RCMs either via Circuit 1 or Circuit 2. The heat supply in the RCMs was calculated for these four days (Table 4), according to equation 2. Considering differences in water temperatures between 11.5 K and 12.5 K, heat inputs in the order of 2,800 to 3,000 Wh per day were obtained, which represents an average heating power within the range of 380-440 W or 120-140 W/m², given the total area of the RCMs of 3.24 m².

Table 4: Indoor and outdoor temperatures, energy supplied to the RCM, average heating power for the period.

	Outdoor Temperatures			Indoor Temperatures			ΔTw7	Q (Wh)	P (W)
Data/Hora	Max	Min	Avg	Max	Min	Avg			
May 20	19,9	4,3	10,6	24,2	13,6	18,5	12,21	2,990	407
May 21	20,9	5,0	12,1	25,4	14,7	19,6	12,27	3,000	439
May 22	21,3	5,3	12,6	25,8	15,9	20,4	11,32	2,770	378
May 23	22,6	11,5	15,5	24,2	18,0	20,9	6,58	1,610	327
Average	21,2	6,5	12,6	24,9	15,5	19,8	10,6	2,592	388

As for the Decrement Factor, due to additional heating, the average FD was 0.64, higher than CB1 (FD = 0.42) when in free-running mode in the cold season.

4. FUTURE PERSPECTIVES FOR A COMPARATIVE STUDY

Some of the authors of this article (members of the Eduardo Torroja Institute of Construction Sciences, and belonging to the Higher Council for Scientific Research (IETCC-CSIC) of Spain), are currently participating in a European research project, EURAMET 21GRD03, called Metrological framework for passive radiative cooling technologies (PaRaMetriC). The overall goal of this project is to establish a metrological framework for comparable performance assessments of passive radiative cooling technologies. One of its specific objectives is "To develop setups and protocols for on-site testing of PRC materials, with a target uncertainty below 10% for the figures of merit."

Within the framework of this project, the development of a prototype of a radiative cooling system is currently underway, based on the RC-HCS developed in Curitiba, Brazil, described in the present work. The new prototype will allow the thermal performance of the system to be analyzed in two

modes: 1. with nighttime radiative cooling and 2. with radiative cooling taking place 24 hours/day through the use of “passive radiative cooling material” (PRC).

One of the aims of this research is to carry out a comparative study of the thermal performance of the two cooling systems accounting for differences between the components of the systems, the climatic conditions and the experimental cells used for their implementation. Figure 9 shows the experimental cells of the IETCC-CSIC, located in Arganda del Rey, Madrid, where the prototype of the radiative cooling system shall be implemented.

Figure 9: Experimental cells in Arganda del Rey, Madrid, where the prototype of the radiative cooling system of the European PaRaMetriC project will be installed.

5. CONCLUSION

The study showed the advantages of the Radiant-Capacity Heating and Cooling System used for both cooling and heating, confirming the dual applicability of the system. The smart control system, designed to optimize the operation of the system, contributed to the favourable results obtained.

In cooling mode, average $CP_{SR/SC}$ values have been found between 45 W/m² and 71 W/m², with maximum instantaneous values of up to 114 W/m². The system's capacity to reduce the average internal temperature relative to the CB2 has been confirmed. In heating mode, average internal temperatures between 18.5°C and 22°C were observed, approximately 8°C above average external temperatures of 10-15°C. This is a consequence of the thermal input of around 2,800 to 3,000 Wh per day, which represents an average heating power between 120-140 W/m².

ACKNOWLEDGEMENTS

This research was carried out within the framework of EDITAL Nº 11/2018 - PROPPG - Visiting Professor (PV) of the Department of Civil Construction, Federal University of Technology of Paraná - UTFPR, Curitiba, Brazil. To the Eduardo Torroja Institute of Construction Sciences (IETCC-CSIC), partner of the European research project EURAMET 21GRD03, PaRaMetriC (Metrological framework for passive radiative cooling technologies), for their support to the future comparative study.

REFERENCES

1. Smith, G., Gentle, A. Radiative cooling: energy savings from the sky, Nature Energy 2 (2017) 17142. https://doi.org/10.1038/nenergy.2017.142

2. Zhang, F., Guo, H-A., Liu, Z., Zhang, G. A critical review of the research about radiant cooling systems in China. Energy and Buildings 235 (2021) 110756. https://doi.org/10.1016/j.enbuild.2021.0756

3. Karmann, C.; Schiavon, S.; Bauman, F. Thermal comfort in buildings using radiant vs. all-air systems: A critical literature review. Building and Environment. 2017 111, 123-131. https://doi.org/10.1016/j.buildenv.2016.10.020

4. Lehmann, B.; Dorer, V.; Gwerder, M.; Renggli, F.; J. Tödtli, J. Thermally activated building systems (TABS): Energy efficiency as a function of control strategy, hydronic circuit topology and (cold) generation system. Applied Energy, 2011, 88 pp. 180–191. https://doi.org/10.1016/j.apenergy.2010.08.010

5. Kyu-Nam Rhee, Kwang Wookim. A 50-year review of basic and applied research in radiant heating and cooling systems for the built environment. Building and Environment. Vol 91, September 2015, Pages 166-190. https://doi.org/10.1016/j.buildenv.2015.03.040

6. Trevisan, L. Y. I.; Tamura, C. A.; Ribeiro, D. A.; Gomes, B. De L. M.; Drach, P. R. C.; Hara, M. M.; Krüger, E. Construção de câmara bioclimática de baixo custo para estudos de ambiência térmica no brasil. In: ENCONTRO NACIONAL DE TECNOLOGIA NO AMBIENTE CONSTRUÍDO, 2018. Anais [...]. Porto Alegre: ANTAC, 2018. p. 588–595.

7. Kyu-Nam Rhee, Bjarne W. Olesen, Kwang Woo Kim. Ten questions about radiant heating and cooling systems. Building and Environment. 112 (2017) 367-381. http://dx.doi.org/10.1016/j.buildenv.2016.11.030

8. ASHRAE Standard 55 - Thermal environmental conditions for human occupancy, Refrigerating and Air-Conditioning Engineers, 2017, Atlanta

9. ISO 7726. Ergonomics of the thermal environment - Instrument for measuring physical quantities". Geneva, Switzerland: International Organization for Standardization. November 1998.

10. Erell, E.; Etzion, Y. Radiative cooling of buildings with flat-plate solar collectors, Building and Environment 35 (4) 2000, 297–305. https://doi.org/10.1016/S0360-1323(99)00019-0

11. Gonzalez Cruz, E.; Krüger, E. Experimental study on a low energy radiant-capacitive heating and cooling system. Energy and Buildings, 255 (2022) 111674. https://doi.org/10.1016/j.enbuild.2021.111674

PLEA 2024 WROCŁAW
(Re)thinking Resilience

Towards Resilient Neighborhoods
Impact of Block Morphology on Outdoor Comfort

AFEEFA ADEEBA RAHMAN[1,2], MD. MIZANUR RAHMAN[1], KHANDAKER SHABBIR AHMED[1]

[1]Bangladesh University of Engineering and Technology, Dhaka, Bangladesh
[2] Military Institute of Science and Technology, Dhaka, Bangladesh

ABSTRACT: Comfort is one of the main determinants of sustainable living with minimum resources. Urban built environment is responsible for the excessive energy use to ensure thermal comfort. In Dhaka (the capital of Bangladesh), the building guidelines can be rethought to affect the block morphology to facilitate outdoor comfort and reduce energy demand to improve the indoor environment. This paper aims to address the scope of change in Dhaka city's existing development policies that affect resilience through changes in the morphology for outdoor comfort affecting the existing neighborhoods. The methodology includes comfort analysis, parameter identification, study of the existing development policies, selection of the sample site; and simulation and analysis. Based on the simulation studies, the findings show a clear scope of possible change in the existing plot division policies. Implementing proposed guidelines in the building codes in existing neighborhoods to check the comfort situation of present and changed conditions for further validation, and exploring other parameters like shading devices, trees, waterbody, etc. for enhancing comfort are identified as the scope of the research. In conclusion, the research can be a database of urban coding and guidelines of building construction regulations of Dhaka city as the basis of future resilient design.
KEYWORDS: Energy Efficiency, Comfort, Urban policies, Building Plot division, Simulation.

1. INTRODUCTION

Urban resilience depends on the ambient environment it provides for the users. In an urban context, the urban elements and their arrangement influence the morphology and ensuing microclimate impacting the environmental factors leading to outdoor thermal comfort [1]. Ensuring outdoor thermal comfort leads to sustainability and resilience by reducing energy demands while facilitating a comfortable environment [2]. This is particularly important in situations where urban heat islands tend to become a regular phenomenon.

The four main factors affecting thermal comfort identified by ASHRAE (American Society of Heating, Refrigerating, and Air-Conditioning Engineers) are Temperature, wind movement, humidity, and solar radiation which can be controlled using urban morphology to lead to a resilient neighborhood by reducing the energy demand necessary for comfortable living [3].

To accommodate the overgrowing population of Dhaka, the population density is progressively challenging the urban infrastructure and affecting the environment with the Heat Island Effect with increasing demands on energy to ensure comfort [4]. The existing building code of the country has been updated since its first publication in 1993 to incorporate development and growth but still lags in addressing the environmental resilience issues [5].

Most of the planned residential areas of Dhaka city are compact with rows of buildings having similar plot sizes and similar height ranges with only set back as the open space between the buildings. Figure 1 shows a typical residential area of Mirpur DOHS.

Figure 1: View of Mirpur DOHS (planned area of Dhaka) [6].

But the latest gazette DAP 2022 (Detailed Area Plan) provides a scope towards block-based development by creating an opportunity to plot unification to consider the unified plot as a block-based development rather than a plot-based approach [7].

This paper aims to analyze the existing urban development policies of Dhaka City and identify the potential scope to rethink the guidelines based on urban morphology to ensure resilience through energy efficiency by enhancing thermal comfort in urban neighborhood block morphology.

The outcome concludes by proposing changes in the planning guidelines for urban blocks in a residential neighborhood considering thermal comfort.

2. METHODOLOGY

The methodology includes mixed methods of experimental and simulation. Literature review and

weather study are used for contextual climatic analysis to identify the thermal comfort parameters of Dhaka city. Existing building codes are studied to identify development policies. Urban and environmental parameters are identified for simulation studies to analyze various combinations and identify the optimized case of urban microclimate to ensure comfort. Software used for simulation studies are ENVI MET (version 5.0.1), Rhinoceros (version 7.13) with additional plugins of climatestudio (version 1.8), and EDDY 3D [8–11]. Analyzing and comparing the simulation results of different case scenarios of the same site with varying parameters helps to provide specific guidelines for Dhaka city considering the climate and the context.

2.1 Comfort and Context

In the tropics, considering the bioclimatic chart of thermal comfort by Olgay, wind flow and solar heat gain by radiation can extend the thermal comfort range. Introducing wind flow can help tolerate higher air temperatures and increasing radiation can help tolerate lower temperatures [12]. So, in tropical climates when air temperature mostly remains higher than the comfort range, it can be extended by introducing wind flow and reducing heat gain by solar radiation. The wind flow will extend the comfort range to a higher temperature and the radiation decrease will extend it to a lower temperature.

In Dhaka (the capital of Bangladesh), outdoor comfort has been reported to vary between 28.5°C and 32°C [2]. Analyzing the existing weather EPW (EnergyPlus Weather File) files of Dhaka, in Rhinoceros (version 7.13) with Climatestudio (version 1.8) the maximum summer temperatures are often higher than the comfort range indicating the cooling need (Figure 2) [10, 13, 14].

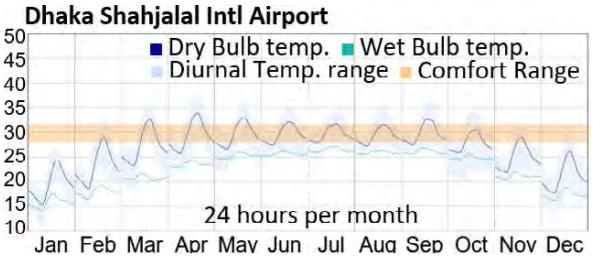

Figure 2: Hourly average dry bulb, wet bulb, diurnal temperature range, and comfort range with weather EPW files of Shahjalal International Airport in Rhino-ClimateStudio throughout the year. [13].

Universal Thermal Climate Index (UTCI) with weather EPW file of Dhaka Shahjalal International Airport from ClimateStudio analysis in Rhinoceros (version 7.13) shows thermal stress conditions where heat stress days are 63.4% (Figure 3) considering extreme heat stress, very strong heat stress, strong heat stress and moderate heat stress [10, 13].

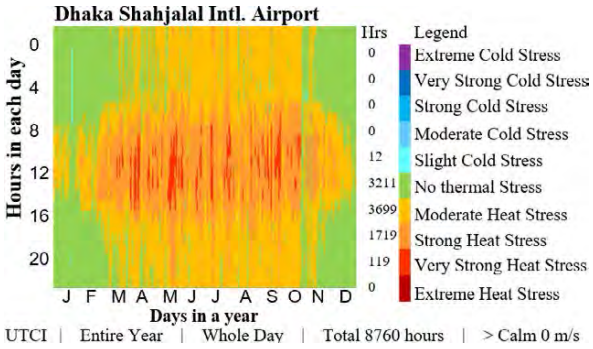

Figure 3: UTCI analysis with weather EPW file of Dhaka Shahjalal International Airport in climatestudio. [13].

In the tropics, the outdoor temperature influences indoor energy demand [2]. So, to reduce energy needs, the outdoor microclimate should be controlled by regulating urban block parameters.

2.2 Parameter Identification

Considering the tropical hot and humid climate of Dhaka city, the two main parameters affecting comfort are solar radiation and wind flow. The hot temperature feels even hotter due to heat gain by solar radiation, so it should be reduced; and wind flow can flow away hot humid air and facilitate evaporative cooling, so wind flow should be introduced to keep the temperature within the comfort range [12].

The elements affecting the urban microclimate are buildings, roads, and open spaces [1]. For environmental considerations, control of solar radiation, and promoting wind flow; and for urban elements, orientation, building height, and open space must be considered. Of these, the environmental parameter of open space in different variations is considered to be the future research scope of this paper. The analysis of other parameters is simulated accordingly in this paper.

2.3 Selecting the sample site

The sample is a hypothetical site of 118.5m X 120 m dimension (14220 sqm) with 60 plots of 3 katha (201 sqm) each for A2 (Residential apartment and flat) type buildings according to the Building Construction Regulations 2008 of Dhaka City [15].

The site is prepared considering the general criteria of a planned urban residential neighborhood of Dhaka (like Figure 1) representing the urban morphology of the city. From Dhaka's Building Construction Regulations of 2008, access roads of 6m and 1.5m footpaths are considered. Building masses are included considering regulations of FAR (Floor Area Ratio) and MGC (Maximum Ground Coverage) (Figure 4) [15]. For the plot size of 201 sqm, FAR is 3.5 and MGC is 62.5% of the lot area for buildings of A1-A4 type.

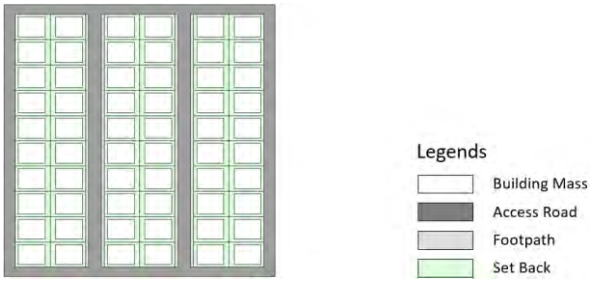

Figure 4: Hypothetical site considering building regulations of Dhaka (2008) [15].

The site with buildings is rotated at an interval angle of 22.5^0 to analyze the effect of building and road orientation on heat gain by solar radiation and wind movement using ENVI-MET (demo version 5.0.1) and Rhinoceros with Ladybug for holistic and solar radiation respectively [8–11]. The building heights are changed based on the FAR and MGC using plot accumulation to simulate the effect of height variation on wind movement by increasing surface roughness and porosity.

3. ANALYSIS AND FINDINGS

A total of eight sights are considered after rotation to simulate wind velocity and solar radiation and compare the analysis results to select the optimized solution of orientation and building height.

3.1 Orientation

The initial rotation angle is the site is considered 0 degrees where the roads are elongated in East-West and the buildings have larger façade to North-South that is, the building orientation is North-South. The other sites are 22.50 from North-South, 450 from North-South, 67.50 from North-South, 900 from North-South (East-West oriented Buildings), 112.50 from North-South, 1350 from North-South, and 157.50 from North-South.

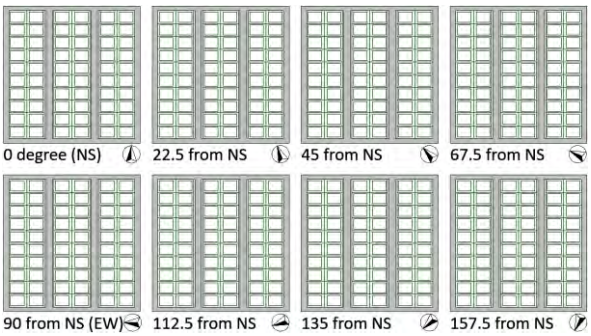

Figure 5: Hypothetical sites with a rotation of 22.5-degree intervals for environmental impact analysis.

Now, the effect of solar radiation is analyzed to identify the site (/s) with minimum solar gain. The primary concern of solar heat radiation is the hottest months of the year, and so, the simulation period is considered to be from March to October and the considered hours are from 5 am to 7 pm. The software used is Rhinoceros (version 7.34) with Ladybug tools (version 1.6) as the plugin for simulation along with Shahjalal International Airport weather EPW (Energy Plus Weather file) for weather data of Dhaka City. For each site, the ground (road, footpath, setback), building façade, and roof are considered as the context, and all the elements and individual elements are considered as the analysis geometry. Dividing all the surfaces in a grid size of 0.2 meters each, the mean radiation for each grid is analyzed and the results are added to get the total radiation for each element. The visualized radiation simulation is shown in Figure 6. The results are shown in Table 1.

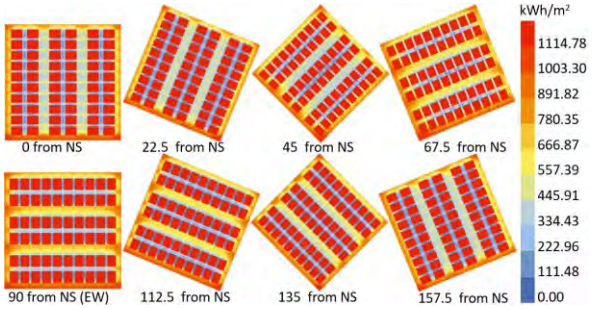

Figure 6: Solar radiation analysis for each site from March to October, from 5 am to 7 pm in Ladybug- Rhinoceros.

Table 1: Solar radiation and Wind velocity change due to the variation in site orientation.

Site Rotation Degrees	Total Rad kWh/m²	Ground Rad kWh/m²	Façade Rad kWh/m²	Avg velocity m/s
0^0 from NS	21009000	4219000	8690000	1.35
22.5^0 from NS	20990000	3980000	8910000	1.21
45^0 from NS	21010000	4150000	8760000	1.13
67.5^0 from NS	21065000	4380000	8585000	1.05
90^0 from NS (EW)	20956500	4776500	8080000	0.83
112.5^0 from NS	21008000	4360000	8548000	0.97
135^0 from NS	21022000	4134000	8788000	1.43
157.5^0 from NS	21020000	3990000	8930000	1.73

The results show that the radiation for the roof surface (without any vegetation and external elements) is constant and the total radiation for the simulation period is 8100000 kWh/m²-year. Variation is seen in the case of ground and façade surfaces due to variations in shadow angle due to the change in orientation. The three orientations for total minimum radiations are 22.5^0 from NS, 90^0 from NS,

and 112.5^0 from NS. Orientations for minimum ground radiation are 22.5^0 from NS, 45^0 from NS, and 157.5^0 from NS. The orientations 67.5^0 from NS, 90^0 from NS, and 112.5^0 from NS get the minimum façade radiation for the simulation period.

For wind simulation, ENVI-MET (demo version 5.0.1) is used with the same eight sites. The location is set to Dhaka with a model geometry of 43 grids along the x-axis with 3 meters, 43 grids along the y-axis with 3 meters, and 38 grids along the z-axis with 3 meters. The simulation is carried out on June 21, 2023, for the hottest hour of 16:00-17:00 considering the temperature, relative humidity, wind speed (3 m/s at 10-meter height from constant average wind direction at 180 degrees), direction, and cloud situation of the simulation date from the weather database of Dhaka City [16]. The average summation of velocities at each grid is considered and visualized in Leonardo of ENVI-MET (Figure 7). The total velocity at the human perception height (1.5 meters) is considered, shown in Table 1.

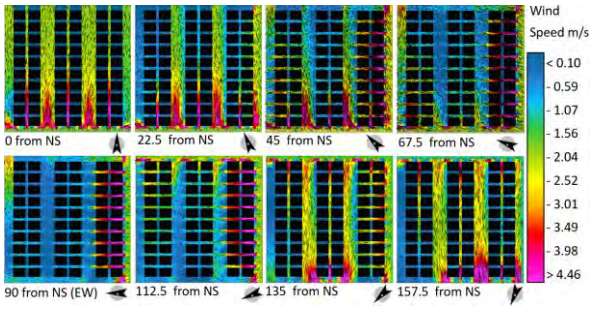

Figure 7: Wind simulation visualization for each June 21, 2023 site in Leonardo-ENVI-MET [11].

From Table 1, considering the maximum wind velocity at a plan level of 1.5 meters the sites 157.5^0 from NS, 135^0 from NS, and 0^0 from NS perform better chronologically. However, the sites have higher total solar gain from radiation, and site 0^0 from NS receives direct solar radiation from the west (the direction of maximum solar gain). So, to get optimized solar radiation and wind velocity, the site with a rotation of 22.5^0 from NS can be considered for developing building codes for resilient neighborhoods and is also considered for simulation analysis for building height parameters.

3.2 Building Height

The building height parameter is analyzed by simulation results for height constant and variation cases for the site with 22.5^0 rotation from NS to simulate the effect of height variation on wind penetration in the neighborhood block.

For site variation cases, considering the FAR and MGC, buildings of similar plot sizes have a maximum limit of height. So, to create height variation, plot variation is necessary. Conceptually, to create variation in plot size, the plots of the existing site are merged in a combination of 1 plot, 2 adjacent plots, and 4 adjacent plots accordingly to maintain the approximate total volume (constant case: 71968.5 m^3, variation case: 71957 m^3) of building masses after considering the building height according to FAR and MGC. The plot unification concept towards block-based development of DAP 2022 is maintained [7].

Figure 8: Sites with constant building height (left) and variation in building height (right).

Two sites (one with constant building height, another with height variation) at an orientation of 22.50 with the North are simulated with a similar setup as mentioned in 3.1 in ENVI-MET (demo version 5.0.1). The results are visualized in Leonardo (in ENVI-MET) in three different planes for comparing changes in wind velocities (Figure 9) [11]. The average velocity along the xy-plane at 1.5 meters is 1.37 m/s for the height variation case which is greater than 1.21 m/s for the height constant case. Results are also considered along the yz-plane along the windward-leeward axis to calculate the wind velocity along the façade towards the wind. The considered area is from the grid at the base and 2 grids above the roof of the buildings for each case and the average is shown in Table 2. In the yz-plane also the wind velocity has increased in the height variation case which is 1.98 m/s whereas the height constant case has an average wind velocity of 1.70 m/s.

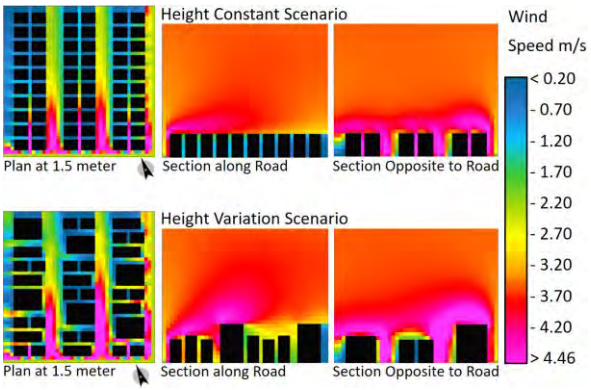

Figure 9: Variation of wind flow in the urban block with height constant and variation case (in ENVI MET 5.0.1) [11].

To analyze the impact of height variation in heat gain by solar radiation, the sites are again simulated for solar radiation comparison in Rhinoceros (version 7.34) with Ladybug Plugin (version 1.6). The analysis results are shown in Table 2 and visualized in Figure 10 [9].

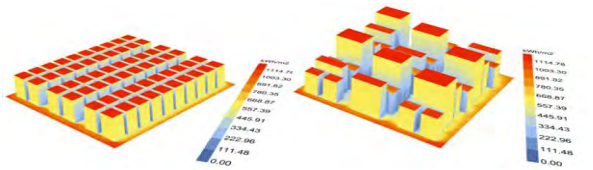

Figure 10: Solar radiation analysis from March to October, from 5 am to 7 pm in Ladybug- Rhinoceros for height constant and height variation cases [9, 10].

Table 2: Solar radiation and Wind velocity change in height constant and variation scenario.

	Height Constant (at 22.5 rotation)	Height Variation (at 22.5 rotation)
Total Radiation (kWh/m2)	20990000	20977972.65
Ground Radiation (kWh/m2)	3980000	3990000
Total Roof Radiation (kWh/m2)	8100000	6910220
Façade Radiation (kWh/m2)	8910000	10077753
Average velocity XY plane m/s	1.21	1.37
Average velocity YZ plane m/s	1.7	1.98

The results of solar radiation simulation show that, although the façade radiation for the height variation case has increased, the overall radiation for the analysis period has decreased compared to the height constant case.

4. FINDINGS

Findings show that the orientation of buildings and roads impacts solar radiation and wind penetration. The change in building and road orientation impacts overall solar heat gain by radiation due to the variation in solar gain by building facades, roofs, and the ground and the road by creating variation in shadows and solar gain by direct, diffused, and indirect solar radiation. The building orientation also affects the road orientation for giving access to the road to a greater number of buildings. Thus the site orientation (building and road) has an impact on overall heat gain by solar radiation by the neighborhood residential buildings. The orientation also affects wind penetration due to having a proper channel for wind penetration. Considering the climate, the wind direction in different seasons is almost predictable. So, to ensure maximum wind, the building and road orientation should be aligned to the wind direction especially in summer to enhance wind penetration and cooling due to wind. Better wind flow will also ensure evaporative cooling if there are shaded waterbody or greenery while passing through the waterbody and trees. Considering the climate of Dhaka City concerning solar heat gain and wind flow, a site rotation of 22.50 can be an optimized solution for both heat minimization and wind maximization to optimize energy demand.

In the case of building height, when the adjacent plots are of the same size, the buildings are also of the same height considering the maximum allowable height according to FAR and MGC as we can see in the planned residential areas of Dhaka City. These buildings restrict wind penetration inside the neighborhood and trap the heat in the in-between space of the buildings by restricting sky view and night-time radiative cooling [17]. The height variation creates porosity in the urban block to improve the wind flow in the neighborhood. The height variation also creates better sky-view opportunities to facilitate night-time radiative cooling to reduce the energy demand for cooling for comfortable living.

5. CONCLUSION

The paper concludes the extent to which the existing building codes can be altered to impact the urban morphology to ensure outdoor thermal comfort vis-a-vis energy demand by designing a block morphology that may help achieve resilience.

A site orientation (with road and buildings) with a rotation of 22.5^0 with the north can be an optimum site to ensure both minimum solar radiation and maximum wind flow. So, the primary consideration for the master plan should be the site orientation. To maximize wind flow, and increase sky view for radiative night cooling the building height needs variation so that turbulent patterns evolve within the canopy layer. However, similar plot sizes will have a constant height range considering FAR and MGC. As opposed to the existing practice of having identical plot sizes, plot size needs variation to ensure height variation and wind penetration in the neighborhood to ensure comfort and reduce energy demand towards a resilient future.

The guidelines proposed in this paper can help review the existing Building construction regulations to develop future development codes for urban neighborhood design of Dhaka city to ensure resilience considering the comfort and urban microclimate. These can also be implemented in the various planned existing and proposed residential neighborhoods to compare the environmental impact in the existing situation and the situation with implemented guidelines through comfort and resilience.

ACKNOWLEDGEMENTS

The authors express their gratitude to the Department of Architecture, of their affiliated Institutions.

REFERENCES

1. Ignatius, M., Wong, N. H., & Jusuf, S. K., (2015). Urban microclimate analysis with consideration of local ambient temperature, external heat gain, urban ventilation, and outdoor thermal comfort in the tropics. Sustainable Cities and Society: p. 19, 121–135, [Online], Available: https://doi.org/10.1016/j.scs.2015.07.016

2. Ahmed, K. S., (2003). Comfort in urban spaces: Defining the boundaries of outdoor thermal comfort for the tropical urban environments. Energy and Buildings, 35(1), 103–110. https://doi.org/10.1016/S0378-7788(02)00085-3

3. ASHRAE, (2021). 2021 ASHRAE Handbook—Fundamentals, ASHRAE.

4. Mortuza, S., (2022). The cooling conundrum, The Daily Star July 29, [Online], Available: https://www.thedailystar.net/opinion/views/blowin-the-wind/news/the-cooling-conundrum-3082711

5. Zawad, S., (2020). Bangladesh National Building Code (BNBC) Explained—Bproperty. A Blog about Homes, Trends, Tips & Life | Bproperty , May 29, [Online], Available: https://www.bproperty.com/blog/bangladesh-national-building-code/

6. Mirpur DOHS, (n.d.). Google Earth. Retrieved August 30, 2023, from https://earth.google.com/web/@23.83753278,90.36884921,10.32008543a,777.20711521d,35y,-2.60251531h,9.65457505t,-0r?utm_source=earth7&utm_campaign=vine&hl=en

7. RAJUK, (2022). Detailed Ares Plan (Vol. 1).

8. Eddy3D (3.8), (2021). [Computer software], Available: https://www.eddy3d.com/

9. Ladybug Tools (1.6), (2022). [Computer software], Available: https://www.ladybug.tools/

10. Rhinoceros 3D (7.13), (2021). [Computer software], Available: https://www.rhino3d.com/

11. ENVI-met, (2022). ENVI-met Decoding Urban Nature (5.0.1) [Computer software].

12. Koenigsberger, O., Ingersoll, T., Mayhew, A., & Szokolay, S., (1975). Manual of tropical housing. y Orient Blackswan Private, [Online], Available: Limitedhttps://www.academia.edu/30105808/Manualoftropicalhousing_koenigsberger_150824122547_lva1_app

13. ClimateStudio—Solemma (1.8), (2022). [Computer software] , Available: https://www.solemma.com/climatestudio

14. EPW Map, (n.d.). Retrieved August 27, 2023, from https://www.ladybug.tools/epwmap/?fbclid=IwAR2-iVw3_CIMCgZ0ZQ5Bqq8wzKWMyxhet-KJD5Mi12K8r2BUQbszJ_8g178

15. Ministry of Housing and Public Works, (2008). Dhaka mohanagar imarat nirman bidhimala 2008. Government of the People's Republic of Bangladesh, [Online], Available: http://rajuk.portal.gov.bd/sites/default/files/files/rajuk.portal.gov.bd/page/20b761b8_ab9c_4ec7_8692_0877fe834afd/2022-06-23-09-46-0de2c16f0eab9b2884a3d4c1d9696c80.pdf

16. Weather Spark., (2023). Dhaka June 21, 2023 Historical Weather (Bangladesh)—Weather Spark.

17. Sharmin, T., Steemers, K., & Humphreys, M., (2019). Outdoor thermal comfort and summer PET range: A field study in tropical city Dhaka. Energy and Buildings: p. 198, 149–159, [Online], Available: https://doi.org/10.1016/j.enbuild.2019.05.064

PLEA 2024 WROCŁAW
(Re)thinking Resilience

Seven Rs and Eleven Zs for climate responsive living.

Enhancing regenerative architecture through low-tech innovations

MARWA DABAIEH[1,2]

[1]Malmo University, Malmo, Sweden
[2]Aalborg University, Aalborg, Denmark

ABSTRACT: In the face of escalating environmental concerns and resource limitations, the building sector plays a pivotal role, necessitating sustainable and adaptive solutions. This paper presents an experimental research project in Sweden that addresses pressing global challenges of climate change and resource scarcity through the innovative design and construction of a regenerative tiny house, known as the Z Free Home. The Z Free Home is based on the integration of 7 R (Refuse, Reduce, Rethink, Reuse, Renewable, Regenerative, and Respect) and 11 Z (Zero Energy, Zero material waste, Zero waste water, Zero emissions, Zero deforestation, Zero toxins, Zero poverty, Zero injustice, Zero exclusion, Zero ignorance, Zero displacement) principles. This paper provides an overview of the design and design development stages, with a primary focus on the current methodological stage for the building structure and construction. The paper aims to contribute to the discourse on regenerative architecture by offering a practical and experimental solution to mitigate the impact of climate change and environmental degradation. By emphasizing the sustainable principles embodied in the Z Free Home, this research seeks to inspire a paradigm shift in the construction industry, fostering a future where architectural endeavours align harmoniously with the imperative challenges of our times.
KEYWORDS: Z Free Home, 7Rs, 11Zs, Regenerative architecture, low-tech.

1. INTRODUCTION

In an era defined by unprecedented technological advancements, rapidly shifting environmental landscapes, and socio-economic transformations, the field of architecture finds itself at a critical crossroads [1]. As architectural creations continue to shape the world we inhabit, the imperative for buildings and structures to exhibit resilience has become increasingly evident. Resilience, in this study context as defined by several scholars, refers to the capacity of architectural designs to withstand, adapt to, and recover from the multifaceted challenges that define our contemporary reality [2]. The urgency of resilient architectural approaches is underscored by the pressing need to mitigate and respond to the uncertainties of the future [3]. Urbanization, climate change, resource scarcity, and the unpredictable trajectories of technological advancements have rendered static, inflexible architectural designs obsolete [4&5]. Buildings must no longer be conceived as isolated entities, but rather as integral components of a dynamic and interconnected ecosystem [4&6]. The ability of architectural solutions to endure and evolve alongside these emerging challenges is the litmus test for their relevance and longevity [6].

As architects and academics grapple with these complexities, the realm of resilient architecture offers a promising yet underexplored avenue. Resilient architecture entails envisioning structures that possess the versatility to accommodate shifting demands and unforeseen disruptions while maintaining functionality, sustainability, and aesthetic integrity. To achieve this, a departure from traditional paradigms is imperative, inviting a re-evaluation of established design philosophies and the incorporation of innovative materials, technologies, and spatial configurations [1&3].

This research paper delves into the intricate tapestry of regenerative architectural resilience, unravelling its importance in a world characterized by binate change. By scrutinizing the existing approaches to regenerative architecture and proposing innovative strategies through a case application of Z free home. This study seeks to shed light on the dynamic interplay between architectural design and the challenges of the future. As we navigate uncharted territories in a rapidly evolving world, the quest for architectural resilience stands as a beacon guiding us towards built environments that not only endure but thrive in the face of uncertainty.

2. Synergizing the 7 R and 11 Z Principles for Holistic Resilience of Z free home Regenerative concept

In the pursuit of architectural resilience, the convergence of ethical, environmental, and economic imperatives has driven the integration of sustainable design principles into architectural practice. Within this transformative paradigm, the 7 R principles — *Refuse, Reduce, Rethink, Reuse, Renewable, Regenerative, and Respect*— along with the 11 Z

principles —Zero Energy, Zero waste water, Zero material waste, Zero emissions, Zero deforestation, Zero toxins, Zero poverty, Zero injustice, Zero exclusion, Zero ignorance, Zero displacement — stand as fundamental pillars, providing a comprehensive framework for crafting environmentally responsible and resilient architectural solutions.

In this project, the integration of the 7 R principles encompasses a holistic and sustainable approach that transcends conventional paradigms. The first three principles—Refuse, Reduce, and Rethink—emphasize the judicious use of materials, urging architects to repurpose existing elements, minimize waste through thoughtful design, and incorporate reclaimed materials. Rethinking challenges architects to question established norms, fostering innovative and eco-friendly design solutions. The inclusion of renewable materials and renewable energy underscores the imperative of harnessing sustainable energy sources, mitigating environmental impact. Regenerative introduces a dynamic dimension, urging architects to design structures that are regenerative in response to climate change and capable of fostering and enhancing ecological systems. Finally, the principle of Respect underscores the ethical and cultural dimensions, emphasizing the incorporation of designs that honour local traditions, communities, and the environment. The synthesis of these principles not only fosters environmental stewardship but also results in architectural solutions that harmonize with their surroundings and contribute to a more sustainable and resilient built environment.

The incorporation of the 11 Z principles in in the Z free home signifies a commitment to a comprehensive and sustainable built environment. Zero Energy design ensures that buildings generate or harvest as much energy as they consume, contributing to a net-zero energy balance. Zero Waste emphasizes minimizing and repurposing waste, fostering a circular economy within the design. Zero Wastewater promotes efficient water management, striving to achieve water self-sufficiency and eliminate water wastage. Zero Emissions prioritizes the reduction of carbon emissions, striving for carbon-neutral or even carbon-negative structures. The principle of Zero Deforestation underscores the importance of sustainable sourcing and conservation of natural resources. Zero Toxins advocates for building materials and processes that are devoid of harmful substances, ensuring a healthy indoor environment which results in zero indoor air pollutants. Addressing societal concerns, Zero Poverty, Zero Injustice, and Zero Exclusion advocate for designs that contribute to social equity, poverty alleviation, and inclusivity. Simultaneously, Zero Ignorance encourages educational aspects within the project steps, fostering awareness and knowledge dissemination. Lastly, Zero Displacement underscores the importance of designing spaces that do not contribute to the displacement of communities. The synthesis of these principles forms a blueprint for conscientious architectural design that not only minimizes environmental impact but also actively contributes to social well-being and equity.

The amalgamation of the 7 R and 11 Z principles fosters a dynamic synergy that transcends mere sustainability, pivoting towards a holistic approach to architectural resilience. This integration requires a profound shift in architectural thinking, necessitating an understanding that design decisions reverberate through time, space, and communities. As the field of architecture grapples with the complexities of binate change and the uncertainties of the future, the interplay between these principles offers a robust framework for shaping built environments that are not only responsive to evolving challenges but also generative of positive impact. Through the lens of these principles, architects and academics are empowered to be stewards of a more resilient, regenerative, and harmonious architectural practice.

This paper follows a research by design methodological approach, offering a dynamic process of iteratively conceptualizing and refining design solutions, guided by the 7 R and 11 Z principles. Central to this approach is the utilization of advanced simulation tools and building modelling techniques, enabling to explore various scenarios and predict the performance of designs in a controlled virtual environment. Through these simulations, insights are gained into energy consumption patterns, indoor environmental quality, and the interplay between design elements. Generally, the synthesis of research by design and simulation-based experimentation empowers architects and researchers to tailor resilient architectural solutions. Below are sketches in figures 1&2 of the combination of the seven Rs and eleven Zs principles in the Z Free Home. The project is currently in its conclusive phase, gearing up for the impending implementation of the proof of concept 1:1 physical prototype. This scholarly contribution aims to elucidate the intricacies of the design process, specifically focusing on the final stage of the structural design solution. Furthermore, it will provide insights into the forthcoming implementation phase and the subsequent monitoring stage, offering a comprehensive exploration of the project's evolution and methodological intricacies.

Figure 1. Axonometric showing the Z free tiny home exterior.

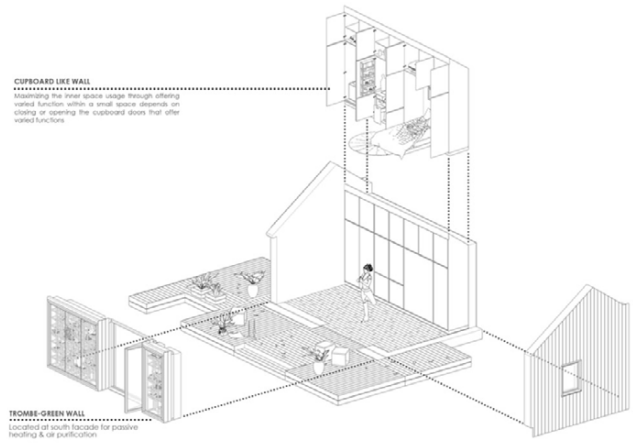

Figure 2. Blown up axonometric showing the plug and play elements in the house design that follows the 7Rs and 11Zs principles

3. Methodology

The study adopts an experimental innovation proof of concept methodology, integrating research by design and development methods with lab testing and a 1:1 physical prototype. This multi-faceted approach ensures a comprehensive exploration of the Z Free Home's design principles and resilience to global challenges. Below the detailed steps of the methodological approach:

3.1 Investigative Phase: Interviews and Literature Review

The investigative phase initiates with targeted interviews of architects, engineers, builders, and bio-based materials experts. This process aims to discern challenges related to resilient and regenerative building and low impact living, establishing a foundation for subsequent design considerations. Simultaneously, a thorough desk literature review delves into influential books and scientific journal articles on regenerative design, climate-responsive architecture, and passive zero-carbon design. This dual-pronged approach ensures a comprehensive understanding of existing knowledge in the field.

3.2. Design Phase

Building upon insights gained from interviews and literature, the design phase involves the generation of intricate design and development sketches for the Z Free Home proposal. These sketches serve as the blueprint for the integration of the 7 Rs and 11 Zs principles, defining the design strategies and requirements essential for achieving project goals.

3.3. Experimental Virtual Reality Workshop

In this phase, an experimental virtual reality mini workshop is conducted to visualize the Z Free Home. This immersive experience aids in rectifying design decisions and rigorously testing passive interactive eco-cycle systems within the house, ensuring their seamless integration.

3.4. Verification Stage: Simulation

The verification stage employs simulation, primarily the ClimateStudio software, complemented by numerical calculations. This phase rigorously assesses energy performance, carbon emissions, and overall environmental impact. Validation of the zero goals—zero energy, zero carbon, and zero environmental impact—is paramount in confirming design objectives.

3.5. Implementation Preparation

The final methodological step involves preparing for implementation, where a detailed inquiry into design technicalities related to the construction process is undertaken. Extensive meetings with construction engineers and builders prioritize considerations such as time, cost, and overall environmental impact. A deliberate emphasis on a low-tech approach aims to reduce labor costs, facilitating the possibility of a do-it-yourself construction method for homeowners seeking active involvement in the building process. This meticulously structured methodology, encompassing interviews, literature review, design, virtual reality testing, simulation, and implementation preparation, positions the Z Free Home project at the intersection of innovative design, sustainability, and resilience against the backdrop of global challenges.

The comprehensive methodology detailed herein underscores the multifaceted approach employed in the design and development of the Z Free Home. From strategic shifts in construction materials to meticulous load-bearing considerations and thermal performance optimizations, each step contributes to the creation of a resilient and sustainable housing solution. The impending implementation in the Lund Urban Living Lab in south Sweden marks a significant milestone, offering a tangible manifestation of this research project innovative outcomes. The subsequent one-year monitoring and assessment period will provide invaluable data to further refine and validate the Z

Free Home's efficiency in addressing global challenges in sustainable and low-impact living.

4. Results and Discussion

The outcomes of the multifaceted design and development phases, including the virtual reality interactive workshop and simulation of design and design development, have been extensively elucidated in prior publications [7-11]. These antecedent steps were of paramount significance, providing the necessary groundwork for an in-depth exploration into the pivotal realm of construction detailing. Some of the simulation outcomes are presented below in table (1). That is to show the values that the project reached prior to the implementation phase.

Table 1: Energy and thermal comfort simulation results

Parameter	Value
EUI, kWh/m^{2}y	73.28
Overheating ratio during the summer, %	0.31%
Heating load after using passive heating systems, kWh/m^{2}y	10.25
Cooling load after using passive cooling systems kWh/m^{2}y	13.03
Equipment load, kWh/m^{2}y	30.00
Hot water load, kWh/m^{2}y	20.00
Total electricity consumption, kWh/y	1465.67

4.1 Construction Detailing Methodology

The ramifications of construction detailing, as gleaned from intensive interviews and workshops involving adept builders and esteemed building manufacturers in Sweden, coalesced into the formulation of a straightforward, do-it-yourself modular structure system. Initially contemplating a modular wooden frame infused with bio-based materials, it became evident that wood, despite its ubiquity, succumbed to sustainability concerns owing to the energy-intensive manufacturing process. Rigorous investigations and a scholarly revisitation of pertinent literature on natural materials in construction led to the proposition of a modular frame constructed from shredded waste reeds, augmented by other high-cellulose biomaterials for binding. This paradigmatic shift aims not only to minimize environmental impact but also leverages the prolific availability of reeds, often deemed invasive species, their rapid growth, and ease of harvest and shredding.

The primary challenge lay in ensuring robust binding force and the production of structurally sound frames capable of bearing loads. Given the experimental context of a single-story design, the roof load emerged as the paramount consideration. The integration of load-bearing walls within the structural system facilitated the continued use of frames made from reeds, with the filling material contributing significantly to load-bearing capacity. Future iterations necessitate comprehensive load-bearing compression strength tests to ascertain structural viability in multi-story configurations.

4.2 Filling Material Challenges and Innovations

The second challenge centred on selecting a filling material that strikes a delicate balance between light weight and robust load-bearing capacity for the roof structure. To achieve this, a judicious mix of straw, kenaf, jute and shredded reeds was proposed. While kenaf and jute presented commendable thermal performance, they were not readily available in the Swedish context where the pilot 1:1 model is slated for construction. Consequently, the chosen blend comprises straw from wheat, oat, and barley, combined with shredded reeds and seaweeds. The lightweight nature of these materials, especially dried seaweeds, mirrors the desired thermal performance synonymous with kenaf and jute. An added advantage is the high fireproofing resistance conferred by the substantial salt content in seaweeds.

4.3 Challenges in Cladding Materials Selection

The third set of challenges pertained to the inner and outer cladding for the modular panel elements. Clay emerged as an optimal choice for interior plastering due to its commendable thermal properties, humidity regulation capabilities, and high fire resistivity. However, for exterior plastering, considerations of resistance against rain and snow necessitated supplemental additives. Consequently, the decision was made to employ clay for both interior and exterior surfaces, fortified with an additional layer of lime plaster or casein protein for the exterior surfaces.

4.4 Optimization of Panel Size

Extensive discussions unfolded regarding the dimensions of the panels, with an emphasis on accommodating low-tech do-it-yourself construction practices. Recognizing the potential drawbacks of small-sized panels—primarily the creation of thermal bridges and the necessity for additional layers to close gaps between joints—a judicious compromise between size and weight was sought. The finalized optimal panel dimensions stand at 40 cm in width, 90 cm in length, and 135 cm in height, weighing between 13 to 16 kilograms. This adheres to safety standards, allowing for manual transport without risk of injuries.

4.5 Implementation Plans and Future Assessments

While the accompanying sketches illustrate the generic design for the modular system and the building skeleton, detailed drawings are withheld due to copyright considerations, given the project's ongoing pre-construction status. The implementation phase is planned for August 2024 at Lund Urban Living Lab (Labbet). A proposed one-year standing period for the constructed house aims to facilitate comprehensive year-round monitoring and assessment. This extended monitoring duration is pivotal for capturing nuanced performance metrics, providing empirical insights into the Z Free Home's resilience and sustainability under diverse climatic conditions and define performance gaps.

The Z Free Home, presently existing as a conceptual idea, eagerly anticipates transitioning into the conclusive phase of the proof of concept building stage. The overarching objective is to subject the dwelling to an exhaustive one-year monitoring period, planned to assess its operational efficiency comprehensively. This comprehensive evaluation spans diverse facets, encompassing energy production, consumption patterns, waste management intricacies, and the efficacy of its passive heating and cooling systems. While simulation tools offer preliminary insights and contribute to anticipatory efficiency predictions, it is imperative to underscore that empirical performance, derived from an amalgamation of real-world conditions, often deviates from simulated projections. This variance is notably pronounced, especially in the context of passive systems for heating and cooling, where performance is intricately intertwined with fluctuating outdoor weather conditions. Furthermore, a noteworthy facet of passive systems lies in their manual operation, often necessitating direct user engagement. The reliance on users for manual control adds an additional layer of complexity to the evaluation of these systems.

Recognizing these inherent intricacies, it is imperative to integrate a pre and post occupancy evaluation into the assessment framework to provide a more understanding of the Z Free Home's operational efficiency. Such an evaluation serves as a complementary tool, offering a qualitative and quantitative lens through which to scrutinize the holistic performance of the dwelling. This dual-pronged approach, combining empirical monitoring with user-centred assessments, ensures a robust and comprehensive depiction of the house's functionality and efficiency.

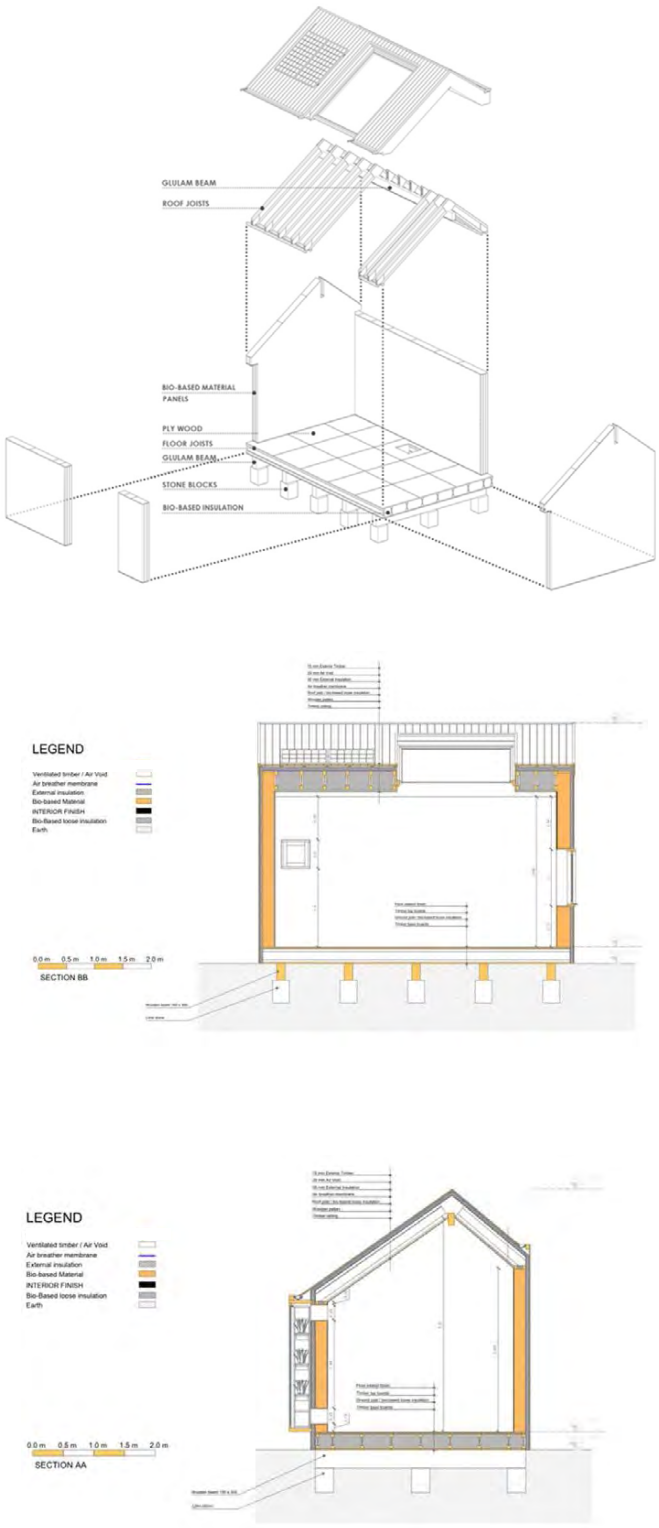

Figure 3. The Z free home structure system proposal.

CONCLUSION

The Z Free Home project, presented as a pilot study, embodying a commitment to a comprehensive and sustainable built environment. The amalgamation of the 7 R principles— *Refuse, Reduce, Rethink, Reuse, Renewable, Regenerative, and Respect* —with the 11 Z principles—Zero Energy, Zero Waste, Zero Water waste, Zero Emissions, Zero Deforestation, Zero Toxins, Zero Poverty, Zero Injustice, Zero Exclusion, Zero Ignorance, and Zero Displacement, forms a dynamic synergy that transcends mere sustainability. This integration fosters a holistic approach to architectural resilience, demanding a profound shift in architectural thinking to consider the far-reaching implications of design decisions.

The methodology employed in this research, characterized by a research-by-design approach, advanced simulation tools, and a experimental proof-of-concept process, positions the Z Free Home project at the forefront of innovative and sustainable architectural solutions. The construction detailing methodology, particularly the selection of materials and the formulation of a do-it-yourself modular structure system, exemplifies a departure from conventional practices. Challenges such as load-bearing considerations, filling material selection, and cladding materials were systematically addressed, culminating in an optimized panel design.

In essence, the synthesis of these principles and methodologies not only propels architectural practice towards resilience but also positions architects and academics as stewards of a more resilient, regenerative, and harmonious built environment. As we navigate the uncertainties of the future, the interplay between the 7 R and 11 Z principles offers a robust framework for shaping built environments that endure, adapt, and thrive in the face of multifaceted challenges. Through the lens of these principles, architects are empowered to usher in a new era of architectural practice—one that is responsive, sustainable, and generative of positive impact.

Moreover, the implementation phase will serve as a platform for experimental proof-of-concept, where innovative ideas and techniques will be put into practice. From the selection of sustainable materials to the construction of the modular structure system, every aspect of the Z Free Home will be scrutinized and refined to ensure optimal performance and durability. Challenges encountered during this phase, whether technical, logistical, or regulatory, will be met with ingenuity and determination, driving the project towards its ultimate goal of creating a truly resilient and regenerative built environment.

ACKNOWLEDGEMENTS

The author expresses sincere gratitude to The Swedish Crafoord Foundation for their generous research grant, which has been instrumental in advancing the Z Free Home project. Profound appreciation is extended to all the interviewees who willingly shared their valuable insights and experiences during the meticulous interview process. The successful culmination of the project's two-year journey owes much to the dedicated contributions of research assistants Ilia Larkov, Douglas Barcley, and Mohamed Elbangy. Their unwavering support has significantly enriched the project, contributing to its successful realization.

REFERENCES

1. Dabaieh, M. (2023). Circular design for zero emission architecture and building practice: it is the green way or the highway. Cambridge, MA: Woodhead Publishing.

2. Trogal, K., Bauman, I., Lawrence, R. & Petrescu, D. (eds.) (2019). Architecture and resilience: interdisciplinary dialogues. Abingdon, Oxon: Routledge.

3.Watson, J. (2019). Lo-TEK: design by radical indigenism. Cologne: Taschen.

4.Roaf, S., Crichton, D. & Nicol, F. Adapting buildings and cities for climate change: a 21st century survival guide. (2nd ed.) Amsterdam: Architectural Press.

5.Boswell, M.R., Greve, A.I. & Seale, T.L. (2019). Climate Action Planning A Guide to Creating Low-Carbon, Resilient Communities. (1st ed. 2019.) Washington, DC: Island Press/Center for Resource Economics.

6.Newman, P., Beatley, T. & Boyer, H. (2017). *Resilient cities: overcoming fossil-fuel dependence*. Washington: Island Press

7. Dabaieh, Marwa (2022). The Z Free Home. inspired by vernacular architecture. Valencia: Editorial Universitat Politècnica de València. Available on Internet: http://urn.kb.se/resolve?urn=urn:nbn:se:mau:diva-54951

8. Dabaieh, Marwa & Iarkov, Ilia (2022). The Z free home from conceptual design to simulation results. E3S Web of Conferences. 362. Available on Internet: http://urn.kb.se/resolve?urn=urn:nbn:se:mau:diva-56493

9. Dabaieh, M., & Iarkov, I. Rodil,K., (2022). Z-free home: A circular practice. In, Bustamante et., el (Eds). Proceeding of the 36th PLEA 2022 conference: The future of *sustainable buildings and urbanism in the age of emergency. Will cities survive?.* ISBN: 978-956-14-3069-3

10.Dabaieh, M., Iarkov, I., & Rodil, K. (2023). The 'Z-Free' Home: A Circular Thinking and Eco-Cycle Design Practice. Energies, 16(18). https://doi.org/10.3390/en16186536

11.Rodil, K., Bisbo, K., Kronborg, K. T., Kristensen, L. B., Atkinson, P. B., & Dabaieh, M. (2022). Using Virtual Reality to Demonstrate Sustainable Architecture Concepts: Making Passive Systems Interactive. ACM International Conference Proceeding Series. https://doi.org/10.1145/3547522.3547718

PLEA 2024 WROCŁAW
(Re)thinking Resilience

Robotic additive manufacturing of lichen composites for air quality monitoring

Digital fabrication of responsive and resilient material systems from lichens

ANNA NIKOLAIDOU[1] SONNY LIGHTFOOT[2] TAVS JORGENSEN[2]

[1]Unconventional Computing Laboratory, UWE, Bristol, UK
[1]School of Architecture and Environment, UWE, Bristol, UK
[2]Centre for Print Research, UWE, Bristol, UK

ABSTRACT: In the light of an unprecedented climate emergency, there is an urgent need to reconsider the materials we use for the construction of our buildings and to explore alternative material systems that are abundant, easy to source, and exhibit increased climate resilience and adaptability. Materials with these attributes have been developed by living systems. We propose the development of hybrid materials from living lichens and abiotic components for air pollutant sensing, using a 3D digitally driven paste delivery system. Lichens are excellent indicators of air pollutants, they present resilience to extreme environmental conditions and are abundant, can self-grow and self-regulate. The lichen species Flovoparmelia caperata, Parmotrema perlatum and Xanthoria parietina were used for the production of the samples. We employed a robust photographic recording system that allowed the morphological monitoring of the samples. We assessed colonisation tendencies and performed statistical analysis of changes in pigmentation distribution to understand substrate-lichen correlations and the metabolic activity change over time. Our findings demonstrated that three combinations of lichen species-substrates presented optimal integration and were selected as most suitable for 3D printing. We also report that one sample demonstrated excellent colonisation behaviour and less changes in its metabolic activity over time.
KEYWORDS: hybrid living materials, lichens, robotic 3D printing, biosensing, sustainability

1. INTRODUCTION

The building industry accounts for one of the largest negative impacts on the planet, significantly contributing to the depletion of natural resources and raw materials. In addition to this, we are already experiencing pressure on living conditions and an increase in damage to buildings from extreme weather events, attributed to climate change [1]. In the light of this unprecedented climate emergency, there is an urgent need to reconsider the materials we use for the construction of our buildings, their production and assembly processes. We therefore need to explore alternative material systems and fabrication processes that allow the use of materials that are not only abundant in our planet, readily available and easy to source, but also exhibit increased climate resilience and adaptability, mitigating the impact of extreme climate change events and responding to the ever-changing environmental conditions.

Materials with responsive capabilities have already been developed by living systems over the last 4.5 billion years, as they have created biological structures for the modification of their environment and survival [2]. Natural biological systems are capable of sensing environmental conditions and responding to them on multiple scales [3]. Living systems possess distinctive features that endow them with intrinsic advantages for the manufacture of responsive materials such as their ability to grow autonomously into structured bulk materials without human effort, to self-regenerate and degrade the components that they make, thereby possessing a sustainable life cycle for the entire material and to provide complex responses to environmental stimuli [4]. In addition to the above features, they exhibit living attributes such as self-growth, self-regulation, self-repair and self-replication, making them excellent candidates for the development of materials with reduced environmental impact as compared to conventional materials. The above exceptional properties and capabilities make living materials attractive as functional components for the development of responsive materials.

An emerging area of materials that has attracted interest in the scientific community is Living Hybrid Materials. This class of materials can be defined as materials composed of living cells that form or assemble the material itself, or modulate the functional performance of the material in some manner [2]. Living hybrid materials contain both living organisms and abiotic components. They retain the living attributes while the incorporated abiotic materials enhance the material structure and

performance such as responsive and sensing functionalities [4]. Living hybrid materials with sensing and information processing capabilities usually incorporate a substrate, and functional or active layers [5]. The functional layers include the active elements where the main activity takes place while the substrate is a solid substance upon which the functional layers are deposited [6, 7].

This research project aims to contribute to an emerging and growing body of work that recognises the potential of living cells as functional layers for the development of materials with responsive capabilities such as sensing external stimuli. We propose the development of hybrid living materials from lichens, using a novel robotic additive manufacturing process for paste 3D printing of the lichen substrate matrix.

Lichens are symbiotic organisms, usually composed of a fungal partner and one or more photosynthetic partners [8]. They are found on trees, rocks and in soils [9] and are perennial, resilient and able to live for many years in extreme conditions [10,11]. They are abundant, providing easy accessibility, they can self-grow, self-repair and they are self-regulating. Unlike plants, lichens lack vascular organs to directly control their water loss or uptake [12], their water content equilibrates with atmospheric conditions and as a result, lichens range between desiccated and water-saturated states on a daily basis throughout much of their lifetime [13]. Lichens can survive in harsher environments compared to their constituting fungi and algae as individual living microorganisms due to passing nutrients and metabolites to each other which ensures better adaptability [14]. This astonishing capability to survive and remain living and healthy under extreme environmental changes, makes them promising candidates to be used as a sustainable alternative to conventional materials currently used in the building industry.

In addition to exhibiting resilience to extreme environmental conditions, lichens are excellent biomonitors for air pollutants. The use of lichens as biomonitors is attributed to their ability to respond to air pollutants at different levels, their slow growth rate, longevity as well as their ability to indicate the presence and the concentrations of these pollutants [15,16]. Although lichens have been used extensively in the field for the detection and monitoring of air pollutants such as metals and organic air pollutants, to our best knowledge, integration of lichens into substrates for the development of building material composites has not been reported yet. We therefore present a scoping study in which we investigate the integration of lichens into various substrate matrices using a digitally driven paste delivery system.

2. HYPOTHESIS AND OBJECTIVES

Drawing from the existing literature demonstrating lichen's ability to respond to extreme environmental changes as well as sense and report the presence of air pollutants, we hypothesise that it might be possible to 3D print lichen composites that can perform the above functions. Our aim is to develop living hybrid material systems from lichens that exhibit responsive capabilities when exposed to environmental pollutants, using a novel digital fabrication method of paste delivery.

The hypothesis is sought to be verified through the following objectives:

- To assess and establish protocols of lichen/substrate colonisation for the development of the hybrids.
-To 3D print substrates that present optimal colonisation behaviour using a digitally driven paste delivery system.
-To evaluate gas absorption rates of hybrid materials upon exposure to pollutants.
-To develop a framework for deploying lichen hybrid material systems.

3. METHODS

3.1 Experimental set up and material synthesis

The lichen species Flovoparmelia caperata, Parmotrema perlatum and Xanthoria parietina were collected from three tree trunks of an outdoor area with average pollution levels in Bristol, United Kingdom. For each of the species, the same tree trunk site was used for the collection. The rationale for this decision was that since the same site was used, it was most likely that the specific lichen species benefitted from the same secondary metabolites such as nutrients and water intake, environmental stress, moisture content and sun exposure, allowing the development of conclusions by excluding these parameters when performing morphological characterisation and statistical analysis.

Seventeen samples of different substrates- lichen species combinations were produced (Fig. 1). The substance choice and concentrations were based on an already established protocol of material mixture and concentrations used for 3D printing. The materials used were Cellulose Fibre Scarva, Methyl cellulose, Chitosan, Glycerin, Agar, Coffee grounds, Rice Starch, Sodium alginate, Hemp Shive and Clay (Smooth Terracotta). Table 1 shows the composition and quantities of the developed substrate samples.

The samples were kept at ambient room temperature in a hydroponic growing tent with the provision of artificial daylight (Fig. 2) and monitored every 2-3 days. Additional moisture was added manually as required with de-ionised water.

Figure 1: Inoculated substrate samples. Flovoparmelia caperata, Parmotrema perlatum and Xanthoria parietina lichen species were used for the inoculation. *Photograph by Simon Regan 2023.*

3.2 Pigmentation distribution

A photographic recording system incorporating a customised 3D printed base for the positioning of a camera at an angle and distance that allows the morphological monitoring and characterisation of the samples was established.

Sample 8
Lichen species: Parmotrema perlatum

Material	Weight (g)
Cellulose Fibre Scarva	10
Methyl cellouse	50 dry
Chitosan	80
Glycerin	40

Sample 10
Lichen species: Flovoparmelia caperata

Material	Weight (g)
Cellulose Fibre Scarva	12
Sodium alginate	50
Rice Starch	4
Glycerin	20
Cellulose Fibre Scarva	12

Samples 9
Lichen species: Parmotrema perlatum

Material	Weight (g)
Cellulose Fibre Scarva	5
Bio bean	20
Chitosan	30
Additive 5	40
Fine Hemp Shive	5

Samples 11, 12
Lichen species: Xanthoria parietina, Parmotrema perlatum

Material	Weight (g)
Cellulose Fibre Scarva	12
Sodium alginate	50
Rice Starch	4
Agar	20
Cellulose Fibre Scarva	5

Sample 13
Lichen species: Flovoparmelia caperata

Material	Weight (g)
Cellulose Fibre Scarva	10
Methyl cellulose	30
Sodium alginate	20

Sample 15, 16, 17
Lichen species: Flovoparmelia caperata, Parmotrema perlatum, Xanthoria parietina,

Material	Weight (g)
Clay [Valentines Smooth Terracotta VC10]	200
Hemp Shiv	5

Samples 14, 14a
Lichen species: Parmotrema perlatum, Flovoparmelia caperata

Material	Weight (g)
Cellulose Fibre Scarva	10
Methyl cellouse	50 dry
Chitosan	80
Glycerin	40

Table 1: Substances and concentrations used for the development of the substrate samples.

Images of each sample were taken for 6 consecutive weeks prior to the implementation of data analysis (Fig. 3). We performed colour distribution statistical analysis. The rationale behind the selection of this method is the described below

Figure 3: Recordings of sample 16 for 6 consecutive weeks. Pigmentation distribution changes have been analysed to understand correlations between lichen species and substrate composition.

The parameters that may affect the distribution of the lichen pigmentation over time can be attributed to the following factors: 1. Fungal partner pigments 2. Algal or cyanobacteria pigments 3. Secondary metabolites 4. Interaction of lichens with the substrate 5. Type of lichens 6. Environmental stress 7. Moisture content. Since the inoculation of the substrates was performed in controlled conditions, factors 3, 6 and 7 remain the same for all samples and therefore can be eliminated from the parameters taken into consideration. Changes to pigmentation distribution over time may therefore be attributed to the interaction of the lichens with the different substrates as well as the composition of the fungal and photosynthetic partners in each sample. Conclusions may lead to a better understanding of how lichens interact with the substrates and which lichen species- substrate combinations could lead to integration and adherence of the lichens to the substrate substances and therefore to self-assembly formation mechanisms. For the interpretation of the data set depicting pigmentation change over time, the data of the same lichen species samples were analysed and compared to allow the elimination of the impact of factor 5 on our possible conclusions. MATLAB was used for the analysis.

Figure 2: Hydroponic tent used for the lichen-substrate inoculation to allow controlled conditions of light, humidity and temperature for all samples. Photograph by Simon Regan 2023.

3.3 Robotic 3D printing test system

The Robotic 3D printing test system used in this research project consists of an UR collaborative Robotic Arm which is connected to an Arduino based

micro controller hardware unit. This unit operates a stepper motor which is integrated within Poseidon open-source syringe pump fixture that facilitate the delivery of the paste, synchronised with the movement of the robotic arm. The Poseidon fixture has been modified to fit the UR end-effector bracket and adapted to hold a 60ml syringe tightly. The syringe itself has been modified with a set of interchangeable set of nozzles 3D printed in 5, 8 and 10mm diameter.

The workflow of processing test prints starts with forms designed in a CAD software and saved in the STL format. The STL files are then sliced into 3D printing paths using the CURA software. These paths are saved as G code data, which can be interpreted by the integrated robot arm and paste delivery system. To facilitate the interpretation, the CURA G-code commands are loaded into the RobotDK software running on a laptop which is connected to the UR control box via an ethernet cable – enabling real time data flow. Data is relayed from the UR control box to an Arduino microcontroller which in turn send commands to stepper motor driver that controls movement of the stepper motor which pushes the plunger of the syringe and ultimately deliver the paste in amounts that are synchronised with the movement of the robotic arm (Fig. 4).

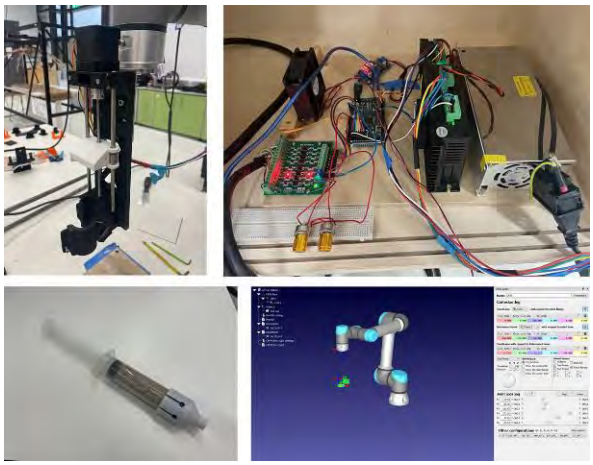

Figure 4: Images of the development of the robotic 3D printing test system. The system consists of an UR collaborative Robotic Arm connected to an Arduino based micro controller hardware unit using a syringe paste delivery printing process.

4. RESULTS

Samples 1, 2 and 11 presented optimal colonisation and the lichen species were fully integrated with the substrate, forming a hybrid material from the fusion of the living and synthetic particles. By optimal colonisation, we refer to the binding and attachment of the lichen species to the substrate in such a manner that the components are coalesced and cannot be separated.

It is worth noting that for the image classification via statistical analysis of changes in pigmentation distribution implemented in the analysis below, the red, green and blue mean values are the average values of the red, green and blue channels of the image pixels. In regard to the species Xanthoria parietina and for the course of 6 weeks, sample 2 presented the highest red and green mean values of 177.9 and 170.9 with standard deviation values of 49.4 and 55.0, skewness of 2.52 and 2.47 and kurtosis 8.97 and 8.55. This indicates that the sample presents leptokurtic distribution and the kurtosis is therefore positive. Additionally, the skewness is negative. On the other hand, sample 1 showed the lowest red and green mean values of 157.2 and 150.2, with 70.3 and 76.2 standard deviation values, skewness of 2.56 and 2.48 and kurtosis 8.77 and 8.53, also presenting leptokurtic distribution with positive kurtosis and negative skewness. Sample 11 showed the highest blue mean value of 158, 48.6 standard deviation value, with skewness 0.86 and kurtosis 2.60. This may be interpreted as negative skewness but the kurtosis is platykurtic. In contrast, sample 1 demonstrated the lowest blue value of 140.2 with standard deviation of 78.5 and 1.97 skewness and 6.05 kurtosis with leptokurtic distribution. The above statistical analysis indicates that for sample 1 (Fig. 5), modification in pigmentation distribution remains the lowest compared to the other samples inoculated with the Xanthoria parietina species which may be attributed to the living cells retaining their nutrients and functional exchanges between the fungal and photosynthetic components. Sample 2 contains cellulose fibre scarva, methyl cellouse and chitosan, same particles used in sample 1. In addition to the above particles, sample 1 substrate also contains glycerine and additive. It may therefore be possible that the glycerine and additive contributed to the living cells presenting lowest pigmentation modifications and thus retaining their original living state and metabolic activity.

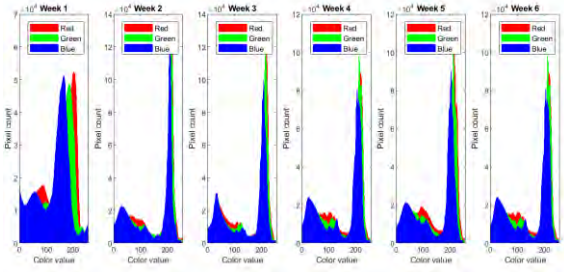

Figure 5: Plots depicting pigmentation distribution changes over 6 consecutive weeks for sample 1.

A similar trend can be observed in regard to the species Parmotrema perlatum. Sample 14 presented the highest red mean value of 169.6, standard deviation of 58.3, a negative skewness of 1.65 and a

positive kurtosis of 4.46 with leptokurtic distribution. Sample 8 showed the highest green mean value of 165.4, standard deviation of 45.1, a negative skewness of 1.69 and a positive kurtosis of 5.80 with leptokurtic distribution. Finally, sample 12 showed the highest blue mean value of 157.2, standard deviation of 45.8, a negative skewness of 0.86 and a kurtosis of 2.22 with platykurtic distribution. On the contrary, sample 9 displayed the lowest red, green and blue mean values of 155.2, 148.7 and 139.9 (Fig. 6). The standard deviation values were 73, 78.3 and 79 respectively, with negative skewness of 2.84, 2.62 and 2.44 and positive kurtosis of 10.67, 9.45 and 8.92, also with leptokurtic distribution. From the above analysis, it is demonstrated that from the substrates inoculated with Parmotrema perlatum lichen species, sample 9 displayed the lowest pigmentation distribution modifications and therefore its substrate might have contributed to the living lichens maintaining their original state and metabolic activity in comparison to the other samples. By comparison of the substances used in the samples, it may be possible that this behaviour is attributed to Bio bean and Additive and/or Fine Hemp Shive.

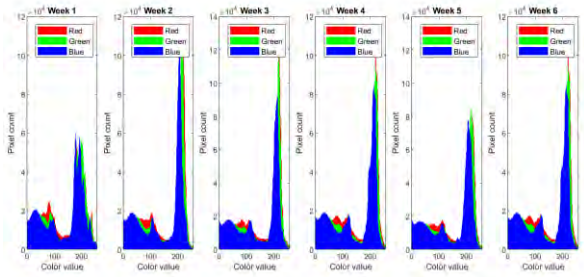

Figure 6: Plots depicting pigmentation distribution changes over 6 consecutive weeks for sample 9.

Lastly, for the species Flovoparmelia caperata, sample 14a showed the highest red mean value of 173, standard deviation of 46.7, a negative skewness of 1.08 and a negative kurtosis of 2.73 with platykurtic distribution. These findings are consistent with sample 14 discussed above, where the same substrate is inoculated with the lichen species Parmotrema perlatum and also show the highest red mean value. It is therefore possible that the particles used in substrates 14 and 14a have a maximum impact on the lichen species and more specifically on their metabolic activity. Table 1 shows in detail the substances used for each sample. Sample 14a also presents the highest green mean value which is 167.1 with 49.2 standard deviation, a negative skewness of 0.70 and a negative kurtosis of 2.16 with platykurtic distribution. Finally, three samples showed the same blue mean value of 156.2 which was the highest between the discussed samples of this lichen type. These samples are 3, 13 and 14. Standard deviation is 59.3, 45.1 and 53 respectively. The skewness is negative for all three samples and is 1.58, 1.43 and 0.45 respectively. The kurtosis is positive for samples 3 and 13 and is 4.28, 3.80 with a leptokurtic distribution and negative for sample 14 with a value of 2.34 and platykurtic distribution. It is therefore evident that the substrate components of sample 14 may impact most the metabolic activity of the lichens and therefore exhibit highest change of the pigmentation distribution. Regarding the lowest mean values, sample 5 demonstrated the lowest mean values for all three pigments (Fig. 7). These are 154.5, 148.9 and 141, showing standard deviation of 74.1, 79.8 and 80.9 respectively. The skewness is negative and the values are 2.99, 2.87 and 2.50 for red, green and blue pigments. The kurtosis is positive and is 12.20, 11.39 and 9.11 with a leptokurtic distribution.

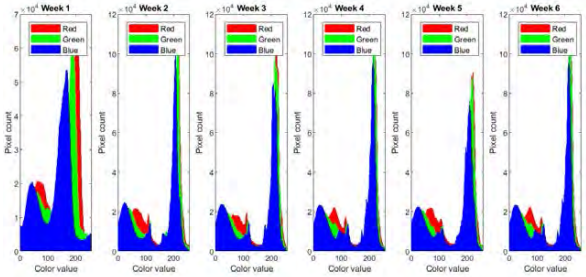

Figure 7: Plots depicting pigmentation distribution changes over 6 consecutive weeks for sample 5.

5. DISCUSSION

Our findings demonstrated that three combinations of lichen species-substrates presented optimal colonisation (1, 2, 11) and were therefore selected as most suitable for 3D printing using the system mentioned above (Fig. 8). Additionally, the data analysis contributed to a better understanding of the substrate-lichen correlation and more specifically the metabolic activity change over time. We can report that the three samples that showed lowest change of the pigmentation distribution are 1, 5, 9 and therefore their metabolic activity was more similar to their initial state than the other samples. On the other hand, most pigmentation distribution changes were observed in samples 2, 11, 14, 14a, 3 and 13 indicating that the metabolic activity of the living cells has been most impacted. We can therefore report that from the data analysis and physiological monitoring, sample 1 presents the most ideal candidate for the development of the new hybrid living material since it exhibits excellent colonisation behaviour and less changes in its metabolic activity over time. Further research needs to be undertaken to better understand the impact of the concentrations of the substrate components on the metabolic activity, the implication of metabolic changes to the living cells and substrate as well as the

specifics of the substances used so that a more accurate mapping can be achieved.

6. CONCLUSION

This research project marks a ground-breaking investigation of incorporating lichens into substrate matrices aimed at robotic 3D printing. To our best knowledge, this is the first time that such approach has been tested, opening up exciting opportunities for the development of a new class of hybrid materials using living components that are truly resilient to environmental stress, sustainable, can self- assemble, self-heal and self-regenerate. Our findings so far contribute to a better understanding of lichen species- substrates correlations as well as 3D printing approaches that can lead to the production of lichen hybrid living materials with scalability potentials for applications in the building industry through integration and self- assembly of their components.

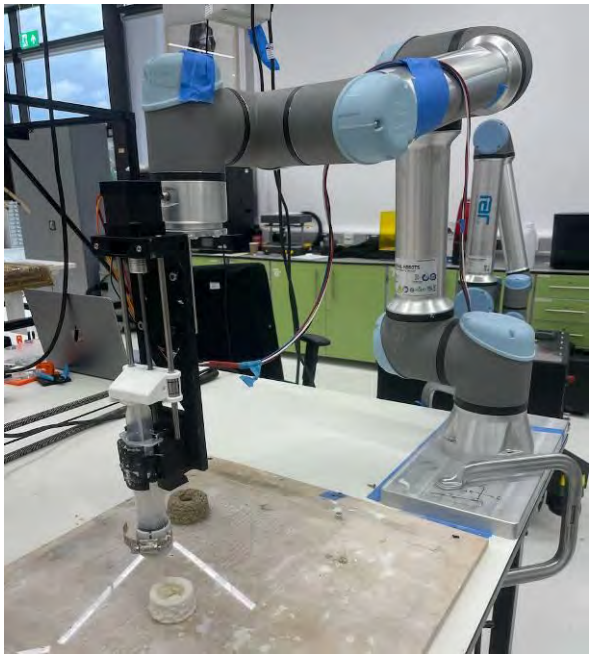

Figure 8: Small scale 3D printing studies of optimal substrates for lichen inoculation.

Following the above studies, we will use our findings for the next phase of this research project which includes the assessment of the responsiveness of the developed hybrid living materials to air pollutants exposure. For assessing gas absorption, the inoculated 3D printed hybrid living materials will be subjected to distinct gases in bespoke chambers and quantitative data will be collected for analysis of absorption. The findings of this phase will be included in the conference presentation. Challenges that need to be considered in this next research phase is minimising contamination risks and deterioration of the substrate material as well as monitoring the lichen hybrid materials for any pathogen growth.

REFERENCES

1. United Nations Environment Programme (2021). A Practical Guide to Climate-resilient Buildings & Communities. [Online], Available: https://www.unep.org/resources/practical-guideclimate-resilient-buildings [28 August 2023].
2. Nguyen, P. Q., Courchesne, N. M. D., Duraj-Thatte, A., Praveschotinunt, P., & Joshi, N. S. (2018). Engineered living materials: prospects and challenges for using biological systems to direct the assembly of smart materials. Advanced Materials, 30(19), 1704847.
3. Teague, B. P., Guye, P., & Weiss, R. (2016). Synthetic morphogenesis. Cold Spring Harbor perspectives in biology, 8(9), a023929.
4. Wang, Y., Liu, Y., Li, J., Chen, Y., Liu, S., & Zhong, C. (2022). Engineered living materials (ELMs) design: From function allocation to dynamic behavior modulation. Current Opinion in Chemical Biology, 70, 102188.
5. Li, W., Liu, Q., Zhang, Y., Li, C. A., He, Z., Choy, W. C., ... & Kyaw, A. K. K. (2020). Biodegradable materials and green processing for green electronics. Advanced materials, 32(33), 2001591.
6. Piro, B., Tran, H. V., & Thu, V. T. (2020). Sensors Made of Natural Renewable Materials: Efficiency, Recyclability or Biodegradability—The Green Electronics. Sensors, 20(20), 5898.
7. Cao, Y., & Uhrich, K. E. (2019). Biodegradable and biocompatible polymers for electronic applications: A review. Journal of Bioactive and Compatible Polymers, 34(1), 3-15.
8. Nash, T. (2008). Introduction. In T. Nash, III (Ed.), Lichen Biology (pp. 1-8). Cambridge: Cambridge University Press.
9. M.E. Hale, M.E. (1974) The Biology of Lichens, 2nd ed., Edward Arnold, London.
10. L. Bergamaschi, L. et.al. (2003) Determination of baseline element composition of lichens using samples from high elevations, Chemosphere 55, p. 933–939.
11. Maphangwa, K.W. et.al. (2012) Differential interception and evaporation of fog, dew and water vapour and elemental accumulation by lichens explain their relative abundance in a coastal desert, J. Arid Environ. 82, p.71–80.
12. Proctor MCF, Tuba Z (2002) Poikilohydry and homoihydry: antithesis or spectrum of possibilities? New Phytol 156(3), pp. 327–349.
13. ten Veldhuis, MC., Ananyev, G. and Dismukes, G.C. (2020) Symbiosis extended: exchange of photosynthetic O2 and fungal-respired CO2 mutually power metabolism of lichen symbionts. Photosynth Res. 143, 287–299.
14. Wöstemeyer, J. (1997) MT Madigan, JM Martinko, J. Parker, Biology of Microorganisms, Prentice Hall International Inc.
15. Sloof, J.E., de Bruin, M., Wolterbeek, H. (1988) Critical evaluation of some commonly used biological monitors for havy metal air pollution, in: Environmental Contamination: Proceedings of the international Conference Venice (Italy), Edinburgh, pp. 296–298.
16. Nimis, P.L. et al. (1993) Lichens as bioindicators of heavy metal pollution: a case study at La Spezzia, VHC, New York, pp. 265–284.

The Environmental Performance Of Contemporary Bamboo Architecture In The Tropics

A case study of an educational building designed by Ibuku in the warm and humid climate of Bali, Indonesia

OLIVIER DAMBRON[1]

[1]Atmos Lab, London, UK

ABSTRACT: This research critically examines the environmental performance of contemporary bamboo architecture in tropical regions, focusing on a case study of an educational building designed by Ibuku in Bali, Indonesia. Amidst the rapid development and modernization affecting tropical countries, traditional architectural practices often get overshadowed. This paper highlights the importance of local materials, craftsmanship, and innovative designs for sustainable living. It specifically explores bamboo's potential as a sustainable construction material in tropical climates – as the vegetal rod that comes out of the ground -, highlighting the significance of bamboo species selection, processing techniques, and the application of durable design principles in bamboo architecture. The paper presents an in-depth analysis of The Green School near the town of Ubud, a project that exemplifies the innovative use of bamboo in contemporary architecture. The study investigates various aspects of its environmental performance, including daylighting, natural ventilation, and thermal comfort. The school's thermal performance was rigorously evaluated through fieldwork employing data loggers and spot measurement tools, complemented by user interviews. The research provides both qualitative and quantitative insights into the efficacy of bamboo architecture in ensuring comfort with minimal energy consumption.
KEYWORDS: bamboo, vegetal rod, warm and humid climate, fieldwork, thermal performance

1. INTRODUCTION

The hasty development of emerging tropical countries has led to the proliferation of inappropriate architectural practices that replicate designs intended for very different cultures and environmental conditions. These uncontextualized practices, create built environments in the tropics which rely heavily on mechanical systems, consume non-renewable energy all year long and thus pose significant environmental threats. To counteract this trend, the use of local ecological materials, local craftmanship and innovative environmental designs is crucial for sustainable living. This paper delves into the case of Bali, Indonesia, a region, heavily impacted by tourism and rapid modernization, which holds rich examples of vernacular and contemporary bamboo architecture. For the past decades “ruthless” developers have focused on the southern part of the island, building fully airconditioned high rise resorts, encouraging foreigners to maintain their customs from abroad. Not only has this phenomenon gentrified the local Balinese population away, but also constitutes a real threat by gradually separating locals from their culture. A direct consequence is the decrease of tolerance from the Indonesians regarding their perception of comfort. However, further inland, lies the Balinese cultural capital town of Ubud where genuine traditions are perpetuated and relation to nature kept strong. Abundant around the tropics, bamboo has traditionally been used as a construction material for the warm and humid climate. Although varied uses and applications in building construction have established bamboo as an environment-friendly, energy efficient and cost-effective option, recent transformation techniques of the material have derived it from its natural state. Therefore, drawing attention of designers away from its initial potential as a vegetal rod. Reporting guidelines for bamboo selection, preservation and processing in Indonesia is necessary to set the conditions in which bamboo holds its best potential to generate sustainable architecture. A significant challenge that has slowed the development of bamboo architecture resides in its social perception. Bamboo remains widely misunderstood and attributed exclusively to extreme contexts, either for old traditional uses (vernacular architecture, scaffolding, etc) or temporary emergency sheltering. However, several noticeable examples of bamboo buildings have achieved to elevate the material to more contemporary and modern uses, at locations where the strongest bamboo species grow abundantly. The focus of this paper will be on Indonesia, as it detains a strong handcrafting heritage combined with a traditional know how regarding the use of bamboo. This set of conditions creates new possibilities to generate

sustainable and environmental architecture using natural bamboo rods for contemporary lifestyles.

2. CONTEXT

2.1 The climate of Indonesia

Indonesia lies between latitudes of 11°S and 6°N and experiences a tropical warm and humid climate characterized by annually consistent temperatures around 27°C with little diurnal variations and high incident solar radiation reaching 1000 Wh/m². Humidity levels are high averaging around 84% and winds are moderate averaging at 2.5m/s, hence the majority of the population living in naturally ventilated houses to ensure thermal comfort. Winds are generally predictable, usually blowing in from the south-east during the dry season (May to September), and from the northwest during the rainy season (November to March).

2.2 The local climate of Ubud, Bali

Figure 1: Location of Ubud on the island of Bali (source: Google Maps)

Ubud is centrally located on the island of Bali at 220 meters in altitude, with the nearest coast at more than 10 km (figure 1). Annual temperatures (figure 2) are slightly cooler than in the coastal areas, ranging from 20 to 30°C with a narrow diurnal temperature range of +/- 7°C. Relative humidity levels remain above 80% and natural ventilation is permanently needed to relieve from heat stress. Sky illuminance is high with frequent overcast sky conditions which can easily cause disturbing glare [1]. Rainfall is substantial with an annual average of 2244mm mostly occurring during the wet season facilitating a dense vegetation. The dry season has fewer rainy days, lower humidity levels and clearer skies.

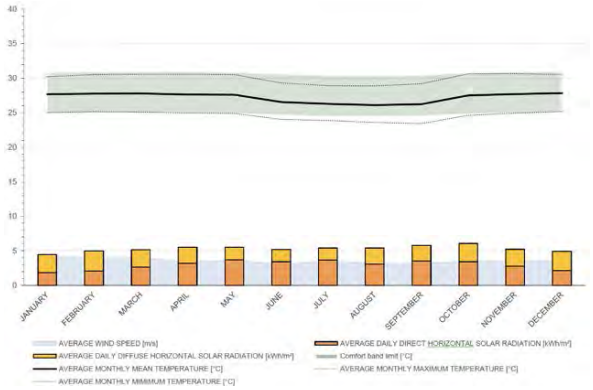

Figure 2: Climate analysis of Bali

Indonesians reckon witnessing climate change as conditions have now become less predictable. Historically, an annual sudden change of wind direction occurred during a week in April and another in September, these events were traditionally the object of social gatherings in the rice fields and a celebration for the kite festivals. Although wind patterns are now more scattered, prevailing winds can still be considered to be south-eastern and north-western, respectively during the dry and wet season.

3. BAMBOO A VIABLE RESOURCE IN BALI

3.1 Overview on bamboo

This study highlights the potential of bamboo as a traditional construction material well-suited for warm and humid tropical climates. Despite its historical significance, bamboo has been overlooked due to modern material preferences. A shift towards bamboo architecture in the tropics offers benefits such as being affordable and widely available. It is a lightweight material with the tensile strength of steel and compression resistance of concrete which can be used to build structural cores, columns, beams, staircases, slabs, roofs, facades, partitions, frames and furniture [2].

3.2 Bamboo a locally abundant natural resource

Over 1000 bamboo species flourish between the latitudes of 50° North to 20° South, with Asia accounting for 67% of the global distribution. This rapid-growing grass demands meticulous harvesting to ensure optimal construction performance. Culms attain their full height within an eight-month period, exhibiting their maximum diameter upon emergence. A two-year maturation period is essential for the outer layer to shed and branches to develop. The prime harvesting window for a bamboo culm is post three years, coinciding with peak internal density, verifiable via sonic testing. Post-harvest, the culms undergo a two-week solar drying phase, during which they experience shrinkage. Minimizing shrinkage is crucial to avert cracking. Subsequently, the culms are immersed in a heated boron solution for a full day, a step imperative for eliminating natural sugars and deterring insect infestation. The final stage involves

exposing the green poles to sunlight until they achieve a yellow hue, indicating the depletion of chlorophyll. Selecting species that are highly adaptable to the local climatic, soil, and topographic conditions is essential to meet the expectations of rapid growth, superior quality, and robustness. Traditional practices, now substantiated by contemporary research [6], recommend three specific species for construction in Indonesia (figure 3), capitalizing on their wide availability, proven adaptability and structural integrity.

1- Petung (Dendrocalamus Asper):

Height of culm: 18-25 m
Diameters: 10-20 cm
Thickness: < 2 cm
Timber bamboo used for structural elements and furniture.

2- Tali (Gigantochloa Apus):

Height of culm: 10-20 m
Diameters: 10 cm
Thickness: < 2 cm
Straight bamboo used for roof structures, furniture and scaffolding.

3- Duri (Bambusa blumeana):

Height of culm: 10-15 m
Diameters: 6-12 cm
Thickness: < 2 cm
Curvy bamboo used for flooring, railings and furniture.

Figure 3: Species used for construction in Indonesia.

3.4 Durable bamboo design principles

Bamboo is acknowledged as a sustainable construction resource within tropical regions. Nonetheless, the inherent variability of bamboo culms precludes standardization, making the quality of craftsmanship a determinant of structural integrity. The irregularity of bamboo's anatomical structure complicates the development of uniform mechanical joints for assembling construction components. However, this challenge is mitigated in countries like Indonesia, where a rich heritage of handcrafting tradition empowers designers with the ability to devise efficient, bespoke solutions. Adherence to fundamental principles is essential for optimizing the longevity of bamboo construction elements. Joinery, being a critical aspect of bamboo construction, demands meticulous attention. Joints are the most susceptible to damage and cracking if not properly executed. A prevalent method involves sculpting the end of the receiving pole into a 'fish mouth' shape to snugly accommodate the adjoining pole and facilitate effective load distribution [3]. While traditional construction utilized bamboo pegs and rope to secure joints, contemporary methods employ threading and bolting for enhanced stability. For principal structural components, infilling with concrete is an additional measure that is taken to augment their strength.

Figure 4: Picture of fish mouth joint with bamboo pin (source: courtesy of Pt. Bamboo Pure)

Bamboo's porous nature allows it to absorb and release moisture, and significant changes in moisture levels can negatively impact its durability [3]. Hence, implementing protective measures against precipitation and direct, intense solar radiation becomes imperative, particularly on the building's windward side where water penetration is more profound. These protective strategies can be realized through various approaches. One effective method is to design the roof overhang to extend sufficiently such that the extremity forms a 45° angle to the ground when viewed in relation to the base of the bamboo structural component. Should achieving this angle be impractical, an alternative is to elevate the base of the bamboo culms. This can be done by creating a concrete foundation or placing a stone beneath the base, thereby diminishing the exposure relative to the roof's overhang.

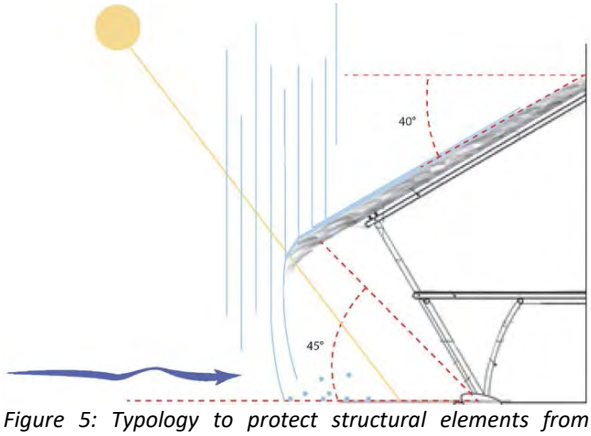

Figure 5: Typology to protect structural elements from weathering effects.

4. CASE STUDY: THE GREEN SCHOOL BY IBUKU

Situated near Ubud in Bali, The Green School, constructed in 2007 and designed by Ibuku, stands as a contemporary example of bamboo architecture in the tropics. It serves approximately 500 students, ranging from kindergarten through high school,

drawn from both international and local backgrounds. This institution fosters a unique educational milieu, immersing students within an architecture entirely made of a natural material.

4.1 Overview of the Heart Of School

Figure 6: Aerial and west & elevation view of HOS (source: courtesy of Ibuku)

Figure 7: Ground floor view & offices of HOS

The master plan's spacious design facilitates wind flow, and the eastward descending slope of the terrain helps prevent wind blockage between structures. At the core of the HOS's design is the hyperbolic shape that supports the roof's load. This principle is central to the building's structure, as detailed in the study. Constructed from three bamboo species identified in this research, the building utilizes bamboo for floors, ceilings, stairs, railings, furniture, and versatile blinds, all handcrafted from bamboo culms, resulting in a notably lightweight construction. Roof pitches and extended overhangs are specifically designed for efficient water runoff and to shield the bamboo's foundation. Additional adaptive features, such as the bamboo blinds (figure 6), address rain, sunlight, and glare. The building is confined only by its roof as there are no walls, allowing the building to be opened to more than 80 % of its elevation. With floors and partition made extremely permeable to maximise air movement (figure 7), and considering acoustic limitations of the material, the program is distributed to prioritise privacy of classrooms and avoid disturbance by adjacent users. A practical remedy for the squeaking caused by footsteps on multiple stories bamboo structures is the use of repurposed rubber from old tires as dampers. The school operates from 8:30 am to 3:30 pm, Monday through Friday. Break times are scheduled for a 15-minute snack at 10 am and an hour-long lunch at noon, during which significant activity is permitted on the ground floor. Throughout the day, classrooms and offices are in continuous use, with study areas experiencing higher occupancy in the afternoons.

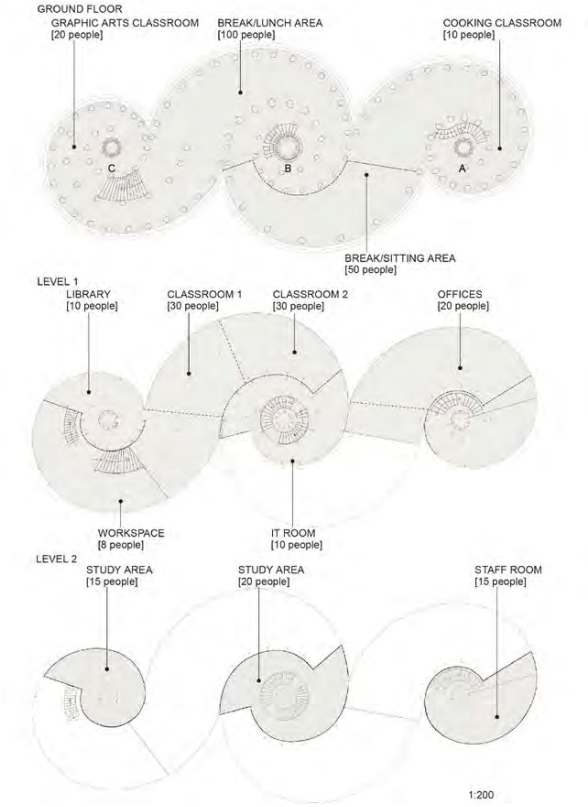

Figure 8: Floor plans, program and occupancy of HOS (courtesy of Ibuku)

The HOS has its longer facades set perpendicular to the prevailing North-West and South-East winds, prioritizing natural ventilation potential over easier solar control. Extensive openings facilitate effective cross ventilation, enhancing comfort regardless of wind direction. Positioned atop a hill and adjacent to a river to the East, the HOS benefits from the cooling effect of the South-Eastern wind, which accelerates as it moves up the hill, delivering a cooling breeze at its peak [7]. The North-western side opens onto a grass-covered sports field, where wind can develop over cooler surfaces prior to entering the school.

Figure 9: Aerial views comparing vegetation growth

Furthermore, rapid and dense vegetation growth means the landscape conditions at the design stage likely differed considerably from the current ones. This temporal discrepancy is illustrated by comparing aerial photos from 2012 and 2016 (figure 11).

Vegetation, including bushes, mid-sized plants, and tall palm trees, now encircles parts B and C of the Heart of the School (HOS), significantly impeding breezes at the level of the openings and reducing comfort during peak temperatures. This observation is corroborated by interviews with two teachers who report a lack of air circulation in these areas. Conversely, another teacher on the ground floor of part A experiences frequent cool breezes.

4.2 Methodology

The potential for natural ventilation is investigated through wind speed spot measurements. The thermal performance is investigated through temperature spot measurements and recordings from four temperature and humidity dataloggers placed on site. The daylight performance is investigated through lux spot measurements. The application of the durable bamboo design principles is analysed based on photographs of the construction elements.

4.3 Results: HOS environmental performance

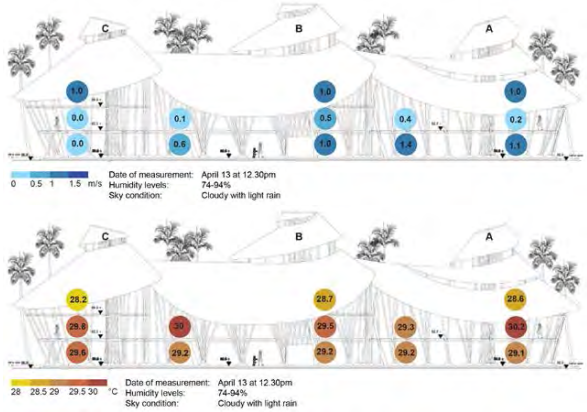

Figure 10: Wind speed & air temperature measurements (after: elevation by Ibuku)

Spot measurements across the HOS showed low to moderate wind speeds ranging from near 0 to 1.4 m/s and temperatures from 28.2°C to 30.2°C (figure 12), pinpointing that higher temperatures occur in zones with calmer wind conditions and conversely. Airflow does improve at higher floors, but lengthy windward roof spans could deflect breezes unless openings are strategically placed. Surrounding vegetation hinders airflow on both the ground and first floors of part C. There's a slight increase in air movement near part A, where vegetation is less dense. The first floor across all three parts of the HOS experiences more stagnant air compared to other levels due to the roof overhangs extending to the first floor's height, which, while shielding against sun and rain and reducing glare, also impede the desired direct airflow. To monitor further these conditions, four data loggers were placed, one on each of the three floors of part B - the central and most occupied section - and one outdoors. Air temperatures were recorded over a school week in April 2016, from Monday to Friday (figure 13). The analysis focuses on the last three recorded days which show diverse climatic conditions: (i) Wednesday 13/04, precipitation between 11:30 am and 1 pm, (ii) Thursday 14/04, intermittent cloud cover during the day's warmest hours, (iii) Friday 15/04, clear skies and consistent solar radiation.

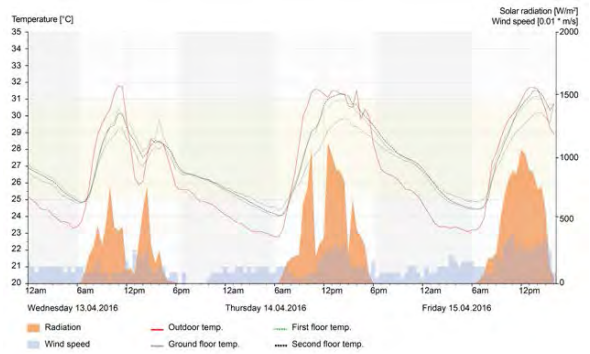

Figure 11: Wind speed & air temperature measurements (after: elevation by Ibuku)

These observations highlight the building's responsive lightweight structure, as evidenced by the semi-internal temperatures mirroring outdoor temperature fluctuations without delay. Daytime temperature differentials were observed as follows: a 1° difference between the ground floor and the first floor, and an additional 0.5° increase from the first to the second floor. This gradual temperature rise confirms the presence of a stack and buoyancy effect, facilitated by the high permeability of most vertical elements. Furthermore, the building's structural hyperbolic core functions as a conduit (figure 14), allowing warm air to ascend to higher openings. Consequently, warm air accumulates at upper levels, potentially causing discomfort in low wind conditions.

Figure 12: Permeable hyperbolic structural core

While temperatures generally fall within a comfortable range, during peak daylight hours, intense solar radiation significantly warms the surrounding ground and the surfaces of the building's roof. This results in overheating on the first and second floors. Although thatched roofs typically do not retain much heat, a portion of the heat is captured by the winds on the windward side and channelled into the interior spaces. This issue can be mitigated to some extent using existing retractable blinds. Solar radiation heats the soil, creating significant air movement and influencing wind speed. It peaks shortly after noon and diminishes by 6 pm, leaving the warm air trapped under the roof to cool down gradually overnight. During this time, there is a consistent 1 to 2°C difference between the ground floor and outdoor temperatures, persisting until morning. This phenomenon highlights the ground's thermal storage capacity, which releases heat via conduction and convection as the outdoor temperature decreases. The building's temperatures are significantly affected due to the extensive surface area of the roof covering the ground, enhanced further by extended overhangs. These overhangs channel the heat indoors, demonstrating the thermal dynamics in play [8].

4.4 Daylight analysis

The yellow bamboo's light reflectance is nearly 50%, enhancing the building's interior with a unique roughness that scatters daylight effectively. A key design feature is the circular top opening above each spiral's structural core, with a diameter of 2 to 3 meters, allowing ample sunlight to penetrate the interior. In regions with high sun paths and humidity, glare can become overwhelming, but due to its elevated position, rarely within users' direct line of sight, this opening minimizes glare issues. To preserve the bamboo's durability and mitigate direct sunlight exposure, a white translucent canvas covers the top opening, ensuring diffused daylight. Additionally, the core structure's reflective coating prevents the bamboo poles from cracking.

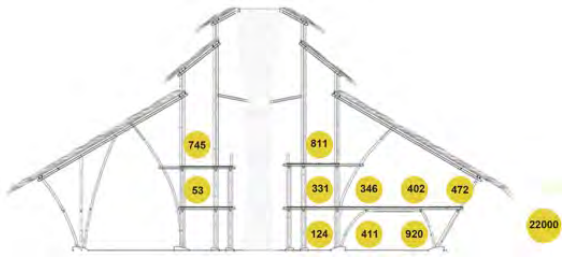

Figure 13: Lux spot measurements (after: section by Ibuku)

During a sunny day, spot measurements indicated that most areas achieve the necessary 300 lux for educational buildings (figure 15). The building's extended overhangs, essential for the HOS design, restrict sky visibility, further reducing ground reflections. This results in most daylight being indirect, leading to the necessity of artificial lighting in deeper areas of the plan, even on sunny days.

4. CONCLUSION

Bamboo, in its natural form, presents a wealth of sustainable options for creating contemporary environmental architecture that is not only cost-effective and functional but also fosters a connection between users and nature. This is exemplified by the Green School in Bali, which is constructed entirely from bamboo and demonstrates exceptional thermal performance. The school consistently maintains internal temperatures that are lower than the outdoor temperature during the day's warmest hours. Future enhancements, such as wind-driven modifications to the roof and strategic arrangement of nearby vegetation, are poised to further improve internal airflow, thereby elevating the comfort level for occupants. It's crucial to comprehensively educate users on these adaptive strategies to empower them with greater control over their environment. Bamboo's potential as a primary material for tropical architecture is readily achievable in regions where it has naturally thrived. In these areas, cultural practices and knowledge have evolved in tandem with the growth of bamboo, making it a fitting and accessible choice for sustainable building.

ACKNOWLEDGEMENTS

I would like to thank Ibuku for granting me access to the Green School and to the archives. I would also like to thank Jorg Stamm for sharing generously his knowledge and expertise in Bamboo construction.

REFERENCES

1. Koch-Nielsen, H. (2002). Stay Cool. A design guide for the built environment in hot climates. James & James Ltd.
2. Hidalgo, L, O. (2003). Bamboo - The Gift of the gods. Bogotá. ISBN 958 – 33 – 4298
3. Kramer, K. (1985). Bamboo as a building material. Institute for Light weight structures. Nr.31, Stuttgart.
4. Stamm, J. (2006). Manual for bamboo selection, classification, preservation and processing. Colombia.
5. Stamm, J. (2008). Following the natural advantage of the giant Grass. Colombia.
6. Rabik, A. (2003). Towards resilient bamboo forestry. A reference guide for improved management of clumping bamboo for timber bamboo. Environmental Bamboo Foundation. Bali, Indonesia.
7. Koenigsberger, O. Ingersoll, T. Mayhew, A. Szokolay, S. (1973). Manual of Tropical Housing and Building. Longman Group Ltd., London.
8. Szokolay, S. (2003). The role of Thermal Mass in Warm-Humid Climate Housing. pp55-61, PLEA 2003, Santiago.

PLEA 2024 WROCŁAW
(Re)thinking Resilience

Psychophysiological Effects of Vertical Greening Systems:
Patterns between Green Facade Design Variables and Effects

XIAOJIE SHEN[1], FENG YANG[2]

[1] College of Architecture and Urban Planning (CAUP), Tongji University, Shanghai, China
[2] Key Laboratory of Ecology and Energy-Saving Study of Dense Habitat, College of Architecture and Urban Planning (CAUP), Tongji University, Shanghai, China

ABSTRACT: The Vertical Greening System (VGS), which can be divided into Green Façade (GF) and Living Wall (LW), is supported as an effective method for increasing exposure to nature in dense urban areas, potentially reducing stress and improving emotional well-being. However, while studies have explored the psychophysiological benefits of VGS through field and simulation experiments, questions remain regarding whether VR-observed effects are akin to those in the real world. Furthermore, the relationships between VGS design variables and their effects have not been fully elucidated. By utilizing data from self-report and biosensing measures collected through real-world and virtual reality experiments, this study sought to explore these relationships. The results indicate that virtual GF exposure evoked psychophysiological responses similar to those from real-world GF exposure; the dose-response curve, illustrating the relationship between the GF dose and an increase in stress levels and negative affect, was U-shaped in the presence of a stressor; the threshold GF dose likely varies across different built environments; the buffering effects of green facades that were close to the pedestrian level, and decentralized in layout were more effective.
KEYWORDS: Vertical greening system, Psychophysiological responses, Buffering effect, Restorative effect, Emotion.

1. INTRODUCTION

Intensive urbanization has led to the development of oppressively dense streetscapes, posing challenges to creating liveable, pleasant urban environments and threatening the mental health of city residents. Exposure to natural elements has been recognized for its substantial benefits in reducing the adverse impacts of densely built environments and the stress of urban living on cognitive function, stress levels, and emotional well-being [1-2]. Chan et al. identified three categories of psychophysiological effects of nature [3], namely, 1) buffering effects, which mitigate negative outcomes in the presence of stress; 2) restorative effects, which help return psychophysiological states to baseline levels following stress; and 3) instorative effects, which enhance psychophysiological states even without stressor exposure.

However, land use constraints are an obstacle to increasing ground-level green space in dense urban areas. The Vertical Greening System (VGS), which can be divided into Green Façade (GF) and Living Wall (LW) [4], has attracted increasing attention in recent decades, as it offers the potential to increase exposure to nature without the cost of land.

The psychophysiological benefits of VGS have been supported by several empirical and experimental studies [3,5-6]. However, although two studies of indoor VGS have investigated the correlations between green dose/size of VGS and its psychophysiological benefits through experiments in virtual reality (VR) [7-8], the patterns between more VGS design variables (especially outdoor VGS design variables) and effects have not yet been elucidated. And the question remains whether the effects observed in VR are the same as in the real world.

To address this gap, this study aims to provide evidence on the relationships between spatial design variables of outdoor VGS and the psychophysiological effects of VGS during the experience of a stressor. The category of VGS in this study is green façade, and the research questions are as follows:

- Question 1: Would exposure to green façade in VR evoke similar psychophysiological responses as in real-world settings?
- Question 2: Does the spatial arrangement (e.g., amount/dose, height distribution, centralised/decentralised layout, plant diversity, etc.) of green façade affect the psychophysiological states of pedestrians? If so, what are the patterns?

2. METHODOLOGY

This study comprised two experiments and was approved by the Science and Ethics Committee. Experiment 1 (Expt. 1) was conducted in late October 2023. Experiment 2 (Expt. 2) was conducted in May 2023. The experiments were numbered based on the research questions they addressed rather than the order in which they were conducted.

2.1 Experiment design

In Expt. 1 (Fig. 1), which was designed to address the first research question, two comparable visual stimuli (i.e., a green façade versus a bare façade) in the real world were captured as virtual versions using an Insta360 panoramic camera and could be viewed through VR devices. Participants' psychophysiological responses were tested in both virtual and real visual exposure, and efforts were made to keep participants' sensory experiences other than visual (such as smells, auditory sensations, etc.) as consistent as possible.

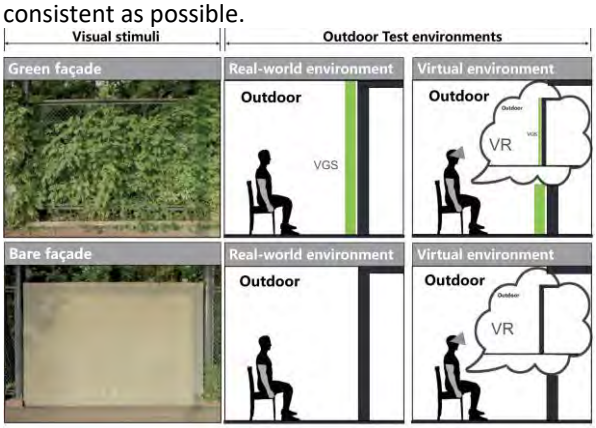

Figure 1: Virtual and real-world test environments in Expt. 1.

In Expt. 2, which was designed to answer the second research question, fifteen VR scenes with different spatial arrangements of green façade were created as visual stimuli (Table 1, Fig. 2), i.e., panoramic photographs with different GF doses (measured by 360-degree Green View Index), height distributions, plant configurations and layouts (centralized or decentralized). Scenes 1 to 9 are linear streets in high density neighbourhoods, and 10 to 15 are pocket plazas. The streets and plazas in these scenes are surrounded by six-story buildings of the same form.

Table 1: Design variables of green façade in VR scenes.

No. of Scenes		GF Dose (%)	Height distribution	Layout	Diversity
Street	1	0	-	-	-
	2	5	Low floor	Centralized	Unitary
	3	5	Low floor	Decentralized	Unitary
	4	10	Low floor	Centralized	Unitary
	5	10	Low floor	Decentralized	Unitary
	6	20	High floor	Centralized	Unitary
	7	20	Low floor	Centralized	Unitary
	8	35	High floor	Centralized	Unitary
	9	35	High floor	Centralized	Diverse
Plaza	10	0	-	-	-
	11	10	Low floor	Centralized	Unitary
	12	10	High floor	Centralized	Unitary
	13	15	All Floor	Centralized	Unitary
	14	15	All Floor	Decentralized	Unitary
	15	20	All Floor	Centralized	Unitary

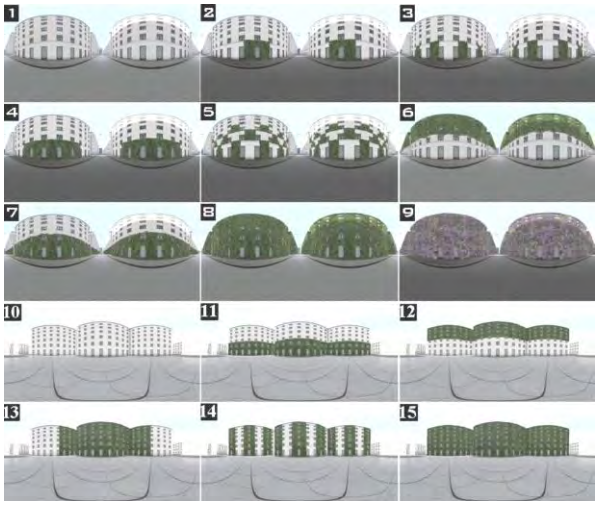

Figure 2: Fifteen VR scenes in Expt. 2.

In both experiments, recordings of traffic noise were used as a stressor for stress induction.

2.2 Participants

Participants were recruited from the university and were aged between 18 and 32 years. Individuals who had used tobacco, alcohol, drugs, or caffeinated beverages within 24 hours of the experiment, and who had participated in intensive exercise within 6 hours prior to the experiment were excluded.

2.3 Outcome measures

As shown in Table 2, the Visual Analog Scale (VAS) and Skin Conductance Level (SCL) were used to measure the psychological and physiological responses of the participants, respectively. The VAS contained 23 items, of which the average of 3 items was used to measure stress levels, the average of 10 items (e.g., interested, excited, Inspired) was used to measure positive affect, and the average of the other 10 items (e.g., upset, hostile, nervous) was used to measure negative affect.

Table 2: Measures of psychophysiological data.

Psychological and physiological data		Description	Relationship with the stress level	Expt.1	Expt.2
Modified VAS (0 to 100)	Anxiety Tension Avoidance	Stress level	Positive	●	●
	20 items from PANAS	Positive and negative affection	-	-	●
EDA	SCL (μS)	Arousal and anxiety level	Positive	●	●

Note, PANAS: Positive and Negative Affect Schedule.

2.4 Procedure

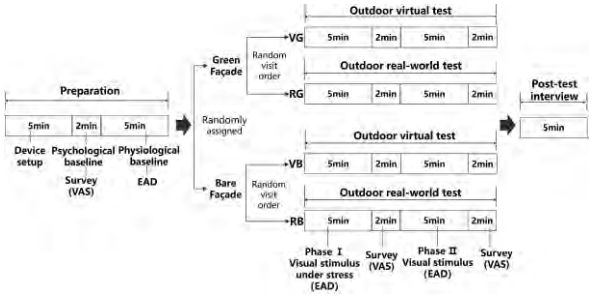

Figure 3: Procedure of Expt. 1. VG: Virtual green façade, RG: Real-word green façade, VB: Virtual bare façade, RB: Real-word bare façade.

As shown in Figure 3, Expt. 1 includes three parts: preparation, test and post-test period.

In the preparation period, participants signed the informed written consent and were assisted in wearing the VR devices and biomonitoring sensors. Their psychophysiological baselines were then obtained through a pre-test survey (VAS) and physiological monitoring.

During the test period, participants were divided into two groups and randomly assigned to experience either a green facade or a bare facade. Meanwhile, each participant visited the same test location twice to separately evaluate both virtual and real environments, with the order of testing randomized to eliminate any order effects. For the first 5 minutes of each test, noise was played along with the visual stimulus. After that, participants were asked to complete a survey (VAS) to obtain their psychological responses. They were then given the same visual stimulus as before for 5 minutes recovery. After that, a survey (VAS) was administered again. The EDA sensors were used to collect SCL data during the whole test period.

In the post-test period, participants were interviewed about their feeling during the test.

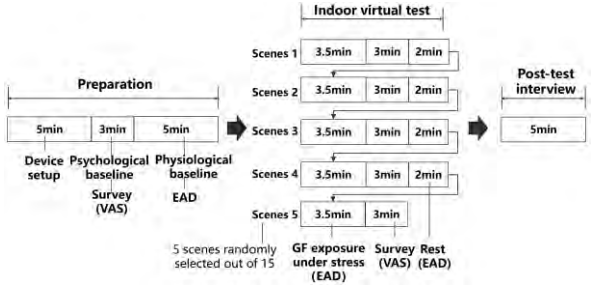

Figure 4: Procedure of Expt. 2.

As shown in Figure 4, Expt. 2 involves a similar procedure to Expt. 1, except that in the test period, participants were randomly assigned 5 out of 15 VR scenes for testing, including three street scenes and two pocket plaza scenes. And participants were asked to visit only once.

2.5 Statistical analysis

The change in psychological and physiological data (ΔVAS and ΔSCL) was used to measure the buffering effects of different visual stimuli under stress and the restorative effects after stressor exposure. In addition, using ΔVAS and ΔSCL as outcome variables may adjust for potential differences in baseline level for different participants and for the same participant across two visits. Buffering effects and restorative effects were calculated as (1), (2) (3) and (4), (5), (6) respectively. VAS data (in Expt.1 and Expt.2) and SCL data (in Expt.1) were log transformed.

Buffering effects:

$$\Delta SCL_b = SCL_{post\_stressor} - SCL_{pre\_stressor} \quad (1)$$

$$\Delta Log\,(SCL)_b = Log\,(SCL)_{post\_stressor} - Log\,(SCL)_{pre\_stressor} \quad (2)$$

$$\Delta Log\,(VAS)_b = Log\,(VAS)_{post\_stressor} - Log\,(VAS)_{pre\_stressor} \quad (3)$$

Restorative effects:

$$\Delta SCL_R = SCL_{post\_recovery} - SCL_{post\_stressor} \quad (4)$$

$$\Delta Log\,(SCL)_R = Log\,(SCL)_{post\_recovery} - Log\,(SCL)_{post\_stressor} \quad (5)$$

$$\Delta Log\,(VAS)_R = Log\,(VAS)_{post\_recovery} - Log\,(VAS)_{post\_stressor} \quad (6)$$

First, the randomization effectiveness of the experiment design was checked. Second, the difference in the psychophysiological measures before and after stress induction in each group/scene was assessed. In Expt.1, the difference before and after recovery in each group was also assessed. Third, the buffering effects (in Expt.1 and Expt.2) and the restorative effects (in Expt.1) were compared between groups/scenes.

Paired t-tests (for normally distributed data) and Wilcoxon signed-rank tests (for non-normally distributed data) were used to analyse within-subject group data, i.e., VG vs. RG and VB vs. RB in Expt. 1. Independent-sample t-tests (for normally distributed data) and Mann-Whitney U tests (for non-normally distributed data) were used to analyse between-subject group data, i.e., VG vs. VB and RG vs. RB in Expt. 1. One-way ANOVA was used to compare data across 15 scenes in Expt. 2.

All data were expressed as the mean. In all comparisons, a p-value < 0.05 was considered statistically significant.

3. RESULTS

3.1 Quality of randomization

In Expt.1, 33 participants generated a total of 66 visits, with randomization resulting in a balanced sequence of visits for the four groups, i.e., 15 (RB) :18(RG): 15 (VB): 18 (VG). The outdoor environment, demographic information, and

psychophysiological baseline, as shown in Table 3, were compared across the four groups to assess the effectiveness of randomization.

Table 3. Characteristics of four groups and outdoor environment in Expt. 1.

Characteristics	Test environments, Mean (± SD) or Number			
	RB	RG	VB	VG
Number of visits	15	18	15	18
Number of males	4	11	4	11
Number of females	11	7	11	7
Good sleep quality	14	16	14	16
Poor sleep quality	1	2	1	2
Self-reported health condition (1-poor to 5-excellent)	3.47 (±0.99)	3.50 (±1.04)	3.53 (±0.99)	3.50 (±0.92)
Self-reported stress level (1-lowest to 5-highest)	3.00 (±0.93)	2.72 (±0.96)	2.93 (±0.80)	2.72 (±1.02)
Solar radiation (W/m^2)	83.59 (±122.25)	131.72 (±139.82)	72.54 (±103.31)	129.63 (±123.62)
Wind speed (m/s)	1.61 (±1.00)	0.49 (±0.21)	1.45 (±1.04)	0.46 (±0.24)
Temperature (°C)	24.68 (±2.58)	25.15 (±2.65)	24.44 (±2.15)	25.61 (±2.60)
Humidity (%)	64.41 (±10.60)	62.54 (±11.77)	66.46 (±10.65)	62.11 (±11.10)
Physiological baseline: Log (SCL) $_{Baseline}$	0.28 (±0.40)	0.39 (±0.26)	0.30 (±0.33)	0.37 (±0.30)
Psychological baseline: Log (VAS) $_{Baseline}$	0.67 (±0.51)	0.71 (±0.53)	0.56 (±0.45)	0.80 (±0.58)

The within-subject analysis showed that the difference between the RB and VB groups, and the difference between the RG and VG groups on demographic, environmental, and psychophysiological measures was not statistically significant. The between-subjects analysis also showed that there were no statistically significant differences between the RB and RG, the VB and VG groups on most demographic and environmental measures. One exception is that mean wind speed was lower in the green façade test environment compared to the bare façade environments. And, due to the unbalanced male-to-female ratio, the physiological baseline was statistically different between the RB and RG groups (Fig. 6).

Table 4: Physiological measures of baseline and rest periods, Mean (± SD)

Period	Baseline	Rest 1	Rest 2	Rest 3	Rest 4
SCL (μS)	1.35 (±0.28)	3.03 (±0.49)	3.43 (±0.57)	3.31 (±0.48)	3.35 (±0.50)

In Expt.2, a total of 20 participants (9 male, 11 female) were recruited for testing. Physiological measures between the baseline and four rest periods were compared to assess the effectiveness of randomization.

The ANOVA showed that the differences in subjects' physiological baseline across the 15 scene groups were not statistically significant (except for 2&4; 2&5; 2&6; 2&7), indicating that randomization was effective in 14 scene groups, except for scene 2. However, the difference in physiological measures between baseline and the 4 rest periods, as shown in Table 4, was statistically significant, indicating that the 2-min rest period was insufficient.

3.2 Expt.1: Changes in psychophysiological data after stressor and recovery

As shown in Figures 5 and 6, the significant difference in psychophysiological data following the stressor confirms its effectiveness. Compared to the under-stress phase, the changes in psychological data after recovery were statistically significant, whereas the changes in physiological data were not. This indicates that physiological recovery may lag behind psychological recovery, and a 5-minute recovery period may be inadequate for physiological recuperation.

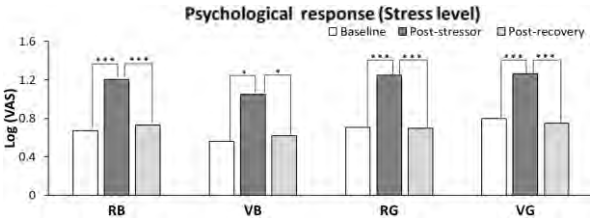

*Figure 5: Pre-post changes of the psychological data. * = p < 0.05, *** = p < 0.001.*

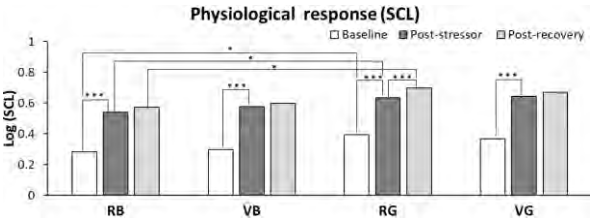

*Figure 6: Pre-post changes of the physiological data. * = p < 0.05, *** = p < 0.001.*

3.3 Expt.1: Buffering and restorative effect

As shown in Figure 7, there was no statistically significant difference in the buffering and restorative effects between the virtual stimuli and the real-world stimuli (comparing RB vs. VB, RG vs. VG), indicating that the virtual green/bare façade stimuli elicited similar psychophysiological responses as in the real world.

The differences in the buffering effects between green façade and bare façade (comparing RB vs. RG, VB vs. VG) were not statistically significant, as were

the differences in restorative effects. However, it was appealing that the 'ΔLog $(VAS)_R$' of the green façade, as shown in Figure 7(d), was lower compared to the bare façade, indicating the more effective restorative effect of the green façade. In Figure 7(c), the 'ΔLog $(SCL)_R$' displays a trend opposite to that of the 'ΔLog $(VAS)_R$', which is understandable given that the physiological baseline of the participants in the RG and VG groups was statistically higher than that of the RB and VB groups, respectively, as shown in Table 3 and Figure 6.

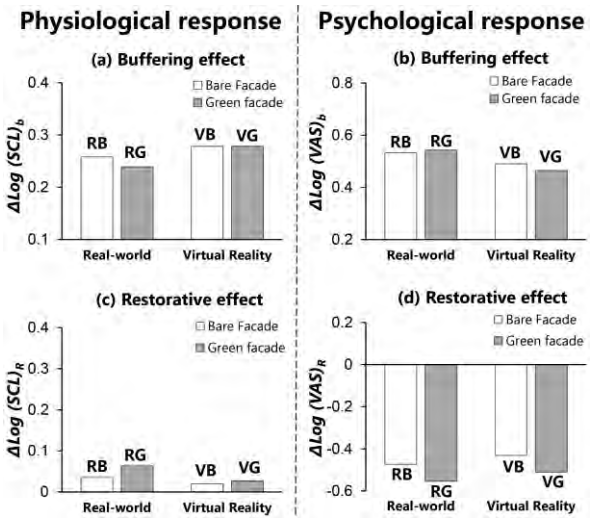

Figure 7: Psychophysiological buffering and recovery.

3.4 Expt.2: Psychophysiological responses across scenes

ANOVA showed that the differences in physiological measures between scenes were not statistically significant, but the comparison between scenes still reflected important trends.

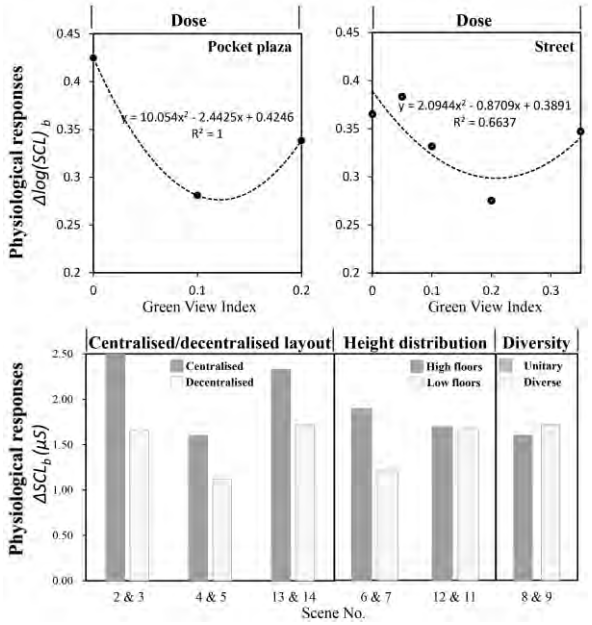

Figure 8: Patterns between the design of green façade and participants' physiological responses.

As shown in Figure 8, the dose-response curve between green façade dose and participants' 'ΔSCL_b' was U-shaped, indicating that the stress-buffering effects (negative to the ΔSCL_b) of GF increased with the dose of green facades and began to decline after a certain threshold was reached. The green facade dose corresponding to the inflection point of the dose-response curve was higher in the dense street compared to the open plaza, indicating that the psychophysiological effects of the green facade are influenced by the built environment. Green facades located close to the pedestrian level and decentralized in layout were more effective in buffering stress.

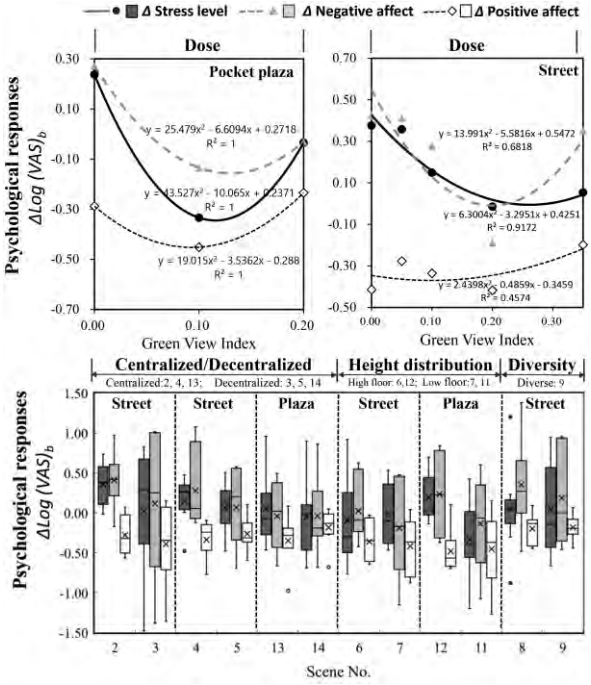

Figure 9: Patterns between the design of green façade and participants' physiological responses.

The curve between the GF dose and the increase in stress levels under stressor, as shown in Figure 9, was U-shaped, as was the curve between the dose and the increase in negative affect, while the association between the GF dose and positive affect was not significant. Green facades that were close to pedestrian level and decentralized in layout were more effective in buffering stress and negative affect, and in reducing the attenuation of positive affect.

4. DISCUSSION

This study investigated the patterns between green façade design variables and participants' psychophysiological responses through VR simulation experiment in Expt.2, and validated the effectiveness and feasibility of conducting VR experiment as an alternative to field experiment in Expt.1, which would ensure the credibility of the conclusions obtained in Expt. 2.

In Expt.2, conducted in May 2023, we found important patterns between green façade design (GF dose, height distribution, centralized or decentralized layout) and its buffering effects. However, there are several limitations in this experiment. First, we did not perform a statistical power calculation before the experiment to ensure an adequate sample size. Second, the rest time (2 minutes) in the Expt.2 was insufficient for washing out the effect of previous stressor. Due to the insufficient number of subjects and rest time, the study did not provide statistically significant quantitative results.

Therefore, in Expt.1, conducted in October 2023, we set a 5-minute test after stress exposure to investigate the restorative effects of different visual stimuli (virtual vs. real, green facade vs. bare facade). Our findings indicate that although 5 minutes has been supported by previous studies as a sufficient time to induce the restorative effect of greenery after stress-inducing tasks (e.g., visual reaction time task, memory task, and arithmetic task) [9-10], it was insufficient for physiological recovery from a green façade after exposure to a noise stressor. The sufficient time for stress recovery may vary depending on the type of greenery and the stressor. By analysing within-subject data, we found that the effects observed in VR were similar to those observed in the real world. However, the different restorative effects between the green façade and the bare façade were not observed, likely due to ineffective randomization of between-subject groups, as indicated by statistically significant differences in baseline data and wind environment across the groups.

Drawing on the data and insights from this study, it's feasible to optimize experiments for statistically significant quantitative results. For instance, allowing sufficient test time to study restorative effects after noise exposure and ensuring adequate rest time in within-subject experiments are crucial. Additionally, conducting statistical analysis prior to the experiment is necessary to ensure an adequate sample size and effective randomization between subject groups. Finally, more biosensors and indicators should be used to measure subjects' physiological responses. It was found that there may be heterogeneity among physiological outcome measures; for example, heart rate and heart rate variability may have higher sensitivity than SCL [11].

5. CONCLUSION

Main findings of this study were as follows:

1) Virtual GF exposure evoked similar psycho-physiological responses to GF exposure in the real world.

2) When exposed to a stressor, the dose-response curve between green façade dose and the increase in stress levels and negative affect was U-shaped. The threshold dose of green façade may vary across the built environment.

3) The buffering effects were more effective for green façades that were close to the pedestrian level and decentralized in layout.

ACKNOWLEDGEMENTS

The study was supported by the National Natural Science Foundation of China (NSFC) Project (Grant No: 52178022).

REFERENCES

1. Kaplan, S., (1995). The restorative benefits of nature: Toward an integrative framework. *Journal of Environmental Psychology*, 15(3): p. 169-182.

2. Ulrich, R. S., et al., (1991). Stress recovery during exposure to natural and urban environments. *Journal of Environmental Psychology*, 11(3): p. 201-230.

3. Chan, S. H. M., et al., (2021). Vertical greenery buffers against stress: Evidence from psychophysiological responses in virtual reality. *Landscape and Urban Planning*, 213: Article 104127.

4. Pérez, G., et al., (2011). Green vertical systems for buildings as passive systems for energy savings. *Applied Energy*, 88(12), 4854-4859.

5. van den Bogerd, N., et al., (2020). Greening the classroom: Three field experiments on the effects of indoor nature on students' attention, well-being, and perceived environmental quality. *Building and Environment*, 171: Article 106675.

6. Elsadek, M., et al., (2019). Green façades: Their contribution to stress recovery and well-being in high-density cities. *Urban Forestry and Urban Greening*, 46: Article 126446.

7. Yeom, S., et al., (2021). Psychological and physiological effects of a green wall on occupants: A cross-over study in virtual reality. *Building and Environment*, 204: Article 108134.

8. Li, Z., et al., (2022). Physiological and psychological effects of exposure to different types and numbers of biophilic vegetable walls in small spaces. *Building and Environment*, 225: Article 109645.

9. Yin, J., et al., (2018). Physiological and cognitive performance of exposure to biophilic indoor environment. *Building and Environment*, 132: p. 255-262.

10. Yin, J., et al., (2020). Effects of biophilic indoor environment on stress and anxiety recovery: A between-subjects experiment in virtual reality. *Environment International*, 136: Article 105427.

11. Gaekwad, J. S., Sal Moslehian, A., & Roös, P. B. (2023). A meta-analysis of physiological stress responses to natural environments: Biophilia and Stress Recovery Theory perspectives. *Journal of Environmental Psychology*, 90, 102085.

PLEA 2024 WROCŁAW
(Re)thinking Resilience

Energy Efficient Ceiling Fans- Perceptions and Popularity in Indian Households

JAYASREE TK[1], SREEJITH UNNIKRISHNAN[2,3]

[1]National Institute of Technology Calicut, Kozhikode, India
[2] Avani Institute of Design, Kozhikode, India
2 Eulerforms- Architecture, Structure and Sustainability, Kozhikode, India

ABSTRACT: Ceiling fans are the most commonly used appliance for residential cooling demands in India irrespective of the climate zone. The government of India have initiated many policies and guidelines for the star rating of ceiling fans and dissemination of awareness regarding the benefits using the same. However, there is an apprehension or lack of awareness among various stakeholders of building industry towards the use of BLDC fans. The current study explores the perception and awareness of various stakeholders regarding the use of BLDC fans. The methods involved interviews, questionnaire surveys among vendors, building professionals and home owners. The sample size was 206 and 75 respondents among them were not aware of BLDC fans. This indicates that 31.45% of the building professionals from the respondents were unware of the BLDC fans. Further questions included the user experience of BLDC fans. The major disadvantage was identified to the high initial investment compared to a regular fan. Other apprehensions included the unfamiliarity in the use of remote controller, lack of technical expertise for installation and possible repairs etc. The study highlights the need for extensive policies at national level along with the dissemination of information and education to building professionals along with the general public.
KEYWORDS: BLDC fans, Energy efficient fans, Thermal Comfort, Residences, Indian households

1. INTRODUCTION

Ceiling fans are used for attaining cooling and ventilation in more than 90% of the Indian households as per the India Residential Energy Survey [1]. Increase in purchasing power, urbanisation and several other factors have contributed to a rapid rise in the sales of room air conditioners in India. However, even with the rapid increase in the purchase of room air conditioners, fans and coolers are projected to maintain a substantial contribution in the year 2037-38 compared to the energy consumption by air conditioning systems [2].

Also, it is interesting to note that approximately 70% of the homes that use air conditions for thermal comfort operate ceiling fans simultaneously [2]. Ceiling fans contributed to 30%-40% share of the residential energy consumption in India [3,4] and ceiling fans are operated for about 2000 hours annual in households [5].

It has been also accepted that in a developing country like India, a large population will not be able to afford air conditioning and depend on natural ventilation or ceiling fans for better thermal conditions [2,6]. These conditions have projected ceiling fans as a major appliance to be focused on for attaining better thermal environment, especially in the warm and humid conditions. The Indian government has introduced various policies and standards to strive towards energy efficiency. Unnat Jyoti by Affordable LEDs for All (UJALA) launched in 2015 by Ministry of Power was a key scheme which transformed the national market in India. As part of this scheme 37 Crore LED bulbs, 73 lakhs LED tube-lights and 25.92 lakhs energy efficient fans were distributed till March 2022 with subsidised rates. This scheme brought down the retail price of LED bulbs from Rs. 300 - Rs. 350 per bulb to Rs. 70 – Rs. 80 per bulb [7,8]. However, certain surveys have identified the use of energy consuming fans and lamps even after focused campaigns [5].

The Bureau of Energy Efficiency have introduced rating systems for ceiling fans. Though earlier introduced as an optional rating criteria for ceiling fans, the BEE has recently made the rating of ceiling fans as mandatory criteria [3]. A typical ceiling fan used to consume 70-80W and a BLDC (Brushless Direct Current) ceiling fan with 5 Star rating consumes only 30-35W energy. BLDC fans can provide energy savings up to 46.3% [9].

However, despite the energy saving potential, it is observed that the use of the energy efficient fans is limited to certain sectors or economic class. A recent study [1] tried to assess the reasons as:

i. Issues in maintaining logistics.
ii. Lack of technical support and services
iii. Lack of awareness
iv. Unavailability of finance options.

It is essential to explore further into the issues and concerns of various stakeholders in the adoption of energy efficient fans.

This study intends to explore the various factors influencing the adoption of energy efficient fans in the households of various economic backgrounds. The study is limited to warm humid climates where the airflow can have a significant influence on the thermal conditions.

2. METHODS

The study was initiated by discussions/interviews with various vendors in the market. Based on the insights from vendors, a questionnaire was developed to gather the information regarding awareness, perception and user experiences of BLDC fans. The questionnaire was further revised based on the expert opinions from architects and various other stakeholders. The questionnaire consisted of 4 parts. The first part collected the basic demographic characteristics including age, profession and economic status. The part 1 concluded with a question "Have you heard of BLDC ceiling fan?". Only those who responded "Yes" were directed to further questions in the upcoming sections. The part 2 consisted of questions regarding the source of information about BLDC fans. This section also seeks whether the respondents have used a BLDC fans. Based on the answers to this questions, the respondents are redirected to 3rd or 4th part of the questionnaire. The Part 3 was intended at respondents who have never used a BLDC fan, but have heard of the same. Whereas Part 4 of the questionnaire is intended at the user experience of BLDC fans. The respondents included architects, contractors, electricians and similar building professionals as well as occupants who are not professionally related to building industry. The random survey ensured almost equal responses from all the income categories considered.

3. RESULTS

The initial market study involved the collection of data regarding the brands, wattage and price range of BLDC fans. Around 21 brands of BLDC fans, namely, Impex, Usha, Atomberg, Luker, Crompton, Orient, Havells, Bajaj, Activa, Lifelong, KUHL, GM, Candes, Tropiko, Amazon basics, Nex glyde, V guard, Hindware, Anchor, Syska, Milton were identified to be available in either offline or online Indian market. The wattage ranged from 26- 42 watts and the price range varied from Rs. 2,000- Rs. 10,000.

This was followed by discussions and interviews with various vendors in the market. The prices in offline market started from Rs. 3,000 with the basic models. In many base models, remote controller facility was not integrated and were limited to very few brands. The high end models had features like Wi-Fi connectivity, integrated light fixtures etc. It was mentioned that most of these models are a preferred gift choice for 'House warming ceremony', which is a common practice in India.

The questionnaire survey collected responses from 206 people with varying age groups and professions. 60.6% of the respondents belonged to the age group between 23 years to 35 years (Figure 1).

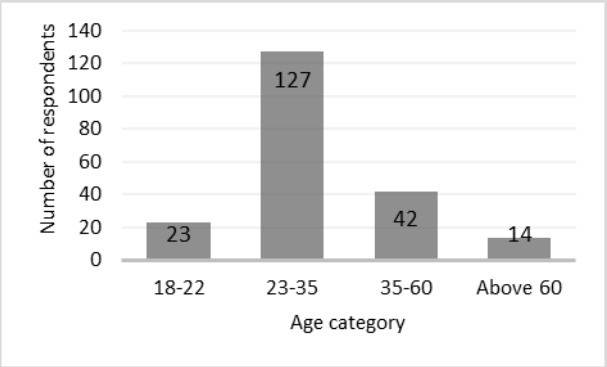

Figure 1. Age group

Also 77.8% (159) of the respondents belonged to building profession (Table 1). Table 1 also provides and overview of the age characteristics combined with the profession. Majority of the respondents belonged to building professionals within the age of 23 years to 35 years.

Table 1. Details of age and profession

		Profession		Total
		Building professional	Other Professions	
Age	18-22	15	8	23
	23-35	107	20	127
	35-60	28	14	42
	Above 60	9	5	14
Total		159	47	206

All the income categories considered were covered fairly (Table 2). The distribution of respondents varied from 16.0% to 27.7% across different categories.

Table 2. Income characteristics

Income Range	Number	Percent
Less than Rs. 25,000	35	17.0
Rs. 25,000 - Rs. 50,000	47	22.8
Rs. 50,000 - Rs. 1,00,000	33	16.0
Above Rs. 1,00,000	34	16.5
Not Applicable	57	27.7
Total	206	100.0

The last two questions from Part 1 were "Have you heard of energy efficient fans?" and "Have you heard of BLDC ceiling fan?". 24 respondents had not heard of energy efficient fans and 75 respondents had not heard of BLDC fans. Further questions after Part 1 were asked only to the 131 respondents who are aware of BLDC fans (Table 3).

Table 3. Awareness on energy efficient fans and BLDC fans

		Have you heard of BLDC ceiling fan?		Total
		No	Yes	
Have you heard of energy efficient fans?	No	24	0	24
	Yes	51	131	182
Total		75	131	206

However, it is interesting to note that out of the 75 respondents who are unaware of BLDC fans, 50 respondents were from building profession. This indicates that 50 out of 159, i.e., 31.45% building professionals from the selected sample were unaware of the BLDC fans. This scenario urges for the increased awareness and self-updating for the building professionals to educate the clients for the incorporation of energy efficient or BLDC fans.

It was observed from the Part 2 of the questionnaire that most of the respondents (131) who have heard about BLDC fans were aware about the same from various sources in internet, friends/ family/ colleagues, newspapers/ magazines, shops and as part of academics.

However, 57 among the 131 respondents have not used a BLDC fan ever, though some of them have seen it in shops or other residences.

Questions from part 3 tried to explore the understanding of those who have never used a BLDC fan and their perception towards it. The major advantage pointed out was the lower electricity consumption. Other pros as per their understanding were Longer backup on Inverters, Reliability, Noise reduction, aesthetically appealing, Remote control, Green and sustainable, less maintenance, Timer for fan speed based on requirement etc. The highlighted disadvantages include high initial expenses, lack of technical expertise for installation, limited availability, complex installation, vibrations at lower speeds, limited repair options, Installation and issues with remote controller like replacement of batteries, inconvenience in using remote controller and worry about the remote being misplaced, maintenance, etc.

It is encouraging to note that 33 among the 54 respondents who have never used a BLDC fan have thought of buying one at some point of time. However, various factors like initial expenses, unavailability of technicians with expertise, difficulty in incorporating in existing electrical layout, unavailability of good options in remote areas, apprehension in adopting a new technology restricted the purchase of a BLDC fan.

Questions from Part 4 were intended at the users of BLDC fans. The 74 respondents purchased the BLDC fans over the last four years- 2020, 2021, 2022, 2023 and most of them have been using since more than a year (Table 4).

Table 4. Details of usage history

Year	Number	Percent
1-2 years	45	60.8
2-5 years	10	13.5
Less than a month	10	13.5
Less than an year	9	12.2
Total	74	100.0

The purchase decision was based on the recommendations by friends/ family, shopkeepers/ vendors, architect/ contractor or as a self-decision based on awareness from various media. It is observed from Table 5 that only 8.1% of the decisions were based on the recommendation from architect. This aligns with the unawareness of building professions about BLDC fans as discussed earlier.

Table 5. Decision maker for purchase of BLDC fan

	Number	Percent
Architect/ Contractor	6	8.1
Friends/ Family	29	39.1
Self-decision based on awareness from various media.	33	44.6
Shopkeeper/ Vendors	6	8.1
Total	74	100.0

Also, it is interesting to note that the brands of BLDC fans used by the respondents were majorly four, namely, Atomberg, Crompton, Havells and Usha. Out of these, Atomberg covers 67.65 of the users in the study.

Table 6. Brands of BLDC fans

	Number	Percent
Atomberg	50	67.6
Crompton	7	9.4
Havells	15	20.3
Usha	2	2.7
Total	74	100.0

The price ranges of the fans are given in Table 7. Most of the fans were priced between Rs. 3000- Rs. 5000 whereas regular ceiling fans are available in the market from Rs. 1000 onwards. The prices in offline market for BLDC fans were much higher compared to the online platforms.

Table 7. Price range of BLDC fans

	Number	Percent
Above Rs. 8000	4	5.4
Less than Rs. 3000	11	14.9
Rs. 3000 - Rs. 5000	35	47.3
Rs. 5000- Rs. 8000	10	13.5
Not aware	14	18.9
Total	131	100.0

The wattage of the BLDC fans ranged from 26 watts to 35 watts and 44.5% of the respondents were not aware of the wattage of their fans. The users are prompted to buy BLDC fans based on various factors as discussed earlier- low electricity consumption, longer backup on Inverters, reliability, noise reduction, aesthetically appealing, remote control, green and sustainable and Less maintenance.

39.2% of the responses reported that they have not faced any issues with the fan yet. However, others have issues like misplacement of remote controller, unconformable in the use of remote controller, limited access to technical expertise, maintenance, vibrations at lower speeds etc.

Apart from the initial expenses and installation services, most of the issues were regarding the remote controller. It is assumed that these issues were probably due to the unfamiliarity with the same. Further questions focused on the remote controller were asked to these respondents. 87.8% of the BLDC fan owners had a remote controller with the fan. Most of the respondents reported that they are comfortable with the operation of remote controller. However, it was not very comfortable for some users until getting familiarised with the technology. The elders and guest were also very unfamiliar with the use of remote controller. Also, 39% of the respondents have lost or misplaced the remote controller at some point of time.

Most of the BLDC owners have not kept a track regarding the power consumption and electricity bills, though they are aware of the savings. Some have noticed a reduction of 4-5 units of electricity consumption while few others have noticed 25% in electricity bills.

82.4% of the users were happy about the BLDC fans and would recommend to their friends and family whereas 14.8 users were not very sure about recommending the same.

4. CONCLUSION

The current study explored the awareness and perception towards BLDC fans across various stakeholders. The questionnaire survey collected responses from 206 individuals and 75 respondents among them were not aware of BLDC fans. This also indicates that 31.45% of the building professionals from the respondents were unware of the BLDC. Further questions included the user experience of BLDC fans. The major disadvantage was identified to the high initial investment compared to a regular fan. Other apprehensions included the unfamiliarity in the use of remote controller, lack of technical expertise for installation and possible repairs etc. Availability of technical support and services should be extended to the households of all economic background. The current consumers of energy efficient fans are very limited. This is also due to the unfamiliarity and apprehension to adopt a new technology. Certain measures like mandatory installation of BLDC fans in government buildings or offices can pave way to familiarising the same to general public. Along with that, awareness or technology upgradation programs to educate building professionals can popularise the use of BLDC fans in their projects. The findings of the study indicate that policy level initiatives are necessary to create awareness on the energy efficiency aspects of the ceiling fans.

REFERENCES

1. D. Aggarwal, S. Agrawal, A Deep Dive on Ceiling Fans in India Business Model for Scaling Up Super-Efficient Appliances Centre for Energy Finance, 2022.
2. India Cooling Action Plan, India Cooling Action Plan, India Cooling Action Plan- ICAP. Ozone Cell. Ministry of Environment, Forest & Climate Change, New Delhi, 2019.
3. A.S. Aditya Chunekar, Shweta Kulkarni, Mandatory S & L for Ceiling fans : Potential game-changer but needs follow-through, Perspect. Power. (2022) 1–6.
4. M. Indraganti, Behavioural adaptation and the use of environmental controls in summer for thermal comfort in apartments in India, Energy Build. 42 (2010) 1019–1025. https://doi.org/10.1016/j.enbuild.2010.01.014.
5. S. Thapar, Energy consumption behavior: A data-based analysis of urban Indian households, Energy Policy. 143 (2020) 111571. https://doi.org/10.1016/j.enpol.2020.111571.
6. T.K. Jayasree, B.S. Jinshah, T. Srinivas, The effect of opening windows on the airflow distribution inside naturally ventilated residential bedrooms with ceiling fans, Build. Serv. Eng. Res. Technol. 1 (2021) 23–39. https://doi.org/10.1177/01436244211024084.
7. A. Garg, J. Maheshwari, D. Mukherjee, Transitions towards energy-efficient appliances in urban households of Gujarat state, India, Int. J. Sustain. Energy. 40 (2021) 638–653. https://doi.org/10.1080/14786451.2020.1837132.

BEE, Impact of Energy Efficiency measures for the year 2020-21, 2023.

8. A. Sendrayaperumal, S. Mahapatra, S.S. Parida, K. Surana, P. Balamurugan, L. Natrayan, P. Paramasivam, Energy Auditing for Efficient Planning and Implementation in Commercial and Residential Buildings, Adv. Civ. Eng. 2021 (2021). https://doi.org/10.1155/2021/1908568.

PLEA 2024 WROCŁAW
(Re)thinking Resilience

Thinking Outside the Glass Box:
Creating Carbon-Neutral Work Environments in Developing Nations

RAGHAV SWARUP[1], SIMOS YANNAS[1]

[1]Architectural Association School of Architecture, London, United Kingdom

ABSTRACT: With almost 40% of global energy use and emissions associated with the building sector, the architectural community is deeply intertwined with energy, materials, and ideas that relate to climate change – both in its causes and solutions. Developing nations play a significant role at both ends of this spectrum, being responsible for almost two-thirds of global emissions over the last decade, as well as being identified by the United Nations as the highest at-risk regions from the impact of climate change due to warmer climates, relative financial shortcomings and poorer infrastructure. Substantial solar radiation and large areas of exposed glazing in the already warm climates of most developing nations, coupled with the elevated occupancy densities and intensive equipment in its workplaces, leads to exceptionally high space cooling demands to lower internal temperatures and provide thermal comfort to its occupants. While recognising that there may not be a single answer to these multifaceted challenges, the paper aims to challenge the current trends of office building design in developing nations by presenting a set of guidelines encompassing architectural features and environmental strategies for innovative, energy-efficient, healthy and comfortable buildings that can reduce building operation related emissions to net-zero.
KEYWORDS: Net Zero Buildings, Operational Energy, Warm Climates, Office Buildings, Developing Nations

1. INTRODUCTION

With climate change being more imminent, rapid and discernible than ever before, the environmental dimension has taken center stage in the discussion around sustainable development [1]. Global carbon emissions over the last 30 years (831 $GtCO_2$) have been greater than those over the previous 250 years (784 $GtCO_2$), with the built environment emerging as the most critical sector representing nearly 40% of all energy and process related emissions [2,3]. Historically, developed nations or nations with greater means and concentration of wealth & industry had been considered responsible for almost 80% of global carbon emissions, however, in just the last 10 years or so, this trend has reversed with developing nations now being responsible for nearly two-thirds of these emissions [4].

Within these developing nations, the workplace sector is the most rapidly growing market, contributing up to 60% of the Gross Domestic Product (GDP) is some cases [5]. This growth is often characterised with the development of a number of new office buildings, which often follow ill-conceived and unsustainable architectural & environmental practices, leading to the "glass box" typology. Despite a vast majority of developing nations being located in warm climates, many new office buildings simply duplicate both the building archetype as well as comfort standards from developed nations, many of which have much cooler climates. These unsuitable practices have substantiated the conversation around the climate emergency, and led to each such typical office building consuming a staggering 33 million kWh in energy, emitting 13 million $kgCO_2$ and having a social cost of carbon of $4.5 million over its lifecycle. Accounting for almost 80% of these emissions is the energy demand for building operations through the building's lifecycle, emitting 4.2 tCO_2e/m^2 as against around 1 tCO_2e/m^2 coming from embodied carbon [6]. Additionally, with most of these office buildings being located within city centres, the resultant heat island effect has further underlined the need for intervention.

This paper summarises the findings of an investigation carried out to determine whether a mutually feasible architectural and environmental framework can be created to achieve an operationally carbon-neutral future for new build office buildings across all developing nations.

2. RESEARCH METHOD

With a challenge to create a functional framework applicable across all developing nations, a literature review was conducted to identify analogous traits within the context of developing nations in terms of climatic conditions, primary building features, and occupational patterns and behaviours.

This was followed by performative studies of alternative scenarios using space cooling demand as a comparative metric. Finally, the design applicability of these strategies was investigated and the resulting guidelines are presented below.

2.1 Contextual Analysis

- **Workplace Characteristics:**
  Construction styles, materials, equipment, lighting, modes of ventilation, envelope design, thermal performance and occupant behaviour – a thorough examination of the factors leading to the prevalent "glass box" office building typology was undertaken.
- **Challenges Specific to Developing Nations:**
  Factors such as economic vulnerability, pollution, heterogenous (non-vernacular) design language, occupant density, 24-hour working hours and the paradoxical "glass box" building type itself were closely considered.
- **Climate Analysis:**
  Geographically, developing nations are concentrated between 30°N and 30°S. According to the Köppen-Geiger climate classification, there are largely only three climate types within these regions: Tropical (Aw), Temperature (Cwa) and Arid (BWh). For an in-depth analysis of the climate, one representative city was chosen from each of these three climatic zones. These were selected in the same country, India, ensuring a similar context and high demand for the office building typology. Figure 1 shows a comparative summary of the climates of the three representative cities: Kolkata (Aw), New Delhi (Cwa) and Jaisalmer (BWh), highlighting central aspects of their primary seasons as well as their associated percentage of outdoor comfort. It was seen that there are only two distinct seasons of high energy use between them – the Hot-Dry period, characterised by high dry-bulb temperatures, low relative humidity and high diurnal swings, and the Warm-Humid period of moderate to high dry-bulb temperatures, very high relative humidity and low diurnal swings. Although these occur at different times of the year in the different climates, these are the primary seasons of discomfort across all three [6].

2.2 Performative Studies

From the contextual analysis, a 'base case' was established for a defined set of parameters encompassing building geometry, materiality, internal heat gains and occupancy schedules.

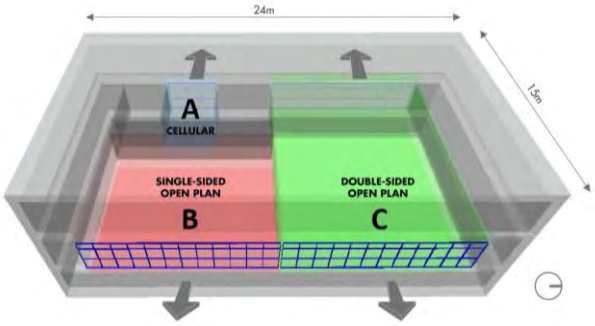

Figure 2: Spaces within an office selected as the base case

This base case was modelled spatially with three spaces representing typical office buildings:

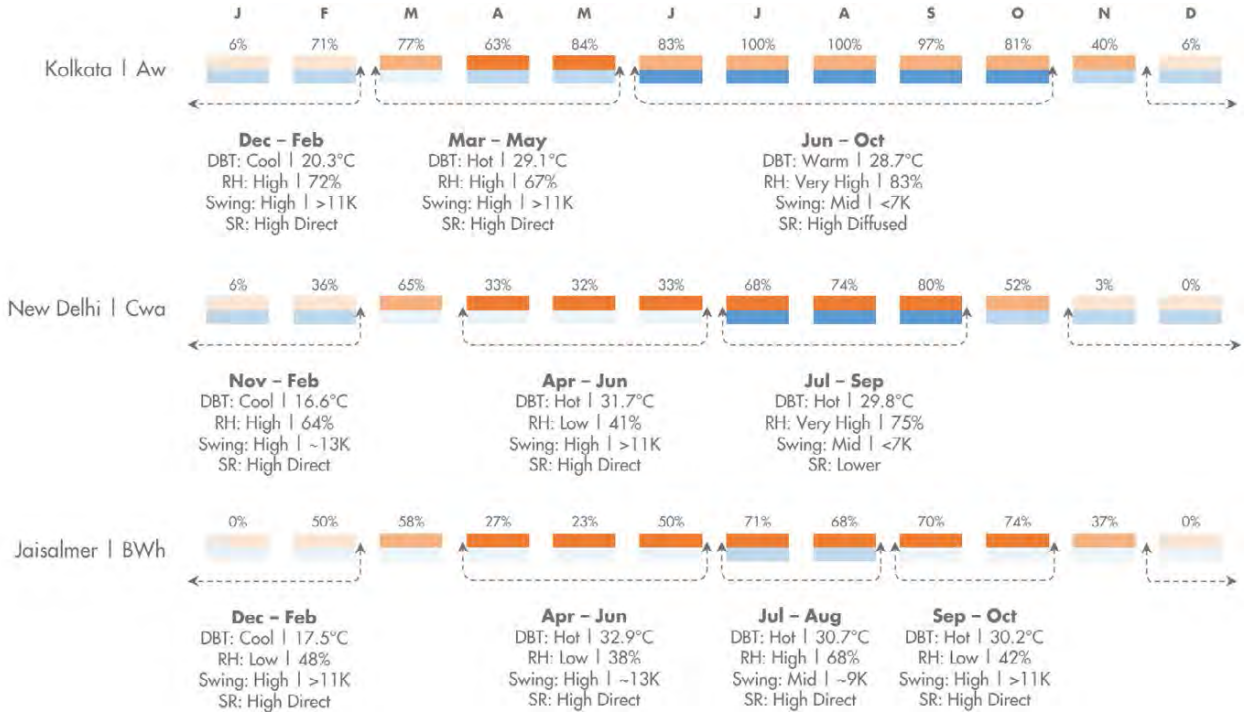

Figure 1: Comparative summary of the three analysed climate types found within developing nations – Aw, Cwa & BWh

(A) cellular office, (B) single-sided open-plan office and (C) double-sided open-plan office (refer Fig. 2).

Energy modelling and simulation studies were undertaken with Energy Plus and Ladybug Tools, which included the following optimisation studies:

- OP1- Process Optimisation: set-point temperature and occupant density & patterns.
- OP2- Design Optimisation: orientation, ventilation, shading, window-to-wall ratio and glazing properties.
- OP3- Passive Cooling Strategies: thermal mass and night ventilation, evaporative cooling, radiant cooling and ground cooling.
- OP4- ZNE Strategies: potential of outdoor workspaces and integration of renewable energies.

Each of the aforementioned optimisation studies was carried out for all three space types and representative climates (refer Fig. 3). This is believed to be an important consideration to help support the far-reaching applicability of this study.

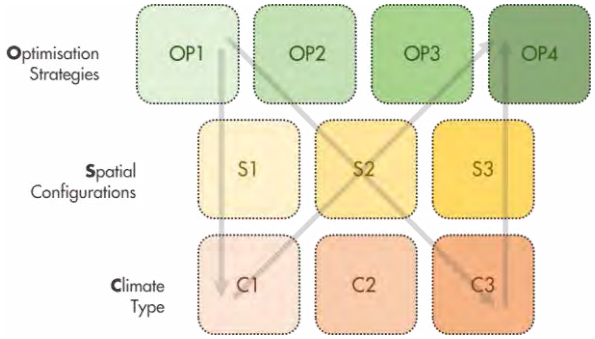

Figure 3: Method for performative studies – testing four optimisation strategies across three spatial configurations for three climate types

3. RESULTS & DISCUSSION

Averaged across the three spatial configurations, the base case yielded an annual space cooling demand of 341 kWh/m^2/yr for Aw; 281 kWh/m^2/yr for Cwa and 300 kWh/m^2/yr for BWh. Although all three represent substantial loads, it is interesting that the 'milder' Tropical (Aw) climate had a 14% higher space cooling demand than the 'harsh' Arid (BWh) climate. This seems to be due to a longer cooling period required by the Aw climate, coupled with large internal gains. On the other hand, the winter period is significantly cooler in the Cwa and BWh climates, which when coupled with internal heat gains of the work environment does not require space cooling during this period.

The optimisation studies to reduce this massive space cooling demand were tested first in isolation to determine their individual impact on the space cooling demand for the three spaces in the three climates, and then later combined systematically. The key findings are listed in Table 1.

3.1 Base Case

- For the base case, the space cooling demand averaged across the three spatial configurations and three climates was found to be 307 kWh/m^2/yr.
- The Aw climate and cellular office space emerged as those with the highest climatic and spatial space cooling demands respectively.

Table 1: Space cooling demand for the three climates averaged across the three spatial configurations (in kWh/m^2/yr) when testing various optimisation studies in isolation [6].

	Aw	**Cwa**	**BWh**
Base Case	*341*	*281*	*300*
Set-Point Temperature	172	160	178
Orientation	292	223	235
Natural Ventilation	138	216	247
Shading	289	229	243
WWR	280	223	236
Glazing Properties	279	220	231
Combined Reduced	**86**	**75**	**79**

3.2 Process Optimisation

- **Set-Point Temperature:**
  In the absence of country specific comfort standards, it was found that offices in developing nations are typically designed to operate at 22.5±1°C all year round to meet specifications outlined by international standards. On the basis of studies conducted for the Indian Model for Adaptive Comfort (IMAC) [7], however, it was found that indoor operative temperatures up to 30°C may be considered comfortable in such climates. On increasing the cooling set-point temperature to 30°C, a reduction of 45% on the space cooling demand was observed.
- **24-Hour Workplaces:**
  Offices in developing nations often have to work at all hours to match times in developed nations, and therefore a multi-shift hot-desking system was explored. It was found that 24-hour operation (three 8-hour shifts) had negligible increase on the space cooling demand.

3.3 Design Optimisation

- **Building Orientation:**
  Using a North-South orientation instead of East-West for the Base Case resulted in a cooling demand reduction of close to 19%

across all the tested climates for all spatial configurations.

- **Natural Ventilation:**
  Natural or mixed-mode ventilation methods were explored. It was found that especially in the warm & humid period of the Aw climate, natural ventilation could be extremely successful, effectively removing the need for further cooling. Across the entire year, it was found that these methods could reduce space cooling demands by almost 35% across all climates.
- **Shading:**
  Shading devices, both horizontal and vertical, of varying depths and angles were tested to reduce incident solar radiation on exposed glazed facades of the buildings. Reducing the large radiation on East and West using 45° angled vertical fins and horizontal shading for the North & South, resulted in a reduction of 17%.
- **Window-to-wall Ratio (WWR):**
  The WWR was optimised from the 75% of the base case to 25% leading to a reduction of around 20% in space cooling demand. It was found, through simulations using Ladybug Tools and Radiance, that a 25% WWR would provide sufficient illumination (350-450 lux) in all the tested office spaces all throughout the day.
- **Glazing Properties:**
  Glazing u-values and Solar Heat Gain Coefficients (SHGC) were studied for reduction in heat gains through the glazing. Triple glazed units (TGU) were found to reduce space cooling demand by 21%.

The combination of these process and design optimisation strategies (OP1 + OP2) showed very promising results, reducing the average space cooling demand across all three climates and all three spatial configurations from 307 kWh/m^2/yr to 80 kWh/m^2/yr); a 74% reduction. Looking at the case of the Aw climate (refer Fig. 4), which had the largest space cooling demand to begin with, it can be seen that the indoor operative temperature is reduced by almost 8°C across the three spatial configurations, thereby reducing the required space cooling demand significantly.

3.4 Passive Cooling Strategies

- **Thermal Mass:**
  Combined with night ventilation, thermal mass helps delay the ingress of heat and ensures that the building is pre-cooled naturally in the mornings, allowing for over 88% annual comfort hours across all climates with nearly 95% comfort hours in the Aw climate.
- **Evaporative Cooling:**
  Evaporative cooling has a large potential, especially in the hot & dry season. It is believed it can reduce space cooling demand by 60-80% [8]. In the particular cases studied, it was seen that the Aw climate

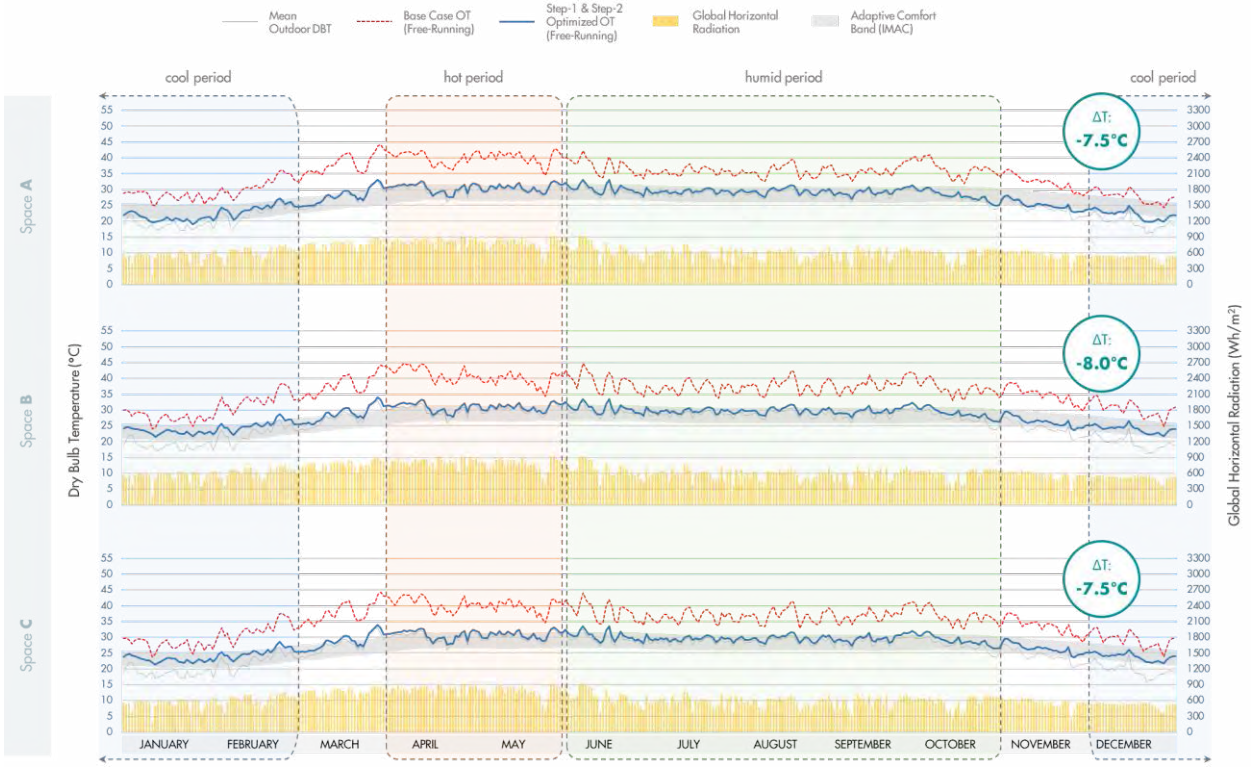

Figure 4: Thermal performance when combining process & design optimisation (OP1+OP2) strategies for the Aw climate

experiences a peak operative temperature (OT) of 32°C and relative humidity (RH) of 65% in its period of discomfort. The Cwa and BWh climates, on the other hand, experience a peak operative temperature (OT) of 38°C and relative humidity (RH) of 35%. Studies conducted by the Office of Energy Efficiency & Renewable Energy have shown that the resultant effective temperature for both these cases with evaporative cooling can be as low as 28°C, allowing for 100% comfort hours.

- **Radiant Cooling:**
  Radiant cooling has been found to provide the same level of comfort with higher air temperatures as compared to a conventional cooling system [9]. Various examples of studies in similar climates have shown between 35-50% reduction in space cooling demand when using radiant cooling systems [10].
- **Ground Cooling:**
  Studies show that ground cooling systems can reduce the energy required by space heating, space cooling and water heating cumulatively in commercial buildings by as much as 50%, while reducing indoor operative temperatures by almost 10°C as compared to the outdoor dry bulb temperature [11].

3.5 Zero Net Energy (ZNE) Strategies

- **Outdoor Workspaces:**
  The need for spatial diversity and access to outdoor spaces and nature is part of a growing office trend proven to benefit employee mental health and productivity. Additionally, provision of outdoor workspaces could aid demand minimization by reducing the strain on internal workspaces. Therefore, the feasibility of outdoor (or semi-outdoor) workspaces was assessed. It was found that a 4m deep semi-outdoor space with a southern orientation would achieve 88% comfort hours in the Aw climate, 77% in Cwa climate and 71% in the BWh climate – an average of comfort across more than 3/4th of the year. It was observed that this can be further improved upon through the provision of solar control in the form of adaptive shading devices and the addition of adaptive opportunities such as ceiling fans to facilitate air flow (refer Fig. 5).
- **Renewables:**
  An important aspect of ZNE buildings apart from demand minimisation, is the supply or generation of alternative/ renewable sources of energy as well as efficient use and conservation of resources. Drawing from the high solar radiation typically received in developing nations due to their geographic location and warm climate, a system with Building Integrated Photovoltaics (BIPVs) as well as roof mounted PV was considered. Even with conservative calculations, this system showed potential of easily generating more than 70 kWh/m^2/yr.

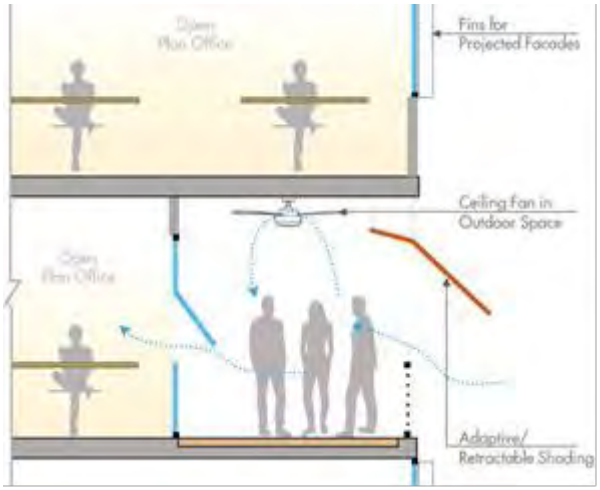

Figure 5: Potential Adaptive Opporunties for thermal comfort in semi-outdoor workspaces

To access the overall combined impact of these optimisation studies, it was imperative to map out the results against existing benchmarks. The base case had a total energy demand (cooling/ heating + equipment + lighting) of 377 kWh/m^2/yr as against the Indian Energy Conservation Building Code (ECBC) benchmark of 175 kWh/m^2/yr. As discussed in sections 3.2, 3.3 & 3.4, it was seen that a combination of the process and design optimisation (OP1 + OP2) could reduce the space cooling demand by around 74% while the remaining 26% could be reduced through passive cooling strategies (OP3), hence achieving net-zero on space cooling demand. Additionally, as seen from section 3.5, the renewable energy systems (OP4) could suffice the demand for equipment and lighting, allowing for a holistic net-zero on energy demand (refer Fig. 6).

4. CONCLUSIONS

In 2022, global carbon emissions saw an all-time high of around 38.5 $GtCO_2e$ of which 28% or 10.8 $GtCO_2e$ came from energy required for building operations alone [12]. To further substantiate this problem in developing nations, many of them rely on coal-fired electricity generation for up to three-quarters of their power supply, which is one of the primary factors for rising emissions in these nations [13]. Drawing from the various strategies discussed in the above sections, there is a strong case for the

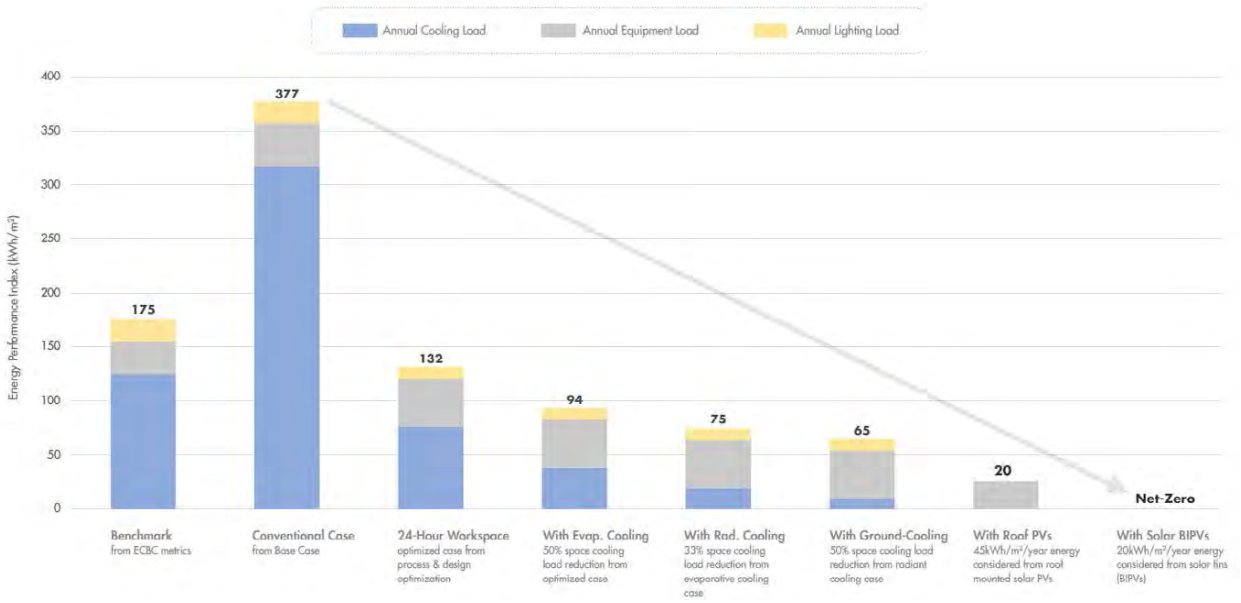

Figure 6: Potential for reduction in overall energy demand – Net Zero Operational Energy

ability to create workplaces in developing nations that consume net zero operational energy; exhibiting huge potential to significantly reduce energy production, thereby reducing carbon emissions.

Through the contextual analysis, it was established that developing nations possess several analogous traits, not least in which is their climate, which allows for a similar design approach to be used across them. The performative studies revealed the potential of various optimisation strategies, which when combined, reduced a massive initial space cooling demand of 307 kWh/m^2/yr by around 74% across various spatial configurations and climates, while creating a thermally comfortable 24-hour workspace. The use of passive cooling strategies such as evaporative, radiant and ground cooling allowed for a net-zero cooling demand and 100% occupant comfort even in a completely free-running environment. Taking this even a step further, the ZNE strategies of using semi-outdoor workspaces and using renewable sources of energy showed the potential of achieving a truly holistic operational net-zero office building.

This paper does not advocate a 'one size fits all' approach, but in considering applicability across the varying climates within developing nations and varying spatial configurations within a typical office building to test its hypothesis, it is believed that a successful framework can be developed to design operationally carbon-neutral workplaces across all developing nations.

REFERENCES

1. United Nations Framework Convention on Climate Change (UNFCCC), (2015). What Is the United Nations Framework Convention on Climate Change?
2. Institute for European Environmental Policy, (2020).
3. Global Alliance for Buildings and Construction, (2018).
4. Hoornweg, D. & K. Pope, (2014). Socioeconomic Pathways and Regional Distribution of the World's 101 Largest Cities. *Global Cities Institute*. Toronto.
5. The World Bank, (2019). World Development Indicators.
6. Author, (2022). Thinking Outside the Glass Box: Creating Carbon-Neutral Work Environments in Developing Nations Through Climatic Adaptation.
7. Manu, S. et al, (2015). Field Studies of Thermal Comfort Across Multiple Climate Zones for the Subcontinent: Indian Model for Adaptive Comfort. *Building & Environment*.
8. Evapoler, (2021). Evaporative Cooling Concept.
9. Mohamed, S.E.S.E.S, (2018). Radiant Cooling System Between Theory and Practice. Higher Institute of Engineering, Cairo. *Internal Journal of Current Engineering and Technology.*
10. Fairconditioning, (2022). Radiant Cooling.
11. Omer, A.M., (2016). Cooling and Heating with Ground Source Heat Pumps. *Cooling India*.
12. European Commission, Joint Research Centre, Crippa, M. et al, (2023). GHG Emissions of All World Countries.
13. Bhattacharya, S., (2022). Report At COP27: India Records Highest Emissions Increase Among Top Global Contributors. *Outlook India*.

PLEA 2024 WROCŁAW
(Re)thinking Resilience

Challenging the suitability of French energy regulations for unconventional renovations:

A Case study of the underground spaces of La Defense in Paris

RAFAEL ALONSO CANDAU[1], FLORENCIA COLLO[1], OLIVIER DAMBRON[1]

[1]Atmos Lab, London, United Kingdom

ABSTRACT: This paper focuses on the suitability of energy efficiency regulations for the renovation of unconventional buildings. The authors present a case study in Paris, the formerly abandoned underground spaces below La Defense, which are under renovation to host cultural, artistic and sport uses. Rather than requiring a performance level, French energy regulations for renovations impose prescriptions to all buildings that must be achieved. The authors evaluated the existing condition, the regulatory scenario and alternative insulation strategies using a dynamic thermal model calibrated with temperature data recorded on site. The results show that meeting regulations has the largest carbon footprint – even larger than the existing uninsulated condition - and generates an overheating problem. Based on the findings and the upcoming wave of building renovations in the EU, the authors argue the need for performance-based options in energy regulations.
KEYWORDS: Renovation, energy efficiency, calibrated thermal model, underground spaces, carbon emissions

1. INTRODUCTION

The EU must renovate 35 million inefficient buildings by 2030[1] to meet its emissions target and achieve climate neutrality by 2050[2]. This unprecedented wave of renovations is subjected to efficiency requirements by country, which are often set as prescriptive regulations to reduce the technical burden on the industry: projects must meet certain rules rather than achieve a level of performance.

This paper challenges the suitability of these prescriptive regulations for certain building renovations and exposes the need for a performance-based alternative. The problem is illustrated by a case study in France, the renovation of the underground spaces in La Defense (LD) designed by Baukunst. The main Business district in Paris, LD is organised around a central square with some 10,000m^2 unoccupied spaces below it. The spaces will host cultural, sport and artistic uses: programmes usually characterised by a dense occupancy and high internal heat gains. An aerial view of the project can be seen on the right (Fig. 1).

The residual spaces of LD extend over an area 380m long and 100m wide and are distributed in two levels. They are the leftover space between multiple highway tunnels on each side and the ground, and form a series of broken underground volumes partially connected to each other, each of them some 15m high. The project connects these leftover spaces through a semi outdoor promenade that becomes the main circulation axis on level -1 (Fig. 2). As a result, each space has a different degree of exposure to the new semi outdoor promenade, the ground, the surrounding roads or outdoors.

The unique characteristics of the spaces below LD give them a large thermal stability: all the spaces have at least two sides in direct contact with the ground (or other underground tunnels), and are delimited by large infrastructure-sized concrete walls and slabs, 30cm thick or more. Indoor temperatures are remarkably stable and completely decoupled from outdoor variations, which makes them ideal to host intense uses such as those proposed by the project, especially during Parisian summers when temperatures easily exceed 30°C. Furthermore, the underground spaces in LD are exceptional candidates for the existing local network of heatwave refuges[3].

Figure 1: Aerial view of the spaces below ground (Cathedrale above, promenade below). Source: Baukunst

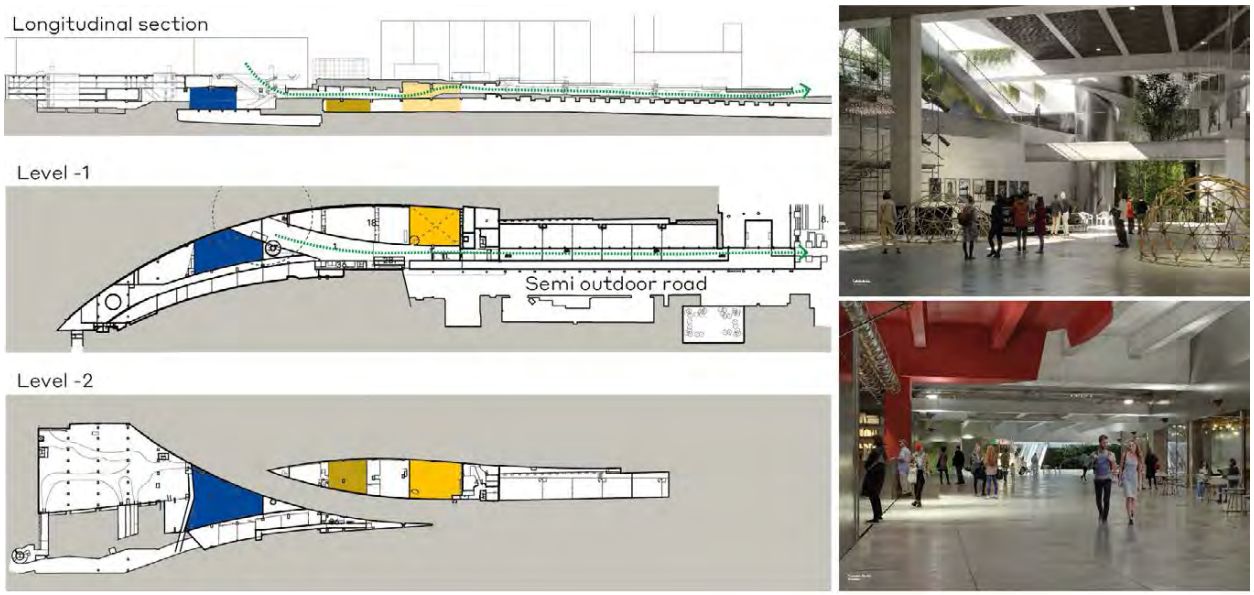

Figure 2: Longitudinal section and plans of levels below ground (Spaces: Cathedrale in blue, Atelier bas in dark yellow and Espace Moretti in lighter yellow. Promenade in dashed green). Source: Baukunst

2. COMMON PRACTICE WITH ENERGY REGULATIONS

As in many European countries, French regulations for building renovations (RT-Existant) [4] establish maximum U-values required in all areas of the project under any regulatory route. These maximum U-values, reproduced in Table 1 below, are defined as minimal thermal insulation exigences on article 43 and usually referred to as *garde-fous* by the industry.

Table 1: Maximum U-values required by French building regulations for renovations [4]

Element	U-value (W/m^2K)
Wall in contact with outdoors or ground	0.45
Wall in contact with an unheated space	0.45/b*
Floor slab in contact with outdoors/collective parking	0.36
Floor slab in contact with sanitary void/unheated space	0.40
Concrete/masonry floors and sheet metal roofs waterproofed	0.34
High floors with metal sheet roofing	0.41
Other high floors	0.28
Bare windows and patio doors to outside	2.60
Curtain walls	2.60
Roller shutter boxes	3.0

* b is the reduction coefficient for the heat loss to unheated spaces, defined on the French national calculation method TH-C-E ex [5].

As shown in table 1, walls in contact with the ground have the same thermal insulation requirements as those facing outdoors (U = 0.45 W/m^2K). Similarly, no specific mention is made to floor slabs in direct contact with the ground, which are subjected to outdoor requirements (U = 0.36 W/m^2K). For the underground spaces of LD, these U-values translate into the following insulation requirements (thermal conductivity = 0.035 W/mK): 7cm for walls and 9cm for slabs. Due to the configuration of the spaces, this thermal insulation can only be installed on the internal side of the perimeter walls and slabs of the existing building, a common problem in numerous building renovations. Some other smaller internal partitions must also be insulated, although they are considered irrelevant for the content of this paper.

As a result of regulatory requirements, all the underground spaces must be wrapped with thermal insulation, a counterintuitive strategy from an environmental point of view: the large thermal inertia of concrete walls and slabs in direct contact with the ground is now blocked by insulation installed on their inner side. The lack of thermal inertia, and its temperature stabilisation effect, is particularly impactful on spaces destined to intense indoor uses, such as those proposed by the project.

An European Standard exists that regulates heat transfer via the ground, EN ISO 13377 [5] and, in most cases, reduces or eliminates the need for thermal insulation for underground elements by considering the thermal stability of the ground. However, the regulatory text [4] or the national calculation method [6] make no reference to this standard, and traditional U-value calculations are usually performed for all elements disregarding their position.

Alternative routes for compliance [7] exist in the French context: the ELAN law [8] and the exclusion list from RT-Existant[4], both of which are discussed in some detail in section 5 of this paper.

3. METHODOLOGY

The methodology to evaluate the existing building and develop the project from an environmental point of view was based on fieldwork conducted on site, a

calibrated thermal model, and the evaluation of different project scenarios both in free running conditions and active mode.

3.1 Fieldwork

Temperature and humidity were recorded in five rooms and outdoors during autumn of 2019 (8th to 17th of October) and a summer week in 2020 (25th of June to 2nd of July) using Dataloggers TESTO 174-H. Temperature recordings can be seen in Figure 3, overlaid with solar radiation data from a local weather station (Wunderground ID IHOUILLE89). The graphs show the large thermal stability of the spaces in both seasons. In autumn, indoor temperature always remained within 17.5 and 21°C in all spaces while outdoors it fluctuated between 11 and 24.5°C. In summer, despite outdoor temperatures reaching 32 and 30°C on the first two days of the recordings, indoor temperature remained always below 24°C. Monitoring was also performed in winter but is not included in this paper for brevity.

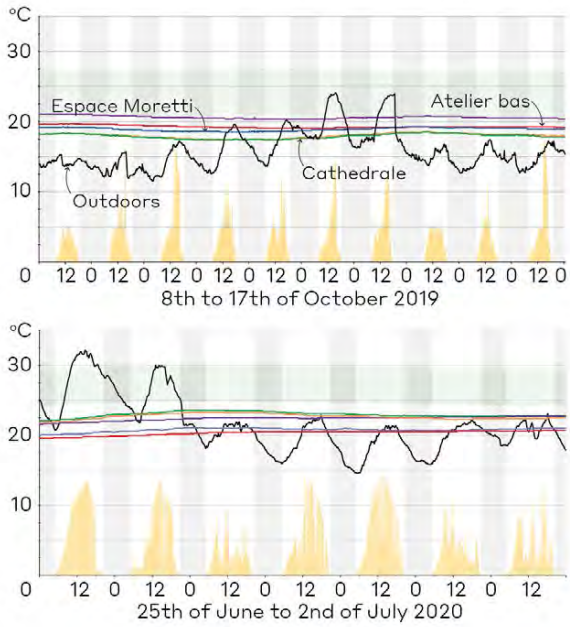

Figure 3: Recorded air temperatures during a week in autumn (above) and a summer week (below).

3.2 Calibrated thermal model

A thermal model of the underground spaces of LD and all the surrounding areas was built in Energy+ v.9.2, using Honeybee plugin [9] for grasshopper and Rhinoceros. These were built following a survey of the existing spaces and images of the thermal model can be seen in Figure 4.

Temperatures recorded on site during the summer week were used to calibrate the thermal model: properties of the ground heat transfer algorithm in Energy+ (Basement Preprocessor), soil (thermal conductivity) and air infiltration were adjusted iteratively until the resulting indoor mean air temperatures for the five thermal zones followed the recordings. Results of the calibration can be seen in Figure 5, which shows a maximum difference between simulated and measured temperatures of some 1.5°C, while it remains within +-0.5°C during most of the time.

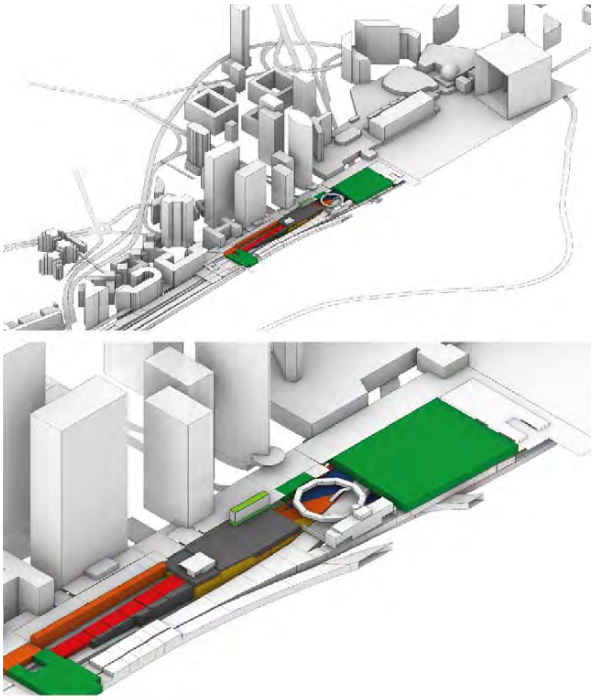

Figure 4: Image of thermal model and surrounding context to the southwest (context in grey, and thermal zones in different colours).

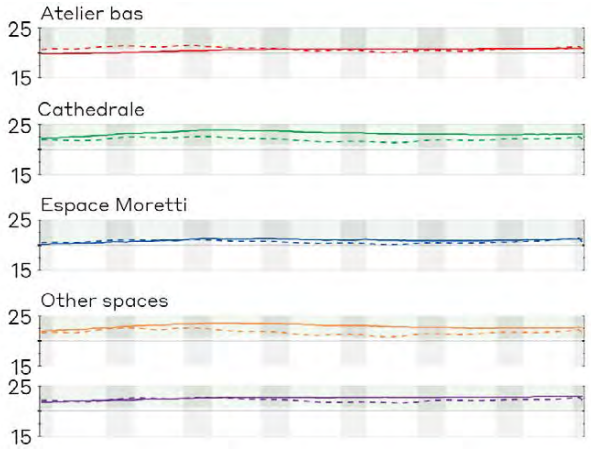

Figure 5: Graphs show simulated temperature from the calibrated model (dashed) and recordings (constant) for five selected spaces.

3.3 Simulated project scenarios

Thermal simulations were performed using the calibrated model and the weather file for Paris Montsouris, extracted from Meteonorm 7.0. Detailed inputs used for the simulations can be seen in Table 2. Five project scenarios were developed in collaboration with the project architects, of which only the following two are included in this paper in

addition to the uninsulated existing building: a fully insulated scenario following regulatory requirements, and the retained solution for the project insulating only the external roof. These can be seen in Figure 6.

Table 2: Thermal simulation inputs

Element	Value	Unit
Envelope (internal insulation)		
Walls - ground and exterior	0.25	W/m²K
Walls - interior	0.25	W/m²K
Slabs - exterior	0.25	W/m²K
Slabs - ground	0.33	W/m²K
Beam thermal bridge	1	W/mK
Windows	1.5	W/m²K
	0.6	SHGC
	0.77	VLT
Internal heat gains		
Occupancy	5	m²/person
Lights	10	W/ m²
Equipment	30	W/ m²
Adjacent parking areas	8	W/m²
Infiltration via exposed envelope	1.7	m³/m²h
Ventilation	36	m³/hperson
Natural ventilation		
Operable windows	35	%
Opening temperature	24	°C
Heating and cooling		
Heating setpoint	19	°C
Cooling setpoint	26	°C
Heat recovery	80	%
COP heating/cooling	2.6/3.25	
Carbon intensity heating*	0.132	$kgCO_2/kWh$
Carbon intensity cooling*	0.143	$kgCO_2/kWh$
Embodied carbon factors		
Semi rigid mineral wool	25.6	$kgCO_2/m^2$
Cellular glass insulation	43.65	$kgCO_2/m^2$
(*) District heating/cooling from Enertherm		

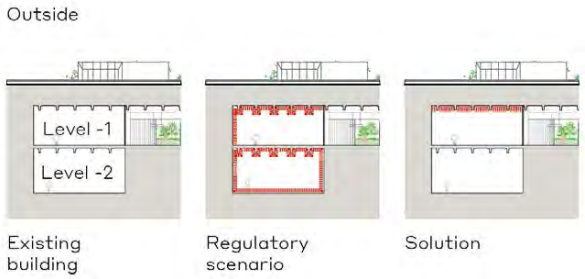

Figure 6: Section with new thermal insulation (dashed red)

The authors evaluated the performance of the selected scenarios under free running conditions through their indoor operative temperatures during a typical summer week and the number of hours they exceed 28°C over the year. Indoor conditions were evaluated in detail in three representative spaces (highlighted in Fig. 2): these were plotted during a typical summer week and compared with those outdoors and the thermal comfort criteria as defined by EN 16798 cat. II. Additionally, the authors calculated the energy demand for heating and cooling and the total carbon emissions including heating and cooling energy consumption over a 50-year period and the embodied footprint of any additional insulation added to the space.

4. RESULTS

4.1 Summer performance and overheating under free running conditions

Atelier Bas: indoor operative temperatures vary by up to 7K during the central hours of the day between the regulatory scenario and the other two scenarios (Fig. 7). The regulatory scenario has the highest indoor temperatures, which are 1 to 2K higher than outdoors and exceed the upper threshold of the comfort band every day for a few hours. Both the existing uninsulated condition and the adopted solution have indoor temperatures some 7K below outdoors during the warmest hours of the day and demonstrate the effectiveness of the existing thermal inertia in reducing indoor overheating. Indoor temperatures drop to a similar level in the early morning in the three scenarios, although it takes a few hours longer for the regulatory one to cool down.

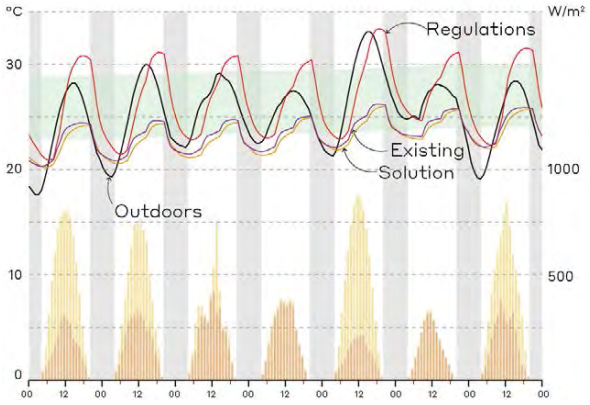

Figure 7: Operative temperatures in Atelier bas during a typical summer week.

Espace Moretti: indoor operative temperatures are very similar to those in Atelier bas and vary by up to 7K depending on the thermal insulation scenario (Fig. 8). As in Atelier bas, the regulatory insulated scenario has the highest indoor temperatures, which exceed the upper threshold of the comfort band every day and are above outdoors by some 4K during the early evenings. Similarly to Atelier bas, the existing uninsulated condition and adopted solution never exceed the upper threshold of the comfort band and only exceed 25°C on very hot days when outdoor temperatures are above 32°C.

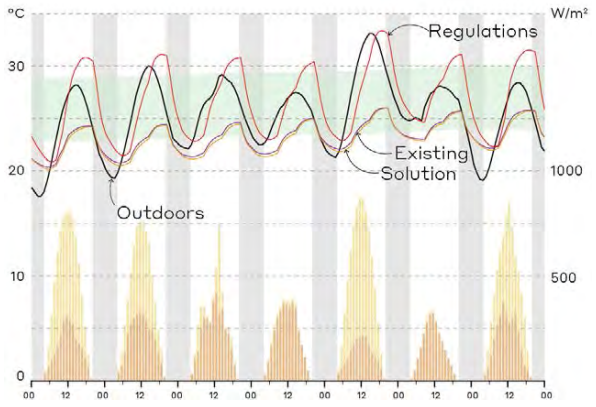

Figure 8: Operative temperatures in Espace Moretti during a typical summer week.

Cathedrale: Operative temperatures in this space are less affected by the thermal insulation scenario, but can still vary up to 5K (Fig. 9). As in the other two spaces, the fully insulated condition induces the highest indoor temperatures, although they are slightly lower in this space and only exceed the comfort band on three days. The adopted solution has the lowest temperatures, some 0.5 to 1 K lower than the existing condition during most of the time, especially at night: unlike the other spaces, Cathedrale's roof is directly exposed to outside.

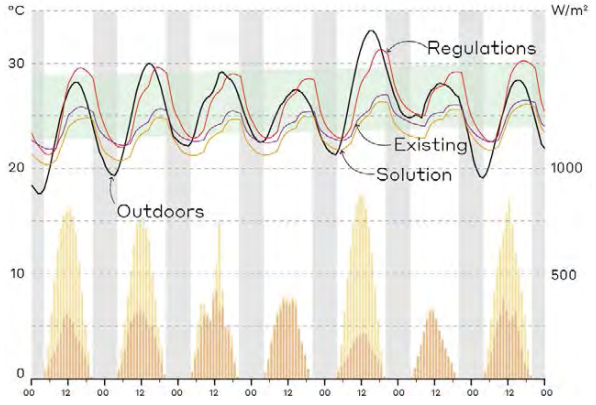

Figure 9: Operative temperatures in Cathedrale during a typical summer week.

The upper chart in Figure 10 shows the average number of hours above 28ºC for all the underground spaces in LD for each of the three scenarios previously described. Results are conclusive: the existing building does not have any overheating problem, which is only induced by insulating the entire envelope to meet regulations. The regulatory scenario has more than 400 hours above 28ºC, while both the existing building and the adopted solution keep the number of hours above 28ºC to 9 or less.

4.2 Energy demand and carbon emissions

A summary of the results from the thermal simulations can be seen on the graphs in Figure 10:

1) Heating and cooling annual demands are shown on the chart in the centre. Results for the existing building show heating and cooling demands of 20 and 6 kWh/m^2 respectively. Wrapping all the spaces in thermal insulation to meet regulations increases their cooling demand by 11 kWh/m^2 (+183%) while it only reduces their heating demand by 8 kWh/m^2 (-40%) when compared to the existing uninsulated condition.

In comparison to regulatory requirements, results for the adopted solution show the impact of removing the thermal insulation and keeping it only in the upper slab, the best performing scenario, as it reduces both heating and cooling demand to 9 and 6 kWh/m^2 respectively. This equals to a 55% reduction in heating demand, without increasing cooling needs.

2) Total carbon emissions are shown on the graph in the bottom (Fig.10). Results show that the carbon footprint of the regulatory insulated case is the highest of them all: 1229 tCO_2 mostly caused by the embodied carbon of the thermal insulation (76%). Leaving the spaces as they are nowadays would reduce the overall carbon footprint by 789 tCO_2 (-64%): even if the operational emissions are higher by some 140 tCO_2 (440 tCO_2 in total), no carbon emissions arise from manufacturing any thermal insulation. The adopted solution has the lowest carbon emissions of them all: insulating the upper slab reduces the footprint by 924 tCO_2 as a very small amount of insulation installed on the right location reduces winter heat loss towards outdoors.

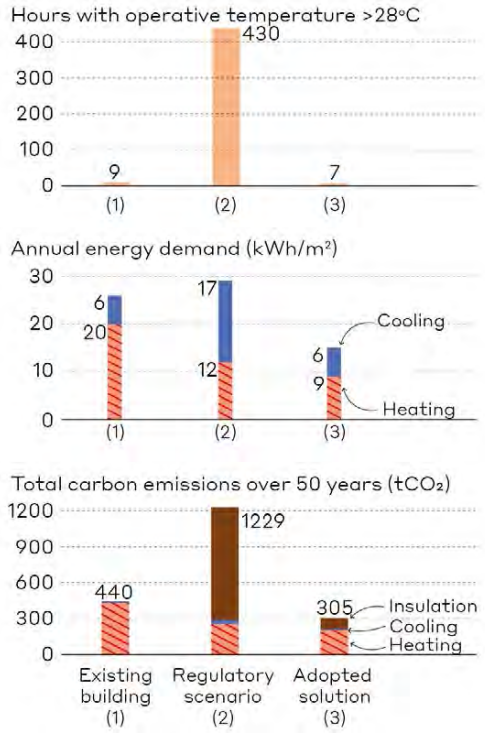

Figure 10: Graphs showing overheating hours (upper) heating and cooling energy demand (centre) and total carbon emissions (bottom) for the three scenarios.

It must be noted that any of the other project scenarios developed during the project and not included in this paper also had a lower carbon footprint than the regulatory one by some 300 to 900 tCO_2 (-25 to 75%). These included insulating only the lower slab, the walls on level -1, or all of the walls (level -1 and -2).

5. DISCUSSION

The analysis of the underground spaces of LD shows that despite the large investment in thermal insulation required by regulations (~€300k), this scenario: (i) has the highest carbon emissions of all the scenarios tested, even higher than not insulating at all, (ii) generates a large overheating problem (>400 hours above 28ºC, and indoor operative temperatures above the upper threshold of the comfort band every day) due to the lack of thermal inertia, a non-existent problem in any of the other scenarios, and (iii) retains heat indoors much longer during summer evenings: temperatures at 10pm are 3 to 5K higher than the other scenarios.

Considering the results and the architectural implications of covering all the internal elements with insulation, the team explored two alternative routes for compliance [7]: (i) ELAN law [8] and (ii) the exclusion list from RT-Existant[4], both unfruitful.

The ELAN law allows to derogate the requirements imposed by national regulations in France until 2025, as long as the objectives of these regulations are satisfied. However, the objectives of national French regulations are the reduction of operational energy consumption and the insulation of existing walls, rather than an overall improvement in the environmental performance of buildings and reduction of carbon emissions.

The exclusion list of French regulations (RT-Existant) [4] includes several typologies that do not require compliance, such as buildings for agricultural or industrial use, those without mechanical equipment other than fireplaces, or those that are usually open to outside. Only the latter one could be applicable to the underground spaces of LD and remains under evaluation, although it imposes certain restrictions to the overall functioning of the project, architecture, safety and HVAC design.

A new, more ambitious, French energy efficiency regulation for new buildings was rolled out in 2022, although its counterpart for existing buildings has not been announced at the time or writing. It is essential for the industry that this new regulation includes a performance-based compliance route, to avoid the pitfalls of prescriptive rules imposed on unconventional renovations described in this paper.

6. LESSONS EXTRACTED FOR UNCONVENTIONAL RENOVATIONS

1) Building regulations might be too focused on prescriptive rules and miss common performance trade-offs (operational vs embodied carbon, or heating vs overheating). Thus, they might create new overheating problems without completely solving the existing ones, especially in existing buildings where thermal inertia plays a key role (ie. churches, castles, ancient buildings, or concrete structures).

2) It must be emphasized that temperature monitoring carried out before the design of a building renovation and calibrated thermal modelling can provide valuable information and help identify existing issues. Accurate data extracted from the building and scenario modelling enables the design team to develop custom solutions for the project, rather than applying generic ones (ie. over insulation, or over reliance on mechanical equipment).

3) Leaving some elements of the building uninsulated could mitigate most of the newly created overheating problem without a large increase in heating demand. However, such specific solutions must be developed on a case-by-case basis, based on accurate modelling.

7. CONCLUSIONS

French energy efficiency regulations are unfit for unconventional building renovations due to their prescriptive approach: projects must meet generic insulation rules even if they induce higher energy demand, carbon emissions and generate overheating indoors. While the existing approach certainly suits many renovations, a performance-based alternative is required for the unconventional ones. With the large upcoming wave of building renovations, the current prescriptions risk locking in underperforming buildings that will undermine progress for decades.

REFERENCES

1. European Comission, 2020. The European Green Deal - Renovation Wave factsheet.
2. European Comission, 2020. 2030 Climate Target Plan.
3. Ville de Paris, 2019. EXTREMA Paris.
4. Ministere de la transition Écologiqe, 2018. Arrêté du 13 juin 2008 relatif à la performance énergétique des bâtiments existants de surface supérieure à 1 000 mètres carrés, lorsqu'ils font l'objet de travaux de rénovation importants.
5. CEN, Brussels (2019) EN ISO 13377. Thermal performance of buildings. Heat transfer via the ground. Calculation methods
6. Ministere de la transition Écologiqe, 2018. Méthode de calcul TH-C-E ex (annexe de l'arrêté du 8 août 2008)
7. Design team, 2020. Espaces résiduels de la Défense, NOTE ENERGETIQUE ENVIRONNEMENTALE.
8. République Française, 2018. LOI n° 2018-1021 du 23 novembre 2018 portant évolution du logement, de l'aménagement et du numérique.
9. Honeybee plugin, part of ladybug tools suite, [Online], available on https://www.ladybug.tools/.

PLEA 2024 WROCŁAW
(Re)thinking Resilience

Improving Indoor Air Quality in UK Classrooms through Enhanced Natural Ventilation

SARA MOHAMED[1] OLUTOLA OYEBANJI[1,2] JOHN CALAUTIT[1], SIDDIG OMER[1] LUCELIA RODRIGUES[1]

[1]University of Nottingham, Nottingham, UK
[2]Kwara State University Malete, Kwara State Nigeria

ABSTRACT: In this study, the authors explored the optimization of cross-stack height (CSH) for enhancing indoor air quality through natural ventilation, utilizing computational fluid dynamics (CFD) simulations. We thoroughly examine the crucial role of inlet-to-outlet positioning and the strategic placement of openings on classroom façades. Our analysis of CO2 concentration contours across various CSH configurations assesses their impact on indoor air quality (IAQ). The results indicate that an increased CSH significantly enhances air circulation, effectively lowers indoor CO2 levels, and ensures a more uniform distribution of fresh air throughout the classroom. Notably, the configurations with CSH at 1.5 meters and 2.0 meters achieved the lowest observed CO2 concentrations, ranging between 400 to 550 ppm. These figures are in stark contrast to the baseline scenarios, where CO2 levels exceeded 2500 ppm. The study highlights the pivotal importance of ventilation design in classrooms for managing CO2 dispersion and demonstrates the efficacy of CSH in optimizing airflow patterns, thereby promoting a healthier indoor environment.
KEYWORDS: Natural ventilation, IAQ, CO2 concentration, classroom ventilation, Cross Stack Height (CSH)

1. INTRODUCTION

Ventilation in buildings is necessary for refreshing polluted and contaminated indoor air and cooling. Previous studies have reported on the benefits of natural ventilation for school buildings. For example, Daisey, Angell [1] used an extensive range of sources to assess the importance of ventilation in classrooms and revealed that ventilation levels in schools affect thermal comfort, indoor air quality (IAQ) and health, indirectly impacting student learning ability and performance. Meanwhile, according to Haynes et al [2], poor air quality is often associated with inadequate ventilation, and excessive ventilation may cause undesirable draughts. Ultimately, the ventilation rate should be sufficient to maintain both indoor air quality and thermal comfort.

Indoor CO_2 is produced by the metabolic breathing of occupants and can be decreased through increased ventilation. This means that CO_2 levels and corresponding ventilation rates are good indicators of indoor air pollution, with studies demonstrating that 'natural ventilation rates[…] have an impact on indoor deposition rate, which can result in different indoor exposure levels in case occupants have all windows closed' [3]. The outcomes of high CO_2 concentrations in humans vary from breathing and respiration problems to immediate death. Thus, it is important to predict the CO_2 concentration caused by equipment usage, occupant behaviour and external sources, and it is critical that the upper allowable limit not be exceeded.

Although providing a good level of IAQ in schools is critical for both the health of the pupils and their learning outcomes, it is common for school classrooms to be significantly under-ventilated, promoting high levels of CO_2 and other pollutants. The concentration of CO_2 in classrooms can rise to high levels around 4,000 ppm, substantially exceeding the Chartered Institution of Building Services Engineers (CIBSE) suggested threshold of 1,000 ppm [4]. It is a matter of considerable priority given children spend long periods inside school buildings and are more vulnerable to the adverse effects of indoor pollutants. Additionally, classrooms often experience unsuitably high temperatures due to poor ventilation, even during cold winters [5, 6].

Numerous studies have highlighted the importance of ventilation in heavily populated environments such as schools, with Myhrvold et al [7] presenting a three-year analysis indicating a correlation between student performance, health issues, and classroom CO_2 levels. The placement of operable elements (e.g. windows) on a façade requires careful consideration of (i) the exterior wind environment, including its interaction with building or classroom components, and (ii) the essential characteristics of room airflow patterns, which define the magnitude of local heat transfer from interior surfaces, occupants and ICT with significant thermal capacity. Other studies have evaluated the number of cross-ventilation windows on a classroom façade in terms of the impact on the internal temperature in classroom buildings, showing that uniformity of cross-ventilation in buildings with significant numbers of openings improves pressure and mean velocity values or the internal environment [8] [9].

There is currently limited or no consensus in the literature regarding which cross-stack height (CSH) method provides the best ventilation outcomes, and there exists no research examining the relationship between classroom geometry (i.e. area and height), cross-ventilation, the internal environment (i.e. occupants and ICT), and future climate conditions. Although buildings with a single dominant opening are most common in UK schools, accurate evaluation of the internal environment in classrooms with cross-ventilation and realistic wall porosity is essential. Evaluation of the internal environment in classrooms with different façade openings introduces additional complexities regarding the internal flow and temperatures and demands attending to classroom geometry and area, the inlet-to-outlet CSH effect and the relative location of openings, aspects that few studies have examined and a gap addressed by this research's case study. The work presented in this paper is therefore a novel contribution offering a potential solution for cross stack driven ventilation that addresses issue critical to using natural ventilation to reduce indoor pollutants and enhance IAQ in the classroom environment.

The first step involved predicting ventilation airflow, and the second step focused on the design of the CSH effects of windows, particularly their location on classroom façades. The results are compared with those of a reference classroom with single-side ventilation.

2. METHODS

2.1 Classroom Ventilation Geometry

Measuring CO_2 concentration has become a viable approach to calculating the appropriate ventilation of a room and, thus, its air quality. This section analyses and identifies appropriate measuring zones for mean CO_2 concentration in a classroom full of pupils to determine the effect of different cross stack height (CSHs) on a classroom's indoor environment using CFD modelling.

The existing literature on CO_2 in classrooms has typically been based on in-situ measurements. With a limited number of CO_2 sensors and the limitation of CO_2 measuring precision, measurements can only be collected at a few points in a given space. Meanwhile, a numerical simulation provides CO_2 concentrations at all locations in the calculation domain, which are important for designing new classrooms. Hence, for this research's case studies, a three-dimensional classroom representation of the classroom's interior was generated based on the dimensions of a real room from a model classroom described by CIBSE.

The floor dimensions were 7.5 m × 7.5 m and the height was 3.0 m. The CSH of the window and one inlet and outlet were assigned to simplify the model. Ten geometries were considered for the calculations, with one used as the baseline classroom, based on a field study of the one-window classroom, and one considering a full-occupancy classroom. Due to large variations in classroom configurations and inlet/outlet locations, a simplified but representative occupancy situation was selected to reflect possible patterns at much larger spatial scales. The classroom geometry features a simplified inlet opening (1.0 m x 0.5m) (w x h) and outlet opening (1.0m x 0.5m) (w x h) for a total area of 1 m^2 (Figure 1). The classroom was occupied by eight pupils seated around the table in the middle of the classroom, with the pupils represented by cylinders 0.8 m tall and 0.24 m in diameter [10].

One previous study [11] produced similar modelling results for simplified and precise human geometry, while another [12] applied the geometry of a person in a bedroom using a simplified cuboid shape. Figure 2 shows a 3D view of the physical model used by the CFD simulation model for the modular classroom and the various CSH configuration scenarios.

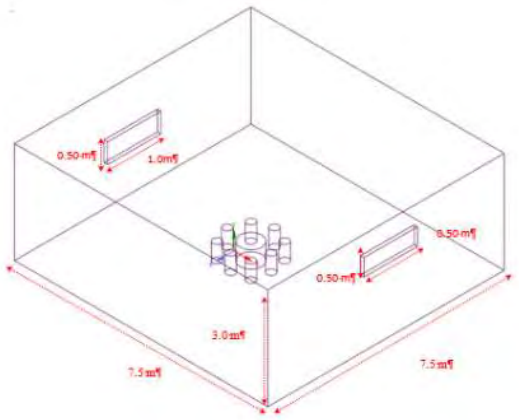

Figure 1: The geometric model of the classroom, including dimensions.

2.2 Solver Setting and Boundary Conditions

The CFD code ANSYS Fluent 2021R was used to examine and conduct the classroom simulations. Classrooms with different CSH configurations were also analysed to examine the effect on the classroom, including on occupant breathing and CO_2 levels (i.e. indoor pollutants) and the indoor climate, according to the position of the opening and the activity level of the pupils and the field tests. For the solver settings, Reynolds-Averaged Naiver–Stokes flow simulations were used [13] to produce accurate results for the wall-bounded flows that are frequently found in room airflows [14].

For the turbulence model, the Shear Stress Transport k–ω turbulence model was employed to consider prediction performance for turbulent indoor airflow in association with thermal plumes and wall-bounded flows in indoor environments [15, 16].

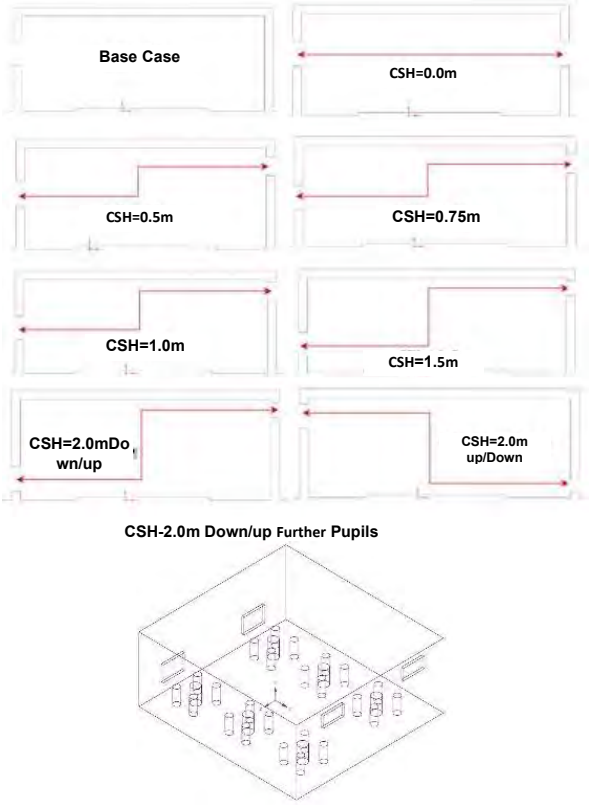

Figure 2: The window opening configurations used to study the effects of CSH on CO_2 inside the classroom.

The boundary condition of the room was modelled in terms of airflow and CO_2 [17], with CO_2 production modelled as a low-velocity, low-volumetric air-CO_2 mixture flowing from the top surface of the cylinders representing the classroom's occupants. Subsequently, CO_2 boundary conditions were set to 0.008 kg/s with temperatures of 30°C [12], considering a constant exhalation and a full breathing cycle for occupants. Exhalation velocity from a person varies between 0.6 and 0.8 m/s [17]. To focus solely on the impact of room airflows on the indoor environment – that is, air quality and CO_2 – outdoor conditions were excluded by making the model's envelope adiabatic except for the airflow from inlet and occupant simulators. For boundary conditions, the air supply and outlet were modelled as a velocity inlet and a pressure outlet. The airflow boundary condition was set to 1.2 m/s, with a constant air temperature value of 20°C. Figure 3 and Table 1 summarise the boundary conditions of the classroom domain.

Table 1: Summary of boundary conditions

Turbulence model	RNG k–ε model
Numerical scheme	Upwind second-order difference, transient state with full buoyancy effect, enhanced wall treatment
Pressure–velocity coupling	SIMPLE
Room air inlet	Velocity=1.2 m/s, T=22°C
Classroom outlet	Pressure outlet
CO2 from occupants	Mass flow rate 0.008 kg/s

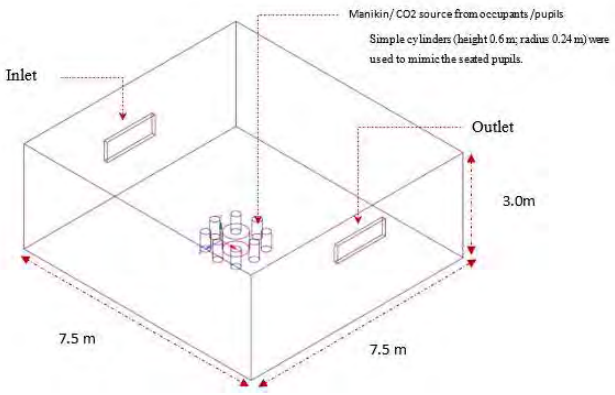

Figure 3: The simulation domain and boundary conditions of the classroom (featuring cylindrical occupant simulation).

2.3 Grid Setup and Analysis

To test 3D IAQ, the computational mesh was constructed based on the predefined classroom CSH configuration. The rectangular shape of the windows and the classroom geometry, including the various cylindrical blocks, required the use of a structured Poly-Hexacore mesh. Because the second phase of airflow and CO_2 testing required buoyancy forces, cell sizes were refined near the surface of the windows and cylinders to estimate the convective CO2 level and the transfer rate more accurately to the indoor environment.

For natural ventilation dominated by supply jet momentum, the inlet and outlet were refined along with the whole domain to provide correct computational results for airflow between the two openings. These refinements were processed with the aid of a surface remaster to improve and enhance cell quality. Cells above CO_2 sources were refined to capture turbulent entrainment of the thermal plume of the CO_2, which can be considered a pollutant Figure 4. The simulation results considered the average air velocity results in the domain, showing less than a 2% difference for each of the refined meshes.

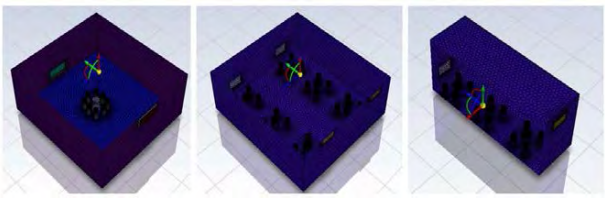

Figure 4: Details of the computational grid for the classroom domain.

Three different mesh sizes were studied, varying from coarse to fine, using the simulation results presented in Figure 5.

Mesh-1	Mesh-2	Mesh-3
318,370	858,680	3,150,219

Figure 5: Perspective view of the grids pertaining to the grid sensitivity analysis: coarse grid (318,370 cells), baseline grid (858,680 cells) and fine grid (3,150,219 cells).

Given velocity was the factor most pertinent to this study, it was used for the mesh-independence study for 3D indoor airflow. When the cell number was increased from 318,370 to 3,150,219 cells, the values for air velocity and temperature remained nearly constant, with a maximum variation of 7%. Additionally, the differences in the average air velocity across the whole classroom was about 1% between the baseline grid and the fine grid. Hence a total cell number of 858,680 was chosen.

3. RESULTS

These case studies use eight occupants in two postures (standing and sitting) to evaluate inhalation of CO_2. The sitting posture represents an occupant working at the centre of a classroom and different CSH configurations are used, with the only constant being the simulation of the exhalation process. The air supply jet enters the classroom to initially form a layer of fresh air throughout the classroom. The results simulate the airflow pattern for the baseline case and configurations CSH-0.0m, CSH-0.5m–CSH-0.75m, CSH-1.0m, CSH-1.5m, and CSH-2.0m. For configurations CSH-2.0m, the plume of fresh air entering the classroom at the lower inlet produced a breathing zone at 0.6 m that moved into the buoyant plume of CO_2 that formed above the occupants. The spatial distribution of CO_2 and air velocity showed only small differences for the areas surrounding the different occupants. One study [18] has notably demonstrated that a simplified constant exhalation model can be used effectively for the CFD analysis of IAQ. The velocity contours of the described different scenarios of CSH ventilation strategies and CO_2 level are depicted for the classroom. The results illustrate the mean turbulent velocity vector field under steady flow conditions for different CSH configurations with dispersion of CO_2 from pupils. Clearly, the air supply from the opening formed a jet that extended across the room and generated a large region of circulating flow. As the CSH increased, the jet flow and accompanying circulation flow increased, pushing the CO_2 particles outside. Figure 6 represents the velocity of the streamlined air and the streamline of the CO2 from the pupils in the classroom for the baseline case and cross-ventilation cases of CSH-0.0m, CSH-0.5m and CSH-0.75 m.

Figure 6 also shows that ventilation airflow significantly impacts CO2 dispersion, especially in the CSH-1.0m to CSH-2.0m range.

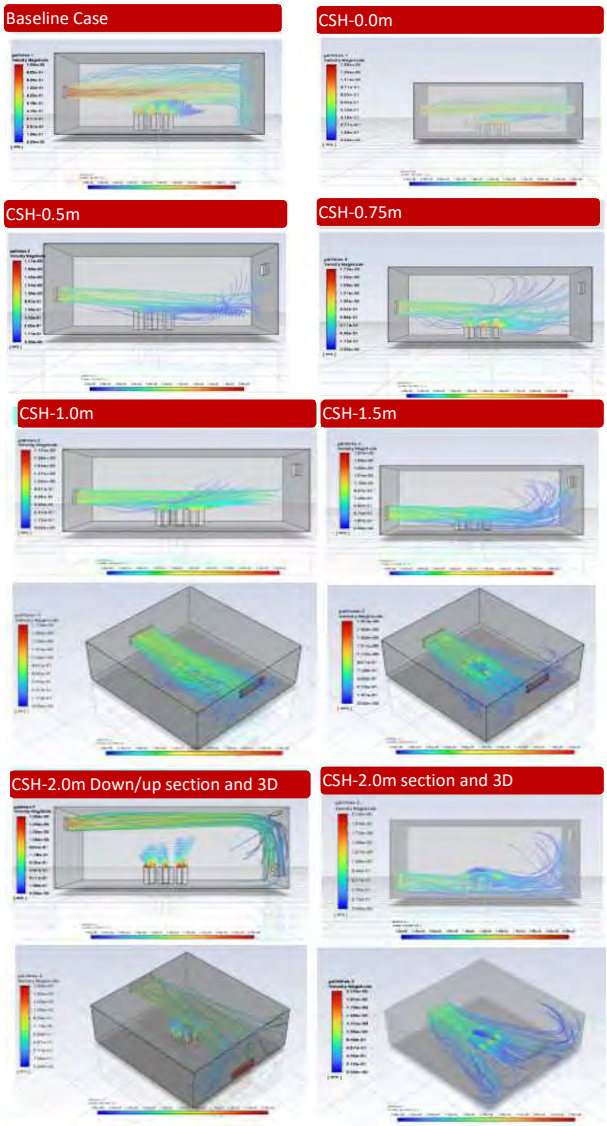

Figure 6: Section view and 3D classroom view with path lines for air velocity in the rooms, indicating CO_2 levels for the following different CSH configurations: CSH-1.0, CSH-1.5, CSH-2.0 and CSH-2.0 Up/Down.

In the CSH-2.0 scenario, fresh air reaches the sitting occupants and rises, pushing CO_2 particles towards the outlet, resulting in cleaner air around the occupants with average concentrations of 400–500 ppm, meeting CIBSE standards. Conversely, in the CSH-2.0 Up/Down ventilation scenario, CO_2 particles remain near the face area, dispersing throughout the room as ventilation flows horizontally and vertically, raising overall CO_2 levels**.** Figure 8 shows CO_2 levels on the Y horizontal plane for eight pupils under various CSH configurations: baseline, CSH-0.0 to CSH-2.0, including

Down/Up and Up/Down variations. The CO_2 concentration differences are influenced by thermal plumes from occupants, which move CO_2 upwards. For CSH-0.0, CSH-0.5 and CSH-0.75, average horizontal concentrations range from 1,500 to 2,000 ppm, with specific levels at 1.2 m and 1.0 m. Higher CSH levels (1.0 m, 1.5 m and 2.0 m) reduce maximum concentrations to 1,200, 900, and 400 ppm at sitting level. At CSH-2.0, despite CO_2 stratification, concentration is around 400 ppm, with a smaller vertical gradient due to increased CSH and adequate ventilation. In the full exhalation model, CO_2 plumes disperse rapidly above occupants, with the highest concentrations observed in the CSH-2.0 Up/Down configuration near and above occupants.

Figure 8: CO_2 levels in the classroom at the level of the measurement plane (1.0m).

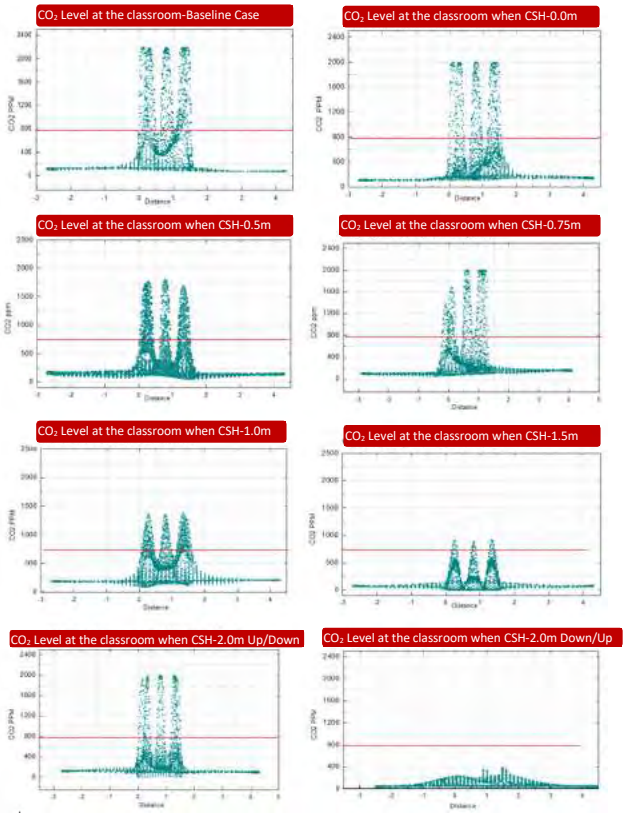

Figure 9 visualises how varying CSH levels affect the classroom's CO_2 concentration at 1.0 m (seated level). Student bodies and their heat are not included in the IAQ model, but CO_2 concentrations are evaluated at different STs. High-momentum supply air mixes with CO_2 in the room. Increased CSH results in CO_2 levels below 500 ppm despite higher concentrations near occupants due to thermal plumes. In the baseline scenario, CO_2 concentrations range from 1,200 to 2,000 ppm. However, with increased CSH, the average CO_2 concentration decreases. The CSH-2.0 Down/Up configuration effectively minimises CO_2, pushing it from occupants towards the exhaust. Conversely, in the CSH-2.0 Up/Down setting, fresh air at the supply opening concentrates more CO_2 around the breathing zone, creating a higher CO_2 concentration area.

Figure 9: The non-dimensional contour of CO_2 concentration

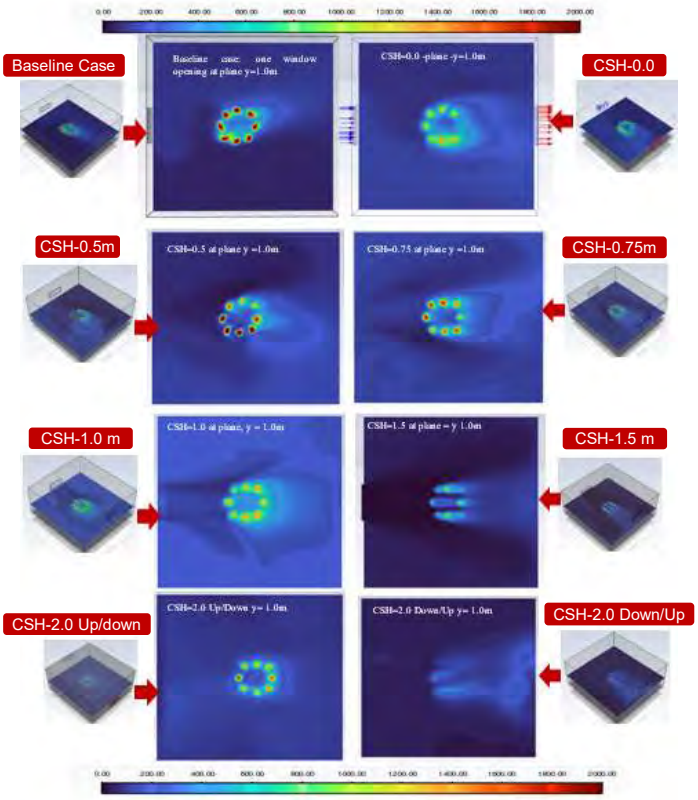

in the classroom for each CSH case at a height of 1.0 m.

Figure 10 considers the CSH-2.0 Down/Up scenario in the context of an entire classroom (30 pupils), highlighting streamlined airflow and CO_2 inhalation patterns. Here, the inlet air jet creates a low CO_2 region around occupants, pushing the emitted CO_2 towards the outlet. This results in cleaner air for occupants, with an average CO_2 concentration of around 450 ppm in the inhalation region.

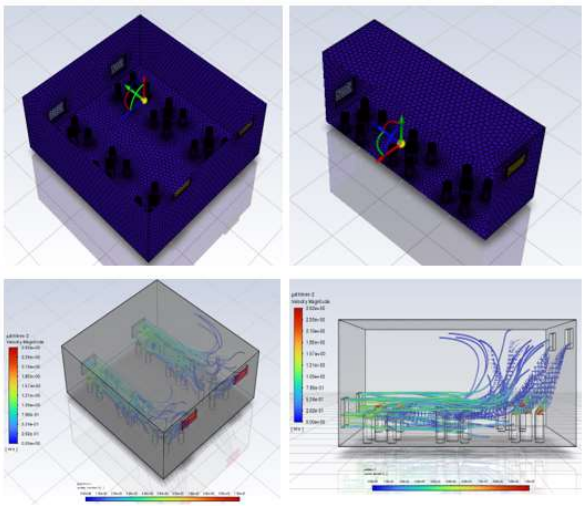

Figure 10: The configuration CSH-2.0 Up/Down for a completely occupied classroom showing the streamlined airflow with CO_2 concentration.

4. MAIN FINDINGS AND DISCUSSION

Inlet-to-outlet positioning and the relative location of openings on a classroom façade are important parameters to be considered in the context of improving IAQ. This study provides new insights that enable improved design and control of operable façade elements to enhance the indoor environment using natural ventilation.

The results obtained enable us to assess IAQ based on the distribution of CO_2 concentration in the classroom. CO_2 concentration contours for different CSH effect configurations selected for classroom cases/breathing models have been analysed. At the occupancy level, the breathing model has an influence that is limited to the local CO_2 distribution in the room. The most discrepancies in terms of CO_2 concentration were observed in the baseline case. Comparison between CSH configurations shows some different effects on CO_2 concentration, with the lowest concentrations appearing in the contexts of configurations CSH-1.5m and CSH-2.0m, with average concentrations between 400 ppm and 500 ppm observed in the baseline case (but exceeding 2,000 ppm near the ceiling). As CO_2 concentrations increased, CSH impacted the streamlining of CO_2 from classroom occupants, demonstrating that airflow streamlining reduces the spread of CO_2, with the baseline case's poor performance providing further evidence, with increased CSH generally increasing the inlet airflow jet, reducing the level of CO_2 and allowing fresh air to penetrate deeper into the classroom before pushing CO_2 to the outlet. When CSH increased, the fresh air from the inlet entered the region of inhalation, drawing CO_2 upwards thermally and resulting in metabolic heating. The air in the region extending from the occupants to the outlet opening hardly reaches the region of inhalation or the seated occupants at all, instead moving towards the outlet. The geometry of classroom inlets and outlets and the CSH between them is very important for the distribution of the room's CO_2. Differences in ventilation effectiveness and the reduction of CO_2 levels by the different CSH configuration scenarios reveal the importance of distributing fresh air in classroom spaces. Furthermore, higher STs increase the supplied air, enabling the conclusion that certain opening positions could help to boost wind-induced ventilation, reduce temperatures, and enhance IAQ, especially in the context of densely populated classrooms.

5. CONCLUSION

In this work, the authors optimised CSH to improve IAQ in classrooms using natural ventilation, with CFD simulations employed for testing. The approach involved managing air circulation to reduce indoor pollutants such as CO_2. Key factors include positioning inlets and outlets on classroom façades to harness the impact of different CSH levels. The results show that CO_2 concentrations vary between CSH configurations, with the lowest levels observed for CSH-1.5m and CSH-2.0m. By contrast, baseline scenarios showed CO_2 levels exceeding 2,000 ppm near the ceiling. Increased CSH helps draw fresh air into the breathing zone, moving CO_2 upwards and aiding in metabolic heating. However, the air between occupants and the outlet was observed to have a limited impact on the breathing zone. Notably, this study has had to simplify certain aspects due to computational limitations. The building envelope and internal heat gains were reduced in complexity, and classroom obstacles – such as desks and chairs – were omitted to minimise the computational load. Nonetheless, the study highlights the importance of inlet and outlet placement and CSH for distributing fresh air and managing CO_2 levels in classrooms. Enhanced CSH effectively brings fresh air into the inhalation region and helps in the upward thermal movement of CO_2, emphasising the critical role of classroom ventilation geometry.

REFERENCES

1.Daisey, J.M., W.J. Angell, and M.G. Apte, *Indoor air quality, ventilation and health symptoms in schools: an analysis of existing information.* Indoor air, 2003. 13(LBNL-48287).

2.Haynes, J., et al., *Air Quality and Heat-related Health Issues*, in *Earth Observation, Public Health and One Health: Activities, Challenges and Opportunities*. 2022, CABI GB. p. 38-52.

3.Shrestha, P.M., et al., *Impact of outdoor air pollution on indoor air quality in low-income homes during wildfire seasons.* International journal of environmental research and public health, 2019. 16(19): p. 3535.

4.Turanjanin, V., et al., *Indoor CO2 measurements in Serbian schools and ventilation rate calculation.* Energy, 2014. 77: p. 290-296.

5.Wyon, D.P. and P. Wargocki, *How indoor environment affects performance.* thought, 2013. 3(5): p. 6.

6.Gil-Baez, M., et al., *Natural ventilation in classrooms for healthy schools in the COVID era in Mediterranean climate.* Building and Environment, 2021. 206: p. 108345.

7.Myhrvold, A.N., E. Olsen, and O. Lauridsen, *Indoor environment in schools - Pupils health and performance in regard to CO2 concentrations.* Indoor Air, 1996. 4(4): p. 369-374.

8.Karava, P., T. Stathopoulos, and A.K. Athienitis, *Wind-induced natural ventilation analysis.* Solar Energy, 2007. 81(1): p. 20-30.

9.Karava, P., T. Stathopoulos, and A.K. Athienitis, *Airflow assessment in cross-ventilated buildings with operable façade elements.* Building and Environment, 2011. 46(1): p. 266-279.

10.Ahn, H., D. Rim, and J. Lo, *Ventilation and energy performance of partitioned indoor spaces under mixing and displacement ventilation.* Building Simulation, 2017. 11.

11.M. Deevy and N. Gobeau, *CFD modelling of Benchmark Test Cases for Flow Around a Computer Simulated Person* 2006.

12.Bulińska, A., Z. Popiołek, and Z. Buliński, *Experimentally validated CFD analysis on sampling region determination of average indoor carbon dioxide concentration in occupied space.* Building and Environment, 2014. 72: p. 319-331.

PLEA 2024 WROCŁAW
(Re)thinking Resilience

Assessing the effect of Nature-Based Solutions on Air Quality in a Residential Area of Delhi using ENVI-met

Assessment of Nature-Based Solutions on Air Quality

AMARNATH SHARMA[1], MAHUA MUKHERJEE[1,2]

[1]Department of Architecture and Planning, Indian Institute of Technology Roorkee, India
[2] Centre of Excellence in Disaster Mitigation and Management, Indian Institute of Technology Roorkee, India

ABSTRACT: Air pollution is a huge global concern, particularly in Indian metropolitan areas. Nature-based solutions (NbS) are recognized as cost-effective and sustainable solutions. However, the effectiveness of NbS strategies relies on the built system, which influences airflow. Therefore, comprehending air pollution distribution in open spaces is crucial before implementing NbS. This study assesses the impact of a built system on pollutant patterns and evaluates 14 NbS scenarios (involving green roofs, walls, grass, and trees) on six air pollutants ($PM_{2.5}$, PM_{10}, O_3, SO_2, NO, and NO_2) in the residential block of Dwarka, Delhi by applying the microclimatic CFD-based high-resolution simulation model using ENVI-met 5. The results show that changing street canyons and building distribution influence pollutant distribution in varying quantities. The results show that distribution patterns of all air pollutants, in varying quantities, are affected by the varying street canyons and distribution of buildings. NbS have varied effects, with limited impact on PM_{10} and $PM_{2.5}$. While some positively reduce pollutant concentrations, others exhibit negative or negligible impacts. Combining NbS or changing vegetation type led to a notable rise in pollution deposition. This study highlights the necessity for future research to evaluate the effectiveness of additional NbS with diverse vegetation species.
KEYWORDS: Air Pollution, Residential Area, Built System, Nature-Based Solutions, ENVI-met.

1. INTRODUCTION

Urban air pollution poses a significant threat to public health and quality of life, and it is a critical issue in many urban areas in India. According to the Central Pollution Control Board (CPCB), 38 out of 51 million-plus cities in 2019 did not meet the National Ambient Air Quality Standards (NAAQS) Regarding air pollution indices[1]. Delhi stands out as one of the most severely affected cities. In 2019, the Government of India Launched a National Clean Air Programme focusing on improving the air quality in cities that are unable to meet NAAQS by focusing on a green recovery model. A similar commitment is stated in the Master Plan-2041 for Delhi[2].

Urban air quality may be improved in two ways: by reducing air pollution at its source or removal from the urban atmosphere. While it is important to reduce pollution at the source, it is also necessary to take measures to reduce air pollutants from the urban atmosphere as the air quality of an urban area is impacted by numerous sources and the regional airshed it is a part of [3].

For enhancing air quality in metropolitan settings, NbS are regarded as cost-effective and sustainable air pollution mitigation techniques [4,5]. NbS are implemented at multiple scales in urban areas, from green roofs at the facet scale to urban forests at the city Scale. Stuttgart, a German city, used to have bad air quality, but they could fix it by retrofitting it with NbS-like green roofs[6].

NbS applications within a neighbourhood include but are not limited to green façade, green roofs, street trees, pocket gardens/parks, vegetation barriers, private and community gardens, pre-existing vegetation, and vegetated grid pavement [7].

A review indicates that numerous studies have reported a substantial reduction of up to 60% in traffic-generated $PM_{2.5}$ and 40% in NO_2 concentration with the introduction of vegetation in urban street canyons.[5].

However, not every NbS will probably function identically in varying urban environments; air pollutant behaviour changes with varying urban settings and meteorological conditions [8]. To have a well-planned and constructed strategy of NbS for urban areas, it is crucial to understand the influence of different NbS strategies on the specific type of urban setting.

2. OBJECTIVES

This study aims to conduct a Computational Fluid Dynamics (CFD) simulation using ENVI-met to assess the pollution pattern and effectiveness of NbS in mitigating air pollution at the neighbourhood level for a residential block of Dwarka, Delhi.

The objectives of this research are:

- To evaluate the pollution dispersion pattern in a residential area at a street canyon scale.

- To identify the appropriate NbS strategies, focusing on compact residential areas in metropolitan cities.
- To compare the base scenario to NbS scenarios to evaluate the impact of relevant NbS on pollutants' concentration and deposition.

3. METHODOLOGY

First, a literature review identifies the appropriate NbS for metropolitan cities focusing on Delhi. Then, one of the significant air pollution hotspots, in a residential area, is selected from the identified hotspots by H. Yadlapalli in 2021 [9] based on the air pollution data given by CPCB from 2019-21. The 3D modelling of urban features is carried out utilizing physical surveys and geospatial data. Meteorological information and air pollution concentrations are obtained from the CPCB app (https://app.cpcbccr.com/).

CFD simulation of the base scenario (no greening) is conducted. Insights into the relationships between pollutants and the built form are sought by doing this. Various NbS techniques are subsequently introduced, considering the needs and limitations of the study area. Given the time-consuming nature of CFD simulation, the simulations incorporating various NbS strategies are conducted on a specific segment (shown in Figure 3) of the study area. The selected segment reflects the study area, which has similar built patterns such as variations in street canyons and wind flow and height of roughness elements. The outcomes of diverse NbS strategies are analyzed and compared across all air pollutants.

3.1. Simulation methodology

ENVI-met software, a holistic three-dimensional non-hydrostatic model (https://www.envi-met.info/doku.php?id=intro:modelconcept), is used for simulation with active chemistry dispersion module and simple forcing meteorological strategy. During the test simulation, it was found that within 4 hours lower limit of O_3 concentration goes down by 99%. Thus, simulations are conducted for 4 hours from 02:00 pm to 06:00 pm. The grid resolution is taken 1 m X 1 m X 1 m, which is a higher resolution than previously conducted studies [10,11]. An additional 5 cells to each side of the models are added to increase the stability of the model.

4. STUDY AREA

The study area is in Delhi, which is one of the most polluted cities. Air pollution in Delhi caused 54,000 estimated premature deaths and an economic loss of $8.1 billion in 2020 [12]. One of the significant challenges facing the city in controlling air pollution is deforestation and saturated sinks [13]. Figure 1 shows the boundary of the site & location of the CPCB station.

The study area with the size of 513 m X 468 m, can be classified as the Compact Low Rise Local Climate Zone-3 (LCZ-3) [14], which is one of the city's leading hotspots for air pollution [9] and features a wide variety of building types, including low-rise to mid-rise structures up to six floors high and about forty-five percentage of urban cover.

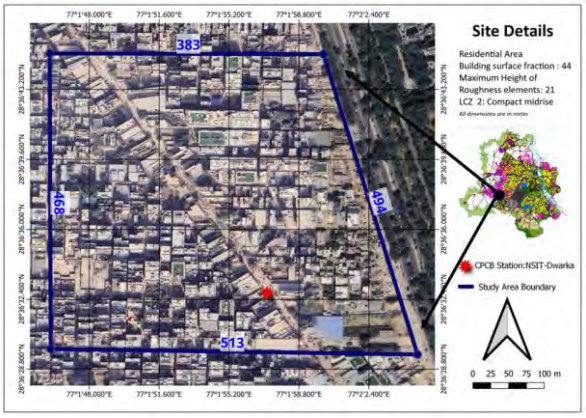

Figure 1 Google Earth image of the Study area with the location of CPCB Air quality station (Source: Google Earth; https://app.cpcbccr.com/)

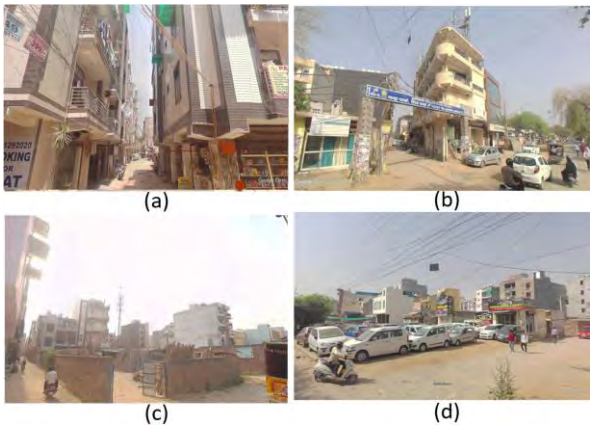

Figure 2 View of varying urban canyon: (a) 5-meter-wide street with most of the buildings of 5-6 stories. (b) 9-meter-wide main road with negligible vegetation, most of the buildings of 3-4 stories and some vacant plots. (c) 3 & 5-meter-wide streets with buildings of varying heights. (d) Open space used as parking space (Source: Google Earth)

The maximum height of roughness elements in the study area is 21 meters. The streets range in width from 3 to 5 meters, while the main road is 12 meters wide. Figure 2 shows graphic renderings of the many street canyons, while Figure 3 presents a conceptual 3D picture of the overall built structure inside the area.

The study uses average air pollution and data for 09th January 2023, when pollution was at its peak, from the NSIT-DWARKA monitoring station (Coordinates: 28°36'32.7"N, 77°01'57.2"E), which is situated inside the study area. Relative humidity

varies from 79% to 98 % throughout the day, and air temperatures range from 7 to 15 °C. The prevailing wind is from the southwest direction with an average wind speed of 0.30 m/s; Clear sky conditions are assumed.

The average pollution concentrations for $PM_{2.5}$, PM_{10}, O_3, SO_2, NO, and NO_2 are recorded as 411, 529, 21, 7, 43, and 34 ($\mu g/m^3$), respectively, which are used in the CFD simulation model as the background pollutant concentrations. It is assumed that this measurement includes emissions connected to traffic as well as other types of pollution.

Figure 3 Image of 3d model of the study area -Dwarka Residential area-sector 15 and marked (red Dash line) part of study area used for analyzing the impact of varying NbS strategies (Source: Author)

Below are the surface details considered to conduct the simulation for the base scenario:

Table 1 Surface details for the base scenario.

Surface Type	Surface Details
Wall	Typical wall -10 mm default plaster (inner and outer layer) on 200 mm bright brick burnt wall
Roof	Typical roof 10 mm default plaster (inner and outer layer) on 100 mm default concrete
Road	Asphalt road
Soil	Default unsealed soil (sandy loam)

NbS like green roofs, green walls, grass on the ground, and trees along the main road and on vacant plots [15–17] are strategically employed individually and in combination for maximizing green elements in the urban landscape, without obstructing wind flow, overcoming limitations posed by the lack of pubic green space and narrow street dimensions.

Table 2 Scenarios-wise details of NbS strategies. LAD- Leaf Area Density, SLF- Sessional Leaf Factor.

SN	Scenario name	LAD	SLF	NbS details
0.	Base scenario			No Greening/NbS
1.	All green roof	0.15	1	0.3 m funkia with sand loam substrate
2.	All green wall- 1	0.15	1	0.3 m funkia with sand loam substrate
3.	All green wall- 2	0.15	1	0.3 m hedera helix
4.	All green wall- 3	0.3	1	0.25 m grass
5.	Flow side green wall	0.15	1	0.3 m ivy (hedera helix) -wall
6.	Flow side green wall and all green roof	0.15; 0.15	1	0.3 m ivy (hedera helix) -wall; 0.3 m funkia with sand loam substrate --roof
7.	All green wall and roof- 1	0.15; 0.15	1	0.3 m ivy (hedera helix) -wall; 0.3 m funkia with sand loam substrate --roof
8.	All green wall and roof- 2	0.3; 0.3	1	0.25 m grass- wall; 0.5 m grass with sand loam substrate- roof
9.	All green wall and roof- 3	0.3; 0.3	1	0.5 m mm grass- wall; 0.5 m grass with sand loam substrate- roof
10.	All green wall and roof- 4	0.15; 1	1	0.3 m ivy (hedera helix) for flow side wall; 1 m hedge green sandy loam substrate for roof
11.	Trees on the main road only	1	0.2	15 m heart-shaped, large trunk, dense, medium trees
12.	Trees on all vacant plots	1; 1; 1	0.2; 0.2; 0.2	15 m heart-shaped, large trunk, dense, medium trees on the main road; 15 m heart-shaped, medium trunk, dense, medium trees on the primary vacant plots; 5 m heart-shaped, small trunk, sparse, small trees on the marginal vacant plots
13.	Trees and grass on all vacant plots with	0.3; 1; 1; 1	1; 0.2; 0.2; 0.2	0.25 m grass on vacant plots; 15 m heart-shaped, large trunk, dense, medium trees on the main road; 15 m heart-shaped, medium trunk, dense, medium trees on the primary vacant plots; 5 m heart-shaped, small trunk, sparse, small trees on the marginal vacant plots
14.	Trees on all vacant plots with grass for the whole open space	0.3; 1; 1; 1	1; 0.2; 0.2; 0.2	0.25 m grass on whole open space (other than roads); 15 m heart-shaped, large trunk, dense, medium trees on the main road; 15 m heart-shaped, medium trunk, dense, medium trees on the primary vacant plots 5 m heart-shaped, small trunk, sparse, small trees on the marginal vacant plots

Subsequently, 14 scenarios involving NbS strategies have been developed to assess its pollution reduction effectiveness in comparison to the base scenario. Table 2 provides information on NbS used in these scenarios. Deciduous trees are employed in

NbS strategies, with a Leaf Area Index (LAI) of 1.5 across all NbS strategies.

5. RESULTS AND DISCUSSION

5.1 Dispersion and deposition pattern of varying air pollutants in existing conditions (base scenario)

Built spaces with high canyon ratios show higher pollutant concentrations than those with low canyon ratios, as shown in the SO_2 concentration map at 2:30 pm at the human level (1.5 m) in Figure 4. Pollutant concentration in front of airflow facing surface is observed to increase due to obstruction of the flow of wind by built envelopes. Interestingly, there are greater concentrations along sections of the main road that go through the entire area linearly. This phenomenon is more evident at locations with higher canyon ratios and irregularly shaped building formations.

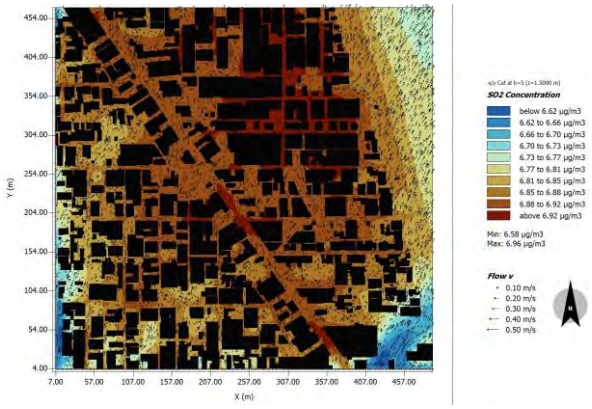

Figure 4 Dispersion patterns of SO_2 in the base scenario at 1.5 m height.

Figure 5 illustrates the recorded lower and upper limits of pollutant concentration at a height of 1.5 meters, for a time interval of 3 and a half hours.

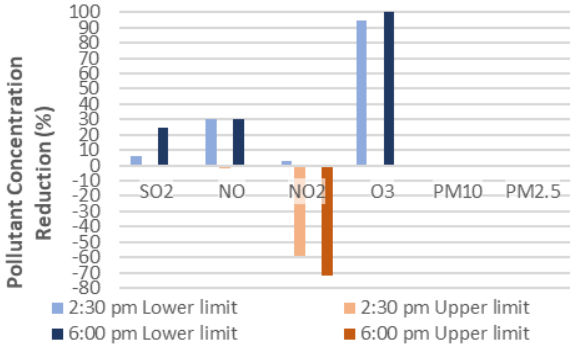

Figure 5 Pollutants' concentration reduction (%) in both lower and upper limits across the study area in the base scenario.

There is negligible variation in the $PM_{2.5}$ and PM_{10} concentrations, despite the presence of substantial deposition of pollutants on the ground.

Within 30 minutes of simulation, the concentration of NO and O_3 reduces by 30% and 94% respectively, in spatial dispersion. At the end of the 4-hour simulation, NO concentration remains relatively stable, whereas a further reduction of 5% is observed in the O_3 pollutant. Conversely, NO_2 concentration demonstrates an increase of up to 59% within the initial 30 minutes, followed by an additional increase of 13% after 4 hours of simulation. These dynamics highlight the varying responses of different pollutants to spatial and temporal dispersion. Figure 6 displays the corresponding deposition at the ground surface.

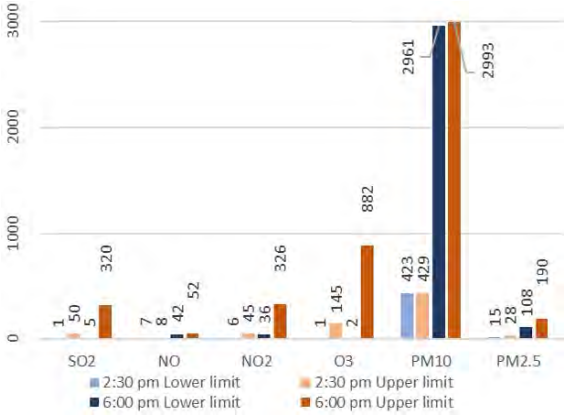

Figure 6 Deposition of pollutants on the ground in both the lower and upper limits across the study area in the base scenario.

It is observed that in 3 and a half hours, the deposition of pollutants on the ground increased by 7 times at ground. SO_2 deposition is observed to be minimal on hard surfaces (Road). NO shows no deposition on soft surfaces (Soil), but maximum deposition is observed on hard surfaces. NO_2 exhibits 5-6 times greater deposition on soft surfaces in comparison to hard surfaces. Furthermore, ozone (O_3) deposition is markedly higher on soft surfaces like soil, reaching up to 60 times the deposition observed on hard surfaces. Deposition of PM_{10} and $PM_{2.5}$ appears across all surfaces and is prominently affected by the surrounding built form. These results highlight the complex interaction between ground surface properties and changing air pollutant deposition.

5.2 Change in dispersion and deposition pattern of varying air pollutants with NbS scenarios.

The alterations in air pollution concentrations are graphically depicted for 14 NbS scenarios in comparison to the base scenario in Figure 7,Figure 8, and Figure 9. Where the Pollutants show varying behavioural patterns for the upper limit and lower limit of concentration across the area.

NO_2 experiences a substantial change in the upper limit of concentration from +9% to -3.5% at 02:30 pm. Conversely, the other pollutants show negligible to no variation in the upper limit of concentration of varying NbS scenarios.

For the lower limit at 02:30 pm, PM_{10} and $PM_{2.5}$ observed a slight reduction in the concentration by 0.13% and 0.01%, respectively. The concentration of

NO, O_3, SO_2 and NO_2 showed a diverse range of change from 2.67% to -6.72%, 13.77% to -30.82%, 1% to 0%, and -0.48 % to 0.09% respectively, for this study, at 2:30 pm.

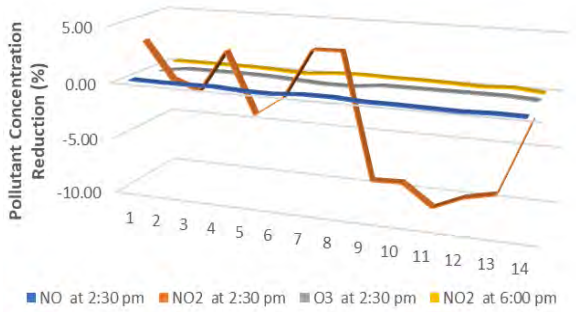

Figure 7 Pollutants' concentration reduction (%) in the upper limit of pollutants by varying NbS strategies in comparison to the base scenario at 2:30 pm and 06:00 pm.

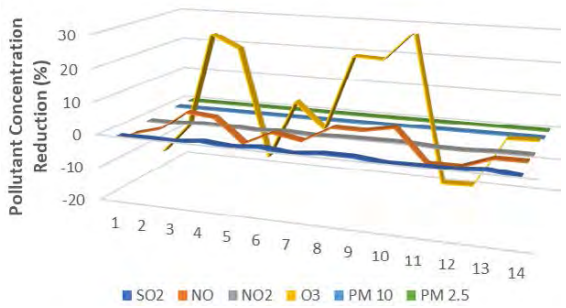

Figure 8 Pollutants' concentration reduction (%) in the lower limit of pollutants by varying NbS strategies in comparison to the base scenario at 2:30 pm.

The concentration of NO, O_3, and SO_2 showed a diverse range of change from 0.5% to -0.46%, 46.67% to -42.22%, and 1% to -1.4% respectively, at 6:00 pm and NO_2 showed no change.

For the lower limit at 06:00 pm, PM_{10} and $PM_{2.5}$ observed a slight reduction in the concentration by 0.22% and 0.01%, respectively. Overall, the major impact of NbS is evident in the concentration of NO, NO_2 & O_3 pollutants.

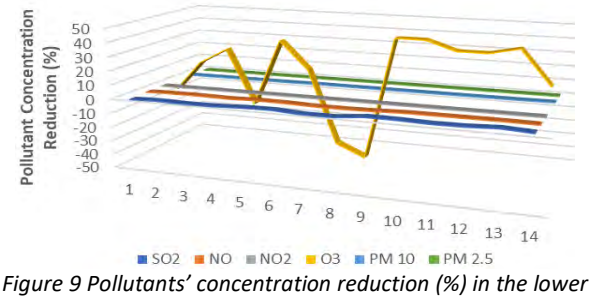

Figure 9 Pollutants' concentration reduction (%) in the lower limit of pollutants by varying NbS strategies in comparison to the base scenario at 6:00 pm.

Among the studied scenarios 3, 4, 8, 9, and 10 demonstrate superior performance in overall pollution reduction. Conversely, scenarios 1, 5, 11, and 12 lead to a significant increase in overall pollution, while scenarios 2, 6, 7, 13, and 14 have a negligible impact on overall pollution levels.

However, the impact of an individual NbS strategy changes across pollutants. Scenarios 9 and 10 demonstrated the most effective concentration reduction for NO, NO_2, and O_3. Figure 10 shows the spatial pattern of reduction of concentration of O_3 at 06:00 pm for NbS Scenario 10. In the case of SO_2, scenario 13 exhibited the best performance, while for PM_{10} and $PM_{2.5}$, scenario 14 proved to be the most effective.

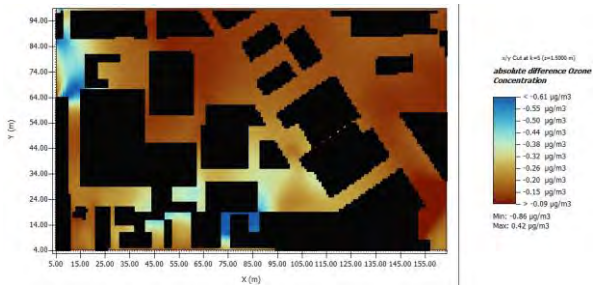

Figure 10 Comparison O_3 concentration of base scenario with scenario 10 at 06:00 pm

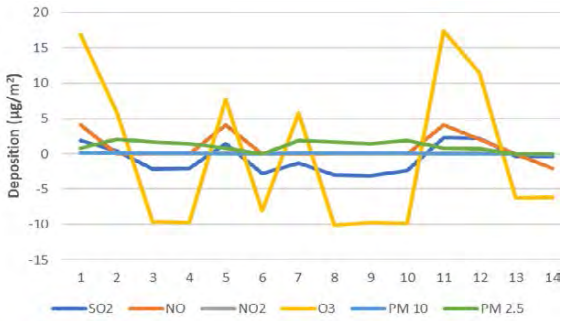

Figure 11 Air pollutant deposition increases in the lower limit across the NbS scenarios in comparison to the base scenario at 6:00 pm.

At 2:30 pm only scenario 6 outperformed other NbS strategies in increasing the overall lower limit of pollutants' deposition on the ground as rest caused the negligible change in it. The upper limit of pollutants' deposition on the ground increases by 6,7 and 14 scenarios.

At 06:00 pm (Figure 11) scenarios 1,2,5,7,11,12 increased the lower limit of the overall deposition rest causing a reduction and the upper limit increased by scenarios 13 and 14 only. Scenarios 1, 2, 5, 7, 11, and 12 increased the lower limit of overall deposition, while the remaining scenarios caused a reduction. For the upper limit, an increase is observed in scenarios 13 and 14. The results emphasize the need to reduce or maintain low canyon ratios in an urban area to improve air quality.

Surface properties and NbS types have varying effects on varying pollutant deposition, suggesting no one-size-fits-all solution.

Some NbS positively impact pollution reduction and increase deposition which confirms previous

studies [4, 5,11,15]. Despite a multiple-fold increase in deposition caused by certain NbS Scenarios, by combining NbS or changing vegetation type, the actual impact on pollution reduction was notably low, particularly for PM_{10} and $PM_{2.5}$. This study focuses not only on road traffic pollutant sources but on collectively accumulated urban air pollution where each grid of the urban area behaves as a pollutant source. It is possible that for such cases NbS is not very effective.

1. CONCLUSION

This research is limited to specific NbS and vegetation species, prompting the need for further exploration, to find more effective NbS solutions. Further studies can explore the avenues for integrating technology with NbS strategies that need exploration to enhance the overall reduction of air pollution.

Conclusively, air pollution concentration is impacted by built systems, especially by an obstruction in wind flow patterns and canyon ratio. This study demonstrates the air pollution spatial distribution among neighbourhoods. NbS has great potential for minimizing the harmful effects of air pollution, which can be used effectively.

REFERENCES

1. CPCB, “National Ambient Air Quality Status & Trends 2019,” New Delhi, Sep. 2020. Accessed: Apr. 14, 2023. [Online]. Available: https://cpcb.nic.in/upload/NAAQS_2019.pdf

2. A. Chatterji, “Air Pollution in Delhi: Filling the Policy Gaps,” Obs. Res. Found., vol. 291, no. December, pp. 1–48, 2020.

3. I. Khanna and S. Sharma, “Could the National Capital Region serve as a control region for effective air quality management in Delhi ? Edited by,” Policy Brief, CCAPC/2020/02, Collab. Clean Air Policy Centre, New Delhi, no. May, 2020, [Online]. Available: https://www.teriin.org/sites/default/files/2020-11/capc-pf.pdf

4. S. Janhäll, “Review on urban vegetation and particle air pollution - Deposition and dispersion,” Atmospheric Environment, vol. 105. Elsevier Ltd, pp. 130–137, Mar. 01, 2015. doi: 10.1016/j.atmosenv.2015.01.052.

5. B. K. Biswal, N. Bolan, Y. G. Zhu, and R. Balasubramanian, “Nature-based Systems (NbS) for mitigation of stormwater and air pollution in urban areas: A review,” Resour. Conserv. Recycl., vol. 186, no. November 2021, p. 106578, 2022, doi: 10.1016/j.resconrec.2022.106578.

6. ICLEI, “Nature-based solutions for sustainable urban development (ICLEI Briefing Sheet),” Iclei, no. March, pp. 1–6, 2017, [Online]. Available: http://www.iclei.org

7. J. A. C. Castellar et al., “Nature-based solutions in the urban context: terminology, classification and scoring for urban challenges and ecosystem services,” Sci. Total Environ., vol. 779, p. 146237, 2021, doi: 10.1016/j.scitotenv.2021.146237.

8. T. R. Oke, G. Mills, A. Christen, and J. A. Voogt, Urban climates. 2017. doi: 10.1017/9781139016476.

9. P. Goyal, S. Gulia, and S. K. Goyal, “Identification of air pollution hotspots in urban areas - An innovative approach using monitored concentrations data,” Sci. Total Environ., vol. 798, p. 149143, 2021, doi: 10.1016/j.scitotenv.2021.149143.

10. J. Lu et al., “A micro-climatic study on cooling effect of an urban park in a hot and humid climate,” Sustain. Cities Soc., vol. 32, no. April, pp. 513–522, 2017, doi: 10.1016/j.scs.2017.04.017.

11. L. Rui, R. Buccolieri, Z. Gao, E. Gatto, and W. Ding, “Study of the effect of green quantity and structure on thermal comfort and air quality in an urban-like residential district by ENVI-met modelling,” Build. Simul., vol. 12, no. 2, pp. 183–194, 2019, doi: 10.1007/s12273-018-0498-9.

12. Greenpeace, “PM2.5 air pollution behind an estimated 160,000 deaths in world’s 5 biggest cities in 2020 - Greenpeace Southeast Asia,” 2021. https://www.greenpeace.org/southeastasia/press/44319/pm2-5-air-pollution-behind-an-estimated-160000-deaths-in-world-5-biggest-cities-in-2020/ (accessed Jul. 24, 2023).

13. M. H. Rahman et al., “High-Resolution Mapping of Air Pollution in Delhi Using Detrended Kriging Model,” Environ. Model. Assess., vol. 28, no. 1, pp. 39–54, 2023, doi: 10.1007/s10666-022-09842-5.

14. H. Yadlapalli, “WUDAPT Level 0 training data for delhi (India, Republic of), submitted to the LCZ Generator,” This dataset is licensed under CC BY-SA, and more information is available at, 2022. https://lcz-generator.rub.de/factsheets/3f8459e865000cc0dbe1c851bec34c6b4861be45/3f8459e865000cc0dbe1c851bec34c6b4861be45_factsheet.html

15. K. V. Abhijith et al., “Air pollution abatement performances of green infrastructure in open road and built-up street canyon environments – A review,” Atmospheric Environment, vol. 162. pp. 71–86, 2017. doi: 10.1016/j.atmosenv.2017.05.014.

16. K. Vijayaraghavan, “Green roofs: A critical review on the role of components, benefits, limitations and trends,” Renewable and Sustainable Energy Reviews, vol. 57. pp. 740–752, 2016. doi: 10.1016/j.rser.2015.12.119.

17. IGBC, “IGBC Green Residential Societies Rating System Ver 1.0,” no. July, 2020.

PLEA 2024 WROCŁAW
(Re)thinking Resilience

Urban Heat Island Resilience in Athens: Analysing the Effectiveness of Green Roofs for Current and Future Climates

ASMAA SADOU AMMAR[1], STEPHEN SHARPLES[1]
[1]School of Architecture, Liverpool, United Kingdom

ABSTRACT: Athens, Greece, has a Mediterranean climate, characterized by very hot summers and cool winters that present microclimate challenges both indoors and outdoors. The city's concrete construction exacerbates the situation, making it difficult to maintain a comfortable temperature. Green roofs could be one possible solution, but it is uncertain if they are a reliable and effective strategy to positively affect the city's microclimate. Climate change is also a growing concern in Athens, and its impact on the city's infrastructure has become a significant challenge. Maintenance of homes and roads has also been problematic. The city's Mediterranean climate, combined with inadequate preparation for extreme weather, has resulted in unforeseen fires and unusual snowfall. To improve Athens' future, adapting to these changes is essential. One proposed solution is to transform certain city areas with green roofs. However, it is necessary to assess whether this approach is effective in improving the microclimate. This study used the ENVI-met software to explore the potential benefits of adding green roofs in mitigating the urban heat island effect and enhancing overall thermal comfort and well-being. The results were encouraging, suggesting that green roofs could be an effective solution for microclimate adaptation in Athens.
KEYWORDS: Climate change, green roofs, Microclimate, Urban Heat Island.

1. INTRODUCTION

Cities are dealing with a range of issues because of increased urbanisation and climate change, including urban heat island (UHI) effects, reduced air quality, declining biodiversity, and a lack of green space. Green roofs can counter these problems by converting rooftops into dynamic and sustainable urban environments and generating pockets of cooler, very localised microclimates [1-5]. This research examined, through simulations using the microclimate simulation software ENVI-met, the possible benefits of green roofs as a sustainable urban solution to a neighbourhood in Athens, Greece. Global temperature increases disproportionately influence metropolitan areas via the urban heat island effect. Athens is a city that already experiences hot summers and faces various issues because it has not developed and adapted to the environmental challenges posed by a warming climate. This study has explored the hypothesis that implementing green roofs could reduce the impact of the urban heat island by cooling outdoor air temperatures. By simulating the effects of green roofs in the current climate and projecting their impact into the years 2050 and 2080, the effectiveness of these solutions in mitigating the effects of climate change on the city and improving the well-being of its residents can be evaluated. Greece faces economic challenges, necessitating a pragmatic approach to climate adaptation. It is necessary to reconcile the need for climate adaptation with the constraints of Greece's economic landscape. Through diligent research, innovative solutions, and simulation-based assessments, a sustainable approach can be found to foster a better future for Athens and its inhabitants.

2. METHODOLOGY

This research used the commercial software ENVI-met (https://www.envi-met.com/), which is a high-resolution microclimate modelling system capable of simulating interactions between surfaces, vegetation, and air in urban environments with a typical resolution down to 0.5m in space and 1- 5 sec in time. 3D models of buildings and neighbourhoods can be created, and weather data can be imported for current and future climates. This study obtained current, 2050 and 2080 weather data for Athens from the climate generation software Meteonorm (https://meteonorm.com/en/) Meteonorm is a software that generates accurate and representative typical years for any location on Earth. You have the option to choose from over 30 different weather parameters. The database comprises more than 8,000 weather stations, five geostationary satellites, and a globally calibrated aerosol climatology. Using this information, advanced interpolation models provide highly accurate results worldwide. An analysis of Athens took a historical overview of how the modern city was created (materials used and identified heights). It was decided to work in the Piraeus area in Eleftheriou Venizelou for this study, which focused on the use of green roofs for microclimate mitigation in this district. In this study, the contemporary climate was analysed by the data of temperatures, wind speeds and directions, solar radiation and the sky cover range. Once the district had been identified, using Google Maps enabled the

areas of individual roofs to be estimated, while the heights of the green roof plants were based on previous similar studies. For the analysis of the microclimate in general, current, 2050 and 2080 weather data for Athens were obtained from the climate generation software Meteonorm. Finally, a digital twin of the district was developed in ENVI-met v5.1.1.

3. CLIMATE CONTEXT

Athens has a Mediterranean climate with hot, dry summers and mild, wet winters. The city is influenced by the eastern shore of the Mediterranean resulting in hot, dry winds from North Africa during summer. Spring (March - May) is hotter than winter, with average temps between 15 to 18°C and lighter precipitation. Summer (June - August) can be very hot with average monthly temps ranging from 29°C to 32°C, with very little rainfall. Autumn (September - November) has mild temperatures and lower humidity. Figure 1 predicts that monthly average air temperatures in Athens are expected to increase by 2 to 3°C in 2050 and by 3 to 4°C in 2080 compared to current conditions.

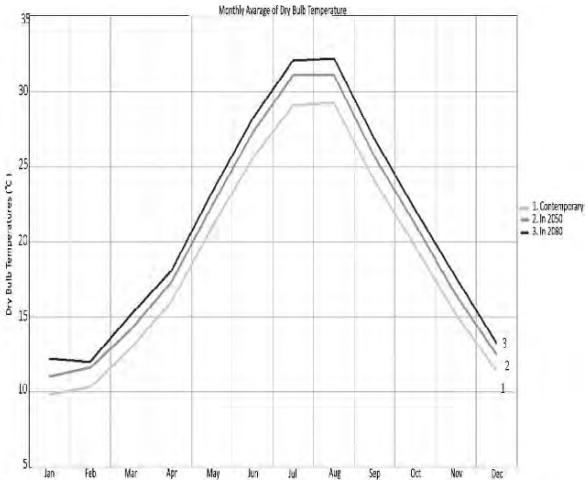

Figure 1: Monthly average dry bulb air temperature in Athens

When comparing the relative humidity levels of the years 2050 and 2080, it was observed that they follow similar patterns throughout most months. However, there is a noticeable change in February 2080, where the humidity levels increase. In contrast, the winter months of 2050 show a slight increase, but there is a significant decrease in the summer months. The humidity levels in 2050 are 2% lower than those in 2080 during the summer months. Nevertheless, the humidity levels for both years never go below 42% or exceed 71% (Figure 2).

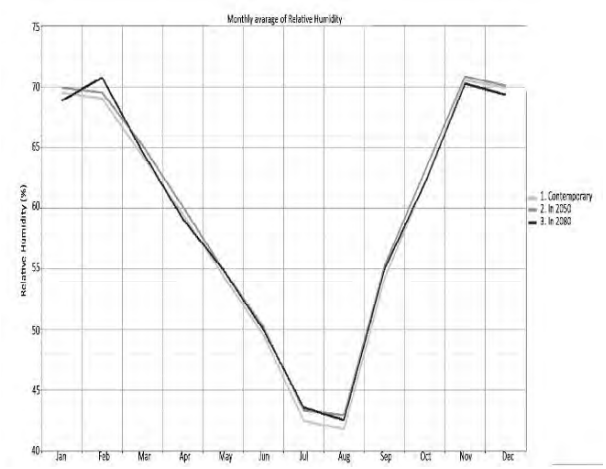

Figure 2: Monthly average of relative humidity in Athens

Figure 3 shows that there is a range of values related to wind speed. The changes in wind speed for the years 2050 and 2080 are concentrated in different months. Overall, there are no noticeable changes between contemporary wind speeds and 2050. At the same time, the comparison (Figure 3) shows an increase of approximately 0.1 m/s in February, a decrease of approximately 0.08 m/s in March, and a decrease of 0.1 m/s in June. This analysis reveals that the most notable changes are occurring between February and March, and June and July. However, all three graphs exhibit similar behaviour, with the year 2080 showing the most significant changes.

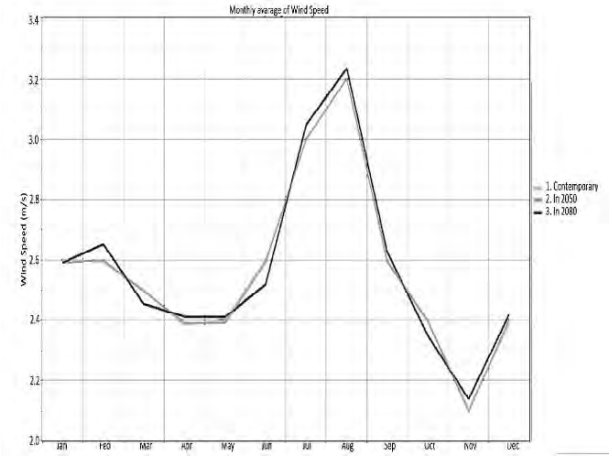

Figure 3: Monthly average wind speed in Athens

2.1 Simulation by ENVI-met.

A 3D recreation of the Piraeus Venizelou area of Athens, located near the coast and mountains, was generated through ENVI-met (Figures 4 and 5) and microclimate conditions were simulated without and with green roofs added to all flat roofs in the area. Analysis was undertaken using current, 2050 and 2080 climate data. The study focussed on the 15th of July since, according to the data, this would be the hottest day.

Figure 4: Pireaus Venizelou area of Athens, Greece

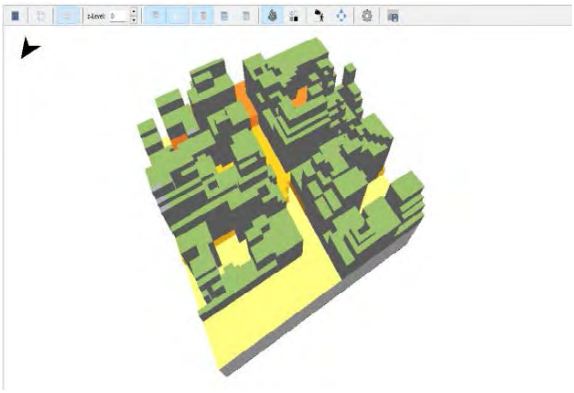

Figure 5: 3D model of the location in ENVI-met

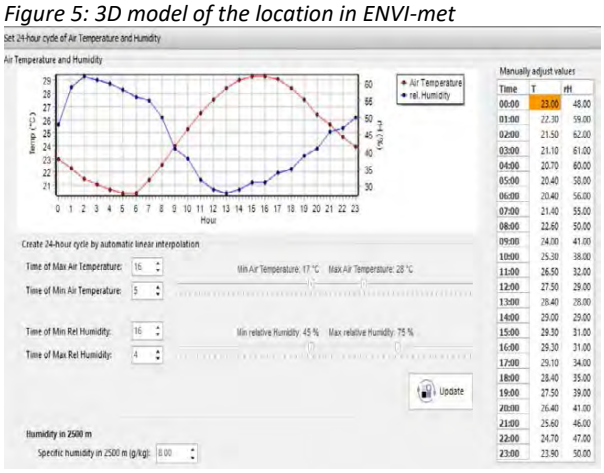

Figure 6: Input data in ENVI-met

The Meteonorm software provided temperature (°C) and humidity(%) data for the contemporary, 2050, and 2080 scenarios. This data was added to the ENVI-met simulation program, as shown in Figure 6.

3. DISCUSSION AND RESULTS

Based on the results obtained from ENVI-met (shown in Figure 7, Figure 8, Figure 9 and Table 1), the use of green roofs had a positive impact on the microclimate. By analysing the changes in the current weather, it can be inferred that the hourly temperature reduction was 1.5°C. Furthermore, the data for 2050 suggest that this reduction will be maintained. On the other hand, for current climatic conditions with a green roof, the wind speed and relative humidity increased by 0.36m/s and 2% respectively. However, in the year 2050, this increase was predicted to be 0.76m/s and 7%. In 2080 the data showed a clear rise in temperatures, with an increase of 3.3°C compared to 2005 and a projected increase of 2.7°C by 2050 with the implementation of green roofs. At the same time, there has been a decrease in relative humidity, with a reduction of 1% compared to current data, but with a significant increase of 5% anticipated by 2050.

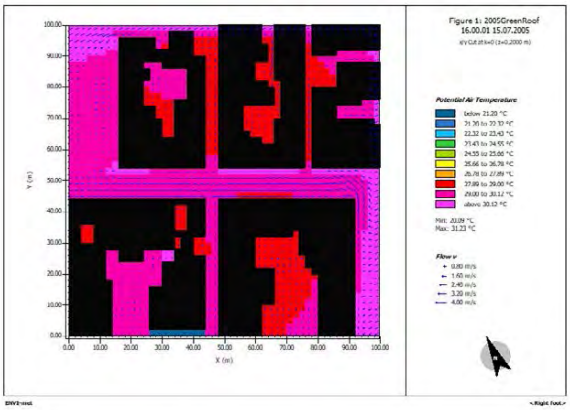

Figure 7: Simulation of contemporary climate ENVI-met

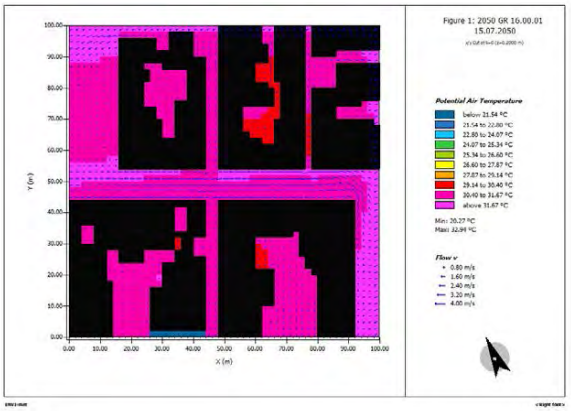

Figure 8: Simulation of 2050 climate ENVI-met

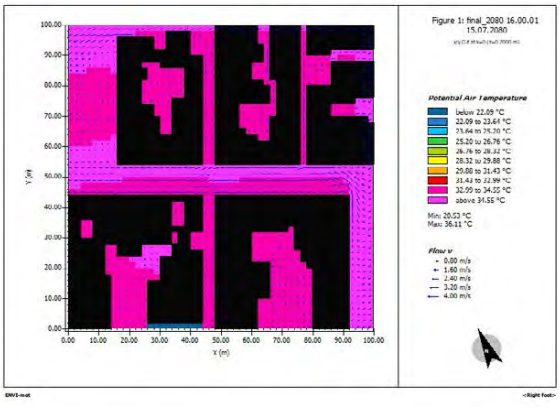

Figure 9: Simulation of 2080 climate ENVI-met

Considering the impact of structures, placement, and orientation on green roofs, the green roof placement

must be studied carefully. The absorption of heat, the increase in wind speed and relative humidity have physical relationships with the building structure in which it is located, regardless of the location. It is important to consider the significant impact and the need for different adaptations as climate changes over the years, especially if green roofs become widely adopted.

Table 1: Average hourly results with and without green roofs.

Time	AT(°C)	RH(%)	WS(m/s)
July current without green roofs			
15:00	29.4	32	0.51
16:00	29.4	32	0.51
July current with green roofs			
15:00	27.9	34	0.87
16:00	27.9	34	0.85
July 2050 with green roofs			
15:00	28.5	39	1.27
16:00	28.6	39	1.25
July 2080 with green roofs			
15:00	31.2	39	1.29
16:00	31.7	37	1.27

AT: Air Temperature; RH Relative Humidity; WS: Wind speed

3.1 Comparison of contemporary, 2050 and 2080 with green roof.

To obtain a deeper analysis of the results, changes in temperature, relative humidity, and wind speed were studied in different years. It is crucial to understand how climate change affects the solution since cities act as structures that both absorb and emit heat. Therefore, it is essential to study the changes and behaviour of these structures with natural materials such as green roofs. The results of this study are as follows:

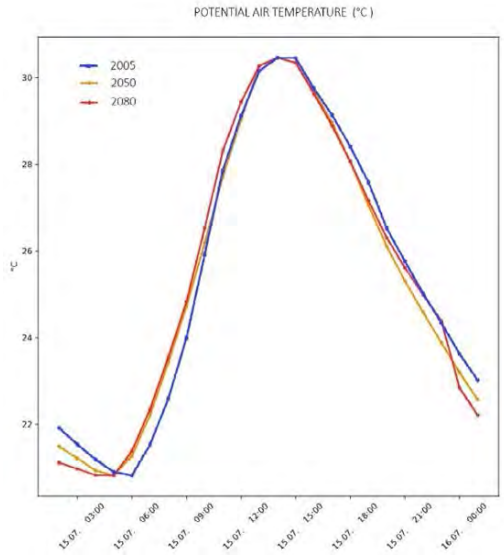

Figure 10: Comparison of Potential air temperature between contemporary climate, 2050 and 2080 with green roof

Figure 10 clearly illustrates the difference between the years. July 15th was chosen to observe changes in temperature between current, 2050 and 2080 data. The highest temperature was recorded in the year 2080, at 20°C, while 2050 recorded a temperature of 21°C and current temperature was 22°C. The difference in temperature during the day is positive. Initially, it was expected that the year 2080 would exceed the temperature by 4°C, but the application of a green roof has improved it by 1 to 2°C. There are no significant changes in temperature in the year 2050, and the temperature drops by one degree after 4 p.m. The temperature is much lower in 2080 during daylight hours.

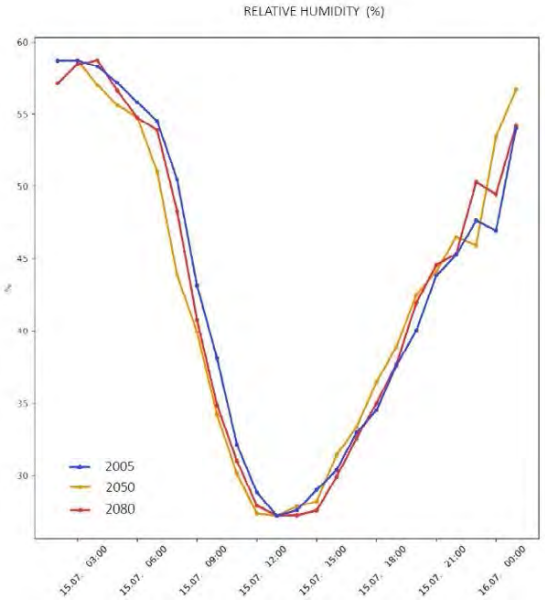

Figure 11: Comparison of relative humidity between contemporary climate, 2050 and 2080 with green roof

Figure 11 displays how relative humidity levels change when a green roof is implemented in the years 2050 and 2080, as compared to current data. Overall, relative humidity will decrease more in 2050 compared to 2080 and current when it arrives at 58%. Initially, there is a 3% decrease in 2050 and a 2% decrease in 2080. Throughout the day, the decrease in relative humidity is 3% and 2% for 2050 and 2080, respectively. There are some specific changes throughout the day, such as no difference at 12:00 am and higher levels in 2050 during the hours of 3:00 p.m. being this lower than 30%. to 9:00 p.m. In contrast, 2080 is only 1% higher during those same hours. During the night, relative humidity levels are lower in both 2050 and 2080, with 2050 being higher.
Based on Figure 11, there is a decrease in wind speed during the early morning hours and a noticeable increase during the daytime hours until nighttime, which is the same as the years 2005 and 2080.
It is worth noting that the wind speed during the afternoon hours, which are the hottest, has the most

significant increase. In 2050, the wind speed will increase by 0.05 m/s, while in 2080 it will increase by 0.1 m/s compared to current data. At 3:00 p.m. in 2080, the wind speed reached 2 m/s.

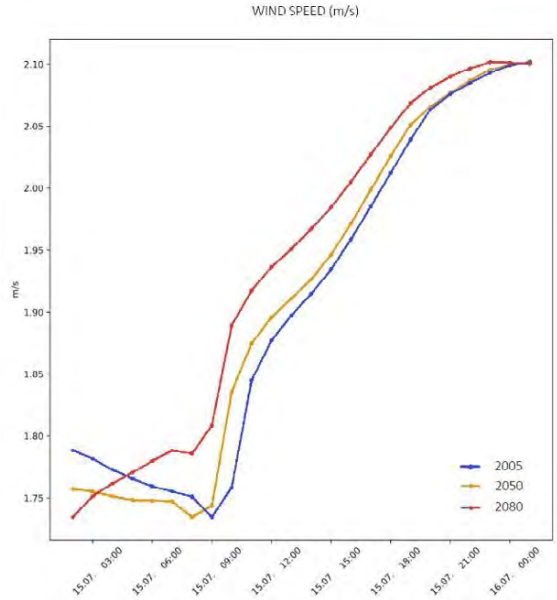

Figure 12: Comparison of Wind speed between contemporary climate, 2050 and 2080 with green roof

After conducting an analysis, it was observed that the green roof affected the relative humidity (RH) in comparison to the reference roof. On average, the RH on the green roof was higher due to its soil composition, which absorbs more rainwater and water during rainfall or irrigation. This feature promotes more evapotranspiration of water from green roofs, increasing the relative humidity in the surrounding air. The benefits of increased relative humidity levels are numerous, including reducing the risk of respiratory infections, reducing static electricity, and preventing wooden furniture from splitting. It can also aid in the prevention of airborne viruses and bacteria, which thrive in dry air. Moreover, increased relative humidity levels can make the air feel warmer, reducing the need for heating during colder months and, in turn, lowering energy expenses.

3.2 Physiological Equivalent Temperature (PET)

The Physiological Equivalent Temperature (PET) is a measure of the air temperature that balances the heat budget of the human body in a typical indoor setting, without wind and solar radiation. This temperature is the same as the core and skin temperature under the complex outdoor conditions being assessed. By analyzing the findings of the PET and evaluating current, 2050, and 2080 climate conditions, a concerning pattern becomes evident. There is an observed increase in temperature during the day and heat spreading throughout the city, attributed to the greenhouse effect.

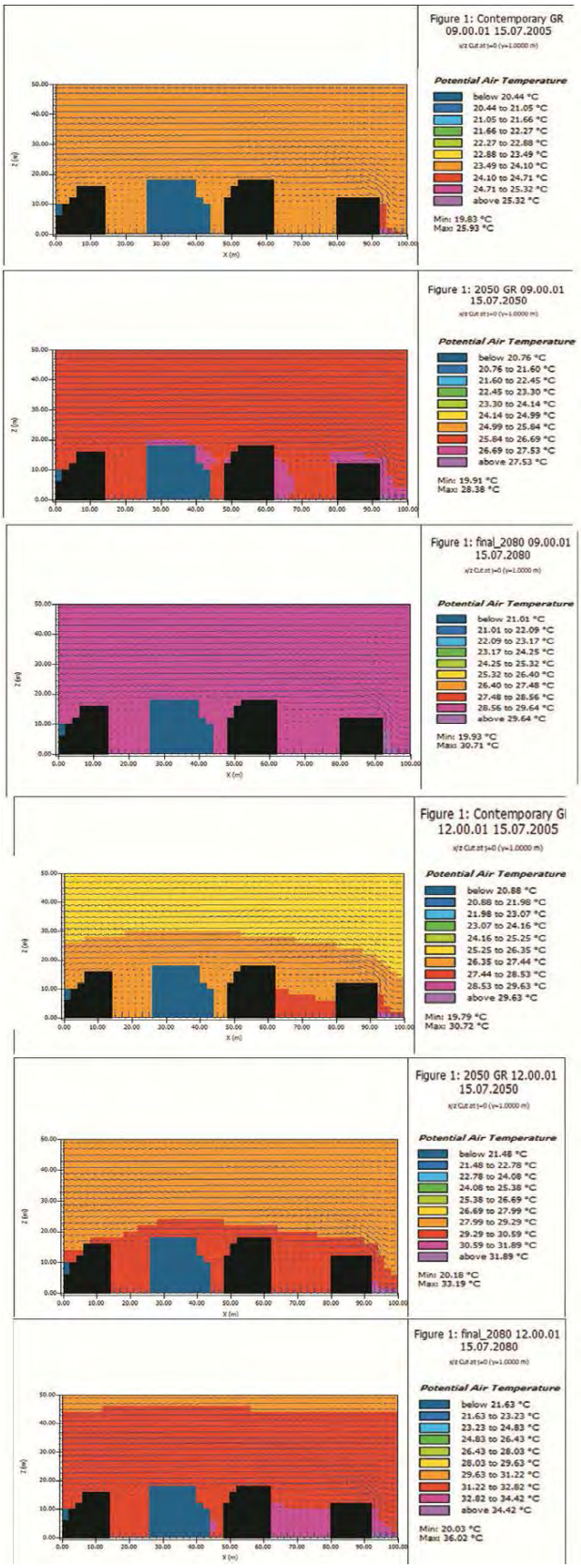

Figure 13: Temperature section, Greenhouse effect in Venizelou (Athens, Greece)

Figure 13 further illustrates this phenomenon, showing an increase in temperature during the day and heat spreading throughout the city. As temperatures continue to rise, there will be a growing

demand for microclimate-modifying components, such as green roofs. Therefore, it is critical to conduct urban planning studies to assess the impact of these changes on the climate and surroundings.

4. CASE STUDIES

This research focuses on the use of green roofs as a means of mitigation. The case studies examine how these changes are being implemented in a specific climate and city. To provide a clearer approach, a real project involving a green roof on the Ministry of Economics and Finance building in Athens, Greece is chosen. The green roof, which covers 650m² and 1.4 hectares, was installed on the rooftop of a ten-story building. The project aimed to study the impact of the green roof on thermodynamics in hot Athens. The building was constructed to provide a research roof to study the thermal effects of green roofs in Athens. The objective was to create a portable green roof to investigate the impact of rooftop gardens on biodiversity and the local microclimate, with the challenges of resilience, mitigation, biodiversity, and environmental quality in mind.[7]

There was a case study conducted in Turkey, which has a similar climate to Greece. The study aimed to investigate how green roofs impact microclimates and outdoor thermal comfort. It was carried out on a university campus and focused on determining whether green roofs can create a comfortable environment. The researchers surveyed users and used ENVI_met modelling to evaluate the influence of various roof terrace flooring materials on thermal comfort. The study found that green roofs and vegetation can help reduce high temperatures and improve outdoor thermal comfort on hot summer days. ENVI_met was used to estimate the effect of roof terrace flooring material on human thermal comfort. It was discovered that variation in flooring material can improve the outdoor thermal environment, depending on building geometry and the presence of trees. The comparison between trees and grass showed that trees improve thermal perception in the summer.[8]

5. CONCLUSION

This study aimed to assess the impact of green roofs on the microclimate of Athens. To achieve this, several case studies were analysed about the use of green roofs to combat urban heat islands (UHIs). The results of this study were encouraging and suggest that green roofs can be an effective solution. Further research is required to understand the necessary adaptations. The research indicates that the implementation of green roofs has a positive impact. This assertion is supported by observed changes in temperature, humidity levels, and wind speed between 2050 and 2080, which demonstrate the stabilization of temperatures compared to areas without vegetation cover. Although this study focused on rooftop alterations, it highlights the importance of wider building refurbishments, including walls and other architectural elements. The ultimate aim of this study was to demonstrate the impact of changes that can encourage the construction industry to reconsider its approach to resilience. It is hoped that the findings of this study will lead to further research and implementation of green roofs as a potential solution to combat urban heat islands.

REFERENCES

1. Santamouris, Matthaios, and Paul Osmond. “Increasing Green Infrastructure in Cities: Impact on Ambient Temperature, Air Quality and Heat-Related Mortality and Morbidity.” Buildings 10, no. 12 (2020): 233. https://doi.org/10.3390/buildings10120233.

2. Kitsopoulou, A., Bellos, E., Lykas, P., Vrachopoulos, M. G., & Tzivanidis, C. (2023). Multi-objective evaluation of different retrofitting scenarios for a typical Greek building. Sustainable Energy Technologies and Assessments, 57, 103156. https://doi.org/10.1016/j.seta.2023.103156

3. Battista, G., Mauri, L., Basilicata, C., & De Lieto Vollaro, R. (2016). Green Roof Effects in a Case Study of Rome (Italy). Energy Procedia, 101, 238-245. doi: 10.1016/j.egypro.2016.11.134

4. D. Mazzeo, N. Matera, G. Peri, G. Scaccianoce, "Artificial neural network for the prediction of green roof thermal behaviour in Mediterranean climate," Applied Thermal Engineering, vol. 222, p. 119879, Dec. 2022. Available online:
https://doi.org/10.1016/j.applthermaleng.2022.119879

5. Giannaros, Christos, Nenes, Athanasios, Giannaros, Theodore M., Kourtidis, Konstantinos, and Dimitrios Melas. "A comprehensive approach for the simulation of the Urban Heat Island effect with the WRF/SLUCM modelling system: The case of Athens (Greece)." Atmospheric Research 201, (2018): 86-101. Accessed June 21, 2023.

https://doi.org/10.1016/j.atmosres.2017.10.015.

6. Höppe, P. “The physiological equivalent temperature - a universal index for the biometeorological assessment of the thermal environment”. Int J Biometeorol, (1999) Oct;43(2):71-5

7. “The Green Roof of the Ministry of Economics and Finance.” Urban Nature Atlas. Published

October 2021. Accessed May 15, 2023. https://una.city/nbs/athens/green-roof-ministry-economicsand-

finance.

8. Bakovic, Mujesira & Gocer, Ozgur. (2017). ENVI_ met Modeling of green roof effects
on microclimate and outdoor thermal comfort.

PLEA 2024 WROCŁAW
(Re)thinking Resilience

Daylighting and Energy Optimisation in Tropical Offices
Performance of Climate Adaptive Kinetic Façades over Static Designs

FABIHA TAHMINA[1] MD ASHIKUR RAHMAN JOARDER[1]

[1]Department of Architecture, Bangladesh University of Engineering and Technology (BUET), Dhaka, Bangladesh

ABSTRACT: Energy consumption in tropical buildings is increasing rapidly due to solar heat gain and glare. Buildings are also affected by dynamic climatic factors, such as daylight and wind. Research showed that compared to static facades, climate adaptive kinetic facades offer potential opportunities for daylighting and energy efficiency by adapting to changing outdoor conditions. Most of the research in adaptive design has been conducted for temperate and seasonal climates, and little information is available on tropical climates. A few studies attempted simultaneous analysis of adequate daylighting, energy savings and energy generation. Little attention is provided in the context of Dhaka, where office buildings face high energy demands due to the popularity of the use of glass facades without shading and air conditioning for thermal comfort. This research aims to find out the optimised configurations of climate adaptive kinetic facades for office buildings in Dhaka by optimising daylighting and energy performance. The result of multi-objective optimisation showed the significant positive impact of kinetic facades and identified 12 different configurations, varying in shading depths (0.83 to 1.00 meters) and angles (1^{o} to 29^{o}) for 12 months. The study can potentially be useful for implementing climate adaptive kinetic façades in tropical office buildings.
KEYWORDS: Kinetic Facades, Heat Gain, Daylighting, Energy Performance, Office Buildings.

1. INTRODUCTION

The energy consumption in buildings accounts for approximately one-third of the total energy demand in the world and is expected to grow by 2.1% per year by 2040 [1]. Among diverse types of buildings, office buildings in tropical cities often have the maximum energy concerns due to the use of large glass facades and air conditioners, resulting in solar heat gain and glare. These results in high energy consumption and increased operational costs. Therefore, energy efficiency measures with optimised daylighting for office buildings are necessary [2].

The weather pattern shifts continuously, and pronounced seasonal variations are noticed. Daylighting and energy requirements are changing with the change in the outdoor environment. It can be argued that static passive building designs are not often effective for adequate daylight and energy efficiency. Relatively passive strategies and active technologies need to be integrated to achieve effective daylighting, reduce energy consumption, and increase the energy generation of office buildings [1,3]. By integrating photovoltaic films with the kinetic elements, the façade system can increase energy performance [4].

For the high temperature and humidity, glass façades trap heat and increase the energy demand for cooling in tropical cities [5]. In Bangladesh, the increased use of glass facades results in the creation of air-conditioned office spaces with artificial lighting, resulting in increasing energy demands. These induce the energy crisis and frequent power disruptions in Dhaka. As a result, both optimised daylighting and energy efficiency measures are urgently required for Dhaka city [5,6].

2. AIM AND OBJECTIVES

This study aims to determine the optimised configurations of the climate adaptive kinetic facades for daylighting and energy performance of office buildings in Dhaka. Objectives of the study are the following.

- To explore the effectiveness of climate adaptive kinetic facades under tropical climatic conditions.
- To find out the optimised configurations (angle and depth) for the south façade for office buildings in Dhaka.

3. LITERATURE REVIEW AND CASE STUDY

Climate adaptive kinetic facades consist of transformative elements that can change parameters, such as shape, size and angle, to adapt to the outdoor environment [7]. Studies showed that there are varying sky conditions and solar angles in tropical climates. Therefore, conventional static solar shading systems are less effective in ensuring adequate daylight and energy efficiency [6,7]. In tropical climates, climate adaptive kinetic facades can improve daylighting by reducing glare and saving energy use by 20-30% for commercial buildings. Kinetic photocells can produce 30-40% more energy than a fixed photocell by tracking the sun's position [8].

A study in Melbourne showed that climate adaptive facades can reduce energy consumption by 14.2% to 29% for office buildings. The study was based on computational optimisation by EnergyPlus and Eppy to show the comparative energy consumption of office buildings under a temperate climate [9]. Another research used parametric simulation and multi-objective optimisation by Rhinoceros, Grasshopper, Ladybug, Honeybee and Octopus showed the simultaneous optimisation of visual and thermal comfort achieved by adaptive facades for a hypothetical space in Tehran under an arid climate [10]. A residential building in Taiwan, which has a dynamic shading screen, was analysed under a tropical climate [11]. Research on readymade garments in Dhaka was done towards the path to net zero energy building using Rhinoceros, Grasshopper and ClimateStudio. The optimisation of thermal comfort and energy consumption provides an optimised result for static shading devices [12].

In Al Bahar Tower, Abu Dhabi, United Arab Emirates, the external kinetic façade reduces solar heat gain by 50% and cooling costs by 15%. The climate adaptive façade of GSW Headquarter, Berlin, Germany, controls heat gain, daylight and airflow and can reduce energy consumption by 40%. The climate adaptive kinetic façade of Q1 Thyssen Krupp Headquarter, Essen, Germany, can reduce glare and heat gain with improved daylight performance. Thus, it can maximise energy performance [13].

Research has already been conducted on climate adaptive kinetic facades in temperate and seasonal climates. Multiple examples of real-life applications in buildings are also available in those regions. Only a little research and hardly any application are available for tropical climates, particularly for Dhaka City [5-7, 12]. The knowledge of the effects of climate adaptive kinetic facades in tropical climates remains inadequate. Consequently, research on the application of this façade system for Dhaka is urgently required.

4. METHODOLOGY

A field survey was conducted to select a case building and collect data. Simulation analysis was incorporated for performance measures and comparisons. 3D modelling and multi-objective optimisation of daylighting and energy performance simulations were conducted by the Rhinoceros (version 7) with its plugins (e.g. Grasshopper, ClimateStudio, Octopus and Wallecei). Rhinoceros and its plugins are validated successfully for energy simulation [14]. Design Explorer was used for multi-objective optimisation considering maximum spatial daylight autonomy (sDA), minimum annual sunlight exposure (ASE), minimum energy use intensity (EUI) and maximum energy harvest. In this research, sDA measures the percentage of floor area in a building that receives standard daylight (300 lux) during office hours (9:00 AM to 5:00 PM). ASE measures the percentage of a floor area that receives direct sunlight exceeding 1000 lux for 250 hours in a year. The simulation procedure was conducted using Dhaka's weather data, which is available on the web in EnergyPlus weather (EPW) format [energyplus.net].

4.1 Selection of case building

The NCC Bank Head Office, located at Motijheel, Dhaka, Bangladesh, was selected as the case building by purposive sampling method. The building has an exterior shading system on a curtain glass façade oriented to the south (Fig. 1).

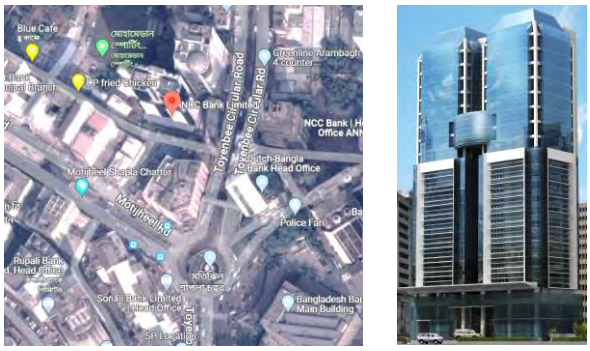

Figure 1: Google map location (L) and south elevation (R) of NCC Bank Head Office, Motijheel, Dhaka

The office building is situated at a latitude of 23.727° and a longitude of 90.421° in the context of tropical urban climate. In Dhaka, the annual average temperature is 26°C, and the average daily solar radiation is 4.65kWh/m^2. The temperature often increases above 40°C, and solar radiation increases above 5.5 kWh/sqm/day in the pre-monsoon period [15].

4.2 Field survey and data collection

Data about the geometry and dimensions of the shading devices were collected from the field survey (Fig. 2 and Fig. 3). There are two office blocks connected with a common service block. Both open office block's dimensions are 15 m x 15 m (Fig. 2). It is a 22-story building with shading devices on the 4th to 14th floors. There are two intermediate shading devices (500 mm) attached to the outer glass façade with extended floor planes (750 mm) (Fig.3).

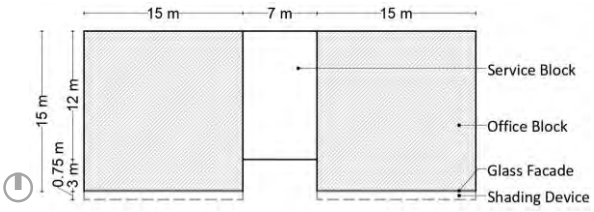

Figure 2: Basic zoning in typical floor layouts of the case office building

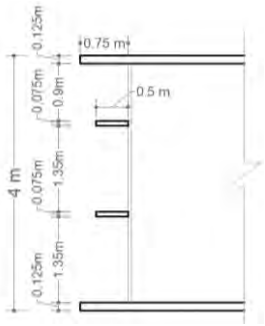

Figure 3: Typical schematic south façade section of the case office building

4.3 Creating 3D model

A 3D model was generated based on the field survey data using Grasshopper and Rhinoceros (Fig. 4). The multi objective simulation procedure was conducted for one office block to the east side (Fig. 2) located on the 4th floor of the case building oriented towards the south. The office space is considered to have an open-plan layout. On the south façade, four shading devices are considered outside the curtain glass façade (Fig. 3). The other three facades are considered to be solid and opaque.

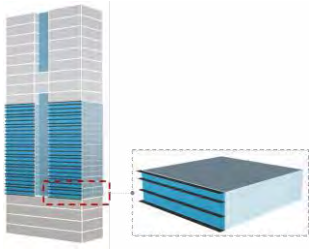

Figure 4: Case building model created in Rhinoceros (L) and space module (15m x 15m) of 4th floor (R)

4.4 Simulation

During simulation, the existing façade with existing shading devices was analysed first, considering the shadings as PV panels. After that, for the multi-objective optimisation, the shading devices were considered static and kinetic. The angle and depth were analysed for the kinetic façade system. Research showed that a maximum 30° tilt angle was optimum for energy harvest in the Dhaka context. Therefore, in this research, angles ranged from -30° to 30° and depth ranged from 0.3m to 1.0m [16]. The simulation methodology flow diagram is shown in Fig. 5.

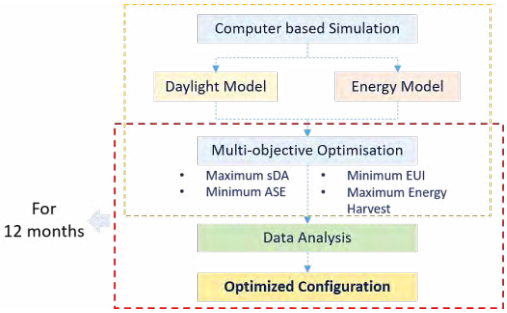

Figure 5: Methodology flow diagram for multi-objective optimisation

4.4.1 Daylight and energy modelling

Rhinoceros and Grasshopper were used to create the daylight and energy models for the simulation analysis. Detailed parameters with the generated model are shown in Table 1. The shadings are selected as PV panels to generate energy (Fig. 6).

Table 1: Basic Simulation Parameters

Indoor Space Parameters	
Room size	15m x 15m
Room area	225 m²
Floor level	12m above the ground
Shading façade orientation	South
Analysis grid	2 x 2 m
Working plane height	0.75 m

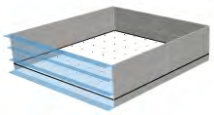

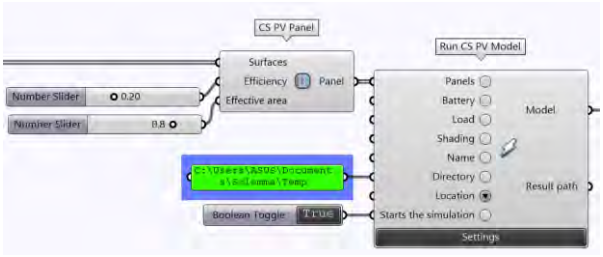

Figure 6: PV panel settings for simulation

4.4.2 Multi-objective optimisation

ClimateStudio was used to input weather data files for daylight and energy simulations. Daylight simulation provided the result of LEED credit, sDA and ASE (Fig. 7). Energy simulation provided the result of EUI, energy harvest data (the amount of energy harvested from the shading devices set as PV panels) and extra energy requirement (the gap between the EUI and energy harvest data) (Fig. 8). Octopus was used for multi-objective optimisation considering maximum sDA, minimum ASE, minimum EUI and maximum energy harvest (Fig. 9). The full script is shown in Fig. 10.

Figure 7: Daylight analysis result by ClimateStudio [LEED credit (L), sDA (M), ASE (R)]

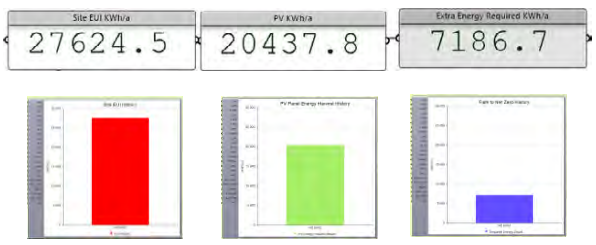

Figure 8: Energy performance analysis by ClimateStudio [EUI (L), energy harvest (M), extra energy required (R)]

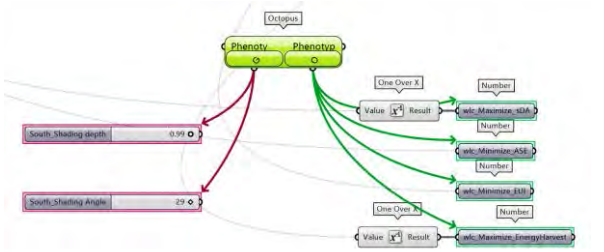

Figure 9: Multi-objective optimisation by Octopus

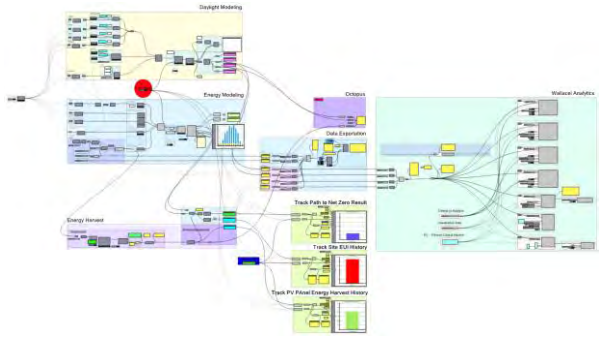

Figure 10: Grasshopper script for modelling, simulation and optimisation

The output data of Octopus was generated as an Excel file (Table 2). Finally, the output data was analysed in Design Explorer (Fig. 11, 12). The simulation procedure was conducted for annual average data, considering the shading as static for the whole year. The simulation process is conducted 12 times to find out the optimised configuration for 12 months of a year.

Table 2: Excel file created by Octopus and Wallecei

	in:Depth_South	in:Angle_South	out:sDA	out:ASE	out:EUI	out:EnergyHarvest
2	1	23	1	0	2567.4	1480.8
3	0.84	-20	1	0.2222	2615.9	1271.5
4	0.39	6	1	0.2099	2770.8	836.6
5	0.69	-14	1	0.2222	2647.4	1137.4
6	0.47	-24	1	0.2222	2695.8	893.7
7	0.91	-14	1	0.2222	2551.5	1351.8
8	0.9	23	1	0.037	2529.6	1382.2

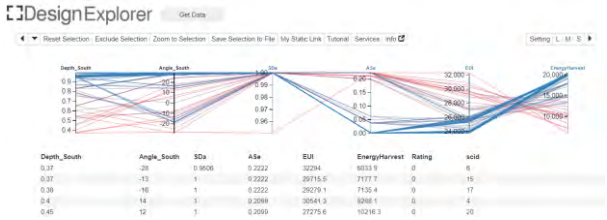

Figure 11: Design Explorer analysis using the Excel file

Figure 12: Optimised result considering the dependent variables

5. RESULTS

Results are presented in three portions: existing configurations, optimised static shading configurations and optimised kinetic shading configurations.

Firstly, the existing glass façade integrated with static shading devices was analysed. Secondly, the optimised shading configurations were analysed by multi-objective optimisation, considering the shading is static for the whole year. The simulation results, according to the annual average data, are shown in Table 3.

Table 3: Analysis results for the existing façade and optimised static façade configurations

Parameters	**Existing shading configurations**	**Optimised static shading configurations**
Depth (m)	0.75, 0.50, 0.50, 0.75	0.99
Angle (°)	0°	29°
sDA	1	1
ASE	0.1	0
EUI (kWh)	30112.2	27624.5
Energy Harvest (kWh)	12850.9	20437.8
Extra energy required (kWh)	**17261.3**	**3321.8**
3D model view	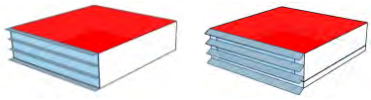	

The comparative results showed that after the optimisation of daylight and energy performance, the EUI is reduced from 30112.2 kWh to 27624.5 kWh and energy harvest is increased from 12850.9 kWh to 20437.8 kWh. Results showed that energy generation is increased to a greater number for the optimised static shading configurations.

Thirdly, when the façade is considered kinetic, rotating and scaling every month of a year, multi-objective analysis differs from one to another. For example, Fig. 13 and Fig. 14 show the Design Explorer analysis for January and February.

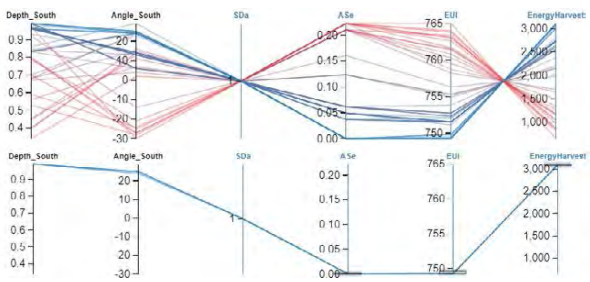

Figure 13: Design Explorer analysis for January

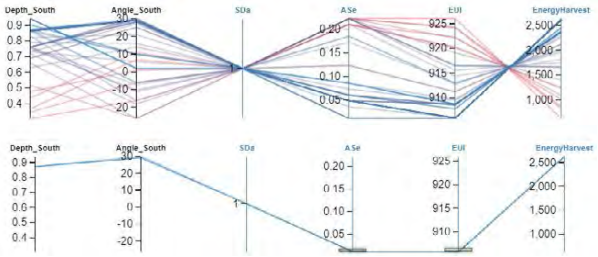

Figure 14: Design Explorer analysis for February

The optimisation analysed 50 iterations. Among them, considering maximum sDA, minimum ASE, minimum EUI, and maximum energy harvest, the optimum result for January showed that the depth should be 0.99m and that the angle should be 25° for the shading device. For February, the optimum depth was 0.87m, and the optimum angle was 29°. For two continuous months, the optimised depth and angle of shading varied from 0.99m to 0.87m and 25° to 29°.

The same simulation procedure was followed for 12 months of the year (Fig. 15). The summarised results for the studied 12 months are presented in Table 4. The results showed that after the optimisation of daylighting and energy performance, the optimised depth and angle of shading differed from month to month.

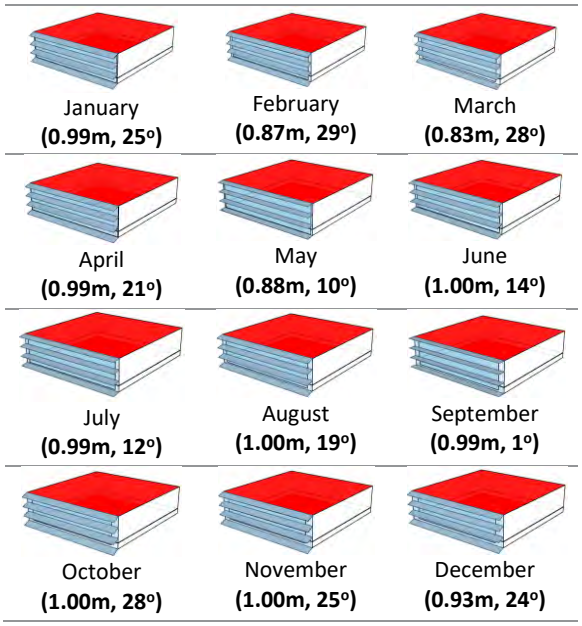

Figure 15: Depth (m) and Angle (°) of optimised results for climate adaptive kinetic shading for 12 months of a year

Figure 16 presents the summary of the three studied conditions: existing configurations, optimised static shading configurations and optimised kinetic shading configurations.

It is evident that the EUI of the existing façade system is the highest (30112.2 kWh) and requires more extra energy (17261.3 kWh) than the others. If the shadings are fixed for the whole year, 7186.7 kWh of extra energy is required. Supposing the shading is considered kinetic and rotating every month, the extra energy requirement is reduced to a greater degree and 914.4 kWh of energy is required for the specific office room, considering the climate of Dhaka. Energy requirements can be further reduced by analysing the optimised configurations for every day or even every hour of the year.

Table 4: Optimum depth and angle for shading device corresponding sDA, ASE, EUI and energy harvest values for kinetic façade.

Month	Depth (m)	Angle (°)	sDA (% area)	ASE (% area)	EUI (kWh)	Energy harvest (kWh)
Jan	0.99	25	1	0	749.2	3106.2
Feb	0.87	29	1	0.0123	905.9	2619.7
Mar	0.83	28	1	0.037	1698.2	2402.8
Apr	0.99	21	1	0	2303.6	1472
May	0.88	10	1	0.0494	2558.1	1160.6
Jun	1.00	14	1	0.0123	3259.8	1130.6
Jul	0.99	12	1	0.0494	3106.4	1081.8
Aug	1.00	19	1	0	3466.4	1578.7
Sep	0.99	1	1	0.0864	3007.6	1852.8
Oct	1.00	28	1	0	2473.2	2700.2
Nov	1.00	25	1	0	1407.8	2903
Dec	0.93	24	1	0	860.8	2874.2
			Total		**25797**	**24882.6**
			Extra energy required		**914.4** kWh	

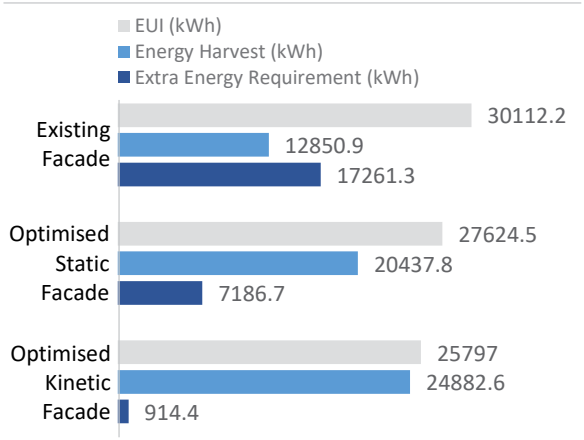

Figure 16: Analysis results for the three studied façade configurations

6. DISCUSSION

The literature review and simulation analysis provide a comprehensive picture of the effectiveness of using climate adaptive kinetic facades for daylighting and energy performance. The optimised configurations of the climate-adaptive kinetic façade system for the south façade of the case office buildings were analysed in the context of Dhaka. The results showed 12 different depths and angles of shading for 12 months throughout the year to reduce the extra

energy requirement while maintaining effective daylight. The static shading device cannot make the best use of daylighting and energy consumption throughout the year. Thus, an optimum solution is essential for every month, even for days and hours, to achieve energy efficient building solutions.

Shifting from static shading devices to climate adaptive kinetic facades that can rotate and change dimensions according to external weather conditions is apparent. Different studies have shown that office buildings are rapidly growing with glass facades, artificial lighting, and air conditioners, which results in high energy demands in tropical climates such as Dhaka. The existing office buildings with larger glass facades in the south direction can be renovated with external climate adaptive kinetic facades. The future office buildings can also be designed accordingly. Successful application of climate adaptive kinetic façade is vital for adequate daylighting and energy efficiency.

While numerous studies and examples are available for temperate climates, only a little study has been found for tropical climates. Therefore, the knowledge acquired by the literature review and case studies is limited to climates different from those in tropical regions. Due to software and time constraints, there are limitations to input diversified data available from the surroundings. Time constraints lead this research to focus on optimisation on a monthly basis instead of analysing individual days.

7. CONCLUSIONS

The necessity of considering the climate adaptive kinetic façade system as an alternative to the traditional static shading systems has been acknowledged throughout this study. This study will help the architects and create the opportunity to think of future façade designs for office buildings. This study can be the basis for further research on using and implementing climate adaptive kinetic facades for different types of buildings, particularly office buildings in tropical climates. Future research can be conducted by including several optimisation options, such as LEED credit, illuminance level, and glare analysis, and increasing the variables such as material, rotation axis, aesthetic, and technical requirements.

ACKNOWLEDGEMENTS

This paper is based on the research done in the Department of Architecture, Bangladesh University of Engineering and Technology (BUET), Dhaka, Bangladesh. The authors gratefully acknowledge the support provided by BUET.

REFERENCES

1. Mahmoud, A. H., Dewidar, M. and Ahmed, S. (2022). The role of intelligent facades in energy conservation. In *International Conference on Sustainability and the Future*. Cairo, Egypt, December 13-15.

2. Al-Masrani, S. M., Al-Obaidi, K. M., Zalin, N. A. and Isma, M. I. A. (2018). Design optimisation of solar shading systems for tropical office buildings: Challenges and future trends. *Solar Energy*, *170*: 849–872.

3. Rodriguez, C. S. and D'Alessandro, M. (2014). Climate and Context Adaptive Building Skins for Tropical Climates: a review centered on the context of Colombia. In *Advanced Building Skins*. Bresssanone, Italy, October 28-29.

4. Jayathissa, P., Caranovic, S., Hofer, J., Nagy, Z. and Schlueter, A. (2018). Performative design environment for kinetic photovoltaic architecture. *Automation in Construction*, *93*: 339–347.

5. Bari, N. (2020). The Impact of Building Facade on Cooling Efficiency and Related Thermal Comfort for West Oriented Offices in Dhaka City. Thesis (M.Arch). Department of Architecture, Bangladesh University of Engineering and Technology (BUET), Dhaka, Bangladesh.

6. Rana, J., Hasan, R., Sobuz, H. R. and Tam, V. (2020). Impact assessment of window to wall ratio on energy consumption of an office building of subtropical monsoon climatic country Bangladesh. International Journal of Construction Management, 22(3): 1-26.

7. Ahmad, J. and Alibaba, H. Z. (2019). Kinetic façade as a tool for energy efficiency. *International Journal of Engineering Research and Reviews*, 7: 1-7.

8. Ramzy, N., and Fayed, H. (2011). Kinetic systems in architecture: New approach for environmental control systems and context-sensitive buildings. *Sustainable Cities and Society*, *1*(3): 170–177.

9. Bui, D. K., Nguyen, T. N., Ghazlan, A., Ngo, N.-T. and Ngo, T. D. (2020). Enhancing building energy efficiency by adaptive façade: A computational optimisation approach. *Applied Energy*, *265*, 114797.

10. Rizi, R. A., and Eltaweel, A. (2021). A user detective adaptive facade towards improving visual and thermal comfort. *Journal of Building Engineering*, *33*, 101554.

11. Dow, B. H. (2020). Applications of Dynamic Shading Screens for Residential Buildings in Taiwan. Thesis (M.Arch). University of Washington, Seattle, Washington.

12. Joarder, M.A.R., Hossain, M.M., Bach, A.J.E., Palutikof, J.P. and Tonmoy, F. (2022) Optimisation of Thermal Comfort and Energy Consumption in Bangladesh Readymade Garment Factories: An Approach towards the Path to Net Zero Energy Buildings. In Hviid, C.A., Khanie M.S. and Petersen S. (Eds.). *E3S Web of Conferences 362.*

13. Edupuganti, S. R. (2013). Dynamic Shading: An Analysis. Thesis (M.Arch). University of Washington, USA.

14. Cachat, E. T. and Goia, F. (2020). Co-simulation and validation of the performance of a highly flexible parametric model of an external shading system. *Building and Environment*, *182*, 107111.

15. Rahman, A. (2007). Performance Evaluation of Shading Devices Used in Tall Office Buildings of Dhaka City. Thesis (M.Arch). Department of Architecture, Bangladesh University of Engineering and Technology (BUET), Dhaka, Bangladesh.

16. Ghosh, H. R., Bhowmik, N. C. and Hussain, M. (2010). Determining seasonal optimum tilt angles, solar radiations on variously oriented, single and double axis tracking surfaces at Dhaka. *Renewable Energy.* 35(6): 1292-1297.

PLEA 2024 WROCŁAW
(Re)thinking Resilience

Performance Based Dynamic Shading Module

Exploring fold adaptive mechanisms for tropical office façades

HASIBUL HOSSAIN[1], NISHAT JAHAN ITU MIAJI[1], MD ASHIKUR RAHMAN JOARDER[1]
[1]Department of Architecture, Bangladesh University of Engineering and Technology (BUET), Dhaka, Bangladesh

ABSTRACT: Rising energy consumption in tropical buildings, driven by solar heat gain and glare, necessitates innovative design solutions. Despite extensive research, a gap still needs to address unique tropical challenges. This study focuses on dynamic shading to combat radiation and energy issues. Beginning with an existing case building, it considers local context and environmental analysis, progressing to dynamic shading design using evolutionary tools and parametric scripting. These shadings adapt to climatic conditions, improving daylighting and energy efficiency. The research involves a physical model with photo-sensitive dynamic shading, demonstrating adaptive mechanisms. It is further virtually utilized by the multi-objective optimization simulation approach to the case office building to quantify the performance. The research studied multiple alternative linear actuator vertical displacements in the shading module ranging from 0-50 cm for January and identified that 47.5 cm is the ideal depth for effective performance. This paper presents a unified design strategy for enhancing indoor environmental quality in tropical office spaces. The findings highlight the potential of climate-adaptive dynamic shading, particularly for office buildings in Dhaka. It contributes to sustainable urban design, advocating using adaptive shading technology in tropical regions to balance energy efficiency with aesthetics.
KEYWORDS: Dynamic Shading, Tropical Architecture, Multi-Objective Optimisation, Energy Efficiency, Sustainable Design

1. INTRODUCTION

Building design confronts significant challenges in tropical climates, notably managing high solar radiation, ensuring adequate ventilation while minimizing heat gain, and coping with high humidity. Traditionally, buildings in tropical areas used natural ventilation to keep a comfortable indoor environment. Before the 21st century, air conditioning was rarely used because it uses more energy than passive cooling. Recent trends in tropical cities (e.g., Dhaka) show a shift towards Western architectural styles, marked by extensive use of glass façades in commercial buildings, which inadvertently has led to heightened energy consumption [1].

The widespread use of glass façades in Dhaka has resulted in unintended consequences. The root of the problem lies in the intense solar radiation that penetrates the glass, significantly raising indoor temperatures. To combat this, occupants often close blinds or curtains, which reduce heat and diminish daylight. Furthermore, closing windows to mitigate glare and solar radiation eliminates the possibility of natural ventilation, exacerbating the indoor heat. This situation compels more reliance on artificial lighting and cooling, leading to heightened energy consumption and electricity costs [2]. The increased energy usage worsens Dhaka's existing energy issues, further complicating the city's efforts to fulfil its electricity requirements. It is crucial to promptly adopt efficient daylight utilization and energy conservation strategies in Dhaka to tackle the city's severe energy challenges [3]. Dynamic shading can reduce heat gains and glare, enhancing thermal and visual comfort. They alter heat exchanges via the building's screen and lower yearly solar radiation. The dynamic façade has a favourable impact on the building's energy performance regarding heating, cooling, ventilation, and lighting [4]. Responsive dynamic shading can increase building energy efficiency by changing its behaviour and features by utilizing stimulus-responsive materials and intelligent control systems that can make a significant and valuable contribution to the success of the building system as a whole [5].

Climate-adaptive dynamic shading has emerged as an innovative solution, significantly enhancing energy efficiency, daylighting, and occupant comfort across various climates [6]. Despite their proven effectiveness in temperate and seasonal settings, a noticeable gap exists in understanding their performance in tropical environments such as Dhaka. A study in Melbourne demonstrated that dynamic shading could reduce energy consumption by 14.2% to 29% using EnergyPlus and Eppy [7]. Another study in Iran has focused on optimizing smart shading blinds for office buildings. Utilizing EnergyPlus and jEPlus + EA with NSGA-II for the optimization process, the goal was to decrease energy consumption, reduce discomfort, and lower glare, thereby enhancing energy efficiency and occupant comfort. The findings revealed energy savings ranging from 2.8% to 47.8% and notable reductions in glare and discomfort, showcasing the advantages of improved shading control in building performance [8]. Real-world applications further validate their benefits: the Al Bahar Tower in Abu Dhabi significantly reduced solar

heat gain by 50% and cooling expenses by 15% [9]. These advancements have yet to be fully realized in tropical settings, such as Dhaka, where high costs and challenges in controlling daylight deter their adoption, emphasizing a substantial research and application gap.

This paper aims to bridge the said gap by showcasing the capabilities of dynamic shading in tropical regions. We present a comprehensive design strategy, including integrating fold-adaptive mechanisms, solar responsiveness, and Arduino IDE, aiming to refine shading performance while reducing energy demands. The development and demonstration of a fully functional prototype under this research illustrate the practical implementation of the dynamic shading concept, setting a precedent in sustainable architectural solutions tailored for the unique challenges of tropical climates.

2. METHODOLOGY

To ground our research in real-world scenarios, we initiated our study by selecting an actual room within an existing office building as our case study. An office building was chosen for our research because office buildings often have a high percentage of glass surfaces. These glass facades, while aesthetically pleasing and good for visibility, also lead to significant challenges in terms of energy efficiency and solar heat absorption [10]. Furthermore, it is observed that densely built high-rise commercial areas in Dhaka tend to experience higher temperatures compared to districts with varied types of architecture, underscoring the relevance of office buildings for this research [11].

Upon opting for the room, we deployed advanced analysis technologies. Rhinoceros for precise 3D modelling and Grasshopper for algorithmic design allowed us to simulate daylight and energy performance [12]. We used ClimateStudio to evaluate and improve our models based on critical performance criteria. Octopus was pivotal in automating optimal solution selection. This stage was essential for analyzing energy use intensity (EUI), spatial daylight autonomy (sDA), annual sunlight exposure (ASE), mean illuminance level, spatial disturbing glare (sDG), daylight glare probability (DGP) and human comfort with predicted percentage of dissatisfied (PPD) [13]. Informed by the insights garnered from our simulations and optimizations, we then developed a shading concept—a fold-adaptive responsive shading designed to enhance energy efficiency and indoor comfort. This shading was strategically designed to lower EUI, maximize sDA, reduce ASE, improve illumination, and ensure optimal human comfort. Its adaptability to changing environmental conditions showcases a balance between indoor light quality and energy efficiency.

To validate the practicality and effectiveness of our design, we constructed a physical prototype showcasing the dynamic, light-responsive exterior shading. This step illustrated how fold-adaptive mechanisms and solar responsiveness, managed through Arduino IDE, can be applied in natural settings. The successful implementation of the prototype underlines the design's potential to reduce energy consumption and enhance indoor comfort. The findings of this research demonstrated the substantial benefits of combining computational tools with responsive design to achieve sustainable, efficient, and comfortable building environments.

3. CASE STUDY SELECTION

For our case study, we selected the corporate office building of Bank Asia Limited, located in Gulshan, Dhaka (Figure 1). We intentionally chose this building for its west-facing orientation, highlighting the challenges of tropical climates. The western facade, subjected to intense afternoon sunlight, presents increased cooling needs and glare, significantly impacting occupant comfort and productivity.

Figure 1: Corporate office building of Bank Asia Limited, Gulshan, Dhaka.

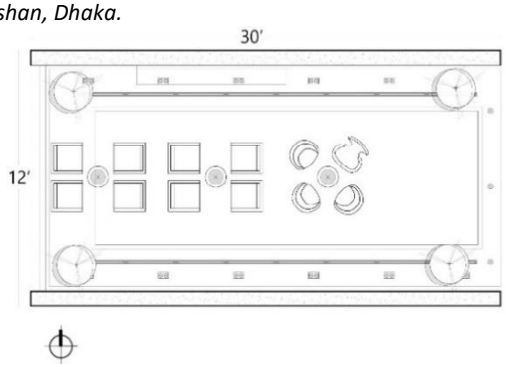

Figure 2: The case office room on the 3rd floor of the case building

An office area on the third level (Figure 2) with a glass facade on its west side caught our attention. This space has office walls on the north and south sides and an aperture on the east side. The exclusive west exposure intensifies solar gain, making natural illumination questionable. This position and the

room's deep floor layout make daylight distribution challenging. This design makes the room a good example for studying office daylighting and energy efficiency, revealing flexible strategies that improve comfort while reducing energy use.

4. SHADING DESIGN

The study focused on developing a dynamic shading module specifically for tropical office buildings, aiming to address the limitations of fixed glass facades. Traditional shading devices often fail to adapt to varying sunlight throughout the day, leading to excessive light, causing glare and overheating, or insufficient light, necessitating artificial lighting.

The term "static performance" describes the typical issue with these systems: their inability to respond to changing weather conditions, which can compromise comfort and increase energy consumption. A flexible shading system was designed to resolve these issues. This system features a modular design with individual pieces that adjust autonomously, allowing for precise control of sunlight entering the building. Daylight simulation was used to determine the best placement for each module, ensuring optimal light conditions and energy efficiency. This approach is not only expected to reduce the building's energy usage but also will enhance occupant comfort by providing a more adaptable shading solution.

4.1 Façade Design Process

The design incorporates a fold-adaptive mechanism, activated by sunlight intensity, which triggers the linear actuator's vertical movement and the consequent folding of the plate. The actuator can move within a range of 0 to 50 cm (Figure 3). This movement allows for angles up to 30 degrees between the folded plates, providing precise control over the penetration of light.

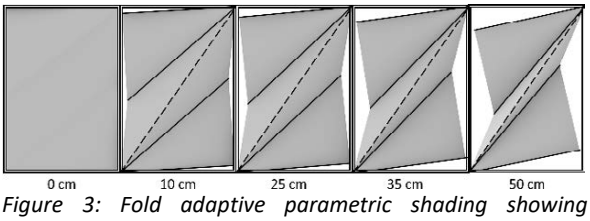

Figure 3: Fold adaptive parametric shading showing opening based on linear actuator movement.

The shading system utilizes an origami-inspired, fold-adaptive mechanism, enhancing functionality by mimicking the transformative nature of paper folds. This functionality is crucial for the module's dynamic response to environmental changes. Renowned for its quick and precise adaptations, this technology is essential for regulating the indoor environment. The module, compact and efficient, measures 0.9 meters in length and 0.5 meters in width (Figure 4).

A complex linear actuator system drives the module's fundamental mechanism. These actuators must be strategically moved to manipulate the module's triangle folding panels. The constructed panels may tilt from 0 to 30 degrees. This angular modulation dynamically forms façade openings, regulating natural light into the building interior. These apertures are sensitively tuned to sunlight intensity, interacting with the light resistor to balance visibility and thermal comfort.

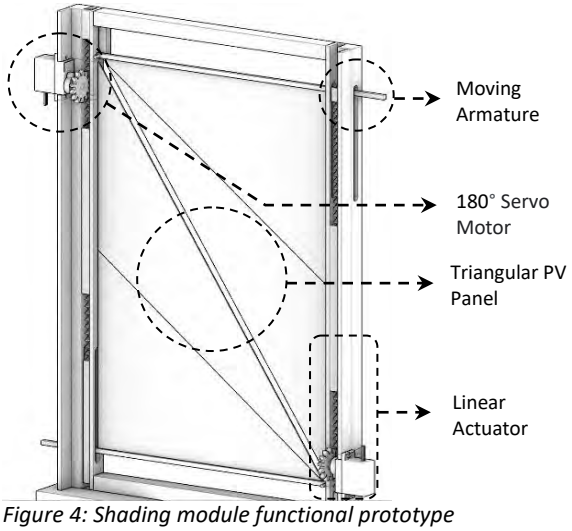

Figure 4: Shading module functional prototype

Integrating the open-source Arduino Software (IDE) platform is an essential component of the system's functionality, as it acts as the central control mechanism for the linear actuator system. The utilization of Arduino IDE (Figure 5) highlights the advanced technological capabilities of the module, enabling accurate manipulation and flexibility in controlling the movements of the façade. This integration not only improves the operational efficiency of the module but also provides a foundation for future customizations. Figure 6 shows photos captured during real-scale shading experimentation in the studio setting. Figure 7shows impression of the elevation of the full-scale façade generated from proposed dynamic module.

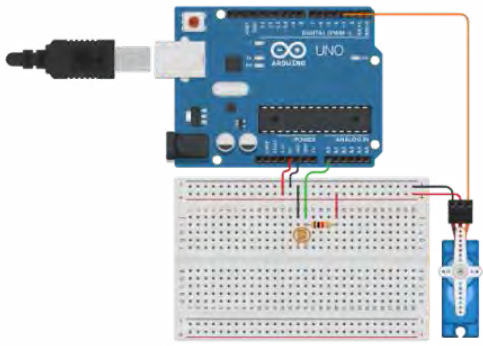

Figure 5: Arduino IDE mechanism with a photoresistor and servo motor.

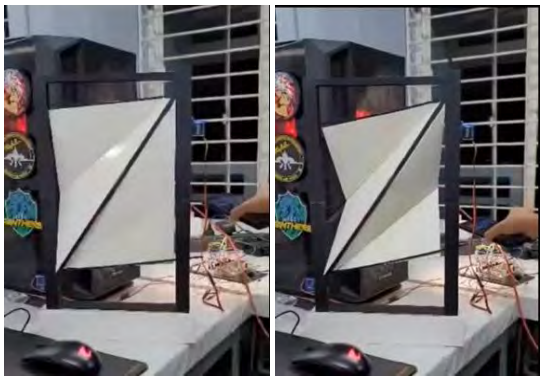

Figure 6: Real-scale dynamic shading experimentation in the studio setting.

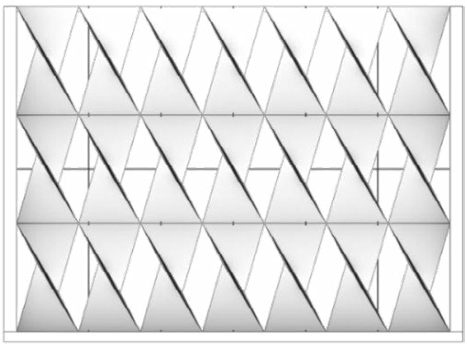

Figure 7: Elevation of full-scale façade generated from proposed dynamic module.

4.2 Multi Object Optimisation

Table 1 presents the indoor space parameters. Simulations were conducted to compare the proposed dynamic shading system (Figure 8 [R]) with typical static shading (Figure 8 [L]), both designed for west-facing orientations, using the specific case office room. The static shading comprised clear sun gate 400 (krypton) glass with wooden louvers measuring 2.75m x 0.25m x 0.02m, oriented at a 45-degree angle. In contrast, the dynamic shading system utilizes metalized fabric panels.

Table 1: Indoor space parameters

Room size	*9 m x 3.65 m*
Floor level	10 m above the ground
Shading façade orientation	West
Sensor Spacing	0.2 m x 0.2 m
Working plane height	0.75 m

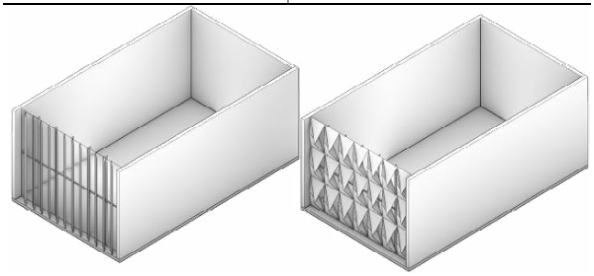

Figure 8: Daylight and energy models with typical static shading suitable for west orientations [L] and with the modified dynamic façade [R].

ClimateStudio was used to input weather data files into daylight and energy simulations. Figure 9 displays the results of the LEED Credit, sDA, ASE, and mean illuminance level for static shading appropriate for west orientations. The Octopus plugin was used for multi-objective optimization, accounting for the lowest EUI and ASE, the maximum sDA, and the mean illuminance level (Figure 10).

Figure 9: The outcome of static shading suitable for west orientations.

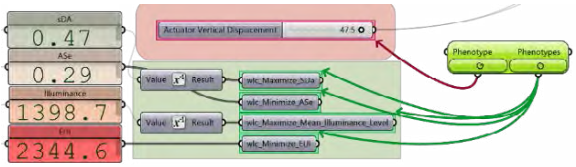

Figure 10: Multi-objective optimization script for Octopus.

The Octopus generates output data as an Excel file (Table 2). The optimization examined 100 iterations considering the maximum sDA, mean illuminance level, minimum ASE and EUI. The analysis determined that the optimal depth for the linear actuator displacement in January was 47.5 cm. Figure 11 shows the values for modified dynamic shading.

Table 2: Excel file created by Octopus for modified façade.

In: Actuator Displacement	*Out: EUI*	*Out: sDA*	*Out: ASE*	*Out: Illuminance*	*Out: Extra Energy Required*
50	1690.78	1	0.17	1117.5	696.67
25	1911.03	0.29	0	384.02	916.95
02	2285.01	0	0	4.15	1291.6
47.5	1702.87	0.93	0.13	1398.7	708.65
38.5	1727.06	0.59	0.03	774.09	732.99
26	1908.01	0.32	0	410.09	913.85
8.5	1920.69	0	0	603.48	897.15
44	1842.31	0.83	0.05	944.93	848.24
16.5	1914.25	0.03	0	181.7	920.13
40.5	1909.82	0.66	0.04	837.55	915.64
21.5	1984.37	0.02	0	295.67	788.73
48	1852.79	0.97	0.13	1070.9	858.67
33	1891.27	0.46	0	603.48	897.15
05	2293.07	0	0	18.49	1299.2

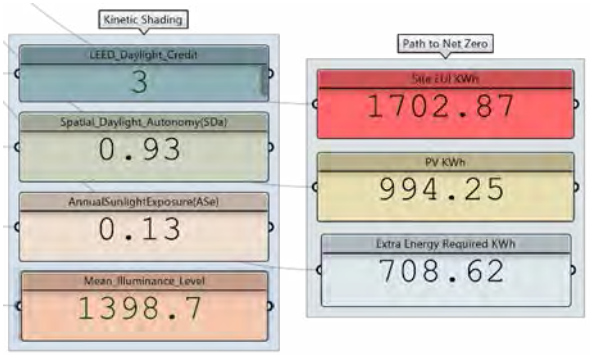

Figure 11: The outcome of dynamic shading recommended for west orientations.

4.3 Comparison

The static shading configuration (i.e. consistent shading throughout the year) exhibited a higher EUI of 2344.6 kWh compared to the kinetic shading configuration (i.e. adjustable to change with weather conditions), which had an EUI of 1702.87 kWh (Figure 12), achieving a 27% overall reduction. The PV panel harvest capacity showed that the kinetic shading configuration generated 994.25 kWh of energy, surpassing the 745.68 kWh generated by the static shading configuration. This highlights the superior energy harvesting capability of the kinetic shading configuration, contributing to its lower EUI. When considering the extra energy required beyond what is harvested by PV panels, the static shading configuration demanded 1598.92 kWh, while the kinetic shading configuration required 708.62 kWh (Figure 13). This suggested that the kinetic shading configuration was more self-sufficient in meeting its energy needs, requiring less additional energy. These insights underscore the superior energy efficiency and self-sustainability of the kinetic shading configuration compared to the static shading configuration. Energy demands can be further reduced by tweaking the configuration of the shading on a daily or even hourly basis throughout the year.

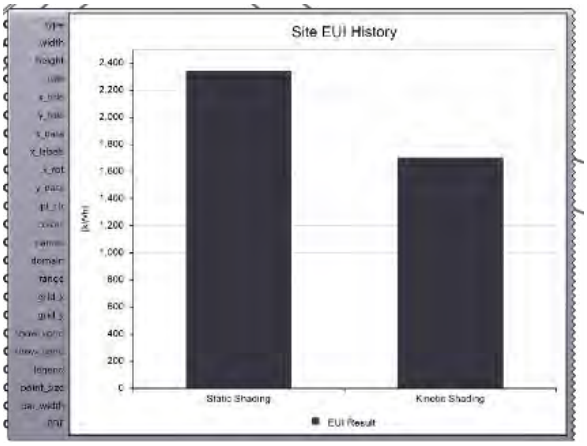

Figure 12: EUI comparison for static and dynamic shading configurations.

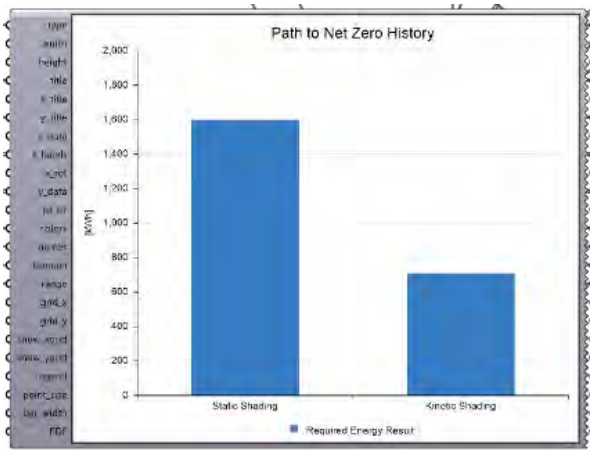

Figure 13: Required extra energy comparison for static and dynamic shading configurations.

The dynamic shading system significantly improved sDA from 0.47 to 0.93 and decreased ASE from 0.29 to 0.13. The mean illuminance level increased from 1046.39 to 1398.7, indicating improved daylight availability (Figure 14).

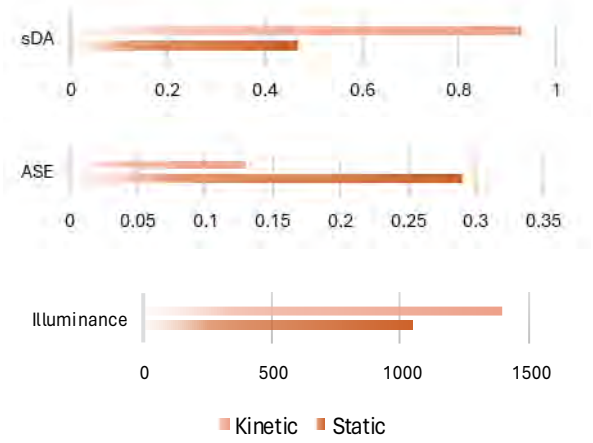

Figure 14: Comparison of daylight performance metrics between static and dynamic shading configurations.

Further analysis of glare and spatial thermal comfort revealed advantages of the dynamic shading system. While the static shading had intolerable glare at 32.4%, the dynamic shading reduced it to 14.1% (Figure 15 and Figure 16).

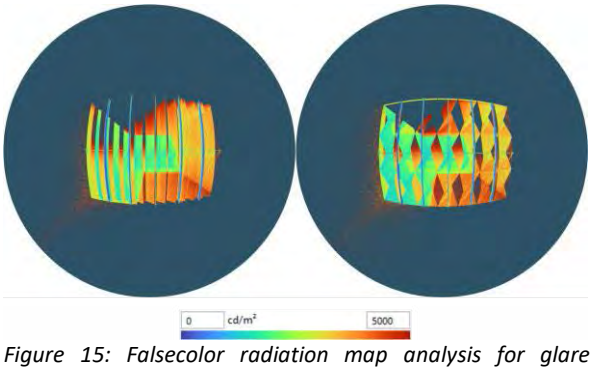

Figure 15: Falsecolor radiation map analysis for glare comparison for static [L] and dynamic [R] shading configurations on 15th March at 09:30 am.

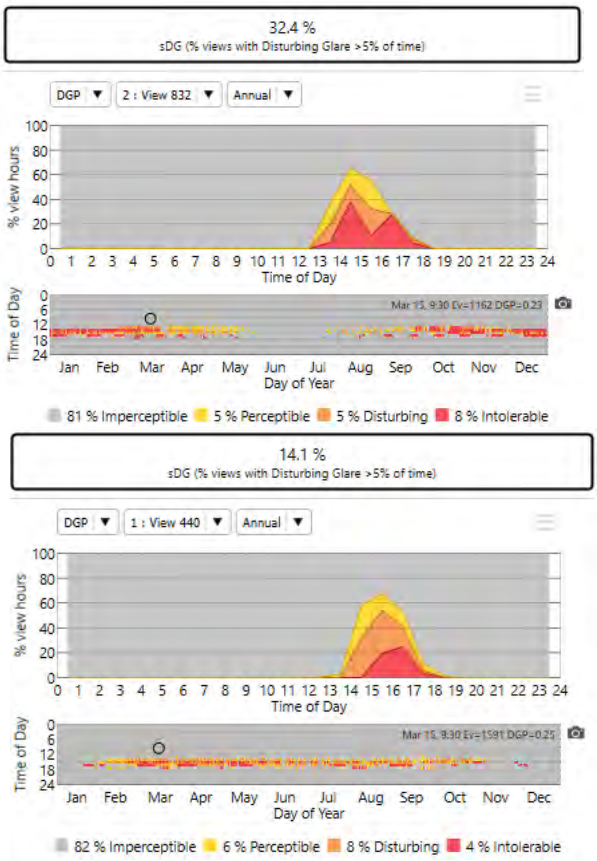

Figure 16: Spatial disturbing glare (sDG) and daylight glare probability (DGP) for static [top] and dynamic [bottom] shading configurations.

Similarly, the static shading exhibited a PPD value of 22.6 for thermal comfort, whereas the dynamic shading lowered it to 15.4 (Figure 17). The reduced PPD value does not comply with American Society of Heating, Refrigerating and Air-Conditioning Engineers (ASHRAE) standard 55-2020; however, it complies with Bangladesh Standard [10].

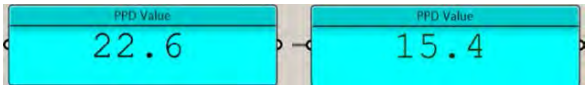

Figure 17: PPD analysis comparison for static [L] and dynamic [R] shading configurations.

5. CONCLUSIONS

The research examined various alternative linear actuator vertical displacements within the shading module, spanning from 0 to 50 cm, specifically for the month of January. The study concluded that a vertical displacement of 47.5 cm emerged as the optimal depth for achieving effective performance. This paper outlines a strategy to improve the indoor environmental quality of office spaces in tropical climates, showcasing the benefits of climate-adaptive shading. It contributes to sustainable urban design by promoting the use of adaptive shading technology in tropical regions.

ACKNOWLEDGEMENTS

This paper is based on the research done in the Department of Architecture, Bangladesh University of Engineering and Technology (BUET), Dhaka, Bangladesh. The authors gratefully acknowledge the support provided by BUET.

REFERENCES

1. Bari, N. (2020). The Impact of Building Facade on Cooling Efficiency and Related Thermal Comfort for West Oriented Offices in Dhaka City. Thesis (M.Arch). Department of Architecture, Bangladesh University of Engineering and Technology (BUET), Dhaka, Bangladesh, p. 17-18.
2. Amin, A. (2019). Façade design for energy-efficient buildings: analysis of architectural façades through functionality and simplified forms approach, The Architectural Science Association (ANZAScA) Conference.
3. Rana, J., Hasan, R., Sobuz, H. R. and Tam, V. (2020). Impact assessment of window to wall ratio on energy consumption of an office building of subtropical monsoon climatic country Bangladesh. *International Journal of Construction Management*. 22(3): p. 1-26.
4. Hassooni A. and Kamoona G. (2023). Effects of Kinetic Façades on Energy Performance: A Simulation in Patient's Rooms of a Hospital in Iraq. *Journal of the International Society for the Study of Vernacular Settlements*. 10 (7).
5. Wanas, A., Aly, S., Farghal, A., and El-Dabaa, R. (2015). Use of kinetic facades to enhance daylight performance in office buildings with emphasis on Egypt's climate. *Journal of Engineering and Applied Sciences*. 62(1), p. 339-361.
6. Hartman, P., Cehel'ová, D., Bielek, B. (2019). Principal solutions for sustainable adaptive Façades providing suitable indoor environment for inhabitants. *Appl. Mech. Mater*. 887, p. 435–442.
7. Bui, D.-K., Nguyen, T. N., Ghazlan, A., Ngo, N.-T., and Ngo, T. D. (2020). Enhancing building energy efficiency by adaptive façade: A computational optimization approach. *Applied Energy*. 265, p. 114797.
8. Naderi, E., Sajadi, B., Behabadi, M. A., Naderi, E. (2020). Multi-objective simulation-based optimization of controlled blind specifications to reduce energy consumption, and thermal and visual discomfort: Case studies in Iran. *Building and Environment*. 169, 106570.
9. Karanouh, A., and Kerber, E. (2015). Innovations in dynamic architecture. *Journal of Facade Design and Engineering*. 3, p. 185-221.
10. Aman, J., (2017). Impact of windows for daylighting on thermal comfort in architecture design studios in Dhaka (M.Arch. Thesis). BUET, Dhaka.
11. Ahmed, Z. N., (1994). Assessment of Residential Sites in Dhaka with respect to Solar Radiation Gains, PhD thesis, De Montfort University, UK.
12. Ratajczak, J., Siegele, D., Niederwieser, E. (2023). Maximising Energy Efficiency and Daylight Performance in Office Buildings in BIM through RBFOpt Model-Based Optimization: *The GENIUS Project. Buildings*. 13(7), 1790.
13. Showkatbakhsh, M., Kaviani, S. (2021). Homeostatic generative design process: Emergence of the adaptive architectural form and skin to excessive solar radiation. *Int. J. Archit. Comput.* 19, p. 315–330.

PLEA 2024 WROCŁAW
(Re)thinking Resilience

Sustainable 3D Modular Social Housing

Process- and Energy-Efficient Construction

KINGA RACOŃ-LEJA[1] ANNA PORĘBSKA[1] BARTŁOMIEJ HOMIŃSKI[1] KRZYSZTOF BARNAŚ[1]

[1]Cracow University of Technology, Kraków, Poland

ABSTRACT: This paper presents a brief overview of major developments made over the course of the Process- and Energy-Efficient Construction project's social housing track, which was aimed at developing a technology package that would combine 3D modular construction with the latest in energy efficiency and climate change mitigation. The project culminated in a proposal of a technology demonstrator building, which has been constructed and, as of the writing of this paper, was waiting for its first tenants to move in. We outline the major contributions and advancements made to both the technologies forming the package and how they play to each other's strengths within the package, resulting in a comprehensive offering of environmentally friendly social housing. The package was centered around the RESHeat system, which was coupled with a selection of environmental and building services solutions targeting indoor comfort and rainwater and stormwater retention.
KEYWORDS: modular housing, sustainability, energy efficiency, process efficiency

1. INTRODUCTION

This paper presents a proposal of a sustainability-focused approach to collective housing design which involves the use of 3d modular construction solutions coupled with energy generation and storage, energy-saving and low-carbon-footprint material solutions as well as rainwater retention solutions integrated with the building's green surroundings. The proposal was initially drafted and later developed as a part of a research-to-application project entitled Energy- and Process-efficient Construction which received funding from the Polish National Centre for Research and Development (NCBR) and culminated in the design and construction of a technology demonstration building completed at Karola Miarki Street in Mysłowice, Poland. The proposal was developed as a part of the project's social housing track.

The proposal presented was selected as a part of a three-stage competition process as outlined in the Project Regulation [1], in which it cleared all three stages and was selected as the sole winner.

1.1 Relevance and literature review

The proposal presented in this paper was formulated as a response to a specific set of guidelines put forth by the funding institution. The intent behind these guidelines was to produce an actionable and repetitive solution to Poland's housing shortage [2] while adhering to high energy standards, whose improvement has been dubbed insufficient in the literature [3]. The energy system employed in the proposal was based on the output of the RESHeat project, which was initially modeled for the energy retrofit of relatively new [4, HH5] (also with a technology demonstrator) and 1970s post-communist housing stock [6] sectors of Poland, and the NCBR project was deemed as a good fit for exploring the system's capabilities in new housing.

The project is therefore a part of a string of larger efforts to bring a comprehensive energy-efficiency and climate-friendliness technology package, and is therefore relevant to contemporary academic discourse.

1.2 Project background

The NCBR adapted the program for the purposes of social housing for rent, for which there is demand in Poland [17]. The proposal was formulated to meet a set of very strict and highly specific criteria provided by the funding institution. These ranged from number and size of the apartments (27 apartments, 15 with a minimum floor area of 45 m², suitable for a family of three, and 12 with a minimum floor area of 60 m² suitable for a family of four), to spatial layout (smaller ones with a kitchenette, smaller ones with a separate kitchen, larger ones with a kitchenette, and larger ones with a separate kitchen), to built-in elements of the reference building to be constructed as a technology demonstrator. These conditions were intended by the funding institution to ensure applicability within Polish urban settings, and upon analysis were found suitable for application in low-density housing areas typical of Polish housing estates. The conditions also allowed for comparing different proposals submitted by other applicants (consortia) in the project's early proposal submission phase.

The proposal was evaluated based on energy efficiency, carbon emissions, material recycling and reuse as well as the cost of the building. Site plan and architectural design quality were also assessed. It was critical to provide solutions that could reduce all on-site works to as few as three months. The solution proposed by the consortium, formed by DMD Modular p.s.a. (project leader and main implementation entity), Lightoffo sp. z o.o. (partner) and the Cracow University of Technology (research institution), was selected for the application stage. At the time of the writing of this paper, the first implementation of the technology, namely the technology demonstrator, has been completed and awaits for the first tenants to move in.

The proposal aims to alleviate key problems that currently affect Polish housing. These problems include:

- A pervasive housing shortage in general and that of apartments suitable for families with children, people with special needs, and seniors in particular, coupled with a steep rise in property prices, which, when combined with the influx of refugees fleeing from the Russo-Ukrainian War, has negatively affected the availability of affordable housing [28];
- Climate change associated phenomena such as the increased incidence of droughts and flash floods, which creates greater demand for on-site water retention [39];
- Rising average temperatures, long-lasting heat waves [39] and biome shifts;
- A wider and deeper implementation of sustainability goals, including, but not limited to, greywater treatment, on-site energy generation and storage, zero-energy and zero-carbon housing;
- The need for the top-down transfer of advanced building technologies and smart solutions such as Building Management Systems (BMS), which are necessary to control energy-efficient buildings, to affordable housing;
- The transfer of knowledge about and awareness of our impact on energy consumption as individuals, to enhance more sustainable habits among the general population.

2. METHODOLOGY

The proposal was formulated, prepared and assessed based on the methodology imposed by the funding institution and specified in Appendices 1 and 4 to the Project Regulation [10, 11] and were grouped into qualitative and quantitative architectural, environmental, energy and building services requirements. These requirements were supplemented with detailed methodology and verification guidelines and were assessed by the funding institution at the end of each competition stage. Each stage culminated in a report that each participating consortium submitted to the institution.

The authors did not have access to the reports by other entrants and therefore no meaningful comparison was possible during the writing of this paper. The Regulation, its Appendices and the funding institution's final assessments in the form of a final score for each stage are available on the project's website.

2.1 Trade secret clause

Many of the solutions featured in the proposal are company trade secrets of DMD Modular p.s.a. and Lightoffo sp. z o.o. and therefore could not be published here.

3. MAJOR ELEMENTS OF THE PROPOSAL

The proposal was formulated to leverage the capabilities and know-how of the consortium that included industry and academic entities, and to deliver a set of technological solutions that could be used to quickly and efficiently erect zero or energy-plus multi-family residential buildings.

The project leader, who as a company has significant experience in delivering 3D modular single-family and hotel buildings both in Poland and abroad, but had not previously had multi-family buildings in its portfolio, developed a dedicated version of its 3D modular technology. The implementation partner was responsible for smart solutions, including digital tools that allow users to monitor their individual carbon footprint, and the concept of managing production, distribution, heat recovery and energy storage systems. The CUT's interdisciplinary team was responsible for formulating the building's energy supply system, which utilized a diverse array of heat reservoirs / low-temperature heat sources, including ground heat exchangers [12], along with heat recovery from each building services system [13], the integration of technological solutions with architectural and urban design solutions, as well as building design alternatives (research by design), qualitative solutions for climate change adaptation (including an analysis of various forms of rainwater and stormwater retention and the capture of water from torrential rains, and alternative means of improving the water balance [14, 15]), in addition to a multi-criteria analysis aimed at selecting the best of the alternatives formulated.

3.1 Flexibility enhancements

One of the main disadvantages of 3D modular construction is it can make standardized plans inflexible and hard to adapt [16]. The proposed technology aimed

to alleviate this by allowing for greater flexibility and prototyping.

In buildings like hotels or dormitories, the housing unit is typically fully contained in a two-bay module (room–hallway) or in a three-bay module (room–hallway–room). This also concerns building services distributed via shafts, typically located between a bathroom and a hallway. The consortium set out to develop a version of 3D modular technology based on a steel frame that would allow for the module boundary to be crossed and to build multi-module housing units while maintaining high process effectiveness while reducing the scope of on-site work to a minimum.

To ensure wider applicability, the consortium proposed flexible module layouts to enhance the potential for introducing a wide range of custom configurations, which means that more spatial situations are now suitable for buildings based on the proposed technology. In addition, the proposed module configurations were optimized to ensure that the highest possible percentage of the building's structure consists of 3D modules and to minimize standard structural elements that require on-site construction, such as stairwells, that were replaced with prefabricated concrete technologies.

In the project's second stage, two versions of the technology were developed. The open version enabled changing the stratification of each story and provided freedom in selecting the number of apartments of a given type in future projects. The closed version focused on the maximum optimization in terms of the assumptions of the funding institution, which acted as a project sponsor in line with the mass customization principle, namely adapting the technology to a specific project. The production and on-site assembly optimization featured a building layout in which kitchens and bathrooms were placed in service modules, so-called wet modules, while the residential spaces were placed in dry modules. This solution, due to eliminating a portion of on-site fit-out works, was found to be optimal in terms of assessment criteria.

The funding institution also tasked the competition participants with ensuring that apartments could have their interiors rearranged. The CUT team proposed solutions that allowed for the adaptation of all the apartments to wheelchair-bound persons with special needs and to seniors, although this was not a specific requirement. All the design alternatives were compliant with universal design principles and widely understood accessibility to persons with special needs. Keeping in mind the experience of the Covid-19 pandemic, all the apartments were designed so that the number of rooms corresponded to the number of users, and so that each user would have access to a dedicated work zone. Attention was also paid to providing suitably large rest and dining areas, in which the residents could spend time together.

The integration of user perspectives in every aspect of the building's operation with technical and technological solutions allowed for attaining the target level of energy and process efficiency without compromising the quality of living spaces. The apartments were also designed to be adaptable to changing user needs.

The scalability of the proposed solutions was analyzed on an architectural and urban scale. The potential for the construction of low- and mid-rise buildings in core-, corridor- and gallery-type buildings, infill buildings, and of vertical building extensions was found.

Another benefit of the proposed technology is its compatibility with essentially all currently available facade finish technologies. On the one hand, it allows for the use of the most cost-efficient solutions, which does lower process efficiency, such as the light wet method, and offers freedom in adapting the building's appearance to the character of its neighborhood, local traditions or climate specificity (clinker cladding, wooden siding, etc.).

3D modular technology based on steel frames can cooperate with all foundation types. In the case of the technology demonstrator building, which was located in an area suffering from subsidence due to underground mining and non-continuous faults, it was necessary to use indirect footing in the form of piles that connected directly to the modules, without a reinforced concrete slab or beam grid. This indicates that buildings using the proposed technology can be constructed in essentially any soil conditions.

3.2 Sustainable building services

A range of sustainability-focused building services solutions were incorporated into the proposal. The proposal of the building's energy-efficiency systems consisted of:

- combining a variety of low-temperature heat sources / temperature heat reservoirs such as vertical solar collectors, underground thermal storage, heat recovery from mechanical ventilation and plumbing;
- the development of high-performance ground-sourced heat regeneration and boreholes, which meant that the heat pump's EER coefficient does not drop over the course of the building's operation;
- passive indoor cooling supported by cooling from dedicated ventilation units with heat recovery;

- cooling using air heat exchangers (stage 2) or capillary matting (stage 3);
- a system of cascade domestic hot water heating during periods with low insolation;
- underground thermal storage for heating and cooling, allowing the storage of the thermal energy of water, ranging from high temperatures to zero degrees Celsius, that can operate in sub-zero temperatures using the latent heat of freezing;
- electrical energy storage coupled with electric vehicle charging stations as elements of distributed electrical energy storage systems;
- greywater purification system with heat recovery [6], with an efficiency that eliminates the need to flush toilets with potable water;
- rainwater and stormwater retention tanks and rain gardens that can capture water from torrential rains, including from neighboring areas [614, 715].

A total of fifteen boreholes for vertical ground heat exchangers were created for use by the building, with a total length of 1500 m, which factored in the limited effectiveness to a depth of ca. 15 m. The planned borehole density, confirmed by TRT ground tests, allowed for the use of a narrow strip of stable soil and the keeping of most of the site's pre-existing trees.

3.4 Occupant wellbeing

A key project requirement was to ensure temperature comfort not only in terms of code-compliant minimal indoor temperature, but also ensuring cooling during summer. Innovative ventilation units with heat recovery were designed for this purpose, adapted for fitting in service ducts. Indoor sensors control both temperature, air humidity and pollutant concentration.

To limit the energy required for attaining thermal comfort, additional external covers were added to prevent overheating during summer, as well as external textile covers from high-insulation materials. Both systems are steered by the building's energy management systems, and when a user wants to override the system, they are informed how this will alter energy consumption.

The integration of residential spaces with the site played an essential role in the demonstrator building's conceptual design. The technology that allowed for minimum interference with pre-existing greenery, a compact massing with a beneficial A/V coefficient (0.37) and energy storage in the multi-element power system allowed for large, floor-to-ceiling glazing, thanks to which the residential interiors open towards balconies with support structures for climbing plants and offer a view of the building's green surroundings.

The proposal also consisted of a range of solutions intended to enhance occupant wellbeing, and generally associated with creating a pleasant housing environment around the building. These features included:

- A quiet recreation zone, insulated by trees and featuring a meandering path delineated in such a way as to create small, intimate spaces;
- A loud recreation zone that is open and can accommodate a range of open-air activities such as those typical of a playground, a calisthenics exercise yard, and chess tables.

The common spaces featured in the design are to contribute to forming neighborly ties. The decision not to fence the property, which went against the requirement of the funding institution, and incorporating the building into the pre-existing pedestrian circulation system was intended to not only integrate new and current residents, but is also a voice against the gated community model that had embedded itself into the Polish landscape.

Figure 1: The technology demonstrator building during construction, prior to external facade finish application; photo courtesy of DMDmodular p.s.a.

The Covid-19 pandemic and the full-scale invasion of Ukraine by Russia have contributed to the redefinition of what gives us a sense of safety. In this context, the building, which is self-sufficient in terms of energy, lowers potable water consumption, allows for the storage of rainwater and stormwater and its use, and in which residents have full control over resource consumption, gives these residents a sense of control and empowerment. It is also a potential key to building resilient communities.

3.5 Carbon footprint minimization guidelines

Due to the use of steel framing elements in the modular components of the building other avenues of carbon footprint minimization had to be sought [817]. Reuse of post-demolition materials among which discarded brick to be used for the facade or wooden siding boards to be incorporated on site were taken into consideration. Unfortunately, none of the materials recovered on the construction site or other construction sites in the area was suitable for implementation due to poor quality and/or contamination.

The embodied carbon footprint of the volumetric modular technology based on steel framing is balanced, to some extent, by the use of recycled steel and the structure remaining a recyclable material. One of the features of the technology is that construction waste from panel materials is minimized and is limited to interior finishes such as wall cladding and flooring. Construction waste from gypsum boards, OSB boards, chipboards and insulation materials is minimized during the shop drawing stage.

The optimization of the building and minimization of the number of modules allowed to reduce the cost of transports. Furthermore, the 3D module technology implemented in the design allows for the disassembly and reassembly of modules in either an identical or different configuration. This solution was a requirement of the funding institution.

4. DISCUSSION

The technology demonstrator developed by the design and research team presents a sustainability-focused approach to collective housing while implementing a range of guidelines set by the funding institution while also adding additional enhancements.

Over the course of research and development in stages 2 and 3 of the project, a high adaptation potential to local project determinants was found. The model three-story building, designed for two hypothetical plots that met the requirements set by the funding institution during the application submission stage was, over the course of a few weeks, adapted to a four-story version and a forested plot with complex soil conditions.

The building offers public housing for rent – it is affordable, inclusive, energy-plus multi-family housing and is within reach of current technology readiness levels. As a collective housing building that can be built quickly it can become key to attaining resilient and adaptable urban settlements. This takes on a key significance in the light of the Ukrainian refugee crisis spurred on by the Russo-Ukrainian War [18].

The building offers social housing that can be rented out by the municipality – it is affordable, inclusive, energy-positive multi-family housing that is within reach of current technology readiness levels.

As intended, the solution is suitable for low- and mid-rise development. The surface area of photovoltaic panels and solar collectors per square meter and resident remains a problem, as is the shade of the plot. Due to evapotranspiration and minimizing the urban heat island effect, the building should be sited in a green context, especially in an area with trees. Dual panels, which offer photovoltaic functionality with heat recovery, as well as tracking panels, could be an alternative solution here. we are also aware that photovoltaic panel solutions are becoming increasingly effective.

4. CONCLUSIONS

Resilience is a concept introduced back in the 1990s when narrowly understood sustainability was discovered to be inefficient in making cities last in the face of economic, demographic, and environmental crises, along with climate change and rapid urbanization [19]. Derived from physics and engineering, resilience refers to the (potential) “ability of an urban system—and all its constituent socio-ecological and socio-technical networks across temporal and spatial scales—to remain or rapidly return to desired functions in the face of a disturbance, to adapt to change, and to quickly transform systems that limit current or future adaptive capacity” [20].

Adaptability, flexibility, inclusiveness and empowerment as precepts for building a resilient built environment formed a framework into which the CUT team strived to fit the design. The coming months and years, when the demonstrator building will be subjected to tests, and the data from its systems will be analyzed, when we will be listening to its users and investigate their satisfaction levels, will verify the results. However, it appears that in the face of the energy crisis and the worsening consequences of climate change, reorienting the housing sector towards energy-efficient, zero-energy buildings should be done without delay.

ACKNOWLEDGEMENTS

The authors would like to thank the National Centre for Research and Development for funding this research as a part of Commission no. 84/20/PU/P79 – Process- and Energy-Efficient Construction and the city of Mysłowice (strategic partner) as well as to the implementation entities: DMD Modular p.s.a. and Ewelina Woźniak-Szpakiewicz, PhD (project leader), Lightoffo sp. z o.o. and Dariusz Stolarczyk. Special thanks go to the remaining members of the interdisciplinary team of the Cracow University of Technology team not listed as authors: Prof. Paweł Ocłoń, Prof. Elżbieta Radziszewska-Zielina, Prof. Michał Zielina, Marzena Nowak-Ocłoń, PhD, DSc, Izabela Godyń PhD, Bartosz

Dendura, PhD, Olga Kania, PhD, Grzegorz Ojczyk, PhD, Filip Suchoń, PhD, Bartłomiej Szewczyk, PhD, and Grzegorz Śladowski, PhD.

REFERENCES

1. Narodowe Centrum Badań i Rozwoju (2020). Regulamin przeprowadzenie postępowania nr 84/20/PU/P79 o udzielenie zamówienia na usługi badawczo-rozwojowe w ramach Przedsięwzięcia: „Budownictwo efektywne energetycznie i procesowo", [online], Available: https://www.gov.pl/web/ncbr/8420pup79---budownictwo-efektywne-energetycznie-i-procesowo [25 April 2024].
2. Barchoń, K.; Ciesielski, T.; Bobrzyński, M. (2021). *What's behind the boom? Changes in the Polish housing market*, [Online], Available: https://www.pwc.pl/pl/pdf-nf/2022/PwC_Report_What_is_behind_the_boom.pdf (24 April 2024).
3. Attia, S.; Kosiński, P.; Wójcik, R.; Węglarz, A.; Koc, D.; Laurent, O. (2022). Energy efficiency in the polish residential building stock: A literature review. *Journal of Building Engineering*, 45, 103461, [Online], Available: https://doi.org/10.1016/j.jobe.2021.103461, [30 April 2024].
4. Vallati, A.; Fiorini, C.V.; Grignaffini, S.; Ocłoń, P.; Di Matteo, M.; Kobylarczyk, J. (2023). Energy retrofit optimization for social building in temperate climate zone. *Energy and Buildings*, 282, 112771, [Online], Available: https://doi.org/10.1016/j.enbuild.2023.112771 [25 April 2024].
5. Yildirim, M.A.; Bartyzel, F.; Vallati, A.; Woźniak, M.K.; Ocłoń, P. (2023). Efficient energy storage in residential buildings integrated with RESHeat system, *Applied Energy*, 335, 120752, [Online], Available: https://doi.org/10.1016/j.apenergy.2023.120752, [30 April 2024].
6. Barnaś, K.; Jeleński, T.; Nowak-Ocłoń, M.; Racoń-Leja, K.; Radziszewska-Zielina, E.; Szewzcyk, B.; Śladowski, G.; Toś, C.; Sabev Varbanov, P. (2023). Algorithm for the comprehensive thermal retrofit of housing stock aided by renewable energy supply: A sustainable case for Krakow. *Energy*, 263, Part D, 12774, [Online], Available: https://doi.org/10.1016/j.energy.2022.125774 [25 April 2024].
7. Przymeński A. (2021). Mieszkalnictwo socjalne w Polsce w procesie zmian. *Ruch prawniczy, ekonomiczny i socjologiczny*, Year LXXXIII, z. 3: 355-372, [online], Available: https://doi.org/10.14746/rpeis.2021.83.3.23 [20 December 2023].
8. Trojanek, R. and M. Głuszak, (2022). Short-run impact of the Ukrainian refugee crisis on the housing market in Poland. Finance Research Letters, 50: 103236, [Online], Available: https://doi.org/10.1016/j.frl.2022.103236 [30 August 2023].
9. Narodowe Centrum Badań i Rozwoju (2020). Załącznik nr 1 do regulaminu – wymagania: obligatoryjne, opcjonalne, konkursowe i jakościowe, [online], Available: https://www.gov.pl/web/ncbr/8420pup79---budownictwo-efektywne-energetycznie-i-procesowo [25 April 2024].
10. Narodowe Centrum Badań i Rozwoju (2020). Załącznik nr 4 do Regulaminu – Harmonogram Przedsięwzięcia, opis Wyników Prac Etapu oraz założeń testów, [online], Available: https://www.gov.pl/web/ncbr/8420pup79---budownictwo-efektywne-energetycznie-i-procesowo [25 April 2024].
11. AA.VV. (2021) Climate Change in Poland: Past, Present, Future. Falarz, M. (Ed.). Springer. https://doi.org/10.1007/978-3-030-70328-8.
12. Ocłoń, P., (2021). Renewable Energy Utilization Using Underground Energy Systems. In *Lecture Notes in Energy*, 84, [Online], Available: https://doi.org/10.1007/978-3-030-75228-6 [30 August 2023].
13. Nagpal, H., J. Spriet, M. Krishna Murali and A. McNabola, (2021). Heat Recovery from Wastewater—A Review of Available Resource. *Water*, 13(9): 1274, [Online], Available: https://doi.org/10.3390/w13091274 [30 August 2023].
14. Vijayaraghavan, K., B.K. Biswal, M. Gerrit Adam, S. Hong Soh, D.L. Tsen-Tieng, A.O. Davis, S. Hoe chew, P. Yok Tan, V. Babovic, and R. Balasubramanian, (2021). Bioretention systems for stormwater management: Recent advances and future prospects. *Journal of Environmental Management*, 292: 112766, [Online], Available: https://doi.org/10.1016/j.jenvman.2021.112766 [30 August 2023].
15. Vaculová, V. and J. Fuska, (2017). Rain gardens – Case study of potential locations identification using GIS. *Acta Scientiarum Polonorum: ormatio Circumiectus – Kształtowanie Środowiska*, 16(2): p. 217–230, [Online], Available: https://doi.org/10.15576/ASP.FC/2017.16.3.217 [30 August 2023].
16. Ghannad, P. and L. Yong-Cheol, (2022). Automated modular housing design using a module configuration algorithm and a coupled generative adversarial network (CoGAN). *Automation in Construction*, 139: 104234, [Online], Available: https://doi.org/10.1016/j.autcon.2022.104234 [30 August 2023].
17. Huisingh, D., Zh. Zhang, J.C. Moore, Q. Qiao and Q. Li, (2015). Recent advances in carbon emissions reduction: policies, technologies, monitoring, assessment and modelling. *Journal of Cleaner Production*, 103: p. 1–12, [Online] Available: https://doi.org/10.1016/j.jclepro.2015.04.098 [30 August 2023].
18. Milert, M., Nowak, K., Sroka, B. (2022). Kwestia mieszkaniowa a kryzys uchodźczy. Wspólne wyzwania i rozwiązania dla równoważenia sektora mieszkalnictwa w Polsce, In K. Nowak, H. Milewska-Wilk (Eds.), Mieszkalnictwo i polityki społeczne. Raport o stanie polskich miast. Warszawa-Kraków - Instytut Rozwoju Miast i Regionów.
19. Porębska, A., Rizzi, P., Otsuki, S., Shirotsuki, M. (2019) Walkability and Resilience: A Qualitative Approach to Design for Risk Reduction. *Sustainability*, 11(10): 2878, [Online], Available: https://doi.org/10.3390/su11102878 [30 August 2023].
20. Meerow, S.; Newell, J.P.; Stults, M. Defining Urban Resilience: A review. *Landsc. Urban. Plan.* **2016**, *147*, 38–49 [Online] Available: https://doi.org/10.1016/j.landurbplan.2015.11.011 [30 August 2023].

PLEA 2024 WROCŁAW
(Re)thinking Resilience

Earthen architecture

The rammed earth walls as a sustainable resource in architecture

Dominga Zuleica Chávez Pérez [1], Jorge Armando Ojeda Sánchez[1], Javier Esparza López[1]
José Ricardo Moreno Peña[2]

[1]Universidad de Colima, Colima, México.
[2] Tecnológico Nacional de México, campus Colima, Colima, México.

ABSTRACT: The use of land in construction, ancestrally present in civilizations, is experiencing a resurgence today due to the environmental and economic benefits. Current research seeks to reintegrate it to address housing issues, especially in vulnerable areas. The UN highlights the importance of reducing CO2 emissions in buildings, with land being an ecological option. Construction systems with earth are explored, focusing on the rammed earth, its process, and benefits. Although it is not common in warm subhumid climates, its application is considered in rural homes in Colima, Mexico. The study includes testing of materials and construction methods. The results indicate feasibility for the construction of rural housing in Colima with rammed earth walls. These have good thermal, acoustic and fire resistance behavior. Environmental and economic benefits are highlighted, with significantly lower CO2 emissions compared to conventional materials. A rural housing design is proposed based on the analysis of local needs and resources. The conclusion highlights the relevance of the use of local materials for sustainability and accessibility in housing construction.
KEYWORDS: Earth, rammed earth, wattle and daub, bamboo, housing.

1. INTRODUCTION

Earth is one of the most used materials in the architectural development of ancient civilizations. Earthen constructions dating back to 7,000 BC have been discovered [1]. Construction systems with earth present characteristics depending on the degree of humidity and the manufacturing process; Notable examples include adobe and rammed earth.

Currently, construction systems with earth have been falling into disuse due to various social, economic, and technological phenomena in the construction industry. However, thanks to the emergence of new materials, earth or clay still offers important environmental, economic and health benefits to users.

Currently, various research efforts are being developed on earth construction and its reintroduction into current architecture as a response to current housing challenges, especially invulnerable areas.

According to the United Nations [UN], 38% of CO2 emissions are derived from the operation and construction of buildings [2]. This includes the manufacturing process of materials such as steel and cement, transportation, execution, and operation of buildings. The UN set goals to raise awareness about the conscious use and management of natural resources, as well as the adoption of technologies [3], with the aim of combating climate change applied in different fields, in this case, construction.

Finally, in Mexico, the issue of low-carbon construction has potential, since it can follow paths towards the decarbonization of the construction sector, energy savings and the implementation of technologies with the involvement of public and private organizations [4], focusing this Analysis on rural housing.

According to the 2020 National Housing Survey [ENVI], in terms of housing quality, the factors that cause dissatisfaction include the quality of roofs, walls, finishes and protection against wind, rain, cold and weather. heat. Nationally, 58.5% of the population needs to make repairs or remodels in their homes, such as installing or repairing floors, doors, or windows; 58.1% need to build or expand spaces such as bedrooms, bathrooms and kitchens [5].

By providing the opportunity to use natural building materials, the goal is not only to reduce CO2 emissions during construction processes, but also to significantly improve the quality of life of users. Choosing these materials, such as earth and bamboo, not only promotes environmental sustainability by minimizing the carbon footprint, but also provides economic benefits by taking advantage of local resources. This strategy not only focuses on construction efficiency but also comprehensively addresses the well-being of communities, combining architectural functionality with environmentally friendly practices. In this approach, construction with natural materials becomes a catalyst for

environmental improvement and the promotion of accessible and sustainable housing.

2. THE BENEFITS OF A HOME WITH LAND

The Earth is produced because of the erosion process of the rocks found in the Earth's crust, as well as organic processes of plants, water and oxygen [1]. It is composed of different layers or horizons, each one with characteristics. The first group, called "solum", is formed by the superficial layer where all the vegetation is located, followed by an organic layer where some minerals accumulate because of the decomposition of plant matter. The third layer contains mineral material with accumulation of humus, followed by the layer where the greatest accumulation of silt and clay occurs, and finally a deeper layer with a greater concentration of materials [6].

This first layer is used for construction and must meet specific granulometry requirements depending on the construction system to be used.

The main benefits of construction with earth are the following: it regulates environmental humidity, stores heat, provides interior thermal conditions that favor habitability, reduces environmental pollution, is a reusable material and economizes construction processes, in addition to being a good insulator. acoustic and thermal. [1,7]. Recent studies have demonstrated the thermal balance inside spaces built with adobe, demonstrating that when considering a comfortable space, the use of electrical energy of some appliances is reduced to achieve said comfort. This is shown in Figure 1 taken from [7].

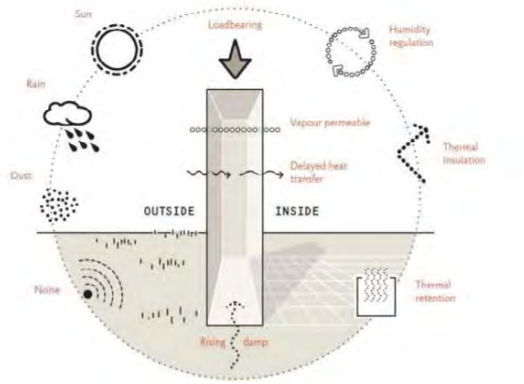

Figure 1: Benefits of Earth Walls

2.1 Characteristics of rammed earth

Rammed earth is a construction system that primarily utilizes earth extracted directly from the site or even from excavation for foundations. This is achieved through a process of modular formwork, typically consisting of two wooden planks spaced no less than 30 cm apart. Between these planks, layers of earth measuring between 10 and 20 cm are poured, with an appropriate moisture content allowing for compaction of the material in a dry state, ultimately reducing this layer to centimeters [1,8,9].

The construction system includes a foundation, generally made of stone, a superstructure that must reach up to 30 cm above ground level to protect the walls from water, horizontal and vertical structural reinforcements, typically of plant origin such as thin branches, bamboo or wood, and a roof.

The appropriate granulometry for the construction of rammed earth walls is 0-15% gravel, 40-50% arena, 20-35% sand and 15-25% clay [6]. As for humidity, it should range between 10-15% [10],

2.2 Decent housing

According to the UN, housing is a human right that must meet certain aspects to be classified as adequate housing: security of tenure, availability of services, materials, facilities and infrastructure, affordability, habitability, location and cultural appropriateness [11].

Furthermore, the connection of decent housing with each of the Sustainable Development Goals [SDGs] shows that housing improves the conditions of people in extreme poverty, thus promoting access to necessary services. Housing promotes food security, improving health and well-being, as long as it is equipped with appropriate materials and makes responsible use of resources [12].

In Mexico, housing policies address the fulfillment of these objectives. Therefore, considering the existing climate in the territory, construction with materials that help improve indoor climatic conditions is recommended.

In very dry and dry climates found in the north, center and, to a lesser extent, south of the country, the use of massive construction systems is recommended. These systems are thicker than lightweight systems, with the aim of storing and releasing heat with a time lag and in smaller quantities. This recommendation applies to natural materials such as rammed earth, stone, cob and adobe. For the warm subhumid climate, observed mainly in coastal areas, the use of natural materials such as adobe, cob and stone are conditioned.

For humid and subhumid temperate climates, rammed earth, stone, adobe, and cob are recommended, as well as for cold mountain climates, which are rare in Mexico. In warm subhumid climates such as that of the state of Colima, the use of light natural materials is recommended, such as acacia, clay straw, straw panels, bamboo lattice and palm. The use of heavy systems, such as rammed earth or super adobe, is not recommended, mainly due to external weather conditions. However, it has been found within the state that there are soil types suitable for this type of construction. Furthermore, one of the recommendations is to use finishes,

whether with natural or industrial materials, that preserve this type of materials [13].

All of this aims to provide affordable and participatory self-construction alternatives for rural areas of the state. According to the National Council for the Evaluation of Social Development Policy [CONEVAL], the municipalities with the greatest housing gap are: Ixtlahuacán 10.3%, Minatitlán 8.3%, Armería 7.4%, Tecomán 6.0% and Comala 5.3% [14]. Taking these characteristics into account and considering that the most used construction materials in the state are block, brick, concrete and, in some cases, galvanized sheets or asbestos.

With this information, a housing proposal has been developed to meet the needs of vulnerable communities, analyzing the thermal and mechanical characteristics of rammed earth walls for an area with high seismic activity and abundant summer rains.

3. MATERIALS AND METHODS

Despite recommendations that do not favor the use of rammed earth for warm subhumid climates, a study was carried out to demonstrate the benefits it could bring to the construction of housing, particularly in rural areas of the region, using local natural materials.

3.1 Materials

In the state of Colima there is a variety of soils suitable for construction with earth. According to previous studies, soil types such as sandy loam, clay loam, sandy loam, sandy and loam have been identified, suitable to produce adobes, bricks and rammed earth [15].

Bamboo of the Guadua species is also available in large plantations in the northern part of the state. Due to its physical and mechanical characteristics, bamboo becomes one of the most resistant natural materials for construction.

Calcium oxide or lime is used as a material stabilizer.

Finally, coconut fiber or coir is used as a material, coming from the hard and fibrous layer of the coconut, Colima being the second producer of this fruit, used for food, aesthetic, and construction purposes.

3.2 Methods

- Granulometry tests of materials and determination of proportions of lime and coconut fiber. Manufacture of formwork for rammed earth.
- Preparation of the foundation.
- Construction of the walls with the following proportions: Wall A) 100% earth, Wall B) 80% earth, 20% lime and Wall C) 60% earth, 32% lime and 8% coconut fiber.
- Physical analysis of the walls.

3.3 Wall Construction Process

First, the selection and extraction of land was carried out, prioritizing materials with higher sand and clay content and lower silt content. A sieving process was carried out to remove larger stones and plant materials such as seeds, roots, branches or leaves that could affect the process. Then the mixtures were prepared for each type of wall.

For Wall A, with dimensions of 2.44 m long, 0.40 m wide and 1.22 m high, with a volume of 1.19 m³ and an expansion factor of 1.37, it was calculated a total of 1.63 m³ of material.

For Wall B, with 80% soil and 20% lime, 36 kg of lime was added to the total soil mix.

Finally, for Wall C, with 60% soil, 32% lime and 8% coconut fiber, 0.71 m³ of soil, 91 kg of lime and 1.40 kg of coconut fiber were considered. This information was taken from previous studies [16], where the thermal and mechanical behavior of the proportions of each soil sample was analyzed.

Simultaneously, a sliding wooden mold was designed with light metal tubes, screws, plastic wheels to facilitate horizontal movement and two sheets of 15 mm plywood to facilitate the construction of earth walls. The dimensions of the mold are 2.44 m long by 1.22 m high, and due to its structure, it can reach up to three meters high.

Subsequently, a stone foundation 0.60 m high and 0.50 m wide was built and the vertical bamboo structure was installed. Additionally, the greased wooden mold was assembled. Figure 2 shows the plan with the dimensions of the foundation and the exact placement of horizontal bamboos to trace the experimental module on the ground and take reference levels.

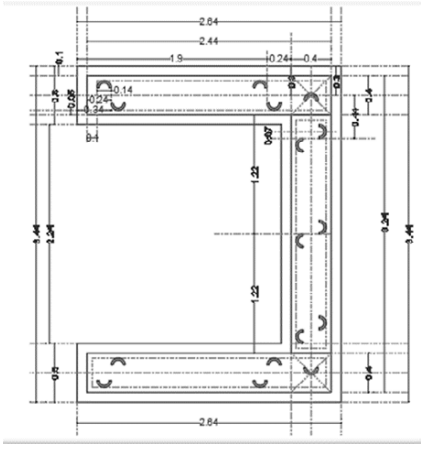

Figure 2: Plan of the walls

The walls were built using the conventional technique, filling 20 cm of previously sifted soil with the appropriate quantities of clay, silt, sand, and

moisture. Subsequently, it was compacted by 0.05 m. This process was repeated for all walls until reaching a height of 1.20 m, as shown in Figure 3.

Figure 3: Experimental Rammed Earth Module.

4. RESULTS

The results obtained showed that the construction of rural housing for vulnerable families within the state of Colima is feasible. Aesthetically, the three walls only presented small cracks that do not represent structural damage but were a result of the quality of compaction in some areas, as well as the aggregates used in the earth mixture.

The physical condition of the walls was evaluated through a guide in which four important aspects were assessed:

- Presence of cracks and fissures derived from the bamboo structure, compaction, or the amount of moisture.
- Material detachment caused by the mold or structural failure.
- Material compaction, uniform layers.
- Setting of each wall.

In wall "A" with 100% earth, some cracks were found caused during mold removal and some generated by the vertical bamboo reinforcements. Additionally, cracks were generated between the wall and the mold, causing material detachment in the corners. Earth compaction was uniform; however, in the area where the bamboos were placed, compaction became complicated. Regarding the amount of applied moisture, according to the literature, this caused loose material and evaporation a few hours after removing the formwork.

In wall "B" with 80% earth and 20% lime, the main results of the physical evaluation included the presence of cracks on the wall's surface derived from the location of the bamboo reinforcements. Compaction was adequate between the mold and the bamboos due to minimal space between them, making this work difficult and generating material detachment in some areas, which was only aesthetic without causing structural damage. In this wall, the amount of added water was increased, and the formwork was removed after 24 hours, favoring moisture retention for a longer time and uniform setting.

Finally, for wall "C" with 60% earth, 32% lime, and 8% coconut fiber, cracks of 1 to 3 cm thickness were identified only on the surface, arising from the compaction difficulty between bamboo spaces and the mold. Additionally, the addition of coconut fiber was also a fundamental factor that complicated this procedure, resulting in a slight detachment of material at the corners and the base of the wall. A greater amount of moisture was applied, and the formwork was removed after 48 hours, generating greater benefits to setting and solidification.

A good thermal performance was demonstrated, as earth allows for lower heat transmittance compared to materials such as concrete, brick, and block, which were the materials used for comparison. Developing the Fourier equation:

$$Q/t=-\lambda A((Tb-Ta)/L) \quad (1)$$

Where Q/t, is the heat flux; λ, is the conductivity coefficien; A is the wall area; Ta, is the initial temperature; Tb, is the final temperature, and L, is the length or thickness. According the results obtained previously in an experimental models [16] and applying λ de 0.43 W/mK,(Wall A) 0.27 W/mK (Wall B) y 0.23 W/mK (Wall C) , an área of 2.97 m2 , a temperature difference of 5°C and a wall length of 0.40 m for earth walls applied theoretically, the thermal calculations showed that the thermal conductivity for each wall was: for wall “A”, Q/t = 16.00 W, wall“B”, Q/t = 10. 04 W, wall “C”, Q/t = 8.55 W.

Compared to block walls with a λ= 0.91 W/mK, maintaining the area of 2.97 m2, a temperature difference of 5°C, and a length of 0.15 m, the result is Q/t = 90.29 W.

In a reinforced concrete wall with a thickness of 0.10 m and a λ =2.3 W/mK, maintaining the area and the temperature difference, the result is λ = 342.33 W/mK. Whereas in a brick wall with λ =1.04 W/mK and a thickness of 0.15 m, λ = 103.19 W/mK. In a reinforced concrete wall with a thickness of 0.10 m and a λ =2.3 W/mK, maintaining the area and the temperature difference, the result is λ = 342.33 W/mK. Whereas in a brick wall with λ =1.04 W/mK and a thickness of 0.15 m, λ = 103.19 W/mK.

Similarly, it exhibited good acoustic performance, significantly reducing the amount of external sound that can enter the interior of the homes.

Regarding fire resistance, it is known that earth is one of the most fire-resistant materials. Therefore, theoretical comparison demonstrated that it can withstand up to 2,500 minutes (41 hours) before

presenting any significant damage. However, this applies when the material does not have additives such as coconut fiber or wooden structure.

The analysis of structural behavior is based on experimental compression strength results from prior research [16], where wall "A" has a strength of 46.82 kg/cm^2, wall "B" 20.37 kg/cm^2, and wall "C" 20.14 kg/cm^2. Thus, wall "A" has better structural behavior and compression strength similar to that of a concrete wall.

Regarding environmental and cost-benefit analysis, the obtained results were as follows: CO_2 emissions. It is estimated that wall "A" emits approximately 3.8 kg of CO_2, wall "B" 4.8 kg of CO_2, and wall "C" 4.4 kg of CO_2 per element, well below conventional materials. Regarding the cost of manufacturing 1 m^3 of earth walls, considering preliminary concepts of layout, leveling, excavation, material extraction, as well as labor, mold, and additives, wall "A" has a cost of 38.05 USD, wall "B" 53.79 USD, and wall "C" 65.55 USD, approximate prices for 2022.

Finally, a housing proposal was derived for vulnerable communities in the state of Colima, taking into account factors such as the classification of existing materials in the area [15], spatial distribution for housing on larger plots than those in urban areas, and an analysis of users and their spatial needs. The conclusion was an architectural program comprising three bedrooms, one bathroom, kitchen, living room, and dining room with an approximate area of 144 m^2.

Figure 4: Rural housing proposal

5. CONSIONS

The use of construction materials that can be obtained locally will always be a sustainable option, as it requires minimal energy to obtain them. Materials like earth and bamboo offer economic and environmental benefits. Rammed earth walls are not only structural elements but also thermal and acoustic components adaptable to various climatic regions, addressing economic challenges in accessing decent housing.

Earth facilitates the construction of walls easily and quickly, with a low budget, and is particularly suitable for self-construction. Following the recommendations of SEDATU and CONAVI, construction with earth walls can be employed across most of the Mexican territory, incorporating other materials like lime and coconut fiber to enhance the strength of these elements. This approach allows for the utilization of natural resources, reducing material costs, and lowering CO2 emissions by avoiding industrial processes and material transportation.

Providing an opportunity to use natural construction materials that reduce CO2 emissions in construction processes and improve users' quality of life promotes the adoption of more sustainable and environmentally friendly construction practices. Opting for local resources such as earth and bamboo not only contributes to mitigating climate change by minimizing the use of materials with a large ecological footprint but also stimulates the local economy by utilizing readily available materials in the region.

This conscious choice of materials not only results in environmental benefits but also fosters community resilience by facilitating self-construction and offering affordable housing solutions. By incorporating these natural elements into architecture, a balance between functionality, efficiency, and environmental respect is established, laying the foundation for a more holistic and sustainable approach to the design and construction of homes.

ACKNOWLEDGEMENTS

To my thesis advisors, both for my master's and to Dr. Jorge Ojeda, thesis director of the Interinstitutional Doctoral Program in Architecture [PIDA], and to the people who supported me in the construction of the experimental module, to the University of Colima, and to PLEA for the opportunity to present a work that will surely benefit people in need.

REFERENCES

1.Minke, G. (2005). Manual de construcción en tierra: La tierra como material de construcción y su aplicación en la arquitectura actual.

2. United Nations Environment Programme (2020). 2020 Global Status Report for Buildings and Construction: Towards a Zero-emission, Efficient and Resilient Buildings and Construction Sector. Nairobi

3. United Nations. (2023). Sustainable Development Goals. https://www.un.org/sustainabledevelopment/

4. Mackres, E., Loutfi, F (16 de octubre de 2020). El potencial de México para liderar en edificaciones cero carbonos. WRI MÉXICO. https://wrimexico.org/bloga/el-potencial-de-m%C3%A9xico-para-liderar-en-edificaciones-cero-carbono

5. INEGI: Encuesta Nacional de Vivienda (2020). https://www.inegi.org.mx/programas/envi/2020/

6. Lepsch, I. (2010). Formación y Conservación del suelo.
7. Gatti, F. (2012). Arquitectura y construcción en tierra. Estudio comparativo de las técnicas contemporáneas en Tierra. Universidad Politécnica de Catalunya, 101. http://mastersuniversitaris.upc.edu/tecnologiaarquitectura.
8. Rodríguez, L. M. (2015). El uso del tapial en la arquitectura de las haciendas de Tlaxcala, México. In Congreso.indb (pp. 1461–1470).
9. AIS. (2004). Manual para la rehabilitación de viviendas construidas en adobe y tapia pisada. Asociación Colombiana de Ingeniería Sísmica, 90.
10. Ministerio de Vivienda, Construcción y Saneamiento, G. de P. (2017a). Diseño y construcción con tierra reforzada NORMA E. 080. In Resolución Ministerial, el Peruano. (Vol. 1, p. 24). https://procurement notices.undp.org/view_file.cfm?doc_id=109376#:~:text=La norma se orienta al,confortables y de fácil difusión.
11.Naciones Unidad, Derechos Humanos, el derecho a una vivienda adecuada (2010) https://www.ohchr.org/sites/default/files/Documents/Publications/FS21_rev_1_Housing_sp.pdf
12. Naciones Unidas- ONU-HABITAT, contribución de la vivienda al cumplimiento de la agenda 2030. ONU-Habitat - Contribución de la vivienda al cumplimiento de la Agenda 2030 (onuhabitat.org.mx)
13. Comisión Nacional de Vivienda (2020) Estrategias de Diseño arquitectónico con Enfoque bioclimático. Criterio técnico para una vivienda adecuada.https://siesco.conavi.gob.mx/doc/tecnicos/diseno/Estrategias%20de%20Dise%C3%B1o%20Arquitectonico.pdf.
14. Consejo Nacional de Evaluación de la Política de Desarrollo Social (2020). Estadísticas de pobreza en Colima.https://www.coneval.org.mx/coordinacion/entidades/Colima/Paginas/principal.aspx.
15. Chávez, D, Moreno, J, Castellanos, M, Navarro, J, G. L. y A. S. . (2022). Caracterización de los suelos del estado de Colima para la construcción con tierra mediante pruebas de campo. 2004, 336–363.

PLEA 2024 WROCŁAW
(Re)thinking Resilience

Adobe stabilized with coconut fiber and lime

Compressive strength and thermal behaviour

PEDRO CIPRIANO MAGANA MENDOZA[1], JOSE RICARDO MORENO PEÑA[2], CARLOS JAVIER ESPARZA LOPEZ[1], ELIA MERCEDES ALONSO GUZMAN[3], MARIO FILOMENO CABRERA SANDOVAL[1]

[1] University of Colima, Colima, Mexico
[2] National Technological of Mexico, Colima, Mexico
[3] Michoacan University of San Nicolas of Hidalgo, Michoacan, Mexico

ABSTRACT: The following investigation analyzes construction with raw materials, specifically that of adobe. Based on the diagnosis obtained and in the pursuit of innovation, it is proposed that coconut fibers and lime be integrated into aggregates, to perform as soil stabilizers, and thus determine the material's behavior when exposed to compression and temperature stress.

There were many considerations involved in the development of the specimens. The factors contemplated during this study include: the characteristics and specifications of each specimen, the design and sizing of the mold for their preparation, and the development of laboratory tests regarding compression stress, thermal behavior, moisture absorption and retention.

The experimental model used to determine the different mixtures produced was based on the Completely Random Design (CRD). This model determines the percentage of lime and coconut fiber to be combined with the aggregate and distributes it into 5 treatments. Each treatment has a percentage of integration, which generates four experimental units in each.

The results obtained in this study reveal values that surpass those established by the international regulations NTE E-080 Peruvian, as well as the thermal tests carried out with the specimens.
KEYWORDS: Adobe, Coconut fiber, Calcium oxide, Sustainable materials, Sustainable architecture.

1. INTRODUCTION

The emission of Greenhouse Gases (GHG) into the Earth's atmosphere has significantly increased since the Industrial Revolution began in the second half of the 18th century. These concentrations affected the natural balance of the greenhouse effect.

As the concentration of greenhouse gases increased, more UV rays that were reflected by the Earth's surface towards the atmosphere became trapped, leading to a rise in the global average temperature [1,2]. This temperature increase reached its historical peak in 2016, with subsequent years, including 2020, being the warmest since 1880 [3].

Currently, global warming is primarily caused by humanity's unsustainable development, characterized by excessive growth in population centers and the exploitation of natural resources at the expense of the environment.

The construction sector should prioritize research on sustainable materials with low emissions throughout their life cycle. This approach not only reduces GHG emissions but also promotes sustainable construction alternatives aimed at minimizing Construction and Demolition Waste (CDW) and fostering a circular economy within the sector.

2. GREENHOUSE GASES (GHG)

Global warming is the result of transgressions made to the environment due to humanity's development, which has excessively and unsustainably exploited natural resources to satisfy its needs. This development has primarily occurred in population centers, leading to an exclusive focus on satisfying immediate needs at the expense of long-term environmental health; generating the emission of GHG, whose main six gases are:

- Carbon Dioxide (CO^2).
- Methane (CH^4).
- Nitrous Oxide (N^2O)
- Fluorinated: Hydrofluorocarbons (HFC), Perfluorocarbons (PFC) and Sulfur Hexafluoride (SF^6).

GHG emissions into the atmosphere experienced a notable increase during the industrial revolution in the second half of the 18th century. This period marked the beginning of the overexploitation of natural resources to fuel industrial development and satisfy growing needs.

Since 1750, atmospheric GHG concentrations have increased by 47% for carbon dioxide (CO^2), 156% for methane (CH^4), and 23% for nitrous oxide

(N^2O). Despite efforts to curb emissions, these pollutants continue to rise; This resulted in GHG levels reaching 410 ppm, which exceeded the limit of 350 ppm considered safe [4].

3. POLLUTING SECTOR

The main polluting sectors include agriculture, accounting for 23% of total global GHG emissions [5], and forest deforestation, which contributes up to a third of total global emissions. This significantly affects the ecological balance of the planet, directly impacting global warming and climate change [6]. Finally, the most polluting sector is the construction industry, with buildings responsible for 36% of global GHG emissions worldwide [7].

The construction industry is estimated to also consume 50% of natural resources as well as 40% of primary energy worldwide [8].

The construction industry currently requires 43 gigatons of mineral materials to meet demand [9]. The use of cement in architectural and civil works accounts for 8% of total CO^2 emissions worldwide [10], while steel represents another 8% [9]. Consequently, the industry generates 35% of the total industrial waste worldwide [11]. In 2020 alone, 600 million tons of Construction and Demolition Waste (CDW) were generated, with only 22% being recycled [12].

This aspect of the construction sector should focus on researching sustainable materials with low emissions. These materials not only reduce GHG emissions but also promote constructive alternatives that foster a circular economy within the sector.

4. EARTH ARCHITECTURE

One of the most environmentally friendly options for sustainable construction, which contributes to reducing GHG emissions, is construction using raw earth as the primary material, which can be used in 12 different methods or techniques (figure 1) illustrated in Figure 1, include adobe, which is one of the most representative.

Classified according to the function of the plasticity of the earth with respect to its use within the construction system used [13]:

- Solid and/or dry: Excavate, cover, fill, and cut.
- Wet: Compact.
- Plastic: Mold, pile up, modular and extrude.
- Liquid: Adhere, pour, and coat.

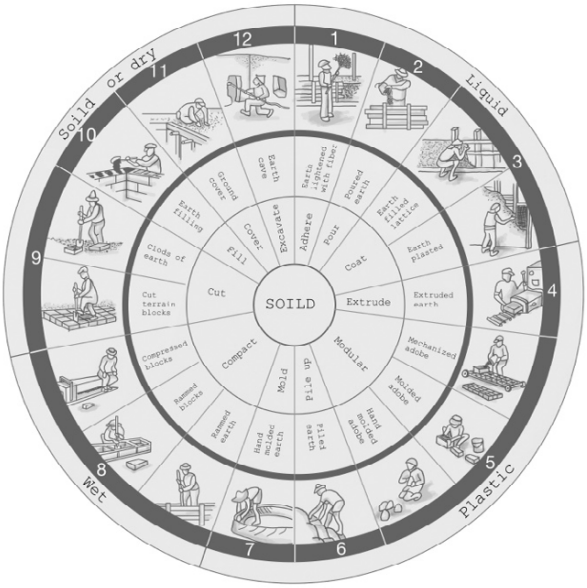

Figure 1: Methods or techniques, Huben & Guillaud, 1994.

4.1 The Adobe

This construction technique is one of the oldest, with a history spanning over 10,000 years. According to Bautista (1992), it is defined as a solid block made of uncooked clay, which may contain straw or other material that improves its stability against external agents.

Land stabilization can occur through consolidation, friction, or waterproofing. This is achieved by adding fibrous materials and/or natural or artificial binders of vegetable, animal, or mineral origin [14].

In the case of the mineral materials used in various investigations, lime is often present. While its production process generates considerable CO^2 emissions due to the combustion of limestone, it acts as a natural carbon sink when used. When lime comes into contact with water, a chemical process called carbonation occurs, permanently capturing CO^2 from the environment in the same amount as emitted during its manufacturing process.

In this process, lime permanently captures CO^2 from the environment in the same amount as was emitted during its manufacturing process [15]. Therefore, it makes it feasible as an alternative stabilizing material for consolidation and waterproofing.

Mexico ranks eighth in coconut production worldwide, with production spanning 124.3 thousand hectares across nine entities of the national territory; The state of Colima holds the second position in the country's coconut production [16].

According to statistics from the Agri-Food and Fisheries Information Service (SIAP) and the Secretariat of Agriculture, Livestock, Rural Development, Fisheries and Food (SAGARPA), Colima has 14,440 hectares of coconut palm cultivation, with

65 palms per hectare, established in the municipalities of Tecoman, Armeria, Manzanillo, and Coquimatlan.

With this, the use of the fibers present in the leaves of palm trees is established as a viable option, which will give optimal use to this natural and renewable resource in a short cycle of time, and an alternative economy for the sector.

5. EXPERIMENTAL SAMPLE DESING

The experimental design for this research was the Completely Random Design (CRD) [17], which considers variations in terms of the percentage integration of aggregates, including lime and coconut fiber.

The mixture design allowed for the determination of 5 different treatments, each with 4 different percentages of aggregates, and 1 control. This resulted in a total of 21 different mixtures for the preparation of experimental units or test tubes (Table 1); For compression tests, 3 test tubes were prepared for each mixture, along with 1 test tube for thermal, absorption, and moisture retention tests. This resulted in 4 test tubes for each treatment and mixture, totaling 84 experimental units.

Table 1: Completely randomized sample design.

EXPERIMENTAL MIXTURE DESIGN																	
INTEGRATION PERCENTAGES		Experimental Unit	Treatment A		Experimental Unit	Treatment B		Experimental Unit	Treatment C		Experimental Unit	Treatment D		Experimental Unit	Treatment E	
Soil	Agregated		CaO	Fiber		CaO	Fiber		CaO	Fiber		CaO	Fiber		CaO	Fiber
%			0%	100%		20%	80%		50%	50%		80%	20%		100%	0%
100%	0%		0%	0%		0%	0%		0%	0%		0%	0%		0%	0%
80%	20%	A1	0%	20%	B1	4%	16%	C1	10%	10%	D1	16%	4%	E1	20%	0%
60%	40%	A2	0%	40%	B2	8%	32%	C2	20%	20%	D2	32%	8%	E2	40%	0%
40%	60%	A3	0%	60%	B3	12%	48%	C3	30%	30%	D3	48%	12%	E3	60%	0%
20%	80%	A4	0%	80%	B4	16%	64%	C4	40%	40%	D4	64%	16%	E4	80%	0%

6. RESULTS

6.1 Compression

According to the Peruvian technical standard NTE E 080 [18] specifies that the minimum allowable compression stresses in adobe blocks are 12 kg/cm^2; Several experimental units in the research exceeded the minimum allowable compression stress value specified by the regulations.

The best resistance was observed in experimental units “1” (made with 20% aggregates), which exceeded the minimum requirement in four out of five treatments (Figure 2). However, the best results in treatments “A” were dismissed due to the high level of fiber, causing them to behave like sponges; The most optimal treatments were “D” (80% calcium oxide and 20% coconut fiber), with experimental units “D1” achieving a compression stress of 21.68 kg/cm^2 and “D2” achieving 20.37 kg/cm^2.

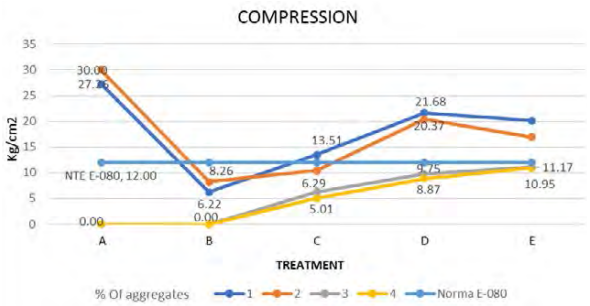

Figure 2: Resistance to compression.

6.2 Thermal behavior

6.2.1 Specific heat

Regarding specific heat, 76.92% of the tested specimens outperformed the control specimen (Figure 3), which had a value of 1,686 MJ/m^3.K. Only “B1”, “C1,” and “D1” exhibited higher values, with 1,994, 1,994, and 2,461 MJ/m^3.K respectively.

Among the tested experimental units, the “B2” specimen (composed of 40% aggregates, 8% lime, and 32% coconut fiber) achieved the best result, with a specific heat of 0.602 MJ/m^3.K. This value represents a 36% decrease in performance compared to the control specimen.

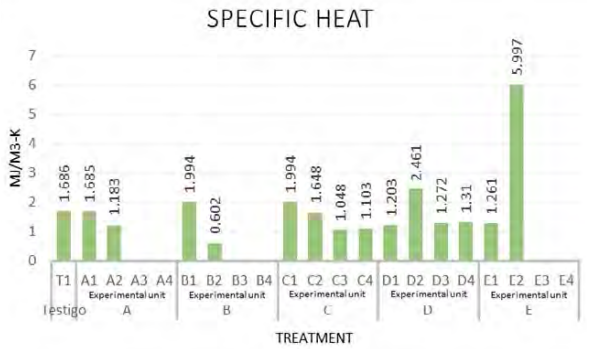

Figure 3: Specific heat.

6.2.2 Thermal conductivity

In traditional adobe, the thermal conductivity coefficient typically ranges between 0.46 and 0.81 W/m.K, as stated by Cecilia Aching and Soledad Moscoso. However, in this investigation, all mixtures exceeded these values by up to 50%.

Regarding thermal conductivity values (Figure 4), improvements were observed in 93% of the tested specimens compared to the average value of 0.435 W/m.K for the control specimens. The best performance was achieved by the “C4” treatment (composed of 80% aggregates, 40% lime, and 40% coconut fiber) with a value of 0.142 W/m.K.

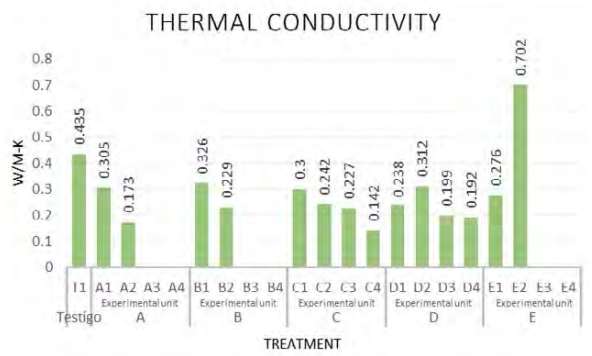

Figure 4: Thermal conductivity.

6.2.3 Thermal resistivity

In terms of thermal resistivity, the control registered a value of 229.6 oC.cm/W. Improvements were obtained in 93% of the specimens tested compared to the control (Figure 5), with the range of improvement spanning from 33.66% to 307.72%. The experimental unit "B1" achieved a minimum value of 306.9 oC.cm/W, while the specimen "C4" (composed of 80% aggregates, 40% lime, and 40% coconut fiber) reached a maximum value of 706.533 oC.cm/W.

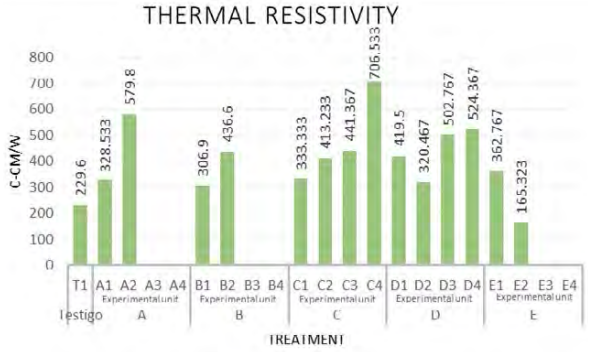

Figure 5: Thermal resistivity.

6.2.4 Thermal diffusivity

In terms of thermal diffusivity, 84.61% of the specimens showed values below the control (Figure 6). The best result was obtained in the experimental unit "D2" with 0.127 mm^2/s. Only two specimens achieved higher values: the experimental units "B2" with 0.381 mm^2/s and "C4" with 0.513 mm^2/s.

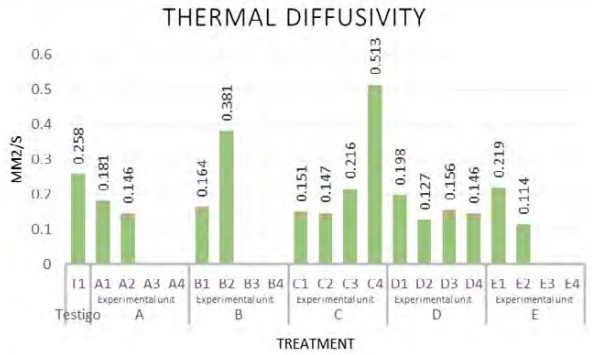

Figure 6: Thermal diffusivity.

6.3. Moisture absorption and retention

One of the most contentious aspects when discussing the use of adobe in construction is the weight of the material. Therefore, it was deemed important to analyze this characteristic in the research.

This new mixture presents a viable option that significantly addresses this concern, as there is an improvement in weight reduction across all treatments. The decrease compared to the control ranges from 11.37% to 42.96% in the best cases, depending on the chosen mixture and treatment (Figure 7).

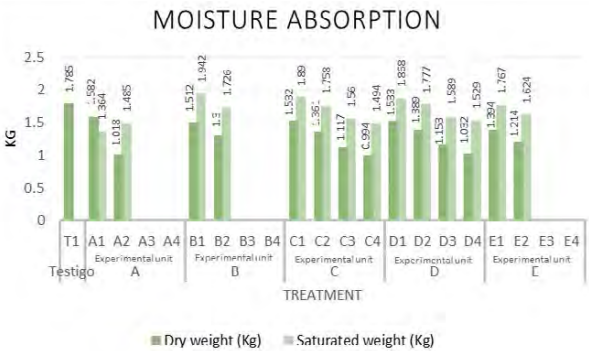

Figure 7: Moisture absorption.

The results obtained from subjecting the test tubes to the water saturation process revealed their moisture absorption capacity and the subsequent increase in weight for the different mixtures. Similar increases were observed for all experimental units tested, which were weighed once the saturation process was completed to continue with the analysis of moisture retention and loss.

In the case of treatment "A", the experimental unit "A1" with 20% aggregates managed to lose the retained moisture in 10.5 days of drying, while the specimen "A2" composed of 40% aggregates presented an increase of 45.87% in weight compared to its dry state, which it managed to lose in nine and a half days of drying.

For treatment "B", the specimen "B1" reached its maximum drying process in 18.5 days, while "B2" took only 10.5 days to reach its dry weight.

In treatment "C", the experimental units "C2", "C3", and "C4" dried in 13.5, 12.5, and 9.5 days respectively, while the specimen "C1" had the fastest moisture loss with a duration of 10.5 days.

Treatment "D" showed drying durations of 10.5 days for experimental unit "D1", 12.5 days for "D2", 15.5 days for "D3", and 13.5 days for "D4".

For treatment "E", the experimental units "E1" and "E2" required 12.5 and 11.5 days respectively to dry.

The moisture retention tests showed that the specimens were able to dry between 10 and 19 days,

indicating that these mixtures do not require the 28 days of drying as required by international regulations. This difference in drying time is attributed to the climatic conditions of the Colima region during the spring season when the analysis was conducted.

Therefore, there was a nine-day difference in the drying of the specimens compared to what is established in international regulations, reflecting the specific climatic conditions of the study area.

7. CONCLUSION

As emphasized throughout the article, there is a growing interest in the architectural and construction sectors to explore new construction material mixtures that address energy efficiency, economic demand, and resource conservation, ultimately contributing to sustainable architecture.

The results of our research demonstrate that the analyzed adobe mixture, incorporating soil with coconut fiber and lime as stabilizers, significantly enhances the material's mechanical and compression characteristics, along with improvements in its thermal properties.

This provides the construction industry with a sustainable material that boasts shorter production times compared to traditional mixtures and has a reduced carbon footprint. Moreover, at the end of its useful life, this material can be fully reintegrated into the environment or completely reused, thereby not only mitigating construction waste but also promoting a circular economy with its 100% recyclable nature.

With this, the construction sector would be part of the global resilience to the changes and strategies established to achieve the mitigation of climate change and its effects.

ACKNOWLEDGEMENTS

To carry out the entire process that the research involved, we had the intellectual support of the collaborators belonging to the educational departments of the National Technology of Mexico, Campus Colima, the University of Colima and the Michoacana University of San Nicolas of Hidalgo; which in turn provided the equipment and tools necessary to carry out each of the laboratory tests applied.

Likewise, I thank the National Council of Humanities, Sciences and Technologies (CONAHCYT) of the government of Mexico, which through its support was able to finance the research.

REFERENCES

1. National Aeronautics and Space Administration (NASA), (2023). "Earth's atmosphere". [Online]. Available: https://spaceplace.nasa.gov/atmosphere/sp/#:~:text=La%20atm%C3%B3sfera%20de%20la%20Tierra,en%20las%20im%C3%A1genes%20de%20abajo.

2. National Aeronautics and Space Administration (NASA), (2023). "Global Climate Change". [Online]. Available: https://climate.nasa.gov/faq/70/que-es-el-efecto-invernadero/#:~:text=El%20efecto%20invernadero%20es%20la,lo%20que%20ser%C3%ADa%20sin%20ella [10 of june 2023].

3. NASA, Goddard Institute for Space Studies, (2023). "Temperature". [Online]. Available: Global.https://climate.nasa.gov/vital-signs/global-temperature/ [10 of june 2023].

4. World Meteorological Organization (WMO), (2019). "The concentration of greenhouse gases in the atmosphere reaches a new record". WMO.

5. IPCC, (2020). "Sixth Assessment Report". [Online]. Available: https://www.ipcc.ch/report/ar6/wg2/.

6. IPCC, (2007). [Online]. Available: https://www.ipcc.ch/site/assets/uploads/2018/02/ar4_syr_sp.pdf.

7. OECD, (2019). "Development Co-operation Report 2019". [Online]. Available: https://www.oecd-ilibrary.org/development/development-co-operation-report-2019_9a58c83f-en.

8. Institute of Construction Technology of Catalonia, (2021). [Online]. Available: https://iaac.net/?utm_source=google&utm_medium=cpc&utm_id=19739902527&utm_campaign=worldwide_ong_architecture-courses_adquisicion_prs_text&gad_source=1&gclid=Cj0KCQiAv8SsBhC7ARIsALIkVT0cp9AOMyGqoGccANvpbcLQx7wl_orjnvYTTL2umwKlUE4EmT2v0LwaArymEALw_wcB

9. Krausmann F., Lauk C., Haas W & Wiedenhofer, (2018). "From resource extraction to outflows of wastes and emissions: The socioeconomic metabolism of the global economy, 1900–2015". [Online]. Available: https://doi.org/10.1016/j.gloenvcha.2018.07.003.

10. IEA, (2022). "World Energy Outlook 2022". [Online]. Available:https://www.iea.org/reports/world-energy-outlook-2022.

11. . World Steel Association, (2017). "Steel Statistical Yearbook 2017", [Online]. Available: https://worldsteel.org/wp-content/uploads/Steel-Statistical-Yearbook-2017.pdf [10 of june 2023].

12. C.F. Hendriks, H.S. Pietersen, (2000). "Sustainable Raw Materials - Construction and Demolition Waste - State-of-the-Art Report of RILEM TC 165-SRM", ISBN: 2-912143-17-9.

13. . EPA, (2020). "Construction and Demolition Debris: Material-Specific Data", [Online]. Available: https://www.epa.gov/facts-and-figures-about-materials-waste-and-recycling/construction-and-demolition-debris-material [10 of june 2023].

14. Houben, H. y Guillaud, H. (1994). "Earth construction : a comprehensive guide". Londres: ITDG Publishing.

15. Alavéz, R., Montes, P., Martínez, J., Altamirano, D. C., & Gochi, Y. (2012). "The use of sugarcane bagasse ash and lime to improve the durability and mechanical properties of compacted soil blocks". Construction and Building Materials, 34, 296–305. doi:10.1016/j.conbuildmat.2012.02.

16. Alavéz, R., Montes, P., Martínez, J., Altamirano, D. C., & Gochi, Y. (2012). "The use of sugarcane bagasse ash and lime to improve the durability and mechanical properties of compacted soil blocks". Construction and Building

Materials, 34, 296–305. doi:10.1016/j.conbuildmat.2012.02.
17. Ibarra, E.L. (1988). “Completely randomized design and comparisons between treatment means”, Tegucigalpa (Honduras). p. 31-41.
18. Ministry of Housing Construction and Sanitation, Government of Peru ,(2017). “NTE E 080, Design and construction with reinforced earth (adobes)”, [Online]. Available: https://procurement-notices.undp.org/view_file.cfm?doc_id=109376 [10 of june 2023].

PLEA 2024 WROCŁAW
(Re)thinking Resilience

The Environmental Performance of The Contemporary Residential Building

A case study in São Paulo

LARISSA AZEVEDO LUIZ[1], JOANA CARLA SOARES GONÇALVES[1]

[1]University of São Paulo, São Paulo, Brazil

ABSTRACT: Aiming to evaluate the thermal and daylight performance of residential architecture production in the city of São Paulo between 2000 and 2020, the article presents the main strategies used in the design of the facades of this set of buildings identified through data collection and evaluates, in a combined way, the performance of the most relevant design strategies. Computational simulations were used to evaluate thermal and daylight performance through the shoebox methodology, using as performance metrics the percentage of hours in the comfort zone according to the adaptive model of ASHRAE 55 and the percentage of hours with at least 50% of the area of the environment between 300 and 3000 lux. The results allow us to present, in this way, a reading on the best way (types and dimensions), from the performance point of view, to apply the strategies proposed in this new emerging architectural language. Among the main results, it was possible to observe that the simulations of the 224 scenarios studied resulted in a variation of 13% in terms of thermal performance and a variation of 100% in terms of daylight. In other words, daylighting proved to be an aspect much more influenced by the proper design of the facade than thermal performance.
KEYWORDS: Thermal comfort, Daylight, Residential Architecture, Contemporary Architecture.

1. INTRODUCTION

The recent production of residential architecture of medium and high standard in the city of São Paulo has been marked by the appearance of a new architectural language, based on the valorisation of authorial architecture and a discourse of promoting user comfort through the maximization of views and natural lighting, for example.

Classical architectural elements of the facades of modernist buildings, built in the 1950s and 1960s, such as brise-soleil in different formats, exposed structure, garden terraces, balconies, and large floor-to-ceiling windows, have increasingly appeared in a renewed way in this new architectural production that found in the political-economic scenario of the city a market niche from the 2000s.

However, despite preaching a valorisation of architecture that values comfort and using a series of design strategies, mainly about facades, related to adaptation to the local climate, it is rare to see studies that prove the environmental performance of this set of buildings and demonstrate the effectiveness of the application of these strategies.

The lack of studies that support the use of one facade strategy over another in the design process may be an indication that, despite the overvaluation of modernist architecture and the discourse of resuming its elements of bioclimatic value, there is only the use of resources, which could have great importance in the performance of buildings, as a way to add aesthetic appeal and to seek differentiation from the excessively standardized buildings that are characteristic of national architectural production since the crisis faced by Brazil in the 1980s.

In order to evaluate the thermal and daylight performance of this recent architectural production, the research was developed in a way to identify the main characteristics of this set of buildings and taking into account the most striking strategies in the design of the envelope of the set, evaluate, in a combined way, the performance of the most relevant design strategies through computational simulations. Being possible to present, in this way, a reading about the best way (types and dimensions), from the point of view of performance, to apply the strategies proposed in this new emerging architectural language.

2. METHODOLOGY

To evaluate the thermal and daylight performance of this recent architectural production, the methodology was based on two main stages (Fig. 1.). The first stage consisted of enumerating, through the analysis of a set of 51 projects of residential buildings launched in São Paulo after 2000, the main characteristics and design strategies related to the envelope of this group of projects. The second stage consisted of evaluating, through computational simulations in shoebox models, the thermal and

daylight performance of these design strategies independently and combined.

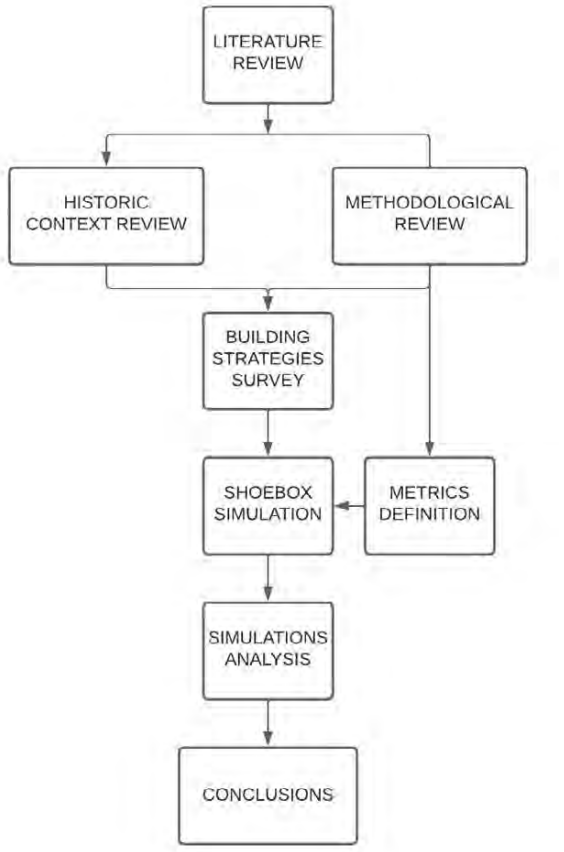

Figure 1: Flowchart illustrating the methodology of the study.

The computational simulations for the evaluation of thermal and daylight performance had their results evaluated using performance metrics. Several metrics can be considered in parallel during a performance evaluation, or in other words, a space may have as requirements to meet a regulatory standard on minimum annual illuminance levels, glare control, and energy consumption.

Performance metrics become especially useful as a design tool when combined with a performance target, as, thus, various design options can be compared through the application of the metric in order to obtain a design result based on the best performance.

The computational study carried out in this research allowed the daytime spaces to be evaluated, from the point of view of natural lighting, using the Useful Daylight Illuminance (UDI) index as a parameter.

The UDI uses a range with minimum and maximum levels, thus it is possible to divide the year into three ranges, one range with the hours below the minimum level, therefore with insufficient light, a range that comprises the hours within the limits, therefore with adequate lighting, and a last range that comprises the hours above the maximum limit, that is, with a high risk of glare due to excess of light.

Thus, the evaluation of the daylight performance was based on the analysis of the UDI by checking the percentage of the analysed space area that was in the range of hours between 300 and 3000 lux in at least 50% of the annual daylight hours. For the evaluation of thermal performance, the percentage of hours per year within the range of operative temperature considered as the comfort zone according to the adaptive model of ASHRAE 55:2020 was used as a metric for the city of São Paulo climate.

3. RESULTS

During the first phase of the research, through the analysis of a set of 51 projects of residential buildings of medium/high standard launched in São Paulo between 2000 and 2020, it was possible to identify the main characteristics of this set, mainly the characteristics related to the design of the envelope that can have an impact on the thermal and daylight performance of the housing units.

The first point observed during the reading of the projects was the typology of the housing units. It was observed that, among the 51 buildings studied, in 88% of the buildings, it was possible to identify the presence of traditional apartments, while in 59% it was possible to identify type Duplex units and in 45% type Studio units, which indicates the overlap of different apartment typologies in the same building.

In addition to the typologies, the set was analysed in order to understand what envelope characteristics the contemporary buildings have (Fig. 2). The most present items in the set were balconies, shading elements, and floor-to-ceiling windows in at least one of the environments. On a smaller scale, it was also possible to identify two other elements, the presence of double height and vegetation on the facades covered 35% of the projects and, despite not reaching 50%, they proved to be a trend.

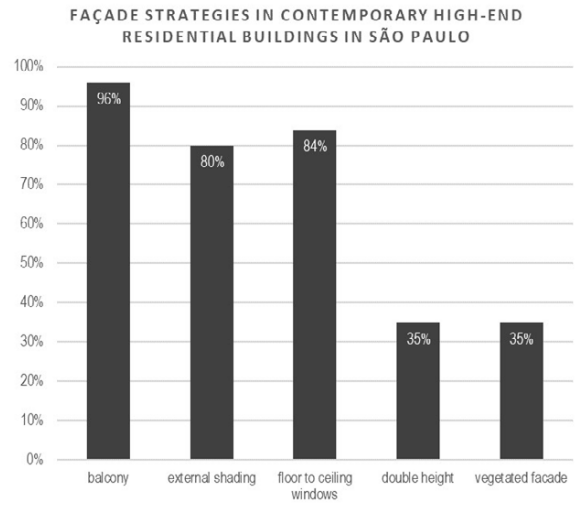

Figure 2: Graph showing the main facade strategies in contemporary high-end residential buildings in São Paulo according to the analysis of a set of 51 projects.

Balconies can be identified as the main element in the design of the facades of these buildings, appearing with different typologies and linked to different architectural elements (with or without shading function), but appearing in almost 100% of cases, sometimes even in more than one environment within the same housing unit.

Regarding the typologies of balconies, it was possible to identify three typologies with a direct relationship to the level of solar exposure (Fig. 3), namely:

- Exposed balcony: characterized by open sides with high solar exposure of the glazed areas and present in 41% of the buildings studied.
- Semi exposed balcony: characterized by one open side and one closed side, resulting in intermediate solar exposure with partial shading of the glazed area and present in 67% of the buildings studied.
- Unexposed balcony: characterized by closed sides throughout the depth of the balcony, resulting in greater shading of the glazed area and lower solar exposure in relation to the other typologies and present in 71% of the buildings studied.

Figure 3: Illustrative scheme showing the different types of balconies identified according to solar exposure.

As with balconies, shading elements appear in more than 80% of the projects analysed. Therefore, it was also necessary to identify, more than their presence, the typology of these elements. For this purpose, they were separated into fixed shading, regardless of their position in relation to the facade, movable shading, and metal meshes.

In 55% of the buildings, it was possible to identify the presence of fixed shading elements that consist of horizontal flaps, eaves, fixed louvers, or vertical elements. In 51% of the cases, it was possible to identify the presence of movable panels with the most diverse typologies of perforation and materiality, normally associated with balconies. Metal meshes, despite appearing on a smaller scale, were identified in 27% of the projects.

This analysis helped to understand the main characteristics of this set of contemporary buildings related to the high-standard neighbourhoods of the city of São Paulo. The identification of these characteristics allowed the definition of the simulation scenarios for the next stage.

Thus, to understand the impact of these facade design strategies on the performance of the internal space, shoebox models were executed to simulate the thermal and daylight performance of the strategies considering different combinations between the following factors (Fig. 4):

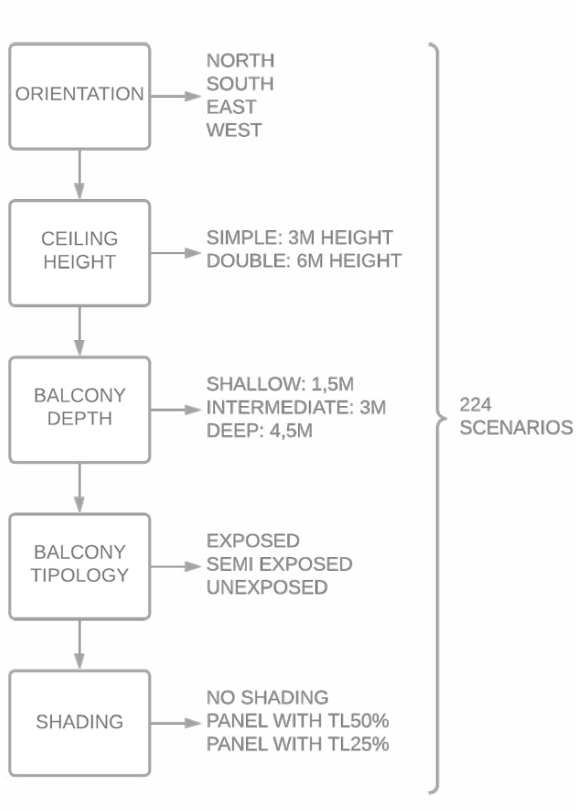

Figure 4: Flowchart showing the parameters used in the performance simulations of the facade design strategies.

- Four main orientations were considered: north, south, east, and west.

- Two options for ceiling height were considered: simple (3 meters high) or double (6 meters high).
- Balconies with three variations in depth were considered: shallow (1.5 meters), intermediate (3 meters), and deep (4.5 meters).
- Balconies with different levels of solar exposure were considered according to the identification in the previous phase survey: exposed, semi exposed, and unexposed.
- Three shading scenarios were considered: no protection, with an external protection element of the panel type with a light transmission of 50%, and with an external protection element of the panel type with a light transmission of 25%.

From then on, through the combination of the different strategies, the thermal and daylight performance simulations of the 224 resulting scenarios were carried out and the results could be evaluated.

Among the main results, it was possible to observe that the thermal performance simulations of the scenarios studied resulted in a difference of 13% between the scenario with the most and the scenario with the least hours within the comfort zone according to the adaptive model of ASHRAE 55.

When it comes to daylighting performance, the scenarios resulted in a variation of 100%, with the worst scenario presenting 0% of the annual hours with at least 50% of the area between 300lux and 3000lux and the best scenario presenting 100% of the annual hours with at least 50% of the area between 300lux and 3000lux.

In other words, from a methodological point of view, by giving the same importance to the two variables (thermal performance and natural lighting), the best and worst results of the analysis were directly related to the most extreme natural light results. Thus, it is possible to conclude that natural lighting proved to be an aspect much more influenced by the adequate design of the facade than thermal performance.

It is also worth noting that various strategies, such as the use of solar control glasses, insulation materials, reflective materials, or automated blinds, can be used to improve thermal performance, while improving access to natural light requires increasing the opening area.

The graph presented in Figure 5 shows the results of the scenarios and the relationship between thermal performance and natural lighting performance. The vertical axis indicates the daylight performance and the horizontal axis the thermal performance. Thus, each point represents a scenario and the closer it is to the upper right corner, the better the scenario performed in relation to the two variables under analysis.

By reading the results, it is possible to identify two main clusters of points. The first, in the upper left corner, refers to the group of scenarios that performed well in natural light, but not in thermal performance. The second, in the lower right corner, refers to the opposite situation. A small group of nine points shows the scenarios with the best combined results for the two variables.

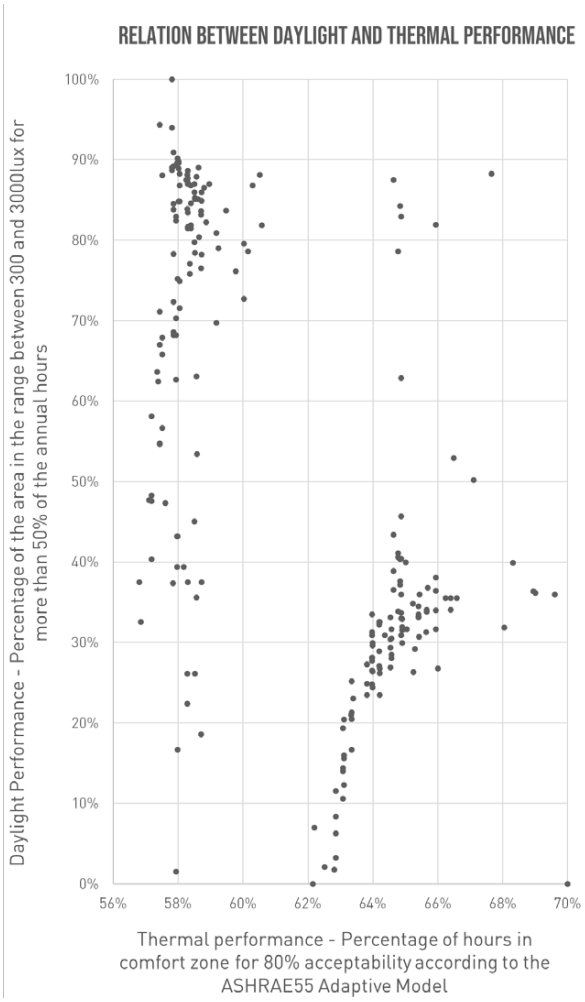

Figure 5: Graph showing the relation between daylight and thermal performance according to the results of the simulation of combined facade design strategies.

It was possible to observe that the best combined scenarios are those with a north orientation (favourable for natural light entry in the latitude of the city of São Paulo) combined with double height, deep balconies, and the presence of shading elements. Meanwhile, the worst scenarios are those with a combination of low ceiling height, the presence of shading elements, and deep balconies with lateral closures. The low levels of natural light, regardless of the orientation, made this combination the worst choice.

Balconies provide adequate shading when the correct orientation is observed. Shorter balconies,

with a depth between 1.5 and 3 meters, provide adequate shading for north and south orientations. However, for east and west facades, balconies with at least 3 meters of depth are necessary or should be associated with shading elements.

On the one hand, balconies with more than 3 meters, up to 4.5 meters, of depth can provide more adequate shading. On the other hand, they are responsible for very low levels of natural light and are only recommended in situations where there is no lateral closure, there is double height, and preferably in west-facing facades.

Shading elements have a significant impact on the final performance, especially in the case of scenarios with an east or west orientation due to the angles of solar incidence.

The results indicate that the variation in the light transmission of shading elements influences the final performance, however, the greatest influence comes from the presence or absence of the panel and its combination with the morphology of the balcony.

Shading panels showed better performance in scenarios with exposed or semi-exposed balconies, as they allow shading without drastically reducing the entry of daylight. The combination of panels, regardless of light transmission, with unexposed balconies, closed on the sides, culminated in results that are not recommended, as it greatly reduces the penetration of daylight, despite resulting in good thermal performance.

The use of double height should not be disregarded, being a relevant strategy in situations where there is a need to maximize the entry of natural light, mainly in facades facing south or east, and being a great strategy when combined with shading on the north façade (Fig. 6).

The results indicate that despite the double ceiling height results in scenarios with higher internal operating temperature compared to scenarios with single ceiling height, the reduction in the percentage of hours in the comfort zone according to the adaptive model is very small compared to the gain in daylighting performance.

It is possible to conclude, therefore, that double height ceilings can be a great strategy to improve the overall performance of housing units by increasing daylighting levels, but the envelope should be designed in such a way as to provide the necessary shading for adequate control of internal thermal loads.

4. CONCLUSION

The analysis of a set of 51 medium to high-end residential buildings launched in São Paulo between 2000 and 2020 identified the facade elements that characterize the contemporary residential architecture of the city.

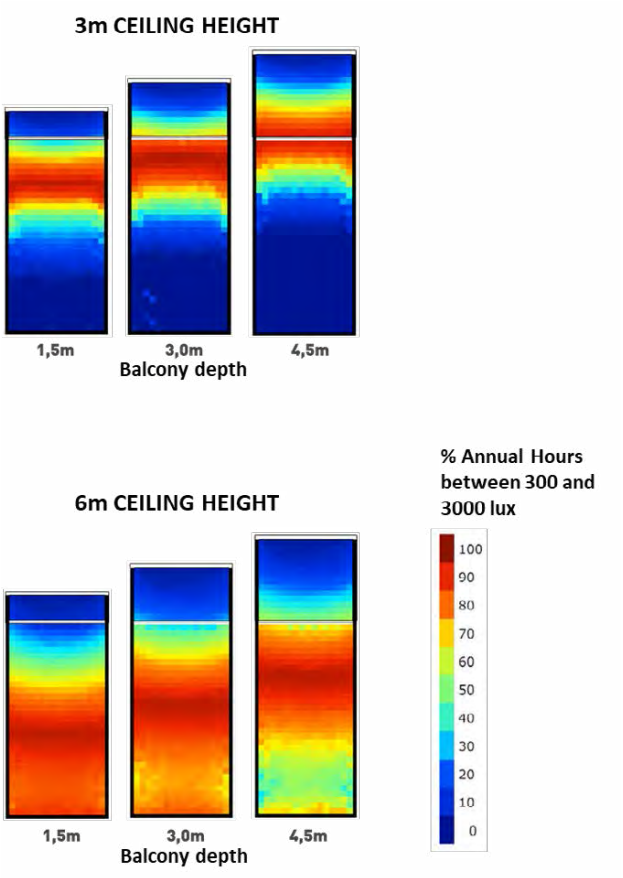

Figure 6: Simulation results for daylight performance of the scenarios for north orientation with single and double ceiling height and unexposed balcony with different depths and no shading showing the benefits of the double ceiling height for the daylight performance.

Elements such as balconies, floor-to-ceiling windows, fixed or movable sunshades, panels, metal mesh, and planters are responsible for delineating the aesthetics of these facades and can be used as performance enhancers.

As a result of the analysis, it was possible to conclude that balconies are the main elements in the design of these facades, appearing in different typologies and associated with different architectural elements.

The analysis of the strategies applied in the design of the facades reinforced some known points, such as the need to protect the north and west facades. However, it was also possible to identify some new factors, such as the enormous potential of using double-height ceilings, which is usually not recommended for the local climate due to the extensive glazed areas associated with it, but which can result in good performance when used in conjunction with balconies and shading elements.

Another pertinent observation is that balconies with a depth of more than 3 meters, up to 4.5 meters, can provide adequate shading, but they are

responsible for very low levels of natural light. Thus, it is possible to observe that in the case of residential units in which the balconies are subsequently closed, a common practice in São Paulo, forming a new facade line with exposed glass, there will be a serious loss in thermal and luminous performance. In these cases, the use of the closure will result in an increase in thermal load, with high temperatures in the perimeter zone.

Finally, the analyses concluded that, considering the various facade strategies, the variation in thermal performance is around 13% between all the scenarios evaluated, including the starting scenarios without the use of balconies.

Meanwhile, the variation in luminous performance ranged from 0 to 100%. In other words, natural lighting proved to be an aspect much more influenced by the proper design of the facade than thermal performance.

It is concluded that, despite the extreme relevance of thermal performance in the qualitative impact on the end user, it is essential that projects are designed in a way that maximizes light entry, with adequate shading and protection during the hottest periods.

REFERENCES

1,2. Reinhart, C., (2011). Daylight performance predictions. In: HENSEN, J. L. M.; LAMBERTS, R. *Building Performance Simulation for Design and Operation*: p. 235-276.

3. American Society of Heating, Refrigerating, And Air-Conditioning Engineers (ASHRAE), (2020). *ASHRAE Standard 55-2020 – Thermal Environmental Conditions for Human Occupancy*.

4. Serapião, F., (2014). Moderno nas Alturas. In: SERAPIÃO, F. *Revista Monolito*: p. 14-26.

5. Mendes, M. R. A. V., (2018). Idea!Zarvos: O mercado imobiliários e a arquitetura autoral.

6. Gonçalves, J. C. S., (2015). Edifício Ambiental. *Oficina de Textos.*

PLEA 2024 WROCŁAW
(Re)thinking Resilience

Improving thermal safety, comfort and indoor air quality in public schools in Nepal

Design solutions for improving thermal conditions, resiliency and ventilation in present and future climate scenarios

SHREEJAYA TULADHAR [1], ARUNIMA DEV[1]

[1]ArchSolar Designs, Kathmandu, Nepal

ABSTRACT: Schools in Nepal are built with little consideration for thermal comfort and safety ignoring the local climate and materials with similar prototype designs adopted throughout the country despite the diversity in geography and climates. There are reports of the extreme conditions hindering the learning environment and tragically harming the health of the pupils, a solution is critical. The study aims to use thermal simulation to evaluate the adaptive thermal comfort of these public schools. Evaluation was done in the three distinct climatic/geographic regions of Nepal i.e. the mountainous Himalayan (cold/temperate), Hilly (mild), and the plains terai (hot & humid) regions with the cities Jumla, Kathmandu, and Nepalgunj representing the climatic geographical regions respectively. Passive design intervention using low-cost, bio based improvised insulation such as agricultural waste (rice husk) was explored. Natural ventilation potential of the classroom was also evaluated and enhanced using a high operable clerestory window. Projected climate scenarios such as 2050, and 2080 were also evaluated to test their climate adaptation potential in terms of changing climate.
KEYWORDS: Thermal Comfort, Thermal Safety, Resilience, Climate Change, Natural Ventilation

1. INTRODUCTION

1.1 Background

Nepal ranks 127th in the world education ranking with an education index of 0.52 which is a component of the Human Development Index, [10] The ranking shows Nepal needs a lot of improvement in its education system and infrastructure.

There is a growing body of literature and field data from around the world that links classroom conditions and (IAQ) with the health, absenteeism, and educational performance of pupils. Inadequate thermal conditions and poor IAQ in school environments cause an increased risk for respiratory illnesses and other health-related symptoms such as asthma and affect children's cognitive performance and learning [12]. One such study has shown providing enhanced ventilation rate of around 10 L/S per pupil over the ASHRAE-62.1 [1] standard recommended rate of 6.7 L/s per pupil demonstrated improved performance with a study from South-western United States showing 3% more pupils passed tests and math score improved by 0.6 for every 1L/s per pupil increase in ventilation rate and a 13% increase in math scores for every 1°C decrease of classroom temperature. [12]

The geography and climate in Nepal can be divided into three distinct regions i.e. the mountainous Himalayan (cold/temperate), Hilly (mild), and the plains terai (hot & humid) regions. The selected cities and their location on the map of Nepal is shown in figure 3 below.

1.2 Typical public school design for Nepal

Public school buildings in Nepal are simple and elongated in plan with single-loaded corridors that act as semi-outdoor spaces with open facades on one side and classrooms on the other. They are usually 1-2 storeys with rural ones being single storey. A typical single-story classroom design is shown in Figure. 1 and 2 below. It has 2 classrooms each of size 5m X 8m meant for 40 pupils in each classroom.

Typical materials used in school construction are burnt brick masonry walls with concrete floors and structure in the Hilly region and the hot & humid Terai region. Stone masonry walls are used mostly in the Himalayan region where stone is available. For roofs, CGI (Corrugated Galvanized Iron) sheets are typically used all over Nepal with CGI sheets being commonly exposed; and a false ceiling being rarely used. The design shown in Figure. 1 is a reference from the Government of Nepal's Reconstruction Authority website.

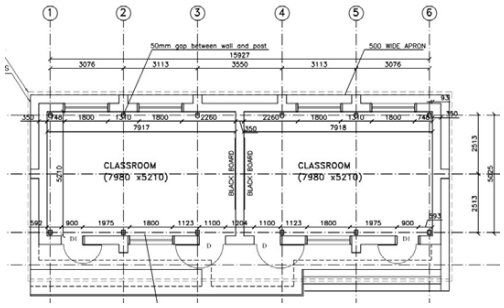

Figure 1: Plan of Typical classroom [4]

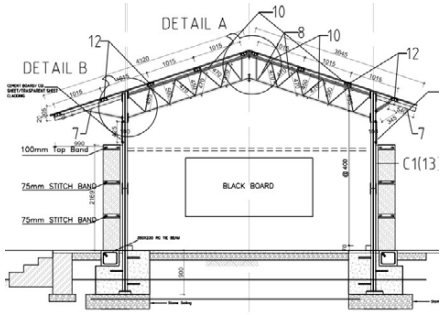

Figure 2: Section of Typical classroom [4]

The Department of Education, Ministry of Education Nepal (2016) also published a guideline for school design. It is clearly influenced by the aftermath of the Nepal 2015 Earthquake (moment magnitude 7.8) prioritizing earthquake disaster resilience while omitting hot/cold waves.

The guideline mentions the use of insulation and climate-responsive strategies such as proper orientation, window sizes, and maximization of natural ventilation without providing any details and there is no mention of any thermal comfort or ventilation rate standards.

Recent news of hot and cold waves leading to week-long school closures have been reported [13] with the heat wave of summer 2023 in Nepalgunj reported of students falling sick, fainting, vomiting, and nausea. The school authorities complained about the CGI roofing overheating. [5]

1.3 Parameters of the study

In this study, a typical 1-story classroom building will be evaluated using thermal simulation in the three cities in Nepal representing the three distinct geography and climates of Nepal. The cities: Jumla (JUM), Kathmandu (KTM), and Nepalgunj (NPJ) represent the cool/temperate Himalayan region, the mild Hilly region, and the hot and humid Terai region respectively.

Figure 4 graphically compares the dry-bulb temperatures of the selected cities. Figure 5 compares the cold and hot degree days. It is clear from the comparisons in figure 4 and 5 that Kathmandu is milder with warm summer and cool winters whereas Nepalgunj is hot and humid, and Jumla is colder.

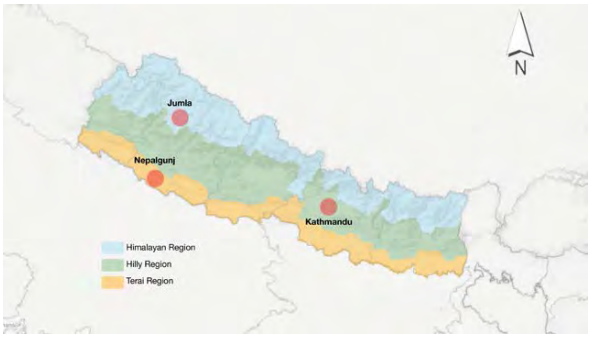

Figure 3: Geographical and climatic map of Nepal

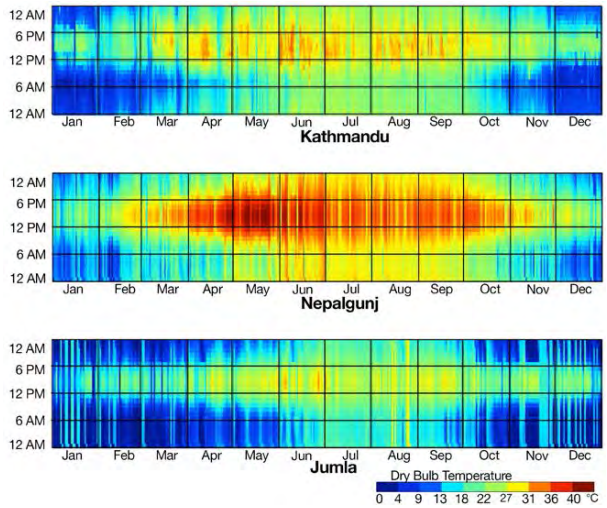

Figure 4: Graphical field view of dry bulb temperatures

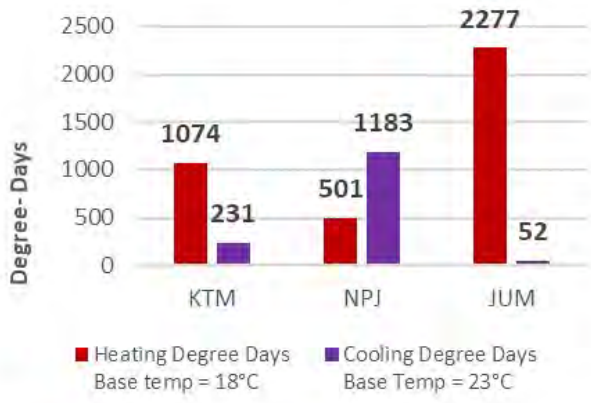

Figure 5: Heating and Cooling Degree Days of evaluated cities in Nepal

Past research by the authors [13] demonstrates that interior evaluation based on ASHRAE-55 adaptive thermal comfort [1] is insufficient as the interior conditions far exceed the adaptive thermal comfort standards and health risk conditions. In the absence of agreed-upon standards for thermal safety, Indoor temperatures of 35°C and 12°C are set as upper and lower thresholds. These are based on statistical data of increased mortality rates in heat waves over

temperatures of 35°C [14] and data suggesting that vulnerable populations, i.e. the elderly, sick, and small children, are susceptible to cardiovascular problems and strokes in sustained conditions below 12°C [2]. A similar evaluation was performed on future projected climate scenarios of 2050, and 2080 to evaluate the performance of the building in terms of adaptation to future climate scenarios and resiliency to extreme weather events.

Envelope design solution was tested using simulation tools to improve thermal comfort and safety to produce design guidelines. The Solutions tested was wall and roof insulation using repurposed wastes such as rice husks (agricultural waste) and shredded denim (fabric waste).

Alternative waste materials have been proposed as insulation in place of more conventional commercial insulation materials such as glass wool, mineral wool, Polystyrene, and EPS (Expanded Polystyrene) as they are readily available even in remote rural areas. Conventional insulation materials are not readily available and are extremely expensive in Nepal. For comparison, mineral wool of similar thickness (150mm) costs at least five times the cost of rice husk based insulation attached to the building.

Rice husk/hull insulation has been used for the study as the material is a low-cost, bio based, and carbon neutral insulation material. Even in its raw stage it has been classified as a Class A or I insulation material [9].

The authors based on previous research [13] built a prototype temporary shelter with rice husk insulation for Western Nepal 2023 earthquake victims (moment magnitude 6.4, Nov 3rd). Its thickness 150mm was determined based on this research. The insulation and methods of attaching it to the building can be seen in figure 6. The resulting performance of the rice husk insulated shelter was promising. The interior surface and air temperature was 13°C when the minimum outdoor temperature was 7°C showing a difference of 5°C. The surface temperature for the control uninsulated shelter was 2°C, thus the rice husk insulation showed an 11°C difference.

For this simulation study, the same material and thickness of 150mm rice husk insulation was used with thickness determined due to diminishing returns on increased thickness beyond it.

The natural ventilation rate will also be evaluated based on the size and position of the window openings using hand calculations. To enhance the ventilation rate and provide natural cooling, design solutions ranging from size and position of the added window openings will be synthesized.

Figure 6: Rice husk packed into jute tubes to act as insulation for a prototype temporary shelter for earthquake victims. Source: Author

2. METHODOLOGY

A typical 1-storey classroom building (see Figure 1) was selected. A typical Brick masonry wall 230mm thick was used for evaluation on Kathmandu in the mild Hilly region and Nepalgung in the Hot and humid Terai region. Stone masonry wall of 350mm thickness typical of the Himalayan region was evaluated for Jumla. For all regions concrete floor and CGI (Corrugated Galvanized Iron) sheet roofing was be used.

Thermal simulations was performed using the US Department of Energy's EnergyPlus (DOE, 2015) simulation engine, via the Honeybee interface [7], a plug-in for Grasshopper [6], a visual scripting plug-in for the Rhinoceros 3D modelling software [6].

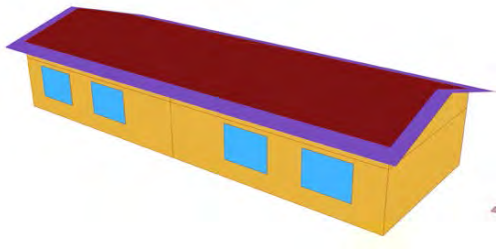

Figure 7: 3d Energy model geometry of classroom building.

Table 1: material property of rice husk insulation used for simulation.

parameter	Value	Unit
Roughness	Rough	-
Thickness	0.15	m
Thermal conductivity	0.05	W/m-°K
Density	120	kg/m3
Specific Heat	1000	J/kg-°K
Thermal Absorptance	0.9	-
Solar Absorptance	0.6	-
Solar Absorptance	0.6	-

Occupancy was set at 40 pupils per classroom (1 pupil/m^2) based on government of Nepal's guidelines discussed previously on introduction section. Equipment load and Lighting load was set at 15W/m^2 and 7.64W/m^2 respectively based on Energy plus and Honeybee plugin default profile for primary schools classroom [7]. Occupancy profile was also set based on the same default profile. The infiltration rat was set at 0.006m3/s[1.27cfm] per m2 of exposed area, as recommended for leaky buildings [1]. Natural ventilation was modelled to provide air flow and ventilation with window controls set assuming the operable windows would be closed when interior temperatures dropped below 20°C [68°F]. EnergyPlus calculates natural ventilation using the simple ventilation equations same as equations 1, 2, and 3. The weather data, typical meteorological weather (TMY) files was obtained from the Climate.One.Building.Org website based on the regional airport data.

For the projected future climate scenario of 2050, 2080, the TMY files were morphed using the CCWorldWeatherGen, a tool developed by the University of Southampton's Energy and Climate Change Division to morph weather files according to IPCC (Intergovernmental Panel on Climate change) HadCM3 A2 experiment scenarios.

As evaluation of interior conditions using just the ASHRAE-55 adaptive thermal comfort might not explain the extent to which the interior conditions might exceed the comfort zones, the metric of Degree-hours is used where the number of hours and degrees above or below the adaptive comfort were added up. This metric gives a more nuanced idea of the interior condition especially when considering future climate scenarios.

For a closer ventilation analysis, hand calculation was done using following equations 1, 2, 3 for buoyancy ventilation to evaluate the ventilation of the classroom.

$$\dot{V} = [(AC_d)_{eff} \sqrt{\beta . \Delta H . q}]^{2/3} \quad (1)$$

$$\beta = 2g/(\rho . C_p . Tr_{ef)} = 0.0000545\ m^4/s^4 \quad (2)$$

Where $\dot{V}$ - Volumetric Flow rate (m^3/s);

$(AC_d)_{eff}$ – effective area of window openings;
A – Area of operable window openings – 7.2m^2;
C_d – discharge coefficient [0.65 for open window, 0.45 for window with insect screens];
ΔH – height difference between inlet, outlet (m2);
q – Internal heat gain,[40 pupils X 70W per pupil];
ρ – Density of air [1.2kg /m^3];
C_p – specific heat capacity of air [1000J / (Kg.°K)];
T ref – 300°K;
g – Acceleration due to gravity [9.81 m/s^2];

$$\Delta T = q/(\rho . C_p . \dot{V}) \quad (3)$$

Where ΔT – overheating due to internal heat gain (°C);
The resulting volumetric flow rate ($\dot{V}$) was converted to ACH (Air changer per hour) metric for comparisons using following equation 4.

$$ACH = (\dot{V} \times 3600s) / V \quad (4)$$

Where ACH – Air changer per hour;

V – Volume of room (m^3)
s - Seconds

For the ventilation hand calculations, only buoyancy ventilation was calculated and wind driven ventilation ignored. The reasoning was that winds are sporadic and unreliable and highly dependent upon contextual factors such as wind direction and surrounding terrains and obstacles to wind. Since in this study we are evaluating typical designs applied without site context, winds was ignored. Solar heat gain and thermal mass gains was also ignored to keep the ventilation calculations simple.

3. RESULTS

As can be seen in the results below in figure 6, the adaptive comfort levels in the classroom interiors remain poor. This could mainly be due to the un-insulated metal CGI roofing which is subject to extreme diurnal temperature swing during the day and night. Figure 8 also clearly shows gradual warming of the indoor conditions in future climate scenarios.

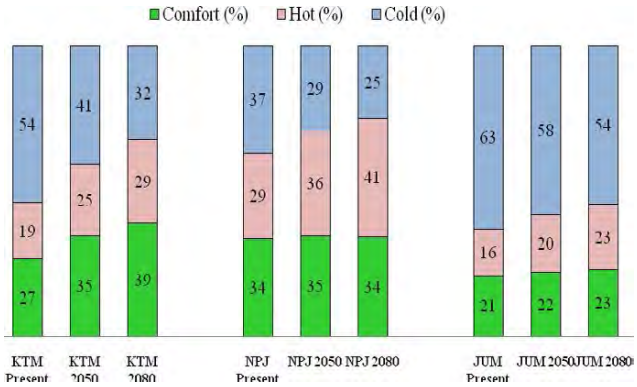

Figure 8: Adaptive comfort evaluation of baseline classroom interior conditions in present and future scenarios

Figure 9 below shows the degree-hours metric exceeding cold health risk (<12°C) and hot health risk (>35°C). Is shows that the climate of hot-humid Nepalgunj (NPJ) poses a risk which will get dire in future climate scenarios. Conditions in Kathmandu (KTM) are milder while that of Jumla (JUM) in the mountainous Himalayas faces risk due to cold which will decrease in future climate scenarios.

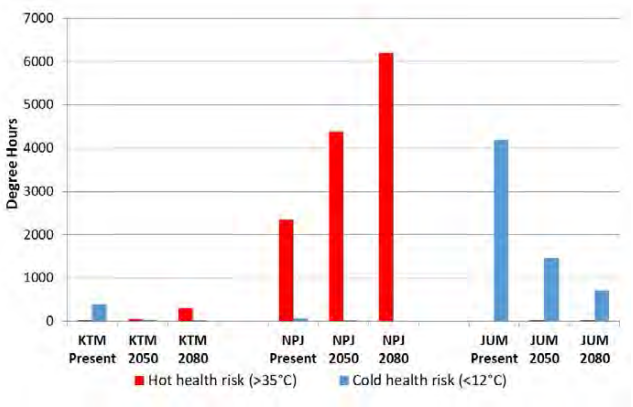

Figure 9: Hot and Cold Health risk Degree-hours in present and future climate scenarios

Insulation using risk husk of 150mm in roof and 75mm in the walls greatly improved the interior conditions of the classroom. Figure 10 below shows doubling of the adaptive thermal comfort levels in all the studied locations.

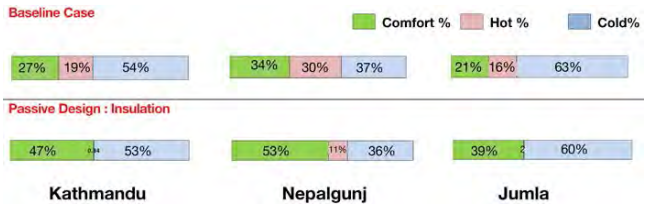

Figure 10: Hot and Cold Health risk Degree-hours in present and future climate scenarios

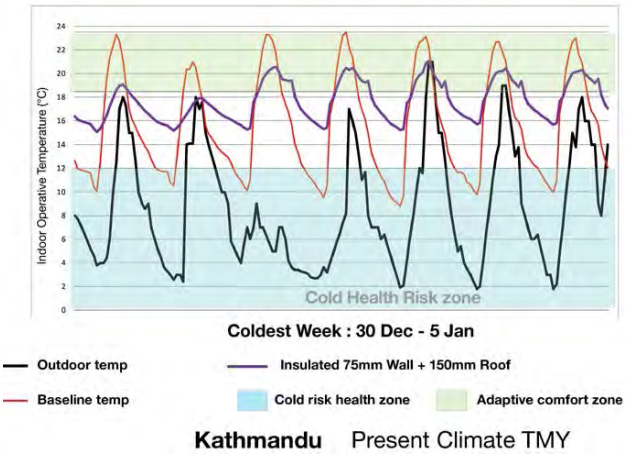

Figure 11: Temperature curves showing indoor and outdoor temperatures during coldest week.

Taking an in-depth look at the temperature curve comparison of the coldest week in the location of Kathmandu, we can observe from figure 11 that adding insulation moderates the diurnal temperature swings. In the baseline case there is high diurnal swing of over 12°C with high daytime temperature and gradual lowering of the indoor temperature in the morning and late afternoon mirroring the outdoor temperature dipping in the cold health risk zone of below 12°C. In the scenario with the use of roof and wall insulation, the interiors are either inside the adaptive thermal comfort limits or close to it. Lower temperature in the very early mornings and late nights can be ignored as classroom will be unoccupied during those hours. However mornings and late afternoons must not be too cold.

For ventilation analysis, equations 1-4 for used to evaluate the flow rate into the classroom.

Results for the baseline design based on size of window openings are as follows

<u>Baseline design</u>

$\dot{V}$ - Volumetric Flow rate = 0.5m^3/s

ACH = 12

ΔT – Overheating = 4°C

The volumetric flow rate or ventilation rate of the existing classroom is well and above the minimum ventilation rate according to ASHRAE 62.1 [1].

The minimum ventilation rate for the classroom which has 40 pupils was determined to be 0.224m^3/s (5L/s per pupil + Area rate 0.6L/s .m^2).

However typical naturally ventilated buildings designed with natural ventilation in mind have ventilation or flow rates much higher ranging from 20-30 ACH and up to 50 [15]. As seen from the Overheating of 4°C that the existing window design is not sufficient to naturally cool the classroom especially as it has an occupancy of 40 pupils.

However if insect screens were to be added to the window openings to keep insects out and reduce mosquito transmitted tropical illness such as malaria and dengue, the ventilation rates are further reduced as follows.

<u>Baseline design with insect screen</u>

Where, c_d – discharge coefficient – 0.45

$\dot{V}$ - Volumetric Flow rate = 0.292m^3/s

ACH = 7

ΔT – Overheating = 6.84°C

Therefore, in order to enhance ventilation and reduce overheating providing natural cooling, a 1m high pop-up clerestory window facing north was proposed as shown in figure 12 below. The height difference between the proposed north facing clerestory window at top and the existing windows was 2m centre to centre. The height difference was created to increase the ventilation or flow rate based on equation 1.

<u>Proposed enhanced natural ventilation design</u>

$\dot{V}$ - Volumetric Flow rate = 2.169m^3/s

ACH = 52

ΔT – Overheating = 0.92°C

<u>Proposed enhanced natural ventilation design with insect screen.</u>

Where, c_d – discharge coefficient – 0.45

$\dot{V}$ - Volumetric Flow rate = 1.242m^3/s

ACH = 29.8

ΔT – Overheating = 1.6°C

The proposed clerestory window does greatly enhanced the ventilation rate and provide natural cooling and avoid overheating due to internal occupant heat gain. The enhanced ventilation or volumetric flow rate with increased air changes means the air inside the classroom is frequently changed as much as 52 times per hour. It can be assumed with high certainty that it results in much improved indoor air quality as indoor air pollutants are frequently flushed out of the space. Addition of insect screens will decrease the ventilation rates. However as the ventilation rate is high, a slight decrease in ventilation rates should not greatly decrease the ventilation rates.

The addition of north facing clerestory windows should also greatly enhance the natural lighting in the classrooms.

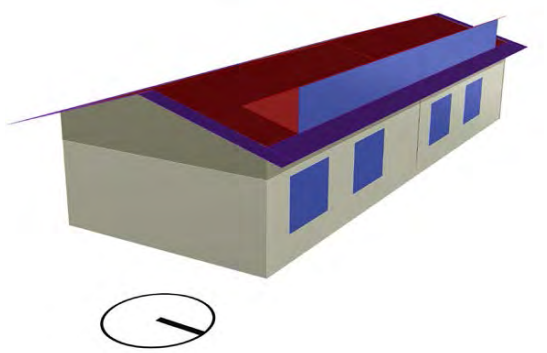

Figure 12: Addition of north facing pop-up clerestory window.

3.1 limitations

Although the high north clerestory window is highly effective in enhancing the ventilation rate, there are limitations as to its application. This type of solution is more suitable to single storied designs.

However for 2-3 storied school designs, dedicated thermal chimneys can be added to provide the enhanced ventilation. It must be noted that the addition of thermal chimney will not provide extra natural lighting.

Addition of insect screens will decrease the ventilation rates. However the ventilation rate is also satisfactory as the ventilation rate is 29.8 ACH and overheating is limited to 1.6°C.

4. CONCLUSION

Simulations can be a useful tool to evaluate and improve thermal safety and comfort, improving resiliency to extreme weather events, including in future climate change scenarios.

The interior thermal conditions of the classrooms far exceeds the adaptive thermal comfort standards for majority of the time i.e. less than 50% of the time extending into the Health risk temperatures of above 35°C and below 12°C in evaluated cities. The conditions are exacerbated in future climate scenarios. Additionally, low cost improvised insulation can be sufficient to improve thermal safety and comfort in classrooms thus also improving the learning environment. Addition of high operable clerestory window can enhance ventilation rate in the classrooms providing natural cooling. The enhanced ventilation also improves the indoor air quality of the classrooms by flushing out indoor air pollutants. It also allows good ventilation rate despite addition of insect screens as insect screens reduces air flow as compared to open window openings.

REFERENCES

1. American Society of Heating, Refrigerating and Air-Conditioning Engineers (2016) Standard 55, Handbook fundamentals: 2001, Standard 62.1: 2010, Thermal Environmental Conditions for Human Occupancy. ASHRAE, Atlanta.
2. Collins K. J. (1986). Low indoor temperatures and morbidity in the elderly. Age and ageing, 15(4), 212–220. https://doi.org/10.1093/ageing/15.4.212
3. Department of Energy. (2015).EnergyPlus. Version 8.3.0.
4. Department of Education, Ministry of Education Nepal (2016). Guidelines for Developing Type Design for School Buildings. Available: http://www.moepiu.gov.np/rules/School-Design-Guidelines_FINAL_1474869069-1668077971.pdf
5. Ghatraj, R. et. Al (2023, June 14). Hot weather makes life difficult in Terai. The Kathmandu Post. https://kathmandupost.com/climate environment/2023/06/14/hot-weath..
6. McNeel and Associates.(2020) Rhinoceros 3D. Version 7. Massachusetts Institue of Technology. (2012). CoolVent. Available: http://coolvent.mit.edu/download/
7. Rousdari M.S and Mackey C. (2022). Honeybee.Version 1.6.
8. Climate.One.Building, [Online], Available: https://climate.onebuilding.org/WMO_Region_2_Asia/NPL_Nepal/index.html [30 Aug2023].
9. Rankedex, Countries by education Index, https://rankedex.com/society-rankings/education-index [30 Aug 2023]
10. Rice hulls in construction". Appropedia. 2006–2023. Retrieved December 29, 2023.
11. RSS (2023, Jan 3). Schools closed to avoid cold. The Rising Nepal. https://risingnepaldaily.com/news/20911
12. Sadrizadeh, S., et al. (2022). Indoor Air Quality and health in schools: A critical review for developing the roadmap for the Future School Environment. Journal of Building Engineering, 57, 104908. https://doi.org/10.1016/j.jobe.2022.104908
13. Tuladhar, S. et al. (2019,), Tempering the temporary: Improving thermal safety and comfort in relief shelters, Proceedings of the 16th IBPSA Conference, Rome, 2-4 Sep 2019.
14. World Health Organization Europe. (2009). Improving Public Health Responses to Extreme Weather and Heat-Waves.[Online],http://www.euro.who.int/__data/assets/pdf_file/0010/95914/E92474.pdf?ua=1[19 March 2017].
15. Atkinson J, Chartier Y, Pessoa-Silva CL, et al., editors. (2009). Natural Ventilation for Infection Control in Health-Care Settings. World Health Organization. https://www.ncbi.nlm.nih.gov/books/NBK143277/

Policy insights from a financial analysis of energy retrofit with heat pumps compared with PV.

Paybacks range from 6 years to over 100 years - which investment makes most sense?

SHANE COLCLOUGH[1,3] OLIVER KINNANE[1] PAUL OSULLIVAN[2] NIAMH POWER[2]

[1] University College Dublin, Dublin, Ireland
[2] Munster Technological University, Cork, Ireland
[3] Energy Expertise Ltd, Naas, Ireland

ABSTRACT: There is a pressing need to carry out energy upgrades on the European residential building stock. This paper looks at examples of challenges and opportunities within the largest cohort of dwellings (i.e. those with a Building Energy Rating of C) within the member state (Ireland), through a case study analysis of two properties. The paper shows that there are low barriers to entry and clear financial benefits for the stakeholders associated with installing photovoltaic installations for the case study dwelling considered (financial payback of 5.9 to 12 years). Conversely, there were significant challenges, both financial and project-related in upgrading the gas fired heating system to a heat pump in a separate case study dwelling (with a financial payback of over 100 years). While both decarbonising routes may be necessary and beneficial, the analyses highlight a need for further supports in the case of HP deployment for a cohort of the targeted dwellings.
KEYWORDS: Energy retrofit, heat pump, photovoltaic, PV, financial analysis.

1. INTRODUCTION

The Irish Government's policy is to install 400,000 heat pumps and carry out 500,000 home energy upgrades by 2030 (1), with the National Retrofit Plan assuming that by 2025 up to 88% of upgrades will involve the installation of a heat pump (2).

There are clear advantages for the retrofit of old energy inefficient homes, e.g., those with a Building Energy Rating (BER) of F and G, where homes are made more healthy and comfortable, and heating costs are significantly reduced following the energy retrofit. The considerable energy retrofit and heat pump grants available are key enablers in this respect.

The installation of heat pumps in new energy efficient homes also continues apace with over 96% of dwellings built since 2015 having a BER of A, and with the majority using electric heat pumps (3).

However, there is a cohort of Irish homes for which installing a heat pump may make a poor financial case, fitting neither in the new build group nor the energy inefficient group. The problem is that this cohort is large (exemplified as homes with a middle-of-the-road C BER which comprises 35% of Irish homes (3). Without addressing the impediments including those identified in this paper, it seems apparent that the government will struggle to achieve the stated national targets.

In parallel with carrying out energy upgrades to the building fabric and installing heat pumps, the installation of photovoltaic (PV) is also being carried out at a national scale. PV also offers an opportunity of reducing the net energy demand of the dwellings, and therefore contribute to achieving improved BER's, in line with the government's objectives. Moreover, PV can represent a less disruptive means of improving the energy efficiency of the home, and potentially offer a lower cost and more financially attractive proposition.

This paper presents financial analyses for two C rated case study dwellings:

1. A 1998 Deep Energy Retrofit (DER) in combination with installing a HP in a 167m^2 dwelling with an annual gas consumption of 19,380 kWh and an annual electricity consumption of 4636 kWh excluding Electric Vehicle (EV).
2. A 2004 100m^2 holiday home with an annual electricity consumption of 2,910 kWh including space and Domestic Hot Water (DHW) heating and excluding EV.

A summary of the findings for the DER with HP previously presented (4) is below in addition to the PV analysis for the holiday home.

2. METHODOLOGY

Heat pumps have the advantage of theoretically producing between three and four units of space heating for each unit of electricity consumed (i.e. the Coefficient

of Performance, COP). If this is equivalent to the price differential between gas and electricity, it means that, once installed, the cost of running a heat pump should be comparable with mains gas (5). But is this the case in reality? For example the COP for heating hot water is typically only 2. Also space heating COPs can vary widely depending on many variables, including the specific heat pump, the energy efficiency of the home in which they operate, the difference between the internal and external temperatures and how well they were installed and operated, etc (6). Further, what is the cost of upgrading to a heat pump, and are the costs justifiable compared with the less disruptive and less costly option of installing a condensing gas boiler? Also how does this compare with the relatively straightforward energy upgrade alternative prospect of installing PV panels instead of or in addition to the Heat Pump?

These questions are being addressed in research projects being run by University College Dublin (UCD), Munster Technological University (MTU) and industry partner Energy Expertise Ltd.

Monitoring of over 50 Irish HP (7) & also over 50 PV installations (8) is being carried out nationally. The actual amount of heat produced by the HP's for each unit of electricity input is being measured in real-world conditions. In addition, the contribution of PV generated electricity in Irish homes is also being measured and analysed with a view to increasing the self-consumption percentage. The financial analysis for PV, based on recorded data and up to date financials illustrates potentially superior financial returns with significantly less financial outlay and disruption compared with a Deep Energy Retrofit and HP deployment, as outlined below.

3. RESULTS

3.1 DER in combination with HP

The deep energy retrofit (DER) and heat pump installation was found to be financially unattractive for a C-rated case study dwelling in a recently presented analysis (4):

1. Overall, the analysis found that the lowest Total Cost of Ownership (TCO) was achieved by heating with a condensing gas boiler rather than a heat pump.

2. The cost of improvements to the fabric (to reduce the heat loss to the necessary 2.0 W/°Cm^2 required to attain a national grant) amounted to €41k (net of grant), yet resulted in a reduced space heating demand of only 21%, of 2,730 kWh, equivalent to an annual gas cost reduction of €380. This gives a simple payback of over 100 years for the DER (Fig 1).

3. The cost of the heat pump installation (net of grants) amounted to €16.5k, compared with a cost of 3.5k for the installation of a condensing gas boiler (Fig 1).

4. The annual running costs for the heat pump (assuming the DER was carried out) compared with the condensing gas boiler reduced from €2,631 to €2,576, or €55 annually, assuming the best case scenario of lowest cost electric smart tariffs and the HP manufacturers stated COP.

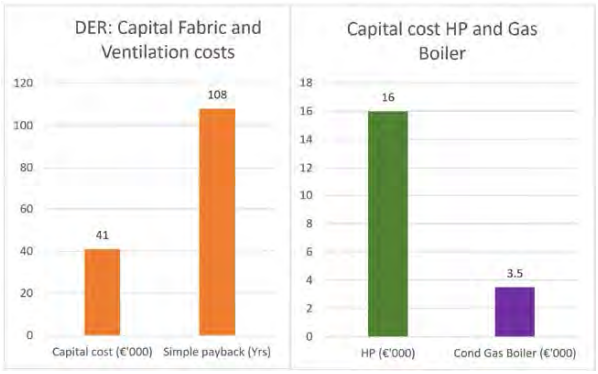

Figure 1: Capital cost comparisons – DER and HP Vs gas boiler

Even if the HP installation was grant aided at current levels without requiring a deep energy retrofit, (and assuming the COP is the same with or without the DER) the additional annual TCO of the heat pump compared with the condensing gas boiler are in excess of €800 per annum (assuming the dwellings' smart electricity tariffs being used at the time of the study, March 2023).

So, it is seen that the financial analysis highlights the fiscal challenge of performing a DER upgrade to the relatively well performing case study dwelling to one which will accept a heat pump (with a payback of circa 100 years). It is seen that a large expenditure is required to reduce the energy consumption by a relatively small amount, resulting in high payback periods.

Moreover, Ireland continues to have the highest consumer electricity prices in Europe (9), a factor which is considered by many to discourage the adoption of electric heat pumps.

However, based on the same Household Energy Price Index report (9), Ireland also has among the highest natural gas prices in Europe. Therefore it is worthwhile trying to understand the factors which influence the financial viability of heat pumps such as the (most common) air to water heat pumps being deployed in the UK and Ireland.

The annual running costs of a Heat Pump compared with a gas boiler are directly related to:

1. The HP COP (which is the subject of the current research (7))
2. The Gas Boiler Efficiency
3. The price differential between electricity and gas.

The reason for this is that while heat pumps offer an advantage of high values of output heat per unit of electricity (e.g. a COP of between 2 and 3), if the cost of electricity is higher than the multiplier value of the COP, it is more expensive to heat with electricity than with gas. The issue is compounded in that the COP for DHW heating is often significantly lower than that for space heating, leading to a lower average COP.

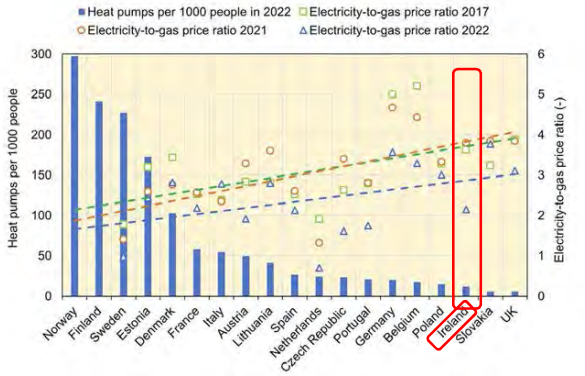

Figure 2: No. of electrically driven heat pumps per 1000 households in 2022 and ratio of electricity to natural gas price for domestic consumers in major European economies between 2017 and 2022 (10)

Figure 2 indicates that, for the countries considered, the price differential between natural gas and electricity favours the installation of heat pumps (10). Where the electricity to gas price ratio is high, the concentration of heat pumps is low, with Ireland, Slovakia and the UK respectively having the lowest densities per capita and among the most disadvantageous electricity to gas ratios.

Figure 2 shows that Ireland has had disadvantageous electricity to gas price ratios over the years 2017, 2021 and 2022 (see the broken trendlines in figure 2). Specifically, the electricity to gas price ratios were between 3.5 and 4 in 2017 and 2021, before falling to 2.1 in 2022.

The most recent data (11) from the Sustainable Energy Authority of Ireland (SEAI) was analysed (Fig 3). It indicates that the ratio of the standard tariffs for the most common electricity and gas consumption bands (12) were high (2.8 to 3.4) between 2017 and Q1 2022, before falling to c. 2 in Q3 2023. The ratio of electricity to gas prices has remained relatively stable at approximately 2 since the Ukraine war commenced (Mar 2022).

Therefore, despite the high cost of electricity, based on the SEAI unit prices, the HP COP appears to currently make the electric Heat Pump more cost competitive than gas boilers in Ireland, if the HP COP's are greater than a very realistic 2.0.

However, based on the case study actual electricity and gas tariffs and the recorded DHW and space heating demand, servicing costs etc, HP's remain less attractive in reality (Table 1).

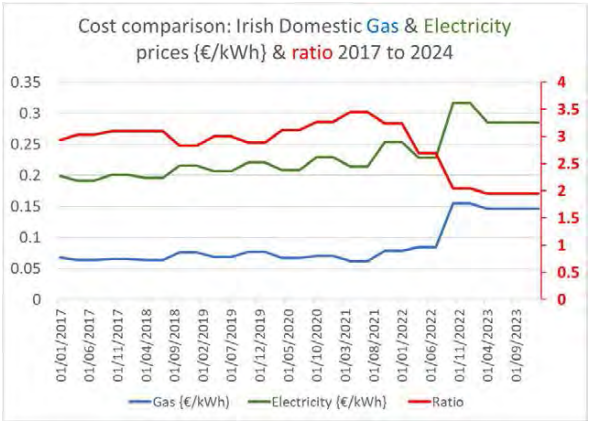

Figure 3: Irish domestic electricity and gas prices and ratio of electricity to natural gas price between January 2017 and January 2024

Table 1 shows that an electric heat pump (with COP of 2.6) has in the region of €100 additional total annual cost for DHW and space heating. These costs are based on choosing the most competitive rates available in the marketplace for gas and electricity (Smart meter tariff).

Table 1: Case Study Electricity and gas costs 2023 and 2024

Year	Gas {€}	Electricity {€}	Difference
2024	1935	2046	€111 (5.7%)
2023	2631	2728	€97 (3.7)

Investigation revealed a significant discrepancy between the average unit prices in the SEAI report and those available in the marketplace. SEAI's applicable figures at March 2023 were 14.65c (gas) and 28.52c (electricity), and "are based on a selection of suppliers that publish their prices online". SEAI rates also exclude standing charges and any discounts and result in a electricity/gas price ration of 1.95 at Mar 2023. This compares with the case study actual standard rates of 14.37c (gas – SSE Airtricity) and 43.59c (electricity) recorded at March 2023 (electricity/gas price ratio 3.0). The SEAI stated rate for electricity was considerably lower than that actually available in the marketplace, even without considering the complicating factor of individual supplier discounts and also didn't consider standing charges (which can be high for smart tariff. It is noted that SEAI included two €200 credits under the Government Electricity Costs Emergency Benefit

Scheme. Similar credits were not applied to gas accounts, and there is no plan to apply future credits to either gas or electricity (and therefore none have been included in the case study figures).

A key finding of the analysis is the variance between stated unit prices and those available in the marketplace, and the impact of high standing charges for smart meter tariffs. This underlines the value in catting out detailed analysis based on actual case studies in order to obtain accurate comparisons between gas and heat pump actual annual costs.

3.2 PV Installation

An alternative proposition is considered below (in relation to the installation of PV for the case study holiday home). It is potentially also a challenging case study in that it will use a lot less PV generated electricity than a typical home, given the low occupancy profile of holiday homes.

The PV case study dwelling presented below also has a middle-of-the-road C BER, and a 4.2 kW PV system was installed at the start of 2023. A diverter was installed which enabling PV electricity surplus to the instantaneous demands of the dwelling to be diverted to the Domestic Hot Water (DHW) in the first instance and then to an electric space heating storage heater. An Electric Vehicle (EV) is charged from the PV array when the owners are in residence (subject to 1.1kW of surplus power being available), and the EV is topped up using night rate electricity. It is noted that there is no domestic battery storage.

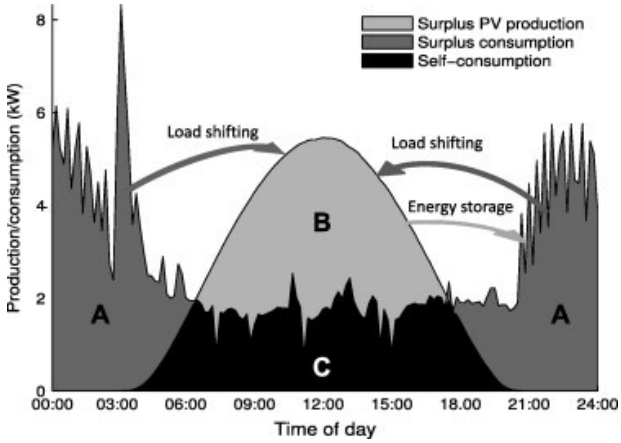

Figure 4: Outline of daily net load (A + C), net generation (B + C) and absolute self-consumption (C) in a building with on-site PV (13).

The amount of PV generated electricity used within the dwelling is defined as the self-use fraction β. The value of β depends on the coincidence of electricity generation and electricity demand. At present, in the absence of measured data, a value of β = 0.30 is used when performing fuel cost calculations by the Sustainable Energy Authority of Ireland (SEAI).

Fig. 4 shows a schematic outline of the power profiles of on-site PV generation and power consumption. The areas A and B are the total net electricity demand and generation, respectively. The overlapping part in area C is the PV power that is utilized directly within the building. There are varying definitions of self-consumption (13), and in this paper the self-use fraction β is defined as the self-consumed part relative to the total production, which in the simplified nomenclature of Fig. 3 is:

Self-use fraction β = C/(B+C)……eq 1

For the 3371kWh PV electricity generated, the recorded self-use fraction β for the case study was 51.16%, considerably higher than the 30% (0.30) assumed by SEAI.

Factors which influenced this self-use fraction for the case study dwelling include:

1. The relatively low annual energy consumption of the dwelling (2,910 kWh) compared with the national average (4,200 kWh).
2. The inclusion of a diverter which makes use of surplus PV electricity to heat DHW and electric storage radiators.
3. EV charging which increased the β value to 85% (0.85) even on cloudy days.

These factors have resulted in an atypically large fraction of the dwellings energy consumption being met by PV.

Table 2 gives details of the case study cost of electricity supply and the applicable feed in tariffs (FIT) (based on the Electric Ireland Home Saver rate at 31 Dec 2023 (14)).

Table 2: Case Study Electricity costs and FIT (at Mar 2023)

Electric Ireland	€	% (est)	kWh
Day Rate	0.3816	0.64	1862
Night Rate	0.1882	0.36	1048
Standing charge pd	0.8978		
Feed In Tariff	0.21		

Of note in Table 2 is the high cost of daytime electricity compared with night rate electricity and the feed in tariff rate.

Fig 3 shows that attractive financial returns are being achieved in the case study dwelling based on the self-use fraction β of 51% compared with the other options.

The three scenarios presented in Fig 3 include:

1. The null option of no PV,

2. The extreme option where no PV electricity is used within the dwelling, but all is exported at €0.21 / kWh
3. The actual case, where 51% of the PV electricity is consumed within the dwelling, and the remainder exported to the grid.

Fig 5 demonstrates that the lowest net annual electricity cost is achieved by using PV electricity within the dwelling rather than exporting it (as is the case in scenario 2). In order to understand why this is the case, Table 3 shows the calculations for the net cost of electricity.

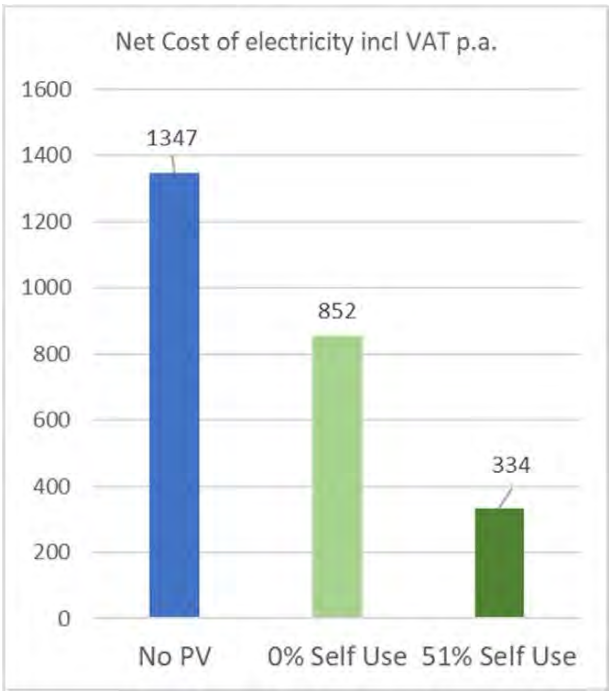

Figure 5: Annual case study electricity cost for three scenarios.

The costs, as outlined in the three rows at the top of the table, remain the same for all scenarios apart from the 51% self-use, where the costs of daytime electricity is reduced from €711 to €55. The significant reductions are achieved primarily given that the use of the PV electricity avoids an expenditure of €656 at the expensive daytime rate of €0.39 (Table 2).

However, in addition to the daytime cost of electricity being significantly reduced due to the high β factor, the payment of income tax and VAT is also reduced (Table 3).

Currently, €200 p.a. FIT contribution is allowed per dwelling tax free. In the case study, the high rate of income tax is charged, resulting in an effective tax rate of c.50% (including PRSI & Universal Social Charge) for PV electricity returns in excess of €200 per annum.

Thus, scenario 2 results in an income tax liability of €254, while the relatively high self-use fraction in scenario 3 results in a tax liability of only €73.

Table 3: PV Case study costs, benefits and paybacks

Costs / benefits p.a. (€)	PV Scenario		
	No PV	0% Self Use	51% Self Use
Cost - Standing charge	328	328	328
Cost - night	197	197	197
Cost - Day	711	711	55
Day cost avoided	0	0	656
PV contribution	0	708	347
tax	0	254	73
PV Value net of tax	0	454	273
Net cost excl VAT	1236	782	306
Net Cost of elect'y incl VAT p.a.	1347	852	334
Savings due to PV		495	1013
Simple payback (years)		12.0	5.9

The combination of avoiding high day rate electricity, and the generation of a tax (and associated VAT) liability means that savings of €1,013 are possible under scenario 3 compared with savings of €495 for scenario 2 (where all of the PV electricity is exported to the grid).

The cost of the PV system (including diverter) was €5,959 net of grant and VAT benefits. Therefore the payback period varies between 5.9 years (where the self-use fraction is 51%) and 12 years (where all of the PV electricity is exported to the grid).

4. DISCUSSION AND CONCLUSION

This paper looked at two very different scenarios for two dwellings with mid-range energy efficiency (with a Building Energy Rating of C). The analysis was carried out for the case of a country with electricity prices which are the highest in Europe (15) and gas prices 4th highest in Europe (16).

In the case of the 167m^2 1998 home considering installing a heat pump, a €41,000 energy upgrade was required to the building fabric as a precursor to receiving a HP grant, resulting in a payback of over 100 years. In addition, the (net of grants) €16,500 cost of installing the HP did not compare favourably with the €3,500 cost of installing a condensing gas boiler.

Finally, the running costs of the HP were comparable with the running costs of the condensing gas boiler, meaning that there was no period within which payback would be achieved.

This paper demonstrates, that there are real challenges in appropriately incentivising investment in deep energy retrofit and heat pump deployment, particularly in the case of dwellings with mid-range energy efficiency.

It should however be noted that the financial attractiveness of electric HP's compared with gas boilers while directly related to the efficiency of the gas boiler, and the efficiency (COP) of the heat pump, is also crucially, dependent on the differential between residential electricity and gas tariffs. If a policy initiative enables the electricity/gas price differential to exceed the heat pump/gas boiler efficiency differential, the financial case for electric heat pumps is made stronger.

In the case of the second residential unit studied, the price of electricity in combination with attractive capital grant aid, elimination of VAT for the PV installation and the introduction of feed-in tariffs combine to make a strong financial argument for the deployment of PV.

For the 100m^2 2004 holiday home, the installation of the €5,959 PV system resulted in an electricity cost reduction of over €1,000 pa - a payback of 5.9 years.

It is noted that the DER and HP installation would take approximately six weeks and also would require the residents to decamp from the property. The PV installation took place over a two-day period and did not impact on the occupants.

In summary, there is a clear imperative and desire for improving the energy efficiency of Irish dwellings among the vast majority of stakeholders – residents, homeowners, government, industry etc.

With 35% of the residential dwelling stock having a BER of C, the contribution of this paper is to highlight some of the challenges and opportunities which are faced by the stakeholders within the largest cohort of dwellings.

A clear finding from the analysis was the financial challenges faced by stakeholders in carrying out a deep energy retrofit in buildings which are already relatively thermally efficient. In order to achieve grant aid for installing heat pumps, costly additional renovation was required.

In addition, policy needs to address the price differential between gas and electricity, in order to improve the financial attractiveness of electric heat pumps compared with gas boilers.

The other clear finding from the analysis relates to the significant benefits of PV. In particular it's important to maximise the amount of PV generated electricity which is used directly within the dwelling, rather than incur income tax charges through on FiT payments received.

ACKNOWLEDGEMENTS

This paper has been supported with financial contribution from Sustainable Energy Authority of Ireland under the SEAI Research, Development & Demonstration Funding Programme 2022, Grant number 22/RDD/866 and Grant number 21/RDD/744.

REFERENCES

1. Government launches updated Climate Action Plan accelerating ambition in reaching climate goals [Internet]. 2022 [cited 2023 Apr 26]. Available from: https://www.gov.ie/en/press-release/c2114-government-launches-updated-climate-action-plan-accelerating-ambition-in-reaching-climate-goals/
2. Sustainable Energy Authority Of Ireland [Internet]. [cited 2022 May 6]. Government launches the National Retrofitting Scheme. Available from: https://www.seai.ie/news-and-media/government-launches-the-n/
3. Domestic Building Energy Ratings Quarter 4 2022 - CSO - Central Statistics Office [Internet]. CSO; 2023 [cited 2023 Mar 3]. Available from: https://www.cso.ie/en/releasesandpublications/ep/p-dber/domesticbuildingenergyratingsquarter42022/
4. Retrofit – Public Policy [Internet]. 2023 [cited 2023 Dec 30]. Available from: https://publicpolicy.ie/tag/retrofit/
5. Sustainable Energy Authority of Ireland. https://www.seai.ie/publications/Domestic-Fuel-Cost-Comparison.pdf. Domestic Fuel Cost Comparison. 1 July [Internet]. 2019 Jul. Available from: https://www.seai.ie/publications/Domestic-Fuel-Cost-Comparison.pdf
6. O'Hegarty R, Kinnane O, Lennon D, COLCLOUGH S. Air-to-water heat pumps: Review and analysis of the performance gap between in-use and product rated performance. Renewable and Sustainable Energy Reviews. 2022 Mar 31;155, Article 111887.
7. macairh.ie [Internet]. [cited 2023 Apr 26].
8. PVResearch.ie [Internet]. [cited 2023 Dec 31].
9. HEPI [Internet]. [cited 2024 Mar 14]. HEPI. Available from: https://www.energypriceindex.com
10. Olympios AV, Hoseinpoori P, Markides CN. Toward optimal designs of domestic air-to-water heat pumps for a net-zero carbon energy system in the UK. Cell Reports Sustainability. 2024 Feb 23;1(2):100021.
11. Sustainable Energy Authority Of Ireland [Internet]. [cited 2024 Mar 14]. Energy Data Downloads. Available from: https://www.seai.ie/data-and-insights/seai-statistics/key-statistics/energy-data/index.xml
12. Sustainable Energy Authority Of Ireland [Internet]. [cited 2024 Mar 14]. Prices. Available from: https://www.seai.ie/data-and-insights/seai-statistics/key-statistics/prices/
13. Luthander R, Widén J, Nilsson D, Palm J. Photovoltaic self-consumption in buildings: A review. Applied Energy. 2015 Mar 15;142:80–94.
14. Switch electricity price plans today | Electric Ireland [Internet]. [cited 2023 Dec 31]. Available from: https://www.electricireland.ie/switch/new-customer/price-plans?priceType=E
15. Electricity price statistics [Internet]. [cited 2023 Apr 26]. Available from: https://ec.europa.eu/eurostat/statistics-explained/index.php?title=Electricity_price_statistics
16. Natural gas price statistics [Internet]. [cited 2023 Apr 26]. Available from: https://ec.europa.eu/eurostat/statistics-explained/index.php?title=Natural_gas_price_statistics

Influence of Pavements on Microclimatic Comfort of Public Spaces:

Reference of an urban transformation area in Brasilia, Brazil

GUSTAVO CANTUARIA[1], JULIANA IAHN[2], MANUEL GUEDES[3]

[1]Gustavo A. C. Cantuaria, IST and LaSus/UnB, Brasilia, Brazil
[2] Juliana L. de Oliveira Iahn, CEUB, Brasilia, Brazil
[3]Manuel Correia Guedes, IST University of Lisbon, Lisbon, Portugal

ABSTRACT: Enjoyment, and habitability of public spaces is directly linked to microclimatic comfort. Considering that the thermal and permeability properties of pavement materials are strongly related to heat intensity perceived in public spaces, the objective of this research is to investigate thermal behaviour of different pavement materials for the thermal comfort of pedestrians. Microclimatic studies were done on the requalification of an urban area in Brasilia, namely the South Hospital Sector. Studies were performed in both the dry and rainy season. The methodological procedures for this were: literature review; case study fieldwork, with environmental analysis of surface variables, and superficial temperature of selected spaces. For data corroboration, simulated scenarios with ENVI-met 5.0 software were also performed and confronted. Results show that material temperatures in the rainy season have a different behaviour in relation to the dry period, and a constant relation to the increase in temperature according to the material used, and if exposed to sun or sheltered by shade. During the dry season, "cold" materials performed better in a sun exposed space. Significant differences of up to 22°C were recorded. The simulations corroborated with the fieldwork investigation
KEYWORDS: Microclimatic comfort; Pavements; Public Spaces.

1. INTRODUCTION

Thermal comfort in public spaces is one of the main indicators that provide their enjoyment, attractiveness and habitability. Thinking of the microclimatic scale, the one closest to everyday life, it is necessary to treat climate variables when planning these spaces. Regarding this adaptation, the choice of the type of pavement in urban redevelopment projects must be conditioned by the characteristics of the environment, in addition to taking advantage of the surface qualities of the materials.

The role of construction materials is decisive in reducing thermal gains and heating in these spaces. In this sense, studies compared the thermal performance of 93 paving materials commonly used in open spaces. For the same material, temperatures varied between 33.4ºC and 54ºC, with the minimum value being observed for white and the maximum for black painted surfaces. Regarding texture, smoother surfaces presented lower temperatures than rough surfaces. High temperatures were observed on black and gray pebble surfaces, in the order of 45ºC. Regarding the type of material marble, stones and mosaics were colder than other materials [1].

Therefore, 'cold' materials can be characterized as those that have a smooth and light-colored surface, such as materials made from marble, stone and mosaics (natural raw material). In the same way as hot materials can be defined those that have a rough and dark-colored surface and with materials made of pebble and paving stone.

Dimoudi et al. (2014) monitored thermal fluctuations in the city of Serres in Greece, a place where traditional construction materials are used. Simulations of replacement with 'cold' materials accompanied by other mitigating techniques resulted in a reduction in the average street surface temperature by up to 6º C [2].

In addition to thermal and radiative properties, the permeability properties of floor covering materials also influence human thermal discomfort in spaces. Replacing natural soil and vegetation with impermeable surfaces, such as asphalt and concrete, reduces the cooling effect of the air through evaporation, further increasing the surface temperature. The impermeability of pavements reduces the possibility of heat release through evapotranspiration.

Studies carried out in China have demonstrated the effectiveness of permeable pavements in urban thermal comfort through evaporative cooling [3]. After testing two types of permeable materials (permeable concrete and drainage ceramic block), the results indicated that pavements with high capillary strength can improve thermal comfort above the pavements by up to 3°C.

Considering that the thermal and permeability properties of the types of paving materials used have a strong relationship with the heat intensity in public spaces, this research aims to investigate elements that contribute to the treatment of pavements for the thermal comfort of users. through microclimatic studies of the implementation of the requalification project of the Southern Local Hospital Sector in Brasília. This sector was chosen because it is undergoing an urban intervention process, which includes changing ground cover materials.

2. CONTEXT

With Brasília, the capital of Brazil, located in the centre of the country, has two well-defined seasons, the rainy season (October to March) and the dry season (April to September). The hottest period occurs in September and October, with temperatures reaching 36° C; and the coldest period occurs in June and July, when the lowest temperatures reach 13°C;

As for the urban context, inaugurated in 1960, the city became a landmark in urban planning with Lucio Costa's Pilot Plan, which was designed under modernist urban planning principles.

More than sixty years later, corrections, adaptations, and upgrades have become necessary, to conform to current demands, especially the streets and sidewalks, which are vital for locomotion. However, the modern heritage of the city of Brasília, certified by UNESCO, must be taken into account.

In this sense, the PPCUB - Brasília Urban Complex Preservation Plan, provides for the urban qualification of public spaces in cities in order to intensify urban dynamics and promote the continuous conservation of these spaces according to urban scales; and landscaping, through strategies that promote bioclimatic comfort.

The Southern Hospital Sector Requalification Project (SHLS), the object of study in this work, was executed and inaugurated in 2020. With the aim of requalifying the sector and promoting the use of public transport and pedestrians, the project reduced the size of the lanes road, regulated parking lots, changed the texture of the pavements, installed pergolas, planted trees, among other changes. As for the floors, more permeable and 'cold' floors were proposed (Fig.1).

Figure 1: Before and after pavement change

3. METHODOLOGY

To achieve the scope of the research objective, which relates the treatment of pavements in public spaces and the urban microclimate, an investigation was developed from a qualitative perspective with technical case study procedures suggested and based on the theoretical conception.

3.1 Definition of measuring points and climate variables

Three (3) measurement points were selected in these spaces (Fig. 2). The definition of the points was based on the surface type, seeking to include the types existing in the areas under study: Asphalt; Concrete floor; Natural soil; Lawn; Interlocking concrete blocks; Pisogram (perforated concrete blocks with grass); and Fulget flooring (a coating mix of very small stones and adherents).

Figure 2: Measuring points.

Furthermore, measuring points were chosen according to Romero's (2015) classification: A- Shaded areas during the day and open at night; B – Shaded areas during the day and covered at night; and C – Open areas.

To characterize the spaces in terms of ground covering, an area of approximately 4,000 m² of influence was traced to determine the percentage of covering materials at each measuring point.

Based on literature review, the following variables were chosen for measurements: Air temperature (ºC) – Ta; Relative air humidity (%) - %RH; Surface Temperature (ºC) – Ts. For data collection, a thermo-hygrometer and a thermographic camera were used. In addition to the data provided from the INMET meteorological station.

Measurements were taken during three consecutive days, in the dry and rainy season, in a month belonging to each of the periods. Due to recording the lowest percentages of %RH, in the dry period, the records were made in September and October 2021. On the other hand, in the rainy period, the surveys were carried out in January 2021, due to recording the highest rainfall rates. The variable records were taken at 9h, 15h and 21h.

3.2 Envi-met simulations

For data corroboration, simulated scenarios with ENVI-met 5.0 software were performed. Three-dimensional models were created corresponding to the selected locations with their urban morphology, and the different pavements covering the ground was identified.

During this phase, three situations were created. Firstly, the original scenario, prior to the urban intervention, was simulated. The construction of this scenario aimed to fill the gap of the impossibility of collecting data before the SHLS urban transformation and to estimate the bioclimatic strategies through the treatment of pavement coverings. Secondly, the current scenario, (Modified Scenario) with the interventions already carried out, was simulated. In addition to these, a third scenarios was also simulated, the Green Scenario. This case focuses on the possible inclusion of urban vegetation as proposed by the design projects (Fig.3).

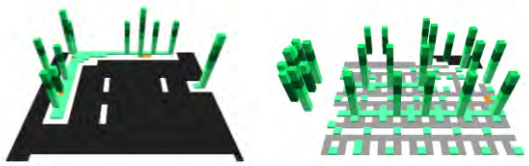

Figure 3 – Models before and after intervention on Point 2.

4. RESULTS

4.1 Climatic Variables

Fieldwork was performed, in an attempt to compare the air temperature between points and its relationship with the existing ground cover, nevertheless, it was not possible to estimate the cooling potential, due to the air fluidity of open spaces. On the other hand, surface temperature measurements showed satisfactory results. Furthermore, the fieldwork demonstrated the cooling potential through vegetation. Both in the dry and rainy periods, the point shaded by trees with high leaf density, recorded a temperature 3.8°C lower than the less vegetated point, and higher humidity, at 3pm.

It was observed that materials in the rainy season have a different behavior in relation to the dry season and a constant relationship with the increase in temperature depending on the material and the sun or shade situation (Fig. 3).

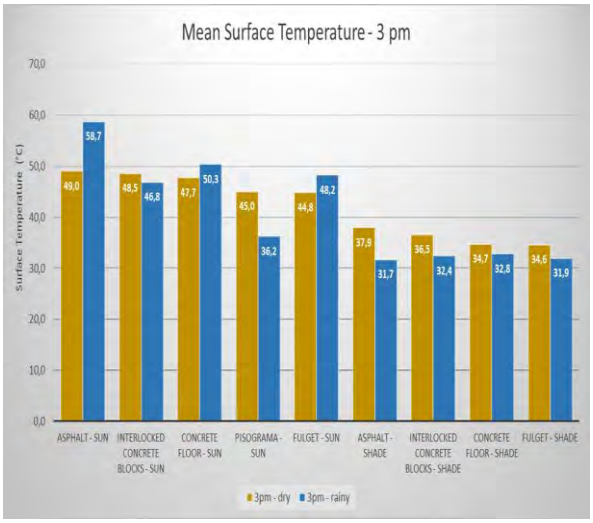

Figure 3 – Comparative graph of the average temperature of different surface materials at 3pm

Among the 'cold' materials, the mix of small stones and adherents (Fulget Flooring) performed the best when exposed to the sun, being 5°C cooler than asphalt at 3pm, the most critical time for pedestrians. Among the permeable materials, the hollow concrete blocks with grass (Pisograma), which at 3pm recorded a temperature average of 36.2°C, was 22°C colder than Asphalt. Also to be mentioned is the Interlocking Concrete Floor, which was 12°C cooler than Asphalt. It is noteworthy that in both periods, the Pisograma presented a lower temperature at 9 pm, revealing that its natural portion (soil and grass) can contribute to the mitigation of urban heat islands.

Ground surfaces analysis in situations of sun exposure and shade demonstrated the cooling potential caused by the shading of tree canopies and pergolas, in which the surfaces were significantly warmer when exposed to the direct sunlight. Shading reduces the absorption of solar radiation from the surface and decreases the transfer of sensible heat to the air.

4.2 Simulation

The modified scenario was designed with the following bioclimatic proposals and its respective cooling mechanisms: modification of the thermal properties of materials and permeability; increased reflection of solar radiation; and evapotranspiration; and more shading through trees and pergolas, reducing the absorption of solar radiation.

Thus, the original scenario was built with the original characteristics before the interventions. In general, the roads and parking lots were asphalted, with concrete sidewalks, some grassy areas with exposed soil and few trees. The modified scenario was built with cold (higher albedo) and permeable pavements. The new proposed afforestation was disregarded, so that it would be possible to estimate the potential of the surfaces in cooling the environment. The green scenario was designed to study the combination of the Modified Scenario's more reflective pavement techniques, with shading of surfaces through vegetation and pergolas.

As for air temperature, the simulations revealed zones up to 1.5°C cooler depending on the pavement type. Areas covered by Asphalt and Concrete surface were hotter than those covered by Fulget, Pisograma and Interlocking Concrete Flooring (Fig. 4).

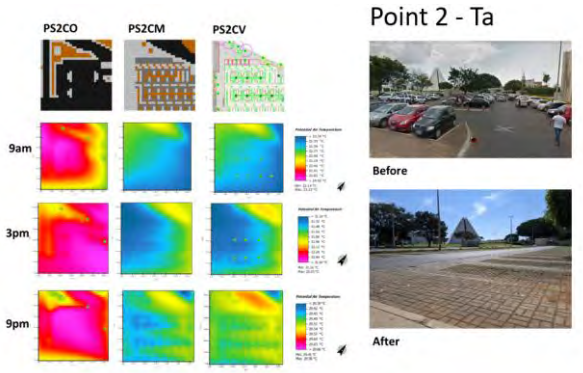

Figure 4: Simulation analysis of Point 2 – Ta.

The results for reducing surface temperature (Ts) were superior when compared to reducing air temperature (Ta), proving to be the parameter with the greatest impact.

For Point 2, this change covered almost the entire parking lot. The highest temperatures were found on the Asphalt, represented by the wine color, and the lowest under the Pisograma and areas shaded by trees. When compared to the Original Scenario, at 3pm, the Modified Scenario showed a temperature reduction of up to 10.15°C, and in the Green Scenario of up to 17.69°C (Fig.5).

The specific effect of shading from trees stands out at both points, which reduces solar absorption from the surface and reduces the transfer of sensible heat to the air. Furthermore, the potential of vegetation was observed for the night period, as with the same floors as in the modified Scenario, the temperature of these was lower, mitigating the formation of heat islands.

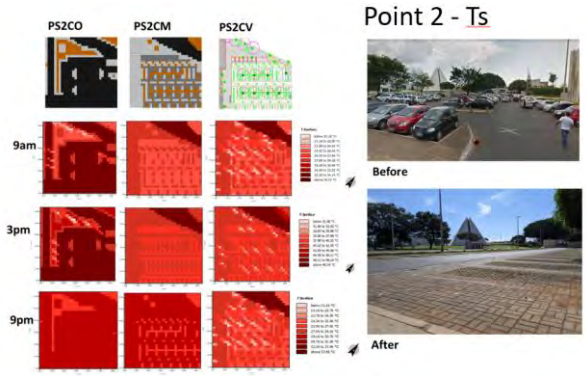

Figure 5: Simulation Analysis of Point 2 – Ts

5. CONCLUSION

Through data collection, it was possible to highlight on the microclimatic scale the influence of the two characteristic annual periods, one dry and the other rainy, given the different behavior of pavement surface materials in relation to water.

The results showed that the temperature of materials in the rainy season has a different behavior in relation to the dry period and is constantly related to the increase in temperature depending on the material and the sun or shade situation. During the dry period, materials with a lower albedo had a higher temperature when exposed to the sun, and materials with a higher albedo were colder. During the rainy season, permeable and natural materials performed better, because the retained water is available for evaporation and cooling of the pavement.

As for the simulation process, the results corroborated the experimental investigation, as it made it possible to estimate bioclimatic proposals as a cooling mechanism for public spaces, simulating each point before and after the intervention, for the same day, at the same time. Based on the results of the simulations, just by changing the ground surface material already has a cooling effect on the air temperature. Furthermore, heat mitigation is significantly enhanced when associated with the inclusion of vegetation.

The results on the use of cold and permeable pavements confirm, regarding the reduction in surface temperature, what has already been raised by research on the subject in other climatic contexts. Therefore, the implementation of these pavement materials, from the point of view of reducing air temperature and surface temperature, can be adopted. In addition, shading should be proposed through afforestation and the installation of pergolas, as their implementation provided an even greater specific temperature reduction.

From the above, it is reinforced that the thermal, radiative and permeability characteristics of the ground surface materials that make up public spaces must be designed in order to benefit the pedestrian's

thermal microclimatic environment. The Surface Temperature (Ts) parameter was the most suitable for this type of analysis, in addition to thermal comfort indices (not estimated in this research). Actions that promote the use of vegetation in the studied context are recommended because they reduce heat gain and thus thermal exchanges between the human body and the surrounding environment. In this sense, public space redevelopment projects, which adopt a combined strategy of cold, permeable pavement and medium-density afforestation, deliver better conditions than just cold, permeable pavements. Even with slightly lower air temperatures due to the change of ground surface, with additional afforestation the potential for heat mitigation at a microclimatic level is more promising.

Finally, the results clearly indicate the need to be translated into viable urban planning actions, resulting in more comfortable and livable spaces.

ACKNOWLEDGEMENTS

This paper acknowledges the sponsoring support received from FAP/DF, CNPQ from Brazil, and IST of Lisbon.

REFERENCES

1. Doulos, L et al, (2004). Passive cooling of outdoor urban spaces. The role of materials. *Solar Energy*, v. 77, n. 2, p. 231–249.

2. Dimoudi, A et al (2014). Use of cool materials and other bioclimatic interventions in outdoor places in order to mitigate the urban heat island in a medium size city in Greece. *Sustainable Cities and Society*, v. 13, p. 89–96.

3. Wang, J et al (2018). Experimental investigation on the influence of evaporative cooling of permeable pavements on outdoor thermal environment. *Building and Environment*, v. 140, n. January, p. 184–193

PLEA 2024 WROCŁAW
(Re)thinking Resilience

Thermal Comfort In Megastructures Using Hybrid Cooling:
Building resilience for diamond industry

MANIT RASTOGI[,1] SONALI RASTOGI[,1] ALOK DECRUZ[,1] ABHISHEK ARORA[,1]
SHRADHA GODYA[,1] PAVITHRA LAKSHMI[,1]

[1]Morphogeneis, Mumbai, India

ABSTRACT: Paradoxically, as world trade becomes increasingly complex, concentrated trading hubs have emerged, consolidating production, storage, documentation, and trade all under one roof. Large structures synonymous with the region comprehensively integrate the seamless flow of people, goods, data, and energy. While these mega structures economize function at scale, they present an architectural opportunity to relook at energy efficiency from the lens of cultural and regional identity. Two key parameters define this approach – regionalism and scale. While regionalism brings to the fore - adaptive thermal comfort, local material, craftsmanship and culture; scale realizes the potential of such measures combined in hybrid systems translating to substantial energy and cost savings. Using the example of one such megastructure in Surat, India, a hot and humid climate zone, we examine if hybrid cooling technologies in conjunction with adaptive thermal comfort parameters and passive strategies can offer a novel approach to efficient cooling of megastructures. Climate data, thermal comfort, capital, and operational cost and building performance are tracked to arrive at the conclusions. The success of these strategies must be measured not only through energy data and cost savings but also cultural relevance and adaptation.
KEYWORDS: Radiant Cooling, Thermal Comfort, Hybrid Cooling, Hot and Humid, Office Design, Cultural Impact

1. INTRODUCTION

The diamond industry in Surat was facing a crisis amidst its booming business. Despite housing production and certification capacity within its regional limits, the trading centre was located almost 300 kilometres away in Mumbai. This forced traders to commute 6-7 hours for daily transactions. Realizing the potential to redefine the centre, an elected representation of traders decided to build a new trading facility within Surat city limits as part of DREAM (Diamond Research and Mercantile) city masterplan. The resultant megastructure was designed to also house trading facilities, storage, and customs functions. Occupying an area of 35.5acre site and a built-up area of 7.1 million square feet, it eventually earned the title of the world's largest office building. [1,2]

2. CONTEXT

Surat (21.2° N, 72.8° E), situated in Gujarat, India, experiences a tropical savanna climate. Strong cultural aspects related to trade, community, and informality within the workspace typify the city.

2.1 Climate

The climate of Surat is characterised by hot and dry summers, warm-humid monsoons, and comfortable winters. Climate data and the psychrometric chart (Fig. 1) shows temperature exceeding 30^{0}C for 6-8 months (March - October) and humidity above the 60% mark. Solar shading and wind movement can help with thermal comfort. Increased air movement can induce physiological comfort of up to 5-6^{0}C as the region experiences high wind speed above 1.5 m/s speed during the uncomfortable period.

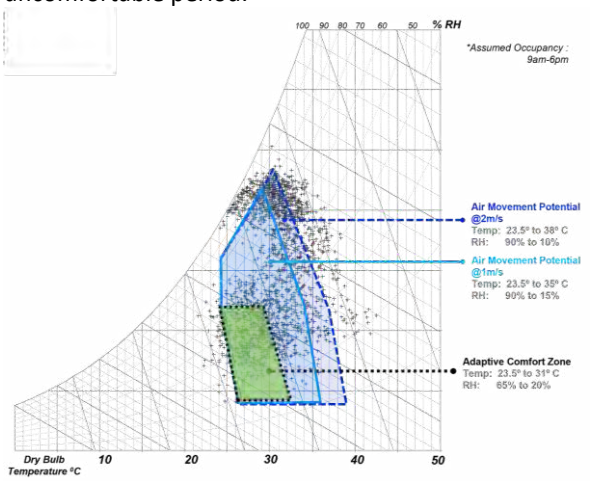

Figure 1: Psychrometric chart of Surat indicating need of air movement to achieve thermal comfort for most of the operational hours due to high humidity.

2.2 Social and Cultural background

Diamond trade in Surat evolved organically, conducted in informal environments, in the marketplace and even under the shade of trees in the old city. (Fig. 2) Small business transactions were often made in the outdoors over a shared meal. The community of diamond traders in Gujarat is close knit

fostering strong interpersonal bonds. Trade and social relationships intermingle seamlessly and form the backbone of business and societal culture. [3]

Figure 2: Typical diamond district. [4,5]

3. DESIGN STRATEGY

One of the prime challenges while designing an office building for 67,000 end users is to create a seamless flow of people and goods within stipulated time periods. Multiple access points into the premises are strategically located at optimal proximity to the office tower lobbies which enables pedestrians and vehicle users to reach their destinations in under 5 and 7 minutes of site entry respectively. A key element aiding this secure but free internal flow of people is a large "central spine" (Fig. 3) connecting the nine office towers separated by open to sky courtyards (Fig. 4).

Figure 3: Natural light and air filters through the landscaped courts through the punched openings at all levels.

Figure 4: Landscape courtyards - schematic on left; actual photograph on right

The central spine thus comprising of 30% of the total built-up area, these corridors and common areas are fully naturally ventilated, punctured with landscaped pockets and supplemented with radiant cooling system for thermal comfort. The ambience of the space and equitable access from offices makes it ideal for carrying out trade in an informal setup, reminiscent of the erstwhile marketplace setting. It is the space where relationships within the community are built, deals are struck, and trusted bonds are nourished.

4. PASSIVE STRATEGY

4.1 Macroclimate

The relationship between the built form and outdoor spaces are carefully crafted to create a positive impact on the macroclimate (Fig. 5). Thematic landscaping with water bodies and strategically planted vegetation aid in the reduction of radiant heat. The courtyards are sized equal to building height to allow shading. Extensive vegetation is planned along the western edge for added shade and thermal-visual comfort while the Eastern courts support functions like the food courts, recreational and interaction spaces. Since all courtyards are equally accessible to the occupants, the usage of the outdoor areas is maximised. Based on the time of the day and purpose, different subsets of the courtyard spaces become activated.

Figure 5: Typical floor plan showing the central spine connecting office towers segregated by landscaped courtyards.

4.2 Microclimate

Multiple strategies influence the microclimate and cause variations across spatial zones.

4.2.1 Central Spine

The central spine functions within a range of microclimatic conditions that changes as per outside temperature aided by low tech passive strategies and landscape elements. The conspicuous curved blade walls (Fig. 6) cutting across the site calling out the north-south axis capture prevailing winds through venturi effect. The green courts work to direct warm air upwards ensuring enhanced wind movement which can temper harsh climatic outdoor conditions through stack effect (Fig. 7). The landscaped pockets aid in thermal visual comfort and help improve IAQ. The Western walls have large, punched opening into the courts allowing for daylight penetration into the spine and wind movement from multiple directions adding to thermal comfort (Fig. 8). Radiant cooling system is installed along the entire stretch of

common areas which amount to 30% of the built-up area ensures thermal comfort for 90% of the year.

Figure 6: Top view of spine walls – a naturally Ventilated, micro- climate tempered community corridor through "Venturi effect ".

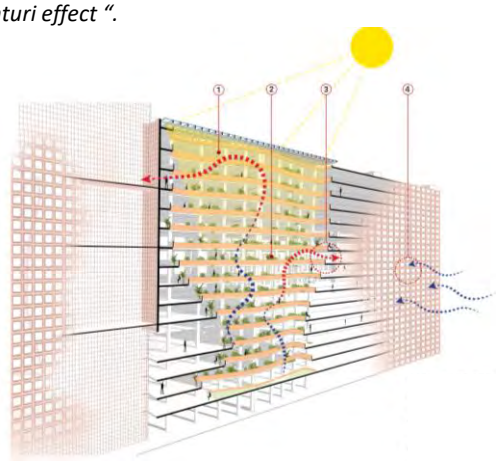

Figure 7: Sketch showing wind flow along tne staggered atria integrated with the landscape using Stack effect.

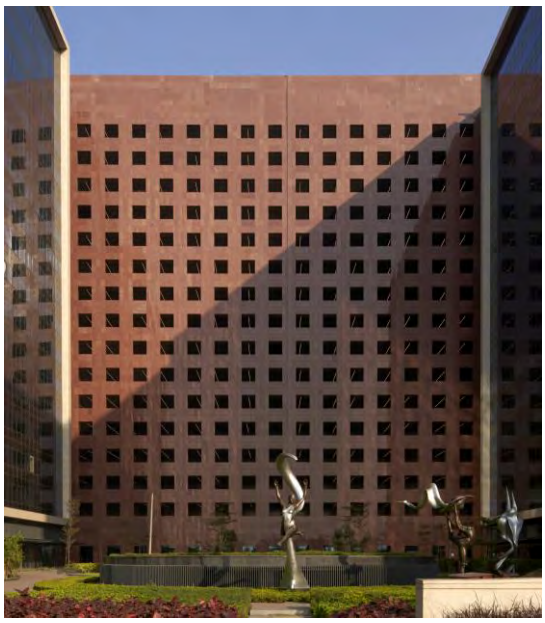

Figure 8: External image of the building highlighting punched opening on Western wall for natural light and ventilation along spine.

4.2.2 Office and ancillary spaces

The office towers have a narrow floor plate separated by proportionately sized courtyards whose widths of are equal to the tower heights to allow maximum daylight penetration (Fig. 9). 75% of the office spaces can be naturally lit. The north-south orientation of the towers and screened east-west surfaces minimise heat gain which has a direct impact on air conditioning loads. To cool the passages outside of the offices, the system allows the return air from the offices to leak into the passages and then directs it to the return air ducts.

Figure 9: Shaded landscaped courts between towers accessed equitably by all occupants.

5. ACTIVE STRATEGY

The active strategy is a combination of a dual chilled water loop and variable flow chiller system for office, lobbies, dining and ancillary spaces and radiant floor cooling system for common areas. A dedicated outdoor air system (DOAS) is integrated in both, which helps improve Indoor air quality (IAQ) as well separates sensible and latent cooling loads. Varying temperature set points vary for spaces driven by functionality and architectural intent. (Table 1)

Table 1: Temperature set point for Indoor conditions.

Space	Indoor Conditions	
	Temp °C	Relative Humidity
Official spaces, Meeting & Conference, Food and Beverage	24±1°C	Less than 60%
Common Lift lobby + circulation	26±1°C	Less than 60%
Central Spine	31°C	Less than 60%

5.1 Dual chilled water system - offices and ancillary spaces

A central variable flow dual chilled water recirculation system with 6.8 Coefficient of Power cools the offices and ancillary spaces. The total air conditioning load is separated into sensible and latent load. Two sets of chillers with different set points cater to each load, thereby achieving overall higher efficiency than conventional systems (Fig. 10). It also ensures efficient operations at part-load conditions. The air conditioning peak load is estimated at 7000 TR served by:

1000 X 4 - Low Temperature Chillers for Sensible load.
1000 X 3 - High Temperature Chillers for Latent load.

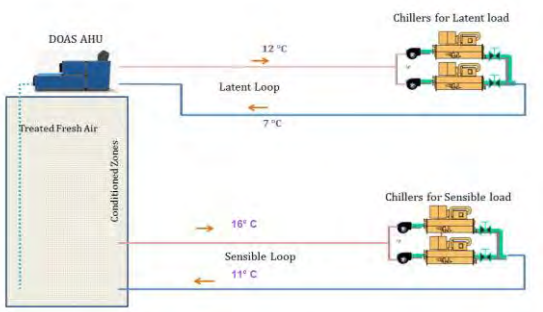

Figure 10: Diagram showing dual loop chiller and DOAS relationship with air-conditioned space.

5.2 Radiant cooling for spine

To achieve adaptive thermal comfort under natural ventilation, maximum operative air temperature of 32°C with wind speed in range of 0.94 to 1.59 m/sec needs to be maintained. [6] In the case of Surat, the outside air temperature is uncomfortable 40% of the time (>32°C) and wind speeds are favourable for inducing thermal comfort 90% of the time (Fig. 11, 12). Additionally, fresh air is induced with a DOAS system and wind speeds are enhanced using ceiling mounted angular air fans. These factors support the use of radiant cooling to supplement natural ventilation to achieve adaptive thermal comfort. Cultural factors play an important role in acceptability of naturally ventilated spaces in office buildings. In the case of Surat, cultural references work in favour of natural ventilation as diamond traders prefer informal spaces to conduct transactions as business depends on building strong community bonds which happens outside the office in an informal setting.[2]

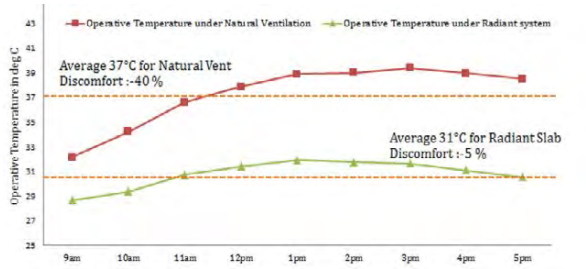

Figure 11: Comparison of operative temperature during the typical summer day

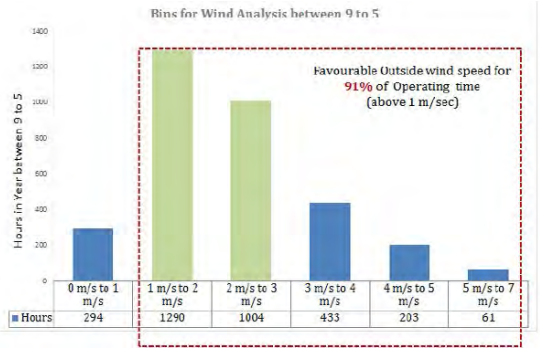

Figure 12: Graph showing hours during which wind speed are favourable for inducing thermal comfort.

5.3 Air-conditioning loads and efficiencies

Based on simulations, the total connected load was found to be 2.19 KW/TR on the built-up area compared to 4.15 KW/TR using conventional systems (Fig. 13). The Air conditioning efficiency is 685 Sft/TR on total built up area. (Table 2)

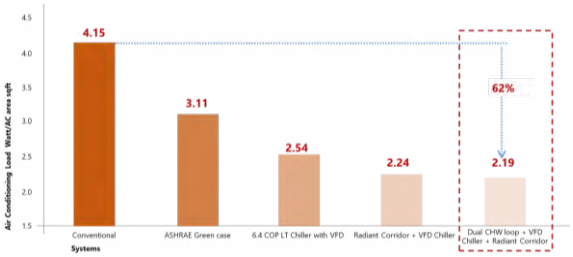

Figure 13: Graph mapping reduction of air conditioning load

Table 2: Comparison of cooling loads for HVAC system.

Air conditioning Efficiency	
Built up area / TR	685 sft/TR
Conventional Building	150-200 sft/TR

6. CHALLENGES AND MITIGATION

One of the primary challenges while using radiant cooling systems is condensation. In the case of Surat, the design temperature for naturally ventilated radiant cooled corridor is set at 28°C-32°C which is above the dew point temperature of 26°C (average). Hence, condensation in the corridors within the radiant cooled space was of lesser concern. The primary concern was when outside fresh air flows against the walls of the air-conditioned office spaces where the temperature is set at 24°C ±1°C. The analysis of the outside dew point temperature indicates that 40% of the operating time will experience dew point temperature between 24°C and 29°C, during which the likelihood of condensation is high. (Fig. 14, 15)

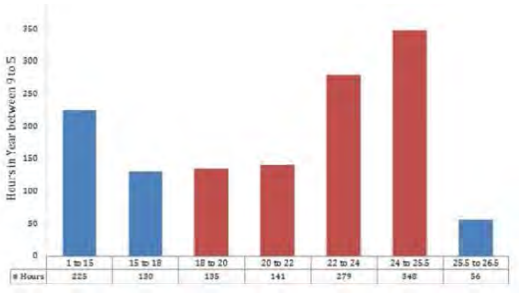

Figure 14: Pattern of dew point temperature during summer season.

Certain mitigation measures were employed in the design to reduce the chances of condensation.

1. Provision of an air lock lobby or a revolving door at office corridor entry: The air lock provides a buffer between the two spaces

and prevents any fresh air from directly coming contact with office spaces.

2. Enhanced air movement by installing hanging angular air fans in the spine: This prevents warm humid air from settling down near conditioned spaces.
3. Landscaped courts for increased air movement via stack effect and blade walls for venturi effect.

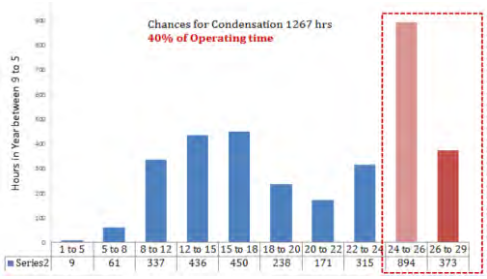

Figure 15: Bins for Outside Dew Point temperature.

System Design: 20mm PEX pipes placed 150mm apart were embedded within the slab screed for approximately 20 kms of running length per floor for a cumulative length of ~300kms. A temperature delta of 5°C is maintained at inlet and outlet at 25°C and 30°C respectively. The cooling tower lowers the water temperature to 27°C, and the mixing chamber ensures that the water temperature does not fall below 25°C. (Fig. 16, 17)

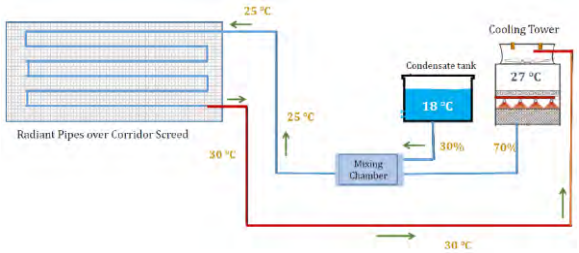

Figure 16: Diagram of radiant cooling system

Figure 17: Installation of radiant cooling pipes on spine slab

7. RADIANT COOLING SYSTEM SIMULATION

Multiple simulations were conducted to establish the structural composition of slab with and without insulation. The simulation for surface temperature for radiant cooling system assumes a six-inch-thick slab, 20 mm PEX pipe within the screed at 150 mm pitch and finished with tile.

7.1 Simulation scenario 1: without insulation

Since no insulation is installed, the cooling effect permeates below the slab through a thermal mass of 225 mm and above the slab through a thermal mass of 75 mm (Fig. 18). The time is set at 14:00 hours on 20th April which has the highest wet bulb temperature and dry bulb temperature of the year. The resultant capacity is 26 W/sqm upward and 20 W/sqm downward.

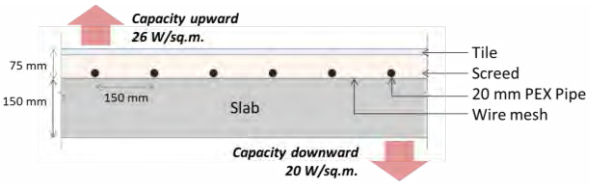

Figure 18: Scenario 1, Simulation of radiant cooling capacity on slab without insulation for highest DBT on 20TH April at 14:00 hours

7.2 Simulation scenario 2: with insulation

The simulation is repeated for the same time of the year but includes a 25m thick expanded polystyrene layer for insulation. The cooling effect permeates only above the slab through a thermal mass of 75mm (Fig. 19). There is no change in the cooling capacity of the system.

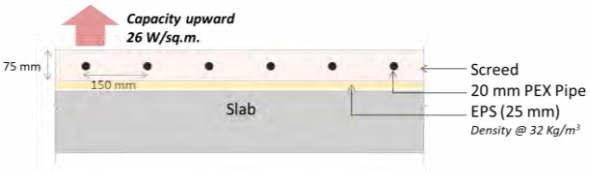

Figure 19: Scenario 2, Simulation of radiant cooling capacity on slab without insulation for highest DBT on 20TH April

In conclusion, a multistorey structure scenario, insulation for radiant cooling was not found to be effective and hence not recommended for installation.

8. COST AND ENERGY REDUCTION

The use of a dual chilled water loop with variable flow chiller and radiant cooling system for Surat amounted to a 23% reduction in capex + opex (3 years) cost compared with conventional systems (Fig. 20). 45% lower energy consumption with energy performance of ≤48 kWh/sqm./yr. compared to local benchmark (Energy Conservation Building Code) of 90 kWh/sqm./yr [7] is noted based on simulation data. The efficiency of the combined system is 685 sft/TR for air conditioning in comparison to conventional benchmarks at ~250sft/TR.

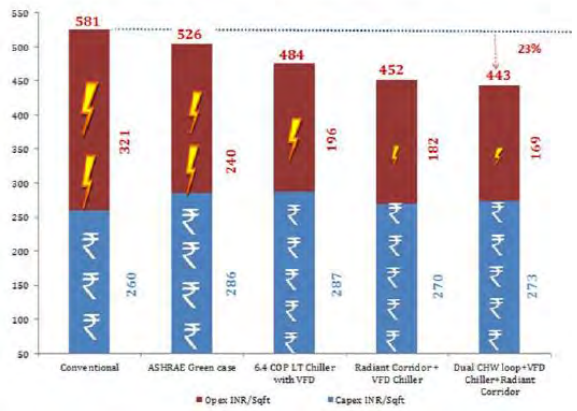

Figure 20: Graph comparing the capex and opex (over 3 years) for different cooling systems.

9. ENERGY PERFORMANCE

The results of energy performance simulation carried out at design stage are presented for comparitive purpose. The simulation was carried out as per appendix G of ASHRAE 90.1-2010 as an IGBC (Indian Green Building Council) requirement. The design case is compared to a baseline case (comply with ASHRAE Standard 90.1-2010). Following the methodology defined by IGBC, the simulation involves modeling the baseline building with its actual orientation. Subsequently, the entire building is rotated by 90, 180, and 270 degrees, and the results are averaged to determine the baseline energy consumption. The simulation results in 30.19% reduction in a total energy consumption compared to baseline case. Of this, HVAC chillers form 18%; HVAC pumps form 5% and HVAC fans form 9% of the energy savings. (Fig. 21)

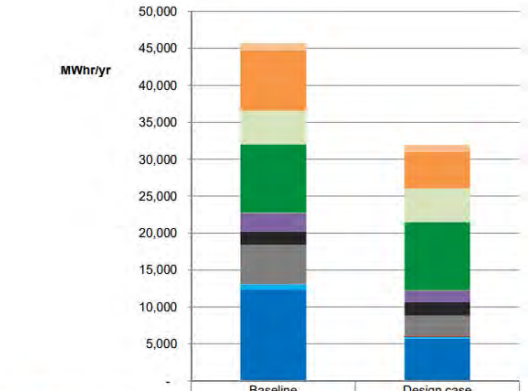

	Baseline	Design case
Basement Lighting	935	921
Lighting (Air-conditioned areas)	8,244	4,942
Process Load	4,555	4,555
Main Building Equipment	9,146	9,146
External Lighting	44	29
HVAC Water Pump	2,557	1,647
Basement Ventilation	1,789	1,791
Air-system fans (AHU FCU)	5,309	2,891
Hot Water	-	-
Space Heating	-	1
Heat Rejection	702	235
Chillers	12,431	5,753
Total	45,711	31,911
Savings		30.19%

Figure 21: Comparison between Baseline Case and Design Case Energy Use Characterization

10. CONCLUSION

In very large structures where diverse functions are brought together, usage of hybrid cooling systems can aid in creating varying environmental conditions considering the local climate while improving building performance. The integration of various cooling technologies can address the complex cooling needs of expansive constructions, contributing to an energy-efficient future for megastructures. By integrating cultural relevance into the design and operation of hybrid cooling systems, megastructures can not only achieve enhanced efficiency but also foster a sense of connection and acceptance within the communities they serve.

ACKNOWLEDGEMENTS

We would like to thank the project team Neelu Dhar, Nishtha Dewan and Akanksha for their hard work and dedication towards realising the project.

REFERENCES

1. Guiness world records, [Online], Available: https://www.guinnessworldrecords.com/news/2023/8/surat-diamond-bourse-surpasses-the-pentagon-as-worlds-largest-office-building-757334 [22 August 2023]
2. India Briefing, [Online], Available: https://www.india-briefing.com/news/indias-surat-diamond-bourse-a-game-changing-hub-for-global-diamond-trade-30571.html/ [19 December 2023]
3. Quartz, [Online], Available: https://qz.com/282999/how-the-gujaritis-took-over-belgiums-diamond-trade.html/ [17 October 2014]
4. Outlook, [Online], Image retrieved from: https://www.outlookindia.com/magazine/story/bloodied-diamonds/277666 [05 February 2022]
5. India Today, [Online], Image retrieved from: https://www.indiatoday.in/magazine/nation/story/20141201-best-cities-2014-surat-diamonds-806028-2014-11-20 [01 December 2014]
6. BUREAU OF INDIAN STANDARDS. (2016). IS SP 7-NBC National building code of India 2016, (2 volume set, part 8, section 5, table 9). BIS.
7. Energy Conservation Building Code-2017, Bureau of Energy Efficiency (BEE), 2017

PLEA 2024 WROCŁAW
(Re)thinking Resilience

From Theory to Everyday Life in Low Energy Home of Own Design:

energy use, IAQ and technology domestication

MAGDALENA BABORSKA-NAROŻNY[1], MARIA KOSTKA[2], KAROL BANDURSKI[3]

[1]Wrocław University of Science and Technology, Faculty of Architecture, Wrocław, Poland
[2] Wrocław University of Science and Technology, Faculty of Environmental Engineering, Wrocław, Poland
[3] Poznań University of Technology, Faculty of Environmental Engineering and Energy, Poznań, Poland

ABSTRACT: The discussion on optimum technical solutions in construction to address climate emergency is far from over. Studies taking sociological or psychological approach provide evidence, that technology driven energy demand reduction in housing needs to be aligned with user needs, their routines and home use practices. To explore if an exceptional alignment of technology and household characteristics actually leads to outstanding performance, case study houses inhabited by their designers are examined, against the background of non-designer households. The results, based on one year of intense monitoring and occupant feedback, focus on household as designed versus measured energy consumption and indoor air quality (IAQ) outcomes. The results show areas of clear advantage of high expertise within a household, e.g. in relation to IAQ issues prevention. However overall within the studied sample no clear connection between expertise and performance was established. The experience of domestication of self-designed technology influenced professional decisions of the involved engineers in their design practice.
KEYWORDS: Household Energy, Thermal Comfort, Indoor Air Quality, BPE, Domestication

1. INTRODUCTION

The responsibility to address the root causes and mitigate the risks associated with climate emergency has in part been assigned to the stakeholders of the design and construction sector. Over the last several decades an EU policy shift towards 2050 climate neutral aims indicated ambitious energy efficiency targets for new built and retrofit housing, enabled by varied innovative materials, heating and ventilation systems (HVAC) and design strategies. Passive House is one of the established strategies developed around energy efficiency. It requires deployment of certified products and following specific and quantified design, construction and commissioning guidelines to achieve the ambitious energy efficiency aims and question the inevitability of the performance gap. And even within the well-defined Passive House framework there are unresolved technology related questions, in particular in the housing retrofit domain. As Welch et al. put it “It’s easy to say “do it right” but harder to answer “what is right”?” [1]. The discussion on optimum technical solutions in construction to address climate emergency is far from over, as there are competing strategies for material use, heating or ventilation presumably leading to environmentally beneficial outcomes and new complexity levels coming into focus, e.g. embedded energy, circular economy or sufficiency [2-5], as well as a recurring theme of the need for simplicity and usability [6] of buildings. Within the changing conceptual and regulatory framework design teams adopt strategies and make specification choices that contribute to mainstreaming or side-tracking novel technologies [7] based on their professional knowledge. Ideally, the design knowledge is accumulated through engineering education, professional trainings focused on specific products or systems, modelling as well as findings of building performance evaluation (BPE), closing the loop of constructive feedback between the operational and design stages of buildings’ life cycle [8]. However, in most countries, including Poland, the BPE studies are not routinely embedded into the design process. What’s more the BPE findings may not be directly transferable between countries due to specific climatic or cultural factors. This puts not only users but designers in a vulnerable position, encouraging business-as-usual approach despite climate emergency, as proposing new technologies caries a greater risk of in-use liability or performance issues.

Where available, the in-depth BPE studies provide insight into the actual roles of technologies in shaping domestic indoor environment and the related energy consumption. The ergonomics and usability of controls or residents’ awareness and understanding of a technology were identified as relevant factors shaping its actual use, e.g. in an apartment block where 40% of the over 100 surveyed households were unaware that their dwellings rely on continuous mechanical ventilation for healthy indoor air quality (IAQ), only ca. 10% had it “on” across the seasons as designed, with negative IAQ consequences [9].

Numerous studies taking sociological or psychological approach provided evidence, that the potential effectiveness of energy demand reduction in housing to be achieved by the means of designer led technology choices would be undermined if the technology did not match user needs, their routines and home use practices. Given that the lack of overlap between design intentions and user needs has been linked with housing underperformance it is interesting that no studies to date, the authors are aware of, explore the opposite scenario, i.e. effectiveness of technology and the alignment of its intended and actual use in households living in homes of the designers themselves. In such case both the rationale for a given technology and its intended use is well understood within a household and the household routines are known at the design stage. Two key research questions are explored here:

Can the houses occupied by a design team member, having in-depth understanding of energy efficiency strategy for their home be linked with outstanding performance outcomes in terms of IAQ parameters and energy performance?

Is living in self designed home used to verify the assumptions about energy efficiency strategy adopted?

2. METHOD

To address the above questions a socio-technical approach has been adopted involving an in-depth building performance evaluation of 10 case study low energy homes, located in and around Wrocław, Poland (Table 1). There were two main selection criteria for the purposive (non-probability) sampling, suitable for exploring ideas and developing understanding (Ritchie & Lewis, 2004). First, a house needed to be equipped with some technology exceeding standard practice in Poland at the time of construction, e.g. mechanical ventilation with heat recovery or a heat pump. Secondly, the occupancy period at the recruitment stage must have been at least two years. The rationale for the latter was to observe settled home use practices well after early occupancy. As the recruitment started in early 2021 a house needed to be occupied at least by early 2019, i.e. before the nearly zero emissions (nZEB) requirements for all new built housing were implemented in Poland. Such timeline meant that the recruited sample was not representative for standard new built, but focused on voluntary early adopters of novel energy efficiency technologies. Nevertheless, the households and their individual members represent contrasting levels of understanding and varied focus in relation to their home performance (Table 1). Three households are neither connected with construction sector or engineering disciplines. However, four households involve engineers (three environmental and one automation engineers) responsible for the design and partly also the installation of the heating and ventilation systems in their homes. Also two houses are occupied by the architects responsible for their design, and one by an engineer not engaged in the construction sector but having a very good understanding of technology.

Data collection, between August 2021 and October 2022, included one year of regular home visits, interviews, walk-through, surveys and extensive monitoring of IAQ as well as energy use and thermal comfort analysis. More details about the methods, preliminary quantitative monitoring results for selected households and other aspects of the broad study have been previously reported in [10,11]. Here the focus is on comparing performance of all houses in connection with the professional expertise present within each household. The conclusions draw on both quantitative and qualitative data.

Table 1: Key household member roles in shaping energy efficiency strategy and in-use performance focus.

Household member responsible for:		Design/in-use focus on:
EH	HVAC design	ZEB standard with natural ventilation; high thermal mass/closing the performance gap
EK	HVAC design	ground source heat exchanger; MVHR/ added PVs, utility costs
EZ	Maintenance (engineer)	n/a (second owner)/ thermal comfort, added PVs
WA1	-	n/a (not an engineer)/ individual thermal comfort needs
WA2	-	n/a (not an engineer)/ utility costs
WZ1	Architecture	Building form and structural material (CLT)/ plug & play HVAC
WZ2	Housing developer	Material choice (CLT)/ plug & play HVAC
WZ3	HVAC design	bespoke heating & hot water automation/ fine grained control over heating and natural + MVHR ventilation practices for efficient
NA1	HVAC design + Architecture	Envelope + heat pump & hybrid ventilation/ IAQ + energy use monitoring; tailored energy tariffs
NA2	-	n/a (not an engineer)/ affordable thermal comfort + good IAQ

3. RESULTS

The following sections provide a comparison of energy standard of the studies houses, as well as key monitoring results to understand in-use environmental standard achieved in the designer vs. non designer households and the overall energy consumed. Next, key designers' experience based insights into technology domestication process, their awareness of own house performance against assumptions and the intended further energy efficiency improvements are explored.

3.1 As designed energy standard

As a starting point for comparison of energy standard between the analyzed houses energy certificates were developed. The certificates were intended to represent household size, and the operational stage conditions as closely as the relevant guidance allowed, to capture the impact of introduction and use of varied HVAC solutions or photovoltaics (PVs), even if these were unaccounted for during initial design. The resulting usable (EU), final (EF) and primary energy (EP) values, as well as the share of renewable energy in annual energy balance is presented in Table 2.

Table 2: Case study houses energy standard.

	Construction	Usable area	EU	EF	EP*	U_{RES}
		m^2	kWh/(m^2·y)			%
EH	2015/2016	213,5	64.8	32.2	7.4	97.4
EK	2012/2015	265,1	111.4	197.3	164.6	77.4
EZ	2012/2015	168,3	159.9	69.6	64.0	89.2
WA1	2012/2018	149,8	42.9	32.8	98.5	44.6
WA2	2012/2015	149,8	42.1	46.7	89.0	64.9
WZ1	2012/2016	149,8	37.6	30.6	91.8	43.7
WZ2	2012/2016	149,8	42.5	33.0	99.0	44.7
WZ3	2012/2016	149,8	40.6	53.6	61.6	75.4
NA1	2015/2017	141,8	42.5	29.0	86.9	47.1
NA2	2015/2018	175,7	102.5	49.9	141.2	60.7

* value required by EP regulations < 120kWh/(m^2·y)

Diverse results can be seen for five neighboring household built by one constructor to same building envelope specifications (WA1-WZ3) but using different HVAC solutions. The building envelope specifications exceeded by far energy efficiency standard of the time of their construction, though fell short of the Passive house standard mentioned by the architect (WZ1) and developer (WZ2) as an energy efficiency inspiration. In these high performing buildings the final energy demand varies by up to 75% between least efficient HVAC solution in WZ3 and the three comparable technologies, namely heat pumps and mechanical ventilation with heat recovery (MVHR) in WA1, WZ1 and WZ2. However the opposite can be observed in terms of primary energy, perceived as the key measure of environmental impact. The energy efficient heat pumps, lead to worse EP results as they rely exclusively on grid electricity, while a less effective wood burner with water jacket often used as a substitute for the heat pump (WZ3) performs best in terms of EP. The system designer and at the same time its user, well aware of the actual energy sources, claims in the interview: ”I have a stove running on the energy of the sun [referring to wood] and a heat pump running on coal [referring to electricity]”.

However, three households within the sample did install the PVs. One of these houses (EH) has been designed to achieve an almost zero energy standard (ZEB) with EP=7.4 kWh/m^2·y. Two other highest EP scoring households are EZ and NA1. Three out of four of the top EP values in the certificates are in HVAC designers’ households. Also in the fourth household there is an engineer with good understanding of heat pump technology, however not involved in developing energy strategy for his house, as it was bought complete with the system from previous owner. The fourth HVAC designer did not secure an ambitious EP result, as for the studied sample, despite the PVs and unique technologies introduced with energy saving in mind, namely ground source heat exchanger feeding preheated (or precooled) air into the MVHR. The advanced ventilation technology could not counterbalance the standard approach to building envelope energy efficiency for the time of its construction as well as a standard gas boiler for heating and hot water.

3.2 Indoor environment quality

The energy efficient envelope and HVAC technologies are intended to secure healthy indoor environment at a minimum energy and environmental cost. Here the measurement results of indoor environment parameters regarded as key for a robust representation of IAQ, i.e. air temperature, relative humidity and CO_2 concentration, are shown against the existing regulatory or best practice guidelines for healthy domestic environment [12]. Thermal environment evaluation is underpinned by adaptive comfort model [13].

Unlike with the expected environmental impact of energy use expressed in EP value, where the engineer/designer households overall scored higher than the non-designer households (except for EK), the indoor parameters evaluation does not provide a clear picture of superior IAQ in designers’ homes. For thermal environment (Figure 1a) the evaluation based on adaptive comfort thresholds, defined as predicted percentage of dissatisfied (PPD), adjusted to outdoor running mean temperatures [13] shows that both the highest (over 80% of time within the top comfort threshold of PPD<10%) and lowest (ca. 40% of time with threshold of PPD<10%) performing households represent all three energy proficiency household categories, i.e. HVAC designers, other engineers and non-engineers. For indoor temperatures no correlation between technology expertise level and in-use outcomes can be established. However a broader analysis and discussion on the comfort criteria, that is not within scope of this paper, could shed light on actual satisfaction of some households with their thermal environment, despite presented results suggesting comfort criteria exceedances. In particular lower than

typically expected indoor temperatures were advocated as desirable in EH. The HVAC designer suggested the culturally underpinned expectation of indoor temperatures exceeding 20°C in Poland is irrational and should be challenged.

The results for relative humidity (RH) and CO_2 are similarly ambiguous, with no clearly better conditions observed in the designers' households. What stand out however, is that the underperforming outliers for both IAQ parameters were the non-designer households. What's more the persistent underperformance remained unnoticed until it was flagged as a part of post data collection research findings reporting. On the other hand, the instances of IAQ related underperformance detected in designer households came as no surprise to the home owners and was either deemed as acceptable regardless of the standard guidance or there was an plan in place to address the issue.

3.3 In-use energy consumption

Diminishing domestic energy consumption and its related environmental impact are in focus of climate emergency debate. Nevertheless understanding own household energy consumption in connection with home practices and the technology performance proves highly challenging to implement even for experts, whenever deeper analysis is attempted. For non-expert households energy as such has not been a matter of investigation, whereas opinions on comfort and costs were robustly assessed against expectations. Data on electric energy consumption, and where applicable export of PV generated electricity was obtained from utility provider. Where applicable the residents were asked to assess the amount of solid fuel (wood) burned and gas bills were analyzed. Detailed understanding of PV generation and self-consumption was modelled [14,15].

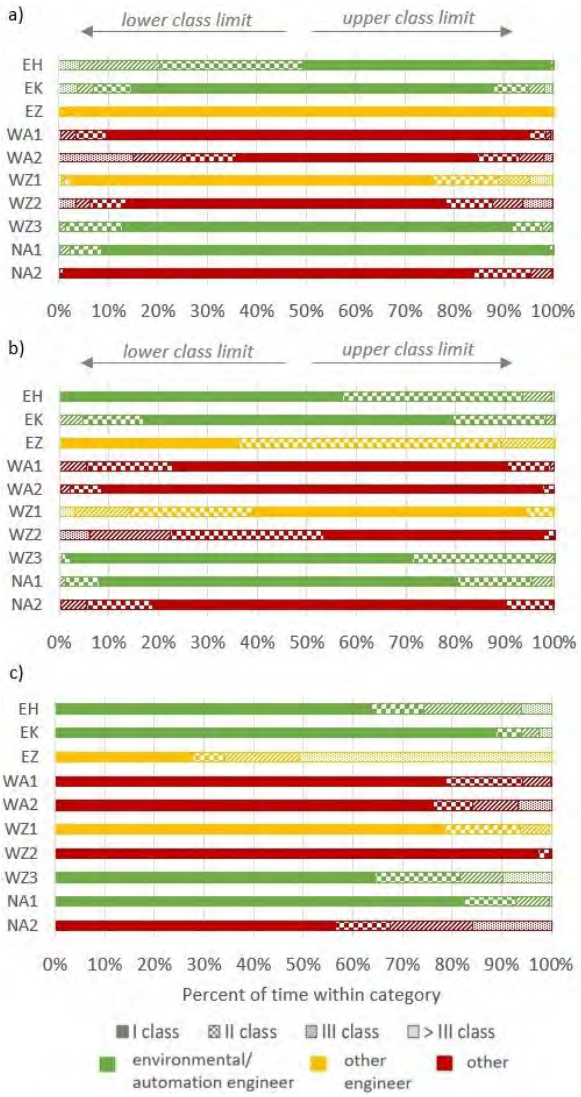

Figure 1. Percent of time within indoor air quality thresholds defined according to: [12,13]. a) Adaptive thermal comfort, b) RH, c) CO_2 .

One way to understand the final and primary energy results (Figure 2) is to compare them with the expectations built on energy certificates. Only broadly the trend of highest and lowest energy performance is aligned between the certificates and in use consumption, e.g. high EH energy performance is confirmed by in-use EP results and so is the best EP performance of the WZ3. However within the sample hierarchy of the expected EP levels changes for certificate and in-use results, e.g. for WA1, NA1 and NA2. Also, in use data shows much higher impact of PV generation on annual primary energy balance than assumed at certificate stage. Overall as with IAQ parameters energy consumption results do not show a clearly better results for expert households as both the highest and lowest in-use EP is identified in HVAC designers' homes.

3.4 Domestication and verification of design assumptions

Domestication theory provides a framework to understand the complex process of "taming"

technology and its incorporation into daily routines. Importantly the theory links the perceived success or failure of the incorporation with subsequent contribution of an individual to speeding or hindering technology adoption in wider society (Silverstone et al., 1992). The theory distinguishes four phases of the process: appropriation, focusing on technology choices and ownership, objectification centring on giving meaning and place for technology in the space of one's home, incorporation referring to everyday use, its temporality and the perceived functionality of a technology. The final conversion stage describes how the technology perceived status is disseminated to the outside world. Domestication theory provides a framework to understand the unique and wide reaching impact of an experience with technology used in own domestic setting, if perceived as meaningful and positive. Here, focus on the perceived success of domestication of specific low energy strategies by designers in particular, but also other construction stakeholders is particularly relevant given their unique professional impact on technology choices.

In the designers' households the appropriation stage in some cases reveals a clear alignment of decisions with professional interests: the architects focused their attention on the building form, specific envelope material and its energy standard. As to the heat pump the architect (WZ1) recalls its specification and purchase was an ad hoc decision guided by retailer's advice on a special offer. On the other hand within the studied sample there are two catalogue houses (EK, EZ). The HVAC designer owner decided to improve the insulation and invest in better windows than the standard for that time, however his particular focus was on unique ventilation solutions, i.e. ground source heat exchanger coupled with MVHR. There are also examples of high performing envelopes aligned with high performing HVAC technology. However in each case of a designer owner the in-use attention shifts towards own professional expertise area, e.g. securing air tightness and installing check valves in ventilation ducts to prevent heat loss, where the design ambition was to prove natural ventilation as a viable option for ZEB standard. The objectification and incorporation stages are key in verification of the design assumptions. Varied attention and effort was observed between households to obtain evidence base for assumptions assessment. Overall the designers were significantly more engaged than non-designers, at least at early occupancy, in some form of data collection, mostly aiming to understand energy consumption based on bills or meter readings, but also some assessment of indoor temperatures and controls' settings. In one HVAC designer household CO_2 was monitored to understand ventilation performance. Most enquiries were concluded, either when the findings were deemed satisfactory or too complex to be followed up with the resources available. A more detailed enquiry attempting to understand the share of energy use for heating (and ventilation) was performed in two HVAC designer households only (EH, NA1). An overview of the scope of performance assessment of own homes and the resulting plans for further improvement is presented in Table 3. Overall, expert households have targeted plans for future interventions to improve their home performance. In the long term perspective this is a significant advantage. The notable planned improvements in HVAC designer households include installing CO_2 monitoring for informed natural ventilation control. Also, awareness and willingness to act on IAQ issues proved specific to expert households. Non-experts retained in unknown unknowns state and were not concerned until the research project findings revealed exceedances in high CO_2 or extremely low humidity levels.

The reported impact of experience of living in self designed home on the evolution of design approach and professional practice varies. Not overly positive

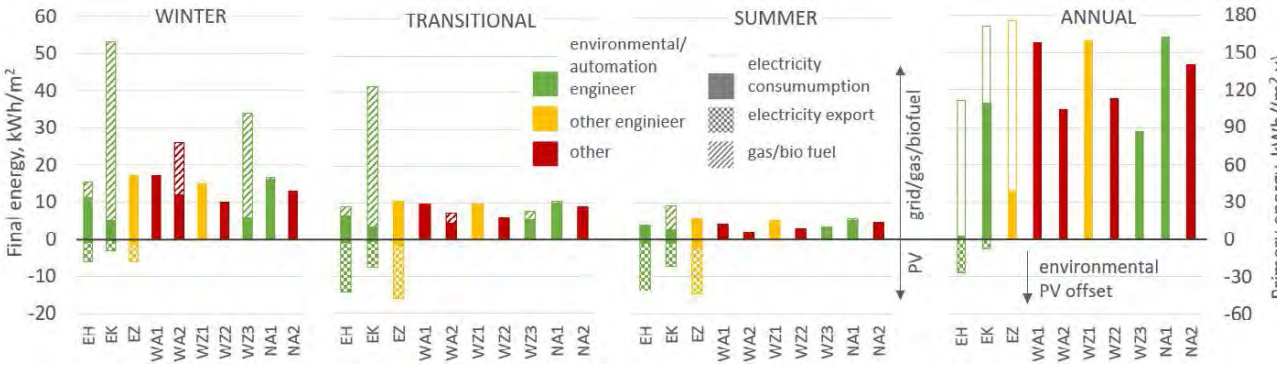

Figure 2. Seasonal final energy consumption and annual primary energy balance.

perception of own outcomes coincided with a professional decision not to engage in HAC design for individual home owners, due to understanding the complexity of the challenge, that is not reflected in fees. On the other hand the designers satisfied with natural or hybrid ventilation performance in their

houses claim to be reassured about the applicability of the approach in energy efficient housing in Poland, despite regulations pushing for MVHR.

Table 3: Key learning methods implemented and further plans.

	Testing implemented by the household	Planned adjustments
EH	early occupancy spreadsheets on metered energy /HP active time; regular checking of internal temperatures	CO_2 level controlled natural ventilation
EK	early occupancy notes on metered energy (gas +electricity) + water consumption + bills	damper actuator on a ground source HP; control over heating between spaces
WA2	energy bills	-
WZ1	first year of occupancy notes of metered energy	-
WZ3	internal temp. monitored to adjust floor heating valves in rooms; bespoke automation for heating/ hot water settings	CO_2 level controlled natural ventilation
NA1	submetering on HP + MVHR, monitoring of IAQ; adjusting floor heating valves in rooms	PV; green roof; external shading

5. CONCLUSIONS

Owner occupied low energy houses representing varied energy efficiency strategies participated in an in-depth case study building performance evaluation. In five out of 10 homes owners were responsible for some aspect of own home design: architecture or HVAC systems. The parameters assessed for the studied sample do not allow to conclude, that expert knowledge within a household guarantees securing outstanding results in terms of energy consumption savings or IAQ fully aligned with regulatory or literature derived guidelines. Contrary, some experts question the rationale of the standard IAQ targets. However, the results suggest that in-depth understanding of environmental issues and technology within home helps to avoid extreme exceedance, in particular for RH or CO_2 that go unnoticed for none experts. Also despite limited capacity to develop detailed assessment of own house performance, the expert knowledge allows to plan relevant and targeted future interventions. Domestication of solutions is perceived as a relevant experience informing future design decisions.

ACKNOWLEDGEMENTS

The research was supported by the National Science Centre Poland, OPUS15 No. 2018/29/B/HS6/02958. The authors gratefully acknowledge the generous time commitment by the voluntary participants of the study.

REFERENCES

1. Welch S., Obonyo E., Memari A., (2023). A review of the previous and current challenges of passive house retrofits. *Building and Environment*, 245, 110938.
2. Sakiyama N., Calro J., Frick J., Garrecht H., (2020). Perspectives of naturally ventilated buildings: A review. *Renewable and Sustainable energy Reviews,* 130, 109933.
3. Tognon G., Marigo M., De Carli M., Zarrella A., (2023). Mechanical, natural and hybrid ventilation systems in different building types: Energy and indoor air quality analysis. *Journal of Building Engineering*, 76: p.107060.
4. Berril P., Wilson E., Reyna J., Fontanini A., Hertwich E., (2022). Decarbonization pathways for the residential sector in the United States. *Nature Climate Change,* 12: p.712-718.
5. Saheb Y., (2021). COP26: Sufficiency Should be First. *Buildings & Cities*, [Online], Available: https://www.buildingsandcities.org/insights/commentaries/cop26-sufficiency.html [16 January 2024]
6. Leaman A., Bordass B., (1993). Building Design, Complexity and Manageability. *Facilities*, 11(9).
7. Coma Bassas E., Patterson J., Jones P., (2020). A review of the evolution of green residential architecture. *Renewable & sustainable energy reviews,* 125, 109796.
8. Stevenson F., (2019). Housing Fit For Purpose, RIBA Publishing, London.
9. Baborska-Narożny M., Stevenson F., (2017). Mechanical ventilation in housing: understanding in-use issues. *Engineering Sustainability*, 170(1): p.33-46.
10. Baborska-Narożny M., Kostka M., (2022). Seasonal air quality in bedrooms with natural, mechanical or hybrid ventilation systems and varied window opening behavior – field measurement results. *Energies*, 15, 9328.
11. Baborska-Narożny M. Grudzińska, M., Bandurski, K., (2023). Capturing Building Fabric Thermal Performance and Solar Heat Gains Through a Whole House Heat Loss Test – an In-Situ Study in Poland. *Journal of Physics: Conf. Series,* 2654, 012118.
12. CEN EN 16798-1:2019 Energy performance of buildings - Ventilation for buildings - Part 1 - Module M1-6
13. Boerstra A.C., van Hoof J., van Weele A.M., (2014). A New Hybrid Thermal Comfort Guideline for the Netherlands, *Proceedings of 8th Windsor Conference 2014: Counting the Cost of Comfort in a changing world*, pp. 967-978, Cumberland Lodge, Windsor, UK, London: NCEUB.
14. Gracia, A. M., Huld, T. (2013). Performance comparison of different models for the estimation of global irradiance on inclined surfaces: Validation of the model implemented in PVGIS. *JRC Technical Reports*.
15. Jastrzębska, G. (2013). *Ogniwa Słoneczne. Budowa, technologia i zastosowanie*. Wydawnictwo Komunikacji i Łączności.

PLEA 2024 WROCŁAW
(Re)thinking Resilience

Expatriate Behaviour in Hot Arid Countries:
Understanding conditioned environments to assess resilience.

MONAYA SYAM[1], CLARICE BLEIL DE SOUZA[1], ELENI AMPATZI[1]

[1]Welsh School of Architecture, Cardiff University, Cardiff, UK

ABSTRACT: This paper aims to provide insights into thermal comfort perception of expatriate households living under very hot climatic conditions. It explores perceptions of indoor thermal sensation, thermal preference, and decisions of self-declared Air Conditioning (AC) setpoint temperatures of 372 expatriate households in typical apartments and villas in the Al Ain city (United Arab Emirates), using a questionnaire survey. Results show that expatriates do not appear resilient to very hot climates in summer, as most of them seem to feel satisfied with narrow setpoint ranges, while stating setpoints above 25°C are not tolerable. Further studies are needed to properly assert adaptive comfort indoor temperatures and investigate expatriates' tolerances to extreme heat to assess hybrid and passive design strategies.
KEYWORDS: Expatriate housing occupants, Thermal comfort, Air-conditioning setpoint temperatures, Indoor environmental control, Hot-arid countries

1. INTRODUCTION

The impact of occupant behaviour on energy policy effectiveness is currently not well understood, primarily due to lack of sufficient representative data (1,2). Typical assumptions about standard behavioural patterns may not be appropriate in informing energy saving strategies (3), potentially contributing to uncertainties or inaccuracy in building energy use prediction. This is particularly true in new housing developments in hot arid countries, where Air Conditioning (AC) is used indiscriminately, and the demographics are varied due to migrations from different parts of the world (4,5).

The United Arab Emirates (UAE) is considered one of the highest electricity consumers in the world (6). Due to extreme high summer temperatures, air-conditioning is the major electricity end-user in buildings, accounting for more than 65% of the energy consumption (4). The rapid economic growth, high living and working standards have led to around 81% of Abu Dhabi Emirate's population (UAE's capital) to be of expatriates (7). In fact, the average annual growth rate of this group in relation to the overall population is 6% (7). At present, thermal comfort perceptions, heat acclimatization levels and adjustment behaviours of the expatriate population are not understood, neither for the UAE context nor for the gulf region in general.

Considering that expatriates constitute around 51% of the gulf countries' population and are key to supporting economic and social development (8), understanding their climatic experiences, thermal comfort perceptions and acclimatization levels becomes fundamental if energy savings are to be achieved. Differences in thermal acceptability levels between local people and migrants from different climatic regions indicate that thermal histories have a strong influence on their indoor thermal comfort levels (9).

Therefore, this paper explores thermal comfort perception of expatriate households living under very hot climatic conditions in typical apartments and detached houses (locally called 'villas'). Through a questionnaire survey, it assesses the behavior of 372 households in the extreme hot climate of Al Ain city, which is part of Abu Dhabi Emirate in the UAE, to assess expatriates' resilience to extreme hot climates. For the analysis, residences are grouped into two categories; those that have individual room controls and those that do not.

Results suggest that expatriates do not seem resilient to very hot climates as they appear to locate their thermal comfort levels away from what is broadly recognized as "neutrality" (10), stating they prefer 'cooler' and 'much cooler' environments while already feeling 'neutral' or 'slightly cool'. AC setpoint ranges are quite narrow particularly for homes with no individual control (around 2°C) whereas setpoints around 25°C are already deemed uncomfortable, making the implementation of passive strategies questionable and difficult to be accepted alone.

2. METHODOLOGY

Demographics and behavioural data were collected through an online survey from randomly reached expatriate who are aged 18 years old and above during summer 2023. The survey consisted of two parts; the first part collected respondents' place of origin, previous place of living and housing type.

Table 1: Second part of survey questions.

	Survey questions*
Thermal sensation	How do you feel at home in general during summer season under typical circumstances (Example: with air conditioning on at home)?
Thermal preference	Would you prefer to have your home…
AC setpoint temperature	At what temperature do you usually set your air conditioning during summer season? (˚C = Degree Celsius)
AC control type	Are you able to control the air conditioning in each room separately?

The second part collected information about respondents' thermal perceptions as shown in Table 1. A link to the survey (done in Microsoft Forms (11)) was shared with the targeted population group via social networks with requests for further circulation. The survey was prepared in English and translated into Arabic, as it was expected that some expatriates would be native Arabic speakers. Questions requiring voting on scales related to thermal sensation and preference were developed based on the ISO 10551 (12), also used in (13) in English and Arabic.

Initially, descriptive statistics analysis was applied to all data collected. Data was then grouped so results could be analyzed based on building typology and AC control type, respectively apartments or villas with or without individual room control (14). AC self-declared setpoint temperature ranges were identified for each case. Responses were then checked for consistency. Thermal sensation and thermal preferences were analyzed individually and then paired as shown in Table 2. Frequency distribution of AC setpoint temperatures in each case were connected with preference and sensation to identify patterns of preferences from expatriates. Lastly, thermal preference, sensation and setpoints results were aggregated from the four cases, shedding light in how resilient expatriates potentially are to very hot climates.

3. RESULTS AND ANALYSIS

Survey responses were collected online from 515 participants. After filtering, 402 complete sets were obtained. Any responses with "prefer not to say" answers on housing type and/or AC setpoint temperature were excluded, to enable data grouping based on typology and AC control type. The resulting dataset included 372 responses. All Arabic responses were translated to English for data analysis.

3.1 Descriptive analysis

Out of the 372 participants surveyed, 169 respondents live in apartments whereas 203 live in villas. A larger dataset was obtained for villas and apartments with individual AC controls, 178 and 142 respectively. Homes with individual room controls have wider temperature setpoint ranges than those without (Fig. 1). The widest setpoint ranges are observed for villas with individual room controls whereas narrowest setpoint ranges are observed for villas without it. Nine responses out 372 were considered outliers as they stated either very low (such as 9˚C) or very high temperatures (35˚C).

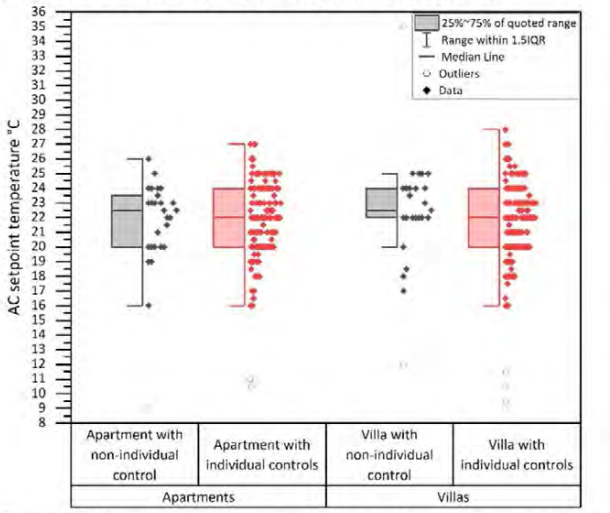

Figure 1: AC setpoint temperature ranges for apartments and villas with non-individual and individual AC controls.

Table 2: Total number of votes obtained for each pairwise combination of thermal sensation and thermal preference.

		Thermal preference						
		Much warmer	Warmer	Slightly warmer	**Without change**	Slightly cooler	Cooler	Much cooler
Thermal sensation	Hot						1	2
							3	
	Warm					1		1
					1	2		
	Slightly warm					2 4	1	1
						2	2 3	1
	Neutral				3 11	3 11	1 7	1 3
					2 19	1 11	1 9	1 7
	Slightly cool				2 7	2 6	1 10	11
				1	12	2 12	1 12	5
	Cool				3 23	3 14	1 17	1
			2	1	8 26	11	3 26	1 5
	Cold			1 3	1 4	1	1 2	2
				1 1	1 5			2

*Survey questions: DOI 10.5281/zenodo.10970285

Reasons for different temperature setpoints were investigated by further disaggregating data and analysing pairwise combinations of thermal sensation and thermal preference, followed by their respective AC setpoint temperatures. Table 2 illustrated pairing thermal sensation with thermal perception for apartments (shaded cells) and villas (white cells) with individual controls (in red) or without them (in black). Empty cells represent no cases.

3.2 Apartments with no individual control (n=27)

Thermal sensation votes for apartments with no individual control range mainly from 'neutral' to 'cold' in 89% of votes. Note that more than half of the respondents, around 59%, usually feel either 'slightly cool', 'cool', or 'cold' with only 11% feeling from 'slightly warm' to 'hot'.

All respondents who feel neutral, prefer either not to change or change to a 'slightly cooler' to a 'much cooler' environment. Two of the respondents feeling 'slightly cool' prefer not to change, whereas the rest prefers going 'slightly cooler' to 'cooler'. Three people feeling 'cool' prefer not to change whereas the rest wants to go to 'slightly cooler' or lower. Only one person feeling 'cold' wishes for a 'slightly warmer' environment. Everyone feeling from 'slightly warm' to 'hot' prefers to go from 'slightly cooler' to 'cooler'.

AC setpoint temperatures, as stated by residents of apartments without individual control, range between 9°C and 26°C, with most of the responses within the range of 20°C to 24°C (78% of responses) (Fig. 2).

Setpoint temperatures for the nine respondents that claim no change is needed range from 20°C to 25°C, with mostly reported temperatures are 23°C and 24°C. Mostly reported setpoint temperatures by the eleven respondents that prefer a 'slightly cooler' environment range between 19°C to 24°C, whereas setpoints for the five that prefer a 'cooler' environment range between 19°C and 26°C. One respondent setting the thermostat at 16°C, prefers a 'much cooler' environment whereas the setpoint for the respondent preferring a 'slightly warmer' environment is 23°C. Interestingly, the only respondent claiming to feel hot sets the thermostat at 19°C.

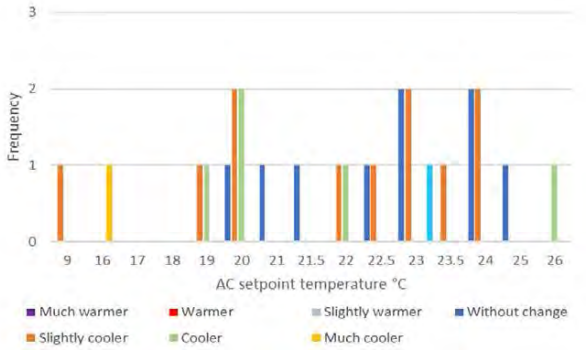

Figure 2: Frequency distribution of AC setpoint temperatures in apartments without individual room control for different residents' thermal preferences.

Looking at setpoint against thermal preference and sensation, one could conclude that 18.5% of residents feel temperatures between 23°C and 25°C need not to be changed, whereas 18.5% of residents feel these temperatures need to be 'cooler' or 'colder'. 11% of residents feel temperatures between 20°C and 22°C need not to be changed, whereas 22% of residents feel these temperatures need to be 'cooler' or 'colder'. Interestingly, 11% of residents felt temperatures between 16°C and 19°C needed to be 'cooler'. Overall, results show that setpoints between 20°C and 22°C are either OK or need to be lower for around half of the expatriates.

3.3 Apartments with individual room control (n=142)

93% living in apartments with individual AC controls, feel 'neutral' to 'cold', with 70% of respondents feeling between 'slightly cool' and 'cold' and 39% of respondents feeling 'cool'.

Only 7% of respondents feel between 'slightly warm' and 'hot'. All respondents who feel 'neutral', prefer either not to change or change to a 'slightly cooler' to a 'much cooler' environment. From those feeling 'slightly cool', seven prefer not to change whereas the rest prefers going 'cooler' or 'much cooler'. From those feeling 'cool', twenty-three prefer not to change whereas fourteen prefer a 'slightly cooler' environment and eighteen prefer an even 'cooler' environment. Four people feeling 'cold' prefer not to change whereas three want to go 'slightly warm'. Respondents claiming to feel from 'slightly warm' to 'hot' all want to go from 'slightly cooler' to 'cold'.

A wide range of AC setpoint temperatures was stated by residents living in apartments with individual AC controls, between 10.5°C and 27°C (Fig. 3). The most frequently stated setpoint temperatures are 22°C, followed by 24°C, 20°C, and 25°C.

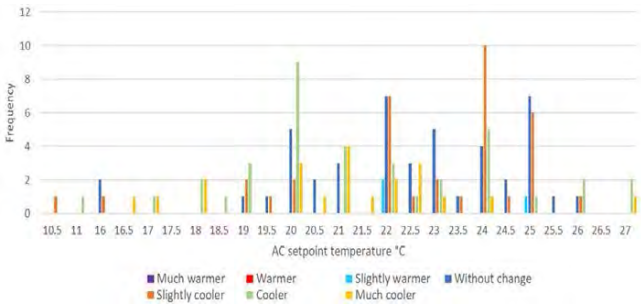

Figure 3: Frequency distribution of individual AC setpoint temperatures in apartments for different thermal preferences.

Setpoint temperatures for those needing no change vary between 16°C and 26°C, with the most reported temperatures between 20°C and 25°C. Setpoint temperatures for the thirty-six respondents that prefer a 'slightly cooler' environment range

between 10.5°C and 26°C, with concentration of temperatures on the range between 22°C and 25°C. Setpoints for the thirty-seven respondents that prefer a 'cooler' environment range between 11°C and 27°C, but predominantly varying between 20°C and 24°C. Setpoints for the twenty preferring 'much cooler' environments vary from 16.5°C to 27°C but with a predominant distribution between 20°C and 22.5°C. The three respondents willing to feel 'slightly warmer' are currently with their setpoints at 22°C and 25°C.

Looking at setpoints against thermal sensation and preference, it can be noted that around 27% of residents feel temperatures between 20°C and 25°C need not to be changed whereas 50% prefer them to be from 'slightly cooler' to 'much cooler'. Overall results show that setpoints between 20°C to 25°C are either OK or need to be lower for 77% of expatriates.

3.4 Villas with no individual control (n=25)

In villas with no individual control, most households, 92%, state they feel between 'neutral' and 'cold', with nearly half of households (48%) reporting feeling 'cool' and 20% feeling 'neutral'.

All respondents who feel 'neutral', prefer either not to change or change to a 'slightly cooler', a 'cooler' or a 'much cooler' environment. Three respondents feeling 'slightly cool' prefer either a 'slightly cooler' or 'cooler' environment, whereas one of them prefers a 'slightly warm' environment. Eight people feeling 'cool' prefer not to change, whereas three prefer a 'cooler' environment. The two respondents feeling 'Slightly warm' prefer a 'cooler' environment and one of the respondents feeling 'cold' asks for a 'slightly warmer' environment.

AC setpoint temperatures of villas with no individual control range between 12°C to 35°C, with most temperatures set between 22°C to 24°C. Figure 4 shows that setpoint temperatures for the eleven respondents that want no change, range between 18.5°C and 24°C, with most of them falling between 22°C and 24°C. Setpoints for those who want a 'slightly cooler' environment fall again between 22°C and 24°C, whereas setpoints for those wanting a 'cooler' environment are scattered on 12°C, 17°C, 20°C, 25°C and 35°C. Two individuals preferring a 'much cooler' environments use setpoints in 18°C and 25°C, whereas the two preferring 'slightly warmer' environments set their thermostats at 22°C and 25°C.

Looking at setpoints against thermal sensation, one can see that 40% of households are happy with setpoints between 22°C to 24°C whereas 16% think these temperatures should be 'cooler' or 'colder'. 20% think temperatures should be equal to or 'cooler' than 20°C whereas 16% think they should be 'cooler' than 25°C. Overall, results show that setpoints between 22°C to 24°C are either OK or need to be lower for 76% of expatriates.

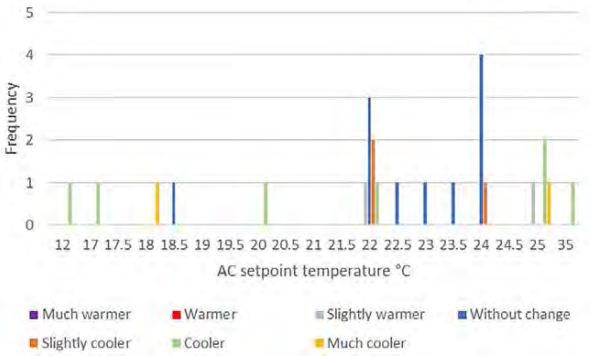

Figure 4: Frequency distribution of AC setpoint temperatures in villas without individual room control for different residents' thermal preferences.

3.5 Villas with individual room control (n=178)

Thermal sensation votes for villas with individual AC controls show that around 93% of respondents usually feel 'neutral' to 'cold', with 67% of respondents feeling between 'slightly cool' and 'cold' and a bit less than half of respondents (40%) feeling 'cool'. Only 6% of respondents feel from 'slightly warm' to 'hot'.

All respondents who feel 'neutral', prefer either not to change or change to a 'slightly cooler' to a 'much cooler environment'. Twelve people feeling 'slightly cool' prefer not to change whereas the rest prefers to go from 'cooler' to 'much cooler'. Twenty-six people feeling 'cool' prefer to not to change, whereas eleven prefer a 'slightly cooler' environment and three a 'slightly warmer' to 'warmer' environment. Only one person feeling 'cold' wishes for a 'slightly warmer' environment. Everyone feeling from 'slightly warm' to 'hot' prefers to go from 'slightly cooler' to 'much cooler'.

Figure 5 illustrates that villas with individual AC controls have the widest range of AC setpoint temperatures, from 9°C to 28°C. Most frequently stated temperatures vary between 18°C and 25°C, with many people reporting 20°C, followed by 22°C, 23°C, 24°C, and 25°C as their setpoints.

Setpoint temperatures for the sixty-three respondents who need no change are mainly between 20°C to 25°C with five individuals feeling happy with lower ranges and four with higher ranges. The thirty-five respondents preferring a 'slightly cooler' environment state their setpoints are mostly between 20°C and 26°C whereas the fifty-two respondents preferring a 'cooler' environment set their thermostats between 11.5°C and 26°C, but predominantly varying from 20°C to 24°C. AC setpoint temperatures stated by the twenty respondents that prefer a 'much cooler' environment were mainly in the range from 9.5°C to 25.5°C and concentrated at around 18°C.

On the other hand, the only two respondents that reported preferring a 'slightly warmer' environment, state they set their thermostats at 24°C and 25°C,

respectively whereas respondents who reported preferring a 'warmer' environment have their setpoints at 18°C. Interestingly, no respondent with setpoints below 18°C reported preferring a 'slightly warmer' to 'Much warmer' environment. Most respondents with setpoints above 25°C report preferring from a 'slightly cooler' to 'much cooler' environment, except for four who feel no need to change.

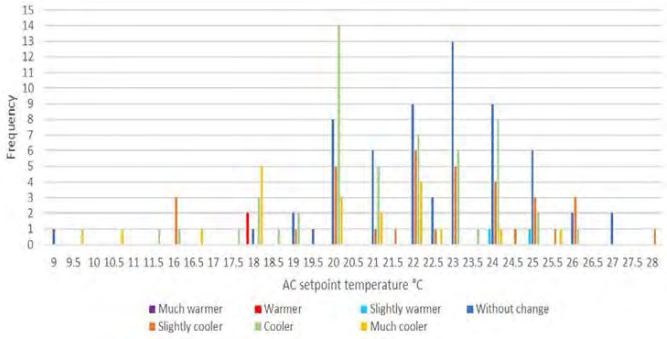

Figure 5: Frequency distribution of individual AC setpoint temperatures in villas for different residents' thermal preferences.

Looking at setpoints against thermal preference and sensation, one can conclude that 29% of the residents feel temperatures between 20°C and 25°C do not need to change, whereas 45% of residents feel these temperatures need to be 'slightly cooler' up to 'much cooler'. Overall, results show that setpoints between 20°C and 25°C are either OK or need to be lower for most of the expatriates**.**

4. CONCLUSIONS

This paper explored thermal comfort perception and setpoint temperature of 372 expatriate households living in the typical villas and apartments in Al Ain city in the UAE, under very hot climatic conditions, using a questionnaire survey, considering individual and non-individual AC controls. The survey queried on typical thermal sensation and thermal preference when at home as well as self-declared AC temperature setpoints for the summer.

As expected, most respondents typically feel 'neutral' to 'cool' (86%), as they can control their indoor environment using AC. Few people feeling 'cold' wish for a 'slightly warmer' environment and all respondents who feel 'neutral', prefer either no change or change from 'slightly cooler' to 'much cooler' environment. As expected, given the hot climate, everyone feeling from 'slightly warm' to 'hot' prefer anything from 'slightly cooler' to 'much cooler', except one respondent. These findings suggest that, in this climate and for this season, expatriates seem to be finding expressions of 'slightly cool' and 'cool' synonymous to comfortable, something which agrees to the results by Al-khatri et al. (15) for Oman which has an even milder climate than the UAE.

Around 62% of people feeling 'neutral' prefer to change to a 'slightly cooler', 'cooler', or 'much cooler' environment. These results confirm the distance between expressed neutrality and comfort, which was also proven in previous research for Oman (10). The findings reveal that neutrality is perceived as being warmer than comfort in this study context, an effect which can potentially be related to its extreme hot summer.

Furthermore, results show nuances in the understanding of 'slightly cool', 'cool' and 'cold'. Linguistic discrepancies could be a significant impacting factor of respondents' misinterpretation of thermal scales, both for non-native English participants and those completing the survey in Arabic, as previously flagged by (13). In relation to the latter, Al-Khatri and Gadi (10) noted that the Arabic thermal sensation scale, after being translated, makes votes that are out of the three middle levels of the scale perceived as comfortable (10). This was also noticed in this study as the most frequently stated thermal sensation level was 'cool', and it appeared to mean comfortable for almost half of the respondents (41%). In addition, the direction of writing in Arabic is the opposite of English, which could bring out some level of inconsistency in response patterns (13). Future research could analyse English and Arabic responses separately and even examine native-language effects within the English sample to disentangle this.

Results also show that the percentage of people dissatisfied with individual controls (6% to 7%) is lower than those dissatisfied with non-individual controls (8% to 11%). The average setpoint for all cases was found to be 22°C. This figure agrees with the study of Al Mumin et al. (16) which explored through a survey the setpoints for 30 homes of local residents in Kuwait (16) with similarities in AC system control type, economic status, high living standards, and cultural diversity (16) to this study**.**

The cooling setpoint range proposed by Abu Dhabi International Building Code (ADIBC) that is also linked to ASHRAE standards, is 20°C to 24°C (17). Survey results from apartments and villas without individual room controls show ranges of setpoint choices, between 20°C to 22°C and 22°C to 24°C. On the other hand, apartments and villas with individual control show larger setpoint ranges for most expatriates, respectively between 20°C to 25°C.The study did not record the residents' understanding of and overall perceptions related to AC controls' use but previous research has shown that there are significant misconceptions around such features affecting user interactions with them (18). The self-declared

setpoints quoted here do not provide information on the users' 'ideal' indoor temperature, but rather reflect on their choices when interacting with these controls.

It is important to highlight that for homes with individual controls, the survey did not request or record the rooms for which setpoints are set. Thus, respondents might well be reporting averages, temperatures for the room they either feel more comfortable or more discomfortable with, temperature for the room they are sitting when responding to the survey, etc. Further work is needed to match setpoints stated with actual room temperatures and thermal preferences.

Overall, the declared setpoint choices which go as low as 9°C indicate that many of the expatriates in this context may not be resilient to the hot summer climate. This raises further concerns over potential passive design options suited to the region may carry as well as their acceptability by building occupants. Hybrid systems that make optimised use of passive and active design solutions are needed to address the demands especially in summer to properly assert adaptive comfort indoor temperatures and investigate expatriates' tolerance and resilience to extreme heat.

REFERENCES

1. Hu S, Yan D, Azar E, Guo F. A systematic review of occupant behavior in building energy policy. Build Environ. 2020 May 15;175:106807.
2. O'Brien W, Tahmasebi F, Andersen RK, Azar E, Barthelmes V, Belafi ZD, et al. An international review of occupant-related aspects of building energy codes and standards. Build Environ. 2020 Jul 15;179:106906.
3. Schweiker M, Shukuya M. Comparative effects of building envelope improvements and occupant behavioural changes on the exergy consumption for heating and cooling. Energy Policy. 2010 Jun 1;38(6):2976–86.
4. Afshari A, Nikolopoulou C, Martin M. Life-Cycle Analysis of Building Retrofits at the Urban Scale—A Case Study in United Arab Emirates. Sustainability. 2014 Jan;6(1):453–73.
5. The United Arab Emirates' Government Portal [Internet]. 2022 [cited 2022 Nov 9]. The United Arab Emirates' Government Portal. Available from: https://u.ae/en/about-the-uae/fact-sheet
6. UAE State of Energy Report [Internet]. Ministry of Energy and Industry; 2019 [cited 2022 Oct 20] p. 106. Available from: file:///C:/Users/20135/Downloads/Energy%20Report-2019-Final-Preview-1%20(1)%20(5).pdf
7. Statistics Centre-Abu Dhabi. Statistical Yearbook of Abu Dhabi 2020 [Internet]. Statistics Centre-Abu Dhabi; 2020 [cited 2022 Sep 20] p. 272. Available from: https://www.scad.gov.ae/Release%20Documents/Statistical%20Yearbook%20of%20Abu%20Dhabi_2020_Annual_Yearly_en.pdf
8. Al flaiti A. Poster session presented at: 64th ISI World Statistics Congress; 2023 July 19; Canada.
9. Gautam B, Rijal HB, Imagawa H, Kayo G, Shukuya M. Investigation on adaptive thermal comfort considering the thermal history of local and migrant peoples living in sub-tropical climate of Nepal. Build Environ. 2020 Nov 1;185:107237.
10. Al-Khatri H, Gadi MB. Collective understanding of ASHRAE thermal sensation phrases among Arab students: 10th International Windsor Conference 2018: Rethinking Comfort. Nicol F, Roaf S, Brotas L, Humphreys MA, editors. Proc 10th Windsor Conf. 2018;357–70.
11. Microsoft Forms [Internet]. [cited 2024 Jan 31]. Microsoft Forms. Available from: https://forms.office.com/Pages/DesignPageV2.aspx?origin=shell
12. ISO. ISO 10551 Ergonomics of the physical environment — Subjective judgement scales for assessing physical environments [Internet]. 2019 [cited 2023 May 19]. Available from: https://www.iso.org/standard/67186.html
13. Schweiker M, André M, Al-Atrash F, Al-Khatri H, Alprianti RR, Alsaad H, et al. Evaluating assumptions of scales for subjective assessment of thermal environments – Do laypersons perceive them the way, we researchers believe? Energy Build. 2020 Mar 15;211:109761.
14. Verbeke S, Aerts D, Reynders G, Ma Y, Waide P. FINAL REPORT ON THE TECHNICAL SUPPORT TO THE DEVELOPMENT OF A SMART READINESS INDICATOR FOR BUILDINGS. 2020.
15. Al-Khatri H, Gadi MB. Investigating the behaviour of ASHRAE, Bedford, and Nicol thermal scales when translated into the Arabic language. Build Environ. 2019 Mar 15;151:348–55.
16. Al-Mumin A, Khattab O, Sridhar G. Occupants' behavior and activity patterns influencing the energy consumption in the Kuwaiti residences. Energy Build. 2003 Jul 1;35(6):549–59.
17. Abu Dhabi International Building Code. 2014 p. 699.
18. Peffer T, Pritoni M, Meier A, Aragon C, Perry D. How people use thermostats in homes: A review. Build Environ. 2011 Dec 1;46(12):2529–41.

3.6. Together we can – think, learn, teach and take the leadership (e.g., education and training, environmental activism)

PLEA 2024 WROCŁAW
(Re)thinking Resilience

Sustainable Beauty:
Sustainability and Aesthetics Indicators for Buildings and Spaces

BARBARA WIDERA[1], MATTHEOS SANTAMOURIS[2]

[1]Wrocław University of Science and Technology, Faculty of Architecture, Wrocław, Poland
[2] Anita Lawrence Chair High Performance Architecture School Built Environment Faculty Art Design and Architecture University New South Wales Sydney Australia

ABSTRACT: The research aimed to develop theoretical foundations for selecting a set of quantitative indicators allowing to assess the aspects of sustainability and aesthetics in the context of the New European Bauhaus initiative. The authors analysed currently used indicators of sustainability (SI) and aesthetics (AI) and conducted research on their mutual relationships. The study revealed interdependencies between AI and SI and their positive but also potentially negative correlations. It was noted that in the technical assessment tool the SI and AI should be analysed together. In the case of a positive corelation between SI and AI, the highest possible percentage score in each criterion is desirable. The targets complement each other and the same targets apply to all defined categories, i.e. heritage buildings and spaces aimed at temporary use, renovated buildings and spaces aimed at regular use, and new buildings and spaces aimed at everyday use. In the case of negative corelation SI and AI might be contradictory or partially contradictory. Therefore, the balanced targets are preferred to definite targets, and various targets apply to different categories of buildings and spaces.

KEYWORDS: New European Bauhaus, Sustainability, Aesthetics, Indicators, Climate resilience

1. INTRODUCTION

Achieving climate goals and limiting global warming requires radical steps in transforming the built environment and preserving the nature. The critical importance of these activities has been reflected in recent political and social initiatives. On 19 July 2023, The European Commission proposed a sixth Horizon Europe Mission dedicated entirely to the New European Bauhaus (NEB). If endorsed by the Member States and the community, this Mission would be added to the existing five which cover adaptation to climate change, cancer, climate neutral and smart cities, the restoration of our oceans and waters, and soils. With a focus on research and innovation solutions, the proposed NEB mission would aim to transform neighbourhoods across Europe and worldwide [1].

In the analysis of architecture and space in the context of NEB, three basic values are taken into account: Sustainability, Inclusiveness and Aesthetics [2]. In this article, we focus on the complex interdependencies between aesthetics and environmental sustainability, and attempt to identify indicators that will allow for an objective assessment how a given building or space implements these values. It should be noted that it is impossible to achieve the climate goals without fully implementing the goals of sustainable development [3], an integral part of which is inclusiveness and combating social inequalities, including energy poverty [4].

2. SUSTAINABILITY AND AESTHETICS IN NEB

According to the GreenComp The European Sustainability Competence Framework [5], 'Sustainability means prioritizing the needs of all life forms and of the planet by ensuring that human activity does not exceed planetary boundaries". The Building sector is one of the most dynamic economic sectors, generating wealth and income, and contributing highly to the global European development. The budget associated with the construction, renovation and management of buildings, development of urban projects, and extension of assets currently represent a huge budget close to 1.7 trillion Euros. In parallel, the construction sector is one of the most important employment sectors in Europe employing directly almost 4.1 million workers. In addition to the direct employment capacity of the building sector a very high number of employees in other sectors depend on the growth and activities of the building sector such as materials and systems manufacturing.

Buildings protect the health and wellbeing of humans. The built environment is not just a collection of buildings though, but the physical expression and manifestation of numerous economic, social, and environmental processes strongly related to the human activities and the changing needs of the society. To reflect these needs, various elements of user comfort are analysed, including thermal, acoustic, and visual comfort. Still, the of quality of experience beyond technical aspects are often

underestimated. This involves aesthetical acceptance of buildings and spaces by the end-users.

Aesthetics brings extraordinary value to our lives. We tend to visit buildings and places that we consider beautiful more often, we take better care of them and we are more willing to retrofit and preserve them. If necessary, we look for new functions that will allow us to re-use them and maintain for the equally pleasant aesthetic experience of subsequent generations. Some cultural and natural landscapes represent such a unique value that they are protected by the law and it is often the case that their beauty is prioritised above other aspects. Heritage buildings might be even exempted from commonly adopted regulations so that different rules are applied for example to their energy efficiency requirements. In Wrocław townhall renovation (2003) (Fig.1) the improvement of energy efficiency was partially sacrificed to emphasise traditional methods and building techniques. In particular the very thin lime plaster was used to manifest the medieval origins of the edifice. In this case Aesthetics was prioritised above Sustainability but it was also noted that selected lime plaster did not create negative environmental impact so the Sustainability have not been compromised. There is on-going discussion how to preserve cultural heritage in the most sustainable way, but all actors agree that the recognition and maintenance of heritage representing accumulated creative achievements of the past are an integral responsibility of contemporary society. The same applies to the natural environment as a vital part of heritage of humanity. Therefore, ensuring a high quality urban environment, composed of both cultural and natural landscapes, is essential for the economic success, cultural vitality and social well-being of cities and regions [6].

Meyer [7] and Lenzholzer [8] believe that the real beauty results from sustainability and in particular from skilful landscaping (Fig.2). Building symbiotic relations between nature and architecture, and applying nature-based solutions for natural cooling can be observed is several completed large-scale projects such as PARKROYAL on Pickering (2013, Singapore) designed by WOHA (Fig.3). However, sometimes Aesthetics and Sustainability in architecture are perceived as contradictory [9]. In many cases the contradiction might result from overexposure of infrastructural and technological elements, while the authors of renovations seek for

the balance between the aesthetic and historical values, and the sustainability. NEB promotes deeper understanding of user needs, analysed not only through the prism of momentary "wants", but also in the context of long-term needs, the most important of which is the survival of the planet and counteracting climate change. Can these values be reconciled? The authors of this paper believe that this is absolutely possible. Greater understanding of aesthetic value can lead to more sustainable and strategic approach to the design of not only products but also of buildings and spaces [10].

Figure 1: Wrocław Townhall after renovation (2003). Authors

Figure 2: Arboretum in Wojsławice (2018, Poland). Authors

Figure 3: Hotel PARKROYAL on Pickering (2013, Singapore) by WOHA. Source: Authors

The first tool designed specifically to facilitate evaluation of NEB values (Sustainability, Aesthetics and Inclusiveness) of the project is a NEB Compass [11]. In this tool NEB values are combined with working principles: participatory process, multi-level engagement and a transdisciplinary approach. These principles describe the process through which a project should operate and work to achieve the highest level of ambition in the three values. The

Compass allows to assess how the project promotes a fair transformational outcome which is not only accepted, but also beneficial for everyone and mindful of the systemic and close relationships between complex social, environmental and structural factors. The authors of this paper build on the Compass with aim to manifest deeper interrelations and potential contradictions between Aesthetics and Sustainability.

The European building sector is facing serious economic, environmental, technical, and social challenges caused mainly by the unprecedent global and local climate change, intensive urbanisation, excessive use of resources and social vulnerability and inequalities. The responses to these challenges will shape the present and future quality of life of several hundred million of Europeans and will define to a great extend the future socioeconomic pathways and the magnitude of the economic, technological and social growth In Europe.

3. EXISTING INDICATORS FOR SUSTAINABILITY AND AESTHETICS

2.1 Quantitative indicators

Among the main, commonly used indicators with which we can measurably determine the level of sustainability, the following can be listed: energy efficiency, management, recycling and storage; operational energy consumption; balance between RES and non-RES used in the buildings / neighbourhoods / cities; embodied energy and carbon footprint of the built environment; GHG emissions; heat emissions. All above indicators can be demonstrated in a measurable (quantifiable) way and their achievement might be verified in a given time.

For aesthetics dimension, it is much more difficult to extract quantifiable indicators, because most aspects are analysed using qualitative indicators. Part of the assessment of space quality can be measured by considering comfort aspects such as:

- Thermal comfort assessed with the range of acceptable temperatures measured in relation to relative humidity and the type of clothing and activities performed [12];
- Air quality - measured by the percentage of individual gases in the breathing mix, the amount of pollutants, pathogens, etc. [13]
- Acoustic comfort - measured by the number of decibels, frequency [14]
- Visual comfort - daylight intensity in connection with cultural aspects, activities performed, glare, number of windows, field of vision, contact with space, nature and art, colour intensity in the visible spectrum of light [15].

Other aspects related to comfort include security, availability and functionality of solutions.

3.2. Qualitative indicators

The most difficult to measure values are context, sense of place and beauty. These are qualitative criteria and qualitative methods are used to assess them, allowing for drawing conclusions from multiple subjective assessments. However, conducting surveys and polls is time-consuming and in some situations similar methods cannot be used. This applies, for example, to the criteria used in green public procurement for the construction sector [16].

While the use of sustainability indicators in this area is a common practice today, an attempt to select adequate indicators in relation to beauty and the level of acceptance is extremely difficult. On the other hand, without proper consideration of aesthetic parameters, we will not achieve the expected level of acceptance for the built environment and the transformation will not become widespread. Consequently, the achievement of climate goals will be slowed down or even impossible.

4. PROPOSED APPROACH TO INDICATORS DESIGN

The authors of the article analysed currently used indicators of sustainability and aesthetics, and conducted research aimed at determining their mutual relationships in such a way that they could be used to assess the sustainability and aesthetics of buildings and spaces as objectively as possible [17].

Defined quantitative assessment is mainly related to cultural and natural ecosystem, such as landscape aesthetics. In landscape metrics-based assessment approach, naturalness and landscape diversity can establish some baselines for assessment criteria, where Shannon's Diversity Index (SHDI), Shape Index (SHAPE) and Patch Density (PD) can be used as indicators [18]. It should be noted that while some indicators complement each other, e.g. distance to green areas as Aesthetics Indicator (AI) / biodiversity as Sustainability Indicator (SI), others may be contradictory, e.g. visual index of pro-environmental technologies as (SI) can be seen as disturbance in harmony of cultural and natural landscape (AI). The first couple of indicators illustrates that in order to assess the attractiveness of a space, it is necessary to include an indicator from the areas of sustainability. On the other hand, in the second case, sustainable technologies must be controlled in terms of beauty, visual appeal and acceptability by end users.

4.1 Key objectives of Aesthetics assessment

In purpose to select the key performance indicators for Aesthetics the key assessment areas were identified. They include:

- Quality of experience, covering such aspects as safety and resilience to extreme events, versatility and functionality, all aspects of user

comfort as well as the use of novel materials, structures, technologies and design methods;
- Context and sense of place, covering spatial coherence (planning and design), preservation of cultural and natural heritage, renovation and reuse of buildings and spaces as well as *genius loci* and sense of belonging;
- Beauty, covering aesthetical acceptance of space and architecture including sensory aesthetic experience, spatial experience, cognitive, emotional and attentive response of users as well as intellectual experience resulting from comparison to actual styles and tendencies.

The most important objective of the Aesthetics self-assessment methodology is to ensure high level of aesthetical acceptance of space and architecture. This refers both to new and renovated spaces. The main goals are aimed at increasing the number of renovations, greater acceptance of sustainable technologies and improving their aesthetic appearance. To meet the social need for beauty and improve acceptance of the transformations in the built environment necessary to counteract climate change, seven primary targets relating to the assessment of aesthetic values have been defined:

1. Ensuring high level of aesthetical acceptance of buildings and spaces;
2. Providing spatial coherence in planning and design;
3. Improving preservation of cultural and natural heritage;
4. Enhancing renovation and reuse of buildings and spaces;
5. Increasing *genius loci* and improving sense of belonging;
6. Facilitating aesthetic perception of contemporary buildings and spaces through comparison to actual styles and tendencies in art and architecture [19].

Several existing tools, norms and standards offer methods to assess the quality of experience with a particular focus on safety and functionality [20]. In this paper we focus on indicators allowing for quantitative assessment of less explored areas such as aesthetical acceptance, context and sense of belonging.

4.2 Key objectives of Sustainability assessment

The proposed self-assessment methodology developed in the frame of the NEB, aims to promote sustainability in the European built Environment. Advanced and inclusive targets, methodologies, tools and indices are designed and proposed to assess all aspects of sustainability in buildings and cities, promote sustainable economic and financial activities, overcome local constraints and improve the quality of life of the European citizens indoors and outdoors. The main objectives of the designed self-assessment methodology and of the related indicators:

1. To setup the requirements of the private and financial market sectors to support NEB projects.
2. To support the private sector in implementing NEB transformation projects, addressing financing schemes.
3. To quantify sustainable business practices for NEB projects.
4. To improve sustainability in the production, use and management of energy.
5. To minimise the emissions of greenhouse gases and mitigating the impact on global and local climate change.
6. To minimise the non-energy related environmental impact of the building sector.

In order to properly reflect the objectives in the planned self-assessment system, performance Indicators have been proposed towards the optimisation of the environmental quality in the built environment and the minimisation of the potential negative impacts, and the optimisation of the economic and financial environment to accelerate the sustainable development in the built environment. It was noted that indicators allowing us to assess the optimisation of economic and financial environment and its influence on the transformation of the built environment towards sustainability do not demonstrate direct corelation with the Aesthetics.

4.3 Proposed set of indicators for Aesthetics

The selection of AI was based on their relevance to key objectives of assessment, considering potential corelations with SI. Indicators cover: maintaining proportions, scale and visual coherence with surroundings, preservation and conservation of original historical buildings and their elements, preservation of cultural and natural landscapes, distance to green areas, overall feeling of coherence and harmony including seamless integration of technological elements, aesthetical acceptance for renovations, new functions adopted for re-use of buildings and spaces, use of traditional materials and techniques, application of living systems and bio-based materials, time spent on pedestrian walking routes, satisfaction from sensory experience.

4.4 Proposed set of indicators for Sustainability

Indicators aimed to assess the optimisation of the environmental quality in the built environment and the minimisation of the potential negative impacts were selected for further analysis due to their potential corelation with aesthetic perception of space and architecture. These indicators cover in

particular optimisation of the built environment ability to remove and store carbon in the smart and efficient way as well as minimisation of Greenhouse Gas (GHG) Emissions using Life Cycle Assessment (LCA). The indicators consider also facilitation of sustainable mobility and increasing the amount of green areas absorbing carbon dioxide. Specific group of indicators are focused on energy sources (renewable and non-renewable energy balance), consumption (embodied and operational), storage and recovery. The last proposed set of indicators represents several aspects of circular economy, such as water and waste management, recycling and reuse of building parts and materials.

4.5 Interdependencies between aesthetic and sustainable indicators

Examples of positive and potentially negative correlations between SI and AI are presented in Table 1. In the case of a positive corelation between SI and AI indicators, the highest possible percentage score in each criterion is desirable. The targets complement each other and the same targets apply to all defined categories, i.e. heritage buildings and spaces aimed at temporary use, renovated buildings and spaces aimed at regular use, and new buildings and spaces aimed at everyday use.

In the case of negative corelation SI and AI might be contradictory or partially contradictory. Therefore, the balanced targets are preferred to definite targets, and different targets apply to the categories of buildings and spaces defined above.

4. CONCLUSIONS

The research on Sustainability and Aesthetics Indicators for buildings and spaces confirmed the need to apply SI and AI indicators in the technical assessment in relationships resulting from their mutual interdependence. In pursue to enable technical assessment how the NEB values are addressed in examined buildings and spaces, the authors performed preliminary tests of the set of SI and AI on selected case-studies for verification and self-calibration. The first results shown that for the projects aimed at the symbiotic relations between natural and architectural landscapes, such as Arboretum in Wojsławice, there is no contradiction between SI an AI and the highest scores can be achieved. In new large-scale buildings, applying nature-based solutions for natural cooling, while simultaneously increasing the amount of green spaces in the building and improving biological diversity, such as in Hotel PARKROYAL on Pickering, AI and SI were very well balanced. In Wrocław townhall renovation the improvement of energy efficiency was partially sacrificed to emphasise traditional methods

Table 1: Examples of correlation between Sustainability and Aesthetics indicators and targets for various buildings and spaces

Sustainability Indicator (SI)	Correlation	Aesthetics Indicator (AI)
Optimisation of the built environment ability to remove and store carbon, minimisation of GHG Emissions using LCA	Positive	Natural and bio-based materials, living systems applied in the built environment
Increasing biodiversity and the amount of green areas absorbing carbon dioxide		Distance to green areas, skillful landscaping
heritage buildings and spaces aimed at temporary use → renovated buildings and spaces aimed at regular use → new buildings and spaces aimed at everyday use		
The targets complement each other – the same targets apply to all categories defined above		
Minimal target	Acceptable target	Desired target
SI >30%; AI >30%	SI >50%; AI >50%	SI >70%; AI >70%
Facilitation of sustainable mobility	Potentially negative	Preference to pedestrian walking routes
Renewable and non-renewable energy balance, embodied and operational energy consumption, storage and recovery; visual index of pro-environmental technologies;		Harmonious compositions of natural and cultural environment; seamless integration of technological elements
Innovative materials and techniques; deep renovation for energy efficiency		Traditional materials and techniques, sensory experience
Recycling and reuse of building parts and materials; water and waste management		An amount of preserved original building materials, elements and functions
new buildings and spaces aimed at everyday use → renovated buildings and spaces aimed at regular use → heritage buildings and spaces of unique value		
Targets might be contradictory - balanced targets are preferred to definite targets, different targets apply to the categories defined above		
Desired targets	Acceptable targets	Balanced target
SI >50%; AI > 50%	~50%	AI > 50%; SI < 50%

and building techniques, but the selected solution did not create negative environmental impact so the proposed approach to SI and AI targets allowed for the high scores for the project.

The study shown that even if the same indicators are used for assessment of aesthetic values and sustainability of particular building (or space), when the analysis is conducted separately for aesthetics and sustainability, for some aspects we will obtain different results than in the case of an analysis conducted jointly for both dimensions. Therefore, in order to assess the attractiveness of a space, it is necessary to include indicators from the area of sustainability. On the other hand, sustainable technologies, materials, approaches or building techniques must be controlled in terms of their beauty, visual appeal and acceptability by end users.

At the moment of development of this article the technical assessment framework for the New European Bauhaus has been still in the preliminary phase. While the first results are promising, further tests are necessary for the full calibration of the method.

REFERENCES

1. JRC (2023), *New European Bauhaus: Horizon Europe EU Mission in the pipeline*; New European Bauhaus: Horizon Europe EU Mission in the pipeline (europa.eu) [16.08.2023]
2. European Union, *New European Bauhaus* (2023) https://new-european-bauhaus.europa.eu/about/about-initiative_en [access 10 Jul 2023]
3. United Nations (2023), THE 17 GOALS | Sustainable Development (un.org) [access 10 Jul 2023]
4. Santamouris, M. (2019), Minimizing Energy Consumption, Energy Poverty and Global and Local Climate Change in the Built Environment: Innovating to Zero Casualties and Impacts in a Zero Concept World, Elsevier, http://dx.doi.org/10.1016/C2016-0-01024-0
5. Bianchi, G., Pisiotis, U. and Cabrera Giraldez, M. (2022) GreenComp *The European sustainability competence framework*, Punie, Y. and Bacigalupo, M. editor(s), Publications Office of the European Union, Luxembourg.
6. UNESCO (2005). Vienna Memorandum on World Heritage and Contemporary Architecture - Managing the Historic Urban Landscape and Decision 29 COM 5D, 15th session of the General Assembly of States Parties.
7. Meyer, E.K, Sustaining beauty. The performance of appearance: a manifesto in three parts. *Journal of Landscape Architecture*, spring 2008, p. 6-24.
8. Lenzholzer, S., A city is not a building - architectural concepts for public square design in dutch urban clinute contexts, *Journal of Landscape Architecture*, Spring 2008, p. 44-56.
9. Daniels T.L. (2009) A Trail Across Time: American Environmental Planning From City Beautiful to Sustainability, *Journal of the American Planning Association*, 75:2, 178-192, DOI: 10.1080/01944360902748206
10. Harper, K. (2018). Aesthetic Sustainability: Product Design and Sustainable Usage (R.R. Simonsen, Trans.; 1st ed.). Routledge. https://doi.org/10.4324/9781315190419
11. Joint Research Centre (2023), New European Bauhaus Compass, NEB Compass V 4.pdf (europa.eu) [1.12.2023]
12. Givoni, B. (1994) *Passive Low Energy Cooling of Buildings*, Wiley.
13. Dodd, N., Donatello, S., Cordella. M. (2020) Level(s) indicator 4.1: Indoor air quality, User manual: overview, guidance and instructions. 20201013 New Level(s) documentation Indicator 4.1 Publication v1.0.pdf (europa.eu) [access 14.12.2023]
14. Bluyssen, P.M., (2014). *The healthy indoor environment: how to assess occupants' wellbeing in buildings,* Routledge, London; New York
15. Bluyssen, P.M., Towards an integrated analysis of the indoor environmental factors and its effects on occupants *Intell Build Int*, 12(2020), pp. 199-207
16. Dodd N., Garbarino E., Gama Caldas M. (2016); Green Public Procurement Criteria for Office Building Design, Construction and Management. Procurement practice guidance document; doi:10.2791/858761
17. Thomas, W.A., (2013) *Indicators of Environmental Quality*, Springer US
18. Frank S., Fürst C., Koschke L., Witt A., Makeschin F., Assessment of landscape aesthetics - Validation of a landscape metrics-based assessment by visual estimation of the scenic beauty, *Ecological Indicators*, 32(2013), 222-231, https://doi.org/10.1016/j.ecolind.2013.03.026
19. Santamouris, M., Maloutas, T., Lourenço P.B., Widera, B., Ansaloni, F., Balaras, C., Katurić, I., Kolokotsa, D., Medeiros, E., Rossetto, T, Senatore, G., Tomaszewicz, A. (2024). *A practical guide to the New European Bauhaus self-assessment method and tool*. Luxembourg: Publications Office of the European Union, 2024 Ispra: European Commission
20. Lützkendorf, T., Lorenz, D.P. (2006) Using an integrated performance approach in building assessment tools, *Building Research & Information*, 34:4, 334-356, DOI: 10.1080/09613210600672914.

PLEA 2024 WROCŁAW
(Re)thinking Resilience

Carbon Pasts, Low Carbon Futures:
Teaching Low Energy Architecture Through Adaptive Reuse of Heritage Sites in the South Wales Coalfield

CHRISTOPHER J. WHITMAN[,1]

[1]Welsh School of Architecture, Cardiff University, Cardiff, Wales, UK

ABSTRACT: As we rethink resilience in the face of the climate emergency, it becomes increasingly important to consider embodied carbon, and not only the reduction of operation carbon emissions. Whilst it has been acknowledged for some time that we must retain and reuse our current building stock, architectural education predominantly maintains it focus on the teaching of the design of new-build construction. This is despite the fact that within the construction industry, over half of construction work engages with existing buildings. Architectural students are now requesting the opportunity to engage with design work exploring adaptive reuse, building conservation, and retrofit. This paper presents the development and delivery of a final year architectural design unit that has come about through such demands. For the past three academic years the unit "Carbon Pasts, Low Carbon Futures" has challenged students to propose sustainable reuse strategies for former mining infrastructure within the South Wales Coalfield, transforming these sites once responsible for the UK's carbon legacy into part of the solution to its devastating effects. To date, proposals have included renewable energy production, storage and distribution; reuse and recycling centres; low carbon manufacture; education and knowledge sharing; wellbeing facilities; and innovation and research centres.
KEYWORDS: Education, embodied carbon, low energy design, adaptive reuse, industrial heritage

1. INTRODUCTION

It is now over sixteen years since the then president of the American Institute of Architects (AIA), Carl Elefante, famously stated that "The greenest building is…one that is already built" [1], and yet architectural education continues to focus on new-build design [2, 3], even when teaching passive and low energy architecture. This is despite estimates that between 50-70% of global construction work is on existing buildings [4], and the growing importance of embodied carbon, as highlighted by the Architects' Journal's RetroFirst campaign [5], the RIBAs' new "Reinvention" prize [6], and the recent outcome of the public inquiry against the proposed demolition and replacement of Marks & Spencer's Oxford Street store [7].

Set against this context, it is encouraging that "Conservation and Retrofit" was in 2019 voted 3rd by Master of Architecture (MArch) students at the XXX School of Architecture with regards to areas of key interest for their final year design thesis. This came just above "Zero/ Low Caron Design", as also reflected in their free text comments (Fig.1).

On the basis of this, the author was approached to create a design unit combining reuse, retrofit, and passive and low energy design. The development and results of which are presented in this paper.

Figure 1: Word cloud from free-text requests from MArch students requests for final year design thesis unit topics 2019 highlighting high interest in sustainable conservation and retrofit.

2. CARBON PASTS, LOW CARBON FUTURES

The South Wales Coalfield was chosen as the studio unit's focus to immediately engage the students with the UK's carbon legacy, and the current climate emergency. At its peak in 1913, the South Wales Valleys were one of the largest sites of carbon extraction in the world [8]. However, the subsequence decline and eventual end of the coal industry's dominance in the region [8], has led to a continued period of economic hardship.

As in other communities who have lost their primary industry, the impact of this on collective memory and identity has still yet to be fully understood [9], and there is the danger of "Smokestack Nostalgia" [10]. Yet at the same time, industrial heritage has been argued by some as the key to these communities future [11]. The remaining evidence of coal mining in the South Wales Valleys sits at the border of what is viewed as heritage and what is viewed as waste. For some they are symbols of pride, yet for others they embody exploitation, of people and natural resources, and economic and political disenfranchisement. This dichotomy provides the ideal springboard for finding alternative uses that transform these remnants into key components in the areas low carbon future. They provide the opportunity to explore the major challenges facing 21st century society, including circular economy; social inclusion; passive and low energy design; the UK's carbon legacy; and our role in tackling the climate emergency.

3. LIVE PROJECT SITES

For the each of the three academic years that the unit has so far run (2021/22, 2022/23 and 2023/24), a different site within the South Wales Coalfield has been selected for study. These have been selected using the following criteria; i. they have a historical link to the coal industry; ii. they have substantial surviving built heritage; and iii. they have real and ongoing challenges currently leading to an uncertain future.

For the academic year 2021/22, unit focused on the grade II* listed Crumlin Navigation Colliery (fig.2), located in the heart of the Welsh Valleys. Once the source of high-quality steam coal, the site now offers low carbon opportunities, including the low enthalpy geothermal energy in the flooded mines [12].

Figure 2: Crumlin Navigation Colliery (Whitman, 2021)

In 2022/23 the unit studied the grade II* listed Cefn Coed Colliery (Figure 3), in the west of the Valleys Region. At one point the world's deepest anthracite mine, it ceased operation in 1968, and became a museum in 1986. Today its future is uncertain having failed to reopen following the pandemic due to maintenance and financial concerns. A complementary use is therefore crucial and yet again mine water heat recovery could hold the key.

Figure 3: Cefn Coed Colliery (Whitman, 2022)

For the academic year 2023/24, the attention shifts from sites of carbon extraction to the social infrastructure that grew up during the 19th and 20th centuries to meet the needs of the miners and their families. Pontypridd Market Quarter (Fig.4) is a complex mixture of a working market, high street shops, underused office spaces, a lost chapel, and an abandoned theatre.

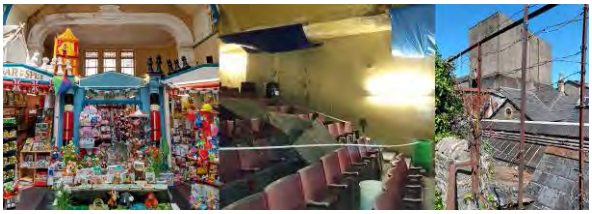

Figure 4: Pontypridd Market and Town Hall Theatre (Whitman, 2023)

4. PEDAGOGICAL METHODOLOGY AND THEORIES

The pedagogical approach followed in the development and delivery of this teaching have been incrementally developed over a period of more than 15 years by the author. This has parallels with "The Double-layered Asymmetrical Model" [13], especially as it is understood and presented by Salama [14], which provides a systemised, yet personal approach to complex existing contexts. The process starts (Fig.5 (A)) with a period of information gathering in groups.

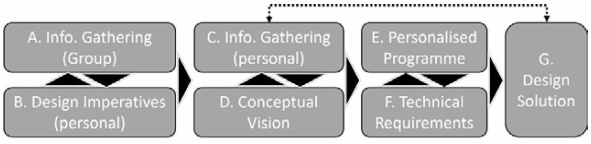

Figure 5: Process of student design, adapted from [14]

This involves desktop review of secondary sources (including archival research and literature review), original data collection (including building surveying, sketching, photography, and community engagement in the form of surveys and semi-structured interviews). This stage results in the production of a dossier of information that is then shared as unit-wide resource to inform the subsequent stages. Simultaneously students are asked to develop and record an initial personal response (B) which begins to define individual design imperatives. For this the students are encouraged to experiment with the capturing of subjective, often abstract and intangible

ideas through a range of artistic mediums from painting to sculpture, and creative writing.

This first stage is then followed by further individual information gathering (C), whilst simultaneously developing a conceptual vision and an intellectual position to test through the design thesis (D). In turn this leads the development of personalised programmes (E) informed by the previous stages and the definition of technical requirements (F), from which the design solution is developed (G). Further cyclical iterations then follow, refining the design solution and increasing in detail. As stated by Salama, the model encourages students to provide their own interpretations, with the tutor supporting in this process [14].

Given that the teaching uses existing sites, with real-life problems, and the involvement of third parties (communities and owners), the pedagogical approach can also be categorised under the umbrella of Live Project Teaching [15]. These projects offer the potential to bridge between mainstream architectural education and professional practice [16], and by doing so bring many benefits. However, care must be taken to avoid unintended consequences, such as false expectations from non-academic partners, and extractive or exploitative research [17]. With the aim of overcoming, or minimising these risks, promoting transparency and clarity from the start, the School has co-created an online induction module for students, staff, teaching practitioners and community partners [xx], a key component of which is promoting appreciative inquiry. This places the emphasis on identifying and building upon strengths [18], rather than focusing on weaknesses, which often student projects are unable to address. As such, it is hoped that students benefit from applying their design skills to real life scenarios, whilst non-academic partners are provided with new ideas that challenge preconceptions and innovate.

At the end of each academic year the work is shared with the non-academic partners. The work of the first year (2021/22) was presented on-site as a public exhibition, open to both the local community, the current site custodians, and local and regional government representatives. The second year (2022/23) was presented only to the site owner, the local Borough Council, however, it is hoped this year (2023/24) a public onsite exhibition will once again be possible.

5. IMPLEMENTATION AND RESULTS

The richness of the existing contexts have inspired students to go on an develop very different building programmes and architectural responses that are technically advanced and highly creative, despite each year sharing a common site**.** These have included renewable energy production; renewable energy storage and distribution; reuse and recycling centres; low carbon manufacture; education and knowledge sharing; wellbeing facilities; nature conservation; and innovation and research centres. Equally, through individual investigation and initiatives, key low energy design strategies have been incorporated (Table 1). Whilst implicit in the brief, it is the students' engagement with the existing buildings that has ultimately led them to adopt these low carbon technologies.

Table 1: Key low energy themes tackled by unit members (2021/22 and 2022/23 only).

Theme	No. of students
Renewable Energy	16
Design for Disassembly	13
Low Carbon Materials	12
Retrofit	9
Biophilia	4
Phytoremediation	2

There follow four examples of students' work, that foreground the possibilities of students engaging with existing buildings with a common focus on low energy architecture.

5.1 Example 1 – MedTech Research Centre

For this project the student, Jordan Grady, took inspiration from the heritage theories explored by historian David Lowenthal in his book, "The Past is a Foreign Country" [19], exploring the notion of building conservation and heritage as a continuous narrative. As such, the industrial legacy of Crumlin Navigation Colliery perpetuated through the proposed reuse for one of South Wales's emerging key industries, Medical Technology, or MedTech. To achieve this, the new programme was conceived as the insertion of new "machinery" (Fig.6).

Figure 6: Internal render of proposal at Crumlin Navigation Colliery for MedTech Research Centre, showing inserted "machinery" (Grady, J., 2022)

This employed box-in-box construction for laboratory and research spaces, to meet their high environmental specification, whilst allowing the less onerous requirements of circulation spaces to be met by the historic fabric itself, with limited interventions. U-values of 0.1 W/m^{2}K, excellent airtightness, controlled ventilation with heat recovery, acoustic separation and reverberation times of 1.2 sec, were all achieved within these new insertions.

5.2 Example 2 – Renewable Energy Storage Facility

This time the student, Rowan Luckman, took as a starting point Crumlin Navigation Colliery's history as a past store of solar energy in the form of coal, and explored this through Burke's notions of the sublime [20] and subsequent ideas of the post-industrial sublime [21]. The result was a storage facility for renewable energy investigating alternatives to chemical batteries and their inherent environmental impact and use of non-renewable resources. Technologies incorporated included pumped hydroelectric using the abandoned mine workings as the lower reservoir, winch-based gravity batteries in the south upcast mine shaft, and subterranean compressed air storage (Fig.7).

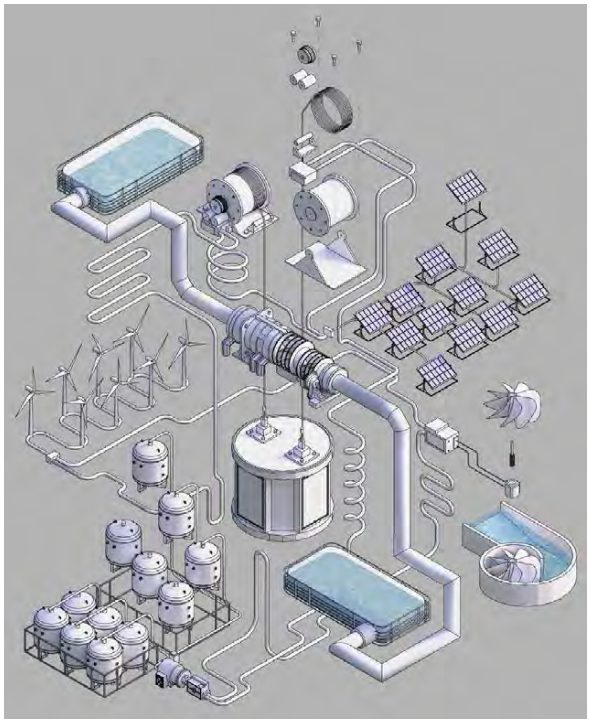

Figure 7: Conceptual image of energy storage technologies for proposal at Crumlin Navigation Colliery for Renewable Energy Storage Facility (Luckman, R., 2022)

This linked to a wider landscape masterplan, integrating photovoltaic, wind and small-scale hydro energy production. For the interventions on the existing buildings, lightweight materials were explored to reduce the loads on the historic fabric (Fig.8).

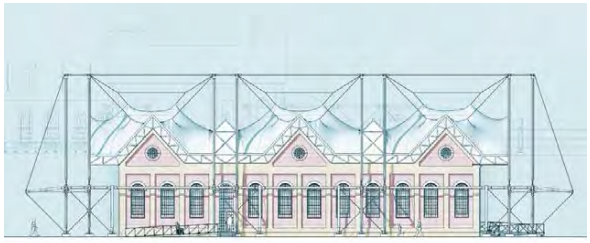

Figure 8: Elevation of renovated Power House, part of a proposal at Crumlin Navigation Colliery for Renewable Energy Storage Facility (Luckman, R., 2022)

However, due to the structural forces involved in both energy production and storage, the use of low carbon materials was limited, however a calculation was undertaken offsetting the new embodied carbon against that saved through increased renewable energy injection at peak-demand hours. This showed a carbon payback of just 2.7 days. There are potentially some oversimplifications in these calculations, however the basic precepts and methodology is correct.

5.3 Example 3 – Mine Water Heat Recovery Research Centre and National Coal Archives

The third proposal for Crumlin Navigation Colliery presented in this paper emerged from a detailed study undertaken by the student, Alexander McCormick, into the subterranean elements of the site (Fig.9), using historic mine plans, borehole logs, geological data, personal histories of former miners and their families, and peer reviewed research documents.

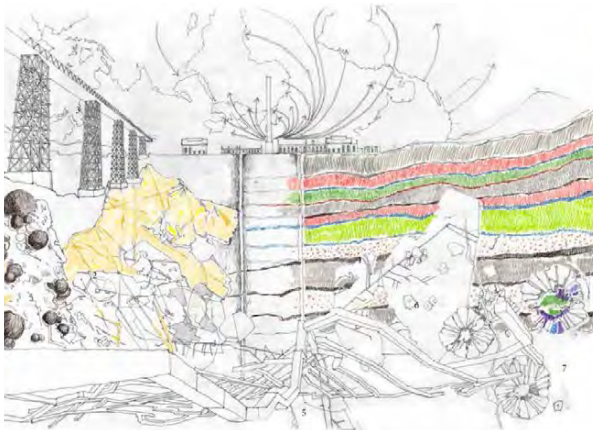

Figure 9: Conceptual collage of subterranean and global connections, leading to the proposal at Crumlin Navigation Colliery for Mine Water Heat Recovery Research Centre and National Coal Archives (McCormick, A., 2022)

This led to the design of a research centre for mine water heat recovery, combined with a National Coal Archives (Fig.10). Part of the project was designed as an earth sheltered building, using compressed earth blocks and charred Welsh larch. With the rest of the programme being incorporated

into the refurbished existing buildings, connected by a timber framed roof, the geometry of which was derived from principal coal seams present below the site. Across the site, space heating was provided from mine water sourced heat pump, based on a mean temperature of the mine water of 15.2^{o}C [12].

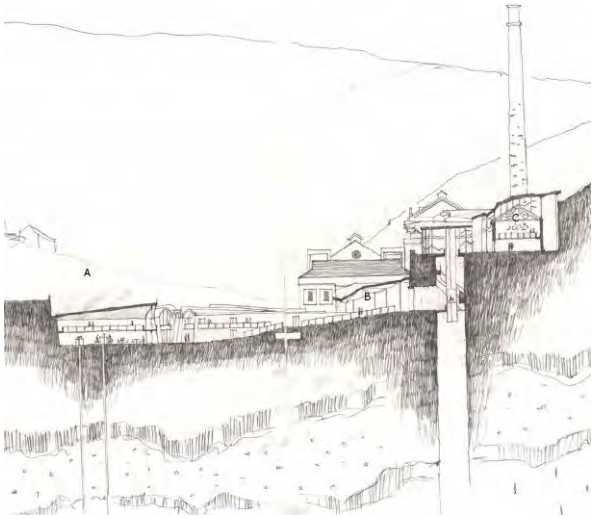

Figure 10: Cross section of proposal at Crumlin Navigation Colliery for Mine Water Heat Recovery Research Centre and National Coal Archives (McCormick, A., 2022)

5.4 Example 4 – National Museum of Energy and Renewable Energy development Park

The final example is one from the academic year 2022/23 by Morgan Taylor and looks at Cefn Coed Colliery Museum. Again, the theme of energy is taken as the focus of the project, this time proposing a National Museum of Energy, as part of the *Amgueddfa Cymru* (National Museum of Wales) portfolio, accompanied by a renewable energy development park (Fig.11).

Figure 11. Aerial axonometric of proposal at Cefn Coed Colliery for a National Museum of Energy and Renewable Energy development Park (Taylor, M., 2023)

The museum exhibits depict industrial, transportation and domestic uses, and are curated to into three themed areas covering energy past, present and future. Energy past is displayed in the renovated existing historic buildings, energy present takes the form of demonstration low energy dwellings based on current new-build and retrofit technologies, and energy future incorporates a mine water heat recovery and ambient loop and creates a new enclosure for the grade II* listed range of boilers, replacing the current condemned asbestos shelter (Fig.12). All this lies at the centre of a low carbon mobility masterplan, thereby considering low energy design at the full range of scales.

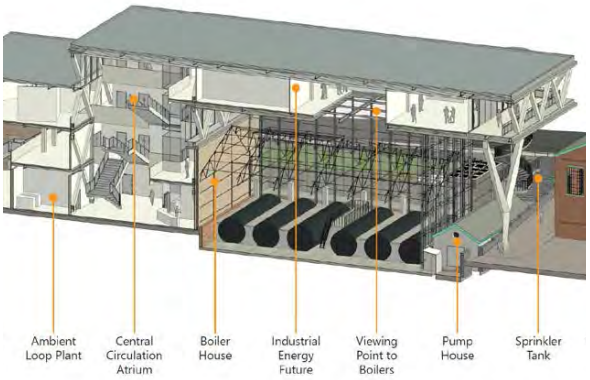

Figure 12. Sectional axonometric of the "Energy Futures" building, enclosing the grade II listed boiler house, as part of the proposal at Cefn Coed Colliery for a National Museum of Energy and Renewable Energy development Park (Taylor, M., 2023)*

5.5 Outcomes

As these four examples have demonstrated, there is a high level of engagement with low energy architecture engendered by working with these examples of industrial heritage. At the same time the quality of architectural creativity and complexity has not been restricted by the constraints posed by the existing buildings and structures, with a higher percentage than the year average of students being awarded a 1st or 2:1 degree. The work of the first year 2021/22 was unprecedently nominated as an entire unit by the School for the RIBA Silver Medal, whilst the top student from the second year 2022/23 was awarded the School prize for best in year and was nominated for the RSAW medal.

Following this success, and recognising the growing interest and need for designing with existing buildings, work has been undertaken, as part of a wider undergraduate curriculum redesign, to extend engagement with adaptation and reuse throughout the undergraduate BSc Architecture course.

The work of this academic year, 2023/24, is still in its early stages, however initial work is showing interesting new areas of investigation emerging, with a growing emphasis on social sustainability, and the role that communities can play in tackling climate change.

6. CONCLUSION

The work presented in this paper has highlighted the value of engaging with existing buildings in architectural pedagogy, and the level of success that is possible, especially with regards to the teaching of low energy architecture. It has shown how working specifically with sites that form part of the historical UK carbon legacy can inspire students to provide innovative solutions to the resultant climate emergency. It is hoped that the increased acknowledgement by the architectural profession of the need to challenge demolition and new-build, now also being seen in our students and teaching, will continue to grow and expand to encompass the global construction industry as a whole. If we are to meet our ambitious targets of limiting anthropogenic climate change, it is essential that our focus shifts to making the most of the built assets that already exist and maximising their embodied carbon. In these six pages it has not been possible to share all details and fully reflect on the benefits of working with existing buildings. The author looks forward to the opportunity to expand on this and share their experience with the PLEA community in Wrocław!

ACKNOWLEDGEMENTS

The author wishes to thank all those who have been involved in the preparation and delivery of the teaching covered by this paper. There are too many individuals to name, however special thanks go out to our non-academic partners, including Friends of the Navigation, The Coal Authority, Neath Port Talbot Council, Rhondda Cynon Taf County Borough Council, Pontypridd Markets Fairs and Town Hall Company Ltd, Max Fordham Building Service Engineers and Mann Williams Consulting Civil and Structural Engineers. The author is also indebted to all the students who have chosen this unit, and to their enthusiasm and engagement. The students whose work is presented as examples in this paper have specifically given their permission for their work to be included and for them to be named. Thank you all.

REFERENCES

1. Elefante, C. *The greenest building is... one that is already built*. in *Forum Journal*. 2007. NATIONAL TRUST FOR HISTORIC PRESERVATION.

2. Grant, E.J., *Mainstreaming environmental education for architects: the need for basic literacies.* Buildings and Cities, 2020. 1(1).

3. Waite, R., *'Students told to ignore existing building' – survey reveals retrofit teaching gap.* Architects' Journal (London), 2022.

4. Cramer, J. and S. Breitling, *Architecture in existing fabric: Planning, design, building*. 2012: Walter De Gruyter.

5. Hurst, W., *Introducing RetroFirst: a new AJ campaign championing reuse in the built environment.* Architects' journal (London), 2019.

6. Harrabin, R., *Riba launches Reinvention prize to encourage refurbishment over demolition*, in *The Guardian*. 2023.

7. Gove, M., *Called-in decision: 456-472 Oxford Street, London W1 (ref: 3301508 - 20 July 2023)*, H.C. Department for Levelling Up, Editor. 2023, HMG: Online.

8. Hughes, S.R., *Collieries of Wales: Engineering and Architecture*. 1994: Royal Commission on the Ancient and Historical Monuments in Wales.

9. Berger, S. and C. Wicke, *Introduction: Deindustrialization, Heritage, and Representations of Identity.* The Public Historian, 2017. 39(4): p. 10-20.

10. Strangleman, T., *"Smokestack Nostalgia," "Ruin Porn" or Working-Class Obituary: The Role and Meaning of Deindustrial Representation.* International labor and working class history, 2013. 84(84): p. 23-37.

11. Smith, L. and G. Campbell, *'Nostalgia for the future': memory, nostalgia and the politics of class.* International Journal of Heritage Studies: Nostalgia and Heritage: Potentials, Mobilisations and Effects, 2017. 23(7): p. 612-627.

12. Farr, G., et al., *Low enthalpy heat recovery potential from coal mine discharges in the South Wales Coalfield.* International Journal of Coal Geology, 2016. 164: p. 92-103.

13. Goldschmidt, G., *Doing design, making architecture.* Journal of Architectural Education, 1983. 37(1): p. 8-13.

14. Salama, A.M.A., *Spatial design education : new directions for pedagogy in architecture and beyond*. 2015, Farnham, Surrey ;: Ashgate.

15. Brown, J.B., *Learning theories for live projects*, in *Architecture Live Projects: Pedagogy into Practice.*, Harriet Harriss and L. Widder, Editors. 2014, Routledge: New York. p. 18-23.

16. Morrow, R., *Live Project love: building a framework for Live Projects*, in *Architecture Live Projects: Pedagogy into Practice*. 2014, Taylor and Francis. p. xviii-xxiii.

17. Almond, C. *Tackling the Unintended Consequences of Live Projects: Co-creating*
an induction module towards better practice. in *Architecture 101: Questioning the Fundamentals*. 2023. Newcastle: Newcastle University.

18. Hall, J. and S. Hammond, *What is appreciative inquiry.* Inner edge newsletter, 1998: p. 1-10.

19. Lowenthal, D., *The past is a foreign country-revisited*. 2015: Cambridge University Press.

20. Burke, E., *A Philosophical Inquiry into the Origin of Our Ideas*. 2012: Simon and Schuster.

21. Baptist, K.W., *The Post-Industrial Sublime or Forgetting Love Canal*, in *Dialectics of Space and Place across Virtual and Corporeal Topographies*. 2016, Brill. p. 325-339.

PLEA 2024 WROCŁAW
(Re)thinking Resilience

Tools and Methods for "Quantifying" Urban Liveability:
two Parallel University Teaching Experiences

VALENTINA DESSÌ[1], LAVINIA CHIARA TAGLIABUE[2]

[1]Politecnico di Milano, Dept DASTU, Milan, Italy
[2] University of Turin, Computer Science Department, Turin, Italy

ABSTRACT: The paper describes a specific educational experience carried out at two Italian universities within distinct academic programs.
At the Politecnico di Milano, within the School of Architecture AUIC, an architectural design studio was held with the aim to identify urban regeneration opportunities near to an area undergoing significant enhancement and repurposing. Meanwhile, at the Faculty of Computer Science at the University of Turin a course in a master's program on Digital Innovation for Living Environments, introduced students to spatial environments with diverse functionalities. The students analysed these environments to identify ways of supporting user needs through digital and innovative technologies. In both cases, spaces within public and private buildings, and urban spaces, were considered. Students were involved in qualitative and quantitative assessments of urban spaces' livability using a methodology based on the approach developed by the Barcelona Ecology Agency (AEUB). This approach aimed to synthesize, with a single indicator, the blend of qualitative and quantitative aspects contributing to the attractiveness and environmental well-being of places.
KEYWORDS: Urban liveability index, Public space, Tools & methods, Computing sustainability

1. INTRODUCTION

The paper describes a specific educational experience at two Italian universities within distinct academic programs driven by a shared goal of promoting sustainability evaluation for urban spaces. These programs can converge in transdisciplinary approaches and methods to enhance the implementation of strategies and tools aimed at improving livability in both existing and newly developed urban environments. A semester-long architectural design studio was held at the Politecnico di Milano, within the School of Architecture AUIC. Its objective was to identify opportunities for urban regeneration of the site around the Porta Romana Rail Yard in Milan. A significant part of the design process presented to student groups involved assessing, including quantitatively, the livability of public and urban spaces using a methodology derived from the approach implemented for many years by the Barcelona Ecology Agency (AEUB). During the same semester, a course on Digital Innovation for Living Environments was conducted at the Faculty of Computer Science at the University of Turin. This course, offered within the master's program, introduced students to spatial environments with diverse functionalities. The students analyzed these environments to identify ways of supporting user needs through digital and innovative technologies to enhance environmental conditions and livability. Spaces within both public and private buildings, as well as open spaces, were considered. During this course, the indicators from the AEUB were introduced, and methodologies and digital tools (i.e., customized codes) were developed to calculate the livability indicators. These tools are aimed at supporting the assessment of various elements contributing to the quantification of spatial quality and the degree of livability in public spaces.

2. TOOLS AND METHODS FOR "QUANTIFYING" URBAN LIVABILITY

A common ground between the educational activities conducted in the Architectural Design Studio for future architects and those for future computer scientists lies in the necessity to translate a concept, often exclusively qualitative, into a numerical indicator to compare different conditions (before and after a project, different spaces, design options, etc.). This process aims to identify the best acceptable solution while considering the various aspects of the urban realm.

When the concept of livability is concerned, it can be defined as the combination of a number of variables [1], including safety, sustainability, environmental comfort, services, walkability and public transport, which can generate different livability conditions. In this context, the livability concept meets the users' needs without sacrificing the functionality requirements of the spaces. The sustainability challenge is quantifying exquisitely qualitative aspects, such as the architectural quality of a space or its attractiveness, which is crucially important as it would allow us to consider all aspects in the overall evaluation of an area. It is hence

interesting how the contribution of computer science comes in support of automizing the process [2] of quantification. It defines a possible objective assessment structure that would otherwise be subjective and naive. The evaluation approach, developed by the AEUB, aims to synthesize, in a single indicator, the blend of qualitative and quantitative aspects contributing to the attractiveness and environmental well-being related to urban spaces [3,4]. All measurements are standardized on a score scale from 1 to 5 to combine the different parameters (1 is the worst, 5 is the best condition). In some cases, it is pretty easy to translate a value, like the thermal comfort indicator, in a score scale from 1 to 5. In other cases, it is more complex, for instance, when we need to evaluate the impact of the greenery in terms of attractiveness or the effect of the suited mix of commercial activities.

2.1 The work of the Architecture students

It is increasingly important to clarify to architecture students involved in designing livable, attractive, and sustainable urban space that the city is a system that integrates many aspects at different levels and that the design is the synthesis of acceptable solutions that the systemic, and therefore complex, vision poses, which often require different points of view, approaches and skills. The approach of the AEUB is particularly intriguing, as it considers 9 indicators to calculate urban space livability, plus additional 3 indicators for estimating the livability of the surrounding urban area of the selected public space (Table 1). The categories of parameters considered are:

1. Ergonomic characteristics;
2. Attractiveness;
3. Environmental features.

The additional three parameters used for calculating the:

4. Surrounding livability are:
   - Number of services (i.e., schools, clinics, libraries, etc.) within a 300-meter radius;
   - Number of daily-use commercial activities within a 300-meter radius;
   - Number of public transportation networks within a 300-meter radius.

Table 1 lists the parameters considered for the liveability assessment; the first 9 only related to a specific space, while the 12 parameters assess the liveability at urban level.

Although the AEUB methodology was adopted for data collection and the final indicator calculation, in the case study selected by the architecture students, adjustments were made to adapt it to specific contexts and the availability of open data in the City of Milan [5]. This occurred, for instance, in assessing the best dimensional ratio, such as the view of the sky from the streets or the evaluation of functional mix and thermal comfort.

Table 1: Parameters considered for the liveability assessment.

Parameters	mu	How to assess
1.1 Pedestrian/vehicular areas ratio	%	Proportion between pedestrians and the whole area
1.2 Accessibility	%	Sidewalk wideness and slope
1.3 Dimensional ratio (H/D; SVF)	Deg	Degree of Sky View factor
2.1 Functional mix	Bit	Shannon formula
2.2 Attractivity	N.	Typology of activity
2.3 Green volume	%	The ratio between green volume and the street volume (below 8m)
3.1 Thermal comfort	n. hours	The number of hours of t. comfort
3.2 Acoustic comfort	Dec	Decibel level revealed with app
3.3 Air quality	NO_2;	Pollutant data available from open data

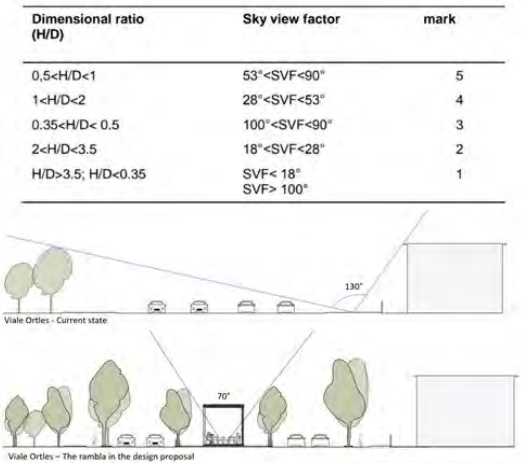

Figure 1: Table of correspondence of dimensional ratio and sky view factor of a street and score associated with different values, and below, two different sky view factor values of the same street, Ortles road at Milan, before and after a design proposal.

Although the students of Politecnico worked on all the parameters to define the liveability indicator, the paper reports the analysis of some aspects which were then analyzed by the students of University of Turin.

Among the works developed within the Design Studio, which aims to work within the city of Milan, an interesting case can be considered, in which the the location for evaluating the degree of livability of the public space focuses on a particularly significant road within the design strategy identified by the student's groups. The road, viale Ortles, in the southern part of the city, is a traffic-devoted space with very low quality from every point of view.

Nevertheless, it has the potential to be an important green corridor and an important arterial road that enables the connection of existing urban spaces and gardens.

Figure 2: The current state of Ortles road in Milan, Italy.

An accurate analysis of the area's current state is an integral part of the site knowledge process, preliminary to the project phase and necessary to assess the increase in the livability value achieved by the project proposal. One of the necessary elements to be investigated concerns the type of present plants (regarding bearing and height). Vegetation is an aspect impacting several parameters that contribute to the indicator calculation. In particular, in the section "attractiveness," we find the volume of greenery. At the same time, in the group of environmental variables, it is important mainly for thermal comfort but also air quality. Vegetation can also be considered as a design strategy to change the dimensional ratio of the street 1.3), at least from the point of view of perception of the vertical limits of the space. The volume of greenery parameter (2.3) is calculated by considering the section of the street, possibly divided into parts if the section or the size/shape of the trees changes, up to the height of 8 meters, which takes into account the real field of view of a person walking down the street. In the case of Ortles road in Milan, the analysis of the existing situation shows a relevant absence of vegetation, which is evident from Figures 1 and 2. The design proposal for vehicular traffic reduction and the livability and attractiveness enhancement of the street consists of a mix of actions, including the increase of pedestrian areas, new paved and vegetated surfaces, commercial activities and trees (considering the road section up to the height of 8 meters, from the 7% to 25%, i.e., from the score of 1 to 4). The street becomes a sort of "Rambla," where the green areas support different functions, including diverse types of plants characterized by specific shapes and sizes. Figure 3 reports the street and the facing built environment, the section with the line at 8 m high for the calculation of the percentage of green and the plan of the area. With the proposed renovation, final users are attracted to and can fully enjoy the improved livability from several points of view. The improvement due to the vegetation increase on the final score is very evident; for other parameters, the increase in the score is not so strong. For example, the commercial activities on the ground floor of buildings facing the road (2.1) were weighted in terms of attractiveness (2.2), by those who worked with direct observations (e.g., site visits, Google Street map, etc.) and design analysis of plan instruments.

Figure 3: Design proposal for revitalizing the Ortles road in Milan that use an adequate number of trees in the central pedestrian area (the Rambla) and along the sidewalks.

The weight of each type of activity is performed as defined by AEUB, and it was calculated and averaged every 500 meters. The increase, from the initial score of 2.6 to 3, in the proposed renovation of the case study is due to the rise of some retail commercial activities within the Rambla, particularly ice cream kiosks, bars, and others in the buildings facing the road. The appropriate choice of both the types of activities and their location along the entire street axis also positively affected the diversity, the functional mix that ensures the presence of multiple users with different characteristics creates the livability of the area throughout the day. In this case, the calculation was done using the Shannon Diversity Index (2.1) formula, which calculates the bits of information based on the calculation of the types of activities present and their occurrence (1):

$$H = - \sum p_i \log_2 p_i \qquad (1)$$

where H is the Diversity (bit)
p_i is the proportion of the entire community made up of species i.

The higher the value of H, the higher the diversity of species (in this case, the attractive commercial activities in a particular location). According to the design proposal, the functional mix increased from 1.5 to 2.6. Considering the whole strategy, the road livability increases from 2.6 to 3.7.

2.4 The Work of Computer Science Students

In the case of the architecture students, the primary purpose was a design proposal to improve

the livability conditions of the streets, while the computer science students focused on methods and tools to speed up and promote process automation in the evaluation procedure.

In fact, the computer science students collected data on the city of Turin as case study and developed specific methodologies and codes to support verifications related to the following indicators:

- Pollution/acoustic comfort;
- Presence of trees in surveyed areas;
- Percentage of green spaces;
- Quantity of commercial services;
- Diversity of activities in the test area.

These methodologies can also be applied to verify the following indicators:

- Air quality;
- Thermal comfort.

The students' activities primarily focused on collecting robust open data, enabling the identification of areas with acoustic pollution in the city of Turin, used as case study, and the mapping of existing trees in the urban area. They used an urban scale approach and then focused on district and street level. The use of open data allowed them to create maps for assessing critical areas and identify possible strategies for improving the situation [6], such as:

- Areas in need of traffic control;
- Acoustically critical areas that need specific strategies (e.g. limited traffic zones).

The analysis allows to define where to promote the creation of new green areas supporting city-level decision-making processes with key local policies.

The methodology is suitable for conducting a primary screening and general assessment of the conditions however, the precision and accuracy is reduced in specific streets where possibly some measurements can be required to define hourly scenarios.

Open data and the translation in maps of the acoustic risk have been implemented using digital tools and data available as open source (Figure 2). To assess the trees in the Turin area, the students used the Treepedia [7] of the MIT Senseable City Lab of Boston to obtain an image containing the different trees in the city. Through this open resource, they can obtain the approximate number of trees on different streets using a very robust source and implement the possibility to automate the task.

However, with this procedure, it is impossible to define the trees' and the tridimensionality. To overcome the first issue, the students developed a method to automate the process of counting the trees starting from the available open-source information (Figure 5).

For trees counting, an "image classifier" was developed using a code that takes an image of a street as input, allowing the calculation of the percentage of pixels corresponding to the trees. The RGB value of the pixels is considered. When the pixel has a value with a prevailing green color, it is counted as public green, allowing the percentage of green automatic calculation in the street (Figure 4).

Figure 4: Acoustic pollution map, city of Turin, Italy.

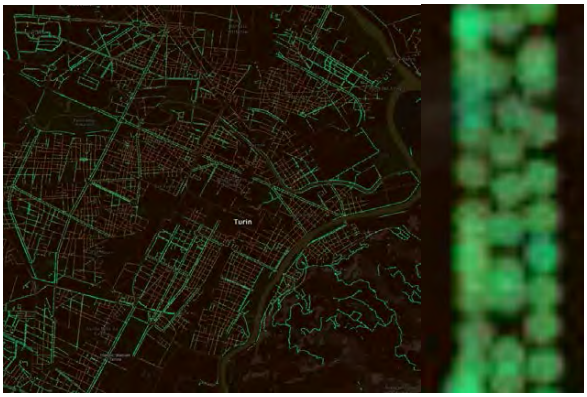

Figure 5: Map of the trees in Turin and Pixel analysis to detect the green areas and the number of trees through the image classifier in a street.

A possible future development uses the convolutional neural networks (CNN) to detect trees from images to include information related to the tridimensionality.

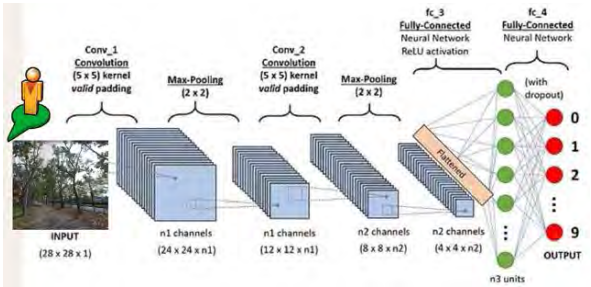

Figure 6: Scheme of the image recognition performed through neural networks (CNN).

To assess the value of the commercial activities and functional mix indicator, a python dashboard was organized to use the collected data, regarding all

commercial activities in Turin through CSV files downloadable as open data. This dashboard enables filtering based on street or postal code. All the calculated indices can be visualized on an interactive dashboard. A customized code has been realized for extracting and elaborating the information by the open data of the city of Turin

```
import pandas as pd
import math
import matplotlib.pyplot as plt
```

Uploading the file: This portion of the code loads the csv file that contains the information on business activities. The second line specifies the fields in the table that are kept and are useful for the calculations to be performed. The other fields in the file were not useful for the purpose of the project. The result is shown in the table below the code.

```
df = pd.read_csv('attivita_commerciali.csv', encoding='latin-1', lineterminator='\n', delimiter=';')
df = df.loc[:, ['INDIRIZZ', 'TIPO_MER', 'DESC_RIP', 'DETT_RIP', 'CAT_MER', 'CAP']]
df.head()
```

	INDIRIZZ	TIPO_MER	DESC_RIP	DETT_RIP	CAT_MER	CAP
0	VIA PIETRO PALMIERI 61/A		Somministrazione	D	Nessuna	10138.0
1	VIA PASQUALE PAOLI 9		Acconciatori/estetisti	Acconciatori	Nessuna	10134.0
2	VIA PASQUALE PAOLI 9	EXTRALIMENTARI	PICCOLE STRUTTURE	Vend.dettaglio con superf. fino a mq 250	Bigiotteria	10134.0
3	VIA PASQUALE PAOLI 26/A		Somministrazione	B	Nessuna	10134.0
4	VIA PASQUALE PAOLI 33/A	EXTRALIMENTARI	PICCOLE STRUTTURE	Vend.dettaglio con superf. fino a mq 250	Serramenti	10134.0

Filter Table: In this portion of the code it is possible to filter the initial table on a specific city area. We can focus on a portion of a street, defined by a range, or on an area defined by a certain zip code.

Search_address:

Input:

String min_integer -> interior here the considered street section begins

String max_integer -> interior in here the considered street segment ends

String address -> name of considered life e.g. street/course name

DataFrame table -> table of business activities

Output: table with activities between [address + min_integer, address + max_integer]

search_CAP (zip code)

Input:

Int postal_office_code -> zip code that you want to consider in the search

DataFrame table -> table of business activities

Output: table with the business activities that have postal_code == zip_code

```
# Definire qui i valori per le ricerca che si vogliono usare
indirizzo = 'corso sebastopoli'
min_interno = '214'
max_interno = '343'
cap = '10135'

filtered_df, used_cap = search_address(min_interno, max_interno, indirizzo, df)        # search_CAP(cap, df)
filtered_df.head()
```

	INDIRIZZ	TIPO_MER	DESC_RIP	DETT_RIP
9129	CORSO SEBASTOPOLI 214/A	ALIMENTARI	FORME SPECIALI DI VENDITA	Vend.dettaglio a mezzo apparecchi autom.
9130	CORSO SEBASTOPOLI 214/A	MISTA	PICCOLE STRUTTURE	Vend.dettaglio con superf. fino a mq 250
9131	CORSO SEBASTOPOLI 214/A	MISTA	PICCOLE STRUTTURE	Vend.dettaglio con superf. fino a mq 250
9132	CORSO SEBASTOPOLI 214/A	MISTA	PICCOLE STRUTTURE	Vend.dettaglio con superf. fino a mq 250
9133	CORSO SEBASTOPOLI 216/A	MISTA	PICCOLE STRUTTURE	Vend.dettaglio con superf. fino a mq 250

Histogram: we can print an histogram that shows for each business category how many stores are in the chosen area.

df_cat_mer -> Dataframe where we have for each category the total number of occurrences found in the table filtered above tot_shop -> I count how many businesses there are in total.

```
# Dataframe dove ho per ogni categoria il numero totale di occorrenze trovate
df_cat_mer = pd.DataFrame(filtered_df['CAT_MER'].value_counts()).reset_index()
df_cat_mer.columns = ['CAT_MER', 'count']
# Conto quante attività commerciali ci sono in totale
tot_shops = df_cat_mer['count'].sum()

print("Numero attività commerciali: ", tot_shops)
print("Numero di categorie: ", len(df_cat_mer.index))

df_cat_mer.plot(kind='barh', figsize=(8, 10))
if used_cap:
    plt.ylabel('CAP: ' + str(df['CAP'].iloc[0]))
else:
    plt.ylabel(indirizzo + ' ' + min_interno + ' - ' + max_interno)
plt.xlabel('Numero di attività')
plt.title('Numero di attività per ogni categoria')
plt.show()
```

```
Numero attività commerciali:  18
Numero di categorie:  10
```

The code can calculate the diversity of activities for the street.

Urban diversity: A function that calculates the urban diversity index related to the specific equation is defined. It adds the probability of occurrence and information values to the filtered table for each row.

urban_diversity

Input:

Dataframe table -> filtered table of categories and the number of stores belonging to them

Int val -> number of total businesses

Output: bit/person information value and updated table with two new columns: one for probability of occurrence and one for information

urban_diversity_score

Input:

Int ud_index -> bit/person index value

Output: urban_diversity_score

```
def urban_diversity(table, val):
    table['p'] = table['count'].apply(lambda x: round(x / val, 6))
    table['H'] = table['p'].apply(lambda x: round(x*math.log(x), 6))
    return round(-table['H'].sum(), 4), table

def urban_diversity_score(ud_index):
    if urban_diversity_index <= 1 :
        return 1
    elif 1 < ud_index <= 1.9:
        return 2
    elif 2 < ud_index <= 2.9:
        return 3
    elif 3 < ud_index <= 3.4:
        return 4
    else:
        return 5
```

```
urban_diversity_index, df_ud = urban_diversity(df_cat_mer, tot_shops)
print("Diversità urbana: ", urban_diversity_index)
print('Punteggio: ', urban_diversity_score(urban_diversity_index))
```

```
Diversità urbana:  2.0582
Punteggio:  3
```

Hence, we can have the Urban diversity index (2.0582) and the score (3) for the selected test area, collecting all the activities that can be then displayed as aggregated per area (Figure 7).

```
df_ud
```

	CAT_MER	count	p	H
0	Extralimentari	5	0.277778	-0.355815
1	Alimentari	4	0.222222	-0.334239
2	Mobili	2	0.111111	-0.244136
3	Tabacchi	1	0.055556	-0.160577
4	Gastronomia	1	0.055556	-0.160577
5	Supermercato	1	0.055556	-0.160577
6	Autoveicoli e motoveicoli	1	0.055556	-0.160577
7	Vendita al dettaglio di cose antiche ed usate	1	0.055556	-0.160577
8	Tessuti	1	0.055556	-0.160577
9	Macelleria	1	0.055556	-0.160577

Save the last table to a csv file

```
if used_cap:
    indirizzo_completo = f'{cap}'
else:
    indirizzo_completo = f'{indirizzo}_{min_interno}-{max_interno}'
df_cat_mer.to_csv('cat_mer_{}.csv'.format(indirizzo_completo), sep=';', encoding='latin-1', index=True)
```

The last code command allows the use of the information to create a table to be exported or it is possbile to plot the histogram of the activities used to calculate the index (Figure 7).

Possible future development of this approach has been suggested as follows:

- Adapt the code to calculate the remaining indices (thermal and acoustic, air quality, urban livability index, and morphological indices);
- Dashboard creation for greater accessibility of data;
- Ability to expand the system to other cities.

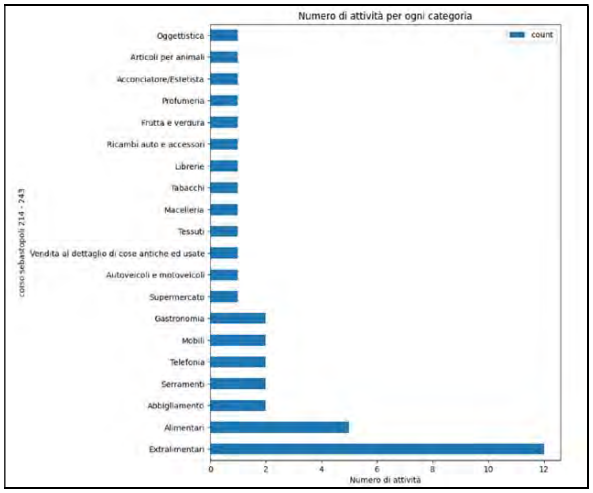

Figure 7: Number of activities per each category for a test zip code (10136).

3. THE DEVELOPMENT OF A SHARED APPROACH

Based on the conducted analyses, it is conceivable that a collaborative pathway among students from different degree programs would be highly beneficial regarding knowledge increase and cultural and language cross-fertilization. This could promote co-creation and interdisciplinary cooperation, enhancing students' possibilities and capabilities. It could also initiate a fresh collaborative approach concerning the sustainability of urban spaces on a novel basis [8]. The first aspect of systematizing to continue an effective transdisciplinary collaboration is related to the case study. Precisely, because of the need to "calibrate" the method and develop an approach that is useful to both groups, in the next step, we should work on the same case study, allowing the teams to interact and tune the calculation and design solutions according to the possibility of performing several iterations, in the early stages of the site investigation. A second relevant aspect is to enable students of Architecture, who are not prepared to develop ad hoc tools for the evaluation of specific parameters to have access to simplified calculation and simulation systems, allowing for quick verifications during the design process to enable more appropriate and informed design choices.

4. CONCLUSION

The paper delineates a dual experience carried out across two distinct universities and academic programs. However, this experience should ideally continue, as the genuine effectiveness becomes evident when these tools are put into practical use, tested, adjusted, and adapted to real-world cases, specifically when applied to the architectural design of an urban space. It is intriguing to consider that this process was initiated by the designer's requirement, then evaluated and observed from the different perspective of a computer scientist. Ultimately, through a transdisciplinary approach, it can return to the realm of design, where the product is "tested" and contributes to its refinement.

ACKNOWLEDGEMENTS

This paper reports the works carried out during the II semester at Politecnico di Milano and University of Turin. The final design studio at the Politecnico, School of Architecture AUIC was held by professors V. Dessi', L. Dondi, I. Mariotti. Architectural proposal by E.Carubelli, I. Cavallotti, O.Radu, S.Sabellini, C.Sangalli. Code and Maps: G. Frumento, A. Fontana, S. Monestirolo, E. Calvi, L. Grassi.

REFERENCES

1. Bosselmann, P. (2008), Urban Transformation: Understanding City Design and Form, Island Press, Washington.
2. De Lotto, R., Sessi, M., & Venco, E. M. (2022). Semi-automatic method to evaluate ecological value of urban settlements with the biotope area factor index: sources and logical framework. Sustainability, 14(4), 1993.
3. Rueda et al., (2012). El urbanismo ecólgico. Su aplicación en el diseño de un ecobarrio en Figueres. Agencia Ecologia urbana de Barcelona, Barcellona
4. Echave C., Rueda S., (2008). "Habitability index in the public space". In The annual international conference on walking and liveable communities. Barcelona
5. Dessi V., Astolfi L., (2020). "Qualità vs quantità. È possibile quantificare la qualità dello spazio pubblico?". In: Techne, 19: p. 114-124
6. Wu, A. N., & Biljecki, F. (2021). Roofpedia: Automatic mapping of green and solar roofs for an open roofscape
registry and evaluation of urban sustainability. Landscape and Urban Planning, 214, 104167.
7. Cai, B. Y., Li, X., Seiferling, I., & Ratti, C. (2018, July). Treepedia 2.0: applying deep learning for large-scale quantification of urban tree cover. In 2018 IEEE International Congress on Big Data (BigData Congress) (pp. 49-56). IEEE.
https://senseable.mit.edu/treepedia/cities/turin
https://senseable.mit.edu/treepedia/cities/turin
8. Zhang, Y., Lu, H., Luo, S., Sun, Z., & Qu, W. (2017). Human-scale sustainability assessment of urban intersections based upon multi-source big
data. Sustainability, 9(7), 1148.

PLEA 2024 WROCŁAW
(Re)thinking Resilience

Shaping the Thermal Comfort in Semi-outdoor Spaces with the Roof Canopy

A Design-Simulation Feedback Responsive Method

GAO WEIZHI[1] SUN JINGFEN[2] CHU YINGNAN[1] SONG YEHAO[1]

[1] Tsinghua University, Beijing, China
[2] Architectural Design and Research Institute of Tsinghua University, Beijing, China

ABSTRACT: This paper introduces a design-simulation feedback responsive method based on the architectural design methodology of integrating functional and engineering requirements under the control of a prototype. The aim is to provide a building environment that is better aligned with human activities and comfort needs through design strategies prioritizing methods preceding energy and equipment solutions. Employing an in-process project as a case study, the interactive design and research process focuses on the overall form design and constructional design strategies of the roof canopy, investigating their impact on thermal comfort in the semi-outdoor space beneath. During crucial decision points in the design process, the study conducts simulated research on the UTCI index and its distribution in the study area, offering theoretical references for design decision.
KEYWORDS: roof canopy, thermal comfort, semi-outdoor space, feedback method, sustainable design

1. INTRODUCTION

As a comprehensive expression, architecture is intricately interconnected with its site and environment. Whether manifesting itself as a sculptural and abstract entity, or a metaphorical and decorative structure, a building's form is fundamentally rooted in its context. Irrespective of its aesthetic manifestation, the underlying commonality lies in the imperative task of shaping the built environment in harmony with the site.

Within the realm of architecture, particularly in the context of climate change and the energy crisis, a shift in methodology is necessitated. Architectural design must not only respond to the urgency of reducing negative environmental impact but must concurrently elevate architectural quality. Aligned with the 10R principles of the circular economy, with a prioritized focus on refuse, rethink, and reduce, the goal is to reduce energy consumption through judicious pathways [1]. Reducing the building volume requires heating and cooling through holistic utilization of outdoor spaces emerges as effective strategies for achieving emission reduction. Given the lesser need for stringent control in outdoor space, the passive strategy of formal design exerts a more discernible impact.

This study delves into the intrinsic process within architectural practice, shaping spatial environment through architectural form, employing a design-simulation feedback responsive method. The response of the architectural form to the environment is a blend of creativity, empiricism, and comprehensive value judgment. The overall direction of the project takes shape through this process, meanwhile scientific simulations serve as valuable reference points. Upon this foundation, architectural performance simulation guides design optimization, ensuring that design outcomes are objectively verified through systematic feedback methods.

2. RESEARCH BACKGROUND

2.1 Methodology background: a prototype-controlled design method

The research is accompanied by the design of the roof canopy for the Jiaxing High-speed Railway New Town Cultural Centre. (Figure 1-a)

The project locates in Jiaxing High-speed Railway New town, Zhejiang, China. The location holds significance as a crucial landscape and ecological node within the city. Therefore, a response of elevated standards is imperative, addressing both urban identity and site ecology considerations.

(a)

(b)

Figure 1: The project rendering (a); the semi-public space beneath the roof canopy(b)

Jiaxing is in ⅢA zone (hot summer and cold winter) within the north subtropical monsoon climate category, characterized by concurrent rainfall and high temperatures, abundant sunshine, short spring and autumn seasons, and extended durations of winter and summer.

The team practices a design methodology that address intricate functional demands and engineering challenges under the guidance of a priori prototype. The prototype, serving as a comprehensive control mechanism, encapsulates various design strategies in accordance with the specific project. Providing a high-quality thermal comfort environment for semi-outdoor spaces (figure 1-b) is a crucial goal in this project. The design-simulation feedback responsive method seeks to offer directional insights for design decisions through quantitative or semi-quantitative research at pivotal stages of the design process.

Building mass reduction and thermal comfort enhancement are parts of the framework of the project's carbon neutrality strategies, complemented by other space organization strategies, construction system design considerations, and equipment system strategies (figure 2).

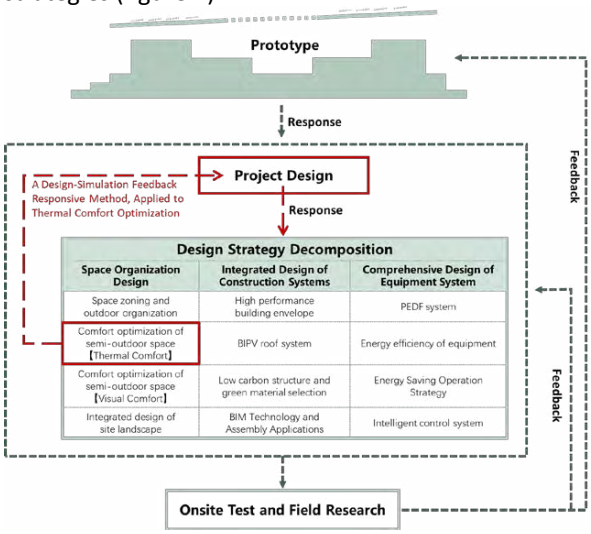

Figure 2: The prototype-controlled methodology framework and the project's strategy framework

2.2 Gap between theory and practice: integrating design and research for formal engineering projects

While numerous studies and completed projects have explored under-roof semi-outdoor spaces, a noticeable gap exists in establishing a cohesive correlation between theory and practical application.

Theoretical research on semi-outdoor spaces beneath roofs highlights a specific focus on the thermal comfort impact of shading facilities. For instance, a study in the arid climate of Arizona indicates that the type of shading structure (trees or pergolas) has no significant effect on thermal comfort. Meanwhile, it emphasizes that outdoor thermal perception is influenced by non-meteorological factors, including physiological, psychological, and behavioural aspects.[2]

Researches also delve into human thermal comfort perception and adaptability, exploring the neutral temperature, acceptable thermal comfort range, and preferred temperature in specific regions. Current studies suggest that in humid and hot environments, semi-outdoor spaces can significantly reduce perceived body temperatures, improving environmental thermal comfort compared to outdoor spaces. [3,4,5] Moreover, users demonstrate higher tolerance for thermal comfort in semi-outdoor and outdoor environments than in indoor settings [3]. During excessively warm summer conditions, users tend to feel more comfortable when the perceived temperature is slightly lower [4].

In the realm of existing architectural projects, there are cases intended to optimize the thermal environment in semi-outdoor spaces with roof canopies. For instance, the Barcelona's Flea Market employed a vernacular approach using sunshade canopies to enhance thermal comfort through sun shading and wind guidance. Similarly, the Metropol Parasol in Seville, Spain, aimed to optimize the thermal comfort of the plaza beneath with the roof canopy. However, according to a field study, compared to another traditional plaza in the same city, it is evident that the latter provides a more comfortable micro-climate and a more appealing outdoor space with the inclusion of trees and shadows [6]. Consequently, a thorough examination of the thermal comfort performance of outdoor spaces beneath the roof canopy is imperative during the design phase to prevent potential deviations from initial assumptions.

An exemplary illustration of integrating research and practice is the Elytra Filament Pavilion, a project completed by ICD-ITKE University of Stuttgart and the climate engineering consultant Transsolar. During the installation, visitor behaviours were monitored, and the subsequent installation of the canopy units were based on the observed occupancy behaviour patterns

of tourists [7]. An empirically responsive design method was explored.

However, in larger-scale formal projects, the responsive on-site design method is no longer feasible. In this context, responsive Investigations and design decisions must be concluded before the commencement of construction.

The proposed methodology in this study aims to assist formal engineering projects in achieving climate adaptation and sustainable goals.

3. METHODOLOGY

3.1 Simulation-Design interactive design method

(1) Overall form concept of roof canopy

The form of the roof canopy is inspired by the metaphor of traditional Chinese large roof eaves, utilizing contemporary architectural language to create a lightweight and graceful curved surface. This design seeks to establish an iconic landmark.

The architectural prototype, integrating the main building with a roof canopy, strategically utilizes outdoor spatial organization to reduce the volume of air-conditioned areas, thereby achieving energy consumption reduction. Concurrently, the prototype aims to optimize the environmental comfort of semi-outdoor spaces through the environmental regulation function of the roof canopy.

(2) outdoor thermal comfort optimization oriented overall form control

Roof canopy has the potential to improve comfort in the semi-outdoor space in summer, but it may also impact the sunlight exposure for occupants during winter. Therefore, how to balance the comfort effects between seasons while enhancing overall comfort is the issue to be addressed.

Hence, the overall form control process emerges as a crucial decision point in the design process, necessitating research-backed assistance for informed judgment.

(3) Deepening and comparison of design schemes

Based on the overall shape, a comprehensive examination involving geometric construction scheme comparisons and parametric design is conducted, considering the requirements of functional integration, structural design, and construction implementation.

(4) Thermal comfort evaluation and design feedback

By conducting the performance evaluation and visualizing the design outcomes, the impact of the roof canopy on the thermal environment will be verified. The feedback information is instrumental for design optimization. This stands as the second decision point in the design process, requiring more detailed research results to guide pertinent design decisions such as the arrangement of spatial functionalities and visitor's spatial usage preferences.

3.2 Index selection

In this study, the UTCI index is used to assess the outdoor thermal comfort under the influence of the roof canopy. [8,9]

3.3 Simulation Platform Selection

This study uses the Rhino-Grasshopper platform to simulate the UTCI index in various zones of the semi-outdoor platform for corresponding analysis and optimization. In the overall form control stage, the emphasis is on examining the conceptual roof form and its variations for the overall thermal comfort impact on all beneath spaces. The Ladybug UTCI Comfort operator is used in this stage. In the design feedback stage, a more detailed consideration of the effects of roof construction details and platform morphology is required. The Honeybee_energy module UTCI_Comfort_Map operator is employed in this stage.

4.RESULTS

4.1 Overall form control

Referring to the local annual UTCI index chart, the outdoor discomfort conditions are mainly overheating in summer and overcooling in winter.

(1) Preliminary thermal comfort simulation setting: The study selects a typical day in summer and in winter respectively, calculating hourly changes in comfort during the main activity period from 9:00 to 18:00. It involves two preliminary scenarios: no roof mode(a), total roof mode(d) (figure 3).

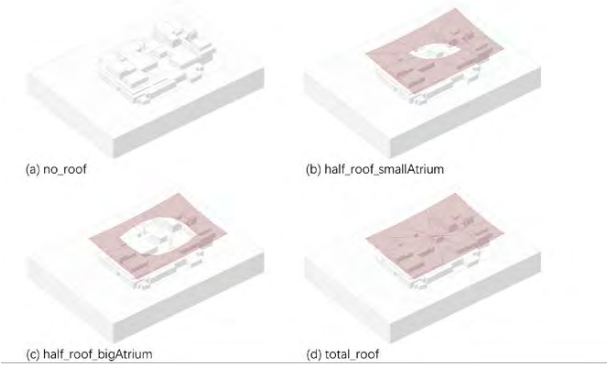

Figure 3: Simulated canopy mode

(2) Comparison of roof canopy geometry based on outdoor thermal comfort

Experimenting with openings to reduce roof coverage area and find a form that balances summer and winter comfort, two gradients of openings are selected besides the preliminary scenarios to investigate the impact on UTCI index: small atrium mode (b), big atrium mode (c).

Expanding the roof atrium openings attenuate the perceived temperature reduction of the UTCI index in winter, while reducing the cooling effect in summer The thermal comfort difference between the no-opening mode and the no-roof mode is significant.

The operational conditions between the small atrium model and the big atrium model both fall within the range capable of balancing thermal comfort effects between winter and summer. (Figure 4)

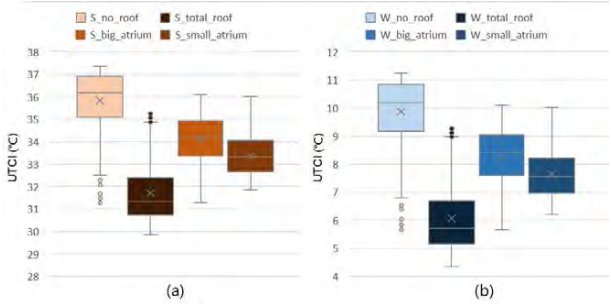

Figure 4: Box plot of summer UTCI data for simulation scenarios(a); Box plot of winter UTCI data in four simulation scenarios(b)

Adjust the scope of the atrium and obtain comfort data in real time. The base form (e) for further design development is selected comprehensively considering the function of the main part of the building and the architectural form. (Figure 5)

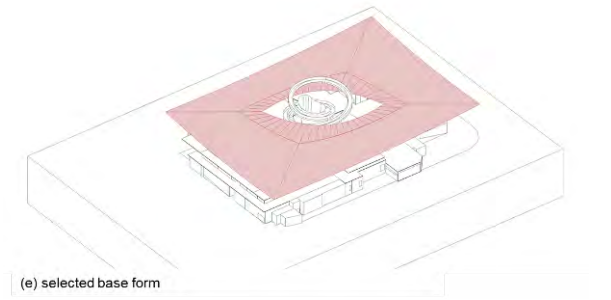

Figure 5: The selected canopy mode

4.2 Comparison of Roof Unit Forming Schemes

On the basis of the overall roof canopy form, the subsequent design deepening should adhere to the coherence of construction and geometric logic of construction. Therefore, a space grid method is used to fit the three-dimensional curved surface; at the same time, the design must account for upcoming technical integrations, including construction, photovoltaics, drainage, lightning protection, construction implementation, etc. To ensure the feasibility of subsequent technological integration, a unitized design strategy is employed.

In light of the above two strategies, several options are compared (Figure 6):

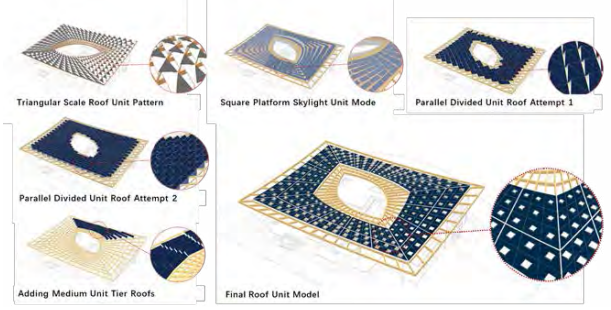

Figure 6: Comparison of roof unit forming schemes

The model of small grid units superimposed on medium-sized roof units is chosen for further development. This approach allows for independent control of the visual aesthetics of the space beneath canopy and the fifth facade of the building. In technical aspect, it enables uniform control over the size and type of grid units, thereby simplifying the deepening design and construction implementation.

In the chosen canopy mode, an integrated strategy combining sunshades, courtyard atrium and skylight components is proposed to adjust semi-outdoor space comfort.

4.3 Comfort evaluation of the semi-outdoor space

To optimize the spatial and functional organization of the platform with the physical environment, a thermal comfort simulation of the semi-outdoor space underneath is conducted. This process aims to validate the actual impact of pertinent design strategies, as well as to provide insights for further design optimization, function settings, and space utilization.

A Honeybee Energy Model including details of building envelope, thermal parameter and canopy construction details is constructed. UTCI_Comfort_Map operator in the Honeybee_energy module is used for a more precise simulation (Figure 7).

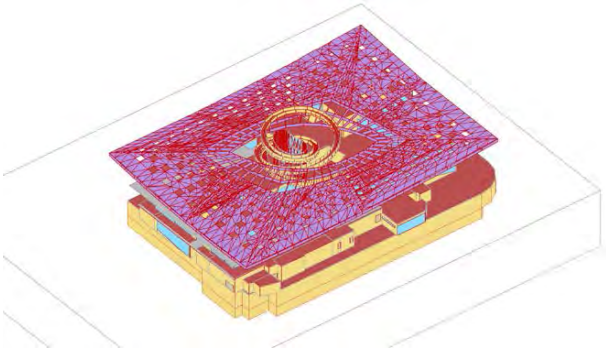

Figure 7: Thermal comfort Honeybee model

The typical sunny days and overcast days in four seasons are selected to compare the annual thermal comfort performance under representative scenarios.

UTCI equivalent temperatures of the semi-outdoor platform are calculated at 12:00 noon on typical sunny days and overcast days in the four seasons. Drawing from researches in Wuhan and Shenzhen, this study adopts a UTCI thermal neutral temperature of around 25°C, with a thermal comfort range between 21 and 32°C and a preferred temperature of approximately 24°C.

(1) Typical days in spring (Figure 8)

Select April 17th as the typical sunny day:

a. The UTCI equivalent temperature in the atrium area surpasses that in the platform area, with the

atrium area consistently falling within the thermal comfort range.

b. Despite the overall lower UTCI equivalent temperature, scattered regions within the platform area experience enhanced thermal comfort due to the solar radiation received through the skylights, thereby improving the thermal comfort in the semi-outdoor space beneath the roof canopy.

Select April 14th as the typical overcast day:

a. The influence of skylight components in the roof canopy on the thermal comfort of the platform is not evident;

b. The UTCI equivalent temperatures in the atrium and outer unobstructed areas are higher, but both remain below the thermal comfort range.

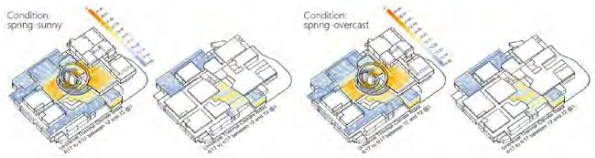

Figure 8: Visualization of UTCI equivalent temperature on typical days in spring

(2) Typical days in summer (figure 9)

Select August 18th as a typical sunny day:

a. The roof canopy notably lowers the UTCI equivalent temperature, substantially enhancing thermal comfort. Additionally, the sunlight radiation penetrating through the skylight components does not cause overheating in the platform area.

b. The UTCI equivalent temperature in the atrium area is excessively high.

Select August 17th as a typical overcast day:

a. Overheating is observed in the atrium area and some unsheltered sections on the outer perimeter of the platform, while the majority of the platform area beneath the canopy falls within the thermal comfort range.

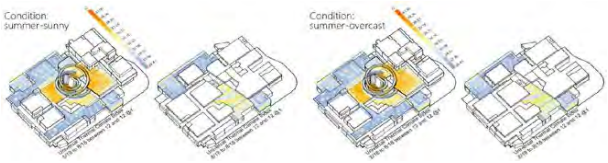

Figure 9: Visualization of UTCI equivalent temperature on typical days in summer

(3) Typical days in autumn (figure 10)

Select November 3rd as the typical sunny day:

a. The surrounding area of the atrium and partial platform sections are in the thermal comfort zone;

b. The majority of the platform beneath the roof canopy registers temperatures lower than the comfort zone.

c. The lighting from the skylight contributes to the distribution of point-like areas with enhanced thermal comfort, thereby improving overall comfort performance.

Select November 4th as a typical overcast day:

a. All areas are below the thermal comfort zone.

b. The UTCI temperature in the atrium and the outer edge of some platforms is relatively high.

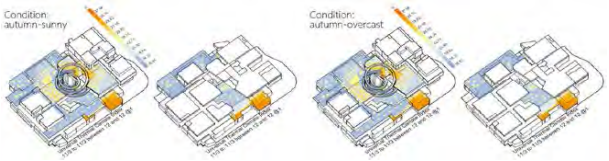

Figure 10: Visualization of UTCI equivalent temperature on typical days in autumn

(4) Typical days in winter (figure 11)

Select December 23rd as a typical sunny day:

a. The majority of areas fall below the comfort range, with some sections along the outer edge of the platform situated within the comfort zone.

b. Skylights and atriums significantly improve thermal comfort.

Select December 22nd as a typical overcast day:

a. All areas are below the thermal comfort zone;

b. The UTCI temperature in the atrium and the outer edge of some platforms is relatively high.

Figure 11: Visualization of UTCI equivalent temperature on typical days in winter

5.CONCLUSION

The preliminary design simulations indicate that the roof canopy exhibits a pronounced shading effect during the summer months, whereas temperatures tend to be lower in spring, autumn and winter. Therefore, the further design aims to minimize the loss of shading effectiveness during summer while enhancing thermal radiation absorption in other seasons, achieving a balanced shading effect for the canopy.

Further investigation during the deepening process reveals that atrium openings can improve comfort except in summer. Skylight components contribute to an improved thermal experience in sunny weather throughout spring, autumn, and winter, mitigating the adverse impacts of roof canopy shading. Skylights do not exert a negative effect on thermal comfort in any scenarios. As is shown in table 1. In summary, the roof canopy integrating the strategies of sun shading, atrium openings, and skylight components, proves effective in enhancing the thermal comfort of the semi-outdoor public space in most scenarios.

Table 1: The impact of roof canopy form strategies on thermal comfort under different research scenarios

Roof canopy form strategy		overall sunshade	courtyard atrium	skylight component
Spring	Sunny	-	+	+
	Overcast	-	+	○
Summer	Sunny	+	-	○
	Overcast	+	-	○
Autumn	Sunny	-	+	+
	Overcast	-	+	○
Winter	Sunny	-	+	+
	Overcast	-	+	○

+ represents a positive effect；
- represents a negative effect；
○ means no obvious effect.

Additionally, the results can guide further design adjustments and layout of functional areas. For instance, to address overheating in outer perimeter areas, planting greenery can cool the space while unconsciously restricting activities in uncomfortable areas. The next stage of the research will test comfort index and users' comfort perceptions under typical weather conditions in the actual built condition, examining preferences for activity areas and behavioural types, to verify the thermal comfort adjustment capability of the canopy.

This study provides a framework and offers examples for the design-simulation responsive design method, providing a basis for assessing the building performance post-implementation. Additionally, it provides a basis for further on-site research.

6.DISCUSSION

Contemporary life is reliant on artificial physical environments, often taking for granted the convenience based on excessive energy consumption. In architectural practices within regions with favourable outdoor climatic conditions, there is value in bridging the gap between humans and the environment. Through methods other than energy and equipment, we aim to provide physical environments that better align with the habits and comfort needs of human activities.

Architectural design, under the control of a prototype, comprehensively addresses complex functional and engineering demands. The prototype, functioning as an integrated design control mechanism, accommodates various possibilities of design strategies. In this decision-making process, quantitative or semi-quantitative research targeting specific objectives can provide theoretical support for design at various levels. For example, in this project, regarding outdoor thermal comfort, simulations are conducted during the early stages of the canopy form control and the later stages of platform functional organization, providing conclusive findings to support design directions. In this process, parallel goals collectively contribute to the development of the project.

The method of simulation has limitations of simplified boundary condition settings and idealized scenario setups; therefore, the research aims not to exert fine-grained control over design through simulation calculations. Under the feedback mechanism of post-occupancy evaluation of the built environment, the research team engages in more refined studies by means of on-site testing, subjective questionnaires, etc., providing feedback into the prototype and strategies for application in subsequent projects.

ACKNOWLEDGEMENTS

This work was funded by The National Natural Science Foundation of China (Grant No. 52394225), and the National Natural Science Foundation of China (Grant No. 52078264).

REFERENCES

1. Potting, J., Hekker, m., Worrell, E., Hanemaaijer, A., (2017). Circular economy: Measuring innovation in the product c hain, [Online], Available: https://www.pbl.nl/sites/default/f iles/downloads/pbl-2016-circular-economy-measuring-inno vation-in-product-chains-2544.pdf [January 2017].
2. Middel, A., Selover, N., Hagen, B. Chhetri, N., (2016). Imp act of shade on outdoor thermal comfort—a seasonal field study in Tempe, Arizona. International Journal of Biometeor ology, 60: p. 1849–1861.
3.Hwang, R., Lin, T., (2007). Thermal Comfort Requirements for Occupants of Semi-Outdoor and Outdoor Environments in Hot-Humid Regions, Architectural Science Review, 50(4): p. 60-67.
4. Zhou, Z., Chen, H., Deng, Q., Mochida, A., (2013) A Field S tudy of Thermal Comfort in Outdoor and Semi-outdoor Envi ronments in a Humid Subtropical Climate City, Journal of As ian Architecture and Building Engineering, 12(1): p. 73-79.
5. Xie, X., Liao, H., Wang, R., Gou, Z., (2022) Thermal Comfor t in the Overhead Public Space in Hot and Humid Climates: A Study in Shenzhen. Buildings 2022, 12(9): p.1454.
6. Guayo, P. M., (2014) Improving Outdoor Urban Environm ents: Three Case Studies in Spain. Proceedings of PLEA 2014 Conference. Ahmedabad, India, December 2014.
7. Daniele, S., Plotnikov, B., Mildenberger, E., (2017). An inv estigation on the relation between outdoor comfort and pe ople's mobility: the Elytra Filament Pavilion survey. PowerS kin 2017. München, Germany, January 2017.
8. Fiala, D., Havenith, G., Bröde, P., Kampmann, B., Jendritzk y, G., (2012) UTCI-Fiala multi-node model of human heat tra nsfer and temperature regulation. International journal of b iometeorology 56 (3): p. 429-441.
9. Kumar, P., Sharma, A., (2020) Study on importance, proce dure, and scope of outdoor thermal comfort –A review. Sus tainable cities and society 61: 102297.

PLEA 2024 WROCŁAW
(Re)thinking Resilience

Educational Buildings as Educational Tools:
A Building Performance Post-Occupancy Evaluation Course in a Subtropical Climate

MILI KYROPOULOU[1]

[1]University of Houston, Houston, USA

ABSTRACT: In the era of climate change and increased focus on sustainability, health, and wellbeing, it becomes imperative that architecture students own the fundamentals of building physics and human comfort. This paper delineates the integration of a student-centered Post Occupancy Evaluation (POE) project into architectural pedagogy, redefining traditional learning approaches. It illuminates the potential of immersive, research-informed POEs as a learning tool within Environmental Technology courses for graduate students. Thermal comfort, air quality, lighting, and acoustics are studied through the lens of occupants' experience and measured data in existing built environments. Students navigate the convergence of theoretical knowledge and real-world application through systematic data acquisition and analysis. Focused on studying the students' own college building, the project extended beyond the boundaries of the course, engaging stakeholders and demystifying the space through data dissemination. This paper advocates for integrating POE as a cornerstone in architectural education, poised at the intersection of academic exploration and practical implementation, ushering architects toward a more responsive and evidence-based architectural future.
KEYWORDS: Post-occupancy evaluation, Architectural Education, Student-centered Instruction, Learning-by-doing

1. INTRODUCTION

Diverting from over-concentration to new construction, Bordass and Leaman advocated for a fresh approach to professionalism within the built environment field, emphasizing the importance of deepening their understanding of buildings that are already in use [1, 2]. Studying precedents has always been a favorite topic in architectural pedagogy [3, 4], particularly in sustainable environmental design [5, 6]. Internet resources for studying existing buildings are plentiful today but often lack depth and validity or are inconsistent in providing evidence of performative statements [7]. Additionally, cognitive psychology has shown that episodic and semantic knowledge are not stored together and are difficult to combine. Lawson, in his article "Design and the Evidence" [8], says, "It is quite possible, for example, for a student to pass a theoretical examination in structural mechanics with flying colours, and yet apparently unable to use that knowledge creatively in design." Students report learning faster and better when engaging in first-hand applications [9], especially when understanding and quantifying invisible or intangible parameters, such as thermal sensation and light. Combining the benefits of precedents' study analytical methods with learning-by-doing can provide a dynamic educational framework for teaching environmental technology fundamentals.

Post Occupancy Evaluation (POE) is the process of obtaining feedback about the performance of existing buildings. Although a substantial part of the life-cycle of the building is feedback, POEs are not mandated or regulated, and the design profession has not fully appreciated their importance [10]. Most green building certification systems base their criteria on design documentation, with only a few relying on actual performance. As a result, it is mostly research initiatives that drive the application of POEs. POE projects have been used as teaching tools for educational purposes, adopting a more experiential learning-by-doing approach [11, 12] and engaging students actively in real-world scenarios to maximize their understanding and critical thinking abilities [6, 12, 13]. The students return to understanding buildings as physical objects with physical processes, a concept exponentially getting lost since buildings started being designed on computer screens.

This paper presents the development and implementation of a student-centered, research-informed POE project as part of a core Environmental Technology (ET) course for first-year Master of Architecture (MArch) students with no former architectural education. The project aims to maximize student engagement, optimize learning efficiency, enhance understanding of "invisible" microclimatic properties, and increase awareness of environmental parameters that impact energy performance and user experience.

2. OVERVIEW OF THE POE PROJECT

The case study building was the college building of architecture situated in a humid subtropical climate, explicitly focusing on the studio spaces where the students spend a significant amount of their time. The building was built in 1985 and is fixed on a central 40' x 80' (~12m x 24m) atrium. The atrium is sky-lit from above and acts as the central life to those in the college. The three upper levels are occupied by open-plan studio spaces clustered around the atrium, which is the core of the architecture students' lives. The studio spaces are laid out on north and south-oriented facades, and the floors differ in window size, access to the skylight, and height (Table 1 and Fig. 1).

Table 1: Summary data of study areas

ID*	Area (m^2/ft^2)	Avg. height (m/ft)	w/w (%)	Access to skylight
2S	812/8,735	4.26/14	4.1	No
2N	812/8,735	4.26/14	4.1	No
3S	465/5,000	4.26/14	48.6	No
3N	465/5,000	4.26/14	48.6	No
4S	653/7,028	9.1/30	8.5	Yes
4N	653/7,028	9.1/3o	8.5	Yes

*ID name depicts floor number and cardinal orientation

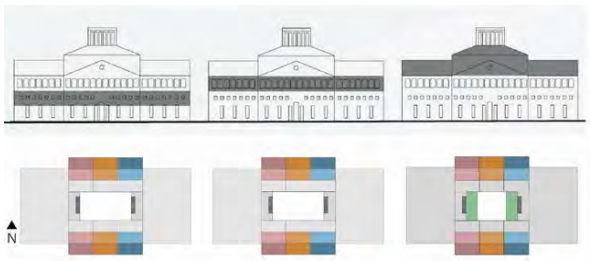

Figure 1: Building's schematic plans and elevations

3. THE POE DESIGN

The project was divided into two distinct phases. During phase 1, the eleven enrolled students worked in groups of 3-4 people on one of the three floors. The findings of this phase became the basis for formulating individual research agendas on which the students worked during phase 2 (Fig. 2). Collaboration among students and teams became critical in reinforcing a holistic understanding of the building technologies and occupants' interaction.

3.1 Phase 1 – teamwork

Phase 1 comprises four progressive assessment tasks designed based on time and resource availability. The studied properties were thermal comfort, air quality, lighting, and acoustics (Fig. 2).

Task 1 - Secondary data collection: Energy consumption and operational data collection, building documentation, material properties, and envelope composition. The collection of this material helps formulate research hypotheses and questions.

Task 2 - User perception and satisfaction (PS): The students collectively designed an anonymous survey in six sections: i) demographics and studio space identification, ii) thermal PS, iii) air quality PS, iv) visual PS, v) acoustical PS, and vi) general PS. They used the ASHRAE 55 [14] thermal sensation 7-point scale based on Fanger's heat balance equation [15] and the ASHRAE 55 3-point preference scale.

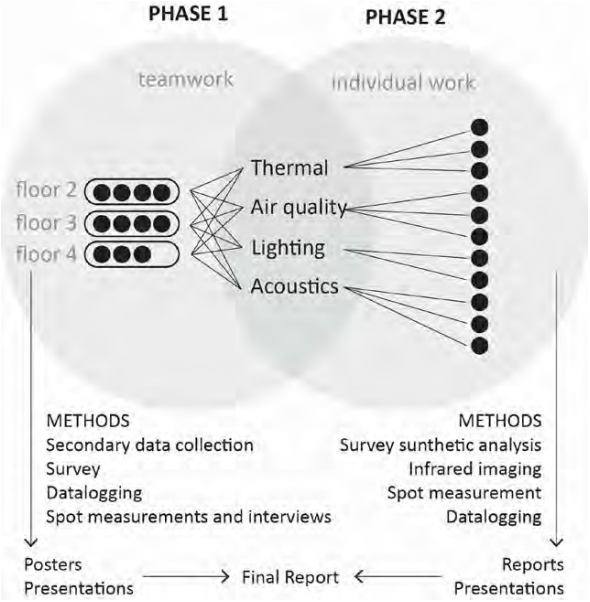

Figure 2: Project organization around two subsequent phases. Every dot represents one student.

Task 3 - Datalogging: Two data loggers (item 1 in Table 2) were installed centrally on each floor on the northern and southern sides, away from direct sun and air-conditioning (AC) outlets. They recorded dry bulb temperature (DBT), Relative Humidity (RH), and carbon dioxide (CO_2) levels at 5-minute intervals between March 2nd and 10th, 2023.

Task 4 - Interviews and spot measurements: Forty-six students were interviewed on February 14 (cloudy - daily average temperature 21.3°C/70.41°F) and February 20 (sunny - daily average temperature 20°C/68.03°F), 2023. The students took simultaneous DBT, RH, and airspeed measurements (using items 2 and 3 in Table 2). All questions were designed based on the ASHRAE 55 [7] questionnaire so students can compare occupant subjective thermal comfort and computed comfort using the Predicted Mean Vote (PMV) calculation per Fanger's equation [15]. Measured values were used in the calculation, together with observed or self-reported metabolic rate (met) and clothing levels (clo) values. For this initial study, it was assumed that DBT values equal operative temperatures.

Air quality assessment included CO_2 and VOC measurements using items 4 and 5 in Table 2, which were evaluated against ASHRAE 62 thresholds. Sound measurement evaluations using item 6 in Table 2 used the World Health Organization (WHO) threshold recommendations to define noise pollution.

Illuminance levels (using item 7 in Table 2) were mapped independently from the interview times on a

horizontal level at desk height across the spaces during two days (one sunny and one overcast). Lighting was assessed as combined daylighting and artificial since the fixtures operated with motion sensors, and the students did not have access to controls.

Table 2: List of environmental sensing equipment

#	Instrument	Quantity	Range
1	Extech SD800	CO_2	0 to 4000 ppm
		Temp	32 to 122°F (0 to 50°C)
		RH	10 to 90% RH
2	Extech 407119	Air Speed	40 to 3346ft/min, 0.2 to 17.0m/s
3	RH 101	RH	10% to 95%
		Temp	-4 to 140 °F (-20 to 60 °C)
		IR Temp	-58 to 932 °F (-50 to 500 °C)
4	VFM200	TVOC	0.00 to 9.99ppm (mg/m^3)
5	Extech CO260	CO_2	0 to 5000, 5001 to 9999ppm
6	Extech SDL600	Sound	30 to 80, 50 to 100, and 80 to 130dB
7	Extech 33	Illuminance	99.99, 999.9, 9999, 99990, 999900
8	Flir One Pro	Temp	-20° to 120°C (-4°F to 248°F)

3.2 Phase 2 – individual agendas

Students used the preliminary evaluation reports to synthesize a holistic understanding of building design and operations. This shared knowledge assisted students with identifying areas of interest and formulating their individual agendas on one of the study areas (Fig. 2). Phase 1 also exposed students to the methods and tools available to them to refine their methodology and approach to their individual research questions. The research methodologies used by the students at this stage spanned a variety of media and tools. Examples are further survey analysis, infrared imaging (using item 8 in Table 2) to assist thermal comfort analysis, infrared imaging to assist mechanical systems' inspection, and focused controlled experiments on reported issues on one of the four studied parameters.

3.3 Project modules

The course was spread across twelve 1.5-hour sessions led by one instructor and designed around five modules:

1) Introduction to POE (three sessions): An overview of the origins, value, and examples of POE introduces the students to the process of investigating existing buildings. This lecture-based module takes place parallel to task 1.

2) POE tools (three sessions): This module includes familiarization with the tools used to obtain occupant feedback (task 2) and collect environmental data (tasks 3 and 4). Leveraging primarily student-led workshops of collaborative learning, it results in substantial in-class work. Students design anonymous mass surveys and formulate interview questions for individuals. By the end of this module, students distribute the survey, and they install the dataloggers. Before collecting the data from those two tasks, which require a minimum of two weeks, students have time to perform targeted interviews with occupants and additional spot measurements.

3) Benchmarking (one session): A key aspect of POE studies is benchmarking. This lecture-based module provides students the resources to evaluate their measurements against standards.

4) Research hypothesis and methodologies (two sessions): Following the findings presentations at the end of phase 1, students are presented with a relevant research paper and are asked to analyze it, identifying its core structure. Through collaborative workshops, they learn to distinguish between the main components of a research project. This module is deemed essential for formulating their own research hypothesis for phase 2 and for identifying the analytical methods and tools critical to carrying out their individual research agendas.

5) Data analytics and case studies (three sessions): This hybrid module (lectures and workshops) focuses on visualization techniques for the collected data using various media, such as combined graphs, 2D heat maps, and compiled images. The module's goal is to bridge the gap between data collection, data representation, and data interpretation. Figures 3-7 show examples of student work during the semester, including phase 1 survey analysis and environmental data collection, as well as phase 2 individual studies and experiments.

4. RESULTS

Secondary data collection: The building operates at 22.7°C/73°F with two air handlers per floor. The R-values are estimated for the cavity walls at 4.7 ft^2·°F·h/BTU, for the roof at 5.1 ft^2·°F·h/BTU, and the windows/skylight U-value is estimated at 1.2 ft^2·°F·h/BTU. The initial hypothesis was that the central atrium exemplifies air stratification, generating a vertical gradient thermal environment. In addition, it was expected that different orientations and façade treatments per floor substantially affect the corresponding spaces. Being exclusively mechanically ventilated without economizers could result in low ventilation rates and air quality challenges during the studied mid-season.

Survey: The survey was sent to 816 students and completed by 139, almost equally distributed among the three floors. The highest level of dissatisfaction pertained to noise levels across all floors, with 49% of participants reporting dissatisfied or very dissatisfied. Regarding thermal comfort during mid-season (when the data collection occurred), the greatest dissatisfaction appears on the 3rd and 4th floors. 42.1% of the 3rd floor respondents reported feeling

cool or cold, and 36.8% preferred a warmer environment. On the 4th floor, 40% reported feeling warm or hot, and 51.4% preferred a colder environment. 75% of all participants reported having had to change their environment to improve thermal comfort. On the 2nd floor, most participants feel comfortable (72.2%), but only 55.6% prefer no change, with the rest of the respondents favoring warmer (19.4%) or colder (25%) environments. Examples of representations of survey results can be seen in Figure 3.

Measurements - whole building: There was great variability in environmental conditions among spaces. The air stratification was not observed as expected, with the 3rd floor consistently exhibiting the lowest temperatures. The 2nd and the 3rd floors reach the highest CO_2 levels (>1000ppm) during high occupancy times. The south studios have slightly higher humidity and CO_2 levels than the north. High CO_2 concentration and VOC levels affect all open spaces on the same floor, usually with a small lag after occupancy increases. Examples of data logging and spot measurement representations can be seen in Figures 4 and 5. The high dissatisfaction with noise at the open-floor studios directed the design of a controlled experiment across all floors. A 65-dB loud noise was generated centrally in the studios. Noise levels dropped to 39dB in areas with partitions and carpet floors (3rd floor), while they only dropped to 48dB for the same distance from the source in areas without partitions and vinyl floors (2nd floor). On the 4th floor, sound levels were measured on a perimeter around the sound source. It was observed that the atrium's open space diffuses sound to 49dB while the walls reverberate it to 56dB (Fig. 7 left).

Measurements - 2nd floor: The south-facing spaces are consistently warmer than the north-facing ones. Temperatures show the smallest diurnal variation compared to the other floors, and occupancy patterns only moderately affect temperatures. Averaged surface temperatures at the north studios are lower than the south ones during morning and evening. Even though radiant temperature analysis was done on a cloudy day and the windows are small, surface temperatures by the windows are much higher than those close to the corridors (Fig. 6). The 2nd floor reaches the highest CO_2 levels (> 1000 ppm). Lighting levels are sufficient across the floor, and on a sunny day, they are higher next to the south-facing windows. The inconsistent light distribution in the rest of the space is unrelated to the distance from the windows.

Measurements - 3rd floor: The 3rd floor was the coldest floor during the recorded period. The north-facing studios are consistently warmer than the south-facing ones, and the air always moves from the south side of the building to the north side, that is, from cold to warm, contrary to expectations. The vents on the 3rd floor south hall operate at much lower temperatures, ranging from 55°F to 66°F, with no predictable pattern (Fig. 7 right). Occupancy does not statistically relate to temperature variations. The correlation between CO_2 levels and occupancy is moderate, with R^2=.52. VOC levels were consistently elevated and related to the proximity of studio deadlines, measuring 0.4-2.2 ppm. An experiment was conducted using a LEVOIT LV-H132 HEPA Filter in each studio space. The unit dropped VOC levels by as much as 0.1 ppm with just 30 minutes of operation time. Lighting levels are generally sufficient on the 3rd floor. On a sunny day, light levels are significantly higher next to the large south-facing windows, which may cause glare.

Measurements - 4th floor: On the 4th floor, thermal and air-quality responses in the north and south-facing studios are almost identical due to minimal vertical windows. Temperatures show the largest diurnal variation compared to the other floors. Indoor dry bulb temperatures fluctuate relative to outdoor temperatures. Occupancy patterns only moderately affect temperatures. The 4th floor shows the lowest CO_2 levels during high occupancy times.

5. DISCUSSION

The fully mechanically ventilated spaces dominated the thermal experience in most spaces, explaining that the middle floor (3rd) was consistently the coldest against any expectations. The fully exposed to the skylight 4th floor was an outlier to this observation, with solar gains through the dome dictating diurnal temperature fluctuations. On the other two floors, solar gains had a profound impact on radiant temperatures, distinctly differentiating thermal comfort profiles on different orientations and envelope configurations. Occupancy patterns moderately affected indoor temperature fluctuations, but were the driving force behind elevating CO_2 levels. The low CO_2 levels on the 4th floor are attributed to its large height. Lighting was above recommended levels; however, the spaces were not uniformly lit by electrical lighting, and direct sunlight often became the cause of glare. The biggest cause of occupant dissatisfaction was noise due to open-plan space design. Simple partitions were proven effective.

The study motivated the students to seek innovative research methods to interpret the building's performance. Their recommendations included in no particular order: window replacement, shading on the 3rd floor south façade, mechanical system inspection and maintenance, acoustic tiles' replacement, acoustic movable partitions, replacement of lighting fixtures and upgrade to LEDs, banning aerosols, and integrating indoor vegetation.

Figure 3: Examples of student work: Phase 1 survey analysis

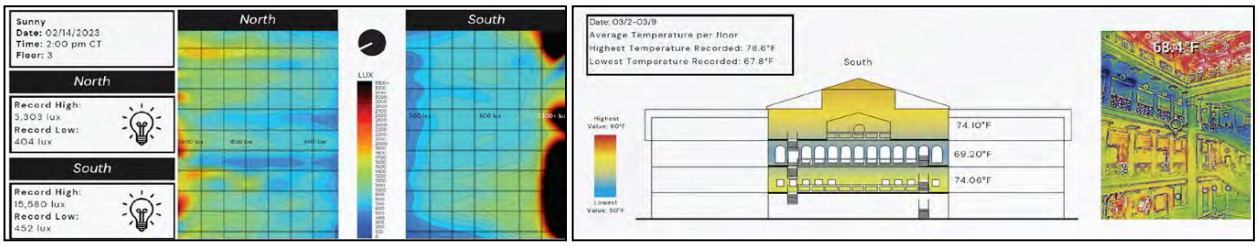

Figure 4: Examples of student work: Phase 1 spot measurements, illuminance (left), and thermal (right)

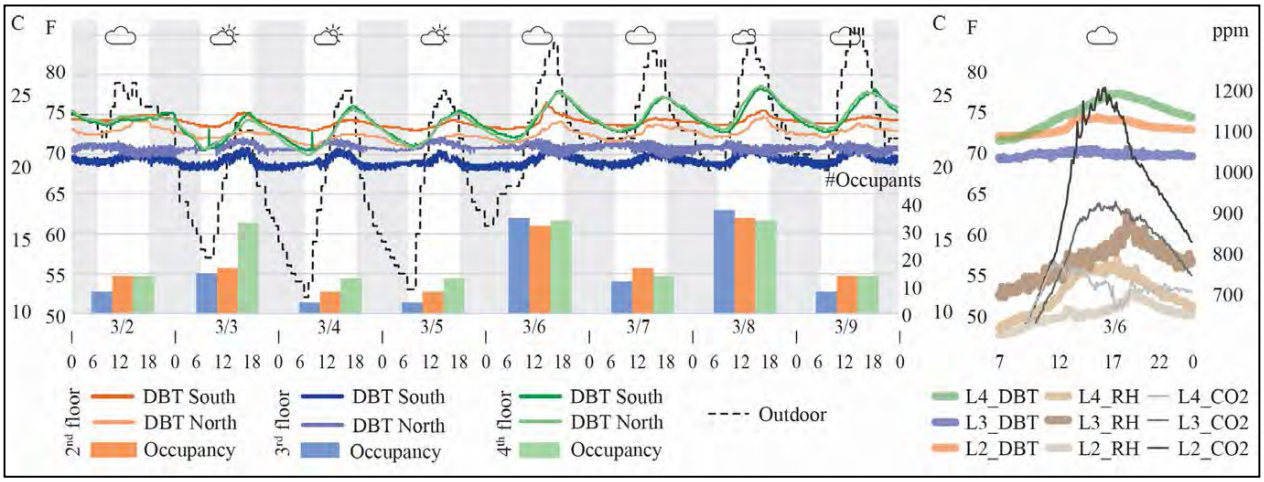

Figure 5: Examples of student work: Phase 1 data logging

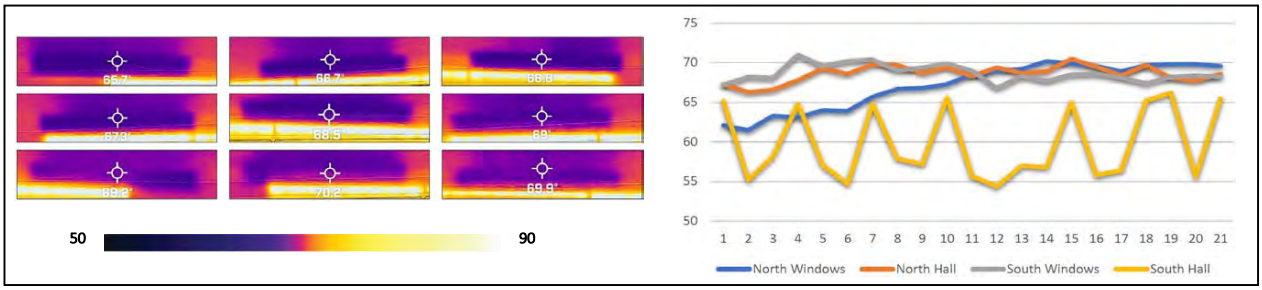

Figure 6: Examples of student work: Phase 2 mechanical systems – diffusers' operational temperature

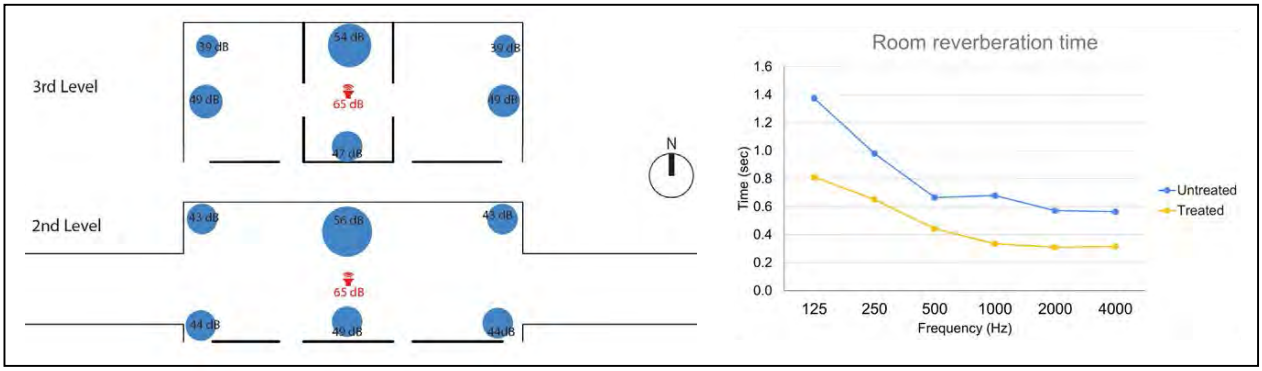

Figure 7: Examples of student work: Phase 2 acoustics experiment (left), acoustic treatment calculations (right)

The students also recommended the undertaking of similar studies during the cooling season.

6. CONCLUSION

This article outlines the implementation of a student-centered, research-informed environmental POE project, employing hands-on experiential education to assist in learning building physics and human comfort fundamentals. It highlights the transformative potential of POE as an educational tool within architectural pedagogy by emphasizing learning from existing built environments. Ultimately, it redefines the paradigm of architectural education, bridging theory with experiential learning.

The POE project is embedded within an environmental technology course for graduate architecture students. By blending collaborative teamwork and individualized research agendas, it is grounded in systematically examining the students' college building. The course is developed around five modules: Introduction to POE, POE Tools, Research Hypothesis and Methodologies, Benchmarking, and Data Analytics and Case Studies. Thermal comfort, air quality, lighting, and acoustics are explored through four designed tasks: secondary data collection, user perception and satisfaction, data logging, and interviews and spot measurements. Through data postprocessing methods and self-driven research, students gained insights into the building's functional, technical, and environmental performance, as well as occupants' perception and satisfaction. The students acquired hard and soft skills, practicing data processing, research questions and methods formulation, presentations, summary reporting, and evidence-based design ideation. The process yielded an impressive learning leap attributed only to the hands-on, learning-by-doing approach.

The outcomes of the project extended the course's requirements, fostering conversations about building design and operations through active engagement with the academic community and college leadership. Choosing the college as a case study intuitively created a sense of ownership and personal investment for the students. The physical presence of students as researchers around the college assisted with the project's propagation across the community. This paper strongly supports the integration of POE into architectural education, emphasizing its pivotal position where academic study meets hands-on application. By embracing POE as a learning tool, architectural education moves toward a more informed future grounded in evidence-based, responsive designs.

ACKNOWLEDGEMENTS

The author would like to express her gratitude to the University of Houston Equipment Grant for equipment funds. She also thanks graduate level 1 students 2023 for participating in the project.

REFERENCES

1. Bordass, B. and A. Leaman, *Making feedback and post-occupancy evaluation routine 3: Case studies of the use of techniques in the feedback portfolio.* Building Research & Information, 2005. 33(4): p. 361-375.
2. Bordass, B. and A. Leaman, *A new professionalism: remedy or fantasy?* Building Research & Information, 2013. 41(1): p. 1-7.
3. Grover, R., S. Emmitt, and A. Copping, *The typological learning framework: the application of structured precedent design knowledge in the architectural design studio.* International Journal of Technology and Design Education, 2018. 28(4): p. 1019-1038.
4. Eilouti, B.H., *Design knowledge recycling using precedent-based analysis and synthesis models.* Design Studies, 2009. 30(4): p. 340-368.
5. Ye, C., et al., *Post-Occupancy Evaluation of Green Technologies for a High-Rise Building Based on User Experience.* Sustainability, 2022. 14(15): p. 9538.
6. Yannas, S., *What Can Buildings Tell Us, What Can We Tell Back*. 2009.
7. Paul Kenny, V.B. *A Methodology to Develop Judgment Skills in Sustainable Architectural Education*. in *World Sustainable Building Conference*. 2011. Helsinki: VTT Technical Research Centre of Finland.
8. Lawson, B., *Design and the Evidence.* Procedia - Social and Behavioral Sciences, 2013. 105 (2013): p. 30-37.
9. Freeman, S., et al., *Active learning increases student performance in science, engineering, and mathematics.* Proceedings of the National Academy of Sciences, 2014. 111(23): p. 8410-8415.
10. Durosaiye, I., K. Hadjri, and C. Liyanage, *A critique of post-occupancy evaluation in the UK.* Journal of Housing and the Built Environment, 2019. 34.
11. Beaudin, B.P. and D. Quick, *Experiential learning: Theoretical underpinnings.* Fort Collins, CO: Colorado State University, High Plains Intermountain Center for Agricultural Health and Safety, 1995.
12. Gupta, R. and S. Chandiwala. *A student-centred POE approach to provide evidence-based feedback on the sustainability performance of buildings*. in *PLEA2009, 26th Conference on Passive and Low Energy Architecture*. 2009. Quebec City, Canada.
13. Woo, J. *Building as a learning tool: a student-centred POE approach to the Swanston Academic Building (SAB)*. 2015. Living and Learning: Research for a Better Built Environment: 49th International Conference of the Architectural Science Association 2015: The Architectural Science Association and The University of Melbourne.
14. *ANSI/ASHRAE Standard 55-2010: Thermal Environmental Conditions for Human Occupancy*. 2010, American Society of Heating, Refrigerating Air-Conditioning, Engineers American National Standards, Institute: Atlanta, Ga.
15. Fanger, P.O., *Calculation of thermal comfort-introduction of a basic comfort equation.* ASHRAE Transactions, 1967. 73.

PLEA 2024 WROCŁAW
(Re)thinking Resilience

Fusing Environmental Technologies with Attached Housing in Rural Vietnam:
A Synergistic Approach

LILIANA O. BELTRÁN[1], LUMING XIAO[1], GHAYDA ALHABIB[1], ANTONIO A. VAZQUEZ MOLINARY[1]

[1]Texas A&M University, Department of Architecture, College Station, USA

ABSTRACT: This paper presents the design, development, and performance evaluation of a Net-Zero attached housing project in the hot and humid climate of Northern Vietnam. Integrating bioclimatic design principles, contemporary environmental technologies, and local building materials. The project aimed to minimize energy consumption while improving the quality of life for the local Tay ethnic group with respect to their traditional lifestyles. A careful examination and adaptation of the traditional local house layouts enabled the integration of efficient passive design strategies such as natural cross-ventilation, shading, solar heating, thermal mass, and daylighting. The use of indigenous building materials and renewable energy sources, including solar panels, was crucial in achieving optimal thermal and lighting performance, resulting in net-zero energy consumption. The successful outcome of this project demonstrates the potential of environmentally friendly, economically viable, and culturally sensitive building practices in achieving sustainable development in the region.
KEYWORDS: Energy, Comfort, Net-Zero, Bioclimatic Design

1. INTRODUCTION

The project is situated in a rural village within the mountainous region of Cao Bang, at an elevation of 289 m above sea level. This village is inhabited by members of the Tay ethnic group, and its population consists of 14 multigenerational families. The local economy predominantly depends on agricultural and forestry activities, along with providing homestays for tourists.

Our team had the opportunity to visit the village and conduct surveys on neighbouring houses. Measurements were taken for indoor illuminance, dry bulb temperature, and air velocity to evaluate the indoor environmental quality in November 2022. The findings revealed that the residents inhabit poorly ventilated spaces with dim interiors (127-136 lux) and cold environments (with no auxiliary heating).

The project is in a region characterized by a temperate climate, experiencing a dry winter season and a hot summer season (Cwa) at a latitude of 22°N, according to the Koppen-Geiger climate system. It falls under the International Energy Conservation Code (IECC) climate zone 2A, which is categorized as hot and humid. The average highest temperature reaches 31°C, while the lowest temperature can drop to 11°C. Additionally, the global horizontal radiation can reach up to 503 W/m². By employing a modified comfort range tailored explicitly for Vietnamese individuals [1], which is 20°C-27.7°C, we have determined that passive design strategies such as internal heat gains and natural ventilation can effectively provide thermal comfort for approximately 80% of the year. Supplementary heating and cooling measures would be necessary only during the remaining 20% of the year. This approach ensures minimal reliance on energy consumption (refer to Figure 1).

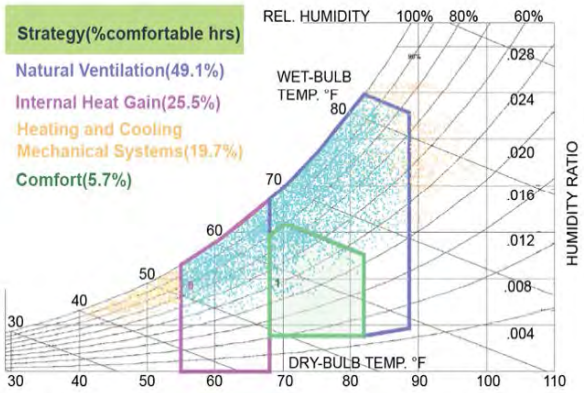

Figure 1: Adapted psychrometric chart for Vietnam.

Our design approach encompasses five overarching objectives. Firstly, in terms of "quality of life," our focus is on enhancing the well-being of the local community in Khuoi Ky Village. This involves addressing issues related to indoor environmental quality, with a particular emphasis on improving daylighting, natural ventilation, and thermal comfort.

Secondly, sensibility plays a crucial role in our design philosophy. We acknowledge and respect local people's unique way of life and specific building attributes. Thus, our project aims to incorporate and honour local customs and architectural features seamlessly. Thirdly, passive design is integral to our strategy. We employ natural ventilation, daylighting,

and shading strategies to ensure occupant comfort, reduce energy consumption, and enhance indoor environmental quality. Fourthly, constructability considerations were meticulously studied, considering the village's location, community setting, and accessibility. We prioritized utilizing locally sourced materials and low-skilled construction techniques while still achieving the desired insulation levels. Lastly, resilience is a crucial aspect of our design, with the project aptly responding to common hazards like flooding and landslides in the area. This holistic approach ensures a comprehensive and sustainable solution that aligns with the unique context of Khuoi Ky Village.

2. METHODOLOGY

The optimization of energy and lighting performance of the three attached housing units involved utilizing software tools, such as ClimateStudio [2], Sefaira SketchUp [3], ALFA, IESVE [4], Meteonorm [5], Rhino, OneClickLCA [6], and Ekotrope [7]. These programs facilitated a comprehensive assessment and refinement of environmental technologies to enhance the overall project. Performance metrics included Energy Use Intensity (EUI) for energy consumption efficiency, Home Energy Rating System (HERS) for overall energy efficiency, and Spatially Daylight Autonomy (sDA) and Annual Sunlight Exposure (ASE) for natural lighting assessment. Equivalent Melanopic Lux (EML) addressed circadian lighting impacts, while Daylight Glare Probability (DGP) ensured visual comfort. Air quality was evaluated through Air Changes per Hour (ACH) and Local Mean Age of Air (LMA) using the CFD tools available in IESVE. Lighting Power Density (LPD) gauged lighting efficiency, Solar Production (kW) measured solar energy generation, and Carbon Footprint Target (LCA) provided an environmental impact assessment.

3. RESULTS

This project is a sensible intervention aimed at addressing existing issues regarding access to energy, living conditions, lifestyle, and the economy. The houses were conceptualized to accommodate a multi-generational family, following the typical pattern of development in the local village. Additionally, they were designed to be an adaptable and affordable housing prototype for future development in the region. Due to the growing tourist homestay market, the project also lends itself to a homestay typology that a family could administer from one of the housing units.

The houses were designed to adapt to future weather changes, explicitly considering the years 2050 and 2090 (see Figure 2). The building envelope, shading, and ventilation systems were carefully designed to respond and adapt effectively to variations in solar radiation, temperature, and relative humidity. This was accomplished through detailed simulations to assess the future thermal loads and optimize the design accordingly.

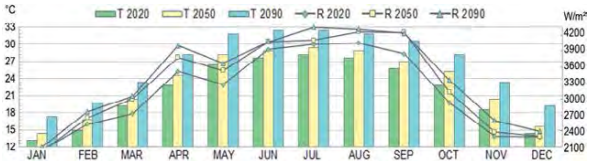

Figure 2: Future climate projections 2020-2090, temperature (T) and global horizontal solar radiation (R).

3.1 Architecture

3.1.1 Site & Programming

The Khuoi Ky Houses consist of three independent housing units attached to an outdoor veranda that serves as the main entrance, a gathering space, and a shaded area. The houses are labelled as Modules A, B, and C in Figure 3. Modules A and C have a living room, dining room, two bedrooms, bathroom, and kitchen for a total internal net area of 90.6 m^2. Module B has the same programming but with only one bedroom for a total of 76.6 m^2.

The site is elongated along the NE- SW axis and can only be accessed from a road on the eastern side. A vegetated mountainside borders the western side of the site. Importance was given to the south-eastern orientation due to local customs, access to views, and prevailing winds during the hot season.

Figure 3: Site Plan.

3.1.2 Architectural Strategies

The building massing aligns with the NE-SW axis of the site's geometry. The three housing units are intentionally separated from each other to allow the placement of windows on opposite sides of each room, promoting natural cross-ventilation and uniform daylighting. The massing of the three units was deliberately kept as a shallow floor plate to allow for cross-ventilation and daylighting, with the deepest space being 4.5 m. The northern facade of the houses has an azimuth angle of 31° offset from True North. The houses cast shade on each other to help regulate solar heat gains. An outdoor veranda

facing southeast connects the units and acts as a shading device while promoting access to morning circadian light.

Figure 4: Main design features

Given that the users rely on agricultural practices, the backside of the housing units was designed as planting terraces. This helped to create a buffer zone to avoid landslide hazards. The initial site survey also revealed that the locals use exterior gathering spaces. Thus, the front side of the project was designed as a veranda that connects all the housing units.

The decision to elevate the building responds to natural hazards and local customs, where the ground level is often used for storage and multifunctional spaces. Elevating the building also provides a better sense of privacy, access to unobstructed views, and a summer breeze. The roofs were designed for efficient solar power generation and to provide an area for north-facing clerestories. The operable clerestory windows provide even distribution of daylighting and take advantage of the stack effect to enhance natural ventilation further.

3.2 Integrated Performance

3.2.1 Structure and Building Materials

The project adopts a hybrid structural system tailored to meet the unique requirements of the rural Cao Bang region, focusing on efficient thermal insulation, low embodied carbon, and resilience against natural hazards. Also, the construction system is designed to be implemented by low-skilled laborers.

Structural System: We incorporated a stone foundation and frame to elevate the ground floor. This decision was influenced by the local availability of materials and techniques and the reduced need for specialized labour and long-haul transportation. The stone foundation is environmentally sustainable and offers superior flood resistance and waterproofing capabilities. For the upper structure, a wooden and bamboo frame was selected.

Insulation System: The project features a thermal insulation system comprising two key concepts:

1. Continuous building envelope insulation. Rigid insulation panels (Expanded Polystyrene, EPS) were used over the envelope to minimize heat transfer, eliminate thermal bridging over shading devices, and reduce dependency on air conditioning.

2. R-values of series heat transfer. The R-value for each building component (roof, floor, and wall) and U-value for windows were determined based on climate characteristics, parametric energy simulations, and future climate change.

Table 1: R-values for various building components.

Building components	R-value SI (IP)
Wall	3.79 (21.54)
Roof	5.37 (30.52)
Floor	4.71 (26.76)
Windows	**U-value:** 1.42 (0.25)

3.2.2 Mechanical Equipment

In Khuoi Ky homes, all equipment, including a mini-split air conditioner, is Energy Star certified, offering 30% more energy efficiency compared to standard models. Advanced exhaust fans equipped with humidity and temperature sensors efficiently regulate moisture levels. The air conditioning system, rated at 21 SEER and 1.16 kW, alongside fans with varied CFM and Sones ratings, dynamically adjusts to human activities, conserving energy. Compliant with ASHRAE, LEED, and other local standards, this setup ensures optimal performance and energy conservation in varying humid conditions.

3.2.3 Energy Use Intensity

The Khuoi Ky houses will consume 93-99% less source energy than the LEED Source Energy Budget limit. The American Institute of Architecture (AIA) 2030 Challenge serves as a viable climate strategy, outlining a comprehensive framework of benchmarks and objectives aimed at achieving net-zero emissions within the built environment. Khuoi Ky houses' Energy Use Intensity (EUI) exceeds the current AIA 2030 Challenge target of 8, signifying a remarkable energy efficiency standard that represents a 94% to 97% improvement compared to the RESNET's Home Energy Rating System (HERS) [see Table 2]. Electric lighting was distributed based on the visual tasks and use of each space, resulting in 0.2 LPD. The thermal comfort simulation included the natural ventilation and air conditioning operating hours.

Table 2: Rating systems & energy targets.

Rating System	Target	Results		
		A	B	C
AIA 2030 Challenge Energy Use Intensity	8	0	0	0
HERS index	0	-1	-5	-1
Zero tool	-	100%		
Carbon footprint	Less than 500 $kgCO_2e/m^2$			

3.2.4 Solar Panel Design

The photovoltaic panel (PV) capability is 675-700W, and its capacity lasts at least 30 years. The PV

panels are placed on the roof and are oriented Southeast, at 211° and tilted 22° to maximize the incident solar radiation. The total collector irradiance is 1,232 kWh/m², producing 2,868 kW per house annually. The total operational hours of the PV panels in Khuoi Ky Village are 4,616 hours a year. The module type BSM700PMB-70SDC has an efficiency of 22.81%, and the energy production for locations A, B, and C is 8.4 kW.

3.2.5 Solar Water Heater

The solar water heater was designed to preheat water to minimize energy consumption during the heating process. The solar water heater features a durable SUS 304 stainless steel insulated tank. The interior of the tank is equipped with a 2-inch-thick layer of polyurethane foam insulation, which can maintain heat for up to 72 hours. The solar water heater is oriented southeast, at 211°, tilted 22 °, and placed on the roof to maximize the performance [Table 3]. The electric water heater is tankless, resulting in lower energy usage.

Table 3: Solar water heater characteristics.

Demand for hot water in households	110 l/day
Hot water supply flow in 1 second	5.766 l/s
Required heat capacity	603 kW
Hot water heating needs of households	3.2 kWh/day
Hot water demand for the whole year (200 days)	640 kWh/year
Total heat required in a year	914 kWh/year

3.2.6 Life Cycle Assessment

We conducted the three houses' life cycle assessment (LCA), adhering to EN 15978 guidelines and ISO 14044 framework. We evaluated the environmental impacts across the entire lifecycle, from raw material extraction to end-of-life stages [Table 4]. Our analysis aimed to scrutinize the environmental efficiency of these houses and explore avenues for diminishing their ecological footprints. Achieving the design goal, each house and its shared veranda successfully maintained a carbon footprint below 500 $kgCO_2e/m^2$.

Table 4: Embodied carbon rating of LCA for House A&C, House B, and the shared space - Veranda.

Structures	$kgCO_2e/m^2$	Rating
Module A & C	291	B
Module B	243	B
Veranda	140	A

3.3 Durability and Resilience

The project's unique location, adjacent to a river and a mountain, required strategies to mitigate natural hazards like floods and landslides, inherent due to the area's topography and rainy climate. Conversely, this setting offered an opportunity for sustainable water management through rainwater harvesting, enhancing environmental sustainability.

3.3.1 Flooding Measures

To combat flooding risks, the project integrated architectural and landscaping measures. Elevating the main living areas was a crucial architectural step to minimize flood damage. A strategically placed drainage system diverts the mountain runoff into the river, preventing water accumulation near the buildings. Additionally, a retaining wall built from local stone along the river's north bank was designed to prevent river overflow and floodwater encroachment, combining architectural foresight with effective landscaping.

3.3.2 Landslides Prevention

Bamboo is used for soil stabilization for landslide prevention, leveraging its strength, resilience, and extensive root system. This approach, proven in various Asian countries, effectively prevents landslides. To control bamboo spread, a root barrier system and the integration of native trees like Teak and Acacia were employed. Additionally, minimal retaining walls offered extra protection against landslides, blending biological and structural methods for comprehensive risk management.

3.3.3 Rainwater Harvesting System

The rainwater harvesting system was calculated in two steps. The first one quantified the potential rainwater collection from the roof based on the local average monthly rainfall, roof catchment area, roofing material's collection efficiency, and a conversion factor, estimating a monthly harvest of approximately 31,000 liters.

The second step assessed the outdoor water needs, particularly for the planting area. It was estimated that the natural rainfall is sufficient for irrigation, eliminating the need for a supplemental irrigation system. Therefore, all harvested rainwater is allocated for indoor use, such as in bathrooms, laundry, and car washing. This efficient use of rainwater enhances the project’s sustainability and water resource management.

3.4 Occupant experience and environmental quality

3.4.1 Daylighting & non-visual comfort

The predominant annual sky types of the local EPW weather file, generated by Meteonorm, were evaluated. It revealed predominantly cloudy sky conditions for approximately 81% of the year, whereas clear days constituted less than 1%, as illustrated in Table 5 and Figure 5. The evaluation of sky types by hours confirmed similar annual percentages.

Table 5: Annual sky types of Khuoi Ky Village.

Annual Sky types	Days (%)	Hours (%)
Clear	3 (1%)	44 (1%)
Partly cloudy	66 (18%)	892 (19%)
Cloudy	296 (81%)	3,699 (80%)

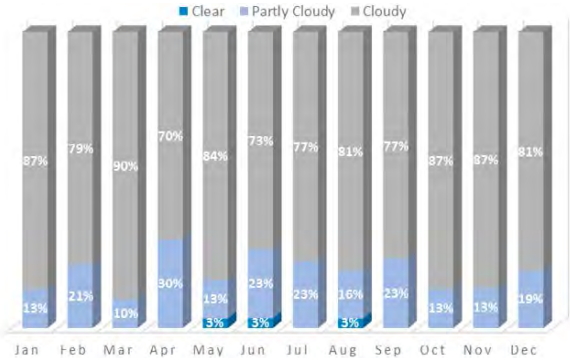

Figure 5: Monthly sky types in Khuoi Ky Village.

Due to the reduced annual daylight availability, multiple daylighting systems were integrated to provide high indoor daylighting levels throughout the year. This strategy entailed installing high-performance windows positioned strategically in various orientations in conjunction with high-operable clerestories for natural ventilation. These measures guarantee extensive natural light penetration within the houses, consequently reducing dependence on electric lighting and augmenting healthy circadian light for occupants. The effectiveness of these interventions was evaluated using climate-based daylight modeling, yielding the results summarized in Table 6, Figures 6 and 7.

Table 6: Summary of dynamic daylighting simulation results.

	House A	House B	House C
UDI (% hrs)	77.4 %	68.8 %	77.0 %
sDA (% space)	99.5 %	92.8 %	96.8 %
ASE (% space)	3.3 %	0 %	1.6 %
DGP (% space)	5.9 %	2 %	5.6 %
EML (% space)	81.5 %	75.5%	78.7 %

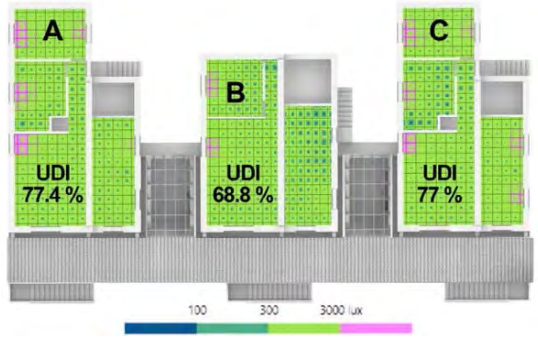

Figure 6: Useful Daylight Autonomy (UDI) results.

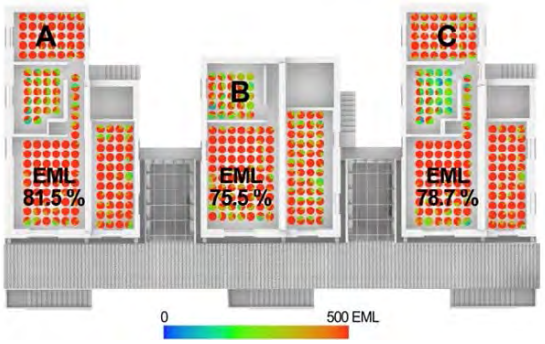

Figure 7: EML simulation results for December 21, 9 AM.

3.4.2 CFD analysis

In the design phase, an in-depth examination of indoor air quality was conducted for the housing units, with a particular focus on natural ventilation. This analysis involved the use of IESVE's CFD tools to simulate indoor air conditions with fully open windows. A key aspect of this simulation was enhancing air circulation through the introduction of operable clerestory windows. Figure 8 presents the velocity vectors in the living room on a typical summer day, illustrating that high windows promote air streams of greater velocities, thereby enhancing the efficiency of air exchange rates.

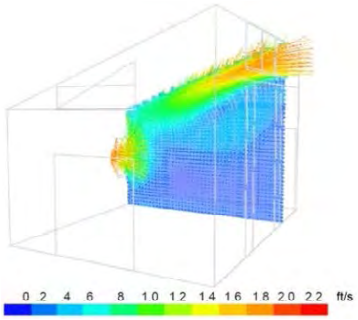

Figure 8: Velocity vectors in living room on a summer day.

Further analysis was carried out to examine the air changes per hour (ACH), a crucial metric for assessing ventilation efficacy. Our simulations for June conditions revealed that several window openings in the living room yielded an average of 25 ACH (Figure 9.) This result underscores the effectiveness of natural ventilation in maintaining recommended ventilation levels during the warmer seasons.

The Local Mean Age (LMA) of air quantifies the average time required for air to traverse from the supply inlet to various locations within a typical kitchen. Figure 10 depicts a maximum LMA value of 2.4 minutes on a typical summer day (June 21). The LMA simulation confirms an efficient air turnover and mitigates the risk of stagnant air conditions within the housing units.

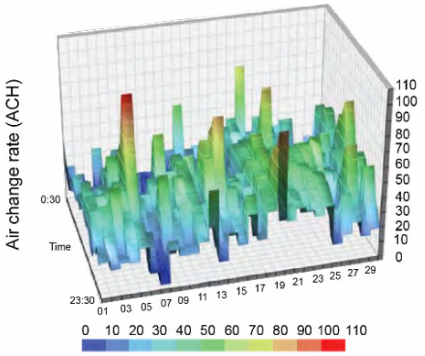

Figure 9: ACH results in the living room of house C.

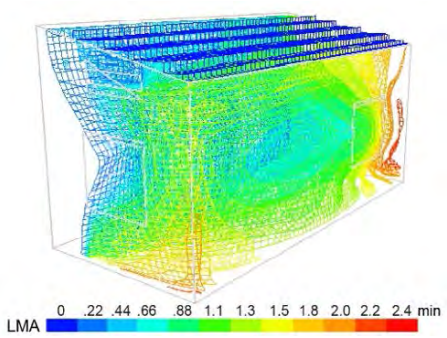

Figure 10: LMA contours in the typical kitchen.

4. DISCUSSION

4.1 Natural Ventilation and Humidity Control

In the humid climate of Cao Bang, our project leverages natural ventilation, particularly operable clerestory windows, to reduce high humidity, as confirmed by CFD analysis (refer to Figure 6). This approach cools the indoor environment and manages humidity, which is essential for comfort. Smart systems with humidity-sensitive exhaust fans automatically adjust to humidity and temperature changes, although they may pose maintenance challenges in Khuoi Ky Village.

4.2 Daylighting and Its Impacts

Addressing limited natural light in a cloudy region (see Table 5), our design uses high-performance and clerestory windows to maximize daylight, improving visual comfort and circadian health, as shown by daylighting simulations (Table 6). The night-time lighting selected is also crucial for circadian rhythm and energy efficiency.

4.3 Local Material Use and Low-skilled Labor

Emphasizing community engagement and sustainability, our approach was centered on using locally sourced materials and straightforward construction techniques accessible to low-skilled labour. This strategy bolsters the local economy and encourages residents to partake in constructing their homes, easing economic pressures. The chosen materials and thoughtful design enhance thermal efficiency and comfort. Considering the rural areas of northern Vietnam, local biodiversity offers a significant opportunity for future housing projects.

4.4 Net-Zero and Climate Adaptation for Future

Our design considered the future climatic changes up to the year 2090 (Figure 2), incorporating adaptable daylighting and ventilation systems for resilience. Strategic solar panel placement contributes to economic and ecological benefits, aligning with our net-zero goal and ensuring the long-term adaptability of the housing units.

5. CONCLUSION

In summary, the Khuoi Ky Houses project in rural Vietnam is an example of innovation in local, sustainable housing development. This project skilfully balances energy efficiency, environmental quality, and community engagement using advanced architectural and technological solutions. Key achievements include exceptionally low EUI, optimized natural lighting and ventilation, and enhanced occupant comfort while respecting local cultural contexts. The use of local materials and construction methods has bolstered the economy and encouraged community participation. Looking ahead, the project's design response to future climatic change ensures long-term resilience and sustainability. This initiative sets a precedent for the future of rural housing in Vietnam, combining traditional practices with modern technology to create a sustainable and culturally sensitive future.

ACKNOWLEDGEMENTS

The authors would like to thank to all the members of the 2023 Solar Decathlon TAMU-HUCE team. To Dr. Pham Thi Hai Ha and her team at Hanoi University of Civil Engineering for their invaluable support. Special thanks to our TAMU students: Na Wang, Sejal Sanjay Shanbhag, Li Chloe, Jumana Naser, and Quynh Le for their contribution to the project.

REFERENCES

1. Ha, P.T.H., Hoa, N.T., Binh, P.T. (2021). Simple method to improve the TCXDVN 306:2004 indoor climate standard for closed office workplaces in Vietnam. Scientific Review Engineering and Environmental Sciences, 30 (1) p.117-133.
2. Solemma, (2021). ClimateStudio Software. [Online], Available: https://www.solemma.com/climatestudio.
3. Sefaira, (2023). Sefaira Software. [Online], Available: https://support.sefaira.com/hc/en-us.
4. Integrated Environmental Solutions, (2023). IES VE Software. [Online], Available: https://www.iesve.com/.
5. Meteotest (2023). Meteonorm Software. [Online]. Available: https://meteonorm.com/.
6. One Click LCA, (2023). OneClickLCA Software. [Online], Available: https://www.oneclicklca.com/.
7. Ekotrope, (2023). Ekotrope Software. [Online], Available: https://www.ekotrope.com/.
8. RESNET, (2023). HERS Index. [Online], Available: https://www.hersindex.com/.

PLEA 2024 WROCŁAW
(Re)thinking Resilience

Transforming a European Commission's Building into Beautiful, Sustainable and Inclusive Spaces

Renovation and adaptation aligned to the New European Bauhaus principles

EVANGELIA BEKTASIADOU[1]

[1] European Commission, Joint Research Centre, Directorate R, Support Services Geel, (JRC.R.6), Geel, Belgium

ABSTRACT: Rethinking buildings' resilience can be achieved by renovating and adapting existing buildings into sustainable, beautiful and inclusive spaces. This has been the ambition for the hero of this paper, the Conference Building, a European Commission's building located at the European Commission's Joint Research Centre in Geel, Belgium. Aiming to give the building a new lease of life and adapt it to current and future needs, a deep renovation and extension concept was proposed. Simultaneously, a participatory and multidisciplinary journey was launched with identified stakeholders, to co-create, brainstorm and collaborate in generating ideas to enhance the building's performance. This co-creation journey towards the final design effectively aligned the building project with the New European Bauhaus initiative. The project and its approach can serve as a role model in practice for deep renovation and adaptation of existing structures into buildings resilient to future challenges and in line with the New European Bauhaus values and working principles.
KEYWORDS: deep renovation, environmental impact, NEB Compass, co-creation, Level(s)

1. INTRODUCTION

In the view of a building project at the Joint Research Centre (JRC) in Geel, Belgium, a distinctive approach to respond to the project's challenges has been introduced. This paper demonstrates the chosen process towards reuse and efficient renovation of an existing building versus demolition and replacement by a new building. In addition, it highlights the essential role of a participatory and multidiscipline collaboration in identifying the building's purpose, co-creating ideas, evaluating sustainability and brainstorming design outcomes.

A unique co-creation journey started during the predesign phase of the *Conference Building* project, (Fig. 1). The ambition was to engage identified stakeholders, share visions and expertise, and co-design sustainable, beautiful and inclusive spaces, aligned to the New European Bauhaus initiative. It is anticipated that this journey and the design outputs could inspire future renovation projects, and the renovated building itself could become a role model in practice of renovating and adapting the existing building stock into buildings that can be resilient and adapted to future challenges.

Figure 1: The Conference Building at the JRC - Geel site

2. CONTEXT

2.1 The joint research centre (JRC)

The Joint Research Centre (JRC) is the European Commission's science and knowledge service. It provides "*independent, evidence-based knowledge and science, supporting European Union's policies to positively impact society*", [1]. The JRC facilities, are sited in Belgium, (Brussels and Geel), Germany (Karlsruhe), the Netherlands (Petten), Italy (Ispra), and Spain (Seville).

2.2 JRC-Geel and the Conference building

The JRC-Geel site in Belgium was founded in 1962 within an area of nearly 40 hectares, in the Antwerp province. At the JRC-Geel site, approximately 280 employees contribute daily in the fields of biotechnology, reference materials, food and feed safety, food fraud detection, healthcare, nanotechnology, nuclear safety and security, threat detection, support services, etc. Throughout the multi-disciplinary scientific work, the goal is to promote standardisation and harmonisation across the European Union to stimulate innovation and to protect consumers and citizens, [2]. These main activities take place in fifteen buildings, owned by JRC. Many of these buildings are new, constructed during the past fifteen years, while a few others are very old and at the end of their service life.

The JRC-Geel *Conference Building* is one of those later buildings, present at the JRC-Geel site for nearly 45 years. Over the years, it has been adapted to meet the demands of its time, but still it lacks resilience to further adaptations. Its future is currently quite

uncertain mainly due to excessive energy consumption, deterioration of materials and non-compliances with legal obligations.

3. RENOVATION VERSUS DEMOLITION

Up to recently, demolition of buildings and replacement by new buildings has been common practice. While environmental experts, activists, and architects have been campaigning on climate change and sustainability, building demolition was implemented in favour of new buildings and without consideration of the negative environmental cost.

Fortunately, the tides are changing. Since the beginning of our century, environmental legislation and guidelines are in place, encouraging building renovation, caring for nature, boosting the economy, people's wellbeing and quality of life. The European Green Deal, 2019, towards a sustainable future and Europe, [3], the renovation wave strategy, 2020, [4] and the New European Bauhaus initiative, 2021, [5], are but a few of the initiatives going ahead today.

4. THE DESIGN CONCEPT

Demolition and constructing an entirely new building, was not an option to be deliberated for this project. Instead, the focus was on improving building resilience, minimising the environmental impact, and reducing life cycle costs. Essential considerations involved redefining the building's purpose and required functionalities.

We aimed to renovate in depth, adapt and expand the *Conference Building*, with respect to our needs, teaching new working methods and implementing EU policies and initiatives. The current structure and plan of the building could be fortunately adapted without significant modifications in the existing structural part, offering flexibility even to future adaptations.

The initial approach and design concept favoured openness, beauty, sustainability, inclusivity and collaboration. Setting the objective of transforming the building into a place, where JRC staff, scientists, students, universities, start-ups and citizens could meet, interact, co-create, innovate and work together for the European Citizen's well-being, we had to envisage with new challenges. The vision for this building has been to evolve it into a multifunctional building for all, which has being provisionally named "*Citizen's Centre for the citizen's well-being".*

5. WORKING METHODS AND OUTCOMES

5.1 Participatory approach with staff

Following our initial design concept within the Support Services Geel Unit (R.6), a bottom up approach was launched. We wanted to brainstorm on the *Conference Building's* needs and functionalities and to include JRC-Geel staff to be innovative and design together with us their visions. Staff became voluntarily part of a co-creation experimental journey and a key stakeholder, participating actively in a variety of events, such as co-creation workshops, online informative sessions and surveys. During this period, we collaborated with archipelago architects to brainstorm and co-develop our initial idea, while decoding the workshops' deliverables. Soon, three main functionalities for the *Conference Building* were distinguished: an auditorium, a visitor's centre and social spaces. In addition, an aspiration towards sustainable, beautiful and inclusive spaces, accessible to staff, collaborators and citizens was clearly underlined by staff.

Subsequently, we developed three design proposals and asked staff to endorse the most preferred option. In parallel, a stakeholder's analysis assisted us to identify internal European Commission's stakeholders, as well as additional ones from the academia, Belgian research organisations and industry. Emphasising the importance of stakeholders in co-creation, and decision-making, we wanted to engage additional partners, looking for insights and expertise to enhance the process.

5.2 Assessing Sustainability in Level(s)

To assess the building's sustainability, we applied the Level(s) European framework, [6]. By applying Level(s), we could support the New European Bauhaus in the fields of EU climate, circular economy, and healthy and comfortable living spaces [7]. Moreover, with Level(s), we aimed to experience a multidisciplinary collaboration together with our architects and stakeholders involved in the project.

The Level(s) framework can be implemented in three levels (phases), which are Level 1_ Predesign, Level 2_ Design and Construction, and Level 3_ Building in use. This framework is based on six macro objectives, which cover in total sixteen sustainability indicators. Depending on the project and expectations, the related levels of Level(s) and indicators for assessment and reporting, can be thoroughly assessed. The Level(s) indicators are:

1.1 Use stage energy performance (kWh/m²/yr.)
1.2 Life Cycle Global Warming Potential CO_{2eq} /m²/yr.
2.1 Bill of quantities, materials and lifespans
2.2 Construction & Demolition waste and materials
2.3 Design for adaptability and renovation
2.4 Design for deconstruction, reuse and recycling
3.1 Use stage water consumption (m³/occupant/yr)
4.1 Indoor air quality
4.2 Time outside of thermal comfort range
4.3 Lighting and visual comfort
4.4 Acoustics and protection against noise
5.1 Protecting occupier health and thermal comfort
5.2 Increased risk of extreme weather
5.3 Sustainable drainage
6.1 Life cycle costs (€/m²/yr.)
6.2 Value creation and risk factors

For the project concerned, reporting on Level 1 (Predesign phase) and part of Level 2 (Design phase) have been finalised. The complete Level 2 and Level 3, which are related to the subsequent phases of the project (construction and building in use), will be examined in the future and are not within the scope of this paper.

5.2.1 Level(s), Level 1 workshop, (Predesign phase)

During the Level 1 workshop, the Level(s) indicators were deliberated. Together with the architects, engineers and our identified stakeholders, we brainstormed and discussed the interest in addressing all the Level(s) indicators. Additionally, the project's plan was set up, and the Level 1 checklist was completed. Understanding the methodology, led us to fruitful insights on how Level(s) could be implemented to improve the project.

5.2.2 Level(s), Level 2 workshop (Design phase)

Subsequent to the Level 1 workshop, various meetings and brainstorming sessions aimed at better defining the design concept, monitoring the evolution of the environmental studies and reporting on specific indicators. To determine how material mass, openings, natural ventilation, shading and natural light, could affect the building's energy efficiency, comfort and resilience, archipelago architects worked on various dynamic energy simulation models. Factors such as the building's occupancy, as well as current and future weather data, were also taken into consideration influencing the outcomes. The data derived throughout these studies were deliberated at the Level 2 workshop. Simultaneously, we brainstormed on building materials and construction implementations (build-ups), Life Cycle Assessment (LCA), Life Cycle Costs (LCC), heating and cooling, flexibility, health and thermal comfort, etc.

During the Level 2 workshop, we decided to explore alternative design solutions through a comparative analysis and make essential decisions prior to the final design. Finalising one design proposal and assessing its sustainability would have prevented the opportunity to evaluate and compare different design alternatives. Therefore, we decided to reflect on different materials and construction choices (build-ups) at element level (impact per m²). This approach, in combination with various design scenarios, enable us to enrich the results at building-level and shape the final design.

In line with this decision to work at element level, and aligned to the Level(s) assessment process, various construction implementations (build-ups) were chosen. Our main goal has been to examine and evaluate these build-ups, for renovating the existing walls, floors, and roofs, and for constructing newly walls, floors and roofs at the building envelope level. Following, we could implement these results at building level, (impact for the total m²).

The environmental impact of the different build-ups was studied by KU Leuven, (University of Leuven - Research division Architectural Engineering). For these studies, the LCA assesses all life cycle stages of the building over a 50 years' service life. Both the Global Warming Potential, (GWP) and a total environmental impact have been assessed. For these later studies the Belgian MMG method was applied, [8]. This is the Belgian LCA method of construction products and buildings. It considers a broad list of environmental indicators in line with the EN15804+A1 standard, and expresses the impacts in an aggregated single score, expressed in a monetary value, reflecting the "*cost to prevent or repair the environmental damage*" in €/m² (surface of wall, roof, floor, etc.).

Part of the process we followed will be demonstrated through an example of the energetic renovation of the existing non-insulated cavity walls, (Table 1). For these studies, the insulation values and the bearing capacity were kept identical to ensure objective results. Factors such as the environmental impact of materials, heat storage capacity and investment cost, were taken into consideration. The possible build-ups we examined are listed below:

_BT : Existing cavity wall without insulation
_BT1: Replacing brick veneer & installing insulation
_BT2: Replacing brick veneer with brick strips & installing insulation
_BT3: Replacing brick veneer by a panel façade and installing insulation
_BT4: Adding additional insulation & rendering
_BT5: Internal insulation and internal finishing

For each of these build-ups, the indicators 1.2 (LCA Global Warming (CO_{2eq}/m² wall) and 6.1 (LCC, Euro/m² wall) have been assessed.

T*able 1: Renovation options (build-ups) for renovating existing cavity walls (_BT), (archipelago architects)*

The analysis shows that the environmental impact LCA (in €/m²) of renovating the existing non-insulated cavity wall (_BT), can be reduced up to 65% (build-up _BT3) and up to 73%, (build-up –BT5), depending on our choices, (Fig. 2). Analysing the Life Cycle Global Warming Potential (GWP), (Fig. 3), it appears that _BT3 and _BT5 build-ups have the lowest impact for both the total environmental impact and the GWP.

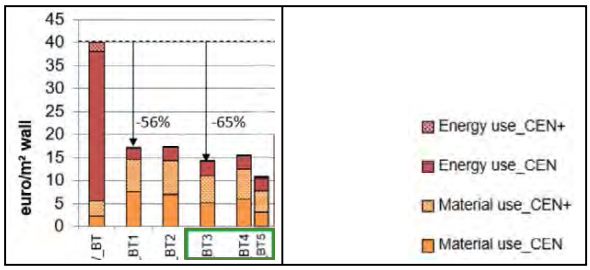

Figure 2: Total environmental impact LCA in €/m² wall, (KU Leuven)

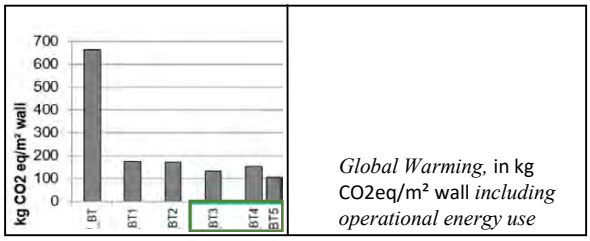

Figure 3: Life Cycle Global Warming Potential operational energy use included, (KU Leuven)

Considering the Life Cycle Cost (LCC), (Fig. 4), it is the lowest for the build-ups _BT4 and _BT5. It is also noticeable that the option of not renovating the wall (_BT) has the lowest Life Cycle Cost, as the energy use for renovation stays quite high, (Fig. 4). Nevertheless, such an option cannot improve the energy performance of the building envelope.

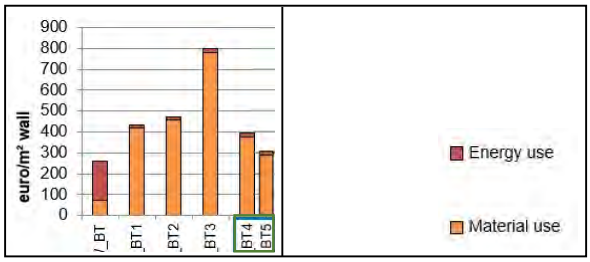

Figure 4: Life Cycle Cost (KU Leuven)

While the conclusion of the LCA and LCC analysis have been that the _BT4 and _BT5 solutions scored higher from an environmental point of view, additional parameters in consideration adapted the data and our decisions. For instance, the use of internal insulation to improve the energy performance of the existing walls was not in favour, due to lack of air tightness and thermal mass. Furthermore, reporting on the indicator 2.4, (deconstruction - massed based circularity cost and ease of recovery and recycling), contributed towards diverse decisions.

Focusing in the build-ups of the existing walls, the studies made by VITO (Independent Flemish Research Organisation, Belgium) on the later 2.4 indicator, illustrate that the built-up of the wall _BT1, was a better choice, as this type of build-up could be easily recycled and reused, and with the appropriate lime-mortar could be slightly reversible, (Table 2).

Table 2: Mass-based circularity score – comparison between different options of renovating the existing non-insulated cavity wall (_BT), (VITO)

Element	Element name	Mass-based circularity score
Wall _BT	existing wall	25.00%
Wall _BT1	new cavity wall	54.21%
Wall _BT2	brick strips	24.83%
Wall _BT3	soft insulation with panel facade	29.90%
Wall _BT4	existing wall with extra insulation	24.53%
Wall _BT5	existing wall with internal insulation	25.96%

Additional studies demonstrated that the total environmental impact of the _BT1 build-up could be even less, by reusing the existing brick veneers or using recycled ones. For all these reasons, the _BT1 build-up was selected as the most efficient option.

We adequately implemented this methodology for the newly added walls, the new and renovated roofs and the new and renovated floors. The investment cost per build-up, the aesthetics of numerous materials and their availability at the market have been also examined and influenced our decisions. Trying to consolidate our findings and the impact of the chosen build-ups for the total surfaces of walls, roofs and floors (renovated and new), of the building envelope, two scenarios of comparison were set. At the table below, (Table 3), there is a comparison between renovation and extension of the building envelope (option 1) and the option of an entire new building envelope, (option 2).

Table 3: Selected build-ups for the building envelope-comparison table, (Archipelago architect)

Initial cost €/m² - total surface of all build-ups	indicator 6.1: LCC (€/m²)	LCA Envir. Impact (€/m²)	indicator 1.2: LCA Global warming (kg CO2 eq/m²)
1. Renovation & extension (build-ups - building envelope)			
804 792.00€	2 203.28€	68 258.00€	679 290.00
2. Implementation of new build-ups - building envelope			
966 715.00€	2 340.80 €	70 489.00€	672 580.00
Comparison of the build-ups -building envelope			
- 161 923.00 (€) **- 20%**	-137527.00 (€) **- 6%**	- 2 232.00 (€) **- 3%**	6,710.00 **1%**

Between these two choices, the renovation and extension option resolves in a lower LCC (6%) and LCA (3%), and a significant lower investment cost (20%). The CO_2 emissions are almost the same but slightly higher at the renovation option, (1%) mainly due to specific design choices, as for example to keep the uninsulated existing floor of the auditorium, (increased embodied carbon footprint, which should be distinguished to the total environment footprint).

The above methodology and the comprehensive analysis aligned to the Level(s) process, inspired us to derive discussions and take thorough decisions, focusing on the building's energy performance, comfort, adaptability and aesthetics. The financial impact of our choices have been also considered and shaped our final decisions.

6. NEW EUROPEAN BAUHAUS (NEB) ALIGNMENT

The design of the potential building project has been aligned to the New European Bauhaus (NEB) values, that of sustainability, beauty and inclusivity. Additionally, the whole process, journey, following a participatory, multidisciplinary and transdisciplinary approach and methodology has been aligned to the NEB working principles. This journey has been a great example of collaboration across numerous departments and Directorates within the European Commission. Co-creation and brainstorming with managers and peers was challenging and productive, supporting the multi-level engagement of different partners. Collaboration with external stakeholders has also been inspiring and rewarding. The whole approach became a transdisciplinary journey, bringing together knowledge of different fields towards a better understanding, implementation and dissemination of EU values and policies.

Evaluating the project under the NEB Compass, [9], our ambitions successfully reach the highest score, both for the NEB working principles and values. A brief description on how the NEB values fulfil the NEB Compass, is given below.

6.1 Sustainability (NEB Compass -AMBITION III)

The goal to minimise the environmental impact of the building has been very ambitious. By applying Level(s), working on energy simulation models, and implementing additional studies aligned to national legislation, the building's sustainability has been thoroughly enhanced. Supplementary studies such as analysis of construction materials and built-ups reuse and ease of recycling, also guaranteed a positive impact on the building's environmental footprint.

The sustainability ambition has been set even higher, considering the fact that our goal was to renovate, extent and preserve the largest part of the existing building versus demolition and a new construction. This approach will allow us to implement and disseminate our findings within the premises of the European Commission and even beyond. Introducing this building and process as a role model for future renovation projects, sets a more ambitious sustainability goal, with an overall Compass score of AMBITION III.

6.2. Beauty (NEB Compass -AMBITION III)

The design concept of the project is well integrated within the natural setting, and a continuous strong dialogue between the new and old building volumes strengthens the building's antiquity and authenticity. Through the implementation of *Level(s)* and simulation models, attention has been given to studying the use of light, shading, thermal and visual comfort, and air quality, assuring for the users comfortable, healthy and beautiful spaces.

The proposed extension surrounds the existing dominant volumes like an external caring skin, creating flexible spaces to wonder around, work, meet and interact. The auditorium keeps its leading role to host beautiful scientific and cultural events, while a few private places are accessible only for staff establishing the sense of ownership. The proposed carefully chosen materials, add an extra layer of beauty, promising an attractive and cosy atmosphere. This ambiance extends through the glazed façade, connecting in harmony the building with its neighbourhood and natural surroundings, (Fig. 5, 6).

Overall, the building has been designed to offer new ways of interaction, communication and collaboration. This new experience of interaction, learning and evolving, could create the sense of "us", setting overall according to the NEB Compass, the NEB beauty value score to AMBITION III.

Figure 5: Sustainable design, interaction with nature and the neighbourhood. Garden view (archipelago architects)

Figure 6: Beautiful, inclusive spaces, honesty of materials, ease of movements (archipelago architects)

6.3. Inclusivity (NEB Compass - AMBITION III)

Accessibility and inclusivity have been our major concerns. Therefore, a single level plan has been proposed to guarantee ease of moments within the building and pleasant connections with nature. The circulation areas are carefully designed to give access to all. For the second level, access is gained through a wide staircase and a lift. A green roof terrace ensures additional connections to nature for the occupants of the upper level, (Fig. 5, 6).

The prospective building will provide staff and collaborators access to knowledge of JRC scientific achievements and EU policies. It can become a *Hub*, offering diverse activities and spaces, accessible to staff and stakeholders to collaborate and interact. This building has the potential to make a positive impact on our society, which is fully aligned to JRC's role. Therefore, the ambition is set at level III, (Fig. 7).

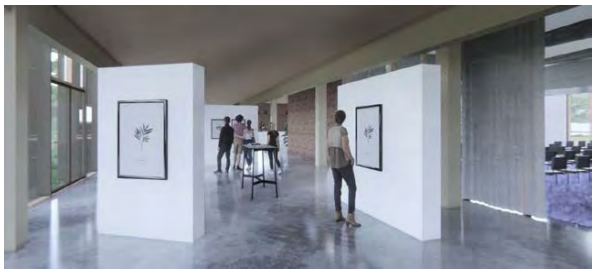

Figure 7: Diversity and inclusivity (archipelago architects)

7. CONCLUSIONS

The implemented approach of this building project has been distinct and innovative compared to previous procedures. Assessing and reporting the building's sustainability through the Level(s) framework and alternative tools, initiating essential discussions and evaluating a variety of build-ups at element level per square meter, supported collaboration, respectable choices and decisions.

Throughout this project, sustainability, beauty and inclusivity have been embraced. Furthermore, the participatory, transdisciplinary and multi-level engagement has profited the project's outcomes aligning it successfully to the NEB initiative.

Underlining the importance of deep renovation over demolition, this NEB project aims to become a role model in renovation approaches, inspiring diverse approaches in building projects. The preliminary assumptions will be confirmed during the Level(s) Level 2 and 3 phase (building in construction and in use), but still, the knowledge gained during this experimental journey can be implemented in future infrastructure projects and shared to disseminate knowledge on EU values and policies. Our ambition is to persist in this journey and create a New European Bauhaus multifunctional building, resilient to future challenges, fit for purpose, and prepared to affect positively our society, (Fig. 8).

Figure 8: Transforming the Conference building, into beautiful and sustainable multifunctional spaces, inclusive to all, (by archipelago architects)

ACKNOWLEDGEMENTS

This paper synopsises part of the predesign and design phase of the project, during which numerous stakeholders have actively contributed in the process. It has been a wonderful team work. Sincere thanks to all of them, with special acknowledgement to:

- archipelago architects, Tractabel engineers, VITO (Flemish Institute for Technological Research), KU Leuven, (Catholic University of Leuven), Socotec, and INTER Accessible Flanders.
- European Commission colleagues, specifically to DG JRC, JRC Directorate R, and to all JRC-Geel colleagues for their input, engagement, and becoming an essential part of this inspiring co-creation journey.
- In the content of this paper, a heartfelt thank you for their contributions to Verlinden Marijn, Haremans Veerle and Declercq Joost, (archipelago architects), Allacker Karen and Van de moortel Els, (KU Leuven), with special appreciation to my Head of Unit Wellens Marc, (JRC, Support Services Geel, R.6), for his active involvement, support and constant collaboration.

REFERENCES

1.European Commission, EU Science Hub, JRC, available: https://joint-research-centre.ec.europa.eu/index_en

2.European Commission, EU Science Hub, JRC, avaliable: https://joint-research-centre.ec.europa.eu/jrc-sites-across-europe/jrc-geel-belgium_en>

3. European Commission, Directorate-General, European Green Deal, avaliable: https://commission.europa.eu/strategy-and-policy/priorities-2019-2024/european-green-deal_en

4. European Commission, Directorate-General for Energy, avaliable: https://energy.ec.europa.eu/topics/energy-efficiency/energy-efficient-buildings/renovation-wave_en

5. European Commission, Joint Research Centre, New European Bauhaus, avaliable: https://new-european-bauhaus.europa.eu/index_en

6. European Commission, Directorate-General for Environment, Level(s), avaliable: https://environment.ec.europa.eu/topics/circular-economy/levels_en

7. European Commission, Directorate-General for Environment, Level(s) and the new European Bauhaus, Publications Office of the European Union, 2022, https://data.europa.eu/doi/10.2779/104409

8. TOTEM 2023, OVAM, Brussels Environment and the Public Service of Wallonia available: https://www.totem-building.be/

9. European Commission, Joint Research Centre, General Publications 2022, The New European Bauhaus Compass, avaliable: https://new-european-bauhaus.europa.eu/get-involved/use-compass_en

10. Declercq, J., Ramon D., Dermy F., Allacker K., The feasibility of natural ventilative cooling in na office building in a Flemish urban context and the impact of climate change, 17th IBPSA Conf., Bruges, Belgium, Sept. 1-3, 2021, DOI: https://doi.org/10.26868/25222708.2021.30811 p.910

11. Allacker K., Environmental and economic optimisation of the floor on grade in residential buildings, The International Journal of Life Cycle Assessment, 2018, p. 813–827. https://doi.org/10.1007/s11367-012-0402-2

12. Van de moortel E., Allacker K., De Troyer F., Stijnen L., Schoofs E., Development Of A Guidance Tool For Sustainable Renovation Of Social Housing In Flnders, 4th Building Simulation and Optimization Conf., Cambridge, UK: 11-12 Sep 2018, https://lirias.kuleuven.be/retrieve/644475

PLEA 2024 WROCŁAW
(Re)thinking Resilience

Coding Olgyay:
Exploring the pedagogical potential of parametric modelling tools for teaching bioclimatic design

LUCA FINOCCHIARO[1], MARIYA BOND STOYANOVA[1], ANSHUMAN MISHRA[1], LEIF MARTIN HOKSTAD[2]

[1]NTNU, Department of Architecture and Technology, Trondheim, Norway
[2] NTNU, Department of Education and Lifelong Learning, Trondheim, Norway

ABSTRACT: "Climate and built form" is a combined theory and design course at the MSc in Sustainable Architecture at NTNU where architecture and engineering students collaborate in the analysis and design of climate adapted buildings. The course is structured in a series of pedagogic modules where students are trained in the use of digital simulation tools for environmental performance analyses. Teaching experiences show that an extensive use of these tools risk to reduce complexity behind architectural design to a discrete number of parameters. Researchers agree moreover that analog tools such as sketching and physical models still represent a valuable tool for processing knowledge and let students better grasp theory. In order to enable students to more effectively handle holistic design process and enhance students learning environment, we developed the pedagogic module about form and sun and tested it in the form of an experimental workshop. During the workshop the use of analog and digital tools have been balanced in a reasoned way. Research was conducted following action research methods and the workshop analysed for the potential of experiments to enhance students learning environment, facilitating the translation of theory for climate adaptive design into skills.

KEYWORDS: Coding, Bioclimatic, Design, analog, tools

1. INTRODUCTION

"Climate and built form" is a combined theory and design course at the MSc in Sustainable Architecture, at the Norwegian University of Science and Technology - NTNU - where architecture and engineering students are called to collaborate in the design of climate adapted buildings [1]. The course is structured in a series of pedagogic modules where students are trained in the use of digital simulation tools. Those are used to analyze the environmental performance of case studies or to cope with complex computational analyses in integrated energy design processes. Teaching experiences showed, however, that an extensive use of digital tools risk to simplistically reduce the complexity behind architectural design to a discreet number of quantitative parameters, limiting the attention addressed to social sustainability or functional efficiency of the project [2]. The most courageous and innovative proposals, generally based on intuitive approaches, are often the most difficult to simulate. Students therefore often need to choose if to follow a purely qualitative approach through sketching and physical models or abandoning courageous ideas in favor of more numerically convincing analyses. Such condition limits the potential of the course for the development of holistic and innovative concepts and processes.

Researchers suggest moreover that hands-on activities, such as sketching and model making, still represent a powerful tool for processing knowledge and letting students to better grasp theory [3-6]. Question is therefore how to combine digital and analog tools in a way to take advantage of the computational capabilities of the first, while exploiting values of hands-on approaches for handling holistic design processes and enhancing the learning environment. With this purpose, in 2016, thanks to the support of NTNU, we initiated the development of the Climate HubLab (figure 1), as a pedagogical laboratory collecting a series of analog machines for environmental performance analyses (such as heliodons and streamlines visualization tools) and equipment for facilitating the transfer of information between the digital to the analog environment.

The ultimate intention of the climate HubLab is that of transforming courses in climate and built form into an experimental laboratory where theory is grasped by involving students in a series of activities or experiments were analog and digital tools are balanced in a reasoned way. This transition requires three fundamental ingredients:

- Understand how digital tools can be used not only for their computational capabilities but also to enhance the learning potential of hands-on activities.
- facilitate the transfer of information from the analog to the digital environment, distinguishing values and potential on each side.

- moving from cumulative to formative assessment practices, leaving space to "learning from failure".

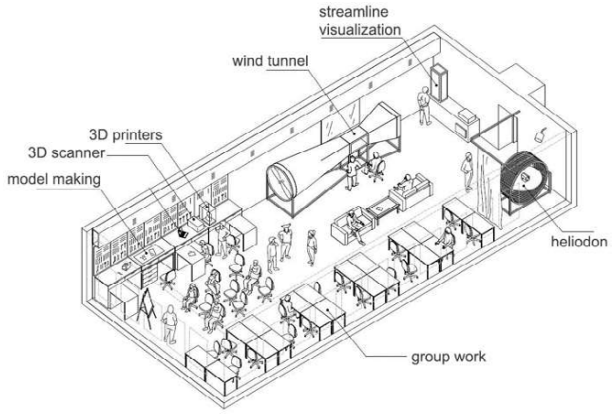

Figure 1: The climate HubLAB at NTNU was conceived and developed with the purpose of exploring the pedagogical potential of equipping conventional design studios with equipment for testing physical models.

This paper focuses on the first of these points and it is built over the premises hereby described and experiences gained during the last ten years of teaching bioclimatic design at NTNU. Results and discussions are the result of activities run, with the help of a PhD student, inside a multidisciplinary research project focusing on pedagogics of environmental design, and involving students, teachers and a pedagogist. Teaching and learning activities tested in the form of a experimental workshop have been built as result of feedback collected from students on the use of digital simulation tools, with an insight on their beneficial or adverse role for creatively handling holistic architectural design processes.

2. TEACHING BIOCLIMATIC DESIGN

Since 2013, courses in "Climate and built form" have been structured in a sequence of pedagogic modules where theory, generally transferred through a lecture, is used as the basis for the use of simulation tools. Looking at Bloom's taxonomy [7], learning in the course was assumed as a linear process (Figure 2) where students introduced to knowledge through lectures would gain the ability to apply it in practice by simply taking part in multidisciplinary design tasks. A comparison between grading in the theory and in the design course, conducted from 2010 to 2014, showed however that students could master knowledge in climate adaptive design without necessarily developing the ability to apply it in practice.

For this reason, from year to year, focus on the development of the pedagogic modules moved from content to the process of learning: from refining knowledge transferred through lectures, to the development of activities that could enhance student learning by involving them in experimental hands-on activities. Such transition is represented in Figure 2. Assignments in the course have been moved from cumulative assessment to formative ones, where progression of the students is monitored during the analysis of the case studies. Following experiential learning theories [8], pedagogic modules have been turned into a series of experiments where knowledge is grasped by involving students in numerical exercises and solve numerical problems related to the adaptation of form, construction, and systems of a building to a specific climatic context.

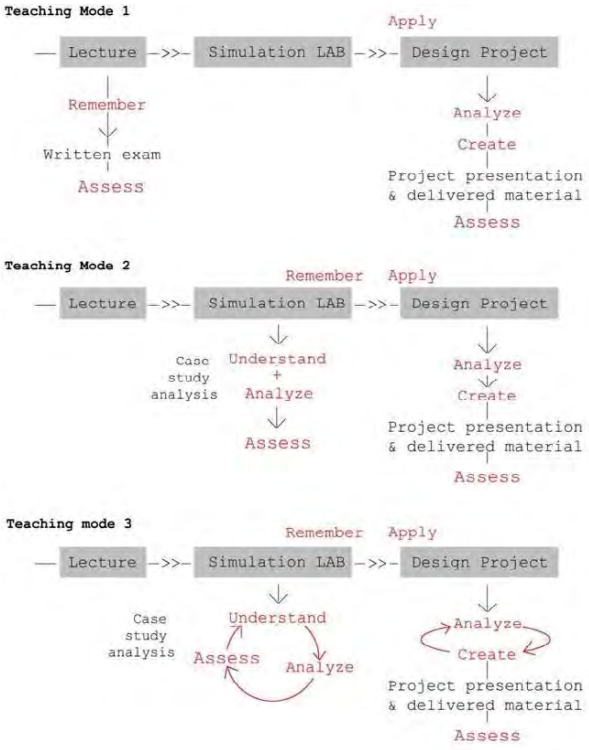

Figure 2: Evolution of teaching and learning activities in the course in the last years.

Moreover, in order to enhance the phases of reflective observation and abstraction of principles for bioclimatic design, structure of the pedagogic module have been flipped. After the lecture, students receive a video tutorial on how to build a script and a task to solve. Students use the script independently and with the possibility of looking at the video several times. After that, students gather in the class and discuss with peers their analyses and difficulties. This general structure is represented in Figure 3, where the three phases of experimentation, reflection and abstraction are represented as the premise for a more conscious active experimentation during the design process.

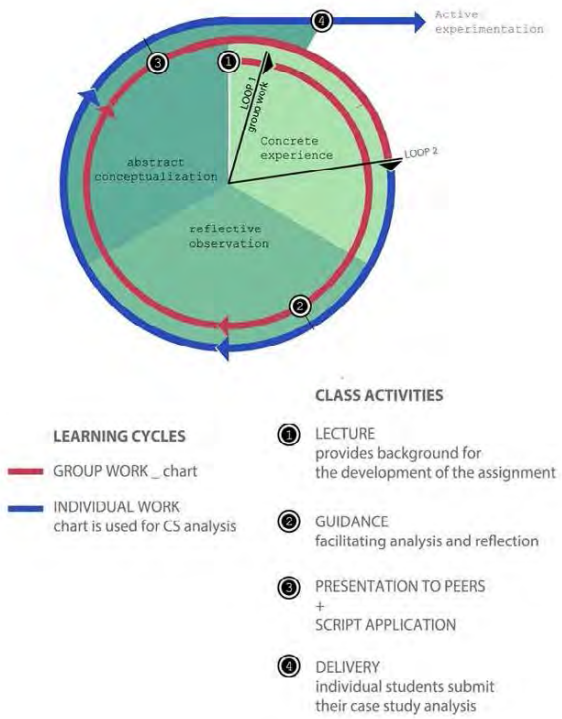

Figure 3: a graphic representation of teaching and learning activities in the revised pedagogic model

3. THE EXPERIMENTAL WORKSHOP

In 2023, with the purpose of analyzing the pedagogical potential of combining analog and digital tools for environmental design, we designed an experimental workshop where digital tools were used to support the learning potential of hands-on activities, rather than as mere computational tools. The workshop focused on the revision of the pedagogic module about "sun and form". During the workshop, students were asked to question and reflect over specific aspects of their project through a series of experiments.

The workshop was developed as an intensive experimental activity of the regular design course where students, distributed in five different climatic conditions, were asked to design a prefabricated climate adaptive shelter for post disaster recovery. Concepts were developed on a purely intuitive basis in the time of one before the workshop started. In defining the concept students had to compromise specific functional and dimensional requirements while embedding solutions for improving the project environmental performance, involving form, construction, and systems to employ throughout the year. In this stage students were asked to only look at climatic data without building any model for digital simulations. Once concept was developed, students were asked to expose their concepts to three experiments, where the first and third were based on hands-on activities, and the second one on the use of a digital parametric modeling tool. In the first step, students were asked to formulate three climate-specific questions to investigate through the use of a manual heliodon (i.e. optimize form to minimize self-shading; identify orientation ensuring maximum exposure in winter, etc.). In the second step, students were asked to use a digital script for relating the morphological characteristics of their project to the assigned climatic context on quantitative basis. Finally, students were invited to run a more detailed analysis in an automated heliodon equipped with micro-cameras to analyze solar access and adjust detailed components within the project (i.e. distribution of thermal mass, effectiveness of a solar shading system, etc.).

3.1 The revised digital module

The second stage of the workshop represented the only "digital step" in a sequence of hands-on activities, involving sketching, model making and testing in two different kinds of heliodons. In this second stage, thanks to a premade script in grasshopper, students could calculate the optimal proportions and orientation of a hypothetical box in the specific climatic context where they were working. This exercise was voluntarily included as an intermediate step such that students would rather use this piece of information to reflect over their proposal, developed on a purely intuitive basis in a more holistic setting. Students would be exposed to learn from failure and adjust the form, rather than get a specific answer from the computer at the beginning of the process and risk to not use their own critical abilities.

As each step in the workshop, also this second one was structured following the four steps internal to the experiential learning cycle: (1) Using the script students would get a concrete experience about the use of simulation tools for morphological optimization; (2) the results would give them the possibility to reflect over their proposals, being able to quantify implications of choices taken in the concept stage; (3) comparing numerical result and their concept morphology, students can now more easily abstract principles for climate adaptive design and (4) enter an active experimentation stage where they can more consciously adjust form of their project on the basis of knowledge gained through the processed experience.

3.2 Coding Olgyay

The adaptation of morphological characteristics of a building to a specific climatic context represents one of the very fundamental steps for ensuring a proper passive environmental performance. Form determines the ability of a building to take advantage of external resources, limiting or enhancing the efficiency of passive strategies such as passive solar heating and natural ventilation.

The original pedagogic module about sun and form in the course aimed to equip students with the ability to calculate and analyze heat quantities in a building.

Through digital simulation tools, students could analyze heating and cooling demand as the result of the building thermal budget and adjust morphological characteristics in a way to increase solar intake or construction and schedules to improve airtightness or facilitate natural ventilation. The limit of such an approach was that of working on refining a form without being aware of how much that form is close or not to the ideal, or optimal, one, in terms of thermal balance. For this reason, in the digital step of the experimental workshop, we decided to develop a code that could make it possible to identify the optimal form on a numerical basis. The script was developed following the sol-air approach, as defined by Victor Olgyay [9], according to which the optimal form of a building is the one able to take maximum advantage of solar radiation whenever temperatures are below the comfort zone, while ensuring minimum intake while outdoor temperatures are above it.

The sol-air temperature - $T_{sol\text{-}air}$ - is a fictitious temperature value that makes it possible to quantify the heat exchange through the envelope as result of both temperature difference and extra contribution due to the solar radiation. $T_{sol\text{-}air}$ can be calculated as:

$$T_{sol\text{-}air} = T_{out} + I_{sol} \times \alpha \times R_{s,e} \quad (1)$$

where:

T_{out}=outdoor temperature

I_{sol}=incident solar radiation

$R_{s,e}$, the surface's exterior air thermal resistance commonly assumed as 0,04 m^2/kW

α is the absorbance assumed as 0.8 for opaque surfaces.

Once $T_{sol\text{-}air}$ is known, heat exchanges through the envelope can be calculated as:

$$Q_{surface} = A \times U \times \Delta T = A \times U \times (T_{sol\text{-}air} - T_i) \quad (2)$$

Thus, for a given form, the total heat exchange through an exposed surface Qc is calculated as:

$$Q_C = Q_{walls} + Q_{roof} \quad (3)$$

In building the script we referred to the dimensional requirements of the given task, according to which the shelter should have been characterized by a gross area of 64sqm and a maximum height of 6 meters. As input students had to define the number of floors, orientation, characteristics of the envelope and targeted design-days. As an output students would get two diagrams: a first one (Figure 4), showing the distribution of sol-air values throughout the day, giving a preliminary understanding of the contribution of solar radiation from different orientations; and a second one, showing heat exchanges for a range of forms and making it possible to identify the ideal form as the one characterized by minimal heat gains in the summer and maximum heat gains in the winter (Figure 5).

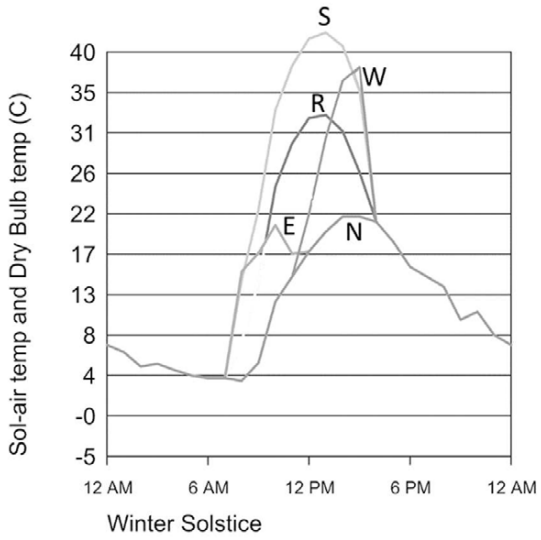

Figure 4: The script made it possible to calculate $T_{sol\text{-}air}$ for the identified design days, showing values for the different orientations and the roof.

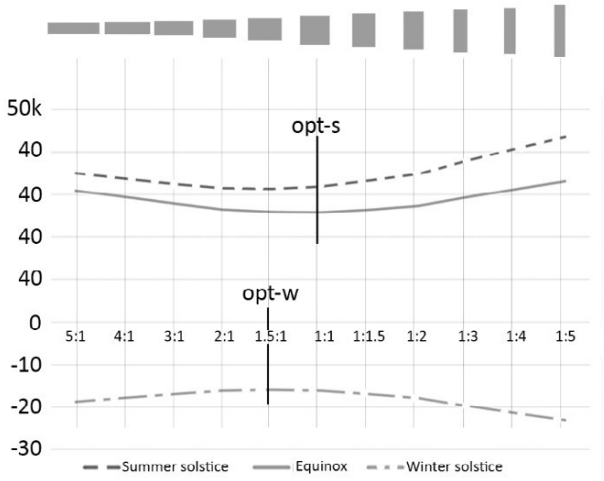

Figure 5: Thanks to the script it is possible to identify the optimal form as the one characterized by maximum solar intake in the underheated period and minimum intake in the overheated one.

4. WORKSHOP ANALYSIS

In order to evaluate the impact of the revised digital module on students' learning we looked at experiential learning theories while taking advantage of action research methods. Before the workshop, students learning style was mapped following Kolb's theories [10] asking students to fill a questionnaire about their attitudes when approaching learning tasks. During the workshop, action research methods were used as "a form of systematic inquiry, prioritizing reflection and bridging the gap between theory and practice" [11]. Following action research methods, we did not only observe but interacted with students and intervened whenever a good opportunity for learning arose. Finally, after the workshop, we collected relevant feedback from students through a questionnaire and an interview in design groups.

5. RESULTS

Results of the workshop's analyses are collected in Table 1. The upper part of the table was developed over the analysis of the material delivered by students and and complemented with information collected during the interview. In this part it is described how students approached the use of the digital script, if the experiment provided unexpected results or supported a more holistic understanding of "sun and form", a reflection or a design choice influencing the design process. Finally it is also added a mark whenever the digital module opened to more active experimentation. In the second part of the Table, it is collected other relevant comments given at the interviews about timing, concept and administration of the workshop.

Besides it is not easy to identify a pattern in the analysis of the results, a few reflection points can be drawn. Four of five groups made use of the digital script developed on the basis of the sol-air approach in order to relate their proposals to the optimal as calculated following the sol-air approach. Only the group working in the cold climate of Oslo recurred to a different software. Students working in the hot-arid and mediterranean climate, where shading in the overheated season is a relevant concern, claimed to have used the script to test alternative solutions and came into unexpected results that affected their design choices and process ahead. People working in warm-humid climatic contexts such as Kuala Lumpur and Trivandrum, where houses needed mostly to be shaded from the zenith and where natural ventilation and wind patterns played a stronger role for the concept development, got a broader understanding of climate adaptive design issues related to sun and form; none of them claims that the experiment influenced their design process anyway. The group working in the cold climatic context of Oslo, focusing on maximizing passive solar heat gains, used the script to identify the proportion of the ideal box in their climatic context but preferred to leave the project as originally planned (anyway close to the optimal) because of other concerns related to aesthetics and prefabrication of the project.

The groups working in Rome, Kuala Lumpur and Oslo wished that the digital tool module could be implemented earlier and, among them, students from the group working in Rome felt that the digital tool limited their creativity and possibility for exploring alternative design solutions. Together with them, the group working in Trivandrum reported that the digital tool was more difficult to grasp than the use of heliodons and four out of five groups preferred hands-on activities to the digital module.

Table 1: A resume of the analysis of the workshop showing a reflection over activities and feedback provided by students.

		Rome	Cairo	Kuala Lumpur	Trivandrum	Oslo
Experiment	initial design	●	●		●	●
	bondary conditions	●		●	●	●
	alternative solutions	●	●			
Discovery	as expected	●		●		●
	unexpected	●	●		●	
	broader understanding			●	●	
Reflection	initial design	●		●		●
	on discovery	●	●		●	
	on possible solutions	●				
Design choice	due to experiment	●	●			●
	due to discovery					
	due to reflection	●		●		
experiment influenced the project development		●	●			
Followed more active experimentation on Sun and form		●	●	●		●
Feedback	wished the digital script earlier	●		●		●
	the digital tool limited my creativity	●				
	digital tool was more difficult to grasp than heliodons				●	
	rather pointed at hands-on activities as more valuable	●	●			●
	the workshop facilitated critical reflection	●	●	●	●	

It is important to notice that only groups working in Rome and Cairo claimed to have used the script to test alternative design solutions, developing choices that affected the design process forward. This might be due to the fact that the climatic context, in comparison to others, resulted more inspiring and brought them to unexpected results that were then translated into concepts. Evaluation criteria of the design course prized anyway those projects that gave evidence of a systematic effort for the adaptation of their projects to climate and context and those two projects seemed to have gained the most from the experimental arena tested in the workshop.

6. DISCUSSION

Analyses conducted at the end of the workshop highlighted that those students for which the content of the sun and form was more aligned to the concept got the highest benefit from the workshop. Those groups that in their concept put the premises for a

more detailed analysis about wind and form naturally perceived the workshop as a distraction and ended up not exploiting the activity or underestimating its potential contribution for the development of the project. This should have be more attention in the next round of the course. The tested experimental framework will be used however next year to define a new module about wind and form where the use of CFD tools will be combined with a water based streamline visualization tool for testing alternative morphological solutions and wind patterns.

This work represented the first attempt to define a clear methodology for the analysis and discussion of experimental workshops combining analog and digital tools for environmental design. The methodology included also mapping of students' learning style in a way to understand if different kind of learners approached or benefited from the workshop in different ways. However, collected information did not make easy to overlap and compare learning style and the way the workshop was approached and perceived. Questionnaire and interviews will be refined in the next round to tackle this issue.

7. CONCLUSION

The revision of the digital module with a coding of Olgyay's sol-air approach served the purpose of facilitating the process of reflection and understanding of general principles of climate adaptive design. 60% of students claimed that the script was useful or very useful, while 5% rated it as informative and 5% as not useful. Remaining 20% did not express their opinion. However, the planning of the activities did not success in exploiting the connection between analog and digital tools and the three steps seemed to be perceived as independent attempts rather than part of a one flow. Finally, the way activities have been planned and monitored, did not make it easy to understand the connection between the use of the digital script and the desire to follow active experimentation through the automated heliodon or other tools. Interviews seemed to suggest on the other hand that hands-on activities became so attractive that the digital tool ended up into a side activity. This clearly limited the intention of exploiting the potential of using digital tools as a computational tool for more qualitative analyses run through the use of hands-on activities.

ACKNOWLEDGEMENTS

This work has been developed within the DigiHands project supported by NTNU through the toppundervisning program. We would like to thank moreover all students that supported the workshop development and administration.

REFERENCES

1. https://www.ntnu.edu/studies/courses/AAR4532
2. Sustainability in Architecture education. Re-harmonizing built and natural environment.. I: Formation - Architectural Education in a Nordic Perspective: Architectural Publisher 2018 ISBN 978-87-92700-24-7. s. 217-226
3. Fernandes, M. A., Wammes, J. D., & Meade, M. E. (2018). The Surprisingly Powerful Influence of Drawing on Memory. *Current Directions in Psychological Science*, *27*(5), 302-308.
4. Heideman PD, Flores KA, Sevier LM, Trouton KE. Effectiveness and Adoption of a Drawing-to-Learn Study Tool for Recall and Problem Solving: Minute Sketches with Folded Lists. CBE Life Sci Educ. 2017 Summer;16(2):ar28. doi: 10.1187/cbe.16-03-0116. PMID: 28495932; PMCID: PMC5459246.
5. Sunalini Esther Devadas and Sheeba Chander 2023 *IOP Conf. Ser.: Earth Environ. Sci.* 1210 012018
6. Newman, D.L., Stefkovich, M., Clasen, C., Franzen, M.A. and Wright, L.K. (2018), Physical models can provide superior learning opportunities beyond the benefits of active engagements. Biochem Mol Biol Educ, 46: 435-444.
7. Bloom, B.S. (1956) Taxonomy of Educational Objectives, Handbook: The Cognitive Domain. David McKay, New York
8. Kolb, D. A. (1984). Experiential learning: Experience as the source of learning and development. Englewood Cliffs, N.J: Prentice-Hall.
9.V. Olgyay, Design with Climate: bioclimatic approach to architectural regionalism. Princeton University Press, 2015. Chapter IV.
10. Kolb, D. A. (1976). *The Learning Style Inventory: Technical Manual*. Boston, MA: McBer.
11. Daniel Selener, Participatory Action Research and Social Change. Published by the Cornell Participatory Action Research Network, Cornell University, USA, 1997

PLEA 2024 WROCŁAW
(Re)thinking Resilience

Urban Green Infrastructure for Resilient Urban Transformations:

A System Dynamics Modelling Approach for Streets as Multifunctional Spaces

JULIA MICKLEWRIGHT [1]; MAHTAB BAGHAIE POOR [2]; ELIZAVETA FAKIROVA [3]; ANDREW J. FAIRBAIRN [4]; HADI YAZDI [5]; MOHAMMAD A. RAHMAN [3]

[1]Chair of Sustainable Urbanism, School of Engineering and Design, Technical University of Munich, Munich, Germany
[2]Chair of Urban Structure and Transport Planning, School of Engineering and Design, Technical University of Munich, Munich, Germany
[3]Chair for Strategic Landscape Planning and Management, School of Life Science, Technical University of Munich, Freising, Germany
[4]Terrestrial Ecology Research Group, Department for Life Science Systems, School of Life Science, Technical University of Munich, Freising, Germany
[5]Professorship for Green Technologies in Landscape Architecture, School of Engineering and Design, Technical University of Munich, Munich, Germany

ABSTRACT: In pursuing resilient urban transformations, streets must be transformed into multifunctional spaces integrated into the urban green infrastructure (UGI), but there is a lack of systemic understanding of synergies and trade-offs of UGI in streetscapes. System dynamics (SD) modelling is a method to better understand complex interconnections between indicators in a multidisciplinary context and, therefore, can help achieve multifunctional streets. We propose here a SD model focusing on four sub-projects of a Research Training Group (active mobility comfort, private yard morphology, bird community composition, and tree canopy growth) and centred around two urban planning goals, i.e. enhancing Active Mobility Comfort (AMC) and increasing Bird Biodiversity (BBD). The resulting model allowed us to exemplify relevant indicators, synergies and trade-offs of UGI elements, indirect paths to reach urban planning objectives and high-impact indicators serving as a lever for street transformations. Through this endeavour, we gained a more holistic understanding of street UGI interactions, which is beneficial for interdisciplinary research and effective decision-making.
KEYWORDS: Streets, Multifunctional, System dynamics, Modelling, Multidisciplinary

1. INTRODUCTION

In the face of current climate change projections, Urban green infrastructure (UGI) is seen as a critical component in creating resilient and sustainable cities [1]. More than just the ecosystem services that UGI provides, its multifunctional character makes it a central component of resilient urban spaces [2]. For this reason, developing UGI demands a multi-scalar and multidisciplinary approach [2]. This is the challenge that the Research Training Group (RTG) "Urban Green Infrastructure – Training Next Generation Professionals for Integrated Urban Planning Research" at the Technical University of Munich aims to address since its start in 2022. The RTG comprises 14 departments from the natural sciences, engineering, and planning disciplines. We strive to address part of this challenge here.

Streetscapes, defined here as the areas between building facades that include public streets and adjacent spaces, represent a convergence point of the research projects of the RTG as they are increasingly recognised as pivotal components within urban ecosystems to achieve a continuous UGI in densely built areas [3]. Moreover, they are already undergoing transformations around the world significantly in part due to a shift in the mobility paradigm - from car-based mobility towards active mobility, i.e. walking and cycling [3]. These current transformations can be an opportunity to integrate more elements of the UGI, therefore becoming multi-functional spaces and helping to achieve resilience and sustainability goals. Nonetheless, these transformations represent a challenge because of the variety of actors involved and the lack of a multidisciplinary approach leading to a common understanding of the benefits and trade-offs of UGI in streets [4]. To contribute to this, we focused our study on urban transformations taking place in streets and considered the integration of UGI elements crucial to achieving resilient urban streetscapes.

1.1 Opportunities of a System Dynamics Modeling Approach

To achieve a better understanding of the benefits and trade-offs of UGI in streets, a method applicable to studying complex problems, such as sustainable development with a multidisciplinary approach, is needed [1]. System dynamics models (SD) do just that [5,6] by describing complex systems through time by illustrating stocks, flows, feedback loops, and time delays [5]. SD models frequently find application within the domain of urban development as a foundation for formulating policies and exchanges with decision-makers [5] and can, therefore, be a tool to facilitate the planning of multifunctional street spaces.

Our SD model aims to identify critical indicators and types of connections between the four identified project focuses to analyse synergies and trade-offs relevant to reaching two selected urban planning goals. Our model aims to facilitate a holistic understanding in the context of interdisciplinary research and pave the way for the planning of multifunctional, resilient streetscapes.

2. METHODS

2.1 Model Context and Boundaries

Here we present a conceptual framework for developing a SD model of urban streets. Our aim is to allow a systemic understanding between domains within UGI. As a lack of clear model boundaries is identified as a research gap [5], we limited our model to encompass the following domains: 1) Active mobility comfort, 2) Private yard morphology, 3) Bird community composition and 4) Tree canopy growth. These represent sub-projects focuses within the Research Training Group and are described in more detail below.

In the active mobility domain, the project focuses on the interactions of UGI with active mobility modes due to the direct exposure of pedestrians and cyclists to the urban environment, making them the group of users to profit the most from the benefits of vegetation in streetscapes. [4] Within the domain of private frontage morphology, the focus lies on the role of frontages as a buffer area between public and private urban spaces that contain a significant share of green elements and hold great potential in contributing to the integration of UGI in streetscapes. [7] The bird community composition is relevant as the complex interactions between different taxa and urban green are just beginning to be understood [8]. Birds are one of the best-studied urban taxa and are nearly ubiquitous in urban environments. Lastly, the domain of tree canopy growth is particularly relevant in streetscapes as trees are a decisive factor for microclimate [9] and bird habitat in otherwise highly sealed streetscapes [10].

To further reduce the scope of this specific endeavour, this model was developed to gain a further systemic understanding of two specific urban planning objectives which are, among others, relevant in achieving resilient cities, i.e. (1) enhancing Active Mobility Comfort (AMC) and (2) increasing Bird Biodiversity (BBD). Indeed, these two urban planning goals are two significant points defined by The New Leipzig Charter under the dimension of a “green city”, which contributes to developing resilient cities in the European context [11].

2.2 Model Development

We used a three-step process to develop the system model (Fig. 1). First, we identified relevant indicators for the four domains using relevant literature and domain expertise. To identify the influence of the indicators, we categorised them into adjustable, affected, or linked types. This facilitated result analysis for determining loops in the model. "Affected" indicators undergo changes mostly indirectly through other indicators in the model (e.g., Walking/Cycling comfort). "Adjustable" indicators represent potential levers within the system that can be changed or adjusted directly (e.g., Tree Species). Finally, "linking" indicators are crucial for illustrating indirect relationships between adjustable and affected indicators.

In the second step, we looked for connections between the identified indicators in step one. The connection between indicators could be either directed or mutual, exemplifying the causes and consequences of the model. In addition to the direction of these connections, they were categorised by the connection types, which can be ++, +-, --, and +/-. Table 1 explains all possible types and directions of connections in the model.

Type	Direction	Interpretation
++ or +-	Directed	Increasing index X will increase/ decrease index Y.
+/-	Directed	One index influences the other, but the positive or negative effect is not apparent. (e.g., categorical indicators)
+/-	Mutual	Both indicators influence each other reciprocatively, but the indicators are qualitative or categorical.
++ or --	Mutual	Both indices influence each other reciprocatively and will increase /decrease correspondingly

Table 1: Typology of connections between indicators.

In the third step, we visualised the indicators and connections through a causal-loop diagram using

"Kumu"[1]. The resulting causal-loop diagram captures the indicators' causal connections (Fig.2). We used this tool to define the causal loops by focusing on two urban planning goals: 1) enhancing Active Mobility Comfort (AMC) and 2) increasing Bird Biodiversity (BBD). To improve the readability of the model, indicators were grouped into eight thematic categories: 1) Active mobility, 2) Bird community composition, 3) Urban Typology, 4) Network Structure, 5) Vegetation properties, 6) Individual characteristics, 7) Climate conditions, and 8) Spatial conditions. The thematic categories linked to urban planning goals (AMC and BBD) were set at the two extremities of the model. This visual organisation allowed for highlighting cross-discipline connections and indirect, unforeseen relationships (Fig. 2).

The causal-loop diagram was iteratively developed, involving a continuous process of refinement based on expert assessment to ensure its accuracy and alignment with established literature. Therefore, the result of step 3 helped adjust the indicators and connections along steps 1 and 2 to increase the model's accuracy (Fig.1).

The resulting model was then interpreted by observing direct and indirect connections between indicators which are relevant to the urban planning goals (Fig.2). We also identified high-impact indicators, which are indicators that are characterised as adjustable and related at the maximum second-degree to indicators of the two urban planning goals. Each connection was backed up by a literature reference, which is cited in the interpretation of the results.

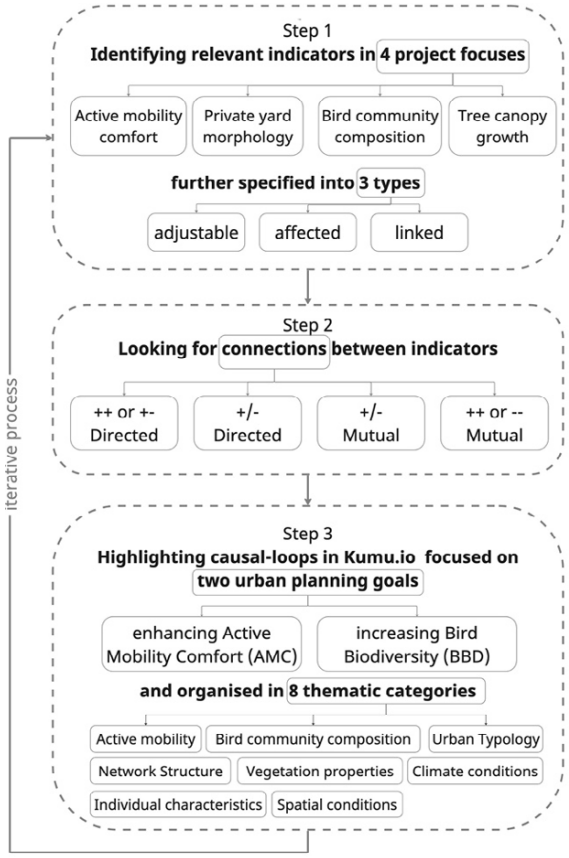

Figure 1: Flow chart of the methodological process

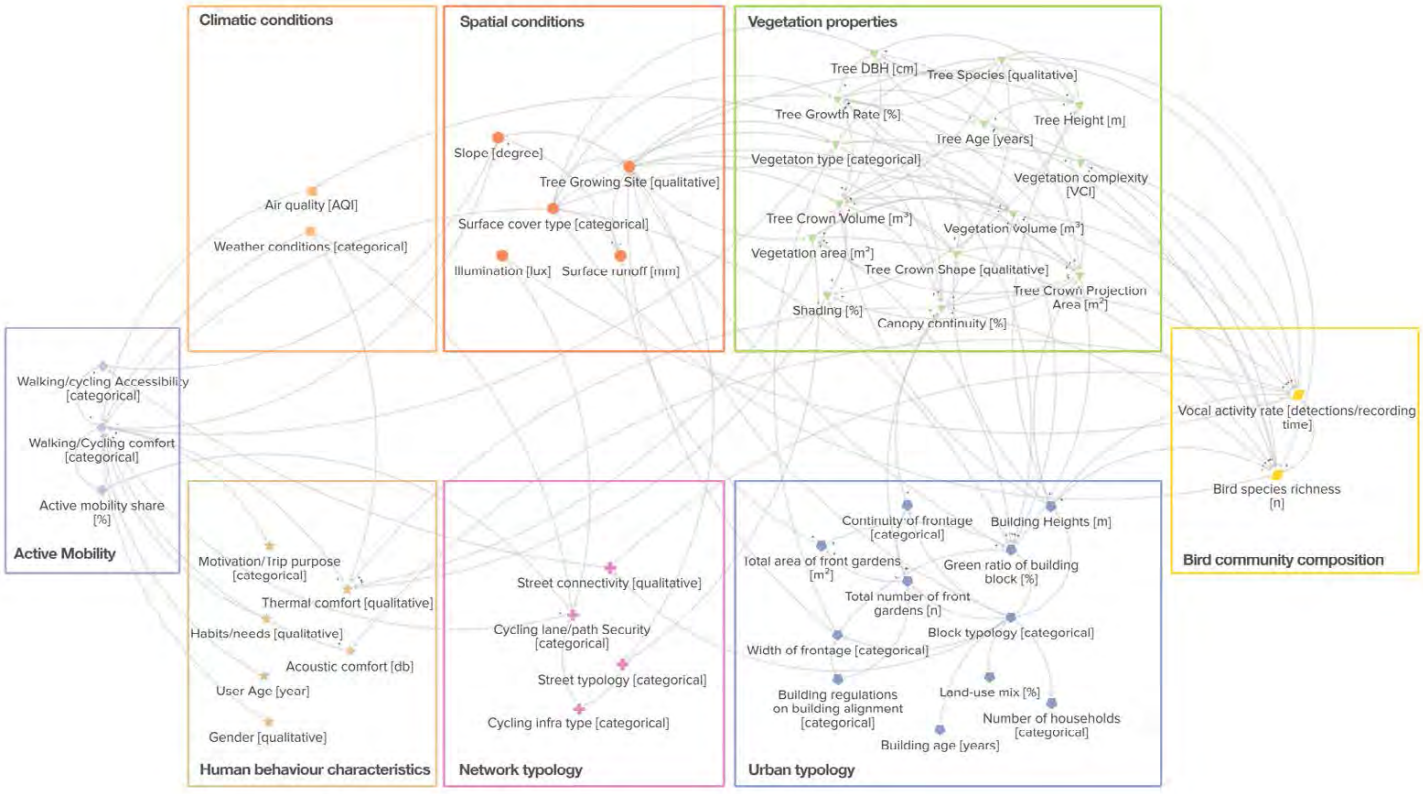

Figure 2: Visualisation of the SD model using the tool Kumu depicting the connections between indicators grouped into 8 thematic categories.

3. RESULTS AND DISCUSSION

3.1 Pursuit of Urban Planning Objectives

While The SD model illustrated known direct relationship indicators, it also highlighted indirect ones that are more surprising.

When focusing on indicators relevant to the first objective, AMC, the model illustrates indicators and relationships that are commonly described in the literature, such as the Vegetation area (Fig.3). This indicator indeed is known to participate in improving the microclimate thanks to evapotranspiration and shading [12, 9]. Our model additionally helped identify other, less obvious indirect relationships. For example, the Width of frontages is indirectly related to the indicator Walking and Cycling comfort through its influence on Vegetation type and Surface cover type (Fig. 3). Indeed, narrow frontages do not allow to plant certain tree species, and various widths of frontages allow for different usages such as parking and therefore have different surface cover types [7]. Another example of an indirect relationship is that of the Vocal activity rate of birds, which affects Active mobility comfort through its impact on Acoustic comfort (Fig. 3) [13-14].

When focusing on the second objective, BBD, the model illustrates connections between obvious indicators, also identified in the literature, such as Tree age and Species, Vegetation area, Type and Volume, and Canopy continuity. [10] Additionally to these, the results show that Building height has an unexpectedly significant relationship with Bird activity as it not only has a direct impact on bird mobility [15] but also affects Tree growth [16], which affects Vegetation volume, which then affects Bird species as identified earlier [10] (Fig.2).

3.2 Discovery of High-impact Indicators

The SD model allowed us to identify high-impact indicators that are adjustable and impact both pursued urban planning goals simultaneously. We observed ten high-impact indicators: Vegetation type, Vegetation volume, Tree species, Tree growing site, Surface cover type, Illumination, Width of frontages, Green ratio of building block, Street typology and Illumination (Fig.2). For example, the Vegetation area and the Tree growing site quality both substantially impact the Canopy continuity indicator [16, 17], which is a linking indicator related to both urban planning goals (Fig.4). Indeed, the Canopy continuity is significant for the Shading percentage and consequently affects Thermal comfort [12], which in turn affects Walking/ cycling comfort and Bird species richness by affecting their habitat [10]. This means that to achieve the urban planning goals, planners or policymakers can focus on these two adjustable high-impact indicators to achieve significant results.

Street typology is another one of these high-impact indicators as it affects the Tree growing site by changing the distance and height of the surrounding buildings [16] and the Vegetation area as different street typologies will impact the tree planting design [18]. Those indicators then have an impact on both pursued urban planning goals.

Another discovery pertains to the dual relationships of artificial light at night, represented by the indicator Illumination: it both has a positive influence on Cycling lane/path security and a negative influence on bird-related indicators, i.e. Vocal activity rate. While crucial for the safety of nocturnal pedestrians and cyclists, it represents a trade-off regarding bird habitat quality [19-20] and, therefore, requires particular attention.

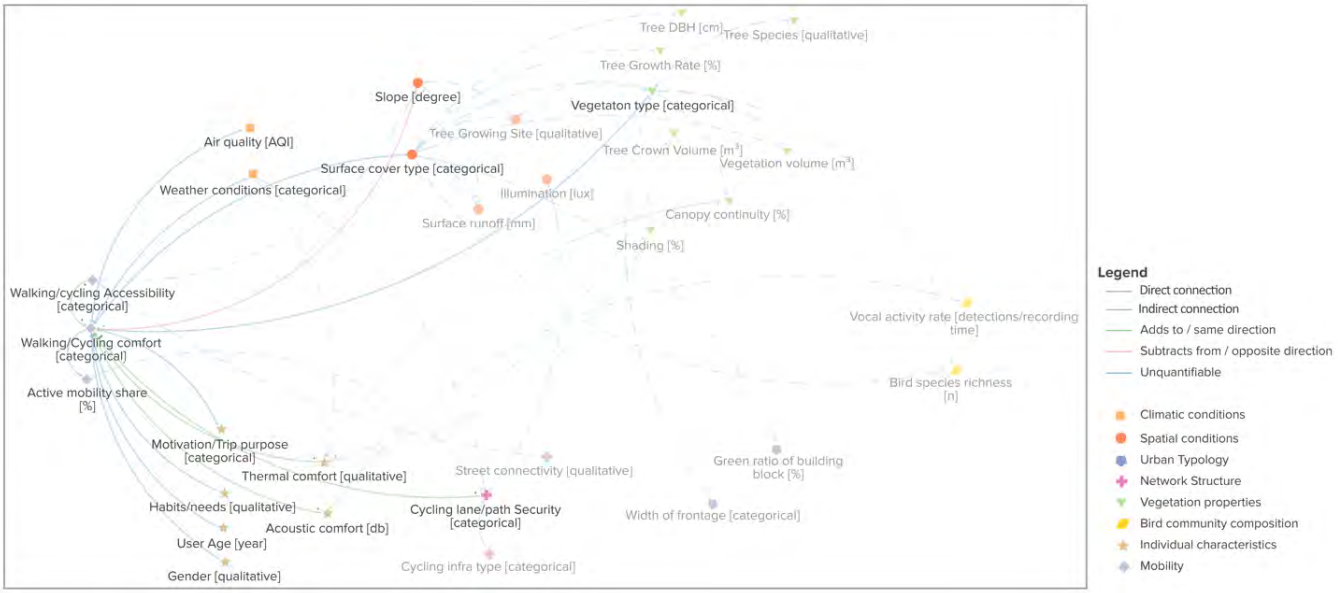

Figure 3: Direct and indirect stressors on Active mobility comfort

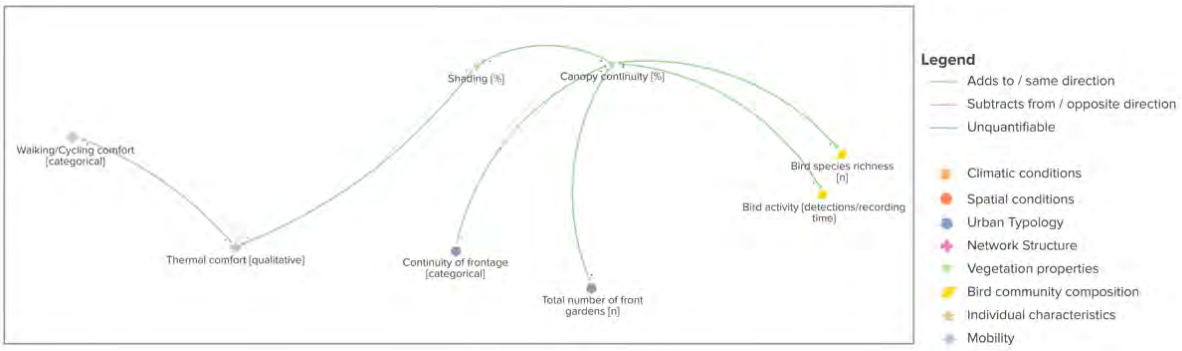

Figure 4: High impact of Canopy continuity

3.3 Implications for Interdisciplinary Research

This SD model allowed us to connect components specific to four sub-projects of a Research Training Group at the Technical University of Munich. This interdisciplinary visualisation facilitates the comprehension of correlations between research outcomes across sub-projects and scientific domains. The empirical evidence produced by each sub-project can gain meaningful interpretation through its insertion in the larger SD model, enabling the validation of anticipated correlations and the discovery of new ones. This strategic approach effectively contributes to developing a comprehensive knowledge framework specific to the interdisciplinary research group and is seen for this matter as a powerful tool for interdisciplinary collaboration. Moreover, it allows for results that are explored in a fundamental manner to be put into perspective with urban planning goals, making these results more applicable.

3.4 Process Governance

This SD model can be used as a framework for the governance of various ecosystem services that are difficult to manage by highlighting high-impact indicators that wield a substantial effect. The visualisation of the interdependencies among different indicators of the model can help decision-makers choose appropriate strategies and actions that lead to the pursued urban planning goals in practice. This is particularly important in UGI planning, where decisions can have long-term impacts.

The integrative and multidisciplinary character of the model allows for more informed policymaking, taking into consideration also indirect effects that can be overlooked in other circumstances. This aids in the effective allocation of resources to domains that may seem distantly connected to the goal but wield substantial impact. Assessing the feasibility of such changes further allows for prioritising interventions and optimising the pathway toward achieving the overall urban planning goals. Moreover, the risk of overlooking relevant actors is diminished, offering a more transparent and holistic perspective on stakeholder engagement.

3.5 Limitations and Outlook

While the proposed SD model has inherent limitations due to its scope centred around two specific urban planning objectives and four project focuses of the RTG, this deliberate framing provides clarity. It also allows the identification of potential interfaces of the model with other disciplines not presently incorporated but which can be potentially considered in the future. An illustration of this is evident in the omission of urban water systems, which would significantly impact many indicators in the Vegetation properties category. This illustrates potential connection points for further extending this model. Additionally, it's worth noting that another limitation of this system model lies in its conceptual nature. In the subsequent stage, it necessitates being populated with measurements to advance towards conducting behaviour reproduction tests, thereby verifying and quantifying the relationships between indicators within a local context.

4. CONCLUSION

In conclusion, the system dynamics model discussed in this paper proves to be a valuable tool for interdisciplinary research by elucidating high-impact indicators and highlighting synergies, trade-offs, and potential side effects of UGI in streetscapes. Focusing on two urban planning objectives — enhancing Active Mobility Comfort and increasing Bird Biodiversity — serves as a proxy to illustrate complex relationships and interdependencies between disciplines. This model can serve as a basis for further models integrating more domains and illustrating increasingly complicated relationships between indicators. The developed conceptual framework aids decision-making by identifying adjustable indicators within urban spaces and creating a baseline for interdisciplinary collaborative governance. This enhanced understanding, facilitated by system dynamics modelling in interdisciplinary research, is crucial for addressing complex challenges, such as transforming urban streets into integral components of Urban Green Infrastructure and enhancing urban resilience.

ACKNOWLEDGMENTS

This research is funded by the German Research Foundation through the Research Training Group (GRK 2679/1) “Urban Green Infrastructure - Training Next Generation Professionals for Integrated Urban Planning Research”.

REFERENCES

1. McPhearson T., Iwaniec D.M., Hamstead Z.A., Berbés-Blázquez M. A., Muñoz-Erickson T.A., Mannetti L., Grimm N., (2021). Vision for Resilient Urban Futures. In Hamstead, Z. A., Iwaniec D. M., McPhearson T., Berbés-Blázquez M., Cook E. M., and Muñoz-Erickson T. A., eds. Resilient Urban Futures. The Urban Book Series. Cham: *Springer International Publishing*.

2. Jato-Espino, D., Capra-Ribeiro, F., Moscardó, V., del Pino, L. E. B., Mayor-Vitoria, F., Gallardo, L. O., Carracedo, P., & Dietrich, K. (2023). A systematic review on the ecosystem services provided by green infrastructure. *Urban Forestry & Urban Greening.*

3. Pogačar, K., & Šenk, P. (2021). Sustainable Transformation of City Streets – Towards a Holistic Approach. In: Rotaru, A. (eds) Critical Thinking in the Sustainable Rehabilitation and Risk Management of the Built Environment. *CRIT-RE-BUILT 2019. Springer Series in Geomechanics and Geoengineering*.

4. Eisenman, T. S., Coleman, A. F., & LaBombard, G. (2021). Street Trees for Bicyclists, Pedestrians, and Vehicle Drivers: A Systematic Multimodal Review. *Urban Science*, 5(3): p. 56.

5. Pejic Bach, M., Tustanovski, E., Ip, A.W.H., Yung, K.-L. and Roblek, V. (2020). System dynamics models for the simulation of sustainable urban development: A review and analysis and the stakeholder perspective*. Kybernetes*, 49(2): p. 460-504.

6. Schwarz, N., Haase, D. and Seppelt, R. (2010). Omnipresent sprawl? A review of urban simulation models with respect to urban shrinkage. *Environment and Planning B: Planning and Design*, 37(2).

7. Blanc-Reibel, C., and Haegel. O. (2018). Vorgärten, Privative Green Spaces in Neustadt (Strasbourg, France). A Century of Practices in the Heart of the City. In The Urban Garden City, edited by Sandrine Glatron and Laurence Granchamp*. Cities and Nature*. Cham: Springer International Publishing, p. 33–51.

8. Fairbairn, A., Meyer.& Mühlbauer, M, Jung, K.,& Apfelbeck., , Berthon, K., , Bungenstock, P., Frank, A., Guthmann, L., Jokisch, J., Kerler, K., Matejka, J., Müller, N., Obster, C., Unterbichler, M., Webersberger, J., Weisser, W. (in prep). Urban biodiversity is affected by human-designed features of public squares.

9 Morakinyo, T. E., Kong, L., Lau, K. K.-L., Yuan, C., & Ng, E. (2017). A study on the impact of shadow-cast and tree species on in-canyon and neighborhood’s thermal comfort.*Building and Environment*, p. 115, 1–17.

10. Beninde J, Veith M, Hochkirch A (2015). Biodiversity in cities needs space: a meta-analysis of factors determining intra-urban biodiversity variation. *Ecology Letters,* 18: p. 581–592.

11. The New Leipzig Charter, the transformative power of cities for the common good. *Adopted at the Informal Ministerial Meeting on Urban Matters* on 30 November 2020.

12. Moser, A., Rötzer, T., Pauleit, S., & Pretzsch, H. (2015). Structure and ecosystem services of small-leaved lime (Tilia cordata Mill.) and black locust (Robinia pseudoacacia L.) in urban environments. *Urban Forestry & Urban Greening,* 14(4): p. 1110–1121.

13. Chau, C.K., Leung, T.M., Chung, W.K., Tang, S.K. (2023). Effect of perceived dominance and pleasantness on the total noise annoyance responses evoked by augmenting road traffic noise with birdsong/stream sound. *Applied Acoustics,* 213:109650.

14. Liu, J., Wang, Y., Zimmer, C., Kang, J., & Yu, T. (2019). Factors associated with soundscape experiences in urban green spaces: A case study in Rostock, Germany. *Urban Forestry & Urban Greening*, 37: p. 135–146.

15. Merkens, L., Mimet, A., Bae, S., Fairbairn, A., Mühlbauer, M., Lauppe, L., Mesarek, F., Stauffer-Bescher, D., Wehrmaker, P., Hauk, T.E., Weisser, W.W. (in prep). Connectivity at home: A data-driven connectivity modeling framework for home range movements in fragmented landscapes.

16. Franceschi, E., Moser-Reischl, A., Rahman, M.A., Pauleit, S., Pretzsch, H., and Rötzer, T. (2022). Crown Shapes of Urban Trees-Their Dependences on Tree Species, Tree Age and Local Environment, and Effects on Ecosystem Services. Forests.

17. Rötzer, T., Rahman, M. A., Moser-Reischl, A., Pauleit, S., & Pretzsch, H. (2019). Process based simulation of tree growth and ecosystem services of urban trees under present and future climate conditions. *Science of The Total Environment*, 676: p. 651–664.

18. Ng, WY., Chau, C.K., Powell, G., and Leung, T.M. (2015) Preferences for Street Configuration and Street Tree Planting in Urban Hong Kong. *Urban Forestry & Urban Greening* 14(1): p. 30–38.

19. Dominoni, D. M., Carmona-Wagner, E. O., Hofmann, M., Kranstauber, B., & Partecke, J. (2014). Individual-based measurements of light intensity provide new insights into the effects of artificial light at night on daily rhythms of urban-dwelling songbirds. *Journal of Animal Ecology*, 83(3): p. 681–692.

20. McLaren, J. D., Buler, J. J., Schreckengost, T., Smolinsky, J. A., Boone, M., Emiel van Loon, E., Dawson, D. K., & Walters, E. L. (2018). Artificial light at night confounds broad-scale habitat use by migrating birds. *Ecology Letters*, 21(3): p. 356–364.

PLEA 2024 WROCŁAW
(Re)thinking Resilience

Bridging urban planning and just energy transition strategies

Key urban framework of Sustainable Energy Action Plans for Polish Tricity

JULIA KUREK[1], JUSTYNA MARTYNIUK-PĘCZEK[1], NATALIA SOKÓŁ[1]

[1]Gdańsk University of Technology, Gdańsk, Poland

ABSTRACT: The imperative to integrate urban planning with sustainable energy management is increasingly recognized as vital in addressing contemporary environmental and energy challenges. Sustainable Energy Action Plans (SEAPs) have been instrumental in facilitating this integration, successfully implemented by numerous European cities. These plans play a crucial role in defining urban energy strategies, setting objectives for renewable energy usage, and reducing greenhouse gas emissions. This paper explores the integration of SEAPs within the Tri-City Metropolitan Area in Poland, which is characterized by significant environmental issues including pollution and high heat energy import dependency, making it a critical case study. We applied critical case studies analysis and comparative methods to analyze SEAPs from twelve European alongside the existing plans from Tricity (Gdańsk, Gdynia, Sopot). Our analysis revealed divergent approaches to local energy strategies, highlighting the successes and gaps in Tricity's current plans. Based on our findings, we propose a novel urban framework for updated SEAPs in Tricity. This framework emphasizes integrated energy management, grassroots actions, and structured regulatory approaches. It aims to enhance local energy autonomy and foster robust community engagement, providing a model that could be adapted globally for sustainable urban energy development.
KEYWORDS: Energy, Energy Transition, Sustainable Energy Action Plans (SEAPs), Urban Planning, Energy Management Strategies

1. INTRODUCTION

In the face of rapid urbanization, growing global environmental challenges, the integration of urban planning and sustainable energy management also at city level has become more crucial than ever. This need for integration is made even more urgent by the global imperative for energy transformation, highlighted by international climate agreements. Furthermore, the ongoing war in Ukraine has added to the urgency, particularly in the context of energy security and the increasing challenges related to natural resources. These issues, coupled with the impacts of climate change, underscore the importance of aligning urban development with energy-efficient and environmentally conscious practices. Cities, as hubs of innovation and economic activity, must therefore play a crucial role in shaping these sustainable futures. In light of these facts, EU energy and environmental policies aim for sustainability and climate neutrality, focusing on reducing emissions, enhancing renewable energy, and improving efficiency. The Paris Agreement [1] and the European Green Deal [2] are central, targeting a climate-neutral EU by 2050 and addressing climate change. Initiatives also promote sustainable energy use in cities and buildings, contributing to an integrated strategy for a resilient and green future.

This paper addresses the integration of sustainable urban planning and energy management at city level, focusing on the comparison of current cities energy and climate strategies among 8 European cities leading in this area and Tricity Metropolitan Area (TMA) located in northern in Poland. Poland is actively pursuing an energy shift, yet the transition from its long-established coal reliance is complex, influenced by economic and cultural factors, and a robust coal industry infrastructure. The situation is further strained by the war in Ukraine and gas supply issues, adding to the challenges of diversifying Poland's energy mix and moving towards more sustainable sources.

The Polish Tricity exhibits a unique morphology and is characterized by the contiguous urban layout of Gdańsk, Sopot, and Gdynia. **Tricity** faces also significant environmental and energy challenges such as environmental pollution and reliance on energy imports [3]. In Tricity there is also **lack of updated Sustainable Energy Action Plans (SEAPs).**

This study aims to provide clear guidelines for sustainable urban and energy development by applying a novel methodology for creating effective, updated SEAPs for Tricity, and taking insights and general trends from successful plans across European cities.

1.1 The importance Sustainable Energy Action Plans (SEAP) and analogical cities strategic energy and climate plans

Sustainable Energy Action Plans (SEAPs) are strategic frameworks guiding cities to reach energy and climate goals, including emissions reduction and energy efficiency. These plans, essential for

facilitating a city's transition to a low-carbon economy, are typically driven by commitments to initiatives like the Covenant of Mayors for Climate and Energy in Europe (SEAPs). Particularly, SEAPs were initiated as a response to global climate change challenges, SEAPs have gained prominence, particularly with the Covenant of Mayors for Climate and Energy in Europe, starting in 2008. This initiative motivates cities to aim for at least a 40% reduction in CO_2 emissions by 2030. Regardless of their varied names (SEAP, Climate and Energy Plans etc.), they all aim for a sustainable, low-carbon future. SEAPs and analogical documents are essential for cities to contribute to national and international climate goals, offering local benefits like improved air quality and energy security. Initially focusing on energy consumption and renewable energy, recent SEAPs have evolved to include sustainable transportation, waste management, and water conservation.

The effectiveness and importance of SEAPs (and analogical documents) in energy transition and climate change mitigation are well-documented in scientific literature. For instance, Kona and others [4], analysed the climate mitigation trajectory of Covenant of Mayors (CoM) signatories, highlighting the significant role of these initiatives in adhering to the Paris Agreement commitments. Similarly, Palermo and others [5] assessed 315 SEAP policies in cities participating in the CoM initiative, shedding light on the various types of policies adopted and their effectiveness. Despite the frequent coverage of Sustainable Energy Action Plans (SEAPs) in academic literature, there remains a notable research gap in the detailed examination of SEAPs in the Tricity area, whose unique morphological layout, ecological considerations, economic factors, and social dynamics present a distinct case study yet to be thoroughly explored.

2. METHODOLOGY

We used critical case studies analysis and comparative analysis methods to study successfully implemented SEAPs (Sustainable Energy Action Plans) and analogical documents of European cities. Based on them we drew conclusions and proposed a novel urban framework (including trends and 7 common areas of change) for creating updated SEAPs in Tricity. In total we analysed 12 municipal and cities sustainable energy, climate and urban plans of following European cities: Malmö [6], Stockholm [7], Oslo [8], Grenoble [9], Rennes [10], Freiburg [11], Vienna [12], London [13] along with Tricity SEAPs of: Gdańsk [14], Gdynia [15] and whole Tricity [16] (Fig.1.). The SEAP (Sustainable Energy Action Plan) of Sopot was not available at the time of analysis due to technical reasons. It is important to note that each city in the Tricity area - Gdańsk, Sopot, and Gdynia - has its own individual SEAP, and they collectively share a common SEAP as part of the Tricity metropolis. The criteria of choosing such international examples for case studies were: similar planning culture in Europe, location in cool temperate climate zone as Tricity (according to Passsivhaus Institute 2016), accessibility of existing updated policies and continuation of their municipal energy policy on district level (erecting new sustainable energy housing district according to this policy).

Figure 1: Map with locations of cities whose SEAPs were analysed in this study.

2.2 Tricity as a main case study area

Tricity metropolis is the fastest growing area of northern Poland, an internationa rar k, thus interweaving in the network of metropolitan connections occupies a place in networks of various scales. It has developed connections both regionally, nationally and internationally. According to Central Statistical Office [17], **Tricity is experiencing the most dynamic suburbanization in whole Poland**. This intense growth in residential areas, is driven by a significant housing market deficit. Unfortunately it is leading to a rapidly and chaotically evolving suburban landscape that is not adequately supported by corresponding infrastructural expansion. A large part of the metropolis is covered by landscape parks and nature reserves, with large share of Natura 2000 protected areas located within the city of Gdańsk. In Tricity, the number of certified green buildings, primarily LEED and BREAM, is steadily increasing. Additionally, the opening of a waste incineration plant at the Szadółki landfill is planned for 2024. This facility will enable the disposal of large amounts of high-energy waste while simultaneously generating clean energy (Fig. 2).

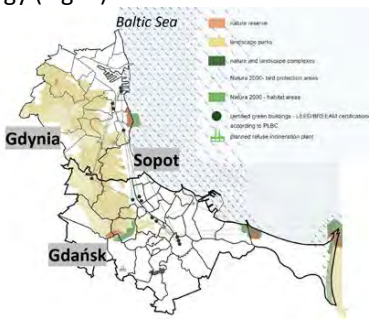

Figure 2: Environmental protection in Tricity metropolis. Authors' elaboration.

Several major plants contributing significantly to environmental pollution in Gdańsk were identified in a recent study on Tricity's environmental issues. These facilities have contributed to **exceeding the**

annual PM10 dust concentration standards, with the most critical levels observed during both the heating and summer seasons [18]. The primary sources of air pollutants in this region are identified as the high-speed roads traversing the Tricity and low emission form heating. Furthermore, the study highlights a significant flood risk, particularly in the coastal areas of Gdynia and the downtown regions of Gdańsk. These areas are notably vulnerable to the impacts of climate change, emphasizing the urgent need for comprehensive climate strategies (Fig.3.). Tricity faces energy **challenges due to its reliance on external electricity supplies from other Polish regions (up to 50%),** while simultaneously holding significant potential for local renewable energy development [18].

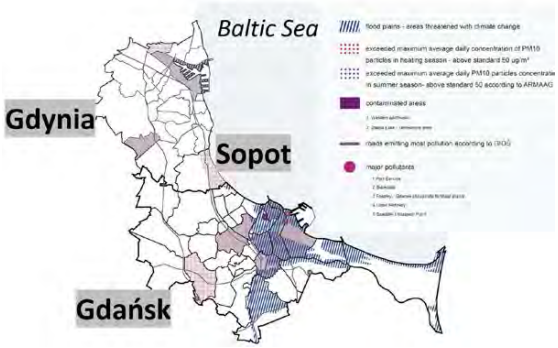

Figure 3: Environmental hazards and pollution in Gdańsk Metropolis. Authors' elaboration.

2.3. European Reference Cities: Comparing Tricity's Opportunities and Challenges

The chosen European cities leading in sustainable urban and energy planning and having developed plans similar to SEAP- Malmö, Stockholm, Oslo, Grenoble, Rennes, Freiburg, Vienna, and London - share common characteristics with Tricity, such as a European planning culture and a temperate climate. However, they **differ in having established sustainable housing districts which Tricity currently lacks (Tab.1.)**. We used this these cities as case studies to assess SEAPs, providing insights for Tricity, using comparative analysis (presented in further tables). While the analysed cities differ from the Tricity area in many aspects such as exact population size and geographical location, there are similarities that make them relevant for comparison in ecological, energy, and urban planning contexts, such as: commitment to sustainable development:, development of sustainable public transport, initiatives for energy efficiency, urban planning challenges (i.a. need for the revitalization of degraded areas, spatial development, and ensuring affordable housing amidst rising real estate prices).

Table 1: Comparative Analysis of basic information on cities chosen for further studies.

City	*Country*	*Number of inhabitants of the city*	*Sustainable districts located in the city*
Malmö	SE	344 166	Bo01, Västra Hamnen
Stockholm	SE	975 551	Hammarby Sjöstad
Oslo	NO	634 293	Pilestredet Park
Grenoble	FR	158 198	Zac de Bonne
Rennes	FR	215 366	La Courrouze
Freiburg	DE	230 241	Vauban
Vienna	A	1 920 949	Seestadt Aspern
London	UK	9 541 000	BedZED
Gdańsk	PL	486 345	**not present**
Gdynia	PL	242 141	**not present**
Tricity	PL	~1 500 000	**not present**

3. RESULTS

3.1 Seven common areas of sustainable urban and energy development in analysed SEAP documents

During our critical analysis of SEAPs of chosen cities we observed the occurrence of 7 common areas of interdisciplinary approach. We identified these 7 areas as critical for sustainable urban and energy development:

- **Sustainable planning and spatial management (1)**
- **Building structures and their surroundings (2)**
- **Sustainable energy systems (3).**
- **Sustainable transport (4),**
- **Environmental protection (5),**
- **Research and Cooperation (B&R) (6),**
- **Fair policy and society (7).**

3.1. SEAPs and analogical documents in European Cities – comparative analysis of results in tables.

Table 2: Basic characteristics on SEAP plans – sustainable planning and spatial management (1).

City	I Type of SEAP plan	II SEAP validity period	III Main scales of SEAP interventions	IV Building interventions
Malmö	P, W	-2030	C (D)	E, N
Stockholm	P, W	-2040	C (D)	E, N
Oslo	P	-2030	C	E, N
Grenoble	W, M	-2030	C,D ,G, B	E, N
Rennes	P,W	-2024	C,D, G, B	E, N
Freiburg	P,W, M	- 2050	C, D, G, B	E, N
Vienna	P, W	n.d. 'future'	C, D, G, B	E, N
London	P, W	-2047	C, D, G, B	E, N
Gdańsk	P	2018 **expired**	**C,B**	**E**
Gdynia	P, W	2018 **expired**	**C,B**	**E**
Tricity	P	2018 **expired**	**C,B**	**E**

Abbreviations:
I - masterplan (M), sustainable energy plan (P), webpage (W)
III- city (C), district (D), neighbourhood, group of buildings (G), building (B)
IV- existing (E) and new (N) residential buildings

*Table 3: Cities main sustainable energy goals in their SEAPs**.(1)***

City	Energy autonomy	Reduction of GHG	Carbon neutrality	Climate neutrality	Use of RES
Malmö	by 2030	+	+	+	+
Stockholm	n.d.	+	by 2040	+	+
Oslo	n.d.	+	-	+	+
Grenoble	n.d.	+	-	+	+
Rennes	n.d.	+	-	+	+
Freiburg	by 2050	+	+	+	+
Vienna	by 2050	+	+	+	+
London	n.d.	+	by 2030	+	+
Gdańsk	n.d.	+	-	-	+
Gdynia	n.d.	+	-	-	+
Tricity	n.d.	+	-	-	+

*Table 4: Building Structures and Surrounding Environment - main goals of cities SEAPs **(2).** Builidings':*

City	Energy Demand Reduction	Energy retrofitting	Energy Efficiency	Materials' LCA
Malmö	+	+	+	+
Stockholm	+	+	+	
Oslo	+	+	+	
Grenoble	+	+	+	
Rennes	+	+	+	
Freiburg	+	+	+	
Vienna	+	+	+	+
London	+	+	+	+
Gdańsk	+	+	+	+
Gdynia	+	+	+	
Tricity	+	+	+	+

*Table 5: Sustainable Energy System cities' SEAPs **(3)**. The use of renewable energy sources (RES):*

City	PV and solar collectors	Wind Energy	Biomass/Bio gas	Geothermal Energy	Wave Energy	Hydrogen Electrolysis	Hydropower
Malmö	+	+	+	+	+	+	
Stockholm	+		+	+		+	
Oslo	+		+				
Grenoble	+		+	+			
Rennes	+		+				
Freiburg	+	+	+	+			
Vienna	+	+	+	+		+	
London	+		+			+	
Gdańsk	+	+	+	+			+
Gdynia	+	+	+	+			
Tricity	+	+	+	+			+

*Table 6: Sustainable Energy System of cities' SEAPs **(3).** The use at the city scale of:*

City	Utilization of waste heat/ cooling	Local energy generation	Smart energy systems	Urban district heating network
Malmö	+	+	+	+
Stockholm		+	+	+
Oslo		+	+	+
Grenoble	+	+	+	+
Rennes		+		+
Freiburg		+		+
Vienna	+	+	+	+
London	+	+	+	+
Gdańsk			+	+
Gdynia		+	+	+
Tricity			+	+

Abbreviations: H.C. - Housing cooperatives

*Table 7: Sustainable transportation issues in cities' SEAPs. **(4)***

City	Priority to pedestrian and bicycle movement	Eco-Public transportation*	Promotion of individual vehicles powered by biofuels and electricity**
Malmö	+	+	+
Stockholm	+	+	+
Oslo	+	+	+
Grenoble	+	+	
Rennes	+	+	
Freiburg	+	+	+
Vienna	+	+	+
London	+	+	+
Gdańsk	+	+	
Gdynia	+	+	
Tricity	+	+	

Eco-public transportation: support for ecological transport using biofuels, hydrogen, or electrified transport utilizing locally generated renewable energy sources; support for convenient and frequent public connections

****powered by local renewable energy sources***

*Table 8: Major environmental protection issues in SEAPs **(5).***

City	Sustainable Water Management*	Supporting Biodiversity	Waste Recycling, Circular Economy
Malmö	SP	SP	SP
Stockholm	SP	SP	+
Oslo	+	+	+
Grenoble	SP	SP	SP
Rennes	+	+	+
Freiburg	+	+	+
Vienna	+	+	+
London	+	+	+
Gdańsk	+	SP	+
Gdynia	+	-	-
Tricity	+	+	+

Abbreviations: SP – The City has formulated and disseminated separate program addressing this issue (not included in SEAP).

****Sustainable Water Management: utilization of grey and/or black water and rainwater retention***

Table 9: Research and cooperation. Interdisciplinary collaboration among stakeholders from various sectors in cities' SEAPs. (6) Sectors:

City	Energy	Construction	City / Municipality	Research	Business	Citizens
Malmö	+	+	+	+	+	+
Stockholm	+	+	+		+	+
Oslo	+	+	+	+	+	+
Grenoble	+	+	+	+	+	+
Rennes	+	+	+	+	+	+
Freiburg	+	+	+	+	+	+
Vienna	+	+	+	+	+	+
London	+	+	+	+	+	+
Gdańsk	+	+	+	+	+	H.C.
Gdynia			+			
Tricity	+	+	+	+	+	H.C.

Abbreviations: H.C. - Housing cooperatives

Table 10: Fair Policy and Society in cities' SEAPs (7).

City	Support programs for eco-solutions	Resident participation	Ecological education for residents	Publicly accessible guidance*
Malmö	+	+	+	+
Stockholm	+	+	+	+
Oslo	+	+	+	+
Grenoble	+	+	+	+
Rennes	+	+	+	+
Freiburg	+	+	+	+
Vienna	+	+	+	+
London	+	+	+	
Gdańsk	+		+	SP
Gdynia	+		+	SP
Tricity	+		+	SP

Abbreviations: SP – The City has formulated and disseminated separate program addressing this issue (not included in SEAP).

****advisory on planning and design for residents regarding ecological building practices***

3.3 Comparative analysis of cities' SEAPs (Tables 2-10).

Assessing SEAPs across Europe: trends, challenges, and opportunities.

The Sustainable Energy Action Plans (SEAPs) analyzed in various European cities, including Tricity, reveal a range of strategies and priorities. A prevailing form of SEAP presentation is the plan format, while webpages and maps are less common. The majority of these plans are set to be active until at least 2030, contrasting with the outdated plans of Tricity, which currently lack prospects for updates (Tab. 2.). SEAPs interventions primarily focus on the city level, occasionally extending to districts, neighbourhoods, and buildings. The guidelines typically address both new and existing residential buildings, but in Tricity, they are limited to existing structures only (Tab. 2.)

Cities like Malmö, Freiburg, and Vienna stand out for their ambitions towards local energy independence and carbon neutrality, an approach not as commonly observed elsewhere. All cities commit to reducing greenhouse gas emissions and utilizing renewable energy sources (RES) (Tab. 3.). This

commitment extends to buildings, where energy demand reduction, retrofitting, and efficiency are universally prioritized. However, the inclusion of buildings material's Life Cycle Assessment (LCA) in SEAPs is not as widespread (Tab. 4.). The plans universally endorse the use of renewable energy, particularly photovoltaics (PV), solar collectors, biomass, and biogas (Tab. 5.). Urban district heating networks are consistently featured across all cities. Local energy generation is a common goal, though not shared by Gdańsk and Tricity. Most cities, excluding Rennes and Freiburg, are keen on implementing smart energy systems (Tab. 6.). A consistent theme across all cities is also the prioritization of pedestrian and bicycle movement, alongside eco-friendly public transportation. The promotion of biofuel and electric-powered individual vehicles, using local renewable sources, is prevalent, although not uniformly adopted by cities like Tricity, Grenoble, and Rennes (Tab. 7.).

Programs for Sustainable Water Management and biodiversity support are commonplace, with Gdynia being an exception in terms of biodiversity initiatives. All cities, except Gdynia, incorporate waste recycling and circular economy strategies in their plans (Tab. 8.). Interdisciplinary collaboration among various sectors, including energy, construction, city/municipality, research, business, and citizens, is a key feature, with Gdynia again being the outlier for not declaring such collaboration (Tab. 9.). Support for eco-solutions, ecological education, and publicly accessible guidance on ecological building practices is a unanimous focus in these cities. However, resident participation in the SEAP process is almost universally emphasized, with Tricity as the notable exception (Tab. 10).

This comprehensive analysis highlights the diverse approaches and focuses of SEAPs across Europe, underscoring the similarities and differences between these cities and the Tricity area, and reflecting the range of opportunities and challenges in pursuing sustainable urban energy development.

4. DISCUSSION

4.1 Divergent approaches to SEAPs and their impact on local energy strategies

The analysis of Sustainable Energy Action Plans (SEAPs) in various European cities, including Tricity, demonstrates significant divergences in sustainable development planning and implementation. Cities like Malmö, Freiburg, and Vienna, with their ambitious strides towards energy independence and carbon neutrality, contrast with other regions. This disparity likely results from variations in local governmental policies, public awareness, economic capabilities, or environmental priorities. A deeper understanding of these determinants is crucial for tailoring effective SEAPs, particularly for areas like Tricity, which show a lag in updating their plans.

4.2. The role of interdisciplinary collaboration and citizen engagement in SEAPs

The study highlights the significance of interdisciplinary collaboration and resident participation in SEAPs. Cities engaging actively in cross-sector partnerships and involving citizens in the SEAP process tend to demonstrate more comprehensive and inclusive strategies. The absence of such collaboration in areas like Gdynia suggests a gap in maximizing SEAP effectiveness. The barriers to collaboration and participation might relate to policy limitations, a lack of awareness, or insufficient infrastructure to facilitate engagement. Addressing these barriers could enhance the inclusivity and effectiveness of SEAPs.

5. CONCLUSION

5.1. Enhancing Tricity's Sustainable Energy Action Plans (SEAPs): a comprehensive approach

Tricity should undertake several key steps to enhance its Sustainable Energy Action Plans (SEAPs). Firstly, there is a need to update the existing SEAPs, expanding their scope from not just the city and individual buildings but also to include districts and neighbourhoods. This should involve creating guidelines for new residential constructions, which could aid in energy transition and potentially lead to the creation of eco-districts. Furthermore, Tricity should explore strategies for energy autonomy to reduce its dependence on centralized energy supplies, a move that is particularly crucial for suburban areas. Local energy generation needs to be a focus, especially in Gdańsk and the wider Tricity region, along with the utilization of waste heat and cooling. Lastly, emphasizing resident participation in the SEAP process across the entire Tricity area is vital for ensuring community engagement and support for these sustainable initiatives.

5.2. Key urban framework for sustainable energy action plans in Tricity

Based on our study and conclusions from comparative analyses we created updated key urban framework for creating SEAPs in Tricity (Fig.4.).

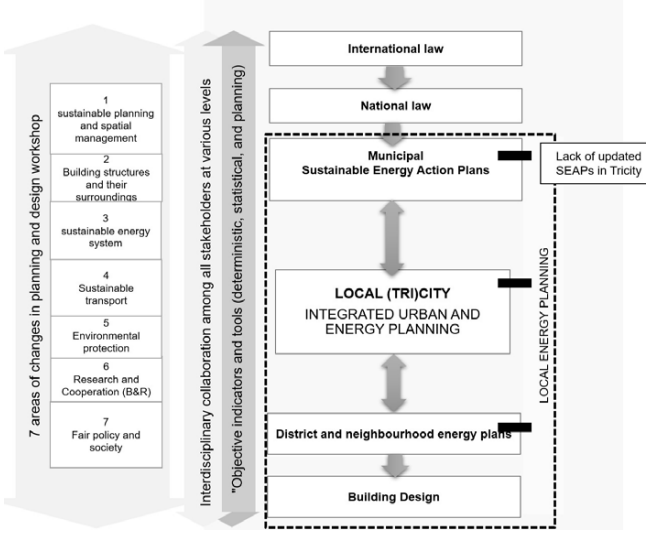

Figure 4: Key urban frameworks for TMA, detailing the elements of local integrated urban and energy planning at the municipal, city, and district levels.

The key urban framework in the just energy transition era should include

- Integrated energy management initiatives.
- Grassroots actions that involve stakeholder cooperation across sectors, including participation and education of end-users.
- Top-down strategies implementing structured regulations, standards, and programs.
- An integration of issues from the seven common areas of European SEAPs into the planning process.
- A local focus that includes the development of city-wide Sustainable Energy Management Plans.
- Use of objective tools: planning, statistical, and energy, which when skilfully integrated, can help achieve set goals.

Our research presents significant key urban framework as a starting point for sustainable energy management, that can be applicable globally with local adjustments. The findings emphasize the need for integrated urban and energy planning, and the adoption of sustainable energy action plans, highlighting the role of collective thinking in sustainable urban development. Our research underlines the necessity of adopting comprehensive, forward-looking, and sustainable energy action plans, and it affirms the importance of fostering a culture of collective thinking, learning, teaching, and leadership in sustainable urban development.

REFERENCES

1. Paris Agreement," United Nations, Paris, France, Dec. 2015. [Online]. Available: https://unfccc.int/process-and-meetings/the-paris-agreement/the-paris-agreement

2. European Commission, "The European Green Deal," Brussels, Belgium, Dec. 2019. [Online]. Available: https://ec.europa.eu/info/strategy/priorities-2019-2024/european-green-deal_en

3. Board of the Pomeranian Voivodeship. (2021). Regional Strategic Program in the Field of Energy and Environment, Resolution No. 756/271/21, July 29.

4. Kona, A., Bertoldi, P., Monforti-Ferrario, F., Rivas, S., Dallemand, J. F. (2018). "Covenant of mayors signatories leading the way towards 1.5 degree global warming pathway," Sustainable Cities and Society.

5. Palermo, V., Bertoldi, P., Apostolou, M., Kona, A., Rivas, S. (2020). "Assessment of climate change mitigation policies in 315 cities in the Covenant of Mayors initiative," Sustainable Cities and Society.

6. Emanuelson, J., Olsbäck, M. (2022). "Energy Strategy for Malmö 2022–2030." Available: https://malmo.se [15 May 23]

7. City Executive Office of Stockholm. (2016). "Strategy for a fossil-fuel free Stockholm by 2040." Available: http://international.stockholm.se [15 May 2023]

8. Oslo City Council. (2020). "Climate Strategy for Oslo towards 2030." Available: https://www.klimaoslo.no [15 May 2023]

9. Grenoble Alpes Métropole. "Climate / Air / Energy." Available: https://www.grenoblealpesmetropole.fr [15 May 2023]

10. Rennes Métropole. "The climate plan of Rennes Métropole." Available: https://metropole.rennes.fr [15 May 2023]

11. Freiburg. (2002). Greencity.

12.Wien. "Wiener Klimafahrplan bis 2040." Available: https://www.wien.gv.at [15 May 2023]

13. London City Hall. "Energy Planning Guidance." Available: https://www.london.gov.uk [15 May 2023]

14. Rackiewicz, I., Bartocha, A., Jaśkiewicz, J., Płuska, E., Rosicki, M., Mostowska, A., Schönfelder, T., Szatkowska, I., Załupka, M., Hutyra, K., Sicińska, W. (2015). "Low-Emission Economy Plan for the Gdańsk Metropolitan Area." ATMOTERM S.A., Gdańsk.

15. BMTcom Sp. z o.o. (Leader), PVO Sp. z o.o. (2016). "Low-Emission Economy Plan for the City of Gdynia 2015-2020."

16. Gdańsk, Gdynia, Sopot Program. (2016). "Low-Emission Economy Program for the Gdańsk-Gdynia-Sopot Metropolitan Area."

17. Polish Central Statistical Office. (2014). "Population Projection 2014-2050." Demographic Surveys and Labour Market Department (Ed.).

18. Board of the Pomeranian Voivodeship. (2021). Resolution No. 756/271/21 of July 29, 2021, on the Adoption of the Regional Strategic Program in the Field of Environmental and Energy Security, Rationale to Regional Strategic Program.

PLEA 2024 WROCŁAW
(Re)thinking Resilience

Perceive The Mechanism of Air Movement of Classroom
Teaching Trials for Understanding Built Environment After COVID-19

GENKU KAYO[1] NOBUE SUZUKI[2]

[1] Tokyo City University, Yokohama, Japan
[2] Freelance, Tokyo, Japan

ABSTRACT: The interest in indoor air quality (IAQ) to keep a healthy condition gets more popular in the wake of COVID-19 pandemic. The article describes the challenge to add the content of ventilation in which students can realise the mechanism of air movement and perceive the actual volume of air change happening in the classroom where the student stayed during the lecture. The article reported the application cases for two student groups one with non-engineering background, and another with engineering background. The figure generated by the trial clearly shows the behaviour and applicable to explain the necessity of ventilation. The result of answer against the question "the contents of the lecture were understandable." shows that more than 60% of students evaluated the contents positively. It is supposed that the procedure of the lecture made the students easy to understand the mechanism of air movement and the model. By providing the opportunity to follow the process from knowledge development to demonstrate the application of mathematical modelling through involving students in the classroom, the student can achieve the requirement. Considering the limitation for appropriate set up, the proposed method is pedagogically feasible and beneficial for both student groups.

KEYWORDS: Classroom, Indoor Air Quality, Ventilation, Mathematical Modelling, Onsite Measurement

1. INTRODUCTION

1.1 Awareness raising for ventilation

The interest in indoor air quality (IAQ) to keep a healthy condition gets more popular in the wake of the COVID-19 pandemic. The trend can be observed as, for example, CO_2 concentration monitoring devices become easy to get on the market. It is supposed that it's a good opportunity to raise awareness for our own built environment and act for our behavioural changes. Ventilation aims to exhaust polluted air outside of the room and to get fresh air into the room. In case a mechanical ventilation system (MVS) is applied, occupants have less chance to be aware of the status of air change. To help it, CO_2 concentration monitoring devices can be used. However, it provides us with the status of air quality but doesn't show us the flow of air. Therefore, the device application is not enough to be aware of dynamic air movement by ventilation.

Proactive user behaviour for managing IAQ is recommended and promoted more and more in COVID-19 guidelines. However, there are a lot of issues which are out of perception in the situation of a room controlled by mechanical ventilation systems. To open the black box, understanding the mechanism of system and flow, and raising awareness for ventilation are essential. The article describes the challenge of adding the content of ventilation in which students can realise the mechanism of air movement and perceive the actual volume of air change happening in the classroom where the student stayed during the lecture. The article reported the challenge of teaching a built environment focusing on ventilation for two student groups, one doesn't have engineering knowledge, and another has.

1.2 Guideline for ventilation after COVID-19

REHVA, ASHRAE or SAGE-EMG publish the guidelines for epidemic [1, 2, 3]. These guidelines show the acceptable limitation of CO_2 concentration rate for managing safe indoor air quality, such as a value under 1000 ppm in ASHRAE or 1500 ppm in REHVA. However, these guidelines don't show the air change rate as an indicator. The reason is that it is hard to estimate it in daily activity, or mechanical ventilation systems work correctly to keep IAQ safe. So, there is no demand to monitor IAQ with air flow rate. On the other hand, according to the Japanese guideline for COVID-19 based on SHASE (the Society of Heating, Air-Conditioning, and Sanitary Engineers of Japan) [4], the air change rate is also shown as one of the monitoring indicators. In addition, enhancing natural ventilation is strongly recommended. This is one of the reasons why the study focuses on estimating air change rate instead of CO_2 concentration for perceiving air movement.

2. METHODOLOGY

2.1 Air flow rate estimation model

Regarding airflow, CFD simulation is often applied. It is an appropriate method to understand the streamline of air movement visibly or distribution of air speed in the classroom. However, a high engineering knowledge is required to apply. It is so-

called black box method, is applied as a post evaluation phase in many cases, and interactive use in classroom is difficult because of a high calculation load. Also, simulated result affects variable settings, such as wind direction of surrounding and initial state of calculation.

The aim of the trial is to show the phenomenon in the classroom with stimulating student's imagination. The balance model to simulate mass flow, which is CO_2 in the study, is written with the basic formula (eq. 1). The equation describes that the amount of mass incoming to the system is balanced with the mass which is stored in the system and that of mass outgoing from the system to the environment through the focused system boundary, classroom in this case. Based on the basic concept of the balance model, the mass balance equation regarding CO_2 concentration to estimate the behaviour of air change is written as equation (2). The terms on the left side of the equation show the input to the boundary, including coming in by ventilation and generated by occupants. The first term on the right side shows the stored in the boundary, and the second term does the output to the boundary which is outgoing by ventilation. The V_o is the target value to estimate, and C_r is the measured value. CO_2 concentration rate of outdoor (C_o) is given as a constant value (400 ppm) for the study. The number of people (m) who were in the classroom was counted by manual.

$$[\,Input\,] = [\,Stored\,] + [\,Output\,] \tag{1}$$

$$\boldsymbol{V_o C_o dt + mGdt = V_r dC_r + V_o C_r dt} \tag{2}$$

where

V_o	[m^3/s]	Air flow rate by ventilation
V_r	[m^3]	Volume of classroom
C_r	[mg/m^3/s]	CO_2 concentration rate, indoor
C_o	[mg/m^3/s]	CO_2 concentration rate, outdoor
G	[mg/s/p]	CO_2 generation rate from body
m	[person]	Number of people

2.2 Trials applying the studied method

Case1: Trials for non-engineering students

The lecture was done in the course entitled "Mathematics in Environmental Study" for bachelor-level students (1st year) in the Faculty of Environment Studies in Japan. The course consists of fourteen modules (100 minutes for each) and two modules were provided continuously every week. The trial of the study was demonstrated using four modules of those through two weeks (Fig 3). The trials were done in 2021, 2022 and 2023. The volume of the classroom is 1750 m^3 (V_r) and the article shows the result of 2023 when 176 people (m) were in the classroom (Fig 1).

Case2: Trials for engineering students

The studied method was also applied at the lecture in the Department of Architecture and Built Environment in Sweden. The course was titled "Sustainable Buildings" for master-level students. Using two modules (two hours for each), the contents of the studied method were provided. The classroom was operated only by mechanical ventilation systems. The demonstration was done in 2022 and the volume of the classroom was 360 m^3 (V_r) and the number of people (m) was 27 (Fig 2).

Figure 1: Case 1, 176 persons in 1750m^3 classroom

Figure 2: Case 2, 27 persons in 360 m^3 classroom

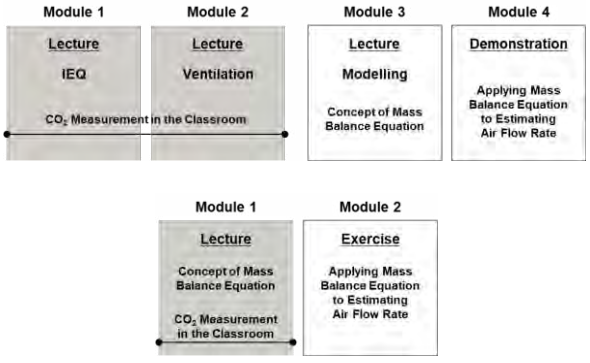

Figure 3: Structure of lecture (upper: Case 1, lower: Case 2)

2.3 Structure of lecture

Figure 3 shows the modules of two cases. Case 1 was done in two weeks using four modules. Case 2 applied two modules in one day, which included two-hour lecture session and three-hour exercise session. The lecture consists of two parts. In the first part, CO_2 concentration measurement in the classroom is conducted during providing lecture about the importance of IAQ and ways of ventilation in a building. The lectures construct a basic understanding of why ventilation is needed. The students can see the measurement devices but no explanation regarding the sensors was provided. The concept of the mass balance equation is described in the second part showing the result of the measurement. The process of transforming the mass balance equation to a difference equation is explained step by step. Applying the measured dataset, the estimation of ventilation is shown for the student group tangibly. In the second step, the simplified spreadsheet and measured dataset were provided to the student group to do exercise work.

3. RESULTS AND DISCUSSIO

3.1 Visualizing the behaviour of air movement

The upper plot of Figure 4 shows the results of the CO_2 concentration rate through two modules in Case 1. In the first 110 minutes, which includes one module and 10-minute break, the mechanical ventilation system was stopped by the lecturer intentionally for the purpose of showing the change of CO_2 concentration rate. The figure clearly shows the behaviour and is applicable for explaining the necessity of ventilation. The lower plot of Figure 4 shows the result of estimating air flow rate by using the CO_2 concentration rate shown in the upper plot in Figure 4. Since the air flow rate of the classroom by mechanical ventilation system is 1.67 m^3/s, which is equal to 6000 m^3/h, the result was slightly overestimated. The difference is caused due by CO_2 generation rate by the body being lower than supposed. It can be a part of lecture content to study the model. It provides enough information to understand the trend of air movement.

3.2 Resolution of balance equation

Figure 5 shows the results of the estimated air flow rate in Case 2. The upper figure is the estimation calculated by 1-minute difference, and the lower is that by 5-minute difference. Scattering in 5-minute difference is smaller than 1-minute difference. Both are applicable to illustrate the outline of air movement behaviour, but 5 minutes interval is more appropriate to see the tendency clearly than that of 1-minute interval. It also can be a learning content to understand the feasibility of the mass balance equation model. Therefore, time scale can be one of the key factors in developing the difference models.

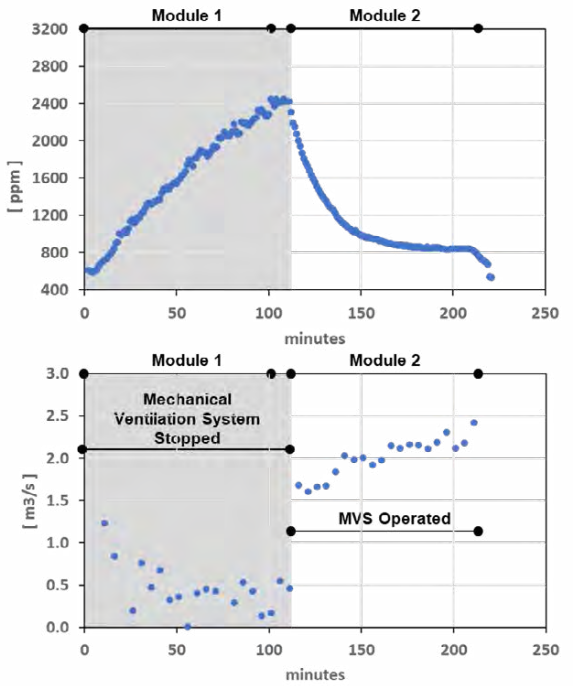

Figure 4: CO_2 concentration rate (upper) measured during the lecture in Case 1 and the air flow rate estimated by the measured dataset (lower).

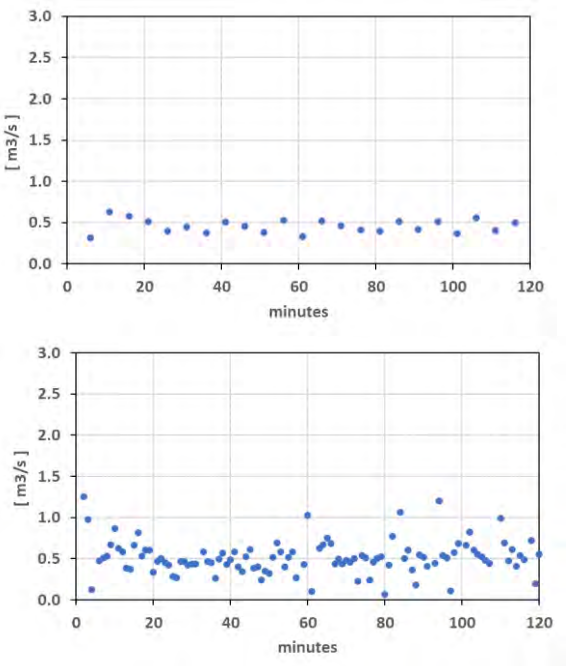

Figure 5: Estimation of the air flow rates estimation using difference equation by 1 minute interval (upper) and 5 minutes interval (lower) in Case 2

3.3 Reflection from the students

To evaluate the feasibility of the studied method, two questions were asked of the student group in Case 1. The question was asked at the end of the course each year. Figure 6 is the result of the answer to the question "The contents of the lecture were understandable." The result shows that more than 60% of students evaluated the contents positively. It is

supposed that the procedure of the lecture made it easy to understand the mechanism of air movement and the model. Also, Figure 7 shows the result of the answer to the question "The skill development required in the course was achieved". The required skill written in the syllabus was defined as, for example, the scope of mathematical modelling. Almost 40% of students answered as "agreed", and 80% of students answered positively. By providing the opportunity to follow the process from knowledge development to demonstrate the application of mathematical modelling by involving students in the classroom, the student can achieve the requirement.
The open-ended comments collected from the students were, for example, "I was surprised that the balance equation can describe the behaviour of air change in the classroom", "I could understand that mathematical modelling can be applied in our built environment" or "the importance of ventilation can be understood through the application of mathematical modelling. It supports us to learn the air movement." etc.

3.4 Limitation of the approach

The method cannot estimate the exact air flow rate because the uncertainties are included in the process of calculation, for example, undetectable air leakage in the room, exact supplied air volume by mechanical fans or the exact amount of CO_2 generation from the body considering body size or metabolism. However, it is enough to grasp the behaviour of airflow. The advantage of the approach is to generate and provide additional information and views through the actual space where they are. The trials in the study were done in the classroom without natural ventilation. Because the balance equation calculates the air flow rate using the difference of two timestep values, the balance is collapsed in cases with extremely high flow rates, for example, large volume flow by natural ventilation. The applicable range of air flow movement should be considered. Also, the distribution of CO_2 concentration is one of the influential factors of this method. In case the extremely low air movement, the layout of students in the classroom causes the biased distribution of CO_2 concentration.

4. CONCLUSION

The proposed method in the classroom is the challenge to perceive the airflow volume rate instead of the CO_2 concentration rate. The article reported the application cases for two student groups one with a non-engineering background, and another with an engineering background. Considering the limitation for appropriate set-up, the proposed method is pedagogically feasible and beneficial for both student groups.

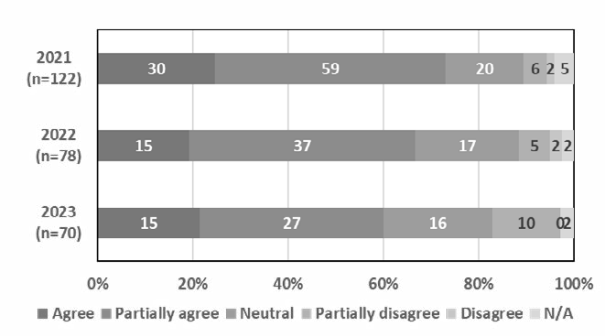

Figure 6: Answer distribution against the question asking, "the contents of the lecture were understandable"

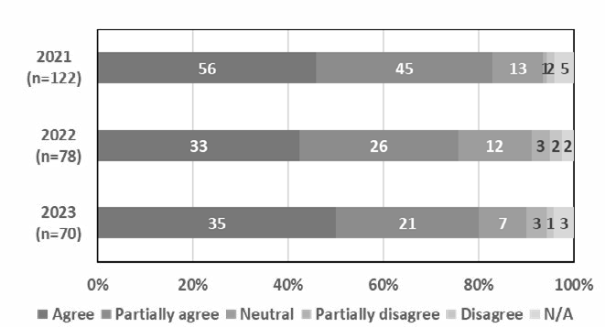

Figure 7: Answer distribution against the question asking, "the skill development required in the course was achieved"

ACKNOWLEDGEMENTS

The study is supported by Tokyo City University Advance Research Laboratories through the research project entitled "Positive Energy Lab Leading Resilient Carbon Neutral Communities". The authors would like to extend their gratitude for the financial assistance, which was instrumental in conducting experiments, acquiring necessary resources, and disseminating the findings in PLEA2024.

REFERENCES

1. REHVA, COVID-19 GUIDANCE Ver.4.1, 15 April 2021
2. ASHRAE, COVID-19: ONE PAGE GUIDANCE DOCUMENTS, 24 June 2021
3. SAGE-EMG, Role of Ventilation in Controlling SARS-CoV-2 Transmission, 23 October 2020
4. Kurabuchi T, Yanagi U, Ogata, M, et al. Operation of air-conditioning and sanitary equipment for SARS-CoV-2 infectious disease control. Jpn Archit Rev. 2021;00:1–13. https://doi.org/10.1002/2475-8876.12238

PLEA 2024 WROCŁAW
(Re)thinking Resilience

Environmental Comfort Teaching - from design to built environment:

the *Escola da Cidade* case and the Itinerant School

EDUARDO GASPARELO LIMA[1,2], LAÍS DE GUSMÃO COUTINHO[1,2,3], MONICA DOS SANTOS DOLCE UZUM[1], CRISTINA KANYA CASELLI CAVALCANTI[1]

[1] Escola da Cidade, São Paulo, Brazil
[2] School of Architecture and Urbanism of USP, São Paulo, Brazil
[3] National Council for Scientific and Technological Development scholarship holder, São Paulo, Brazil

ABSTRACT: The Escola da Cidade *is an architecture and urbanism college that has been integrating innovative didactic-pedagogical approaches into its program. The Itinerant School is one of these initiatives, in which students embark on a meticulously planned itinerary for destinations across Brazil and Latin America. This article details a pedagogical experience during an Itinerant School to Belo Horizonte. Preparatory classes focusing on bioclimatic strategies for the city were organized and a booklet was created to direct attention towards various aspects related to environmental comfort. A noteworthy outcome of these activities was a significant rise in student engagement in learning throughout the semester. According to some reports, there has been an improvement in the way students perceive and analyse buildings, as well as internal and external spaces.*
KEYWORDS: Environmental Comfort, Teaching, School trip, bioclimatic project

1. INTRODUCTION

The *Escola da Cidade Association*, established in 1996 in São Paulo, is a non-profit organization dedicated to the education of architects and urban planners. It brings together professionals from diverse fields who share the common goal of fostering an environment conducive to intellectual freedom and reflection. Presently, the institution boasts a distinctive educational approach compared to most of the architecture and urbanism programs in Brazil. It is characterized by the integration of innovative didactic and pedagogical practices in architectural and urban planning education.

Among these notable practices is the *Vertical Studio*, a research and project workshop that collaborates with students across different academic years. Additionally, there is an external experience exclusively available to fifth-year students, who are granted a six-month absence from *Escola da Cidade* for extracurricular activities. The institution also hosts the *Contemporary Reality and Culture Seminar*, held weekly, inviting students to engage in discussions and reflections on topics beyond the scope of traditional architecture.

The *Itinerant School* is an integral part of this educational context, organizing national and international trips to provide students with direct experiences, on-site observations, and in-depth analyses. This approach aims to foster a comprehensive understanding of the social and cultural dynamics of the visited locations, activating all human senses in a manner challenging to achieve within the confines of a traditional classroom setting [1]. Aligned with the Course Pedagogical Project, this initiative contributes to shaping architects equipped with critical and reflective capacities, ready to confront the complexities of the ever-evolving global reality. The itineraries are guided by historical context and draw upon architectural and urban repertoires.

Throughout the six years of their undergraduate education, students undergo a series of six one-week trips, featuring diverse itineraries and destinations across Brazil and Latin America. These selections are tailored to accommodate the specific needs and possibilities of each cohort. The cost associated with participating in the Itinerant School is encompassed within the monthly tuition fees, ensuring the inclusion of all students in the program, including those on scholarships. The success of these activities relies on the mobilization of numerous teachers who guide students, and a meticulously prepared script is studied and defined in advance.

As part of the broader initiative to redefine the landscape of architectural and urban planning education in Brazil, *Escola da Cidade* has actively contributed to the restructuring of the teaching of environmental comfort. This involves the construction of models, engagement in external experiences, the organization of laboratories, and an attempt to establish a horizontal alignment between disciplines related to environmental comfort and design. This approach aims to move away from

traditional methods, reducing the emphasis on purely expository classes dominated by calculations.

It is noteworthy that, since 1994, with the enactment of Ordinance Nº 1,770 by the Ministry of Education (then known as the Ministry of Education and Sports), environmental comfort has been mandated as a compulsory professional subject in all Brazilian architecture and urban planning courses [2]. Despite its well-intentioned connection to the imperative of sustainable development, this mandate inadvertently led to a disconnection between bioclimatic architecture concepts and architectural design. Consequently, there is a need to establish a counterpoint by bridging the teaching of comfort with design practice. The Itinerant School emerges as a crucial instrument in this endeavour, providing a tangible understanding of environmental comfort in the built environment when appropriately directed.

In the second semester of 2023, first-year students were programmed to participate in the Itinerant School, with Belo Horizonte as the chosen destination – a Brazilian state, capital of Minas Gerais, renowned for its cultural, historical, and patrimonial richness. Simultaneously, these students were immersed in the Environmental Comfort 1 course throughout the semester. The primary aim of this endeavour is to convey the experience of integration, both within and beyond the classroom. It offers students a unique opportunity to perceive space in a multisensorial manner, fostering an appreciation for the development of bioclimatic projects with a specific emphasis on the well-being and health of end-users. This integrated approach aims to enhance students' understanding by connecting theoretical knowledge with real-world experiences, encouraging a holistic perspective on architectural and environmental considerations.

This paper will introduce the environmental comfort activity that was devised for first-year students who took part in the Belo Horizonte Itinerant School, along with its principal outcomes concerning the teaching and learning process of the students. It is noteworthy that this current experience represents an enhancement compared to a previous Itinerant School held in 2022 and the identified issues highlighted through feedback from previous students have been addressed and rectified [3].

2. INSTRUMENTAL PREPARATORY CLASSES

Environmental comfort classes at *Escola da Cidade* are conducted on a weekly basis. Each session is designed to incorporate concepts and strategies from bioclimatic architecture, along with references to various projects for climate analysis and sustainability-focused solutions. For the upcoming second semester of 2023, all classes are strategically structured to contribute significantly to the success of the Itinerant School, particularly from the perspective of environmental comfort.

The three classes the preceded the Minas Gerais trip have had a heightened focus on the locations to be visited and key aspects that warrant observation and analysis during the journey. In the initial class, students were introduced to the tools (psychrometric charts, software, and national regulations) and resources essential for climate diagnosis. Subsequently, in the second class, students actively conducted this diagnosis for Belo Horizonte. Finally, in the third class, students were encouraged to explore bioclimatic strategies pertinent to the specific climatic conditions of the city. This sequential approach aims to equip students with the necessary knowledge and skills to engage effectively with the environmental aspects of the upcoming Itinerant School experience.

The objective of this approach is to sensitize students to architectural design by imparting a comprehension of fundamental techniques. These include understanding the surroundings, determining optimal orientation based on sunlight and prevailing winds, implementing sun protection devices, optimizing the use of natural light, and strategically positioning rooms for noise attenuation, among other considerations. It is important to note that the intention is not to transform students into environmental consultants. Rather, the goal is to instil an intuitive awareness of these elements so that students can naturally incorporate them into their design process. This approach seeks to cultivate a holistic understanding of environmental factors that should inform and enhance their architectural designs.

2.1 Climatic context

In terms of climate, the city of Belo Horizonte (Latitude 19.82° S; Longitude 43.96° W) is situated in the South tropical zone, and the Köppen-Geiger climate classification for the region is tropical, with a dry winter season (Aw). Elevated at 869 meters above sea level, Belo Horizonte experiences a notable cooling effect attributed to its relatively high elevation, mitigating the high maximum air temperatures observed in nearby cities at lower altitudes. The climate is characterized by warm-humid summer days featuring partially or cloudy skies, and mild-drier winter days with predominantly sunny conditions. Prevailing wind directions are Southeast and East throughout the year. Air temperatures remain moderate for the most part, with an annual average temperature of 21.75 °C, according to data from the climatological bank of the National Institute of Meteorology [4]. On typical extremely hot days with clear skies, temperatures can reach 32 °C in the early afternoon. On the other hand, under a cloudy sky, air temperatures on warm days hover around 20 °C. During the winter season, temperatures can drop

below 15 °C, and on cooler days, they may rise to around 24 °C due to the impact of solar radiation.

2.2 Recommendations and strategies

In accordance with the Brazilian Bioclimatic Zoning [6], the city of Belo Horizonte is situated within Bioclimatic Zone 3 and the technical-constructive guidelines for this zone are succinctly outlined in Table 1, adapted from ABNT NBR 15220 [5].

Assisted by the Climate Consultant 6.0 software and utilizing the ASHRAE Adaptive Model and Standard 55 [6] as an assessment parameter, the students observed that natural ventilation, coupled with shading, significantly contributes to achieving comfort during warmer periods of the year. Additionally, the analysis revealed a noteworthy percentage of hours necessitating dehumidification, accounting for almost 30% of the year. Conversely, cold discomfort during lower temperatures could be mitigated by leveraging the internal thermal load generated through occupation complemented by the presence of thermal inertia. Solar heat also assumes a pivotal role during this period.

Table 1: Technical-constructive guidelines for Bioclimatic Zone 3.

PASSIVE THERMAL CONDITIONING STRATEGIES					
Summer			*Winter*		
(I) Cross-ventilation			(I) Solar heating (II) Heavy internal seals (thermal inertia)		
APERTURES					
For ventilation		*A (in % of floor area)*		*Shading*	
Medium		15% < A < 25%		Sun access during winter	
EXTERNAL SEALS					
Walls			*Roof*		
Light and reflective			Light and insulated		
U-Factor (W/m²K)	*Thermal Lag (h)*	*Solar Factor (%)*	*U-Factor (W/m²K)*	*Thermal Lag (h)*	*Solar Factor (%)*
U ≤ 3.60	φ ≤ 4.30	FS_o ≤ 4.0	U ≤ 2.00	φ ≤ 3.30	FS_o ≤ 6.5

3. ITINERANT SCHOOL

The last trip primary focus centred around the city of Belo Horizonte, supplemented by visits to the surrounding areas. The itinerary commenced as students and teachers arrived in Belo Horizonte on October 2nd in the morning. In the afternoon, they explored *Praça da Liberdade* and its environs, including the Niemeyer Building.

The subsequent morning was dedicated to the historical city centre, featuring a visit to the Santa Tereza Viaduct – constructed in 1929 with reinforced concrete – and the Museum of Arts and Crafts, situated within the historical complex of the former Central Station of Brazil's Estrada de Ferro Central, one of the nation's inaugural railways. The group acquainted themselves with the JK complex, a structure from 1952 consisting of two mixed-use blocks that also serves as a symbol of modern architecture [7].

The third day encompassed a tour of another section of the city's historical center, highlighting notable buildings such as Acaica, Sulacap, and Cine Brasil, and the Municipal Park. In the afternoon, an activity unfolded in collaboration with students from the Federal University of Minas Gerais (UFMG), during which *Escola da Cidade* and local teachers presented their studio productions.

On the following day, the morning was dedicated to visiting the *Serra do Curral*, a national heritage site listed by the National Historical and Artistic Heritage Institute and situated in the transition between the Brazilian biomes of *Cerrado* and *Mata Atlântica*. This location is characterized by conflicts arising from environmental issues stemming from indiscriminate mining. The afternoon was reserved for a visit to the *Pomar do Cafezal* House and the *Lá da Favelinha* Cultural Centre – an independent artistic-cultural organization promoting cultural activities and professional training for favela residents [8].

On the fifth day, the students journeyed to Brumadinho and explored the Inhotim Institute, an esteemed open-air Contemporary Art Museum and Botanical Garden. The last day was dedicated to the Pampulha neighbourhood, home to the iconic Church of São Francisco de Assis, designed by Oscar Niemeyer.

4. PROPOSED EXERCISE: ENVIRONMENTAL BOOKLET

With the intention of guiding students' attention towards specific parameters or strategies, a notebook was developed for them to respond to during the Itinerant School. This material was crafted in A5 size in the most inviting and friendly manner possible, encouraging students to feel stimulated to fill it out, incorporating the use of various icons. Some questions had a response scale ranging from 0 to 100, reflecting each student's comfort perception. This allowed for a subsequent quantitative evaluation.

It is emphasized that this notebook was developed based on the previous experience of the Itinerant School in the *Vale do Paraíba*, where three buildings were analysed at the students' choice. For this edition in Belo Horizonte, two buildings were pre-selected through a classroom draw – presented in next subsection –, along with two urban routes, to also include sensations perceived in different parts of the city. However, this article presents only the observations related to the interior of the buildings.

For the students perceived analysis, the notebook was divided into the following items: (I) general project data; (II) overall perception; (III) lighting and daylight; (IV) thermal and ventilation aspects; (V) environmental sketch and detail of an environmental strategy; and (VI) identified strategies and notes.

In the first section, the identification of the case study is conducted, along with information such as latitude, day, time, air temperature, and sky conditions. In the second item, the student is required to document their sensations concerning environmental variables. In parts 3 and 4, the student is tasked with responding to more technical questions about lighting and thermal aspects, connecting their perception of the environment to these factors. Subsequent sections provide spaces for sketches representing the studied building and a bioclimatic strategy present in it. There is also an area for notes and the identification of other, more complex environmental strategies. This material was handed out to the students during the final class before the trip to Belo Horizonte, along with instructions for its proper completion.

4.1 Selected buildings

The JK Complex (Fig. 1), designed by the architect Oscar Niemeyer and inaugurated in 1951, stands as an exemplary representation of modern architecture and was provisionally listed as a cultural heritage site in 2021. The complex is structured into two distinct scales: a monumental scale at the ground level supported by pillars, aligning with the city's scale, and a human scale established by the streets that interconnect the floors.

The complex consists of two mixed-use blocks. Block A, with 23 floors, has its longer facades to the north-south axis, featuring glass windows to facilitate natural ventilation, along with blind walls facing east and west. Block B, consisting of 36 floors, orients its longer facades to the east and west, incorporating iron windows for natural ventilation. Notably, the west-facing facade is equipped with vertical shading devices. The north and south facades of Block B are structured as a closed system of enclosure.

The *Pomar do Cafezal* House (Fig. 2), designed by the Levante Collective and completed in 2020, occupies a 70 m² space in a neighbourhood characterized by predominantly self-built structures. The construction materials and techniques employed align with the local context, utilizing a reinforced concrete structure with precast slabs and unfurnished ceramic block walls. The house is situated on a steep plot and follows a 3 x 3 m construction module, with its main facades oriented towards the northeast and southwest.

The internal spaces are distributed across three levels: the entrance level encompasses a combined living room and kitchen, a bathroom, and a laundry area; the middle floor accommodates a bedroom, bathroom, and balcony; and the upper level serves as a terrace. The windows, designed in a casement style, are strategically positioned to facilitate ventilation. Additionally, the ceramic blocks were laid in a non-conventional manner, contributing to enhanced thermal inertia within the structure.

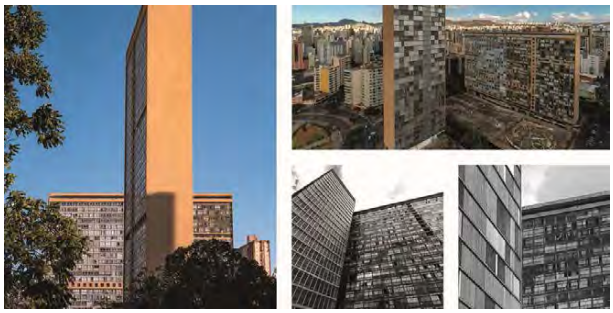

Figure 1: JK Complex in Belo Horizonte. On the left, image of the complex - Photo: Thiago Giardini. Above, urban context in which it is located - Photo: Viva JK. Below, details of the facades (Photos: Igor Fracalossi and Viva JK).

Figure 2: Pomar do Cafezal House in Belo Horizonte. On the left, image of the project. Above, urban context in which it is located. Below, details of the shaded main access and the interior of the bedroom. Photos: Leonardo Finotti.

5. RESULTS

The outcomes of this experience can be assessed through various means: (I) return of the experience booklet by the students, encompassing numerous questions and observations regarding the built environment; (II) a satisfaction and learning questionnaire, featuring inquiries related to the overall experience and the integration between the Itinerant School and the classes conducted throughout the semester; (III) field observations and reports, given that in this edition of the Itinerant School, there was an environmental comfort teacher accompanying the students and guiding their senses and attention towards the adopted bioclimatic strategies.

5.1 Answered booklets

Upon the arrival from the trip, the notebooks were returned to the teachers for evaluation and analysis. Multiple-choice questions and those with a scaled response were tabulated, while sketches and notes were individually reviewed.

The tabulation of responses recorded by students in their notebooks is a crucial procedure as it allows for the analysis of questions with higher levels of comprehension difficulty, marked by significant divergence in responses. This aids in adjusting the activities for the future Itinerant Schools. It also

facilitates an understanding of the diverse perceptions of users regarding the built environment and its variables, demonstrating practically the substantial degree of subjectivity inherent in environmental comfort. Furthermore, by employing environmental variable measurement equipment, another scientific study can be conducted to compare measurements with perceptions, accompanied by an interpretation of these results. The intention is to carry out this comparison in future research endeavours.

A total of 44 students participated in the Itinerant School, and 40 notebooks were returned to the teachers. In general, due to the divergence in responses, it was evident that there were difficulties in understanding the layout of the building on the plot, the orientation of the main facade, the extent to which the surroundings mask the building, the relationships between opaque and transparent materials, the thickness of the walls (which needed to be answered in palms to accommodate the potential absence of a ruler or tape measure), and issues related to accessibility. Given that these students were in their first year, some design concepts were not yet well-defined. On the other hand, the students demonstrated ease in identifying types of natural ventilation, as well as recognizing openings in buildings, solar shading devices, and lighting control mechanisms (Fig. 3).

In the *JK Complex*, when asked to respond regarding their perception of natural ventilation, 79% of the students provided answers ranging from 30 to 50 on a scale of 0 to 100, where 0 represents no wind, 50 is a breeze, and 100 is a strong wind. However, perceptions regarding the presence of noise varied significantly. When questioned about overall comfort, 75% of the students reported feeling comfortable, while the remaining students, who expressed discomfort, attributed it to a sensation of heat and stuffiness.

Regarding the *Pomar do Cafezal House*, in the question about thermal ambiance on a scale of 0 to 100, where 100 represents warmth, 50 neutrality, and 0 cold, more than 80% of the students provided responses above 80 points. However, when evaluating the comfort question "do you feel comfortable?", also more than 80% of the responses were affirmative. This suggests that the perception of thermal comfort is not solely related to environmental variables but also to the environmental quality of the building and the user's current experience, in this case, a relaxed occasion among friends. For instance, one student mentioned feeling uncomfortable due to fatigue from the trail they had undertaken. Perceptions regarding natural ventilation and noise varied widely, once again highlighting the subjective nature of environmental comfort.

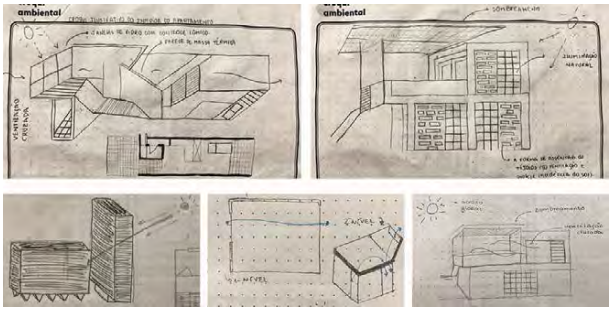

Figure 3: Student sketches identifying bioclimatic strategies.

5.2 Questionnaire results

To enhance future experiences, a satisfaction survey was conducted with the students. The questionnaire was divided into four sections, with the first pertaining to the preparatory classes conducted before the trip, the second focusing on the provided booklet, the third addressing the activities during the Itinerant School, and the last concentrating on the impact generated by the immersion week. More than 77% of the respondents found that the content covered in the classes was sufficient for completing the notebook, and nearly 90% stated that the activities were clear. Additionally, 80% of the students deemed the execution of the climate diagnosis before the trip to be important or very important.

Regarding the notebook, 100% of the respondents found the layout and organization to be excellent, and likewise, 100% believed that the clarity of information in the material was excellent or good, resulting in a 100% satisfaction rate with the printed material. Concerning the Itinerant School, nearly 90% of the students indicated that the presence of a professor specializing in environmental comfort was necessary or very necessary. Some mentioned difficulties in completing the material during the trip. Regarding the impact felt from the external experience, the most important aspects brought by the Itinerant School included the broadening of repertoires and references, the training of senses for understanding architectural and urban space, and the knowledge of new cultures and societies. Additionally, almost 80% of the respondents stated that they feel this activity has made them more familiar with and receptive to the discipline of environmental comfort.

5.3 Field observations and classroom discussions

The essence of the Itinerant School's richness lies in the interplay between individuals and the climate, the city and its structures, and the simultaneous stimulation of the senses. Students had the opportunity to experience sensations provoked by the relationship between space, whether built or open, and their own bodies.

Throughout the week, the temperature remained consistently around 30°C, significantly influencing the perception of discomfort due to the extreme heat. The breaks provided for students to document their experiences in booklets played a crucial role in

fostering their awareness of comfort and discomfort in various locations, whether urban or rural.

One notable instance occurred during a stroll in an underground passage between Sapucaí streets and a train station, where students were captivated by a refreshing breeze generated by a wind corridor. The visit to the municipal park underscored the significance of green and shaded areas: along the lake's perimeter, students could discern temperature variations between exposed and shaded zones.

The trek along the *Serra do Curral* presented intense heat (ranging from 28.9 °C to 30.6 °C), but the overcast day offered relief. Students acknowledged that on a clear day, without shade and considering the local vegetation, the experience would be even more overwhelming.

The students' prompt adaptation to the climatic conditions was evident in their choice of attire. While some initially wore pants on the first day, the prevailing choice in subsequent days became shorts and dresses.

Armed with prior knowledge, students could concretely address technical aspects of comfort. Recognizing that everyone experiences comfort and discomfort in different manners, the architect's role is to adeptly translate these sensations into projects that align with local needs.

In the first class that followed the trip, a discussion session was conducted, during which students were invited to reflect on their experiences and connect them with the topics previously covered in the classroom and the climate diagnosis that had been carried out by them. It was observed that the discussion was particularly insightful at this juncture, as the trip possessed the capacity to stimulate and further engage them in the semester's content. However, the students were unable to correlate the climate diagnosis they had formulated with their observations in the visited city, given that the trip coincided with the days of the heatwaves that occurred in Brazil in 2023 [9], making issues related to climate change and global warming tangible.

6. CONCLUSIONS

In this paper, the entire experience gained by the Environmental Comfort group at *Escola da Cidade* during the Itinerant School in the city of Belo Horizonte, in southeastern Brazil, has been shared. The organization commenced prior to the trip with preparatory classes and the development of an activity booklet. The week-long journey resulted in a noticeable increase in student engagement with the discipline's activities upon their return to regular classes. This demonstrates that such experiences, in addition to enriching their repertoire, provide a moment of relaxation combined with learning during the semester, thereby enhancing the teaching-learning process. In addition, the exercise also brought contributions to the academic and professional future of these students, as indicated by some reports on the change in the way they perceive and analyse buildings and internal and external spaces.

The inclusion of a professor specializing in environmental comfort accompanying the students during the trip was essential for addressing doubts and guiding the perspectives of first-year students who are not yet accustomed to perceiving and analysing certain components, systems, and design decisions. For the upcoming editions of the Itinerant School, it is necessary to review certain aspects of the proposed activity, considering reports of insufficient time to answer all questions and draw sketches.

REFERENCES

1. Escola da Cidade. Escola Itinerante. 2021. Available: <https://escoladacidade.edu.br/graduacao/escola-itinerante/>. [20 December 2023].
2. Leite, M. A Aprendizagem Tecnológica do Arquiteto. Thesis (PhD). University of São Paulo, 2005.
3. Cavalcanti, C.; Lima, E.; Coutinho, L.; Uzum, M. (2023) Sensibilização aos Conceitos de Conforto Ambiental: experiência didático-pedagógica em Escola Itinerante. In ENCAC/ELACAC. São Paulo, Brazil, October 30-31 and November 1.
4. Climate data. [Online], Available: http://climate.onebuilding.org [12 December 2023].
5. Associação Brasileira de Normas Técnicas. 2005. ABNT NBR 15220: Desempenho térmico de edificações. Rio de Janeiro, Brazil.
6. American Society of Heating, Refrigerating and Air Conditioning. 2020. ANSI/ASHRAE Standard 55-2013. Thermal environmental conditions for human occupancy.
7. Vivajk. Por um JK vivo, harmônico e plural. [Online], Available: https://vivajk.org/ [26 August 2023].
8. Lá da Favelinha. [Online], Available: https://ladafavelinha.c om.br/quem-somos/centro-cultural/ [26 August 2023].
9. Reuters. Climate change drove deadly winter heat wave in South America, study says. 2023. [Online], Available: https://www.reuters.com/world/americas/climate-change-drove-deadly-winter-heat-wave-south-america-study-says-2023-10-10/. [20 December 2023].

PLEA 2024 WROCŁAW
(Re)thinking Resilience

Natural Ventilation Awareness Through Wind-Tunnel Tests:
A didactic experience

LAÍS DE GUSMÃO COUTINHO[1,2,3], EDUARDO GASPARELO LIMA[1,2], ALESSANDRA RODRIGUES PRATA SHIMOMURA[1], MICHELE MARTA ROSSI[1], RANNY LOUREIRO XAVIER NASCIMENTO MICHALSKI[1]

[1] School of Architecture and Urbanism of USP, São Paulo, Brazil
[2] Escola da Cidade, São Paulo, Brazil
[3] National Council for Scientific and Technological Development scholarship holder, São Paulo, Brazil

ABSTRACT: The wind tunnel is an important tool to evaluate the behaviour of wind flow in urban arrangements, as well as to assess the design process focused on environmental aspects – in this case, natural ventilation strategies. The aim of this paper is to describe a didactic experience of a workshop about natural ventilation in urban scale to incoming students of the Architecture and Urbanism course at the University of São Paulo and its preparatory stage. The didactic-pedagogical process includes the presentation of theoretical concepts and the application of wind-tunnel tests (simulations with erosion figure technique). The adopted approach allows analyses, discussions, and comparisons of the technical and the visual understanding of the students, proving valid the application of practical activities and experiments to teach and to better illustrate theoretical concepts during the early design stages.
KEYWORDS: Natural Ventilation, Wind-tunnel, Didactic Experience

1. INTRODUCTION

Effective air flow is imperative for achieving thermal comfort, especially in hot and humid climates, such as those prevalent in a substantial part of Brazil. The removal of heat generated by users, equipment, building envelope, and activities is essential to maintain acceptable air temperatures within a structure. Natural ventilation emerges as a viable solution to assist in this process [1].

Furthermore, this strategy significantly contributes to air renewal, a critical factor in any built environment, regardless of weather conditions. It directly influences the dispersion of carbon dioxide and the dissipation of air humidity – key elements in preserving user health and indoor air quality [2, 3, 4]. Notably, since 2020, amidst the SARS-CoV-2 pandemic, building ventilation has gained greater relevance and was acknowledged by society and political authorities as a means of minimizing the spread of the virus.

According to Lawson [5], the act of designing can be explained considering the scope of the product or based on the process. In the first case, the focus is on producing a solution; in the latter, it is about solving problems. Additionally, an adequate environmental design includes parameters imposed by a given climate to achieve good building performance.

Nowadays, architects and urban planners are increasingly engaged with environmental design, but are still looking for robust information on how to implement certain aspects during the early stages of design.

Considering this, wind-tunnel tests emerge as valuable resources, encompassing both qualitative (smoke tests and erosion technique) and quantitative methods (measurements with hot wire anemometers or pressure transducers). Silva [6] asserts that aerodynamic tunnels facilitate a quick understanding of current and future scenarios of the urban fabric using reduced-scale physical models. Hence, wind tunnels serve as valuable tools during the early stages of design, providing a swift and didactic means to comprehend wind patterns without the complexity of computer simulations.

To verify this hypothesis, a workshop on natural ventilation, incorporating wind-tunnel tests (basic qualitative experiments applying the erosion figure technique), was proposed for first-year Architecture and Urbanism students. This paper aims to delineate this didactic experience, bringing natural ventilation concepts closer to the design process during the early stages. It includes a brief theoretical explanation and more extensive practical activities. Encouraging the adoption of wind tunnels by students during their design process and throughout their undergraduate course is also an objective.

The paper is organised as follows: Section 2 comprehensively outlines the methodology, which is divided into two distinct stages: the workshop preparation phase and the execution of the workshop itself. Subsection 2.1 provides insights into the development and preparation of the workshop, encompassing the definition of its program, activities, and the creation of didactic materials to support its objectives. Subsection 2.2 delves into the experience

of presenting natural ventilation concepts through the application of wind-tunnel tests.

In Section 3, the qualitative results, derived from the observations made by professors and monitors, are discussed alongside the quantitative outcomes obtained through a questionnaire completed by the students. Finally, Section 4 consolidates and summarizes the principal findings of this didactic experience.

2. METHODOLOGY

The methodology employed in formulating the event encompassed two phases: a preparatory stage and the workshop.

2.1 Workshop Preparation

The workshop preparation was summarised in two main stages: (1) the development of workshop programme and (2) the elaboration of didactic material.

The first stage comprises some definitions such as: the objective of the workshop, its programme, and the complexity of natural ventilation concepts to be addressed during the proposed activities.

The aim of the workshop was to raise students' awareness about natural ventilation through wind-tunnel tests with a programme divided into theoretical and practical activities. Due to the limited time available for the workshop (around four hours), natural ventilation concepts were focused on the urban scale.

Some pre-tests in the wind tunnel defined the tests' typology, the number and duration of each take, the wind attack angles, and the wind speed controlled by fan operating frequencies - revolutions per minute (RPM).

Based on that, an erosion test was carried out with wooden solid generic blocks (3 cm x 3 cm x 2 cm in height), forming a mesh. Those pre-tests guided some improvements in the preliminary design of the practical activity such as:

1. the number of two urban configurations tests per group of students, varying wind attack angle (0° and 45°) or the arrangement (dense or spread out);
2. the adoption of three minutes for each wind-tunnel trial, considering this period as the time to stabilise the airflow and to produce the visualisations and captures;
3. the selection of wooden solid generic cubes of 3 cm, using black colour to increase the contrast between the blocks and the pink-coloured sand;
4. the definition of four fan operating frequencies: 650, 750, 850 and 950 RPM; and
5. the application of cork on the base-test area.

It is important to emphasise that test definitions were based on the available time to develop the practical activity as well as the adequate number of groups, or students per group, and the test accuracy and precision in illustrating the basic aerodynamic phenomena in urban scale for the students.

The second stage covered the didactic material elaboration (Fig. 1). For the theoretical part of the workshop, a slide presentation (to be used by the professors) and a textbook (to be given to the students) were developed concerning the fundamentals of natural ventilation on urban scale.

The textbook included seven main topics: (1) welcome text; (2) workshop programme; (3) a "did you know?" section; (4) a "why is natural ventilation important?" section; (5) types of natural ventilation systems and phenomena; (6) possible tools to aid the analysis and the verification of natural ventilation efficiency in the design process; and (7) bibliography. The primary objective of this booklet was to provide accessible and compiled basic theoretical information. In this way, the importance of natural ventilation for the Brazilian context, as well as stack-effect and wind-induced ventilation, were more prominently emphasized.

For the development of the exercise and understanding of the results that would be obtained in the wind tunnel tests, it was important to include explanations of the following aerodynamic effects: pilotis effect, corner effect, wake effect, wise effect, barrier effect, Venturi effect, staggered buildings, channel effect, pyramid effect, and mesh effect. Several drawings were also developed to illustrate these effects.

Additionally, two reduced physical models (scale 1:12) of a 9 m² bedroom area and 2.7 m ceiling height were created. One of them had only a wooden frame and the 5 surrounding faces were filled with plastic material to easily illustrate the pattern of the faces facing airflow. The other was a solid wooden block with printed wind distribution contour graphs on windward and leeward faces. This last model was previously proposed to support a natural ventilation class at the Institute of Architecture and Urbanism from the University of São Paulo (IAUUSP) based on data provided by Rossi [7].

Figure 1: Didactic materials: textbook and two physical reduced models (scale 1:12).

2.2 The Workshop

The workshop, entitled "Awareness of Natural Ventilation Concepts through Wind-Tunnel Experiments", occurred on March 15th, 2023 during the welcome week for beginning students of the Architecture and Urbanism course. Consequently, it was designed to present basic and qualitative concepts about natural ventilation, in order to familiarise students with this subject and to enable them to apply these preliminary concepts to their designs throughout the course.

This didactic workshop comprised three distinct stages: a theoretical presentation, a practical activity and a final discussion about students' findings.

The theoretical stage encompassed a presentation to highlight three key aspects: (1) the role of natural ventilation in promoting health, well-being, and thermal comfort for occupants; (2) the aerodynamic effects on the built environment; and (3) the introduction of support tools for assessing and evaluating natural ventilation strategies during the design process. Among the tools was the open-circuit wind-tunnel of the Environmental Comfort and Energy Efficiency Laboratory (LABAUT) at the Faculty of Architecture and Urbanism of the University of São Paulo and housed in the Technical Section of Models, Tests and Constructive Experiments (STMEEC).

The equipment allows to evaluate the impacts in a reduced model caused by the artificial aspiration of air by a fan through a duct with suitable dimensions [8]. Presently, the LABAUT apparatus spans approximately 8.5 metres, featuring a configuration that includes a contraction, three primary testing modules, and a diffuser (Fig. 2).

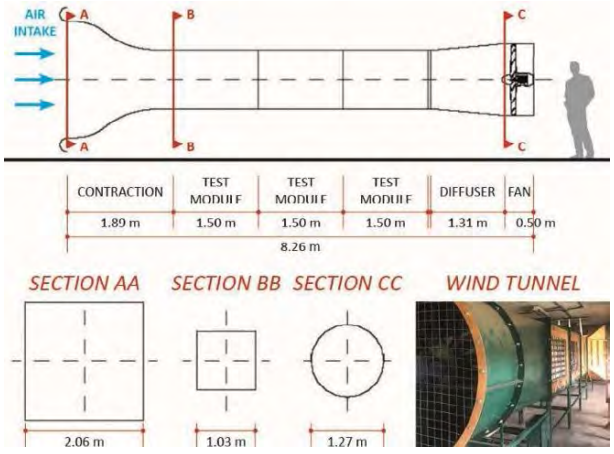

Figure 2: Composition of the wind-tunnel of the Environmental Comfort and Energy Efficiency Laboratory (LABAUT).

During the practical activity (second stage) the students could apply and observe the concepts learned in the theoretical presentation. The students were divided into two teams and invited to create volumetric models. Then, these proposed models were tested in the wind tunnel using sand deposition technique.

This technique provides a qualitative assessment of the wind behaviour at pedestrian level in a specific direction by applying a thin layer of sand on the horizontal surfaces of the model. The sand is eroded or remains undisturbed, depending on wind speed.

By gradually increasing the wind speed, it is possible to determine the airflow trajectories in the studied geometry. This assessment is based on identifying points where the sand has been eroded (indicating the presence of airflow) and areas where there is no alteration or accumulation of sand (indicating a wind shadow). The movement of particles is influenced by three factors: air speed, terrain roughness, and sand grain size. In this regard, red-dyed sand with a particle size of 0.3 mm, standardised according to NP EN 196-12, was utilised [9].

The models were constructed using cubic wooden blocks with 3 cm sides. They were black to ensure a clear contrast with the coloured sand. A squared plan with 63 cm side and a regular grid with intervals of 3 cm was the base for the exploration of each group, considering (1) geometry and (2) spacing.

After establishing the model volume and before conducting the wind-tunnel tests, the students were asked to draw the expected wind trajectories.

The workshop instructors only intervened during the model definition phase, guiding the students with some observations about the expected flows and the representation by drawings.

The first group, that was responsible for geometry, simulated the same configuration considering two different wind attack angles (0° and 45°). This prompted discussions on how the building's orientation can influence its exposure to winds.

Conversely, the second group prioritised an investigation varying the spaces between volumes in the proposed scenario. Based on that, students simulated two cases of arrangement, one was dense and the other was sprawled. It can be asserted, therefore, that this group operated on an urban scale in their models, examining the distances between building blocks and streets, for instance.

Thus, four scenarios were meticulously examined, constructed, anticipated, and tested.

At the end of the tests, the third and last stage was conducted, the final discussion on students' findings. The first group (geometry) examined the correlation between geometry and the wind attack angle, while the second one (spacing) observed the relationship between spacing and aerodynamic effects.

In this collaborative session, they compared three kinds of differences between: (1) the typology of the tests (i.e. geometry vs. spacing); (2) the inner scenarios developed by each group (scenarios 01 and 02), and (3) the final obtained visualisations and the

preliminary drawings in which they illustrated the expected wind pattern.

Ultimately, the expectation was to contribute to increase students' visual repertoire on the impact of design changes on the wind pattern obtained. Although the compositions were simple, they were fundamental in introducing the importance of thinking about orientation, arrangements, geometries, and other parameters since the initial stages of design.

3. RESULTS

The outcomes of the workshop were derived from: (1) the results of wind-tunnel tests, and (2) the observations made by professors, instructors, and students during the event and through a virtual survey (online form) conducted just after the workshop.

About the results of wind-tunnel tests and the observations captured during the workshop, it was noted that the students were intrigued by the sand erosion patterns around the elements as the wind speed increased. They were motivated to comprehend and elucidate the divergences and convergences observed in the instrument. This approach allowed to prove the hypothesis that the initial exposure to theoretical concepts (Fig. 3) and wind tunnel experiments (Fig. 4) would be satisfactory.

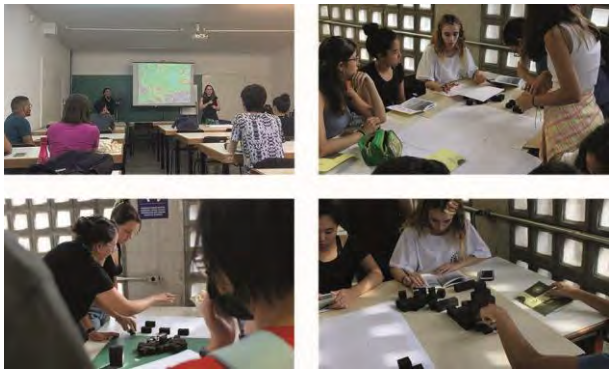

Figure 3: Theoretical elaboration of the arrangements to be simulated.

Additionally, during the workshop, numerous observations were conducted regarding students' reactions, interest, and engagement (Fig. 5).

Due to the small size of both the classroom and the wind tunnel room, the students were divided in two groups. Half of them first received the theoretical explanation and later visited the wind tunnel, while the other half were familiarised with the tool before attending the theoretical class. There was a noticeable increase in engagement, during the theoretical part, among students who had already seen the wind tunnel. Knowing what to expect from the activity motivated and made them more receptive.

A virtual questionnaire was provided to students to gather feedback on their workshop experience, including questions about their interests or satisfaction about the knowledge area (environmental comfort), the topic (natural ventilation), the workshop programme and organization; the quality of theoretical topics (natural ventilation phenomena and aerodynamic effects in built environment), explanation about the tool (wind tunnel); the proposed exercise (qualitative wind-tunnel tests); the produced didactic materials (textbook and models to support the tests and also the explanations) or, finally, the desire to have more workshops concerning comfort environment topics.

Regarding the motivation for enrolling in the workshop, the majority (66.7%) expressed interest in environmental comfort. Approximately 80% of respondents reported being satisfied or very satisfied with the theoretical explanations and the workshop organization (Fig. 6A).

Figure 4: Wind-tunnel tests of the configurations elaborated.

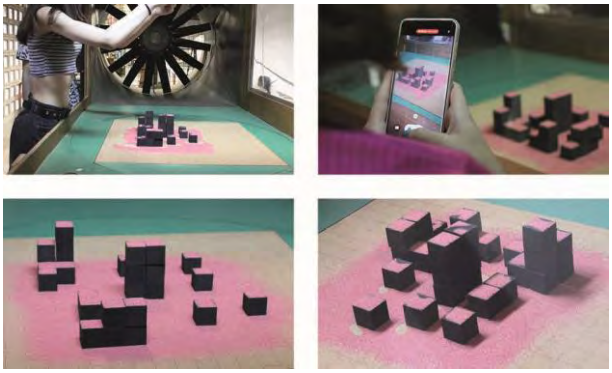

Figure 5: Observations resulting from visualisation using the erosion figures technique.

All participants expressed satisfaction or high satisfaction with the practical explanation of the tool, as well as with the proposed exercise. Furthermore, all participants were very satisfied with the textbook. In addition, 78% of respondents assessed the workshop as highly important for introducing fundamental

concepts related to natural ventilation, while the remaining 22% considered it important (Fig. 6B).

Furthermore, all students expressed a desire for more workshops of similar topics.

It is necessary to emphasise that, as only one base test area was produced, students had to reconstruct the entire setup already defined in the wind tunnel. This, coupled with a lack of practice in depositing sand around the model, resulted in a delay in the schedule, making it impossible to carry out the final team presentations.

During these presentations, the expected outcomes were supposed to be compared with those obtained in the wind tunnel tests. Additionally, the delay led to some impatience among students who had already conducted their experiments and did not stay to observe and learn from subsequent group trials.

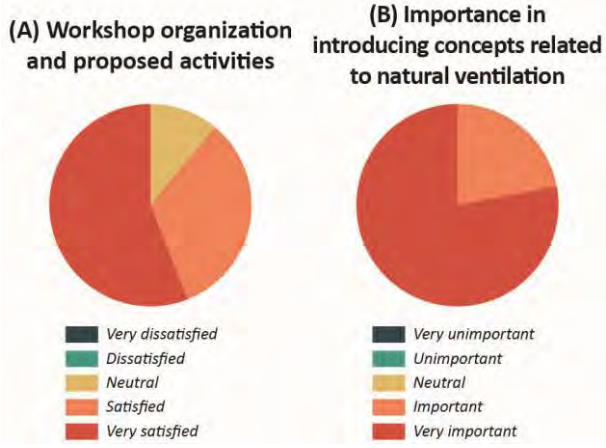

Figure 6: (A) Chart depicting responses regarding the organization of the workshop and proposed activities. (B) Chart depicting responses regarding the importance in introducing concepts related to natural ventilation.

Regarding limitations, the authors highlight some improvements (for next editions) below:

1. To produce more than one test-based area to reduce the time between the tests.
2. To prepare a short instruction, during the wind tunnel presentation, about how depositing the sand could help minimize the delay in the preparation for the tests, due to the lack of practice of the students in this process.
3. To better structure the final discussion, in order to emphasise the comparison between the expected and the obtained results.
4. To reduce the number of participants to permit just one group per workshop.
5. To initiate the workshop with wind tunnel presentation.
6. To present more design cases, during the explanations, to better illustrate the aerodynamic effects with real cases.
7. To reproduce the same qualitative tests in wind tunnel and water table apparatus during the workshop.

4. CONCLUSION

This article presented a workshop about natural ventilation concepts, design process and use of practical exercises with students from the first year of Architecture and Urbanism course, focusing on the use of wind tunnel tests. The didactic-pedagogical process, when supported by practical studies, awakens the gaze and interest to know phenomena, in this case related to environmental comfort, applicable in the development of projects and evaluations of built spaces.

Practical activities, such as the one described here, have an essential role in the teaching-learning of environmental comfort, since it is a discipline that deals with human senses and cannot be fully learned only through lectures. In addition, these experiences should be aimed at bringing concepts of bioclimatic architecture and sustainability closer to design practice. It is important that all tools and instruments are introduced to students at the beginning of the graduation, since they already start the course motivated to learn more and knowing that these tools can be used to help the work and design decisions throughout the course.

This experience was a pioneering workshop and brought very positive results, encouraging the development of other practical workshops that aim to present and understand the existing instruments in the Environmental Comfort and Energy Efficiency Laboratory (LABAUT) at FAU USP – such as the water table and the heliodon, for example. It is worth mentioning that the wind tunnel workshop also needs to be improved, as mentioned above, with the inclusion of active learning methods and longer duration.

ACKNOWLEDGEMENTS

The authors gratefully acknowledge technicians from both the Environmental Comfort and Energy Efficiency Laboratory (LABAUT) and the Technical Section of Models, Tests and Constructive Experiments (STMEEC) of Faculty of Architecture and Urbanism of University of São Paulo (FAUUSP) for helping in the pre-tests and tests during the workshop.

REFERENCES

1. Bhagat R. K.; Linden, P. F. Displacement ventilation: a viable ventilation strategy for makeshift hospitals and public buildings to contain COVID-19 and other airborne diseases. *Royal Society Open Science*, 7, 2020.

2. Frota, A. B.; Schiffer, S. R. *Manual de Conforto Térmico*. 7ª ed. São Paulo: Editora Nobel, 2003.

3. Marcondes, M. P., 2010. *Soluções Projetuais de Fachadas para Edifícios de Escritórios com Ventilação Natural em São Paulo.* Thesis. University of São Paulo, São Paulo.
4. Field, C.; Cuthbert, G. Acoustically Treated Dual Vented Window System. In: *Inter-noise*, 2019. Madrid, Spain, 2019.
5. Lawson, B., 1980. *How Designer Think. The design process demystified*. The Architectural Press, London.
6. Silva, F. A. G., 1999. *O vento como ferramenta no desenho do ambiente construído: Uma aplicação ao nordeste do Brasil.* Thesis. University of São Paulo, São Paulo.
7. Rossi, M. M., 2021. *Dispositivos de Sombreamento: avaliação do Impacto no Desempenho da Ventilação Natural.* Thesis. University of São Paulo, São Paulo.
8. Pope, A.; Rae, W. H. *Low-speed wind tunnel testing*. New York: Wiley, 1984.
9. Shimomura, A. R. P., 2005. *Impacto da altura de edifícios nas condições de ventilação natural do meio urbano.* Thesis. University of São Paulo, São Paulo.

PLEA 2024 WROCŁAW
(Re)thinking Resilience

Towards A Reduction Of The Impact On The Universities' Activities

Project Nearly Zero Emissions Campus–University of Colima

CARLOS J. ESPARZA-LÓPEZ[1], OSCAR F. VÁZQUEZ-VUELVAS[2], JORGE A. OJEDA-SÁNCHEZ[1], ALFONSO CABRERA-MACEDO[1], JUAN CARLOS TEJEDA-GONZÁLEZ[3]

[1]Faculty of Architecture and Design, University of Colima, Colima, México
[2] Faculty of Chemical Sciences, University of Colima, Colima, México
[3] Faculty of Civil Engineering, University of Colima, Colima, México

ABSTRACT: University centers serve as hubs for significant human interaction. The activities conducted within these spaces necessitate substantial resources and generate considerable waste. In Mexico, more than 3.65 million students are enrolled in over 3,000 universities at the higher education level. Situated along the Pacific coast, the University of Colima stands as the primary higher education institution in the region, catering to the needs of 65% of students across six extensive campuses. This document outlines the methodology employed to gather information from these areas, aiming to define a diagnosis of the impact generated from one the campuses in order to formulate proposals that alleviate the impacts associated with these activities. The study focus areas include energy, indoor environmental quality, waste, and water. The outcomes of these studies will inform implementation plans, programs, and actions geared towards minimizing the university's environmental footprint and aligning with the Sustainable Development Goals (SDGs) in the short term.
***KEYWORDS**: Carbon emissions, Methodology, Educational building, Impact reduction, Net Zero.*

1. INTRODUCTION

Universities serve as hubs for meaningful human knowledge and interactions. The various activities undertaken within these environments necessitate substantial resources and generate considerable waste. Lifestyles have undergone changes that have transformed the environment, leading to permanent consequences and jeopardizing essential assets.

These impacts on resource consumption, as well as waste production, contribute to the overall emission of greenhouse gases, adding to the international emergency of climate change. To address the impacts of climate change, it is crucial to decrease carbon dioxide emissions across all sectors [1].

Decarbonization entails reducing the reliance on carbon as an energy source. It is linked with the carbon footprint, which assesses the amount of carbon utilized for energy generation through human-driven activities. This metric encompasses the total CO2 emissions, primarily from fossil fuel combustion for energy production, subtracting the amount of atmospheric CO2 used, such as through plant absorption or their derivatives like biofuels. When the sum of CO2 emissions and the quantity of reabsorbed atmospheric carbon reaches equilibrium, the process can be termed as achieving net-zero carbon emissions [2].

This document outlines the procedural framework employed to amass data about different areas of impact, such as energy, water, indoor air quality, and waste, to formulate recommendations aimed at mitigating the repercussions engendered by said activities. The focal areas of study encompassed energy usage, indoor environmental quality, waste generation, and water utilization. The energy team appraised the energy consumption and the inventory of electrical apparatuses deployed on campus. The faction devoted to indoor environmental quality examined variables such as ambient temperature, relative humidity, acoustics, and lighting preferences of occupants. The waste division scrutinized the volume and nature of refuse produced. Lastly, the water cohort investigated water resource sourcing, distribution, and application.

The findings will serve as the foundation for strategies, initiatives, and measures intended to curtail the impact on the university while concurrently advancing the attainment of the Sustainable Development Goals in the near term.

2. PROJECT NEARLY ZERO EMISSIONS CAMPUS-UNIVERSITY OF COLIMA (GENERAL METHOD)

Institutional policy to address environmental problems is delineated in the University of Colima Development Plan 2022-2025 [3]. These documents align with the United Nations Sustainable Development Goals (SDGs) and promote environmental policies focused on legislation managing all natural resources. It is essential to

mention that The University of Colima is centered on an environmental management policy, described by the sustainability of forestry and hydric resources.

The University of Colima is segmented into six extensive campuses, with three located within the capital city's metropolitan region, two in coastal municipalities (Manzanillo and Tecoman), and an additional one in the central area of Coquimatlan. This last campus is designated explicitly for studies related to exact sciences and serves as the focal point for the project (refer to Figure 1).

The campus has four faculties: Architecture and design [FAD], chemical sciences [FCS], civil engineering [FCE], and mechanical and electrical engineering [FMEE], a two-shift high school (morning and evening), and administrative and services areas.

The "Towards a nearly zero emissions campus- the University of Colima" project began in August 2022 and is currently completing its first stage. The main objective is to "Develop a comprehensive management plan for implementing a campus with low consumption of resources and highly efficient (Nearly Zero Emissions Campus) that allows serving as an example and leverage for the community where the processes are implemented and established to be able to extrapolate its execution to other campuses and areas." It was planned to work in 4 stages in 4-5 areas depending on the stage, as shown in Figure 2.

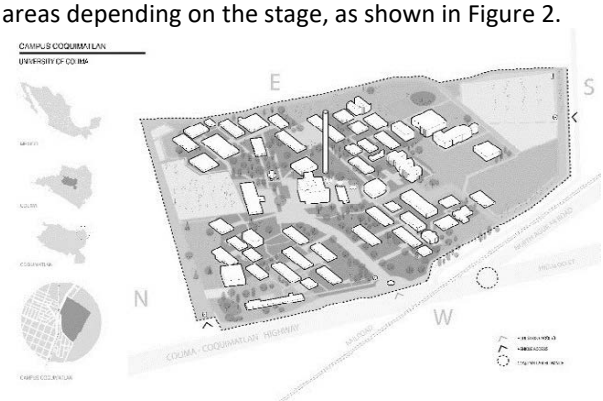

Figure 1: Location of the University campus and distribution of faculties.

To assess the repercussions arising from activities conducted on this university campus, a consortium of over 80 researchers and students representing diverse fields of expertise convened to evaluate the effects of human endeavors across four primary domains. This investigation intended to scrutinize the influence of human actions within the university precinct.

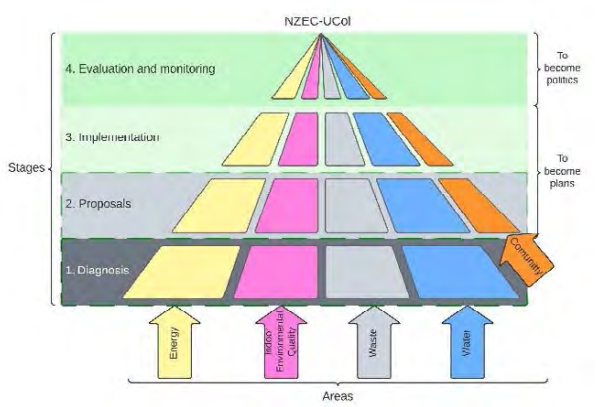

Figure 2: General method of the NZEC-UdeC project.

The initial phase, termed "diagnosis," encompassed four focal areas: energy, indoor environmental quality, waste, and water. Subsequent phases, labelled as "proposals," "implementation and evaluation," and "monitoring," introduced a fifth area known as "community." Each area featured a dedicated workgroup, with each team devising a tailored methodology for conducting the diagnostic assessment based on specialization. As such, the faculty of chemical sciences concentrated on waste-related matters, the faculty of civil engineering centered on water management, the faculty of mechanical and electrical engineering addressed energy-related aspects, and the faculty of architecture and design tackled indoor environmental quality. Nonetheless, this arrangement did not preclude cross-area participation by team members, allowing them to contribute to other areas based on their expertise or personal interests.

2.1 Energy method

The work method developed directly inspects the equipment, power outputs, and lighting systems installed on the Campus. The objective was to define in a particular way the general operation of each of the buildings, laboratories, and workshops, among other buildings, that the faculties and dependencies must determine their correct operation and functionality based on the established requirements in the reference standards.

Lighting: In this section, both the type of lighting and its quality on the work surfaces will be quantified, taking as reference the equipment or machinery that will be working in the building to reduce the risk of accidents. For this system, surveys were carried out by type of lamp, power, and distribution of lighting points according to the NOM-025-STPS-2008 standard [4], Lighting requirements in work centers, which refers to the quantity of Minimum lighting depending on the activity to be carried out in the reference building.

Strength: the connection points for the equipment that will be installed were accounted for so that the

required energy is supplied and reduces the risk of failure and breakdown and its correct operation. Tension measurements were carried out for each power output, as well as a visual inspection of the cable gauge and physical condition for each output following the NOM-001-SEDE-2012 standard [5], Electrical distribution systems, use, which governs everything related to the installation of electrical circuits, from cable gauge, ampacity, conduits, to types of feeders for load centers and their protections.

Load centers: It is essential to verify that each building has a center in good condition, that the feeder circuits can supply the connected load, and that the protections are by it. To comply with this section, a visual inspection and voltage measurement were carried out in each load center, reviewing installed gauges and functionality and their interruption capacity according to the same standard NOM-001-SEDE-2012 [5].

2.2 Indoor Environmental Quality method

A survey was carried out to know the perception of the inhabitants of educational spaces. The variables that define the space environment were addressed, such as dry bulb temperature, relative and absolute humidity, wind, sounds, lighting, air quality, and hygiene.

The approximate study universe of the campus was 2767. The process of applying surveys to determine the perception of the quality of the indoor environment in university spaces began on October 28, 2022, and concluded in May 2023. One thousand sixty-eight surveys were applied, giving a sample of close to 39% of the population that lives on campus. However, filtering the responses and eliminating those with discordant values resulted in 534 (19%) valid surveys for statistical analysis.

The process for applying surveys and environmental monitoring in classrooms complied with the recommendations of the following standards: ISO 7726 ergonomics of the thermal environment. Instruments for measuring physical quantities (ISO 7726, 1998); and ANSI/ASHRAE Standard 55:2017 Thermal environmental conditions for human occupancy (ANSI - ASHRAE Standard 55, 2017).

The survey was designed in several sections:

-Identification data.
-General data and hygrothermal history.
-Hygrothermal comfort.
-Acoustics.
-Lightning.
-Air pollution
-Closing.

The following table shows the recorded variables, the equipment used for each of them, and the general measurement units for each.

Table 1. Variables and equipment used.

#	Variable	Equipment	Unit
1	Dry Bulb Temperature	Data logger U12-012, onsetcomp	°C
		Thermal stress station HD32.2, Delta OHM	°C
2	Black globe temperature	Thermal stress station HD32.2, Delta OHM	°C
3	Relative humidity	Data logger U12-012, onsetcomp	%
		Thermal stress station HD32.2, Delta OHM	%
4	Surface temperature	Thermal camera i5, flir	°C
5	Wind speed	Thermal stress station HD32.2, Delta OHM	m/s
6	lightning	Data logger U12-012, onsetcomp	Lumen/ ft^2
7	Sound	Decibelimeter SLM-25 Sound lever meter	Db
8	CO_2	Air quality monitor BEYHT001, ym	ppm
		Air quality monitor ML4-154, KAMYSEN	ppm

2.3 Waste method

The methodology for sampling solid waste considered municipal (office garbage, schools, houses, and similar non-chemical-biological hazardous waste) was based on the NMX-AA-015-1985 standard [7]. The collection was planned so that an amount was accumulated for 24 hours, one typical day of the week.

The population of people who use the facilities in the study was considered for selection on the sampling day. Quantification was carried out with mechanical weighing equipment. Once the initial containers were weighed, sampling was carried out for separation and classification, considering the quartering method indicated in [7] Environmental protection - Soil contamination - Municipal solid waste - Selection and quantification of byproducts.

2.4 Water method

A lifting of all the hydraulic furniture of the campus was made in all buildings. In addition, hydraulic planes for irrigation systems were reviewed. Because there were no water flow meters, the amount of potable water and drainage was estimated from the counting of furniture and outputs for irrigation systems.

3. RESULTS

The results are presented for each work area designed in the diagnostic stage. Each area presented an extensive diagnosis of those found. The general

results indicated areas of opportunity in each of them.

3.1 Energy results

Figure 3 shows the quantities of lamps by technology and their installed capacity throughout the Coquimatlán Campus. About 50% of the lighting technology in spaces comprises fluorescent lamps. LED lamps have already replaced 40% of the technology.

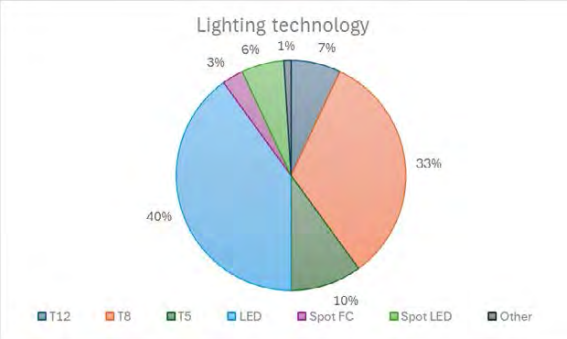

Figure 3. Percentage of lighting technology.

The installed power capacity for luminaires by technology is shown below in Figure 4, with fluorescent technology once again making up the most significant percentage.

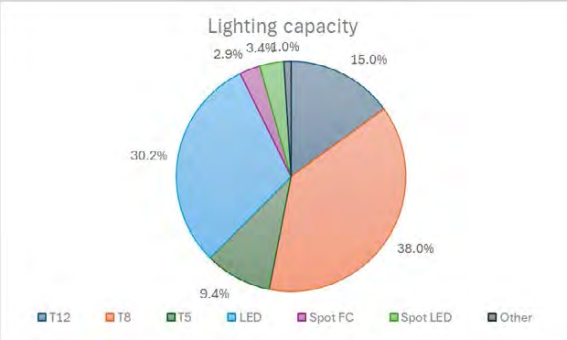

Figure 4. Percentage of lighting capacity.

3.2 Indoor Environmental Quality results

According to the climatic characteristics of the area, three climatic seasons described below were considered: warm and humid, which includes the months of June to November; temperate from December to March, and warm and dry in April and May. For the hot-humid season, temperatures ranged between 24°C and 32°C inside the spaces. In Figure 5, the distribution of temperatures related to the users' responses regarding the sensation they perceived of their space can be seen, with -3 being very cold, 0 being neither cold nor hot, and +3 being very hot.

Figure 5 shows that the neutral temperature value is close to 27°C, above the standard of 25°C for naturally ventilated spaces.

For the acoustic variable, the values for background noise ranged between 47 dB and 77 dB in the recorded measurements; however, when the passing of the train was recorded, unrecorded values of up to 85 dB were achieved, as well as values close to 90 dB in the FMEE workshops. Regarding the acoustic sensation, it can be seen in the trend line that the values considered comfortable were close to 50 dB, higher than those indicated by the standards for educational spaces, which are around 30 dB at 35 dB. dB [8].

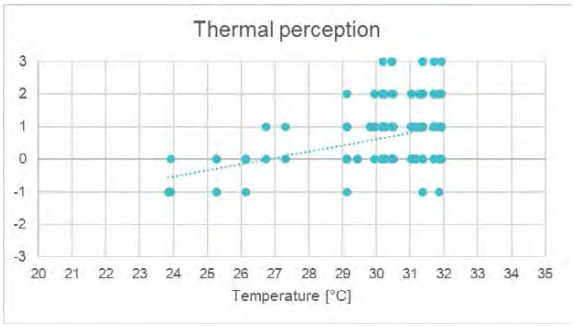

Figure 5. Distribution of the thermal perception and the logged temperature.

The values observed during the survey ranged from 10 lux to 710 lux for the lighting variable. In terms of the sensation on the student's part, it is generally observed that, regardless of the value recorded, low lighting values were perceived in the spaces. It can even be seen that the trend line remains constantly close to the value -1 as low illumination.

Finally, for the last variable analyzed, the average values of CO_2 concentrations in the spaces used at the time of the survey, for the most part, remained close to 500ppm, which, according to the occupational risk prevention department of the Complutense University of Madrid [9] and the environmental health department for the same locality [10] are within the permissible limits for this type of spaces. However, a considerable percentage of spaces presented values higher than the said mark, even reaching almost 2,000 ppm, requiring, according to said technical reports, immediate ventilation to maintain the hygiene of the space. According to the above, it is necessary to implement effective ventilation strategies that guarantee the health of its occupants.

3.3 Waste results

The results showed that 245.5 kg of solid waste was counted in 24 hours (See figure 3). The most abundant component was organic material, mainly from food and kitchen waste, which comprised 48.8% of the identified components, constituting 119.9 kg. Secondly, plastic from bags and jars or bottles, both polyethylene and PET, accounted for 26.3% of the total quantified waste, constituting 64.5 kg daily. Thirdly, paper constituted 10.8% of the total

quantified waste, having an estimated emission of 26.5 kg in 24 hours. Subsequently, cardboard and glass presented a similar composition of 4.2% and 5.2% of the total waste, and plastic from expanded polystyrene, which is generally used as food packaging, represented 2.3% by weight of the total.

Figure 3. Waste quantification for 24 hours.

The annualized projection represents a total of 39,344 kg of solid waste. The materials with the highest emissions projected annually correspond to food waste material and kitchen waste at 19,179 kg, PET and Polyethylene plastics at 10,327 kg, paper at 4,242 kg, and cardboard at 1,660 kg.

3.4 Water results

A starting from the lifting of each space of the campus, a final count of all hydraulic furniture was made. Table 1 can see that the most useful furniture on campus is toilet with 120 units that represents 23% of the total furniture, followed by the bath sinks with 109 (21%), laboratory faucets with 84 units (16%), kitchen sinks with 79 units (15%) and migitory with 60 units (12%). To a lesser extent are the faucet, shower and eye-showers.

Table 1. Quantity of water furniture in the campus.

Furniture	**Quantity**
Toilet	120
Bath sink	109
Migitory	60
Kitchen sink	79
faucet	38
Laboratory faucet	84
shower	23
Eye-shower	6

To calculate the estimated consumption of water in the campus, the provision of water per minute is presented in table 2.

Table 2. Provision of water per minute for each type of furniture.

Furniture	Provision (l/min)
Toilet	10
Bath sink	5
Migitory	10
Kitchen sink	10
faucet	15
Laboratory faucet	5

Based on previous information, the estimated water consumption of the campus per year, considering 210 days of effective activity on the campus, following the calendar of the University of Colima for the period 2022-2023, and with a use factor daily of 52.5% of the devices, and a 40% loss due to distribution was 408,410,100 liters of water per year (408,410.1 m3 of water per year).

While, for irrigation, its consumption was estimated considering an effective irrigable area of 60,000 m^2 and an ideal expenditure of 5 l/m^2/day, with an over-irrigation factor of 3 and a 40% loss due to distribution, taking as a result 264,600,000 liters of water per year (264,600 m^3 of water per year).

Therefore, the estimated final consumption of the campus was 673,010,100 liters per year (673,010 m^3 per year).

4. CONCLUSION

Specific initiatives pursued by university institutions entrusted with spearheading the journey toward carbon neutrality involve generating greenhouse gas-free energy. These practices have seamlessly integrated into curricula, projects, research endeavors, infrastructure modifications, and equipment upgrades. This concerted effort ensures that upcoming generations have enhanced prospects for residing in an improved environment. The general conclusions for each area are presented next:

For energy, the high consumption of artificial air conditioning and the operation of computers and specialized equipment require changing the energy source towards renewable sources. In addition, it is necessary to update practically the entire infrastructure with more efficient equipment.

For the quality of the indoor environment, the comfort temperatures indicated differences in terms of more remarkable adaptation of the inhabitants concerning standards such as ASHRAE 55. For the quality of the environment, the values remained below the dangerous range, between 500 ppm and 700 ppm.

For the waste area, the amount of municipal solid waste was concentrated in Styrofoam from the food area and waste from pruning green areas. It is

presented as an opportunity to create policies to reduce waste production.

For water, it is necessary to update the bathroom furniture for those with low consumption, create mechanisms for rainwater harvesting, and reconsider green areas with high water consumption.

The impact of human activities on the environment is undeniable, as observed in the results of the diagnosis presented here. The pressure exerted on resources such as water or energy to adapt our spaces to the daily activities of the campus is enormous, coupled with the large amount of waste produced of which few are treated to reincorporate them in productive or usable cycles.

ACKNOWLEDGEMENTS

The authors would like to thank the authorities of the University of Colima for their support to develop of the research project "Hacia una Universidad de bajo impacto NZEC-UdeC".

REFERENCES

1 Filho, W.L., Vidal, D.G., Dinis, M.A.P., Lambrechts, W., Vasconcelos, C.R.P., Molthan-Hill, P., Abubakar, I.R., Dunk, R.M., Salvia, A.L., Sharifi, A., 2023. Low carbon futures: assessing the status of decarbonisation efforts at universities within a 2050 perspective. Energy. Sustain. Soc. 13, 1–18. https://doi.org/10.1186/s13705-023-00384-6.

2 Ahmed, A., Ge, T., Peng, J., Yan, W.C., Tee, B.T., You, S., 2022. Assessment of the renewable energy generation towards net-zero energy buildings: A review. Energy Build. 256, 111755. https://doi.org/10.1016/j.enbuild.2021.111755

3 Universidad de Colima, 2021. Plan Institucional de Desarrollo 2020-2025. Colima, México.

4 Comité Consultivo Nacional de Normalización para la Seguridad y Salud en el Trabajo, 2008. Lighting requirements in workplaces. México.

5 Comité Consultivo Nacional para la Normalización de Instalaciones Eléctricas, 2019. Electrical distribution systems, use.

6 ANSI - ASHRAE Standard 55, 2017. Thermal Environmental Conditions for Human Occupancy. Atlanta, GA.

7 Secretaría de Desarrollo Urbano y Ecología, 1985. Protección al ambiente - contaminación del suelo - residuos sólidos municipales - muestreo - método de cuarteo. Diario Oficial de la Federación, México.

8 Infraestructura Educativa INIFED. (2014). Normas y especificaciones para estudios, proyectos, construcción e instalaciones, Tomo IV acondicionamiento acústico. In Normatividad e Investigacion (Vol. 3, Issue Tomo IV). https://www.gob.mx/cms/uploads/attachment/file/105400/Tomo4_Ac_stica.pdf.

9 Universidad Complutense Madrid. (2020). Recomendaciones para la utilización de medidores de CO2 para evaluar la eficiencia en el escenario COVID de la pauta de ventilación de los espacios de la UCM con ocupación de personas manteniendo la capacidad máxima que corresponda cumpliendo la distancia.

10 Doremalen, N., Morris, D., & Holbrook, M. (2020). Medición de la concentración de CO2 como indicador de una ventilación adecuada de edificios y locales. COVID19. In Departamento de Salud Ambiental Subdirección General de Salud Pública. www.madridsalud.es-www.madrid.es

PLEA 2024 WROCŁAW
(Re)thinking Resilience

Fostering In-Depth Learning in Daylighting Design
Insights from two summer schools

FEDERICA GIULIANI[1,2], NATALIA SOKOL[3], NIKO GENTILE[4], VALERIO R. M. LO VERSO[5], MANDANA SAREY KHANIE[6,7]

[1]Università degli Studi della Tuscia, Viterbo, Italy
[2]Università degli Studi Niccolò Cusano, Rome, Italy
[3]Gdansk University of Technology, Gdansk, Poland
[4]Lund University, Lund, Sweden
[5]Politecnico di Torino, Turin, Italy
[6]The Bartlett, Faculty of the Built Environment, University College London, London, England
[7]Technical University of Denmark, Kgs. Lyngby, Denmark

ABSTRACT: This paper reports on the educational model undertaken in two specialized summer schools in Denmark (2022) and Poland (2023) on daylighting in buildings. As a part of a European educational initiative, these schools aimed to deepen participants' understanding of the impact of daylight on building design. The programme, a collaborative effort between universities, companies, associations, professionals, and students, integrated an online platform for theoretical knowledge with practical summer schools. The paper presents the objectives and results of the summer schools, the project-based learning outcomes, topics and the structure of the teaching activities. The participants' positive responses highlight the summer schools' success and suggest future improvements.
KEYWORDS: Daylighting design, Educational model, Project-based learning, Multidisciplinary education, Participant feedback

1. INTRODUCTION

With the implementation of the daylight assessment method in compliance with the EN 15193 standard [1], and particularly with the adoption of EN 17037 for the assessment of daylight in buildings [2], a clear trend is emerging in the field of built environment design, which increasingly considers daylighting. Designers are at the forefront of this change, committed to the challenge of creating energy-efficient buildings for the next generations. It underlines the importance of fully understanding daylight regulations, their design implications, and beyond the standards. However, studies highlight a widespread lack of knowledge regarding lighting retrofitting and the energy performance evaluation of modern lighting systems [3, 4]. Moreover, other studies reveal how designers still rely on simplified methods and rules of thumb in the early stages of the project [5, 6]. Others show that there is a growing need for better daylight education [7-10].

In response to these challenges and recognizing the evolution of the building design, this article shows the vital role of specialized summer schools in teaching daylight. These educational initiatives aim to bridge the knowledge gap, provide designers with insights and cutting-edge tools, and prepare them to meet the increasing demand for sustainable and energy-efficient building practices.

2. PROJECT STRUCTURE

The educational project "New Level of Integrated Techniques for Daylighting Education" (NLITED) was introduced within the Erasmus+ funding program in 2020, with the participation of four European universities in Denmark, Italy, Poland, and Sweden. The project's main goal was to increase knowledge of daylighting in the construction sector to benefit professionals and university students.

2.1 The educational package

The educational project involved a synergy between *theoretical* knowledge, provided through a free e-learning platform based on independent modules, and *applied* knowledge, provided through intensive study programmes in summer schools. The combination of these two learning approaches was designed to enrich the educational experience and offer the opportunity to deepen specialized knowledge that can contribute significantly to understanding environmental sustainability.

Networks of stakeholders played a strategic role in defining the project's goals. The networks, including other universities, consulting and design companies, trade associations, (day)lighting associations, and technical publishing houses, were created nationally.

The networks of stakeholders were a vital part of the project, actively contributing to the creation of the

curriculum, participating in the implementation of the teaching modules, and realizing the summer schools. For the definition of the curriculum, fourteen workshops (three or four in each country) were held between January and February 2021, involving 63 experts. Besides, 98 opinions were collected from other professionals through an online questionnaire. The experts' views and the 98 professionals' responses were influential in defining educational needs and gaps [12].

2.2 The NLITED eLearning Platform

The NLITED educational platform is free and open access, designed to fill knowledge gaps and tailored to learners' educational needs [11]. The curriculum is structured into five thematic areas ("blocks") covering (1) health, (2) daylighting design, (3) energy aspects, (4) daylight assessment, and (5) daylighting simulation. Each block includes coordinated lectures ("eModules") that provide theoretical knowledge and practical case studies. Interactive self-assessment exercises are integrated with engaging participants. Each module has a final knowledge assessment test for issuing the attendance certificate. Additionally, each module undergoes a quality evaluation test ("eModule evaluation", EE). Overall, 32 modules were developed with the involvement of stakeholders from the strategic network, who serve as instructors and present case studies.

The NLITED online learning platform was launched on January 31, 2022. After over two years (data as of February 29, 2024), the platform has over 800 registered users. The introduction of the educational platform is detailed in publications [12, 13], and initial results have also been reported [14, 15].

3. THE NLITED SUMMER SCHOOLS

Two summer schools, 'Daylighting in buildings', were implemented within the NLITED project. The first occurred in Copenhagen at the Technical University of Denmark (DTU) from 16 to August 22 2022. The event was closely connected to the BuildSim Nordic Conference, held in Copenhagen on August 22-23, 2022. During this event, the summer school participants presented their projects in a poster session as part of the scientific discourse. The second summer school was held in Gdańsk, Poland, at the Technical University of Gdańsk from 25 to August 31 2023. With a similar structure to the previous one, the participants presented their final work at a public event explicitly organized by the Polish institution to promote the design initiatives PPNT (Pomeranian Science and Technology Park).

The main objectives and peculiarities of the summer schools, which make them a unique learning approach to foster the interaction between students and experts, were:

1) Foster an Engaging Learning Experience. Develop an interactive and captivating approach to learning. All elements of the summer school, i.e., lectures, group discussions, pitches, and presentations throughout the week and the directed project-based work in collaboration with teachers, lecturers, and industry experts, were designed to allow for interaction and knowledge exchange in every detail of the project.

2) Provide Comprehensive Work Exposure. Participants gain holistic work experience. The project-based approach and group work were the two significant elements of the summer schools that allowed for a real-life representation of a task in industry. Projects, addressed in groups, expose the group members to diverse experiences, study backgrounds, and knowledge. Throughout the conceptualization of the training program adopted in the two summer schools, we ensured that the main elements of a real working environment were adopted in the training process, i.e.,

- Troubleshooting and comparison with standards
- Exchange of knowledge
- Communication in group and teamwork
- Diverse expertise and skills
- Dissemination

3) Facilitate networking with experts from studios, industries, and firms. Create opportunities for participants to connect with professionals from studios and companies in the industry. The teachers at the summer school were a team of experienced daylighting professionals from different European universities and industry partners. The participants had the opportunity to learn from the experts, gain practical experience in daylighting design, and network with other professionals in the field.

4) Designed for Both Master's and Ph.D. Students and Professionals. This program is tailored to benefit both master's and Ph.D. students and professionals seeking an immersive study experience.

5) Culminate in a Presentable Final Product (Event/Competition). The projects were to be concluded by creating a tangible and presentable final output, presented at a more significant event and with a larger audience of peers in the building industry with possibly different backgrounds and fields.

3.1 Summer School n.1: Copenhagen 2022

The week-long program included training, technical tours of laboratories and actual buildings, and a final poster competition at the BuildSim Nordic conference. The 24 participants included students and professionals. The primary aim of the summer school was to carry out an entire daylighting design project.

Students were divided into groups, with two teachers accompanying each group throughout the project.

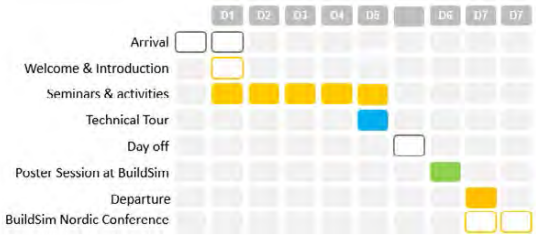

Figure 1: Overview of the summer school.

The training program took place over four days, with daily lectures addressing the task at hand, supervised by various lecturers. The fourth day was allocated for project finalization and presentation/communication aspects. The program included a guided Technical Tour across the city.

3.1.1 The training concept

The students were grouped and completed a set of tasks with clear learning objectives: understanding photometric measurements, design approaches, technologies, and interventions to enhance a building's daylight conditions, and finally, evaluating the design through simulation.

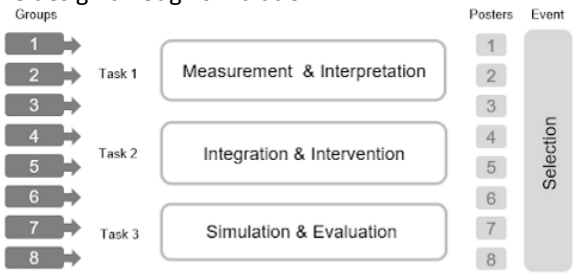

Figure 2: The NLITED educational program was defined to complement the ePlatform content for a more hands-on and realistic experience.

The teaching and learning activities were structured around three core tasks designed to provide a more hands-on and realistic experience:

- **Task 1: Measurement and Interpretation**

The learning objectives of this task were to familiarise the students with the basics of the physics of light and photometry through measurement to understand the quantities behind the numbers. Light intensity, colour, spectral distribution, and visual comfort-related parameters were measured.

- **Task 2: Integration and Intervention**

This task focused on integrating daylighting concepts and interventions into the design process. The participants and the tutors defined the problems in the buildings to study and theoretically examined different architectural solutions.

- **Task 3: Simulation and Evaluation**

The strategies, solutions, and design scenarios examined in the previous task were tested and evaluated through simulations to evaluate their impact. The learning objectives at this stage were focused on understanding the results from daylighting simulation and strategies through hands-on work, listing & remembering the daylighting metrics, evaluating the metrics through a comparative assessment, and finally evaluating the daylighting design.

Figure 3: The planned distribution of knowledge exchange and group work throughout the program.

3.1.3 Summer School Features

- **Scientific Board**

The Consortium coordinators primarily undertook the operational responsibilities and active engagement in the scientific board. Additionally, select teachers from the network were invited to serve as Lecturers and Mentors, playing a vital role in guiding participants throughout the enriching summer school experience.

- **Boot camp**

The summer school was structured as an immersive boot camp. Participants and teachers shared the same venue and communal meals, fostering a sense of community. This approach was aimed to facilitate a cohesive learning environment and contribute significantly to creating a community spirit among all participants.

- **Final Event**

As a culmination of the programme, the NLITED summer school hosted a final event, which served as a platform for participants to showcase their work through scientific posters. The event was a formal presentation during the popular scientific BuildSim Nordic conference. Participants presented their results and engaged in academic discussions, enriching their learning experience.

- **Admission Criteria**

An essential requirement was a fundamental understanding of the physics of light, daylight assessment principles, and building simulation. To do this, significant emphasis was placed on completing at least four eModules of the [name] platform, highlighting the programme's commitment to building a solid knowledge base on daylighting.

- **Projects and Presentation Preparation**

Eight projects tackled real daylighting problems at the DTU campus. One day was dedicated to preparing the posters, with lessons on scientific reporting and communication skills. The groups evaluated their work and designed the posters to communicate findings.

3.2 Summer School n.2: Gdansk 2023

The second summer school occurred in Gdansk, Poland, in August 2023. It attracted 19 in-presence persons and seven online participants, including MSc and PhD students alongside professionals. Retaining the thematic divisions from the first summer school (Daylight Quality, Design, Simulation, Dissemination), the students worked in groups of three (totalling six groups). The critical modification was in the afternoon student-teacher interaction, which allowed independent work, with consolidated feedback sessions at the end of each day. The schools started with a technical tour to visit different districts of Gdansk and the university campus that hosts the buildings used as case studies, plus the day of the open-to-public presentations at the Gdansk University of Technology. Similarly to the first summer school, the participants presented their final work in a public event at the Pomeranian Science and Technology Park (PPNT). The event was co-hosted by Gdynia Design Days, promoting sustainable design solutions.

3.2.1 Schedule

The summer school lasted from August 26 to August 31, 2023. It started with a technical tour of the Gdansk area to learn about local architectural and urban solutions, emphasizing daylight for residential areas in Gdansk over the last 250 years, and to visit the case studies. The tour was guided by the local architects and urban planners, who explained how urbanists and architects designed residential areas for people through the centuries and how daylight was treated in buildings and at an urban scale.

The training program started with an open-to-public lecture on daylight quality at the Gdansk University of Technology. Like the previous year, the second edition had a boot camp formula: the training sessions were held in the university resort centre in Sopot, where students and teachers worked for a week. The participants presented their projects as a video clip at an open-public event co-organized in the neighbouring city of Gdynia with the local design organization called 'Gdynia Design Days'. This event was hybrid, and many emphases were placed on disseminating daylight topics to a diverse audience.

3.2.2 The Role of Chronobiology Lectures

The novelty proposed during this summer school was that chronobiology lectures focused on interactive lighting, daylight exposure, and well-being were offered. At the beginning of the school, an introductory lecture on non-visual aspects of light was delivered. Then, a critical session with an invited chronobiology expert was offered at the end of the week. The idea was to allow students to evaluate their projects from a chronobiological point of view after considering all other aspects. The chronobiology expert also delivered a dissemination lecture on the circadian aspects of light and its impact on our lives at the final hybrid event.

3.2.3 Projects

The summer school proposed to the students a choice among seven projects focusing on two buildings - a dormitory and an office building - located at the Gdansk Tech campus. These projects explored various aspects of daylighting design:

(1) Dormitory Building:

- Façade Design: Investigated changes in window size, glazing type, and facade design for improved indoor lighting conditions.
- Interior Layout: Explored furniture settings, room sizes, and view direction to enhance visual and non-visual aspects.
- Solar Shading: Examined the impact of solar control devices on indoor lighting.

(2) Urban Densification:

- Explored how to achieve higher urban density around the dormitory building while ensuring compliance with daylight standards.

(3) Office Building:

- Façade Design: Investigated changes in window size, glazing type, and facade design for improved indoor lighting conditions.
- Interior Layout: Explored furniture settings, room sizes, and view direction to enhance visual and non-visual aspects.
- Solar Shading: Examined the impact of solar control devices on indoor lighting.

These projects aimed to provide students with hands-on experience by designing spaces, prioritizing daylighting, and fostering innovative solutions within established standards.

3.2.4 Presentation and Communication Preparation

The summer school participants discussed their progress on design tasks daily, except for the day allocated to prepare the final video clip and event. Different tutors asked the groups daily to evaluate their work, create an explanatory movie to convey their findings from the practice and communicate the selected design solutions to the general audience. The emphasis was put on suggesting design solutions concerning both visual and non-visual effects of light.

3. RESULTS

Activity satisfaction surveys were conducted at the end of each summer school. The questionnaire covered satisfaction with the training offer, agenda structure, training objectives and involvement aspects. Approximately 25 responses were collected from the 41 participants in both editions, representing a response rate of 61%.

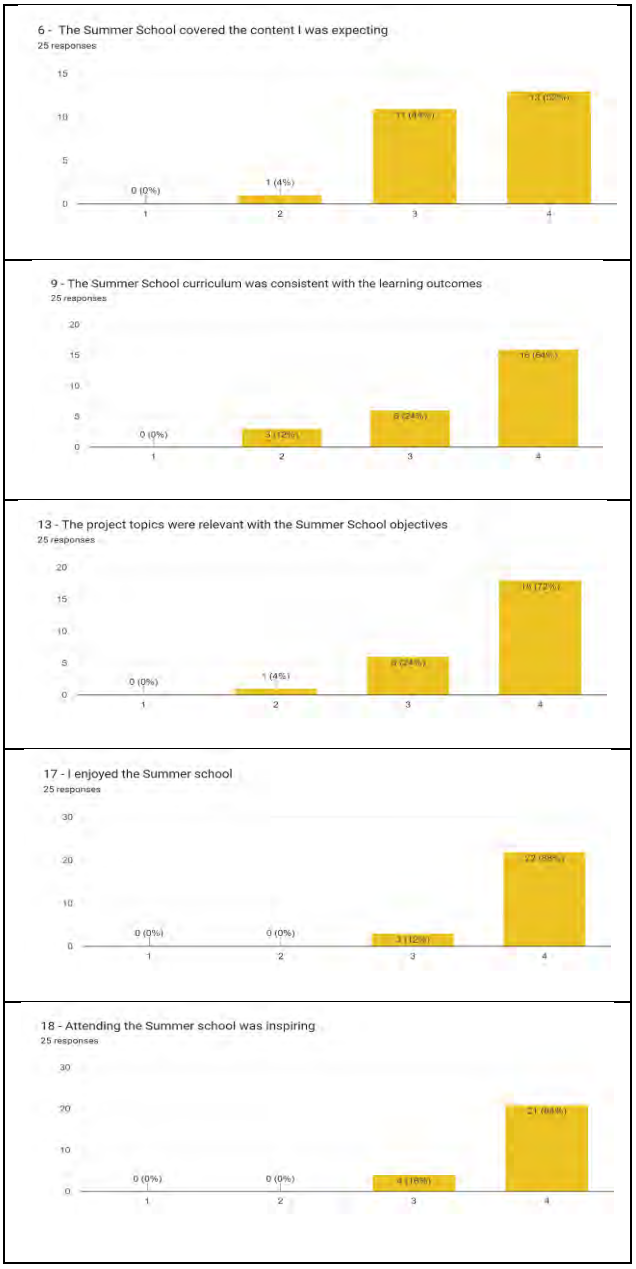

Figure 4: Some of the results of the satisfaction questionnaire administered to the participants of both summer school editions.

The survey responses generally showed positive feedback from participants, highlighting the many strengths of the summer school programme (Fig. 4):

- **Appreciation for the Educational Model**: 65% of participants expressed a score of 4, reflecting their appreciation. This positive feedback underscores the effectiveness of the program in delivering educational content.
- **Collaboration Between Architects and Engineers**: 75% of participants found the summer school curriculum consistent with the learning outcomes and the workload adequate. These findings highlighted the program's success in promoting collaboration between architects and engineers, fostering a comprehensive understanding of daylighting principles, and balancing creativity and performance.
- **Interaction Between Students and Experts:** One of the key aspects of summer school is the interaction between students and experts. An outstanding 100% of participants found the tutoring provided by teachers valuable and helpful.
- **Inspiration and Enjoyment:** 100% of participants found attending the summer school inspiring, and 95% reported enjoying it. This positive feedback emphasizes the program's ability to motivate and engage participants, making it an enjoyable and fulfilling educational experience.
- **Relevance to Career and Academic Development:** 90% of participants felt confident about the knowledge they gained, indicating that the educational content was relevant to their career and academic development. Additionally, 85% found that the concepts they learned were helpful in their academic curriculum or professional careers.
- **Recommendation:** 95% of participants expressed willingness to recommend the summer school to colleagues, underscoring their confidence in the program's quality and value.

4. DISCUSSION

Both editions received highly favourable responses from participants. The participants appreciated the educational model and the opportunity for close interaction with their instructors. While design topics were well-developed, specific weaknesses surfaced. The participants expressed concerns about the limited time following afternoon reviews in the first edition. Educators expressed doubts about the demanding pace. The second edition aimed to specialize case studies and optimize time management; however, feedback still indicated ongoing time constraints. Additionally, teachers observed overly simplistic projects, lacked creativity, and focused excessively on verification, according to the mere project guidelines.

From the experiences of the summer schools, valuable insights have emerged regarding teaching daylighting principles to young students and professionals in architecture and building design. The summer school format represented a unique learning model, where participants had the chance to work on

daylighting side by side with specialists to develop a project like building practitioners and daylighting specialists do in the current practice. Besides, visiting real buildings during the dedicated tours and designing their daylighting retrofitting was also a unique experience. This learning approach is far more productive and enriching than any other approach offered in standard academy courses.

Results underline that there is not a single teaching approach for daylighting. Enhanced collaboration between architects and engineers is offered to yield a more holistic proposal in upcoming editions, effectively reconciling creative and performative knowledge. Notably, the most compelling aspect of these summer schools remains the interaction between students and experts, facilitating deeper knowledge acquisition and delivering a valuable educational experience for all participants.

The integrated educational model, combining online modules and hands-on summer schools, forms a robust framework for knowledge dissemination on daylighting. The synergy between theoretical e-learning and practical summer sessions enriches the learning experience and caters to diverse participant needs. Besides, stakeholder involvement in curriculum development ensures relevance.

5. CONCLUSION

From the experiences of the first summer schools, valuable insights emerged on teaching daylighting principles to young students and professionals in architecture and building design. The results, as reflected in participant feedback and its broader impact on sustainable construction practices, highlight the urgency of expanding educational initiatives in daylighting design.

The most significant contribution has been addressing a crucial educational gap, promoting sustainable construction practices, encouraging multidisciplinary learning, and fostering a community of educated professionals through a unique learning approach that bridges the gap between the academic and professional worlds.

Areas for improvement remain, especially concerning a closer collaboration between architects and engineers to produce a more holistic proposal in future editions to effectively reconcile creative and performative knowledge. However, as all the participants emphasized, the most engaging aspect of these summer schools lies in the interaction between students and experts, which facilitates deeper knowledge acquisition and provides a valuable educational experience.

In addition, even after the conclusion of the funding, new intensive study experiences have been planned for 2024: a Winter School has taken place in Viterbo, Italy, in January, while the third summer school will take place in Lund, Sweden, in August. The fact that the NLITED group has managed to continue without direct funding but through the strength of the network attests to the group's resilience and ongoing interest in the subject, as well as the interest in the new funding agencies, such as the Swedish TO BE COMPLETED.

ACKNOWLEDGEMENTS

The NLITED project was co-financed with support from the European Commission's Erasmus+ programme. Project ref.: 2020-1-IT02-KA203-079527.

REFERENCES

1. EN 15193 - Energy performance of buildings — Module M9 — Energy requirements for lighting, 2014-2017.
2. EN 17037 - Daylight in buildings, 2018.
3. M.-C. Dubois et al., Daylighting and lighting retrofit to reduce energy use in non-residential buildings: A literature review. IEA SHC Task 50, Tech. Rep. T50.D2, Feb. 2016.
4. M.-C. Dubois et al., Retrofitting the Electric Lighting and Daylighting Systems to Reduce Energy Use in Buildings: A Literature Review. *Energy Res. J.*, vol. 6, no. 1, 25–41, 2015.
5. C. Reinhart and A. Fitz, "Findings from a survey on the current use of daylight simulations in building design," Energy Build., vol. 38, no. 7, 824–835, 2006.
6. A. D. Galasiu and C. F. Reinhart, "Current daylighting design practice: a survey," *Build. Res. Inf.*, vol. 36, no. 2,159–174, 2008.
7. Giuliani, F. et al. (2018). Daylighting Education in Practice Verification of a new goal within a European knowledge investigation. *PLEA 2018: Smart and Healthy Within the Two-Degree Limit*. Hong Kong, December 10-12.
8. Giuliani, F. et al. (2021). A study about daylighting knowledge and education in Europe. Results from the first phase of the DAYKE project. *Architectural Science Review.* Taylor & Francis, 64 (1–2), 169–181.
9. Lo Verso, V.R.M., et al. (2021). A survey on daylighting education in Italian universities. Knowledge of standards, metrics and simulation tools. *Journal of Daylighting*, 8(1), 36–49.
10. Lo Verso, V.R.M., et al. (2021). Questionnaires and simulations to assess daylighting in Italian university classrooms for IEQ and energy issues. *Energy and Buildings* 252.
11. The NLITED ePlatform is available at lms.nlited.eu
12. Gentile, N. et al. (2022). A shared curriculum for daylighting education to meet the educational needs of society. *PLEA 2022, Will Cities Survive?* Santiago de Chile, November 22-25.
13. Giuliani, F., et al. (2020). Discussing daylight simulations in a proposal for online daylighting education. *IBPSA- Nordic Conference*. Oslo, October 13-14.
14. Guliani, F., et. Al (2022). NLITED - New Level of Integrated Techniques for Daylighting Education: Preliminary Data on the Use of an E-learning Platform. *LUX EUROPA 2022*, Prague, September 20-22.
15. Sokol, N., et al. (2023). Training on sustainable daylighting: the NLITED project. *The 30th Quadrennial Session of the CIE,* Lubiana, September 15-23.

PLEA 2024 WROCŁAW
(Re)thinking Resilience

Building Science Learning Toolkit:
Integration of building physics and performance simulation subject teaching in Architecture curricula

PARAG WATE[1]

[1]School of Architecture, The University of Sheffield, Sheffield, UK

ABSTRACT: In a multi-disciplinary Architecture education, students may often have a gap in their physics and mathematics skills set, which may render their low energy design proposals as under-developed ones. This skills set is however required to provide building physics and performance simulation based scientific evidence for drafting of the design costing with clients and property developers. A good building science learning toolkit should support students in reinforcing this skills set and should be based on comprehensive assessment of joint design-technology pedagogy that prepares students for working as a performance simulation expert or consultant in multi-disciplinary practices. This educational research paper provides such toolkit and attempts to establish the inter-relationship between pedagogical tools [: an instrument to teach a subject], models [: an approach that understands how students learn and tutors teach], employability skills [: a potential learning outcomes of a study programme should have] and fit-for-purpose building science learning toolkit [: a teaching resource that facilitates students' and tutors' learning] that demonstrates how to teach BPS to architects as an assisting tool for performance evaluation of their design intents. In addition to the learning toolkit, this paper presents a holistic assessment criteria that evaluates suitability of a pedagogical model based on levels and a range of employability skills a student may attain.
KEYWORDS: Building performance simulation, Architectural Technology, Low energy design Pedagogy, Decarbonisation, Overheating risks

1. INTRODUCTION

Architecture education is an interdisciplinary journey where a student who embarks on it, to be highly knowledgeable and competent practitioner in their future career, would have to possess knowledge and skills in diverse subjects ranging from artistic designs, humanities and building science and technology disciplines. Throughout the journey as per student's interests and inclination, they go on developing their set of skills and expertise in either of these broad subject areas, which opens different employability avenues for them as architectural designer, historian, and environmental consultant / technologist. The pedagogical approaches to teaching of the last skills set to Architecture students is of interest for this research paper under 'Together we can' topic to learn and teach building resilience and energy sustainability. This is because Architecture students often have skills gap in their mathematics and physics subject training and these skills are the most important ones when they work in sustainable building and urban design simulation practice and performance research discipline.

So, when working in practice and / or research discipline one would expect a strong collaboration culture between architects and other specialists i.e., say environmental consultants to be able to design and deliver low-zero energy buildings. Ideally, fostering such a diverse work environment and culture should start from early on from their undergraduate and postgraduate programme of studies. In that vein, one could find a kind of an evolution in the teaching of building science and technology with BPS tools from no interaction between building design studio and technology modules [1] [2] to collaborative teaching of the modules, attempting to apply BPS in the design projects [3][4][5]. As analysed from the related literature, there are however few key challenges in thoroughly implementing the studio-technology collaborations and integration of building physics and performance science subjects teaching (with BPS software and tools) in Architecture curricula.

1.1 The THREE key challenges for integration

Firstly, depending upon the academic expertise of a tutor, the practices around building science and related performance modelling and simulation teaching to Architects would vary e.g., when studio tutors who don't necessarily come from Science and Engineering education background.

Secondly, pedagogic technique: teaching building science and engineering subjects i.e., physics of heat, air, light and acoustics and its thermodynamic applications in buildings requires adapting problem-based learning technique, which has widely been

practised, well-developed and acknowledged by academics in teaching a Science and Engineering discipline subject [6]. The technique that motivates the learner to actively learn and then self-learn how to solve a problem using the iterative trial-and-error method. Using the BPS tools, students can develop their problem-solving skills based on the evidence and feedback of performance implications that their design interventions would generate – resembling the iterative design principle with trial-and-error problem-solving nature. The studio tutors from non-Engineering background may not be well familiar with the flipped way of teaching building physics with BPS tools in the discipline.

Thirdly, students' way of learning: Architecture students being highly visual and experiential in the way they learn throughout majority of their modules, the experimental way of building physics teaching using computer simulation wouldn't initially appear as straightforward application of their previous skills. On tutors' part, this would involve encouraging and motivating students in getting on with the learning curve and making them understand the benefits the learning would bring when working with or themselves as environmental consultants in practice. When tasked with designing low energy buildings in the face of climate emergency [7], the future Architects will have to be well-equipped with the experimental, technical and analytical skills in building physics and performance simulation, for to be able to deliver zero energy buildings.

Along with accounting for the challenges, this research work consolidates previous published works in building physics education research to provide holistic insight on what pedagogical tools and models exist and how suitable are they when teaching in joint and collaborative context of studio design and technology modules to Architecture and Architectural Engineering cohorts. This research work attempts to address these by developing and demonstrating a building science learning toolkit, based on robust understanding of pedagogy and related fit-for-purpose model implementation.

1.2 Research aim and objectives.

The aim of this educational research piece is to develop a learning toolkit, that demonstrates how building physics and performance simulation teaching can be integrated in sustainable architectural and urban design and engineering programmes. And the objectives are:

1. Present a synthesis of the existing pedagogical tools and models.
2. Propose a criteria for assessing suitability of the reviewed joint models.
3. Develop and demonstrate a learning toolkit, based on fit-for-purpose pedagogical model.

1.3 Paper structure

The paper starts with analysing what different pedagogical tools are being used to teach Architects and Architectural Engineers different subjects, assessing how different building physics and performance simulation teaching is and what pedagogical tool may work best for such teaching. Drawing on the experimental tool that can be used, the subsection next derives from the literature the different ways to teach building simulation by illustrating pedagogical models that have been practised in design-technology collaborative teaching [8] [9]. The dedicated section on toolkit development proposes the criteria for assessing the suitability of the pedagogical models for simulation teaching (Fig. 1). The subsection next proposes the fit-for-purpose model that's been implemented, along with the presentation of a prototype of learning toolkit. The paper concludes with the next steps on how the scope of the toolkit can be extended, to include teaching and learning of advance developments in building simulation brought by development of statistical and machine learning techniques in recent years [10] [11].

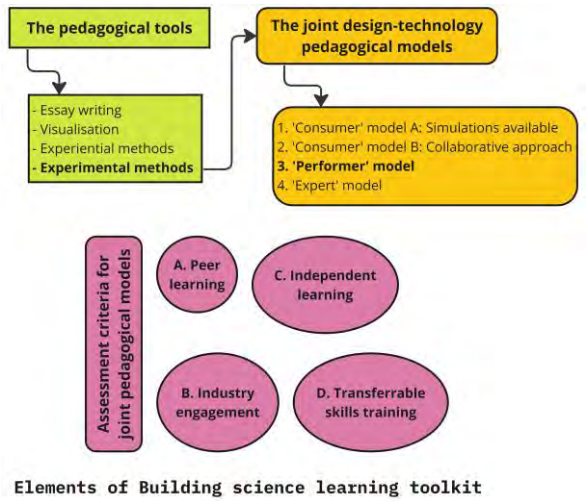

Figure 1: Elements of Building science learning toolkit: The pedagogical 1) tools and 2) models, 3) Assessment criteria

2. JOINT DESIGN-TECHNOLOGY PEDAGOGY

The literature review that follows presents current practices in teaching building physics with performance simulation software to Architecture and Architectural Engineering students. It discusses what the related pedagogical practices and implementation challenges faced across UK [3] [13] and overseas higher education providers [4] [5] are, the progress that's been made so far [12], and further investigates and presents learning from the practices [9] [14].

Following a range of search techniques to perform systematic literature review [15], conventional subject searching, reference list checking and citation

searching were adopted for the review of papers that involved keywords as 'Building physics', 'Architectural Technology', 'Simulation based approach' and 'Architectural education'. The Web of Science, ScienceDirect and Google Scholar platforms were searched with the keywords. Only handful of papers that are highly relevant for this research work are selected and cited. The sections and subsections present the synthesis of the literature references.

The pedagogical tools that's been used to teach students different subjects do vary significantly [16] – for instance –

1. the essay stories in classroom lecture-based format to teach humanities-oriented subjects like history of solar technology or Energy use in Society.
2. more visual tools e.g., drawing, model making and painting in studio environment to teach sustainable design speculation and imagination as project-based pedagogy,
3. experiential tools – observation, questionnaire surveys and interviews - to teach accounting of human behaviour and their energy practices in design and its feedback on their behaviour and practices as a result,
4. experimental tools – in-situ field and lab measurements and experiments, computer experiments using building performance modelling and simulation tools - to teach evidence-based assessment of effectiveness of design and technology interventions in improving indoor and outdoor comfort conditions and in reducing building's likely energy use and environmental impact.

A precedent analysis of a case study building design done using the first three tools may develop students' 'thermal intuition' about a sustainable design project and its massing (e.g., size, shape, glazing and orientation) but only in a speculative, abstract and imaginative way. Inherently, these three teaching tools don't provide students with a building physics-based evidence and an ability to make predictions about how their design might perform and what might like the likely performance be particularly in the contexts of overheating risks, solar gain and thermal mass against insulation type and position analyses, evaluation of night time natural ventilation for passive cooling, fabric energy efficiency analysis using synthetic vs bio-based materials and sizing of HVAC systems and renewable energy technologies. The fourth tool however can develop students' ability to quantify and give scientific rigour to their abstract 'thermal intuition and ideas' and assess the performance implications of their thought design interventions in the varying contexts of environmentally conscious design decision making. The joint teaching of the simulation skills set has been experimented in the past, to foster collaborative working in interdisciplinary groups. As per [8] and [9], the below joint pedagogical models have been practised toward including building physics and performance simulation teaching with BPS software in studio environment.

The [8] and [9] propose two teaching approaches – 'domain'-specific and 'User'-centric to teach BPS subject. Each of them has got different teaching goals and pedagogical models. The 'domain'-specific one focuses on training a student as a BPS tool creator and a simulation expert / simulationist where students may likely come with Engineering background due to the understanding of how heat phenomena are dealt is required. The 'User'-centric one rather focuses on training a student as a BPS consumer and performer where students may likely be from Architecture due to interpretation and evidence-based skills set needed to inform design decision making. This research work focuses on teaching BPS to Architects it is therefore reviews 'User'-centric approach to the teaching, which is also the widely employed approach [17].

2.1 The joint pedagogical models

2.1.1 'Consumer' model A: Simulation outputs made available by an expert.

This model allows more close collaboration between a consultant and architecture students, where the consultant provides simulation models and takes the role of an expert. Apart from introducing Climate and indoor comfort analysis tools, no further BPS software training is provided in the studio and the consultant does the simulations iteratively for students. The consultant's role is to prepare simulation models and teach them how to interpret and analyse the results (e.g., energy demand and temperature peaks) in the context of their design intents.

This model has been found to be consistent with an undergraduate programme where students were given an opportunity to fully focus on their designs with BPS results available as a 'service'. This model allowed to resemble the architect/consultant collaboration in professional practices more closely. On the other hand, however bringing in an expert consultant can help students in gaining knowledge about practice examples and receiving expert's advice on their design projects. This could involve interactions in the form of individual and / or group portfolio reviews by experts in lectures and workshops.

2.1.2 'Consumer' model B: Collaborative approach

This model has a focus on bringing architecture and engineering students as consultants together to

work in interdisciplinary environment. Consultants are expected to use a BPS software, by asking a group of students to volunteer for training themselves. It has got advantages in having an opportunity to develop some 'in-house' expertise among the cohort and as well as reducing the workload on instructor's part in preparing simulations. The saved time can effectively be used to advise and supervise a group of volunteers instead.

This model was better at encouraging peer learning among students than the previous ones because the volunteers have been tasked to prepare simulations for their own as well as their peers' designs – the architect/consultant collaboration one would expect in practice. Overall, the approach received a mixed response from students because more able designers were confident enough to integrate BPS in their design pipeline than the less able ones who expressed learning a BPS software was an added burden.

2.1.3 'Performer' to 'Expert' model

The format for this model is split in two stages: first stage provides the basic training to all students and second stage provides more confident students to do in-depth analysis with a BPS software. The approach was found to be most suited for students enrolled on dual degree courses, due to the nature of workshop format split into group of students taking roles as architect and simulation performer.

The model allowed problem-based learning environment for students to learn from each other, encouraged closely interlinked design synthesis and related simulation analysis. Given how self-elected volunteers in the second stage further develop their simulation and performance analysis skills, they could really be a good resource as a teaching assistant training junior students and as well as can act as internal expert for the first two models.

3. DEVELOPMENT OF AN ASSESSMENT CRITERIA FOR JOINT PEDAGOGICAL MODELS

It is highly important to establish the effectiveness of the pedagogical models in achieving the programme level goals and outcomes, which are mostly about assessing of how their degree level modules have prepared students in gaining meaningful employment and first professional experiences after they graduate. In addition to BPS and analytical skills it is important to know and understand about how good students' communication, collegial and transferrable skills are. Following a questionnaire survey sent to recent graduates in Spain [18] and review of the literature that's been identified earlier, the below assessment criteria is proposed. The criteria allow us to better understand the effectiveness of different joint pedagogical models that have been practised by UK and overseas higher education providers.

A. Collaborative working and peer learning: the level of interaction within and between study groups, ranging from precedent analysis to evaluating design interventions.
B. Industry engagement: amount of time invested in developing and teaching BPS by an expert / external consultant.
C. Independent learning: the range of opportunities provided - from basic scaffolding, self-learning to making own interpretations and understanding of the performance feedback from environmental design interventions.
D. Transferrable skills training: the level of attainment - from confidence in applying to a real-life projects in practice to become a provider of a similar collaborative problem-based learning environment elsewhere as an instructor / external expert.

3.1 Assessment of pedagogical models

This subsection assesses the models as per the proposed criteria, to guide selection of a model for our proposed toolkit development.

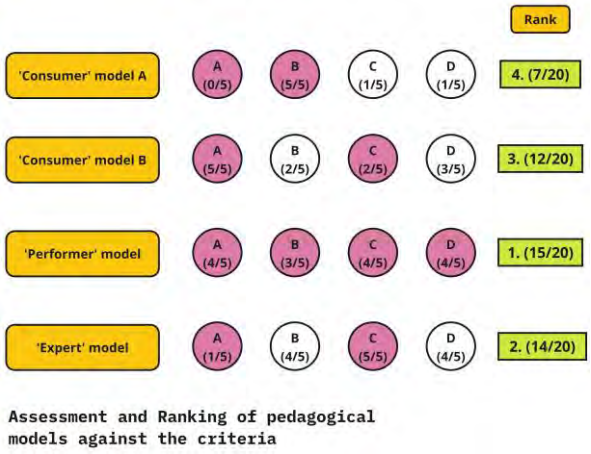

Figure 2: Assessment and Ranking of pedagogical models against the criteria. Please refer Fig. 2 for colour coding.

'Consumer' model A where simulation results are provided by an expert ranks amongst the lowest because of only Industry experience students may gain. It doesn't do well in supporting peer learning among students as there is a direct interaction with an expert and less so among students. It doesn't score well either on independent learning and transferrable skills criteria as the tasks involved are only about developing simulation interpretation skills without developing actual performing skills.

'Consumer' model B on collaborative approach support highly conducive environment for peer learning as engineering students as consultant providing simulations to architects and adapting the

simulation as per design decisions. It does well on remaining three criteria on students gaining Industry exposure with an expert mentoring engineering students; they are being given good opportunities to learn independently and will be able to apply their consultancy skills to other similar projects.

'Performer' model is being ranked one of the best to teach BPS to architecture students. Given a student is performing simulations and they are also the ones responsible for making sense of the results they get in view design performance targets, it is a well-rounded approach to BPS teaching. Students also learn problem solving skills in an environment that supports both peer and independent learning. Students can also be given Industry exposure when expert advice is needed, allowing them to think about how they can apply their newly learned simulation and analysis skills to different real-world projects.

'Expert' model from 'domain'-specific approach in general performs well across the criteria, except when in case of collaborative / peer learning. It is due the fact that only very few among architecture student cohort are enthusiastic to bridge their maths and physics skills gap to learn how to engineer / model different design decisions (e.g., natural ventilation and passive cooling) using one or more BPS tools (for the example it will require simulating both thermal and airflow using EnergyPlus and ANSYS). Based on the assessment and ranking analysis, the 'Performer' model is selected for the purposes of learning toolkit development.

3.2 Development of the learning toolkit

Based on the 'Performer' model, the teaching format involved demonstration of DesignBuilder interface to EnergyPlus and its related features that students can use to test performance criteria. The brief involved zero energy design of a Mixed-use University building, which may have outdoor seating area, café, computer and classrooms. The performance criteria included avoiding overheating risks in summer months and minimal utilisation of heating systems in Winter months with requirement to maintain desirable comfort temperatures.

As inherent to the pedagogic model, the demonstration of BPS software and subsequent interpretation of results followed developing incremental understanding of BPS by experimenting with the design interventions and evaluating their impact on performance. A total of 4 hours of contact time with the instructor was provided. An hour of 2 hours long session involved enhancing students' understanding on how their theoretical knowledge apply to estimating energy balances and performing overheating risks and related energy demand calculations. The second hour of the session involved teaching iterative design-and-evaluate approach using University building as a case study, by showing how different design components (e.g., varying air flow rates by changing openable window area), allowing parametric way of assessing their design interventions. This way it allowed them to understand how to generate evidence for their design intentions and how to assess effectiveness of them in achieving the target performance.

Another 2-hour long session in that week was structured in a flipped way where students were given time and asked in advance of the session to begin modelling their design proposals and interventions and use the session time to seek support from the tutor, who assisted them in solving the design problem the students started working on. The approach also allowed them to realise how designs can be modelled in iterative way and how their design solution feeds back in for the next intervention. The format each week ran for few more weeks giving students an opportunity to focus on thermal mass effect, heating and cooling system sizing. The assessment brief also involved an open-ended component where students were asked to present a critical report of the sustainable design strategy they evaluated. This way it facilitated excellent student learning in applying building physics concepts, experimenting design strategies using BPS and making evidence-based interpretation of simulation results.

3.3 Prototype implementation of the learning toolkit

MIRO platform was used to design tutorial sheets, which were shared each week after first 2-hour long session. Students were asked to use the time between the release of this and the 2-hour long flipped session to practising the BPS tool and start modelling their design intents. The tutorial sheet had links to video recording and lecture slides of the sessions, independent learning resources including building physics theory from book [19] and software tutorial videos, tutorial models from the session and summary of key teaching and learning topics covered.

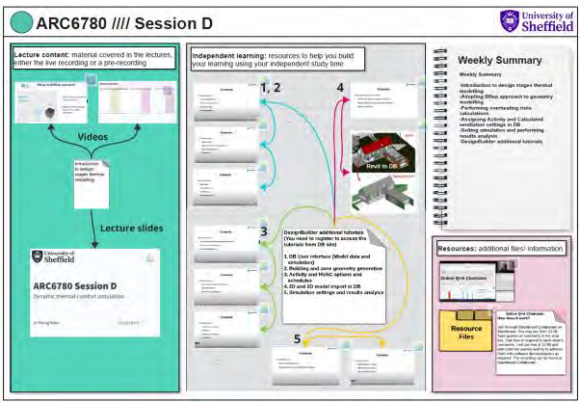

Figure 3: Prototype of learning toolkit: Typical tutorial sheet

3.4 Beyond learning toolkit.

Currently, this toolkit is a part of simulation teaching on MSc Sustainable Architecture Studies (SAS) programme at the University of Sheffield. This toolkit philosophy can be extended for a programme level approach that University adapts when developing a new curriculum. In view of this, this toolkit has a potential to be developed into a whole new curriculum on building and urban performance science and engineering simulation, that's based on application of building physics and related machine learning methods [10] [11].

4. CONCLUSION

This paper delivers below tangible outcomes:

- A synthesis of 'Consumer', 'Performer' and 'Expert' pedagogical models that have been developed to deliver BPS teaching (Section 2.1) and how they have been worked out in teaching practice.
- A holistic assessment criteria that's been demonstrated to evaluate how good a pedagogical model performs in developing different levels and range of employability skills in students (Section 3, 3.1).
- A building science learning toolkit that demonstrates how the best of four 'Performer' model have been implemented to deliver building overheating risks evaluation teaching using BPS tool (Section 3.2, 3.3).

ACKNOWLEDGEMENTS

I'd like to thank my PGCertTLHE mentors for their encouraging discussions about pedagogy.

REFERENCES

1. Celadyn, W., 2018. Postgraduate studies and sustainable architecture. Glob. J. Eng. Educ, 20, pp.54-58.
2. Boarin, P., Martinez-Molina, A. and Juan-Ferruses, I., 2020. Understanding students' perception of sustainability in architecture education: A comparison among universities in three different continents. Journal of Cleaner Production, 248, p.119237.
3. Basavapatna Kumaraswamy, S. and De Wilde, P., (2016). Simulation in education: application in Architectural Technology design projects. In Proceedings of BS2015: 14th Conference of International Building Performance Simulation Association, Hyderabad, India, Dec. 7-9, 2015: p. 2733-2780.
4. Gamble, J.M., Gentry, R., Augenbroe, G. and Stephen Taul with students from the Georgia Institute of Technology, 2015. Architecture and high performance building at Georgia tech: teaching design+ technology in the environmental context. Journal of Green Building, 10(3), pp.67-86.
5. Rajagopalan, P., Wong, J.P.C. and Andamon, M.M., 2016, December. Building performance simulation in the built environment education: Experience from teaching two disciplines. In Proceedings of the 50th International Conference of the Architectural Science Association (pp. 359-368).
6. Velegol, S., Zappe, S., & Mahoney, E. (2015). The Evolution of a Flipped Classroom: Evidence-Based Recommendations. Advances in Engineering Education.
7. RIBA 2030 Climate Challenge. Available: https://www.architecture.com/about/policy/climate-action/2030-climate-challenge [29 August 2023]
8. Charles, P.P. and Thomas, C.R., (2009). Four approaches to teaching with building performance simulation tools in undergraduate architecture and engineering education. Journal of Building Performance Simulation, 2(2), pp.95-114. https://doi.org/10.1080/19401490802592798
9. Alsaadani, S. and Bleil De Souza, C., 2019. Performer, consumer or expert? A critical review of building performance simulation training paradigms for building design decision-making. Journal of Building Performance Simulation, 12(3), pp.289-307.
10. Paterson, G., Mumovic, D., Das, P. and Kimpian, J., 2017. Energy use predictions with machine learning during architectural concept design. Science and Technology for the Built Environment, 23(6), pp.1036-1048.
11. de Wilde, P., 2023. Building performance simulation in the brave new world of Artificial Intelligence and Digital Twins: a systematic review. Energy and Buildings, p.113171.
12. Fernandez-Antolin, M.M., del Río, J.M. and Gonzalez-Lezcano, R.A., 2022. Building performance simulation tools as part of architectural design: Breaking the gap through software simulation. International Journal of Technology and Design Education, 32(2), pp.1227-1245.
13. Weng, Z., Coley, D., and Gonzalez, A. R. (2016). ROOM–A Web-based Interactive Educational Tool on Building Physics. In PLEA2016 Los Angeles–32nd International Conference on Passive and Low Energy Architecture. Cities, Buildings, People: Towards Regenerative Environments (pp. 1442-1446).
14. Reinhart, C., Geisinger, F., Dogan, T., and Saratsis, E. (2015). Lessons learnt from a simulation-based approach to teaching building science to designers. In Proceedings of the 10th IBPSA conference and exhibition (pp. 1126-1133).
15. Papaioannou, D., Sutton, A., Carroll, C., Booth, A. and Wong, R., 2010. Literature searching for social science systematic reviews: consideration of a range of search techniques. Health information & libraries Journal, 27(2), pp.114-122.
16. Brainard, G. and Correa, C., 2019. Classroom as laboratory: engaging architecture students in hands-on building science research. Building Technology Educator's Society, 2019(1), p.22.
17. Soebarto, V., Hopfe, C., Crawley, D. and Rawal, R., 2015. Capturing the views of architects about building performance simulation to be used during design processes.
18. Fernandez-Antolin, M.M., del-Río, J.M., del Ama Gonzalo, F. and Gonzalez-Lezcano, R.A., 2020. The relationship between the use of building performance simulation tools by recent graduate architects and the deficiencies in architectural education. Energies, 13(5), p.1134.
19. Robinson, D., 2023. Science and technology of low Carbon design: Physical principles. An open-source textbook published as pressbook by University of Sheffield. https://sheffield.pressbooks.pub/scienceandtechnologyoflowcarbondesign/

PLEA 2024 WROCŁAW
(Re)thinking Resilience

Digital and Analog Tools for Bioclimatic Design
Learning Potential and Limitations

MARIYA STOYANOVA BOND[1] ANSHUMAN ABHISEK MISHRA[1] LEIF MARTIN HOKSTAD[1] LUCA FINOCCHIARO [1]

[1]NTNU Norwegian University of Science and Technology, Trondheim, Norway

ABSTRACT: This article summarizes the first attempt of a series of experimental workshops aiming to build a comprehensive methodology for conducting systematic investigations of bioclimatic design strategies through the utilization of analog and digital tools. The workshop was conducted within the "Climate and Built Form" course, part of the MSc in Sustainable Architecture at NTNU. The study investigated the impact of integrating both digital and analog tools in architectural education and explored the pedagogical potential of combining them in different teaching and learning activities. The goal was to offer educators insight into the teaching and learning potential, as well as the limitations, of these tools.
KEYWORDS: analog tools, bioclimatic design, digital tools, experimental workshop, pedagogic potential

1. INTRODUCTION

Digital tools have significantly transformed many aspects of architecture, from the design processes and methods to the educational approaches and curricula [1-2]. This shift from traditional analog tools to software-based approaches has revolutionized fields like environmental and bioclimatic design, among others. Digital tools developed in the last decades allow architects and engineers to experiment with complex forms and to simulate and explore buildings' environmental and energy performance in detail. Software programs make the computational analysis of the complex numerical aspects of architecture easier and more effective while minimizing the related costs.

However, this transition also has an impact on architectural education. There is an ongoing debate about the implications of the teaching methods and learning outcomes of architecture students across different architectural domains because of this shift [3-4].

Digital tools often have embedded predefined solutions readily available for improving environmental performance. While this can be very useful in the practice, in education it can potentially limit students' creativity and capacity to explore different ideas. It can further make students reliant on these tools instead of on their own knowledge, experience, and intuition.

Studies [5] show that hands-on activities in the early stages of design allow students to build a better understanding of new concepts and frameworks and develop the ability to implement them in their work.

While digital technologies are already dominating the mental and operational landscape of our lives [6], effective learning often requires a blend of analog and hands-on methods [7]. On one side, hands-on engagement with analog tools sparks creativity, facilitating rapid idea sketching, prototyping, and testing. On the other hand, digital simulations empower students to explore a wider range of scenarios and variables, fostering a deeper understanding of complex climatic interactions in the built environment.

This study investigates the impact of integrating both digital and analog tools in architectural education and explores the pedagogical potential of combining them in different teaching and learning activities.

An experimental workshop has been set up, balancing the use of both sets of tools. The workshop has been designed to create an engaging learning environment, enabling students to define their own design processes where analog and digital tools for environmental design can be freely combined.

Seeking to strike a balance between these approaches, particularly in the context of bioclimatic design education, the workshop prompts critical thinking about different design drivers and processes by allowing students to actively experiment.

Students were not only encouraged to experiment with both physical and virtual simulation tools, but also to record and reflect on their findings. This was done to encourage the completion of the learning cycles [8] embedded in the research design and test the students' capacity to define innovative design processes with those tools and to develop their design projects systematically on the basis of evidence. The goal was to offer educators insight into the teaching and learning potential, as well as the limitations, of these tools.

Our hypothesis is that digital tools can not only be used as mere computational tools but also as tools enhancing the learner's experience when integrated into hands-on learning activities.

2. EXPERIMENTAL WORKSHOP DESIGN: THEORETICAL BACKGROUND

Following Kolb's Learning Cycle [8] and Action research framework [9], the investigation aimed to shed light on the role of tools in design processes developed as part of educational activities at NTNU.

Research shows [10-12] that hands-on experimentation is an appropriate tool for developing creativity and innovative thinking.

Kolb, building upon Dewey, Lewin, and Piaget's theories [8], developed the theory of experiential learning and upgraded the previously mentioned pedagogical theorists' ideas of learning cycles. His take on these theories led him to establish four main categories, defining the main steps within the learning cycles – 'concrete experience' (CE), 'reflective observation' (RO), 'active conceptualization' (AC), and 'active experimentation' (AE).

In his theory, the cycle can be entered and exited at any stage. Furthermore, the cognitive learning style of each individual influences the way they approach the learning cycle and their tendency to rely on some categories more than others. However, for knowledge to become fully embodied, even transformed later into what we call tacit knowledge and intuition, the learner must go through the full cycle. Often, this cycle is not completed or is completed on a superficial level, meaning that the instructions might be followed, and all tasks might be completed, but the stages of reflection do not lead to any abstraction of principles or internalization of any particular knowledge.

One potential problem could be that many times, the experimentation phase is replaced by an exercise. Exercises are useful in theoretical courses, where the acquiring of factual knowledge and related specific competencies are desired as learning outcomes. However, design education is about developing the capacity to bring about changes in the "made" world [13]. In the framework of Kolb's Learning Cycle, an exercise is rather a "concrete experience" that allows for reflections, but it has limited learning potential.

The architect's education might begin with hierarchical or goal-oriented knowledge being taught where exercises have an important role. However, Vowels [14] argues that inevitably, in the later stages, especially once one reaches the master's level, the knowledge becomes process-oriented. In the architectural design studio, exercises cannot be sufficient in replacing the step of 'active experimentation' when the desired learning outcomes include developing the ability to creatively design or develop innovative concepts.

Another potential problem could be the complete lack of experimentation as an established step in the design process. One of the key concerns is that grades can stagnate the design process by encouraging students to focus solely on achieving high scores rather than exploring innovative and creative solutions and thus discourage them from performing experiments on their own, outside of the curriculum, that might not yield results. Furthermore, it can lead to a cautious, formulaic approach to design, where students prioritize producing safe, predictable outcomes that they believe will earn them higher grades. This phenomenon is called "design fixation" [15].

The centuries-old culture of master-apprentice dynamics in architecture education, paired with the largely implicit and untaught criteria of what constitutes the culturally prevailing image of an architect, pose serious challenges for many learners when it comes to taking alternative approaches to design [14].

Building on Kolb's theories, Jeb Schenck and Jessie Cruickshank developed the Co-Constructed Developmental Teaching Theory [16]. This theory simply repeats Kolb's Learning Cycle as a basis. However, the learning cycles are not perceived as separate events but rather as a part of a continuous spiral where every next inquiry increases in complexity.

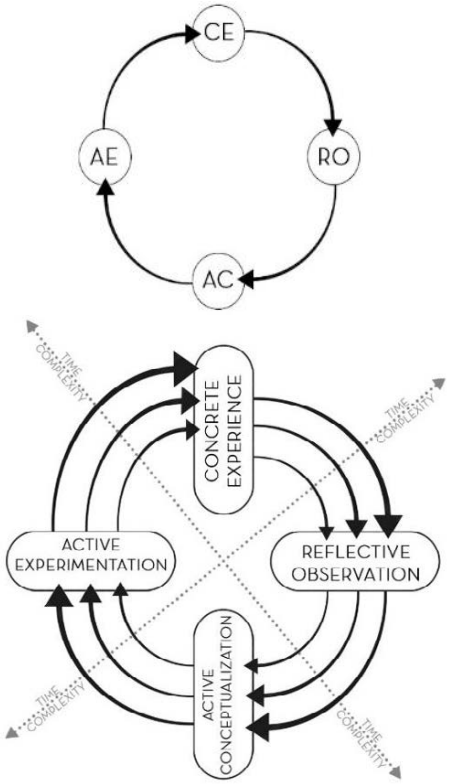

Figure 1. Kolb's Learning Cycle and Jeb Schenck's and Jessie Cruickshank's Co-Constructed Developmental Teaching Theory

To summarize the theoretical background and research drivers for this inquiry, we focused on Kolb's experiential learning theory, Kolb's Learning Cycles (Fig. 1), and Jeb Schenck's and Jessie Cruickshank's Co-Constructed Developmental Teaching Theory (Fig. 1) to investigate the pedagogical potential of analog and digital tools by implementing "active experimentation" as an additional step in the design studio.

Using an Action research framework, we revised the conventional structure of one pedagogic module of the Climate and Built Form course. The module focuses on the relationship between sun and form, where originally theory was first transferred through a lecture, and then students were trained to use digital tools. The experimental workshop instead was designed in a way to ensure that students would complete three learning cycles alternating between analog and digital tools, breaking the original structure of the course. Encouraging students to engage with the theory repeatedly and enabling them to experiment by introducing hands-on activities at every cycle of the learning design process and alternating between different analog and digital tools used to investigate the same problems, the workshop activities allowed students to understand the vast possibilities of investigative tactics for environmental performance problems.

By creating an environment where students can actively manipulate and observe both physical and virtual simulations, the workshop stimulates critical thinking about design solutions. Focusing on the sun as a design driver, the workshop employs a conceptually clear heliodon, an automated heliodon, and digital parametric modeling tools. This juxtaposition of physical and digital simulations highlights their strengths and weaknesses.

Our main aim was to deepen the students' understanding of real-world climatic phenomena, to gain firsthand insight into how different simulation tools replicate these real-world phenomena, and to master the nuances of simulation results.

Furthermore, by encouraging the students to run more structured experiments with various simulation tools, the workshop activities enabled them to improve their designs on the basis of evidence in a systematic manner.

3. METHODOLOGY

Given the provided background information, we suggest that distinctions exist between the pedagogical potential of digital and analog tools in the design studio, significantly influencing the educational outcomes depending on how those tools have been integrated into different teaching and learning activities. While analog tools facilitate a more holistic approach to design, they have limitations to the complexity of the simulations that can be performed with them. Similarly, while the computational capabilities of digital tools can provide strong evidence for strengthening one's concept, they can also stagnate creativity by offering predefined solutions or specific numerical answers.

To test our hypothesis, we planned a three-week-long experimental workshop restructuring the pedagogical framework of the existing module called 'Sun and Form' of the 'Climate and Built Form' course and introducing various analog and digital simulation tools.

This section details the workshop design conditions and theoretical framework, the teaching and learning activities embedded in the workshop, the participants, the data collection process, and the data interpretation process.

3.1. Workshop design conditions

The experimental workshop was designed as part of the semester design project of the 'Climate and Built Form' due to the time limitations of the semester and to avoid the workshop becoming an extra task for the students. We decided to keep the main focus of the workshop on the semester project to allow the students to be able to give their full attention to the workshop activities at hand even though they were not graded.

For the semester design project, students were split into five groups and asked to design a prefabricated climate adaptive shelter for post-disaster recovery. Each group was given a different climatic context to work with. Before the workshop started, the students were asked to develop design concepts on a purely intuitive basis without using any simulation tools. To develop their designs, they had to take into consideration spatial requirements, functional distribution, environmental performance, construction, and infrastructure requirements.

The workshop was designed in three connected cycles. Each cycle built in complexity, encouraging students to see the same problems through different lenses and systematically improve their design based on the evidence gathered. The cycles further allowed students to reflect on their findings, conceptualize ideas, and later test them through active experimentation, including hands-on activities. Kolb's Learning Cycle was used as a basis for the individual activities, and the whole workshop followed the Co-Constructed Developmental Teaching Theory (Fig. 1).

The framework of the workshop design can be seen in (Fig. 2), where the starting point is the theory circle near the center.

3.2 Theoretical framework: Action research

Action research has been selected for the research design because this framework allows us as researchers to engage in ongoing situations and take

an active role in influencing the unfolding events while at the same time measuring the impact of our interventions. Action research focuses on assessing deliberately planned change. This framework has also allowed us to actively participate in the planning and implementation phases [9].

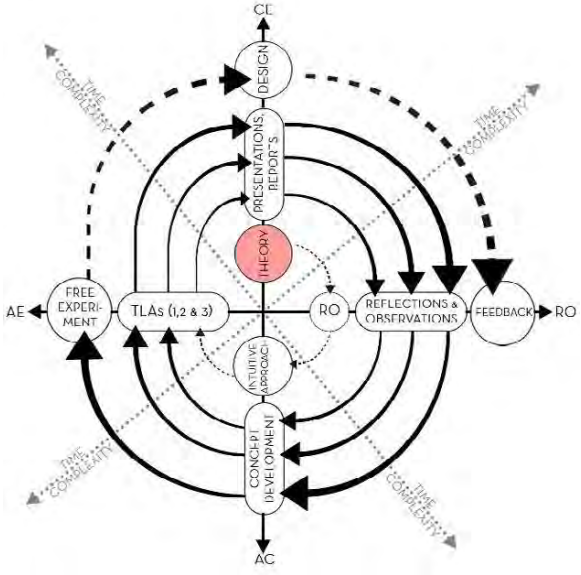

Fig. 2 Pedagogical Loop

This approach led us to develop a double-loop Action research design (Fig. 2) and (Fig. 3), where the same didactics we used for the workshop activities were applied to the research structure itself. This was done in order to be able to structure our interventions, data collection, and data interpretation protocols.

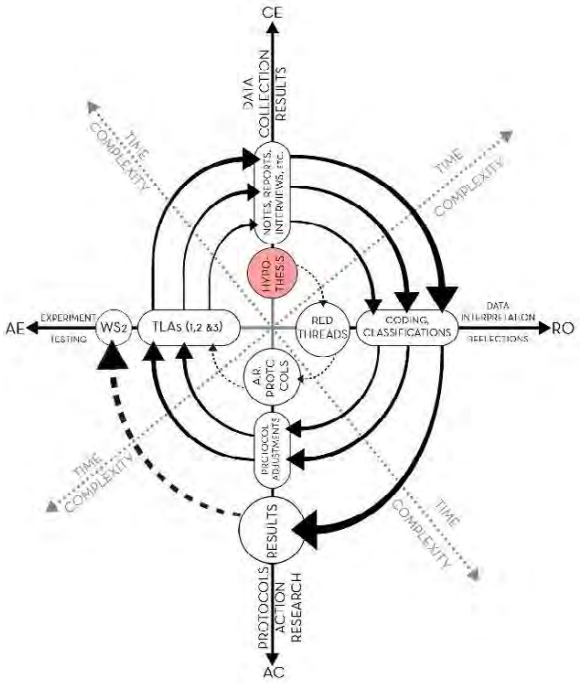

Fig. 3 Research Design Loop

We began our own learning cycle with a hypothesis. Based on this hypothesis, we established a series of “red threads” (Fig. 3) or, in other words, patterns we wanted to investigate. We incorporated the “red threads” in the research protocols at every level.

The teaching and learning activities in the workshop served as experiments, where we actively engaged with the students in hands-on activities.

The data collected gave us a concrete basis for reflections and adjusting the research protocols if needed.

This loop allowed us to revise our objectives with every activity, to understand the results better, and to recognize many factors that might influence those results. Furthermore, by creating this double-loop Action research design, we established a strong foundation for further improvement of the course activities and a basis for further investigations in the next planned workshop. The research design loop is represented in the graph in (Fig. 3).

3.3 Teaching and learning activities

There were three teaching and learning activities in the workshop, and each activity included a different simulation tool.

In the first week of the workshop, the students were introduced to a conceptually clear heliodon. They were asked to develop three research questions regarding their own design in relation to the sun's geometry and try to answer them by performing experiments in the heliodon. At the end of the week, the students were asked to present their findings.

In the second week, the students were introduced to Grasshopper, a parametric modeling tool, and Ladybug, an environmental analysis plugin, and given an exercise following the Sol-Air approach [17]. The exercise followed a pre-written script for form optimization and orientation of a hypothetical box in the same climatic context as their design task. The task was intentionally not applied directly to the students’ design concepts in order to avoid a specific software-generated answer influencing the design choices from the outset and undermining the students’ critical thinking abilities. At the end of the week, the students were once more asked to present their findings.

In the third and last week, the students were introduced to an automated heliodon equipped with micro-cameras for solar access analysis. No specific task was given, but the students were encouraged to investigate in more detail the solar-responsive design solutions they have integrated into their projects.

3.4 Participants

There were twenty participants in total, all of them master students. The participants had different educational backgrounds since the course is interdisciplinary.

The majority of the students, 70%, had an architecture background, 20% an engineering background, and 10% a mix of the two.

The students were from 10 different countries, where 35% were from Norway.

About 40% of the students had some prior knowledge about the digital tools introduced in the workshop, and 60% had no prior knowledge. One person had in-depth knowledge, 55% had some basic knowledge, and 40% had no prior knowledge about bioclimatic design theory.

3.5 Data collection

While a large number of data was recorded throughout the workshop using different data collection methods, the scope of this article is to investigate the pedagogical potential, as well as the limitations, of digital and analog simulation tools for environmental performance. Because of this, certain data is not included in the data analysis in this paper.

Since we used a mixed-methods approach in this research, we were able to collect and interpret both qualitative and quantitative data.

The data collected consists of:

- Mapping sheets (educational background of each student and country of previous education degree, prior knowledge of the digital tools introduced in the workshop, and prior knowledge about bioclimatic design and environmental performance). Ethical approval for collecting this data was not required since no names, ages, or other distinguishable information was collected.
- Likert scale charts mapping the students' satisfaction with the different teaching and learning activities
- Field notes from semi-structured round table discussions with each group
- Field notes from four group presentations
- Project reports concluding the workshop.

Protocols were established for the data collection procedures. These protocols allowed us to put constraints on the collected material in order to put the data in context. We called these constraints 'red threads,' as mentioned earlier, which were directly integrated into the data collection protocols and later served as a 'start list' [18] for the first cycle of coding the data by using a Provisional Coding method.

3.6 Data interpretation

The collected data was manually coded in three cycles using different coding methods. The coding methods were selected in accordance with what is appropriate for the Action research framework and the type of data collected. Later, the data was 'themed' [18] and reflected upon through analytical memos in order to be visually represented in a matrix.

A separate matrix was used for each cycle of the workshop in order to be able to compare and contrast the outcomes of the use of the different tools. Furthermore, the matrices were aligned with the learning cycle steps for further coherence.

By using these categories in matrices, we managed to analyze to what degree each group of students engaged in the learning cycles, if they conducted experiments, whether those experiments yielded results, if the students reflected on the results, and if the results influenced their design choices.

4. RESULTS

The results of the workshop data analysis were collected into matrices and visually represented on the framework scheme of the workshop, which was presented in (Fig. 2). This visual representation of the results can be seen in (Fig. 4), where one group's performance is given as an example.

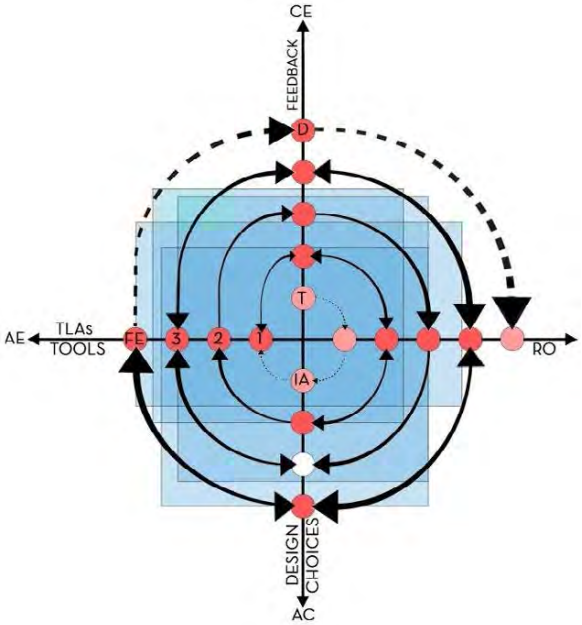

Fig. 4 Example of results graph (Group 5) (red – completed task, white – not completed task, pink – outside of workshop timeframe)

In the first module, with the conceptually clear heliodon, all five groups conducted experiments by using the tool, "made a discovery," engaged in thorough reflections, and claimed that the use of the tool impacted their design choices. 75% of the students found this module very useful or useful. 10% found the activities informative, and the remaining 15% did not express opinions.

In the second module, following the Sol-Air approach with the digital tools, one group was discarded from the statistic because even though they completed the exercise, they opted for another software for optimizing their design. However, all four other groups conducted experiments in the

software after the exercise, they all claimed to have "made discoveries" or have "seen the bigger picture."

They further claimed that the second task allowed them to reflect on their design. However, only two groups claimed that this module influenced their design choices. 60% of students found this module useful or very useful, 5% found the activities informative, and 5% rated them as not useful. The remaining 20% did not express any opinion.

Unfortunately, due to time constraints and the approaching final semester presentations, only two groups used the tool and completed the TLA in the third and final module of the workshop. Only one group claimed that the activity influenced their design choices.

5. DISCUSSION

The analysis conducted after the workshop emphasized a few reflection points that require heightened attention in the further development of this study in order to refine the methodology and strengthen the basis for drawing conclusions.

For example, the climatic context the students worked with determined certain attitudes toward the workshop activities. Seeing that the main topic of the workshop was "Sun and Form," naturally, groups that aligned their concept development with other bioclimatic strategies, like the relationship between wind and form, for example, perceived the workshop as a distraction, either not fully utilizing the activity or underestimating its potential contribution to their project development.

6. CONCLUSIONS

This article summarizes the first attempt of a series of experimental workshops aiming to build a comprehensive methodology for conducting systematic investigations of bioclimatic design strategies through the utilization of analog and digital tools.

Some patterns were detected, but the sample of 5 groups was too small to draw conclusions. A second workshop is planned for the autumn semester of 2024, which will repeat the study with refined protocols based on our current findings. It will expand the sample size and will span over another module, combining CFD tools with a water-based streamline visualization tool focusing on the relationship between wind and form.

7. ACKNOWLEDGEMENTS

The authors would like to thank NTNU for the opportunity to hold these workshops within the DigiHands project with financial support from Toppundervisning and SO Stilling. We would also like to thank all the participants who willingly contributed with their information and work.

8. REFERENCES

1. Picon, A. (2010) Digital Culture in Architecture: An Introduction for the Design Professions. Basel: Birkhaeuser.
2. Scheer, D.R. (2014) The death of Drawing: Architecture in the age of simulation. London: Taylor & Francis Group/Routledge.
3. Oxman, R. (2008) 'Digital Architecture as a challenge for design pedagogy: Theory, knowledge, models and Medium', Design Studies, 29(2), pp. 99–120. doi:10.1016/j.destud.2007.12.003.
4. Aydemir, A.Z. (2018) 'Learning from Pedagogical Experiments,' Eurau18 Alicante: Retroactive research: Congress Proceedings [Preprint]. doi:10.14198/eurau18alicante.
5. Ibrahim, R. and Pour Rahimian, F. (2010) 'Comparison of CAD and manual sketching tools for teaching architectural design', Automation in Construction, 19(8), pp. 978–987. doi:10.1016/j.autcon.2010.09.003.
6.Spiridonidis, C. and Voyatzaki, M. (2007) Teaching and experimenting with architectural design: Advances in technology and changes in pedagogy.
Thessaloniki, Greece: EAAE.
7. Scheer, D.R. (2014) The death of drawing: Architecture in the age of simulation. London: Taylor & Francis Group/Routledge.
8. Kolb, D.A. (2021) Experiential learning: Experience as the source of learning and development. Upper Saddle River (New Jersey): Pearson Education
9. Cohen, L., Manion, L. and Morrison, K. (2018) 'Action research', in Research methods in education. London: Routledge, Taylor & Francis Group, pp. 297–313.
10. Trnova, E. (2015). Hands-On Experiments and Creativity. In Proceedings of the 12th International Conference Hands-On Science pp. 103-109.
11. Caper, R. (1996). Play, experimentation and creativity. The International journal of psycho-analysis, 77(5), 859.
12. Shieh, R.-S., & Chang, W. (2014). Fostering student's creative and problem-solving skills through a hands-on activity. Journal of Baltic Science Education, 13(5), 650–661. https://doi.org/10.33225/jbse/14.13.650
13. Kimbell, R., & Perry, D. (2001). Design and technology in a knowledge economy. London: Engineering Council.
14. Nicol, D., Pilling, S., & Vowels, H. (2000). The "crit" as a ritualised legitimation procedure in architectural education. In Changing Architectural Education: Towards a new professionalism pp. 259–264. essay, E & FN Spon.
15. Altés Alberto, Jara, A., and Correia, L. (2016) "On the infinite demands of responsible architectural practice," in The power of experiment: Artéria - humanizing architecture: 4th edition of Lisbon Architecture Triennale. Lisboa/Portugal: Edition Artéria - humanizing architecture, pp. 37–49.
16. Schenck, J., & Cruickshank, J. (2014). Evolving Kolb. Journal of Experiential Education, 38(1), 73–95. https://doi.org/10.1177/1053825914547153
17. Olgyay, V. (2015). Sol-Air Orientation. In Design with climate: Bioclimatic Approach to architectural regionalism (pp. 54–62). essay, Princeton University Press.
18. Saldaña, J. (2016). The coding manual for qualitative researchers. SAGE.

PLEA 2024 WROCŁAW
(Re)thinking Resilience

(Re)thinking Sustainability in Architecture and Urban Design Education and the urgency of climate action.

Case study of the Tunisian schools of Architecture
The AKSA Matrix as an assessment tool and an instrument for change

KHANSA DHAOUADI[1] PIERRE LECLERCQ[1]

[1]Faculty of Applied Sciences, University of Liège, Belgium

ABSTRACT: This paper focuses on architecture and urban design education facing climate change, and the urgent need to integrate sustainability within university programs at Tunisian architecture schools.
Our methodology is structured around two important phases. First, the literature review examines several pedagogical experiences and case studies to identify emerging trends to build the AKSA Matrix (Awareness, Knowledge, Skills, And Attitude) as an assessment tool.
Secondly, we confront this matrix with the local pedagogical context. The investigation is conducted to determine the level of the current implementation of sustainability issues at the macro (academic program) and micro (design studio) levels from the first to last year. This involves analyzing the content of the courses and examining the whole design process, teaching methods, and students' outcomes.
The findings reveal that the challenges are to deal with multiple difficulties at different levels especially when it comes to knowledge delivered, and skills needed. Despite some efforts, Sustainability issues are not taken seriously and are still looked at as a facultative matter in the Tunisian academic curriculum.
This research suggests the AKSA model as an instrument for change to enhance the integration of sustainability within the local context, taking into consideration the unique specificities and needs.
KEYWORDS: Sustainability, Architecture, education, knowledge, skills.

1. INTRODUCTION

The growing global focus on incorporating sustainable development into architecture and urban design education is a worldwide concern. This emphasizing situation indicates the urgent need to rethink and acknowledge that the built environment plays a vital role in dealing with the interconnected challenges of the 21st century. The Commission of the European Communities has defined Sustainable Development as a strategy aimed at ensuring the continuity over time of economic and social development while respecting the environment and ensuring that it meets the needs of the present without compromising the ability of future generations to meet their own needs [1].

This emerging paradigm admits several definitions and various ambiguities that can be seen from diverse angles and multidisciplinary visions. It cannot be implemented as additional knowledge but asks us to rethink outside disciplinary boundaries and limits. A substantial shift in policies is needed to facilitate the transfer of knowledge and enhance the implementation of environmental sustainability within the creative design [2].

In this context, many strategies, initiatives, and experiences have been conducted to integrate sustainability issues into architectural education. They shed light on new teaching methods and approaches to successfully integrate these issues into academic curricula and programs. The accreditation requirements and regulatory bodies worldwide play a role in supporting and promoting sustainability in architectural education.

The aim is to improve understanding and develop awareness, knowledge, skills, and attitudes needed to face this challenge so students can act and develop solutions to environmental, social, and economic problems. The UNESCO-UIA Charter for Architectural Education declares that educators must prepare future architects to formulate new solutions for the present and the future as the new era will bring with it grave and complex challenges concerning the social and functional degradation of many human settlements [3].

This paper focuses on architecture and urban design education facing climate change, and the urgent need to integrate sustainability within university programs at Tunisian architecture schools.

2. METHOD

The purpose of the study is to determine the level of the current implementation of sustainability in the Tunisian architecture program and specifically the National School of Architecture and Urbanism on

both macro (academic curriculum) and micro (design studio) scales from the first to last year.

Our methodology is structured around two phases. First, the literature review examines several pedagogical experiences to identify emerging trends and build the AKSA matrix (Awareness, Knowledge, Skills, And Attitude) as an assessment tool. It explores the 'what' (content and structure of courses and programs) and the 'how' (pedagogies and implementation processes for teaching methods and curriculum development purposes) worldwide. Secondly, we confront this matrix with the local current pedagogical context based on data collected at different levels from the first to the final year. On the macro-scale, our study involves document analysis of program syllabi and courses materials within the curriculum. On the micro-scale, observations are conducted within the design studio to analyze the whole design process, teaching methods, and students' learning outcomes (Fig. 1).

By studying both scales, The AKSA matrix will be used to enhance the integration of sustainability within the Tunisian context, taking into consideration the unique specificities and needs.

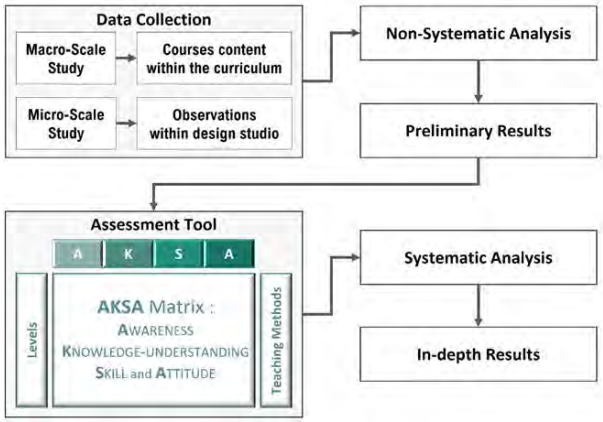

Figure 1: Research Method, Data Collection and Analysis.

3. CASE STUDY

We choose to focus our study on academic curricula at The National School of Architecture and Urban Planning in Tunis (ENAU). It is the first and only public school of architecture in Tunisia. Over the years, other private institutions offering architectural studies, have emerged, and we have also chosen to examine their programs. It should be mentioned that the curriculum and structure at (ENAU) have been reproduced by most, if not all, of these institutions.

Returning to history of the architectural education in Tunisia has allowed us to understand local specificities and contextualized performance criteria underlying Architectural Education. The first institution established was the School of Fine Arts of Tunis, founded in 1923. Since then, it has been followed by the establishment of the National School of Architecture and Urbanism in 1994. From the pedagogical reform of 1997 till today, several attempts to restructure programs have taken place to set up pedagogical content, which adapts to the needs and expectations of teachers and students.

The system of the School of Fine Arts has had an impact with its emphasis on classical aesthetics, historical references, principles of proportion, and harmony in design. It has shaped pedagogical practices in Tunisian architectural schools.

4. THE AKSA MATRIX: AWARENESS, KNOWLEDGE, SKILLS, AND ATTITUDE

4.1 Literature review

Since the 1990s, education has adopted the Competency-Based Approach, which focuses on "knowing how to act". This approach focuses on the object of learning, what we want the learner to develop or acquire: skills. The search for skills is the main object of learning in active and dynamic teaching methods. In educational science, a skill is an identifiable situation that corresponds to a task that the student can solve in an effective way [4].

In Architectural education, students are equipped with a wide range of knowledge and skills essential for both academic learning and professional practice. Procedures for validation and accreditation in architectural education are outlined by national and international organizations, such as the European Association for Architectural Education (EAAE) or the National Architectural Accrediting Board (NAAB) in the United States [5].

These entities not only specify the necessary knowledge but also outline the required skills for individuals to become competent professionals capable of meeting market demands. The UNESCO-UIA validation system aims to establish an international standard of excellence and assessment of the quality of architectural education ensuring the integrity of validated schools. This charter, created in 1996, outlines a set of guidelines that architects should acquire through their education to meet the professional, social, and cultural challenges of the modern world. When it comes to sustainability issues, this calls for a reconsideration of the integration of complexity within this paradigm. The Education Commission of the International Union of Architects has made significant progress in recent years towards a sustainable future [6].

The literature highlights different case studies throughout the world from North and South America, Europe, Asia, Africa, and Australia conducted to incorporate sustainability in architectural education.

According to the University Leaders for a Sustainable Future association, since 1990, more than 300 universities have signed the Talloires Declaration, committing themselves to the pursuit of a sustainable future. This declaration serves as a comprehensive

framework for universities to integrate sustainability into their missions and operations.

In Canada, some universities have successfully implemented significant initiatives to genuinely transform their campuses, incorporating sustainability into their teaching and research. Several of these institutions have chosen to take control of their built environment, while others have established transdisciplinary research laboratories focused on sustainable development.

In Europe, the EDUCATE Initiative (Environmental Design in University Curricula and Architectural Training in Europe) stands out among others as an academic project to promote environmental design education in university curricula and architectural education. One of the goals was to define and test a curriculum and pedagogical framework that bridges current divides between sustainability-related technical information and the design studio at different levels and stages of architectural education to meet current professional demands and expectations [7]. Integrating sustainability into education requires a foundational understanding of key concepts, principles, and frameworks.

On one hand, the assessment methodologies and Environmental quality certifications such as the BREEAM (Building Research Establishment Environmental Assessment Method), NF HQE (High Environmental Quality), and LEED (Leadership in Energy and Environmental Design) have emerged to guide in ensuring the responsible nature of the building, with variations depending on construction types, countries, climates, cultures, regulations [8].

On the other hand, there are additional considerations to consider, such as the 17 Sustainable Development Goals (SDGs) covering various dimensions of societal, economic, and environmental well-being. In the field of architecture, these targets offer a roadmap for fostering sustainable practices and conscious principles [9] to face poverty and hunger, ensure decent work for all, achieve prosperity, peace, gender equality, justice, and protection of human rights, tackle climate change and environmental degradation, and afford water and clean energy. These tools are alternatives to ensure the learning and awareness of students [10].

Several teaching methods are employed in shaping these learning experiences including Knowledge-based Process, learning by doing, Collaborative Learning, Performance-based design, and the Integrated approach also known as Integrated Pedagogy, the interdisciplinary approach encourages students to draw from diverse knowledge areas, fostering a holistic understanding of sustainability [11, 12]. Despite these variations, a shared global concern for environmental issues exists, fostering common ground.

4.2 The AKSA Matrix as an assessment tool

This leads us to the AKSA matrix, which represents various criteria in terms of awareness, knowledge, skills, and attitude (Table 1), as an assessment tool for the investigative study. It is structured around three levels of complexity: sensiblization, validation, and reflection taking into account the progression of education from the first to the fifth year (Table 2).

The AKSA Matrix stands as a holistic comprehensive model encompassing key dimensions critical to evaluating the efficacity of educational programs, particularly within the field of architecture.

Table 1: AKSA Matrix Criteria (Part 1).

Guidelines for the Proposed AKSA Criteria within the Local Tunisian Pedagogical Context	**Awareness**	**Knowledge**	**Skills**
Awareness of environmental and contextual factors in sustainable design			
Awareness of site-specific characteristics vernacular architectural solutions			
Understanding Tunisian context and site dynamics for sustainable design			
Knowledge of human-environment interaction, social context, accessibility			
Understanding built environment materials, construction, climate comfort			
Skills in Multidisciplinary approach to sustainable design challenges			
Skills in environmental design strategies considering various factors and contexts			

Table 2: AKSA Matrix Criteria (Part2).

Levels	**The Proposed AKSA criteria by levels**
Sensibilization	**A**1-**A**3-**A**4-**A**5-**A**6-**A**7-**A**8-**A**9-**A**11-**A**14 **K**1-**K**2-**K**3-**K**5-**K**8-**K**9-**K**10
Validation	**A**2-**A**4-**A**10-**A**11-**A**12-**A**13-**A**14 **K**1-**K**2-**K**3-**K**4-**K**5-**K**7-**K**8-**K**9-**K**10-**K**11-**K**12-**K**13 **K**14-**K**15-**K**16-**K**17-**K**18-**K**19-**K**20-**K**21-**K**22 **K**23-**K**27-**K**28-**K**29-**K**30 **S**2-**S**3-**S**4-**S**5-**S**6-**S**7-**S**9-**S**10-**S**11-**S**12 **S**13-**S**14-**S**15-**S**16
Reflection	**K**1-**K**6-**K**7-**K**8-**K**9-**K**10-**K**11-**K**12-**K**13-**K**14 **K**15-**K**16-**K**17-**K**18-**K**19-**K**20-**K**21-**K**22-**K**23-**K**24 **K**25-**K**26-**K**27-**K**28-**K**29-**K**30-**K**31-**K**32-**K**33 **S**1-**S**2-**S**3-**S**4-**S**5-**S**6-**S**7-**S**8-**S**9-**S**10-**S**11 **S**12-**S**13-**S**14-**S**15-**S**16

Sustainability awareness requires a conscious recognition of environmental, social, and economic challenges. This recognition fosters an understanding of the relationship between human activities and the well-being of our planet. Acquiring knowledge in sustainability is essential for a comprehensive understanding of sustainable principles, including eco-friendly practices, conservation strategies, and the broader implications of human actions on ecosystems. Developing skills in sustainability represents the application of this understanding and

empowers students to implement and incorporate sustainable solutions into their projects. Attitude towards sustainability reflects the student's values, beliefs, commitment, and mindset to adopting environmentally responsible practices.

We mention, for example among the AKSA Matrix articulating around the environmental, sociocultural, contextual, and economic, dimensions :

Awareness related to:

- The ecological and environmental issues involved in architectural practice.
- The socio-economic and cultural context in which built environments are created.
- Vernacular architecture and contribution to the creation of sustainable environments.
- The potential of traditional and new materials and technologies to inform design.

Knowledge related to :

- Relation to Tunisia's climatic identity.
- History and practice of landscape architecture, ecological urban planning, and sustainable cities
- knowledge of the key values and principles of vernacular architectural design.
- Local and regional priorities in relation to environmental issues.
- Understanding the social context in which built environments are created, ergonomic and spatial requirements and needs, and issues of equity and access, User accessibility.
- Understanding of traditional vernacular building materials and processes.
- Knowledge of traditional and bioclimatic technical systems for heating, cooling (Capture, distribute and regulate, protect against heat)

Skills related to:

- Ability to adopt a multi/inter/transdisciplinary approach to sustainable design issues.
- Ability to design the architectural project concerning its geographical and contextual requirements, typography, climate...
- Ability to propose innovative technical solutions inspired by vernacular architecture.
- Ability to meet the requirements and needs of building users within the constraints of cost, building regulations, and sustainability.
- Ability to meet the indoor comfort requirements and needs of building users: The ability to create a satisfactory indoor environment.
- Ability to develop a project by defining the needs and requirements of society and users in terms of ergonomic and spatial requirements and issues of equity and access / User accessibility.

5. RESULTS AND DISCUSSION

By using the AKSA Matrix, the analysis of data is both quantitative and qualitative framework.

The findings reveal that at the macro level, our focus is on scrutinizing the entirety of the academic programs, spanning from the foundational to advanced levels.

In this context, we can identify that there is a limited number of courses that explicitly address sustainability in their content. Even these courses only focus on the social aspect of sustainability while neglecting the consideration of environmental and economic aspects. These courses rarely appear during the early years but become more concentrated in the fifth and final year (Table 3) Instead of approaching it by levels of complexity in terms of awareness, knowledge, skills, and attitudes needed (Fig. 2).

Table 3: Track of Sustainability Awareness, Knowledge, and Skills within program content over the years.

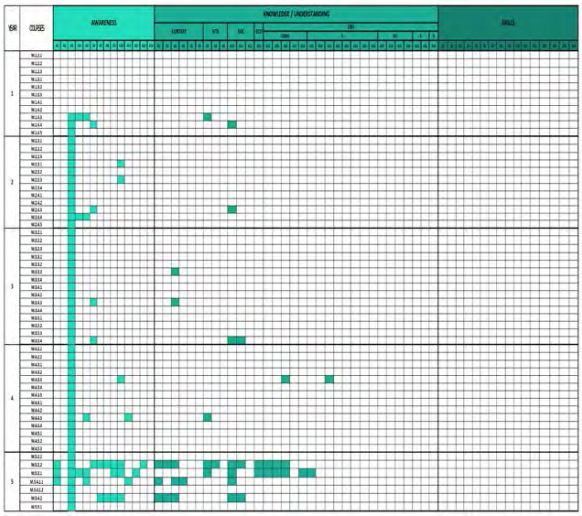

One of the challenges lies in the disconnection between various theoretical courses and design studios, as well as the lack of coordination between theoretical principles and their application within the same academic year, and from one year to the next.

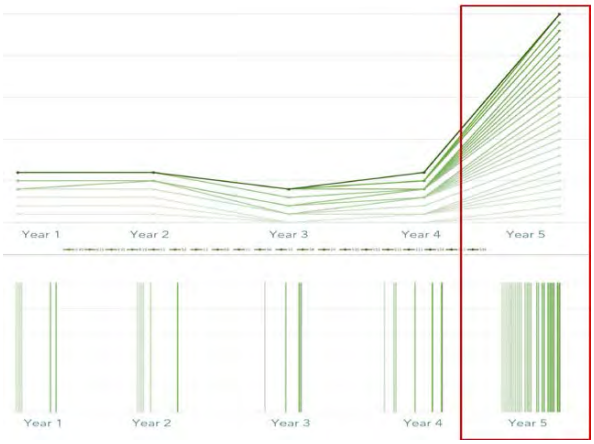

Figure 2: Track of Complexity of Sustainability within Program Content Over the Years.

Transitioning to the micro level, we carefully analyze the pedagogical landscape within design studios. This is where theoretical principles meet practical application. It involves an in-depth exploration of the design process, teaching

methodologies employed, and the student's learning outcomes. In this context, we can identify dysfunctions at two levels: the design process and the learning outcomes. The design process mainly prioritizes the exploration of form and volume and focuses on functional programs, with limited emphasis on sustainability.

Within the design studio of the 1st year (Fig. 3), we can identify some awareness levels among students but a total absence of knowledge, understanding of skills, and attitude related to sustainable design principles.

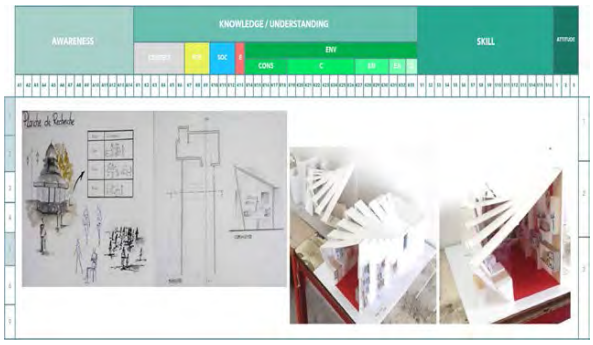

Figure 3: Assessment of student's outcome using AKSA Matrix (Year 1).

Within the design studio of 2nd as well as 3rd years (Fig. 4), many students are environmentally aware, and they can have the knowledge and the attitude needed but not the skills acquired.

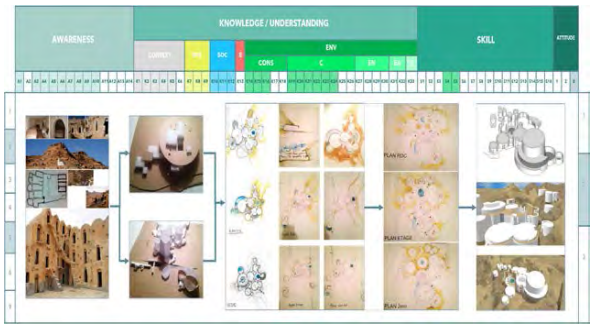

Figure 4: Assessment of student's outcome using AKSA Matrix (Year 3).

In other cases, and especially in the fifth and final year during our first observation conducted (Fig. 5), students express the intention to integrate sustainability into their projects but encounter difficulties in doing so due to various factors. They may face many challenges such as limited resources, complex projects, time management… The primary focus remains on providing information and awareness about sustainability, rather than integrating it deeply. In addition to that, students generally receive minimal encouragement to incorporate sustainability and instructors often do not consider it essential. Philosophy statements and objectives of programs refer to relating design artifacts to the social aspect of sustainability. Each instructor follows their own methods, guided by their own ideologies, principles, and beliefs in design.

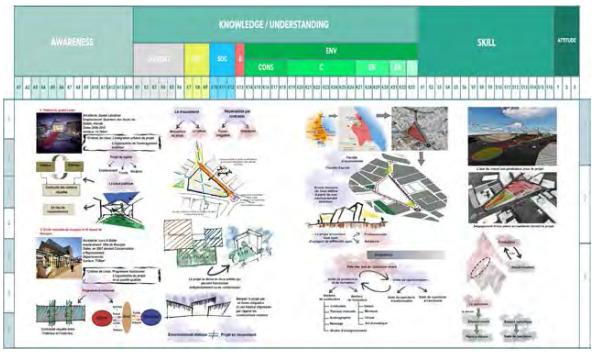

Figure 5: Assessment of student's outcome using AKSA Matrix (Year 5 (Case 1)).

Even if sustainability is introduced at the beginning of the instruction, its presence is often not evident in the learning outcomes, revealing a disconnect between the teacher's pedagogical intentions and the students' reception.

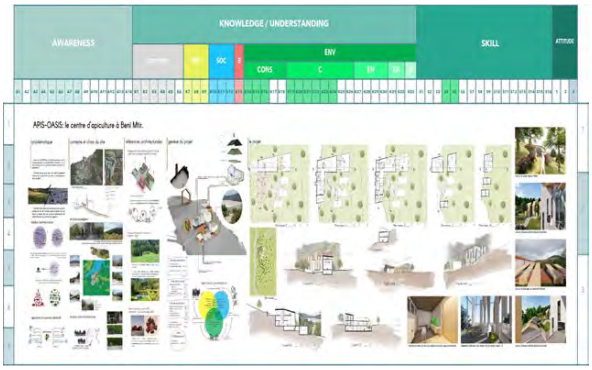

Figure 6: Assessment of student's outcome using AKSA Matrix (Year 5 (Case 2)).

This is different from the 2nd observation conducted (Fig. 6), where students were encouraged but they faced constraints such as conflicting and complex project requirements, and time management…(Fig. 7).

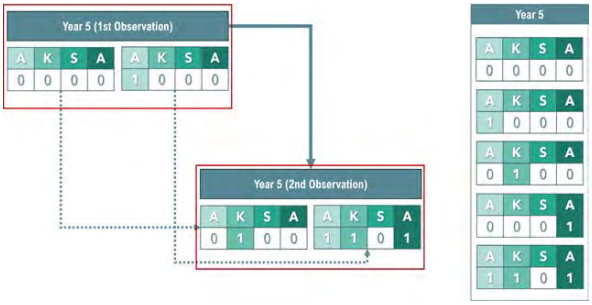

Figure 7: Categories of dysfunctions (Year 5).

One concern with this matrix is that we have had considerable difficulty in assessing students' work across levels, particularly in terms of dealing effectively with the increasing complexity from the 1st

year to the final year. This area requires more careful attention and development.

Based on the AKSA Matrix, constructed from a literature review, the findings have provided an analysis of sustainability implementation across Awareness, Knowledge, Skills, and Attitude dimensions in the Tunisian pedagogical context.

Beyond its role as an assessment tool, this Matrix stands out as a powerful instrument for change. Approaching the different dimensions of the Sustainability Paradigm involves considering various factors such as different levels of complexity, including the aspects of Year, Content, Knowledge, Skills, Ability, and teaching methods (Fig. 8).

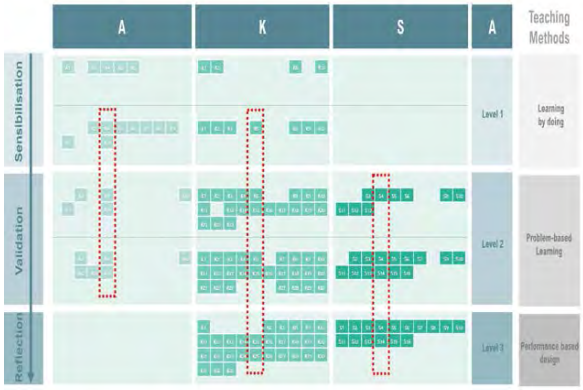

Figure 8: The Framework proposed based on AKSA Matrix.

6. CONCLUSION

In light of the research results, the findings show a focus on knowledge and skills specific to design and aesthetics within the Fine Arts system that has shaped the educational landscape over the years in Teaching architecture in Tunisia. This situation reveals several challenges of integrating sustainability despite some efforts and experiences and how it is taught, learned, and practiced in Tunisia.

The research highlights the importance of Sustainability paradigm in architectural education from the first to the final years of study, as well as the need to improve teaching methods and resources to promote sustainability in the practice of architecture. It is imperative to adapt content taught to the job market, and industry and to new issues, particularly environmental ones.

The aim is to suggest revisions, reformulations, and restructuring of the performance criteria and teaching methods that shape architectural education in Tunisia concerning the sustainability paradigm on both levels of curriculum and design studio taking into consideration the unique specificities and needs of the local context.

And because Integrating sustainability is an ongoing process that requires continuous evaluation and adaptation, the outcome of this study provides potential solutions to dressing the difficulties, and complex issues that can be dealt with.

Therefore, The AKSA matrix is designed to be adapted and transferred to other pedagogical contexts. However, it is important to discuss how these adaptations can be carried out and achieved effectively, considering the differences between educational systems and settings.

ACKNOWLEDGEMENTS

We would like to express our deepest thanks and gratitude to the Tunisian instructors and students for their contributions.

REFERENCES

1. CMED. (1989). Notre avenir à tous. Les éditions du fleuve, Montréal.
2. S. Altomonte et al. (2012).« Educate! Sustainable Environmental Design in Architectural Education and Practice ».
3. UNESCO-UIA Validation Council for Architectural Education. (2017). Architectural Education Charter. Revised Edition. p.2-4.
4. GILLET Perre. (1991). Construire la formation. Editions ESF, Paris 1991.p.45.
5. Attia, A. (2019). International accreditation of architecture programs promoting competitiveness in professional practice. AEJ - Alexandria Engineering Journal, 58, 877 883. https://doi.org/10.1016/j.aej.2019.08.002
6. L. O. Burton et A. M. Salama. (2023). « Sustainable Development Goals and the future of architectural education – cultivating SDGs-centred architectural pedagogies », Archnet-IJAR Int. J. Archit. Res., vol. 17, no 3, p. 421-442, doi: 10.1108/ARCH-08-2023-0201.
7. S. Altomonte. (2009). « Environmental Education for Sustainable Architecture », Rev. Eur. Stud., vol. 1, doi: 10.5539/res.v1n2p12.
8. Serra, S. (2013). Methodology for the assessment of environmental certification in construction : A case study.
9. Morton, S., Pencheon, D., & Squires, N. (2017). Sustainable Development Goals (SDGs), and their implementation : A national global framework for health, development and equity needs a systems approach at every level. British medical bulletin, 124, 1 10. https://doi.org/10.1093/bmb/ldx031.
10. O. Erdogdu Erkarslan et Y. Akgün. (2022). « Incorporating United Nations 2030 Sustainable Future Agenda into the Architectural Studio: A Graduation Studio Case », Int. J. Art Des. Educ, doi: 10.1111/jade.12435.
11. D. Gulec Ozer et B. Turan. (2015) « Ecological Architectural Design Education Practices Via Case Studies », MEGARON Ildız Tech. Univ. Fac. Archit. E-J., vol. 10, juill, doi: 10.5505/megaron.2015.20592.
12. N. Demirbilek, V. Garcia-Hansen, et S. Gard. (2009). « Daylighting design in the architectural design studio ».

PLEA 2024 WROCŁAW
(Re)thinking Resilience

Building Resilience: Examining the Impact of Cultural Behaviour on Air Quality in British Asian Homes

SATISH BK

Welsh School of Architecture, Cardiff University, Cardiff, UK

ABSTRACT: There is a limited understanding of householders' cultural differences, resultant energy behaviour and its impact on indoor air quality. Indoor air quality directly impacts the health and well-being of occupants. The airborne COVID-19 epidemic has highlighted shortcomings of controlled ventilation systems in recent reports. The recently published works including National Design Guide (Jan 2021) are underpinned by the quality of life for the occupants and users of buildings. However, there is a lack of reference to the socio-cultural background of the occupants and how it informs the way we use spaces and hence its impact on indoor thermal comfort, overheating and air quality. The main aim of this research is therefore to develop insights into the realities associated with the social and physical context of one of the key cultural practices, cooking, in kitchens. The impact of cultural behaviour on indoor thermal conditions is examined by studying the impact of cooking on indoor air quality in British-Asian homes in comparison with white British homes through a detailed study of households in Plymouth and Cardiff, UK. This project lays the foundations for larger-scale research working with diverse ethnic minority communities to promote a resilient, inclusive, low-carbon society.

KEYWORDS: Indoor air quality, energy behaviour, Ethnic minority, Indoor thermal comfort Energy, low-carbon society

1. INTRODUCTION

The housing sector is responsible for around 27% of carbon emissions [1] therefore to hit the 2050 carbon target, new homes need to be built to '2050' ready standards [2]. This will mean homes are built with high insulation and controlled ventilation, with no or limited window openings for natural ventilation, to avoid heat loss. The success of these highly insulated houses is determined by many factors including occupants' behaviour and lifestyle. As households in the UK spend nearly 80% of their time indoors, air quality in homes is increasingly responsible for respiratory issues associated with nitrogen dioxide emitted from heating and cooking appliances [3].

Indoor air pollution is one of the key environmental causes of death globally accounting for about 4 million premature deaths. The indoor air pollution further exuberates the condition of women and children below the age of five as they spend more time indoors in homes leading to up to 60 per cent of premature deaths [4]. Poor air quality in terms of an increase in exposure to PM will lead to an increase in hospital admissions, especially in the elderly and people with comorbidity [5]. Recent studies have demonstrated that Indoor Environmental Quality (IEQ) could significantly affect occupant's cognitive skills and in the process their learning and working abilities [6]. PM exposure is also linked to cognitive deficits and oxidative stress [7, 8].

Indoor air pollution is believed to cause respiratory health problems and cancer deaths. Further effects include irritation, Nero toxicological behaviour and other adverse effects. According to the US Environmental Protection Agency (EPA), the associated economic cost is considerable; in 2001 alone, it was likely to be 150 – 200 billion dollars (in the USA) [9]. Exposure to PM2.5 is a major health concern, as they are small and damage airway cells. The Short-term effects include suffocation, burning eyes, and headaches. Long-term effects include chronic disease and premature death [4].

Our research indicates that British- Asians use their homes differently than White-British in terms of spatial organisation, cooking habits and ventilation strategies, all of which impact indoor air quality [10]. However, data and research linking behaviour to indoor air quality is relatively sparse and understanding the energy behaviour of ethnic minorities is itself a relatively new area.

Recent studies have demonstrated that household culture and ventilation behaviour will have a major impact on indoor air quality [4, 12]. There is a limited understanding of householders' cultural differences and their impact on spatial organisation and energy behaviour in dwellings. Indoor air quality directly

impacts the health and well-being of occupants. The airborne COVID-19 epidemic has highlighted shortcomings of controlled ventilation systems in recent reports [11]. While efficiency interventions can make homes more affordable to heat, they can exacerbate conditions such as asthma, due to reduced indoor air quality and ventilation.

Extensive scientific literature has demonstrated that people (users/ occupants) play an important role in determining the energy consumption of a building and therefore research concerned with indoor air quality and ventilation must consider the socio-cultural behaviour of users [4].

Further, households have a limited understanding of potential health and comfort conditions due to their actions [12]. Indoor activities like cooking, cleaning etc will result in the generation and re-suspension of particulate matter (PM2.5) [13, 14]. Cooking generates a range of organic and inorganic compounds, including species that are identified as possible carcinogens such as polycyclic aromatic hydrocarbons (PAHs). Studies have shown that the risk of lung cancer increases three-fold with the increasing number of meals prepared per day [15]. Certain types of cooking related to the culture of the people such as frying, roasting, and grilling can exert a significant impact on pollutant emissions [16].

The main aim of this research is therefore to develop insights into the realities associated with the social and physical context of cooking within given cultural and environmental circumstances and it is achieved by studying the impact of cooking on indoor air quality in British-Asian homes in comparison with white British homes through a detailed study of households in Plymouth and Cardiff, UK.

2. METHODOLOGY

To achieve the objectives of this study, the behaviour patterns and spatial usage, specifically related to cooking practices and associated spaces are reviewed by comparing British-Asian households and native- British households. Survey questionnaires are deployed to collect data related to cooking patterns and associated issues from 120 homes. Measurements of air quality are taken in the homes in summer and winter with data loggers to quantify the difference in mean daily temperature, relative humidity, and air quality index (Figure 1).

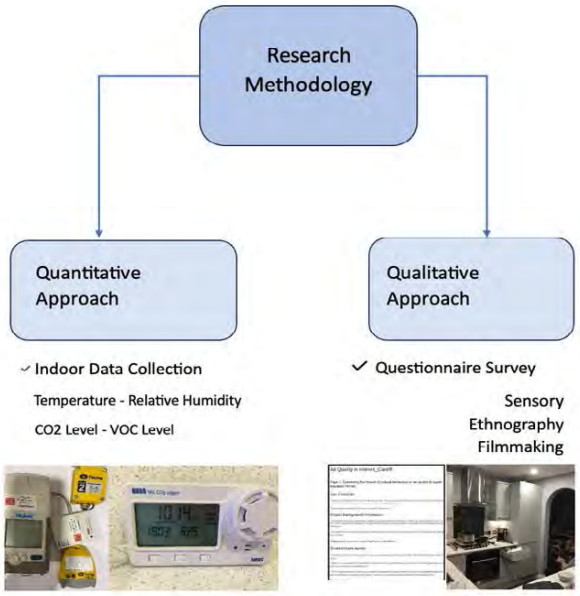

Figure 1: Research Methodology

This paper focuses on the quantitative data collected during this project (Figure 1) which is triangulated by the qualitative and quantitative information gathered during the questionnaire survey.

2.1 Measurements

The HOBO and Tiny tag data recorders were placed in strategic locations in the kitchens in Plymouth and Cardiff, UK to collect indoor climate quality-related variables. The data is collected at 10-minute intervals over a minimum of fifteen days. These loggers were positioned in such a way that they would be shielded from any potential sources of heat and sunshine. The calibrated Testo 480 IAQ Pro loggers were used to measure the interior environment temperature (0.3 °C), humidity (1.0%), CO2 levels (50 ppm CO2), and airflow (59 fpm). The temperature was found to be within the acceptable ranges for all these factors.

3 ANALYSIS AND DISCUSSION

Using the data loggers in neighbouring houses, nearly 4100 sets of data are collected over 15 days, including daily temperature, relative humidity, and air quality in terms of CO2 level.

3.1 Indoor temperature level

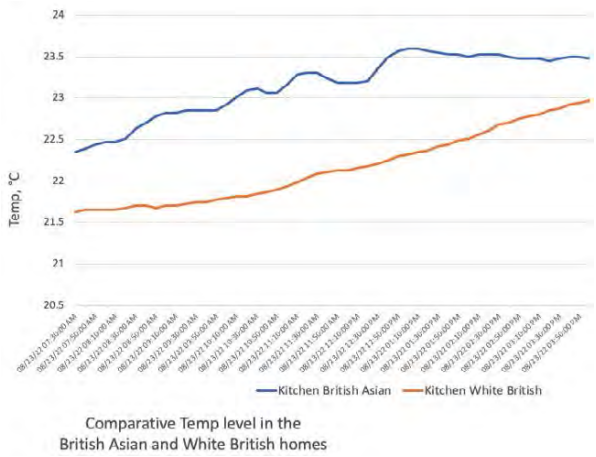

Figure 2: Comparative Temperature Level

In the two sets of houses compared, the dry bulb temperatures of the British Asian homes were consistently higher than the White British Houses (Figure 2). The temperature reached nearly 24 degrees C in August in a British Asian house whereas it was two degrees lower at the same time in the White British House (Figure 2). Considering the similar building typology with building fabric (U Value) and spatial organisation, in terms of orientation, opening sizes, etc. it is evident that the increased temperature in the British Asian Kitchens is due to the way they use the kitchen, i.e. the amount of time spent in kitchens, especially cooking.

The questionnaire survey has revealed that British Asians spend nearly four times more time in the kitchen than white British residents. The overheating will have a serious impact on the health of the occupiers, particularly the elderly and the very young.

3.2 Humidity

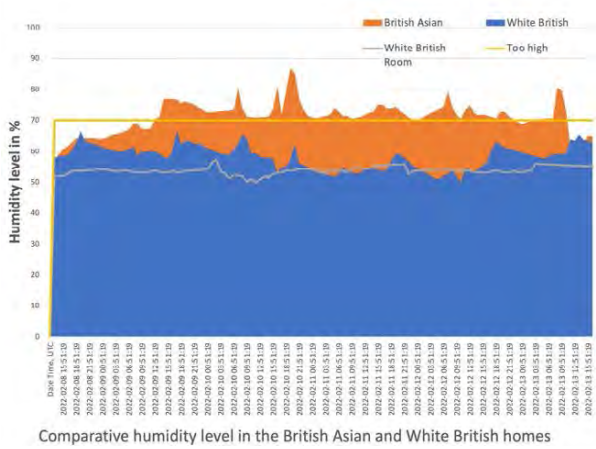

Figure 3: Comparative humidity level in the British Asian and White British homes

The user behaviour, activities, and how we use space will have a major impact on the humidity level in the kitchen. When it comes to humidity, humidity below 70 per cent is considered an acceptable level [17]. The humidity level is around 55 per cent in the rooms of white British homes. Due to the cooking activities, the humidity level fluctuates but has remained below 65 per cent. However, in the case of British Asian homes, the humidity level in the kitchens is much higher than 70 per cent and at times, it is closer to 90 per cent (Figure 3).

The higher level of humidity is due to the type and duration of cooking. Further, it is also due to the user behaviour; for instance, whether they open the windows while cooking would have a major impact on the indoor humidity level in the kitchens (Figure 4).

With super-insulated houses, without proper attention to the build-up of steam and humidity would have major implications on health in terms of including respiratory infections, asthma, and malaise. Higher humidity for longer periods will also impact the building condition in terms of the corrosion of metal components, decayed timber, damp damage and mould growth. Further, higher humidity levels, if not properly addressed can lead to interstitial condensation and lead to hidden structural damage.

Figure 4: Comparative humidity level in the British Asian and White British homes

3.3 Indoor Carbon Dioxide (CO2) level

The literature review suggests that there will be a normal background concentration of 250 – 400 ppm in outdoor ambient air and up to 1000 ppm of CO2 in occupied indoor spaces. Once the CO2 concentration increases beyond 1000 ppm, occupants will experience health effects in buildings.

In the case of the two kitchens compared, the CO2 level was below 90 per cent of the time below 1000 ppm in the White British home (Figure 6), whereas only 45 per cent of the time the kitchen air quality was below 1000 ppm. The comparison of air quality in the British Asian and White British house kitchens clearly demonstrates the poor air quality in the British Asian homes as nearly 13 per cent of the time the CO2 level is more than 1500 ppm in the kitchen (figure 5).

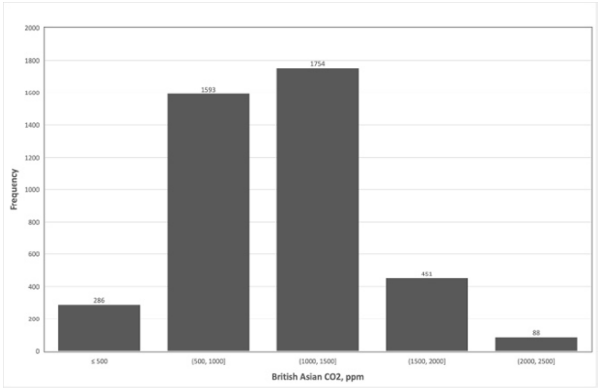

Figure 5: CO2 concentration in the kitchen of a British Asian home

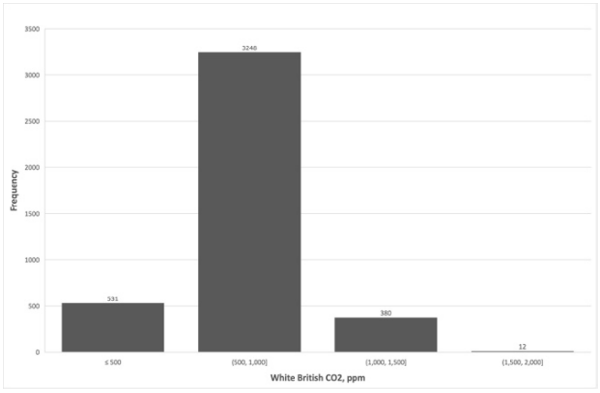

Figure 6: CO2 concentration in the kitchen of a White British home

While comparing the CO2 levels in the British Asian and White British homes. Barring a couple of days, the CO2 level has been consistently higher in British Asian homes with many days CO2 touching 2000 ppm and dangerously reaching 2500 ppm on three occasions (figure 7).

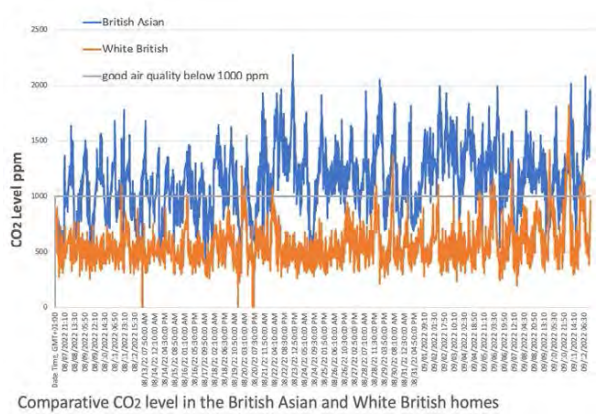

Figure 7: Comparative CO2 level in the British Asian and White British home

Analysis of one representative day clearly demonstrates the impact of cooking on CO2 levels in kitchens. The CO2 level is nearly the same in both British Asian and White British homes early morning between 2.00 am to 6.30 am (figure 8). The CO2 level starts rising in the British Asian home with morning kitchen activities and due to the nature of cooking activities, stays above 1000ppm for most of the day and reaches a peak by 8.00 pm, by the end of cooking evening meals.

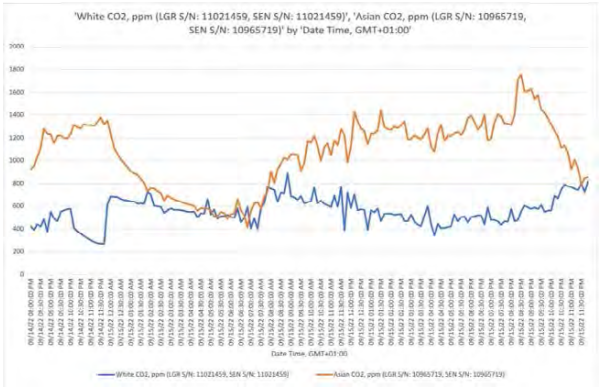

Figure 8: Comparative CO2 level in the British Asian and White British home - one day

The marked difference in the CO2 levels in British Asian and White British homes is due to many reasons but could be mainly attributed to the cooking and ventilation habits of the households. The higher and prolonged levels of CO2 in British Asian homes are due to the duration of cooking. Based on the survey conducted in Plymouth and Cardiff, UK, British Asians spend 3.3 hours per day in the kitchen during the weekday, while White British spend around 1.5 hours per day in the kitchen. The gap further widens during the weekend, wherein, White British cook around 1.75 hours/ day while British Asians spend nearly 4.16 hours/day cooking.

All the White British respondents (100 per cent) said that in summer, during the weekdays, most of the time they keep the windows open. Whereas only about 16 per cent of the British Asians responded that they keep the windows open in the morning. Further, 22 per cent of the British Asian respondents hardly ever open the windows and nearly 40 per cent of them open the windows for one to two hours in the morning. Although it is slightly better during the weekend as it has dropped to 30 per cent. During the weekend, British Asians tend to open their windows more than during the weekdays with nearly 30 per cent of them opening the windows most of the time. Concern for heat loss is evident as they tend to keep the window closed most of the time. As 30 per cent of them never open the windows and nearly 25 per cent open only 1 to two hours in the evening, whereas most of the White British keep them open for most of the time.

4 CONCLUSION

4.1 Applications for the research

The results of this study will be of key interest to government policymakers and building industry stakeholders. The study identifies the specific areas where homeowners' cultural behaviour impacts the air quality.

4.2 Summary

While acknowledging the need to develop air-tight homes, emphasis needs to be given to the importance of lifestyle and cultural preferences. This research focuses on cooking and associated indoor air quality as a social and cultural phenomenon that can allow insights into the effective formulation of localised and relevant indoor air quality and low-carbon strategies and thus provide a bottom-up tool to implement the policies and targets set by the professional bodies and the UK government.

The study in this paper, using a literature review and survey fieldwork, has highlighted the similarities and differences in the socio-cultural value systems of British and British Asian households and the resultant indoor air quality. From the outcome of the IAQ Data Loggers and questionnaire survey, this paper examined one key aspect of lifestyle and cultural preferences.

The particular points are as follows:

1. Particularly higher levels of CO2 in British Asian homes for a prolonged period of time are alarming and as discussed in the literature review, poor air quality in BA homes could put them at severe health risk.
2. Consistently higher level of temperature and humidity in BA Houses has to be closely studied as lack of ventilation due to lack of window opening and cooking preferences could lead to mould and risk the health and wellbeing of the households.

4.3 Limitation and further research

From the outcome of the survey questionnaires and IAQ Data Loggers, this paper examined the impact of one of the homeowners' cultural behaviours, cooking, and associated behaviours on indoor air quality. Further studies with the ethnographic survey and interview of households triangulated with environmental analysis would be helpful to further develop this research and develop a healthy living environment for ethnic minority households.

The research has shown that there is a direct correlation between the social and cultural values and energy behaviour of households. Further examination of specific aspects like hourly activities in the kitchen and other spaces within the house, would provide greater insight into the extent of the impact of behaviour on indoor air quality and would go a long way in designing the built environment for the health and wellbeing of the households and sustainable communities for the future.

This study reviewed selected elements and the survey was limited to two cities, Cardiff and Plymouth and British Asians. Further examination of other places in the UK and other ethnic minority groups would be helpful to develop an exhaustive understanding of the indoor air quality in ethnic minority homes to enable a more sensible and inclusive understanding of indoor air quality requirements and inform policy decisions.

ACKNOWLEDGEMENTS

This paper is part of the ongoing research made possible by the RIBA Research Fund.

REFERENCES

1.DECC and H. Treasury, *Policy paper - 2010 to 2015 government policy: greenhouse gas emissions*. 2015, https://www.gov.uk/government/publications/2010-to-2015-government-policy-greenhouse-gas-emissions/2010-to-2015-government-policy-greenhouse-gas-emissions: Committee on Climate Change, Department of Energy & Climate Change.

2.Trust, E.S. *Save energy at home*. 2017 [cited 2017 15 Nov 2017].

3.Parliament, U., *UK indoor air quality, November 2010, Postnote 366*, post-parliament-uk.abc.cardiff.ac.uk/research-briefings/post-pn-366, Editor. 2010, UK Parliament.

4.Lueker, J., et al., *Indoor air quality among Mumbai's resettled populations: Comparing Dharavi slum to nearby rehabilitation sites.* Building and environment, 2020. **167**: p. 106419.

5.Buczyńska, A.J., et al., *Composition of PM2.5 and PM1 on high and low pollution event days and its relation to indoor air quality in a home for the elderly.* The Science of the total environment, 2014. **490**: p. 134-143.

6.Wang, C., et al., *How indoor environmental quality affects occupants' cognitive functions: A systematic review.* Building and environment, 2021. **193**: p. 107647.

7.Amato, F., et al., *Sources of indoor and outdoor PM2.5 concentrations in primary schools.* The Science of the total environment, 2014. **490**: p. 757-765.

8.Wan, M.-P., et al., *Ultrafine particles, and $PM_{2.5}$ generated from cooking in homes.* Atmospheric environment (1994), 2011. **45**(34): p. 6141-6148.

9.Crump, D., A. Dengel, and M. Swainson, *Indoor air quality in highly energy efficient homes - a review*, N.F.-Z.C. Hub, Editor. 2009, IHS BRE Press: Bucks.

10.Satish, B.K. and J. Brennan, *Understanding the energy use behaviour of British Indian households to shape optimised sustainable housing strategies in existing housing stock.* Sustainable Cities and Society, 2019: p. 101542.

11.*Women and Equalities Committee 3rd Report. Unequal impact? Coronavirus and BAME people Volume 1. Report: HC 384*. 2020, Dandy Booksellers.

12.Behar, C. and L.F. Chiu, *Ventilation in energy efficient UK homes: A user experience of innovative technologies*. 2013, ECEEE Summer Proceedings. p. 2389 - 2399.
13.Wang, L., et al., *Characterization particulate matter from several Chinese cooking dishes and implications in health effects.* Journal of environmental sciences (China), 2018. **72**: p. 98-106.
14.Escobedo, L.E., et al., *Indoor air quality in Latino homes in Boulder, Colorado.* Atmospheric environment (1994), 2014. **92**: p. 69-75.
15.Gao, J., et al., *Indoor emission, dispersion and exposure of total particle-bound polycyclic aromatic hydrocarbons during cooking.* Atmospheric environment (1994), 2015. **120**: p. 191-199.
16.Kim, K.-H., et al., *The modern paradox of unregulated cooking activities and indoor air quality.* Journal of hazardous materials, 2011. **195**: p. 1-10.
17.Rojas, G., et al., *Applying the passive house concept to a social housing project in Austria - evaluation of the indoor environment based on long-term measurements and user surveys.* Advances in building energy research, 2016. **10**(1): p. 125-148.

PLEA 2024 WROCŁAW
(Re)thinking Resilience

An Evidence Based Educational Framework:
Passive architecture to reduce agitation in people living with Dementia

NEVEEN HAMZA [1], AND STUART FRANKLIN[2]

[1] Newcastle University, Newcastle Upon Tyne, United Kingdom
[2] JDDK Architects, Newcastle Upon Tyne, United Kingdom

ABSTRACT: This paper shares experiences of setting the design brief and teaching a graduation project using integrational and experiential architectural studio pedagogy. This is a live project that will inform decision makers in the University of Newcastle, UK, and its estates department. This paper aims to show how insights from environmental psychology and advances in building and urban performance simulation modelling can inform a dementia user-centric, energy efficient and sustainable architectural design approach in the pedagogy of the design studio. The educational framework, based on the Structure of Observed Learning Outcome (SOLO), allows the students to design buildings that provide meaningful multi-sensory experiences that compensate for cognitive decline, loss of agency to control personal comfort, while enhancing social engagement in an environmentally comfortable and energy efficient environment.
KEYWORDS: Architectural pedagogy, Dementia, SOLO framework

1. INTRODUCTION

Inclusive Design for people living with mental health conditions, and specifically Dementia (PLWD), is rarely seen as an architectural project in architecture schools. The World Health Organization defines 'dementia' as a progressive syndrome leading to a set of symptoms that lead to deterioration in memory, difficulties with thinking, problem solving, verbal communication and the ability to perform daily tasks. These changes are often incremental at the beginning, progressing to a stage where patients need to be hospitalized or taken into care homes. The mid to late onset of the syndrome, leads to an inability to express personal discontent in a socially acceptable manner. This necessitates a building designed to compensate for sensory, cognitive, and physical impairments. Designing purpose-built facilities that educate, re-habilitate, provide thermal and visual therapeutic environments is a need for both patients and their carers.

Literature suggests that well designed environments for a small group of patients in a home like environment influences dementia patients' behavioural attitude and aids in retention of physical abilities to move within the spaces [1,2] The term 'well designed environment' is used here to refer to the physical attributes of a building and its sensory thermal, visual, and acoustic environments. Thermally comfortable and well daylit indoor and outdoor environments alleviate symptoms of depression, sleep disturbances, and agitation, that are commonly treated with antipsychotic drugs. Studies show that antipsychotic treatments of PLWDs are modestly effective and produce a variety of serious side effects [3]

The prevalence of Dementia is alarming with 55 million people living with dementia worldwide, and 10 million new cases diagnosed every year. The rates of this syndrome are expected to continually rise, with estimates at 75.6 million cases by 2030 and an expected rise to 135.5 million by 2050 [4] The proportion of people diagnosed with Dementia doubles for every five years in age and one in six people over the age of 80 will be diagnosed with the disease. Unfortunately, it also affects a younger age group, 42,000 people in the UK under 65 are diagnosed with dementia. Globally dementia is believed to have cost approximately $1.3 trillion. Approximately 50% of these costs are associated with direct medical care while the other 50% is attributed to unpaid care by family members, social care [4]. There are currently around 900,000 people with dementia in the UK. This is projected to reach 1.6 million people in the UK living with dementia in 2040.This sharp rise is due mainly to accelerated population ageing [5]. This positions Dementia as the seventh cause of death globally and care strategies as a pressing societal issue to provide care strategies and homely and comfortable facilities when needed.

Considerations for designing for PLWD coupled with climate change, leads to the need to integrate the understanding of desperate knowledge domains into architectural conceptualization. Proposed architectural designs need to reduce building energy demand by adopting sound passive design strategies that harnesses the natural energy of the site. Passive

designs strategies then need to be enhanced by the integration of renewable energy technologies in the building design process as an architectural feature not an add on.

The School of Architecture, Planning and Landscape, Newcastle University, UK has piloted a pedagogy of integrating a design centric approach for PWLD and sustainability approaches in the design studio, since 2019. The aim is to educate a distinct graduate, capable of relational and critical thinking combining architectural design vision with targeted and specialised knowledge, to create environments that promote wellness for vulnerable users.

Critical to an increasing population with dementia, is a need to change the social perceptions of mental health facilities, commonly confused in the popular imagination with Victorian asylums and prisons. The availability of facilities that educate, re-habilitate, provide therapeutic and healing environments **is** a need for both patients and their carers. This paper aims to show how insights from environmental psychology and advances in building and urban performance simulation modelling can inform a dementia user-centric, energy efficient and sustainable architectural design approach in the pedagogy of the design studio. The educational framework allows the students to design buildings that provide meaningful multi-sensory experiences that compensate for cognitive decline, loss of agency to control personal comfort, while enhancing social engagement in an environmentally comfortable and energy efficient environment.

2. A METHODOLOGY FOR SETTING PEDAGOGICAL TARGETS AND COMPETENCIES

This paper shares experiences of setting the design brief and teaching a graduation project in an integrational and experiential architectural studio pedagogy. This is a live project that will inform decision makers in the University of Newcastle and its estates department. The site is part of a multi-million intended development of the Health and Innovation Neighbourhood (HIN) located in the heart of the city.

The teaching team aimed to:

- Create a design brief where the building and its surroundings offer a delicate balance between memorable sensory experience, while reducing information overload for PLWDs.
- Integrate an architectural design programme, with the environmental psychology theories of ‘affordance’ and ’Salutogenesis’, the latter delineating the psychology of human transactions with their environment [6]
- To amplify the intellectual and analytical capabilities of students to visualize and work with the invisible environmental energies that influence occupants’ comfort and can be reiterated into early architectural decision- making processes.
- An understanding that one software will not deliver the required indoor and outdoor environmental analysis. Instead, a process of building the students capabilities for using two industry standard software (IESVE and ENVI-met) that will require time and dedication from the students added to their usual commitments in the studio.
- As the outputs of simulation tools are tables and graphs, students need to transfer this data into graphical visualization images to facilitate design decisions and communication with non-experts [7] in this case external assessors who may be other tutors, medics and members of the public in the design team

The brief was constructed based on evidence-based research on psycho-spatial effects of space design on the vulnerable frail older people living in age care facilities [7,8,9], while investigating the use of building and urban environmental early-stage assessment tools, how to communicate their analytical outcomes to be used to develop an inclusive design for PLWDs [10]

The studio trajectory focused on engaging with targeted user requirements, the complexity of surrounding socio-economic neighbourhood, local climate, sustainability, and climate change to deliver an integrating interpretation of these driving factors into a holistic, situated in place architecture.

Established Dementia design guidelines [2], attempt to highlight the need to address contrasting design brief requirements when designing Dementia facilities. Contrasting a feeling of ‘home away from home’ while providing a hospital secure and easily sterilized accommodation. Other contrasting requirements include provision of outdoor spaces where external environments reduce the effects of high wind speed and provides sunny areas, with reduced visual contrast in shaded areas, to extend the free use of outdoor space for the ‘wandering’, while easily being observed by staff and carers.

Considering time limitations and an aspirational studio brief, the teaching team took the view that supporting cognitive and experiential thinking requires a pedagogical framework. The aspiration was that design projects can incorporate designed environments that require deeper levels of relational thinking of existing knowledge domains. The Structure of Observed Learning Outcomes (SOLO) taxonomy proposed by Biggs and Collis [11] identifies five levels of increasing competence and knowledge acquisition for learners to reach an expert-like level of

dealing with complex propositions. SOLO is a general model of intellectual development concerned with assessing learning based on the quality of the learner's response. SOLO had its origins in the stage development ideas of Piaget and information processing concepts of the 1970s. SOLO is referred to broadly as a neo-Piagetian framework, where a structured pedagogical experience that involves the learner as an active participant in the process, and co-generator of knowledge and its application into individual design propositions.

The SOLO framework is progressive in its structural complexity towards developing the learners 'ability to handle increased cues to handle a sophisticated design brief**.** We have adapted the SOLO model to the design studio as:

- Pre-structural: Understanding the medical conditions of PLWD, that leads to research into neurological specific requirements of space.

  Being able to list definitions, and basic understanding of dementia, its types, and progression of the condition, sensory materials and assistive living technologies for PLWD. Students were asked to work in groups at this stage and present (in a student led event), to the teaching team and each other, their bibliographical research and think of creative data visualizations to present their findings.

  This stage also includes understanding of design criteria development over time from a 'History of Madness' [12] understanding to listing current knowledge of indoor and outdoor design criteria that can be used to provide a sensory environment.
- Unistructural: being able to connect principles understood from the previous level into critically analysing precedents of built Dementia specific facilities, in terms of their programmatic interpretation of individual, communal and medical staff requirements. Precedents were analysed for their success in providing spaces for care and what could be improved. This stage also investigated the provision of intergenerational spaces, and how the facilities integrate to their climatic and social specific contexts. This was followed by each group presenting a designed 'sensory experience' wall of textures and edible fragrancies in a 1:1 installation.
- Also analysing built precedents based on what was learnt from the principles of designing for PLWD, and how these facilities provide for individual lifestyles and cultures in non-institutionalized buildings.
- Multi structural: In this stage different building performance simulation tools are introduced. Students are asked to start 'designing from the pillow' of a resident's bed.

  In this stage, the design of the 'Dementia Pod', Figure 3, as the residential individual room is designed with a late stage PLWD in mind, maintaining 5 visual axis from the patients pillow. Namely, a direct visual access to an external view, to a TV, to a carer seating area, to the door and to the toilet. The latter is recommended for more dignity, speed of access and reminding the person to use it. 'Dementia pod' were tested in peak seasonal conditions over a day to test the varying levels of daylight and their impact on patient vision and perception of space. Design iterations were undertaken to reduce sharp contrasting shadows on floors that could be perceived by PwD as a hole in the ground. In this level, IESVE was used to test year-round iterations of the project massing, for shadowing and external environmental conditions, to provide solar access to all 'Dementia Pods' and to ensure that Photovoltaics (PV) positioning on the roof will not be overshadowed by the massing of buildings.

An operational matrix, presented in (Figure 1), where tutor structured milestones are mapped to the SOLO taxonomy (*X*-axis). Expected student's competence and learning outcomes towards a consolidated proposal of architectural merit are presented on the (*Y*-axis).

Two students massing proposals, were presented in (Figure 2), showing a competence in synthesizing multiple knowledge domains, from understanding of the environmental psychology theories of dementia as a health condition, to lessons learnt from precedents and integration with results of the building and outdoor environmental condition simulations in a coherent whole.

The top proposal moves from an abstract massing to accommodate the user requirements to creating indoor courtyards for wandering to moving the patient rooms to respond to the sun path.

The second proposal (bottom) shows how outdoor environmental condition simulations let to the building form, creating a sheltered indoor courtyard, while strategically positioning trees to allow for patient rooms view out while sheltering from high wind speeds in winter.

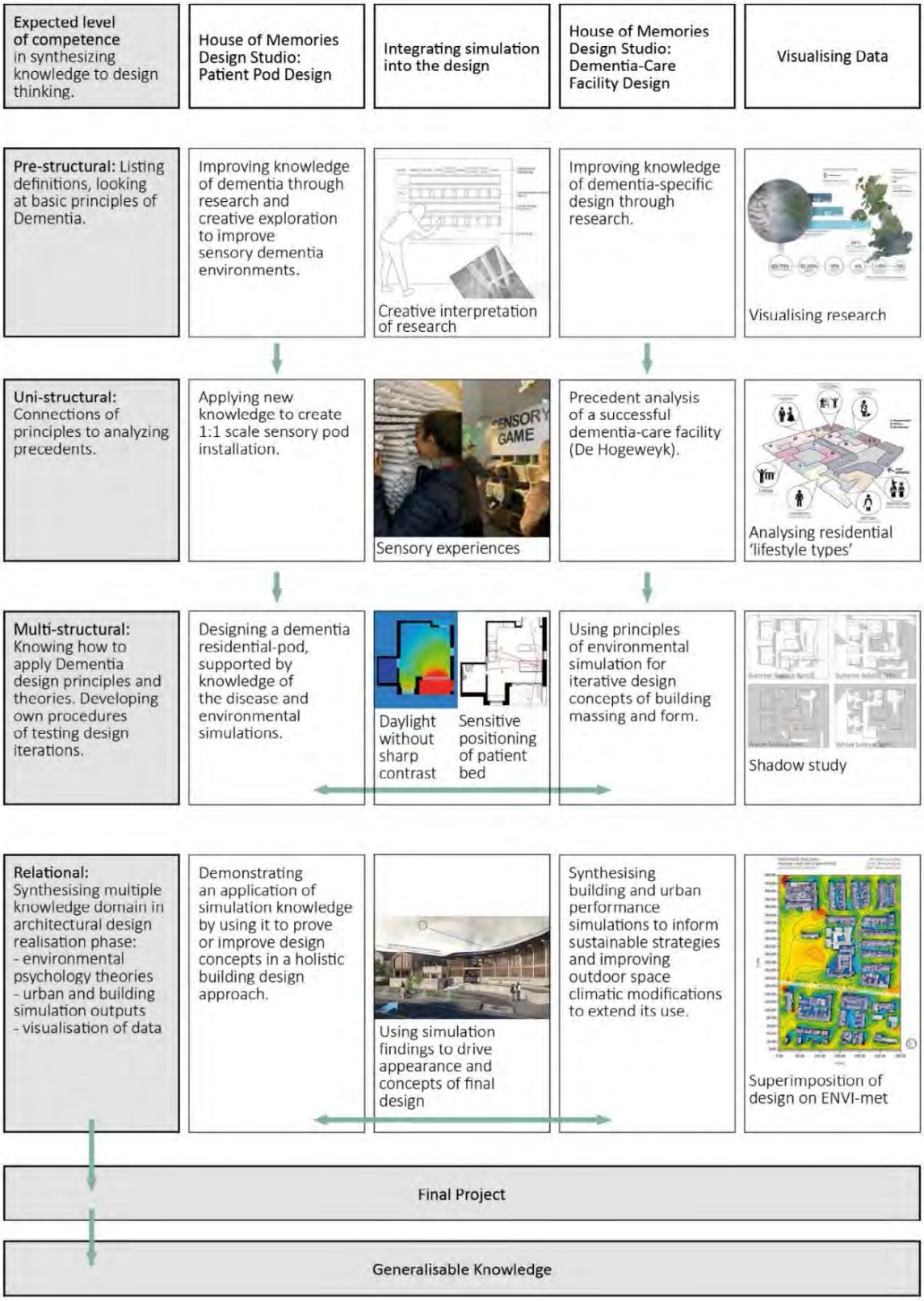

Figure 1: Mapping aspirations for students' attainment against the SOLO Taxonomy[12]

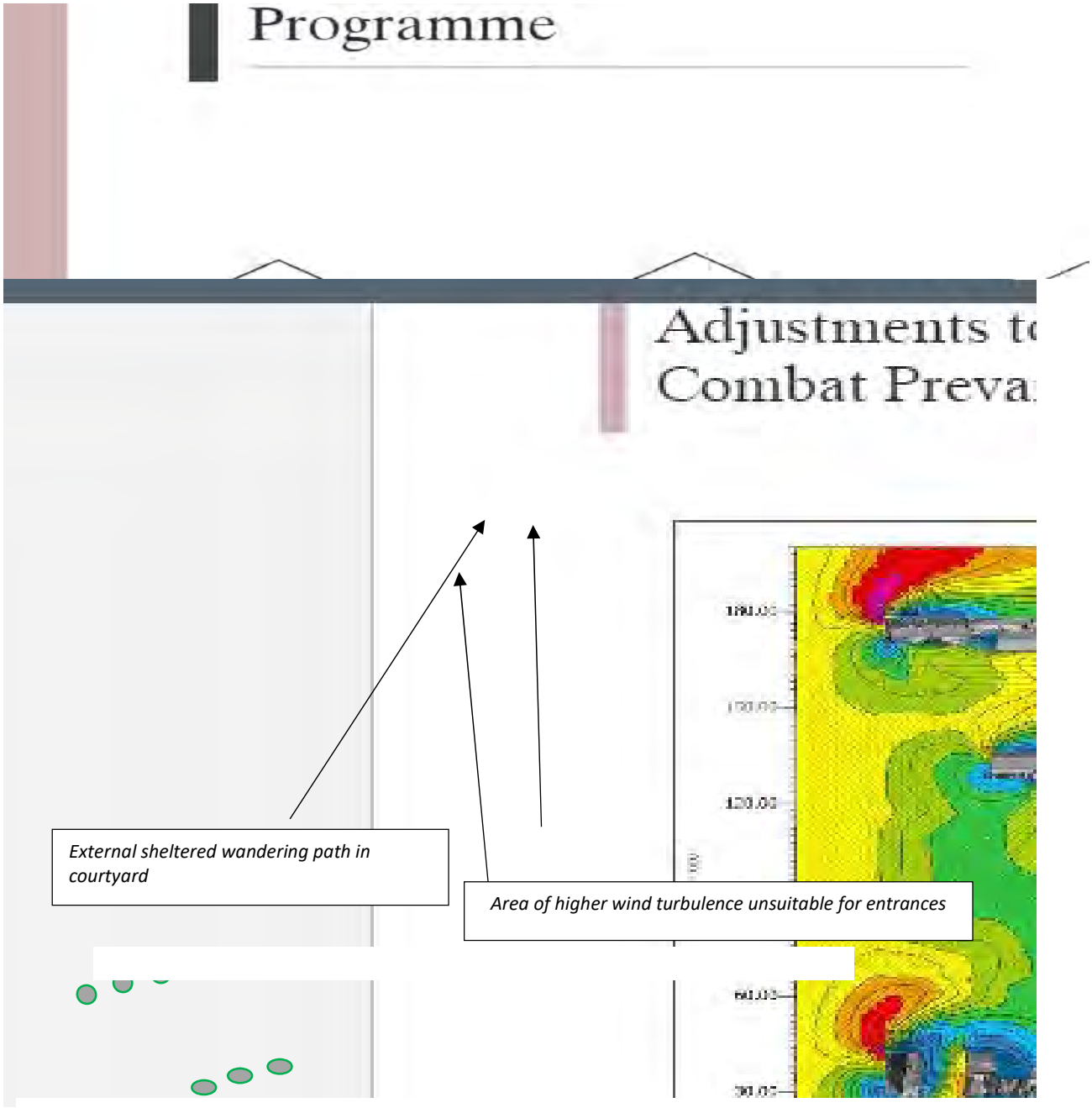

Figure 2: ENVI-MET simulation and how it changed massing proposals-Students' work [12]

Figure 3: testing room design with daylight contour maps.

Simulation of daylight levels and contours (Figure 3), shows how a PWLD perceives sharp contrasts of light on the floor as holes, which requires a careful consideration of placing windows and furniture. The patient room is designed so a person laying on the bed would have direct visual access to the toilet, a TV, a view out and to the room's door.

3. CONCLUSION

A structured pedagogy framework to advance architectural education is presented in this paper. However, this methodology can also be used in practice to optimize the environmental performance of buildings for PLWD. In this methodology a design from the inside to outside is proposed, that introduces environmental assessment tools at conceptual stage.

The design of buildings and outdoor environments can have a long term and significant impact on PWD behaviours and the progression of the disease. This chapter presents a pedagogical methodology based on the SOLO educational model in the design studio to educate a new generation of architects on how to design for vulnerable building users.

Designing for dementia requires the integration of different knowledge domains, linking environmental psychology theories of 'space perceptions', 'space affordance' 'Salutogenesis' to building and urban environmental performance modelling, in the architectural design process. Visualizing the differences in environmental and space perception between a cognitively sound person and a Person Living With Dementia (PLWD) helps reduce agitation. Design iterations, based on environmental simulations results, provides easier environments for care provision and works towards a better integration with local climatic conditions to maximize renewable energy integration.

Reflecting on our experience, we thought there is no better way than including students' feedback and letting them write our conclusion. Initially as tutors we were pleasantly surprised by the level of enthusiasm and continuous appetite to work with the integration methodology and the co-generation of knowledge in our studio. We asked the students: why they decided to choose our studio and to give us feedback on the process. All 36 students concurred that it was a steep learning curve on how to use the two softwares. The external help of the two graduate tutors, and the student champion was acknowledged. However, feedback suggests that it was an enjoyable experience although at times stressful and challenging when software crashed. Feedback suggests that they were happy to prove how their designs could work to quantitively comply with design standards rather, than just speculations based on aesthetics judgements.

'I was excited at the prospect of working on a project that felt 'rooted in reality'; dealing with a live site, official regulations and scientific research, and with vulnerable end-users who form a significant part of our society – users for who empathetic design can be instrumental to their well-being and understanding of the world around them. In addition, the studio's intent on using environmental simulation to guide the project felt invaluable, as we prepared to enter the working world – a world where climate change and the environment are finally becoming of utmost importance across all industries and disciplines.'

'Using IESVE and EnviMET demanded a basic understanding of light, wind and other environmental factors, while the outputs were purely factual and informative, once again providing a refreshing difference to large proportions of architectural education which seem driven by aesthetics. It was interesting to learn not only how to produce the right diagrams or images, but to gain an understanding as to why certain results occur, and how changes can be made so that more optimal results can be achieved.'

REFERENCES

1. Lawton M. (2001). The physical environment of the person with Alzheimer's disease. Aging and mental health, May5, Suppl1:S56-64
2. HBN 08-02, Dementia-friendly health and social care environments https://www.gov.uk/government/publications/dementia-friendly-health-and-social-care-environments-hbn-08-02
3. Singleton, M. (2013). Understanding Alzheimer's Disease. A review of medical advancements and efforts to address the societal, economic, and personal toll of an impending public health crisis, California Senate Office of Research
4. World Health Organization (WHO, March 2023). Dementia Key facts online.Dementia (www.who.int). retrieved 14/12/2023
5. Wittenberg R, l. Hu, L.Barraza-Araiza, and A. Rehill (2019). Projections of older people with dementia and costs of dementia care in the United Kingdom, 2019–2040, Publisher LSE (alzheimers.org.uk)
6. Antonovsky A.(1979). Health, Stress and Coping, SanFrancisco, Jossey-Bass Publishers, 1979.
7. Feddersen E. and I. Ludtke (2014). Architecture and Dementia, Lost in Space, Birkhauser Igawa, N. and H. Nakamura, (2001). All Sky Model as a standard sky for the simulation of daylight environment. *Building and Environment*, 36: p. 763-770.
8. Nagari K, N. Hamza (2016) Assessment of Daylight in Relation to the Agitation Levels of People with Dementia. In Hamza, N and C. Underwood.(Ed) Building Simulation and Optimization, Sept 12-14th Newcastle University, Newcastle
9. Rodriguez M, and N. Hamza(2016) Assessment of Indoor Visual Environments Using Dementia Friendly Design Criteria in Day Care Centres, in Hamza, N and C. Underwood (Ed) Building Simulation and Optimization, Sept 12-14th Newcastle University, Newcastle
10. Hamza N, and P. De Wilde (2014) Building simulation Visualization for the boardroom: an exploratory study, Journal of Building Performance Simulation 7 (1),p. 52-67
11. Foucault M.(2001) Madness and Civilization: The history of Insanity in the age of reason, Routledge
12. Hamza N, S. Franklin, and C. Elkington(2022) An Evidenced-Based Approach to Optimise Age-Care Facility Design for People with Dementia, In Pozo-Menéndez E, Higueras -García E (eds.), Urban Design and Planning for Age-Friendly Environments Across Europe: North and South

PLEA 2024 WROCŁAW
(Re)thinking Resilience

Transforming transportation infrastructure into inclusive spaces

Sustainable urban revitalization in line with the New European Bauhaus ambitions

AGATA WOŹNICZKA[1] BARBARA WIDERA[1]

[1] Architecture Faculty, Wrocław University of Science and Technology, Wrocław, Poland

ABSTRACT: The aim of this paper is to explore the potential of transforming transportation hubs into high-quality public spaces with ambition to strengthen both local communities and sustainable development of urbanized areas. The research address such issues as scarcity of emerging public spaces in cities all over the world resulting from limited public resources and rapid transformation of existing green areas into new housing estates, parking lots or commercial developments. Recognizing the need to ensure the proposals' multi-threaded and multifunctional character, the authors utilize the New European Bauhaus Compass as a research tool. This political instrument not only audits the current state of selected case studies but also shapes the redesign guidelines. The analysis of chosen sites demonstrated the effectiveness of transforming transportation hubs into public spaces that support public engagement. The multi-directional New European Bauhaus design framework proves to be an effective approach in addressing formal, functional, societal, and economic challenges in contemporary cities. The research proves that development of a climate-resilient city aligned with New European Bauhaus ambitions is achievable by identifying and strategically utilizing underestimated resources, such as transportation infrastructure, as potential public spaces.
KEYWORDS: New European Bauhaus, NEB Compass, Public Space, Public Infrastructure, Sustainable Mobility

1. INTRODUCTION

Political programs and bottom-up initiatives emphasize the role of high-quality public spaces in strengthening both local communities and sustainable development of urbanized areas. Conversely, limited public resources and rapid transformation of existing green areas into new housing estates, parking lots or commercial developments, result in scarcity of emerging public spaces in cities all over the world. Even though there is a tendency to group the elements of functional program into multifunctional layouts, such programs are rarely continued outside one typology or merged with the surrounding areas. There is a need for trans-functional compositions, so that the urban tissue is truly multi-threaded and effective in terms of providing both an efficient infrastructure and inclusive public spaces. The literature review revealed a research gap related to societal inclusiveness and sustainability of transit infrastructure which typically represents an important part of contemporary cities, but is seldom perceived as attractive, safe and welcoming [1-4].

In the search for available spaces in cities that can be transformed into accessible, welcoming and inclusive areas serving society, the authors focus on transportation hubs as a functional typology. Already effective in terms of programmatic layout, the selected spatial typology – by being enriched with additional forms, functions and working methodologies – has a potential of becoming a multi-threaded public space.

To guarantee most versatile public characteristics, the chosen infrastructure type is analysed in line with the New European Bauhaus (NEB) ambitions. This particular initiative has been chosen because it responds to the awareness, needs and aspirations of 21st century citizens. 'Beautiful, Sustainable, Together' values established the basis for the transformation strategy, while looking for a multi-faceted approach to design. The research presented in this paper was carried out for the two transportation hubs in Warsaw (Poland): Bemowo and Olszynka Grochowska. The hubs vary in novelty and multi-modality, size, importance in the municipal context and the status. While Bemowo is a newly-transformed transportation hub in a centre of the busy housing estate and includes a metro station, Olszynka Grochowska is a modest station that lacks any public characteristics, but has a potential of becoming a vibrant local centre. The two hubs were chosen because of their contrasting features, so that the research method is tested for varying entry characteristics. Furthermore, because of the adverse case studies' selection, the obtained results cover a wider range of applications, advocating for multifunctional urban spaces of different characteristics and socio-cultural basis.

2. METHOD

2.1. The NEB Compass as a research tool

In order to analyse the selected sites in accordance with the NEB ambitions the authors employed the New European Bauhaus Compass [5] as both the analysis tool and the re-design framework. Chosen Warsaw transportation hubs were analysed with the NEB Compass. While several existing assessment frameworks, guidance and recommendations, including 'Towards a Shared Culture of Architecture' [6], 'The Davos *Baukultur* Quality System' [7] or 'European quality principles for EU-funded interventions with potential impact upon cultural heritage: Main Recommendations & Selection Criteria' [8] were carefully studied, the NEB Compass was selected as the most relevant tool capturing the ethos of contemporaneity. While the assessment process generated site-specific design guidelines for selected case studies, the ultimate purpose of the study was to explore the general potential of transportation hubs revitalisation and their transformation into contemporary public spaces that promote high levels of social acceptance, beauty understood as an enriching experience, inclusiveness, safety and climate resilience [9]. Furthermore, applying a review tool as the design-support framework helped diagnosing the revitalization potential and showed directions for rehabilitation.

This diagnosis strategy is graphically summarized in Figures 1 and 2, where the NEB Compasses present both the existing situation and the ambitions of target, yet realistic revitalization. To generate the presented graphs, data gathered from official information sources and an on-site surveillance was put into a structured table, which was prepared by the authors on the basis of the NEB Compass framework.

2.2. Analysis of transportation hubs using NEB Compass

After filling the assessment table, the SWOT analysis performed in a consecutive phase helped us to describe the existing characteristics (sections: Strengths and Weaknesses) and identify design and organizational proposals (sections: Opportunities and Threats). The results directed the authors towards possible revitalization solutions and, therefore, indicated the potential for a multi-threaded urban renewal of transportation hubs. Even though the process was conducted for specific locations, is was concluded that the similar approach can be applied across the whole typology being the subject of this research.

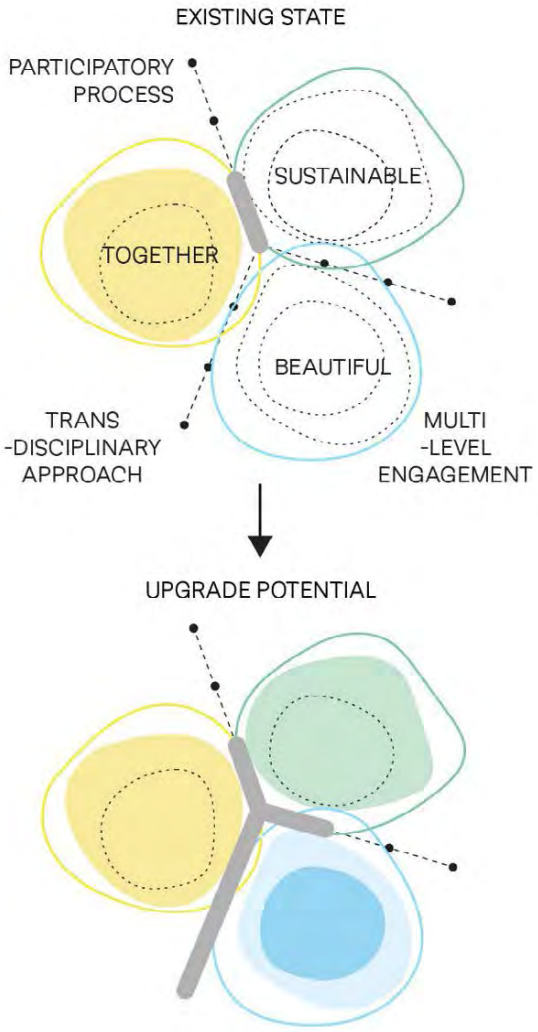

Figure 1: The New European Bauhaus Compasses for Bemowo transportation hub, presenting the existing state and the upgrade potential (based on [5]).

To summarise the process the authors upgraded the existing levels of NEB ambitions and working principles, which was followed by developing the recommendations that were later transformed into rendered visions of the future city. Those exemplary design solutions are presented as sketches in Figures 3-7. These drawing demonstrate how specific target ambitions from the NEB Compass are translated into site-specific holistic renovation projects or designer add-ons.

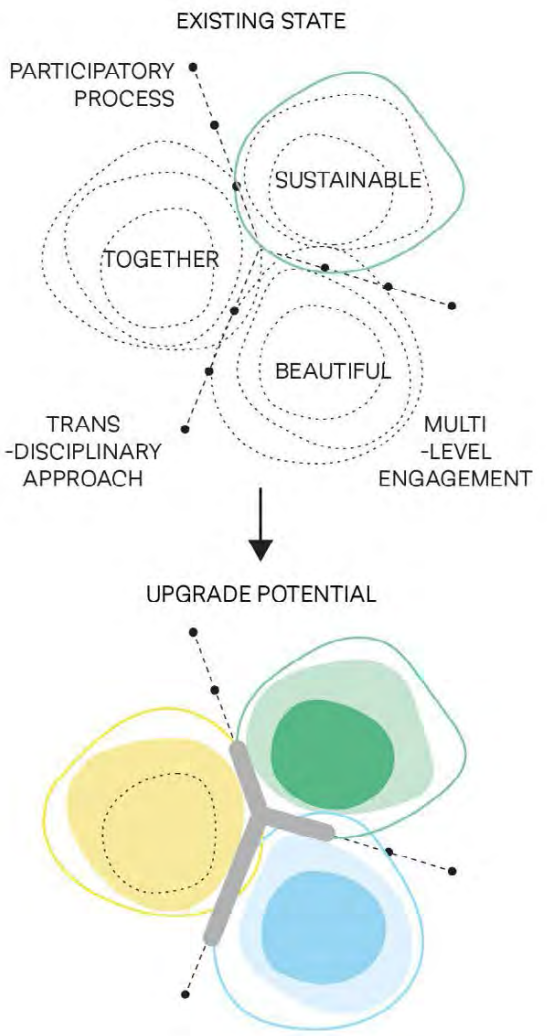

Figure 2: The New European Bauhaus Compass for Olszynka Grochowska transportation hub, presenting the existing state and the upgrade potential (based on [5]).

In the Bemowo transportation hub, the design proposals (Figures 3,4,5) emphasize the enhancement of sustainability and incorporation of nature-based solutions. These suggestions carefully acknowledge the recency of the performed revitalization of the area by introducing design plug-ins into the newly-completed volumes. Eco-conscious retrofitting becomes a leitmotif of a Bemowo hub revitalization. Additionally, the authors define both formal and programmatic adjustments of the existing architectural design to facilitate the introduction of the NEB values of beauty and inclusivity. Such a strategy can enhance locality as well, creating a unique public space in the city tissue.

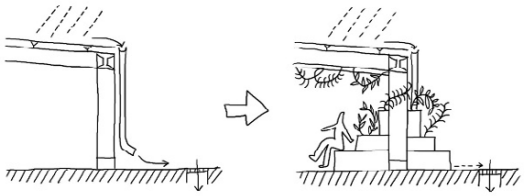

Figure 3: Proposal to improve the existing canopy and expand its functionality by capturing rainwater, introducing a rain pot / rain garden and supplementing the structure with seating (image by Authors).

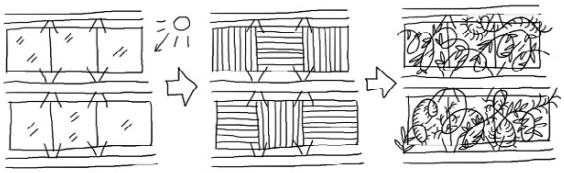

Figure 4: Proposal to improve the canopy and provide shade by applying graphics, additional grate or planting climbing greenery (image by Authors).

Figure 5: Complementing the empty and inefficient covered space with small architecture objects and design solutions promoting sustainability (image by Authors).

Conversely, at the Olszynka Grochowska station, the recommendations focus on using design to revitalize the social structure and strengthen community bonds. This case study adheres to NEB guidelines, emphasizing the expression of formal and material locality while seeking beauty through enriching experiences.

Through the utilization of the terrain reserve and the implementation of site-specific, tailored architectural projects, along with thoughtful arrangement of surrounding greenery, the authors successfully transform an undefined site area into an open-air local centre characterized by a distinctive formal language (Figure 6) and effectiveness, both socially and programmatically. Moreover, the terrain serves a dual purpose, not only enhancing local urban biodiversity but also effectively mitigating communication noise from the upcoming trains, as illustrated in Figure 7.

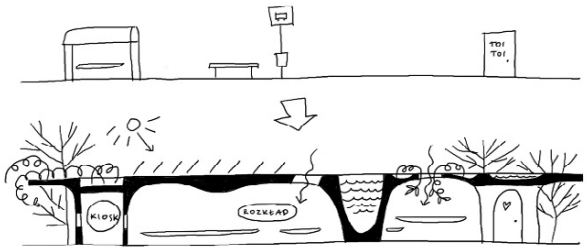

Figure 6: Linear stop - public pavilion instead of disjointed elements and fragmented landscape (image by Authors).

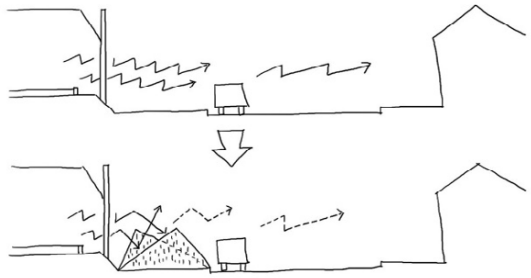

Figure 7: Proposal to establish an above-ground green linear acoustic barrier along Makowska Street, where it is impossible to plant trees because of the underground network infrastructure (image by Authors).

The article delves into the transformative potential of harnessing the New European Bauhaus Compass for an in-depth examination of existing transportation hubs, subsequently crafting precise design recommendations. Through the exploration of two carefully selected case studies, each employing diverse design solutions and adhering to distinct themes, the article compellingly argues for the effectiveness of the New European Bauhaus Compass in evaluating a range of sites and establishing bespoke revitalization guidelines. The cases not only serve as practical examples but also underscore the adaptability of the NEB Compass in addressing the unique characteristics of different locations.

Moreover, the article posits that the conversion of existing transportation hubs into public spaces, guided by the principles of the New European Bauhaus, is not merely a theoretical concept but a feasible and worthwhile avenue for research. The authors believe that such transformations hold promise not only for contributing to sustainable urban revitalization but also for enhancing the overall management of urban assets. By contemplating the intersection of design innovation and sustainable urban development, the article advances the discourse on the multifaceted role of transportation infrastructure in shaping vibrant and resilient urban environments.

3. RESULTS

The authors noted that even though there are multiple examples of multidisciplinary public spaces, a challenge to create contemporary urban spaces using interdisciplinary process and employing a trans-typological layout is often overlooked. Additionally, less evident functional mergers are not commonly explored. In response, the authors advocate for the adoption of one of the New European Bauhaus model working methods – trans-disciplinary collaboration. This approach aims to ensure both formal and programmatic innovation in urban planning.

Through trans-disciplinary collaborations, the authors contend that formal and programmatic innovation can be achieved by merging seemingly contradictory functions, diverse effectiveness goals, opposite intensity levels, or conflicting target users within new multidisciplinary program compositions. The research, therefore, focuses on analysing and comparing various solutions to identified problems, utilizing the NEB Compass as a tool to audit the project's alignment with the initiative's ambitions, values, and exemplary working methods.

The authors observed that when applied with a focus on spatial, environmental, and social enhancement, the NEB Compass guides urban space revitalization toward multifunctional and multi-directional solutions. A noteworthy aspect of this approach is that the assessment process, detailed and multi-faceted, narrows down several potential solutions, transforming specific limitations into project benchmarks. Consequently, each proposal derived from the NEB Compass analysis is bespoke, tailored to address the unique challenges and opportunities presented by the specific urban context.

Furthermore, completed case studies covering expertly converted, popular urban infrastructure [10, 11] were analysed with NEB Compass for comparative purposes. Then, the characteristics that allowed for trailblazing the new interdisciplinarity of public domain were identified. These features showed how to utilize transport infrastructure to realize NEB postulates, within the chosen sites benefitting from a design intervention and fulfilling the initial intention of a transformation from an urban groundwork into public space. Moreover, the study diagnosed

transportation hubs as areas of limited interest and attractiveness. To change the state of the play the design framework was developed and tested for the places covered by the research. Using the NEB Compass for an audit of purely utilitarian functional areas resulted in rendering a new typology of a public space and creating a site-specific revitalization project that targets various architectural, social, environmental and organizational challenges.

What is more, the NEB-driven analytic exercise proved valuable in aspects of both academic research and design implementation.

As a reminder, Figures 8 and 9 depict the current state of the Bemowo transportation hub and Olszynka Grochowska stop, emphasizing their contrasting challenges. In the recently renovated Bemowo site [Figure 8], there is a notable absence of both an enriching experience for visitors and the incorporation of sustainable solutions to mitigate climate impact. Conversely, the latter case study [Figure 9] exhibits deficiencies in terms of effectiveness, quality, and overall urban definition.

Figure 8: Desolated and inefficient architecture of a newly renovated Bemowo hub (photo by the authors).

Figure 9: Disorganized and redundant area of the Olszynka Grochowska stop (photo by the authors).

The research findings suggest that an effective communication area has the potential to evolve into a distinctive public space when supplemented with additional recreational or climate-change-mitigating features. This transformation is notably exemplified in the case of the Bemowo hub, where the revitalization could turn it into a local center within a district lacking a central public space. Similarly, at the Olszynka Grochowska stop, the potential for individual character emerges through the transformation of typical urban street furniture.

Moreover, the research, supported by the NEB Compass, played a crucial role in defining the revitalization themes for the two sites: sustainable retrofitting for the Bemowo hub and Innovative Locality for Olszynka Grochowska. In conclusion, the results underscore the effectiveness of the employed method in ensuring distinctive character and trans-program multifunctionality for these urban spaces.

4. CONCLUSIONS

The research revealed that the most disquieting issues related to the analysed areas that limit their potential for being sustainable, beautiful and inclusive spaces concern:

- One-way, Monofunctional Perception: The space's manager perceives the hub in a one-way, monofunctional manner, leading to the adoption of purely utilitarian design solutions and a functional layout that may limit the space's aesthetic and social potential,
- Quantitative Effectiveness Metrics: There is a tendency to measure the effectiveness of the hub solely based on quantitative characteristics, overlooking the qualitative aspects of the experience and the impact on the urban biotope. This narrow focus may neglect the nuanced qualities that contribute to the overall well-being and vibrancy of the public spaces,
- Lack of Community Engagement: Limited or insufficient involvement of the local community in the design and decision-making processes can hinder the creation of spaces that truly reflect the needs and preferences of the people who use them,
- Insufficient Recognition of Terrain Reserve Potential: The current perception of the existing and often expansive terrain reserve does not acknowledge its potential as a temporary site, for instance, until further infrastructure development utilizes the reserve. This overlooks the possibility of leveraging the terrain reserve as a more intricate urban biotope area in the interim,

- Neglect of Cultural Heritage: Failure to recognize and integrate elements of cultural heritage into the infrastructure design may result in a loss of identity, undermining the potential for creating spaces that resonate with the local community,
- Short-Term Planning Perspective: Overemphasis on short-term planning without considering long-term sustainability may lead to design choices that lack resilience and fail to adapt to evolving urban needs and environmental challenges.

These issues can be overcome with reformulating the programmatic scope of typology and rearranging the structure of hub's both design and governance team.

On the other hand, the most promising opportunities for transportation hub revitalisation include:

- Innovative Public Functions: The potential exists to introduce innovative public functions in transit areas without causing disruption,
- Ample Flat Surfaces for Eco Solutions: The extensive flat surfaces available provide opportunities for incorporating eco-friendly solutions without compromising the efficiency of transit operations,
- Community-Focused Spaces: Transportation hubs hold the potential to evolve into popular spaces for local communities, given their inherent popularity and centrality,
- Cultural and Artistic Integration: Showcasing local art, cultural installations, and public spaces for community events can transform transportation hubs into vibrant cultural hubs, fostering a formally innovative locality, a sense of place and community identity,
- Safety and Security Enhancements: Implementing advanced yet discreet security measures and, especially, well-lit and easily accessible spaces fosters a sense of safety for passengers, encouraging increased usage of public transportation facilities,
- Community Engagement Initiatives: Involving local communities in the planning and decision-making processes ensures that the revitalized transportation hubs meet the specific needs and preferences of the people they serve. Incorporating external feedback fosters trans-disciplinary program connections.

The ultimate conclusion from the research is that envisioning extended program for sustainable, inclusive and beautiful transportation hubs brings invaluable benefits for the city. Multi-directional NEB design framework allows to effectively address formal and functional challenges of the contemporary city, as well as societal and economic problems.

A development of climate resilient city in line with NEB ambitions is possible if the underestimated resources such as transportation infrastructure as potential public space are identified and correctly targeted.

Recognizing the intricate relationship between urban design and climate resilience underscores the significance of adopting a holistic approach for creating vibrant, resilient, and harmonious urban environments. In conclusion, transforming transportation infrastructure into inclusive spaces emerges as a pivotal strategy for fostering sustainable urban development in alignment with the principles of the New European Bauhaus.

5. ACKNOWLEDGMENTS

This study was possible due to Warsaw grant for doctoral students: Transportation hubs as the elements of public infrastructure that realize ambitions of the New European Bauhaus - multifaceted design guidelines [12].

REFERENCES

1. Hutton, B., (2013). *Planning Sustainable Transport*.
2. Boglietti, S. and M. Tiboni, (2022). Analyzing the Criticalities of Public Spaces to Promote Sustainable Mobility. *Transportation Research Procedia*, 60: p. 172-179.
3. Bertolini, L., (2017). *Planning the Mobile Metropolis Transport for People, Places and the Planet.*
4.Wefering, F., Rupprecht, S., Bührmann, S., and S. Böhler-Baedeker, (2014). *Guidelines. Developing and implementing a sustainable urban mobility plan.*
5. Joint Research Centre, *New European Bauhaus Compass*, [Online], Available: https://www.urbaninitiative.eu/sites/default/files/2022-12/NEB_Compass_V1.pdf [16 May 2023].
6. European Union (2021). *Towards A Shared Culture of Architecture Investing in a High-Quality Living Environment For Everyone*. Report Of The Omc (Open Method Of Coordination) Group Of Eu Member State Experts, Luxembourg: Publications Office of the European Union.
7. Swiss Federal Office of Culture (2021). *The Davos Baukultur Quality System*, Berne.
8. ICOMOS (2020) European quality principles for EU-funded interventions with potential impact upon cultural heritage: Main Recommendations & Selection Criteria. Paris.
9. Semken, S., Butler Freeman, C. (2008) Sense of place in the practice and assessment of place-based science teaching. *Science Education*, November 2008.
10. Park'n'Play by jaja architects, [Online], Available: https://jaja.archi/project/konditaget-luders/ [25 August 2023].
11. *The Cineroleum,* [Online], Available: https://assemblestudio.co.uk/projects/the-cineroleum [25 August 2023].
12. Woźniczka A., (2023). Węzły przesiadkowe jako elementy infrastruktury publicznej realizujące ambicje Nowego Europejskiego Bauhausu – wytyczne do projektowania wieloaspektowego, [Online], Available: DOI: 10.13140/RG.2.2.26166.47680 [16 November 2023].

PLEA 2024 WROCŁAW
(Re)thinking Resilience

Architectural Education – The Case Study

The Living Laboratory of Sustainability

ANNA BAĆ[1], LEA KAZANECKA-OLEJNIK[1]

[1] Wrocław University of Science and Technology, Wrocław, Poland

ABSTRACT: Higher education institutions are currently facing enormous challenges in transforming didactics to meet the needs of a changing world. Teaching and learning methods need to strengthen students' individual value system and give them motivation to change for a better tomorrow. Of particular importance is didactics oriented toward the built, social and natural environment, which must now respond to the 2030 Sustainable Development Goals. A sustainable, adaptive, resilient and regenerative approaches to architecture and urban design require changes in teaching methods. Innovative approach to architectural education should help students find personal mastery and gain skills to share it with the community. The article describes a case study of didactic of tomorrow carried out at the Faculty of Architecture at the Wroclaw University of Science and Technology. The analysed first experimental course was conducted for the 5th semester of the bachelor's degree, and was entitled Architectural Design - Studio Habitat - complex residential structures.
KEYWORDS: Education, Didactic, Sustainability, Architecture

1. INTRODUCTION

Institutions for higher education are currently facing challenges in transforming didactics to meet the needs of a changing world. Teaching and learning methods need to strengthen students' individual value system and give them motivation to change for a better tomorrow. Of particular importance are didactics oriented toward the built, social and natural environment, which must now respond to the 2030 Sustainable Development Goals [1, 2]. A sustainable, adaptive, resilient and regenerative approaches to architecture and urban design require changes in teaching methods to implement them in everyday design. Innovative architectural education should help students find personal mastery and gain the skills to share it with the community.

The article describes a case study of the didactic of tomorrow carried out at the Faculty of Architecture at the Wroclaw University of Science and Technology (FA-WUST). The first experimental course, analysed in this article, was conducted for the 5th semester of the bachelor's degree, in the year 2022/2023, as an *Architectural Design - Studio Habitat - Complex Residential Structures (Studio Habitat*).

In order to find a didactic answer to contemporary issues and help students establish their value system based on sustainability, a concept of *Living Laboratory of Sustainability* (LLoS) was developed as a baseline for the analysed course. LLoS concept adheres to rules guiding a didactic approach as well as a design process. Students and teachers are exchanging knowledge and creating a horizontal organization system where students take part in creating a didactic process and are responsible for their growth during the course. Additionally, external specialists and practitioners are invited to teach during the semester, to incorporate transdisciplinary approach and the Integrated Design Process – IDP [3]. LLoS is based on well-established knowledge and many years of experience of the authors of the course, and is supported by unique needs of a specific group of students. The selected design problem for the course is a real site with development plans supported by the city government. Through those solutions LLoS meets conditions set by current and important university teaching concepts [4] such as Service Learning [5] and Research Based Design.

2. DESIGN CHALLENGE

The course Studio Habitat, is based on the concept of a habitat created in FA-WUST in the 1980s [6]. This idea promotes housing design as an ideal space to live – work – play, with consideration of socio-cultural and spatial conditions, and understanding that architecture influences a human being. Under this condition, mostly intuitive design methods were individually implemented by teachers of the course.

The design task at the time was dedicated to real plots in Wrocław, where students set out to improve the existing environment through creation of a habitat's community.

In 2019, the course's design task was changed and is now dedicated to Saint-Gobain's student competition. Each year the organizer selects a city and together with local authorities prepares a comprehensive design challenge for a selected plot.

Participants are asked to find a creative, architectural answer to real problems through sustainable solutions. Over the years, students' winning designs had a chance of being implemented in development plans for such cities as Dubai, Madrid or Warsaw.

In 2022/2023 participants were asked to create a proposal for revitalization of the Boavista Landfill, part of the Lisbon's urban fabric alongside the river Tag. The existing infrastructure consists of two buildings with a parking lot. The revitalization is supposed to provide new cultural activities complemented by residential functions [7].

According to the task, the area should become a part of the larger city system, a local cultural centre focused on promoting and developing audio-visual art. The challenge was based on three main items. Firstly, one of the existing buildings will become the new Lisbon Video Library, connecting functionally to nearby art schools and the House of Cinema in Bairro Alto. Secondly, the other building will be demolished and, in its place, a multifamily housing with commercial and community services will be provided. Thirdly, the site should become a good place for community development, living, working and leisure.

Baseline for the functional program, maximum and minimum dimensions, as well as volume parameters for the new building were provided by the organiser. Within a given scope certain deviations from the program and parameters were acceptable, depending on the projects unique design.

Organisers created a comprehensive pack of information about the site. Together with Lisbon's urban planners and local authorities they provided guidelines focused on the environmental issue, urban development, sustainability, economic feasibility, users' needs. Creating a proposal based on environmental and energy sustainability, as well as user's comfort, was crucial for this competition.

3. DIDACTIC APPROACH

3.1 Standard design course at FA-WUST

Commonly, design courses at FA-WUST are carried out in groups of maximum 15 people with one tutor. There are usually 2 groups in one classroom. At the beginning students work individually and in later stages of education, also in pairs or small groups.

Throughout the years, design courses lasted 90 hours per semester and were based mostly on individual consultations, with 3-4 evaluations with the whole group. Those classes were supported by 30 hours-long theoretical lecture about architectural design, conducted through "ex cathedra teaching". For Studio Habitat, the lecture referred to creating multifamily housing based on the theory of the habitat. Both types of coursers were dedicated to sustainable design in a limited way.

Since 2019, after a reform of standards of teaching architecture [8], design courses began to last 195 hours per semester, and incorporate the design process as well as the lecture part.

3.2 Standard of the LLoS course

Innovation of the LLoS is encompassed in five new didactic approaches compared to the common course:

1. Organisation of the course
2. Structure of each class
3. Design tools
4. Sustainable approach
5. Group dynamics.

3.2.1 Organisation of the course

The LLoS was conducted for two design groups by 2 main teachers and 8 experts of various specialties. External experts were not commonly a part of the didactic team. They were selected and introduced to the LLoS at the discretion of the main teachers.

Guest specialists were: sustainability and residential design practitioner, Smart City and time management specialist, HVAC and MEC engineer, structural and technical specialist, LCA and energy efficiency specialist, landscape architect, inclusive design specialist. Guests were instructed about LLoS didactic approach and way of working.

The course lasted one semester, that is 15 weeks and 195 hours, with classes twice a week, each 6 or 7 teaching hours long. Out of a total of 30 meetings, 10 were given to selected specialists and the rest was led by the two main teachers. The semester began with strategies enhancing good group dynamics: getting to know each other, defining roles and responsibilities, integrating the team and ensuring open communication, which are described below. The work ended with a final ceremony with presentation of the design to invited guests, e.g. other students, parents.

The course was attended by 28 students, who formed 14 pairs. Each pair was working on the same task, and based on the same entry data from the competition organisers, followed by their own additional research. Each group individually developed their own goal and design strategy.

3.2.2 Structure of each class

Each class followed similar organisation plan and a time schedule. Every week students received information booklets, reading list to familiarize themselves with before the next meeting. Classes started with a short lecture based on upside down learning, and a Q&A session regarding their reading materials. Next, students received a design task, that needed to be completed within an assigned time frame. At the end of the class, results of the tasks were presented and discussed. This organisation

allowed to spend time actively and productively during classes. Also, interactive teaching and learning methods were used (detailed description in subsection 3.2.5 – A).

3.2.3 Design tools

In the fifth semester, students use computer programs in their design process. For the LLoS, students are required to start with hand drawings and physical models at the initial, conceptual stage.

Furthermore, the task for the competition required deep analysis, rigorous design based on sustainable solutions, providing simulations and calculations proving effectiveness of the introduced solutions. Learning to use computer tools for these purposes is not a part of the bachelor's studies at FA-WUST. Hence, classes on how to use such programs as One Click and energy simulators were introduced as a part of LLoS curriculum, thanks to Saint-Gobain's input.

Methods used to present projects also extended beyond the basic drawings and boards preparation. As part of the competition recording of a presentation was required and for that students created slide presentations as well as movies and animations.

3.2.4 Sustainable approach

The authors' didactic focused on an interdisciplinary and sustainable approach to architectural and urban design [9]. Special attention was dedicated to the users need's and their comfort (Table 1). It was key from teachers' perspective as well as for the topic of the competition.

Table 1: Key didactic topics and related strategies, worked through during the course

	Key topic	Key didactic strategies
S	sustainability	- 10 fields approach - research based design - analysis - verification - diagrams
U	users' needs	- Service Learning

Sustainability (distinguished in the paper with letter S, as per Table 1) is understood as creating the best possible space for living while reducing the negative environmental impact and ensuring the lowest economic cost throughout the building's whole life cycle. As a main strategy, students learned what a sustainable design is based on the author's 10 fields approach: energy, materials, waste, water, greenery, transport, cost, place, community and process [10]. By understanding those crucial aspects, they could easily identify which design solutions they can incorporate in their own concept.

Furthermore, research based design was a crucial part of the LLoS and replaced intuitive design methodology. Students carried out the analysis stage and in-depth research in pairs in order to understand environmental, landscape, cultural, social and functional conditions of the chosen plot. This strategy allowed them to fully comprehend their design context, make informed design decisions as well as find a "clue" – key element of their project.

Saint-Gobain's competition, as a design challenge, has facilitated didactic goals for the course very well. Organizers offered detailed information regarding environment, local history and future plans for a chosen plot. They have also set precise sustainability requirements. Students had to provide user's comfort requirements such as thermal, visual and acoustic comfort and appropriate air quality. They also needed to achieve low CO_2 emissions and low carbon footprint. For those purposes, organizers offered free access to programs such as One Click, which helped with verification of effectiveness of incorporated solutions. This way, concepts became measurable and easier to comprehend.

Students were also tasked with preparing a set of schemes. They represented how 10 fields approach works in their project. They created energy diagrams, showing building's energy, air flow, sun control during day and night, for summer and winter, as well as water management and other schemes. The visual representation supported students' understanding of incorporated solutions.

The idea of sustainability encompasses community centred design, where understanding and incorporating needs of people are crucial to achieve effective spatial solutions. Users' needs (U, as per Table 1) were important for students' projects, the topic was not theoretical but grounded in a real place and community. Students prepared questionnaires for local people, created scenarios relating to how users will live in a designed space. They also addressed issues of local flora and fauna. Those methods helped in incorporating Service Learning in the curriculum.

3.2.5 Group dynamics

LLoS is on the one hand based on didactic approaches 1-5, which are described above. On the other hand, the laboratory is based on innovative pedagogical approaches. Their synergy creates author's concept of didactic of tomorrow based on group dynamic [11]. The authors have been working for years on methods of cooperation with students, supporting their activity and involvement. Students have a possibility to co-create the course, take full responsibility for their own development process, as designers and as people.

At the beginning of the course the introductory, open interview was conducted with the whole group to find out about students' previous educational experiences, their needs and potential issues. Two general questions were asked to prompt a discussion:

- What issues/problems did you encounter during your educational process?

- What were the most positive aspects of your educational process?

In the discussion, a set of potential threats and opportunities was pointed out (Table 2). They were issues common for the whole group, or at least commented on by several students, rather than being individual experiences.

Table 2: Key group issues, based on main threats (-) and opportunities (+), worked out during the course

	Key group issues	Key didactic strategies
A	choice: - inability to make a choice - difficulty to begin drawing + having many options	- quick design tasks reviewed at the end of each class - time management - semester schedule
B	hierarchy: - fear of hierarchy + feeling one's own value	- creating community - upside down learning - research based design
C	criticism: - inability to offer or receive constructive criticism - strong criticism - lack of open communication + having strong opinions and passions	- discussion at the end of every design task - open and nonviolent communication
D	cooperation: - lack of openness and cooperation + having a chance to work together	- working in pairs - working in bigger groups of a few pairs - working all together

As a result of the interview, 4 main groups of didactic interest were discussed (distinguished with letter A-D, as per Table 2). Those issues are mostly common among students, nevertheless discussing them helped tailoring the well-established didactic process to this particular group of students. The interview led to the creation of didactic strategies outlined below.

The first important aspect (A) is related to students wanting to have an impact. They see that they have many options and possibilities but it can sometimes be overwhelming. As a result, it is difficult for them to make a choice or start the design process. Those abilities are crucial to conduct a professional work.

In order to help students make a choice and begin their design, a set of rules was established. Each class included short design task that needed to be finished and discussed by the end of it. They were obligated to quickly start and encompass their ideas about subsequent parts of architectural design. The short "bursts" of a design process were planned as easier to manage than looking at a project in its entirety.

Furthermore, at the beginning of the semester, plan for the whole course was laid out, including design steps and specialists' visits. Every part was planned within a time limit. Usually, a design task took about 2-3 hours, presentation of an idea 5 min., short discussions 15 min., and group project analysis 45 min. per project. Over time, students became more and more proficient in finishing tasks within a time limit.

The second issue (B) is related to the fear of authority. Students claimed that at times they felt like they needed to do what the professor said and were not sure what they thought themselves. Moreover, they were unable to make their own decisions. This idea of hierarchy led to their believes and concepts being dismissed, and they wanted to work on that. This particular issue was very important to students, more than the authors have initially anticipated.

As a response, achieving a sense of community was the goal for the group development. It was important to create mutual trust and respect, to ask questions and encourage further research for design, rather than solve problems for (or instead of) students. By asking questions and requiring to deepen the research, the upside-down learning was established. Students were explaining to teachers the rules by which their projects were created, and teachers guided them through results of their analysis.

The next major issue (C) was connected to giving and receiving comments about design. It is a crucial ability for architects to honestly talk about architecture and the way it shapes the society. On the one hand, students have strong opinions and believes, but on the other, they find it hard to communicate in a constructive way without hurting, or feeling hurt by, their colleagues. As a result, communication is often limited and dishonest.

Working on the ability to discuss projects was based on open and nonviolent communication [12], which means to enhance empathy in a conversation. The goal of discussion is not to be right, but to understand what guides the other person, to empathise with their way of thinking, and then offer one's won perspective. On the design level, this leads toward searching for reasoning behind design decisions, grounding them within rules of sustainability, users' needs and specificity of a surrounding. Thus, answering a question "why is something created in a certain way" is vital for making design decisions.

Furthermore, to help students practice open communication, each class contained an individual consult, discussions in pairs or bigger groups, as well as short presentations. This repetitive practice was intended as a key to get proficient and uninhibited with receiving and providing constructive criticism.

The last key subject, cooperation (D), is related to the previous one. Up to this point in students' architectural education they were often working alone, or were not satisfied with their previous experiences. Cooperation is basis for architectural design process, hence it is crucial to work on this ability during studies.

As a baseline, students worked on the course's project in pairs and discussed it with teachers. However, they also consulted each other's projects, and had group tasks (dedicated to 2 or 3 pairs). This was intended as a way to help them bond, and as an encouragement to support each other, even though they were all trying to win the same competition. They all influenced each other's designs and creative processes.

As the result of an interview the Code of work for this particular group of students was created. It motivated the group to actively respond to their own needs and issues. Code included two main parts:

1) Mission and vision for the semester, willingness to seize opportunities, with such goals as: "being proactive", "having an impact", "being responsible for the planet".

2) Acceptance and willingness to act upon discussed threats.

4. RESULTS

The effectiveness of the LLoS was assessed in three ways. Both, teachers' and students' opinions were taken into account, as well as results of the competition.

The students' opinion about the course was surveyed at the end of the semester using a multi-criteria questionnaire. The survey consisted of 42 items: 12 questions based on the scale from 1 to 5, and 30 open questions for long responses. All students participated in the survey.

Students generally appreciated the concept of the Living Laboratory of Sustainability. They felt that new organization of the course, group dynamics, routine design tasks, keeping time limit, expert visits and open communication were crucial for their development during the semester.

(S) Students pointed out that gathering knowledge related to sustainability and IDP was the most important for them during this course. Even though they see the importance of sustainable design the topic is not usually included in course's curriculum, hence those classes were quite unique for them, and they would like that topic to be included more often.

(D) Another crucial aspect for students was related to different types of cooperation. They worked in pairs, in small and bigger groups, had individual and group consultations. Even though they found individual consults to be very important, they noted that cooperation in smaller groups (2-3 pairs) was very helpful in their design process. They preferred it to working as a one whole group, where too many people were involved.

(C)(B) Most of the students were very satisfied with open communication and working above hierarchy during classes. The results show that the most limiting factor for students was „the fear of authority". This was related to the anxiety that arises while debating with an authority figure, someone who is believed to "know everything better". Such situations were noted by students and were connected with receiving a limiting response to their inquiries, e.g. not discussing an idea because it is deemed not appropriate by the person with authority. Instead, the preferred and well-received action was to try to find a possible solution based on emphasising positive aspects of an idea, and helping students to overcome their shortcomings themselves.

(A) Time management, immersive process with a fast pace helped students with decision making. They appreciated this kind of approach and it supported their design process.

From authors perspective the LLoS was crucial for that semester's success. Through implemented didactic strategies – both didactic topics and issues – students achieved well working sustainable designs dedicated to site-specific needs. In general, the group has created a well-organized community (Table 3).

Table 3: Teachers' assessment of incorporated strategies

	A	B	C	D	S	U
AVG.	4,0	5,0	4,0	4,5	4,5	4,0

The biggest difficulty throughout the semester was sometimes keeping within the assumed time limit. It helped organising the workflow but it also required a lot of focus and dedication.

Another difficulty was implementing methodology by all guest specialists, not only the main teachers. This required a lot of people following the same guidelines. The main structure of each class was much easier to implement by many different people than following didactic strategies regarding hierarchy, open communication and keeping group dynamics. It was harder for specialists, who come only ones or twice during the whole semester, to make the same connection with students as full-time teachers. Because of that open communication have not always been easily formed.

The structure of this course allowed students to improve in areas set out at the beginning. Most

students got a very good understanding of sustainability and how to shape it through architecture. The most notable improvement was visible regarding understanding one's own value and getting confidence as architectural designers.

The results of the implementation of the LLoS were highly satisfactory, 4 projects were among the Top 10 qualified for the national stage of the competition. 37 projects from all over Poland were sent at this stage. One of this course's projects won the national stage, and won the student's prize at the international finals in Lisbon (Figure 1).

Figure 1: Project Yellow, visualisations, top – street view, bottom – front elevation, authors: Magda Kazulak, Konstancja Staniecka.

5. CONCLUSION

Teaching in the approach of the Living Laboratory of Sustainability is based on finding each student's own mastery, as well as helping them understand sustainable design as a part of a larger process of creating the built, social and natural environment. This is determined by 3 main aspects: exploring students' own value system, training their communication skills, practicing their time management skills. Throughout the course, those aspects seemed to be most crucial and most challenging at the same time.

The LLoS gave students the opportunity to understand sustainability issues most successfully through working together on a non-theoretical project, incorporating Research Based Design. Those facets proved to be fundamental in gaining knowledge on how a site specific architecture should be build. Without that basis, searching for a concept, comprehending sustainability and making conscious design decisions proved to be difficult for students.

The biggest challenges of the course were to invite students to open communication, and to taking full responsibility for their own development process, as designers and as people. It proved to be a difficult but positive experience that offered a lot of diverse wisdom and allowed them to learn how to honestly discuss architectural concepts, problems and solutions. The process also showed that this way of working and introduced didactic changes do not suit all teachers, some prefer different approaches. The formed concept needs to be explored further and continued.

ACKNOWLEDGEMENTS

We want to thank all the students, specialists and professionals participating in the Living Laboratory of Sustainability for willingness to take on the challenge of this collaboration.

REFERENCES

1. Architectural Education For A Sustainable Future, [Online], Available: https://uia2023cph.org/program/architectural-education-for-a-sustainable-future/ [13 Dezember 2023].
2. Savic, M. and Kashef, M., (2013). Learning outcomes in affective domain within contemporary architectural curricula. International Journal of Technology and Design Education, 23: p. 987–1004.
3. Kalpkirmaz Rizaoglu, I. and Voss, K., (2020). Building Performance Simulation to Simulate Architectural Early Design: Integrating Design and Simulation, PLEA 2020: p. 1525-1530.
4. Nicol, D. and Pilling, S. (Eds.), (2005). Changing architectural education: Towards a new professionalism. Taylor & Francis.
5. Bringle, R. and Hatcher J., (1996). Implementing Service Learning in Higher Education. The Journal of Higher Education, 67(2): p. 221-239.
6. Bać, Z. (Ed.), (2018). Theory of Habitat. Oficyna Wydawnicza Politechniki Wrocławskiej.
7. Contest Task by Saint-Gobain, Architecture Student Contest 2023, Lisbon, Portugal, [Online], Available: http://architecture-stuednt-contest.saint-gobain.com/ [20 August 2023].
8. Rozporządzenie Ministra Nauki i Szkolnictwa Wyższego z dnia 18 lipca 2019 r. w sprawie standardu kształcenia przygotowującego do wykonania zawodu architekta, [Online], Available: https://isap.sejm.gov.pl/isap.nsf/DocDetails.xsp?id=WDU20190001359/ [13 Dezember 2023].
9. Auad Proenca, M., Balducci, A., Cognetti De Martis F., (2022). The role of universities on forming social inclusive and sustainable environments, PLEA STGO 2022: p. 94-99.
10. Bać, A., (2016). Zrównoważenie w architekturze. Od idei do realizacji na podstawie doświadczeń kanadyjskich. Oficyna Wydawnicza Politechniki Wrocławskiej.
11. Forsyth, D., (2019). Group Dynamics. Cengage Learning.
12. Rosenberg, M. B., (2003). Life-Enriching Education. Nonviolent Communication. PuddleDancer Press.

WUST Publishing House prints can be obtained
via mailorder: zamawianie.ksiazek@pwr.edu.pl;
www.ksiegarnia.pwr.edu.pl

ISBN 978-83-7493-275-2